













TS  
200  
15



THE JOURNAL OF THE INSTITUTE OF METALS





Digitized by the Internet Archive  
in 2024



# THE JOURNAL OF THE INSTITUTE OF METALS

VOLUME LXXXII

1953-54

EDITOR

N. B. VAUGHAN, M.Sc.

*The Right of Publication and of Translation is Reserved.  
The Institute of Metals is not responsible for the statements  
made or for the opinions expressed in the following pages.*



LONDON

PUBLISHED BY THE INSTITUTE OF METALS

4 GROSVENOR GARDENS, S.W.1

1954



## PAST-PRESIDENTS

Sir WILLIAM HENRY WHITE, K.C.B., LL.D., D.Eng., Sc.D., F.Inst.Met., F.R.S., 1908–1910 (*deceased*).

Sir GERARD ALBERT MUNTZ, Bart., 1910–1912 (*deceased*).

WILLIAM GOWLAND, A.R.S.M., F.R.S., 1912–1913 (*deceased*).

ALFRED KIRBY HUNTINGTON, A.R.S.M., 1913–1914 (*deceased*).

Engineer Vice-Admiral Sir HENRY JOHN ORAM, K.C.B., F.Inst.Met., F.R.S., 1914–1916 (*deceased*).

Sir GEORGE THOMAS BEILBY, LL.D., D.Sc., F.R.S., 1916–1918 (*deceased*).

Sir HENRY CORT HAROLD CARPENTER, M.A., Ph.D., D.Sc., D.Met., A.R.S.M., F.Inst.Met., F.R.S., 1918–1920 (*deceased*).

Engineer Vice-Admiral Sir GEORGE GOODWIN GOODWIN, K.C.B., LL.D., F.Inst.Met., 1920–1922 (*deceased*).

LEONARD SUMNER, O.B.E., M.Sc., J.P., F.Inst.Met., 1922–1924 (*deceased*).

THOMAS TURNER, M.Sc., A.R.S.M., F.Inst.Met., 1924–1926 (*deceased*).

Sir JOHN DEWRANCE, G.B.E., F.Inst.Met., 1926–1928 (*deceased*).

WALTER ROSENHAIN, D.Sc., B.C.E., F.Inst.Met., F.R.S., 1928–1930 (*deceased*).

RICHARD SELIGMAN, Ph.nat.D., F.Inst.Met., 1930–1932.

Sir HENRY FOWLER, K.B.E., LL.D., D.Sc., 1932–1934 (*deceased*).

HAROLD MOORE, C.B.E., D.Sc., Ph.D., F.Inst.Met., 1934–1936.

WILLIAM ROBB BARCLAY, O.B.E., F.Inst.Met., 1936–1938 (*deceased*).

CECIL HENRY DESCH, D.Sc., LL.D., Ph.D., F.Inst.Met., F.R.S., 1938–1940.

The Hon. RICHARD MARTIN PETER PRESTON, D.S.O., 1940–1942.

Lieut.-Colonel Sir JOHN HENRY MAITLAND GREENLY, K.C.M.G., C.B.E., M.A., F.Inst.Met., 1942–1944 (*deceased*).

Sir WILLIAM THOMAS GRIFFITHS, D.Sc., 1944–1946 (*deceased*).

Colonel Sir PAUL GOTTLIEB JULIUS GUETERBOCK, K.C.B., D.S.O., M.C., T.D., D.L., J.P., M.A., A.D.C.,  
F.Inst.Met., 1946–1948 (*deceased*).

Sir ARTHUR JOHN GRIFFITHS SMOUT, J.P., F.Inst.Met., 1948–1950.

HUBERT SANDERSON TASKER, B.A., F.Inst.Met., 1950–1951.

ALFRED JOHN MURPHY, M.Sc., 1951–1952.

COLIN JAMES SMITHELLS, M.C., D.Sc., 1952–1953.

FRANK CHARLES THOMPSON, D.Met., M.Sc., 1953–1954.



# COUNCIL AND OFFICERS

FOR THE YEAR 1954-55

## PRESIDENT

S. F. DOREY, C.B.E., D.Sc., F.R.S.

## PAST-PRESIDENTS

Professor A. J. MURPHY, M.Sc.

C. J. SMITHELLS, M.C., D.Sc.

Professor F. C. THOMPSON,  
D.Met., M.Sc.

## VICE-PRESIDENTS

G. L. BAILEY, C.B.E., M.Sc.

Major C. J. P. BALL, D.S.O.,  
M.C.

MAURICE COOK, D.Sc., Ph.D.

L. B. PFEIL, O.B.E., D.Sc.,  
A.R.S.M., F.R.S.

Professor G. V. RAYNOR, M.A.,  
D.Phil., D.Sc.

Major P. L. TEED, A.R.S.M.

## HONORARY TREASURER

J. C. COLQUHOUN, M.B.E.

## ORDINARY MEMBERS OF COUNCIL

ALFRED BAER, B.A.

W. A. BAKER, D.Sc.

N. I. BOND-WILLIAMS, B.Sc.

K. W. CLARKE

E. R. GADD

The Hon. JOHN GRIMSTON, M.P.

R. D. HAMER, B.Sc.

N. P. INGLIS, Ph.D., M.Eng.

IVOR JENKINS, D.Sc.

E. H. JONES

A. G. RAMSAY, Ph.D., B.Sc.

CHRISTOPHER SMITH

H. SUTTON, C.B.E., D.Sc.

W. J. THOMAS

G. P. TINKER, M.Sc.

## EX-OFFICIO MEMBERS OF COUNCIL

S. S. SMITH, M.Met.

(*Birmingham Local Section*)

J. C. CHASTON, B.Sc., Ph.D., A.R.S.M.

(*London Local Section*)

B. T. PARKER, B.Sc., Ph.D.,

A.R.S.M.

(*Oxford Local Section*)

G. MacDONALD, O.B.E., B.Sc.

(*Scottish Local Section*)

W. R. MADDOCKS, B.Sc., Ph.D.

(*Sheffield Local Section*)

J. S. WALTON

(*South Wales Local Section*)

---

## REPRESENTATIVES OF OTHER BODIES

The following, in accordance with Article 32, represent Government Departments and allied societies at Council meetings, for purposes of liaison

ADMIRALTY . . . . . Captain (E.) W. F. B. LANE, D.S.C., R.N.

WAR OFFICE . . . . . Major-General W. A. LORD, C.B.E.

IRON AND STEEL INSTITUTE . . . . . The Hon. R. G. LYTTTELTON

INSTITUTION OF METALLURGISTS . . . . . L. NORTHCOTT, Ph.D., D.Sc.; E. G. WEST, B.Sc., Ph.D.

---

## SECRETARY

Lieut.-Colonel S. C. GUILLAN, T.D.

## ASSISTANT SECRETARY

Major R. E. MOORE

## EDITOR OF PUBLICATIONS

N. B. VAUGHAN, M.Sc.



# CHAIRMEN, HONORARY SECRETARIES, AND TREASURERS OF THE LOCAL SECTIONS

at 31 December 1954

## Birmingham

*Chairman* : S. S. SMITH, M.Met., Imperial Chemical Industries, Ltd., Metals Division, Kynoch Works, Birmingham 6.

*Hon. Secretary* : A. W. MATTHEWS, 124 Hay Green Lane, Birmingham 30.

*Hon. Treasurer* : R. CHADWICK, M.A., 5 Fairmead Rise, King's Norton, Birmingham 30.

## London

*Chairman* : J. C. CHASTON, Ph.D., B.Sc., A.R.S.M., Johnson, Matthey and Co., Ltd., Wembley, Middx.

*Hon. Secretary* : J. R. KNIGHT, B.Sc., The Mond Nickel Company, Ltd., Development and Research Department, Bashley Road, London, N.W.10.

*Hon. Treasurer* : E. G. V. NEWMAN, B.Sc., A.R.S.M., The Royal Mint, London, E.C.3.

## Oxford

*Chairman* : R. T. PARKER, B.Sc., Ph.D., A.R.S.M., Aluminium Laboratories, Ltd., Banbury, Oxon.

*Hon. Secretary* : O. R. SMITH, B.Sc., Aluminium Laboratories, Ltd., Banbury, Oxon.

*Hon. Treasurer* : J. C. ARROWSMITH, M.Met., Pressed Steel Company of Great Britain, Ltd., Oxford.

## Scottish

*Chairman* : G. MACDONALD, O.B.E., B.Sc., E. Chalmers and Co., Ltd., 36 Newhaven Road, Edinburgh 6.

*Hon. Secretary* : MATTHEW HAY, A. Cohen and Co., Ltd., Craigton Industrial Estate, Barfillan Drive, Cardonald, Glasgow, S.W.2.

*Hon. Treasurer* : N. J. MACLEOD, Steven and Struthers, Ltd., 86 Eastvale Place, Kelvinhaugh, Glasgow, C.3.

## Sheffield

*Chairman* : W. R. MADDOCKS, B.Sc., Ph.D., The University, St. George's Square, Sheffield 1.

*Hon. Secretary and Treasurer* : A. J. MACDOUGALL, M.Met., The University, St. George's Square, Sheffield 1.

## South Wales

*Chairman* : J. S. WALTON, Bay View, The Crest, Pentyla, Port Talbot, Glam.

*Hon. Secretary* : P. W. A. CUNNIFFE, Thirlmere, Mansel Road, Bonymaen, Swansea.

*Hon. Treasurer* : P. J. LIPROT, M.Eng., The National Smelting Co., Ltd., Swansea Vale Works, Llansamlet, Swansea.



# CORRESPONDING MEMBERS TO THE COUNCIL

at 31 December 1954

## Australia

Professor H. K. WÖRNER, D.Sc.,  
Professor of Metallurgy, University of Melbourne, Carlton, N.3, Melbourne, Victoria.

## Belgium

H. P. A. FÉRON,  
Administrateur-Directeur, Société Anonyme Visseries et Tréfileries Réunies, 2 Avenue Général Leman, Haren, Bruxelles.

## Canada

G. S. FARNHAM, B.A., M.Sc., Ph.D.,  
Chief, Development and Research Section, The International Nickel Co. of Canada, Ltd., 25 King St. W., Toronto 1, Ontario.

Professor F. A. FORWARD, B.A.Sc.,  
Head of the Department of Mining and Metallurgy, University of British Columbia, Vancouver, B.C.

Professor G. LETENDRE, B.A., Ph.D.,  
Professor of Metallurgy and Director, Department of Mining and Metallurgical Engineering, Faculty of Sciences,  
Laval University, Boulevard de l'Entente, Quebec City, P.Q.

## France

Professor P. A. J. CHEVENARD,  
Administrateur et Conseiller Scientifique, Société Anonyme de Commentry-Fourchambault et Decazeville, 84 rue de Lille, Paris 7e.

JEAN MATTER,  
Vice-Président et Directeur-Général, Société Centrale des Alliages Légers, 66 Avenue Marceau, Paris 8e.

## India

N. P. GANDHI, M.A., B.Sc., A.R.S.M., D.I.C.,  
183 Lam Road, Devlali.

## Italy

Professor LENO MATTEOLI, Dott.chim.,  
Centro di Ricerche Metallurgiche, Lungodora Voghera 82, Torino.

## Netherlands

M. HAMBURGER,  
Managing Director, N.V. de Koninklijke Nederlandsche Lood- en Zinkpletterijen voorheen A.D. Hamburger,  
Leidschekade 30, Utrecht.

## South Africa

G. H. STANLEY, D.Sc., A.R.S.M.,  
24 Duncombe Road, Forest Town, Johannesburg, Transvaal.  
Professor L. TAVERNER, A.R.S.M., D.I.C.,  
Professor of Metallurgy and Assaying, University of the Witwatersrand, Johannesburg, Transvaal.

## Spain

Professor J. ORLAND, M.Sc., M.A., Ph.D., D.D.,  
Head of the Department of Metallography and Strength of Materials, Instituto Católico de Artes e Industrias,  
Alberto Aguilera 23, Madrid.

## Sweden

Emeritus Professor CARL BENEDICKS, Fil.Dr., Dr.-Ing.e.h., Dr.Techn.h.c.,  
Drottninggatan 95 B., Stockholm.  
Emeritus Professor AXEL HULTGREN,  
Valevågen 49, Djursholm 2, Stockholm.

## Switzerland

O. H. C. MESSNER, Dipl.Ing., Dr.sc.techn.,  
Consulting Metallurgical Engineer, Stauffacherquai 40, Zürich 4.  
Professor A. VON ZEERLEDER, Dr.-Ing., Dr.Mont.h.c.  
Director, Research Laboratories, Société Anonyme pour l'Industrie de l'Aluminium, Neuhausen a./Rheinfall.

## United States of America

Professor R. F. MEHL, Ph.D., Eng.D., Sc.D.,  
Director, Metals Research Laboratory, Carnegie Institute of Technology, Pittsburgh, Pa.  
Professor C. S. SMITH, Sc.D.,  
Professor of Metallurgy and Director of the Institute for the Study of Metals, University of Chicago, Chicago 37, Ill.  
Dr. R. A. WILKINS,  
Vice-President, Research and Development, Revere Copper and Brass, Inc., Rome, N.Y.



INSTITUTE OF METALS  
PUBLICATION DEPARTMENT

---

*Editor*

N. B. VAUGHAN, M.Sc.

*Editorial Assistants*

T. H. L. GRAFF, Dr.Ing.

A. E. KING, B.A.

*Indexer*

R. C. BOHENER

*Secretary*

J. M. FRYER







S. F. DOREY, C.B.E., D.Sc., F.R.S.  
(*President 1954-55*)

*Frontispiece, to face p. ix.*



# CONTENTS

## MINUTES OF PROCEEDINGS

	PAGE
General Meeting, Birmingham, 6 January 1954 . . . . .	xiii
Annual Spring Meeting, London, 26 April–4 May 1954 (Joint Meeting with the Société Française de Métallurgie) . . . . .	xiii
General Meeting, London, 27 May 1954 . . . . .	xvii
General Meeting, London, 30 June 1954 . . . . .	xvii
Annual Autumn Meeting, Switzerland, 6–14 September 1954 . . . . .	xvii
General Meeting, London, 25 and 26 November 1954 . . . . .	xx

## PAPERS, NOTES, AND DISCUSSIONS

	PAGE	
	<i>Paper</i>	<i>Discn.</i>
1487. The Mechanism of Residual-Stress Formation in Sand Castings. By R. N. Parkins, B.Sc., Ph.D., A.I.M., and A. Cowan, B.Sc., Ph.D. . . . .	1	
1488. The Constitution of Aluminium–Copper–Silicon Alloys. By H. W. L. Phillips, M.A., F.R.I.C., F.Inst.P., F.I.M. . . . .	9	
1489. The Structure and Mechanical Properties of Copper–Manganese–Tin Alloys. By J. C. Blade, B.Sc., Ph.D., and J. W. Cuthbertson, D.Sc., F.I.M. . . . .	17	
1490. The Preparation and Properties of Magnesium Alloy Sheets of Controlled Impurity Content. By H. G. Cole, B.Sc., A.R.I.C., A. E. L. Tate, A.I.M., and B. Walters, M.A. . . . .	25	
1491. The Behaviour of the Crystal Boundaries of Aluminium at Temperatures Near the Melting Point. By W. I. Pumphrey, M.Sc., Ph.D., and J. V. Lyons, Ph.D. . . . .	33	598
1492. A Slide-Rule for the Interconversion of Atomic and Weight Percentages for Any Binary Alloy System. By W. A. Rachinger, Ph.D., M.Sc. . . . .	38	
1493. Structural Studies of the Creep of Lead. By R. C. Gifkins, B.Sc., A.I.M. . . . .	39	603
1494. The Re-Investigation of a Nickel–Titanium Alloy and Observations on $\beta/(\alpha + \beta)$ Boundaries in Titanium Systems. By A. D. McQuillan, Ph.D., B.Sc. . . . .	47	644
1495. An Investigation of Thickening and Metal Entrapment in a Light Alloy Melting Flux. By A. H. Sully, Ph.D., M.Sc., F.Inst.P., F.I.M., H. K. Hardy, Ph.D., M.Sc., A.R.S.M., A.I.M., and T. J. Heal, B.Sc., F.Inst.P. . . . .	49	601
1496. Constitution of the Copper-Rich Copper–Aluminium–Germanium Alloys. By Professor G. V. Raynor, M.A., D.Sc., and P. Greenfield, Ph.D., B.Sc. . . . .	59	
1497. Some Observations on the Mechanism of Pitting Corrosion. By R. May, A.R.S.M. . . . .	65	
1498. The Effect of Iron, Manganese, and Chromium on the Properties in Sheet Form of Aluminium Alloys Containing 0.7% Magnesium and 1.0% Silicon. By R. Chadwick, M.A., F.I.M., N. B. Muir, B.Sc., A.I.M., and H. B. Grainger, B.Sc., A.I.M. . . . .	75	621
1499. The Copper–Indium Eutectoid at 31.36 Weight Per Cent. Indium. By Chester W. Spencer, Ph.D., and Associate Professor David J. Mack, Ph.D. . . . .	81	
1500. The Free-Energy Diagram of the System Titanium–Oxygen. By O. Kubaschewski, Dr.phil.habil., and W. A. Dench . . . . .	87	644
1501. The Effect of Cold Work on an Iron–Manganese Alloy. By J. Gordon Parr, Ph.D., B.Sc. . . . .	92	
1502. The New Metal Titanium. Twenty-Fourth Autumn Lecture. By Maurice Cook, D.Sc., Ph.D., F.I.M. . . . .	93	
1503. The Oxidation of Aluminium–Magnesium Alloys by Steam : A Contribution to Research on Mould Reaction. By Marjorie Whitaker, B.Sc., A.I.M. With an Appendix on The Constitution of Oxide Films Formed at High Temperature on Aluminium–Magnesium–Beryllium Alloys. By A. R. Heath, B.Sc. . . . .	107	
1504. Some Creep Characteristics of a Group of Precipitation-Hardening Alloys Based on the Alpha-Copper–Aluminium Phase. By J. P. Dennison, B.Sc., Ph.D. . . . .	117	603
1505. The Computation of Loads in Metal Strip Rolling by Methods Involving the Use of Dimensional Analysis. By Maurice Cook, D.Sc., Ph.D., F.I.M., and R. J. Parker, A.M.I.Mech.E. . . . .	129	
1506. A Survey of the Uranium–Nickel System. By J. D. Grogan, B.A., and R. J. Pleasance. With an Appendix on An X-Ray Examination of Some Uranium–Nickel Alloys. By Betty E. Williams . . . . .	141	
1507. The Low-Stress Torsional Creep Properties of Pure Aluminium. By W. Betteridge, Ph.D., F.Inst.P. . . . .	149	603
1508. The Copper–Silicon Eutectoid Transformation. By A. D. Hopkins, M.Sc. . . . .	163	
1509. The Melting Point of Titanium. By T. H. Schofield, M.Sc., F.I.M., and A. E. Bacon . . . . .	167	
1510. Lamellæ in Chromium. By W. E. Carrington . . . . .	170	
1511. The System Uranium–Lead. By B. R. T. Frost, B.Sc., Ph.D., and J. T. Maskrey . . . . .	171	
1512. The Effects of Some Constitutional Factors on the Creep and Fatigue Properties of Lead and Lead Alloys. By L. M. T. Hopkin, Ph.D., A.R.S.M., A.I.M., and C. J. Thwaites, B.Sc., A.R.S.M. . . . .	181	603
1513. The Constitution of Alloys of Aluminium, Copper, and Iron. By H. W. L. Phillips, M.A., F.R.I.C., F.Inst.P., F.I.M. . . . .	197	568

	PAGE	
	Paper.	Discn.
1514. The Oxidation of Titanium at High Temperatures in an Atmosphere of Pure Oxygen. By A. E. Jenkins, M.Eng.Sc. . . . .	213	
1515. The Structure of Titanium-Silver Alloys in the Range 0-80 Atomic Per Cent. Silver. By H. W. Worner, M.Sc. . . . .	222	644
1516. The Metallographic Detection of Gamma Phase in Beta-Brass. By L. E. Samuels, B.Met.E. . . . .	227	
1517. Mechanism of Creep Deformation in High-Purity Aluminium at High Temperatures. By Hsing C. Chang, M.S., Sc.D., and Nicholas J. Grant, B.S., Sc.D. . . . .	229	603
1518. Ageing Curves at 110° C. on Binary and Ternary Aluminium-Copper Alloys. By H. K. Hardy, M.Sc., Ph.D., A.R.S.M., A.I.M. . . . .	236	610
1519. Structural Ageing Characteristics of Binary Aluminium-Copper Alloys. By (Miss) J. M. Silcock, B.Sc., T. J. Heal, B.Sc., F.Inst.P., and H. K. Hardy, M.Sc., Ph.D., A.R.S.M., A.I.M. . . . .	239	610
1520. Changes of Damping Capacity in Quench-Ageing Aluminium-Rich Alloys. By K. M. Entwistle, M.Sc., Ph.D. . . . .	249	610
1521. Some Metallographic Observations of the Creep of Aluminium-Copper Alloys. By A. H. Sully, M.Sc., Ph.D., F.Inst.P., F.I.M., and H. K. Hardy, M.Sc., Ph.D., A.R.S.M., A.I.M. . . . .	264	
Report of Council for the Year Ended 31 December 1953 . . . . .	266	
Report of the Honorary Treasurer for the Year Ended 30 June 1953 . . . . .	276	
SYMPOSIUM ON THE CONTROL OF QUALITY IN THE PRODUCTION OF WROUGHT NON-FERROUS METALS AND ALLOYS. II.—THE CONTROL OF QUALITY IN WORKING OPERATIONS		
1522. Problems of the Control of Dimension, Shape, and Finish in the Rolling of Sheet and Strip and in the Drawing of Wire. By Hugh Ford, D.Sc. (Eng.), Ph.D., Wh.Sch., and J. G. Wistreich, M.Sc. (Eng.), D.I.C. . . . .	281	
1523. The Control of Quality in the Hot and Cold Rolling of Aluminium and Aluminium Alloys. By F. King, A.I.M., and A. N. Turner, B.Sc., Ph.D., A.R.S.M., A.I.M. . . . .	291	
1524. The Control of Properties and Structure in the Hot and Cold Rolling of Copper and Copper-Base Alloys. By W. W. Kee, B.Sc., F.I.M. . . . .	307	
1525. Some Factors Affecting the Quality of Extrusions. By Christopher Smith, F.I.M., and Norman Swindells, M.A., Ph.D., F.I.M. . . . .	323	
1526. Statistical Control in Metal-Working Operations. By M. Whyte, B.Sc. . . . .	335	
Joint Discussion . . . . .		581
<hr/>		
1527. The Forgeability, Creep Strength, and Ductility of Molybdenum and Some of Its Alloys. By J. H. Rendall, B.Sc., A.R.S.M., A.I.M., S. T. M. Johnstone, B.Met.E., A.I.M., and W. E. Carrington . . . . .	345	599
1528. The Arc Melting of Metals and Its Application to the Casting of Molybdenum. By G. L. Hopkin, O.B.E., B.Sc., F.I.M., (Mrs.) J. E. Jones, B.Sc., D.R.T.C., A. R. Moss, and D. O. Pickman, B.A. . . . .	361	599
1529. The Pressure Welding of Molybdenum. By A. R. Moss . . . . .	374	599
1530. Factors Influencing Brittleness in Aluminium-Magnesium-Silicon Alloys. By I. R. Harris, D.R.T.C., A.I.M., and P. C. Varley, M.B.E., M.A., F.I.M. . . . .	379	621
1531. Techniques for the Investigation of Thermal Conditions in Continuous Casting. By D. M. Lewis, B.Sc., A.I.M. . . . .	395	615
1532. The Use of Autoradiography for Finding the Solidification Boundary in Continuously Cast Aluminium. By J. L. Putman, M.A. . . . .	414	615
1533. The Domain Structure of Ferromagnetic Metals. Forty-Fourth May Lecture. By Professor L. F. Bates, Ph.D., D.Sc., F.R.S. . . . .	417	
1534. The Influence of Extrusion Direction on the Corrosion and Stress-Corrosion of Aluminium-Copper-Magnesium Alloys. By E. A. G. Liddiard, M.A., F.I.M., and Winifred A. Bell, B.A. . . . .	426	635
1535. A Redetermination and Interpretation of the Titanium-Rich Region of the Titanium-Chromium System. By (Mrs.) M. K. McQuillan, M.A. . . . .	433	644
1536. Resistivity Anomalies in the Nickel-Chromium System as Evidence of Ordering Reactions. By Rolf Nordheim, Chem.Eng., Sc.D., and Nicholas J. Grant, B.S., Sc.D. . . . .	440	
1537. X-Ray Determination of the Alpha-Phase Boundary of the Copper-Indium System. By R. O. Jones, B.Sc., and Professor E. A. Owen, M.A., D.Sc. . . . .	445	
1538. Some Further Observations on the Fatigue Process in Pure Aluminium. By P. J. E. Forsyth, A.I.M. . . . .	449	
1539. The System Uranium-Mercury. By B. R. T. Frost, B.Sc., Ph.D. . . . .	456	
1540. The Ternary Compound <i>E</i> in the System Aluminium-Chromium-Magnesium. By (Miss) K. Little, M.A., D.Phil. . . . .	463	
1541. Staining of Clad Aluminium Alloy Sheets During Salt-Bath Heat-Treatment. By E. C. Williams, M.Sc., A.Inst.P., and H. J. G. Challis, F.R.I.C., A.I.M. . . . .	465	641
1542. The Constitution of Gold-Molybdenum Alloys, with Particular Reference to the Solubility of Molybdenum in Gold. By G. A. Geach, M.Sc., Ph.D., F.I.M., and D. Summers-Smith, B.Sc., Ph.D., A.R.T.C. . . . .	471	
1543. Metallographic Observations on Cell Formation and Development in Aluminium. By J. W. Kelly, M.Sc., and R. C. Gifkins, B.Sc., A.I.M. . . . .	475	



	PAGE	
	<i>Paper</i>	<i>Discn.</i>
1544. <b>Some Observations on the Deformation of Zinc at High Temperature.</b> By R. W. Cahn, Ph.D., (Miss) I. J. Bear, A.M.T.C., and R. L. Bell, B.Sc. . . . .	481	
1545. <b>Methods for Determining the Liquidus Points of Titanium-Rich Alloys.</b> By W. Hume-Rothery, O.B.E., F.R.S., and D. M. Poole, B.Sc., M.Sc. . . . .	490	644
1546. <b>Isothermal Transformations of Hypo-Eutectoid Aluminium Bronzes.</b> By R. Haynes, B.Met., Ph.D., A.I.M. . . . .	493	
1547. <b>Metals and Marine Engineering.</b> Presidential Address. By S. F. Dorey, C.B.E., D.Sc., F.R.S. . . . .	497	
1548. <b>Note on the Constitution of the Titanium-Gold System in the Region 0-6 Atomic Per Cent. Gold.</b> By (Mrs.) M. K. McQuillan, M.A. . . . .	511	644
1549. <b>Grain-Refining Additions for Cast Copper Alloys.</b> By A. Cibula, M.A., A.I.M. . . . .	513	632
1550. <b>Exploratory Creep Tests on Metals of High Melting Point.</b> By N. P. Allen, M.Met., D.Sc., F.I.M., and W. E. Carrington . . . . .	525	652
1551. <b>The Constitution of the Titanium-Rich Alloys of Titanium, Iron, and Oxygen.</b> By N. P. Allen, M.Met., D.Sc., F.I.M., T. H. Schofield, M.Sc., F.I.M., and (Mrs.) B. Mellish, B.Sc. . . . .	534	644
1552. <b>The Constitution of the Copper-Rich Copper-Zinc-Gallium Alloys.</b> By T. B. Massalski, B.Sc., and Professor G. V. Raynor, M.A., D.Sc. . . . .	539	
1553. <b>A Study of Preferred Orientation in Extruded, Drawn, and Annealed Copper.</b> By Professor Paul G. Bastien, Dr.ès.Sci., and Dr. J. Pokorný . . . . .	545	653
1554. <b>The Cleavage Fracture of Pure Polycrystalline Zinc in Tension.</b> By G. W. Greenwood, B.Sc., Ph.D., and Professor A. G. Quarrell, D.Sc., Ph.D., A.R.C.S. . . . .	551	
1555. <b>Preferred Orientation in Rolled Uranium Sheet.</b> By J. Adam, B.Sc., Ph.D., A.Inst.P., and J. Stephenson, B.Met., A.I.M. . . . .	561	653
1556. <b>The Constitution of the System Silver-Lithium.</b> By W. E. Freeth, Ph.D., B.Sc., and Professor G. V. Raynor, M.A., D.Sc. . . . .	569	
1557. <b>The Systems Magnesium-Lithium and Magnesium-Lithium-Silver.</b> By W. E. Freeth, Ph.D., B.Sc., and Professor G. V. Raynor, M.A., D.Sc. . . . .	575	
<b>Obituary: Sir PAUL GUETERBOCK, K.C.B., D.S.O., M.C., T.D., D.L., J.P., M.A., F.Inst.Met.</b> . . . .	658	
<b>Name Index</b> . . . . .	659	

# LIST OF PLATES

S. F. Dorey, C.B.E., D.Sc., F.R.S., President 1954-55 . . . . .	<i>frontispiece</i>
Arms of the Institute of Metals . . . . .	<i>facing p. xiii</i>
I-II. Paper by Dr. J. C. Blade and Dr. J. W. Cuthbertson . . . . .	<i>between pp. 48 and 49</i>
III. Paper by Mr. H. G. Cole, Mr. A. E. L. Tate, and Mr. B. Walters . . . . .	<i>between pp. 48 and 49</i>
IV-VI. Paper by Mr. R. C. Gifkins . . . . .	<i>between pp. 48 and 49</i>
VII. Paper by Dr. A. D. McQuillan . . . . .	<i>between pp. 48 and 49</i>
VIII. Paper by Dr. A. H. Sully, Dr. H. K. Hardy, and Mr. T. J. Heal . . . . .	<i>facing p. 92</i>
IX-XIII. Paper by Mr. R. Chadwick, Mr. N. B. Muir, and Mr. H. B. Grainger . . . . .	<i>between pp. 92 and 93</i>
XIV-XV. Paper by Dr. C. W. Spencer and Associate Professor D. J. Mack . . . . .	<i>between pp. 92 and 93</i>
XVI-XVII. Lecture by Dr. Maurice Cook . . . . .	<i>between pp. 148 and 149</i>
XVIII. Paper by Miss M. Whitaker . . . . .	<i>between pp. 148 and 149</i>
XIX. Paper by Dr. J. P. Dennison . . . . .	<i>between pp. 148 and 149</i>
XX-XXI. Paper by Mr. J. D. Grogan and Mr. R. J. Pleasance . . . . .	<i>between pp. 148 and 149</i>
XXII. Paper by Dr. W. Betteridge . . . . .	<i>facing p. 196</i>
XXIII. Paper by Mr. A. D. Hopkins . . . . .	<i>between pp. 196 and 197</i>
XXIV. Paper by Mr. W. E. Carrington . . . . .	<i>between pp. 196 and 197</i>
XXV. Paper by Dr. B. R. T. Frost and Mr. J. T. Maskrey . . . . .	<i>between pp. 196 and 197</i>
XXVI-XXVIII. Paper by Dr. L. M. T. Hopkin and Mr. C. J. Thwaites . . . . .	<i>between pp. 196 and 197</i>
XXIX-XXX. Paper by Mr. H. W. L. Phillips . . . . .	<i>between pp. 228 and 229</i>
XXXI. Paper by Mr. A. E. Jenkins . . . . .	<i>between pp. 228 and 229</i>
XXXII. Paper by Mr. H. W. Worner . . . . .	<i>between pp. 228 and 229</i>
XXXIII. Paper by Mr. L. E. Samuels . . . . .	<i>between pp. 228 and 229</i>
XXXIV-XXXVIII. Paper by Dr. H. C. Chang and Dr. N. J. Grant . . . . .	<i>between pp. 280 and 281</i>
XXXIX-XLI. Paper by Miss J. M. Silcock, Mr. T. J. Heal, and Dr. H. K. Hardy . . . . .	<i>between pp. 280 and 281</i>
XLII-XLIII. Paper by Dr. A. H. Sully and Dr. H. K. Hardy . . . . .	<i>between pp. 280 and 281</i>
XLIV. Paper by Dr. H. Ford and Mr. J. G. Wistreich . . . . .	<i>facing p. 344</i>
XLV. Paper by Mr. F. King and Dr. A. N. Turner . . . . .	<i>between pp. 344 and 345</i>
XLVI. Paper by Mr. W. W. Kee . . . . .	<i>between pp. 344 and 345</i>
XLVII-XLVIII. Paper by Mr. J. H. Rendall, Mr. S. T. M. Johnstone, and Mr. W. E. Carrington . . . . .	<i>between pp. 416 and 417</i>
XLIX-L. Paper by Mr. G. L. Hopkin, Mrs. J. E. Jones, Mr. A. R. Moss, and Mr. D. O. Pickman . . . . .	<i>between pp. 416 and 417</i>
LI-LIV. Paper by Mr. A. R. Moss . . . . .	<i>between pp. 416 and 417</i>
LV-LVI. Paper by Mr. I. R. Harris and Mr. P. C. Varley . . . . .	<i>between pp. 416 and 417</i>
LVII-LIX. Paper by Mr. D. M. Lewis . . . . .	<i>between pp. 416 and 417</i>
LX. Paper by Mr. J. L. Putman . . . . .	<i>facing p. 417</i>
LXI-LXVI. Lecture by Professor L. F. Bates . . . . .	<i>between pp. 464 and 465</i>
LXVII. Paper by Mr. E. A. G. Liddiard and Miss W. A. Bell . . . . .	<i>between pp. 464 and 465</i>
LXVIII. Paper by Mrs. M. K. McQuillan . . . . .	<i>between pp. 464 and 465</i>
LXIX-LXXI. Paper by Mr. P. J. E. Forsyth . . . . .	<i>between pp. 464 and 465</i>
LXXII-LXXIII. Paper by Mr. E. C. Williams and Mr. H. J. G. Challis . . . . .	<i>between pp. 496 and 497</i>
LXXIV-LXXVII. Paper by Mr. J. W. Kelly and Mr. R. C. Gifkins . . . . .	<i>between pp. 496 and 497</i>
LXXVIII-LXXX. Paper by Dr. R. W. Cahn, Miss I. J. Bear, and Mr. R. L. Bell . . . . .	<i>between pp. 496 and 497</i>
LXXX. Paper by Dr. W. Hume-Rothery and Mr. D. M. Poole . . . . .	<i>between pp. 496 and 497</i>
LXXXI. Paper by Dr. R. Haynes . . . . .	<i>facing p. 497</i>
LXXXII. Paper by Mr. A. Cibula . . . . .	<i>facing p. 544</i>
LXXXIII. Paper by Dr. N. P. Allen and Mr. W. E. Carrington . . . . .	<i>between pp. 544 and 545</i>
LXXXIV-LXXXV. Paper by Dr. N. P. Allen, Mr. T. H. Schofield, and Mrs. B. Mellish . . . . .	<i>between pp. 544 and 545</i>
LXXXVI-LXXXVII. Paper by Professor P. G. Bastien and Dr. J. Pokorny . . . . .	<i>between pp. 630 and 631</i>
LXXXVIII. Paper by Dr. G. W. Greenwood and Professor A. G. Quarrell . . . . .	<i>between pp. 630 and 631</i>
LXXXIX-XCVII. Discussion on Various Papers . . . . .	<i>between pp. 630 and 631</i>
XCVIII-CI. " " . . . . .	<i>between pp. 646 and 647</i>
CII. Sir Paul Gueterbock, K.C.B., D.S.O., M.C., T.D., D.L., J.P., M.A., F.Inst.Met. . . . .	<i>facing p. 658</i>



## ARMS OF THE INSTITUTE OF METALS

*Official Blazon of the Arms :* Per pale Or and Argent an open book proper thereon the alchemical signs for the non-ferrous metals Sable And for the Crest on a Wreath Or and Sable, Issuant from flames a crucible emitting Oxide vapour proper.

*Supporters :* Griffins, traditional guardians of treasure.

*Motto :* De Re Metallica.



ARMS OF THE INSTITUTE OF METALS



# THE INSTITUTE OF METALS

## MINUTES OF PROCEEDINGS

### GENERAL MEETING

6 January 1954

A GENERAL MEETING of the Institute of Metals was held in the University, Edgbaston, Birmingham, on Wednesday, 6 January 1954. The Chair was taken by Mr. W. J. THOMAS, Chairman of the Metallurgical Engineering Committee.

#### INFORMAL DISCUSSION ON "LUBRICANTS FOR METAL-WORKING OPERATIONS IN THE NON-FERROUS METALS INDUSTRY"

An all-day Informal Discussion took place, to which numerous contributions were made. A report of the discussion is published in the *Bulletin*, 1953-55, vol. 2, pp. 100-104 (April 1954).

At the conclusion of the meeting, a vote of thanks was passed to the University authorities for permission to use the Chemistry Lecture Theatre for the meeting.

### ANNUAL SPRING MEETING

26 April to 4 May 1954

THE FORTY-SIXTH ANNUAL SPRING MEETING of the Institute of Metals took the form of a Joint Meeting with the Société Française de Métallurgie, held in London from Monday to Saturday, 26 April-1 May 1954, and in Provincial Centres on Monday and Tuesday, 3 and 4 May 1954.

Monday, 26 April

#### VISITS

During the afternoon, members of the Société Française de Métallurgie visited the laboratories of the British Non-Ferrous Metals Research Association and of the British Iron and Steel Research Association, the works of the Britannia Lead Co., Ltd., Northfleet, and the precious-metal refinery of The Mond Nickel Co., Ltd., at Acton, while other members and ladies made a coach tour of London.

#### OPENING CEREMONY

The President, Professor F. C. THOMPSON, D.Met., M.Sc., occupied the Chair at an Opening Ceremony in the Lecture Theatre of The Royal Institution, Albemarle Street, London, W.1, at 6.30 p.m.

On behalf of the Institute of Metals, Professor Thompson welcomed the President, Dr. E. DUPUY, and members and ladies of the Société Française de Métallurgie.

Professor Sir Cyril HINSHELWOOD, F.R.S., Foreign Secretary of The Royal Society, welcomed the Institute's guests on behalf of British Science.

The President of the Société Française de Métallurgie replied to the addresses of welcome.

#### MAY LECTURE

Professor L. F. BATES, Ph.D., D.Sc., F.R.S., Lancashire-Spencer Professor of Physics and Deputy Vice-Chancellor of the University of Nottingham, then delivered the Forty-Fourth Annual May Lecture on "The Domain Structure of Ferromagnetic Metals".

At the conclusion, Professor Sir Lawrence BRAGG, O.B.E., F.R.S. (Honorary Member), proposed a vote of thanks to Professor Bates for his lecture, which is printed on pp. 417-425 of this volume of the *Journal*.

A vote of thanks was passed to the Managers of The Royal Institution for permitting the use of their Lecture Theatre for the meeting.

Later in the evening, the Council entertained the Lecturer to dinner at the United Service Club, Pall Mall, S.W.1.

Tuesday, 27 April

#### ANNUAL GENERAL MEETING

THE FORTY-SIXTH ANNUAL GENERAL MEETING of the Institute of Metals was held in Convocation Hall, Church House, Great Smith Street, London, S.W.1, at 10.0 a.m. The retiring President, Professor F. C. THOMPSON, D.Met., M.Sc., occupied the Chair at the opening of the meeting.

The minutes of the previous General Meetings, held in Southport on 21-25 September 1953, in London on 27 November 1953, and in Birmingham on 6 January 1954 were taken as read and signed by the Chairman.

#### Elections of Members, Junior Members, and Student Members

The Secretary (Lieut.-Colonel S. C. GUILLAN, T.D.) announced that, since the Annual Autumn Meeting held at Southport in September 1953, a total of 240 Ordinary Members, Junior Members, and Student Members had been elected on 19 October, 9 November, 23 November, and 31 December 1953, and 25 January, 26 February, 30 March, and 26 April 1954, the lists of whose names are printed in the *Bulletin*, 1953-55, vol. 2, pp. 24, 25, 63, 77, 85, 95, 110, and 117.

#### Report of Council for the Year Ended 31 December 1953

The Chairman moved, Dr. N. SWINDELLS seconded, and there was carried unanimously, a motion for the adoption of the Report of Council for the year ended 31 December 1953, which is printed on pp. 266-275 of this volume of the *Journal*.

#### Report of the Honorary Treasurer and Accounts for the Financial Year Ended 30 June 1953

The Honorary Treasurer presented his Report and the accounts for the financial year ended 30 June 1953, and moved their adoption. Dr. S. F. DOREY, C.B.E. (Senior Vice-President and Chairman of the Finance and General Purposes Committee) seconded the motion, which was carried without dissent.

The Report and accounts are printed in this volume of the *Journal*, pp. 276-280.

#### Re-Election of Auditors

It was proposed, seconded, and carried unanimously that Messrs. Poppleton and Appleby be re-elected auditors to the Institute for the year 1954-55.

#### Election of Officers for 1954-55

The Secretary announced that the following officers had been elected to fill vacancies on the Council for the year 1954-55:

#### President:

S. F. DOREY, C.B.E., D.Sc., F.R.S.

#### Vice-Presidents:

Maurice COOK, D.Sc., Ph.D.

L. B. FREIL, O.B.E., D.Sc., A.R.S.M., F.R.S.

Major P. Litherland TEED, A.R.S.M.

*Ordinary Members of Council :*

R. D. HAMER, B.Sc.  
G. P. TINKER, M.Sc.

*Senior Vice-President for 1954-55*

The Secretary announced that the Council had elected Dr. Maurice COOK to be Senior Vice-President for 1954-55, and that he would be its next nominee for the Presidency.

*Vote of Thanks to Retiring Officers*

Dr. J. C. CHASTON, B.Sc., A.R.S.M., proposed, and there was carried with acclamation, a hearty vote of thanks to the following retiring officers for their services on the Council: Mr. H. S. Tasker, B.A., Past-President; Mr. A. B. Graham and Mr. P. V. Hunter, C.B.E., Vice-Presidents.

*Presentation of a Presidential Badge*

Mr. Donald McDONALD, B.Sc., on behalf of the Directors of Johnson, Matthey and Co., Ltd., presented to the Institute a Presidential Badge, an illustration of which is printed in the *Bulletin*, 1953-55, vol. 2, p. 141 (August 1954). After having been invested with the Badge, the President, on behalf of the Institute, thanked the donors warmly for their very welcome and beautiful gift.

*Induction of the New President*

The Chairman (Professor F. C. THOMPSON, D.Met., M.Sc.) then introduced the new President, Dr. S. F. DOREY, C.B.E., F.R.S., invested him with the Presidential Badge, and inducted him into the Chair.

*Vote of Thanks to the Retiring President*

Dr. IVOR JENKINS (Member of Council) proposed, Dr. R. T. PARKER, B.Sc., A.R.S.M. (Chairman of the Oxford Local Section) seconded, and there was carried unanimously a hearty vote of thanks to the retiring President, Professor F. C. Thompson, D.Met., M.Sc. Professor Thompson briefly responded.

*Presidential Address*

Dr. S. F. DOREY, C.B.E., F.R.S., then delivered his Presidential Address, entitled "Metals and Marine Engineering", which is printed on pp. 497-510 of this volume of the *Journal*.

A vote of thanks to the President for his Address was proposed by Mr. G. L. BAILEY, C.B.E., M.Sc., and carried with acclamation.

*Institute of Metals (Platinum) Medal*

The President presented to Dr. Leslie AITCHISON, M.Sc. (Honorary Member), the Institute of Metals (Platinum) Medal for 1954, in recognition of his services to metallurgy in industry, in education, and in public service.

*Rosenhain Medal*

The President presented to Professor A. H. COTTRELL, B.Sc., Ph.D., the Rosenhain Medal for 1954, in recognition of his outstanding contributions to knowledge in the field of physical metallurgy, with special reference to the deformation of metals.

*Students' Essay Prize*

The President presented to Mr. Derek HULL, B.Sc., of University College, Cardiff, the Students' Essay Prize for 1953, for an essay on "The Characteristics of the Martensite Transformation", which is printed in the *Bulletin*, 1953-55, vol. 2, pp. 134-139 (July 1954).

## COCKTAIL PARTY

The meeting was followed by a cocktail party, held in the Hoare Memorial Hall, Church House, to enable members of the Institute of Metals to meet the President, members, and ladies of the Société Française de Métallurgie.

## DISCUSSION OF PAPERS

The meeting was resumed in the afternoon in Convocation Hall, Church House, when Dr. Maurice COOK (Senior Vice-President) occupied the Chair.

The following papers, which had previously been published in the *Journal*, were discussed:

"An Investigation of Thickening and Metal Entrapment in a Light Alloy Melting Flux", by A. H. Sully, Ph.D., M.Sc., F.Inst.P., F.I.M., H. K. Hardy, Ph.D., M.Sc., A.R.S.M., A.I.M., and T. J. Heal, B.Sc., F.Inst.P.

"The Effect of Iron, Manganese, and Chromium on the Properties, in Sheet Form, of Aluminium Alloys Containing 0.7% Magnesium and 1.0% Silicon", by R. Chadwick, M.A., F.I.M., N. B. Muir, B.Sc., A.I.M., and H. B. Grainger, B.Sc., A.I.M.

"Factors Influencing Brittleness in Aluminium-Magnesium-Silicon Alloys", by I. R. Harris, D.R.T.C., A.I.M., and P. C. Varley, M.B.E., M.A., F.I.M.

The two latter papers were discussed jointly.

At the conclusion of each discussion, a vote of thanks to the authors was proposed by the Chairman and carried with acclamation.

## VISITS

During the afternoon, members and ladies of the Société Française de Métallurgie paid visits to the National Gallery; a large London Store; the Chemical Research Laboratory, D.S.I.R., Teddington; the National Physical Laboratory, D.S.I.R., Teddington; and the works of Frederick Braby and Co., Ltd., Crayford; Fraser and Chalmers, Ltd., Erith; and the Telegraph Construction and Maintenance Co., Ltd., Greenwich.

## RECEPTION BY H.M. GOVERNMENT

In the evening, Her Majesty's Government gave a reception at Lancaster House in honour of the President and members of the Société Française de Métallurgie.

## Wednesday, 28 April

At the resumed meeting, at 10.0 a.m. in Church House, Great Smith Street, London, S.W.1, three simultaneous scientific and technical sessions were held, (i) an all-day Symposium on "The Control of Quality in the Production of Wrought Non-Ferrous Metals and Alloys." Part II.—The Control of Quality in Working Operations; (ii) discussion on papers published in the *Journal*; (iii) discussion on papers arranged by the Société Française de Métallurgie.

SYMPOSIUM ON "THE CONTROL OF QUALITY IN THE PRODUCTION OF WROUGHT NON-FERROUS METALS AND ALLOYS".  
PART II.—"THE CONTROL OF QUALITY IN WORKING OPERATIONS".

At the morning session in the Hoare Memorial Hall the Chair was taken by the President, Dr. S. F. DOREY, C.B.E., F.R.S.

Professor A. J. MURPHY, M.Sc. (Past-President) as rapporteur, introduced the following five papers (see this volume of the *Journal*, pp. 281-344), which had been contributed to the Symposium.

In the afternoon the Chair was taken by Mr. W. J. THOMAS, Chairman of the Metallurgical Engineering Committee.

There was an all-day discussion, a report of which is printed on pp. 581-597 of this volume of the *Journal*.

"Problems of the Control of Dimension, Shape, and Finish in the Rolling of Sheet and Strip and in the Drawing of Wire", by H. Ford, D.Sc.(Eng.), Ph.D., Wh.Sch., and J. G. Wistreich, M.Sc.(Eng.), D.I.C.

"The Control of Quality in the Hot and Cold Rolling of Aluminium and Aluminium Alloys", by F. King, A.I.M., and A. N. Turner, B.Sc., Ph.D., A.R.S.M., A.I.M.

"The Control of Properties and Structure in the Hot and



Cold Rolling of Copper and Copper-Base Alloys", by W. W. Kee, B.Sc., F.I.M.

"Some Factors Affecting the Quality of Extrusions", by Christopher Smith, F.I.M., and Norman Swindells, M.A., Ph.D., F.I.M.

"Statistical Control in Metal-Working Operations", by M. Whyte, B.Sc.

At the conclusion of the Symposium, a hearty vote of thanks to the authors and to the rapporteur was proposed by the Chairman and carried with acclamation.

#### DISCUSSION ON "PRECIPITATION-HARDENING"

At the morning session in Convocation Hall the Chair was taken by Dr. L. B. Pfeil, O.B.E., A.R.S.M., F.R.S. (Vice-President).

Dr. A. H. Sully, M.Sc., as rapporteur, introduced the following five papers, which had previously been published in the *Journal*.

"The Effect of Minor Additions on the Age-Hardening Properties of a High-Purity Lead-Antimony Alloy", by L. M. T. Hopkin, Ph.D., A.R.S.M., A.I.M., and C. J. Thwaites, B.Sc., A.R.S.M.

"Some Metallographic Observations on Aged Aluminium-Copper Alloys", by I. J. Polmear, B.Met.E., and H. K. Hardy, M.Sc., Ph.D., A.R.S.M., A.I.M.

"Ageing Curves at 110° C. on Binary and Ternary Aluminium-Copper Alloys", by H. K. Hardy, M.Sc., Ph.D., A.R.S.M., A.I.M.

"Structural Ageing Characteristics of Binary Aluminium-Copper Alloys", by (Miss) J. M. Silcock, B.Sc., T. J. Heal, B.Sc., F.Inst.P., and H. K. Hardy, M.Sc., Ph.D., A.R.S.M., A.I.M.

"Changes of Damping Capacity in Quench-Ageing Aluminium-Rich Alloys", by K. M. Entwistle, M.Sc., Ph.D.

#### DISCUSSION OF PAPERS ON FERROUS METALLURGY, ARRANGED BY THE SOCIÉTÉ FRANÇAISE DE MÉTALLURGIE

Mr. James MITCHELL, C.B.E. (President of the Iron and Steel Institute) took the Chair in the Bishop Partridge Hall, at the morning session, when a discussion, arranged by the Société Française de Métallurgie in association with the Iron and Steel Institute, took place on the following papers, previously published in the *Journal of the Iron and Steel Institute*:

"Diffusion of Nitrogen in Iron", by J. D. Fast and M. B. Verrijp.

"Assessment of Weldability by Rapid Dilatation Tests", by C. L. M. Cottrell, M.Sc., Ph.D.

"Continuous-Cooling Transformation Diagrams of Steels", by W. Steven, Ph.D., F.I.M., and G. Mayer, B.Sc., A.I.M.

"The Effect of Hydrogen on the Continuous-Cooling Transformation Diagram for a Manganese-Molybdenum Steel", by C. L. M. Cottrell, M.Sc., Ph.D.

At the conclusion of each discussion, a vote of thanks to the authors and rapporteur was proposed by the Chairman and carried with acclamation.

The meeting was resumed in the afternoon, when there were two simultaneous scientific and technical sessions, including the symposium on "The Control of Quality in Working Operations", referred to above.

#### DISCUSSION ON "CREEP"

At the afternoon session in Convocation Hall the Chair was taken by Professor F. C. THOMPSON, D.Met., M.Sc. (Past-President).

Dr. W. BETTERIDGE as rapporteur, introduced the following six papers:

"Some Observations on Creep and Fracture from Investigations on Lead Cable-Sheath Alloys", by A. Latin, Ph.D., M.Eng., F.I.M.

"Structural Studies of the Creep of Lead", by R. C. Gifkins, B.Sc., A.I.M.

"Some Creep Characteristics of a Group of Precipitation-Hardening Alloys Based on the Alpha-Copper-Aluminium Phase", by J. P. Dennison, B.Sc., Ph.D.

"The Low-Stress Torsional Creep Properties of Pure Aluminium", by W. Betteridge, Ph.D., F.Inst.P.

"The Effects of Some Constitutional Factors on the Creep and Fatigue Properties of Lead and Lead Alloys", by L. M. T. Hopkin, Ph.D., A.R.S.M., A.I.M., and C. J. Thwaites, B.Sc., A.R.S.M.

"Mechanism of Creep Deformation in High-Purity Aluminium at High Temperatures", by H. C. Chang, M.S., Sc.D., and N. J. Grant, B.S., Sc.D.

At the conclusion of the discussion a vote of thanks to the authors and rapporteur was proposed by the Chairman and carried with acclamation.

#### VISITS

During the morning, ladies and members of the Société Française de Métallurgie visited the Tower of London.

In the afternoon, visits were paid to the Victoria and Albert Museum; the Wallace Collection; the research laboratories of the British Iron and Steel Research Association, the British Non-Ferrous Metals Research Association, and The General Electric Co., Ltd.; and the works of J. Stone and Co. (Charlton), Ltd.

#### BANQUET AND DANCE

In the evening a Banquet and Dance was held in the Great Room, Grosvenor House, Park Lane, W.1, at which the President, members, and ladies of the Société Française de Métallurgie were the guests of the Institute of Metals.

#### Thursday, 29 April

At the resumed meeting, at 10.0 a.m. at Church House, three simultaneous scientific and technical sessions were held, as follows:

#### DISCUSSION ON "RECOVERY AND RECRYSTALLIZATION"

A general discussion on this subject took place in the Hoare Memorial Hall, under the Chairmanship of Professor G. V. RAYNOR, M.A., D.Phil., D.Sc. (Vice-President and Chairman of the Metal Physics Committee).

Dr. R. W. K. HONEYCOMBE and Professor P. LACOMBE delivered, by invitation, introductory contributions.

#### DISCUSSION ON "CONTINUOUS CASTING"

At the morning session in Convocation Hall the Chair was taken by Mr. G. L. BAILEY, C.B.E., M.Sc. (Vice-President). A discussion took place based on the following two papers previously published in the *Journal*.

"Techniques for the Investigation of Thermal Conditions in Continuous Casting", by D. M. Lewis, B.Sc., A.I.M.

"The Use of Autoradiography for Finding the Solidification Boundary in Continuously Cast Aluminium", by J. L. Putman, M.A.

#### DISCUSSION ON "MOLYBDENUM AND MOLYBDENUM ALLOYS AND THE ARC WELDING OF METALS"

There followed a discussion on three papers dealing with molybdenum and its alloys:

"The Forgeability, Creep Strength, and Ductility of Molybdenum and Some of its Alloys", by J. H. Rendall, B.Sc., A.R.S.M., A.I.M., S. T. M. Johnstone, B.Met.E., A.I.M., and W. E. Carrington.

"The Arc Melting of Metals and its Application to the

Casting of Molybdenum", by G. L. Hopkin, O.B.E., B.Sc., (Mrs.) J. E. Jones, B.Sc., D.R.T.C., A. R. Moss, and D. O. Pickman, B.A.

"The Pressure Welding of Molybdenum", by A. R. Moss.

#### DISCUSSION OF FRENCH PAPERS

In the Bishop Partridge Hall the Chair was taken by Professor G. CHAUDRON, Past-President of the Société Française de Métallurgie, when the following papers were discussed:

"Recherches sur la Cinétique de la Transformation Martensitique dans un Acier hypereutectoïde", by J. Philibert and Professor C. Crussard.

"Influence des Joints intergranulaires des Métaux et Alliages sur certains Propriétés mécaniques au Voisinage du Point de Fusion", by Ch. Boulanger.

"Recherches sur l'Oxydation sélective des Alliages Nickel-Chrome aux Températures élevées", by J. Moreau, Ing.Dr., and Professor J. Bénard.

At the conclusion of each discussion, a vote of thanks to the authors was proposed by the Chairman and carried with acclamation.

#### VISITS

In the afternoon, visits were paid to the Wallace Collection; the research laboratories of The British Aluminium Co., Ltd., Gerrards Cross, and of The General Electric Co., Ltd., Wembley; and the works of The A.P.V. Co., Ltd., Crawley.

Members and ladies of the Société Française de Métallurgie took part in an all-day visit to Windsor Castle, St. George's Chapel, Windsor, Eton College, and Hampton Court Palace.

#### RECEPTION BY H.E. THE FRENCH AMBASSADOR

In the evening, His Excellency the French Ambassador gave a reception for the President, members, and ladies of the Société Française de Métallurgie.

#### Friday, 30 April

##### VISITS

All-day visits were paid to: (a) Cambridge and the Colleges; (b) Research Laboratories of Associated Electrical Industries, Ltd., Aldermaston; (c) Enfield Rolling Mills, Ltd., and Enfield Cables, Ltd., Brimsdown; (d) Ford Motor Co., Ltd., Dagenham; (e) Fulmer Research Institute, Stoke Poges, and High Duty Alloys, Ltd., Slough; (f) Northern Aluminium Co., Ltd., and Aluminium Laboratories, Ltd., Banbury; and (g) Stewarts and Lloyds, Ltd., Corby.

#### Saturday, 1 May

Members and ladies of the Société Française de Métallurgie, the Institute of Metals, and the Iron and Steel Institute took part in an all-day tour of the Kent countryside visiting Canterbury Cathedral and Rochester.

#### Monday and Tuesday, 3 and 4 May

##### PROVINCIAL VISITS

Members and ladies of the Société Française de Métallurgie spent two days at one of the following provincial centres: Birmingham, Cambridge, Sheffield, and Swansea. They paid visits as detailed below and on the Monday were entertained at a dinner by local industries or, in the case of Cambridge, by local members.

*Birmingham.*—Visits were paid to the works and laboratories of Birmetals, Ltd.; Birmingham Aluminium Casting (1903) Co., Ltd.; James Booth and Co., Ltd.; Imperial Chemical Industries, Ltd., Metals Division; McKechnie Brothers, Ltd.; The Mond Nickel Co., Ltd.; and Henry

Wiggin and Co., Ltd. The ladies visited Stratford-on-Avon, Warwick Castle, and Broadway.

*Cambridge.*—Visits were paid to: British Welding Research Association Laboratories, Abington; Cambridge Instrument Co., Ltd.; Cavendish Laboratory; the Engineering and Metallurgy Departments of the University of Cambridge; and the Colleges. The ladies visited the Colleges and Ely Cathedral.

*Sheffield.*—Visits were paid to the works and laboratories of Samuel Fox and Co., Ltd.; The Brightside Foundry and Engineering Co., Ltd.; British Iron and Steel Research Association; Davy and United Engineering Co., Ltd.; Edgar Allen and Co., Ltd.; and Hadfields, Ltd. Ladies visited the Dukeries, and Chatsworth and Haddon Hall.

*South Wales.*—Visits were paid to the Research Laboratories of the British Iron and Steel Research Association and to the works of the Aluminium Wire and Cable Co., Ltd., Swansea; Imperial Chemical Industries, Ltd., Metals Division, Wauarlwydd; The Mond Nickel Co., Ltd., Clydach; The National Smelting Co., Ltd., Llansamlet; the Northern Aluminium Co., Ltd., Rogerstone; and the Steel Company of Wales, Ltd., Margam and Trostre.

The meeting then concluded.

#### COMITÉ D'HONNEUR

The following were Patrons of the Joint Meeting (Members of a Comité d'Honneur):

ADRIAN, Dr. E. D., O.M., M.A., F.R.S. (President, The Royal Society).

AUSTIN, Professor G. Wesley, O.B.E., M.A., M.Sc. (Professor of Metallurgy, University of Cambridge).

BAILEY, Mr. G. L., C.B.E., M.Sc. (Director, British Non-Ferrous Metals Research Association, London).

BALL, Major C. J. P., D.S.O., M.C. (Chairman and Managing Director, Magnesium Elektron, Ltd., Manchester).

BARNARD, Mr. H. B. (Managing Director, H. B. Barnard and Sons, Ltd., London).

BOOTH, Mr. G. W. (President, The British Bronze and Brass Ingot Manufacturers' Association).

BRABY, Mr. F. C., M.C., B.Sc. (Chairman and Managing Director, Frederick Braby and Co., Ltd., London).

BROWN, Mr. A. J. S., B.Sc. (Managing Director, J. Stone and Co. (Deptford), Ltd., London).

BRUCE, Mr. Fraser W., B.A.Sc. (Managing Director, Northern Aluminium Co., Ltd., Banbury).

CAMPBELL, Mr. D. F., M.A., A.R.S.M. (Chairman, Electric Furnace Co., Ltd., Weybridge).

CLARKE, Mr. Horace W., Hon.D.Sc. (Chairman and Managing Director, James Booth and Co., Ltd., Birmingham).

COLQUHOUN, Mr. J. C., M.B.E. (Chairman and Managing Director, Manganese Bronze and Brass Co., Ltd., Birkenhead).

COOPER, Mr. L. H., M.B.E. (Chairman, The Mond Nickel Co., Ltd., London).

CUNLIFFE, The Hon. Geoffrey (Chairman, The British Non-Ferrous Smelters' Association).

DANNATT, Professor C. W., A.R.S.M., D.I.C. (Head of the Department of Metallurgy, Royal School of Mines, London).

FIENNES, Mr. M. A. (Managing Director, Davy and United Engineering Co., Ltd., Sheffield).

FLECK, Dr. Alex. (Chairman, Imperial Chemical Industries, Ltd., London).

GARRETT, Sir Ronald (Chairman, Lloyd's Register of Shipping, London).

GOVETT, Mr. J. R. (Chairman, The Consolidated Zinc Corporation, Ltd., London).

GRIMSTON, The Hon. John, M.P. (Managing Director, Enfield Rolling Mills, Ltd., Brimsdown).

GUETERBOCK, Colonel Sir Paul, K.C.B., D.S.O., M.C., T.D., A.D.C. (Managing Director, Copper Pass and Son, Ltd., Bristol).

HAMER, Mr. R. D., B.Sc. (President, The Aluminium Development Association, London).



HERRINGTON, Mr. H. G. (Managing Director, High Duty Alloys, Ltd., Slough).

HUMPHREYS, Mr. O. W., B.Sc. (Director, The General Electric Co., Ltd., and Director of the Company's Research Laboratories, Wembley).

HUNTER, Mr. P. V., C.B.E. (Joint Deputy Chairman, British Insulated Callender's Cables, Ltd., Prescott).

IRELAND, Mr. John, M.C., B.Sc. (Director, The Tin Research Institute, Greenford).

JACKSON, Mr. H. E. (President, The British Non-Ferrous Metals Federation).

JONES, Sir Lewis, J.P. (Secretary, The South Wales Siemens Steel Association, Swansea).

LIDDIARD, Mr. E. A. G., M.A. (Director of Research, Fulmer Research Institute, Stoke Poges).

MC CONNELL, Mr. J. L., M.C. (Chairman, Goodlass Wall and Lead Industries, Ltd., London).

MCDONALD, Mr. Donald, B.Sc. (Joint Managing Director, Johnson, Matthey and Co., Ltd., London).

MC KECHNIE, Mr. J. D. (Chairman and Managing Director, McKechnie Brothers, Ltd., Birmingham).

MITCHELL, Mr. James, C.B.E. (President, The Iron and Steel Institute).

MURPHY, Professor A. J., M.Sc. (Head of the Department of Metallurgy, University of Birmingham).

PFEL, Dr. L. B., O.B.E., A.R.S.M., F.R.S. (President, The Institution of Metallurgists).

PLAYER, Mr. Edward (Managing Director, Birmid Industries, Ltd., Smethwick).

PORTAL OF HUNGERFORD, Marshal of the Royal Air Force The Right Hon. The Viscount, K.G., G.C.B., O.M., D.S.O., M.C. (Chairman, The British Aluminium Co., Ltd., London).

PRESTON, Mr. G. W., M.B.E. (General Manager, Copper Development Association, Radlett).

RANDALL, Mr. W. F., B.Sc., A.R.S.M. (Director, Metals Division, The Telegraph Construction and Maintenance Co., Ltd., London).

ROBERTSON, Mr. W. H. A. (Managing Director, W. H. A. Robertson and Co., Ltd., Bedford).

SANDERS, Mr. Spence (Managing Director, Almin, Ltd., Farnham Royal).

SELIGMAN, Dr. Richard (Chairman, The A.P.V. Co., Ltd., London).

SLATER, Mr. W. F., B.Sc. (Director and General Manager, Thomas Bolton and Sons, Ltd., Stoke-on-Trent).

SMOUT, Sir Arthur, J.P. (Chairman, Murex, Ltd., Rainham).

STEDEFORD, Mr. I. A. R. (Chairman and Managing Director, Tube Investments, Ltd., Birmingham).

STUBBS, Mr. R. Lewis, O.B.E. (Director, Zinc Development Association, Oxford).

STURDEE, Mr. A. H., M.B.E. (Chairman, Light Metal Founders' Association).

TREBUCC, Mr. A. (Deputy Chairman, H. J. Enthoven and Sons, Ltd., London).

## EXECUTIVE COMMITTEE

The arrangements for the meeting were made with the assistance and advice of an Executive Committee constituted as follows:

DOREY, Dr. S. F., C.B.E., F.R.S. (Chief Engineer Surveyor, Lloyd's Register of Shipping, London) *Chairman*.

BAER, Mr. Alfred, B.A. (Vice-Chairman, The Consolidated Zinc Co., Ltd., London).

BAILEY, Mr. G. L., C.B.E., M.Sc. (Director, The British Non-Ferrous Metals Research Association, London).

BRABY, Mr. F. C., M.C., B.Sc. (Chairman and Managing Director, Frederick Braby and Co., Ltd., London).

COOK, Dr. Maurice (Joint Managing Director, Imperial Chemical Industries, Ltd., Metals Division, Birmingham).

DANNATT, Professor C. W., A.R.S.M. (Head of the Department of Metallurgy, Royal School of Mines, London).

HEADLAM-MORLEY, Mr. K. (Secretary, The Iron and Steel Institute, London).

HUNT, Dr. L. B. (Manager, Industrial Division, Johnson, Matthey and Co., Ltd., London).

JONES, Mr. E. H. (Joint Managing Director, Capper Pass and Son, Ltd., Bristol).

PARKER, Dr. R. T., B.Sc., A.R.S.M. (Director of Research, Aluminium Laboratories, Ltd., Banbury).

PFEL, Dr. L. B., O.B.E., A.R.S.M., F.R.S. (Director, The Mond Nickel Co., Ltd., London).

THOMPSON, Professor F. C., D.Met., M.Sc. (President of the Institute of Metals; Professor of Metallurgy, University of Manchester).

*Secretary:* GUILLAN, Lieut.-Colonel S. C., T.D.

## GENERAL MEETINGS

## 27 May 1954

A GENERAL MEETING of the Institute of Metals was held at 4 Grosvenor Gardens, London, S.W.1, on Thursday, 27 May 1954, at 5.30 p.m. The Chair was taken by Professor G. V. RAYNOR, M.A., D.Phil., D.Sc., Vice-President and Chairman of the Metal Physics Committee.

Dr. W. BOAS, of the Division of Tribophysics, C.S.I.R.O., Melbourne, delivered a lecture on "Lattice Defects and Energy Stored in Deformed Metals", after which there was a discussion.

A vote of thanks to the lecturer was proposed, seconded, and carried with acclamation.

## 30 June 1954

A GENERAL MEETING of the Institute of Metals took place at 4 Grosvenor Gardens, London, S.W.1, on Wednesday, 30 June, 1954, at 5.0 p.m. Dr. S. F. DOREY, C.B.E., F.R.S. (President) was in the Chair.

Professor E. OROWAN, F.R.S., of the Massachusetts Institute of Technology, delivered a lecture on "The Brittle Fracture of Metals", followed by a discussion.

A vote of thanks to the Lecturer was proposed, seconded, and carried with acclamation.

## ANNUAL AUTUMN MEETING

## 6 to 14 September 1954

THE FORTY-SIXTH ANNUAL AUTUMN MEETING of the Institute of Metals was held in Switzerland from Monday 6 to Tuesday 14 September 1954, by invitation of the Verein Schweiz. Maschinen-Industrieller and the Schweiz. Verband für die Materialprüfungen der Technik.

## Monday, 6 September

## OFFICIAL WELCOME TO SWITZERLAND

The meeting opened at 9.30 a.m. in the Eidgenössische Technische Hochschule, Zürich, Professor Dr.-Ing. A. von ZEERLEDER, Corresponding Member to the Council for Switzerland, took the Chair when representatives of the Institute's hosts and other organizations offered a welcome to members of the Institute of Metals, to which the President, Dr. S. F. DOREY, C.B.E., F.R.S., replied.

## GENERAL MEETING

The President having taken the Chair, it was agreed that the minutes of the last General Meetings held in London on 26 April-1 May, 27 May, and 30 June 1954, be taken as read and signed by the Chairman.

*Elections of Members, Junior Members, and Student Members*

The Secretary (Lieut.-Colonel S. C. GUILLAN, T.D.) announced that, since the 1954 Spring Meeting, a total of 56 Ordinary Members, Junior Members, and Student Members had been elected on 9 June, 1 July, 13 August, and 1 September 1954, the lists of whose names are printed in the *Bulletin*, 1953-55, vol. 2, pp. 142, 152, and 160.

*Election of Officers for 1954-55*

The Secretary announced that the following members would retire from the Council at the 1955 Annual General Meeting, as required by the Articles of Association :

*President :*

S. F. DOREY, C.B.E., D.Sc., F.R.S.

*Past-President :*

C. J. SMITHELLS, M.C., D.Sc.

*Vice-President :*

G. L. BAILEY, C.B.E., M.Sc.

*Honorary Treasurer :*

J. C. COLQUHOUN, M.B.E.

*Ordinary Members of Council :*

K. W. CLARKE  
CHRISTOPHER SMITH

He stated that, in accordance with Article 19, Dr. S. F. DOREY, C.B.E., F.R.S., would fill the vacancy as Past-President; that Mr. J. C. COLQUHOUN, M.B.E., having been appointed by the Council to fill a vacancy occurring during the year 1954-55, in accordance with Article 28, was eligible for re-election as Honorary Treasurer; and that, in accordance with Article 22, the Council had nominated the following members to fill the vacancies :

*As President :*

MAURICE COOK, D.Sc., Ph.D.

*As Vice-Presidents :*

E. H. JONES  
W. J. THOMAS

*As Honorary Treasurer :*

J. C. COLQUHOUN, M.B.E.

*As Ordinary Members of Council :*

L. E. BENSON, M.Sc.  
C. F. J. FRANCIS-CARTER, O.B.E.  
D. P. C. NEAVE, M.A.  
Professor H. O'NEILL, M.Met., D.Sc.

*Senior Vice-President for 1955-56*

The Secretary announced that, in accordance with Article 42, the Council had elected Major C. J. P. BALL, D.S.O., M.C., to be Senior Vice-President for 1955-56, and that he would be their nominee for the Presidency in 1956-57.

*Institute of Metals (Platinum) Medal for 1953*

The President presented to Dr. Georg MASING—who had been unable to attend a meeting previously, owing to ill-health—the Institute of Metals (Platinum) Medal for 1953. Dr. Masing briefly acknowledged the honour that had been conferred on him.

The President then vacated the Chair, which was taken by Professor F. C. THOMPSON, D.Met., M.Sc. (Past-President).

## DISCUSSION ON "GRAIN REFINEMENT"

A discussion was then held on the theme "Grain Refinement", based on the following papers previously published in the *Journal* :

"The Application of Grain-Refinement to Cast Copper-Aluminium Alloys Containing the Beta Phase", by J. P. DENNISON, B.Sc., Ph.D., and E. V. TULL, B.Sc., A.I.M.

"Grain-Refining Additions for Cast Copper Alloys", by A. CIBULA, M.A., A.I.M.

At the conclusion of the discussion, a vote of thanks to the authors was proposed by the Chairman and carried with acclamation.

## VISITS

In the afternoon members paid visits to the works of Escher-Wyss Engineering Works, Ltd., Zürich; Micafil, Ltd., Zürich-Alstetten; Oerlikon Machine Tool Works Bührle and Co., Machine Tool and Electrode Manufacture Divisions, Zürich-Oerlikon; and the Swiss Car and Elevator Manufacturing Corp., Ltd., Schlieren-Zürich. Other members and ladies made a sight-seeing tour of Zürich.

## OFFICIAL RECEPTION

In the evening a Reception was given for members at the Rathaus by the President of the Cantonal Government, Dr. P. MEIERHANS.

## Tuesday, 7 September

## VISITS

All-day visits were paid by members to : (a) Brown-Boveri and Co., Ltd., the Hydraulic Power Station, Wildeggen-Brugg, and the Gas Turbine Station, Beznau; (b) A. G. Oederlin and Co., Ltd., and the power stations mentioned in (a) above; and (c) Oerlikon Engineering Co., Zürich-Oerlikon, and the Hydraulic Power Station, Etzel. Members were entertained to lunch by the Companies.

In the afternoon, ladies visited the Uetliberg for tea.

## BANQUET

In the evening, members and ladies were the guests of the two host associations at a banquet at the Grand Hotel Dolder, Zürich.

## Wednesday, 8 September

The meeting was resumed at 9.30 a.m. at the Eidgenössische Technische Hochschule, Zürich. The Chair was taken by Professor Dr.-Ing. A. von ZEERLEDER.

## DISCUSSION ON "CORROSION AND STAINING OF ALUMINIUM ALLOYS"

A discussion was held on the following two papers, previously published in the *Journal* :

"The Influence of Extrusion Direction on the Corrosion and Stress-Corrosion of Aluminium-Copper-Magnesium Alloys", by E. A. G. Liddiard, M.A., F.I.M., and Winifred A. Bell, B.A.

"Staining of Clad Aluminium Sheets During Salt-Bath Heat-Treatment", by E. C. Williams, M.Sc., A.Inst.P., and H. J. G. Challis, F.R.I.C., A.I.M.

At the conclusion of the discussions, a vote of thanks to the authors was proposed by the Chairman and carried with acclamation.

## VISITS

In the afternoon, members visited the works of Sulzer Brothers, Ltd.; the Swiss Locomotive and Machine Works (S.L.M.); J. J. Reiter and Co.; and the Metallarbeiterschule and Werkmeisterschule, all at Winterthur. Ladies visited the Reinhart Art Gallery, Winterthur.

## DINNER

In the evening members and ladies were the guests of Sulzer Brothers, Ltd., the Swiss Locomotive and Machine Works (S.L.M.), and J. J. Reiter and Co., Ltd., at dinner at Kyburg Castle.

## Thursday, 9 September

## VISITS

Members and ladies made all-day visits to Schaffhausen and Neuhausen. In the morning ladies visited the "Allerheiligen" Museum at Schaffhausen, while members visited :



(a) the Research Laboratories of the Société Anonyme pour l'Industrie de l'Aluminium, Neuhausen-am-Rheinfall; (b) the works of the Swiss Industrial Company, Neuhausen-am-Rheinfall; (c) the Steel Foundry Division "Ebnat" of Georg Fischer, Ltd., Schaffhausen; (d) the Machine Works "Ebnat" of Georg Fischer, Ltd., Schaffhausen; and (e) the works of Alfred J. Amsler and Co., Schaffhausen.

After lunch at the Casino, Schaffhausen, by invitation of the companies whose works and laboratories had been visited, members and ladies were also the companies' guests on a trip on the Rhine to Stein-am-Rhein and back.

#### AUTUMN LECTURE

The President occupied the Chair when, at 8.30 p.m. in the Auditorium Maximum of the Eidgenössische Technische Hochschule, Zürich, Professor Dr.-Ing. A. von ZEERLEDER, Corresponding Member to the Council for Switzerland, delivered the Twenty-Fifth Autumn Lecture on "Attempts to Improve Aluminium Reduction Since Héroult and Hall". (The lecture is printed in the *Journal*, 1954-55, 83, (7), 321.)

A vote of thanks to the Lecturer was proposed by Mr. R. D. HAMER, B.Sc., Member of Council, and carried with acclamation.

After the lecture, members and ladies were offered light refreshments by the Interessengemeinschaft der Schweizerischen Aluminiumhütten-Walz und Presswerk.

#### Friday, 10 September

##### VISITS

At 9.0 a.m., members paid visits to: the Eidgenössische Materialprüfungs- und Versuchsanstalt and the Physical, Metallurgical, Cryogenic, Photoelasticity, and Mechanical Engineering Departments, and the Institute for Hydraulic Machines and Hydraulic Power Installations, at the Eidgenössische Technische Hochschule, Zürich.

#### DISCUSSION ON "THE CONSTITUTION OF TITANIUM ALLOYS"

The meeting was resumed at 10.30 a.m. in the Eidgenössische Technische Hochschule, when Dr. Maurice Cook (Senior Vice-President), occupied the Chair.

A discussion was held on "The Constitution of Titanium Alloys", based on the following series of eight papers previously published in the *Journal*. Mr. E. A. G. LIDDIARD, M.A., introduced the papers, as rapporteur.

"The Structure of Titanium-Tin Alloys in the Range 0-25 Atomic Per Cent. Tin", by H. W. Wörner, M.Sc.

"The Re-Investigation of a Nickel-Titanium Alloy and Observations on  $\beta(\alpha + \beta)$  Boundaries in Titanium Systems", by A. D. McQuillan, Ph.D., B.Sc.

"The Free-Energy Diagram of the System Titanium-Oxygen", by O. Kubaschewski, Dr.phil.habil., and W. A. Dench.

"The Structure of Titanium-Silver Alloys in the Range 0-30 Atomic Per Cent. Silver", by H. W. Wörner, M.Sc.

"A Redetermination and Interpretation of the Titanium-Rich Region of the Titanium-Chromium System", by (Mrs.) M. K. McQuillan, M.A.

"Methods for Determining the Liquidus Points of Titanium-Rich Alloys", by W. Hume-Rothery, O.B.E., F.R.S., and D. M. Poole, M.Sc.

"Note on the Constitution of the Titanium-Gold System in the Region 0-6 Atomic Per Cent. Gold", by (Mrs.) M. K. McQuillan, M.A.

"The Constitution of the Titanium-Rich Alloys of Titanium, Iron, and Oxygen", by N. P. Allen, M.Met., D.Sc., F.I.M., T. H. Schofield, M.Sc., and (Mrs.) B. Mellish, B.Sc.

At the conclusion of the discussion, a vote of thanks to the authors and rapporteur was proposed by the Chairman and carried with acclamation.

At 12 noon, the President, Dr. S. F. DOREY, C.B.E., F.R.S., took the Chair.

#### PRESENTATION TO MR. W. VON ORELLI

On behalf of the Council, the President made a presentation to Mr. W. von ORELLI, as a mark of appreciation of his services as Honorary Secretary to the Executive Committee of the Meeting.

#### VOTE OF THANKS

Dr. Maurice Cook, Senior Vice-President, proposed and Mr. W. G. HISCOCK seconded: "That the best thanks of the Institute of Metals be, and are hereby, extended to:

(i) The Presidents and Councils of the Verein Schweiz. Maschinen-Industrieller and the Schweiz. Verband für die Materialprüfungen der Technik for their kind invitation to the Institute to hold this Autumn Meeting in Switzerland, and for their most generous hospitality.

(ii) Professor Dr.-Ing. A. von ZEERLEDER, Chairman of the Reception Committee, the Honorary Secretary, Mr. W. von ORELLI, and the members of the Reception Committee and the Ladies' Committee for the excellent arrangements made for this meeting.

(iii) The representatives of the Canton and City of Zürich and of the Eidgenössische Technische Hochschule for their welcome and hospitality.

(iv) The Rector of the Eidgenössische Technische Hochschule for kindly placing accommodation for this meeting at the disposal of the Institute.

(v) The Interessengemeinschaft der Schweizerischen Aluminiumhütten-Walz und Presswerke, for their hospitality.

(vi) The Directors of numerous Swiss establishments and companies for their invitations to members and guests to visit their works and laboratories and for their hospitality.

(vii) All others who have contributed in any way to the success of this meeting."

The motion was put to the meeting and carried with acclamation. Professor Dr.-Ing. A. von ZEERLEDER, on behalf of the two host associations, briefly acknowledged the vote of thanks.

The business meeting then concluded.

#### COCKTAIL PARTY

In the evening, the members of the Institute of Metals present at the meeting gave a cocktail party for their hosts on the M/S "Linth", during a trip on the Lake of Zürich.

#### Saturday and Sunday, 11 and 12 September

Members and ladies proceeded on Saturday, 11 September, by special train to Montreux, via Lucerne, Interlaken, and the Bernese Oberland. Tea was taken at Zweisimmen.

#### Monday, 13 September

##### VISITS

Members paid visits to the works of the Société Anonyme pour l'Industrie de l'Aluminium, Chippis; and the Société Anonyme des Câbleries et Tréfileries de Cossonay, and were entertained to lunch by the companies. Other members and ladies took part in an all-day tour of Gruyère and the Pilon Pass.

#### Tuesday, 14 September

##### VISITS

Members paid visits to the works of the Fonderie Boillat S.A., Reconvilier, Metallwerke A.G., Dornach, and Louis de Roll Iron Works, Ltd., Gerlafingen and Choindéz, and were entertained to lunch by the companies.

The meeting then terminated.

The arrangements for the meeting were made with the assistance and advice of a Reception Committee and a Ladies' Committee constituted as follows:

#### RECEPTION COMMITTEE

VON ZEERLEDER, Professor Dr.-Ing. A. (*Chairman*)  
 BRANDENBERGER, Dr. E.  
 MESSNER, Dr. O. H. C.  
 VON ORELLI, Mr. W. (*Hon. Secretary*)

#### LADIES' COMMITTEE

AMSTUTZ, Mrs. E.  
 FISCHER, Mrs. G.  
 MESSNER, Mrs. O. H. C.  
 MEYLAN, Mrs. C.  
 VON ORELLI, Mrs. W.  
 SPEISER, Mrs. E.

### GENERAL MEETING

25 and 26 November 1954

A GENERAL MEETING of the Institute of Metals was held at 4 Grosvenor Gardens, London, S.W.1, on Thursday and Friday, 25 and 26 November 1954.

The President, Dr. S. F. DOREY, C.B.E., F.R.S., occupied the Chair at the opening of the meeting, at 2.30 p.m., on Thursday, 25 November.

#### Thursday, 25 November

It was agreed that the minutes of the previous General Meeting, held in Switzerland from 6 to 14 September 1954 be taken as read and signed by the Chairman.

#### ELECTIONS OF ORDINARY MEMBERS, JUNIOR MEMBERS, AND STUDENT MEMBERS

The Secretary (Lieut.-Colonel S. C. GUILLAN, T.D.) announced that since the Annual Autumn Meeting a total of 92 Ordinary Members, Junior Members, and Student Members had been elected on 3 November and 25 November, 1954, the lists of whose names are printed in the *Bulletin*, 1953-55, vol. 2, pp. 176 and 208.

The President then vacated the Chair, which was taken by Mr. G. L. BAILEY, C.B.E., M.Sc. (Vice-President).

#### DISCUSSION ON "THE CONSTITUTION OF TITANIUM ALLOYS"

A discussion was held, based on the following series of eight papers previously published in the *Journal*. Mr. E. A. G. LIDDIARD, M.A., introduced the papers, as rapporteur.

"The Structure of Titanium-Tin Alloys in the Range 0-25 Atomic Per Cent. Tin", by H. W. Wörner, M.Sc.

"The Re-Investigation of a Nickel-Titanium Alloy and Observations on  $\beta/(\alpha + \beta)$  Boundaries in Titanium Systems", by A. D. McQuillan, Ph.D., B.Sc.

"The Free-Energy Diagram of the System Titanium-Oxygen", by O. Kubaschewski, Dr.phil.habil., and W. A. Dench.

"The Structure of Titanium-Silver Alloys in the Range 0-30 Atomic Per Cent. Silver", by H. W. Wörner, M.Sc.

"A Redetermination and Interpretation of the Titanium-Rich Region of the Titanium-Chromium System", by (Mrs.) M. K. McQuillan, M.A.

"Methods for Determining the Liquidus Points of Titanium-Rich Alloys", by W. Hume-Rothery, O.B.E., F.R.S., and D. M. Poole, M.Sc.

"Note on the Constitution of the Titanium-Gold System in the Region 0-6 Atomic Per Cent. Gold", by (Mrs.) M. K. McQuillan, M.A.

"The Constitution of the Titanium-Rich Alloys of Titanium, Iron, and Oxygen", by N. P. Allen, M.Met., D.Sc., F.I.M., T. H. Schofield, M.Sc., F.I.M., and (Mrs.) B. Mellish, B.Sc.

At the conclusion of the discussion, a vote of thanks to the authors and rapporteur was proposed by the Chairman and carried with acclamation.

The meeting was then adjourned.

#### Friday, 26 November

The meeting was resumed at 4 Grosvenor Gardens, at 10.0 a.m., when Dr. L. B. PFEIL, O.B.E., A.R.S.M., F.R.S. (Vice-President) took the Chair.

#### DISCUSSION ON "PREFERRED ORIENTATION"

A discussion took place, based on the following three papers previously published in the *Journal*. Professor A. H. COTTRELL, Ph.D., B.Sc. introduced the papers, as rapporteur.

"A Theoretical Investigation of the Deformation Textures of Titanium", by D. N. Williams, Ph.D., and Professor D. S. Eppelsheimer, D.Sc.

"A Study of Preferred Orientation in Extruded, Drawn, and Annealed Copper", by Professor P. G. Bastien, Dr.ès.Sci., and Dr. J. Pokorny.

"Preferred Orientation in Rolled Uranium Sheet", by J. Adam, B.Sc., Ph.D., A.Inst.P., and J. Stephenson, B.Met., A.I.M.

The meeting was resumed at 2.30 p.m., when Dr. H. SUTTON, C.B.E. (Member of Council) occupied the Chair.

#### DISCUSSION ON "CORROSION AND STAINING OF ALUMINIUM ALLOYS"

A discussion was held, based on the following two papers, previously published in the *Journal*. Dr. R. T. PARKER, B.Sc., introduced the papers, as rapporteur.

"The Influence of Extrusion Direction on the Corrosion and Stress-Corrosion of Aluminium-Copper-Magnesium Alloys", by E. A. G. Liddiard, M.A., F.I.M., and Winifred A. Bell, B.A.

"Staining of Clad Aluminium Alloy Sheets During Salt-Bath Heat-Treatment", by E. C. Williams, M.Sc., A.Inst.P., and H. J. G. Challis, F.R.I.C., A.I.M.

At the conclusion of each discussion, a vote of thanks to the authors and rapporteur was proposed by the Chairman and carried with acclamation.



# THE MECHANISM OF RESIDUAL-STRESS FORMATION IN SAND CASTINGS\*

1487

By R. N. PARKINS,† B.Sc., Ph.D., A.I.M., JUNIOR MEMBER,  
and A. COWAN,‡ B.Sc., Ph.D., STUDENT MEMBER

## SYNOPSIS

Experiments on cast iron, brass, and Y alloy show that residual stresses in sand castings may result from: (a) temperature differences set up during cooling, (b) phase transformations in the alloy, and (c) resistance to contraction offered by the sand. The magnitude of the contribution by each of these varies according to the type of casting produced, but a qualitative interpretation of the present results indicates that minimizing temperature differences in the casting usually promotes low stresses. This is because the contributions of phase transformations and sand resistance to the total residual stresses depend largely upon the presence of temperature differences in the casting.

## I.—INTRODUCTION

THE stresses remaining in sand castings after removal from the mould arise from inhomogeneous plastic deformation, so that to enable the parts of the casting to fit together elastic strains corresponding to the residual stresses must be introduced. Non-uniform deformation may be expected to be due to variations in cooling rates in different parts of the casting, or to hindrance to free contraction by the mould material. Phase transformations may also affect the magnitude of the residual stress, since, if temperature differences are present, a transformation, with its accompanying heat and volume changes, will occur at different times in different sections of the casting, thereby possibly causing varying amounts of plastic deformation.

The relative contributions of these three factors to the total residual stress in any casting will be dependent upon the shape of the casting; in extreme cases the stress may be due to either non-uniform cooling rates or sand hindrance alone. The object of the present work was to determine the relative effects of these factors in a casting in which both temperature differences and restricted contraction occurred.

Although the presence of residual stresses in castings had been appreciated many years previously, it was not until 1897 that Schumann,<sup>1</sup> in a discussion of stresses in cast iron, stated that they were caused by unequal cooling rates in various sections of the casting. This effect was further studied by Heyn,<sup>2,3</sup> whose work represented the first serious attempt to make quantitative determinations. Schüz,<sup>4</sup> in a study of the contraction of chill-cast iron rolls, also associated the residual stresses with temperature gradients, as well as with the differing coefficients of contraction of grey and white iron.

A framework-type casting, similar to that shown in

Fig. 2, and consisting of three members of equal length, joined at their extremities by rigid yokes, the two outer members having smaller cross-sections than the central member, has been used extensively in researches on residual stresses. Von Steiger<sup>5</sup> showed that increasing the difference between the cross-sectional areas of the members of a cast-iron framework (and hence the temperature difference between them) caused an increase in the stresses; no temperature measurements were made, however. This result has been confirmed in work with an aluminium alloy.<sup>6</sup> In a modified form (similar to that shown in Fig. 1), the framework-type casting has recently been used to show that the stresses in an aluminium alloy casting increased as the moisture content of the moulding sand, the pouring temperature, and runner diameter increased.<sup>7</sup> Castings in an aluminium alloy and a steel were stripped from the mould at various intervals after pouring, the stress being found to increase with the time allowed to elapse before stripping. This provided confirmation of previous work on cast iron.<sup>8</sup> These effects were attributed to the temperature variations caused by the factors studied, but again no temperatures were quoted.

In 1927 Malzacher,<sup>9</sup> discussing the origin of internal stresses in sand castings, stated that they might arise from (a) mould resistance and (b) thermal gradients due to variations of metal thickness. He considered that the stresses were largely due to sand resistance. Phillips,<sup>10</sup> however, showed that sand cores, of the varying degrees of hardness commonly found in industrial practice, had no influence on crack-formation in a steel casting designed to be susceptible to hot-tearing. This has been confirmed with framework-type castings of steel and aluminium alloy, using moulding sands having a wide range of compressive strengths.<sup>6,7</sup> More recently,<sup>11</sup> how-

\* Manuscript received 23 February 1953.

† Lecturer in Metallurgy, King's College, University of Durham, Newcastle-upon-Tyne.

‡ Ministry of Supply (Division of Atomic Energy); formerly research student at King's College, University of Durham, Newcastle-upon-Tyne.

ever, it has been shown that sand resistance can be considerable in castings of certain design. By making castings of uniform and small cross-section, temperature differences can be minimized, and the effect of sand resistance can be studied by making the shape of the casting such that its contraction is restrained by the sand. A straight bar with flanges at each end, or a thin-walled hollow cylinder, conforms to these requirements. To a first approximation, it was shown that the degree of restraint was proportional to the sand strength, although it was also shown that the grain-size distribution of the sand could have quite a marked effect upon the amount of restraint and upon the stresses remaining in certain castings.

Machin and Oldham<sup>12</sup> advocated the use of hot moulds to reduce residual stresses, since temperature differences in the casting would be less and the sand would be crushed more readily at a high temperature, so that a condition of almost free contraction would

operative at the same time, each being varied in turn and the contributions of the other two kept constant. While the first method is undoubtedly of some value, and indeed the initial experiments in the present work<sup>11</sup> followed these lines, it is doubtful whether it can give an accurate estimate of the relative importance of transformation, thermal, and mould effects in castings where all three are present. Consequently, in the work described here, castings have been used in which the stresses arose from a combination of all three effects, and the importance of each has been assessed by casting into various sands, by comparing different alloys, and by conducting certain cooling experiments in air.

The framework-type of casting (Fig. 2), first used by Heyn,<sup>3</sup> is ideally suited to this purpose. The thicker section of the centre member, as compared with the outer members, gives rise to unequal cooling rates, while the overall contraction of the casting is hindered by the sand between the end yokes and the centre and

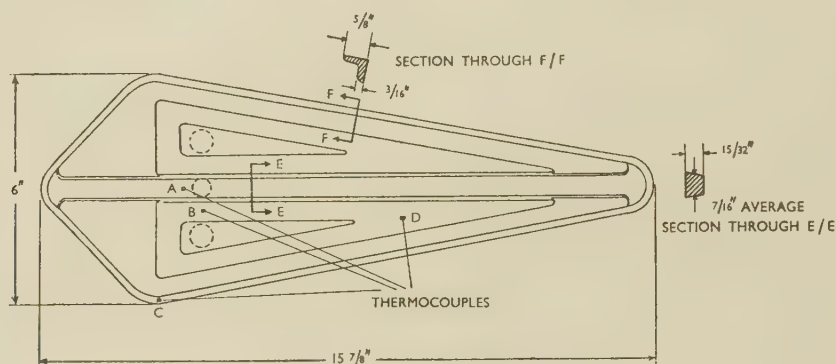


FIG. 1.—Ferranti-Type Framework.

exist. Davies and Rees,<sup>13</sup> however, later showed that the compressive strengths of moulding sands generally increased to a maximum at temperatures of the order of 1000° C., and then rapidly decreased with further increase of temperature.

No attempt has apparently been made hitherto to determine the effect of phase transformations on residual stresses in castings, although stresses in quenched cylinders have been considered in relation to the volume changes accompanying transformation.<sup>14, 15</sup> Moreover, although the majority of residual-stress measurements on castings have been made on ferrous alloys in which a phase transformation occurs, no assessment of the relative importance of transformation, thermal, and mould stresses has been attempted.

## II.—EXPERIMENTAL TECHNIQUE

### 1. CASTING DESIGN

The problem of determining the relative contributions of the three effects mentioned may be approached in two different ways. Thus, castings can be made in which residual stresses will arise from any one of these sources separately; or else all three factors may be

side limbs. The formation of stress in castings of this type is usually considered to be a two-stage process. In the earlier stages of contraction the lighter (outer) members cool more quickly than the centre member, and hence cause the latter to deform plastically in compression, so that its actual length at any temperature during this stage is less than its "free" length, i.e. its length if it had been allowed to contract freely. As cooling continues, the centre member, owing to its higher temperature, tends to contract faster than the lighter members, but the latter, now relatively rigid, hinder contraction, and for equilibrium to be attained a tensile stress is set up in the centre member, balanced by compressive and bending stresses in the outer members. It should be made clear, however, that this is an oversimplified description of the mode of stress formation.

In a comparative study of the present nature it was preferable that only unidimensional stresses should be set up in the centre member. This condition demands that the casting be as rigid as possible and not prone to bending. Of the various designs described in the literature, based on that of Heyn but incorporating modifications to produce a unidimensional stress system, the Ferranti type<sup>8</sup> (Fig. 1) was



selected initially. The usual end sections were eliminated by the use of shaped outer limbs, of angular section, which were joined directly to the centre member by thin webs. In the pattern plate used, two V-shaped blocks were inserted to reduce the temperature variation between the centre and outer members and so reduce the risk of hot-tearing. These were poured simultaneously with the framework from a common pouring basin, using separate downgates.

In order to determine the cooling rates at different points in the casting, Chromel/Alumel (or noble metal in the case of cast iron) thermocouples were inserted in the sand during moulding, so that their hot junctions were in contact with the surface of the casting. The junctions were coated with an alcoholic suspension of alumina to prevent contamination by the molten metal.

In spite of the advantageous rigidity of the Ferranti framework, however, it was found necessary, for certain experiments, to use a simple rectangular

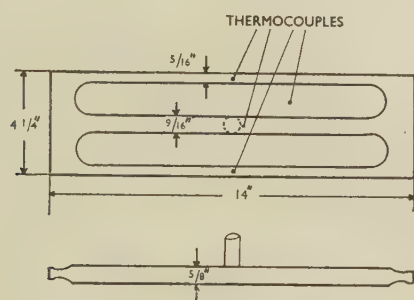


FIG. 2.—Rectangular-Type Framework.

framework (Fig. 2). In this design, the three members were straight and of rectangular section, the combined cross-sectional area of the outer members being very slightly greater than that of the centre member. The end yokes were in the form of a heavily filleted I section, thus providing maximum strength for a given amount of metal.

The use of this design enabled more accurate temperature measurements to be made, since the heavier cross-sections allowed thermocouple junctions to be inserted to the centre of the members, whereas with the lighter-section Ferranti framework only mould/metal interface temperatures could be measured. Platinum/platinum-rhodium couples were used for these experiments and, to overcome any effect which the presence of the thermocouple might have had upon the development of the stress, a "blank" casting without thermocouples was poured at the same time. The residual stress in the centre member of the blank casting was of the order of 0.2 tons/in.<sup>2</sup> less, and the stress values quoted are those for the blank casting.

## 2. AIR-COOLING EXPERIMENTS

By allowing framework castings to cool in air and establishing cooling conditions similar to those

observed as the casting cools in the mould, the effect of sand restraint may be eliminated, since the residual stresses arise from thermal effects only.

Rectangular frameworks were cast and allowed to cool in the mould. After removal of the runner, they were stress-relieved by slow heating, to 650° C. for cast iron and to 450° C. for the aluminium alloy, followed by slow cooling.

To achieve appreciable temperature differences between the members during the subsequent cooling in air, it was found necessary to lag them with 1/4-in.-thick asbestos rope. Suitable temperature differences were finally obtained by winding one layer of rope around each of the outer members and two layers around the centre member. The end sections were not lagged. Temperatures were measured by means of Chromel/Alumel thermocouples situated under the lagging, with their hot junctions mechanically attached close to the centre of the upper surface of each member.

After lagging, the frameworks were heated to varying temperatures, up to a maximum of 1000° C. for the cast iron and 475° C. for the aluminium alloy. During cooling they were supported only by their end sections.

## 3. SAND CONTROL

To obtain as high a degree of reproducibility as possible in the test results, routine sand-control tests, i.e. hardness, moisture, and permeability, were employed throughout. Determinations of green and hot compressive strength were also made, using a machine and technique similar to those adopted by Davies and Rees.<sup>13</sup>

Although it was not intended to study the effects of specific moulding sands, representative naturally bonded, synthetic, and core sands were used. To obtain a wider range of sand strengths, a dried floor sand with varying initial moisture contents, and hence appreciably differing dry strengths, was used. Addition of sawdust caused further lowering of the sand strength owing to charring at high temperatures. For the sake of greater clarity in discussion, the sands have been designated by their initial letter, followed by a number relating to their compressive strength, as given in Table I. The results of the hot compression tests are shown in Fig. 3.

The tests were not carried out at temperatures above 800° C., since measurements on castings showed that only a small amount of sand surrounding the metal was at a temperature above this. The curves for sands N.13, S.14, F.300, and F.180 show a similar relationship between strength and temperature to that obtained for like sands by Davies and Rees.<sup>13</sup> The sawdust of F.60 gradually charred as the temperature of testing was increased, thus leaving voids in the test-piece and causing the strength to diminish to a value of approximately 15 lb./in.<sup>2</sup> at 600° C. At a temperature of 250° C., the linseed oil of C.2000 began to char, the compressive strength rapidly diminishing as the temperature increased. Above

600° C. complete charring had occurred throughout the test specimen during the standard soaking time, with the result that the strength had too low a value to be measurable.

TABLE I.—*Sands Used in the Experiments.*

Sand Type	Composition of Sand Mix	Condition	Compressive Strength, lb./in. <sup>2</sup>	Designation
Naturally bonded	Northallerton sand + 5% moisture.	Green	13	N.13
Synthetic	Southport sand + 5% Bentonite + 3% moisture.	Green	14	S.14
Core	Southport sand + 2% cereal bond + 3% linseed oil + 3% moisture.	Baked at 220° C. for 1 hr.	2000	C.2000
Floor	Floor sand + 10% moisture.	Dried at 200° C.	300	F.300
Floor	Floor sand + 5% moisture.	Dried at 200° C.	180	F.180
Floor	Floor sand + 5% sawdust + 5% moisture.	Dried at 200° C.	60	F.60
Floor	Floor sand + 5% moisture.	Green	13	F.13
Floor	Floor sand + 5% sawdust + 5% moisture.	Green	10	F.10

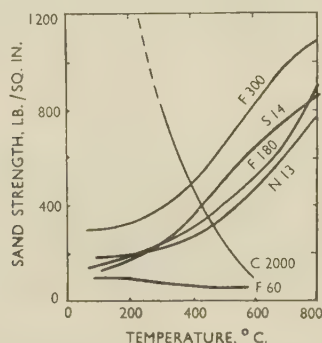


FIG. 3.—High-Temperature Compression Strengths of Moulding Sands.

#### 4.—MELTING, CASTING, AND PROPERTIES OF METALS

The castings were made in grey cast iron, brass, and Y alloy, these being chosen as representative of the ranges of contraction, temperature, and properties commonly found in practice. Their chemical analyses are given in Table II.

TABLE II.—*Analyses and Properties of Alloys Used.*

Alloy	Composition, %	Yield Stress, tons/in. <sup>2</sup>	U.T.S., tons/in. <sup>2</sup>	Elastic Modulus, tons/in. <sup>2</sup>
Cast iron	C 3.01, Si 1.90, Mn 0.86, P 0.18, S 0.04	8.4	18.8	6500
Brass	Cu 66, Zn 34	5.2	13.0	6160
Y alloy	Cu 4, Ni 2.5, Mg 1.5, Al remainder	5.2	11.0	4420

Melting was carried out in a gas-fired crucible furnace according to the usual practice, i.e. with additions for melting losses, fluxes where appropriate, and degassing treatment for the aluminium alloy.

The casting temperature varied according to the casting, but was kept constant for any one series of experiments.

The mechanical properties of the alloys were determined at room temperature and at elevated

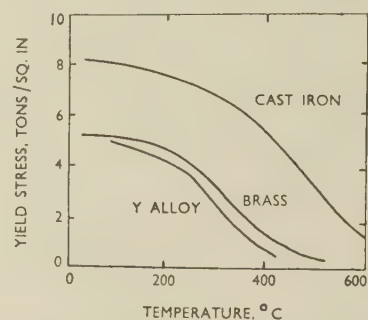


FIG. 4.—Variation of the Yield Stress of the Alloys with Temperature.

temperatures, since the maximum amount of residual stress at any temperature is governed by the yield point of the alloy at that temperature. The yield stress and the modulus of elasticity were determined, the accuracy of measurement decreasing at the higher temperatures of testing. The yield stress, which was poorly defined, was taken as that stress at which rapid plastic deformation took place, as opposed to slow steady creep.

The mechanical properties at room temperature and their variation with temperature are shown in Table II and Fig. 4, respectively. The curves of Fig. 4 indicate that, above 650°, 550°, and 420° C. for cast iron, brass, and Y alloy, respectively, measurable stresses cannot exist, owing to the low value of the yield stress.

#### 5. STRESS MEASUREMENT

The residual-stress determinations were made by electrical-resistance strain-gauges, which measured the change in strain associated with relieving the stress by sawing through the centre member of the casting. Details of the method have been given elsewhere.<sup>16</sup>

### III.—EXPERIMENTAL RESULTS

#### 1. STRESSES IN FERRANTI-TYPE FRAMEWORK

The stresses developed in Ferranti-type framework castings in the three alloys made in various moulds are given in Table III. All the stress values are averages of measurements on at least two castings, which invariably agreed to within 0.15 tons/in.<sup>2</sup> in the case of cast iron, and 0.3 tons/in.<sup>2</sup> in the case of the non-ferrous metals.

The highest stresses were obtained by casting in green sands N.13 and S.14. The core sand, C.2000, gave stresses approximating to those observed when using an average dry sand. The high dry strength was diminished by charring, which occurred across the



whole area of the casting immediately after pouring, and was more pronounced with the cast iron than with the non-ferrous alloys, owing to the higher pouring temperature.

With sands F.300, F.180, and F.60, the effect of different cooling rates was eliminated, and the difference in stress values was entirely due to the varying sand strengths. Temperature measurements were made during the cooling of all castings. The distribution of the thermocouples was such that the temperatures of the hottest and coldest parts of the surface of the casting were measured, as well as the temperature of the sand at two points in the region

TABLE III.—*Residual Tensile Stress (tons/in.<sup>2</sup>) in Centre Member of Ferranti Framework.*

Sand	Cast Iron	Brass	Y Alloy
N.13	4.7	3.0	3.8
S.14	4.8	3.2	3.9
C.2000	2.9	2.7	2.5
F.300	4.6	2.4	Hot tear
F.180	3.5	2.6	1.4
F.60	1.7	1.9	1.0
F.10	2.7	2.6	3.5

between the centre member and one of the outer members, as indicated in Fig. 1. For any specific alloy, the cooling rates for each member of the framework were found to be approximately constant, and varied only according to whether a green or dry sand was used. The maximum temperature of the sand between the centre and outer members (point *B* in Fig. 1) approached the surface temperature of the centre member, while the average temperature was similar to that of the coldest part of the outer member (point *C* in Fig. 1).

Although the stresses observed in the castings made in the three dry sands varied, the values did not bear a simple relationship to the sand strengths at room temperature. This is to be expected in a casting of this design, since the non-uniform plastic deformation that causes the stress occurs at elevated temperatures, so that it is the high-temperature strength of the sand which is of importance. Moreover, even though the deformation is cumulative over a range of temperature, the sand strength/temperature curves (Fig. 3) indicate that the variation produced by these three sands is likely to be greater with cast iron than with the non-ferrous alloys because of the higher temperatures involved.

A comparison of the effect of cooling rates produced by a similar sand in the green and dry states is afforded by sands F.10 and F.60. The strengths are not very dissimilar initially, and they are likely to be even closer shortly after pouring, because of the drying of the sand and charring of the sawdust in F.10. Thus the predominant factor in causing the increased stress with F.10 must be the greater temperature differences produced by the initially different cooling rates.

## 2. STRESSES IN RECTANGULAR FRAMEWORK

The primary object of the experiments with rectangular frameworks was to study the formation of stresses in the absence of sand resistance, i.e. by cooling in air. However, for purposes of comparison, a few experiments were conducted on the lines of

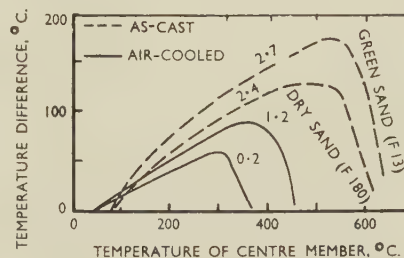


Fig. 5.—Temperature-Difference Curves for As-Cast and Air-Cooled Y Alloy Frameworks.

(The residual tensile stress is indicated in tons/in.<sup>2</sup>.)

those followed with the Ferranti frameworks. The results of some of these are mentioned in the following paragraphs, but collectively they indicated the same conclusions as those observed with the Ferranti frameworks, although the predominance of thermal differences over sand strength appeared to be more pronounced.

Temperature measurements were made during the cooling of these castings with thermocouples reaching to the centre of the metal sections, and in the positions indicated in Fig. 2. The results are most conveniently represented by a plot of the temperature difference between the outer members and the centre member against the temperature of the centre member. Some of the results, both for the air-cooling and for the as-cast experiments, are indicated in Figs. 5 and 6,

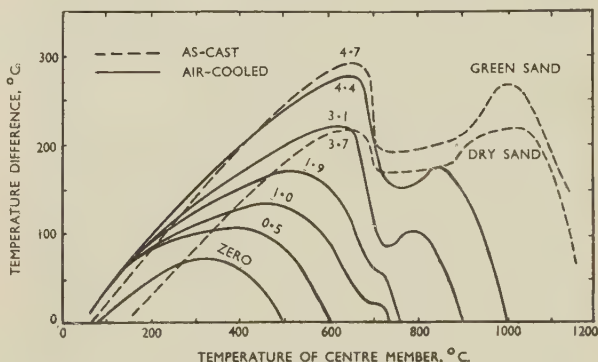


Fig. 6.—Temperature-Difference Curves for As-Cast and Air-Cooled Cast-Iron Frameworks.

(The residual tensile stress is indicated in tons/in.<sup>2</sup>.)

which refer to Y alloy and cast iron, respectively. The temperature-difference curves for the Y alloy frameworks rise rapidly to a maximum in each case and then gradually decrease to a zero value near room temperature. Castings were also made in the dry sands F.300 and F.60, the former resulting in a hot

tear, the latter in a stress of 2.3 tons/in.<sup>2</sup> and both yielding temperature-difference curves practically coincident with that obtained with sand F.180.

The temperature-difference curves for cast iron when cast or when cooled from above 725° C. are of a different form. The difference rapidly rises to a maximum and then decreases or remains steady until the centre member is at approximately 725° C. This preliminary decrease is due to the outer members passing through the  $Ar_1$  point, with its accompanying heat evolution. When the centre member reaches the  $Ar_1$  point, its slower cooling rate and greater mass give rise to a comparatively long and steady heat evolution while the outer members continue to cool. Thus the temperature difference rapidly increases to a final maximum and then gradually falls to zero as room temperature is approached. In those experiments where castings were air-cooled from below

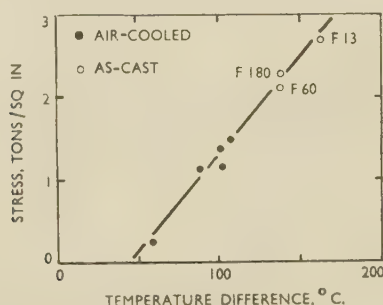


Fig. 7.—Residual-Stress/Maximum-Temperature-Difference Relationship in Y Alloy Frameworks.

725° C., the temperature-difference curves resemble those for Y alloy.

The effect of a relatively weak green sand in producing high stresses by promoting greater temperature differences is again shown. As in the case of Y alloy, castings were made in dry sands F.300 and F.60, which gave temperature-difference curves coincident with that shown for sand F.180 and stresses of 4.7 and 3.5 tons/in.<sup>2</sup>, respectively.

If the maximum temperature differences observed on the air-cooled and as-cast Y alloy frameworks are plotted against the residual stresses developed, as in Fig. 7, the results lie about a straight line. This would appear to indicate the small effect of sand strength, as compared with the effect of temperature difference, on the magnitude of the residual stress under the particular experimental conditions. The hot-tearing resulting from casting in sand F.300 is attributed to the high sand strength preventing contraction of the weak metal immediately after casting, so that the result cannot be considered as equivalent to the development of a high residual stress.

The results, plotted similarly, for cast-iron frameworks are shown in Fig. 8. The linear relationship applies to air-cooled castings at high and low temperature differences, but, at differences of about 180° C., the stress increases rapidly for small increases in temperature difference. This discontinuity

is associated with the  $Ar_1$  transformation, since to achieve temperature differences of this and greater values under the conditions of these experiments, it was found necessary to cool from above the trans-

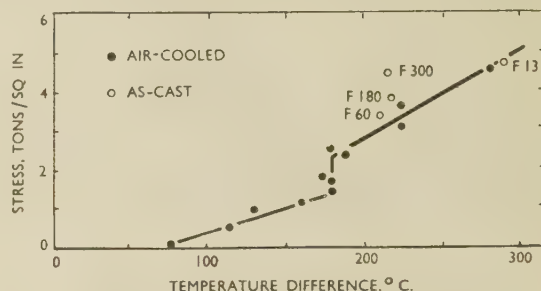


Fig. 8.—Residual-Stress/Maximum-Temperature-Difference Relationship in Cast-Iron Frameworks.

formation. The as-cast experiments appear to indicate that sand strength has a positive effect in the case of cast iron, as opposed to the results obtained with Y alloy.

#### IV.—DISCUSSION

The stages in the formation of stress may be considered in relation to the cooling-rate curves for each member of the framework; Fig. 9 (a) shows typical curves for a casting in Y alloy. The outer members cool more rapidly initially, but after attaining a maximum value the rate decreases until the centre member is cooling more quickly and the curves intersect, as occurs again at room temperature. These intersections mark a maximum or minimum

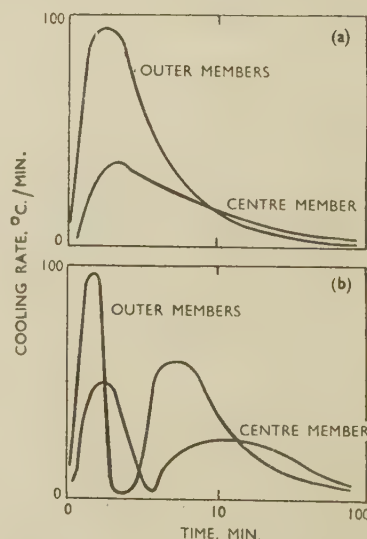


Fig. 9.—Typical Cooling-Rate Curves for Rectangular Frameworks. (a) Y alloy; (b) Cast iron.

temperature difference between the members, and their significance from the point of view of stress formation is that they indicate a point of maximum or minimum strain. Thus, before the intersection,



the outer members are cooling more rapidly than the centre member, so that they will be subjected to tension; but when the temperatures of the members begin to approach one another, the centre member will be subjected to tension and the outer ones to compression. Whether these strains are elastic or plastic in nature will depend upon the temperature of the casting considered with respect to the highest temperature at which elastic strain may exist within the material. Therefore, the intersection point need not necessarily indicate a state of zero stress in the casting; if it occurs when the temperature of the hottest part of the casting is below the maximum temperature at which elastic strains can exist, the latter will be present. In this case there will be a temperature lag before zero stress obtains, depending on the amount of contraction of the alloy necessary to reduce the elastic strain to zero value and then reverse it to give the room-temperature distribution. In the case where the thermal intersection occurs when the temperature of the hottest member is above the temperature at which elastic strain can exist, the directions of the plastic deformations will reverse at the intersection, and the centre member will undergo plastic extension until elastic strain can be withstood. In both cases, however, the most important single quantity affecting the magnitude of the final stress will be the maximum temperature difference attained when the hottest part has cooled to a temperature at which elastic strains can exist. It is to be expected, then, that a plot of the residual stresses against the maximum temperature differences observed should show a significant relationship, although why this has the linear form of Figs. 7 and 8 is not clear.

When cast iron is cooled from above the transformation temperature, the form of the cooling curves obtained is as shown in Fig. 9 (b). Three intersections occur, corresponding to the maximum and minimum temperature differences set up by the thermal effect of the transformation; this takes place first in the outer members and then in the centre member, reducing the respective cooling rates to a zero or negative value. Initially, the difference in cooling rates results in compression in the centre member and tension in the outer members. Since the cooling rate of the outer members is reduced as they approach the transformation, the stress changes to compression and the accompanying volume increase tends further to increase the stress value. The question of whether these temperature differences cause plastic deformation or the build-up of elastic strains is further complicated in the case of cast iron by its differing behaviour under tensile and compressive forces. Thus, when the outer members are passing through the transformation and are in compression, it appears likely that the deformation is concentrated in the hotter centre member, as in the case of Y alloy frameworks. But, when the cooling rate of the outer members increases after the transformation and exceeds that of the centre member, the stress in the latter reverts to compression, and as the temperature

of the outer members is now approaching that at which elastic tensile strains can exist, the framework is elastically stressed. The subsequent transformation of the centre member results in its expansion, so that the magnitude of the stresses is further increased, almost certainly causing some plastic flow. After this arrest, the cooling rate of the centre member increases and finally exceeds that of the outer members. This final reversal causes the centre member to develop a tensile stress, though not until the compressive stress present at the point of reversal is removed.

Thus the important point, so far as the transformation is operative in increasing the residual stresses, is that the deformations which it causes are not completely reversed, owing to the high temperature of the centre member when the outer members transform as compared with the relatively low temperature of the outer members when the centre transforms. As shown in Fig. 6, on cooling from 730° C., the transformation in all three members occurs over a very short time range, so that the heat and volume changes take place when cooling conditions are similar and consequently have no effect upon the final stress. On cooling from higher temperatures, however, the transformation occurs when a considerable temperature difference between the members has already been established, with the result that the deformations associated with the transformation are not completely reversed. This would also appear to account for the greater slope of the line at temperature differences higher than those at which the discontinuity in the stress/temperature-difference curve occurs (Fig. 8), the effect of the transformation being more marked the higher the temperature difference existing when it begins.

The effect on the residual stress of the sand in which a casting is made would also appear to be related to temperature differences between the members of the framework. Thus, Figs. 6 and 7 show that the increased stress observed on casting into a green sand, indicated by the results from both Ferranti and rectangular frameworks, is explicable by the higher temperature differences set up in the casting. Dry sands of differing strengths are not markedly effective in producing different stresses except in grey-iron castings; this indicates that it is only when the temperatures involved are high, and the difference between the strengths of the sands F.300, F.180, and F.60 is therefore large (cf. Fig. 3), that their contributions to the stress are sufficiently different to be noticeable. However, the effective contribution of sand restraint to the residual stress cannot be merely a question of developing sufficient strength at high temperatures to cause plastic deformation of the metal, because for the effects of this to be observed in the stress measured, the deformation must be inhomogeneous. If the sand is assumed to operate by supporting the member in compression, or by increasing the magnitude of the stress in the member in tension, its effects above and below any stress-reversal point will not be equal, because of the changing mechanical properties of the

metal and sand with temperature. Thus the resistance to contraction offered by the sand is likely to be more effective in increasing the final stress when temperature differences are present in the casting at high temperatures; for if the temperature is uniform, the only possible source of inhomogeneous deformation is the varying stress arising from equal amounts of restraint being imposed on the different cross-sectional areas of the members. The contribution from such a source is likely to be very small in the castings used in the present work.

A surprising feature of the results, and also of results obtained on similar castings by other workers, is that the observed stresses have such low values. The temperature differences established and the deformations undergone by the members would be expected to give values of the order of the yield stress of the material, but such values are rarely approached. It can only be assumed that this is the result of a lack of rigidity in the framework, causing bending of the outer members, and/or creep at high temperatures leading to stress relaxation.

#### V.—CONCLUSION

It is apparent that the relative contributions of temperature differences, sand strength, and phase transformations to the residual stresses in metal castings vary to a considerable extent. Thus, in the case of the non-ferrous alloy frameworks, the

stresses may be attributed almost entirely to the temperature differences established. In grey-iron castings, however, the contributions of the phase transformation and of the sand may be of the same order as that due to temperature differences, although it is clear that transformation and sand restraint are likely to have an appreciable effect only if temperature differences exist within the casting. The frequent suggestion, then, that the mechanical properties of the mould have little influence upon the magnitude of the final stress is not always true, and indeed it has been shown elsewhere<sup>11</sup> that the stresses in rectangular frameworks can be controlled to some extent by the use of a facing sand, on either the centre or outer members, having a grain-size distribution such that close packing of the grains results. It is evident, however, that the practical means of reducing residual stresses in castings to low values must lie in an attempt to give careful consideration to the shape of a casting in order to reduce temperature differences established during cooling.

#### ACKNOWLEDGEMENTS

The authors wish to record their indebtedness to Mr. G. Elston, Messrs. R. and W. Hawthorn, Leslie and Co., Ltd., for the supply of certain materials used in the work; to their colleagues for helpful discussion; and to Professor A. Preece for provision of laboratory facilities.

#### REFERENCES

1. F. Schumann, *Trans. Amer. Soc. Mech. Eng.*, 1897, **18**, 394.
2. E. Heyn, *Stahl u. Eisen*, 1907, **27**, 1309, 1347.
3. E. Heyn, "Metallographie", Leipzig: 1909 (G. J. Goschen).
4. E. Schütz, *Stahl u. Eisen*, 1922, **42**, 1773.
5. R. v. Steiger, "Ueber Gussspannungen". Thesis, Zürich, 1913; and *Stahl u. Eisen*, 1913, **33**, 1442.
6. R. A. Dodd, *J. Inst. Metals*, 1952-53, **81**, 77.
7. Report of Sub-Committee T.S. 32, *Proc. Inst. Brit. Found.*, 1952, **45**, A179.
8. Report of Sub-Committee T.S. 18, *Proc. Inst. Brit. Found.*, 1949, **42**, A61.
9. H. Malzacher, *Stahl u. Eisen*, 1927, **47**, 2108.
10. W. J. Phillips, *Foundry*, 1940, **68**, 27, 87.
11. R. N. Parkins and A. Cowan, *Inst. Brit. Found. Preprint*, 1953, (1062).
12. W. Machin and M. Oldham, *Foundry Trade J.*, 1936, **54**, 343.
13. W. Davies and W. J. Rees, *J. Iron Steel Inst.*, 1945, **152**, 61.
14. H. Bühler and H. Buchholtz, *Arch. Eisenhüttenwesen*, 1933, **6**, 335.
15. J. E. Russell, *Inst. Metals: Symposium on Internal Stresses in Metals and Alloys*, 1947, 95.
16. "Note on Construction and Use of N.P.L.-Type Strain Gauges", N.P.L. (E), T.P. No. 244, (1943).



# THE CONSTITUTION OF ALUMINIUM-COPPER-SILICON ALLOYS\*

1488

By H. W. L. PHILLIPS,† M.A., F.R.I.C., F.Inst.P., F.I.M., MEMBER

(Communication from the Research Laboratories of The British Aluminium Co., Ltd., Gerrards Cross, Bucks.)

## SYNOPSIS

The constitution of the aluminium-rich alloys of the aluminium-copper-silicon system has been investigated both as slowly cooled and under conditions of equilibrium, the range covered being 0-40% copper and 0-15% silicon.

The system is eutectiferous, with a eutectic of aluminium,  $\text{CuAl}_2$ , and silicon containing 26.70% copper and 5.25% silicon, freezing at 524° C. The aluminium-rich apex of the ternary eutectic plane was found to lie at 4.9% copper and 1.1% silicon, under conditions of equilibrium, and at 0.25% copper and 0.25% silicon, under conditions of cooling likely to be met with in industrial practice. The section  $\text{CuAl}_2$ -Si is quasi-binary, with a eutectic containing approximately 50% copper and 4.4% silicon, freezing at 571° C.

The solid solubility of copper and silicon in aluminium was determined at 500° and 400° C. At these temperatures, the composition of the solid solution, fully saturated with respect to both components, was found to be 4.1% copper and 0.85% silicon (500° C.) and 1.5% copper and 0.25% silicon (400° C.). The solid solubility of either copper or silicon in aluminium was little, if at all, affected by the presence of the other component.

## I.—HISTORICAL INTRODUCTION

It has long been known that alloys of the aluminium-copper-silicon system containing less than about 45% copper consist of three constituents only, an aluminium-rich solid solution, the binary compound  $\text{CuAl}_2$ , and elementary silicon. The identity of these constituents was first established by Hanson and Archbutt<sup>1</sup> and almost simultaneously by Wills.<sup>2</sup> Shortly afterwards, systematic studies covering a fairly wide range of composition were reported by Wetzel<sup>3</sup> and by Sterner-Rainer,<sup>4</sup> both of whom found that the aluminium-rich alloys formed a simple eutectiferous system with a eutectic of aluminium,  $\text{CuAl}_2$ , and silicon containing 29-30% copper and 5% silicon, and freezing at 520°-525° C.

The general correctness of this picture of the structure has been confirmed by all subsequent investigators, but agreement has not yet been reached

on the composition and freezing point of the ternary eutectic, as Table I will show.

Recent investigations on the solid solubility of copper and silicon in the aluminium-rich phase have shown that the solubility of one element is but little affected by the presence of the other. Values reported for the composition of the aluminium-rich apex of the three-phase triangle Al-Si- $\text{CuAl}_2$  at 400°, 460°, and 520° C. are quoted in Table II.

TABLE II.—Composition of Aluminium-Rich Solid Solution Fully Saturated with Respect to Both Copper and Silicon at the Temperature Stated.

Investigators	Ref.	400° C.		460° C.		520° C.	
		Cu, %	Si, %	Cu, %	Si, %	Cu, %	Si, %
Wiehr . . .	12	1.8	0.30	3.3	0.67	4.9	1.1
Hanemann and Schrader . .	11	1.5	0.25	3.6	0.6	4.6	1.15
Axon . . .	13	...	...	2.9	0.5	...	...

TABLE I.—Composition and Freezing Point of the Ternary Eutectic of Aluminium,  $\text{CuAl}_2$ , and Silicon

Investigators	Ref.	Cu, %	Si, %	Temp., °C.
Gwyer, Phillips, and Mann . .	5	26	6.5	525
Hisatsune . . . . .	6	23.8	5	522
Urazov, Pogodin, and Zomoruev . .	7	27	5	525
Matsuyama . . . . .	8	31	5	522
Hisatsune . . . . .	9	27	5	522
Petrov and Nagorskaya . . . .	10	29	5.2	525
Hanemann and Schrader . . . .	11	26.7	5.8	520.3

## II.—SCOPE OF INVESTIGATION

In the previous investigation of this system made in these Laboratories,<sup>5</sup> aluminium of 99.67% purity had been used, and some of the liquidus temperatures then reported did not link up well with those found in an investigation now proceeding on the quaternary alloys of aluminium, copper, silicon, and magnesium. It was therefore decided to make a fresh survey of the

\* Manuscript received 8 April 1953.

† Research Laboratories of The British Aluminium Co., Ltd., Gerrards Cross, Bucks.

liquidus surface over the range 0–40% copper and 0–15% silicon with alloys made from super-purity aluminium, and with special precautions to minimize undercooling. Initially, series of alloys were prepared of which the composition was varied in steps of 5.0% copper and 2.5% silicon. In the neighbourhood of phase boundaries, additional alloys were made, where necessary, in steps of 1%, 0.5%, or 0.25%. In order to determine the composition of the ternary eutectic, six alloys were made, bracketing the anticipated composition, and drillings taken from the ternary eutectic areas of the microsections were analysed.

Determinations of solid solubility were made at 400° and 500° C. To determine the composition of the aluminium-rich corners of the three-phase triangles at these temperatures, series of alloys were made up bracketing the expected composition, and covering the range  $\pm 1\%$  copper and  $\pm 1\%$  silicon in steps of 0.2% copper and 0.1% silicon. To fix the positions of the isothermals in the two-phase fields, series of alloys were prepared containing 2% silicon with copper varying in steps of 0.2%, and 10% copper with silicon varying in steps of 0.1%, in each case over a range of  $\pm 1\%$  of the expected composition. Microsections of these alloys were afterwards used for determinations of the solidus, the heating quench method being employed.

### III.—MATERIALS AND METHODS

#### 1. MATERIALS USED

Copper and silicon were added as hardeners made up from super-purity aluminium and electrolytic copper and elementary silicon, respectively. The silicon carried a rather heavy iron contamination, and attempts to purify it by prolonged boiling in hydrochloric acid met with only limited success. The amount of iron introduced into the alloys by the use of the hardener varied, of course, with the silicon content of the final product, but in no case was it sufficient to give rise

TABLE III.—*Typical Analyses of Raw Materials Used.*

	Super-Purity Aluminium	Copper Hardener	Silicon Hardener
Aluminium, %	99.996	By diff.	By diff.
Silicon, %	0.0020	0.005	19.85
Iron, %	0.0010	0.005	0.17
Copper, %	<0.0005	54.20	0.006
Manganese, %	<0.0005	<0.001	0.005

to additional arrests on the cooling curves, and its effect on the microsections could be disregarded. At the maximum, iron contamination reached 0.14%, and judging from previous work on the quaternary system Al-Cu-Si-Fe,<sup>5</sup> the error introduced into the primary arrest temperatures would not be likely to exceed 1° C.

Typical analyses of the super-purity aluminium used, and of the hardeners, are given in Table III.

#### 2. THERMAL ANALYSIS AND MICROGRAPHY

For cooling curves, quantities of about 200 g. were melted and allowed to cool in an electric furnace, the rate of cooling being adjusted in general to about 5° C./min., and the melt was stirred until the primary arrest was clearly defined. For alloys lying in the primary-silicon phase field, under-cooling was very liable to occur, so that the rate of cooling was decreased, and stirring carried out vigorously; it was not, however, found necessary to have recourse to "seeding". Heating curves were taken on representative alloys in the various phase fields. Where they were used solely to verify the liquidus temperatures, the heating curves were taken immediately after the completion of solidification. In all other cases, however, the alloys were given a homogenizing treatment of 3–4 hours' duration at the eutectic temperature before the heating curve was begun. After removal of a sample for micro-examination, the ingots were remelted and cast into a small chill mould in order to obtain samples as uniform in composition as possible for analysis. Every melt was analysed for copper, silicon, and iron, and representative samples were tested for manganese contamination.

In alloys containing high percentages of copper, it proved very difficult to take large amounts of silicon into solution, so that the percentage of silicon found by analysis often fell well below the intended amount. To correct for errors in composition, the procedure advocated by Haughton<sup>14</sup> was followed. Sectional diagrams were plotted for alloys of nominally constant silicon content, in which the arrest temperatures were plotted against copper contents as found by analysis, and liquidus curves were drawn as evenly as possible through the points. From these curves it was easy to calculate the change in temperature in °C. per 1% copper,

$\left(\frac{\partial \theta}{\partial C_{\text{Cu}}}\right)_{\text{Si}}$ . The corresponding coefficient

$\left(\frac{\partial \theta}{\partial S_{\text{Si}}}\right)_{\text{Cu}}$  was obtained from similar diagrams for alloys of nominally constant copper content. To allow for the iron contamination, the coefficient  $\left(\frac{\partial \theta}{\partial F_{\text{Fe}}}\right)_{\text{Cu, Si}}$  was

derived from the sectional diagrams for the quaternary system, published in 1928.<sup>5</sup> Table IV has been included to show the extent of the discrepancy between the nominal and the actual composition, the degree of contamination, and the method of making the corrections, for a few representative alloys. The partial differential coefficients are expressed in °C. per 1%, and the effect of the manganese contamination has been ignored.

New sectional diagrams were then prepared, in which the corrected temperatures were plotted against nominal compositions, and the liquidus isothermals and phase boundaries transferred to a triangular diagram representing the basal projection of the liquidus surface. Smooth isothermal and phase-boundary curves were drawn, and all the diagrams checked for consistency. Repeat curves were taken, on fresh samples, to check any doubtful points.



TABLE IV.—Nominal and Actual Compositions, and Temperature Corrections.

Nominal Composition: Cu, % Si, %	10	10	20	20	40	40
	2½	10	5	15	7½	2½
Analysis:						
Cu, %	10.00	10.70	20.30	20.40	39.90	40.20
Si, %	2.25	9.80	5.15	14.10	7.70	2.50
Fe, %	0.015	0.06	0.04	0.14	0.10	0.04
Mn, %	<0.001	<0.001	<0.001	<0.001	<0.001	<0.001
Primary Field	Al	Si	Al	Si	Si	CuAl <sub>2</sub>
( $\partial\theta/\partial\text{Cu}$ ) <sub>Si</sub>	-3	+3	-4	+4	+5	+2
( $\partial\theta/\partial\text{Si}$ ) <sub>Cu</sub>	-7	+17	-9	+19	+28	-1
( $\partial\theta/\partial\text{Fe}$ ) <sub>Si, Cu</sub>	-1	-0.5	-2	-0.5	+3	+0.5
Liquidus, observed	618°	570°	555°	700°	653°	567°
Correction for Cu		-2.1°	+1.2°	-1.6°	+0.5°	-0.2°
Correction for Si	-1.8°	+3.4°	+1.4°	+17.1°	-5.6°	Nil
Correction for Fe	Nil	+0.3°	+0.1°	+0.1°	-0.3°	Nil
Liquidus, calculated	616°	571°	558°	715°	648°	567°

Microsections were examined in the unetched condition, and there was rarely any difficulty in distinguishing between the microconstituents. The

sufficient for the attainment of equilibrium. One of the duplicate sets was afterwards annealed at 400° C. for a total period of 8 days, with similar checks at intervals. No particular difficulty was encountered in identifying precipitated particles of CuAl<sub>2</sub> and silicon in these re-annealed specimens, and constituents due to iron could easily be distinguished.

### 3. CHEMICAL ANALYSIS

Copper, if present in amounts less than 0.25%, was estimated colorimetrically by the sodium diethyl-dithiocarbamate process. In the range 0.25–25%, it was determined volumetrically, by means of thio-sulphate, while for amounts greater than 25% the electrolytic process was followed.<sup>15</sup>

Silicon, in amounts less than 1.5%, was estimated photometrically by the development of the yellow colour with ammonium molybdate and the use of a Spekker absorptiometer.<sup>15</sup> For all higher percentages of silicon, the Weiss-Sieger gravimetric process was used. This is a variant of the Regelsberger process in which the SiO<sub>2</sub> is precipitated in the presence of

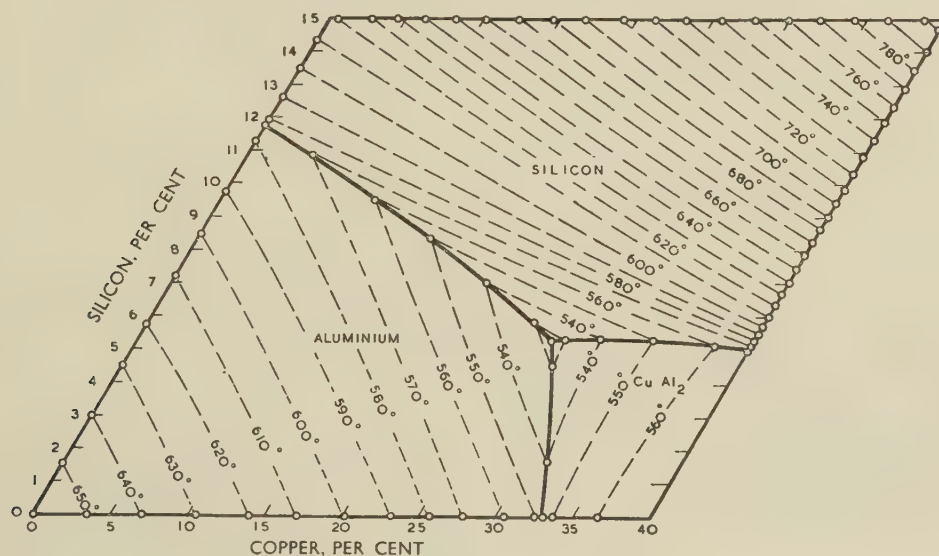


Fig. 1.—Liquidus Surface.

CuAl<sub>2</sub> could be darkened, if needed, by treatment with 20% nitric acid at 70° C., or with 12½% sodium hydroxide solution, used cold.

For solidus determinations, microsections cut from small chill-cast ingots, which had previously been annealed for 8 days at 500° C., were slowly heated until the first signs of melting could be detected, specimens being examined at temperature intervals of 2° C. beginning some 10° below the expected solidus temperature.

Estimates of the limits of solid solubility were based on the microscopic examination of annealed and quenched chill-cast samples. Duplicate sets of specimens were first heated at 500° C. for a total period of 8 days, the examination of random samples at intervals having shown that this length of time was

gelatin, and in which the final fuming with HF is not needed.<sup>16</sup>

Iron and manganese were both estimated colorimetrically, the former by means of thiocyanate, and the latter by oxidation to permanganate. In both cases the colours developed were matched visually against standard samples.<sup>15</sup>

### IV.—THE LIQUIDUS SURFACE

The liquidus surface, for the range 0–40% copper and 0–15% silicon, is shown in Fig. 1. There was some difficulty in determining the position of the isotherms in the primary CuAl<sub>2</sub> field and in locating the valley between this field and that due to primary silicon. The primary arrest points, near the valley, were not

well defined, and massive silicon and massive  $\text{CuAl}_2$  could be seen in the microsections on both sides of the valley. It proved necessary to examine series of alloys containing 45 and 50% copper, with silicon contents covering the range 0–7% in small steps, so that interpolation could be used. This examination confirmed that the section  $\text{CuAl}_2$ -silicon was quasi-binary, with a eutectic containing approximately 50% copper, and 4.4% silicon, and freezing at  $571^\circ\text{C}$ .

It was impossible to determine the composition of the ternary eutectic from either cooling curves or microsections. In the immediate neighbourhood of the eutectic, primary arrests tended to be suppressed, and a microsection might contain, in different regions, segregates of large silicon crystals, dendrites of aluminium, and dendrites of  $\text{CuAl}_2$ . The eutectic areas in six such microsections were analysed, and the

melt. Where, owing to slowness of diffusion, equilibrium is not reached during solidification, the locus of the point on the projection of the liquidus surface representing the composition of the liquid phase will meet the binary valley at a point which may differ appreciably from the equilibrium value. Where solid solubility is appreciable, as in the primary aluminium field, cooling curves can therefore not be relied upon for accurate determinations of the secondary isothermals. Heating curves, taken on homogenized samples, are essential. Since the compositions of the two extremities of a secondary isothermal can be established with accuracy from the liquidus and solidus diagrams (Figs. 1 and 2) and since, at equilibrium, the isothermals themselves are rectilinear, direct determinations at intermediate compositions are needed only as checks. Heating curves

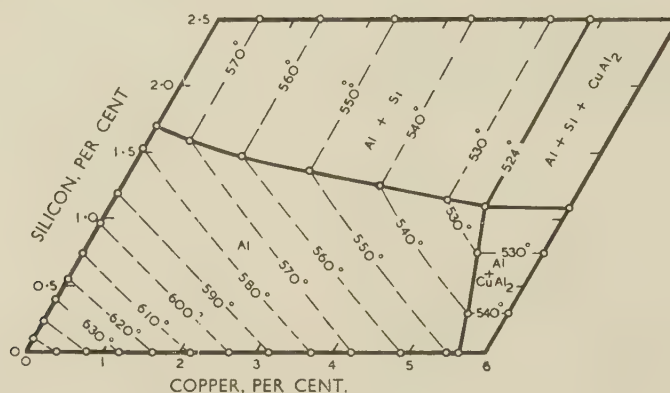


Fig. 2.—The Solidus.

figures for copper lay within the range 26.4–26.9%, and for silicon 5.1–5.4%. The best estimate of the composition was 26.70% copper, and 5.25% silicon, with the freezing point  $524^\circ\text{C}$ . This temperature was derived from cooling curves, and from heating curves on homogenized samples, the temperature range so found being  $523^\circ$ – $524.5^\circ\text{C}$ . The iron contamination in these ternary eutectic samples was 0.015%.

## V.—THE SURFACES OF SECONDARY SEPARATION

There is no necessity to include a diagram of the secondary isothermals. In the primary-silicon and  $\text{CuAl}_2$  fields, the secondary isothermals may be assumed to run from points on the appropriate binary valleys to 100% silicon and 52.5% copper, 47.5% aluminium, respectively, the latter point being the limit of the homogeneity range of the  $\text{CuAl}_2$  constituent on the aluminium side. In the primary-aluminium field, the secondary isothermals terminate on the appropriate boundary of the single-phase field of the solidus diagram, shown in Fig. 2.

It should be remembered that the tie-lines, during the primary separation, pass through the instantaneous composition of the solid crystallizing from the

were therefore taken at a few compositions only, in the 4% copper, 10% copper, and 1% silicon series.

## VI.—THE SOLIDUS

In the alloys solidified slowly, free  $\text{CuAl}_2$  could be detected in the microsections at a copper content of 0.25%, and free silicon at 0.25%, so that the ternary eutectic plane extended almost to the bounding faces of the triangular model. Evidently equilibrium is far from being attained under these conditions of cooling.

The basal projection of the true solidus is shown in Fig. 2, in which the lettering in the various fields indicates the solid phase or phases in equilibrium with the liquid. Part of the ternary eutectic plane ( $524^\circ\text{C}$ .) is to be seen in the upper right-hand corner of the diagram; its apex was found to lie at 4.9% copper and 1.1% silicon.

In the temperature range  $524^\circ$ – $548^\circ\text{C}$ ., any isothermal section through the solidus model would have six phase fields. Beginning at the aluminium corner and proceeding in a clockwise direction round the section, these would be:

(1) A single-phase field (solid aluminium), extending upwards as far as the thick line separating it from the (Al + Si) field, to the right as far as the thick line



limiting the  $(\text{Al} + \text{CuAl}_2)$  field, and intermediately as far as the broken "contour line" appropriate to the temperature.

(2) A two-phase field  $(\text{Al} + \text{Si})$ , bounded on the right by the appropriate "contour line".

(3) A three-phase field  $(\text{Al} + \text{Si} + \text{liquid})$ . This field must be a triangle of which the apices are the compositions of the three phases in equilibrium. One of these, Al, has a composition given by the point on the  $\text{Al}/(\text{Al} + \text{Si})$  line appropriate to the temperature, the second is silicon, possibly containing some aluminium and copper in solid solution, and the third, the liquid phase, having the composition shown on the liquidus diagram (Fig. 1) for the point at which the liquidus isothermal for the temperature in question cuts the aluminium-silicon binary valley.

(4) A two-phase field  $(\text{Al} + \text{liquid})$  bounded on the left by the solidus isothermal, and on the right by the appropriate liquidus isothermal.

(5) A three-phase triangle  $(\text{Al} + \text{CuAl}_2 + \text{liquid})$ .

aluminium, the aluminium-rich limit of the homogeneity range of the  $\text{CuAl}_2$  phase.

## VII.—THE LIMITS OF SOLID SOLUBILITY

Fig. 3 is a basal projection of the solid solubility surfaces. At any temperature below that of the ternary eutectic separation ( $524^\circ \text{C.}$ ), any isothermal section through the model will contain four phase fields:

(1) A quadrilateral—almost a true parallelogram—in which the only constituent present is the aluminium-rich solid solution.

(2) An area in which the constituents are aluminium and silicon.

(3) A three-phase triangle  $(\text{Al} + \text{CuAl}_2 + \text{Si})$ , the apices of which are the upper right-hand corner of the aluminium quadrilateral, silicon, and  $\text{CuAl}_2$ .

(4) A two-phase area  $(\text{Al} + \text{CuAl}_2)$ .

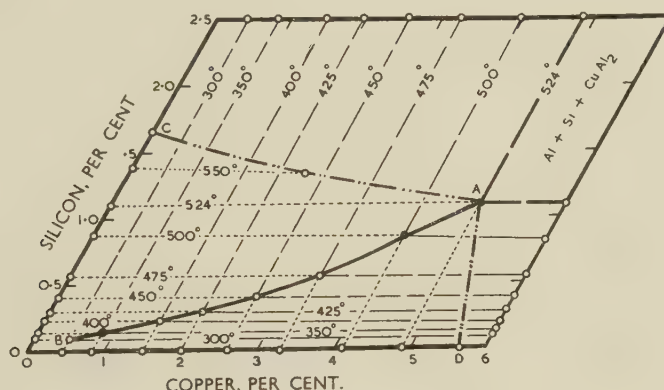


Fig. 3.—Limits of Solid Solubility.

The apices of this field will be  $\text{CuAl}_2$  containing some aluminium and possibly some silicon in solid solution, and the point of intersection of the  $\text{Al}-\text{CuAl}_2$  binary valley and the liquidus isothermal.

(6) A two-phase field  $(\text{Al} + \text{CuAl}_2)$ .

At  $548^\circ \text{C.}$  the two phase fields containing solid  $\text{CuAl}_2$  disappear, and at  $578^\circ \text{C.}$  so do those containing solid silicon. Above  $578^\circ \text{C.}$ , therefore, only two phase fields remain, those associated with solid aluminium and with aluminium plus liquid.

In drawing Fig. 2 it has been assumed that silicon is capable of taking little, if any, copper into solid solution at the temperatures in question. The isothermals in the field labelled " $\text{Al} + \text{Si}$ " have therefore been drawn as though they met at the point representing 100% silicon. It was also assumed that  $\text{CuAl}_2$ , though capable of dissolving aluminium, was incapable of dissolving silicon to any marked extent. Attempts to verify this assumption, by direct experiment or by solidus determinations on alloys of high copper content, proved inconclusive. In the absence of evidence to the contrary, the isothermals of the " $\text{Al} + \text{CuAl}_2$ " field have been drawn as meeting at the point representing 52.5% copper and 47.5%

These four fields have one point in common, the aluminium-rich apex of the three-phase triangle. The locus of this point, for temperatures in the range  $524^\circ$ – $300^\circ \text{C.}$ , is shown in the diagram by the full line  $AB$ . The sides of the three-phase triangles for various temperatures are shown by thin broken lines, whilst the lines separating the aluminium field from the adjacent two-phase fields have been drawn as dotted lines. The only field lettered in the diagram is the ternary eutectic plane,  $524^\circ \text{C.}$

The thick broken lines  $CA$  and  $DA$  have been taken from the solidus diagram (Fig. 2); they represent the limits of occurrence of solid silicon and solid  $\text{CuAl}_2$ , respectively, at temperatures above that of the ternary eutectic.

In making use of Fig. 3, it may be found helpful to remember that, in tracing the constitution of a series of alloys of constant silicon content, each isothermal crossed on proceeding from left to right indicates the temperature at which a field free from  $\text{CuAl}_2$  is left, and one containing  $\text{CuAl}_2$  is entered. The horizontal isothermals provide similar information about the temperatures at which silicon first appears in alloys with constant copper.

The isothermals for 524°, 500°, and 400° C. were determined experimentally, and their intersections with the curve *AB* have been distinguished by the use of solid circles. They confirm the findings of previous investigators that the solid solubility of copper or silicon in solid aluminium is hardly, if at all, affected by the presence of the other element. The iso-

### VIII.—VERTICAL SECTIONS

It has not been thought necessary to include vertical sectional diagrams for series of alloys with high copper or silicon contents; the liquidus, solidus, and solid-solubility curves can be drawn from the data presented in Figs. 1, 2, and 3, whilst the lines represent-

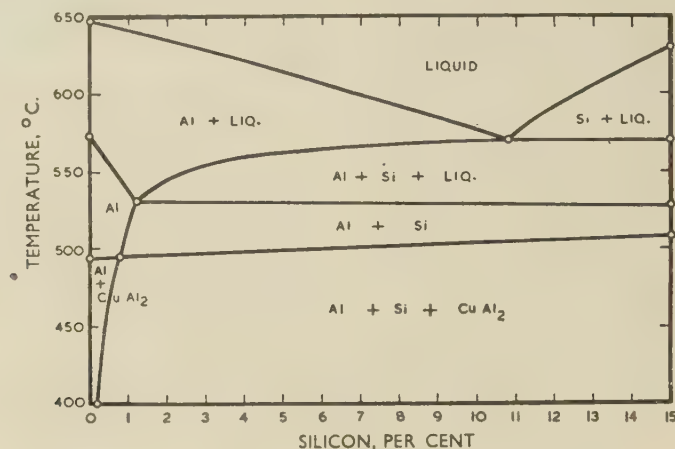


Fig. 4.—Vertical Section for Alloys Containing 4% Copper.

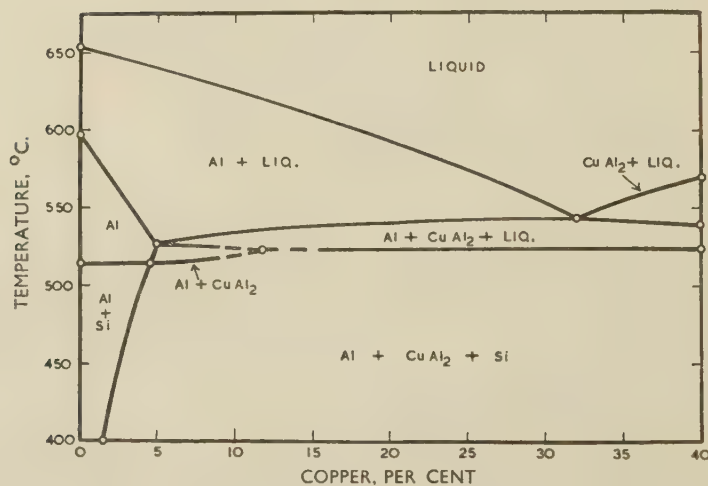


Fig. 5.—Vertical Section for Alloys Containing 1% Silicon.

thermals bounding the single-phase aluminium field have therefore all been drawn as true parallelograms. The isothermals drawn as broken lines, which are sides of three-phase triangles, have been drawn as though they ran to points representing 100% silicon and pure  $\text{CuAl}_2$ .

The isothermals for 460° C. reported by Axon<sup>13</sup> are fully consistent with those shown in Fig. 3, as are those found by Hanemann and Schrader<sup>11</sup> for 400° C. Values found by the latter investigators for other temperatures, and those published by Wiehr,<sup>12</sup> differ somewhat from those plotted in Fig. 3.

ing secondary arrests can be derived by following the procedure indicated in Section V.

Fig. 4 shows the constitution, under equilibrium conditions, of a series of alloys containing 4% copper with increasing silicon. This section is of interest in connection with alloys of the Duralumin type. In alloys containing less than 1.2% silicon, solidification is completed on the single-phase region of the solidus surface, and this single-phase structure can be retained by quenching from a temperature of, say, 525° C. It will be seen that annealing the quenched alloys at a low temperature would result in the precipitation of



both  $\text{CuAl}_2$  and silicon, so that both constituents take part in the age-hardening process.

Fig. 4 does not represent the constitution of the alloys as ordinarily cast. On cooling at rates of the order of  $5^\circ \text{C./min.}$  or faster—rates which may be expected in ordinary chill or sand casting— $\text{CuAl}_2$  separates as a eutectic constituent across the whole of the diagram, while silicon appears as a eutectic constituent from about 0.25% silicon upwards. A sectional diagram appropriate to industrial cooling rates would therefore show a ternary eutectic horizontal extending to the left to 0.25% silicon. The line of secondary arrests, associated with the separation of the aluminium-silicon eutectic complex, would begin from the end of the ternary eutectic horizontal, and would merge eventually into the equilibrium secondary arrest curve. Cooling curves followed by heating curves on homogenized samples show that the metastable and equilibrium curves merge at about 5% silicon. The solidus, at 0% silicon, lies at the  $\text{Al-CuAl}_2$  binary eutectic temperature of  $548^\circ \text{C.}$ , and falls to the ternary eutectic temperature,  $524^\circ \text{C.}$ , at 0.25% silicon. No attempt has been made to determine the exact course of the solidus between these two points, but quenching experiments lead to the conclusion that it may be rectilinear. At the moment that solidification is complete, the aluminium-rich phase will be highly cored; the centre of each dendrite may well be unsaturated with respect to both copper and silicon, and the extreme outer layers fully saturated. Homogenization will tend to occur, but with rapid rates of cooling its extent is certain to be small. As the temperature falls, the outer layers will become supersaturated, but whether they remain in this condition or deposit their excess will again depend on the rate of cooling and the rate of diffusion. Eventually, the centres of the dendrites will, in their turn, become supersaturated. In the series of alloys containing 4% copper, cooled at  $5^\circ \text{C./min.}$ ,  $\text{CuAl}_2$  will occur as a constituent of the eutectic generation

at all concentrations of silicon, and may also occur, principally in the neighbourhood of the crystal boundaries, as a precipitate from solid solution. Similarly, silicon may occur in both forms; as a eutectic constituent, in large particles from 0.25% upwards, and as a finely dispersed precipitate at all concentrations.

Fig. 5 shows the equilibrium constitution of a series of alloys containing 1% silicon with increasing copper. It was not possible to determine exactly the point at which the solidus and the  $\text{CuAl}_2$  solid-solubility curve merge into the ternary eutectic horizontal, and therefore this portion of the diagram has been drawn in broken lines. Here again the diagram is not applicable to industrial rates of solidification. In such circumstances, in a series of alloys containing 1% silicon, this element would always separate as a eutectic constituent, though further precipitation would probably take place from the aluminium-rich solid solution as the temperature fell. The point of first appearance of  $\text{CuAl}_2$  as a constituent of the eutectic depends very much on the rate of cooling. With extremely rapid rates, it may appear at a copper content as low as 0.25%. At the eutectic temperature, aluminium is capable of dissolving nearly 5% copper, so that precipitation at 0.25% indicates conditions so far removed from equilibrium that even a small retardation of the cooling rate would result in appreciably more copper being retained in solution. In these alloys, precipitation of  $\text{CuAl}_2$  from solid solution would occur only at comparatively low temperatures.

The diagram representing the constitution of a series of alloys containing 1% silicon as cooled at  $5^\circ \text{C./min.}$  would show the ternary eutectic horizontal prolonged to about 0.25% copper, with the solidus line sloping sharply upwards from this point to  $578^\circ \text{C.}$  at 0% copper, and the line of secondary arrests beginning at the termination of the eutectic horizontal and merging into the equilibrium secondary arrest curve at about 10% copper.

#### REFERENCES

1. D. Hanson and S. L. Archbutt, *J. Inst. Metals*, 1919, **21**, 299.
2. L. J. Wills, *ibid.*, p. 316 (discussion), and *J. B'ham Met. Soc.*, 1920, **7**, 475.
3. E. Wetzels, *Metallbörse*, 1923, **13**, 936.
4. R. Sterner-Rainer, *Z. Metallkunde*, 1924, **16**, 362.
5. A. G. C. Gwyer, H. W. L. Phillips, and L. Mann, *J. Inst. Metals*, 1928, **40**, 297.
6. C. Hisatsune, *Suiyōkwaishi*, 1928, **5**, 559.
7. G. G. Urazov, S. A. Pogodin, and G. M. Zomoruev, *Mineral'noe Syr'e i Tsvet. Metally*, 1929, **4**, 160.
8. K. Matsuyama, *Kinzoku no Kenkyū*, 1934, **11**, 461.
9. C. Hisatsune, *Mem. Coll. Eng. Kyōtō. Imp. Univ.*, 1935, **9**, 18.
10. D. A. Petrov and N. D. Nagorskaya, *Zhur. Obshch. Khim.*, 1949, **19**, 1994.
11. H. Hanemann and A. Schrader, "Ternäre Legierungen des Aluminiums". (Atlas Metallographicus, Band 3, Teil 2). Düsseldorf: 1952 (Verlag Stahleisen).
12. H. Wiehr, *Aluminium-Archiv*, 1940, (31).
13. H. J. Axon, *J. Inst. Metals*, 1952-53, **81**, 209.
14. J. L. Haughton, *ibid.*, 1939, **65**, 447.
15. British Aluminium Co. Ltd. Publication No. 405 (1949).
16. L. Weiss and H. Sieger, *Z. anal. Chem.*, 1940, **119**, 24.





# THE STRUCTURE AND MECHANICAL PROPERTIES OF COPPER-MANGANESE-TIN ALLOYS\*

1489

By J. C. BLADE,† B.Sc., Ph.D., JUNIOR MEMBER, and  
J. W. CUTHBERTSON,‡ D.Sc., F.I.M., MEMBER

## SYNOPSIS

The metallography and mechanical properties of copper-base alloys containing 1.5–23% manganese and 4–14% tin have been investigated. It is found that manganese reduces the primary solid solubility of tin in copper, particularly below the eutectoid temperature. The tempering of quenched alloys below this temperature results in the precipitation of a new phase, designated  $\delta'$ .

The effect of heat-treatment on the quenched alloys, with or without previous cold working, has been examined, and it is found that good mechanical properties are obtained if the quenched alloys are cold worked before tempering. In the absence of cold work, considerable brittleness may develop on tempering, owing to the preferential precipitation of  $\delta'$  at the grain boundaries or along crystallographic planes.

The mechanical properties appear to be governed more by the total manganese-plus-tin content than by the contents of the individual metals, although, of the two alloy additions, tin seems to exert more influence than manganese. Within the composition range investigated, it is possible by suitable treatment of the alloys to obtain ultimate tensile strengths of up to 30 tons/in.<sup>2</sup> with elongations of up to approximately 45%. The tensile strength can be further increased to a maximum of about 40 tons/in.<sup>2</sup>, though above 33 tons/in.<sup>2</sup> there is a progressive and fairly rapid fall in the elongation.

Alloys containing not less than 15% manganese with not less than 6% tin are almost white in colour.

## I.—INTRODUCTION

A CONSIDERABLE amount of study has been devoted to the effect of adding small amounts of manganese to other metals and alloys, but less work has been done on the possible uses of manganese as a major alloying constituent. Many binary and ternary systems containing manganese as one component have been worked out, but from the practical viewpoint some high-manganese alloys have proved to be rather disappointing. Melting and casting difficulties increase rapidly as the manganese-rich field is approached, and this is probably one reason why high-manganese alloys have not yet been widely used. Moreover, until a few years ago high-purity manganese was not obtainable at an attractive price. The development of the electrolytic manganese industry in America has radically altered this position, and the ready availability of high-purity manganese is now stimulating interest in manganese-containing alloys.

The possibilities of using manganese as an alternative to other metals, notably to those that are at present scarce, are receiving consideration. In this respect the use of manganese as an alternative to nickel is an obvious possibility. There is a demand for a white alloy having good mechanical properties and good corrosion-resistance, which is at present largely

met by nickel silver. The work about to be described, which is still in its early stages, has indicated that copper-manganese-tin alloys of suitable composition compare favourably in colour and mechanical properties with copper-nickel-zinc alloys. The corrosion-resistance of the new ternary alloys has not yet been systematically examined, but preliminary tests suggest that the alloys will adequately meet service requirements in this respect.

## II.—PREVIOUS WORK

### 1. THE BINARY ALLOY SYSTEMS

#### (a) Copper-Tin System

Raynor's diagram<sup>1</sup> summarizes all earlier work on this system. The primary solid solubility of tin in copper at 600° C. is given as 15.8%. The  $\beta$  phase, which is stable only above 590° C. and has a body-centred cubic structure, decomposes at that temperature into  $\alpha + \gamma$ . The  $\gamma$  phase decomposes eutectoidally at 520° C. to give  $\alpha$  and  $\delta$ . Structurally, the  $\gamma$  phase is similar to  $\beta$ ; neither  $\beta$  nor  $\gamma$  can be fully retained by quenching, which leads to the appearance of a metastable transition structure.

#### (b) Copper-Manganese System

This system has been investigated by Persson,<sup>2</sup> Grube,<sup>3</sup> Dean,<sup>4</sup> and Naylor.<sup>5</sup> Copper and manganese

\* Manuscript received 16 January 1953.

† Research Metallurgist, Tin Research Institute, Greenford, Middlesex.

‡ Assistant Director of Research, Tin Research Institute, Greenford, Middlesex.

form a continuous series of solid solutions at elevated temperatures. The solubility of manganese in copper decreases as the temperature falls, and below 685° C. the decrease is very rapid. At room temperature, alloys containing up to just over 20% manganese consist of the  $\gamma$  solid solution. The higher-manganese alloys are duplex and consist of the  $\gamma$  solid solution plus the  $\alpha$  modification of manganese.

### (c) Tin-Manganese System

The equilibrium diagrams of Williams<sup>6</sup> and of Nial<sup>7</sup> differ considerably in respect of the compounds identified. Williams identifies the compounds  $\text{MnSn}$  and  $\text{Mn}_4\text{Sn}$ , whereas Nial reports the existence of a  $\beta'$  phase ( $\text{MnSn}_3$ ), a  $\gamma'$  phase, and a  $\delta$  phase ( $\text{MnSn}_2$ ). Other investigators have identified the compounds  $\text{Mn}_{11}\text{Sn}_3$ <sup>8</sup> and  $\text{Mn}_2\text{Sn}$ .<sup>9</sup> The solid solubility of tin in manganese has been reported both as very small,<sup>7</sup> and as 17%.<sup>8</sup>

## 2. THE TERNARY SYSTEM

The ternary system in the composition range 0–15% manganese and 0–30% tin has been investigated by Verö,<sup>10</sup> who concluded that only the constituents of binary tin bronzes and a manganese-rich phase were formed in the region examined. He found that the primary solid solubility of tin in copper was considerably lowered by manganese, decreasing from 15.8% with no manganese to approximately 11% with 15% manganese. With more than 5% manganese the  $\beta$  phase, and the transformations associated with it, disappear, and the  $\beta$  phase is replaced by  $\gamma$ . A manganese-rich phase, designated  $X$  (possibly  $\text{Mn}_4\text{Sn}$ ) is present when the manganese content exceeds 4%. An apparently new lamellar constituent ( $\alpha + \delta + X$ ) appears if the alloys are slowly cooled from the ( $\alpha + \gamma$ ) region. This lamellar constituent is not considered to be a true eutectoid, however, since if the alloys are slowly cooled from the  $\gamma$  region only agglomerated  $X$  crystals and the normal binary bronze constituents are found.

Verö's equilibrium diagram does not appear to be completely reliable. If  $\text{Mn}_4\text{Sn}$  does come into equilibrium with the copper-rich solid solution, the solubility of tin should be more restricted than is shown in this diagram. Moreover, in an X-ray investigation of the magnetic properties of these alloys, Carapella and Hultgren<sup>11</sup> have shown that above 625° C. the  $\beta$  phase extends over a considerable range of composition, in contradiction to the findings of Verö. Carapella and Hultgren found that the  $\beta$  phase could be retained by quenching and that if the manganese content exceeded 20 at.-% long-range ordering occurred. The atomic distribution in the superlattice formed corresponded to the composition  $\text{Cu}_2\text{MnSn}$ . This phase was found to have ferromagnetic properties, and it would seem to resemble the  $\beta$  ( $\text{Cu}_2\text{MnAl}$ ) phase of the Heusler alloys.

## 3. MECHANICAL PROPERTIES

Little information is available on the mechanical properties of bronzes containing manganese. Hanson and Wheeler<sup>12</sup> examined  $\alpha$ -phase alloys containing 1–8% manganese and 1–6% tin. These alloys could all be cold rolled satisfactorily, although some of the more highly alloyed materials required homogenizing at 800° C. before rolling. The hot-rolling properties were not affected by manganese, and all the alloys hot rolled easily at 780° C.

The mechanical properties of both annealed and quenched alloys varied little with composition, indicating that the influence of manganese on the properties of the  $\alpha$  phase is small. However, the annealing temperature for complete softening after cold work was raised by manganese.

## III.—EXPERIMENTAL PROCEDURE

### 1. MELTING AND CASTING

The alloys were prepared from high-conductivity copper (max. impurity 0.04%, excluding oxygen), electrolytic manganese (99.97%), and tin (99.99%). Melting was carried out in either Salamander or carbon crucibles in a high-frequency induction furnace. To reduce contamination, no flux or cover was used; when making the higher-manganese alloys, the manganese was charged at the beginning of the run before the copper was molten. Some difficulty was experienced in melting the manganese, owing to the pieces floating upwards and becoming entrapped in the oxide skin on the surface of the melt. This and oxidation losses account for the difference between the nominal and actual manganese contents of some of the alloys.

Deoxidation with a small quantity of magnesium was carried out before casting, except in the case of four alloys which were deoxidized with phosphor-copper.

The alloys were cast into a 10 × 2 × 1-in. cast-iron chill mould, using a tundish to ensure an even rate of pouring. The surfaces of the four ingots to which phosphor-copper had been added were better than those of the corresponding alloys deoxidized with magnesium. The compositions of the alloys are given in Table I.

The colour of the alloys varied from yellow to white, according to composition. They were white when 15% manganese and 6% tin were present; with less manganese or less tin whiteness could be restored by increasing the percentage of the other alloying metal.

### 2. ROLLING

The ingots were machined to remove surface defects, homogenized for 16 hr. at 650° C. to remove coring, and quenched in water in order to retain the high-temperature second phase present in the duplex alloys. Little difficulty was encountered in cold



rolling homogenized alloys falling within the composition ranges given in Table II. It was possible to cold roll all these alloys by as much as 80% reduction

TABLE I.—Composition of Alloys.

Nominal Composition		Actual Composition		
Mn, %	Sn, %	Mn, %	Sn, %	P, %
3	10	1.42	9.85	...
3	12	1.42	12.25	...
3	14	1.57	13.75	...
5	10	4.63	10.25	...
5	12	4.71	12.5	...
5	14	4.10	13.9	...
10	8	7.15	8.4	...
10	8 *	7.35	8.1	0.082
10	10	8.0	10.0	...
10	10 *	9.0	9.9	0.114
10	8	9.6	8.1	...
10	10	9.5	9.7	...
10	12	9.6	11.6	...
10	14	10.2	13.3	...
15	6	11.5	6.2	...
15	6 *	14.3	6.0	0.135
15	8	14.15	8.2	...
15	8 *	13.1	8.1	0.134
15	6	14.8	5.8	...
15	8	15.9	7.9	...
15	12	15.5	12.0	...
15	17	15.1	16.8	...
20	4	19.9	3.90	...
20	5	17.5	5.7	...
20	6	20.5	5.8	...
20	8	20.0	8.2	...
25	4	23.3	4.6	...

\* Indicates alloys to which phosphor-copper was added.

TABLE II.—Limiting Compositions for Cold Rolling.

Mn Content, %	Approx. Sn Content, %
5	> 14
10	12
15	10
20	8

in thickness, and in some cases even greater reductions were possible.

#### IV.—THE EQUILIBRIUM DIAGRAM

The approximate phase boundaries have been determined in the temperature range 400°–700° C. by micro-examination, cooling curves, quenching treatments, and hardness determinations. From the results obtained, the approximate pseudo-binary sections for 5, 10, 15, and 20% manganese shown in Fig. 1 were constructed. The positions of the vertical boundaries between the  $\alpha$  and the  $(\alpha + \beta)$  fields have been estimated from the observation that alloys shown close to these boundaries contained only a trace of the  $\beta$  constituent.

Increase in the manganese content rapidly causes

a decrease in the primary solid solubility of tin in copper above 600° C., the limit falling from 15.8% in the absence of manganese to approximately 5.8% with 20% manganese. These values are considerably lower than those reported by Verö,<sup>10</sup> and suggest that 2% manganese is approximately equivalent to 1% tin.

In alloys of composition exceeding the primary solubility limit, only one other phase was observed above the eutectoid temperature. This phase was unattacked by any of the etchants used. Since quenched alloys containing large amounts of this constituent were found to be feebly magnetic, it is probable that the phase in question is the  $\beta$  phase referred to by Carapella and Hultgren,<sup>11</sup> and not the  $\gamma$  phase as suggested by Verö.

The structure of the 20% manganese–8% tin alloy quenched from 600° C. (Fig. 2, Plate I) is typical of an alloy quenched from the  $(\alpha + \beta)$  region. At lower temperatures, the  $\beta$  phase decomposes eutectoidally into  $\alpha$  and a phase that we shall designate  $\delta'$ . Metallographically, the  $\delta'$  phase resembles the  $\delta$  phase of the copper–tin system, but whereas the latter phase has a  $\gamma$ -brass structure, the new phase,  $\delta'$ , is hexagonal, having the parameters  $a = 2.852$ ,  $c = 4.014$  Å. (these parameters refer to the  $\delta'$  phase present in a heat-treated sample containing 15% manganese and 17% tin). Funk and Rowland, in a very recent publication,<sup>13</sup> refer to the  $\delta'$  phase as  $\theta$ , in conformity with the terminology used by Eash and Upthegrove in the latter's description of the copper–nickel–tin system.<sup>14</sup> Funk and Rowland find that their phase  $\theta$  has an X-ray diffraction pattern resembling that of  $\beta$ -manganese, but they state that positive agreement could not be obtained.

The temperature at which the eutectoid transformation occurs varies considerably with the manganese content of the alloy, increasing slowly from 520° C. with no manganese to 530° C. with 5% manganese, and then more rapidly to 595° C. with 10% manganese. A maximum of about 610° C. is reached with 13% manganese, beyond which the transformation temperature falls to 600° C. with 15% manganese and to 550° C. with 20% manganese. Fig. 3 (Plate I) shows the structure of an alloy containing 15% manganese and 17% tin quenched from 550° C. The structure is duplex, consisting of  $\alpha + \delta'$ ; there is no evidence of the presence of a third phase,  $X$ , as reported by Verö.

The appearance of the eutectoid is markedly affected by the rate of cooling through the transformation temperature and by the temperature of tempering if the  $\beta$  phase is decomposed isothermally. Thus, a coarse, lamellar structure is obtained if the alloy is either very slowly furnace-cooled (Fig. 4, Plate I), or if it is tempered very close to the eutectoid temperature (Fig. 6, Plate I). On the other hand, the structure of the eutectoid becomes progressively finer as the tempering temperature is reduced, or if the cooling rate is increased. Thus, the chill-cast 15% manganese–17% tin alloy was

cooled insufficiently rapidly to suppress the transformation, but sufficiently so to give an unresolvable sorbitic type of structure (Fig. 5, Plate I).

Below the eutectoid temperature, the solid solubility of tin in copper decreases rapidly, resulting in the precipitation of  $\delta'$  from the  $\alpha$  solid solution. If the supersaturated  $\alpha$  phase in an alloy containing 10% or more of manganese is furnace-cooled, a dark-etching constituent having a lamellar structure develops (Figs. 7 and 8, Plate I). This phase

On tempering alloys quenched from 650° C., this leads to the precipitation of  $\delta'$  and thus permits a wide variation in properties to be obtained, as shown later.

## V.—EFFECT OF TEMPERING

Tempering at 500° C. alloys previously quenched from 650° C. causes a rapid precipitation of  $\delta'$  both within the grains and at the grain boundaries (Figs. 9, Plate I, and 10, Plate II). As the tin content

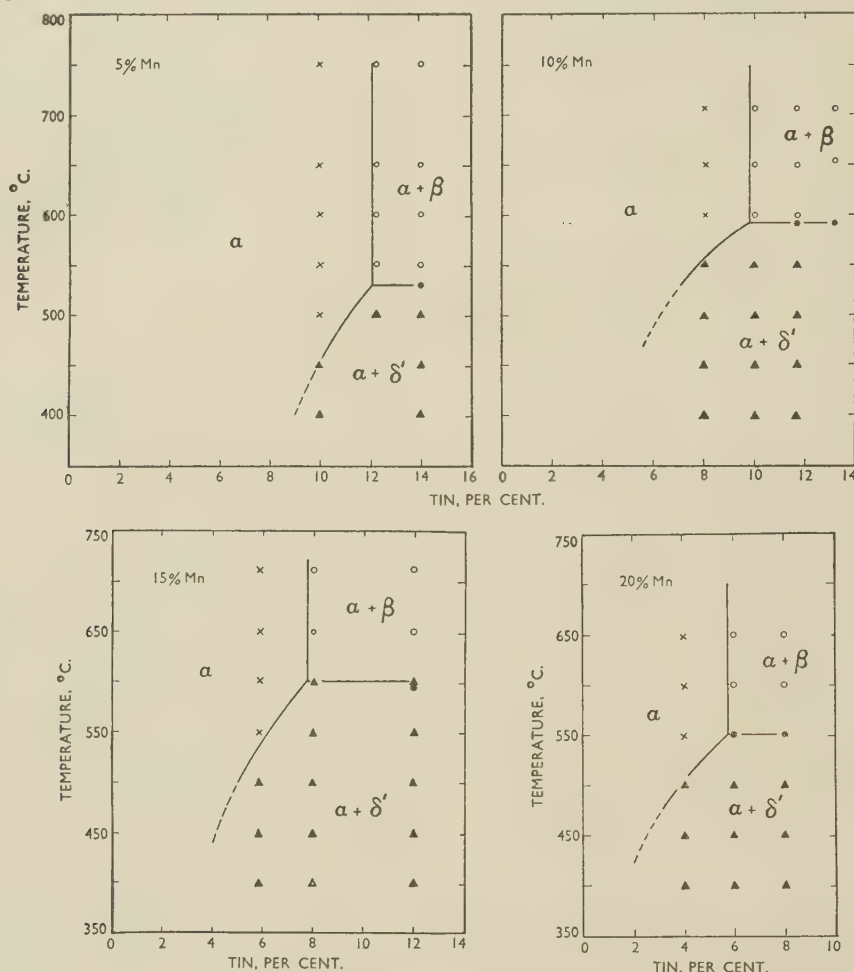


FIG. 1.—Pseudo-Binary Sections of Copper-Manganese-Tin Alloys at 5%, 10%, 15%, and 20% Manganese.

appears to correspond to a transition stage, as not all of the  $\alpha$  phase stable at the high temperature is decomposed. Thus, a furnace-cooled alloy containing 10% manganese and 14% tin shows coarse ( $\alpha + \delta'$ ) eutectoid resulting from the decomposition of the  $\beta$  phase, some undecomposed  $\alpha$ , and the dark-etching lamellar constituent (Fig. 7, Plate I). It is significant that the incidence of the lamellar constituent coincides with a marked fall in the ductility of the alloy as compared with the ductility after quenching.

The ternary system possesses interesting possibilities as a result of the rapid decrease in the primary solid solubility of tin below the eutectoid temperature.

of the alloy is increased beyond the solubility limit, the distribution of the  $\delta'$  changes progressively, from discontinuous particles to grain-boundary films which ultimately become continuous. At and below 450° C. the precipitation sequence is somewhat modified; there is an increasing tendency for the precipitation of  $\delta'$  at the grain boundaries to take precedence in the early stages of tempering, particularly in alloys of low tin content. Grain-boundary precipitation is followed by precipitation within the grains. Two forms of the latter precipitation have been discerned. In the first, precipitation occurs as resolvable particles; at 500° C. the distribution of



these particles is more or less random, but at 450° C. they tend to separate along the crystallographic planes. In the second, the dark-etching, lamellar constituent mentioned in the preceding section develops from the grain boundaries, and gradually penetrates into the grains (Fig. 11, Plate II). In contrast to furnace-cooling, tempering causes a marked alteration in the structure of this phase, which becomes less lamellar in appearance as the tempering time is extended. After tempering for 65 hr. at 400° C., there is considerable coarsening of the structure, and the  $\delta'$  phase is readily resolvable as continuous bands following the crystallographic planes (Fig. 12, Plate II).

The  $\beta$  phase decomposes very rapidly into  $\alpha + \delta'$  on tempering between 400° C. and the eutectoid temperature.

Quenched and tempered alloys containing  $\delta'$  at the grain boundaries or along the crystallographic planes are brittle. It was thought that brittleness might be reduced by cold working before tempering with the aim of obtaining a random distribution of the  $\delta'$  phase. Figs. 13, 14, and 15 (Plate II) show the structures of an alloy containing 10% manganese and 10% tin, quenched from 650° C. and cold worked before tempering. Figs. 13 and 14 show the structure of alloys cold worked 50% and 80% respectively and tempered for 1 hr. at 550° C. The resulting structure consists of evenly dispersed particles of  $\delta'$  in a matrix of  $\alpha$ . In the case of Fig. 15 the alloy was cold worked 50% and tempered for 2 hr. at 500° C. The distribution of the  $\delta'$  is seen to be less uniform, and there is a tendency for this constituent to separate along the grain boundaries. It thus seems that the tempering should be 50°–100° C. below the critical temperature (i.e. the eutectoid temperature or the temperature corresponding to the solid-solubility limit).

In those alloys to which phosphorus had been added, the phosphorus appeared as an unidentified light-grey phase, which may be either copper phosphide or manganese phosphide.

## VI.—MECHANICAL PROPERTIES

### 1. QUENCHED ALLOYS

The tensile properties of alloys in the form of strip approximately 0.07 in. thick after soaking for 1 hr. at 650° or 750° C. and quenching are quoted in Table III. There is comparatively little variation in properties over the wide range of composition studied, and manganese has less influence than tin on the tensile properties. There is a tendency for the ultimate tensile strength to increase when an appreciable amount of the  $\beta$  phase is present. The presence of  $\beta$  has little effect on the ductility, provided that the  $\beta$  phase does not become continuous.

### 2. QUENCHED AND TEMPERED ALLOYS

Alloys were quenched from 650° C. and then tempered for various times at 400°, 450°, and 500° C., the

times being so chosen as to obtain the maximum hardness in as many of the alloys as possible.

Hardness/tempering-time curves are shown in Fig. 16. The maximum hardness obtainable increases with the total amount of manganese plus tin, the tin exercising rather more influence than the manganese. On tempering at 400° C., the maximum hardness is reached in 1–30 hr., according to the

TABLE III.—*Mechanical Properties of Quenched Alloys.*

Composition			Quenching Temp., °C.	U.T.S., tons/in. <sup>2</sup>	Elongation, % on 2 in.	Structure
Mn, %	Sn, %	P, %				
1.4	9.85	...	750	24.8	65	$\alpha$
1.4	12.25	...	750	26.9	60	$\alpha$
1.6	13.75	...	750	26.5	33	$\alpha + \beta$
4.6	10.25	...	750	25.2	74	$\alpha$
4.1	13.9	...	750	32.4	47	$\alpha + \beta$
7.15	8.4	...	650	22.9	57	$\alpha$
7.35	8.1	0.082	650	27.1	67	$\alpha$
8.0	10.0	...	650	26.5	40	$\alpha$
9.0	9.9	0.114	650	28.8	54	$\alpha$
9.6	8.1	...	650	24.3	47	$\alpha$
9.5	9.7	...	650	27.0	63	$\alpha + \beta$
9.6	11.6	...	650	31.0	45	$\alpha + \beta$
11.5	6.2	...	650	23.7	56	$\alpha$
14.3	6.0	0.135	650	26.4	41	$\alpha$
13.1	8.1	0.134	650	27.6	58	$\alpha$
14.15	8.2	...	650	26.1	43	$\alpha$
14.8	5.8	...	650	23.3	46	$\alpha$
15.9	7.9	...	650	25.7	48	$\alpha$
19.9	3.9	...	650	25.1	46	$\alpha$
17.5	5.7	...	650	26.1	55	$\alpha$
20.0	8.2	...	650	31.8	47	$\alpha + \beta$
23.3	4.6	...	650	27.3	43	$\alpha$

TABLE IV.—*Mechanical Properties of Alloys Quenched from 650° C. and Tempered.*

Composition		Tempered for 4 hr. at 500° C.		Tempered for 8 hr. at 450° C.		Tempered for 16 hr. at 400° C.	
Mn, %	Sn, %	U.T.S., tons/in. <sup>2</sup>	Elongation, % on 2 in.	U.T.S., tons/in. <sup>2</sup>	Elongation, % on 2 in.	U.T.S., tons/in. <sup>2</sup>	Elongation, % on 2 in.
4.6	10.25	n.d.	n.d.	26.7	48	26.5	28
4.1	13.9	n.d.	n.d.	29.2	11	25.4	2
9.6	8.1	27.8	15	23.1	2	28.2	1
9.5	9.7	29.0	7	35.1	2	34.4	0
9.6	11.6	25.4	2	Brittle		24.6	0
14.8	5.8	24.3	34	25.2	17	26.1	35
15.9	7.9	26.0	5	31.7	3	34.2	4
19.9	3.9	n.d.	n.d.	24.9	40	26.1	36
17.5	5.7	30.0	33	30.8	15	31.6	23
20.0	8.2	26.7	5	26.7	3	17.8	0
23.3	4.6	27.2	45	27.2	37	29.2	32

n.d. = not determined.

composition of the alloy. The cause of the secondary hardening after tempering for more than 30 hr., shown by the alloys containing 20% manganese and 4% and 6% tin, respectively, has not yet been fully elucidated. On tempering at 450° C., maximum hardness develops in all alloys in 12 hr. or less.

Over-tempering effects are shown by some of the more highly alloyed samples on prolonged treatment.

The tensile properties of quenched and tempered alloys are reported in Table IV. Tempering quenched

Such brittle alloys were difficult to test owing to a tendency to shatter in the grips, and because of this the fall in tensile strength may be apparent rather than real. This brittleness may explain the very low values of the ultimate strength obtained with some of the alloys after tempering at 400° C.

### 3. COLD-WORKED ALLOYS

Alloys containing 7–20% manganese, with varying amounts of tin, were quenched from 650° C. and cold rolled to either 50% or 80% reduction in cross-section. Tensile tests carried out on the rolled material gave the results in Table V. It will be seen that little

TABLE V.—Mechanical Properties of Alloys Quenched from 650° C. and Cold Worked.

Composition			Cold Worked 50%		Cold Worked 80%	
Mn, %	Sn, %	P, %	U.T.S., tons/in. <sup>2</sup>	Elongation, % on 2 in.	U.T.S., tons/in. <sup>2</sup>	Elongation, % on 2 in.
7.15	8.4	...	47.3	5	52.5	0.5
7.35	8.1	0.082	50.6	1	44.6	1
8.0	10.0	...	49.0	3.5	60.2	1.5
9.0	9.9	0.114	52.1	6	53.7	1.5
9.6	8.1	...	46.5	3	45.3	1
9.5	9.7	...	49.2	5.5	54.4	1
9.6	11.6	...	52.9	3.5	42.5	1
11.5	6.2	...	46.8	4	51.6	0
14.3	6.0	0.135	48.5	1	47.5	0
13.1	8.1	0.134	51.3	2	43.6	0
14.15	8.2	...	50.2	2	44.4	0
14.8	5.8	...	43.3	4	50.7	2
15.9	7.9	...	47.8	2	57.0	1.5
19.9	3.9	...	43.1	2.5	50.1	1.5
17.5	5.7	...	47.6	2	50.4	2
20.0	8.2	...	54.0	3	60.6	1.5
23.3	4.6	...	45.8	2	52.5	1.5

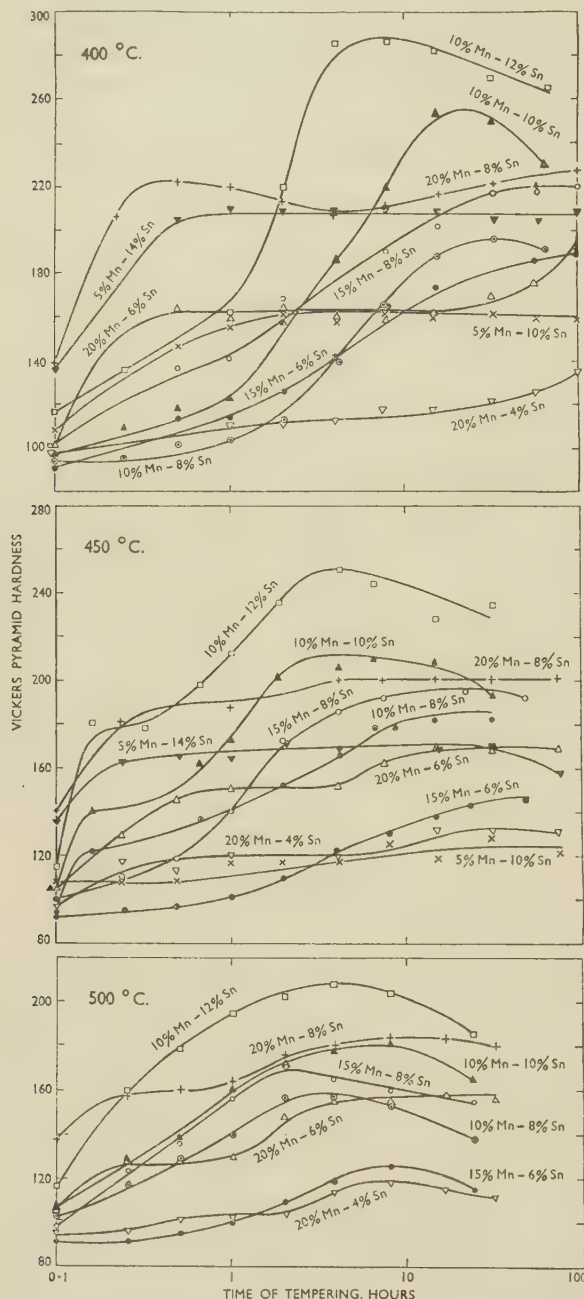


FIG. 16.—Hardness/Tempering-Time Curves for Copper-Manganese-Tin Alloys Quenched from 650° C. and Tempered at 400°, 450°, and 500° C.

alloys to precipitate  $\delta'$  from the solid solution leads to an increase in tensile strength, except when the alloy content of the quenched solid solution greatly exceeds the equilibrium composition at the tempering temperature. In the latter circumstances,  $\delta'$  separates at the grain boundaries and the alloys are very brittle.

advantage is to be gained by cold work in excess of 50%. The decrease in tensile strength sometimes detected after 80% cold work suggests that in these cases the alloys may have been rolled to the point of incipient failure. As in the case of the quenched alloys, the mechanical properties of the cold-rolled alloys appear to be influenced rather more by tin than by manganese.

### 4. COLD-WORKED AND TEMPERED ALLOYS

Table VI gives the tensile properties of alloys cold-worked 50% or 80% and then tempered at various temperatures and for increasing lengths of time. Comparison of the figures in Tables IV and VI indicates that the quenched alloys show superior mechanical properties when cold worked and tempered than when tempered alone. In particular, the worked and tempered alloys are less brittle.

By cold working and tempering, the ductility at a given tensile strength is improved. For instance, by quenching and tempering alone the maximum elongation obtainable with a tensile strength of 33–35 tons/in.<sup>2</sup> is approximately 4%, whereas by



cold working the quenched alloy before tempering the ductility is raised to 10–20%.

Cold work seems to accelerate the precipitation of  $\delta'$ , since the tensile strength of quenched and tempered alloys that temper slowly at 500° C. is much higher than that of similar alloys cold worked and tempered at the same temperature. Comparison of the tensile test results for alloys containing 4% tin with 20% and 23% manganese, respectively, clearly illustrates this difference.

There is little noticeable difference between the effects of 50% and 80% cold work except when, as mentioned previously, the degree of supersaturation

(d) The ( $\alpha + \delta'$ ) eutectoid temperature varies considerably with manganese content, increasing from 520° C. with no manganese to a maximum of approximately 610° C. with 13% manganese and then falling to 550° C. with 20% manganese.

(e) Below the eutectoid temperature the quenched  $\alpha$  solid solution is metastable and precipitates  $\delta'$  on tempering. The solid solubility of tin at 400° C. varies from approximately 9–10% with 5% manganese to 4% with 20% manganese. It is this latter feature which offers the greatest advantages from the point of view of mechanical properties, since the effect of manganese on these properties in the quenched,

TABLE VI.—Mechanical Properties of Alloys Quenched from 650° C., Cold Worked, and Tempered.

Composition			Cold Worked 50%						Cold Worked 80%					
			Tempered for 1 hr. at 550° C.		Tempered for 2 hr. at 500° C.		Tempered for 20 hr. at 450° C.		Tempered for 1 hr. at 550° C.		Tempered for 2 hr. at 500° C.		Tempered for 20 hr. at 450° C.	
			U.T.S., tons/in. <sup>2</sup>	Elong., % on 2 in.	U.T.S., tons/in. <sup>2</sup>	Elong., % on 2 in.	U.T.S., tons/in. <sup>2</sup>	Elong., % on 2 in.	U.T.S., tons/in. <sup>2</sup>	Elong., % on 2 in.	U.T.S., tons/in. <sup>2</sup>	Elong., % on 2 in.	U.T.S., tons/in. <sup>2</sup>	Elong., % on 2 in.
Mn, %	Sn, %	P, %												
7.15	8.4	...	25.1	54	29.3	45	29.9	14	24.8	65	29.6	41	33.3	18
7.35	8.1	0.082	27.6	54	31.2	33	32.0	13	26.6	53	32.1	33	33.4	13
8.0	10.0	...	34.1	21	36.9	5	38.4	3	29.9	14.5	36.0	7	36.7	4
9.0	9.9	0.114	31.7	34	36.3	12	36.8	6	32.6	39	37.3	13	35.1	3
11.5	6.2	...	25.5	43	31.0	25	32.8	11	25.6	48	34.2	18	33.6	11
14.3	6.0	0.135	25.4	30	32.7	17	35.1	14	28.2	33	35.8	17	36.0	19
14.15	8.2	...	32.9	17	38.7	4	39.5	3	33.5	19	34.6	3	37.9	3
13.1	8.1	0.134	32.2	24	37.9	7.5	38.1	4	27.4	14	36.8	6	33.5	2
19.9	3.9	...	26.9	31	28.0	30	...	...	26.6	35	30.1	37	...	...
17.5	5.7	...	27.7	37	32.3	24	...	...	27.6	34	34.0	27	...	...
20.0	8.2	...	30.5	15	35.1	6	...	...	29.9	22	37.6	10	...	...
23.3	4.6	...	31.2	31	32.0	28	...	...	30.3	35	32.6	34	...	...

is sufficiently low for precipitation to occur slowly from the quenched condition. Under these circumstances, the tendency is for 80% cold work before tempering to lead to higher strengths than 50% cold work.

## VII.—SUMMARY AND CONCLUSIONS

The approximate phase boundaries of the copper-manganese-tin system have been determined over the range 400°–700° C. for alloys containing 5–20% manganese and 4–14% tin. The chief structural features were as follows:

(a) The  $\alpha$  and  $\beta$  phases are analogous to those found in binary tin bronzes. The  $\delta'$  phase resembles the  $\delta$  phase in the copper-tin system metallographically but appears to have a hexagonal structure.

(b) Manganese considerably decreases the solid solubility of tin in the  $\alpha$  copper-rich phase; thus at 650° C. the solubility falls from approximately 16% with no manganese to 12.5% with 5% manganese and to 5.8% with 20% manganese.

(c) Only two solid phases were found at temperatures above the eutectoid temperature, the  $\alpha$  phase and a second phase thought to be the  $\beta$  phase identified by Carapella and Hultgren and not the  $\gamma$  phase as suggested by Verö.

i.e. soft, condition is relatively small. Tempering many of the quenched alloys results in extreme brittleness, owing to unfavourable distribution of the precipitated  $\delta'$  phase. However, this can be overcome by cold working the alloys before tempering, which leads to a much improved distribution of  $\delta'$  as evenly dispersed particles in an  $\alpha$  matrix. The optimum treatment to obtain this type of structure would involve cold working the quenched alloy between 50% and 80%, followed by tempering at approximately 50°–100° C. below the critical temperature. Tensile strengths of 35–38 tons/in.<sup>2</sup> with elongations of 10–20% can be obtained in this way.

(f) Alloys containing not less than 15% manganese with not less than 6% tin are almost white in colour.

## ACKNOWLEDGEMENTS

This work was carried out in the laboratories of the Tin Research Institute. The authors are indebted to the International Tin Research Council for permission to publish this paper. Grateful acknowledgement is made to Dr. E. C. Ellwood, who carried out the X-ray work on the  $\delta'$  phase, and to Dr. J. W. Price, who undertook the numerous chemical analyses.

## REFERENCES

1. G. V. Raynor, *Inst. Metals Annotated Equilib. Diagr. Series*, 1944, (2).
2. E. Persson, *Z. physikal. Chem.*, 1930, [B], **9**, 25.
3. G. Grube, E. Oestreicher, and O. Winkler, *Z. Elektrochem.*, 1939, **45**, 776.
4. R. S. Dean, J. R. Long, T. R. Graham, E. V. Potter, and E. T. Hayes, *Trans. Amer. Soc. Metals*, 1945, **34**, 443.
5. B. F. Naylor, *U.S. Bur. Mines, Rep. Invest.*, 1946, (3835).
6. R. S. Williams, *Z. anorg. Chem.*, 1907, **55**, 1.
7. O. Nial, "X-Ray Studies on Binary Alloys of Tin with Transition Metals", University of Stockholm: **1945**; summarized in *Svensk. Kem. Tidskr.*, 1947, **59**, 172.
8. H. Nowotny and K. Schubert, *Metallforsch.*, 1946, **1**, 17.
9. A. S. Russell, T. R. Kennedy, and R. P. Lawrence, *J. Chem. Soc.*, **1934**, 1750.
10. J. Verö, *Mitt. berg- u. hüttenmänn. Abt. Kgl. ung. Hochschule Berg- u. Forstwesen Sopron*, 1933, **5**, 128.
11. L. A. Carapella and R. Hultgren, *Trans. Amer. Inst. Min. Met. Eng.*, 1942, **147**, 232.
12. D. Hanson and M. A. Wheeler, *J. Inst. Metals*, 1935, **57**, 93.
13. C. W. Funk and J. A. Rowland, *Trans. Amer. Inst. Min. Met. Eng.*, 1953, **197**, 723.
14. J. T. Eash and C. Upthegrove, *ibid.*, 1933, **104**, 221.



# THE PREPARATION AND PROPERTIES OF MAGNESIUM ALLOY SHEETS OF CONTROLLED IMPURITY CONTENT\*

1490

By H. G. COLE,† B.Sc., A.R.I.C., A. E. L. TATE,‡ A.I.M.,  
and B. WALTERS,§ M.A., MEMBER

## SYNOPSIS

A description is given of the preparation and rolling of ingots of three commercial types of magnesium alloy sheet, each in three grades of purity with respect to iron, and containing: (i) 1.7% manganese; (ii) 3.5% aluminium, 1% zinc (AZ31); and (iii) 6.5% aluminium, 1.5% zinc (AZ61). Corrosion and mechanical tests were made on the sheets. High corrosion-resistance was shown by all the sheets of 1.7% manganese alloy, irrespective of iron content, by high-purity AZ31, and by intermediate- and high-purity AZ61 sheets. The mechanical properties of the sheets were independent of iron content; those of the aluminium-containing sheets were good.

Protective treatments were much more effective on sheets of high-purity aluminium-bearing alloys than on those of ordinary purity.

## I.—INTRODUCTION

WHEN this investigation was begun, interest in magnesium alloys in sheet form was restricted because no one type of sheet existed which combined the desired properties of high strength, high corrosion-resistance, and weldability. Of the two types of sheet commonly available at that time, the magnesium-manganese alloy had good corrosion-resistance, was easily welded, but had comparatively poor strength; the magnesium-aluminium type of alloy had good strength and could be gas welded,<sup>1</sup> but had hitherto shown poor corrosion-resistance.

The critical effect of impurities, notably iron and nickel, on the resistance of magnesium alloys to attack by chloride solutions was demonstrated in 1941 by Beerwald<sup>2</sup> and shortly afterwards confirmed by the much more exhaustive experiments of Hanawalt and his colleagues.<sup>3</sup> The alloys used by these workers represented the general types of magnesium-manganese and magnesium-aluminium-zinc alloys, but did not include the exact compositions of the sheet materials in common use.

It was, therefore, decided to prepare two commercial types of magnesium-aluminium sheet in each of three grades of iron content and to determine the mechanical properties and corrosion-resistance of the sheets. It was also decided to include the magnesium-manganese type of sheet to see whether the good corrosion-resistance of the commercial-purity sheet could be further improved by reducing the iron content.

The three types of sheet selected for study were:

(i) D.T.D. 118 (1.7% manganese) corresponding to AM503 and Dowmetal M.

(ii) D.T.D. 120A (3.5% aluminium, 1% zinc) corresponding to AZ31 and Dowmetal FS.

(iii) D.T.D. 120A (6.5% aluminium, 1.5% zinc) corresponding approximately to AZ61, AZM, and Dowmetal J.

The zinc content of the last alloy was chosen as a compromise between the high content necessary for good corrosion-resistance and the low content desirable for easy rolling.

In addition to these alloys, others containing 3.5% aluminium were prepared with high copper content (0.1%) with and without the normal 1% zinc. This was to test a suggestion that copper of this order had little effect on corrosion-resistance, provided that zinc was present.

It was intended to prepare each alloy in three grades of purity, high, intermediate, and ordinary, with respect to iron. These designations were applied as follows:

High purity	. . . . .	<0.004% iron
Intermediate purity	. . . . .	0.0040-0.0099% iron
Ordinary purity, good grade	. . . . .	0.010-0.019% iron
„ „ poor grade	. . . . .	>0.020% iron

These limits are somewhat more rigorous than those quoted by Fox and Bushrod.<sup>4</sup>

## II.—PREPARATION OF INGOTS FOR ROLLING

### 1. METHODS OF OBTAINING SPECIFIC IRON CONTENTS

#### (a) Alloys Containing Aluminium

Preliminary work showed that the use of steel crucibles coated with protective washes, steel foundry tools similarly treated, pure fluxes, and pure raw materials were unreliable in preventing iron pick-up;

\* Manuscript received 25 February 1953.

† Royal Aircraft Establishment, Farnborough, Hants.

‡ Metallurgy Division, National Physical Laboratory,

Teddington, Middlesex.

§ Formerly of Magnesium Metal Corporation, Ltd., Swansea; now at Imperial Smelting Corporation, Ltd. Avonmouth.

this method of preparing high-purity ingots was, therefore, abandoned in favour of the known method of reducing iron by settlement.<sup>5</sup>

Since all ingots were cast before the work by Fox, Bushrod, and Mayer<sup>6</sup> had been published, it was necessary to carry out preliminary experiments to determine the precise conditions under which the

TABLE I.—*Treatment Temperatures for Intermediate- and High-Purity Alloys.*

Alloy Composition				High-Purity		Intermediate-Purity	
Al, %	Zn, %	Mn, %	Cu, %	Fe, %	Temp., °C.	Fe, %	Temp., °C.
6.5 ± 1	1.5	0.3	...	0.001–0.0025	630	0.006	700
3.5 ± 0.5	1.0	0.3	...	0.002–0.0035	640	0.007	700
...	...	1.7	...	...	640	0.004–0.007	660
3.5 ± 0.5	1.0	0.3	0.1	0.002–0.0035	640	0.007	700
3.5 ± 0.5	...	0.3	0.1	0.002–0.0035	640	0.007	700

required iron contents could be achieved. By maintaining melts at temperatures between the liquidus and 730° C., approximate solubility/temperature curves for iron in the alloys were obtained. Very low

(ii) Aluminium and zinc contents were not affected by the settlement process.

(iii) Small additions of copper, up to 0.1%, did not hinder the removal of iron by settlement.

#### (b) Magnesium–Manganese Binary Alloys

The solubility of iron in binary magnesium–1.7% manganese alloys is considerably higher than in aluminium-containing alloys at corresponding temperatures. Settlement at 660° C. consistently gave an iron content of 0.004–0.006%, and this intermediate purity was adopted as the best obtainable.

Reproducible iron content could not be achieved easily in the intermediate range (0.008%) by settlement, and it was found easier to make an alloy of manganese content higher than that required and to dilute with pure magnesium.

For ordinary-purity alloys, some superheating was necessary to ensure that sufficient iron was dissolved.

## 2. MELTING AND CASTING

The materials used are given in Table II. Alloying was carried out according to established practice;

TABLE II.—*Materials Used in Manufacture of Ingots.*

Material	Description	Al, %	Zn, %	Mn, %	Si, %	Pb, %	Cu, %	Fe, %
Magnesium	"Domal" made by the Dominion Magnesium Corp., Canada, by the ferro-silicon process.	0.003	0.004	0.003	0.006	0.005	0.0005	0.0015
Aluminium	Commercial grade.	Rem.	0.002	0.003	0.1	...	0.002	0.2
Zinc	High-purity commercial grade	...	99.9(N)	...	...	...	...	...
Manganese–aluminium hardener:								
No. 1	War-time quality, found to contain copper; used only for copper-containing alloys.	Rem.	...	10(N)	...	...	0.3	...
No. 2	Low copper content, obtained for the investigation.	Rem.	...	9.75	0.4(N)	...	0.05(N)	0.6
Manganous chloride (anhydrous)	Commercial grade.	...	...	40	...	...	...	0.4
Copper	High purity.	0.007	Tr.	Tr.	0.005	0.004	Rem.	0.025
Fluxes	Melrasal "E" and "Z".	...	...	...	...	...	...	...

(N) indicates nominal content; all other figures were determined chemically or spectrographically.  
Rem. = remainder. Tr. = trace.

iron contents (0.001% and below) were easily achieved by maintaining the melts at a temperature near the liquidus for 1 hr.; for iron contents corresponding to intermediate purity a rather higher temperature was necessary. Because of the different aluminium contents, temperature conditions varied slightly for the two alloys; they are given in Table I.

After treatment, the melts were heated quickly to the casting temperature (730° C.) and poured without delay to minimize re-solution of iron. For ingots of ordinary purity, no precautions were taken to reduce the iron contents.

In the preparation of high- and intermediate-purity ingots, the following observations were made:

(i) During treatment the manganese content fell at the same time as the iron content, because of decreased solubility at the lower temperatures. This effect was greater in alloys of higher aluminium content. High-purity alloys therefore had a manganese content below 0.3%

in the case of aluminium-containing alloys, manganese was added as aluminium–manganese hardener, and in binary magnesium–manganese alloys as anhydrous manganous chloride.

Previous experience and published work had shown that microporosity could be considerably reduced by presolidification, microporosity being due to a combination of shrinkage and of separation of dissolved hydrogen. At each presolidification, which progressively removed dissolved hydrogen, the tendency to microporosity was found to decrease, and all aluminium-containing alloys were presolidified three times by pouring into ingots before being used for ingot casting.

The casting procedure was modelled on that used at the National Physical Laboratory.<sup>7</sup> The alloys were made in a gas-fired furnace, and ingots 15 × 7 × 1½ in. were cast. Rapid solidification at the mould face, which was essential to avoid microporosity in the alloys high in aluminium, was achieved by keeping the



metal and mould temperatures as low as was consistent with the satisfactory filling of the mould, and by the use of a thick cast-iron mould having a mould-section to casting-section ratio of 4 : 1. The most favourable casting and mould temperatures were, respectively, 710°–730° C. and 150° C. for the aluminium-containing alloys, and 730° C. and 200° C. for the 1.7% manganese alloys. A thin graphite film produced by a commercial grate-polish was found to be a satisfactory mould dressing, largely because it gave a sound

were therefore pickled in dilute sulphuric acid after sawing into small pieces, or drilled with a copper-beryllium drill.

### III.—ROLLING OF CAST INGOTS TO SHEET

#### 1. PREPARATION OF INGOTS AND ROLLING PROCEDURE

After cropping to 12 in., the ingots were halved to give pieces  $6 \times 7 \times 1\frac{1}{2}$  in. and machined on the faces

TABLE III.—Summary of Rolling Procedure for Magnesium Alloy Ingots.

Purity	Alloy Type	Grain Structure	Homo-genizing Treatment	Rolling Procedure											
				Stage 1				Stage 2				Stage 3			
				Rolling Temp., °C.	Reduction, in.	No. of Passes	Reduction, %	Rolling Temp., °C.	Reduction, in.	No. of Passes	Reduction, %	Rolling Temp., °C.	Reduction, in.	No. of Passes	Reduction, %
High Inter. Ord.	1.7% Mn	Coarse Less coarse with increasing iron content	430° C. for 20 hr.	430–170	1.38–0.25	5	82	430–300	0.25–0.125/0.100	4/5	50/60	430–220	0.125/0.100–0.06/0.05	2	50
Rolling Behaviour.—All three grades rolled easily; the grain-size had no apparent effect.															
High Inter. Ord.	AZ31 (3.5% Al + 1% Zn)	Coarse	360° C. for 30 hr.	360–260	1.38–0.5	7	65	370–260	0.5–0.25	7	50	370–230	0.25–0.125/0.100	4/5	50/60
High Inter. Ord.	AZ31 + 0.1% Cu	Coarse				13									
High	3.5% Al + 0.1% Cu	Coarse				13									
Rolling Behaviour.—The material rolled well, but some edge-cracking occurred. In the first stage of rolling the coarse-grained ingots did not respond satisfactorily to the heavier reductions given to ingots of normal purity.															
High Inter. Ord.	AZ61 (6.5% Al + 1.5% Zn)	Grain-size decreasing with increase in iron content	390° C. for 20 hr.	360	1.4–0.70 (press-forged)	...	50	320–260	0.70–0.25	8	65	320–250	0.25–0.125	2	50
Ord.												320–250	0.25–0.07	2	60
Rolling Behaviour.—There was considerable cracking at all stages of rolling.															

surface zone which minimized cracking during subsequent rolling.

#### 3. SAMPLING FOR ANALYSIS

In each case sufficient alloy was prepared to cast four ingots. The composition of a dip-sample was taken to represent the aluminium and zinc contents of all ingots cast from the batch. In the case of manganese and iron in the medium- and high-purity ingots and of copper in all ingots in which it was included, dip-samples were taken from the melt for each ingot before casting. Although the medium- and high-purity ingot melts were sampled for iron and manganese during non-equilibrium conditions, i.e. when heating after settlement, a few check analyses of samples taken before and after pouring, of drillings taken from ingots, and of the sheets after rolling, showed that all agreed reasonably well, there being a slight increase in iron content of the slabs as compared with the dip-sample because of the rapidity of iron pick-up at the pouring temperatures.

It was found, as expected, that drilling and milling with steel tools introduced notable and unpredictable iron contamination. Samples for iron determination

to remove casting skin and superficial defects. Generally about 0.06 in. was removed from each face.

Rolling was carried out with lubricated rolls heated to about 100° C. and driven at a peripheral speed of 120–180 ft./min. A lubricant consisting of a mixture of 70 parts of transformer oil and 30 parts of paraffin was applied by means of a felt pad, weighted against the rolls. Special attention was given to the prevention of contamination of the sheets from the rolls, and frequent roll cleaning was carried out during the operations. The rolls were two-high and each weighed 15 cwt.

#### 2. TREATMENT OF MATERIALS AND ROLLING BEHAVIOUR

The grain-structure of the ingots was influenced by the iron content, and usually the grain-size increased with decrease in iron content. The range of grain-size in the 1.7% manganese alloy ingots was substantially larger than that in the alloys containing aluminium and zinc. The ingots were given a suitable homo-genizing treatment before they received any mechanical treatment, and all except those of the AZ61 type were rolled direct from the cast ingot.

The AZ61 alloy ingots had to undergo a preliminary reduction by press-forging in a hydraulic press between dies heated to about 100° C. The rolling procedures used for all the materials are summarized in Table III. In the initial rolling reductions it was found that the high-purity binary manganese alloy, which had the coarsest grain structure, could be given heavy reductions per pass, but that with the other alloy ingots less heavy reductions per pass were necessary to avoid cracking. The ingots were given alternate passes in the longitudinal and transverse directions with intermediate heating until the sheets were 11 in. in width, after which they were generally rolled to a thickness of between 0.125 and 0.100 in.

The sheets were thoroughly cleaned with coarse emery paper, and then scoured with alumina and paraffin (kerosene) to remove any surface contamination left by the emery. They were then trimmed, halved, and rolled finally to give sheets about 0.06 and 0.04 in. thick, respectively. With the AZ61 alloy, severe cracking occurred, and it was not possible to produce reasonable areas of sound sheet less than 0.07 in. thick. Many rolling experiments were carried out, but it became clear that 6.5% aluminium with 1.5% zinc exceeded the limit of composition for satisfactory rolling.

No attempt was made to roll any of the materials to optimum mechanical properties.

#### IV.—CORROSION TESTS

The actual compositions of the sheets selected for test are given in Table IV. The nickel contents of the 1.7% manganese sheets were found to be rather high (0.008%). Hanawalt's work<sup>3</sup> suggests, however, that in this type of alloy up to 0.01% nickel has little effect on the corrosion-resistance. The source of the nickel is not known.

##### 1. PREPARATION OF SPECIMENS

Specimens 10.5 × 4.5 cm. were cut from each sheet, and prepared for exposure in three conditions: unprotected, chromate-treated, and chromate-treated and painted.

When the 1.7% manganese alloy specimens selected for chromate treatment were cleaned with moist pumice powder, degreased by immersion for 15 min. in a boiling 5% solution of Zonax metal cleaner, and treated in the hot half-hour chromate bath (bath (iii) of D.T.D. 911A), the resulting chromate film was streaky. This effect, which was probably due to contamination of the surface of the metal by oxidized oil, has been found<sup>8</sup> to lead to reduced corrosion-resistance. To remove the contaminated surface, all the test specimens, including those to be exposed without protective treatment, were rubbed with moist pumice powder, immersed for 15 min. in a boiling 5% caustic soda solution, dipped for 10 sec. in a cold 10% nitric acid solution, and again rubbed with pumice. The specimens to be chromate-

treated were then degreased in Zonax and treated in bath (iii). The films on the 1.7% manganese alloy were a uniform light straw brown in colour, and those on the AZ61 specimens were uniform black. On the 3.5% aluminium specimens the films were mottled light and dark brown; this appearance was evidently connected with the structure of the metal, as further rigorous cleaning and retreatment did not change it. A similar effect has been found on Dowmetal FS1 sheet, though on this material the mottling was much finer.

Specimens to be exposed painted, were sprayed with two coats of an oil-type primer pigmented with zinc chrome, followed by a coat of matt cellulose black to D.T.D. 754.

The specimens were exposed to the R.A.E. intermittent sea-water spray test. In this test the specimens are hung by glass hooks from glass rods in a shed open to the air on one side. They are sprayed three times a day for five days a week with sea-water from the English Channel.

At the end of the exposure, the specimens were freed from gross corrosion product by brushing in running water, and were then immersed overnight in a cold 10% ammonium chromate solution through which a stream of air bubbled. This treatment removed the last traces of corrosion product without appreciable effect on the metal or the chromate film. Paint films were removed with a paint solvent of the methylene chloride type, followed by a rinse in benzol. The specimens were then weighed and the losses of weight due to corrosion, calculated as g./dm.<sup>2</sup>, were taken as a measure of the corrosion.

##### 2. RESULTS OF TESTS

The detailed results are given in Table V. Fig. 1 (Plate III) shows some of the corroded AZ31 specimens after removal of the corrosion product and paint.

###### (a) 1.7% *Manganese Alloy*

The corrosion-resistance of all three grades was good in the partly and wholly protected conditions, the response to chromate treatment being particularly high even in the absence of paint.

The similarity of the corrosion-resistance of the three grades is remarkable, because the iron contents lay on each side of the tolerance limit of 0.017% found by Hanawalt<sup>3</sup> and supported by Jones and Petch<sup>9</sup> from results obtained on D.T.D. 118 sheet. The results do not, of course, indicate what the corrosion-resistance of this alloy with really low iron and nickel content would be.

###### (b) 3.5% *Aluminium*, 1% *Zinc Alloy*

When unprotected, the high-purity sheets had an appreciably higher corrosion-resistance than the intermediate-purity sheets, which in turn were rather more resistant than the ordinary-purity sheets. The efficiency of the protective treatments increased markedly with increasing purity of sheet, however, so



TABLE IV.—Actual Composition by Analysis of Magnesium Alloy Sheets.

Alloy	Purity	Gauge	Composition by Analysis, %								
			Al	Zn	Mn	Fe	Cu	Ni	P	Si	Mg
1.7% Manganese	Ordinary, poor	16	0.05	<0.03	1.72	0.0225	0.003	0.008	<0.001	0.005	Rem.
	„ good	16	<0.02	None	1.66	0.0120	0.003	0.008	<0.001	0.005	„
	Intermediate	16	<0.01	„	1.72	0.007	0.004	0.008	<0.001	0.005	„
3.5% Aluminium, 1% Zinc	Ordinary	20	3.83	1.02	0.31	0.018	0.009	0.002	0.001	0.025	Rem.
	„	16	3.73	1.02	0.30	0.018	0.009	0.0017	0.001	0.02	„
	Intermediate	20	3.87	1.01	0.22	0.0088	None	0.0005	0.001	0.019	„
	„	16	3.85	0.92	0.33	0.0072	0.001	0.002	<0.001	0.007	„
	High	20	3.80	1.01	0.30	0.0025	0.0035	0.0015	0.001	0.012	„
	„	16	3.60	0.91	0.29	0.0020	0.0035	0.0013	0.001	0.012	„
	Intermediate Fe, high Cu	16	3.57	0.70	0.30	0.0050	0.092	0.0017	0.001	0.014	„
	Low Fe, high Cu, no Zn	16	3.60	<0.02	0.29	0.003	0.104	0.005	<0.001	...	„
6.5% Aluminium, 1.5% Zinc	Ordinary, poor	17	6.80	1.55	0.28	0.022	0.0095	0.0035	<0.001	0.012	Rem.
	„ good	18	6.60	1.45	0.29	0.0175	0.003	0.0035	<0.001	0.010	„
	Intermediate	16	6.55	1.45	0.28	0.008	0.0095	0.0035	<0.001	0.012	„
	High	16	6.55	1.50	0.22	0.003	0.0045	0.0035	<0.001	0.010	„

TABLE V.—Results of Sea-Water Spray Corrosion Tests on Magnesium Alloy Sheets.

Purity	Gauge	Iron and Nickel Contents		Untreated		Chromate Treated		Chromate Treated and Painted				
		Fe, %	Ni, %	Period of Exposure, months	Losses Due to Corrosion, g./dm. <sup>2</sup> *	Period of Exposure, months	Losses Due to Corrosion, g./dm. <sup>2</sup>	Period of Exposure, months	Losses Due to Corrosion, g./dm. <sup>2</sup>			
1.7% <i>Manganese Alloy</i>												
Ordinary, poor	16	0.023	0.008	4½	1.026 1.610 1.158 0.901	1.17	21	0.332 0.363 0.365 0.231	0.32	27	0.009 0.005 0.014 Trace	0.01
„ good	16	0.012	0.008	4½	1.161 0.963 1.224 0.515	0.97	21	0.772 0.683 1.237 0.382	0.52	27	0.116 0.109 0.036 0.005	0.07
Intermediate	16	0.007	0.008	4½	0.692 0.340 0.554 0.784	0.59	21	0.197 0.207 0.210 0.230	0.21	27	0.009 0.005 0.016 0.011	0.01
3.5% <i>Aluminium, 1% Zinc Alloy</i>												
Ordinary	20	0.018	0.002	2	1.690 1.534 1.318 1.302	1.46	4½	2.820 2.295 2.181 1.562	2.21	...	...	...
„	16	0.018	0.0017	2	1.158 1.342 1.212 1.033	1.19	4½	3.478 2.771 2.445 2.495	2.80	27	1.724 1.572 1.883 1.686	1.72
Intermediate	20	0.0088	0.0005	2	1.350 1.055 0.974 0.969	1.09	21	1.457 1.470 1.187 1.752	1.47	...	...	...
„	16	0.0072	0.002	2	0.803 0.770 0.816 0.720	0.78	21	1.773 1.890 2.093 1.542	1.82	27	0.030 0.103 0.120 0.038	0.07
High	20	0.0025	0.0015	2	0.172 0.132 0.135 0.360	0.20	21	0.320 0.171 0.161 0.131	0.20	...	...	...
„	16	0.0020	0.0013	2	0.528 0.180 0.198 0.159	0.27	21	0.344 0.301 0.269 0.256	0.29	27	0.003 0.008 0.001 Trace	<0.01
Intermediate iron but high copper	16	0.0050	0.0017	2	1.307 1.018 0.887 0.910	1.03	21	1.046 1.292 1.040 1.032	1.10	...	...	...
Low iron but high copper; no zinc	16	0.003	0.005	2	1.157 1.170 1.056 0.720	1.02	4½	0.439 0.396 0.365 0.594	0.45	...	...	...
6.5% <i>Aluminium, 1.5% Zinc Alloy</i>												
Ordinary, poor	17	0.022	0.0035	2	1.389 1.201 1.052 1.124	1.19	4½	6.340 7.810 4.640 8.400	6.8	27	2.350 3.000 1.629 1.962	2.24
„ , good	18	0.018	0.0035	2	0.900 0.974 0.968 1.035	0.97	4½	2.851 2.582 3.149 3.357	3.0	...	...	...
Intermediate	16	0.008	0.0035	21	1.217 1.458 1.229 1.290	1.30	21	0.214 0.270 0.225 0.186	0.23	27	0.007 0.002 0.003 0.005	<0.01
High	16	0.003	0.0035	21	0.516 0.543 0.569 0.623	0.56	21	0.151 0.111 0.108 0.091	0.12	27	Trace 0.003 Trace 0.023	0.01

\* Mean losses are indicated in heavy type.

that in the protected conditions the differences between the three grades of sheet were very much greater. When chromate-treated and painted, the high-purity sheet showed only very slight corrosion after 27 months' exposure. On the whole, the 20-gauge sheets were a little more resistant than the 16-gauge sheets.

in the period of exposure. These results tend to confirm the suggestion that copper of this order can be tolerated provided that zinc is present.

(c) 6.5% Aluminium, 1.5% Zinc Alloy

When unprotected, the high-purity sheet was somewhat more resistant than that of intermediate purity,

TABLE VI.—Mechanical Properties of Magnesium Alloy Sheets.

Material	Purity	Gauge	Longitudinal Properties						Transverse Properties					
			L.P., tons/in. <sup>2</sup>	0.1% P.S., tons/in. <sup>2</sup>	U.T.S., tons/in. <sup>2</sup>	Elong., % on 2 in.	E, lb./in. <sup>2</sup> × 10 <sup>6</sup>	Bend Radius	L.P., tons/in. <sup>2</sup>	0.1% P.S., tons/in. <sup>2</sup>	U.T.S., tons/in. <sup>2</sup>	Elong., % on 2 in.	E, lb./in. <sup>2</sup> × 10 <sup>6</sup>	Bend Radius
1.7% Manganese Alloy														
Sheet made as described	Ordinary, poor	16	1.3 2.1	6.5 6.3	11.4 10.7	3.0 3.0	6.0 5.2	>6t ...	1.7 2.1	7.4 7.5	16.2 16.2	8.3 8.5	6.6 6.5	6t ...
" "	" good	16	2.2 2.2	6.8 6.7	12.5 12.8	2.5 2.8	5.8 6.2	>6t ...	2.4 2.2	8.5 8.3	16.6 16.7	9.0 9.5	5.9 6.4	6t ...
" "	Intermediate	16	1.6 1.6	6.2 7.0	12.8 12.7	2.5 2.5	6.8 5.7	>6t ...	2.7 1.9	8.9 7.7	16.4 16.2	10.0 9.5	6.0 6.5	6t ...
Dowmetal Mh	"	16	3.9	10.7	16.8	7.0	6.1	7t	2.1	8.0	15.6	14.0	6.3	6½t
" Ma	"	16	3.2	7.0	14.7	20.0	5.9	4½t	2.7	6.2	14.1	20.5	6.1	3t
Specification D.T.D. 118A.	Iron >0.03%	...	...	<6.0	<13.0	...	...	>6t	...	...	...	...	...	...
3.5% Aluminium, 1% Zinc Alloy														
Sheet made as described	Ordinary	20	3.8 4.3	12.5 12.7	20.4 18.3	4.5 8.5	7.1 6.9	>8½t ...	2.2 4.3	16.7 14.0	21.6 21.0	17.0 17.0	6.9 6.7	...
" "	"	16	3.4 4.0	10.7 11.4	19.4 20.0	6.0 10.5	7.1 6.5	>6t ...	2.7 2.0	15.2 14.6	20.8 20.8	17.0 16.3	6.6 6.7	6t ...
" "	Intermediate	20	3.6 2.7	13.9 14.2	20.5 20.5	3.3 5.0	6.5 6.3	>8t ...	4.0 3.1	15.7 15.7	20.5 21.5	13.5 14.0	6.4 6.4	6½t ...
" "	"	16	2.0 2.0	11.8 11.8	18.5 18.3	19.0 17.0	6.4 6.7	5t ...	2.2 3.0	14.0 14.4	18.9 19.0	17.0 18.5	6.4 6.4	5½t ...
" "	High	20	3.9 4.4	10.2 12.7	20.8 19.4	6.0 9.25	7.0 6.4	5½t ...	4.5 4.9	14.8 15.8	20.0 20.4	18.0 18.0	6.6 6.3	5½t ...
" "	"	16	3.1 4.7	10.4 12.1	18.5 18.0	14.0 11.0	6.8 5.6	5½t ...	2.3 2.6	13.9 13.8	18.4 18.6	9.3 22.5	6.6 6.9	5½t ...
Dowmetal FS 1h	"	19	5.3	12.2	19.4	8.0	6.2	7t	5.5	13.2	20.5	14.0	6.2	6½t
" "	"	16	5.5	13.1	19.8	11.0	6.3	8t	5.5	12.8	16.9	15.0	6.5	8t
Dowmetal FS 1a	"	19	2.8	7.2	16.4	17.0	6.2	3t	3.1	9.1	17.2	18.0	6.3	3t
" "	"	16	5.5	10.2	16.7	20.0	6.2	4½t	6.9	10.2	17.0	21.0	6.3	3½t
6.5% Aluminium, 1.5% Zinc Alloy														
Sheet made as described	Ordinary, poor	17	3.0 2.9	14.3 13.8	22.8 23.4	14.5 9.0	6.5 6.6	7½t ...	7.6 2.8	14.8 12.5	22.6 22.4	15.0 16.0	6.1 7.0	7½t ...
" "	Intermediate	16	3.0 3.2	15.5 15.5	22.6 22.7	5.5 8.0	6.3 6.4	7½t ...	1.7 4.5	13.9 15.0	23.0 23.0	14.0 15.0	7.0 6.4	6t ...
" "	High	16	2.7 3.3	13.3 12.2	19.8 20.8	10.5 21.0	6.4 6.4	>7t ...	1.5 2.7	14.0 14.3	20.9 20.6	21.8 20.0	6.7 6.4	7t ...
Dowmetal J 1h	"	16	6.0	13.0	20.3	9.5	6.3	10t	4.7	13.7	20.8	8.0	6.3	10t
" J 1a	"	16	2.8	10.2	19.4	11.0	6.3	7t	3.5	11.6	19.8	11.0	6.4	7t
D.T.D. 120A (Mg-Al-Zn-Mn sheet)	...	...	...	< 7.0	<16.0	...	...	...	...	...	...	...	...	>6t
D.T.D. 707 (high-purity sheet)	...	...	...	<10.0	<18.0	...	...	>4t	...	...	...	...	...	...
Draft 1945	...	...	...	...	...	...	...	...	...	...	...	...	...	...
D.T.D. 626 (Mg-Zn-Zr sheet)	...	...	...	<11.0	<17.0	...	...	>4t	...	...	...	...	...	...

The sheet with high copper content (0.10%) behaved as would be expected from its iron content (0.005%), the copper apparently having little influence. A similar alloy with 0.1% copper but without zinc appeared to be rather less resistant, in spite of a somewhat lower iron content (0.003%). Comparison is, however, difficult owing to differences

which in turn was very much more resistant than the ordinary-purity sheet. When chromate-treated and painted, both the high-purity and intermediate-purity grades showed only very slight corrosion after 27 months' exposure. Chromate treatment alone gave good protection to the high- and intermediate-purity grades; it gave none to the ordinary-purity grade.



## V.—MECHANICAL PROPERTIES

The results of mechanical tests are given in Table VI. Results on some commercial Dowmetal sheets and a list of relevant specification requirements are also included in the table.

## (a) 1.7% Manganese Alloy

The longitudinal strength and ductility were appreciably less than the transverse, the longitudinal U.T.S. being below the limit laid down by the latest D.T.D. 118A specification. This was in contrast with the two types of Dowmetal M sheet (hard rolled and annealed, respectively), which showed a strength and ductility independent of direction. The transverse strength of the sheets was equal to that of the Dowmetal, but the ductility was rather lower transversely and much lower longitudinally. The properties of the sheets were independent of the iron content.

## (b) 3.5% Aluminium, 1% Zinc Alloy

The transverse 0.1% proof stress and elongation values were higher than the longitudinal values, but there was no appreciable difference in the U.T.S. The 20-gauge sheets were stronger, but on the average less ductile, than the 16-gauge sheets.

The sheets showed good mechanical properties, which were, on an average, as good as or better than those of Dowmetal FS1. The sheets complied with the draft D.T.D. 707 specification (high-purity sheet) in strength and ductility, though not in the limiting bend radius. Most of the sheets also complied with D.T.D. 626, the new specification covering magnesium-zinc-zirconium alloy sheet. The properties were independent of the iron content.

## (c) 6.5% Aluminium, 1.5% Zinc Alloy

With the exception of the ductility of the intermediate grade, the properties of these sheets were independent of the direction of rolling. The properties were as good as or better than those of Dowmetal J1, and in strength and ductility they complied with draft specification D.T.D. 707 and also with D.T.D. 626. The high-purity sheet was a little less strong and more ductile than the intermediate- and ordinary-purity sheets. The sheets had slightly better properties than those containing 3.5% aluminium and 1% zinc.

## VI.—CONCLUSIONS

Magnesium alloy sheets containing 1.7% manganese (D.T.D. 118 or AM503 type) showed, in the protected condition, a very high corrosion-resistance as measured by weight loss, independent of variation in the iron content from 0.007 to 0.023%.

Sheets containing 3.5% aluminium, 1% zinc, and 0.3% manganese (AZ31 type) of ordinary purity (0.02% iron) showed comparatively poor corrosion-resistance. In the fully protected state the intermediate-purity alloy (0.008% iron) showed high resistance (25 times that of the ordinary-purity) and the high-purity alloy (0.002% iron) a very high resistance (200 times that of the ordinary purity). The successive improvements were due partly to increased intrinsic resistance of the metal but mainly to a great increase in the effectiveness of the protective treatment. The mechanical properties of the sheet were good and were independent of iron content. The transverse properties were somewhat higher than the longitudinal ones. A high copper content (0.10%) had no effect on the resistance of intermediate-purity sheet; omission of zinc from such an alloy appeared to lower the corrosion-resistance.

Sheets containing 6.5% aluminium, 1.5% zinc, and 0.3% manganese (AZ61 type) of ordinary purity (0.02% iron) showed poor resistance. In the protected state both intermediate- (0.008% iron) and high-purity (0.003% iron) grades showed very high resistance (200 times that of the ordinary purity). The intermediate-purity grade, in contrast to the AZ31 sheet, was on the average only slightly less resistant than the high-purity grade. Increased intrinsic resistance, as well as increased effectiveness of chromate treatment, contributed to the great improvement over the ordinary-purity grade. The mechanical properties were good, being slightly better than those of the AZ31 sheets, and were independent of direction of rolling or of iron content.

## ACKNOWLEDGEMENTS

The authors acknowledge with thanks the part played by Mr. J. Harper in the initiation of this work.

Acknowledgement is made to the Chief Scientist, Ministry of Supply, the Director of the National Physical Laboratory, and the Controller of H.M. Stationery Office for permission to publish this paper.

## REFERENCES

1. J. G. Ball and A. E. L. Tate, *Weld. Research*, 1952, **6**, 13r.
2. A. Beerwald, *Z. Metallkunde*, 1941, **33**, 28.
3. J. D. Hanawalt, C. E. Nelson, and J. A. Peloubet, *Trans. Amer. Inst. Min. Met. Eng.*, 1942, **147**, 273.
4. F. A. Fox and C. J. Bushrod, *J. Inst. Metals*, 1944, **70**, 325.
5. British Patents Nos. **336,498** and **411,324**.
6. F. A. Fox, C. J. Bushrod, and S. E. Mayer, *J. Inst. Metals*, 1947, **73**, 55.
7. A. E. L. Tate, *ibid.*, 1950, **78**, 71.
8. L. Rakowski, *Metallurgia*, 1950, **42**, 362.
9. E. R. W. Jones and M. K. Petch, *J. Inst. Metals*, 1947, **73**, 129.

# NOTICE TO AUTHORS OF PAPERS FOR THE "JOURNAL" AND CONTRIBUTORS TO DISCUSSIONS

1. **Papers will be considered for publication from non-members as well as members of the Institute.** They are accepted for publication in the *Journal* and not necessarily for presentation at any meeting of the Institute. MSS. should be addressed to The Editor of Publications, The Institute of Metals, 4 Grosvenor Gardens, London, S.W.1.

2. **Papers suitable for publication** may be classified as:

(a) Papers recording the results of original research.  
(b) First-class reviews of, or accounts of progress in, a particular field.

(c) Papers descriptive of works methods, or recent developments in metallurgical plant and practice.

(d) Papers in classes (a), (b), and (c) above, previously published in languages other than English, French, German, or Italian, if of sufficient merit.

3. **Manuscripts and illustrations** should be submitted in duplicate. MSS. must be typewritten (*double-line spacing*) on one side of the paper only, and authors are requested to sign a declaration that neither the paper nor a substantial part thereof has been published elsewhere. Exceptions may be made in certain cases where a paper has been published in a language other than English, French, German, or Italian (see 2(d) above). MSS. not accepted are normally returned within 6 months of receipt.

In the interests of economy, all papers must be written as concisely as possible; in general, internal research reports are not in suitable form for publication as papers in the *Journal*. All but the simplest mathematical expressions should be written by hand, with capital and small letters clearly distinguished. Superscript and subscript letters should also be plainly indicated. Greek letters and special signs should be identified in the margin. For style, spelling, and abbreviations used, any recent issue of the *Journal* may be consulted.

4. **Synopsis.** Every paper must have a synopsis (not exceeding 250 words in length) which, in the case of a paper reporting original research, should state its objects, the ground covered, and the nature of the results. The synopsis will appear at the beginning of the paper, and should be in a form suitable for use by abstracting organizations. Extracts from a "Guide for the Preparation of Synopses" drawn up by the Abstracting Services Consultative Committee are reproduced below.

5. **References** must be collected at the end of the paper and must be numbered in the order in which they occur in the MS. Initials of authors must be given, and the Institute's official abbreviations for periodical titles (as used in *Metallurgical Abstracts*) should be employed, where known. References to papers should be set out in the style:

A. L. Dighton and H. A. Miley, *Trans. Electrochem. Soc.*, 1942, 81, 321 (i.e. year, volume, page).

References to books should be in the following style:

C. Zener, "Elasticity and Anelasticity of Metals". Chicago: 1948 (University of Chicago Press).

6. **Illustrations.** Each illustration must have a number and description; only one set of numbers must be used in one paper, and it is desirable to number the half-tone illustrations consecutively, rather than to interperse them with the line figures. The captions should be typed on a separate sheet.

The set of **line figures** sent for reproduction must be drawn (about twice the size to appear in the *Journal*) in Indian ink on smooth white Bristol board, good-quality drawing paper, co-ordinate paper, or tracing cloth, which are preferred in the order given. Co-ordinate paper, if used, must be blue-lined, with the co-ordinates to be reproduced finely drawn in Indian ink. Curves should be drawn boldly (i.e. at least twice the thickness of the frame). Experimental points should be indicated by open or closed circles, triangles, squares, &c. (preferably not crosses). Curves should be broken on each side of such symbols and plenty of allowance should be made for closing up in blockmaking. All lettering and numerals, &c., should preferably be in *pencil*, so that the Institute's standard lettering may be affixed, and ample margins must be left outside the framework of the figures to enable this to be done. The second set of line illustrations may be photostat copies.

**Photographs** must be restricted in number, owing to the expense of reproduction, and photomicrographs should be trimmed to the smallest possible of the following sizes consistent with adequate representation of the subject: 4 in. deep by 3 in. wide: 2 in. deep by 3 in. wide: 2 in. square. Magnifications of photomicrographs must be given in each case. Photographs for reproduction should be loose, not pasted down (and not fastened together with a clip, which damages them), and the figure number and author's name should be written on the back of each. Captions should be given to the photomicrographs, but these should be kept as brief as possible.

Because of the present high cost of printing and paper it is imperative that authors restrict illustrations (particularly photographs) to the absolute minimum deemed necessary to support their argument. Only in exceptional cases will illustrations be reproduced if already printed and readily available elsewhere.

7. **Tables or Diagrams.** Results of experiments, &c., may be given in the form of tables or figures, *but* (unless there are exceptional reasons) *not both*. Tables should bear Roman numbers, and each should have a heading that will make the data intelligible without reference to the text.

8. **Corrections.** A certain number of corrections in proof are inevitable, but any modification of the original text is to be avoided. Since corrections are very expensive, the Institute reserves the right to require authors to contribute towards their cost if the Editor deems them to be excessive. The Institute also reserves the right to require a contribution to the cost of remaking any block where this is necessitated by an error on the author's part.

9. **Reprints.** Individual authors are presented with a maximum of 25, and two or more authors with a maximum of 50 reprints from the *Journal*, without covers. Limited numbers of additional reprints can be supplied at the author's expense, if ordered before proofs are passed for press. (Orders should preferably be placed when submitting MSS.)

10. **Discussion.** Except in the case of special symposia, shorthand records of discussions are not taken at meetings. Written discussion may be submitted on any paper, preferably typewritten (*double-line spacing*). References should be given in the form of footnotes. Paragraphs 6 and 7 above are also applicable to such contributions. Reprints of discussion cannot be supplied to contributors.

## GUIDE FOR THE PREPARATION OF SYNOPSES

(As recommended by the Abstracting Services Consultative Committee)

1. **Purpose.** The synopsis is not part of the paper; it is intended to convey briefly the content of the paper, to draw attention to all new information, and to the main conclusions. It should be factual.

2. **Style of writing.** The synopsis should be written concisely and in normal rather than abbreviated English. It is preferable to use the third person. Where possible use standard rather than proprietary terms, and avoid unnecessary contracting.

It should be presumed that the reader has some knowledge of the subject, but has not read the paper. The synopsis should therefore be intelligible in itself without reference to the paper; for example, it should not cite sections or illustrations by their numerical references in the text.

3. **Content.** The title of the paper is usually read as part of the synopsis. The opening sentence should be framed accordingly and repetition of the title avoided. If the title is insufficiently comprehensive, the opening should indicate the subjects covered. Usually the beginning of a synopsis should state the objective of the investigation.

It is sometimes valuable to indicate the treatment of the subject by such words as: brief, exhaustive, theoretical, &c.

The synopsis should indicate newly observed facts, conclusions of an

experiment or argument and, if possible, the essential parts of any new theory, treatment, apparatus, technique, &c.

It should contain the names of any new compound, mineral species, &c., and any new numerical data, such as physical constants; if this is not possible, it should draw attention to them. It is important to refer to new items and observations, even though some are incidental to the main purpose of the paper; such information may otherwise be hidden, though it is often very useful.

When giving experimental results the synopsis should indicate the methods used; for new methods the basic principle, range of operation, and degree of accuracy should be given.

4. **References.** If it is necessary to refer to earlier work in the summary, the reference should always be given in full and not by number. Otherwise references should be left out.

When a synopsis is completed, the author is urged to revise it carefully, removing redundant words, clarifying obscurities, and rectifying errors in copying from the paper. Particular attention should be paid by him to scientific and proper names, numerical data, and chemical and mathematical formulæ.



# THE BEHAVIOUR OF THE CRYSTAL BOUNDARIES OF ALUMINIUM AT TEMPERATURES NEAR THE MELTING POINT\*

1491

By W. I. PUMPHREY,† M.Sc., Ph.D., MEMBER, and  
J. V. LYONS,‡ Ph.D., JUNIOR MEMBER

## SYNOPSIS

The tensile strength of aluminium of 99.988 and of 99.998% purity decreases progressively with increase in the temperature of testing. At a temperature some 4° C. below the generally accepted melting point, a sudden fall in strength occurs, and it is suggested that this may be attributed to the melting of the crystal boundaries. Reasons are considered for melting taking place in the crystal boundaries at a temperature some 4° C. below that at which melting of the crystals begins, and it is concluded that this may be due to the high strain energy in the boundaries.

## I.—INTRODUCTION

DURING an investigation of the mechanical properties at elevated temperatures of aluminium-silicon alloys containing 0–12% silicon, Singer and Cottrell<sup>1</sup> found that the strength of each alloy decreased gradually with increasing temperature until the solidus temperature of the alloy was reached, at which point a sudden fall in strength occurred as a result of the appearance of liquid metal at the crystal boundaries. At temperatures below the solidus, the alloys were ductile, whereas at temperatures immediately above the solidus the appearance of liquid at the crystal boundaries caused the specimens to break with a brittle, intercrystalline fracture having a shiny surface appearance. With aluminium of high purity, however, although the normal decrease in strength with increasing temperature was observed, intercrystalline fractures, accompanied by the sudden fall in strength, occurred at a temperature of 655° C., some 4° C. below the generally accepted melting point of pure aluminium.

Chaudron, Lacombe, and Yannaquis,<sup>2</sup> in connection with work on the relationship between intercrystalline corrosion and the behaviour of the crystal boundaries of aluminium during melting, published a photograph which illustrated an effect similar to that observed by Singer and Cottrell. A temperature difference of 10° C. was established between the ends of a thin strip of pure aluminium, so that one end was liquid whilst the other was still solid. The photograph showed that, at positions between the two ends of the strip, melting of the crystal boundaries occurred before the melting of the body of the crystals.

A possible explanation of the phenomenon was mentioned by Varley<sup>3</sup> during the discussion of the

paper by Singer and Cottrell. He suggested that the melting point of the crystal boundaries of high-purity aluminium may be lower than that of the body of the crystals because of the higher strain energy of the crystal boundaries. This suggestion had previously been advanced by Chalmers<sup>4</sup> for pure tin.

In order to obtain further information on this problem, tensile tests have been carried out at elevated temperatures on aluminium of 99.988 and of 99.998% purity, and also on aluminium of 99.988% purity after various annealing treatments.

## II.—EXPERIMENTAL TECHNIQUE

The apparatus used for the tensile tests consisted of a Hounsfield horizontal tensometer with motor drive, together with a resistance-tube furnace arranged to slide along the tie-bars of the testing machine. The design of the furnace was such that the tube could be placed coaxially with the pulling rods in order to eliminate friction between the grips and the inside of the furnace tube. It was not found necessary to modify the tensometer in any way, the normal beams and the mercury-column-displacement method of load measurement being used throughout the tests. A  $\frac{1}{2}$ -H.P. electric motor, driving through a worm-reduction gear and chain wheels, provided a constant rate of travel of the cross-head of 0.25 in./min. This speed was chosen to ensure that the results obtained in the present investigation should be comparable with those of Singer and Cottrell, who carried out their tensile tests on high-purity aluminium at this rate of straining.

The designs of the grips and test-piece used are illustrated in Figs. 1 and 2. The tubular pulling rods permitted the insertion of thermocouples into the

\* Manuscript received 7 January 1953.

† Research Manager, Murex Welding Processes, Ltd., Waltham Cross.

‡ Research Metallurgist, Department of Development and Research, Tube Investments, Ltd., Birmingham.

thermocouple holes at each end of the test-piece, which was so designed that, whilst being sufficiently short to minimize sagging of the gauge-length and the development of thermal gradients, it was adequate for the measurement of elongation and of the reduction of area.

Chromel/Alumel thermocouples were used to measure the specimen and furnace temperatures. Possible thermal gradients along the length of the test-piece were investigated by drilling a hole axially through the length of the specimen and advancing a search thermocouple, the readings of which were compared with those of a second placed in the normal position at one end of the test-piece. No temperature difference greater than  $1^{\circ}\text{C}$ . was detectable after the heating cycle of 20 min. used in the tests. The thermocouples were checked regularly against the bulk melting point of aluminium of 99.988% purity; the absolute accuracy of the temperature measurements was better than  $\pm 1^{\circ}\text{C}$ .

The test-piece attained the required testing temperature approximately 15 min. after insertion in the furnace and was maintained within  $\pm 1^{\circ}\text{C}$ . of this temperature for a further 5 min. After completion of the 20-min. heating cycle, the thermocouples, at the ends of the specimen agreed to within  $1^{\circ}\text{C}$ . The specimen was then extended to fracture; the autographic recorder incorporated in the tensometer was used to take a load/extension curve during the

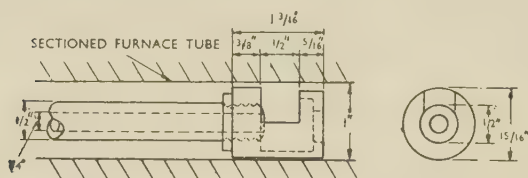


FIG. 1.—Design of Test-Piece Grips.

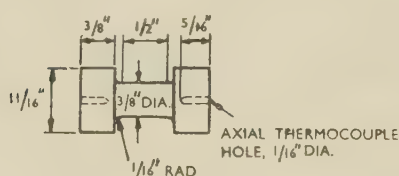


FIG. 2.—Design of Test-Piece.

course of each test, and measurements of elongation and of reduction of area were finally made on the broken specimen.

### III.—EXPERIMENTAL RESULTS

#### 1. TESTS ON CAST SPECIMENS

A series of specimens machined from cast bars of high-purity aluminium to the form shown in Fig. 2 were subjected to tensile tests. The aluminium used had a purity of 99.988%, which was nominally the same as that used by Singer and Cottrell, and contained silicon 0.005, iron 0.0015, copper 0.0005, and

magnesium 0.005%, giving a total impurity content of about 0.012%.

The curve showing the variation of tensile strength with testing temperature published by Singer and

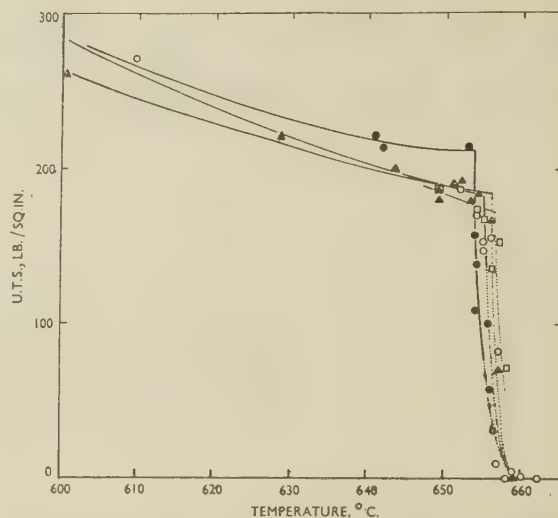


FIG. 3.—Strength of High-Purity Aluminium Near the Melting Point.

KEY.  
 — Normal fracture, i.e. no liquid present.  
 ..... Short fracture, i.e. liquid present.  
 ○ Aluminium of 99.988% purity, as cast (present work).  
 ● " " " " (Singer and Cottrell<sup>1</sup>).  
 ▲ " " " " annealed at 630°C. for 7 weeks.  
 □ " " " " 99.988% purity.

Cottrell is compared in Fig. 3 with the curve obtained on the same material in the present investigation.

The ductility of the cast specimens was found to increase to a maximum of 100% with increase in the temperature of testing to 640°C. Between 640° and 654°C., intercrystalline fractures were obtained, attended by a progressive decrease in ductility, but not accompanied by any sudden fall in strength. A sudden fall in strength occurred at 654°C. Singer and Cottrell found that a sudden fall in tensile strength occurred at 655°C. The agreement between these two figures is satisfactory.

#### 2. TESTS ON ANNEALED SPECIMENS

A number of test specimens of aluminium of 99.988% purity were annealed at 630°C. for 7 weeks to remove, as far as possible, any concentrations of impurities at the crystal boundaries. This treatment brought about some increase in the crystal size, but it is unlikely that this increase affected, to any marked extent, the temperature at which brittle fracture occurred.

The strength/temperature curve obtained with the annealed test-pieces is plotted in Fig. 3. The curves in Fig. 3 indicate that, at any one temperature, the strength of aluminium of 99.988% purity is reduced by annealing and that with annealed specimens the rapid fall in strength does not occur until a temperature of 656°C. has been reached. The form



of the strength/temperature curve for the annealed specimens above 656° C. is, however, very similar to that for the as-cast specimens.

With the annealed specimens, intercrystalline fractures associated with low ductility, but not accompanied by any sudden fall in strength, were obtained between 649° and 656° C.

### 3. TESTS ON ALUMINIUM OF EXCEPTIONALLY HIGH PURITY

To enable an examination to be made of the effect of purity of the aluminium on the temperature at which the rapid fall of strength occurs, a small quantity of aluminium of exceptionally high purity was supplied to the authors by Major P. C. Varley of The British Aluminium Co., Ltd. The metal was stated to be 99.998% pure, the silicon, iron, copper, and magnesium contents each being less than 0.0005%. Tensile test-pieces were machined directly from the ingot in order to avoid the possibility of contamination by further melting and casting.

The results obtained in tests on this material are plotted in Fig. 3. The sudden fall in strength occurs at 656° C.; this temperature is higher than that for the specimens of cast aluminium of 99.988% purity and the same as that for the annealed specimens of 99.988% purity. The difference of 2° C. between the temperature of the fall in strength of some of the cast test-pieces and that of the annealed and the very high-purity test-pieces is, however, approaching the limit of experimental accuracy of the measurements.

Intercrystalline fractures not accompanied by any sudden fall in strength but associated with low ductility were obtained with the material of 99.998% purity between 649° and 656° C.

## IV.—DISCUSSION

The results in Fig. 3 show that the tensile strength of pure aluminium gradually decreases with increase in the temperature of testing up to a temperature some 4°–5° C. below the generally accepted melting point of the metal. Then the strength drops suddenly to a small, but measurable, value, which is retained up to a slightly higher temperature.

Intercrystalline fractures, associated with low ductility but not accompanied by any sudden fall in strength, were encountered in many specimens at temperatures some 5°–20° C. below the accepted melting point. The surfaces of fracture in such specimens had a glazed and rounded appearance. The occurrence of this type of fracture, accompanied by a sudden fall in strength some 4°–5° C. below the generally accepted melting point, is anomalous and permits of two possible explanations. It may be due either to viscous flow of the crystal boundaries of the metal under the application of stress at a high temperature, or to the occurrence of melting in the crystal boundaries at some temperature below that at which melting occurs in the body of the crystal. It is of interest to consider both possibilities further.

At temperatures well below the melting point of a polycrystalline metal, the viscosity of a crystal boundary is high, and, unless the rate of straining is exceptionally slow, deformation of the crystals always occurs in preference to viscous flow of the crystal boundaries. The viscosity of the crystal boundaries decreases with increasing temperature, and it is probable that, at some temperature nearer the melting point, it becomes low enough to permit viscous boundary flow to take place in preference to crystal deformation. This condition, of course, arises only if the imposed rate of straining is not too great. When a temperature is reached at which viscous flow of the crystal boundaries has begun to cause the appearance of intercrystalline fractures, the rate of fall in strength with increase in temperature would be expected to be similar to the rate of fall in the viscosity of the crystal boundaries, since this is then the factor which determines the overall strength of the test-piece. Results obtained by Kê,<sup>5</sup> however, indicate that the coefficient of viscosity of the crystal boundaries of aluminium decreases slowly with increase in temperature near the melting point, so that a rapid fall in strength with increase in temperature would not be expected from these considerations alone. If, however, the crystal boundaries were to melt at a temperature somewhat below that at which melting occurs in the crystals, then a rapid fall in strength at this temperature would be expected.

It seems probable, therefore, that the observed occurrence of intercrystalline fracture, unaccompanied by any sudden fall in strength, is due to viscous flow at the crystal boundaries, and that the sudden fall in strength and the total loss of ductility (accompanied by the glazed type of fracture) with progressive increase in the temperature of testing is associated with incipient melting of the crystal boundaries some 4° C. below the temperature at which melting occurs in the body of the crystals.

In seeking an explanation of this phenomenon, the most obvious point to examine is the likely effect of the small percentage of impurities present in high-purity aluminium on the temperature at which brittle fracture occurs. Pumphrey and Jennings<sup>6</sup> found that on rapidly reheating a cast test-piece of pure aluminium, incipient fusion did not occur at the crystal boundaries below 656° C., even though the time taken to reheat the specimen to this temperature was as short as 20 sec. The lowest temperature at which these workers observed brittle fractures in reheated tensile specimens was thus the same as that observed in the present investigation. It appears, therefore, that the period for which cast aluminium of high purity is maintained at a high temperature before tensile testing, whether it be 20 sec., 20 min., or 7 weeks, has a negligible effect upon the temperature at which intercrystalline fracture and a sudden fall in strength occur. This conclusion suggests that the incipient fusion of the crystal boundaries is not caused by a segregation of impurities in such regions.

It may be argued, however, that even though there

is no especially marked concentration of impurities in the crystal boundaries of aluminium of 99.988% purity in the cast and annealed conditions, the amount of impurity normally present in the boundaries of the material is sufficient to cause incipient melting of the boundaries some 4° C. below the generally accepted melting point of the metal in the mass.

The results given in Table I show the effect on the melting point of pure aluminium of the addition of 0.01% of a number of elements singly and together.

TABLE I.—*The Effect of Impurities on the Melting Point of Pure Aluminium*

Impurity Addition	Melting Point Depression, °C.	Reference
0.01% Fe + 0.01% Si	2.0	7
0.01% Cu + 0.01% Mg	0.5	8
0.01% Mg <sub>2</sub> Si	0.5	9
0.01% Fe	1.7	10
0.01% Cu	0.23	11
0.01% Si	0.6	7, 10
0.01% Mg	0.16	12

These figures are necessarily somewhat approximate and do not give any complete indication of the combined effect of all the impurities, but if the effects of the several elements are assumed to be roughly additive, it would seem just possible that, if 0.01% of each of the four separate elements listed were present in pure aluminium, their cumulative effect would produce a depression of about 3° C. in the melting point. However, since the depression of the melting point of the crystal boundaries was observed not only with aluminium of 99.988% purity but also with that of 99.998% purity (which contained less than 0.0005% of each of the same four elements), it may be concluded that the small amount of impurity present in the aluminium of 99.988% purity cannot account satisfactorily for the observed depression of the temperature at which melting begins.

The preceding considerations have been based on the assumption that the metal is in a homogeneous condition at the moment of testing, so far as distribution of impurities is concerned. It is possible, however, that, even after annealing for seven weeks, such a condition is not attained, because the impurities may, for physical reasons, always be concentrated to some extent at the crystal boundaries. A crystal boundary may be thought of as a series of dislocations, and it seems possible that a local concentration of impurities may exist at a boundary because of the formation of "solute atmospheres" of foreign atoms around the dislocations.<sup>13</sup> It may be imagined that the impurities attracted to the crystal boundaries in this way will remain there even when the mass has been homogenized for some considerable time and that such a concentration may lead, in the normal manner, to incipient melting of the boundaries at a temperature below that at which melting begins in the crystals. In this connection, however, it should be remarked that the addition of a small quantity of an

alloying element to a pure metal causes the melting point of the latter to be lowered because the foreign atoms increase the strain energy of its lattice. It may not be valid to assume, therefore, that impurities will have the same effect on the melting point when they are in the crystal boundaries as when they are distributed throughout the mass of the crystals, since impurities concentrate at the boundaries because they do not cause such a large increase in strain energy there as when distributed in the crystals themselves.

These considerations confirm the view that the difference between the melting points of the crystal boundaries and of the crystals in pure aluminium is not due to a concentration of impurities at the boundaries. A more probable explanation of the phenomenon is that advanced by Chalmers,<sup>4</sup> namely that the melting point of a crystal boundary may be lower than that of a crystal because of the interatomic tensional stresses in the boundary due to the atomic disorder at an interface between metal crystals.

Chalmers calculated the stress necessary in a crystal boundary of tin to account for the observed occurrence of melting in the boundary 0.14° C. below the generally accepted melting point of the metal in the mass. For this calculation Chalmers made use of the following expression :

$$\frac{L}{T} \cdot \frac{1}{(V_2 - V_1)} = \frac{dp}{dT}$$

In the expression  $L$  is the latent heat of fusion of the metal,  $T$  is the absolute temperature in °K.,  $V_2$  is the specific volume of the liquid metal,  $V_1$  is the specific volume of the solid metal, and  $\frac{dp}{dT}$  is the stress necessary in the boundary to depress the melting point of the boundary by 1° K. For pure aluminium,  $L = 94.6$  cal./g.,  $T = 933^\circ$  K.,  $V_1 = 0.394$  c.c./g., and  $V_2 = 0.420$  c.c./g.

Hence,  $\frac{dp}{dT} = 1.67 \times 10^2$  kg./cm.<sup>2</sup>/°C.

For a depression of 4° C. in the melting point of the crystal boundary, the stress,  $p$ , necessary in the boundary is 668 kg./cm.<sup>2</sup> or 4.24 tons/in.<sup>2</sup>

It is somewhat difficult to decide whether this calculated value is of the correct order of magnitude. Some information on this point is provided by a consideration of the relationship between the stress in the crystal boundary calculated in the above way and the surface energy or surface tension of a crystal boundary in pure aluminium. It is reasonable to assume that the surface tension per cm. of crystal boundary is equal to the stress in the crystal boundary multiplied by the thickness of the crystal boundary. If it is assumed that the stress in the crystal boundary is 668 kg./cm.<sup>2</sup> and that the boundary is 10–15 Å. thick, then the surface tension of the boundary is, by calculation, between 65.5 and 98.3 dynes/cm.

Although the actual value of the surface tension of a crystal boundary in aluminium is not known, it is most probably less than the surface tension of a free



surface of aluminium. Portevin and Bastien<sup>14</sup> found the maximum value of the surface tension of an oxide-free surface of molten aluminium to be 420 dynes/cm.

The surface tension of a free surface of a molten metal just above its melting point is reported<sup>15</sup> to be similar to that of the same metal just below its melting point. As already mentioned, however, the surface tension of a crystal boundary of aluminium is likely to be less than that of a free surface, and thus a value of between 65.5 and 98.3 dynes/cm. for the surface tension at the crystal boundary is probably of the correct order of magnitude. This, in turn, suggests that the figure of 668 kg./cm.<sup>2</sup> for the internal stress required in a crystal boundary in pure aluminium to produce a depression of 4° C. in the melting point at the boundary is also of the correct order of magnitude.

### V.—CONCLUSIONS

The occurrence of brittle, intercrystalline fractures accompanied by very low values of strength in aluminium of high purity at temperatures of testing between 655° and 660° C. may possibly be attributed to melting occurring in the crystal boundaries some 4°–5° C. below the generally accepted melting point of the metal in the mass. It is suggested that the difference in the melting points of the crystal boundaries and the body of the crystals is associated with the physical properties of the crystal boundary rather than with the presence of impurities in the metal. A calculation has been made of the internal stress required in a crystal boundary in pure aluminium to produce a depression of 4° C. in the melting point at the boundary. By assuming that the surface tension of a crystal boundary is a reflection of the stress in the

boundary, the surface tension in a crystal boundary in aluminium has been calculated, and it is concluded that the calculated value of the surface tension, and hence of the stress in the crystal boundary, is of the correct order of magnitude.

### ACKNOWLEDGEMENTS

The work described in this paper was undertaken for the Aluminium Development Association, and is published by kind permission of that Association.

### REFERENCES

1. A. R. E. Singer and S. A. Cottrell, *J. Inst. Metals*, 1947, **73**, 33.
2. G. Chaudron, P. Lacombe, and N. Yannaquis, *Nature*, 1948, **162**, 854.
3. P. C. Varley, *J. Inst. Metals*, 1947, **73**, 732 (discussion).
4. B. Chalmers, *Proc. Roy. Soc.*, 1940, [A], **175**, 100.
5. Ting-Sui Kê, *Phys. Rev.*, 1947, [ii], **71**, 533.
6. W. I. Pumphrey and P. H. Jennings, *J. Inst. Metals*, 1948–49, **75**, 203.
7. V. Fuss, "Metallography of Aluminium and Its Alloys." 1936: Cleveland, O. (Sherwood Press).
8. H. Nishimura, *Nippon Kinzoku Gakkai-Si*, 1937, **1**, 8.
9. D. Hanson and M. L. V. Gayler, *J. Inst. Metals*, 1921, **26**, 321. H. W. L. Phillips, *ibid.*, 1941, **67**, 257.
10. L. F. Mondolfo, "Metallography of Aluminium Alloys." 1943: New York (John Wiley and Sons Inc.).
11. G. V. Raynor, *Inst. Metals Annotated Equilib. Diagr. Series*, 1944, (1).
12. G. V. Raynor, *ibid.*, 1945, (5).
13. A. H. Cottrell, "Progress in Metal Physics", Vol. 1, p. 77. 1949: London (Butterworths Scientific Publications).
14. A. Portevin and P. Bastien, *Compt. rend.*, 1936, **202**, 1072.
15. H. Udin, A. J. Shaler, and J. Wulff, *Trans. Amer. Inst. Min. Met. Eng.*, 1949, **185**, 186.

# 1492 A Slide-Rule for the Interconversion of Atomic and Weight Percentages for Any Binary Alloy System \*

By W. A. RACHINGER,† Ph.D., M.Sc., JUNIOR MEMBER

## SYNOPSIS

A slide rule is described which permits direct interconversions of atomic and weight percentages, a single setting of the rule corresponding to one particular alloy system.

IN studies of alloy systems, the interconversion of atomic and weight percentages is a frequent and tedious task. A slide-rule has been devised which will allow a direct interconversion, a single setting of the rule corresponding to one particular alloy system.

If  $w$  is the weight percentage and  $a$  the atomic percentage of element  $A$  in a binary alloy of elements of atomic weights  $A$  and  $B$ , then :

$$\frac{w}{100 - w} = \frac{A}{B} \times \frac{a}{100 - a} \quad (1)$$

of  $\log A$ ,  $\log B$ ,  $\log \frac{a}{100 - a}$ , and  $\log \frac{w}{100 - w}$ . Equation (1) is automatically satisfied, the reading on the  $D$  scale corresponding to  $[\log A - \log B + \log \{a/(100 - a)\}]$ .

A portion of the face of this rule is illustrated in Fig. 1. The setting is for a lithium-sodium alloy, the Li and Na graduations on the  $A$  and  $B$  scales, respectively, being brought into coincidence. The direct interconversion of atomic and weight percentages of lithium is given on the two lower scales (e.g. 40 at.-% = 16.7 wt.-%).

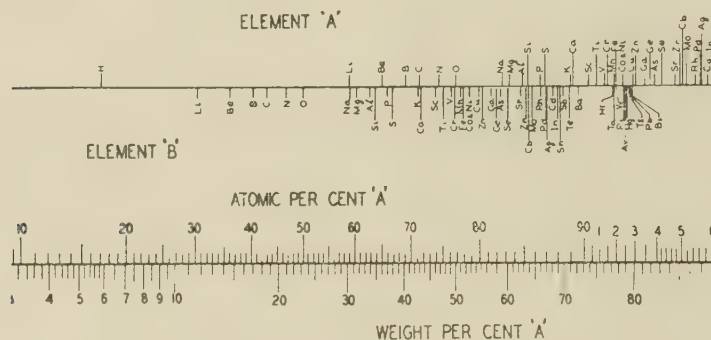


FIG. 1.—Interconversion for the Lithium-Sodium System.

Hermann<sup>1</sup> has described a slide-rule for making the necessary calculations, in which the usual  $A$  scale is replaced by one having the atomic weights of the elements plotted on a logarithmic scale. The distance between the graduations is therefore proportional to  $\log A/B$ . The  $B$  scale on the slider is graduated with values of  $\log \frac{x}{100 - x}$  covering the range  $x = 3$  to  $x = 75$  on one side and  $x = 0.3$  to  $x = 23$  on the reverse. This rule has the disadvantage that it must be reset for every conversion. This can be avoided by the use of all four slide-rule scales, the usual  $A$ ,  $B$ ,  $C$ , and  $D$  scales being replaced respectively by scales

It is impracticable to construct a rule capable of converting very small percentages, because of the large length of scale involved. However, in these circumstances a sufficiently accurate conversion is usually obtained on multiplication by the ratio of the atomic weights. With the 24-in. rule constructed in these laboratories, conversion can be effected if both the atomic and weight percentages lie within the range 0.4–99.6.

## REFERENCE

1. C. Hermann, *Metallwirtschaft*, 1933, 12, 104.

\* Manuscript received 7 May 1953.

† Aeronautical Research Laboratories, Department of Supply, Melbourne, Australia.



# STRUCTURAL STUDIES OF THE CREEP OF LEAD\* 1493

By R. C. GIFKINS,† B.Sc., A.I.M., MEMBER

## SYNOPSIS

Metallographic and X-ray-diffraction observations have been made during the creep of extruded specimens of high-purity lead and lead-thallium alloys, at stresses of 500–200 lb./in.<sup>2</sup>. The thallium additions were below 10%, and thus their effect was due almost entirely to grain-refinement (see *J. Inst. Metals*, 1952–53, **81**, (8), 417). A multiple-beam interference-fringe technique and the phase-contrast microscope have been used to study grain-boundary migration, triple-point folds, intragranular slip, and the tilting of grains. The movement of marker lines has revealed bodily rotation of grains of up to 30°, and measurements have shown the distance between grains 0.1 mm. apart to increase by 30–40% without significant change in their shape.

Specimens repolished after large creep strains show an interlocking structure, some grains having unusual peninsula-like features. There was considerable evidence of inhomogeneous strain within grains, which could account for the observed occurrence of arcs in the X-ray reflections. There was no metallographic evidence of a cell sub-structure, although sub-reflections were observed in the X-ray diagrams of certain very coarse-grained specimens. It is suggested that relative grain movement occurs readily in lead and the dilute lead-thallium alloys because it is assisted by grain-boundary migration and inhomogeneous deformation within the grains. The internal adjustments to grains all appear to be associated with intragranular slip. These features are contrasted with those found in other metals, particularly those like aluminium which form cell sub-structures.

## I.—INTRODUCTION

DETAILS of the structural changes which occur during the creep of high-purity lead and a series of lead-thallium alloys have been described recently and correlated with the variations in creep characteristics<sup>1</sup> and with the lattice-spacing determinations of Tang and Pauling.<sup>2</sup> During these creep experiments, a number of new observations of relative grain movement and grain rotation were made, together with observations of other metallographic features, such as slip, boundary migration, and strain marks, each of which has been noted and studied previously in other metals and alloys. In the present paper these features are described in order to show how they contribute to the general deformation at low rates of strain. On the basis of evidence from previous work,<sup>1</sup> it is assumed that thallium additions below 10% have no important effect on creep, except through their grain-refining influence. It has been possible, therefore, to study features which predominate in both coarse- and fine-grained specimens and to compare and contrast these with those occurring in other metals and alloys.

The phenomenon of creep has received considerable attention recently, both from those undertaking fundamental investigations into its mechanism and from those seeking to develop high-temperature alloys by more or less direct methods (see, e.g., Edwards<sup>3</sup>). Earlier work in both fields has been extensively reviewed,<sup>4–7</sup> but a large number of papers have since appeared, in which specific features associated with structures developed during creep have been studied.

Particular attention has been paid to aluminium, partly because of the simple techniques involved in its use at high temperatures,<sup>8–19</sup> and also because of the development of a cell sub-structure in specimens deformed under specific conditions. Cells have also been found in zinc,<sup>20,21</sup> magnesium,<sup>22</sup> and certain aluminium alloys.<sup>13,23</sup> A number of observations made at various times suggest that similar sub-structures are present in other metals and alloys.<sup>24</sup>

Some evidence for the presence of cells was found in a tin-antimony alloy studied by Betteridge and Franklin,<sup>25</sup> but they were not found in lead by Greenough and Smith.<sup>12</sup> The present author has been unable to detect their presence in lead or lead-thallium alloys,<sup>1</sup> although it had been suggested in an earlier paper<sup>26</sup> that the zones formed by coarse slip in a lead-thallium alloy were analogous to cells; this suggestion has not been confirmed by further work reported in the present paper. Coe,<sup>27</sup> working with a lead-tellurium alloy at room temperature and 100° C., has found no indication of cells; he demonstrated that, as visible slip diminished with decreasing rate of strain or increased temperature, grain-boundary flow increased, but led to the initiation of intercrystalline cracks at low strains.

In previous papers<sup>1,26</sup> the structural changes occurring during the creep of lead and lead-thallium alloys have been considered in relation to the thallium concentration and rate of strain. The course of the changes considered proceeded, broadly, from structures in which slip predominated, at high rates of strain or in very dilute alloys, to structures in which the evidence for grain-boundary flow was marked, at

\* Manuscript received 16 February 1953.

† Research Officer, Physical Metallurgy Section, Common-

wealth Scientific and Industrial Research Organization, The Baillieu Laboratory, University of Melbourne, Australia.

low rates of strain or in alloys containing higher concentrations of thallium. In the present paper the development of these structures is described in order to show how the deformation depends on a number of fundamental processes. In Section II the changes occurring in the relatively coarse-grained pure lead are considered; these include: (1) slip, (2) grain-boundary migration, (3) strain marks from triple points, and (4) evidence of inhomogeneous strain within grains. In Section III additional features associated with the creep of the fine-grained alloys are presented; these include: (1) the tilting and bodily rotation of grains, (2) evidence for relative movement of grains, obtained by measurements on specific areas, and (3) the structures associated with specimens after fracture at large extensions. Some X-ray back-reflection observations are also presented in the various sections.

The methods of preparing and testing the extruded specimens have been described previously,<sup>1, 26</sup> together with relevant creep data; details of the optical techniques<sup>28</sup> have also been published. The specimens were prepared in a standard manner and polished in a 70 : 30 mixture of acetic acid and hydrogen peroxide, except where the movement of surface marks was being followed, when the specimens were not etched or polished. Creep was induced by direct loading at initial stresses of 500–200 lb./in.<sup>2</sup> at room temperature.

## II.—CREEP OF PURE LEAD (MEAN GRAIN DIA. 0.4 MM.)

The specimens described in this section consisted of high-purity lead; similar changes occur, however, in specimens of dilute alloys containing less than about 0.5% thallium. With pure lead at 500 lb./in.<sup>2</sup> initial stress, there was a short period of minimum creep rate of  $30 \times 10^{-4}$  mm./mm./day; at about 3–4% extension, recrystallization occurred, and then accelerating creep rate and fracture. At 400 lb./in.<sup>2</sup> initial stress, the minimum creep rate of  $3.5 \times 10^{-4}$  mm./mm./day lasted until recrystallization took place at about 3.5% extension in 30 days; after about 5% extension there was a further period of steady-state creep up to about 7% extension. At 300 lb./in.<sup>2</sup> initial stress, recrystallization occurred at about 3% extension in 200 days, and the minimum creep rate was  $1.5 \times 10^{-4}$  mm./mm./day.

### 1. OCCURRENCE OF SLIP TRACES

Immediately after loading, some faint slip traces were observed on all specimens; at the higher stresses double and treble slip was often present. Figs. 1 and 2 (Plate IV) show an area typical of specimens stressed at 400–500 lb./in.<sup>2</sup>, after about 1% extension. Fig. 1 is a normal bright-field micrograph, and Fig. 2 is the interferogram of the same area, obtained with the unsilvered specimen. It is important to note that Fig. 1 and all micrographs in this paper at magnifications of  $\times 100$  or  $\times 150$  were obtained using a

16-mm. objective of small numerical aperture (0.28); a consequence of the small numerical aperture is loss of detail in areas which are slightly tilted. This gives rise to the characteristic “broadened” dark grain boundaries.

Fig. 2 shows that the slip steps are of various heights up to about 500 Å., and this was confirmed by the appearance of such slip under phase-contrast illumination; a change from positive to negative phase-contrast gave a reversal in intensity, a result obtained only with features less than about 500 Å. in height. Some of the slip lines (indicated by arrows) in Figs. 1 and 2, which consist of steps larger than the rest, continue the line of one of the boundaries at a triple point. They probably represent a simple form of the markings (triple-point steps) found by Wyon and Crussard<sup>10</sup> in aluminium, and explained by Betteridge and Franklin<sup>25</sup> in terms of relative movement of two grains causing the step in the third. Slip traces or groups of slip traces were often found emphasized in this manner.

On further extension, the height of the existing slip steps increased in some grains and new slip appeared progressively. Figs. 3 and 4 (Plate IV) show the area in Fig. 1 after further extension to 3.5% in 7 days, just before recrystallization began. Groups of slip lines were often present in localized areas of grains, as in the large grain of Fig. 3.

Fig. 5 (Plate IV) illustrates the type of slip which developed at the higher strains; it shows a specimen after 7.5% extension in 20 days in an area in which recrystallization did not appear to have taken place. The slip is less uniform than at lower strains. Cross-slip is present, producing curved slip traces, especially adjacent to the boundary, as between grains *A* and *B*. The angle between the slip traces in these grains increased with extension between 1 and 7.5%, thus indicating some tilting or bodily rotation of the grains. There is also evidence in Fig. 5 of slip occurring in groups of marked traces from triple points, and of areas within grains in which there is very little slip.

After recrystallization during creep and further deformation, the slip at the higher stresses was fairly straight and widely spaced; the slip traces were often slightly displaced at the original boundaries. Fig. 6 (Plate IV) shows an area of the same specimen as that shown in Figs. 1–4, after 10% extension in 99 days; there was a complex pattern of slip in three directions, and subsequently the surface was too heavily marked for areas to be clearly recognized. It was possible, however, to see that some of the original grains elongated in the direction of the applied stress. The original grain boundaries are indicated by arrows. It would appear, therefore, that slip was the main mechanism of deformation in the recrystallized specimens after about 7–10% extension, when further recrystallization and tertiary creep began.

At the lower stresses (300 and 200 lb./in.<sup>2</sup>), slip was very much less marked, and the initial faint slip,



comparable to that shown in Fig. 1, did not increase in intensity very greatly. After recrystallization, the coarse, wavy slip which occurred in the new grains was rarely duplex. An example is shown in Fig. 7 (Plate IV), which was taken after 10% extension in 740 days.

## 2. GRAIN-BOUNDARY MIGRATION

Grain-boundary migration was present to a marked degree in all the coarse-grained specimens, and the amount of migration increased with decreased stress. Examples are given in Figs. 1-12 (Plates IV and V).

In Figs. 1-4 there are examples of the commonest types of migration. At the boundary between the two grains on the left of the photograph, there are numerous traces; the fringe pattern shows these to have formed terrace-like areas on which there are small steps similar to those formed by faint slip. There were indications of even fainter traces and presumably of smaller steps between those revealed by the fringes. This is illustrated by Fig. 17 (Plate VI), which was obtained using positive phase-contrast illumination; very faint traces down to the limits of sensitivity of the phase-contrast microscope are shown. Sometimes the traces formed in this way were remarkably straight and nearly parallel, as on the right-hand side of grain *B* in Fig. 5. It is possible that similar fine migration traces form the origin of the marks seen near the grain boundaries of aluminium slowly deformed at elevated temperatures; such marks have been observed by Garrod, Suiter, and Wood<sup>29</sup> by means of the electron microscope.

Dark, broadened grain boundaries, such as those at the lower, right-hand corner of Figs. 1-4 and the upper, right-hand corner of Figs. 9-12 (Plate V), were shown by the fringe patterns to consist of sloping areas between grains. The inclination of these slopes to the grains was usually of the order of 4° or 5°. A fine structure could often be discerned in these boundaries, as in Figs. 1 and 3, and this structure was readily seen with the phase-contrast microscope. Fig. 18 (Plate VI) shows an example which, although obtained on a 2.45% thallium alloy, is quite typical of the appearance of coarse-grained pure lead. Moreover, presumably because of the diffraction effects due to the very fine structure, such dark boundaries appeared bright with dark-field illumination. Similarly, they showed changes in brightness when the specimen was rotated between crossed nicols, whereas with normal bright-field illumination there was very little variation in their intensity. Sometimes a dark boundary appeared bright when an objective of higher numerical aperture was used. Thus it seems certain that the darkness of these broadened boundaries was not associated with shadows from relatively steep "cliff faces" between grains, and that they usually consisted, not of smooth facets, but of numerous small steps, sometimes too small to be detected except with the electron microscope. Observations with a stereo-microscope confirmed this conclusion.

Often boundary migration appeared to be held up at a triple point, when a fan-like group of traces resulted, or at some point within a grain, when cusps were formed (Fig. 11). Where numerous cusps were present, a complex interlocking pattern was formed, similar to that commonly found in zinc<sup>21</sup> and magnesium<sup>22</sup>; this is illustrated in Fig. 6, on the right-hand side, where there has been migration at a boundary of a new grain formed in recrystallization. This type of migration was much more usual after recrystallization, probably because the surface was then considerably modified by slip and other features which could hold up migration locally.

Another type of boundary migration observed was that in which a boundary appeared to jump a comparatively large distance without intervening traces; this was particularly common at 500 lb./in.<sup>2</sup> stress. An example occurs in the grain at the top right of Figs. 1 and 3, and there are others in Fig. 5.

These observations confirm previous suggestions<sup>11, 16, 18</sup> of the importance of grain-boundary migration during slow deformation.

## 3. STRAIN MARKS FROM TRIPLE POINTS

This type of strain mark, previously noted in other metals and alloys,<sup>11, 16, 25, 30</sup> has been found in pure lead at all stresses, particularly at the lowest.

Figs. 9-12 (Plate V) show the development of a mark of this kind, Figs. 9 and 11 being normal micrographs taken after 1% extension in 36 hr. and 3.5% extension in 7 days, respectively, and Figs. 10 and 12 being the corresponding multiple-beam interferograms. This particular strain mark continued across the grain as a group of slip steps which were larger than those in the rest of the grain, as Fig. 10 shows. Cross-slip is present in this group, and the appearance of the main fold suggests that it might also consist of complex cross-slip. Fig. 10 also reveals that the step at the grain boundary at which relative grain movement had occurred and that of the strain mark it generated were of about the same height and slope, for the number and spacing of the fringes is the same for each. This observation confirms the explanation of such triple-point marks advanced by Betteridge and Franklin.<sup>25</sup> Both steps developed similarly on further extension to 3.5% in 7 days, as Figs. 11 and 12 show, but the triple-point mark did not extend any further across the grain.<sup>30</sup>

Besides the examples already noted in Figs. 1 and 2 of emphasized slip replacing the more general type of triple-point steps, there were many examples in which groups of similar, roughly parallel marks were present, as in grains *C* and *D* in Fig. 5. Triple-point marks of this character were frequently observed in fine-grained alloys. Fig. 8 (Plate IV) shows a typical group, photographed under phase-contrast illumination; the marks are shown to be the result of undulations on the surface, rather than steps produced by slip. This was confirmed by the interference microscope, as shown, for example, in grain *D* of Figs. 13 and 14 (Plate V). Fig. 8 also shows that very

fine slip was present at a high angle to the marks, the direction of the fine slip being different on the two sides of the group of marks, suggesting rotation of the lattice. From this evidence it seems likely that the marks are deformation bands rather than coarse slip, although recently McLean<sup>19</sup> has interpreted similar folds in aluminium as bundles of fine slip which form locally intensified slip-traces.

It thus appears that triple-point marks are generally manifestations of local slip, which form the folds by complex, intimate cross-slip as in Figs. 9-12, by deformation bands as in Fig. 8, or by simple slip as in Figs. 1-4.

#### 4. INHOMOGENEOUS STRAIN WITHIN GRAINS

There was considerable evidence that the strain within the grains of the pure lead specimens was not homogeneous. Earlier in this section, the bending of slip traces and their non-uniform distribution were noted, and the triple-point folds are further evidence of inhomogeneous deformation. The fringe patterns in Figs. 10 and 12 also indicate the formation of distorted areas near grain boundaries. The closer fringe spacing near boundaries indicates that "drag" occurred with relative grain movement, so that some grains, like the central one in Figs. 10 and 12, became slightly dome-shaped. Further evidence of inhomogeneous strain was found in the bending of groups of originally straight marker lines, often into S-shaped curves. Fig. 19 (Plate VI) shows some marker lines, formed during extrusion and therefore straight and parallel originally, which have become bent during creep to 10% in 25 days.

Perhaps the most general evidence of inhomogeneity was found in the peripheral spread of X-ray back-reflection spots before recrystallization,<sup>1</sup> and in the splitting of reflections into smaller spots during creep after recrystallization. The appearance of arcs in the X-ray photographs before recrystallization occurred even at the lower stresses when comparatively little evidence of slip was seen. The sub-reflections were not sharp and separate, as are those due to cells in aluminium, but diffuse and superimposed on a general background reflection (Fig. 20, Plate VI).

These sub-reflections were similar to those found by Hirst<sup>31</sup> in single crystals and in very coarse-grained specimens of lead during creep. Hirst's results have been quoted as an early example of polygonization,<sup>32</sup> but, as will be shown, this is entirely on the evidence of the X-ray pattern, and no metallographic confirmation of a discrete sub-structure in lead has been found. The techniques of polishing and etching lead are perhaps not as advanced as those for aluminium, but the following experiments indicate that the X-ray observations are best explained on the basis of inhomogeneous strains, similar to those found in aluminium by various workers by X-ray and metallographic methods (see, e.g., Urie and Wain<sup>33</sup>).

No sub-structure was found on deeply etching specimens which gave rise to sub-reflections. Other specimens were repolished at this stage and then

further strained at the same or a slightly lower rate, in order that any traces due to relative movement of cells or change in size by sub-boundary migration might be revealed,<sup>34</sup> but no marks other than slip were observed within the grains.

A similar specimen was repolished and then etched in the polishing solution, to which an excess of about 2% of acetic acid had been added. This produced fine, closely-packed pits, and it has been found that specimens etched in this way yield colour contrasts from grain to grain when examined under polarized light with a wave-plate between the specimen and analyser.<sup>28</sup> The effect is similar to the well-known one with anodized aluminium, and it appears that the colours are similarly an indication of orientation. Examination of the repolished creep specimen by this technique did not show any variation of colour within the grains that could be identified as a definite sub-structure, even during rotation of the specimen, when small changes in colour show very clearly at the extinction angle.

Since the number and size of the sub-reflections were similar to those from the original grains, it was possible that the latter might constitute the cells within the new grains, but the original boundaries showed no further changes after recrystallization was complete, and they did not etch again on repolishing.

Finally, a specimen which had extended a few per cent. after recrystallization during creep was repolished and then further strained 3% rapidly. Although the slip traces produced did not show curvatures or changes in direction which could be associated with either a sub-structure or any regular disorientation, they were exceedingly complex. In some grains, bands or bundles of coarse slip alternated with apparently undeformed areas, and the bands were not quite parallel to the slip traces, very like Honeycombe's "secondary slip bands"<sup>35</sup>; in other grains, unusually stepped and coarse cross-slip was present. Neither of these features occurred to such a marked degree in an annealed specimen of about the same grain-size similarly strained.

### III.—CREEP OF LEAD-THALLIUM ALLOYS (MEAN GRAIN DIA. 0.1 MM.)

Some evidence of relative grain movement has been given in previous papers;<sup>1, 26</sup> in this section more detailed observations will be described to demonstrate its extent and nature.

#### 1. TILTING AND BODILY ROTATION OF GRAINS

The evidence of previous workers for the tilting and bodily rotation of grains has depended to a great extent on indirect methods, such as observation of the shadowing and broadening of grain boundaries and the formation of triple-point folds. Some more direct evidence has been advanced from time to time in the movement of marker lines, the first example being that of Moore, Betty, and Dollins,<sup>36</sup> who worked with a lead-tin alloy.



In the present work the marks formed during extrusion were used for this purpose on a number of the fine-grained specimens. At the lower stresses this technique indicated very considerable bodily rotation of grains. Figs. 21 and 22 (Plate VI) show typical fields on a specimen of a 4.81% thallium alloy, stressed initially at 300 lb./in.<sup>2</sup>, after 10% extension in 35 days and 45% in 122 days, respectively. In Fig. 21 it will be seen that the marks near the right-hand edge have been displaced step-wise; this type of movement of a group of grains was often observed. In Fig. 22 rotations of about 20° from the original direction are present and were general at this extension. At about 75% extension some grains had rotated 30°. Rotations of about 15° have been found in other fine-grained specimens deformed 20–30%. The maximum displacements of marker lines at grain boundaries were found to be of the order of those predicted by Rachinger's<sup>17</sup> formula for longitudinal grid lines.

The tilting of grains can be clearly demonstrated at low strains by the use of the multiple-beam interference-fringe technique. At high extensions the movements were usually too great to allow the production of sharp fringes; slight tarnishing also reduced reflectivity, and thus the intensity of fringes, so that photography was not possible. Figs. 23 and 24 (Plate VI) show an area of a 4.81% thallium alloy after 4% extension in 14 days, under normal illumination and with interference fringes, respectively. The straight, parallel, and evenly spaced fringes, which change direction from grain to grain, show that the grains have tilted in many directions but remained remarkably flat. The angles of tilt at this extension were not large, but after about 50% extension, tilting was very marked and the appearance of the grains under the stereo-microscope most striking, for they appeared as bright facets tilted in all directions, and the "broadened" grain boundaries appeared as dark, granular material. An example of the tilting of grains at a higher extension is given in Figs. 13 and 14, which are micrographs of the 2.45% thallium alloy, after 13% extension in 243 days. Beyond extensions of about 50% it was not possible to continue systematic microscopical observations, because the tilting and movement of grains were usually too great for many of them to be observed with a low-power objective; with a higher power, the depth of focus was not great enough. Numerous individual grain facets could be seen, however, at extensions up to nearly 400%; an example is given in Fig. 25 (Plate VI).

## 2. RELATIVE MOVEMENTS OF GRAINS

On a few specimens it was possible to follow the development of selected areas over a long period of time and to measure the movements of grains. The clearest examples were found on a specimen of the 2.45% thallium alloy, initially stressed at 200 lb./in.<sup>2</sup>;

its minimum creep rate of  $4.8 \times 10^{-4}$  mm./mm./day lasted until about 25% extension in 500 days.

During the first 5% extension the changes were almost entirely at the boundaries, which broadened; the phase-contrast microscope showed this broadening to be due to boundary migration (Fig. 18), and the formation of slopes between grains was indicated by interference fringes. Faint slip traces were seen with normal illumination in about one grain in 25; very fine slip could be detected with the phase-contrast microscope in many grains, but, as Fig. 18 shows, even this slip was far from general. On further extension to 10%, slip and slip-like traces were found in about one grain in five, but there was apparently little increase in the amount of very fine slip. Figs. 13 and 14 show an area of this specimen under normal illumination and the corresponding interferogram, respectively, after 13% extension in 243 days.

A common feature is also shown in Figs. 13 and 14, where the fringe pattern reveals a small tilt at the twin boundary in grain *C*. Such twins were formed during annealing, and were only just visible on the polished specimens. The twin boundaries became clearly marked on extension during creep, and then tilting about them was observed; usually, the tilts did not appear to increase during further deformation. The phase-contrast image of such twins also indicated tilting, for the twin and matrix appeared as having different intensities, as Fig. 26 (Plate VI) shows. Such an intensity variation usually denotes a difference in level, but when large areas are involved, according to Ramsay,<sup>37</sup> the difference must be ascribed to tilting; the fringe patterns confirm this. The diffraction lines along the twin boundary in Fig. 26 may be due to a small step at the boundary, but they are probably the result of a slight misalignment of the phase-retarding annulus and the image of the annular diaphragm. Very faint slip was usually present in the twinned areas (as on the left of Fig. 26), and the tilting of the twins is probably the result of slip, as Miller<sup>38</sup> has shown recently in  $\alpha$ -brass. Thus, the tilting of the twins in the lead alloys may be evidence of a greater amount of very fine slip than other observations suggest. Fig. 26 also shows broad undulations of a slip-like character in the lower right-hand corner; these appear to be intermediate between the folds shown in Fig. 8 and normal slip.

Figs. 15 and 16 (Plate V) show the same area as Fig. 13 after further deformation to 18% extension in 351 days and 38% in 757 days, respectively. The relative movement of grains *B* and *C* has been measured on these and on an intermediate photograph, and the results are recorded in Table I. It can be seen from Figs. 13–16 that the grains *A* and *B* have not changed size or shape measurably, and that grain *C* has not changed along the direction of the applied stress. The table shows, however, that there has been an increase in the distance between grains *B* and *C*.

It should be noted that the small square-shaped grain between grains *B* and *E* moved so that it was not

visible in Fig. 15, but tilted back to become partly visible in Fig. 16. Table I also records the change in length of the grain *E* between the moving grains *B* and *C*.

TABLE I.—Measurements of Grain Movement in Figs. 13–16 (Plate V).

Duration of Test, days	Extension of Specimen on Original Gauge-Length, %	Extension of Specimen on Gauge-Length at 243 Days, %	Distance on Photographs* Between Grains <i>B</i> and <i>C</i> , mm.	Extension of Distance Between <i>B</i> and <i>C</i> , %	Grain <i>E</i> Between <i>B</i> and <i>C</i>	
					Length on Photograph, mm.*	Extension, %
243	13	...	17	...	13	...
351	18	4.4	18.5	8.4	13	0
562	28	13.2	22.0	35.5	16	23.1
757	38	22.1	25.0	47.2	18	38.5

\* Reduced by  $\frac{1}{8}$  in reproduction.

It will be seen that *B* and *C* have moved apart a greater amount than the overall extension of the specimen, the difference being greatest at 562 days, at the end of the stage of secondary creep. At 351 days, grain *E* had not extended, but after 562 days it had done so sufficiently to make an important contribution to the extension *BC*, and during tertiary creep a large proportion of the extension of *BC* could be ascribed to that of grain *E*, although there were no conventional slip traces present on it. Measurements on further areas of this and other specimens have shown similar, but smaller grain movements; no other examples being so obviously associated with the extension of an intermediate grain have been found. It is, of course, uncertain how far such superficial changes can be assumed to be typical of changes in the interior of specimens, but until techniques are developed which allow direct observation of the latter, results such as these have to be taken as an illustration of the possible extent and mode of occurrence of relative grain movements. Since measurements have been made on relatively few areas, too much importance should not be attached to the numerical values.

### 3. EXAMINATION OF SPECIMENS AFTER LARGE CREEP EXTENSIONS

When fine-grained specimens which had extended by large amounts were repolished, the structure revealed was different from that of the annealed material, although the number of grains per unit area had not changed significantly.<sup>39</sup> Fig. 27 (Plate VI) shows a typical area on a specimen of the 7.87% thallium alloy which had fractured at 372% extension after 221 days; the photograph was taken on an area several inches from the fracture. The interlocking grain boundaries and peninsula-like extensions to many grains were found in numerous specimens of this and other alloys. The slight pitting and thickening of the grain boundaries in Fig. 27 was the result of the method of repolishing; this consisted

of immersing the specimen in the standard polishing reagent for 10 sec. some 40 or 50 times and thoroughly washing and drying after each immersion. This procedure avoided modifying the structure by the heat of chemical reaction; it produced an undulating surface, but numerous areas comprising several grains were usually flat enough for photography.

#### (a) Inhomogeneous Strain Within Grains

Although specimens were repolished cleanly occasionally, the difficulty of obtaining sharp boundaries, with grains free from etching and pitting, suggested that the polishing difficulties might be due, in part, to variations of strain within the grains. Hardness measurements did not show appreciable work-hardening, but there were prominent arcs in the X-ray reflections. Accordingly, some repolished specimens were rapidly given a slight strain, either by bending around a cylindrical mandrel and re-straightening or by a tensile extension of about 2%. Both methods produced faint slip in which the traces were ill-defined and curved, particularly near the grain boundaries; often S-shaped slip traces were observed. This is illustrated in Fig. 28 (Plate VI), which was taken with conical-stop illumination to show the slip more clearly. Such slip was not found on annealed specimens similarly deformed or on specimens rapidly strained by a few per cent., repolished, and further strained at a high rate; in the latter case, some complex cross-slip was present, but not the ill-defined, wavy traces characteristic of the repolished creep specimens.

The curvature of the slip traces was not due to surface undulations, for individual grains were flat. This was confirmed in two ways. Firstly, part of a fractured creep specimen was carefully ground flat with wet carborundum papers, then repolished to remove the worked layer and rapidly strained to produce slip, which was similar to that shown in Fig. 28. Secondly, the profile of specimens showing the slip was examined using a sensitive device due to Tolansky,<sup>40</sup> and no surface curvature was found, although the slip and boundary steps were clearly indicated. This profile device consisted of a straight fine wire (about 0.001 in. in dia.) mounted close to the field stop of the projection microscope; its image, projected on to the specimen, could be observed, distorted to form a profile of the surface, the magnification in depth being of the order of the lateral magnification. The device could be used on a specimen having undulations, where multiple-beam fringes could not be produced readily; in addition, the wire could be turned to give the profile in any direction.

#### (b) Examination for Preferred Orientation

Specimens showing the interlocking structure of Fig. 27 were examined for evidence of preferred orientation, but none was revealed by glancing-angle X-ray-diffraction photographs. Although this technique is not very sensitive, it was thought that after



such large extensions, any tendency to a preferred orientation should have been revealed.

Results obtained with the etching and polarized-light techniques described in Section II indicated that the large grains with the peninsula-like extensions tended to a preferred orientation. These grains were seen to have one of two colours, and changed colour simultaneously on rotation of the specimen. If this can be taken as evidence of preferred orientation in these grains, it suggests that their elongation resulted from the action of sufficient slip to bring about the observed preferred orientation.

#### (c) X-Ray Back-Reflection Observations

At the high extensions with fine-grained specimens, prominent arcs occurred in the X-ray reflections, although even at more than 100% extension there were usually some blurred traces of discrete spots (see, e.g., Fig. 16, Plate LXV of ref. 1). There was no evidence that the arc reflections broke down into smaller reflections, as with the coarse-grained pure lead and dilute alloys, although collimation errors might well have masked any fine sub-division; there was also no evidence of sharp new reflections due to recrystallization during creep. The latter observation is supported by the metallographic and creep-data records. On etching the specimens after about 50% extension or after fracture, there was some sharpening of the X-ray reflections, thus indicating that the grains in the interior of the specimen were less distorted than those on the surface. This is in keeping with Rachinger's observations on aluminium.<sup>17</sup>

### IV.—DISCUSSION

The observations recorded in the present paper show that there are many features of deformation common to both coarse- and fine-grained specimens. With the coarse-grained specimens, however, the relatively small number of grains per cross-section reduces the freedom for mutual adjustment of the grains, and slip is much more predominant. It would be of interest to compare the changes in coarse-grained specimens of large cross-section with those in the normal specimens described in this paper.

The terrace-like zones at grain boundaries are particularly marked in coarse-grained lead, and are similar to those found in aluminium.<sup>9, 10, 16</sup> The fringe patterns confirm their step-like character, and thus the suggestion that they are formed by alternations of grain-boundary flow and migration.<sup>9, 16</sup> With finer grain-sizes the importance of this feature has been somewhat overlooked because of the use of objectives of small numerical aperture, but Rachinger<sup>9</sup> has noted the importance of migration in fine-grained aluminium. The present results show that "broadened" grain boundaries are generally associated with grain-boundary migration.

Triple-point steps are also a very common feature in specimens of all grain-sizes, but again, because of

the comparatively restricted freedom of adjustment, this feature is more marked with coarse grain-sizes. Such steps are often associated with, or even replaced by, marked slip traces or groups of deformation bands; it seems likely that such steps always either consist of complex cross-slip or are the result of fine slip and the formation of deformation bands. Fine slip was also detected with the phase-contrast microscope in fine-grained specimens, often in association with deformation bands, and it seems possible that the observed tilting about twin boundaries may be the result of a significant amount of fine slip, even at very low rates of strain. McLean<sup>18, 19</sup> has found that fine slip contributes extensively to the deformation of aluminium at 200° C.; this temperature for aluminium is roughly equivalent to room temperature for lead.

There was considerable evidence for inhomogeneous deformation within grains in all specimens, both from the tendency of the X-ray back-reflection spots to form arcs and from metallographic observations. The breaking up of the large X-ray reflections from grains formed by recrystallization during creep does not appear to be associated with a discrete sub-structure analogous to cells in other metals. Rather, it would seem that the large grains become distorted in such a way that some areas remain sufficiently perfect to give rise to the sharp sub-reflections, whilst curved or fragmented zones between these units are responsible for the diffuse background reflection. Except that he identified the sub-reflections with the blocks formed by coarse slip, this is the explanation originally put forward by Hirst.<sup>31</sup>

It should be noted that there does not appear to be any tendency for grains in this state to recrystallize *in situ* at room temperature or to form perfect cells by "stress-recovery".<sup>34</sup> Recrystallization took place on annealing such a specimen at 70° C. for a short period. It is possible that in a metal such as lead, which is so near to its melting point at room temperature, the more perfect areas of the grains are themselves of relatively high internal disorder. Thus, there is little tendency for them to grow at the expense of the more disordered curved or fragmented areas. If, however, a driving force for this is provided either by stress or temperature, it would seem that recrystallization is initiated so readily that it inevitably occurs. In other words, either nothing happens to the embryo cells or complete recrystallization takes place.

Other metallographic evidence of inhomogeneous strain within the grains was found in the type and distribution of slip traces and deformation bands, in surface curvatures, particularly near grain boundaries, and in the curved slip on specimens repolished and rapidly strained. Another possible explanation of the arcs in the X-ray reflections is that they are due to grain-boundary "debris"; Suiter and Wood<sup>22</sup> have advanced this concept to explain similar but less marked arcs with magnesium deformed at elevated temperatures. They suggest that the appearance of the boundaries in this metal before and after repolishing supports their view. However, this

broken appearance is very similar to that of the recrystallized boundary in Fig. 7, and it can also be explained on the basis of numerous overlapping cusps formed by boundary migration. The granular material which can be seen with the stereo-microscope between grain facets in lead-thallium specimens at high strains is certainly suggestive of fine "debris"; however, repolished specimens show only normal or very slightly broadened boundaries, and it does not seem that these would give rise to the observed arcs. On the other hand, the evidence for inhomogeneous strain is strong, and this would appear to be sufficient to account for the diffuse reflections.

Despite the arcs in the X-ray reflections, there is clear evidence of bodily rotation, tilting, and actual movement apart of grains in fine-grained specimens. Rotation of grains by as much as  $30^\circ$  has been observed, and  $15^\circ$  twists were common; small but significant rotations in the coarse-grained specimens have also been recorded. The relative movement of surface grains can occur without change in shape of many of them, in contrast to the results with aluminium, reported by Rachinger.<sup>17</sup> He found by a statistical counting method, that surface grains extended more or less in conformity with the aggregate at elevated temperatures, although the X-ray reflections remained sharp; grains in the interior remained equi-axed, but were shown to move relatively to one another.

A further difference between the lead alloys and aluminium is the formation of the elongated grains with peninsula-like tongues in the former during creep to high extensions. The general structure of these specimens was extensively interlocked or "sutured". MacGregor<sup>41</sup> has pointed out the similarity of these sutured structures to those found in the quartz of dynamically metamorphosed sandstones and in ice crystals in deep tunnels in glaciers; he suggests that all result from recrystallization under stress. Somewhat similar sutured structures are indeed found in pure lead which recrystallizes during creep, but these do not show the peninsula-like extensions to grains. Moreover, the evidence against recrystallization during creep of the fine-grained alloys is very strong, being based on (a) metallographic and X-ray observations during creep, (b) the similarity of grain-sizes before and after creep for a number of alloys over a range of rates of strain, and (c) the shape of the creep curves. The sutured structure and the peninsula-like portions of the grains could be produced by a diffusion mechanism, possibly in association with grain-boundary migration. However, it appears that the grains having the peninsula-like features may extend and produce the peninsulas by slip, whilst the smaller neighbouring grains rotate and move; such slip would contribute to the occurrence of arcs in the X-ray reflections and explain the observed tendency to a preferred orientation of the larger grains. It is possible that grain-boundary migration can assist relative movement of grains by taking place in stages around the perimeter of a grain;

the wavy boundaries seen in lead and other metals might, therefore, be the result of such partial migration (as well as being due to the formation or envelopment of small sub-grains in some metals<sup>16, 17, 21, 22</sup>).

Andrade and Jolliffe<sup>42</sup> have recently postulated intragranular glide as the sole mechanism of creep of polycrystalline lead under simplified conditions of pure shear. The evidence is mainly from an extensive and convincing analysis of creep curves, but it is claimed that microscopic examination supports the conclusion. In the published micrograph, however, there appears to be evidence of grain-boundary flow in the presence of "broadened", dark boundaries and also in the displacement of slip or scratch marks at some of them. This and the results of the present paper, which show marked interdependence of boundary flow and intergranular slip, suggest that the identification of these processes with the constants of Andrade's equation must be viewed with caution.

## V.—CONCLUSIONS

At all rates of strain over a fairly wide range, lead deforms by a combination of boundary migration and various internal adjustments, such as clearly visible slip, fine or micro-slip, and local bending, possibly to give deformation bands or triple-point marks; recrystallization is a factor only with grain-sizes greater than 0.1 mm. dia. The net effect of these adjustments is to bring about relative movement of grains and permit "grain-boundary flow", whilst generating the minimum of internal strain in the grains. The latter is sufficient, however, to cause arcs to appear in the X-ray reflections. When grains become interlocked at irregularities in the boundaries, particularly in fine-grained specimens at lower stresses, the stresses are redistributed within the aggregate, and other grains move by small amounts. Eventually the originally locked grains may be free to move again, possibly in the reverse direction to that taken at first. When a large number of grains becomes locked, the stress on a particular grain may not have to rise greatly before local visible slip, micro-slip, or deformation bands are formed and further relative movement is permitted. It may be this similarity of activation energies for various mechanisms which distinguishes lead from metals which form sub-grains; quantitative experiments to test this hypothesis would be of very great interest, for there seems to be no *a priori* reason why cells should not sometimes form in lead.

It also seems probable that, when lead is sufficiently hardened by a suitable alloying addition (e.g. more than 10% thallium<sup>1</sup> or 0.05% tellurium<sup>27</sup>), although the tendency is still for grain-boundary flow to take place, the stress necessary to activate slip is relatively high, and so the probability of the mutual adjustments outlined is correspondingly low. Local stress concentrations may then lead to the initiation of cracks at the boundaries.



## ACKNOWLEDGEMENTS

The work reported in this paper formed part of the programme of research of the Physical Metallurgy Section of the Commonwealth Scientific and Industrial Research Organization, and was carried out at the Baillieu Laboratory under the general direction of

Professor J. N. Greenwood, whose encouragement and advice, based on a wide experience in the study of the creep of lead, are gratefully acknowledged. The author also wishes to thank his colleagues for helpful discussions which saw the genesis of many of the ideas expressed in the paper.

## REFERENCES

1. R. C. Gifkins, *J. Inst. Metals*, 1952-53, **81**, (8), 417.
2. Y. Tang and L. Pauling, *Acta Cryst.*, 1952, **5**, 39.
3. A. R. Edwards, *Australasian Eng.*, 1952, (June), 42.
4. A. H. Sully, "Metallic Creep and Creep-Resistant Alloys". London: 1949 (Butterworths Scientific Publications).
5. G. V. Smith, "The Properties of Metals at Elevated Temperatures". New York and London: 1950 (McGraw-Hill).
6. E. G. Stanford, "The Creep of Metals and Alloys". London: 1949 (Temple Press).
7. L. Rotherham, "Creep of Metals". London: 1951 (Institute of Physics).
8. W. A. Wood, G. R. Wilms, and W. A. Rachinger, *J. Inst. Metals*, 1951, **79**, 159.
9. W. A. Rachinger, *ibid.*, 1951-52, **80**, 415.
10. G. Wyon and C. Crussard, *Rev. Mét.*, 1951, **48**, 121.
11. D. McLean, A. E. L. Tate, and M. H. Farmer, *Nature*, 1950, **165**, 70.
12. G. B. Greenough and E. M. Smith, *J. Inst. Metals*, 1950, **77**, 435.
13. G. B. Greenough, C. M. Bateman, and E. M. Smith, *ibid.*, 1951-52, **80**, 545.
14. I. S. Servi and N. J. Grant, *Trans. Amer. Inst. Min. Met. Eng.*, 1951, **191**, 917.
15. H. C. Chang and N. J. Grant, *ibid.*, 1952, **194**, 619.
16. I. S. Servi, J. T. Norton, and N. J. Grant, *ibid.*, 1952, **194**, 965.
17. W. A. Rachinger, *J. Inst. Metals*, 1952-53, **81**, 33.
18. D. McLean, *ibid.*, 1951-52, **80**, 507.
19. D. McLean, *ibid.*, 1952-53, **81**, 133.
20. A. H. Cottrell and V. Aytakin, *ibid.*, 1950, **77**, 389.
21. J. A. Ramsey, *ibid.*, 1951-52, **80**, 167.
22. J. W. Suiter and W. A. Wood, *ibid.*, 1952-53, **81**, 181.
23. W. A. Rachinger, Ph.D. Thesis, Melbourne University, 1952.
24. A. Guinier, "Imperfections in Nearly Perfect Crystals", p. 402. Edited by W. Shockley *et al.* 1952: New York (John Wiley); London (Chapman and Hall).
25. W. Betteridge and A. W. Franklin, *J. Inst. Metals*, 1951-52, **80**, 147.
26. R. C. Gifkins, *ibid.*, 1951, **79**, 233.
27. H. C. Coe, M.Sc. Thesis, Melbourne University, 1952.
28. R. C. Gifkins, *Australasian Eng.*, 1952, (May), 63.
29. R. I. Garrod, J. W. Suiter, and W. A. Wood, *Phil. Mag.*, 1952, [vii], **43**, 677.
30. E. C. W. Perryman, *J. Inst. Metals*, 1951-52, **80**, 587 (discussion).
31. H. Hirst, *Proc. Australasian Inst. Min. Met.*, 1941, [N.S.], (121), 11, 29.
32. R. W. Cahn, *J. Inst. Metals*, 1949-50, **76**, 121.
33. V. M. Urie and H. L. Wain, *ibid.*, 1952-53, **81**, 153.
34. W. A. Wood and J. W. Suiter, *ibid.*, 1951-52, **80**, 501.
35. R. W. K. Honeycombe, *ibid.*, 1951-52, **80**, 45.
36. H. F. Moore, B. B. Betty, and C. W. Dollins, *Univ. Illinois Bull.*, 1935, (272).
37. J. V. Ramsay, private communication.
38. D. R. Miller, M.Sc. Thesis, Melbourne University, 1953.
39. R. C. Gifkins, *Nature*, 1952, **169**, 238.
40. S. Tolansky, *ibid.*, 1952, **169**, 445.
41. A. G. MacGregor, *J. Glaciology*, 1952, **2**, 100.
42. E. N. da C. Andrade and K. H. Jolliffe, *Proc. Roy. Soc.*, 1952, [A], **213**, 3.

# THE RE-INVESTIGATION OF A NICKEL-TITANIUM ALLOY AND OBSERVATIONS ON $\beta/(\alpha + \beta)$ BOUNDARIES IN TITANIUM SYSTEMS \*

By A. D. McQUILLAN,† Ph.D., B.Sc., MEMBER

## SYNOPSIS

The possible causes of disagreement in reported  $\beta/(\alpha + \beta)$  boundaries in titanium-rich systems are considered. Examination of a 2.4 at.-% nickel-titanium alloy has shown that the deposition of  $\alpha$  from  $\beta$  can occur extremely rapidly by a process of nucleation and growth. It is concluded that delay in quenching of alloy specimens is the most probable cause of error.

RECENT workers on the binary systems of titanium with vanadium,<sup>1, 2</sup> chromium,<sup>3, 4, 5</sup> manganese,<sup>6</sup> and nickel<sup>7</sup> have reported positions of the  $\beta/(\alpha + \beta)$  boundaries in these systems, which, besides disagreeing among themselves in cases where a system has been

studied by more than one group, also disagree with the results obtained by the hydrogen-pressure method<sup>8</sup> for the same systems. To discover the reason for these differences, a titanium alloy containing 2.4 at.-% nickel was re-examined. This alloy was chosen

\* Manuscript received 2 May 1953.

† Metallurgy Department, Birmingham University.

because there is a considerable discrepancy between the temperatures at which the  $\beta/(\alpha + \beta)$  boundary has been reported for it by Margolin, Ence, and Neilsen,<sup>7</sup> who carried out microscopic examinations of quenched specimens, and by McQuillan,<sup>8</sup> using the hydrogen-pressure method.

The alloy, prepared by melting spectroscopically-pure nickel and van Arkel titanium in an argon-arc furnace, was subjected to a hydrogen-pressure determination as a check on the author's previously reported results. The  $\beta/(\alpha + \beta)$  boundary was found to occur at 805° C., in good agreement with previous hydrogen-pressure determinations, but considerably at variance with the value of 873° C. obtained from the diagram of Margolin *et al.* A further confirmation of the hydrogen-pressure result was obtained by examining the structure of a specimen of this alloy which had been instantaneously quenched from 820° C. in the type of direct-radiation furnace described by M. K. McQuillan.<sup>9</sup> The microstructure of this specimen (Fig. 1, Plate VII) shows the typical martensite-like decomposition product of unretained  $\beta$  phase which has formed during quenching, and indicates that at 820° C. the alloy consisted entirely of the  $\beta$  phase.

Since both Margolin *et al.* and McQuillan used alloys of high purity and took adequate precautions to prevent contamination of their specimens at elevated temperatures, the possibility that the large disagreement in the experimental results was due to impurities can be discounted. In the experiments of Margolin *et al.*, however, the specimens were sealed in silica tubes and quenched by breaking these under water. This procedure must have given rise to a delay of several seconds between removal of the specimens from the annealing furnace and the contact of the specimens with the quenching water, during which time slow cooling inevitably occurred. The effect of a progressively increased delay in quenching on the microstructure of the 2.4 at.-% nickel alloy was, therefore, examined.

After heating four specimens of the homogenized alloy to 820° C. in a bath of tin for 30 min., the specimens were withdrawn, allowed to air-cool for 0.4, 3, 6, and 10 sec., respectively, and water-quenched. The resulting microstructures, shown in Figs. 2-5 (Plate VII), indicate a progressive increase in the amount of  $\alpha$  grains which have been deposited by a

process of nucleation and growth during the brief period of air-cooling immediately before quenching. There is little doubt, therefore, that significant amounts of coarse-grained  $\alpha$  phase of sufficient size to be mistaken for grains of the primary  $\alpha$  solid solution, can be formed during air-cooling of specimens of titanium-rich alloys at temperatures within the  $(\alpha + \beta)$  region. Since in all the work reported<sup>1-7</sup> experimental methods were used which would be expected to give a delayed quench, it seems probable that extremely rapid nucleation and growth of the  $\alpha$  phase is a factor which has not been taken into consideration by these workers. As the duration and rate of cooling during a delayed quench are influenced by many factors, the wide disagreement between the various  $\beta/(\alpha + \beta)$  boundaries in titanium-rich systems is only to be expected, if this theory is valid. Unless great care has been taken to obtain an instantaneous quench, the interpretation of microstructures of titanium-rich alloys, especially those cooled from a high initial homogenizing temperature to an annealing temperature close to the  $\beta/(\alpha + \beta)$  boundary, must in future be regarded with some caution.

#### ACKNOWLEDGEMENTS

Thanks are due to M. K. McQuillan, of Imperial Chemical Industries, Ltd., Metals Division, for carrying out the instantaneous-quench experiment. The author wishes also to acknowledge his indebtedness to the late Professor D. Hanson.

#### REFERENCES

1. H. K. Adenstedt, J. R. Pequignot, and J. M. Rayner, *Trans. Amer. Soc. Metals*, 1952, **44**, 990.
2. P. Pietrokowsky and P. Duwez, *Trans. Amer. Inst. Min. Met. Eng.*, 1952, **194**, 627.
3. R. J. van Thyne, H. D. Kessler, and M. Hansen, *Trans. Amer. Soc. Metals*, 1952, **44**, 974.
4. F. B. Cuff, N. J. Grant, and C. F. Floe, *Trans. Amer. Inst. Min. Met. Eng.*, 1952, **194**, 848.
5. P. Duwez and J. L. Taylor, *Trans. Amer. Soc. Metals*, 1952, **44**, 495.
6. D. J. Maykuth, H. R. Ogden, and R. I. Jaffee, *Trans. Amer. Inst. Min. Met. Eng.*, 1953, **197**, 225.
7. H. Margolin, E. Ence, and J. P. Nielsen, *ibid.*, 243.
8. A. D. McQuillan, *J. Inst. Metals*, 1951-52, **80**, 363.
9. M. K. McQuillan, *ibid.*, 1951, **79**, 379.



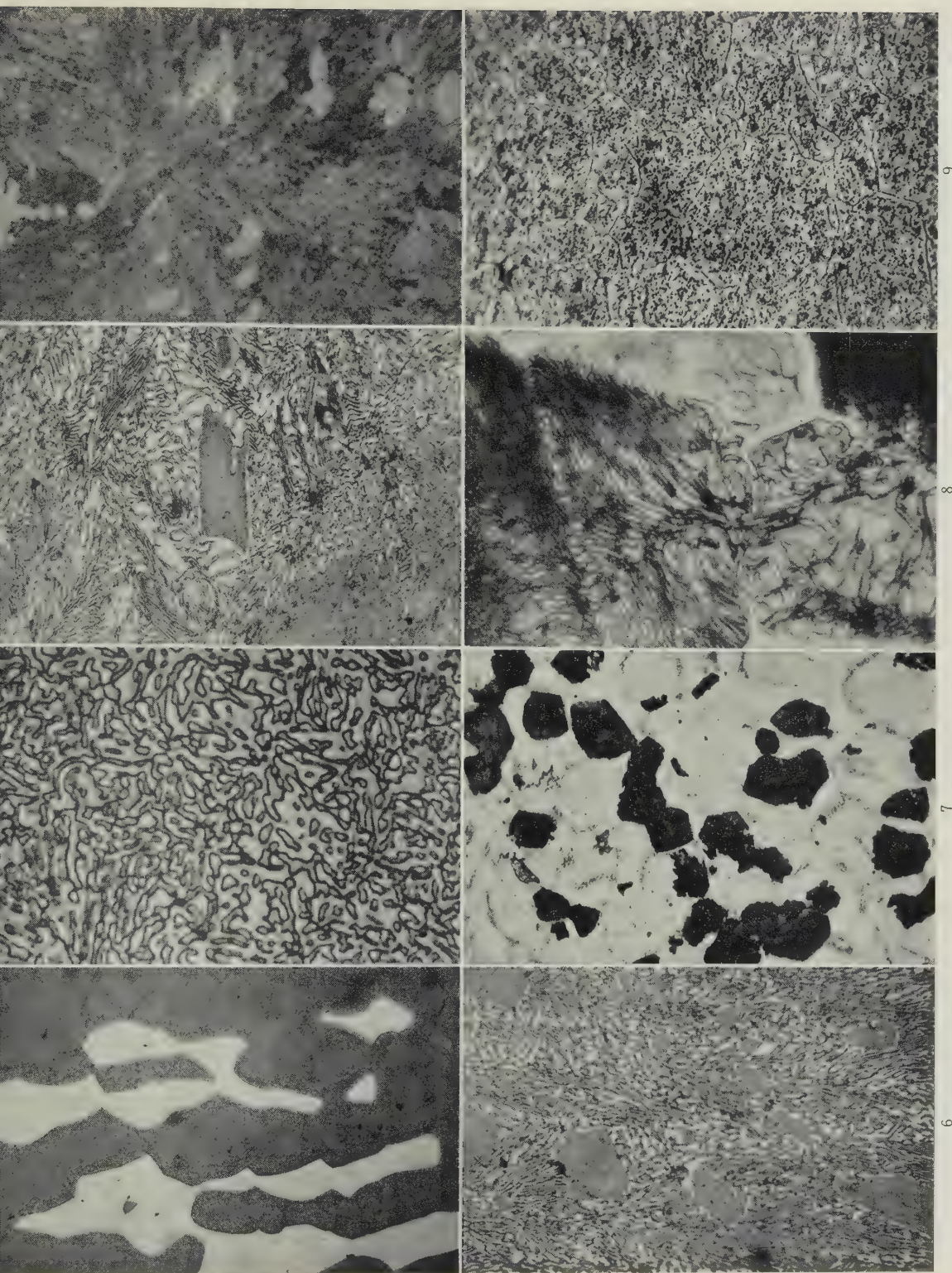


FIG. 2.—20% Mn, 8% Sn.  $\alpha$ , dark;  $\beta$ , light.  $\times 500$ .  
 FIG. 3.—15% Mn, 17% Sn. Q. 550° C. ( $\alpha + \delta'$ ) eutectoid.  $\times 1850$ .  
 FIG. 4.—15% Mn, 17% Sn. Very slowly cooled from 650° C. Coarse grains of  $\alpha$  (dark) surrounded by lamellar ( $\alpha + \delta'$ ) eutectoid.  $\times 500$ .  
 FIG. 5.—15% Mn, 17% Sn. Chill cast.  $\alpha$  grains in unresolvable matrix.  $\times 500$ .  
 FIG. 6.—15% Mn, 17% Sn. Q. 600° C.  $\alpha$  (dark) in matrix of lamellar ( $\alpha + \delta'$ ) eutectoid.  $\times 500$ .  
 FIG. 7.—10% Mn, 14% Sn. Furnace-cooled from 720° C.  $\alpha$ , eutectoid, and a dark-etching constituent.  $\times 500$ .  
 FIG. 8.—10% Mn, 14% Sn. The lamellar structure of the dark-etching constituent shown in Fig. 7 is revealed.  $\times 1500$ .  
 FIG. 9.—10% Mn, 8% Sn. Q. 650° C. + 2 hr. at 500° C. Precipitated  $\delta'$  in matrix of  $\alpha$ .  $\times 500$ .  
 All specimens etched in 10% solution of ammonium persulphate in dilute ammonia.



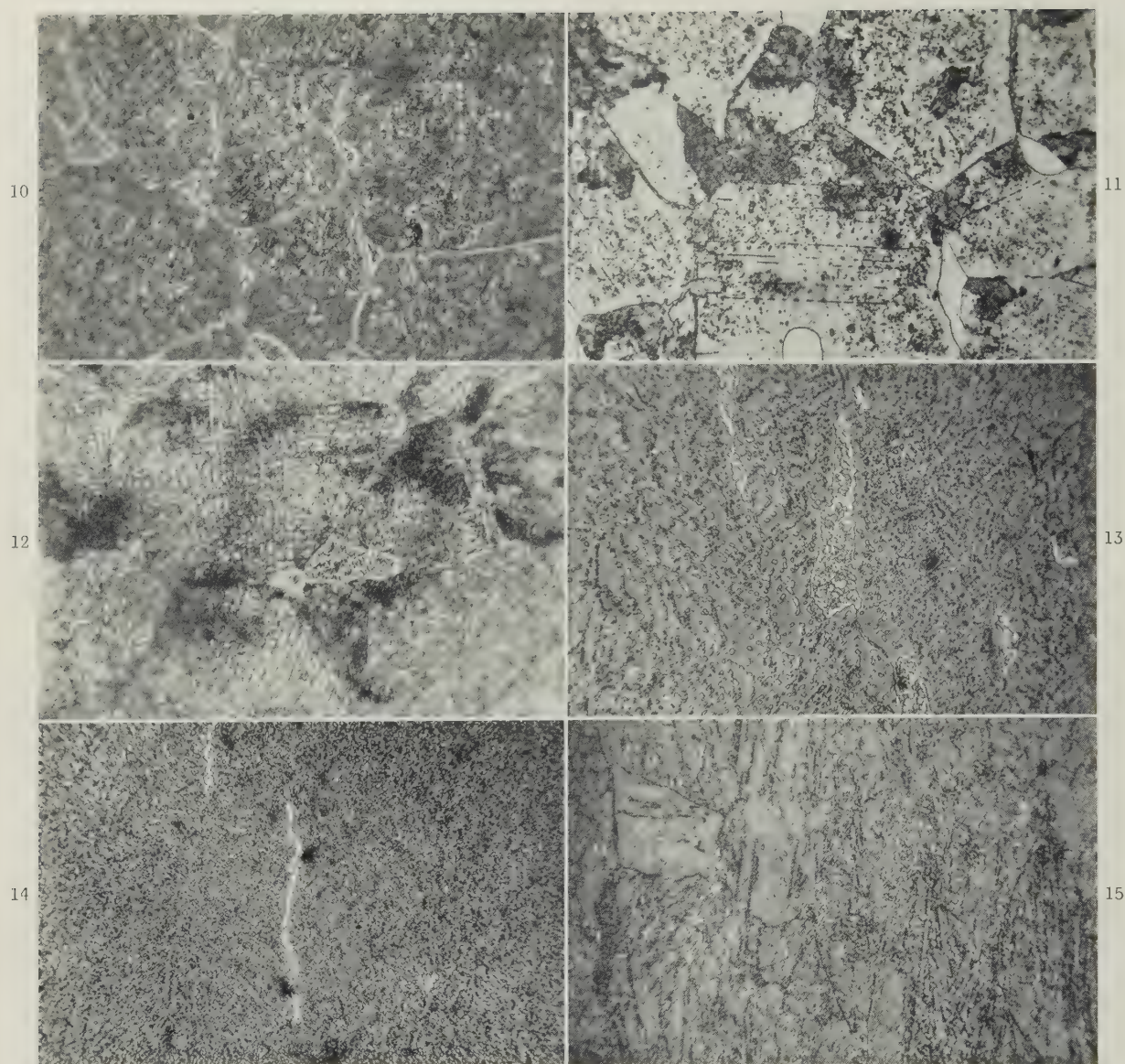


FIG. 10.—15% Mn, 8% Sn. Q. 650° C. + 2 hr. at 500° C. Precipitated  $\delta'$  in matrix of  $\alpha$  with some  $\alpha + \delta'$  eutectoid resulting from the decomposition of  $\beta$  during quenching. Continuous grain boundaries of  $\delta'$ .  $\times 500$ .

FIG. 11.—10% Mn, 10% Sn. Q. 650° C. + 2 hr. at 400° C. Penetration of lamellar constituent into the  $\alpha$  grains.  $\times 500$ .

FIG. 12.—10% Mn, 10% Sn. Q. 650° C. + 65 hr. at 400° C. Heavy precipitation of  $\delta'$  along crystallographic planes.  $\times 500$ .

FIG. 13.—10% Mn, 10% Sn. Q. 650° C., cold worked 50% and tempered 1 hr. at 550° C. Uniformly distributed particles of  $\delta'$  in matrix of  $\alpha$ . Some eutectoid is also present.  $\times 500$ .

FIG. 14.—10% Mn, 10% Sn. Q. 650° C., cold worked 80%, and tempered 1 hr. at 550° C. Structure is similar to that of Fig. 13, but grain-size is much finer.  $\times 500$ .

FIG. 15.—10% Mn, 10% Sn. Q. 650° C., cold worked 50%, and tempered 2 hr. at 500° C. Distribution of  $\delta'$  is less satisfactory than that resulting from tempering at 550° C.  $\times 500$ .

All specimens etched in 10% solution of ammonium persulphate in dilute ammonia.



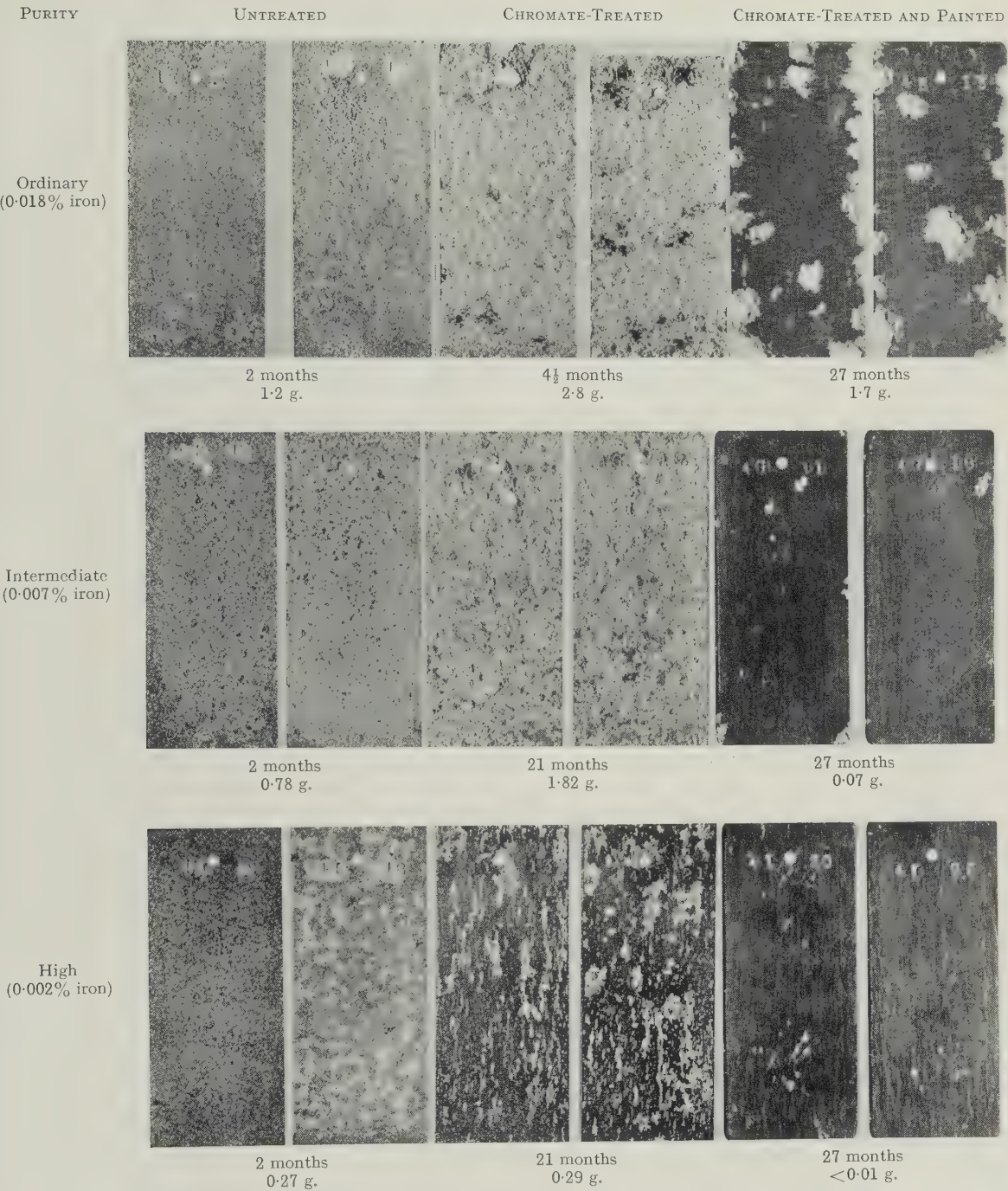
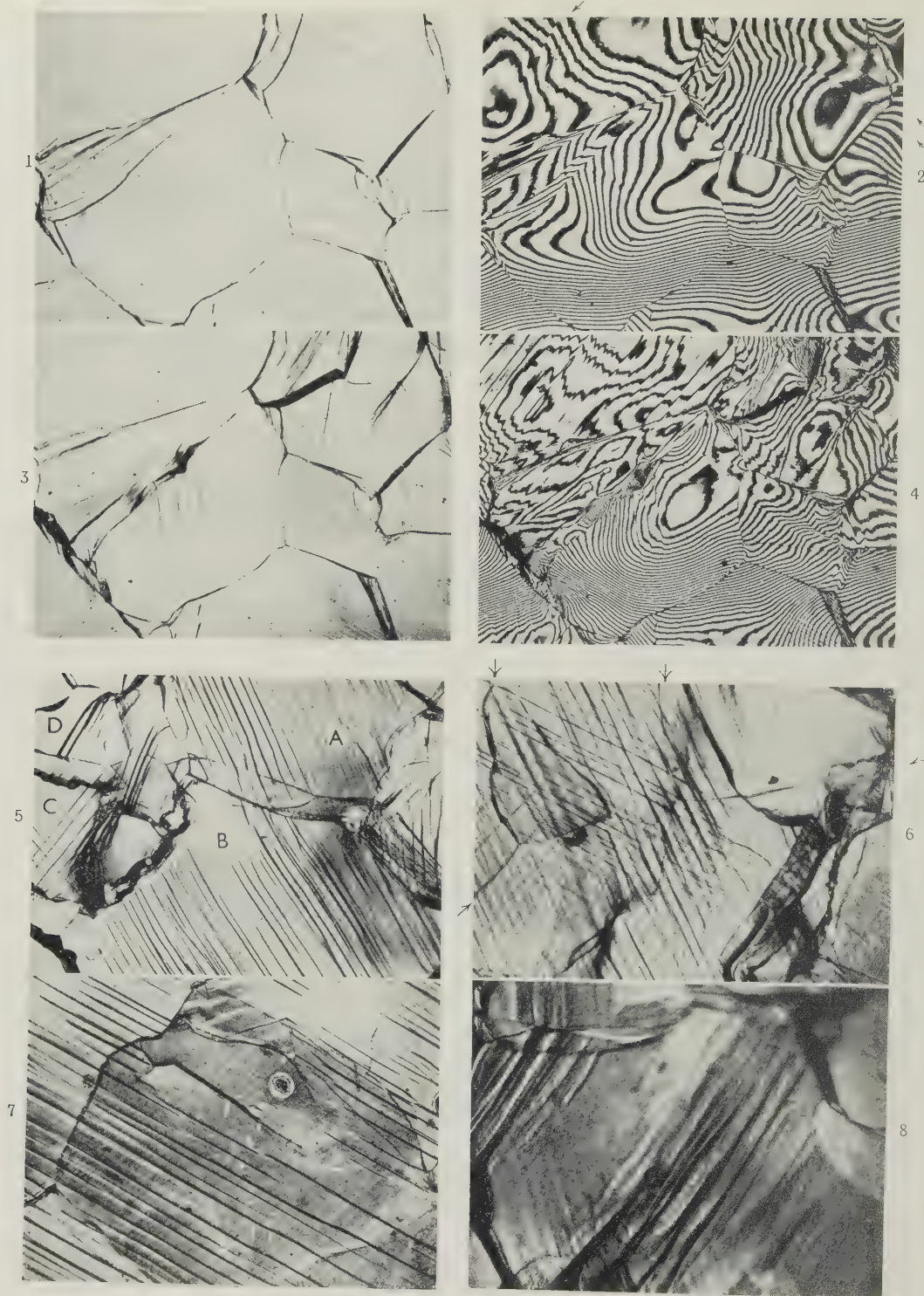


FIG. 1.—Magnesium Alloy (AZ31) Specimens After Sea-Water Spray Corrosion Test, Corrosion Product and Paint Having Been Removed.  
Mean weight losses are indicated in g./dm.<sup>2</sup>.

← APPLIED STRESS →



FIGS. 1-6.—Development of Slip and Boundary Migration in Pure Lead at High Stresses.

FIG. 1.—Stress 400 lb./in.<sup>2</sup>; 1% extension in 36 hr.  $\times 150$ .

FIG. 2.—As Fig. 1. Multiple-beam interferogram.  $\times 150$ .

FIG. 3.—As Fig. 1. 3.5% extension in 7 days.  $\times 150$ .

FIG. 4.—As Fig. 3. Multiple-beam interferogram.  $\times 150$ .

FIG. 5.—Stress 450 lb./in.<sup>2</sup>; 7.5% extension in 20 days.  $\times 100$ .

FIG. 6.—Stress 400 lb./in.<sup>2</sup>; 10% extension in 99 days.  $\times 150$ .

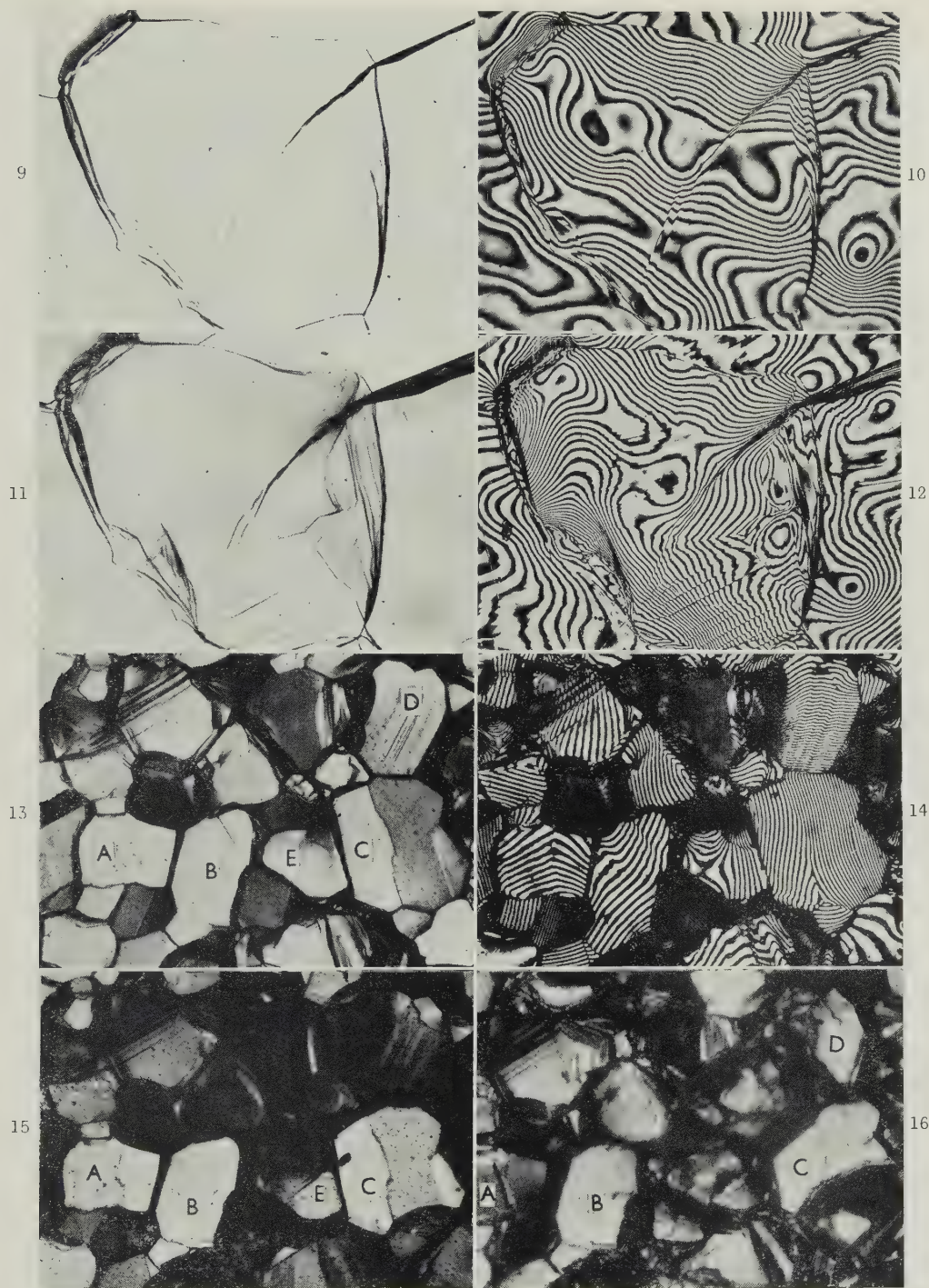
FIG. 7.—Pure lead. Stress 300 lb./in.<sup>2</sup>; 10% extension in 740 days.  $\times 150$ .

FIG. 8.—1.25% Ti Alloy. Stress 500 lb./in.<sup>2</sup>; 20% extension in 103 days. Positive phase contrast. Triple-point folds and fine slip.  $\times 600$ .

Reduced by  $\frac{1}{3}$  in reproduction



← APPLIED STRESS →



FIGS. 9-12.—Development of Triple-Point Fold in Pure Lead under Stress of 400 lb./in.<sup>2</sup>.  $\times 150$ .

FIG. 9.—1% extension in 36 hr.

FIG. 10.—As Fig. 9. Interferogram.

FIG. 11.—As Fig. 9. 3.5% extension in 7 days.

FIG. 12.—As Fig. 11. Interferogram.

FIGS. 13-16.—Relative Movement of Grains B and C, and Tilting of Grains and at Twin Boundaries in 2.45% Thallium Alloy under Stress of 200 lb./in.<sup>2</sup>.  $\times 150$ .

FIG. 13.—13% extension in 243 days.

FIG. 14.—As Fig. 13. Interferogram.

FIG. 15.—As Fig. 13. 18% extension in 351 days.

FIG. 16.—As Fig. 13. 38% extension in 757 days.

Reduced by  $\frac{1}{4}$  in reproduction.





Fig. 17.—Pure Lead. Stress 500 lb./in.<sup>2</sup>; 1% extension in 6 hr.; positive phase contrast; boundary migration.  $\times 300$ .  
 Fig. 18.—2.45% Ti. Stress 200 lb./in.<sup>2</sup>; 2.5% extension in 40 days; negative phase contrast; boundary migration.  $\times 550$ .  
 Fig. 19.—Pure Lead. Stress 500 lb./in.<sup>2</sup>; 10% extension in 25 days; bending of marker lines.  $\times 150$ .  
 Fig. 20.—Pure Lead. Stress 400 lb./in.<sup>2</sup>; 8% extension in 100 days; X-ray back-reflection photograph: sub-reflections after recrystallization.

Fig. 22.—As Fig. 21. 45% extension in 122 days.  $\times 250$ .  
 Fig. 23.—4.81% TI. Stress 300 lb./in.<sup>2</sup>; 4% extension in 14 days.  $\times 150$ .  
 Fig. 24.—As Fig. 23. Multiple-Beam Interferogram.  $\times 150$ .  
 Fig. 25.—7.87% TI. Stress 300 lb./in.<sup>2</sup>; 373% extension in 221 days.  $\times 500$ .  
 Fig. 26.—2.45% TI. Stress 200 lb./in.<sup>2</sup>; 13% extension in 243 days; negative phase contrast.  $\times 300$ .  
 Fig. 27.—As Fig. 25, repolished.  
 Fig. 28.—3.92% TI. Stress 300 lb./in.<sup>2</sup>; repolished after fracture and rapidly





FIG. 1.—Instantaneous quench.



FIG. 2.—0.4 sec. delay.

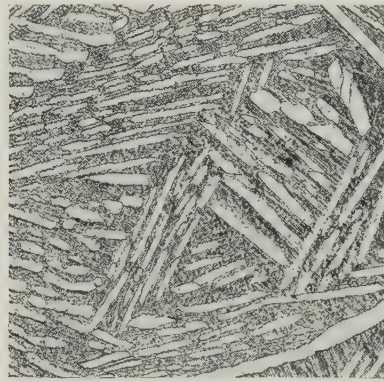


FIG. 3.—3 sec. delay.

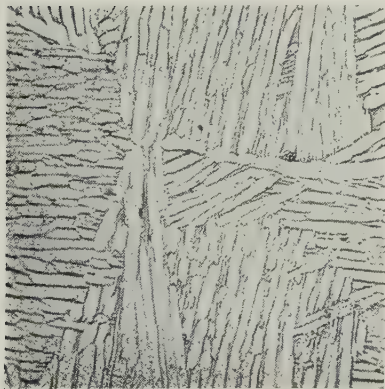


FIG. 4.—6 sec. delay.

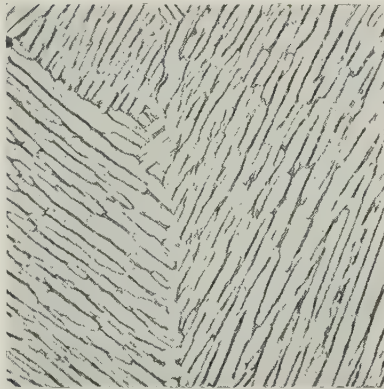


FIG. 5.—10 sec. delay.

FIGS. 1-5.—Microstructures of Titanium-2.4 At.-% Nickel Alloy After Delayed Quenching. Etched in 2% HF + 2% H<sub>2</sub>O<sub>2</sub> in water. × 235.





# AN INVESTIGATION OF THICKENING AND METAL ENTRAPMENT IN A LIGHT ALLOY MELTING FLUX \*

1495

By A. H. SULLY,† Ph.D., M.Sc., F.Inst.P., F.I.M., MEMBER,  
H. K. HARDY,‡ Ph.D., M.Sc., A.R.S.M., A.I.M., MEMBER,  
and T. J. HEAL,§ B.Sc., F.Inst.P.

## SYNOPSIS

Fluxes based on alkali chlorides used in remelting aluminium alloys become thickened and dry in service, especially when the charge is in the form of finely divided metal. The thickened flux contains trapped within it an appreciable proportion of metal. An investigation has been made of flux samples taken from industrial furnaces and of synthetic fluxes to determine the reason for flux thickening and metal entrapment. The latter is attributed to an increase in viscosity due to the presence of alumina films, stripped by the flux by surface-tension forces from the metal surface. Measurements of viscosity of molten fluxes at 850° C. have shown that the increase of viscosity caused by a dispersion of alumina in molten flux is critically dependent upon the shape of the alumina particles, being very great for particles that are thin and flat. Such dispersions exhibit thixotropy, and the viscosity of the thickened flux can be reduced by stirring. Agglomeration of all but the smallest particles of aluminium trapped in the flux can be effected by stirring, and the efficacy of the treatment in practice is determined by the range of particle sizes and by the practicability of stirring.

## I.—INTRODUCTION

IN remelting secondary aluminium alloys, particularly when the charge is in a finely divided form, e.g. swarf or foil, it is common practice to use a cover of molten flux, usually based on sodium chloride. This flux prevents oxidation of the metal during melting and also assists the running together of the metal once the melting point is exceeded. The sponsors of this work have always held the view that the action of the flux in assisting agglomeration of the metal was due to stripping of the oxide films from individual particles by surface-tension forces, rather than to actual dissolution of the oxide. During the melting process the flux deteriorates. An initially thin and fluid flux becomes progressively thicker until eventually it must be renewed. The spent and thickened flux carries a considerable amount of aluminium in particles of a wide range of sizes. Although a proportion of this can be recovered by tapping the molten flux into a container, so that the larger aluminium globules settle to the bottom before the flux solidifies, a considerable amount of aluminium remains entrapped.

## II.—REVIEW OF LITERATURE

An account of the problem of melting finely divided aluminium was given by Gillett and James <sup>1</sup> as early as 1916. They pointed out that two properties of finely divided aluminium must be taken

into account, namely the readiness with which it oxidizes and the difficulty with which tiny globules coated with oxide coalesce. They gave an account of the industrial fluxing methods in use at that time, together with a full description of various methods tried and recoveries obtained on a laboratory scale. Chlorides were stated to have no dissolving action on the oxide, whereas fluorides had. Good recoveries were of the order of 70% of the weight of aluminium chips charged, which consisted of about 90% metal. The best results were obtained by using a large quantity of flux, which acted as a molten cover and promoted coalescence by soaking up dirt and oxide. A flux consisting of 85% sodium chloride and 15% calcium fluoride was recommended for this purpose.

The use of oxide-dissolving fluxes, such as cryolite, has been the subject of many patents, among which may be mentioned one by Robison,<sup>2</sup> who recommended charging aluminium scrap, mixed with cryolite, into molten salt. A series of patents on fluxes for remelting magnesium alloy scrap<sup>3,4,5</sup> provides examples of methods in which thickening of the flux is deliberately sought and artificially accelerated in order to obtain good separation from the metal and to prevent flux inclusions.

Anderson<sup>6</sup> reviewed the literature on fluxes for aluminium alloys up to 1930, and discussed the subject fully. A few years later Irrmann<sup>7</sup> gave the following compositions of fluxes said to dissolve oxide: cryolite 15%, NaCl 85%; cryolite 15%, NaCl 60%, KCl 25%; cryolite 50%, Na<sub>2</sub>CO<sub>3</sub> 15%, NaCl 35%.

\* Manuscript received 19 March 1953.

† Principal Physicist; ‡ Senior Metallurgist; § Head of

Physics Section, Fulmer Research Institute, Ltd., Stoke Poges, Bucks.

Tronstad and Reimers<sup>8</sup> examined the behaviour of cryolite and sodium silicofluoride in fluxing aluminium and found that cryolite would dissolve small quantities of alumina above 565° C. Sodium silicofluoride reacted with alumina and also decomposed to form volatile silicon tetrafluoride, which would have a scavenging action on the melt.

Discussing fluxes for welding aluminium, West<sup>9</sup> reviewed the literature exhaustively and listed the physical properties of possible fluxing materials. In a further paper<sup>10</sup> he discussed the action of welding fluxes. He found that the solubility of alumina in most of the fluxes (alkali chloride and fluoride type) was extremely small, and he considered it to play no part in the fluxing process. He suggested that the function of these fluxes, the most successful of which were alkali halide mixtures, was to attack the basis metal at the oxide/metal interface, thus detaching the oxide film mechanically, and then to remove the alumina, possibly as a suspension. This action might be due to halide ions penetrating the oxide film and lifting it, owing to the formation of volatile aluminium compounds at the oxide/metal interface.

Feuer<sup>11</sup> suggested the use of a 50:50 NaCl-KCl flux, which has a lower melting point than NaCl. The chlorides can be recovered separately, since the solubility of KCl in water increases with rising temperature whereas that of NaCl is relatively unaffected by increasing temperature. That melting fluxes become tacky in use owing to the presence of suspended particles and loss of volatile constituents, was noted by Einerl and Neurath.<sup>12</sup>

### III.—PHYSICAL AND CHEMICAL EXAMINATION OF SLAG SAMPLES

Samples of a flux were taken at various stages during melting aluminium-silicon alloy scrap at about 850° C. in an oil-fired rotary furnace. The appearance of the flux varied with the stage of the process at which the sample was taken. The flux was run out of the furnace and solidified in flat shallow troughs. In this condition it was a greyish-black colour, and when it was fractured trapped aluminium globules of various sizes could readily be seen.

#### 1. DETERMINATION OF METAL CONTENT OF FLUX

The size distribution of aluminium particles inside a typical "slag out" flux was determined on an 80-lb. sample, which was crushed and sieved and then analysed to determine the metal content. The method of analysis was based on that of Ehrenberg.<sup>13</sup> The water-soluble portion was determined by the loss in weight after solution. The insoluble portion was treated with aqueous cupric chloride solution, in which the aluminium dissolves, replacing the copper; aluminium is then determined in the filtrate. If required, the non-metallic portion of the insolubles

can be determined by weighing the residue after adding nitric acid to dissolve the precipitated copper and filtering.

The results of this examination are given in Table I. The total metal content shown by this analysis was 6.72%, of which approximately equal amounts were present as particles of size greater and smaller than 8 B.S., the majority of the latter being particles smaller than 200 B.S. An analysis on an unscreened sample gave a total metal content of 6.34%, in fair agreement with the above total.

TABLE I.—*Size Distribution of Aluminium Particles in Spent Flux.*

Size	Weight on Sieve, % of Total Weight of Flux	Metal † in Sieve Sample, % of Total Weight of Flux
> ½ in.	1.76	1.76 *
½ in.—8 B.S.	1.31	1.31 *
8—30 B.S.	0.56	0.11
30—44 B.S.	0.93	0.04
44—72 B.S.	4.30	0.23
72—150 B.S.	7.18	0.48
150—200 B.S.	3.10	0.17
< 200 B.S.	80.74	2.62
Total metal content 6.72		

\* Hand-picked and assumed 100% metal.

† Calculated from analysed aluminium content  $\times 9/8$  to allow for silicon content of alloy.

The content of water-insoluble material, excluding calcium fluoride, was about 40–60% by weight of the dry and thickened flux and about 20% of the diluted, "slag out" flux. X-ray-diffraction examination of the insoluble portion did not give a diffraction pattern of any form of alumina.

#### 2. MICROSCOPICAL EXAMINATION

A microscopical examination was made by transmitted light of the water-insoluble portion of various samples of flux. Needles of calcium fluoride were identified particularly in samples taken during the early stages of melting (Fig. 1, Plate VIII), but in later stages the insoluble portion of the flux consisted mainly of yellowish flat plates (Fig. 2, Plate VIII). By examination in mounting media of different refractive indices, the refractive index of most of the particles was found to be approximately 1.65, which was consistent with that of  $\beta$ -alumina or of  $\gamma$ -alumina in the hexagonal form as prepared by the decomposition of alum.

#### 3. EXPERIMENTS ON REMELTED FLUXES

Samples of spent flux, corresponding to "slag out" flux and prepared by the same methods as for the determination of metallic content, were remelted and held at 850° C. in silica crucibles, particles > ½ in. dia. being removed by hand before melting. After being held at temperature for 24 hr., the samples were allowed to solidify and were then broken out of the crucibles. No settling of alumina or aluminium



had occurred, and metal particles were visible right to the top of the solidified cake.

Dilution of the slag with 10% of fluorspar, sodium fluoride, or cryolite did not have any marked effect on the viscosity of the slag or on the settling of alumina or aluminium. Dilution with 50% of sodium chloride increased the fluidity of the slag, and after holding at temperature for 20 hr. there was a gradation vertically through the sample from a clean salt layer at the top to the normal dirty grey colour at the bottom. There was, however, no appreciable settling or agglomeration of metal.

During these experiments the incidental, but significant, observation was made that if the molten flux was stirred it appeared to become appreciably more fluid. After vigorous stirring some settling and agglomeration of metal had occurred, metal beads being found at the bottom of the crucible.

#### IV.—QUALITATIVE EXPERIMENTS ON SYNTHETIC FLUXES

##### 1. VISCOSITY OF PURE FLUXES

Molten 90 : 10 NaCl-CaF<sub>2</sub> flux was found to have a viscosity very similar to that of water and was unaffected, as far as could be ascertained from its appearance and by stirring, either by solidification and remelting up to six times or by being held molten for up to 24 hr.

##### 2. EFFECT OF ALUMINA ON THE VISCOSITY OF 90 : 10 NaCl-CaF<sub>2</sub> FLUX

The effect of various quantities of different types of alumina on the viscosity of the flux was determined by simple stirring tests. The types of alumina used are listed in Table II, and the results of the tests are summarized in Table III.

TABLE II.—Types of Alumina Used in Tests of Flux Thickening.

Description	Results of X-Ray Examination	Results of Microscopical Examination
$\alpha$ -Alumina. British Aluminium Co. pure calcined alumina	$\alpha$ -Al <sub>2</sub> O <sub>3</sub>	Fine particles.
White Bauxilite abrasive (500 mesh)	$\alpha$ -Al <sub>2</sub> O <sub>3</sub>	Coarse, angular particles.
Aloxite. Grade H	$\alpha$ -Al <sub>2</sub> O <sub>3</sub>	Medium-sized flattish particles.
Micronized alumina (40% under 4 $\mu$ )	$\alpha$ -Al <sub>2</sub> O <sub>3</sub>	Medium-sized, platelike particles.
Micronized and ball-milled alumina (89% under 4 $\mu$ )	$\alpha$ -Al <sub>2</sub> O <sub>3</sub>	Much finer particles.
Corrosion alumina. Commercial-purity Al corroded in contact with mercury; corrosion product heated 20 hr. at 300° C. and 2 hr. at 600° C.	Too fine or thin to produce diffraction pattern	Exceptionally small and extremely thin plates.
Alum alumina ( $\gamma$ ). Alum decomposed by heating $\frac{1}{2}$ hr. at 1100° C.	$\gamma$ -Al <sub>2</sub> O <sub>3</sub>	Very thin plates, less than 0.0005 in. thick.
Alum alumina ( $\alpha$ ). Alum decomposed by heating $\frac{1}{2}$ hr. at 1425° C.	$\alpha$ -Al <sub>2</sub> O <sub>3</sub>	Thin, opaque plates.

Increasing quantities of  $\alpha$ -alumina in the form of fine calcined powder up to 30% changed the consistency of the molten flux from that of a thin liquid

to that of a fairly thick cream, which was, however, very much more fluid than the thickened practical flux. Bauxilite abrasive, although rather coarser, gave very similar results. Equivalent amounts of Aloxite grade H gave slightly more thickening.

Micronized and ball-milled  $\alpha$ -alumina of very fine particle size gave results very similar to  $\alpha$ -alumina

TABLE III.—Summary of Results on the Effect of Alumina Additions on the Viscosity of 90 : 10 NaCl-CaF<sub>2</sub> Flux.

Type of Alumina	Description	Appearance of Flux with :			
		10% Alumina	15% Alumina	20% Alumina	30% Alumina
Calcined $\alpha$ -alumina	Fine particles	Thin	Fairly thin	...	Creamy
Bauxilite abrasive, 500 mesh	Coarse, angular particles	Thin	Creamy	...	Somewhat viscous
Aloxite. Grade H	Medium-sized particles	Slight increase in viscosity	...	Thin cream	Fairly thick
Micronized and ball-milled	Very fine particles	Slight increase in viscosity	...	Very thin cream	Not very thick cream
Micronized	Medium-sized, plate like	Fairly thin	...	Thin cream	Thick cream
Corrosion alumina	Extremely small and thin plates	Creamy consistency approximating to 20-25% of micronized alumina	...	...	...
$\gamma$ -alumina from alum	Very thin plates	Creamy	...	Thick and viscous	Very pasty, never molten
$\alpha$ -alumina from alum	Thin plates	Thin cream	...	Viscous fluid	Very pasty, never molten

in the calcined form, but the alumina which had been micronized only gave markedly more thickening in spite of its larger average particle size.

The alumina which had been prepared by heating the corrosion product of aluminium in contact with mercury produced much greater thickening than equivalent quantities of the types described above, the thickening produced by 10% being about equivalent to 20-25% of micronized alumina.

$\gamma$ -Alumina produced by the decomposition of alum was a very effective thickening agent, 20% producing a mass too pasty to be stirred, while 10% produced a viscosity very similar to that of "slag out" flux.  $\alpha$ -Alumina produced by the decomposition of alum at higher temperatures was somewhat less effective in thickening the flux, but nevertheless increased the viscosity in equivalent amounts much more than any of the other forms of  $\alpha$ -alumina investigated.

##### 3. BEHAVIOUR OF FLUX IN CONTACT WITH ALUMINIUM

A small pellet of aluminium was melted on the surface of powdered 90 : 10 NaCl-CaF<sub>2</sub> flux in a crucible and was observed while the flux melted. When molten, the aluminium pellet was almost spherical and covered with a dirty grey oxide film.

As the flux melted it crept over the surface of the aluminium. By tapping the crucible gently, tears could be made to appear in the oxide film, which remained floating in a very thin layer of flux. The oxide film could easily be detached from the surface of the aluminium, leaving the bead with a very bright surface covered with a layer of flux. This was too thin to prevent oxidation, so that the metal surface gradually tarnished. As the whole of the flux melted, the aluminium sank through it to the bottom of the crucible. This type of experiment was repeated several times with slight variations.

In two tests a piece of aluminium was maintained in contact with molten flux for 24 hr., the liquid in one crucible being occasionally stirred while the other was not stirred at all. On breaking up the solidified cake, the aluminium bead in the unstirred sample was found to be perfectly clean, but the film of oxide was trapped in the flux immediately surrounding it. In the sample which had been stirred, the oxide had been more uniformly dispersed throughout the flux. Two small pieces of aluminium melted below a layer of powdered flux were found to have run together at the end of the test. A similar result was also obtained when the pieces of aluminium were melted on top of the flux layer.

Pellets of aluminium were melted on top of powdered flux containing 10 and 20%  $\gamma$ -alumina prepared from alum. The molten aluminium remained as a globule on the flux containing 20% alumina, but was covered with a layer of salt, which had crept over it even though the flux had never properly melted. The molten aluminium partially sank into the 10% alumina flux mixture, and in this case the oxide film was stripped from the aluminium by the salt which crept over the surface. In a similar experiment in which the flux was stirred, the aluminium pellet sank through the flux.

## V.—DISCUSSION OF RESULTS OF QUALITATIVE EXPERIMENTS

### 1. FLUX THICKENING

The degree of flux thickening observed in practice is very many times greater than that which would be expected from the known concentration of insoluble matter in the flux, which is about 40% for a very dry flux and about 20% in the diluted "slag out" flux. The viscosity of a fluid containing a volume fraction  $V_1$  of dispersed particles is related to the original viscosity  $\eta_0$  of the fluid by Einstein's formula:<sup>14</sup>

$$\eta = \eta_0(1 + 2.5V_1)$$

Thus a 40% volume concentration of particles should result in only a doubling of the viscosity of the flux. Einstein's formula, however, assumes that the particles are spherical and that there is no mutual interaction between them. Vand<sup>15</sup> has treated the case where particle interaction occurs, and calculation from his formula predicts an increase in viscosity

by a factor of eight for a 40% volume concentration of insoluble particles. This increase in viscosity is, however, very many times smaller than that required to cause appreciable thickening of pure molten salt (the difference in viscosity between water and fairly thick syrup represents an increase by a factor of about  $10^3$ ).

Microscopical examination showed that when alumina caused a high degree of thickening, it was present in the flux in the form of thin films or flat plates. No X-ray-diffraction patterns could be obtained from these residues; this is consistent with their small dimension in one direction. On the other hand, forms of alumina, which when added to pure flux produced only slight thickening, were shown by microscopic examination to be considerably more rounded and gave X-ray-diffraction patterns typical of well-formed crystals. Alumina prepared in plate-like form by the decomposition of alum or by corrosion produced a degree of thickening of the flux very similar to that occurring in practice.

These results suggest that the anomalous behaviour of the industrial flux is due to the fact that the form of the alumina films is such that the conditions under which Einstein's and Vand's formulæ may be applied do not obtain. The derivation of these formulæ assumes a roughly spherical particle shape. It appears that in the presence of flat, plate-like particles of alumina wide deviations from the formulæ are to be expected. The experiments with micronized and with micronized and ball-milled alumina provide an interesting confirmation of this. It was found that for equivalent amounts of these materials the flux thickening caused by the ball-milled material was less than that due to the original micronized sample, although the former had an appreciably smaller particle size. Ball milling breaks down to smaller particles the initial rather plate-like particles of the micronized material and yields a product for which the assumption of roughly spherical particles is more nearly justified.

### 2. MECHANISM OF FLUXING

Stripping of the oxide film was observed to proceed by penetration of the flux between the aluminium and the alumina, the latter being carried into the flux. For this to occur the sum of the interfacial tensions, aluminium/flux plus alumina/flux, must be less than the interfacial tension alumina/aluminium. Thus, a more stable state is reached when the alumina is completely immersed in a flux which completely wets the aluminium. The marked tendency for this to occur is well brought out by the experiments in which aluminium pellets were melted on flux containing as much as 30%  $\gamma$ -alumina. Although the flux was so thick that the aluminium could not settle through it, the flux still crept over the surface of the molten aluminium, removing the oxide coating.

The practical significance of this tendency is that the failure to agglomerate of metal particles in the



thickened flux is in no way connected with surface-tension effects, as the thickened flux is still capable of stripping films from aluminium particles.

### 3. TRAPPING OF METAL PARTICLES

The experimental work strongly supported the view that the trapping of aluminium particles in the pasty industrial flux was primarily due to the high viscosity induced by alumina in the form of thin films. However, the increased density of the flux, due to its alumina content, must also be a contributory factor militating against settling of aluminium droplets through the flux.

The qualitative experiments described above also suggested that the viscosity might show a thixotropic anomaly, i.e. it might vary with the rate of shear. It was noticed that stirring resulted in an apparent thinning of the flux and assisted agglomeration of the metal particles trapped in the flux.

In order to assess the relative importance of these factors, measurements of density and of viscosity were made on synthetic and practical fluxes and are described below.

## VI.—MEASUREMENTS OF DENSITY

### 1. EXPERIMENTAL METHODS

Density determinations by the conventional methods of weighing a sinker in air, water, and flux and of weighing a constant volume of flux were not satisfactory, owing to the viscous drag of the thickened flux and the trapping of air in the  $\gamma$ -alumina. The method finally adopted was that described by Greenaway,<sup>16</sup> and consisted in measuring the pressure required to bubble a slow stream of nitrogen up through the flux against the pressure head of the liquid itself. The experimental arrangement comprised a silica tube of uniform circular bore, dipping vertically into the flux, the tube being connected via a water manometer and a needle valve to a nitrogen cylinder. Two pressure readings,  $p_1$  and  $p_2$ , were taken at heights  $h_1$  and  $h_2$ , from which the density was obtained by the formula :

$$d = \frac{p_1 - p_2}{h_1 - h_2}$$

Measurements were made on a 90 : 10 NaCl-CaF<sub>2</sub> flux with 10%  $\gamma$ -alumina. It was found that, provided that the nitrogen stream was kept flowing continuously to prevent a reduction in the bore of the tube by deposited alumina, and provided that the melt was stirred frequently to prevent settling of the alumina, consistent and reliable results could be obtained. The results showed that the freshly prepared flux on melting had a density of 1.6 g./c.c., which increased on holding at 850° C. and stirring to 1.8-1.9 g./c.c. after 2-4 hr. Allowing a melt to solidify and then remelting caused the density to

assume its final stable value immediately after remelting.

The density values obtained by this and by the conventional methods are given in Table IV.

TABLE IV.—Results of Density Measurements.

Material	Method	Density, g./c.c. at 850° C.	Remarks
NaCl	Weighing sinker	1.50	Values from International Critical Tables :
	Weighing known volume	1.47 at 950° C. 1.49 " 912° C. 1.51 " 850° C.	950° C. 1.45 912° C. 1.48 850° C. 1.51
Synthetic flux	Weighing sinker	1.60	
90% NaCl : 10% CaF <sub>2</sub>	Weighing known volume	1.59	
Water + 20% $\gamma$ -alumina	"	1.05 at 20° C.	Should be 1.48
Synthetic flux + 5% $\gamma$ -alumina	"	1.59	Immediately after melting.
	"	1.78	After solidifying and remelting.
Synthetic flux + 10% $\gamma$ -alumina	"	1.62	Immediately after melting.
	"	2.00	After solidifying and remelting.
" Slag out " practical flux corresponding to analysis of Table I	"	2.00	Small quantity NaCl added to promote fluidity — allowed for in calculation.
Synthetic flux + 10% $\gamma$ -alumina	Bubble method	1.62	20 min. after melting
		1.66	40 " "
		1.76	60 " "
		1.84	120 " "
		2.00 *	300 " "

\* This value is probably rather high, owing to volatilization of NaCl.

### 2. DISCUSSION OF DENSITY MEASUREMENTS

The most reliable figures are as follows :

	g./c.c. at 850° C.
(a) 90 : 10 NaCl-CaF <sub>2</sub> flux.	1.60
(b) 90 : 10 NaCl-CaF <sub>2</sub> flux + 10% $\gamma$ -Al <sub>2</sub> O <sub>3</sub>	1.84
(c) Practical "slag out" flux	2.00

Calculation of the density of  $\gamma$ -alumina from (a) and (b) gives a value of 4.0. This is of the same order as the values for  $\alpha$ -alumina and is higher than the values given by Jellinek and Fankuchen,<sup>17</sup> of 3.42 measured and 3.4 calculated, on the basis of the crystal structure which they proposed. Taking this value of 4.0 for the density of  $\gamma$ -alumina, the calculated density of the "slag out" flux, assuming it to contain 6.5% aluminium and 15% alumina, is 2.004, in good agreement with the observed experimental value.

The anomalously low initial density of the synthetic flux plus alumina samples is probably due to absorbed gas films on the oxide films stripped from the metal particles. This is considered to have little relevance to the problem of metal entrapment, since, even if the phenomenon also occurs in the practical flux, the stirring to which the flux is subjected in a rotary furnace should soon increase the density to the normal value.

Since the density measurements on the practical flux never exceeded 2.0, while the density of aluminium at 850° C. is 2.34, there is no reason, based on considerations of density alone, why aluminium globules should not settle through the molten slag.

## VII.—MEASUREMENTS OF VISCOSITY

## 1. EXPERIMENTAL METHOD AND RESULTS

The measurements were made with a rotating-outer-cylinder viscometer in which the rate of rotation of the outer cylinder could be varied, in order to investigate the thixotropic anomaly in the thickened fluxes by measurements of viscosity at various shear gradients. The marked thixotropy of the suspensions of  $\gamma$ -alumina in 90:10 NaCl-CaF<sub>2</sub> flux made it essential to adopt the rotating-outer-cylinder method, despite constructional difficulties, so that a wide range of shear rates could be obtained.

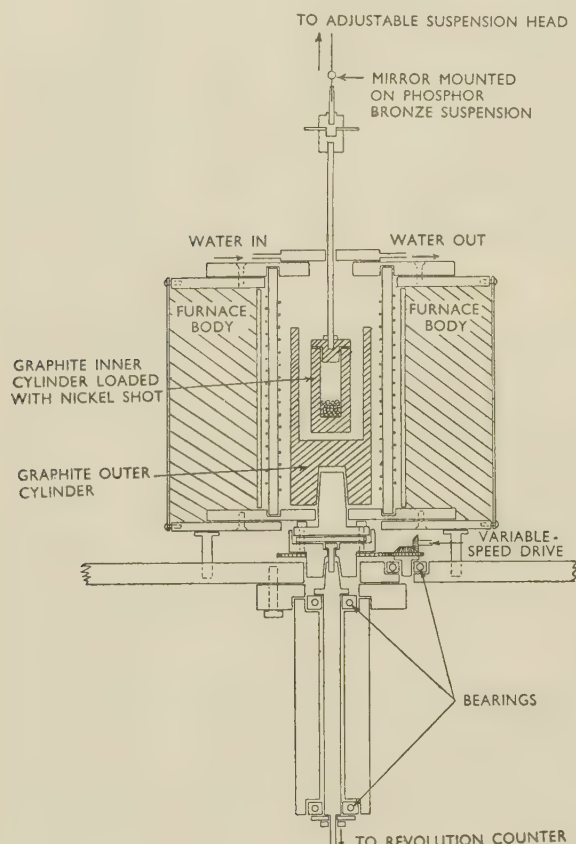


FIG. 5.—Diagram of Apparatus for High-Temperature Viscosity Measurements.

The major difficulty in construction lay in the choice of materials for the inner and outer cylinders. The material had to be such that the finished product could be produced to close tolerances, and it had to resist the attack of the fluxes at temperatures up to 900° C. for a sufficiently long period. After experiments with various materials it was found that graphite fulfilled these requirements reasonably well. Fig. 5 shows the arrangement of the viscometer in its final form. The outer cylinder could be rotated at speeds up to 160–180 r.p.m. without loss of stability. With cylinders of the dimensions used, of approxi-

mately 2 and 3 cm. radii, this meant a shear rate of 50–60 cm./sec./cm. separation.

To determine the torsional rigidity of the phosphor bronze suspensions, as a necessary prelude to viscosity measurements, the inner-cylinder assembly was replaced by cylinders of aluminium and steel of different sizes for the different gauges of suspension wire and the period  $T$  of torsional oscillation of small amplitude determined. The torsional rigidity of the suspension  $\tau$  was then calculated from the formula:

$$T = 2\pi\sqrt{\frac{I}{\tau}}$$

where  $I$  is the moment of inertia of the suspended system.

The inner-cylinder assembly was replaced and the experiments repeated, assuming the values of  $\tau$  for the suspensions obtained as above. This gave a mean value for the moment of inertia of the inner-cylinder assembly, which was later used to determine the torsional rigidity of the suspension under operating conditions at high temperature. It was found that the torsional rigidity was little affected by the slight rise in temperature of the suspension occurring during operation of the viscometer at 800°–900° C.

Calibration measurements at room temperature on water and on 25, 50, and 70% sucrose solutions gave results within 15% of the accepted values for these liquids, which ranged in viscosity from 10 to 1100 millipoises. The values obtained were always on the high side of the correct values. All the measurements at high temperature were made at 850° ± 10° C. A first determination of the viscosity of molten sodium chloride at this temperature gave a value consistently 50% higher than the value given in standard tables. On remelting the charge on the following day the viscosity was found to be over 100% above the standard value. Graphite powder was visible in the melt, and it was clear that the high values obtained for sodium chloride and, also in the measurements at room temperature, were probably attributable to an increase in viscosity caused by small particles of graphite washed off the crucible and suspended in the liquid. This effect was greater at high temperatures, and was aggravated by allowing the sodium chloride to solidify and cool, since the high degree of contraction pulled a skin of graphite away from the inner wall of the outer cylinder.

Provided that this solidification was avoided, the error introduced was insignificant in relation to the viscosities of the thickened fluxes. A 50% error in the viscosity of sodium chloride at 850° C. is only 6 or 7 millipoises, and the expected viscosities of the thickened fluxes were of the order of 10<sup>2</sup>–10<sup>3</sup> millipoises. A note on factors affecting the accuracy of the viscosity measurements is given in an Appendix (p. 58).

Since there was no reason to suppose that the presence of 10% of calcium fluoride would alter the



viscosity of the synthetic fluxes to any large extent, these were made up from commercial sodium chloride, which contains calcium fluoride as impurity, with additions of various amounts of alumina.

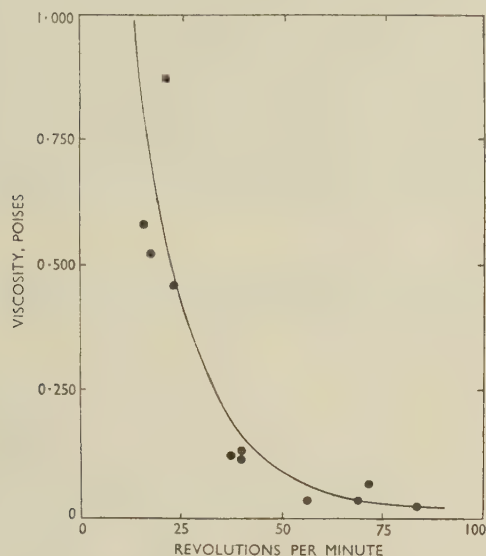


FIG. 6.—Variation of Viscosity with Rate of Shear for a Synthetic Flux Containing 3%  $\gamma$ -Alumina.

The results obtained on a flux containing 3%  $\gamma$ -alumina (Fig. 6) showed it to be markedly thixotropic. The viscosity was 680 millipoises at 20 r.p.m., and this decreased to 25 millipoises at 84 r.p.m., a value near to that of pure sodium chloride. Further confirmation of thixotropy followed from results obtained with a flux containing 7.7%  $\gamma$ -alumina which had a viscosity of 4700 millipoises at 13 r.p.m., falling to 400 millipoises at 100 r.p.m. Attempts to measure the viscosity of fluxes with higher contents of alumina were a failure, the rigidity of the stiffest available suspensions being insufficient to overcome the initial high viscosity.

Attention was then turned to a sample of practical "slag out" flux. In this the viscosity decreased from 23 poises at 40 r.p.m. to 3.5 poises at 140 r.p.m., the highest speed at which stability could be maintained under the particular experimental conditions.

Some further experiments were made with sodium chloride containing a 5% suspension of three different grades of  $\alpha$ -alumina—micronized and ball-milled alumina, Aloxite grade H, and white Bauxilite abrasive (500 mesh)—in order to relate the anomalous thickening of the flux to particle shape in a more quantitative manner than in the experiments reported above. Fig. 7 shows the variation of viscosity with the rate of revolution for these fluxes and for the flux containing 7.7%  $\gamma$ -alumina. Each flux was analysed for insoluble content at the completion of the measurements; the values were higher than the 5% original addition, owing to volatilization of

sodium chloride during the experiment. Micro-examination, described earlier, had shown that the Aloxite had small flattish particles, the micronized and ball-milled alumina small and more rounded particles, and Bauxilite comparatively large, angular particles. The results are in good agreement with the theory that it is the flat plate-like particles that cause the maximum increase in viscosity and lead to thixotropy. Neither the Bauxilite nor the micronized and ball-milled alumina showed any appreciable thixotropy. The Aloxite did, but on a very small scale compared with the effect obtained with  $\gamma$ -alumina, which consists of very thin films. The degree of thixotropy can, therefore, be correlated, without inconsistencies, with the particle shape.

Fig. 8 shows a plot of viscometer deflection against time, from the moment of starting the driving motor, in the determination of the viscosity of the synthetic flux containing 3%  $\gamma$ -alumina. It illustrates (AB) the rise in deflection as the outer cylinder accelerates from rest to a constant speed of 38 r.p.m., the rapid thixotropic breakdown (BC), and the slow continuation of the breakdown (CD). DE was a rest period during which a substantial recovery of the high viscosity occurred. At E the motor was started again. The apparently greater decrease in viscosity along EF than along BC is due to the fact that the speed of the motor was initially somewhat higher (40 r.p.m.). This was adjusted to 38 r.p.m. and the final value of the viscosity at G approaches that at D.

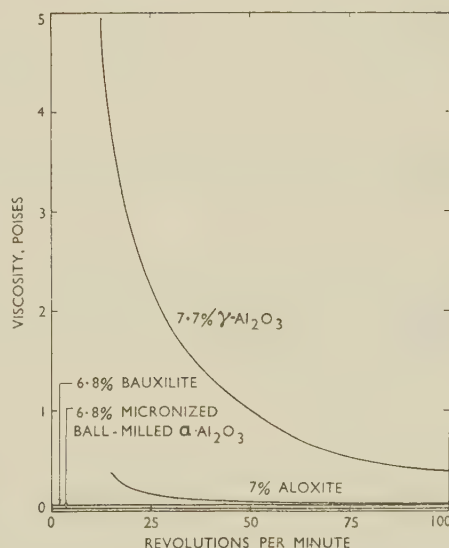


FIG. 7.—Variation of Viscosity with Rate of Shear for a Flux Containing Additions of Different Types of Alumina.

It must be noted that the measured values of viscosity all relate to specific shear rates and do not enable the viscosity of the fluxes when at rest to be deduced. Even at the lowest speeds attainable with the motor and gearing used, some breakdown of

the thixotropic structure in layers adjacent to the wall of the inner vessel is to be expected. This is a well-known limitation of the use of rotating-cylinder viscometers, or in fact of any viscometer, for the study of systems exhibiting anomalous viscosity. The viscosity of undisturbed samples of flux is probably very much greater than the values recorded. This is substantiated by the shape of the viscosity/rate-of-shear plots, which show viscosity increasing rapidly with decreasing rate at low rates of shear. This point has an important bearing on the recovery of metal to be expected on stirring the practical flux, and is discussed later.

An interesting feature of the viscosity measurements on the "slag out" flux was that a small ingot of aluminium was found at the bottom of the outer

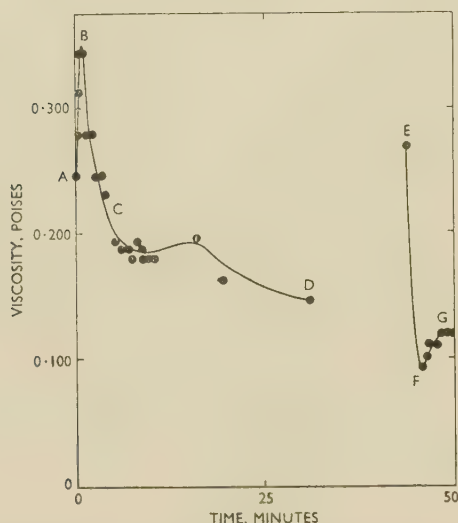


Fig. 8.—Variation of Viscosity with Time at Constant Rate of Shear for 3%  $\gamma$ -Alumina Flux. AD, 38 r.p.m.; DE, motor stopped; EF, 40–38 r.p.m.

cylinder after solidification, the mass being 4–4.5% of the total weight of charge (about 300 g.). The total proportion of aluminium contained in this flux was about 6.5% (Table I).

#### VIII.—SETTLING OF ALUMINIUM PARTICLES IN THE SYNTHETIC FLUX

A few experiments were made to determine the size ranges of aluminium particles which could be recovered by stirring to reduce the viscosity and permit the settling of the particles through the flux. The experiments were made with aluminium particles of known sizes mixed with pure 90:10 flux before melting. Additions of 5 and 10% of aluminium particles cut from  $\frac{1}{4}$ ,  $\frac{1}{8}$ ,  $\frac{1}{16}$ , and  $\frac{1}{32}$  in. wire and 36–60, 100–150, and <200 mesh aluminium powder were mixed with the 90:10 flux and the recoveries were

determined on heating to 900° C. with and without stirring.

The results are given in Table V. With 5% metal addition only  $\frac{1}{4}$ -in. particles were recovered without stirring. With 10% metal addition some recovery occurred without stirring of particles of sizes down to  $\frac{1}{32}$  in. For both 5 and 10% metal addition stirring produced a marked increase in recovery. No recovery was achieved for powder finer than 100 mesh. The striking nature of the results on the larger sizes is illustrated by Figs. 3 and 4 (Plate VIII). These illustrate a 10% addition of aluminium initially as  $\frac{1}{8}$ -in. dia. particles, melted without and with stirring,

TABLE V.—Percentage Recoveries Obtained on Aluminium Particles of Different Sizes, Melted in 90:10 NaCl-CaF<sub>2</sub> Flux at 850° C., With and Without Stirring.

Size of Aluminium Particle	Quantity of Aluminium and Treatment				Calculated Alumina Content, % of Flux for 10% Metal Addition
	5% Unstirred	5% Stirred	10% Unstirred	10% Stirred	
$\frac{1}{4}$ in. dia.	76	82.5	31.5	94	0.04
$\frac{1}{8}$ in. dia.	Nil	82	{ Nil 68	{ 93	0.08
$\frac{1}{16}$ in. dia.	Nil	78	{ 39.4 20.8	{ 92.5	0.16
$\frac{1}{32}$ in. dia.	...	82	{ 37.5 20.2	{ 94	0.32
36–60 mesh	...	25.5	{ Nil Nil	{ 80	1.0
100–150 mesh	Nil	...	Nil	Nil	2.5
<200	Nil	...	Nil	Nil	5.0

Unstirred—held molten for 1 hr. at 900° C.

Stirred—5 min. gentle stirring with a refractory rod halfway through holding period.

respectively. Only slight agglomeration occurred in the unstirred sample, but in the stirred sample the metal globules ran together to form one large lump of aluminium, and there was also a marked settling of alumina towards the bottom of the crucible.

#### IX.—DISCUSSION OF VISCOSITY MEASUREMENTS AND SETTLING EXPERIMENTS

The viscosity measurements can be used to predict the recovery of aluminium particles of various sizes to be expected on standing or on stirring. Fig. 9 gives the variation of the velocity of fall with the viscosity of the slag for various particle sizes. The terminal velocities of fall are all calculated from Stokes' law, assuming the density of the molten slag to be 2.00, the value for the "slag out" flux.

The horizontal lines correspond to rates of fall of 1 mm., 1 cm., and 10 cm./min., respectively. The experimental viscosity values for the various dispersions studied are also shown. It must be remembered that these values refer only to specific



rates of shear, and it is not possible to predict, from the measured values, the viscosity of the various dispersions when they are static. For this reason the information summarized in Fig. 9 does not enable any accurate deductions to be made about the settling of aluminium particles of various sizes in unstirred flux.

Reference will first be made to the experiments on the pure 90:10 NaCl-CaF<sub>2</sub> flux with additions of aluminium particles of various sizes. No deliberate addition of alumina was made to these fluxes, but alumina was, nevertheless, present because of the removal by the flux of the oxide film on the particles.

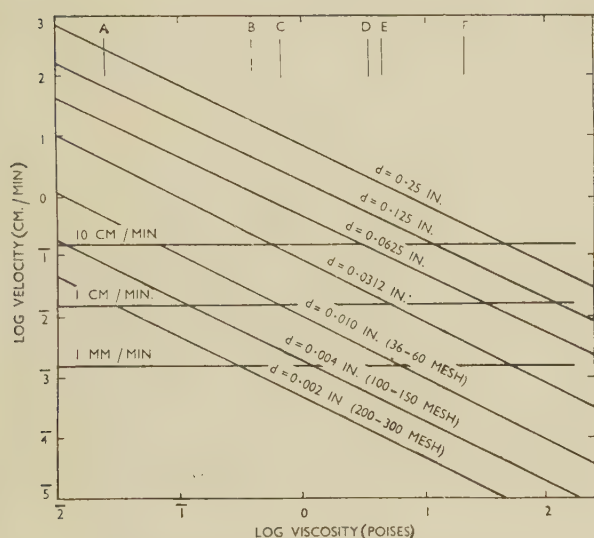


Fig. 9.—Variation of Rate of Fall of Aluminium Particles of Various Sizes with Viscosity of Suspension.

KEY.

- A, viscosity of 3%  $\gamma$ -alumina flux at 84 r.p.m.
- B, viscosity of 7.7%  $\gamma$ -alumina flux at 100 r.p.m.
- C, viscosity of 3%  $\gamma$ -alumina flux at 20 r.p.m.
- D, viscosity of "slag out" flux at 140 r.p.m.
- E, viscosity of 7.7%  $\gamma$ -alumina flux at 13 r.p.m.
- F, viscosity of "slag out" flux at 33 r.p.m.

The metal particles were mixed with the powdered flux in the crucible, which was then heated in a furnace. The aluminium thus had ample opportunity to oxidize before the temperature reached the melting point of the flux. An estimate can be made of the alumina content of the flux if the thickness of the oxide film is known. According to the authors' colleague, Mr. D. L. Levi,<sup>18</sup> the weight of oxide film formed in the first hour at 750° and 900° C. is  $0.5 \times 10^{-3}$  g./cm.<sup>2</sup> and  $3.0 \times 10^{-3}$  g./cm.<sup>2</sup>, respectively, in excess of the film formed at room temperature, which is negligible by comparison.

The alumina content of the flux calculated for a 10% metal addition is given in Table V. It will be seen that for particles down to  $\frac{1}{32}$  in. dia. this is small, but for powders 36-60 mesh and finer the consequent alumina additions are substantial. For particle

sizes of  $\frac{1}{4}$  to  $\frac{1}{32}$  in. dia. the viscosity may be taken as not very different from that of the pure flux. The predicted rates of fall in stirred or unstirred flux are, therefore, greater than 10 cm./min., and substantial recovery would be expected in both cases. For 36-60-mesh powder the alumina addition is approximately 1%. The unstirred viscosity is unpredictable, but it is reasonable to assume that it is at least 100 millipoises. This infers a rate of settling between 1 and 10 cm./min. In the stirred condition it may be assumed that the viscosity is reduced to a value approaching that for the pure flux, and a rate of fall greater than 10 cm./min. is predicted.

For suspensions of 100-mesh and finer powder the alumina additions amount to 2.5-5%, and appreciable quantities of aluminium are lost by oxidation before the flux melts. Unstirred values of viscosity will be higher than that shown in Fig. 9 for a 3%  $\gamma$ -alumina suspension stirred at 20 r.p.m. Settling rates will therefore be less than 1 mm./min., and no recovery is to be expected. On stirring, the viscosity of the suspension containing 100-150-mesh powder will approach that of the stirred 3%  $\gamma$ -alumina flux and a settling rate of about 5 cm./min. might be expected. The viscosity of the suspension of 200-300 mesh powder on stirring will not be much lower than the value shown for 7.7%  $\gamma$ -alumina, and the rates of fall will be less than 1 mm./min., so that no recovery would be expected. In practice, no recovery was achieved with either 100-150- or 200-300-mesh powders.

These predictions, moreover, ignore three considerations which militate against settling and agglomeration even when conditions appear to be favourable.

(1) The fluxed-off alumina films probably stay suspended in the flux close to the particles from which they are stripped, so that the particles move in a medium which has a much higher local concentration of alumina than the average content of the suspension.

(2) The effects of convection currents in the flux and of volatilization of sodium chloride from fairly small samples, which increases the effective alumina content, both reduce the predicted amount of settling.

(3) The calculations are based upon terminal velocities of fall, and with small depths of flux these are probably not attained.

For the "slag out" flux, the determined value of viscosity for a shear rate corresponding to 140 r.p.m. is 3600 millipoises. From Fig. 9 it will be seen that particles of sizes of  $\frac{1}{32}$  in. or greater would settle at rates greater than 1 cm./min. and should be recoverable on stirring. Table I shows that particles of this size range correspond to 3-10% by weight of the flux, i.e. about half the total aluminium content. Dilution with an equal quantity of salt would reduce the stirred viscosity to a value approximating to that of the suspension of 7.7%  $\gamma$ -alumina and settling of 36-60-mesh powder would be expected. This additional yield, however, represents only a very small weight increment, since the aluminium content in this size fraction is small (Table I). No large

difference in recovery between undiluted flux and flux diluted with an equal quantity of salt is, therefore, to be expected, and the recovery in both cases should be of the order of 3% of the weight of the flux.

Experimental agreement with these predictions is satisfactory. In small-scale stirring experiments, 2.5% aluminium was recovered from undiluted "slag out" flux and 3.5% from flux diluted with an equal quantity of salt. In larger-scale experiments on 5 lb. of flux, a recovery of 2.8% was obtained on dilution with an equal quantity of salt and 3.8% on dilution with only half this quantity. Allowing for some scatter from the average analyses of the flux, the recovery results are all grouped around 3%, in reasonable agreement with the predicted values.

Unfortunately, the present work does not suggest any means whereby the agglomeration and recovery of particles of aluminium of 100 mesh and finer, which account for the remaining half of the metal content of the practical flux, could be accomplished.

#### ACKNOWLEDGEMENTS

This investigation was sponsored at the Fulmer Research Institute by International Alloys, Ltd., Aylesbury, to whom the authors are indebted for permission to publish this account. They are particularly grateful to Dr. E. Scheuer (Head of International Alloys Laboratory), for his interest in the work and for many helpful suggestions, and to Dr. G. J. Thomas (Manager, Birmingham Branch), for assisting in the provision of samples of industrial flux. They also acknowledge advice and assistance in chemical analyses of flux samples from Dr. W. Stross of International Alloys, Ltd., and their colleague Mr. H. H. Smith.

#### REFERENCES

1. H. W. Gillett and G. M. James, *U.S. Bur. Mines Bull.*, 1916, (108).
2. C. S. Robison, U.S. Patent No. 1,180,435 (1916).
3. Chemische Fabrik Greisheim-Elektron and A. Beielstein, Brit. Patent No. 182,948 (1921).
4. A. Beielstein and Chemische Fabrik Greisheim-Elektron, Brit. Patent No. 219,287 (1923).
5. I.G. Farbenindustrie A.-G. and A. Beck, Brit. Patent No. 287,360 (1927).
6. R. J. Anderson, "Secondary Aluminium". Cleveland, O.: 1931 (Sherwood Press Inc.).
7. R. Irmann, *Giesserei*, 1937, **24**, 597.
8. L. Tronstad and J. H. Reimers, *Aluminium*, 1939, **21**, 834.
9. E. G. West, *Trans. Inst. Weld.*, 1940, **3**, 93.
10. E. G. West, *ibid.*, 1941, **4**, 50.
11. E. Feuer, *Metal Ind.*, 1942, **61**, 406.
12. O. Einerl and F. Neurath, *Chem. Age*, 1942, **46**, 181, 235.
13. W. Ehrenberg, *Z. anal. Chem.*, 1932-3, **91**, 1.
14. A. Einstein, *Ann. Physik*, 1906, **19**, 289; 1911, **34**, 591.
15. V. Vand, *Nature*, 1945, **155**, 364.
16. H. T. Greenaway, *J. Inst. Metals*, 1948, **74**, 133.
17. M. H. Jellinek and I. Fankuchen, *Indust. and Eng. Chem.*, 1945, **37**, 158.
18. D. L. Levi, unpublished information.

#### APPENDIX

##### *Factors Affecting the Accuracy of Viscosity Measurements in a Rotating-Cylinder Viscometer*

The well-known relationship between the viscosity  $\eta$  and the viscometer constants in a rotating-cylinder viscometer is:

$$\eta = \frac{\tau_1(R_2^2 - R_1^2)(\theta_1 - \theta_2)}{4\pi\Omega R_1^2 R_2^2 (l_2 - l_1)} \quad (1)$$

where  $\tau_1$  is the torsional rigidity of the suspension,  $\Omega$  the angular velocity of the outer cylinder,  $R_2$  the internal radius of the outer cylinder,  $R_1$  the external radius of the inner cylinder, and  $\theta_1$  and  $\theta_2$  the angular deflections of the suspension for depths of immersion  $l_1$  and  $l_2$  of the inner cylinder.

If  $(h_1 - h_2)$  is the difference between cathetometer readings of the height of a fixed mark on the suspension for the depths of immersion  $l_1$  and  $l_2$ , it can be shown that:

$$l_2 - l_1 = \frac{R_2^2(h_1 - h_2)}{(R_2^2 - R_1^2)} \quad (2)$$

Substituting in (1):

$$\eta = \frac{\tau_1(\theta_1 - \theta_2)(R_2^2 - R_1^2)^2}{4\pi\Omega R_1^2 R_2^4 (h_1 - h_2)} \quad (3)$$

$\tau_1$ ,  $\Omega$ ,  $R_1$ ,  $R_2$  and  $(h_1 - h_2)$  are readily and accurately determined, but the main source of experimental error lies in the determination of  $(\theta_1 - \theta_2)$ . Provided that the suspended system is critically damped and also very accurately centred, a perfectly stable reflected spot of light can be obtained and  $(\theta_1 - \theta_2)$  determined with considerable accuracy.

The condition for critical damping of the suspended system is:

$$\frac{\eta^2}{4IS^2} = \frac{360}{2} \tau_1, \text{ where } S = \frac{R_2^2 - R_1^2}{4\pi R_1^2 R_2^2 l},$$

$l$  being the depth of immersion and  $I$  the moment of inertia of the suspended system. The system is, therefore, critically damped for only a very limited range of values of  $\eta$ , and with the wide range of values of viscosity of the synthetic and practical fluxes a compromise has to be adopted. Values of the constants were selected which gave over-damping for the high values of  $\eta$  and under-damping for the majority of the readings at high shear rates. The continuous oscillation of the under-damped suspended system reduced considerably the accuracy of individual observations, but, by taking the mean of a number of values, consistent results were obtained. In addition to this source of inaccuracy, an additional source of error arose from the difficulty of accurately centring the inner cylinder at high temperatures.

In view of these factors it is considered that a better accuracy than  $\pm 50\%$  cannot be claimed for the viscosities obtained for the synthetic and practical fluxes, although the majority of the values may be expected to have errors of  $\pm 25\%$  or less. Fortunately, the variation of viscosity with alumina content is generally so great that probable errors even of this magnitude have little significance.



# CONSTITUTION OF THE COPPER-RICH COPPER-ALUMINIUM-GERMANIUM ALLOYS\*

1496

By PROFESSOR G. V. RAYNOR,† M.A., D.Sc., VICE-PRESIDENT,  
and P. GREENFIELD,‡ Ph.D., B.Sc., STUDENT MEMBER

## SYNOPSIS

The constitution of the copper-rich alloys of the system copper-aluminium-germanium has been examined by metallographic and X-ray methods at 700°, 600°, and 550° C. At 700° and 600° C., the solubilities of aluminium in the close-packed hexagonal copper-germanium  $\zeta$  phase, and of germanium in the body-centred cubic copper-aluminium  $\beta$  phase are considerable, and the homogeneous  $\zeta$  and  $\beta$  areas in the isothermal diagrams are separated by a comparatively narrow two-phase region. At 550° C., the  $\beta$  phase is no longer stable, and the copper-rich solid solution ( $\alpha$ ) enters into equilibrium with  $\zeta$  and the copper-aluminium  $\gamma_2$  phase. In spite of this, however, the range of compositions over which  $\zeta$  is stable remains almost unchanged from that at 600° C. At all three temperatures the  $\alpha$  solid-solubility isothermal is slightly convex in the direction of increasing solute concentration. The results of the investigation are discussed, with particular reference to the comparison with previously established constitutional diagrams for alloys of a similar type.

## I.—INTRODUCTION

THE constitution of copper-rich alloys of the system copper-zinc-germanium has already been reported.<sup>1</sup> For comparison with the results of this work, a similar examination has been made of the system copper-aluminium-germanium, and the results are reported in the present paper. Since the aims of the work, the techniques employed, and the general metallographic characteristics of the alloys were identical with those discussed in the earlier paper, it is not considered necessary to repeat this information.

Experimental work on a ternary system involves an accurate knowledge of the three binary systems involved. Details of the copper-germanium system have already been summarized,<sup>1</sup> while the most probable equilibrium diagram for the copper-aluminium alloys has been presented as an Annotated Equilibrium Diagram,<sup>2</sup> to which reference should be made. The aluminium-germanium system has been examined by Stöhr and Klemm;<sup>3</sup> it is of the simple eutectiferous type, with limited mutual solid solubilities of the components in each other. Since no stable intermediate phases are formed, the system is of little importance to the present work.

Isothermal diagrams for temperatures of 700°, 600°, and 550° C. have been established by micrographic and X-ray examination of a large number of alloys, prepared from the copper and germanium used in the earlier work<sup>1</sup> and super-pure aluminium (99.997%) supplied by The British Aluminium Co., Ltd. Most of the alloys were chemically analysed after examination, either in the authors' laboratory or by Messrs. Johnson, Matthey and Co., Ltd.; the analytical totals of the three components were satis-

factory (99.96–100.06%), and since the specimens included several which had been remelted with copper additions to conserve germanium, it may be concluded that no significant contamination occurred during repeated remeltings. Results from the two laboratories agreed excellently.

The results are best presented as isothermal diagrams, involving the ternary  $\alpha$  solid solution, the  $\beta$  and  $\gamma_2$  phases of the copper-aluminium system, and the  $\zeta$  and  $\epsilon$  or  $\epsilon_1$  phases of the copper-germanium system. Individual alloys are referred to in terms of their atomic percentages of aluminium and germanium; thus the symbol 1.98/13.85 denotes an alloy containing 1.98 at.-% aluminium and 13.85 at.-% germanium.

## II.—EXPERIMENTAL RESULTS

### 1. THE 700° C. ISOTHERMAL

Fig. 1, in which unanalysed alloys are distinguished by vertical bars, shows the constitutions of the copper-rich alloys at 700° C. The chill-cast specimens were annealed for a minimum of four days and quenched; the usual tests of further annealing and examination were applied to ensure equilibrium. The  $\alpha$  solid-solubility isothermal is adequately defined, and is slightly convex in the direction of higher solute concentration. There is no observable discontinuity at the junction of the  $\alpha/(\alpha + \beta)$  and  $\alpha/(\alpha + \zeta)$  branches. The outstanding features of the diagram are the marked extension of the copper-germanium  $\zeta$  phase into the ternary system, and the considerable homogeneity range of the ternary  $\beta$  phase. The  $\zeta$  phase dissolves a maximum of 15.4 at.-% aluminium

\* Manuscript received 4 May 1953.

† Professor of Metal Physics, University of Birmingham.

‡ Research Associate, University of Illinois, Urbana, Ill., U.S.A.; formerly, Research Student, University of Birmingham.

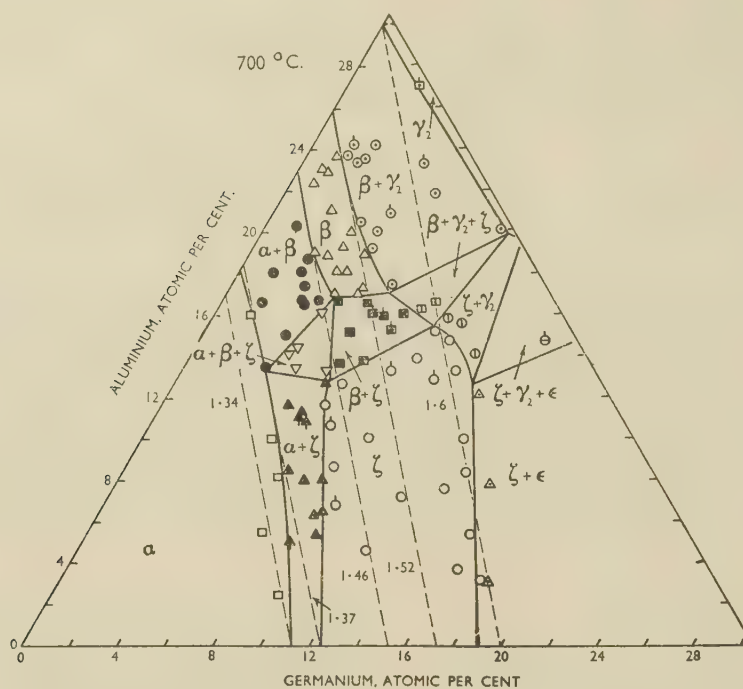


FIG. 1.—The 700° C. Isothermal. The fine broken lines represent constant electron : atom ratios.

KEY TO FIGS. 1-3.

$\alpha$   $\square$ ;  $\beta$   $\triangle$ ;  $\zeta$   $\circ$ ;  $\gamma_2$   $\square$ ;  $\alpha + \beta$   $\bullet$ ;  $\alpha + \zeta$   $\blacktriangle$ ;  $\beta + \zeta$   $\blacksquare$ ;  $\beta + \gamma_2$   $\odot$ ;  $\zeta + \gamma_2$   $\oplus$ ;  $\alpha + \gamma_2$   $\nabla$ ;  $\zeta + \epsilon(\epsilon_1)$   $\triangle$ ;  $\alpha + \beta + \zeta$   $\nabla$ ;  $\beta + \zeta + \gamma_2$   $\square$ ;  $\alpha + \zeta + \gamma_2$   $\nabla$ ;  $\zeta + \gamma_2 + \epsilon(\epsilon_1)$   $\ominus$ . Unanalysed alloys distinguished by vertical bars.

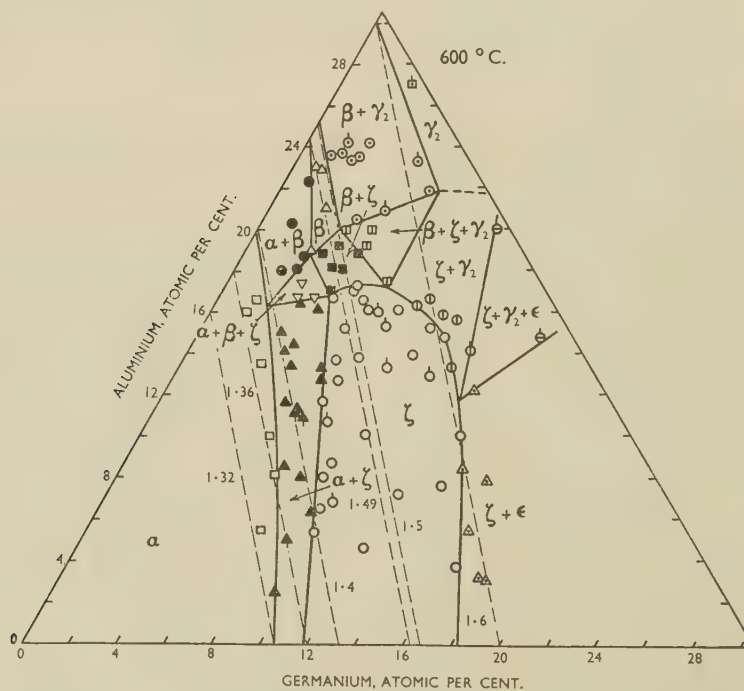


FIG. 2.—The 600° C. Isothermal. The fine broken lines represent constant electron : atom ratios. Key as for Fig. 1.



without losing its close-packed hexagonal structure; at this limit the germanium content is only 9.4 at.-%. The  $\beta$  phase dissolves a maximum of 6.7 at.-% germanium. The phase boundaries which define the homogeneous  $\beta$  and  $\zeta$  areas are well established, and it may be noted that the boundaries of the ( $\zeta + \beta$ ) and ( $\alpha + \zeta + \beta$ ) regions cannot be moved appreciably from their positions in Fig. 1 without violating the results obtained in adjacent phase fields.

The form of the solute-rich boundary of the  $\zeta$  phase is of interest. Taking into account the relative amounts of phases in the ( $\zeta + \epsilon$ ) alloys, the  $\zeta/(\zeta + \epsilon)$  branch cannot deviate appreciably from a straight

but that of germanium in copper falls from 11.2 to 10.7 at.-%. Consequently the  $\alpha$  boundary in the ternary system pivots about the approximate composition 4/9, but is still almost a straight line joining the two binary limits. Though the boundary is less well established than at 700°C., the results suggest a slight convexity in the same sense.

The  $\zeta$  phase projects much further into the ternary diagram than at 700°C., and its aluminium-rich limit is represented by the composition 17.3/5.5; the hexagonal structure thus persists until the phase contains more than three times as many aluminium atoms as germanium atoms. It may be noted that

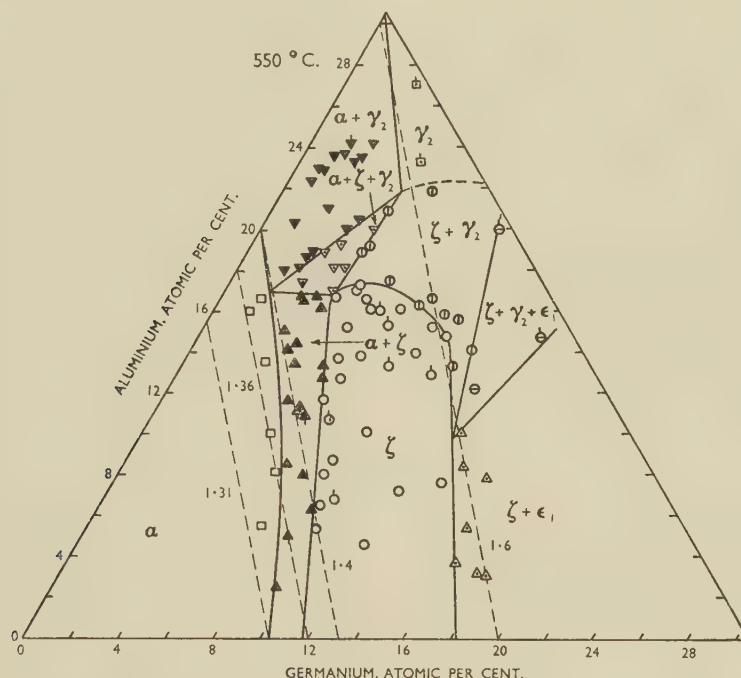


Fig. 3.—The 550° C. Isothermal. The fine broken lines represent constant electron : atom ratios. Key as for Fig. 1.

line. At aluminium contents exceeding 12.5 at.-%, however,  $\zeta$  enters into equilibrium with the copper-aluminium  $\gamma_2$  phase, which must therefore have a considerable homogeneity range in the ternary system. The boundary between the  $\zeta$  and ( $\zeta + \gamma_2$ ) fields bends sharply round towards lower germanium contents.

The phase fields shown in Fig. 1 have all been confirmed by X-ray analysis of filings prepared from the annealed alloys.

## 2. THE 600° C. ISOTHERMAL

Alloys already annealed to equilibrium at 700°C. were re-annealed for a minimum of five days at 600°C. These specimens were examined, with the results shown in Fig. 2. The general form of Fig. 1 is maintained, but differences in detail exist. On cooling from 700° to 600°C., the solid-solubility limit of aluminium in copper rises from 18.2 to 19.9 at.-%,

all the ( $\alpha + \zeta + \beta$ ) and ( $\zeta + \beta$ ) alloys of the 700°C. isothermal become ( $\alpha + \zeta$ ) or  $\zeta$  at 600°C. In contrast, the  $\beta$  field narrows considerably, as expected from the existence of the eutectoid reaction  $\beta \rightleftharpoons \alpha + \gamma_2$  in the copper-aluminium system. A maximum of 3.5 at.-% germanium is dissolved at 600°C.

The solute-rich boundary of the  $\zeta$  phase again shows a marked curvature when  $\zeta$  enters into equilibrium with  $\gamma_2$ ; the  $\zeta/(\zeta + \gamma_2)$  boundary is more extensive at 600°C. than at the higher temperature. The solute-rich alloys plotted in Fig. 2 suggest that the solubility of germanium in the copper-aluminium  $\gamma_2$  phase is smaller than at 700°C.

The phase fields plotted were again confirmed by X-ray methods.

## 3. THE 550° C. ISOTHERMAL

Since the eutectoid decomposition of the copper-aluminium  $\beta$  phase occurs at 565°C., this phase does

not appear at 550° C. Some alloys which had been quenched from 600° C. were re-annealed at 550° C., but it was found that the martensitic decomposition of  $\beta$  on quenching from 600° C. resulted in the  $(\alpha + \gamma_2)$  structure produced at 550° C. taking the form of a very intimate mixture of the two phases in which the acicular appearance of the decomposition structure was maintained. This caused difficulty in interpretation, so that the procedure adopted was to re-anneal alloys quenched from 600° at 700° C. for 24 hr. before cooling them slowly to 550° C., at which temperature they were held for a minimum of six days. This treatment was given to all alloys represented in Fig. 3, which shows the 550° C. isothermal. The primary solid-solubility isothermal changes very little from that at 600° C., and is again slightly convex in the direction of increasing solute concentration. It is of great interest to note that the  $\zeta$  phase area also remains almost unchanged in passing from 600° to 550° C., in spite of the disappearance of the  $\beta$  phase. The substitution of an  $(\alpha + \zeta + \gamma_2)$  field in place of the  $(\alpha + \zeta + \beta)$ ,  $(\zeta + \beta)$ , and  $(\zeta + \beta + \gamma_2)$  fields which occur at 600° C. is accompanied by an enlarged  $(\zeta + \gamma_2)$  field, and, as at higher temperatures, the  $\zeta/(\zeta + \gamma_2)$  boundary is markedly curved. At 550° C., the  $\zeta$  phase is no longer in equilibrium with  $\epsilon$ , but with the  $\epsilon_1$  phase of the copper-germanium system. The  $\zeta/(\zeta + \epsilon_1)$  boundary lies slightly to the copper-rich side of the  $\zeta/(\zeta + \epsilon)$  boundary at 600° C., but the difference is small.

### III.—DISCUSSION

It is of interest to compare the results described above with those for the copper-zinc-germanium alloys, and for other recently investigated alloys of a similar type.<sup>4, 5</sup>

#### 1. THE PRIMARY SOLID-SOLUBILITY ISOTHERMALS

In the system copper-zinc-germanium the  $\alpha$  solubility boundaries at 600° and 550° C. are convex towards the copper-rich corner of the isothermal diagrams. The curvature shown in Figs. 1, 2, and 3 is slight, but in the opposite sense. For the zinc-bearing alloys, the curvature was interpreted in terms of the increase both in the total lattice distortion and in the number of centres of distortion when zinc replaces germanium at the solid-solubility limit of the latter, and the introduction of a number of centres of intense distortion in the already severely strained lattice at the copper-zinc solubility limit when zinc is replaced by germanium. In the copper-aluminium-germanium system, both solutes again expand the lattice of copper, and again it is to be expected that the electron:atom ratio will tend to remain approximately constant along the solid-solubility isothermal. When, therefore, aluminium replaces germanium in the saturated solution in copper of the latter, three aluminium atoms replace

two of germanium; since the distortion of the copper lattice produced by one atom of aluminium is approximately 0.7 of that produced by one atom of germanium, the total lattice distortion is increased only very slightly, if at all. The solid solution of germanium in copper is relatively dilute, and the number of centres of distortion correspondingly small; this number is increased somewhat by replacing germanium by aluminium, but, since the total distortion is almost unchanged, the general result is to distribute the strain to be accommodated more evenly through the lattice. It is thus possible to understand how an increase in the ternary solid-solubility limit may be produced, and we may contrast the case where zinc is substituted for germanium; three atoms of zinc replace one of germanium, and since the distortions produced in copper by equal atomic percentages of zinc and germanium are in the approximate ratio 0.6:1, the increase in total distortion is much more serious, leading to a decrease in solubility.

Similar arguments indicate that the total distortion decreases considerably when germanium replaces zinc at the solubility limit of the latter in copper, and remains almost unchanged when germanium is substituted for aluminium at the corresponding limit. The solute concentration in the latter case is, however, only half that attained at the solubility limit of zinc in copper, and the distortion of the copper lattice at saturation is only 1.36% for aluminium as solute, as opposed to 2.47% for zinc. The intense local distortions in the region of the introduced germanium atoms will therefore be more easily accommodated when these atoms replace aluminium than when they replace zinc in the already highly distorted copper-zinc saturated solid solution, and any tendency towards a solubility decrease will be considerably reduced in the copper-aluminium-germanium system. The difference between the forms of the solid-solubility isothermals in the two cases may therefore be understood in terms of the relative valencies of the solute metals, and the extent to which they distort the copper lattice.

It would be expected that the precise form of the primary solid-solubility isothermals would depend upon the nature of the phases with which the solid solution enters into equilibrium. If the equilibrium changes from  $(\alpha + 3/2 \text{ electron compound})$  to  $(\alpha + \text{normal valency compound})$ , marked discontinuities in the  $\alpha$  boundary may occur.<sup>5</sup> If, however, the primary solid solution is in equilibrium with  $3/2$  electron compounds over the whole length of the boundary, there is little or no discontinuity where the equilibrium changes. This is illustrated in Figs. 1 and 2 of the present paper, while Fig. 3 shows that there can be little change of direction on passing from the  $(\alpha + \zeta)$  to the  $(\alpha + \gamma_2)$  branch of the  $\alpha$  boundary. Where equilibrium with  $3/2$  electron compounds is involved, evidence at present available suggests that the influence of lattice-distortion effects on the  $\alpha$  boundary greatly outweighs that of factors connected with the second phase.



## 2. THE 3/2 ELECTRON COMPOUNDS

The work described in the present paper shows that the close-packed hexagonal  $\zeta$  phase of the copper-germanium system projects considerably into the ternary model, even when it is no longer in equilibrium with  $\beta$ , which, at the appropriate temperatures, also projects appreciably into the ternary model. As previously suggested,<sup>1,4</sup> the  $\zeta$  phase in a ternary system of this type would be expected to persist from low negative size-factors to an effective size-factor of approximately +2,\* while the  $\beta$  phase (body-centred cubic) would not be expected to persist below a positive effective size-factor of approximately +3. It is of interest to compare the effective size-factors at the solubility limits of zinc and aluminium in  $\zeta_{\text{Cu-Ge}}$ , and of germanium in  $\beta_{\text{Cu-Zn}}$  and  $\beta_{\text{Cu-Al}}$ . These values are given in Table I; the size-factors in the systems Cu-Ge, Cu-Zn, and Cu-Al are, respectively, -4.15, +4.23, and +6.62, the last value being based on an atomic diameter of 2.71 Å. for aluminium, as generally assumed for structures in which no overlap occurs from the first Brillouin zone.

TABLE I.—Effective Size-Factors at Limits of Stability.

Phase	Temp., °C.	System Cu-Zn-Ge		System Cu-Al-Ge	
		Solute-rich limit	Cu-rich limit	Solute-rich limit	Cu-rich limit.
$\zeta$	700	...	...	+2.5	+3.0
	600	...	...	+3.4	+4.2
	550	+0.6	+1.6	+0.9	+4.2
	400	+0.9	+1.6	...	...
$\beta$	700	...	...	+3.7	+4.4
	600	...	...	+5.0	+5.1
	550	+2.8	+3.38	...	...
	400	+2.8	+2.9	...	...

The figures in Table I are in good qualitative agreement with the suggestion that the extent of the projection of a 3/2 electron compound into the body of a ternary model is governed by the effective size-factor, in such a way that the ranges of effective size-factors over which the close-packed hexagonal and body-centred cubic phases are stable are closely similar to the ranges of size-factor over which the same structures exist in binary copper or silver alloys. It may be noted that, especially at the lower temperatures, the  $\zeta$  phase in the copper-aluminium-germanium system extends slightly further into the ternary model than would be expected from comparison with the copper-zinc-germanium system. In terms of atomic percentages the difference between the observed and expected homogeneity ranges is small, and is probably to be interpreted in terms of the effect of solute valency on the structure of 3/2 electron compounds. It is known that decreasing

solute valency favours the cubic structure;<sup>6</sup> dilution of the  $\zeta$  copper-germanium phase with two-valent zinc will therefore tend to bring about a breakdown of the hexagonal structure at an earlier stage than in the case of dilution with aluminium, which is three-valent. Hence, the ternary  $\zeta$  phase containing aluminium atoms may be expected to persist to an effective size-factor higher than that in the copper-zinc-germanium system, as observed. This interpretation implies that the  $\beta$  phase in the copper-zinc-germanium system should persist to lower effective size-factors than in the copper-aluminium-germanium system, which again is observed.

The data for this and other systems support the general hypothesis that a qualitative guide to the extent of the projection of a 3/2 electron compound into the body of a ternary isothermal diagram may be obtained by considering the effective size-factor variations in the ternary system, in conjunction with the relationship between structure, size-factor, and valency in the relevant binary alloys.

## 3. THE RELATIONSHIP OF PHASE BOUNDARIES TO ELECTRON : ATOM RATIOS

For the copper-zinc-germanium alloys, it was found that there was no tendency for the ternary isothermal boundaries to follow lines of constant electron:atom ratio, or to approximate to the electron:atom ratios characteristic of the corresponding limits of homogeneity in the binary systems. In Figs. 1, 2, and 3, the relationship between phase boundaries and electron:atom ratios in the copper-aluminium-germanium alloys is summarized; the fine broken lines represent electron:atom ratios as indicated. Fig. 1 is analogous to the corresponding diagram for copper-zinc-germanium alloys at 550° C.; the most significant feature is the general movement of the phase boundaries of the  $\zeta$  and  $\beta$  phases to higher electron:atom ratios than those characteristic of the corresponding homogeneity ranges in the binary systems, as the effective size-factor decreases numerically. This is entirely consistent with the behaviour exhibited by binary 3/2 electron compounds, the homogeneity ranges of which are shifted to higher electron:atom ratios as the numerical magnitude of the size-factor decreases. At 600° C., the main features of Fig. 1 are reproduced, except that the  $\beta$  phase area tends to move towards lower electron:atom ratios; the  $\beta/(\beta + \gamma_2)$  boundary in this case does approximate to a constant electron:atom ratio of 1.50. Fig. 3 indicates that the electron:atom ratios associated with the  $\zeta$  phase are almost unaffected by the disappearance of the  $\beta$  phase, and the general movement to higher electron:atom ratios as aluminium replaces germanium is maintained.

The maximum electron:atom ratios attained at the solute-rich boundaries of the 3/2 electron com-

\* The effective size-factor is defined as  $(xF_B + yF_G)/(x + y)$  for a system ABC, in which the atomic percentages of B and

C are, respectively,  $x$  and  $y$ ;  $F_B$  and  $F_G$  are the size-factors of B and C with respect to A.

pounds are very similar in both the copper-zinc-germanium and copper-aluminium-germanium systems; the appropriate values are given in Table II.

TABLE II.—*Maximum Electron : Atom Ratios of 3/2 Electron Compounds.*

Temp., °C.	System Cu-Zn-Ge	System Cu-Al-Ge
700	...	1.63
600	...	1.61
550	1.63	1.61
400	1.59	...

As would be expected from the behaviour of binary 3/2 electron compounds, these maximum values occur at very low, or zero, effective size-factors. It may be noted that, in the copper-aluminium-germanium system, the maximum electron:atom ratio at which the  $\zeta$  phase exists exceeds the minimum electron:atom ratio for the  $\gamma_2$  phase in the copper-aluminium system. It is doubtful whether this could be attributed to any factor other than the lowering of the effective size-factor on adding

aluminium to the copper-germanium system, or germanium to the copper-aluminium system.

#### ACKNOWLEDGEMENTS

This research was carried out in the Metallurgy Department of the University of Birmingham, and forms part of a programme which has received the generous support of the Department of Scientific and Industrial Research, the Royal Society, the Chemical Society, and Imperial Chemical Industries, Ltd. The authors gratefully acknowledge this assistance.

#### REFERENCES

1. P. Greenfield and G. V. Raynor, *J. Inst. Metals*, 1951-52, **80**, 375.
2. G. V. Raynor, *Inst. Metals Annotated Equilib. Diagr. Series*, 1944, (4).
3. H. Stöhr and W. Klemm, *Z. anorg. Chem.*, 1939, **241**, 305.
4. G. V. Raynor and B. R. T. Frost, *J. Inst. Metals*, 1949, **75**, 777.
5. B. R. T. Frost and G. V. Raynor, *Proc. Roy. Soc.*, 1950, [A], **203**, 132.
6. W. Hume-Rothery, P. W. Reynolds, and G. V. Raynor, *J. Inst. Metals*, 1940, **66**, 191.



# SOME OBSERVATIONS ON THE MECHANISM OF PITTING CORROSION \*

1497

By R. MAY,† A.R.S.M., MEMBER

(Communication from the British Non-Ferrous Metals Research Association.)

## SYNOPSIS

The mechanism of pitting attack on copper is discussed, and the factors which lead to the formation of pits are outlined. The conditions necessary for the maintenance of an active pit are then described in more detail, with particular reference to the circumstances in which abnormally rapid pitting, such as occasionally occurs in service, can develop. It is shown that the nature of the corrosion products formed is of prime importance, and the controlling factors at different stages are discussed. The effects of water movement and of traces of accelerating agents, such as organic sulphur compounds, are mentioned. The construction and operation of a reproducible and active "artificial pit" are described, such cells providing a useful tool in the study of the mechanism of pitting.

## I.—INTRODUCTION

A METHOD sometimes applied in the laboratory investigation of corrosion problems is to set up a suitably arranged cell with electrodes of the metal concerned immersed in the appropriate electrolyte, and to observe the current and voltage changes when the factors relating to the particular problem are varied experimentally. The method yields much information, but it has often proved difficult to start cells intended to simulate the localized types of corrosion or pitting, and they may fail to remain in the desired state of activity long enough to form a reliable basis for experimental work. The present paper is concerned with attempts to make cells or "artificial pits" which reproduce the essential features of pitting reactions in copper and are sufficiently stable for use as a laboratory test, suitable, for example, for comparing the corrosiveness of different waters and for experimental study of factors which control or prevent pitting.

The emphasis was concentrated chiefly upon what happens when a pit reaches the active stages of its development and less upon the conditions which cause its natural start, since it is the slow and uncertain early stages which have to be by-passed if an artificial pit is to be of use as a laboratory test. The conditions at different stages of activity were observed mainly by the dissection and microchemical examination of numerous pits encountered in practical investigations and in laboratory tests, and it emerged that the increase in rate of growth which some pits undergo after an indefinite period of slow development coincided with well-defined changes in the character of the corrosion products formed inside the pit, and in some cases, with the disappearance

of features known to be essential during the early stages. The observations suggested that some of the difficulties in obtaining rapid pits experimentally might be due to maintaining the starting conditions too rigidly, on the assumption that they were equally necessary in the rapid stages. This conclusion made it possible to set up artificial pits with copper electrodes in which the slow early stages are eliminated, so that a high rate is attained in a short time and can be kept up indefinitely. Some of the properties and uses of such artificial pits are briefly described.

At the present stage it cannot be claimed that the detailed mechanism of pitting is clear in all circumstances. This applies particularly to pitting in the more concentrated chloride solutions, such as seawater. However, the fact that rapid artificial pits can be made to start and continue working in more dilute chloride solutions, indicates the correctness of some of the deductions regarding the mechanism by which the pitting of copper develops beyond the initial stages.

## II.—FACTORS INVOLVED IN THE START AND ACCELERATION OF PITTING

The essential principle involved in starting a cell which simulates a corrosion pit has been known ever since U. R. Evans demonstrated that pitting depended fundamentally upon differences of oxygen distribution, and that a pit could be started on a metallic surface at a point where the oxygen concentration was kept below that at the surrounding areas. As is well known, the effect can be shown by means of a very simple cell with two electrodes of the same metal, one of them being screened from the free access of oxygen, e.g. under a deposit of sand. Immediately

\* Manuscript received 21 March 1953. The work described in this paper was made available to members of the B.N.F.M.R.A. in a confidential research report issued in

September 1952.

† Corrosion Adviser, British Non-Ferrous Metals Research Association, London.

after such a cell is set up, some of the dissolved oxygen in the liquid at the surfaces of both electrodes is consumed by the initial reaction, and its renewal by diffusion and convection is hindered in the case of the screened electrode, which then becomes the anode and undergoes corrosion. The other electrode, to which dissolved oxygen has access, becomes covered with some kind of protective film of corrosion products which ennobles the surface so that it functions as the cathode, the dissolved oxygen acting as the depolarizer. The ennoblement due to this cathodic film is a most important feature of the pitting process.

If the cell is kept short-circuited, the current gradually rises to a more or less steady value, which, in most cases, corresponds to a rather low rate of pitting. In this state the cell readily shows the effects of experimental changes, and much has been learnt about the factors which stimulate or retard pitting from experiments with such cells. However, experimental factors may affect slow and fast pits in different ways, and it is clearly desirable that fast pits should be studied.

The much higher rates sometimes observed in practice may develop naturally in laboratory tests, but it is more usual to find that when attempts are made to hurry through the slow initial stages the cell becomes stifled or polarized before the rapid rate is attained. It is of some importance to note that this uncertain behaviour of a laboratory corrosion cell or "artificial pit" is not inconsistent with that of actual pits under practical conditions; examination of failed samples often shows that, in the same environment, for each rapid pit there are many more which have become stifled or have remained at a low level of activity. Obviously this uncertainty of behaviour is of great importance in corrosion testing, and it is essential that its causes should be recognized; otherwise attempts to remove it may easily introduce conditions not found in practice.

From the wide differences of rate observed in a common environment, it has long been recognized that pitting must in some respects (or at certain stages) be a cumulative action, the working of the pit itself tending to produce conditions which stimulate its greater activity. Two factors of undoubted importance in the early stages are the using up of oxygen diffusing towards the anode by reaction with corrosion products diffusing away from it, and the deposition of solid corrosion products to give more effective screening of the anodic areas. However, the anode potential built up cumulatively by these conditions necessarily approaches a limit, mainly determined by factors such as the chlorine-ion concentration at the anode surface and the solubility of the anodic corrosion products; consequently, as this limit is approached, any further increase of rate becomes increasingly dependent upon a reduction of internal resistance and a rising efficiency of cathode depolarization, both of which can become cumulative, as described below, and may permit the development of very high rates.

Although features in the development of pits are common to many metals and alloys, the present paper is almost entirely confined to the narrow field of copper in dilute chloride solutions. As indicated in the introduction, the work has not yet been extended satisfactorily to include solutions of higher chloride content. However, the field covered is of much practical interest, since nearly all public supply waters contain chlorides, and in all cases so far examined in which such waters have caused pitting of copper pipes, there has been evidence that chlorides were involved in the pitting reactions.

### III.—THE PITTING OF COPPER IN WATERS CONTAINING CHLORIDES

#### 1. INITIAL STAGES OF PIT FORMATION

When a clean copper surface is exposed to a sufficiently corrosive water containing dissolved

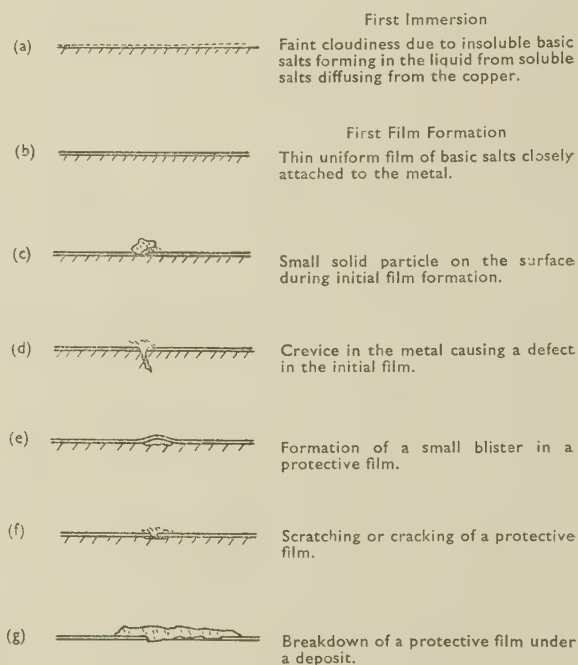


FIG. 1.—The Development of Pits. Factors which start the first local attack.

oxygen, such as sea-water or diluted sea-water, there is for a brief period a rapid and uniform formation of soluble copper corrosion products, and the visible conversion of some of these to insoluble basic salts which appear as a cloudiness in the layer of liquid on the surface of the copper (Fig. 1 (a)). The initial rate falls rapidly, and the basic salts, instead of continuing to appear in the layer of liquid, are formed on the metal surface as a visible film which becomes increasingly protective and reduces the rate of attack (Fig. 1 (b)).



Later stages of film formation can follow two alternative courses:

(i) The initial film of basic salts continues to thicken and becomes a protective film of a kind not commonly associated with pitting.

(ii) A layer of cuprous oxide appears under the initial film and replaces it, gradually becoming a comparatively thick and often non-uniform oxide scale, which is much more cathodic and therefore favourable to pitting at any local defect which may be formed.

In the less-corrosive waters, which may nevertheless be capable of supporting pitting, these stages cannot be observed unless the specimen is dried, the first change seen generally being the formation of a film consisting largely of cuprous oxide.

Local inequalities in the rate of attack, which may develop into pitting, may be initiated even at an early stage by a solid particle or deposit on the surface (Fig. 1 (c)), by a crevice in the metal (Fig. 1 (d)), by blistering (Fig. 1 (e)) or mechanical damage to the protective film (Fig. (f)), or by deposits of various kinds (Fig. 1 (g)). The essential feature in each case is that a small pocket of liquid is held in contact with a small area of metal where film formation is incomplete. The building up of a protective film on the metal inside such a pocket can proceed only if dissolved oxygen can diffuse in rapidly enough to replace that used up in the formation of insoluble basic salts close to the corroding surface. A slightly lower rate of oxygen diffusion means that soluble copper salts diffuse from the surface and basic salts are formed in the liquid, so that film-formation slows down and the oxygen concentration inside the pocket falls. Film formation on the areas of copper surrounding the pocket, at which the oxygen concentration is high, then takes the lead, and these areas eventually become sufficiently ennobled to act as cathodes, while the copper inside the pocket, exposed to a lower oxygen concentration, is still in an incompletely protected condition and can act as the anode. In other words, an oxygen concentration-cell has been started, and can develop into a more or less active pit as discussed below.

## 2. THE DEVELOPMENT OF PITS

Although they may differ in the way in which they are initiated and in the details of development, over a wide range of chloride content of the water, including that of sea-water, active pits in copper and copper alloys have certain features in common which must be taken into account in discussing their mechanism. These are:

(a) The presence of porous, crystalline cuprous chloride in varying amounts next to the metal at the anodic areas. The actual amount does not seem to be of direct importance; highly active pits are found with little cuprous chloride on the anode surface,

whereas others, equally active, may be nearly filled. There is some indication that waters with a high sodium chloride content, e.g. sea-water, tend to produce pits with less solid cuprous chloride and vice versa, but this is by no means an invariable rule. Irrespective of the amount, the cuprous chloride in active pits is invariably porous or has the appearance of a compact layer which has become broken up.

(b) The presence of crystalline cuprous oxide in varying amounts on top of the cuprous chloride inside the pit or as a deposit at the entrance, and often as a compact layer in direct contact with the metal at cathodic areas. As cuprous oxide is readily produced by the hydrolysis of cuprous chloride, it would be expected to appear at some point in the pit in which this salt is being formed at the anode. There is little doubt that much of the porous crystalline cuprous oxide often found in pits is produced in this way. The origin of the compact, strongly adherent cuprous oxide layers sometimes found on the metal at cathodic areas is less obvious. In a few cases its formation has been observed at small cathodic areas which became abnormally active, apparently owing to some depolarizing action of copper corrosion products diffusing from the nearby anode; this matter is referred to later. Alternatively, Campbell<sup>1</sup> has shown that copper pipes sometimes bear a highly cathodic cuprous oxide scale produced during manufacture, and that this can be the cause of rapid pitting. Carbonaceous films sometimes formed during manufacture can have a similar effect.

Active pits with these common features may develop in a variety of forms, some examples of which are sketched in Fig. 2.

The changes of shape which pits undergo during development give an indication of changes in the local rates of anodic attack within the pit, and microscopic examination of the corrosion products and their distribution can give information on the reactions which have been in progress at different points. Examination from the outside of pits in action usually shows little more than the growth and perhaps the cracking of a mound of corrosion products over the pit, but in some very rapid pits this mound breaks up and exposes an open network of crystals. By using a microscope with a water-immersion objective, it is sometimes possible to see small portions of the anode surface between the crystals and to watch the growth of cuprous chloride crystals upon it. Some metals, including various copper alloys but not copper itself, may show a deep and narrow type of pit (Fig. 2 (a)), in which practically the whole of the attack is clearly concentrated at the deepest part, with little or no attack on the walls, and the depth soon becomes many times greater than the diameter. With such pits the rate of penetration can become very rapid; rates of 1 mm. in 20 days and occasionally even up to 1 mm. in 5 days have been observed in flowing aerated sea-water containing organic sulphur compounds. In the case of copper, such narrow pits have never been observed; the pits become wider as

well as deeper, and the highest rate of attack seems to be associated with a roughly hemispherical shape (Fig. 2 (b)-(j)). Rates of penetration of up to 1 mm. in about 50 days are observed in sea-water, and the same rate may at times be reached in the corrosive fresh waters. Pits are often of larger diameter in the interior than at the entrance (Fig. 2 (f)-(j)), and in extreme cases this may be associated with the undermining of a strong cathodic scale so that a large pit can develop and remain roofed over with scale containing a single small hole corresponding to the initial pit.

It is sometimes difficult to believe that either in the deep narrow pit or in the scale-covered pit the

#### IV.—THE CONDITIONS IN PITS AT DIFFERENT STAGES OF ACTIVITY

Assuming that a pit has started and that the corrosion current leaving the anode flows out through the mouth of the pit to cathode areas upon which a suitable film or scale is present, where depolarization by oxygen takes place, then at all stages essential factors to be considered include: (i) the migration of chloride ions into the pit to take part in the anode reaction, (ii) the diffusion of oxygen into the pit at a rate controlled by the screen of solid corrosion products deposited at the entrance, and (iii) the diffusion of soluble cupric chloride out of the pit.

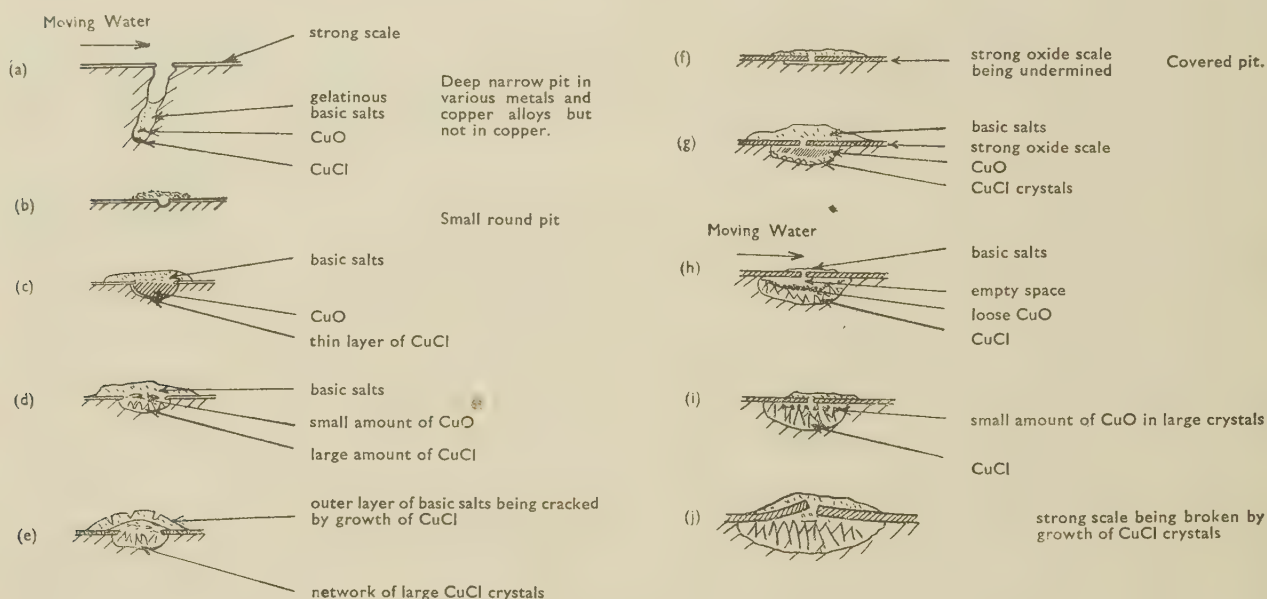


FIG. 2 (a-j).—Ways in Which Pits Develop.

corrosion current leaving the anode necessarily flows entirely to the external cathodic areas. It may be surmised that when such a pit is at its most active stage part of the current flows to cathodic areas on the walls of the pit nearer the entrance, or to the underside of the scale in the case of the covered pit just described.

The depolarization of such small internal cathodes must be extremely active, and it is highly probable that the corrosion products diffusing from the anode play an important part, possibly that of oxygen carriers, in the reaction between cathodic hydrogen and the dissolved oxygen diffusing from outside the pit.\*

#### 1. EARLY STAGES OF PIT DEVELOPMENT

In the early stages, when the rate is low, the primary corrosion product, cuprous chloride, formed at the anode diffuses from the anode surface in dilute solution and at some point reacts with the inward-diffusing oxygen to form cuprous oxide, insoluble basic salts, and soluble cupric chloride. If the screening is insufficient, so that oxygen diffuses in too readily, the cuprous chloride is oxidized and cupric chloride is formed too close to the anode, and the activity of the pit is kept low by any cupric chloride or oxygen which diffuses to the anode surface itself. The deposition of the insoluble products from the

\* In this connection appearances suggest that dezincification of brass can be regarded as an extreme example of pitting in which a high proportion of the corrosion current flows to cathodic areas inside the pit, cathodic depolarization in this case taking place by deposition of spongy copper from the copper salts produced by corrosion at the adjacent anodic

areas. The energy needed to supply the losses presumably comes from corrosion of the zinc in the brass, with a corresponding amount of cathodic depolarization by oxygen at some point nearer the entrance of the pit, or at the external surface.



oxidation and hydrolysis of cuprous chloride gradually makes the screening more effective; the concentration of cupric chloride able to reach the anode is thus reduced and the pit gradually becomes more active. Thus, in the early stages, the rate is very closely dependent upon the effectiveness of the screen in hindering the diffusion of oxygen into the pit and towards the anode areas, and the effectiveness of the screen is itself dependent upon corrosion products formed gradually as the attack proceeds. Consequently, the early development of a pit tends to be a slow process, becoming more and more rapid as favourable conditions are established.

## 2. LATER STAGES OF PITTING

In pits which have attained a higher rate, the anode surface is usually seen to be covered with a porous layer of crystalline cuprous chloride. This salt is sparingly soluble in fresh water or dilute chloride solutions. Hence it is to be expected that, after a pit has become sufficiently active to maintain a saturated solution of cuprous chloride at the anode, the metal-ion concentration at the anode and the back-e.m.f. due to it cannot increase further, and the pit ought not to become polarized on this account, however great the rate of attack. Any higher degree of activity, producing cuprous chloride more rapidly than it can diffuse away in solution, must lead to its deposition at the anode in the solid state. There is little doubt that the outward diffusion of cuprous chloride in solution from the anode is a most important factor in maintaining rapid pitting, since by reacting with the oxygen diffusing into the pit it can maintain the oxygen concentration at the anode at the lowest possible value. Thus, when the rate has increased beyond a certain point, pitting may reach a stage at which the exclusion of oxygen from the anodic areas becomes much less dependent upon the presence of a screen or obstruction of solid substances. In these circumstances, the whole of the inward-diffusing oxygen would be used up by the outward-diffusing cuprous chloride well clear of the anode, so that only a small concentration of cupric chloride, representing the last of the oxygen, could reach the anode surface. A pit could not reach this stage by natural means without an oxygen screen to enable it to pass through the slow earlier stages.

The stage at which cuprous chloride is formed at the anode more rapidly than it can diffuse away in solution, so that it appears in the solid state, is highly critical. In some pits, particularly those in which too much cupric chloride diffuses to the anode, the cuprous chloride rapidly forms a compact layer with a high electrical resistance, and such pits remain almost stifled for long periods. In others, the cuprous chloride appears in a fairly dense but porous form, under which some attack continues, and later at intervals causes the layer to crack, with corresponding temporary increases in corrosion rate. In still others, the cuprous chloride first appears as

coarse crystals growing from a comparatively small number of points on the anode surface. The spaces between the crystals remain open, and much of the growth appears to take place from below, the crystals being pushed outwards with sufficient force to deform and crack the outer layer of basic salts, &c. This often breaks up the original screening layer upon which the earlier development of the pit depended, and the solid substances in the pit then become remarkably open in structure and the rate may become very high.

Some important consequences also follow from the outward movement of solid cuprous chloride; in particular the zone in which the last of the inward-diffusing oxygen reacts with the saturated cuprous chloride is kept at a distance from the anode surface, so that the possibility of cupric chloride formed by the reaction diffusing to the anode surface is further lessened; the rate of attack becomes more firmly established and the pit more stable.

## 3. THE CONTROLLING FACTORS AT DIFFERENT STAGES OF PITTING

The factors controlling pitting at different stages may be summarized as follows: (i) In the slow stages cathode depolarization by dissolved oxygen is usually more than adequate, so that anodic polarization and the internal resistance are the controlling factors, and it is the gradual reduction of these which permits the rate to increase. (ii) The early increments of rate react cumulatively in the way described, gradually producing conditions of constant e.m.f. at the anode; when this point is reached a further increase of rate can come only from a reduction of the resistance of the cell and by depolarization of the cathode. Some pits become resistance-controlled at this point by the deposition of impervious cuprous chloride on the anode and are practically stifled. Those which proceed to the higher rates associated with the formation of cuprous chloride in a highly porous state must come increasingly under cathodic control.

It is significant that the highest rates of pitting observed (in copper alloys but not in copper) in practice or in the laboratory, have occurred only when there was impingement of rapidly moving aerated water on the cathodic areas very close to the pit. Earlier experiments, also with copper alloys, have shown that in these circumstances the cathodic area can be made quite small before the rate is much reduced, indicating the high efficiency of cathodic depolarization under these conditions. The possibility that the outward-diffusing soluble copper salts assist in such cathode depolarization has been mentioned and requires further study.

For the development of rapid pitting of copper in nearly stagnant conditions, on the other hand, cathode areas have to be a good deal larger, and this is possibly the chief reason why large rapid pits in a pipe tend to be widely separated, and are sometimes found distributed at curiously regular intervals along the

pipe. There may be many smaller pits in the spaces between the larger ones, but all in a more or less stifled condition. A possible explanation is that, in a given area, the large pit happened to be that which reached the critical stage first and by its rapid increase of rate partially polarized the available cathode area, so that other pits sharing the same area were hampered in their further development by a permanent reduction in the available e.m.f.

## V.—INFLUENCE OF WATER MOVEMENT AND ACCELERATING AGENTS

In the foregoing discussion of the salient features of pitting, little has been said about the influence of rate of water movement and the effects of accelerating agents. This is because it was desired to avoid over-emphasizing factors which may be necessary to maintain the very highest rates of pitting, but are not essential for the important increase of rate at the conclusion of the primary stages of development.

### 1. THE RELATIONSHIP BETWEEN PITTING AND IMPINGEMENT ATTACK

At one time, repeated failure to obtain artificial pits with rates approaching those commonly observed in practice, together with many observations of rapid pitting associated with moving water, created the impression that pitting in stagnant conditions was necessarily a slow process and that water movement was essential before the rate could increase. The present view is that water movement is better considered as an important accelerating factor. It is not a controlling factor where the primary increase of rate is concerned, because this increase can take place quite well under stagnant conditions, but further increases necessarily demand more effective cathodic depolarization, and in cases where the available cathode area is being used to its limit under stagnant conditions, movement of the water is a means by which such depolarization can be effected. In the case of copper the issue can be greatly confused by the ease with which the metal undergoes impingement attack when exposed to rapidly moving water, sea-water in particular. It is, in fact, common to find some pits in which breaking of the screening layer of basic salts has enabled moving water to sweep away the comparatively loose cuprous oxide and remove the porous cuprous chloride. If this does not take place too rapidly, there may be time for an impervious film of solid cuprous chloride to form on the anode and become oxidized to a protective layer of basic salts, so that attack stops. More often, the removal is rapid and continuous, so that cuprous chloride can be present only as a film of dilute solution which is continually being carried away by movement of the water and renewed by corrosion of the anode. In these circumstances the back-e.m.f. due to the concentration

of copper ions at the anode can be very low, depolarization of the nearby cathode areas by oxygen in the moving water continues as before, and attack can remain rapid but without any visible formation of corrosion products at the anode. This is the main characteristic of impingement attack (see Fig. 3 (a)), which in copper can occur in the absence of entrained air bubbles. The characteristic of alloys which are more resistant than copper to impingement attack is that the solid film upon which resistance depends is stronger than that which tends to form upon copper. It thus requires a more vigorous and continuous mechanical action, e.g. the impingement and collapse of air bubbles, to hinder its development. This difference between pitting and impingement

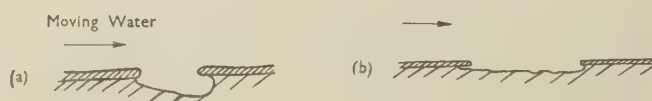


FIG. 3.—Pit with Shape Changed by Impingement Attack.

attack is well known, and is described in some detail because of the insight it gives into the relationship between the two important corrosion processes. The change can also take place in the reverse direction during a period of slow water movement, but it takes much longer for the conditions needed for pitting corrosion to become re-established. The change from impingement attack to pitting is also complicated by the rapid alteration in the shape of the cavity while impingement attack is in progress. With copper the tendency is for the original, approximately hemispherical pit to widen much more rapidly than it deepens, so that it becomes a large shallow depression (Fig. 3 (b)), and if pitting starts up again the whole process has to be repeated, from perhaps only a few points on the attacked area.

### 2. THE EFFECT OF ACCELERATING AGENTS

Similar considerations account for the omission of specific reference to the part played by traces of accelerating agents, mainly organic sulphur compounds, which may be present in some waters as a result of biochemical processes. The very highest rates of concentrated pitting, occasionally observed with copper alloys but never with copper, can probably occur only when such agents are present and when there is vigorous impingement of aerated water as well. The latter condition favours the change to impingement attack discussed above, so that in this case also copper may be saved from very rapid pitting by the development of large shallow areas of impingement attack. From this point of view it might be inferred that the highest rates of pitting would be found among alloys which resist impingement attack, as is indeed the case. This does not mean that such alloys have a low resistance to pitting; resistance may be good except when the alloy encounters an unusual combination of harmful



factors and then pitting is intense. The explanation is connected with the fact that resistance to impingement attack demands that the alloy should form a mechanically strong protective film but that such films tend to be rather highly cathodic. This, while promoting rapid healing if the film is damaged under normal conditions, can also promote rapid highly localized corrosion if some abnormal factor is present which either interferes with the healing process or makes the film abnormally cathodic, or both. Organic accelerating agents are factors of this kind, but their exact mode of action has not yet been decided. This is one of the problems awaiting the development of a suitable type of artificial pit for its investigation.

In the case of copper, the first effect of accelerating agents is greatly to increase the number of small pits which start and which remain in a moderately active state, and these seem to develop uniformly until sometimes most of the surface is covered with shallow pits. However, the early stages of pitting and the increase of rate following them can be obtained quite well in waters in which the presence of organic accelerating agents is most unlikely, so that they cannot be regarded as essential controlling factors so far as the basic pitting reactions are concerned.

## VI.—REPRODUCIBLE, ACTIVE ARTIFICIAL PITS

### 1. CONDITIONS NECESSARY FOR RAPID PITTING

These may be summarized as follows:

(i) An adequately depolarized cathodic area, e.g. an area of copper on which a suitable scale is present, to which oxygen in solution has access. When pitting is rapid, cathode depolarization tends to become the main controlling factor.

(ii) Formation of cuprous chloride at the anode more rapidly than it can diffuse away in solution.

(iii) Deposition of the excess of cuprous chloride in the solid state close to the anode in a form which does not stifle the pit, so that while the pit is in action there is an outward movement of solid cuprous chloride from its zone of formation to the zone where it is oxidized nearer the entrance.

(iv) The presence of no more screening between the solid cuprous chloride and the outside of the pit than is necessary to stop convection in the liquid and to give a suitable rate of diffusion.

Even when all these conditions are attained, the resistance of the cell remains to limit the rate. The resistance at the anode is an important part of this, depending greatly on the way in which the cuprous chloride is deposited. A compact layer on the anode surface gives a resistance of perhaps 100,000 ohms, whereas an open honeycomb structure of coarse crystals may give a resistance of only a few thousand ohms. Such low values are associated with the highest observed rates of pitting. As already indicated, the establishment of the highest rates

depends on the breaking up of the screening layer of insoluble basic salts, &c., at the entrance of the pit by the growth of cuprous chloride crystals in the pit, and it is surmised that the maintenance of these rates depends on the continuous formation of cuprous chloride sufficiently rapidly to balance the increased rate of oxygen diffusion. This means that when a critical rate of pitting is exceeded the cuprous chloride is formed quickly enough to establish a diffusion zone where the oxygen, diffusing rapidly into the entrance because of the breaking up of the screen of solid materials, is equally rapidly used up by the cuprous chloride. This condition tends to be unstable, since any momentary fall in the rate of attack at the anode, such as might follow varying cathode depolarization, allows oxygen to diffuse deeper, so that cupric chloride is produced further in and some of it readily diffuses to the anode zone because of the open condition of the cuprous chloride network in pits of this kind. The fall in the rate thus tends to become cumulative, so that the pit may be anodically polarized. It is probably because of their instability, and the critical nature of the conditions required, that pits of the most rapid type are rare in practice. Those with somewhat lower rates are correspondingly more stable and are much more common. In such pits there is no need for such a low resistance, and a certain amount of screening is essential, the required degree of porosity being produced and maintained by cracking of the screening layer rather than by its complete break-up.

### 2. EARLY ATTEMPTS TO PRODUCE ARTIFICIAL PITS

These considerations make it clear why early attempts to produce artificial pits were unsuccessful, and what lines should be adopted for a fresh attack on this problem.

In original experiments the artificial pit usually consisted essentially of two electrodes of copper, or copper alloy, one inside some sort of small compartment into which cuprous chloride could be introduced and covered by a porous screen, and the other, intended to form the cathode, freely exposed. Both were immersed in a vessel of the water in which the pit was to be started. Arrangements were made for measuring the current, the potential of the electrodes, and the open-circuit e.m.f. of the cell. If the enclosed electrode was simply covered with sand or other screen, low rates of attack slowly developed, sometimes to the stage at which solid cuprous chloride could be recognized under the sand; but all attempts to eliminate the very slow early stages by introducing cuprous chloride were unsuccessful. The cuprous chloride was introduced as a freshly washed suspension in a saturated solution (necessarily containing the equilibrium concentration of cupric chloride and hydrochloric acid), precautions being taken against oxidation and exposure to light. Apparently because of the initial higher concentration of copper ions,

the enclosed electrode or "pit" usually became cathodic instead of anodic. If the two electrodes were connected together in this condition, the cell supplied a current in the wrong direction until the supply of chloride had been used up by oxidation, by deposition of copper, and by losses by diffusion. Meanwhile the external electrode, intended as cathode, acted as anode and was correspondingly corroded. If, on the other hand, the electrodes were not connected together, the concentration of cupric chloride was reduced by reaction with the copper electrode (provided there was a screen of some sort to hinder the access of oxygen) and the enclosed electrode became anodic, but on connecting the electrodes the cell failed to supply any appreciable current because the anode had become covered with a high-resistance layer of cuprous chloride.

### 3. NEW METHOD OF ESTABLISHING ARTIFICIAL PITS

In the earlier attempts, partial success was achieved if a cathode of a more noble metal was used. This led to a consideration of the possibility of ensuring that the first formation of cuprous chloride took place electrolytically at the correct current density as calculated from the observed rates of typical pits. It was hoped that this might yield cuprous chloride in crystals of the same type as those formed in pits, instead of the impervious layer produced by reaction between the copper and the excess cupric chloride. This simply meant passing the appropriate current from an external source in the required direction, i.e. connecting the intended anode to the positive pole, immediately after adding the solid cuprous chloride to the anode compartment. To avoid disturbing the conditions at the cathode, an auxiliary cathode was used to carry the starting current, although it was later found that this was not essential unless the cathode processes were to be investigated. Provided that the resistance of the cell is not too high (e.g. owing to an unsuitable screening layer) and that the cathode has a suitable film and is adequately depolarized, the e.m.f. across the cell, which at first opposes the external source, gradually falls to zero and then builds up in the opposite direction, assisting the external source. The cell can now be short-circuited and the external source disconnected and the current will continue to flow at an anodic current density comparable with that in an active natural pit functioning in the same water.

Development was carried out with cells of various designs. Experiment was needed to establish suitable conditions of screening and size of cathode, for instance, and it was during this work that observations were made leading to some of the conclusions and surmises embodied in the foregoing discussion.

In considering the practical details of these experiments, it seemed obvious that the critical conditions of diffusion and movement of the corrosion products associated with the correct working of a pit would be

easier to establish if the anode compartment, and in particular the area of the anode, were made of about the same size as in an actual pit. The same conclusion had been reached in connection with the earlier work on impingement attack; in that case it was much easier to obtain uniform conditions by using a very small surface for the anode.

As many highly active pits have anodic areas as small as 1 mm.<sup>2</sup>, it was convenient to make electrodes for the experimental cell of high-conductivity copper wire passing through narrow glass tubes, held together and sealed with "Okerin" wax. Some of these cells were made using 28-S.W.G. wire with 1 mm. length exposed to form an electrode surface with an area of about 2 mm.<sup>2</sup>. A convenient design is shown in Fig. 4. This is for a cell with two

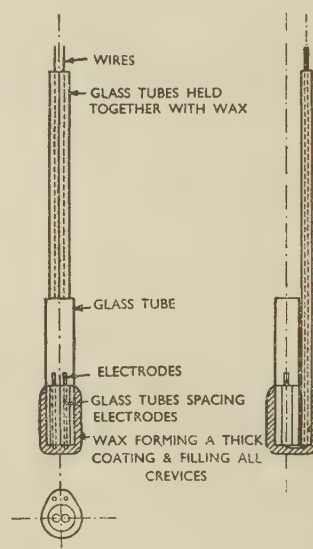


Fig. 4.—Anode Compartment of Corrosion Cell. Approx. natural size.

electrodes side by side in the anode compartment. One of the electrodes can be used as the cathode for the starting current, so that the excess concentration of copper ions due to the presence of cupric chloride in the pit can be rapidly reduced by the deposition of metallic copper with the formation of the equivalent amount of cuprous chloride at the anode. Thereafter, the auxiliary cathode can be left disconnected and is available as a reference electrode for measuring the resistance of the cell and the extent of polarization at the working anode. The working cathode of the cell, representing the external cathodic area associated with an actual pit, is made of a suitable length of 18-S.W.G. wire, coiled if necessary, upon which a film has been allowed to form by immersion during the period while the anode of the cell is being started by means of the auxiliary cathode, or it may be formed by a wire which has had a longer previous immersion in the same water.

In starting this type of cell it does not seem to be necessary to take extreme precautions in preparing



the cuprous chloride to be used. Rapid washing by decantation, using dilute hydrochloric acid followed by freshly boiled distilled water, has given satisfactory results. After washing, the cuprous chloride is allowed to settle, and a small portion is taken up in a narrow glass tube used as a pipette and is transferred to the anode compartment, previously filled completely with freshly boiled distilled water. This is a simple operation which involves lowering the pipette vertically on to the top of the anode compartment, when the cuprous chloride, which has already settled to the lower end of the pipette, at once settles further through the water in the anode compartment.

To provide a screening layer it has been found convenient to use about  $\frac{1}{4}$ -in. thickness of acid-washed Kieselguhr (from which the fines have been discarded) on top of the cuprous chloride. This is transferred to the anode compartment in exactly the same way. These operations should not be carried out in bright sunlight, and as soon as they are completed the electrode assembly should be placed in the vessel of water to be used. This is kept in the dark throughout the experiment. A large test-tube about 1 in. in dia., surrounded with a tube of black paper, has been found convenient. The potential of the electrodes may then be measured if required, after which the starting current is passed without delay.

Experiments with a cell of this type having an anode area of 2 mm.<sup>2</sup>, using distilled water, with an external cathode on which an oxidized film had been previously formed, showed that before passing the starting current, the intended anode was 23 mV. cathodic to the external oxidized electrode. A starting current of 2 microamp., applied by way of the auxiliary electrode, raised this potential to 75 mV. while the current was flowing, corresponding to a resistance at the anode of 26,000 ohms. The potential gradually fell, as did also the open-circuit e.m.f. to the external electrode when the starting current was interrupted. The open-circuit e.m.f. became zero at about 65 hr. from the start, at which point the potential drop with 2 microamp. flowing was 45 mV., corresponding to a resistance at the anode of about 22,500 ohms. At about 90 hr. from the start the open-circuit e.m.f. was 10 mV. in the reverse direction, i.e., the cuprous-chloride-covered electrode was now anodic to the external cathode and the potential drop with 2 microamp. flowing was 40 mV., corresponding to a resistance at the anode of 25,000 ohms.

In order to find what current the anode was capable of carrying without polarization, the starting current was reduced gradually until the potential drop remained steady at zero. This occurred with a current of about 0.5 microamp., from which it was concluded that if short-circuited at this stage the cell would have acted correctly as a pit generating a current of this value, provided cathode depolarization was adequate. However, it was noticed that the open-circuit e.m.f. of the cell had increased as a

result of the lower current, and it was thought advisable to find if there was an optimum value for the starting current giving the highest e.m.f. on open circuit. Over several days the current was limited to various values between 0.1 and 0.5 microamp., and it was found that the highest value of the open-circuit e.m.f., 66 mV., was obtained after passing a current of 0.3 microamp., but the resistance at the anode rose to 66,000 ohms.

At this stage the starting current was discontinued and the anode connected to the working cathode through a low-resistance microammeter. The current now supplied by the cell was at first 0.7 microamp., falling in a few hours to 0.5 microamp. The cell having started in distilled water contaminated with atmospheric carbon dioxide and a little chloride diffusing from the anode compartment, it was of interest to find how it behaved in a water known to produce pitting. With this object the liquid was changed to a mixture of 1 part sea-water and 9 parts distilled water. The current at once increased to 1.0 microamp. and after a short time reached about 1.5 microamp., becoming sensitive to the slightest movement of the cathode. Moderate stirring around the cathode raised the current to 2.3 microamp. The cell was allowed to stand short-circuited and continued to supply a current of 1.6–1.0 microamp. for about 9 months, falling to 0.5 microamp. after 14 months.

The maximum rate, calculated from the anodic current density when the current was 2.3 microamp., represents a rate of penetration of approximately 1 mm. in 160 days. This may be compared with the observed rate of natural pits in rapidly moving sea-water of 1 mm. in about 60 days.

In further experiments with similar cells it was found that they could be transferred to diluted sea-water for periods of up to an hour and that, on replacing the diluted sea-water by distilled water, they rapidly resumed their original distilled-water rate.

The experiments thus showed that a cell started with distilled water in the way described could be brought to a relatively stable state of activity in the medium in which it was started. Moreover, the electrode assembly could be transferred to a more corrosive liquid and would not only continue active over a long period, but would indicate by its greater activity the more corrosive nature of the new medium. Further, cells could be transferred for short periods to a more corrosive medium and would resume a lower rate when transferred back to distilled water.

It appeared that such a cell might form a valuable test for the rapid and direct demonstration of whether or not a given water would support pitting corrosion. This problem existed in the Association's investigation of pitting corrosion of copper pipes in domestic cold-water supply systems. These investigations indicated that certain waters are capable of supporting pitting because of the absence of an inhibitor present in waters which do not cause pitting. It was found that waters thought to contain inhibitor stopped the

working of the cell in a few minutes and that the action started up again in waters from which inhibitor was thought to be absent.

At this stage, further work on the starting of artificial pits became part of the investigation of pitting in supply waters. In this work, it was found that a pit can often be started without using an external source of current, provided that the cuprous chloride is prepared by first dissolving it in strong hydrochloric acid and re-precipitating by dilution with de-aerated distilled water. The earlier work had always used A.R. cuprous chloride freshly washed with dilute hydrochloric acid but not re-precipitated. Similar precautions as regards washing and exposure to light and oxidation were observed in each case, and it would appear that re-precipitation gives the correct form of crystal which can act as a nucleus and prevent the deposition of the fine-grained resistant layer on the anode.

It also appeared possible that artificial pits would assist in the study of factors accelerating pitting

corrosion in sea-water. Attempts to start a pit directly in sea-water have so far been unsuccessful, but the results obtained have indicated the extreme importance of the cathodic processes and suggested reasons for the formation of internal cathodes and, consequently, of deep narrow pits. For instance, pits started in distilled water should continue to work when transferred to sea-water, and so provide a basis for further study in this field.

#### ACKNOWLEDGEMENT

The author is indebted to the Director and Council of The British Non-Ferrous Metals Research Association for permission to publish this paper.

---

#### REFERENCE

1. H. S. Campbell, *J. Inst. Metals*, 1950, **77**, 345.



# THE EFFECT OF IRON, MANGANESE, AND CHROMIUM ON THE PROPERTIES IN SHEET FORM OF ALUMINIUM ALLOYS CONTAINING 0.7% MAGNESIUM AND 1.0% SILICON \*

1498

By R. CHADWICK,† M.A., F.I.M., MEMBER, N. B. MUIR,‡ B.Sc., A.I.M., MEMBER, and H. B. GRAINGER,‡ B.Sc., A.I.M., MEMBER

## SYNOPSIS

As part of a systematic investigation of alloys hardened by magnesium silicide precipitation, the effects of 0.0-0.4% iron and 0.0-0.6% manganese or chromium have been assessed in materials of constant magnesium and silicon content.

The alloys were hot and cold rolled to sheet; after solution heat-treatment and room-temperature ageing the properties varied only slightly with composition, strengthening being brought about by all three alloying additions. After subsequent artificial ageing at 160° C., alloys free from manganese or chromium were brittle and exhibited intercrystalline fracture in tension. Alloys containing manganese or chromium were both stronger and more ductile, fractures being mainly transcrystalline. Corrosion-resistance was high in the room-temperature-aged materials, but susceptibility to intercrystalline attack was induced by artificial ageing.

Micrographic studies were particularly concerned with precipitation occurring at different stages in processing and heat-treatment. By analogy with existing equilibrium data in related systems, the probable identities of the precipitate phases, and their significance in relation to the properties of the alloys, are discussed.

## I.—INTRODUCTION

WROUGHT heat-treatable aluminium alloys in which age-hardening is associated with the precipitation of magnesium silicide have assumed considerable importance as structural materials, and a comprehensive investigation has been undertaken into the effect of composition and heat-treatment on the constitution and properties of the materials broadly covered by British Standard 1470/HS10 and related specifications. The present paper is concerned with alloys containing 0.7% magnesium and 1.0% silicon with varying amounts of iron, manganese, and chromium.

The first important investigation of the aluminium-magnesium-silicon alloys was made by Hanson and Gayler,<sup>1</sup> who suggested that age-hardening could be simply considered in terms of the quasi-binary system Al-Mg<sub>2</sub>Si, the maximum solid solubility of Mg<sub>2</sub>Si being about 1.65% at 590° C. and diminishing rapidly with falling temperature. A more detailed investigation of quasi-binary alloys by Dix *et al.* followed.<sup>2</sup> There have been several later investigations of the ternary equilibrium and of the properties of cast and wrought ternary and more complex alloys in which magnesium silicide precipitation

occurs, and it has been established that age-hardening behaviour is more complicated than the simple quasi-binary picture would indicate. Thus, Phillips<sup>3</sup> showed that at equilibrium in alloys containing magnesium and silicon in the proportions necessary to form Mg<sub>2</sub>Si, some of the magnesium is in solid solution in the aluminium, while silicon is present as a separate phase. Since, moreover, magnesium in solid solution reduces the maximum solubility of magnesium silicide at the temperature of solution heat-treatment, and consequently diminishes age-hardening potentialities,<sup>1,3,4</sup> it is necessary to have excess of silicon to obtain the highest tensile properties.<sup>5</sup>

Manganese and chromium are both added to commercial alloys to increase strength,<sup>6</sup> but the effect of these elements has not been investigated in detail. Iron is generally regarded as having only a slight influence on strength, although there is some evidence that it affects corrosion-resistance adversely.<sup>7</sup>

## II.—MATERIALS INVESTIGATED

Three series of alloys were prepared. The first made from high-purity aluminium, was iron-free; the second, made from commercial aluminium, con-

\* Manuscript received 14 May 1953.

† Assistant Research Manager, Imperial Chemical Industries, Ltd., Metals Division, Birmingham.

‡ Technical Officer, Imperial Chemical Industries, Ltd., Metals Division, Birmingham.

tained about 0.2% iron as impurity, while the third had a further amount of added iron. About 0.7% high-purity magnesium was added to all the alloys, and silicon was adjusted according to the amounts already present as impurity, to give a total content of 1%. Manganese or chromium was introduced

TABLE I.—*Composition of the Alloys.*

Nominal Composition, %			Actual Composition, %				
Fe	Mn	Cr	Mg	Si	Fe	Mn	Cr
...	...	...	0.77	1.09	0.03	...	...
...	0.2	...	0.71	0.95	0.04	0.20	...
...	0.4	...	0.72	0.89	0.03	0.40	...
...	0.6	...	0.74	1.06	0.03	0.60	...
...	...	0.2	0.82	0.98	0.04	...	0.20
...	...	0.4	0.81	0.95	0.05	...	0.40
...	...	0.6	0.86	0.99	0.08	...	0.55
0.2	...	...	0.76	1.07	0.20	...	...
0.2	0.2	...	0.67	0.94	0.13	0.19	...
0.2	0.4	...	0.74	0.95	0.24	0.40	...
0.2	0.6	...	0.72	0.89	0.24	0.58	...
0.2	...	0.2	0.81	1.07	0.19	...	0.21
0.2	...	0.4	0.79	0.92	0.20	...	0.38
0.2	...	0.6	0.77	1.05	0.21	...	0.59
0.35	...	...	0.74	1.14	0.32	...	...
0.35	0.2	...	0.74	0.97	0.34	0.20	...
0.35	0.4	...	0.70	0.87	0.40	0.40	...
0.35	0.6	...	0.75	1.10	0.34	0.60	...
0.35	...	0.2	0.86	1.12	0.36	...	0.20
0.35	...	0.4	0.80	1.11	0.33	...	0.42
0.35	...	0.6	0.81	1.13	0.35	...	0.58

The following impurity limits were established by spectrographic examination: Ti 0.01–0.015%, Zn <0.02%, Cu <0.03%.

in the form of commercial hardeners. The compositions of the alloys as determined by chemical and spectrographic analyses are given in Table I.

### III.—PREPARATION AND HEAT-TREATMENT OF ALLOYS

Charges of 4 kg. each were melted in a gas-fired furnace, degassed at 750° C. by injecting a vigorous stream of chlorine gas, cooled to 700° C., and cast by the Durville method into a cast-iron mould of  $4\frac{1}{2} \times 1\frac{1}{4}$  in. section. Pieces from the gate ends of the castings were retained for chemical analysis, micro-examination, and heat-treatment experiments; the remainder was hot and cold rolled to strip. Preheating was carried out at 500° C., and the slabs were rolled across their length to strip 8 in. wide  $\times$  0.25 in. thick. After pickling in caustic soda solution, washing, and drying, the strips were annealed for 2 hr. at 400° C. in a forced-circulation air furnace, cold rolled to 0.1 in., re-annealed, and finally cold rolled to 0.050 in., all rolling being in the one direction.

Optimum temperatures of solution heat-treatment and ageing were established on individual representative alloys by means of hardness measurements. Differences in response were slight, and all were therefore given the same solution-treatment of  $\frac{1}{2}$  hr. at 540° C., with subsequent ageing at 160° C. for 18 hr. or at room temperature. Solution heat-treatment was carried out in a nitrate salt bath, and artificial ageing in a forced-circulation air furnace.

### IV.—MICROSTRUCTURE

Microsections were prepared from alloys in the cast state and at various stages in fabrication. A mixed acid etch (Keller's reagent) was used to study the changes brought about by thermal treatments and to identify the phases present. Boiling 1% caustic soda solution was used to a limited extent on the wrought alloys to reveal grain boundaries. Typical microstructures observed in iron-free alloys are shown in Figs. 1–9 (Plate IX), while a similar series containing 0.35% iron is shown in Figs. 10–18 (Plate X). Results of thermal treatment are illustrated in Figs. 19–27 (Plate XI) and Figs. 28–31 (Plate XII).

#### 1. CAST ALLOYS

In the basis alloy in the as-cast condition, islands of the Al–Mg<sub>2</sub>Si eutectic were observed together with small particles of elementary silicon (Fig. 1). Manganese in the iron-free alloys was present as  $\alpha$ -(MnSi)Al (Fig. 2) and chromium as the isomorphous  $\alpha$ -(CrSi)Al (Fig. 3).

In the absence of either chromium or manganese, iron occurred in the cast alloy mainly as  $\beta$ -(FeSi)Al, in the well-known plate-like form which is so deleterious to the hot-working properties.  $\alpha$ -(FeSi)Al was present in small amounts and can be detected in Fig. 10 (Plate X) by its characteristic "Chinese-script" formation. With either manganese or chromium present, the  $\alpha$  phase predominated, and striking examples of "Chinese script" are shown in Figs. 11 and 12 (Plate X). The suppression of the  $\beta$  phase by the addition of manganese to aluminium–silicon–iron alloys is well known from work by Gwyer and Phillips<sup>8</sup> and by Phillips and Varley.<sup>9</sup> It is apparent from the present series of microstructures that, in the more complex alloys containing magnesium, both manganese and chromium have this effect.

In the basis alloy (Fig. 4) and the quaternary alloy with 0.35% iron (Fig. 13), no marked change in the cast microstructure was brought about by reheating. In alloys containing manganese or chromium, with or without iron, reheating caused the primary phase to develop a mottled structure, indicating that some form of precipitation had occurred. The effect of heating to progressively higher temperatures an alloy containing 0.6% manganese is shown in Figs. 19–21 (Plate XI). Mottling is at first general, but later becomes more pronounced near the centre of the grains



and, finally, at 500° C. (Figs. 5 and 14), the edges of the grains appear free from precipitate. A similar effect was observed in chromium-bearing alloys (Figs. 6 and 15), but the appearance of the mottling suggests that the precipitated particles are larger than in the manganese-bearing alloys.

The solubilities of manganese and chromium in aluminium fall off rapidly with temperature even in the binary alloys.<sup>10, 11</sup> However, the retention of these elements in large excess of their solid solubilities in heavily chilled castings of the binary alloys and reprecipitation in subsequent annealing has been reported by Hofmann.<sup>12, 13</sup> Furthermore, structures similar to those shown in Figs. 5 and 14 have been observed to occur as a result of annealing a cast heat-treatable aluminium-copper-magnesium alloy containing 1% manganese<sup>14</sup> and are attributed to the precipitation of a manganese-rich phase.

In the present series of alloys, the phases first precipitated during slow cooling or prolonged heating just below the melting point are probably  $\text{MnAl}_6$  or  $\text{CrAl}_7$  in both binary and more complex alloys, or, where iron is present, the compounds of indefinite composition  $(\text{Mn, Fe})\text{Al}_6$  or  $(\text{Cr, Fe})\text{Al}_7$ . According to existing data on the aluminium-manganese-silicon-iron<sup>9</sup> and aluminium-magnesium-silicon-iron<sup>15</sup> systems,  $(\text{Mn, Fe})\text{Al}_6$  would be converted at lower temperatures to  $(\text{Mn-Fe, Si})\text{Al}$ , but the concentration is too low for identification by X-ray-diffraction techniques.

The clearance of the precipitate from the areas in the neighbourhood of the residual eutectic phases would seem to indicate that a diffusion process has occurred, involving reaction with and constitutional changes in the intermetallic compounds present.

## 2. WROUGHT ALLOYS

The hot- and cold-rolling operations led to the usual breaking up of the grain-boundary phase into stringers of intermetallic particles, which were well distributed and too slight in quantity to have any significant effect on the general properties of the alloys.

Within the primary grains all the alloys showed evidence of structural changes having taken place during the rolling operation. In the ternary alloy, for example, a precipitate of large and well-distributed particles had been thrown down (Fig. 22), and on heat-treatment at 540° C. was reabsorbed into solid solution (Fig. 23, Plate XI). From known equilibrium data on the system it would seem that this precipitate was  $\text{Mg}_2\text{Si}$ , which would be present in excess of solid solubility below 500° C. The quaternary iron-bearing alloys behaved in a similar manner, and again after heat-treatment the precipitate was taken into solid solution. In the manganese- and chromium-bearing alloys the structures were characterized by the presence of dark and light bands arising from the dark and light areas in the cast structure (Fig. 24). After solution heat-treatment, the dark bands changed in appearance, the precipitate

becoming smaller in quantity and more finely dispersed, so that the appearance was uniformly grey rather than mottled (Fig. 8). It would appear, in fact, that in the as-rolled condition the precipitate was duplex, consisting of coarse particles of  $\text{Mg}_2\text{Si}$  thrown down during the rolling operation and of the original unchanged finer particles of  $(\text{Mn, Fe})\text{Al}_6$  or  $(\text{Cr, Fe})\text{Al}_7$ . In the subsequent heat-treatment the  $\text{Mg}_2\text{Si}$  was redissolved.

A further significant change in microstructure was brought about by artificial ageing at 160° C. Dark, uneven lines appeared on the grain boundaries in the ternary alloy and in the quaternary aluminium-magnesium-silicon-iron alloy (Figs. 7 and 16), but were absent from the manganese- and chromium-bearing alloys (Figs. 8, 9, 17, and 18). However, after more prolonged etching treatments, darkening of the grain boundaries was detected under high magnification in all the alloys. Typical structures are shown in Figs. 25, 26, and 27 (Plate XI). In the manganese-free alloy (Fig. 25) relatively large and numerous particles are present on the grain boundaries, in the low-manganese alloy (Fig. 26) particles are fewer, and in the high-manganese alloy the grain boundaries are visible only within the light bands, and are less intense and free from precipitate.

Seemann and Dudek<sup>16</sup> showed that banded structures could be removed in aluminium-copper-magnesium-manganese alloys by prolonged soaking above 500° C. In alloys of the present series a temperature of about 600° C. was necessary to achieve a similar result and only those free from iron were subjected to this treatment, because when iron was present a substantial amount of liquid was formed at 560° C. and above. The progressive changes at 600° C. are illustrated in Figs. 28-30 (Plate XII). After 6 hr. the original banded structure is still apparent, but after more prolonged heating it has disappeared, the particles increasing in size and coalescing into comparatively large and widely spaced aggregates. No further precipitation occurred on reheating at 500° C., but at 160° C. (Fig. 31) grain-boundary precipitation occurred with all the characteristics of the manganese-free alloy (Fig. 7) subjected to normal processing.

## V.—MECHANICAL PROPERTIES OF WROUGHT ALLOYS

Mechanical properties were determined in two conditions of heat-treatment, i.e. after solution heat-treatment at 540° C., and after either room-temperature ageing or artificial ageing for 18 hr. at 160° C. The room-temperature-aged alloys were tested 5 days after quenching; however, age-hardening was by no means complete after this short period, but continued at a diminishing rate so that ageing could be detected for periods of up to 1 year.

Standard tensile test-pieces of  $\frac{1}{2}$  in. width and 2-in. gauge-length were cut from the hard-rolled

strip transverse to the rolling direction and heat-treated subsequently.

The bend test is of practical importance in the the commercial aluminium-magnesium-silicon alloys, and as a testing procedure is particularly useful where elongation values are small and therefore affected by slight inaccuracies of alignment during tensile testing. Specimens for the bend test were  $3 \times 0.6$  in., cut across the direction of rolling, the axis of bending being in the rolling direction. Bending was carried out on a rubber bed, the desired radius being obtained by contact with the semicircular tip of one of a series of steel former bars. The bend properties of the material were characterized by the ratio of the smallest radius ( $R$ ) of bending through  $180^\circ$  without cracking, to the metal thickness ( $T$ ).

The mechanical properties of the room-temperature-aged alloys are plotted in Fig. 40. Both proof and ultimate tensile stress increased progressively with either manganese or chromium additions to the ternary iron-free alloy, while elongation values were correspondingly diminished. Iron additions also increased strength in both series, and where iron was present with manganese or chromium the effects were roughly additive. Iron, however, appeared to have a less consistent effect on ductility as measured by elongation values. Bend-test results on the room-temperature-aged alloys are not shown, for all the ratios obtained were small, generally less

alloying with manganese or chromium was to increase strength progressively as in the room-temperature-aged alloys, while iron additions again produced further increments in strength in both series.

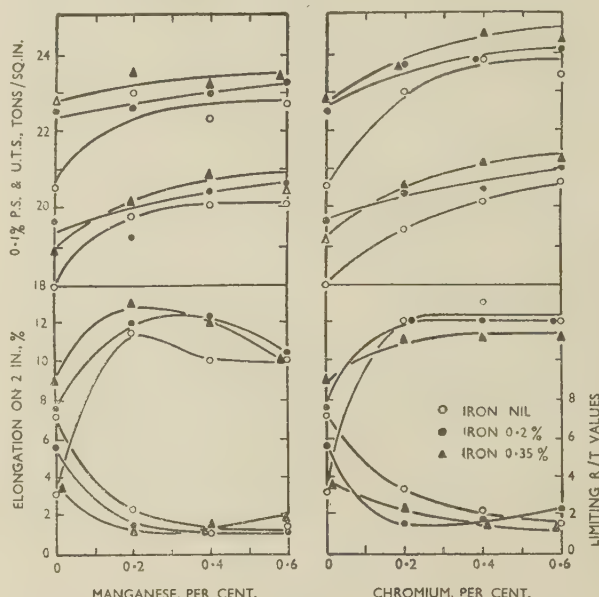


FIG. 41.—Mechanical Properties of Fully Heat-Treated Alloys.

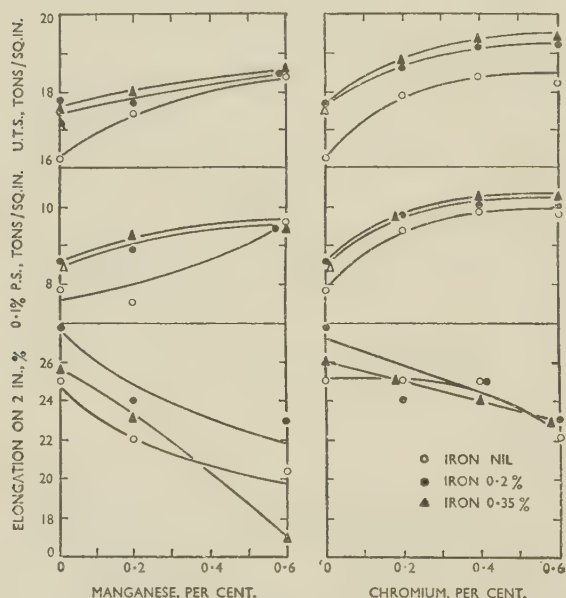


FIG. 40.—Mechanical Properties of Room-Temperature-Aged Alloys.

than 1.0, and comparisons were therefore of little significance.

By artificial ageing (Fig. 41) the proof-stress values were raised substantially, and the ultimate-stress values slightly, ductility as measured in both tensile and bend tests being diminished. The effect of

Elongation values of artificially aged alloys did not exhibit the usual inverse relationship to ultimate tensile stress and proof stress. In fact the basis alloy was quite brittle, but ductility, as measured by either elongation or bending properties, was increased by additions of iron and still further improved by manganese or chromium, maximum elongation and minimum  $R/T$  values being obtained with 0.2% or more of either manganese or chromium.

In the further investigation of anomalies in ductility, fractured bend-test specimens were sectioned and examined under the microscope. Caustic soda etching of these specimens revealed that in the basis ternary alloy and the iron-bearing quaternary alloys fractures were entirely intercrystalline (Fig. 32, Plate XII). In iron-free alloys containing 0.2% of either manganese or chromium, fractures were mainly but not wholly intercrystalline. In all iron-bearing alloys with manganese or chromium and in iron-free alloys with 0.4% or 0.6% of either manganese or chromium, fractures were mainly transcrystalline (Fig. 33, Plate XII). It was, however, impossible to say with certainty that any of the alloys was completely free from all grain-boundary fracture in tensile or bend tests.

Comparison of these observations on bend-test specimens with the micrographic studies in Figs. 1-27 can leave little room for doubt that the brittle fractures were associated with the presence of a strongly marked grain-boundary precipitate. Where well-developed banded structures were present, the fractures appeared to be mainly, if not entirely, trans-



crystalline. Bend tests on the alloy containing manganese 0.6%, iron nil, after prolonged soaking to remove the banded structure followed by artificial ageing (Fig. 31), were of particular significance, for the specimens fractured in an intercrystalline manner indicating that, in the absence of the banded structure, manganese as an alloying element was ineffective.

## VI.—CORROSION-RESISTANCE

The most generally applicable and reproducible accelerated-corrosion test for making a critical comparison of an experimental series of alloys is the salt-

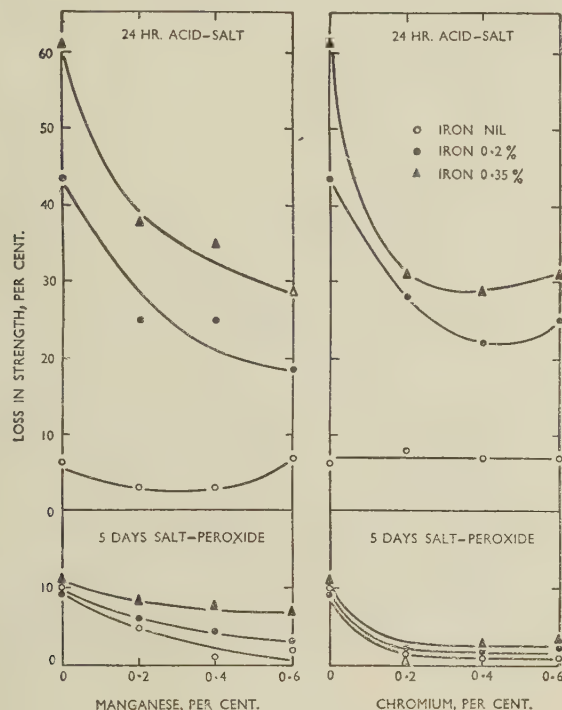


Fig. 42.—The Effect of Iron, Manganese, and Chromium on Loss of Strength in Accelerated-Corrosion Tests.

peroxide test. This is widely used, although there is no universally accepted standard for it. The procedure generally adopted by the authors is to immerse tensile test-pieces, each in a separate jar containing 330 c.c. of solution kept at 30° C. by a water bath. The solution, which contains 3% sodium chloride and 0.3% hydrogen peroxide in distilled water, is renewed completely every 24 hr., to ensure that it is in an active condition throughout the period of testing, which ranges from 1 to 5 days. The present series of alloys showed such a high resistance to this corroding medium that, after the full five days, the greatest reduction in strength of any alloy in either condition of heat-treatment was 13%, while most suffered negligible loss of strength. Additional tests were therefore carried out by the more aggressive acid-salt test, in which the corroding medium contains 1% hydrogen chloride and 3% sodium chloride. The

same procedure with individual jars was adopted, and the tests were terminated after 24 hr. Both salt-peroxide and acid-salt tests were carried out in triplicate.

The characteristic of both methods of accelerated testing is that any susceptibility to intercrystalline attack is brought out, while loss in strength on prolonged immersion in these testing media is generally significant only where intercrystalline attack occurs. In the room-temperature-aged condition none of the alloys suffered a loss of strength sufficiently great to be measurable with any degree of accuracy, and no intercrystalline attack could be detected on micro-sections of corroded specimens. After artificial ageing, attack was generally more severe and intercrystalline in character.

The degree of attack, as indicated by the loss in strength of tensile test-pieces, is plotted in Fig. 42, and some typical microsections of corroded specimens are reproduced in Figs. 34–39 (Plate XIII). In salt-peroxide solution the greatest loss of strength was suffered by alloys containing neither manganese nor chromium. Chromium reduced attack to a greater extent than manganese, and only in the manganese-bearing series did iron appear to have any significant adverse effect.

In acid-salt solution iron caused a substantially increased attack. For example, in the manganese- and chromium-free alloys, 0.2% iron increased attack by about 7 times, and 0.35% iron by 10 times. Manganese and chromium additions to alloys containing iron reduced attack to about half. The very slight loss in strength of the iron-free alloys, with or without manganese or chromium, is noteworthy. The microsections (Figs. 34–39) showing the attack on alloys of the 0.35% iron series, confirm that in salt-peroxide solution chromium is more beneficial than manganese in preventing intercrystalline attack, while in acid-salt solution chromium and manganese have about the same effectiveness.

## VII.—DISCUSSION

It is evident that the properties of the alloys in different conditions of heat-treatment are influenced in a very considerable measure by precipitation processes, the nature and effect of which depend on both the thermal and mechanical treatments to which the alloys are subjected. Precipitation at grain boundaries during final low-temperature thermal treatment is especially undesirable, since it results in a brittle condition in which intercrystalline fracture in tension or bending occurs.

Three distinct types of precipitation have been observed, and in each one the particles are sufficiently large to be easily resolved under the optical microscope; they are thus quite distinct from the sub-microscopic particles associated with age-hardening. The first type is brought about in manganese- and chromium-bearing alloys when the casting is reheated at 500° C. before hot rolling, and the pre-

precipitates, which when first formed are presumably  $(\text{Fe}, \text{Mn})\text{Al}_6$  or  $(\text{Fe}, \text{Cr})\text{Al}_7$ , remain throughout the subsequent rolling and heat-treatment operations, giving rise to a banded structure. The second type of precipitate is of markedly larger particle size, and is thrown down in all the alloys during hot- and cold-rolling operations, presumably by nucleation on slip planes, being taken into solid solution again on subsequent heat-treatment at  $540^\circ\text{C}$ .; it would appear to be  $\text{Mg}_2\text{Si}$ , which, according to existing equilibrium data, would be present in excess of its solid solubility in this series of alloys below about  $500^\circ\text{C}$ . The third type occurs on final artificial ageing at  $160^\circ\text{C}$ . and is probably also  $\text{Mg}_2\text{Si}$ , since this compound is strongly supersaturated at that temperature. In the absence of manganese or chromium it occurs at grain boundaries, causing pronounced mechanical weakness. As manganese and chromium are increased, the amount of precipitation at the grain boundaries, and the associated intercrystalline weakness diminish. No grain-boundary precipitation can be detected in the dark banded areas associated with the first type of precipitation referred to above, and it seems possible that this precipitation provides alternative sites for the nucleation of  $\text{Mg}_2\text{Si}$ .

Intercrystalline fracture could result either from a brittle phase at the grain boundaries, or from a stress-corrosion effect associated with a grain-boundary phase or composition gradient. The following observations are relevant in this connection:

(i) The basis alloy, in which strong grain-boundary precipitation was associated with intercrystalline failure in tension, was not severely attacked in either of the highly aggressive corroding media, and its tensile strength was only slightly reduced by them. Other alloys containing iron and manganese or iron and chromium suffered more pronounced intercrystalline attack.

(ii) Bend test-pieces protected by a layer of grease fractured in an intercrystalline manner.

(iii) A limited series of stress-corrosion tests on representative alloys under direct tensile stresses of up to 90% of the proof stress indicated that stress had no marked effect on the rate of corrosion.

The conclusion would appear to be that grain-boundary fracture is caused by the low mechanical strength of a precipitate thrown down at the grain boundaries.

#### ACKNOWLEDGEMENTS

The authors gratefully acknowledge the inspiration and encouragement of Dr. N. P. Inglis and the assistance of various colleagues.

#### REFERENCES

1. D. Hanson and M. L. V. Gayler, *J. Inst. Metals*, 1921, **26**, 321.
2. E. H. Dix, Jr., F. Keller, and R. W. Graham, *Trans. Amer. Inst. Min. Met. Eng.*, 1931, **93**, 404.
3. H. W. L. Phillips, *J. Inst. Metals*, 1941, **67**, 257.
4. F. Keller and C. M. Craighead, *Trans. Amer. Inst. Min. Met. Eng.*, 1936, **122**, 315.
5. W. Geller, *Z. Metallkunde*, 1939, **31**, 9.
6. C. Panseri and M. Monticelli, *Alluminio*, 1945, **14**, 51.
7. M. Bosshard and H. Hug, *Metallwirtschaft*, 1939, **18**, 6.
8. A. G. C. Gwyer and H. W. L. Phillips, *J. Inst. Metals*, 1927, **38**, 29.
9. H. W. L. Phillips and P. C. Varley, *ibid.*, 1943, **69**, 317.
10. E. Butchers and W. Hume-Rothery, *ibid.*, 1945, **71**, 87.
11. G. V. Raynor and K. Little, *ibid.*, 1945, **71**, 481.
12. W. Hofmann, *Aluminium*, 1938, **20**, 865.
13. W. Hofmann and H. Wiehr, *Z. Metallkunde*, 1941, **33**, 369.
14. M. Dudek, H. Mahl, and H. J. Seemann, *Metall*, 1948, **75**.
15. H. W. L. Phillips, *J. Inst. Metals*, 1946, **72**, 151.
16. H. J. Seemann and M. Dudek, *Z. Metallkunde*, 1948, **39**, 319.



# THE COPPER-INDIUM EUTECTOID AT 31.36 WT.-% INDIUM \*

1499

By CHESTER W. SPENCER,† Ph.D., and ASSOCIATE PROFESSOR  
DAVID J. MACK,‡ Ph.D.

## SYNOPSIS

The structure of the copper-indium eutectoid alloy at 31.36 wt.-% indium is similar in appearance to pearlite in the iron-carbon eutectoid alloy. During isothermal transformation of the  $\beta$  phase just below the eutectoid temperature ( $574^{\circ}\text{C.}$ ), the eutectoid pearlite forms into nodules. This lamellar pearlite, on continued isothermal transformation, develops into a much coarser second two-phase structure, described as a secondary pearlite. This transformation is not identical with spheroidization of iron-carbon pearlite. The manner in which the secondary pearlite forms is believed to indicate that one of the phases in the parent pearlite is of non-equilibrium composition. During isothermal transformation below approximately  $547^{\circ}\text{C.}$ , a portion of the  $\beta$  phase is not consumed by the nodules; instead, a new reaction occurs which gives the  $\beta$  phase a herring-bone appearance. In the areas which have developed a herring-bone appearance, particles of the  $\alpha$  phase are then observed to precipitate as the parent matrix gradually assumes the appearance of the  $\delta$  phase. At the completion of this process, a two-phase structure, resembling the final two-phase structure formed at higher temperatures, is observed. A time-temperature-transformation diagram is proposed for this alloy.

## I.—INTRODUCTION

As part of a general investigation into the mechanism of eutectoid transformations, the eutectoid at 31.36 wt.-% indium in the copper-indium system has been studied intensively. Since eutectoid transformations are in general complicated, isothermal techniques, as introduced by Davenport and Bain,<sup>1</sup> were principally used in this study.‡ This method eliminates the temperature variable, and therefore allows more information to be obtained about the sequence of the changes occurring during the progress of a transformation than may be obtained by the more widely used method of continuous cooling.

## II.—EARLIER WORK

Weibke and Eggers<sup>3</sup> proposed the first comprehensive diagram for the copper-indium system. Fig. 1 shows the area of this system in which the  $\beta$  phase, which has approximately a 3/2 electron : atom ratio, undergoes a eutectoid transformation. The two equilibrium phases produced on cooling  $\beta$  are  $\alpha$  and  $\delta$ , having a face-centred cubic and a  $\gamma$ -brass structure, respectively. The  $\delta$  phase is described as hard, brittle, and silver-coloured. Weibke and Eggers indicated that the  $\beta$  phase was stable above  $574^{\circ}\text{C.}$ , and they considered it to be retainable to room temperature on quenching. X-ray investigations showed that this retained  $\beta$  phase had a body-

centred cubic structure with a superlattice similar to that of  $\beta$ -brass.

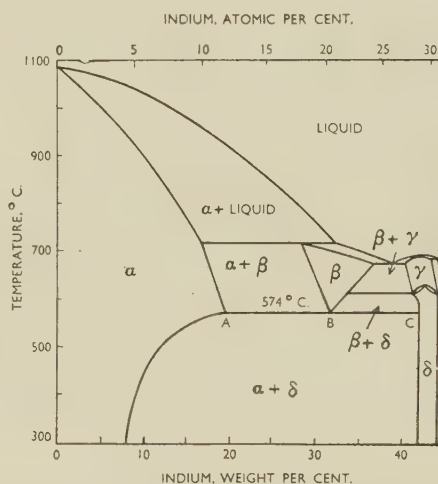


FIG. 1.—The Copper-Indium Equilibrium Diagram (after Weibke and Eggers).

KEY.  
A 18.1 wt.-% (10.9 at.-%) indium.  
B 31.36 wt.-% (20.15 at.-%) indium.  
C 34.23 wt.-% (28.9 at.-%) indium.

Hume-Rothery, Raynor, Reynolds, and Packer<sup>4</sup> later studied in detail the copper-rich end of the copper-indium diagram, and as a result the phase-

\* Manuscript received 27 May 1953.

† Sylvania Electric Products Inc., Bayside, New York, U.S.A.

‡ Department of Mining and Metallurgical Engineering, University of Wisconsin, Madison, Wisconsin, U.S.A.

§ It is interesting to note that, although Davenport and Bain were the first to make formal use of the isothermal transformation method in the study of eutectoids, Hanson and Gayler<sup>2</sup> had made incidental use of it some years earlier in their study of the aluminium-zinc eutectoid.

field limits in Weibke and Eggers' diagram were somewhat altered. The eutectoid composition and temperature were given as 31.36 wt.-% (20.15 at.-%) indium and 574° C. The decrease in solubility of indium in the  $\alpha$  phase with falling temperature was found to be more rapid than the diagram of Weibke and Eggers indicated. It was shown that the  $\beta$  phase area extended up to 25 at.-% indium, but did not exceed this limit. This was considered to be the result of short-range order in the  $\beta$  phase, a composition of less than 25 at.-% indium enabling the atoms to be so arranged that no solute atom has another solute atom as its first- or second-zone neighbour.<sup>5</sup>

X-ray data obtained by Hume-Rothery, Raynor, Reynolds, and Packer indicated that the  $\beta$  phase had a simple body-centred cubic structure, and it was suggested that the extra lines that Weibke and Eggers considered as superlattice lines were the result of quenching. It was found that the  $\beta$  phase always decomposed to some extent on quenching to room temperature.

### III.—EXPERIMENTAL PROCEDURE

The copper-indium alloy was received from the Indium Corporation of America in the form of chill castings  $\frac{1}{2}$  in. in dia.  $\times$  4 in. long. These ingots were hot worked to 75% reduction while in the  $\beta$ -phase field. They were then homogenized for 72 hr. at 630° C. Chemical analysis, using the iodometric method for copper, showed 68.6 wt.-% copper and 31.4 wt.-% indium by difference.

Small specimens, approximately  $\frac{1}{4} \times \frac{1}{4} \times \frac{1}{8}$  in., were used for the isothermal studies. The isothermal salt bath consisted of 50 : 50 potassium nitrate and sodium nitrite. After the specimen had been held in the salt bath for the predetermined period, the transformation was stopped by quenching into water at 21° C. All specimens were held for 2 hr. at 650° C. before undergoing further heat-treatment, i.e. quenching, isothermal transformation, or continuous cooling.

### IV.—EXPERIMENTAL RESULTS

After furnace-cooling from the  $\beta$  phase area, a fine pearlite (Fig. 2, Plate XIV) is formed.\* On quenching to room temperature from 650° C., a structure which appears to be composed of large grains of  $\beta$  phase is formed. However, some areas of the  $\beta$  grains near the grain boundaries show optical activity when viewed under polarized light. Careful etching of the specimen brings out a rough-etching surface in these optically active areas.

Fig. 3 (Plate XIV) shows the structure of a specimen transformed for 2 hr. at 573° C. (eutectoid tem-

perature, 574° C.). A nodule of extremely coarse pearlite can be seen at an old  $\beta$ -phase grain boundary. A transitional area is present between the pearlite lamellae and the  $\beta$  phase on portions of the surface of the nodule. It should be noted that the remaining  $\beta$  phase has a rough-etching and, in areas adjacent to the pearlite nodule, a cross-hatched appearance; this is observed to grow more pronounced during isothermal transformation.

Fig. 4 (Plate XIV) shows under high magnification the edge of a large pearlite nodule after isothermal transformation for 8 min. at 570° C. The lighter lamellae are probably the  $\alpha$  phase. The transitional area between the pearlite lamellae and the  $\beta$  phase is clearly shown. Although most of the resulting eutectoid structure is lamellar in form, a small amount of granular pearlite was observed. The rough-etching or cross-hatched appearance of the  $\beta$  phase is not apparent in Fig. 4, because of the light etching treatment necessary to permit good resolution of the two-phase structure. However, a heavy etching treatment was found to bring out a faint cross-hatched appearance in the retained  $\beta$  phase.

Fig. 5 (Plate XIV) shows the structure after 7 hr. at 570° C. The fine lamellae are the same as those present in Fig. 4. The coarse lamellae are the product of a new reaction that occurs in the original pearlite. After longer times of transformation, the entire structure consists of this coarse two-phase mixture, which itself has a pearlitic appearance.

The pearlite nodules in this alloy are very similar in appearance at low magnification to the nodules of fine pearlite that are observed in the iron-carbon eutectoid alloy. This suggests that the manner in which they are formed may be similar. Since a transitional structure of the nature described above is not observed in the iron-carbon eutectoid alloy, the possibility must be considered that in the copper-indium eutectoid alloy it is formed during quenching. In order to explore this possibility, specimens were quenched from the transformation temperature in boiling water and iced brine. A significant difference was apparent in the structure at the surface of the nodules after the two quenching treatments. The faster quench, in iced brine, gave rise to a structure in which the nodules possessed almost no transitional band at their surface, but in which, in most instances, the lamellae extended to the surface of the nodules. The slower quench, in boiling water, produced a structure in which the nodules were surrounded by a transitional band somewhat larger than that shown in Fig. 4.

Isothermal transformation at 547° C. produces a large number of small nodules, which have the same shape as those produced at 570° C. Fig. 6 (Plate XIV) shows their appearance, under polarized light, in a structure formed after 12 sec. at 547° C. A dark area in the centre of the photomicrograph

\* All metallographic specimens were etched with a bichromate solution containing:  $K_2Cr_2O_7$ , 2 g.; NaCl, 1.5 g.;  $H_2SO_4$  (conc.), 8 ml.; water, 100 ml.



indicates an area of untransformed  $\beta$  phase. Fig. 7 (Plate XIV) shows the specimen at higher magnification under ordinary light. The nodules grow indiscriminately across the  $\beta$  grain boundaries; this was found to occur at all transformation temperatures.

Examination of the nodules formed at 547° C. shows that they are not composed of a resolvable two-phase structure. However, their extreme optical activity, which gives them an "interwoven" appearance, and their rough-etching surface indicate that they are not composed of a single homogenous phase. The entire nodule can be compared to the transitional area which is present between the lamellar pearlite and the retained  $\beta$  phase during transformation at higher temperatures (Fig. 4).

Fig. 8 (Plate XV) shows the structure developed after 16 hr. at 547° C. Some areas have etched darker than others, and there is a well-defined interface between the grey phase and the lighter phase in the darker-etching areas. In the lighter-etching areas, sharp colour differences are visible, but it is not possible to distinguish two separate phases. All areas develop a well-defined interface between the grey phase and the lighter phase, which are believed to be  $\delta$  and  $\alpha$ , respectively, after longer times of transformation.

At transformation temperatures below 547° C., a portion of the high-temperature  $\beta$  phase is not consumed by the nodules before it undergoes a new reaction, which gives it a "herring-bone" appearance. Fig. 9 (Plate XV) shows the edge of a nodule, which appears light, and the adjacent area with the herring-bone pattern. It was found that the nodules continued to consume the  $\beta$  phase during the early stages of the development of the herring-bone pattern.

Specimens transformed at 512° C. developed the greatest amount of pre-eutectoid  $\delta$  phase. Fig. 10 (Plate XV) shows the structure developed after 10 sec. at 512° C. By this stage in the transformation, the growth of the pre-eutectoid  $\delta$  particles has practically ceased.

The entire  $\beta$  phase develops the herring-bone pattern if the specimen is immersed for approximately 1 sec. in the isothermal bath just below 500° C. and then quenched. Fig. 11 (Plate XV) shows a specimen which was heated for about 1 sec. at 476° C. before quenching. The herring-bone structure has begun to develop dark-etching areas, which spread from the grain boundaries. It is seen that, as this structure develops, the old  $\beta$  grain boundary becomes irregular in appearance.

Some nodules were found to form at 476° C. However, these do not have the same appearance as the nodules formed at higher temperatures; they are light-etching, but have an extremely rough surface after etching (Fig. 12, Plate XV). It was observed that the nodules ceased to grow when the

herring-bone structure developed the dark-etching appearance seen in Fig. 11. It is believed that the dark-etching characteristic of the "herring-bone" structure indicates the precipitation of a second phase.

Fig. 12 shows that particles of a new phase have formed in the herring-bone structure. Close examination of this and later structures showed the precipitated phase to be  $\alpha$ . Fig. 12 also shows that the light-etching nodules are preparing to separate into two phases. It is thought that some of the segregation that has taken place in the area occupied by the

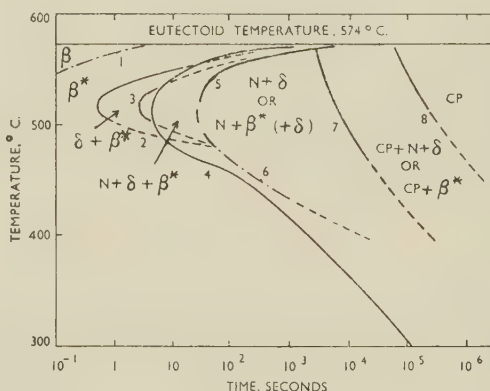


Fig. 15.—Time-Temperature-Transformation Diagram for the Copper-Indium Eutectoid Alloy at 31.36 wt.% Indium.

KEY.

- $\beta^*$  Cross-hatched  $\beta$ .
- $\delta$  Pre-eutectoid  $\delta$ .
- N Nodules.
- CP Coarse pearlite.
- Curve 1 Beginning of cross-hatching of  $\beta$ .†
- Curve 2 Beginning of precipitation of pre-eutectoid  $\delta$ .
- Curve 3 End of precipitation of pre-eutectoid  $\delta$ .
- Curve 4 Beginning of formation of nodules.
- Curve 5 End of formation of nodules.
- Curve 6 (Not an extension of Curve 5) Cross-hatching of  $\beta$  reaches a point where nodules will not grow.
- Curve 7 Beginning of formation of coarse pearlite.
- Curve 8 End of formation of coarse pearlite.

† Since it is not possible completely to retain the  $\beta$  phase to room temperature, this curve indicates the approximate times of transformation at which, after quenching, the cross hatching of the  $\beta$  becomes appreciably greater.

nodules occurred before the nodule consumed the herring-bone structure.

Fig. 13 (Plate XV) shows the structure after 18 hr. at 476° C. The darker areas result from the herring-bone reaction, whereas the lighter areas are remnants of the nodules. The darker areas are essentially in equilibrium; they are composed of small rounded particles of  $\alpha$  in a matrix of  $\delta$ . The lighter areas are approaching equilibrium by two processes; particles of  $\alpha$  are breaking away from the matrix in the interior of the nodules, and the interface between the light-etching area and the dark-etching area is advancing into the light area. As the interface moves into the light area the  $\alpha$  particles become sharply defined, and there is a darkening

\* As used here, the term "pre-eutectoid" refers to a single phase rejected from a eutectoid alloy during isothermal holding at sub-eutectoid temperatures. Pre-eutectoid rejection

occurs very commonly in isothermally transformed eutectoid aluminium bronzes.<sup>6</sup>

of the background  $\delta$  phase. After longer transformation times, the entire structure has the appearance of the darker portions of Fig. 13.

Isothermal transformation at 322° C. does not result in a well-defined herring-bone structure as it does at 476° C. Instead there is a gradual darkening of the high-temperature  $\beta$  grains as a fine precipitate of  $\alpha$  phase appears in them. A grain-boundary reaction begins early in the transformation and proceeds slowly into the old  $\beta$  grains.

After 67 hr. at 322° C., the grain-boundary reaction becomes well-defined (Fig. 14, Plate XV). Some small nodules have formed in the interior of the grains. This structure gradually approaches equilibrium in a manner similar to that observed at 476° C.; however, no well-defined two-phase structure is observed at transformation times up to 150 hr.

Fig. 15 (Plate XV) shows the proposed time-temperature-transformation diagram for the copper-indium eutectoid alloy at 31.36 wt.-% indium.

## V.—DISCUSSION

The structure resulting from the continuous cooling of the copper-indium eutectoid alloy closely resembles the pearlite formed in the iron-carbon and copper-aluminium eutectoid alloys.<sup>6</sup> However, study of the eutectoid transformation in this alloy by isothermal-transformation methods shows significant differences in the mechanism of the transformation under certain conditions.\* Some features not noted in the eutectoid transformation in the iron-carbon and copper-aluminium alloys are: (a) the transitional structure which may appear at the surface of the growing pearlite nodules; (b) the manner in which a visible two-phase structure forms in the nodules that appear at the intermediate transformation temperatures; (c) the transformation of the fine pearlite to a coarser pearlite; and (d) the development of a cross-hatched or herring-bone structure in the parent  $\beta$  phase. These features will be discussed and a possible explanation for their presence will be proposed.

On isothermal transformation within approximately 20° C. of the eutectoid temperature, pearlite nodules consume the  $\beta$  phase. When the transformation is interrupted by quenching the specimen before the reaction is complete, a transitional structure is observed at the surface of the growing pearlite nodules (Fig. 4). The breadth of the transitional band is found to be dependent on the quenching rate. Examination under high magnification ( $\times 2000$ ) shows that the transitional structure is composed of a single phase near the advancing surface of the nodule, but at a small distance behind the advancing surface, a second phase, in a finely dispersed form, is observed. The rough-etching or cross-hatched ap-

pearance of the retained  $\beta$  phase is most pronounced just ahead of the advancing surface of the nodules (Fig. 3). It is possible that the quenching process enhances the appearance of the cross-hatched structure, but, since this becomes more pronounced as the transformation progresses, some compositional change or segregation is believed to occur in the parent  $\beta$  phase near the surface of the growing nodules. These considerations suggest that the transitional structure observed in the quenched specimens is the result of rapid growth of the nodules into the surrounding  $\beta$  phase during quenching.

During isothermal transformation at about 547° C., the nodules that are formed in the parent  $\beta$  phase do not possess a resolvable two-phase structure, but one that resembles the transitional structure observed on the surface of the pearlite nodules formed at the higher transformation temperatures. Their extreme optical activity, which gives them an "interwoven" appearance under polarized light, and their rough-etching surface indicate that the nodules are not composed of a single homogeneous phase. The nodules are thought to be composed of fine particles of the  $\alpha$  phase distributed throughout a matrix of the  $\delta$  phase which is supersaturated with copper. As the transformation proceeds, the fine particles of the  $\alpha$  phase appear to agglomerate, while more  $\alpha$  phase forms as the  $\delta$  phase approaches the equilibrium composition. When the  $\delta$  phase reaches the equilibrium composition, the final step in the transformation is the formation of the visible interface between the two phases at the point where the colour interface was seen earlier.

Upon continued isothermal transformation of the fine pearlite which is formed at the higher transformation temperatures, a coarsening reaction is observed in which the fine lamellar structure is transformed to a coarser lamellar structure. This reaction is not identical with the spheroidization of the iron-carbon eutectoid pearlite. The transformation of a fine, pearlitic structure to another, coarser, pearlitic structure will be referred to as the formation of a secondary pearlite. A similar reaction has been reported for the copper-beryllium eutectoid alloy.<sup>7</sup> Probably two forces contribute to the formation of secondary pearlite in the copper-indium eutectoid: (a) the surface-energy forces which tend to cause agglomeration and spheroidization of the eutectoid constituents; and (b) the forces which result from one of the eutectoid constituents possessing a non-equilibrium composition. It is thought, therefore, that the difference between this reaction and spheroidization of the iron-carbon eutectoid lies in an adjustment of composition in one of the phases during the formation of the secondary pearlite.

During isothermal transformation at intermediate and lower temperatures, a reaction occurs in the untransformed  $\beta$  phase which is described as giving

\* The pearlites in the copper-aluminium and iron-carbon eutectoid transformations seem to form in an identical

manner. In this paper the iron-carbon pearlite is referred to as the prototype of this type of transformation.



the  $\beta$  phase a "herring-bone" appearance. As the transformation proceeds, this appearance becomes more pronounced. In the later stages of the reaction,  $\alpha$  particles precipitate on a sub-microscopic scale and grow in the pattern of the herring-bone structure, while the parent structure gradually assumes the appearance of the  $\delta$  phase. Approximately at the point in the transformation where precipitation of the  $\alpha$  particles is first noted, the nodules cease to grow.

All the features of this transformation which have been discussed seem to possess one factor in common: the presence of a transitional phase or phases of non-equilibrium composition. As a possible explanation of these features, it is suggested that a transitional phase, having a series of compositions and crystal structures intermediate between that of the  $\beta$  phase at eutectoid composition and that of the  $\delta$  phase, may exist. This suggestion is based on the close crystallographic relationship between the  $\beta$  phase, which has the body-centred cubic structure, and the  $\delta$  phase, with the  $\gamma$ -brass structure. The latter can be derived from the body-centred cubic structure by arranging 27 body-centred cubes to form a large cube; if two of the 54 atoms present are removed, the  $\gamma$ -brass structure can be represented by the remaining 52 atoms.

The wrinkled or cross-hatched appearance of the retained  $\beta$  phase at higher transformation temperatures and its herring-bone appearance at lower transformation temperatures can be explained on the basis of a transitional phase of this nature. These markings in the  $\beta$  phase indicate the segregation of copper atoms on preferred crystallographic planes. As a result of this segregation, the parent phase becomes a transitional phase with a composition and crystal structure slightly removed from those of the  $\beta$  phase. The appearance of  $\alpha$  particles in the pattern of the herring-bone structure during transformation at lower temperatures supports this belief (Fig. 12). Apparently the segregation of the copper atoms occurs at a rate sufficient to cause the reaction to show up on X-ray photographs of specimens quenched from the  $\beta$  field. This might account for the lines, interpreted as superlattice lines, found by Weibke and Eggers in quenched  $\beta$  alloys.

The transitional structure on the surface of the pearlite nodules formed at the higher transformation temperatures and the rough-etching nodules formed at the intermediate temperatures are structures in which the transition from the  $\beta$  to the  $\delta$  phase has progressed further. Composition changes occurring in the  $\beta$  phase just ahead of the surface of the growing nodules have permitted the corresponding portions of the interior structure of the nodules to be much nearer to the equilibrium composition of the  $\alpha$  and  $\delta$  phases than is the case in the adjacent cross-hatched  $\beta$  phase. However, at this point, it is probable that only a small amount of the  $\alpha$  phase has precipitated in the interior of the nodules. It is only on continued

isothermal transformation of the nodules formed at the intermediate temperatures that the equilibrium composition of the  $\delta$  phase is reached.

In the fine pearlite formed at temperatures slightly below the eutectoid temperature, composition changes occurring just ahead of the surface of the growing nodules permit the  $\delta$  phase to form only slightly supersaturated with copper. The transformation to the equilibrium  $\gamma$ -brass structure of the  $\delta$  phase results in the formation of the secondary pearlite, as has been discussed.

## VI.—CONCLUSIONS

Although the pearlite which forms in the copper-indium eutectoid alloy is similar in appearance to the pearlite which forms in the iron-carbon eutectoid, a significant difference is observed between the two transformations. During the formation of the iron-carbon pearlite, nodules of pearlite, in which the  $\alpha$ -iron and iron carbide are virtually of equilibrium composition, nucleate and grow in the parent austenite; all the adjustments in composition are made directly *ahead* of the advancing pearlite/austenite interface.<sup>8</sup> During the formation of the copper-indium pearlite, however, some of the adjustments are made *behind* the advancing interface between the growing nodule and the parent  $\beta$  phase; the extent of the adjustments of composition occurring in the interior of the growing nodule increases as the temperature of transformation decreases below the eutectoid temperature. Evidence of composition adjustments in the nodules is found in the formation of the secondary pearlite and in the manner in which the visible two-phase structure forms in the interior of the nodules appearing at the intermediate temperatures of isothermal transformation.

## ACKNOWLEDGEMENTS

The authors wish to thank Dr. L. L. Seigle of the Sylvania Electric Products Inc. Metallurgical Laboratories for his helpful discussions. This work was part of a study made possible by a grant from the International Nickel Company.

## REFERENCES

1. E. S. Davenport and E. C. Bain, *Trans. Amer. Inst. Min. Met. Eng., Iron Steel Div.*, 1930, 117.
2. D. Hanson and M. L. V. Gayler, *J. Inst. Metals*, 1922, 27, 267.
3. F. Weibke and H. Eggers, *Z. anorg. Chem.*, 1934, 220, 273.
4. W. Hume-Rothery, G. V. Raynor, P. W. Reynolds, and H. K. Packer, *J. Inst. Metals*, 1940, 66, 209.
5. W. Hume-Rothery, P. W. Reynolds, and G. V. Raynor, *ibid.*, 1940, 66, 191.
6. D. J. Mack, *Trans. Amer. Inst. Min. Met. Eng.*, 1948, 175, 240.
7. R. H. Fillnow and D. J. Mack, *ibid.*, 1950, 177, 1229.
8. R. F. Mehl, *J. Iron Steel Inst.*, 1948, 159, 113.





# THE FREE-ENERGY DIAGRAM OF THE SYSTEM TITANIUM-OXYGEN\*

1500

By O. KUBASCHEWSKI,† Dr.phil.habil., MEMBER, and  
W. A. DENCH †

(Communication from the National Physical Laboratory.)

## SYNOPSIS

Titanium-oxygen alloys of various compositions were equilibrated with calcium, magnesium, or barium mixed with its respective oxide in bombs of titanium or steel at temperatures between 950° and 1380° C. After leaching, the concentrations of oxygen in the titanium were determined by the vacuum-fusion method. The analytical data, the free energies of formation of the oxides of the alkaline-earth metals, and the heats and entropies of formation of the titanium oxides have been used to construct the free-energy concentration curves of the titanium-oxygen system at 1000° and 1200° C.

## I.—INTRODUCTION

SYSTEMS of transition metals with oxygen or sulphur are generally treated by thermochemists as though they strictly obeyed Dalton's law. The thermochemical data for certain "compounds" whose existence has been established by X-ray analysis are determined, and the intermediate concentration ranges are neglected. The fact is constantly overlooked that these systems closely resemble certain alloy systems having phases of variable composition. The thermochemical investigation should, therefore, extend over the whole system and not be limited to a few compositions which may not even be of any particular significance. An example of an investigation over a whole range of compositions is afforded by the free-energy diagram of the vanadium-oxygen system, recently published.<sup>1</sup>

The formation of solution ranges instead of compounds of constant composition has considerable practical importance. The production of a pure metal is not simply a question of reducing a certain compound by a straightforward reaction with a reducing agent, for a given agent can remove the negative component only to the extent that it is able to overcome the gradual increase of affinity of the negative component for the metal in the solution range; i.e. with each reducing agent there will be a certain *equilibrium* concentration, below which no further reduction can occur under the given conditions.

A knowledge of the complete free-energy curve of the system, particularly in the concentration range near the pure metal, is therefore indispensable in any discussion of the production of a metal from its oxides or sulphides. The method usually employed for establishing such free-energy curves is to determine the oxygen or sulphur content of the metal after it

has been held in contact with mixtures of various compositions of hydrogen and water vapour or hydrogen sulphide. This method has, for instance, been applied successfully to the iron-oxygen and iron-sulphur systems. The metals of Groups IVA and VA, however, have much higher affinities for oxygen and sulphur, and the method is not applicable in these cases. On the other hand, the determination of the heats of formation, standard entropies, and specific heats would be rather laborious; accordingly, a new method was suggested by Dr. N. P. Allen for the system vanadium-oxygen, and this has already been described.<sup>1</sup> This method has been further developed and has now been applied to the titanium-oxygen system.

## II.—EXPERIMENTAL PROCEDURE

The experimental method involves heating a sample of titanium containing oxygen for some time at a known temperature with calcium, magnesium, or barium. Under these conditions the oxygen content of the titanium should be reduced until its pressure equals the dissociation pressure of the oxide of the alkaline-earth metal. The surplus reducing metal and its oxide are removed, and the oxygen content of the titanium is determined.

Titanium-oxygen alloys containing 3–12 wt.-% oxygen were prepared by melting mixtures of Kroll titanium and pure titanium dioxide in an arc furnace. The Kroll titanium contained as impurities Si 0.025, Fe 0.2–0.4, Al 0.007, Mg 0.035, C 0.05, O 0.24, H 0.02, and N 0.02–0.05%. The titanium-oxygen alloys were ground in a tungsten-carbide mortar to various particle sizes. The fine powder (*f*) was 0.4–0.12 mm. in dia., the very fine powder (*vf*) represented the portion with a particle size of less than 0.12 mm. dia., and the third

\* Manuscript received 18 March 1953.

† Metallurgy Division, National Physical Laboratory, Teddington, Middlesex.

grade (vuf) was obtained by further grinding the *vf* powder for  $\frac{1}{4}$  hr. in an agate mortar.

Samples of 2.5–5 g. of these powders were mixed with one to two times this amount of calcium, barium, or magnesium. The purities of these metals were 99.8, 98.5, and 99.97%, respectively. Calcium and barium were used in the form of small lumps; the magnesium was turned into hollow cylinders, which were filled with the titanium powder and closed by a magnesium plug. In other cases the magnesium was in the form of turnings (No. 18, Table I) or powder (No. 15 and 17, Table I). The mixtures were sealed in cylinders of mild steel of length 6.5 cm., dia. 2.5 cm., and wall thickness 3 mm.

Iron is virtually insoluble in liquid calcium and barium,<sup>2</sup> and its solubility in liquid magnesium is

gently knocked; finally they were quenched in water and opened by turning off the bottom part on a lathe. The contents generally collected at the bottom in a solid mass, which was either crushed, if brittle, or turned off. The products were then leached in dilute hydrochloric acid (generally 5%) for 20–75 min. to dissolve the alkaline-earth metal and its oxide. The undissolved titanium powder was filtered, washed with distilled and de-aerated water, and dried at room temperature in an evacuated desiccator. At this stage some of the powders were analysed chemically for titanium and iron, and in a few cases spectrographically for calcium or magnesium. It was observed that the powders picked up considerable amounts of hydrogen during leaching, and before gas analysis these were removed by heating the powder

TABLE I.—*Experimental Details and Analyses of Reduction of Titanium Containing Oxygen by Calcium, Magnesium, and Barium.*

Experiment No.	Initial Oxygen Content of Ti, wt.-%	Relative Powder Size	Reactant	Crucible Material	Re-action Time, hr.	Re-action Temp., °C.	Analysis of Reduced Powder, wt.-%							Remarks
							O	N	H	Fe	Ca + Mg	Ti	Total	
1	3	vf	Ca	Steel	8	900	0.095	0.05	0.005	1.57	n.d.	98.5	100.2	
2	3	vf	Ca	"	16	1000	0.24	<0.1	0.1	~5	<0.1	n.d.	...	
3	4	vf	Ca	"	8	1000	0.23	0.1	0.1	3.65	<0.1	n.d.	...	
4	3	vuf	Ca	"	$\frac{1}{2}$	1020	0.10	0.14	0.01	0.84	n.d.	n.d.	...	
5	4	vf	Ca	"	$\frac{1}{2}$	1020	0.125	0.14	0.005	n.d.	n.d.	n.d.	...	
6	3	vuf	Ca	Titanium	4	1020	0.12	0.18	0.01	0.27	n.d.	98.42	99.0	
7	3	vf	Ca	"	5	1020	0.13	0.1	0.01	n.d.	n.d.	n.d.	...	
8	3	vf	Ca	"	7	1020	0.10	0.11	0.01	n.d.	n.d.	n.d.	...	
9	3	vf	Ca	"	8	1020	0.07	0.08	0.21	0.34	n.d.	98.9	99.6	
10	3	vf	Ca	Steel	8	1050	0.23	0.12	0.14	3.5	n.d.	96.1	100.1	
11	3	vuf	Ca	Steel*	5 $\frac{1}{2}$	1100	0.14	0.06	0.06	0.3	0.08	99.4	100.04	* low contact area with wall
12	3	vf	Ca	Titanium	7 $\frac{1}{2}$	1100	0.08	0.35	0.1	n.d.	n.d.	n.d.	...	
13	3	vf	Ca	"	1	1380	0.21*	0.30	0.01	n.d.	0.21	n.d.	...	* 0.08% as CaO, leaving 0.13% O
14	3	vf	Mg	"	8	960	2.8	0.07	0.01	n.d.	n.d.	n.d.	...	
15	TiO <sub>2</sub>	...	Mg	Steel	3	975	2.74*	0.24	0.03	2.30	0.83	93.7	99.8	* 0.54% as MgO, leaving 2.20% O
16	4	vuf	Mg	"	5	1000	1.5	<0.1	0.5*	4.70	n.d.	92.0	98.8	* not degassed
17	0.1	vf	Mg + MgO	Titanium	8	1000	2.22	0.4	0.01	0.34	n.d.	95.32	98.3	Ti by Ca reduction
18	3	vf	Mg	"	8	1020	2.5	0.7	0.4*	n.d.	n.d.	n.d.	...	* not degassed
19	4	vf	Mg	Steel	8	1100	2.0	<0.1	0.2	24.11	n.d.	73.65	100.0	
20	3	vf	Mg	Titanium	8	1200	2.03*	0.12	0.006	n.d.	0.45	n.d.	...	* 0.30% as MgO, leaving 1.73% O
21	4	f	Mg	Steel	14	1250	2.3	0.1	<0.1	n.d.	n.d.	n.d.	...	
22	12	vf	Ba	Titanium	8	1000	6.5	1.34	0.025	n.d.	n.d.	n.d.	...	
23	3	vuf	Ba + BaO	Steel	8	1100	6.85	3.52	0.29	n.d.	n.d.	n.d.	...	0.36% C

n.d. = not determined.

small (0.3% at 1000° C., increasing with temperature<sup>3</sup>); however, the titanium picked up considerable amounts of iron (see, e.g., No. 19, Table I), except in experiment No. 11, which was carried out in an exceptionally large steel bomb, so that the area of contact between the reaction mixture and the container was relatively small. Since the iron content might affect the activity of oxygen in titanium, a series of experiments was carried out in titanium cylinders turned from a titanium bar (containing O 0.22, H 0.02 and N 0.09 wt.-%, according to a vacuum-fusion analysis). The titanium cylinders were of the same size as the steel cylinders, but were closed by a tightly fitting plug of titanium and enclosed in steel bombs, which were then sealed by welding, the space between the titanium and the steel being packed with calcium oxide.

The bombs were heated to temperatures between 900° and 1380° C. for  $\frac{1}{2}$ –16 hr., during which they were removed from the furnace from time to time and

to 850° C. in a silica tube connected to a mechanical vacuum pump. The powders were then analysed for oxygen, nitrogen, and hydrogen by the vacuum-fusion method.<sup>4</sup>

The solubility of titanium in liquid magnesium is very small (0.0025% at 650° C.<sup>5</sup>), and so in all probability is its solubility in liquid calcium and barium.

### III.—EXPERIMENTAL RESULTS

The results of the various analyses, together with some of the experimental details, are summarized in Table I. In addition to the elements listed in the table, the reduced samples contained 0.03–0.2% manganese, 0.02–0.1% silicon, traces of other metals, such as chromium and vanadium, and occasionally some carbon. The total content of these impurities was 0.2–0.4% when steel bombs were used, but less



with the titanium bombs. Apart from analytical inaccuracies, another reason for the varying deviations from a total of 100% in Table I is the fact that chemical analysis was carried out before, and vacuum-fusion analysis after, degassing, and the amounts of hydrogen contained in the leached powders varied greatly.

The nitrogen contents were largely due to the starting materials. After melting in the arc furnace, the titanium-oxygen alloys contained small but varying amounts of nitrogen and, in addition, any nitrogen contained in the alkaline-earth metals would be absorbed by the titanium. This was to be expected from the thermochemical data for the nitrides<sup>6</sup> and was confirmed by an experiment in which titanium containing 17.4% nitrogen was found still to give the same analysis after being in contact with liquid calcium for 8 hr. at 1000° C. The high nitrogen contents of the last two samples in Table I are due to the nitrogen contained in the barium and barium oxide used in the reaction mixtures. It was also observed that the slightest leak in the degassing apparatus caused a pick-up of nitrogen and oxygen by the powder; such results were, of course, rejected.

As mentioned above, the iron contents of the reduced powders were found to be considerable when steel bombs were used, particularly when magnesium was the reducing agent. When titanium bombs were used, the iron contents were assumed to be equal to or less than the original amounts in the titanium, i.e. <0.35%.

It was found in a separate series of experiments that the rate of solution of magnesium oxide and calcium oxide in hydrochloric acid was slower the higher the temperature from which the powders were quenched. Some samples were therefore analysed to determine the calcium and magnesium remaining after leaching. The residual calcium and magnesium was low when the reaction temperature was 1000° or 1100° C. (No. 2, 3, and 11), but high in samples (No. 13 and 20) that had reacted above 1200° C. The residual magnesium was also high when large amounts of magnesium oxide were present, as in sample No. 15, where titanium dioxide was reduced by magnesium. The most favourable procedure for the whole-range reduction of titania, however, requires separate investigation and is not the object of the present paper. It appears justifiable to assume that the remaining amounts of alkaline-earth metals are present in the form of their oxides and therefore to subtract the equivalent amounts of oxygen from the contents given in column 8 of Table I to derive the oxygen dissolved in titanium.

Since the oxygen contents found by analysis might have been not the equilibrium concentrations but due largely to adsorption during the wet treatment of the powders, the particle size was varied, but this had no effect on the results within the limits of error, and it was concluded that the amount of adsorbed oxygen could be neglected.

Owing to the relatively high sensitivity of titanium to nitrogen, the irregular amounts of nitrogen in the

powders could hardly be avoided. Generally they were fairly small. For the reduction by calcium, there appears to be slight tendency, if any, to higher oxygen values the higher the nitrogen content. This is hardly likely to be due to equilibrium conditions, and it could be explained by slight adsorption during leaching or degassing. It is therefore assumed that the lowest figures for oxygen in the calcium reductions are closest to the actual equilibria.

A dependence on temperature cannot be deduced from Table I within the limits of error, but on thermochemical grounds reduction should be favoured by lower temperature; it is seen, however, that this dependence cannot be very pronounced. The time of reduction appears to have no effect on the result; equilibrium is virtually attained after  $\frac{1}{2}$  hr.

Table I indicates that the reduction of titania by magnesium can be carried far below the composition TiO, contrary to the findings of Chrétien and Wyss,<sup>7</sup> and the statements in an earlier patent by Dominion Magnesium, Ltd.<sup>8</sup> Later, this firm published another patent,<sup>9</sup> in which a higher degree of reduction of titanium oxides by magnesium is claimed, substantially in agreement with the present findings. There is agreement between the present results and those of the three papers mentioned<sup>7, 8, 9</sup> that calcium reduces titanium oxides almost to the pure metal.

The equilibrium concentration of oxygen in titanium in contact with calcium oxide and liquid calcium is 0.07–0.12 wt.-% at the temperatures studied. The presence of several per cent. of iron increases this figure to more than 0.2% (No. 2, 3, and 10). The oxygen concentrations for magnesium lie between 1.5 and 2.8 wt.-%; those for barium at about 6.7%. In order to ascertain that these are true equilibrium values, equilibrium was established "from both sides" by reduction as well as by oxidation (No. 17 and 23). The agreement was satisfactory.

The results for the reduction by magnesium may be compared with the phase diagram for the titanium-oxygen system determined by Bumps, Kessler, and Hansen.<sup>10</sup> At 1000° C. the ( $\beta + \alpha$ ) field extends from 0.6 to 2.1 wt.-% oxygen, and at 1200° C. from 1.4 to 3.6%. The reduction and oxidation experiments carried out in titanium bombs at about 1000° C. lead to an equilibrium concentration of  $2.4 \pm 0.2\%$  oxygen, just inside the  $\alpha$  phase. When iron was picked up in considerable quantities, the equilibrium concentrations of oxygen tended to be lower, but, as iron is expected to have an effect on the activities of oxygen in titanium, the results of experiments Nos. 16 and 19 should be disregarded. The same would apply to No. 21, though the iron content of the powder has not been determined; owing to the increase of solubility of iron in magnesium with temperature, the iron content of this sample is probably high. The analysis of No. 20, however, is interesting. Taking into account the amount of oxygen combined with magnesium, only 1.7% is found in the titanium. This is in agreement with the phase diagram: since the ( $\beta + \alpha$ ) field extends to higher oxygen concentrations

at 1200° C., reduction, carried through the whole of the heterogeneous field, should result in a maximum concentration of 1.5%, a value that was not quite attained.

These considerations do not apply to the results obtained with barium; the oxygen contents in samples 22 and 23 correspond to concentrations well within the  $\alpha$  phase field. The results with barium are somewhat uncertain because of the relatively high nitrogen contents.

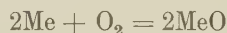
There are thus three equilibrium values for the activity of oxygen in solid solutions of oxygen in titanium for a temperature of about 1000° C. which may be used in thermochemical calculations. The following concentrations are suggested (1000° C.):

Reduction by:	Ca	Mg	Ba
Oxygen, wt.-%.	0.07	2.3	6.6

It is very difficult to estimate the probable errors. Inaccuracies due to temperature measurement, &c., may be neglected. The accuracy of the vacuum-fusion analysis may be taken to be within  $\pm 10\%$  of the given values. The effect of nitrogen and other impurities on the oxygen concentration can probably be neglected. A possible major source of error is the adsorption of oxygen during leaching and degassing. Since the particle size of the starting materials does not appear to have had any great influence, and since the oxygen contents were substantially confirmed when analyses were carried out with undegassed samples, the error due to adsorption was taken to be within the scatter of the analytical results. Some account has been taken of the possible effect of adsorption by selecting figures somewhat below the average.

#### IV.—THERMOCHEMICAL EVALUATION

The dependence on temperature of the standard free energies of formation of the alkaline-earth-metal oxides according to the reaction



are known.<sup>6, 15</sup> The values for 1000° C. are –241,800 cal. for 2CaO, –224,000 cal. for 2MgO, and –204,300 cal. for 2BaO. The estimated limits of accuracy of these values are  $\pm 1500$  cal.,  $\pm 800$  cal., and  $\pm 6000$  cal., respectively. These values and the oxygen concentrations given above have been used to plot circles in Fig. 1 relating the *partial* free energies  $\Delta\bar{G}_{\text{O}_2} = -RT \ln p_{\text{O}_2}$  to the percentage of oxygen in the titanium–oxygen system. It is seen that the free energy of dissociation increases with decreasing concentration of oxygen, as is required by the conditions of thermodynamics. The limitations of the phase fields, which are also plotted, have been obtained from the papers by Hansen *et al.*<sup>10</sup> and (beyond TiO) by Ehrlich.<sup>11</sup> It should be remembered that the partial free energy of dissociation must decrease with increasing oxygen concentration within the homogeneous ranges and remain constant within the heterogeneous

ones. On the basis of these considerations, together with the present results and the integral free energies at the “compound” compositions TiO, Ti<sub>2</sub>O<sub>3</sub>, Ti<sub>3</sub>O<sub>5</sub>, and TiO<sub>2</sub>, the complete partial-free-energy curve can be worked out with fair accuracy. The latter values can be obtained from the heats of formation,<sup>12</sup> the entropies,<sup>13</sup> and the molar heats<sup>14</sup> of the compounds mentioned and of pure titanium. Earlier results of thermochemical and equilibrium measurements in-

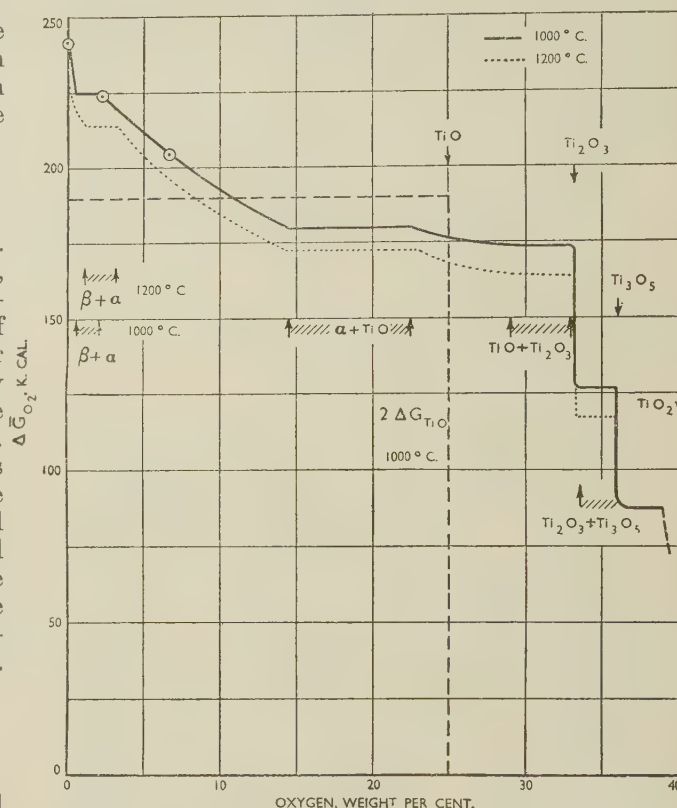
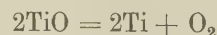


FIG. 1.—Partial Free Energies in Titanium–Oxygen System.

volving titanium oxides<sup>6</sup> are considered to be less accurate and have been neglected.

Calculation of the integral free energy of dissociation of the monoxide, according to the reaction:



leads to

$$\Delta G^0_T = 244,600 - 42.6T \quad (600^\circ\text{--}1800^\circ \text{K.})$$

The connection between partial and integral thermochemical values is given by:

$$\Delta G = N_{\text{Ti}} \int_0^x \Delta\bar{G}_{\text{O}_2} dx,$$

where  $x = N_{\text{O}}/N_{\text{Ti}}$  and  $N_{\text{O}}$  and  $N_{\text{Ti}}$  represent atomic fractions of oxygen and titanium, respectively ( $N_{\text{O}} + N_{\text{Ti}} = 1$ ). Thus the area under the curve in Fig. 1 (if plotted against the concentration scale  $N_{\text{O}}/N_{\text{Ti}}$ ) must be equal to the integral value given above, and is represented by the dashed curve in



Fig. 1. The experimental part of the curve was extrapolated to the phase boundary  $\alpha/(\alpha + \text{TiO})$ , thus determining the horizontal part in the  $(\alpha + \text{TiO})$  range. There can be no more than a slight drop in the value of  $\Delta\bar{G}_{\text{O}_2}$  within the homogeneity range of TiO if the condition that the two areas given by the full and dashed lines should be equal is to be satisfied. It was found that the experimental data and the thermodynamical conditions permit only a small range of deviation of the values, so that the  $\Delta\bar{G}_{\text{O}_2}$  curve as drawn probably agrees closely with the true one. The partial free energy of dissociation,  $\Delta\bar{G}_{\text{O}_2}$ , of 2TiO at 1000° C. is found to be 176,000 cal., as compared with its integral free energy of dissociation of 190,000 cal.

Using the data mentioned,<sup>12-14</sup> the remaining part of the curve beyond the composition TiO has been obtained in a similar manner which need not be discussed in detail. As an example of such an evaluation, the free-energy diagram of the system vanadium–oxygen was discussed more fully in an earlier paper.<sup>1</sup>

The continuous curve in Fig. 1 is valid only for 1000° C. The present results do not allow a derivation of values for the entropies or heats of solution. Since the oxygen concentrations after reduction at various temperatures between 950° and 1200° C. do not vary substantially with temperature, the temperature coefficients for the free energies of formation of the alkaline-earth-metal oxides may be used for calculations in that temperature range. In doing this, the phase diagram of the titanium–oxygen system<sup>10</sup> should be consulted. Using the high-temperature values found in the present investigation, a free-energy curve has been drawn as a dotted line in Fig. 1. The present data should not be used, however, for other than rough calculations above, say, 1300° C.

## ACKNOWLEDGEMENTS

The work described above has been carried out as part of the research programme of the National Physical Laboratory, and this paper is published by permission of the Director of the Laboratory.

The authors wish to acknowledge the comments and suggestions received from Dr. N. P. Allen and Mr. H. A. Sloman, and also the assistance given by Mr. T. H. Schofield in preparing the titanium–oxygen alloys and Mr. C. A. Harvey in carrying out the vacuum-fusion analyses.

## REFERENCES

1. N. P. Allen, O. Kubaschewski, and O. von Goldbeck, *J. Electrochem. Soc.*, 1951, **98**, 417.
2. M. Hansen, "Der Aufbau der Zweistofflegierungen". 1936: Berlin (J. Springer).
3. E. Fahrenhorst and W. Bulian, *Z. Metallkunde*, 1941, **33**, 31.
4. H. A. Sloman, *J. Inst. Metals*, 1945, **71**, 391.
5. K. T. Aust and L. M. Pidgeon, *Trans. Amer. Inst. Min. Met. Eng.*, 1949, **185**, 585.
6. O. Kubaschewski and E. Ll. Evans, "Metallurgical Thermochemistry". 1951: London (Butterworth-Springer).
7. A. Chrétien and R. Wyss, *Compt. rend.*, 1947, **224**, 1642; *Ann. Chim.*, 1948, [xii], **3**, 215.
8. Dominion Magnesium Ltd., Brit. Patent No. **664,061**, 1952.
9. Dominion Magnesium Ltd., Brit. Patent No. **675,933**, 1952.
10. E. S. Bumps, H. D. Kessler, and M. Hansen, *Trans. Amer. Soc. Metals*, 1953, **45**, 1008.
11. P. Ehrlich, *Z. Elektrochem.*, 1939, **45**, 362; *Z. anorg. Chem.*, 1941, **247**, 53.
12. G. L. Humphrey, *J. Amer. Chem. Soc.*, 1951, **73**, 1587.
13. C. H. Shomate, *ibid.*, 1946, **68**, 310.
14. B. F. Naylor, *ibid.*, 1946, **68**, 1077.
15. L. Brewer, *Chem. Rev.*, 1953, **52**, 1.

Continued from p. 92.

The conclusions drawn from this work are:

(a) Cold-working an iron–manganese alloy containing 19.0% manganese produces the metastable phases  $\alpha'$  and  $\epsilon$ .

(b) The amounts of metastable phases formed on filing increase with decreasing particle size, i.e. as the amount of cold work increases.

(c) Greater quantities of  $\gamma$  are transformed if the

temperature of the samples is prevented from rising by filing under a liquid.

## REFERENCES

1. M. Gensamer, J. F. Eckel, and F. M. Walters, Jr., *Trans. Amer. Soc. Steel Treat.*, 1931–32, **19**, 599.
2. J. G. Parr, *J. Iron Steel Inst.*, 1952, **171**, 137.
3. A. R. Troiano and F. T. McGuire, *Trans. Amer. Soc. Metals*, 1943, **31**, 340.

# 1501 The Effect of Cold Work on an Iron-Manganese Alloy\*

By J. GORDON PARR,† Ph.D., B.Sc., JUNIOR MEMBER

## SYNOPSIS

Cold-working an iron-manganese alloy produces metastable phases in quantities which depend upon the extent of cold working. This effect—and the different constitutions of filings made in air and under liquid—is demonstrated by phase analyses made on filings of different sizes.

THE effect of cold working iron-manganese alloys containing 10–30% manganese has been reported by some workers<sup>1,2</sup> to increase the amount of  $\epsilon$  phase (close-packed hexagonal). Others<sup>3</sup> have reported an increase in the amount of  $\alpha'$  phase (body-centred cubic, supersaturated with manganese). As both  $\alpha'$  and  $\epsilon$  are produced from the  $\gamma$  phase (face-centred cubic) by martensite-type reactions, it seems reasonable to expect an increase in the amounts of both phases on cold working.

As a preliminary stage of an investigation into the effect of cold work, filed samples from a 19 at.-% manganese alloy were examined by the X-ray spectrograph. Filings of a wide range of sizes, made simultaneously with a fine file, were screened into four fractions between 65 mesh and about 400 mesh. Etched and unetched filings showed the same phase ratios (computed from line intensities), and it was therefore assumed that the stress imparted by cold work was transmitted throughout each particle. (Presumably, the first few atom layers at the surface are extremely distorted, but these contribute only to the scattered “background” reflections.)

Although the filings do not have a uniform shape, nor are they similar to any simple geometrical solid, it is assumed as a rough approximation that each filing is cylindrical. The amount of work done on each filing to sever it from the main body of metal is proportional to its surface area, and hence the work done per unit volume of particle is proportional to area/volume, i.e. inversely proportional to diameter. It is to be expected, therefore, that filings of smaller diameter are more highly stressed.

This conclusion has been borne out by measuring line breadths of different size fractions of pure iron filings. Line broadening is due, in this case, either to lattice strain or to crystal fragmentation, both of which result from cold working. The observed consistent increase in line breadth as the particle size decreases indicates an increasing amount of cold work.

The factor that decides whether or not a filing passes through a screen aperture is length rather than diameter; but examination under a low-power microscope shows that filings that pass through smaller apertures have smaller diameters as well as shorter

lengths. Hence it may be deduced that the amount of work done on a filing depends upon its screen size.

Screened samples of the 19.0 at.-% manganese alloy were exposed to  $\text{FeK}_\alpha$  radiation and the amounts of the phases present were assessed. Results given in Table I are roughly reproducible and always show the same trend.

TABLE I.—*The Amounts of Phases in Different Size Fractions of Filings Made in Air.*

	Phases, %		
	$\alpha'$	$\gamma$	$\epsilon$
Original ingot . . . .	10	60	30
65–200 mesh (Tyler screen) .	17	48	35
200–250 mesh . . . .	19	36	45
250–325 mesh . . . .	25	25	50
325–400 * mesh . . . .	27	23	50

\* Assessed by microscopical examination.

Heat is evolved during filing, and it was thought possible that less transformation of  $\gamma$  might occur at elevated temperatures, for the  $\gamma \rightarrow \alpha' + \epsilon$  driving force decreases as the temperature rises. A further set of samples was therefore cut under toluene. Results are given in Table II. It will be seen that the

TABLE II.—*The Amounts of Phases in Different Size Fractions of Filings Made Under Toluene.*

	Phases, %		
	$\alpha'$	$\gamma$	$\epsilon$
Original ingot . . . .	10	60	30
65–200 mesh . . . .	36	16	48
200–250 mesh . . . .	40	11	49
250–325 mesh . . . .	41	8	51
325–400 * mesh . . . .	42	5	53

\* Assessed by microscopical examination.

same trend is observed, but that greater quantities of  $\gamma$  are transformed.

*Concluded on previous page.*

\* Manuscript received 8 June 1953.

† Post-Doctorate Research Fellow, British Columbia Research Council, Vancouver, B.C., Canada.



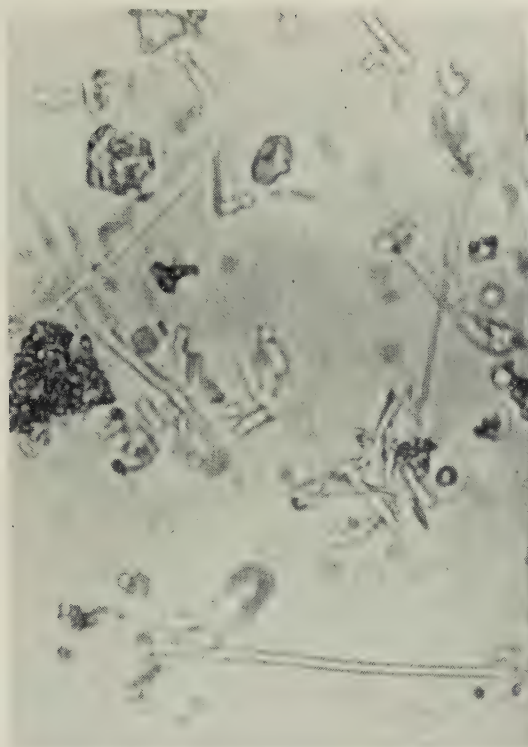


FIG. 1.—Water Insolubles from Flux Immediately After Melting Down in Furnace. Needles of  $\text{CaF}_2$  and a few films of alumina.  $\times 700$ .

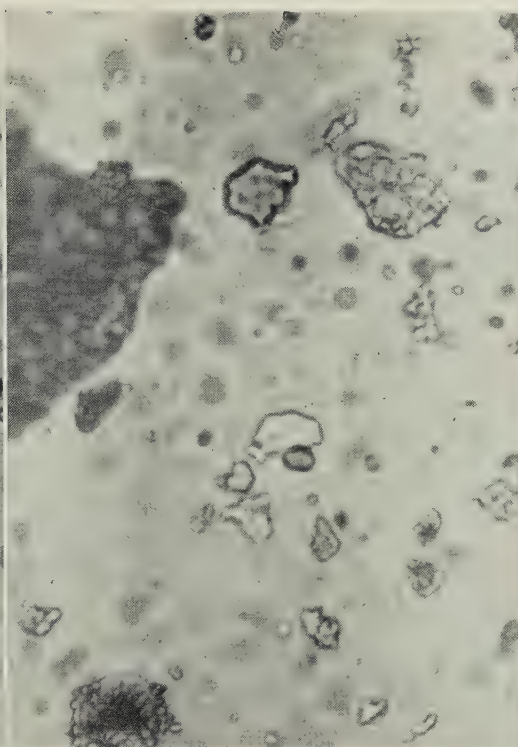


FIG. 2.—Water Insolubles from "Slag Out" Sample of Flux. Alumina films and plates of various sizes.  $\times 700$ .



FIG. 3.—Product Recovered from 10%  $\frac{1}{8}$ -in.-Dia. Aluminium Particles Melted in 90:10  $\text{NaCl-CaF}_2$  Flux Without Stirring. Fireclay crucible.  $\times 1$ .



FIG. 4.—Product Recovered from 10%  $\frac{1}{8}$ -in.-Dia. Aluminium Particles Melted and Stirred in 90:10  $\text{NaCl-CaF}_2$  Flux. Fireclay crucible.  $\times 1$ .

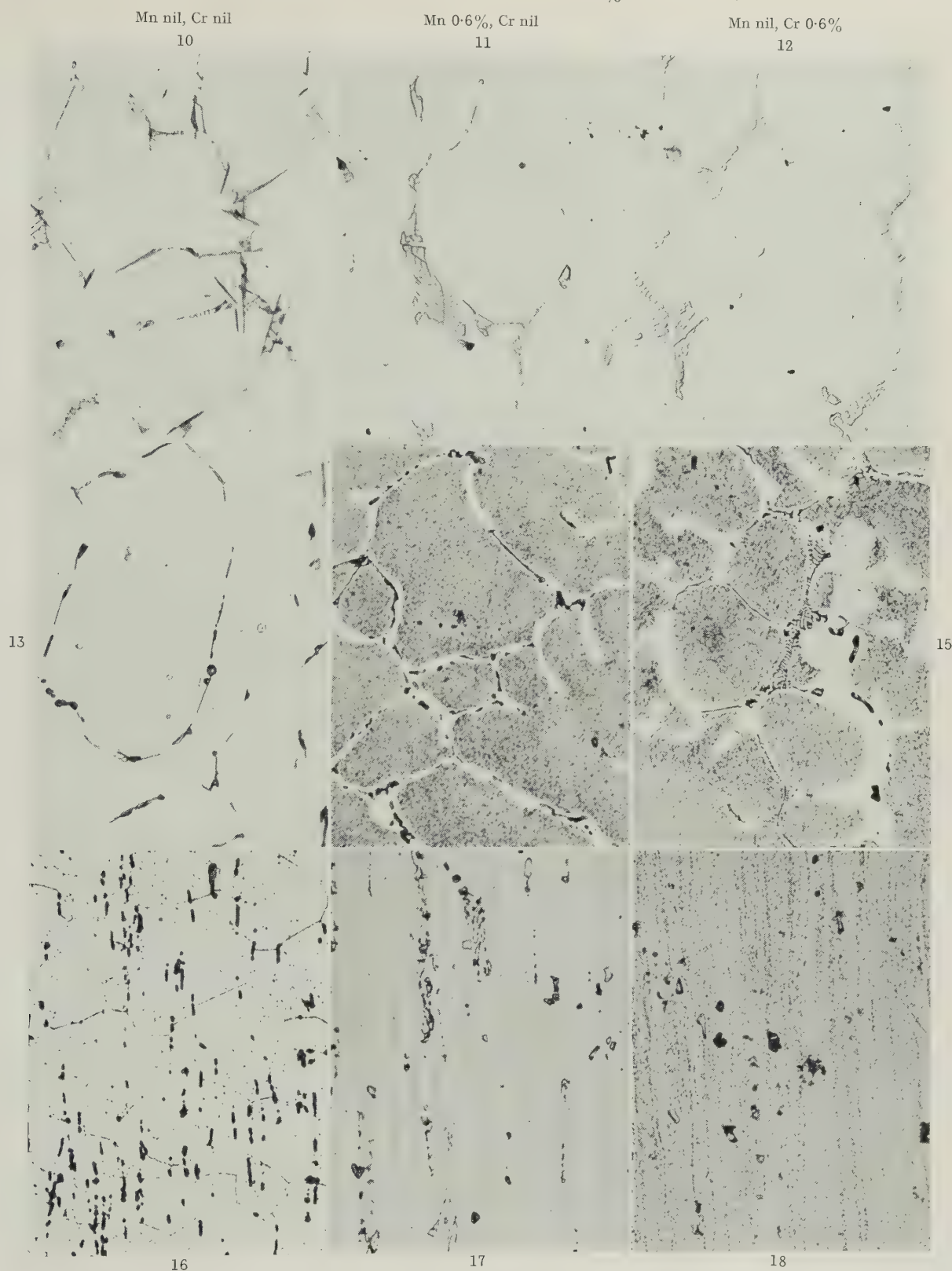
MICROSTRUCTURES OF IRON-FREE ALLOYS.  $\times 250$ .

FIGS. 1-3.—As cast.

FIGS. 4-6.—Cast and reheated to 500° C.

FIGS. 7-9.—Rolled, solution-treated at 540° C., quenched and aged at 160° C. Etched with Keller's reagent.



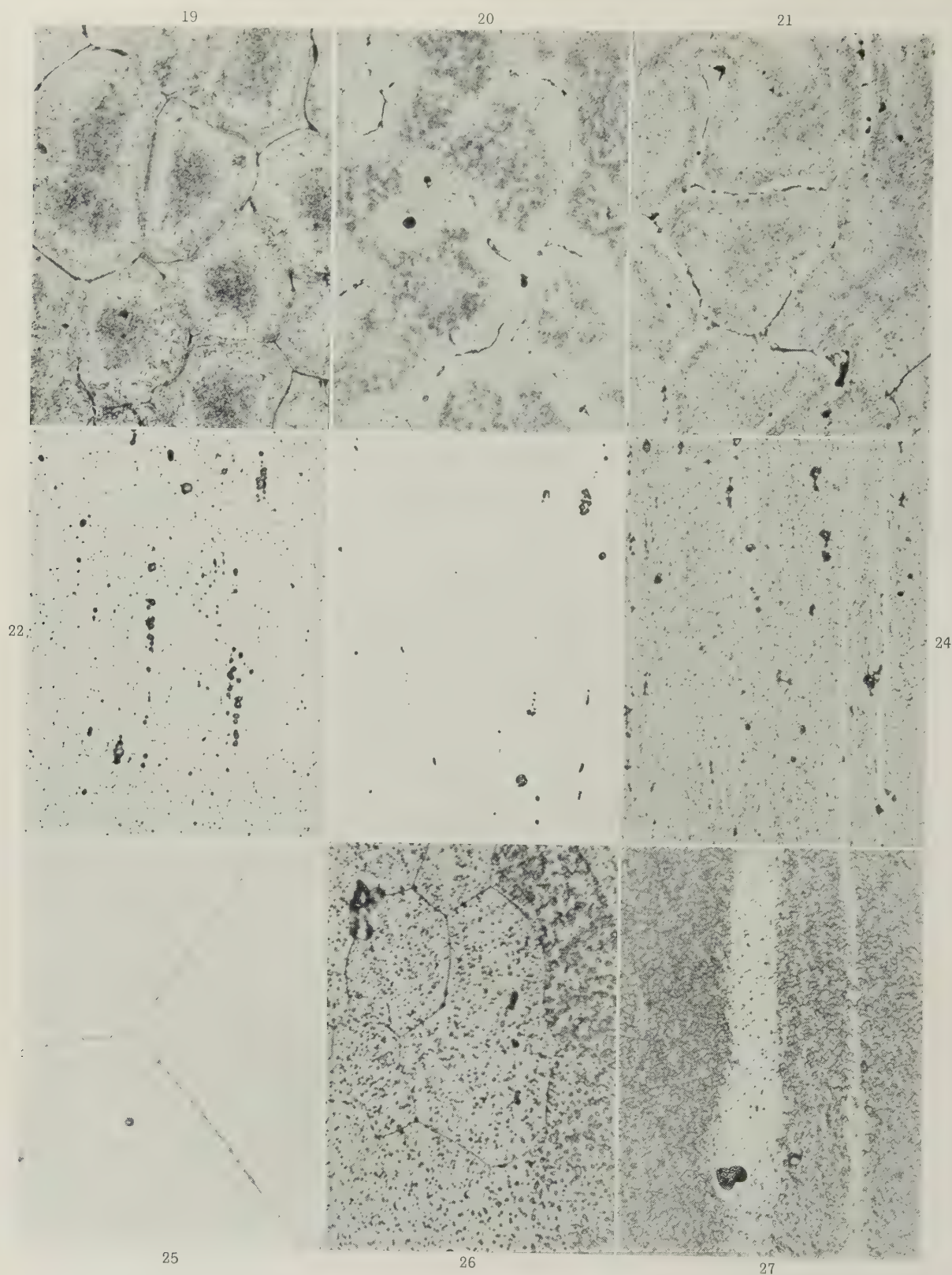
MICROSTRUCTURES OF ALLOYS CONTAINING 0.35% IRON.  $\times 250$ .

FIGS. 10-12.—As cast.

FIGS. 13-15.—Cast and reheated to 500° C.

FIGS. 16-18.—Rolled, solution-treated at 540° C., quenched and aged at 160° C. Etched with Keller's reagent.

## STRUCTURAL CHANGES ASSOCIATED WITH HEAT-TREATMENT.



FIGS. 19-21.—Fe nil, Mn 0.6%, Cr nil. Cast and reheated to 200°, 300°, and 400° C., resp.  $\times 250$ .  
 FIG. 22.—Fe nil, Mn nil, Cr nil. As rolled.  $\times 250$ . FIG. 23.—As 22, solution-treated at 540° C., and water-quenched.  $\times 250$ . FIG. 24.—Fe nil, Mn 0.6%, Cr nil. As rolled.  $\times 250$ .  
 FIGS. 25-27.—Alloys rolled, solution-treated, quenched, and aged at 160° C.  $\times 1500$ .  
 FIG. 25.—Fe nil, Mn nil, Cr nil. FIG. 26.—Fe nil, Mn 0.2%, Cr nil. Etched with Keller's reagent. FIG. 27.—Fe nil, Mn 0.6%, Cr nil.



ALLOY CONTAINING Fe NIL, Mn 0.6%, Cr NIL AFTER THERMAL TREATMENT.  $\times 250$ .

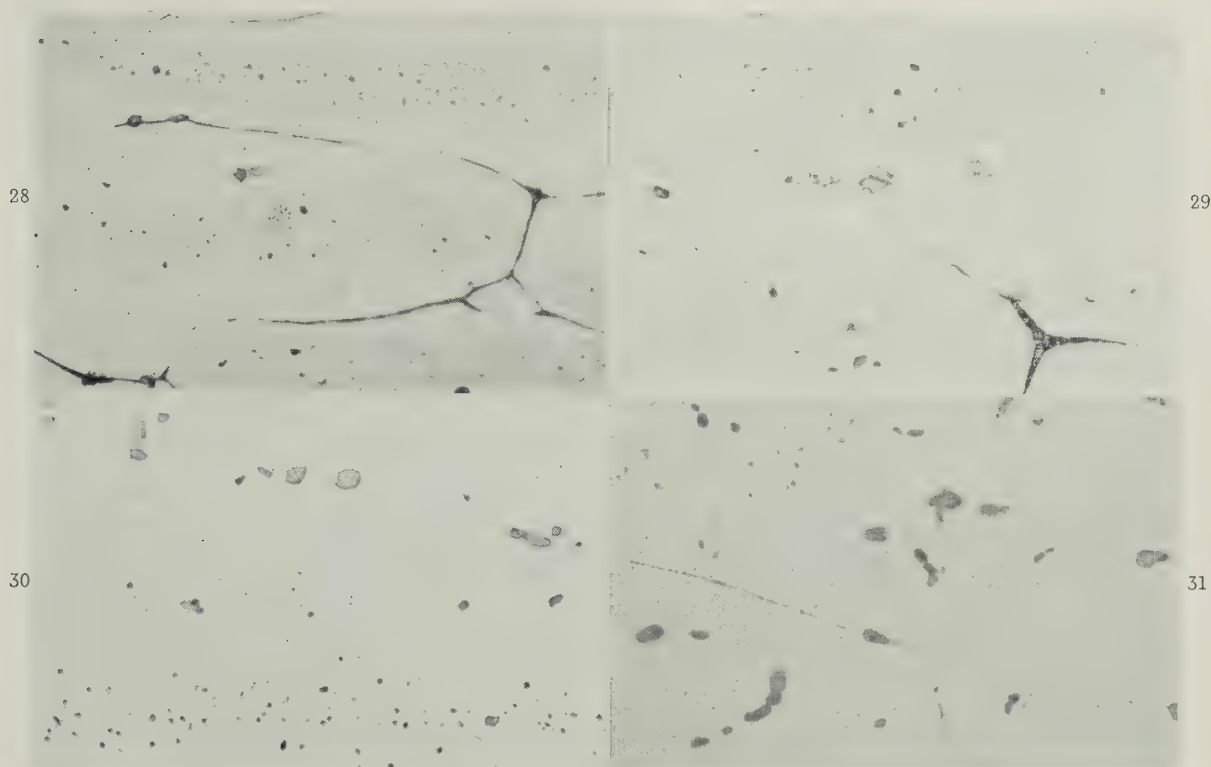


FIG. 28.—Temperature raised from  $0^{\circ}$  to  $600^{\circ}$  C. in 6 hr. Water-quenched.

FIG. 30.—Water-quenched after 120 hr. at  $600^{\circ}$  C.

FIG. 29.—Water-quenched after 15 hr. at  $600^{\circ}$  C.

FIG. 31.—Water-quenched after 120 hr. at  $600^{\circ}$  C., then aged for 18 hr. at  $160^{\circ}$  C.

Etched with Keller's reagent.

BEND-TEST SPECIMENS.  $\times 100$ .

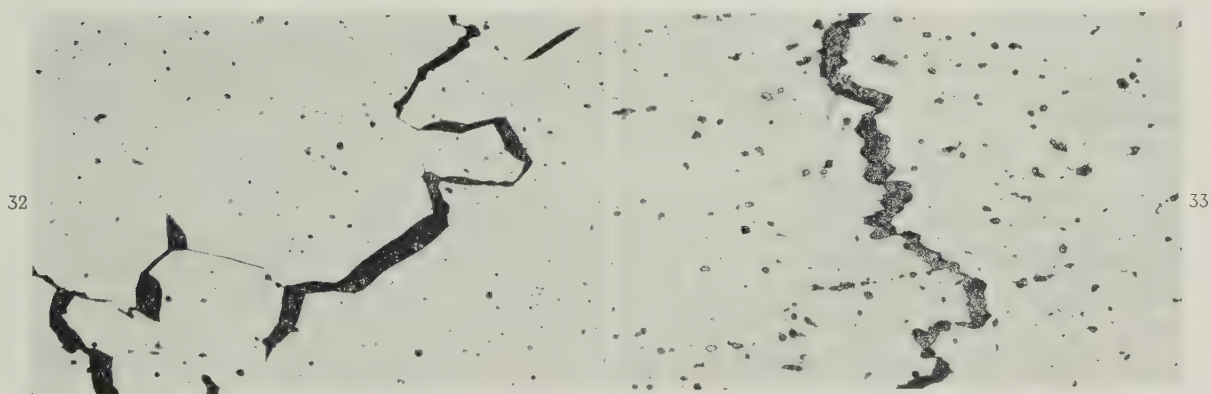


FIG. 32.—Fe nil, Mn nil, Cr nil. Intercrystalline crack.

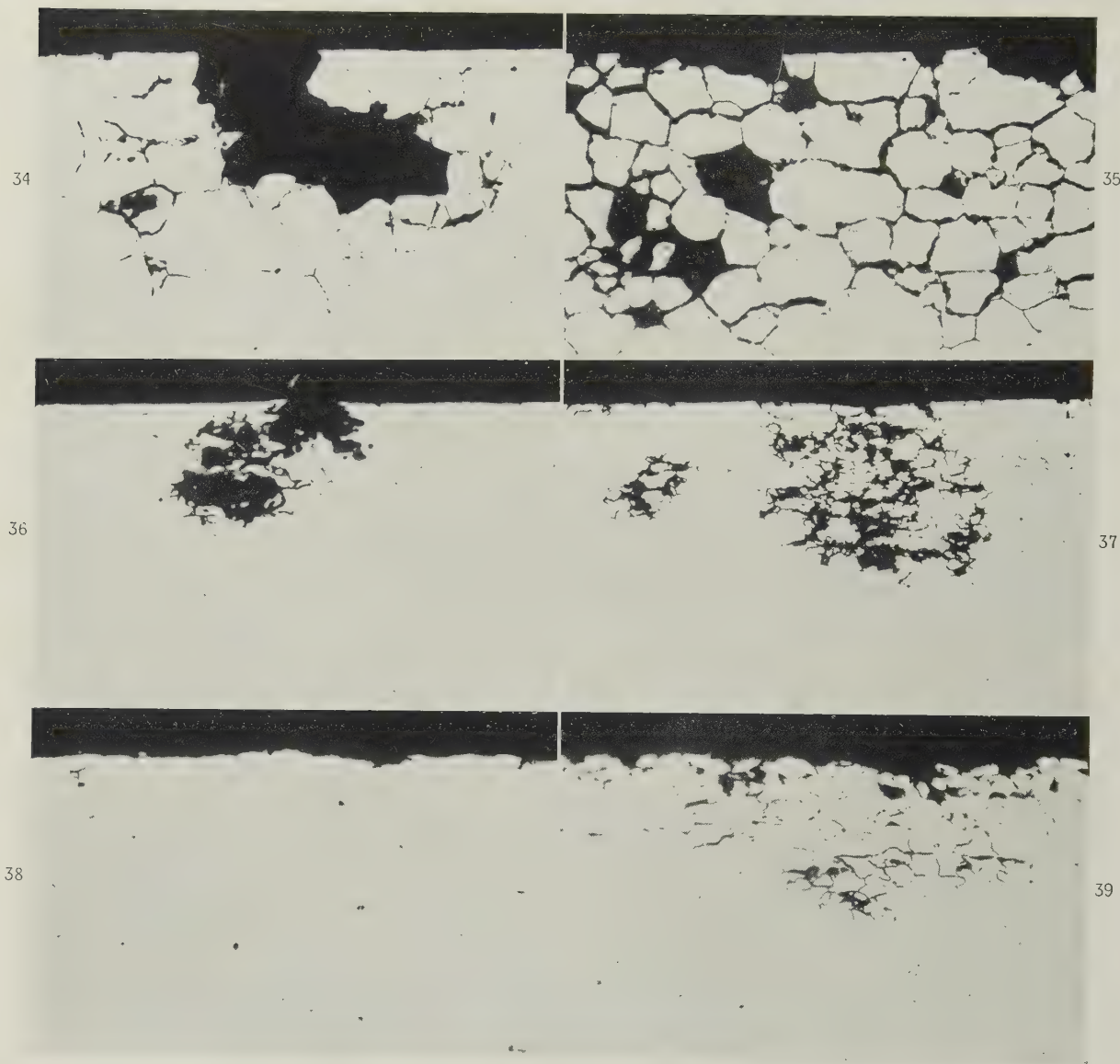
FIG. 33.—Fe nil, Mn 0.6%, Cr nil. Mainly transcrystalline crack.

Etched with 1% boiling NaOH solution.

SECTIONS THROUGH CORRODED SURFACES OF FULLY HEAT-TREATED ALLOYS.  $\times 100$ .

Corroded 5 Days in Salt-Peroxide Solution

Corroded 24 Hours in Acid-Salt Solution



FIGS. 34 AND 35.—Fe 0.35%, Mn nil, Cr nil.  
 FIGS. 36 AND 37.—Fe 0.35%, Mn 0.6%, Cr nil.  
 FIGS. 38 AND 39.—Fe 0.35%, Mn nil, Cr 0.2%.  
 Unetched.



## COPPER-INDIUM EUTECTOID ALLOY.

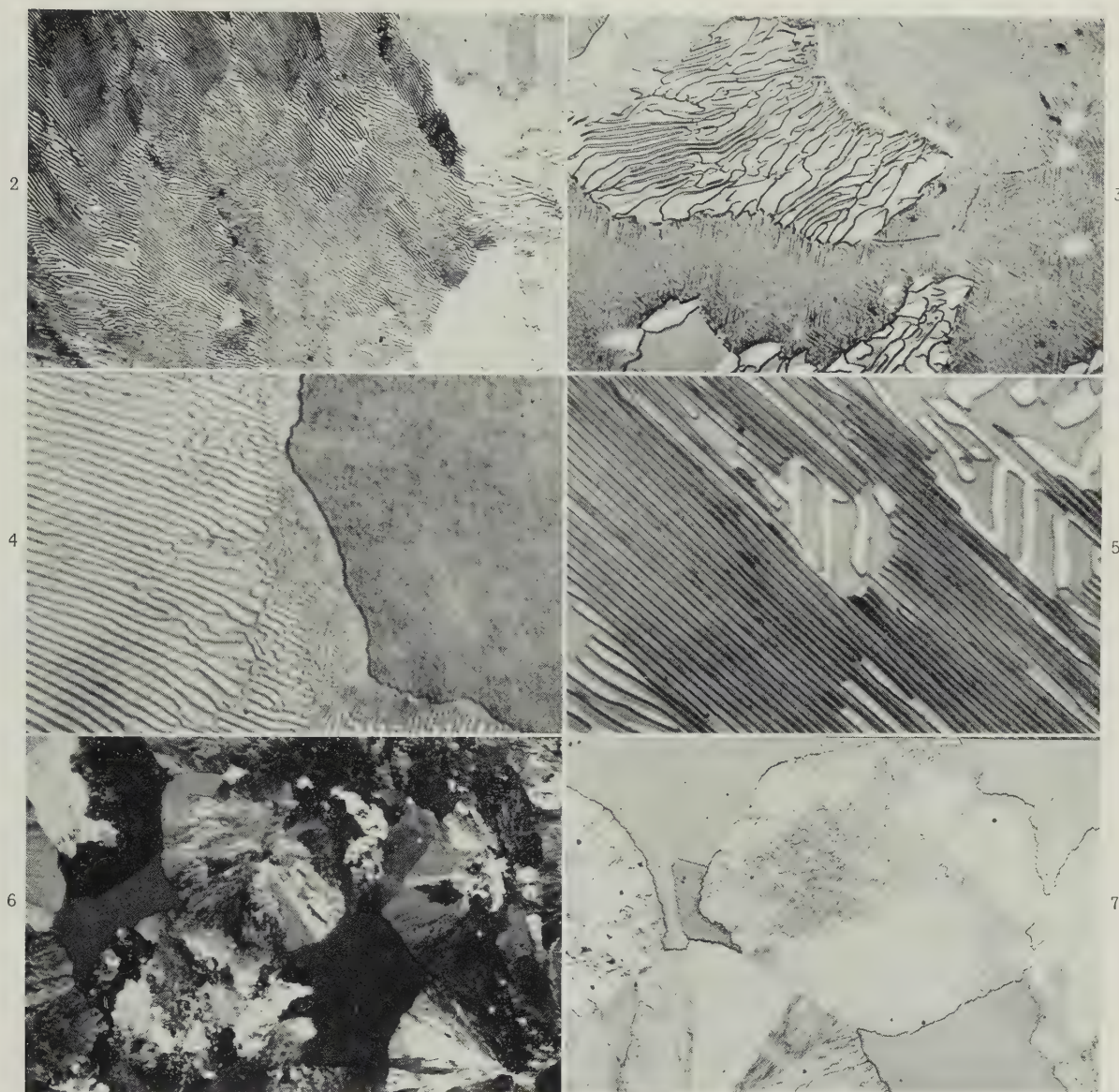


FIG. 2.—Fine Pearlite Formed by Furnace Cooling at  $1\frac{1}{2}^{\circ}\text{C./min.}$  from  $650^{\circ}\text{C.}$   $\times 250$ .

FIG. 3.—2 Hr. at  $573^{\circ}\text{C.}$  Pearlite nodule where pearlite lamellæ are separated from retained  $\beta$  by transitional area. Indirect illumination.  $\times 750$ .

FIG. 4.—8 Min. at  $570^{\circ}\text{C.}$  Edge of growing pearlite nodule. Pearlite lamellæ are separated from retained  $\beta$  by transitional area.  $\times 2000$ .

FIG. 5.—7 Hr. at  $570^{\circ}\text{C.}$  Coarse lamellar structure forming from the original fine lamellar pearlite. The light phase is  $\alpha$ ; the dark phase  $\delta$ .  $\times 2000$ .

FIG. 6.—12 Sec. at  $547^{\circ}\text{C.}$  Nodules under polarized light.  $\times 75$ .

FIG. 7.—12 Sec. at  $547^{\circ}\text{C.}$  Nodules under direct light.  $\times 150$ .



## COPPER-INDIUM EUTECTOID ALLOY.

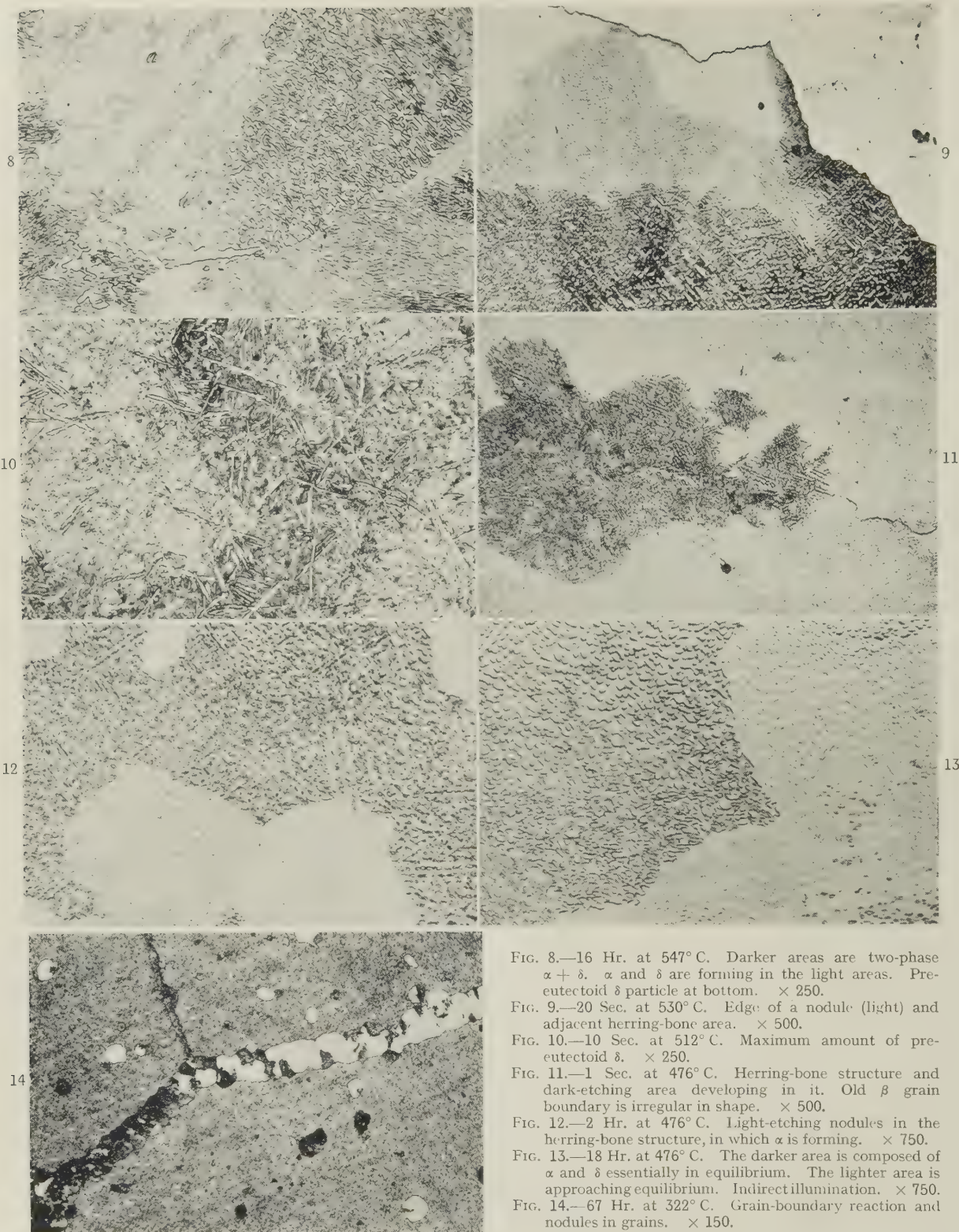


FIG. 8.—16 Hr. at 547° C. Darker areas are two-phase  $\alpha + \delta$ .  $\alpha$  and  $\delta$  are forming in the light areas. Pre-eutectoid  $\delta$  particle at bottom.  $\times 250$ .

FIG. 9.—20 Sec. at 530° C. Edge of a nodule (light) and adjacent herring-bone area.  $\times 500$ .

FIG. 10.—10 Sec. at 512° C. Maximum amount of pre-eutectoid  $\delta$ .  $\times 250$ .

FIG. 11.—1 Sec. at 476° C. Herring-bone structure and dark-etching area developing in it. Old  $\beta$  grain boundary is irregular in shape.  $\times 500$ .

FIG. 12.—2 Hr. at 476° C. Light-etching nodules in the herring-bone structure, in which  $\alpha$  is forming.  $\times 750$ .

FIG. 13.—18 Hr. at 476° C. The darker area is composed of  $\alpha$  and  $\delta$  essentially in equilibrium. The lighter area is approaching equilibrium. Indirect illumination.  $\times 750$ .

FIG. 14.—67 Hr. at 322° C. Grain-boundary reaction and nodules in grains.  $\times 150$ .



## THE NEW METAL TITANIUM\*

1502

By MAURICE COOK,† D.Sc., Ph.D., F.I.M., MEMBER

## SYNOPSIS

The history of titanium and the present developing production position are reviewed with reference to the technological problems peculiar to the metal in regard to its extraction and processing. The abundance of titanium ores and the properties of the metal and those of its alloys so far developed, indicate its possibilities as a basic or large-tonnage metal, but the essential requirement for its eventually attaining this position is the devising of cheaper production methods.

After a brief survey of the extent and availability of titanium ores, methods for its production by dissociation of the tetraiodide and reduction of the tetrachloride with metallic magnesium are described, and details are given of its purification by vacuum treatment. Various other possible methods of extraction are mentioned, and the technology of arc melting titanium is described.

The effect of impurities, particularly oxygen, nitrogen, carbon, and hydrogen, on the properties of the metal and its fabrication, its physical, mechanical, and corrosion-resistance characteristics are broadly considered. After noting the early work on alloy development, the structural features and properties of alloys now available are briefly described in the light of the constitutional effect of the elements used, and an indication is given of some of the chief differences between single-phase and duplex alloys.

## I.—HISTORY

It may seem somewhat odd to refer, as I do in the title of this lecture, to titanium as a new metal when, in fact, its existence was known more than 150 years ago. Since that time it has, of course, been familiar to chemists as a metallic element with a recognized place in the Periodic Table, many of its compounds have long been used in quantity commercially, and for some years metallurgists have made use of it as a minor but not unimportant constituent in the production of both ferrous and non-ferrous alloys. It is, however, only within the last five years or so that the metal has been produced on a tonnage basis by industrially worked processes. Until a few years ago few people had even seen it, it is not yet a common metallurgical commodity, and few metallurgists have experience of it or know much about it. This, therefore, is the justification for referring to it as a new metal, which it is, in as much as we are just now witnessing its industrial birth.

In 1790, a Cornish clergyman named Gregor recognized that titanium dioxide was the oxide of a hitherto unknown metal, and in 1795 the Austrian chemist Klaproth came to the same conclusion, and although he did not isolate the metal, he called it titanium. It was, however, the famous Swedish chemist Berzelius who first produced titanium, albeit in a very impure state, in 1825, the same year as that in which the Danish chemist Oersted is credited with having first isolated aluminium. Metal of about 95% purity was produced in 1887 by Nilson and

Pettersson by reducing titanium tetrachloride with sodium, and in 1895 Moissan, by reduction in an electric arc, made metal of 98% purity, but it was brittle, and although in 1910 Hunter, in the U.S.A., made titanium of about 99.5% purity, which was ductile when hot, it was brittle in the cold state. It was in 1925 that van Arkel and de Boer produced experimentally, by the dissociation of the tetraiodide, metal sufficiently pure to establish the fact that titanium was ductile when cold. This indeed was the outstanding discovery made about titanium since its isolation in a crude form a hundred years earlier, and the discovery which indicated its potentialities. The assessment of the characteristics of titanium that could be made, following its experimental production in a pure form, provided a far different picture of the metal and its industrial future than it had previously been possible to visualize. The technique used by van Arkel and de Boer was one which on the grounds of cost and technological difficulties could not readily be translated into an industrial process, but their achievement provided the spur for other work on methods of producing titanium which might constitute the basis of industrial processes for its manufacture in quantity and at much lower cost.

In 1940, Kroll described a route for the production of titanium which, with some modifications, is the method by which most of the current output is produced, and it was, in fact, the first process which provided the prospect of manufacturing ductile titanium on an industrial scale. I will refer to it in a little more detail later, but essentially it con-

\* Delivered at the Annual Autumn Meeting, Southport, 21 September 1953.

† Joint Managing Director, Imperial Chemical Industries, Ltd., Metals Division, Birmingham.

sisted of reducing titanium tetrachloride with metallic magnesium. This pioneer work was followed up in the United States by research teams of the Bureau of Mines, who were responsible for an immense amount of valuable work which was the prelude to the first commercial production of the metal in the U.S.A. in 1948, in which year about 30 tons were made. This figure was almost doubled two years later, and in 1952 it is reported to have been about 1000 tons. Various figures have appeared for the estimated U.S. production for this year, and they range up to about 10,000 tons, but much lower figures have been more recently quoted for what the actual production is likely to be. It has been suggested that outputs of the order of 20,000 tons per annum may be reached within the next two or three years in the U.S.A., to which country most of the titanium production has hitherto been confined. In Great Britain commercial production so far has been on a very limited scale, but within the next two or three years it may well reach a figure approaching 2000 tons, and interest is also being shown in its manufacture in other countries. That broadly and briefly is the history of the metal to date.

## II.—GENERAL

During the past six or seven years or so, an enormous amount of scientific and technological work has been carried out on titanium, mostly in the U.S.A., but not only there. On work of this kind many millions of pounds have been spent, and not only is the effort still proceeding, but it is being intensified. Never before has there been in so short a time so much research activity directed to a single industrial metal.

Clearly there must be a reason and a justification for this, and indeed there is. Briefly, it is that the metal has attractive physical and mechanical properties, a high strength:weight ratio, and outstandingly good resistance to corrosion generally. Its importance as a very desirable if not uniquely suitable material for several aircraft components was recognized as soon as sufficient of it had been made to enable its properties to be determined, if only approximately, and for evaluation tests to be made. Much of this work was done on metal compacted from powder before techniques for melting in quantity were devised and developed. Limited though they were at the time, the results were enough to open up to the imagination a vista of possibilities extending far beyond such immediate and current uses as the properties of the metal and some of its alloys justify even at present prices. The early results and the picture of future possibilities which they unfolded, stimulated the vast volume of work which has since gone on concerning methods of production and fabrication of titanium and its alloys.

Although the future is unpredictable, the possible position of titanium in relation to other metals is a matter of no small interest to both metal producers and consumers alike. Of all the known chemical elements more than seventy are classified as metals.

About half of these are so rare and comparatively unknown that no appreciable use is made of them. Many of the remainder have significant and indeed important uses for specialized applications, even though in small quantity, whilst a number are used quite widely for many purposes in fairly large quantities. The remarkable advances in transport, communications, and various other branches of engineering activity in the last decade or two have necessitated the use of such a wide variety of metals and new alloys—one of the most notable features in the metallurgy of our time—that we can regard ourselves as living in an age of new metals.

But of all these there are only eight which are normally regarded as basic in the sense that they form what might be called massive metallurgical industries, in which primary metal production has reached annual figures of 100,000 tons or more, and so far as five of them are concerned, individual outputs extend to millions of tons. These eight metals are all well known to you for they are iron, copper, zinc, aluminium, lead, tin, nickel, and magnesium, and some of them have served the needs of mankind through centuries of time. The consumption of metals both new and old is proceeding at a greater rate than ever, and it has, in fact, been reported, for example, that in the U.S.A. alone since the First World War most metals have been used in quantities exceeding the total world consumption for all time up to 1914.

Although its current production runs to an annual level of a few thousand tons, the use of titanium, because of its price, is limited at present to special purposes. This indeed may long continue to be the position. On the other hand, if more convenient and cheaper methods of extraction were devised, so enabling its cost to be very substantially reduced, then it might well become a large-tonnage basic metal. In these days of high metal consumption which have witnessed temporary shortages, unbalances, and high costs amongst some of the older strategic materials, as well as uncertainties regarding the future availability of some of them, the advent of a new metal is a matter of no little interest and moment. Especially is this so when it is known that the metal and its alloys possess properties which make them not only attractive for special uses, but suitable also for ordinary and more general applications involving large tonnage consumption.

It is, however, a far cry from the present position of expensive production and processing to what still is the purely imaginative one of manufacture at price levels even approaching those of the more costly basic metals. All the major problems connected with the extraction, melting, and fabrication of titanium, and there are indeed many, stem from its very high degree of reactivity when hot and particularly when it is molten. Its great affinity for oxygen, the extremely low free energy of its lower oxides, the solubility of oxygen, and the marked embrittling effect which quite small traces of it have on the metal, have proved major obstacles in the production of



titanium of satisfactory quality by direct reduction of its oxide, and in the reduction processes so far developed and worked industrially it has been found necessary to start with oxygen-free compounds. Since the molten metal attacks all the known refractory materials used for lining metal-melting furnaces and for making crucibles, because of the solubility of nitrogen and oxygen in titanium, and to a lesser extent because of its high melting point, which is at present accepted as  $1725^{\circ}\text{C}$ ., special equipment and procedures involving melting *in vacuo* or in argon, far more costly to operate than the techniques usually employed for melting other metals, have had to be developed. I will refer later in a little more detail to reduction and melting operations, but what I have already said will make it clear enough that many serious problems will have to be solved before titanium can become a readily available metal. Formidable as many of these are, there is justification for a reasonable measure of optimism. Notwithstanding the difficult and complicated nature of the most important extraction process so far developed and which was first used on an industrial scale so very few years ago, the amount of progress both in metal production and in improvements to the process itself are quite impressive. It may well be that eventually other routes, more attractive either economically or technically, or both, will be devised. Although this is not the occasion for speculating in detail on future price trends of titanium, it is clear that success in any such developments as the scaling up and substantial improvement of existing production methods, or the devising of superior new ones, would undoubtedly result in price reductions and conceivably, in due time, bring titanium into the range of basic metals which its general properties and its abundant and wide distribution over the world in the form of workable ores would make possible.

### III.—OCCURRENCE

In Fig. 1 is shown the relative abundance of some of the important metallic elements in the lithosphere, from which it can be seen that of the so-called common or basic metals, that is, those which are or can be used in quantity for a wide range of ordinary purposes and form the basis of major alloy groups, only aluminium, iron, and magnesium are more plentiful than titanium. The extent of its occurrence is many times greater than that of several well-known metals, such as copper, zinc, lead, and tin, put together, the extensive use of which, in addition to the obvious one of suitability, is also associated with the fact that their ores are fairly readily obtainable or accessible and yield up their metal content relatively easily. Titanium ores, on the other hand, whilst plentiful and accessible enough, are most discouragingly resistant to reduction.

In view of the present great interest in the metal and its potential importance, the sources from which it is obtained justify some mention. The chief ores of

titanium are ilmenite ( $\text{FeTiO}_3$ ), a combination of iron and titanium oxides, and the oxide rutile, both of which derive originally, as decomposition products, from granites and pegmatites. Titanium ores have long been used as a source of titanium dioxide for the paint and other industries, the world production of ilmenite concentrates amounting in 1951 to no less than 1,183,000 tons. This mineral occurs as massive deposits in Canada, U.S.A., Norway, and Russia, and as beach sands in Queensland, Travancore, and Florida. Rutile, which occurs to a much lesser extent, is found principally in Australia and the U.S.A. From information already known about deposits, it is evident that abundant supplies of ore exist. For example, one deposit in Eastern Quebec alone is estimated to contain the equivalent of about 25 million tons of titanium metal, but in addition to rich

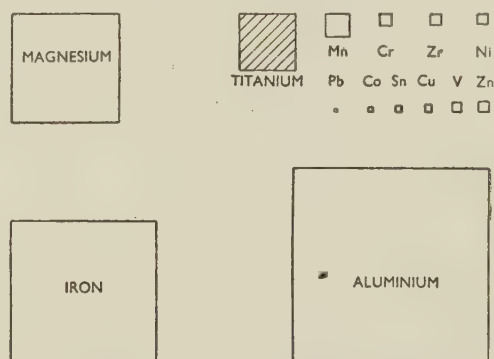


FIG. 1.—Relative Abundance of Structural Metals.

ores, there are vast quantities of lower-grade ores in every part of the world. In short, and as far as the future can be foreseen, there are supplies of titanium ores to meet production levels comparable with those of to-day's basic metals.

### IV.—REDUCTION PROCESSES

#### 1. THE VAN ARKEL PROCESS

In turning now to a brief survey of some of the techniques by which metallic titanium is produced, the iodide method of van Arkel and de Boer merits a description, however brief, since it was by its use, although as a laboratory experiment, that the first ductile titanium was made and because it is still the method employed for producing the metal in its purest form. In principle, it is an elegant process and in theory quite simple, for its operation turns on the fact that at relatively low temperatures titanium reacts with iodine to form titanium tetraiodide, which at higher temperatures dissociates into metallic titanium and iodine vapour, which is then available for continuing the cycle.

The reaction is carried out in a vacuum-tight vessel such as that shown in Fig. 2, through the lid of which pass the necessary electrical connections for heating a

thin filament of titanium wire and connections to vacuum pumps and an argon supply. Pieces of the material, usually the crude metal, from which the

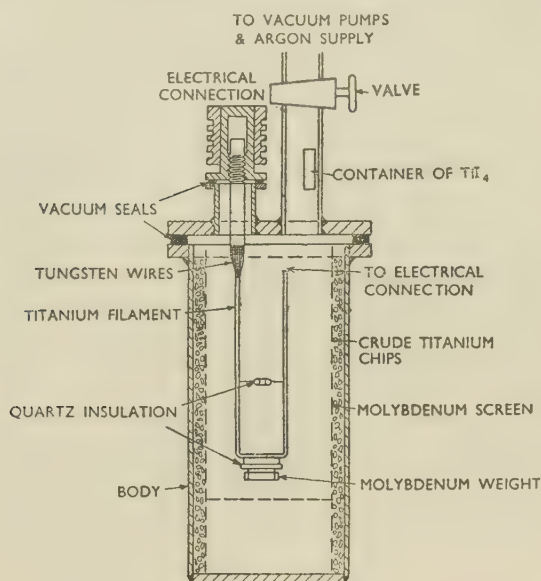


FIG. 2.—Plant for Production of Titanium by Thermal Decomposition of Titanium Tetraiodide.

pure titanium is to be extracted, are packed into the annular space between the wall of the chamber and an inner refractory-metal radiation screen, usually made of perforated molybdenum sheet. The lid with its attachments is then fitted to the vessel which is heated to about  $600^\circ\text{C}$ ., kept under vacuum until all gases are removed, and the temperature then reduced to about  $200^\circ\text{C}$ ., when the iodine or titanium tetraiodide is released from a capsule and commences to react with the crude titanium. By the passage of an electric current, the filament of fine pure titanium wire, disposed as will be seen in the form of what has fancifully become known as a "hairpin", is heated to  $1400^\circ\text{C}$ . On to this, under these conditions, titanium from the tetraiodide is deposited, the liberated iodine diffuses back through the perforated screen to combine with more titanium, and so the process continues. It ceases when the filament has grown to such dimensions that either the electrical seals cannot carry the increased current required to maintain the filament at the temperature of decomposition, or the total amount of heat liberated in the container becomes too great to be effectively dissipated, and, in consequence, overheats the interior of the reaction vessel. When the operation is finished, cooling is effected as quickly as possible, argon gas being simultaneously admitted, until normal temperature is reached.

Since neither oxygen, nitrogen, or carbon, nor other non-metallic impurities normally present in crude titanium metal take part in the reaction, the metal deposited on the filament is almost completely free from these impurities. On the other hand, some

metals, notably iron, which form volatile iodides, become involved in the reaction if present and are found in the purified metal of the filament.

This iodide-dissociation method is usually operated as a purification process, but it clearly has possibilities for primary-metal production, and some consideration has naturally been given to these, although no major new developments have been reported. It would, for example, be possible to extract the metal content in this way from titanium carbonitride, which is made by heating ilmenite with carbon in an electric furnace. In its present form, the thermal-dissociation process has several limitations including those of slowness and the use of expensive iodine, small losses of which on large-scale working would materially affect costs. It would, however, be possible, for example, to have alternatives to a heated filament for effecting dissociation and, moreover, on such heated surfaces other compounds could possibly be used as the source of metal.

## 2. THE KROLL PROCESS

The process by which practically all of the titanium now being made industrially is produced is that developed by Kroll, although the plant and operational details have been much improved and modified since it was first introduced. The basis for extraction is titanium tetrachloride, a colourless liquid with a density

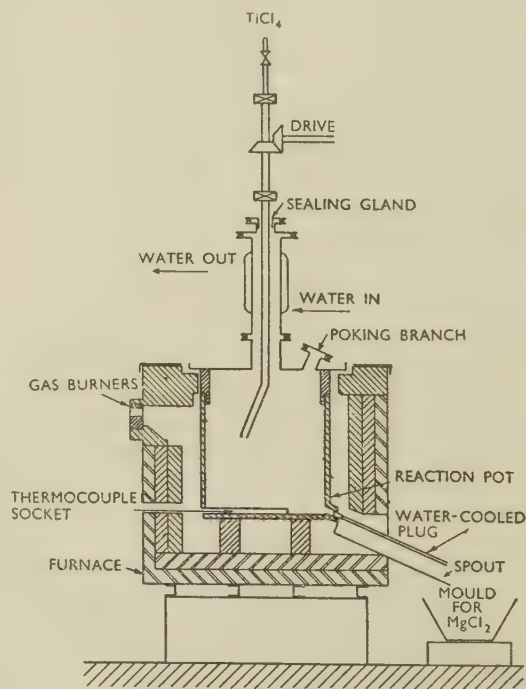


FIG. 3.—Plant for Magnesium-Reduction Process.

of  $1.76\text{ g./c.c.}$  and a boiling point of  $136^\circ\text{C}$ ., made by heating titanium dioxide with carbon at  $800^\circ\text{C}$ . in chlorine, after which it is purified by distillation. In Fig. 3 is shown the type of equipment in which the



reduction of titanium tetrachloride by metallic magnesium is carried out. The vessel, which is constructed of mild steel, is charged with high-purity magnesium, and the lid with its connections to the titanium tetrachloride feed, vacuum pump, and argon supply, is fitted into position. The system is then purged of air by evacuating and filling with argon, and throughout the operation a small positive pressure of argon is maintained. The whole is then externally heated to the melting point of magnesium, when titanium tetrachloride is slowly introduced through the rotary feed pipe. This pipe, which passes through a sealing

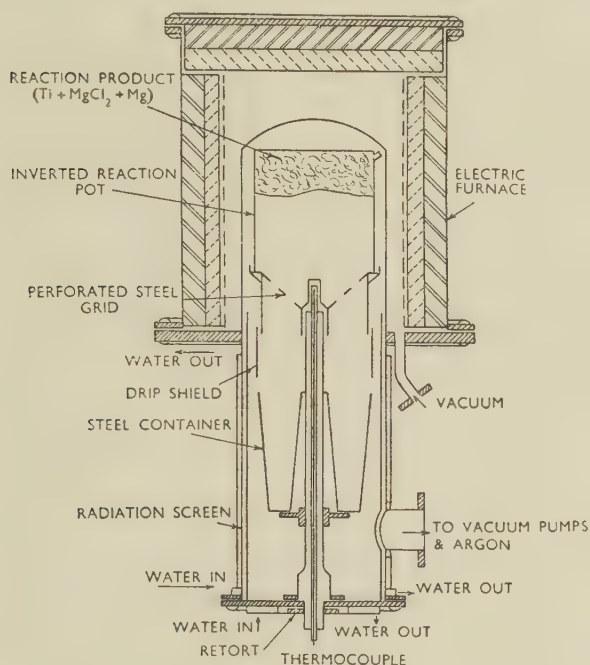


Fig. 4.—Plant for Vacuum Purification of Product of Magnesium-Reduction Process.

gland, is bent at the delivery end, and it is rotated during the reaction to ensure even distribution of the tetrachloride. The reaction is strongly exothermic, and as there is a risk of iron contamination from the containing vessel at temperatures of the order of 900° C., the temperature is carefully controlled and only permitted to rise to about 800° C., at which it is maintained by regulating the supply of tetrachloride and the external heating. Molten magnesium chloride which is formed collects at the bottom of the reactor and is tapped off during the operation. On completion of the run, the reactor, still under a positive pressure of argon, is allowed to cool to room temperature, after which the lid is removed and the vessel transferred to the purification unit.

It contains a mass of titanium mixed with magnesium chloride and magnesium, and in the early days of the process this was chipped out and extracted with dilute hydrochloric acid, washed, and dried. The coarse titanium powder so produced contained considerable quantities of both hydrogen and oxygen.

The former could be, and was, removed by heating *in vacuo* at 800°–900° C., but the oxygen remained, making the metal hard, brittle, and consequently difficult to fabricate. As a method of separation from reaction products and purification, leaching has given place to the more effective treatment at high temperature under high vacuum, a process previously developed in the manufacture of zirconium. In this, as shown in Fig. 4, the steel reactor containing its charge of intermixed sponge metal is introduced in an inverted position into a vertical retort which can be made gas-tight and connected either to vacuum pumps or an argon supply. The upper portion of the retort is surrounded by a removable electric furnace and the lower part by a water-cooled jacket. Mounted within the retort is a steel container for collecting the magnesium chloride, which is driven off from the sintered mass in the reaction pot and falls through a perforated grid, the magnesium being volatilized and condensing on the radiation screen. The operation is carried out under high vacuum, the pressure inside the retort being reduced initially to 1 micron and held at a low value thereafter. After removal of the gas, the temperature of the retort is raised to about 800° C., maintained there for several hours, and then allowed to cool, argon being admitted during the final stages of cooling. At the finish there is left in the reactor only metallic titanium, a coke-like mass to look at, which is then broken up and ground to a suitable size for melting.

Involving as it does initially expensive materials, that is, pure titanium tetrachloride, magnesium metal of high purity, argon gas, and difficult operational techniques, the process is inevitably an expensive one. Nevertheless, it is workable industrially, and it has been the means of providing, even if so far in relatively small quantity at comparatively high cost, metal that has been wanted. Among the further improvements to the method that are envisaged is the removal of some of its limitations as a batch process by transforming it into a continuous operation.

### 3. POSSIBLE ALTERNATIVE REDUCTION METHODS

Because of the obvious desirability of producing titanium more cheaply, great interest centres round other methods of extraction, and a good deal of work is going on with this object. For example, further consideration has been given to the method of reducing the tetrachloride with sodium which, as already noted, was first done experimentally several years ago, and another method that has been worked is the two-stage reduction process of the oxide. This latter provides the exception to the general understanding that chemical reduction cannot be effected in the presence of oxygen. If titanium-oxygen compounds or titanium containing appreciable amounts of dissolved oxygen are held in contact with metallic calcium at temperatures of the order of 1000° C., oxygen reacts with the calcium to form calcium oxide, and the equilibrium amount of oxygen remaining in solution in the titanium is sufficiently small for the

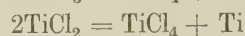
metal to be relatively soft and ductile. Theoretically, this means that the whole reduction process can be carried out without recourse to the intermediate stage of forming a halide compound, one of the costly steps in present methods. It has not, however, so far proved economically possible to effect the whole of the reduction by calcium alone, but by reacting the oxide with magnesium a lower oxide of titanium is produced. When the product of this reaction is leached to remove magnesium and magnesium oxide, the purified lower oxide of titanium remains. This is reduced by calcium and the residual calcium oxide removed by a second leaching. Metallic titanium is thus produced, but the oxygen content of metal hitherto so made on an industrial scale appears to have been too high for it to be suitable for ordinary fabrication processes.

Titanium powder can also be made by processes involving the preparation and subsequent decomposition of the hydride, but such routes so far have not resulted in the production of pure metal at reduced cost.

Where chemical methods are outstandingly difficult or otherwise unattractive, attention naturally directs itself to processes of electrolysis on which, for the extraction of titanium, large sums of money have been spent, but up to the present no industrial process of this kind has been developed. The same restriction which the ruinous solubility of oxygen in metallic titanium imposes on materials for reduction by chemical processes, would seem to render unlikely the successful electrolysis of aqueous solutions, as can be done for copper, or the use of oxides dissolved in molten salts, as, for instance, in the extraction of aluminium. Furthermore, no suitable oxygen-free non-aqueous organic solvents have been disclosed, and titanium tetrachloride itself is a very poor conductor of electricity.

Experimentally, titanium has been produced in small quantities by electrolysis of titanium trichloride and other lower halides dissolved in fused lithium and potassium chlorides and similar electrolytes, but as the deposit is in the form of flakes or dendrites, the problem still remains of the satisfactory separation of the metal from the electrolyte. This has, in fact, proved a serious limitation in the electrolytic process as applied to high-melting-point metals with high affinity for oxygen, since it has not been possible to produce metal in massive form from fused-salt electrolytes unless the metals are molten at the temperature of electrolysis, as, for instance, sodium, magnesium, and aluminium, and even the higher-melting-point metals such as calcium and Mischmetall. Modifications of the electrolytic process in which the metal is dissolved in another low-melting-point metal which acts as a liquid cathode is possible, as, for example, in cells using mercury or molten zinc, but these again would involve a subsequent distillation process for the separation of the solvent metal comparable with the Kroll vacuum-purification method.

The lower chlorides of titanium undergo disproportionating reactions resulting in the formation of titanium tetrachloride and titanium metal as follows:



Titanium trichloride, which is formed when excess titanium tetrachloride is allowed to react with magnesium, consists of violet-coloured crystals, and is always accompanied by the black, unstable dichloride produced by the first reaction just referred to. Titanium trichloride can also be formed by the direct reduction of the tetrachloride by hydrogen, forming HCl as a co-product. Some attempts have been made to produce titanium metal by this disproportionation reaction, but little success has yet been achieved. At present, the conditions under which these reactions occur are not sufficiently understood to indicate how much promise they hold as the basis of a workable process.

Because of the very low free energy of its oxides, titanium metal in the presence of water vapour reacts at elevated temperatures almost irreversibly to form oxide and hydrogen. It is, however, theoretically possible at extremely high temperatures for this reaction to be reversed. A very large excess of hydrogen would be required to remove the water vapour and prevent recombination with the titanium and for the same reason the reaction would have to be carried out at fairly low pressures. Moreover, the necessity for operating at very high temperatures would require the solution of metallurgical engineering problems of a major character.

These are but a few examples of the many possible approaches that are being considered, and, in some instances, actually investigated, as alternative routes on which industrial processes for the production of titanium might be based.

## V.—MELTING

The great affinity of titanium for oxygen and nitrogen, which necessitates the carrying out of extraction processes in the complete absence of air, also demands the same conditions for melting. Metal produced by thermal decomposition on a heated filament can be worked directly into small-diameter rod or wire, but the product of the chemical reduction processes now being used needs to be consolidated for further fabrication. In the pioneer days, this was done by compacting titanium powder, but the limitations of that technique for the production of the metal and its alloys in quantity in wrought forms made the development of melting techniques imperative. Since, as already mentioned, titanium attacks all the refractory materials normally associated with metal melting, methods not involving their use had to be devised or adapted.

The one partly exceptional refractory material is carbon, and methods of melting *in vacuo* or in an atmosphere of argon in graphite crucibles heated by



high-frequency induction or graphite resistors were developed and used. When molten, however, titanium dissolves carbon, and although in small quantities the presence of this element is not seriously detrimental, the extent of carbon contamination when melting in graphite is considerable and uncertain.

The technique now generally employed is based on the discovery of von Bolton in 1905 that high-melting-point metals—his experiments were conducted on tantalum—can be melted in a water-cooled copper receptacle by striking an arc between an electrode and the metal to be melted. Thus the particular feature of this method is that the problem

with argon. The arc is then struck between the electrode and the charge, and as the latter melts more metal is fed in from the hopper and the electrode progressively raised. In this way the ingot is built up, although at any moment the pool of metal in the molten state is quite small. At the end of the run the metal is allowed to cool in argon, and thereafter withdrawn by lowering the retractable base of the crucible. Modifications to the process, such as utilizing consumable electrodes of pressed titanium powder or sponge in order to eliminate impurities derived from the electrode, and the continuous retraction of ingots, are being developed, but even so it involves high capital expenditure and working costs, and to obtain uniformity of composition under such conditions of melting requires careful operational control. Although, as already noted, relatively large ingots are being made as the basis for the production of titanium and its alloys in wrought forms, nevertheless, the problem of devising cheaper and better melting techniques is second only in importance to developing cheaper and improved extraction processes.

## VI.—PROPERTIES

The vast amount of published matter relating to titanium which has already appeared covers much detailed information concerning the properties of the metal and its alloys, and, therefore, these and other factors I propose to consider only broadly and generally.

Titanium undergoes an allotropic transformation at 882° C., above which temperature it has a body-centred cubic structure, known as the  $\beta$  phase, and below this temperature it has an hexagonal close-packed structure, known as the  $\alpha$  phase. Pure titanium, such as that produced by the dissociation of titanium tetraiodide, is a relatively soft metal with high ductility. The  $\alpha$  phase has a  $c/a$  ratio of 1.587, a value which is significantly lower than the theoretical value of 1.633 corresponding to ideal close packing. In this regard it differs from other hexagonal close-packed metals, such as magnesium, zinc, and cadmium, the  $c/a$  ratios of which are 1.624, 1.86, and 1.89 respectively, and in these metals the dominant deformation mechanism is slip on the basal planes. A low  $c/a$  ratio implies that prismatic and pyramidal planes are, relative to the basal plane, more closely packed, and consequently in titanium the former are slip planes.

High-purity titanium can be easily cold worked, and it can sustain deformation to the extent of reductions in area of more than 95% before annealing becomes necessary for further working. Its ultimate tensile strength is, however, only of the order of 15 tons/in.<sup>2</sup>, with an elongation value on 2 in. of between 40 and 60%, and, therefore, as an engineering material or as a constructional metal in a wider and more general sense, its possibilities are not comparable with those of commercial grades of titanium or of titanium alloys.

Commercially pure titanium as produced by

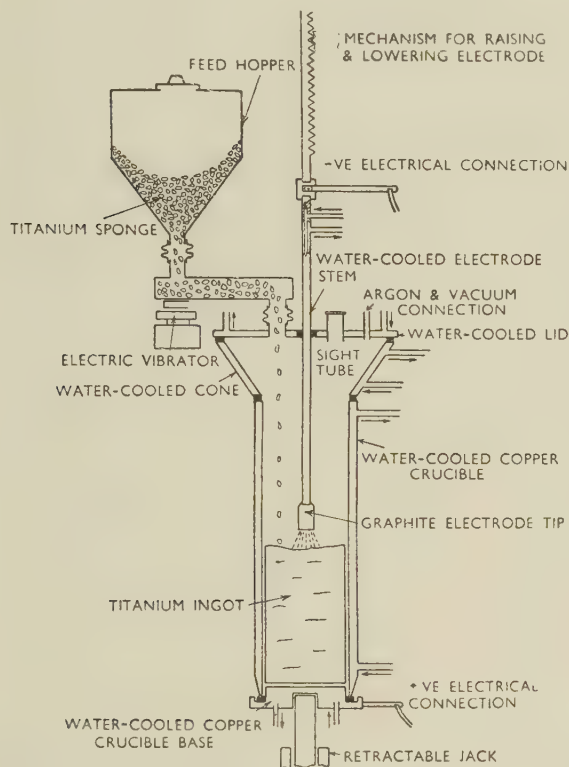


Fig. 5.—Titanium Arc-Melting Unit.

of finding a stable refractory material is avoided, rather than solved, by melting titanium in a vessel which can conveniently and effectively be kept cold enough to prevent any bonding or interaction between the two.

It has been developed in a comparatively short time from laboratory-scale equipment to units capable of producing ingots weighing up to 4000 lb. This type of melting plant is illustrated in Fig. 5. It consists of a water-cooled copper crucible fitted with a water-cooled electrode having either a tungsten or a graphite tip, a hopper for feeding in crushed vacuum-purified titanium sponge together with any alloying ingredients that may be required, a sight tube, and connections to vacuum pumps and to argon and water supplies. In operation a quantity of sponge is placed in the crucible, which is then evacuated and filled

chemical reduction methods, as, for example, the Kroll process, has considerably greater strength and lower ductility than iodide titanium, although the

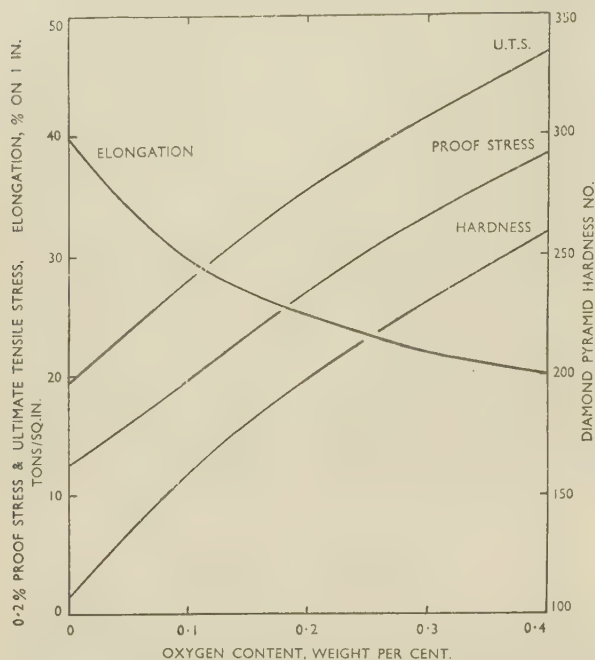


FIG. 6.—Effect of Oxygen Content on Mechanical Properties of Titanium.

crystallographic features of the deformation mechanism are maintained. Ultimate tensile strength values of about 35–40 tons/in.<sup>2</sup>, with 30–25% elongation, are typical of this quality of metal. The marked difference between these properties and those of the iodide metal is attributable to the presence of impurities, some of which in titanium have effects of unusual magnitude. Indeed, the technology of titanium is dominated by four impurities—oxygen, nitrogen, hydrogen, and carbon—all of which form interstitial solid solutions up to the limits of their solid solubilities, which for the first three are about 30, 15, and 30 at.-%, respectively, while that of carbon is very limited. They find their way into the metal at various stages of processing and, in fact, most of the major problems arising in the production, melting, and subsequent working of the metal are associated with the necessity for excluding, or at least minimizing as far as possible, contamination by these impurities.

So far as production technology is concerned, oxygen is, so to speak, in the light of present knowledge, titanium enemy number one, with nitrogen quite well behind in second place. Although their effects on processing and properties are pronounced, hydrogen and carbon are less significant impurities, since the former can be removed from the metal without recourse to remelting by heating to 800°–1000° C. *in vacuo*, while contamination by the latter can be limited to tolerable proportions by effective control of the purity of raw materials and melting

conditions. Once in solution, there is no established method yet by which oxygen and nitrogen can be removed, short of reconversion of the metal to the halide. In commercial grades of metal, oxygen may be present up to about 0.25% and nitrogen to about 0.1%. Both bring about hardening with corresponding increase in strength and loss of ductility, and the effect of progressively increasing amounts of these two elements are shown in Figs. 6 and 7, which are based on the work of Jaffee, Ogden, and Maykuth. Weight for weight, the effect of nitrogen is much greater than that of oxygen, but normally it is present in much smaller amounts, and furthermore, in processing by hot working, the extent and liability to nitrogen contamination is negligible in comparison with that of oxygen. In the production of titanium, the overriding factor affecting the hardness of the metal is generally its oxygen content.

On heating in air at comparatively low temperatures, oxides and nitrides are formed on the surface of titanium, and at higher temperatures these diffuse into the metal. In the early days of titanium metallurgy it was thought necessary to carry out hot-working operations in the absence of air to avoid embrittlement, and to this end elaborate techniques were devised which involved enclosing the metal in gas-tight welded sheaths of steel. However, further experience in hot working and the more precise information which has been obtained on the rates of diffusion of these gases and their dependence on

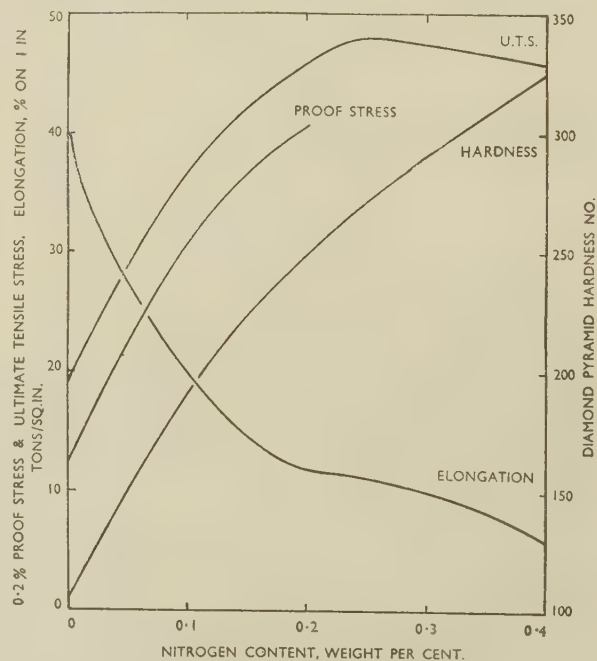


FIG. 7.—Effect of Nitrogen Content on Mechanical Properties of Titanium.

temperature, which has been shown to be approximately exponential, has indicated that titanium can be processed without an intolerable degree of oxygen contamination at temperatures in the range of about



850°–1000° C., according to circumstances and with certain reservations. While this is generally true, the fact remains that some oxygen is taken up, and to that extent the metal is deteriorated. Hence the compelling need for precise control of hot-working and annealing operations to ensure the least possible contamination by oxygen because of its adverse effect both in further cold working and on the properties of the final product. The curves in Fig. 8 show the increase in hardness at and below the surface due to oxygen pick-up as a result of heating the metal for 1 hr. at various temperatures.

The maximum solubility of carbon in  $\alpha$ -titanium is about 0.2%, and it is less in the  $\beta$  phase, any present in excess assuming the form of discrete particles of titanium carbide. In amounts up to about 0.5%, the effects of carbon are not pronounced, except in so far as both machining and the production of ductile welds are more difficult. Metal containing up to this

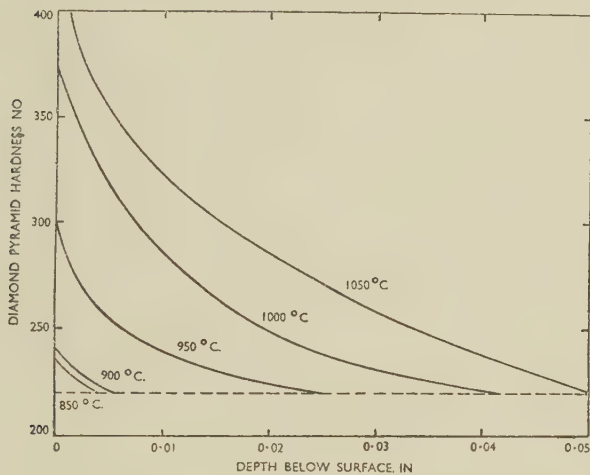


FIG. 8.—Hardness Gradient in Titanium on Heating for 1 Hr. in Air.

limiting quantity of carbon can be quite readily fabricated in the hot and cold states, but with greater amounts the hot-working properties seriously deteriorate. As will be seen from Fig. 9, which is based on the work of Finlay and Snyder, carbon, like oxygen and nitrogen, but to a markedly less degree, increases the strength and reduces the ductility of titanium.

Although it has been known since the early days of titanium production that a large content of hydrogen give rise to hardening and embrittlement, the amounts normally present were not considered to have any appreciable effect on the physical or mechanical properties of the metal. Recently, however, evidence has been obtained which indicates that a hydrogen content as small as 0.02% may reduce the impact strength from about 25 ft.-lb. on a standard Izod test-piece to as low a figure as 5 ft.-lb., as shown in Fig. 10, without the tensile strength or elongation being affected.

Commercially pure titanium can be readily hot worked by forging, rolling, extrusion, and other

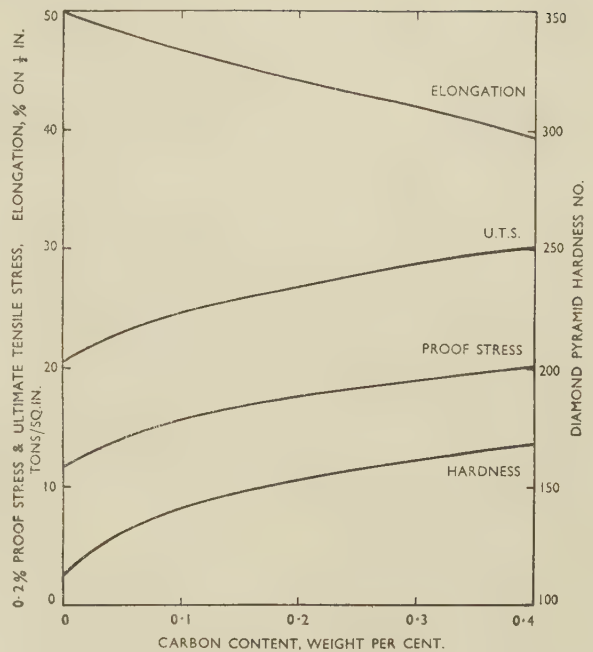


FIG. 9.—Effect of Carbon Content on Mechanical Properties of Titanium.

conventional methods, but in general, it is more resistant to cold working than are most non-ferrous alloys usually produced in wrought forms. One feature of titanium which adds seriously to the difficulty of such cold-working operations as drawing of various kinds and deep pressing, is its unfortunate tendency to seize on other metals during sliding contact with them under pressure. So far no lubricant has been found which will prevent seizure of metal-to-metal surfaces, but this can be overcome to some extent through avoiding metal-to-metal contact by oxidizing the surface of the titanium or depositing on to it layers of other substances to serve as vehicles for the lubricant. Even under these conditions, only highly viscous or semi-solid lubricants can be used with any measure of success. Thus, for example, in drawing wire or tubes the metal surface can be oxidized and then carefully

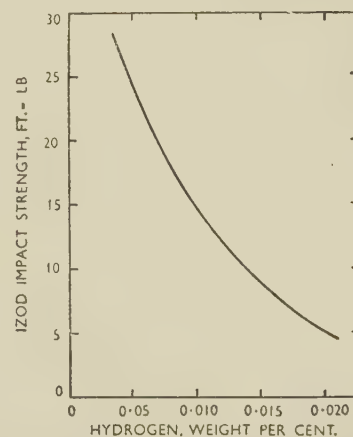


FIG. 10.—Relationship Between Impact Strength and Hydrogen Content of Commercially Pure Titanium.

coated with molybdenum disulphide or a mixture of soap and calcium stearate. Alternatively, where circumstances necessitate it, recourse can be made to the technique of sheathing with another metal, which is removed by pickling towards the end of the cold-working operations.

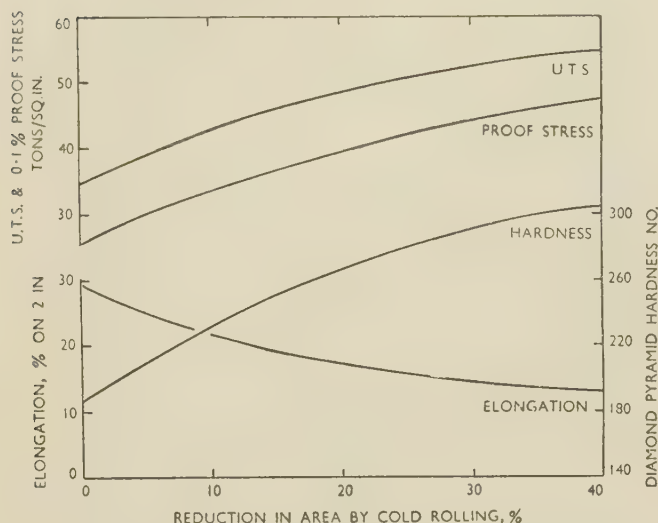


FIG. 11.—Effect of Cold Working on Commercially Pure Titanium.

In addition to the need for minimizing contamination in processing and for special techniques for drawing, such as those just referred to, another factor which looms large, if indeed not largest, in the economics of current wrought-titanium production, is that scrap metal cannot be remelted and returned to the production cycle. This arises partly from the fact that massive scrap cannot be fed into arc furnaces of the type at present employed for melting titanium, and partly from the necessity of avoiding cumulative contamination which would result from repeated melting and fabrication. Considerable effort is therefore being directed towards developing furnaces capable of melting scrap in the charge and in devising processes for the removal of at least some of the contamination before remelting.

The effect of cold working on some of the mechanical properties of commercially pure titanium is illustrated in Fig. 11, and the annealing curves in Fig. 12 on metal reduced 40% in thickness by cold rolling show that complete softening is effected by heating at 700° C. The generally accepted value for the elastic modulus of isotropic material is  $15 \times 10^6$  lb./in.<sup>2</sup>, but like many other metals, titanium develops pronounced directional properties as a result of plastic deformation and, according to the crystal orientation in relation to the direction of testing, modulus values may vary between  $14$  and  $20 \times 10^6$  lb./in.<sup>2</sup>.

The fatigue properties of titanium are unlike those of most non-ferrous metals for the *S/N* curve shows an approach to a true fatigue limit. The ratio of fatigue to tensile strength is generally greater than

0.5, but the most notable feature in which titanium excels other non-ferrous and ferrous alloys in respect of fatigue-resistance is the degree to which this ratio is maintained under corrosive conditions.

The impact strength of commercially pure titanium is of the order of 20–25 ft.-lb., and whilst, as already noted, this property is very susceptible to the presence of impurities, notably hydrogen, very much higher values characterize the pure metal.

Even at room temperature the creep properties are disappointing, and tests which have been carried out so far indicate that creep occurs when the metal is stressed near to its proof stress, which is unusual in a metal having so high a melting point.

The only mechanical properties which have been studied at high temperature in any great detail are the tensile and creep properties. As will be seen from Fig. 13, the strength falls away fairly uniformly as the temperature is raised, but the proof stress falls much more rapidly at first and then remains approximately constant between 200° and 350° C. Examples of stress-rupture tests, including for comparison the short-time ultimate tensile stress curve, are illustrated in Fig. 14. These curves show the various stresses and temperatures at which failure will occur in 1, 10, 100, and 1000 hr. It can be seen that the rupture-strength curve for 1000 hr. begins to fall abruptly at 350° C., and even for periods as short as 1 hr., further increase in temperature of no more than 50° C. causes rapid decrease in rupture strength. Despite the expectations there may have been in view of its

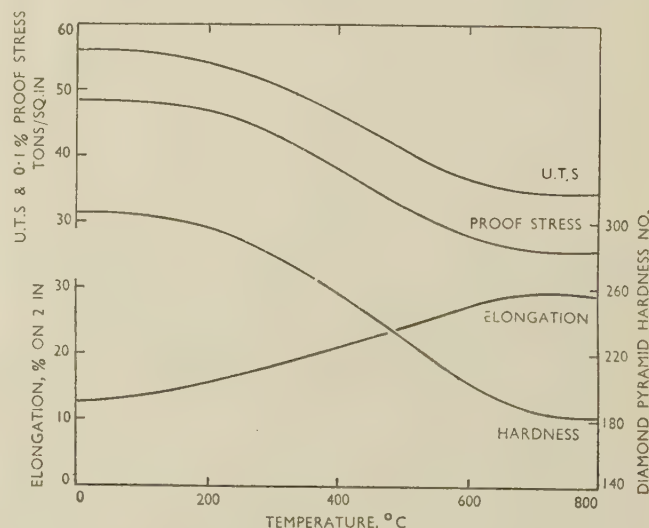


FIG. 12.—Effect of Annealing Commercially Pure Titanium 40% Cold Rolled (1 hr. soak at temperature.)

high melting point, commercially pure titanium is not suitable for applications involving long-continued stresses at temperatures exceeding 350° C.

Joining presents numerous problems, many of which, especially those concerned with brazing and soldering and with the welding of alloys, are not yet solved. Commercially pure titanium can, how-



ever, be readily welded by electrical-resistance methods and also by means of argon-arc techniques, provided that precautions are taken to shield from atmospheric contamination not only the molten welded metal, but also all heated parts of the base metal, including the back of the weld. In the welding

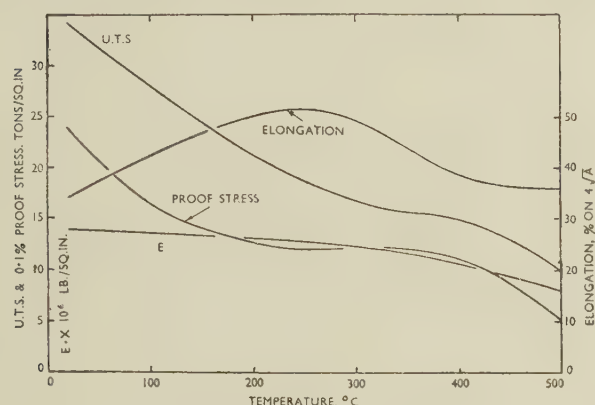


FIG. 13.—Short-Time Elevated-Temperature Tensile Properties of Commercially Pure Titanium.

operation the metal runs easily, and there is no difficulty in consistently producing sound ductile welds of good appearance.

The attractive strength : weight ratio is the feature of titanium and its alloys chiefly responsible for their demand and use in aircraft, but the other excellent characteristic of the metal is its resistance to corrosion. The early optimism about this has been abundantly justified, and a broad indication of it in comparison with a few other well-known metals is provided in Table I and by Fig. 15 (Plate XVI),

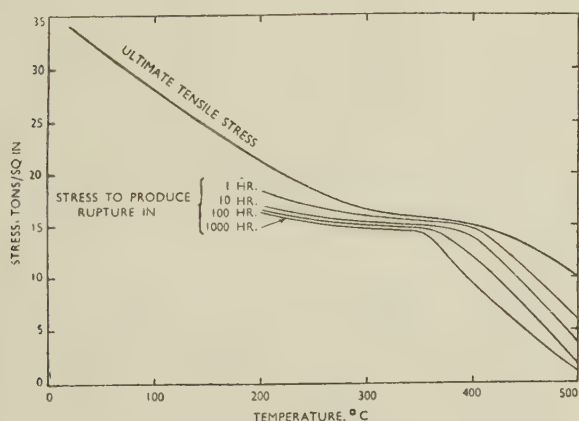


FIG. 14.—Elevated-Temperature Stress-Rupture Properties of Commercially Pure Titanium.

which suggest its possible usefulness in chemical engineering. The latter shows specimens that have been rotated for periods up to 500 hr. in 40% boiling cupric chloride, cold *aqua regia*, boiling concentrated nitric acid, and heavily polluted sea-water containing erosive silt, and it will be seen that while the titanium is practically unaffected after the full period, the

stainless-steel specimens were all seriously corroded, some after much shorter periods of time.

This outstanding resistance to corrosion is attributed to the presence of a protective oxide film which is most stable in oxidizing environments, and under such conditions the behaviour of the metal is similar to that of stainless steel, but additionally the film on titanium is resistant to penetration by the chlorine ion, and so the metal is resistant to moist chlorine and aqueous solutions of many chlorine-containing compounds. Its resistance to sea-water and to marine conditions generally is of a very high order indeed, and its behaviour in a standard jet-impingement test, in comparison with a range of alloys widely used for condenser tubes, is illustrated in Fig. 16 (Plate XVI). Within 1000 hr. all the specimens, except titanium, which was not sensibly affected, were completely penetrated over a considerable area. Further-

TABLE I.—Resistance to Corrosion in Various Media.

Corrosion Medium	Titanium	Austenitic Stainless Steel	Aluminium	Copper
Cold 10% sulphuric acid	●	●	●	●
Boiling 65% nitric acid	●	●	●	●
Cold 5% hydrochloric acid	○	●	●	●
Cold <i>aqua regia</i>	○	●	●	●
Boiling 20% acid chloride solutions	○	●	●	●
Hot fatty acids	○	●	○	●

KEY.

- Suitable for use where little dimensional change is tolerable; corrosion rate <0.005 in./year.
- Suitable for use where some corrosion is tolerable; corrosion rate 0.005–0.05 in./year.
- Not ordinarily suitable for use; corrosion rate >0.05 in./year.

more, it is not corroded by fouling organisms in sea-water, nor is it corroded in this medium when it is coupled, for example, to stainless steel or cupronickel.

It is resistant to cold nitric acid up to 98% concentration, sulphur compounds, strong alkalis, many organic acids, chlorinated solvents, and cold *aqua regia*. It is not affected by most foods and food products, or by body fluids, and being non-toxic it could be used for many purposes in surgery. In those solutions which do attack the metal, such as certain hot strong acids, the corrosion always appears to be general without evidence of either intercrystalline or stress corrosion.

## VII.—TITANIUM ALLOYS

As soon as ductile titanium became available, even in small quantities, attention was immediately turned to a consideration of alloying possibilities. In those early days, although they were only a few years ago, when little or nothing was known about the theoretical background or constitution of titanium alloys, this

work was in the main of an *ad hoc* nature, and consisted largely of making and testing a great many alloys containing varying amounts of one or more elements that could conveniently be added to the metal, with the object of making a rapid assessment of the effect of such additions on the more commonly determined mechanical properties.

A lot of work of this type was carried out by a large number of research teams, but as titanium of various grades and purity and various methods of consolidation by powder compacting and melting were employed, it is not surprising that comparison and assessment of the different claims of the many alloy compositions was difficult. Nevertheless, it became clear from these investigations that some elements showed promise as alloying ingredients, and at that time these were known to include iron, chromium, manganese, molybdenum, and aluminium, and from this work emerged a limited number of quite useful alloys which

niobium, depress the transformation, are more soluble in the  $\beta$  phase than in the  $\alpha$  phase, and tend to stabilize it. Two metals, namely aluminium and tin, have just the opposite effect. They are more soluble in the  $\alpha$  phase, with which they form substitutional solid solutions, tend to stabilize it, and raise the transformation. Other elements, such as oxygen, nitrogen, carbon, and boron, which form interstitial solid solutions have the same effect.

On slow cooling, the phase transformation takes place by a process of nucleation and grain growth at high temperatures, but rapid cooling suppresses this type of transformation, and the  $\alpha$  phase is formed at lower temperatures as a result of a martensitic type of change. Alloying additions influence not only the relative stability of the two phases, but also the cooling rate necessary to suppress the transformation, the temperature of the martensitic change and the nature of the decomposition products of that change.

TABLE II.—*Approximate Compositions and Properties of  $\alpha/\beta$  Titanium Alloys.*

Alloy Type	Nominal Alloy Content, %						Condition	Typical Mechanical Properties		
	Cr	Fe	O <sub>2</sub>	Mo	Mn	Al		0.2% P.S., tons/in. <sup>2</sup>	U.T.S., tons/in. <sup>2</sup>	Elonga- tion, %
Titanium-chromium-iron	1.8	0.9	0.15	...	...	...	Hot-worked and annealed at 700° C.	35-45	50-60	15-25
	2.7	1.3	0.25	...	...	...		55-65	65-75	10-20
	3.0	1.5	0.5	...	...	...		65-75	75-85	5-15
Titanium-chromium-iron- molybdenum	2.0	2.0	0.2	2.0	...	...	Hot-worked and annealed	50-60	60-70	10-20
	4.5	4.5	0.2	4.5	...	...		55-65	65-75	5-15
Titanium-manganese	...	...	...	...	7.0	...	Annealed sheet	60-65	65-70	10-20
Titanium-manganese-aluminium	...	...	...	...	4.0	4.0	Hot-worked bar	60-65	65-70	15-25
Titanium-chromium-aluminium	5.0	...	...	...	...	3.0	Hot-worked bar	60-75	70-85	5-10

have been developed on a production scale since about 1950. In the meantime, not only has much more information been obtained about the properties and characteristics of these alloys, but several new and extremely promising compositions are being developed as a result of recent and current researches on the structure and constitution of a great number of binary and more complex titanium alloys. Although this has led to a fuller understanding of the behaviour and characteristics of existing alloys and pointed the way to new and improved alloys, it has also made it abundantly clear that the whole subject of the constitution of titanium alloys, quite apart from their technology, is a complicated one, and our present limited knowledge is itself an indication that a great deal yet remains to be found out.

The role which various alloying elements play is becoming more clearly defined. It is possible in this regard to classify them into several groups on the basis of relative solubility in the two phases, but in considering them more generally and broadly it has been established that most of the metallic elements so far investigated, including iron, chromium, manganese, molybdenum, vanadium, tantalum, and

Depending, therefore, on the amount and type of element or elements added, it is possible to produce alloys with structures consisting entirely of the  $\alpha$  or  $\beta$  phases, or mixtures of these phases with or without such decomposition products as eutectoids, intermetallic compounds, and others, the precise nature of which is not yet understood. Four different types of structure are shown in Figs. 17-20 (Plate XVII).

The sort of alloys that have so far been available are indicated, together with some room-temperature properties, in Table II, which is based on data from various sources. They are all much stronger but less ductile than commercially pure titanium, their tensile strengths and elongation values ranging up to 85 tons/in.<sup>2</sup> and 25%, respectively. They retain their properties somewhat better at high temperatures and have superior creep properties. As a result of alloying, the superlatively good corrosion-resistance of the metal does not appear to be impaired, and, in general, the alloys possess the excellent fatigue and corrosion-fatigue properties that characterize the metal. Impact-strength values range from about 5 to 15 ft.-lb., according to composition, grain-size, structure,



and impurity content, and although these are relatively low, they increase rapidly with temperature, values of 100 ft.-lb. being obtained with titanium-chromium-iron alloys at temperatures over 250° C., whilst alloys have been produced experimentally with room-temperature impact strengths of over 50 ft.-lb. Although some doubt has been expressed about the

by interstitial alloying elements and, moreover, they have improved creep properties. Recent evidence indicates that molybdenum may be a beneficial addition in improving ductility and strength at elevated temperatures. The short-time elevated-temperature tensile properties of several duplex titanium alloys with those of some other metals, are shown in Figs. 21-23.

Although all of the alloys which have so far been developed beyond the experimental stage are of the  $\alpha/\beta$  type, attention is now being turned to single-phase alloys, since from results now being obtained it is evident that they, at least in certain respects, are better than the duplex alloys. Thus alloys containing metallic stabilizers, such as aluminium or tin, in sufficient amount are not affected by cooling rate from high temperatures, and so are free from the limiting disadvantages which beset duplex alloys so far as welding is concerned. In addition to having improved properties at high temperature and being far less sensitive to hot-working conditions, such alloys, if stabilized by aluminium, have the further merits of lower density than alloys containing such elements as iron, chromium, or manganese, and improved resistance to oxidation which in hot working is a most useful attribute. It would thus seem that alloys of the  $\alpha$  type may prove to have the best possibilities for high-temperature applications. On the other hand, they are less ductile and cannot be so readily cold worked.

The interstitial solutes which stabilize the  $\alpha$  phase have a different effect on mechanical properties, for

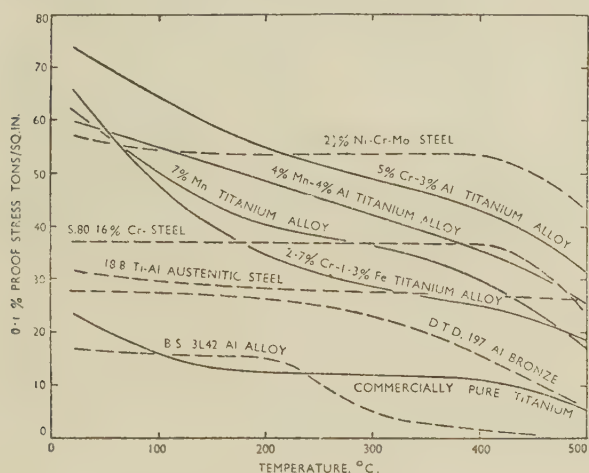


FIG. 21.—Effect of Temperature on Ultimate Tensile Stress of Commercially Pure Titanium and Titanium Alloys.

notch sensitivity of high-strength titanium alloys, particularly when subjected to fluctuating stresses, recent evidence suggests that some at least of the duplex alloys are equal to or better than high-tensile steels in this respect.

Such alloys as those in Table II have essentially similar structures in as much as they consist of a mixture of the two phases. The quantities of  $\beta$ -stabilizing elements present are sufficient to effect the retention of some  $\beta$  at room temperature, and the presence of  $\alpha$  stabilizers, such as oxygen, carbon, and aluminium, modifies without basically changing the mixture of  $\alpha/\beta$  phases. The optimum mechanical properties of these duplex alloys are developed by hot working them in the transformation-temperature range, when a structure of the kind shown in Fig. 20 (Plate XVII) is produced. If the working is not continued down to comparatively low temperatures, there is a risk that some loss of ductility will result. Rapid cooling from temperatures above that of the transformation has an embrittling effect, so although these  $\alpha/\beta$  alloys have shown themselves to be useful engineering materials, they are not suitable for welding.

Duplex alloys containing aluminium, having a considerably higher transformation range, permit of more latitude in hot-working conditions, and the presence of this element also has the important effect of increasing the strength of the  $\alpha$  phase at elevated temperatures. They thus retain a greater proportion of their strength at temperatures up to about 600° C. than do alloys in which  $\alpha$  stabilizers are not present or where the  $\alpha$  phase is strengthened only

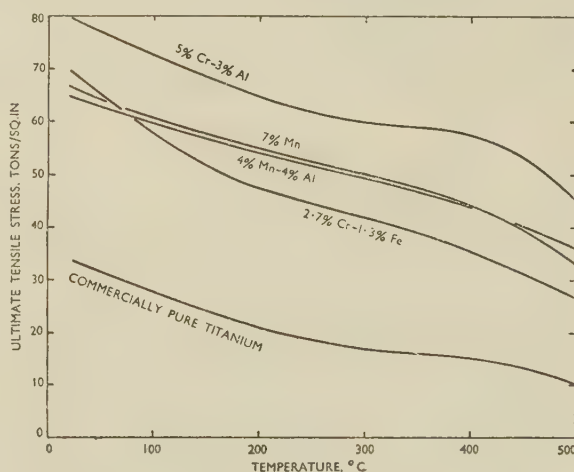


FIG. 22.—Effect of Temperature on Proof Stress.

quite small additions give rise to pronounced hardening, and consequently marked changes result from small variations in alloy concentration. So far there has been no evidence to indicate that the addition of these elements alone would be likely to give rise to useful titanium alloys.

Alloys composed wholly of the  $\beta$  phase appear to be much more ductile and to have a lower rate of work-hardening than single-phase  $\alpha$  alloys, and are potenti-

ally therefore much more suitable for the manufacture of strip and sheet. Furthermore, fully stabilized  $\beta$  alloys, not being sensitive to rate of cooling, might be expected to hot work and weld as easily as  $\alpha$  alloys. The development of satisfactory all- $\beta$  alloys, however,

seriously reduced by achieving complete stability. Alloys of this type would not be expected to have high-temperature properties as good as those of  $\alpha/\beta$  alloys, and therefore are not so suitable for service under such conditions, especially as they are particularly sensitive to contamination by small amounts of oxygen, for example, which could give rise to localized instability and the formation of small amounts of embrittling decomposition products.

It is too early yet to suggest what the relative importance of alloys of different structural types might eventually be or to forecast the possible pattern of alloy development. The fact that in so short a time and in the almost complete absence of detailed basic knowledge, alloys have been produced with a strength : weight ratio better than that of any other available material, is, however, I would submit, most encouraging and augurs well for the future. The additions that have been made to our knowledge in the meantime, and the clarifying information that is being obtained from current studies on alloy constitution and properties, warrant the confident expectation of much progress in the development of new alloys in the near future.

## VIII.—APPLICATIONS

So much as already been said and written on many occasions recently about the present use of titanium and its alloys in the construction of aircraft that no further comment is called for regarding this well-known application, which can, on technical and economic grounds, justify the consumption of all the titanium that is being made now or is likely to be made in the immediate future. Neither is it necessary to speculate on other uses, for it seems sure enough that the consumption of the metal in much greater quantities for other applications—and already there are many for which titanium and its alloys are well suited—will quickly follow when it is more readily and more cheaply available.

As I see it, the advent of titanium as an industrial metal provides metallurgists with yet another field of endeavour and further scope and opportunity for adding importantly to their many notable achievements and contributions to progress in the past.

## ACKNOWLEDGEMENTS

Finally, I wish to express my very sincere thanks to many colleagues in the General Chemicals and Metals Divisions of Imperial Chemical Industries, Limited, who have so willingly and generously provided me with much valuable help.

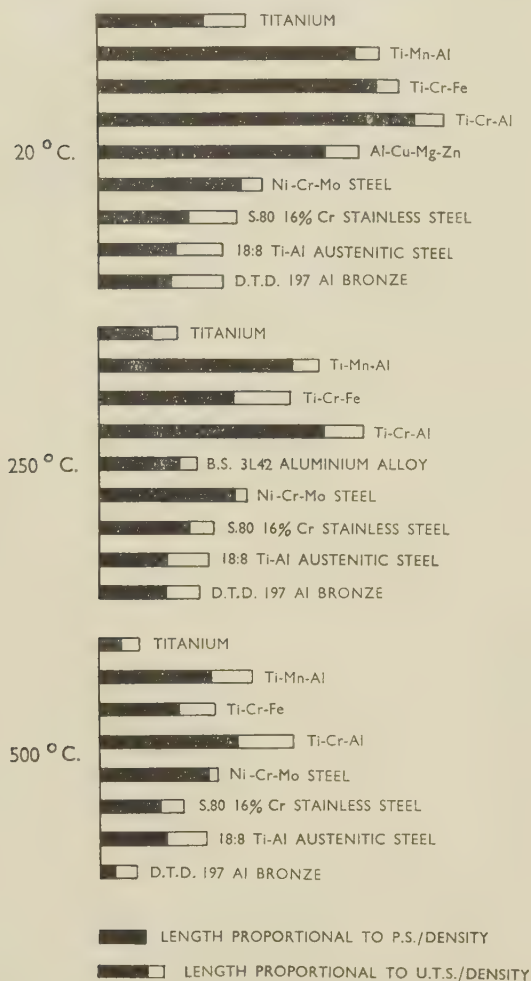


FIG. 23.—Ratio of Proof Stress and Ultimate Tensile Stress to Density of Various Alloys.

presents many difficulties, several of which have not yet been resolved. For instance, in order to avoid the formation of embrittling martensitic decomposition products when the alloys are heated to quite low temperatures, the  $\beta$  phase must be thoroughly stabilized, and this necessitates the addition of substantial amounts of alloying elements. This, of course, increases the density, but what is more important, it results in the formation of a highly alloyed phase which is much less ductile than a less heavily alloyed but incompletely stabilized  $\beta$  alloy. Thus the desired cold ductility is



# THE OXIDATION OF ALUMINIUM-MAGNESIUM ALLOYS BY STEAM: A CONTRIBUTION TO RESEARCH ON MOULD REACTION \*

1503

By MARJORIE WHITAKER,† B.Sc., A.I.M., MEMBER

With an Appendix on

## THE CONSTITUTION OF OXIDE FILMS FORMED AT HIGH TEMPERATURE ON ALUMINIUM-MAGNESIUM-BERYLLIUM ALLOYS

By A. R. HEATH,† B.Sc., JUNIOR MEMBER

(Communication from The British Non-Ferrous Metals Research Association.)

### SYNOPSIS

The work described formed part of a research on methods of preventing the reaction between aluminium-10% magnesium alloy and the steam atmosphere generated in a sand mould, a reaction causing surface oxidation and gas porosity in the casting. To reproduce conditions giving rise to this reaction, small cylinders of alloys were heated in steam in a laboratory apparatus, and the amount of reaction was assessed by the change in weight. Tests on alloys containing 0.0001-0.15% beryllium, the element usually added to inhibit mould reaction, disclosed minimum reactivity at 0.004% beryllium, suggesting that this is the optimum addition. The rate of oxidation in the laboratory test obeyed a logarithmic law. Reducing the moisture content of the atmosphere in the apparatus by dilution with argon decreased the reaction. Investigation of the effect of impurities on the inhibiting action of beryllium showed sodium to be the only harmful one, iron, silicon, copper, calcium, potassium, and carbon being innocuous. Prior degassing of the metal with nitrogen, chlorine, and hexachlorethane, the use of melting fluxes based on chlorides of potassium and magnesium, and grain-refining additions of titanium and boron were also harmless. Small additions of cerium, niobium, tantalum, thorium, vanadium, and zirconium, selected on account of the properties of their oxides, had some inhibiting effect on the reaction, both in the presence and absence of beryllium, but it was too small to have any practical application in the foundry. From the results of electron-diffraction and electron-microscope examinations of oxide films it appeared unlikely that the protective action of beryllium could be attributed to a single-phase layer of beryllia in the film.

### I.—INTRODUCTION

WHEN a metal is poured into a sand mould, it is confronted with an atmosphere of steam vaporized from the mould, and, with few exceptions, the metal reacts with the steam to form the oxide of the metal and liberates hydrogen in the process. If the oxide forms a protective film on the metal surface, the reaction rapidly ceases, and its occurrence is of no practical consequence. In many cases, however, the reaction is not stifled in this way, and, because the hydrogen formed in the reaction is liberated in the nascent state, the metal may then absorb large amounts of gas, which are subsequently rejected from solution again as the metal continues to cool; the reaction may thus give rise to more or less severe gas unsoundness. Owing to the presence in the clay bond of combined moisture which is liberated on

heating, the reaction cannot be prevented by oven drying of the mould.<sup>1</sup>

Slight mould reaction may occur in aluminium alloys containing as little as 0.5% magnesium. It becomes greater as the magnesium content increases, and at 10% magnesium it is so severe that its control is one of the major problems of foundry practice.

The oxidation of the surface of the casting, frequently called "sand attack", has often been described in the literature, but the equally or more important effect of the accompanying gas absorption has received little attention, apart from work on copper alloys containing phosphorus.<sup>2</sup> The work described in the present paper formed part of a research on mould reaction in light alloys, in which gas porosity was the primary concern, and among other things it has been shown that pronounced porosity may result from mould reaction, even when there is no visible oxidation.<sup>1</sup>

\* Manuscript received 30 April 1953. The work described in this paper was made available to members of The British Non-Ferrous Metals Research Association in confidential

reports issued during the period February 1951-January 1953.

† Investigator, The British Non-Ferrous Metals Research Association, London.

The usual method of inhibiting mould reaction in the 10% magnesium alloy is to add a small amount of beryllium to the metal and at the same time to add boric acid or ammonium bifluoride to the moulding sand. Gauthier<sup>3</sup> recommended in 1938 that the beryllium addition should be 0.02%, and for a long time this appears to have been accepted as the most suitable amount. In 1952 Calvet and Potemkine<sup>4</sup> recommended as little as 0.0001% beryllium to prevent oxidation stains on small sand castings of aluminium-8% magnesium alloy, but they did not examine the gas porosity of their castings.

The purpose of the present work was to examine, with laboratory precision, the way in which mould reaction in aluminium-10% magnesium alloy is influenced by various additions to the metal. First, the effect of varying the beryllium content within the range 0.0001-0.15% was investigated; secondly, the effect of common impurities, grain-refining elements, degassing agents, and fluxes upon the inhibiting action of beryllium was examined; and, thirdly, an attempt was made to find another element which might enhance the effect of beryllium. These three portions of the work are described in Sections III, IV, and V, respectively. Finally, the constitution and structure of films formed on alloys with different beryllium contents were examined, using electron diffraction and the electron microscope, and the results are given in an Appendix (p. 114).

This laboratory work was carried out in conjunction with experimental foundry work, an account of which has recently been published.<sup>1</sup>

## II.—EXPERIMENTAL TECHNIQUE

To reproduce mould reaction in the laboratory, small cylinders of the alloy were heated in a current of pure steam and the reaction was assessed by the weight increase. A steady temperature of 580° C. was selected for most of the experiments, as Swain<sup>5</sup> had shown that the reaction between aluminium-10% magnesium and steam was greatest at that temperature. Slow-cooling tests were also carried out.

### 1. PREPARATION OF ALLOYS

The alloys were made from aluminium of 99.99% purity and magnesium of 99.96% purity. They were melted in an alumina-lined Salamander pot in an electric furnace, under an atmosphere of argon, without a flux cover, degassed with argon, and poured at 710° C. into stick moulds of iron or graphite. Certain of the alloys required a higher pouring temperature to retain the constituents in solution. Different degassing and other treatments were applied in certain cases.

### 2. METHODS OF ANALYSIS

Magnesium, iron, silicon, copper, and titanium were determined by chemical methods, calcium and boron

by spectrographic solution methods, and beryllium by a spectrographic arc method. Sodium was determined by vacuum distillation, using a method based on that described by McCamley, Scott, and Smart.<sup>6</sup> Cerium, niobium, tantalum, thorium, vanadium, and zirconium were determined approximately by spectrographic arc methods.

### 3. APPARATUS AND TECHNIQUE

Cylindrical specimens, 5.0 cm. long and 1.00 cm. in dia., were machined dry from the as-cast alloy, care being taken to avoid surface contamination; any with porosity greater than 2% were rejected. A longer specimen (8.0 cm.) was used for certain of the experiments described in Section V. A thermocouple was inserted in an oxidized nickel sheath\* into the centre of the specimen, as shown in Fig. 1 (a).

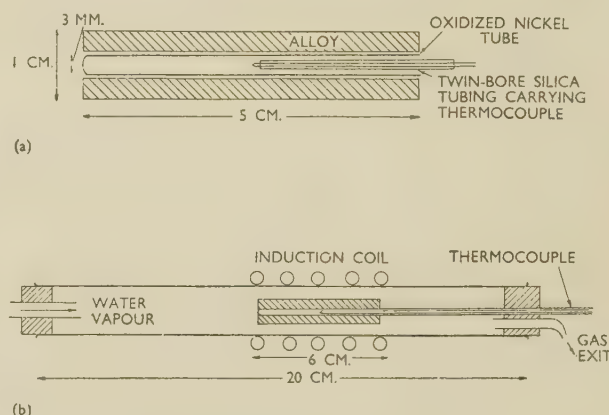


FIG. 1.—Diagrams of (a) Specimen and (b) Reaction Tube with Specimen in Position.

A high-frequency induction coil heated the specimen in a horizontal reaction tube carrying a current of pure steam. By using specimens of equal surface area and supporting them as shown in Fig. 1 (b) so that the whole surface was in contact with the steam, measurement of the weight increases gave comparative figures for the amount of reaction.

The specimens were washed with acetone, weighed to  $\pm 0.1$  mg., and preheated to 120° C., to prevent condensation, before insertion into the reaction tube. Application of the full available power raised the temperature of the 5-cm. specimen to 580° C. in 20 sec., and this temperature was then maintained for specified times, with occasional fluctuations of not more than  $\pm 3^\circ$  C. Modifications of the technique are described in the appropriate sections of the paper.

## III.—THE EFFECT OF BERYLLIUM

The main purpose of this part of the work was to determine the optimum beryllium content for inhibiting mould reaction in sand castings of aluminium-10% magnesium alloy. In addition, the possibility

\* The weight of the oxidized nickel sheath did not change during the experiment.



of preventing the reaction by reducing the steam pressure in the mould was explored by testing alloys in an argon atmosphere containing only a little water vapour.

## 1. ALLOYS

Eighteen aluminium-10% magnesium alloys, with beryllium contents in the range 0.0001-0.15% were tested. Eleven had been degassed with argon, six with nitrogen under a flux cover, and the remaining two, which were of commercial purity, had been degassed with chlorine. The two latter contained iron 0.18, silicon 0.09%, and traces of copper and titanium. Owing to melting losses, the magnesium contents of the alloys varied in the range 8.2-10.6%, but there was no evidence that the results were significantly affected by this variation.

## 2. EXPERIMENTS AND RESULTS

### (a) Optimum Beryllium Content

To examine the effect of beryllium content, a test specimen of each alloy was held in the apparatus at 580° C. for 30 min.

The results are plotted on a logarithmic scale in Fig. 2, which shows that after falling rapidly the reactivity passed through a minimum at 0.004% beryllium and then increased, reaching a small peak at about 0.035% beryllium, followed by a second decrease. The shape of the curve was in keeping

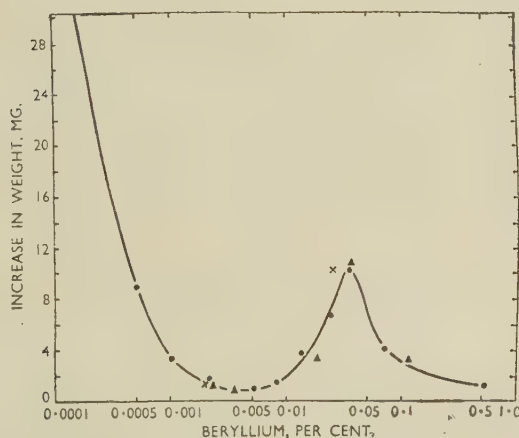


FIG. 2.—Influence of Beryllium Content on the Reaction with Steam at 580° C. (Log Scale).

KEY.

● High-Purity Alloys Degassed with Argon.  
▲ " " " " " Nitrogen.  
× Commercial-Purity "Alloys" Degassed with Chlorine.

with the appearance of the specimens after test, those containing 0.002-0.004% and 0.07-0.15% beryllium being clean, whereas the others were discoloured.

The beryllium-free alloy and the alloy containing 0.0001% beryllium reacted so vigorously that 5 minutes' exposure was the maximum for reproducible results, giving weight increases of 90 and 20 mg., respectively. It is clear that as little as 0.0001% beryllium has a

pronounced inhibiting effect. If the reaction-rate curves are assumed to have the same shape as those obtained for the other alloys (see Fig. 3), these increases would correspond to increases of the order of 300 and 50 mg., respectively, after 30 minutes' exposure.

The alloys degassed with nitrogen under a flux cover and the two commercial-purity alloys degassed with

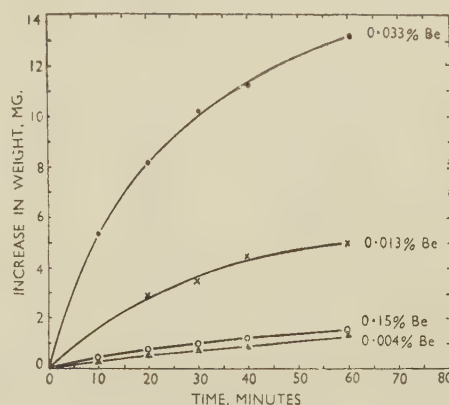


FIG. 3.—Rate of Reaction with Steam at 580° C.

chlorine gave results which fitted on the curve for the main series of alloys.

### (b) *Slow-Cooling Test*

To compare the test at 580° C. with conditions more closely resembling the solidification of a casting, three of the alloys were tested by melting in dry argon in a recrystallized alumina boat, using a modified form of the apparatus, and cooling slowly in steam through the solidification range 615°–450° C. The rate of cooling was controlled to reproduce that of a sand casting in this alloy 10 in. long  $\times$  5 in. dia., which takes about 50 min. to solidify.<sup>7</sup>

The weight increases of alloys containing 0.004, 0.035, and 0.15% beryllium were 2.0, 8.0, and 2.0 mg., respectively, showing that the peak in the reaction curve at 0.035% beryllium, observed at a steady temperature, is also present when the temperature falls as in a solidifying casting.

### (c) Reaction-Rate Curves

The rate of reaction of four alloys was examined by holding specimens at 580° C. in steam for periods of 10, 20, 30, 40, and 60 min. Increase in weight is plotted against time in Fig. 3, and the same results are plotted on a logarithmic scale in Fig. 4. The linear relationship shown in Fig. 4 suggests that the rate of oxidation obeys a logarithmic law of the type :

$$\Delta m = C_1 \log (C_2 t + C_3)$$

where  $\Delta m$  is the weight increase,  $t$  is time, and  $C_1$ ,  $C_2$ , and  $C_3$  are constants.

#### (d) *Effect of Steam Pressure*

Steam at atmospheric pressure in the reaction tube was replaced by argon saturated with water vapour at (1) 25° C. and (2) 0° C., thus reducing the partial

pressure of water vapour to 24 and 4.6 mm. of mercury, respectively.

The weight increases on heating specimens of beryllium-free alloy for 5 min. at 580° C. in these two atmospheres were 19 and 18 mg., respectively, and

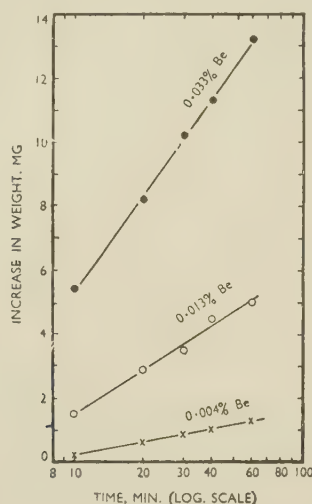


FIG. 4.—Rate of Oxidation by Steam at 580° C. (Log Scale).

rapid blackening occurred. In comparison with the 90 mg. obtained normally, this shows that the reaction was lessened.

A smaller reduction, from 3.2 mg. at atmospheric pressure to 2.5 mg. at 4.6 mm. of mercury, occurred when the alloy containing 0.018% beryllium was heated for 30 min. at 580° C.

#### (e) *Relation Between Weight Increase and Hydrogen Absorbed*

The volume of hydrogen generated in the reaction  $\text{Me} + \text{H}_2\text{O} \rightarrow \text{MeO} + \text{H}_2$  is proportional to the

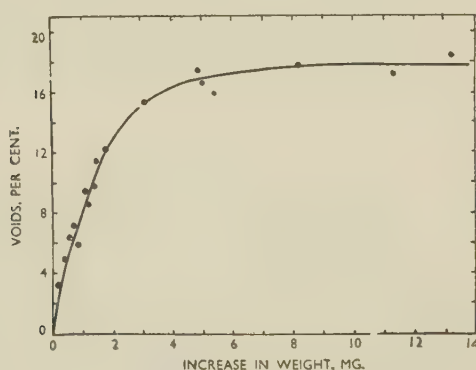


FIG. 5.—Relationship Between Increase in Weight and Increase in Porosity.

weight increase of the specimen, each milligramme increase being equivalent to the generation of 1.4 c.c. hydrogen at S.T.P. But the important consideration in foundry work is the amount of hydrogen absorbed by the casting, which is only a part of the total amount generated. To examine the relationship between

weight increase and hydrogen absorbed, the densities of a number of test specimens with random beryllium content were measured after test. Increase in porosity is plotted against weight increase in Fig. 5, which shows that the porosity increase was at first approximately proportional to the weight increase, but eventually (above about 5 mg. increase) became nearly constant at about 17%.

### 3. DISCUSSION AND INTERPRETATION OF RESULTS

Fig. 2, relating beryllium content to amount of reaction, suggests that within the commercially practicable range of additions 0.0001–0.1% the optimum content would be 0.004%. This amount had a greater inhibiting effect, in the laboratory test, than the 0.025% which had previously been recommended by the Association and by others. To test this conclusion, sand castings of aluminium–10% magnesium alloy containing 0.004 and 0.025% beryllium were made in the foundry, using commercial-purity materials, and it was found that the smaller addition gave sounder castings.<sup>1</sup> The smaller addition also has the advantage that production costs are reduced, and, as reported elsewhere,<sup>1</sup> the melting loss of beryllium is low.

Even when beryllium is added to the metal and either boric acid or ammonium bifluoride to the moulding sand, castings of heavy section in this alloy are not entirely free from mould reaction. Such castings take a long time to solidify, and the reaction-rate curves in Fig. 3 suggest that the porosity is caused by prolongation of the slight residual reaction.

Lowering the partial pressure of water vapour in the atmosphere surrounding the alloy reduced the reaction to a certain extent, but the results suggest that no readily applicable measures to reduce the partial pressure of water vapour in the mould would adequately inhibit mould reaction.

### IV.—EFFECT OF IMPURITIES AND OTHER MINOR CONSTITUENTS

Erratic results had sometimes been obtained in experimental foundry work, and it was thought that impurities or other constituents might be interfering with the action of the beryllium.<sup>8</sup> The purpose of this section of the work was to examine, under laboratory conditions, the effect of impurities, grain-refining elements, fluxes, and degassing agents.

#### 1. ALLOYS

Iron, silicon, copper, calcium, sodium, and potassium were selected as impurities, titanium and boron as grain-refining elements, and chlorine and hexachlorethane as degassing agents, the latter introducing carbon as an impurity into the metal. Degassing with nitrogen had been found innocuous in the experiments described above in Section III. Two fluxes were tested, one a commercial flux, based on carnallite and con-



taining up to 1½% sodium chloride and about 3% calcium chloride as impurities, and the other a high-purity flux, prepared in the laboratory, containing 60% magnesium chloride, 20% magnesium fluoride, and 20% potassium chloride. Twenty-four high-purity alloys were made up, with beryllium contents (verified spectrographically) in the range 0.003–0.004%. The control alloy, free from added impurities, contained 0.002% iron and 0.02% silicon. When these alloys had been tested, the influence of sodium was further examined by means of additional alloys containing 0.004, 0.035, and 0.18% beryllium. The compositions of the alloys are given in Tables I and II. Alloys containing more than 0.01% potassium could not be prepared, presumably because of the low solubility of this element in aluminium and magnesium.

## 2. EXPERIMENTS AND RESULTS

Specimens of 5 cm. length were heated in steam at 580° C. for 15 min., longer heating being impossible

TABLE I.—*Effect of Impurities and Other Minor Constituents on the Inhibiting Action of 0.004% Beryllium.*

Analysed Composition,* %		Weight † Increase, mg.	Porosity † Increase, % Voids
Addition Element	Magnesium		
None (control alloy)	10.9	0.4	4.3
0.02 iron	10.3	0.2	5.1
0.13 "	10.7	0.1	5.7
0.94 "	10.8	0.3	4.8
0.06 silicon	10.5	0.2	3.7
0.15 "	10.5	0.4	3.9
1.05 "	10.8	0.3	3.8
0.01 copper	10.6	0.2	3.7
0.11 "	10.8	0.2	3.6
1.08 "	10.7	0.1	3.2
0.01 calcium	10.7	0.3	4.5
0.10 "	11.0	0.0	3.9
1.0 "	10.5	0.2	2.2
~0.01 potassium	11.0	0.3	5.2
0.01 boron	10.2	0.1	3.3
0.12 "	11.2	0.1	3.2
0.01 titanium	10.9	0.2	3.3
0.08 "	10.3	0.2	3.7
<i>Melting Fluxes</i>			
Commercial flux	10.3	0.4	3.9
High-Purity Flux	10.9	0.3	4.2
<i>Degassing Agents</i>			
Chlorine	10.7	0.2	3.6
Hexachlorethane	10.9	0.4	3.7

\* All alloys contained 0.003–0.004% beryllium, determined spectrographically.

† Mean of two tests.

because of the failure of coherence in some of the alloys. Increases in weight and in porosity were measured.

The results obtained with alloys other than those containing sodium are given in Table I. There was no significant variation in either weight increase or porosity increase in this group of alloys, all of which contained 0.004% beryllium.

TABLE II.—*Influence of Sodium on the Inhibiting Action of Beryllium.*

Analysed Composition, %			Weight Increase,† mg.
Sodium	Beryllium	Magnesium	
0.001 *	0.004	10.9	0.4
0.002	0.003	10.6	0.2
0.003	0.003	10.5	0.8
0.006	0.004	11.0	2.7
0.060	0.004	10.5	88.2
not determined*	0.044	11.0	3.5
0.03	0.040	10.7	23.8
0.06	0.038	10.8	67.3
0.0015 *	0.18	11.0	0.2
0.025	0.17	10.5	16.2
0.035	0.18	11.0	22.3

\* Sodium was not added to these three alloys.

† Mean of two tests.

The influence of sodium, shown by the results given in Table II, was increasingly harmful from 0.003% upwards, until at 0.06% the inhibiting effect of beryllium was almost nullified. Increasing reactivity was accompanied by the formation of a pale grey coating. Increasing the beryllium content to 0.18% did not overcome the effect of sodium.

## 3. DISCUSSION AND INTERPRETATION OF RESULTS

The results show that, with the exception of sodium, none of the impurities, grain-refining elements, degassing agents, or fluxes had a harmful effect on the inhibiting action of beryllium. The absence of harmful effects resulting from the use of titanium and boron to refine the grain has been confirmed by foundry work.<sup>1</sup>

Calcium might be regarded with suspicion, since it increases the porosity of gas welds in aluminium–7% magnesium alloy sheet,<sup>9</sup> but, although there is a certain similarity between porosity in gas welds and porosity in castings, both being caused by reaction with water vapour, there are certain fundamental differences, and beryllium does not prevent porosity in welds. The present work showed that calcium did not reduce the inhibiting effect of beryllium, in fact it may be beneficial. Other workers<sup>4, 8</sup> have found that calcium additions reduce burning and the reaction with moisture.

Carbon had previously been suspected of interfering with the inhibiting action of beryllium in castings.<sup>8</sup> In the present work the amount introduced by a single degassing treatment with hexachlorethane had no such effect, and this agrees with the results of foundry experiments.<sup>1</sup>

Very slight contamination with sodium, as represented by an increase from 0.001 to 0.002%, had no detectable effect, which suggests that pre-treating the metal to remove traces of sodium below 0.003% would not improve the inhibition. Nevertheless, it was concluded that slight contamination of the melt with sodium from fluxes or other sources would be likely to increase the amount of mould reaction in sand castings of this alloy.

### V.—SEARCH FOR ANOTHER INHIBITING ELEMENT

This part of the work was an attempt to find another inhibiting element. Lees<sup>8</sup> had tested thorium and found a moderate inhibiting effect, and Hall and Liddiard<sup>8</sup> had found that calcium and zirconium

volume of metal from which it was formed, a ratio less than unity being associated with a discontinuous film of low protective power.

The oxide films on alloys are complex. Elements with small ionic radius and high free energy of formation tend to diffuse outwards and oxidize preferentially; for example, de Brouckère<sup>12</sup> has shown that under certain circumstances double oxide layers, with MgO at the outer surface, can form on aluminium-magnesium alloys, and Keil<sup>13</sup> has detected a concentration of beryllium at the surface of sand castings of a magnesium alloy containing 8% aluminium and 0.005% beryllium. Heath (see Appendix, p. 114) detected at least two phases (magnesia and beryllia) in oxide films on aluminium-magnesium-beryllium alloys; he did not find any evidence of a single-phase layer of beryllia in the film.

TABLE III.—*Properties of Oxides.*

Element	Atomic Weight	Goldschmidt Ionic Radius, Å.	Oxide Formed at 650° C.	Standard Free Energy of Formation of Oxide at 650° C., K. cal./mole O <sub>2</sub>	Melting Point of Oxide, °C.	Electrical Resistivity of Oxide		Pilling-Bedworth Ratio
						Temp., °C.	Resistivity, ohm/cm.	
Al	27.0	0.57	Al <sub>2</sub> O <sub>3</sub>	—217	1999–2032	830 1095	10 <sup>8</sup> 10 <sup>6</sup>	1.3
Mg	24.3	0.78	MgO	—242	2800	555 782	6.9 × 10 <sup>5</sup> 9.6 × 10 <sup>4</sup>	0.8
Be	9.0	0.34	BeO	—253	2585	630 1100	3.9 × 10 <sup>8</sup> 5.2 × 10 <sup>6</sup>	1.6
Ce	140.1	1.18	CeO <sub>2</sub>	—193	1950	800 1000	6.5 × 10 <sup>4</sup> 2.1 × 10 <sup>2</sup>	1.2
Nb	92.9	0.69	Nb <sub>2</sub> O <sub>5</sub>	—185 at 25° C.	1520	Room temp.	11.4 × 10 <sup>4</sup>	2.6
Ta	180.9	0.68	Ta <sub>2</sub> O <sub>5</sub>	—164	1470 (dissociation)	No information		2.3
Th	232.1	1.10	ThO <sub>2</sub>	—253	>2800	550 950	2.6 × 10 <sup>7</sup> 3.9 × 10 <sup>4</sup>	1.3
V	51.0	0.65	V <sub>2</sub> O <sub>3</sub>	—163	1970	No information		1.8
Zr	91.2	0.87	ZrO <sub>2</sub>	—217	2700	340 700	2.1 × 10 <sup>6</sup> 2.3 × 10 <sup>4</sup>	1.5

reduced the reaction of aluminium-7% magnesium with moist air at 600° C.

#### 1. THEORY OF OXIDATION

Mould reaction is a matter of oxidation by steam, the rate of reaction being controlled by the properties of the oxide film.

One generally accepted theory of oxidation suggests that the system can be regarded as an electrolytic cell of the type metal|metal oxide|oxygen, and that progressive oxidation occurs as a result of the diffusion of metal ions, electrons, and possibly oxygen ions through the oxide film.<sup>10</sup> With pure metals the principal factors governing the rate of oxidation are the electrical resistivity of the oxide, a high value signifying a low rate of oxidation, and the Pilling-Bedworth<sup>11</sup> ratio, i.e. the ratio of volume of oxide to

The film on a solidifying casting may be ruptured by contraction stresses, even when the Pilling-Bedworth ratio is favourable. High mechanical strength should help to prevent this, and it was, in fact, observed in the present work that oxide films removed from molten aluminium-magnesium alloys containing 0.004 and 0.15% beryllium were stronger than the less protective film from the alloy containing 0.035% beryllium. When fissuring is responsible for the growth of an oxide film, the increase in weight,  $\Delta m$ , often follows a logarithmic law of the type:

$$\Delta m = C_1 \log (C_2 t + C_3)$$

where  $t$  is time, and  $C_1$ ,  $C_2$ , and  $C_3$  are constants. Since Fig. 4 shows that the rate of oxidation in the laboratory test was logarithmic, it may be tentatively suggested that oxidation of these alloys under these



conditions proceeds as the result of fissuring. A parabolic rate of growth is generally associated with continuous films.

## 2. SELECTION OF ELEMENTS

Information on the relevant properties of all the likely elements was reviewed, and from the data obtained six were selected: cerium, niobium, tantalum, thorium, vanadium, and zirconium (see Table III). The most likely oxides of niobium and tantalum at the casting temperature of aluminium-magnesium alloy are  $\text{Nb}_2\text{O}_5$  and  $\text{Ta}_2\text{O}_5$ , and, according to Gulbransen and Andrew,<sup>14</sup>  $\text{V}_2\text{O}_3$  is the oxide formed on vanadium at 600° C.

## 3. ALLOYS

To examine the effect of the six addition elements with and without beryllium, three groups of high-purity alloys were made. The first group was free

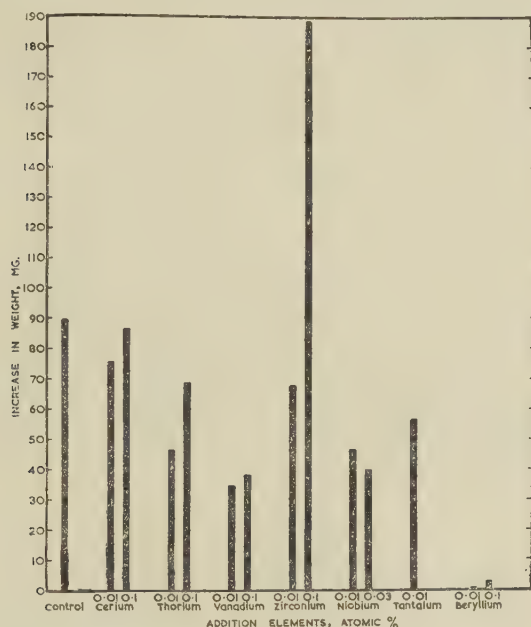


FIG. 6.—Influence of Addition Elements on Reaction of Plain 90:10 Aluminium-Magnesium Alloy with Steam at 580° C. (Specimens 5 cm. long; 5 min. exposure.)

from beryllium, the second contained 0.003–0.004% (nominally 0.004%), and the third 0.03–0.04% beryllium (nominally 0.035%). These beryllium contents were selected from the curve in Fig. 2 as the optimum and least effective additions within the range 0.0005–0.1%. The six other elements were added in the same atomic proportions as the beryllium, i.e. 0.01 and 0.1 at.-%, since protective action is more likely to be related to the number of atoms present than to the percentage by weight. Because of low solubility the higher addition of tantalum was omitted, and the highest possible addition of niobium was 0.03 at.-%, which was made to an alloy poured at 850° C. to keep the niobium in solution. Alloys containing

0.1 at.-% zirconium also required a high pouring temperature (800° C.). There was a control alloy in each group, making 36 alloys in all.

## 4. EXPERIMENTS AND RESULTS

Two specimens of each alloy were heated in steam at 580° C. in the laboratory apparatus. Alloys free

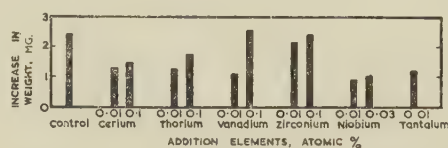


FIG. 7.—Influence of Addition Elements on Reaction of 90:10:0.004 Aluminium-Magnesium-Beryllium Alloy with Steam at 580° C. (Specimens 8 cm. long; 30 min. exposure.)

from beryllium blackened rapidly, and tests were restricted to 5 min. because of the tendency to form exudations on longer exposure. The weight increases of the beryllium-free group are given in Fig. 6, which shows that all the additions except 0.1 at.-% zirconium reduced the reaction. Two lines representing the much greater effect of beryllium additions have been inserted in this figure for comparison.

With alloys containing beryllium, particularly 0.004% of it, the weight increase was so small that a longer specimen was used (8.0 cm.) and the test was prolonged to 30 min. In the presence of 0.004% beryllium, all the additions except 0.1 at.-% vanadium and 0.1 at.-% zirconium had a beneficial effect (Fig. 7), and in the presence of 0.035% beryllium all

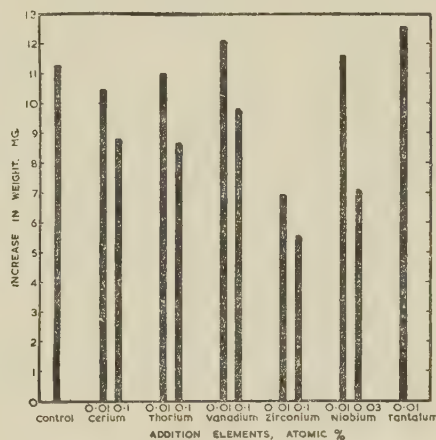


FIG. 8.—Influence of Addition Elements on Reaction of 90:10:0.035 Aluminium-Magnesium-Beryllium Alloy with Steam at 580° C. (Specimens 8 cm. long; 30 min. exposure.)

except 0.01 at.-% each of vanadium, niobium, and tantalum were beneficial (Fig. 8).

## 5. DISCUSSION AND INTERPRETATION OF RESULTS

The six elements cerium, niobium, tantalum, thorium, vanadium, and zirconium had an inhibiting effect upon the reaction of aluminium-10% magnesium

with steam at 580° C., but it was much less than that of beryllium. When used in conjunction with beryllium some improvement in inhibition was produced, in comparison with that afforded by beryllium alone.

Comparison of the effect of 0.01 and 0.1 at.-% of an added element is of theoretical interest, as it has been shown in Fig. 2 that 0.01 at.-% beryllium (0.004 wt.-%) is more effective than 0.1 at.-% (0.035 wt.-%). From Figs. 6 and 7 it can be seen that with each of the four elements cerium, thorium, vanadium, and zirconium (the only four added in these two atomic proportions) 0.01 at.-% was more effective than 0.1 at.-%, both in the group of beryllium-free alloys and in the group of alloys containing 0.004% beryllium.

When 0.035% beryllium was present, however, the relationship was reversed (Fig. 8), and 0.1 at.-% beryllium plus 0.1 at.-% of another element (total 0.2 at.-%) was more effective than the same amount of beryllium plus only 0.01 at.-% of the other element (total 0.11 at.-%). Assuming that the effects of the elements are additive, this links up with the observation (Fig. 2) that when the beryllium content is increased beyond the peak at 0.1 at.-% there is an increase in the inhibiting action. In other words, there is a certain amount of evidence that the minimum and the peak in Fig. 2 may occur with other added elements.

From the practical point of view of reducing mould reaction in sand castings of aluminium-10% magnesium alloy, it is clear from these results that, although the six elements had some effect, they were much less effective than beryllium alone. The most promising additions, for use in conjunction with 0.004% beryllium, were 0.01 at.-% of thorium, niobium, or vanadium. Vanadium was selected for further investigation in the foundry, and two sets of sand castings, with dia. 1, 2, and 4 in., were made. Mould reaction in the castings was examined by density measurements, following the technique usually employed in the research,<sup>1</sup> and it was found that the vanadium had not conferred any detectable improvement on the inhibition provided by 0.004% beryllium alone. The small improvement detected in the more sensitive laboratory test was evidently masked by other factors in foundry work.

It was concluded that the inhibiting action of 0.004% beryllium in castings would not be improved substantially by adding any of the other six elements to the alloy.

## VI.—CONCLUSIONS

The principal conclusions are as follows:

(1) Within the range of additions 0.0001–0.1% beryllium, the greatest inhibition of the reaction of aluminium-10% magnesium alloy with pure steam at 580° C. occurs at 0.004% beryllium, and a peak in the curve relating reaction to beryllium content occurs at 0.035% beryllium. The conclusion that 0.004% beryllium was the optimum addition for the inhibition

of mould reaction in castings of this alloy has been confirmed by foundry work.

(2) Reducing the moisture content of the atmosphere to a partial pressure of 4.5 mm. of mercury, by dilution with argon, reduces the amount of reaction to a certain extent.

(3) The inhibiting action of beryllium is not reduced by degassing the melt with chlorine, nitrogen, or hexachlorethane, nor by the use of melting fluxes based on chlorides of magnesium and potassium. The impurities carbon (introduced by degassing with hexachlorethane), iron, silicon, copper, calcium, and potassium, and the grain-refining elements boron and titanium are also harmless.

(4) Sodium reduces the inhibiting effect of beryllium, 0.003% or more having a detectable effect in the laboratory test and 0.06% practically destroying the inhibition. Contamination of the melt with sodium from fluxes or other sources is likely to increase the amount of mould reaction occurring in sand castings of this alloy.

(5) Small additions of cerium, niobium, tantalum, thorium, vanadium, or zirconium have some inhibiting effect in the presence and absence of beryllium, but it is too small to have any practical application in sand castings of this alloy.

(6) The rate of oxidation of alloys containing up to 0.15% beryllium by steam at 580° C. obeys a logarithmic law.

(7) The beryllia content of the oxide film increased with increasing beryllium content of the metal, and there was no evidence of a single-phase layer of beryllia to account for the protective effect of beryllium (see Appendix). Oxide films from alloys containing 0.004 and 0.15% beryllium are mechanically stronger than the less protective film from the alloy containing 0.035% beryllium.

## APPENDIX

### THE CONSTITUTION OF OXIDE FILMS FORMED AT HIGH TEMPERATURE ON ALUMINIUM-MAGNESIUM-BERYLLIUM ALLOYS

By A. R. Heath, B.Sc.

#### (a) *Experimental Work*

Films formed on aluminium-10% magnesium alloys containing 0.0001–0.15% beryllium were examined in an attempt to find an explanation for the inhibiting effect of beryllium on mould reaction, and for the shape of the curve reproduced in Fig. 2, which shows that 0.035% beryllium has less inhibiting effect than 0.004 or 0.15%.

Surface films on chill-cast specimens and on specimens which had been metallographically polished and then exposed to pure steam at 580° C. were examined by the reflection method in the electron-diffraction camera. In addition, oxide skins were removed from the surface of molten alloys by means of a wire loop



and examined by transmission in the electron-diffraction camera. Transparent portions of these films were also examined in the electron microscope at a magnification of  $\times 27,000$ .

### (b) Results

The results of the electron-diffraction examinations are given in Table IV. These show that the beryllia content of the film increases as the beryllium content of the alloy increases. No alumina, as such, could be identified in any of the electron-diffraction plates, but all the films contained isolated portions which gave rise to a complex spotty pattern, possibly caused by some spinel-like complex of alumina and magnesia, since a similar pattern was observed when a beryllium-free aluminium-10% magnesium alloy was examined. Numerous measurements of the spots showed that they arose in each case from a similar structure, but it could not be identified. An example of the pattern of spots is reproduced in Fig. 11 (Plate XVIII), where it is superimposed on the lines of beryllia and magnesia which are shown separately in Figs. 9 and 10 (Plate XVIII).

TABLE IV.—*Results of Electron-Diffraction Examination of Oxide Films.*

Type of Specimen	Be Content, %	Time of Steam Treatment at 580° C., min.	Phases Shown in Electron-Diffraction Pattern *
Steam-treated surface	0.004	5	MgO with faint trace BeO
	0.004	10	MgO
	0.013	5	MgO with trace BeO
	0.013	10	MgO with about 30% BeO
	0.035	2	MgO
	0.035	10	MgO with about 40% BeO
	0.15	2	MgO with small amount BeO
	0.15	10	MgO with about 45% BeO
Chill-cast surface	0.004	None	MgO
	0.013	"	MgO with about 30% BeO
	0.033	"	MgO with about 40% BeO
Films taken from surface of melts	0.0001	None	MgO
	0.0005	"	MgO
	0.004	"	MgO
	0.013	"	MgO with small amount BeO
	0.033	"	MgO with about 25% BeO
	0.15	"	MgO with about 45% BeO

\* Parts of all specimens gave rise to a spotty pattern superimposed on the pattern caused by phases listed in this column.

Electron micrographs of the transparent parts of oxide films taken from the surface of molten alloys showed, in general, a granular appearance of varying grain-size, of which a typical example is shown in Fig. 12 (Plate XVIII). It is similar to an electron micrograph of the surface of a magnesium alloy con-

taining 2% aluminium plus 0.012% beryllium published by Burns.<sup>15</sup> The dark-grey area in the plate is probably due to folds in the oxide film and is therefore of no significance. No systematic change could be found in the appearance of micrographs of films from alloys with different beryllium contents.

### (c) Discussion of Results

In the electron-diffraction technique used in reflection, the electron beam penetrates to a depth of about 300 Å. The diffraction pattern obtained from the alloy containing 0.004% beryllium indicated that only a trace (<5%) of beryllia was present in that part of the oxide layer penetrated by the beam. If this beryllia were present as a homogeneous layer in the film, it could be only about 15 Å. thick. It is not expected that a layer of this thickness would give rise to diffraction rings which are continuously sharp. The pattern is more likely, therefore, to have arisen from beryllia present as discrete particles in the oxide layer than as a single-phase layer on the surface. No evidence was found for the presence of an amorphous layer of beryllia. Furthermore, if the beryllia formed a single-phase protective layer, there would be no apparent reason why the protective effect should decrease at 0.035% beryllium in the manner shown in Fig. 2. It therefore seems reasonable to conclude that the inhibition does not occur through the formation of a single-phase layer of beryllia, and probable that the film consists of a multi-phase layer containing magnesia, beryllia, and possibly a third complex.

It is possible that the lower protective power of the film formed on the alloy containing 0.035% beryllium may be the result of a phase change in the layer of oxide immediately adjacent to the metal surface, and undetected in the electron-diffraction examination. Work by de Brouckère<sup>12</sup> has shown that double oxide layers can form on aluminium-magnesium alloys under certain conditions.

An alternative explanation of the shape of the curve in Fig. 2 is that the mechanical strength of the film varies as the beryllium content of the alloy increases. When films were removed from melts for examination, it was observed that those from the two with a high resistance to oxidation (0.004 and 0.15% beryllium) were markedly tougher than those from two with less resistance to oxidation (0.013 and 0.035% beryllium). Thus toughness of the oxide film appears to be linked with high protective power.

### ACKNOWLEDGEMENT

The authors are indebted to the Director and Council of the British Non-Ferrous Metals Research Association for permission to publish this paper.

## REFERENCES

1. Marjorie Whitaker, *Inst. Brit. Found. Preprint*, 1953, (1072); and *Found. Trade J.*, 1953, **95**, 195.
2. W. A. Baker, F. C. Child, and W. H. Glaisher, *J. Inst. Metals*, 1944, **70**, 373.
3. G. Gauthier, *Found. Trade J.*, 1938, **59**, 373.
4. J. Calvet and V. Potemkine, *Recherche aéronaut.*, 1952, (29), 21.
5. A. J. Swain, *J. Inst. Metals*, 1951-52, **80**, 125.
6. W. McCamley, T. E. L. Scott, and R. Smart, *Analyst*, 1951, **76**, 200.
7. R. W. Ruddle and A. L. Mincher, *J. Inst. Metals*, 1950-51, **78**, 229.
8. B.N.F.M.R.A., unpublished work.
9. J. Pendleton, *Weld. Research*, 1949, **3**, 74r.
10. O. Kubaschewski and B. E. Hopkins, "Oxidation of Metals and Alloys". 1953: London (Butterworths Scientific Publications).
11. N. B. Pilling and R. E. Bedworth, *J. Inst. Metals*, 1923, **29**, 529.
12. L. de Brouckère, *ibid.*, 1945, **71**, 131.
13. A. Keil, *Z. Metallkunde*, 1951, **42**, 13.
14. E. A. Gulbransen and K. F. Andrew, *J. Electrochem. Soc.*, 1950, **97**, 396.
15. J. R. Burns, *Trans. Amer. Soc. Metals*, 1948, **40**, 143 (see particularly p. 150).



# SOME CREEP CHARACTERISTICS OF A GROUP OF 1504 PRECIPITATION-HARDENING ALLOYS BASED ON THE ALPHA-COPPER-ALUMINIUM PHASE \*

By J. P. DENNISON,† B.Sc., Ph.D., JUNIOR MEMBER

## SYNOPSIS

The creep and creep-rupture characteristics of precipitation-hardening alloys based on the  $\alpha$ -copper-aluminium phase and containing cobalt, chromium, iron, nickel, titanium, or zirconium, have been examined. Hardness and metallographic data have been used to investigate the structural changes occurring on reheating solution-treated alloys, including specimens cold worked before ageing. Variation of the condition of the alloy before testing has provided information on the effect of these changes on creep behaviour under specific conditions of test.

Alloys which exhibited a form of discontinuous precipitation, mainly along grain boundaries, were found to fracture after very small extensions. An even distribution of precipitate along slip planes favoured considerable extension before fracture.

The results indicate the importance of such ductility in assessing creep performance, and the necessity for including experiments continued to fracture when creep-testing precipitation-hardening alloys.

The tensile properties of the alloys investigated are recorded, together with observations on their resistance to scaling.

## I.—INTRODUCTION

THE high oxidation-resistance of the copper-aluminium alloys makes them suitable for use in air at temperatures in the region of 400°–500° C., providing that the necessary mechanical properties and resistance to creep can be obtained. These alloys may be heat-treated in air at all temperatures up to the melting point without serious surface deterioration. The single-phase alloys, containing up to 8% aluminium, may be worked satisfactorily either hot or cold. The principal immediate application of such alloys is in the production of heat-interchanger tubes for gas turbines.

A number of precipitation-hardening alloys based on the copper-7% aluminium alloy were prepared, with the object both of developing a potentially useful industrial alloy and of making a metallographic study of the effect of precipitation phenomena on creep characteristics. Resistance to scaling under severe conditions, comparable to those encountered in the gas turbine, was also noted.

The selection of alloys was limited to those which could be obtained as primary solid solutions alone; the choice was complicated by the absence of information on the ternary diagrams. Additions were made of metals reported to give precipitation-hardening binary alloys when added to copper, without markedly lowering its melting point, namely cobalt, chromium, iron, titanium, and zirconium. In addition to ternary alloys of copper-aluminium with each of these metals, quaternary alloys containing cobalt and iron, and cobalt and nickel were prepared.

The alloys listed in Table I were prepared from 99.98% aluminium and M.C.3-grade fire-refined copper. The other alloying elements were added as master

TABLE I.—*Composition of Alloys.*

Nominal Composition		Actual Composition			
Al, %	Alloying Element, %	Cu, %	Al, %	Alloying Element, %	Re-remainder (mainly Ni and Fe), %
7	...	92.83	7.15	...	0.02
6	1.5 Co	92.58	6.03	1.37 Co	0.02
6	3 Co *	...	...	...	...
7	1.5 Co	91.58	6.85	1.54 Co	0.03
7	2.0 Co	91.48	6.37	2.12 Co	0.03
7	1 Co, 1 Fe	91.23	6.71	1.09 Co, 0.96 Fe	0.01
7	1.5 Co, 5 Ni	86.41	6.88	1.72 Co, 4.97 Ni	0.02
6	0.75 Cr	93.15	6.09	0.74 Cr	0.02
7	1.5 Cr *	...	...	...	...
6	1.5 Fe	92.30	6.16	1.52 Fe	0.02
7	3.0 Fe *	...	...	...	...
7	1.0 Ti	91.79	7.05	1.14 Ti	0.02
7	2.0 Ti	90.99	6.94	2.04 Ti	0.03
7	1.0 Zr	92.51	6.86	0.60 Zr	0.03
7	1.0 Ni, 1.0 Fe †	...	...	...	...

\* Two-phase alloy, not further examined.

† Industrial alloy tested for comparison.

alloys. An industrial alloy containing aluminium 7, iron 1, and nickel 1%, which has been used for heat-interchanger tubes, was included for comparison.

## II.—PREPARATION OF ALLOYS

The alloys were cast by the Durville process as ingots of approx.  $8 \times 6 \times 1\frac{1}{2}$  in. Each ingot was sectioned and hot rolled, with 80% reduction in area to  $\frac{1}{8} \times 1$  in. strip or  $\frac{1}{8} \times 1\frac{1}{4}$  in. strip. Sample pieces

\* Manuscript received 23 February 1953.

† Lecturer in Metallurgy, University College, Swansea.

were then solution-treated for 1 hr. at 1000° C. (950° C. for the copper-aluminium-titanium alloys), quenched, and examined under the microscope.

The alloys containing 3% cobalt, 1.5% chromium, and 3% iron, respectively, proved to have appreciable amounts of second phase present and were discarded. The remaining alloys were found to be single-phase, with the exception of the 2.12% cobalt, the 2% titanium, and the 0.6% zirconium alloys, which however, showed only traces of a second phase after solution-treatment. Hot rolling presented little difficulty, the titanium- and zirconium-bearing alloys being particularly amenable to this method of fabrication.

Strip for the preparation of specimens was fabricated as above, solution-treated for 3 hr. at 900° C., quenched in water, and given a variety of treatments, which included cold working, solution-treatment, and precipitation-hardening. The strip, before machining, was obtained in final sizes of  $4 \times 1 \times \frac{1}{16}$  in. for creep-rupture tests,  $6 \times 1 \times \frac{1}{16}$  in. for the investigation of mechanical properties, and  $8 \times 1 \frac{1}{4} \times \frac{1}{16}$  in. for creep tests. All solution-treated specimens were capable of being cold worked to at least 60% reduction in area without cracking.

It was noted that the oxidation-resistance during fabrication, which was already high in the basis alloy, was markedly improved by both titanium and zirconium additions, which also made the scale fully adherent even on quenching.

### III.—SCALING BEHAVIOUR

Service conditions in the gas-turbine interchanger involve exposure to an atmosphere containing small amounts of carbon dioxide and water in addition to approximately 17% oxygen. The presence of 2% sulphur in the fuel leads to 0.05% sulphur dioxide in the products of combustion, and to sulphurous or sulphuric acid in the condensate. Copper oxide scales are soluble in these acids; the formation of non-adherent or partially adherent scales may, in consequence, lead to catastrophic exfoliation, due to a combination of scale dissolution during shut-down periods and exposure of fresh surfaces during periodic reheating.

TABLE II.—Scaling Tests at 450° C.

Alloying Element, %	Number of 48-Hr. Cycles Before First Appearance of Exfoliation
7 Al . . . . .	15
7 Al, 1 Fe, 1 Ni . . . . .	11
7 Al, 1.5 Co . . . . .	9
7 Al, 2 Ti . . . . .	>21 Adherent scale
7 Al, 0.6 Zr . . . . .	>21 Adherent scale

Qualitative cyclic heating and cooling tests (alternate 24-hr. on and 24-hr. off periods) on the Al 7%; Al 7, Fe 1, Ni 1%; Al 7, Co 1.5%; Al 7, Ti 2%; and Al 7, Zr 0.6% alloys, in such an atmosphere at 450° C., showed the alloys containing iron, nickel, and cobalt to form an exfoliating scale, with heavy surface

deterioration, more rapidly than the binary alloy (Table II). The tests were discontinued after 1000 hr., when the scales on the alloys containing 2% titanium or 0.6% zirconium were found to have remained tightly adherent, and to have very low copper contents. Specimens used in this test were in the form of  $1 \times 1 \times \frac{1}{16}$  in. strip, finished to 000 grade emery.

### IV.—PRECIPITATION-HARDENING

Specimens of  $1 \times 1 \times \frac{1}{8}$  in. were prepared in the following initial states:

- Solution-treated for 1 hr. and water-quenched from 1000° C.
- Solution-treated for 3 hr. and water-quenched from 900° C.
- Solution-treated and water-quenched as above, then subjected to 30% cold work.

Each alloy was reheated for varying periods up to 1000 hr., at 350°, 400°, 500°, and 600° C., changes in hardness being followed by carrying out Vickers tests at 10-kg. load. At 350° C., with the exception of the alloy containing chromium, no significant change took place within the test period.

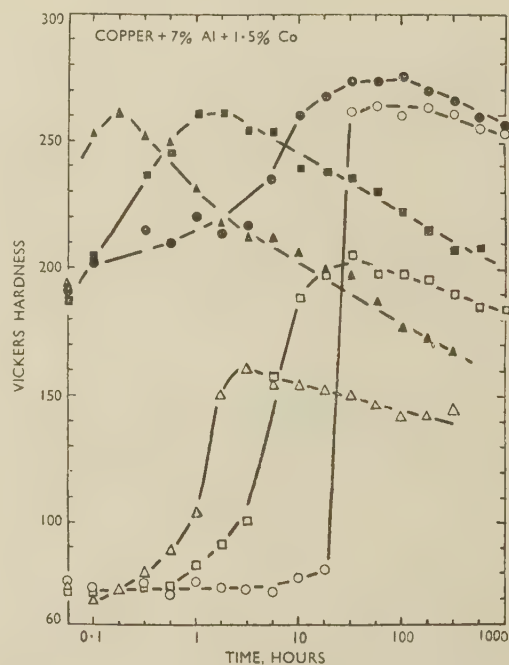


Fig. 1.—Precipitation-Hardening of 7% Aluminium, 1.5% Cobalt Alloy.

KEY.  
 ○ Aged at 400° C.    □ Aged at 500° C.    △ Aged at 600° C.  
 Open points—soln.-treated at 1000° C.  
 Solid points—soln.-treated at 1000° C., cold worked 30%.

Hardness in the solution-treated states varied from 70 to 100 D.P.N., depending on the alloy composition, and from 180 to 210 D.P.N. after 30% cold work. Specimens up to  $\frac{3}{16} \times 1 \times 1$  in. could be air-cooled



without increase in hardness, again with the exception of the alloy containing chromium; however, all specimens were in fact quenched from a vertical furnace,



FIG. 2.—Precipitation-Hardening of 7% Aluminium, 1% Cobalt, 1% Iron Alloy. (Key as for Fig. 1.)

dropping 12 in. into cold water contained in a tube 5 in. in dia. and 30 in. high.

The results obtained for one alloy of each class are recorded in Figs. 1–7; curves for the alloys solution-treated at 900° C. have been omitted for the sake of clarity, and the results summarized in Table III.

### 1. COBALT SERIES (FIGS. 1–3)

Alloys containing cobalt showed unusual hardening characteristics. The solution-treated material had a considerable incubation period (Fig. 1), during which no change in hardness occurred, followed by a sudden and large increase to maximum hardness. The latter value was then maintained for the duration of the ageing experiments at 400° and 500° C. The hardening characteristics were not measurably affected by a change in aluminium content from 6.85 to 6.03%. The alloy containing 2.12% cobalt attained a maximum hardness of 320 D.P.N. at 400° C.

The quaternary alloy containing iron showed a lower rate of hardening—maximum hardness was not developed in 1000 hr. at 400° C.—and a lower rate of softening from the cold-worked state at 600° C. (Fig. 2). The presence of nickel increased the maximum hardness attainable (Fig. 3). In the solution-treated state, all the alloys containing cobalt were obtained as single-phase solid solutions at 900° and 1000° C., with the exception of the 2% cobalt, and the 1.5% cobalt, 5% nickel alloys. The former showed a regularly distributed second phase even on quenching from 1000° C., whilst the latter showed traces of a second phase after quenching from 900° C.

In all cases the attainment of maximum hardness coincided with the first signs of precipitation shown by microscopic examination at a magnification of  $\times 1500$ . The precipitate at this stage appeared as a thickening of the grain boundaries in disconnected areas. Further ageing had the effect of linking together the areas of grain-boundary precipitate, and after solution-treatment at the higher temperature this was accompanied by the formation of small zones of a new phase at the boundaries (Figs. 8 and 9, Plate XIX). This new phase could not be detected after solution-treatment at 900° C. With pronounced over-ageing (as defined by decrease in hardness) precipitation took place along preferred lattice planes at each temperature. The zones of the newly formed phase and original precipitate continued to extend inwards from the grain boundaries. At 900° C., precipitation within the grains left a marked zone around the boundaries free from precipitate (Fig. 10, Plate XIX).

Continued ageing, accompanied by a decrease in hardness to approximately the original value, gave rise to spheroidization of these precipitates.

Apart from its effect on the rate of precipitation, a change in the temperature of ageing did not significantly affect the initial appearance of the precipitate.

Cold work before ageing decreased the time taken for the formation of a visible precipitate, the appearance of which was still coincident with the attainment of maximum hardness. The appearance of a lattice



FIG. 3.—Precipitation-Hardening of 7% Aluminium, 1.5% Cobalt, 5% Nickel Alloy. (Key as for Fig. 1.)

precipitate, however, took place after an interval greater than that in specimens not subjected to cold work, i.e. there was an alteration in the relative rates of growth of grain-boundary and internal precipitates.

## 2. CHROMIUM ALLOY (FIG. 4)

After solution-treatment at 900° or 1000° C., the first precipitate appeared at the grain boundaries;

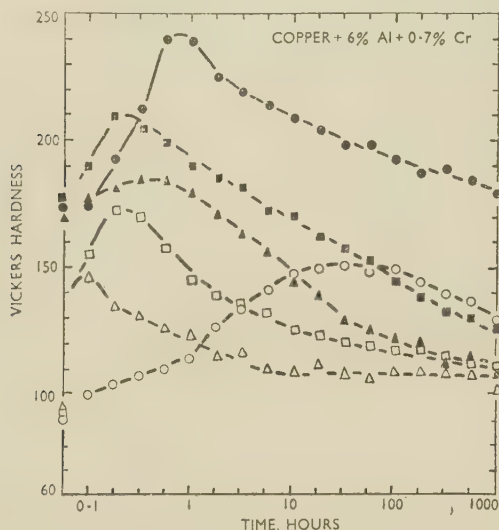


FIG. 4.—Precipitation-Hardening of 6% Aluminium, 0.7% Chromium Alloy. (Key as for Fig. 1.)

with over-ageing, a lattice precipitate appeared. Considerable zones adjacent to the initial grain-boundary precipitates remained free from precipitate, suggesting that diffusion from these zones to the boundaries took place in the earlier stages.

## 3. IRON SERIES (FIG. 5)

Precipitation was slow and not extensive, being confined to the grain boundaries for most of the periods in question, though after cold work it was

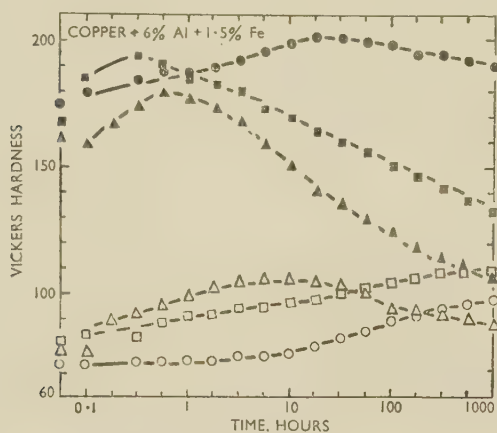


FIG. 5.—Precipitation-Hardening of 6% Aluminium, 1.5% Iron Alloy. (Key as for Fig. 1.)

possible to detect a new phase at the grain boundaries on prolonged exposure. Previous workers<sup>1,2</sup> on binary copper-iron alloys have emphasized the slow rate of precipitation.

## 4. TITANIUM SERIES (FIG. 6)

The two alloys were characterized by exceptionally slow over-ageing, even at 600° C.; both showed similar hardening characteristics. The alloy with the lower titanium content gave maximum hardness values approximately 30 D.P.N. lower than those shown in Fig. 6.

Microscopic examination showed precipitation to be continuous; the appearance of a precipitate along slip planes could be detected during the period of increase to maximum hardness. This precipitate gradually coarsened as ageing proceeded without, however, changing in form (Fig. 11, Plate XIX).

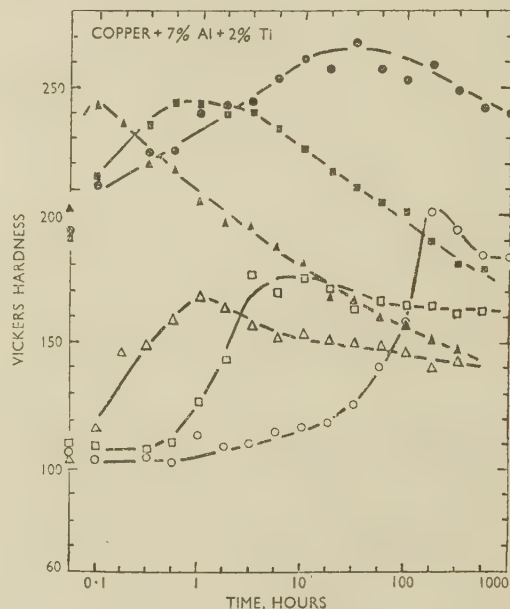


FIG. 6.—Precipitation-Hardening of 7% Aluminium, 2% Titanium Alloy.

## KEY.

○ Aged at 400° C.    □ Aged at 500° C.    △ Aged at 600° C.  
Open points—soln.-treated at 950° C.  
Solid points—soln.-treated at 950° C., cold worked 30%.

Only specimens which had previously been subjected to cold work showed spheroidization within the period of the tests.

## 5. ZIRCONIUM ALLOY (FIG. 7)

Although appreciable hardening has been reported for the binary copper-zirconium alloys,<sup>3</sup> only slight hardening was shown by the ternary alloy examined. The amount of precipitate was much less than with the titanium alloys, though it followed a similar pattern.

In the case both of the alloy containing 0.6% zirconium and of that containing 2.04% titanium, solution-treatment at the higher temperature (1000° C.) gave rise to the formation of a new phase round the grain boundaries (Fig. 12, Plate XIX). The nature and amount of this phase was unaffected by the rate of cooling after solution-treatment, whilst microscopic



evidence and cooling-curve determination of the solidus (980° C. for the 2% titanium alloy and 1020° C. for the 0.6% zirconium alloy) indicated that there was apparently no melting in these regions. It is

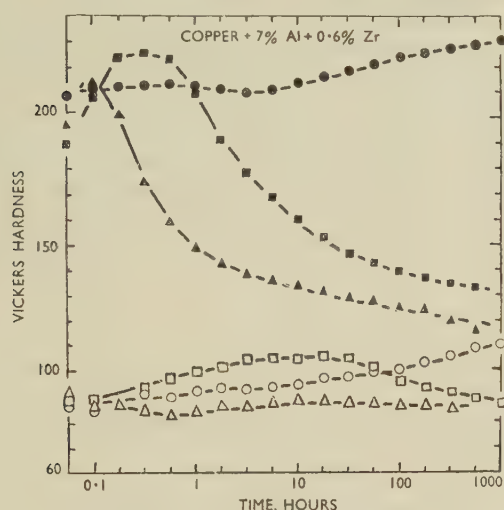


FIG. 7.—Precipitation-Hardening of 7% Aluminium, 0.6% Zirconium Alloy. (Key as for Fig. 1.)

possible that an increase in the solution-treatment temperature caused the alloy to enter a two-phase region, analogous to the behaviour of the normally single-phase 35% zinc-copper alloy at 825° C. This new phase remained unchanged during both ageing

Specimens were hot rolled to 30% over size, soaked for 3 hr. at 900° C., water-quenched and cold-worked to size. Final treatment temperatures were taken at 50° intervals from 650°–1000° C. The period of the final reheating at each temperature was chosen in accordance with previous hardness measurements, in order to give complete stability as defined by the attainment of constant hardness; the actual times of reheating were double those observed to correspond with a constant hardness value. The periods necessary varied slightly with the compositions of the alloys, particularly at the lower temperatures; all specimens were reheated for the maximum period found necessary at each temperature, as shown in Table IV.

Grain-size measurements were carried out by counting linear intercepts on sections of strip before machining to size and are also reported in Table IV. These observations show that grain-size is affected to a far greater extent by variations in temperature than by variation of the alloying element, except in the alloys containing iron.

The latter alloys, containing Al 7, Fe 1.5%; Al 7, Co 1, Fe 1%; and Al 7, Fe 1, Ni 1%, showed grain-sizes closely comparable to the other alloys after reheating to above 800° C., but reheating to below this temperature resulted in extremely uneven grain-sizes, the average of which was rather larger than for the other alloys. Attempts to obtain even grain-sizes in these alloys by variation in time of treatment were unsatisfactory. Grains of reasonably even size

TABLE III.—Precipitation-Hardening After Initial Solution-Treatment at 900° C.

Nominal Composition		Hardness as Solution- Treated and Water- Quenched, D.P.N.	Maximum Hardness Attained and Time Taken During Ageing						Hardness After 1000 Hr., D.P.N.		
			400° C.		500° C.		600° C.				
Al, %	Alloying Element, %		D.P.N.	Time, hr.	D.P.N.	Time, hr.	D.P.N.	Time, hr.	400° C.	500° C.	600° C.
7	1.5 Co	108	170	800	170	100	145	10	170	155	135
7	1 Co, 1 Fe	77	Not reached		165	130	152	10	140	162	140
7	1.5 Co, 5 Ni	130	285	800	220	20	205	3	285	195	160
6	0.7 Cr	108	132	24	138	0.3	130	0.1	120	113	103
6	1.5 Fe	78	Not reached		103	1000	100	12	98	103	81
7	2 Ti	122	170	200	163	7	154	2	154	154	131
7	0.6 Zr	90	Not reached		110	8	No change		118	100	90

and cold-working treatments. Solution-treatment at 900° C. was in each case insufficient to take all the original second-phase material into solid solution. A structure similar to that illustrated has been obtained in a 1.08% zirconium binary alloy treated at 950° C.

## V.—CREEP-RUPTURE TESTS

### 1. EXPERIMENTAL METHOD

#### (a) Preparation of Specimens

As a first and rapid method of comparing creep behaviour, a broad survey of the creep-rupture properties of selected alloys was made.

were obtained by variations in fabrication technique, but in the present experiments it was decided to keep the latter factor constant.

The only other significant variation in grain-size was found in specimens showing traces of a second phase at 900° C., before the final working to size, namely the alloys containing Al 7, Zr 0.6%; Al 7, Ti 2%; and Al 7, Co 1.5, Ni 5%. As shown in Table IV, the grain-size of the former was very slightly less than average at all temperatures, whilst for the alloys containing titanium, and cobalt plus nickel, grain-sizes were approximately one-third to one-quarter of those of the other alloys. It is noteworthy that the grain-size of the copper-aluminium-cobalt-nickel

alloy increased to the "average" value at 1000° C., the temperature at which all traces of a second phase disappeared.

Specimens reheated at temperatures up to about 750° C. were probably in a stable state at test temperature (450° C.) during the period of the creep-rupture tests, whilst precipitation was likely to occur in those treated at higher temperatures, owing to the increasing solubility of other phases. This was shown by hardness tests on each specimen before and after exposure.

### (b) Testing Procedure

The creep-rupture tests were carried out on specimens  $\frac{1}{2}$  in. thick, having a gauge-length of  $2\frac{1}{2}$  in. The specimens were prepared in a manner similar to that described below for the creep tests, and the stainless-steel suspension shackles were of a similar design, except that the micrometer extensometers were omitted. Direct loading was employed, the load being applied immediately the test temperature was reached.

testing, local elongation being expressed as percentage elongation on the section in which it occurred, after subtracting the general elongation for that section as determined on the whole specimen. The measurements of elongation after fracture were estimated to be accurate to  $\pm 0.25\%$  elongation on the  $2\frac{1}{2}$ -in. gauge-length employed. Surface oxidation occurring during tests was in all cases limited to the formation of a film not greater than  $10^{-4}$  in. in thickness.

A representative number of specimens of each alloy were prepared for microscopic examination in the following conditions: (a) specimen before testing, (b) unloaded specimen exposed for life of test specimen, and (c) fracture showing longitudinal and transverse sections.

## 2. RESULTS OF CREEP-RUPTURE TESTS

The results of the creep-rupture tests are given in Table V.

With the binary 7% aluminium alloy, an increase

TABLE IV.—Grain-Size\* (Grains/Mm.) After Recrystallization.

Recrystallization		Nominal Composition, %										
Temp., °C.	Time, hr.	7 Al	6 Al, 1.5 Co	7 Al, 1.5 Co	7 Al, 2 Co	7 Al, 1 Co, 1 Fe	7 Al, 1.5 Co, 5 Ni	6 Al, 0.7 Cr	6 Al, 1.5 Fe	7 Al, 2 Ti	7 Al, 0.6 Zr	7 Al, 1 Fe, 1 Ni
650	100	150 ± 10	170 ± 10	160 ± 10	185 ± 10	15-150 *	300 ± 20	160 ± 10	15-150 *	320 ± 20	205 ± 20	15-150 *
700	50	125 ± 5	...	130 ± 10	140 ± 10	15-100 *	275 ± 20	135 ± 10	15-100 *	290 ± 20	180 ± 20	15-100 *
750	16	60 ± 5	...	55 ± 5	...	10-50 *	210 ± 20	...	10-50 *	185 ± 10	70 ± 5	10-50 *
800	9	35 ± 3	33 ± 3	38 ± 3	...	10-50 *	110 ± 10	41 ± 4	10-50 *	78 ± 10	35 ± 4	10-50 *
850	5	17 ± 2	...	19 ± 2	21 ± 2	16 ± 2	55 ± 5	...	14 ± 1	52 ± 5	26 ± 3	21 ± 2
900	3	12 ± 1	14 ± 1	12 ± 1	...	10 ± 1	28 ± 3	11 ± 1	11 ± 1	30 ± 3	19 ± 2	13 ± 1
950	1	9 ± 1	...	10 ± 1	...	8 ± 1	12 ± 1	...	9 ± 1	18 ± 1	11 ± 1	10 ± 1
1000	1	3.5	4	4	...	3.5	5	5	5	...	5	3.5

\* Material appears to be composed of grains of two types, sizes being of the order indicated. Scatter  $\pm 25\%$  on each of the alloys containing iron at temperatures below 850° C.

The specimen assembly, with a calibrated thermocouple bound lightly to the specimen with asbestos string, was lowered into a stainless-steel furnace tube, which was slightly above the test temperature.

The furnace tubes were of  $1\frac{1}{4}$  in. internal dia. and carried central, upper, and lower windings each connected to independently variable external resistances. By this means a satisfactory constant-temperature zone was obtained, extending over more than three times the gauge-length. The upper end of the tube was packed with asbestos wool. Operating temperature was reached in 20-30 min. and maintained to  $\pm 1^\circ$  C. by a mechanical temperature controller, actuated by a thermocouple fixed between tube and winding and capable of varying the current supplied by 20%.

Fracture of the specimen was arranged to interrupt the continuous recording of temperature against time on a six-point recorder. The tests were carried out in air; life under load, and percentage elongation, including both local and total elongation, were noted. In order to measure local elongation, ten equal divisions were lightly marked on the gauge-length before

in temperature of reheating was accompanied by a steady increase in life and decrease in extension during tests. Grain-size was the only variable in this case, and a consideration of its effect may help in assessing the degree to which the changes in creep properties of the other alloys with temperature of heat-treatment are due to an increase in grain-size. It will be noted that the very large increase in grain-size produced by increased temperatures of reheating in the binary alloy has apparently only a minor effect on creep-rupture life under these conditions of test.

McKeown<sup>4</sup> and Clark and White<sup>5</sup> have concluded that at high testing temperatures a coarse-grained alloy is more resistant to creep than a fine-grained one, though the reverse may be true at low temperatures.

The alloys recrystallized in the lower temperature ranges, up to 800° C., showed considerable extension, both locally at fracture and generally during exposure. Presumably, this was due partly to the increased number of boundaries for grain-boundary flow, and partly to the spheroidized nature of the second phase.

Table V shows that the presence of iron, which was associated with a grain-size that was uneven but larger



than average, after reheating at temperatures up to and including 800° C., was accompanied by marked reductions in elongation, particularly local elongation at fracture.

The alloys containing titanium and zirconium showed evidence of recrystallization as a result of deformation during the test, after previous treatments at temperatures up to 700° C. The structure after testing had a reduced grain-size, which was accompanied by "tearing" cracks parallel to the direction of the axial stress (Fig. 13, Plate XIX). The final fracture appeared to be transcrystalline, and was accompanied by considerable necking.

The copper-aluminium-cobalt alloys also showed recrystallization during test after prior heating at

these showed that internal cracking had already begun after half the expected life period.

It is believed that the cracks were the result of conditions analogous to those described by Perryman<sup>6</sup> for the stress-corrosion of aluminium-zinc alloys. Boundary flow may have occurred during the initial stages of creep and have been rendered easier by either of the conditions observed during precipitation: viz. the formation of a new "soft" phase at the boundaries, or a precipitate-free zone adjoining the boundaries. This flow may have resulted in the concentration of stress across those boundaries originally perpendicular, or approximately perpendicular, to the direction of loading, exceeding the strength of the bond between the boundary phases. The cracks

TABLE V.—Creep-Rupture Tests at Stress of 4 Tons/in.<sup>2</sup> at 450° C.

Recrystallization Temp., °C.		Nominal Composition, %										
		7 Al	6 Al, 1.5 Co	7 Al, 1.5 Co	7 Al, 2 Co	7 Al, 1 Co, 1 Fe	7 Al, 1.5 Co, 5 Ni	6 Al, 0.7 Cr	6 Al, 1.5 Fe	7 Al, 2 Ti	7 Al, 0.6 Zr	7 Al, 1 Fe, 1 Ni
650	L	10	5	6	3	43	10	...	15	20	61	50
	TE	10	12	12	28	2	20	...	7	54	25	8
	LE	2	2	4	8	...	3	...	2	22	8	2
700	L	18	10	9	5	60	65	3	25	15	60	80
	TE	9	14	15	20	1	7.5	18	4	78	28	6
	LE	3	2	5	4	...	1.5	4	<1 >0.5	43	10	1
750	L	25	10	...	...	70	121	...	30	28	94	120
	TE	5	14	...	...	3	4	...	3	60	21	5
	LE	1	4	...	...	...	<0.5	...	...	24	5	0.5
800	L	20	12	12	6	108	160	7	30	55	330	145
	TE	2	12	16	14	2	5	3	2.5	30	16	6
	LE	<1 >0.5	1	1	3	...	<0.5	1	...	13	3	0.5
850	L	32	15	...	5	100	80	15	40	108	700	83
	TE	2	6	...	12	1	3	3	1.5	18	20	2.5
	LE	<0.5	1	...	1	...	...	<0.5	...	3	2	...
900	L	30	45	49	20	121	55	29	51	350	880	33
	TE	1.5	1	<1 >0.5	2	<0.5	2	4	1	4	4	1
	LE	...	...	...	...	...	...	<0.5	...	1	<1 >0.5	...
950	L	37	9	...	...	35	28	15	15	1000 + 0.6	1000 + 0.2	...
	TE	<1 >0.5	<0.5	...	...	<0.5	<1 >0.5	2	<0.5	No failure	No failure	...
1000	L	49	8	14	4	21	24	14	9	...	1000 + 0.1	20
	TE	<1 >0.5	<0.5	<0.5	<0.5	<0.5	<0.5	1	<0.5	...	No failure	<1

L = Life in hr.

TE = Total extension, %.

LE = Local extension at fracture, %.

temperatures up to 700° C., but only slight necking was observed, and the fractures were intergranular.

Where recrystallization did not occur during test, fractures were all intergranular. In the alloys containing titanium and zirconium, the cracks were confined to the region of fracture and presumably originated after the beginning of the tertiary-creep period or period of local reduction in cross-section. With the above exceptions, cracks formed at temperatures at which precipitation occurred during test were approximately perpendicular to the direction of axial stress and had a regular distribution over the entire gauge-length (Figs. 14 and 15, Plate XIX).

The appearance and location of the cracks suggested that they originated internally as well as at the surface of the specimen, and arose mainly at the grain boundaries of the specimen, where the initial precipitates formed. Duplicate tests were carried out on selected alloys and discontinued before rupture;

produced then linked up to give minimum total elongation and no local elongation at fracture.

It was found that, allowing for grain-size and solid-solution effects, the more rapidly precipitation occurred in this series of alloys, the shorter was their creep-rupture life. The time taken to fracture coincided with the appearance of the initial grain-boundary precipitate. Particularly close correlation was obtained with the alloys containing cobalt, in which there was a sudden change in hardness.

### 3. EFFECT OF PRECIPITATION BEFORE TEST ON CREEP-RUPTURE PROPERTIES

Increase in the temperature of the previous heat-treatment caused the creep-rupture life to increase to a maximum, followed by a rapid decrease in those alloys in which grain-boundary precipitation occurred. The increase in grain-size and in solid solubility of

the alloying element should tend to give an increase in life, whereas precipitation, which followed the higher-temperature treatments, would lead to early fracture. Each of these factors would result in a reduction in elongation.

It did not appear that under these conditions precipitation was markedly accelerated by strains introduced during testing. The elongation occurring before fracture was in all cases very small after solution-treatment, and the rapid fracture resulting may have masked such an effect. Later tests have shown that with this type of precipitation very rapid fracture may occur at temperatures as low as 300° C. with

ness at 500° and 600° C. before testing reduced creep-rupture life. Extension remained of the same order, and the actual temperature of pre-ageing had no significant effect. The second group showed considerable increases in total elongation with ageing temperatures above the temperature of testing, whilst the creep-rupture life was relatively unchanged.

#### 4. EFFECT OF WORK-HARDENING BEFORE TESTING

The binary copper-aluminium alloy, the 1.54% cobalt, 6.85% aluminium, and the 2.04% titanium, 6.94% aluminium alloys were tested at the standard

TABLE VI.—Creep-Rupture Tests: Effect of Pre-Treatment.

Nominal Composition, %	Stress, 4 tons/in. <sup>2</sup> at 450° C.				Stress, 6 tons/in. <sup>2</sup> at 450° C.															
	S.T. 900° C., Aged 600° C.		S.T. 900° C., Aged 500° C.		S.T. 900° C., C.W. 15%		S.T. 1000° C., C.W. 15%		S.T. 900° C., C.W. 30%		S.T. 900° C., C.W. 30%, Aged 500° C.		S.T. 900° C., C.W. 30%, Aged 600° C.		S.T. 1000° C., C.W. 30%		S.T. 1000° C., C.W. 30%, Aged 500° C.		S.T. 1000° C., C.W. 30%, Aged 600° C.	
	L	E	L	E	L	E	L	E	L	E	L	E	L	E	L	E	L	E	L	E
7 Al	...	...	...	...	16	3	33	1	29	2	...	...	...	...	37	1	...	...	...	...
7 Al, 1.5 Co	25	1	32	1	15	1	2	1	190	2	140	1.5	168	1.5	53	0.5	72	0.5	38	0.5
7 Al, 1 Co, 1 Fe	36	1	25	1	10	1	3	1	260	2	238	2.5	315	1.5	65	1	140	0.5	70	0.5
7 Al, 1.5 Co, 5 Ni	44	5	48	3	40	4	14	1.5	70	4	80	3.5	100	3	160	1	119	1.5	150	1.5
7 Al, 0.7 Cr	16	3	24	1.5	10	2	2	1	38	2	13	3	5	1	12	1	26	1.5	15	1.5
7 Al, 1.5 Fe	8	0.5	7	1	8	1	5	1	30	1	16	1.5	11	2	23	1	18	1	12	0.5
7 Al, 2 Ti	360	19	550	16	160	5	257	1	180	3	160	6	136	11	140	4	120	6	130	6
7 Al, 0.6 Zr	620	24	1000	8	180	4	480	1	116	5	93	11	78	29	100	2	39	5	43	6
7 Al, 1 Fe, 1 Ni	...	...	...	...	18	2	11	1	103	2.5	...	...	...	...	47	1	...	...	...	...

All ageing treatments to produce maximum hardness.

L = Life in hr.

E = Total extension, %.

S.T. = Solution-treated.

C.W. = Cold work.

TABLE VII.—Creep-Rupture Tests: Effect of Work-Hardening on Specimens Tested at 4 Tons/in.<sup>2</sup> at 450° C.

Nominal Composition, %	S.T. 900° C., C.W. 5%		S.T. 900° C., C.W. 15%		S.T. 1000° C., C.W. 15%		S.T. 1000° C., C.W. 20%		S.T. 900° C., C.W. 25%		S.T. 900° C., C.W. 30%		S.T. 1000° C., C.W. 30%		S.T. 900° C., C.W. 40%		S.T. 1000° C., C.W. 40%		S.T. 900° C., C.W. 60%		S.T. 1000° C., C.W. 60%	
	L	E	L	E	L	E	L	E	L	E	L	E	L	E	L	E	L	E	L	E	L	E
7 Al	33	<1	45	<1	49	<0.5	78	<0.5	62	<1	78	<1	60	<1	23	5	25	8	10	15	5	18
7 Al, 1.5 Co	15	<0.5	19	<0.5	9	<0.5	33	<0.5	168	<1	219	<1	238	<1	279	<1	252	1	43	3	58	5
7 Al, 1.5 Co *	...	...	11	<0.5	...	...	8	<0.5	...	...	180	<1	...	...	239	<1	...	...	49	5	...	...
7 Al, 2 Ti	385	3	313	2	>1000	No failure	...	...	...	...	405	4	>1000	No failure	291	6	...	...	...	...	...	...
Al, 2 Ti *	...	...	297	5	...	...	...	...	...	...	326	6	...	...	...	...	...	...	...	...	...	...

\* Pre-aged 500° C.

L = Life in hr.

E = Total extension, %

S.T. = Solution-treated.

C.W. = Cold work.

an applied stress of 6 tons/in.<sup>2</sup>, although an unstressed specimen would show no signs of precipitation after 1000 hr. at that temperature.

Where precipitation was confined to slip planes and was apparently continuous, creep-rupture life increased rapidly with the temperature at which recrystallization has been carried out. Precipitation in this manner was not associated with grain-boundary cracking before fracture. Comparison with the binary alloy indicated that this increase in creep-rupture life was only partly due to an increase in grain-size.

The alloys may be divided into two groups: those containing cobalt, chromium, iron, and nickel, and those containing titanium or zirconium. In the first group, Table VI shows that ageing to maximum hard-

ness at 4 tons/in.<sup>2</sup>, after solution-treatment at 900° and 1000° C., followed by cold working with varying reductions in area. The results are summarized in Table VII.

The binary alloy showed a steady increase in life after subjection to up to 25–30% cold work. After greater amounts of cold work, recrystallization set in during test, resulting in early fracture with appreciable elongation.

Specimens of the cobalt alloys subjected to less than 20% cold work fractured in times corresponding to those necessary to attain maximum hardness. This was corroborated by hardness tests before and after fracture. Elongation at fracture was in all cases very slight. With 20–30% cold work a rapid increase in



creep-rupture life occurred, time to rupture being considerably in excess of the time required to reach maximum hardness, but elongation remained of the same order. Microscopic examination showed the form of precipitation to be unchanged. In specimens that had undergone more than 50% cold work, recrystallization began before fracture. Presumably, as with the binary alloy, grain-boundary flow is impeded in the cold-worked material, so that fracture across the new boundary phases occurs at a later stage. The existence of an optimum amount of pre-strain in relation to subsequent creep properties

led to rapid fracture, and the larger to a considerable improvement in creep-rupture properties, the difference being particularly marked with specimens that had been solution-treated at the higher temperature. Pre-ageing had little effect when carried out on the more heavily cold-worked alloys of this type. The titanium-aluminium-copper alloys were again only slightly affected by cold work, but ageing following cold work resulted in an increase in general elongation without a significant change in time to fracture. After 30% cold work the alloy containing zirconium showed signs of recrystallization at fracture in all cases. Pre-

TABLE VIII.—Creep Tests at 450° C. Under Stress of 2 Tons/in.<sup>2</sup>.

Nominal Composition, %	Solution-Treated at 900° C.			Solution-Treated at 1000° C.		
	2nd Stage Steady Rate after 500 hr., %/day $\times 10^{-3}$	Total Extension after 500 hr., %	Approx. Total Extension Measured in Primary Stage, %	2nd Stage Steady Rate after 500 hr., %/day $\times 10^{-3}$	Total Extension after 500 hr., %	Approx. Total Extension in Primary Stage, %
7 Al . . . . .	70	1.9	0.5	...	...	...
7 Al, 1.5 Co . . .	7	0.30	0.15	Fracture at 150 hr.	0.05 after 144 hr.	...
7 Al, 1.5 Co. : Pre-aged 450° C.	5	0.22	0.12	...	...	...
" 500° C..	9	0.28	0.10	...	...	...
" 600° C..	(400 hr.) 7	0.23 after 430 hr.	0.10	...	...	...
7 Al, 1 Co, 1 Fe .	1	0.09	0.07	0.7	0.05	0.035
7 Al, 1.5 Co, 5 Ni	33	0.85	0.20	6	0.19	0.07
6 Al, 1.5 Fe . . .	(250 hr.) 19	0.48 after 360 hr.	0.12	Fracture at 100 hr.	0.07	...
7 Al, 2 Ti . . . .	35	0.26	0.19	(950° C.) 0.8	0.15	0.12
7 Al, 2 Ti : Pre-aged 400° C.	4	0.16	0.12	...	...	...
" 500° C.	11	0.38	0.16	...	...	...
" 600° C.	20	0.56	0.16	...	...	...
7 Al, 0.6 Zr . . .	8	0.25	0.09	1	0.12	0.08
7 Al, 1 Fe, 1 Ni .	15	0.42	0.14	Fracture at 300 hr.	0.10	...

has been demonstrated by Greenwood and Worner<sup>7</sup> and McKeown<sup>4</sup> for lead, and by Zschokke and Niehus<sup>8</sup> for steels. It may be concluded from their experiments that the optimum degree of cold work will decrease as the temperature of testing is increased, and that recovery or recrystallization during testing is mainly responsible for the deterioration in properties after larger amounts of pre-strain. Pre-ageing of the cold-worked material at 500° C. before the test decreased the creep-rupture life considerably after reductions in area up to 30%. With greater amounts of cold work, any change was within the limits of experimental error.

No recrystallization during test occurred in copper-aluminium-titanium specimens which had received up to 40% cold work, nor were the creep-rupture life and total elongation markedly affected.

A series of tests, at 6 tons/in.<sup>2</sup>, were carried out with specimens which had received 15 and 30% cold work (Table VI). The alloys were tested as worked, after quenching from 900° and 1000° C., and as pre-aged to maximum hardness at 500° and 600° C. after 30% cold work. Where grain-boundary precipitation occurred, behaviour was similar to that of the cobalt series described above. The smaller amount of work

ageing this alloy resulted in a decrease in creep-rupture life and a marked increase in elongation.

## VI.—CREEP TESTS

Creep measurements were carried out at 450° C. and a stress of 2 tons/in.<sup>2</sup> (Table VIII). The majority of the tests were discontinued after 500 hr. The creep equipment used was based upon that developed by the British Non-Ferrous Metals Research Association for strip specimens.

Stainless-steel specimen shackles operated through universal-joint systems, the load being applied through a 10:1 lever arm. The specimen,  $\frac{1}{16}$  in. thick and approximately 8 in. overall length, with a 5 in. gauge-length, was held by two  $\frac{1}{4}$ -in.-dia. stainless-steel bolts at each end, the holes in both holders and specimen having been drilled from a master jig to ensure axial loading. These bolts served to clamp the stainless-steel holding plates to the flat specimen. Two  $\frac{1}{8}$ -in.-dia. holes between the shackles and the ends of the gauge-length enabled the extensometer system to be attached. These holes were drilled from the same jig. The upper end of the specimen carried an Inconel rod at each side, aligned parallel to the gauge-

length, whilst the lower end carried Inconel tubes in which the rods were slotted, attached in a similar manner. Vernier micrometers, fixed to the ends of the tubes, outside the furnace, enabled the relative movements of rod and tube, and hence the changes in length over the gauge-length, to be read to  $10^{-4}$  in.

The furnace ends were closed with asbestos wool. The specimen assembly was then lowered into the 2.5 in. internal dia. silica furnace tube, the temperature being about  $50^{\circ}$  C. above test temperature. Thermocouples were attached at the centre and ends of the gauge-length by asbestos string. The test temperature was attained within 45–60 min., the load was then applied, and readings were started. Readings were taken every 15 min. during the first 3 hr., and afterwards at increasing intervals up to 48 hr., after which they were recorded twice daily.

The furnace tube was provided with three separate windings, upper, central and lower, each of which was connected to an independently variable external resistance in order to obtain an even temperature over the gauge-length. An electronic temperature controller, actuated by a thermocouple fixed between tube and winding, enabled the current supplied to be varied between maximum and minimum values differing by 20%. In this manner the temperature was controlled to within  $\pm 1^{\circ}$  C. with not more than  $2^{\circ}$  C. variation along the gauge-length.

The alloys were examined as solution-treated (at  $900^{\circ}$  and  $1000^{\circ}$  C.), total extension (elastic plus plastic strain) being plotted against time. In each case, except where prior fractures occurred, the creep rate had reached a constant steady value. Selected alloys of each type were tested as pre-aged to maximum hardness at  $450^{\circ}$ ,  $500^{\circ}$ , and  $600^{\circ}$  C. after solution-treatment at  $900^{\circ}$  C. The steady-rate, total extension after 500 hr., and the approximate total extension in the primary stage of creep are reported as determined by plotting extension against time.

All the alloys showed considerably reduced steady rates when compared with the binary alloy, but it was apparent that a low rate of creep might be accompanied by early fracture, as was the case with the 1.54% cobalt, 6.85% aluminium alloy and the 1.52% iron, 6.16% aluminium alloy. These alloys showed only slight deviation from a linear creep/time relationship immediately before fracture. Creep tests on this material, interrupted at a suitable time before fracture, during the second-stage creep period, provided evidence of internal cracking along isolated grain boundaries. The presence of iron was effective in further reducing the creep rate of the copper-aluminium-cobalt alloys, whilst that of nickel appreciably increased both steady-rate and transient creep. The steady rates of creep of the alloys containing titanium and zirconium were comparable with those of the copper-aluminium-cobalt series and were appreciably lower than those of the copper-aluminium-iron and copper-aluminium-iron-nickel specimens.

A marked difference in behaviour was apparent on pre-ageing. With the 6.85% aluminium, 1.54%

cobalt alloy pre-ageing had little effect on the second-stage steady rate of creep, but reduced both transient creep and total elongation at fracture. Time to fracture was also reduced. Transient creep was also reduced with the copper-aluminium-titanium alloy, but second-stage creep rate and total elongation during test were considerably increased as a result of the higher temperatures of pre-ageing.

After solution-treatment at  $1000^{\circ}$  C., the alloys containing cobalt, exhibiting a long incubation period before hardening began, showed an initial contraction under load of up to 0.15%; this immediately changed to extension when hardening began.

## VII.—DISCUSSION OF CREEP BEHAVIOUR

The alloys fall into two types, in which creep behaviour may be explained tentatively on the basis of their precipitation characteristics. The addition of each alloying element produces changes in the solid solution which must not be neglected when considering changes due to precipitation. Greater lattice distortion is caused by the introduction of titanium or zirconium than by that of cobalt, iron, or chromium, and the enhanced creep performance of the former alloys may in some measure be due to the increase in lattice strain.

The group of alloys containing cobalt, iron, and chromium, in which the grain-boundary precipitates appeared to be discontinuous, exhibited low elongations under load, very low total elongations at fracture, and short times to fracture under comparable tests. The second group, containing titanium and zirconium, in which precipitation occurred on slip planes, had equally low creep rates, but gave very much longer creep-rupture lives and permitted much greater elongations before fracture.

The low extensions of the first series may be connected with the formation of a new phase along the grain boundaries, or, after lower solution-treatment temperatures, with diffusion of the components of the precipitating intermetallic compound towards the grain boundaries, leaving an impoverished zone around those boundaries. Assuming that creep in the steady state is due partly to grain-boundary flow, it appears that precipitation of this type would enhance boundary flow, whilst lattice slip would be retarded by the presence of a non-equilibrium solid solution. Although the rate of boundary flow and the proportion of total creep movement due to it may thus be increased, the capacity of the material for extension would be decreased. Rapid flow along boundaries originally parallel to the direction of stress, without corresponding slip within the grains, would result in a concentration of stress across boundaries almost perpendicular to the direction of stress. Movement of the latter would be hampered by the presence of the precipitate, and fracture could then occur with very limited extension. The actual rate of creep in such a case appears to be dependent on the relative roles of grain-boundary flow and lattice slip. McLean<sup>9</sup> has



indicated that for super-purity aluminium the relative magnitude of these components of flow is affected by the grain-size and by the stress applied.

With the series of alloys under investigation the discontinuous type of grain-boundary precipitation led to rapid failure under high stress and to deceptive results in tests carried out at low stress and discontinued before fracture.

The results of Jenkins, Bucknall, and Jenkinson<sup>10</sup> on the creep-rupture behaviour of a precipitation-hardening copper-nickel-silicon alloy provide additional evidence that precipitation during testing may produce deterioration rather than improvement in creep properties.

The effect of increasing grain-size on the behaviour of the copper-aluminium alloys was masked by precipitation effects in all but the binary alloy, but it appeared far less important for these alloys than that due to corresponding increases in grain-size reported for aluminium-base alloys.

The "tearing cracks" produced in boundaries parallel to the applied stress during creep-rupture tests of fully over-aged material of this type may be an indication of very rapid deformation by lattice slip without correspondingly rapid boundary movement.

Above a certain minimum value cold work appeared to impair grain-boundary flow in those alloys in which a new grain-boundary phase was formed; this resulted in longer life under load, owing to an increase in the time necessary to reach the total extension permissible before fracture. Below this value, which is dependent on stress, the overall effect of cold work was to speed up the precipitation process and thus cause rapid fracture.

Only slight improvement in creep properties resulted from cold working an alloy which underwent continuous lattice precipitation; this may be offset by the possibility of recrystallization with extended test periods.

It appears that the most satisfactory creep-resistance

TABLE IX.—*Tensile Properties.*

Nominal Composition, %	Annealed 650° C.		Annealed 800° C.		Soln.-treated 900° C. Aged to max. hard- ness 400° C.		Soln.-treated 1000° C. Aged to max. hard- ness 400° C.		Soln.-treated 900° C. C.W. 30%. Aged to max. hardness 400° C.		Soln.-treated 900° C. C.W. 30%. Aged to max. hardness 500° C.		Soln.-treated 1000° C. C.W. 30%. Aged to max. hardness 400° C.		Soln.-treated 1000° C. C.W. 30%. Aged to max. hardness 500° C.	
	U.T.S.	E.	U.T.S.	E.	U.T.S.	E.	U.T.S.	E.	U.T.S.	E.	U.T.S.	E.	U.T.S.	E.	U.T.S.	E.
7 Al . . . . .	28	50	...	...	...	...	...	...	40	13	...	...	...	...	...	...
7 Al, 1.5 Co . . . .	38	50	35	45	41	23	47	16	49	17	46	21	51	12	...	...
7 Al, 1 Co, 1 Fe . .	34	43	31	37	...	...	48	17	...	...	43	28	52	13	46	11
7 Al, 1.5 Co, 5 Ni .	36	37	37	39	49	15	65	8	54	12	60	4	61	6	62	8
6 Al, 0.7 Cr . . . .	30	66	29	62	46	30	46	25	42	25	38	30	42	19	42	33
6 Al, 1.5 Fe . . . .	...	...	31	39	...	...	35	8	...	...	33	32	32	11	...	...
7 Al, 2 Ti . . . . .	37	42	34	38	51	25	49	20	51	12	53	16	55	11	56	14
7 Al, 0.6 Zr . . . .	...	...	30	59	39	16	40	13	...	...	36	21	38	10	...	...

U.T.S. in tons/in.<sup>2</sup>.

E = Extension, % on 2 in.

Over-aged structures stable at test temperature resulted in creep-rupture extensions comparable with those of the binary alloy, except in cases where recrystallization occurred through elongation during exposure. With fully over-aged material the basic lattice may differ from that of the binary 7% aluminium alloy if aluminium is present in the precipitates.

Evidence of precipitation taking place before creep and creep-rupture tests indicated that, where discontinuous precipitation occurred, the creep-rupture life would be affected adversely, variations in the temperature of pre-ageing having little effect. This supports the concept that creep properties are determined by the nature of the new boundary phase, rather than by the form of the precipitate itself.

When continuous precipitation takes place within the grains, the overall effect on creep behaviour mainly depends on the restriction of lattice slip. Presumably a critical particle size exists at which the rate of flow produced by a given stress is a minimum. The increasing coarseness of precipitate produced either by over-ageing or by a high temperature of ageing thus results in increased extension during test, as noted in Tables IV-VI.

under these conditions is obtained in an alloy exhibiting continuous slip-plane precipitation, in the solution-treated state. The transient creep of such an alloy may be reduced by hardening at a temperature not exceeding the test temperature; hardening at higher temperatures would cause an increase in the second-stage creep rate.

The development of an alloy for use in gas turbines as heat-interchanger tubes requires an increase in resistance to specific conditions of corrosion; the presence of titanium or zirconium offered considerable improvement on other alloys in this respect.

## VIII.—TENSILE PROPERTIES

Tensile tests were carried out on the alloys, and values of the ultimate tensile strength and percentage elongation on 2 in. are given in Table IX. The alloying additions lead to a marked improvement in the properties of the binary single-phase alloy. The results were obtained on strip specimens machined according to British Standard recommendations, and are the average of three tests on the Hounsfield testing machine.

## IX.—FURTHER WORK

It is intended to study the creep behaviour at temperatures where the alloys in question will be completely stable during testing. This should enable the dependence of the various stages of creep on the size and extent of precipitates to be assessed more completely. Similar work is in hand for binary precipitation-hardening copper-base alloys.

It is hoped to be able to increase the optimum hardening temperature of the alloys containing

titanium and zirconium, so that they may be obtained in a completely stable state at 450° C.

## ACKNOWLEDGEMENTS

The author wishes to express his thanks to the British Non-Ferrous Metals Research Association, whose staff prepared and analysed a number of the alloys used, and to Messrs. N. C. Ashton, Ltd., Huddersfield, who provided material for the remainder and facilities for the development of promising alloys on an industrial scale.

## REFERENCES

1. D. Hanson and G. W. Ford, *J. Inst. Metals*, 1924, **32**, 335.
2. R. B. Gordon and M. Cohen, *Age-Hardening of Metals* (*Amer. Soc. Metals*), 1940, 161.
3. G. F. Comstock and R. E. Bannon, *Metals and Alloys*, 1937, **8**, 106.
4. J. McKeown, *J. Inst. Metals*, 1937, **60**, 201.
5. C. L. Clark and A. E. White, *Proc. Amer. Soc. Test. Mat.*, 1932, **32**, (II), 492.
6. E. C. W. Perryman and J. C. Blade, *J. Inst. Metals*, 1950, **77**, 263.
7. J. N. Greenwood and H. K. Worner, *ibid.*, 1939, **64**, 135.
8. H. R. Zschokke and K. H. Niehus, *J. Iron Steel Inst.*, 1947, **156**, 271.
9. D. McLean, *J. Inst. Metals*, 1952-53, **81**, 287.
10. C. H. M. Jenkins, E. H. Bucknall, and E. A. Jenkinson, *ibid.*, 1944, **70**, 57.



# THE COMPUTATION OF LOADS IN METAL STRIP ROLLING BY METHODS INVOLVING THE USE OF DIMENSIONAL ANALYSIS\*

1505

By MAURICE COOK,<sup>†</sup> D.Sc., Ph.D., F.I.M., MEMBER, and  
R. J. PARKER,<sup>‡</sup> A.M.I.Mech.E.

## SYNOPSIS

The method devised and previously reported (Cook and Larke, *J. Inst. Metals*, 1948, **74**, 55) for calculating loads involved in metal strip rolling has been checked by reference to the results of a series of load measurements made for H.C. copper and 70 : 30 brass strip reduced on  $8\frac{1}{4} \times 10$ -in. and  $14 \times 20$ -in. rolling mills. Calculated load values were found to be in good agreement with measured results for conditions where the ratio of initial strip thickness to roll diameter was greater than about 1 : 200, but when the ratio was less than this value computed data were not so accurate. The method has, therefore, been modified to extend its applicability and, in consequence, accurate rolling-load data can be calculated for any rolling condition where the ratio of initial strip thickness to roll diameter falls between such wide limits as 1 : 40 and 1 : 800.

The method requires relevant load data for a range of strip thicknesses and roll diameters, but dimensional analysis of the factors influencing the magnitude of rolling loads has made possible the formulation of a technique for deriving the necessary information from measurements on one mill only, and the validity of the dimensional analysis, described in the paper, is demonstrated by reference to published data for mild steel.

The procedure involving the modified method and dimensional analysis has been applied to the rolling of H.C. copper and 70 : 30 brass rolled on an  $8\frac{1}{4} \times 10$ -in. mill. The data so obtained have been used to calculate load values for these two metals reduced on mills with larger-diameter rolls, and the standard of agreement between measured and calculated results indicates that this procedure permits the rapid and accurate computation of rolling-load data for widely varying conditions of reduction, initial strip thickness, and roll diameter.

## I.—INTRODUCTION

FOR the purpose of producing optimum designs of mill plant and auxiliaries, the importance of a knowledge of the loads developed when the thickness of metal strip or sheet is reduced by rolling needs no emphasis. Such information is equally valuable to the rolling-mill technician, since the determination of pass reductions in rational practices involving a minimum number of passes is possible only from a consideration of loading conditions.

Much investigational work on the subject of rolling loads has been carried out in recent years, and several methods for calculating them have been developed. Most of these, however, are laborious and involve complex calculations. For practical purposes they are, for this reason, not particularly well suited, or convenient, although they may be very accurate. In practice, extreme accuracy is not necessary, and methods which require the least amount of data in the form of actual load measurements, and calculations which can be readily and quickly made, are therefore likely to commend themselves as being of more immediate and direct value for everyday use.

With this in mind, a simple method for the compu-

tation of rolling loads, applicable to conditions where strip tension is not employed, was developed and has been described in an earlier paper.<sup>1</sup> The degree of applicability of the method over a wide range of rolling conditions has been checked by a comprehensive series of load measurements which are described in the present paper. Accuracy of calculated load values was found to be good for conditions where the ratio of initial strip thickness to roll diameter was between about 1 : 40 (0.025) and 1 : 200 (0.005), but when it fell below the smaller value computed data were no longer completely satisfactory. The method has therefore been modified, as a result of which, and as will be seen from data illustrated, for example, in Figs. 4-7, the agreement between measured and calculated results is satisfactory for ratios ranging from 1 : 40 (0.025) to values as small as 1 : 800 (0.00125).

The method collectively includes the effects of such variables as resistance to deformation of the material being rolled, frictional conditions in the roll throat, and the elastic distortion of the roll face over the arc of contact, and it requires only a relatively small amount of measured load data for its application. A systematic consideration of the data recorded in the present paper has, however, indicated that by using dimen-

\* Manuscript received 17 April 1953.

<sup>†</sup> Joint Managing Director, Imperial Chemical Industries, Ltd., Metals Division, Birmingham.

<sup>‡</sup> Technical Officer, Imperial Chemical Industries, Ltd., Metals Division, Birmingham.

sional analysis it is possible to compute rolling loads for a wide range of initial thicknesses and roll diameters by making reference to data obtained on one mill only, thus still further reducing the amount of measured load data necessary.

## II.—DETAILS OF EXPERIMENTAL WORK

### 1. MATERIALS AND ROLLING CONDITIONS

Samples of H.C. (high-conductivity) copper and 70 : 30 brass were produced in the fully annealed condition at nominal thicknesses of 0.01, 0.018, 0.025, 0.036, 0.05, 0.1, and 0.2 in., typical diamond pyramid hardness values of the annealed materials in these gauges varying from about 45 to 50 and 65 to 70 for the copper and 70 : 30 brass, respectively.

Load measurements were carried out on two rolling mills of the 2-high type, fitted with steel rolls measuring  $8\frac{1}{2} \times 10$  in. and  $14 \times 20$  in., the rolling speed of each unit being constant at about 70–80 ft./min. The rolls of both mills were smoothly ground to a mean axial surface finish of about 10–12 micro-in., and since the same standard mineral rolling oil was applied to rolls and strip during all experiments, frictional effects set up on both units can be regarded as similar.

### 2. LOAD-MEASURING EQUIPMENT

Rolling loads were determined by reference to the elastic compression of cylindrical steel blocks placed between the top roll chocks and each mill screw, the deformation being measured by the use of electric resistance wire strain gauges bonded to the surface of each block. This method of load measurement has been widely used for a number of years, and a recent description of it has been given by Sims, Place, and Morley.<sup>2</sup> The load cells were calibrated under conditions of static loading, data being reproducible to about  $\pm \frac{1}{2}$  ton over the whole measuring range. Subsequent tests carried out at regular intervals during the rolling experiments indicated that the calibration curves did not change significantly.

### 3. EXPERIMENTAL PROCEDURE

During the experiments test lengths of the various materials were subjected to single-pass reductions of increasing magnitude until the maximum reduction for any particular metal, initial thickness, and roll diameter had been reached. Strips which had been reduced in thickness by 10% in a single pass were then subjected to further reductions of 10%, relative to the thickness before each pass, until an overall reduction of between 50 and 80%, depending upon the test specimen, had been effected. The material which had been reduced by 20, 30%, &c., in the first pass was also subjected, in a similar manner, to successive reduction of 20, 30%, &c., respectively, relative to the thickness before each pass. Finally, a number of other strips was reduced in a series of passes of varying magnitude until an overall reduction was reached

comparable with that obtained in effecting reductions by regular, i.e. 10 or 20%, &c., decrements. In all experiments a standard mineral rolling oil was applied to both strip and rolls, and loads were recorded for every pass, a total of approximately 1000 measurements being made.

## III.—COMPUTATION OF ROLLING LOADS

The derivation of a simple method for calculating rolling-load values, based on the assumption that the pure work of rolling is independent of the number of passes required to effect a given reduction in strip thickness, has been described in a previous paper.<sup>1</sup>

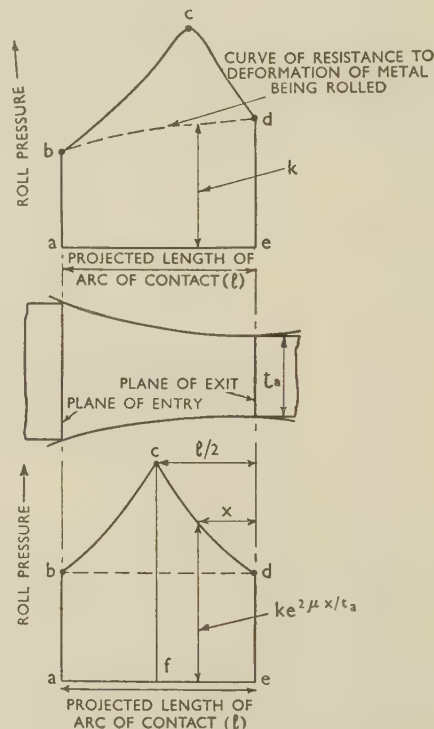


FIG. 1.—Curves Illustrating Distribution of Roll-Face Pressure.

To simplify the method it was assumed that the influence, on the magnitude of rolling loads, of the frictional forces generated in the roll throat would be small. When, however, the ratio of initial strip thickness to roll diameter is less than about 1 : 200, the influence of frictional forces becomes increasingly significant, and it has been found that load values computed under such conditions are not acceptably accurate.

The method has, therefore, been modified to include an allowance for the effects of these frictional forces, and it is based on simplified considerations of the distribution of working pressure developed during passage of metal through the roll throat. In the hypothetical roll-pressure curve drawn in the upper portion of Fig. 1, heights  $ab$  and  $ed$  represent, respectively, the resistance to plane homogeneous deformation of the metal before and after passage through the rolls, while point  $c$  indicates the magnitude of the



maximum pressure generated. Area  $abcde$ , which is usually termed the friction hill, and which represents the total rolling load per unit width of the material, may conveniently be divided into two parts, viz. the base—area  $abde$ —and the roof—area  $bcd$ . It is apparent that area  $abde$  represents the contribution  $P_c$  to the total rolling load, arising from the basic resistance to deformation of the metal being reduced, while area  $bcd$  indicates the additional roll force developed as a result of frictional effects.

Although the accurate evaluation of roll pressure is complex and protracted,<sup>3</sup> Orowan and Pascoe<sup>4</sup> have determined that variation of this pressure from the neutral plane to the point of exit may be approximately defined by the equation :

$$p = ke^{2\mu x/t_a} \quad . \quad . \quad . \quad (1)$$

where  $p$  = roll-face pressure,

$k$  = resistance to plane homogeneous deformation,

$\mu$  = coefficient of friction,

$x$  = distance from plane of exit,

and  $t_a$  = thickness after pass.

To keep the method of calculation as simple as possible, equation (1) has been used to define change in pressure on both sides of the neutral plane, and it has been assumed that the resistance to plane homogeneous deformation  $k$  remains constant during passage of metal through the roll throat. It follows that the pressure curve then becomes similar to that which is drawn in the lower portion of Fig. 1, and the total rolling load  $P_t$  may, therefore, be calculated from the equation :

$$P_t = 2kw \int_0^{l/2} e^{2\mu x/t_a} \quad . \quad . \quad . \quad (2)$$

where  $w$  = width of material

and  $l$  = projected length of arc of contact.

Integrating,

$$P_t = \frac{kwt_a}{\mu} \{e^{\mu l/t_a} - 1\} \quad . \quad . \quad . \quad (3)$$

This equation is the same as one recently reported by Stone.<sup>5</sup> Although  $\mu$  has been defined as the coefficient of friction, it is more satisfactory, in view of the simplifications made in the present analysis, to regard this as a factor which can be empirically adjusted—as indicated below—to ensure increased accuracy of computation.

The area of the base  $abde$  of Fig. 1 is simply  $kl$ , so that the ratio of the total rolling load  $P_t$  to the load  $P_c$  associated with plane homogeneous compression of the metal is

$$\frac{P_t}{P_c} = \frac{t_a}{\mu l} \{e^{\mu l/t_a} - 1\} \quad . \quad . \quad . \quad (4)$$

If  $P_{c1}$ ,  $P_{c2}$ , . . . . .  $P_{cn}$ , associated with the first, second, and  $n$ th passes, respectively, represent loads, as defined above—the total percentage reduction effected during these passes being  $R_n$ —and if  $P_{cs}$

represents the load generated during one heavy pass of magnitude  $R_n$ , it can be shown<sup>1</sup> that

$$\begin{aligned} \frac{P_{c1}\sqrt{R_1}}{100 - R_1} + \frac{P_{c2}\sqrt{R_2 - R_1}}{100 - R_2} + \dots + \\ + \frac{P_{cn}\sqrt{R_n - R_{n-1}}}{100 - R_n} = \frac{P_{cs}\sqrt{R_n}}{100 - R_n} \quad . \quad (5) \end{aligned}$$

where  $R_1$  = percentage reduction after first pass,

$R_2$  = total percentage reduction after second pass,

and  $R_n$  = total percentage reduction after  $n$ th pass. Thus, combining equations (4) and (5) :

$$\begin{aligned} \frac{P_{t1}}{\frac{t_{a1}}{\mu l_1} \{e^{\mu l_1/t_{a1}} - 1\}} \cdot \frac{\sqrt{R_1}}{100 - R_1} + \frac{P_{t2}}{\frac{t_{a2}}{\mu l_2} \{e^{\mu l_2/t_{a2}} - 1\}} \cdot \frac{\sqrt{R_2 - R_1}}{100 - R_2} + \dots + \\ + \frac{P_{tn}}{\frac{t_{an}}{\mu l_n} \{e^{\mu l_n/t_{an}} - 1\}} \cdot \frac{\sqrt{R_n - R_{n-1}}}{100 - R_n} \\ = \frac{P_{ts}}{\frac{t_{an}}{\mu L_n} \{e^{\mu L_n/t_{an}} - 1\}} \cdot \frac{\sqrt{R_n}}{100 - R_n} \quad . \quad (6) \end{aligned}$$

It should be noted, in this equation, that  $l_1$ ,  $l_2$ , and  $l_n$  represent the projected lengths of arcs of contact associated with first, second, and  $n$ th light passes, respectively, while  $L_n$  is the length associated with a single heavy pass  $R_n$ .

It can be shown that if  $D$  = roll diameter and  $t_b$  = initial thickness of strip,

$$\frac{l_1}{t_{a1}} = 100 \sqrt{\frac{D}{200t_b}} \cdot \frac{\sqrt{R_1}}{100 - R_1} = c.b_1,$$

$$\frac{l_2}{t_{a2}} = 100 \sqrt{\frac{D}{200t_b}} \cdot \frac{\sqrt{R_2 - R_1}}{100 - R_2} = c.b_2,$$

$$\frac{l_n}{t_{an}} = 100 \sqrt{\frac{D}{200t_b}} \cdot \frac{\sqrt{R_n - R_{n-1}}}{100 - R_n} = c.b_n,$$

$$\text{and} \quad \frac{L_n}{t_{an}} = 100 \sqrt{\frac{D}{200t_b}} \cdot \frac{\sqrt{R_n}}{100 - R_n} = c.B_n$$

and, accordingly, equation (6) may be simplified considerably. Thus,

$$\begin{aligned} \frac{P_{t1}}{\frac{P_{c1}}{e^{\mu c b_1} - 1}} \cdot b_1 + \frac{P_{t2}}{\frac{P_{c2}}{e^{\mu c b_2} - 1}} \cdot b_2 + \dots + \\ + \frac{P_{tn}}{\frac{P_{cn}}{e^{\mu c b_n} - 1}} \cdot b_n = \frac{P_{ts}}{\frac{P_{cs}}{e^{\mu c B_n} - 1}} \cdot B_n \quad . \quad (7) \end{aligned}$$

Using this equation, together with a curve relating  $P_{ts}$  to corresponding reductions  $R_n$ , effected, on any particular mill, in a single pass—the first-pass curve—it is possible to calculate such loads as  $P_{t1}$ ,  $P_{t2}$ , &c., which would be developed when the same overall reduction is effected in several passes. From a practical point of view, it is necessary for the curve to cover reductions as large as 60–80%, and although it is not

usual to make such heavy reductions in one pass—particularly when rolling thin strip—it is possible to construct a suitable curve using the above equation and load data  $P_{11}$ ,  $P_{12}$ , &c., determined experimentally for a series of successive passes. Thus it is necessary to measure rolling loads for a series of passes of, say, 20% each, until the total reduction effected is of the order of 60–80% and, in addition, loads must be measured for a few first-pass reductions up to about 50%. Measured load values for the successive passes, together with appropriate data for  $c$ ,  $b_1$ ,  $b_2$ , . . . .  $b_n$  are then substituted into the left-hand side of equation (7), the numerical value of the factor  $\mu$  being adjusted by a few trials until calculated data for first-pass

reductions of 30% per pass, and the degree of accuracy of computed results is shown by the figures in columns 16 and 17 of this table, which are the calculated and measured load data, respectively.

By using the procedure indicated in Tables I and II, together with measured load values for the series of passes in which successive reductions of 20% were effected, first-pass curves were constructed for all the rolling conditions investigated, the numerical value of the factor  $\mu$  being adjusted to give the best agreement between measured and calculated data. From an examination of the results, it was established, for the range investigated, that the value of  $\mu$  varied, for H.C. copper, from 0.03 to 0.07, the corresponding

TABLE I.—Construction of First-Pass Curve.  
Annealed H.C. Copper 3 in. Wide  $\times$  0.0175 in. Thick.  $8\frac{1}{4}$ -in.-Dia. Rolls.

$R_n$	$100 - R_n$	$R_n - R_{n-1}$	$\frac{\sqrt{R_n - R_{n-1}}}{100 - R_n} = b_n$	$\mu c b_n$	$\frac{\mu c b_n}{e}$	$\frac{\mu c b_n - 1}{e} = E_n$	$P_{1n}$ , tons	$P_{1n} = \frac{P_{1n}}{E_n}$	$\frac{P_{1n} \sqrt{R_n - R_{n-1}}}{100 - R_n}$	Sum	$\frac{\sqrt{R_n - R_{n-1}}}{100 - R_n} = b_n$	$P_{1n} = \frac{\text{Sum}}{b_n}$ , tons	$\mu c b_n$	$\frac{\mu c b_n}{e}$	$\frac{\mu c b_n - 1}{e} = E_n$	$P_{1n} = \frac{P_{1n}}{E_n}$ , tons
20.0	80.0	20.0	0.0559	0.517	0.677	1.31	9.9	7.56	0.422	0.422	0.0559	7.56	0.517	0.677	1.31	9.9
34.9	65.1	14.9	0.0594	0.549	0.731	1.33	12.6	9.46	0.562	0.984	0.0907	10.8	0.841	1.32	1.57	17.0
48.3	51.7	13.4	0.0709	0.655	0.924	1.41	18.2	12.9	0.915	1.899	0.1345	14.0	1.24	2.46	1.98	27.7
59.8	40.2	11.5	0.0845	0.780	1.18	1.52	23.3	15.3	1.397	3.196	0.1920	16.6	1.775	4.90	2.76	45.9
67.8	32.2	8.0	0.0879	0.810	1.25	1.54	24.4	15.8	1.393	4.589	0.2553	17.9	2.365	9.65	4.08	73.0

TABLE II.—Computation of Rolling Loads.  
Successive 30% Passes. Annealed H.C. Copper 3 in. Wide  $\times$  0.0175 in. Thick.  $8\frac{1}{4}$ -in.-Dia. Rolls.

$R_n$	$R_n - R_{n-1}$	$\frac{\sqrt{R_n - R_{n-1}}}{100 - R_n} = b_n$	$\mu c b_n$	$\frac{\mu c b_n}{e}$	$\frac{\mu c b_n - 1}{e} = E_n$	$\frac{\sqrt{R_n - R_{n-1}}}{100 - R_n} = b_n$	$\mu c b_n$	$\frac{\mu c b_n}{e}$	$\frac{\mu c b_n - 1}{e} = E_n$	$P_{1n}$ , tons (from Fig. 2)	$P_{1n} = \frac{P_{1n}}{E_n}$	$\frac{P_{1n} \sqrt{R_n - R_{n-1}}}{100 - R_n}$	Difference between Successive Values of $\frac{P_{1n} \sqrt{R_n - R_{n-1}}}{100 - R_n} = D$	$P_{1n} = \frac{D(100 - R_n)}{\sqrt{R_n - R_{n-1}}}$	$P_{1n} = \frac{E_n P_{1n}}{E_n}$ , tons	Measured Load, tons
30.3	30.3	0.0790	0.730	1.075	1.47	0.0790	0.730	1.075	1.47	14.4	9.80	0.775	0.775	9.80	14.4	13.8
50.3	20.0	0.0900	0.832	1.30	1.56	0.1425	1.32	2.74	2.08	30.1	14.5	2.065	1.290	14.35	22.4	23.8
62.9	12.6	0.0958	0.885	1.42	1.60	0.2135	1.97	6.17	3.14	55.0	17.5	3.74	1.675	17.5	28.0	27.3

loads  $P_{1n}$  are in good agreement with measured results. The curve relating  $P_{1n}$  and  $R_n$  so obtained may then be used, together with the corresponding value for  $\mu$ , to calculate rolling loads for any given sequence of passes.

A numerical example of the construction of a typical first-pass curve relating to the rolling of annealed 3-in.-wide  $\times$  0.0175-in.-thick H.C. copper on an  $8\frac{1}{4} \times 10$ -in. mill, should clarify the details of the method of computation. Table I shows the step-by-step method of calculation using values of 154 and 0.06 for  $c$  and  $\mu$ , respectively. The computed data have been plotted in Fig. 2, which also includes measured load values, and it is apparent that agreement between measured and calculated load values is satisfactory.

The method of computing rolling loads is shown in Table II, which refers once again to 3-in.-wide  $\times$  0.0175-in.-thick annealed H.C. copper rolled on an  $8\frac{1}{4} \times 10$ -in. mill. Loads have been calculated for

values for 70 : 30 brass being 0.04 and 0.10. Curves showing the variation of  $\mu$  with the ratio initial thickness : roll diameter are plotted in Fig. 3, where the upper limit of this ratio is 0.006, since for values greater than this  $\mu$  remained constant at 0.03 and 0.04 for the H.C. copper and 70 : 30 brass, respectively. Data taken from the first-pass curves were then used, in conjunction with the appropriate value for the factor  $\mu$ , to determine the degree of accuracy, when applied to the whole range of experimental conditions, of rolling loads calculated from equation (7). A number of typical curves showing computed and measured loads are recorded in Figs. 4–7, from which it will be seen that agreement between them is good over the whole range of conditions considered.

The satisfactory standard of agreement between measured and calculated results effectively demonstrates the applicability of this simple method of load computation to a wide range of rolling conditions. Before loads can be calculated for any particular



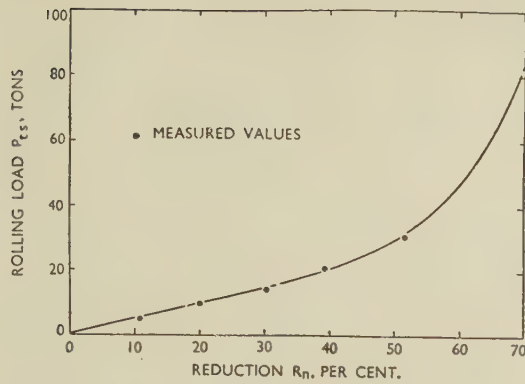


FIG. 2.—First-Pass Curve for Annealed 3-in.-Wide  $\times$  0.0175-in.-Thick H.C. Copper. Roll dia. =  $8\frac{1}{4}$  in.

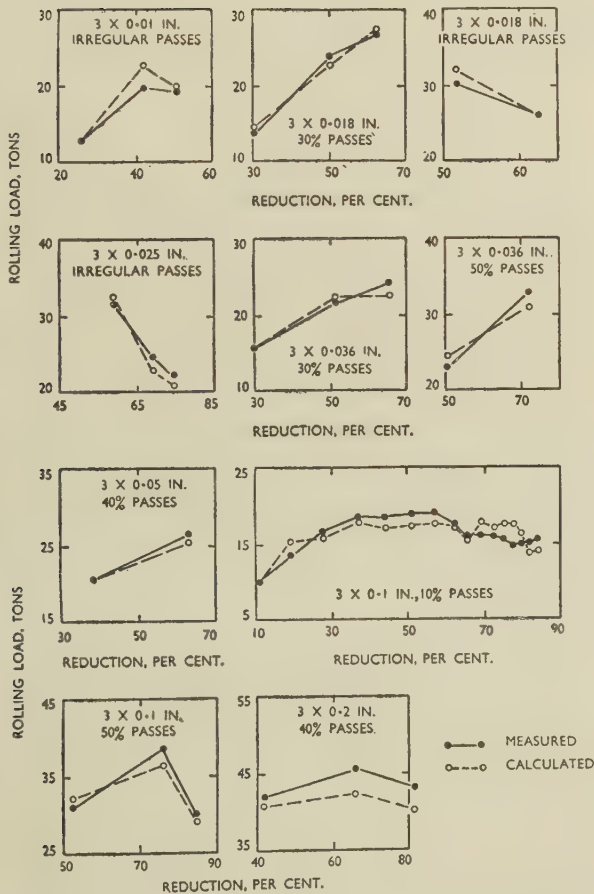


FIG. 4.—Measured and Calculated Load Data for Annealed H.C. Copper. Roll dia. =  $8\frac{1}{4}$  in.

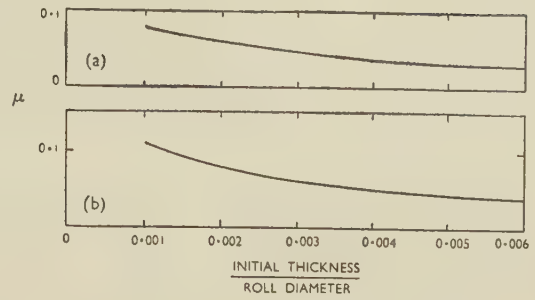


FIG. 3.—Variation of Values for Factor  $\mu$  for  
(a) Annealed H.C. Copper, and  
(b) Annealed 70 : 30 Brass.

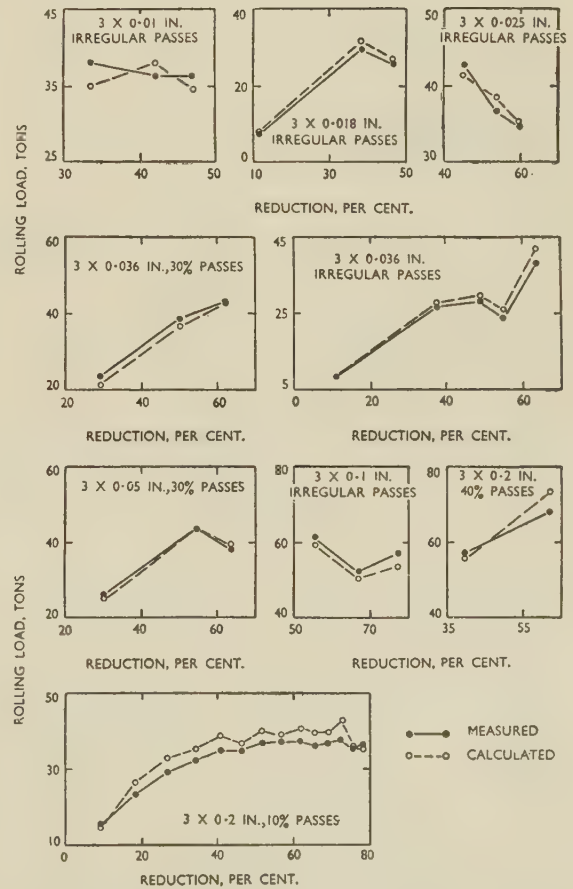


FIG. 5.—Measured and Calculated Load Data for Annealed 70 : 30 Brass. Roll dia. =  $8\frac{1}{4}$  in.

metal, roll diameter and strip thickness, however, appropriate first-pass curves are required. The establishment of such curves by load measurement necessitates the use of several mills fitted with rolls of different diameters. If the measurements could be limited to one mill and the load values so obtained made applicable for the calculation of rolling loads for mills of different sizes, the amount of data needed would be substantially reduced.

Dimensional-analysis methods are frequently used to facilitate the solution of physical and mechanical problems, and can be applied to the determination of rolling loads. A dimensionless formula has, in fact, been suggested by Ford,<sup>6</sup> but no supporting experimental evidence has so far been produced.

A detailed study by methods of dimensional analysis has, therefore, been made of the factors affecting rolling load, and a procedure has been evolved whereby first-pass curves for any thickness and roll diameter within the range subsequently indicated can be derived, after which equation (7) can be used as

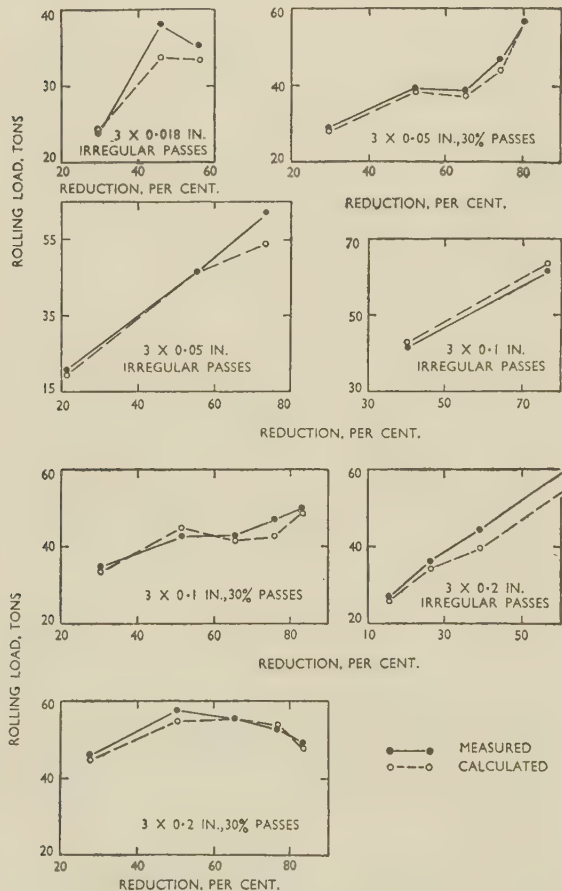


FIG. 6.—Measured and Calculated Load Data for Annealed H.C. Copper. Roll dia. = 14 in.

previously described. As a result of this work it is possible to calculate rolling loads for a wide range of conditions from a comparatively small amount of experimentally determined load-measurement data,

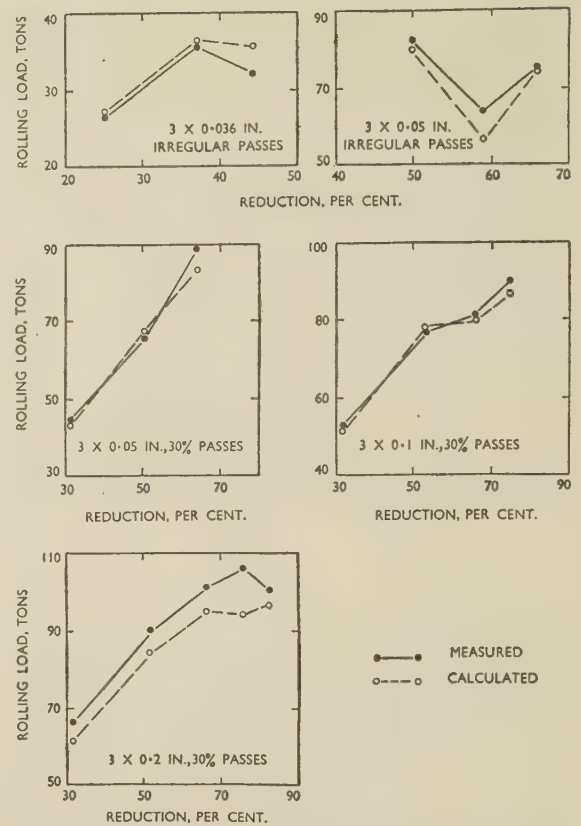


FIG. 7.—Measured and Calculated Load Data for Annealed 70:30 Brass. Roll dia. = 14 in.

and full details of the method of analysis and its application are recorded in the following section.

#### IV.—DIMENSIONAL ANALYSIS OF ROLLING-LOAD DATA

The magnitude of the loads developed on a rolling mill is influenced by such dependent variables as initial strip thickness, roll diameter, width of material, resistance to homogeneous deformation, and frictional effects, and the form of the relationship between these variables can be determined by methods of dimensional analysis.

Let  $P$ ,  $D$ ,  $w$ ,  $\sigma$ ,  $t_b$ , and  $\mu$  denote rolling load, roll diameter, strip width, resistance to deformation, initial thickness of stock, and coefficient of friction, respectively. Then, for constant frictional conditions, a dimensionless grouping of the variables  $P$ ,  $D$ ,  $w$ ,  $\sigma$ , and  $t_b$  can be deduced<sup>7</sup> by equating a factor,  $K$ , to the product of these variables with unknown exponents. Thus,

$$K = P^a \times D^b \times w^c \times \sigma^d \times t_b^e \quad (8)$$

or if the dimensions of each quantity are written in place of its symbol:

$$K = \left(\frac{ML}{T^2}\right)^a \times L^b \times L^c \times \left(\frac{M}{LT^2}\right)^d \times L^e \quad (9)$$

where  $M$  = mass,  $L$  = length, and  $T$  = time.



In order that the grouping,  $K$ , should be dimensionless, the sum of the exponents of the individual terms  $M$ ,  $L$ , and  $T$  in equation (9) must be equal to zero. Hence,

$$\text{for } M, \quad a + d = 0 \quad (10)$$

$$\text{for } L, \quad a + b + c - d + e = 0 \quad (11)$$

$$\text{and for } T, \quad -2a - 2d = 0 \quad (12)$$

If these conditions are satisfied, a dimensionless grouping results, and because there are five unknowns in equations (10) to (12) the numerical values of three of them can be conveniently fixed<sup>7</sup> and values thereby obtained for the remaining two.

Denoting the value of  $a$  by 1 and  $b$  and  $c$  by 0, it follows that  $d = -1$  and  $e = -2$ . Under these conditions,

$$K_1 = P/\sigma t_b^2 \quad (13)$$

Next let  $b = 1$  and  $a$  and  $c = 0$ , when  $d = 0$  and  $e = -1$ .

Then,

$$K_2 = D/t_b \quad (14)$$

To introduce  $w$  into the grouping, let  $c = 1$  and  $a$  and  $b = 0$ , from which  $d = 0$  and  $e = -1$ .

Hence,

$$K_3 = w/t_b \quad (15)$$

Equations (13), (14), and (15) are now combined to provide a complete dimensionless grouping of  $P$ ,  $D$ ,  $w$ ,  $\sigma$ , and  $t_b$  by writing:

$$K_1 = f(K_2, K_3)$$

$$\text{i.e.} \quad P/\sigma t_b^2 = f(D/t_b, w/t_b)$$

$$\text{or} \quad \sigma t_b^2/P = f'(t_b/D, t_b/w) \quad (16)$$

The above analysis indicates, for constant frictional conditions, that the factor  $\sigma t_b^2/P$  is a function of both  $t_b/D$  and  $t_b/w$ , and it follows, since the ratio  $t_b/D$  covers both initial thickness and roll diameter, that if the relevant values for any individual mill are plotted against an appropriate function of the measured loads, the curves derived can also be used to determine the loads developed on mills fitted with rolls of other diameters.

If the ratio  $t_b/w$  remains constant,  $\sigma t_b^2/P$  can be expressed as a function of  $t_b/D$  only, but for  $t_b/w$  to be constant for stock of different initial thickness, the strip width must differ with thickness. On the other hand, experimental technique would be greatly simplified if load data from stock of uniform width could be used in the analysis. Although it is generally accepted that rolling load is, in fact, proportional to strip width, very little corroborative data have been recorded in the literature, except those of Lueg and Pomp.<sup>8</sup> Because of this, and in view of the importance attached to an accurate knowledge of the above relationship, further work was carried out on an  $8\frac{1}{4}$ -in. mill. Rolling loads were measured for annealed

0.05-in.-thick 70 : 30 brass strip, 1, 2, 3, 5, and 8 in. wide, subjected to single-pass reductions of increasing magnitude. The first-pass curves so obtained are plotted in Fig. 8 (a), data taken from this graph being used to construct Fig. 8 (b), which indicates the effect of strip width on rolling load. These results show that over the range 1–8 in. load is directly proportional

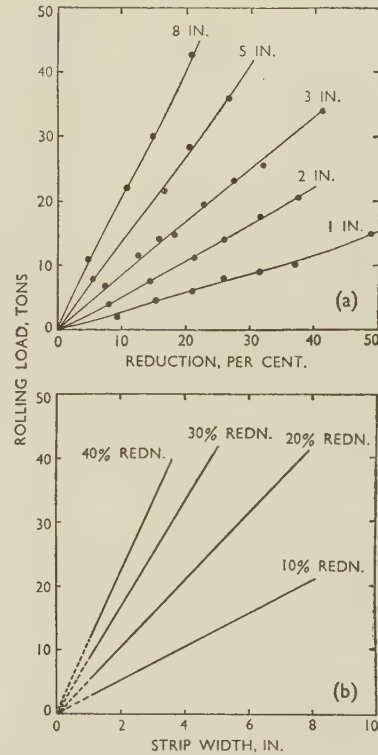


FIG. 8.—Effect of Strip Width on Rolling Load for 0.05-in.-Thick 70 : 30 Brass.

to width, and rolling loads for various widths of material can, therefore, be calculated by simple proportion from a single width.

#### V.—APPLICATION OF ANALYSIS TO DATA OBTAINED ON AN $8\frac{1}{4}$ × 10-IN. MILL

Since, for a given metal or alloy in a defined condition, the resistance to homogeneous deformation corresponding to a given percentage reduction in a single pass is constant, application of dimensional analysis is facilitated by writing equation (16) in the form:

$$t_b^2/P = f''(t_b/D, t_b/w) \quad (17)$$

The procedure used to apply the analysis can probably be most clearly illustrated by an actual example, and data which refer to annealed H.C. copper reduced on  $8\frac{1}{4}$ -in. rolls are recorded in Table III. To make  $t_b^2/P$  a function of  $t_b/D$  only, it is necessary to keep the factor  $t_b/w$  constant, and this has been arbitrarily





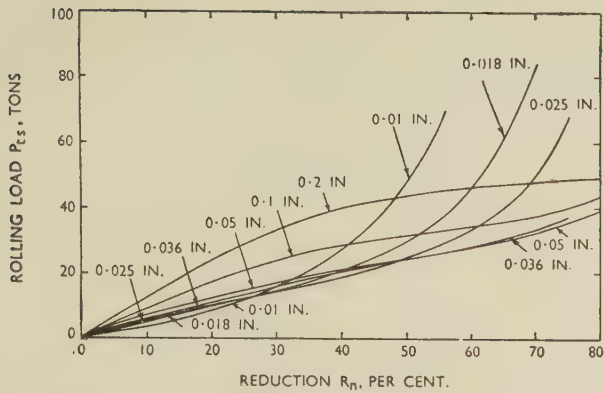


FIG. 9.—First-Pass Curves for Annealed 3-in.-Wide H.C. Copper Strip Rolled on an  $8\frac{1}{4} \times 10$ -in. Mill.

fixed at 0.0167, i.e. the value corresponding to 3-in.-wide  $\times$  0.050-in.-thick material. The initial thicknesses of the copper strips which were rolled on the  $8\frac{1}{4}$ -in. mill are recorded in the second column of Table III, and the widths, corresponding to  $t_b/w = 0.0167$ , associated with these thicknesses are recorded in column 3.

Load data  $P_{ts}$  for 3-in.-wide material, taken from

first-pass curves established for annealed H.C. copper (see Fig. 9) are given in column 4, the loads calculated by simple proportion for the various strip widths being detailed in columns 5–10. Columns 11–17 contain values of  $t_b^2/P_{ts}$  which have been established by reference to the load data for these strip widths.

Values for the ratio  $t_b/D$ , with  $D = 8\frac{1}{4}$  in., corresponding to the various initial strip thicknesses, are recorded in column 18, and these have been used in conjunction with appropriate data for  $t_b^2/P_{ts}$  to plot the family of curves in Fig. 10. Similar sets of curves have been constructed from results established for annealed 70 : 30 brass, and these are plotted in Fig. 11.

## VI.—CONSTRUCTION OF THE FIRST-PASS CURVE FOR ANY STRIP THICKNESS AND ROLL DIAMETER

Data from the families of curves included in Figs. 10 and 11 can be used to construct a first-pass curve for any strip thickness and roll diameter, within the range covered, and roll-force values may then be computed, for any rolling schedule, using equation

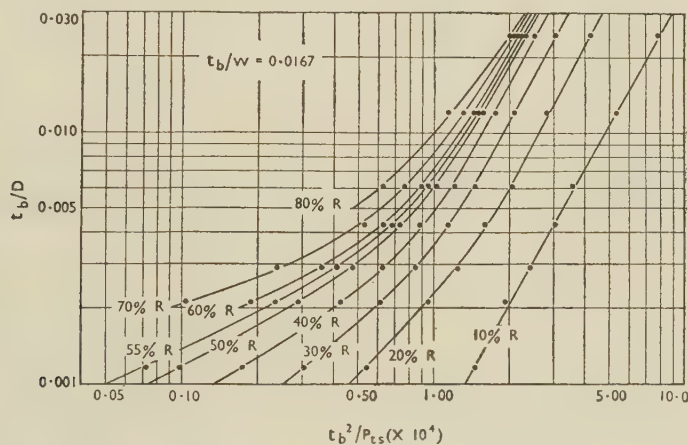


FIG. 10.—Data for Constructing First-Pass Curves for Annealed H.C. Copper.

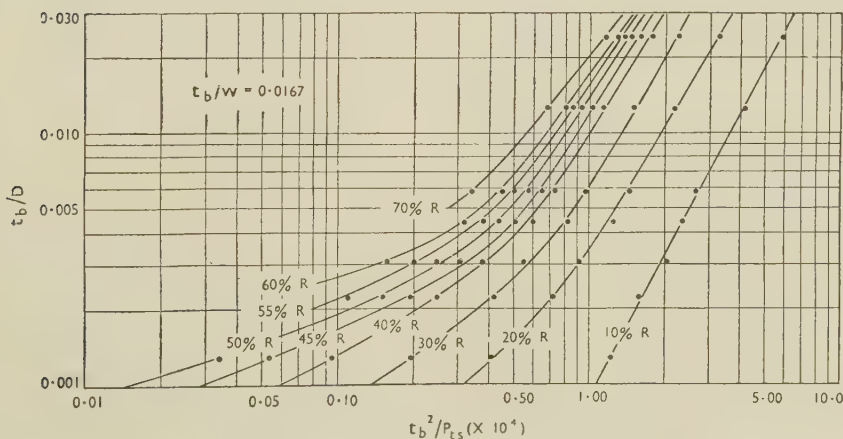


FIG. 11.—Data for Constructing First-Pass Curves for Annealed 70 : 30 Brass.

(7). The method of establishing such a curve is most conveniently demonstrated by considering a particular thickness and roll diameter, and data will be derived, for example, for 24-in.-wide  $\times$  0.2-in.-thick 70:30 brass strip reduced on a mill fitted with 16-in.-dia. steel rolls ground to a mean axial surface finish of about 11 micro-in. The value of  $t_b/D$  corresponding to these conditions is  $0.2/16 = 0.0125$ , and appropriate figures for the ratio of  $t_b^2/P_{ts}$  at single-pass reductions of 10–70% can be read from the family of curves in Fig. 11. Since  $t_b = 0.2$  in. and  $t_b^2 = 0.04$  in.<sup>2</sup>, first-pass load data  $P_{ts}$  can be calculated from the equation :

$$P_{ts} = 0.04/t_b^2/P_{ts}$$

and these values are given in column 3 of Table IV. As these figures refer to a  $t_b/w$  value of 0.0167, i.e.  $w = 0.2/0.0167 = 12$  in., the data for plotting the

TABLE IV.—Method of Constructing First-Pass Curve.

Annealed 70:30 brass, 24 in. wide  $\times$  0.2 in. thick; 16-in.-dia. rolls.

Reduction, %	$t_b^2/P_{ts} (\times 10^4)$ (from Fig. 11)	$0.04 \div t_b^2/P_{ts}$ $= P_{ts}$ , tons (12 in. width)	Load Data for 24-in.-Wide Strip, tons
10	4.10	98	196
20	2.20	182	364
30	1.51	265	530
40	1.15	348	696
50	0.930	430	860
60	0.790	507	1014
70	0.675	593	1186

required first-pass curve, included in the last column of the table, are twice those recorded in the third column.

## VII.—VALIDITY OF THE DIMENSIONAL ANALYSIS

The validity of the analysis has been checked by reference to the results of load measurements made by Ford,<sup>9</sup> Lueg and Pomp,<sup>10</sup> and Lueg and Schultze<sup>11</sup> and confirmed by data obtained from experiments on a 14-in. rolling mill given earlier in the paper.

Ford<sup>9</sup> has carried out numerous tests on 0.10-in.-thick H.C. copper strip rolled on a 10-in. mill fitted with rolls ground to a mirror finish. From a consideration of mechanical properties,<sup>9</sup> it was estimated that slitting and coiling had work-hardened the copper strip by the equivalent of about 4% reduction by rolling, so that before constructing a first-pass curve some allowance for this work-hardening had to be made. The initial thickness of the strip was accordingly increased by 4%, and, using the data of Fig. 10, a first-pass curve was constructed as described in the previous section of the paper, for this adjusted initial thickness, i.e. 0.104 in. A further correction was also necessary before loads could be calculated for the various practices, since total percentage reductions relative to the adjusted initial thickness were not identical with those recorded by

Ford<sup>9</sup> relative to the actual initial strip thickness. These corrections are not required if the material is initially in the fully annealed condition.

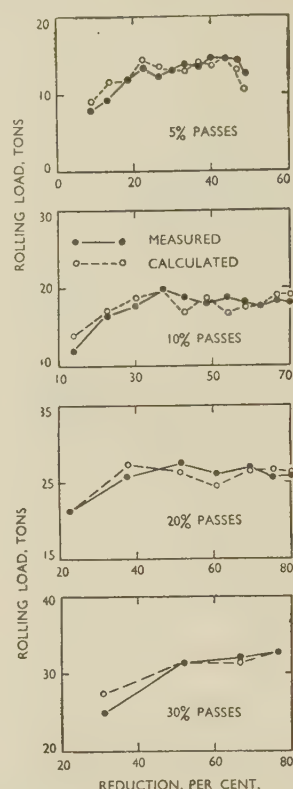


FIG. 12.—Comparison Between Measured Loads and Results Calculated from Data Obtained on an  $8\frac{1}{2} \times 10$ -in. Mill for 3-in.-Wide  $\times$  0.1-in.-Thick H.C. Copper Strip. Roll dia. = 10 in.

Data from the first-pass curve, together with a value of 0.03 for the factor  $\mu$ , were then employed in conjunction with the corrected percentage reduction values to calculate rolling loads for the various

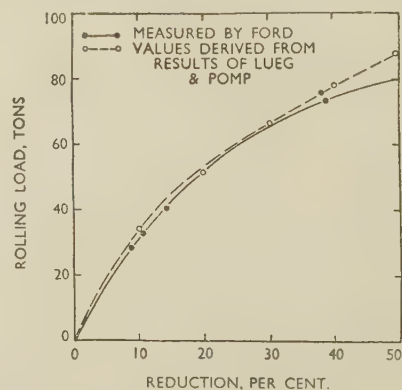


FIG. 13.—Comparison of Annealed Mild Steel, 3 in. wide  $\times$  0.1 in. Thick. Roll dia. = 10 in.

practices. Typical comparisons between these calculated results and those measured by Ford<sup>9</sup> are indicated graphically in Fig. 12, and it will be seen that the measure of agreement is good. Since the



calculated values were established using a  $\mu$  value determined on the  $8\frac{1}{4}$ -in. mill, this good agreement demonstrates that the frictional conditions on both  $8\frac{1}{4}$ - and 10-in. mills were reasonably uniform.

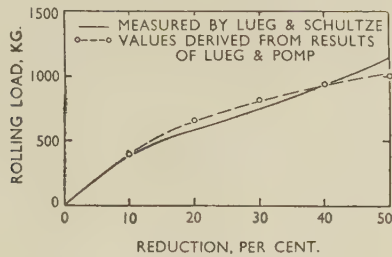


Fig. 14.—Comparison of Annealed Mild Steel, 0.6 in. Wide  $\times$  0.02 in. Thick. Roll dia. = 0.4 in.

Ford<sup>9</sup> also measured loads for annealed 3-in.-wide  $\times$  0.1-in.-thick mild-steel strip rolled on a 10-in. mill, and similar material 1.18 in. wide  $\times$  0.079 in. thick has been rolled by Lueg and Pomp<sup>10</sup> on 1.81-

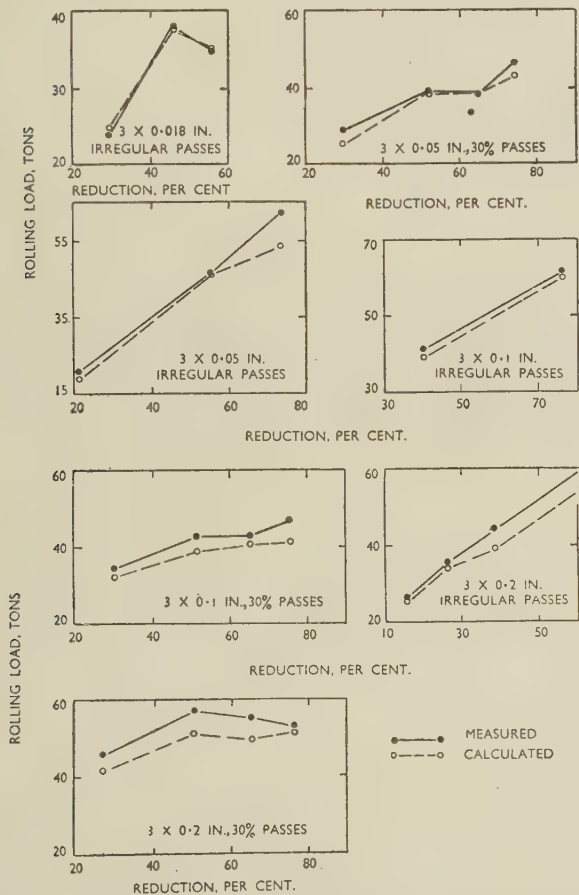


Fig. 15.—Comparison Between Measured Loads and Results Calculated from Data Obtained on an  $8\frac{1}{4} \times 10$ -in. Mill for Annealed H.C. Copper Strip. Roll dia. = 14 in.

2.44-, 3.66-, and 7.28-in.-dia. rolls. Both investigations were carried out without the use of lubricants, and frictional conditions were, it is assumed, reasonably similar. The work of Lueg and Pomp<sup>10</sup> provides

load data corresponding to different  $t_0/D$  values, and these have been analysed as described above, and the plotted curves were similar in form to those shown in Figs. 10 and 11. By the aid of these curves, rolling loads, developed when reducing 0.1-in.-thick material by 10, 20, 30, 40, and 50% in one pass on 10-in.-dia. rolls, were established and compared with the load data actually measured by Ford.<sup>9</sup> The results, plotted in Fig. 13, show an excellent measure of agreement.

Lueg and Pomp<sup>10</sup> have also carried out corresponding experiments on another grade of 1.18-in.-wide  $\times$  0.079-in.-thick mild-steel strip, and Lueg and

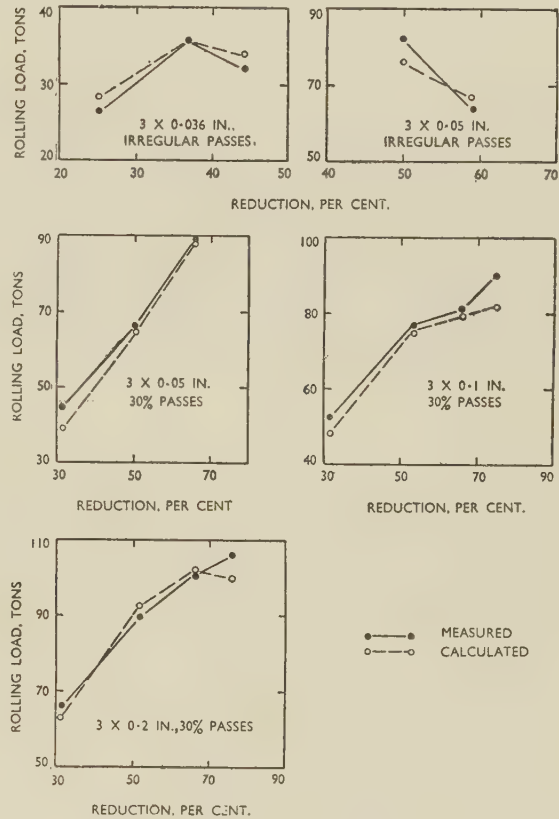


Fig. 16.—Comparison Between Measured Loads and Results Calculated from Data Obtained on an  $8\frac{1}{4} \times 10$ -in. Mill for Annealed 70 : 30 Brass Strip. Roll dia. = 14 in.

Schultze<sup>11</sup> have made load measurements when rolling similar material 0.59 in. wide  $\times$  0.02 in. thick on a 12-high Rohn mill, the working rolls of which were only 0.4 in. in dia. The method of dimensional analysis has been applied to the results published by Lueg and Pomp<sup>10</sup> and the data obtained were then used to determine loads for comparison with those measured by Lueg and Schultze.<sup>11</sup> The corresponding values are plotted in Fig. 14, from which it will be seen that agreement is again very satisfactory. The two comparisons illustrated in Figs. 13 and 14 are important, since they provide independent confirmation of the validity of the method of dimensional analysis.

The results of the experiments carried out by the authors on a 14-in. rolling mill enable further comparisons between calculated and measured loads to be made. For example, the curves plotted in Figs. 10 and 11 were used to construct appropriate first-pass curves for 14-in.-dia. rolls, and values from these were then used, in conjunction with equation (7), to calculate rolling loads for all conditions of varying initial thickness and reduction involved in the experimental work on the 14-in. mill. Computed and measured values are shown in Figs. 15 and 16, which indicate a very satisfactory standard of agreement.

#### VIII.—GENERAL APPLICATION OF THE METHOD OF COMPUTATION

The comparisons which have been made between calculated and measured load data demonstrate that the method of dimensional analysis as described permits a wide application of equation (7) for computing rolling loads. For example, curves such as those plotted in Fig. 10 are applicable to material initially 0.004–0.75 in. thick and to rolls from 4 to 24 in. in dia. To establish these curves for any one material, only about five series of annealed strips are needed, each series being of different initial thickness. First-pass reductions of about 10, 20, 30, 40, and 50%

are made for each series, the strips reduced by 20% then being given successive passes of this magnitude until overall reductions of about 80% have been effected. The relevant load data are plotted as first-pass curves, e.g. Fig. 9, and graphs are established giving the relationship between the factor  $\mu$  and the ratio of initial thickness to roll diameter. The first-pass curves, however, are valid only for the particular rolling conditions employed, but the dimensional analysis described has made it possible to construct curves such as those plotted in Figs. 10 and 11, and from these, first-pass curves can be derived for any initial strip thickness: roll diameter ratio within the range covered by the experiments.

The data included in this paper relate to rolling conditions in which strip tension is not applied, and to mills fitted with steel rolls having a mean axial surface finish of about 11 micro-in., although it might be noted that results obtained by Ford<sup>9</sup> suggest that even fairly marked differences in frictional condition may have no great effect on roll force.

#### ACKNOWLEDGEMENT

The authors are indebted to Mr. E. C. Larke for much valuable help in connection with the work described in this paper.

#### REFERENCES

1. M. Cook and E. C. Larke, *J. Inst. Metals*, 1948, **74**, 55.
2. R. B. Sims, J. A. Place, and A. D. Morley, *Engineering*, 1952, **173**, 116.
3. E. Orowan, *Proc. Inst. Mech. Eng.*, 1943, **150**, 140.
4. E. Orowan and K. J. Pascoe, *Iron Steel Inst. Special Rep.*, 1946, (34), 124.
5. M. D. Stone, *Iron Steel Eng.*, 1953, **30**, 61.
6. H. Ford, *J. West Scotland Iron Steel Inst.*, 1944–45, **52**, 59.
7. W. C. Johnson, "Mathematical and Physical Principles of Engineering Analysis", p. 224. 1944.
8. W. Lueg and A. Pomp, *Mitt. K.-W. Inst. Eisenforsch.*, 1935, **17**, (20), 219.
9. H. Ford, *Proc. Inst. Mech. Eng.*, 1948, **159**, 115.
10. W. Lueg and A. Pomp, *Mitt. K.-W. Inst. Eisenforsch.*, 1935, **17**, (5), 63.
11. W. Lueg and F. Schultze, *ibid.*, 1940, **22**, (7), 93.



By J. D. GROGAN,<sup>†</sup> B.A., MEMBER, and R. J. PLEASANCE<sup>†</sup>

With an Appendix on

## AN X-RAY EXAMINATION OF SOME URANIUM-NICKEL ALLOYS

By BETTY E. WILLIAMS<sup>†</sup>

(Communication from the National Physical Laboratory.)

## SYNOPSIS

The liquidus of the system uranium-nickel takes the form of two eutectic troughs; one is composed of  $U_6Ni$  and a compound approximately  $U_7Ni_3$ , melting at  $740^\circ C.$  and containing about 10.5 wt.-% (33 at.-%) nickel, the other of  $UNi_5$  and nickel, melting at  $1110^\circ C.$  and containing about 71 wt.-% (91 at.-%) nickel. These are separated by a peak which rises to  $1305^\circ C.$ , the melting point of  $UNi_5$ . The following compounds are formed by peritectic reactions:  $U_6Ni$  at  $790^\circ C.$ ; compounds approximately of compositions  $U_7Ni_3$  and  $U_5Ni_3$ , at  $785^\circ$  and  $820^\circ C.$ , respectively;  $UNi_2$  at  $985^\circ C.$  and a compound containing 78–79 at.-% nickel at  $1290^\circ C.$  Another compound occurs, containing approximately 77 at.-% nickel. The exact ranges of composition and the formulae of the compounds have not been determined; the formulae suggested are adopted for the sake of convenience. The existence of compounds  $U_6Ni$ ,  $UNi_2$ , and  $UNi_5$  has been established elsewhere by X-ray methods. The solid solubility of nickel in uranium is nearly 0.5 wt.-% (2 at.-%) at  $790^\circ C.$  and decreases with temperature. The solid solubility of uranium in nickel is about 0.75 wt.-% (0.18 at.-%) at  $1000^\circ C.$  and decreases with temperature.

## I.—PREVIOUS WORK

No equilibrium diagram of the system uranium-nickel has so far been published; Baenziger and his colleagues<sup>1</sup> state that four compounds— $U_6Ni$ ,  $UNi$ ,  $UNi_2$ , and  $UNi_5$ —occur in the system, and give the structures of all but  $UNi$ , which, they say, is complex.

## II.—MATERIALS USED AND PREPARATION OF ALLOYS

The nickel was specially selected material of over 99.9% purity, kindly supplied by The Mond Nickel Co., Ltd. The uranium was of similar high purity. The alloys were prepared in stabilized zirconia crucibles *in vacuo* in a spark-operated induction furnace. The crucibles were not visibly attacked by the molten metal, and chemical analysis did not indicate any pick-up of zirconium.

The general form of the diagram was determined with uranium of rather lower quality. Arrest points obtained with this material were generally somewhat below those given by the pure material, particularly at the uranium end of the diagram; for this reason the values were not used in Fig. 1, though the information obtained from them reduced the number of alloys it was necessary to prepare in order to establish the less-complex portions of the diagram.

## III.—EXPERIMENTAL PROCEDURE

The system was examined by thermal analysis, by heat-treatment and microscopical examination, and by X-ray analysis of the alloys. The thermal arrests at the liquidus in certain areas of the system are discussed below. Elsewhere the liquidus arrests on cooling were generally small, and on heating were replaced by small changes in the heating rate that were difficult to distinguish from irregularities caused by the settling of the molten metal in the crucible.

Owing to the slow rate of diffusion, prolonged annealing was necessary for equilibrium to be reached in the middle portion of the system. Annealing was carried out in sealed silica capsules *in vacuo*. To avoid reaction with the silica, the alloy specimens were placed in thin alumina tubes inside the capsules. There was no evidence of changes taking place during the cooling of the annealed material, except at the uranium end of the system and at the compound  $UNi_5$ . In the uranium-rich alloys, the change from  $\gamma$ - to  $\alpha$ -uranium could not be suppressed, in accord with experience of the uranium-iron alloys; at the compound  $UNi_5$ , alloys slightly deficient in nickel developed a Widmanstätten structure.

Polishing was carried out with alumina followed by chromic oxide. A final electrolytic etch for a few seconds at 20 V. in a bath of equal portions of ethylene

\* Manuscript received 2 May 1953.

<sup>†</sup> Metallurgy Division, National Physical Laboratory, Teddington, Middlesex.





glycol, phosphoric acid, and alcohol helped to outline the various phases in some alloys.

X-ray examination of powder samples greatly assisted in the elucidation of the diagram. The results obtained are given in the Appendix.

The compositions of alloys quoted in this paper were obtained by analysis of samples of ingots, except where they are stated to be "nominal", in which cases no analyses were made.

#### IV.—THE EQUILIBRIUM DIAGRAM (FIG. 1)

##### 1. URANIUM-RICH ALLOYS

This area of the diagram is very similar to that of the uranium-iron system.<sup>2,3</sup> Addition of nickel lowers the liquidus to 740° C., the melting point of a eutectic which contains about 10.5 wt.-% (33 at.-%) nickel. The solidus falls rather slowly at first and then very steeply, and meets the U<sub>6</sub>Ni peritectic horizontal at 790° C.

##### 2. SOLID SOLUBILITY OF NICKEL IN URANIUM

The solid solubility of nickel in uranium is just under 0.5 wt.-% (2 at.-%) at the peritectic temperature. The presence of nickel depresses the  $\beta \rightarrow \gamma$  transformation temperature from 780° to 760° C. at about 0.26 wt.-% (1.1 at.-%) nickel. The area in which  $\gamma$ - and  $\beta$ -uranium exist together is smaller in this system than in that of uranium and iron. Below 790° C., the temperature of the U<sub>6</sub>Ni peritectic, the solubility of nickel in  $\gamma$ -uranium decreases steadily with temperature and then suddenly at the  $\gamma \rightarrow \beta$  transformation. Fig. 2 (Plate XX) shows an alloy containing 0.28 wt.-% nickel in which this sudden change has taken place. This alloy had previously been cooled from the  $\gamma$  range slowly enough for segregation to take place into  $\gamma$  areas rich in nickel and  $\beta$  areas poorer in nickel; on further cooling the  $\gamma$  areas had decomposed into  $\beta$  in which particles of U<sub>6</sub>Ni were embedded. The alloy was then reheated to 760°–763° C. for 8 days and quenched from 760° C. The figure shows areas of indefinite structure where the  $\beta$  had retransformed into  $\gamma$  in a matrix of untransformed  $\beta$  containing particles of U<sub>6</sub>Ni.

The solubility of nickel falls rapidly with decreasing temperature in the  $\beta$  range, and is very low in  $\alpha$ -uranium. The temperature of the  $\alpha \rightarrow \beta$  transformation of uranium is not appreciably altered by the presence of nickel. The lamellar structure characteristic of uranium-iron alloys of low iron content did not appear in the low-nickel alloys, U<sub>6</sub>Ni separating in small rounded particles.

##### 3. THE U<sub>6</sub>Ni PERITECTIC AT 790° C.

The compound U<sub>6</sub>Ni is formed by reaction between solid uranium and liquid alloy. Fig. 3 (Plate XX) shows massive U<sub>6</sub>Ni with uranium containing particles of precipitated U<sub>6</sub>Ni, in a crucible-cooled alloy containing 1 wt.-% nickel. In this system, as in that of uranium and iron, the reaction between the solid

uranium and the liquid is not complete in alloys close to the peritectic composition cooled at normal rates; on annealing, the excess-phase uranium or the eutectic is absorbed. An alloy containing 4.03 wt.-% (14.6 at.-%) nickel, rather more than that required to form U<sub>6</sub>Ni, annealed for 28 days at 720° C., consisted almost entirely of U<sub>6</sub>Ni. This compound is not as brittle as U<sub>6</sub>Fe, but is similar to it in appearance under the microscope. The horizontal line of the U<sub>6</sub>Ni peritectic meets the liquidus curve at about 8 wt.-% (27 at.-%) nickel. On the addition of more nickel, the liquidus falls to 740° C., the temperature of the eutectic of U<sub>6</sub>Ni and U<sub>7</sub>Ni<sub>9</sub>.

##### 4. U<sub>6</sub>Ni–U<sub>7</sub>Ni<sub>9</sub> EUTECTIC

This eutectic is very similar in appearance to that of U<sub>6</sub>Fe and UFe<sub>2</sub>. The structure is shown in Fig. 4 (Plate XX).

##### 5. U<sub>7</sub>Ni<sub>9</sub> AND U<sub>5</sub>Ni<sub>7</sub>

The liquidus in this area rises increasingly steeply with increasing nickel content. Inverse-rate cooling curves, instead of showing a sharp break at the liquidus, form a bulge increasing rather slowly to a maximum and then decreasing, the bulge extending over 10°–15° C. Heating curves are normal in form, and show only a change of slope at the liquidus. Thermal curves show a large arrest at 820° C., a small one at 785° C. on heating and at a rather lower temperature on cooling, and an arrest at 740° C. which is due to the eutectic. All ingots containing more than 20 wt.-% nickel, cooled at normal rates, were found to contain particles of UNi<sub>2</sub>, eutectic and a rather indefinite phase which appeared heavily twinned when etched with 50% nitric acid solution in water (Fig. 5, Plate XX). X-ray examination showed the presence of two phases which were neither U<sub>6</sub>Ni nor UNi<sub>2</sub>, the one in alloys containing less than about 25 wt.-% nickel and the other in alloys containing higher proportions of nickel. The horizontal arrest at 820° C. was due to a peritectic reaction in which one of these compounds was formed. The arrest at 785° C. was small for a peritectic arrest, and extended as far into the nickel-rich area as the 820° C. arrest.

In order to investigate these arrest points further, alloys of nominal contents of 24 and 27 wt.-% nickel, respectively, were prepared, broken up, and remelted in crucibles fitted with thermocouple tubes in the bases. Owing to the very tough skin that these alloys develop on melting, the metal did not run well round the thermocouple tubes and consequently no great accuracy in the temperature measurements was to be expected. The crucibles were heated *in vacuo* for some days and heating and cooling curves plotted daily. Care was taken to keep the temperature below that of the peritectic change, at 820° C., in order to limit segregation and prevent the reformation of UNi<sub>2</sub>, which was known to be tedious to eliminate.

In the alloy containing 24 wt.-% nickel (corresponding to U<sub>7</sub>Ni<sub>9</sub>) the eutectic arrest at 740° C. gradually

grew shorter and finally disappeared, while the arrest at 785° C. increased and remained very sharp. Finally, after the temperature had been raised to above 820° C., the arrest at 740° C. re-appeared and that at 785° C. became very small. In the alloy containing 27 wt.-% (60 at.-%) nickel, which exceeded the content required to form  $U_5Ni_7$ , the eutectic arrest at 740° C. rapidly disappeared, while the arrest at 785° C. remained; after annealing for several days, the temperature of the arrest rose slowly to about 810° C., but it did not disappear. On heating through the arrest to above 820° C. the alloy reverted to its original state, arrests occurring at 785° C. and 740° C.

These results show that (1) the eutectic horizontal at 740° C. does not extend beyond 24 wt.-% nickel; and (2) the temperature of the solidus, 785° C. in the alloy containing 24 wt.-% nickel, increases on the further addition of nickel until it reaches the peritectic horizontal at 820° C.

#### (a) Annealing

As alloys in this area contain eutectic which melts at 740° C., preliminary annealing experiments were carried out below this temperature. Under these conditions equilibrium was attained in 5-6 weeks, and the eutectic disappeared from alloys in which it was present as a metastable constituent.

An alloy containing 23.7 wt.-% nickel, after annealing for 6 weeks at 735°-738° C., consisted of a heavily twinned phase,  $U_7Ni_9$ , together with a small quantity of eutectic. The alloy contained many short fine cracks which widened on etching, a characteristic of the phase  $U_7Ni_9$ . On heating to 785° C. the structure showed little change (Fig. 6, Plate XX). Reheating to 798° C. for 1 hr. and moderately slow cooling profoundly altered the structure; this was found to consist of untwinned crystals surrounded by crystals which had been molten and were strongly twinned, embedded in which were patches of eutectic (Fig. 7, Plate XX).

After prolonged heating at 735° C. an alloy containing 26.7 wt.-% nickel consisted of crystals of an untwinned phase,  $U_5Ni_7$ , and pieces of the compound  $UNi_2$ . This material also developed some cracks, though not as many as the previous sample. The alloy was heated to progressively higher temperatures up to 810°-813° C. without the appearance of liquid (Fig. 8, Plate XX). In this and the previous alloy the composition was determined of samples taken from the ingots, but not of the pieces used for heat-treatment. The compositions found by analysis were close to those intended.

Three further alloys were prepared. Pieces cut from these were heat-treated and examined, and then analysed. Analysis showed that they contained 24.1, 24.75, and 25.65 wt.-% nickel, respectively.

The alloy containing 24.1 wt.-% (56.2 at.-%) nickel, annealed at 735°-738° C., consisted almost entirely of twinned  $U_7Ni_9$  with a small amount of untwinned  $U_5Ni_7$  (Fig. 9, Plate XX). No visible change occurred on reheating to 780° C. The alloy containing

24.75 wt.-% (57.1 at.-%) nickel consisted mainly of untwinned  $U_5Ni_7$ , but contained also a quantity of  $U_7Ni_9$ . No visible change occurred on re-annealing at 780° C. (Fig. 10, Plate XX). On re-annealing at 788° C., the structure of both alloys changed profoundly and became similar to that shown in Fig. 7, consisting mainly of crystals of  $U_5Ni_7$  surrounded by eutectic and a little  $U_7Ni_9$ .

The alloy containing 25.65 wt.-% (58.3 at.-%) nickel was quenched from 791°-792° C. after annealing and was then found to contain some liquid. After annealing at 780° C., it consisted almost entirely of  $U_5Ni_7$  with a little  $U_7Ni_9$ . Subsequent annealing at 740° C. did not appreciably alter the relative proportions of these two compounds.

#### (b) Polishing and Etching $U_5Ni_7$ and $U_7Ni_9$

After hand-polishing, alloys in this area of the diagram showed the  $U_5Ni_7$ - $U_7Ni_9$  eutectic and  $UNi_2$  if these were present, but it was not possible to distinguish between  $U_5Ni_7$  and  $U_7Ni_9$ . On electrolytic polishing in a bath containing orthophosphoric acid, alcohol, and ethylene glycol, the surface became covered by a yellow-brown film, which by subsequent very gentle hand-polishing was removed from the  $U_5Ni_7$  while the  $U_7Ni_9$  remained stained. Better results were obtained by etching with a solution of 50% nitric acid, in water or in acetic acid. With both reagents a surface film formed and was removed by gentle hand-polishing. The aqueous solution was the better agent for the development of the twinned structure of the  $U_7Ni_9$ ; the acetic acid solution gave a more uniform yellow colour to that compound, but showed up the boundaries between it and the  $U_5Ni_7$ . Preparation of the surface had the effect of cold working, and caused some twinning in the  $U_5Ni_7$ ; this disappeared in the final stages of grinding and polishing.

#### (c) The Phase Boundaries of $U_5Ni_7$ and $U_7Ni_9$

The arrest at 820° C. observed on thermal analysis of all alloys in this area was of long duration, and represented the peritectic formation of  $U_5Ni_7$ .

The arrest which occurred at 785° C. on heating was short in thermal curves obtained in the usual way, but increased when the alloy containing 24.1 wt.-% nickel was annealed. It extended horizontally at least as far as 25.65 wt.-% nickel, but rose in the alloy containing 26.7 wt.-% nickel, though not to 820° C. It is assumed, therefore, that the line joining these two peritectic lines is not quite vertical but slopes upwards towards the nickel-rich area, as is shown by the broken line in Fig. 1.

No positive indication of ranges of composition in the compounds  $U_7Ni_9$  or  $U_5Ni_7$  has been observed. The fact that equilibrium can be obtained on annealing shows that there must be some such range in each, but the slowness with which equilibrium is attained suggests that it is very small. There is no indication of change of composition with temperature in either compound below 785° C.



6.  $\text{UNi}_2$  (33.0 Wt.-% NICKEL)

This compound is formed at  $985^\circ\text{C}$ . by a peritectic reaction between liquid and a compound  $X$  described below. In alloys containing excess uranium  $\text{UNi}_2$  separates as rather rounded crystals; these are not coloured by 50% nitric acid solution, which colours the ground-mass of  $\text{U}_5\text{Ni}_7$  yellow-brown. In alloys containing excess nickel it separates as very long plates, which are extensively cracked (Fig. 11, Plate XXI) and stain yellow with 50% nitric acid.

There is no evidence that  $\text{UNi}_2$  dissolves excess uranium. Alloys containing  $\text{UNi}_2 + \text{U}_5\text{Ni}_7$  annealed just below  $800^\circ\text{C}$ . and slowly cooled showed no signs of precipitation inside the  $\text{UNi}_2$  crystals. A number of alloys were prepared of composition close to that corresponding to  $\text{UNi}_2$ ; none was found to consist only of a single phase.

There is little range of solubility of nickel in  $\text{UNi}_2$  on the nickel-rich side of the system. Fig. 11 shows an alloy containing 33.3 wt.-% nickel, 0.3% in excess of that required to form  $\text{UNi}_2$ . This alloy was annealed for 70 days at  $720^\circ\text{C}$ ., then for 24 hr. at  $900^\circ\text{C}$ ., and finally quenched. The cast structure appeared unaltered and still contained long narrow plates of  $X$ . There appears, however, to be some range of solubility. An alloy containing 41.1 wt.-% nickel and consisting of  $\text{UNi}_2$  with much  $X$  was heated to  $940^\circ\text{--}950^\circ\text{C}$ . and slowly cooled; it was observed that the  $\text{UNi}_2$  phase contained a precipitate separating in fine parallel lines (Fig. 12, Plate XXI) identical in colour to that of the surrounding  $X$  phase and almost certainly consisting of that phase. On reheating to  $950^\circ\text{C}$ . and quenching, this structure disappeared. The amount of this precipitate was small.

7. AREA BETWEEN  $\text{UNi}_2$  AND COMPOUNDS  $X$  AND  $Y$ 

The liquidus rose very steeply at first as the nickel content was further increased, reaching  $1280^\circ\text{C}$ . at about 42 wt.-% nickel. The liquidus slope then flattened out, and in this area very anomalous thermal curves were obtained. Sometimes a small recalescence occurred at the liquidus on cooling, but, whether this happened or not, the rate of subsequent cooling was very irregular, the curves showing a series of haphazard breaks which indicated that irregular heat evolutions were taking place over a range of temperature. This phenomenon disappeared at about  $1200^\circ\text{C}$ ., below which the curves were quite normal. The abnormal area is shown shaded in Fig. 1. Both heating and cooling curves behaved in this way; alloys containing 45 wt.-% nickel or more behaved normally.

8. COMPOUNDS  $X$  AND  $Y$ 

Ingots were prepared of a series of alloys of compositions lying between the compounds  $\text{UNi}_2$  and  $\text{UNi}_5$ . Metallurgical examination of the specimens showed that alloys towards the  $\text{UNi}_2$  end of the series consisted of parallel plates of  $\text{UNi}_2$  and another compound, designated  $X$ ; the proportion of  $X$

increased with increasing nickel content. The structure is illustrated by Fig. 11 (Plate XXI).

At the other end of the series the type of structure was quite different. These alloys consisted of  $\text{UNi}_5$  and a compound  $Y$  (Fig. 15, Plate XXI). The proportion of  $Y$  increased with decreasing nickel content of the alloys. These observations pointed to the existence of a compound of composition lying between those of  $\text{UNi}_3$  and  $\text{UNi}_4$ .

X-ray examination of the series indicated the occurrence of two compounds in addition to  $\text{UNi}_2$  and  $\text{UNi}_5$ ; the phase in contact with  $\text{UNi}_2$  gave a different pattern from that in contact with  $\text{UNi}_5$  (Appendix, Table II). The compositions and methods of formation of these two compounds have not been completely determined. The available evidence is summarized below.

(a) Compound  $Y$ 

Thermal analyses were made of a series of alloys with contents of nickel ranging from 47.25 wt.-% (78.5 at.-%) to 55.5 wt.-%; the latter slightly exceeds the composition of  $\text{UNi}_5$ . The liquidus temperature increased slowly with increasing nickel content. All the alloys gave a definite arrest at  $1290^\circ\text{C}$ ., which has been interpreted to be the temperature of the peritectic reaction  $\text{UNi}_5 + \text{Liquid} \rightarrow Y$ . All the ingots had the structure of  $\text{UNi}_5 + Y$  (Fig. 15) except the first, which contained 47.25 wt.-% (78.5 at.-%) nickel and had the parallel-plate structure of  $\text{UNi}_2 + X$  (Fig. 11). X-ray examination, however, showed that it contained  $Y$  with a little  $\text{UNi}_5$ .

A piece of this ingot was heated to  $1100^\circ\text{C}$ . *in vacuo*, with the primary purpose of proving that no melting occurred below this temperature. The specimen was then found to consist of one peculiarly cracked phase,  $Y$  (Fig. 13, Plate XXI), with rows of dark spots where the second phase had been. It was then annealed for 10 days at  $1000^\circ\text{C}$ . On prolonged etching in 50% nitric acid it appeared duplex, with approximately equal amounts of an uncoloured phase and of another phase coloured a light brown. Grinding with emery papers removed the darker phase, but this tended to remain in the parallel areas where the original second phase, thought to be  $\text{UNi}_2$ , had been. Fig. 14 shows this structure after 8 days at  $1000^\circ\text{C}$ . After annealing for 10 days at  $1000^\circ\text{C}$ ., the temperature was raised for 6 hr. to  $1100^\circ\text{C}$ . and the capsule containing the specimen then quenched in water. On polishing, the material appeared duplex as before, but on further grinding the darker-etching phase gradually disappeared, leaving  $Y$  only. The identity of this phase was confirmed by X-ray analysis.

These observations can be explained on the assumption that slight superficial loss of nickel occurs on heating the alloy *in vacuo* at high temperatures. As the  $X$  compound contains over 46.1 wt.-% and  $Y$  47.25 wt.-% nickel, a slight loss of nickel would convert  $Y$  into  $X$ . It has been observed that, in this series, the phase in the duplex alloys lower in nickel is coloured preferentially by nitric acid. It follows that

the darker-etching phase observed in these annealing experiments may well have been X.

#### (b) Compound X

The X-ray evidence for the existence of this compound is given in the Appendix. Some chemical evidence was also obtained. In the chemical analysis of alloys in the range 33 wt.-% ( $\text{UNi}_2$ ) to 47 wt.-% nickel, it was observed that part of the material was rapidly attacked by nitric acid of  $d$  1.2 and that thin plates remained which were much more resistant to attack. This method was used to isolate the more resistant phase. Small pieces of alloy were treated with warm acid for 7 hr., and the residue was analysed. The following results were obtained:

Composition of alloy (Ni, wt.-%)	38.9	41.1	41.1*	41.1†	44.8
Ni content of residue (wt.-%)	46.12	46.19	46.12	46.79	47.65
	46.15	46.04	45.64	45.47	47.86
	46.08				

\* Heated 4 hr. at 950° C. and quenched.

† Heated 24 hr. at 950° C. and slowly cooled.

These figures fall into three groups. The two specimens that are poor in nickel may be suspected to contain some unattacked  $\text{UNi}_2$ . Six analyses agree well and give a mean value of 46.12 wt.-% nickel; 46.3 wt.-% nickel corresponds to  $\text{U}_2\text{Ni}_7$ , and this composition is probably close to that of the compound X. Three results definitely exceed this value and are difficult to explain, though it is possible that some of the more resistant phase was attacked, with preferential solution of nickel; this reaction was known to occur when hot acid was used. The high nickel contents may also be due to the presence of untransformed Y. It is possible that X is formed by a peritectic reaction between Y and liquid at 1260° C., as is suggested by the broken line in Fig. 1. The alloy containing 44.8 wt.-% nickel gave sharp arrests at this temperature, both on heating and cooling. Arrests occurring in this temperature range in alloys poorer in nickel would be obscured by the irregular heat evolutions already described. If this suggestion is correct, X and Y comprise a pair of compounds of very similar composition, analogous to the pair  $\text{U}_7\text{Ni}_9$  and  $\text{U}_5\text{Ni}_7$ .

Alloys in the region of 40–47 wt.-% nickel possessed some malleability in that, when struck with a hammer, they did not fly to pieces as do most of the alloys of the system, but flattened, though with much cracking.

#### 9. THE Y- $\text{UNi}_5$ AREA

The alloy containing 50.9 wt.-% nickel was examined after crucible-cooling. Its structure was found to be entirely different from those of the alloys described above, and to consist of irregular particles of Y and  $\text{UNi}_5$ . The Y particles were ragged in outline, as if they had been produced by a peritectic reaction (Fig. 15). No etching reagent was found to colour either phase;  $\text{UNi}_5$  was identified by its characteristic Widmanstätten structure. The relative amount of  $\text{UNi}_5$  present increased with increasing

nickel content until the composition corresponding to that compound was reached. Thermal analysis showed that the liquidus rose very slowly with increasing nickel content up to the melting point of  $\text{UNi}_5$ .

#### 10. $\text{UNi}_5$ (55.2 Wt.-% NICKEL)

An alloy containing 55.5 wt.-% nickel gave a very large arrest at 1305° C., no arrest at 1290° C., and a very small arrest at the uranium-nickel eutectic. These results indicated that the nickel content just exceeded that required by  $\text{UNi}_5$ . A Widmanstätten structure was observed in  $\text{UNi}_5$  in all alloys containing that compound associated with Y; this indicates some range of solubility of uranium in  $\text{UNi}_5$ . The range is small; an alloy containing 54.85 wt.-% nickel and cooled in the crucible contained a quantity of Y particles (Figs. 16 and 17, Plate XXI). Annealing for 3 days at 1000° C. did not visibly alter the amount of massive Y, but caused the precipitate in the  $\text{UNi}_5$  to ball up. Low-temperature annealing, e.g. 60 days at 680° C., rendered the material extremely brittle and increased the amount of Widmanstätten precipitate. Annealing at higher temperatures, 800° C. and above, caused the precipitate to ball up, and appeared to reduce its amount progressively. Fig. 18 (Plate XXI) shows the Widmanstätten precipitate in this alloy annealed for 20 days at 950° C., then 3 days at 1000° C. and finally quenched. No Widmanstätten precipitate was observed in any alloy containing nickel in excess of the amount needed to form  $\text{UNi}_5$ . This suggests that  $\text{UNi}_5$  can contain a slight excess of uranium, but not of nickel.

#### 11. THE NICKEL-RICH AREA

With increasing nickel contents the liquidus fell sharply to a eutectic containing about 71 wt.-% (91 at.-%) nickel melting at 1110° C. (Fig. 19, Plate XXI) and then rose to the melting point of nickel.

There is a slight range of solid solubility of uranium in nickel. An alloy containing 0.74 wt.-% (0.18 at.-%) uranium quenched from 1000° C. contained only one phase, but when reheated to 950° C. and quenched showed some precipitated phase.

### APPENDIX

#### AN X-RAY EXAMINATION OF SOME URANIUM-NICKEL ALLOYS

By Betty E. Williams

Some thirty uranium-nickel alloys were examined by X-ray-diffraction methods. All the patterns were obtained with a powder camera of 19 cm. dia., using filtered cobalt radiation. The results are summarized in Table I. Results obtained on alloys made from the less-pure uranium are not reported, except in the case of alloy UN C, which gave a particularly good picture.

Neither UN 39.5 nor UN 90 showed the lines of the compound  $\text{U}_6\text{Ni}$  stated to exist by Baenziger *et al.*<sup>1</sup> The intermetallic compounds  $\text{UNi}_2$  and  $\text{UNi}_5$ , previously reported by the American workers, were



TABLE I.—X-Ray Identification of Phases Present.

Number	Analysis Ni, wt.-%	Heat-Treatment	U	U <sub>2</sub> Ni	U <sub>7</sub> Ni <sub>5</sub>	U <sub>5</sub> Ni <sub>7</sub>	UNi <sub>5</sub>	X	Y	UNi <sub>5</sub>	Ni	UO <sub>2</sub>	NiO	Extra Lines A
UN 39-5	4.0	63 days at 720° C.	Mainly											
UN 90	(9.0)	43 days at 720° C.	Mainly											
UN 198A	(19.8)	4 weeks at 680° C.			Mainly	P.T.								2-20 s
UN 198B	(19.8)				Mainly	P.T.								
UN 237C	23.7				Mainly	P.T.								
UN 240	24.1				Mainly	P.T.								
UN 250	24.75	39 days at 735° C.			Mainly	P.T.								
UN 255	24.65	17 days at 735° C.			Mainly	P.T.								
UN C	25.8	28 days at 735° C.			Mainly	P.T.								
UN 258	25.8	70 days at 720° C.			Mainly	Pure								
UN 270B	26.65	70 days at 720° C.			Mainly	Pure								
UN 330	33.3	7 days at 785° C.				Some								
2UN 425	42.5	None				Pure								
7UN 425	42.5	4 hr. at 950° C.					Mainly	Mainly						
UN 425 (Ann.)	42.5	4 hr. at 950° C.					Mainly	Mainly				L.A.	L.A.	
UN 450	44.8	2 hr. at 1100° C.					Mainly	Mainly				L.A.	L.A.	
UN 450X	44.8	2 days at 950° C.										L.A.	Some	{ 3-10 vw 2-06 vw
UN 475X	46.1*											L.A.		
UN 500	47.25	2 days at 950° C.										L.A.		
UN 552	50.9	None							Mainly	Some				
UN 742	56.0	"										P.T.		
	72.35	"									Mainly			

\* Plates extracted from UN 400.

P.T. = possible trace.

L.A. = large amount.

TABLE II.—Interplanar Spacings of Compounds.

Y		X	U <sub>5</sub> Ni <sub>7</sub>		U <sub>7</sub> Ni <sub>5</sub>
UN475 X	UN500	7UN425	UN C	UN258	UN240
4.25 w	4.25 w	4.2 w	3.65 m	3.65 m	3.65 m
3.20 w	3.20 w	4.0 w	2.48 mw	2.48 m	3.25 w
2.09 m	2.09 m	3.10 w	2.41 vw		2.50 vw
2.03 m	2.03 m	2.92 m	2.35 m	2.35 ms	2.43 m
	1.89 vw	2.48 m	2.30 w		2.20 s
1.87 vw		2.28 m	2.28 m	2.28 m	2.18 vw
	1.80 vw	2.36 mw	2.22 ms	2.23 ms	2.05 vw
1.74 vw		2.28 vw	2.20 w	2.20 w	1.94 vw
1.69 w		2.24 vw	2.18 w	2.18 w	1.87 w
1.33 <sub>5</sub> vw		2.12 mw	2.16 m	2.17 m	1.83 w
1.28 <sub>5</sub> m	1.28 <sub>5</sub> vw	2.06 m	2.13 w	2.14 m	1.75 vw
1.18 <sub>5</sub> vw		2.04 vw	2.08 w	2.08 w	1.55 ms
1.17 vw		1.97 vw	2.06 vw	2.05 w	1.51 w
1.15 <sub>5</sub> vw		1.90 w	2.04 w		1.49 w
1.09 <sub>5</sub> vw		1.72 <sub>5</sub> w	1.92 vw		1.47 w
1.07 vw		1.62 <sub>5</sub> w	1.83 vw		1.46 w
1.04 m		1.56 w	1.74 vw		1.43 w
		1.54 w	1.65 vw		1.38 <sub>5</sub> w
		1.45 m	1.63 <sub>5</sub> vw		1.35 m
		1.42 <sub>5</sub> m	1.55 w	1.55 mw	1.33 w
		1.41 m	1.52 <sub>5</sub> w		1.32 w
		1.39 m	1.49 w	1.50 vw	1.27 <sub>5</sub> ms
		1.38 vw	1.48 w	1.48 w	1.26 <sub>5</sub> ms
		1.36 w	1.44 w	1.44 w	1.23 <sub>5</sub> mw
		1.35 w	1.40 m	1.40 m	1.21 vw
		1.32 <sub>5</sub> w	1.38 vw		1.17 <sub>5</sub> mw
		1.32 vw	1.37 <sub>5</sub> vw	1.37 <sub>5</sub> w	1.16 mw
		1.27 s	1.35 vw	1.35 <sub>5</sub> w	1.12 <sub>5</sub> w
		1.24 s	1.33 vw	1.33 <sub>5</sub> w	1.11 <sub>5</sub> w
		1.21 m	1.32 w	1.32 w	1.10 m
		1.18 <sub>5</sub> vw	1.31 <sub>5</sub> w	1.31 m	1.08 <sub>5</sub> w
		1.18 vw	1.28 w	1.28 w	1.08 vw
		1.17 <sub>5</sub> w	1.27 w	1.27 w	1.06 vw
		1.16 mw	1.26 <sub>5</sub> vw		1.05 w
		1.15 <sub>5</sub> mw	1.24 <sub>5</sub> mw	1.24 <sub>5</sub> mw	1.01 w
		1.11 <sub>5</sub> w	1.19 vw	1.19 vw	
		1.10 w	1.17 <sub>5</sub> m	1.17 <sub>5</sub> mw	
		1.08 <sub>5</sub> ms	1.16 <sub>5</sub> w	1.16 <sub>5</sub> mw	
		1.04 m	1.15 <sub>5</sub> w	1.16 w	
		1.03 <sub>5</sub> w	1.12 w	1.14 vw	
		1.02 m	1.08 vw	1.11 <sub>5</sub> vw	
			1.07 vw	1.09 <sub>5</sub> w	
			1.06 vw		
			1.04 <sub>5</sub> vw		
			1.01 vw		
			0.994 w		

present in the alloys numbered UN 270 B, UN 330, UN 450, and in UN 475 X, UN 500, UN 552, UN 742, respectively. The compound UNi<sub>5</sub> has a hexagonal structure, while UNi<sub>7</sub> is face-centred cubic. Baenziger also reported a compound UNi, which was stated to have a complex structure, though no spacings were given. In the present investigation four additional compounds have been observed by the X-ray-diffraction method; their approximate spacings are listed in Table II. As the structure types have not been determined, it is not possible to be certain that all the lines listed in Table II can be ascribed to the particular compound. There is always the possibility of the presence of a small amount of a further constituent. For example, the two lists of spacings for U<sub>5</sub>Ni<sub>7</sub> are in excellent agreement, except that the pattern from alloy UN C shows a number of lines in addition to those in the pattern from UN 258. All of these are, however, of very low intensity. UN C was a piece of a segregated thermal-analysis sample; the nickel content of 25.8 wt.-% was based on analysis of the piece submitted to X-ray examination. In Table I, the compositions in brackets are intended compositions; other figures are based on chemical analysis.

## ACKNOWLEDGEMENTS

The work described above was carried out in the Metallurgy Division of the National Physical Laboratory as part of a programme of the Division of Atomic Energy, Ministry of Supply. This paper is published on the recommendation of the Division of Atomic Energy and by permission of the Director of the National Physical Laboratory.

## REFERENCES

1. N. C. Baenziger, R. E. Rundle, A. I. Snow, and A. S. Wilson, *Acta Cryst.*, 1950, **3**, 34.
2. P. Gordon and A. R. Kaufmann, *Trans. Amer. Inst. Min. Met. Eng.*, 1950, **188**, 182.
3. J. D. Grogan, *J. Inst. Metals*, 1950, **77**, 571.

# NOTICE TO AUTHORS OF PAPERS FOR THE "JOURNAL" AND CONTRIBUTORS TO DISCUSSIONS

1. **Papers will be considered for publication from non-members as well as members of the Institute.** They are accepted for publication in the *Journal* and not necessarily for presentation at any meeting of the Institute. MSS. should be addressed to The Editor of Publications, The Institute of Metals, 4 Grosvenor Gardens, London, S.W.1.

2. **Papers suitable for publication** may be classified as:

(a) Papers recording the results of original research.

(b) First-class reviews of, or accounts of progress in, a particular field.

(c) Papers descriptive of works methods, or recent developments in metallurgical plant and practice.

(d) Papers in classes (a), (b), and (c) above, previously published in languages other than English, French, German, or Italian, if of sufficient merit.

3. **Manuscripts and illustrations** should be submitted in duplicate. MSS. must be typewritten (*double-line spacing*) on one side of the paper only, and authors are requested to sign a declaration that neither the paper nor a substantial part thereof has been published elsewhere. Exceptions may be made in certain cases where a paper has been published in a language other than English, French, German, or Italian (see 2(d) above). MSS. not accepted are normally returned within 6 months of receipt.

In the interests of economy, all papers must be written as concisely as possible; in general, internal research reports are not in suitable form for publication as papers in the *Journal*. All but the simplest mathematical expressions should be written by hand, with capital and small letters clearly distinguished. Superscript and subscript letters should also be plainly indicated. Greek letters and special signs should be identified in the margin. For style, spelling, and abbreviations used, any recent issue of the *Journal* may be consulted.

4. **Synopsis.** Every paper must have a synopsis (not exceeding 250 words in length) which, in the case of a paper reporting original research, should state its objects, the ground covered, and the nature of the results. The synopsis will appear at the beginning of the paper, and should be in a form suitable for use by abstracting organizations. Extracts from a "Guide for the Preparation of Synopses" drawn up by the Abstracting Services Consultative Committee are reproduced below.

5. **References** must be collected at the end of the paper and must be numbered in the order in which they occur in the MS. Initials of authors must be given, and the Institute's official abbreviations for periodical titles (as used in *Metallurgical Abstracts*) should be employed, where known. References to papers should be set out in the style:

A. L. Dighton and H. A. Miley, *Trans. Electrochem. Soc.*, 1942, **81**, 321 (i.e. year, volume, page).

References to books should be in the following style:

C. Zener, "Elasticity and Anelasticity of Metals". Chicago: 1948 (University of Chicago Press).

6. **Illustrations.** Each illustration must have a number and description; only one set of numbers must be used in one paper, and it is desirable to number the half-tone illustrations consecutively, rather than to intersperse them with the line figures. The captions should be typed on a separate sheet.

The set of **line figures** sent for reproduction must be drawn (about twice the size to appear in the *Journal*) in Indian ink on smooth white Bristol board, good-quality drawing paper, co-ordinate paper, or tracing cloth, which are preferred in the order given. Co-ordinate paper, if used, must be blue-lined, with the co-ordinates to be reproduced finely drawn in Indian ink. Curves should be drawn boldly (i.e. at least twice the thickness of the frame). Experimental points should be indicated by open or closed circles, triangles, squares, &c. (preferably not crosses). Curves should be broken on each side of such symbols and plenty of allowance should be made for closing up in blockmaking. All lettering and numerals, &c., should preferably be in *pencil*, so that the Institute's standard lettering may be affixed, and ample margins must be left outside the framework of the figures to enable this to be done. The second set of line illustrations may be photostat copies.

**Photographs** must be restricted in number, owing to the expense of reproduction, and photomicrographs should be trimmed to the smallest possible of the following sizes consistent with adequate representation of the subject: 4 in. deep by 3 in. wide: 2 in. deep by 3 in. wide: 2 in. square. Magnifications of photomicrographs must be given in each case. Photographs for reproduction should be loose, not pasted down (and not fastened together with a clip, which damages them), and the figure number and author's name should be written on the back of each. Captions should be given to the photomicrographs, but these should be kept as brief as possible.

Because of the present high cost of printing and paper it is imperative that authors restrict illustrations (particularly photographs) to the absolute minimum deemed necessary to support their argument. Only in exceptional cases will illustrations be reproduced if already printed and readily available elsewhere.

7. **Tables or Diagrams.** Results of experiments, &c., may be given in the form of tables or figures, *but* (unless there are exceptional reasons) *not both*. Tables should bear Roman numbers, and each should have a heading that will make the data intelligible without reference to the text.

8. **Corrections.** A certain number of corrections in proof are inevitable, but any modification of the original text is to be avoided. Since corrections are very expensive, the Institute reserves the right to require authors to contribute towards their cost if the Editor deems them to be excessive. The Institute also reserves the right to require a contribution to the cost of remaking any block where this is necessitated by an error on the author's part.

9. **Reprints.** Individual authors are presented with a maximum of 25, and two or more authors with a maximum of 50 reprints from the *Journal*, without covers. Limited numbers of additional reprints can be supplied at the author's expense, if ordered before proofs are passed for press. (Orders should preferably be placed when submitting MSS.)

10. **Discussion.** Except in the case of special symposia, shorthand records of discussions are not taken at meetings. Written discussion may be submitted on any paper, preferably typewritten (*double-line spacing*). References should be given in the form of footnotes. Paragraphs 6 and 7 above are also applicable to such contributions. Reprints of discussion cannot be supplied to contributors.

## GUIDE FOR THE PREPARATION OF SYNOPSES

(As recommended by the Abstracting Services Consultative Committee)

1. **Purpose.** The synopsis is not part of the paper; it is intended to convey briefly the content of the paper, to draw attention to all new information, and to the main conclusions. It should be factual.

2. **Style of writing.** The synopsis should be written concisely and in normal rather than abbreviated English. It is preferable to use the third person. Where possible use standard rather than proprietary terms, and avoid unnecessary contracting.

It should be presumed that the reader has some knowledge of the subject, but has not read the paper. The synopsis should therefore be intelligible in itself without reference to the paper; for example, it should not cite sections or illustrations by their numerical references in the text.

3. **Content.** The title of the paper is usually read as part of the synopsis. The opening sentence should be framed accordingly and repetition of the title avoided. If the title is insufficiently comprehensive, the opening should indicate the subjects covered. Usually the beginning of a synopsis should state the objective of the investigation.

It is sometimes valuable to indicate the treatment of the subject by such words as: brief, exhaustive, theoretical, &c.

The synopsis should indicate newly observed facts, conclusions of an

experiment or argument and, if possible, the essential parts of any new theory, treatment, apparatus, technique, &c.

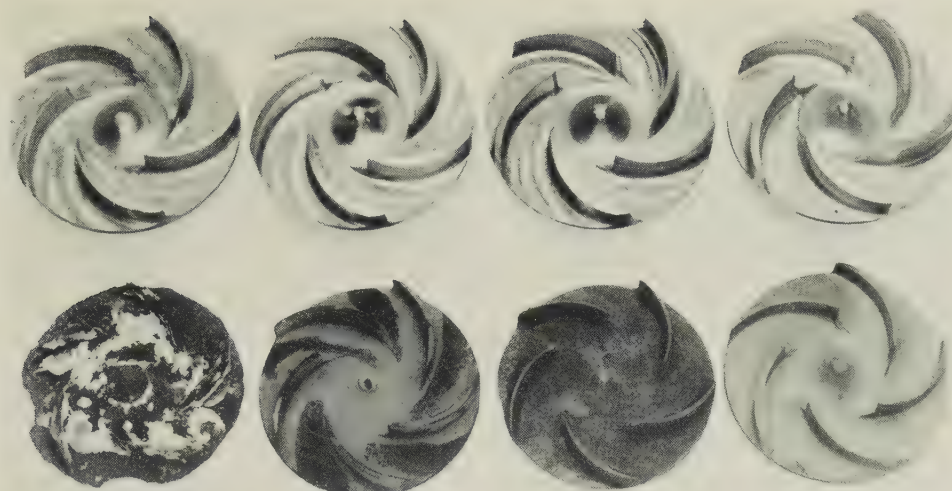
It should contain the names of any new compound, mineral species, &c., and any new numerical data, such as physical constants; if this is not possible, it should draw attention to them. It is important to refer to new items and observations, even though some are incidental to the main purpose of the paper; such information may otherwise be hidden, though it is often very useful.

When giving experimental results the synopsis should indicate the methods used; for new methods the basic principle, range of operation, and degree of accuracy should be given.

4. **References.** If it is necessary to refer to earlier work in the summary, the reference should always be given in full and not by number. Otherwise references should be left out.

When a synopsis is completed, the author is urged to revise it carefully, removing redundant words, clarifying obscurities, and rectifying errors in copying from the paper. Particular attention should be paid by him to scientific and proper names, numerical data, and chemical and mathematical formulæ.





40% Cupric  
chloride, boiling

Concentrated nitric  
acid, boiling

*Aqua regia*, room  
temperature

Sea-water, room  
temperature

Top row : Titanium after 500 hr.

Bottom row : Stainless steel, reading left to right, after 110, 250, 8, and 500 hr.

FIG. 15.—Corrosion Tests with Titanium and Molybdenum-Bearing Stainless Steel Impellers Rotated at 300 R.P.M. in Various Liquid Media.

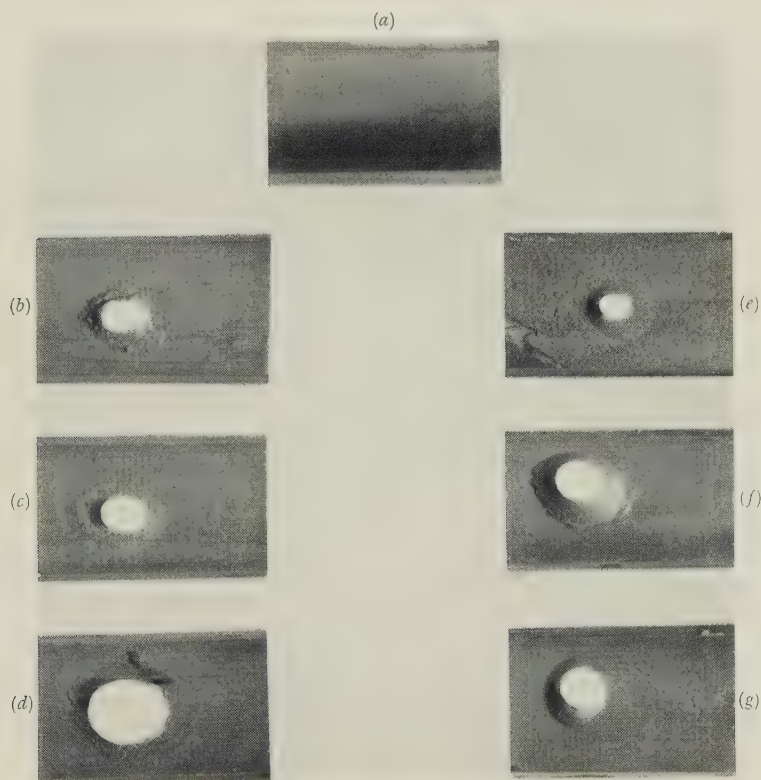


FIG. 16.—Specimens from Jet-Impingement Apparatus After 1000 Hr. in Estuarine Sea-Water.

- (a) Commercially pure titanium.
- (b) 66 : 30 : 2 : 2 copper-nickel-iron-manganese alloy.
- (c) 68 : 30 : 1 : 1 copper-nickel-iron-manganese alloy.
- (d)  $87\frac{1}{2}$  : 10 : 2 :  $\frac{1}{2}$  copper-nickel-iron-manganese alloy.
- (e) 91 : 7 : 2 copper-aluminium-nickel alloy.
- (f) 76 : 22 : 2 copper-zinc-aluminium alloy.
- (g) 70 : 29 : 1 copper-zinc-tin alloy.

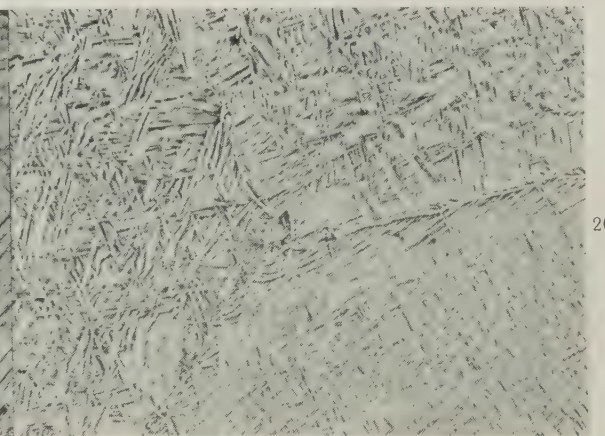
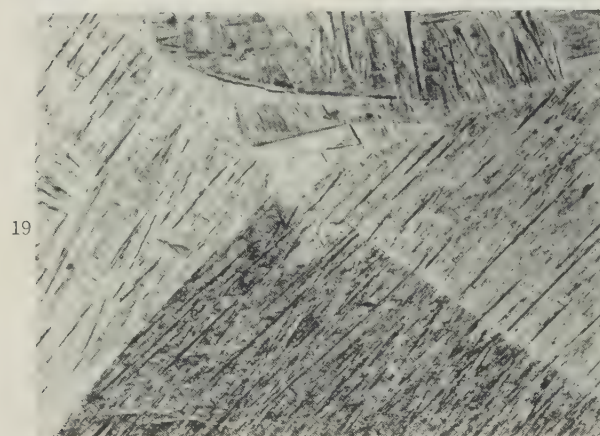
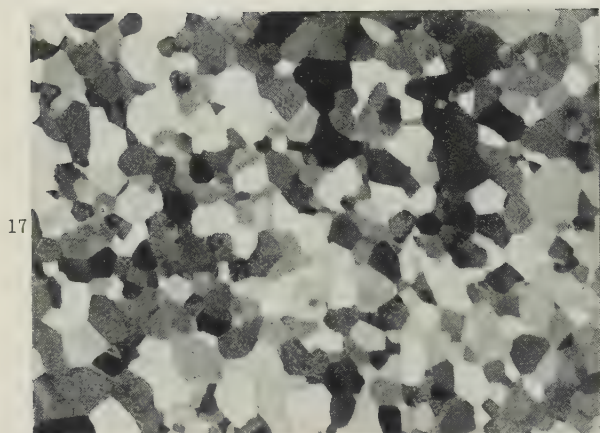


FIG. 17.—Titanium-4% Aluminium Alloy, Annealed at 900° C. and Slowly Cooled.  $\alpha$  phase.  $\times 100$ .  
 FIG. 18.—Titanium-5½% Manganese Alloy, Quenched from 950° C.  $\beta$  phase.  $\times 100$ .  
 FIG. 19.—Titanium-3½% Manganese Alloy, Quenched from 950° C. Martensitic  $\alpha$ .  $\times 100$ .  
 FIG. 20.—Titanium-4% Manganese-4% Aluminium Alloy, As Forged.  $\alpha + \beta$ .  $\times 500$ .



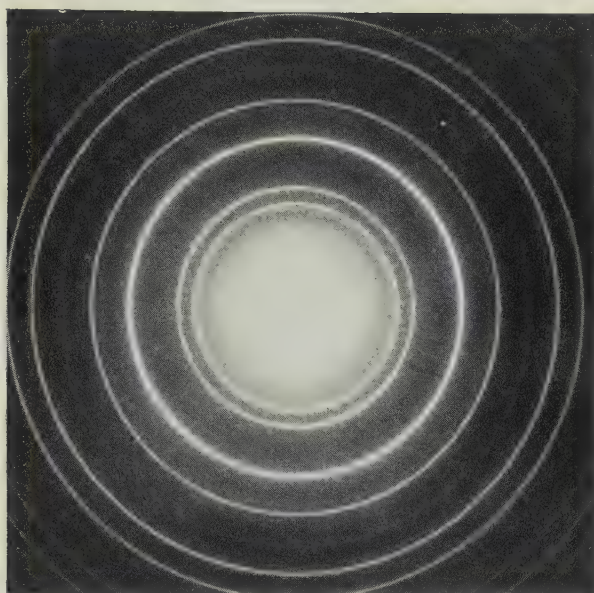


FIG. 9.—Magnesium Oxide Pattern Obtained from an Alloy Containing 0.004% Beryllium.

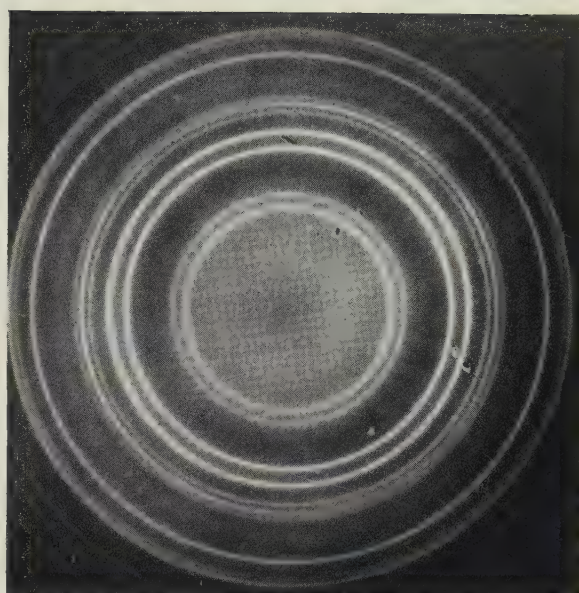


FIG. 10.—Magnesium Oxide Pattern with Beryllium Oxide Pattern Superimposed. Obtained from an Alloy Containing 0.15% Beryllium.

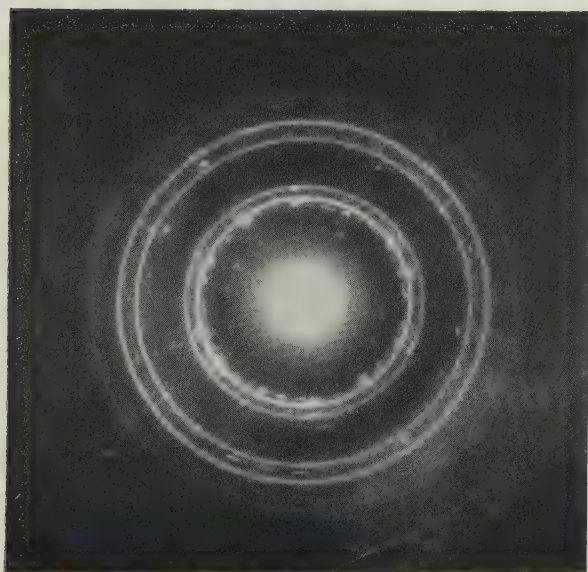


FIG. 11.—An Example of the Spotty Pattern Given by the Specimens (0.15% Beryllium).

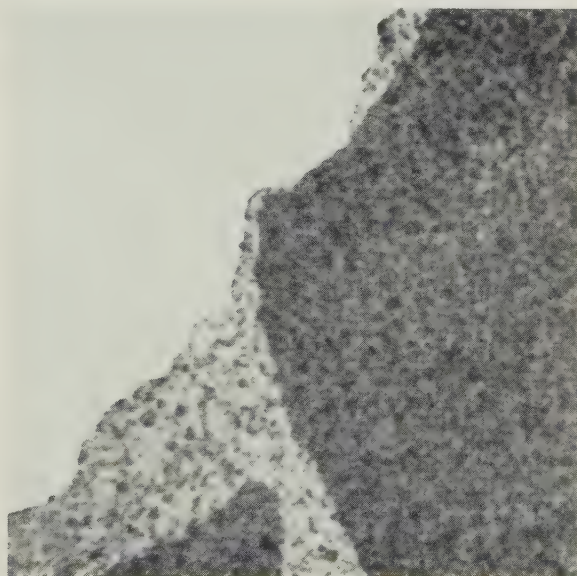


FIG. 12.—Electron-Micrograph of Film Stripped from Alloy Containing 0.035% Beryllium.  $\times 27,000$ .

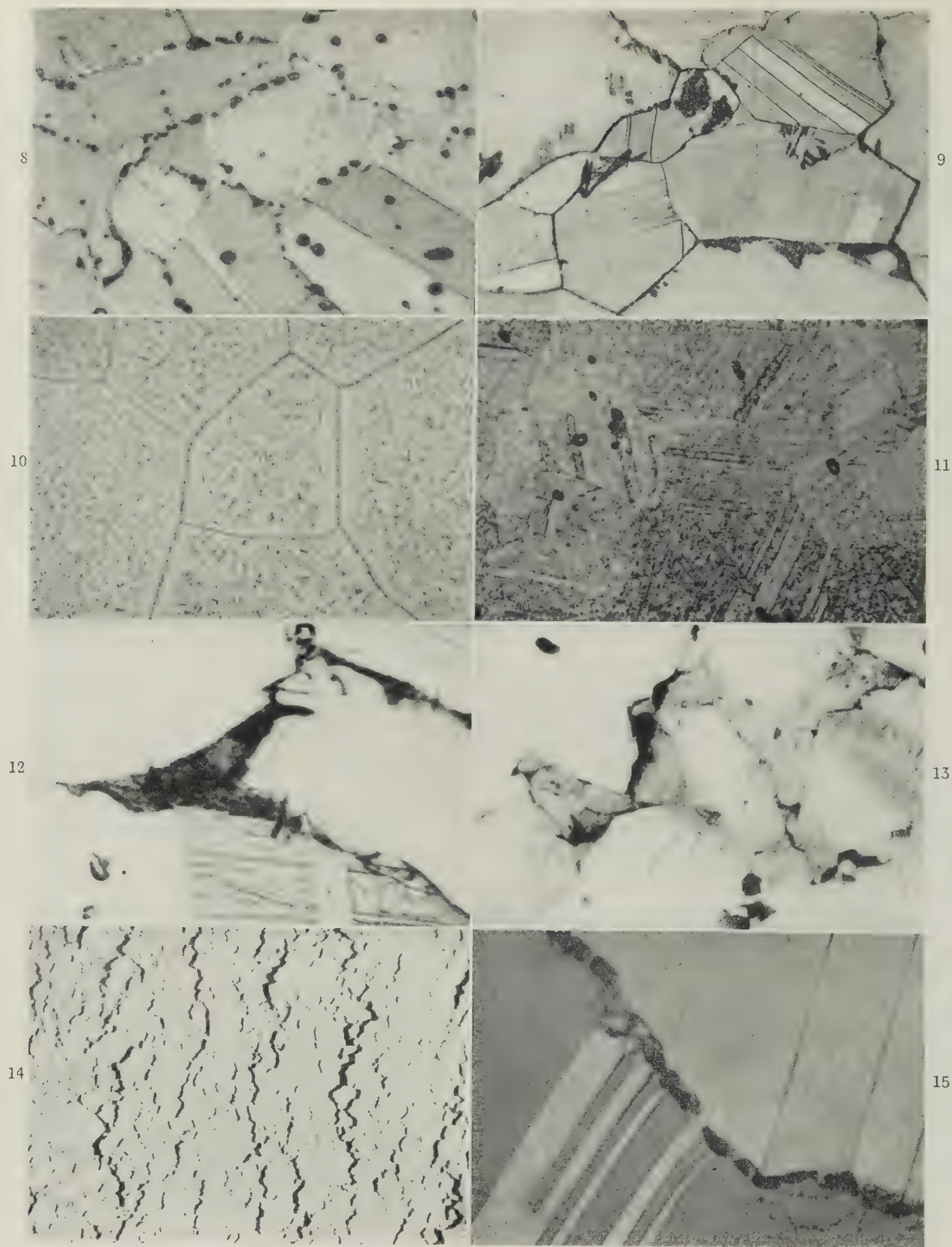


FIG. 8.—7% Al, 1.5% Co, 5% Ni. Soln.-treated 900° C., aged 24 hr. 500° C. New phase and precipitate at grain boundaries with spheroidized particles not taken into solution.  $\times 250$ .

FIG. 9.—7% Al, 1.5% Co. Soln.-treated 900° C., aged 500 hr. 500° C. Inward growth of discontinuous precipitation from grain boundaries.  $\times 250$ .

FIG. 10.—7% Al, 1% Co, 1% Fe. Soln.-treated 800° C., aged 1000 hr. 500° C. Original grain-boundary precipitate appears after 50–100 hr., subsequent lattice precipitate after 600–700 hr.  $\times 500$ .

FIG. 11.—7% Al, 2% Ti. Soln.-treated 900° C., aged 100 hr. 500° C. Mainly lattice precipitation; small zones of second phase not taken into solution.  $\times 250$ .

FIG. 12.—7% Al, 0.6% Zr. Soln.-treated 1000° C. Grain-boundary phase formed at 1000° C. and retained on quenching.  $\times 1000$ .

FIG. 13.—7% Al, 0.6% Zr. Soln.-treated 700° C.; tested at 4 tons/in.<sup>2</sup> at 450° C.; test discontinued before failure. Grain-boundary cracks in random directions.  $\times 1000$ .

FIG. 14.—7% Al, 1.5% Co. Soln.-treated 900° C.; tested to fracture at 4 tons/in.<sup>2</sup> at 450° C. General distribution of cracks along gauge-length perpendicular to applied stress.  $\times 50$ .

FIG. 15.—As Fig. 14. Grain-boundary crack across new phase produced by discontinuous precipitation.  $\times 1000$ .



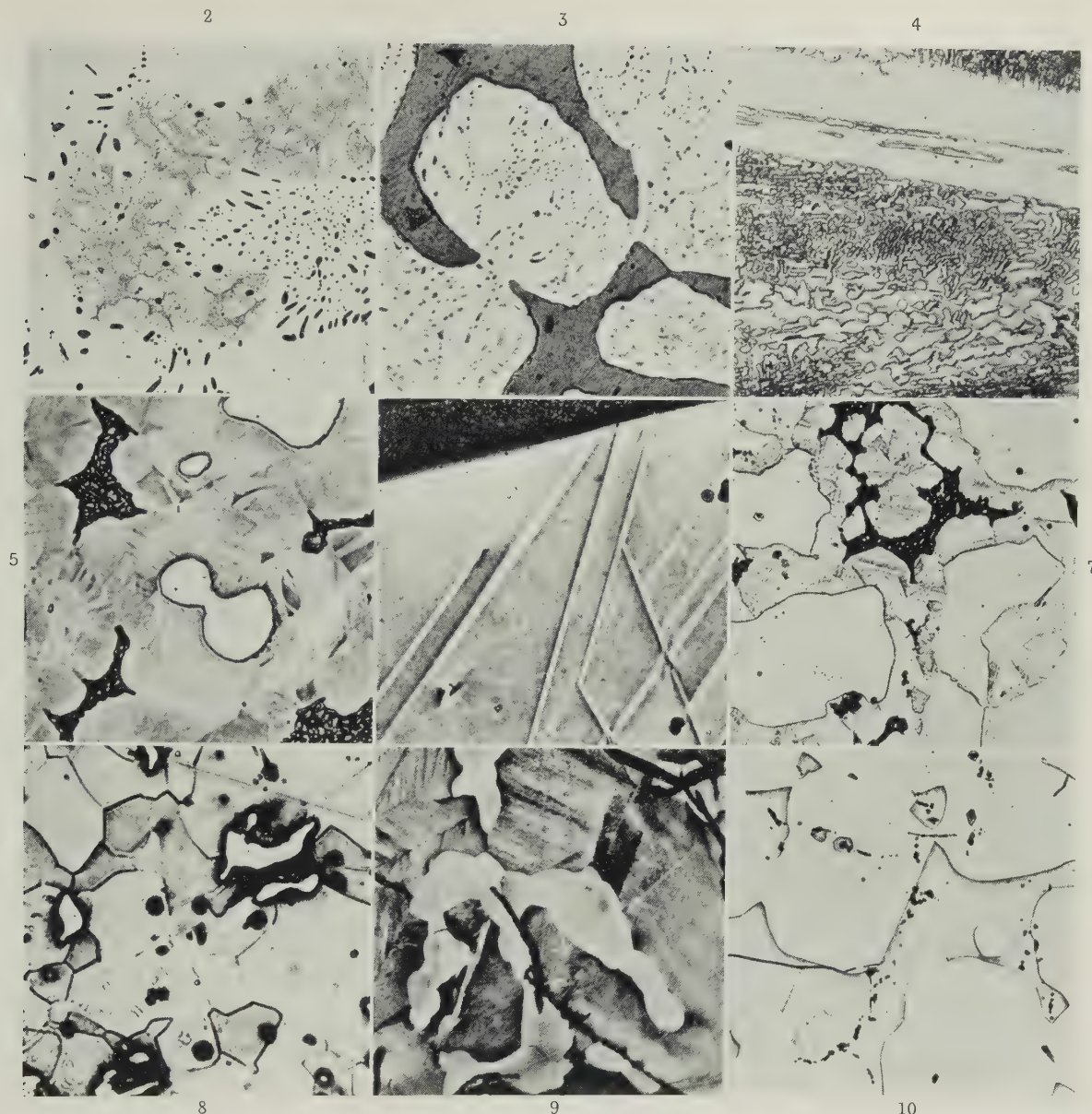


FIG. 2.—Nickel 0.28 wt.-% (1.2 at.-%). Etched 50%  $\text{HNO}_3$  in water. 8 days at  $763^\circ\text{--}760^\circ\text{C}$ . Q.  $760^\circ\text{C}$ .  $\beta$ - + decomposed  $\gamma$ -uranium +  $\text{U}_6\text{Ni}$ .  $\times 150$ .

FIG. 3.—Nickel 1 wt.-% (4 at.-%). Etched 50%  $\text{HNO}_3$  in water. Crucible-cooled ingot. Uranium +  $\text{U}_6\text{Ni}$  +  $\text{UO}_2$  (black).  $\times 500$ .

FIG. 4.—Nickel 9 wt.-% (28.5 at.-%). Crucible-cooled ingot. Unetched.  $\text{U}_6\text{Ni}$  +  $\text{U}_6\text{Ni--U}_7\text{Ni}_9$  eutectic.  $\times 150$ .

FIG. 5.—Nickel 23.9 wt.-% (56 at.-%). Electrolytic etch. Crucible-cooled ingot.  $\text{UNi}_2$  (white),  $\text{U}_7\text{Ni}_9$ , and  $\text{U}_5\text{Ni}_7$  (grey); eutectic dark.  $\times 600$ .

FIG. 6.—Nickel 23.7 wt.-% (55.7 at.-%). Etched 50%  $\text{HNO}_3$  in water. Heated 62 days at  $720^\circ\text{--}725^\circ\text{C}$ , then 2 days at  $783^\circ\text{--}785^\circ\text{C}$ . Coarse twinned  $\text{U}_7\text{Ni}_9$  + liquid.  $\times 600$ .

FIG. 7.—As Fig. 6. Reheated 1 hr. at  $798^\circ\text{C}$ . and slowly cooled to  $700^\circ\text{C}$ .  $\text{U}_5\text{Ni}_7$  (white) +  $\text{U}_7\text{Ni}_9$  (grey); eutectic black.  $\times 150$ .

FIG. 8.—Nickel 26.7 wt.-% (59.6 at.-%). Etched 50%  $\text{HNO}_3$  in water. Heated 12 days at  $720^\circ\text{--}725^\circ\text{C}$ , 7 days at  $785^\circ\text{C}$ , and 4 hr. at  $810^\circ\text{--}813^\circ\text{C}$ .  $\text{U}_5\text{Ni}_7$  (grey) +  $\text{UNi}_2$  (white).  $\times 150$ .

FIG. 9.—Nickel 24.1 wt.-% (56.2 at.-%). Etched 50%  $\text{HNO}_3$  in water. Heated 32 days at  $735^\circ\text{--}738^\circ\text{C}$ .  $\text{U}_7\text{Ni}_9$  (grey) +  $\text{U}_5\text{Ni}_7$  (light). Black lines are cracks.  $\times 600$ .

FIG. 10.—Nickel 24.75 wt.-% (57.1 at.-%). Etched 50%  $\text{HNO}_3$  in acetic acid. Heated 39 days at  $735^\circ\text{--}738^\circ\text{C}$ , 5 days at  $785^\circ\text{--}788^\circ\text{C}$ , 12 days at  $780^\circ\text{C}$ .  $\text{U}_5\text{Ni}_7$  (white) +  $\text{U}_7\text{Ni}_9$  (grey). Black lines are cracks.  $\times 150$ .

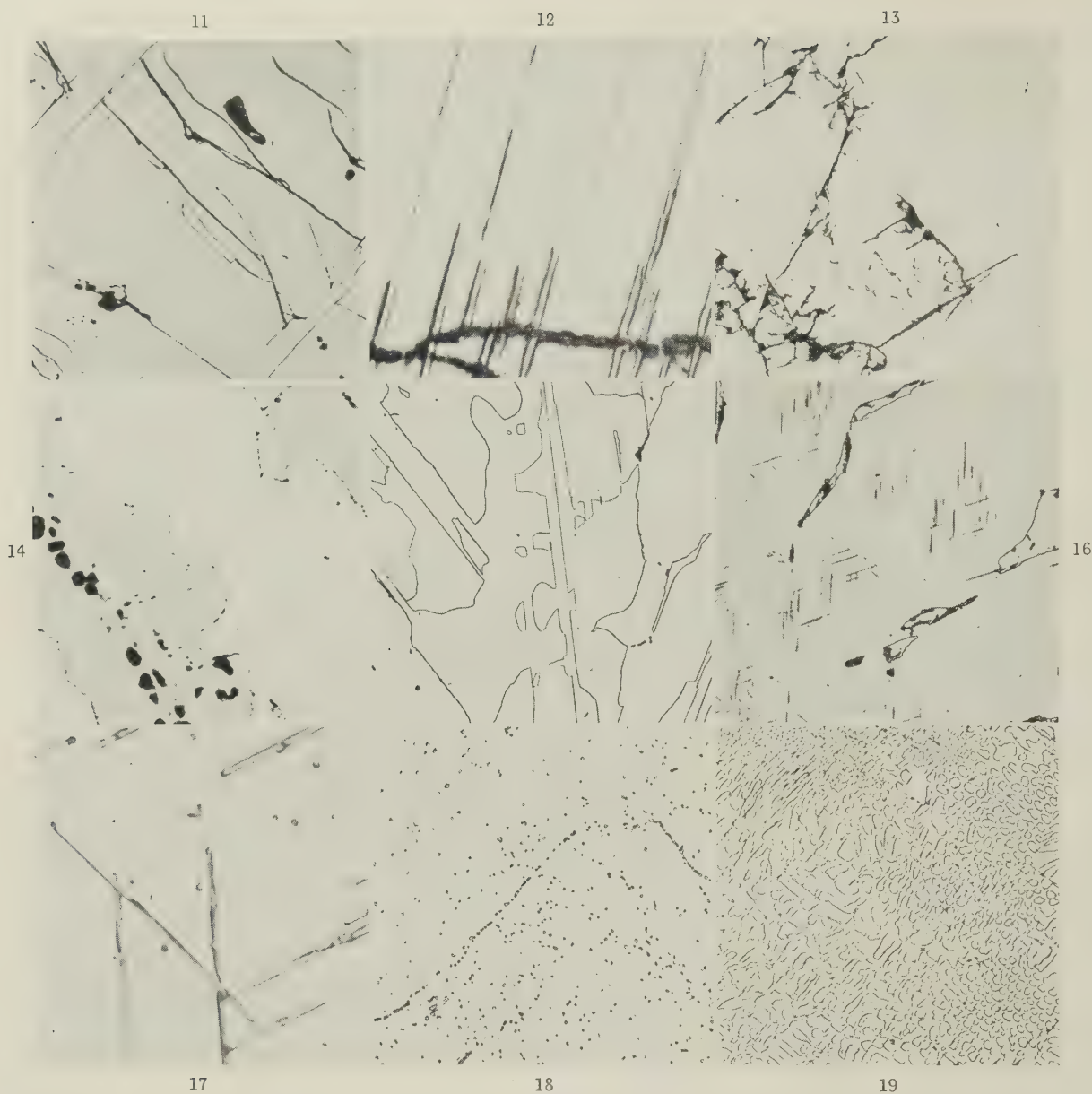


FIG. 11.—Nickel 33.3 wt.-% (67.0 at.-%). Finished electrolytically. Heated 24 hr. at 900° C. and quenched.  $\text{UNi}_2$  cracked and needles of X.  $\times 150$ .

FIG. 12.—Nickel 41.1 wt.-% (73.9 at.-%). Finished electrolytically. Slowly cooled from 950° C. Precipitate in  $\text{UNi}_2$ .  $\times 2000$ .

FIG. 13.—Nickel 47.25 wt.-% (78.5 at.-%). Finished electrolytically. Heated to 1100° C. and quenched. Cracking in Y.  $\times 500$ .

FIG. 14.—Nickel 47.25 wt.-% (78 at.-%). Etched 10 min. in 50%  $\text{HNO}_3$ . 8 days at 1000° C. X + Y.  $\times 150$ .

FIG. 15.—Nickel 50.9 wt.-% (80.8 at.-%). Finished electrolytically. Y +  $\text{UNi}_5$  with Widmanstätten structure.  $\times 150$ .

FIG. 16.—Nickel 54.85 wt.-% (82.8 at.-%). Finished electrolytically.  $\text{UNi}_5$  with Widmanstätten structure + a little Y.  $\times 150$ .

FIG. 17.—As Fig. 16.  $\times 2500$ .

FIG. 18.—As Fig. 16. Heated to 1000° C. and quenched. Widmanstätten structure balled up.  $\times 500$ .

FIG. 19.—Nickel 70.9 wt.-% (90.8 at.-%). Etched 20%  $\text{HNO}_3$ . Eutectic  $\text{UNi}_5$  + Ni.  $\times 150$ .



# THE LOW-STRESS TORSIONAL CREEP PROPERTIES OF PURE ALUMINIUM\*

1507

By W. BETTERIDGE,† Ph.D., F.Inst.P., MEMBER

## SYNOPSIS

The creep properties of pure aluminium at 200° C. have been determined by a high-sensitivity torsion method, at a torque producing a maximum elastic shear strain of  $2.8 \times 10^{-5}$ . The creep strain has been shown to be primarily dependent on the amount of cold work applied to the material and on the time and temperature of annealing treatments given before the creep test. The strain can be reduced to very small amounts by annealing at 600° C., but in order to prevent it completely annealing at a temperature very close to the melting point would appear to be necessary. The creep strain is proportional to a simple fractional power of the time; the exponent lies between 0.1 and 0.6, the exact value depending primarily on the annealing temperature. There is evidence that the sum of two such power terms might be preferable in some cases. In the standard conditions of test, single crystals grown from the molten metal do not creep at all, but a small amount of initial plastic strain in torsion induces creep. A similar amount of strain in tension is ineffective.

The results are interpreted as indicating that the mechanism by which the creep strain is produced is the movement of the dislocations existing in the material before test, and that it is not associated with viscous movement at the grain boundaries.

## I.—INTRODUCTION

It has been shown by a number of investigators (Hanson and Wheeler,<sup>1</sup> Moore, Betty, and Dollins,<sup>2</sup> Rachinger,<sup>3</sup> and McLean<sup>4</sup>) that intergranular movement makes an important contribution to the overall strain observed in the creep of metals, particularly in pure metals at relatively high temperatures and low rates of strain. The isolation of this mechanism from others which operate at the same time, e.g. distortion of the grains of the metal, is necessary in studying the factors which control the grain-boundary properties.

Kê<sup>5</sup> has published results of investigations on the anelastic properties of metals, from which he deduced that some of the anelastic behaviour was due to viscous flow at the grain boundaries. The experimental method used was primarily the determination of the internal friction of a 0.033-in.-dia. wire which formed the suspension of a torsion pendulum, with a period of about 1 sec., and the same apparatus was also used to determine the creep in torsion when a small steady couple was applied to the wire. Kê's interpretation of his observations was that a peak in the curve relating damping coefficient to temperature was due to energy lost as a consequence of viscous flow at the grain boundaries, and that the creep strain observed with a small couple within the range in which the creep strain was linearly proportional to the stress was due solely to grain-boundary flow. It appeared that, if this interpretation were correct, the technique should make possible a useful study of commercial creep-resisting alloys. With this in mind, an apparatus was constructed with which torsional creep at very low stresses could be determined on

samples  $\frac{1}{4}$  in. in dia. and 15 in. long. The rod sample was chosen instead of the wire used by Kê, since it was desired to investigate materials having grain-sizes up to about 1 mm. dia., and it is important to have the diameter of the sample appreciably larger than the diameter of the grains; in addition, it is not always possible to heat-treat alloys without some surface oxidation, and whereas wires cannot subsequently be cleaned satisfactorily rod samples can be centreless-ground.

Zener<sup>6</sup> has considered theoretically the case of an assembly of uniform equi-axed grains which are perfectly elastic, but of which the grain boundaries are viscous, so that no shearing stress can be maintained across them. He deduced that:

$$\frac{E_R}{E_U} = \frac{7 + 5\sigma}{2(7 + \sigma - 5\sigma^2)}$$

where  $E_R$  is the Young's modulus when shearing stresses across the boundaries are completely relaxed,  $E_U$  is the modulus when no relaxation occurs, and  $\sigma$  is Poisson's ratio. The corresponding expression for the rigidity modulus, which applies to a torsion test, has been given by Kê<sup>5</sup> as:

$$\frac{G_R}{G_U} = \frac{2(7 + 5\sigma)}{5(7 - 4\sigma)}$$

When a constant stress is applied to a specimen, the strain corresponding to the modulus  $G_U$  is the immediate elastic strain, while the additional strain to raise the total to correspond with the modulus  $G_R$  is observed as creep strain. Thus we find that:

$$\frac{\text{Final Creep Strain}}{\text{Elastic Strain}} = \frac{G_U}{G_R} - 1 = \frac{21 - 30\sigma}{2(7 + 5\sigma)}$$

\* Manuscript received 9 May 1953.

† The Mond Nickel Co., Ltd., Birmingham.

With Poisson's ratio in the usual range of 0.3–0.4, this ratio of final creep strain to elastic strain varies between 0.7 and 0.5, and is independent of the grain-size. The rate at which the creep strain grows depends upon the effective viscosity of the grain boundaries and on the grain-size, being faster the finer the grain-size. The shearing stress acting at a grain boundary at any instant will be proportional to the amount of flow still to occur before reaching the equilibrium displacement at which the shearing stress becomes zero. Hence the shape of the extension/time curve to be expected on the basis of uniform polyhedral grains with constant grain-boundary viscosity is an exponential of the form:

$$\gamma = \gamma_0 (1 - e^{-kt})$$

where  $\gamma_0$  is the final creep strain given by the expression above.

The creep curves determined for various samples of creep-resisting alloys bore no resemblance to this shape of curve, and consequently some doubt was felt as to whether the creep strain observed was due solely to grain-boundary flow. An examination of Kê's curves obtained on pure aluminium showed that they also did not conform to this shape. Furthermore, although Kê claimed that his curves obtained at different temperatures within the range 150°–300° C. all showed a tendency to flatten out to a constant value of strain approximately 0.5 times the initial elastic strain, as predicted by the theory, this was not at all convincing. It appeared that the maximum creep strain increased continuously with increasing temperature of test.

For these reasons an investigation of the creep of super-purity aluminium was planned, with the object of repeating some of Kê's work and of extending it to determine, as far as possible, the factors which control the characteristics of the creep curve.

## II.—EXPERIMENTAL PROCEDURE

### 1. APPARATUS

A sectional view of the apparatus used for the low-stress torsional-creep experiments is shown in Fig. 1. The upper end of the  $\frac{1}{4}$ -in.-dia. test-bar was clamped in a shackle which fitted in a socket in the upper cross-member of the frame, where it could be locked in position by a screw. The lower shackle was clamped to the test-bar and carried at its lower end a  $5\frac{1}{2}$ -in. length of 0.036-in.-dia. piano wire by means of which torsional stress was applied to the specimen.

The strain was measured by an optical method. The lower shackle carried at its lower end a small plane mirror, and a cover tube, clamped to the top end of the specimen and extending over the specimen and the lower shackle, also carried a mirror adjacent to the first one. An illuminated scale was fixed at a distance of approximately 150 in. from the mirrors, and the images of the scale in the mirrors were observed with a single telescope. The torsional strain of the test-

bar was measured by the relative deflection of the two images; the magnification was such that a 1-in. deflection was equivalent to a maximum shear strain of  $3.5 \times 10^{-5}$ .

A tubular furnace was used which could be swung in and out of position to enable the specimen assembly to be inserted and suspended from the upper cross-member of the frame. The temperature of the furnace was controlled by a platinum resistance element, used in conjunction with an electronic circuit. The temperature of the specimen was measured

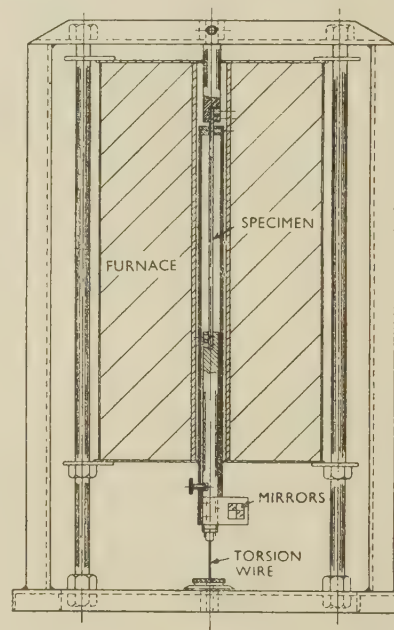


FIG. 1.—Torsion Creep-Testing Apparatus.

by three platinum/platinum-rhodium thermocouples, placed in holes in the cover tubes at intervals along its length. In practice it was found that, by careful adjustments, the specimen assembly could be put in the hot furnace and brought up to the normal test temperature of 200° C. in approximately  $2\frac{1}{2}$  hr., with a temperature gradient of less than 5° C. In most experiments the test temperature was within 2° of 200° C. and the temperature gradient was within the same range. In all cases the temperature was never allowed to vary by more than 5° C. in either direction.

When carrying out a creep experiment, the temperatures were stabilized, the torsion head was set at zero, and the stress wire was locked into position in the lower shackle. Mirror readings were taken just before application of the creep stress. This was applied as quickly as possible, by turning the dial to the required figure and locking it into position. Readings were taken 5 sec. after application of the stress, and at subsequent suitable intervals of time.

The standard torsional stress used was that produced by a 50° twist of the torsion wire, which gave an elastic deflection of 0.80 in., corresponding to a maximum elastic shear strain of  $2.8 \times 10^{-5}$ . The



weight of the lower shackle was 600 g., which imposed a tensile stress corresponding to an elastic strain of  $2.7 \times 10^{-6}$ , i.e. about one-fifth of the equivalent tensile strain produced by the torsional stress. The results are normally recorded in terms of arbitrary units of stress and strain, the former as degrees twist of the torsion wire, the latter as the scale deflection in inches.

## 2. MATERIAL

The material used throughout this investigation was high-purity aluminium, nominally 99.99%, supplied by The British Aluminium Co., Ltd., in the form of notched ingot. Ingots were hammer-forged to about  $1\frac{1}{4}$  in. dia., annealed, and machined to  $1\frac{1}{8}$  in. dia. to remove surface defects. The material was then cold-rolled to  $\frac{3}{8}$  in. dia., and finally drawn to  $\frac{1}{4}$ -in.-dia. rod. A sample of each batch of rod was analysed spectrographically, and the figure of 99.99% purity confirmed in all cases. In the course of the work eight batches of material were prepared, and in order to obtain varying degrees of cold work some batches were annealed at suitable stages in the processing. The details of the batches are given in Table I, and the amount of cold reduction applied after the final anneal

TABLE I.—Processing Details of Batches of Cold-Drawn Aluminium Rod.

Batch	Reduction of Area, %	$\ln(A_0/A)$	Hardness, D.P.N.	Annealing Treatment before Cold Work
A	Approx. 95	3.00	33.0	...
B	88.9	2.20	33.6	
C	75.0	1.39	36.4	
D	55.6	0.71	33.5	
E	29.2	0.35	22.3	1 hr. at 500° C.
F	15.4	0.17	24.4	
G	97.2	3.58	...	1½ hr. at 450° C.
H	97.2	3.58	33.1	2 hr. at 600° C.

is expressed in the conventional manner, as percentage reduction of area, and also in the form  $\ln(A_0/A)$ , where  $A_0$  and  $A$  are the initial and final cross-sectional areas, respectively. The latter expression is derived from the concept that a given fractional reduction in cross-section produces a constant increment of cold work, so that the total cold work can be expressed as :

$$\int_{A_0}^A \frac{dA}{A} = \ln\left(\frac{A_0}{A}\right)$$

## III.—EXPERIMENTAL RESULTS

The results obtained can be understood most readily by describing and considering each series of tests separately. As will be explained later, it was found that the curves conformed very closely to a simple power law of the form  $\gamma = \beta t^n$ . The constants  $\beta$  and  $n$  have been calculated in all cases, and are quoted in the tables of results, the time being measured in minutes.

## 1. INFLUENCE OF CREEP STRESS

Tests were carried out on bars of batch H, which were all annealed together for 1 hr. at 300° C. before testing. They were made at torques varying between  $12\frac{1}{2}^\circ$  and  $75^\circ$  twist of the torsion wire. Results are summarized in Table II, and in Fig. 2 the creep

TABLE II.—Influence of Stress on Creep Strain.

All specimens annealed for 1 hr. at 300° C.

Bar	Grain Dia., mm.	Stress, Degrees torque	Creep Strain, Deflection, in.		$\beta$	$n$
			1 hr.	3 hr.		
H 76	0.04	75°	1.75	2.64	0.39	0.37
H 78	0.06	62.5°	1.43	2.18	0.30	0.38
H 75	0.04	50°	1.09	1.63	0.23	0.38
H 77	0.06	37.5°	0.66	0.94	0.18	0.32
H 73	0.05	25°	0.45	0.67	0.10	0.36
H 74	0.05	12.5°	0.19	0.27	0.05	0.32

strains after a period of 3 hr. are plotted against the applied torque. The relationship is seen to be approximately linear throughout the range of stresses

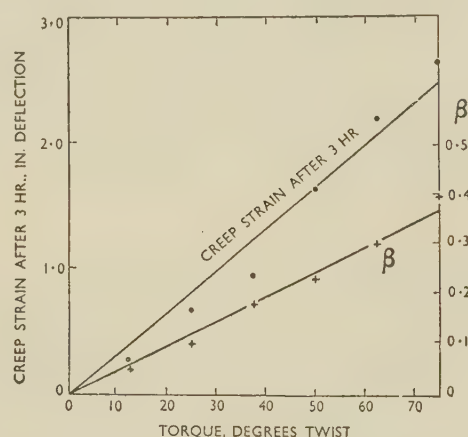


FIG. 2.—Influence of Applied Torque on Creep Strain for Specimens with 97.2% Rolling Reduction. Annealed for 1 hr. at 300° C.

examined, although plotting on double logarithmic paper shows that the strain is more accurately proportional to the torque to the power of 1.30. Analyses of the creep curves in terms of the expression  $\beta t^n$  yielded the values of  $\beta$  and  $n$  given in Table II, from which it is seen that  $n$  is sensibly constant and  $\beta$  is proportional to the torque. The values of  $\beta$  are plotted against torque in Fig. 2. In torsion tests of this character, interpretation of the results is much simplified if the maximum shearing stress is within the range in which the creep strain is linearly proportional to the stress, since the stress distribution along the radius of the test sample will not then vary during the course of the test. Except in two tests on a single crystal specifically referred to later, all the subsequent tests were carried out with  $50^\circ$  twist of the torsion wire.

## 2. SHAPE OF THE CREEP CURVE

Many attempts have been made to derive, either theoretically or empirically, mathematical expressions which represent the shape of a creep curve. Perhaps the most widely accepted formula, at least for pure metals, is that proposed by Andrade,<sup>7</sup> which for a tensile test under constant stress has the form:

$$l = l_0 (1 + \beta t^{\frac{1}{3}}) e^{\kappa t}$$

where  $l$  is the length of the test-bar and  $l_0$  a constant. For a uniform-stress torsion test, which involves no change in shape of the specimen with progressive strain, the formula can be expressed in the form given by Cottrell and Aytakin<sup>8</sup>:

$$\gamma = \gamma_0 + \beta t^{\frac{1}{3}} + \kappa t$$

where  $\gamma$  is the torsional strain and  $\gamma_0$  a constant, and this will also apply in the case of torsion of a solid rod, provided that the strain is proportional to the stress. The Andrade formula has been shown to apply reasonably accurately to a wide variety of materials at various stresses and temperatures of test. Several formulæ for transient creep have been derived from considerations of the theory of the movement of dislocations in crystal lattices, notably those by Orowan<sup>9</sup> and by Mott and Nabarro,<sup>10</sup> which reduce, under certain conditions, to the transient component of the Andrade formula, i.e.  $\gamma = \beta t^{\frac{1}{3}}$ , but wide confirmation of the applicability of these theoretical formulæ is lacking. Other workers have suggested that creep curves are closely represented by a simple power law of the type:

$$\gamma = \gamma_0 + \beta t^n$$

and this approach has been strengthened by a recent paper by Bhattacharya, Congreve, and Thompson,<sup>11</sup> who showed that it was applicable over a wide range of stresses and temperatures to several metals, although some deviation was apparent at the very early stages of a test. Johnson and Frost<sup>12</sup> have also shown recently that a formula involving two power terms of this type closely fits the creep properties, between 20° and 250° C., of an aluminium alloy.

Examination of all the creep curves determined in the present work has shown that they are very closely represented by the simple power law, and although the exponent of time is usually near to  $\frac{1}{3}$ , the best agreement is obtained if it is chosen arbitrarily. When this exponent was  $\frac{1}{3}$  or greater, the constants of the Andrade formula could be adjusted to give a close fit with the experimental curve, although the agreement was not quite as satisfactory as could be obtained with the simple power law. A comparison of a typical experimental curve and calculated curves is shown in Fig. 3; this relates to sample No. G 58, which was reduced 97.2% in area by cold working and was annealed for 141 hr. at 200° C. before test, to ensure that the shape of the curve was not disturbed by any annealing occurring during test. In this case, as in the remainder of the experiments, the first strain reading, made 5 sec. after the application of the

stress, was initially taken as the strain zero, and the strain increments were plotted against time on double logarithmic paper. This usually gave a very close approximation to a straight line, except for the readings made within the first 1 or 2 min. and, by extrapolation, a value for the creep strain at 5 sec. could be obtained. Correction of all the strain readings by this amount then usually yielded a very satisfactory straight line, although sometimes a second approximation was required. The adjustment for strain in the first 5 sec. was always small compared with the subsequent strain, and when, as is done later in this work, the strain at 3 hr. is taken as a measure of the amount of creep, the correction is of little significance. When  $n$  was lower than  $\frac{1}{3}$ , it was impossible to obtain close agreement by adjustment of the Andrade constants. This is illustrated in Fig. 4, for specimen No. C 37, which was reduced by 75% by cold working and was annealed for 1 min. at 500° C. A good fit is obtained with the power law with  $n = 0.17$ , but with  $n = \frac{1}{3}$  agreement is poor, and could only be improved in the early stages of the test with negative values of  $\kappa$ , which would lead to a decreasing creep strain at longer times.

It was stated in the introduction that the concept of viscous grain boundaries leads to the expectation, in a sample consisting of uniform equi-axed grains with constant boundary viscosity, of a creep curve of an exponential form. The time constant  $k$  will be inversely proportional to the grain-size  $x$ , so that the expression becomes:

$$\gamma = \gamma_0 (1 - e^{-mt/x})$$

If, however, the grain-size is not uniform, the creep curve could be expressed as the summation of a series of such terms, i.e.:

$$\gamma = \int \gamma_0 (1 - e^{-mt/x}) \cdot f(x) \cdot dx$$

where  $f(x)$  is a distribution function for the volume of material having grain-size  $x$ . A similar distribution function for the viscosity of the grain boundaries could be introduced, but recent work<sup>13</sup> has indicated that grain-boundary properties are roughly constant over a wide range of relative orientations of the adjacent grains and depart seriously from this level only when the orientations of the grains approach each other. With the normal random distribution of grain orientations, it is unlikely that variation in grain-boundary viscosity could have any appreciable effect on the shape of the creep curve. Reverting to the variation of grain-size, distribution functions of the form  $f(x) = x^n$  have been tried, and it appears that approximate agreement with the observed shape of curve could be obtained if  $n$  is about  $-1$  and the integration is carried out over a range of variation in grain-size of 100 times. Such a distribution of grain-size is most unlikely, for it implies that the total volume of grains of a given small range of sizes is proportional to the reciprocal of the grain diameter, i.e. there would be a vast preponderance of the smallest grains of the total range considered. A



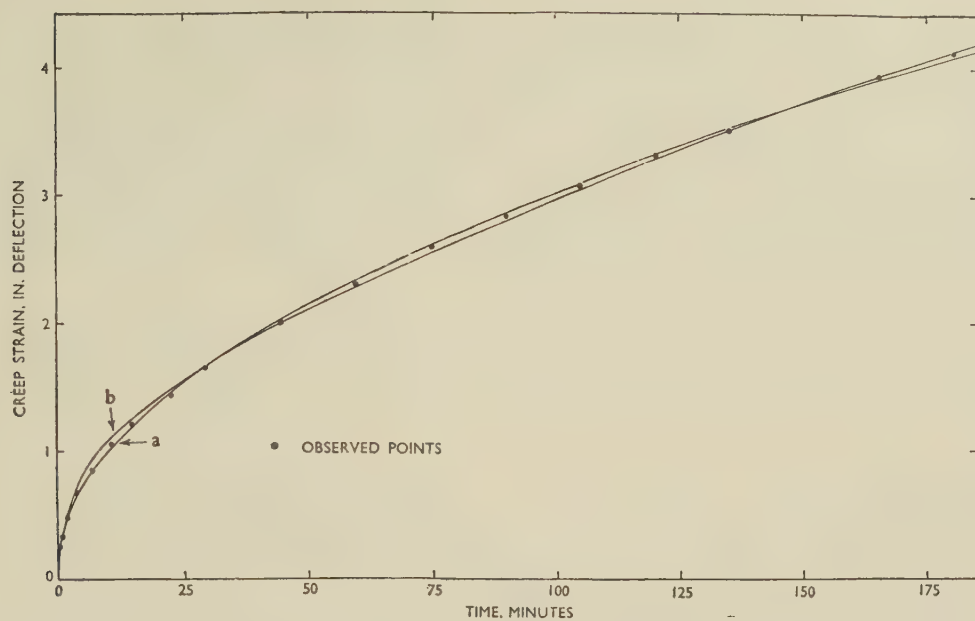


FIG. 3.—Experimental Creep Strains for Sample No. G 58 Compared with Expressions giving Closest Fit of Form : (a)  $\gamma = 0.305 t^{0.5}$ ; (b)  $\gamma = 0.453 t^{1/3} + 0.0088 t$ .

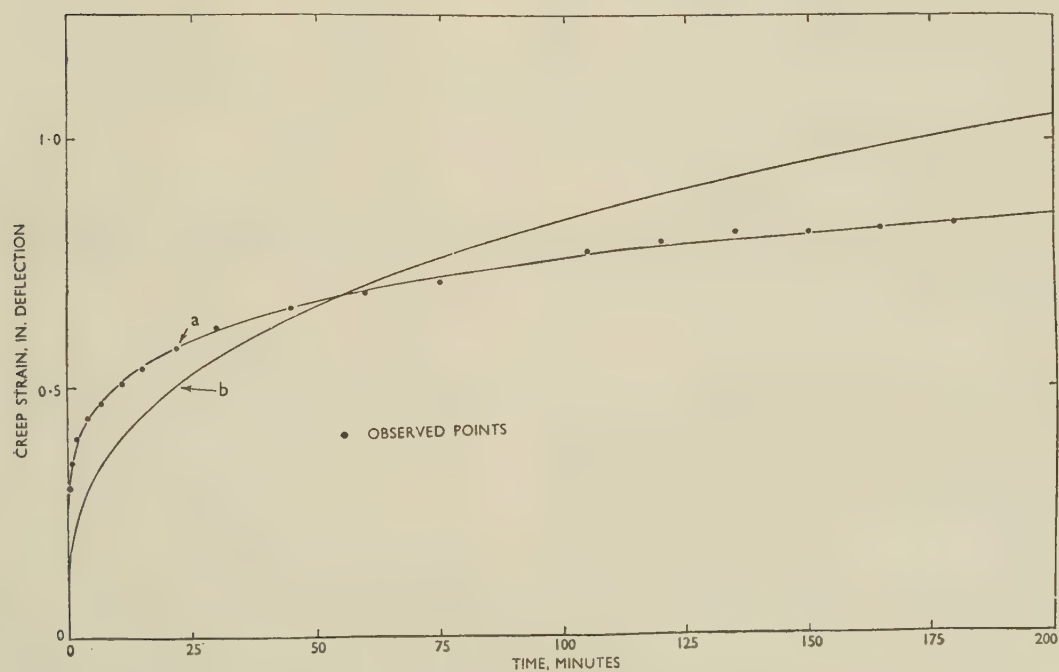


FIG. 4.—Experimental Creep Strains for Sample No. C 37 Compared with Expressions giving Closest Fit of Form : (a)  $\gamma = 0.345 t^{0.17}$ ; (b)  $\gamma = 0.18 t^{1/3}$ .

reduction of the range of grain-sizes over which the integration is carried out would require that the distribution function should increase still more the proportion of small grains. In view of the very unlikely distribution factors required, it was decided that the observed form of creep curve could not be explained as the sum of exponential curves.

In the analyses of the shape of creep curves, consideration of recovery of creep is helpful. Johnson and Frost<sup>12</sup> have recently shown, for an aluminium alloy, that recoverable creep was expressed by a

in shape to the first, but at a lower strain level. A similar analysis of the results for sample No. A 1, for which the forward creep continued for 50 hr., also showed that the recovery creep did not follow a simple power law. Mathematically it is not to be expected that such a law would apply, for the recovery creep is limited by the extent of the prior forward creep, whereas the simple power term can increase to infinity. It appears reasonable, however, to consider recovery creep as proceeding under a decreasing stress in a manner similar to that observed in relaxation

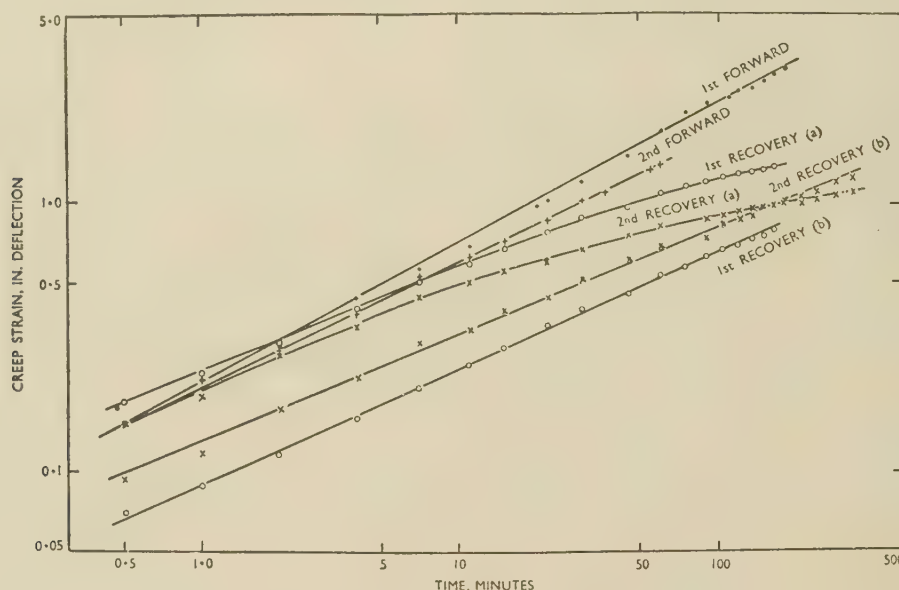


FIG. 5.—Forward and Recovery Creep Results for Sample No. H 65: (a) Creep Strain,  $\gamma_R$ ; (b)  $\frac{\gamma_R}{\gamma_F - \gamma_R}$ .

formula of the type  $\gamma_R = K_2 t^{m_2}$ , and that the forward creep was composed of the sum of this term and another similar one representing non-recoverable creep, i.e.:

$$\gamma = K_1 t^{m_1} + K_2 t^{m_2}$$

The period of forward creep was sufficient to carry the test into the region of constant creep rate, and the recovery creep term became constant within this region. Attempts were made to fit the pure aluminium torsion-creep curves to a formula of this type, but it was found that the recovery creep curves were not a simple power function of time and that the forward creep curves were, in general, quite satisfactorily represented by a single power term. Fig. 5 shows the results for sample No. H 65, which was annealed at 200° C. for 165 hr. before test, the log creep strain being plotted against log time. The first forward creep curve, as stated earlier, could be plotted as a straight line, but the recovery curve, after 3 hours' forward creep, did not give a straight line. A second forward curve, determined after 20 hours' recovery, again gave a straight line, with essentially the same slope as the first one, and after 1 hour's forward creep the second recovery curve was similar

tests. Consider that the creep process is governed by a power law of time and is linearly related to the stress, i.e.:

$$\gamma = \beta \cdot S \cdot t^n$$

The effective stress at any time in the recovery test will be proportional to the unrecovered portion of the forward creep strain, so that we can write:

$$\gamma_R = \beta(\gamma_F - \gamma_R)t^n$$

or

$$\frac{\gamma_R}{\gamma_F - \gamma_R} = \beta t^n$$

where  $\gamma_F$  is the forward creep strain at which the stress was removed, and  $\gamma_R$  is the recovery creep strain. The results for sample No. H 65 were analysed in this manner, the expression  $\gamma_R/(\gamma_F - \gamma_R)$  being plotted against  $t$  on double logarithmic paper, and satisfactory straight lines were obtained for each of the recovery curves. These are shown in the plots marked (b) in Fig. 5. The slopes of the two recovery creep lines were essentially the same, but were lower than those for the forward creep lines, the values of  $n$  being 0.53 and 0.47 for the forward curves and 0.43 and 0.39



for the recovery curves. Similar agreement was found for the results on sample No. A 1, except that in this case the exponent was slightly higher for the recovery curve than for the forward creep curve, 0.44 compared with 0.39.

The recovery creep curves were also examined on the basis of superposition theory, as originally put forward by Boltzmann.<sup>14</sup> If the forward creep follows the expression  $\gamma = \beta t^n$ , the superposition theory indicates that the recovery curve would be of the form:

$$\gamma_{F_1} - \gamma_R = \beta[(T_1 + t)^n - t^n]$$

where  $T_1$  is the period of action of the forward creep stress. Similarly if, after recovering for a time  $T_2$ , the stress is re-applied for a time  $T_3$ , the second recovery curve will be of the form:

$$\gamma_{F_2} - \gamma_R = \beta[(T_1 + T_2 + T_3 + t)^n - (T_2 + T_3 + t)^n + (T_3 + t)^n - t^n]$$

The experimental recovery creep strains for specimen No. H 65 were plotted against the appropriate functions of time, which were calculated using the value of  $n$  derived from the initial forward curve, as shown in Fig. 6. Very satisfactory straight lines were obtained.

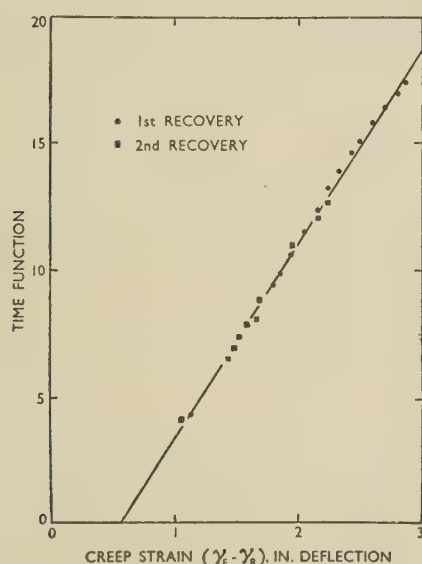


Fig. 6.—Creep Recovery Results for Sample No. H 65 Plotted against Appropriate Time Function from Superposition Theory.

The two sets of recovery readings fall on the same straight line, but the slope of the line indicated that  $\beta$  had fallen from 0.17, for the first forward curve, to 0.13. Moreover, the straight line did not pass through zero strain at zero time function (infinite  $t$ ), indicating that the forward creep strain was not all recoverable.

### 3. FACTORS INFLUENCING THE CREEP STRAIN

The concept that grain-boundary flow is the origin of the observed creep strain indicates that the creep

curves should be related to grain-size, the initial creep rate (but not the final creep strain) being inversely proportional to the grain diameter. Although the shape of the creep curves did not appear to conform to the theory of viscous grain boundaries, an investigation of the effect of grain-size variation on the creep behaviour was planned. Unfortunately the grain-size of a metal cannot be varied without changes in the cold-working or annealing conditions, which in themselves may influence the shape of the creep curve. It was, therefore, considered desirable to investigate the effects of variations in degree of cold working, and of time and temperature of annealing, on the creep properties, and to make parallel measurements of hardness and of grain-size, in the hope that it would be possible to determine the factors controlling creep behaviour.

#### (a) Influence of Cold-Working Reduction

Tests were carried out without any prior annealing treatment on samples from the batches of material which had undergone different cold-working reductions. It will be shown later that annealing takes place at the test temperature of 200° C., although this is relatively slow. The tests were, therefore, begun as soon as possible after the samples had reached the test temperature and become stabilized, and, to ensure uniformity, the total period from inserting in the furnace to the beginning of the test was fixed at 3 hr. The results obtained are given in Table III, and in Fig. 7 are plotted against the reduction of

TABLE III.—Influence of Cold Work on Creep Strain.

Bar	Anneal	Hardness, D.P.N.	Grain Dia., mm.	$\ln(A_0/A)$	Creep Strain, Deflection, in.		$\beta$	$n$
					1 hr.	3 hr.		
C 39	1 hr. at 500° C.	15.2	0.32	0	0.50	0.58	0.27	0.14
F 51	Nil	...	...	0.17	0.95	1.44	0.16	0.37
E 50	"	23.2	0.60	0.35	1.37	2.12	0.27	0.40
D 36	"	30.9	0.54	0.71	2.58	4.14	0.44	0.43
O 41	"	...	...	1.39	3.87	6.48	0.56	0.47
B 31	"	...	...	2.20	6.20	10.08	0.87	0.48
G 44	"	28.3	0.05	3.58	10.43	25.00	1.79	0.50

area and the expression  $\ln(A_0/A)$ . It will be seen that, except for sample G 44, which had undergone the highest reduction, a very satisfactory linear relationship between the creep strain and the expression  $\ln(A_0/A)$  is obtained. X-ray and microscopic examination of the samples after test indicated that in the case of sample G 44 the material had recrystallized during test, and this fact possibly explains the anomalously high creep strain observed in that case. On the other hand, this batch of material was annealed, before the cold work, for 1½ hr. at 450° C., compared with 1 hr. at 500° C. for the other batches, and this may have resulted in a generally higher level of cold work than is represented by the subsequent reduction. Glancing-incidence-rotation X-ray photographs, taken before and after the creep test, showed that consider-

able preferred orientation existed in all the specimens of the series, mainly with the [111] direction parallel to the axis of the rod, but with a small proportion of [100] also. The direction or amount did not alter appreciably during the creep experiment.

The hardness values given in Table III indicate the increasing hardness which would be expected with

essentially constant except for the sample annealed at 200° C. A similar series of tests was carried out on

TABLE IV.—Influence of Annealing Temperature on Creep Strain.

Bar	Cold-Working Reduction, %	Anneal	Hardness, D.P.N.	Grain Dia., mm.	Creep Strain, Deflection, in.			$\beta$	n
					1 hr.	3 hr.	50 hr.		
A 1	ca. 95	1 hr. at 300° C.	16.4	0.07	0.97	1.35	3.22	0.29	0.30
A 2	ca. 95	1 hr. at 400° C.	15.9	0.22	0.74	0.99	2.13	0.26	0.26
A 3	ca. 95	1 hr. at 445° C.	15.7	0.35	0.58	0.72	1.31	0.26	0.20
A 9	ca. 95	1 hr. at 450° C.	17.0	0.43	0.60	0.72	1.18	0.31	0.16
A 4	ca. 95	1 hr. at 500° C.	16.0	0.64	0.58	0.68	1.07	0.30	0.15
A 5	ca. 95	1 hr. at 550° C.	15.8	1.19	0.38	0.38	0.52	0.23	0.10
A 6	ca. 95	1 hr. at 600° C.	15.8	0.89	0.36	0.37	0.52	0.21	0.11
G 58	97.2	141 hr. at 200° C.	23.0	0.02	2.41	4.10	...	0.35	0.48
G 55	97.2	3 hr. at 302° C.	16.7	0.06	0.88	1.26	...	0.24	0.31
G 62	97.2	3 hr. at 400° C.	15.2	0.53	0.48	0.61	...	0.21	0.21
G 61	97.2	2 hr. at 500° C.	14.6	1.05	0.32	0.39	...	0.15	0.23
G 59	97.2	1 hr. at 610° C.	15.1	2.47	0.23	0.29	...	0.10	0.20
F 51	15.4	145 hr. at 200° C.	19.7	0.66	0.42	0.56	...	0.14	0.28
F 63	15.4	3 hr. at 400° C.	15.0	1.05	0.29	0.34	...	0.14	0.16
F 24	15.4	1 hr. at 480° C.	16.8	0.63	0.47	0.55	...	0.15	0.25
F 29	15.4	1 hr. at 600° C.	...	1.13	0.27	0.34	...	0.12	0.18
F 30	15.4	1 hr. at 610° C.	16.0	1.58	0.30	0.38	...	0.12	0.20

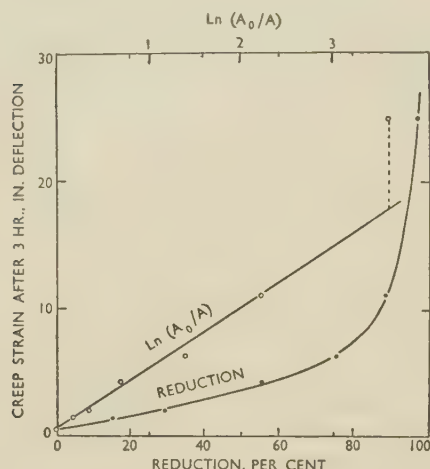


FIG. 7.—Creep Strain after 3 hr. of Unannealed Samples with Varying Amounts of Cold Work.

increasing cold work, although sample D 36 is out of line in this respect. The measurements of grain-size are, of course, of little significance, since the grains were not equi-axed after cold working. Hardness and grain-size measurements are not available for all specimens, since a few were used later for other tests after annealing.

#### (b) Influence of Annealing Temperature

The influence of annealing before the creep tests was first investigated on material of batch A, prepared before the importance of the amount of cold working was appreciated, and consequently an accurate determination of the reduction of area had not been made. Samples of this batch of material were annealed for 1 hr. each at temperatures varying between 300° and 600° C.; the results are recorded in Table IV. The creep strain falls steadily with increase of annealing temperature and, in general, there is a corresponding rise in grain-size, although sample A 6 falls out of line. The hardnesses all lie between 15.7 and 17.0, with no indication of a fall with rise in annealing temperature. It was realized from the results of subsequent work that an annealing time of 1 hr. was not sufficient to obtain equilibrium at the lower temperatures, and this series was later repeated, using batch G with a 97.2% reduction of area and with the annealing times increased at the lower temperatures to periods which had been shown to be adequate. The results of these tests are also given in Table IV and are plotted in Fig. 8. Again a steady fall of creep strain and a corresponding increase in grain-size follows the rise in annealing temperature, while the hardnesses are

material which had had a reduction of area of 15.4%; the results are given in Table IV. In this case the creep strain was always low, and only a general indication of reduction of creep with rise in annealing temperature was apparent. The grain-size was always large, although it varied irregularly from sample to sample within the range 0.63–1.58 mm. No relation

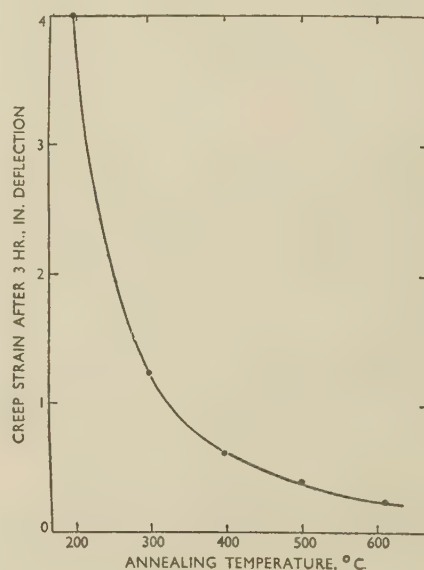


FIG. 8.—Creep Strain after 3 hr. of Samples of Batch G after Fully Annealing at Various Temperatures.

between the grain-size and the creep strain was apparent. The sample annealed at 200° C. was significantly harder than those annealed at higher temperatures.

Glancing-incidence-rotation X-ray photographs taken on all the specimens in these series showed that there was considerable preferred orientation of the [100] direction and slight preferred orientation of the



[111] direction parallel to the rod axis. Thus it appears from the X-ray results already given in the previous section that annealing before test changes the preferred orientation from mainly [111] and slight [100] parallel to the rod axis to mainly [100] and slight [111]. Both treatments of 141 hr. at 200° C. and of 1 hr. at 300° C. were sufficient to bring about this change, and increasing the temperature or duration of annealing had no further effect.

(c) Influence of Time of Annealing

It became apparent during some early tests on unannealed samples that the samples were undergoing annealing while being held at the test temperature of 200° C. In order to investigate the manner in which this was occurring, three series of tests were carried out at annealing temperatures of 200°, 302°, and 500° C. For the first two series material of batch G with a reduction of 97·2% was used, and the third series of tests was made on material of batch C reduced by 75%. The annealing times of different samples were

TABLE V.—Influence of Annealing Time on Creep Strain.

Bar	Cold-Working Reduction, %	Anneal	Hardness, D.P.N.	Grain Dia., mm.	Creep Strain, Deflection, in.		$\beta$	$n$
					1 hr.	3 hr.		
G 44	97·2	Nil	28·3	...	10·43	25·0	1·79	0·50
G 45	97·2	3½ hr. at 200° C.	27·4	...	9·90	17·4	1·17	0·52
G 48	97·2	8½ hr. at 200° C.	27·1	...	7·02	12·7	0·78	0·54
G 54	97·2	26 hr. at 200° C.	23·3	...	5·18	9·2	0·61	0·52
G 47	97·2	46 hr. at 200° C.	23·9	...	4·28	7·1	0·63	0·42
G 58	97·2	141 hr. at 200° C.	23·0	...	2·41	4·1	0·31	0·50
G 56	97·2	3 min. at 302° C.	19·9	0·02	4·18	7·60	0·45	0·55
G 52	97·2	10 min. at 302° C.	18·5	0·03	1·94	3·17	0·34	0·44
G 57	97·2	20 min. at 302° C.	18·0	0·05	1·32	1·99	0·29	0·37
G 53	97·2	1 hr. at 302° C.	16·9	0·05	1·10	1·63	0·24	0·37
G 55	97·2	3 hr. at 302° C.	16·7	0·06	0·88	1·26	0·24	0·31
C 41	75·0	Nil	...	...	3·87	6·48	0·56	0·47
C 37	75·0	1 min. at 500° C.	14·8	0·28	0·68	0·82	0·34	0·17
C 38	75·0	10 min. at 500° C.	15·4	0·50	0·60	0·73	0·29	0·18
C 39	75·0	1 hr. at 500° C.	15·2	0·32	0·50	0·58	0·27	0·14
C 40	75·0	10 hr. at 500° C.	14·9	0·59	0·52	0·61	0·27	0·15

varied over a suitable range at each temperature, the treatments at 302° and 500° C. being carried out in molten liquid baths, so that short annealing times, of the order of 1 min., could be obtained with a reasonable degree of accuracy. The results obtained are recorded in Table V, and for temperatures of 200° and 302° C. are plotted in Fig. 9. The curves are typical of published annealing curves for other properties such as hardness, thermoelectric power, &c., in which the measured property falls rapidly at first and finally becomes steady at a residual value which is lower the higher the annealing temperature. The hardness values show a similar trend at the three temperatures. At 302° C. increasing times of annealing result in progressive increase in grain-size, but at 200° C. the grains were always small and had not fully recrystallized. It was, therefore, impossible to make measurements of grain-size. The change in preferred orientation on annealing described in the previous section

was confirmed in X-ray photographs of these series. In the case of annealing at 200° C., the change was completed in approximately 5 hr., whereas the corresponding figure at 302° C. was approximately 3 min. The grain-sizes after annealing at 500° C. were irregular and were not related to the measured creep strains. They were too coarse for any interpretation of X-ray photographs.

The process of recovery of a cold-worked metal has been dealt with by various authors (van Liempt,<sup>15</sup> Krupkowski and Balicki,<sup>16</sup> Burgers,<sup>17</sup> Cook and Richards<sup>18</sup>), and the work has been summarized by Brindley.<sup>19</sup> The simplest suggestion is that recovery is a single-stage process, in which rate of recovery at any moment is proportional to the fraction of cold-worked metal remaining and to an activation term

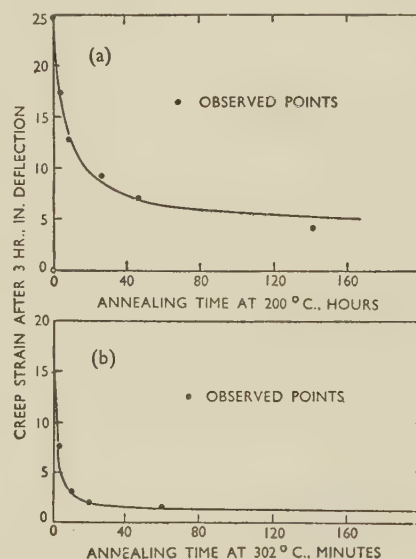


Fig. 9.—Creep Strain/Annealing Curves for Batch H.

$$(a) \frac{1}{\gamma - 4.25} = \frac{1}{25 - 4.25} + 0.0075t$$

$$(b) \frac{1}{\gamma - 1} = \frac{1}{25 - 1} + 0.046t$$

$e^{-Q/RT}$ . Thus if the physical property  $P$ , the recovery of which is being observed, is proportional to the amount of cold-worked metal present, we have :

$$-dP/dt = c \cdot P \cdot e^{-Q/RT}$$

and at a constant temperature

$$P = P_0 \cdot e^{-ct}$$

or

$$\ln (P/P_0) = -ct$$

Cook and Richards suggested that recovery and recrystallization form a two-stage process which leads to the expression :

$$\ln (P/P_0) = -ct^2$$

for isothermal treatment. The observed values of creep strain were examined in the light of these suggestions, plotting  $\log (\gamma/\gamma_0)$  against  $t$  on double

logarithmic paper, but straight lines did not result, and in any case the approximate slope of the curves indicated an exponent for  $t$  in the region of 0.5, so that the results did not agree with either of the suggested formulæ.

An alternative formula for recovery, based on an assumed linear relationship between the activation energy for dislocations and their density, has been proposed by Kuhlmann, Masing, and Raffelsieper,<sup>20</sup> and independently by Cottrell and Aytakin,<sup>8</sup> and this leads to the following relationship between the density of dislocations,  $N$ , and the time of annealing at any fixed temperature:

$$N = N_0 - K \log(t + t_0)$$

At the suggestion of Professor Cottrell, the curves relating the creep strain to the time of annealing were examined on this basis, but good agreement was not obtained.

If recovery is regarded as due to the reduction of the number of dislocations in the cold-worked metal, it would be expected, as was proposed by W. G. Burgers,<sup>17</sup> that this would be a consequence primarily of the combination of dislocations of opposite signs. Dislocations are thought to be composed of irregular mixtures of screw and edge dislocations, so that any one dislocation of a particular shape and extent would not be expected completely to cancel another. Nevertheless, in a statistical treatment of the problem, it is convenient to regard the complex dislocations as made up of unit lengths of simple dislocations which can completely cancel one another when of opposite signs, and in the subsequent discussion the term "number of dislocations" refers to the number of such unit lengths. It seems possible that the factor controlling the rate of combination of dislocations of opposite signs might be the chance of activated dislocations meeting, rather than the activation energy needed to move a dislocation from a stable position. If it is assumed that equal numbers of positive and negative dislocations exist in the cold-worked condition, the rate of decay of dislocations will then be proportional to the square of the total number of dislocations, i.e.:

$$-dN/dt = \alpha N^2$$

$$\text{or} \quad \frac{1}{N} = \frac{1}{N_0} + \alpha t$$

On the assumption that the observed creep strain was proportional to the number of dislocations present in the metal, attempts were made to fit the results to an expression of this type, but good agreement was not obtained, largely because of the finite creep strain still observed after relatively long periods of annealing. The implication was that some of the dislocations which gave rise to the creep strain could not be thermally activated to allow them to combine with dislocations of the opposite sign. A modified formula of the type:

$$-dN/dt = \alpha(N - x)^2$$

was therefore tried,  $x$  being the number of dislocations not available for combination. This leads to the formula:

$$\frac{1}{N - x} = \frac{1}{N_0 - x} + \alpha t$$

By choice of  $x$  to correspond with the creep strain observed after long annealing, it was found possible to obtain excellent agreement with the observed curves, although the value of  $x$  fell as the annealing temperature rose. This is quite reasonable, since a higher annealing temperature would be expected to activate dislocations which are too firmly anchored to be mobile at lower temperatures. The good agreement between the last formula and the observed curves is illustrated in Fig. 9.

The assumption that equal numbers of positive and negative dislocations are present in the cold-worked material cannot be strictly true in the case of inhomogeneously strained material, for it is known that polygonization is due to the alignment of the excess dislocations of a single sign after combination has proceeded as far as possible. If the numbers of the dislocations of opposite signs are initially  $N_1$  and  $N_2$ , the rate of combination, as in the Law of Mass Action controlling the rate of reaction of chemical molecules, is proportional to the product  $N_1 N_2$ , i.e.:

$$-dN/dt = \alpha N_1 N_2$$

A reasonably close fit to the experimental values for any one of the annealing temperatures could be obtained on the basis of this formula, but the final value after long annealing would be dependent on the original excess of one type of dislocation and should, therefore, be independent of the annealing temperature. It was thought that this difficulty might be overcome by introducing a further term for the rate of decay of dislocations during annealing, proportional to the number present. This term could be regarded as representing the diffusion of dislocations to positions of stability from which they could not be removed by the stress applied during the creep test. The equation then becomes:

$$-dN/dt = \alpha N_1 N_2 + \beta(N_1 + N_2),$$

the solution of which again gave a formula which, by suitable choice of constants, fitted very closely the experimental values for any one annealing temperature, but constant values of  $N_1$  and  $N_2$  for the cold-worked state still would not give agreement with the annealing curves for all temperatures.

#### (d) *Influence of Prior Plastic Strain*

The close correlation found between the creep strain and the degree of reduction in cold working, and the agreement of the curves of creep strain relative to annealing time with a plausible formula based on the reduction of the number of dislocations by a process of combination, suggested that the observed creep might be due solely to dislocations



originally present in the sample. On this basis it was considered that the amount of creep observed with a highly annealed sample should be increased by a small amount of plastic strain before the creep test. If the creep were due solely to grain-boundary flow, such an effect would be less likely to be observed, although it might be argued that plastic strain, even though due to slip within the grains, could influence the effective viscosity of the boundaries. To investigate this effect, several samples, all initially annealed together for 1 hr. at 600° C., were subjected to progressively increasing amounts of plastic torsion by completing the specimen assembly and turning the lower shackle through a known angle while at room temperature. The creep test was then carried out under the standard conditions, and was begun as soon as the test temperature was reached and stabilized, the total time required being standardized at 3 hr. The results obtained are recorded in Table VI. Although creep strain did not increase progressively with increasing amounts of plastic strain, all the strained samples gave higher creep strains than the unstrained specimens, the increase being approximately two-fold for the largest amount of plastic deformation. With the hope of obtaining more regular results, a similar series of tests was carried out on a single

TABLE VI.—*Effect of Cold Plastic Strain Before Creep Test.*

Bar	Cold-Working Reduction, %	Anneal	Plastic Twist of Bar, degrees	Grain Dia., mm.	Creep Strain, Deflection, in.		$\beta$	$n$
					1 hr.	3 hr.		
H 68	97.2	1 hr. at 600° C.	0	2.04	0.24	0.29	0.13	0.17
H 69	97.2	" "	30	1.87	0.30	0.36	0.15	0.16
H 70	97.2	" "	90	1.81	0.28	0.34	0.13	0.19
H 71	97.2	" "	180	1.79	0.38	0.52	0.12	0.28
H 72	97.2	" "	360	1.79	0.40	0.54	0.13	0.27
D 32	55.6	1 hr. at 600° C.	0	...	0.32	0.37	0.16	0.18
			30	...	0.47	0.56	0.14	0.24
			90	...	0.47	0.56	0.14	0.24
			180	...	0.56	0.75	0.26	0.19
			360	...	0.58	0.80	0.31	0.17

sample, the forward creep after each stage being allowed to recover over a period of about 24 hr; this allowed almost complete recovery to occur. The results are included in Table VI. A close correlation between the two series was obtained, and it appears that the check in the increase of creep strain at approximately 90° plastic strain may be real. A similar effect has been obtained by other workers, in relations between hardness and amount of cold work.

#### (e) Influence of Grain-Size

Much of the work already described had indicated that, although the amount of creep strain observed with any sample was not rigorously related to the grain-size, there was a general tendency for the creep strain to be lower with the samples of larger grain-size. In order to examine this factor more closely, samples were prepared by annealing in different ways material

which had undergone varying amounts of cold work, thus producing, by different strain-annealing processes, specimens having similar grain-sizes. By including specimens which have already been described under different headings, three groups, each consisting of specimens having similar grain-sizes, were obtained. The creep test results of these are quoted in Table VII.

TABLE VII.—*Influence of Grain-Size on Creep Strain.*

Bar	Cold-Working Reduction, %	Anneal	Grain Dia., mm.	Hardness, D.P.N.	Creep Strain, Deflection, in.		$\beta$	$n$
					1 hr.	3 hr.		
B 20	88.9	1 hr. at 610° C.	0.74	...	0.33	0.38	0.19	0.14
C 41	75.0	1 hr. at 610° C.	0.70	14.8	0.34	0.40	0.19	0.14
E 21	29.2	1 hr. at 570° C.	0.78	15.7	0.25	0.30	0.13	0.15
F 27	15.4	1 hr. at 295° C.	0.69	19.8	0.31	0.43	0.08	0.31
A 9	ca. 95	1 hr. at 450° C.	0.48	17.0	0.60	0.72	0.31	0.16
D 23	55.6	1 hr. at 530° C.	0.45	15.1	0.29	0.35	0.14	0.17
E 25	29.2	1 hr. at 425° C.	0.42	16.3	0.35	0.41	0.19	0.15
G 62	97.2	3 hr. at 400° C.	0.33	15.2	0.48	0.61	0.21	0.21
A 3	ca. 95	1 hr. at 445° C.	0.35	15.7	0.58	0.72	0.26	0.20
B 22	88.9	1 hr. at 560° C.	0.52	16.2	0.50	0.55	0.17	0.14
C 39	75.0	1 hr. at 500° C.	0.52	15.2	0.50	0.58	0.27	0.14

Within each group of similar grain-size, the observed creep strains varied over a range of about 2 to 1, indicating that the creep strain under the standard test conditions is not dependent solely on grain-size. On the other hand, the average creep strain for each group of samples increases systematically with decrease in the average grain-size, confirming the general trend previously observed.

#### 4. PROPERTIES OF SINGLE CRYSTALS

Kê put forward, as one of his arguments in favour of the grain-boundary origin of the peak in the damping curve and of the creep strain, the fact that neither of these phenomena was observed in the case of a single-crystal specimen. However, the strength of this evidence was much reduced by the fact that his single crystal was of commercially pure aluminium, instead of the high-purity metal which he used for his polycrystalline specimens, and he showed elsewhere<sup>21</sup> that the peak in the damping curve was much lower with lower-grade than with high-purity aluminium. He did not state whether the single crystal which he used was prepared by a strain-annealing procedure, or was grown from the melt, but in either case it would have been subjected to a high-temperature anneal which, as the present work has shown, leads to low values of creep strain. To examine the behaviour of single crystals more closely and to compare their properties with those of similar polycrystalline material, a number of crystals, 15 in. long and  $\frac{1}{4}$  in. in dia., were grown by progressive solidification in a graphite mould, the material used being the  $\frac{1}{4}$ -in.-dia. drawn rod used for the work already described. After growth in this manner, all the crystals were annealed at 600° C. for 1 hr. before testing. The first experiment was carried out on a

crystal as grown, and, under the standard conditions of test, no creep strain, within the accuracy of observation, was detected after 50 hr. A plastic twist of 2.2° was then applied to the crystal, and the creep test was repeated. In this case a strain of 0.11 in. deflection was observed after 3 hr., a quite significant amount, although still less than had been found even for the most highly annealed polycrystalline rod. A second crystal was tested after abrading the surface with emery paper, the idea being that this treatment might introduce dislocations into the lattice which would lead to creep strain. However, no significant creep strain was observed under the standard test conditions. A third crystal was plastically strained 2% in tension at room temperature before test, but again no creep strain was observed.

A fourth crystal was tested, primarily to determine the minimum stress at which creep occurred. A stress/strain curve at 200° C. was first determined, with torque increments of 25° up to 200°, and thereafter of 10°, applied at approximately 1-min. intervals. The "limit of proportionality" was clearly defined at a torque of 240°. The test was concluded at a torque of 260°. After resting at 200° C. for 24 hr., to allow recovery to take place, a creep test was carried out at a torque of 220°, i.e. just below the short-time "limit of proportionality". The results are recorded in Table VIII. The test was continued for 50 hr.,

TABLE VIII.—*Creep Observations on Single Crystals.*

Sample	Condition	Stress, Degrees torque	Creep Strain, Deflection, in.		
			1 hr.	3 hr.	50 hr.
SC 1	(a) Annealed 1 hr. at 600° C.	50	0.01	0.01	0.01
	(b) Plastic twist 2.2°	50	0.06	0.11	...
SC 2	Abraded surface	50	0.01	0.02	...
SC 3	2% Linear plastic strain	50	0	0	...
SC 4	(a) After short-time test	220	0.03	0.11	0.31
	(b) After recovery from (a)	260	0.83	1.20	4.56
	(c) Annealed 68 hr. at 600° C.	50	0.01	0.03	...
	(d) Plastic twist 30°	50	0.16	0.24	...
	(e) " " 90°	50	0.13	0.23	...
	(f) " " 180°	50	0.17	0.38	...
	(g) " " 360°	50	0.16	0.29	...

and the bar was then allowed to recover at 200° C. for a further 50 hr. A second test was then carried out, at a torque of 260°, i.e. just above the "limit of proportionality". The creep strain observed at the higher torque was over 10 times that at the lower torque, and since the increase of torque was less than 20%, this observation is a clear indication of a "limiting creep stress". The crystal was then annealed for 68 hr. at 600° C., to restore it as closely as possible to its original unstrained condition, and the effect of plastic strain before the creep test was investigated.

The crystal was first tested without prior strain, and then after successively increasing amounts of plastic torsional strain, up to a total of 360°; the maximum torsional plastic strain is equivalent to a tensile strain of 3.3% in the surface layer of the rod. In these tests the creep strain was allowed to recover for

24 hr. after each period of forward creep, the recovery being essentially complete at each stage.

Results obtained on all the single crystals are summarized in Table VIII. It is clear from these figures that slight tensile strain of a single crystal does not promote creep strain under the conditions of test used, but that an equivalent torsional strain is effective. The explanation is probably that tensile strain takes place by pure slip, involving the generation and movement of dislocations right across the section of the crystal, so that after plastic straining they have reached the surface of the sample, where they remain anchored so far as small applied creep stresses are concerned. Torsional plastic strain, on the other hand, must involve dislocations remaining within the lattice, in order to accommodate the change in orientation along the length of the rod, and these are able to move under small stresses and so to produce creep strain. These suggestions are borne out by the Laue photographs shown in Fig. 10 (Plate XXII). The clusters of sharp spots given by the original unstrained crystal (Fig. 10 (a)), are unchanged after 2% tensile strain (Fig. 10 (b)), but become spread into a number of smaller spots after 360° torsional twist (Fig. 10 (c)).

#### IV.—DISCUSSION

The results provide evidence which, although not conclusive, points to the fact that the creep strain observed in the low-stress torsional tests described is due to distortion within the grains, rather than to viscous flow of the grain boundaries. The evidence against the mechanism of the creep being viscous flow of the boundaries is primarily that the shape of the creep curve obtained—a simple power function of the time—is widely different from the exponential curve to be expected from an assembly of uniform polyhedral grains with constant grain-boundary properties, and the curve could not be obtained by any reasonable distribution of grain-sizes or of grain-boundary viscosities. Furthermore, the theory that the grains are perfectly elastic, and the boundaries viscous, leads to the conclusion that the initial creep rate should be inversely proportional to the grain-size, and that the asymptotic value of creep strain at infinite time should be independent of grain-size. Creep tests of 50 hours' duration have shown no deviation from the power law, and there is thus no evidence of the strain reaching an asymptotic value. The results given in Table VII show that, while the exponent of time is reasonably independent of grain-size, there is a general, although not exact, trend for  $\beta$  to increase with reduction of grain-size. The creep strain throughout the whole period of the creep test will therefore tend to be higher with smaller grain-sizes, and there is no evidence of a common asymptote.

The results generally support the suggestion that the strain mechanism operating during the creep test is the movement of dislocations within the crystals, the density of dislocations at the beginning of the



test controlling the magnitude of the observed strain. The linear relationship between the creep strain after 3 hr. and the amount of cold work introduced after the last anneal provide important evidence in support of this theory. The fact that the time exponent  $n$  recorded in Table III increases somewhat with increasing amounts of cold work suggests that a linear relationship cannot apply to the strains at all times of test, but the markedly lower value of  $n$  for sample C 39, which received no cold work after annealing, points to a probable solution of this difficulty. It has been suggested<sup>12</sup> that creep curves can be expressed as the sum of two, or more, power terms of time. The curves of the cold-worked samples were, therefore, analysed in this manner, on the assumption that the term  $\beta_1 t^{n_1}$ , fixed by the results for sample C 39, was due to the residual strain after annealing, and that an additional term  $\beta_2 t^{n_2}$  was introduced by the cold work. The results obtained are given in Table IX and

TABLE IX.—Analysis of Results from Table III in Terms of the Expression  $\gamma = \beta_1 t^{n_1} + \beta_2 t^{n_2}$ .

Bar	$\ln(A_0/A)$	$\beta_1$	$n_1$	$\beta_2$	$n_2$
C 39	0	0.27	0.14	0	0
F 51	0.17	0.27	0.14	0.05	0.57
E 50	0.35	0.27	0.14	0.08	0.52
D 36	0.71	0.27	0.14	0.25	0.52
C 41	1.39	0.27	0.14	0.32	0.56
B 31	2.20	0.27	0.14	0.70	0.52
G 44	3.58	0.27	0.14	1.50	0.54

indicate that the exponent  $n_2$  is remarkably constant and that  $\beta_2$  is roughly proportional to the amount of cold work. The value of  $\beta_2$  for sample G 44 is rather high, probably owing to the term  $\beta_1 t^{n_1}$  being incorrect, in view of the different annealing treatment given to this batch of material before cold working.

The influence of annealing before test also conforms to the theory that the creep strain is due to the movement of pre-existing dislocations. The effect of increasing the annealing temperature is, of course, to reduce the number of remaining dislocations, and thus to reduce the magnitude of the creep, but more quantitative support is given by the isothermal annealing curves, which conform very closely to an expression based on the removal of dislocations by the combination of pairs of opposite sign. The influence of annealing on the constants  $\beta$  and  $n$  is not very clearly established, largely because there is a reasonable tolerance in the selection of the constants to give a good fit with the experimental curve, particularly in the case of well-annealed samples giving small creep strains. Nevertheless, there is some indication that with isothermal annealing increasing time reduces  $\beta$ , with little effect on  $n$ , but that with isochronal annealing at varying temperatures  $n$  falls with increasing temperature, and  $\beta$  is less affected.

The introduction, into a well-annealed test-bar, of slight plastic strain, insufficient to cause recrystallization during the creep test, has been shown to increase

the creep subsequently observed, which still conforms to the usual power law. This provides further evidence that the strain is due to the movement of dislocations. The similar observations on single crystals are particularly important in this respect, since the X-ray photographs confirm that a small tensile strain, which occurs by pure slip, without leaving residual distortion within the lattice, does not lead to subsequent creep, but that similar torsional strain, which leaves a slightly distorted lattice, results in creep.

Much further work is required in this field, particularly with regard to the effect of higher creep stresses. It is suggested that at the stress used for the present work the creep is due to the pre-existing dislocations only, but that with increasing stress a level is eventually reached at which either the applied stress itself or the movement of the existing dislocations leads to the generation of new ones. The creep strain is then related to a high power of the stress, and it is in this region of behaviour that the greatest practical interest lies, since all commercial creep-resisting alloys are used at such stress levels. Torsional methods are unsuitable for fundamental studies in this region of stress.

#### ACKNOWLEDGEMENTS

The author wishes to thank Mr. H. W. G. Hignett for many stimulating discussions during the course of the investigation and Mr. H. C. Rose for help with the experimental work. Thanks are also due to The Mond Nickel Co., Ltd., for permission to publish.

#### REFERENCES

1. D. Hanson and M. A. Wheeler, *J. Inst. Metals*, 1931, **45**, 229.
2. H. F. Moore, B. B. Betty, and C. W. Dollins, *Univ. Illinois Bull.*, 1935, **32**, (23).
3. W. A. Rachinger, *J. Inst. Metals*, 1952–53, **81**, 33.
4. D. McLean, *ibid.*, 1951–52, **80**, 507.
5. T.-S. Kê, *Phys. Rev.*, 1947, [ii], **71**, 533.
6. C. Zener, *ibid.*, 1941, [ii], **60**, 906.
7. E. N. da C. Andrade, *Proc. Roy. Soc.*, 1910, [A], **84**, 1.
8. A. H. Cottrell and V. Aytekin, *Nature*, 1947, **160**, 328.
9. E. Orowan, *J. West Scotland Iron Steel Inst.*, 1946–47, **54**, 45.
10. N. F. Mott and F. R. N. Nabarro, *Proc. Phys. Soc.*, 1940, **52**, 86.
11. S. Bhattacharya, W. K. A. Congreve, and F. C. Thompson, *J. Inst. Metals*, 1952–53, **81**, 83.
12. A. E. Johnson and N. E. Frost, *ibid.*, 1952–53, **81**, 93.
13. B. Chalmers, "Progress in Metal Physics", Vol. III, p. 298. 1952: London (Pergamon Press).
14. L. Boltzmann, *Pogg. Ann. Physik u. Chem.*, 1876, **7**, 624.
15. J. A. M. van Liempt, *Z. anorg. Chem.*, 1931, **195**, 366.
16. A. Krupkowski and M. Balicki, *Ann. Acad. Sci. Tech. Varsovie*, 1937, **4**, 270.
17. W. G. Burgers, *Proc. K. Ned. Akad. Wetensch.*, 1947, **50**, 452.
18. M. Cook and T. Ll. Richards, *J. Inst. Metals*, 1947, **73**, 1.
19. G. W. Brindley, *Phys. Soc.: Rep. Conf. on Strength of Solids*, 1948, 95.
20. D. Kuhlmann, G. Masing, and J. Raffelsieper, *Z. Metallkunde*, 1949, **40**, 241.
21. T.-S. Kê, *J. Appl. Physics*, 1949, **20**, 274.





# THE COPPER-SILICON EUTECTOID TRANSFORMATION\*

1508

By A. D. HOPKINS,† M.Sc.

## SYNOPSIS

Hardness and metallographic studies have been made of the eutectoid transformation in a copper-5% silicon alloy over the range 275°–500° C. The curve showing the temperature at which transformation begins against time has the usual C shape. The transformation is extremely sluggish. It is accompanied by an increase in hardness, and a small increase also takes place before any change is observable in the microstructure. Transformation at 400° C. gives rise to a pearlitic structure.

## I.—INTRODUCTION AND PREVIOUS WORK

INTEREST in eutectoid transformations generally was stimulated by the paper of Davenport and Bain<sup>1</sup> published in 1930. Their studies were extended by Mehl<sup>2</sup> and his co-workers to include quantitative measurements of nucleation and growth in iron-carbon alloys. While there exists considerable literature on the decomposition of austenite in both plain carbon and alloy steels, it is only recently that there have been extensive studies of eutectoid transformations in other systems, e.g. copper-aluminium (Mack<sup>3</sup> and Klier and Grymko<sup>4</sup>), copper-beryllium (Fillnow and Mack<sup>5</sup>), iron-nitrogen (Bose and Hawkes<sup>6</sup>), and aluminium-zinc (Garwood and Hopkins<sup>7</sup>).

The copper-silicon alloys<sup>8</sup> undergo a eutectoid transformation in which the  $\kappa$  solid solution containing 5.23% silicon transforms to the  $(\alpha + \gamma)$  solid solution at 552° C. The system is interesting in that the form of the equilibrium diagram<sup>11</sup> is unusual in the eutectoid region; the relevant portion of the diagram is given in

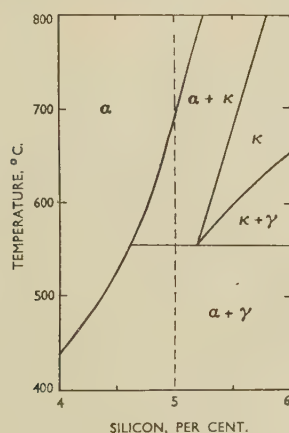


Fig. 1.—Eutectoid Region of Copper-Silicon System.

Fig. 1. Although it is possible to obtain a homogeneous  $\kappa$  structure by quenching alloys containing more

than 5.2% silicon, pro-eutectoid  $\gamma$  must separate before the remaining  $\kappa$  transforms to  $(\alpha + \gamma)$ . Alloys containing less than 5.2% silicon can be termed truly hypoeutectoid. Experimental work on the decomposition of the  $\kappa$  phase has not been extensive. In his paper on the constitution of copper-silicon alloys, C. S. Smith<sup>8</sup> observed that the transformation was extremely sluggish. Hibbard, Eichelman, and Saunders<sup>9</sup> studied the transformation of a hypereutectoid alloy containing 5.56% silicon and noted that decomposition of  $\kappa$  was preceded by the precipitation of Widmanstätten  $\gamma$ . The transformation products were shown to have none of the morphological characteristics generally associated with eutectoid transformations. Instead of a lamellar pearlitic product being formed, the structures generally consisted of particles of proeutectoid  $\gamma$  plus relatively large particles of  $\gamma$  set in a ground mass of  $\alpha$  solid solution. The transformation was shown to be slow, taking over a week for completion.

The paucity of experimental data on the kinetics of transformation in the copper-silicon system has stimulated the present work, in which the transformation of a hypo-eutectoid alloy has been studied to see whether the form of the transformation product is different from that obtained in hypereutectoid alloys.

## II.—EXPERIMENTAL PROCEDURE

### 1. CASTING

The alloy was made from high-purity cathode copper and high-grade silicon. The silicon, originally of 98% purity, was further purified by acid washing in the manner developed by Tucker.<sup>10</sup> The copper was melted in a Salamander crucible and the silicon added under a flux of sodium fluoride. The metal was chill cast, remelted, and cast again to yield an ingot 1 in. in dia. and weighing  $1\frac{1}{2}$  lb. The alloy was analysed by standard methods<sup>10</sup> and found to contain copper 95.0, silicon 5.0, and iron <0.02%.

\* Manuscript received 4 June 1953.

† G.K.N. Group Research Laboratory, Wolverhampton.

## 2. WORKING

After the extensive pipe had been removed, the ingot was lightly forged and homogenized by annealing for 24 hr. at 780° C. The circular bar was reduced to a flat strip, 0.2 in. thick, by a combination of rolling and forging at 780° C., and finally reduced to 0.1 in. by cold rolling without intermediate annealing. The cold-rolled strip was annealed for 36 hr. at 780° C. and water-quenched.

## 3. HEAT-TREATMENT

It was considered unnecessary to employ the orthodox technique of studying isothermal transformation, because of the sluggish decomposition of  $\kappa$  and the low critical cooling rate. The "classical" method generally adopted is to heat the specimen at the homogenization temperature to obtain the parent solid solution and then to transfer the specimen rapidly to another furnace maintained at the lower transformation temperature. The transformation can be arrested by removing the specimen and quenching it. In the present series of experiments it was possible to simplify this technique; the strip was water-quenched from 780° C. and then cut into small specimens which were heated at 275°, 330°, 375°, 400°, and 500° C., respectively, for various times. The heat-treatment was carried out in a nitrate salt-bath at all temperatures except 275° C., for which an air oven was used. Temperatures were maintained accurate to  $\pm 2^\circ$  C.

## III.—EXPERIMENTAL RESULTS

## 1. MICROSTRUCTURE

The specimens were mounted in Bakelite for micro-examination. The etching reagent was Smith's modified reagent of ammonia, hydrogen peroxide, and potassium hydroxide, except in the case of specimens containing pearlitic structures, for which acid ferric chloride was used as it gave better definition. The structure of the quenched untransformed material consisted of a ground mass of  $\alpha$  solid solution showing twinning. Though this structure was slow-etching and might be confused with a heavily twinned structure, Smith has conclusively shown that it is truly duplex. This point was confirmed during the present investigation, when it was found that as the transformation progressed the ground mass lost its heavily striated appearance, indicating that the plates of  $\kappa$  decomposed into  $\alpha + \gamma$ . After heat-treatment the structure was rapid-etching. Thus, the final structure consisted of the  $(\alpha + \gamma)$  eutectoid set in a matrix of  $\alpha$ , free from the heavily twinned appearance characteristic of the untransformed alloy.

On treatment at 500° C. particles of  $\gamma$  became visible at the boundaries of the grains after 2 hr. These particles grew, and the structure after 80 hr. was as shown in Fig. 2 (Plate XXIII). Fig. 3 (Plate XXIII) shows the appearance of the structure after one week

at 500° C.; the  $\gamma$  particles are much larger, although no more numerous. No lamellae are apparent, the structure consisting of particles of  $\gamma$  set in a ground mass of primary  $\alpha$  solid solution. After 21 days at this temperature, the breakdown of  $\kappa$  was almost complete; little trace of the Widmanstätten structure remained. The grain-boundary deposits were larger, and in a few areas a vaguely lamellar structure could be seen.

At 400° C. traces of  $\gamma$  were visible at the grain boundaries after 40 min. The grain-boundary deposit

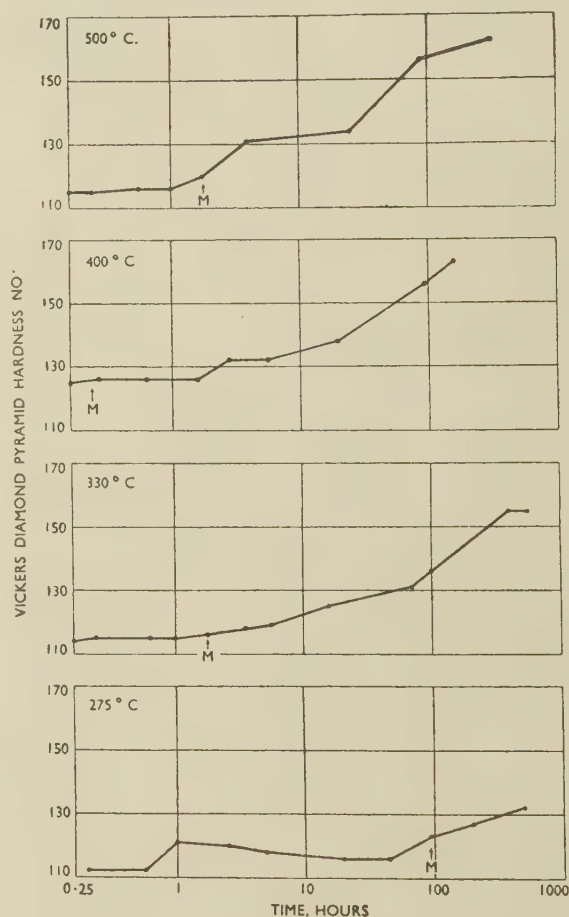


FIG. 9.—Variation of Hardness with Time of Transformation. M denotes first appearance of microstructural change.

was much finer than that obtained at 500° C. The structure after 5½ hr. at 400° C. is shown in Fig. 4 (Plate XXIII). No trace of a lamellar structure was seen until 21 hr. had elapsed, but after 93 hr. at 400° C. the pearlitic nodules were general and clearly visible (Fig. 5, Plate XXIII). After 172 hr. the structure was wholly pearlitic, in places coarse and partly spheroidized; a completely pearlitic area is shown in Fig. 6 (Plate XXIII).

Transformation began most rapidly at 375° C., grain-boundary deposits being visible after 20 min. At 330° C. decomposition at the grain boundaries began only after 1¼ hr. (Fig. 7, Plate XXIII). The



amount of transformation product had increased, and the structure showed pearlitic areas. Fig. 8 (Plate XXIII) (16 hr.) shows a structure typical of the earlier stages of transformation at all temperatures.

At 275° C. the transformation was even more sluggish. Grain-boundary deposits were visible after 96 hr. After 216 hr. the deposits of  $\gamma$  were relatively few and small in size. Because the time necessary for heat-treatment at this temperature was so long, the behaviour of the alloy below 275° C. was not investigated.

## 2. HARDNESS

The results of the Vickers diamond pyramid hardness tests (5-kg. load) are shown in Fig. 9. The points *M* denote the first appearance of  $\gamma$  in the structure. At all temperatures there is an increase in hardness after the transformation product becomes visible under the microscope. The total hardness change recorded at any particular temperature is relatively small, but it is probable that complete transformation has not been achieved within the period of an experiment. The increase in hardness during transformation is caused by the greater hardness of the  $\gamma$  of the transformation product. A smaller increase in hardness can be detected before precipitation becomes visible, indicating that some pre-precipitation processes are occurring within the parent solid solution. Since the hardness of the quenched untransformed material was 112 V.P.N., the increased hardness obtained before visible transformation took place can be ascribed to atomic movements occurring before decomposition of  $\kappa$ . The specimen treated at 275° C. showed a marked increase in hardness, followed by a drop, before the presence of the transformation product caused the hardness to increase again. No corresponding change was noted in the microstructure.

## IV.—CONCLUSIONS

The times required at each temperature for the transformation to begin, i.e. for the first trace of  $\gamma$  phase to appear in the microstructure, have been plotted in Fig. 10 on a log time base. The results yield a curve of the C-type found in similar studies of other eutectoid systems. Because the transformation is so sluggish at all the temperatures investigated, it is not possible to include a corresponding curve in Fig. 10 for its completion. Transformation starts most rapidly at 375° C., and this point forms the "nose" of the C curve. Within the range 400°–350° C. the transformation product is of a lamellar nature, and the structure can be described as pearlitic. The

growth mechanism in this temperature range is by group-nodules nucleated by particles of  $\gamma$ . At all temperatures the initial deposit of  $\gamma$  is in the form of relatively large particles. At later stages the particles become finer and show a greater tendency to take up a lamellar habit.

The separation of  $\kappa$  from  $\alpha$  takes place relatively rapidly. It was difficult to measure the time at which separation of  $\kappa$  began with accuracy, because, even in the water-quenched specimen, faint markings

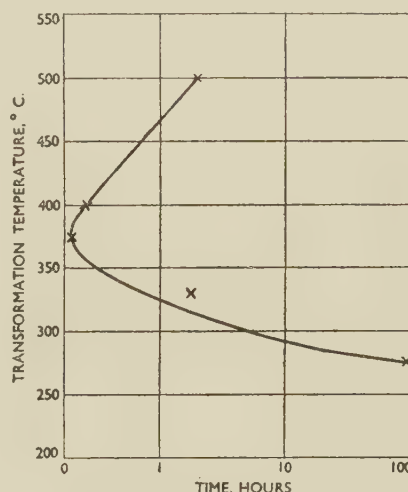


FIG. 10.—Time at Which Microstructural Change Begins.

were visible, although the structure was slow-etching. On transformation, however, even for 10 min., at all temperatures,  $\kappa$  precipitation became definite. The changes in hardness before the eutectoid decomposition begins are probably connected with this precipitation. Further work on this stage of the transformation would be of value, especially if X-ray techniques were used.

## REFERENCES

1. E. S. Davenport and E. C. Bain, *Trans. Amer. Inst. Min. Met. Eng. (Iron Steel Div.)*, 1930, 117.
2. R. F. Mehl, *J. Iron Steel Inst.*, 1948, 159, 113.
3. D. J. Mack, *Trans. Amer. Inst. Min. Met. Eng.*, 1948, 175, 240.
4. E. P. Klier and S. M. Grymko, *ibid.*, 1949, 185, 611.
5. R. H. Fillnow and D. J. Mack, *ibid.*, 1950, 188, 1229.
6. B. N. Bose and M. F. Hawkes, *ibid.*, 1950, 188, 307.
7. R. D. Garwood and A. D. Hopkins, *J. Inst. Metals*, 1953, 81, 407.
8. C. S. Smith, *Trans. Amer. Inst. Min. Met. Eng.*, 1940, 137, 313.
9. W. R. Hibbard, Jr., G. H. Eichelman, Jr., and W. P. Saunders, *ibid.*, 1949, 180, 92.
10. N. P. Tucker, *J. Iron Steel Inst.*, 1927, 65, 412.
11. — *Copper Development Assoc. Publ.*, 1951, (44), 37.





By T. H. SCHOFIELD,† M.Sc., F.I.M., MEMBER, and  
A. E. BACON †

(Communication from the National Physical Laboratory.)

### SYNOPSIS

The melting point of titanium has been re-determined using a technique which reduces the possibility of contamination by refractories. Under approximately black-body conditions the melting point is found to be  $1660^{\circ} \pm 10^{\circ} \text{C}$ .

### I.—INTRODUCTION

BECAUSE of the highly reactive nature of titanium it is understandable that the accurate determination of the melting point is difficult and that results reported by different workers show wide discrepancies. A technique is required in which contact with refractories, metals, and reactive gases is reduced to a minimum. Since no refractory is known which does not seriously contaminate molten titanium, the standard method of determining the melting point, which consists essentially of maintaining a relatively large mass of metal at the melting point for a sufficiently long period to enable a number of observations to be carried out, cannot be used.

In the development of the method described below, particular attention has been paid to minimizing the surface area and time of contact of the titanium with refractory material and also to maintaining approximation to black-body conditions in the measurement of temperature.

The earliest determination of the melting point of titanium appears to have been that carried out by Burgess and Waltenberg,<sup>1</sup> using a micropyrometer and a sample of metal prepared by Hunter.<sup>2</sup> They reported a temperature of  $1795^{\circ} \pm 15^{\circ} \text{C}$ . Later Zwikker at Eindhoven, using material prepared by the van Arkel process, obtained a value of  $1727^{\circ} \pm 10^{\circ} \text{C}$ . The method he used is not known, and a report of his experiments is not now available.<sup>3</sup> Recently Hansen, Kessler, and McPherson<sup>4</sup> and Maykuth, Ogden, and Jaffee,<sup>5</sup> using optical-pyrometer techniques, have reported the melting point to be  $1720^{\circ} \pm 25^{\circ} \text{C}$ . and  $1680^{\circ} \pm 10^{\circ} \text{C}$ ., respectively. It appears that none of the above investigators has employed the classical method of obtaining close approximation to black-body conditions, which entails the measurement of the temperature at the base of a small deep hole in a uniformly heated specimen by means of an optical pyrometer.

### II.—APPARATUS

The furnace used for the experiments is similar to that described by Alberman,<sup>6</sup> and consists essentially

of a spiral of tungsten wire enclosed in a series of molybdenum radiation screens. A cylindrical water-cooled brass cover fits over the furnace assembly and rests on an O-ring located in the water-cooled furnace base. Water-cooled current leads and a pipe connected to a vacuum system are led in through the base. The furnace current is supplied from 230-V. A.C. mains through a Variac and step-down transformer. The vacuum obtained in the cold is between 1 and  $5 \times 10^{-4}$  mm. mercury.

An alumina tube, one end of which rests on the furnace base, passes through the lower radiation shield into the heating coil and supports a molybdenum platform on which a zirconia crucible rests. The crucible is about 1 in. long and  $\frac{1}{2}$  in. in dia., and is fitted with a lid having a central hole  $\frac{3}{16}$  in. in dia.

The cylindrical specimen, about  $\frac{11}{16}$  in. long and  $\frac{1}{4}$  in. in dia., has a recess  $\frac{1}{32}$  in. deep and  $\frac{3}{16}$  in. in dia. in its base, so that only a ring of metal  $\frac{1}{32}$  in. wide is in contact with the crucible. During an observation the filament of an optical pyrometer is sighted through a glass window in the top of the furnace cover on the base of an axial hole drilled in the specimen. Buckley has shown that, provided that the temperature of the specimen is uniform and the ratio of length to diameter of the hole is at least 5, the temperature observed closely approaches the true temperature.<sup>7</sup>

The optical pyrometer of N.P.L. design was calibrated in the Physics Division against a standard tungsten-strip lamp at temperatures between  $1200^{\circ}$  and  $2000^{\circ} \text{C}$ . A check of the calibration was carried out after completion of the experiments, and no change was observed. The accuracy of the instrument within the temperature ranges  $1300^{\circ}$ – $1500^{\circ}$  and  $1600^{\circ}$ – $1900^{\circ} \text{C}$ . was estimated to be  $\pm 7^{\circ}$  and  $\pm 10^{\circ} \text{C}$ ., respectively.

### III.—EXPERIMENTAL PROCEDURE AND RESULTS

In determining a melting point, the furnace chamber was first evacuated. In some experiments (see Table I) sufficient argon (99.8% purity) was then introduced to give a pressure of about 4 mm. mercury. This

\* Manuscript received 30 June 1953.

† Metallurgy Division, National Physical Laboratory, Teddington, Middlesex.

TABLE I.—*Melting Points of Nickel, Iron, Platinum, and Titanium.*

Metal	Experiment No.	Length of Specimen, in.	Diameter of Hole, in.	Length of Hole Diameter of Hole	Melting Point, °C.
Nickel	11	0.625	0.08	5	1448
	12	0.625	0.08	5	1455
	13	0.625	0.08	5	1452
	37	0.656	0.063	6	1448
					mean 1451 (1453)
Iron	33 *	0.688	0.08	6	1534
	34 *	0.688	0.10	5	1540
	35 *	0.688	0.08	6	1534
	36 *	0.688	0.08	6	1531
					mean 1535 (1533)
Platinum	21	0.625	0.08	5	1776
	40 *	0.625	0.063	6	1756
					mean 1766 (1769)
Iodide Titanium, Sample A	14	0.656	0.08	5	1654
	15	0.656	0.08	5.5	1658
	20	0.688	0.063	6	1652
	22	0.75	0.10	5	1658
					mean 1655
Iodide Titanium, Sample B	27	0.688	0.063	6	1662
	28	0.688	0.063	6	1657
	30	0.531	0.063	6.5	1658
	31	0.688	0.063	6	1661
	50 *	0.656	0.063	7	1661
					mean 1660

\* Experiments were carried out in an atmosphere of argon under reduced pressure (4 mm. mercury).

The melting points for nickel, iron, and platinum shown in parentheses are those generally accepted. The values for nickel and platinum are taken from the International Temperature Scale 1948,<sup>8</sup> and the value for iron from papers by Adcock<sup>9</sup> and Bristow.<sup>10</sup>

prevented film formation on the cover glass above the furnace. The use of argon was necessary in determining the melting point of iron because the dense film on the glass produced in these experiments gave rise to considerable errors which could not readily be cor-

rected. The use of argon (or other inert gas) for the experiments on nickel and titanium was not necessary, since the films, if present in these experiments, were so thin that the correction amounted to no more than 2°–3° C. The furnace was then slowly heated, the rate of heating being reduced as the melting point was approached. The duration of an experiment, i.e. the total time of heating from the cold to the melting point, was approximately  $\frac{1}{2}$  hr. When the temperature was about 200° C. below the point at which melting was expected, pyrometer readings were begun. The pyrometer-filament current was measured by observing the voltage change across a standard 0.02- $\Omega$  resistance by means of a Tinsley vernier potentiometer.

When melting of the specimen occurred, liquid metal in the sighting hole began to rise. Simultaneously the apparent temperature in the hole fell rapidly owing to departure from black-body conditions. The melting point was calculated from the highest potentiometer reading immediately before rise of molten metal in the hole. Before complete collapse of the specimen, the furnace current was shut off; this procedure enabled crucibles to be used for more than one experiment, since sticking of the metal to the crucible was prevented.

The melting points of three metals—nickel, iron, and platinum—the values of which are known accurately, were also determined. The results of these experiments and the results on two samples of iodide titanium are given in Table I. The analyses of the metals are given in Table II.

It was expected that the titanium specimens might be contaminated during the experiments owing to adsorption of traces of oxygen and nitrogen. This was confirmed by hardness measurements, which indicated that the surface layers contained about 0.2% oxygen or nitrogen. A vacuum-fusion analysis of one of these specimens (exp. 28) showed that the mean gas content of the specimen was: oxygen 0.06, nitrogen 0.009, and hydrogen 0.001%.

TABLE II.—*Analyses of Metals Used in Melting-Point Determinations, Wt.-%.*

Metal	Pt	C	Si	Fe	Cu	Ni	Cr	Mo	Mn
Nickel * (Mond Nickel)	...	0.096	0.004	0.001	0.04	...	...	0.001	...
Iron (18AF2) (Nat. Phys. Lab.)	...	0.0025	0.009	...	0.007	0.007	0.002	...	0.004
Platinum (Johnson Matthey)	99.995	...	...	...	...	...	...	...	...
Titanium A (I.C.I. Metals)	...	0.006	0.05	0.17	...	...	...	...	...
Titanium B (New Jersey Zinc Co.)	...	...	...	0.0045	0.002	...	...	...	0.0055
Metal	Al	Mg	Pb	Sn	S	P	O	N	H
Nickel * (Mond Nickel)	<0.001	...	...	...	...	...	0.10	...	...
Iron (18AF2) (Nat. Phys. Lab.)	<0.001	...	...	...	0.0055	<0.001	0.016	0.003	...
Platinum (Johnson Matthey)	...	...	...	...	...	...	...	...	...
Titanium A (I.C.I. Metals)	...	...	...	...	...	...	0.015	<0.01	tr.
Titanium B (New Jersey Zinc Co.)	0.0065	0.0005	0.0025	0.0025	...	...	0.03	0.001	0.03

\* This sample was originally in powder form and was subsequently briquetted and arc-melted; a large volume of gas evolved during melting was presumably due to interaction between the carbon and oxygen present in the sample; consequently the carbon and oxygen contents are lower than that of the powder given above. The copper content, which was low in the powder, was introduced during arc melting.



## IV.—CONCLUSION

The melting point of iodide titanium has been determined by a technique which reduces the possibility of contamination with refractories. The melting point appears to be  $1660^{\circ} \pm 10^{\circ} \text{C}$ . The melting points of nickel, iron, and platinum have also been determined by the same technique and, since good agreement between the observed and accepted melting points of these metals was obtained, it is assumed that the result obtained for titanium is not likely to be greatly in error.

## ACKNOWLEDGEMENTS

The work described in this paper has been carried out as part of the General Research Programme of the National Physical Laboratory, and this paper is

published by permission of the Director of the Laboratory. The authors wish to acknowledge the assistance of their colleagues in carrying out the analyses.

## REFERENCES

1. G. K. Burgess and R. G. Waltenberg, *Z. anorg. Chem.*, 1913, **82**, 361.
2. M. A. Hunter, *J. Amer. Chem. Soc.*, 1910, **32**, 330.
3. Private communication from Dr. J. D. Fast, Eindhoven.
4. M. Hansen, H. D. Kessler, and D. J. McPherson, *Trans. Amer. Soc. Metals*, 1952, **44**, 518.
5. D. J. Maykuth, H. R. Ogden, and R. I. Jaffee, *Trans. Amer. Inst. Min. Met. Eng.*, 1953, **197**, 231.
6. K. B. Alberman, *J. Sci. Instruments*, 1950, **27**, 280.
7. H. Buckley, *Phil. Mag.*, 1934, [vii], **17**, 576.
8. —, *Trav. Mém. Bur. Internat. Poids Mesures*, 1952, **21**; Neuvième Conférence Générale Annexe VI, 89.
9. F. Adcock, *J. Iron Steel Inst.*, 1937, **135**, 281.
10. C. A. Bristow, *Iron Steel Inst. Special Rep.*, 1939, (24), 1.

# 1510 Lamellæ in Chromium \*

By W. E. CARRINGTON †

(Communication from the National Physical Laboratory.)

## SYNOPSIS

Lamellæ of acicular, irregularly indented form have been observed in arc-melted 99.8% chromium (nitrogen content 0.11%) after it had been lightly hammered; they were bent in zones of heavy distortion.

A BUTTON of 99.8% chromium metal was made by melting a pressed-powder compact in a water-cooled copper vessel in an atmosphere of argon.<sup>1</sup> The button was sectioned and was then broken up by blows with a light hammer; the fragments were mounted in Bakelite, polished with diamond dust, and etched. Fig. 1 (Plate XXIV) shows the microstructure in a heavily distorted fragment; Figs. 2, 3, and 4 (Plate XXIV) show fragments which had been less distorted.

The grain-size of the metal was large. Oriented needles of nitride and small globules of oxide were visible in the crystal grains. Various amounts of cracking were present, as may be seen in the photomicrographs, the cracks having been enlarged by successive etching and polishing processes. In some areas lamellæ were observed, typical examples being illustrated in Figs. 1-4 inclusive, and the general pattern shown in Fig. 1 persisted after four repolishings, as did the single lamella in Fig. 3. The lamellæ were of acicular form, usually starting at a grain boundary, and differed from the Neumann lamellæ occurring in  $\alpha$ -iron in being irregularly indented along their long axes. When examined under phase-contrast illumination the bands were seen to be at a different and constant level from the matrix material. The lamellæ were bent in heavily distorted areas, as shown in Fig. 1, and where cracking or slip had taken place in the interior of a grain they were displaced along the crack or slip line, e.g. the lamella crossing Figs. 3 and 4 appears to have been shifted by slip occurring along a line crossing the top left-hand corner of these figures. This indicated that the

lamellæ had been formed before the apparent slip occurred.

Chromium is generally regarded as being brittle at room temperature; instances have been recorded of the occurrence of slip markings in chromium,<sup>2,3</sup> but no mention has been found of Neumann lamellæ. Since such lamellæ are generally assumed to be twins, it is possible that twinning can occur in chromium. Barrett<sup>4</sup> lists three body-centred cubic metals and alloys in which twinning has been recorded, i.e.  $\alpha$ -iron, tungsten, and  $\beta$ -copper-zinc alloy. In these instances conditions unfavourable to slip within the grains were produced by such means as cooling to sub-zero temperatures, the addition of silicon or phosphorus to iron, and shock.

The nitrogen content of the sample of chromium studied was found by chemical analysis to be 0.11%; the presence of nitride may have favoured the occurrence of lamellæ or twinning in chromium.

## ACKNOWLEDGEMENT

This paper is published by permission of the Director of the National Physical Laboratory.

## REFERENCES

1. W. J. Kroll, *Trans. Electrochem. Soc.*, 1940, **78**, 38.
2. E. S. Greiner, *Trans. Amer. Inst. Min. Met. Eng.*, 1950, **188**, 891.
3. H. B. Goodwin, R. A. Gilbert, C. M. Schwartz, and G. C. T. Greenidge, *J. Electrochem. Soc.*, 1953, **100**, (4), 152.
4. C. S. Barrett, "The Structure of Metals". 1943: New York and London (McGraw-Hill).

\* Manuscript received 30 July 1953.

† Metallurgy Division, National Physical Laboratory, Teddington, Middlesex.



By B. R. T. FROST,† B.Sc., Ph.D., JUNIOR MEMBER, and  
J. T. MASKREY†

## SYNOPSIS

The system uranium-lead has been investigated over the whole composition range and up to 1250° C. by micrographic, X-ray, and thermal-analysis methods. Owing to the pyrophoric nature of the alloys at all except very dilute concentrations and to the tendency towards segregation, experimental techniques have been developed which contain novel features; in particular, use is made of a hot centrifuge to determine liquidus points.

The solid solubilities at the uranium-rich and lead-rich ends of the phase diagram are very small, so that lead has little effect on the transformation temperatures of uranium. Two inter-metallic compounds are formed, to which the formulae UPb and UPb<sub>3</sub> have been assigned; they melt congruently at 1280° and 1220° C., respectively. X-ray studies show UPb<sub>3</sub> to have a cubic structure. A subsidiary investigation revealed that a similar structure is formed at the composition UX<sub>3</sub>, where X is silicon, germanium, indium, or gallium. The reason for the high melting points of these compounds, and for those of the other isomorphous compounds UAl<sub>3</sub> and USn<sub>3</sub>, cannot be explained by consideration of size-factors.

## I.—INTRODUCTION

THE investigation of the uranium-lead system formed part of a programme being carried out at the Atomic Energy Research Establishment, Harwell, to examine the binary alloys of uranium for their theoretical and practical applications. Work on this system was nearing completion when a paper describing a similar investigation was published by Teitel.<sup>1</sup> His phase diagram was similar in general form to that arrived at by the present authors, although certain differences are discussed below. It is of interest to compare the techniques adopted in the two investigations to overcome the experimental difficulties encountered in this work due to the pyrophoric nature of many of the alloys and to the tendency to segregation.

A series of subsidiary experiments on the inter-metallic compounds formed by uranium with Group III and IV elements were carried out for the reasons discussed in Section III, 4.

The physical and chemical properties of uranium are now well known, as a result of several years of intensive research, and details have been widely published.<sup>2</sup> Of the three allotropic forms in which uranium can exist, the body-centred cubic  $\gamma$  form is the only one in which the bonding is purely metallic. The closest distance of approach of the atoms in this structure (3.0 Å.) gives the atomic diameter of uranium that is used for comparison with the atomic diameters of other metals.

The valency of uranium under alloying conditions (as distinct from chemical combination) is not known with certainty, but is believed to be either 4 or 6. Lead is partially ionized in the solid state and probably exerts a valency of 2. On melting, the metal becomes fully ionized with a valency of 4. The position of

uranium in the electrochemical series has been established as lying between aluminium and beryllium; a high electrochemical factor between lead and uranium therefore exists.

## II.—EXPERIMENTAL METHODS

## 1. MATERIALS

The uranium was 99.96–99.98% pure (by weight). The principal impurities were iron, carbon, silicon, nickel, and oxygen, with smaller amounts of aluminium, copper, nitrogen, and hydrogen. The lead, which was in lump and powder form, was supplied by Messrs. Hopkins and Williams and was of Analar quality. The purity was 99.97% (by weight), principal impurities being silver, copper, iron, arsenic, and metal sulphates.

## 2. PREPARATION OF THE ALLOYS

(a) *Direct Melting*

The first attempts to prepare alloys consisted of melting together weighed lumps of uranium and lead in graphite crucibles in a vacuum furnace. The crucibles, of internal dimensions  $1\frac{1}{4}$  in. dia. by  $1\frac{1}{2}$  in. high, were machined from pure graphite in such a way as to leave a re-entrant thermocouple sheath in the base. A crucible containing the metal lumps was placed on an alumina tube inside a molybdenum-wound furnace. The whole furnace assembly is shown in section in Fig. 1.

The usual procedure was to evacuate to about  $10\ \mu$  pressure via a 2-in. outlet in the base-plate, before melting. When it became evident that much lead vaporized in the melting process, purified argon was admitted to a pressure of about 70 cm. before melting

\* Manuscript received 10 June 1953.

† Metallurgy Division, Atomic Energy Research Establishment, Harwell, Berks.

began. The alloys produced by this means were segregated, owing to the uncertain method of stirring and were slightly attacked on the outside by the carbon of the crucible.

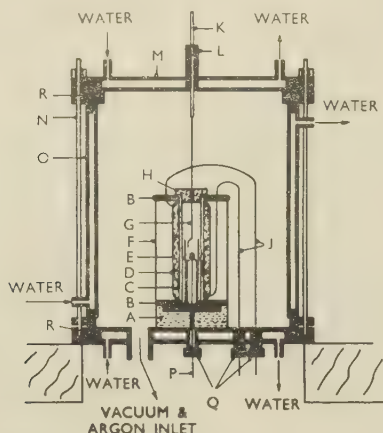


FIG. 1.—Molybdenum-Wound Thermal-Analysis Furnace.

KEY.

- |   |                                    |
|---|------------------------------------|
| A. Alumina block.                               | J. Furnace leads.                  |
| B. Graphite ends.                               | K. Stirring rod.                   |
| C. Molybdenum-wound alumina tube (1½-in. bore). | L. Wilson seal.                    |
| D. Alumina.                                     | M. Water-cooled top plate (brass). |
| E. Crucible with thermocouple in base.          | N. 6 clamping rods.                |
| F. Nickel shield.                               | O. Water-cooled cylinder.          |
| G. Stirrer.                                     | P. Thermocouple.                   |
| H. Alumina plug.                                | Q. Vacuum seals.                   |
|   | R. Rubber gaskets.                 |

Another resistance-wound vacuum furnace (Fig. 2) was constructed for melting uranium-rich alloys and for carrying out thermal analyses. Two arrangements were possible. Either a thermocouple-in-base crucible was used, in which case the stirrer hung down into the crucible, or the thermocouple tube itself hung down into the melt and acted as a stirrer. With the latter arrangement it was possible to stir the melt by rotating the crucible by attaching a motor drive to the supporting rod. The stationary sheath was thereby made to agitate the melt. The former arrangement was used mainly for thermal analysis.

(b) Soaking Method

Lead-rich alloys were made by a "soaking" method which did not involve raising the alloys to the melting point of uranium. This had the advantage of minimizing the vaporization of the lead.

Uranium turnings were cleaned in the electropolishing bath (described in Section II, 4) or in dilute nitric acid, washed in water, dried in alcohol, and placed in an alumina crucible after weighing. Lumps of lead were added, and the crucible was put into a Pyrex tube, which was then attached to a vacuum system. When a good vacuum ( $\sim 10^{-4}$  mm. mercury) had been attained, the lead was melted by a gas torch and the tube was sealed off at a constriction. The tube was held in a furnace at 500° C. for about 5 days. On removal from the furnace, the tube was well shaken and allowed to cool in air. The resulting ingot was fairly homogeneous, and no traces of free uranium were detected.

This technique was modified for the examination of alloys in the region of the compound  $UPb_3$ , the formation of which tended to be strongly exothermic, marked vaporization of the lead occurring in alloys of this composition. Lead and uranium powder finer than -200 mesh were weighed and thoroughly mixed. The material was then compressed in a ½-in.-dia. die under a pressure of 4000 lb./in.<sup>2</sup> to give a pellet about  $\frac{3}{16}$  in. in thickness. A pellet was placed in an alumina crucible inside a silica tube, which was then evacuated to about  $10^{-4}$  mm. mercury. The tube was warmed until the lead just melted, and the reaction would then proceed quietly. The sample could be annealed at any temperature up to 1100° C. Some samples were heated to above the melting point of the compound in a tungsten-coil furnace of the type designed by Alberman<sup>3</sup> or in an "Efco" spark-gap induction furnace.

(c) Hydride Method

A further refinement of the "soaking" technique was used to obtain good samples for X-ray analysis. This was a modification of the "hydriding" method developed for preparing uranium-mercury alloys.<sup>4</sup> The uranium turnings were cleaned, weighed, and placed in a Pyrex reaction tube to which was attached a side arm in which a weighed quantity of lead powder was placed. The uranium was converted to the hydride  $UH_3$  by heating to 250° C. in an atmosphere

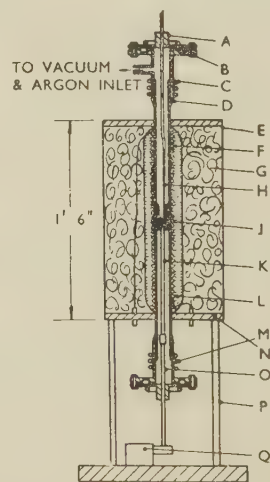


FIG. 2.—Platinum-Wound Thermal-Analysis Furnace.

KEY.

- |                                  |  |
|----------------------------------|--|
| A. Wilson seal.                  | K. Alumina rod.  |
| B. Rubber seal.                  | L. 1-in.-bore mullite tube wound with 22-S.W.G. platinum wire. |
| C. Brass end tubes and plates.   | M. Cooling coils.  |
| D. Wax seal.                     | N. Sindanyo ends.  |
| E. Brass tube.                   | O. Steel rod.  |
| F. Alumina.                      | P. Support rods.   |
| G. Asbestos lagging.             | Q. Motor for rotating crucible.                                |
| H. Off-set-thermocouple sheath.  |  |
| J. Crucible in graphite furnace. |  |

of pure hydrogen. Evacuating for  $\frac{1}{2}$  hr. at 300° C. converted the hydride to a finely divided, reactive form of uranium. After cooling, the lead was added to the uranium, and the tube was shaken to mix the powders, which reacted on warming. The product



was removed without oxidation, since one end of the reaction tube was sealed by a glass membrane or septum. To this end was sealed another Pyrex tube on to which capillary tubes for X-ray samples were attached as in Fig. 3 (c). This second tube was evacuated, the membrane was broken with a glass striker, and the powder transferred to a capillary, which was then sealed in a flame and removed.

#### (d) X-Ray Samples

To obtain filings for X-ray analysis from block specimens, a small dry-box was constructed. To admit specimens to the box, one of the rubber gloves was temporarily removed.  $\text{CO}_2$  was passed through the system for  $\frac{1}{2}$  hr., after which the taps were closed and the operator pushed his hands into the gloves. The specimen was filed over a

were placed inside alumina containers before being sealed off in silica tubing under vacuum.

#### 4. MICROGRAPHIC WORK

After annealing, samples were quenched in cold water and polished for micrographic examination. The lead-rich samples were carefully sectioned, and polishing was begun on grade 0 emery papers, using copious quantities of paraffin. Final polishing was with metal polish on a Selvyt cloth. Lead-rich alloys were etched in a 5% solution of nitric acid in alcohol, and uranium-rich alloys in a mixture of equal volumes of concentrated nitric acid and glacial acetic acid. A final electrolytic polish was given to some of these alloys in a bath containing a mixture of 40% concentrated sulphuric acid, 20% orthophosphoric acid, and 40% water<sup>5</sup> at a current density of about 0.1 amp./cm.<sup>2</sup>. It was found that a light smear of low-vapour-pressure Apiezon oil protected the polished surfaces from corrosion for several hr. without impairing microscopic examination.

The phases identified consisted of a lead-rich solid solution;  $\text{UPb}_3$ , which appeared as bright yellow cubes;  $\text{UPb}$ , which oxidized very rapidly and generally appeared blackish, except in the uranium-rich alloys, in which it was present as greyish polyhedra; and finally the uranium-rich solid solution. Some microstructures are shown in Fig. 4 (Plate XXV). In most cases the different rates of oxidation of the phases gave sufficient contrast in duplex alloys, so obviating the need for etching.

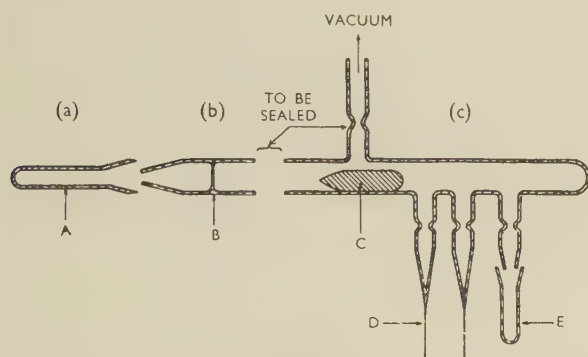


FIG. 3.—Pyrex Tubes for Handling of Dry-Box Specimens.

#### KEY.

- A. Tube from dry-box containing specimen filings.
- B. Tube with septum.
- C. Septum breaker.
- D. Capillaries for X-ray specimens.
- E. Tube for chemical-analysis specimen.

funnel, and the filings were collected in a tube with a ground-glass cone top (Fig. 3 (a)). This tube was removed from its clamp and another tube (Fig. 3 (b)), having a septum at one end and a ground-glass socket at the other, was fitted to it. This arrangement was removed from the box and sealed to an "analysis sample" tube (Fig. 3 (c)). The latter was evacuated and sealed off at the constriction. The filings were then transferred to the capillaries and to the analysis tube. The reason for this procedure was that the X-ray capillary specimens could not be sealed in a flame under an atmospheric pressure of  $\text{CO}_2$ , since the tubes would blow out and burst; the pressure inside the tube therefore had to be reduced.

#### 3. ANNEALING

Lead-rich specimens were homogenized by heavily deforming the ingot in a vice, sealing the sample in a Pyrex tube under vacuum, and annealing. Annealing was carried out in a furnace controlled to  $\pm 1^\circ \text{C}$ . At the lead-rich end of the system the standard annealing temperature was  $290^\circ \text{C}$ . To prevent reaction between the uranium and the silica tubing, uranium-rich alloys

#### 5. THERMAL ANALYSIS

The furnace in which the thermal analysis of the alloys was carried out has been described above, and is shown in Fig. 2. Power for the furnace was supplied through a Variac transformer, the spindle of which was turned at a constant rate by an electric motor to give a temperature change of approximately  $5^\circ \text{C./min}$ . The time/temperature relationship was a smooth curve, not a straight line. It was quite easy to detect thermal arrests on a potentiometric-recorder chart, a more accurate determination being made with a potentiometer on a subsequent temperature cycle.

Two disadvantages in this method of thermal analysis, as applied to uranium-lead alloys, became apparent. Firstly, considerable undercooling took place while determining liquidus curves, and true recalescence did not occur. Secondly, at high temperatures, significant quantities of lead vaporized from the alloy and were deposited at the ends of the furnace. Principally to overcome the first of these difficulties, a method was developed to determine liquidus points without using a thermal-analysis furnace. This method is based on the fact that an alloy of composition  $X$  at a given temperature  $T_1$ , which is between the solidus and liquidus temperatures, will consist of solid of composition  $A_1$  and liquid of composition  $B_1$ . If these two components can be separated and analysed, two points on the

diagram are established, viz. the position of the liquidus curve at temperature  $T_1$  and the composition of the solid phase (usually an invariable compound). In the case of the uranium-lead system, this separation was achieved by centrifuging the alloy at high temperatures between the liquidus and solidus. An advantage of this method is that the whole of the liquidus curve can be determined from one fixed composition. A large quantity of alloy of one composition can be made up in one melt, and will suffice for the complete determination, samples being centrifuged at increasingly higher temperatures above the solidus temperature.

The centrifuge employed is shown in Fig. 6. A

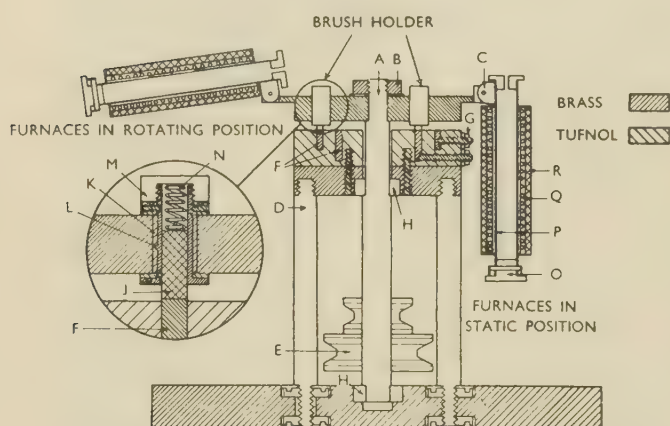


Fig. 6.—Hot Centrifuge for Separation of Solid and Liquid Phases in Alloys.

#### KEY.

- |                            |   |
|----------------------------|---|
| A. Rotating steel shaft.   | L. Brass brush sheath.                                    |
| B. Locking nut.            | M. Terminal nut.  |
| C. Pivots.                 | N. Spring.  |
| D. 4 steel support rods.   | O. Furnace bottom with fixing pin and pin-retaining ring. |
| E. Pulleys for belt-drive. | P. Stainless steel furnace tube with welded flanges.      |
| F. Slip rings.             | Q. Nichrome windings set in alumina.                      |
| G. Terminals.              | R. Asbestos string binding.                               |
| H. Roller bearings.        |   |
| J. Graphite brushes.       |   |
| K. Tufnol insulation.      |   |

specimen of the alloy was sealed under vacuum in a silica tube of fairly large wall thickness. The tube was placed in the furnace, which was fitted with a quick-release cap at the lower end. In the other furnace, which was not supplied with current, was placed a piece of lead so that the weights at the ends of the rotating arm were balanced. To allow for cooling in the air stream, the furnace containing the alloy was heated to about  $50^{\circ}\text{C}$ . above the required operating temperature before the motor was started. The centrifuge was run with a steady furnace current and at a constant rate of rotation (about 2500 r.p.m., which gave a force about 900 times that of gravity) for about 15 min. It was then stopped and a thermocouple rapidly inserted in the furnace. This method of checking the temperature was considered to be as accurate as having a thermocouple permanently in the furnace and taking off the e.m.f. by slip rings. The total run

lasted about 2 hr., at the end of which time the temperature was finally checked. On removing the cap from the end of the furnace, the specimen dropped into a beaker of cold water. The ingot so obtained was sectioned longitudinally and polished. In such a section the line of demarcation between the two constituents was clearly visible to the naked eye, as evidenced by the specimen in Fig. 5 (Plate XXV), which shows photographs of the interface at (a) high and (b) low magnification. A specimen for chemical analysis was then removed from both regions of the ingot.\*

## 6. X-RAY TECHNIQUES

The majority of the X-ray specimens were enclosed in Pyrex capillaries, the presence of the glass having no serious effect on the diffraction patterns. A few lead-rich specimens were obtained by filing a block under paraffin, treating the filings with benzene and drying them, and finally mixing them with "Durofix" and rolling into a rod 1 cm. long by 0.02 cm. dia.

Nine- and 19-cm.-dia. Unicam powder cameras were employed on a Metrovick Raymax demountable-tube set running at 35 kV. and 20 millamp. and on a Muller MC60 sealed-tube set running at 40 kV. and 30 millamp. The copper radiation was filtered through nickel foil to select  $K\alpha$  radiation.

## 7. RESISTIVITY EXPERIMENTS

As a final check on the shape of the lead-UPb<sub>3</sub> liquidus curve, and in order to develop methods for the determination of liquidus curves in other systems, a resistivity method was devised. Insufficient data exist to enable the form of resistivity/temperature curves in the liquid, semi-liquid, and solid regions of an alloy to be predicted accurately. It is reasonable to assume, however, that the curve in the region between the solidus and the liquidus has a different slope from the curves of the solid and the liquid.

A sample of alloy was melted in an alumina crucible (E) (Fig. 7), and a twin-bore alumina thermocouple insulator (B) was pushed down into the melt. Iron wires (G) were inserted in the tops of the two bores to form contacts, since iron is not attacked by lead or by uranium in dilute solution. When solid, the alloy was sealed inside a silica tube, which was evacuated. The iron wires were taken out through rubber seals (J). The tube was then placed in a furnace and a series of readings of the resistivity of the alloys were taken at different temperatures, read on the thermocouple (D). Errors due to expansion of the alloy were eliminated by the fact that the iron wire contacts remained fixed. This method has the advantage that the specimen, which is virtually a wire, is surrounded by a large bulk of alloy at the same temperature, so that temperature fluctuations are very small.

\* While these experiments were in progress, it was learned that the British Non-Ferrous Metals Research Association had

built a similar device,<sup>6</sup> the purpose of which was to separate out the crystals of a compound for X-ray analysis.



Fig. 8 shows a typical resistance/temperature curve; in this case the alloy contained 0.2 at.-% uranium. A change of slope occurs between 720° and 735° C. The

resistance value. The liquidus is taken as the point at which the change begins.

### 8. CHEMICAL ANALYSIS

Samples for chemical analysis were examined by the Analytical Section, Metallurgy Division, A.E.R.E. An ether-separation method was employed for the earlier samples; later, a gravimetric separation was developed. Samples containing very small amounts of uranium were determined colorimetrically. Usually both constituents were determined.

## III.—EXPERIMENTAL RESULTS

The phase diagram of the uranium-lead system is given in Fig. 9 (a). The liquidus on either side of the

TABLE I.—Micrographic Results.

Alloy Composition, at.-% Pb	Annealing Temp., °C.	Structure	
		Micrographic	X-Ray
0.4	500	U + UPb	U
1.5	500	"	U
9.4	500	"	...
15.0	500	"	...
41.0	500	"	...
50.5	...	UPb (heavily oxidized)	...
58.2	290	UPb + UPb <sub>3</sub>	UPb <sub>3</sub> + ?
71.6	500	"	"
71.6	290	"	"
71.6	500	"	"
80.5	290	UPb <sub>3</sub> + Pb	UPb <sub>3</sub> + Pb
85.1	290	"	"
90.0	290	"	"
91.0	290	"	"
92.5	290	"	Pb + ?
97.5	290	"	"
99.4	290	"	"

\* A number of additional alloys were examined which gave results in accord with those given above, but which had to be discarded owing to excessive oxidation.

TABLE II.—Thermal Analysis Results.

Alloy Composition, at.-% Pb	Thermal Arrest, °C.		Alloy Composition, at.-% Pb	Thermal Arrest, °C.	
	Heating	Cooling		Heating	Cooling
0.4	640	636	50.0	...	1280
0.4	766	760	58.2	1212	...
0.4	1120	...	65.0	1208	...
9.4	645	640	71.6	1215	1200
9.4	765	760	77.5	320	...
9.4	1130	1125	80.5	328	...
15.0	640	642	85.1	320	...
15.0	758	761	90.0	325	...
15.0	1128	1124	90.0	1190	1186
15.0	...	1190	91.0	327	...
41.0	638	640	95.0	325	323
41.0	770	765	97.5	1023	...
41.0	1127	1124	99.4	902	897
41.0	...	1275			

composition of the compound UPb has not been accurately determined owing to the experimental difficulties involved in carrying out thermal analysis

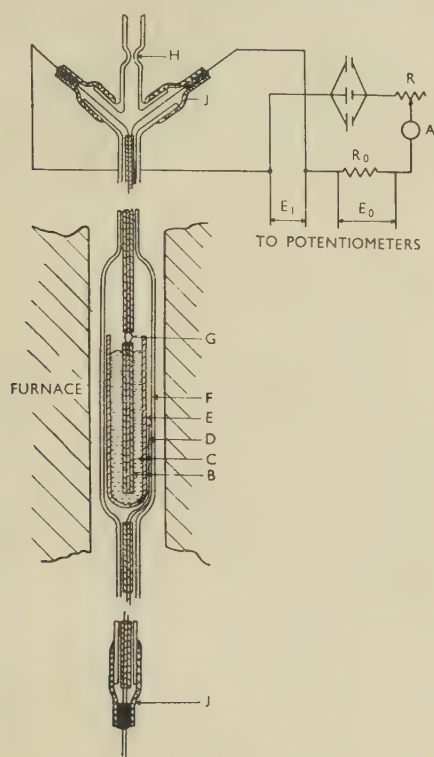


Fig. 7.—Resistivity Method for Finding Liquidus Points in Lead-Rich Uranium-Lead Alloys.

#### KEY.

- |                             |                                       |
|-----------------------------|---------------------------------------|
| A. Ammeter.                 | G. Iron wire leads.                   |
| B. Twin-bore alumina quill. | H. For sealing under vacuum.          |
| C. Uranium-lead alloy.      | J. Rubber and wax seals.              |
| D. Thermocouple.            | R. Rheostat.                          |
| E. Alumina crucible.        | R <sub>0</sub> . Standard resistance. |
| F. Silica container.        |                                       |

rate of change of temperature was low, but equilibrium was attained slowly, as it involved the solution of the residual solid particles of UPb<sub>3</sub>; hence there is a range over which the curve turns towards the liquid

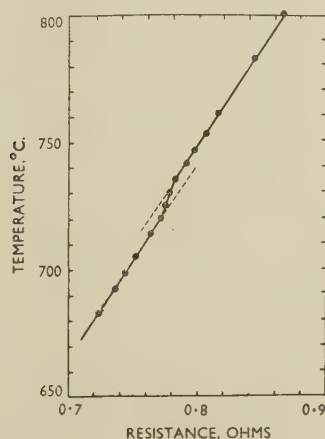


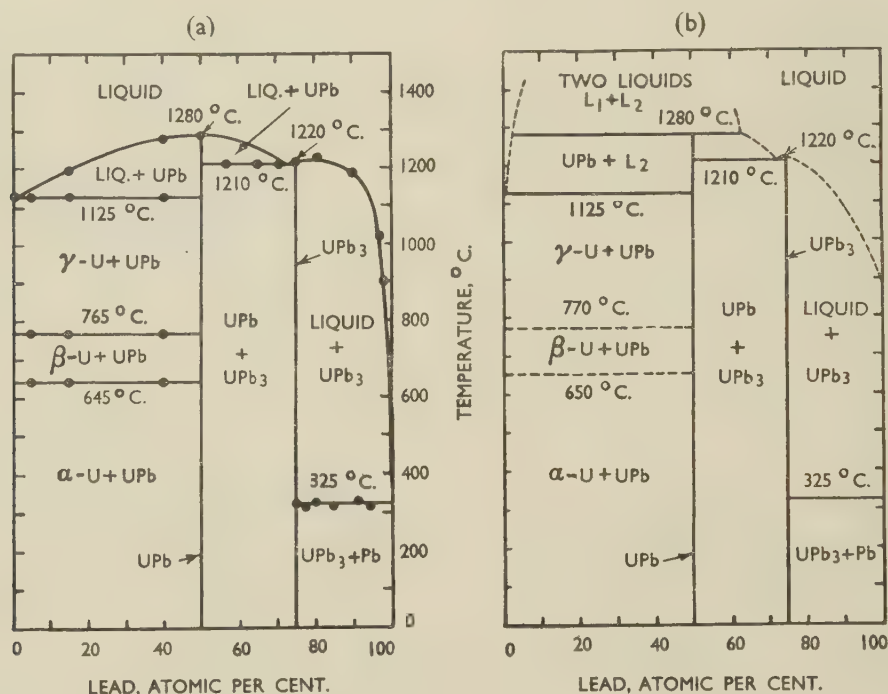
Fig. 8.—Resistivity/Temperature Curve for 0.2 at.-% Uranium.

TABLE III.—*Determination of Lead-Rich Liquidus by Resistivity Measurements.*

Run	Temp., °C.	Solubility, at.-% U in Pb	Run	Temp., °C.	Solubility, at.-% U in Pb
1	500	0.02	4	720	0.25
2	691	0.06	5	615	0.10
3	895	0.59	6	782	0.29

on alloys containing lead, which has a very appreciable vapour pressure above 1200° C. Results are given in Tables I-IV.

approximately 25 at.-% uranium gave a face-centred cubic X-ray pattern with a lattice parameter of 4.75 Å. This was interpreted as meaning that the uranium formed an extensive solid solution in lead. The microstructures of all lead-rich alloys subsequently examined were, however, two-phase in character. An X-ray film of an alloy in this range was finally obtained on which two face-centred cubic patterns occurred. This was at first thought to be an effect similar to that obtaining in the system aluminium-zinc, i.e. a splitting of the solid solution into two face-centred

FIG. 9.—Uranium-Lead Equilibrium Diagram after: (a) Frost and Maskrey; (b) Teitel.<sup>1</sup>TABLE IV.—*The X-Ray Pattern of UPb<sub>3</sub>.*  
19-cm. Camera.

Indices	$\sin^2 \theta$	$a$ , Å.
111	0.0782	4.7663
200	0.0986	4.8448
220	Too faint for accurate measurement	
311	0.2858	4.7752
222	0.3114	4.7739
400	0.4135	4.7852
331	0.4925	4.7787
420	0.5157	4.7822
422	0.6193	4.7868
511, 333	0.7066	4.7859
440	0.8267	4.7868
531	0.9086	4.7825
442, 600	0.9347	4.7826

$a_0$  = as extrapolated = 4.7834 Å.

### 1. LEAD-RICH ALLOYS

The initial examination of lead-rich alloys led to erroneous conclusions, since an alloy containing

cubic phases of different parameters. The subsequent thermal-analysis results tended to contradict this point of view, since alloys containing 100–75 at.-% lead gave arrests at about 325° C., indicating that this was the eutectic temperature. Accurate measurement of the parameters of a series of alloys in this composition range showed that the parameters of the two phases were the same at all compositions, suggesting little or no range of composition for either phase. After a few liquidus results had been obtained for alloys in the region 100–75 at.-% lead, it became evident that the second face-centred cubic phase was a compound, since its melting point was found to be about 1200° C. and the stoichiometric composition was found micrographically to be UPb<sub>3</sub>. Comparison with the system uranium-tin led to the proposal that the structure of UPb<sub>3</sub>, as shown by X-ray results, was similar to that of USn<sub>3</sub>, i.e. face-centred cubic ordered, the additional reflections being so faint as to be undetected, since the scattering powers of uranium and lead are similar. The uranium atoms



are probably situated at the corners of a cube, with the lead atoms occupying the face-centred positions.

It was difficult to determine the exact position of the eutectic by metallographic methods. However, the value of the eutectic arrests at 325° C. and the fact that the lead face-centred cubic parameter remained virtually unchanged with the addition of uranium imply that there is a very small solid solubility of uranium in lead and that the eutectic composition must lie very near to the 100% lead axis of the diagram.

The determination of the liquidus between 0 and 20 at.-% uranium presented many problems. Of the early thermal-analysis experiments one or two produced results thought to be reliable, these being in the range 10–20% uranium. Centrifuge experiments in the temperature range 350°–600° C. indicated zero solubility, the upper sections of the ingots showing no uranium even by colorimetric analysis. However, the presence of a fine precipitate in the microstructure of the upper section of the ingot indicated that a very small amount of uranium was present. Subsequently resistivity determinations (Table III) showed the centrifuge results to be of the correct order of magnitude. The solubility limit at 600° C. is 0.03 at.-% uranium in lead. The liquidus rises very steeply, reaching 0.6 at.-% uranium at 900° C., after which the slope decreases until at 1190° C. the liquidus composition is 10 at.-% uranium.

## 2. URANIUM-RICH ALLOYS

The uranium end of the diagram did not present any great difficulties in investigation. The lattice spacings derived from X-ray-diffraction patterns indicated little solubility of lead in uranium. The micrographic and thermal-analysis results also showed no evidence of marked solubility of lead in any of the modifications of uranium. The addition of lead did, however, cause the  $\alpha \rightarrow \beta$  and  $\beta \rightarrow \gamma$  transformations to be slightly depressed, to the extent of about 5° C. in each case. The eutectic temperature of 1125° C. indicated that the eutectic composition must be quite near to pure uranium, since the depression of the freezing point of uranium by lead obeys the law for dilute solutions.<sup>7</sup> It was not found possible accurately to determine this composition, since it was difficult to prepare alloys with a small, accurately known percentage of lead in uranium.

## 3. THE COMPOUND UPb

Difficulty was experienced in examining alloys in the region of the compound UPb, owing to their pyrophoric nature. The melting-point data are not very accurate, since traces of oxygen react very readily with the compound, displacing the composition towards the lead axis. Offsetting this is the fact that the rate of evaporation of lead at these temperatures is fairly high. It was not found possible to devise a method of obtaining a suitable X-ray photograph of UPb. As the compound could be formed only at

high temperatures, it could not be prepared under vacuum in sealed Pyrex or silica tubes. Attempts to extract samples from the induction furnace by protecting them from oxidation with a layer of Apiezon oil were not successful, since oxidation occurred during the crushing of the lumps of compound in preparing the X-ray specimen.

The composition of the compound was fixed by two methods. Firstly, the few liquidus arrests indicated a maximum at the UPb composition, and secondly the estimation of the relative proportions of the two phases in the (U + UPb) and (UPb + UPb<sub>3</sub>) fields also gave this formula.

## 4. EXPERIMENTS ON THE UX<sub>3</sub> SERIES OF COMPOUNDS

Of the two compounds formed, only UPb<sub>3</sub> could be examined in any detail and compared with other similar compounds. Before this investigation, two compounds similar to UPb<sub>3</sub> were known—UAl<sub>3</sub><sup>8</sup> and USn<sub>3</sub>.<sup>9</sup> These both have face-centred cubic ordered structures (*L1*<sub>2</sub>), giving a simple cubic diffraction pattern. With the discovery of UPb<sub>3</sub> it was decided to determine whether similar compounds existed in the systems formed by uranium with the remaining Group IIIB and IVB elements, viz. gallium, indium, thallium, silicon, and germanium. Accordingly, samples having the stoichiometric composition UX<sub>3</sub> were prepared. Weighed quantities of metal were placed in small beryllia crucibles and melted in a tungsten-coil vacuum furnace of the type described by Alberman.<sup>3</sup> The ingots, which did not oxidize in air, were crushed, formed into X-ray-diffraction specimens with Durofix, and examined in the normal manner. As a great deal of effort would have been involved in devising methods of chemical analysis for these systems, care was taken to prevent loss of metal during melting, and the assumption was made that

TABLE V.—*Properties of the Compounds UX<sub>3</sub>.*

Formula	<i>a</i> , Å.	X-Ray Density, g./c.c.	Freezing Point, °C.
UAl <sub>3</sub>	4.27	6.8	1350
UGa <sub>3</sub>	4.2475	9.686	ca. 1300
UIn <sub>3</sub>	4.6013	10.12	...
USi <sub>3</sub>	4.0353	8.298	1500
UGe <sub>3</sub>	4.2062	10.37	ca. 1200
USn <sub>3</sub>	4.626	10.00	1350
UPb <sub>3</sub>	4.7834	13.24	1220

the ingots had the composition corresponding to the metals as weighed before melting. As none of the metals had a low boiling point, evaporation was not expected to be excessive.

The freezing points of the compounds were estimated roughly by sighting an optical pyrometer on the melt.

In four of the five systems examined reactions occurred. Thallium failed to react owing to excessive oxidation, probably caused by oxygen dissolved in the metal, which reacted on heating. Compounds with

the formulæ  $UGa_3$ ,  $UGe_3$ ,  $UIn_3$ , and  $USi_3$  were obtained, and all gave diffraction patterns which could be indexed as face-centred cubic ordered ( $L1_2$  type). The seven  $UX_3$  compounds, together with their lattice parameters, X-ray densities, and freezing points, are listed in Table V.

#### IV.—COMPARISON WITH AMERICAN RESULTS

The present experimental work on the uranium-lead system had almost been completed when Teitel's results were published.<sup>1</sup> His diagram is redrawn in Fig. 9 (b) to permit direct comparison with the authors' diagram in Fig. 9 (a). The principal difference between the two lies in the miscibility gap in Teitel's diagram, the existence of which was proposed on the evidence of segregated alloys, from which the limiting compositions of the gap were determined. Several thermal arrests were reported at the syntectic temperature of 1280° C. The present authors, who obtained only two arrests in this region—1275° C. at 41 at.-% Pb and 1280° C. at the composition of UPb—interpreted their results in terms of a flattened liquidus to be consistent with the 1190° C. arrest at 15.0 at.-% Pb. It was believed that such segregated alloys as were obtained were the result of prolonged holding at a high temperature, which permitted gravitational separation, rather than of immiscibility. For reasons given in the discussion below, the authors still prefer their interpretation of the results to those of Teitel.

Comparison of the experimental methods in the two investigations shows that the present authors decided to develop new techniques for possible use in subsequent work on similar alloy systems, rather than rely on speed of manipulation and the wide use of dry-boxes as in Teitel's work. In neither investigation was it possible to prepare a specimen of UPb suitable for X-ray-diffraction purposes, because the method of preparation of the compound precluded the use of the handling techniques which were developed for  $UPb_3$ .

#### V.—DISCUSSION

##### 1. SOLID SOLUBILITY

The form of equilibrium in the system uranium-lead is largely determined by the two high-melting-point compounds. Hume-Rothery<sup>10</sup> has shown that in such a case the solid solubilities will be restricted on free-energy considerations. Moreover, the size-factor of lead with respect to uranium, as defined by Hume-Rothery, has a value of +16.7%, which is outside the empirical limit of 14–15% for extensive solid solubility.

##### 2. $UPb_3$ AND $UX_3$ SERIES OF COMPOUNDS

A unit cell of the  $L1_2$  type of structure, the general formula of which is  $AB_3$ , is shown in Fig. 10. Each A atom has 12 nearest neighbours of type B at a distance  $a/\sqrt{2}$ , where  $a$  is the length of the unit-cell side. Each

B atom has 8 nearest neighbours of type B and 4 of type A at a distance  $a/\sqrt{2}$ . In the group of seven compounds of this type listed in Table V, variable size-factors, electro-chemical factors, and valencies are operating, yet the melting points all lie within the range 1200°–1500° C. The reason for this is difficult to find. The arrangement of the atoms permits a high co-ordination, and hence an opportunity for strong metallic binding. However, aluminium and lead have equally high co-ordination numbers in the elemental form and yet have much lower melting

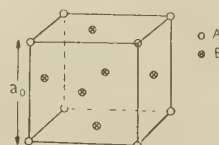


FIG. 10.—Unit Cell of  $L1_2$ -Type Compound with Formula  $AB_3$ .

points than the  $UX_3$  compounds. In these compounds, although three-quarters of the atoms are of the low-melting-point Group IIIB and IVB elements, the melting points are high. In an attempt to solve the problem, the interatomic distances in the compounds were calculated and are listed in Table VI. The figures given are:  $a$  (column 2),

TABLE VI.—Interatomic Distances in  $UX_3$  Compounds:

Compound	Cell Side $a$ , Å.	U-X Distance Calculated, Å.	U-X and X-X Dis- tance in Compound, Å.	X-X Dis- tance in Element, Å.	Size- Factor, %
$UAl_3$	4.27	2.88	3.01	2.75	− 8.3
$UGa_3$	4.2475	2.85	2.995	2.7	−10.0
$UIn_3$	4.601 <sub>3</sub>	3.12	3.25	3.24	+ 8.0
$USi_3$	4.035 <sub>3</sub>	2.67	2.85	2.346	−22.0
$UGe_3$	4.206 <sub>2</sub>	2.72	2.97	2.445	−18.5
$USn_3$	4.626	3.00	3.27	3.01	+ 0.3
$UPb_3$	4.783 <sub>4</sub>	3.25	3.28	3.49	+16.7

$a/\sqrt{2}$  (column 4), the sum of the atomic radii ( $r_u + r_x$ ), which are derived from the closest distances of approach of the atoms in their crystals (column 3), the atomic diameters of the elements X (column 5), and the size-factors (column 6). Two conclusions can be stated: (i) There is no U-X contraction in any compound (comparing column 3 with column 4); on the contrary, there is an expansion. This implies that the electrochemical factor is not responsible for the high stability of the phases. (ii) Only in the case of  $UPb_3$  is the X-X distance less than in the elements, i.e. only in this case is there a compression of the X atoms. This is probably due to the large positive size-factor of lead with respect to uranium, which is higher than in any other compound. To accommodate the large lead atoms in the lattice, a compression is necessary along the Pb-Pb bonds.

These data present a picture of a group of compounds in which the atoms do not touch or overlap, except in the case of the lead atoms in  $UPb_3$ , and the electro-



chemical factor does not appear to be playing a part; yet some factor is operating that makes for great stability of the structure as shown by the high melting points. Strictly speaking, this group of compounds, with their open packing, cannot be described as size-factor compounds, although the term is often loosely applied to all compounds which are not electron compounds or valency compounds.

It is difficult to compare the uranium compounds with the other 32 compounds of type  $L1_2$  listed by Smithells,<sup>11</sup> since there are no groups based on one common metal analogous with uranium in  $UX_3$ . Tin and lead form  $L1_2$  type compounds with some rare-earth metals, e.g.  $LaPb_3$  and  $CeSn_3$ . In these cases the melting points, where known, are considerably higher than those of tin or lead, showing that a similar factor must be operating. At present the correlation between the structures and melting points is not well understood, and explanations cannot be readily given for their behaviour until the whole problem of the stability of size-factor compounds has been examined.

### 3. MISCIBILITY GAP

The evidence for the existence of this gap is not, in the opinion of the authors, very strong. Apart from there being two possible interpretations of the experimental facts, the existence of a compound (UPb)—on which both publications agree—raises an anomaly. It is generally agreed that a miscibility gap in an alloy system is due to a dissimilarity between the two species of atom concerned.<sup>12</sup> In the system  $A-B$ , the  $A-A$  interaction and  $B-B$  interaction are both greater than the  $A-B$  interaction, so that segregation into two layers will occur. At the syntectic temperature of 1280° C. in the system uranium-lead, the interaction energies so change that a compound, UPb, can be formed. The only possible interpretation of this is that a higher entropy results from a regular geometric arrangement of atoms, e.g. in two interpenetrating networks, than from a complete segregation of U and Pb atoms.

A search of the literature revealed that only two alloy systems exhibiting miscibility gaps had inter-metallic compounds under the gap. These were potassium-zinc and sodium-zinc, in which the compounds  $KZn_{12}$  and  $NaZn_{12}$ , respectively, were reported. It will be seen that these compounds, which are built on geometric packing considerations (i.e. size-factor), are close to the zinc axis and not almost under the miscibility maximum, as in the uranium-lead system. It follows that the phenomenon proposed in Teitel's diagram is, as far as is known, unique.

### 4. THE LIQUIDUS

Of the two methods used, only the resistivity method gave quantitative results for the liquidus curve at the lead-rich end of the diagram. The results, listed in Table III, are plotted in Fig. 11 (b). With the

exception of point 2, a smooth curve can be drawn through these points. A further check on these results can be made by application of the Clausius-Clapeyron equation to this equilibrium curve. In this case the curve represents the separation of a compound of fixed composition from a liquid, and the treatment of Fink and Freche<sup>13</sup> can be applied. The Clausius-Clapeyron equation can be reduced to the form:

$$\log N_A = \frac{L_{sol.}}{RT} + K$$

where  $N_A$  is the mol. fraction of the solid  $A$  separating from liquid  $B$ .  $L_{sol.}$  is the latent heat of solution,  $T$  is the absolute temperature,  $R$  the gas constant, and

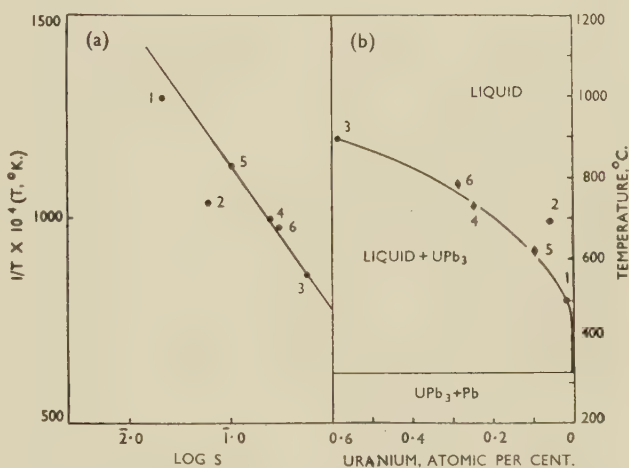


FIG. 11.—(a) Graph of  $\log S$  against  $1/T$  for the Lead-Rich Liquidus; (b) The Lead-Rich End of the Uranium-Lead System up to 900° C.

$K$  a constant. Reduced to its simplest terms, if the log of the atomic per cent. of solute  $S$  is plotted against the inverse of the absolute temperature, a straight-line relationship should be obeyed. The plot is shown in Fig. 11 (a). Points 3, 4, and 5 lie on a straight line, and points 1 and 6 are not far from this line. At higher temperatures and concentrations, the  $\log S/\frac{1}{T}$  curve begins to deviate from a straight line and ideal conditions, which can be treated thermodynamically, no longer apply.

### ACKNOWLEDGEMENTS

This work was carried out in the Metallurgy Division, Atomic Energy Research Establishment, Harwell. Thanks are due to the Director of the Establishment for permission to publish this paper.

The analytical work of Mr. C. E. Austing is gratefully acknowledged. The authors would also like to thank Professor G. V. Raynor, Dr. H. M. Finnieston, and many of their colleagues at A.E.R.E. for helpful discussions while this work was in progress.

## REFERENCES

1. R. J. Teitel, *Trans. Amer. Inst. Min. Met. Eng.*, 1952, **194**, 397.
2. J. J. Katz and E. Rabinowitch, "The Chemistry of Uranium" (National Nuclear Energy Series, Part VIII, Vol. 5). 1951: New York (McGraw-Hill).
3. K. B. Alberman, *J. Sci. Instruments*, 1950, **27**, 280.
4. B. R. T. Frost, unpublished work.
5. B. W. Mott and H. R. Haines, *Metallurgia*, 1951, **43**, 255.
6. W. A. Baker and M. D. Smith, *B.N.F.M.R.A. Research Rep.*, 1945, (**A694**).
7. J. Lumsden, "Thermodynamics of Alloys" (Institute of Metals Monograph No. 11). 1952: London.
8. P. Gordon and A. R. Kaufmann, *Trans. Amer. Inst. Min. Met. Eng.*, 1950, **188**, 182.
9. R. E. Rundle and A. S. Wilson, *Acta Cryst.*, 1949, **2**, 148.
10. W. Hume-Rothery, "The Structure of Metals and Alloys" (Institute of Metals Monograph No. 1). 1949: London.
11. C. J. Smithells, "Metals Reference Book", p. 220. 1949: London (Butterworths Scientific Publications).
12. J. H. Hildebrand and R. L. Scott, "The Solubility of Non-Electrolytes". 1950: New York (Reinhold Publishing Corp.).
13. W. L. Fink and H. R. Freche, *Trans. Amer. Inst. Min. Met. Eng.*, 1934, **111**, 304.



# THE EFFECTS OF SOME CONSTITUTIONAL FACTORS 1512 ON THE CREEP AND FATIGUE PROPERTIES OF LEAD AND LEAD ALLOYS\*

By L. M. T. HOPKIN,† Ph.D., A.R.S.M., A.I.M., MEMBER, and  
C. J. THWAITES,‡ B.Sc., A.R.S.M., JUNIOR MEMBER

(Communication from The British Non-Ferrous Metals Research Association.)

## SYNOPSIS

Alloying elements were added to a basis lead of the highest purity so that some of the resulting alloys were single-phase (lead-tin alloys), some two-phase (lead-copper alloys), and others were amenable to heat-treatment causing age-hardening or precipitation (lead-antimony alloys). All the materials were laboratory extruded; the effect of grain-size was investigated, mostly by extruding at different temperatures.

Creep-resistance markedly decreased, and the ductility at failure increased, as the grain-size was made smaller, but these effects were sometimes obscured by grain-size changes resulting from recrystallization during test. In the single-phase alloys of a given grain-size, creep-resistance increased with the amount of alloying addition and, for additions of similar atomic percentage, with resistance to recrystallization. The presence of a dispersed phase increased the creep-resistance. In these alloys the effect of a decrease of grain-size, produced by lowering the extrusion temperature, was offset to some extent by the effect of fragmentation of the grains which increased as the extrusion temperature was lowered. Age-hardening to maximum hardness before test reduced transient creep. The solution-treated materials aged markedly during test, and their steady-state creep rates were therefore not different from those of specimens aged before test. Overageing increased the steady rate of creep of fine-grained, but not of coarse-grained, specimens. Grains twinned and irregular in shape were associated with a higher creep-resistance than grains of uniform shape containing few twins.

For a given grain-size, the fatigue-resistance of the single-phase alloys increased markedly as the alloying content was increased, but the effect in the two-phase alloys was only slight. The fatigue-resistance of the age-hardened antimony-bearing alloy was higher than that of the solution-treated material and the overaged material, the fatigue-resistance of the two last-mentioned materials being similar. Decreasing grain-size of the materials increased the fatigue-resistance, but the effect was only slight compared with that for creep-resistance.

A suggestion is made as to the constitution of an alloy likely to have good creep and fatigue properties.

## I.—INTRODUCTION

THE creep and fatigue properties of metallic materials at elevated temperatures have assumed increasing significance with progress in the development of jet and gas-turbine engines. The importance of creep and fatigue behaviour, however, is by no means limited to such applications, since all metals and alloys exhibit these phenomena to an extent dependent on the material and on the prevailing stress and temperature. In general, there is a rough relationship between the melting point of a material and its resistance to creep and fatigue, the resistance decreasing as the temperature approaches the melting point of the material. Thus the creep and fatigue behaviour at atmospheric temperature of low-melting-point materials such as lead and tin are

similar to that of higher-melting-point materials at elevated temperatures. It is, therefore, understandable that creep and fatigue behaviour is of importance in the design of lead water pipes and electric cable sheaths.

Although great advances have been made in the development of materials having a high resistance to creep and fatigue, the effect of constitutional factors on these properties is not completely understood. For instance, there is little existing information as to the effect of adding elements to a basis metal to form alloys of various types, such as single-phase, two-phase, and age-hardenable alloys. The present investigation was therefore carried out to examine the effect of constitutional factors on creep and fatigue behaviour to make possible the selection of lead alloys suitable for service as water pipes and cable sheaths.

\* Manuscript received 12 June 1953. The work described in this paper was made available to members of the B.N.F.M.R.A. in a confidential research report issued in November 1952.

† Formerly Investigator, B.N.F.M.R.A.; now at National Physical Laboratory, Teddington, Middlesex.

‡ Formerly Investigator, B.N.F.M.R.A.; now at Tin Research Institute, Greenford, Middlesex.

A short account of relevant published information is given in Appendix I (p. 193).

## II.—SCOPE OF THE INVESTIGATION

The tests were designed to show the influence of additions of various elements to a basis lead of high purity. The alloying elements were so chosen that some of the resulting alloys were single-phase, (lead-tin alloys), some two-phase (lead-copper alloys), and others were amenable to heat-treatment causing age-hardening or precipitation (lead-antimony alloys).

All the test specimens were prepared in the form of rod by extrusion on a small laboratory extrusion press. Since grain-size was considered to be of importance, it was generally most convenient to study the effect of this factor by producing specimens of different grain-sizes by extruding each alloy at a series of temperatures.

## III.—PREPARATION OF THE EXTRUDED ROD

### 1. MATERIALS

The composition of the basis lead, which was specially refined by Consolidated Mining and Smelting Co. of Canada, Ltd., for the present work, is shown in Table I. This table shows the analysis given by the suppliers and a check analysis made by the American Smelting and Refining Co. The purities of the alloying elements, as given by the suppliers, are shown in Table II.

TABLE I.—*Analysis of the Basis Lead.*

Element	Analysis by Consolidated Mining and Smelting Co., %	Analysis by American Smelting and Refining Co.	
		Spectro-graphic, %	Chemical, %
Ag . . .	0.00003	<0.0001	...
Cu . . .	0.0001	0.0001	0.00016
Zn . . .	0.0001	n.d.	0.0001
Fe . . .	0.0001	trace	0.0001
Bi . . .	0.0001	0.0001	0.00008
Tl . . .	0.0002	n.d.	...
Sb . . .	0.0001	"	0.00004
Cd . . .	<0.0001	"	<0.0001
As . . .	trace	"	n.d.
Se and Te . .	"	...	...
Au . . .	"	n.d.	...
In . . .	"	"	...
Ni . . .	nil	"	0.000006
Co . . .	"	...	...
Sn . . .	"	n.d.	...

n.d. = not detected.

TABLE II.—*Purity of Alloying Elements.*

Element	Purity, %	Element	Purity, %
Tin . . .	99.996	Indium . . .	99.9
Copper . . .	99.999	Thallium . . .	99.9
Antimony . .	99.975	Arsenic . . .	99.95
Cadmium . . .	99.995		

Alloys containing the following additions were made up:

0.05, 0.2, 0.5, and 1 wt.-% tin  
 0.005, 0.01, 0.05, and 0.1 wt.-% copper  
 0.05, 0.5, and 0.85 wt.-% antimony  
 0.9 wt.-% antimony + 0.001 wt.-% arsenic  
 0.09 at.-% each of indium, thallium, and cadmium.

Analysis of the first and last billets cast from each melt showed them to be of uniform composition, with nominal and actual compositions similar. The oxygen content of all these materials was less than 0.0001%, this figure being the limit of accuracy of the method of analysis.<sup>1</sup>

### 2. PREPARATION OF BILLETS FOR EXTRUSION

The basis lead and the alloys were melted in a mild-steel pot from which they were bottom-poured, through an atmosphere of nitrogen, into a cast-iron mould  $2\frac{1}{2}$  in. in dia.  $\times$  10 in. long. The molten metal was maintained at 400° C., except for the 0.1% copper alloy, for which a casting temperature of 500° C. was necessary to obtain a homogeneous melt.

Sufficient billets were cast from one melt to carry out all the creep and fatigue tests required on a material of one composition.

The cast billets were homogenized at 300° C. and surface-machined before extrusion.

### 3. EXTRUSION

The materials were extruded by the inverted method as straight  $\frac{7}{8}$ -in.-dia. rods, which were cooled freely in air. A closely controlled extrusion speed of 10.5 in./min. was used, unless otherwise stated. Several extrusion temperatures were used for most of the materials to obtain rods with a range of grain-sizes.

## IV.—EXPERIMENTAL PROCEDURE

All tests, both creep and fatigue, were carried out at  $20^\circ \pm 1^\circ$  C. The extruded rods were tested in creep under constant stress as described elsewhere.<sup>2,3</sup> Fatigue tests were carried out on a 3000-r.p.m. rotating-beam (Wöhler) testing machine modified for testing lead rod.<sup>2</sup> The specimens, which were carefully machined from the extruded rod, were prepared for testing by rubbing the reduced sections with "Bluebell" metal polish on Selvyt cloth until all machining marks had been removed. They were then thoroughly degreased with trichlorethylene.

The stress corresponding to a life of  $20 \times 10^6$  reversals, termed in this work "the endurance limit", has been taken as a measure of fatigue-resistance.

Longitudinal sections of the extruded rods were prepared, as described elsewhere,<sup>4</sup> for grain-size determinations, using comparison screens. In determining the grain-size, a twinned grain was counted as one grain.



The grain-size of each material was reasonably uniform, although, generally, the uniformity slightly decreased, and the crystals contained more twins, the lower the extrusion temperature. The extent of twinning, however, was only small even at the lowest temperatures of extrusion.

Only small amounts of oxide or other insoluble impurities were observed in the basis lead and the single-phase alloys. The particle size of the insoluble copper was about the same in all the alloys containing this element. Even the 0.005% copper alloy, extruded at 250° C., contained insoluble copper. It was confirmed metallographically that the solubility of copper in lead at 300° C. is much less than 0.005%.

X-ray examination showed that only a slight amount of preferred orientation existed in the 1% tin and the 0.1% copper alloys extruded at 100° C. It is, therefore, unlikely that the creep or fatigue properties of any of the materials were affected by variations in the extent of preferred orientation.

## V.—CREEP TESTS

### 1. REPRODUCIBILITY OF TESTS

Tests on specimens taken from the same extrusion and from different extrusions showed that the reproducibility of test results was good enough for the results of single tests on a material in each condition to be accepted with confidence.

### 2. GENERAL FEATURES OF THE CREEP CURVES

Many of the creep curves showed an inflection which is now generally regarded as being associated

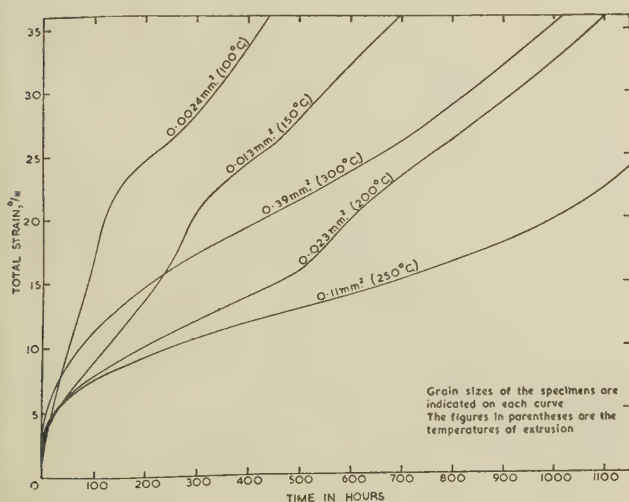


FIG. 1.—Creep Tests at 1000 lb./in.<sup>2</sup> on the Lead-1% Tin Alloy of Various Grain-Sizes.

with recrystallization<sup>5,6</sup> (see e.g. Fig. 1.) Recrystallization occurred at lowest strains and after shortest times in the basis lead; increasing alloy content retarded the occurrence of the inflection at

equal stresses and grain-sizes. The smaller the grain-size, and alternatively the larger the stress, other things being equal, the lower the strain and the shorter the time necessary for recrystallization.

Although the curves of the basis lead clearly showed the inflection characteristic of recrystallization only

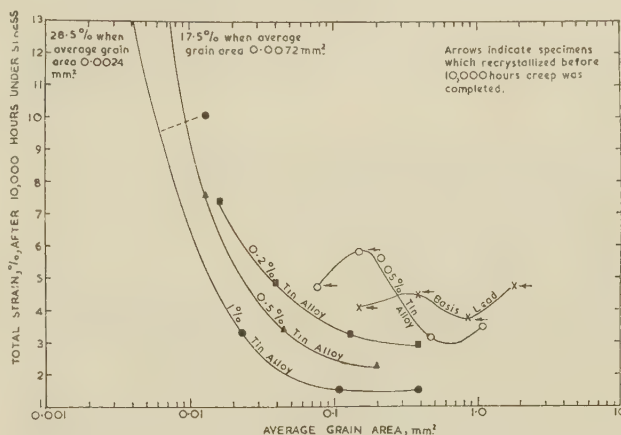


FIG. 2.—Effect of Grain-Size on the Creep-Resistance of the Lead-Tin Alloys at 300 lb./in.<sup>2</sup>.

at low stresses, it is considered that the beginning of tertiary creep in the specimens tested at high stresses was also associated with recrystallization, since metallographic examination of these specimens after failure showed that this phenomenon had occurred. Intercrystalline cracking, which also increases creep rate, was absent. Recrystallization may, also, have contributed to tertiary creep in the coarse-grained specimens of the various lead-tin and lead-copper alloys tested at the highest stresses.

In the basis lead and the alloys the instantaneous extension on loading a specimen in creep at any one stress became smaller as the grain-size decreased.

### 3. EFFECT OF TYPE OF ALLOY SYSTEM ON CREEP-RESISTANCE

#### (a) Effect of Amount of Addition in Single- and Two-Phase Alloys

The results of tests on the single-phase (lead-tin) and two-phase (lead-copper) alloys are shown in Figs. 2 and 3, where the total strain after 10,000 hours' creep at 300 lb./in.<sup>2</sup> has been used as a measure of creep-resistance. The results obtained at this relatively low stress show most clearly the effects of the amount of added element and of initial grain-size, since recrystallization during test occurred less readily at this than at the higher stresses used. In Figs. 2 and 3 arrows mark the points corresponding to those specimens which recrystallized before the 10,000-hr. period was completed.

Fig. 2 shows that the creep properties of the single-phase alloys tested are little affected by grain-size when the latter exceeds some critical value, about

0.02 mm.<sup>2</sup>, but that below this value grain-size has a marked effect, the creep-resistance decreasing rapidly with decreasing grain-size. In specimens of one grain-size, in the range 0.02–0.4 mm.<sup>2</sup>, creep-resistance increased almost linearly as the alloying

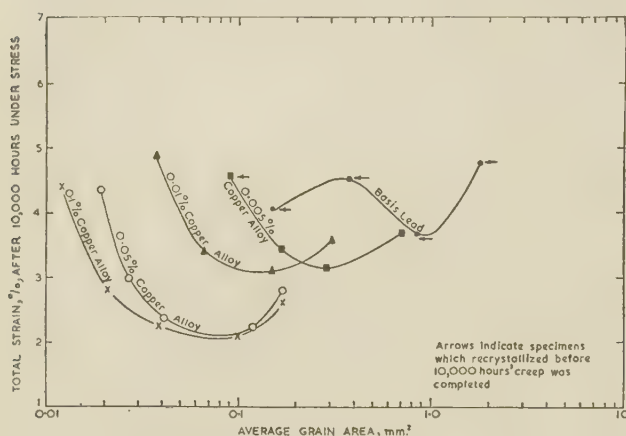


FIG. 3.—Effect of Grain-Size on the Creep-Resistance of the Lead-Copper Alloys at 300 lb./in.<sup>2</sup>.

addition increased, as shown in Fig. 4. Some points are not included in Fig. 4, since the specimens had recrystallized before the 10,000-hr. period was completed.

Detailed examination of Fig. 2 shows that for large

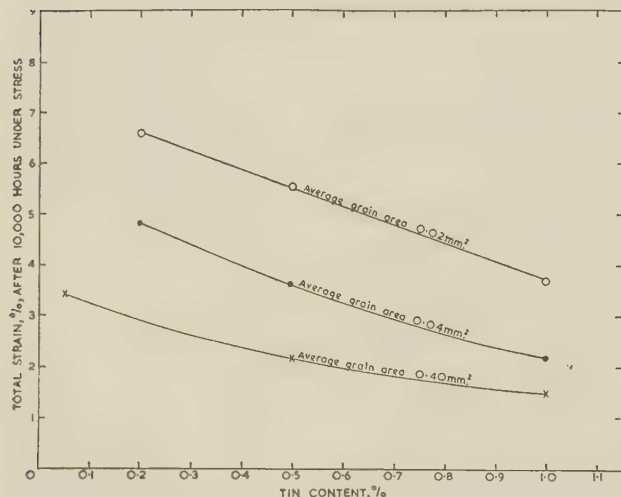


FIG. 4.—Effect of Tin Content on the Creep Resistance of Specimens of Similar Grain-Size at 300 lb./in.<sup>2</sup>.

grain-sizes in the 0.05% tin alloy there was a slight decrease in creep-resistance with increasing grain-size; an effect contrary to the relationship observed for fine-grained material. This effect was also found in the creep curves of some of the other materials and

was most marked at the highest stresses (see e.g. Fig. 1). By analogy with the behaviour of the lead-copper alloys, this anomalous behaviour may have been associated with slight fragmentation of the grains of the materials resulting from the extrusion process, although the X-ray technique described in Appendix II (p. 194) failed to reveal it.

The results of tests on two-phase alloys are shown in Fig. 3. In none of the alloys was the creep-resistance markedly dependent on grain-size. Creep-resistance tended to increase up to a point with increasing grain-size and then to decrease. This decrease of creep-resistance with increasing grain-size suggested that some variable with an effect opposite to that of grain-size was affecting the behaviour of these alloys.\* X-ray examination (see Appendix II) showed that this variable was fragmentation of the grains † resulting from the extrusion process. For these specimens the conditions favouring fine grain-size also favoured fragmentation, which is shown later to increase creep-resistance.

Fig. 3 shows that the creep-resistance of the alloys increased with increasing copper contents, and further tests described later show that this was also true when the fragmentation variable was eliminated.

#### (b) Effect of Alloying Additions Which Cause Age-Hardening

Commercially produced lead-antimony alloys age-harden readily, and it was intended that an alloy of 0.85% of the high-purity antimony with the basis lead should be used to study the effect of age-hardening, but, as shown elsewhere,<sup>7</sup> this alloy did not age-harden after appropriate heat-treatments. It was found that the addition of a small amount of impurity, notably arsenic, was necessary to bring about age-hardening. It was also shown that for the impurity to be most effective in promoting age-hardening, it must be in solid solution.

The present tests were accordingly carried out on the lead + 0.9% antimony + 0.001% arsenic alloy extruded at 160° C., the alloy being single-phase at this temperature. Specimens were heated for various times at 250° C. and water-quenched to produce large and small grain-sizes. The temperature of 250° C. was employed for solution of the arsenic.

Tests were carried out on the materials in the solution-treated condition and after ageing to maximum hardness at both 20° and 50° C. It was originally intended that specimens should be tested after overageing at 50° C., but little overageing had occurred at this temperature after about 7000 hr. Overageing was obtained by further heat-treatment at 100° C.

Metallographic examination of the materials before

\* It was shown that the observed relationships between grain-size and creep-resistance were in no way affected by the variations in solubility of copper in lead which must occur, however slightly, with change of extrusion temperature.

† This fragmentation does not necessarily mean that the grains were in a polygonized condition, since rapid plastic straining at atmospheric temperature produced similar fragmentation (see Appendix III, p. 194); rapid polygonization is unlikely at this temperature.



test showed that in the solution-treated and quenched condition there was slight discontinuous precipitation at the grain boundaries but no continuous precipitation within the grains. Ageing to maximum hardness at 20° and 50° C. did not affect the extent of discontinuous precipitation, but produced extensive continuous precipitation which was only just resolvable at a magnification of 2000 times. Overageing, partly at 50° and partly at 100° C., produced no change in structures from those corresponding to the condition of maximum hardness.

Hardness and grain-size data for the specimens tested are shown in Table III.

TABLE III.—Hardness and Grain-Size of Creep Specimens of 0.9% Antimony-0.001% Arsenic Alloy After Various Heat-Treatments.

Condition	Vickers Pyramid Hardness Number	
	Fine-Grained Material	Coarse-Grained Material
As solution-treated . . . . .	6.0	5.8
Aged to max. hardness at 20° C.	11.5	13.5
Aged to max. hardness at 50° C.	9.3	10.1
Overaged at 50° and 100° C. . .	7.4	8.0
Average grain area, mm. <sup>2</sup> . . .	0.015	1.8

The creep curves obtained at 1000 lb./in.<sup>2</sup> are shown in Fig. 5 for both the fine- and coarse-grained specimens. It can be seen in Fig. 5 that age-hardening

of creep, which was almost linear from the moment of loading, was similar to the rate of steady-state creep of the solution-treated specimens, but it must be remembered that by the time the latter specimens had reached the stage of steady-state creep they also would have aged, at 20° C., to a maximum hardness. Overageing slightly lowered the creep-resistance of the fine-grained specimen, as compared with the age-hardened condition, but did not affect the creep-resistance of the coarse-grained specimens.

The same general features were observed in tests at lower stresses.

#### (c) Relative Creep-Resistance of the Lead-Tin, Lead-Copper, and Lead-Antimony-Arsenic Alloys

Although the lead-tin, lead-copper, and lead-antimony-arsenic alloys are respectively typical of solid-solution, two-phase, and age-hardenable-type alloys, their creep-resistances should not be regarded as being entirely indicative of the types of alloy systems which they represent, since later sections show that variables other than type of alloy system are important. In Table IV, however, some idea can be obtained as to the effect of these alloying elements on the relative creep-resistances of materials of one grain-size.

TABLE IV.—Relative Creep Resistances of the Lead-Tin, Lead-Copper and Lead-Antimony-Arsenic Alloys.

Average grain area = 0.015 mm.<sup>2</sup>.

Alloy	Creep Strain, % after 500 hr. at 1000 lb./in. <sup>2</sup>	Creep Strain, % after 10,000 hr. at 800 lb./in. <sup>2</sup>
Lead-1% Tin . . . . .	28	4.5
Lead-0.1% Copper . . . . .	Broken *	3.5
Lead-0.9% Antimony-0.001% Arsenic (age-hardened) . .	0.6	1.5

\* 23% general extension.

The table shows that comparison of creep-resistances at high stresses can be misleading. Thus, at 1000 lb./in.<sup>2</sup>, the age-hardened lead-antimony-arsenic alloy appears greatly superior to the other two, while at the lower stress the respective creep strains in a given time differ, at the most, by a factor of only 3 to 1. This effect of stress on relative creep-resistances is due not only to fundamental differences in creep behaviour, but also to recrystallization during test which occurs readily at the higher stress, especially in the lead-copper alloy.

#### 4. EFFECT OF OTHER FACTORS ON CREEP-RESISTANCE

##### (a) Effect of Different Additions Entering into Solid Solution

An attempt was made to determine whether the effects of different solutes were dependent on the differences between their melting points and atomic

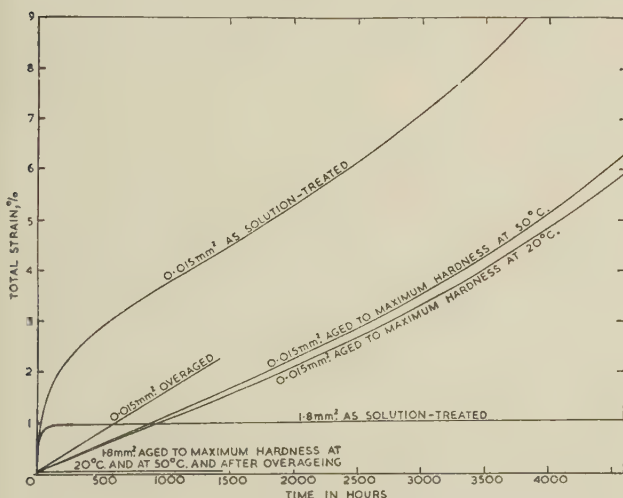


Fig. 5.—Creep Tests at 1000 lb./in.<sup>2</sup> on the Lead-0.9% Antimony-0.001% Arsenic Alloy Showing the Effect of Age-Hardening and of Overageing.

at 20° or 50° C. completely removed the stage of transient creep, which was clearly defined in the curves for the as-solution-treated material. Moreover, although the specimens heat-treated at 20° and 50° C. were aged to different maximum hardnesses, they had a very similar creep-resistance. Their rate

diameters and those of the basis metal. For this purpose tests were carried out on five binary alloys containing cadmium, thallium, tin, indium, and antimony, respectively. The first three elements in this list have melting points not very different from that of lead, but their apparent atomic diameters,

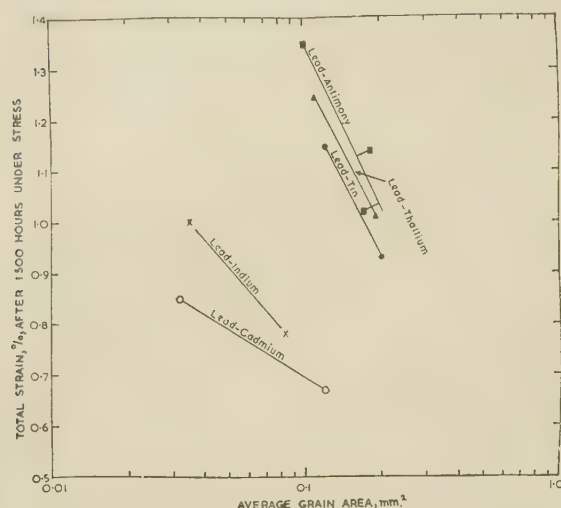


Fig. 6.—Relative Creep-Resistances, at 300 lb./in.<sup>2</sup> of Single-Phase Alloys Containing Equal Atomic Percentages of Various Elements.

according to X-ray data given in the literature,<sup>53</sup> differ by 14.6, 1.4, and 3.4%, respectively, from that of lead. The apparent atomic diameters of the last three differ by about 4% from that of lead, but their melting points (232°, 156°, and 630° C., respectively) lie above and below that of lead.

Metallographic examination showed that antimony is the least soluble of these elements and has a solid solubility at 20° C. of between 0.05 and 0.1 wt. % (0.09–0.18 at.-%). Each alloy was, therefore, made up to contain 0.09 at.-% of alloying element, so that all were single-phase at 20° C. The alloys were extruded at 100° C., plastically strained in tension, and then annealed to produce in each material two specimens with different grain-sizes. The specimens were examined after annealing, by the X-ray technique described in Appendix II, and were found to be fully recrystallized.

The result of creep tests on the materials so prepared are shown in Fig. 6, where the strain in 1500 hr. has been used as a measure of creep-resistance. Up to the end of 1500 hr. none of the materials had recrystallized during test.

Inspection of Fig. 6 shows that there is no relationship between the creep properties of the alloys and the melting points of the solutes and therefore some uncontrolled factor was affecting the creep behaviour of these alloys. This invalidates the indication in Fig. 6 that creep-resistance increases with difference in atomic diameter between solute and basis metal. However, during preparation of the test specimens it was found that for similar amounts of prior strain,

higher annealing temperatures had to be used to produce complete recrystallization in the cadmium and indium alloys than in the others; also, for specimens of similar grain-size (0.1 mm.<sup>2</sup>), the cadmium and indium alloys had a greater resistance to recrystallization, as measured by the time to the beginning of the characteristic inflection in the creep curves, than the other alloys.

The cadmium and indium alloys were presumably more resistant than the others to the structural changes which precede recrystallization, and this may account for their relatively good resistance to creep.

#### (b) Effect of Second Phase Precipitated from a Supersaturated Solid Solution

As mentioned earlier, the lead-antimony alloys made from the high-purity metals used in this work do not age-harden. These high-purity alloys were, therefore, used to study the influence of a second phase precipitated from solid solution.

High-purity 0.5 and 0.85% antimony alloys were extruded at 120° and 160° C., respectively, and air-cooled. At these temperatures the two alloys were just within the single-phase region of the equilibrium diagram. The extruded alloys had similar grain-sizes, and X-ray examination showed that their grains were not fragmented. Both alloys were heat-treated at 100° C. to precipitate antimony present in excess of its solubility at this temperature. Hardness tests confirmed that age-hardening did not occur. Tests at 500 lb./in.<sup>2</sup> were begun after various times of heat-treatment.

The results of the creep tests are shown in Fig. 7,

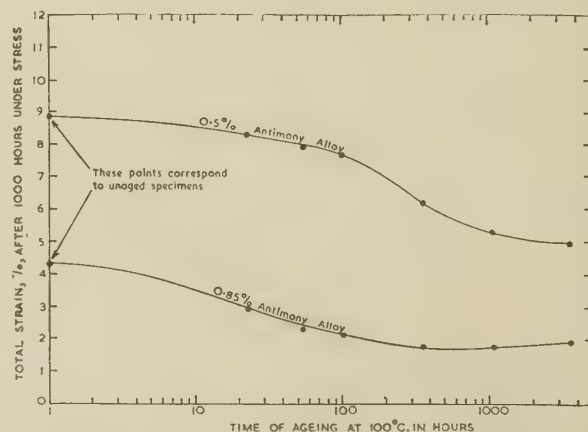


Fig. 7.—Effect of Time of Ageing at 100° C. on the Creep-Resistance of the Lead-0.5% and the Lead-0.85% Antimony Alloys at 500 lb./in.<sup>2</sup>.

where the strain in 1000 hr. has been plotted against time of ageing at 100° C. It can be seen that the creep properties of the alloys were improved when some of the antimony was precipitated from solid solution. In these alloys, therefore, the reduction in the amount of antimony in solid solution, which accompanies precipitation, was more than offset by the beneficial effect of the precipitated second



phase. Comparison of the creep-resistances of the 0.5 and 0.85% antimony alloys when they consisted of a single phase and when they were fully precipitated at 100°C. confirms that solid-solution hardening and the presence of a second phase both increase creep-resistance (Fig. 7).

(c) *Effect of Fragmentation of the Grains in the Two-Phase Alloys*

(i) *Effect of Speed of Extrusion.*—X-ray examination showed that the extent of fragmentation of the grains of a lead-copper alloy extruded at a given temperature increased as the speed of extrusion was lowered (see Appendix II). Experiments were, therefore, carried out on specimens extruded at various speeds to determine the effect of fragmentation of the grains on creep-resistance.

The 0.1% copper alloy was extruded at speeds of 2.6 and 42 in./min. at each of the temperatures 100°, 200°, and 300°C. The specimens obtained were tested at 500 lb./in.<sup>2</sup>. The results of these tests are compared in Fig. 8 with those obtained from the specimens extruded at the "normal" speed of 10.5 in./min. Comparison of the behaviour of the specimens with similar grain-sizes shows that creep-resistance was raised by decreasing the speed of extrusion, which increased the fragmentation of the grains.

(ii) *Creep-Resistance of Recrystallized Specimens.*—Specimens of each lead-copper alloy and of the basis

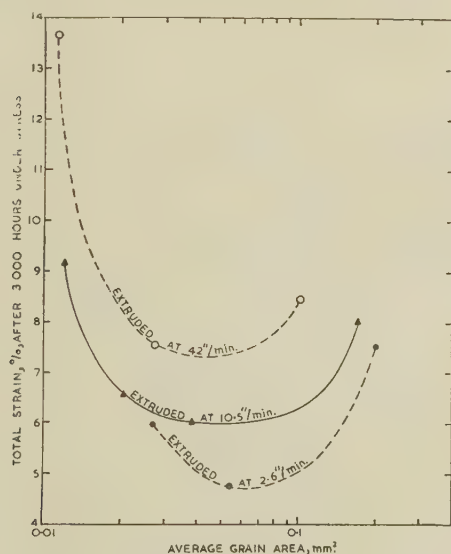


FIG. 8.—Effect of Speed of Extrusion on the Creep-Resistance of the Lead-0.1% Copper Alloy at 500 lb./in.<sup>2</sup>.

lead were overstrained by various amounts and then annealed at 100°C. to provide specimens of different grain-size in each material. X-ray examination showed that these specimens were not fragmented and were work-free. Metallographic examination revealed that the extent of twinning had increased during annealing and that the grain shape had become

irregular. The extent of twinning was much the same for all the materials.

The materials were tested at 300 lb./in.<sup>2</sup>, and in Fig. 9 the strains at 10,000 hr. are plotted against the logarithms of the grain-sizes of the materials. It can be seen that creep-resistance increased as the copper content was increased, as for these materials in the

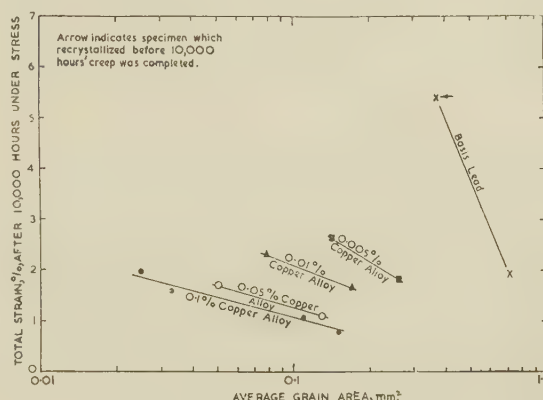


FIG. 9.—Effect of Grain-Size on the Creep-Resistance at 300 lb./in.<sup>2</sup> of the Lead-Copper Alloys After Recrystallization.

as-extruded condition. Moreover, in each material the creep-resistance was lowest in the finest-grained specimens. Comparison of Figs. 3 and 9 shows the unexpected result that, for specimens of the same grain-size, the recrystallized, and consequently work-free materials, had a higher creep-resistance than the as-extruded materials which contained fragmented grains. The other major difference between the two groups of materials was that the grains were more extensively twinned and irregular in shape in the recrystallized than in the as-extruded specimens. This suggests that a twinned and irregular structure has higher creep-resistance than one which is not twinned and has grains of uniform shape.

(d) *Effect of Twinning and of Grain Shape*

The effect of twinning and of grain shape was further investigated, using the 1% tin alloy. Specimens of this material extruded at 100°C. were

TABLE V.—Effect of Twinning and of Grain Shape on the Creep-Resistance of the Lead-1% Tin Alloy.

Condition	Average Grain Area, mm. <sup>2</sup>	Creep Strain (%) at Various Times, hr.				
		500	1000	2000	3000	5000
Grains of regular shape containing few twins	0.12	1.51	1.95	2.69	3.26	4.26
	0.30	1.63	2.03	2.61	3.07	3.83
Grains twinned and of irregular shape	0.04	0.88	1.07	1.55	1.81	2.53
	0.098	1.07	1.29	1.62	1.86	2.35

plastically strained in tension and recrystallized, some by flash-annealing at 300°C. in a salt bath and others by heating in air at 100°C. Photomicrographs

illustrating the structures obtained are shown in Figs. 15 and 16 (Plate XXVI). Two specimens of different grain-sizes were produced by each method of recrystallization. All specimens were found by X-ray examination to be fully recrystallized. They were tested at 500 lb./in.<sup>2</sup>, and the results are shown in Table V.

It can be seen that the specimens with regularly shaped grains containing few twins have a significantly lower creep-resistance than those specimens with twinned and irregularly shaped grains.

### (e) Effect of Prior Plastic Strain

An investigation was made of the relative effects of plastic strain, before creep testing, on the single-phase 1% tin alloy and the two-phase 0.1% copper alloy. While the general effect of increasing prior plastic strain was to reduce progressively the transient stage of creep, as has been shown by several investigators, there were features of the creep curves which have not been reported before. For this reason the results of this work are recorded in Appendix III.

## 5. EFFECT OF TYPE OF ALLOY SYSTEM ON LIFE AND GENERAL EXTENSION AT FAILURE

The life and general extension at failure for the basis lead, the single- and two-phase alloys in the as-extruded condition, are shown in Tables VI and

TABLE VI.—*The Life and General Extension at Failure of the Basis Lead and the Lead-Tin Alloys.*

Material	Temp. of Extrusion, °C.	Average Grain Area, mm. <sup>2</sup>	General Extension (%) at Failure for Various Stresses, lb./in. <sup>2</sup>			Life in Hours at Various Stresses, lb./in. <sup>2</sup>		
			1000	750	500	1000	750	500
Basis lead	100	0.15	67	50	37	<24	<119	1060
	150	0.38	62	48	26	<24	80	1210
	200	0.86	29	47	22	<24	<120	1010
	250	1.8	35	37	15	<24	<144	1160
Lead-0.05% tin alloy	100	0.077	32	38	19	6½	63	2544
	150	0.15	32	22	12	9	61	2040
	200	0.47	22	20	21	12½	<120	2330
	250	1.1	26	23	19	15½	<120	2800
Lead-0.2% tin alloy	100	0.016	55	28	18	36	295	11,057
	150	0.04	45	32	...	38	415	...
	200	0.13	34	31	20	47	460	12,400
	250	0.39	27	33	...	54	630	...
Lead-0.5% tin alloy	100	0.0072	57	35	...	230	2475	...
	150	0.013	50	39	...	264	2480	...
	200	0.045	40	36	...	266	3130	...
	250	0.20	39	33	...	284	2720	...
Lead-1% tin alloy	100	0.0024	59	68	250*	1656	2840	7944
	150	0.013	66	98	260*	1968	5125	17,380
	200	0.023	64	56	53*	2095	4084	28,600
	250	0.11	45	29*	...	1896	6630	...
	300	0.39	59	31*	...	1536	6000	...

\* Specimens in which little or no recrystallization occurred during test.

VII. No failures occurred at 300 lb./in.<sup>2</sup>. Most of the specimens of the lead-antimony-arsenic alloy broke in the grips, so that these results are not significant and therefore are not included.

In most cases the general extension at failure of the single-phase (lead-tin) alloys at any one stress increased as the grain-size became smaller, although there was no similar effect in the two-phase (lead-copper) alloys. Most of the specimens recrystallized during test, as indicated by the characteristic in-

TABLE VII.—*The Life and General Extension at Failure of the Basis Lead and the Lead-Copper Alloys.*

Material	Temp. of Extrusion, °C.	Average Grain Area, mm. <sup>2</sup>	General Extension (%) at Failure for Various Stresses, lb./in. <sup>2</sup>			Life in Hours at Various Stresses, lb./in. <sup>2</sup>		
			1000	750	500	1000	750	500
Basis Lead	100	0.15	67	50	37	<24	<119	1060
	150	0.38	62	48	26	<24	80	1210
	200	0.86	29	47	22	<24	<120	1010
	250	1.8	35	37	15	<24	<144	1160
Lead-0.005% copper alloy	100	0.091	79	39	20	14	81	3576
	150	0.17	44	46	33	12	85	3100
	200	0.29	44-64	39	16	16	93	2568
	250	0.71	48	40	20	<24	90	2740
Lead-0.01% copper alloy	100	0.037	64	33	14	16	148	9820
	150	0.067	54	27	12	17	131	7620
	200	0.15	42	23	19	15	127	10,458
	250	0.31	52	28	14	17	130	6120
Lead-0.05% copper alloy	100	0.019	27	19	...	75	2500	...
	150	0.027	32	23	...	<96	3500	...
	200	0.041	21	14	...	60	2100	...
	250	0.12	27	14	...	56	1700	...
	300	0.17	27	24	...	49	1800	...
Lead-0.1% copper alloy	100	0.012	23	18	33	68	2360	16,220
	150	0.021	21	21	...	76	3000	...
	200	0.038	21	20	...	51	2340	...
	250	0.10	29	17	...	62	1700	...
	300	0.17	25	29	...	46	1800	...

flexion in the creep curves. This recrystallization during test occurred in any one material after shorter times and at lower strains as the grain-size became smaller. Metallographic examination of failed specimens showed that all the 1% tin alloy specimens and the 0.1% copper specimen tested at 500 lb./in.<sup>2</sup> were the only ones to contain intercrystalline cracking. The extent of this cracking in the 1% tin alloy became less as the grain-size decreased (Fig. 17, Plate XXVI), and in the finest-grained specimens the cracks were short and, judging from their shape, had little tendency to spread.

In the single- and two-phase materials, of any one grain-size, the general extension at failure usually became less with decreasing stress. This might be associated with recrystallization occurring less readily as the stress was decreased. In the 1% tin alloy, however, the effect can be associated, also, with intercrystalline cracking, which was more severe the lower the stress (Fig. 18, Plate XXVI). The exception to this general behaviour occurred in the extremely fine-grained 1% tin alloy specimens extruded at 100° and 150° C., and possibly the 0.1% copper alloy extruded at 100° C., where the general extension increased with decreasing stress, despite the fact that intercrystalline cracking, also, became more extensive as the stress was lowered (Fig. 18). The 1%



tin alloy was the only one which did not recrystallize to a coarser grain-size during test.

Generally, at each stress, the life to failure was greater the larger the alloying addition in both the single- and two-phase alloys. Increasing grain-size, at each stress, increased the life to failure of the single-phase alloys, but had no effect on the two-phase alloys.

## VI.—FATIGUE TESTS

The same series of materials were used to study the influence of constitutional factors on fatigue-resistance.

### 1. EFFECT OF TYPE OF ALLOY SYSTEM ON FATIGUE-RESISTANCE

#### (a) Effect of Amount of Addition in Single- and Two-Phase Alloys

The endurance limits of the basis lead, the single-phase (lead-tin), and two-phase (lead-copper) alloys

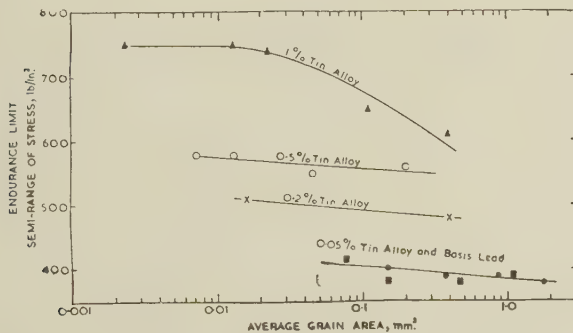


FIG. 10.—Effect of Grain-Size on the Fatigue-Resistance of the Lead-Tin Alloys.

are related to grain-size in Figs. 10 and 11. For similar grain-sizes it is seen that the endurance limits of the single-phase alloys increased as the amount of addition was made larger, but this effect was small in the two-phase alloys. It can be seen also that the endurance limits of the 1% tin and the 0.05% and the 0.1% copper alloys increased as the grain-size became smaller. In the basis lead and the remaining alloys the effect of grain-size was not significant, although, for each material, the endurance curves of specimens of the finest grain-size were slightly but consistently above those of the coarsest grain-size, as shown for the basis lead in Fig. 12.

Metallographic examination of failed specimens showed that the fractures were all intercrystalline. Recrystallization had occurred in some of the materials during test in those regions which had been subjected to the highest stress. There was less recrystallization, for any one grain-size, the higher the amount of the addition (Figs. 19 and 20, Plate XXVI) and, for any one material, the larger the grain-size (Figs. 21 and 22, Plate XXVII). In all the fine-grained materials,

recrystallization was extensive and resulted in an increase of grain-size.

To determine when recrystallization occurred during test, several of the finest-grained specimens of the

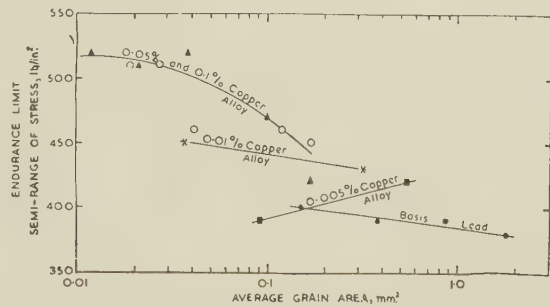


FIG. 11.—Effect of Grain-Size on the Fatigue-Resistance of the Lead-Copper Alloys.

lead-tin and lead-copper alloys were tested at stresses just above their endurance limits and the tests discontinued after various fractions of the time required for failure. Recrystallization occurred in all these alloys after about one-tenth of the time required for failure. These results indicate that for most of each test the fine-grained materials had a grain-size larger than that at the start of the test. Such increases of grain-size would lower the endurance limit, as is shown by the coarse-grained specimens of the 1% tin and 0.05% and the 0.1% copper alloys, which did not recrystallize. The effect of grain-size on endurance limit was confirmed by tests, described later, on another alloy which did not recrystallize during test.

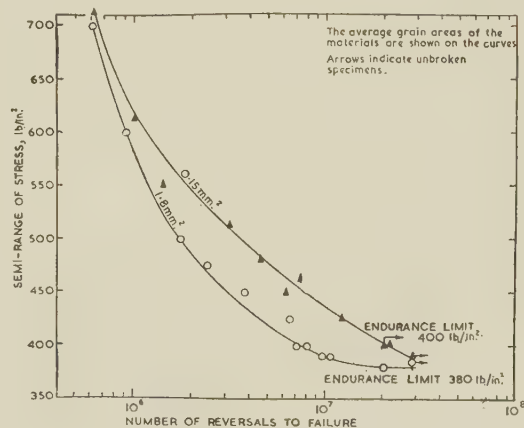


FIG. 12.—Endurance Curves for the Basis Lead of Two Grain-Sizes.

#### (b) Effect of Second Phase Precipitated from a Supersaturated Solid Solution

To examine further the effect of composition in single- and two-phase alloys which do not recrystallize during test, the 0.5 and 0.85% antimony alloys were extruded at temperatures such that they were single-phase during extrusion and produced materials with

similar grain-sizes, as described for the creep tests. Fatigue tests were made on these materials immediately after extrusion, when they were wholly single-phase, and after 3600 hr. at 100° C., when precipitation was complete. In the latter condition the alloys contained different amounts of insoluble phase, but similar amounts of antimony in solid solution. Hardness tests confirmed that age-hardening did not occur during the ageing treatment.

The endurance limits of the alloys in the two conditions are shown in Table VIII, where it can be seen that increasing the antimony content by 0.35% improved fatigue-resistance extensively in the single-phase materials, but only slightly in the two-phase materials.

In each alloy precipitation from supersaturated solid solution decreased the fatigue-resistance. Thus the lowering of fatigue-resistance by a decrease of

TABLE VIII.—Effect on the Fatigue-Resistance of Lead-Antimony Alloys of a Precipitated Second Phase.

Condition	Endurance Limit, Semi-Range of Stress, lb./in. <sup>2</sup>	
	Lead-0.5% Antimony Alloy	Lead-0.85% Antimony Alloy
As extruded (single-phase) . . . .	1100	1400
After complete precipitation (two-phase)	1000	1125

solid-solution hardening was not offset by the formation of a second phase.

### (c) Effect of Alloying Additions Which Cause Age-Hardening

The lead-0.9% antimony-0.001% arsenic alloy was extruded at 160° C., at which temperature it consisted of a single phase. Lengths were solution-treated for various times at 250° C. and water-quenched to produce materials with large and small grain-sizes, as for the creep tests. Specimens of both grain-sizes were tested in the following conditions: (i) as-solution-treated and water-quenched; (ii) after ageing to a maximum hardness at 20° C.; (iii) after ageing to a maximum hardness at 50° C.; and (iv) after overageing partly at 50° C. and partly at 100° C. The endurance limits of these materials are shown in Table IX.

Hardness measurements on failed specimens from these tests showed that the solution-treated coarse-grained material had hardened during test to about the same extent as that aged to maximum hardness at 20° C. before test. The solution-treated, fine-grained material did not harden very much during test.

These observations account for the apparent anomaly in Table IX, namely that while age-hardening before test markedly improved the endurance of

the fine-grained material, it had little effect on the coarse-grained alloy.

TABLE IX.—Effect of Age-Hardening and of Overageing on the Fatigue-Resistance of the Lead-0.9% Antimony-0.001% Arsenic Alloy.

Condition	Fine-Grained Material		Coarse-Grained Material	
	Hardness (V.P.N.)	Endurance Limit, Semi-Range of Stress, lb./in. <sup>2</sup>	Hardness (V.P.N.)	Endurance Limit, Semi-Range of Stress, lb./in. <sup>2</sup>
As-solution treated . . . . .	5.9	1400	5.9	1375
Aged to max. hardness at 20° C. . . . .	12.9	1850	14.2	1425
Aged to max. hardness at 50° C. . . . .	11.8	1700	12.2	1425
Overaged at 50° C. and 100° C. . . . .	7.4	1400	8.1	1275
Average grain area, mm. <sup>2</sup> . . . . .	0.015		1.8	

The overaged materials had lower endurance limits than the age-hardened alloys. In the fine-grained material the overaged and the solution-treated specimens had similar endurance limits. In the coarse-grained material the endurance limit of the overaged specimens was lower than that of the solution-treated specimens, probably because the latter had age-hardened during test.

The specimens tested in the solution-treated condition were shown, by metallographic examination, to have failed partly by transcrystalline and partly by intercrystalline cracking. The specimens aged to maximum hardness at 20° and 50° C. and after overageing, failed entirely by intercrystalline cracking, as in the case of the basis lead and the lead-tin and the lead-copper alloys.

## 2. EFFECT OF GRAIN-SIZE

Some of the foregoing tests suggested that the endurance limit is higher for fine- than for coarse-

TABLE X.—Effect of Grain-Size on the Fatigue-Resistance of the Lead-0.85% Antimony Alloy.

Extrusion Temp., °C.	Average Grain Area, mm. <sup>2</sup>	Endurance Limit, Semi-Range of Stress, lb./in. <sup>2</sup>
160	0.0039	1400
200	0.012	1250
250	0.043	1175
300	0.19	1025

grained materials, whereas in others any such effect was obscured by recrystallization during test. A lead-0.85% antimony alloy which did not recrystallize during test was therefore used to confirm the effect of grain-size on endurance limit.



The alloy was extruded at four temperatures, at which it was single-phase, to obtain materials with a range of grain-sizes. The results of tests on these materials are shown in Table X, where it can be seen that the endurance limit increased as the grain-size became smaller.

## VII.—SUMMARY AND DISCUSSION

An attempt has been made to show how the creep and fatigue properties of lead-base alloys are affected by their constitution and other metallurgical characteristics. Most of the materials were extruded on a laboratory press at extrusion rates much lower than those normally used in practice, but some were cold worked and recrystallized after extrusion. The results show that many factors are at work, some in opposition to others, so that it becomes very difficult to generalize in a quantitative way. However, it is possible to generalize in qualitative terms, and no more than this is attempted.

### 1. CREEP

#### (a) *Effect of Grain-Size*

In general, the creep properties of the alloys are markedly dependent on their grain-size. Except where other factors interfere, creep-resistance, as measured by the creep strain occurring in a given time under a given stress, decreased rapidly as the extrusion temperature was lowered and as the grain-size consequently became smaller.

This finding is in agreement with McKeown's work on lead<sup>8</sup> and with the main body of evidence on the effect of grain-size on other metals at temperatures where they show continuous creep. Some authors have paid insufficient attention to this factor of grain-size,<sup>9-14</sup> and their observation that additions of other elements sometimes impair the creep properties of the basis metal conflicts with the results of the present work for that reason. Thus the effect of grain-size can be as great as any other constitutional factor, and the influence of other constitutional factors can be discussed only by comparing materials of similar grain-size.

#### (b) *Effect of Type of Alloy System*

In most of the work lead-tin alloys were tested as representative of solid-solution-type materials, and their resistance to creep improved continuously and approximately linearly as the amount of alloying addition was increased up to 1% tin. This indicates that the more extensive the solution-hardening the greater the improvement in creep-resistance. It would, therefore, be expected that, for additions of similar atomic percentage, an increase in solution-hardening resulting from an increase in the difference of atomic diameter between solute and solvent would also increase the creep-resistance. Experiments failed, however, to establish this effect conclusively.

A few supplementary tests on various solid solu-

tions showed that the creep-resistance of the lead-tin alloys was not representative of that of all solid-solution systems. For example, for very dilute alloys at least, much greater resistance to creep was conferred by additions of indium or cadmium than by additions of tin or antimony. The effects of these solutes were not clearly related to the difference between their atomic diameters or melting points and those of the basis metal. However, the first two elements named greatly increased the resistance of the material to recrystallization, whereas the second two elements did not. This finding is in agreement with that of Austin, St. John, and Lindsay,<sup>15</sup> who consider that the influence of resistance to recovery or recrystallization on creep-resistance is more important than that of solution-hardening.

The presence of a dispersed phase in the basis material increased its resistance to creep. In the lead-copper alloys examined, the size of the particles of the dispersed phase was roughly constant, and no observations were made on the influence of this variable. In these alloys particularly, the effect of grain-size was often more than offset by the effects of fragmentation of the grains, to which reference is made later.

It has been shown that the age-hardened specimens of the fine-grained lead-antimony-arsenic alloy had a higher creep-resistance than the solution-treated or overaged specimens. In the coarse-grained alloy, however, overageing did not lower the creep-resistance of the age-hardened specimens, although age-hardening increased the creep-resistance of the solution-treated specimens. Jenkins, Bucknall, and Jenkinson<sup>16</sup> working with a copper-nickel-silicon alloy also found that age-hardened specimens possessed the best creep-resistance providing that the tests were carried out under conditions where the age-hardened structure was stable. In the present tests it was found that the age-hardened lead alloy was stable at the temperature of test, 20° C., and overaged only slowly at 50° C.

Many variables other than type of alloy system, such as resistance to recrystallization and fragmentation of the grains, have been shown in this work to affect creep-resistance. Thus the creep-resistance of the lead-tin, lead-copper, and lead-antimony-arsenic alloys tested in the present programme should not be regarded as being entirely typical of the creep-resistance of single-phase, two-phase, or age-hardenable types of lead alloy systems. The comparison made in Table IV indicates only the relative properties of the three alloys produced under laboratory conditions.

#### (c) *Effect of Fragmentation of the Grains*

The effect of fragmentation of the grains in the two-phase lead-copper alloys in some cases more than offset the effect of grain-size. This fragmentation, which increased creep-resistance, resulted from the process of extrusion used to produce the test specimens. The extent of the fragmentation in-

creased as the temperature and speed of extrusion were lowered and as the copper additions were made larger. Consequently, the resistance to creep of the extruded two-phase lead-copper alloys was not simply related to the extrusion temperature and the resultant grain-size.

This fragmentation is believed to be due to polygonization, although it was shown by X-ray examination to be similar to that obtained by plastic straining at room temperature where rapid polygonization was unlikely to have occurred. The creep curves show that there is a difference between these two fragmented structures. All the curves from the as-extruded two-phase alloys show normal transient creep, whereas this stage of creep is initially missing from specimens plastically strained at room temperature (see Appendix III). This difference suggests that the as-extruded materials were in a polygonized condition. Although micrographic examination of the as-extruded alloys failed to reveal polygonization, it has been observed in similarly produced lead alloys not reported upon in this paper. McLean and Tate<sup>17</sup> also found that specimens with a polygonized structure, obtained by hot rolling, had a much higher creep-resistance than the fully recrystallized material.

#### (d) *Effect of Twinning and of Grain Shape*

Cold-worked and recrystallized specimens of a 0.1% copper alloy had higher creep-resistances than the as-extruded materials, which contained fragmented grains, and which, on the evidence set out above, should have had the higher creep-resistance. However, the grains in the recrystallized specimens were more twinned and irregular in shape than those in the as-extruded specimens, and further tests, on a lead-1% tin alloy, confirmed that materials with grains twinned and irregular in shape have a higher creep-resistance than those with grains of uniform shape containing few twins.

This effect of twinning and irregularity of grain shape is to be expected for several reasons. Slip or any other mechanism by which grains deform under creep conditions would be impeded by the presence of twins because they differ in orientation from the parent grain. The irregularity of the shape of the grains would reduce the rate of relative movement of one grain past another at grain boundaries; a mode of deformation which is of the greatest importance in creep. It is unlikely that similar relative movement occurs on twin boundaries, since cracking has never been observed along these boundaries after failure.

#### (e) *Effect of Various Factors on Life and General Extension at Failure*

The general extension at failure of the single-phase lead-tin alloys, at any one stress, was generally greater for fine- than for coarse-grained specimens. For the coarse-grained specimens of these alloys, the general extension decreased as the stress was lowered. In the finest-grained specimens of the 1% tin alloy, however, the general extension markedly increased

as the stress was lowered. In many cases this feature of fine-grained alloys was obscured by recrystallization to a coarse grain-size during test. This general effect of grain-size is in agreement with the findings of McKeown and Hopkin.<sup>4</sup>

## 2. FATIGUE

### (a) *Effect of Grain-Size*

In some of the fatigue tests on single-phase (lead-tin) and two-phase (lead-copper) alloys the endurance limits of fine-grained alloys were higher than those of coarse-grained materials, but in others any effect of initial grain-size was masked to some extent by recrystallization and grain growth occurring during test. Other tests on a binary lead-antimony alloy which did not recrystallize or age-harden during test, confirmed that a decrease in grain-size can markedly increase fatigue-resistance. Generally, however, the effect of grain-size was not as great as that of alloying additions which hardened the basis lead.

The absence of an effect of grain-size on the fatigue-resistance found by Beckinsale and Waterhouse<sup>19</sup> in pure lead might have been due to recrystallization during test, which obscured the effect, as in some of the present tests. Several other workers<sup>20, 21</sup> have shown that the fatigue-resistance of copper-base alloys increases as the grain-size is reduced.

### (b) *Effect of Types of Alloy System*

In the single-phase lead-tin alloys of any one grain-size, fatigue-resistance generally increased as the alloying addition was made larger; that is, with increasing solid-solution hardening. This agrees with the work of Riches, Sherby, and Dorn,<sup>18</sup> who showed that the elements producing the most solid-solution strengthening in single-phase binary aluminium alloys also produced the highest fatigue-resistance.

In the two-phase lead-copper alloys of any one grain-size, fatigue-resistance increased only slightly as the amount of addition was increased up to 0.1% copper. However, the extent of fragmentation of the grains also increased with the amount of alloying addition, so it is not possible to say whether it was the discrete particles or the fragmentation of the grains which produced the increased fatigue-resistance. In either case the effect was small over the range of composition studied.

An age-hardened lead-antimony-arsenic alloy had a higher fatigue-resistance than the solution-treated material. The overaged materials had fatigue-resistances comparable with that of the solution-treated materials.

## VIII.—CONCLUSIONS

The results of this investigation show that, for lead alloys of equal grain-size, the creep- and fatigue-resistances are increased by additions which form single-phase alloys, or two-phase alloys, or which cause age-hardening. However, all alloying additions



to lead cause grain refinement, for similar temperatures of extrusion, and this is shown to lower creep-resistance but enhance fatigue-resistance. Thus, a creep-resistant alloy must contain alloying elements whose strengthening effect on the grains more than offsets the attendant effect of the decrease of grain-size. It is, therefore, suggested that this requirement is likely to be met in lead alloys containing additions causing as much solid-solution hardening, or age-hardening, as possible and forming a relatively large amount of a hard second phase. The solid-solution hardening or age-hardening additions would strengthen the grains, while the presence of the second phase would add to this strengthening directly and, possibly, indirectly by promoting fragmentation of the grains during a fabrication process. The fine grain-size produced by the large amount of additions would ensure that the elongation at failure, under creep conditions, increased rather than decreased as the stress was lowered, thus avoiding the danger of a "short" failure. Such alloys would also have good fatigue-resistance.

#### ACKNOWLEDGEMENTS

The authors wish to thank the Director and Council of The British Non-Ferrous Metals Research Association for permission to publish this paper and to acknowledge the helpful advice received from Dr. J. McKeown and Dr. W. A. Baker in the course of many discussions.

#### APPENDIX I PREVIOUS WORK

##### 1. CREEP

There is little existing information on the effect of constitutional factors on the creep and fatigue behaviour of lead and its alloys. For this reason, and because the behaviour of lead-base materials at atmospheric temperature is similar to that of higher-melting-point materials at elevated temperatures, this survey considers the literature referring to all metals and alloys.

Although, generally, it has been found that alloying additions to a pure metal increase its creep-resistance, some workers have shown a contrary effect. Among these are Greenwood and his colleagues,<sup>9-14</sup> who found that small quantities of alloying elements either increased or decreased the creep-resistance of pure lead.

Hanson and Sandford<sup>22</sup> investigated the effects of various amounts of alloying elements on the creep properties of tin. In all cases the addition of a solute element resulted in increased creep-resistance. A similar effect has been shown by Clark and White<sup>23</sup> in the case of steels. Austin, St. John, and Lindsay<sup>15</sup> found that the order of merit of the effects of various solute elements in ferrite was quite dissimilar from that

for solid-solution strengthening, as obtained from tensile data or hardness tests at atmospheric temperatures. There was, however, a direct correlation between the effect of alloying elements on creep-resistance and their effect on resistance to recrystallization. Robinson, Tietz, and Dorn,<sup>24</sup> found that in aluminium the solute elements which produced the greatest solid-solution strengthening and the greatest resistance to recrystallization also produced the highest creep-resistance.

Increasing the proportion of second phase in a plain carbon steel by increasing the carbon content has been found by Tapsell<sup>25</sup> and Clark and White<sup>26</sup> to increase creep-resistance. Addition elements or heat-treatment producing finely dispersed carbides have been shown, also, to increase the creep-resistance of steels.<sup>23, 27, 28, 29</sup> Greenwood and Orr<sup>12</sup> found that the creep-resistance of lead was increased by additions of copper, an element which is almost completely insoluble in lead.

The effect of age-hardening on creep properties has been studied for a copper-nickel-silicon alloy by Jenkins, Bucknall, and Jenkinson.<sup>16</sup> In long time-to-rupture tests maximum strength was obtained from the condition of maximum hardness at temperatures where atomic mobility was low and overageing did not occur. At high temperatures, where overageing occurred during test, the maximum time to rupture was obtained from specimens which had been overaged before test.

Most workers have found that creep-resistance decreases markedly as the grain-size is made smaller,<sup>8, 30, 31, 32</sup> although Parker and Riisness<sup>33</sup> found no such effect. Clark and White<sup>34</sup> showed that coarse-grained material is more creep-resistant than fine-grained material at high temperatures and that at low temperatures the reverse is the case. They suggested that this reversal of the effect of grain-size occurs at the minimum temperatures of recrystallization. Stress, as well as temperature, has also been found to reverse the effect of grain-size. Von Hanffstengel and Hanemann<sup>35</sup> showed that below a critical stress coarse-grained lead was more creep-resistant than fine-grained lead, while the reverse was true above this stress.

McKeown and Hopkin,<sup>4</sup> have shown that increasing amounts of plastic strain, before test, up to a limiting value, progressively increase the creep-resistance of lead. Beyond this limiting value, further prestrain lowered the creep-resistance owing to recrystallization occurring during test. Zschokke and Niehus<sup>36</sup> also found that there was an optimum amount of prior cold work for the maximum creep-resistance of austenitic steel. Other workers<sup>31, 32</sup> have shown that prior cold work increases creep-resistance, providing that recrystallization does not occur during test. Frey and Freeman<sup>37</sup> consider that cold work improves creep-resistance, by setting up elastic stresses in the crystal lattice, only up to the point where internal stresses become so high that rapid relaxation occurs during test.

## 2. FATIGUE

Although there is extensive literature on the fatigue properties of metals and alloys, the individual effects of constitutional factors have received little attention. Waterhouse<sup>38</sup> and others<sup>39-42</sup> have shown that the fatigue-resistance of lead is increased by increasing additions of alloying elements. In much of this work no account was taken of the constitution of the materials.

The effect of composition in solid-solution alloys has been investigated by Burghoff and Blank,<sup>20</sup> who found that the fatigue-resistance of  $\alpha$ -brasses increased with zinc content. Epremian and Nippes<sup>43</sup> found the fatigue-resistance of ferrite to be inversely proportional to the limit of solid solubility of the addition elements, while Riches, Sherby, and Dorn<sup>18</sup> showed that, in aluminium, the effectiveness of solute additions was in the same order as their effect on solid-solution strengthening and resistance to recrystallization.

The presence of a second phase, according to Greenall and Gohn<sup>44</sup> and Forrester, Greenfield, and Duckett,<sup>45</sup> increases fatigue-resistance; the latter workers found that the effect was most marked when the second phase was present as a eutectic and hence finely dispersed.

No effects of age-hardening have been found, either by Gohn and Ellis<sup>42</sup> for lead alloys or by Templin<sup>46</sup> and Chevigny<sup>47</sup> for aluminium alloys. Sopwith,<sup>48</sup> Gohn and Arnold,<sup>49</sup> and Greenall and Gohn<sup>44</sup> showed that the fatigue-resistance of copper-beryllium alloys was only slightly increased by an age-hardening treatment, although the other mechanical properties were greatly improved.

In most of the work described above grain-size has been an uncontrolled factor. Beckinsale and Waterhouse<sup>19</sup> found no effect of grain-size on the fatigue-resistance of pure lead, although several workers<sup>20, 21, 44, 50</sup> have shown that fatigue-resistance increases with smaller grain-size.

## APPENDIX II

## X-RAY EXAMINATION OF MATERIALS TESTED

The materials tested in both creep and fatigue were examined by the X-ray technique devised by Barrett,<sup>51</sup> in which the specimen and the film are oscillated synchronously. This method has the advantages over the standard Laue method that the complications due to the variation of intensity with wave-length are avoided, and that the angular resolution is much higher.

In the method as used, the angle of oscillation was  $10^\circ$  and the radiation was the filtered characteristic emission from a copper target. The cylindrical surface of an extruded rod was examined after it had been deeply etched, the X-ray beam being in a horizontal plane containing the axis of the specimen.

The X-ray photographs of the 0.1% copper alloy extruded at the "normal" speed (10.5 in./min.) at

$100^\circ$  and  $300^\circ$  C. are shown in Figs. 23 and 24 (Plate XXVII). Since this alloy extruded at the lower temperature had the finer grain-size, Fig. 23 contains more spots than Fig. 24. Comparison of the two plates, however, also indicates that generally more grains were fragmented in the alloy extruded at  $100^\circ$  C. than in the alloy extruded at  $300^\circ$  C. The extent of this fragmentation was uniform across the diameter of the rods in any one material.

At any one temperature of extrusion the number of fragmented grains and the extent of their fragmentation increased as the proportion of second phase became larger, as can be seen by comparing Figs. 25, 26, and 23 (Plate XXVII). Fig. 25 is of the basis lead extruded at  $100^\circ$  C., which had nearly perfect grains. It will also be observed that the grain-size became smaller as the copper content was increased. Figs. 27-30 (Plate XXVIII) show the effect of speed of extrusion on the extent of fragmentation of the grains in the 0.1% copper alloy. The grains of the alloy extruded at 2.6 in./min. at  $100^\circ$  C. were severely fragmented (Fig. 27), while that extruded at 42 in./min. contained much less fragmentation (Fig. 28). The material extruded rapidly at  $300^\circ$  C. was almost completely work-free (Fig. 30) while that extruded slowly contained some fragmented grains (Fig. 29). These photographs also show that at both temperatures of extrusion the grain-size was reduced by an increase in speed of extrusion.

The fragmentation of the grains in the 0.1% copper alloy and the 1% tin alloy resulting from plastic straining at atmospheric temperature can be seen in Figs. 31 and 32 (Plate XXVIII).

## APPENDIX III

## EFFECT OF PRIOR PLASTIC STRAIN ON THE CREEP BEHAVIOUR OF THE LEAD-1% TIN AND LEAD-0.1% COPPER ALLOYS

The single-phase 1% tin alloy and the two-phase 0.1% copper alloy were extruded at  $250^\circ$  C. and had similar grain-sizes. Specimens were given tensile strains of 0, 0.5, 1, 2, and 3% before testing in creep at 500 lb./in.<sup>2</sup>.

The creep curves obtained are shown in Figs. 13 and 14. Specimens prestrained by amounts greater than 0.5%, corresponding to the instantaneous extension of the unstrained specimens, showed no transient stage of creep immediately after loading but entered directly into what appeared to be the stage of tertiary creep (see insert to Fig. 14). This stage was not true tertiary creep, since it was followed by a period of decreasing rate of creep, as in transient creep, which began after longer testing times as the amount of prestrain was increased. The inflections in the creep curves produced by the change from one stage of creep to the other, were not due to recrystallization, since this phenomenon would have occurred after the shortest times in specimens prestrained by the largest amounts.



X-ray examination of the specimens was made before test and after unloading during creep. Before test the X-ray reflections from both materials pre-

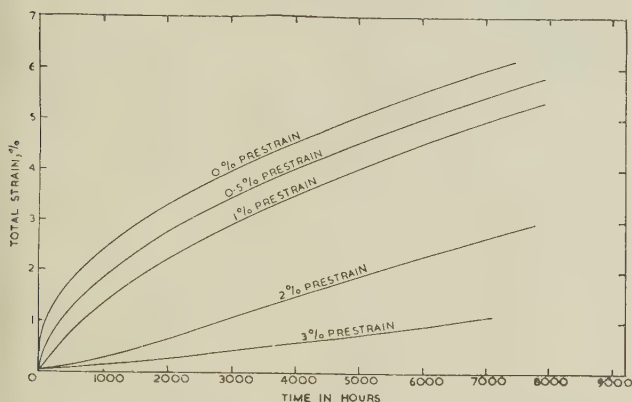


FIG. 13.—Effect of Prior Plastic Strain on the Creep-Resistance of the Lead-1% Tin Alloy at 500 lb./in.<sup>2</sup>.

strained 3% were diffuse and contained intensity maxima; the latter indicating that the grains were fragmented. The effect of creep on these specimens was to reduce the diffuseness of the reflections and to increase the distance between the intensity maxima. After creep the distance between the intensity maxima was greater in the initially unstrained than in the prestrained specimens. It would, therefore, seem that the initially increasing creep rate in the creep curves of the prestrained specimens was associated with a decrease in the diffuseness of the X-ray reflections.

Comparison of the creep curves of the 1% tin and the 0.1% copper alloys shows that the rate of creep of the prestrained specimens increased and became similar to that of the unstrained specimens, more slowly in the single-phase than in the two-phase alloy. It can be concluded, therefore, that the changes within cold-worked grains brought about by creep occurred more slowly in the former than in the latter materials.

The result that small plastic strains before test increase creep-resistance by removing the transient stage of creep is in agreement with the findings of several workers. The initially low rate of creep of prestrained specimens which gradually increased and eventually became similar to that of the unstrained

specimens is, however, an effect which has not been reported before. Frey and Freeman,<sup>37</sup> working on an austenitic alloy, concluded that cold work increases creep-resistance because of the presence of elastic stresses and that relaxation of these stresses lowers creep-resistance. Relaxation of internal stresses is unlikely to be the explanation of the present findings, since locked-up elastic stresses must be small in the case of lead. A more likely explanation is that put forward by Greenough and Smith<sup>52</sup> to explain the effect, on X-ray photographs, of creep of cold-worked aluminium. These workers showed that creep broke up all the initially blurred X-ray reflections, resulting from cold work. They attributed the effect to diffusion of randomly distributed dislocations, resulting from cold work, to form a polygonized structure.

In the prestrained alloys polygonization, if indeed this is the explanation of the observed phenomenon, took place more rapidly in the lead-copper alloy than in the lead-tin alloy. This is considered to be the

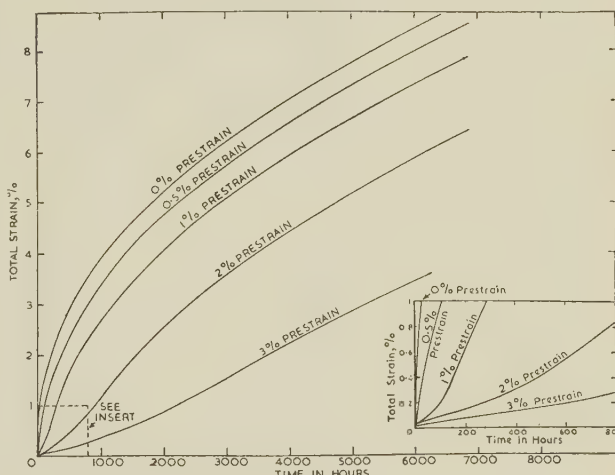


FIG. 14.—Effect of Prior Plastic Strain on the Creep-Resistance of the Lead-0.1% Copper Alloy at 500 lb./in.<sup>2</sup>.

explanation of the creep-resistance of the former alloy being lower than that of the latter alloy when both are in the unstrained condition, polygonization taking place in these specimens by diffusion of randomly distributed dislocations formed during initial extension and transient creep.

## REFERENCES

1. W. A. Baker, *Metallurgia*, 1949, **40**, 188.
2. J. McKeown, *ibid.*, 1950, **42**, 189.
3. L. M. T. Hopkin, *Proc. Phys. Soc.*, 1950, [B], **63**, 346.
4. J. McKeown and L. M. T. Hopkin, *Metallurgia*, 1950, **41**, 135, 219.
5. J. N. Greenwood and H. K. Worner, *J. Inst. Metals*, 1939, **64**, 135.
6. E. N. da C. Andrade, *Nature*, 1948, **162**, 410.
7. L. M. T. Hopkin and C. J. Thwaites, *J. Inst. Metals*, 1952-53, **81**, 255.
8. J. McKeown, *ibid.*, 1937, **60**, 201.
9. J. N. Greenwood, *Proc. Australasian Inst. Min. Met.*, 1934, [N.S.], (95), 79.
10. J. N. Greenwood and H. K. Worner, *ibid.*, 1936, [N.S.], (101), 57.
11. J. N. Greenwood and H. K. Worner, *ibid.*, 1936, [N.S.], (104), 385.
12. J. N. Greenwood and C. W. Orr, *ibid.*, 1938, [N.S.], (109), 1.
13. J. N. Greenwood and C. W. Orr, *ibid.*, 1938, [N.S.], (112), 287.
14. J. N. Greenwood and C. W. Orr, *ibid.*, 1939, [N.S.], (113), 1.
15. C. R. Austin, C. R. St. John, and R. W. Lindsay, *Trans. Amer. Inst. Min. Met. Eng.*, 1945, **162**, 84.
16. C. H. M. Jenkins, E. H. Bucknall, and E. A. Jenkinson, *J. Inst. Metals*, 1944, **70**, 57.
17. D. McLean and A. E. L. Tate, *Rev. Mét.*, 1951, **48**, 763.
18. J. W. Riches, O. D. Sherby, and J. E. Dorn, *Trans. Amer. Soc. Metals*, 1952, **44**, 882.
19. S. Beckinsale and H. Waterhouse, *J. Inst. Metals*, 1928, **39**, 375.
20. H. L. Burghoff and A. I. Blank, *Proc. Amer. Soc. Test. Mat.*, 1948, **48**, 709.
21. A. R. Anderson, E. F. Swan, and E. W. Palmer, *ibid.*, 1946, **46**, 678.
22. D. Hanson and E. J. Sandford, *J. Inst. Metals*, 1936, **59**, 159; 1938, **62**, 215.
23. C. L. Clark and A. E. White, *Trans. Amer. Soc. Metals*, 1936, **24**, 831.
24. A. T. Robinson, T. E. Tietz, and J. E. Dorn, *ibid.*, 1952, **44**, 896.
25. H. J. Tapsell, "Creep of Metals". 1931: Oxford (University Press).
26. A. E. White, C. L. Clark, and R. L. Wilson, *Trans. Amer. Soc. Metals*, 1935, **23**, 995.
27. R. F. Miller, R. F. Campbell, R. H. Aborn, and E. C. Wright, *ibid.*, 1937, **26**, 81.
28. D. A. Oliver and G. T. Harris, *J. West Scotland Iron Steel Inst.*, 1946-47, **54**, 97.
29. C. Sykes, *J. Iron Steel Inst.*, 1947, **156**, 321.
30. D. Hanson, *Trans. Amer. Inst. Min. Met. Eng.*, 1939, **133**, 15.
31. H. L. Burghoff, A. I. Blank, and S. E. Maddigan, *Proc. Amer. Soc. Test. Mat.*, 1942, **42**, 668.
32. N. D. Benson, J. McKeown, and D. N. Mends, *J. Inst. Metals*, 1951-52, **80**, 131.
33. E. R. Parker and C. F. Riisness, *Trans. Amer. Inst. Min. Met. Eng.*, 1944, **156**, 117.
34. C. L. Clark and A. E. White, *Proc. Amer. Soc. Test. Mat.*, 1932, **32**, 492.
35. K. v. Hanffstengel and H. Hanemann, *Z. Metallkunde*, 1938, **30**, 41.
36. H. R. Zschokke and K. H. Niehus, *J. Iron Steel Inst.*, 1947, **156**, 271.
37. D. N. Frey and J. W. Freeman, *Trans. Amer. Inst. Min. Met. Eng.*, 1951, **191**, 755.
38. H. Waterhouse, *B.N.F.M.R.A. Research Rep.*, 1937, (440).
39. J. R. Townsend, *Proc. Amer. Soc. Test. Mat.*, 1927, **27**, 153.
40. J. R. Townsend and C. H. Greenall, *ibid.*, 1930, **30**, 395.
41. J. C. Chaston, *Elect. Communication*, 1934, **13**, (1), 31.
42. G. R. Gohn and W. C. Ellis, *Proc. Amer. Soc. Test. Mat.*, 1951, **51**, 721.
43. E. Epremian and E. Nippes, *Trans. Amer. Soc. Metals*, 1948, **40**, 870.
44. C. H. Greenall and G. R. Gohn, *Proc. Amer. Soc. Test. Mat.*, 1937, **37**, 160.
45. P. G. Forrester, L. T. Greenfield, and R. Duckett, *Metallurgia*, 1947, **36**, 113.
46. R. L. Templin, *Proc. Amer. Soc. Test. Mat.*, 1933, **33**, 364.
47. R. Chevigny, *Rev. Mét.*, 1946, **43**, 330.
48. D. G. Sopwith, *Aeronaut. Research Council, R. and M.*, 1950, (2486).
49. G. R. Gohn and S. M. Arnold, *Proc. Amer. Soc. Test. Mat.*, 1946, **46**, 741.
50. H. Habart and R. H. Caughey, *Metal Progress*, 1939, **35**, 469.
51. C. S. Barrett, *Metals and Alloys*, 1937, **8**, 13.
52. G. B. Greenough and E. M. Smith, *J. Inst. Metals*, 1950, **77**, 435.
53. E. Jenckel and H. Mäder, *Metallwirtschaft*, 1937, **16**, 499.
- I. Obinata and E. Schmid, *ibid.*, 1933, **12**, 101.
- A. Ölander, *Z. physikal. Chem.*, 1934, [A], **168**, 274.
- N. Ageew and V. Ageewa, *J. Inst. Metals*, 1936, **59**, 311.
- N. Ageew and I. W. Krotow, *ibid.*, 1936, **59**, 301.



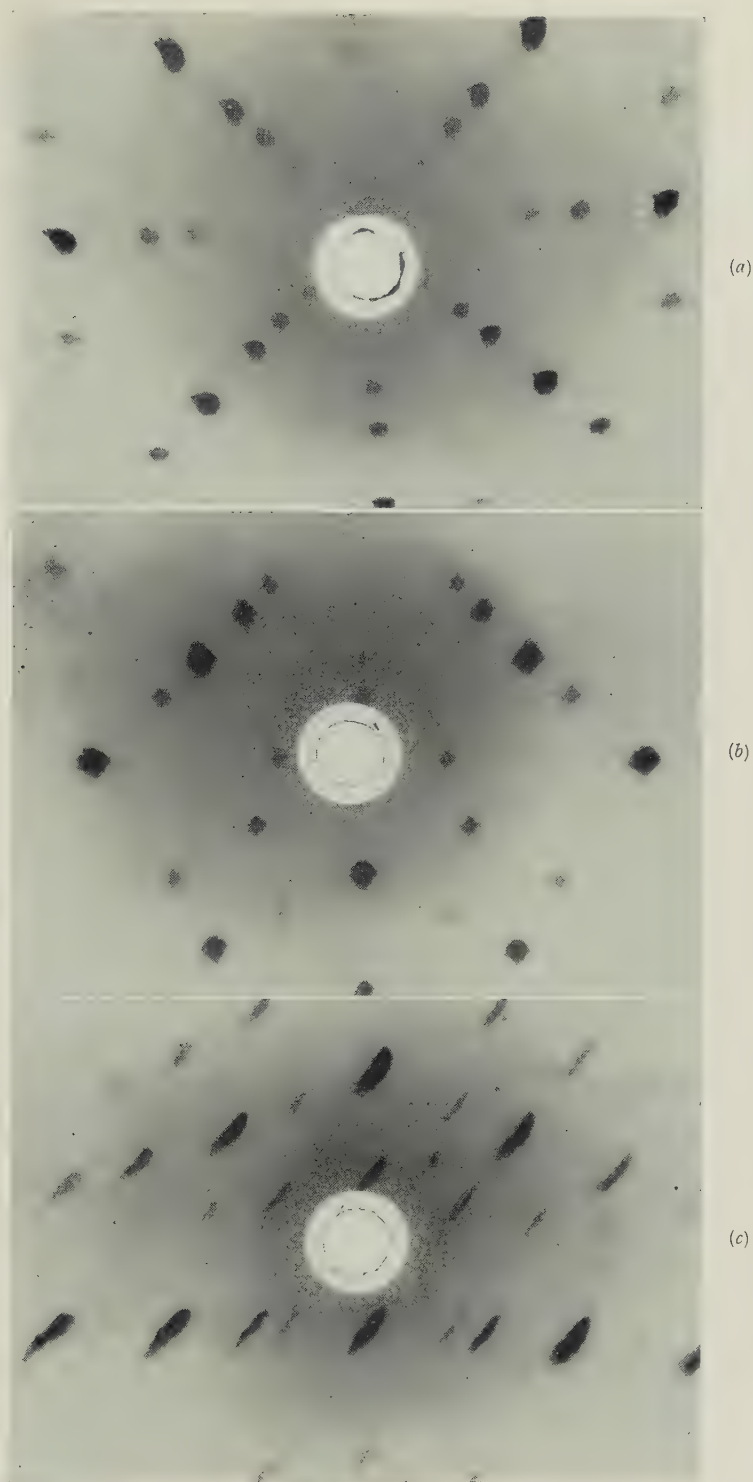


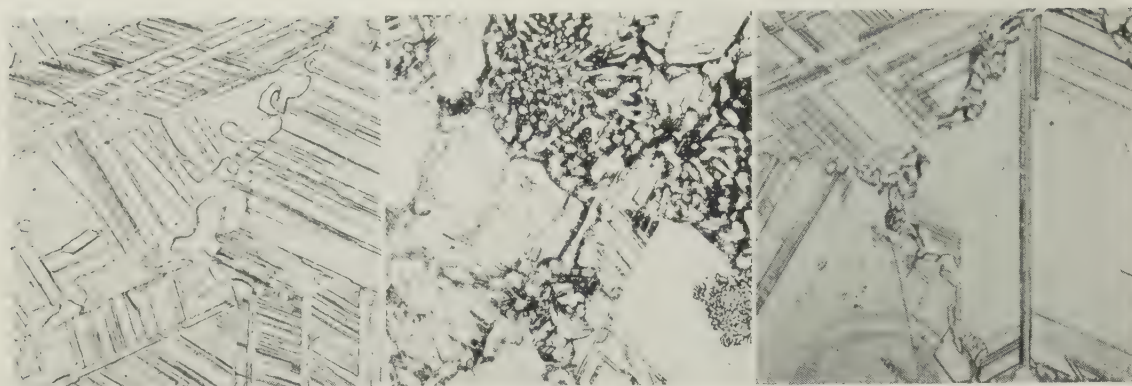
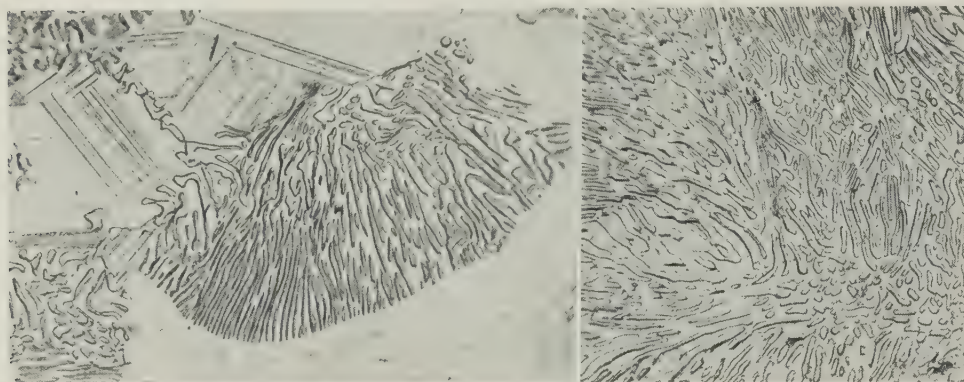
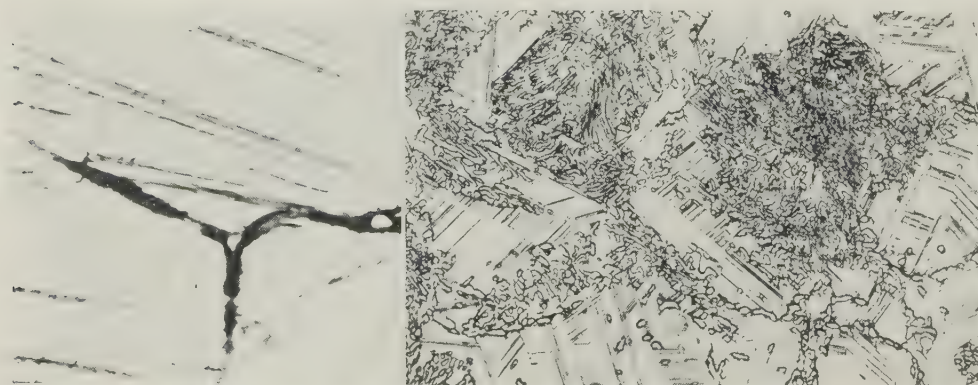
FIG. 10.—Back-Reflection Laue Photographs of Aluminium Single Crystal.

(a) As grown and annealed.

(b) After 2% tensile strain.

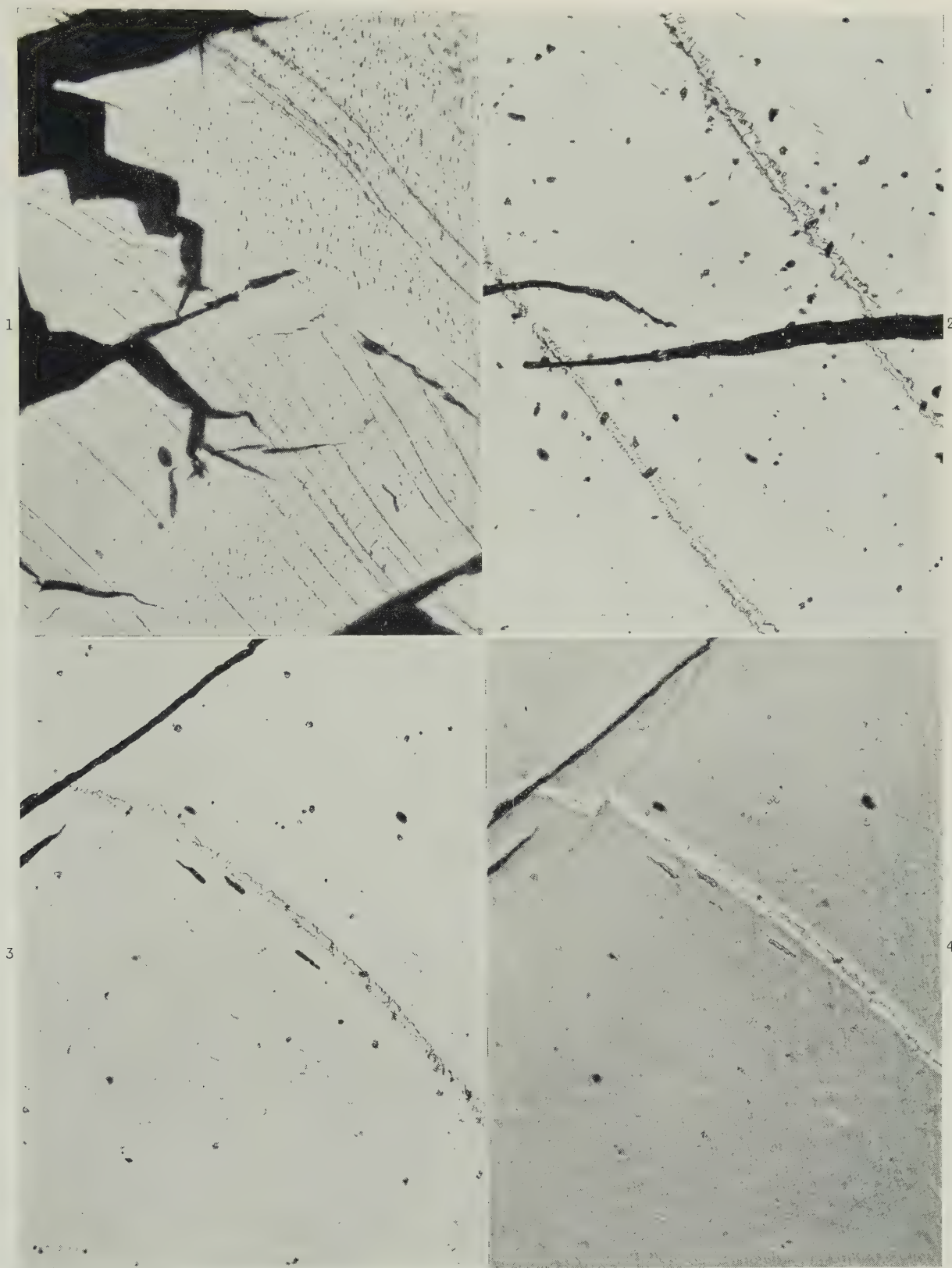
(c) After torsion equivalent to 3.3% tensile strain.

## MICROSTRUCTURES OF COPPER-SILICON EUTECTOID.

FIG. 2.—80 hr. at 500° C.  $\times 375$ .FIG. 3.—168 hr. at 500° C.  $\times 200$ .FIG. 4.—5½ hr. at 400° C.  $\times 375$ .FIG. 5.—93 hr. at 400° C.  $\times 375$ .FIG. 6.—172 hr. at 400° C.  $\times 375$ .FIG. 7.—1½ hr. at 330° C.  $\times 1500$ .FIG. 8.—16 hr. at 330° C.  $\times 150$ .



## OCCURRENCE OF LAMELLÆ IN DISTORTED CHROMIUM.

FIG. 1.—Heavily Hammered Fragment.  $\times 150$ .FIG. 3.—Stepped Lamella Crossing Line of Shear. Normal illumination.  $\times 500$ .FIG. 2.—Stepped Lamellæ Crossing Crack.  $\times 500$ .FIG. 4.—As Fig. 3. Phase-contrast illumination.  $\times 500$ .

Etched electrolytically in alkaline ferricyanide.

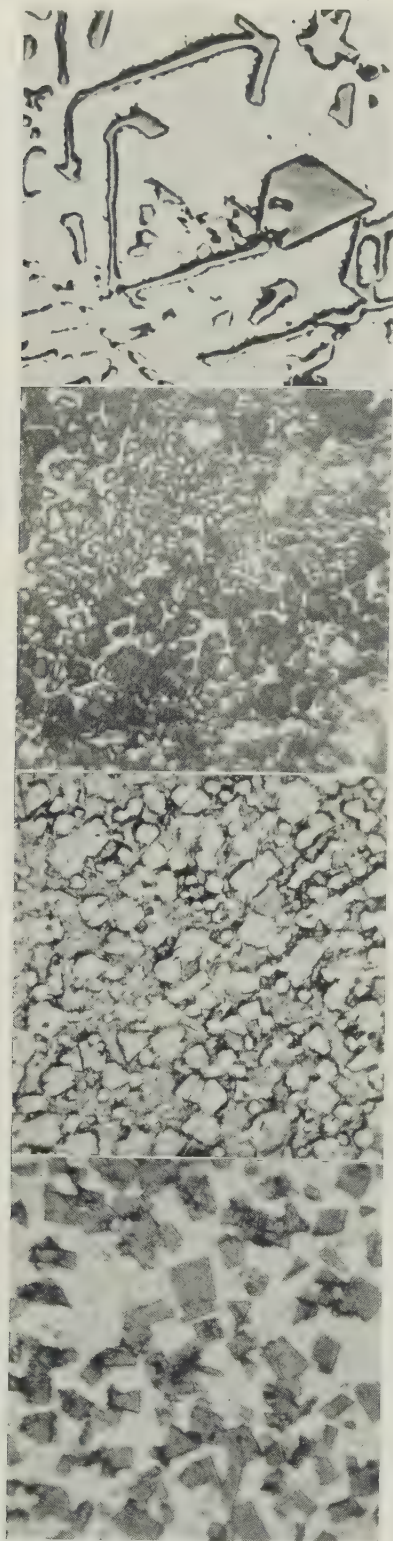


FIG. 4.—Photomicrographs of Uranium-Lead Alloys Containing Various Amounts of Lead.

(a) 90% Lead.  $UPb_3$  particles in Pb eutectic. Long air etch.  $\times 200$ .

(b) 85% Lead.  $UPb_3$  particles in Pb eutectic. Short air etch.  $\times 150$ .

(c) 60% Lead. Dark grains of UPb in matrix of UPb +  $UPb_3$ . Air etch.  $\times 150$ .

(d) 0.4% Lead. UPb in uranium matrix. Air etch.  $\times 750$ .

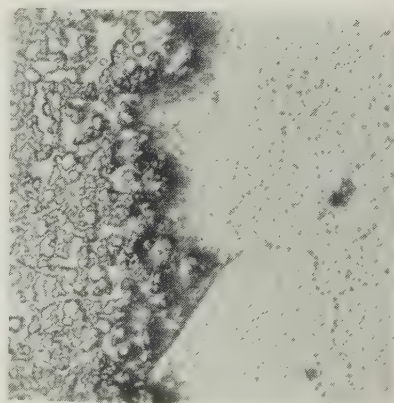


FIG. 5 (a).—Interface Between Uranium-Rich and Lead-Rich Portions of Centrifuged Ingot.  $\times 100$ .



FIG. 5 (b).—Longitudinal Section of Centrifuged Ingot.  $\times 2$ .





FIG. 15.—Pb-1% Sn Alloy Recrystallized in Air at 100° C. Grains twinned and irregular in shape.  $\times 12$ .

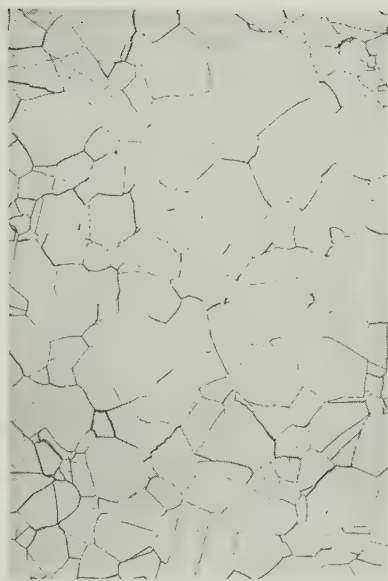


FIG. 16.—Pb-1% Sn Alloy Recrystallized in Salt Bath at 300° C. Grains comparatively free of twins and regular in shape.  $\times 20$ .

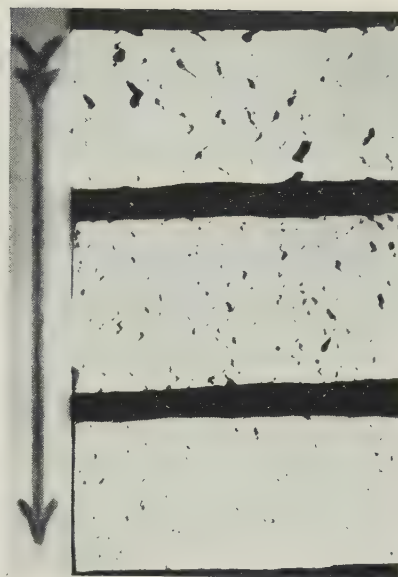


FIG. 17.—Pb-1% Sn Alloy Tested in Creep at 1000 lb./in.<sup>2</sup>. Effect of grain-size on intercrystalline cracking; grain-size decreasing in the direction of the arrow.  $\times 2.5$ .

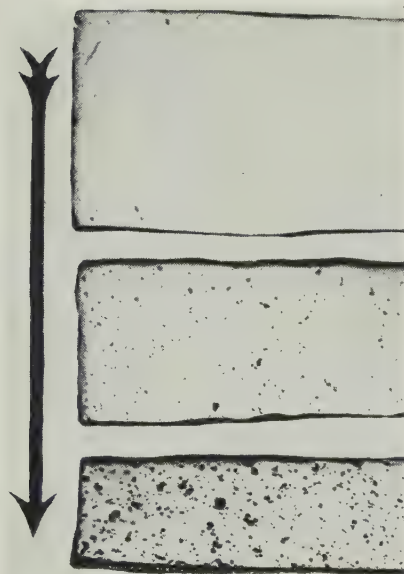


FIG. 18.—Pb-1% Sn Alloy Extruded at 100° C. Effect of creep stress on intercrystalline cracking; stress decreasing in the direction of the arrow.  $\times 3.5$ .



FIG. 19.—Pb-0.05% Sn Alloy (Grain-Size 0.47 mm.<sup>2</sup>). Recrystallization caused by testing in fatigue at a stress near the endurance limit.  $\times 8$ .

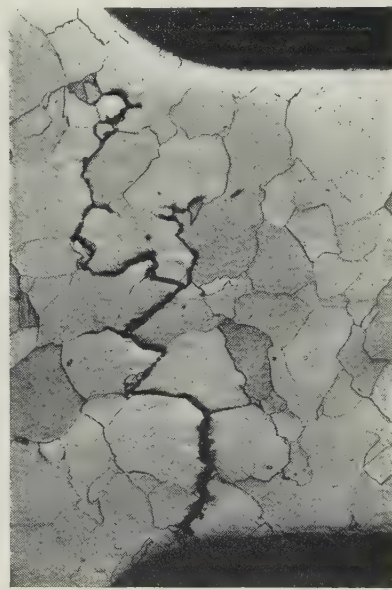


FIG. 20.—Pb-1% Sn Alloy (Grain-Size 0.39 mm.<sup>2</sup>). Absence of recrystallization after testing in fatigue at a stress near the endurance limit.  $\times 8$ .

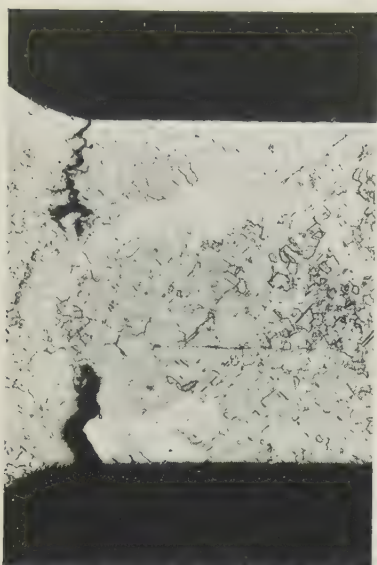


FIG. 21.—Pb-0.1% Cu Alloy (Grain-Size 0.0084 mm.<sup>2</sup>). Recrystallization caused by testing in fatigue at a stress near the endurance limit.  $\times 6$ .

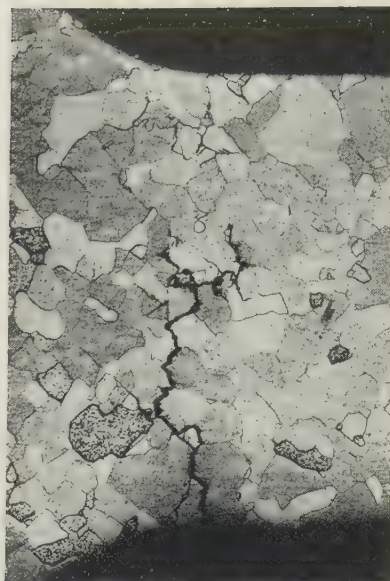


FIG. 22.—Pb-0.1% Cu Alloy (Grain-Size 0.17 mm.<sup>2</sup>). Absence of recrystallization after testing in fatigue at a stress near the endurance limit.  $\times 8$ .



FIG. 23.—Pb-0.1% Cu Alloy Extruded at 100° C.  $\times 2$ .



FIG. 24.—Pb-0.1% Cu Alloy Extruded at 300° C.  $\times 2$ .



FIG. 25.—Basis Lead Extruded at 100° C.  $\times 2$ .



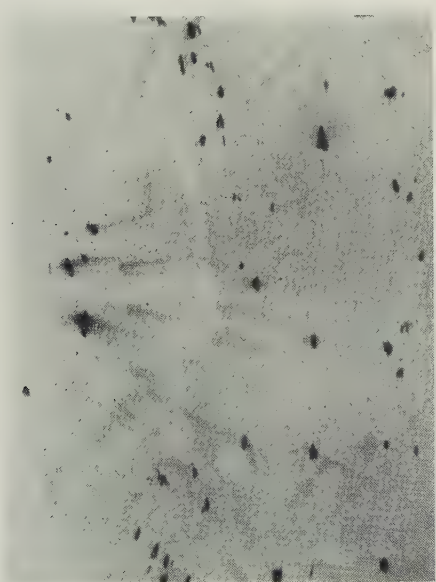
FIG. 26.—Pb-0.01% Cu Alloy Extruded at 100° C.  $\times 2$ .

FIGS. 23-26.—Oscillating-Beam X-Ray Photographs Showing Effect of Temperature of Extrusion and Composition on the Fragmentation of the Grains in As-Extruded Materials.



FIG. 27.—Extruded Slowly at 100° C.  $\times 2$ .FIG. 28.—Extruded Rapidly at 100° C.  $\times 2$ .FIG. 29.—Extruded Slowly at 300° C.  $\times 2$ .

FIGS. 27-30.—Oscillating-Beam X-Ray Photographs Showing Effect of Speed of Extrusion on the Fragmentation of the Grains in the Pb-0.1% Cu Alloy Extruded at Two Temperatures.

FIG. 30.—Extruded Rapidly at 300° C.  $\times 2$ .FIG. 31.—Pb-0.1% Cu Alloy (Grain-Size 0.08 mm.<sup>2</sup>).  $\times 2$ .FIG. 32.—Pb-1% Sn Alloy (Grain-Size 0.1 mm.<sup>2</sup>).  $\times 2$ .

FIGS. 31-32.—Oscillating-Beam X-Ray Photographs Showing Fragmentation of the Grains Resulting from 3% Rapid Plastic Straining in Tension at Atmospheric Temperature.





# THE CONSTITUTION OF ALLOYS OF ALUMINIUM, COPPER, AND IRON \*

1513

By H. W. L. PHILLIPS,† M.A., F.R.I.C., F.Inst.P., F.I.M., MEMBER  
(Communication from the Research Laboratories of The British Aluminium Co., Ltd.)

## SYNOPSIS

The constitution of the aluminium-rich alloys of the aluminium-copper-iron system has been investigated over the range 0-40% copper, 0-3.5% iron by the methods of thermal analysis and microscopic examination, supplemented by measurements of liquid solubility.

The constituents occurring over this range are aluminium, containing copper and iron in solid solution, the two binary phases  $\text{CuAl}_2$  and  $\text{FeAl}_3$ , and two ternary bodies:  $\alpha$ , isomorphous with  $\text{MnAl}_6$ , and  $\beta$ , originally designated  $N$ , and more recently  $\text{Cu}_2\text{FeAl}_7$ . Depending on the composition, the constituents  $\alpha$  and  $\beta$  may separate independently, or they may be formed as the result of peritectic reactions,  $\alpha$  from  $\text{FeAl}_3$  and  $\beta$  from either  $\text{FeAl}_3$  or  $\alpha$ . The reaction involving the formation of  $\alpha$  rarely proceeds to completion during solidification, and takes place very slowly on annealing, even if the iron content is low and the  $\text{FeAl}_3$  finely dispersed. The reactions resulting in the formation of  $\beta$  take place more rapidly, and may proceed to completion during slow solidification.

The liquidus surface contains five invariant points:

Reaction	Temp., °C.	Composition of Participating:			
		Liquid		Al-Rich Solid Phase	
		Cu, %	Fe, %	Cu, %	Fe, %
Peritectic: $\text{Al, FeAl}_3 + \text{liq.} \rightarrow \alpha$	620	10.8	1.36	1.48	0.034
Peritectic: $\text{Al, } \alpha + \text{liq.} \rightarrow \beta$	590	20.0	1.00	3.00	0.022
Peritectic: $\text{FeAl}_3 + \text{liq.} \rightarrow \alpha + \beta$	622	23.6	1.50	...	...
Maximum on $\text{FeAl}_3$ - $\alpha$ boundary	626	~20	1.55	...	...
Eutectic: $\text{Al, } \beta, \text{CuAl}_2, \text{liq.}$	548	32.55	0.23	5.60	0.013

It is believed that  $\text{FeAl}_3$  is capable of taking only a small amount of copper into solid solution, possibly 0.5%; that  $\alpha$  has the approximate composition copper 7, iron 25%, with formula  $\text{Fe}(\text{Cu}_{0.04}\text{Al}_{0.96})_6$  and electron/atom ratio of 2.12; and that  $\beta$  has an appreciable range of homogeneity, extending approximately from copper 26.5, iron 17.5% to copper 33, iron 13.5%.

The solid solubility of copper in aluminium is slightly reduced by the addition of iron and that of iron by the addition of copper. The compositions of the aluminium-rich apices of the three-phase triangles at 500° C. were found to be:

$\text{Al, FeAl}_3, \alpha$ : Cu 0.4, Fe 0.0055%  
 $\text{Al, } \alpha, \beta$ : Cu 1.3, Fe 0.0055%  
 $\text{Al, } \beta, \text{CuAl}_2$ : Cu 4.1, Fe 0.0040%

## I.—HISTORICAL INTRODUCTION

UNTIL recently, it has been believed that, under conditions of equilibrium, four constituents may occur in the aluminium-rich alloys of the aluminium-copper-iron system, namely aluminium containing up to 5.65% copper and 0.052% iron in solid solution, two binary constituents often termed  $\text{FeAl}_3$  and  $\text{CuAl}_2$ , and a ternary constituent which was designated  $N$  by Gwyer, Phillips, and Mann,<sup>1</sup> who were the first to make a systematic survey of the alloys over a fairly extensive range. These authors, using as a basis aluminium of purity 99.67%, determined the boundaries of the primary phase fields in alloys

solidified at rates likely to be encountered in industrial practice, and reported that whilst primary  $N$  separated over a certain range of compositions, elsewhere it was formed as the result of a peritectic reaction between  $\text{FeAl}_3$  and liquid. Owing to envelopment, this reaction rarely proceeded to completion. They found the peritectic invariant point, at which  $\text{FeAl}_3$ ,  $\text{Al}$ ,  $N$ , and liquid were in equilibrium, to lie at 21.5% copper, 1.0% iron, and 590° C. The system contained a ternary eutectic, which solidified at 542° C.; the constituents present were  $\text{Al}$ ,  $\text{CuAl}_2$ , and  $N$ , and the composition 32.5% copper, 0.3% iron. No attempt was made to determine the solid solubility of copper and iron in aluminium, or to find the chemical com-

\* Manuscript received 20 August 1953.

† Research Laboratories of The British Aluminium Co., Ltd., Gerrards Cross, Bucks.





three-phase structures of Al, FeAl<sub>3</sub>, and N, and the second to three-phase structures of Al, N, and CuAl<sub>2</sub>. From these curves, the authors derived isothermal diagrams showing the phases present in solid alloys at 475°, 500°, and 525° C., the range covered being 0·8% copper, 0·1% iron. The apices of the two three-phase triangles Al-FeAl<sub>3</sub>-N and Al-N-CuAl<sub>2</sub> were found to lie at 1·3 and 3·8% copper, respectively, at 500° C. The iron contents were not determined, but are known to be extremely small. These apices have been plotted in Fig. 1, as the points *D* and *E*, respectively, along the aluminium-copper axis, and have been joined, by dotted lines, to the appropriate points *A*, *B*, and *C* of the quasi-binary section, in order to show the various phase fields present in the ternary alloys at 500° C.

It is convenient here to depart from the chronological sequence and to refer to the work of Hanemann and Schrader,<sup>9</sup> whose diagram is the most recent to have been published. It is of the general form shown in Fig. 1, the chief differences being that FeAl<sub>3</sub> is stated to be incapable of taking much copper into solid solution, and that *N* is considered to have only a small homogeneity range and to correspond with the formula Cu<sub>2</sub>FeAl<sub>6</sub> (37·7% copper, 15·63% iron). Hanemann and Schrader's values for the co-ordinates of the liquidus invariant points and for the aluminium-rich apices of the three-phase triangles in the solid alloys are included in Tables I and II.

TABLE I.—Composition and Temperature of Invariant Points on the Liquidus Surface.

Investigators	Ref.	Peritectic FeAl <sub>3</sub> , Al, N, liquid			Ternary Eutectic Al, N, CuAl <sub>2</sub> , liquid		
		Cu, %	Fe, %	Temp., °C.	Cu, %	Fe, %	Temp., °C.
Gwyer, Phillips, and Mann	1	21·5	1·0	590	32·5	0·3	542
Archer and Fink	2	...	...	585	...	...	545
Yamaguchi and Nakamura	4	20·0	1·5	590	32·5	0·3	545
Hanemann and Schrader	9	15·4	1·5	600	32·5	0·49	546

Before 1943, there had been no evidence, from constitutional investigations, of the existence of more than one ternary phase in the aluminium-rich alloys of the system, although microscopic studies of etched alloys had suggested that there might be a second. Thus Keller and Wilcox,<sup>10</sup> in a paper on the etching characteristics of aluminium alloys generally, had listed two constituents, α(Al-Cu-Fe) and β(Al-Cu-Fe), differing slightly in behaviour towards etching reagents. Thus they stated that, with a 0·5% HF solution, swabbing for 15 sec. would result in α being blackened, but β would be unattacked; whereas with a 1% NaOH solution, swabbing for 10 sec. would result in a slight darkening of β but would leave α unattacked. Mondolfo<sup>11</sup> expressed the opinion that alloys, rapidly solidified, often contained a metastable phase which he designated ω, which tended to react with aluminium to form Cu<sub>2</sub>FeAl<sub>7</sub>. The etching behaviour of Mondolfo's ω corresponded in all

respects with that given by Keller and Wilcox for α(Al-Cu-Fe). For convenience, the designation α will be retained for this intermediate constituent, and the designation β for the phase richer in copper, originally termed *N*, and later Cu<sub>2</sub>FeAl<sub>7</sub>.

TABLE II.—Aluminium-rich Apices of the Three-phase Triangles in Solid Alloys at Temperatures Specified.

Investigators	Ref.	Equilibrium Al, FeAl <sub>3</sub> , N		Equilibrium Al, N, CuAl <sub>2</sub>	
		Temp., °C.	Cu, %	Temp., °C.	Cu, %
Brown, Fink, and Hunter	8	475	1·0	475	3·1
		500	1·3	500	3·8
		525	1·6	525	5·0
Hanemann and Schrader	9	500 *	1·3	400	1·6
		550	1·75	500 †	4·2
		560	1·80	520	4·94
		575	2·0	530	5·05
		600 *	2·35	546 *	5·25

\* Extrapolated.

† Interpolated.

NOTE: Iron contents were not determined.

The first evidence that the α compound was a stable constituent of the system was published by Phragmén,<sup>12</sup> whose diagram showed a small primary α field lying between those due to Al, FeAl<sub>3</sub>, and β. He found that α was formed peritectically from FeAl<sub>3</sub>, and itself reacted peritectically to form β. Exact co-ordinates were not given in his paper, but from his diagram the compositions of the invariant points were approximately:

Peritectic: Al, FeAl<sub>3</sub>, α, liquid . . . Cu 10, Fe 1·5%  
 Peritectic: Al, α, β, liquid . . . Cu 16, Fe 1·2%  
 Peritectic: FeAl<sub>3</sub>, α, β, liquid . . . Cu 21, Fe 2·2%  
 Ternary eutectic: Al, β, CuAl<sub>2</sub>, liquid . . . Cu 31, Fe 0·8%

Phragmén was able to extract crystals of α, and found that their composition was copper 8, iron 22, aluminium 70%; they were orthorhombic with *a* = 7·449, *b* = 6·428, *c* = 8·768 kX. These parameters are almost identical with those reported for MnAl<sub>6</sub>,<sup>13</sup> which α resembles in crystal habit. Phragmén therefore assigned to α the formula (Fe,Cu)(Al,Cu)<sub>6</sub>, regarding it as being derived from an imaginary compound FeAl<sub>6</sub>, of which the lattice could be stabilized by substituting copper atoms for some of the iron and some of the aluminium atoms. Phragmén also isolated crystals of the β constituent, and confirmed Wiehr in finding tetragonal symmetry. He found, however, that the chemical analysis corresponded with the formula Cu<sub>2</sub>FeAl<sub>7</sub>, thus confirming the work of Yamaguchi and Bradley and their colleagues, but he suggested that β had only a small range of homogeneity.

Raynor<sup>14</sup> has shown that in alloys of aluminium with at least one of the transitional elements, stable intermetallic phases frequently occur in which the ratio of electrons to atoms is approximately 2·05. In calculating this ratio he assumes that each aluminium atom contributes 3 electrons to the structure, whilst





decreases in width until, at the point *K*, it becomes a straight line. Beyond this point, it opens out again, becoming a mirror image of its former self. This suggests that the line  $P\alpha K$ , at high temperatures at least, is a quasi-binary section. One would expect the primary  $\alpha$  field  $BCH$  to have the form of a saddle, with its ridge roughly coinciding with the prolongation of the line  $P\alpha K$ .

It can readily be shown that, if the compositions of *P*,  $\alpha$ , and  $BH$  are roughly as plotted in Fig. 2, then the temperatures along  $BH$  must pass through a maximum.

Fig. 3 (a) represents an isothermal section, not drawn to scale, based on the assumption that temperatures along the  $FeAl_3/\alpha$  valley fall on proceeding to the left from *H*. If so, then a given isothermal

the isothermal equilibria leads to the conclusion that temperatures must rise along the whole length of the  $FeAl_3/\alpha$  valley, from the point *B* to the point *H*. Exact determinations of these temperatures would therefore furnish an independent check on Phragmén's findings.

The dotted lines in Fig. 2 indicate the probable limits of occurrence of the phases in the solid alloys at 500° C. The points *U* and *V*, which are the apices of the three-phase triangles  $Al, FeAl_3, \alpha$  and  $Al, \alpha, \beta$  have been inserted arbitrarily, and lines have been drawn from them to the appropriate points of the diagram. If Phragmén is correct in stating that  $\beta$  has a negligibly small homogeneity range, then the two-phase area  $Al, \beta$  must be a triangle  $WV\beta$  and not a quadrilateral  $WVQR$  as drawn.

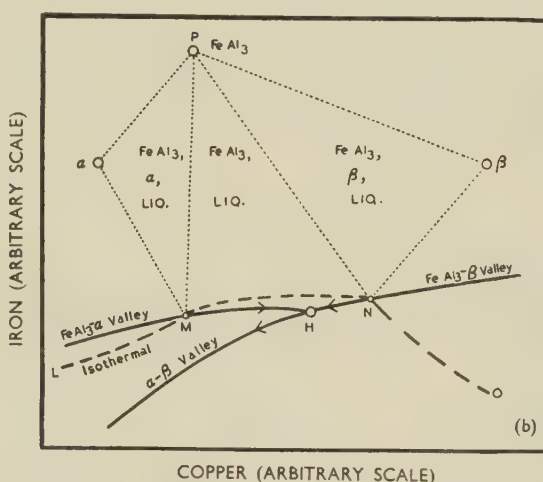
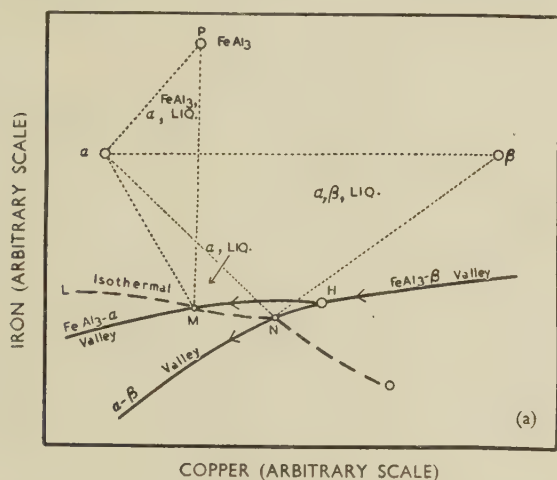


FIG. 3.—Isothermal Sections at Temperatures Close to that of the Peritectic Invariant  $FeAl_3 + liq. \rightarrow \alpha + \beta$ .

(a) Impossible; (b) Correct.

$LMNO$  must cross the primary  $\alpha$  field at  $MN$ , and give rise to a three-phase triangle  $P\alpha M$ , ( $FeAl_3, \alpha$ , liquid *M*); a two-phase region  $\alpha MN$  ( $\alpha$ , liquid varying in composition between *M* and *N*); and a second three-phase triangle,  $\alpha\beta N$  ( $\alpha, \beta$ , liquid *N*). As will be seen, these phase areas overlap, so that the diagram cannot possibly be correct. Fig. 3 (b) has been drawn on the assumption that temperatures rise on proceeding to the left from *H* along the  $FeAl_3/\alpha$  valley. In these circumstances an isothermal  $LMNO$  must cross the  $FeAl_3$  field at  $MN$ , and the various two- and three-phase areas fall into their correct sequence. In a similar way it may be shown that on proceeding to the left from *H* along the  $FeAl_3/\alpha$  boundary, the temperatures will continue to rise only until the point *K* in Fig. 2 is reached, and will then fall steadily until the end of the boundary is reached at *B*. The sharpness of the maximum at *K* will depend on the degree of dissociation of  $\alpha$  and on the extent of its homogeneity range.

If it is assumed that Phragmén's estimate of the composition of  $\alpha$  is in error, and that its true composition lies to the right of the line  $PH$ , then a study of

It is clear that the constitution of these alloys cannot be regarded as satisfactorily established. Four points in particular call for further investigation:

- (1) Does the  $\alpha$  constituent exist? If so, is it a stable or a metastable phase, and if the former, is Phragmén's estimate of its composition approximately correct?
- (2) Is the constituent designated  $FeAl_3$  capable of dissolving much or little copper?
- (3) Does the constituent  $\beta$  exist over a wide range of homogeneity?
- (4) What is the solid solubility of iron in the aluminium-rich phase in the ternary alloys?

The present work was undertaken in the hope of obtaining answers to these four questions.

## II.—SCOPE OF INVESTIGATION

In the previous investigation made in these Laboratories,<sup>1</sup> aluminium of 99.67% purity had been used, and no attempt had been made to study equilibrium conditions; the diagrams published were applicable

only to rates of solidification likely to occur in industrial practice. It was therefore decided to make a fresh survey of the liquidus surface over the range 0–40% copper 0–3.5% iron, with alloys made from super-purity aluminium. Series of alloys were first prepared with copper varying in steps of 5%, and iron in steps of 0.5%, but intermediate compositions were used in the neighbourhood of all phase boundaries, and particularly on crossing the region in which primary  $\alpha$  was expected to occur.

Determinations of solid solubility were limited to one temperature, 500° C. Two series of alloys were prepared, containing 0.25 and 0.05% iron, with copper varying in steps of 0.5% up to a maximum of 6%: these were used to determine the limits of occurrence of the iron-bearing phases and the solid solubility of  $\text{CuAl}_2$ . To find the limiting solubility of iron in the ternary alloys, additional series were made with iron ranging from 0.003 to 0.008% in steps of 0.001%, with copper constant at 0.0, 0.5, 1.0, 1.5, 2.0% and thence in steps of 1% to a maximum of 6%. These alloys were afterwards used for solidus determinations.

### III.—MATERIALS AND METHODS

#### 1. MATERIALS USED

Copper and iron were added as hardeners made up from super-purity aluminium, electrolytic copper, and Armco iron. Typical analyses were as follows:

	Fe, %	Si, %	Cu, %	Mn, %
S.P. aluminium	0.001	0.002	<0.0005	<0.0005
Iron hardener	7.89	0.002	0.001	0.003
Copper hardener	—	0.003	54	0.001

In analysing ternary alloys, the only contaminants estimated were silicon and manganese; both averaged 0.003%.

#### 2. THERMAL ANALYSIS AND MICROGRAPHY

Quantities of about 200 g. were used for cooling curves, and were allowed to cool at a rate of about 5° C./min., the melt being well stirred until a well-marked arrest occurred. In the primary  $\text{FeAl}_3$  field, the primary arrests were often difficult to distinguish, and therefore reliance was placed on solubility measurements for the determination of liquidus temperatures. In these experiments the alloy was held molten at a constant temperature, and samples of the liquid portion were taken for analysis after 1 and 2 hr. Heating curves were taken on selected samples only, such as those in the neighbourhood of invariant points. For determining the temperatures of secondary arrests, considerable use was made of a furnace of the constant-gradient type described by Smith.<sup>16</sup>

Microsections were examined unetched in ordinary and in polarized light, and also after etching for 10–15 sec. with solutions of 0.5% HF or 12½% NaOH, used cold. In the unetched sections, and under ordinary illumination, it was easy to identify  $\text{FeAl}_3$  by its dark

grey colour and tendency towards relief, but it was difficult to decide whether one or two ternary phases existed. Examination under polarized light showed unmistakably that over a certain range of compositions two ternary bodies could occur, both strongly birefringent;  $\alpha$  either crystallized independently or was formed peritectically from  $\text{FeAl}_3$ , and itself reacted peritectically to form  $\beta$ . With the acid etch,  $\text{FeAl}_3$  was tinted straw yellow and the ternary compounds brown,  $\alpha$  being generally, though not consistently, the more heavily attacked. With the alkaline etch,  $\text{FeAl}_3$  acquired a deep brown and the ternary compounds a fawn colour, and in general  $\beta$  was the more deeply tinted.

For solidus determinations, the heating-quench method was employed on small chill-cast specimens which had previously been annealed to equilibrium at 500° C. The sections were examined at temperature intervals of 2° C., commencing some 5° C. below the expected solidus temperature.

Estimates of solid solubility were based on the microscopic examination of sections cut from chill-cast samples, annealed for 8 days at 500° C. and quenched in cold water. It proved to be extremely difficult, and in many cases impossible, to decide which of the iron-bearing constituents were present in any section; the tints developed on the small particles by etching reagents were not consistent, and the colour changes on rotation of the specimen between crossed Nicols were not pronounced. It was, however, fairly easy to decide whether a specimen contained one iron-bearing constituent, or two, and in this way to locate the boundaries of the phase fields.

All alloys used for cooling or heating curves were remelted, chill cast, and analysed. In general, the composition found by analysis agreed very closely with that intended. In the rare instances where arrest temperatures required correction for errors in composition, the procedure advocated by Haughton<sup>17</sup> was followed. Silicon contamination was of the order of 0.003% and was ignored.

#### 3. CHEMICAL ANALYSIS

Copper was estimated colorimetrically, volumetrically, or electrolytically, according to the amount present. For quantities of less than 0.25%, the sodium diethyldithiocarbamate colorimetric process was used, and for quantities of 25% or over, the electrolytic. Intermediate amounts were estimated volumetrically, by means of thiosulphate.<sup>18</sup>

Iron, in amounts less than 0.05%, was estimated colorimetrically, by means of thiocyanate. In larger amounts, it was estimated volumetrically, against titanous chloride.<sup>18</sup>

Silicon and manganese, present as contaminants, and in minute amounts only, were estimated colorimetrically, the former by means of the yellow colour developed with ammonium molybdate and the latter by oxidation to permanganate.<sup>18</sup>



## IV.—THE LIQUIDUS SURFACE

## 1. GENERAL TOPOGRAPHY

The basal projection of the liquidus surface for the range studied is shown in Fig. 4. The diagram is of the same general form as that published by Phragmén,<sup>12</sup> having five primary phase fields, although it differs somewhat from his in the positions of the binary valleys and their intersections. The observations on which it is based confirm his view that the constituent  $\alpha$  is formed peritectically from  $\text{FeAl}_3$  along  $BH$ , reacts peritectically along  $HC$  to form  $\beta$ , and separates as a eutectic complex with aluminium along  $BC$ . The reactions along the remaining valleys have been reinvestigated and the earlier findings<sup>1, 2, 4, 9</sup> have been confirmed;  $AB$ ,  $CD$ ,  $DE$ , and  $DF$  (Fig. 4) are all

high figures for iron were recorded, due almost certainly to the primary  $\text{FeAl}_3$  not having settled out completely; where this occurred repeat experiments were made.

The positions of most of the eutectic valleys were determined without difficulty from cooling curves and micro-examination, but in the case of the  $\text{CuAl}_2/\beta$  valley,  $DF$ , the latter method proved unreliable, because massive crystals of both constituents occurred simultaneously over a range of iron contents on both sides of the boundary as determined from the cooling curves. It was, therefore, necessary to extend the investigation to include alloys containing 45 and 50% copper with 0.1–0.5% iron, so that interpolation could be used.

In the case of the peritectic valleys, the approximate positions were plotted from the presence or absence of

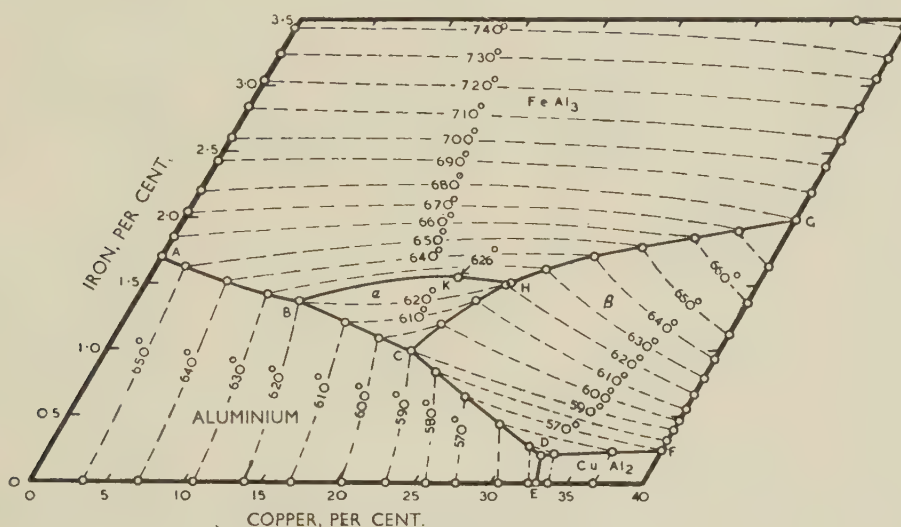


FIG. 4.—The Liquidus Surface.

eutectic in character, whilst  $GH$  is associated with the peritectic reaction between  $\text{FeAl}_3$  and liquid to form  $\beta$ . The co-ordinates of the ternary invariant points are listed in Table III.

TABLE III.—Ternary Invariant Points.

Ref.: Fig. 4	Reaction	Composition		Temp., °C.
		Cu, %	Fe, %	
B	Peritectic; $\text{Al}, \text{FeAl}_3 + \text{liq.} \rightarrow \alpha$	10.8	1.36	620
C	Peritectic; $\text{Al}, \alpha + \text{liq.} \rightarrow \beta$	20.0	1.00	590
D	Eutectic; $\text{Al}, \beta, \text{CuAl}_2, \text{liq.}$	32.55	0.23	548
H	Peritectic; $\text{FeAl}_3 + \text{liq.} \rightarrow \alpha + \beta$	23.6	1.50	622
K	Maximum on $\text{FeAl}_3/\alpha$ boundary	~20	1.55	626

The isothermals of the primary  $\text{Al}$ ,  $\alpha$ ,  $\beta$ , and  $\text{CuAl}_2$  fields were determined by means of cooling curves only. Those of the primary  $\text{FeAl}_3$  field were based on solubility measurements from 625° C. upwards. Analysis was carried out of samples of supernatant liquid from alloys containing 4% iron with copper increasing in steps of 5% up to 40%. Occasionally very

coring in the slowly cooled microsection, and by extrapolation to the liquidus of the peritectic arrest lines in the vertical sectional diagrams. Neither method proved reliable in the case of the  $\alpha/\beta$  boundary: the reaction tended to go to completion, and coring occurred but rarely, whilst the peritectic line on the sectional diagram was too short to permit of extrapolation. For this and other peritectic boundaries, reliance was placed on quenching experiments, and on cooling curves taken at very slow rates, preferably in the constant-gradient furnace. Three of these cooling curves are shown in Fig. 5. In Fig. 5 (a), representing the solidification of an alloy containing 5% copper, 2% iron, both the peritectic arrests occur after the aluminium has commenced to solidify, and the earlier one, due to the  $\text{FeAl}_3 \rightarrow \alpha$  reaction, could not be detected at all on an inverse-rate curve taken in the usual way. In the constant-gradient furnace, the heat evolution due to the separation of the aluminium caused the cooling of the furnace to be retarded, with the result that the arrests associated with both

peritectic reactions were clearly revealed. Fig. 5 (b), the cooling curve of an alloy containing 22.5% copper, 1.55% iron, has been included to show the smallness of the arrest due to the separation of ( $\text{FeAl}_3 + \alpha$ ), and the indefinite, rounded, character of the arrest due to the  $\alpha \rightarrow \beta$  reaction. Quenching experiments showed that owing to envelopment, a high proportion of the  $\text{FeAl}_3$  took no part in the  $\alpha$  reaction, and was converted to  $\beta$ , with the  $\alpha$ , at the lower arrest. In Fig. 5 (c), the curve for an alloy containing 26% copper, 2% iron, the primary arrest due to  $\text{FeAl}_3$  at 665° C.—as determined from solubility measurements—is not

$\text{FeAl}_3$  was complete; thereafter  $\alpha$  separated from the melt as if it were primary. In Fig. 7,  $\alpha$  is primary, and has crystallized in the form of rhomboids apparently identical in crystal habit with those formed by primary  $\text{MnAl}_6$  in binary aluminium-manganese alloys. Some of these rhomboids have been superficially converted to  $\beta$ , and numerous needles of  $\beta$  can also be seen in the micrograph. Figs. 8 and 9 show the same area of a specimen in which  $\alpha$  is primary, photographed in polarized light. The large  $\alpha$  rhomboid has been extensively converted to  $\beta$ : the difference between the two constituents is strikingly

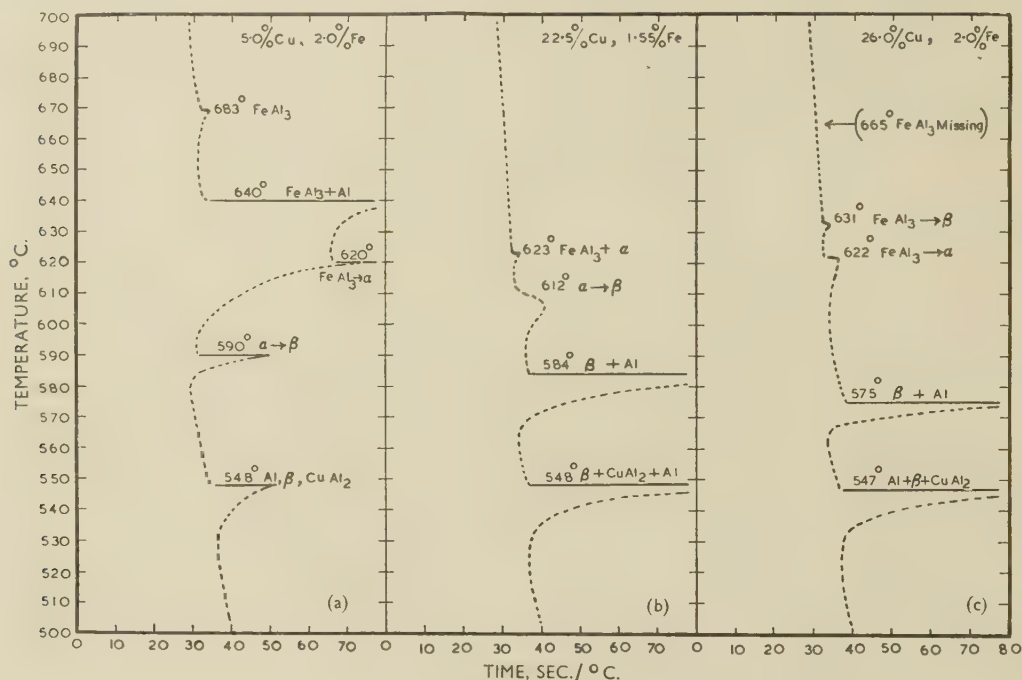


FIG. 5.—Inverse-Rate Cooling Curves of Three Alloys Taken in a Constant-Gradient Furnace.

visible; the  $\text{FeAl}_3 \rightarrow \beta$  arrest at 631° C. is quite small, and there is an arrest at 622° C., which quenching experiments showed to be due to some unconverted  $\text{FeAl}_3$  reacting with liquid to form  $\alpha$ .

The composition of the ternary eutectic was found by analysing eutectic areas in a set of four micro-sections bracketing the expected value. The figures ranged from 32.4 to 32.65% copper and 0.21 to 0.25% iron. The mean of the four analyses has been included in Table III.

Figs. 6–9 (Plate XXIX) show typical microsections of slowly cooled alloys which deposit  $\alpha$  during solidification. In Fig. 6,  $\text{FeAl}_3$  is primary, and a mass of this constituent can be seen as a core in a large crystal of  $\alpha$ . The extreme edge of the  $\alpha$  crystal has reacted to form  $\beta$ , which has crystallized in its usual needle form. It seems probable that only a small proportion of the  $\alpha$  body has been formed peritectically. Experiment showed that the peritectic reaction virtually ceased as soon as the envelopment of the

revealed on rotating the specimen between the crossed Nicols.

## 2. TOPOGRAPHY OF THE $\alpha$ FIELD

As explained in Section I, it is a matter of some interest to know whether the temperature along the  $\text{FeAl}_3/\alpha$  boundary passes through a maximum, and whether the  $\alpha$  field itself is saddle-shaped. Series of cooling curves were therefore taken, employing very slow cooling rates, (a) of alloys lying along the  $\text{FeAl}_3/\alpha$  boundary and (b) of alloys containing 15, 17.5, and 20% of copper, with iron increasing in steps of 0.25% across the field. The arrest temperatures of the alloys lying in the boundary are shown in Fig. 14. The figures in parentheses show the iron contents of the alloys used, and the lettering along the lines of arrests indicates the constituents separating. It is clear that the valley passes through a flat maximum at 626° C. in the region 19–21% copper: this confirms



Phragmén's view that  $\alpha$  has only a limited homogeneity range. The arrest temperatures of the series of alloys across the  $\alpha$  field have been utilized in preparing the liquidus diagram Fig. 4; they show that the field is, in fact, saddle-shaped.

### 3. COMPOSITION OF THE INTERMETALLIC PHASES

#### (a) Composition of $\text{FeAl}_3$

Attempts were made to determine the composition of the phase designated  $\text{FeAl}_3$  by the chemical analysis of primary crystals extracted electrolytically from two alloys, one containing 5% iron, 5% copper, and therefore lying well to the left of the  $\text{FeAl}_3/\alpha$  line, and the other 5% iron, 30% copper, lying well to the

right of this line. Micro-examination showed that the  $\text{FeAl}_3$  crystals in both alloys, quenched from 700°C. in both cases, and therefore well above the peritectic reaction temperatures, were free from reaction rims, but the alloy richer in copper contained many large  $\beta$  crystals, some of them adhering to the  $\text{FeAl}_3$ . The electrolytic extraction was done in 2-N nitric acid solution, an electrolyte which experiment had shown to be capable of dissolving  $\beta$  but not  $\text{FeAl}_3$ . The larger crystals extracted were picked out by hand, washed in stronger nitric acid to remove any deposited copper, and analysed. The results, on triplicate samples, were:

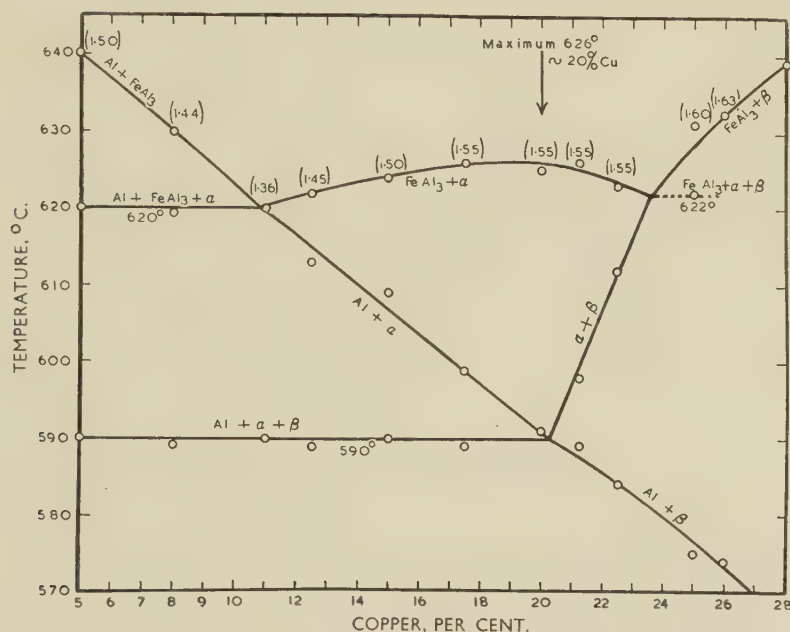


FIG. 14.—Arrest Temperatures of Alloys Lying in the  $\text{FeAl}_3/\alpha$  Boundary.

right of this line. Micro-examination showed that the  $\text{FeAl}_3$  crystals in both alloys, quenched from 700°C. in both cases, and therefore well above the peritectic reaction temperatures, were free from reaction rims, but the alloy richer in copper contained many large  $\beta$  crystals, some of them adhering to the  $\text{FeAl}_3$ . The electrolytic extraction was done in 2-N nitric acid solution, an electrolyte which experiment had shown to be capable of dissolving  $\beta$  but not  $\text{FeAl}_3$ . The larger crystals extracted were picked out by hand, washed in stronger nitric acid to remove any deposited copper, and analysed. The results, on triplicate samples, were:

Crystals extracted from 5/5 alloy: iron 36, copper 0.50–0.55%  
Crystals extracted from 5/30 alloy: iron 33, copper 6.1–8.0%

X-ray powder-diffraction patterns were taken, with cobalt radiation in a 19-cm. camera, and found to be identical, line for line, within a small fraction of a millimetre, with the pattern of  $\text{FeAl}_3$  containing

seems improbable that contamination of this type is responsible for the 0.5% copper found in the crystals extracted from the 5/5 alloy. Any crystals of the matrix present would contain about 5% copper, 2% iron, and experiment shows that an alloy of this composition floats readily, whereas  $\text{FeAl}_3$  sinks, in tetrabromethane ( $d$  2.96). Since the crystals extracted from the 5/5 alloy sank in this reagent, and appeared to be completely free from adherent matter, there seems to be no reason to question their uniformity. Their analysis, 36% iron, 0.5% copper, has been taken to be that of the  $\text{FeAl}_3$  separating over the whole primary field, a view which is consistent with the X-ray-diffraction patterns and with the direction of the secondary isothermals.

#### (b) Composition of $\alpha$

It has not yet been possible to make a direct determination of the composition of  $\alpha$ , as attempts to

grow large primary crystals and to make electrolytic extractions have proved unsuccessful. All that can be said at present is that the composition must lie along the line joining the composition of  $\text{FeAl}_3$  to the maximum point along the  $\text{FeAl}_3/\alpha$  binary valley. This line is shown as  $ABCD$  in Fig. 15. If, by analogy with  $\text{MnAl}_6$ ,  $\alpha$  has an electron/atom ratio of 2.05, its composition should lie at the point  $B$ , which is the intersection of the  $\text{FeAl}_3/\alpha$  maximum line with the locus  $PQ$  of compositions having this ratio. Raynor<sup>14</sup> has shown, however, that in  $\text{MnAl}_6$ , iron can replace manganese, atom for atom, up to a limiting composition of  $(\text{Mn}_4\text{Fe}_2)\text{Al}_6$ . At this composition the electron/atom ratio is 2.12, and it is possible that this corresponds with the limit of stability of the  $\text{MnAl}_6$  type of structure. If so, then the composition

the copper replaces the aluminium is inherently the most probable. In  $\text{MnAl}_6$ , one set of eight aluminium atoms lie very close together, at 2.57–2.62 Å., and not 2.71–2.86 as expected, and these aluminium atoms also lie very close to the manganese atoms, at 2.435 Å., as against the expected distance of 2.68 Å. He infers that these particular aluminium atoms may be the donors of electrons to the manganese atoms, as postulated by the Pauling-Raynor theories. If now we replace manganese by iron, this will reduce the electrons accepted by the transition-metal atoms from 3.66 to 2.66/atom, and thus tend to increase the spacing between the aluminium atoms, and between them and the transition-metal atoms. It is possible that it is the inability to tolerate such increased spacing that accounts for the non-existence of  $\text{FeAl}_6$ .

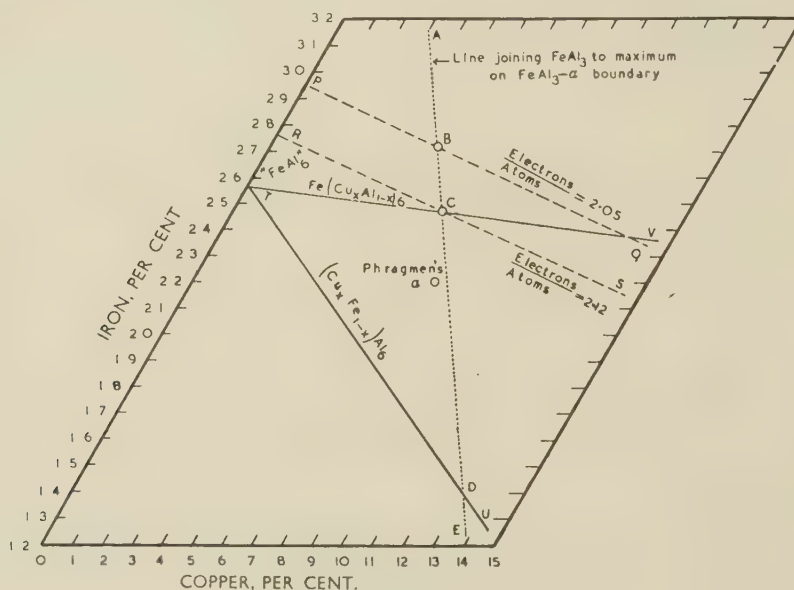


Fig. 15.—Estimated Composition of  $\alpha$ .

of  $\alpha$  may be represented by the point  $C$  of Fig. 15, the intersection of the  $\text{FeAl}_3/\alpha$  maximum line with the 2.12 electron/atom locus  $RS$ .

Phragmén<sup>12</sup> has suggested that the formula of  $\alpha$  is  $(\text{Cu},\text{Fe})(\text{Cu},\text{Al})_6$ . The locus of alloy compositions, in which all the copper enters the first bracket, partially replacing the iron, is shown in Fig. 15 as  $TU$ , intersecting  $AE$  in  $D$ , whilst the locus of compositions in which all the copper is in the second bracket, partially replacing the aluminium, is shown as  $TV$ , intersecting  $AE$  in  $C$ . Thus the point  $C$  satisfies Raynor's views as regards electron/atom ratios, and Phragmén's as regards the formula. Phragmén's suggested composition of  $\alpha$ , based on the extraction of crystals from an alloy containing magnesium, copper, and iron, corresponds with a formula in which roughly half of the copper is replacing the iron, and half the aluminium.

From Nicol's work on the crystal structure of  $\text{MnAl}_6$ ,<sup>19</sup> it would seem that a formula for  $\alpha$  in which

Replacing some of the iron atoms by copper would be expected to increase the strain, since copper does not accept electrons, so that the aluminium atoms would tend to retain more of their electrons and hence to revert to their normal spacing. Replacing aluminium by copper, however, might tend to relieve the strain, since the copper atom with the smaller radius of 1.27 Å. might fit more easily into the structure.

Attempts were made to check the composition of  $\alpha$  by making an alloy of composition  $C$  (Fe 24.7, Cu 7%), annealing it for a prolonged period just below the peritectic reaction temperature, and quenching. These attempts to produce a single-phase alloy were not successful. After 96 hr. at 620° C. the reaction rims on the primary  $\text{FeAl}_3$  crystals were nowhere more than 0.001 mm. in thickness, representing at the most a 1% conversion: they had only doubled in thickness after a further 300 hr., and the alloy still contained a large amount of a liquid phase which, on quenching, solidified to aluminium,  $\beta$ , and  $\text{CuAl}_2$ .



(c) Composition of  $\beta$ 

Up to the present, all attempts to extract  $\beta$  electrolytically have failed. Nitric and hydrochloric acids at various dilutions, and also tartaric acid, have been tried as electrolytes. Although crystals have been extracted, X-ray powder-diffraction patterns showed them to be essentially aluminium. This suggests that the interlacing network of  $\beta$  crystals is being preferentially attacked, allowing crystals of the matrix to become dislodged.

Phragmén and others have analysed  $\beta$  crystals picked from cavities in cast alloys, and Hanemann and others have prepared single-phase alloys consisting of  $\beta$ . No attempt has been made to repeat any of

mined by Bradley and Goldschmidt,<sup>5</sup> and on the right, to the copper-rich end of this range. In the aluminium field they are tie lines joining corresponding points on the binary valleys and the solidus curves.

## 2. LATER SEPARATIONS

During the primary separation, the point representing the composition of the liquid phase crosses the primary field, running in the general direction of the secondary isothermals of the region in question, and when the secondary separation begins, the point has reached one of the binary valleys. If this valley is eutectic in character, the point will follow it until either the supply of liquid is exhausted or an invariant

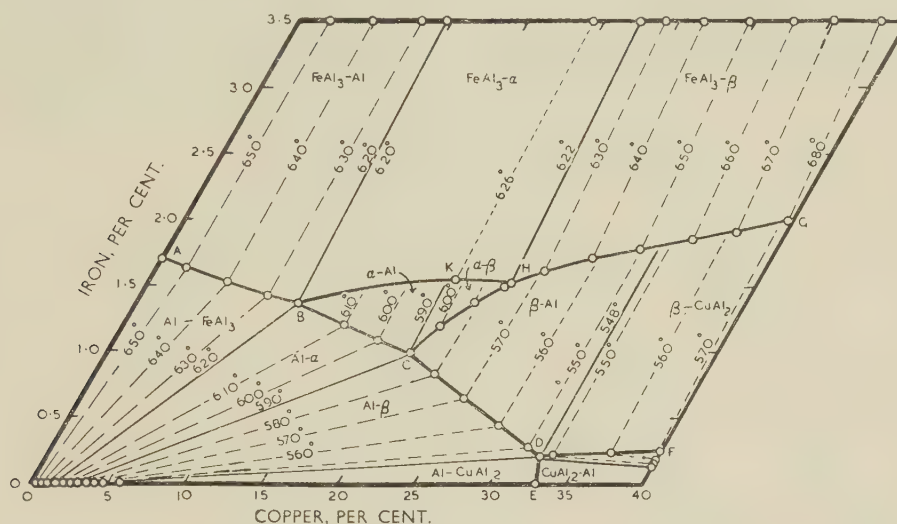


FIG. 16.—Isothermals of the Secondary Surface.

this work or to ascertain directly whether  $\beta$  has a large or small homogeneity range.

## V.—SECONDARY AND LATER SEPARATIONS

## 1. THE SECONDARY ISOTHERMALS

The isothermals of the secondary surface, under conditions of equilibrium, are shown in Fig. 16. Each primary field has two or more secondary fields associated with it; these have been indicated in Fig. 16 by appropriate lettering.

In the primary  $\text{FeAl}_3$  field, the isothermals appear to run from the points on the binary valleys to the point representing  $\text{FeAl}_3$  containing about 0.5% dissolved copper. The primary  $\alpha$  field is too small to permit of the course of the secondary isothermals being accurately determined, but the experimental points are consistent with the view that  $\alpha$  contains about 25% iron, 7% copper. In the  $\beta$  field, the secondary lines do not appear to radiate from a fixed point. On the left of the field, they can best be represented as running to the point representing the iron-rich end of the homogeneity range of  $\beta$  as deter-

mined by Bradley and Goldschmidt,<sup>5</sup> and on the right, to the copper-rich end of this range. In the aluminium field they are tie lines joining corresponding points on the binary valleys and the solidus curves.

point is reached. Here the ternary separation commences. In the case of a peritectic invariant depending on the rate of cooling, the reaction will proceed to completion or until the solid reactant has become completely enveloped. The residual liquid, which will be reduced in amount but unchanged in composition, will then complete its solidification along the lower branches of the eutectic valley or at the ternary eutectic. In these circumstances the complete course of solidification can be followed from the liquidus, secondary, and solidus diagrams.

Where the secondary separation occurs as the result of a peritectic reaction, the point representing the composition of the liquid will only remain in the valley while the reaction is proceeding; during this process the temperature will fall and the liquid will be reduced in amount and changed in composition. When the reaction is brought to a close, either by completion or envelopment, the point representing the liquid composition will leave the valley and traverse the field associated with the solid reaction product as if the latter were primary, until it reaches another binary valley. With rapid rates of cooling, such as those likely to be met with in semi-continuous and

chill casting, there is little opportunity for a peritectic reaction to occur. The point representing the liquid composition therefore crosses a peritectic valley, without proceeding along it, and the subsequent course of solidification can be predicted from the secondary and solidus diagrams.

Under conditions of equilibrium, the point representing the liquid composition will remain in a peritectic valley until the peritectic reaction is completed. The temperature and liquid composition at which this occurs, and the point leaves the valley, cannot be ascertained from the secondary diagram. For this purpose, it is necessary to construct series of isothermal sections through the ternary model.

### 3. ISOTHERMAL SECTIONS

It has been thought sufficient to reproduce one isothermal diagram, that for  $624^\circ\text{C.}$ , shown in Fig. 17.

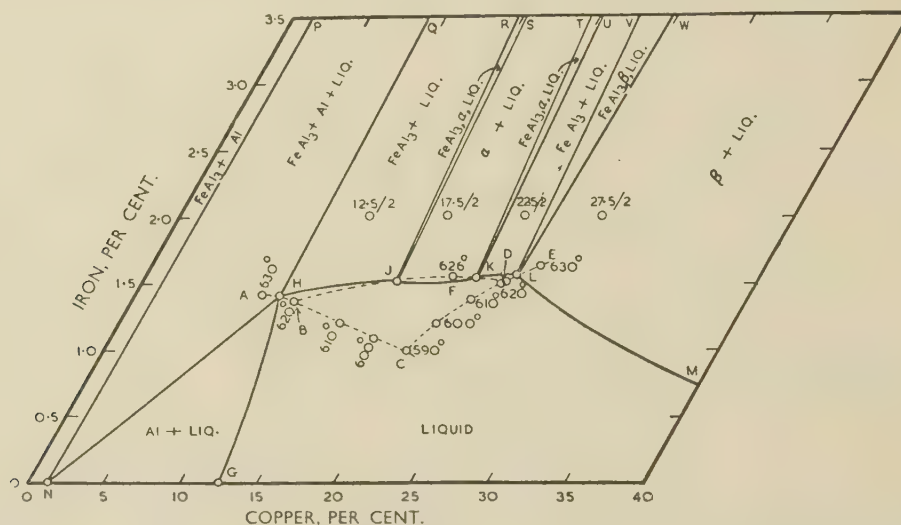


FIG. 17.—Isothermal Section at  $624^\circ\text{C.}$

The broken lines *AB*, *BC*, *CD*, *DE*, *BFD* represent part of the liquidus diagram including the primary  $\alpha$  field. The full line *GHJKLM* is the  $624^\circ\text{C.}$  liquidus isothermal. The branch *GH* separates the (*Al* + liquid) from the (liquid) field and terminates on the  $\text{FeAl}_3/\text{Al}$  binary valley at *H*. The isothermal cuts the  $\text{FeAl}_3/\alpha$  boundary at two points, *J* and *K*, and the  $\text{FeAl}_3/\beta$  boundary at *L*, thereby generating a succession of two-phase and three-phase fields as shown in the diagram. The branch *LM* separates the ( $\beta$  + liquid) from the (liquid) field. Of the remaining lines, *NP* is the solidus, experimentally determined by means of heating quenches, for which composition and temperature brackets were employed. *NH*, *HQ*, and *LV* are secondary isothermals crossing the  $\text{Al}-\text{FeAl}_3$ ,  $\text{FeAl}_3-\text{Al}$ , and  $\text{FeAl}_3-\beta$  fields of Fig. 16, from which they were derived by interpolation. They are therefore based on the results of cooling curves. The lines meeting in *J* and *K* were drawn in accordance with the theoretical requirements: *JR* and *KU* run to the composition of  $\text{FeAl}_3$  and *JS* and

*KT* to the composition of  $\alpha$ . The line *LW* runs to the high-iron end of the homogeneity range of  $\beta$ .

It was realized that it would be very difficult, if not impossible, to verify experimentally the existence of the two three-phase fields *JRS* and *KTU*. They are both narrow, and their positions must be very sensitive to temperature. An increase in temperature of  $2^\circ\text{C.}$  would cause the points *J* and *K* to merge into *F*, and a similar decrease would displace *K* to *D* and *J* nearly to *B*. It was therefore decided to attempt only to confirm the existence of the four two-phase fields. Alloys were prepared containing 2% iron with 12.5, 17.5, 22.5, and 27.5% copper, as indicated by the small circles in Fig. 17, and were annealed first for 96 hr. at  $624^\circ \pm 2^\circ\text{C.}$ , and then for a further period of 300 hr. at  $623^\circ \pm 2^\circ\text{C.}$  Micrographs of the four alloys after this treatment are reproduced in Figs. 10–13 (Plate XXX). In the

2 Fe/12.5 Cu and 2 Fe/22.5 Cu alloys, the only constituent solid at the moment of quenching was  $\text{FeAl}_3$ , and the structures were unaltered by annealing. Few of the  $\text{FeAl}_3$  crystals were free from adherent crystals of  $\beta$ ; these, however, did not appear to be reaction rims but material deposited during quenching. The existence of the two ( $\text{FeAl}_3$  + liquid) fields has therefore been established. The 2 Fe/27.5 Cu alloy contained cores of  $\text{FeAl}_3$  in large  $\beta$  crystals before annealing, but these cores disappeared completely after 96 hours' annealing, leaving  $\beta$  as the only phase solid at the moment of quenching.

The evidence for the existence of the intermediate ( $\alpha$  + liquid) field is not quite so satisfactory. Before annealing, the 2 Fe/17.5 Cu alloy contained large  $\text{FeAl}_3$  crystals with purely superficial reaction rims, together with a few small rhomboidal crystals of  $\alpha$ . During the anneal, the reaction rims increased progressively in thickness, but even after 400 hr. a considerable amount of  $\text{FeAl}_3$  remained. The  $\alpha$  reaction product appeared to be somewhat disinte-



grated, possibly as a result of the fluctuations in temperature during annealing. Although it was not possible in the time available to eliminate the  $\text{FeAl}_3$  cores completely, the difference in behaviour between the 2 Fe/17.5 Cu alloy on the one hand, and the 2/12.5 and 2/22.5 alloys on the other, suggests very strongly that the  $(\alpha + \text{liquid})$  field does exist at the temperature in question, and occupies a position between two  $(\text{FeAl}_3 + \text{liquid})$  fields.

It was relatively easy, by means of quenching experiments, to check the accuracy of isothermal sections for temperatures above  $626^\circ\text{C}$ ., where the two  $(\text{FeAl}_3 + \text{liquid})$  fields had merged into one. The structures obtained resembled those reproduced in Figs. 12 and 13. It was also easy to verify, by quenching and annealing experiments, the existence of the  $(\alpha + \text{liquid})$  field in sections for temperatures in the range  $590^\circ$ – $620^\circ\text{C}$ .; it was, however, necessary to use alloys the composition of which lay in the primary

intersection with the boundary  $AB$  are also the terminations of the isothermals of the secondary surface, which again are rectilinear. Thus the independent determination of the solidus furnishes a useful check on the accuracy of the work from which the secondary

TABLE IV.—Solidus Invariant Points.

Ref.: Fig. 18	Equilibrium	Composition		Temp., $^\circ\text{C}$ .
		Cu, %	Fe, %	
<i>B</i>	Al, $\text{FeAl}_3$ , $\alpha$ , liq.	1.48	0.034	620
<i>C</i>	Al, $\alpha$ , $\beta$ , liq.	3.00	0.022	590
<i>D</i>	Al, $\beta$ , $\text{CuAl}_2$ , liq.	5.60	0.013	548

isothermals were plotted. Similar remarks apply, of course, to the other fields of the solidus diagram.

Table IV gives the co-ordinates of the invariant points of the solidus surface.

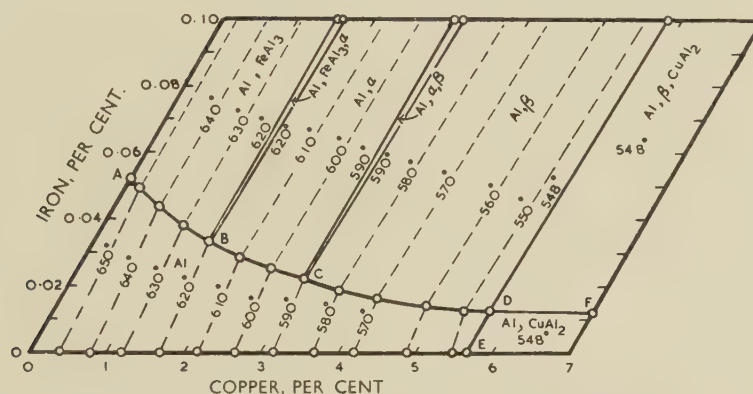


FIG. 18.—Solidus Isothermals for Alloys of Low Iron Content.

$\alpha$  field, thereby avoiding the persistent  $\text{FeAl}_3$  coring. No trouble was experienced from  $\alpha$  or  $\text{FeAl}_3$  cores in  $\beta$ : these rapidly disappeared during annealing.

## VI.—THE SOLIDUS

The solidus isothermals for alloys of low iron content are shown in Fig. 18. The diagram includes eight phase fields, all of which have been lettered to indicate the solid phases in equilibrium with the liquid. It has been plotted on a large scale for clarity, and does not cover the whole range of compositions investigated, which included series of alloys containing 0.25% and 2% iron, and a few alloys containing 10% copper. It is based on the results of quenching experiments on microsections previously annealed to equilibrium at  $500^\circ\text{C}$ .

In the field representing the equilibrium between aluminium,  $\text{FeAl}_3$ , and liquid, the solidus isothermals are straight lines running from their points of intersection with the boundary  $AB$  to the composition of  $\text{FeAl}_3$ , and hence a limited number of observations, on alloys containing 0.05, 0.10, 0.25, and 2.0% iron, sufficed to establish their positions. The points of

## VII.—THE LIMITS OF SOLID SOLUBILITY

### 1. SOLID SOLUBILITY AT $500^\circ\text{C}$ .

Fig. 19 (a) shows the phase boundaries in alloys containing 0.0–0.25% iron, 0–6% copper, annealed to equilibrium at  $500^\circ\text{C}$ . As it is impossible to show on this scale the exact limits of the single-phase aluminium field, Fig. 19 (b), plotted on a much larger scale, has been included.

It will be appreciated that at these extremely low concentrations of iron it was rarely possible to identify each minute particle of constituent, but it was relatively easy to say whether one or two species were present in any microsection. The phase boundaries have been drawn from these observations, and the fields lettered in the usual sequence. Table V gives the co-ordinates of the apices of the three-phase triangles.

The solid solubility of iron in pure aluminium at  $500^\circ\text{C}$ . was determined in the course of these experiments, and estimated to be 0.0055%, in almost exact agreement with the figure of 0.006% reported by Edgar.<sup>20</sup> The figure of 4.1% for the copper co-ordinate of point *C* agrees fairly well with that (3.8%)

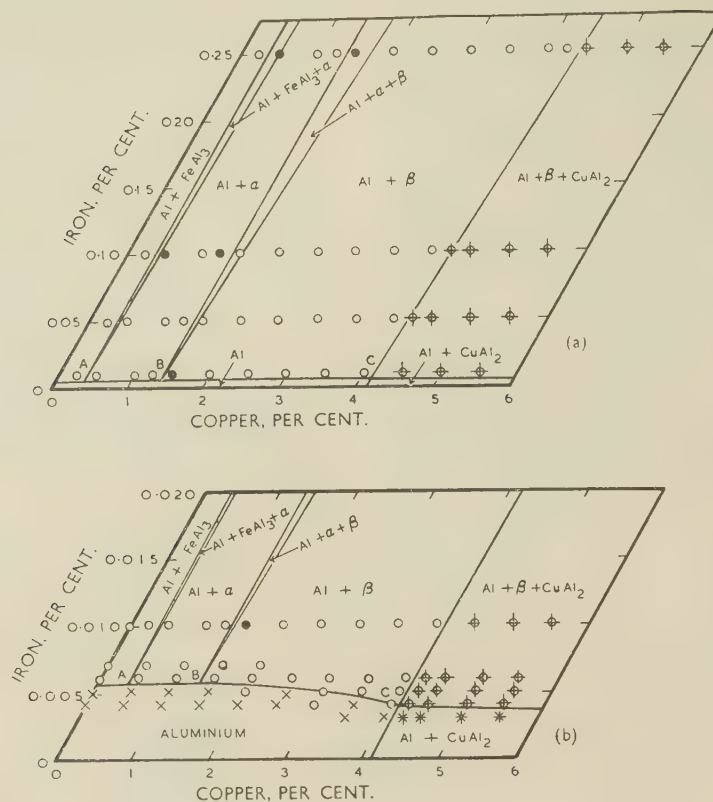


FIG. 19.—Solid Solubility at 500° C.

## KEY.

× No iron constituent present.  
 ○ One iron constituent present.

● Two iron constituents present.  
 +  $\text{CuAl}_2$  present.

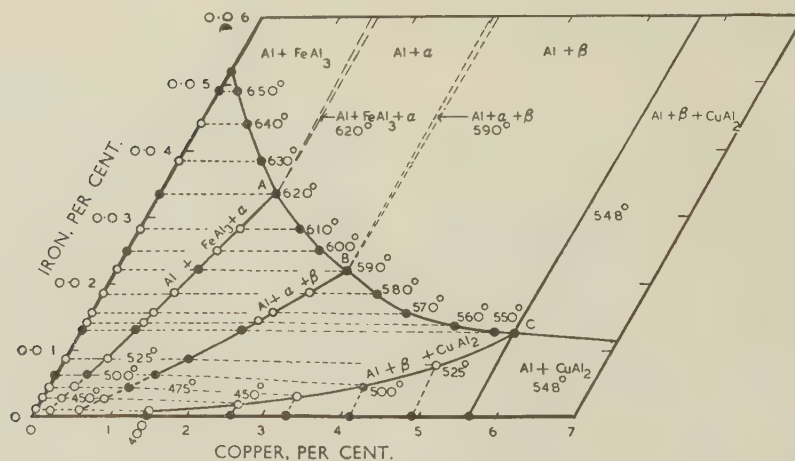


FIG. 20.—Solid Solubility at Various Temperatures Between 400° C. and the Solidus.



determined directly by Brown, Fink, and Hunter,<sup>8</sup> and even more closely with that of 4.2% derived by interpolation from the data published by Hanemann and Schrader.<sup>9</sup> Both groups of authors report an

TABLE V.—Apices of 3-Phase Triangles at 500° C.

Ref. : Fig. 19	Phases	Composition	
		Cu, %	Fe, %
A	Al, FeAl <sub>3</sub> , $\alpha$	0.4	0.0055
B	Al, $\alpha$ , $\beta$	1.3	0.0055
C	Al, $\beta$ , CuAl <sub>2</sub>	4.1	0.0040

apex at 1.3% copper, but ascribe it, not to the triangle (Al +  $\alpha$  +  $\beta$ ), but to one with which the associated constituents are Al, FeAl<sub>3</sub>, and  $\beta$ .

the logarithm of the atomic percentage and the reciprocal of the absolute temperature. Points along the copper axis have been taken from recent investigations in these Laboratories on the aluminium-copper-silicon system.<sup>21</sup> The points plotted on the three loci for 500° C. have been taken from Fig. 19, and those for 550°, 590°, and 620° C. were derived from similar diagrams constructed for those temperatures, which it has not been thought necessary to publish. The curved line, commencing at 0.052% iron on the axis, and terminating at the point C, has been taken from the solidus diagram (Fig. 18).

At these four temperatures, the boundaries between the Al and (Al + FeAl<sub>3</sub>) fields and between the Al and (Al +  $\alpha$ ) fields are apparently straight lines parallel to the copper axis of the diagram. This relationship has been assumed to hold for other temperatures;

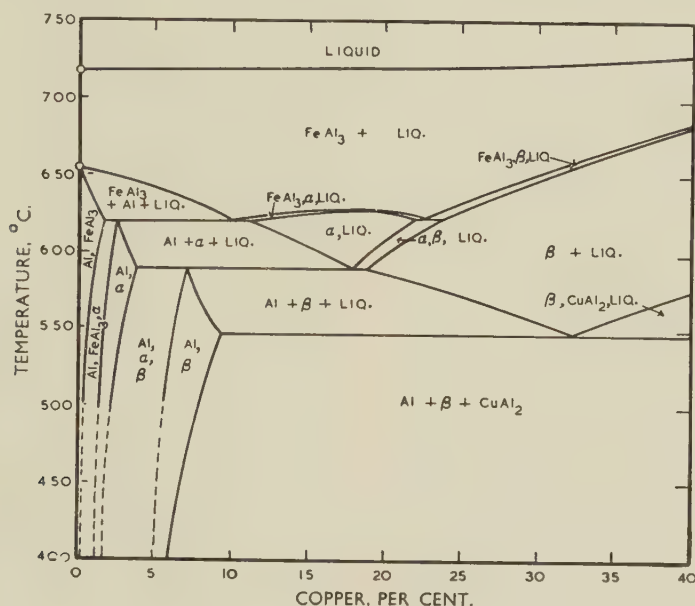


FIG. 21.—Alloys Containing 3.0% Iron.

## 2. SOLID SOLUBILITY AT OTHER TEMPERATURES

It is impossible to show, on a single diagram, the full solid-solubility data for a range of temperatures. Fig. 20 shows the estimated co-ordinates of the loci of the three apices of the three-phase triangles for selected temperatures, together with the boundaries of the single-phase field associated with the aluminium-rich solid solution at these temperatures. The three-phase triangles themselves have been drawn at the appropriate solidus temperatures only. For other temperatures, no serious error would be introduced by drawing the sides of the triangles parallel to those at the solidus temperatures.

The diagram is a composite one. The points along the iron axis have been taken from Edgar's data.<sup>20</sup> His observed points have been shown as solid circles, whilst points derived by interpolation or extrapolation have been plotted as open circles. In deriving these points, a linear relationship was assumed between

some confirmation of this assumption is afforded by the fact that it leads to copper co-ordinates for the 475° and 525° C. points on the Al- $\alpha$ - $\beta$  line in exact agreement with those directly determined by Brown, Fink, and Hunter.

The boundary between the Al and (Al +  $\beta$ ) field appears to be parallel to the copper axis for temperatures of 550° C. and upwards, but to slope slightly towards the axis at lower temperatures. The boundary between the Al and (Al + CuAl<sub>2</sub>) fields is slightly inclined to the iron axis, indicating that the solubility of copper in aluminium is reduced to a small extent by the presence of iron.

## VIII.—VERTICAL SECTIONAL DIAGRAMS

It has been thought sufficient to include two diagrams, Fig. 21 representing alloys with 3% iron, and Fig. 22 those with 5% copper. Both diagrams have

been drawn to represent equilibrium conditions, and it has been assumed that the two peritectic reactions have gone to completion and that the aluminium-rich solid solution has reached full saturation. Neither of these assumptions is true for alloys cast under industrial conditions, so that diagrams applicable to such

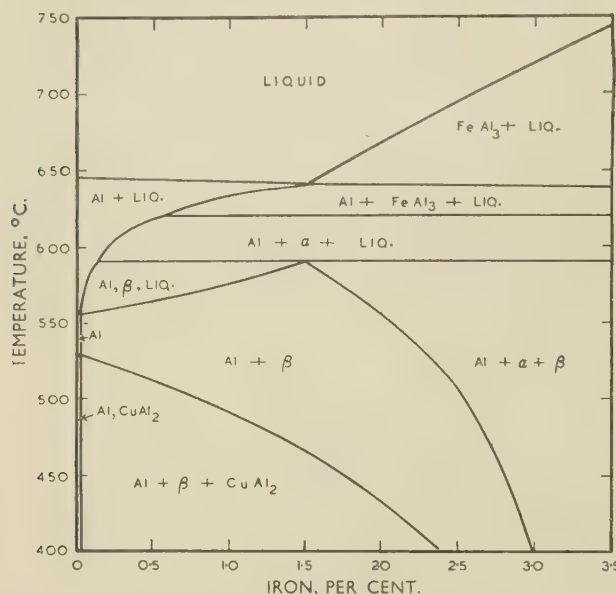


FIG. 22.—Alloys Containing 5.0% Copper.

conditions differ appreciably from those representing equilibrium.

The reaction between  $\text{FeAl}_3$  and liquid to give  $\alpha$  will proceed to completion only if the iron content is low, the  $\text{FeAl}_3$  finely dispersed, and if prolonged annealing has been given, so that diagrams representing alloys produced under industrial conditions would have to show residual  $\text{FeAl}_3$  as a constituent in all fields in which  $\alpha$  had been formed peritectically. This residual  $\text{FeAl}_3$ , with any  $\alpha$  formed peritectically or

deposited as such from the liquid, would react in due course to form  $\beta$ , and this reaction would go to completion with slow rates of solidification or on annealing for a short time, so that the areas in the equilibrium diagrams in which  $\beta$  is shown as the only iron-bearing constituent would require little or no modification to render them applicable to industrial conditions.

Under conditions of equilibrium,  $\text{CuAl}_2$  occurs as a constituent of the ternary eutectic in alloys containing 5.6% copper and upwards in the absence of iron, and in those containing 9.3% copper or more with iron contents of 3%. In alloys solidified rapidly,  $\text{CuAl}_2$  first becomes visible as a eutectic constituent at 0.25% in the absence of iron and at about 1.1% with 3% iron. In a diagram applicable to alloys as cast, the ternary eutectic horizontal would therefore have to be shown as commencing at a correspondingly lower copper content. In Fig. 21, for example, it would begin at 1.1% copper; the solidus line would have to be shown as running from this point to the Al- $\text{FeAl}_3$  binary eutectic point at 655°C., and the two peritectic horizontals lengthened correspondingly. The phase fields below the solidus containing no  $\text{CuAl}_2$  would be reduced in width, and those shown as containing  $\alpha$  would have to be shown as containing  $\text{FeAl}_3$  as well. In Fig. 22, the ternary eutectic horizontal would have to be introduced, extending across the whole diagram, and this would be the solidus. The (Al +  $\beta$  + liquid) field, shown in Fig. 22 as a triangle with its right-hand apex lying at 1.5% iron, would also extend across the whole diagram, and the presence of residual  $\text{FeAl}_3$  would have to be indicated for iron contents exceeding about 1%, the precise figure depending upon the rate of solidification and the duration of any anneals. Below the solidus, all the fields would have to be shown as containing  $\text{CuAl}_2$ , and for the higher iron contents, the presence of residual  $\text{FeAl}_3$  would also have to be indicated.

#### REFERENCES

1. A. G. C. Gwyer, H. W. L. Phillips, and L. Mann, *J. Inst. Metals*, 1928, **40**, 318.
2. R. S. Archer and W. L. Fink, *ibid.*, 350 (discussion).
3. V. Fuss, Dissertation, Berlin: 1922.
4. K. Yamaguchi and I. Nakamura, *Rikwagaku Kenkyu-jo Iho* (Bull. Inst. Phys. Chem. Research, Tokyo), 1932, **11**, 815.
5. A. J. Bradley and H. J. Goldschmidt, *J. Inst. Metals*, 1939, **65**, 403.
6. G. V. Raynor and P. C. L. Pfeil, *ibid.*, 1947, **73**, 397.
7. H. Wiehr, *Aluminium-Archiv*, 1940, (31).
8. R. H. Brown, W. L. Fink, and M. S. Hunter, *Trans. Amer. Inst. Min. Met. Eng.*, 1941, **143**, 115.
9. H. Hanemann and A. Schrader, "Ternäre Legierungen des Aluminiums" (Atlas Metallographicus, Band 3, Teil 2). 1952: Düsseldorf (Verlag Stahleisen).
10. F. Keller and G. W. Wilcox, *Metal Progress*, 1933, **23**, (2), 44; (4), 45; (5), 38.
11. L. Mondolfo, "Metallography of Aluminium Alloys". 1943: New York (John Wiley and Sons, Inc.).
12. G. Phragmén, *J. Inst. Metals*, 1950, **77**, 489.
13. W. Hofmann, *Aluminium*, 1938, **20**, 865.
14. G. V. Raynor, *J. Inst. Metals*, 1944, **70**, 531.
15. L. Pauling, *Phys. Rev.*, 1938, [ii], **54**, 899.
16. C. S. Smith, *Trans. Amer. Inst. Min. Met. Eng.*, 1940, **137**, 236.
17. J. L. Haughton, *J. Inst. Metals*, 1939, **65**, 447.
18. British Aluminium Co., Ltd., Publication No. 405 (1949).
19. A. D. I. Nicol, *Acta Cryst.*, 1953, **6**, (3), 285.
20. J. K. Edgar, *Trans. Amer. Inst. Min. Met. Eng.*, 1949, **180**, 225.
21. H. W. L. Phillips, *J. Inst. Metals*, 1953, **82**, (1), 9.



# THE OXIDATION OF TITANIUM AT HIGH TEMPERATURES IN AN ATMOSPHERE OF PURE OXYGEN\*

1514

By A. E. JENKINS,† M.Eng.Sc., MEMBER

## SYNOPSIS

The oxidation of titanium has been investigated in the temperature range 600°–925° C., at an oxygen pressure of 700 mm. of mercury. The process of oxidation was followed by determining the gain in weight of separate specimens after various periods. The distribution of oxygen between the scale and remaining metal core was determined in the temperature range in which physical stripping of the scale was possible, and in such instances an examination of the oxidation products was undertaken.

The scales were found to be porous to oxygen and the oxidation process has been shown to occur at the metal-oxide/metal interface. A glancing-angle X-ray-diffraction technique was used to establish the nature of the scales and surface layers on the metal cores; the rutile modification of  $\text{TiO}_2$  was the only oxide observed in the scales. The surface layers of the metal cores were found to be composed of titanium–oxygen solid solutions, the surface concentrations and internal oxygen gradients of which were dependent on the oxidation temperature.

A mechanism has been suggested for the oxidation of titanium at high temperatures, which involves the diffusion of oxygen within the metal core as an accelerating factor.

## I.—INTRODUCTION

In recent years a number of papers<sup>1-6</sup> dealing with the oxidation of titanium have been published, but the main emphasis of the work described in them has been directed towards establishing the kinetics of the process under conditions of varying temperature and pressure. In a recent paper dealing with the scaling of titanium in air, Morton and Baldwin<sup>6</sup> have presented a very useful summary of previous investigations. Davies and Birchenall,<sup>5</sup> studying the oxidation of titanium between 650° and 950° C. for a maximum period of 24 hr. in an atmosphere of pure oxygen, found the behaviour to be less complex. By neglecting a short initial period, they were able to express their oxidation results in the form of a linear law.

The present paper is concerned with the oxidation of both commercial and refined titanium in the temperature range 600°–925° C., in an atmosphere of pure oxygen. Some oxidation-rate results have been obtained, which agree quite well with those of Davies and Birchenall; however, the investigation has been concerned mainly with a study of the reaction product formed as a result of oxidation.

## II.—EXPERIMENTAL PROCEDURE

### 1. MATERIALS

Titanium refined by the iodide process in the Philips Laboratories, Eindhoven, and commercial titanium produced by the Kroll process at the Boulder City

plant of the United States Bureau of Mines have been used throughout this investigation. Impurities present in the two grades of metal have been reported recently by Corbett<sup>7</sup> and by Worner.<sup>8</sup>

### 2. PREPARATION OF SPECIMENS

Sheet specimens were cut transversely from cleaned rolled strip. The strip was produced from arc-melted titanium ingots by a sequence of hot-swaging and rolling operations performed in air at 600° C. Scale was removed first by abrading the surface with a wire brush and then by immersing the whole sheet for a suitable period in a 10%  $\text{HF-HNO}_3$  solution. The commercial titanium specimens measured approximately  $1.75 \times 1.5 \times 0.2$  cm., and those made from the refined metal about  $1.0 \times 0.5 \times 0.1$  cm.

The specimens were placed in a titanium boat and annealed at 700° C. for 4 hr. in a continuously evacuated system maintained at a pressure of  $<10^{-5}$  mm. of mercury. They were then given a final surface treatment to remove any superficial contamination produced in the anneal. The treatment consisted of immersion for 15 sec. in a warmed 10%  $\text{HF-HNO}_3$  solution, followed by an immediate cleansing in a fast stream of water. An excellent polish, free of pitting, resulted from this treatment, and a slight etching of the surface, visible under the microscope, permitted a check to be kept on the grain-size of the specimens.

As a result of this polishing treatment, it is believed that the ratio of real to apparent surface area of the specimens was kept close to unity and, more important still, held fairly uniform from specimen to specimen.

\* Manuscript received 16 June 1953.

† Research Officer, Physical Metallurgy Section, Common-

wealth Scientific and Industrial Research Organization, Baillieu Laboratory, University of Melbourne, Australia.

The average grain-sizes of the commercial and refined titanium specimens were  $2 \times 10^3$  grains/mm.<sup>2</sup> and  $10^3$  grains/mm.<sup>2</sup>, respectively. Specimens examined by means of the back-reflection X-ray-diffraction technique showed no evidence of preferred orientation.

### 3. OXIDATION PROCEDURE

The oxidation apparatus was of simple design, consisting of a fused silica combustion tube, which could be evacuated to a pressure of  $10^{-2}$  mm. of mercury, flushed with pure oxygen, and then refilled to the required 700 mm. pressure. A two-litre oxygen reservoir attached to the combustion tube ensured that the oxidation runs were carried out under essentially constant-pressure conditions. The oxygen was produced by heating potassium permanganate in a vessel which had been evacuated and flushed with pure oxygen. The fine powder produced in the process was effectively removed by passing the gas through a series of glass-wool and sulphuric-acid filters.

The titanium specimens rested horizontally on four points in a platinum-lined glazed porcelain boat. The furnace was controlled by a Cambridge regulator utilizing a thermocouple placed between the combustion tube and the furnace walls.

### 4. X-RAY-DIFFRACTION TECHNIQUE

Extensive use of a glancing-angle X-ray-diffraction technique was made in determining the structure of the oxidation products. Filtered cobalt  $K_\alpha$  radiation was used in conjunction with a circular 14.6-cm.-dia. camera. The specimens were inclined at  $125^\circ$  to the incident beam and oscillated  $\pm 10^\circ$  about this mean position.

## III.—EXPERIMENTAL RESULTS

### 1. OXYGEN WEIGHT-GAIN MEASUREMENTS

The total oxygen gain/unit area of original metal surface was determined for a series of commercial

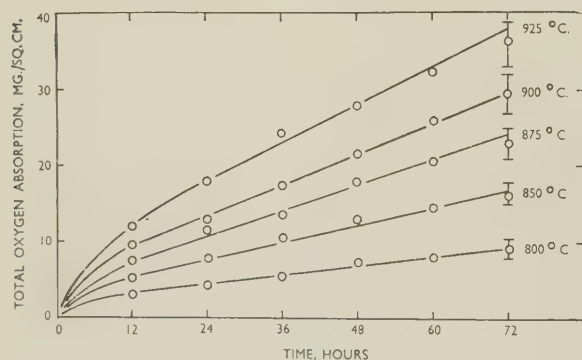


Fig. 1.—Total Oxygen Absorbed by Commercial Titanium During Oxidation at 800°–925° C. The points represent average values. The range of observations is indicated for 72 hr.

titanium specimens (Figs. 1 and 2). The points on these curves represent a simple arithmetic mean of at least four observations, the scatter of which could

be quite large, as is indicated in Fig. 1 for the results of oxidation for 72 hr. A separate investigation still in progress, which involves the continuous recording of oxygen absorption of single specimens over a

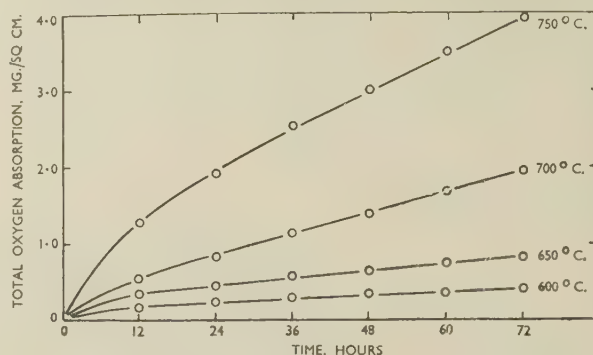


Fig. 2.—Total Oxygen Absorbed by Commercial Titanium During Oxidation at 600°–750° C.

period of 72 hr., shows that deviations from the linear oxidation rate can occur at irregular intervals (Fig. 3). At this stage, therefore, any further mathematical analysis of the oxidation results for titanium as expressed in Figs. 1 and 2 must be considered premature; it is necessary to obtain further information on the events occurring during the actual formation of the scales.

It has been found that during the oxidation of titanium, as distinct from most other metals, oxygen taken up by the specimen is distributed between a scale and the metal core. It was possible to remove the scales from the underlying cores in most instances where oxidation was carried out above 750° C. Oxygen absorbed in the cores was confined to the outer layers, penetrating to a depth which depended on the oxidation temperature. Table I presents the

TABLE I.—Calculated Oxygen Distribution for Titanium Oxidized 36 Hr. at 800° C.

	Total Oxygen Gain, mg./cm. <sup>2</sup>	Scale Formed, mg./cm. <sup>2</sup>	Assuming TiO <sub>2</sub> Scale		Oxygen Distribution		Percentage Distribution of Oxygen	
			Oxygen, mg.	Titanium, mg.	To Scale, mg.	To Metal Core, mg.	To Scale	To Metal Core
Commercial Titanium	5.83 5.91	11.3 11.6	4.5 4.6	6.8 7.0	4.5 4.6	1.3 1.3	77 78	23 22
Refined Titanium	7.63	16.2	6.5	9.7	6.5	1.1	85	15

method of calculating the oxygen distribution. In Fig. 4, the calculated oxygen absorption by the cores has been plotted for different temperatures as a function of the time of oxidation. In Fig. 5, similar results after oxidation at 900° C. have been expressed as a percentage of the total amount of oxygen absorbed in each case.

Specimens of refined titanium were included in all oxidation runs and, compared with commercial



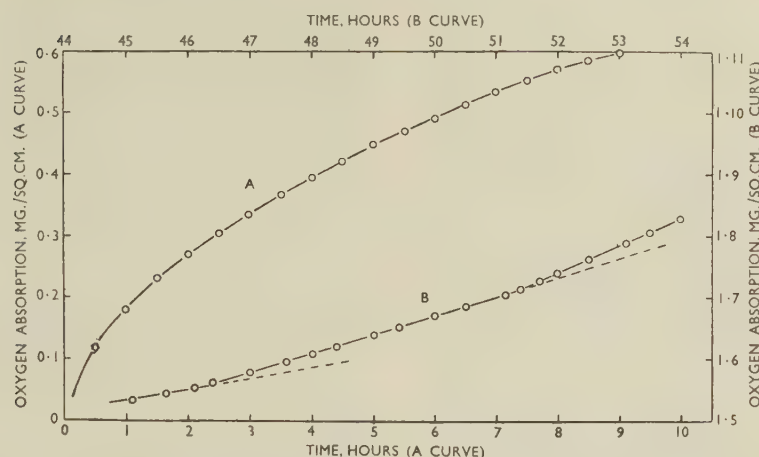


Fig. 3.—Oxygen Absorption During Oxidation of a Specimen of Refined Titanium at 700° C.

A Oxidation period 0–9 hr.

B Oxidation period 45–54 hr.

titanium, showed a greater total oxygen absorption. The scales formed were thicker, leaving less oxygen to enter the cores (see Table I). The difference in total

Scales formed on titanium specimens oxidized in region A, Fig. 6, could be completely removed from the underlying cores, for the scale and core separated on cooling. By fracturing the scale along the sides it could be removed in complete sheets from the main faces and the sides of the specimen (Fig. 13, Plate XXXI). The outer surfaces of the scales were a pale yellow-brown and, in the case of refined titanium, were noticeably darker in some areas than in others. The

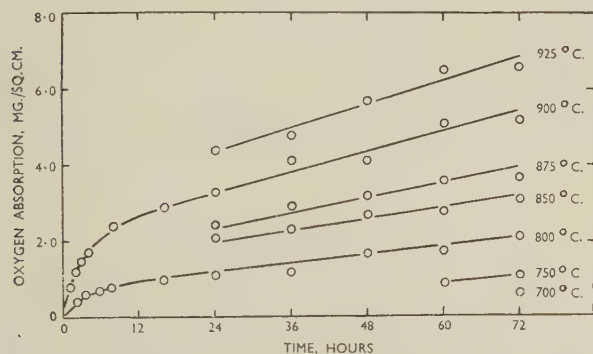


Fig. 4.—Calculated Oxygen Absorption by Metal Cores During Oxidation of Commercial Titanium Between 700° and 925° C.

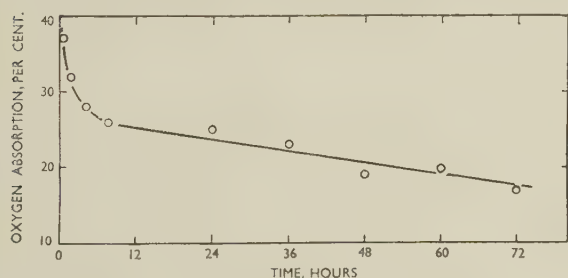


Fig. 5.—Oxygen Absorption by Metal Core at 900° C. Expressed as a Percentage of Total Oxygen Absorption.

oxygen absorption was never greater than 30%, and appeared to be negligible for oxidation in the vicinity of 850° C.

## 2. EXAMINATION OF OXIDATION PRODUCTS

The appearance of the scales and underlying cores varied according to the oxidation conditions, but in general a simple division could be drawn along the lines presented in Fig. 6.

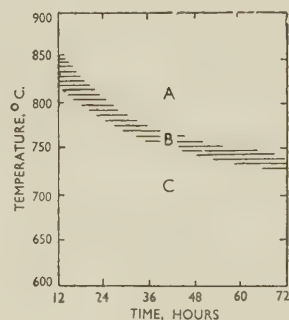


Fig. 6.—Division of the Oxidation of Commercial Titanium into Regions Illustrating Certain Properties of the Oxidation Products at Room Temperature.

- A Oxide scales porous to oxygen, light yellow-brown. Scales strip easily, exposing black metal-core surface.
- B Oxide scales thin and grey. Tendency to flake off core on cooling. Core surface shows beginnings of thin black layer.
- C Oxide scales dark slate-grey. Extremely adherent to metal.

white under-surfaces which had been in intimate contact with the cores during oxidation were flecked with a fine black scale, the distribution density of which remained fairly constant on all specimens. The cores after stripping appeared to be thinly covered with the same black scale, which adhered tenaciously to the metal beneath. This black scale could be rapidly dissolved in dilute sulphuric acid, giving a bright metallic appearance to the core and a white under-surface to the stripped scale.

By means of a diamond polishing technique, specimens of scale were examined both in plane and in

cross-section. The scales were essentially chalk-like in structure and were extremely porous. There were large fissures within the scales lying parallel to the metal surface, as shown by Fig. 14 (Plate XXXI); these were apparently caused by growth stresses arising from a decrease in density as the metal oxidized. The densities of typical scales are given in Table II. It will be noticed that these are consistently

TABLE II.—*Densities of Oxide Scales Formed on Commercial and Refined Titanium.*

Oxidation Conditions		Density, g./c.c.	
Temp., °C.	Time, hr.	Scales Formed on Commercial Titanium	Scales Formed on Refined Titanium
925	72	* † 3.44-3.90	* † 3.81-4.02
	48	3.51-3.80	3.80-3.98
	24	3.68-3.84	4.00-4.15
900	72	3.50-3.78	3.82-3.92
875	72	3.63-3.97	3.74-3.94
850	72	3.82-4.03	3.96-4.05

\* Density after 2 min. immersion.

† Density after 30 min. immersion.

lower than the value (4.2 g./c.c.) for the compact oxide; this is further evidence of scale porosity. Fig. 14 also shows that the scale is thinner at the edges. For this reason, measurements of scale thickness were in all cases taken across the centre of the main faces of the scales. The thickness was found to increase linearly with time of oxidation, as shown in Table III.

TABLE III.—*Average Thickness of Oxide Scales Formed on Commercial Titanium.*

Oxidation Conditions		Scale Thickness, mm.
Temp., °C.	Time, hr.	
925	72	0.36
	24	0.13
900	72	0.25
	24	0.10
875	72	0.18
	24	0.08
850	72	0.11
	24	0.05
800	72	0.08
	24	0.03

During the oxidation of specimens within region *A* of Fig. 6, a number of observations were made which suggested an oxidation mechanism involving the inward growth of oxide scale. In numerous instances scratches and other surface markings placed upon

metal specimens were observed on the outer surfaces of thick scales after oxidation. Similarly, fine platinum wire looped tightly around the original metal specimen was not buried in the growing oxide scale. The wire extended slightly and remained on the outer surface of the oxide layer. Again, when a thin specimen was allowed to oxidize almost to completion (Fig. 15, Plate XXXI) a complete oxide-to-metal contact was maintained from the initial to the final stage of oxidation.

The scales formed under conditions represented by region *C* of Fig. 6 were extremely thin and adherent. They appeared slate-grey whilst in contact with the core, although, once removed, small pieces appeared light grey in colour. These scales could be scraped from the specimen surface, exposing a metallic core apparently unchanged by the oxidation treatment. A feature of all scales formed in this region was the existence of ridges of white oxide along specimen edges and surface scratches. With scales formed on refined titanium a peculiar white mosaic ridge pattern was often observed (Fig. 16, Plate XXXI). This pattern was not related to any surface feature visible on the original metal specimen.

Within the transition region *B* of Fig. 6, scales were light grey in colour and were easily removed from the major portion of the specimen surface. The surfaces of the underlying cores became progressively darker as the amount of thin black scale mentioned previously increased.

### 3. X-RAY-DIFFRACTION EXAMINATION OF OXIDATION PRODUCTS

The majority of specimens examined by this method were in sheet form, and this required the use of a glancing-angle X-ray-diffraction technique. For purposes of comparison, X-ray-diffraction patterns were also obtained from a series of synthetic titanium-oxygen compositions produced by melting together the required amounts of titanium and rutile in an argon-arc furnace. In agreement with the results obtained by Ehrlich,<sup>9</sup> oxygen was found to expand the hexagonal titanium lattice, the extension being greatest along the *c* axis. Diffraction patterns were also obtained for the oxides TiO, Ti<sub>2</sub>O<sub>3</sub>, Ti<sub>3</sub>O<sub>5</sub>, and TiO<sub>2</sub>.

The lattice expansion produced by oxygen solution in the surface layers of the core could be followed by observing the shift in the reflection 11.4 to lower Bragg angles; the results are summarized in Table IV. This high-angle reflection was chosen to reveal the extent of oxygen solution because of its high intensity and its sensitivity to changes in dimension parallel to the *c* axis. The broadening of the reflection 11.4 decreased considerably with increase in oxidation time. Scales from specimens oxidized at 650° C. could not be stripped very easily; however, satisfactory X-ray-diffraction patterns were taken through the thin oxide layer. During the early stages of oxidation at 650° C., the width and position of the



reflection 11·4 indicated that the X-ray beam was actually penetrating to pure metal through an oxygen-affected surface layer. Sharply defined high- and low-angle extremities to the reflection 11·4 corresponded, respectively, to pure metal and a metal-oxygen solid solution. In all cases, a high value for the solution of oxygen at the surface was attained during the earliest stages of oxidation, and this increased very slowly throughout the remainder of the oxidation period.

X-ray-diffraction examination of stripped scales showed that these layers possessed a rutile structure. No structural or orientation differences could be detected between the outer and inner surfaces of such

affected surface zone. This is deduced from the continued existence of the high-angle portion of the reflection 11·4 after long periods of oxidation.

#### 4. REHEATING OF OXIDATION PRODUCTS

A number of commercial titanium specimens oxidized at 650°, 800°, and 900° C. for 72 hr. were reheated in vacuum without stripping the scale, in order to investigate the possibility of transport of material other than oxygen across the scale/core interface. Experimental results obtained from these reheating runs are given in Table V.

These X-ray-diffraction results, when compared with

TABLE IV.—X-Ray Results for the Surfaces of Metal Cores Remaining After the Oxidation of Commercial and Refined Titanium at 650°, 800°, and 900° C.

Photographed with Co K $\alpha$  radiation. All results for the reflection 11·4.

Oxidation Time, hr.	Oxidation of Commercial Titanium						Oxidation of Refined Titanium					
	650° C.		800° C.		900° C.		650° C.		800° C.		900° C.	
	$\theta^\circ$	d, Å.	$\theta^\circ$	d, Å.	$\theta^\circ$	d, Å.	$\theta^\circ$	d, Å.	$\theta^\circ$	d, Å.	$\theta^\circ$	d, Å.
0 *	77·1	0·918	77·1	0·918	77·1	0·918	77·2	0·917	77·2	0·917	77·2	0·917
1	77·1– 74·6	0·918– 0·928	74·5	0·928	74·1	0·930	77·3– 74·7	0·917– 0·927	74·5	0·928	73·9	0·930
2	77·1– 74·5	0·918– 0·928	74·4	0·929	74·0	0·930	77·2– 74·5	0·917– 0·928	74·4	0·929	73·8	0·931
4	77·1– 74·4	0·918– 0·929	74·4	0·929	73·9	0·931	77·2– 74·5	0·917– 0·928	74·3	0·929	73·8	0·931
8	74·6	0·928	74·2	0·930	73·8	0·931	77·2– 74·5	0·917– 0·928	74·1	0·930	73·8	0·931
24	75·0	0·926	74·1	0·930	73·7	0·932	76·8– 74·5	0·919– 0·928	73·9	0·931	73·6	0·932
72	74·9	0·926	74·0	0·930	73·5	0·933	75·3– 74·5	0·925– 0·928	73·9– 72·8	0·931– 0·936	73·6– 72·8	0·932– 0·936

\* Pure Metal.

scales. The average grain diameter determined by X-ray back-reflection methods proved to be less than  $10^{-4}$  cm. Although diffraction patterns of the thin adherent scales formed at low temperatures of oxidation showed them to be rutile, the patterns were weak and incomplete, with many of the high-angle reflections absent.

Although a large number of titanium specimens oxidized for various times in the range 600°–950° C. were examined, rutile was the only oxide observed. Apparently the lower oxides of titanium are either unstable under these oxidation conditions or they are formed in exceedingly small quantities.

Oxidation of the refined titanium gave results similar to those obtained for the commercial metal. Comparison of the two sets of results in Table IV shows a slightly higher oxygen concentration in the surface layers of the purer-metal cores. Oxidation of the pure metal at 650° C. produces a thinner oxygen-

the values for the oxidized specimens given in Table IV, show that the oxygen concentration at the surface of the cores changed considerably after vacuum heating.

At 1000° C. the scales were reabsorbed by the cores, in each case to an extent depending on the original scale thickness. The specimens originally oxidized at 650° and 800° C. completely absorbed their scales, and further diffusion of oxygen into the cores lowered the original surface oxygen concentration. The thicker scale, originally formed at 900° C., however, was not completely reabsorbed, and illustrates what may be termed a transition stage in reabsorption. The oxygen concentration at the surface was slightly higher in this case, and the X-ray pattern of the scale remaining showed that it possessed a complex distorted rutile structure. An approximate composition TiO<sub>1.9</sub> could be attributed to this scale by comparison with the series of synthetic alloys mentioned previously.

During these reheating experiments, oxygen was absorbed by the core from the scale, presumably across an interface at which oxide-to-core contact existed throughout, for, if this were not the case, the outer scale layers would undoubtedly have fallen away from the specimen. The appearance, on the outer surface of scales, of markings that were originally on the unoxidized metal specimens has been mentioned above. These markings remained on the metal surface when the scales had been reabsorbed into the

TABLE V.—Results of Reheating Oxidized Commercial Titanium Specimens in Vacuum.

All X-ray results from reflection 11·4.  
Co  $K\alpha$  radiation.

Reheating Conditions	Previous Oxidation	After Heating in Vacuum		
		Metal Core		Comments
		$\theta^\circ$	d., Å.	
1000° C., 18 hr., 10 <sup>-3</sup> mm. Hg oxygen	900° C., 72 hr., 700 mm. Hg oxygen	73·0	0·935	Scale quite black on outer and inner surfaces. Decreased approx. 50% in thickness. Complex X-ray-diffraction pattern. Metallic appearance of surface of metal core.
	800° C., 72 hr., 700 mm. Hg oxygen	74·7	0·927	No trace of original oxide scale. Metallic surface appearance. Final specimen dimensions intermediate between un-oxidized and oxidized states.
	650° C., 72 hr., 700 mm. Hg oxygen	77·1– 76·7	0·918– 0·919	No trace of original oxide scale. Similar to previous specimen. Grain growth at surface of specimen revealed by vacuum etching.

core, thus excluding the possibility of an absorption process that involved the movement of metal ions outwards through the scale.

To determine the extent to which the cores were affecting changes in the scales, the behaviour of single specimens of stripped scale when heated in vacuum and in oxygen was briefly investigated. Oxidation in an atmosphere of pure oxygen at 700 mm. mercury pressure and at a maximum temperature of 1000° C. produced no detectable increase in weight. The yellow-brown appearance of the outer layers of the scale remained unchanged, while the slight flecking of dark scale on the under-surfaces turned white and could no longer be distinguished from the main body of scale. Heating under similar temperature conditions but in vacuum produced scales which were dark slate-grey in colour; again no significant weight change was recorded. It was apparent that these vacuum-heated scales were slightly deficient in oxygen, because their original white appearance could be restored by reheating in oxygen. The structure of the scales, as determined by standard X-ray-diffraction analysis, proved to be rutile in all cases.

##### 5. OXYGEN PENETRATION INTO METAL CORES

The presence of oxygen in the titanium lattice could be detected by an increase in hardness. Measurements were made on a specimen cross-section, utilizing

a Leitz microhardness instrument with a standard 124° diamond indenter. The hardness curves given in Figs. 7–9 reveal the increased depth of penetration

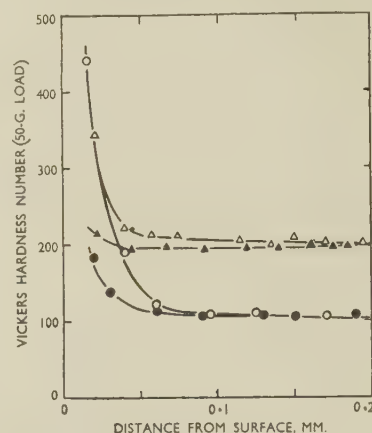


Fig. 7.—Oxygen Penetration into Metal Cores During Oxidation of Commercial and Refined Titanium at 700° C. for 24 and 72 hr.

KEY.  
 $\Delta$  Commercial Titanium 72 hr.     $\circ$  Refined Titanium 72 hr.  
 $\blacktriangle$  " " 24 hr.     $\bullet$  " " 24 hr.

associated with higher oxidation temperatures and also indicate a change in oxygen distribution in the cores with increase in the oxidation time. These hardness curves necessarily begin at a small distance below the core surfaces because the oxygen-rich

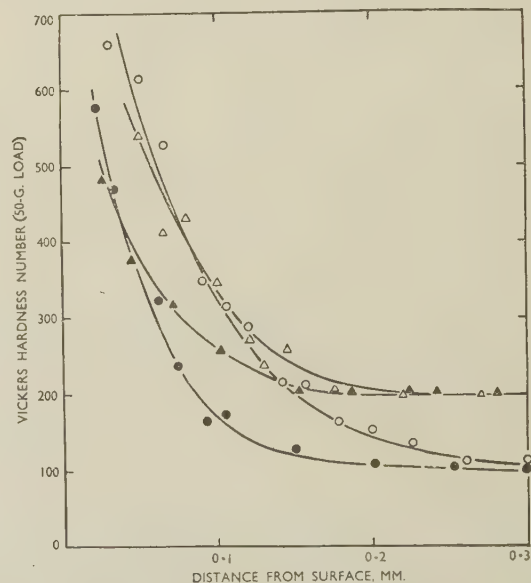


Fig. 8.—Oxygen Penetration into Metal Cores During Oxidation of Commercial and Refined Titanium at 800° C. for 24 and 72 hr. Key as for Fig. 7.

surface layers, owing to their extreme brittleness, were removed during the preparation of the specimens for examination.

A series of cores were examined for oxygen penetration by X-ray-diffraction analysis at successive



distances from the surface. Thin layers were removed from the specimen with fine metallographic polishing papers. Because of the extreme hardness of the oxygen solid solutions involved, X-ray-diffraction patterns

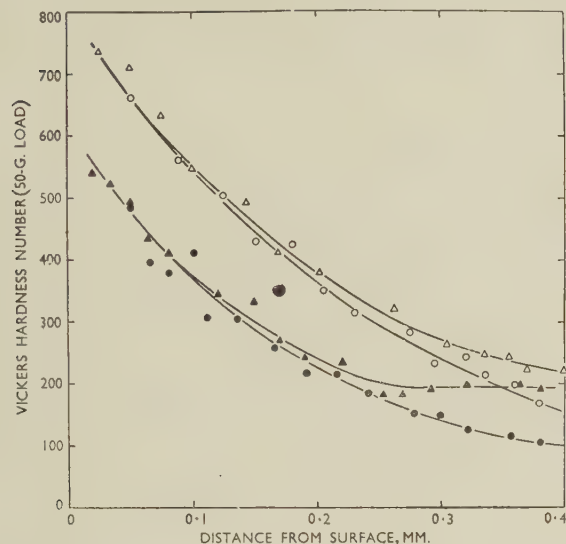


Fig. 9.—Oxygen Penetration into Metal Cores During Oxidation of Commercial and Refined Titanium at 900° C. for 24 and 72 hr. Key as for Fig. 7.

suitable for the determination of the position of the reflection 11·4 could be obtained at each stage during the polishing of the specimens. The oxygen concentration values given in Fig. 10 were derived by com-

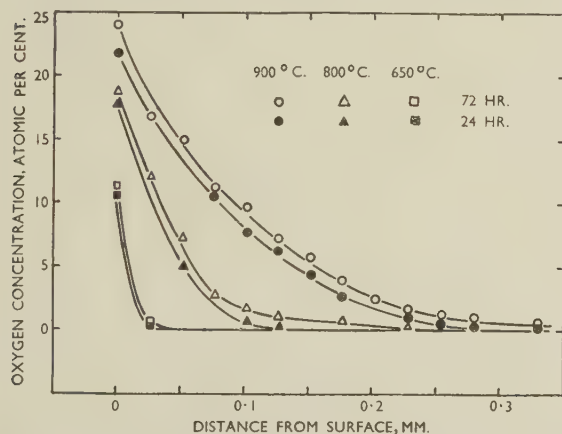


Fig. 10.—The Penetration of Oxygen in Oxidized Titanium Cores. Determined by X-ray-diffraction analysis on layers at varying depths from surface.

paring the X-ray-diffraction results for this series of experiments with those obtained from the synthetically produced titanium-oxygen alloy series.

#### IV.—DISCUSSION

In agreement with the results of previous investigations,<sup>3,5</sup> it has been shown that the oxidation rate of titanium below about 650° C. continually decreases

during the progress of oxidation, whereas in the range 650°–925° C. it becomes constant after a short initial period.

Observations on the structure of scales formed on titanium indicate that the thin, dense, slate-grey scale formed at low temperatures is replaced at high temperatures by a thick, porous, yellow-brown scale. This scale is largely composed of layers of oxide which have been twisted and shattered like natural rock strata (Fig. 14, Plate XXXI). The transformation in scaling behaviour is believed to occur when the thin, dense scale grows beyond a certain maximum thickness; when this has been attained, growth stresses established within the scale could partially shatter the outer layers. These stresses result from the growth of fresh oxide at the interface between scale and core.

Assuming that the inward passage of oxygen through the dense portion of the scale occurs by a process of anion-vacancy diffusion through the oxide lattice,<sup>10,11</sup> the formation of an outer, porous scale layer would produce a change in the oxidation rate. Fig. 11 shows a diagrammatic representation of the oxidation behaviour of titanium. A third division—region A—has been added to this figure on the assumption that at very high oxidation temperatures a complete sintering of the scale will occur which will prevent the establishment of a porous scale layer. The oxidation rate under these conditions will return to the parabolic form, since diffusion of either oxygen or titanium through the *complete* scale layer will be necessary in order to maintain an oxidation reaction. In this connection, it is interesting to note that an empirical law due to Tamman<sup>12</sup> gives the lowest temperature for complete sintering of the oxide as approximately 0·6  $T_M$ ,  $T_M$  being the melting point of the oxide. In the case of rutile, this temperature would be about 1000° C. Moreover, at these temperatures the growth stresses would be more easily relieved by plastic deformation of the scale, and this would prevent the formation of cracks in the outer layers.

The investigations into the structure of the titanium core after oxidation have shown that oxygen enters the surface layers of the core during the reaction. Moreover, when the supply of gaseous oxygen has been withdrawn, the metal redissolves the oxide scale. Since oxygen must diffuse through a dense scale layer for reaction at the interface between scale and core, it is concluded that the scale thickness at any instant during oxidation must be related in some way to the oxygen concentration-gradient existing in the core. Ehrlich<sup>13</sup> has shown that when oxygen dissolves in the hexagonal titanium lattice it enters the octahedral interstices, and hence it is accepted that oxygen diffuses interstitially through the metal lattice. It is reasonable to assume that oxygen diffuses through rutile according to a vacancy mechanism.

Thus, if the reactions at the metal oxide/metal interface could be considered to have established a state of quasi-equilibrium during the course of oxidation, the ratio of scale thickness to depth of pene-

tration of oxygen in the core may well prove to be constant, depending on the ratio of the respective oxygen diffusivities in rutile and titanium and on the oxygen concentration gradient in the core. From theoretical considerations it would seem that the

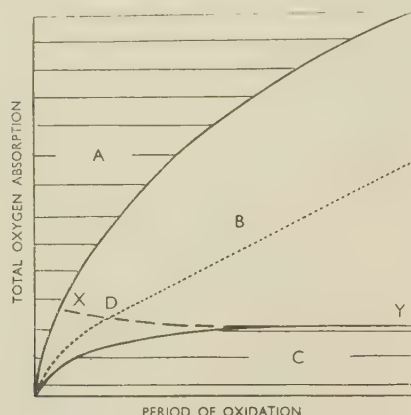


Fig. 11.—An Empirical Division of the Oxidation Behaviour of Titanium.

Region A.—High-temperature oxidation according to a parabolic law. Diffusion through a compact scale which has grown beyond a critical thickness is necessary because of the complete sintering of the scale at high temperatures.

Region B.—Oxidation at intermediate temperatures. Change from a parabolic to a linear relationship at D, when the compact scale reaches a critical thickness. The scale produced by further growth is porous.

Region C.—Low-temperature oxidation according to a parabolic law, caused by the diffusion of oxygen through a compact, growing oxide scale.

The oxygen required in the formation of the compact scale is represented by the curve XY.

interstitial diffusivity is the greater of the two; this would offer an explanation for the observed early establishment of an oxygen solution in the metal phase during the oxidation reaction.

These considerations suggest that, in the early stages, the scaling of titanium is controlled by the diffusion of oxygen within the core, this control ceasing only when a critical scale thickness has been reached. The role of the diffusion of oxygen in the metal core during oxidation can best be illustrated by examining the oxidation of a titanium specimen under conditions expressed by region B of Fig. 11.

Immediately after the first contact between pure oxygen and the surface of a titanium specimen at high temperature, oxygen must pass through a thin oxide barrier in order to produce fresh oxide or to be dissolved interstitially in the core. Because of the relative diffusivities of oxygen in the scale and metal, the early stages of oxidation are characterized by the establishment of an oxygen concentration gradient in the core. This initial stage is followed by a joint process of scale growth and oxygen solution in the core. The scale growth is controlled by the oxygen concentration gradient in the core; scale will be absorbed or reformed if its thickness becomes too large or too small for the existing gradient. With the

growth of the dense scale to a critical thickness, the oxidation rate becomes linear. The rate constant derived from this portion of the oxidation curve depends on the diffusion of oxygen through a rutile scale, under the influence of an approximately constant concentration gradient. From the temperature coefficient of the reaction rate an activation energy of 30.5 kg.cal./g. mole may be derived for the process (Fig. 12).

After the establishment of a critical dense scale thickness, the amount of oxygen available for reaction at the interface between scale and core remains constant. It should be possible to reach a final stage where a static oxygen gradient exists within the core, if a balance is established between the rate of advancement of the interface and the rate of diffusion of oxygen away from the interface. The observed total oxygen absorption rate will then be equivalent to the actual scaling rate. Under all other conditions, the total oxygen absorption curve is the resultant of two separate curves, one for actual scaling and the other for solution in the metal.

A similar analysis could be made of the oxidation behaviour of titanium under the conditions represented by regions A and C of Fig. 11. These conditions are not suitable for the attainment of a linear oxidation rate. In region A it is possible that the oxidation mechanism may eventually involve the passage of metal ions outwards through the non-porous scale. This high-temperature oxidation change may be the

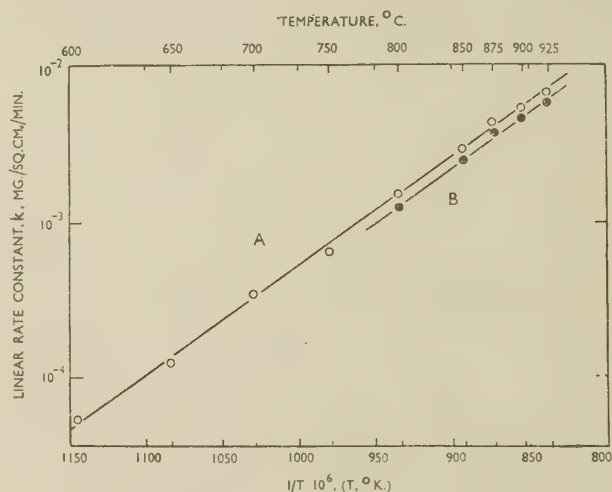


Fig. 12.—Variation of the Oxidation Linear Rate Constant with Temperature.  $E = 30.5$  kg.cal./g.mole.

A Total oxygen absorption.

B Oxygen absorption in actual scaling reactions.

$$\text{Equation for Curve A: } k = 2.5 \times 10^3 \cdot e^{-\frac{30,500}{RT}}$$

result of a change in the relative diffusivities of the anion and cation in the rutile scale.

The theory put forward in this discussion is partly based on the assumption that oxygen diffusion within the core is an accelerating factor in the oxidation of titanium. Presumably any process which will decrease



the diffusion rate of oxygen in the metal will decrease its oxidation rate, and this could be of some practical importance. Diffusion is a structure-sensitive process, and hence oxidation of titanium could well be affected by specimen properties such as grain-size, recrystallization, and the degree of texturing associated with previous cold working or annealing. The oxidation of ridges or of sharp corners on specimens would tend to be very rapid initially, but would slow down when an oxygen gradient was established in the metal. The elimination of physical porosity in the scales formed during oxidation in the intermediate temperature range would seem to be necessary in any attempt to decrease the oxidation rate of titanium. It is suggested that the sintering properties of deliberately contaminated rutile could be investigated with this object in view. On the other hand, the diffusivity of titanium ions outward through these scales may be increased by such treatment, and this could introduce complications into the oxidation action. Further experimental work along these lines is continuing, and there is some evidence that the diffusion of titanium

ions outwards through a compact scale occurs at temperatures above 1000° C. Under these conditions, the lower oxides of titanium are produced in the scale.

#### ACKNOWLEDGEMENTS

This investigation was conducted as part of the programme of the Physical Metallurgy Section, Commonwealth Scientific and Industrial Research Organization, Australia. This Section forms part of the Baillieu Laboratory, University of Melbourne.

The author gratefully acknowledges the experimental facilities made available by Professor J. Neill Greenwood, under whose general direction this work was performed. The very helpful assistance of Mr. J. A. Corbett, who performed the necessary analytical work, is much appreciated.

The spectrographic analysis was performed by the Defence Research Laboratories, Maribyrnong. The "commercial" titanium was donated by the U.S. Bureau of Mines.

#### REFERENCES

1. L. G. Carpenter and F. R. Reavell, *Metallurgia*, 1948, **39**, 63.
2. J. W. Hickman and E. A. Gulbransen, *Analyt. Chem.*, 1948, **20**, 158.
3. E. A. Gulbransen and K. F. Andrew, *Trans. Amer. Inst. Min. Met. Eng.*, 1949, **185**, 741.
4. D. J. McPherson and M. G. Fontana, *Trans. Amer. Soc. Metals*, 1951, **43**, 1098.
5. M. H. Davies and C. E. Birchenall, *Trans. Amer. Inst. Min. Met. Eng.*, 1951, **191**, 877.
6. P. H. Morton and W. M. Baldwin, *Trans. Amer. Soc. Metals*, 1952, **44**, 1004.
7. J. A. Corbett, *Analyst*, 1951, **76**, 652.
8. H. W. Worner, *J. Inst. Metals*, 1952-53, **81**, 521.
9. P. Ehrlich, *Z. Elektrochem.*, 1939, **45**, 362.
10. H. Pfeiffer and K. Hauffe, *Z. Metallkunde*, 1952, **43**, 364.
11. K. Hauffe, H. Grunewald, and R. Tränckler-Greese, *Z. Elektrochem.*, 1952, **56**, 937.
12. G. Tammann, *Z. anorg. Chem.*, 1926, **157**, 321.
13. P. Ehrlich, *Z. anorg. Chem.*, 1941, **247**, 53.

# 1515 THE STRUCTURE OF TITANIUM-SILVER ALLOYS IN THE RANGE 0-30 AT.-% SILVER \*

By H. W. WORNER,† M.Sc., MEMBER

## SYNOPSIS

Metallographic and X-ray-diffraction methods have been used to determine a partial phase diagram between 0 and 30 at.-% silver, in the temperature range 650°-1100° C. Addition of silver to titanium depresses the  $\alpha \rightleftharpoons \beta$  transformation; there is a eutectoid horizontal at 855° C., the reaction being:  $\beta$  (11.5 at.-% Ag)  $\rightleftharpoons$   $\alpha$  (7 at.-% Ag) +  $\gamma$  (28 at.-% Ag). The  $\beta$ -solid-solution field extends to 23 at.-% silver at 1100° C. Solutions of silver in  $\beta$ -titanium cannot be retained by quenching into water, as a rapid  $\beta \rightarrow \alpha$  change occurs. The solubility of silver in  $\alpha$ -titanium decreases from 7 at.-% at the eutectoid temperature to 6 at.-% at 700° C. The  $\gamma$  phase possesses an ordered structure based on the face-centred tetragonal lattice. The type of ordering appears to be similar to that shown by  $\text{Cu}_3\text{Au}$  ( $L1_2$ -type), but the degree of long-range order is low. Quenching from the  $\beta$ -solution field causes hardening of the alloys, the effect being of the order of 50-90 diamond pyramid hardness units for alloys in the range 6.5-22.3 at.-% silver.

## I.—INTRODUCTION

THE present investigation was undertaken in connection with a study of titanium alloy systems in which the alloying metals have atomic radii close to that of titanium. Previous work on the titanium-silver system had yielded some rather surprising results. Laves and Wallbaum<sup>1</sup> reported that there were no compounds in the system. Craighead, Simmons, and Eastwood<sup>2</sup> found that addition of about 1 at.-% silver to a commercial grade of titanium elevated the  $\beta/(\alpha + \beta)$  phase boundary but depressed the  $\alpha/(\alpha + \beta)$  boundary. Raub, Walter, and Engel<sup>3</sup> reported that silver would not dissolve titanium, even when the two metals were heated together at 1200° C. in an atmosphere of argon. After the work described below had been completed, Van Thyne *et al.*<sup>4</sup> reported a phase  $\text{TiAg}$ , possessing an ordered tetragonal structure of the  $L1_0$  type.

Some preliminary experiments demonstrated that titanium and silver could be readily alloyed with one another in the liquid state by arc-melting in an argon atmosphere. However, loss of silver by vaporization during melting was rapid. Hence it was difficult to make an alloy of any desired composition, and wastage of both titanium and silver was appreciable. In the interests of economy, most of the alloys were made with a commercial grade of titanium; refined titanium was used only to make a few alloys for critical experiments.

## II.—MATERIALS USED AND ALLOYS PREPARED

The commercial grade of titanium, produced by the Kroll process, was supplied by the United States

Bureau of Mines. The refined titanium was made by the iodide process in the Philips Laboratories, Holland. Impurities found in both grades of titanium have been reported in an earlier paper.<sup>5</sup> Silver of 99.98% purity was used in the preparation of all the alloys. The compositions of the alloys used are listed in Table I, all the values stated being analytical results.

TABLE I.—Alloys Used.

Made with Commercial Titanium		Made with Refined Titanium	
Silver, At.-%	Silver, Wt.-%	Silver, At.-%	Silver, Wt.-%
2.8	6.0	2.7	5.6
3.0	6.3	6.5	13.4
6.7	14.0	10.5	20.9
10.3	20.5	13.2	25.4
11.5	22.8		
16.2	30.3		
22.3	39.3		
24.4	42.0		
28.6	47.4		
30.1	49.1		

## III.—EXPERIMENTAL PROCEDURE

In general, the methods of melting, heat-treating, and examining the alloys by metallographic and X-ray-diffraction methods were the same as those described by the author in a paper on titanium-tin alloys.<sup>5</sup> To expedite mixing of the two metals during fusion in the argon-atmosphere arc-furnace, pieces of titanium sheet, 0.5 mm. thick, were used in preference to lumps. Segregation during freezing was kept to a minimum by restricting the "buttons" to 3-5 g. Rapid evaporation of silver during melting caused a fine "fog" of silver to form in the argon atmosphere, and

\* Manuscript received 12 June 1953.

† Physical Metallurgy Section, Commonwealth Scientific

and Industrial Research Organization, Baillieu Laboratory, University of Melbourne, Australia.



this made the quantitative estimation of freezing ranges by optical pyrometry practically impossible.

Alloys with silver contents up to 16.2 at.-% could be deformed very considerably at 700°-800° C. These alloys were hot worked before heat-treatment. The alloys with higher silver contents would withstand only a very small amount of plastic deformation at temperatures in the range 20°-800° C.

The duration of heating necessary to produce equilibrium in an alloy at any given temperature was ascertained by examining specimens heated for different periods at the temperature concerned. Results of such experiments are given in Table II.

TABLE II.—Duration of Heating Necessary To Produce Equilibrium Structures.

Temperature Range, °C.	Duration of Heating, hr.	
	Hot-Forged Alloys (2.7-16.2 at.-% Silver)	Brittle Alloys (22.3-30.1 at.-% Silver)
1000-1100	~1	~5
900-1000	1-3	10-20
800- 900	~ 5	30-50
650- 800	~10	~100

The data shown were based on two types of heat-treatment. In one type, the specimen was simply heated rapidly to the desired temperature and kept at this before quenching; in the other, the specimen was first heated for about 5 hr. at 1000°-1100° C., then cooled and maintained at the required temperature until it was quenched.

#### IV.—EXPERIMENTAL RESULTS

##### 1. AS-CAST ALLOYS

Addition of silver depressed the freezing point of titanium. However, for the reasons stated above, no quantitative measurements of freezing ranges were made.

Examination of as-cast specimens showed that alloys containing 2.7-16.2 at.-% silver crystallized entirely as columnar grains of  $\beta$ -titanium-silver solid solution which, on cooling, transformed to  $\alpha$  solution with the development of a fine, acicular microstructure. In alloys with 22.3-30.1 at.-% silver, small quantities of a phase other than  $\beta$  solid solution apparently formed in the final stage of solidification.

The acicular structure caused by the  $\beta \rightarrow \alpha$  transformation etched darker in the central zone of each columnar grain than it did in the vicinity of boundaries. This suggested that dendritic segregation occurred during freezing of the alloys. Non-uniformity of composition, due to segregation, in the brittle, high-silver alloys was probably the chief reason for the protracted approach to equilibrium which was noted during the heat-treatment of these alloys (cf. Table II).

##### 2. STRUCTURES OF HEAT-TREATED ALLOYS MADE WITH COMMERCIAL TITANIUM

The microstructures of alloys quenched into water from temperatures in the range 650°-1100° C. are represented graphically in Fig. 1, and phases identified

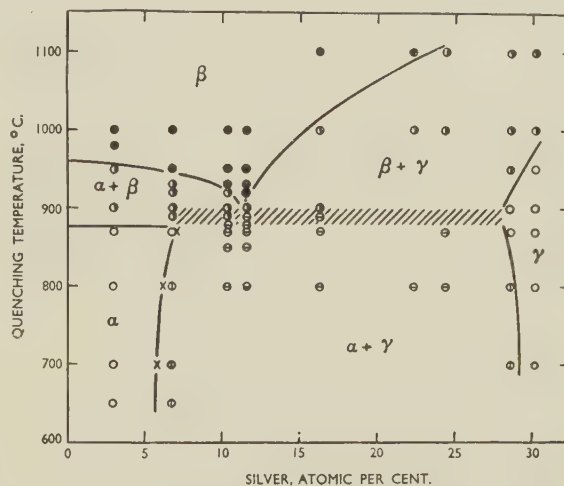


FIG. 1.—Results of Quenching Experiments on Alloys Made with Commercial Titanium.

##### KEY.

- Constituent with fine, acicular structure.
- Single-phase (bright-etching).
- ⊙ Mixture of bright-etching phase and constituent with fine, acicular structure.
- ⊖ Mixture of two bright-etching constituents.
- ⊖ Fine, lamellar mixture plus bright-etching constituent.
- x Derived from X-ray-diffraction results.

TABLE III.—X-Ray-Diffraction Results for Alloys Made With Commercial Titanium.

Silver Content, at.-%	Quenching Temp., °C.	Phases Identified by X-Ray-Diffraction
3.0	1000	Strained $\alpha^*$
	900	Strained $\alpha^*$
	870	$\alpha$
6.7	1000	Strained $\alpha^*$
	900	Strained $\alpha^*$
	870	$\alpha$
	800	$\alpha + \gamma$
10.3	700	$\alpha + \gamma$
	1000	Strained $\alpha^*$
	900	Strained $\alpha^*$
	870	$\alpha + \gamma$
11.5	800	$\alpha + \gamma$
	700	$\alpha + \gamma$
	1000	Strained $\alpha^*$
	900	$\gamma + \text{Strained } \alpha^*$
16.2	870	$\alpha + \gamma$
	1100	Strained $\alpha^*$
	900	$\gamma + \text{Strained } \alpha^*$
22.3	870	$\alpha + \gamma$
	1100	Strained $\alpha^*$
	1100	Strained $\alpha^*$
24.4	950	$\gamma + \text{Strained } \alpha^*$
	870	$\gamma$
	700	$\alpha + \gamma$
28.6	950	$\gamma$
	870	$\gamma$
	700	$\gamma$
30.1	950	$\gamma$
	870	$\gamma$
	700	$\gamma$

\* Strain in lattice evidenced by broad reflections, especially at high reflection angles.

by Debye-Scherrer X-ray-diffraction experiments on heat-treated alloys are given in Table III.

Solid solutions of silver in  $\beta$ -titanium could not be retained by quenching into water. X-ray-diffraction results showed that all quenched alloys which exhibited the fine, acicular structure—represented by solid circles in Fig. 1—possessed a strained, close-packed hexagonal crystal structure. Supersaturated solutions of silver in  $\alpha$ -titanium, formed by quenching alloys from the  $\beta$ -solution field, proved to be surprisingly stable. As far as could be judged from microstructures and X-ray-diffraction results, supersaturated  $\alpha$  solutions containing 10.3-16.2 at.-% silver remained unaltered when heated for 1 hr. at 700° C. A supersaturated  $\alpha$  solution containing 22.3 at.-% silver showed only slight evidence of decomposition after heating for 1 hr. at 500° C.

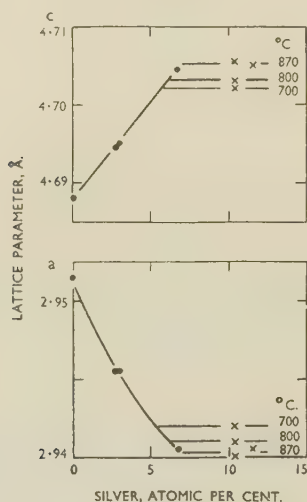
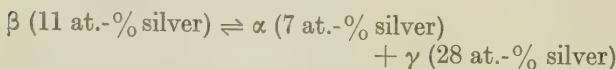


FIG. 2.—Lattice Parameters of  $\alpha$  Phase in Alloys Made with Commercial Titanium.

#### KEY

- Single-phase alloys water-quenched from 870° C.
- × Duplex alloys water-quenched from temperatures shown (°C.).

The eutectoid reaction, which occurs at 880°-900° C. can be represented by:



Eutectoid mixtures similar to that shown in Fig. 6 (Plate XXXII), but having a finer grain texture, were produced from supersaturated  $\alpha$  solutions containing 10.3 and 11.5 at.-% silver by reheating to a temperature just under the eutectoid region (cf. Figs. 6 and 7, Plate XXXII).

The lattice parameters of the  $\alpha$  phase in alloys containing 2.8-11.5 at.-% silver are shown in Fig. 2 as a function of silver concentration. Addition of silver increased the  $c$  parameter of  $\alpha$ -titanium, but decreased the  $a$  parameter. The  $c/a$  ratio for the  $\alpha$  solution saturated with silver at 870° C. was 1.60, as compared with 1.59 for the commercial titanium.

### 3. THE $\gamma$ PHASE

Debye-Scherrer X-ray-diffraction patterns for the 28.6 at.-% silver alloy quenched from 870° C., and the 30.1 at.-% silver alloy quenched from 950°, 870°, 700°, and 400° C. were all very similar. The diffraction data for the 28.6 at.-% silver alloy are listed in Table IV. All the reflections could be indexed on

TABLE IV.—X-Ray-Diffraction Results for  $\gamma$  Phase—28.6 at.-% Silver Alloy, Quenched from 870° C.

Cobalt  $K_{\alpha}$  radiation ( $\alpha_1$  for  $\theta > 65^\circ$ )

$hkl$	$\sin^2 \theta$		Relative Intensity	
	Observed	Calculated	Observed *	Calculated †
100	0.0459	0.0456	W	9
110	0.0917	0.0913	VW	4
101	0.0972	0.0969	W	7
111	0.1429	0.1426	VS	62
200	0.1831	0.1826	VS	21
002	0.2054	0.2051	S	9
201	0.2343	0.2339	VW (B)	2
220	0.3660	0.3652	S	6
202	0.3875	0.3877	S	10
310	0.4617	0.4565	VW (B)	0.7
003		0.4615		0.2
301		0.4621		0.7
103	0.5080	0.5071	VS	0.6
311		0.5078		16
113	0.5529	0.5528	S	7
222	0.5708	0.5703	S	7
400	0.7309	0.7304	M-S	4
410	0.7800	0.7760	VW (B)	0.6
401		0.7816		0.6
004	0.8211	0.8204	M (B)	2
330		0.8217		0.3
223		0.8267		0.6
411	0.8726	0.8273	S	1
303		0.8723		0.6
331		0.8729		10
114	0.9131	0.9117	S	0.8
420		0.9130		13
313	0.9176	0.9180	VS	26
402	0.9359	0.9355	VS	14

\* VS = very strong, S = strong, M = medium, W = weak, VW = very weak, (B) = broad.

$$\dagger \left( \frac{1 + \cos^2 2\theta}{\sin^2 \theta \cdot \cos \theta} \right) \cdot p \cdot |F|^2.$$

the basis of a tetragonal lattice with  $c/a = 0.945$  approximately. The calculated values of  $\sin^2 \theta$  in Table IV were derived from the expression:

$$\sin^2 \theta = 0.04565 (h^2 + k^2) + 0.05127 l^2$$

The lattice parameters calculated from the reflections 222, 400, 313, and 402 by Cohen's method of least squares were  $a = 4.187 \pm 0.004$  Å.,  $c = 3.950 \pm 0.004$  Å.,  $c/a = 0.943_5$ . Assuming 4 atoms/unit cell, the density calculated from the lattice parameters was 6.24 g./c.c.; the observed density was 6.30 g./c.c.

The results given in Table IV indicated that the  $\gamma$  phase possessed an ordered structure based on the face-centred tetragonal structure. The set of superlattice lines suggested ordering of the type shown by ordered  $\text{Cu}_3\text{Au}$  ( $L1_2$  type). Relative intensities calculated for the composition  $\text{Ti}_3\text{Ag}$  with perfect, long-range order (1 Ag in position 000, 3 Ti in  $\frac{1}{2}10$ ,  $\frac{1}{2}01$ ,  $0\frac{1}{2}1$ )



are given together with the observed intensities in Table IV. The calculated intensities were based on the term  $\left( \frac{1 + \cos^2 2\theta}{\sin^2 \theta \cdot \cos \theta} \right) \cdot p \cdot |F|^2$ .

Since the observed intensities were compared by visual inspection, it was not considered necessary to include the temperature and absorption factors in the calculations. The superlattice lines were all of very low intensity, and the few detected at reflection angles greater than  $20^\circ$  were broad. These observations indicated that there was a low degree of long-range order in the  $\gamma$  phase.

#### 4. ALLOYS MADE WITH REFINED TITANIUM

The microstructures of quenched alloys are represented graphically in Fig. 3, and the phases identified

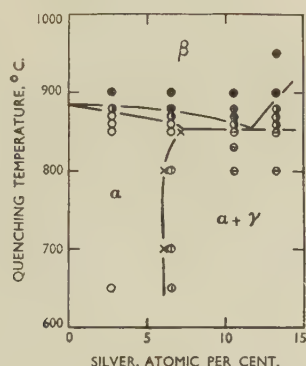


FIG. 3.—Results of Quenching Experiments on Alloys Made with Refined Titanium. Key as for Fig. 1.

by Debye-Scherrer X-ray-diffraction experiments are given in Table V. The lattice parameter/composition relationships for the  $\alpha$  solid solutions are shown in Fig. 4.

TABLE V.—X-Ray-Diffraction Results for Alloys Made With Refined Titanium.

Silver Content, at.-%	Quenching Temp., °C.	Phases Identified by X-Ray-Diffraction
2.7	900	Strained $\alpha^*$
	850	$\alpha$
	650	$\alpha$
	900	Strained $\alpha^*$
6.5	850	$\alpha$
	800	$\alpha + \gamma$
	900	Strained $\alpha^*$
	860	Strained $\alpha^*$
10.5	850	$\alpha + \gamma$
	800	$\alpha + \gamma$
	700	$\alpha + \gamma$
	900	Strained $\alpha^*$
13.2	860	$\gamma + \text{Strained } \alpha^*$
	850	$\alpha + \gamma$

\* Strain in lattice evidenced by broad reflections, especially at high reflection angles.

The results for the purer alloys were similar to those already reported for alloys made from the commercial titanium. The eutectoid temperature

was found to be between  $850^\circ$  and  $860^\circ\text{C.}$ , the eutectoid composition being 11.5 at.-% silver. As was noted in the work on the less pure alloys, a rapid

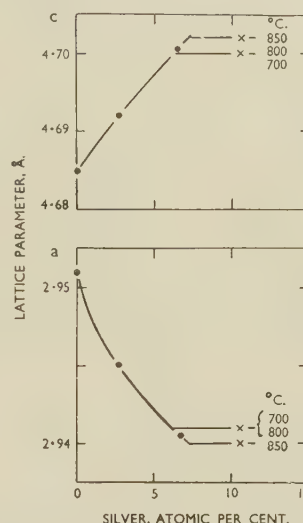


FIG. 4.—Lattice Parameters of  $\alpha$  Phase in Alloys Made with Refined Titanium.

KEY.

- Single-phase alloys water-quenched from  $850^\circ\text{C.}$
- × Duplex alloys water-quenched from temperatures shown ( $^\circ\text{C.}$ ).

$\beta \rightarrow \alpha$  transformation occurred during quenching of alloys from the  $\beta$  solution field.

#### 5. HARDNESS OF ALLOYS MADE WITH COMMERCIAL TITANIUM

As shown in Fig. 5, supersaturated  $\alpha$  solutions produced by quenching from the  $\beta$ -solution field were

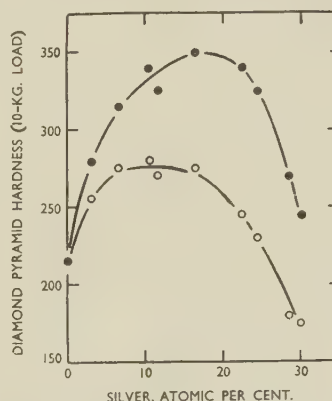


FIG. 5.—Diamond Pyramid Hardness of Heat-Treated Alloys Made with Commercial Titanium.

KEY.

- Water-quenched from  $870^\circ\text{C.}$ , i.e. the  $\alpha$  and  $(\alpha + \gamma)$  fields.
- Water-quenched from  $\beta$  and  $(\beta + \gamma)$  fields ( $1000^\circ\text{C.}$  for 3-11.5 at.-% silver;  $1100^\circ\text{C.}$  for 16.2-30.1 at.-% silver).

a little harder than equilibrium  $(\alpha + \gamma)$  mixtures. Attempts to cause further hardening by heating the supersaturated  $\alpha$  solutions were unsuccessful, as is

shown by the data in Table VI. An interesting feature of these results was the persistence of the hardness at the as-quenched level after heating at a temperature as high as 700° C. for 1 hr. This heat-treatment caused no detectable change in the microstructures or X-ray-diffraction patterns of the alloys (cf. Section IV, 2).

TABLE VI.—Effect of Heating for 1 Hr. at Various Temperatures on the Hardness of Alloys Initially in the Form of Supersaturated  $\alpha$  Solutions.

Temp. of Treatment, °C.	D.P.H. (10-kg. Load)	
	10.3 at.-% Ag *	16.2 at.-% Ag †
As-quenched	345	350
180	350	...
300	340	335
400	345	350
500	360	355
600	350	360
700	365	345
800	325	315
870	305	310

\* Previously water-quenched from 1000° C.

† Previously water-quenched from 1100° C.

## V.—DISCUSSION

Addition of silver causes only a small depression of

the  $\alpha \rightleftharpoons \beta$  transformation temperature in titanium. This is in striking contrast to the marked depression caused by the majority of alloying elements which have atomic radii close to that of titanium.

The crystal structure of the  $\gamma$  phase can be regarded as being based on the  $L1_2$  type (ordered  $\text{Cu}_3\text{Au}$ ), with the important difference that the  $\gamma$  phase has tetragonal symmetry, the  $c/a$  ratio being 0.943. The degree of long-range order is low. Doubtless this is largely attributable to the fact that the silver content of the  $\gamma$  phase is not exactly 25 at.-%; the  $\gamma/(\alpha + \gamma)$  boundary actually lies in the region 28-29 at.-% silver. The  $\gamma$  phase appears to be isomorphous with  $\text{Ti}_3\text{Cu}$ ,  $\text{Zr}_3\text{Cu}$ , and  $\text{Zr}_3\text{Ag}$ , all of which were investigated by Karlsson.<sup>6, 7</sup>

## ACKNOWLEDGEMENTS

This investigation formed part of the programme of the Physical Metallurgy Section of the Commonwealth Scientific and Industrial Research Organization, Australia. The work was carried out in the Baillieu Laboratory, University of Melbourne, under the general direction of Professor J. Neill Greenwood, to whom the author tenders his thanks. Mr. J. A. Corbett performed all the chemical analyses.

The United States Bureau of Mines kindly supplied the commercial titanium.

## REFERENCES

1. F. Laves and H. J. Wallbaum, *Naturwiss.*, 1939, **27**, 674.
2. C. M. Craighead, O. W. Simmons, and L. W. Eastwood, *Trans. Amer. Inst. Min. Met. Eng.*, 1950, **188**, 485.
3. E. Raub, P. Walter, and M. Engel, *Z. Metallkunde*, 1952, **43**, 112.
4. R. J. Van Thyne, W. Rostoker, and H. D. Kessler, *Trans. Amer. Inst. Min. Met. Eng.*, 1953, **197**, (5), 670.
5. H. W. Worner, *J. Inst. Metals*, 1952-53, **81**, 521.
6. N. Karlsson, *ibid.*, 1951, **79**, 391.
7. N. Karlsson, *Acta Chem. Scand.*, 1952, **6**, 1424.



# THE METALLOGRAPHIC DETECTION OF GAMMA PHASE IN BETA-BRASS\*

1516

By L. E. SAMUELS,† B.Met.E., MEMBER

## SYNOPSIS

Mechanical polishing has been successfully used to detect fine grain-boundary precipitates of  $\gamma$  phase in a tin-containing  $\beta$ -brass showing intercrystalline brittleness, but evidence of precipitation is found at only a proportion of the grain boundaries. Electrolytic polishing develops diffuse dark lines at all the grain boundaries of this material, but these indications have a ridge-and-groove contour of a type similar to that previously found in several other copper alloys. The development of this contour at a grain boundary known to contain a discrete precipitate of a second phase is unexpected, and indicates that caution is necessary in interpreting this phenomenon.

## I.—INTRODUCTION

PERRYMAN,<sup>1</sup> in describing the results of examination of a cast  $\beta$ -brass which showed severe intercrystalline brittleness, reported that electrolytic polishing enabled a grain-boundary constituent to be detected, whereas mechanical polishing did not. The appearance of the intercrystalline facets of the fracture surface and the response of the material to heat-treatment suggested that the constituents detected were films of  $\gamma$  phase. It was thought that the system of mechanical polishing developed by the author<sup>2</sup> might enable the precipitates to be detected, and a sample of the material examined by Perryman was kindly made available for this purpose by the British Non-Ferrous Metals Research Association.

## II.—MATERIALS AND METHODS OF EXAMINATION

The material<sup>3</sup> was a tin-containing  $\beta$ -brass made from high-purity metals (cathode copper, Crown Special zinc, and Mellanear tin) and contained 54.00% copper and 3.10% tin.

The preliminary preparation of all surfaces examined was carried out by the method previously described,<sup>2</sup> up to and including the (0.1)  $\mu$ -grade diamond abrasive pad. Finish polishing was carried out either by mechanical methods on a magnesium oxide-water paste (without additions of ammonium persulphate) by the skidding technique,<sup>2</sup> or electrolytically in Jacquet's<sup>4</sup> orthophosphoric acid bath. When required, mechanically prepared surfaces were etched by immersion in a warm 10% ammonium persulphate solution; this was the only one of the usual etching methods for copper alloys which satisfactorily etched the specimens.

## III.—RESULTS OF METALLOGRAPHIC EXAMINATION

After mechanical polishing, clear evidence of a second phase at the grain boundaries was detected,

though only at a relatively small proportion of the total grain-boundary length of the specimen. The phase was present both as discontinuous films (Figs. 1 and 3, Plate XXXIII), and as very fine precipitates which could only just be resolved under an optical microscope (Fig. 5, Plate XXXIII). At some positions, the films were of sufficient width to be discretely resolved (Fig. 3), and here they showed the light-blue colour characteristic of the copper-zinc  $\gamma$  phase.

Electrolytic polishing, on the other hand, developed some indications at all grain boundaries, viz. (a) broad, diffuse, dark bands at those lengths of grain boundary known to contain films of  $\gamma$  phase (cf. Figs. 1 and 2, and Figs. 3 and 4, Plate XXXIII), (b) continuous thinner diffuse lines at the grain boundaries known to contain fine precipitates (cf. Figs. 5 and 6, Plate XXXIII), and (c) similar thin diffuse lines at those grain boundaries at which no evidence of a precipitated phase had been detected after mechanical polishing (cf. Figs. 1 and 2). It was difficult to decide positively from the examination of these electrolytically polished surfaces, however, whether or not a discrete precipitate was present.

The topography of the surface in the neighbourhood of the indications developed by electrolytic polishing was therefore investigated by a taper-sectioning technique. A grain boundary was selected at which marked discontinuous films had been detected after mechanical polishing. The surface was electrolytically polished, heavily copper plated, and taper-sectioned (taper ratio 10:1) so that the taper-section line was approximately perpendicular to the trace of the grain boundary being investigated. The taper-section surface was mechanically polished and lightly etched; the full length of the grain boundary was investigated by repeated polishing treatments. The presence of the copper plating resulted in slight electrolytic etching effects during polishing, and it was not possible to retain the films of  $\gamma$  phase in the taper sections as sharply as before.

It was found that a ridge-and-groove contour had

\* Manuscript received 27 July 1953.

† Senior Scientific Officer, Defence Research Laboratories, N.S.W. Branch, Alexandria, Sydney, Australia.

been developed at all grain boundaries during electrolytic polishing. The effect at positions known to contain a definite film of  $\gamma$  phase was extremely marked (Fig. 7, Plate XXXIII), the step at the grain boundary being more than  $0.8\ \mu$  in true height, and the  $\gamma$  phase appearing to be retained in the edge of the step. The effect was considerably less marked, but was still well developed, at positions at which no precipitation had been detected after mechanical polishing; Fig. 8 (Plate XXXIII) is typical of such areas. These are further examples of the effects previously found in electrolytically polished specimens of a number of brittle copper alloys.<sup>5-9</sup> The present case is somewhat unusual in that the contour is developed very strongly and at all grain boundaries.

It was noted, also, that etching after mechanical polishing developed a halo of dark spots around each length of film of  $\gamma$  phase (Figs. 7 and 8). These spots were developed even more strongly by electrolytic polishing (Fig. 4), and are presumed to be etch pits.

#### IV.—DISCUSSION

The particular method of mechanical polishing was successfully used to detect the precipitation of  $\gamma$  phase with considerable clarity. In this respect, the results were appreciably less ambiguous than those obtained by electrolytic polishing.

Since the finest precipitates observed after mechanical polishing were just within the maximum resolving power of an optical microscope, it would seem reasonable to assume that no resolvable precipitation was obscured by polishing. Although the material presumably was brittle at all grain boundaries, evidence of precipitation was detected at only a small proportion of the total grain-boundary length. Electrolytic polishing, on the other hand, developed indications in the form of a ridge-and-groove contour at all lengths of the grain boundary; this effect has been attributed

to the "equilibrium segregation" of solute atoms at the grain boundaries without actual precipitation, and is frequently associated with intercrystalline brittleness.<sup>6-9</sup>

It is of some interest to note, however, that the ridge-and-groove contour was developed on a very exaggerated scale at the positions of precipitated films of  $\gamma$  phase, whereas it was previously assumed that a second phase would result in a contour symmetrical about the grain boundary.<sup>6, 7</sup> The presence or absence of a discrete precipitate in such cases, therefore, must always be established by independent evidence. It is also to be noted that examination under an optical microscope, even when carried out on well-prepared mechanically polished surfaces, is not completely satisfactory for this purpose, since it is possible that the contour may be associated with sub-microscopic precipitates; this would appear to be a possibility in the present case.

Nevertheless, it is still likely that the asymmetric contour can develop in the absence of discrete precipitation. Schofield and Cuckow's<sup>10</sup> electron-microscope examination, and Kê's<sup>11</sup> internal-friction and elastic-moduli measurements, for example, suggest that precipitation is unlikely in the case of the bismuth-containing coppers. Perryman<sup>8</sup> carried out an electron-microscope examination of the tin bronzes, but did not detect any evidence of precipitation. The most critical evidence is that due to McLean,<sup>9</sup> since there was no possibility of precipitation occurring in the copper-antimony alloys he investigated.

#### ACKNOWLEDGEMENTS

The author wishes to acknowledge the kindness of Mr. R. Eborall of the B.N.F.M.R.A. in making available the specimen examined. This paper is published by permission of the Chief Scientist, Department of Supply, Australia.

#### REFERENCES

1. E. C. W. Perryman, *Metal Ind.*, 1951, **79**, 23.
2. L. E. Samuels, *J. Inst. Metals*, 1952-53, **81**, 471.
3. R. Eborall, private communication.
4. P. A. Jacquet, *Bull. Soc. Franç. Mét.*, 1945, **1**, 1; *Rev. Mét.*, 1945, **42**, 133.
5. D. McLean and L. Northcott, *J. Inst. Metals*, 1946, **72**, 583.
6. D. McLean, *ibid.*, 1947, **73**, 791 (discussion).
7. L. E. Samuels, *ibid.*, 1949-50, **76**, 91.
8. E. C. W. Perryman, *Trans. Amer. Inst. Min. Met. Eng.*, 1953, **197**, 906.
9. D. McLean, *J. Inst. Metals*, 1952-53, **81**, 121.
10. T. H. Schofield and F. W. Cuckow, *ibid.*, 1947, **73**, 377.
11. T. S. Kê, *Phys. Rev.*, 1949, [ii], **75**, 1626.



## ALUMINIUM-COPPER-IRON ALLOYS.

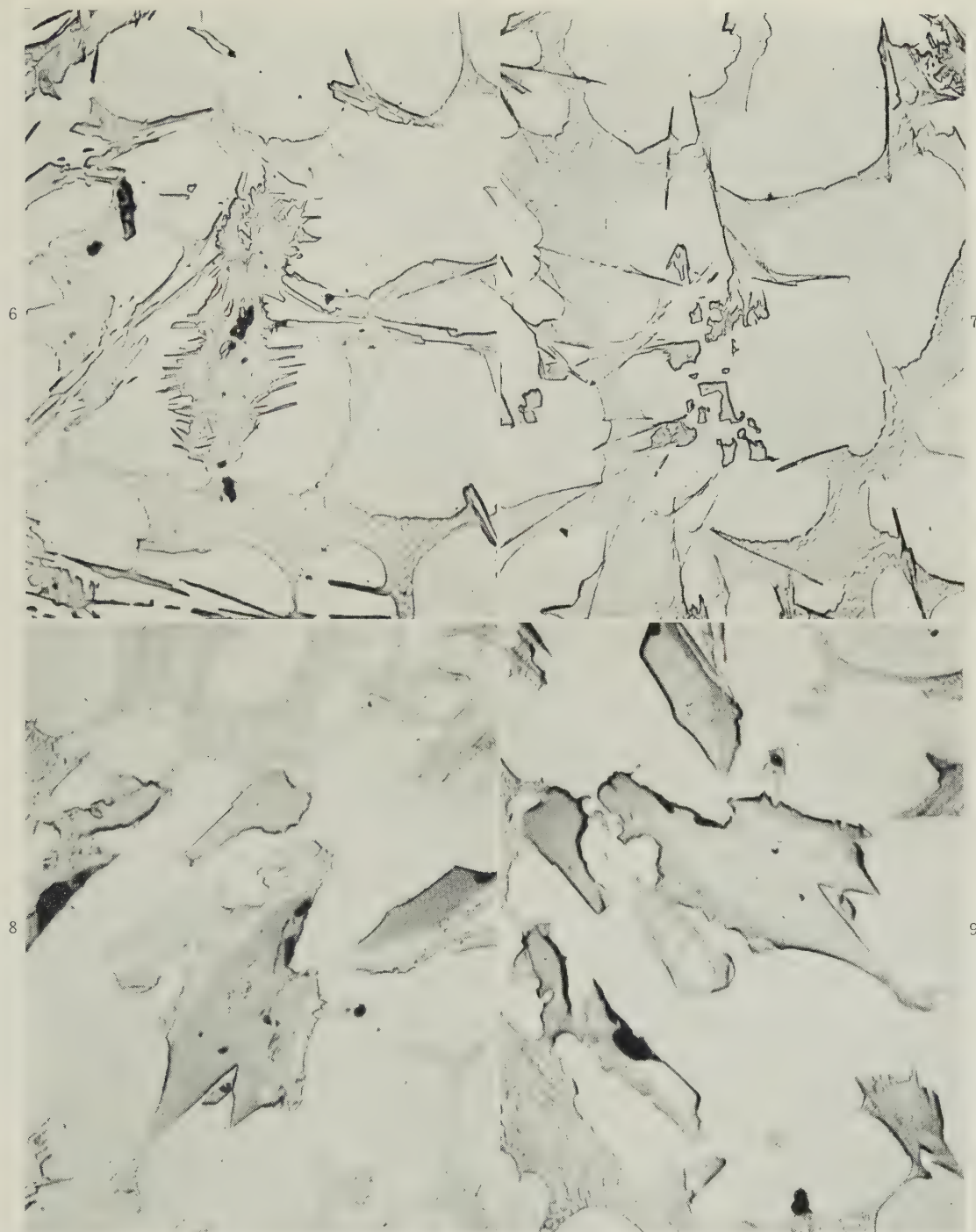


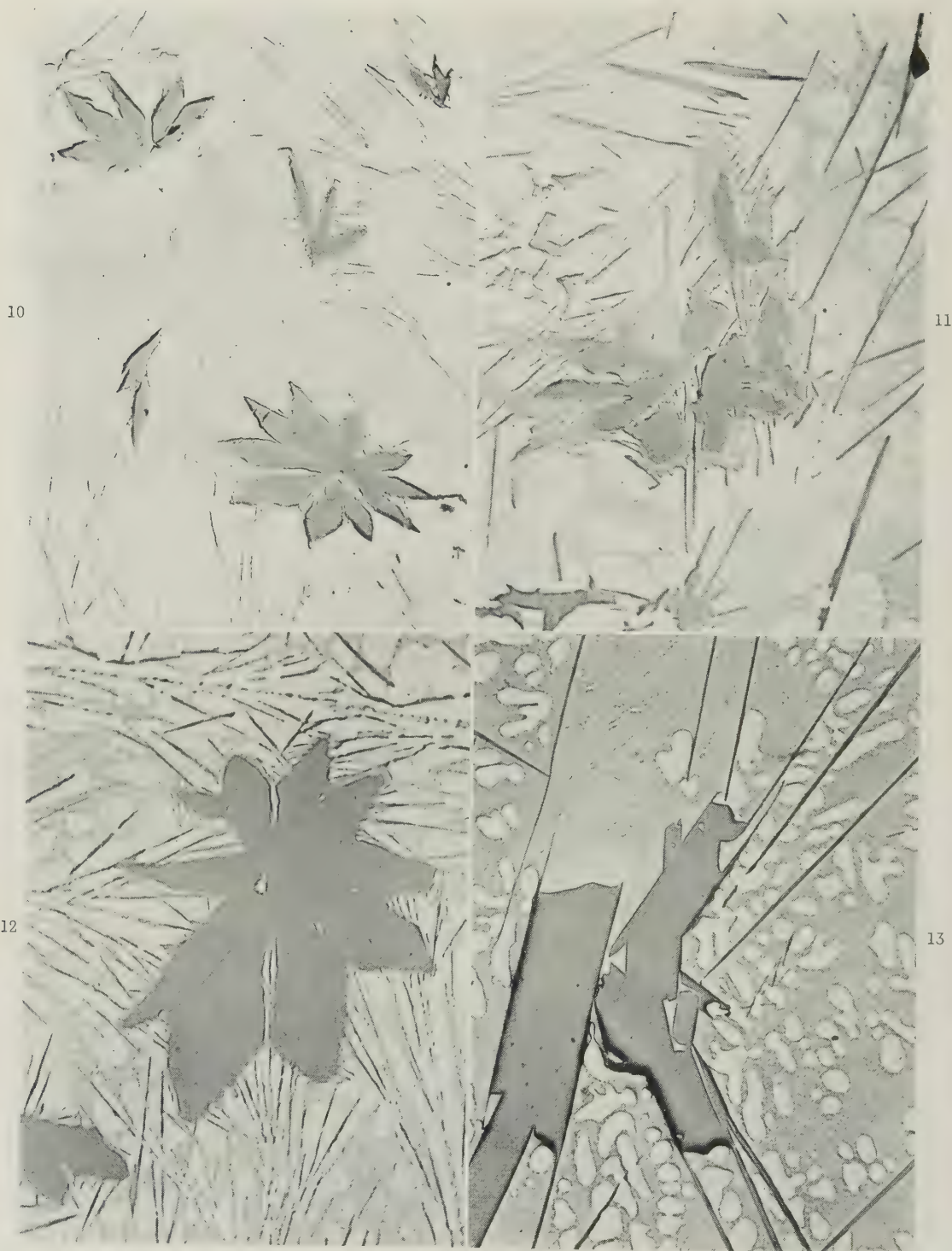
FIG. 6.—Alloy Containing Fe 2, Cu 15% as slowly solidified.  $\text{FeAl}_3$  (grey, in relief) as a core in  $\alpha$ ; the latter with a fringe of  $\beta$  needles. The eutectic areas contain  $\text{CuAl}_2$  (pale grey) and  $\beta$  (long needles). Unetched.  $\times 200$ .

FIG. 7.—Alloy Containing Fe 1.25, Cu 15% as slowly solidified. Primary  $\alpha$  in the form of broken rhomboids. Needles of  $\beta$ , with  $\text{CuAl}_2$ , in the eutectic. Unetched.  $\times 200$ .

FIG. 8.—Alloy Containing Fe 1.5, Cu 15% as slowly solidified. Photographed in polarized light. A large primary crystal of  $\alpha$  (dark), partly converted to  $\beta$  (paler). Unetched.  $\times 200$ .

FIG. 9.—Alloy Containing Fe 1.5, Cu 15% as slowly solidified. Photographed in polarized light. The same area as Fig. 8, but the specimen has been rotated through  $90^\circ$ . The  $\alpha$  is now pale and the  $\beta$  dark. Unetched.  $\times 200$ .

## ALUMINIUM-COPPER-IRON ALLOYS.



- FIG. 10.—Alloy Containing Fe 2, Cu 12.5%. Annealed 96 hr. at 624° C. and quenched. Large crystals of  $\text{FeAl}_3$ , with adherent crystals of  $\beta$ . Unetched.  $\times 500$ .
- FIG. 11.—Alloy Containing Fe 2, Cu 17.5%. Annealed 400 hr. at 623–624° C. and quenched. Spines of  $\text{FeAl}_3$  in  $\alpha$ , the latter with adherent needles of  $\beta$ . Unetched.  $\times 500$ .
- FIG. 12.—Alloy Containing Fe 2, Cu 22.5%. Annealed 96 hr. at 624° C. and quenched. Large crystals of  $\text{FeAl}_3$ . Unetched.  $\times 500$ .
- FIG. 13.—Alloy Containing Fe 2, Cu 27.5%. Annealed 96 hr. at 624° C. and quenched. Large crystals of  $\beta$ . Unetched.  $\times 200$ .



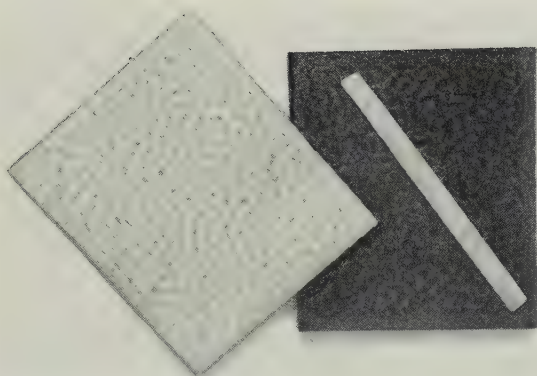


FIG. 13.—Metal Core and Stripped Scale from Commercial Titanium Oxidized at 900° C. for 72 hr.  $\times 3$ .

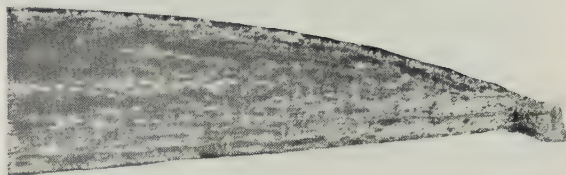


FIG. 14.—Appearance in Cross-Section of Scale Shown in Fig. 13. Tapered portion corresponds to edge of metal core.  $\times 100$ .



FIG. 15.—Specimen of Refined Titanium Oxidized to Near Completion.  $\times 25$ .

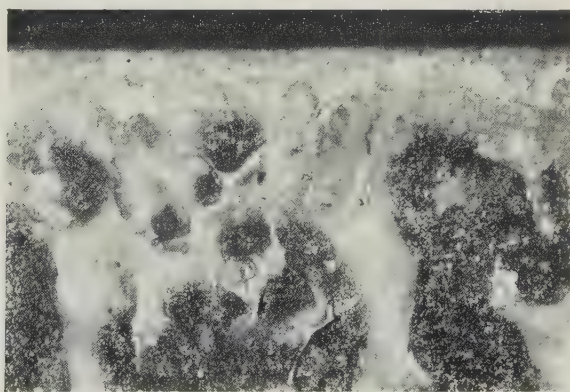


FIG. 16.—Ridge Formation of Oxide Scale on Refined Titanium Oxidized at 750° C. for 12 hr.  $\times 100$ .

## TITANIUM-SILVER ALLOYS

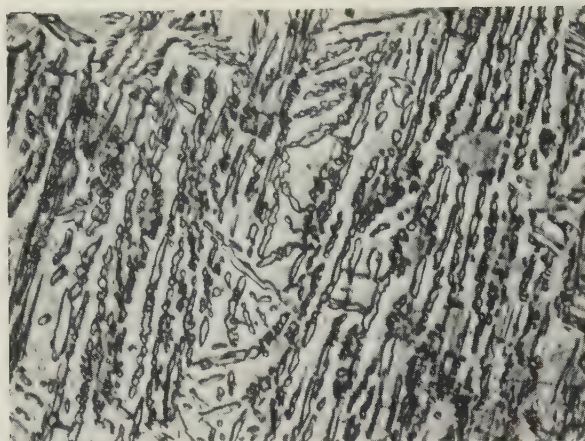


FIG. 6.—10.3 at.-% Silver Alloy (Commercial Titanium).  
Cooled from 950° to 850° C. at 2° C./min. ( $\alpha + \gamma$ ) eutectoid  
mixture; primary  $\alpha$  not shown.  $\times 800$ .

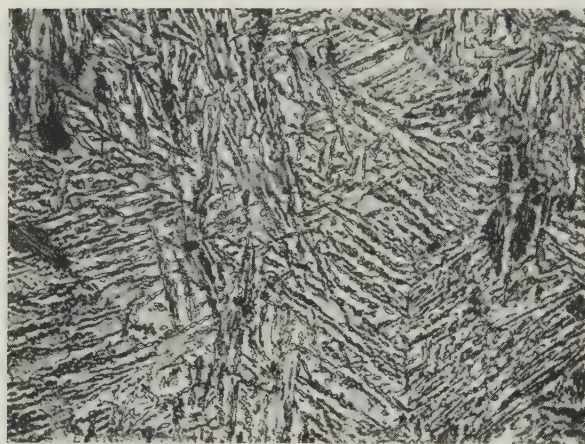


FIG. 7.—10.3 at.-% Silver Alloy (Commercial Titanium).  
Water-quenched from 950° C., then heated 2 hr. at 870° C.  
( $\alpha + \gamma$ ) mixture.  $\times 800$ .

Both specimens were etched in 2 wt.-%  $\text{HNO}_3 + 1$  wt.-% HF in  
water.



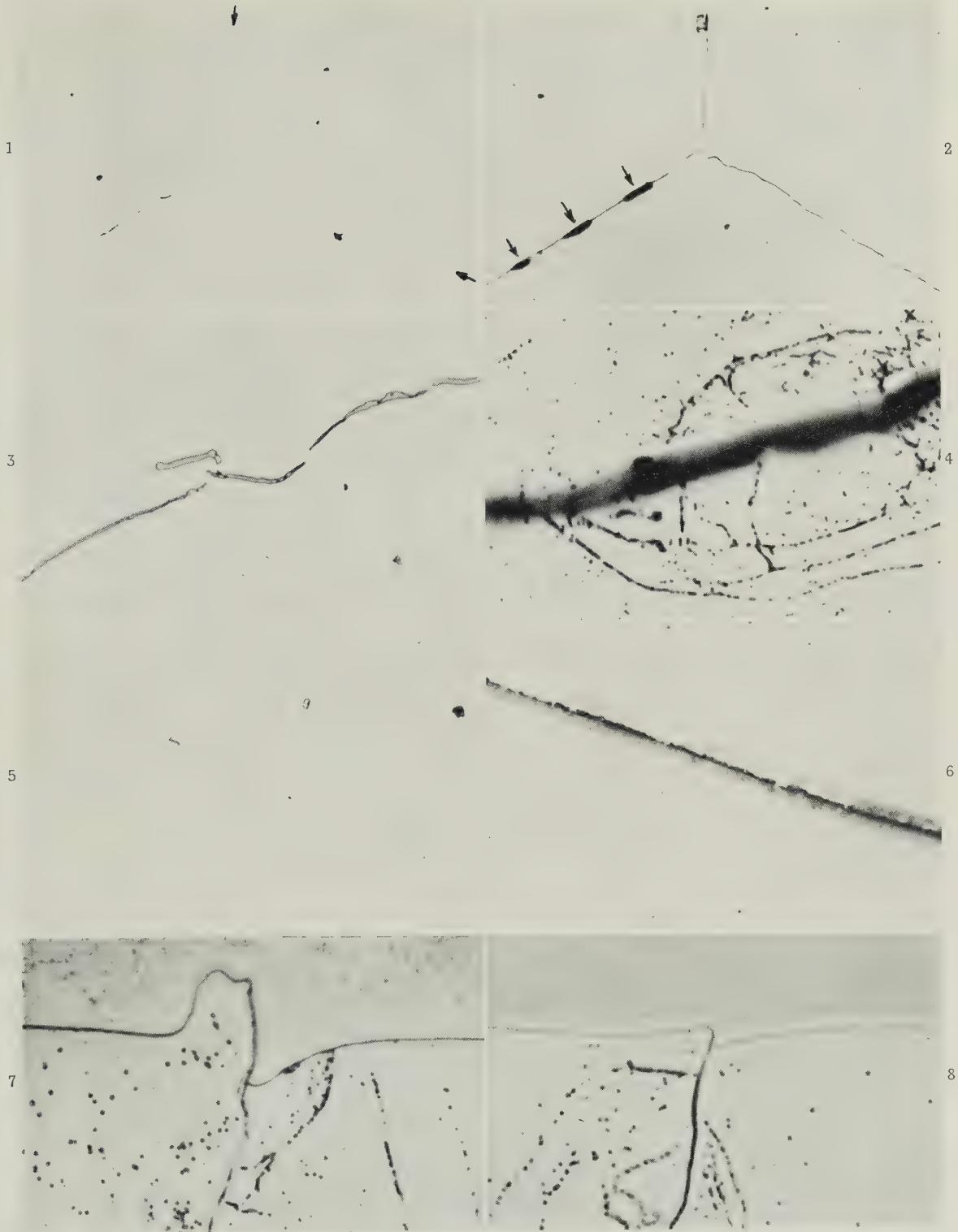
INTERCRYSTALLINE FILMS OF  $\gamma$  PHASE IN  $\beta$ -BRASS.

FIG. 1.—Grain Junction, Mechanically Polished, Light Etch.  $\times 500$ . (Arrows indicate positions of grain boundaries in Fig. 2.)

FIG. 2.—Same Field as Fig. 1, after Electrolytic Polishing.  $\times 500$ . (Arrows indicate positions of films of  $\gamma$  phase in Fig. 1.)

FIG. 3.—Marked Film of Precipitate, Mechanically Polished. Unetched.  $\times 2000$ .

FIG. 4.—Similar Field to Fig. 3, after Electrolytic Polishing.  $\times 2000$ .

FIG. 5. Fine Precipitates, Mechanical Polish, Light Etch.  $\times 2000$ .

FIG. 6. Similar Field to Fig. 5, after Electrolytic Polishing.  $\times 2000$ .

FIGS. 7 and 8. Taper Sections of Electrolytically Polished Surface. Horizontal magnification:  $\times 2000$ ; effective vertical magnification:  $\times 20,000$ .

FIG. 7.—Field Showing Definite Film of  $\gamma$  Phase.

FIG. 8.—Representative Area at which  $\gamma$  Phase was not Detected.





# MECHANISM OF CREEP DEFORMATION IN HIGH-PURITY ALUMINIUM AT HIGH TEMPERATURES\*

1517

By HSING C. CHANG,† M.S., Sc.D., MEMBER, and NICHOLAS  
J. GRANT,‡ B.S., Sc.D.

## SYNOPSIS

Creep of very coarse-grained high-purity aluminium was studied at 400°, 700°, and 1100° F. (205°, 370°, and 595° C.) over a stress range from 50 to 1200 lb./in.<sup>2</sup>. Simultaneous observations and measurements of localized strains on polished specimen surfaces were made by means of a high-temperature microscope. The sequence of the development of various deformation modes, heavy slip bands, kink bands, and subgrains, was followed. Slip is the fundamental mechanism of deformation for both single-crystal and polycrystalline materials even in high-temperature creep. Component creep curves (measured between two closely spaced markings) obtained across grain-boundary-affected slip bands show a periodic behaviour, the significance of which is discussed. Subgrains are shown to be formed under conditions where slip development is restricted. Two types of subgrains, one caused by deformation bands and the other by kinking bands, are observed and discussed.

## I.—INTRODUCTION

THE present paper reports work which is a continuation of that described in two previous publications.<sup>1,2</sup> Its purpose was to investigate the mechanisms of creep, utilizing coarse-grained, high-purity aluminium. The structural changes on polished specimen surfaces were followed during the actual creep process by means of a high-temperature microscope. Closely spaced indentations, made by a sharp needle, permitted creep measurements to be made over short distances in various portions of the grains and across grain boundaries; hence, structural changes in a certain region could be correlated with the local strain measurements in that region.

The behaviour of the grain boundaries has been reported previously.<sup>1</sup> It was shown that grain-boundary sliding can cause the formation of subgrains and folds within the grains. It is proposed in this paper to discuss deformation of the grains during creep at high temperatures, by following the development of heavy slip bands and the manner in which this development is affected by the location of grain boundaries. It is proposed also to show that restriction of the full development of slip bands results in extensive subgrain formation. Finally, the development of kinking bands will be described.

## II.—EXPERIMENTAL PROCEDURE

The experimental procedures and techniques have been described elsewhere.<sup>1</sup> Since the grain-sizes and

the spacing of heavy slip bands were large in comparison with the diameter of the X-ray beam, it was always possible to locate a region on the specimen surface relative either to a known grain boundary or to a known slip band. White radiation from a copper target, a 1-mm.-dia. pinhole, and a camera with a 3-cm. film-to-specimen distance were used in the X-ray work.

The creep-test specimens, which were originally round in section, were prepared for microscopic observation during the creep process by milling two parallel flats over the full gauge length, one of these flats facing the microscope. After polishing and etching, all the grain boundaries were completely delineated. For easy reference, the four surfaces of each test bar were "unrolled" as a structural-development drawing, showing all four faces with the grain boundaries marked out to show the individual grains (Figs. 1 and 4). The nature of the test or observation and the location on the specimen surface are noted on these development drawings. The distance between the needle-point reference marks for component creep curves was about 0.6–0.7 mm. The gauge length was about 1 in., the width of the flat-milled region about 0.180 in., and the thickness about 0.085 in.

## III.—EXPERIMENTAL RESULTS

### 1. SLIP-BAND FORMATION

During this work considerable time was spent in studying the interaction between slip bands and grain boundaries in creep tests at comparatively high tem-

\* Manuscript received 15 December 1952; in revised form 10 August 1953.

† D.I.C. Staff Member and ‡ Associate Professor, Department of Metallurgy, Massachusetts Institute of Technology, Cambridge, Mass., U.S.A.

peratures and low stresses. The deformation patterns under these conditions were clearly revealed in the course of development by an optical microscope.

The results presented below were obtained from the central portion of specimen *P-10*, the surface-development diagram of which is shown in Fig. 1. This specimen was studied during creep at 1100° F. (595° C.) under an initial stress of 50 lb./in.<sup>2</sup>. Fracture occurred after 30 hr. at a total elongation of 33%. The phenomena studied in this test were the deformation of the grains by slip and the restricting effects caused by grain boundaries. In confirmation of the observations made on specimen *P-10*, the same general phenomena were also observed in specimen *P-9*, which was again tested at 1100° F., but at an initial stress of 65 lb./in.<sup>2</sup>, and in specimen *P-8*,<sup>12</sup> which was tested at 700° F. (370° C.) at a stress of 85 lb./in.<sup>2</sup>. Some of the more interesting observations are presented below, and are fairly typical of creep deformation

sake of clarity, only two successively operative slip planes are indicated in Fig. 2 (b) although many slip planes were operative in the wide slip band shown in Fig. 6. After successive slips, the specimen eventually fractured along this band.

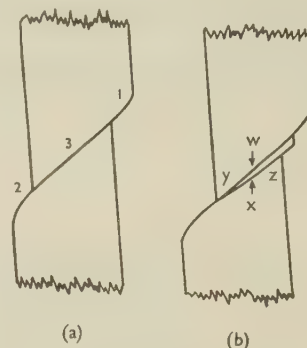


FIG. 2.—Schematic Drawing of the Rotation of the Heavy Slip Band Shown in Fig. 6 (Plate XXXIV) (also slip band I, Fig. 1).

(a) Rotation of portion (3) lagged behind the rotation of portions (1) and (2).

(b) Slip band (x) became operative after slip band (w) had become bent and rotated away from the most favorable position for slip. (y) and (z) indicate the regions of inhomogeneous deformation adjacent to the heavy slip band.

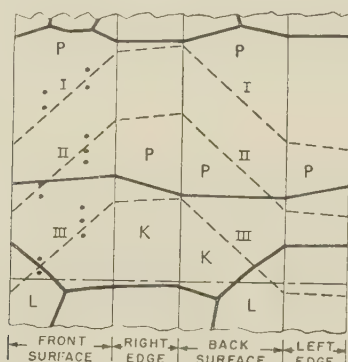


FIG. 1.—Structural-Development Drawing of a Portion of Specimen *P-10*, Tested at 1100° F. and 50 lb./in.<sup>2</sup>.

KEY.  
 — — — Course of slip bands.  
 ● Reference marks for component creep curves (see Fig. 3).

under the above test conditions. The illustrations are selected mainly from specimen *P-10*.

#### (a) The Development of a Heavy Slip Band When It Does Not Encounter a Grain Boundary

The broken line, I, in Fig. 1 shows the course of a heavy slip band in grain *P*, which occupies the whole width and thickness of specimen *P-10*.

Grain *P* started to deform by slip with a fairly uniform slip-band spacing, as shown in the top left-hand region of Fig. 6 (Plate XXXIV). As creep continued, deformation tended to be concentrated in a band about 0.2 mm. wide, shown in the centre of Fig. 6. With further deformation, this wide slip band exhibited an interesting slip and rotation process. Fig. 6 clearly shows the rotation, amounting to about 13°, of the slip bands within this wide band. Schematic drawings, based on observations made both during and after the test, are presented in Fig. 2, to illustrate the stages of this rotation process. For the

Curve I of Fig. 3 shows a component creep curve which was obtained by measuring the extension with time between two reference marks across this slip band (see also Fig. 1). It can be seen that the creep rates increased continuously until fracture occurred along the band.

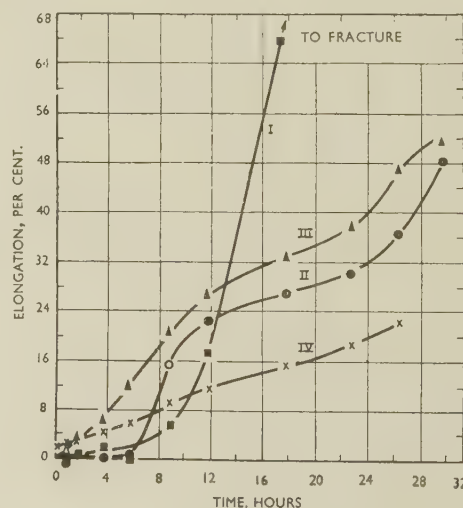


FIG. 3.—Specimen *P-10*, Tested at 1100° F., 50 lb./in.<sup>2</sup>. Three component creep curves across heavy slip bands I, II, and III (Fig. 1) and a total creep curve.

KEY.  
 I. ■ Across slip band I (Fig. 1).  
 II. ● Across slip band II (Fig. 1).  
 III. ▲ Across slip band III (Fig. 1).  
 IV. × Over the entire gauge-length.  
 ○ Extension when offset of grain boundary could be clearly observed (see Fig. 7, Plate XXXIV).



(b) *The Development of a Heavy Slip Band When It Encounters a Grain Boundary Through Which It Can Pass*

The broken line, II, in Fig. 1 shows the position of such a slip band. It can be seen that this crossed the boundary between grains *P* and *K*, both of which occupied the whole cross-section of the specimen.

Figs. 7 and 8 (Plate XXXIV) show a portion of slip band II. These micrographs, of the same field, were taken consecutively during creep (at 1100° F. and 50 lb./in.<sup>2</sup>) after 9.5 and 18.2 hr., respectively.

Fig. 7 shows that slip band II passed through, and segmented the boundary between grains *P* and *K*. This boundary became continuous again only after a period during which boundary migration took place. This gave rise later to a curved grain boundary at the slip band, as indicated by the dashed arrow in Fig. 8.

Two creep curves were obtained across slip band II; the positions of the needle-point marks are shown in Fig. 1. Since the component creep curves were quite similar, it will suffice to present one of them (curve II, Fig. 3). The shape of curve II for the first 9 hr. of creep resembles that of curve I for the first 12 hr., in that the creep rate increases continuously. After this, curve I shows an uninterrupted increase in the creep rate to fracture, whereas curve II shows alternate periods of decreasing and increasing creep rates. From 9 to 18 hr., curve II shows a decreasing creep rate, approaching a steady rate. During this period the grain boundary between grains *P* and *K* migrated from the position shown in Fig. 7 to that in Fig. 8. It can be seen that the amount of offset shown in Fig. 8 along slip band II across the segmented grain boundary, as indicated by the solid arrow, is practically the same as that shown in Fig. 7, as would be expected from the small amount of slip shown in curve II (Fig. 3) during this interval.

(c) *The Development of a Heavy Slip Band When It Encounters a Grain Boundary Through Which It Cannot Pass*

The broken line III (Fig. 1) shows the position of a band of this type. Figs. 9 and 10 (Plate XXXIV) are micrographs of the same region taken after 3.5 and 9.5 hr. of creep, respectively. These show the behaviour of the heavy slip band III on approaching the boundary between grains *K* and *L*. As this slip band developed, the boundary migrated from the original position, (1)–(1), in the direction shown by the solid arrow in Fig. 9 to the final almost horizontal position, (2) (see also Fig. 1).

Fig. 9 shows that the rather sharp slip band is connected across the newly formed boundary between grains *K* and *L* by wavy markings in grain *L*, as indicated by the dashed arrow. From the waviness of these deformation markings, it may be concluded that many slip systems have been operative. With further deformation, these wavy markings developed into a heavy band (Fig. 10), which shows a continuation of the slip band developed in grain *K*. On visual examin-

ation of the specimen after the test, the whole band resembled a regular heavy slip band in the sense that it left offsets on the four surfaces of the specimen, as though this band did not encounter the boundary between grains *K* and *L*.

On comparing Figs. 9 and 7, it can be seen that Fig. 9 shows no clear evidence of shearing of the newly formed boundary, marked (2), between grains *K* and *L* by the slip band, as was the case in Fig. 7.

As regards Figs. 9 and 10, it is interesting to note that the heavy slip band in grain *K* was formed by two separate slip bands which developed early in the test from opposite directions and never merged. This can be seen in the upper right-hand corner of Fig. 9, where a region of cross slip connects the two separate bands. With further deformation, these two bands stayed parallel to each other to form a heavy band (Fig. 10). From the amount of offset produced across the old boundary between grains *K* and *L* (point (*a*) in Fig. 10) by slip band III, it appears that these two initially developed slip bands contributed most of the deformation.

A component creep curve obtained across the heavy slip band III is shown as curve III in Fig. 3. Curve III is similar to curve II in that, after a period of increasing creep rate, both curves show alternate periods of decreasing and constant creep rates. Curve III, however, shows larger elongations than curve II in the early stages of creep. This probably results from the different orientation relationships of grains *P* and *K* and grains *K* and *L*, with respect to the specimen axis.

For the sake of comparison, a total creep curve, IV, is also shown in Fig. 3. It shows a change in rate of elongation after 9 hr. of creep, corresponding to the increases shown in curves II and III.

When two component creep curves were obtained across the same slip band, with one set of measurements taken close to the free edge of the specimen, the shapes of the two curves were qualitatively the same, but the one obtained nearer the free edge almost always showed greater elongations. The fact that the amount of deformation is different across different portions of a heavy slip band indicates that cross slip and bending must both occur in the band to varying degrees.

## 2. SUBGRAIN FORMATION

Subgrain formation was followed easily and clearly during a creep test at comparatively low temperature and high stress. It has already been shown that in order to accommodate the deformation initiated by boundary sliding, subgrains formed both around grain-boundary triple points and along the heavily slid boundary.<sup>1</sup> Two examples are presented to show how subgrains may form extensively in the regions where deformation by slip is restricted by the blocking effect of grain boundaries.

*Example I.*—Fig. 4 shows the development diagram of a portion of specimen *P*-8, tested at 700° F. (370° C.)

and 85 lb./in.<sup>2</sup>. The two broken lines in grain *C* indicate the positions of the two bands developed during the creep test. The appearance of these two bands at different distances from the grain boundaries of grains *A* and *C* on the front, and of grains *C* and *D* on the back surface of the specimen is shown in Figs. 11, 12, and 13 (Plate XXXV), respectively. Fig. 11 was taken close to the centre of the front surface and Fig. 12 closer to the right-hand front edge of the specimen (see also Fig. 4). Since the portions of both bands shown in Fig. 11 were appreciably removed from the influence of the grain boundaries *A/C* and *C/D*, they seemed to follow a specific, parallel direction. However, when the lower band approached the boundary *C/D* on the back surface of the specimen, it deviated away from the grain boundary (Fig. 13). The course of the lower band on the front surface of the specimen was similarly affected, and it merged with the upper band at the extreme right edge of the specimen (Fig. 12).

Examination of the deformation marks left on the specimen surface led to the conclusion that slip had

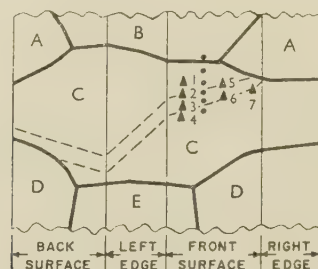


Fig. 4.—Structural-Development Drawing of a Portion of Specimen P-8, Tested at 700° F. and 85 lb./in.<sup>2</sup>.

KEY.

- — — Course of slip bands.
- Reference marks for component creep curves.
- ▲ Positions at which Laue photographs were taken.

taken place on several slip systems within the bands, as indicated by the arrows in Figs. 11–13. It is, therefore, proper to call these bands deformation bands.

Back-reflection Laue photographs were taken at various positions, indicated by numbered small triangles in Fig. 4, on the front surface of specimen P-8. Laue photographs taken at triangles 2 and 3 were similar, and only the one taken at triangle 2 is shown (Fig. 14, Plate XXXVI). This shows that the material situated on the upper band and also that between the upper and lower bands close to the left-hand front edge of the specimen were very slightly distorted. This observation is in agreement with the geometrical condition of the upper band, which was influenced only by the boundary between grains *A* and *C* at the right-hand front surface of the specimen. However, the Laue photograph taken of the lower band, at the position of triangle 4, showed that a Laue spot was broken down into three discrete subgrain spots with a spread of about 2°. This band was influenced both by the boundary between grains *A* and

*C* and by that between grains *C* and *D*, particularly the latter. The influence of the boundary *C/D* must therefore extend through the specimen to the position of triangle 4. As the bands developed across the specimen, they were more strongly subject to the influence of the grain boundaries. The Laue photographs taken at positions corresponding to triangles 5 and 6 (Fig. 4) showed that this was the case. A Laue photograph taken at triangle 6 is similar to that at 5 (Fig. 15, Plate XXXVI) except that the latter shows more severely broken-down Laue spots. It would be expected that the boundary *A/C* would exert a greater blocking effect on the upper band at location 5 than at location 6, owing to the distances involved. Fig. 16 (Plate XXXVI) shows a Laue photograph taken at a position corresponding to triangle 7. This photograph shows that the Laue spots transformed not to discrete subgrain spots, but instead to rather long streaks with a total spread of about 5°. This may mean that, as a result of the restriction by the grain boundaries, this region was deformed by several slip systems and that the subgrains so formed were too small to be resolved distinctly by the X-ray technique employed.

It was noted that the material between the upper band and the grain boundary *B/C* was more severely broken down into subgrains, with a spread of about 6°, than the material within or between the bands. At triangle 1 (Fig. 4), which is quite far from a grain boundary, there was extensive deformation resulting in the formation of subgrains. This is illustrated in Fig. 17 (Plate XXXVI), which was taken at triangle 1. The severe breakdown into subgrains in this region is apparently due to the extensive inhomogeneous deformation which took place there in order to accommodate the deformation taking place in the upper band.

Component creep curves were obtained across both the upper and lower bands. These were similar in shape to curves II and III in Fig. 3. In conformity with the metallographic observations, the elongation measured across the upper band was much larger than that across the lower band.

*Example II.*—Figs. 18–20 (Plate XXXVII) show some interesting deformation patterns for specimen P-11 deformed at 400° F. (205° C.) and 400–750 lb./in.<sup>2</sup>. It should be pointed out that at 400° F., pure aluminium exhibits relatively little grain-boundary sliding but slips readily. In the early stages of creep the specimen deformed initially by slip; three slip systems were operative in grain *G*, but failed to penetrate extensively the region of grain *G* near the boundary with *E*. In the later stages of creep, kinking bands developed in grain *E* and penetrated finally into *G*, causing inhomogeneous deformation in *G* near the triple point. Subgrains were gradually developed in this region, and, as may be seen from the photomicrographs, were formed after some light slip bands had developed in the early stages of creep. At the time of fracture this region was broken down into many subgrains randomly distributed (Fig. 20). Evidence of bound-



ary sliding in the later stages of creep can be obtained on comparing (Figs. 18 and 20) the offset of the continuous slip bands across the boundary between grains *E* and *P*.

The breakdown of grain *G* near the triple point is confirmed by a Laue pattern (Fig. 22, Plate XXXVIII), taken in this region. The random distribution of subgrain spots agrees very well with the metallographic observation in Fig. 20. The range of the subgrain sizes measured metallographically was 0.03–0.12 mm.

### 3. KINK-BAND FORMATION

In connection with Figs. 18–20, it is interesting to note that the kinking bands developed in grain *E* after the development of the slip bands. It is also of interest that the kinking bands that developed in grain *E* and penetrated into grain *G* were almost unaffected by the boundary *E/G*. This is illustrated more clearly in Fig. 21 (Plate XXXVII), which shows the continuous nature of the kinking bands that initially developed in grain *E* and were finally transmitted to another grain, *F*.

Fig. 23 (Plate XXXVIII) shows a Laue pattern from grain *E*. Comparison of this with Fig. 22, the pattern from grain *G*, reveals that grain *G* showed randomly broken-down subgrains, whereas the Laue spots in grain *E* were preferentially broken down.

## IV.—DISCUSSION

### 1. SUBGRAIN FORMATION

The exact mechanism of subgrain formation during creep is still uncertain. Disagreement exists as to whether subgrain formation is a mechanism of deformation in itself<sup>3,4</sup> or the end-product of non-homogeneous deformation.<sup>1,5,6,7</sup> The results presented above clearly show that subgrain formation results when normal slip cannot be fully developed because of blocking effects in the grains and because of the grain boundaries.

In order to establish the sequence of development of the subgrains and slip bands, a single crystal of high-purity aluminium (specimen *P*-12) was subjected to creep at 900° F. (480° C.) and 50 lb./in.<sup>2</sup>. This specimen elongated 33% in 500 hr. As was expected, subgrains first formed close to both ends of the specimen, which were affected by the specimen grips. In the central part, short, seemingly disconnected branches of slip bands, which appeared to occur along the same slip system, developed throughout the width of the specimen. With progressive elongation, these short branches merged and ran continuously across the width of the specimen. In the meantime, subgrains with obscure boundaries formed between the slip bands; these are discussed below. As the amount of displacement along the slip bands increased, both the number of subgrains and sharpness of the subgrain boundaries also increased. With further

creep, other slip bands developed between those already present. These later slip bands were able to segment the existing subgrain boundaries.

The results from the study of creep of a single crystal point to two important facts: (1) In single crystals, as in polycrystalline materials, slip is still the fundamental mechanism of deformation.<sup>7,11</sup> (2) Subgrain formation is the result of the incomplete development of slip bands and is dependent not only on the constitution of the material but also on its crystalline structure and on the creep conditions.

A small part of the strain created by slip along an incompletely developed slip band may be stored as elastic strain in the crystal lattice, but most of it must be relieved by plastic deformation in various slip systems. The existence of an incompletely developed slip band implies that the resistance to slip along the slip plane in which it occurs is not everywhere the same. If the resistance to slip were the same throughout the slip plane, the slip band would have developed fully all across the cross-section of the single crystal.

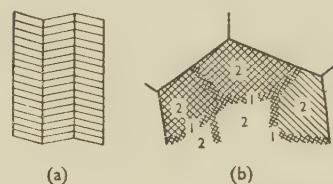


FIG. 5.—Two Types of Subgrain Classified According to the Manner of Their Formation.

- (a) By kinking bands—sharp boundaries.  
 (b) By deformation bands—relatively broad boundaries.  
 (1) Deformation bands. (2) Subgrains.

The places of higher resistance to slip may be the locations of inclusions and mosaic boundaries. When a single crystal is subjected to deformation at high rates of strain in creep or in a conventional tensile test, the high applied stress makes the difference in resistance to slip between the less highly oriented areas and the more perfect ones on the slip planes negligible. Consequently, the slip bands developed under high stress are regular, and in most cases run all the way across the specimen. When, on the other hand, a single crystal is subjected to creep at low strain rates and high temperatures, the difference in resistance to slip at various positions becomes so important that the strains created at the tip of the incompletely developed slip band must be relieved by other slip systems. The operation of different slip systems gives rise to orientation differences, and these result in the formation of subgrains.

Two types of subgrain were observed. The first type is delineated by sharp kinking boundaries which are revealed by electrolytic etching after repolishing. This type of subgrain is formed by kinking bands, and is shown schematically in Fig. 5 (a) (see also Figs. 18–20, grain *E*).

The second type of subgrain is shown schematically in Fig. 5 (b). Owing to the restricting effects of

grain boundaries, extremely inhomogeneous deformation results in localized regions of a grain. This initiates deformation in adjacent regions of the grain by different systems of cross slip. It follows that the amount and direction of rotation in these regions will differ. When the cross slip is restricted to a narrow band, as in region (1) in Fig. 5 (b), this region may properly be termed a deformation band. The regions delineated by these bands, regions (2) in Fig. 5 (b), may have been deformed either by cross slip or by single slip, or have remained practically undeformed. The boundary between regions (1) and (2) is a subgrain boundary and delineates subgrains of the second type. An illustration of the relative areas occupied by the subgrains and the boundaries is shown in Fig. 24 (Plate XXXVIII).

Since cross slip in one region cannot end abruptly at the junction with another region, the change in orientation across the boundaries is not as sharp as that across kinking-band boundaries. It is probably owing to this that subgrains of the second type are not delineated by electrolytic etching after polishing.

The X-ray data show that the grains in which the first type of subgrain is formed (by kinking band) exhibit preferentially broken-down Laue spots (Fig. 23), whereas the grains in which the second type is formed exhibit randomly broken-down Laue spots (Fig. 22). These observations are to be expected from the manner in which these two types of subgrain are formed. It was found by Chen and Mathewson<sup>8</sup> that the orientation relationship across a kinking boundary (Fig. 5 (a)) can be described by a simple rotation about a certain crystallographic axis. When several slip systems operate in various regions of the grain (Fig. 5 (b)) it is obvious that no simple crystallographic relationship can be expected to exist among the subgrains. It was proposed<sup>9</sup> that the collection of edge-type dislocations is responsible for the formation of kinking boundaries, and the simple crystallographic relationship across this kind of boundary can be so explained. Since such a relationship does not exist across the boundaries of the second type of subgrain, the nature of the deformation-band boundaries, and also the orientation relationships of the regions separated by these boundaries, would be expected to be more complicated than in the first type. In polycrystalline materials, as a result of the large range of orientation of the grains and the restriction caused by the grain boundaries, both types of subgrain are formed not only in the same specimen but also in the same grain.

## 2. BEHAVIOUR OF A HEAVY SLIP BAND

It has been shown that the component creep curve obtained across a heavy slip band developing through a single crystal exhibits a continuous increase in creep rate (curve I, Fig. 3 and band I, Fig. 1). This phenomenon may arise from the particular geometry of the crystal studied, in which the grain orientation and length are such that a heavy slip band, such as I

(Fig. 1), is the only slip band which can go through the crystal without encountering any grain boundaries. After a relatively long initial period during which the elongation across band I is small, the deformation rate increases sharply. If the grain containing slip band I had been longer in the axial direction, several unhindered slip bands might have been accommodated. In this event the component creep curve might not have shown the continuous increase in creep rate directly to fracture. It appears that during the initial period of low creep rate the number of slip nuclei<sup>10</sup> (dislocations and Frank-Read sources), which are set free to operate by stress and thermal agitation to initiate slip along the lamellae constituting the wide band, increases with time. The later stages of the component creep curve indicate that the ability of the material in the slip band to impede the motion of dislocations or to stop the operation of Frank-Read sources does not increase with strain. This is probably due to the fact that the dislocations or the dislocation loops generated by Frank-Read sources move out of the interior of the specimen to its surface, since this heavy slip band was developed in a single crystal.

In contrast to the shape of the component creep curve across the heavy slip band I, a periodic behaviour is shown by the component creep curve II (Fig. 3), obtained across the heavy slip band II (Fig. 1), in the path of which there is a grain boundary. The initial portion of curve II is similar to curve I; apparently during this initial period the same processes occur as have been proposed to account for the form of curve I. However, after this initial period of increasing creep rate, as a result of the obstruction by the grain boundary, the sources which initiate slip cease to operate, and the products resulting from their operation accumulate in the new and very unstable segment of the grain boundary between grains *P* and *K* (Fig. 7); this gives rise to a period of decreasing creep rate. During this period, the grain-boundary offset—and therefore the resistance to the operation of the sources—is removed by a recovery process such as boundary migration, thereby permitting another period of increasing creep rate to set in. From the shape of curve II (Fig. 3), it can further be deduced that the rate of accumulation of dislocations in the grain-boundary offset and in the slip band near the obstructing grain boundary is fast, while the removal of these accumulated dislocations is slow.

Though curve II (Fig. 3) was obtained with a specimen which was subjected to creep at a very high temperature (1100° F.), the periodic behaviour of a component creep curve obtained across a slip band may be expected to be a general phenomenon in both high- and low-temperature creep. The period and the amplitude of each cycle can be expected to depend on the orientation relationships of the grains, and on the stress and temperature of testing.

It should be remembered that the component creep curve obtained across a grain boundary also exhibits a periodic behaviour.<sup>1</sup> A satisfactory grain-boundary model is needed to determine whether the process of



boundary sliding and migration, and the process of slip as affected by a grain boundary, differ fundamentally or only in degree.

### V.—CONCLUSIONS

On the basis of a study of creep of very coarse-grained high-purity aluminium at 400°, 700°, and 1100° F., and at an initial stress range of 50–1200 lb./in.<sup>2</sup>, the following conclusions can be drawn:

(1) Slip is the fundamental mechanism of deformation for both single-crystal and polycrystalline specimens, even in high-temperature creep.

(2) Component creep curves obtained across slip bands affected by grain boundaries show a periodic behaviour. This behaviour is found to be associated

with the disregistry regions created in the grains across the grain boundary as a result of slip.

(3) Subgrains are shown to be the result of grain-boundary restriction on the normal development of slip bands and non-homogeneous resistance to slip in the grains.

(4) Two types of subgrain were observed. On the basis of metallographic and X-ray data, the formation of these types of subgrain is associated respectively with kinking bands and deformation bands.

### ACKNOWLEDGEMENTS

The authors wish to express their appreciation to Professor J. T. Norton, Dr. A. R. Chaudhuri, and Mrs. Gloria Johnson, all of whom contributed significantly to this research. Thanks are also due to the U.S. Bureau of Ships for sponsoring the research.

### REFERENCES

1. H. C. Chang and N. J. Grant, *Trans. Amer. Inst. Min. Met. Eng.*, 1952, **194**, 619.
2. H. C. Chang and N. J. Grant, *ibid.*, 1953, **197**, 305.
3. G. R. Wilms and W. A. Wood, *J. Inst. Metals*, 1948–49, **75**, 693.
4. W. A. Wood and W. A. Rachinger, *ibid.*, 1949–50, **76**, 237.
5. G. Wyon and C. Crussard, *Rev. Mét.*, 1951, **48**, 121.
6. R. W. Cahn, *J. Inst. Metals*, 1951, **79**, 129.
7. I. S. Servi, J. T. Norton, and N. J. Grant, *Trans. Amer. Inst. Min. Met. Eng.*, 1952, **194**, 965.
8. N. K. Chen and C. H. Mathewson, *ibid.*, 1951, **191**, 653.
9. E. Orowan, *Nature*, 1942, **149**, 643.
10. J. G. Leschen, R. P. Carreker, and J. H. Hollomon, *Trans. Amer. Inst. Min. Met. Eng.*, 1949, **180**, 131.
11. I. S. Servi and N. J. Grant, *ibid.*, 1951, **191**, 917.
12. H. C. Chang and N. J. Grant, *ibid.*, 1953, **197**, 1175.

# 1518 AGEING CURVES AT 110° C. ON BINARY AND TERNARY ALUMINIUM-COPPER ALLOYS \*

By H. K. HARDY,† M.Sc., Ph.D., A.R.S.M., A.I.M., MEMBER

## SYNOPSIS

Binary aluminium alloys containing 2.5–4.5% copper gave two-stage hardness/ageing-time curves separated by a flat plateau. The incubation values supported the conclusion that the reciprocal-rate curves take the form of two C-curves overlapping in the region 150°–170° C. The inflected form of the peak-hardness/composition relationship was confirmed. The ternary alloys with 0.05% tin or indium gave weak indications of two-stage ageing curves but reached their peak hardness after much shorter ageing times.

## I.—INTRODUCTION

PREVIOUS work<sup>1</sup> had shown that binary aluminium alloys containing 3.5–4.5% copper, aged at 130° C., gave two-stage ageing curves separated by a flat plateau, and that the time to attain peak hardness was almost independent of the copper content. Except for a rather sharp change of slope, the ternary alloys with 4% copper and 0.05% tin or indium gave little indication of a two-stage ageing curve at 130° C. However, they reached their peak-hardness values after much shorter ageing times—about 6–9 days compared with 45–50 days for the binary alloys.<sup>2</sup>

As a further step it was desired to determine whether the binary alloys would also give a flat plateau when aged at a lower temperature and whether the time to reach peak hardness would again be independent of the copper content. Ageing of the ternary alloys at a lower temperature was also undertaken to discover whether they would then show an increased tendency to a two-stage ageing curve. The ageing temperature chosen, namely 110° C., represented the lowest temperature below 130° C. likely to give results in less than three years. Results are also included for the aluminium–2.5% copper alloy aged at 130° C., as this had been omitted from the earlier work.

## II.—EXPERIMENTAL METHODS

As described previously<sup>1,2</sup> alloys of the highest available purity were water-chill-cast to 1½ in.-dia. ingots, scalped, annealed, cold forged to 0.52 in. square, annealed, flattened to 0.22 in. thick and 1–1½ in. wide, scalped, stamped for identification, and cut for hardness specimens. These were prepared as far as possible before heat-treatment. The initial solution-treatment was for not less than 48 hr. in a salt bath at 520° C. (530° C. for the 4.5% copper alloy), followed by quenching in water at 20° C. and immediate ageing in a circulating-air furnace with a close control. In plotting the results, 5 min. were allowed

for the time for the specimens to heat to within 2° C. of the furnace temperature. The hardness/ageing curves are given in Figs. 1 and 2, the former also including the results for the binary aluminium–2.5% copper alloy aged at 130° C.

## III.—DISCUSSION OF RESULTS

The binary alloys with 2.5–4.5% copper showed two stages in the ageing process, separated by a flat plateau. Only single-stage ageing curves were observed for the aluminium–2.0% copper alloy aged at 110° C. and the aluminium–2.5% copper alloy aged at 130° C. Plotting the peak-hardness values against composition (see Fig. 3) showed that the alloys with 2.5–4.5% copper fell into the upper group, whilst the aluminium–2.0% copper alloy aged at 110° C. and the aluminium–2.5% copper alloy aged at 130° C. were intermediate between the upper and lower groups previously established for such alloys. The inflected form of the relationship between peak hardness and composition<sup>1</sup> has thus been amply confirmed. The upper group of peak-hardness values at 130° C. was associated<sup>3</sup> with a structure containing G.P. zones [2] and a little  $\theta'$ .

The time to attain peak hardness was not completely independent of copper content, but lengthened by a factor of 1.6 over the range 4.5–3.0% copper, compared with a factor of 4.0 at 190° C. When the time to reach peak hardness was plotted against the reciprocal of the absolute temperature (as in Fig. 19, p. 339, ref. 1), it was found that the peak hardness of the 2.0% copper alloy at 110° C. occurred at a shorter time than would have been predicted by extrapolation from the results at higher ageing temperatures. The incubation values, plotted in Fig. 4, satisfactorily confirm the existence of two branches to the reciprocal-rate curve, crossing at 140° C. (2.5% copper) to 170° C. (4.0% copper). The lower branch is associated with the formation of G.P. (Guinier–Preston) zones [1] from the matrix and the upper branch with the forma-

\* Manuscript received 20 August 1953.

† Senior Metallurgist, Fulmer Research Institute, Ltd., Stoke Poges, Bucks.



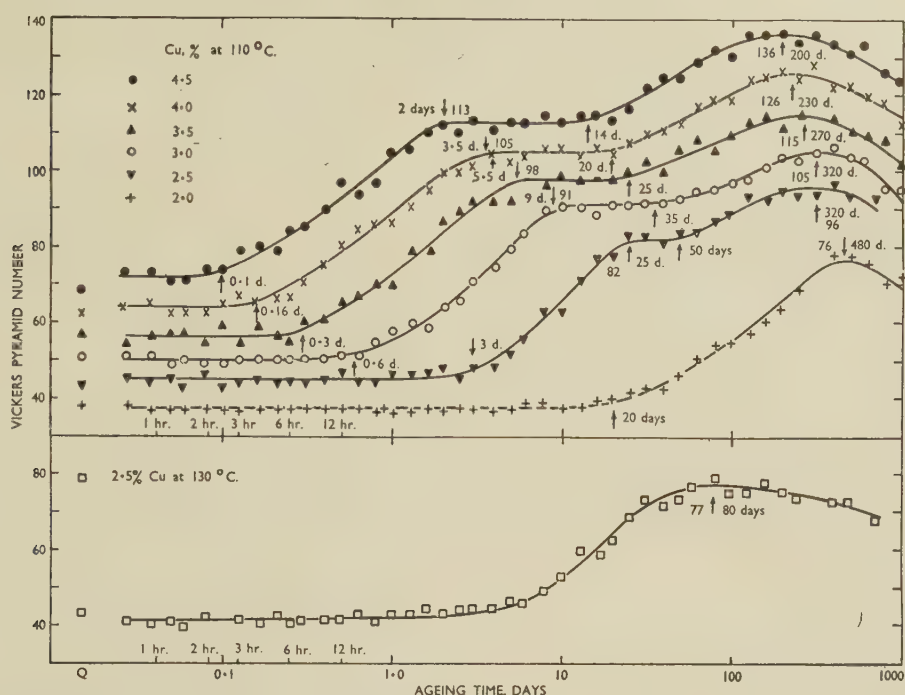


FIG. 1.—Hardness Curves for Binary Aluminium Alloys Containing the Percentages of Copper Shown, Aged at 110° C., and for an Aluminium-2.5% Copper Alloy Aged at 130° C. Up to 200 days each point represents the average of five impressions on each of two specimens; beyond 200 days each point represents the average of five impressions on single specimens.

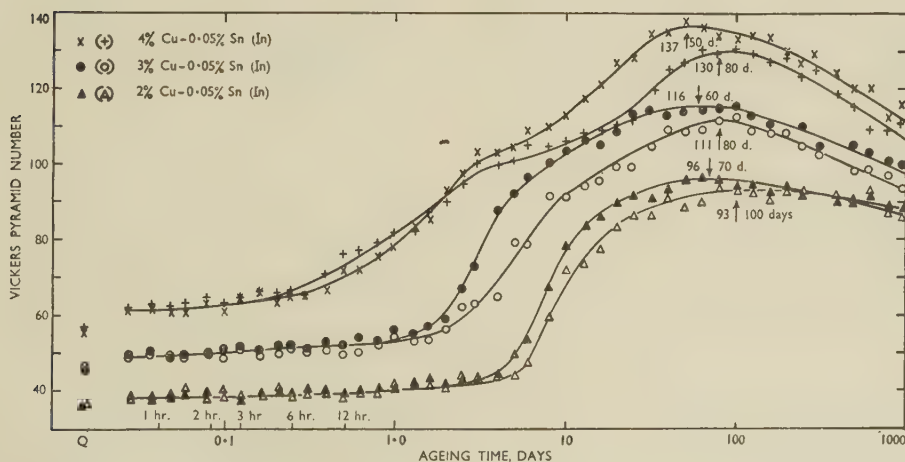


FIG. 2.—Hardness Curves for Ternary Aluminium Alloys Containing the Percentages of Copper and of Tin (or Indium) Shown, Aged at 110° C. Up to 200 days each point represents the average of five impressions on each of two specimens; beyond 200 days each point represents the average of five impressions on single specimens.

tion of  $\theta'$  directly from the matrix. A third C curve may also be included for the formation of G.P. zones [2] directly from the matrix in the case of the 4.5% copper alloy aged at 190° C., but the effect is less marked on the curves for the 4.0% copper alloy.<sup>1, 3</sup>

The ternary alloys with 2.0% copper showed single-stage ageing curves (see Fig. 2). The alloys with 3.0% copper again gave single-stage ageing curves, although they showed a rather abrupt change of slope after about half the hardening, which was identical in appearance with the results on the ternary aluminium-4.0% copper alloys aged at 130° C.<sup>2</sup> A much more marked inflection was found for the 4.0% copper alloys with 0.05% tin or indium, aged at 110° C.,

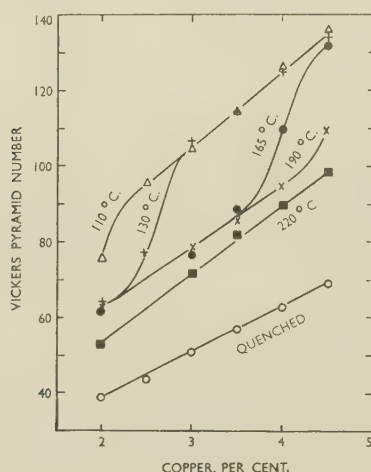


FIG. 3.—Quenched and Peak-Hardness Values for Binary Aluminium-Copper Alloys Aged at Temperatures Indicated.

which gave a similar general impression to that of the aluminium-4.0% copper-0.01% tin or indium alloys aged at 130° C.<sup>2</sup> The time to attain peak hardness was again much shorter in the ternary than in the

corresponding binary alloys and showed a tendency to become independent of copper content. The weak two-stage ageing curves confirm that the additional

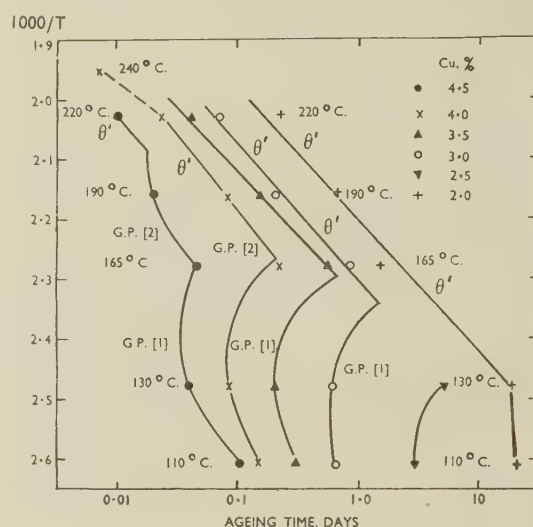


FIG. 4.—Temperature/Incubation-Value Relationships for Binary Aluminium Alloys Containing the Percentages of Copper Shown, with the Decomposition Products First Detected by X-Ray Investigation.<sup>3</sup>

elements do not completely suppress the G.P. zones [1], although the speeding up of the ageing process shows that the ternary elements are still effective at the lower temperature.

#### REFERENCES

1. H. K. Hardy, *J. Inst. Metals*, 1951, **79**, 321.
2. H. K. Hardy, *ibid.*, 1951-52, **80**, 483.
3. J. M. Silcock, T. J. Heal, and H. K. Hardy, *ibid.*, 1953-54, **82**, (6), 239.



# STRUCTURAL AGEING CHARACTERISTICS OF BINARY ALUMINIUM-COPPER ALLOYS \*

1519

By (Miss) J. M. SILCOCK,† B.Sc., T. J. HEAL,‡ B.Sc., F.Inst.P.,  
and H. K. HARDY,§ M.Sc., Ph.D., A.R.S.M., A.I.M., MEMBER

## SYNOPSIS

A systematic X-ray study has been made of the structures formed during the ageing of aluminium-copper alloys over a wide range of supersaturation. The specimens examined included single crystals taken from the polycrystalline hardness specimens used by Hardy (*J. Inst. Metals*, 1951, 79, 321) when obtaining the ageing curves of the alloys. The structures pass through the sequence: G.P. zones [1]  $\rightarrow$  G.P. zones [2] (Guinier's  $\theta'$ )  $\rightarrow$   $\theta' \rightarrow \theta$ , and each of these may in turn be found as the initial decomposition product as the degree of supersaturation diminishes. G.P. zones [1] are responsible for the initial rise in hardness and do not change in size along the "flat plateaux" of the ageing curves. The higher group of peak-hardness values is due chiefly to the presence of the G.P. [2] structure, although a small quantity of  $\theta'$  is also present. The lower group of peak-hardness values is attributable to a structure containing only the  $\theta'$  precipitate. The neat manner in which the X-ray structural data can be correlated with the ageing curves must not obscure the fact that the preferred modes of formation and some of the structural details of the precipitates are still unknown.

## I.—INTRODUCTION

THE sequence of structures occurring in binary aluminium-copper alloys during age-hardening, namely: G.P. [1]  $\rightarrow$  G.P. [2]  $\rightarrow$   $\theta' \rightarrow \theta$ , has been investigated by X-ray methods by Preston<sup>1-3</sup> (4% copper) and by Guinier<sup>4-8</sup> (4 and 5% copper), and their findings are described later. However, no serious attempt has hitherto been made to correlate the structural changes with the hardness/ageing curves on the same alloys, apart from some work, chiefly metallographic, by Gayler.<sup>9</sup>

The present investigation was planned in conjunction with the hardness/ageing curves already reported by Hardy,<sup>10, 11</sup> who found that: (i) hardening occurred in two stages separated by a flat plateau of constant hardness at low ageing temperatures (110° and 130° C.) and high degrees of supersaturation; (ii) single-stage ageing curves were obtained at lower degrees of supersaturation; (iii) the incubation values plotted against temperature gave a family of C-curves; and (iv) the peak-hardness values plotted against composition fell into two distinct groups, the higher of which was associated with the two-stage ageing curves and the lower with the single-stage ageing curves. The principal object of the work now undertaken has been to explore the relationship between the ageing curves and the pattern of the decomposition products over a wide range of supersaturation. Particular importance has been attached to the use of suitable single crystals located in the original polycrystalline hardness specimens.

## II.—EXPERIMENTAL TECHNIQUES

### 1. MATERIALS AND PREPARATION OF SINGLE CRYSTALS

As in the case of the previous work by Hardy,<sup>10, 11</sup> materials of the highest available purity were used to prepare alloys containing 2, 3, 4, and 4.5% copper, whose melt analyses were all satisfactorily close ( $\pm 0.1\%$ ) to the nominal. Billets of  $1\frac{1}{4}$  in. dia. were water-chill cast, scalped to 1.1 in. dia., and used to prepare 1-mm.-dia. wire for the Laue X-ray work and 0.5-mm. strip for the oscillation X-ray work.

Convenient lengths of wire and strip were annealed, strained 2%, slowly heated and held for 48 hr. at 520°–530° C. to produce large-grained material. Short lengths of wire containing crystals 3 mm. or more in length were mounted in aluminium holders and oriented by the back-reflection Laue method due to Greninger.<sup>12</sup> The large-grained sheet specimens were etched and their transmission Laue patterns examined visually on a fluorescent screen. Crystals of suitable orientation were removed from the sheet by exposing the region surrounding them to a mixed-acid reagent.

### 2. HEAT-TREATMENT

The crystals selected were re-solution-treated at 520°–530° C. for 16 hr., quenched, and aged in circulating-air furnaces in the same way as the hardness specimens. The time between quenching and placing in the furnace did not exceed 5 min. The single

\* Manuscript received 20 August 1953.

† Research Metallurgist; ‡ Head of Physics Section;

§ Senior Metallurgist, Fulmer Research Institute, Ltd., Stoke Poges, Bucks.

crystals were used repeatedly with 16-hr. solution-treatments between successive ageing treatments.

The aluminium holders for the wire specimens fitted into the goniometer head, and once a crystal was oriented it could be removed for heat-treatment and then replaced in the goniometer in the required orientation. The sheet specimens were re-oriented after each treatment with the aid of a fluorescent screen.

### 3. X-RAY METHODS

The X-ray techniques suitable for the examination of age-hardening systems have been discussed by Hardy and Heal,<sup>13</sup> who concluded that monochromatic single-crystal methods were essential for a proper understanding of the structural changes. Emphasis was placed on the value of the small-angle scatter method for deciding the shape and size of the precipitates within a suitable size range. The Laue method was recommended for a rapid survey of systems in which the sequence of structural changes had been established by monochromatic means.

#### (a) Monochromatic Oscillation Method

Oscillating-crystal films were taken with  $\text{Mo K}\alpha$  radiation obtained from a Guinier focusing monochromator. Good pictures required a sharp focus in the X-ray tube, and the restriction of the diffuse scattered radiation by three sets of adjustable horizontal and vertical slits. The aged sheet specimens were held in a two-circle goniometer and oriented visually as described above. A  $[100]_{\text{Al}}$  axis was arranged vertically and a  $[010]_{\text{Al}}$  axis parallel to the beam. The crystals were transferred to a Unicam single-crystal structure camera of 3 cm. radius and oscillated around the vertical  $[100]_{\text{Al}}$  axis so that the  $[010]_{\text{Al}}$  axis described an angle of  $0^\circ$ – $15^\circ$  to the X-ray beam. The exposure was 20 m.amp.-hr. at 40 kVp. In addition to the  $\text{Mo K}\alpha$  radiation, the half-wave harmonic ( $\lambda/2$ ) was also diffracted by the monochromator. The spots due to the  $\lambda/2$  radiation were identified by their enhanced relative intensity on a second film placed immediately behind the first, but separated from it by copper foil, which preferentially absorbed the  $\lambda$  radiation. A typical photograph with the  $(002)_{\text{Al}}$  matrix spot indexed is shown in Fig. 1 (Plate XXXIX). The faint streaks running at  $45^\circ$  to the vertical are due to thermal scattering.

#### (b) Small-Angle Scatter Method

The films were taken with  $\text{Cu K}\alpha$  radiation, using a Guinier monochromator and slit systems, as in the oscillation method. The diffraction pattern was recorded on a flat-plate camera, 4.5 cm. from the specimen, the latter being a sheet crystal thinned by etching to  $0.01 \pm 0.002$  cm. thick. A typical film is shown in Fig. 13 (Plate XLI). The method was suitable for examination of the G.P. zones [1] and [2] up to a diameter of 500 Å. The  $\theta'$  platelets were always too large.

#### (c) Laue Method

The single-crystal wire specimens were examined with a  $[100]_{\text{Al}}$  axis parallel to the X-ray beam. Satisfactory films were given by  $\text{Cu}$  radiation with exposures of 30 m.amp.-hr. at 40 kVp., using a lead-glass collimator 6 cm. in length and of 0.65 mm. bore. A typical photograph, with some of the aluminium reflections indexed, is shown in Fig. 14 (Plate XLI).

### 4. SINGLE CRYSTALS IN THE HARDNESS SPECIMENS

The major proportion of the X-ray work was carried out on sheet or rod specimens of dimensions very different from those of Hardy's hardness specimens, which were about 0.16-in. thick. Since the intensity of the quenching strains is known to influence the ageing behaviour, it was regarded as essential to supplement this examination by a further study of crystals obtained from the hardness specimens. This was feasible only where the hardness specimen had fairly large grains on the same surface as that on which the hardness impressions were made. Suitable specimens were sectioned, ground, and electropolished. The Laue method was employed because of the difficulty in applying the monochromatic technique.

### III.—THE STRUCTURE OF THE PRECIPITATES

Before describing the pattern of the decomposition products in relation to the ageing curves, it is necessary to define the structures which they possess. Hardy and Heal<sup>13</sup> have recently discussed the previous X-ray work in some detail and have accepted the sequence obtained by Guinier,<sup>6, 7</sup> namely:



The structural changes are not necessarily allotropic, and two (or more) structures may occur simultaneously in the same specimen.

#### 1. G.P. ZONES [1]

*Previous Work.*—According to Guinier<sup>4</sup> and Preston,<sup>1</sup> the first detectable change in the supersaturated solution during ageing is the formation of Guinier-Preston zones, which consist of copper-rich regions of plate-like shape formed on  $\{100\}$  planes of the aluminium matrix. The net effect of the regrouping is to modify the scattering power of, and spacing between, very small groups of  $\{100\}_{\text{Al}}$  planes throughout the crystals. Owing to their limited thickness, the zones produce the diffraction effects typical of a two-dimensional lattice, e.g. streaks on the diffraction patterns which extend from an aluminium diffraction along  $\langle 100 \rangle_{\text{Al}}$  directions towards the higher indices only. Guinier and Preston have estimated that the zones are a few atomic planes thick and attribute the asymmetry of the streaks to a contraction of the  $(100)_{\text{Al}}$  interplanar spacing. Jagodzinski and Laves<sup>14</sup> have recently claimed to have detected streaks in  $\langle 111 \rangle_{\text{Al}}$  directions.

*Present Work.*—The results of Guinier and Preston have been confirmed. Streaks on the films running



in  $\langle 100 \rangle_{\text{Al}}$  directions are obtained in the early stages of ageing. These streaks represent relrods\* in  $\langle 100 \rangle_{\text{Al}}$  directions in the relplot.\* The streaks obtained on an oscillation picture can be seen in Fig. 1 (Plate XXXIX). The most prominent are those extending from (000) towards  $(002)_{\text{Al}}$ , and vertically from  $(002)_{\text{Al}}$  towards  $(202)_{\text{Al}}$  and  $(\bar{2}02)_{\text{Al}}$ . (The horizontal streak from (000) towards  $(002)_{\text{Al}}$  appears to show an intensity maxima, but this is due to the presence of the  $(002)_{\text{Al}}$   $\lambda/2$  spot.) Fig. 14 (Plate XLI) shows a Laue pattern with streaks running from  $(311)_{\text{Al}}$  towards  $(511)_{\text{Al}}$  and  $(3\bar{3}1)_{\text{Al}}$ . There are also radial streaks towards the  $(301)_{\text{Al}}$  and  $(3\bar{3}1)_{\text{Al}}$  spots. Efforts were made to confirm the claim of Jagodzinski and Laves<sup>14</sup> that streaks existed in  $\langle 111 \rangle_{\text{Al}}$  directions, but none were detected. In some cases such streaks would have been coincident with thermal-scattering streaks.

## 2. G.P. ZONES [2] (or $\theta'$ )

*Previous Work.*—This structure was first detected by Guinier,<sup>6</sup> who reported that the streaks due to G.P. [1] developed intensity maxima. He used the term *surstructure* (later  $\theta'$ ) because he considered that the structure was composed of an ordered arrangement of copper and aluminium atoms within the matrix structure. Guinier<sup>7</sup> first reported the G.P. [2] structure as tetragonal, with  $a = 4.04$  and  $c = 7.7$  Å. The  $c$  value was later<sup>8</sup> changed to 7.9 Å. The structure postulated layers of atoms of the same pattern as the  $\{100\}_{\text{Al}}$  planes of the matrix, but spaced 2.0 : 1.9 : 1.9 : 2.0 Å. apart. The central plane consisted of 100% copper atoms, the next two planes were a mixture of copper and aluminium, and the two basal planes were pure aluminium, giving an overall composition of  $\text{CuAl}_2$ . In Guinier's view the G.P. [2] platelets are coherent with the matrix on their  $\{100\}_{\text{Al}}$  habit planes and are also coherent in the perpendicular  $\langle 100 \rangle_{\text{Al}}$  directions, where there is only a 4% lack of fit. Guinier has obtained sharp G.P. [2] spots corresponding to a platelet thickness of at least 250 Å.

*Present Work.*—The intensity maxima formed in the streaks are visible in Figs. 2–9 (Plates XXXIX and XL), and in Figs. 15 and 16 (Plate XLI). The oscillation films, Figs. 2–6 (Plate XXXIX), show the development of the breaking-up of the streak from (000) to  $(002)_{\text{Al}}$  into three spots whose intensity decreases from the centre outwards. These spots could be given the approximate indices  $(00\frac{1}{2})$ ,  $(001)$ , and  $(00\frac{3}{2})$  with respect to the aluminium lattice. In Fig. 9 (Plate XL), all three spots are indicated. They are slightly displaced towards higher angles. For example, Fig. 6 shows that the central G.P. [2] spot (marked with an arrow) does not exactly overlap the  $\lambda/2$   $(002)_{\text{Al}}$  spot in the  $(001)_{\text{Al}}$  position. In the Laue films the streaks between  $(311)_{\text{Al}}$  and  $(511)_{\text{Al}}$  and between  $(311)_{\text{Al}}$  and  $(3\bar{3}1)_{\text{Al}}$ , (Fig. 14,

Plate XLI), have split into rather long spots (Fig. 15), and into sharper spots (Fig. 16).

All G.P. [2] spots correspond approximately to indices  $(hkl)$  of the aluminium matrix, where  $h + k = 2n$  and  $l = m/2$ . The maxima sharpen during the ageing process and their position alters slightly at 130° C., the  $c$  value changing from 8.0 to 7.6 Å. (see Table I). The  $c$  parameter is constant at 7.6 Å. in alloys aged at 190° C.

TABLE I.—G.P. [2] Parameters in the Aluminium-4% Copper Alloy.

Quenching Medium	Ageing Time	Ageing Temp., °C.	$c$ Parameter, Å., $\pm 0.07$	Remarks
Air	3 days	130	8.08	Very broad maxima
Oil	11 "		7.90	Broad maxima
Water	11 "		7.80	" "
Oil	48 "		7.64	" "
Water	48 "		7.68	" "
Water	1 day	165	7.73	" "
Water	7½ hr.	190	7.66	Fairly broad maxima
"	1 day		7.68	" "
Oil	1 "		7.55	" "

The maximum thickness of the G.P. [2] platelets is of the order of 100 Å., the maximum diameter 1500 Å. Spots as sharp as those recorded by Guinier on ageing at 150° C. have not been obtained.

## 3. THE $\theta'$ STRUCTURE

*Previous Work.*—The structure of  $\theta'$  was investigated by Wassermann and Weerts,<sup>15</sup> using Weissenberg and rotation photographs, and later by Preston,<sup>3</sup> using the oscillation and Laue methods. The German authors established that the unit cell was tetragonal with  $a = 8.2$  and  $c = 11.6$  Å. This large cell was necessary to explain two spots indexed as (550) and (2,5,10); otherwise parameters of half the given values could have been taken. The cell axes were parallel to  $\langle 100 \rangle_{\text{Al}}$  directions. Preston found the unit cell to be tetragonal with  $a = 5.7$  and  $c = 5.8$  Å., and the orientation relationship  $[100]_{\theta'} \parallel [110]_{\text{Al}}$  and  $[001]_{\theta'} \parallel [001]_{\text{Al}}$  resulted in three orientations of  $\theta'$  with respect to the matrix. The atomic arrangement was that of a slightly distorted  $\text{CaF}_2$  structure.

Fink and Smith<sup>16</sup> showed that Preston's atomic arrangement could be fitted to the larger unit cell of the German authors, and concluded that the structures were identical. They ignored the evidence of the (550) and (2,5,10) spots obtained by Wassermann and Weerts.

Guinier<sup>6</sup> indexed his films on Preston's structure and confirmed the orientation relationship. He noted that Preston's structure did not entirely explain his experimental findings. Thus, diffraction spots for  $h + k + l = 4n + 2$  had about 30 times the

\* For convenience and brevity all such terms as "reciprocal lattice point", "reciprocal lattice rod", &c., have been replaced by "relpoint",<sup>13</sup> "relrod", "relplane", "relplot", &c.

calculated intensity, and an extra spot corresponding to  $\theta'$  planes of spacing  $10.1 \pm 0.5$  Å. was recorded. Guinier associated the appearance and variation in intensity of his  $10.1$  Å. spot with that of  $(002)_{\theta'}$ ; the latter was initially stronger than  $(004)_{\theta'}$ , but the intensity relationship was later reversed.

Guinier<sup>17</sup> has given figures for the percentage of the total possible quantity of  $\theta'$  and of G.P. [2] at different ageing times at temperatures of  $150^\circ$ ,  $180^\circ$ , and  $190^\circ$  C. for a 4% copper alloy.

**Present Work.**—The results obtained are very similar to those of Guinier. An unsuccessful search has been made for the  $(550)$  and  $(2,5,10)$  diffractions recorded by Wassermann and Weerts.<sup>15</sup> The parameters of the true unit cell are therefore  $a = 4.04$ ,  $c = 5.8$  Å., and the axes are parallel to  $\langle 100 \rangle_{\text{Al}}$  directions. To

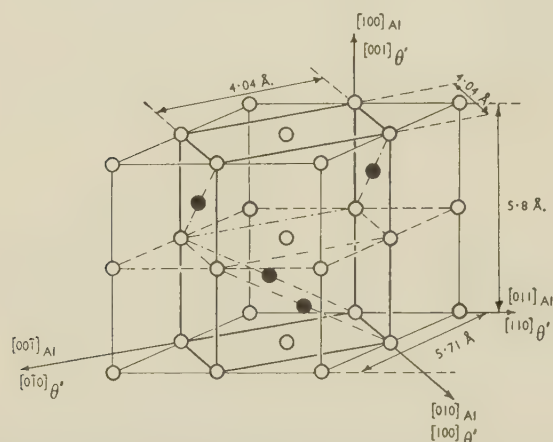


FIG. 19.—Preston's  $\theta'$  Structure, with the Unit Cells Chosen by Preston and the Present Authors Outlined.

○ Al atoms. ● Cu atoms.  
 Preston's unit cell . . . . .  $a = 5.71$  Å.,  $c = 5.8$  Å. ———  
 True unit cell . . . . .  $a = 4.04$  Å.,  $c = 5.8$  Å. - - - - -  
 $(012)_{\theta'}$  and  $(\bar{1}02)_{\theta'}$  planes on which the copper atoms lie - - - - -

The "b" orientation of  $\theta'$  is illustrated. Directions and indices refer to the true cell.

facilitate comparison with the work of Preston and of Guinier, the indices of the  $\theta'$  spots will be given for both unit cells, e.g.  $(111)_{\theta'^P}$ ,  $(101)_{\theta'^T}$ , where they differ.\* Fig. 19 shows Preston's  $\theta'$  structure with the unit cells chosen by Preston and by the present authors outlined.

The two planes  $(\bar{1}\bar{1}2)_{\theta'^P}$ ,  $(\bar{1}02)_{\theta'^T}$ , and  $(\bar{1}12)_{\theta'^P}$ ,  $(012)_{\theta'^T}$ , on which the copper atoms lie, have been shown as dashed-and-dotted lines. The three orientations of  $\theta'$  have been termed  $a$ ,  $b$ , and  $c$ , and the matrix directions in Fig. 19 are with respect to the  $b$  orientation of the true unit cell. The class of diffractions of anomalously high intensities defined by  $h + k + l = 4n \pm 2$  on Preston's unit cell are now defined by the condition that  $2h + l$  and  $2k + l$  must be equal to  $4n \pm 2$ .

In Figs. 10 and 11 (Plate XL) and in Figs. 17 and

18 (Plate XLI) only  $\theta'$  and aluminium matrix spots can be seen. Some of the spots (marked with arrows in Figs. 5 and 17) were elongated or broadened when the  $\theta'$  platelets were thin. (Compare  $b$  and  $c$  orientation  $(111)_{\theta'^P}$ ,  $(101)_{\theta'^T}$ , spots in Fig. 5, Plate XXXIX.) In the Laue photographs, the strongest  $\theta'$  spots lie on ellipses coinciding with those of  $[100]$  zones of the aluminium matrix. Their close coincidence to the G.P. [2] spots (see Fig. 16, Plate XLI) makes the detection of a small quantity of  $\theta'$  difficult by this technique. In the oscillation photographs, strong  $\theta'$  spots occur in entirely new positions and a small quantity of  $\theta'$  can readily be detected. Figs. 4, 5, and 6 (Plate XXXIX) show  $\theta'$  spots of increasing intensity. Fig. 15 (Plate XLI) is a Laue photograph of the same specimen as Fig. 4.

The  $(h + k + l = 4n + 2)^P$  diffractions were found to have an intensity ten times the calculated value. An example is the  $(002)_{\theta'}$  marked with an arrow in Fig. 11 (Plate XL). An extra spot was also obtained at a position corresponding to a spacing of  $10.4 \pm 0.3$  Å. (Fig. 10, Plate XL). The spot frequently occurred even after long ageing times, although a number of the films showed well-developed  $\theta'$ , including the  $(002)_{\theta'}$  and other additional  $4n \pm 2$  spots, without this additional diffraction. The  $(002)_{\theta'}$  spots were always less intense than the  $(004)_{\theta'}$  spots.

Preston<sup>3</sup> had noted the existence of short streaks linking  $\theta'$  and matrix spots on his Laue photographs of well-developed  $\theta'$ . The effect is shown in Fig. 17 (Plate XLI). A faint vertical line was present through the  $(002)_{\text{Al}}$  reflection on the oscillation films (see Fig. 11). The experience can be generalized by stating that reldods<sup>13</sup> occur through  $\theta'$  reldoints<sup>13</sup> in the  $[001]_{\theta'}$  direction, i.e. towards both matrix and other  $\theta'$  points. These are probably attributable to some irregularity in the  $(001)$  planes of the  $\theta'$  lattice due to coherency strains.

Bagaryatsky's<sup>18</sup> claim that one-dimensional diffraction effects are visible at the beginning of the formation of  $\theta'$  has not been confirmed. His observation of a ring on the Laue photographs can be reproduced by diffraction of the white radiation from two-dimensional regions.

#### 4. THE $\theta$ STRUCTURE

The structure is tetragonal, with  $a = 6.066$  and  $c = 4.874$  Å.<sup>19</sup> Guinier<sup>6</sup> has shown that when formed from  $\theta'$  fifteen orientations occur, five from each  $\theta'$  orientation. A complicated pattern is obtained (Fig. 12, Plate XL). When formed by slow cooling of the solid solution the orientation is random.

#### 5. ESTIMATION OF PARTICLE SIZE AND QUANTITY OF PRECIPITATES

Several methods have been used in the course of the work to measure the actual size of the zones or precipitates. Platelet diameters have been obtained

\* The indices of the true cell are related to those of Preston's by the equations  $h^T = \frac{h^P + k^P}{2}$ ,  $k^T = \frac{-h^P + k^P}{2}$ , and  $l^T = l^P$ .



by the small-angle scatter method and thicknesses by measurement of the broadening of the diffraction spots on oscillating-crystal and Laue films. The  $(111)_{\theta^P}$ ,  $(101)_{\theta^T}$  spot (upper arrow in Fig 5) was broadened when the  $\theta'$  platelets were thin (less than 250 Å.). The elongation of the  $(111)_{\theta^P}$ ,  $(101)_{\theta^T}$  relpoint in the  $[100]_{Al}$  direction was calculated from the breadth of this spot and the thickness of the  $\theta'$  platelets calculated on the assumption that the elongation was a particle-size effect. This assumption was justified by the fact that both Laue and oscillating-crystal films gave equivalent elongations, implying that the size of the relpoints was independent of their position in reciprocal space. The quantity of  $\theta'$  present was obtained as a percentage of the total possible quantity (for the alloy in question) by intensity comparisons of appropriate  $\theta'$  reflections. The absolute intensity of the  $\theta'$  spots was greater than that calculated by assuming all the copper to be present as  $\theta'$ . This discrepancy is presumably due to the assumption of the validity of Preston's  $\theta'$  structure in the calculation.

#### IV.—STRUCTURES ALONG THE AGEING CURVES

In relating the structures to the ageing curves it has to be remembered that the rate of ageing varies with the quenching strains, which are a function of the type of specimen and the quenching medium. For this reason greater significance has been attached to the results obtained on crystals from the hardness specimens. However, the single-crystal results on thin sheet and wire specimens were essential for a complete determination of the ageing sequence. The results were repeatable for any combination of specimen type and quenching medium.

##### 1. AGEING AT ROOM TEMPERATURE

Diffuse streaks due to G.P. zones [1] appeared in all alloys and increased in intensity after a few days' ageing. No further change in the intensity of the streaks could be detected in the 4% copper alloy after one year. The zones were about 50 Å. in dia. The precipitation process did not progress beyond the G.P. [1] stage.

##### 2. AGEING AT 110° C. (FIG. 20)

All alloys showed G.P. [1] from ageing times slightly in excess of the incubation value up to ageing times corresponding to the end of the flat. The diameters of the zones were constant at about 80 Å. along the flat plateaux of the alloys with 3–4.5% copper. A rapid increase in the measured zone diameter occurred at the end of the flat and was accompanied by the formation of slight maxima in the streak on the oscillation patterns, i.e. G.P. zones [2] were formed at the beginning of the second rise to peak hardness.

The alloys all showed G.P. [2] with some  $\theta'$  at their

peak hardness. The proportion of  $\theta'$  increased at longer ageing times.

##### 3. AGEING AT 130° C. (FIG. 21)

**2% Copper Alloy.**—Somewhat variable behaviour was encountered. For example,  $\theta'$  only was detected in the wire specimens, but both G.P. [1] and G.P. [2] occurred in the sheet and hardness specimens, whilst the latter gave different structures in different crystals of the same specimen. The G.P. [2] and  $\theta'$  spots on the oscillation photographs were of the same breadth, i.e. the thickness was probably of the same order. 100% of the total possible  $\theta'$  was present at peak hardness. The thickness of the  $\theta'$  platelets was 150 Å.

**3% Copper Alloy.**—G.P. [1] was present up to ageing times of about 4 days (Fig. 14, Plate XLI) and was then replaced by G.P. [2]. The platelet diameter did not vary from 100 Å. between 1 and 4 days (Fig. 13, Plate XLI, and Fig. 21). At peak hardness the G.P. [2] platelets were about 20 Å. thick and more than 500 Å. in dia. and only about 10% of the total possible  $\theta'$  was present.

**4% and 4.5% Copper Alloys.**—G.P. [1] (Fig. 1, Plate XXXIX) was responsible for the initial rise and flat plateau, and gave a constant platelet diameter of 95 Å. (Fig. 21). The intensity maxima due to G.P. [2] developed after ageing times comparable to the end of the flat but varied with the quenching strains, e.g. 1 day in water-quenched and 3 days in acetone-quenched sheet (Fig. 2, Plate XXXIX). Very faint  $\theta'$  spots were also present on these films. A large increase in the measured zone diameter accompanied the appearance of G.P. [2] at ageing times corresponding to the second rise to peak hardness (Fig. 3, Plate XXXIX). The  $c$  parameter of the G.P. [2] structure changed from about 8.0 to 7.6 Å. as the ageing proceeded (see Table I). Faint  $\theta'$  diffractions were usually present on the films and about 5–10% of the possible  $\theta'$  occurred at peak hardness (Fig. 6, Plate XXXIX). Only  $\theta'$  was detected after longer ageing times. The G.P. [2] zones were about 20–30 Å. thick at peak hardness, whereas the  $\theta'$  platelets were about 100 Å. thick at the peak and more than 200 Å. thick at ageing times of 200 days and longer, when all the  $\theta'$  had been precipitated.

##### 4. AGEING AT 165° C.

Only the initial decomposition products and the structures present at peak hardness have been established. A sheet specimen of the 3% copper alloy aged for 1 day (Fig. 17, Plate XLI) showed evidence of thin  $\theta'$  platelets and very little G.P. [2]. A specimen aged to peak hardness (10 days) indicated that all the excess copper had been precipitated as  $\theta'$ . The 4% copper alloy showed G.P. [2] and about 20% of the total possible  $\theta'$  at peak hardness. Single-crystal specimens aged for short times showed streaks with variations in intensity, or separated but elongated G.P. [2] spots. Single-crystal sheet specimens

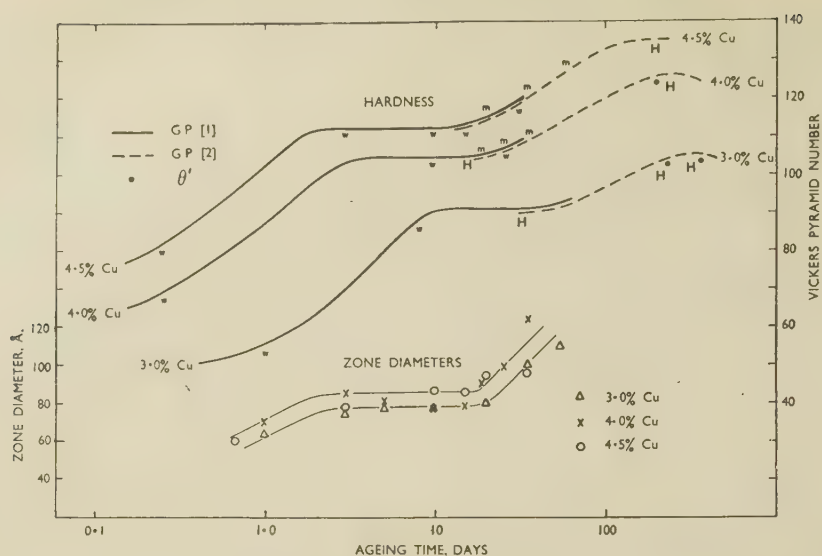


Fig. 20.—Structures and Zone Diameters at 110° C. in Relation to Hardness/Ageing-Time Curves.

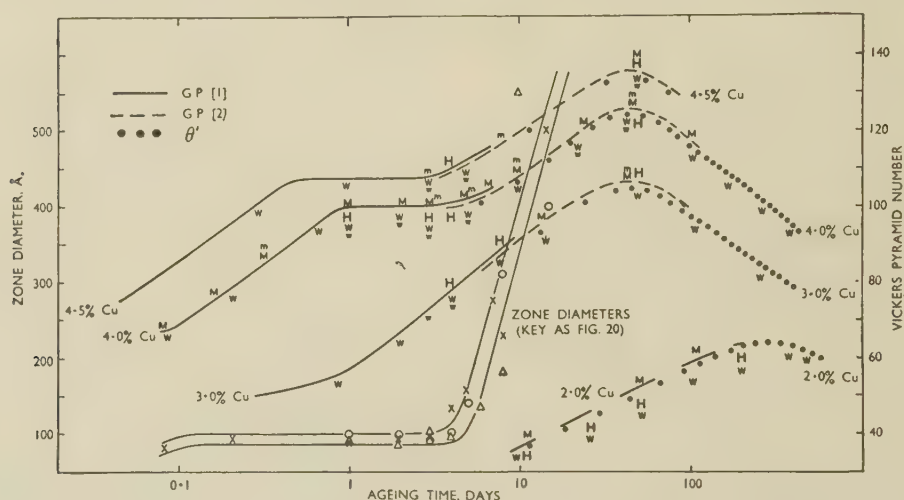


Fig. 21.—Structures and Zone Diameters at 130° C. in Relation to Hardness/Ageing-Time Curves.

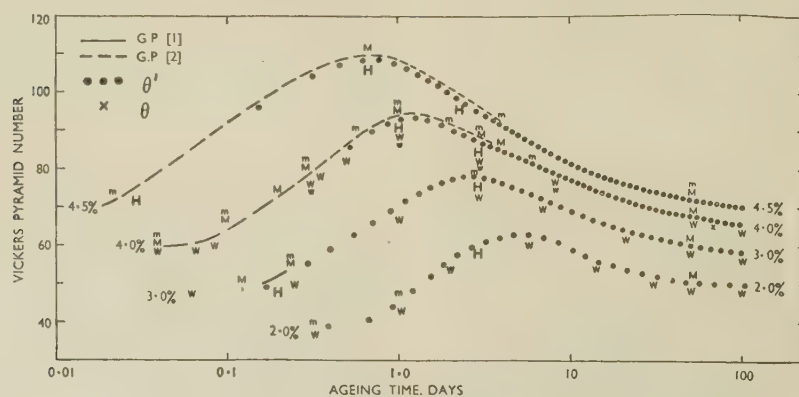


Fig. 22.—Structures at 190° C. in Relation to Hardness/Ageing-Time Curves.

KEY to FIGS. 20-22.

H Hardness specimen.

M } Monochromatic method { Water-quenched.  
m } Acetone-quenched.W } Laue method { Water-quenched.  
w } Acetone-quenched.



of the 4.5% alloy gave very blurred G.P. [2] spots after short ageing times. Clearly defined G.P. [2] spots and about 5% of the possible  $\theta'$  were present at peak hardness times (Fig. 16, Plate XLI).

### 5. AGEING AT 190° C. (FIG. 22)

**2% and 3% Copper Alloys.**—These alloys showed  $\theta'$  only, with the exception of a trace of G.P. [2] found after a short ageing treatment in the 3% alloy examined by the oscillation technique. The maximum possible amount of  $\theta'$  was present at peak hardness. Both alloys showed faint traces of  $\theta$  rods in  $\langle 100 \rangle_{Al}$  directions (see Fig. 11, Plate XL) and had  $\theta'$  platelets about 120 Å. thick as measured on Laue films. The thickness had increased to 250 Å. after 50 days' ageing.

**4% and 4.5% Copper Alloys.**—G.P. [2] was present after short ageing times. Fig. 7 (Plate XL) shows that the G.P. [2] spots were separated and were neither large enough to overlap nor present in a background streak due to G.P. [1]. The  $c$  parameter of the G.P. [2] structure was about 7.6 Å. (see Table I).  $\theta'$  was always present (Figs. 7 and 8, Plate XL). At peak hardness the 4% alloy contained G.P. [2] plus one-third of the possible  $\theta'$  (Fig. 9, Plate XL) whereas the 4.5% copper alloy contained only 10–20% of the possible  $\theta'$  in addition to G.P. [2]. The  $\theta'$  platelets were about 80 Å. thick in the 4% alloy at peak hardness, but had increased to nearly 300 Å. after 50 days' ageing. A little of the stable  $\theta$  structure appeared in this alloy after the same ageing time, but  $\theta'$  was still the predominant precipitate ( $\sim 95\%$  of the total) after 100 days (Fig. 10, Plate XL) and 300 days. After 3 days no G.P. [2] remained and the  $\theta'$  spots had reached maximum intensity.

### 6. AGEING AT 220° AND 240° C.

Only  $\theta'$  was detected up to peak hardness, but all the possible  $\theta'$  was not precipitated. For example, 60% was present in the hardness specimen of 4% copper alloy at peak hardness at 220° C.; the Laue spots indicated a platelet thickness of approximately 150 Å.  $\theta'$  spots were present after very short ageing times in water-quenched sheet specimens, but acetone-quenched specimens aged much more slowly, e.g. one aged for 2½ hr. (time to attain peak hardness) contained only 10%  $\theta'$ . The  $\theta'$  platelet size increased on ageing past the peak.

The water-quenched rod specimens of 4% copper alloy gave a trace of  $\theta'$  after 5 min. at 240° C. and 100%  $\theta'$  after 6 hr., but the spots were not all sharp (thickness  $\sim 300$  Å.). A water-quenched crystal aged for 16 hr. showed only  $\theta'$ , with no  $\theta$ .

### 7. EFFECT OF QUENCHING MEDIUM (FIG. 23)

Quenching in oil or acetone retarded the ageing process as compared with water-quenching. The 4% copper alloy aged at 130° C. showed intensity maxima in the streaks after shorter ageing times if the specimens were quenched in water instead of

oil or acetone. After 11 days' ageing (cf. Figs. 4 and 5, Plate XXXIX) the water-quenched specimen contained more  $\theta'$  than that quenched in oil. Fig. 23 gives the calculated percentage of  $\theta'$  for specimens quenched in different media and aged at 190° C. Guinier's curve<sup>17</sup> for specimens believed to have been air-cooled has been added for comparison purposes. It can be seen that Guinier's curve lies between those for acetone- and oil-quenched specimens and is of very similar slope.  $\theta'$  was formed less rapidly when

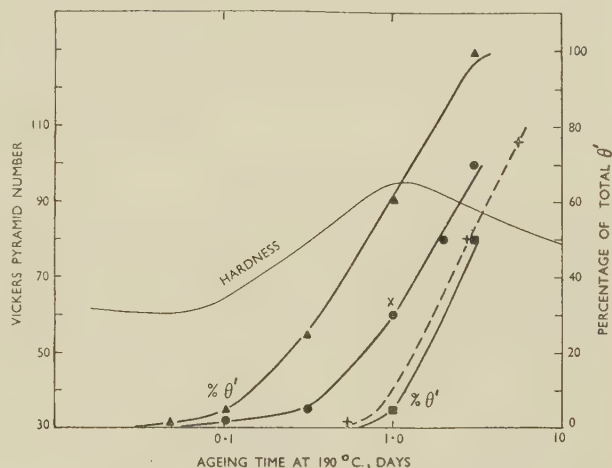


Fig. 23.—Effect on the Quantity of  $\theta'$  in the Aluminium-4% Copper Alloy of Varying the Quenching Medium, in Relation to the Ageing Curves at 190° C. Guinier's<sup>17</sup> curve for the quantity of  $\theta'$  has been added for purposes of comparison.

#### KEY.

- ▲ Water-quenched sheet.
- Oil-quenched sheet.
- Acetone-quenched sheet.
- × Hardness specimen.
- + Guinier's values, air-cooled.

the quenching medium was changed in the sequence water > oil > acetone. The thickness of the  $\theta'$  platelets was less sensitive to the method of quenching.

## V.—DISCUSSION OF RESULTS

### 1. RELIABILITY OF THE X-RAY DATA

The structures obtained on a given alloy were generally the same in the rod, sheet, and hardness specimens. The rate of ageing depended on the quenching strain, but the results were repeatable for any given treatment. Nevertheless, comparison of quantitative measurements from different types of specimens is rendered uncertain. Consequently, the quantities given in Table II and in the text have been taken from the hardness specimens.

The proportions of  $\theta'$  are probably correct to  $\pm 10\%$  for quantities greater than 5%. The estimated accuracy of the thicknesses given is  $\pm 25\%$ . The figures quoted for the diameters of the platelets probably have a relative accuracy of  $\pm 10\%$ , but the absolute accuracy may be considerably lower.

The figures obtained by Polmear and Hardy from an electron-microscope examination of aluminium-4%

copper alloy are pertinent.<sup>20</sup> Thus, they recorded a value of 100 Å. for the thickness of  $\theta'$  platelets at peak hardness at 190°C. This is in reasonable agreement with the value of 80 Å. obtained by the X-ray methods, the discrepancy being within the estimated accuracy. Comparison of the  $\theta'$  platelet diameters is only possible for peak hardness at 130°C. It may be inferred (Fig. 21) that the G.P. [2] diameter is in excess of 500 Å., and hence that the  $\theta'$  diameter is greater than this value. Polmear and Hardy have given a figure of 100 Å. for the same ageing condition. This figure was based on "a few small dots", and as only 10% of  $\theta'$  is present (Table III) the few relatively large particles could easily have been missed.

It appears unnecessary to discuss structural findings other than those that are novel or in conflict with the previous work.

## 2. G.P. ZONES [1]

The findings of Guinier and Preston have been confirmed. Attempts have been made to obtain evidence of the relrods in  $\langle 111 \rangle_{\text{Al}}$  directions reported by Jagodzinski and Laves.<sup>14</sup> Only the thermal-scattering effects found by Preston and by Guinier have been detected.

## 3. G.P. ZONES [2]

As an alternative to the differentiation between G.P. [1] and G.P. [2], it is possible to assume<sup>13</sup> that the streaks interpreted as due to G.P. [1] are in fact due to thin platelets of G.P. [2]. Guinier has always held the view that the structures were distinct, but has not published direct evidence in support of his ideas. Two examples of such evidence have now been obtained:

(i) The development of sharp G.P. [2] spots from G.P. [1] streaks has been studied in some detail. Measurement of the films has shown that the maxima of the diffuse spots which first appear do not coincide with the position of the sharp spots obtained after longer ageing periods at 130°C. The  $c$  parameter of the G.P. [2] structure changes from 8.0 to 7.6 Å., suggesting an ordering process in which aluminium atoms are being removed from the structure and the misfit with the matrix lattice increased. When G.P. [1] is not detected earlier than G.P. [2], during ageing at 190°C., the  $c$  parameter of the structure remains constant at 7.6 Å. (see Table I).

(ii) Consideration of the platelet diameters (as obtained from the small-angle scatter films) in relation to the structures of the same specimens (as determined by oscillation films) and to the relevant hardness curves (Figs. 20 and 21), shows that the G.P. [1] platelet diameters remain substantially constant across the flat of the two-stage hardness curves and that the zone diameters increase rapidly at the end of the flat, concurrently with the appearance of the G.P. [2] structure. If G.P. [1] streaks were due to thin platelets of G.P. [2], there seems to be no logical reason for this marked discontinuity in the growth process.

Guinier first<sup>7</sup> gave 7.7 Å. for the  $c$  parameter of G.P. [2], then later<sup>8</sup> 7.9 Å. for sharp G.P. [2] spots. The difference between this value and the 7.6 Å. obtained in the present investigation is outside the range of experimental error, and no satisfactory explanation of the discrepancy has been found. In confirmation of the finding of the present authors, Köster<sup>21</sup> has stated that he and Gerold have very recently obtained 7.68 Å. for the  $c$  value of G.P. [2] in a 5% copper alloy. The new  $c$  value calls for some modification of Guinier's suggested G.P. [2] structure.

## 4. THE $\theta'$ STRUCTURE

As shown in Fig. 19, the true unit cell of Preston's  $\theta'$  structure has parameters  $a = 4.04$  and  $c = 5.8$  Å., as opposed to the  $a = 5.7$  and  $c = 5.8$  Å. chosen by that author.

Both the present work and that of Guinier<sup>6</sup> have shown that Preston's  $\theta'$  structure is not consistent with all the experimental findings. The departures from that structure can be divided into two categories: (i) those which appear to be permanent and provide evidence that the structure suggested by Preston is not correct, and (ii) those which do not always occur; these are merely evidence of lattice distortion or disorder and have no real bearing on the validity of Preston's structure.

The fact that anomalously high intensities of the  $\theta'$  spots for which  $2h + l$  and  $2k + l$  are equal to  $4n \pm 2$  for the true cell, are consistently found (Guinier  $\sim 30$  times the predicted intensity, present authors  $\sim 10$  times) is the only evidence falling in the first category, but it is sufficient to make it clear that Preston's structure is no more than a very good approximation. A limited number of departures from the stoichiometric composition ( $\text{CuAl}_2$ ) have been considered, but none of these has given a better fit with the observed intensities of  $\theta'$  diffractions than that obtained by Preston.

Guinier has associated the appearance and variation in intensity of his  $(10.1 \pm 0.5 \text{ Å.})_{\theta'}$  spot with the occurrence of  $(002)_{\theta'}$ , i.e. one of the  $(4n \pm 2)_{\theta'}$  spots. The present authors have clearly shown that this is not the case, since the spot occurs irregularly at  $10.4 \pm 0.3 \text{ Å.}$ , while  $(002)_{\theta'}$  is always present. This spot and the relrods through  $\theta'$  reprints in  $[001]_{\theta'}$  directions are category (ii) effects.

Guinier explains his  $(10.1 \text{ Å.})_{\theta'}$  spot by the matching of the 8th  $\theta'$  plane in the  $[001]_{\text{Al}}$  direction ( $7 \times 1.45 \text{ Å.}$ ) with the 6th aluminium matrix plane ( $5 \times 2.02 \text{ Å.}$ ). He assumes that intermediate planes also tend to match, causing modulations of the  $\theta'$  structure over units of 10.1 Å. in the  $[001]_{\theta'}$  direction, and makes the further assumption that only first-order diffractions will be of detectable intensity. The figure of 10.1 Å. required for the spacing of the planes producing the spot lies at the limit of the range of values obtained in the present investigation, i.e.  $10.4 \pm 0.3 \text{ Å.}$ , and Guinier's views afford no explanation of the irregularity of appearance of the spot. We are, however,



unable to offer a more satisfactory account. A number of possibilities have been considered, including an attempt to explain the spot by considering whether a small proportion of the  $\theta'$  sometimes adopts an alternative matching plane. A very good fit is obtained with  $(010)_{\theta'}^T$ , parallel to  $(\bar{1}10)_{Al}$  and the  $[001]_{\theta'}^T$ , parallel to  $[110]_{Al}$ , but such a habit plane would produce new  $\theta'$  diffractions which were not detected.

It is clear from the work of Guinier<sup>6</sup> and the present authors that the atomic arrangement proposed by Preston for  $\theta'$  (Fig. 19) requires some modification. Guinier's G.P. [2] structure<sup>6, 8</sup> is not entirely in accord with the present work, and the G.P. [1] structure is ill defined as regards (i) the extent to which copper atoms have replaced aluminium atoms, and (ii) the extent to which they are sited strictly on aluminium-matrix lattice sites. The problem of elucidating the atomic arrangements of the metastable structures G.P. [1] and G.P. [2], which cannot be isolated and studied in the conventional manner, is very difficult and there seems little possibility of further significant progress with the existing techniques.

## 5. MODES OF FORMATION OF THE PRECIPITATES

In general it is not known whether the sequence of decomposition products occurs by allotropic changes or by independent nucleation from the matrix. Guinier has stated that he never detects G.P. [2] except after the earlier appearance of G.P. [1]. We have shown (Table II) that G.P. [1], G.P. [2], and  $\theta'$ , in turn, can be the structures first detected under suitable conditions of supersaturation. This strongly suggests that G.P. [2] and  $\theta'$  can be nucleated directly from the matrix. Under other conditions G.P. [2] may be nucleated from G.P. [1] and  $\theta'$  from G.P. [2]. This is suggested by two other experimental findings. These are: (i) the change in the  $c$  parameter of G.P. [2] from 8.0 to 7.6 Å. when it is preceded by G.P. [1] during ageing at 130° C., whereas a constant value of 7.6 Å. is obtained during ageing at 190° C., when no G.P. [1] is detected (Table I); and (ii) the finding that  $\theta'$  platelets are thicker, when first detected, than the G.P. [2] platelets concurrently present, except in cases where both structures form simultaneously. Such cases of simultaneous formation are the 2% copper alloy aged at 130° C., and the 3% alloy aged at 165° C. The breadth of the faint  $\theta'$  spots just visible in Fig. 7 (Plate XL) suggests that the 4% copper alloy aged at 190° C. is also a case where G.P. [2] and  $\theta'$  form concurrently. The low intensity prohibited size measurements. Guinier<sup>6</sup> has shown that the X-ray evidence can clearly distinguish between  $\theta$  precipitate formed by nucleation from the matrix and that formed by allotropic change from  $\theta'$ , the orientation relationship with the matrix being different in the two cases. Fig. 12 (Plate XL) is an example of  $\theta$  formed from  $\theta'$ . No such distinction obtains for the other structures, and the preferred mode of formation remains obscure.

## 6. DESCRIPTIVE THEORY OF THE AGEING PROCESS

The present systematic study of the structural changes allows a satisfactory descriptive theory of the ageing process to be formulated. The sequence in which the structures dominate the X-ray patterns is always: G.P. [1]  $\rightarrow$  G.P. [2]  $\rightarrow \theta' \rightarrow \theta$ . In confirmation of the analysis of the ageing curves,<sup>10</sup> Table II shows that the initial decomposition product

TABLE II.—Structures First Detected on Ageing Aluminium-Copper Alloys.

Ageing Temp., °C.	2% Cu	3% Cu	4% Cu	4.5% Cu
110	G.P. [1]	G.P. [1]	G.P. [1]	G.P. [1]
130	$\theta'$ or $\theta'$ and G.P. [2] or G.P. [1]	G.P. [1]	G.P. [1]	G.P. [1]
165	...	$\theta'$ and little G.P. [2]	G.P. [1] and G.P. [2]	...
190	$\theta'$	$\theta'$ and very little G.P. [2]	G.P. [2] and little $\theta'$	G.P. [2]
220	$\theta'$	...	$\theta'$	$\theta'$
240	...	...	$\theta'$	$\theta'$

with decreasing supersaturation passes through the sequence G.P. [1], G.P. [2], and  $\theta'$ , with omission of the earlier products.  $\theta$  can also form the initial precipitate at high ageing temperatures.<sup>6</sup>

Room-temperature ageing is limited to the formation of G.P. [1] for periods up to at least 3 years and probably indefinitely. The initial rise in the two-stage ageing curves (Figs. 20 and 21) is also due to G.P. [1], the platelets of which remain constant in diameter over the flat plateau of the ageing curve. The diameters appear to be independent of the copper content, but increase in size with ageing temperature from  $\sim 50$  Å. at room temperature (Table III) through

TABLE III.—Zone Diameters of Aluminium-Copper Alloys Aged at Room Temperature.

Alloy	Ageing Time	Zone Dia., Å.
3% Cu	4 months	50
4% Cu	1-5 hr.	45
	16-20 "	42
	6 weeks	47
	6 months (at 30° C.)	46

$\sim 80$  Å. at 110° C. (Fig. 20) to  $\sim 100$  Å. at 130° C. (Fig. 21).

The second rise to peak hardness of the two-stage ageing curves is due to the G.P. [2] structure. The G.P. [2] platelets increase in size with ageing time, whilst the  $c$  parameter of the structure contracts. Peak hardness of the two-stage ageing curves is associated with the G.P. [2] structure, together with some  $\theta'$  (see Table IV), whilst  $\theta'$  becomes the dominant structure at longer ageing times. Polmear and Hardy<sup>20</sup>, using the electron microscope, detected no structure before peak hardness of the 4% copper alloy aged at 130° C., which agrees well with Fig. 21 in showing that little  $\theta'$  is formed before this stage is reached.

The flat plateau of the ageing curves becomes less prominent as the supersaturation is reduced and the single- and two-stage ageing curves merge, e.g. the

TABLE IV.—Structures of Aluminium-Copper Alloys Aged to Peak Hardness.

Ageing Temp., °C.	2% Cu	3% Cu	4% Cu	4.5% Cu
110	G.P. [2] + 20% $\theta'$ (150 Å.) *	G.P. [2] + little $\theta'$	G.P. [2] + 3% $\theta'$	...
130	...	G.P. [2] + 10% $\theta'$	G.P. [2] + 10% $\theta'$	G.P. [2] + 5% $\theta'$
165	...	$\theta'$	G.P. [2] + 20% $\theta'$	(G.P. [2] + $\theta'$ ) *
190	100% $\theta'$ (120 Å.) *	$\theta'$ (140 Å.) *	G.P. [2] + 30% $\theta'$	G.P. [2] + 15% $\theta'$
220	( $\theta'$ ) *	...	60% $\theta'$ (150 Å.) *	( $\theta'$ ) *

\* The data in parentheses are from single-crystal work and photographs have not been taken from hardness specimens.  $\theta'$  thicknesses are given where these were measured.

2% copper alloy aged at 110°C., the 3% alloy at 130°C., and the 4% and 4.5% copper alloys at 165°C. and the 4.5% alloy at 190°C. (Figs. 20, 21, and 22). G.P. [1] and G.P. [2] form the initial

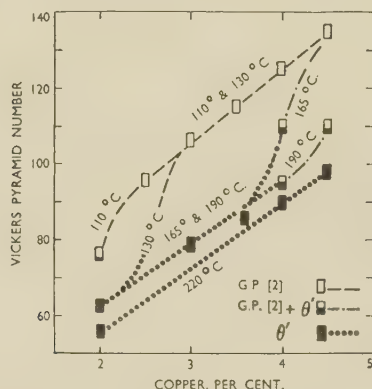


FIG. 24.—Hardness Values (Hardy<sup>10,11</sup>), and Structures (Table IV) of Aluminium-Copper Alloys Aged to Peak at Different Temperatures.

decomposition products (Table II), whilst peak hardness is associated with G.P. [2] and increased amounts of  $\theta'$ .

Single-stage ageing curves are found at the lowest degrees of supersaturation, when  $\theta'$  is the first structure detected.  $\theta'$  is also the only structure present at peak hardness. Peak hardness at 220°C. occurs before the total quantity of copper has been precipitated.

The thickness of the  $\theta'$  platelets at peak hardness appears to be about 140 Å. in all cases when  $\theta'$  is the sole structure present.

Hardy<sup>10,11</sup> had found that the peak-hardness values fell clearly into two groups when plotted against copper content (Fig. 24). The upper group was associated chiefly with the two-stage ageing

process, and it was suggested that the higher peak hardness was due to the formation of G.P. [2] in a matrix already containing G.P. [1]. The lower group of values was associated principally with the single-stage ageing curves and was thought to be attributable to either G.P. [2] or  $\theta'$ . The structures now observed by X-ray analysis have been indicated in Fig. 24, and show that the upper group of peak-hardness values is due to the presence of G.P. [2], whilst the lower group is due almost entirely to  $\theta'$ . Therefore G.P. [2] gives much greater hardening than  $\theta'$ , the occurrence of which leads to softening when it is formed in a matrix already stiffened by G.P. [2]. Some hardening is caused by  $\theta'$  when formed in a matrix free from G.P. [2]. The  $\theta'$  platelets at the peak hardness in the lower group are appreciably thicker than the G.P. [2] platelets of the upper group. It is difficult to be more explicit about the cause of the increased hardness in the presence of G.P. [2] than to say that there is an increased resistance to the motion of dislocations. This could be due to a larger number of G.P. [2] platelets and, consequently a shorter mean free path between the particles.

#### ACKNOWLEDGEMENTS

The authors take pleasure in acknowledging the benefit of helpful discussions with Professor A. Guinier and Dr. A. H. Sully, and thank their colleagues at the Fulmer Research Institute who assisted in the experimental work.

#### REFERENCES

1. G. D. Preston, *Nature*, 1938, **142**, 570.
2. G. D. Preston, *Proc. Roy. Soc.*, 1938, [A], **167**, 526.
3. G. D. Preston, *Phil. Mag.*, 1938, [vii], **26**, 855.
4. A. Guinier, *Nature*, 1938, **142**, 569.
5. A. Guinier, *Ann. Physique*, 1939, [xi], **12**, 161.
6. A. Guinier, *J. Phys. Radium*, 1942, [viii], **3**, 129.
7. A. Guinier, *Compt. rend.*, 1950, **231**, 655.
8. A. Guinier, *Acta Cryst.*, 1952, **5**, 121.
9. M. L. V. Gayler, *J. Inst. Metals*, 1940, **66**, 72.
10. H. K. Hardy, *ibid.*, 1951, **79**, 321.
11. H. K. Hardy, *ibid.*, 1953–54, **82**, (6), 236.
12. A. B. Greninger, *Trans. Amer. Inst. Min. Met. Eng.*, 1935, **117**, 61.
13. H. K. Hardy and T. J. Heal, "Progress in Metal Physics", Vol. V. London: (Pergamon Press) (in the press).
14. H. Jagodzinski and F. Laves, *Z. Metallkunde*, 1949, **40**, 296.
15. G. Wassermann and J. Weerts, *Metallwirtschaft*, 1935, **14**, 605.
16. W. L. Fink and D. W. Smith, *Trans. Amer. Inst. Min. Met. Eng.*, 1940, **137**, 95 (authors' reply to discussion).
17. A. Guinier, *Z. Elektrochem.*, 1952, **56**, 468.
18. Yu. A. Bagaryatsky, *Doklady Akad. Nauk. S.S.S.R.*, 1951, **77**, 261; *Fulmer Research Inst. Translation No. 18*.
19. A. J. Bradley and P. Jones, *J. Inst. Metals*, 1933, **51**, 131.
20. I. J. Polmear and H. K. Hardy, *J. Inst. Metals*, 1952–53, **81**, 427.
21. W. Köster, private communication.



# CHANGES OF DAMPING CAPACITY IN QUENCH-AGEING ALUMINIUM-RICH ALLOYS \*

1520

By K. M. ENTWISTLE,† M.Sc., Ph.D., MEMBER

## SYNOPSIS

Changes of damping capacity recorded during the ageing of quenched Duralumin at constant temperatures up to 65° C. reveal two distinct contributions to the vibrational energy loss. The second of these, which appears as a peak in the curve relating damping and ageing time, has been investigated in detail. The time to reach peak damping was found to vary with ageing temperature ( $T$ , °K.) as  $\exp(H/RT)$ , where  $H$  is 38,000 cal./mole. Further, the damping was established to be of anelastic origin, having a temperature-dependent relaxation time governed by a heat of activation of 13,500 cal./mole.

Simpler, high-purity alloys, namely the binary alloys of aluminium with copper, manganese, or iron, and the ternary aluminium-magnesium-silicon, aluminium-copper-silicon, and aluminium-copper-magnesium alloys, showed neither of these effects, nor did commercial-purity alloys of aluminium-magnesium and aluminium-magnesium-silicon. The damping of a quaternary aluminium-copper-magnesium-silicon alloy rose to a peak during ageing. This is considered to correspond to the second contribution observed in Duralumin, since the activation energies describing the temperature dependence of relaxation time (13,200 cal./mole) and the attainment of peak damping during ageing (38,000 cal./mole) are in good agreement with the corresponding values for Duralumin.

The marked difference between the two activation energies in both alloys is taken to mean that the factor governing the attainment of peak damping during ageing is different from that responsible for the vibrational energy loss, but it is not possible at this stage to identify the precise mechanism by which the damping arises.

## I.—INTRODUCTION

MARKED changes of mechanical vibrational energy loss have been observed in quenched complex aluminium-rich alloys during ageing at room temperature.<sup>1,2</sup> The work now described was undertaken in an attempt to discover the mechanism giving rise to these damping changes, in the hope that this might lead to a method for the investigation of the ageing process itself.

Published information on mechanical damping of age-hardening alloys falls into two categories:

(i) The effect of prolonged vibration at high stress on the damping of ageing alloys in a metastable condition.<sup>3</sup>

(ii) The variation of damping at low vibrational stress of an ageing specimen.

In category (i) the process of vibration has been shown to induce changes akin to natural ageing, thus apparently accelerating the process; as the result of localized plastic deformation. It is the extent of this influence which presents the feature of interest in these experiments. The course of ageing in (ii), on the other hand, is not significantly affected by the mechanical vibrations, if a suitably low stress is selected. No measuring process is completely without influence on the system measured, but in this case the vibrations associated with damping measurement induce only small reversible changes of, for instance, temperature, internal strains, or atom

distribution. Adequate proof that such effects are negligible is obtained by following concurrently the ageing of a vibrated and unvibrated specimen, otherwise identically treated. The damping values can therefore be assumed to reflect the natural ageing process, in the same way, for example, as do electrical-resistivity measurements. The present paper is concerned exclusively with effects of this type.

Previous work in this field on ageing systems has made use of damping contributions from relaxation effects, which arise at low stresses if the equilibrium condition of the metal under stress differs from that in the unstressed state, and further if the change from one condition to the other involves a limited change of strain.<sup>4</sup> Then the vibrational energy loss rises to a peak when the angular frequency of vibration is approximately equal to the reciprocal of the relaxation time for the dimension change. A peak of this type, due to stress-induced modification of the distribution of interstitial solutes in body-centred cubic lattices, has been used by Dijkstra<sup>5</sup> and by Wert<sup>6</sup> to follow quench-ageing in supersaturated iron-carbon and iron-nitrogen alloys and by Kê<sup>7</sup> to follow precipitation from tantalum. It is here assumed that precipitated phases exert no damping effects, and hence that the progressive fall of damping observed during ageing, corresponding to a fall in the height of the relaxation peak, is proportional to the reduction of the number of unprecipitated solute atoms. Harper<sup>8</sup> has used the same method to

\* Manuscript received 11 July 1953.

† Lecturer in Metallurgy, University of Manchester.

follow atom migration to dislocations during strain-ageing.

Although damping from stress-induced diffusion has been identified in substitutional solid solutions which have zinc as one constituent,<sup>9, 10</sup> the author is not aware of any record of the application to the study of atom migration during ageing.

In addition to changes of matrix composition, anelastic measurements appear to be sensitive to the appearance of, or to changes at, incoherent interfaces. Nowick<sup>10</sup> has interpreted anelastic measurements on aluminium-zinc alloys in terms of stress relaxation at the boundaries of discontinuous precipitates, and Kê<sup>11</sup> is of the opinion that the fall of damping observed during ageing of a quenched aluminium-copper alloy at 200° C. arises from segregation of copper at crystal boundaries. This impedes slip between adjacent crystals and reduces the height of the grain-boundary damping peak.

in transverse vibration; all the torsional tests were conducted at room temperature.

### 1. APPARATUS FOR TRANSVERSE VIBRATION

The method consists, in essence, of exciting transverse vibrations in a uniform bar of rectangular section at one of its natural frequencies and measuring the rate of decay of the free vibration after removal of the exciting force. Vibrations are excited by passing current at the vibration frequency through a polarized eddy-current-type exciter at one end of the specimen. The amplitude of vibration is measured by the amplified output voltage from a similar device, arranged to work as a detector at the other end of the specimen.

#### (a) Specimen Assembly

The assembly comprising the specimen, supports, exciter, and detector, shown in Fig. 1, was designed

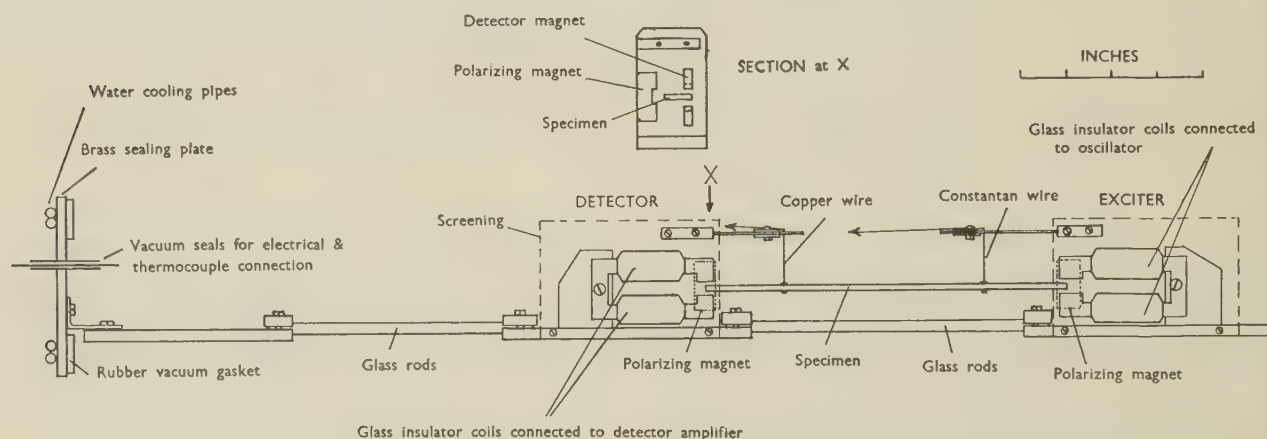


FIG. 1.—Specimen Assembly for Damping Measurement in Transverse Vibration.

The experimental work on aluminium-rich alloys to be described will be discussed against this background of current knowledge on damping of ageing alloys.

## II.—DAMPING-CAPACITY MEASUREMENT

For the elucidation of the fundamental nature of damping contributions in metals vibrating at low stress, the variation of energy loss with frequency and temperature is important. It is often difficult to obtain an adequate range of frequency of vibration using a single technique, and in this work two complementary methods were adopted. All measurements above about 900 c./s. were made on bars of uniform, rectangular section vibrating transversely; lower-frequency results in the range 2–500 c./s. were measured in torsional vibration on specimens which could be loaded to reduce the natural frequency. Torsional vibration was selected for the lower-frequency measurements in order to eliminate damping from macroscopic thermal currents. Measurements over a range of temperature were made only

to fit inside a 3-in.-dia. silica tube, 3 ft. long. The specimens were 8 in. long and varied in section from  $\frac{5}{8} \times \frac{3}{8}$  in. to  $\frac{3}{8} \times \frac{1}{8}$  in. In order to measure the variation of damping capacity during ageing at a constant elevated temperature, it was necessary to be able to heat the specimen and assembly rapidly from room temperature to the ageing temperature. This was effected by induction heating from a coil round the silica tube fed from a 400-kc./s. Philips high-frequency generator. The central part of the assembly was made of glass rods, to avoid partial screening of the specimen from the high-frequency field, and the exciter and detector were screened with aluminium sheet to prevent excessive temperature rise in the ferromagnetic cores.

The coils of the exciter and detector were wound on mica formers with glass-fibre-insulated wire, and the polarizing field was supplied by Alnico magnets. The arrangement was operated satisfactorily up to 350° C.

When testing aluminium-rich alloys in transverse vibration, it is important to eliminate air loss by



making damping measurements at reduced pressure. For this purpose the silica tube was sealed at both ends with water-cooled brass plates faced with rubber gaskets, and could be evacuated with a rotary Speedivac pump to a pressure below  $10^{-3}$  mm. of mercury. Reliable damping readings could be obtained about 2 min. after pumping began at atmospheric pressure.

In order to be able to slide the specimen rapidly into exactly the same position within the furnace tube relative to the high-frequency heating coil, it was rigidly connected to one of the brass sealing plates by glass rods of appropriate length; these reduced heat conduction from the assembly, and associated temperature gradients within it, to negligible proportions.

### (b) Suspension of Specimen

Careful attention was paid to the suspension of the specimen. The first method tried was to use two slings of 0.0048-in.-dia. wire passing under the specimen and each at a node; this was found to be satisfactory for heavier specimens, provided that the plane of vibration was horizontal (see Fig. 2 (a)) and

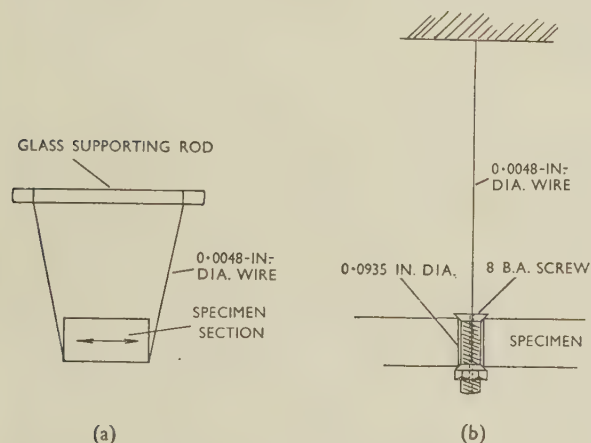


Fig. 2.—Specimen Suspension Details: (a) Sling type showing plane of vibration for minimum loss (arrow); (b) Single-wire type.

that the wires were clear of the upper corners of the bar. For lighter specimens it was found that a slight disturbance while inserting the assembly into the furnace tube, or in some instances higher amplitudes of vibration, caused the wires to move along the specimen into a position in which appreciable additional energy loss occurred. An attempt to prevent this by grinding slight notches in the corners of the bar was unsuccessful; it gave erratic results. The fundamental defect of this arrangement is that the points of support suffer an alternating displacement in the direction of the specimen axis because of the alternating rotation of the specimen section at the node. Relative motion between the specimen and suspension wire is therefore possible, particularly if the frictional force between them is low, as is the case for light specimens. This defect was overcome in the

method finally adopted. The specimen was supported by two single wires, each at a node of vibration and on the neutral axis of bending, that is, at a point which suffered no bodily translation. The wire was attached to the specimen by fixing to the lower end an 8 B.A. screw with tapered head, which fitted into an oversize hole, drilled in the bar with its centre at the node. The screw was secured by a nut with a conical mating surface (see Fig. 2 (b)). The conical faces were the only parts of the bolt in contact with the specimen, and there the normal pressure could be made sufficiently high to prevent interfacial movement, irrespective of specimen size. In each case the upper end of the wire was fixed to a copper clamp, electrically insulated from the assembly with mica sheet. The clamps could be moved along pairs of copper-beryllium supporting rods to adjust the suspension wires for different node positions. In this arrangement the suspension wire was forced into pure torsional vibration of very small amplitude and contributed negligible energy dissipation to the vibrating system. The method of suspension gave consistent results, even if the specimen had to be removed from the apparatus and replaced during a test.

The two suspension wires were made of copper and of Constantan, respectively; these, together with the interconnecting length of specimen material, formed a thermocouple which was used to measure the specimen temperature. The suspension system in its final form was found to have a decided advantage over the earlier sling type for temperature measurement during high-frequency heating. In the sling arrangement high contact resistance often arose between the wire and specimen and led to erratic transient high temperatures during heating. These disappeared on disconnecting the high-frequency power. The effect never arose with the single-wire arrangement, and reliable indications of specimen temperature were obtained while the high-frequency coil was energized.

### (c) Measurement of Decay Time

As the damping capacity increases, the rate of decay of a free vibration becomes so high that the simple method of damping measurement by timing the half-amplitude fall with a stop-watch becomes too inaccurate. There are two ways of increasing the accuracy of the free-decay method: retain the half-amplitude range and use electronic or photographic timing methods, or, alternatively, time the interval for an extended range of amplitude fall. The latter method was found to be adequate for this work. The time for the amplitude of vibration to fall to  $1/n$  of its initial value was measured with a stop-watch; this was started when the amplified detector output voltage reached a reference value and stopped when this voltage was regained after the amplification had been increased by a factor  $n$ . A voltage attenuator in the amplifier, variable in steps, allowed a range of values of  $n$  to be used.

The extension of the range of damping capacities

which can be measured in this way by stop-watch timing is limited. The ratio of:

$$\frac{\text{Time to } 1/n \text{ amplitude}}{\text{Time to } \frac{1}{2} \text{ amplitude}} = \frac{\log n}{\log 2}$$

for an exponential decay. Thus for  $n = 40$  the ratio is 5.3 and  $n$  has to be increased to 130 to increase the ratio to 7. Operation over these extended amplitude ranges is possible only if high maximum amplifications are available, if the specimen vibrates at the highest allowable amplitude, and if the detector has maximum sensitivity, thereby contributing a high input voltage to the amplifier. Maximum practicable amplification is limited by spurious vibration and electrical interference, and the maximum amplitude of vibration is prescribed by the specimen characteristics. In this work a maximum useful amplification of about 50,000 was attained by the introduction of a series of "Twin T" filters tuned to attenuate predominant interference frequencies. Under these conditions it was possible to measure the time for the amplitude to fall to  $\frac{1}{40}$ ; this was found to be adequate.

It is particularly important when using this wide amplitude range to ensure that the logarithmic decrement is constant over the whole range involved. This was determined independently under conditions of low damping capacity where the accurate determination of the half-amplitude time could be made directly at successively increased amplification factors during a single decay. It is convenient that most of the materials tested have a low damping immediately after quenching, that is when amplitude-dependent damping is most likely. Measurements under these conditions gave half-amplitude times independent of the amplitude of vibration.

The damping capacity is expressed here in terms of the logarithmic decrement,  $\delta$  and was calculated from:

$$\delta = 1/f t_{1/n} \cdot \log n,$$

where  $t_{1/n}$  is the time taken for the amplitude to fall to  $1/n$  of its initial value and  $f$  is the frequency of vibration. In the lower damping ranges half-amplitude time measurements gave adequate accuracy. For higher damping values the attenuator method was adopted. Here, the precise attenuation was determined using a low-damping specimen whose half-amplitude time was directly measurable, and  $n$  was calculated from:

$$\log n = \left( \frac{t_{1/n}}{t_{\frac{1}{2}}} \right) \log 2.$$

The calibration for a particular setting was found to vary slightly with frequency because of the amplifier characteristics; in consequence  $n$  was determined at some stage during every test when, as was invariably the case, such conditions were attained that  $t_{\frac{1}{2}}$  could be measured accurately and compared with  $t_{1/n}$ .

#### (d) Spurious Energy Losses

The materials used have been shown to have logarithmic decrements in torsional vibration which

may fall below  $10^{-5}$  at room temperature.<sup>1, 12, 13</sup> For the detection of changes of damping at this level, spurious energy loss must be very small. After paying careful attention to air losses, suspension of the specimen, and the reduction of the eddy-current polarizing field strengths to a minimum value consistent with adequate sensitivity, it was possible in this work consistently to record decrements of the order of  $1.5 \times 10^{-5}$  and often  $1.2 \times 10^{-5}$  for specimens  $\frac{5}{8}$  in. deep in transverse vibration at about 2000 c./s. and under conditions away from anelastic peaks. Since transverse thermal currents contribute about  $0.7 \times 10^{-5}$  under these conditions, the residuum of  $0.8 \times 10^{-5}$  sets an upper limit to apparatus losses. Much of this, however, is likely to be contributed by the specimen.

#### 2. APPARATUS FOR TORSIONAL VIBRATION

The specimens for these tests had a central cylindrical section 0.3 in. in dia.  $\times$  6 in. long, with integral tapered ends of about  $1\frac{1}{8}$  in. dia. Higher-frequency measurements could be made with these specimens freely suspended; lower frequencies were attained by expanding one or both ends into suitable inertias. Both techniques have already been described.<sup>12</sup>

#### 3. RAPID HEATING FOR AGEING TESTS AT ELEVATED TEMPERATURES

It was found that if the 8-in.-long bar specimens for transverse vibration, particularly those of larger section, were put into the silica furnace tube with the wall maintained at the desired ageing temperature, up to about 70° C., at least an hour elapsed before the specimen reached a temperature within 1° C. of that desired. This complicated the damping changes during the initial part of the ageing process. The rate of heating was therefore increased by generating heat in the specimen, using high-frequency current circulating in a coil outside the silica tube. The walls of the silica tube were maintained at the required ageing temperature by passing mains current through a non-inductive Nichrome winding extending over about three-quarters of the total length. The magnetic field within the tube from this winding was always less than 0.1 Oe. and the temperature variation in the empty tube over the length of the specimen was about  $1\frac{1}{2}^\circ$  at 250° C. under vacuum.

At the beginning of an ageing test the quenched specimen and assembly, both at room temperature, were slid into the furnace tube with the wall at the ageing temperature. The high-frequency coil was then energized until the specimen reached the furnace-wall temperature. In the early stages of development it was found that a further rise of specimen temperature took place after high-frequency heating stopped, owing to the assembly heating at a more rapid rate. This difficulty was overcome by adjusting the length of the high-frequency coil so that it embraced the specimen and overlapped only part of the exciter and detector boxes. A position could be found such that, after a short period for temperature equalization in



the assembly, the whole unit was at substantially the same temperature.

It is not easy to arrange for high-frequency heating in a vacuum, because after a short time gas evolved from the heated metal causes the gas pressure to rise and glow discharges develop. These screen the specimen from the high-frequency field and so reduce the heating rate. Glow discharges can be prevented by screening the tube from the electric field with a system of water-cooled conductors running axially down the tube in a direction perpendicular to the lines of force of the electric field, but this also reduces the heating effect. In the present work the high-frequency heating was effected at a pressure of several centimetres of mercury, at which glow discharges do not develop, and pumping-down was completed after the desired specimen temperature had been attained. In general 2-3 min. elapsed between quenching a specimen and the beginning of high-frequency heating, and a further 3 min. before the first reliable damping measurement could be taken.

A heating rate of about 30° C./min. was used. This was found to give rise to temperature differences of less than 0.5° C. between the centre and surface of even the largest specimens. In a vacuum the temperature changes of the specimen are very sluggish. This proved to be a great advantage in controlling the temperature during the early stages of the test, since, if it is arranged for there to be a small time lag between change of mains heating current and furnace-wall temperature, any slight deviations of specimen temperature are immediately checked. This was effected by manual readjustment of the potentiometer-type controller used to regulate the wall temperature. To secure quick response, no lagging was used round the furnace tube; it was merely protected from draughts by an asbestos case. Cyclic fluctuations of specimen temperature of less than  $\pm \frac{1}{2}$ ° C. arose from controller operation, but the long-period control was not as good as this. Throughout all the accepted ageing tests, the temperature was maintained to within  $\pm 1$ ° C. after the first 2 min., during which time temperature changes of not more than 2° C. took place after switching off the high-frequency power.

#### 4. LOW-TEMPERATURE TESTS

Damping measurements down to -70° C. were made by sliding the specimen assembly into a silica tube identical in size with the furnace tube, but fitted with a felt-covered jacket filled with acetone which could be cooled with solid carbon dioxide. This tube was placed alongside the furnace tube so that the specimen could be transferred rapidly from one to the other.

### III.—EXPERIMENTAL RESULTS FOR DURALUMIN

The general plan of the experimental work was first to investigate the temperature- and frequency-

dependence of the damping of ageing Duralumin, in order to establish the nature of the energy dissipation. After this, simpler high-purity alloys were tested to determine the constituents principally responsible for the ageing behaviour; then a more detailed investigation was conducted on the simplest high-purity material exhibiting some of the effects, to obtain



FIG. 3.—Variation of Damping (lower curve) and Indentation Hardness (upper curve) of Duralumin Ageing at Room Temperature, after Being Solution-Treated at 500° C. and Quenched in Water at Room Temperature. Specimens  $8 \times \frac{3}{8} \times \frac{5}{8}$  in. in transverse vibration at 2020 c./s.

+● Specimen 3. ▲■ Specimen 4.

the information necessary for an elucidation of the fundamental mechanism by which the energy loss was produced.

#### 1. RESULTS AT ROOM TEMPERATURE

Specimens were machined from  $1\frac{1}{4}$ -in.-dia. extruded bar of a typical commercial Duralumin of the composition given in Table I.

Fig. 3 shows the variation of damping capacity, measured on  $8 \times \frac{3}{8} \times \frac{5}{8}$  in. bars vibrating transversely, during ageing at room temperature. The specimens were solution-treated in a vacuum for 2 hr. at  $500^\circ \pm 1.5^\circ$  C. and quenched in water at room temperature. The four tests on two different specimens indicate the degree of reproducibility. Later tests showed that the variations evident are entirely

due to variations of ageing temperature. The curves indicate a low damping after quenching, a rise to a point of inflection, and a subsequent more pronounced rise which is still evident at the end of the test. A typical hardness curve is included for comparison; maximum rate of change of damping (with respect

rectangular-section bars vibrating transversely is sensibly independent of the transverse width. This fact was used to investigate the possible existence of mass effects without any troublesome frequency difference. Tests on specimens  $8 \times \frac{3}{8} \times \frac{5}{8}$  in. and  $8 \times \frac{1}{8} \times \frac{5}{8}$  in., quenched and aged at the same

TABLE I.—Composition and Condition of Aluminium Alloys.

Symbol in Fig. 8	Composition, wt.-%					Remarks	Condition	Origin
	Cu	Mg	Si	Mn	Fe			
A.—Duralumin for Tests in Section III.								
...	3.87	0.68	0.38	0.72	0.50 †	...	Extruded	British Non-Ferrous Metals Research Assn.
B.—Alloys for Tests in Section IV.								
■	4.01	...	0.0055	Nil	0.005 †	Super-pure aluminium- base	Extruded	The British Aluminium Co., Ltd. (per B.N.F.M.R.A.)
●	...	...	...	0.72	... *	Super-pure aluminium- base	Cast	Author
▲	...	0.63	0.36	...	... *	Super-pure aluminium- base	Cast	Author
+	3.87	...	0.38	...	... *	Super-pure aluminium- base	Cast	Author
●	3.87	0.68	0.38	...	... *	Super-pure aluminium- base	Cast	Author
▼	3.80	0.67	0.003	...	... †	Front of extrusion	} Extruded	The British Aluminium Co., Ltd.
	3.65	0.68	0.0025	...	... †	Back of extrusion		
×	0.05	0.62	0.37	Trace	0.04 †	...	Extruded	James Booth and Co., Ltd.
Not shown	...	7	...	...	... *	...	...	British Non-Ferrous Metals Research Assn.
Not shown	...	...	...	...	0.5 *	Super-pure aluminium- base	Cast	Author
C.—Quaternary Alloy Used for All Tests in Section V.								
...	3.70	0.63	0.37	...	... †	Front of extrusion	} Extruded	The British Aluminium Co., Ltd.
...	3.81	0.64	0.39	...	... †	Back of extrusion		

\* Not analysed.

† Analysed composition.

to log  $t$ ) appears to correspond to the attainment of maximum hardness, but, as will be shown later, this is fortuitous.

## 2. EFFECT OF AGEING TEMPERATURE

The family of curves in Fig. 4 shows the variation of damping capacity with time during ageing at elevated temperatures up to 63° C. All specimens were solution-treated in a vacuum at 500° C. for 2 hr., quenched in water at room temperature, suspended in the damping apparatus, and heated to the ageing temperature. It was assumed that ageing for 3 min. at room temperature before heating began would have a negligible effect on the elevated-temperature results, and so the times plotted in Fig. 4 were measured from the middle of the heating period.

The important feature brought out by these tests is that the damping appears to be made up of two contributions. The second of these reaches a maximum value which is greater, and occurs later, at lower ageing temperatures. The first corresponds to the point of inflection and is again attained later at lower temperatures but appears to increase in magnitude at higher temperatures.

It is a great advantage that the natural frequency of

temperature, showed maximum damping after exactly the same time, but in the case of the thicker specimen the peak damping was lower. This is consistent with the view, further supported by later work, that the height of the peak depends on the degree of super-saturation, which would be expected to be greater in the thinner specimen because of the more drastic quench.

The time to attain peak damping is proportional to  $\exp(H/RT)$ , where  $T$  (°K.) is the ageing temperature. Fig. 5 confirms this, and gives a value for  $H$  of 38,000 cal./mole.

## 3. EFFECT OF FREQUENCY ON AGEING CURVES

Tests were carried out at different frequencies to determine whether the time-dependent damping effects were of anelastic origin. The results of the first series of experiments, given in Fig. 6, were measured in torsional vibration during ageing at room temperature. All the results were measured on the same specimen which was freshly solution-treated at 500° C. and quenched for each test. For the 2.8 c./s. test the central portion of the specimen was machined down, and the apparatus modified to allow



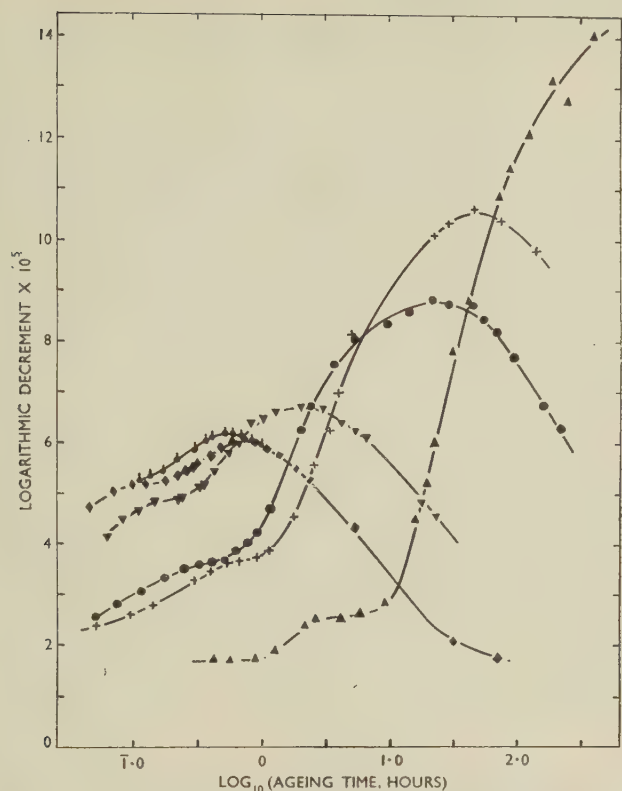


FIG. 4.—Variation of Damping of Duralumin, Solution-Treated for 2 Hr. at 500° C. and Quenched in Water at Room Temperature, Then Aged at Temperatures Between the Limits Indicated:

●	62.7–63.3	} Specimens $8 \times \frac{1}{4} \times \frac{3}{8}$ in.
+	36.4–38.1	
◆	59.4–60.6	
▼	52.3–55.0	} Specimens $8 \times \frac{3}{8} \times \frac{3}{8}$ in.
●	41.0–42.5	
▲	16.0–21.5	

Transverse vibration in frequency range 2050–2150 c./s.

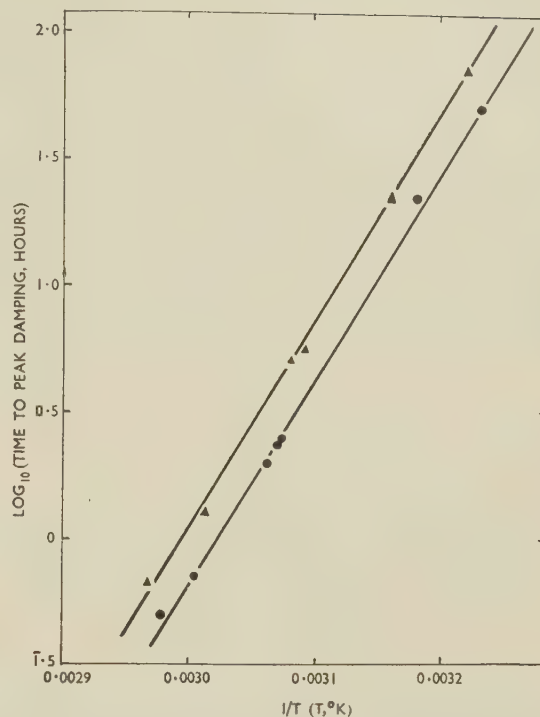


FIG. 5.—Relation Between Logarithm of Time-to-Peak-Damping and Reciprocal of Ageing Temperature (°K.).

● Duralumin. ▲ Al-Cu-Mg-Si alloy.

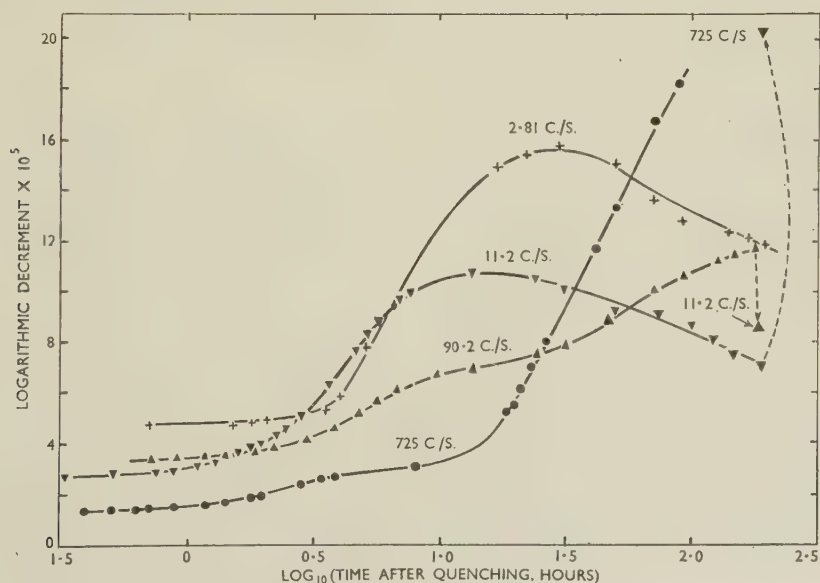


FIG. 6.—Variation of Damping in Torsional Vibration of Duralumin Ageing at Room Temperature After Quenching from 500° C.

+	c./s.	°C.	▼	c./s.	°C.	▲	c./s.	°C.	●	c./s.	°C.
	2.81	(13.9–15.9)		11.2	(20.7–21.0)		90.2	(16.4–17.5)		725	(19.8–23.3)

Damping measured at atmospheric pressure.

the specimen to be tested with the oscillating inertia suspended from the specimen, not in the usual inverted position, which would be near elastic instability for this specimen.

It appears from Fig. 6 that the damping is critically frequency-sensitive. At long ageing times the damping is greater at higher frequencies, and a peak is evident in the low-frequency tests. It was at first suspected that the peak was caused by acceleration of ageing by the rather higher stresses used in the low-frequency damping measurements. Two facts disprove this. Firstly, the intermediate-frequency test at 90.2 c./s. was carried out at the same stress level, and secondly, if, after a low-frequency test, the

in its present form is completely unsuitable for tests at elevated or reduced temperatures.

#### 4. DAMPING/TEMPERATURE CURVES

Although Fig. 6 establishes the frequency-dependence of damping, it is not adequate for the identification of anelastic effects. For this purpose an alternative approach was adopted, using specimens in transverse vibration. These were aged beyond the peak damping at an elevated temperature, and then the damping was recorded as the specimen cooled from the ageing temperature to about  $-60^{\circ}\text{C}$ . It was assumed that the rates of cooling used were insufficient

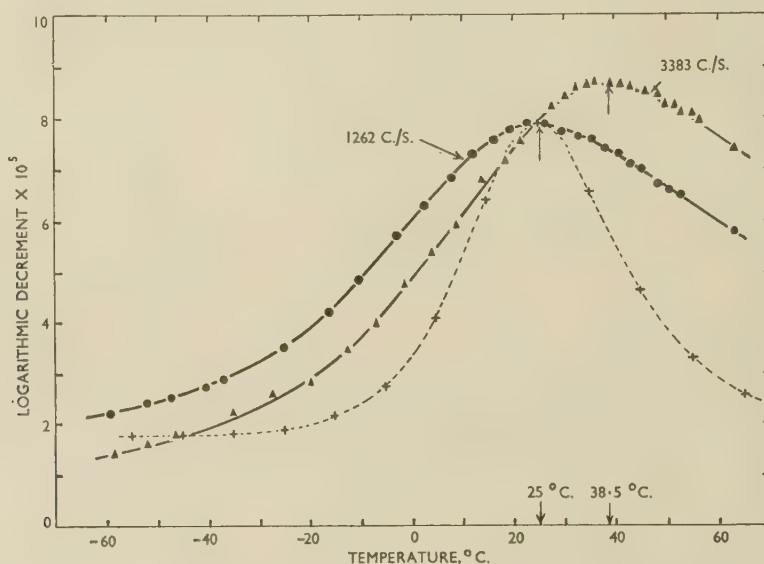


Fig. 7.—Variation of Damping of Duralumin with Temperature After Ageing at  $63.5^{\circ}\text{C}$ . for 4 Hr.

Specimen  $8 \times \frac{3}{8} \times \frac{1}{8}$  in. in transverse vibration.

- 1262 c./s. (fundamental).
- ▲ 3383 c./s. (second mode).
- + Calculated curve for single relaxation effect with  $H = 13,500$  cal./mole, peak at  $25^{\circ}\text{C}$ ., and background damping  $1.75 \times 10^{-5}$ .

specimen was removed from the inertias and tested freely suspended, the damping value showed good agreement with that recorded at the same stage in a test during which the specimen was vibrated only at the higher frequency. It was then considered that the peak might result from an intensification of the effect causing the point of inflection in the higher-frequency tests. Evidence is adduced later which disproves this view and supports the suggestion that the peak is the same as that evident in Fig. 4, but displaced to a shorter ageing time; i.e. it is what has earlier been referred to as the second damping contribution; the first is either absent, masked by the second, or attained after very short ageing times. The increase in height of the peak at 2.8 c./s., against the general trend, is considered to be a mass effect, the more slender specimen receiving a more drastic quench.

The results of Fig. 6 are complicated by variations of room temperature. Unfortunately the apparatus

to allow any significant ageing to take place after cooling began, and therefore that the measured damping/temperature curve is that for the metallurgical condition prevailing at the beginning of the cooling test. This was confirmed by the retraceable form of the curve at the cooling and heating rates used. Cooling was initiated by transferring the specimen assembly from the furnace tube to the low-temperature tube, a procedure which produced a temperature fall of about  $5^{\circ}\text{C}$ . in 1 min. Further cooling then proceeded at not more than  $1^{\circ}\text{C}/\text{min}$ ., controlled by the rate of addition of solid carbon dioxide to the cooling bath. Fig. 7 shows the damping/temperature curve measured during cooling after ageing beyond peak damping at  $63^{\circ}\text{--}64^{\circ}\text{C}$ . The two curves were measured at the fundamental and first harmonic frequencies, respectively, of a specimen  $8 \times \frac{3}{8} \times \frac{1}{8}$  in. The damping rises to a peak during cooling. This occurs at  $25^{\circ}\text{C}$ . at 1262 c./s. and at  $38.5^{\circ}\text{C}$ . at 3383 c./s. This frequency-dependence



establishes the anelastic origin of the damping. The activation energy derived from:

$$H = 2 \log \left( \frac{f_1}{f_2} \right) \cdot \frac{T_1 T_2}{T_1 - T_2},$$

where  $T_1$  and  $T_2$  ( $^{\circ}\text{K}.$ ) are the peak temperatures at frequencies  $f_1$  and  $f_2$ , is 13,500 cal./mole.

The theoretical curve <sup>4</sup> for a single relaxation effect with this value of  $H$ :

$$\delta = 2\delta_m \cdot \frac{\phi}{1 + \phi^2},$$

where  $\delta_m$  is peak damping and

$$\phi = \exp \left[ \frac{H}{R} \left( \frac{1}{T} - \frac{1}{T_p} \right) \right]$$

and  $T_p$  is the peak temperature, is drawn in Fig. 7 for the lower-frequency conditions. The experimental curve is broader. The observed effects must therefore arise from the sum of a series of relaxation effects with peaks over a range of temperature. An alternative possibility is that the effects arise from a series of curves with peaks at the same temperature but with different activation energies, that is, different breadths. In this case change of frequency should shift each constituent curve by differing amounts and alter the shape of the resultant. This is not observed.

#### IV.—DAMPING CHANGES IN SIMPLER HIGH-PURITY ALLOYS

The foregoing experiments sufficed to establish that the damping changes in Duralumin were of anelastic

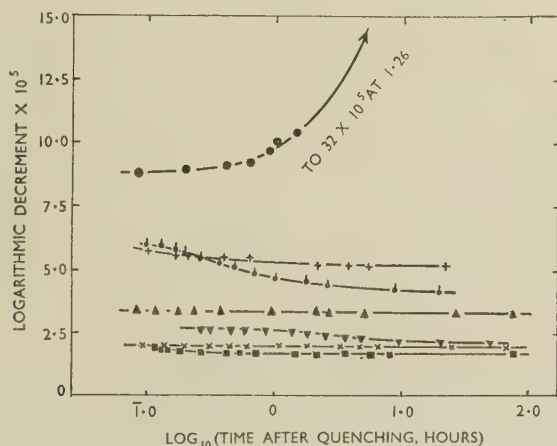


Fig. 8.—Variation of Damping of Aluminium-Rich Alloys During Ageing at Room Temperature After Quenching from 500°C.

- Al-Cu-Mg-Si.
- ▲ Al-Mn.
- + Al-Cu-Si.
- ▲ Al-Mg-Si.
- ▼ Al-Cu-Mg.
- × Al-Mg-Si + 0.05% Cu.
- Al-Cu.

Transverse vibration at  $\sim 2000$  c./s.

origin, but in order to obtain a fundamental explanation of the behaviour it was considered essential to investigate the effect of alloy composition, and if possible to find a simpler alloy exhibiting similar damping changes.

The first specimens tested were binary alloys of

super-pure aluminium with copper, manganese, or iron, and a commercial-purity alloy of aluminium with 7% magnesium. With the exception of magnesium, the percentage by weight of the second constituent was in each case approximately the same

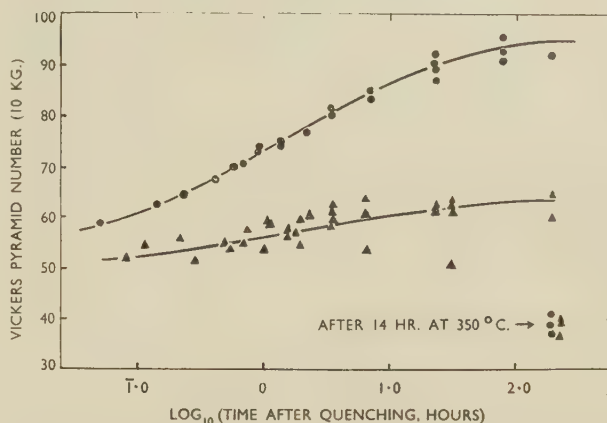


Fig. 9.—Hardness/Time Curves for Aluminium-4% Copper Alloy Solution-Treated at 520°C. for 17 Hr., Quenched in Water at Room Temperature, Then Aged at Room Temperature.

- Specimens  $\frac{1}{8}$  in. thick  $\times \frac{1}{4}$  in. dia.
- + Specimens  $\frac{1}{4}$  in. thick  $\times \frac{1}{4}$  in. dia.

as that in the commercial Duralumin. Later ternary aluminium-copper-silicon, aluminium-copper-magnesium and aluminium-magnesium-silicon alloys and a quaternary aluminium-copper-magnesium-silicon alloy were prepared. The composition, condition, and origin of these alloys are given in Table I.

The variation of damping during ageing at or near room temperature for specimens of some of these alloys, quenched from 500°C., is shown in Fig. 8. The first test was carried out on an aluminium-4% copper specimen,  $8 \times \frac{3}{8} \times \frac{5}{8}$  in., which increased in hardness only slightly. Further investigation confirmed the existence of a hardening mass effect, thin specimens increasing in hardness more rapidly and to a greater degree. The hardness tests shown in Fig. 9 bear this out, and confirm that a bar  $\frac{1}{8}$  in. thick could be expected to harden appreciably during the course of the damping tests. Accordingly, damping tests were made both on  $\frac{1}{8}$ -in.-thick bars and on tubes of  $\frac{1}{8}$ -in. wall thickness, milled with flats to prescribe the planes of vibration.<sup>1</sup> Although appreciable hardness change was observed in these specimens, the changes of damping capacity showed none of the characteristics of Duralumin.

It is clear from Fig. 8 that none of the binary or ternary alloys exhibits changes similar to those observed in Duralumin. The quaternary alloy is the simplest in which an increase of damping was observed. The alloys tested in the cast condition showed a high as-quenched damping due to casting defects, but this was not sufficient to obscure damping changes of the order looked for. Any alloy showing the slightest tendency to damping increase was obtained in the extruded condition and investigated more closely.

The absence of any observed changes in the simpler

alloys is not necessarily taken to mean that relaxation effects are absent. The peak in the damping/temperature curve for quenched aluminium-4% copper alloy observed by Kê<sup>11</sup> at 200° C. and 1 c./s. supports the view that other relaxation effects may exist, though they may be so far removed from the measuring conditions as to be undetectable. For example, in this particular case, assuming a single relaxation time with an activation energy of 34,000 cal./mole, the peak observed by Kê would arise at about 330° C. at a frequency of 2000 c./s. The damping contribution from this effect at 70° C. (the highest temperature used in the present work) would be about  $1/10^9$  of the peak value, a figure which explains its passing unnoticed here.

## V.—BEHAVIOUR OF THE Al-Cu-Mg-Si ALLOY

### 1. EFFECT OF AGEING TEMPERATURE

The damping in transverse vibration of specimens of the aluminium-copper-magnesium-silicon alloy,



FIG. 10.—Variation of Damping During Ageing of the Al-Cu-Mg-Si Alloy; Solution-Treated at 500° C. (2 Hr.) and Quenched in Water at Room Temperature, Then Aged at the following Temperatures:

°C.	°C.
▼ 68.0-70.4	▲ 43.0-44.0
● 63.4-64.5	■ 36.6-38.4
+ 58.0-60.0	× 11.5-16.0
◆ 49.7-50.4	

All specimens  $8 \times \frac{5}{8} \times \frac{1}{8}$  in. in transverse vibration between 1919 and 1940 c./s.

$8 \times \frac{5}{8} \times \frac{1}{8}$  in., quenched from 500° C. was investigated in exactly the same way as for Duralumin. The results are given in Fig. 10. The test at room

temperature shows the absence of the point of inflection corresponding to the first damping contribution in Duralumin; in the higher-temperature tests the

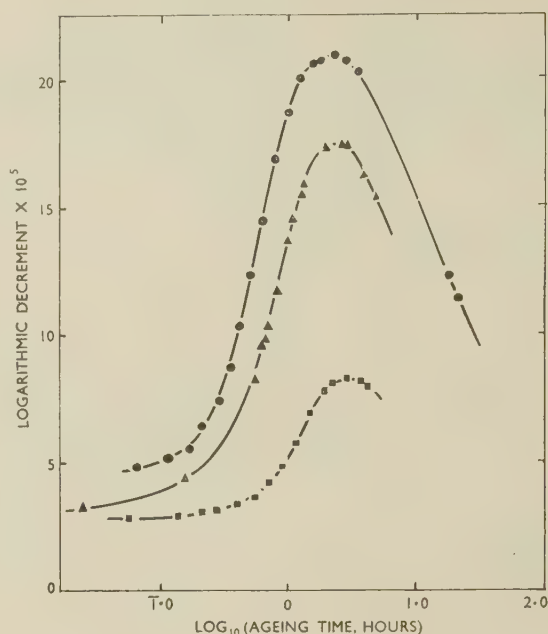


FIG. 11.—Effect of Duration and Temperature of Solution-Treatment on the Variation of Damping After Quenching of the Al-Cu-Mg-Si Alloy.

- Heated to 500° C. in 5 min., quenched, aged at 54.5° C.
- ▲ Solution-treated 2 hr. at 462° C., quenched, aged at 53.5° C.
- Solution-treated 2 hr. at 436° C., quenched, aged at 52.5° C.

Specimen  $8 \times \frac{5}{8} \times \frac{1}{8}$  in. in transverse vibration at  $\sim 1950$  c./s.

subsequent peak is evident and much more pronounced. It is as though some of the constituents responsible for it were rendered inactive in Duralumin by impurities. Again the time ( $t$ ) to attain peak damping varies as  $\exp(H/RT)$  and the plot of  $\log t$  against  $1/T$  in Fig. 5 shows that  $H$  has substantially the same value as for the Duralumin peak, supporting the view that the peaks arise from the same effect. At any temperature the peak is attained in Duralumin slightly before that for the quaternary alloy.

### 2. EFFECT OF TIME AND TEMPERATURE OF SOLUTION-TREATMENT

The two lower curves in Fig. 11 show the effect of solution-treatment temperature. In each case the specimen was held for 2 hr. at the temperature stated. Maximum damping during ageing is attained at the same time, independent of quenching temperature, but the peak is higher for higher temperatures. This is consistent with the view that the height of the peak depends on the degree of supersaturation. The effect of duration of solution-treatment confirms this view. A specimen was overaged for 24 hr. at 350° C. to produce extensive precipitation of solute and was then heated to 500° C. in 5 min. and quenched immediately on attaining that temperature. The upper curve in Fig. 11 shows that a peak damping of  $2.1 \times 10^{-4}$  was reached after about  $2\frac{1}{4}$  hr. ageing at



54.5° C. The same specimen treated for 2 hr. at 500° C. and aged at the same temperature reached a peak of  $2.85 \times 10^{-4}$  after the same period. The specimen which was heated for 5 min. showed an

that it is independent of solution-treatment temperature. The shift of the peak caused by change of frequency is illustrated in Fig. 15, which shows four damping/temperature curves measured on two identi-

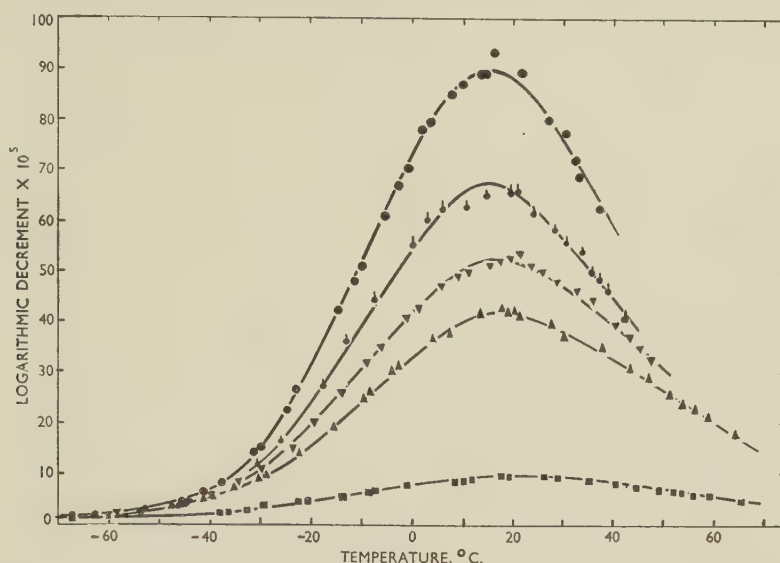


FIG. 12.—Relation Between Damping and Temperature for the Al-Cu-Mg-Si Alloy, Cooled After Ageing for :

● 160 hr. at 37.5° C.    ● 80 hr. at 43.5° C.    ▼ 4 hr. at 54.5° C.    ▲ 1.3 hr. at 64° C.    ■ 18 hr. at 66° C.

Frequency at peak damping 1950 c./s. in all cases. Specimen  $8 \times \frac{3}{8} \times \frac{3}{8}$  in. in transverse vibration.

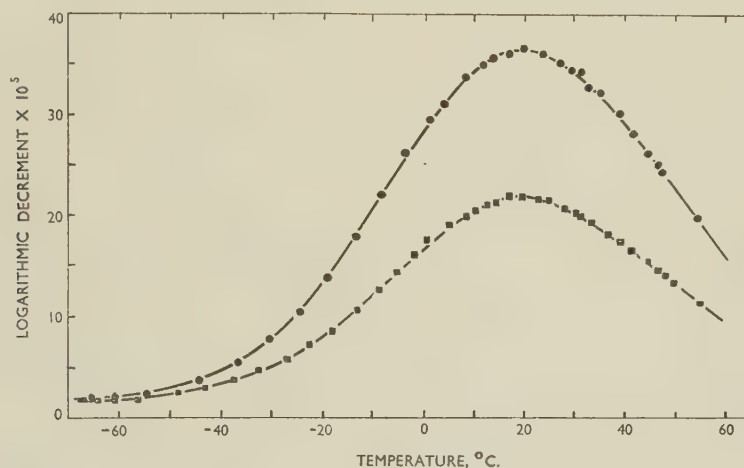


FIG. 13.—Relation Between Damping and Temperature for the Al-Cu-Mg-Si Alloy Quenched from 500° C. (2 Hr.).

● Aged 4 hr. at 54.4° C.    ■ Aged 17 hr. at 54.4° C.

Frequency 1950 c./s.

increase of Vickers pyramid hardness from 54.5 to 96 over a period of 1000 hr. at room temperature.

### 3. DAMPING/TEMPERATURE CURVES

Damping/temperature curves, measured during cooling from a wide range of ageing conditions, are given in Fig. 12. The peak is evident at the same temperature irrespective of the earlier ageing temperature. Fig. 13 shows further that the peak temperature is independent of ageing time and Fig. 14

cally treated specimens of different size in the fundamental and first harmonic frequencies, respectively. Both specimens were suspended at the nodes of the higher-frequency mode and measurements made alternately at the two frequencies during cooling. The measured shift of the peak from the two pairs of curves gives a mean value of 13,200 cal./mole for the activation energy. The observed peaks are broader than the theoretical curves for a single relaxation effect having this value of  $H$ , again in agreement

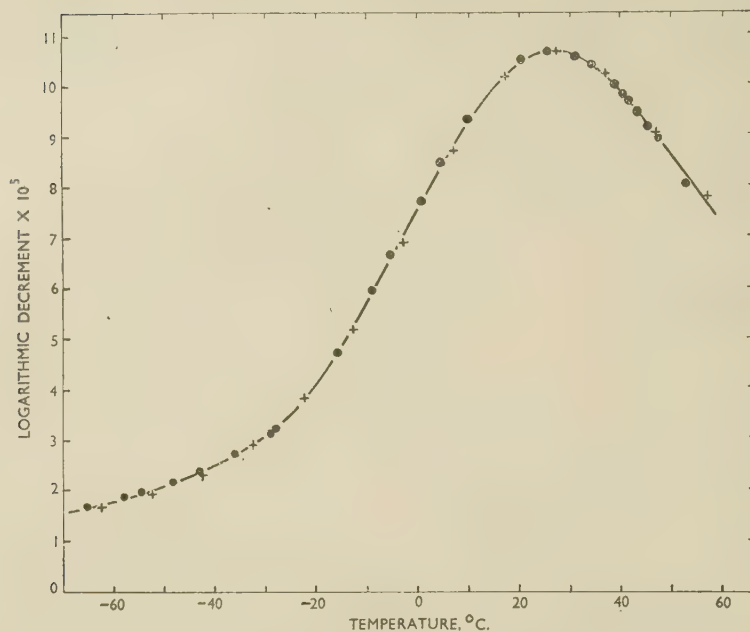


FIG. 14.—Relation Between Damping and Temperature for the Al-Cu-Mg-Si Alloy Quenched from 436° C. (2 Hr.) and Aged 4.5 Hr. at 52.5° C.

● Experimental points. + Calculated points for  $H = 6050$  cal./mole and background damping  $1.49 \times 10^{-5}$ .

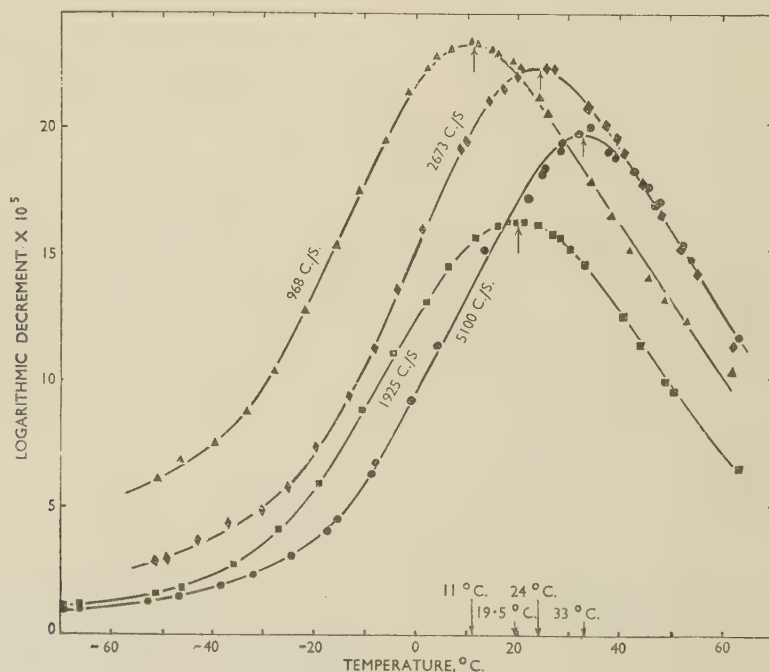


FIG. 15.—Effect of Frequency on the Damping/Temperature Curve for the Al-Cu-Mg-Si Alloy, Aged About 24 Hr. at 63° C., After Quenching from 500° C.

● 5100 c./s. (2nd mode) } Specimen  $8 \times \frac{3}{8} \times \frac{1}{8}$  in.      ◆ 2673 c./s. (2nd mode) } Specimen  $8 \times 0.312 \times \frac{1}{8}$  in.  
 ■ 1925 c./s. (fundamental) }  
 Specimens suspended at nodes of second mode. Arrows indicate peak temperatures.



with the behaviour of Duralumin. The experimental curves illustrate the misleading values which can arise from the determination of activation energy from the geometry of the peak. For a true simple relaxation curve, if  $T_a$  and  $T_b$  are the two tempera-

the suspected trend is supported by damping measurements made concurrently in transverse vibration at 970 and 2650 c./s. on a specimen  $\frac{3}{8}$  in. deep during ageing at 54.8° C. This method eliminates unavoidable slight differences in temperature histories which

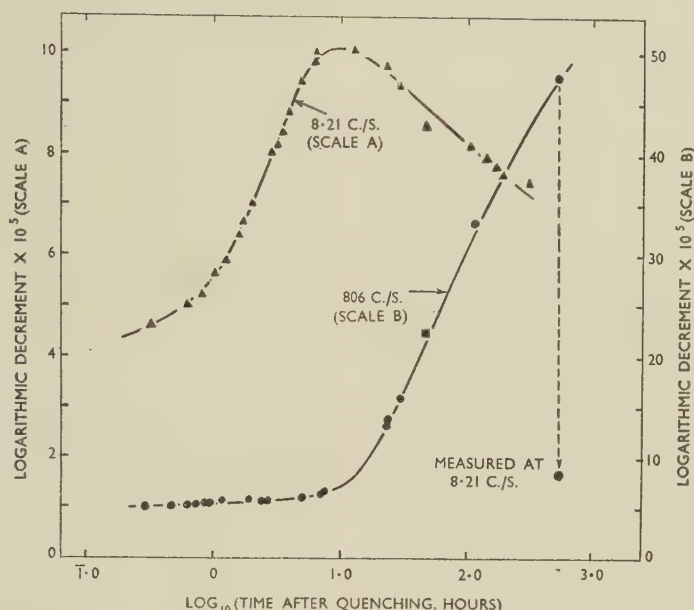


FIG. 16.—Effect of Frequency on the Variation of Damping During Ageing at Room Temperature for the Al-Cu-Mg-Si Alloy.

▲ 8.21 c./s. (left-hand scale) 16.2–18.6° C.

● 806 c./s. (right-hand scale) 13.5–17.5° C.

tures at which the damping is half of the peak value, then :

$$H = 5.28 \frac{T_a T_b}{T_a - T_b}$$

If the curve illustrated in Fig. 14 is assumed to be of this form, a value of  $H = 6050$  cal./mole is deduced. The calculated curve for this value of  $H$  is seen to be in good agreement with the experimental points. The error is evident only if a second curve is measured at a different frequency of vibration.

#### 4. EFFECT OF FREQUENCY ON AGEING CURVES

The variation of damping capacity, measured in torsional vibration, during ageing at room temperature is shown in Fig. 16. A maximum damping is attained after 10 hr. at 8.21 c./s., but at 806 c./s. the damping was still rising after 800 hr. This behaviour is similar to that of Duralumin. The curves for the high-purity alloy, however, do not show the point of inflection of Duralumin, and therefore the peaks evident in Fig. 6 are not caused by an increase of intensity of this first contribution.

It is considered that the low-frequency peak in Fig. 16 is identical with that evident in Fig. 10, but displaced to shorter ageing times. Further work is required to prove this point, involving measurements over a range of temperature at low frequencies, but

would be a source of uncertainty in two separate tests. The peak (Fig. 17) is reached earlier at the lower frequency of vibration and has a reduced height. In this test the bar was supported at the

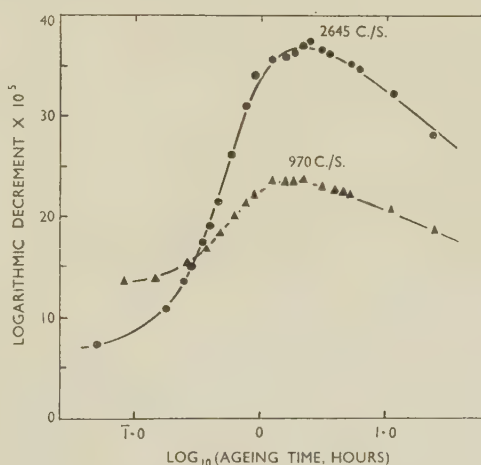


FIG. 17.—Effect of Frequency on the Variation of Damping of the Al-Cu-Mg-Si Alloy During Ageing at 54.5° C.

● 2645 c./s. (transverse vibration). ▲ 970 c./s. (transverse vibration).

nodes of the second harmonic, and part of the discrepancy between the damping values at short times arises from suspension loss.

## VI.—DISCUSSION

A discussion is given here of the merits of possible explanations of the origin of the damping changes, none of which is found to accord completely with the experiments.

The experimental results may be summarized as follows. The changes of damping capacity at 2000 c./s. of Duralumin quenched from 500° C. and aged at constant temperature reflect two damping contributions. The first is a rise to a point of inflection; the second a subsequent rise to a peak followed by a slow fall to a low value. The simplest high-purity alloy in which any similar effects have been observed is a quaternary aluminium-copper-magnesium-silicon alloy which exhibits only the second contribution. The first contribution in Duralumin has not been investigated in detail. The time to reach peak damping in both cases varies with ageing temperature  $T$  as  $\exp(H/RT)$ , where  $H = 38,000$  cal./mole. In the high-purity alloy it was found that the time to attain peak damping during ageing was unaffected by specimen size and solution-treatment temperature and duration, but that the height of the peak was increased by factors favouring high supersaturation on quenching, that is, small specimen section, high temperature of solution-treatment, and long duration. The damping/temperature curve measured during cooling from the ageing temperature in both cases shows a peak, which, although not at the same temperature for the two materials, suffers the same order of shift with change of frequency, characterized by an activation energy of about 13,000 cal./mole. The temperature of this damping peak in the case of the high-purity alloy was found to be almost unaffected by ageing conditions, and in both alloys the measured peak was broader than the theoretical curve for a single relaxation effect.

The peak in the damping/ageing-time curve at constant temperature occurs earlier and has a lower value at lower frequencies of vibration, but further work is required to prove this conclusively. If it is substantiated, no simple correlation between time to peak damping and rate of change of hardness is to be expected, since solution-treatment time and temperature would have no influence on the time to peak damping but are known to affect the rates of change of hardness.

The search for an explanation of the damping changes is complicated by the complex nature of the simplest alloys in which they are observed. It is unfortunate that so little information is available from other techniques on the early stages of ageing in the quaternary alloy.

Attempts are frequently made to identify relaxation effects by comparing activation energies derived from anelasticity measurements with those measured, for example, in conventional diffusion experiments. This procedure may be misleading. For example, in quenched alloys Nowick has shown<sup>14</sup> that activation energies for stress-induced diffusion may be lower in

the quenched condition than in the annealed state, because of a higher vacancy concentration in the former case. In view of effects of this kind it is not surprising that the figure of 13,000 cal./mole measured in this work is not an immediate clue to the origin of the damping. The figure of 38,000 cal./mole for the attainment of peak damping during ageing is a little greater than those for the diffusion of copper, magnesium, and silicon in aluminium, and is of the same order as that for self-diffusion of aluminium. The attainment of peak damping is therefore likely to be controlled by diffusion, but no data for diffusion in the quaternary alloy are available to confirm this view. On the basis of the difference between the two measured activation energies, 38,000 and 13,000 cal./mole, respectively, it is inferred that the factor controlling the attainment of peak damping during ageing differs from that giving rise to the energy dissipation.

An explanation of the damping effects worthy of examination relies on the development of a particular intermediate phase or aggregation of solute atoms which is intrinsically anelastic in virtue of a stress-induced diffusion effect. In this case the relaxation time would be determined by elementary diffusion jumps, presumably of substitutional solvent atoms, giving rise for example to change in orientation of atom pairs. Hence the relaxation time would be of the order of the mean time for which a diffusing atom stays in a particular site. To explain the observed effects this time would have to be of the order of  $10^{-4}$  sec. at 18° C., which is excessively low, even if regard is paid to possible reductions caused by high vacancy concentrations in quenched alloys. Nowick's measurements<sup>14</sup> on a non-ageing alloy of zinc in silver predict a time of  $10^9$  sec. at room temperature for the equilibrium state and  $10^4$  sec. immediately after quenching from 400° C. Even the latter value exceeds the relaxation times measured in this work by  $10^8$ . The most rapidly diffusing atoms are in general interstitial; for example, carbon in  $\alpha$ -iron which has a mean time in a particular site of about 1 sec. at 18° C.; here quenching produces no reduction,<sup>6</sup> in accord with current pictures of the diffusion mechanism for interstitial atoms. It is difficult to imagine, therefore, how the substitutional elements in the aluminium-copper-magnesium-silicon alloy could diffuse between adjacent sites at a rate sufficiently high to explain the observed effects.

This conclusion leads to the suggestion that the effects may arise from a process of atom migration involving a fraction of the interatomic distance. If damping effects from thermal currents are excluded, the only published effect with a relaxation time comparable with that recorded here is for a quenched copper-manganese alloy<sup>15</sup> which exhibits a peak in the damping/temperature curve a little below 0° C. at 700 c./s., that is, the relaxation time is about  $5 \times 10^{-4}$  sec. The necessary frequency-dependence of the peak has not been measured, so that it is not conclusively proved that the effect is of anelastic origin,



and it is therefore impossible to extrapolate the results to 18° C. However, on the assumption that a relaxation effect is likely, the time would be expected to be below  $5 \times 10^{-4}$  sec. at 18° C. and therefore of the same order as that recorded in the present work. A suggested explanation for the suspected copper-manganese relaxation has been put forward,<sup>4</sup> based on the effect of stress on the coherent boundary between tetragonal regions of differing orientation. The application of a tensile strain will favour the extension of a tetragonal region with the longest axis in the direction of strain, and will cause a migration of the boundary with the resultant overall expansion required for the production of anelastic effects. Here the atom translations associated with boundary movement will depend on the degree of tetragonality and difference of orientation, but will always be a small fraction of the interatomic distance. Thus, reduced relaxation times would be expected, compared with those for stress-induced diffusion over the order of one interatomic distance.

The development in the aluminium alloys of adjacent tetragonal regions separated by a coherent boundary requires experimental support. The absence of damping changes in the aluminium-magnesium-silicon alloy with 0.05% copper as "impurity" indicates that trace elements are not responsible for observed effects in the quaternary alloy. It is possible that the damping effects are evident only in alloys in which solute atom concentrations arise leading ultimately to the precipitation of the hexagonal *Q* phase. The absence of the relaxation peak in the annealed state indicates that *Q* (in the form of incoherent precipitates) is not anelastic in the range investigated, but it may well be that in the early stages of solute-atom segregation, before there is any breaking away from the matrix, the effects postulated above may arise. This is being investigated.

The most puzzling feature of the experimental results is the frequency-dependence of the damping/ageing-time curves. On the basis of this information alone it might be suspected that the relaxation time

$\tau$  varies progressively during ageing, as the result, for example, of changes in the distribution of solute atom concentrations. Thus, maximum damping would arise at the instant that the condition  $2\pi f\tau = 1$ , where  $f$  is the frequency of vibration, is satisfied. The earlier peak at lower frequency would require therefore that  $\tau$  falls during ageing. (It is interesting here to note that Nowick has observed a progressive rise following quenching in a silver-zinc alloy.) This is not consistent with the results of cooling tests. On the above hypothesis:

(i) The damping/temperature curve measured during cooling from the ageing temperature should rise to a peak at a progressively lower temperature the longer the ageing time.

(ii) A specimen aged to peak damping at constant temperature should always show a progressive fall of damping on cooling or heating, since the ageing temperature should be the peak temperature for the cooling curve.

Neither of these effects was observed. The cooling-curve peak arose at a temperature substantially independent of ageing conditions, and the damping/temperature curve showed an initial rise for cooling from ageing temperatures above that of the cooling peak. This is being investigated further by extending the low-frequency damping measurements over a range of temperature.

#### ACKNOWLEDGEMENTS

The author wishes to thank The British Aluminium Co., Ltd., and James Booth and Co., Ltd., for the supply of alloys in extruded form, and the British Non-Ferrous Metals Research Association for much material help in the early stages of the work.

He is grateful to Professor F. C. Thompson for encouragement throughout the research, and to his colleagues, Dr. H. J. Axon for preparing the cast alloys, and Mr. B. S. Berry for helpful discussions, particularly on electronic problems, and for the loan of a high-gain amplifier.

#### REFERENCES

1. K. M. Entwistle, *J. Inst. Metals*, 1948-49, **75**, 81.
2. R. F. Hanstock, "The Non-Destructive Testing of Metals" (*Inst. Metals Monograph and Rep. Series No. 10*), p. 87. 1951: London (Institute of Metals).
3. R. F. Hanstock, *J. Inst. Metals*, 1948, **74**, 469.
4. C. Zener, "Elasticity and Anelasticity of Metals". 1948: Chicago (University of Chicago Press).
5. L. J. Dijkstra, *Philips Research Rep.*, 1947, **2**, 357.
6. C. Wert, "Thermodynamics in Physical Metallurgy", p. 178. 1949: Cleveland, O. (American Society for Metals).
7. T. S. Kê, *Phys. Rev.*, 1948, [ii], **74**, 9.
8. S. Harper, *ibid.*, 1951, [ii], **83**, 709.
9. C. Zener, "Elasticity and Anelasticity of Metals", p. 114.
10. A. S. Nowick, *J. Appl. Physics*, 1951, **22**, 925.
11. T. S. Kê, *Chinese J. Physics*, 1950, **7**, 428.
12. G. A. Cottell, K. M. Entwistle, and F. C. Thompson, *J. Inst. Metals*, 1948, **74**, 373.
13. L. Frommer and A. Murray, *J. Inst. Metals*, 1944, **70**, 1.
14. A. S. Nowick and R. J. Sladek, *Acta Met.*, 1953, **1**, 131.
15. A. V. Siefert and F. T. Worrell, *J. Appl. Physics*, 1951, **22**, 1257.

# 1521 SOME METALLOGRAPHIC OBSERVATIONS OF THE CREEP OF ALUMINIUM-COPPER ALLOYS\*

By A. H. SULLY,† M.Sc., Ph.D., F.Inst.P., F.I.M., MEMBER, and  
H. K. HARDY,‡ M.Sc., Ph.D., A.R.S.M., A.I.M., MEMBER

## SYNOPSIS

In aluminium-copper alloys containing 3 and 4% copper, creep at 190° C. occurred preferentially in relatively narrow regions, depleted in solute, on either side of the grain boundary. Plastic flow accentuated the precipitation process in the material immediately adjacent to the grain boundary, thus widening the band of material with a low resistance to deformation. Shear displacement across boundaries favourably oriented to the applied stress was accompanied by the formation of fissures transverse to the stress direction. High-purity alloys showed the effects most prominently and gave intercrystalline fractures. Normal-purity alloys possessed a much better creep-resistance, but also gave intercrystalline failure when previously aged at 190° C. Normal-purity material aged at 300° C. gave ductile fractures associated with longitudinal fissures in the necked region. The results point to the importance of grain-boundary stability in creep-resistant alloys.

## I.—INTRODUCTION

SOME interesting observations have been made of effects localized at and near the grain boundaries during the creep of aluminium alloys with 3 and 4% copper. Both very high-purity (S.P.) and normal-purity (N.P. containing 0.25% iron and 0.11% silicon) alloys were studied. Additional elements, such as

(N.P.) in circulating-air furnaces. The high-purity alloys possessed an appreciably larger grain-size than those of commercial purity. Creep tests were made at 4.5 tons/in.<sup>2</sup> at 190° C. on specimens having a gauge portion 0.564 in. in dia. and 3 in. long; specimens were held in the creep furnace for 24 hr. at 190° C. before loading. The tensile and creep properties of the alloys are summarized in Table I. It will be noted that, apart from the specimens aged at 300° C., the creep properties of the normal-purity alloys were much superior to those of the high-purity material.

TABLE I.—*Tensile and Creep Properties of Aluminium-Copper Alloys.*

Alloy, Cu, %	Ageing Treatment	Tensile Properties at Room Temperature			Creep Properties at 4.5 tons/in. <sup>2</sup> and 190° C.		
		0.1% Proof Stress, tons/ in. <sup>2</sup>	Max. Stress, tons/ in. <sup>2</sup>	Elonga- tion, %	Min. Creep Rate, %/hr.	Time to On- set of Ter- tiary Creep, hr.	Time to Rup- ture, hr.
<i>High-Purity</i>							
3	24 hr. at 190° C.	6.2	13.1	31	0.0090	30	42
3	8 hr. at 250° C.	6.2	13.6	23	0.0133	30	58
4	24 hr. at 190° C.	9.1	17.5	17½	0.0023	125	231
4	8 hr. at 250° C.	7.3	16.6	17	0.0035	210	325
<i>Normal-Purity</i>							
3	24 hr. at 190° C.	6.9	14.1	28	0.00092	360	978
3	8 hr. at 300° C.	4.2	12.3	27	0.00136	...	310
4	24 hr. at 190° C.	11.6	19.0	20½	0.00013	3000	5170
4	8 hr. at 300° C.	5.2	14.7	23	0.0025	270	430

manganese and nickel, frequently present in commercial alloys, were excluded in order to reduce the number of variable factors. The billets were cast to 2½ in. dia., annealed, scalped, and forged to ¾ in. square (S.P. cold forged; N.P. hot forged). The bars were solution-treated in a salt bath at 530° C. and aged for 24 hr. at 190° C. or for 8 hr. at 250° C. (S.P.) or 300° C.

\* Manuscript received 22 July 1953.

† Principal Physicist, Fulmer Research Institute, Ltd., Stoke Poges, Bucks.

‡ Senior Metallurgist, Fulmer Research Institute, Ltd., Stoke Poges, Bucks.

## II.—METALLOGRAPHIC EXAMINATION

### 1. HIGH-PURITY ALLOYS

All the high-purity alloys fractured without necking. Metallographic examination of the creep test-pieces showed that the precipitation process had led to the formation of relatively wide layers, adjacent to the grain boundaries, of solid solution depleted in copper. At a high magnification these regions showed some metallographic evidence of sub-grains; they may be regarded as being equivalent to an artificially widened grain boundary. Evidence for extensive deformation in the layers depleted in copper is provided by the relative movements of crystals by shear displacement across the boundaries favourably oriented to the applied stress and by the formation of fissures at grain boundaries transverse to the applied stress (Figs. 3 and 4, Plate XLII). Fracture occurred in the layer of depleted solid solution (Fig. 5, Plate XLII).

Unstressed specimens of the same alloys aged at 190° C. for periods as long as, and longer than, the duration of the creep test showed layers of copper depletion of very limited width, as may be judged from



Figs. 1 and 2 (Plate XLII). Polmear and Hardy<sup>1</sup> had observed that Gayler's light phenomenon and associated grain-boundary migration occurred only rarely on ageing at 190° C.

## 2. NORMAL-PURITY ALLOYS

Depleted layers adjacent to the boundaries were also a significant feature of the microstructure, but were narrower than in the alloys of high purity.

The alloys aged at 190° C. failed, like the high-purity alloys, by intercrystalline fracture with negligible or only slight necking. Intercrystalline fissures mainly perpendicular to the direction of stress were clearly evident in the microstructure (Fig. 6, Plate XLIII).

The alloys aged at 300° C. and creep-tested at 4.5 tons/in.<sup>2</sup> at 190° C. behaved somewhat differently, in that they necked appreciably before fracture. In the necked region there were numerous small cavities (Fig. 7, Plate XLIII) whose length, in general, was parallel to the direction of applied stress. Away from the fracture small fissures, usually perpendicular to the stress, were occasionally present in the depleted boundary layers (Fig. 8, Plate XLIII). The shape of these fissures was appreciably altered by the localized flow in the necked portion of the specimen, so that they became elongated in the stress direction (Fig. 9, Plate XLIII).

## III.—DISCUSSION

The results provide an interesting example of the interaction of deformation during creep and the precipitation process. Ageing before and during the early stages of the creep test leads to relatively narrow regions, depleted in solute, on either side of the grain boundaries. Creep occurs preferentially in those regions of low resistance to deformation whose presence controls the creep behaviour of the high-purity alloys and of the normal-purity alloys aged at 190° C. The plastic flow accelerates the precipitation process in the material immediately adjacent to the grain

boundary and its thin layers of copper-depleted solid solution, thus widening the band of material with a low resistance to deformation. The precipitation process under creep may be regarded as "discontinuous", since it spreads (slowly) into the grains and probably involves recrystallization (or polygonization) in the flowed layers. Somewhat similar effects have been observed by McKeown and Hopkin<sup>2</sup> in lead-base alloys, but in this case the anomalous precipitation induced by creep was metallographically more typical of normal discontinuous precipitation than that noted here for the aluminium-copper alloys.

The normal-purity alloys gave ductile fractures when tested in the overaged condition. The results suggest that the difference between the creep properties of the depleted layer and crystal centres was less marked. It is not clear whether necking was wholly responsible for the cavities or whether the occurrence of the small cavities perpendicular to the stress direction (Fig. 8) decided the position at which the specimen necked.

The creep behaviour described here illustrates, in an exaggerated form, those effects shown in creep tests on other materials at temperatures and stresses at which grain-boundary flow is an important factor in creep behaviour. These effects are intercrystalline failure, the formation of intercrystalline cavities in boundaries transverse to the applied stress, and the relative movement of crystals by shear displacement across boundaries favourably oriented to the applied stress.

The effects can be minimized in commercial alloys by the presence of elements which raise the recrystallization temperature and stabilize the grain boundaries. Advantages accruing from the impurities present in the normal-purity material are clearly evident.

## REFERENCES

1. I. J. Polmear and H. K. Hardy, *J. Inst. Metals*, 1952-53, **81**, 427.
2. J. McKeown and L. M. T. Hopkin, *Metallurgia*, 1950, **41**, 135.

# REPORT OF COUNCIL

## FOR THE YEAR ENDED 31 DECEMBER 1953

THE year 1953 has been a successful one for the Institute.

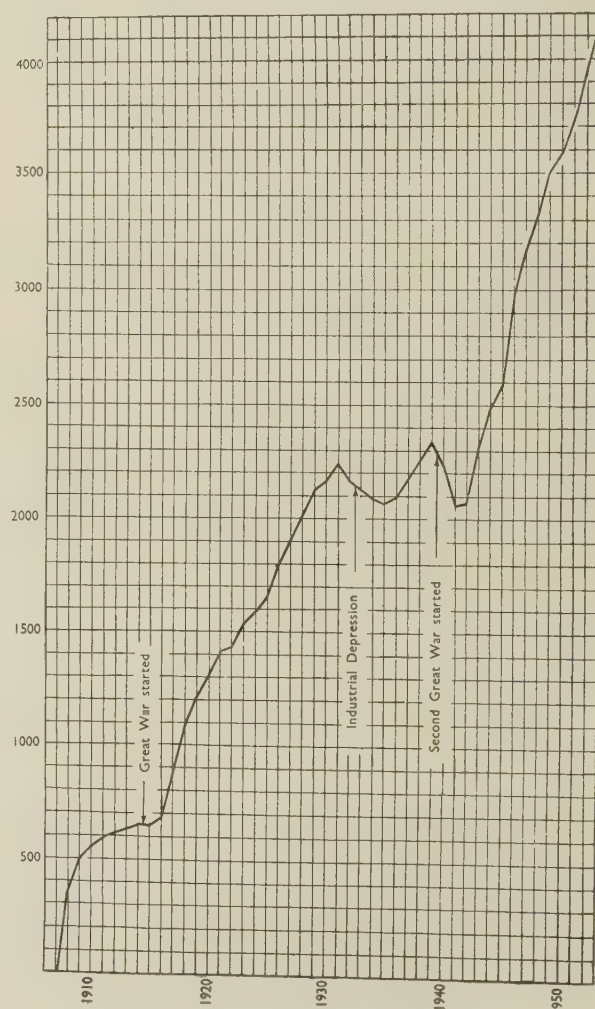
Though the number of papers published during the financial year 1952-53 was greater than that during the previous year (this was made possible by the continuing generous contributions from the metallurgical and engineering industries to the Industrial Donations Fund), the Institute's financial position has shown improvement, as compared with the previous year, as is mentioned in the Report of the Honorary Treasurer on p. 276. The membership showed a steady increase and the Institute's General Meetings were not only well attended but also provided subjects for profitable discussion by members of widely differing interests.

The most notable event of the year was the Autumn Meeting in South Lancashire, which was held at Southport by invitation of the Councils of the Manchester Metallurgical Society and the Liverpool Metallurgical Society. The meeting was well attended, a very interesting series of visits was arranged in connection with it, and members were most hospitably entertained through the generosity of the many firms and individuals who subscribed to the Hospitality Fund. The Council desires to place on record its sense of gratitude to its hosts; to the members of the Reception Committee, under the chairmanship of Lieut.-Commander G. K. Rylands, O.B.E., J.P., R.N. (ret.), and to all others who made this meeting so successful.

The Council has gratefully accepted an invitation from the Société Suisse des Constructeurs de Machines and the Schweizerischer Verband für die Materialprüfungen der Technik for the Institute to hold its next Autumn Meeting in Switzerland from 6 to 14 September, 1954.

During the year, the Société Française de Métallurgie accepted an invitation to hold a Joint Spring Meeting with the Institute from 26 April to 2 May 1954, in London, with extension tours in the Provinces on 3 and 4 May. This is the first time that the Institute (and, so far as is known, any British metallurgical society) will have acted as host to a foreign metallurgical society at a Joint Meeting in the United Kingdom, and the Council hopes that there will be a very large attendance of members and ladies to receive and meet the Institute's guests, for whom an interesting programme has been arranged. In particular, it hopes that there will be a large attendance at a Dinner and Dance which the Institute is holding for the members and ladies of the Société in the Great Room of Grosvenor House, Park Lane, on Wednesday, 28 April.

The Council, in co-operation with the Council of the Iron and Steel Institute and those of other European metallurgical societies, has issued an invitation to certain American metallurgical societies to hold a meeting and tour of some European metallurgical centres in June 1955, and has every hope that this invitation will be accepted. For various reasons, it will be necessary to restrict the numbers attending this meeting to representative members formed into a series of Groups to study European practice in certain branches of industry, with individuals concerned with research and teaching. Particulars of the meeting will be published as early as possible.



Active Membership at 31 December 1908-1953.



## FELLOW

During the year, Sir ARTHUR SMOUT, J.P., F.R.I.C., F.I.M., (Past-President) was elected a Fellow in recognition of his long and eminent services to the Institute.

## MEMBERSHIP

As the following table shows, the steady increase in the Institute's membership has been maintained. There is, however, still scope for a considerable increase in membership, both in the British Isles and overseas, and the Council hopes that members will give the Secretary the names and addresses of potential members of their acquaintance, so that particulars of the Institute's services and a specimen copy of the *Journal* may be sent to them.

At 31 December	1946	1947	1948	1949	1950	1951	1952	1953
Honorary Members	6	9	9	11	11	11	11	11
Fellows	6	7	6	9	10	8	8	9
Ordinary Members	2414	2491	2546	2685	2815	2941	3144	3368
Junior Members	...	...	...	...	291	305	362	363
Associate Members	25	17	19	18	...	...	...	...
Student Members	529	655	746	783	452	462	423	417
Active List	2980	3179	3326	3506	3579	3727	3948	4168
Suspense List	58	36	55	67	97	124	95	131
TOTAL	3038	3215	3381	3573	3676	3851	4043	4299

## OBITUARY

The Council much regrets to record the death of Professor D. Hanson, a former Vice-President of the Institute.

It also records with regret the deaths of the following members, which were notified during the year: Mr. C. F. Aston, Mr. K. J. Forrest, Mr. E. M. Foster, Mr. W. A. Fowler, Sir John French, Mr. W. Waterhouse Gibbins (an Original Member), Mr. G. B. Harris, Mr. A. J. Hawkes, Mr. H. J. Henbrey, Mr. E. N. Hickman, Dr. F. Horster, Dr. O. F. Hudson (an Original Member), Mr. D. Jepson, Captain A. C. Jessup, Mr. S. D. Orr, Wing-Commander E. Parrett, Mr. F. S. Paschek, Professor E. Piwowarsky, Mr. C. E. F. Plutte, Mr. G. B. Salkeld, Mr. W. Singleton, Mr. F. C. Slatford, Mr. W. J. Terry, Dr. Ing. B. Veltman and Mr. A. O. White.

## OFFICERS OF THE INSTITUTE

The following members were declared elected to fill honorary offices of the Institute with effect from the 1953 Annual General Meeting:

*President:*

Professor F. C. THOMPSON, D.Met., M.Sc., F.I.M.

*Vice-Presidents:*

Major C. J. P. BALL, D.S.O., M.C., F.R.Ae.S.  
Professor G. V. RAYNOR, M.A., D.Phil., D.Sc.,  
F.R.I.C., A.I.M.

*Ordinary Members of Council:*

W. A. BAKER, B.Sc., F.I.M.  
J. C. COLQUHOUN, M.B.E.  
E. R. GADD, F.I.M.  
The Hon. JOHN GRIMSTON, M.P.

In accordance with Article 42, the Council elected Dr. S. F. DOREY, C.B.E., M.I.C.E., M.I.Mech.E., F.R.S., as Senior Vice-President for the year 1953-54.

## HONORARY CORRESPONDING MEMBERS TO THE COUNCIL

During the year, Professor B. CHALMERS resigned his appointment as an Honorary Corresponding Member for Canada on taking up a post in the United States, and the Council desires to record its thanks for the services that he has rendered to the Institute.

The following were appointed Honorary Corresponding Members to the Council during the year: Dr. G. S. FARNHAM, B.A., M.Sc. (Canada); Professor F. A. FORWARD, B.A.Sc. (Canada); and Dr. O. H. C. MESSNER (Switzerland).

The Council desires to express to all the Honorary Corresponding Members its appreciation for their help and advice.

The Honorary Corresponding Members to the Council, in addition to those mentioned above, are as follows: *Australia*: Professor H. K. Worner, D.Sc.; *Belgium*: H. P. A. Feron, D.Sc.; *Canada*: Professor G. Letendre, B.A., Ph.D.; *France*: Professor P. A. J. Chevenard and Jean Matter; *India*: N. P. Gandhi, M.A., B.Sc., A.R.S.M., D.I.C.; *Italy*: Leno Matteoli, Dott.chim.; *Netherlands*: M. Hamburger; *South Africa*: G. H. Stanley, D.Sc., A.R.S.M., and Professor L. Taverner, A.R.S.M., D.I.C.; *Spain*: Professor J. Orland, M.Sc., M.A., Ph.D., D.D.; *Sweden*: Professor Carl A. F. Benedicks, Fil.Dr., D.Ing.e.h., Dr.Techn.h.c., and Professor Axel Hultgren; *Switzerland*: Professor A. von Zeerleder, Dr.Ing.; *United States of America*: Professor R. F. Mehl, Ph.D., Hon.Eng.D., Hon.Sc.D., Professor C. S. Smith, Sc.D., and Dr. R. A. Wilkins.

## INSTITUTE OF METALS MEDAL

The Institute of Metals (Platinum) Medal for 1953 was awarded to Professor Dr. GEORG MASING, of the Institut für allgemeine Metallkunde, Universität Göttingen, Germany, in recognition of his outstanding contributions in the field of metallography.

## W. H. A. ROBERTSON MEDAL

The W. H. A. Robertson Medal for 1952 was awarded to Mr. J. F. WRIGHT, for his paper on "Gas Equipment for the Thermal Treatment of Non-Ferrous Metals and Alloys", published in the *Journal*, 1951-52, Vol. 80, pp. 269-285.

## ROSENHAIN MEDAL

The Rosenhain Medal for 1953 was awarded to Dr. CHARLES ERIC RANSLEY, of the Research Laboratories, The British Aluminium Co., Ltd., Gerrards

Cross, in recognition of his outstanding experimental and theoretical work on gas-metal equilibria.

#### CAPPER PASS AWARDS

During the year Capper Pass Awards were made by the Adjudicating Committee as follows: Mr. EDWIN DAVIS, M.Sc., F.I.M., and Mr. S. G. TEMPLE, M.Sc., F.I.M. (£50, jointly) for their paper on "Batch and Continuous Annealing of Copper and Copper Alloys" (*J. Inst. Metals*, 1951-52, Vol. 80, pp. 287-296); Mr. C. P. PATON, B.Eng. (£50) for his paper on "Batch Thermal Treatment of Light Alloys" (*J. Inst. Metals*, 1951-52, Vol. 80, pp. 311-322); Dr. E. C. ELLWOOD, F.I.M., and Mr. T. A. HENDERSON, B.Sc. (£50, jointly) for their paper on "Some Exploratory Experiments on the Formation and Control of Magnetite During Copper Smelting Operations" (*Trans. Inst. Min. Met.*, 1952, Vol. 62, pp. 55-65); Mr. P. M. J. GRAY, B.Sc., A.R.S.M. (£50) for his paper on "The Production of Pure Cerium Metal by Electrolytic and Thermal Reduction Processes" (*Trans. Inst. Min. Met.*, 1952, Vol. 61, pp. 141-170); and Mr. E. A. HONTOIR, B.Sc., A.I.M. (£25) for his paper on "Determination of Sulphur in Iron Pyrites" (*Trans. Inst. Min. Met.*, 1952, Vol. 62, pp. 95-107).

#### STUDENTS' ESSAY PRIZES

The Adjudicators awarded one prize of twenty guineas to be divided between two authors of essays, as follows: Mr. G. THOMAS, for an essay on "Martensitic Transformations in Non-Ferrous Metals and Alloys", and Mr. R. D. STACEY, for an essay on "Some Experimental Evidence for Dislocations".

This competition is open to all Student Members of the Institute and to all Associate Members of Local Sections who are eligible for Student Membership, provided that both are within the normal age-limits for Student Membership, viz. 17 to 25 years. Full particulars may be obtained from the Secretary.

#### PUBLICATIONS

During the financial year 1952-53, 87 papers and addresses were published in the *Journal*, as compared with 75 in 1951-52. Whereas, however, by the end of 1952 the arrears of publication of papers had been overtaken, so that there were in hand only sufficient acceptable papers to maintain the regular monthly publication programme, there has since been a tendency for the numbers of acceptable papers received to increase. Endeavours are being made to keep pace with the publication of such papers, but there are limits to the number of pages that the Institute can afford to print. The Publication Committee appeals to all prospective authors to submit their MSS. in as concise a form as possible, and it is intended to publish a memorandum on this matter at an early date.

*Metallurgical Abstracts* have been brought further up to date. The Subjects volume of the General Index to Volumes 1-10 (1934-1943) is now all in

type, and it should be possible to publish it by 30 June 1954. Both the Subjects and Names indexes to Volumes 11-20 (1944-1953) have now been completed, and it is hoped that the MS. of the Subjects volume will be sent to the printer in 1954.

In the *Monograph and Report Series* there were published No. 13: "Properties of Metallic Surfaces"; No. 14: "Equipment for the Thermal Treatment of Non-Ferrous Metals and Alloys"; and No. 15: "The Control of Quality in the Production of Wrought Non-Ferrous Metals and Alloys. Part I.—The Control of Quality in Melting and Casting".

An *Annotated Equilibrium Diagram* (No. 10) on the System Copper-Silver, by Dr. J. C. Chaston, has been published.

#### GENERAL MEETINGS

On Thursday, 8 January 1953, a General Meeting of the Institute was held in Birmingham, when there was an Informal Discussion, arranged by the Metallurgical Engineering Committee, on "Rolls and Their Maintenance in the Non-Ferrous Metals Industry". There was a large attendance, and a valuable result of the meeting was the bringing closer together of the users and roll manufacturers. A summary of the discussion was printed in the *Bulletin*, 1953, Vol. 1 (May), pp. 199-202.

The Forty-Fifth Annual General Meeting was held in London from 23 to 26 March 1953, when Professor F. C. THOMPSON, D.Met., M.Sc., F.I.M., was inducted into the Chair. The Forty-Third May Lecture was delivered on Monday, 23 March, at the Royal Institution, Albemarle Street, London, W.1, by Sir CHRISTOPHER HINTON, M.A., M.I.C.E., M.I.Mech.E., on "The Present and Future Metallurgical Requirements of the Chemical Engineer". One day of the meeting was devoted to a Symposium on "The Control of Quality in the Production of Wrought Non-Ferrous Metals and Alloys. Part I.—The Control of Quality in Melting and Casting", arranged by the Metallurgical Engineering Committee.

The Forty-Fifth Annual Autumn Meeting was held in Southport from 21 to 25 September, by invitation of the Manchester Metallurgical Society and the Liverpool Metallurgical Society. The meeting was most successful, and there was a good attendance. The Twenty-Fourth Autumn Lecture was delivered on Monday, 21 September, by Dr. MAURICE COOK, F.I.M., on "The New Metal Titanium". During the meeting there was an Informal Discussion on "Damping Capacity", arranged by the Metal Physics Committee.

On Friday, 27 November 1953, an all-day Informal Discussion was held at the Royal Institution, Albemarle Street, London, W.1., on "The Training of Metallurgists for Industry", arranged by the Institute in co-operation with the Institution of Metallurgists.

#### STUDENTS EDUCATIONAL TOUR

An Easter Vacation Tour for Junior and Student Members was held in Birmingham from 13 to 17 April,



inclusive. It was attended by 29 members, and 14 works were visited. The Council records its gratitude to the Directors of the works visited for their co-operation in making this tour a success.

The Joint Spring Meeting with the Société Française de Métallurgie in 1954, closely after the Easter holidays, makes it impracticable for the Institute to arrange an Easter vacation tour for students during that year, and, in view of the decreasing numbers participating in this tour, the opportunity is being taken to ascertain, through the Local Sections, what demand there is for the continuation of these tours in future years.

#### LOCAL SECTIONS AND ASSOCIATED SOCIETIES

The six Local Sections of the Institute (Birmingham, London, Oxford, Scottish, Sheffield, and South Wales) had good programmes for their meetings during the winter session, which were well attended.

Arrangements have been made for meetings of the Sheffield Local Section to be held jointly with those of the Sheffield Society of Engineers and Metallurgists.

Members continued to enjoy the privilege of attending the meetings of the Associated Societies, viz. the Leeds Metallurgical Society, the Liverpool Metallurgical Society, and the Manchester Metallurgical Society, and, during the year, similar arrangements were made with the North East Metallurgical Society.

#### SPECIAL COMMITTEES

The Metal Physics Committee had 3 meetings during the year. It arranged a very successful Informal Discussion at the Spring Meeting on "Liquid Metals" and another at the Autumn Meeting on "Damping Capacity".

The Metallurgical Engineering Committee met 4 times. It arranged an Informal Discussion in Birmingham on "Rolls and Their Maintenance in the Non-Ferrous Metals Industry" on 8 January 1953, and has made arrangements for another to be held in Birmingham on 6 January 1954 on "Lubricants for Metal Working Operations in the Non-Ferrous Metal Industry". It also arranged, at the Spring Meeting, the first of a series of three all-day Symposia on "The Control of Quality in the Production of Wrought Non-Ferrous Metals", this one being on "The Control of Quality in Melting and Casting".

On the recommendation of this Committee, the Institute held, jointly with the Institution of Metallurgists, an all-day Informal Discussion on "The Training of Metallurgists", at the Royal Institution, London, on 27 November 1953.

A Committee has completed its discussions on problems relating to the publication of reviews of progress in metallurgy, and the Council has its report under consideration.

#### STAFF

Miss C. J. Arlidge, B.Sc., has joined the staff as an Editorial Assistant in the place of Mr. S. R. Williams, B.Sc., who resigned to take up a post in industry.

## JOINT ACTIVITIES

### JOINT LIBRARY AND INFORMATION DEPARTMENT

The great use of the Library and Information Department made in previous years continued in 1953; Members, Government Departments, Universities and other teaching establishments, and Research Laboratories availed themselves of the services provided. During the year 13,640 publications were borrowed; the corresponding figure for 1952 was 13,448. The number of text-books acquired was 310, compared with 475 in 1952, and the Council again records its thanks to those donors who presented copies of their works to the Library.

Membership of the Institute carries many privileges with it, and not the least is the use of the Lending Library. Books and periodicals can be borrowed by members resident in the United Kingdom not only from the Joint Library but also, on application through the Librarian, from the Science Library and the National Central Library. Under certain conditions photocopies and microfilms of documents can be obtained for members, both in the United Kingdom and abroad; during the year 119 photocopies (130 in 1952) and 61 microfilms (27 in 1952) were supplied to members.

The Information Department, an important part of the service, is prepared to answer scientific and technical enquiries from members, but members are reminded that it is not its function to give the sort of advice which lies within the field of the metallurgical consultant.

### JOINT COMMITTEE FOR NATIONAL CERTIFICATES IN METALLURGY

The Joint Committee approved four new schemes in England and Wales during 1953, three for Senior Courses and one for an Advanced Course, and other schemes have received preliminary approval of their content. The total numbers of approved Courses in operation during the session 1952-53 were: Senior Courses—Ordinary National Certificate, 33; Contributory Centres, with Courses for the First Year or First and Second Years of the Senior Course, 6; Advanced Courses, Higher National Certificate, 19. A list of the Technical Colleges will be published with the Joint Committee's annual Report.

Final examinations of the course for the Ordinary National Certificate were held during 1953 at 31 Technical Colleges and for the Higher National Certificate at 17 Technical Colleges, for candidates who have satisfied the conditions laid down in Ministry of Education Rules 111, under which the scheme is operated. In addition, 11 Colleges held assessed examinations in mathematics during the year, as part of their courses for the Ordinary National Certificate.

184 candidates have qualified for the award of an Ordinary National Certificate in Metallurgy and 116 candidates have qualified for the award of a Higher

National Certificate as a result of final examinations held in 1953. The records of a further 9 candidates for the Ordinary Certificate and 1 candidate for the Higher Certificate have been approved by the Joint Committee, subject to the fulfilment of certain conditions. Two candidates for the Ordinary and one candidate for the Higher Certificate, who entered the final examinations in previous years and whose records were approved by the Joint Committee subject to certain provisions, qualified for the award of Certificates in 1953.

Distinctions were gained by 17 candidates for the Ordinary and 17 for the Higher Certificate who showed a very good grasp of their subjects, indicating a high degree of training and knowledge in the particular subject in which the distinction has been gained.

Prizes were awarded to 26 successful candidates for the Ordinary and 24 for the Higher Certificate who showed particular merit in the final examinations, from the Prize Fund established by the Iron and Steel Institute, the Institution of Mining and Metallurgy, and the Institute of Metals for the purpose.

#### JOINT COMMITTEE ON METALLURGICAL EDUCATION

Approximately 1800 copies of the Committee's Report on "The Education and Training of Metallurgists" have been circulated since its publication in September 1952, and members of the Committee have reported that comments made to them from the points of view of employers and educational establishments indicate agreement with the Committee's recommendations. There has been a continued demand for copies and for copies of the Committee's previous publications on "Metallurgy—A Scientific Career in Industry" (Second revised edition, 1948); "Recommendations on Qualifications for Entrance to University Schools of Metallurgy" (1948); "Films about Metals" (1949) (compiled jointly with The Scientific Film Association); and "Recommendations on University Full-time Degree Courses in Metallurgy" (1950).

Arising from the recommendations made in para. 40 of the report on "The Education and Training of Metallurgists", the Institution of Metallurgists and the Institution of Mining and Metallurgy (both qualifying professional societies) were invited, and agreed jointly, to make the necessary arrangements to set up a Board of Metallurgical Studies and Examinations. (After a preliminary meeting of representatives of the bodies concerned, a fully representative Committee was formed early in 1953.) Members of the Joint Committee on Metallurgical Education also agreed to give consideration to the question of further implementation of the Report.

It is proposed to hold a meeting of the Joint Committee following on the Informal Discussion on "The Training of Metallurgists for Industry" held by the Institute of Metals and the Institution of Metal-

lurgists in London on 27 November 1953, to consider future work, if necessary, in the light of the discussion at that meeting.

#### MOND NICKEL FELLOWSHIPS COMMITTEE

Mr. E. H. JONES continued to represent the Institute on the Mond Nickel Fellowships Committee.

The Committee held two Meetings in 1953 and made awards of Fellowships to:

J. E. BENSON (Metropolitan-Vickers Electrical Co., Ltd.) to study the technique and interpretation of results and standards of non-destructive testing of metal components in the United Kingdom, on the Continent, and in the U.S.A. and Canada.

K. BLACKBURN (Dorman, Long and Company, Ltd.) to study hot-metal basic open-hearth practice in Great Britain, on the Continent and in the U.S.A. and Canada, with particular reference to mixer furnace operation, refractories, instrumentation and pitside practice.

N. B. PRATT (Broken Hill Proprietary Company, Ltd.) to study the technical and economic aspects of recent advances in the erection and operation of integrated iron and steel works in Great Britain, on the Continent, and in the U.S.A. and Canada.

#### SIR GEORGE BEILBY MEMORIAL FUND

The Administrators of the Sir George Beilby Memorial Fund, representing the Institute of Metals, The Royal Institute of Chemistry, and the Society of Chemical Industry, made an award from the Fund for 1952 of one hundred guineas to Mr. THOMAS VICTOR ARDEN, B.Sc., F.R.I.C., in recognition of his experimental work on the hydrometallurgy of uranium, with particular application to its separation from low-grade ores.

#### SUMMER SCHOOL AT CAMBRIDGE

The Institute arranged, in co-operation with the Board of Extra-Mural Studies of the University of Cambridge, a Summer School in "The Use of Electrons in the Examination of Metals". The Summer School was held in Cambridge from 20–31 July 1953, inclusive.

#### "ACTA METALLURGICA"

The Council agreed that the Institute should become a Co-operating Society in connection with the publication of a new international journal entitled *Acta Metallurgica*. Under this arrangement, members of the Institute are entitled to subscribe to the new periodical at a privileged rate.

Dr. W. A. BAKER has been elected as one of the European representatives on the Governing Board of the new journal.



## APPENDIX I

## LIST OF PAPERS PUBLISHED

The following is a complete list of the papers and lectures published by the Institute during the calendar year 1953 :

1436. High-Temperature Oxidation Characteristics of a Group of Oxidation-Resistant Copper-Base Alloys. By J. P. Dennison, Ph.D., B.Sc., and Professor A. Preece, M.Sc., F.I.M.
1437. A Method of Determining Orientations in Aluminium Single Crystals and Polycrystalline Aggregates. By G. E. G. Tucker, B.Sc., and P. C. Murphy, B.Sc., A.I.M.
1438. Creep at 250° and 300° C. of Some Magnesium Alloys Containing Cerium. By G. A. Mellor, M.Sc., F.I.M., and R. W. Ridley, B.Sc.
1439. New Values of the Coefficients of Equivalence for Manganese, Iron, Cobalt, and Nickel in Copper-Zinc Alloys. By J. B. Haworth, D.Phil., B.Met.
1440. The Effect of Minor Additions on the Age-Hardening Properties of a High-Purity Lead-Antimony Alloy. By L. M. T. Hopkin, B.Sc., A.R.S.M., A.I.M., and C. J. Thwaites, B.Sc., A.R.S.M.
1441. The Effect of Cold Work on the Microstructure and Corrosion-Resistance of Aluminium-5% Magnesium Alloys Containing 0-1% Zinc. By P. Brenner, Dr.Ing., and G. J. Metcalfe, M.Sc.Tech.
1442. Atmospheric Corrosion and Stress-Corrosion of Aluminium-Copper-Magnesium and Aluminium-Magnesium-Silicon Alloys in the Fully Heat-Treated Condition. By G. J. Metcalfe, M.Sc.Tech.
1443. The Measurement of the Relative Hardnesses of Fine Powder Particles. By J. B. Matthews, B.Sc., Ph.D., F.R.I.C.
1444. Crystal Fragmentation in Aluminium During Creep. By D. McLean, B.Sc.
1445. Grain-Boundary Slip During Creep of Aluminium. By D. McLean, B.Sc.
1446. Intercrystalline Corrosion in Cast Zinc-Aluminium Alloys. By C. W. Roberts, B.Sc., A.I.M.
1447. The Constitution of Chromium-Manganese Alloys Below 1000° C. By W. B. Pearson, D.F.C., M.A., D.Phil., and W. Hume-Rothery, O.B.E., F.R.S.
1448. The Principles of Technical Control in Metallurgical Manufacture. By A. R. E. Singer, B.Sc., Ph.D.
1449. The Control of Quality in the Production of Brass Ingots and Billets. By Maurice Cook, D.Sc., Ph.D., F.I.M., and C. L. M. Cowley, B.Sc., A.I.M.
1450. The Control of Quality in Melting and Casting Copper and High-Conductivity Copper-Base Alloys. By J. Sykes, F.I.M.
1451. The Control of Quality in the Casting of Zinc and Zinc Alloy Rolling Slabs and Extrusion Billets. By C. W. Roberts, B.Sc., A.I.M., and B. Walters, M.A.
1452. The Control of Quality in the Melting and Casting of Aluminium Alloys for Working. By R. T. Staples and H. J. Hurst.
1453. The Control of Quality in Melting and Casting Magnesium Alloys for Hot Working. By R. G. Wilkinson, B.Sc., and S. B. Hirst, B.Sc.Tech.
1454. Presidential Address. By Professor F. C. Thompson, D. Met., M.Sc.
1455. The Kinetics of the Eutectoid Transformation in Zinc-Aluminium Alloys. By R. D. Garwood, M.Sc., and A. D. Hopkins, M.Sc.
1456. The Liquid Immiscibility Region in the Aluminium-Lead-Tin System at 650°, 730°, and 800° C. By Morgan H. Davies, B.Sc.
1457. The Influence of Thallium on the Creep of Lead. By R. C. Gifkins, B.Sc., A.I.M.
1458. Some Metallographic Observations on Aged Aluminium-Copper Alloys. By I. J. Polmear, B.Met.E., and H. K. Hardy, M.Sc., Ph.D., A.R.S.M., A.I.M.
1459. The Log-Log Plot of Solubility Data in Ternary Metallic Systems. By H. K. Hardy, M.Sc., Ph.D., A.R.S.M., A.I.M.
1460. Mechanical Anisotropy in Some Ductile Metals. By Professor W. A. Backofen, S.B., Sc.D., and B. B. Hundy, B.Sc., Ph.D.
1461. The Formation of Intracrystalline Voids in Solution-Treated Magnesium-Aluminium Alloys. By E. Lardner, B.Sc., A.I.M.
1462. A Note on the Mathematical Analysis of Creep Curves. By L. M. T. Hopkin, B.Sc., A.R.S.M., A.I.M.
1463. Equilibrium Relations at 460° C. in Aluminium-Rich Alloys Containing 0-7% Copper, 0-7% Magnesium, and 0-6% Silicon. By H. J. Axon, B.Met., D.Phil.
1464. The Constitution of Nickel-Rich Alloys of the Nickel-Chromium-Aluminium System. By A. Taylor, Ph.D., F.Inst.P., and R. W. Floyd, B.Sc., A.I.M.
1465. The Present and Future Metallurgical Requirements of the Chemical Engineer. Forty-third May Lecture. By Sir Christopher Hinton, M.A., M.I.C.E., M.I.Mech.E.
1466. The Use of Diamond Abrasives for a Universal System of Metallographic Polishing. By L. E. Samuels, B.Met.E.
1467. The Solubility of Indium in Copper. By Professor E. A. Owen, M.A., D.Sc., and E. A. O'Donnell Roberts, M.Sc., Ph.D.
1468. Priming Paints for Light Alloys. By J. G. Rigg, Ph.D., and E. W. Skerrey, B.Sc., A.I.M.
1469. The Continuity of Slip Lines Across a Grain Boundary. By G. J. Ogilvie, Ph.D.
1470. Hydrogen Blisters in Brass Sheet. By R. Eborall, M.A., and A. J. Swain, M.A.
1471. Critical-Strain Effects in Cold-Worked Wrought Aluminium and Its Alloys. By W. M. Williams, B.Sc., and R. Eborall, M.A.
1472. The Application of Grain Refinement to Cast Copper-Aluminium Alloys Containing the Beta Phase. By J. P. Dennison, B.Sc., Ph.D., and E. V. Tull, B.Sc., A.I.M.
1473. The Structure of Titanium-Tin Alloys in the Range 0-25 At.-% Tin. By H. W. Worner, M.Sc.
1474. Some Observations on Creep and Fracture from Investigations on Lead Cable-Sheath Alloys. By A. Latin, Ph.D., M.Eng., F.I.M.
1475. Simultaneous Determination of the Surface Tension of Tin and Its Contact Angle with Silica by the Use of Conical Capillaries. By D. V. Atterton, M.A., Ph.D., and T. P. Hoar, M.A., Ph.D., F.I.M.
1476. A Theoretical Investigation of the Deformation Textures of Titanium. By D. N. Williams, Ph.D., and Professor D. S. Eppelsheimer, D.Sc.
1477. The Influence of Composition on the Incidence of Strain Markings in Aluminium Alloys. By W. H. L. Hooper, B.Sc., A.I.M.
1478. The Properties of Cast Chromium Alloys at Elevated Temperatures. I.—The Melting and Casting of Chromium-Rich Alloys. By A. H. Sully, M.Sc., Ph.D., F.Inst.P., F.I.M., E. A. Brandes, B.Sc., A.R.C.S., F.I.M., and A. G. Provan, B.Sc., A.R.T.C., A.R.I.C. II.—Some Properties of Certain Binary Chromium-Rich Alloys. By A. H. Sully, M.Sc., Ph.D., F.Inst.P., F.I.M., and E. A. Brandes, B.Sc., A.R.C.S., F.I.M. III.—The Creep Properties of Ternary and More Complex Chromium-Base Alloys. By A. H. Sully, M.Sc., Ph.D., F.Inst.P., F.I.M., and E. A. Brandes, B.Sc., A.R.C.S., F.I.M.

1479. The Effect of Temperature and Purity on the Ductility and Other Properties of Chromium. By A. H. Sully, Ph.D., M.Sc., F.Inst.P., F.I.M., E. A. Brandes, B.Sc., A.R.C.S., F.I.M., and K. W. Mitchell, B.Sc.(Eng.), Wh.Sch., A.M.I.Mech.E.
1480. The Stepped Stress/Strain Curve of Some Aluminium Alloys. By N. Krupnik, D.I.C., and Professor Hugh Ford, D.Sc., Ph.D.
1481. Discontinuous Flow and Strain-Ageing in a 6% Tin Phosphor-Bronze. By N. H. Polakowski, Dipl.Ing., Ph.D.
1482. Yield-Point Phenomena and Stretcher-Strain Markings in Aluminium-Magnesium Alloys. By V. A. Phillips, A.R.S.M., D.Eng., B.Sc., A.I.M., A. J. Swain, M.A., and R. Eborall, M.A.
1483. Some Methods of Measuring Surface Topography as Applied to Stretcher-Strain Markings on Metal Sheet. By W. H. L. Hooper, B.Sc., A.I.M., and J. Holden, Ph.D.
1484. Effect of Composition and Heat-Treatment on Yield-Point Phenomena in Aluminium Alloys. By V. A. Phillips, A.R.S.M., D.Eng., B.Sc., A.I.M.
1485. Growth of Sulphide Films on Copper. By T. P. Hoar, M.A., Ph.D., F.I.M., and A. J. P. Tucker, M.A., Ph.D.
1486. The Oxidation of Copper in the Temperature Range 200°-800° C. By R. F. Tylecote, M.A., M.Sc., Ph.D., F.I.M.
1487. The Mechanism of Residual-Stress Formation in Sand Castings. By R. N. Parkins, B.Sc., Ph.D., A.I.M., and A. Cowan, B.Sc., Ph.D.
1488. The Constitution of Aluminium-Copper-Silicon Alloys. By H. W. L. Phillips, M.A., F.R.I.C., F.Inst.P., F.I.M.
1489. The Structure and Mechanical Properties of Copper-Manganese-Tin Alloys. By J. C. Blade, B.Sc., Ph.D., and J. W. Cuthbertson, D.Sc., F.I.M.
1490. The Preparation and Properties of Magnesium Alloy Sheets of Controlled Impurity Content. By H. G. Cole, B.Sc., A.R.I.C., A. E. L. Tate, A.I.M., and B. Walters, M.A.
1491. The Behaviour of the Crystal Boundaries of Aluminium at Temperatures Near the Melting Point. By W. I. Pumphrey, M.Sc., Ph.D., and J. V. Lyons, Ph.D.
1492. A Slide-Rule for the Interconversion of Atomic and Weight Percentages for Any Binary Alloy System. By W. A. Rachinger, Ph.D., M.Sc.
1493. Structural Studies of the Creep of Lead. By R. C. Gifkins, B.Sc., A.I.M.
1494. The Re-Investigation of a Nickel-Titanium Alloy and Observations on  $\beta/(\alpha + \beta)$  Boundaries in Titanium Systems. By A. D. McQuillan, Ph.D., B.Sc.
1495. An Investigation of Thickening and Metal Entrapment in a Light Alloy Melting Flux. By A. H. Sully, Ph.D., M.Sc., F.Inst.P., F.I.M., H. K. Hardy, Ph.D., M.Sc., A.R.S.M., A.I.M., and T. J. Heal, B.Sc., F.Inst.P.
1496. Constitution of the Copper-Rich Copper-Aluminium-Germanium Alloys. By Professor G. V. Raynor, M.A., D.Sc., and P. Greenfield, Ph.D., B.Sc.
1497. Some Observations on the Mechanism of Pitting Corrosion. By R. May, A.R.S.M.
1498. The Effect of Iron, Manganese, and Chromium on the Properties in Sheet Form of Aluminium Alloys Containing 0.7% Magnesium and 1.0% Silicon. By R. Chadwick, M.A., F.I.M., N. B. Muir, B.Sc., A.I.M., and H. B. Grainger, B.Sc., A.I.M.
1499. The Copper-Indium Eutectoid at 31.36 wt.-% Indium. By Chester W. Spencer, Ph.D., and Associate Professor David J. Mack, Ph.D.
1500. The Free-Energy Diagram of the System Titanium-Oxygen. By O. Kubaschewski, Dr.phil.habil., and W. A. Dench.
1501. The Effect of Cold Work on an Iron-Manganese Alloy. By J. Gordon Parr, Ph.D., B.Sc.
1502. The New Metal Titanium. Twenty-fourth Autumn Lecture. By Maurice Cook, D.Sc., Ph.D., F.I.M.
1503. The Oxidation of Aluminium-Magnesium Alloys by Steam: A Contribution to Research on Mould Reaction. By Marjorie Whitaker, B.Sc., A.I.M. With an Appendix on The Constitution of Oxide Films Formed at High Temperature on Aluminium-Magnesium-Beryllium Alloys. By A. R. Heath, B.Sc.
1504. Some Creep Characteristics of a Group of Precipitation-Hardening Alloys Based on the Alpha-Copper-Aluminium Phase. By J. P. Dennison, B.Sc., Ph.D.
1505. The Computation of Loads in Metal Strip Rolling by Methods Involving the Use of Dimensional Analysis. By Maurice Cook, D.Sc., Ph.D., F.I.M., and R. J. Parker, A.M.I.Mech.E.
1506. A Survey of the Uranium-Nickel System. By J. D. Grogan, B.A., and R. J. Pleasance. With an Appendix on An X-Ray Examination of Some Uranium-Nickel Alloys. By Betty E. Williams.
1507. The Low-Torsional Creep Properties of Pure Aluminium. By W. Betteridge, Ph.D., F.Inst.P.
1508. The Copper-Silicon Eutectoid Transformation. By A. D. Hopkins, M.Sc.
1509. The Melting Point of Titanium. By T. H. Schofield, M.Sc., F.I.M., and A. E. Bacon.
1510. Lamellæ in Chromium. By W. E. Carrington.
1511. The System Uranium-Lead. By B. R. T. Frost, B.Sc., Ph.D., and J. T. Maskrey.
1512. The Effects of Some Constitutional Factors on the Creep and Fatigue Properties of Lead and Lead Alloys. By L. M. T. Hopkin, Ph.D., A.R.S.M., A.I.M., and C. J. Thwaites, B.Sc., A.R.S.M.



## APPENDIX II

CONTRIBUTIONS TO THE INDUSTRIAL DONATIONS FUND IN, OR FOR, THE FINANCIAL YEAR ENDED 30 JUNE 1953

Donor	Gross, after Recovery of Tax by the Institute
	£ s. d.
United States Copper and Brass Industry: individual subscriptions totalling \$1500, by the following nine companies:	
American Brass Co., The	
Bridgeport Brass Co.	
Bristol Brass Corp., The	
Chase Brass and Copper Co.	
Chicago Extruded Metals Co.	
New Haven Copper Co., The	
Revere Copper and Brass, Inc.	
Scovill Manufacturing Co.	
Wolverine Tube Division, Calumet and Hecla Consolidated Copper Co., Inc.	
*Enfield Rolling Mills, Ltd. (incl. Enfield Copper Refining Co., Ltd.; Enfield Rolling Mills (Aluminium), Ltd.; Holloway Metal Roofs, Ltd.; and London Zinc Mills, Ltd.)	532 17 4
*Mond Nickel Co., Ltd., The (incl. Birlec, Ltd.; Henry Wiggin and Co., Ltd., and associated companies in the United States and Canada)	523 16 0
*Consolidated Zinc Corporation, Ltd., The (incl. The Broken Hill Corporation, Ltd.; Imperial Smelting Corporation, Ltd.; The National Smelting Co., Ltd.; New Broken Hill Consolidated, Ltd.; Northern Smelting and Chemical Co., Ltd.; Sulphide Corporation Ltd.; and The Zinc Corporation, Ltd.)	523 16 0
*Goodlass Wall and Lead Industries, Ltd.; Associated Lead Industries, Ltd.	476 3 9
Fry's Metal Foundries, Ltd. (incl. Antifriction Bearing Co., Ltd., The; Atlas Metal and Alloys, Ltd.; and The Eyre Smelting Co., Ltd.)	£190 9 6
*Mufulira Copper Mines, Ltd.	£95 4 9
*Roan Antelope Copper Mines, Ltd.	285 14 3
*Imperial Chemical Industries, Ltd., and its subsidiary companies	285 14 3
Aluminium Laboratories, Ltd. (incl. Aluminium Union, Ltd.; Northern Aluminium Co., Ltd.; and Stand, Ltd.)	†250 0 0
General Motors, Ltd. (incl. A.C. Sphinx Spark Plug Co., Ltd.; Delco-Remy-Hyatt, Ltd.; and Frigidaire, Ltd.)	200 0 0
Tube Investments, Ltd. (incl. The Chesterfield Tube Co., Ltd.; Mersey Cable Works, Ltd.; Reynolds Light Alloys, Ltd.; Reynolds Rolling Mills, Ltd.; Simplex Electric Co., Ltd.; South Wales Aluminium Co., Ltd.; and T.I. Aluminium, Ltd.)	200 0 0
*British Aluminium Co., Ltd., The (incl. Aluminium Corporation, Ltd.; William Mills, Ltd.; and North British Aluminium Co., Ltd.)	190 9 6
*McKechnie Brothers, Ltd.	190 9 6
*Magnesium Elektron, Ltd. (incl. F. A. Hughes and Co., Ltd.)	190 9 6
*Metallo-Chemical Refining Co., Ltd.	190 9 6
Nchanga Consolidated Copper Mines, Ltd.	150 0 0
Rhodesia Broken Hill Development Co., Ltd., The	150 0 0
Rhokana Corporation, Ltd.	150 0 0
Vickers-Armstrongs, Ltd., and Vickers, Ltd. (incl. A.B.C. Motors, Ltd.; Robert Boby, Ltd.; Cooke, Troughton and Simms, Ltd.; Ioco, Ltd.; George Mann and Co., Ltd.; Palmers Hebburn Co., Ltd.; G. J. Worssam and Son, Ltd.; and Powers-Samas Accounting Machines, Ltd.)	105 0 0
British Insulated Callender's Cables, Ltd. (incl. British Copper Refiners, Ltd.)	100 0 0

Donor	Gross, after Recovery of Tax by the Institute
	£ s. d.
Capper Pass and Son, Ltd. (incl. George Pizey and Co., Ltd.; The Tyne Solder Co., and Victor G. Stevens, Ltd.)	100 0 0
Colvilles, Ltd.	100 0 0
Johnson (Richard) and Nephew, Ltd.	100 0 0
Johnson (Richard) and Nephew, Ltd. for 1951-52	†100 0 0
Johnson, Matthey and Co., Ltd.	100 0 0
Rylands Brothers, Ltd., and The Whitecross Co., Ltd.	100 0 0
*Manganese Bronze and Brass Co., Ltd., The	†95 9 1
*Consolidated Tin Smelters, Ltd. (incl. The Cornish Tin Smelting Co., Ltd.; Eastern Smelting Co., Ltd.; The Penpoll Tin Smelting Co., Ltd.; and Williams, Harvey and Co., Ltd.)	95 4 9
*Enthoven (H. J.) and Sons, Ltd.	95 4 9
*High Duty Alloys, Ltd.	95 4 9
*Venesta, Ltd.	95 4 9
*Whiley (Geo. M.), Ltd.	95 4 9
*Stone (J.) and Co. (Charlton), Ltd.	†90 18 10
General Electric Co. (U.S.A.) \$250	88 19 4
General Electric Co. (U.S.A.) \$250 for 1951-52	†89 7 2
Rubery, Owen and Co., Ltd.	75 6 6
Beralt Tin and Wolfram, Ltd.	52 10 0
Mallory Metallurgical Products, Ltd.	52 10 0
Pyrotex, Ltd.	52 10 0
*Murex, Ltd. (incl. Murex Welding Processes, Ltd.)	52 7 8
*Associated Electrical Industries, Ltd., on behalf of the A.E.I. Group of Companies	50 0 0
Austin Motor Co., Ltd.	50 0 0
Birmingham Small Arms Company, Ltd., on behalf of the B.S.A. Group of Companies	50 0 0
*Dale (John), Ltd.	50 0 0
Fairey Aviation Co., Ltd., The	50 0 0
G.K.N. Group	50 0 0
Lucas (Joseph), Ltd. (incl. Rotax, Ltd.)	50 0 0
*Morgan Crucible Co., Ltd.	50 0 0
Morris Motors, Ltd.	50 0 0
Rolls-Royce, Ltd.	50 0 0
*Simon-Carves, Ltd.	50 0 0
*Tennant (C.), Sons and Co., Ltd.	†50 0 0
*Hopkinsons, Ltd.	49 11 5
*Brown (David) and Sons (Huddersfield), Ltd.	†47 14 6
*A.P.V. Co., Ltd.	47 12 5
*Birmetals, Ltd.	47 12 5
*Birmingham Aluminium Casting (1903) Co., Ltd.	47 12 5
*Bristol Aeroplane Co., Ltd., The	47 12 5
*British Metal Corporation, Ltd., The	47 12 5
*Chloride Electrical Storage Co., Ltd., The	47 12 5
*Essex Aero, Ltd.	47 12 5
*London and Scandinavian Metallurgical Co., Ltd.	47 12 5
*Rotol, Ltd.	47 12 5
*Star Aluminium Co., Ltd. (incl. Anglo-Swiss Aluminium Co., Ltd.)	47 12 5
*Sterling Metals, Ltd.	47 12 5
*Wolverhampton Metal Co., Ltd., The (incl. James Bridge Copper Works, Ltd.)	47 12 5
*Telegraph Construction and Maintenance Co., Ltd., The (incl. Submarine Cables, Ltd.)	†45 9 0
*Telegraph Construction and Maintenance Co., Ltd., The (incl. Submarine Cables, Ltd.) for 1951-52	†47 12 4
Wednesbury Tube Co., Ltd., The	42 0 0
*Hughes-Johnson Stampings, Ltd., The	40 0 0
*Light Metal Forgings, Ltd.	40 0 0
*Ferranti, Ltd.	38 1 11
*Gibbons Brothers, Ltd. (incl. The Thermic Equipment and Engineering Co., Ltd.)	38 1 11

Donor	Gross, after Recovery of Tax by the Institute			Donor	Gross, after Recovery of Tax by the Institute		
	£	s.	d.		£	s.	d.
*Parkinson Stove Co., Ltd., The	†36	7	3	Hoover, Ltd.			
Aluminum Company of America (\$100)	35	5	6	Incandescent Heat Co., Ltd., The (incl. Con- trolled Heat and Air, Ltd.; Metal Porcelains, Ltd.; Metalelectric Furnaces, Ltd.; and Selas Gas and Engineering Co., Ltd.)	10	10	0
*British Tin Investment Corporation, Ltd.	30	0	0	Lawley (Thomas), Ltd., and Jones and Rooke (1948), Ltd.	10	10	0
*Derby and Co., Ltd.	30	0	0	Maudslay Motor Co., Ltd., The	10	10	0
*London Electric Wire Company and Smiths, Ltd., The (incl. Liverpool Electric Cable Co., Ltd.)	†28	12	9	Newey and Tayler, Ltd. (incl. Newey Brothers, Ltd., and D. F. Tayler and Co., Ltd.)	10	10	0
*Barker and Allen, Ltd.	28	11	5	Platers and Stampers, Ltd.	10	10	0
*Bolton (Thomas) and Sons, Ltd.	28	11	5	Rover Co., Ltd., The	10	10	0
*British Lead Mills, Ltd.	28	11	5	Vauxhall Motors, Ltd.	10	10	0
English Electric Co., Ltd., The (incl. D. Napier and Son, Ltd.)	26	5	0	West Yorkshire Foundries, Ltd. (Subsidiary of Leyland Motors, Ltd.)	10	10	0
Head, Wrightson and Co., Ltd.	26	5	0	Allen (W. H.), Sons and Co., Ltd.	10	0	0
*Holroyd (John) and Co., Ltd.	26	3	10	*Central Marine Engine Works (William Gray and Co., Ltd.)	10	0	0
Arkinstall Brothers, Ltd.	25	0	0	*Corfield-Sigg, Ltd.	10	0	0
Braby (Frederick) and Co., Ltd.	25	0	0	Crittall Manufacturing Co., Ltd., The	10	0	0
British Timken, Ltd. (incl. Fischer Bearings Co., Ltd.)	25	0	0	Electric Furnace Co., Ltd. (incl. Electro- Chemical Engineering Co., Ltd.)	10	0	0
British United Shoe Machinery Co., Ltd., The	25	0	0	Electric Resistance Furnace Co., Ltd.	10	0	0
Copper and Alloys, Ltd.	25	0	0	*Harland Engineering Co., Ltd., The	10	0	0
Davy and United Engineering Co., Ltd.	25	0	0	Metro-Cutanit, Ltd.	10	0	0
Gardner (Henry) and Co., Ltd.	25	0	0	Metro-Cutanit, Ltd. for 1951-52	†10	0	0
Plessey Co., Ltd., The	25	0	0	Rothschild (N. M.) and Sons	10	0	0
Pressed Steel Co., Ltd.	25	0	0	Strebor Diecasting Co., Ltd.	10	0	0
Thompson (John) (Wolverhampton), Ltd.	25	0	0	*Wild-Barfield Electric Furnaces, Ltd.	10	0	0
Metal Box Co., Ltd., The	22	1	0	Winfields Rolling Mills, Ltd.	10	0	0
Almin, Ltd.	21	0	0	*Bound Brook Bearings (G.B.), Ltd.	9	10	6
Bull's Metal and Marine Co., Ltd.	21	0	0	*Hoyt Metal Company of Great Britain, Ltd., The	9	10	6
Delta Metal Co., Ltd., The (incl. Heaton and Dugard, Ltd.)	21	0	0	*Hunt and Mitton, Ltd.	9	10	6
Fulmer Research Institute, Ltd.	21	0	0	*Jenkinson (W. G.), Ltd.	9	10	6
Monotype Corporation, Ltd., The	21	0	0	*Shaw, Son and Greenhalgh, Ltd.	9	10	6
Tata Iron and Steel Co., Ltd.	21	0	0	*Stein (John G.) and Co., Ltd.	9	10	6
*International Alloys, Ltd.	20	19	0	*Betts and Co., Ltd.	8	0	0
*Allen (Edgar) and Co., Ltd.	20	0	0	*Glenfield and Kennedy, Ltd.	8	0	0
Brightside Foundry and Engineering Co., Ltd., The	20	0	0	United Wire Works (Birmingham), Ltd.	6	6	0
*British Tin Smelting Co., Ltd., The	20	0	0	Acton Bolt, Ltd.	5	5	0
Deloro Stellite, Ltd.	20	0	0	Barnard (H. B.) and Sons, Ltd.	5	5	0
*General Electric Co., Ltd., The	20	0	0	Bawn (W. B.) and Co., Ltd.	5	5	0
Hall and Pickles, Ltd.	20	0	0	Blackwells Metallurgical Works, Ltd.	5	5	0
Hard Metal Tools, Ltd.	20	0	0	Cheswick and Wright, Ltd.	5	5	0
Park Gate Iron and Steel Co., Ltd., The	20	0	0	Dennison Watch Case Co., Ltd.	5	5	0
*Phosphor Bronze Co., Ltd., The	20	0	0	Easdale (R. M.) and Co.	5	5	0
Renfrew Foundries, Ltd.	20	0	0	Electro-Alloys, Ltd.	5	5	0
*Saunders-Roe, Ltd.	20	0	0	Electroflo Meters Co., Ltd.	5	5	0
Sheffield Smelting Co., Ltd.	20	0	0	Headley, Birch and Co., Ltd.	5	5	0
Sheffield Smelting Co., Ltd. for 1951-52	†20	0	0	Langley Alloys, Ltd.	5	5	0
Société Anonyme pour l'Industrie de l'Alu- minium (Lausanne, Switzerland)	20	0	0	Lead Wool Co., Ltd., The	5	5	0
Wickman, Ltd.	20	0	0	Linread, Ltd.	5	5	0
*Chase Non-Ferrous Metal Co., Ltd.	19	0	6	Miles (John) and Partners (London), Ltd.	5	5	0
*Curran (Edward) Engineering, Ltd.	19	0	6	Ratcliffs (Great Bridge), Ltd.	5	5	0
*Rolle (H.) and Co., Ltd.	19	0	6	Rigby (John) and Sons, Ltd.	5	5	0
*Wolverhampton Die-Casting Co., Ltd., The	19	0	6	Wilkinson (John) and Sons (Saltley), Ltd.	5	5	0
Marconi's Wireless Telegraph Co., Ltd.	15	15	0	Cambridge Instrument Co., Ltd.	5	0	0
Perry Barr Metal Co., Ltd.	15	0	0	Metal Supplies, Ltd.	5	0	0
*Scottish Non-Ferrous Tube Industries, Ltd.	15	0	0	Blakeborough (J.) and Sons, Ltd.	4	4	0
*Loewy Engineering Co., Ltd., The	14	6	0	Kincaid (John G.) and Co., Ltd.	4	4	0
Brotherhood (Peter), Ltd.	12	12	0	*Platt Metals, Ltd.	3	16	2
Belliss and Morcom, Ltd., (incl. W. Sisson and Co., Ltd.)	10	10	0	*Acorn Anodising Co., Ltd.	†3	12	8
Belliss and Morcom, Ltd., (incl. W. Sisson and Co., Ltd.) for 1951-52	†10	10	0	Metal Information Bureau, Ltd.	3	3	0
Carborundum Co., Ltd., The	10	10	0	Mining and Chemical Products, Ltd.	3	3	0
Clifford (Charles) and Son, Ltd.	10	10	0	Walterisation Co., Ltd., The	3	3	0
Elliott Brothers (London), Ltd.	10	10	0	Beryllium and Copper Alloys, Ltd.	2	2	0
Foundry Services, Ltd.	10	10	0	Carobronze, Ltd.	2	2	0
Fry's Diecastings, Ltd.	10	10	0	Follsain-Wycliffe Foundries, Ltd.	2	2	0
G. W. B. Electric Furnaces, Ltd.	10	10	0	Gascoignes Non-Ferrous Foundries, Ltd.	2	2	0
Glynn Brothers, Ltd.	10	10	0	Premier Cooler and Engineering Co., Ltd., The	2	2	0
Harrison (Birmingham), Ltd.	10	10	0	Sheffield Testing Works, Ltd., The	2	2	0
				Jenks (E. P.), Ltd.	1	1	0

\* Annual Donation, Under Covenant, for Not Less Than 7 Years.

† Includes tax recoverable, but not actually recovered in the financial year 1952-53.

‡ Amounts received after the end of the financial year 1951-52 and not included in the list of donations for that year.



## APPENDIX III

## COMMITTEES

The main committees of the Institute which have served during the year were constituted as follows at 31 December 1953 :

## FINANCE AND GENERAL PURPOSES COMMITTEE

BAER, Mr. Alfred ( <i>Chairman</i> ).	<i>Ex-officio :</i>
BAILEY, Mr. G. L.	THOMPSON, Professor F. C.
GRAHAM, Mr. A. B.	( <i>President</i> ).
MURPHY, Professor A. J.	DOREY, Dr. S. F. ( <i>Senior</i>
RAMSAY, Dr. A. G.	<i>Vice-President</i> ).
SMITHELLS, Dr. C. J.	JONES, Mr. E. H. ( <i>Honorary</i>
TASKER, Mr. H. S.	<i>Treasurer</i> ).
TEED, Major P. L.	SMITH, Mr. C. ( <i>Chairman,</i>
	<i>Publication Committee</i> ).

## LOCAL SECTIONS COMMITTEE

PFEIL, Dr. L. B. ( <i>Chairman</i> ).	HAY, Mr. Matthew ( <i>Honorary</i>
ASHTON, Mr. A. B.	<i>Secretary, Scottish Local Sec-</i>
GARSDIE, Dr. J. E.	<i>tion</i> ).
KENNETT, Dr. S. J.	MADDOCKS, Dr. W. R. ( <i>Chair-</i>
WALTON, Mr. J. S.	<i>man, Sheffield Local Section</i> ).
SYMONDS, Mr. H. H. ( <i>Chair-</i>	MACDOUGALL, Mr. A. J.
<i>man, Birmingham Local Sec-</i>	( <i>Honorary Secretary, Sheffield</i>
<i>tion</i> ).	<i>Local Section</i> ).
MATTHEWS, Mr. A. W. ( <i>Hon-</i>	SPRING, Mr. K. M. ( <i>Chairman,</i>
<i>orary Secretary, Birmingham</i>	<i>South Wales Local Section</i> ).
<i>Local Section</i> ).	CUNNIFFE, Mr. P. W. A.
RANSLEY, Dr. C. E. ( <i>Chairman,</i>	( <i>Honorary Secretary, South</i>
<i>London Local Section</i> ).	<i>Wales Local Section</i> ).
RHODES, Dr. E. C. ( <i>Honorary</i>	
<i>Secretary, London Local Sec-</i>	<i>Ex-officio :</i>
<i>tion</i> ).	THOMPSON, Professor F. C.
PARKER, Dr. R. T. ( <i>Chairman,</i>	( <i>President</i> ).
<i>Oxford Local Section</i> ).	DOREY, Dr. S. F. ( <i>Senior</i>
SMITH, Mr. O. R. ( <i>Honorary</i>	<i>Vice-President</i> ).
<i>Secretary, Oxford Local Sec-</i>	JONES, Mr. E. H. ( <i>Honorary</i>
<i>tion</i> ).	<i>Treasurer</i> ).
FOWLER, Mr. E. A. ( <i>Chairman,</i>	
<i>Scottish Local Section</i> ).	

## METAL PHYSICS COMMITTEE

RAYNOR, Professor G. V.	RICHARDS, Dr. T. Ll.
( <i>Chairman</i> ).	RICHARDSON, Dr. F. D.
AXON, Dr. H. J.	SULLY, Dr. A. H.
BAILEY, Dr. G. L. J.	WAKEMAN, Dr. D. W.
CHRISTIAN, Dr. J. W.	
FINNISTON, Dr. H. M.	
FRANK, Dr. F. C.	
GEACH, Dr. G. A.	
HANSTOCK, Dr. R. F.	
HIGNETT, Mr. H. W. G.	
KING, Mr. R.	
MCLEAN, Mr. D.	
NUTTING, Dr. J.	
OLIVER, Mr. D. A. (representing	<i>Ex-officio :</i>
the Iron and Steel Institute	THOMPSON, Professor F. C.
and the British Iron and	( <i>President</i> ).
Steel Research Association).	SMITH, Mr. C. ( <i>Chairman,</i>
	<i>Publication Committee</i> ).

## METALLURGICAL ENGINEERING COMMITTEE

THOMAS, Mr. W. J. ( <i>Chairman</i> ).	SALTER, Mr. J.
BAKER, Dr. W. A.	SINGER, Dr. A. R. E.
BOLTON, Mr. E. A.	SWINDELLS, Dr. N.
BOND-WILLIAMS, Mr. N. I.	WALTON, Mr. J. S.
BOWMAN, Mr. W. H.	WILKINSON, Mr. R. G.
CAMPBELL, Mr. D. F.	
DAVIES, Mr. C. E.	<i>Ex-officio :</i>
FORD, Professor H.	THOMPSON, Professor F. C.
LAKE, Mr. N. C.	( <i>President</i> ).
MILLER, Mr. H. J.	SMITH, Mr. C. ( <i>Chairman,</i>
PATON, Mr. C. P.	<i>Publication Committee</i> ).

## PUBLICATION COMMITTEE

SMITH, Mr. Christopher ( <i>Chair-</i>	<i>Ex-officio :</i>
<i>man</i> ).	THOMPSON, Professor F. C.
BAILEY, Mr. R. W.	( <i>President</i> ).
BAKER, Dr. W. A.	BAER, Mr. A. ( <i>Chairman,</i>
FINNISTON, Dr. H. M.	<i>Finance and General Pur-</i>
FORD, Professor H.	<i>poses Committee</i> ).
HUDSON, Mr. F.	JONES, Mr. E. H. ( <i>Honorary</i>
INGLIS, Dr. N. P.	<i>Treasurer</i> ).
JENKINS, Dr. Ivor.	RAYNOR, Professor G. V.
PARKER, Dr. R. T.	( <i>Chairman, Metal Physics</i>
PFEIL, Dr. L. B. (representing	<i>Committee</i> ).
Local Sections Committee).	THOMAS, Mr. W. J. ( <i>Chairman,</i>
PHILLIPS, Mr. H. W. L.	<i>Metallurgical Engineering</i>
POWELL, Mr. A. R.	<i>Committee</i> ).
SHOWELL, Mr. D. W. D.	

The constitution of certain Committees was fixed by standing orders of the Council, as follows :

## MEDAL COMMITTEE

PRESIDENT ( <i>Chairman</i> ).	lists who are, or have been,
SENIOR VICE-PRESIDENT.	Members of the Council (to
	be selected by the President),
and	with power to the President
Not more than four Institute	to co-opt not more than two
of Metals (Platinum) Medal-	other persons.

## NOMINATIONS COMMITTEE

PRESIDENT ( <i>Chairman</i> ).
TWO IMMEDIATE PAST-PRESIDENTS.
SENIOR VICE-PRESIDENT.

# REPORT OF THE HONORARY TREASURER

## FOR THE FINANCIAL YEAR ENDED 30 JUNE 1953

In the year under review the income and expenditure both reflect a considerable increase in the work of the Institute relative to the previous year. Although a steady growth may be expected, the rate is likely to be less in future years.

The total income increased by £5929, as follows :

	£
Excluding the Industrial Donations Fund, subscriptions and sundry donations increased by . . . . .	1051
Meeting receipts by . . . . .	37
Publications (sales and advertisements) by . . . . .	4841

Total expenditure increased by £4088. The main items of expenditure increased were :

	£
Salaries and wages . . . . .	1283
Printing and stationery, other than publications . . . . .	334
Meeting expenses . . . . .	408
Publications (excluding salaries and overheads) . . . . .	1129

Expenditure exceeded normal Income by £5076; this compares with £6917 for the previous year and is some £1500 less than was allowed for in the estimates submitted to Council a year ago. The sum required to be transferred from the Industrial Donations Fund is, therefore, less than the year before and, if this trend can be maintained, when that Fund is exhausted it will not be necessary to look to Industry for financial support on the present scale. The permanent staff have made great efforts to increase the Institute's income, and the accounts show their success.

The expenditure on the *Journal* and *Metallurgical Abstracts* has been greater than was forecast. It was anticipated that the rate of receipt of MSS. of papers would not increase, but it did increase considerably : 99 MSS. in 1952-53, compared with 89 in the previous financial year. In view of the increases in income, it was found possible (while keeping within the authorized deficit for the year) to continue to carry out the Finance and General Purposes Committee's instruction that all papers reaching the Publication Committee's standards should be accepted and published. Moreover, it was found possible to overtake arrears of publication of the proceedings and *Metallurgical Abstracts* index issues, so that (though

the publication of one of each such issues had been estimated for) two of each such issues were published and paid for during the year. To meet the increased needs of membership and sales, the monthly printing order was increased from 4750 to 5400.

It was anticipated that after the arrears of papers had been published the average number would be around 70 annually. The indications are, however, that this estimate is low; 75 is more likely, and over the years this will probably increase.

In this connection it is pleasing to note that the price of paper has fallen considerably, resulting in a saving at the rate of some £1200 per annum relative to a year ago at the present volume of publication.

Grants in aid of the activities of Local Sections and Associated Societies steadily increase. This is to be expected with the growth of membership. The Council rightly considers the work of the Local Sections of great importance, and requests from their Officers for increased allocations are rarely refused or reduced.

It will be seen that the Industrial Donations Fund had yielded some £9800 in the year, but this figure contains some tax recovery from payments in the previous year. The Fund will probably diminish by about one-sixth of itself each year for the remainder of its term. It is from this Fund, of course, that our deficit is met, and it is essential that the latter should decrease with the fall in yield from the Fund for the Institute to remain solvent.

The decrease in payments in advance for publications from £4701 to £1354 represents a decrease in holdings of stocks of paper. As paper is now much more readily available, it will not be necessary to hold such heavy stocks in the future.

Turning to the Balance Sheet, it will be noted that the paper value of our assets after allowing for the appropriate liabilities is approximately £4500 higher than last year, while the real position is also improved by the market value of our investments having increased by some £2000.

The balance on deposit in the Mond Nickel Fellowships Fund has now been reduced by investing £3000 in a building society and £1000 in Savings Banks.

Financially, the year has been a satisfactory one, having turned out better than the estimates made for it.



## BALANCE SHEET AS AT 30 JUNE 1953

[illegible]

REPORT TO THE MEMBERS OF THE INSTITUTE OF METALS

We have audited the above Balance Sheet dated 30 June 1953, and the annexed Income and Expenditure Account for the year ended 30 June 1953, and report that we have obtained all the information and explanations as far as we are concerned. The accounts are in accordance with the provisions of the Companies Act, 1947. The accounts are in accordance with the provisions of the Companies Act, 1947. The accounts are in accordance with the provisions of the Companies Act, 1947.

The above mentioned Balance Sheet and annexed Income and Expenditure Account are in agreement with the books of account kept by the Institute so far as appears from our examination of those books. In our opinion, and to the best of our information and according to the explanations given us, the said Accounts give the information required by the Companies Act 1946, in the manner so required, and give a true and fair view, in the case of the Institute's affairs as at 30 June 1953, and in the case of the Income and Expenditure Account of the excess of Expenditure over Income for the year ended 30 June 1953.

21 September 1953.

Approved on behalf of the Council: F. C. THOMPSON *President.*  
21 September 1933.

F. O. THOMPSON, *Treasurer*.  
E. H. JONES, *Honorary Treasurer*.  
S. O. GUILLAN, *Secretary*.  
A. DAVIS, *Chairman*, & *moderator*.

POPPLETON AND APPEBY,  
CHARTERED ACCOUNTANTS, BIRMINGHAM AND LONDON.

# THE INSTITUTE OF METALS INCOME AND EXPENDITURE ACCOUNT FOR THE YEAR ENDED 30 JUNE 1953

£	1952	£	1952	£	1952	£	1952	£	1952
<b>ESTABLISHMENT EXPENSES</b>									
Rent, Rates, Services, and Insurance	1,039								
Lighting and Heating	190								
Repairs and Renewals	123								
	1,352								
<b>ADMINISTRATIVE AND PRODUCTION EXPENSES</b>									
Salaries, Wages, and National Insurance	9,056								
Superannuation Fund	769								
Postages, Despatch, and Telephone	626								
Society Expenses	137								
Printing Expenses	498								
Bank Charges	18								
Bank Overcharges	53								
Audit Fee	157								
Professional Charges	365								
Staff Travelling and Secretarial Expenses	194								
Council and Committee Expenses	11,873								
	783								
<b>PENSIONS TO FORMER STAFF AND PAST SERVICE</b>									
	1838								
<b>MEETINGS AND LOCAL SECTIONS, &amp;C.</b>									
Meeting Expenses (Gross)	497								
Local Sections and Associated Societies : Grants, Programmes, and Travelling	21								
Students Essay Prizes	2,356								
<b>JOINT ACTIVITIES</b>									
Official Entertaining	87								
Joint Library Contribution	500								
Joint Committee on National Certificates in Metallurgy	38								
Joint Committee on Metallurgical Education	23								
Subscriptions to Other Bodies	52								
	702								
	50								
<b>BAD AND DOUBTFUL SUBSCRIPTIONS</b>									
	137								
<b>DEPRECIATION: FURNITURE AND EQUIPMENT</b>									
	17,253								
<b>SPECIAL DEVELOPMENT WORK</b>									
	5,670								
	7,387								
	13,057								
	4,196								
<b>LESS PROPORTION ATTRIBUTABLE TO PUBLICATIONS</b>									
Direct Salaries, Superannuation, and Expenses									
Indirect Salaries, Superannuation, and Overheads									
<b>EXPENDITURE ATTRIBUTABLE TO ACTIVITIES OTHER THAN PUBLICATIONS</b>									
<b>PUBLICATIONS</b>									
<i>Journal and Metallurgical Abstracts :</i>									
Production and Despatch Costs	18,559								
Direct Salaries, Superannuation, and Expenses	4,743								
Indirect Salaries, Superannuation, and Overheads	6,199								
	29,501								
<i>Special Publications :</i>									
Production and Despatch Costs and Royalties	2,847								
Direct Salaries, Superannuation, and Expenses	927								
Indirect Salaries, Superannuation, and Overheads	1,188								
	4,962								
	34,463								
	£38,659								
<b>MEMBERS' SUBSCRIPTIONS AND DONATIONS</b>									
	13,391								
<b>INTEREST ON INVESTMENTS</b>									
General Fund	534								
Endowment Fund	769								
	1,303								
<b>MEETING RECEIPTS</b>									
	1,593								
	1,630								
<b>PUBLICATIONS</b>									
<i>Journal and Metallurgical Abstracts :</i>									
Sales (Net)	5,051								
Advertisements, less general charges	6,904								
Postages recovered	279								
	12,234								
<i>Special Publications :</i>									
Sales (Net)	3,109								
Postages recovered	112								
	15,455								
	6,917								
	£38,659								
<b>EXCESS OF EXPENDITURE OVER INCOME FOR THE YEAR</b>									
	30,286								
	5,076								
	£42,747								



THE INSTITUTE OF METALS  
FUND ACCOUNTS FOR THE YEAR ENDED 30 JUNE 1953

ENDOWMENT FUND

1952	1952																																																																																																																																																																																																																																																																																																																																																																																																																																																																																																																																																																																																																																																																																																																																																																																																																																																																																																																																																																																																																																																																																																																																																																																																																																																																																																																																																																																																																																													
------	------	--	--	--	--	--	--	--	--	--	--	--	--	--	--	--	--	--	--	--	--	--	--	--	--	--	--	--	--	--	--	--	--	--	--	--	--	--	--	--	--	--	--	--	--	--	--	--	--	--	--	--	--	--	--	--	--	--	--	--	--	--	--	--	--	--	--	--	--	--	--	--	--	--	--	--	--	--	--	--	--	--	--	--	--	--	--	--	--	--	--	--	--	--	--	--	--	--	--	--	--	--	--	--	--	--	--	--	--	--	--	--	--	--	--	--	--	--	--	--	--	--	--	--	--	--	--	--	--	--	--	--	--	--	--	--	--	--	--	--	--	--	--	--	--	--	--	--	--	--	--	--	--	--	--	--	--	--	--	--	--	--	--	--	--	--	--	--	--	--	--	--	--	--	--	--	--	--	--	--	--	--	--	--	--	--	--	--	--	--	--	--	--	--	--	--	--	--	--	--	--	--	--	--	--	--	--	--	--	--	--	--	--	--	--	--	--	--	--	--	--	--	--	--	--	--	--	--	--	--	--	--	--	--	--	--	--	--	--	--	--	--	--	--	--	--	--	--	--	--	--	--	--	--	--	--	--	--	--	--	--	--	--	--	--	--	--	--	--	--	--	--	--	--	--	--	--	--	--	--	--	--	--	--	--	--	--	--	--	--	--	--	--	--	--	--	--	--	--	--	--	--	--	--	--	--	--	--	--	--	--	--	--	--	--	--	--	--	--	--	--	--	--	--	--	--	--	--	--	--	--	--	--	--	--	--	--	--	--	--	--	--	--	--	--	--	--	--	--	--	--	--	--	--	--	--	--	--	--	--	--	--	--	--	--	--	--	--	--	--	--	--	--	--	--	--	--	--	--	--	--	--	--	--	--	--	--	--	--	--	--	--	--	--	--	--	--	--	--	--	--	--	--	--	--	--	--	--	--	--	--	--	--	--	--	--	--	--	--	--	--	--	--	--	--	--	--	--	--	--	--	--	--	--	--	--	--	--	--	--	--	--	--	--	--	--	--	--	--	--	--	--	--	--	--	--	--	--	--	--	--	--	--	--	--	--	--	--	--	--	--	--	--	--	--	--	--	--	--	--	--	--	--	--	--	--	--	--	--	--	--	--	--	--	--	--	--	--	--	--	--	--	--	--	--	--	--	--	--	--	--	--	--	--	--	--	--	--	--	--	--	--	--	--	--	--	--	--	--	--	--	--	--	--	--	--	--	--	--	--	--	--	--	--	--	--	--	--	--	--	--	--	--	--	--	--	--	--	--	--	--	--	--	--	--	--	--	--	--	--	--	--	--	--	--	--	--	--	--	--	--	--	--	--	--	--	--	--	--	--	--	--	--	--	--	--	--	--	--	--	--	--	--	--	--	--	--	--	--	--	--	--	--	--	--	--	--	--	--	--	--	--	--	--	--	--	--	--	--	--	--	--	--	--	--	--	--	--	--	--	--	--	--	--	--	--	--	--	--	--	--	--	--	--	--	--	--	--	--	--	--	--	--	--	--	--	--	--	--	--	--	--	--	--	--	--	--	--	--	--	--	--	--	--	--	--	--	--	--	--	--	--	--	--	--	--	--	--	--	--	--	--	--	--	--	--	--	--	--	--	--	--	--	--	--	--	--	--	--	--	--	--	--	--	--	--	--	--	--	--	--	--	--	--	--	--	--	--	--	--	--	--	--	--	--	--	--	--	--	--	--	--	--	--	--	--	--	--	--	--	--	--	--	--	--	--	--	--	--	--	--	--	--	--	--	--	--	--	--	--	--	--	--	--	--	--	--	--	--	--	--	--	--	--	--	--	--	--	--	--	--	--	--	--	--	--	--	--	--	--	--	--	--	--	--	--	--	--	--	--	--	--	--	--	--	--	--	--	--	--	--	--	--	--	--	--	--	--	--	--	--	--	--	--	--	--	--	--	--	--	--	--	--	--	--	--	--	--	--	--	--	--	--	--	--	--	--	--	--	--	--	--	--	--	--	--	--	--	--	--	--	--	--	--	--	--	--	--	--	--	--	--	--	--	--	--	--	--	--	--	--	--	--	--	--	--	--	--	--	--	--	--	--	--	--	--	--	--	--	--	--	--	--	--	--	--	--	--	--	--	--	--	--	--	--	--	--	--	--	--	--	--	--	--	--	--	--	--	--	--	--	--	--	--	--	--	--	--	--	--	--	--	--	--	--	--	--	--	--	--	--	--	--	--	--	--	--	--	--	--	--	--	--	--	--	--	--	--	--	--	--	--	--	--	--	--	--	--	--	--	--	--	--	--	--	--	--	--	--	--	--	--	--	--	--	--	--	--	--	--	--	--	--	--	--	--	--	--	--	--	--	--	--	--	--	--	--	--	--	--	--	--	--	--	--	--	--	--	--	--	--	--	--	--	--	--	--	--	--	--	--	--	--	--	--	--	--	--	--	--	--	--	--	--	--	--	--	--	--	--	--	--	--	--	--	--	--	--	--	--	--	--	--	--	--	--	--	--	--	--	--	--	--	--	--	--	--	--	--	--	--	--	--	--	--	--	--	--	--	--	--	--	--	--	--	--	--	--	--	--	--	--	--	--	--	--	--	--	--	--	--	--	--	--	--	--	--	--	--	--	--	--	--	--	--	--	--	--	--	--	--	--	--	--	--	--	--	--	--	--	--	--	--	--	--	--	--	--	--	--	--	--	--	--	--	--	--	--	--	--	--	--	--	--	--	--	--	--	--	--	--	--	--	--	--	--	--	--	--	--	--	--	--	--	--	--	--	--	--	--	--	--	--	--	--	--	--	--	--	--	--	--	--	--	--	--	--	--	--	--	--	--	--	--	--	--	--	--	--	--	--	--	--	--	--	--	--	--	--	--	--	--	--	--	--	--	--	--	--	--	--	--	--	--	--	--	--	--	--	--	--	--	--	--	--	--	--	--	--	--	--	--	--	--	--	--	--	--	--	--	--	--	--	--	--	--	--	--	--	--	--	--	--	--	--	--	--	--	--	--	--	--	--	--	--	--	--	--	--	--	--	--	--	--	--	--	--	--	--	--	--	--	--	--	--	--	--	--	--	--	--	--	--	--	--	--	--	--	--	--	--	--	--	--	--	--	--	--	--	--	--	--	--	--	--	--	--	--	--	--	--	--	--	--	--	--	--	--	--	--

INDUSTRIAL DONATIONS FUND

£.	£.	£.	
To Cost of Appeals, Administration and Stamp Duty . . . . .	215	By Balance at 30 June 1952 . . . . .	6,356
" 10-Year Index to "Metallurgical Abstracts" (Binding) . . . . .	93	" Donations (Gross) . . . . .	10,000
" Amount transferred to General Fund, being Excess of Expenditure over Income for the year ended 30 June 1953 . . . . .	5,076	" Income Tax recovered for previous year . . . . .	9,716
" Balance at 30 June 1953 . . . . .	15,718	" Interest on Investments (including Income Tax recovered for previous year) . . . . .	89
	<u>£21,102</u>		<u>£21,102</u>
	<u>£18,589</u>		<u>£21,102</u>

MOND NICKEL FELLOWSHIPS FUND

£	£	£	
To Grants to Fellows, including Travelling	3,311	By Balance at 30 June 1952	23,837
" Printing, Stationery, Postage, and Publicity	67	" Donations received	7,000
" Bank Charges	3	" Interest on Investments and Bank Interest	559
" Secretarial Expenses	250	" Refund due from Fellow	256
" Balance at 30 June 1953	30,711		
	<u>£34,342</u>		<u>£34,342</u>
	<u>£31,302</u>		<u>£34,342</u>

CAPPER PASS FUND

£	£	£	
To Grants	225	By Balance at 30 June 1952	325
" Balance at 30 June 1953	525	Donations received	200
		" Bank Interest	9
	<u>£750</u>		<u>£534</u>
	<u>£534</u>		<u>£750</u>

W. H. A. ROBERTSON FUND

£	£	£	
33 To Balance at 30 June 1952 due to The Institute of Metals	—	By Donations received	200
3 Expenditure during year	56	" Balance at 30 June 1952 due by The Institute of Metals	100
164 Balance at 30 June 1953 owing by The Institute of Metals	208		164
	<u>£264</u>		<u>£264</u>
	<u>£200</u>		<u>£264</u>

1952		30 JUNE 1960	
£	£	£	£
<i>General Fund :</i>			
5,500	3% Savings Bonds, at cost		5,500
1,010	2½% Treasury Stock, at cost		1,010
4,734	4% Consolidated Loan, at cost		4,734
5,057	2½% National War Bonds, at cost		5,057
500	2½% Defence Bonds, at cost		500
162	£1 War Savings (see Note 1)		162
829	4% Consolidated Loan (see Note 2)		829
17,792			17,792
Note 1. At cost plus accrued interest to 22.11.50.			
Note 2. Transferred at Market Value on 22.11.50 from the War-Time Emergency Fund to the General Fund.			
<i>Endowment Fund :</i>			
525	£525 2½% Defence Bonds, at cost		525
1,285	£1,285 3% Savings Bonds, at cost		1,285
19,482	£17,926 5s. 0d. 4% Consolidated Loan, at cost		19,482
21,292			21,292
<i>Industrial Donations Fund :</i>			
950	£950 3% Funding Stock, at cost		950
1,000	£1,012 8s. 9d. 4% Funding Stock 1960/90, at cost		1,000
1,950			1,950
<i>Mond Nickel Fellowships Fund :</i>			
7,550	Woolwich Equitable Building Society		7,550
1,250	Co-operative Permanent Building Society		1,250
3,500	Halifax Building Society		3,500
5,000	Abbey National Building Society		5,000
17,300			17,300
£58,334			£58,334



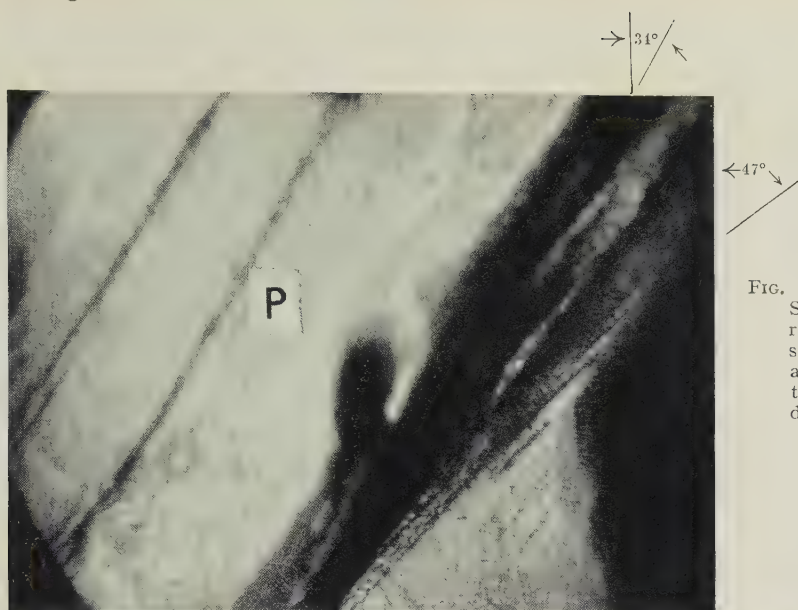
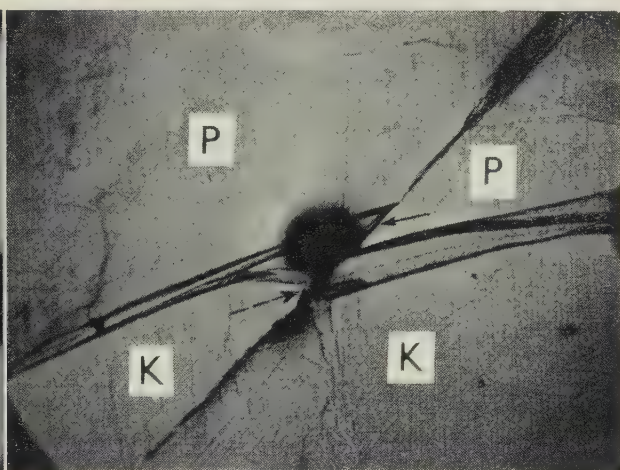
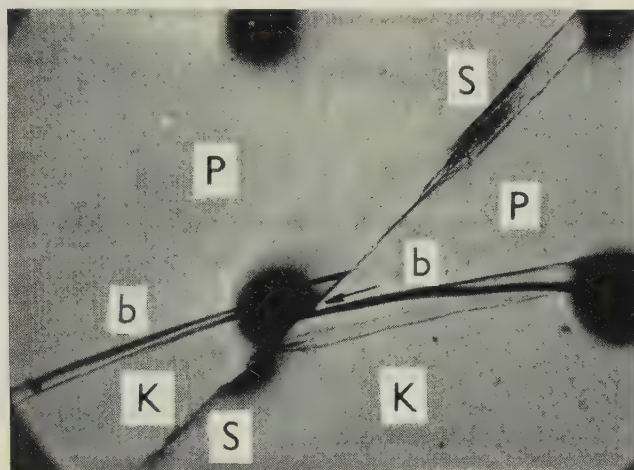


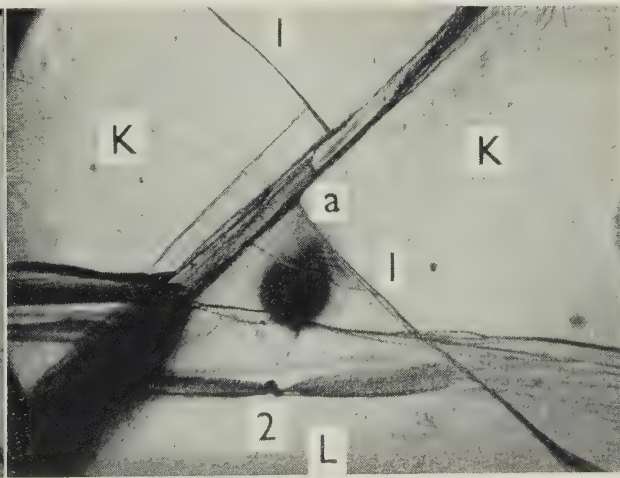
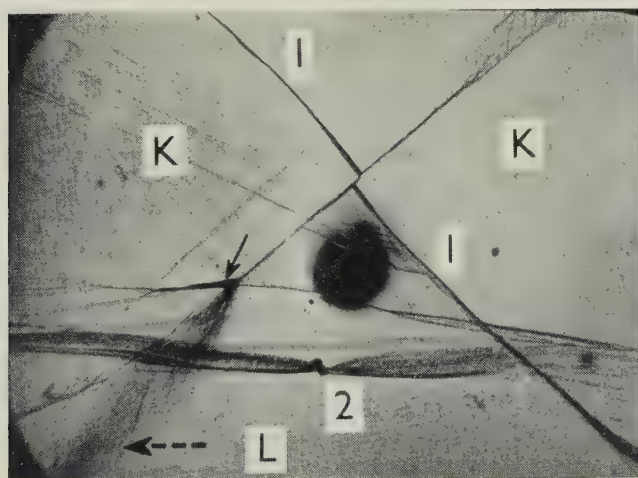
FIG. 6.—Specimen *P*-10. 1100° F., 50 lb./in.<sup>2</sup>, Front Surface. After 29.6 hr. Note slip-band steps at right edge, as a result of shift of the operating slip bands from the upper to the lower bands. The amount of rotation of the slip bands developed in the early stages of creep was greater than that developed in the later stage.  $\times 60$ .



FIGS. 7 and 8.—Specimen *P*-10. 1100° F., 50 lb./in.<sup>2</sup>, Front Surface.  $\times 60$ , reduced by  $\frac{1}{10}$  in reproduction.

FIG. 7.—After 9.5 hr. Slip band *S* passed through the grain boundary (*b*) and segmented it. The offset so produced is indicated by the arrow.

FIG. 8.—After 18.2 hr. The displaced grain boundary of Fig. 7 becomes a continuous boundary bent at the slip band. No further displacement along the slip band has occurred, as is shown by the solid arrow.



FIGS. 9 and 10.—Specimen *P*-10. 1100° F., 50 lb./in.<sup>2</sup>, Front Surface.  $\times 60$ , reduced by  $\frac{1}{10}$  in reproduction.

FIG. 9.—After 3.5 hr. The upper solid arrow indicates the direction of migration of the boundary *K/L*. Note the displacement of the old boundary (1 — 1) by slip and the irregular deformation marks in grain *L* as indicated by the dashed arrow.

FIG. 10.—After 9.5 hr. Same field as Fig. 9. The two original narrow slip bands merged into one wide band at this stage. Note also the steps left across the traces of the old boundary by the two horizontal bands at (*a*). The almost horizontal and vertical marks are oxide cracks.

FIGS. 11-13.—Effect of Grain Boundary on Development of Deformation Bands.

FIG. 11.—Specimen *P-8*. 700° F., 85 lb./in.<sup>2</sup>, Front Surface. The upper band was fully developed throughout, the lower was not. Arrows indicate the regions where cross slip has taken place. (See Fig. 4.)  $\times 50$ .

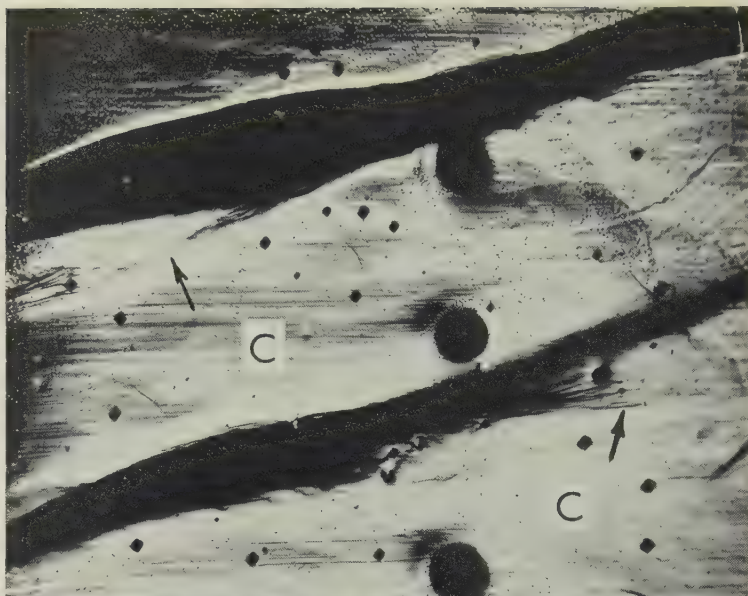


FIG. 12.—Specimen *P-8*. 700° F., 85 lb./in.<sup>2</sup>, Front Surface. A continuation of Fig. 11 to the right. The upper band encountered the grain boundary near the right edge of the specimen; the lower band encountered a grain boundary at the back as well as on the front surface of the specimen and was incompletely developed. (See Fig. 4.)  $\times 50$ .

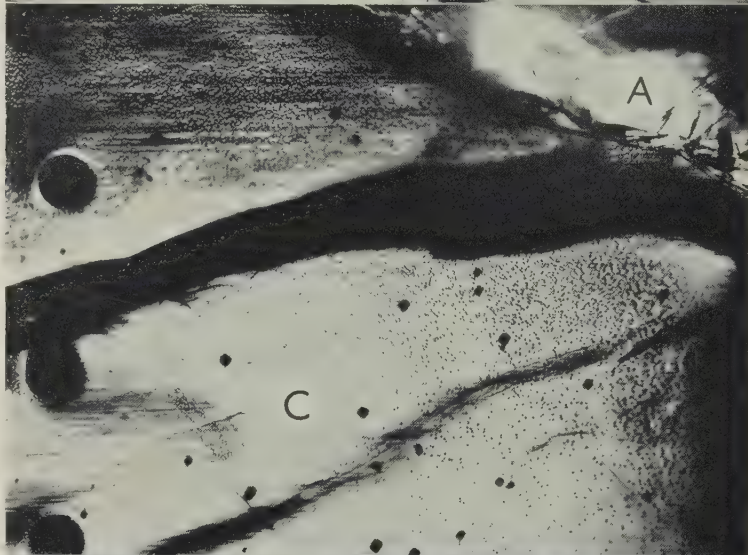
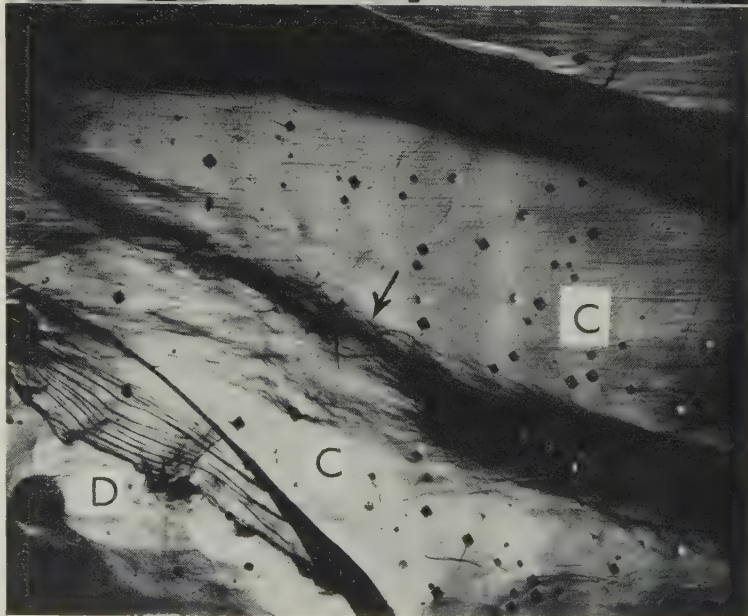
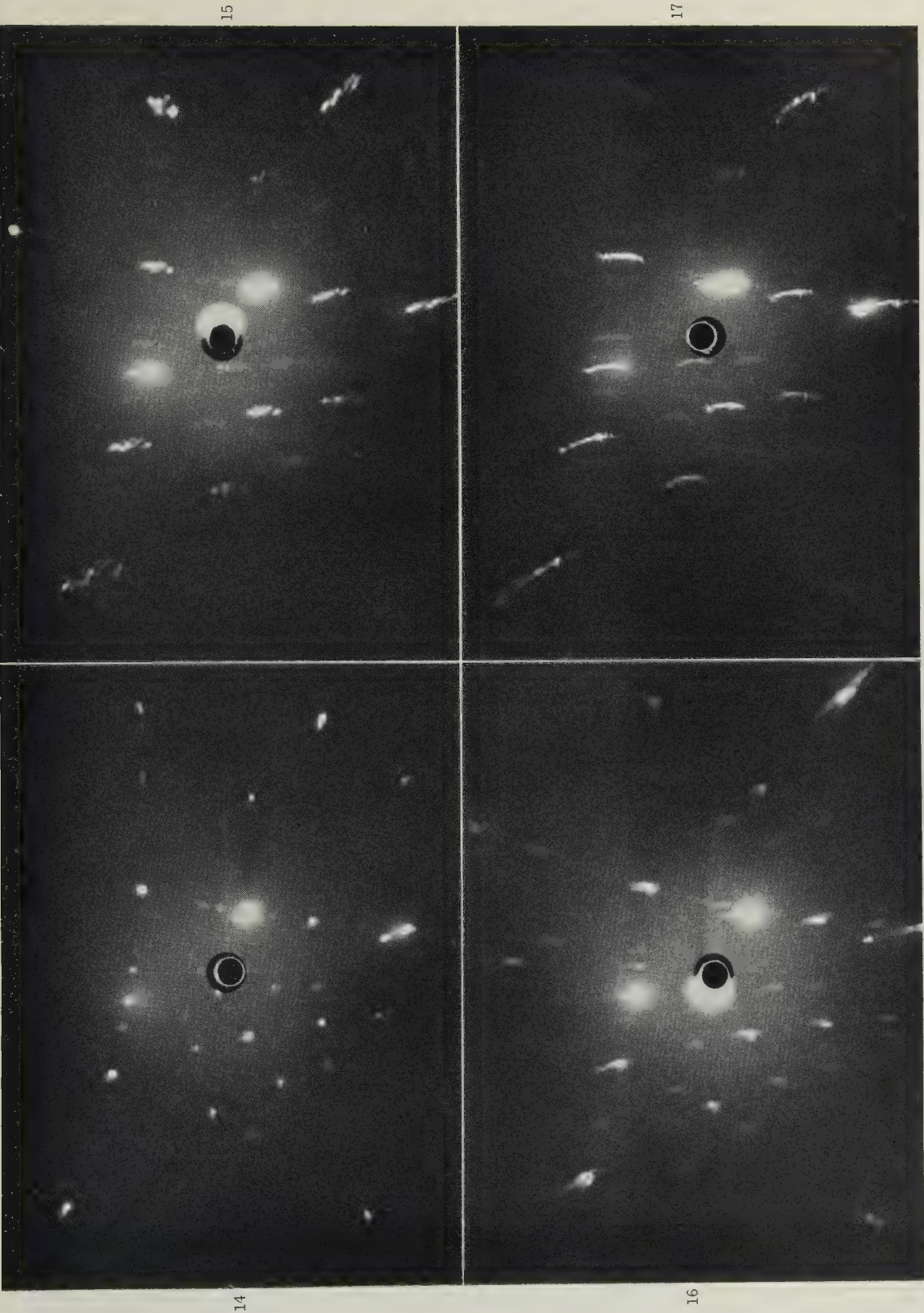


FIG. 13.—Specimen *P-8*. 700° F., 85 lb./in.<sup>2</sup>, Back Surface. The same two bands as shown in Figs. 11 and 12. The lower band deviated on approaching the grain boundary *C/D*. Arrow indicates the region where cross slip has occurred.  $\times 50$ .



Reduced by  $\frac{1}{10}$  in reproduction.

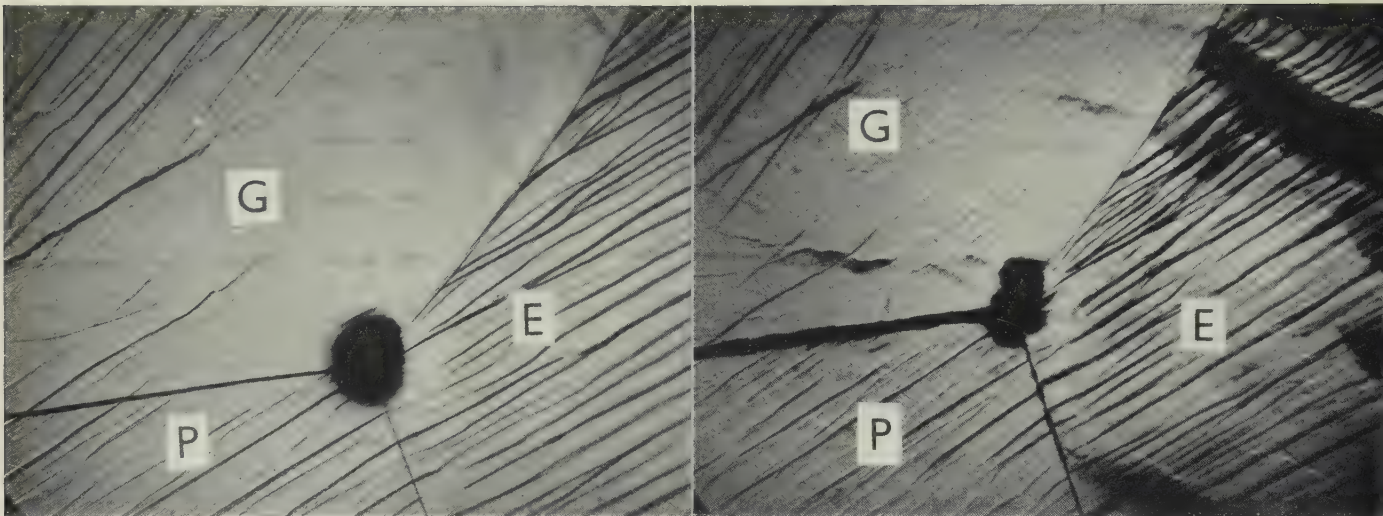




FIGS. 14-17.—Specimen P-8. 700° F., 85 lb./in.<sup>2</sup>, Front Surface. Back-reflection Laue photographs taken at positions indicated by triangles in Fig. 4.

FIG. 14.—Triangle (2). Spots were slightly broken down on the upper slip band.  
FIG. 15.—Triangle (5) on Upper Band. Spots were broken down into about 8 discrete subgrain spots with a spread of 5°. Poorly resolved subgrain spots and streaks show severe inhomogeneous deformation with spread of about 5°.  
FIG. 16.—Triangle (7) on Lower Band. Near a Grain Boundary. Subgrain spots spread up to 6° and show a strong background. This indicates severe inhomogeneous deformation between the upper band and the boundary  $B/C$ .  
FIG. 17.—Triangle (1). Subgrain spots spread up to 6° and show a strong background. This indicates severe inhomogeneous deformation between the upper band and the boundary  $B/C$ .





FIGS. 18-20.—Specimen *P*-11. 400° F., 400-750 lb./in.<sup>2</sup>. Front Surface. Development of kinking bands (grain *E*) and subgrains (grain *G*). Note the continuous nature of the slip bands across the boundary *E/P*. × 60.

FIG. 18.—3.5 hr. After Loading, 400 lb./in.<sup>2</sup>.

FIG. 19.—385 hr. After Loading, 400 lb./in.<sup>2</sup> + 322 hr., 550 lb./in.<sup>2</sup> + 220 hr., 750 lb./in.<sup>2</sup>.

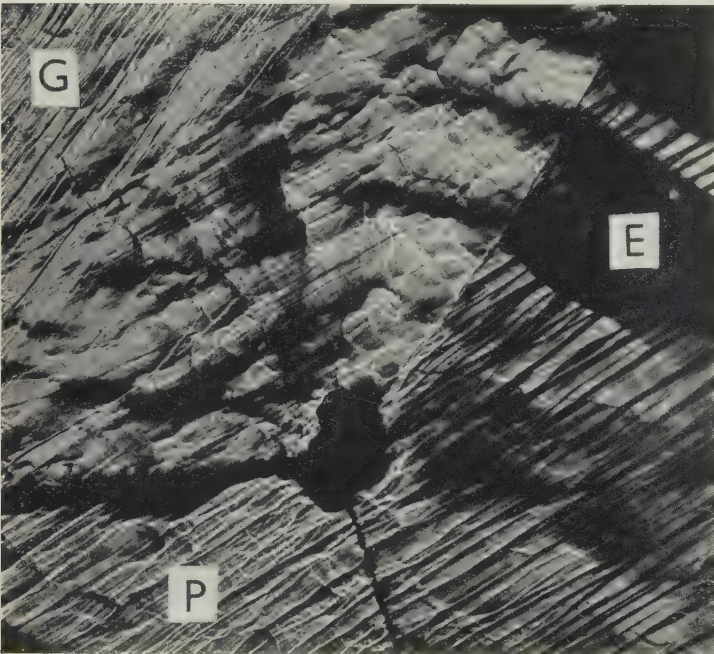


FIG. 20.—After Rupture.



FIG. 21.—Specimen *P*-11. 400° F., 400-750 lb./in.<sup>2</sup>, Front Surface. Illustration of the continuous nature of kinking bands across grain boundary *E/F*. × 60.



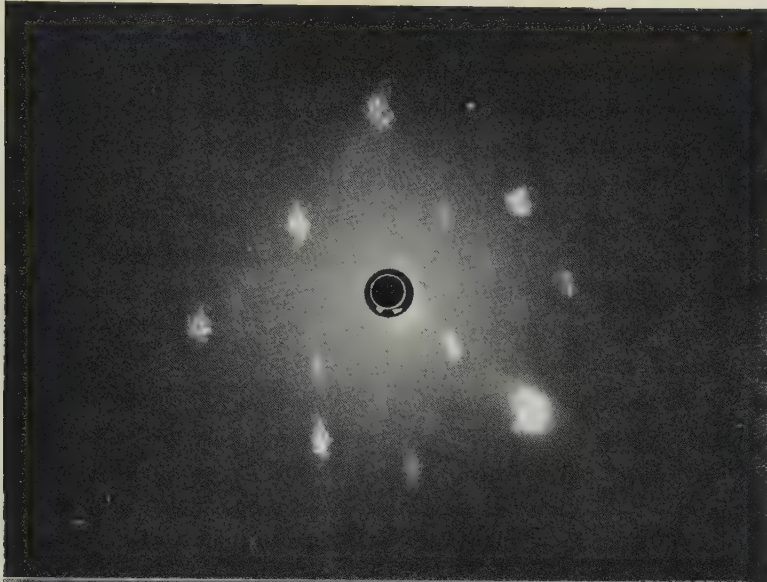


FIG. 22.—Specimen *P-11*. 400° F., 400–750 lb./in.<sup>2</sup>. Back-reflection Laue photograph, taken in grain *G*, close to the boundary *G/E* (see Fig. 20), shows random breakdown into discrete subgrain spots.

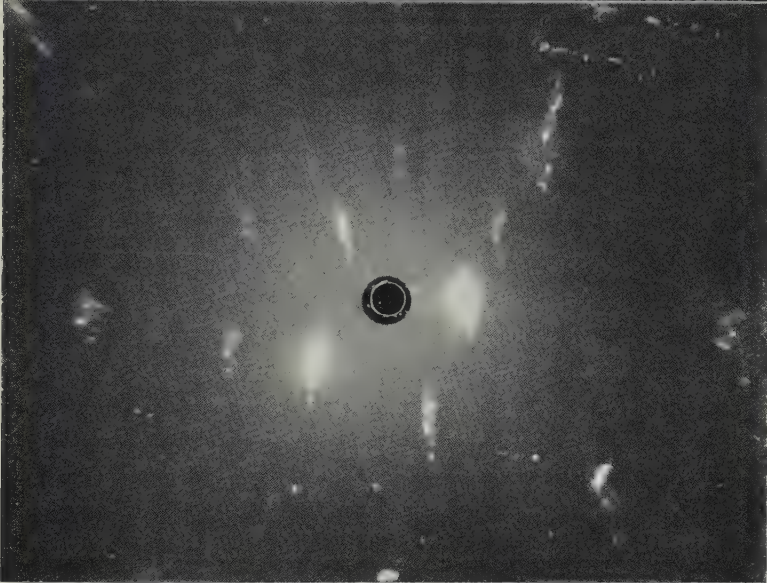


FIG. 23.—Specimen *P-11*. 400° F., 400–750 lb./in.<sup>2</sup>. Back-reflection Laue photograph, taken in grain *E* (see Fig. 20), shows a preferred breakdown into subspots with intense background.

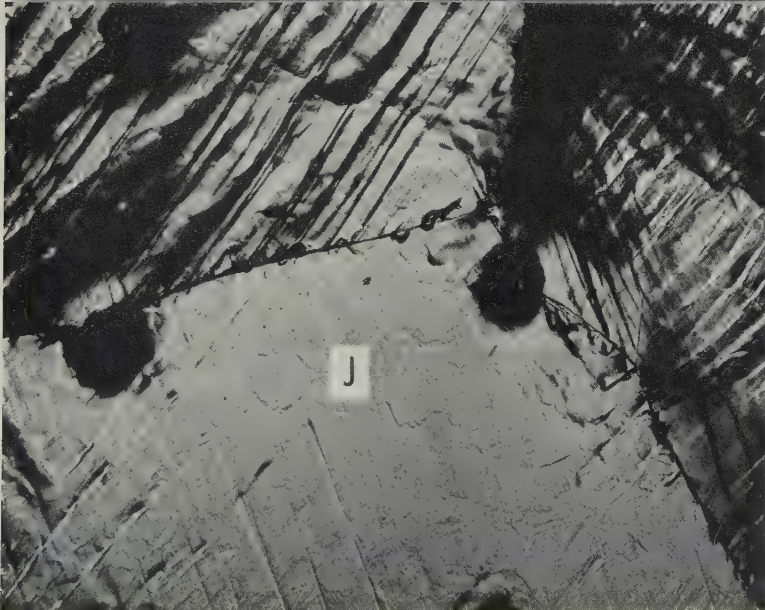


FIG. 24.—Specimen *P-11*. 400° F., 400–750 lb./in.<sup>2</sup>. Subgrains around the triple point in grain *J* delineated by deformation bands. These boundaries cannot be revealed by electro-etching after repolishing.  $\times 100$ .

Reduced by  $\frac{1}{10}$  in reproduction.

OSCILLATION PHOTOGRAPHS TAKEN WITH MONOCHROMATIC MOLYBDENUM RADIATION OF  
ALUMINIUM-4% COPPER ALLOYS AGED AT 136° C. SHEET SPECIMENS.

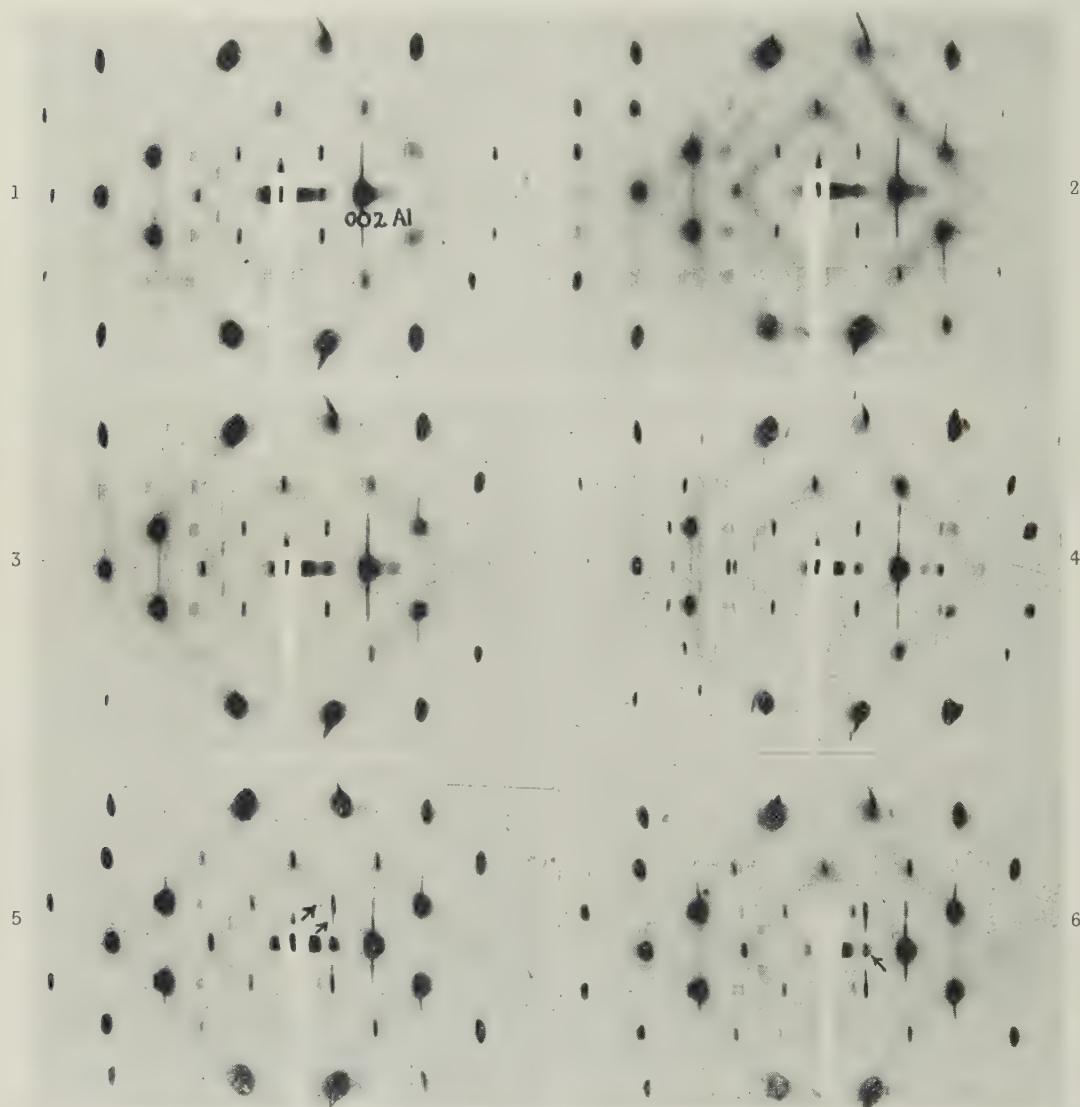


FIG. 1.—Water-Quenched and Aged 8 Hr. Uniform G.P. [1] streaks ( $\lambda/2$  spot in central streak).

FIG. 2.—Acetone-Quenched and Aged 3 Days. Intensity maxima in the streaks.

FIG. 3.—Oil-Quenched and Aged 5 Days. Strong maxima.

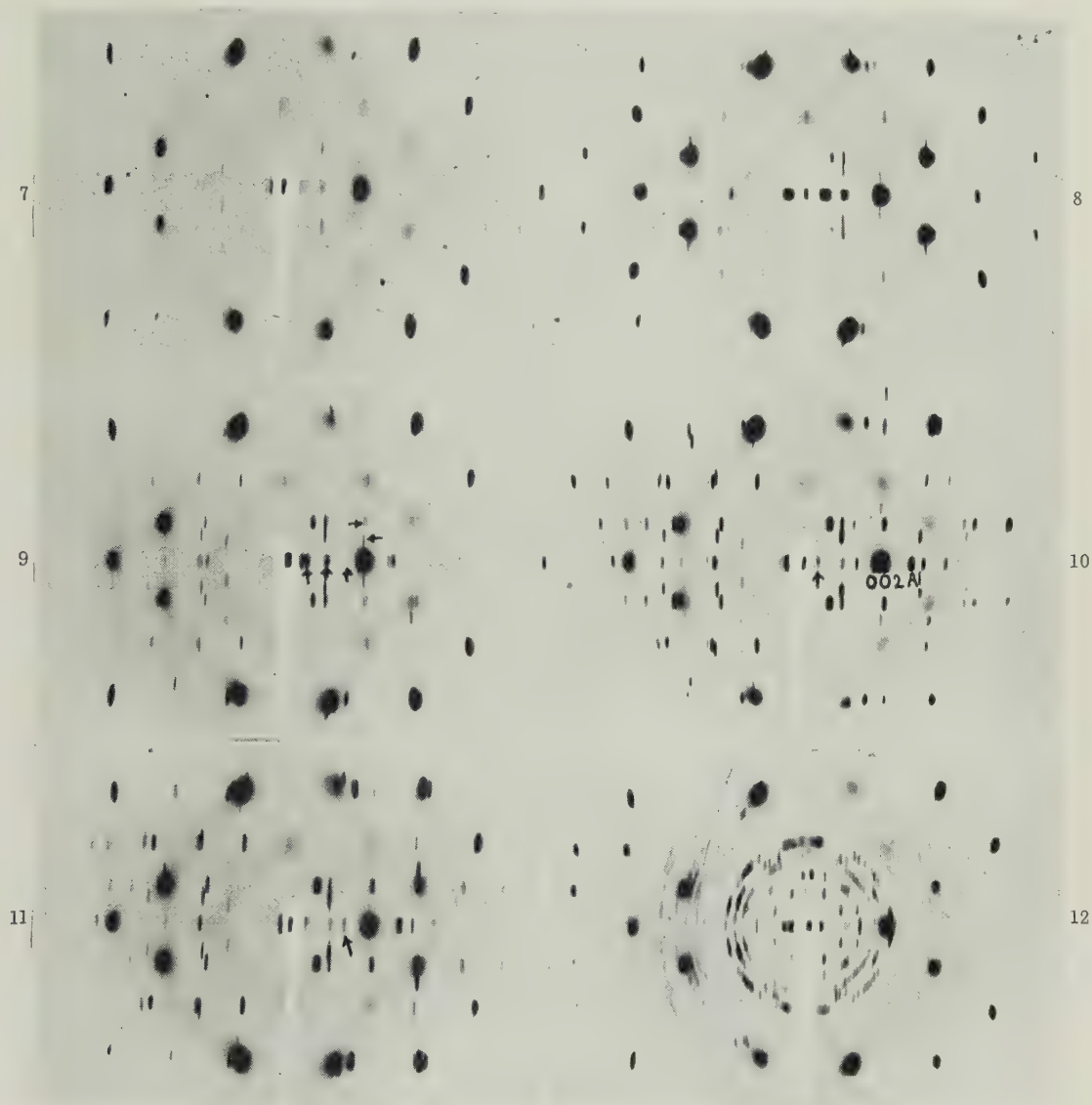
FIG. 4.—Oil-Quenched and Aged 11 Days. G.P. [2].  $\theta'$  spots just visible.

FIG. 5.—Water-Quenched and Aged 11 Days. G.P. [2] and  $\theta'$ .  $(111)_{\theta^P}$ ,  $(101)_{\theta^T}$ ,  $c$  orientation spot (upper arrow) is broad, cf.  $(111)_{\theta^P}$ ,  $(101)_{\theta^T}$ ,  $b$  orientation spot (lower arrow).

FIG. 6.—Water-Quenched and Aged 47 Days. Sharper G.P. [2] spots, more intense  $\theta'$  spots.



OSCILLATION PHOTOGRAPHS TAKEN WITH MONOCHROMATIC MOLYBDENUM RADIATION OF  
ALUMINIUM-COPPER ALLOYS AGED AT 190° C. SHEET SPECIMENS.



FIGS. 7-10.—4% Copper Alloy.

FIG. 7.—Water-Quenched and Aged 30 Min. Faint G.P. [2] and  $\theta'$  spots.

FIG. 8.—Water-Quenched and Aged 8 Hr. G.P. [2] and  $\theta'$ .

FIG. 9.—Oil-Quenched and Aged 1 Day. Sharp G.P. [2] and  $\theta'$  spots. Some G.P. [2] spots marked with arrows.

FIG. 10.—Water-Quenched and Aged 100 Days.  $\theta'$  spots. Spot marked with arrow is from planes of  $10.4 \text{ \AA}$ . spacing.

FIG. 11.—3% Copper Alloy.  $\theta'$  Spots. Spot marked with arrow is  $(002)_{\theta'} c$  orientation. Vertical streak through  $(002)_{Al}$  spot.

FIG. 12.—4% Copper Alloy Aged 3 Days at 350° C.  $\theta$  spots.



FIG. 13.—Small-Angle Scatter Film of Cu Sheet Aged 2 Days at 130° C.  $\text{CuK}\alpha$  radiation.

FIGS. 14-18.—Laue Photographs of Aluminium-Copper Alloys.

FIG. 14.—3% Cu Rod Aged 4 Days at 130° C. G.P. [1].

FIG. 15.—4% Cu Sheet Aged 11 Days at 130° C.; same specimen as Fig. 4. G.P. [2].  $\theta'$  cannot be detected in this film.

FIG. 16.—4.5% Cu Sheet Aged 2.7 Days at 165° C. G.P. [2] and  $\theta'$  (peak hardness reached in 2½ days).

FIG. 17.—3% Cu Sheet Aged 1 Day at 165° C. Elongated  $\theta'$  spots: upper arrow  $(115)\theta'^P$   $(105)\theta'^T$ ; lower arrow  $(331)\theta'^P$   $(301)\theta'^T$ . Stronger Al and  $\theta'$  spots linked.

FIG. 18.—4% Cu Sheet Aged 6 Hr. at 250° C.  $\theta'$  only. Sharp spots.



## HIGH-PURITY ALUMINIUM-4% COPPER ALLOYS.

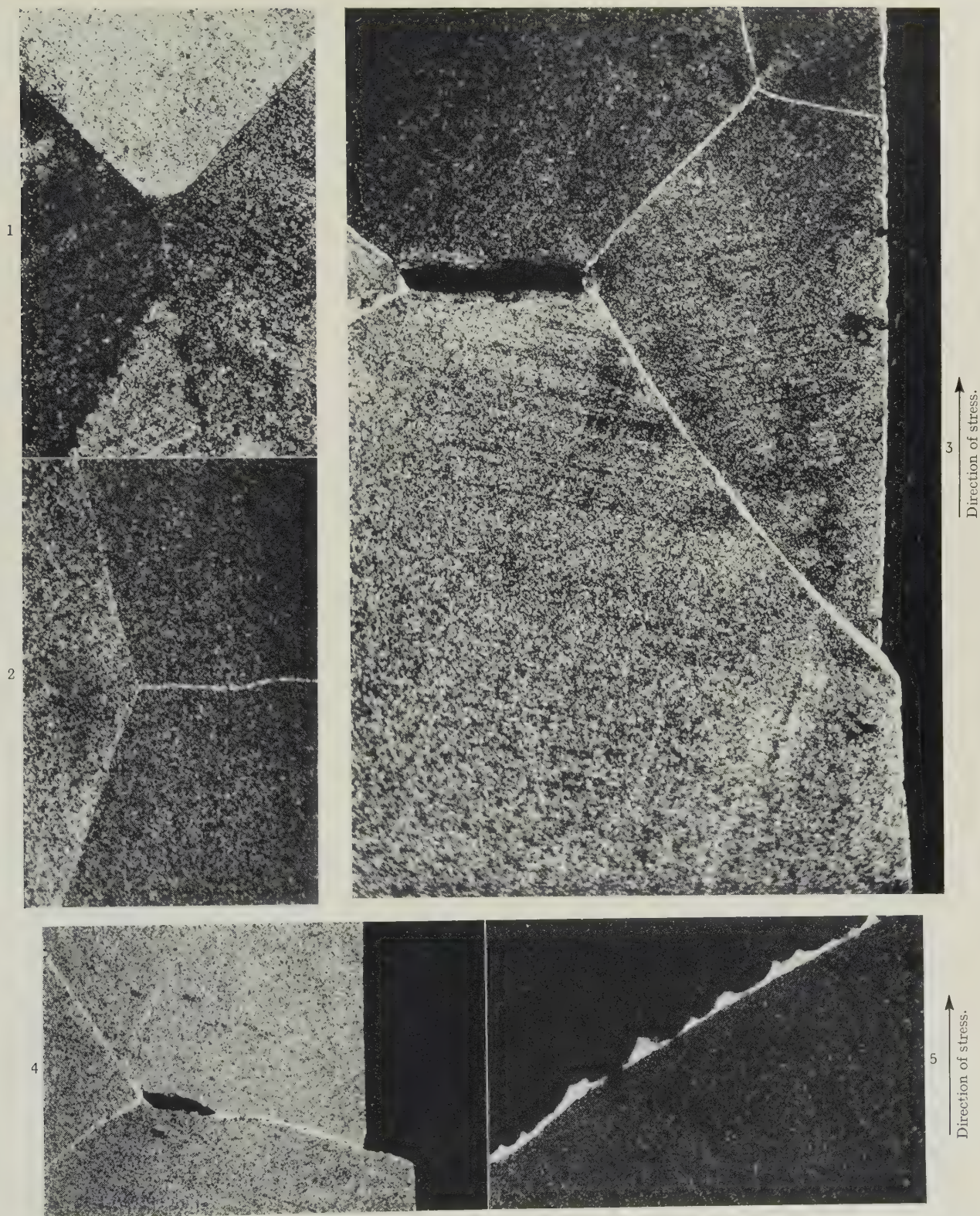


FIG. 1.—Aged 436 Hr. at 190° C. Not creep tested.  $\times 250$ .  
 FIG. 2.—Aged 2740 Hr. at 190° C. Not creep tested.  $\times 250$ .  
 FIG. 3.—Aged at 190° C.; Failed after 231 hr. at  $4\frac{1}{2}$  tons/in.<sup>2</sup> at 190° C.  $\times 250$ .  
 FIG. 4.—Aged at 250° C.; Failed after 325 hr. at  $4\frac{1}{2}$  tons/in.<sup>2</sup> at 190° C.  $\times 250$ .  
 FIG. 5.—As Fig. 3. Fractured Surface.  $\times 250$ .



## NORMAL-PURITY ALUMINIUM-4% COPPER ALLOYS.

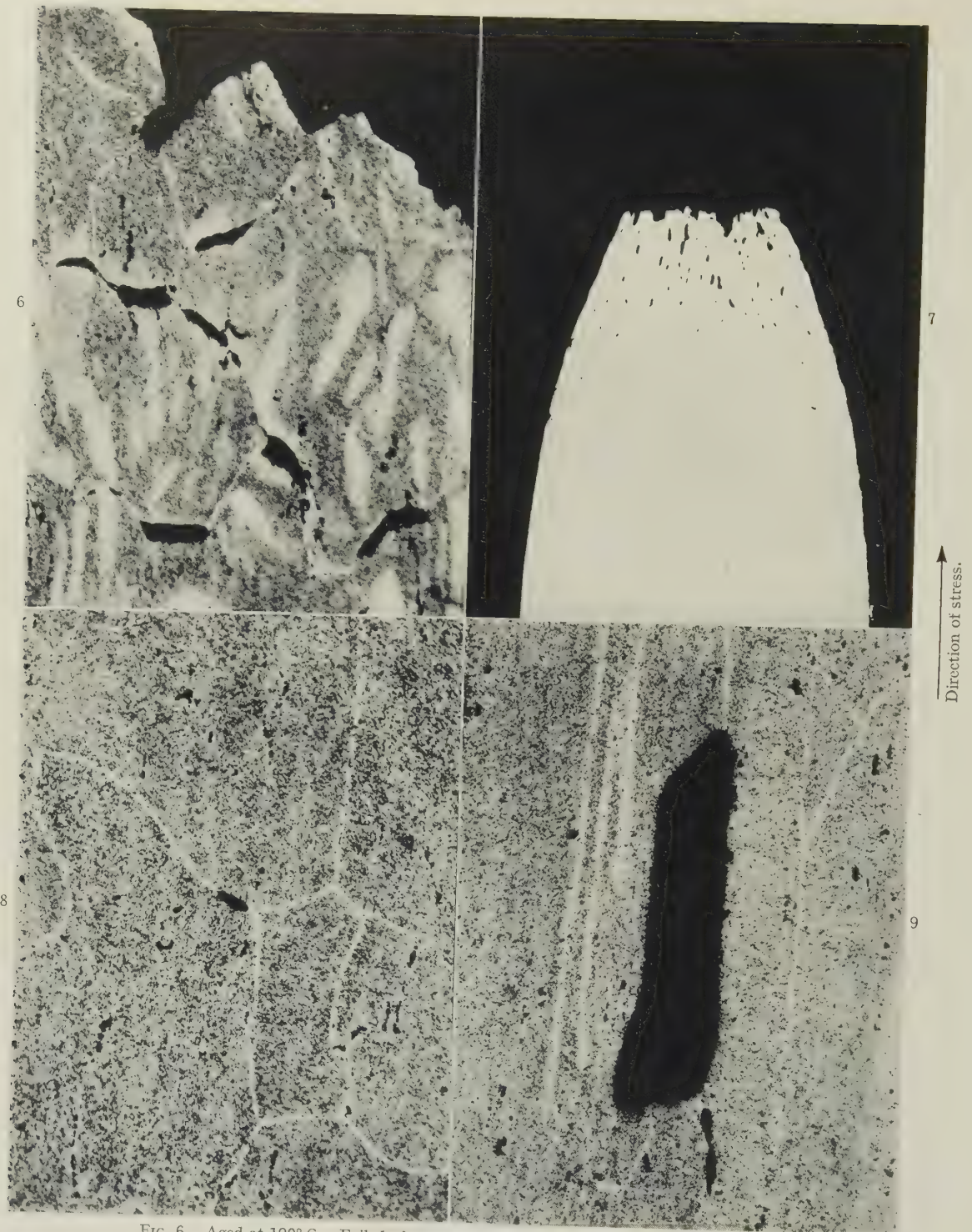


FIG. 6.—Aged at 190° C.; Failed after 5170 hr. at  $4\frac{1}{2}$  tons/in.<sup>2</sup> at 190° C.  $\times 250$ .  
 FIGS. 7-9.—Aged at 300° C.; Failed after 310 hr. at  $4\frac{1}{2}$  tons/in.<sup>2</sup> at 190° C.

FIG. 7.—General appearance of fracture showing small cavities in necked region.  $\times 7$ .  
 FIG. 8.—Structure away from fracture.  $\times 250$ .

FIG. 9.—Structure close to fracture.  $\times 250$ .



# PROBLEMS OF THE CONTROL OF DIMENSION, SHAPE, AND FINISH IN THE ROLLING OF SHEET AND STRIP AND IN THE DRAWING OF WIRE \*

1522

By HUGH FORD,† D.Sc.(Eng.), Ph.D., Wh.Sch., MEMBER, and  
J. G. WISTREICH,‡ M.Sc.(Eng.), D.I.C.

## SYNOPSIS

The general principles of control are examined in relation to the dimensions, shape, and finish of sheet, strip, and wire. The main sources of variations are discussed, and reference is made generally to the problem of hot rolling as it affects both strip and rod.

The control of dimensions in sheet and strip involves the measurement of thickness along the length and across the width. The causes of errors are described, and the methods for manual and automatic control are detailed.

There is a fundamental difference between wire drawing and rolling in the control of dimensions, because the die bore is of fixed dimensions; this is discussed with regard to tolerances on gauge and allowable wear. Difficulties of continuous measurement and problems of ovality are discussed.

The control of shape is shown to depend upon the same factors in wire drawing as in rolling, but the factors are of different degrees of importance.

Of the three properties, surface finish is the least amenable to measurement and control, and the dependence of finish on the forming process is as yet little understood. Roll finish, die polish, and lubricants are discussed in so far as they affect smoothness and lustre.

## I.—GENERAL CONSIDERATIONS

### 1. SCOPE OF THE PROBLEM

THERE are certain general principles underlying every problem of control which need to be stated at the outset. The degree to which a property can be controlled depends upon the methods available for measuring it and for correcting any departure from its desired value, and the degree of control actually realized then depends upon the accuracy and speed of measurement and the particular methods adopted for exercising the control. The latter are usually flexible, and their choice is influenced by both technical and economic considerations, the tolerance allowable from the standard of reference being dictated not only by the importance of the property in question but also by the cost of exercising control within the fixed limits of tolerance.

These general principles have been dealt with in many publications<sup>1-3</sup> and are not examined in detail here. However, the inferences to be drawn for the subject under discussion, need brief indication. Whereas the dimensions and the shape of strip and

wire can be readily and accurately measured, surface finish has, hitherto, not been defined in such a way that an accurate method for its measurement may be adopted. The problem of controlling surface finish is, therefore, in a different category from the control of dimensions and shape.

The methods available for controlling strip dimensions are better understood and more readily used than those available for the control of its shape; it is not surprising, therefore, that dimension-control is in a higher state of development. It will also be shown that the methods available for correcting wire dimensions are much more limited than those available for the correction of strip dimensions, and the two approaches to the problem of control are, therefore, very different.

In general, there are three stages in the enquiry into the control of a property: (i) definition of the property and methods for its measurement; (ii) causes of variation of the property and methods of control; (iii) technical and economic appraisal of possible methods of control, with reference to tolerated variations. The present paper is mainly devoted to the

\* Manuscript received 4 December 1953. Contribution to a Symposium on "The Control of Quality in the Production of Wrought Non-Ferrous Metal and Alloys. II.—Working Operations", to be held in London on 28 April 1954.

† Professor of Applied Mechanics, Imperial College of Science and Technology, London.

‡ Head of Metal Working Laboratory, British Iron and Steel Research Association, Sheffield.

first and second stages, but one aspect of the third requires mention.

The question of control must be related to the allowable tolerances on the finished product. The standard tolerances on sheet and wire laid down in British Standard Specifications may not be difficult to meet, but it must be remembered that the limits depend to some extent on what can be attained in normal practice. Closer limits may be set as control improves, but control of quality must be effected within certain limits of tolerance, these limits acting as a reference standard. The three attributes, dimensions, shape, and finish, to be considered here need, accordingly, to be defined.

The critical dimensions in strip and wire are those of the cross-section, length being usually of secondary importance. In sheet, the length may be critical, but the cutting of the material to length is essentially a separate operation—even in the case of a flying shear which may involve its own problem of control—and it will not be considered as an integral part of the forming process. The thickness of sheet and strip can vary both across the width and along the length, the variations each being dependent upon a number of independent and related factors. Variations in width, whilst not usually as important as those in thickness, can nevertheless have an influence on the general operation of the mill and also involve subsequent operations, e.g. slitting. In the case of wire, the controlling dimension is the diameter; this may vary from point to point along the length, and there may also be departures from circularity.

The shape of strip or wire is taken as the form adopted by a moderately long piece of the material free of constraint, that is, straightness and flatness of sheet and strip, and curvature (cast) in wire. Surface finish is a quality which has not hitherto been precisely defined. For the purpose of this paper, it is taken as meaning smoothness and lustre.

## 2. MAIN SOURCES OF VARIATIONS IN STRIP OR WIRE

There are three main sources of variation in the final product, whether it be strip or wire: (i) variations arising from the raw material itself; (ii) variations arising from the forming process proper; and (iii) variations arising from any auxiliary process.

Variations arising from the forming process proper, (ii), are the subject of this paper.

Examples of (i) were discussed at some length in a previous symposium.<sup>4</sup> Such faults as dross inclusions, hot tears, and surface cracks give rise to unsatisfactory products in the final stages of rolling and drawing, if not removed at an early stage. Hard-scale deposits which will later be rolled into the surface are also to be avoided. A clean and satisfactory ingot is usually obtained by scalping, i.e. machining away the surface on the main faces, and although the finished product of one mechanical-working operation is the raw material of the next (e.g. wire rod), it will be assumed in this paper that the initial raw material is satisfac-

tory, the scalping, &c., being considered as part of the quality control applied to the melting and casting of the raw material, and to the processing of rod.

Variations of the third kind are considered to be outside the scope of the present paper. Examples of faults originating in auxiliary processes include incomplete removal of scale and other surface blemishes in overhauling or pickling, and staining and sticking in heat-treatment.

## 3. HOT ROLLING

Hot rolling is the principal method of ingot conversion and is the first forming operation in the production of sheet, strip, and wire. As an intermediate process, it is, unfortunately, not as closely controlled as cold rolling and drawing; faults starting in the hot-rolling process often persist through all subsequent stages of manufacture, and their rectification in the finishing stage, if possible, is probably costly.

Closer control of hot rolling is most desirable, and this problem has of late received more attention. Similar problems of control arise in flat rolling, whether the process is hot or cold, and they will be discussed together; owing to the greater difficulty of measurement and the addition of temperature as a process variable, control is, however, more difficult in hot rolling. In rod rolling, the most common faults are fins and laps from incorrect roll-pass design. This fault arises from over-filling the pass, and it can cause considerable trouble during wire drawing. An additional source of trouble is the incorrect setting of twist guides and loops, which can lead to bad surface defects.

## II.—CONTROL OF DIMENSIONS

The control of dimensions of sheet, strip, or wire depends upon the following factors: (i) the accuracy with which the dimensions can be measured, (ii) the speed with which the measurements can be made, (iii) the time lag between the origin of the error (or the failure to eliminate a previous error) and the indication of the error, (iv) the causes of the error, and (v) the methods available for correcting the error once it has been indicated.

The relative importance of these factors differs in rolling and in wire drawing and the processes are, therefore, discussed separately.

### 1. ROLLING OF SHEET AND STRIP

#### (a) *Measurement of Strip Thickness*

Until lately the only means of gauging thickness was by hand micrometer. In sheet rolling such measurements can be made only before and after the pass, but in strip rolling in coil form, the thickness can be measured along the length at low speed, and the need for checking the thickness in this way limited, for a long time, the speed in cold rolling to about 60–100 ft./min. The hand micrometer is also limited in that it can measure thickness only near the edge of the strip, and with temperature and camber changes taking place as the rolling proceeds, the edge thickness



may vary from the general thickness, especially in wider strip.

The time interval between taking a reading and correcting, by adjusting the screw-down, any loss of gauge may be of the order of 10 sec. With a power screw-down, the operator almost inevitably over-corrects the first time and the degree of control is limited to correcting gross thickness changes.

Continuous strip-thickness gauging by "flying micrometer" is more accurate than gauging by hand; the hand micrometer can be read by a skilled operator to about  $\frac{1}{20000}$  in. at low rolling speeds, whereas the continuous strip-thickness meter can probably indicate changes from a preset thickness to  $\pm 0.0001$  in., although the absolute measurement may depend upon the rolling speed. Unfortunately, measurements by strip-thickness meter are also confined to a small fraction of the full strip width.

Strip-thickness measurements are usually made on the outgoing side of the stand only, although in reversing mills some indication of incoming variations could be obtained from a measurement on that side. In tandem mills, the outgoing strip of one stand is the ingoing strip of the next.

#### (b) Speed of Response of Measuring Instruments

The possibility of control depends upon the rate of change of thickness and on the speed of measurement; if the thickness changes very rapidly because the speed of rolling is high or because there are rapid cyclical variations, the measuring device may respond too slowly to indicate them. If the strip-thickness meter is to be generally useful, it must have a full-scale response time of a fraction of a second, but the practical difficulties of obtaining both high accuracy and high speed of response coupled with an output signal of sufficient power are considerable. It is possible that between 3 and 30 ft. may pass through the mill before the operator can be certain that the change of gauge which has occurred ought to be corrected.

#### (c) The Causes of Errors in Strip Dimensions

Strip thickness in hot and/or cold rolling depends upon: (i) the yield-stress characteristics of the material, (ii) the entering thickness, (iii) the friction between the roll and strip, (iv) the strip tensions, (v) the roll setting, (vi) roll flattening, (vii) roll bending (and camber), (viii) roll eccentricity, (ix) temperature, (x) speed of rolling, and (xi) stiffness of the mill.

In addition, in hot rolling, the temperature of the strip and the speed of rolling affect the yield stress of the metal, and the temperature of the rolls influences the camber during rolling.

Many of these factors are inter-related, but they can be considered under two main headings: (i) factors connected with the plastic deformation of the strip, and (ii) those connected with the reaction of the mill.

The force necessary to deform the strip from its initial thickness,  $h_1$ , on entering the rolls, to the final thickness,  $h_2$ , on emerging from the rolls, depends mainly upon the yield-stress characteristics of the

strip material and the friction between the roll and strip, together with the intensity of the strip tensions applied. With commercial roll finishes and lubricants, and for normal pass reductions, the coefficient of friction is between 0.04 and 0.08. Its constricting effect in the contact arc causes an increase in roll force by 15–25% over that required for plane plastic deformation in the absence of friction. In rolling thin strip, the contribution of this so-called "friction hill" can be much greater, not because of the plastic behaviour of the strip, but because of the elastic displacements of the mill rolls. The effect of tension, on the other hand, reduces the roll force. It is possible to reduce the roll force to a value less than that represented by the corresponding plane compression.

Any variation in the yield-stress characteristic, i.e. in the hardness of the strip, affects the roll force. Such variations can arise during hot rolling if the temperature is allowed to fall too low in any part, e.g. in the trailing end of a strip, and should be avoided in the hot mill, rather than be allowed to pass to the cold mill for correction.

It is the frictional changes, therefore, which must be most closely examined in cold rolling, and although their effect on roll force may not appear considerable, they do have a serious effect upon strip gauge. Both failure of the lubricant film on the strip or changes in rolling temperature affect friction considerably. Such changes occur during acceleration and deceleration of the mill; with thin hard strip, where roll flattening is extensive and the friction hill becomes a larger part of the total roll force, the strip gauge can show considerable variation and may take as much as 15% of a coil outside the gauge tolerances, depending upon the speed of rolling and size of coil. These problems have been discussed by Mohler,<sup>5</sup> Ford,<sup>6</sup> and Sims;<sup>7</sup> both Ford and Sims give useful bibliographies.

The plastic variables governing the roll force,  $F$ , required to cause the deformation are the yield stress,  $k$ , the entry and exit thicknesses of the strip,  $h_1$ ,  $h_2$ , the coefficient of friction,  $\mu$ , the radius of the contact arc,  $R'$ , and the strip tensions,  $t_1$ ,  $t_2$ .

$$F = f(k, \mu, h_1, h_2, t_1, t_2, R') \quad (1)$$

A change in any of these variables alters the roll force.

The mill components form an elastic link between the upper and lower surfaces of the strip in the contact arc. Hesselberg and Sims<sup>8</sup> have shown that the mill resistance,  $F'$ , can be represented by:

$$F' = M(h_2 - s_0) \quad (2)$$

where  $s_0$  is the roll setting, i.e. the minimum distance between the working faces of the rolls when no strip is in the mill. The quantity  $M$  is almost constant, being made up of the elastic extension of the housings, the elastic compression of the screws, chocks, and bearings, and the elastic flattening and bending of the rolls.

At equilibrium, the roll force is balanced by the elastic reaction of the mill,  $F'$ :

$$F = F' \quad (3)$$

i.e., if the roll is held constant, the outgoing strip remains constant also for a given roll setting,  $s_0$ .

Fig. 1 shows these ideas in graphical form. For a given set of conditions, the line  $P_1$  represents the plastic curve of roll force against  $h_2$  (i.e. against pass reduction, since  $h_1$  is given). If now, for the same entry thickness  $h_1$ , the friction changes or the strip changes in hardness, the roll force for a given reduction changes, and a new plastic curve, e.g.  $P_2$ , can be calculated. A similar modification could follow a change of strip tension.

For a given screw-down setting, i.e. for a given value of  $s_0$ , the relation between the roll force and the actual

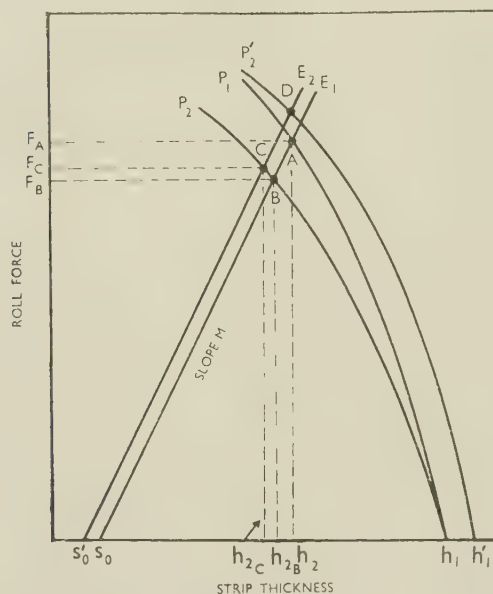


FIG. 1.—The Effect of Roll-Setting and Strip-Thickness Changes on Roll Force.

strip thickness is represented by the line  $E_1$ , having a slope  $M$ . Hence for this given setting and an entry strip thickness  $h_1$ , the roll force will be  $F_A$ , and the final thickness  $h_2$ , these being the co-ordinates of the point of intersection of the lines  $E_1$  and  $P_1$ . If the plastic, frictional, or tension conditions change to line  $P_2$ , then for the same roll setting the new equilibrium is at  $B$ , with co-ordinates  $F_B$  and  $h_{2B}$ .

As the speeds increase in a mill with fluid film bearings, the film thickness increases and the rolls approach each other. According to Sims,<sup>9</sup> this is equivalent to a change in roll setting from  $s_0$  to  $s_0'$ , and in Fig. 1  $E_2$  then becomes the elastic line. Such a change usually takes place with a change in friction, the coefficient falling as the speed increases. The final equilibrium conditions would, therefore, move to  $C$ , and the thickness would decrease to  $h_{2C}$  from the value  $h_2$ .

A change of entry thickness from  $h_1$  to  $h_1'$  under the new conditions results in a new plastic line  $P_2'$  (here an increase in thickness is indicated) and point  $C$  moves to  $D$ .

It can be seen from Fig. 1 that for each change in the plastic variables, a change in both the exit thickness and the roll force occurs. Roll eccentricity can be superimposed on the diagram as a cyclical variation of roll setting, which causes a similar cyclical variation in thickness  $h_2$ .

A change of roll temperature during rolling causes a change in roll diameter, which can also be considered as a change in roll setting; this change is of importance when the thermal changes are not uniform along the roll barrel.

Thus most of the variables cause a decrease in gauge under conditions of both increasing and steady speed, and the question arises as to what the operator can do to minimize these effects and maintain gauge within the specified tolerances.

#### (d) The Control of Strip Gauge

Certain of the plastic variables can be used to control strip gauge. Screw setting is the obvious choice, but if the roll setting is not changed, changing any of the variables in the plastic equation (1) to maintain  $F$  constant, would maintain constant gauge. The possibilities so far realized are the friction and the strip tensions, although they cannot be used in hot rolling, where the screw-down setting presents the only likely solution. The practicability of any control method depends to a large extent on the type of mill.

It need not be pointed out that prevention is the best form of control; i.e. care at every stage to maintain steady conditions of temperature, hardness, and thickness during hot rolling; and strip tension, roll temperature, and roll pressure during cold rolling.

#### (e) Manual Control

In the hot mill, control is limited at present to an occasional check of thickness after rolling. Blain<sup>10</sup> has used the idea of constant roll force to indicate strip thickness, an idea which has been developed by Hesselberg and Sims<sup>8</sup> (see below); apart from this idea, the application of non-contacting strip-thickness gauges represents the only practical attempt at closer indication and control of gauge during hot rolling.

In cold rolling, the usual practice is to employ a continuous strip-thickness meter. When a change of gauge begins, there is a small time interval (which depends upon both the distance of the meter from the rolls and the rolling speed) between the strip leaving the rolls and its arrival at the meter. There is a further lag between the change of meter reading and observation of it by the operator; he has then to decide whether the strip is running off-gauge and whether an adjustment shall be made. Whatever adjustment he applies, a further time lag is involved in making it, and if the operator over-corrects, further changes may be needed before the mill settles down satisfactorily.

In single-stand mills with little coiler tension, or where the coiler drive is not susceptible to adjustment, gauge cannot be corrected by adjusting tension. With medium- and high-speed mills, the speed effect



can be, and is, used to modify the friction, thus representing an effective and readily applied control in most mills. The effect of speed is sizeable only with thin hard strip, where roll flattening is considerable, and this method has not found much application with the normal run of strip thicknesses.

The only method generally available, therefore, is the control of screw-down setting, remembering that the normal gear allows only occasional adjustment during rolling, and that the operator's ability to follow changes in gauge is limited.

The possible alternative method proposed by Hessenberg and Sims<sup>8</sup> involves the maintenance of constant roll force when, if roll temperatures are also constant, the roll gap, and hence strip gauge, is of fixed value. Hessenberg and Sims suggest the control of gauge from roll-force meters as an alternative to the strip-thickness gauge and describe an experiment in which gauge was held very effectively by the adjustment of the coiler tension. With fully electrified drive, the tension is easily and rapidly variable, although the range of control is limited by the coiler power.

In tandem mills, control becomes more complicated, but it can be achieved in a number of ways. The strip provides a connecting link between stands, and by the control of relative roll speeds, the tension can be varied. One method is to control, by the roll setting, the thickness out of stand 1, and to adjust either the speed or roll setting of the last stand to maintain the final gauge; increasing the speed increases the interstand tension, so reducing gauge, which is also decreased at the same time by the speed effect.

#### (f) Automatic Control

Several attempts have been made to control strip gauge automatically from the output signal of a continuous strip-thickness gauge on the exit side of the mill; any change from a preset value is fed, after amplification, to the screw-down gear.

Hessenberg and Sims have suggested two promising methods, both based on holding the roll gap constant; (i) by varying the tension, either between stands or at the wind reel, the signal being given by the roll-force meters, which modify the tension until the roll force is brought back to the preset value; (ii) the same signal is made to vary the roll setting, and this method is suited to hot rolling as well as cold rolling. The former method has given good results in the laboratory and in a works trial,<sup>11</sup> particularly in controlling the effect of speed on gauge during starting and stopping. Fundamentally, the use of the signal from the roll-force meters is sound, since the indication of the error and its correction are both made at the point where the error occurs.

#### (g) Control of Thickness Across the Width

Thickness variations along the length have been described in the above sections; variations across the width, which usually occur more gradually, cause a hollow or wrinkled edge on the strip, or runs to one

side or the other, depending upon roll camber (or bending) or unequal setting of the roll screws. The presence of tension in the strip reduces the extent of these variations which lead to differential elongation over the width, so that the thicker part takes more of the tension and vice versa, thus yielding a higher combination of tension and roll force. The tendency to go off-gauge is therefore partially corrected, although other effects follow and are discussed in Section III.

## 2. WIRE DRAWING

### (a) Factors to be Considered

There is a fundamental difference between drawing and rolling in the maintenance of size. Whereas the roll gap may be adjusted during rolling to compensate for changes in the conditions of rolling and the wear of rolls, the die bore cannot be modified during drawing. Moreover, the wire size is not much affected by changes other than enlargement of the bore. In consequence, the wire size increases more or less continuously from the moment a new die is introduced into the machine until, as the result of die wear, it exceeds the upper limit of gauge tolerance.

Dies should, of course, be kept in the machine as long as possible in order to maintain the rate of machine output, so that ideally, the wire gauge should oscillate throughout the tolerance range. This ideal is rarely achieved in practice because dies may have to be withdrawn from service prematurely for reasons connected with surface finish, or because the wire "sucks down" to less than the lower tolerance limit, owing to blockage by lubricant or metal pick-up. These defects and the great variability of die performance have focused attention on die wear, and the effects of incorrect initial die size and intermittent gauging of wire are usually overlooked. The latter two reduce potential die output, and dies have to be changed more frequently than need be, with a consequent loss of production.

These two factors will be examined in greater detail, the problem of minimizing die wear being considered as outside the scope of the present discussion. It should, however, be noted that variable die wear is itself a sign of insufficient control over the process; the measures designed to achieve a more uniform die performance, such as control of lubrication and of die materials and profiles, indirectly contribute to better control of dimensions.

### (b) Initial Die Size

In the course of die-wear investigations, records were taken of the size of wire when threading up a succession of finishing dies; the allowable lower wire size was 0.0580 in. A typical series of measurements is reproduced in Table I. The allowable upper wire size was 0.0600 in., so assuming (i) that all dies in this example deteriorated at the same rate, and (ii) that all were removed when the allowable upper size was reached, 30% of the potential die performance was lost through faulty initial sizing.

In order to start as close to the lower gauge limit as practicable, the relation between wire size and size of die should be known. Unfortunately, the relation between the two dimensions seems to be more complicated than that between roll gap and strip gauge.

TABLE I.—*Typical Measurements of Die Sizes.*

Die no. . . . .	1	2	3	4	5	6	7	8	9	10
Initial wire size, mils. .	58.8	58.0	58.1	58.5	58.6	58.0	58.5	59.4	59.0	58.3

TABLE II.—*Comparison of Wire Size and Die Size.*

Die . . . . .	A		B	
Die semi-angle . .	4°		10°	
Size of ingoing wire, %	103	131	104	133
Size of outgoing wire, %	100	99.9	100	99.8
Drawing force, % .	100	500	100	310
Die pressure, % .	100	37	100	38

Lueg and Pomp,<sup>12</sup> in an investigation of the drawing of steel bars, found that the difference between the two diameters was independent of the drawing force and that it increased with reduction when the die angle was small, but decreased with reduction in the case of

die are unimportant, and the final wire size is dictated by a combination of plastic deformation continued outside the die and of residual stresses in the wire. The difference between wire and die sizes varies more with die angle than with reduction, which may explain why, in practice, two dies identical in cross-sectional area, but with different profiles of the bore, often produce wires of different sizes. This is clearly a matter deserving further investigation, since at present, die bores are chosen by hit-and-miss methods.

In addition to the uncertainty of wire size for a given size of die bore, the die sizes vary a great deal owing to lack of proper control in the die room. The measurements listed in Table III are typical.

There is much scope for improving the precision of die manufacture. Past shortcomings were largely due to the absence of reliable methods of measurement, or to the use of indirect methods of measurement which have recently been shown to be unreliable.<sup>13</sup> As a result of intensive post-war development, several instruments are now marketed which should ease the problem of inspection.<sup>14-18</sup>

### (c) Measurement of Wire Gauge

At present wire is gauged by hand intermittently during machine stoppages. The desire to increase output by faster drawing and better machine utilization has brought about an increase in the weight

TABLE III.—*Variations in Die Size.*

Die No.	Nominal	Actual									
		1	2	3	4	5	6	7	8	9	10
Bore, mils. . . . .	59.0	58.9	59.0	59.0	59.2	59.3	58.5	59.4	59.5	58.6	59.4
"Parallel," * mils. .	29.0	Nil	5.0	10.0	18.0	Nil	20.0	1.0	25.0	20.0	35.0

\* Length of cylindrical sizing portion.

TABLE IV.—*Die Sizes on Removal from Use.*

Die No.	Upper Gauge Limit	1	2	3	4	5	6	7	8	9	10
Ultimate wire size, mils.	60.0	59.8	59.7	58.1	59.8	60.0	59.8	59.5	59.2	60.3	60.0

large die angles. Comparable data for wire drawing are not available, but the figures in Table II, obtained during experiments with copper wire, confirm that the difference between wire and die size is practically independent of drawing force and die pressure. In these experiments, wires of different initial sizes, but of identical mechanical and metallurgical properties, were drawn through the same dies.

In this case, the wire was invariably smaller than the die, but the reverse is known to happen. These observations should be contrasted with the simple linear relation between strip gauge, roll gap, and roll force. It is evident that, owing to the comparative rigidity of the die, elastic distortions of the wire and

of coils and spools, so that much larger quantities of wire are drawn between checks of gauge. The chance has, therefore, increased of producing an appreciable quantity of off-gauge wire before the fault is detected, or alternatively the die is removed before the upper limit of gauge tolerance is attained. The figures in Table IV, taken from die production records, illustrate the latter point. In this example, 20% of the potential die performance was lost, on the assumption of a uniform rate of wear and a start at the lower tolerance limit, some wire having to be discarded as over-size.

Among various possible techniques for continuous gauging, the pneumatic method appears the most attractive, since there is no contact between the wire



and the gauging instrument. The method has already been applied in the textile industry, and exploratory work has shown it to be suitable for wire.<sup>19</sup>

It has also been suggested that the die load should be used as an indirect measure of gauge, and an instrument for the continuous recording of the die load

#### (d) Ovality

Ovality in the wire may be due to incorrect shaping of the die, or it may develop as the result of asymmetrical wear. An example of a new die with a faulty profile is shown in Fig. 2. The asymmetry has its

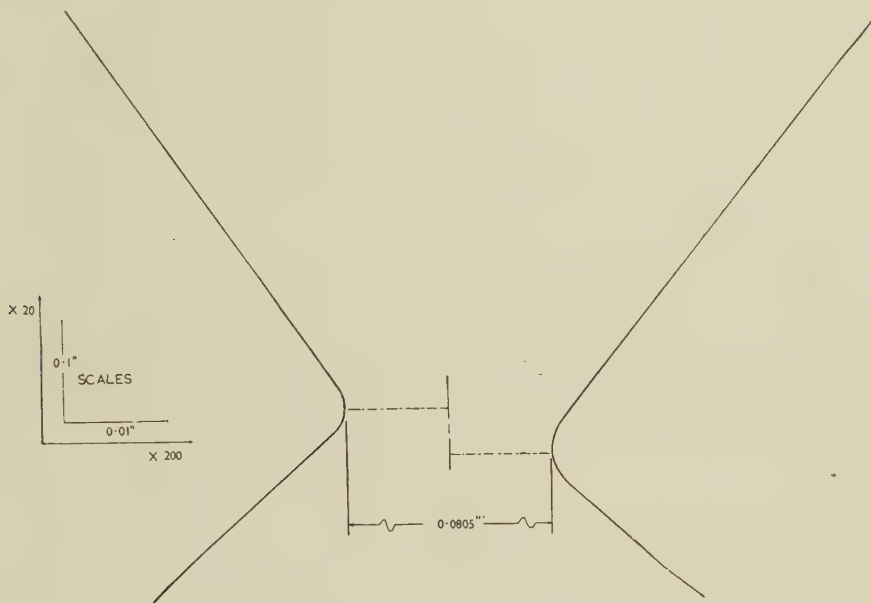


FIG. 2.—Asymmetric Profile of New Die.

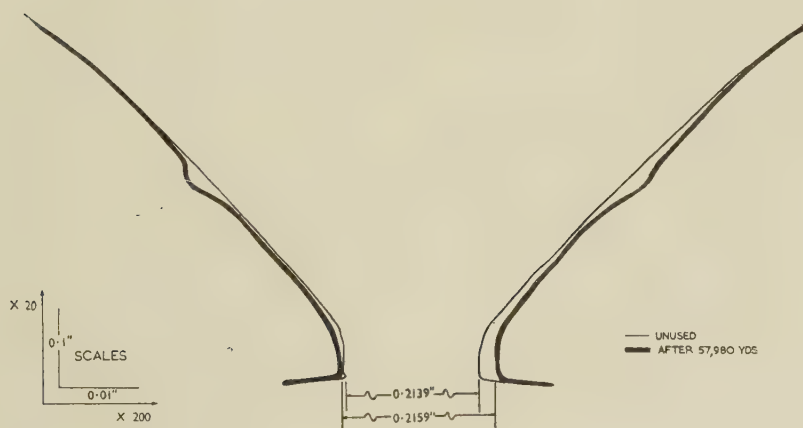


FIG. 3.—Die Worn Asymmetrically.

has been devised.<sup>20</sup> This proposal should be viewed with reserve, since, as was shown above, the wire gauge is not sensitive to changes in the drawing force. Nevertheless, the continuous indication of die load might be helpful in fine wire drawing, where the drawing compartments of fine-wire machines are usually fully enclosed and an appreciable change in drawing force would warn the operator that a change in the conditions of drawing has occurred.

origin in bad alignment of the die in the chuck of the lapping machine. This fault, which is frequently encountered, could be avoided by proper maintenance of lapping machines and occasional trueing up of die cases if the die profiles were properly inspected.

Asymmetrical die wear (see Fig. 3) may be due to a bad wire surface caused by worn drawing cones, excessive slip on the cones, or by misalignment of the die in the machine. The die is often deliberately mis-

aligned for the purpose of controlling the cast of the wire, but this can be avoided if the wire is cast by means of dressing rolls. When this is impracticable, e.g. in fine wire drawing, asymmetrical wear may be eliminated by continuous rotation of the die.

#### (e) *Shaped Wire*

The problem of dimensional control is, of course, much more complicated in the case of shaped wire. The shape of the die bore is known to exert a pronounced influence on the shape of the cross-section of a wire which contains sharp corners. Unfortunately, a relationship between the two is not available. The actual measurement of shaped-wire dimensions also presents considerable difficulties; hence the production of shaped wire is still largely in the hands of highly skilled craftsmen and is done at high cost and at a low rate of output. An application of pneumatic gauging to brass pinion wire, which is in the course of development, promises to ease the problem of inspecting drawn wire and to increase the yield of correctly dimensioned wire; higher precision of die shapes has resulted from the adoption of shadow projection instruments in the die rooms.

#### (f) *Maintenance of Wire Gauge in Intermediate Passes*

The discussion has so far been confined to finished wire, since wire dimensions at intermediate stages of the process are relatively unimportant. It is worth contrasting this consideration with what has been said about rolling. There, it will be recalled, owing to the flexibility of the rolls and housing, the gauge is sensitive to drafting, so that control of the intermediate gauge contributes to the control of the finished gauge; in wire drawing, this is not the case.

This statement needs modification in the case of slip machines, where the wire is allowed to slip on the drawing cones, and the amount of slip varies with drafting. At the same time it is desirable to keep the slip within narrow limits to minimize cone wear and to maintain good surface finish. Moreover, owing to friction between cone and wire, the tension in the latter depends on slip. In drawing very fine wire, the maintenance of constant tension is of cardinal importance, since the wire breaks easily. This is a case where the monitoring of die loads, or of interpass tensions, might conveniently be used as a means of continuous inspection of gauge.

### III.—CONTROL OF SHAPE

The term "shape" in wire drawing normally means the form taken by the wire when free from strain; in sheet and strip rolling, "shape" can be used both in the sense of flatness and straightness and it can also be used to signify the variation of the sheet or strip thickness across the width. All of these are connected with the same variables, the difference between wire drawing and rolling being a question of degree.

#### 1. STRIP

Bad shape in strip rolling arises from comparatively large differences in elongation across the width of the strip, which can be accommodated only by local buckling. In wire drawing these differences are only of elastic order of magnitude, but they have a pronounced effect on shape because of the slenderness of wire.

Bad shape in strip usually originates in hot rolling, where variation in thickness from one edge to the other may be set up in the slab owing to the relative ease in deforming it, and unless corrected by milling, it cannot be removed by subsequent cold rolling, although it may be reduced. High back tension, which can cause strip to narrow instead of spread, can level off "wedgy" strip to some extent, but residual stresses must be left in the strip to hold it straight, and subsequent processing may then lead to bad shape.

The main factors influencing the shape of strip, however, are roll bending and expansion with temperature. High pressures, particularly in the cold mill, cause the rolls to bend as a circular beam, and such bending must be nullified by:

(i) *Reducing the roll force.*—This is realized by using small work rolls to reduce the contact arc, one or more back-up rolls providing stiffness.

(ii) *Cambering.*—The rolls (back-up and work rolls in four-high mills) are ground with a camber to compensate for the deflection due to bending.

(iii) *Maintaining a constant roll force for all passes on the strip.*—The camber on the roll can be correct only for a given loading condition; a flat strip will be maintained throughout only if the pass reductions are so chosen as to keep the roll force, and hence the deflection, the same in all passes.

(iv) *Correct cooling.*—The work done in deforming the metal and in surface friction is partly dissipated through the roll, the heat passing out mainly at the necks. Temperature differences therefore, exist between the middle and ends of the roll, causing differential expansion. A coolant applied as jets on the roll surface can help to maintain steady conditions, or can be used to change the roll camber by suitable adjustment of the jets.

Too much camber causes a hollow strip with a wrinkled edge, while insufficient camber shows a ripple in the centre of the strip or sheet when it is laid out on a flat surface. The reflection of narrow vertical light slits on the surface of thin material is sometimes used as a control test. Normally such differential elongations are to be avoided, since they represent residual stresses. In cold rolling very thin strips, these facts have been used as a means of ensuring a flat strip at the final pass. Roll bending is particularly apparent as a thinning of the edges of the strip, and to avoid this in the earlier passes the rolls are deliberately over-cambered to ensure a slightly hollow centre and to maintain the edge thickness; a final light pass with a nearly plain roll is then made, using sufficient front tension to pull down any incipient wrinkling at the edges.



## 2. WIRE

"Cast" is to wire what "shape" is to strip; it is the form adopted by a moderately long piece of wire free of constraint. Although straight wire is sometimes called for, it has usually to be curved, and invariably the curvature must be in one plane only, i.e. the wire should lie flat when dropped on level ground. The curvature depends on the degree of radial asymmetry of longitudinal residual stresses present in the wire when wrapped round the block or spool.

Wire drawing induces residual stresses which are usually tensile in the skin of the wire and may be quite close to the yield point of the metal, so that very little further stressing is required to cause the surface to yield and to change the original pattern of residual stresses. In practice, the residual-stress pattern arising from deformation in the die is not as a rule axially symmetrical owing to (i) accidental misalignment of the die relative to the direction of drawing, so that the wire does not enter or leave the die axially, and (ii) imperfections of the die profile which frequently lacks axial symmetry (a typical defect is shown in Fig. 2). The shortcomings of die profiles imply that each die needs individual adjustment by tilting so that the desired cast may be obtained.

The dependence of the curvature of cast wire on the angle of tilt of the die has been investigated by Kenneford and Thompson,<sup>21</sup> who have confirmed that the relationship between the two variables depends also upon reduction and die angle. The interesting point about their findings is that curvature is a maximum for intermediate values of the angle of tilt, and in the vicinity of this angle it changes fairly slowly with angle. Clearly, it is desirable to know these "critical" angles, since they might facilitate control of shape. More work, however, is required before knowledge of the subject can be systematized.

Casting by tilting the die is normally to be deprecated, because it leads to asymmetrical die wear and is probably the most frequent cause of ovality in the wire. The use of "dressing" or "killing" rollers is preferable, at any rate for medium-gauge high-tensile wire. In fine wire drawing, casting rollers are impracticable and die tilting must be relied upon. Since profiles of small dies (diamond dies) are particularly variable and often tend to wear asymmetrically, the cast is apt to vary from one spool of wire to another. Continuous rotation of the die during drawing has been found helpful in this case, and wider adoption of this remedy is to be recommended.

## IV.—CONTROL OF SURFACE FINISH

Surface finish is said to be the most important single factor determining the sales value of strip and wire. Of the three attributes here considered, however, it is the one least amenable to measurement and, therefore, to control. The dependence of surface finish upon the forming process is, as yet, little under-

stood. It is evident that excessive roughness of the tool will cause the finish to be poor, but it does not follow that mirror polish of the tool alone is a sufficient condition of good surface finish, since the latter is also known to be affected by the lubricant.

## 1. THE SMOOTHNESS OF THE ROLL IN HOT AND COLD ROLLING

In hot rolling, there is little relative movement between roll and stock, and the smoothness of the roll is a controlling factor in the surface finish of the semi-product. This is of less importance where overhauling is practised, except as it affects the amount which has to be removed. In cold rolling, the roll finish affects the surface roughness and appearance of the strip or sheet, although the effect can be modified by lubricant. A smooth polished roll (i.e. having a Talysurf average roughness figure,  $h_{av}$ , of less than about 10 micro-in.) appears to flatten and smudge the surface asperities to give a burnished or shiny surface, so that with more than one pass and a "good" lubricant, the  $h_{av}$  can be less than the value for the roll. This is particularly marked with some aluminium alloys when pure paraffin and certain proprietary oils are used. On the other hand, a rough roll does not produce a finish better than itself, and the action appears to be one of ploughing and tearing. Whether smoothing over or tearing occurs appears from recent investigations to be not a question of absolute roughness, but whether the roll is smoother or rougher than the entering strip; this effect is markedly influenced by the lubricant.

## 2. THE SMOOTHNESS OF THE DIE IN WIRE DRAWING

It is generally agreed that a mirror polish of the wire-drawing die is conducive to high surface finish in the wire, but owing to the difficulty of measurement, the relation between the two is not properly understood.

## 3. THE EFFECT OF LUBRICANTS

In rolling with no lubricant present, an even surface profile is obtained, but, depending upon the roll surface, a dull or bright finish can equally well be obtained.

It is necessary to distinguish between two factors: surface roughness (Talysurf) readings and appearance. From a large number of tests with different materials, lubricants, and roll finishes, the following general conclusions were reached:

(i) A high coefficient of friction (i.e. 0.1–0.2) usually goes with a bright torn surface, which, depending on roll finish, may be fairly smooth as indicated by Talysurf figure.

(ii) An intermediate coefficient (0.06–0.08) generally gives the optimum results with greatest smearing, burnishing action, and minimum tearing and a low roughness value.

(iii) Some lubricants are better than others; a good lubricant is one which both tends to allow the

burnishing action of a smooth roll, and to act somewhat like a cutting fluid when slight tearings begin to occur, by tending to separate the junctions.

(iv) Generally, while the smoothness in the longitudinal direction of the strip (where relative motion occurs) improves, that in the transverse direction (where there is no relative motion) does not, and with higher friction, roughness tends to increase in this direction, as it decreases in the other.

(v) Lubricants which give low coefficients of friction (0.03-0.05) leave the strip matt and dull, and in most cases surface damage is found to be severe, apparently not so much as a result of ploughing action as by tearing particles out of the surface.

The explanation of these results has not yet been found. The increase in roughness is sometimes spectacular; e.g. with copper having an initial roughness of 14 micro-in. (longitudinal) and 16 micro-in. (transverse), one pass with smooth rolls ( $h_{av} = 9$  micro-in.), using castor oil, raised the corresponding values to 23 and 20, although the coefficient of friction was 0.046. Even worse results were found with brass and lanolin, for which the coefficient was 0.043.

In wire drawing, in spite of high pressures in the die, the surface of the wire deforms fairly unevenly, and in the absence of burnishing tends to wrinkle quite severely (see Fig. 4, Plate XLIV), giving a dull appearance. To enhance the finish of the wire, it is desirable to close up the pits evident in Fig. 4, and this is apparently best achieved when friction is high, i.e. lubrication is "poor" (see Fig. 5, Plate XLIV). Clearly, the right balance between high friction to produce high lustre, and good lubrication to minimize damage of the surface of the die by wear, is precarious and can be maintained only by a careful selection of die profile and lubricant.

#### 4. OTHER EFFECTS

The surface finish improves with the number of passes up to a certain point, depending upon the tool finish and the lubricant. There is a limit to this improvement, and no general rule can be laid down, since the improvement varies with the material and to some extent with the size of pass.

In cold rolling, the surface finish may be impaired by edge marking, particularly where different widths of material are rolled in the same mill. In jobbing mills, this can be avoided to a great extent by scheduling the widths so that the mill works progressively on

narrower strip between roll grinds, but it is preferable to roll at economic widths with subsequent slitting for narrow strip requirements.

In wire drawing, trouble is sometimes experienced with periodic markings on the side of the wire in contact with the block. The cause is lateral vibration of the wire, which is probably induced by a torque ripple originating in the transmission gears of the machine; this effect is most easily suppressed by altering the distance between die and block. Gross surface marking may also be induced by stick-slip on the cones of "slip" machines. This is the outcome of insufficient lubrication, indifferent finish of the cones, or faulty drafting.

Gross roughness is frequently caused by misalignment of the die and the presence of a sharp edge in the die entry; to avoid this, the die entry, the so-called "bell", should be provided with a generous radius. All parts of the machine with which the wire comes into contact should in fact be smooth, and in the case of wires made of soft metals, should be particularly well lubricated.

#### REFERENCES

1. D. P. Eckman, "Principles of Industrial Process Control". 1945: New York (John Wiley and Sons).
2. A. Porter, *Proc. Inst. Mech. Eng.*, 1948, **159**, 25.
3. A. Porter, "Introduction to Servo-Mechanisms". 1950: London (Methuen).
4. —, *J. Inst. Metals*, 1952-53, **81**, 389; also *Inst. Metals Monograph and Report Series*, No. 15.
5. F. Mohler, *Sheet Metal Ind.*, 1940, **14**, 610.
6. H. Ford, *J. Iron Steel Inst.*, 1947, **156**, 381.
7. R. B. Sims and D. F. Arthur, *ibid.*, 1952, **172**, 285.
8. W. C. F. Hessenberg and R. B. Sims, *Proc. Inst. Mech. Eng.*, 1952, [A], **166**, 75.
9. R. B. Sims, *J. Iron Steel Inst.*, 1952, **172**, 415.
10. P. Blain, *Rev. Mét.*, 1948, **45**, 241.
11. R. B. Sims, J. A. Place, and P. R. A. Briggs, *J. Iron Steel Inst.*, 1953, **173**, 343, 354.
12. W. Lueg and A. Pomp, *Mitt. K.W. Inst. Eisenforsch.*, 1941, **23**, 293.
13. J. G. Wistreich, *Wire Ind.*, 1952, **19**, 131.
14. R. M. J. Withers, *J. Iron Steel Inst.*, 1950, **164**, 63.
15. W. Krug, *Feinwerktechnik*, 1949, **53**, 7.
16. W. Lueg, *Stahl u. Eisen*, 1951, **71**, 157.
17. J. G. Wistreich, *Research*, 1953, **6**, 252.
18. S. Werth, *Stahl u. Eisen*, 1952, **72**, 66.
19. J. C. Evans, M. Graneek, and H. G. Loe, *Trans. Soc. Instrument Technol.*, 1950, **2**, (2), 34.
20. O. Herrmann, *Draht*, 1953, **4**, 373.
21. A. S. Kenneford and F. C. Thompson, *Carnegie Schol. Mem., Iron Steel Inst.*, 1933, **22**, 31.



# THE CONTROL OF QUALITY IN THE HOT AND COLD ROLLING OF ALUMINIUM AND ALUMINIUM ALLOYS\*

1523

By F. KING,† A.I.M., MEMBER, and A. N. TURNER,‡ B.Sc.,  
Ph.D., A.R.S.M., A.I.M., MEMBER

## SYNOPSIS

The theoretical and practical implications of the control of the tensile strength, bending and pressing properties, corrosion-resistance, and surface finish of aluminium alloy sheet and strip are considered in the first part of the paper.

In the second part, the effect of each fabricating process on the properties mentioned is described and discussed, and inspection methods are considered.

## I.—INTRODUCTION

ALUMINIUM alloy sheet and strip must be supplied with specific characteristics, according to the particular requirements of the user. The most important properties are tensile, bending, and pressing properties (including earing qualities and grain-size), corrosion-resistance, surface finish, flatness, and uniformity of gauge. Although these properties are not always of equal importance, it is obviously necessary to appreciate both the theoretical and operational factors involved in their control, in order that fabrication practices can be adjusted to give material of the optimum quality for any application.

The first part of this paper deals with each of these properties from the theoretical aspect and also considers the ways in which they are affected by the several operational variables; in the second part the operational variables are discussed, and some factors are mentioned which, in each operation, may influence final quality. This division is made to avoid the necessity of reviewing the control of each of the eight fabricating variables under the six separate "property" headings.

A most important variable dealt with is composition. Although the control of composition is usually considered to be the concern of the casting department, its inclusion in this paper is felt to be justified, as compositional limits must, to a large extent, be governed by considerations of the ease of fabrication and final properties of the material. This may apply particularly to the levels of impurity elements, which often affect the rolling and annealing properties and corrosion-resistance of wrought alloys.

## II.—PROPERTIES OF SHEET AND STRIP

### 1. TENSILE PROPERTIES

Specifications governing the supply of aluminium alloys often require compliance with both maximum and minimum figures for 0.1% proof stress, ultimate tensile stress, and percentage elongation, not only for the intrinsic value of such properties but also to provide evidence that correct fabrication procedures have been employed.

The tensile strength of pure aluminium is increased by the addition of alloying elements which enter into solid solution and confer solution-hardening; such increases are usually not, of themselves, sufficient to give the desired properties. Two main methods of producing further increases are by work-hardening or by precipitation-hardening, and alloys are generally considered to fall into two categories, depending on which of these treatments is applied.

The more important work-hardening alloys are: commercially-pure aluminium, the aluminium-1½% manganese alloy, and the aluminium-magnesium series. In these alloys both the major alloying elements and the impurity elements, such as iron and silicon, influence tensile properties in the work-hardened and annealed conditions.

Annealed aluminium of 99.8% purity is soft and ductile, with a 0.1% proof stress of about 2 tons/in.<sup>2</sup> and an ultimate tensile stress of 4–5 tons/in.<sup>2</sup>. Cold rolling in excess of 70% reduction increases the ultimate tensile stress to a minimum of 8 tons/in.<sup>2</sup>. Less-pure aluminium (99.5 or 99.0% purity) has higher mechanical properties, depending upon the iron and silicon contents.

\* Manuscript received 11 October 1953. Contribution to a Symposium on "The Control of Quality in the Production of Wrought Non-Ferrous Metals. II.—Working Operations", to be held in London on 28 April 1954.

† Works Metallurgist, Northern Aluminium Co., Ltd., Rogerstone, Newport, Mon.

‡ Head of Metallurgical Division, Aluminium Laboratories Limited, Banbury, Oxon.

Fig. 1 illustrates work-hardening curves for commercial-purity aluminium, an aluminium-1.1% manganese alloy, and an aluminium-3.2% magnesium-

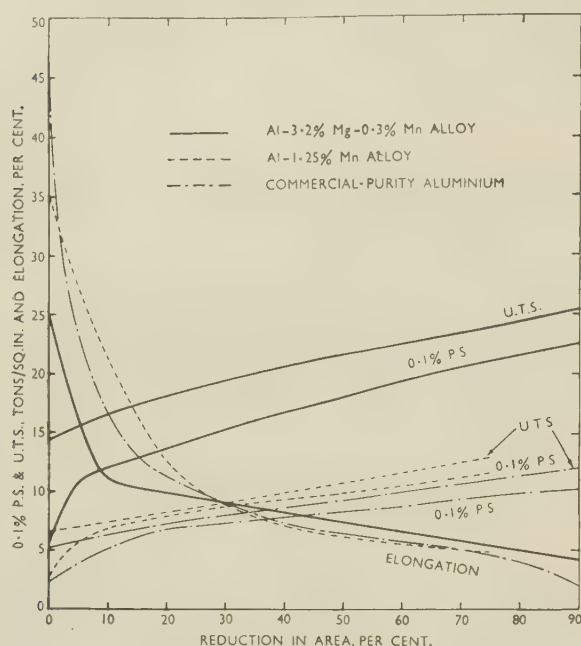


FIG. 1.—Work-Hardening Curves for Commercial-Purity Aluminium, Aluminium-1.25% Manganese Alloy, and Aluminium-3.2% Magnesium-0.3% Manganese Alloy.

0.3% manganese alloy, and shows the increase in strength obtained by the addition of manganese and magnesium, respectively. The amount of cold work required to give a specific temper will depend upon whether the final product is to be obtained by rolling direct from annealed or unannealed hot-mill slab, or whether, as in the case of thin-gauge sheet, it is to be rolled from material which has received two or more intermediate anneals. The degree of cold work is normally controlled to within 5% of nominal. Copper is controlled at a low level, but its presence in amounts of over 0.05% raises tensile properties appreciably.

The tensile properties of the aluminium-1.1% manganese alloy appear to be little affected by the presence of silicon within normal limits. Iron above 0.5, copper above 0.1, and magnesium above 0.2% increase the 0.1% proof stress and ultimate tensile stress and decrease the percentage elongation significantly.

In the aluminium-magnesium series, the presence of silicon slightly decreases all tensile properties; iron increases tensile properties, whilst manganese (which may be added in amounts of up to 1%) affects the tensile properties quantitatively in a manner similar to magnesium.

Intermediate tempers in work-hardening alloys can be obtained either by cold rolling a specified amount after anneal or by "temper annealing". The latter consists of giving an anneal insufficient for complete recrystallization, usually at a temperature between 100° and 300° C., after cold rolling more than the

amount necessary to produce the required temper. This method is valuable in obtaining the softer tempers in the aluminium-magnesium alloys, as higher elongation values may be realized for given tensile strengths. Fig. 2, for example, illustrates the properties obtained from an aluminium-3.2% magnesium alloy (containing iron 0.27, copper 0.05, silicon 0.12, manganese 0.30%) as the result of a variety of temper-annealing treatments. This material was cast by the semi-continuous process, hot rolled after 12-hr. preheat at  $505^{\circ} \pm 5^{\circ}$  C. from a thickness of 6 in. to 0.25 in., cold rolled to 0.2 in., and annealed for 3 hr. at 400° C. with a cooling rate after

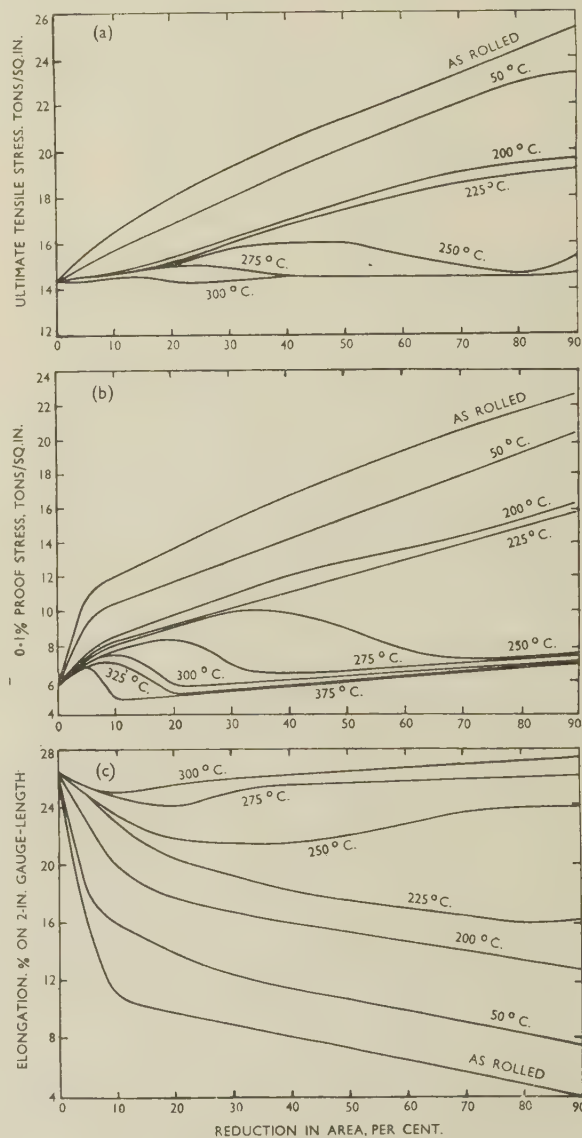


FIG. 2.—Effect of Temper Annealing (5 hr. at temperature indicated) on the Tensile Properties of Aluminium-3.2% Magnesium-0.3% Manganese Alloy.

annealing of 30° C./hr. It was then cold rolled up to 90% and given a 5-hr. temper-annealing treatment between 50° and 375° C. In determining the most suitable temper-annealing treatment for a given



material, it is possible to control both the temperature and time of the annealing treatment, and the degree of cold work imposed before annealing. Thus, there is a considerable latitude both in the properties obtainable and in the precise planning used to obtain those properties.

The tensile properties of heat-treatable alloys are governed by the composition of the solid solution and by its age-hardening characteristics. This may be illustrated by reference to the aluminium-magnesium-silicon system. In these alloys the properties in the annealed or work-hardened conditions are affected by the magnesium content of the solid solution, whilst the response to heat-treatment depends on the  $Mg_2Si$  available for precipitation after solution heat-treatment. The result is that, for a given magnesium plus silicon content, the as-annealed strength is increased by raising magnesium and lowering silicon, whereas the strength in the fully heat-treated condition is (within limits) increased by raising silicon and lowering magnesium.

The equilibrium constitution of aluminium-magnesium-silicon alloys containing iron has been established by Phillips,<sup>1</sup> but under industrial conditions such equilibrium is not attained. Alloys with magnesium in excess of the balanced  $Mg_2Si$  ratio contain  $FeAl_3$  as the only iron-bearing constituent present in appreciable quantities, and those with excess silicon will contain both  $FeAl_3$  and  $\beta(Al-Fe-Si)$ . The presence of normal impurity amounts of iron has an insignificant effect on the strength, though over 0.5% may affect ductility. Manganese is often added to these alloys, and the quaternary system is similar to the aluminium-magnesium-silicon-iron system,  $FeAl_3$  being replaced by  $MnAl_6$  and  $\beta(Al-Fe-Si)$  by  $\alpha(Al-Mn-Si)$ . A general similarity is thus to be expected between manganese-containing and iron-containing alloys. There is, however, a difference in that manganese, unlike iron, has an appreciable solid solubility in aluminium. Thus, the addition of manganese produces two effects on the alloys, first, an increase in the basic solid-solution strength, and secondly, a reduction in the solubility of magnesium and silicon at the solution-treatment temperature, lowering the response to heat-treatment. A further small difference is that  $\alpha(Al-Mn-Si)$ , which corresponds to  $\alpha(Al-Fe-Si)$ , does not decompose to form a phase such as  $\beta(Al-Mn-Si)$  but remains stable down to room temperature.

Similar reasoning may be applied to more complex alloy systems such as the aluminium-zinc-magnesium-copper system, in which variations in the composition affect not only the solid-solution strength but may also result in a difference in the phases in equilibrium with the solid solution at room and elevated temperatures, with a consequent alteration in the age-hardening mechanism.

## 2. BENDING PROPERTIES

For applications such as roll forming or press-brake work, material must be capable of forming without

cracking, and to ensure compliance with this requirement the material may be subjected to one or more of a number of standard bending tests.

Simple bend tests, which are more usually applied, differ from one another principally in the distribution and method of application of the bending moment and in the degree to which "peaking" is restricted. Minor variations in equipment and techniques can lead to an appreciable difference in the results obtained, and the method of test should in every case be closely controlled.

In some applications, the capacity of the material to bend when peaking is allowed is of particular importance. In order to test this characteristic a free bend test in which peaking is not prevented, or is actually encouraged by axial compression, is carried out. A modification of this test, the well-known A.I.D. "free-cone" bend test, attempts to obtain the critical bending radius directly from the test of a single specimen.

It must also be noted that the width-to-thickness ratio of the test-piece can influence the results obtained. In bending, the outer fibres are in tension and the inner fibres in compression; thus the top of the test-piece tends to contract and the bottom to expand, leading to the formation of a saddleback when the material is narrow in relation to its thickness. In wide materials this effect occurs only towards each edge of the plate or sheet, owing to the restraining influence of the rest of the metal, and a transverse tension is induced in the outer fibres parallel to the bending axis. This additional stress reduces the ductility, leading to a higher minimum bend radius (i.e. worse bending properties) than would be obtained on a narrow test-piece.

In the case of sheet or strip, where the width is always considerably greater than the thickness, the minimum bend radius depends upon the local elongation and the rate of work-hardening.

In commercially-pure aluminium, the bend radius for a given thickness depends on the temper of the material and the direction in which the bend is to be made with respect to the rolling direction. In general, fine-grained material is less susceptible to cracking and other defects on bending than coarse-grained material. Greater ductility for any given tensile strength can be obtained in material prepared by temper annealing (as defined previously) than in temper-rolled material.

The aluminium-1½% manganese alloy requires slightly larger bend radii than commercially-pure aluminium, whilst the aluminium-magnesium group require much larger radii, particularly in work-hardened tempers. The aluminium-magnesium alloys respond to temper-annealing treatments at much lower temperatures than commercially-pure aluminium, and a marked improvement in bend characteristics can be obtained by treatment at 100°C. Such low-temperature treatments should, however, be used only with caution on alloys containing 5% magnesium or more, as certain combinations of cold work followed

by a low-temperature treatment can cause grain-boundary precipitation of a type which renders the material susceptible to stress-corrosion.

Table I illustrates the effect of a number of low-temperature annealing treatments (between 80° and 120° C. for times of up to 6 hr.) on an alloy containing 3.6% Mg with Cu 0.02, Fe 0.35, Si 0.18, Mn 0.22%, rolled to the  $\frac{1}{4}$ H (20% cold work),  $\frac{1}{2}$ H (35% cold work), and H (50% cold work) tempers, in the gauge range 0.050–0.080 in. It may be noted that the minimum bend radius increases considerably with increasing cold work but that a flat bend (zero bend radius) is obtained after annealing. Low-temperature treatments lead to a substantial decrease in the bend radius, the previous cold work also being important. It may be seen that the bend radius is more sensitive to changes of temper than are the tensile properties.

load has to be carried as tension in the cup walls. For the greatest reduction in deep drawing, the ultimate tensile stress should be high in relation to the compressive properties, and thus it does not follow that softer and more ductile materials have the optimum drawing characteristics; in commercial-purity aluminium and the aluminium–1 $\frac{1}{4}$ % manganese alloy, for example, the drawing properties improve as the material is work-hardened, although temper-rolled aluminium–magnesium alloys have slightly inferior drawing characteristics. In drawing shapes of cup other than flat-bottomed shells, such as hemispherical-ended, conical, parabolic, &c., the sheet must stretch over the head of the punch to form the contour without puckering, and as considerable general elongation in the material is then required, only the softer tempers are suitable.

Other characteristics of the metal which can affect

TABLE I.—*Mechanical Properties and Bending Characteristics of an Aluminium–3.6% Magnesium Alloy.*

Condition	20% Cold Work				35% Cold Work				50% Cold Work			
	0.1% P.S., tons/in. <sup>2</sup>	U.T.S., tons/in. <sup>2</sup>	Elongation, % on 2 in.	Bend Radius	0.1% P.S., tons/in. <sup>2</sup>	U.T.S., tons/in. <sup>2</sup>	Elongation, % on 2 in.	Bend Radius	0.1% P.S., tons/in. <sup>2</sup>	U.T.S., tons/in. <sup>2</sup>	Elongation, % on 2 in.	Bend Radius
As rolled . . .	16.75	19.7	7	2T	18.0	21.1	5	3 $\frac{1}{2}$ T	19.7	22.9	3	9T
Annealed . . .	6.45	15.15	23	F.B.	6.48	16.95	25	F.B.	7.62	15.4	27	F.B.
Temper-annealed:												
2 hr. at 80° C. .	14.55	18.65	10	1	16.30	20.3	7	2	17.15	21.5	6 $\frac{1}{2}$	5 $\frac{1}{2}$
2 hr. at 100° C.	14.0	18.7	10	$\frac{3}{4}$	15.3	17.95	11	1 $\frac{1}{2}$	17.15	21.45	9	2 $\frac{1}{2}$
2 hr. at 120° C.	13.05	18.35	11	$\frac{3}{4}$	14.2	19.75	10	$\frac{3}{4}$	16.0	20.7	11	1 $\frac{1}{2}$
6 hr. at 100° C.	12.95	18.35	10 $\frac{1}{2}$	$\frac{3}{4}$	15.1	20.1	11 $\frac{1}{2}$	1 $\frac{1}{2}$	16.6	20.95	10	1 $\frac{1}{2}$

F.B. = Flat Bend.

Alloys of the aluminium–magnesium–silicon type containing chromium and copper have appreciably better bending characteristics in the fully heat-treated condition than the basic alloy. Ageing treatments reduce the general elongation and usually increase the minimum tolerable bend radii, and where operations involve stretching and bending it is generally preferable to carry out forming before final precipitation-treatment.

### 3. DEEP-DRAWING AND PRESSING PROPERTIES

Material will deep draw satisfactorily into flat-bottomed cups if three basic requirements are fulfilled. These are, first, that the material possesses sufficient compressive ductility (up to about 55%) to allow the flange to be compressed to form the cup; secondly, that it has sufficient general elongation to bend over the die-and-punch profile radii (usually about 1%); and thirdly, that there is sufficient elongation under combined stress to prevent tensile failure in the upper wall. Generally speaking, if a material has sufficient compressive ductility it will also have sufficient tensile ductility. Providing these conditions are met, the maximum reduction obtainable will depend on the relation between ultimate tensile stress and the compressive properties. The load required to form the cup depends largely on the compressive properties, as the flange has to be shrunk circumferentially; this

drawing properties are surface condition, earring characteristics, grain-size, and structure. As an example of microstructure as a factor affecting deep-drawing quality, the case of two samples of aluminium–1 $\frac{1}{4}$ % manganese alloy may be mentioned; although these had almost identical analyses and hardnesses, only one could be drawn without tearing. Examination of the microstructure showed that the MnAl<sub>6</sub> constituent in the unsatisfactory material was much larger than in the satisfactory material (as can be seen from Figs. 3 and 4, Plate XLV), owing to a difference in rate of cooling during the casting operation consequent on the use of the permanent-mould rather than the semi-continuous process.

#### (a) Earing Characteristics

Any tendency towards directionality leads to the unevenness of cup height known as “earring”, which necessitates excessive trimming and may cause difficulties in drawing. Directionality is usually associated with a non-random crystallographic texture of the sheet material induced during rolling, annealing, and other fabricating operations. Very highly-preferred orientations are seldom obtained in commercial aluminium alloys, remnants of annealing textures remaining even in severely cold-worked sheet and textures similar to rolling textures often occurring after recrystallization during annealing. Rolling



textures usually influence deformation during deep pressing in such a manner that four ears appear at 45° to the rolling direction, whilst most annealing textures lead to four ears at 0° and 90°.

In discussing earing, it is convenient to regard 45° and 90° earing as part of a continuous variate, one being regarded as positive (usually 90° earing) and the other as negative. The zero on this scale is taken to represent both no earing (i.e. a random texture) or eight ears (i.e. where balanced proportions of the two types of textures are present in one sample). It is then found that variation of any operational factor may affect earing in either or both of two different ways. In one case the mean level of earing for any given fabricating condition may be moved a constant amount in either direction along the earing scale; in the other, the range of earing obtained under a variety of fabricating conditions may be altered.

A possible interpretation is that in the first case the factor concerned affects the relative proportions of the rolling textures and annealing textures without affecting the scatter about the ideal orientations, whilst in the second case the factor affects the scatter and not the proportions; both can, of course, occur simultaneously. Thus, to secure sheet material with the minimum amount of earing, a balance between rolling and annealing textures, together with as much scatter about the ideal orientations as possible, must be maintained.

Variables which can affect earing may be divided into the following four groups, according to their positions in the fabricating cycle: (a) composition, (b) casting, (c) hot rolling, and (d) cold rolling and annealing. The influence of variables in each of these groups on the earing behaviour of commercial-purity aluminium sheet serves to illustrate the factors which must be taken into account in the control of earing.

The effect of cold rolling is purely mechanical, and annealing textures usually exhibit a more or less well-defined crystallographic relation to the preceding rolling texture; it therefore appears that their effects on the texture will be substantially independent of the levels of earlier factors, and they will therefore be considered before others which logically precede them in the fabricating cycle.

Increase in cold reduction almost invariably causes sheet textures to approach more closely to a pure "rolling texture", with an increase in 45° earing, whereas annealing normally causes the sheet texture to approach an "annealing texture", with a consequent increase of 90° earing or decrease of 45° earing. For a specific gauge of annealed sheet it appears that variations in cold-rolling reductions and annealing procedures have greater effects than any other production variables in determining the mean level of earing, and can operate independently of variations at earlier stages in fabrication. Some annealing textures are very stable and not easily destroyed by rolling; an inter-anneal at hot-mill slab gauge may therefore result in severe 90° earing in finally annealed sheet,

even though 45° earing would otherwise have been expected. The severe "90° effect" of inter-annealing can be modified by varying the gauge, relative to the slab and final gauges at which it is carried out; reducing the gauge of inter-annealing reduces the "90° effect". This may allow a compromise between a planning which involves no inter-annealing (usually giving 45° earing) and a planning involving an anneal at hot-mill slab gauge (usually giving 90° earing). Variations of slab and final gauge within fairly wide limits affect earing only in so far as they affect the amounts of cold work carried out before and after inter-annealing. The final annealing conditions appear to have relatively little influence, provided that recrystallization is complete and coarse grain is avoided. Similar considerations apply to temper-rolled sheet, where the final cold rolling gives an additional 45° effect.

"Hot-rolling variables" include temperature and time of preheat, cross-rolling, and rate of reduction. Increasing the amount of reduction at high temperatures, (e.g. by greater initial rolling temperatures or rates of reduction) usually results in an enhanced tendency towards 45° earing. A longer preheat time also increases 45° earing, while initial cross-rolling appears to reduce the earing range slightly. These effects are lessened considerably by a subsequent anneal other than the final anneal. Interruption of the hot-rolling process by reheating the material is a factor which increases 90° earing.

As a broad generalization, sheet rolled from permanent-mould ingots gives a narrower range of earing than sheet rolled from continuously-cast ingots, but there is considerable disagreement about the effects of variations in casting conditions within a given process. Thus, it has been claimed by Hug, Siebel, and Buser<sup>2</sup> that casting variables have no effect on the earing of the finished sheet; the present authors' experience, however, does not support this view. Variations in casting procedure may alter the crystallographic texture of the ingot or the degree of supersaturation with respect to alloying or impurity elements. A more random ingot texture reduces the earing range, whilst the retention of elements in solid solution affects the recrystallization characteristics. Variations in composition may affect the range or mean level of earing. High-purity aluminium has a very high earing range, and small amounts of impurities (up to the level of commercial-purity aluminium) reduce this range considerably. Small amounts of iron or manganese increase the tendency towards 45° earing, while silicon appears to reduce the earing range under certain conditions. The effects of larger amounts of manganese, or of additions of magnesium, are much less certain; both elements appear to reduce the earing range in nominally binary alloys. Alloys of the aluminium-magnesium-silicon type give a large earing range and, for comparable methods of production, have a more marked tendency towards 90° earing than commercial-purity aluminium.

The foregoing observations are generalizations, and

exceptions occur; the important consideration is the influence of a factor on texture, and this may not be constant but may itself be affected by the initial texture present; to describe the change in level of a variable as a "45° or 90° factor" is a considerable over-simplification.

The most convenient method of controlling earing industrially is by varying cold-rolling practices to obtain the approximate conditions required, and then making small adjustments of other factors, usually hot-rolling conditions. If the quality of the ingot material can be held constant, it is possible to determine fairly readily the conditions of fabrication suitable for controlling the earing characteristics of each end product; if ingot quality varies, then fabrication details must be altered to suit each batch of material.

### (b) Grain-Size

The final grain-size of aluminium alloy sheet and strip must usually be carefully considered at all stages of fabrication, especially in material to be subjected to deep-drawing and pressing operations. Grain-size control is also of importance in material which is to be formed, as coarse grain may impair not only the appearance but also the ability to bend without cracking. Again, it is usually found that the tensile properties of coarse-grained sheet are inferior to those of fine-grained material. For some applications, such as roofing sheet, the grain-size is of little importance to the user, and in such cases no special effort need be made to control it. There are also applications in which a moderately fine grain-size is preferred, as in aluminium-magnesium alloy sheet for light forming operations, where too fine a grain-size leads to the development of stretcher-strain marks on forming, or in slugs for impact extrusion where the optimum results are again not obtained with the finest possible grain-size.

Methods for the routine determination of grain-size include micrographic or macrographic examination of etched specimens, visual examination of Erichsen domes or the surfaces of bent specimens, and the comparison of these with standards.

Every stage in fabrication from casting to final rolling, annealing, or solution-treatment can to some degree affect grain-size. The following variables are, however, generally recognized as being of importance in the later stages of fabrication: cold work before anneal, rate of heating to annealing temperature, annealing temperature, and time of annealing.

In general, the greater the cold work before anneal, the finer the annealed grain-size, owing to an increased rate of nucleation in the very heavily worked material. There are, however, interesting effects associated with the upper and lower critical strains of the cold reduction/annealed grain-size relationship which cannot be wholly explained in simple terms. If most metals and alloys in the fully soft condition are strained only a very small amount (usually under 2%) they will not recrystallize on subsequent annealing. If the

reduction is slightly greater, they will recrystallize at a critical point to form very coarse grains. If the reduction before anneal is now increased, the grain-size on annealing decreases steadily, though not linearly, until at an upper critical point (usually over 90% reduction) giant grains are formed which may be several inches in diameter. These result from a "secondary recrystallization" and occur principally when adjacent crystals are in certain favourable orientations and when some factor that impedes normal grain growth is removed, as when the last traces of a second phase are taken into solution. In the aluminium-magnesium series, under some conditions, the upper critical point occurs at a surprisingly low degree of cold work. Fig. 5 (Plate XLV) which illustrates the grain-size of an aluminium-5% magnesium-0.3% manganese alloy, cold-worked various amounts and annealed at 500° C., shows that from a reduction of less than 5%, the grain-size decreases progressively until an upper critical point is reached at only 30% cold reduction. The grain-size then decreases again with cold reduction. (It should be noted that large grains could also be developed on annealing after less than 5% reduction, although the photograph does not illustrate this point.) Giant grains are not developed in the aluminium-magnesium alloys if an annealing temperature of 400° C. is not exceeded, while alloys such as commercially-pure aluminium and aluminium-1½% manganese, which have otherwise been correctly fabricated, exhibit giant grains only if annealed at temperatures above 550° C.

A fast rate of heating to annealing temperature generally gives a fine grain, presumably owing to a faster rate of nucleation relative to the increase in growth rate with temperature.

The annealing temperature is not usually of itself a very important factor in affecting grain-size within the limits imposed by commercial practice. It may act indirectly in affecting the rate of rise to temperature of the material undergoing the anneal. If annealing is prolonged beyond the stage where nucleation reactions are complete, a high annealing temperature will cause the grain to grow at a very fast rate and may lead to secondary recrystallization; similar considerations apply to annealing time.

Hot-rolling temperature seems to be of only moderate importance in the control of grain-size except in governing the amount of "residual cold work" present in the hot-rolled slab. Increase in the number of cycles of cold working and inter-annealing appears to refine the grain, especially in strong alloys.

Grain-size may also be affected by what may be described as "constitutional factors". The most obvious of these is composition, which can affect recrystallization characteristics by its effect both on the solid-solution composition and on the constituents in equilibrium with it. This equilibrium can be altered by such fabrication variables as chilling rate during casting, time and temperature of ingot pre-



heating, and temperature of hot rolling and annealing. A high rate of ingot chill will prevent the completion of equilibrium reactions during solidification, and this leads to the development of relatively coarse grain in the final product. An endeavour is made to correct this by preheating the ingot before rolling. A long soak at a high temperature usually leads to grain refinement in the final product.

The aluminium-1½% manganese alloy presents problems in grain-size control. The method of casting has a very considerable effect, and permanent-mould ingots yield sheet and strip of finer grain-size than continuously cast ingots owing to constitutional differences caused by variation in the rates of chilling. Prolonged ingot preheating at temperatures in excess of 575° C., flash or continuous annealing, offer practical remedies. The effects of additions of alloying elements such as copper or magnesium for controlling the grain-size of aluminium-manganese alloys have been referred to by Thomas and Fowler<sup>3</sup>; these, however, introduce other problems, such as increase in staining on annealing.

The grain-size of commercially-pure aluminium and the aluminium-magnesium alloys is also dependent upon the ingot preheat treatment. This is discussed in detail by Phillips<sup>4</sup> for commercially-pure aluminium, and is attributed to constitutional factors.

The heat-treatable alloys supplied in the solution-treated or precipitation-treated conditions present very little difficulty in grain-size control. Flattening subsequent to solution-treatment frequently leaves the material in a critically worked condition, and coarse grain can develop if re-solution-treatment or annealing are carried out without further working. The final annealing of sheet of less than 0.064 in. gauge is frequently carried out by a flash-annealing method; the merits of this process have been outlined by Staples.<sup>5</sup> The grain-size of batch-annealed strong alloy is affected by the amount of work carried out before annealing, the grain-size becoming progressively finer with increasing reduction. This point is dealt with in considerable detail for the case of aluminium-copper-magnesium alloy strip by Chadwick, Richards, and Sumner.<sup>9</sup>

The principles involved in the control of deep-drawing and pressing qualities may be illustrated by consideration of the production of half-hard container sheet in the aluminium-1½% manganese alloy on a modern high-speed continuous strip mill. This commodity calls for a grain-size which is fine, but not so fine as that required for hollow-ware manufacture, good earing characteristics, good appearance, flatness, and gauge. Large-scale production implies the use of large ingots, and this in turn implies the adoption of the semi-continuous casting process; in practice, ingots of 3500 lb. weight may be used. The very rapid chilling imposed causes manganese to be retained in solid solution, leading to a tendency for the rolled material to recrystallize to a coarse grain-size on

annealing. This tendency is corrected by a high-temperature preheat and homogenizing treatment given before hot rolling, which brings the ingot into more uniform constitutional equilibrium. Hot rolling is carried out to a hot-mill slab gauge in the range of  $0.130 \pm 0.030$  in., the finishing temperature being about  $400^\circ \pm 20^\circ$  C. The high finishing temperature necessitates cooling of the slab before coiling. For the greatest economy, the coiled slab must be cold rolled in only one pass through multi-stand breaking-down mills followed by inter-annealing and finish rolling through a single-stand temper mill. Several difficulties arise in endeavouring to implement this: first, the temper of material after hot rolling may vary, leading to difficulties in obtaining uniform flatness and gauge; secondly, owing to the weight of the coil the heating rate will be slow and in addition the annealing time must be long enough to burn off rolling oil, which conflicts with the theoretical requirements for good grain-size; thirdly, the practice of giving as few anneals as possible results in a tendency to 45° earing. Uniformity of temper in material entering the cold-roughing mills could be achieved by a slab anneal, but it is found that this may lead to a coarse grain which persists in the final sheet as "ghosts"—areas of preferred orientation falling within the envelopes formed by the grains of the annealed hot-mill slab which have been elongated by cold rolling. No really satisfactory solution to the problem of degreasing before annealing is available, and hence annealing must be carried out until the rolling oil has been burnt off. The third problem—45° earing—can be solved by introducing an additional anneal; the main objection to this is the expense involved in the extra thermal and rolling operations. However, as an extra thermal treatment reduces the difficulty of maintaining shape and flatness (by reducing the drafts required), in addition to conferring freedom from earing, this solution is usually adopted. As the anneal cannot be introduced at the slab gauge, the strip is given an initial cold reduction of 70–80%; a typical annealing procedure at this stage is to heat for 3 hr. at  $450^\circ \pm 10^\circ$  C. Cold rolling continues in a tandem mill to penultimate gauge (say 0.014 in.) at which stage the coils are annealed for 8 hr. above 400° C. and given approximately 30% cold reduction to, say, 0.010 in. to produce the half-hard temper. The practice outlined above gives a satisfactory product with an average planar grain diameter of less than  $200\mu$  and less than 4% earing under the conditions prevailing at a particular works. Differences in practice and equipment require modifications to this planning, as do alterations in the requirements of the commodity to be produced and the characteristics of the ingot metal being fabricated.

#### 4. CORROSION-RESISTANCE

Although the level of corrosion-resistance of a material is governed mainly by its alloy group, it can be affected by minor variations in composition or fabricating technique.



Commercial-purity aluminium is adversely influenced by the presence of copper; up to 0.05% can be tolerated without substantial detriment to the resistance to atmospheric corrosion.

Aluminium-magnesium alloys containing less than 2.5% magnesium have a very high corrosion-resistance which is little affected by changes in fabricating technique. Impurities, and in particular copper, must be kept to a minimum to preserve this high resistance. In binary alloys containing more than 2.5% magnesium, this element may be retained in solid solution if the rate of cooling from annealing temperature is rapid, but in alloys containing 5% or more, sufficient can be retained to cause grain-boundary precipitation in service at slightly elevated temperatures. If the precipitated phase,  $(\beta) \text{Mg}_2\text{Al}_3$ , lies continuously along grain boundaries, the material will be susceptible to intercrystalline and stress-corrosion. For this reason, rates of cooling from annealing temperatures must be carefully controlled.

The corrosion-resistance of the heat-treatable aluminium-magnesium-silicon alloys is affected by variation in composition principally in so far as such variation affects the amount of free silicon present. Silicon in excess of the amount required to form  $\text{Mg}_2\text{Si}$  can be retained in solid solution after solution-treatment. This will lead to a significant decrease in resistance to corrosion in these alloys after precipitation-treatment unless counteracted by the addition of other alloying elements. The presence of copper and iron within normal impurity limits is also likely to decrease the corrosion-resistance still further, but the effect is small compared with that of free silicon. It should, however, be pointed out that the alloys have a relatively high intrinsic resistance to corrosion and are suitable for use in many applications without protection.

The high-strength aluminium-copper-magnesium-silicon and aluminium-zinc-magnesium-copper alloys are normally protected by cladding; the former with 99.7% purity aluminium, and the latter with an aluminium-1% zinc alloy in order to ensure that the cladding will corrode sacrificially. Thus minor variations in corrosion-resistance of the core material will be of no consequence in service; prolonged thermal treatments which cause diffusion of alloying elements from the core through the cladding, with a consequent destruction of the favourable electropotential relationship, must of course be avoided. Both groups of alloys are affected to some extent by the quenching rate after solution-treatment, the corrosion and stress-corrosion resistance being impaired by slow rates of cooling, which promote intercrystalline corrosion instead of the less harmful pitting attack. This may be of importance if the alloy is to be used unprotected.

##### 5. SURFACE FINISH

Factors influencing the surface finish of rolled aluminium may be considered under the headings: ingot quality, hot rolling, cold rolling, and annealing.

Few ingots can be rolled to sheet or strip without

some form of surface preparation such as scalping. Although the surface blebbing on commercially-pure aluminium and the aluminium-1½% manganese alloy ingots does not affect the hot- and cold-rolling characteristics, it causes a smudged appearance on the finished sheet, and if a bright finish is required, about ¼ in. must be scalped from each face of the ingot.

For anodizing-quality or lustre-finish sheet, it may be necessary in order to obtain uniformity of structure, to remove the outer layer of columnar crystals. Addition of grain refiners is not usually a satisfactory alternative, as they may either cause a grain-boundary etching effect on anodizing (as with titanium additions) or may affect the colour of the anodized film. An additional precaution which may be employed to obtain the optimum surface is to etch the hot-mill slab for the removal of dirt and coating picked up during hot rolling. Another method for the production of uniform structure is to clad the ingot with high-purity aluminium plate. The work carried out on the clad surface in rolling from the original high-purity ingot down to the thickness of the cladding plates, and then to the clad sheet, is usually sufficient to eliminate all traces of the original cast structure.

Blisters generated during heat-treatment or annealing are believed to be caused by the diffusion of gas to a discontinuity which usually originates in the as-cast ingot and may be oxide, porosity, or a hair-crack, but may also result from the liquation of a low-melting-point constituent due to overheating. A gas content above the critical amount necessary for the initiation of a blister is frequently the result of insufficient care during casting, but may also be picked up during preheating or annealing. Prolonged soaking at pre-heat temperatures of the order of 550° C. has been proved to be detrimental to the blistering tendency of commercially-pure aluminium; moisture and products of combustion in the furnace atmosphere have also been shown to be contributory causes of blistering during solution heat-treatment.

During the hot rolling of aluminium sheet and strip there is a tendency for the work rolls to become coated with a film of aluminium and aluminium oxide, which, though useful in that it enables heavy reductions to be given during hot rolling, requires constant attention; too hard a coating will leave imprints which may not be removable on subsequent rolling, and any coating which becomes detached from the roll surface will be rolled into the surface of the slab to the detriment of the final product. This coating can be controlled by the soluble oil emulsions which act also as roll coolants, the choice of the correct oil and the most suitable strength of emulsion depending upon the type of mill and the duty being performed. Four-high hot mills generally give rise to more serious coating problems than two-high reversing mills owing, possibly, to the use of heavier reductions, greater slab lengths, and the direct effect of the back-up rolls on the coating.

Streaks on the sheet surface are usually associated with marks on work rolls caused by the cooling pads or may be due to dirt on the felt-lined bridge pads used



for applying back tension during cold-rolling or slitting operations.

Roll marks on the surface of finished sheet may be caused by roll defects arising from soft rolls, or may be the direct result of damage to the rolls by hard inclusions such as oxide or furnace refractories in the sheet; this form of damage is most likely to occur with thin-gauge material. Such materials are often rolled in packs of two or more sheets, and the surfaces in direct contact with the work rolls have a planished finish, whereas the surfaces in contact with one another have a matt finish; uniformity can be improved by reversing the positions of the sheets between passes.

The surfaces of cold-rolled products are also affected by the type of lubricant used; where bright finishes are required it is customary to use oils of low viscosity blended with additives to improve the load-carrying characteristics and lubricating powers. There is, however, a limit to the extent to which light oils can be used, particularly in the cold rolling of heavy-gauge unannealed hot-mill slab whose temper may vary between batches from soft to three-quarters hard. If an attempt is made to give the harder material heavy reductions using a light oil, the lubrication film may break down and the localized heating of the roll and consequent alteration of the roll camber will give rise to a "herring-bone" defect which cannot be completely removed by further rolling. The tendency can be overcome by the use of blends of oil of higher viscosity; this, however, may impair the colour of the sheet, as the heavier the lubricant the greyer will be the sheet or strip. Heavy oils are, moreover, a potential source of brown stains on annealing, and a compromise must be made between an oil giving little trouble on annealing and one suitable for heavy rolling reductions.

## 6. FLATNESS AND GAUGE CONTROL

For many applications, a high standard of flatness and freedom from localized curvature such as wavy edges, belly, &c., is essential. The production of a flat sheet depends to a very great extent upon the skill of the rolling-mill operators in choosing the correct sequence of roll cambers; good shape must be maintained at all stages of fabrication if a high-class product is to be obtained. Hard alloys give greater roll deflections than commercially-pure aluminium for a given reduction, and hence require greater roll cambers.

Difficulty is often experienced in obtaining flatness in finish-rolling thin-gauge sheet and strip if the material is not flat from the previous stage. A badly buckled sheet can result from a difference in longitudinal extension of as little as 1%, which, for a sheet thickness of 0.010 in., corresponds to an error in gauge in adjacent elements of only 0.0001 in. In modern strip rolling, speeds of the order of 1500 ft./min. may be used, and a considerable amount of heat will be generated in the roll gap. As a rise in temperature of 1°C. throughout the thickness of the rolls may cause a change in the roll gap of up to 0.001

in., the local alteration of camber due to small fluctuations of temperature can be a most important source of buckling. Lack of uniformity of mechanical properties of the material fed into the cold-rolling mill can cause considerable difficulties in maintaining good shape. Heat-treated materials present special problems in regard to flatness, since distortion due to quenching stresses has to be overcome.

As shown by Hessenberg and Sims,<sup>6</sup> the gauge of strip being produced at a given mill setting depends on the plastic properties of the material being rolled and the elastic properties of the mill. For material of any given thickness, the force required to deform it to a lesser thickness depends upon the stress/strain curve of the material. This force increases rapidly at first with increasing reduction in thickness, and then more slowly. The elastic force induced in the

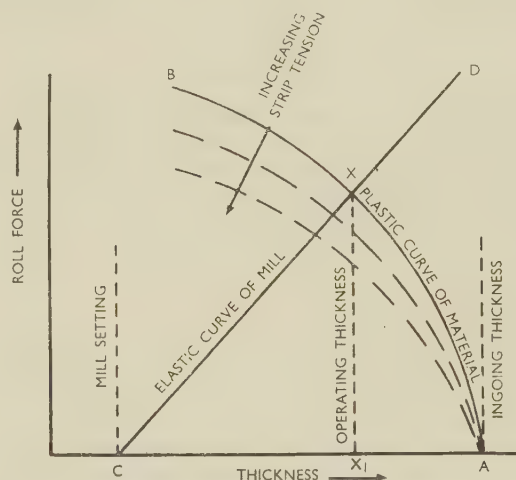


FIG. 6.—Roll Force/Thickness Relationships in Cold Rolling. (Diagrammatic.)

mill by separating the rolls from a given roll setting, increases almost linearly with the roll separation. Consequently, for material of any given starting thickness and for any mill setting, the exit thickness will be such that these two forces are equal. In Fig. 6 the curve *AB* represents the roll-force/thickness curve of the material and *CD* the roll-force/roll-gap curve of the mill. Considering ingoing material of thickness *A* with a mill setting of *C*, and assuming that the thickness of the outgoing material will be equal to the roll gap, this exit thickness is given by *X*, the point where the two curves intersect, the roll force then being given by *XX*<sub>1</sub>.

If tension is applied, the force required to deform the material a given amount is decreased, as shown by the dotted curves, leading to a decrease in both final thickness and roll load. This principle has recently been made the basis of a successful method of gauge control in steel rolling, but probably because of the relatively low modulus and strength of aluminium alloys compared with the high stiffness of modern mills, it does not yet appear to have been applied successfully in the aluminium industry.

As rolling speeds increase, the coefficient of friction falls, leading to a decrease in rolling load, the rolls close slightly, and gauge decreases. This effect is much more noticeable between speeds of 200 and 800 ft./min., than between speeds of 800 and 2000 ft./min. Acceleration and deceleration should therefore be as rapid as possible to avoid production of excessive amounts of off-gauge material.

### III.—THE INFLUENCE OF FABRICATING VARIABLES ON THE PROPERTIES OF SHEET AND STRIP MATERIALS

In the preceding section consideration has been given to the qualities required in wrought aluminium and aluminium alloys in the form of sheet and strip. It is now proposed to deal with the various fabricating operations and to outline their effect on the quality of the finished material.

#### 1. INGOT PREPARATION

The most convenient means of providing the large rolling slabs required for economic operation of modern mills is by the continuous-casting process, although permanent-mould ingots are still used to some extent. It is found, however, that the limited size and lack of operating flexibility renders the permanent-mould method unsuitable for large-scale production.

Extrusion of the ingot provides a possible method of breaking down the as-cast structure and appears to offer a technological advantage in the case of alloys (such as aluminium-7% magnesium) which are difficult to roll direct from as-cast slabs, and also in the breaking down of the as-cast grain for anodizing-quality material. It has, however, the disadvantage of severely limiting the weight of slab that can be obtained in a form suitable for rolling.

Slabs are often supplied to the mill in the full as-cast length, although ingots of alloys such as the aluminium-3½% magnesium, the aluminium-5% magnesium, and the aluminium-zinc-magnesium-copper type, which are prone to "crocodiling", are trimmed by sawing off the base and head. Another factor influencing the pretreatment of continuously-cast ingots is the residual stresses, which will vary with slab size and alloy. These stresses do not cause serious complications in the lower-strength alloys, but as they may cause cracking on sawing of high-strength alloys, such materials are first given a stress-relief anneal (which may be combined with a homogenizing treatment) of 12-24 hours' duration at temperatures of 450°-470° C.

Before preheating for hot rolling, most alloys are machined for the removal of blemishes and surface layers of inverse segregate;  $\frac{1}{4}$ - $\frac{3}{8}$  in. is removed from each face, depending upon the quality of the slab and the nature of subsequent operations, only a very light cut being taken on slabs to be re-machined after breaking down (the initial 50% reduction during hot rolling). Machining to a fine finish makes it possible

to detect any small cracks and imperfections that may have been missed during inspection of the unmachined slab; cracks, porosity, and other defects still visible after a second machining operation are cause for rejection. Immediately after machining, excess soluble-oil emulsion or other coolant is removed and slabs to be clad are degreased with a petrol swab or by other means before fastening the annealed scratch-brushed cladding plates to the faces of the slab by steel bands which retain them in position during preheating. As cleanliness is of the utmost importance for successful cladding, all possible precautions must be taken to prevent oil and dirt becoming entrapped between core and plating, and it is preferable to preheat the material within 24 hr. after plating.

An important point in the preparation of clad material is the choice of a suitable cladding plate thickness. This has an upper limit of  $\frac{1}{2}$  in., as discussed by Kasz and Varley,<sup>7</sup> but there is also a lower limit of about 0.2 in. below which difficulties due to the tendency for thin plates to follow the roll contour may be experienced during "sticking" or welding passes. By choosing suitable core thicknesses and keeping plate thickness within the above limits, it is, however, possible to produce a wide range of coating thicknesses.

#### 2. PREHEATING

The preheating and homogenization of ingots before hot rolling is of the utmost importance, as such treatments have an appreciable effect on the ultimate mechanical properties, grain-size, and directionality of the finished sheet and strip. In some mills, the ingots are first homogenized in one furnace and then reheated for hot rolling in another. This practice has the advantage of increasing the flexibility of mill loading, an important consideration when a number of different alloys has to be catered for. The "double preheating" which this entails also has a metallurgical effect of particular value in the rolling of the aluminium-copper-magnesium-manganese alloys, where it is found that the best results are obtained if, after homogenization, the slabs are reheated to rolling temperature as rapidly as possible and the total time in the furnace is kept as short as is consistent with reaching the required rolling temperature. Slabs treated in this way appear to show less edge cracking and crocodiling than slabs given a prolonged single preheat of equivalent duration.

Close temperature control appears to be of much greater importance than close control of preheating time, provided that 6-12 hours' soaking is given; in general, a control within  $\pm 10^\circ$  C. should be exercised. A standard of  $\pm 10^\circ$  C. uniformity is easier to achieve when operating furnaces continuously than when using a batch system. It is found that with suitable precautions, such as the installation of adequate pyrometric equipment and regular pyrometric surveys, this degree of control can be obtained in modern furnaces of 100 tons' capacity.



### 3. HOT ROLLING

Alloys can be divided roughly into four groups according to the optimum temperature of hot rolling :

Hot-Rolling Temperature °C.	Type of Alloy
(1) ~400 . . . .	Al-Zn-Mg-Cu
(2) ~450-500 . . . .	Al-Cu-Mg-Mn-Si, Al-Mg-Si
(3) ~500-550 . . . .	Al-Mg
(4) ~550 or over . . . .	Al, Al-Mn

This has an obvious bearing on flexibility of operation, especially in regard to loading of preheating furnaces; flexibility is also affected by ingot width, as wide ingots usually take longer to attain soaking temperature than narrow ones. This width factor also influences the planning of rolling schedules as variations in width affect the thermal cambers of the rolls, and it is thus desirable to standardize on one width for as long as possible. It is convenient to standardize ingot widths at 6-in. intervals in order to limit the amount of cross-rolling required to give any desired width of product.

The practice of cross-rolling large slabs early in the hot-rolling cycle is dictated by the limited width and power of any mill. In the fabrication of wide sheet and plate it is usually more convenient to obtain the required width by cross-rolling in excess of the 6-in. limit mentioned earlier, than to cast very wide ingots. In such cases hot rolling may be carried out in two stages, the initial stage consisting of breaking down the cast structure, the amount of cross-rolling at this point being governed by the capacity of the equipment available for machining and reheating the broken-down slab. Even if a light machining operation has been carried out on the as-cast ingot before breaking down, to remove segregates and surface blemishes and to reduce the amount of surface cracking during hot rolling, a further machining operation is often introduced before reheating for the removal of surface defects produced during hot rolling and handling. In the preparation of clad material in alloys, where breaking down is necessary, the cladding plates are usually attached after the second machining operation previous to reheating, in order to avoid handling damage; cladding at this stage is also beneficial in that diffusion from the core to the cladding is minimized.

In rolling narrow material in which the slabs require no cross-rolling, reduction to final hot-mill gauge can be effected with less heat loss than for wide material rolled on the same mill, and consequently as-rolled narrow material tends to be much softer and to have a higher elongation than wide material, particularly in lower gauges.

Hot-rolling temperature has some effect on grain-size, rate of annealing, and directionality; these topics have been discussed by Kasz and Varley,<sup>7</sup> as has also the subject of roll and slab cooling.

It is necessary to exercise close control on the composition of the soluble oil emulsions used in hot rolling by making frequent small additions of pre-mixed emulsion to the main circulating system to com-

pensate for loss of oil and water by drag-out and evaporation. The quantities added are determined by regular checks of emulsion strength and volume. The maintenance of stable conditions during rolling is of particular importance for the control of roll cambers, and hence the shape of the hot-rolled product, and such control is assisted by heating the soluble-oil emulsions before the beginning of, and cooling to a predetermined temperature during, hot rolling. After hot rolling, any soluble oil carried over by the slab is removed by high-pressure jets. Slab which has to be cut to short lengths for cold rolling on flat sheet mills is not usually cooled before shearing to length, but if it is to be coiled for strip rolling it is passed through water sprays and air blasts. This precaution is necessary to reduce damage in handling hot metal and to minimize the risk of staining by decomposition of the oil used during coiling. It is found, however, that water is not suitable for cooling below about 170° C., as at lower temperatures it wets the surface of the slab, and it is then more difficult to remove excess. If water is allowed to evaporate on the surface of the slab, the residual solids will cause staining; on the other hand, if slab is coiled wet, corrosion between adjacent laps of the coil may take place. Air-cooling is therefore employed for reducing slab temperatures below 170° C.

### 4. SLAB ANNEALING

The response of hot-mill slab to annealing varies with the composition of the alloy, the homogenization time and temperature, and the final rolling temperature. As already stated, the aluminium-1½% manganese alloy is particularly sensitive to the foregoing variables, and the grain-size developed on annealing hot-mill slab is frequently very coarse and may be visible as a "ghost" structure even after subsequent cold rolling and annealing; thus, with this alloy, slab annealing may be regarded as of doubtful operational benefit.

An alternative to slab annealing is to insert an inter-anneal after the unannealed hot-mill slab has been given an additional cold rolling; this overcomes the difficulty of coarse grain in aluminium-1½% manganese alloy hot-mill slab, and variation of the gauge of inter-anneal is a very useful means for controlling the earing characteristics of commercial-purity aluminium.

Slab annealing is of great assistance in controlling the grain-size of the aluminium-5% magnesium alloy, the grain-size developed on final annealing at temperatures in excess of 400° C. after cold reduction being smaller in slab-annealed as compared with non-annealed material.

It is usual to anneal strong-alloy slab before cold rolling of the finished sheet; the grain-size at this stage may be coarse, but on subsequent cold rolling and annealing fine grain can be developed. It is generally found that the temperatures required for the annealing and recrystallization of hot-mill slab can be higher by as much as 100° C. than those required

for annealing after further working, and in the case of heat-treatable alloys the relatively high annealing temperatures necessitate control of cooling rates if heat-treatment effects and subsequent age-hardening are to be avoided. In practice, a rate of cooling of 30°–40° C./hr. usually proves satisfactory. A special problem is encountered in the handling of coils of annealed hot-mill slab, as these are not usually very tightly wound and care must be taken to avoid movement between adjacent laps, since chafing and traffic marking which cannot be removed by further working may ensue.

### 5. COLD ROLLING

Before cold rolling, it is desirable to allow material to cool to room temperature.

The practices which can be followed in cold rolling depend upon factors such as the horse-power of the mills, the required temper of the product, the number of passes to be employed, the edge condition of the slab, the type and size of the rolling mill (e.g. two-high or four-high), the type of lubricant, the roll finish, roll cambers, and the surface finish of the slab. Drafting must be limited to suit the hardest material to be encountered in a given production run, and thus variable properties of hot-mill slab can seriously affect production. If excessive drafts are used, the high pressures developed will break down the rolling lubricant, leading to generation of excessive heat and localized thermal cambers which may ruin the shape of the product. The amount of reduction which can be given may be raised by an increase in the viscosity of the cold-rolling lubricant, but as mentioned previously this may lead to a deterioration in the colour of the rolled product; another method is to use rolls with a coarse finish, of say 54 grit, which allow slightly heavier passes than rolls of high-lustre finish. The harder the material, the greater the number of passes required to effect a given total reduction, and beyond a certain point the use of simple equipment, such as two-high flat sheet mills, in which an excessive number of passes would be required, ceases to be economically tolerable. It is also found that a large number of passes affects the shape of the rolled product, tending to reduce the thickness of the edges to a greater extent than the centre, thus leading to wavy edges and increased edge cracking. Other factors influencing the method of production are the width and thickness of the material to be rolled, the final form it is to take, i.e. flat sheet, coiled strip, or circles, the surface finish, and the quantity of material required.

Sheet and strip are not normally rolled in coil form in gauges thicker than 10 S.W.G. (0.128 in.) or in widths exceeding 72 in., as the quantities at present required in the larger sizes do not justify the installation of the heavy rolling, coiling, and ancillary equipment necessary for their production. In modern practice, four-high mills are used for the cold roughing of both strip and flat sheet.

One of the features of products rolled on four-high

mills is the uniformity of gauge across the width; although this is an advantage for most purposes, special cambers have to be used for rolling material to be roughed on four-high mills and finished on two-high flat sheet mills (e.g. strong-alloy sheet), as in this type of finish rolling a certain amount of "centre" is required to compensate for roll deflection and avoid wavy edges.

The shape of material rolled on flat sheet mills depends to a large extent upon the skill of the operator in choosing the optimum roll-pass procedure. A high degree of skill and experience is also required of operators of narrow and wide strip mills; automatic tensioning devices and flying micrometers are of great assistance, but on high-speed mills the ultimate control lies in the maintenance of correct roll cambers by the adjustment of the supply of coolant to the individual sprays across the width of the work rolls.

On the ingoing side of the mill the use of roller bridles or tension frames in conjunction with coil baskets, unwind cones, or mandrels coupled to drag generators or other back-tensioning devices, serves to prevent puckering or pinching of the strip entering the mill; whilst on the outgoing side, tension applied by means of the rewind device helps in the control of shape. All these operations thus require careful attention to control the quality of the product being rolled.

Unless the coil received for cold rolling is tightly wound, the application of back tension during unwinding will cause surface abrasions due to the loose laps moving over one another. Another source of surface markings lies in the felt-lined board bridles, which are liable to pick up small flakes of aluminium and dirt. Excessive back tension applied by means of a multi-roll bridle can cause surface crazing, which appears objectionable on the rolled strip, although it is usually of negligible depth. The lustre of the strip being produced is affected by the angle of entry of the strip into the bite of the work rolls, the more acute the angle of entry, the brighter the lustre of the side of the strip making the more acute angle and the greyer the opposite side.

On the outgoing side of the mill, rewinding may be carried out on a variety of equipment, each of which has its peculiar properties. Strip over 0.128 in. in thickness is usually coiled by means of multi-roll bending machines, the rolls of which must be well lubricated to prevent metal pick-up. Although material of less than 0.128 in. thickness may be coiled on falling-leaf blockers, the time taken to thread them prevents their use on high-speed mills. On these mills collapsing mandrels, with or without steel spools, used in conjunction with belt wrappers are preferable. Steel spools are preferred to plain collapsible mandrels for the coiling of strip under 0.014 in. in thickness, as coils of such material when rolled under tension tend to collapse if not supported internally. These spools, which fit over the collapsible mandrel of the mill rewind gear, are designed to facilitate handling on ancillary equipment, such as



slitters, degreasers, annealing furnaces, and cut-to-length lines. To prevent oxidation and scaling of the spools in passage through annealing furnaces a protective layer of aluminium is applied to them by a metal-spray gun; if these or similar precautions are not taken, rust detached from the spools may be rolled into the strip.

## 6. SLITTING

At some stage in the production of hot-mill slab it is usual to remove edge defects by a slitting operation. Unless the equipment is well maintained, the slit edges may themselves be a source of excessive edge cracking on subsequent cold rolling; in this connection care must also be taken to prevent small slivers of slitting scrap remaining on the surface or edge of the slab where they can be rolled in. Whenever possible thin material should be slit in the hard-rolled, oily condition, rather than in the annealed state, as by this means cleaner edges result, and there is less risk of surface damage.

## 7. ANNEALING

Ideally, annealing can be accomplished by heating for any of a large number of combinations of time and temperature. In practice, however, the temperature must be chosen with regard not only to the characteristics of the alloy but also to the type of furnace used, the heating rate required, and other factors. The most important of the subsidiary factors is the necessity of removing residual rolling oil from the load during the annealing operation so that no stains remain; this residual oil is carried through the mill chiefly as a bead on the edge of the strip.

Many methods of removing this oil before the material enters the furnace have been tried, but none is completely successful. For example, compressed-air jets on the outgoing side of the mill give only partial removal; interleaving with paper is effective, but the price of paper free from hard inclusions and impurities liable to cause corrosion is prohibitive; conventional solvent degreasing methods are effective but expensive and a possible source of handling damage. A light wash pass in kerosene or gas oil, followed by edge trimming or slitting, is also effective, but suitable only for relatively slow-speed mills.

It will thus be appreciated that much high-speed strip mill material must be annealed in an oily condition, and times and temperatures must be adjusted for the removal of oil in addition to the primary function of softening the metal. The cleanliness of the metal after anneal will depend upon that of the oil, suspended oxide and finely divided metal from which will remain as a residue; for this reason mills in which oil is recirculated have provision for filtration, designed to keep the total solids below 0.04%.

The types of filters used and their operation are to some extent governed by the types of rolling additives employed. Oils containing lanolin may require heating before and cooling after filtering, to prevent

removal of the additive. On flat sheet mills the problem of oil staining does not often arise, as the amounts of oil used are very small compared with those necessary for strip mills.

The lowest tensile properties are obtained in material annealed after 10-20% cold reduction, the properties after anneal increasing progressively with prior reductions in excess of this amount; in the aluminium-magnesium alloys, the difference in ultimate tensile strength between materials given 20 and 60% reduction before anneal may be as much as 1 ton/in.<sup>2</sup>. These properties depend also upon the thermal history of the material with regard to preheat time and temperature and number of previous anneals, both high preheat temperatures and a multiplicity of anneals reducing the as-annealed tensile properties.

The rate of cooling from annealing temperature is unimportant in commercially-pure aluminium, the aluminium-1¼% manganese alloy, and the aluminium alloys with low magnesium contents, but rates not exceeding 30° C./hr. are advisable for heat-treatable alloys to prevent a heat-treatment effect. Semi-continuous annealing furnaces having preheating, soaking, and cooling zones have been designed to give the desired cycle of heating and cooling, and have been in use for a number of years. Slow cooling rates are also desirable for aluminium-magnesium alloys in the higher magnesium range to obtain a structure which confers freedom from stress-corrosion susceptibility.

Alloys containing magnesium are subject to the formation of a black oxide coating when annealed at temperatures above 380° C., and for a bright finish a low annealing temperature must be employed. As this will not be high enough to burn off oil, annealing loads must be clean. An additional precaution is to envelop the material in thin sheet to limit the amount of air available for oxidation; this will, however, reduce the rate of heat transfer, and may cause grain coarsening.

The annealing of Alclad materials must be governed by the necessity of avoiding diffusion of alloying elements from the strong-alloy core into the cladding, and if the rolling schedule necessitates a relatively large number of anneals (as in the production of low-gauge sheet or strip) times and temperatures must be reduced to a minimum. More detailed information on the subject of diffusion is given by Keller and Brown.<sup>10</sup> In order to obtain a clean product, excess oil must be removed from the surface of the rolled sheet or strip before anneal, as extended heating periods cannot be tolerated.

Strong-alloy products, particularly if unclad, are susceptible to blistering when annealed at high temperatures in gas- or oil-fired furnaces in which the products of combustion come into contact with the load. Condensation may occur and give rise to surface staining and corrosion, particularly in heavy coils. It is therefore preferable to use muffle-type furnaces with such heating media.

Annealing of aluminium-zinc-magnesium-copper alloys of the D.T.D. 687 type should not be carried

out at temperatures in excess of 400° C., as the solubility of alloying constituents is considerable at higher annealing temperatures, and after repeated annealing at high temperatures constituents may be precipitated on cooling in a form which can impair the ductility and cold-working characteristics. As an alternative to slow cooling after inter-stage annealing of these alloys, it is possible to stabilize the annealed properties by means of a low-temperature treatment at  $210 \pm 10^\circ \text{C.}$  for 2 hr.; for complete stability of as-annealed properties, however, slow cooling is essential.

Annealed aluminium and its alloys are very easily damaged by rough handling. Any defects produced cannot easily be rectified at later stages of fabrication, and may cause ultimate rejection for broken surface, indentations, and scratches.

### 8. SOLUTION-TREATMENT

Some operational problems arising during the solution-treatment of aluminium alloy sheet and coils

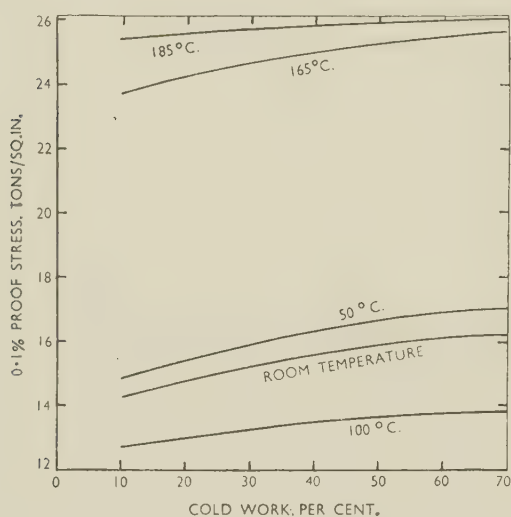


FIG. 7.—Effect of Cold Work Before Solution-Treatment on 0.1% Proof Stress of Aluminium-Copper-Magnesium-Manganese-Silicon Alloy Strip in the Naturally Aged (for 5 days) or Artificially Aged (for 6 hr.) Condition.

have already been dealt with by Paton,<sup>8</sup> and in so far as the control of quality is concerned, only factors affecting the ultimate mechanical properties of the material and the surface appearance of the product need be considered here.

The grain-refining effect of increased cold work before solution-treatment of strong alloys has already been referred to. Similar effects are noted on tensile properties; Fig. 7, for instance, illustrates the influence of cold work before solution-treatment on the 0.1% proof stress of an aluminium-copper-magnesium-manganese-silicon alloy in the naturally and artificially aged conditions. The considerable drop in properties experienced after treating at 100° C. should be noted, as the 0.1% proof stress of material subjected to a treatment at this temperature during

drying would be significantly affected; the influence on ultimate tensile stress would be less. In practice, the drying treatment is limited to a maximum temperature of 60° C.

Owing to the faster rate of heating achieved in a salt bath as compared with an air furnace, a finer grain-size is usually obtained, which in turn has a beneficial effect on the level of mechanical properties. In the case of thin-gauge clad material this faster rate of heating reduces the heat-treatment time, thus minimizing diffusion. On the other hand, air furnaces generally produce a more even colour on sheet.

The purity of the salts used for solution-treatment can affect the appearance of the heat-treated products, as traces of certain impurities such as iodates cause white stains; whilst these may have no detrimental effect on the properties, it is usually considered necessary for the sake of appearance either to reject the sheet or to remove the stains.

Undue delay in transfer from the heat-treatment furnace to the quench tank can cause a serious reduction in ultimate tensile strength and impair the corrosion-resistance of certain alloys. If air furnaces are used, this delay should be limited to a maximum of 10 sec., but with salt baths, lags of up to 30 sec. can usually be tolerated, the film of molten salt affording thermal insulation. Advantage is frequently taken of the increased time lag permissible with salt baths to allow a draining period to minimize drag-out losses of salt. The temperature of the quenching water should not exceed 30° C., as higher temperatures lower the efficiency of the quench, with a consequent reduction in the ultimate mechanical properties.

After quenching material heat-treated in the salt bath, all traces of nitrate must be removed by washing, and it is thus necessary to control the nitrate content of the quench- and wash-waters. If the heat-treatment load is well spaced, washing can be carried out simply by transferring the load from quench- to wash-tank, but if spacing is inadequate the sheets must be separated for final washing and drying.

The temperature used in the drying operation should not exceed 80° C., as temperatures of the order of 100° C. inhibit natural ageing, whilst temperatures in excess of 150° C. will initiate artificial ageing.

Solution-treated material must finally be flattened for the removal of the distortion caused during quenching. This is carried out either by passage through roller-levelling machines or by a small reduction on flat sheet mills, followed by stretching. Before this last operation it is usual to edge-trim to remove small defects and cracks which could cause tearing of the sheet; after stretching, the material is finally sheared to length for the removal of stretcher jaw marks.

A number of special problems are introduced in the heat-treatment of coils. Spacing of the adjacent laps to allow free circulation of the heating or quenching medium renders the material very liable to handling and scratching damage; the heat-



treatment of very large coils is further complicated by difficulties in securing rapid heating and temperature uniformity.

After solution heat-treatment and washing, the coils are usually edge-trimmed and roller-levelled before re-coiling; during this operation, the material may be finally washed with clean water, the excess being removed by squeegees. Final drying may then be carried out by interleaving with paper, which is removed when the coils are unwound for final stretching for the removal of lateral bow; to minimize the risk of staining and corrosion, wet coils should not be allowed to stand for long periods. Another factor limiting the length of solution-treated coil which can be supplied, is the length of the equipment available for the last stretching operation.

The relatively large number of operations carried out between solution-treatment and stretching usually separates these processes by an interval of several hours; if, however, this is for any reason reduced to less than 1 hr., stretching of between  $\frac{1}{2}$  and 1% in length can result in a reduction of  $\frac{1}{2}$  ton/in.<sup>2</sup> or more in the ultimate tensile stress after natural ageing; this drop can, however, be compensated for by an increased amount of stretching.

## 9. INSPECTION AND TEST

The sampling procedures covering the inspection and release of sheet and strip are detailed in the relevant B.S. and D.T.D. specifications, and the general principles laid down are normally followed for commercial materials, even if not ordered to any definite specification. Checks must also be made at all stages of production to ensure that the various processes are under control. At most stages, visual inspection of the product coupled with checks on the pyrometric control of furnaces is usually adequate. Regular pyrometric surveys should also be carried out to ensure that the uniformity of conditions within furnaces is being maintained.

Mention must be made of the technique of statistical experiment or analysis, which is found to be invaluable in investigating the important production factors affecting some final quality of sheet and strip. The statistical approach is valuable, and often indeed essential, because of the large number of variables inherent in the fabrication process and the practical and economic difficulties of conducting carefully controlled experiments on a works' scale. Useful information may usually be obtained by analysis of production results over a limited period of time without the necessity for any planned experimentation. In this case the method of analysis and the value of the results will be determined by the data available considered from the points of view of quantity, completeness, and reliability.

The collection of data entails problems both as regards factors normally recorded and those which are not. In the first case the difficulties involved are principally those of finding the data, which may, of

necessity, be scattered among various documents such as log books, lot tickets, melt sheets, analysis records, &c., and collecting it together in a convenient form. In the second case the difficulties may be practical ones, where the measurement of some quantity would interfere with production, or even be impossible owing to lack of suitable equipment.

The actual method of analysis depends on the type of data available, but in general, where the values are uncontrolled (in the statistical sense), the most satisfactory approach is that of multi-variate correlation. The results of a statistical analysis of this nature are generally in three parts: first, an indication of the *average* numerical effect of varying each factor; secondly, an estimate of the probability that the effect observed is due to pure chance (usually known as the "significance level"); and lastly, an estimate of the variation in the dependent variable to be expected over a range of materials produced by identical fabricating methods (within the limits of accuracy of the data used).

The information gained by the above methods would often be impossible to obtain by controlled experiment except at very great cost, even allowing for the somewhat greater precision of measurement made possible by the latter approach. For this reason it is advisable to record as much information as possible about production details on a routine basis, even when no specific problem requiring analysis is apparent, in such a way that the complete history of any tested material can be ascertained.

An arrangement found to work very well for the control of process quality is for the Production Department supervisors and operators to be responsible at each stage for the quality of the material which they process, the Inspection and Technical Department having certain well-defined obligations and being available to render assistance and to carry out detailed investigations as required.

By this method of operation, prime responsibility for the production of high-quality products is vested in the Production Department, and, since this department has to account for any defective material arising at the inspection stage, there is every encouragement to report faults as soon as they are noted, giving early warning of all matters requiring attention.

## 10. PACKING AND DESPATCH

After the fabricated product has passed inspection and has been released as satisfactory on mechanical test, the remaining task is the delivery of the material in good condition. Two main problems arise in the delivery of material to home consumers. The first is the occurrence of condensation stains; these can be minimized by using waterproof wrapping when packaging and by ensuring that warehousing conditions are suitable in that frequent changes in temperature and humidity are avoided. The second type of defect is caused by the movement of sheets one upon another, giving a form of pitting known as

"traffic markings", which can cause serious disfiguration of heavy sheets shipped in contact with one another. The usual method of preventing this form of damage is by interleaving the sheets with paper or cardboard. Thin material of gauge 0.036 in. and under is less susceptible to damage than heavier gauges, and can usually be despatched without interleaving.

Material to be shipped overseas requires stronger packing cases than those normally employed for home use, and, in addition to the normal precautions of waterproof packing to prevent access of sea-water, it is common practice to apply a protective layer of rolling oil or one of the appropriate proprietary protective coatings before shipping.

#### 11. STANDARD PRACTICE

From the foregoing, it will be appreciated that the considerations affecting the choice of production practices are so numerous that procedures must be tabulated in detail at the plant concerned so that repeat orders can be fabricated to the same quality. Before any change in procedure is made, its effect should be considered on theoretical grounds; if these indicate that the proposed innovation will be advantageous, a small pilot batch should then be fabricated

and tested to minimize the danger of unforeseen complications arising when full-scale production is attempted.

#### ACKNOWLEDGEMENTS

The authors wish to express their thanks to the Managements of the Northern Aluminium Co., Ltd., and Aluminium Laboratories Limited, for permission to publish this paper, and to their colleagues for helpful discussions in the course of its preparation.

#### REFERENCES

1. H. W. L. Phillips, *J. Inst. Metals*, 1946, **72**, 151.
2. H. Hug, G. Siebel, and P. Buser, *Metall*, 1952, **6**, 579.
3. W. J. Thomas and W. A. Fowler, *J. Inst. Metals*, 1948-49, **75**, 921.
4. H. W. L. Phillips, *ibid.*, 1942, **68**, 47.
5. R. T. Staples, *ibid.*, 1951-52, **80**, 323.
6. W. C. F. Hesselberg and R. B. Sims, *Proc. Inst. Mech. Eng.*, 1952, [A], **166**, 75.
7. F. Kasz and P. C. Varley, *J. Inst. Metals*, 1949, **76**, 407.
8. C. P. Paton, *ibid.*, 1951-52, **80**, 311.
9. R. Chadwick, T. Ll. Richards, and K. G. Sumner, *ibid.*, 1948-49, **75**, 627.
10. F. Keller and R. H. Brown, *Trans. Amer. Inst. Min. Met. Eng.*, 1944, **156**, 377.



# THE CONTROL OF PROPERTIES AND STRUCTURE 1524 IN THE HOT AND COLD ROLLING OF COPPER AND COPPER-BASE ALLOYS \*

By W. W. KEE,† B.Sc., F.I.M., MEMBER

## SYNOPSIS

The various phenomena arising during the integrated processes of rolling copper and brass are discussed, and the methods of controlling such factors as grain-size, directionality, shape, gauge, and surface quality are considered in relation to those parts of the process by which they are most affected.

Particular reference is made to the influence of cold rolling and grain-size on properties, and to the effect of annealing on recrystallization and grain growth. In the section on annealing, the importance of atmosphere control is emphasized. Special consideration has been given to gauge-control methods, both established and experimental.

The influence of impurities on processing and structure is outlined, and it is pointed out that every producer should lay down a concentration range for impurities most suitable to his own production methods and requirements.

Brief mention is made of testing and inspection, and the use of production schedules is illustrated.

## I.—INTRODUCTION

IN considering the structure and properties of metals produced by rolling, it is essential to regard the rolling operation as a series of interdependent processes, comprising rolling, annealing, pickling, scalping, handling, &c. Each of these integrated operations contributes to the final properties of the metal, and each requires certain controls in order to produce a satisfactory product. It is the purpose of this paper to discuss these controls, both with regard to their necessity and their implementation.

The paper comprises a review of the phenomena and factors which must be controlled, and an outline of the practical day-to-day methods of exercising control. It deals primarily with the controls exercised in the production of tough-pitch copper and the straight brasses, in sheet and strip form.

The assumption is made that the rolling mill receives structurally sound cakes, which may have slight chemical differences due to the presence of impurities. This means that the first major consideration will be the effect of the impurities on the rolling operations. Emphasis is laid on the fact that the limit of impurities must be regarded in conjunction with the working schedules, and that it is unwise to generalize on the degree of any impurity which affects hot workability.

As the paper deals with the control of structure and properties, a review of the factors influencing grain-size and grain orientation has been made. The

relationship between mechanical properties and grain-size and percentage cold work is illustrated.

The consumer of copper and brass sheets is interested not only in mechanical and physical properties, but also in dimensional uniformity and surface finish. The control of gauge and surface quality is therefore discussed.

## II.—THE EFFECT OF IMPURITIES

The limit for the impurity content of copper and copper-base alloys is governed by the specifications to which they must conform. Certain generalizations have to be made in formulating specifications, and a metal cannot necessarily be produced by a particular plant when certain of the impurities are near the maximum level permitted by the specification. Each mill must decide for itself what range of impurities it can tolerate, giving due consideration to the most economical employment of production methods and schedules. The presence of impurities may affect the workability of the metal as well as its physical characteristics and behaviour during annealing.

### 1. WORKABILITY

In general, the presence of impurities has greater significance in mills employing hot breaking-down than in those which use a cold-working process throughout. Copper is invariably broken down hot, whereas brass is broken down either hot or cold.

\* Manuscript received 16 October 1953. Contribution to a Symposium on "The Control of Quality in the Production of Wrought Non-Ferrous Metals and Alloys. II.—Working

Operations", to be held in London on 28 April 1954.

† Director, Enfield Copper Refining Co., Ltd., Enfield, Middlesex.

Much vital information has been published on the effects of impurities in copper, but it is very unusual for rollers to receive material in which the impurities seriously impair hot workability. Most of the copper produced in rod, sheet, and strip form is of tough-pitch quality, containing between 0.015 and 0.05% oxygen. The presence of oxygen is an important feature in so far as it prevents certain impurities from unduly depressing the conductivity, and also helps to neutralize the deleterious effects of certain minor constituents on hot workability.

Archbutt and Prytherch<sup>1</sup> have indicated that the limit of the lead content which affects the hot workability of copper is a function of the oxygen content. In oxygen-free copper, it would appear that the safe limit for lead in hot working depends upon the working temperature, as lead in solid solution has little embrittling effect. For example, one would expect to be able to tolerate about 0.04% lead, if the rolling temperature does not fall below 800° C. At 700° C., the solubility limit drops to about 0.02% lead, and if hot working is continued into a temperature range which permits precipitation of the lead, difficulties arise. In the case of tough-pitch copper, the presence of oxygen greatly diminishes the harmful effect of lead by altering the character of the precipitating phase, thus permitting lower finishing temperatures on hot rolling. The lead content of high-conductivity coppers is always less than 0.005%, and this causes no difficulty at normal hot-rolling temperatures.

Evidence that antimony resembles lead in its behaviour with respect to oxygen is provided by Archbutt and Prytherch,<sup>1</sup> and by Johnson.<sup>2</sup>

Bismuth is another element which can give rise to serious trouble in hot rolling. It is almost insoluble in copper (0.002% at 980° C.) and forms a low-melting-point intergranular film which causes hot-shortness. The presence of oxygen, or other elements such as arsenic and phosphorus, diminishes the ill-effect of bismuth.

The position regarding the brasses is somewhat different. Zinc acts as a deoxidizer with respect to copper, and the oxide formed is insoluble in the liquid alloy. The brasses, therefore, are mostly free from oxides and often react to impurities in the same way as oxygen-free copper.

The common impurities which have an adverse effect on the hot rolling of brass are lead, bismuth, and antimony, but the amount of such impurities which can be tolerated depends on the basic composition of the alloy. The  $\alpha$ -alloys are particularly sensitive. The amount of lead which can be tolerated increases markedly in ( $\alpha + \beta$ ) or  $\beta$  structures, where the lead shows no preference for the grain boundaries but is uniformly distributed throughout. The presence of small amounts of silicon, however, can cause the lead to collect at the grain boundaries in  $\beta$ -brass, as it does in  $\alpha$ -brass.

Bismuth behaves in a similar manner to lead, and even as little as 0.005% causes hot-shortness in the

$\alpha$  range of brasses. Its effect becomes somewhat less marked as the zinc content of the brass increases to give the ( $\alpha + \beta$ ) or  $\beta$  structure.

There is some disagreement among investigators regarding the effect of antimony on the hot rolling of brass. This is probably due to its various modes of occurrence in the as-cast cake, but there is evidence that the maximum tolerable antimony content decreases as the zinc content of the alloy increases.<sup>3</sup>

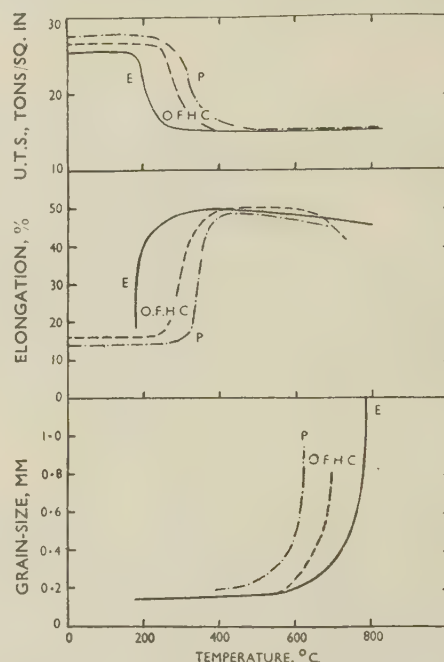


FIG. 1.—The Effect of Increased Annealing Temperature on the Ultimate Tensile Stress, Percentage Elongation, and Grain-Size of Cold-Worked Electrolytic Tough-Pitch Copper (E), Oxygen-Free High-Conductivity Copper (O.F.H.C.), and 0.02% Phosphorus-Deoxidized Copper (P). Material cold worked 62.5% by drawing. Annealing time 1 hr.

It should be noted at this point that it is uncommon to find impurities in such concentration that they affect the cold rolling of either copper or the brasses. Bismuth, lead, and antimony can be tolerated in much larger amounts than in hot rolling.

## 2. STRUCTURE

Apart from the effect of impurities on the hot and cold workability of the metals, the recrystallization temperatures may also be affected. A case in point relates to the difference in the recrystallization temperatures of electrolytic, phosphorus-deoxidized, and oxygen-free high-conductivity (O.F.H.C.) copper. Fig. 1 shows this difference by illustrating the effect of annealing on the tensile strength, percentage elongation, and grain-size of the various coppers, which had previously been reduced 62.5% by drawing.<sup>4</sup>

The fact that O.F.H.C. and phosphorus-deoxidized coppers have higher recrystallization temperatures than electrolytic tough-pitch copper is due to the



absence of oxygen, so that some of the impurities present are in solid solution and thus raise the recrystallization point.

The serious effects of impurities are not confined to troubles arising in rolling. There are certain elements which could cause much inconvenience and expense by upsetting normal mill routine owing to the suppression of grain growth. In brass, for example, iron, chromium, nickel, and phosphorus are amongst such elements. Silver and cadmium have a similar effect in copper, and are often added in order to increase the recrystallization temperatures. Impurities also affect the character and degree of adherence of the oxide layer formed when copper is heated in air.

The control of directionality will be dealt with later, but it should be mentioned here that impurities can have an effect on preferred orientation.

### 3. GENERAL OBSERVATIONS

Little mention has been made regarding the limits of impurities which are injurious—a subject on which many investigators have already written at considerable length and often with apparent disagreement. For example, McLean and Northcott<sup>3</sup> set an upper limit of 0.01% lead in 70 : 30 brass, whereas Cook and Davis<sup>5</sup> point out that 0.025% lead can be borne, if the hot-working conditions are adjusted to suit the composition. This divergence of opinion is typical of many of the reported observations, and is probably due to different conditions of experimentation. The influence of any particular impurity depends also upon other impurities present in the metal. Two cases may be cited to illustrate this point: (i) in copper the deleterious effect of bismuth on hot working is diminished by the presence of oxygen, arsenic, phosphorus, or antimony; and (ii) in  $\alpha$ -brass, tin at normal impurity level has no harmful effect, but a combination of tin and iron above a certain level can lead to fire-cracking.

The realistic approach to the problem of impurities is to establish from experience a concentration range beyond which normal production schedules cannot be applied. To try to work to a fixed limit for any one impurity, without reference to other minor constituents present, may cause unnecessary trouble or even failure.

The first point of control is therefore an analytical one. The production metallurgist must know, not only the basic composition, but also the percentage of all impurities in the raw material. Having established the chemical composition of the stock, it is necessary to identify each cake with its analysis, and with a particular group, according to its prescribed rolling schedule.

Only where special conditions warrant alteration to the normal rolling and heat-treatment routine should one consider handling material where the impurities fall outside the prescribed concentration range.

Although the structure of the castings received by

the mill is of importance, there is usually less significant variation in the cast structure than in impurity levels. This is particularly true in the case of foundries which handle scrap other than that produced in their own rolling mills.

### III.—BREAKING-DOWN

The structure of rolling cakes is under the control of the foundry, and fortunately the technique of casting is so well established that it is very unusual to encounter any difficulties in the primary break-down due to casting defects. The cakes are overhauled before leaving the foundry, any small defects being chiselled out and, in the case of phosphorus-deoxidized copper or the brasses, the shrinkage head cropped.

Metals are more plastic when hot than when cold, so that less power is required to deform them in the hot condition. It would be thought, therefore, that where output justifies the installation of a preheating furnace and a hot-rolling mill, all metals and alloys favourable to hot working would be broken-down hot. This has in fact been the tendency in recent years, but in the U.S.A. several mills still make use of the cold break-down for brass, particularly where the mill rolls both straight and leaded brasses.

Where hot breaking-down is employed, control starts at the preheating furnace. With reasonable handling, no damage occurs to the cakes on their way to the furnace.

The preheat temperature must be controlled, and it is important that all temperature controllers, recorders, and indicators be maintained at a high level of efficiency. Final control on the behaviour of the furnace, at various throughput rates, is made by checking the temperature of the cakes when they have left the furnace and reached the rolling table. A total-radiation pyrometer or a contact pyrometer may be used for this. A controlled atmosphere—in the current meaning of the term—is not required in the preheating furnace, but it is usual to work with furnace atmospheres as near neutral as possible in order to minimize oxidation.

The rate of travel of cakes through the furnace is decided after taking into consideration the rolling temperature required, the speed of rolling, the furnace burden, and the temperature head of the furnace. The aim is to keep the hot breaking-down mill running continuously on cakes which have been in the furnace just long enough to be heated uniformly throughout to the hot-rolling temperature. Although both copper and brasses, except the 67 : 33 alloy, can be hot rolled over a wide range of temperatures, it is important to have a standardized preheating temperature so that a standard series of reductions can be applied for any desired finishing gauge. The factors influencing the selection of temperature have been given by Cook and Davis,<sup>5</sup> as have the hot-rolling temperature ranges for copper and many copper alloys.

Two-high reversing mills are generally employed for hot break-down, and may often reduce 4-6-in.-thick copper or brass cakes to  $\frac{3}{16}$ - $\frac{3}{8}$  in. plate. Plates finished at the heavier gauges are genuinely hot-worked, in that all deformation has occurred above the recrystallization temperature, and the break-down process has little, if any, effect on the properties of the finished cold-rolled material. When the metal is finished to thinner gauges, some cold work may be applied, but the amount is not excessive, and such factors as directionality, &c., in the final cold-rolled strip are not affected. Where heavy brass ingots are not broken down hot, they are usually broken down on non-reversing mills, and the controls used in cold working must be applied. (See Section VIII.)

Uniformity of gauge is important in the hot-rolled plates, as it can affect the subsequent cold rolling. This is true, even if the material is fully soft, as any variations in the gauge will cause variations in the frictional conditions at the rolls of the cold-reduction mill, and unless corrective measures are taken, poor-gauge material may be passed on to the next stage of production. In a similar manner, poor and irregular pickling of hot-rolled plate or coils can result in irregularities in the subsequent cold-rolled strip. A method which has been proposed for gauge control during hot rolling is described in Section VIII, 3.

The main steps to be taken in minimizing the surface defects which arise at the hot mill are to have: (i) clean roller tables, (ii) clean mill housings, and (iii) smooth rolls. The hot cake itself is brushed clean before entry into the rolls, and water or soluble-oil sprays, which are used to maintain roll temperature, have the additional advantage of removing particles of scale loosened during rolling. The hot-rolled plate is visually inspected during, and immediately after, rolling, and any defective plate is laid aside for investigation. Most of the output from the hot mill goes to feed the sheet and strip mills and is, therefore, often overhauled or scalped before cold working.

One of the best-known scalping machines—the Torrington slab-milling machine—has been described and illustrated by Davies.<sup>6</sup> It only remains to mention that all plates from the scalper must be carefully inspected, as it is possible to do more harm than good by milling. For instance, tears can be made in the surface of the metal by a faulty or worn cutter. In the case of copper, in particular, it is possible to get small particles of swarf pressed into the surface, which later fall out and leave pits. These pressed-in particles arise either from metal adhering to the cutter edge, or from defects in the pneumatic swarf-removal system. Where visual inspection reveals such defects, one of two procedures is adopted.

If the defect is rare and at random, it is removed by a hand-operated overhauling machine; if it is frequent and regular, the machine is stopped and the cause of trouble discovered. Only experience can give a guide to the standard thickness to be machined off, as the minimum surface thickness to be removed depends upon the nature of the cast cake and the

breaking-down process. Since, however, these show little significant variation from batch to batch, it is practicable to lay down a standard amount of metal to be removed by scalping. This is usually of the order of 0.010-0.015 in. from each side.

Troubles arising from a well-maintained scalping machine are few, but it should be stressed that inspection at this stage is very important, particularly in the production of finished sheets requiring an immaculate surface, as needed for engraving.

#### IV.—INFLUENCE OF COLD WORK AND GRAIN-SIZE ON PROPERTIES

The general effect of cold rolling is to increase the hardness and strength of the metal and to reduce the recrystallized grain-size and ductility. Some idea of the relationship between grain-size and mechanical properties, obtained by cold rolling, can be seen from Figs. 2-4. It is shown that for similar amounts of

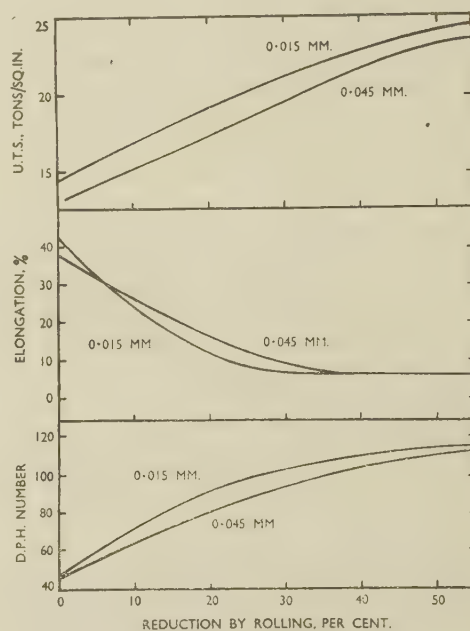


FIG. 2.—The Influence of Grain-Size on the Tensile Strength, Percentage Elongation, and Hardness of Electrolytic Tough-Pitch Copper when Subjected to Various Amounts of Cold Work by Rolling.

cold work, a finer initial grain-size results in an increase in the hardness and ultimate tensile strength of electrolytic tough-pitch copper, 70 : 30 brass, and 63 : 37 brass.

So important is the effect of grain-size on the properties of annealed material, that many A.S.T.M. specifications state that: "Grain-size shall be the standard test for sheet and strip brasses of all thicknesses in annealed tempers, and acceptance or rejection shall depend on the grain-sizes." British Standard Specifications lay the emphasis not on grain-size but on mechanical properties, and to some extent this influences the control methods employed in production in the United Kingdom.



Increase in the grain-size of annealed metal results in a decrease in hardness, and Fig. 5 illustrates the

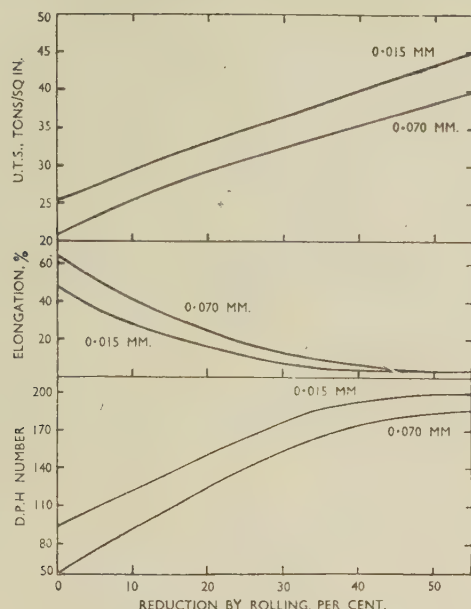


FIG. 3.—The Influence of Grain-Size on the Tensile Strength, Percentage Elongation, and Hardness of 70 : 30 Brass when Subjected to Various Amounts of Cold Work by Rolling.

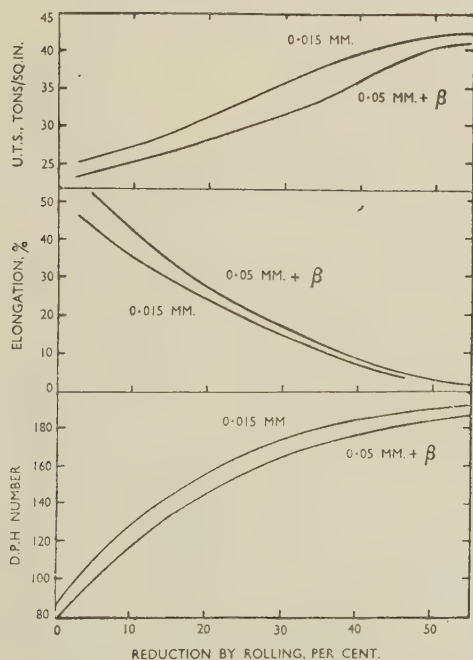


FIG. 4.—The Influence of Grain-Size on the Tensile Strength, Percentage Elongation, and Hardness of 63 : 37 Brass when Subjected to Various Amounts of Cold Work by Rolling. (62.8% copper content in brass.  $\beta$  constituent is present in the 0.05-mm. material.)

effect in the case of tough-pitch copper and 70 : 30 brass. This type of curve serves as a guide for control purposes, but it must be realized that, in practice, a range of hardness values may be obtained with

material annealed to the same nominal grain-size. The degree of scatter in the hardness values, experienced when annealing to a particular grain-size, must be determined for the various types of furnace.

Other properties associated with subsequent processing or service may be influenced by grain-size. Too large a grain-size may result in fracture on pressing or give a rough surface after forming, thus involving extra polishing costs. Such service properties as creep, fatigue, and the tendency to season-cracking in brass are all influenced by grain-size. Morris <sup>7</sup> has

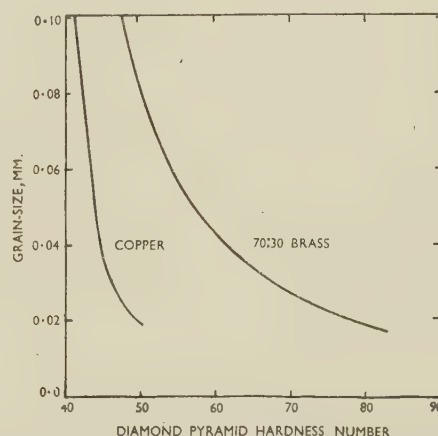


FIG. 5.—The Effect of Increasing Grain-Size on the Hardness of Tough-Pitch Copper and 70 : 30 Brass.

shown that 65 : 35 brass with 0.015 mm. grain-size is much more resistant to stress-corrosion failure in an ammonia atmosphere than material of 0.064 mm. grain-size, and Edmunds <sup>8</sup> has confirmed this relationship for 70 : 30 brass in both an ammonia atmosphere and mercurous nitrate. Burghoff and Blank,<sup>9,10</sup> who studied the effects of grain-size on the fatigue strength and creep strength of brasses, have shown that whereas creep strength increases, fatigue strength decreases with increasing grain-size.

## V.—INFLUENCE OF ANNEALING ON RE-CRYSTALLIZATION AND GRAIN GROWTH

When a cold-worked metal is heated at a suitable temperature for a time appropriate to that temperature, the metal softens, and as it softens several interesting phenomena occur. At least four well-defined and overlapping processes take place during these periods, namely : (i) recovery, (ii) nucleation, (iii) nucleus growth (sometimes called grain growth), and (iv) grain growth (sometimes called coalescence, or collective crystallization). In view of the lack of unanimity with regard to nomenclature, for the purpose of this paper recrystallization will be used to cover the stages of nucleation and nucleus growth, and grain growth will be used to refer to crystal growth which takes place after recrystallization.

## 1. RECOVERY

If a metal which has been cold worked is heated to a sufficiently high temperature for an appropriate length of time, certain changes in properties can be found before there is visible evidence of any structural changes. The metal gradually assumes properties more typical of the annealed state, and "recovery" has taken place. The rate at which the properties are restored increases with increase in temperature. The time lag between recovery and the appearance of structural changes varies from metal to metal.

## 2. RECRYSTALLIZATION

When a metal is cold worked, the crystal lattice is distorted and strains are set up. The residual strain energy in the lattice supplies the force for nucleation and nucleus growth. A minimum deformation appears to be necessary for recrystallization to take place, and the rate of nucleation decreases rapidly with decreasing deformation.

No exact relationship has been established between the critical amount of deformation and the ability to recrystallize. Anderson and Mehl<sup>11</sup> have pointed out that the probability of a nucleus appearing increases with increased annealing time. The critical strain is a function of the annealing conditions, and is defined as the strain necessary to provide the energy for a nucleus to appear in a given time. Thus, when cold deformation just exceeds the critical strain, the number of nuclei will be a minimum and the recrystallized grain-size will be a maximum. In practice, this means that for a standard annealing treatment, the smaller the deformation before annealing, the larger will be the recrystallized grain-size, within certain limits of deformation.

## 3. GRAIN GROWTH

The metal from production rarely has the as-recrystallized grain-size, because annealing treatments go on beyond the moment when the whole structure has just recrystallized. There is, therefore, almost always some grain growth. The average grain-size after annealing usually increases with increased annealing temperature and time, and the rate of grain growth is faster at fine grain-sizes. Grain growth occurs by migration of grain boundaries, and the driving force is provided by the interfacial energies of the grain boundaries. The presence of particles of a second phase hinders grain-boundary migration, and may limit the extent of grain growth, as is the case when  $\beta$  constituent forms round the grains of an  $\alpha$ -brass.

Recent work by Miekkoja<sup>12</sup> has shown that grain growth can also be strongly inhibited in 70 : 30 brass when the iron content is 0.007% or more, and the phosphorus content is in the range 0.002–0.019%. This work is in line with the continental practice, referred to by Jevons,<sup>13</sup> of adding 0.005% phosphorus to prevent excessive grain growth in 70 : 30 brass.

## VI.—THE COMBINED EFFECT OF COLD ROLLING AND ANNEALING

It is essential to note that cold working and annealing are interdependent processes. The purpose of annealing after cold working is either to produce a soft-finished product or to restore the workability of the metal for further reductions in thickness. In the case of brass, a partial anneal may be given to the hard-rolled metal in order to obtain a quarter-hard temper.

The relationship between grain-size and mechanical properties has already been outlined. The various controllable factors in the mill which influence grain-size are discussed below.

(i) *Prior Deformation.*—The recrystallization temperature is lowered with increasing amounts of cold work and the recrystallized grain-size is smaller. The final grain-size will, however, depend on the time and

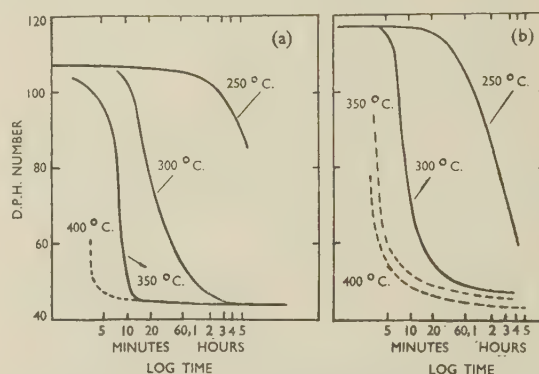


FIG. 6.—The Effect of Annealing Time and Temperature on the Hardness of Electrolytic Tough-Pitch Copper, Previously Cold Rolled to (a) 30% and (b) 50% Reduction.

temperature of the anneal. With short annealing times, heavier reductions tend to give smaller final grain-sizes with tough-pitch copper and 70 : 30 brass. With longer annealing times, the final grain-size of 70 : 30 brass is dependent more on the annealing temperature than on previous deformation, as grain growth has time to become effective. In the case of tough-pitch copper, the rate of grain growth is not so high, and it is insufficient to overcome the refinement occurring immediately on recrystallization. These considerations can be of practical significance in the mill, depending on the subsequent annealing conditions, as previous reductions may vary considerably.

(ii) *Initial Grain-Size.*—A fine initial grain-size results in a greater degree of work-hardening for any given reduction, leading to a lower recrystallization temperature and a finer recrystallized structure.

(iii) *Time and Temperature of Annealing.*—In works practice annealing conditions may be varied either by raising the temperature and decreasing the time, or vice versa. This relationship between time and temperature is illustrated in Figs. 6 and 7. Fig. 6 shows how the hardness of electrolytic tough-pitch copper decreases with increase of annealing time, at



temperatures of 250°–400° C. Fig. 7 shows the decrease in hardness occurring when 70 : 30 brass is annealed for increasing lengths of time at 300°–500° C.

It can be observed from Fig. 6 that at practicable annealing temperatures (say 350° C. and upwards) the softening of copper is almost instantaneous, and it becomes impossible to anneal copper partially, to produce various temper ranges. At the lower temperatures, where the annealing time is very long, it may be possible to anneal copper partially if the temperature is very closely controlled and the grain-size and degree of cold work in the metal are kept within narrow limits. Partial annealing of copper, however, is not considered practicable on an industrial scale, and the various tempers of copper required are produced by appropriate cold reduction after full annealing.

The situation is somewhat different in the case of the brasses (see Fig. 7 for 70 : 30 brass), as the rate of

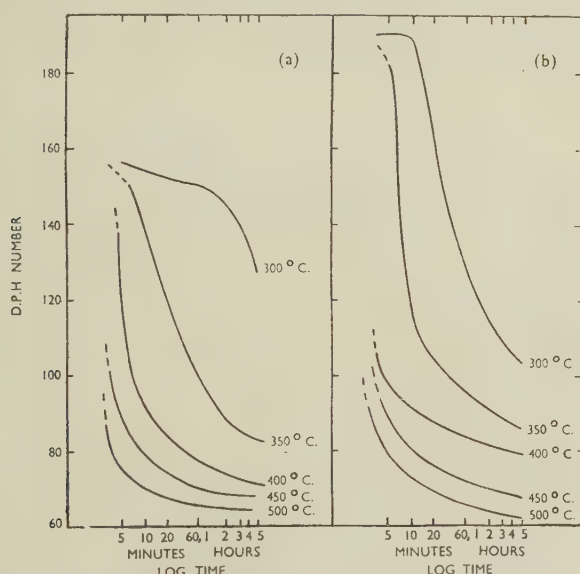


FIG. 7.—The Effect of Annealing Time and Temperature on the Hardness of 70 : 30 Brass, Previously Cold Rolled to (a) 30%, and (b) 50% Reduction.

fall in hardness is more gradual at 350°–400° C. The degree of previous cold work has an effect on the shape of the softening curves, but provided that the reduction before annealing is kept within reasonable limits, partial annealing of brass is a practicable proposition. The quarter-hard temper for brass can be consistently produced by partially annealing the hard-rolled metal.

Although the recrystallized grain-size is almost independent of the annealing temperature, the final grain-size depends upon the time/temperature relationship after recrystallization occurs. In many copper-base alloys, grain growth is very rapid in the range of ordinary annealing cycles, with the result that annealing conditions have a more pronounced effect on the final grain-size than has the amount of cold work before annealing.

Y

## VII.—DIRECTIONALITY

There are two types of directionality, namely, mechanical and crystallographic. The mechanical directionality results from the fibring of inclusions or of a second phase (e.g. cuprous oxide in tough-pitch copper or  $\beta$ -constituent in low-copper brasses). Crystallographic directionality occurs as the result of alignment of the crystallographic axes of grains in definite relationship to the direction of rolling. Such preferred orientation of the crystals is generally most undesirable, particularly where the sheet is to be used for deep drawing. There are, however, a few occasions where maximum directionality is demanded.

The factors which control the degree of preferred orientation have been examined in considerable detail by Cook and Richards<sup>14, 15</sup> and more recently by Baldwin.<sup>16</sup> The principal factors are the amounts of reduction between anneals, particularly at the ready-to-finish and final stages, and the annealing temperatures. These two factors are related in a complex way, but the following generalizations may be made for copper and brass :

- (a) Reductions less than 50% give no directionality.
- (b) Reductions between 25% and 50% help to remove existing directionality in the case of copper.
- (c) A relatively high ready-to-finish anneal and a low final anneal reduce the degree of directionality. The high ready-to-finish anneal provides a relatively large grain-size, which is less likely to give directionality than a fine grain-size.
- (d) Rolling fine-grained annealed material promotes directionality.
- (e) No significant contributions are made to directionality by the rolling procedure. The type of mill, the speed of rolling, and the reduction per pass, do not appear to offer any controllable variable.
- (f) Reverse rolling has no effect on preferred orientation; cross-rolling does have an effect, but the very limited extent to which it is practised does not help in normal production routine.

## VIII.—CONTROL DURING COLD ROLLING

### 1. GENERAL CONSIDERATIONS

The cold-rolling operations must be controlled so that strip or sheet of good shape is produced with a specified accuracy of gauge and temper.

Good shape means that the sheet or strip is free from edgewise bow, wavy or over-rolled edges, or an over-rolled middle. Assuming that the sheet or strip entering the cold-rolling mills is of uniform gauge, good shape is produced only when the roll gap is constant across the whole width of the metal being rolled. In the case of a narrow two-high mill, the roll deflection is small, even at the relatively high mill loads used for heavy reductions. This small deflection, caused at a given roll force, is countered by machining a corresponding camber on the rolls, and it will be apparent that for any particular entry thickness, there

is only one reduction in thickness that results in uniform gauge across the width. If too high a reduction is attempted, the optimum roll force is exceeded, and the rolls deflected and flattened so that the edge of the sheet or strip is wavy or over-rolled, and of lower gauge than the centre. On narrow mills, strip of good shape can be produced even when reductions vary considerably from the optimum reduction for the given entry thickness.

In the case of wide two-high mills, heavy reductions inevitably mean large roll deflections if rolls of a practical diameter are employed. A heavy corrective camber must be employed, and any variations from the optimum roll force for good shape cause more trouble than in the case of the narrow mills. Carefully planned reduction schedules are therefore particularly necessary on wide two-high mills. Where reductions are less than 20% per pass, as is generally the case in temper-rolling, two-high mills are very useful. They have the added advantage that a high polish on the rolls can be maintained more easily than on mills with backing rolls.

In general, four-high mills are able to produce strip or sheet of good shape, under a wider range of rolling conditions. The small-diameter work rolls result in lower rolling loads, because, for the same roll pressure, the contact area is less. Power losses due to frictional effects are also decreased.

The deflection of the work rolls is very small, as support is given by the large backing rolls, and if any camber is employed it is very small. This camber serves to counter effects of roll flattening. It will be seen that relatively large variations in roll force can be tolerated on the four-high mill, without very serious effects on the degree of roll distortion. Strip of good shape can, therefore, be produced over a wider range of reductions for any particular entry gauge. In general, the advantages of the four-high mill, as compared with the two-high mill, increase as the ratio of strip width to strip thickness increases.

It should be noted that an entry strip with a gauge variation across the width can give rise to unusual effects, for the outcoming strip may have uniform gauge across the width but be of poor shape.

Edgewise bow is countered by maintaining the rolls parallel to one another, and in the case of strip by applying a suitable tension from the coiler.

Another type of mill which enables good shape to be maintained, even with heavy reductions on wide strip, is the Sendzimir mill, a high-speed reversing type which makes use of high coiling tension and small, heavily backed, working rolls. As with the four-high mills, gauge variation across the width of the ingoing strip must be a minimum.

The basic need for gauge control is to meet the requirements of standard specifications. However, with the continued development of mass-production methods, customers often demand material to even closer tolerances.

Gauge control across the width of sheet and strip has been considered above. With regard to control

of gauge along the length in the strip-rolling process, factors other than roll distortion must be considered. These factors may be enumerated as follows:

(i) The rolls must be accurately machined so that they are free from eccentricity.

(ii) Rolling-speed variations affect the gauge, as during periods of acceleration and deceleration, other factors remaining constant, off-gauge material is produced. The percentage of off-gauge material is diminished by the use of mills with high rates of acceleration and by running long coils. Where control of gauge, during acceleration and deceleration, is made by adjusting the screw-down, it is necessary to employ relatively slow rates of acceleration, so that the operator has time to make compensatory adjustments. In the case of mills fitted with a variable-speed motor, it may well be expedient to employ a relatively low maximum rolling speed during the early passes, and to increase it only as the length of the coil becomes greater. Many theories have been put forward to account for the effect of speed on the gauge produced, but it is beyond the scope of this paper to consider them in detail. Critical reviews of the literature have been made recently by Ford<sup>17</sup> and by Polakowski.<sup>18</sup> The latter makes the generalization that, all other conditions being equal, a four-high mill is more prone to produce off-gauge material during acceleration and deceleration than is a comparable two-high mill; that an hydraulically loaded mill is most sensitive to speed changes; and that in this case speed variation may be used for gauge correction in foil manufacture. Ford suggests that the effects of mill-speed variations are diminished by the use of high strip tensions.

(iii) The frictional conditions at the rolls must be maintained at a uniform level. A decrease in the frictional effects will result in a lower roll force being required for any particular reduction, and thus if the mill is not reset, low-gauge strip will be produced. Variations in the frictional conditions may be caused by an irregular supply of rolling lubricant, and by variations in the surface characteristics of the incoming strip. An effective and uniform degree of pickling is thus required after annealing and before rolling. Oxidized patches, if present, lead to gauge irregularities. Variations in the gauge of the incoming strip also result in changed conditions, and unless corrective action is applied, the variations are reflected in the finished material.

(iv) The degree of back or front tension can affect the gauge of strip being rolled under otherwise set conditions. Increased strip tension causes a decrease in the roll force required to achieve any given reduction and, as will be seen later, forms the basis for one method of gauge control. Automatic regulation of strip tension is practised and allows for coil build-up on the reel. This may be achieved electrically or hydraulically, and the decoiler can also be arranged as a drag-generator to control the back tension in the strip.

(v) Temperature changes in the rolls can affect



gauge. If roll cooling is efficient, little trouble should be experienced, however.

(vi) The elastic constant of a mill may result in the mill being sensitive, or otherwise, to changes in various other variables. According to Polakowski,<sup>18</sup> a mill with a low elastic constant is more sensitive to changes of rolling speed than one with a high elastic constant, and is more likely to produce off-gauge strip. For the same reason steel rolls, which have a high elastic constant compared with cast iron, are less speed-sensitive.

Efforts have been made to eliminate the spring effects in the mill housings by pre-stressing them to an extent greater than the roll pressure required for any particular reduction, but considerable further experimentation is required.

It will be seen from the above considerations that the gauge of strip produced can be affected by many variables, certain of which can be controlled to correct the bad effect of others. Before the corrections can be applied, some method of gauge measurement is required, and this may be carried out directly or deduced from measurement of the roll force.

## 2. METHODS OF GAUGE MEASUREMENT

On modern high-speed mills it is impossible to use hand micrometers, and some form of continuous measurement is required. Some of the systems employed are:

(a) Electrical systems in which the metal passes between an energized coil and a detector head, and variations in strip thickness result in a change in the output signal. This method has the advantage that there is no physical contact with the strip, and it may be used for gauging foil. It is, however, sensitive to temperature and to changes of alloy composition.

(b) Mechanical types in which there is actual roller contact on the strip. These systems are quite accurate when fairly high strip tensions are employed, and they are widely used. Their percentage accuracy decreases when used on foils, and the roller may cause marking or damage to the strip.

(c) X-ray gauges synchronized with the mill screw-down are employed, particularly in the U.S.A., but the installation tends to be expensive. The gauges rely on the degree of absorption of X-rays by the metal, and the sensitivity may be adjusted to suit the gauge of strip being measured.

(d)  $\beta$ -ray absorption gauges are becoming more popular for use with foils and strip less than about 0.020 in. in thickness. Isotopes are available for a higher range up to 0.035 in. They have the advantage that both the source of radiation and the detector are small, and can normally be accommodated without large modifications to the mill table. The particular isotope employed depends on the range of gauges to be measured, and its useful life may vary from 1 to 10 years. This method may be comparative with respect to a selected standard, or the instrument may be calibrated directly for particular alloys. The sensi-

tivity can be controlled so that high percentage accuracies can be obtained even for foils.

(e) The use of  $\gamma$ -radiation is probably limited to the gauging of quite heavy material, but might find application in the hot-rolling process.

## 3. METHODS AVAILABLE FOR GAUGE CONTROL

Gauge control in sheet rolling is effected by measuring with a hand micrometer, and adjusting the screw-down as necessary.

Manual control of screw-down is still widely practised in strip rolling, but is tending to become inadequate as the speed of rolling increases. The method generally employed is for the operator to control the screw-down mechanism of the mill by reference to the outgoing gauge of strip, as indicated by one of the above-mentioned instruments. The limitations of this method are obvious. The gauge indicator is necessarily on the exit side of the mill, which means that a length of off-gauge strip has already been produced before any indication is given to the operator. The operator's reaction time should be small, but in any event it becomes significant at high rolling speeds. The above system is quite widely employed, however, and is capable of producing strip to very close tolerances at speeds of at least 300 ft./min.

A photograph of a "Flying Mike" micrometer installed on a strip mill, and used for manual gauge control by varying the screw-down, is shown in Fig. 10 (Plate XLVI).

Considerable thought has been given to the subject of automatic gauge control, and a review of various methods has been made by Hessenberg and Sims.<sup>19</sup> They refer to one method in which the back tension is varied by a hydraulic brake on the decoiler. The degree of braking applied is altered by using the amplified output of an electrical strip-thickness gauge. A second method, due to Blain, makes use of a direct measurement of the distance between the rolls, and any variations are automatically corrected by a hydraulic cylinder between the chocks and the mill frame. A third method, developed by E. Meyer, varies the roll setting hydraulically, depending on changes occurring in the roll load.

Hessenberg and Sims also describe two additional methods of gauge control which do not depend on direct measurement of strip gauge, but on continuous measurement of roll force. They call the first of these methods the tension method and this, as its name suggests, is applicable only to cold rolling. If the roll setting remains constant, the thickness of the outgoing strip bears a direct relationship to the roll force. By controlling strip tension the roll force can be kept constant and hence also the gauge of the strip. In practice, load cells are used to indicate the roll force, and the operator adjusts the tension to maintain a constant roll force.

Although there are practical limits to the maximum tension which can be applied without damage to the strip, the variations in tension that would be required

are likely to be within these limits if gauge control has been exercised at all stages. The second method is referred to as the predetermined setting method, and is applicable to hot or cold rolling of sheet and strip. Tension control is not required, and the gauge is controlled by alterations to the screw-down mechanism. The degree of alteration depends upon the elastic characteristic of the mill, and since this varies from mill to mill, it is essential to predetermine the roll setting which will give the roll force necessary to yield the correct gauge. The roll force is again measured by load cells placed between the screws and the roll chocks.

The above two methods would seem to have the advantage that they correct gauge variations caused by changes in the gauge and quality of ingoing metal, and by changes in the frictional conditions in the roll gaps. They are, therefore, able to counter the effects of poor ingoing gauge, temperature variations in hot rolling, temper variations in cold rolling, speed effects in cold strip rolling, and variations in conditions of lubrication. They also lend themselves to automatic as well as manual control.

#### 4. LUBRICATION AND ROLL COOLING

As roll force changes with varying frictional conditions in the roll gap, it is important that lubricating conditions are kept constant. Not only must the supply of lubricant be constant, but the surface of the sheet or strip must be clean to permit even spread of the lubricant. Where the lubricant is also required to act as a coolant, a flood lubricant system is employed, using water with a special soluble oil. In this case it is important that the coolant be settled or filtered before recirculation, so that no foreign particles are brought on to the roll face or stock. Care should be taken to see that no heavy mineral oil pick-up from the mill occurs, as this can give rise to subsequent staining on annealing.

The function of a roll coolant is not primarily to keep the rolls cold, but to maintain a constant level of temperature across the face of the rolls. If this is not done, the roll shape may vary and result in strip of bad shape or poor gauge.

The effects of various types of lubricants on staining are discussed in Sections IX and XI.

#### 5. TEMPER-ROLLING

This is a relatively simple process provided that adequate control has been exercised in preceding operations. If the ready-to-finish grain-size is uniform and the gauge consistent, a prescribed reduction can be made with the certainty of producing the required temper. In temper-rolling, reductions are usually relatively small and polished rolls are generally used to impart a high surface finish.

Gauge control becomes more important as the thickness of the metal to be temper-rolled decreases, since the range of reductions which will give the required temper becomes increasingly small, particu-

larly in the case of quarter-hard material. It is often more convenient to produce thin-gauge quarter-hard brass by partially annealing hard-rolled metal.

### IX.—CONTROL DURING ANNEALING

#### 1. GENERAL CONSIDERATIONS

Many types of furnaces are used for annealing copper and copper alloys. They may be generally classified as batch and continuous, and sub-classified according to the furnace atmosphere and source of heat. Nowadays, it is usual to find electric furnaces employed in the final annealing processes, but gas-fired and oil-fired furnaces are often used for interstage annealing.

Every furnace must be calibrated for each type of material to be handled and for typical weights of charges. The method in which the charge is stacked and the wall thickness of coils must be taken into account in calibration. Another factor of practical significance is the tightness with which a coil is wound. In the case of a semi-continuous furnace, where coils are heated principally by radiation, shorter times are required for tightly wound thin-gauge material than for heavier gauges which have had a comparable degree of cold work. There are economic limits to the weight of coil that can be annealed in this type of furnace, as, unless the rate of heating is very slow, the outer laps of the coil may be over-annealed before the centre has completely recrystallized. For initially heavy or welded coils, better control is achieved with continuous strip-annealing furnaces.

Generally the work being annealed never reaches the nominal furnace temperature, so that there is a "temperature head". This thermal head varies considerably with the type of furnace, usually being fairly low for batch-type furnaces with forced-gas circulation and high for continuous types. The annealing time, which comprises the time to bring the charge to temperature and the time required to attain the requisite grain-size, is affected by the weight of the charge. The rate of heating as experienced in ordinary industrial equipment has little effect on the grain-size of the work, but uniformity of heating is of great importance, and hence forced-circulation furnaces are very popular.

Annealing schedules are constructed from the furnace-calibration experiments, and the successful application of these schedules depends upon the accurate control of furnace temperatures and atmospheres.

#### 2. FURNACE TEMPERATURE

It is not really the temperature of the furnace that requires control, but the temperature of the charge. As it is simpler to control the furnace temperature directly, rather than that of the charge, it is deduced by calibration that a certain nominal furnace temperature gives a reliable indication of the temperature of the charge, under known conditions. To maintain



temperature control we require: (i) a means of measuring temperature correctly over a reasonable range, and (ii) a means of adjusting the temperature.

The primary elements in the measuring devices are thermocouples, and these must be located in a protected position, close to the furnace structure, to avoid damage. Obviously during some stages of the heating cycle the indicated temperature will be very different from the actual temperature of the charge, but the lag is a known characteristic for each furnace, and time becomes the control factor. The electromotive force from the thermocouples is used to operate a temperature indicator, a recorder, and/or a control mechanism. Details of temperature-control devices are outside the scope of this paper, but the following points must be made: the devices should be subject to regular checking, and some visible or audible warning should be arranged in case a thermocouple breaks down. Electric furnaces are always fitted with automatic temperature-control devices, as are the majority of fuel-fired furnaces.

### 3. FURNACE ATMOSPHERE

Control of furnace atmosphere is required to control the surface quality of the annealed material and, in the case of tough-pitch copper, to prevent hydrogen embrittlement during annealing. There are two kinds of atmospheres, namely: natural or combustion atmospheres, and artificially produced atmospheres. The natural atmosphere consists of the products of combustion of the heating fuel, and is of importance only where there is no muffle to shield the work. In such cases, control is exercised by a flue-gas analyser, and consequent proportioning of the air/gas mixtures.

Theoretical considerations involved in atmosphere control have been discussed at length by Jenkins,<sup>20</sup> but an outline of requirements in the case of copper and brass is given below.

Artificial atmospheres are normally produced by burning a nitrogen/hydrogen mixture, obtained by cracking ammonia, or by partially burning ordinary town-gas. The products of combustion after burning cracked ammonia are cooled to approximately 20° C., to give a nominal gas composition of 3% hydrogen, balance nitrogen, saturated with water vapour at 20° C. The nominal gas composition for a partially burnt town-gas atmosphere would be 10–12% carbon dioxide, 1% carbon monoxide, 0.6% hydrogen, balance nitrogen, saturated with water vapour at approximately 20° C.

Whether the atmosphere is produced by partially burning cracked ammonia or town-gas, careful control must be exercised. The control limits vary considerably, however, depending on the type of copper or alloy to be annealed.

Atmospheres must be completely free of oxygen when employed in the bright annealing of all types of copper. To achieve this condition in practice, it is normal to adjust the air/gas ratio entering the generator so that some small amount of hydrogen (or

hydrogen plus carbon monoxide) remains unburnt, and a gas slightly reducing in character is produced.

In the case of a regenerative burnt cracked-ammonia gas plant supplying bell-type furnaces, an excess of hydrogen, upwards from 2%, may be maintained, the balance being nitrogen. If oxygen-free or phosphorus-deoxidized copper is to be annealed, high hydrogen contents can be carried, but would normally not be allowed to rise above 5% for economic and safety considerations. In the case of tough-pitch copper, which contains 0.015–0.05% oxygen, embrittlement is likely to occur on annealing in atmospheres containing much over 4% hydrogen. The actual maximum which can be tolerated decreases as the annealing temperature and time increase, and as the amount of contaminating lubricant on the stock being annealed increases.

A working figure of 2–3% hydrogen, balance nitrogen, has been found satisfactory for annealing tough-pitch copper under a variety of conditions up to temperatures of 550° C., even in the presence of a normal amount of rolling lubricant. Where copper charges vary considerably in type, it is best to set control limits for the gas-generating plant to suit the most stringent conditions likely to be encountered for tough-pitch copper.

Similar considerations hold in the case of a partially burnt town-gas generator when copper is being annealed. This type of atmosphere, however, is controlled by reference to "percentage combustibles" (hydrogen, carbon monoxide, hydrocarbons) remaining in the gas after combustion. The "percentage combustibles", for gas being supplied to a bell-type furnace, would be maintained between 1.3 and 2.0%. The hydrogen content corresponding to this degree of combustion is about 0.6–0.8%; this, it will be noticed, is considerably lower than in the previous case of a burnt cracked-ammonia atmosphere. The presence of carbonaceous gases appears to aggravate the embrittlement by hydrogen.

Although the atmosphere has been produced in such a way that no oxygen should be present, minute traces may occur owing to incomplete combustion. In the case of a burnt cracked-ammonia generator, combustion occurs at heated copper-palladium and copper gauzes, and no oxygen will be present if these are in good order. So far as burnt town gas is concerned, efficient combustion is normally obtained by burning in a refractory-lined chamber in order to obtain a high temperature. However, should oxygen be in the prepared atmosphere, even in amounts undetectable by means of the Orsat apparatus, annealed copper will not be produced with a really bright finish. Oxidation can take place particularly on cooling, owing to trace amounts of oxygen which can be detected by passing a sample stream of gas from the furnace chamber over a copper strip, heated to a low temperature, and enclosed in a Pyrex tube visible to the operator.

Associated with proper combustion is the problem of sulphur removal from town gas. Sulphur burnt

to sulphur dioxide is almost completely removed in the water-cooling chamber, and any remaining is most unlikely to cause staining. Some hydrogen sulphide is present in the burnt gas, and is removed by passing the gas over bog iron ore and/or activated carbon. Details of the size of the bog-ore box required to handle given rates of gas flow have been given by de Coriolis and Lehrer,<sup>21</sup> but whatever size of bog-ore or activated-carbon box is used, it is essential that these media be frequently tested for efficacy.

Gas analyses may be carried out manually by means of the Orsat apparatus, by an automatic Orsat-type instrument, or by a Katharometric instrument. Whichever method is employed, the actual plant control is normally manual. Bradley and Hammond,<sup>22</sup> however, have reported a completely automatic system of atmosphere control in which town gas is burnt to provide an atmosphere containing  $0.5 \pm 0.1\%$  unburnt gases. The presence of sulphur in the form of hydrogen sulphide can be detected by passing the gas sample through a lead acetate, or cadmium chloride, solution.

Very small amounts of hydrogen sulphide show themselves as stains on the outcoming work. These stains may be distinguished from similar blue oxidation stains, as they are insoluble in dilute sulphuric acid, but readily soluble in potassium cyanide.

Assuming that a satisfactory atmosphere is available, it can be used on continuous- or batch-type furnaces. When used with continuous furnaces, it is imperative that no leakage of air into the furnace chamber occurs. On a bell-type batch furnace, very slight leaks can be quite troublesome, as leakage of gas occurs during the heating-up period, resulting in waste; moreover, entry of air is facilitated during the cooling-down period, particularly if the water sprays are applied too vigorously, and causes a reduced pressure in the container. In purging a batch-type furnace, it is normal to allow a total gas flow of 4-5 times the capacity of the bell-cover before heating is begun. The gas flow is left on until the maximum annealing temperature is reached to assist in the removal of rolling lubricants. It is then shut off, and the hearth left under gas pressure of about 3-4 in. W.G., until annealing is completed and the charge cooled to a temperature low enough to permit the removal of the cover without subsequent oxidation of the metal.

Excessive quantities of rolling lubricant may give rise to surface discoloration, or staining, when the stock is annealed in batch-type bell or pit furnaces. This is noticed when a high initial heating rate is employed in the annealing cycle, and insufficient time is allowed for the oil to volatilize before its cracking temperature is reached. In extreme cases, oily tough-pitch copper charges can be embrittled in a controlled atmosphere which under normal conditions would be satisfactory. Stock ready for annealing should be as free from oil as is practicable. If the material tends to be oily, a slow heating rate should be employed up to about 250° C., and the

protective atmosphere allowed to circulate to clear the carbonaceous fume away. The time required to disperse the oil depends on the volume of the furnace cover and the rate of gas circulation, but is usually of the order of  $\frac{1}{2}$  hr. in the range 200°-250° C. After this period, the heating rate can be increased and the charge taken to its full annealing temperature.

Fig. 8 shows the type of heating cycle which may be employed if any oily charge has to be annealed.

On a correctly run plant the surface of copper charges is bright and retains the high degree of finish normally imparted by the final rolling operation. Bright annealing of the common brasses is not possible, as zinc oxidizes in the presence of hot carbon dioxide or water vapour. At a relatively low annealing temperature, it is possible to obtain brass in coil form

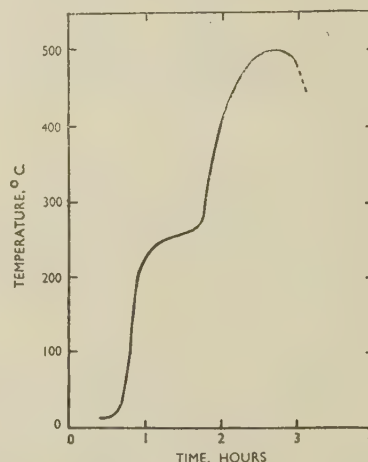


Fig. 8.—Typical Heating Cycle When an Oily Copper Charge Has to be Annealed. (145-kW. bell furnace. Charge weight 3300 lb. in coils.)

with a moderately bright surface in a cracked-ammonia atmosphere, but at normal annealing temperatures of 500°-550° C., a dull surface is obtained, particularly at the edges of coils. Where sheets are concerned, the whole surface is exposed to the atmosphere, and though dull, it is readily cleaned by pickling. This final operation of pickling may not be disadvantageous, particularly when the product is for deep drawing, as the matt surface helps to ensure even lubrication during pressing.

## X.—CONTROL OF PICKLING

The pickling bath itself should never be the direct cause of trouble, particularly where the pickling liquors are circulated through an acid regenerating system. Control of composition of the pickling liquor is exercised by controlling the current passed through the electrolytic recovery plant, and by varying the amount of solution passed through the cells. The copper content of the solution, in the case of a cold pickling system, is maintained at 8-12 g./l. and the acid at 50-100 g./l. The removal of copper by means of the electrolytic cell automatically regenerates an



equivalent amount of sulphuric acid, with the result that acid additions are necessary only to compensate drag-out losses. Both copper and brass are pickled in liquors of the above composition. The pickling bath may be kept at room temperature or heated to about 50° C. Aeration of the pickling solution and the addition of wetting agents is often practised to improve pickling.

Special forms of pickling are sometimes used to give a particular surface finish, or to facilitate the removal of red stain on brass and cuprous oxide from copper. Such methods include electrolytic pickling and the use of baths containing additions of oxidizing agents such as ferric sulphate, or potassium or sodium dichromate. A typical addition to the normal bath would be about 30 g./l. of sodium dichromate, or about 80 g./l. ferric sulphate. Prolonged immersion in these solutions gives undesirable etching of the surface. Pickling solutions should be sampled and analysed daily.

Continuous pickling at fairly high speeds is improved by the use of high-pressure acid sprays instead of direct immersion. Whatever kind of pickling is used, efficient washing and drying must follow to prevent water staining.

## XI.—CONTROL OF SURFACE QUALITY

### 1. GENERAL CONSIDERATIONS

It is not surprising that as there is no general adequate definition of surface quality, there is no standard for this important property of metals. A sample cut from a sheet is reasonably representative of mechanical and physical properties, but the same could not be said of surface quality. Odd spills, blisters, scratches, indentations, stains, or roll marks may occur at random, and may be missing from, or concentrated on, the sample.

Visual examination is the primary method of assessing the surface quality of the sheet. This may be supplemented by bending, polishing, etching, plating, bronzing, or metallographic examination, but, by and large, the bulk of material is passed, or failed, on visual examination. The standard imposed upon inspection is dependent upon the end-use. It is obvious that a surface which may be good enough for roofing copper, will not be suitable for photo-engraving, or even for plating. It can be said that no cold-rolled material should leave the mill unless it is free from blisters, spills, rolled-in oxide, or dirt, and indentations including scratches, or roll marks. Whether the surface is brilliantly lustrous or matt is a question of end-use. Usually a mirror finish aids inspection, because of the ease with which the slightest blemish can be observed. Its attractive appearance has appreciable sales value.

The objective of the producer in relation to surface quality is to try to control his rolling, annealing, pickling, washing, and handling processes, so that the finished material is free from the above-mentioned defects.

Surface troubles which arise from ingot metal, such as blisters, spills, and foreign inclusions, are rare. Defects directly associated with rolling may be roll-marks, rolled-in particles, or pitting.

### 2. DEFECTS ASSOCIATED WITH ROLLING

(a) Roll marks can be avoided by regular inspection of the surface of the rolls and the replacement of any found to be at fault.

(b) Rolled-in particles may be either oxide which has been left as the result of bad pickling or dirt which has been picked up during handling, or which has fallen on the sheet during rolling. The preventive remedy in either case is obvious. Improved pickling or scalping prevents oxide from being present to roll in, and better interstage handling should prevent dirt from being worked into the surface of the metal. The casual dirt found in the air of a rolling mill has little effect when the sheet or strip passes through pads before entering the rolls. The importance of keeping the pads clean cannot be too greatly emphasized.

(c) Pits and indentations arise from the removal of rolled-in particles by pickling or other means.

### 3. DEFECTS ASSOCIATED WITH PICKLING

The inadequate removal of oxide, the etching of the surface of the metal, and development of red stains on brass are the most serious troubles to be encountered in the pickling shop.

(a) Inadequate removal of oxide may be due to the metal not being left sufficiently long in pickle, or else to faulty batch pickling in which one sheet rests so heavily on another that the pickling liquor is excluded.

(b) Etching of the surface may occur if the metal is left too long in pickle, or if the acid strength of the bath is too high.

(c) Red stains on brass. The scale on brass comprises zinc oxide, cuprous oxide, and cupric oxide, and red staining is associated with the presence of cuprous oxide, which reacts with the sulphuric acid in the bath to leave copper. The actual presence of cuprous oxide alone forms another type of red stain.

The incidence of red staining may be greatly minimized by care before and during annealing. Rolled-in oxide should be prevented, and the presence of excessive quantities of oil should be kept to a minimum. Any factors, e.g. greasy marks, chalk marks, &c., which mask part of the sheet may contribute to red staining by preventing complete surface oxidation, so that these partly shielded areas are rich in cuprous oxide when they enter the pickle. Red staining of brass can generally be eliminated by using less viscous oils of high volatility.

### 4. STAINING

A blue-coloured oxide stain on nominally bright-annealed copper may be due to oxygen in the protective atmosphere, to oxygen leakage into the furnace chamber, or to too high a discharge temperature after annealing. Too-rapid cooling in a bell-type furnace,

by the sudden application of the cooling water, may break the water seals and cause air to be sucked in at a temperature high enough to result in oxidation of copper. A discharge temperature of about 50° C. prevents oxidation of the copper after removal of the furnace cover.

Staining on annealing, if not due to oxidation, can usually be traced to alkali or sulphur additives incorporated in the lubricants. Sooting or the formation of a sticky deposit due to decomposition of the lubricant at temperature in the reducing atmosphere may also occur. Chisholm<sup>23</sup> states that rolling oils should have a low and narrow boiling range, and that sulphur contents should be less than 0.5% in order to avoid staining.

Certain materials, such as iron, catalyse the decomposition of lubricants, whereas copper and aluminium do not, and it has been claimed that staining due to lubricants can be avoided by spraying the interior of the furnace container with copper or aluminium.<sup>24</sup>

In general, the lighter oils of high volatility are used in the later stages of reduction by rolling, and this tends to ease the problem of staining on finished work. As has been mentioned previously, a gradual increase of temperature during annealing, with an adequate degree of purging during the warming-up period, minimizes staining. Removal of excessive quantities of oil vapours can also be effected by the use of steam in batch-type furnaces, though conventional controlled atmospheres would be employed during the early stages of heating and the later stages of cooling to avoid water staining. In continuous furnaces it is advantageous to have the direction of gas flow opposite to that of the furnace stock, so that oil vapours come into contact only with the relatively cold incoming metal.

Water staining after pickling is kept to a very low level by passing the sheet or strip through squeegee-rolls, immediately after a hot-water dip, and before entry into the drying unit. The rubber rolls of the squeegee unit must be maintained in good order, so that only the thinnest of water films remains on the metal. Compressed-air jets may be used to achieve a similar result. The drying unit normally consists of a metal box through which warm air is circulated, and the temperature and humidity can be controlled by varying the proportion of fresh air intake to that being recirculated.

In the case of dry-discharge continuous furnaces equipped with controlled atmospheres, the temperature in the externally water-cooled zone must not be allowed to fall below the dew point of the protective atmosphere.

## XII.—TESTING AND INSPECTION

### 1. GENERAL CONSIDERATIONS

It will be apparent from the above considerations of the factors which affect the structure and properties of rolled copper and its alloys, that inspection and testing must be carried out throughout their pro-

duction. There are three major stages in the overall control system.

The first is the general servicing and maintenance of all instruments on which the production metallurgist relies to follow production schedules. This involves the regular testing of temperature regulators and indicators by means of standard thermocouples and/or a potentiometer, and their general cleaning and overhaul. Automatic gas analysers are checked with reference to chemical estimations made by the laboratory, and automatic gauging devices are checked against standard test-pieces.

The second aspect involves interstage testing, which is generally carried out in test-houses in the various mills operating without reference to the central laboratories. These test-houses are used for checking the structure and properties of the metal at various intermediate stages. Testing the effectiveness of annealing, as represented by hardness and grain-size, forms a major part of their work.

The final stage of control is the inspection and testing carried out by the main laboratories and inspection department.

## 2. METHODS OF TESTING AND INSPECTION

### (a) Sampling

Samples are selected in accordance with practice laid down by the governing Standards Institution.

### (b) Analytical

The detailed analysis of the final product can be found by reference to the route card, but since such detail is more than is required for meeting a specification, only the analysis required by the inspection authority is carried out on the final test-pieces. Notes on typical methods of analyses are given in Table I.

### (c) Mechanical Testing

The general mechanical tests made are ultimate tensile strength, percentage elongation, hardness, and bend tests, and often cupping tests.

In the case of copper free from oxygen, bend tests are carried out after the samples have been heated for  $\frac{1}{2}$  hr. at 850° C. in hydrogen. The methods of carrying out these tests are so well known that no elaboration is necessary here.

### (d) Physical Testing

Physical tests comprise: metallographic examination of tough-pitch copper for oxygen content and of 63:37 brass for  $\beta$  constituent, grain-size determinations, and examinations for the degree of directionality. Although X-ray methods for determining directionality are well established,<sup>14</sup> many producers of copper and copper-base alloys still rely on simple mechanical or metallographic techniques. Testing for directionality has been dealt with in detail by Jevons<sup>13</sup> and others, but special mention may perhaps be made of a useful quick laboratory test with the Hounsfield



tensometer. A cupping test is involved, the load at which rupture occurs being measured and related to the thickness of the strip being tested. For a wide range of gauges the load : gauge ratio remains constant

TABLE I.—Notes on the Typical Methods of Analysis Used for Copper and the Straight Brasses.

Material	Elements	Notes on Analytical Method Employed
H.C. Copper	Sulphur	Reduction in hydrogen stream at 900° C. Subsequent estimation of cadmium sulphide using iodine.
	Oxygen	Reduction in hydrogen at 900° C., and absorption of H <sub>2</sub> O evolved in magnesium perchlorate anhydrous.
	Iron	Visual colorimetric estimation, using ferric thiocyanate.
	Bismuth	Visual colorimetric estimation, using thiourea.
Phosphorus-deoxidized copper	Phosphorus	Spekker colorimetric estimation. Reduction of phosphomolybdate with stannous chloride.
Straight brasses	Copper	Volumetric estimation with sodium thiosulphate, or electrolytically.
	Tin	Separation with iron, reduce with nickel, and titrate with iodine.
	Lead	Electrolytic method.
	Iron	As for H.C. copper.
	Phosphorus	As for phosphorus-deoxidized copper.
Copper and brass	General impurities	Spectrographic estimation, using the Hilger medium quartz instrument or direct-reading spectrograph.

for material free from directionality, but a significant drop in the ratio indicates the presence of directional properties.

A useful metallographic technique for the degree of directionality in copper has been described by Baldwin.<sup>16</sup> It involves etching a polished specimen in an acidic aqueous solution of ferric chloride or an aqueous solution of ammonium persulphate. The grains which are cubically aligned remain white, and those of other orientations appear black. This method can be used for estimating quantitatively the percentage of cubically aligned grains in the microstructure. Fig. 11 (Plate LXVI) gives a comparison between photomicrographs of a piece of non-directional copper strip and a piece of highly directional copper strip, both of which had been etched in ferric chloride. The load : gauge ratio for the non-directional strip was 51,000 lb./in. as compared with a value of 25,000 lb./in. for the highly-directional strip (estimated 85% cubically aligned).

### XIII.—PRODUCTION SCHEDULES

Every effort is made to standardize production. A number of standard break-down gauges are adopted, and production to these stages follows an invariable sequence according to the particular break-down gauge required. A typical rolling and annealing schedule for brass to a break-down gauge of 0.070 in. may be as follows :

Cake preheat at 800° C.  
Hot roll to 0.250 in.  
Scalp 0.010 in. from each side (0.230 in.).  
Cold roll plate to 0.140 in. and coil.  
Anneal in coil : heat to 550° C. and soak for 1 hr.  
Pickle.  
Cold roll to 0.070 in. and coil.  
Anneal in coil : heat to 500° C. and soak for 45 min.

From this typical break-down stage, further reductions follow one of several standard sequences. The governing considerations in planning these sequences are the adoption of cold-reduction and annealing cycles, to give material of correct temper and grain-size, and free from directionality.

When an order is received by the mill, the customer's specification is examined to determine whether a standard method of production can be used. It is convenient to record standard methods of production on a card, as illustrated in Fig. 9. When an order

Method No. Customer		Gauge and Tolerances			Alloy	Temper	
Specification No.					Length	Width	Remarks
D.P.N.	Grain Size	U.T.S.	El, %	Erich- sen			
Standard Method of Production							
Hot-rolled gauge							
Scalp/anneal							
Breakdown gauge							
Anneal							
Breakdown gauge							
Anneal							
Ready-to-finish gauge							
Anneal							
Final gauge							
Final anneal							

FIG. 9.—Standard Method-of-Production Card. These cards may also be employed by the production metallurgist to indicate production schedules when special properties or tolerances are required in the final material.

calls for properties or tolerances for which standard production cards are unsuitable, the production or planning metallurgist makes out a special card indicating the latest stage at which it is necessary to deviate from standard practice, and stipulates the

subsequent processing. From the production cards, route cards can be made for each order.

In conclusion, it should be mentioned that there are certain factors influencing the quality of production which have had to be treated rather briefly owing to the limited space available. In particular, detailed reference to cold-reduction passes and detailed annealing cycles have not been given, as these are so dependent upon the type of plant available. The factors and principles involved in the control of

properties and structures have, however, been sufficiently outlined to give a fair idea of the problems confronting rollers of sheet and strip copper and brass.

#### ACKNOWLEDGEMENTS

The author wishes to thank the Directors of Enfield Rolling Mills, Ltd. for permission to publish this paper, and Mr. A. G. Adlington for his very valuable assistance in its preparation.

#### REFERENCES

1. S. L. Archbutt and W. E. Prytherch, "Effect of Impurities in Copper" (*B.N.F.M.R.A. Research Monograph No. 4*), 1937: London (British Non-Ferrous Metals Research Association).
2. F. Johnson, *J. Inst. Metals*, 1912, **8**, 192.
3. D. McLean and L. Northcott, *ibid.*, 1946, **72**, 583.
4. W. R. Webster, J. L. Christie, and R. S. Pratt, *Trans. Amer. Inst. Min. Met. Eng.*, 1933, **104**, 166.
5. M. Cook and E. Davis, *J. Inst. Metals*, 1949-50, **76**, 501.
6. C. E. Davies, *ibid.*, 1950-51, **78**, 501.
7. A. Morris, *Trans. Amer. Inst. Min. Met. Eng.*, (*Inst. Metals Div.*), 1930, 256.
8. G. Edmunds, *A.S.T.M.-A.I.M.E. Symposium on Stress-Corrosion Cracking of Metals*, 1944, 67.
9. H. L. Burghoff and A. I. Blank, *Proc. Amer. Soc. Test. Mat.*, 1947, **47**, 725.
10. H. L. Burghoff and A. I. Blank, *ibid.*, 1948, **48**, 709.
11. W. A. Anderson and R. F. Mehl, *Trans. Amer. Inst. Min. Met. Eng.*, 1945, **161**, 140.
12. H. M. Miekkoja, *J. Inst. Metals*, 1951-52, **80**, 569.
13. J. D. Jevons, "The Metallurgy of Deep Drawing and Pressing". 1945: London (Chapman and Hall, Ltd.).
14. M. Cook and T. Ll. Richards, *J. Inst. Metals*, 1941, **67**, 203.
15. M. Cook and T. Ll. Richards, *ibid.*, 1943, **69**, 351.
16. W. M. Baldwin, *Trans. Amer. Inst. Min. Met. Eng.*, 1946, **166**, 591.
17. H. Ford, *Sheet Metal Ind.*, 1948, **25**, 2189, 2405.
18. N. H. Polakowski, *ibid.*, 1951, **28**, 981, 1077.
19. W. C. F. Hessenberg and R. B. Sims, *ibid.*, 1951, **28**, 1083.
20. I. Jenkins, "Controlled Atmospheres for the Heat-Treatment of Metals". 1946: London (Chapman and Hall, Ltd.).
21. E. G. de Coriolis and W. Lehrer, *Symposium on Controlled Atmospheres (Amer. Soc. Metals)*, 1941, 71.
22. J. H. Bradley and H. J. Hammond, *Indust. Heating*, 1949, **16**, 1158.
23. S. F. Chisholm, *J. Inst. Metals*, 1950-51, **78**, 483.
24. Brit. Patent No. 539,556.



# SOME FACTORS AFFECTING THE QUALITY OF EXTRUSIONS\*

1525

By CHRISTOPHER SMITH,† F.I.M., MEMBER OF COUNCIL, and  
NORMAN SWINDELLS,‡ M.A., Ph.D., F.I.M., MEMBER

## SYNOPSIS

The practice of extrusion is discussed in the light of its effects on the quality of copper and aluminium alloy products made by this process.

## I.—INTRODUCTION

THE present paper is mainly concerned with the manufacture of solid products in copper and aluminium alloys on horizontal presses by the direct process. Many of the factors involved are common to both series of alloys, as well as to other types of extrusion, although the importance of any particular feature varies considerably according to the alloy. It has been found convenient to treat copper and aluminium alloys separately to some extent in order to emphasize certain characteristics, but obviously many of the observations on copper alloys are relevant to aluminium alloys and vice versa. Questions relating to metal flow and the fundamentals of extrusion have already been adequately dealt with in the literature and will be referred to only in so far as they affect the quality.<sup>1-3</sup> Similarly, the general principles governing methods for controlling quality have been discussed at a previous symposium and will not be considered in detail. Skilful judgment is required to produce material of an adequate standard in the most economical manner, especially as extrusion does not readily lend itself to the precise control which is possible with other processes such as rolling and tube drawing. It has been said with considerable truth that there are no major problems with extrusion but a large number of minor ones, and this view is, of course, applicable to most established production processes in which art and science both play their part. Under these circumstances, notwithstanding the technical progress which has been and is being made, the greatest safeguards of quality are still believed to be constant vigilance, intelligent enthusiasm, and attention to apparently insignificant detail.

Modern practices, both here and abroad, have been built up on the basis of experience and shrewd observation, and by any standard must be regarded as reasonably satisfactory, although this does not imply that further progress cannot be made. The same product may be made by different techniques,

but in the absence of irrefutable evidence to the contrary, it seems fair to assume that the overall effect of such differences is comparatively small. Further, it is believed that if the divergent views on the relative importance of many of the details of extrusion practice are considered in conjunction with the variety in equipment, alloys, shapes, and sizes, these differences of opinion may be less serious than would appear at first sight. This variety of conditions is an essential feature of much of the industry, particularly as it influences all stages of manufacture, even to the size of billet used for extrusion, and necessitates that any production scheme must cater for small batches requiring different modes of processing.

This large number of variables is responsible for a fairly considerable factor of ignorance and makes it extremely difficult to obtain data from which completely unambiguous conclusions can be drawn. Inevitably, views based on incomplete knowledge but not always free from dogmatic assertion may receive unmerited attention, and one of the first tasks of scientific control is to expose these "mythologies", though the danger of substituting "technical mythologies" for the more old-fashioned variety cannot be ignored.

In considering the manufacture of extruded products, proper attention should be given not only to planning the processes themselves, but also to plant layout and material flow. With aluminium alloys, for instance, the operations may be most simply described as consisting of extrusion, cooling, cutting, heat-treatment and quenching, straightening, and packing. These alloys are very susceptible to damage when hot, and dents, kinks, scratches, or drag marks may be produced which cannot subsequently be eliminated. The mill should therefore be laid out to reduce the amount of handling to a minimum. To this end, personnel should be trained to appreciate the importance of extreme care and cleanliness at all stages.

In regard to the processes themselves, a full under-

\* Manuscript received 30 October 1953. Contribution to a Symposium on "The Control of Quality in the Production of Wrought Non-Ferrous Metals and Alloys. II.—Working Operations", to be held in London on 28 April 1954.

† Works Superintendent, James Booth and Co., Ltd., Birmingham.

‡ Chief Metallurgist, McKechnie Brothers, Ltd., Birmingham.

standing of the individual details relating to the wide variety of extruded sections can give significant improvements in efficiency. For instance, accurate information on the size and lengths of billets necessary to produce single, double, or multiple lengths of the product can enable considerable economies in metal and handling to be achieved. It is often preferable to produce a job in single lengths for one reason or another, and it cannot be safely assumed that the process which appears most economical on paper is the best in practice, having regard to the quality of the product. It is therefore desirable in the development of standard process sheets that the details used by the works should not be provided by those solely concerned with the production aspect itself. In order that due consideration may be given to the quality of the final product in respect of its mechanical properties, metallurgical characteristics, accuracy of dimensions, and surface appearance, the views of the production department and metallurgists responsible for the quality must both be considered in establishing the methods to be used. If this is not done, apparently economical methods may result in material which is not consistently of the required quality.

As many of the alloys are not easily distinguishable by surface appearance, methods of preventing the occasional mixing of different alloys during processing are obviously of supreme importance and receive appropriate attention. For instance, materials can be segregated by processing in different mills, and identity can be maintained by marking with alloy symbols or by the use of colour codes at all stages of manufacture.

## II.—BILLETS FOR EXTRUSION

### *Copper Alloys*

The  $\alpha + \beta$  brasses, which constitute the most important alloys as far as tonnage is concerned, may be cast in water-cooled moulds, in cast-iron moulds, or by a continuous process. The quality of the billet influences the amount of scrap formed during extrusion, so that casting methods and the skill with which they are carried out are important, particularly as any porosity present in the billet tends to persist in the extruded rod.

### *Aluminium Alloys*

The semi-continuous process is almost universally used, and it has been found advisable to machine billets exhibiting exudations which might get drawn into the extrusion itself. No apparent advantage arises from machining billets of all alloys and sizes; with the Duralumin-type alloys, for instance, it is desirable to machine billets of 12 in. dia. and larger. It is not proposed to discuss billet casting in detail, but billets of fine grain-size free from columnar crystallization will produce the most satisfactory extrusions. In the normal course of events, it is

customary to maintain control of these features by routine selection of samples from the billets for macroscopic examination and ultrasonic scanning. This latter test is necessary because in certain alloys, particularly in the larger sizes of billet, stress-cracks may arise during the casting operation itself. With alloys of the aluminium-zinc-magnesium type, which are particularly susceptible to stress-cracking, it is advisable to place billets of large dimensions in a soaking pit immediately after casting. Maintaining a satisfactory standard of billet quality by methods of this kind has a direct bearing on the elimination of blister and pick-up, as well as on the achievement of good longitudinal and transverse properties in the extruded product.

## III.—PREHEATING OF STOCK FOR EXTRUSION

### *Copper Alloys*

Although the primary object of heating billets uniformly to a desired temperature without surface deterioration might appear to be a relatively simple matter, difficulties arise in practice, and few preheating furnaces in industrial use can be regarded with complacent satisfaction.

In this country, gas or oil firing is normally employed for copper alloys, and the billets travel through the furnace in a variety of ways, which include the use of a rotating hearth or walking beam, being pushed through in parallel rows, and rolling down an inclined hearth. Apart from the questions of economics, ease of maintenance, and obtaining the maximum output from the minimum size of hearth, the nature of the extrusion industry demands other special features in an ideal furnace. In particular, press conditions may introduce variations in the rate at which hot billets are required, so that the furnace should be capable of providing billets at the same temperature with different rates of output. On the other hand, the extrusion of small batches of different alloys may call for rapid changes of temperature from one billet to the next in the range 650°–1000° C. The combination of these two requirements of flexibility of temperature and constancy of billet temperature are not easy to achieve with an automatic unit of conventional design, as in one case a long soaking zone would appear to be necessary and in the other case a low thermal capacity is required. In practice, as extrusion temperature and soaking time are not regarded as critical in many cases, manual control of the furnace provides an acceptable solution to the problem. Careful planning can, of course, considerably reduce the necessity for rapid changes in extrusion temperature from one billet to the next, but such occasions are still likely to arise in practice and will continue to do so as long as small quantities of special alloys are required.

With certain materials, such as tough-pitch copper, oxidation of the billet surface during preheating can have a profound influence on the manner in which



the metal flows during extrusion and increase the amount of scrap due to sub-surface defects. The atmosphere in the furnace is therefore important, although some protection can be given to billet surfaces by coating with whiting or other inert substance which will remain on during the passage through the furnace. Although severe scaling is to be deprecated, it is not easy to define when the scale is excessive, and there is a lack of information as to how much scale can be tolerated without adverse effects. As existing methods entail exposing the hot billet surface to the atmosphere during the transfer from the furnace to the press, the oxidation at this stage must be taken into account when considering the probable efficacy of methods of reducing scaling in the furnace.

With any furnace, special care is required to avoid mistakes in billet identity. In addition to an effective check of the number of billets extruded compared with the number loaded into the furnace, different alloys may be of different billet lengths, separated by dummy billets, or even marked with ordinary chalk, which is legible on the hot billet.

In view of the shortcomings of existing types of furnace, modern developments are of particular interest. Low-frequency induction heating units, for example, possess many attractive features, which in some cases may outweigh the higher cost. Rapid heating can also be achieved in gas-fired surface-combustion furnaces, and these, too, may well find increasing application.

#### *Aluminium Alloys*

In contrast to brass and copper practice, it is inadvisable to "force" the heating of billets, as this may do irreparable harm to some alloys. Preheating is normally carried out in electrically heated air-circulation furnaces, although gas-fired muffle furnaces are also satisfactory. A conveyor-type furnace is preferred, as aluminium alloys are extremely soft at the extrusion temperature and liable to pick up particles of refractory if the billets are rolled along a fire-brick hearth.

The suggestion that preheating in low-frequency induction units may result in greater economy has recently attracted considerable attention, but it should be pointed out that certain of the strong heat-treatable alloys require prior homogenization if ultra-rapid heating is used. With such alloys, and particularly in the case of large-diameter billets, a long soaking period allows extrusion to be carried out at a lower temperature without giving rise to difficulties due to grain growth on subsequent heat-treatment. In addition, small amounts of low-melting-point constituents, which are normally dispersed when preheating is gradual, may be retained with ultra-rapid heating, and may in consequence form zones of weakness leading to the development of shear slits in extrusion, which in their turn give rise to blisters or become apparent in poor transverse properties in the finished extrusion.

#### IV.—PRESS DESIGN

Many of the details of the design of horizontal hydraulic presses have an influence on quality. The range of alloys and sizes which can be extruded on a press depends, of course, on the power of the press in relation to the diameter of the billet. With brass, the nose of the pressing stem reaches a temperature around 500° C., and loads of 75 tons/in.<sup>2</sup> on the stem appear to be as high as is practicable for a reasonable tool life with normal ratios of billet length to diameter. For many types of extrusion, such high unit pressures are unnecessary, and, in fact, few presses are working at these high loadings. On the other hand, the use of very low unit pressures increases the tendency to extrude at temperatures which are undesirably high from the point of view of the quality of the product, and may increase the amount of scrap resulting from failure to extrude complete billets.

As far as the control of extrusion speed is concerned, the influence of which is considered below, the characteristics of the accumulator and direct-drive hydraulic systems have important differences. With the former, the pumps are generally working most of the time to provide a reservoir of pressure water in gas- or weight-loaded accumulators. In this way, high extrusion ram speeds can be obtained without excessive pumping capacity, but this speed depends on the pressure required for extrusion and will vary throughout the extrusion for a given setting of control valves. The valves can, however, be adjusted manually within limits to minimize the variations, with the aid of a ram-speed indicator if necessary. For controlled extrusion speeds, the direct-drive system with positive-displacement pumps offers considerable advantages, and gives a predetermined ram speed which is substantially independent of extrusion pressure. Different ram speeds can be obtained by having a number of pumps which may be used separately or together, giving complete control and being ideally suited to automatic operation. For high ram speeds, however, accumulator presses are still preferred, and they also have the further advantage that the maximum pressure can be sustained, although this can also be achieved with modern direct-pumping equipment.

The alignment of the press is important, as many extrusion defects can arise from the maladjustment of the pressing stem, which should always ride centrally in the container aperture. With aluminium alloys, scraping stems are a cause of blister, and the concentricity of hollow brass extrusions made on presses equipped with piercing mandrels is notoriously difficult to control. It would therefore be of considerable assistance to users of extrusion presses if a method could be devised of ascertaining whether the pressing stem is truly in register during actual extrusion.

Other features of press design which can have an influence on quality include the way in which the billet is put into the press container. If any loose

shell or skull from a previous billet happens to remain in the container, loading the container from the ram end may cause the loose skull to cover the die orifice and subsequently to be extruded as a sheath over the front end of the extrusion. Details of extrusion practice, such as leaving a skull in the container or not, are also influenced by the speed with which auxiliary press movements can be accomplished as well as by purely metallurgical considerations. For instance, with old direct-drive presses in which all ram movements are slow and of the order of 1 in./sec., the extra time taken to withdraw the ram, insert the clearing pad, and clear the container may be held to outweigh any advantages to be gained by this technique.

## V.—EXTRUSION TOOLS

In common with other hot-working processes, the tool materials have to withstand particularly arduous conditions of temperature, stress, and thermal shock. These problems were considered at an informal discussion held by the Institute in January 1952, and although the composition, structure, and heat-treatment of the tools are of major importance, attention is drawn to the appreciable effect of small variations in service conditions on the more or less gradual deterioration of the tools. As far as extruded sections are concerned, dimensional accuracy is one of the main aspects of quality, and it depends on the ability of the dies to maintain their shape without "washing in" or cracking. Cracks are naturally most likely to occur at sharp corners in a die, and can cause a fin or torn surface on the extrusion.

In some cases, thousands of different sections are extruded on the same press, and adequate support for the dies must be provided to reduce deformation and cracking. By having a series of die-holders and bolsters with holes of different shapes, each of which caters for a range of sections, these difficulties can be overcome, although care is required with dies which are used very occasionally owing to the gradual deformation of the supporting pads, which are used more frequently. With multi-hole dies, consideration of metal flow may influence the disposition of the holes,<sup>4</sup> but the desire to make the tools as strong as possible is often an overriding factor. In any case, the holes should be symmetrical about the centre of the die, since if two similar holes are put in a die, metal will flow faster through a hole near the centre of the die than through a hole near the edge. It is, moreover, important to study the orientation and number of apertures to be provided, particularly with sections of irregular shape and thickness. The three-dimensional nature of flow can be simulated by constructing a model press with silver sand as the material being extruded, and gravity as the source of extrusion power. Although this analogy must not be pushed too far, interesting ideas on how to design multi-hole dies may be obtained by varying the layout of the apertures in the die and observing

the sinking surface of the silver sand. The effects of such studies can be extremely valuable, leading to economies in the extrusion process itself and to the production of extrusions of complicated shape which, when subsequently heat-treated and stretched, behave in a docile manner, thus eliminating the necessity for those extra correcting operations which are expensive in man-hours and which often leave a section, though true to dimensions, undesirably stressed internally.

### Tools for Aluminium Alloys

The temperature to which the tools are preheated and maintained during extrusion is of particular importance with aluminium alloys. The electrically heated containers should be maintained at the highest temperature consistent with reasonable life, and a temperature of about 420° C. is found to be suitable in practice. Tools should be heated to about 350° C., and it is good practice to provide furnaces near the presses which will maintain tools at even temperatures. Too often tools are heated over bare gas flames and suffer materially in consequence.

### Tools for Copper Alloys

With copper alloys, the inevitably large temperature difference between the billet and tools makes the temperature to which the tools are preheated less

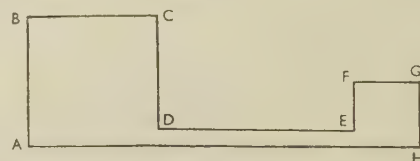


FIG. 1.—Extrusion of Non-Uniform Cross-Section.

critical. Under some conditions, such as where the initial pressure is high, the die temperature can be important in obtaining a satisfactory start to extrusion, and in cases where the finishing pressure is near the maximum, the container temperature may have considerable influence.

The question of die shape is without doubt a very controversial one, although the properties in the extruded condition and the tendency to grain growth on reheating appear to be insensitive to changes of die shape under normal conditions. As far as quality is concerned, therefore, the die design is mainly of importance from the point of view of dimensional accuracy of the extrusion, particularly with sections of irregular cross-section.

The profile through the die may be regarded as consisting of three parts, viz. a lead-in radius, a lead-in taper, and a more or less parallel bearing. It is not unusual for this bearing to have a slight taper, so that the size is a minimum at the exit of the die, in order to obtain the maximum amount of control over the metal during its passage through the die.

In the case of an extrusion having the cross-section shown in Fig. 1, the metal in the area ABCD tends to



flow faster than that at *EFGH*, which in its turn tends to flow faster than the metal between *D* and *E*. If the die were merely a parallel-sided hole of the appropriate shape in the die blank, the section would be almost unrecognizable. The art of die-making is to even out these rates of flow in different parts of the section, and as the influence of friction and temperature gradients, as well as the response of the metal flow to various constraints, is largely unknown, die design is mainly a matter of skilled experience. The part of the die between *D* and *E*, for example, would have a small lead-in radius blended into the bearing, which would be kept short by machining away the die from the back over an area slightly greater than the orifice in the die. In the region *ABCD*, the bearing would be continued right through the die blank and the lead-in radii and approach angles would be greater. This wedging action of tapered entrances to extrusion dies must be used with discrimination if accuracy is to be achieved. The length *DE*, for instance, in the above section can be made greater than the corresponding dimension of the die by improper lead-in shape.

In practice, the tendency of the die to wash in is dependent on the design, so that there is a limitation on possible die shapes if a reasonable number of extrusions are to be obtained from a die. As some die materials are more resistant than others to washing in, it follows that die design can be influenced by the die material. Other methods of controlling flow are by positioning the part of the section where resistance to flow is high in the middle of the die and by encouraging flow by local application of lubricant to the die. Although the shape of the die influences the pressure required for extrusion, this is often a secondary consideration. If the Ugine-Séjournet process becomes popular with copper alloys, some interesting changes in the design of dies for sections may be expected, as a result of the lubricating and insulating properties of the layer of glass between the metal and the tools.

Another aspect of die design is important when extruding shapes in coil form. For example, a hexagon die for use under such conditions must be free from any tendency to spiral. More precisely, each corner in the die must be in a plane perpendicular to the die face, as otherwise the coil itself will have a similar spiral which may interfere with subsequent processing.

## VI.—INFLUENCE OF EXTRUSION SPEED

### Copper Alloys

For most purposes, it is sufficiently accurate to deduce the speed of the metal through the die from the ram speed and the cross-sectional areas of the follower pad and extrusion. With materials extruded in straight lengths down a channel, the speed of the metal through the die is relatively low, and precise control is not normally necessary, except in the case of some special alloys which exhibit transverse

cracking if the speed is too high. For a given extrusion, the higher the speed, the lower the extrusion time, and the greater tendency to uniformity from end to end of an extrusion with respect to properties and dimensions. Although the dies are preheated, they heat up further during extrusion, and the following extreme conditions show the effect of this on diameter in the case of material produced through a single-hole die from billets 8 in. in dia. by 26 in. long, of a leaded 58% copper, free-machining brass at 750° C.

Extrusion Time, sec.	Rod Diameter, in.		
	Front	Middle	Back
57	1.558	1.560	1.570
8	1.559	1.560	1.562

With moderate reductions in area, as in the above case, the speed of the metal through the die does not normally exceed 400 ft./min., and the properties of the metal are not a limiting factor as far as the maximum speed is concerned. When smaller diameter material is produced in coil form, however, the high reduction in area from billet to rod gives high speeds through the die for moderate ram speeds. With direct-drive presses and pan-type coilers near to the press, it is possible to obtain coils of good quality at high speeds of coiling, and in this case the properties of the metal being extruded limit the speed which can be safely used. Many factors influence this maximum speed, which, with  $\alpha + \beta$  brasses, is a complex function of composition, temperature, and size of rod. If the speed or temperature is too high, there is a tendency for the brass to build up around the exit side of the die, and for the rod to emerge

TABLE I.—Limiting Conditions of Extrusion of Leaded Brasses.

Alloy			Billet Dia., in.	Rod Dia., in.	Temp., °C.	Extrusion Speed, ft./min.	Surface of Rod
Cu, %	Zn, %	Pb, %					
61	36	3	5	3:1 hole	780	350	Satisfactory
61	36	3	5	3:1 hole	780	550	Unsatisfactory
61	36	3	5	4:1 hole	780	550	Satisfactory
58	39	3	7	3:2 hole	760	650	Satisfactory
58	39	3	7	3:2 hole	780	650	Unsatisfactory
58	39	3	7	4:2 hole	780	850	Satisfactory

with a grooved surface and under the expected diameter. The brass which builds up may occasionally leave the die and weld itself to the rod, forming an oversize collar which would cause a sheath along the finished rod if subsequently drawn. This effect is presumably due to incipient melting, and tends to be confined to the front end of the extrusion. Like so much else in works practice, it is not possible to define the precise conditions giving rise to a poor surface, which are influenced by the usual variety of factors, so that a reasonable margin is required between standard practice and conditions which are known to give trouble. Brasses with 61% copper are distinctly more critical in this respect than brasses with 58% copper, and smaller sizes can be extruded faster than

larger ones. Some indication of the limiting conditions of extrusion is given by the typical results in Table I.

#### Aluminium Alloys

Extrusions with excellent surfaces may be produced at speeds up to 100 ft./min. without deleterious effects in alloys of the magnesium-silicide type and to a smaller extent in the aluminium-magnesium alloys, which are not prone to liquation at temperatures in the region of 520° C. With the ultra-strong alloys, speeds may have to be as low as 3 ft./min. if a satisfactory product is to be obtained. With alloys falling in the H14, and particularly the H15, classifications, control of extrusion speed is of great importance in avoiding local overheating, which gives rise to blister on subsequent heat-treatment. Control of this factor is not easy, as the effects of friction vary between one shape of extrusion and another, and further consideration is given to this aspect in the section dealing with extrusion temperature.

### VII.—INFLUENCE OF EXTRUSION TEMPERATURE

#### Copper Alloys

The temperature of the billet surface before loading into the container can be measured by means of optical or contact pyrometers. Total-radiation pyrometers have to be calibrated against disappearing-filament pyrometers or by other means, and although they are subject to errors due to variations in emissivity, they appear to give reasonably reproducible readings in practice. Even ignoring any errors of measurement, this temperature is only approximately related to the temperature of the metal as it passes through the die, which may be higher or lower, depending on extrusion conditions. The real extrusion temperature, which may vary across the rod, is therefore only approximately known, and its relationship with the measured temperature is influenced by friction, extrusion speed, rod diameter, die temperature, container temperature, and the time interval between measurement and the start of extrusion. The well-known variation in structure throughout the length of an  $\alpha + \beta$  brass extrusion is, of course, associated with the cooling off of the unextruded part of the billet in the container.

The published literature dealing with the normal temperature ranges used for the extrusion of different alloys needs little amplification.<sup>1,3</sup> Alloys which have a body-centred cubic structure over the whole range of temperatures concerned, may usually be extruded at a pressure which is substantially independent of temperature. Alloys which undergo a phase change resulting in the formation of a face-centred cubic phase as a result of cooling down during extrusion tend to show increases of pressure towards the end of the extrusion. With a 10% aluminium bronze, for instance, the pressure towards the end of extrusion increases very rapidly, being influenced

only slightly by changes in the initial temperature of the billet.

As a general rule, the lowest extrusion temperature consistent with the alloy, extrusion ratio, and power available is preferred for the following reasons:

1. The tendency for deterioration of the surface of the billet during preheating is reduced.
2. Liquid phases at grain boundaries are avoided. Even if these are not sufficiently serious to cause cracking during extrusion, they may impair the impact-resistance of the finished product.
3. A finer structure is obtained in the extruded condition, particularly with alloys which have a substantially all- $\beta$  structure.
4. Transverse cracking with  $\alpha$ -brasses is avoided. ( $\alpha + \beta$  brasses are much less prone to this type of defect.)
5. The mechanical properties throughout the extrusion are more uniform. With a 10% aluminium bronze, for instance, the hardness variation from front to back of an extrusion is markedly dependent on extrusion temperature.
6. The tendency for grain growth to occur on reheating is considerably reduced.

With regard to this last-named effect, an example of widespread practical importance concerns 58:40:2 leaded brass rod for hot stamping. Although different views have been advanced to explain the cracking of leaded brass during hot stamping, there is general agreement that serious intercrystalline cracking is sometimes associated with large grains, which may be of the order of 1 cm. long. It is believed that this effect occurs only when the brass is reheated into the all- $\beta$  range (above approximately 750° C. for 58% copper), and whilst it depends on the lead content of the alloy and the conditions of stamping, it is also markedly influenced by the extrusion conditions. As normal hot-stamping and forging practices introduce complex variables, the effect of different extrusion temperatures on the properties of the rod is more conveniently studied by reheating samples under controlled conditions. Quenching after heat-treatment tends to retain the  $\beta$  structure and greatly improves the effectiveness of a nitric acid etch in showing the grain-size. Typical results of such experiments on 2½-in.-dia. rod extruded from 8-in.-dia. billets and reheated to 800° C. for ½ hr. are:

Extrusion Temp., °C.	Structure	
	Front End	Back End
800	Fine	Coarse
750	Variable	Coarse
700	Fine	Fine
650	Fine	Fine

The grain-size after heat-treatment at 800° C. is regarded as fine if less than 1 mm. and coarse if larger. This somewhat arbitrary distinction is satisfactory in practice, as the coarse grains are usually very much larger, particularly at the outside surface of the rod. The grain-size after heat-treatment of the front end



of rods extruded at high temperatures is usually extremely fine and does not appear to be different from that in the as-extruded condition, except where it has been subject to local cold work, such as identification marking, which may give rise to excessive grain growth. With material extruded at low temperatures, the grain-size after heat-treatment is definitely larger than in the as-extruded condition. The results of the laboratory heat-treatments described above have been found to correlate well with practical stamping experience, and the avoidance of excessive grain growth is believed to be a necessary but not sufficient condition of good stamping rod.

These views on the effect of extrusion temperature are somewhat contrary to those expressed by Hintzmann and Köster,<sup>1</sup> who suggested a high extrusion temperature for stamping rod. Attempts to make complete extrusions with good stamping properties have, however, failed with the normal stamping alloy, even at extrusion temperatures of 825° C., and a ram speed of 3 in./sec., as the back end of the extrusion is still prone to grain growth on reheating. Moderate cold work by drawing or reeling after extrusion increases the tendency to grain growth during heat-treatment, and this effect is much greater with high extrusion temperatures.

As the grain growth occurs only in the all- $\beta$  region, the American practice of using an alloy for forging with 2% more copper is of interest. Although this brass can be stamped at a higher temperature than the 58% copper alloy without danger of grain growth, the pressure required for hot working is significantly greater at a given temperature, and an alloy which will stamp satisfactorily in the all- $\beta$  region is felt to have distinct advantages.

#### *Aluminium Alloys*

Extrusion temperatures should always be as low as practicable; this does not always mean that they should be the lowest which will permit the billet to be extruded. If the extrusion temperature is too low, then in the case of heat-treated alloys, grain growth may occur on subsequent heat-treatment to an extent which will make the product useless.

Temperature measurements should be made by contact thermocouple just before placing the billet in the container, and the billet should be briskly wire-brushed at this time in order to remove any adhering matter. The optimum extrusion temperature naturally varies according to the ratio of reduction in area, the complexity of the shape of the section, and the alloy being extruded. For the softer alloys of the type N4, H9, and H10, a temperature of 420° C. is suitable, whereas 450°–480° C. gives more satisfactory results with the stronger alloys of the H14, H15, and aluminium-magnesium-zinc types.

With the higher-strength aluminium alloys, as indicated earlier, the really significant extrusion temperature is that of the section as it emerges from the die, and this is frequently much higher than the

temperature of the billet placed in the container. In the interests of quality, it would be most valuable if this temperature could be directly controlled. The most obvious difficulty in the measurement of extrusion temperatures in this way is that of coupling the extrusion and the temperature-sensitive element. It is obviously not possible to do this directly, using conductivity, and this limitation naturally enforces the use of some form of radiation.

The temperatures involved in this application are well below 600° C., so that the radiation from the extrusion is confined to the lower wave-lengths in the infra-red band to which most photocells are insensitive. The development of semi-conductor photo-sensitive elements has led to their use as temperature-measuring devices in industry. The commonest type of detector is the lead sulphide cell, and modern cells of this type have a high speed of response, making them suitable for the temperature measurement of moving objects. Although the lead sulphide cell is robust, and can be made small in physical size, it suffers the disadvantage of instability. This defect can be overcome by using two cells, one of which is exposed to the radiation from the hot body while the second cell is exposed to a radiation source which can be varied by known amounts. The outputs of the two cells are then compared and adjusted potentiometrically.

The principal disadvantage of making measurements of this type is their dependence on the surface emissivity of the hot body. With aluminium extrusions this may vary considerably in the minutely small period of time in which the oxide film builds up as the material leaves the die aperture. A method of overcoming this difficulty has been described,<sup>5</sup> but its application piles further complications on the apparatus. To be effective the pyrometer must be sighted on to the surface of the extrusion at the die exit, must be small in size, robust, portable, and protected from heat and dirt.

The problem of temperature measurement of this kind is therefore seen to be one of considerable difficulty, having in mind that one is trying to measure the highest temperature in a temperature gradient, on a material which is rapidly developing a thickening oxide film, and is passing the aperture of the recording instrument at high speed.

## VIII.—EXTRUSION TECHNIQUE

### *Copper Alloys*

One of the main objects of much of the technical effort devoted to the manufacture of rods is to reduce the amount of scrap associated with the occurrence of the "extrusion defect". Whilst this term is sometimes restricted to the central funnel which may form when the amount of billet left unextruded is particularly small, it is more usual to describe as extrusion defect any unsoundness resulting from the metal flow causing the oxidized surface of the billet

to appear inside the extrusion. Unsoundness in the billet can also cause unsoundness in the rod, which is often of a different character, but cannot always be clearly distinguished. An approximate rule, to which there are no doubt numerous exceptions, is that defects at the front end of an extrusion can usually be attributed to internal unsoundness in the cast billet, whereas defects at the back end of an extrusion tend to be due to the type of metal flow. With alloys such as the  $\alpha + \beta$  brasses which extrude with a non-lubricated type of flow, any defects with single-hole extrusions tend to occur centrally in the rod. On the other hand, with the lubricated type of flow exhibited by copper, any defects are likely to be just below the surface and may show up as blisters.

With ordinary brasses, the follower pad is often made smaller in diameter than the bore of the container in order to leave a shell or skull in the container, consisting, it is hoped, of the oxidized billet surface. Although this can be described as the orthodox technique, it does not take care of the oxidized face of the billet against the pressure pad, and in this connection serious attention should be given to the views of France and Thelin, who report better results with a well-brassed container which is not cleaned out between extrusions.<sup>6</sup> The question of the shape of the face of the follower pad receives attention from time to time, and most extruders have no doubt experimented with concave, convex, and other shapes. In practice, it is usual to employ a flat face, partly perhaps because of the ease with which the back-end discard can be separated from the follower pad after extrusion, combined with the difficulties of convincingly proving the advantages of other shapes. Assuming that a skull is being left in the container, the question of the thickness of this skull must be considered. One viewpoint is that the skull should be thick enough to contain all the surface dirt and oxide. This thickness will depend not only on the state of the cast surface, but also on what happens to surface imperfections when the billet is squeezed up to fill the container, as if the initial clearance between the billet and container is large, the squeezing-up operation may increase the depth of wrinkles in the surface. To be effective, the skull must be continuous round the billet diameter and reasonably uniform in thickness. In practice, this may not be achieved without considerable care, because, for instance, of the gradual warming-up of a container during the day and other factors influencing press alignment. Under normal conditions, the skull must be less than  $\frac{1}{8}$  in. thick in order to prevent back extrusion over the follower pad, and it is often about  $\frac{1}{16}$  in. thick.

Although the principle of leaving a skull is perfectly straightforward, lively discussion may be provoked by detailed consideration of precisely what happens under production conditions with more or less imperfect billets and a press container whose bore is no longer an ideal cylinder. It might seem, for example, that the first oxide to enter the extruded

rod originates at the corner of the billet against the follower pad, and that surface blemishes on the billet at this corner are perhaps more serious than greater blemishes further along the billet. It is important to differentiate between two possible effects of leaving a skull, viz:

1. To delay the onset of unsoundness in the rod, which is the real objective.
2. To reduce the total amount of oxide without appreciably affecting the point at which it begins to appear in the rod. In this latter case, the results may depend on the standard of soundness which is regarded as acceptable and may give rise to misleading claims which are not valid for a proper standard of soundness.

With copper and alloys which extrude with a lubricated type of flow, the sub-surface defects are associated with the conditions of flow relatively near the die. It would appear that in these cases, the state of oxidation of the billet surface is more important than whether or not a skull is left in the container. On the other hand, the clearing of a container by removal of the skull avoids contamination of the next billet to be extruded, a point of importance when changing from one alloy to another; for instance, if aluminium bronze is extruded at 900° C., residual brass in the container will give a lubricated type of flow with sub-surface defects.

The influence of the ratio of length to diameter of the billet depends on the alloy being extruded, and in some cases, a higher proportion of sound rod can be obtained by using shorter billets.

Another factor which is not always appreciated is that with the  $\alpha + \beta$  brasses, relatively small variations in composition have a marked effect on the pressure required for extrusion. With the straight brasses in the range 56–62% copper, an increase of 1% in the copper content puts up the pressure required for extrusion under similar conditions by approximately 10–15%. A guide to the behaviour of high-tensile brasses is given by the use of Guillet's equivalents, as the pressures for these alloys are comparable with those required for straight brasses of similar structure. The nickel brasses containing copper 45, nickel 10%, remainder zinc, take about 50% more pressure than a straight 58% copper brass. These inherent differences between alloys not only govern the range of extrusions which can be produced, but also affect the dimensional accuracy which can be achieved, especially with section work. A guide to the usual tolerances for rounds, squares, and hexagons may be obtained from British Standard No. 249.

As the extrusion emerges from the die, care must be taken to avoid damage to the hot metal. Adequate clearance must be allowed in the back die and die-holder, and the channel or run-out table in front of the press must be kept smooth and clean. Occasionally, the surface of extruded brass strip shows zinc-rich areas, which tend to occur on one side only and which project slightly from the surface. These



spots are hard and white in colour, causing difficulties in machining, polishing, and plating. Microscopic examination shows the white area to be surrounded by an all- $\beta$  zone which merges into the  $\alpha + \beta$  structure of the strip. In some cases the small excrescences are yellow in colour and have a  $\beta$  structure. Similar defects can be produced by placing small pieces of zinc on a red-hot strip of brass, and there can be little doubt that the zinc is picked up by the extruded strip after it leaves the die. It is believed that under the reducing conditions associated with an oil and graphite lubricant around the die, and particularly at high extrusion temperatures, zinc volatilizes out of the brass and condenses on the relatively cool support behind the die. If this zinc is allowed to build up, it may melt as the back die warms up during extrusion and fall on to the strip, or the strip itself may touch the deposit. This type of defect can be avoided by keeping the extrusion temperature down to reduce the volatilization of the zinc and by cleanliness on the press to avoid the build up of a zinc-rich deposit.

Apart from the dangers of mechanical damage, brass sections require careful handling whilst they are cooling down after extrusion or annealing, as the leaded  $\alpha + \beta$  brasses, and particularly the leaded nickel brasses, are inclined to be brittle in the range 250°–500° C. The actual brittle range varies with the copper content and alloying additions. Judged by hot impact-bend tests, the lead-free alloys are immune from brittleness, but alloys containing 3% lead are affected only to approximately the same extent as those containing  $\frac{1}{4}$ % lead.

#### *Aluminium Alloys*

The adverse effects of friction are well known; some slight amelioration may be obtained by maintaining the dies in a polished condition and by lubrication of the bearing surfaces. In this field, a great deal of work has been done with colloidal graphite and molybdenum disulphide, but with indifferent results. This must always be so, since a large part of the heat effect arises from the internal friction which occurs in the billet itself just before entry of the metal into the die aperture.

It is apparent, therefore, that a more fundamental approach to this problem is necessary, and this involves a reduction of friction between the metal and the tools, including the container. Since light alloys are by no means fully plastic at their extrusion temperature, the effects of friction are transmitted to the material itself, developing increasing heat effects, and are responsible for the annular grain growth on subsequent heat-treatment. The obvious thing to do is to reduce these frictional effects by isolating the alloy being extruded from the tools by some lubricating method. In the case of the strong light alloys, this may be satisfactorily achieved by the interposition of pure aluminium, which at the extrusion temperature used acts as a truly plastic medium. By this technique, which demands some

modification of the equipment, extrusion pressures are reduced by about 35%, and the mode of flow of the strong light alloy is entirely modified to the lubricated type, with the elimination of shear strains and of the extrusion defect.<sup>7</sup> This method is difficult to apply, particularly in sections of complicated shape and thin cross-section, but it is by careful developments of this nature, by perseverance and observation, that progress is slowly being made.

#### IX.—HEAT-TREATMENT OF ALUMINIUM ALLOYS

A great number of aluminium alloys have to be heat-treated after extrusion. The simple technique of quenching at the die is extremely effective, producing sections of excellent mechanical properties and fine grain-size. Provided that the design of such quenching equipment safeguards the extrusion tools and does not give rise to undue distortion of the product, and provided that the inspection arrangements are adequate, the process may be used with confidence. It has the further advantage that the sections are rapidly cooled and are therefore less sensitive to damage on the press run-out table. In cases where it does not affect the characteristics of the alloy, quenching of non-heat-treatable alloys at the die is on this latter account a good practice.

Solution-treatment of extrusions is carried out in electrically or gas-heated furnaces. It is claimed that distortion on quenching is markedly reduced if vertical furnaces are used, although a great deal of the distortion on quenching from horizontal furnaces may be avoided by proper loading practices. The maintenance of pyrometric equipment at a high standard of accuracy and the intelligent positioning of thermocouples are naturally essential. Controlling the weights of the loads in the furnace and allowing suitable soaking periods are equally necessary. In this field, the routine work of laboratory personnel is important, and their findings should be made available daily to those responsible for production. If this liaison is not maintained and its results acted upon, improper heat-treatment is likely to occur.

As many aluminium alloys are susceptible to corrosion in the unheat-treated condition, it is important to avoid condensation of moisture on work awaiting heat-treatment. Quenching baths should be as large as possible to reduce the amount of steam generated during quenching, and well-ventilated shops assist in the rapid removal of any steam that is formed.

It has been indicated earlier that the previous history of the material may have considerable bearing on the condition of the surface of the extrusion. Apart from defects arising in the casting, in preheating, in the extrusion process itself, in handling, and in the shop atmosphere, it is certain that the atmosphere of the solution-treatment furnace has a profound effect on the development of blister in extruded sections. This has been ascribed to a

variety of causes, but experiments carried out in laboratory furnaces do not appear to give reproducible results, and a discussion on this important aspect of quality control would be most valuable. Vertical furnaces have been reported to induce blister to a greater extent than horizontal furnaces, and it is known that the introduction into the furnace atmosphere of creosote oil or ammonium fluoride vapour or the greasing of sections before being put into the furnace will markedly reduce this blistering effect. As all the wrought alloys contain magnesium and as the intimate contact of water and metal results in a reaction releasing hydrogen which gives rise to blister, it is possible that blistering may arise when cold sections are introduced into the hot humid atmosphere of a furnace and dew is in consequence deposited on the naked metal surface. In support of this view, it is known that the introduction of a hot section into a solution-treatment furnace does not result in blistering of this type, and the action of the so-called inhibitors can be attributed to the deposition of something else on the metal surface before water condenses, thus preventing the necessary intimate contact.

#### X.—FINISHING PROCESSES FOR COPPER ALLOYS

As the amount of extrusion defect tends to vary from billet to billet, it is usual to eliminate defective material before subsequent processing by fracturing the rods or applying some other test for soundness. The examination of a fractured surface is remarkably discriminating and will reveal slight defects which could easily be missed on a polished section of the same material. Non-destructive testing by means of ultrasonic or eddy-current methods has not been developed sufficiently to be used for routine inspection of copper alloy rod. With modern nick-and-break machines, a slight nick is made in the surface of the extrusion near the back end, which is then broken off by reverse bending. Normally, the extrusion is allowed to cool down before fracturing, and the slight distortion which occurs exaggerates the slightest imperfections so that they can easily be observed. If the rod is fractured in the brittle range of temperature, minor defects may not show up, and with very ductile alloys excessive deformation of the fractured surface by reverse bending may also mask small pinholes.

Many extrusions are supplied without further processing apart from straightening, whereas others are given a light cold draw for improved dimensional accuracy or to confer desired mechanical properties. In special cases, a more elaborate schedule of annealing and drawing may be necessary, such as where the extruded size is much larger than the finished size or where a carefully controlled grain structure is required. Operations such as annealing or pickling call for little special comment, except perhaps to emphasize the importance of adequate rinsing after

pickling, particularly with coils, as lack of attention to this point can cause serious pick-up and scoring on drawing.

As far as cold drawing is concerned, the die shape should be related to the reduction in area. With light draws, often not more than 0.020 in., satisfactory results are obtained with an included lead-in angle of about 12° and a short parallel throat. Some commercially available carbide dies have wider approach angles, so that the work is done on the rod over a very short distance. With  $\alpha + \beta$  brass, this causes more abrupt hardness gradients through the stock and, particularly with squares and hexagons, can cause cracking within a few hours of drawing. In order to obtain drawn bars which are reasonably straight and free from bow, it is necessary not only to pay attention to die design but also to the alignment of the die in the draw-bench.

In the case of certain types of section, of which deep channel sections are an example, limitations of die materials prevent their being extruded to the desired shape. They are therefore extruded with the legs splayed apart to give the necessary strength to the tongue of the extrusion die and then cold drawn to the correct form. In these cases, it is important to avoid localized stresses during drawing, particularly at sharp corners, as otherwise cracking is liable to occur.

The final straightening of extruded products depends markedly on the skill of the operator, particularly with those sections which must be straightened by hand methods. It is, of course, important to ensure that the properties of the extrusion are not impaired by the amount of cold work done on it during straightening, especially in the case of material required for subsequent bending. With some methods of straightening, the amount of work done is small, while with others, such as stretching, the applied load may be measured. On the other hand, round rod is often straightened on plate reeling machines which may influence the diameter, surface hardness, and hardness gradients through the rod to an extent which is not fully controlled. With these machines, in which the stock is curved about its own axis between two inclined rotating rolls, one being cylindrical and the other concave, the rod is supported underneath by a stationary plate as it spirals through below the centre line of the rolls. The appropriate plastic deformation must take place to straighten the rod, but the precise effects of the following variables in relation to the diameter and mechanical properties of the rod are not widely understood:

1. Contour and length of barrel of the rolls.
2. Inclination of the rolls to the horizontal.
3. Speed of rotation of the rolls.
4. Helix angle of the rod and time in the rolls.
5. Distance apart of the rolls.
6. Distance of the rod below the centre line.

Many of these factors are interdependent, so that rod of a reasonable degree of straightness may be



obtained with a variety of machine settings. Nevertheless, reliable information on the best procedures to obtain the straightest possible material without change in diameter on reeling would be of considerable interest to many rod producers.

In conclusion, extruded material, being a semi-finished product, must not only perform satisfactorily in service but must also meet the requirements of the maker of the finished article. Although a few specific tests measure a particular property which may be of special interest, such as electrical conductivity, the usual purpose of final testing is to ensure that the material meets specification requirements or to verify that it has been processed in a manner which experience has shown to be satisfactory. For most applications, a knowledge of the chemical composition, the usual mechanical properties, and the results of the mercurous nitrate test gives a sufficient guide to the subsequent behaviour of the material. It should perhaps be pointed out that although measurements of indentation hardness are of some assistance in assessing the uniformity of material, they cannot be used to estimate the tensile properties, as the relationship between hardness and tensile strength is by no means constant.

In spite of the valuable work that has been carried out on such properties as machinability and wear-

resistance, there are no generally accepted laboratory tests which will give a direct measure of these properties.

#### ACKNOWLEDGEMENTS

Papers dealing with works practice are to some extent interim reports on progress made by the authors' colleagues, and it is a pleasure to acknowledge the patient instruction in extrusion equipment and technique readily given by them. Thanks are due to the Directors of both Companies for permission to publish this paper.

---

#### REFERENCES

1. C. E. Pearson, "The Extrusion of Metals." 1953: London (Chapman and Hall, Ltd.).
2. C. Smith, *J. Inst. Metals*, 1949-50, **76**, 429.
3. W. W. Cotter and W. R. Clark, *Trans. Amer. Inst. Min. Met. Eng.*, 1946, **166**, 447.
4. F. Hemmerich and N. Arenz, *Metall*, 1949, **3**, 37.
5. A. F. Gibson, *J. Sci. Instruments*, 1951, **28**, 153.
6. W. D. France and L. E. Thelin, "Rod and Wire Production Practice" (A.I.M.M.E. Inst. Metals Div., Symposium Series, Vol. 3), p. 50. 1949: New York (American Institute of Mining and Metallurgical Engineers).
7. British Patent No. 689,051.

# 1526 STATISTICAL CONTROL IN METAL- WORKING OPERATIONS\*

By M. WHYTE,† B.Sc., MEMBER

(Contribution from the Research Laboratories of The British Aluminium Co., Ltd.)

## SYNOPSIS

In many metal-working processes, a quantitative assessment of variability can be used to gain efficiency without fundamental changes to the processes. Statistical aspects of sampling are discussed, and it is shown that sampling rates should be fixed in relation to the quality and homogeneity of the material being tested. Wherever possible, material processed as a batch should be the unit which is sampled.

The selection, control, and sensitivity of routine tests are considered. The cost of a few relatively expensive tests of high reproducibility is compared with that of a larger number of cheaper tests of low reproducibility. For equal confidence in the final test result, the less reproducible test tends to be the cheaper where the variability in the material being tested is high and if the greater number of tests which are required can be spread over a wide range of samples. Statistical quality control provides a means of ensuring the continuing reliability of routine tests.

The value of error-actuated control throughout an entire production process is emphasized. Statistical methods may be used to assess limits for intermediate variables and qualities which will serve as criteria for the early rejection of material which would finally prove sub-standard. Statistical quality control provides a sound basis for efficient process control at all stages.

A number of applications to specific problems arising in metal-working operations are described. A brief summary of the simpler statistical concepts and formulæ is given in an Appendix.

## I.—INTRODUCTION

STATISTICAL techniques were first applied to industrial problems about twenty-five years ago, and since then steady progress has been made. Cotton spinning, electric lamp manufacture, and beer brewing are among the industrial processes where statistical methods have proved their worth. Each of these processes is basically different, and the success of statistical technique in each case is an indication of the flexibility and general applicability of the statistical approach.

One of the barriers to the successful use of statistics in an industry is the attitude that the problems encountered are not amenable to statistical treatment. This is seldom true. The statistical approach is primarily directed at the quantitative definition of variability and the assessment of probabilities. This information is essential if sound decisions are to be made from the evidence of experimental work or operating-plant data. Decisions have to be made in all industries, and the statistical approach, which provides criteria for making sound decisions, cannot be ignored.

An executive has frequently to decide between two courses of action, and commonly the evidence upon which a forecast of the effects of the alternative courses must be based appears to be equally balanced. In practice he will follow his "hunch". The cautious executive will tend to err on the conservative side, and the impetuous executive will, on average, be too rash. A wiser executive would consult a statistician

who might, from the available evidence, be able to provide a better estimate of the approximate odds for or against the success of a particular course of action.

The present paper has been confined to the illustration of simple statistical techniques, applied in situations which are encountered in metal-working operations. The scope of the paper has deliberately been limited, and it must not be concluded that simple methods only are applicable in this field. In recent years statistical theory and new techniques have been evolved for tackling wider and more complex industrial problems.

A short résumé of the simpler statistical concepts and formulæ is given in an Appendix (p. 342). Those unfamiliar with statistical nomenclature will find there definitions of the special terms used in the text. Workers in the industrial field will find of particular value the three books listed under "Industrial Applications" in the Bibliography (p. 344).

## II.—THE ASSESSMENT OF VARIABILITY AND DIRECT APPLICATIONS

It is now widely recognized that a variable, however well controlled, is subject to some residual variation. A study and assessment of this variation can be as profitable as a similar study of changes in mean level or value. This will be illustrated by the following example, which is pertinent in the majority of metal-fabrication processes.

\* Manuscript received 22 October 1953. Contribution to a Symposium on "The Control of Quality in the Production of Wrought Non-Ferrous Metals. II.—Working Operations", to

be held in London on 28 April 1954.

† The British Aluminium Co., Ltd., Gerrards Cross, Bucks.



In a production process the known quantity is frequently the input weight from which a variable weight of product is recovered. The recovery is controlled as far as possible, and a fairly stable, average level is maintained, but about this mean recovery there is considerable variation which is due to non-assignable process losses and rejections for sub-standard quality. It is also common for a relatively heavy financial loss to be incurred if the recovery falls below a certain value. A fixed weight of product required for a single order may be the objective, and if this is not achieved, a second batch of material may have to be specially processed to make up the order. Under such circumstances, there may be a loss of goodwill due to delay in delivery. On the other hand, there is a loss in production and an increase in "tied" capital if large excess weights are produced. A balance has therefore to be struck.

If the distribution of a group of past weight recoveries from an input weight,  $I_0$ , has the form shown in Fig. 1, and  $M_0$  is the weight recovery below which a serious loss is incurred, the area  $A_1$  represents the proportion of recoveries which fail to achieve  $M_0$ , and the area  $A_2$  represents the proportion of cases where an excess weight is produced.

Proportion of lots failing to achieve  $M_0$

$$= \frac{A_1}{A_1 + A_2} = P,$$

and proportion of lots in which an excess is incurred

$$= \frac{A_2}{A_1 + A_2} = 1 - P$$

The average excess weight produced is the mean abscissa of the area  $A_2$ ; let this be  $X$ .

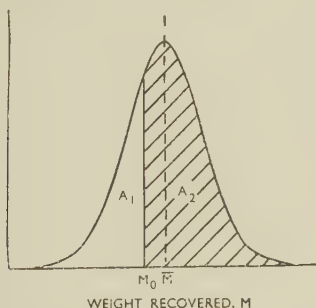


FIG. 1.—Distribution of Weight Recoveries.

Values of  $P$  and  $X$  can now be determined assuming the same frequency distribution of recoveries about different means, and curves of the form I, proportion of lots failing to reach  $M_0$ , and II, mean excess weight, as shown in Fig. 2 are obtained. If relative costs can be allocated to I and II, an overall cost curve, of the type III in Fig. 2, can be plotted, and the minimum on this curve gives the optimum value of the mean weight recovery. The input weight is then adjusted to give this recovery, and this will be the most economical input weight.

An application of this technique to the production of 40-ft.-long bars has been described by Passano.<sup>1</sup>

To avoid bars shorter than 40 ft., which would be rejected, the standard practice had been to work with a billet length which gave bars of average length 41.8 ft. An analysis of production data on the above lines showed that a shorter billet which would yield

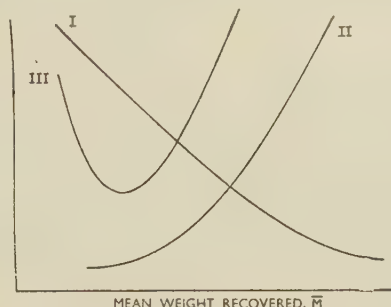


FIG. 2.—Cost Balance of the Proportions Failing to Achieve  $M_0$  and Excess Weight.

- I. Proportion failing to achieve  $M_0$ .
- II. Mean excess weight.
- III. Overall cost.

bars of mean length 41 ft., with one bar in a hundred less than 40 ft., gave an overall increase in output of 0.6%. This gain was achieved without any added cost.

Goodeve<sup>2</sup> commenting on this application, points out the weakness in the original production conditions; namely, that output was being restricted through over-avoidance of the more "sensational" loss (a rejected bar). This is a very common situation in industry.

No assumptions have been made above regarding the characteristic recovery distribution. Where a relatively large number of past results are available, a histogram of results can be constructed, and a simple arithmetical procedure used to obtain the I and II type curves. When adequate past data are not available, it is necessary to assume some form of recovery distribution, and to estimate its parameters from a small sample of past results. If a normal distribution is assumed, estimates of the mean and standard deviation ( $s$ ) may be made and the required area ( $A_1$ ) obtained from reference tables. The mean excess weight (excluding underweight lots) is given by:

$$\text{Mean excess weight} = \frac{sy_0}{1 - A_1} + (\bar{M} - M_0),$$

where  $y_0$  is the ordinate of the normal distribution at  $M_0$ . Values of  $y_0$  can also be obtained from statistical tables.

A similar problem was recently encountered in the extrusion of aluminium section. An extrusion defect occurs towards the end of each billet, and to measure the extent of this defect before cutting into the required lengths is not practicable on a routine basis, since cross-sections have to be cut and etched at small intervals until sound metal is reached. In practice, therefore, the last one or two sections from each billet are rejected.

A means of overcoming this difficulty has been developed. Billet ends after extrusion are process

scrap and are of the shape shown in Fig. 3. Over a period of time, the cross-section (*A*) of butt ends is



FIG. 3.—Sectional Shape of Billet End after Extrusion.

etched, and the presence or absence of extrusion defect recorded, together with the weight of the butt end, expressed as a percentage of the original billet weight. By dividing the butt weights (percentage)

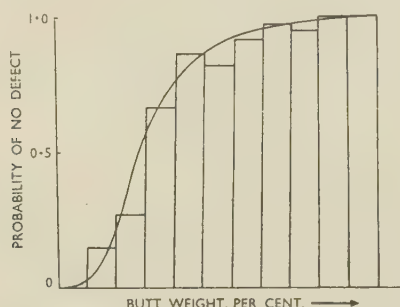


FIG. 4.—The Probability of Freedom from Extrusion Defect.

into relatively small intervals, and computing the ratios of billets showing no defect to the total number examined in each interval (i.e. the probability of "no defect"), a curve such as Fig. 4 is obtained.

From this curve a residual billet weight corresponding to a small probability of defect can be fixed. Extrusion can be arrested at this point, and the effort and cost of extruding defective lengths avoided. In addition, a single etch test on the end of the last section can be carried out, and the relatively small proportion of defective lengths which are produced can be rejected. In this way the output of section can be increased, and the risk of supplying a defective length diminished.

Acceptance of a certain degree of variability is common to each of the above applications. The assessment of this scatter is used to minimize the costs of an existing process. A reduction in scatter, or a change in mean level, would pay even bigger dividends, but such changes, if at all possible, usually involve long-term investigation and probably plant replacement. Whilst fundamental improvement should always be the ultimate objective of research and process development, the immediate saving resulting from correct handling of operational process data should not be overlooked.

### III.—INTERMEDIATE PROCESS LIMITS

Intermediate property or quality limits should be established to avoid processing material that will ultimately prove to be sub-standard. These limits may define the level of a process variable, or may

refer directly to an intermediate characteristic of the material being processed. Divergence from the prescribed limits should be a criterion for rejection. A constant study should therefore be made of the relationships which exist between process variables, and intermediate and final properties.

The statistical techniques of correlation and regression are useful in this field. Regression analysis not only establishes that there is a real association between the variables, but it also defines the relationships quantitatively. It also assesses the remaining variation in the dependent variable, e.g. the final property, when allowance has been made for the effect of the independent variables, i.e. the particular process variables included in the analysis. The assessment of this residual variation is of particular importance, for the probability of final success can only be resolved if it is known. It is on this probability that the decision to reject or pass at the intermediate stage should be made.

A warning is necessary—a relation between two variables may be shown to be statistically significant, but this does not imply the existence of a cause and effect dependence. It is essential that there should be some *a priori* reason for causal association before a regression analysis is started.

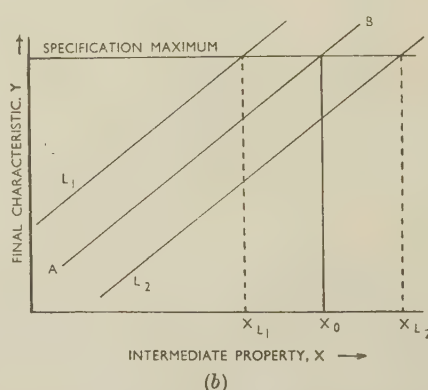
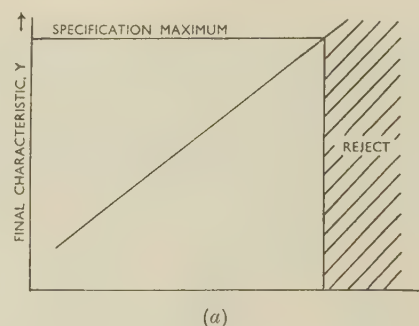


FIG. 5.—Rejection Criteria Based on (a) Linear Relationship and (b) Linear Relationship with Residual Variation.

A final characteristic (*Y*) may be related to an intermediate property (*X*), in the way shown in Fig. 5 (a), and it is easy to fix a limit  $X_0$ , which is the criterion of rejection at the production stage where *X* is measured.



When the relation between  $X$  and  $Y$  is less determinate owing to the effect of later process variables, the situation may be as shown in Fig. 5 (b), where  $L_1$  and  $L_2$  denote the limits for  $Y$  for given values of  $X$ . In this case, the adoption of  $X_0$  as the criterion of rejection may be unwise, as there is obviously an even chance of obtaining a satisfactory product, corresponding to a value  $X_0$  of the intermediate variable. In general, if  $X$  refers to an early stage in the process, i.e. before the cost of production has become heavy, it will pay to use  $X_{L_1}$  as the criterion of rejection. Conversely, if  $X$  refers to a stage late in the process when heavy cost has already been incurred,  $X_{L_2}$  will be a better limit.

Careful scientific determination of the relation  $AB$  may be of little value in determining the limit for  $X$ . This is particularly true if  $X$  refers to a variable early in production, or if it can be held at a fairly steady value while the limits  $L_1$  and  $L_2$  for  $Y$  apply.  $X_{L_1}$  is then required. As  $X_{L_1}$  is mainly a function of later processing, under typical works conditions, it can be determined only from data appropriate to such conditions. This is not an argument against the need to determine  $AB$  or the reasons for the existence of the relationship. The scientific approach to this particular problem is limited, unless it is followed by works trials, preferably with no special control of the rest of the process. A statistical analysis is then necessary to supplement such trials.

The above considerations apply particularly to composition limits, where the decision to pass or fail a heat should almost always be referred to the limit  $X_{L_1}$ . An example of the application of the statistical approach to such a problem will be illustrated.

In the production of high-conductivity aluminium wire for electrical purposes, it is important that only wire-bars likely to lead to wire of the required conductivity should be passed to the wire mills. Conductivity tests on wire-bars are expensive and are not generally a reliable measure of the final conductivity when drawn into wire. It is therefore necessary to have composition limits which will ensure that the final conductivity is attainable.

For many years, composition limits in terms of silicon, manganese, and titanium were used as a criterion of satisfactory purity, but pure metal supplies were recently shown to contain an appreciable content of vanadium, which causes a marked decrease in conductivity. The problem was therefore to redetermine suitable composition limits and to find out if routine analyses for vanadium were necessary on all heats.

Resistivity measurements were made on hard-drawn wire from a number of heats of known composition. The heats were randomly selected over a period of time so that they were representative of metal supplies. The wire was produced under typical works conditions with no special supervision.

The technique of multiple regression was employed and an equation was derived to estimate resistivity from the silicon, manganese, titanium, and vanadium contents:

$$\rho = 2.727 + A(\% \text{ Si}) + B(\% \text{ Mn}) + C(\% \text{ Ti}) + D(\% \text{ V}) \quad (1)$$

The estimate of  $\rho$  from this equation is subject to a standard error of  $\pm 0.0065$  microhm.cm.

To enable the results to be plotted graphically,  $U$  may be defined as:

$$U = A(\% \text{ Si}) + B(\% \text{ Mn}) + C(\% \text{ Ti}) + D(\% \text{ V}) \quad (2)$$

so that equation (1) reduces to:

$$\rho = 2.727 + U \quad (3)$$

The experimental values of resistivity are plotted against  $U$  in Fig. 6. The line represented by equation

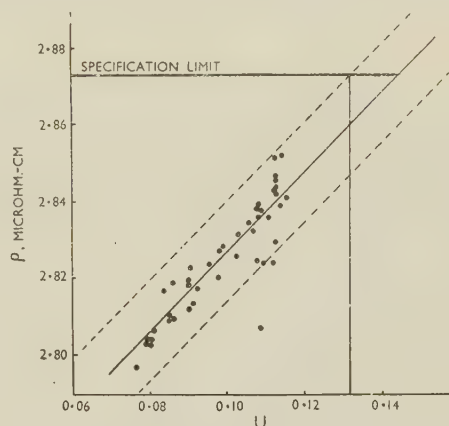


FIG. 6.—The Effect of Impurities on the Resistivity of Electrical-Purity Aluminium Wire.

$$U = A(\% \text{ Si}) + B(\% \text{ Mn}) + C(\% \text{ Ti}) + D(\% \text{ V}).$$

(3) is also shown, and limits have been drawn at  $\pm 0.0130$  microhm.cm. (i.e.  $\pm 2s$ ). These limits are such that they should contain 95% of the observed resistivities. The maximum resistivity, by specification, is also shown, and the point at which the upper limit intersects this line is the maximum value of  $U$ , which was adopted as an upper composition limit. Using this criterion, no wire-bar is released unless the chances of passing the final resistivity specification are 98 in 100 or more.

The need for routine vanadium determinations on all heats was considered and an examination of the distribution of vanadium contents in a representative selection of heats was made. It was shown that the effect of vanadium, in relation to the specified maximum resistivity, could be ignored if the level of the other impurities was low. Composition limits were therefore set in terms of silicon, manganese, and titanium, and vanadium is determined only when a particular heat fails to meet the limit in respect of the other impurities. The vanadium figures obtained on these heats, together with determinations made on a small proportion of normal heats, are used to maintain a control chart which will indicate any adverse trend in purity.

It is worth noting that later results, on metal of lower purity than was encountered in this investigation, confirmed the relation for values of  $U$  up to 0.14.

This investigation set rational composition limits for the purity of heats, and prevented the unnecessary introduction of routine vanadium determinations.

A similar investigation, on a much larger scale, since many more process variables were included, has recently been carried out by Andrew.<sup>3</sup> By an analysis of the process variables in the production of a ferrous rolled product, it was shown that the silicon content of the metal was the major factor giving rise to defects in the final product. By reducing the content of silicon to about one-quarter of its previous level, rejections were reduced from about 4 to 1.5%. In this way the complete scrapping of some 900 tons/annum of finished product was avoided.

#### IV.—SAMPLING AND ACCEPTANCE

A problem common to all industries is that of sampling and testing a batch of material or items to determine whether a specified quality or property is met. The first difficulty often lies in interpreting the terms of a loose specification. If a measurable property is concerned, the specification may simply state " $X$  less than  $X_m$ ," and there are two intrinsically different interpretations. It may be intended that the mean of any batch of material is to be less than  $X_m$ , or, alternatively, that no individual, or at least only a small proportion of items, is greater than  $X_m$ . The latter is undoubtedly the more frequently intended meaning, but although this may seem obvious, current procedures for accepting a batch are not usually compatible with this interpretation. A number of tests are usually made, and if the mean is equal to, or just under,  $X_m$  the lot is accepted.

Taking the limiting case, it is clear that only 50% of the individuals have expected properties less than  $X_m$ . It may be argued that the original specification takes this into account, and is actually intended to ensure that the bulk of the individual items are less than  $X_m + \delta_m$ , where  $\delta_m$  is an appropriate increment to allow for testing, and sampling errors. If this is so, the first interpretation is correct. There will usually be some doubt, and a well-defined specification should state explicitly what is required.

In the above example, it is assumed that correct allowance can be made for  $\delta_m$ . This is true only under certain conditions. If each batch of items represents a production unit, e.g. a batch of sheets heat-treated at the same time, the variability within batches will always be less than that of results from different batches. In most established processes, the standard deviation of results on samples selected from within a batch will be fairly stable and characteristic of the process. If  $s$  is the within-batch standard deviation, the standard error of the mean of  $n$  tests on randomly selected items from the batch is given by:

$$s_{\bar{X}} = \frac{s}{\sqrt{n}}$$

This standard error and the mean of the samples tested can be used to obtain the probability that the batch satisfies the specification requirements. A criterion of acceptance based on this probability is then fixed;  $s$  is taken to refer to all batches, and a fixed sampling scheme is laid down. An allowance  $\delta_m$  can be made, so that the mean of the batch can be used to decide the fate of the batch, rather than the proportion of items which must lie within specification.

The derivation of a sampling and acceptance procedure, covering the grain-size of pure aluminium circles, is outlined below.

The standard deviation of grain-size numbers (which range from 1 to 8 in units of 0.5), on randomly selected circles from batches annealed together, is  $\pm 0.6$  units. Past data have shown that results on samples from within a batch, are approximately normally distributed about their mean in the range 2 to 7 units. A sampling and acceptance procedure is required which will ensure that 95% of the circles in an accepted batch have a grain-size number of 5 or greater.

Consider an individual batch, and let  $\mu$  be the true batch mean.

Let  $\lambda = \frac{\mu - 5}{0.6}$ , i.e. the deviation of the limit from the true mean, expressed as a fraction of the standard deviation.

The proportion of results lying below 5 can be obtained in terms of  $\lambda$ , from tables. When this proportion is 5%,  $\lambda = 1.67$ .

$$\therefore 1.67 \times 0.6 = \mu - 5$$

$$\therefore \mu = 6$$

The minimum batch mean corresponding to 95% of individual results above 5, is 6 (i.e.  $\delta_m = 1$ ).

A sampling procedure to ensure that the batch mean is 6 or greater has now to be found.

If  $n$  samples are selected at random, the mean  $\bar{X}$  has standard error,  $s_{\bar{X}}$ :

$$s_{\bar{X}} = \pm \frac{0.6}{\sqrt{n}}$$

$$\text{Let } \lambda' = \frac{\bar{X} - 6}{\pm \frac{0.6}{\sqrt{n}}}$$

The proportion of sample means greater or less than 6 can then be obtained in terms of  $\lambda'$  from tables. If odds of 1 in 20, i.e.  $P = 0.95$ , are set against accepting a batch of mean less than 6, or rejecting a batch of mean greater than 6,  $\lambda' = 1.67$ .

$$\therefore \bar{X} - 6 = \frac{1.67 \times 0.6}{\pm \sqrt{n}}$$

$$\text{i.e. } \bar{X} = 6 \pm \frac{1}{\sqrt{n}}$$



If  $n = 1$ ,  $\bar{X} = 5$  or 7  
 If  $n = 4$ ,  $\bar{X} = 5.5$  or 6.5

The following sampling and acceptance procedure may therefore be adopted:

Take one sample.

If $\bar{X} \geq 7$	Pass the batch
$\bar{X} \leq 5$	Reject the batch
$\bar{X} = 5\frac{1}{2}, 6$ , or $6\frac{1}{2}$ .	Take three further samples. If the mean of the four is 5.5 or less, reject; if 6.5 or more, pass.

If a decision is not reached from four samples, the same principle is followed and further tests made until the fate of the batch is decided.

This procedure means that the volume of testing increases if the quality is in doubt. This should be true of all sampling schemes. Modern, sequential procedures<sup>4, 5</sup> are based on this latter principle; the sampling of a batch is continued only until a firm decision can be made to pass or fail. If the batch is very good, or very bad, it will quickly be passed or failed; if it is doubtful, sampling will be prolonged. Such schemes minimize the overall sampling for a given degree of testing efficiency, but they have not proved popular in industry, owing to the variable load on testing or inspection departments. The procedure for grain-size control outlined above is a sequential scheme of a type which we have found to work very well in practice.

When lots for testing are made up with no emphasis on segregating production units, varying proportions of different batches will constitute any one lot. If the batch-to-batch variation is great, extensive sampling will be necessary to obtain the information for a basis of acceptance. Under these conditions, the variability within a lot will not be stable, no rational sampling scheme can be laid down, and no reasonable allowance for  $\delta_m$  can be made.

In the situation where the quality level is high, and variation between batches small relative to specification requirements, there may be no need to test all batches. A proportion of batches can be tested, and a quality control chart run, to give early indication of any adverse trend in quality or variability. The need for process batch segregation is not then so apparent, but it is preferable so that process troubles which may develop may be more quickly rectified.

It will be clear that efficient and economical sampling rates can only be assessed correctly by the producer in relation to his particular plant and process. It is useless to lay down generally-applicable sampling rates for material produced in diverse ways.

In the non-ferrous industry as a whole, producers have evaded this responsibility. There seems to be a general feeling that the specification should state explicitly what samples are to be taken. If a released batch of material proves faulty, the producer pleads

compliance with specification sampling in defence. This is a very short-sighted attitude. In the first place, the consumer will be more convinced of the reliability of product release if he is shown a logical sampling plan, together with evidence of its efficient working in the past. The consumer will not generally be impressed by the fact that  $n$  samples (as specified) passed the producer's test, if he has shown, by later testing, that the bulk of the material is outside specification. The second disadvantage of generally specified sampling rates is that sampling is made inflexible, and cannot be varied as quality improves or deteriorates. Products of satisfactory quality are thus over-sampled, with a consequent addition to the final cost, and products of doubtful quality are probably sampled less efficiently than they ought to be.

## V.—TESTING

The selection of a routine control or inspection test is, in the first instance, a purely technical problem. The technician, or scientist, has to decide what is to be measured, and what methods of measurement are available. The cost of possible tests in terms of time, performance, labour, type of sample, and equipment, have to be considered in relation to the precision and accuracy required. An accurate test is one which yields an unbiased result, and the precision of a test is a measure of its reproducibility. In practice, inaccurate tests can be tolerated only if the bias is constant under all conditions. The test can then be calibrated to give true values if required.

It is in the balance of time, cost, and precision that statistical analysis can be of most value. A very precise test may be slow, intrinsically costly, and expensive in terms of lost production, if used for process control or material release. On the other hand, if the inherent variability in a test is large, the test may not be sufficiently sensitive to provide a basis for control. The latter limitation may usually be overcome by testing more frequently, and averaging. In cases where more frequent tests can be made to cover a wider range of samples, an advantage is gained in that the sampling and testing errors are reduced simultaneously.

Consider the sampling and testing of a batch of discrete items. Let  $V_s$  and  $V_T$  be the error components (expressed as variances) in a single test result, due to sampling and testing respectively. If  $n$  items are tested, the mean,  $\bar{X}$ , of the  $n$  tests will have variance  $V(\bar{X})$ , where

$$V(\bar{X}) = \frac{V_s + V_T}{n} \quad . \quad . \quad . \quad (4)$$

Let  $C_s$  = cost of taking and preparing a sample (including cost of item if it is destroyed);

$C_T$  = cost of performing single test.

Then  $C$  = total cost =  $n(C_s + C_T)$ . . . (5)

For a given degree of confidence in the sample estimate of the batch mean, i.e.  $V(X)$  constant, the above formulæ may be used to assess the relative efficiencies of alternative methods of testing.

A hypothetical case will be considered. Suppose we wish to assess the tensile strength of a batch of sheet, and that two test methods are available: (i) a normal tensile test and (ii) a hardness test which can be calibrated, within the range of results which will be encountered, to give an unbiased, but less reproducible, value for the tensile strength.

The data assumed to be characteristic of the two tests are given in Table I.

TABLE I.—Assumed Data for Alternative Tests for Tensile Strength.

Test	Single Test		One Sample from Batch *		Cost of Sample, ( $C_S$ )	Cost of Test, ( $C_T$ )
	Standard Deviation, tons/in. <sup>2</sup>	$V_T$	Standard Deviation, tons/in. <sup>2</sup>	$V_S$		
Tensile	0.1	0.01	0.17	0.03	6	6
Hardness	0.3	0.09	0.17	0.03	1	2

\* The variation in samples from the batch excluding testing errors.

If the error in  $\bar{X}$  is to be constant,

$$\frac{V_S + V_{T_1}}{n_1} = \frac{V_S + V_{T_2}}{n_2}$$

(suffixes 1 and 2 denote the tensile and hardness tests, respectively)

$$\text{i.e.} \quad \frac{0.04}{n_1} = \frac{0.12}{n_2}$$

$$\therefore n_2 = 3n_1$$

Three hardness tests are required to give a mean of the same weight as one tensile test.

$$\begin{aligned} \text{Cost of one tensile test} &= 12 \text{ units} \\ \text{Cost of three hardness tests} &= 9 \text{ units} \end{aligned}$$

The hardness test is therefore to be preferred.

If the batches in the above example were more homogeneous, say  $V_S = 0.01$ , the relative costs would be approximately 12 and 15 for the tensile and hardness tests, respectively. The tensile test would therefore be preferred.

A third situation can be considered. It may be possible to take only one sample from each batch, e.g. the batch may be a single coil. If repeat tests are possible on the one sample, no reduction is made to the sampling-error component, and the equation for equal confidence in  $\bar{X}$  is:

$$V_S + \frac{V_{T_1}}{n_1} = V_S + \frac{V_{T_2}}{n_2}$$

Substituting the data in Table I gives  $n_2 = 9n_1$  with relative costs of 12 and 19 for the tensile and hardness tests, respectively.

The importance of the above is that the efficacy of

a method of testing is not merely a function of its cost and precision characteristics, but depends also on the variability of the product which is being tested, and on the sampling procedure which is possible. The two general principles which emerge are (a) the more heterogeneous the product, the less reproducible need be the test used to measure it, and (b) the wider the range of samples which can be covered by repeat tests, the less is the need for a test of high precision. The comparison of test methods without consideration of the conditions under which they are to be operated should be avoided.

In the control of routine testing, a standard of known properties should be kept in the laboratory, and tests made on this standard simultaneously with routine samples, whenever the test is employed. This procedure provides a safeguard against gross errors, for if an impossible value is obtained on the standard, the routine determinations are immediately shown to be in error. A control chart, of the values determined on the standard, will also show any trends in the results of the test, and will enable remedial action to be taken before the trends reach serious proportions.

Where more than one laboratory is employing the same test, the regular exchange of routine samples between pairs of laboratories will provide an even more rigorous check of the accuracy and precision of the test. These inter-laboratory check-results may also be kept in the form of a control chart.

Both of the above controls have the further advantage that over a period they provide data from which the standard error of the method *under routine conditions* may be calculated. In general, the standard error calculated from the inter-laboratory checks will be higher than that from the internal-standard determinations, since the former are subject to a few additional sources of variation and are relatively free from psychological bias.

Details of the advantages and working of the above control procedure, applied to routine chemical analyses, have been published by MacColl.<sup>6</sup> The scheme has been operating for about ten years and many benefits have been derived. Confidence in chemical analyses is very high in both laboratories and works. Very few complaints from customers regarding composition are received, reliable standard deviations for all the analytical processes employed are known, and by general stabilization of the processes employed, a great deal of unnecessary investigatory work by individual laboratories has been avoided.

The sensitivity of a test in which the result is a function calculated from measurements of a number of independent variables can usually be analysed by applying formula (13) (see Appendix).

Suppose  $Y$  is a test result obtained from measurements  $P$ ,  $Q$ , and  $R$ , and that

$$Y = \frac{PQ}{R}$$

where the errors in  $P$ ,  $Q$ , and  $R$  are independent.



$$\text{Then } V(Y) = \frac{Q^2}{R^2} V(P) + \frac{P^2}{R^2} V(Q) + \frac{P^2 Q^2}{R^4} V(R)$$

If  $P$ ,  $Q$ , and  $R$  have typical values 1, 2, and 4, respectively,

$$V(Y) = \frac{V(P)}{4} + \frac{V(Q)}{16} + \frac{V(R)}{64}.$$

For the values chosen this equation shows the relative effects of  $P$ ,  $Q$ , and  $R$  on the sensitivity. If  $V(P) = V(Q) = V(R)$ , it is obvious that a reduction of the error in  $Y$  will most easily be achieved by some improvement in the measurement of  $P$ , rather than that of  $Q$  or  $R$ . This will usually be effected either by increasing the number of replicate determinations of  $P$ , or by refining the technique which is used to measure  $P$ .

## VI.—STATISTICAL QUALITY CONTROL

In Part I of this Symposium, Singer<sup>7</sup> stressed the advantages of error-actuated control. In many metal-fabrication processes, past developments have been concentrated mainly on streamlining production, increasing output, and reducing costs. On the whole, these developments have made it increasingly difficult to establish error-actuated control. For example, the change from sheet rolling to high-speed strip-rolling has made it almost impossible to locate surface defects early in the rolling process. With sheet-rolling, defects could be traced and eliminated before much material was affected. In high-speed strip-rolling, however, such defects cannot normally be detected until final inspection. Production effort has then been wasted on sub-standard material, time has been lost, and it is usually difficult, if not impossible, to trace specific defects to their source.

The metallurgical engineer is very conscious of the increasing difficulty of controlling the quality of his products. Automatic-control units which provide error-actuated control by mechanical or electrical means are being widely used, developed, and explored. Thermostatically-controlled furnaces, self-compensating gauge recorders, and continuous lamination detectors are a few of the more successful applications. The range of situations in which control can be made automatic is still very limited, and a more generally applicable alternative is necessary. Statistical control is an alternative. Such control is error-actuated and is, in effect, a non-mechanical automatic control.

The real value of both automatic and statistical quality control is that the focal points are the production stages, rather than the final quality of the product. It is obvious that a production process can be successful only if intermediate working conditions and qualities which will ensure that the final standard of acceptance is achieved, can be defined and maintained. This is well recognized, but although the control of these intermediate conditions is regarded

as a desirable objective, too little effort is made to ensure that error-actuated control is achieved.

In metal-fabrication processes, too much emphasis tends to be laid on the testing and final inspection of the product. In some processes, data from such tests can be used as a basis for control, preferably in the form of control charts with limits within those required by specification. Trends can then be followed up and sources of trouble eliminated before the consequences are serious.

Changes in quality have to occur fairly slowly before this rather remote control can be effective. But in most processes changes in quality are liable to occur suddenly if error-actuated intermediate control has not been established. In such circumstances, post-mortems are frequently the *modus operandi*.

The cause of heavy rejections becomes the objective of a large-scale investigation which as often as not does not lead to positive rectification of the trouble. The trouble frequently disappears for no other reason than that attention has been focused on the process. No real cause is found. This is an experience common in most industries and indicates that if stage-by-stage control had been operating in the first place, the heavy rejections would not have been incurred.

A typical process in metal fabrication is strip rolling. At first sight, this is a process which is not amenable to stage-by-stage statistical control. The difficulties in application are obviously greater than in many other processes, but much can be done. In the first place, a production procedure has been defined in terms of roll-passes, intermediate gauges, rolling temperatures, width-allowances, and times and temperatures of annealing. Such properties can be measured, and recorded on simple control graphs. Even if the mills are "jobbing", i.e. dealing with a variety of relatively small orders of different types, comparative values can still be plotted on a basis of divergence from aim. Thus intermediate gauges can be recorded successively as "% deviation from objective gauge".

Singer<sup>7</sup> has illustrated the working of the quality-control chart. Remedial action is invoked when deviations beyond statistically determined limits occur. It is usually convenient to set limits at  $\pm 2s$  and  $\pm 3s$ , where  $s$  is the standard deviation of the variable under satisfactory working conditions. The inner limits provide warning of possible divergence, and two successive points above or below one of these limits should be investigated. The outer limits are action limits and are a criterion for immediate investigation and remedial action.

If the parent distribution is Normal (Gaussian), only one value in twenty should lie outside the range  $\pm 2s$  and three in a thousand beyond  $\pm 3s$ . These are, in fact, the odds against unnecessary investigation or action, so that "tail-chasing" effort is kept to a minimum. At the same time, any serious departure from the desired level is quickly spotted.

If the parent distribution is not Normal, the odds against "tail-chasing" may be rather less, but the

efficacy of control will not generally be impaired. When the chart has been in operation for some time, the limits may be re-set by a direct assessment of the limit probabilities from a histogram of the past results.

If in place of individual values (standard deviation,  $s$ ), the means of  $n$  results are plotted, the above mode of application is unaltered but the corresponding limits will be  $\pm \frac{2s}{\sqrt{n}}$  and  $\pm \frac{3s}{\sqrt{n}}$ . Where individual values are obtained serially in time, it is advisable to run two control charts, one for individual values and the

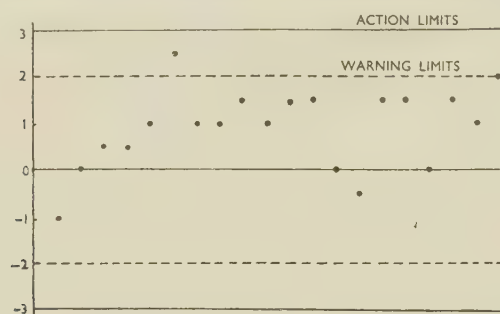


FIG. 7 (a).—Chart of Individual Values (apparently under control).

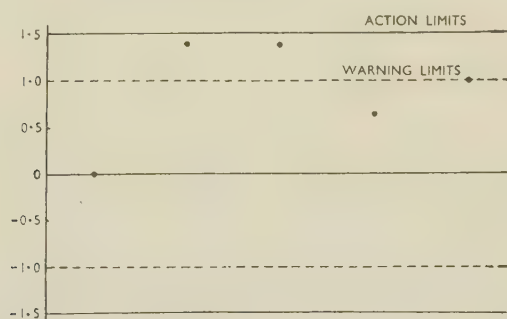


FIG. 7 (b).—Chart of Means of Four Consecutive Values (obviously out of control).

other for the means of a small number of consecutive results. The first chart provides a basis for short-term control, while the second throws into relief any small but persistent trends which occur in time and which may pass unnoticed on the first chart. This is illustrated in Figs. 7 (a) and 7 (b). The means in Fig. 7 (b) correspond to the results plotted individually in Fig. 7 (a).

The reason for the greater sensitivity of the second chart is that the limits based on  $\frac{s}{\sqrt{n}}$  assume that the  $n$  consecutive results, which are averaged, are random samples from the distribution of the individual values. This is not true if time trends are present, and the scatter in the means is then more than anticipated. Action based on the  $\pm \frac{2s}{\sqrt{n}}$  and  $\pm \frac{3s}{\sqrt{n}}$  limits may enable such trends to be repressed.

The value of charts of this type in the control of chemical analysis has been shown by MacColl.<sup>6</sup>

Another situation arises when a group or batch is being tested. If  $n$  samples are taken from each group, it is useful to plot both the batch mean and the range of the  $n$  results. The second chart in this case, controls the variability within the batch or group. This technique, extensively used in mass-producing industries, has been successfully applied by Harding<sup>8</sup> in the control of high-duty iron production in a number of foundries.

#### ACKNOWLEDGEMENT

The author wishes to thank the Directors of The British Aluminium Co., Ltd., for permission to publish this paper.

#### REFERENCES

1. R. F. Passano, *Yearbook Amer. Iron Steel Inst.*, 1949, 192.
2. C. Goodeve, *Manager*, 1953, 21, 257.
3. J. E. Andrew, *Iron Coal Trades Rev.*, 1953, 167, (4464), 1003.
4. A. Wald, "Sequential Analysis". 1947: New York (John Wiley and Sons, Inc.).
5. G. A. Barnard, "Economy in Sampling", Ministry of Supply, Advisory Service on Statistical Method and Quality Control, Tech. Rep., No. Q.C./R/7 (1944).
6. H. G. MacColl, *Chem. and Ind.*, 1944, 418.
7. A. R. E. Singer, *J. Inst. Metals*, 1952-53, 81, 329.
8. E. W. Harding, Suppt. to *J. Roy. Statist. Soc.*, 1946, 8, 233.

#### APPENDIX

##### SIMPLE STATISTICAL CONCEPTS AND FORMULÆ

A few of the simpler statistical concepts and formulæ, are summarized below. Only the basic information necessary to the understanding of very

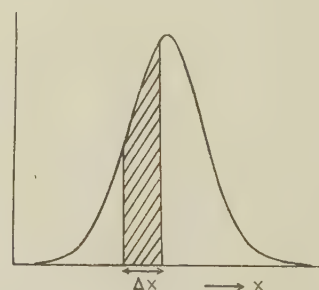


FIG. 8 (a).—Frequency-Distribution Curve.

straightforward applications is included, but a short classified bibliography is given at the end of the Appendix.

Statistics is essentially a study of variation. Theoretically, an infinite number of measurements or estimates of any true value are possible. Each individual measurement is subject to a varying error, and taken together all the individual measurements form a population. This population can be represented by a frequency-distribution curve, which may take the form shown in Fig. 8 (a).

The essential property of the frequency-distribution curve is that the area bounded by it, and any interval



of the measured variable, is proportional to the frequency or probability of values occurring in this interval. When only a finite number of results are available, a histogram which is, in effect, a discontinuous frequency-distribution curve can be drawn. A typical histogram of ultimate tensile strengths is shown in Fig. 8 (b). The heights of the vertical

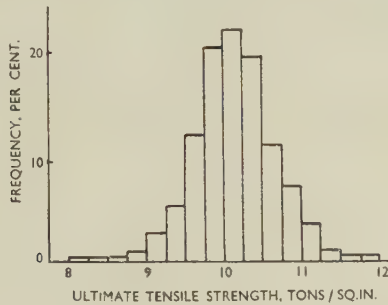


FIG. 8 (b).—Histogram of Ultimate Tensile Strengths.

rectangles are proportional to the observed frequencies in each interval.

The major problem of statistics is the estimation of the characteristics, e.g. mean level, and variability of the population, from finite samples.

Consider a finite sample of observations  $X_1, X_2, \dots, X_n$ . The most common measure of the average level is the arithmetic mean.

$$\text{Arithmetic mean} = \bar{X} = \frac{S(X)}{n} \quad (6)$$

where  $S$  denotes summation from 1 to  $n$ .

If  $X_1, X_2, \dots, X_n$  have weights  $W_1, W_2, \dots, W_n$  (e.g. relative frequencies),

$$\bar{X} = \frac{W_1X_1 + W_2X_2 + \dots + W_nX_n}{W_1 + W_2 + \dots + W_n} = \frac{S(WX)}{S(W)} \quad (7)$$

To measure the variability of the individual values about their mean, the standard deviation ( $s$ ) is defined:

$$s = \sqrt{\frac{S(X - \bar{X})^2}{n - 1}} = \sqrt{\frac{S(x^2)}{n - 1}} \quad (8)$$

where  $x = (X - \bar{X})$ .

Strictly speaking, the denominator in the above expression should be  $n$  when the standard deviation refers to the sample. In practice, the variation in the sample is always used to obtain an estimate of the standard deviation of the population from which the sample is drawn, and the best estimate is given by  $(n - 1)$  in the denominator.

The squared standard deviation is called the "variance", and is denoted by  $s^2$  or  $V(X)$ . The standard deviation and variance are estimates based on  $(n - 1)$  degrees of freedom, i.e. one less than the number of results since a constraint has been imposed by the assumption of the value  $\bar{X}$ .

In many applications it is convenient to assume that the parent distribution is of the Normal (Gaussian)

type. This is often not strictly true, but it proves to be a workable assumption leading to no serious discrepancies. In other cases, a variate transformation can be made which will render the original distribution approximately Normal. The Normal distribution is completely defined in terms of its mean and standard deviation. If these are known, or if estimates are available, the proportion of results lying in any interval can be obtained from tables reproduced in almost all reference books on statistics.

Another property of the Normal distribution is that the mean of a sample of  $n$  randomly selected observations is itself normally distributed about the true mean with standard deviation,  $s_{\bar{X}}$ :

$$s_{\bar{X}} = \pm \frac{s}{\sqrt{n}} \quad (9)$$

The standard deviation of a mean or of any estimated statistic is referred to as its standard error. It should be noted that relation (9) is increasingly true as  $n$  increases for any uni-modal distribution which is not too skew.

The variances of a number of independent variables are additive. Thus if  $X$  and  $Y$  are independent variables with variances  $V(X)$  and  $V(Y)$ ,

$$V(X \pm Y) = V(X) + V(Y) \quad (10)$$

This fact is one of the most important in statistical theory and provides the basis of the "analysis of variance" technique, which in recent years has transformed and improved the general approach to the design of experiments and the interpretation of experimental data.

The following relationship is a corollary of equation (10),

$$V(X_1 + X_2 + \dots + X_n) = n V(X) \quad (11)$$

$$\text{and} \quad V(nX) = n^2 V(X) \quad (12)$$

$$\therefore V(\bar{X}) = V\left(\frac{S(X)}{n}\right) = \frac{n V(X)}{n^2} = \frac{V(X)}{n}$$

$$\text{i.e.} \quad s_{\bar{X}} = \frac{s}{\sqrt{n}}$$

A useful approximation for the variance of a function of variables  $X, Y$ , and  $Z$ , where the errors in  $X, Y$ , and  $Z$  are independent is:

$$V[f(X, Y, Z)] = \left(\frac{\partial f}{\partial X}\right)^2 V(X) + \left(\frac{\partial f}{\partial Y}\right)^2 V(Y) + \left(\frac{\partial f}{\partial Z}\right)^2 V(Z) \quad (13)$$

This expression gives a reliable estimate of the variance of the function, provided that the component errors are independent, and that the standard deviation of each of the variables  $X, Y$ , and  $Z$  is no greater than about one-fifth of its mean level. The formula is useful in determining which components in a calculated function should be most closely controlled if the error variation in the function is to be kept low.

*Correlation and Regression*

If  $X_1, X_2, \dots, X_n$  and  $Y_1, Y_2, \dots, Y_n$  are two sets of variables and if  $X$  is the independent variable, subject to less error than  $Y$ , then the best estimate of  $Y$ , in terms of  $X$ , assuming a linear relationship, is  $Y_E$  in the following equation:

$$Y_E = a + bx \quad (14)$$

where  $a = \bar{Y}$ ,  $x = X - \bar{X}$ ,  $y = Y - \bar{Y}$ ,

$$\text{and } b = \frac{S(xy)}{S(x^2)}.$$

The standard error of the estimated value of  $Y$  is

$$s_{Y_E} = \pm \sqrt{\frac{S(Y_E - Y)^2}{n - 2}} \quad (15)$$

This standard error defines the efficacy of the estimation.  $s_{Y_E}$  may be used to provide limits for the deviations of observed values of  $Y$  from the estimated line, in exactly the same way as the standard deviation provides limits for individual values of a single variable.

The correlation coefficient gives an overall assessment of the statistical significance of the relationship between two variables.

$$\text{Correlation coefficient} = r = \frac{S(xy)}{\sqrt{S(x^2)S(y^2)}} \quad (16)$$

$r$  is associated with  $(n - 2)$  degrees of freedom and varies between 0 and 1 (or 0 and  $-1$  if the relation is inverse). The higher the correlation coefficient, the lower the probability that it has been obtained by chance from samples of two uncorrelated variables. Tables of  $r$  have been compiled, and the probability of a true relationship assessed.  $r^2$  is a measure of the proportion of the total variation in  $Y$ , which is accounted for in terms of a linear correction for  $X$ .

$$\begin{aligned} \text{i.e. } S(Y_E - Y)^2 &= (n - 2) V(Y_E) \\ &= (1 - r^2) S(y^2) \end{aligned} \quad (17)$$

The technique of regression analysis is not confined to the linear case with one independent variable, which is illustrated above. Curvilinear equations can be fitted with more than one independent variable. Where more than one independent variable is included, the technique is called multiple regression analysis. In all cases, an important feature is the estimation of the residual standard error, and the

probability assessment of the need to retain each term included in the analysis.

## BIBLIOGRAPHY

(a) *General Text-books*

- R. A. Fisher, "Statistical Methods for Research Workers". 1950: Edinburgh (Oliver and Boyd).  
 G. W. Snedecor, "Statistical Methods". 1946: Ames, Iowa (Iowa State College Press).  
 G. Udny Yule and M. G. Kendall, "An Introduction to the Theory of Statistics". 1950: London (Charles Griffin and Co., Ltd.).

(b) *Industrial Applications*

- K. A. Brownlee, "Industrial Experimentation". 1949: London (H.M. Stationery Office).  
 O. L. Davies, "Statistical Methods in Research and Production with Special Reference to the Chemical Industry". 1949: Edinburgh (Oliver and Boyd).  
 L. E. Simon, "An Engineers' Manual of Statistical Methods". 1941: New York (John Wiley and Sons, Inc.); London (Chapman and Hall, Ltd.).

(c) *Design of Experiments*

- R. A. Fisher, "The Design of Experiments". 1951: Edinburgh (Oliver and Boyd).  
 W. G. Cochran and G. M. Cox, "Experimental Designs". 1950: New York (John Wiley and Sons, Inc.); London (Chapman and Hall, Ltd.).

(d) *Mathematical Statistics*

- M. G. Kendall, "The Advanced Theory of Statistics", Vols. 1 and 2. 1948-51: London (Charles Griffin and Co., Ltd.).

(e) *Regression Analysis*

- M. Ezekiel, "Methods of Correlation Analysis". 1949: New York (John Wiley and Sons, Inc.).  
 P. Lyle, "Regression Analysis of Production Costs and Factory Operations". 1946: Edinburgh (Oliver and Boyd).

(f) *Quality Control*

- B.S. 600:1935, "Application of Statistical Methods to Industrial Standardization and Quality Control".  
 B.S. 600R:1942, "Quality Control Charts".  
 B.S. 1008:1942, "Guide for Quality Control and Control Chart Method of Analysing Data".  
 B.S. 1313:1947, "Fraction Defective Charts for Quality Control".  
 W. A. Shewhart and W. E. Deming, "Statistical Methods from the Viewpoint of Quality Control". 1939: Washington, D.C. (U.S. Department of Agriculture).

(g) *Tables*

- R. A. Fisher and F. Yates, "Statistical Tables for Biological, Agricultural, and Medical Research". 1953: Edinburgh (Oliver and Boyd).



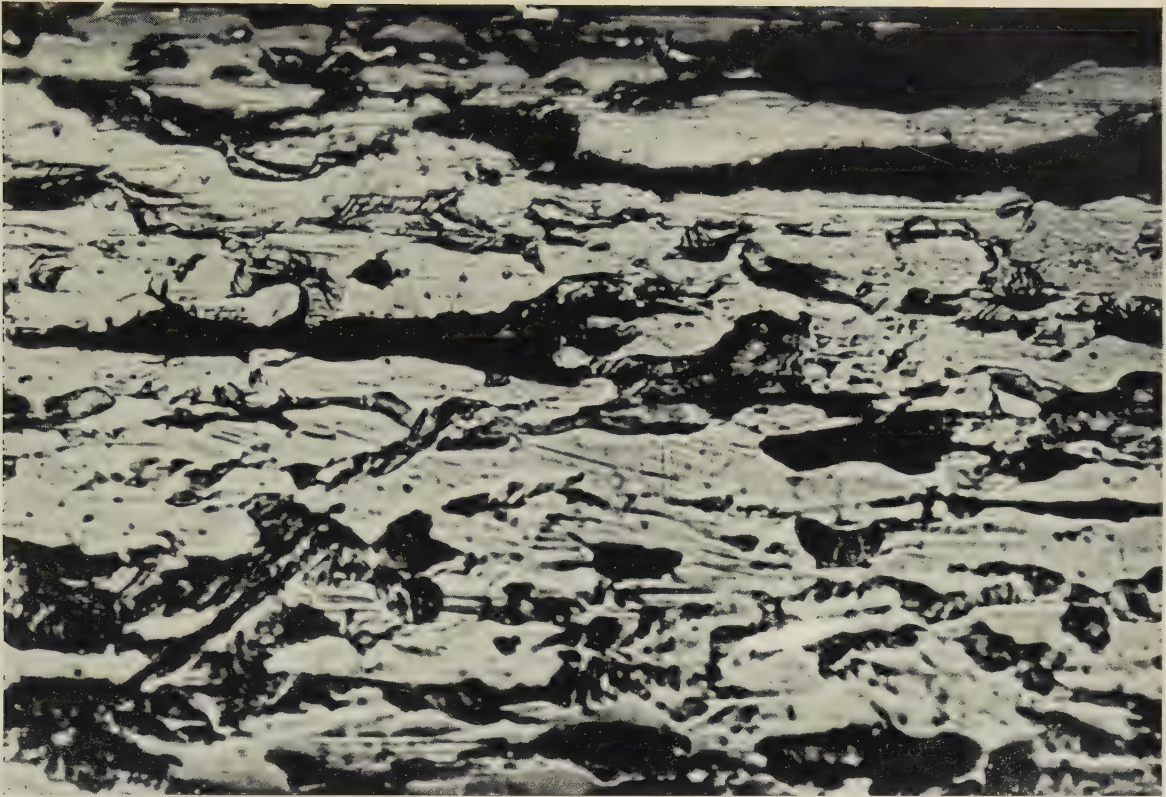


FIG. 4.—Surface of a Bright-Drawn Steel Wire (Medium Finish).  $\times 500$ .



FIG. 5.—Surface of a Bright-Drawn Steel Wire (High Mirror Finish).  $\times 500$ .

[To face p. 344.]



FIG. 3.—Microstructure of Sample of Aluminium-14% Manganese Alloy Strip Which Failed on Pressing, Showing Coarse Intermetallic Constituents. Unetched.  $\times 150$ .

FIG. 4.—Microstructure of Sample of Aluminium-14% Manganese Alloy Strip Which Pressed Satisfactorily, Showing Fine Intermetallic Constituents. Unetched.  $\times 150$ .

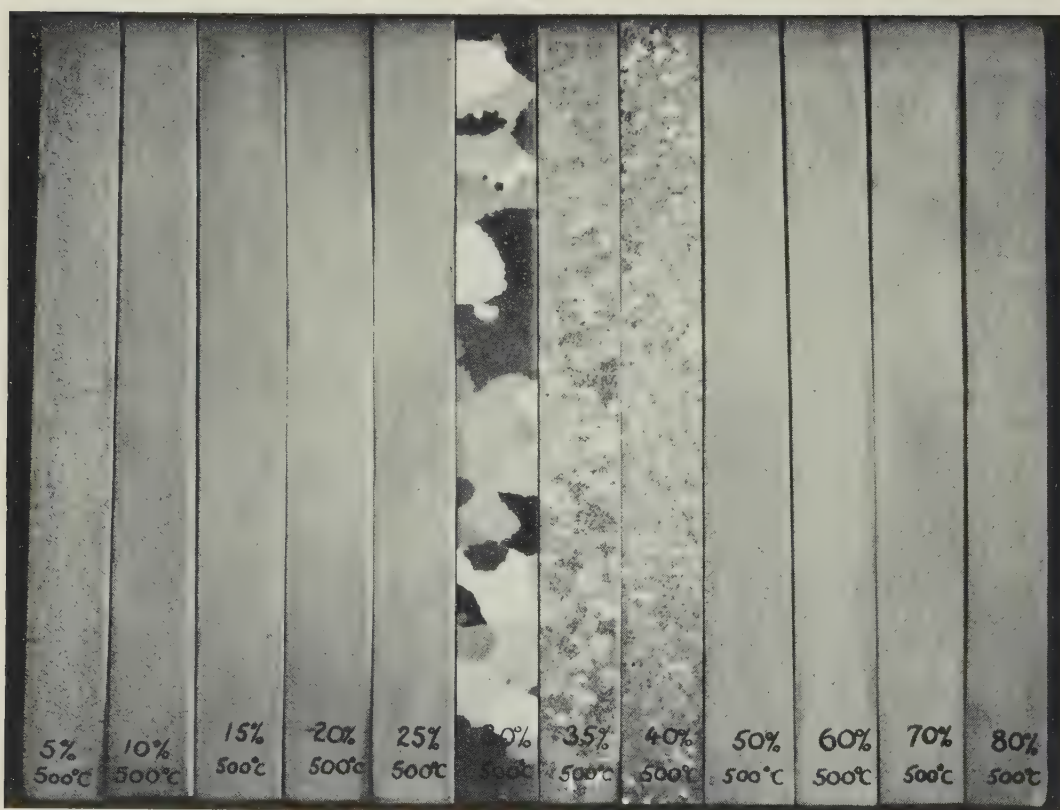
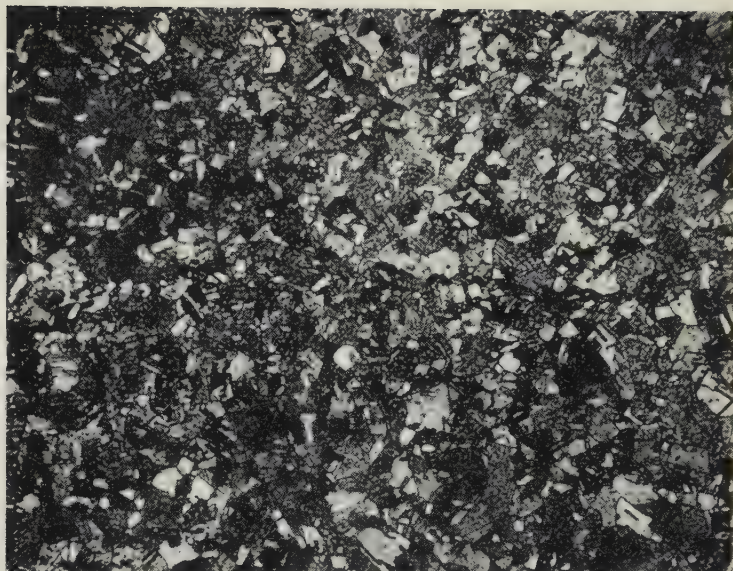


FIG. 5.—Macro-Etched Samples of Aluminium-5% Magnesium-0.3% Manganese Alloy Sheet, Illustrating Relation Between Cold Work Before and Grain-Size After Annealing at 500° C.





FIG. 10.—“Flying Mike” Roller-Type Micrometer Installed on a 300 ft./min. Brass Strip Mill. It is used for the manual control of gauge by varying the mill screw-down. The guide-roll in front ensures correct alignment of the strip passing through the detector head.



(a)



(b)

FIG. 11.—Non-Directional and Directional (85% Cubic Structure) Copper Strip Compared by Etching Polished Specimens in an Acidic Aqueous Solution of Ferric Chloride.  $\times 75$ .

(a) Non-directional.

(b) Directional.





# THE FORGEABILITY, CREEP STRENGTH, AND DUCTILITY OF MOLYBDENUM AND SOME OF ITS ALLOYS\*

1527

By J. H. RENDALL,† B.Sc., A.R.S.M., A.I.M., MEMBER,  
S. T. M. JOHNSTONE,‡ B.Met.E., A.I.M., MEMBER, and  
W. E. CARRINGTON †

(Communication from the National Physical Laboratory.)

## SYNOPSIS

Three aspects of the use of molybdenum and molybdenum-base alloys as heat-resistant materials have been investigated, using powder-metallurgy methods: (1) the forgeability of binary alloys; (2) the creep-resistance at 1000° C. of forgeable binary alloys; (3) the effect of processing variables and alloying additions upon the temperature of transition from ductile to brittle behaviour in a simple bend test. The main conclusions drawn are:

(a) Nearly all alloying additions have an adverse effect on forgeability, the effect being the greater the larger the difference in atomic diameter between the alloying element and molybdenum.

(b) The creep strength of forgeable alloys at 1000° C. is not very much greater than that of molybdenum.

(c) The effects of processing variables on the ductility of molybdenum are very inconsistent, but it appears that increases in oxygen content, grain-size, and porosity decrease the ductility of sintered molybdenum.

(d) All alloying additions, except carbon, aluminium, and titanium, decrease the ductility of molybdenum. The improvement brought about by these elements is not large and is probably due to the resulting reduction of oxygen content.

## I.—INTRODUCTION

INCREASE in the operating efficiency of gas turbines is largely a matter of raising the operating temperature, and has led to a demand from designers for materials capable of withstanding increasingly high temperatures. There are good grounds for believing that no great increase is possible in the operating temperature of the iron- and nickel-base alloys now in use. Thus, it is probable that to develop alloys having a useful creep-resistance at 1000° C., metals such as molybdenum, with a higher melting point than nickel or iron, will have to be used as the major constituents. The main objection to the use of molybdenum at high temperatures is its low resistance to oxidation in air above 400° C. It is believed, however, that should a satisfactory creep-resistant alloy be developed, the problem of finding a suitable protective coating would not prove insoluble.

The present investigation has covered:

(1) The effect of alloying elements on the forgeability of molybdenum.

(2) The effect of alloying elements on the creep strength of molybdenum at 1000° C.

(3) The effect of processing methods and alloying additions on the ductility of fully annealed molybdenum between -50° and +600° C.

Powder metallurgy was chosen as the method of

making the alloys. Molybdenum is easily obtained as a very fine powder (1-10  $\mu$  in size) of high purity (99.9%). A number of other high-melting-point metals which might form useful alloying additions are also available as fine powders, e.g. tungsten and tantalum. In addition, it has been found that alloys made by powder metallurgy are somewhat easier to forge than those made by arc melting,<sup>1</sup> probably as a result of the finer grain-size of the sintered alloys.

On the other hand, there are a number of objections to the use of powder-metallurgy methods, e.g. sintered alloys may not be homogeneous, and, moreover, powders have a large surface area and are easily contaminated, especially by gases. The inhomogeneity of the alloys may be reduced by using fine powders, mixing them well, and sintering at high temperatures; these measures increase the rate of diffusion and also tend to remove gaseous or other volatile impurities of the powders, thus reducing the contamination associated with their large surface areas.

## II.—PREVIOUS WORK

A short review of the work on molybdenum alloys published up to 1947 is given by Schwarzkopf.<sup>2</sup> Work on arc-cast molybdenum alloys is summarized by Ham.<sup>1</sup>

Reliable equilibrium diagrams exist for the binary

\* Manuscript received 6 August 1953.

† National Physical Laboratory, Teddington, Middlesex.

‡ Aeronautical Research Laboratories, Melbourne, Australia; previously attached to the National Physical Laboratory.

systems of molybdenum with chromium,<sup>3,4</sup> cobalt,<sup>5</sup> iron,<sup>6</sup> nickel,<sup>7</sup> tantalum,<sup>8</sup> titanium,<sup>9</sup> and tungsten.<sup>10</sup> The only trustworthy information on the molybdenum-rich side of the diagrams for alloys with aluminium, manganese, and zirconium, is given by Ham,<sup>1,11</sup> who reports limits of solubility.

Sykes<sup>12</sup> gives the tensile strength and elongation, at a series of temperatures, of molybdenum wires after various treatments. Marden and Wroughton<sup>13</sup> quote tensile strengths and elongations of molybdenum wires and point out the wide variations between wires from different sources. Ransley and Rooksby<sup>14</sup> have studied the conditions under which straight-rolled and cross-rolled sheets become brittle. Bruckart, LaChance, Craighead, and Jaffee<sup>15</sup> have measured the forgeability, tensile properties, and hot hardness of a number of binary alloys of molybdenum. American work on the ductility of molybdenum is discussed in Section VII.

When the present work was begun, it was considered that the equilibrium diagrams of the more important alloys were already established, and it was therefore decided to concentrate on forging tests and on creep tests of the forged alloys, aspects concerning which little information seemed to be available.

### III.—EXPERIMENTAL TECHNIQUE

#### 1. POWDERS USED

Powders were of the highest purity obtainable, and, wherever possible, very fine grades were used, in most cases all or the majority of the particles being below  $10\ \mu$  in dia. Table I gives the method of manufacture (where known), analysis (spectrographic or chemical), and an estimate of the particle-size. Determination of the particle-size in the sub-sieve range is difficult; however, only a very approximate determination was needed, sufficient to confirm that there was a reasonable hope of obtaining a homogeneous structure by the sintering process. In the method adopted, due to Green,<sup>16</sup> a little powder was placed on a microscope slide, covered with a drop of turpentine, and the suspension dispersed by rubbing gently with the end of a glass rod. The turpentine was then evaporated off, and a representative area was photographed by transmitted light at a magnification of 1000. The diameter of between 30 and 150 particles was then measured by comparing them with circles drawn on tracing linen. Either the whole of the particles on the photograph were measured, or all those falling inside a circle drawn on the photograph. There are a number of objections to this procedure, but it was believed to be sufficiently accurate for the present purpose.

One of the difficulties, not always satisfactorily overcome, was the uncertainty as to the oxygen and nitrogen contents of the specimens. Pure molybdenum sintered in hydrogen or in vacuum has low contents of these gases, e.g.:

Compact	Sintering Treatment	O <sub>2</sub> , %	N <sub>2</sub> , %
RLW	2 hr. at 2300° C. in H <sub>2</sub>	0.0007	0.0008
RLX	2 hr. at 2300° C. in vacuum	0.0006	0.0005

No trouble arises with metals which do not form very stable oxides or nitrides, such as iron or nickel. Alloys containing metals which form very stable oxides or nitrides may contain oxygen or nitrogen which was either present in the original alloying-element powder or which comes from the hydrogen atmosphere or from surface oxides on the molybdenum powder. Molybdenum powder bears a surface oxide which can be removed by pre-reducing at 800° C. in hydrogen. This fact was not appreciated at the start of the investigation and a number of aluminium and titanium alloys proved unsatisfactory for this reason.

#### 2. MIXING AND SINTERING OF COMPACTS

The compacts were made by cold pressing followed by sintering. They were of two sizes:  $3 \times \frac{3}{8} \times \frac{3}{8}$  in.

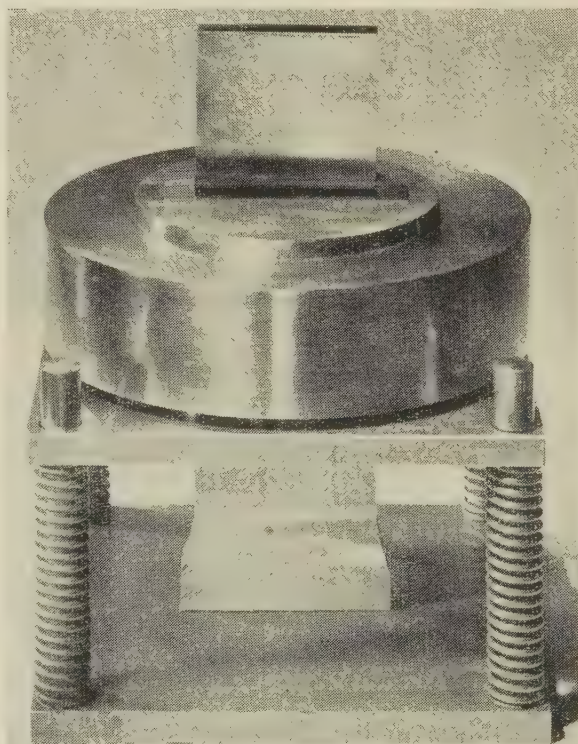


FIG. 1.—Floating Die for Pressing Powders.

and  $3 \times \frac{1}{2} \times \frac{1}{2}$  in. To obtain compacts of molybdenum powder, free from cracks, a strong die which does not deform elastically is essential. The total pressures used were 30 tons on the small compact and 50 tons on the large. Equal pressure must be applied to the top and bottom, if the compact is to remain straight after sintering. This equal pressure was obtained by using the floating die mounted on springs shown in Fig. 1. The heavy ring giving the necessary rigidity should be noted. The powders were mixed on a rotary mixer for 16 hr.

A high sintering temperature (2300° C.) was selected to promote diffusion. Temperatures above



TABLE I.—Details of Powders Used.

Metal	Mark No. of Powder	Method of Manufacture	Analysis, %	Size-Range of Powder		Remarks
				Size, $\mu$	% of Total	
Molybdenum	RBM	Not known; believed to be hydrogen-reduced	Si, 0.017, Fe 0.003, Al 0.006	—1 1-3 4-6 7+	33 37 30 0	Rounded grains with surface oxidation
	REI	Hydrogen-reduced	Si 0.005. Metallic impurities below 0.002 each	—1 1-3 4-6 7+	0 69 28 3	
	RHH	Hydrogen-reduced	Si 0.005, Cu below 0.005, Ni below 0.01. Other metals below 0.002	—1 1-3 4-6 7+	10 65 22 3	From Source A
	RIX	Hydrogen-reduced	Fe 0.005-0.01, Si 0.001-0.05. Other metals below 0.005	—1 1-3	14 86	
	M113B	Hydrogen-reduced	Fe 0.02, Si 0.01-0.02, Al 0.005 approx., Cu 0.001-0.005. Other metals below 0.003	—1 1-3 4-6	32 66 2	From Source B
	M112B	Hydrogen-reduced	Similar to M113B	—1 1-3 4-6	1 80 19	
	Aluminium	REZ	Atomized	Fe 0.1-1.0, Cu 0.01-0.1, Mn 0.01-0.1, Si 0.05-0.5, Mg 0.01-0.1	—10 20-30 40-60 70+	11 52 23 14
Chromium	RBX	Electrolytic, ground	O <sub>2</sub> about 0.5, Fe below 0.01	—1 1-3 4-6 7+	23 42 32 3	Other similar batches also used
Cobalt	RHP	Hydrogen-reduced sponge	On a similar sample: Si 0.39, C 0.010, Ca 0.006, Fe 0.005, Mg 0.005, P 0.004, Al 0.002, Ni 0.002, S 0.002, Pb 0.001	Sieved through 100 mesh		
Iron	RBR	Hydrogen-reduced sponge	C 0.011, S 0.003, Mn 0.046, Ni 0.001	—1 1-3 4-6 7+	19 49 29 3	
Manganese	RID/2	Electrolytic, ground	C 0.008, Si 0.003, S 0.024, P 0.002, Ni <0.001, Cu <0.001, Fe 0.001 *	n.d.		Sieved through 300 mesh
Nickel	RCB	...	C 0.1, Fe 0.001, Si 0.004, O <sub>2</sub> 0.1	—1 1-3 4-6 7+	0 81 16 3	
Niobium	...	...	C 1.2, O <sub>2</sub> 0.17, Ti 0.10, Fe 0.09, Ta trace	n.d.		
Tantalum	RGT	Sponge, electrolytic	Si 0.09, Fe 0.05, Al below 0.01, C 0.11	—1 1-3 4-6 7+	29 69 2 0	
Titanium	RIA	Sponge, ground	Si 0.1, Fe 0.16, Al 0.003, Mg 0.34, C 0.05, V >0.01, O <sub>2</sub> 0.13, N <sub>2</sub> 0.02, H <sub>2</sub> 0.18	—1 1-3 4-6 7+	20 45 20 15	
Titanium hydride	RNU	Hydride, ground	n.d.	—300 mesh		Made from sponge to following analysis, %: Si 0.025, Fe 0.3, Mg 0.035, C 0.05, O <sub>2</sub> 0.3, N <sub>2</sub> <0.01, H <sub>2</sub> 0.019
Tungsten	RHI	Hydrogen-reduced	Fe 0.007-0.04, Cu 0.001-0.01, Si <0.02, Ni <0.01, C 0.0025	—1 1-3 4-6 7+	0 20 64 16	
Zirconium hydride	RNV	...	0.3 Fe. Not very pure	—300 mesh		
Sulphur	...	...	n.d.	n.d.		Flowers of sulphur

n.d. = Not determined.

\* Before ball milling.

2300° C. tended to shorten the life of the heater element of the furnace. The sintering furnace has been described elsewhere.<sup>17</sup> It is designed to run either in hydrogen or in vacuum. The hydrogen is purified by passing it at  $1\frac{1}{2}$  l./min. through a train of palladized asbestos at 200° C., calcium chloride, magnesium at 600° C., solid potassium hydroxide, and phosphorus pentoxide. The magnesium is held in a vertical stainless-steel tube. When operated in vacuum, the furnace is first degassed by running it at 2300° C. with the specimen held above the hot zone, until a pressure of less than  $5 \times 10^{-5}$  mm. of mercury is shown on an ionization gauge. The furnace is then cooled and the specimen lowered into position without opening the furnace. When heating the specimen, the only gas likely to be evolved is that from the specimen and its suspension, the amount given off by the latter being very small.

Pure molybdenum compacts and compacts containing chromium, cobalt, iron, manganese, nickel, tungsten, and sulphur, were normally sintered in hydrogen; those containing aluminium, niobium, tantalum, titanium, and zirconium were sintered in vacuum.

The compacts made from molybdenum powders RIX, REI, and RHH, sintered in hydrogen, except those containing chromium, normally had a density of 9.8–10.0 g./c.c., i.e. 96–98% of the theoretical density. Compacts made from molybdenum powder M112 gave a value of 9.50 g./c.c., and those made with the finer powder M113 from the same source gave 9.88 g./c.c.

When molybdenum powder RIX was sintered in vacuum, the density was only 9.3 g./c.c. However, when the powder was pre-reduced in hydrogen at 800° C., or when about 0.10% carbon in the form of lampblack was added, a figure of 9.9 g./c.c. was obtained by sintering at 2300° C. in vacuum. In spite of the difference in density between the untreated powders sintered in hydrogen and in vacuum, the final oxygen contents of the compacts were very similar, viz. 0.0007% for hydrogen-sintered and 0.0006% for vacuum-sintered metal. This suggests that any impurity which inhibits sintering during the heating-up period may reduce the final density. This conclusion is valid even though the compact is held at a temperature which gives a compact with a high density if the impurity is not present, and results in the removal of the impurity if it is present.

#### IV.—EFFECT OF ALLOYING ELEMENTS ON FORGEABILITY

##### 1 SWAGING TESTS

The decision to make swaging tests arose from the fact that the creep tests were to be carried out on forged material, since this would be stronger and more homogeneous than cast or arc-melted material, and swaging was the most convenient method of making the  $\frac{5}{32}$ -in.-dia. rods required for the compression creep tests. The dies used decreased in diameter in

steps of  $\frac{1}{64}$  in. from  $\frac{23}{64}$  to  $\frac{1}{8}$  in. Compacts for swaging tests were filed in the pressed state to a dia. of  $\frac{25}{64}$  in. and then sintered, giving a suitable bar for the first swaging die.

The specimens were heated for swaging in a molybdenum-wound furnace. Since the compacts were short, about  $2\frac{3}{4}$  in. in length, they would have lost heat while being pulled to the exit of the furnace. To overcome this, a molybdenum block,  $6 \times 1\frac{1}{4} \times 1\frac{1}{4}$  in., with two  $\frac{1}{2}$ -in. holes running through it, was used to carry the specimens. This was pulled to the front of

TABLE II.—*Results of Swaging Tests.*

Compact No.	Nominal Alloy Content, %	Sintering Temperature, °C.	Swaging	
			Starting Temperature, °C.	Result
	Chromium			
RCJ	4	2300	1300	Broke in 2nd die.
RCK	7	2200	1400	Cracked in 4th die.
RCP	3	2150	1400	Swaged to $\frac{5}{16}$ in.
RCQ	4	2150	1400	Cracked in 5th die.
RCS	5	2350	1400	Broke in 1st die.
RHN	3	2300	1500	" " 2nd die.
RIK	2	2300	1350	" " "
RJP	$1\frac{1}{2}$	2300	1500	Swaged to $\frac{5}{16}$ in.
	Aluminium			
RGG	0.5	2300	1350	Swaged to $\frac{5}{16}$ in.
RHF	1	2300	1500	" " "
RHG	2	2300	1350	Broke in 4th die.
	Cobalt			
RHO	0.2	2300	1500	Swaged to $\frac{5}{16}$ in.
RJE	0.3	2300	1500	" " "
RJO	0.4	2250	1500	Broke in 4th die.
RMT	0.3	2300	1500	" 3rd die.
RMX	0.2	2300	1500	Longitudinal crack.
RMV	0.3	2300	1500	Swaged to $\frac{5}{16}$ in.
	Iron			
RHR	0.5	2300	1350	Broke in 2nd die.
RED	0.4	2300	1350	Swaged to $\frac{5}{16}$ in.
	Manganese			
RIU	2	1800	1500	Broke in 2nd die.
RKF	1	1800	1500	Swaged to $\frac{5}{16}$ in.
	Nickel			
RGD	0.2	2300	1350	Broke in 1st die.
RJL	0.1	2400	1500	Swaged to $\frac{5}{16}$ in.
	Tantalum			
RHD	5	2300	1350	Swaged to $\frac{5}{16}$ in.
RHE	10	2300	1350	" $\frac{5}{16}$ in. but longitudinal crack.
	Titanium			
RDS	8	2250	1350	Broke in 4th die.
RHU	4	2300 2000	1350	Swaged to $\frac{5}{16}$ in.
	Tungsten			
RDJ	20	2300	1350	Swaged to $\frac{5}{16}$ in.
RGJ	50	2300	1350	" " "
	Zirconium			
RFY	$1\frac{1}{2}$	2300	1350	Swaged to $\frac{5}{16}$ in.
RKL	$\frac{1}{2}$	2300	1500	" $\frac{5}{16}$ in.
	Carbon			
ROA	0.3 (0.246 residual)	2100	1500	Swaged to $\frac{5}{16}$ in.

the furnace, the specimens meanwhile being picked up with tongs; the large mass of the block conserved the heat. An optical pyrometer was sighted on a blind hole in the block, the temperature thus determined being taken as the swaging temperature. The delay between removing the specimen from the block and putting it into the swaging die was less than 2 sec.

The normal temperature at which swaging started



was 1350° C. For some alloys temperatures of 1500° and 1600° C. were used, but in general it was found that if an alloy could not be swaged at 1350° C. it could not be swaged at 1500° or 1600° C. When the alloy had been reduced by  $\frac{1}{8}$  in. in dia. the swaging temperature was sometimes lowered, so as to finish at some temperature such as 1100° C.

In all, attempts were made to swage about 110 compacts. A selection of the results of swaging tests is given in Table II, the compacts included being those which provided information on the forgeability of the alloys.

The compacts that could not be swaged cracked in two ways. The more common type of crack was transverse and intergranular. The compacts usually, though not invariably, broke in two and some into a number of pieces. This cracking occurred at the beginning of the swaging process, and if the compact could be reduced in diameter by about one fifth, it could normally be swaged right down without any transverse cracking. The other type of cracking was longitudinal, the cracks extending all or most of the way along the bar. Such cracks appeared only towards the end of the swaging process, and might be severe and easily visible, or slight and visible only under a microscope.

## 2. RESULTS

### (a) Chromium Alloys

The first molybdenum-chromium alloys tested, i.e. those up to compact RCS (Table II) were made with molybdenum powder RBM, which had rather more rounded grains and bore more surface oxidation than the molybdenum powders used for subsequent tests on alloys containing chromium and other alloying elements. Compacts made with RBM and containing 3% chromium could be swaged, whereas compacts containing more than  $1\frac{1}{2}$ % chromium and made from the other molybdenum powders could not. This difference was not discovered until supplies of powder RBM were exhausted, but the reason for the difference may be associated with the lower sintered density of compacts made with this powder.

### (b) Aluminium Alloys

The molybdenum-aluminium alloys were made by sintering molybdenum powder and "atomized" aluminium powder REZ. They were not very satisfactory, since the aluminium powder was not of sufficiently high purity and the molybdenum powder was not given a reducing treatment immediately before being mixed with it. The final alloys thus contained a large number of globular inclusions, presumably of alumina. Some sintered alloys made with pre-reduced molybdenum at a later stage of the work were very much cleaner.

Molybdenum alloys with 1% aluminium can be swaged, but not an alloy with 2%.

### (c) Cobalt, Iron, and Nickel Alloys

An alloy with 0.4% iron and one with 0.1% nickel were swaged. Cobalt alloys with 0.2 and 0.3% cobalt were swaged, but tended to develop both longitudinal and transverse cracks.

### (d) Manganese Alloys

Alloys containing 1.0% manganese could be swaged, but not an alloy containing 2.0%. There was, however, a strong tendency for the swaged alloys to contain very fine longitudinal cracks.

### (e) Tantalum Alloys

Alloys containing 5% tantalum could be swaged to give rods free from cracks; the 10% alloys, though they did not show transverse cracks, developed severe longitudinal cracks.

### (f) Titanium Alloys

Two difficulties were experienced when making molybdenum-titanium alloys. First, the alloys contained large amounts of non-metallic inclusions, believed to be titanium oxide, the oxygen of which was derived partly from the titanium used but mostly from the surface oxide of the molybdenum powder. The surface oxide can be removed by pre-reducing the molybdenum, but this procedure was not adopted for the alloys used for swaging tests.

The other difficulty was that molybdenum containing titanium in excess of about 1%, developed during swaging a loose black oxide layer which cracked, the cracks spreading inwards. This oxidation was overcome by spraying molybdenum from a wire-spraying pistol on to the compact, reducing the oxygen content of the coating in hydrogen at 1350° C., and finally re-sintering at 1800° or 1900° C. in vacuum to improve the adhesion of the coating. The coated compact could then be swaged with only slight traces of surface oxide showing. The spraying was carried out by Metallisation, Ltd., Dudley. Coated alloys with 4% titanium were swaged and showed only slight surface cracks in the coating. It is possible that alloys with more than 4% could also be swaged, but this was not tried.

### (g) Tungsten Alloys

Alloys with up to 50% tungsten were swaged.

### (h) Zirconium Alloys

An alloy with  $1\frac{1}{2}$ % zirconium could be swaged, but permanent surface oxidation occurred and the alloy had surface cracks. Coating with molybdenum would no doubt have overcome this.

## 3. HARDNESS OF THE ALLOYS

Vickers pyramid hardness determinations were carried out on most of these alloys, both as swaged and as annealed at 1500° C. A selection of the results is given in Table III.

TABLE III.—*Vickers Pyramid Hardness Determinations (30-kg. Load).*

Compact No.	Analysis, %	Vickers Pyramid Hardness No.		
		Swaged at 1100° C.	Swaged at 1350° C.	Annealed at 1500° C.
RBT . .	Molybdenum	210 *	...	...
RKA . .	"	...	...	164
RCG . .	0.92 Cr	...	289 †	186
RCP . .	3.01 "	...	398 †	278
RGZ . .	0.98 Al	291 ‡	...	216
RHO . .	0.20 Co	261-314	232	200
RED . .	0.41 Fe	304-333 ‡	...	195
RJL . .	0.1 Ni	268	...	169
RGY . .	4.96 Ta	273 ‡	...	181
RHU . .	4 Ti §	...	232	...
RHV . .	4.02 "	210-245	...	...
RHK . .	9.99 W	237	229	168
RHL . .	20.3 "	254	257	234
RHM . .	50.2 "	322	314	292

\* Swaged at 1150° C.

† Swaged at 1300° C.

‡ Swaged at 1000° C.

§ Nominal.

Note: A range of figures is given when the hardness readings have a spread of greater than 20.

#### 4. MICROSTRUCTURE OF ALLOYS

All the alloys considered in this paper except some of the nickel and cobalt alloys, were inside the solid-solution range. Thus there was no reason to expect much useful information from the microstructures at this stage of the investigation, except where impurities were present, e.g. in the titanium and aluminium alloys. Typical microstructures are shown in Figs. 2, 3, and 4 (Plate XLVII).

### V.—EFFECT OF ALLOYING ELEMENTS ON CREEP STRENGTH

#### 1. COMPRESSION CREEP TESTS

The initial series of tests made in this research were for the purpose of finding out whether a binary alloy

could be developed which would have a creep strength substantially greater than that of pure molybdenum and which might, therefore, serve as a useful matrix alloy for the more complex heat-resisting alloys. The maximum amounts of the various alloying elements which could be added to molybdenum without destroying its forgeability had been determined by the work described in Section IV, and the next step was to determine the creep strength of those alloys containing the maximum permissible amount of alloying addition. Some alloys containing less than the maximum amount were also tested.

The miniature compression creep machines described in another paper<sup>18</sup> were employed. The test-pieces,  $\frac{1}{4}$  in. long  $\times$   $\frac{1}{8}$  in. in dia., were tested at 1000° C., generally for about 30 hr.

It is not possible to find a simple relationship between the results of compression creep tests and conventional tensile creep tests. A number of comparison tests have been carried out, and some results are given in Table IV. The comparison creep test-pieces were made either from the shoulder pieces of the tensile creep test-pieces or from the same bar.

It appears that compression creep tests on these machines usually give a greater creep strain than do tensile creep tests, for the same material, load, and time. The ratio of total creep strain or creep rate in compression to the total creep strain or creep rate in tensile testing decreases as the creep strain or creep rate in the tensile test increases. In other words, the tests are more comparable when the specimen shows a fair amount of creep. The stress needed to give 1% creep in 24 hr. was taken as an arbitrary criterion of creep-resistance.

#### 2. RESULTS

##### (a) *Pure Molybdenum*

Some estimate of the creep strength of pure molybdenum was required to act as a standard of comparison for the alloys. Results of some creep tests on molybdenum bars made at the N.P.L. are given in Table V. The figure given in the last column of Table V and other tables giving compression creep results is an approximate estimate of the stress required to

TABLE IV.—*Comparison Between Compression and Tensile Creep Test Results.*

Material	Testing Conditions			Total Creep Strain, %			Creep Rate, %/hr.		Ratio Compression to Tensile Creep	
	Stress, tons/in. <sup>2</sup>	Temp., °C.	Type	0-24 hr.	0-75 hr.	0-100 hr.	10-75 hr.	10-100 hr.	Creep Strain	Creep Rate
Rex 78	4	800	Compression	0.71	...	1.22	...	0.006	3:1 at	2:1 at
	4	800	Tensile	0.15	...	0.4	...	0.003	100 hr.	100 hr.
Nimonic 80	4	815	Compression	0.53	...	0.59	...	0.0007	49:1 at	7:1 at
	4	815	Tensile	0.004	...	0.012	...	0.0001	100 hr.	100 hr.
Nimonic 80A	0.44	1000	Compression	1.31	2.24 *	...	0.021	...	2:1 at	2:1 at
	0.44	1000	Tensile	0.50	1.03	...	0.011	...	75 hr.	75 hr.
Molybdenum	5	1000	Compression	0.76 †	...	0.96 †	...	0.0032	1:1 at	1:1½ at
	5	1000	Tensile	0.65	...	1.00	...	0.0055	100 hr.	100 hr.

\* Mean of 4 tests, range 2.10-2.41% strain.

† Mean of 2 tests.



give 1% creep in 24 hr., obtained by inspection of the figures in the previous two columns.

The results of the tests on molybdenum in the as-swaged condition tend to be rather variable, probably owing to varying amounts of cold work, but taking together the results given in Table V and those of other experiments by one of the authors (W. E. C.)<sup>18</sup> a

stress of 4-5 tons/in.<sup>2</sup> appears to be necessary to give a creep strain of 1% in 24 hr. at 1000° C. As will be seen from Table IV, a tensile stress of 5 tons/in.<sup>2</sup> gives a creep strain of 0.65% in 24 hr. Molybdenum recrystallized at 1500° C. requires a compression stress rather lower than 4-5 tons/in.<sup>2</sup> to give 1% creep in 24 hr.

TABLE V.—Results of Creep Tests on Molybdenum and Molybdenum Alloys.

Compact No.	Alloying Addition, %	Condition of Specimen	Stress, tons/in. <sup>2</sup>	Duration of Test, hr.	Total Creep, %	Stress in tons/in. <sup>2</sup> Giving 1.0% Creep Strain in 24 hr.	Compact No.	Alloying Addition, %	Condition of Specimen	Stress, tons/in. <sup>2</sup>	Duration of Test, hr.	Total Creep, %	Stress in tons/in. <sup>2</sup> Giving 1.0% Creep Strain in 24 hr.		
Carbon							Manganese								
RBT *	n.d. (low)	Swaged at 1150° C. {	3 5	24 24	0.97 0.91	3-5	RKF	0.99	Swaged at 1100° C. {	1 4	24 24	0.41 1.02	4		
RKA *	0.001	Annealed at 1500° C. for 4 hr. {	2 3	24 24	0.49 0.57	Above 3	Cobalt								
RKD *	0.0022	Annealed at 1500° C. for 4 hr. {	2 3	24 24	0.54 0.65	Above 3	RHO	0.20	Swaged at 1100° C. {	2 4 4 4	24 24 46 24	0.59 0.80 1.08 0.50	Slightly above 4		
ROA *	0.246	Annealed at 1500° C. for 4 hr. {	2 3	24 24	0.62 0.99	About 3			Swaged at 1350° C. {	4 6 6	24 24 48	0.50 0.69 0.91	Above 6		
MDB(a) †	0.001	Swaged {	3 4 6	24 24 24	0.54 0.88 † 1.27	4-5			Annealed at 1500° C. for 4 hr. {	3 4	24 24	0.62 0.51	Well above 4		
Tungsten							RMY	0.31	Swaged at 1350° C. {	3 4 2	24 24 24	0.66 0.86 0.42	About 4		
RHK	9.99	Swaged at 1100° C. {	2 4 2	24 24 24	0.58 0.97 0.67	About 4	RGC	1.96	Annealed at 1500° C. for 4 hr. {	4 2 4	24 24 24	0.54	Above 4		
		Swaged at 1350° C. {	4 2	24 24	0.98 0.83	4			Sintered at 1800° C. for 1 hr. in hydrogen. <i>d</i> = 9.37 {	3 4	24 24	1.27 1.65	Below 3		
		Annealed at 1500° C. for 4 hr. {	2 4	24 24	0.83 1.20	Below 4			Iron						
RDJ	18.4	Swaged at 1250° C. {	4 5 6	24 24 24	0.55 0.92 0.74	5-6	RED	0.41	Swaged at 1000° C. {	2 4 5	24 24 24	0.50 0.86 1.15	Below 5		
		Swaged at 1350° C. {	4 2	24 24	0.98 0.83	4			Annealed at 1500° C. for 7½ hr. {	2 4 5	24 24 24	0.49 0.65 1.17	Below 5		
		Annealed at 1500° C. for 8 hr. {	3 4 5	24 24 24	0.45 0.90 0.87	Above 5			Nickel						
RGJ	49.8	Swaged at 1350° C. {	3 4 5	24 24 24	0.90 0.92 1.43	3-4	RFU	0.40	Sintered at 2300° C. for 1½ hr. in hydrogen. <i>d</i> = 9.80 {	3 4	24 24	0.53 0.92	About 4		
		Annealed at 1500° C. for 8 hr. {	2 4	24 24	0.35 0.95	About 4			RGB	1.80	Sintered at 1650° C. for 1 hr. in hydrogen. <i>d</i> = 9.88 {	2 4 6 6	20 24 30 30	1.17 1.80 2.34 2.00	Below 2
		Swaged at 1350° C. {	2 4 5	24 24 24	0.49 0.83 1.25	4-5					Tantalum				
RCG	0.92	Swaged at 1350° C. {	4 5	24 24	0.76 0.71	Above 5	RGX	2.49			Swaged at 1000° C. {	3 4	24 24½	0.70 0.83	Above 4
RCI	1.96	Swaged at 1300° C. {	2 4 5	24 24 24	0.43 0.64 0.78	Above 5	RGY	4.96	Swaged at 1000° C. {	2 4 2	24 24 24	0.56 0.88 0.64	4		
RCP	3.01	Swaged at 1025-1050° C. {	3 4	24 24	0.47 0.45	Presumably above 5			Swaged at 1350° C. {	4 4	24 24	0.99	4		
		Swaged at 1350° C. {	4 5 5	24 24 24	0.39 0.64 0.97	Above 5			Annealed at 1500° C. for 8 hr. {	2 4	24 24	0.31 0.95	4		
		Annealed at 1500° C. for 7½ hr. {	5 6 6	24 24 24	0.95 1.84 0.71	5-6			Titanium						
RDK	20.75	Arc-melted {	5 7	24 24	0.58 0.97	7	RDN	1.78	Swaged at 1000° C. {	4 6 2	24½ 24 24	0.67 1.13 0.65	About 5		
						Annealed at 1500° C. for 7½ hr. {			3 4	24 24	0.57 0.90	About 4			
Aluminium							RHV	4.02	Swaged at 1100° C. {	2 4 2	24 24 24	0.44 1.23 0.37	Below 4		
RGG	0.50	Swaged at 1000° C. {	2 4 4	24 24 24	0.51 0.95 1.36	4	RHU	4 nom.	Swaged at 1350° C. {	2 4 4	24 24 24	0.86 0.59 0.63	Possibly above 4		
		Annealed at 1500° C. for 7½ hr. {	2 4	24 24	0.50 0.62	Above 4			Annealed at 1500° C. for 4 hr. {	4 4	24 24		Above 4		
RGZ	0.98	Swaged at 1350° C. {	2 4 3	24 24 24	0.56 0.79 0.39	Slightly above 4	Zirconium								
		Swaged at 1000° C. {	4 3	24 24	0.94	4	RKL	0.43	Swaged at 1100° C. {	1 4	24 24	0.56 1.30	Below 4		

\* N.P.L. swaged bar.

† Source A swaged bar.

‡ Mean of 3 tests.

(b) *Chromium Alloys*

The results on the alloys are also given in Table V. It will be seen that the chromium alloys tested as-swaged required a stress of rather over 5 tons/in.<sup>2</sup> to give 1% creep, the 3% alloy appearing rather stronger than the 1 and 2% alloys. Alloy RDK was made by arc melting in order to find the strengthening effect of large additions of chromium. It was considerably stronger than pure molybdenum, but had a V.P.N. of over 500 and was completely brittle.

(c) *Aluminium Alloys*

It is apparent that aluminium has little if any strengthening effect.

(d) *Cobalt Alloys*

Tests were carried out on two swaged alloys containing 0.2 and 0.3% cobalt. The 0.2% alloy (RHO) when tested as-swaged at 1350° C. appeared to be considerably stronger than pure molybdenum; it may also be stronger in the annealed condition. However, when tested as-swaged at 1100° C., it gave no indication of an increase in strength. The 0.3% alloy (RMY) tested as-swaged at 1350° C. also showed no increased strength. Thus, the evidence for an increase in the strength of molybdenum from the addition of cobalt is contradictory. The low strength of the sintered alloy with 2.0% cobalt is probably associated with the fact that the alloy is duplex, containing a phase melting at 1620° C.

(e) *Iron Alloys*

Only one alloy was tested (RED, 0.41% iron), and there was no evidence of any substantial increase in strength over pure molybdenum.

(f) *Manganese Alloys*

Only one alloy was tested (RKF, 0.99% manganese), and it appeared that 1% manganese gave no increase in strength over pure molybdenum.

(g) *Nickel Alloys*

No swaged alloys were tested in creep, but tests were carried out on two sintered alloys. The alloy with 1.8% nickel was weaker than that with 0.4%. This may be due to the large proportion of the low-melting-point (1370° C.)  $\gamma$  constituent in the 1.8% alloy.

(h) *Tantalum Alloys*

Neither the 2½ nor 5% alloy showed any increase in strength over pure molybdenum.

(i) *Titanium Alloys*

The figures are very contradictory, but it is probable that titanium does not give an increase in creep strength over pure molybdenum.

(j) *Tungsten Alloys*

It appears that the 20% tungsten alloy gives a slight increase in strength over pure molybdenum, but not the 10% alloy, nor, strangely enough, the 50% alloy.

(k) *Zirconium Alloys*

Only the 0.43% alloy was tested, and this showed no increase in strength over pure molybdenum.

## VI.—EFFECT OF PROCESSING VARIABLES AND ALLOYING ADDITIONS ON DUCTILITY

## 1. BRITTLINESS OF MOLYBDENUM AND ITS ALLOYS

The results reported in Section V suggest that, as far as molybdenum alloys made by powder metallurgy are concerned, there is a limit to the creep strength obtainable by the development of binary alloys, owing to the fact that an amount of the alloying element sufficient to give a useful increase in creep strength cannot be added without destroying the forgeability of the alloys (see Table VI). Complex

TABLE VI.—*Results of Swaging Tests.*

Element Added	Maximum Addition (wt.-%) Giving an Alloy Which Can be Swaged
Aluminium . . . . .	Above 1%, below 2%
Chromium . . . . .	Usually not above 1½%
Cobalt . . . . .	0.3%
Iron . . . . .	0.4%
Manganese . . . . .	Above 1%, below 2%
Nickel . . . . .	0.1%
Tantalum . . . . .	Above 5%, below 10%
Titanium . . . . .	Above 4%
Tungsten . . . . .	Up to 100%
Zirconium . . . . .	Above 1½%

alloys would probably be even less forgeable. When alloying elements were added in amounts which did not destroy the forgeability, the as-forged alloys were often brittle at room temperature. Pure molybdenum, when recrystallized to give an equiaxed annealed structure, is normally brittle at room temperature, but work by Sykes<sup>12</sup> has shown that such material is ductile at 300° C. Thus molybdenum, it appears, has a transition temperature, either sharp or spread over a range, at which in a given test the metal, as the temperature increases, ceases to show a brittle fracture with little or no ductility and exhibits a considerable amount of ductility. The corresponding transition temperature from brittle to ductile failure of iron in the Izod test is very sensitive to small changes in composition or heat-treatment. Experiments showed that the transition temperature of small bars of recrystallized molybdenum, bent as plain un-notched bars, had an equally sensitive transition temperature from brittle fracture, with little or no evidence of ductility, to complete bending without fracture, and thus a useful method of examining the effect of alloying elements and heat-treatment on the ductility of molybdenum is available.



The ductility of molybdenum was studied with two objects, first, in an attempt to overcome the room-temperature brittleness of the annealed metal and its alloys, and secondly, in the hope that if such a remedy could be found it would cure also the lack of forgeability of the alloys. The fact that the room-temperature fractures and the forging fractures both tended to be intercrystalline suggested that there might be a connection between them.

The room-temperature brittleness of annealed molybdenum could not be considered to be overcome unless the transition temperature in a plain bend test was lowered to one well below room temperature, since the presence of a notch or other constraint in a component raises the temperature of brittle failure. In fact, Ham<sup>1</sup> has reported a transition temperature of 315° C. in a V-notch Charpy test on arc-melted and forged molybdenum.

It was therefore decided to investigate the effects of different sintering, swaging, and annealing treatments, and of alloying elements on the transition temperature of molybdenum. Nearly all the tests were carried out on sintered or annealed specimens which had a microstructure composed of equiaxed or almost equiaxed grains. This condition, known to be that in which the metal is most brittle, was selected first, because most heat-treatments leave the metal in this state, and, secondly, because it is probably more easily reproducible than a work-hardened condition.

## 2. PREPARATION AND BEND TESTING OF SPECIMENS

Swaged bars were made in the manner described in Section IV, 1, the final swaging temperature normally being 1100° C. Test specimens,  $\frac{7}{8}$  in. long  $\times$   $\frac{1}{8}$  in. in dia., were ground from the bars, eight usually being obtained from one bar. The specimens were then annealed at 1500° C. for 4 hr. in vacuum. The final microstructure obtained was an annealed structure, the grains being sometimes slightly elongated in the direction of the length of the bar. In tests on sintered material, the test-pieces were ground from sintered bars, a maximum of eight specimens being obtainable from one compact.

The bend tests were carried out in the apparatus illustrated in Fig. 10, in which the specimen is supported on a recessed anvil, the points of support being  $\frac{1}{8}$  in. apart. The load is applied to the mid-point by a tongue of  $\frac{1}{8}$  in. radius, the specimen being free to bend round the radius; the anvil is so shaped that when the tongue has travelled to the bottom of the anvil, the specimen is bent through nearly 180°. A thermocouple runs in a groove between the ram and the sleeve and has its hot junction at the same level as the specimen and within  $\frac{3}{8}$  in. of it. The ram, anvil, and sleeve are of Nimonic. They are held inside a furnace (Brightray wire wound on silica), capable of reaching a temperature of 700° C. Above 400° C. the equipment is heated under vacuum. For tests below room temperature, the furnace is replaced by cotton-waste lagging. The bending jig, carried in

a brass container, is immersed in a Dewar flask of refrigerant (ice, carbon dioxide in acetone, or liquid oxygen) until it reaches a temperature below that required. The brass container is quickly transferred to its position in the mild steel jacket and the load applied when the correct temperature is reached. Under these conditions the temperature of the specimen does not vary by more than 1° C. during the half minute required to make the test.

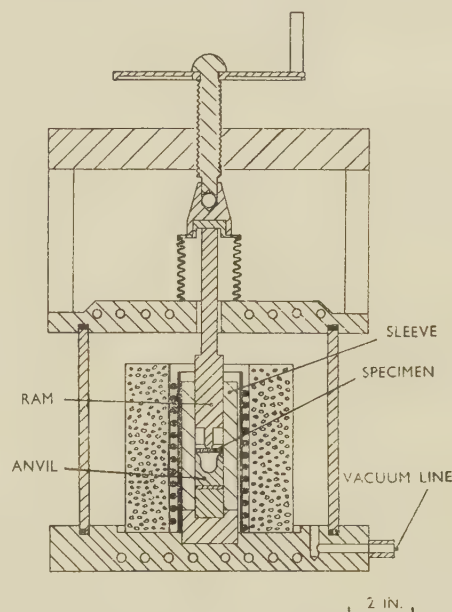


FIG. 10.—Bend-Test Apparatus.

The vertical movement of the ram, and so the deflection at the centre of the specimen, was about 1 in./min.

The transition temperature was taken as the temperature range above which the specimen would bend 120° and below which it would not bend 120°. In the case of any inconsistency in the results, the transition temperature was taken as the range between the lowest temperature at which a bend of 120° or greater was obtained and the highest temperature at which a bend of 120° was not obtained. The angle of bend of a broken specimen was obtained by fitting two pieces together on a protractor. The results on a number of typical compacts are plotted in Fig. 11.

The grain-size of the specimens was measured by comparing them with A.S.T.M. Standard E2-39T, using a projection microscope.

## 3. RESULTS ON SWAGED COMMERCIAL MOLYBDENUM ROD

The first tests were made on  $\frac{1}{8}$ -in.-dia. swaged molybdenum rods supplied by two firms, *A* and *B*, and the results are given in Table VII. The tests were carried out first, to find out whether the transition temperature of molybdenum could be closely defined, and secondly, to obtain a standard with

which to compare rods manufactured at the N.P.L. The rods when received had a worked, fibrous structure (Fig. 5, Plate XLVII) and a transition temperature range of  $-32^{\circ}$  to  $-50^{\circ}$  C. If the specimens were recrystallized by annealing at  $1500^{\circ}$  C. for 4 hr. in vacuum, the transition temperature was raised to  $+30^{\circ}$  to  $+44^{\circ}$  C. for molybdenum from Source *A* and to  $+21^{\circ}$  to  $+24^{\circ}$  C. for molybdenum from Source *B*, the microstructure in both series being mostly equiaxed grains plus a few grains elongated in the direction of working (Fig. 6, Plate XLVIII).

#### 4. TESTS ON SWAGED AND ANNEALED SPECIMENS OF PURE MOLYBDENUM

Rods made at the N.P.L. (Table VIII) had higher transition temperatures than the commercial rods, the values being about  $80^{\circ}$ – $110^{\circ}$  C., while those of the commercial rods were about  $20^{\circ}$ – $40^{\circ}$  C. The powder used came from Source *A*, and was believed to have been similar to that used by the firm concerned when making their own rods. Two series of experiments aimed at investigating this difference were to try the

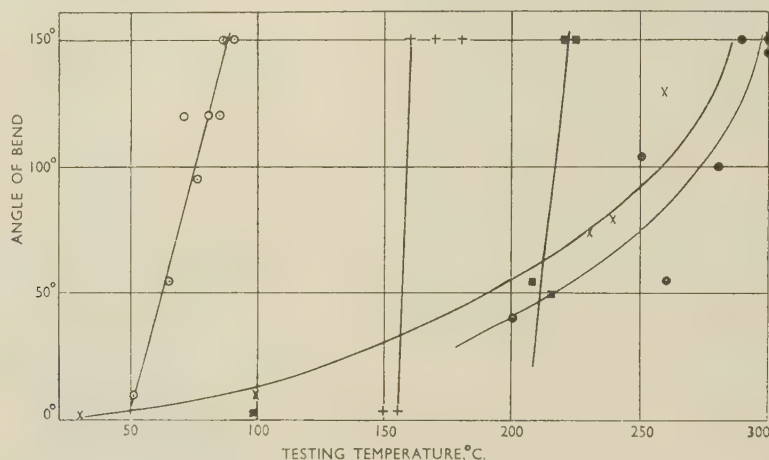


FIG. 11.—Results of Bend Testing on Typical Specimens.

##### KEY.

- RMB. Mo + 0.1% C, sintered for 2 hr. at  $2300^{\circ}$  C. in  $H_2$ .
- × RKH. Pure Mo, swaged at  $900^{\circ}$  C., annealed for 4 hr. at  $1500^{\circ}$  C. in vacuum.
- RNW. Mo + 0.5% TiH, sintered for 2 hr. at  $2300^{\circ}$  C. in vacuum.
- × RKG. Mo + 2% Ta, swaged at  $1100^{\circ}$  C., annealed for 4 hr. at  $1500^{\circ}$  C. in vacuum.
- RIJ. Mo + 1% Cr, swaged at  $1100^{\circ}$  C., annealed for 4 hr. at  $1500^{\circ}$  C. in vacuum.

Annealing molybdenum from Source *A* at  $1300^{\circ}$  or  $1400^{\circ}$  C. instead of at  $1500^{\circ}$  C. reduced the transition temperature by about  $25^{\circ}$  C.; nevertheless, the microstructures were very similar to those of specimens annealed at  $1500^{\circ}$  C. Results on specimen RIP/9 show that water-quenching from  $1500^{\circ}$  C. has no effect on the transition temperature.

TABLE VII.—Results of Bend Tests on Commercial Swaged Rod.

Specimen No.	Source of Supply	Treatment	Transition Temp., °C.	Grain-Size, mm.
RIP/11	A	As-supplied swaged	$-32$ to $-40$	Fibrous structure
RKH/3	A	" " " "	$-32$ to $-50$	" "
RIP/1, 3, 4	A	Annealed for 4 hr. at $1500^{\circ}$ C. in vacuum, furnace-cooled.	30 to 40	0.04
RKH/1	A	" " " "	42 to 44	0.045
RNM	B2 (Powder M113)	" " " "	21 to 24	0.055
RNN	B1 (Powder M112)	" " " "	below 25	0.065
RIP/2, 6	A	Annealed for 4 hr. at $1300^{\circ}$ C. in vacuum, furnace-cooled.	10 to 16	0.045
RIP/5	A	Annealed for 4 hr. at $1400^{\circ}$ C. in vacuum, furnace-cooled.	18 to 22	0.05
RKH/2	A	Annealed for 4 hr. at $1300^{\circ}$ C. in vacuum, furnace-cooled.	15 to 23	...
RIP/9	A	Annealed for 4 hr. at $1500^{\circ}$ C. in vacuum, water-quenched.	40 to 44	0.04

effect of lower final swaging temperatures and of step-sintering, i.e. sintering first at a lower temperature and then at the final temperature of  $2250^{\circ}$ – $2300^{\circ}$  C. In both series of tests, the results were contradictory, since one rod of each series showed a lowering of the transition temperature, while the other showed either no improvement or a raising of the transition temperature.

A further series of experiments was carried out on powder from Source *B*, supplied in two grades, B1 and B2; sintered rods and sintered and swaged rods made from these powders were also provided by the firm. The results of the tests on these materials, either in the as-received condition or after further treatment, are listed in Table IX.

It will be seen that the bars sintered and swaged at Source *B* gave the lowest transition temperature, the next lowest being obtained on the bars sintered at Source *B* and swaged at the N.P.L. Tests were also carried out on bars sintered and swaged at the N.P.L. The results are rather contradictory, but all the bars, particularly those swaged at a final temperature of  $900^{\circ}$  C., had transition temperatures considerably higher than those of bars sintered at Source *B*.

The figures show that, on the whole, inconsistent results, which it has not been possible to explain, were



TABLE VIII.—Results of Bend Tests on Sintered, Swaged, and Annealed Molybdenum from Source A (Powder RIX).

Standard anneal: 4 hr. at 1500° C. in vacuum.

Specimen No.	Sintering Conditions in H <sub>2</sub> Atmosphere	Swaging Conditions	Transition Temp., °C.	Grain-Size, mm.
RKI	2 hr. at 2300° C.	5 dies at 1350° C. 8 " 1100° C.	84-100	0.05
RKJ	2 hr. at 2300° C.	5 dies at 1350° C. 3 " 1100° C. 5 " 1000° C.	100-107	0.045
RLA	2 hr. at 2250° C.	5 dies at 1350° C. 3 " 1100° C. 5 " 900° C.	47-50	0.045
RKK	2 hr. at 2300° C.	5 dies at 1350° C. 3 " 1100° C. 5 " 900° C.	155-160	0.05
RKY	1 hr. at 1600° C. 2250° C.	5 dies at 1350° C. 8 " 1100° C.	190-195	0.06
REZ	1 hr. at 1500° C. 2250° C.	5 dies at 1350° C. 8 " 1100° C.	44-48	0.055
ROV	1 hr. at 1400° C. 2300° C.	5 dies at 1350° C. 8 " 1100° C.	91-99	0.055
ROU	1 hr. at 1300° C. 2300° C.	5 dies at 1350° C. 8 " 1100° C.	77-80	0.045-0.07
ROW	1 hr. at 1500° C. 2300° C.	5 dies at 1350° C. 3 " 1100° C. 5 " 900° C.	80-103	0.045

obtained on bars made at the N.P.L. by sintering, swaging, and annealing. Three processes are involved in making these bars, and variations in any one of them may have an effect on the final transition temperature. The annealing process, being the last, was especially suspect, since calculations suggested that the dissociation pressure of molybdenum dioxide at 1500° C. was approximately equal to the actual oxygen pressure of the vacuum-annealing furnace. It thus might be expected that variations in vacuum obtained in this furnace would affect the oxygen content of the molybdenum. For these reasons it was decided to

carry out further testing as far as possible on sintered specimens, since for any given batch of molybdenum, only one process of manufacture was then involved. Further, because of the high sintering temperature, it was probable that variations in vacuum would have less effect on the oxygen content.

## 5. BEND TESTS ON SINTERED MOLYBDENUM

Two main effects were investigated; first, the effect of carbon additions to the molybdenum powder, before sintering, on the oxygen content and transition temperature of the sintered compact, and secondly, the effect of other addition elements on the transition temperature. The microstructure typical of sintered specimens is shown in Fig. 7 (Plate XLVIII).

It was not easy in this work to carry out measurements of transition temperature and oxygen content on the same sintered compact, so two or more compacts were made, as far as possible similar, and the gas content determined on one compact and the transition temperature on the remainder. This procedure is not entirely satisfactory, but Table X shows that the transition temperatures of equivalent specimens are very similar, e.g. RLY and ROK.

## (a) Effect of Carbon Additions

It will be seen from Table X that the transition temperature of RLY and ROK, without carbon additions and sintered in hydrogen, is 120°-134° C. and the oxygen content is 0.0007%. Step-sintering at 1500° C. before sintering at 2300° C. does not appear to have any effect on transition temperature or oxygen content (RMC, ROX). It is not possible satisfactorily

TABLE IX.—Results of Bend Tests on Materials from Source B.

All swaged bars annealed at 1500° C., for 4 hr. in vacuum at the National Physical Laboratory.

Specimen No.	Sintering Conditions	Where Carried Out	Swaging Conditions	Where Carried Out	Density As Sintered, g./c.c.	Transition Temperature, °C.	Grain-Size, mm.
<i>Powder B1</i>							
RNN	Not known	B	Not known	B	Not known	Below 25	0.065
RMM	"	B	5 dies at 1350° C. 8 " 1100° C.	N.P.L.	9.30	41-48	0.08
RLK	"	B	Not swaged	...	9.30	275-280	0.010
ROZ	2 hr. at 2300° C. in H <sub>2</sub>	N.P.L.	"	...	9.88	130-135	0.035
ROB	" " "	"	5 dies at 1350° C. 8 " 1100° C.	N.P.L.	9.90	179-190	0.085
ROM	" " "	"	Rolled at 1350° C. $\frac{1}{2} \rightarrow \frac{5}{16}$ in. ROM/1 swaged at 1100° C.	...	9.87	...	...
			ROM/2 " 900° C.	N.P.L.	...	70-80	0.065
RON	" " "	"	Rolled at 1350° C. $\frac{1}{2} \rightarrow \frac{5}{16}$ in. RON/1 swaged at 1100° C.	...	9.86	205-220	0.040
			RON/2 " 900° C.	N.P.L.	...	90-95	0.080
RME	1 hr. at 1500° C. in H <sub>2</sub> 2 " 2300° C. in H <sub>2</sub>	"	5 dies at 1350° C. 8 " 1100° C.	N.P.L.	9.89	205-230 130-135	0.035 ...
<i>Powder B2</i>							
RNM	Not known	B	Not known	B	Not known	21-24	0.055
RML	"	B	5 dies at 1300° C. 8 " 1100° C.	N.P.L.	9.33	42-43	0.075
RLJ	"	B	Not swaged	...	9.33	260-268	0.013
ROL	2 hr. at 2300° C. in H <sub>2</sub>	N.P.L.	"	...	9.50	Above 200, below 253	...
RNZ	" " "	"	5 dies at 1350° C. 8 " 1100° C.	N.P.L.	9.66	121-125	0.075

to find the transition temperature of pure molybdenum compacts sintered in vacuum, since the density is too low, but the oxygen content is about the same as for those sintered in hydrogen (RLX).

When 0.16 wt.-% lampblack is added to compacts sintered in hydrogen and in vacuum, there is a reduc-

powder. If this surface oxide is removed by pre-reducing in hydrogen, much less carbon is lost (RPE, Table XI). If the compact is pre-reduced and then sintered in vacuum, a fairly high density is usually obtained, but the transition temperature is raised (RQF, RNL, RPH, RPS, Table X).

TABLE X. *Results of Vacuum-Fusion Analyses and Transition-Temperature Determinations on Sintered Molybdenum.*

Specimen No.	Nominal Carbon Content, %	Sintering Conditions	Residual Carbon Content, %	Density, g./c.c.	Gas Content, wt.-%			Transition Temp. of Equivalent Specimens, °C.	Grain-Size, mm.	Remarks
					O <sub>2</sub>	H <sub>2</sub>	N <sub>2</sub>			
RLU } RMA }	0.16	2 hr. at 2300° C. in vacuum	{ 0.026 0.012	{ 9.98 9.92	0.0003 ...	0.00008 ...	0.0020 ...	... 45-49	... 0.045	Source A molybdenum (RLX)
RLS } RMI }	0.16	2 hr. at 2300° C. in H <sub>2</sub>	{ 0.016 0.042	{ 9.95 9.95	0.0004 ...	0.00016 ...	0.0014 ...	... 80-90	... 0.040	
RLX	Nil	2 hr. at 2300° C. in vacuum	0.0036	9.33	0.0006	0.00007	0.0005	...	...	
RLW } RLY } ROK }	Nil	2 hr. at 2300° C. in H <sub>2</sub>	{ ... 0.0023 ...	{ 9.99 ... 10.01	0.0007 ... ...	0.0002 ... ...	0.0008 ... ...	... 120-127 128-134	... 0.040 0.050	
RMC } ROX }	Nil	1 hr. at 1500° C. in H <sub>2</sub> + 2 hr. at 2300° C. in H <sub>2</sub>	{ ... ...	{ 10.02 ...	0.0006 ...	0.0001 ...	0.0008 ...	... 125-128	... 0.060	
RQF } RNL } RPH } RPS }	Nil Mo preheated at 800° C. in H <sub>2</sub>	2 hr. at 2300° C. in vacuum	{ 0.0005 ... ... ...	{ 9.96 9.93 9.70 9.89	0.0008 ... ... ...	0.00003 ... ... ...	0.0006 ... ... ...	... 215-230 310-322 265-269	... 0.065 0.085 0.075	
RNM	...	Sintered and swaged at Source B	0.0016	...	0.0023	0.0003	0.0038	21-24	0.055	Source B2 molybdenum swaged bend-test specimens
RIP	...	Sintered and swaged at Source A	0.0015	...	0.0029	0.0002	0.0012	30-40	0.04	Source A molybdenum swaged bend-test specimens

TABLE XI.—*Effect of Added Carbon on Transition Temperature in Bend Tests on Molybdenum.*

Specimen No.	Amount and Type of Carbon Added	Sintering Conditions	Residual Carbon Content, %	Density, g./c.c.	Swaging Conditions	Transition Temp., °C.	Grain-Size, mm.	Remarks
RPE	0.16% electrode C added to Mo pre-treated in H <sub>2</sub> at 820° C.	2 hr. at 2300° C. in vacuum	0.134	9.82	...	227-233	0.065	Carbide in boundaries
RMF	1.00% lampblack	2 hr. at 2150° C. in vacuum	0.64	9.98	...	210-348	...	Only two bend samples available
RKC	0.02% lampblack	2 hr. at 2300° C. in H <sub>2</sub>	0.0037	...	{ 5 dies at 1500° C. 3 " 1350° C. 5 " 1100° C. annealed 4 hr. at 1500° C. in vacuum	95-100	0.055-0.095	Very small amount of carbide visible
RKD	0.04% lampblack	" "	0.0022	...				
RKA	0.10% lampblack	" "	0.0010	...				
RKE	0.16% lampblack	" "	0.0029	...	" "	47-48	0.085 and areas of 0.04	No carbide
ROA	0.30% electrode C	2 hr. at 2100° C. in H <sub>2</sub>	0.246	9.80 (before swaging)	" "	30-35	0.06	Some transgranular cracking associated with main fracture
					" "	28-31 34-36	0.055 0.035	Carbide particles mostly in the boundaries

tion both of oxygen content and of transition temperature, which are lower in the compact sintered in vacuum (cf. RLU, RLS, RMA, RMI). The addition of carbon enables a high density to be obtained on the compacts sintered in vacuum. Most of the added carbon is lost during sintering; it is probably used up in reducing the surface oxide on the molybdenum

Most of the preceding results can be explained on the assumption that increase either in oxygen content or in grain-size raises the transition temperature. In Fig. 12 the transition temperatures are plotted against grain-size and the oxygen content of the equivalent specimen, and it will be seen that the explanation given is strongly suggested. It must be realized that



the oxygen determinations at these low oxygen contents cannot be precise and were not made on the bend-test specimens.

There is some evidence in Table X that hydrogen and nitrogen in the quantities present do not affect the transition temperature, since compacts RLU and RMA with the lowest transition temperature have the highest nitrogen content, while compacts RQF, RNL, RPH, and RPS, with the lowest hydrogen content, have the highest transition temperature. However, this evidence is not strong. There is some indication that increase in porosity gives an increase in transition temperature. For example, in Table IX, compact ROZ, sintered at the N.P.L., has a density of 9.88 g./c.c. and a transition temperature of 130°–135° C., while compact RLK sintered at Source B, with a density of 9.30 g./c.c., had a transition tempera-

ture is lowered. The specimens to which 0.10 and 0.16% lampblack were added had transition temperatures similar to those of the commercial swaged and annealed specimens.

#### (b) Additions of Other Alloying Elements

A number of small alloying additions were made, using either elements which are strong deoxidants and thus might lower the transition temperature, or elements which are not deoxidants but which might serve to strengthen the molybdenum in creep. The deoxidants were studied to find out whether they had any tendency to reduce the brittleness of molybdenum, and the other elements to determine how far their effect on the transition temperature correlated with their effect on the forgeability. The results are listed in Table XII. Considering the deoxidants first, additions of 0.2 and 0.5% titanium to pre-reduced molybdenum gave compacts with a transition temperature approximately equal to that of compacts made only with pre-reduced molybdenum. Additions of 0.2% aluminium, with and without 0.2% lampblack, gave a slightly lower transition temperature. Most of the bars containing 0.5% zirconium broke during grinding, but there is no evidence that the addition lowers the transition temperature. It thus appears that none of the deoxidants added in these amounts has any very beneficial effect. It is, of course, possible that the deoxidants were present in more than the critical amounts and that smaller additions might have had a beneficial effect, but it is difficult to add very small amounts of one metal to another, using powder-metallurgy methods, when the added metal cannot be reduced in the compact.

The added metals not normally considered as deoxidants were niobium, tantalum, manganese, nickel, iron, and chromium. Tantalum may in fact act as a deoxidant, since the powder contains a large volume of hydrogen. Table XII shows that all these metals, except 0.3% tantalum in the presence of carbon, tend to raise the transition temperature, and it could be argued that the effect of the carbon was balancing the effect of the tantalum. Nickel, which of the metals tested has the greatest influence on forgeability, also has the greatest effect on the transition temperature. The result on the iron-bearing alloy RIW does not appear to support the suggestion that the lack of forgeability of the alloys with high alloying contents is due to the transition temperature being raised above the forging temperature, since the 0.5% iron alloy cannot be swaged at 1350° C., whereas the 0.38% iron alloy bent easily at 600° C.

Specimen RNQ, containing 0.1% sulphur, was included to test the possibility that sulphur may be one of the causes of the brittleness of molybdenum. The fact that 0.01% residual sulphur raises the transition temperature to over 400° C. supports this suggestion, but owing to the difficulty of analysing very small quantities of sulphur, the point cannot be further investigated.

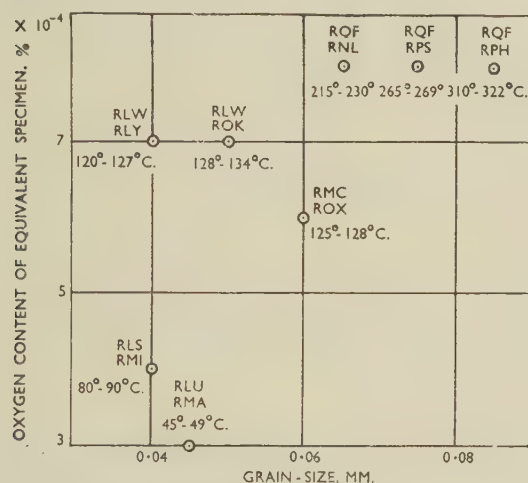


Fig. 12.—Effect of Grain-Size and Oxygen Content on Transition Temperature of Molybdenum.

Note: The top letters above each point are the code number of the equivalent specimen, while the lower letters are the code number of the bend specimen. The figures beneath give the transition temperature range.

ture of 275°–280° C. A rise in transition temperature with increase in porosity would be expected.

It is convenient at this point to consider a number of other tests in which carbon was added; these are listed in Table XI. The molybdenum used was pre-reduced in specimen RPE, thus removing any surface oxide, and this treatment accounts for the high residual carbon content. It is probable that the fairly high transition temperature is not due to the residual carbon, since RNL, RPH, and RPS (Table X), made with pre-reduced molybdenum but without carbon additions, had similar transition temperatures. Further, specimen RMF (Table XI) with 0.64% residual carbon had a transition temperature below 348° C., and the sintered, swaged, and annealed specimen ROA with 0.246% residual carbon had a transition temperature of 34°–36° C.

The remaining specimens in Table XI are sintered, swaged, and annealed specimens to which varying amounts of lampblack were added, and it will be noted that as the addition is increased the transition

TABLE XII.—*Effect of Added Elements on Transition Temperature in Bend Tests on Molybdenum.*

Specimen No.	Nominal Content of Alloying Element, %	Sintering Conditions	Residual Content, %	Density, g./c.c.	Swaging Conditions	Transition Temp., °C.	Grain-Size, mm.	Remarks
RPB	0.2 Ti *	2 hr. at 2300° C. in vacuum	0.21 Ti	10.03	...	192–199	0.06	
RNW	0.5 Ti *	" "	0.52 Ti	9.91	...	215–220	0.055	Clusters of brown constituent in microstructure—probably oxide
RPD	0.2 Al *	" "	0.06 Al	10.01	...	232–235	0.05	
RPQ	0.2 Al + 0.2 C	" "	0.08 Al + 0.076 C	9.88	...	225–226	0.085	Carbide solely at boundaries. Grey massive inclusions of oxide present
ROG	0.3 Nb + 0.2 C	" "	0.043 C	9.92	...	175–185	0.065	
ROF	0.3 Ta + 0.2 C	40 min. at 2300° C. in vacuum	0.042 C	9.88	...	78–84	0.055	
ROD	0.5 Mn	2 hr. at 2300° C. in H <sub>2</sub>	...	9.78	...	Above 410	...	
RNT	0.5 Zr *	2 hr. at 2300° C. in vacuum	...	...	...	Broke (0°) at 125° C.	0.055	Only one specimen available. Grey inclusions, mostly at the boundaries
RNQ	0.1 S	1 hr. at 2300° C. in H <sub>2</sub>	...	...	...	Broke (0°) at 400° C.	0.045	Residual sulphur less than 0.01%
RJL	0.1 Ni	2 hr. at 2300° C. in H <sub>2</sub>	0.1 Ni	...	5 dies at 1500° C. 3 " 1350° C. 5 " 1100° C. annealed 4 hr. at 1500° C. in vacuum	Above 670	0.045	
RIW	0.4 Fe	" "	0.38 Fe	...	" "	Above 300 below 600	0.055	
RKG	2 Ta	2 hr. at 2300° C. in vacuum	...	...	" "	260	...	
RIJ	1 Cr	2 hr. at 2300° C. in H <sub>2</sub>	...	...	7 dies at 1250° C. 6 " 1100° C. annealed 4 hr. at 1500° C. in vacuum	280–290	0.04	

\* Molybdenum pre-reduced in hydrogen at 800° C.

6. *Fracture Characteristics*

The fracture faces of the brittle bend specimens were examined under a binocular microscope at a magnification of  $\times 50$ . Most of the fractures appeared to be intergranular, except when carbon had been added, but the grain-size was too fine for accurate observation. However, micro-examination confirms that unless carbon is present the fracture is almost entirely intercrystalline (Figs. 8 and 9, Plate XLVIII).

## VII.—CONCLUSIONS AND DISCUSSION

The conclusions to be drawn from the swaging and creep testing of molybdenum are fairly definite, namely:

(1) Alloying additions, with the exception of tungsten, decrease the forgeability of molybdenum. Under the conditions of the present investigation, i.e. swaging sintered rods  $\frac{3}{8}$  in. in dia. between 1350° and 1600° C., the maximum amounts of the various alloying elements which can be added without

destroying the forgeability are as given in Table VI (p. 352).

(2) If such maximum amounts of alloying elements are added, then the resulting increase in creep strength is not evident or, if evident, is not large. The only alloys which appear to be definitely stronger than pure molybdenum are those with 1, 2, or 3% chromium and those with 20% tungsten.\*

(3) In a bend test, molybdenum when fairly pure exhibits, with increase in temperature, a sharp transition between brittle fracture and completely ductile bending. Molybdenum-base alloys display a similar transition, but this may not be sharp (see Fig. 11). The transition temperatures of substantially pure molybdenum samples in the annealed state (i.e. not worked) lie between 20° and 300° C., depending on the previous history of the specimen.

(4) In bend specimens prepared from sintered molybdenum compacts, increase in oxygen content, alloy content, grain-size, or porosity all appear to raise the transition temperature.

(5) In specimens tested after being sintered, swaged,

\* With regard to (2), it is known that the mechanical properties of molybdenum are very sensitive to small changes in the constituents present as minor impurities and to small variations in processing. Conclusions drawn from specimens made from the powders used in this investigation may not,

therefore, hold for specimens made from other powders or by a different process, such as arc melting. The same caution must be used in employing results from the work on the ductility of molybdenum, greater caution in fact, since the results tend to be contradictory.



and annealed, the only factor which consistently affects the transition temperature in substantially pure specimens is the addition of small quantities of carbon, which lowers the transition temperature. In sintered specimens such additions lower the oxygen content, and it is reasonable to assume that carbon has the same effect in the sintered, swaged, and annealed specimens. The effects of grain-size and of different manufacturing processes are inconsistent among specimens supposedly similar, and are often inexplicable.

(6) In sintered, and also in sintered, swaged, and annealed specimens, alloying additions of metals considered to be strong deoxidants may slightly reduce the transition temperature. Alloying elements not considered to be strong deoxidants increase the transition temperature. The addition elements tested were: aluminium, chromium, iron, manganese, nickel, niobium (with carbon), sulphur, tantalum, and titanium. Tungsten was not tested, but is reported not to increase the transition temperature markedly.<sup>19</sup>

(7) The fractures in all specimens except those to which carbon had been added were almost entirely intergranular.

(8) Forging carried out at temperatures below the recrystallization temperature appears to lower the transition temperature.

(9) It does not, at the moment, seem possible to develop creep-resistant alloys which are not brittle at room temperature after recrystallization, or to find a means of overcoming the adverse effect of alloying elements on the forgeability of molybdenum.

These conclusions, except (7), dealing with grain-boundary fracture, are in fair agreement with recent work in the United States. There seems to be no American work in which the transition temperature in plain bending has been determined, but transition temperatures have been found in notched-bar tests and in tensile tests.<sup>1, 19</sup> There is apparently some uncertainty with regard to the effect of oxygen. Bechtold and Scott<sup>19</sup> claim that test-pieces made by rolling and annealing a sintered and a cast bar had oxygen contents of 0.006 and 0.0002%, respectively, but in spite of this had very similar properties, including transition temperatures differing only by about 30° C. On the other hand, Rengstorff and Fischer<sup>20</sup> show that cast molybdenum purified by repeated melting in a high vacuum is ductile in bend at room temperature, while cast molybdenum, melted only once, is not. The former contains less carbon and oxygen than the latter.

The only American work on the ductility of molybdenum-base alloys seems to be that of Ham,<sup>1</sup> which shows that increase in alloy content makes forging more difficult and finally impossible. If the limits of forgeability of Ham's alloys are compared with those reported in the present work, it will be found that they tend to be low, e.g. alloys containing 1.5% chromium could be swaged at the N.P.L., whereas Ham could not forge alloys with 1.2%.<sup>11</sup>

It is claimed by Rengstorff and Fischer<sup>20</sup> that carbon increases the brittleness of molybdenum. This is not found to be the case in the experiments now reported, e.g. specimen ROA (Table XI) has a carbon content of 0.246%, but nevertheless has a very low transition temperature. It was found that, unless carbon had been added, the brittle fracture was almost entirely intercrystalline. Bechtold and Scott<sup>19</sup> report transcrystalline fracture even in specimens made by powder metallurgy. However, their powder-metallurgy specimen contained 0.004% carbon. The fracture of arc-cast molybdenum containing

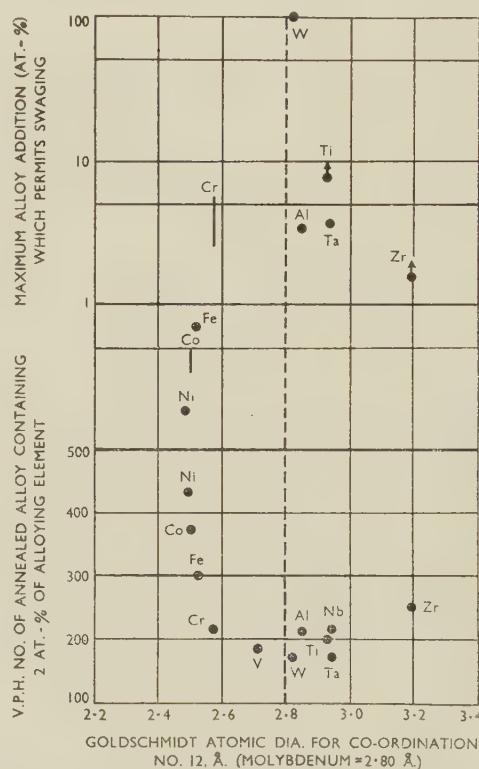


FIG. 13.—Illustrating Relation to Forgeability and Hardness of Molybdenum Alloys of the Ratio Between the Atomic Diameter of the Metal and of the Alloying Element.

carbon was intercrystalline at high temperatures, i.e. during forging, but transcrystalline at low temperature.<sup>1, 11</sup>

In Table VI are listed the maximum quantities of various alloying elements which may be added to molybdenum without destroying its forgeability. These maximum percentages, converted to atomic percentages, are plotted against the Goldschmidt atomic diameters in the top half of Fig. 13. In the lower half of the same figure the hardness, taken from Ham,<sup>1, 11</sup> of annealed alloys of molybdenum containing 2 at.-% of various alloying elements is plotted against the Goldschmidt atomic diameter of these elements. It will be seen that, as the difference between the atomic diameters of the alloying elements and of molybdenum becomes greater, the hardness of the alloy increases and its forgeability decreases.

There are a number of other metals which show a transition from brittle to ductile behaviour with increase in temperature. These are  $\alpha$ -iron, chromium,<sup>21</sup> tungsten,<sup>10</sup> and zinc.<sup>22</sup> It is also said to be shown by  $\beta$ -brass.<sup>23</sup> Most work on this transition has been done in connection with iron. Comparing substantially pure iron, i.e. not steel, with molybdenum, similarities exist. As the oxygen content of iron is increased, the fracture changes from transgranular to intergranular, and the transition temperature becomes rapidly higher.<sup>24</sup> It is reported that the speed of propagation of brittle fracture in iron is very high.<sup>25</sup> It is the present authors' impression, from the sound of the break and from the sudden removal of resistance, that the propagation of fracture during the slow bending of molybdenum is also very fast.

It is often suggested that low-temperature brittleness is a property of body-centred cubic metals, since, except for zinc, the metals exhibiting brittleness have this structure. However, the alkali metals sodium and potassium are not known to show brittleness, and evidence is available which suggests that tantalum and niobium may not do so. A bar of tantalum,  $\frac{7}{8}$  in. long  $\times$   $\frac{1}{8}$  in. dia., was bent through  $170^\circ$  in the bending jig used in this investigation, at  $-177^\circ\text{C}$ . A piece of niobium has been hammered at about the same temperature without any signs of cracking.

If the Ludwik-Davidenkov-Orowan<sup>26</sup> hypothesis for brittle fracture is accepted, the effect of alloying elements and impurities on the transition temperature is explained by assuming that they affect the yield and brittle strengths in such a way that the difference between them is decreased, or that the yield strength is made greater than the brittle strength. Moreover, as the temperature of test is decreased, the yield strength increases more than does the brittle strength.

Thus, a metal or an alloy which is ductile under given conditions of test and temperature, but the brittle strength of which only slightly exceeds the yield strength under the same conditions of test and temperature, will become brittle under these same conditions of test when the temperature is lowered. What the theory does not explain is why lowering the temperature of certain metals, such as copper or nickel, will never bring the brittle strength below the yield strength, even under severe conditions of test such as notch bending, whereas metals such as molybdenum undergo transition at temperatures above room temperature. One partial explanation of the difference is obtained by assuming that the atoms in metallic lattices behave as elastic spheres, and that there are thus smaller holes available in body-centred cubic lattices for accommodating interstitial impurities such as carbon, nitrogen, and oxygen, than in face-centred cubic and hexagonal lattices. Thus when these impurities are present, as they usually are, in the body-centred cubic metals, the lattices are in a state of strain and so are weakened. Support is given to this hypothesis by the fact that the body-centred cubic metals which, as suggested above, do not show a transition temp-

erature, namely, sodium, potassium, tantalum, and niobium, are those with large lattice parameters and thus with the largest holes. Carbon, however, does not appear to act in accordance with this suggestion, since in molybdenum and also, under certain conditions, in iron,<sup>27</sup> it decreases the transition temperature.

#### ACKNOWLEDGEMENTS

The work described has been carried out in part under the research programme of the National Physical Laboratory and in part under that of the Inter-Service Metallurgical Research Council. This paper is published on the recommendation of the Council and by permission of the Director of the Laboratory.

#### REFERENCES

1. J. L. Ham, *Trans. Amer. Soc. Mech. Eng.*, 1951, **73**, 723.
2. P. Schwarzkopf, "Powder Metallurgy", pp. 170-194. 1947: New York (The Macmillan Co.), London (Macmillan and Co., Ltd.).
3. O. Kubaschewski and A. Schneider, *Z. Elektrochem.*, 1942, **48**, 671.
4. W. Trzebiatowski, H. Ploszek, and J. Lobzowski, *Analyt. Chem.*, 1947, **19**, 93.
5. W. P. Sykes and H. F. Graff, *Trans. Amer. Soc. Metals*, 1935, **23**, 249.
6. W. P. Sykes, "Metals Handbook", p. 1210. 1948: Cleveland, O. (American Society for Metals).
7. F. H. Ellinger, *Trans. Amer. Soc. Metals*, 1942, **30**, 607.
8. G. A. Geach and D. Summers-Smith, *J. Inst. Metals*, 1951-52, **80**, 143.
9. M. Hansen, E. L. Kamen, H. D. Kessler, and D. J. McPherson, *Trans. Amer. Inst. Min. Met. Eng.*, 1951, **191**, 881.
10. C. J. Smithells, "Tungsten". 1952: London (Chapman and Hall, Ltd.).
11. J. L. Ham, "Arc-Cast Molybdenum Alloys". 1950: Detroit, Mich. (Climax Molybdenum Co.).
12. W. P. Sykes, *Trans. Amer. Inst. Min. Met. Eng.*, 1921, **64**, 780.
13. J. W. Marden and D. M. Wroughton, *Trans. Electrochem. Soc.*, 1946, **89**, 217.
14. C. E. Ransley and H. P. Rooksby, *J. Inst. Metals*, 1938, **62**, 205.
15. W. L. Bruckart, M. H. LaChance, C. M. Craighead, and R. I. Jaffee, *Trans. Amer. Soc. Metals*, 1953, **45**, 286.
16. H. Green, *J. Franklin Inst.*, 1921, **192**, 637.
17. J. H. Rendall, *J. Sci. Instruments*, 1952, **29**, 248.
18. N. P. Allen and W. E. Carrington, *J. Inst. Metals*, in the press.
19. J. H. Bechtold and Howard Scott, *J. Electrochem. Soc.*, 1951, **98**, 495; 1952, **99**, 277.
20. G. W. P. Rengstorff and R. B. Fischer, *Trans. Amer. Inst. Min. Met. Eng.*, 1952, **194**, 157.
21. A. H. Sully, E. A. Brandes, and K. W. Mitchell, *J. Inst. Metals*, 1952-53, **81**, 585.
22. P. L. Teed, "Properties of Metallic Materials at Low Temperatures". 1950: London (Chapman and Hall, Ltd.).
23. I. R. Kramer and R. Maddin, *Trans. Amer. Inst. Min. Met. Eng.*, 1952, **194**, 197.
24. W. P. Rees and B. E. Hopkins, *J. Iron Steel Inst.*, 1952, **172**, 403.
25. G. Hudson and M. Greenfield, *J. Appl. Physics*, 1947, **18**, 405.
26. E. Orowan, *Rep. Progress Physics*, 1948-49, **12**, 202.
27. N. P. Allen, W. P. Rees, B. E. Hopkins, and H. R. Tipler, *J. Iron Steel Inst.*, 1953, **174**, 108.



# THE ARC MELTING OF METALS AND ITS APPLICATION TO THE CASTING OF MOLYBDENUM\*

1528

By G. L. HOPKIN,† O.B.E., B.Sc., F.I.M., (Mrs.) J. E. JONES,‡  
B.Sc., D.R.T.C., MEMBER, A. R. MOSS,‡ and D. O. PICKMAN,‡  
B.A., MEMBER

## SYNOPSIS

The object of the investigation was to develop a plant and technique for the casting of molybdenum and molybdenum-base alloys.

The difficulties hitherto encountered in the melting of refractory metals are discussed, together with the reasons for the adoption of the present method and its scope and advantages for a range of such metals and alloys, including some of lower melting point. The design and operation of a plant capable of producing 1½-in.-dia. ingots of molybdenum is described, and the metallurgical features of the process are considered.

Experimental observations on the behaviour and characteristics of the metal-depositing arc in vacuum are recorded.

## I.—INTRODUCTION

THERE is a growing demand for metals and alloys with high strength and creep-resistance in the temperature range 850°–1000° C. These properties are most likely to be obtained from alloys based on metals of high melting point. The only metals with melting points above 2000° C. that are available in sufficient quantity to merit consideration for any large-scale application, are molybdenum, tantalum, and tungsten.

The production of solid masses of any of these metals in a high state of purity is not possible at present by a conventional melting and casting process, the fundamental difficulty being the lack of a suitable high-temperature refractory material. Commercially, they are all produced by the powder-metallurgy method of pressing and sintering, and are then hot worked into the required form. This process has limitations, particularly regarding the maximum size of bar that can be pressed and sintered to yield a final product with satisfactory properties.

The heat of the electric arc has been used for melting metals for at least 70 years; the melting of a refractory metal, tantalum, using water-cooled copper as a crucible, was first reported by von Bolton.<sup>1</sup> Since then Kroll<sup>2</sup> has utilized a similar process for melting titanium in an inert atmosphere, the water-cooled copper in this case replacing a refractory owing to the high reactivity of molten titanium with refractory materials.

Parke and Ham<sup>3</sup> developed a consumable-electrode process for arc melting and casting molybdenum in a cylindrical water-cooled copper mould. A similar process with a non-consumable electrode has been

described by Radtke, Scriver, and Snyder<sup>4</sup> for the arc melting of titanium.

In the consumable-electrode arc-melting process the metal to be melted is in the form of a rod, which may be made by powder metallurgy, and is contained in a chamber either under high vacuum or filled with an inert gas. The rod is connected to a source of alternating or direct current and fed down centrally inside a water-cooled copper mould at the base of which is a disc of similar material forming the other electrode. When the two make contact, a metal-depositing arc is initiated, and the rod material melts off, forming a pool of molten metal, on the disc, which eventually extends to the wall of the mould. Owing to the high thermal conductivity of copper and the rapid heat extraction, the molten metal rapidly freezes as it comes into contact with the copper, and no melting of the latter takes place. As more molten metal is added to the pool, progressive solidification takes place from the bottom and sides of the melt, so that at any instant only a small, crescent-shaped pool of metal is molten.

As previously mentioned, the highly refractory metals such as molybdenum and tungsten cannot be cast by any other method. There are also metals of lower melting point, such as titanium, zirconium, and beryllium, for which arc melting presents considerable advantages. These metals are particularly susceptible to embrittlement by impurities, and are highly reactive with the commonly available refractory materials at temperatures above their melting points.

The nature of the process also renders it particularly useful for the melting and casting of a wide range of metals and alloys in a high state of purity. It is

\* Manuscript received 14 July 1953.

† Formerly at Armament Research Establishment; now at

Atomic Weapons Research Establishment, Aldermaston, Berks.

‡ Armament Research Establishment, Fort Halstead.

further possible, by multiple remelting, to reduce the content of gaseous and volatile impurities to a very low level.

Although only the melting of molybdenum and its alloys is considered here, the more general application of the technique to other metals should not be overlooked.

## II.—DESIGN OF THE PLANT

Early experiments to establish the feasibility of arc melting molybdenum in a water-cooled copper mould were made in a simple prototype plant, using a consumable electrode fed manually through a sliding vacuum seal. The mould was mounted inside the vacuum chamber on a steel base-plate.

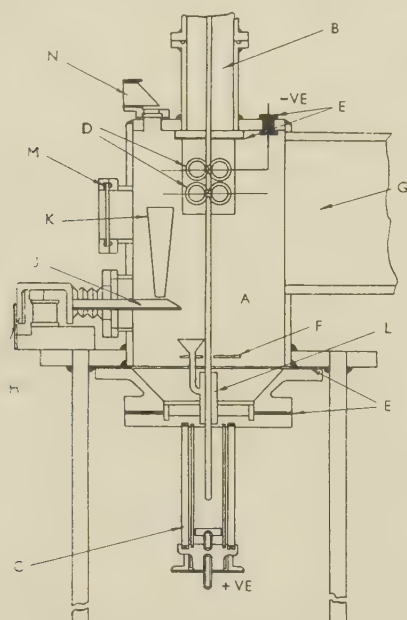


FIG. 1.—Schematic Diagram of Arc-Melting Plant.

### KEY.

- |                                  |                              |
|----------------------------------|------------------------------|
| A. Melting chamber.              | H. Vibrator for powder-feed. |
| B. Extension tube for electrode. | J. Powder-feed trough.       |
| C. Water-cooled copper mould.    | K. Copper hopper.            |
| D. Electrode drive mechanism.    | L. Copper sleeve.            |
| E. Insulator.                    | M. Perspex window.           |
| F. Radiation shield.             | N. Periscope.                |
| G. Vacuum line.                  |                              |

Satisfactory small ingots were prepared in this equipment, and a larger, but essentially similar, plant was then constructed, incorporating a mechanical electrode feed. This plant proved to be electrically unsound and was considerably modified to the form currently in use. The nature of the electrical troubles encountered is of interest and is described in Section VII, 2. The design of the modified plant is shown schematically in Fig. 1, and a photograph of the complete assembly in Fig. 3 (Plate XLIX).

### 1. MELTING CHAMBER AND FEED MECHANISM

The melting chamber (A) is made from 10-in.-dia. steel pipe with a narrower vertical extension tube

(B) to accommodate a 6-ft. length of consumable electrode. The water-cooled copper mould (C) is clamped to a heavy steel base-plate, which is itself connected via a conical adaptor to the flange at the base of the chamber. Both these joints are insulated with  $\frac{1}{8}$ -in. Neoprene gaskets and Tufnol bushes. The electrode is fed down by a drive mechanism (D) attached centrally at the top of the chamber. This comprises two sets of opposed driving rolls with V-shaped edges; the upper and lower rolls on each side are mounted in independent frames, one rigid and the other flexible, which are pulled together by springs to apply pressure on the electrode. Both of the upper and one of the lower driving rolls are made of a copper-chromium alloy, and the other is of steel with case-hardened, knurled V-faces. The steel roll is geared to the opposed copper roll, and is driven through an external gear train, the driving shaft passing through a Wilson seal. The whole drive mechanism is insulated from the chamber, electrical connection to the electrode being made from an insulated terminal (E) on top of the chamber via the two frames holding the driving rolls. Spring-loaded carbon brushes ensure good contact with the copper rolls. A molybdenum radiation shield (F) protects the drive from direct radiant heat.

A 10-in.-dia. pipe (G), bent through 90°, serves as a vacuum line, connecting the side of the melting chamber to the top of the diffusion pump. A small-diameter outlet is connected through a cold trap to a McLeod vacuum gauge.

A vibratory feed (H) is incorporated for making alloying and deoxidizing additions to the melt. A small magnetic coil is supplied with rectified 50-cycle A.C. and vibrates an armature attached through a bellows seal to a shallow horizontal steel trough (J) inside the chamber. A conical copper hopper (K) delivers powder on to the trough, from whence it feeds via a copper guide funnel into an annular copper sleeve (L) around the electrode and drops into the mould. A Perspex window (M) permits observation of the powder feed during melting. The periscope (N) is used to observe the arc.

An alternative top fitting in place of the extension tube (B) may be used. This consists of a modified Wilson seal with three dished rubber seals, the space between the second and third being  $3\frac{1}{2}$  in. long and evacuated by an auxiliary rotary vacuum pump. The consumable electrode may be fed in through this seal, enabling any desired amount of rod to be melted provided a sufficiently large mould is used. Screwed connections between lengths of rod are used, the threads being slotted to allow easy evacuation while passing through the seal. It was found that to prevent undue frictional drag and rapid wear of the rubbers, these had to be dished away from the high-pressure side, a reversal of usual vacuum practice. In spite of this, however, the seal was highly efficient and no deterioration of the vacuum could be detected.



## 2. WATER-COOLED COPPER MOULD

The mould is one of the most critical features of the whole equipment; the design currently in use is shown in Fig. 2.

The copper mould itself (A) is a 7- or 12-in. length of standard tubing, of  $1\frac{3}{4}$  in. internal dia. and  $\frac{5}{32}$  in. wall thickness; the ends are accurately squared up and seat on rubber "O" ring seals in retaining grooves in the steel base-plate (B) and the copper sealing cap (C). A brass water jacket (D) fits closely round the mould, leaving a  $\frac{1}{4}$ -in. annular space for water flow; the jacket is also sealed top and bottom

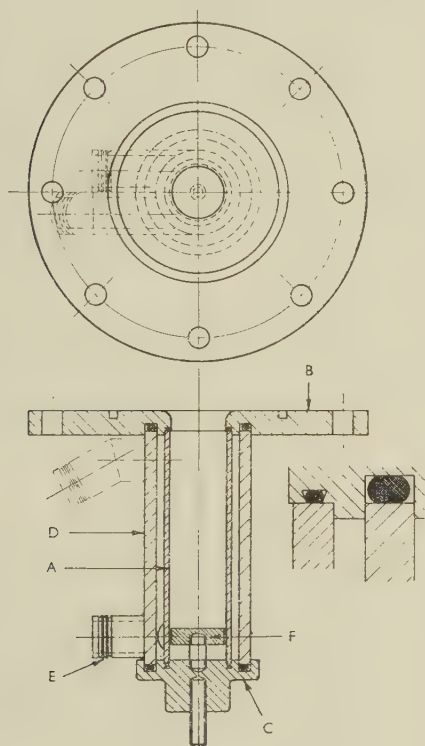


FIG. 2.—Design of Water-Cooled Copper Mould.

## KEY.

- |                  |                        |
|------------------|------------------------|
| A. Copper mould. | D. Brass water-jacket. |
| B. Steel plate.  | E. Water inlet.        |
| C. Copper cap.   | F. Molybdenum disc.    |

by rubber "O" rings free to undergo a large compression. Water enters tangentially through an inlet  $1\frac{3}{16}$  in. in internal dia. (E) at the bottom of the mould and leaves by a similar outlet at the top. Water taken from a 1-in. main can be passed through the jacket at about 12 gal./min.; the desirable flow rate is usually, however, the minimum safe rate, which in this mould, for a power input of 40 kW., is about 6 gal./min. The effect of cooling rate on ingot quality is discussed in Section VI, 5.

The ingot is built up in the mould on a molybdenum disc (F), screwed into the copper sealing cap, this disc forming the other electrode. Electrical connection is made externally to the cap. The whole mould assembly is drawn up and the seals made by

means of a simple clamp attached to the steel base-plate and bearing on steel inserts in the copper cap. This type of mould has the dual advantage that it is inexpensive and that the copper tube can be easily replaced in the event of damage.

## 3. VACUUM SYSTEM

The vacuum system consists of a 9-in., three-stage, silicone oil-diffusion pump, connected via a baffle isolation valve to the vacuum line from the chamber. The speed of this pump with baffle is 1000 l./sec. at pressures of  $1\ \mu$  or lower. The diffusion pump is backed by a rotary oil pump with a displacement of 15 ft.<sup>3</sup>/min. The vacuum obtainable in the apparatus before melting is 0.01–0.05  $\mu$  ( $1 \times 10^{-5}$  to  $5 \times 10^{-5}$  mm.).

During melting, some deterioration of the vacuum invariably takes place. When melting pure molybdenum in rod form, without any powder addition, a steady pressure of about 0.1  $\mu$  is obtained, the higher pressure being due to the evolution of gas from the rod as it is heated and melted. This gas consists largely of oxygen, hydrogen, and carbon monoxide. When powder additions are made, a further deterioration of vacuum occurs owing to liberation of adsorbed gases and breakdown of oxides. This deterioration is generally increased when carbon is included in the powder as a deoxidizer. The extent of this further rise in pressure may be quite small when low-oxygen powders are used, and in the case of additions of molybdenum powder containing about 0.05% oxygen, together with carbon, a vacuum of about 0.3  $\mu$  can be maintained. A gross deterioration of vacuum to the region of 100–150  $\mu$  has been experienced when using powders containing a large amount of adsorbed surface gases or combined surface oxygen. The magnitude of this degradation was due to gas evolution slightly exceeding the capacity of the backing pump, with consequent poor functioning of the diffusion pump.

## 4. ELECTRICAL SUPPLY

The D.C. supply is obtained from two, or sometimes three, D.C. welding generators coupled together in parallel. For melts of short duration, up to 1450 amp. with an arc-stream voltage of 34 V. can be taken with negative polarity on the consumable electrode in vacuum, and up to 2200 amp. with an arc-stream voltage of 23 V. with positive polarity in argon. In both cases the open-circuit voltage is 90 V.

The A.C. supply is obtained from a 90-kVA. multi-operator arc-welding transformer, which has an open-circuit voltage of 100 V.

## 5. AUTOMATIC ARC-LENGTH CONTROL

In order to maintain good melting conditions and prevent damage to the mould, it is necessary to control the arc length within close limits; for the type and sizes of mould described in Section II, 2, the optimum arc length is thought to be  $\frac{3}{4} \pm \frac{1}{8}$  in. From data obtained on the arc, this variation in

length is known to correspond to a variation in arc voltage of approximately 0.4 V. for A.C. and for D.C. with electrode negative, and of 0.8 V. for D.C. with electrode positive.

The principle on which the automatic control operates depends on this relationship between arc length and arc voltage, an increase in voltage resulting in a speeding up of the electrode feed rate and vice versa. The main requirements of the control are, firstly, that it should be sufficiently sensitive to fractional voltage changes to keep the arc length within the required limits, and, secondly, that the response of the driving mechanism should be rapid. The latter condition is particularly necessary during the striking of the arc and while establishing the required arc length.

The control consists of a gas-filled relay which triggers a mercury-vapour thyatron. The arc voltage is applied to the grid of the relay in opposition to a voltage obtained from rectified A.C. such that the grid becomes more negative when the arc voltage rises. The voltage of the applied rectified A.C. can be varied to alter the potential at which the arc voltage causes the relay to stop firing. When the relay fires, the anode current passing through a resistance in the anode circuit causes the grid of the thyatron to become negative, so that it stops firing, and vice versa. A half-wave rectified current is thus available which flows when the arc voltage rises above a set value and ceases when it falls below this value. Within the limits  $\pm 0.12$  V. of the set value, the current flows irregularly. This is well within the minimum sensitivity,  $\pm 0.25$  V., necessary to keep the arc length within the required limits. The rate of response of the control is  $1\frac{1}{2}$  cycles, 0.03 sec. on the 50-cycle supply, since a thyatron continues to pass current whatever the grid voltage until the applied voltage falls below the critical value. Thus, no response will be obtained until the next positive half cycle after the relay has fired.

To ensure rapid response in the driving mechanism, the current from the control device is fed into the field of a magnetic clutch similar in design to a synchronous motor. The stator field, which is fed through a smoothing choke and condenser, is mechanically rotated at a suitable constant speed by means of an electric motor. The rotor is a salient pole, iron keeper. The clutch picks up very rapidly, the inertia of the rotating-field system taking the suddenly increased load from the motor. It has the further advantage that there is no mechanical friction and no wear on the operating parts. In operation the electrode can be driven at full speed into the cold base disc, stopped almost instantaneously when contact is made, allowing the arc to strike, and then restarted as soon as the required voltage is reached.

After some operating experience with this control system, it became apparent that a further modification was required to cater for the fact that the required operating voltage for a particular melt could not be predicted with any certainty. For a given vacuum

pressure and arc length, a variation in arc voltage of as much as 7 V. was found from melt to melt. The reason for this variation is not known, but it is in some way connected with the properties of different batches of molybdenum rod.

An addition was accordingly made to the control system, enabling the actual arc voltage for any run to be measured during the first fraction of a second and the controller to be set to this voltage. Immediately after the arc has been struck, a timing circuit operates a relay that changes over the anode circuit of the thyatron, which in turn energizes a ratchet motor to drive a potentiometer, thus increasing the control-setting voltage until the thyatron is made non-conducting. The time during which this relay is energized is of the order of half a second; by varying this time the controlled arc length can be altered. At the end of the delay period the changeover relay is de-energized and the clutch again put in circuit. The control then begins to function normally and maintains the desired arc length irrespective of the relationship between arc voltage and arc length pertaining to any particular batch of rod.

The control in this form has functioned satisfactorily, but it still suffers from an inability to correct for alterations in arc length due to variation of pressure during the course of a run. The corrections needed can be made manually when the arc can be observed sufficiently well to estimate arc length.

### III.—OPERATION OF THE PLANT

The necessary steps in assembling and operating the plant will now be described.

The required length of electrode is inserted into the feeding mechanism, and the powder addition placed in the hopper. The feed rate of the powder is then adjusted by direct calibration. When alloy additions are made, the rate of powder flow is corrected for melting loss, on the basis of previous experience.

The mould is then clamped in position and the plant evacuated. As a rule, pumping is continued until no further improvement in vacuum is observed, usually for a period of about  $1-1\frac{1}{2}$  hr. The water flow through the mould is then adjusted, and the electrode fed down on open circuit until an arc is struck and melting begins. When the molten pool is well established, after about 5 sec., the powder feed is started. During melting, a close watch is kept on arc voltage and vacuum pressure in conjunction with visual observation of the arc. Any rising trend in arc voltage is corrected by manual adjustment. The powder feed is stopped 5 sec. before the end of melting.

Vacuum-melted ingots are easily removed from moulds, but after considerable use there is a tendency for the moulds to become internally scored and pitted. This gives rise to difficulty in ingot removal, and it is at this stage that the mould is condemned; in the



absence of more severe accidental damage this will be after 30–50 melts.

The procedure when melting in argon is the same, with the additional stage of admitting the argon through a liquid-nitrogen trap after evacuation. The baffle isolation valve is closed immediately before admission. Ingot removal is more difficult with argon-melted ingots and mould wear correspondingly more severe. The reason for this is not clearly understood, but is probably connected with the absence of a spatter shield ahead of the growing ingot.

After removal of the ingot any powder remaining in the feed system is removed and weighed. This, in conjunction with any powder found on the walls of the mould and in some cases with an estimated allowance for powder in the spatter shield, is used to calculate the percentage of alloy or deoxidant added.

Between melts, no regular maintenance of the plant is necessary; the mould is cleared and mould "O" rings checked; apart from this the next melt can be carried out immediately. Periodically the plant must be stripped down for general cleaning and maintenance, including renewal of sight windows and insulation which gradually become metallized. Metallization of insulation can largely be avoided by correct design so that it is screened from the point source of evaporation.

#### IV.—MATERIALS

The consumable electrodes are normally obtained from commercial sources in lengths of approximately 3 ft. and of 10 mm. dia. They are made by powder-metallurgy methods, square-section pressed bars being sintered in hydrogen before forging and swaging. The rods so obtained are straightened and centreless-ground to give electrodes suitable for use with the feed and current pick-up mechanisms previously described.

Initially, the base discs were also made by pressing and sintering molybdenum powder, but it is desirable that they should be of high purity, and they are now generally made from ingots of molybdenum specially cast for the purpose. They are  $\frac{3}{4}$  in. thick and  $\frac{1}{16}$  in. less in dia. than the copper mould.

The consumable electrodes are made from top-grade commercial molybdenum powder and are of about 99.92% purity. The major impurities are carbon ~0.01, iron ~0.02, silicon ~0.005, and oxygen ~0.04%. Other impurities detected spectroscopically in trace amounts are manganese, nickel, tungsten, chromium, vanadium, cobalt, copper, magnesium, calcium, titanium, aluminium, and zinc. The oxygen content has not been determined directly, as no reliable method, other than vacuum-fusion analysis which was not available, is known. The figure of 0.04% has been calculated from loss of carbon in carefully controlled melts, and can be taken as approximate only.

Other materials which have been used in the form of additions to melts are carbon, for deoxidizing vacuum melts, and various metals added for alloying or deoxidizing purposes. Electrode carbon of spectrographic purity with a total ash residue on combustion of 0.009% proves suitable for addition purposes. Other alloying elements have been of the highest purity readily available from commercial sources.

#### V.—METHODS OF ALLOYING

##### 1. FEEDING PROBLEMS

The method of alloying molybdenum ingots to ensure minimum segregation and melting loss has presented a considerable problem. The best method would appear at first sight to be the incorporation of the necessary additions in the consumable molybdenum electrode during manufacture. Unfortunately, this has serious limitations, and in practice can be carried out with only a limited number of metals. In the early days of the work, attempts were made to incorporate carbon in the electrode as a deoxidizer, but the loss of carbon during sintering in hydrogen was so serious and uncontrollable as to rule out this procedure. The incorporation of alloying elements in the electrode was also found to be difficult, as only very small amounts of many elements could be incorporated without rendering the sintered bar unworkable. This meant that only bars pressed and sintered to final electrode size could be used, and the length was limited by the green strength of the bars. Another difficulty then arose in that many alloys were so hard and brittle in the sintered state that joining by any mechanical means was impossible, and, moreover, distortion during sintering made them unsuitable for feeding through the driving mechanism. More fundamentally, even when such bars could be made, difficulties arose from eliquation during melting. The method would, of course, also require the manufacture of special electrodes for each different alloy.

Another method tried was to apply the alloy as an electrodeposit on the molybdenum electrode. This suffers from several drawbacks. First, it cannot be used for all the desired alloys owing to the lack of suitable processes for electrodepositing certain elements, and, secondly, even when only quite small additions of metals forming low-melting eutectics are made, the concentration of the alloy on the surface results in surface melting with the formation of deep longitudinal gouges. This effect is not, in itself, serious, but it results in periodic and relatively large alloy additions which are undesirable from the point of view of homogeneity. Additions of cobalt, nickel, and chromium have been made in this way.

The method finally adopted was to make the additions in the form of a continuous stream of powder fed by a vibrating feed from a hopper inside the melting chamber. The stream of powder was directed into an annular cylinder around the con-

sumable electrode and located just above the top of the mould. The general layout is shown in Fig. 1. This method gives a reasonably even distribution of powder into the molten pool and minimizes build-up of powder on the walls of the mould. In this latter respect the method is more suitable the larger the mould diameter. For the small size of mould used in this work,  $1\frac{3}{4}$  in. internal dia., some powder entrapment in the spatter shield ahead of the growing ingot generally occurs, with a resulting tendency to edge segregation.

When only a deoxidizer is to be added, the difficulty arises of feeding a small amount, say 1 g. in 30 sec., at a uniform rate. This has been overcome by incorporating the deoxidizer in a larger quantity of pure molybdenum powder, which serves as a carrier. Unfortunately, the molybdenum powder is itself a source of oxygen, and allowance must be made for deoxidizing it.

The feeding of ferromagnetic powders is complicated by the powder partially or wholly attaching itself to the electrode on entering the annular cylinder, owing to the magnetic field existing round the current-carrying consumable electrode. This effect, in itself, is not a serious drawback, but it means that a larger amount of molybdenum electrode than is necessary must be melted before the alloys begin to enter the melt and in some cases uneven addition results, in a manner similar to that which occurs with additions in the form of electrodeposited coatings. In extreme cases, such as the addition of pure iron powder, the magnetic attraction is sufficiently strong to influence the feed rate of the powder and to cause some of it to jump directly to the electrode from the end of the vibrating delivery tray. This could be prevented by having the feed remote from the current-carrying portion of the electrode. Some improvement has been effected by making all parts of the feed system of copper.

## 2. PREPARATION OF THE POWDER

It is the aim, when making additions to the melt, to have the powder addition in a form most suitable for feeding and with minimum and known oxygen and moisture contents. All fine metal powders have a relatively high oxygen content due to surface films of oxide, loosely combined oxygen, or both; they also have a tendency to adsorb moisture.

In order to keep the oxygen and moisture content to a minimum, all powders used are either obtained from the manufacturers in containers, flushed with inert gas, into which they are filled immediately after removal from the reduction furnace, or are again reduced in hydrogen after receipt and then stored in a similar manner. Any subsequent exposure to air must be for the minimum possible time. Reduction in hydrogen does not, of course, reduce the oxides of many of the metals used, but it does remove loosely combined surface oxygen, which often, as in the case of molybdenum, forms the major amount. In no case is

hydrogen reduction suitable as an absolute method of determining oxygen, as reduction of internal oxide particles and the removal of oxygen dissolved in the interior of a metal particle take a very long time. Thus, the accurate determination of the oxygen content of the powder addition, especially when appreciable amounts of metals such as chromium or titanium are added, is not possible by any simple method. Vacuum-fusion analysis appears to be the only possible method of total-oxygen determination, but it has not so far been attempted.

The powder mixture is prepared as follows. The alloy powder is taken from its sealed container and weighed as rapidly as possible. If the rate of alloy addition is to be less than about  $\frac{1}{2}$  g./sec., sufficient molybdenum powder is weighed out and mixed with the alloy to bring the feed rate up to this figure. The mixing is done in a sealed bottle flushed with argon. After mixing, the powder is removed and pressed into pellets which are crushed and screened to give a portion between 30 and 50 mesh. All this is carried out as rapidly as possible, and the sized powder is then again stored in a sealed container flushed with argon until required. When an individual check analysis is required, a sample is taken at this stage and similarly stored before the beginning of analysis. The oxygen and moisture contents of the sample are determined, and the moisture figure is corrected for the loss which will take place in the hopper in 1 hr. under vacuum conditions at room temperature. The carbon equivalent of the corrected total oxygen figure is then calculated and, together with the carbon equivalent of the oxygen content of the rod to be consumed and any carbon required as residual, is added to the stored sample and mixed under argon for about 1 hr.

The calculation of carbon addition is reasonably precise for metals with hydrogen-reducible oxides, and an individual check analysis of each melt is not necessary. For metals with non-reducible oxides the amount of carbon to be added can, at the moment, be decided only in the light of experience.

Certain metal powders, when freshly reduced in hydrogen, contain very large amounts of the gas in solution. This hydrogen is rapidly liberated on heating, and the pressure build-up may be sufficient seriously to upset the arc-length control. In such cases the powders are vacuum-degassed after reduction and then stored in the usual way before use.

## VI.—METALLURGY OF THE ARC-MELTING PROCESS

### 1. CRYSTALLIZATION

The melting and casting of molybdenum in the arc-melting process are carried out simultaneously in a water-cooled mould, solidification being progressive from bottom to top. Only a small portion of the ingot is liquid at any given instant during the



process. Both the top and bottom surfaces of this molten pool are concave in form, and its depth decreases from a maximum at the centre to a minimum at the mould wall. The shape and depth of pool depend on the particular alloy being melted, the heat input from the arc, and the arc length. The depth of the pool formed when melting pure molybdenum with D.C., electrode negative, at 1250 amp. and 32 V., with a water flow of 12 gal./min., has been estimated to be about 1 in. in the centre of the ingot. As the vertical mould walls are chilled and the hottest portion of the molten pool is at the centre top, the temperature gradients normal to the growing surface are always greater than those parallel to the growing surface; thus, according to Northcott,<sup>5</sup> conditions favourable to columnar growth exist in the melt. The macro-examination of ingots has shown that except for a small zone of equiaxial crystals at the top of the ingot, the structure of molybdenum cast by this technique is wholly columnar. The crystals initiated at the bottom of the mould are parallel to the vertical mould walls, and those initiated at the walls curve inwards and upwards (Fig. 4, Plate XLIX), the change in direction being in most cases gradual. When the current is switched off and melting ceases, although columnar growth probably continues for a short time, the temperature gradients normal to the growing surface rapidly become less steep, while the parallel gradients are reduced more slowly. This change results in temperature conditions which are no longer conducive to columnar growth and gives rise to a zone of equiaxial crystals. It is in this zone that normal shrinkage cavities are found, owing to the rapid cooling from the top of the ingot.

## 2. POROSITY IN UNDEOXIDIZED INGOTS OF MOLYBDENUM

Ingots melted without a deoxidizing addition have always a high porosity. The addition of a deoxidizer such as carbon, however, results in a much sounder ingot, all other conditions being the same. It is therefore assumed that the porosity is due directly or indirectly to oxygen. Before melting, oxygen may be present in the rod and powder as free oxygen or molybdenum oxides. As the rod and powder are processed under reducing conditions, it is highly probable that any combined oxygen contained in them is in the form of the lower oxide, molybdenum dioxide. Should the raw material contain any molybdenum trioxide, which is highly volatile and unstable, this will either volatilize rapidly and be pumped out of the system, or it will be reduced by the excess of molybdenum to molybdenum dioxide. Careful examination of sectioned ingots has provided no evidence that porosity is due to the entrapment of a volatile oxide. In support of this, it is more likely, under conditions of vacuum melting, when a low partial pressure of vapour or gas can be maintained above the melt, that porosity is due to the slow formation of a gas or vapour in the melt than

to the slow removal of a gas or vapour already existing in the system.

Any free oxygen entering the pool of molten molybdenum will affect locally the equilibrium between molybdenum dioxide, molybdenum, and oxygen and result in the formation of more oxide. This oxide is more stable and also less volatile than the higher oxide, and its decomposition rate is probably slow with respect to the rapid solidification rate of the molybdenum under the conditions of the arc-melting process. Thus, it is probable that oxygen in the melt is mainly in the form of molybdenum dioxide, which gives rise by slow decomposition to free oxygen, the greater part of which comes out of solution on the solidification of the metal, so causing porosity.

## 3. DEOXIDATION

Molybdenum, as-cast or in the form of sintered bars, is generally brittle at normal temperatures. The cause of this brittleness is not at present clearly understood, although it is thought to be associated with the presence of submicroscopic oxide films or oxygen segregation in the grain boundaries. This view is substantiated by the good ductility of individual crystals of cast molybdenum. It has also been shown experimentally that if the oxygen content is reduced to a very low level, the temperature at which the transition from tough to brittle behaviour occurs is appreciably lowered. No exact figure of the critical oxygen content can be given, as the type of test and particular testing conditions by which the ductility is assessed, influence the transition temperature.

To obtain arc-melted molybdenum alloys with the necessary freedom from oxygen, deoxidation is necessary, unless high-purity raw materials can be used. The function of a deoxidizer is either to remove the oxygen as gaseous or volatile compounds, or to redistribute it in a form having no deleterious effect upon the mechanical properties or forgeability of the pure material.

Three possible deoxidation techniques which have been considered are: (i) deoxidation by a gas, such as hydrogen; (ii) deoxidation by a solid, such as carbon, where the product of the deoxidation reaction is gaseous; and (iii) deoxidation by a solid, such as aluminium, where the product of the deoxidation reaction is solid.

The application of these methods to melting in vacuum and in an argon atmosphere will now be discussed.

### (a) Deoxidation in Vacuum Melting

Deoxidation by hydrogen has not been attempted. Owing to the short time interval between melting and solidification, the accurate control of hydrogen input necessary for a balanced reaction would be exceptionally difficult.

Deoxidation by carbon is the method adopted for vacuum melting. The reaction  $C + O \rightarrow CO$  and

the subsequent removal of CO from the melt are governed by the following factors:

- (i) Temperature of the molten metal.
- (ii) Concentration of free carbon present.
- (iii) Time during which the metal remains molten.
- (iv) Partial pressure of carbon monoxide above the molten metal.
- (v) Turbulence of the molten metal.

The high temperature and turbulence of the melt will promote rapid diffusion of carbon and a rapid rate of reaction. According to thermodynamic data, carbon reduces molybdenum dioxide above about 1000° K., the reaction potential increasing fairly rapidly with temperature in a linear manner up to 3000° K., the highest temperature for which experimental results are available. There is every reason to believe, therefore, that reduction of the molybdenum dioxide will be substantially complete in the short time available, if sufficient carbon is present, especially as the carbon monoxide is continually being removed from the region of the free surface and hence also from the reaction zone in the metal. Some carbon monoxide remains in solution in the molten metal until the time of freezing, as a small partial pressure of carbon monoxide always exists above the melt. This equilibrium solubility of carbon monoxide is thought to be responsible for the microporosity found in all deoxidized ingots. The completeness of deoxidation depends on the rate of removal of carbon monoxide, which is determined by the pumping speed of the diffusion pump and is aided by increasing the time during which the metal is molten. It has been shown in this work that a reduction in the water flow through the mould results in ingots of improved soundness.

Deoxidation by other solids such as aluminium, beryllium, calcium, and magnesium, all of which will reduce molybdenum dioxide at high temperatures, is not favoured owing to the large and variable loss of these elements by volatilization under vacuum conditions. These losses make precise control of deoxidation difficult.

#### (b) *Deoxidation in Argon Melting*

The considerations discussed in this section refer only to melting in a static atmosphere of argon at approximately atmospheric pressure.

The arguments against the use of hydrogen as a deoxidizer in an argon atmosphere are the same as those which apply in vacuum melting.

Carbon has again been used as a deoxidizer when melting under argon. The effectiveness of deoxidation has not been assessed by analysis or by any empirical test such as forgeability, but the resulting ingots have all proved unsatisfactory owing to excessive porosity. It is thought that this porosity is due partially to incomplete deoxidation and partially to a higher amount of carbon monoxide in solution in the metal at the moment of freezing.

Both these effects are related to the fact that in these melts carbon monoxide was not removed by pumping away, as in vacuum melting; as a result, an increasing partial pressure of carbon monoxide was present above the molten metal during the melting period. It would appear on theoretical grounds that more efficient deoxidation could be obtained by adding a larger amount of carbon, but even so more porosity would be expected than in a vacuum-melted ingot with the same degree of deoxidation. The undesirable effects of the build-up of carbon monoxide could possibly be overcome if the atmosphere were circulated through a purification train at a speed sufficiently rapid to maintain the concentration of carbon monoxide below a certain level. The difficulty arises, however, that a rapid rate of circulation is not compatible with efficient removal of carbon monoxide in the purification train; whether a compromise rate of circulation could be used to give the required result is not known.

Deoxidation by a solid, such as aluminium, which forms deoxidation products of high melting point, is a promising method when melting under argon, as the loss of deoxidizer is not so great as that which occurs under vacuum conditions. Ingots of molybdenum and several of its alloys have been deoxidized by adding aluminium powder; these ingots were very much sounder than comparable ingots deoxidized with carbon. Particles thought to be alumina have been observed under microscopical examination; they occur as small rounded particles with a random distribution.

#### 4. THE EFFECT OF ALLOYING METALS ON THE GRAIN-SIZE OF MOLYBDENUM

Macro-examinations on sectioned ingots were carried out for a number of molybdenum alloys. No ingots with composition gradients were made for this purpose, and all observations refer to separately cast ingots. As the grain-size of molybdenum varies with melting and cooling conditions and with general purity, the following estimates of the effectiveness of alloying elements can be only approximate.

Some ingots with a carbon content as low as 0.007% exhibited moderate grain refinement, whereas others with contents of 0.05–0.2% showed no refinement at all. In general, however, carbon appears to refine the grain-size when it exceeds 0.05%, but the effect is slight regardless of the amount added.

A study of ingots containing up to 0.3% boron indicated that this element refines the grain-size moderately above 0.05% when the carbon content is greater than 0.01%. As the increase in refinement is greater than would be expected from the relative carbon content, it is probably due to boron carbide, whose presence has been observed during micro-examination of molybdenum–boron alloys to which carbon has been deliberately added. Additions of aluminium to vacuum melts have resulted in very poor alloy recoveries, and no grain refinement was



noted with the small percentage of aluminium retained, but argon-melted ingots with aluminium contents of the order of 1.0% have shown marked refinement. This effect may be associated with the appearance of a second phase, probably the compound  $\text{Mo}_3\text{Al}$ .

The transition elements, titanium, vanadium, and niobium produced only slight refinement when amounts of the order of 0.5% were added. Iron and chromium gave moderate refinement below 1% and very marked refinement above 3%. Cobalt and nickel alloys with upwards of 1.5% showed marked refinement in all ingots, and it is therefore probable that refinement could be effected with lower percentages. Zirconium resulted in fairly good refinement when added in amounts exceeding 0.5%. Ingots containing up to 6% tantalum exhibited no appreciable refinement of structure, nor did alloys containing up to 8% tungsten. Alloys with more than 6% tantalum were not available for examination, but tungsten refined the grain when added in amounts over 11%.

These effects of alloying are illustrated in Figs. 5-9 (Plate XLIX).

### 5. INGOT DEFECTS

Porosity in molybdenum ingots, resulting from oxygen, has already been discussed. Other defects that may be found are shrinkage cavities, internal cracks, lack of flow to the mould wall at the bottom of ingots, and surface imperfections.

Shrinkage cavities are invariably found immediately under the top surface crust of arc-melted ingots. They are, as a rule, confined to the volume of metal which was molten at the time when melting ceased. It is not possible to say definitely that certain larger cavities, sometimes occurring in other parts, are not shrinkage cavities, but the mode of formation of the ingot makes this unlikely. No reliable method of eliminating these shrinkage cavities in the top of the ingot has been found, but it is quite possible that they could be avoided or minimized by allowing the arc to lengthen for a few seconds at the end of the melt, or, alternatively, by melting for a short time with a much reduced current at the end, thus allowing the molten pool to freeze to a large extent while keeping the top molten.

Internal cracks are the most serious of the defects found in ingots. They are undoubtedly caused by an axial tensile stress in the central core, resulting from the temperature gradient across the solidified ingot and the consequent differential post-solidification contraction. These cracks are orientated approximately normal to the axial direction; they are generally straight, indicating that they are cleavage cracks, and they usually stop abruptly within a grain; they also frequently have the step-like formation illustrated in Fig. 12 (Plate L). The incidence of this internal cracking has been reduced by the use of the minimum safe rate of water flow through the mould, but this does not prevent

it in all cases. There is definite evidence that it is also a function of oxygen content, as it occurs rarely, if ever, in properly deoxidized pure molybdenum, but most frequently in undeoxidized molybdenum and molybdenum alloys. It seems probable that oxygen causes a decrease in the cohesion across certain planes and that the internal stress resulting from cooling is sufficient to cause rupture. The mechanism by which oxygen initiates the loss of cohesion is not known, but in general inadequately deoxidized molybdenum fails in tension by cleavage and fully deoxidized molybdenum by intergranular or transgranular fracture.

The minimum safe rate of water flow to prevent dangerous steam-pocket formation is about 6 gal./min. The effect of reducing the flow to this level from 12 gal./min. is unlikely to produce any large change in rate of ingot cooling. Some experiments with rates of 12 gal./min. and 4 gal./min. with an inlet-water temperature of 15° C. gave exit temperatures of 25° and 40° C., respectively, the power input being 42 kW. It appears, however, from the results obtained, that the reduction in cooling rate is significant, its effect being both to reduce the tensile stress built up in the cooling ingot and to give a lower oxygen content as a result of holding the metal molten for a longer time.

The lack of flow to the mould wall at the bottom of ingots is a minor and unavoidable defect always encountered. It is due to the short time delay in forming the molten pool at the start of melting and the lodging of spatter globules in the bottom corner of the mould. These globules are not subsequently remelted when the molten pool forms.

The surface quality of ingots is influenced by the free-flow diameter of the molten pool of metal, by the amount and size of spatter globules thrown out from the arc, and by the atmosphere in the melting chamber.

In order that the mould may be filled satisfactorily, the diameter of free flow in the absence of the containing copper mould must be in excess of the mould diameter. The diameter of free flow for a given power input is greatest for D.C., electrode negative, somewhat less for A.C., and smallest for D.C., electrode positive. This situation is precisely what would be expected from consideration of the distribution of heat between the electrodes, and the relative sizes of the cathode spot and anode area. Thus, when melting with D.C. (negative) more heat is going into the molten pool, and the heated area is greater than with D.C. (positive).

For vacuum melting the amount of spatter does not vary very much for the three electrical conditions, but the size of globules is greatest for D.C. (positive), and least for A.C. This is discussed in more detail in Section VII, 3. Other factors being equal, the smaller the globule size the better, so far as the surface quality is concerned. The action of the spatter is to build a spatter shield on the copper mould ahead of the growing ingot; if this shield is

not subsequently remelted by the molten pool, a poor surface will result. If the arc length is maintained constant, there is a gradual increase in thickness of the spatter shield over the first 3 or 4 in. with a consequent deterioration in surface quality. The quantity of spatter increases with increasing arc length and current density, so that there is an optimum arc length and current density for any size of ingot for best surface quality. Under these conditions pure molybdenum ingots, carbon-deoxidized, melted in the  $1\frac{3}{4}$ -in. mould, need only about  $\frac{1}{16}$  in. turned off the diameter to give sound metal. The surface is as a rule slightly rough and has been found to vary in this respect with different alloys. Fig. 10 (Plate L) shows a typical ingot.

Conditions are altogether different when ingots are melted in argon, as there is an almost complete absence of spatter and the diameter of free flow is considerably reduced for D.C., electrode either positive or negative. The result is that, provided sufficient power is used to fill the mould, the surface quality is good. With the maximum power input of 50 kW. at present available, the free-flow diameter is just sufficient to fill a  $1\frac{3}{4}$ -in.-dia. mould. Fig. 11 (Plate L) shows the poor type of surface which results with a power input of only 34 kW.

#### 6. DENSITY

The theoretical density of molybdenum calculated from X-ray measurements of the lattice parameter is 10.22 g./c.c. The as-cast density of undeoxidized ingots melted in vacuum has varied between 9.8 and 10.1 g./c.c., and when carbon-deoxidized, between 10.1 and 10.22 g./c.c., neglecting ingots with any major defect. Bars and discs forged from cast ingots consistently show densities of over 10.2 g./c.c.

Ingot melted in argon at atmospheric pressure have had densities between 9.3 and 9.6 g./c.c. in the undeoxidized state and between 9.9 and 10.1 g./c.c. when deoxidized with aluminium. Vacuum-melted ingots, showing densities of over 10.2 g./c.c., still exhibit some microporosity, and it is thought that the true density of sound high-purity molybdenum is in excess of 10.23 g./c.c.

#### 7. MICROSTRUCTURE

The present paper does not attempt to deal with the metallurgical examination of ingots of molybdenum and of the various alloys melted. Microscopical examination is, however, essential for a complete assessment of ingot quality and of the effectiveness of the various melting techniques, so the method used is briefly described.

Most of the micropolishing is done electrolytically by a modified version of the method due to Coons.<sup>6</sup> The specimen is made the anode in a solution of 25 ml.  $H_2SO_4$  in 175 ml.  $CH_3OH$ , and is polished for 1 min. at a current density of 0.8–1.2 amp./cm.<sup>2</sup>.

The temperature of the electrolyte is not allowed to rise above 25°C., and it is not agitated; the cathode is of stainless steel.

Small specimens are mounted in Bakelite, ground down to a 000 emery paper, and polished. Frequently, however, when a large section of an ingot is to be examined without further cutting, the section is ground to a 00 emery finish, carefully degreased, and waxed with a stopping-off wax. A window is then cut in the wax as required and the area polished.

This technique has been used for a wide range of alloys with some success, minor adjustments in current density and polishing time being necessary to obtain optimum conditions for most alloys.

In certain cases where difficulty has arisen in deciding whether the porosity revealed is genuine or is a result of the electrolytic-polishing process, conventional metallographic polishing, employing fine diamond powder in filter-paper with a paraffin lubricant, has been used as a check. The results have confirmed that, with the correct conditions, electrolytic polishing gives a true index, although a slight enlargement of the size of the porosity is difficult to avoid.

### VII.—ELECTRICAL CONDITIONS

Little published information exists concerning the behaviour of metal-depositing arcs running at low pressures. Some knowledge of such arcs is, however, necessary for the better understanding of the arc-melting process.

#### 1. THE NATURE OF THE METAL-DEPOSITING ARC AND THE INFLUENCE OF ARC CONDITIONS ON MOLYBDENUM MELTING IN VACUUM AND IN ARGON

The arc consists of three basic parts, the anode area, the cathode spot, and the positive column or plasma. In the cooler zone surrounding the positive column, recombination of atoms takes place with the release of heat; this zone is known as the aureole. The cathode is heated by the bombardment of its surface with positive ions and the anode by electron bombardment. The stability of the cathode spot is greatly influenced by the chemical and physical conditions on the electrode surface.

At the outset it was not known whether direct current, with the consumable electrode negative or positive, or alternating current would be the most suitable for arc-melting molybdenum. Parke and Ham<sup>3</sup> used A.C., and no mention was made in their paper of the use of D.C. The optimum current density and arc voltage were not known, and no information was available about burn-off speed, the effect of spatter, or the effect of very low pressures upon the behaviour of the arc.

Several measurements made in the course of the present work have indicated cathode-spot areas of



less than 1 mm.<sup>2</sup>, corresponding to a current density of the order of 120,000 amp./cm.<sup>2</sup>. There is no clearly defined conducting area at the anode corresponding to that of the cathode spot, so only an approximate current density can be stated. Determinations made from marks left on electrodes showed areas of from 150 to 300 mm.<sup>2</sup>, corresponding to current densities of between 1000 and 500 amp./cm.<sup>2</sup>.

It has been observed that there is a much greater tendency for cathode-spot and consequent arc wandering to take place with the electrode positive than with the electrode negative. When this occurs with the electrode positive, the cathode spot frequently stops tracking and becomes fixed on the copper mould wall. On account of the very high current density, local melting of the water-cooled copper is liable to occur, resulting in complete penetration of the mould wall by the molten molybdenum. Even if penetration is not complete, the mould is badly pitted and ingot removal impeded. Should anode wandering occur when the consumable electrode is negative, the mould does not suffer much damage, as the current density is relatively low and the rapid heat transfer through the water-cooled copper is sufficient to prevent local overheating.

The end of the consumable electrode heats up more quickly than the base disc electrode, because it is of smaller dimensions and is not water-cooled. A stable arc is therefore created more speedily when the former is at negative polarity than when it is positive, because arc stability is dependent on an adequate supply of electrons from the cathode spot, and is therefore a function of temperature. The anode end of an arc is quite stable and rarely wanders unless caused to do so by movement of the cathode spot. With the consumable electrode positive, once molten metal is deposited on the base, there is normally adequate electron emission from it to ensure arc stability.

From the experimental work so far carried out, it can be stated that ability to produce satisfactory ingots is a function of several factors: the type of current supply, the current density, arc stability, and arc length.

With A.C. it was not possible to produce a stable arc using 1-cm.-dia. electrodes until a current of at least 700 amp. was used, with an open-circuit voltage of 100 V. Once started at this current, the arc could be maintained down to about 500 amp. Arc stability increases rapidly above 700 amp., being very good at 900 amp. and over. For ingot production, currents of approximately 1200 amp. A.C. were adopted because of the higher burn-off rate. However, A.C. is not often used, since, although the central cores of the ingots are sound, the outer zones are unsound. The reason for this is not clear, as arc stability is good and the burn-off rate adequate.

Using D.C. with the consumable electrode positive, it was possible to produce an arc at only 200 amp. with an open-circuit voltage of 55 V. Most of the experiments in the original prototype apparatus

were conducted at 500 amp. with fairly good results. Very satisfactory melting takes place at currents higher than 800 amp. so long as cathode-spot wander does not take place. From the standpoint of surface quality of the ingot, a current of between 1000 and 1300 amp. is best, but the surface is inferior to that of ingots produced with D.C. (negative). Apart from this consideration, D.C. (positive) is not recommended owing to the probability of mould damage from cathode-spot wander.

When using D.C. (negative) it was found that currents of over 600 amp., with an open-circuit voltage of 75 V., were necessary before an arc could be struck, but, as with A.C., the arc could be maintained at a lower current once it had been started. Arc stability increases as current increases and is excellent above about 800 amp. Practically all melting is now done at 1200–1300 amp. D.C. (negative), because of higher burn-off speed and improved surface quality of the ingots.

The use of currents below the optimum range results in inferior ingots with poor surface quality. A current somewhat higher than that necessary to produce flow to the mould walls does not cause any noticeable difference in ingot quality or in grain structure as a result of the larger molten pool. A current greatly in excess does, however, cause molten metal to be blasted up the sides of the copper mould, forming an overhang which results in heterogeneous crystal structure and may, in extreme cases, lead to side arcing; in this event the normal molten-pool formation ceases and melting must be stopped to avoid serious damage to the mould. It is also important that the correct arc length should be used in conjunction with a current density within the optimum range. An excessive arc length results in a reduced flow of molten metal, and is analogous to an insufficient current density. Too short an arc is likewise analogous to an excessive current density, and leads to similar undesirable results.

There is a definite relationship, for a given arc length, between current and the free-flow diameter of the molten metal. The maximum mould diameter for satisfactory ingot production is governed by these factors. The minimum mould diameter is controlled by loss of arc stability due to surface deionization and by mechanical choking of the arc in very small moulds. There is also, of course, an increased tendency for side arcing on to the mould in such conditions.

Most of the information given above applies only to arcs in copper moulds of  $1\frac{1}{4}$ – $1\frac{3}{4}$  in. dia.

Summing up, D.C. with the consumable electrode negative is preferable from all points of view. A.C., at least up to a maximum current of 1200 amp. available for this work, is the worst because it leads to poor ingot quality. D.C. (positive) cannot be recommended owing to the possibility of mould damage from cathode-spot wander. The optimum current range for D.C. (negative) is between 1200 and 1300 amp., with an arc length of  $\frac{3}{4}$  in. Higher currents are not advised when using  $1\frac{1}{4}$ -in.-dia. moulds, as

they result in ingot defects and the danger of mould failure.

It was expected that the characteristics of the molybdenum-depositing arc running in argon would differ from those obtaining in vacuum, whatever the pressure of the argon. Some information is available on the behaviour of metal-depositing arcs in various gas atmospheres at atmospheric pressure, as a result of the application of gas-shielded arcs in the welding of metals. When an arc is struck in an atmosphere containing molecules of diatomic gases, whether at high or low pressures, some of the energy of the arc is used in dissociating the molecules, this energy being released again in the outer zones of the arc, where recombination of the atoms takes place. The result of this process is a wider distribution of the heating effect of the arc. For arcs in monatomic gases, such as argon and helium, no such effect can occur, which may be one reason for the small free-flow diameter of the molten pool found in such cases.

The first experiments in argon atmospheres were made at atmospheric pressure using D.C. (negative), the best supply for melting in vacuum. The burn-off speed using 1500 amp. and a voltage of 20 V. was only 3.53 g./sec. Because of this very low speed, the polarity was changed to positive and the test repeated with the same current and voltage. The burn-off speed was almost exactly doubled; in both cases the flow of molten metal to the mould wall was insufficient, resulting in an ingot of irregular surface, as illustrated in Fig. 11 (Plate L); it was concluded that D.C. (positive) was the more suitable for melting in argon.

No evidence of serious cathode-spot wander was encountered in melts in argon, in contrast to the behaviour of D.C. (positive) arcs in vacuum. The reason for this is not known, but the higher currents passing for a given power input may be a contributory cause of the improved stability.

The inadequate flow of molten metal to the mould wall may also be partly due to the additional heat losses by convection; to obtain a total power input higher than that normal in vacuum melting, currents of over 2000 amp. must be used. One of 2200 amp. with the electrode positive gave an ingot which filled the mould, the voltage being 25 V. and the burn-off rate 14 g./sec. It is thought that the use of slightly higher currents would be beneficial, although this is not far from the maximum current which the 10-mm.-dia. electrode will carry without serious overheating.

All ingots produced in argon had an almost flat crater on the top, in contrast to the marked concavity of craters in ingots melted in vacuum. This is illustrated in Figs. 13 and 14 (Plate L).

## 2. SECONDARY ELECTRICAL DISCHARGE IN VACUUM MELTING

The most serious operating trouble encountered in the early development of the technique was an electrical discharge between the electrode and various

parts of the plant. It is now thought that the initial cause of the discharge was the bridging of the gap, between parts at opposite potentials, by a globule of spatter, the temperature of which would be close to the boiling point of molybdenum, and which on passing through the high vacuum would leave a trail of molybdenum vapour which would become positively charged as a result of thermionic emission. This view has recently been substantiated by the work of Gillette and Breymer,<sup>7</sup> who, as a result of motion-picture studies, conclude that the arc contains luminous metal vapour and that droplets of molten metal in free flight are normally surrounded by luminous vapour sheaths.

In the plant now described (see Fig. 1, p. 362), the whole chamber and the larger area of the base-plate have been insulated both from the electrode and drive mechanism and from the mould, so as to cut down the possibility of spatter bridging the gap

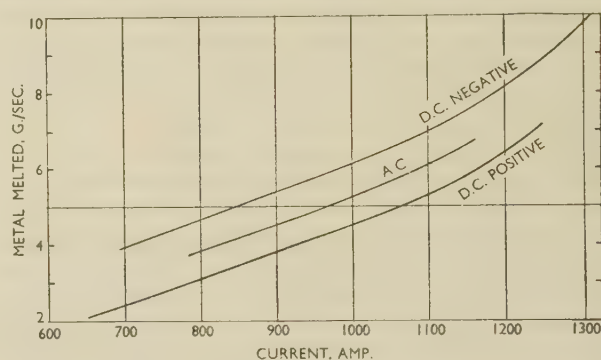


FIG. 16.—Illustrating Burn-Off Rates for Pure Molybdenum Rod (1 cm. dia.).

between parts at opposite potentials. This has eliminated the trouble, except occasionally when large amounts of volatile elements have been added.

In such cases there would appear to be no solution other than melting in an inert atmosphere. This would be desirable in any event, as the high volatility of such elements permits only low melting recovery in vacuum.

## 3. CHARACTERISTICS OF THE BURN-OFF PROCESS

The burn-off rate of the electrode increases with current and is related to other electrical conditions. Fig. 16 shows the burn-off rates for A.C. and D.C. arcs operating in vacuum, plotted against current.

Efforts were made to determine the effect of gas pressure upon the burn-off rate when using negative polarity. Within the pressure range 0.1–0.001 mm., however, no significant difference was observed. Scatter of results was less noticeable at the higher pressures; this may be linked with the fact that the residual gas content of the electrode has a more pronounced effect at low pressures. Calculations of melting efficiency show that this is approximately 22% for D.C. (positive) and 26% for D.C. (negative).



It has been observed that the shape of the electrode tip at the conclusion of a melt is characteristic of the type of electrical supply. The electrode tip or burn-off resulting from a D.C. (positive) melt, has a smooth, almost hemispherical end, as illustrated in Fig. 15 (a) (Plate L). D.C. (negative) burn-offs are of two types, one conical in form (Fig. 15 (b)) and the other characterized by deep valleys cut into the sides, usually at two diametrically opposed positions

burn-off rate, D.C. (negative) the intermediate size spatter and the highest burn-off rate, and A.C. the smallest spatter and an intermediate burn-off rate.

## ACKNOWLEDGEMENTS

The work described in this paper was carried out under the direction of Dr. L. Northcott, to whom the authors are indebted for advice and encouragement. They also wish to thank their colleagues who have helped with the work, in particular, Mr. E. W. Harding, who designed the automatic arc-length control, and those who have given valuable assistance in discussing various aspects of the work. Acknowledgement is made to the Chief Scientist, Ministry of Supply, and to the Comptroller of H.M. Stationery Office, for permission to publish this paper.

TABLE I.—Burn-Off Data for Molybdenum Electrode, Using 950-amp. Arc.

Type of Electrical Supply	Burn-Off Rate, g./sec.	Dia. of Spattered Globules, mm.	Weight of Spattered Globules, g.
D.C. (positive) . . .	4.2	5-7	0.6-1.8
D.C. (negative) * . .	5.8	3-4	0.15-0.35
A.C. . . . .	4.9	2-2½	0.04-0.08

\* Type of burn-off with valleys cut into the sides.

(Fig. 15 (c)). A.C. burn-offs have almost flat ends (Fig. 15 (d)). The burn-off speeds, together with size and weight ranges of spatter collected after melts made with the three types of electrical supply, using a 10-mm.-dia. molybdenum electrode, are given in Table I.

These results show that D.C. (positive) produces the largest globules of spatter and gives the lowest

## REFERENCES

1. W. von Bolton, *Z. Elektrochem.*, 1905, **11**, 45.
2. W. Kroll, *Trans. Electrochem. Soc.*, 1940, **78**, 35.
3. R. M. Parke and J. L. Ham, *Trans. Amer. Inst. Min. Met. Eng.*, 1947, **171**, 416.
4. S. F. Radtke, R. M. Scriver, and J. A. Snyder, *ibid.*, 1951, **191**, 620.
5. L. Northcott, *J. Inst. Metals*, 1946, **72**, 283.
6. W. C. Coons, *Trans. Amer. Soc. Metals*, 1949, **41**, 1415.
7. R. H. Gillette and R. T. Breyemeier, *Weld. J.*, 1951, **30**, 146s.

# 1529 THE PRESSURE WELDING OF MOLYBDENUM\*

By A. R. MOSS†

## SYNOPSIS

The construction and use of a controlled-atmosphere pressure-welding chamber are described. The conditions of temperature and deformation necessary to produce satisfactory welds in commercial sintered molybdenum sheet, in both argon and hydrogen atmospheres, have been determined, and the effect of surface finish and cleanliness upon weldability studied. Welds have been made at temperatures as low as 690° C.; welding below the recrystallization temperature (approximately 1200° C.) is thus shown to be possible.

By using inserts of various materials, the amount of deformation necessary to effect welding can be considerably reduced. Electrodeposited chromium, with which sound welds have been produced, may prove especially valuable in this connection, since chromium and its alloys can also serve as oxidation-resistant coatings on molybdenum. The use of plated sheets to serve a dual purpose is therefore envisaged.

Pressure welds having high strength and ductility at room temperature have been produced on wrought cast molybdenum.

## I.—INTRODUCTION

RECENT advances in arc-melting and powder-metal-lurgy techniques have shown that molybdenum and molybdenum-rich alloys can be produced without difficulty in massive form and that useful engineering properties can be developed. In line with these advances it became necessary to investigate methods of welding molybdenum.

In the cold-worked condition, commercial sintered material, if of a certain minimum purity, is ductile, and it is only by retaining the material at the weld in a substantially unchanged condition that a ductile weld is likely to be obtained. The initial hypothesis for the present work was, therefore, that if such material could be pressure welded without contamination and without recrystallization or appreciable grain growth, a ductile weld would result. The experiments were designed to discover whether, at temperatures and pressures limited by the latter condition, welding could be achieved. The further step of using insert materials to reduce the temperature and pressure necessary was also investigated. Some work carried out on arc-cast molybdenum specimens is also reported.

## II.—PRELIMINARY WORK

In order to establish the practicability of pressure welding on a laboratory scale, preliminary trials were carried out by hammering 1.5-mm.-dia. twisted molybdenum wires at various temperatures in air, argon, and hydrogen atmospheres. The most satisfactory results were obtained on those specimens which had been welded in hydrogen. The wire test-pieces were not suitable for controlled experimental work, chiefly because of the difficulty in determining the extent of deformation at any given position, so a new strip test-

piece, more suitable for pressure-welding investigations, was designed. Strips of sheet molybdenum, 0.5 mm. thick, 10 mm. wide, and 100 mm. long, were used to produce U-shaped specimens, the gap between the two limbs being 2 mm. The ends of the limbs are bent-off at an angle to facilitate clamping in a quick-action clamp. This holds the specimen in position ready for welding and also connects it to the electrical supply used for heating (Fig. 3, Plate LI).

## III.—CONSTRUCTION OF IMPACT PRESSURE-WELDING APPARATUS

To avoid oxidation, it was decided to carry out the welding experiments in a chamber in which a suitable non-oxidizing atmosphere could be maintained.

An all-welded chamber, 3 ft. long, 2 ft. high, and 2 ft. deep, was constructed from  $\frac{1}{4}$ -in.-thick mild-steel plates. After welding, the whole assembly was thoroughly shot-blasted and rough-polished with emery. Into one of the sides was fitted a  $\frac{1}{2}$ -in.-thick Perspex window containing two brass portholes to take long rubber gloves. The chamber was bedded on to a heavy steel bench and securely bolted down. To give access to the inside, one of the ends was fitted with a manhole cover. This could be quickly removed or replaced by means of four quick-action clamps, sealing being effected with a round-section rubber gasket. At a later stage an antechamber was fitted to the manhole cover, so that articles could be passed into or out of the main chamber without interfering with any special atmosphere which it was desired to maintain.

A 2-in.-dia. hole fitted with a seal of special type is provided in the top of the chamber for thermocouple and control wires, as well as for arc-welding electrode holders when these are used. The back and top plates are fitted with non-return valves through which a choice of gases can be led into or out of the chamber.

\* Manuscript received 1 December 1953.

† Armament Research Establishment, Fort Halstead.



All outlet pipes feed into a manifold which ends in a manometer-type non-return valve operating in liquid paraffin; after passing through this last valve the gases are led to a high-speed fan for dispersal. This procedure ensures perfect safety when using inflammable or toxic gases. The general construction is shown in Figs. 1-3 (Plate LI).

An impact-loading mechanism (Fig. 4, Plate LII) fits into the top of the chamber. A steel weight is dropped from a predetermined height inside a brass pipe on to a polished steel rod passing through a Wilson seal. After the blow has been imparted, the steel rod is returned to its original position by a coil compression spring. The end of the steel rod inside the chamber can be fitted with forging tools of various shapes and sizes. In the experiments to be described only one tool was used, 0.13 in. wide and 0.4 in. long. It was made from high-quality tungsten carbide set in an alloy-steel housing of sufficient mass substantially to counteract the inertia of the compression spring. The load is adjusted by altering either the weight or the height from which it is dropped. This impact-loading mechanism was calibrated by the use of copper crushers. These were compressed in a testing machine and compared with similar crushers compressed in the impacting equipment. From appropriate graphs, the equivalent static loads for the various weights, falling from different heights, were determined.

#### IV.—EXPERIMENTAL RESULTS

##### 1. IMPACT WELDING UNDER CONTROLLED CONDITIONS

To obtain data for the construction of curves relating applied load, deformation, and temperature, a series of tests were made, using various loads at specimen temperatures of 20°–1400° C. As these curves were used merely as a guide to the selection of experimental conditions for individual tests, they are not included here. Temperature was measured with a small-diameter platinum/platinum-13% rhodium thermocouple inserted inside the U-shaped specimen at the point of intended weld. Immediately before the welding tool struck the specimen, the thermocouple was removed. To minimize evaporation of the faying surfaces, the time at temperature was restricted to 2 sec., the total heating time being approximately 12 sec. in the high-temperature range. The current supply to the specimen was switched off immediately after impact.

The deformation of the specimens was determined with the aid of a pointed micrometer, the average of ten readings being taken for each test. The formula used was:

$$\text{Deformation (\%)} = 100 \left( 1 - \frac{t}{2T} \right),$$

where  $T$  is the original single sheet thickness, and  $t$  the thickness of specimen remaining after deformation. In some instances the deformation was determined from cross-sections of welds with the aid of a travelling microscope.

In this paper the term "weld" is used rather loosely to include what in some instances, owing to the use of inserts, may more correctly be termed a braze. Whenever an interface fracture showed torn-out pits or particles of additional metal, regardless of size or extent, or whenever micro-examination of the interface area showed substantial continuity of structure, the term "weld" is used. In most cases there was little difficulty in deciding whether or not a specimen was welded.

All specimens were given the same cleaning treatment, the sheet molybdenum being first washed with

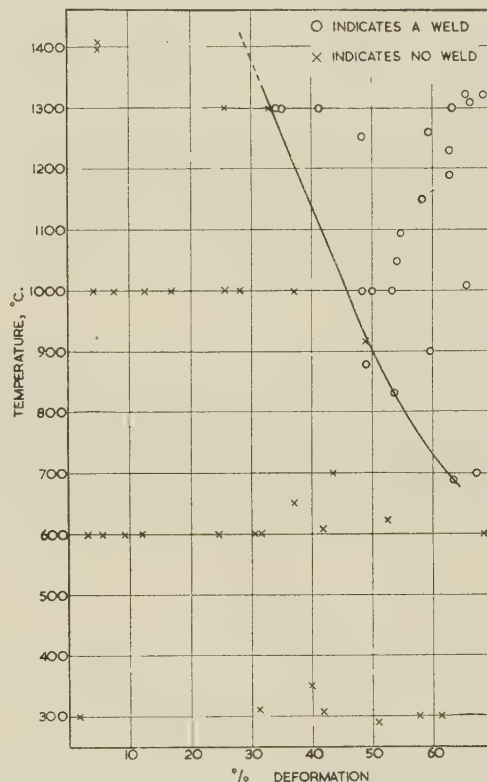


Fig. 5.—Boundary Conditions of Temperature and of Deformation Necessary to Pressure Weld Sheet Molybdenum in Argon.

soap and water and then with acetone; strips were afterwards cut off and placed inside the chamber. Immediately before each experiment the strips were polished with 0 grade emery cloth, bent to shape in a jig, and placed in the clamp; any residual dust was blown away before heating. The time interval between cleaning and welding was approximately 1 min.

Two main series of tests were carried out, one in argon of 99.8% purity, the other in purified oxygen-free hydrogen. Routine gas analysis was not carried out, but heated polished iron wire was regularly employed for detecting oxygen when using the argon atmosphere. Molten magnesium was used as a getter, being melted in a crucible by means of an electric arc. Care was taken when gettering to avoid contamination of the atmosphere and of the weld test-pieces by fine magnesium powder.

After examination of the test-pieces deformed in the argon atmosphere, the results were plotted and the curve in Fig. 5 constructed. This shows the approximate limiting conditions of temperature and deformation required to produce a weld. All conditions to the right of the curve produce welds; conditions to the left do not give welds.

Fig. 6 summarizes the results of welding in a purified hydrogen atmosphere (the curve of Fig. 5 is included for comparison). It will be seen that the deformation required for welding is appreciably less than when an argon atmosphere is used. By expressing the weld/no-weld boundary curves of Figs. 5 and 6 in terms of load rather than of deformation, and plotting these against temperature, the curves shown in Fig. 7 were constructed.

Although welding at 690° C. has been shown to be possible, the use of the highest temperature consistent with absence of recrystallization or appreciable grain growth is recommended. This is advantageous for several reasons: the deformation necessary to produce a weld and the force required are less, and there is more interfacial diffusion and a greater measure of stress-relief.

As surface conditions influence the pressure weldability of most metals, tests were made in a purified hydrogen atmosphere to determine whether molybdenum showed such effects. Four different finishes were used: coarse (2½ grade) emery cloth; fine (1M) emery cloth; electrolytic polish; and electrolytic polishing and etch. No significant differences in weld-

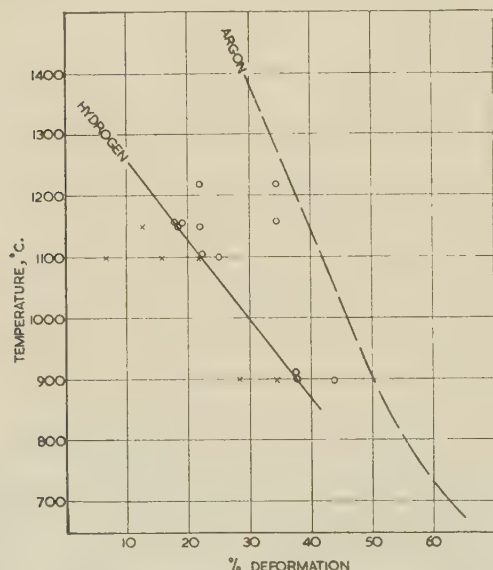


FIG. 6.—Boundary Conditions of Temperature and of Deformation Necessary to Pressure Weld Sheet Molybdenum in Hydrogen. The curve for argon from Fig. 5 is included for purposes of comparison.

ability were observed, but there was some indication that the electrolytically prepared specimens welded a little better than did those prepared with emery cloth.

The time interval between the cleaning and the

welding of a test-piece in argon is important. It was found that welding became more difficult as the time increased, this being especially noticeable when speci-

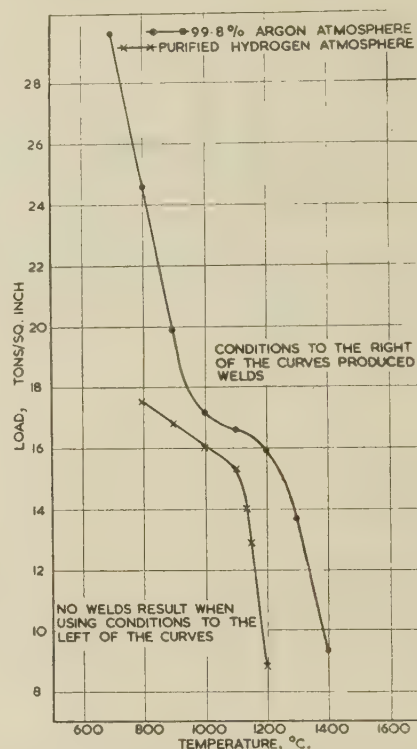


FIG. 7.—Boundary Conditions of Temperature and of Pressure Necessary to Weld Sheet Molybdenum.

mens were cleaned in air and welded in argon. The difference is probably the result of oxide formation, or of gas being adsorbed, on the faying surfaces. The necessity for keeping the time interval as short as practicable was not confirmed for welding in a hydrogen atmosphere, even when the cleaning was done in air and the specimen welded 50 hr. later. This was to be expected, as hydrogen reduces molybdenum oxides when heated. Test-pieces subjected to ionic bombardment did not weld any more easily in hydrogen than did those without this treatment.

## 2. IMPACT WELDING WITH INSERTS

It was thought that welding might be facilitated by placing insert materials between the faying surfaces of the molybdenum, and experiments indicated that it is, in fact, possible to reduce considerably the temperature and the amount of deformation necessary to produce a weld when using an argon atmosphere.

Any element which forms a compound with molybdenum (e.g. iron, cobalt, or nickel) is likely to prove unsuitable unless the compound can be dispersed by diffusion. Elements forming extensive solid solutions with molybdenum (e.g. chromium, tungsten, or tantalum) may be expected to produce alloys having good ductility. Exploratory tests, in an argon atmosphere, were conducted, using metals from both these



with paraffin-soaked emery papers down to 00 grade, and finally polished on diamond-impregnated parchment, using fine oil as a lubricant. In the early part of the last operation, the specimens were etched several times to remove work-hardened areas produced by the emery papers. Alumina and magnesia of various grades were tried without success, especially with insert welds, owing to the relief effect caused by hard zones. Because of the shape of the specimen, coarse powder, produced during the polishing operation, became entrapped in the fine interstices of the joint not filled by the Bakelite mounting material and gave rise to residual polishing scratches. Difficulty was also experienced in etching many of the insert welds, owing to differences in electropotential of the metals concerned. Except where otherwise stated, the etchant used was a potassium ferricyanide/sodium hydroxide solution at room temperature. In the photomicrographs reproduced, small imperfections are purposely included for identification purposes; they are usually to be found close to the end or start of a weld. Where necessary, the weld interface is indicated by arrows.



### (b) *Insert Welds*

Fig. 11 (Plate LIII) shows the microstructure of a weld with an austenitic stainless-steel insert in sheet form, made at 900° C. and 51% deformation. Such welds are generally brittle, probably owing to the presence of a thin layer of an iron-molybdenum intermetallic compound at the interfaces. An extreme example of the brittle nature of such compounds is illustrated in Fig. 12 (Plate LIII), which shows the effect of extensive grain-boundary infiltration of stainless steel into sintered molybdenum.

Fig. 13 (Plate LIII) shows the microstructure of a section taken through a nickel powder insert weld made at 1400° C. with 5% deformation. On the left of the photograph is what appears to be a pure nickel film and on the right, an alloyed film. In Fig. 14 (Plate LIII) the alloyed portion is reproduced in greater detail, the junction being marked by arrows. The thickness of alloying is greater on the lower face, possibly owing to the diffusion of nickel powder during the soaking period. This effect might be minimized

made with a thin platinum-13% rhodium foil insert. The welds produced were especially sound and strong.

In the present work the inserts were applied as thin foils, whenever possible; otherwise a fine film of powder was used. A drawback to the use of powder is its high gas content; it also oxidizes more readily than the corresponding sheet material. Electrodeposited chromium was used with good results.

It is realized that factors may operate which would debar the use of some types of inserts, e.g. chemical attack. It might be possible in most instances to overcome such limitations by joint design or choice of suitable inserts. In the case of structures working at high temperatures, tantalum would probably prove satisfactory, whilst metals of the platinum group might be useful when chemical attack has to be taken into account.

### 3. MICRO-EXAMINATION OF WELDS

Sections of the welds for micro-examination were mounted in Bakelite, surface-ground, hand-polished

by increasing the rate of heating and reducing the soaking time. Part of the extensively alloyed area was split along the interface, and a fractograph of this area (Fig. 15, Plate LIV) exhibits what appear to be dendrites of nickel or of nickel-molybdenum inter-metallic compound.

A photomicrograph of a section of a niobium-foil insert weld made at 1400° C. and with a deformation of 20% is shown in Fig. 16 (Plate LIV).

Although tantalum has a higher melting point than molybdenum, a successful weld was achieved with a tantalum-foil insert at only 900° C. and 41% deformation. A section of this weld is shown in Fig. 17 (Plate LIV).

As the temperature required for the autogenous pressure welding of clean metals greatly increases with melting point, and as it is known that high adhesion values can be obtained between electrodeposited metals and the base metal, it was thought that satisfactory welding might be carried out, at a considerably lower temperature than that necessary for molybdenum/molybdenum welding, by electroplating the faying surfaces with chromium. This proved to be the case, and Fig. 18 (Plate LIV) illustrates a section through such a weld made at only 900° C. and with a deformation of 37%. The specimen was etched with a potassium ferricyanide/sodium hydroxide solution, which revealed the soundness of the molybdenum/chromium junction, but did not etch the chromium/chromium interface. Electrolytic etching with a mixture of chromic and sulphuric acids revealed the chromium/chromium interface, and the grain growth across it (see Fig. 19, Plate LIV), although unfortunately there was rapid attack of the molybdenum. This method of welding is considered important, particularly in the light of the known oxidation-resistance of chromium and its alloys.

#### 4. MECHANICAL PROPERTIES OF MOLYBDENUM WELDS

The quality of a weld is best judged ultimately by its mechanical properties. Although several different tests could be applied to the strip test-pieces used for the welding experiments described above, it was thought that more valuable information would be obtained from tensile tests on butt welds. For this purpose, weld test-pieces in rod form offer advantages, and experiments on these are now proceeding. Some mechanical properties obtained may, however, be worth briefly reporting here.

After welding wrought cast molybdenum without inserts in a vacuum of  $10^{-3}$  mm. Hg, the specimens were machined into standard test-pieces. These comprised: for the bend test, a rod 1 in. long and  $\frac{1}{8}$  in. in dia., and for the tensile test, a No. 11 Hounsfield

Tensometer test-piece. Typical mechanical properties across the weld at room temperature (21° C.) are given below.

Bend Test Piece	Tensile Test Piece
Breaking angle 21°	Y.P., 28.5 tons/in. <sup>2</sup>
	U.T.S., 38.5 tons/in. <sup>2</sup>
	Elongation, 14%
	Reduction of area, 11%

#### V.—CONCLUSION

Commercial sintered molybdenum sheet can be pressure welded, using impact loading, at temperatures as low as 690° C. in atmospheres of oxygen-free argon or hydrogen. The latter is preferred, as appreciably less deformation is required, the time interval between cleaning and welding is not critical, and surface finish of the faying surfaces does not appear to influence weldability.

The temperature and the amount of deformation necessary to produce a weld can be reduced considerably by using insert materials between the faying surfaces. This effect has been produced with a wide range of materials, including niobium and tantalum. The latter possesses a higher melting point than molybdenum, and a sound weld was made in argon at 1000° C. with only 23% deformation, using a 0.002-in.-thick tantalum insert, whereas a weld at 1000° C. without an insert required at least 46% deformation. By electroplating molybdenum with chromium, it is possible to pressure weld chromium/chromium interfaces at low deforming pressures. As chromium can also be used as an oxidation-resistant coating on molybdenum, it may thus be possible to produce coatings to serve a dual purpose.

It must be emphasized that any welding technique ultimately evolved, whether inserts are used or not, may not resemble the present laboratory procedures. Little consideration has yet been given to potential production methods or problems.

Forged and swaged arc-cast molybdenum of high purity can be pressure welded to produce strong and ductile welds.

#### ACKNOWLEDGEMENTS

The work described was carried out in the Metallurgy Branch of the Armament Research Establishment under the direction of Dr. L. Northcott, to whom the author is indebted for advice and encouragement. He also wishes to thank his colleague, Mr. D. O. Pickman, for helpful discussion during the course of the investigation and preparation of the paper for publication. Acknowledgement is made to the Chief Scientist, Ministry of Supply, and to the Comptroller of H.M. Stationery Office, for permission to publish the paper.



# FACTORS INFLUENCING BRITTLINESS IN ALUMINIUM-MAGNESIUM-SILICON ALLOYS\*

1530

By I. R. HARRIS,† D.R.T.C., A.I.M., MEMBER, and P. C. VARLEY,† M.B.E., M.A., F.I.M., MEMBER

(Communication from the Research Laboratories of The British Aluminium Co., Ltd.)

## SYNOPSIS

The effect of composition, heat-treatment, cold work, and structure on the brittleness and mechanical properties of a series of wrought aluminium-magnesium-silicon alloys containing 0-2% silicon and 0-2% magnesium, has been investigated.

It was shown that brittleness in the fully heat-treated alloys which were completely recrystallized with equiaxed grains was dependent on composition. When the alloys were solution-treated at 540° C. and subsequently precipitation-treated at 175° C. for 8 hr., excess silicon was found to be necessary for brittleness, but for the same degree of brittleness, the amount required varied with the percentages of magnesium silicide and iron present.

Microscopic examination after etching indicated that maximum brittleness, as denoted by an Izod impact value of about 3 ft.-lb., was probably associated with the preferential grain-boundary precipitation of either free silicon or magnesium silicide or both, to form a continuous network. The continuity of the grain-boundary network was dependent on the solution-treatment temperature, the rate of cooling from this temperature, and the precipitation-treatment conditions. Grain-boundary precipitation during air-cooling took place more rapidly in alloys containing copper. The interval between quenching and precipitation-treatment also affected the brittleness of some super-purity-base alloys.

The effect of cold work before solution-treatment and before precipitation-treatment is discussed.

Finally, the beneficial inhibiting effect of small additions of manganese and chromium on grain-boundary precipitation is dealt with. In extruded alloys containing either or both of these elements, the notch-sensitivity, as measured by the Izod impact test, was found to be governed largely by the degree of recrystallization and the recrystallized texture of the material.

## I.—INTRODUCTION

It is now fully realized that one of the factors contributing to sudden intercrystalline failure in alloys may be the formation of an extremely thin intergranular film of brittle intermetallic compound or precipitate.

There is also considerable published work indicating that the phenomenon of grain-boundary precipitation usually occurs when a solid-solution range is restricted by the formation of a stable compound and the solubility limit of the restricted solid solution increases with temperature.

Yokoyama<sup>1</sup> has considered the analogy between temper-brittleness in steel due to the precipitation of carbides at the grain boundaries and age-hardening phenomena in non-ferrous alloys. Several steels, including plain carbon steels and those containing nickel and chromium, chromium, and nickel, together with Duralumin, aluminium-5.5% copper alloy, 18:8 stainless steel, and Corson alloy containing 4% Ni<sub>2</sub>Si, were investigated, hardness and impact tests being carried out. As a result brittleness in these materials was stated to be due to the presence

of compounds at the grain boundaries. In addition, Yokoyama divides the age-hardening alloys into two types, according as they have or have not properties similar to temper-brittleness in steels, depending on the relation between the hardness of the phase separated out on the grain boundaries and that of the matrix of the alloys. Copper-iron alloys, with the harder phase on the boundaries, provide an example of the former, while copper-silver and iron-copper alloys, with the softer phase at the boundaries, are examples of the latter.

Earlier, Mishima<sup>2</sup> had investigated the annealing brittleness in nickel, nickel-copper, and nickel-copper-zinc alloys due to the precipitation of free carbon at the grain boundaries. Buehl, Hollomon, and Wulff<sup>3</sup> referred to the carbide precipitation in 18:8 stainless steels, and more recently Hérenghuel and Lacombe,<sup>4</sup> Grogan and Pleasance,<sup>5</sup> and Perryman<sup>6</sup> have investigated brittleness in aluminium-zinc and aluminium-zinc-magnesium alloys after age-hardening. Bailey<sup>7</sup> has encountered brittleness in certain copper-nickel-iron alloys owing to grain-boundary precipitation of the  $\alpha'$ -phase.

Recent theories by McLean<sup>8</sup> and McLean and

\* Manuscript received 31 October 1953.

† Research Laboratories of The British Aluminium Co., Ltd., Gerrards Cross, Bucks.

Northcott<sup>9</sup> postulate that actual precipitation at the grain boundaries is not necessary for brittleness, and suggest that the solute atoms may remain in solution though segregating to the grain boundaries. However, these authors have shown by suitable etching that the low Izod value obtained for steels containing chromium, nickel and chromium, or nickel and manganese, on tempering at certain temperatures, is associated with a definite grain-boundary network suggesting actual precipitation.

It has been shown by Perryman<sup>10</sup> for aluminium-7% magnesium alloys and by Brenner and Metcalfe<sup>11</sup> for aluminium-5% magnesium alloys that grain-boundary precipitation may occur in a continuous form. Although extremely important with regard to intercrystalline corrosion and stress-corrosion, grain-boundary precipitation in these alloys does not produce brittleness as they do not age-harden. If an alloy is both brittle and susceptible to intercrystalline attack, a very serious notch effect may result. A survey of the corrosion-resistance of aluminium-magnesium-silicon alloys of the H10 type has recently been published by Metcalfe.<sup>12</sup>

The purpose of the present paper is to describe the conditions that promote the formation of a continuous brittle grain-boundary precipitate in wrought aluminium-magnesium-silicon alloys and to describe methods for controlling and inhibiting this type of precipitation. There is no indication of any such

work having previously been carried out on this alloy system, with the exception of very brief references by Geisler and Keller<sup>13</sup> and Hume-Rothery.<sup>14</sup>

A study has also been made of the tensile properties of the alloys, regarding which considerable information is already available (see in particular Geller,<sup>15</sup> Brenner and Kostron,<sup>16</sup> and Panseri and Monticelli<sup>17</sup>). A recent paper by Benkö<sup>18</sup> on the tensile properties of the alloys in the cast state illustrates the general effect of variations in composition, but quantitatively the properties differ widely from those obtained on wrought alloys of similar composition, and are of little practical value.

## II.—EXPERIMENTAL PROCEDURE

### 1. MATERIALS USED

The compositions of the alloys used for the systematic survey of mechanical properties and brittleness are given in Table I. The properties of both rolled and extruded material were investigated, and the casting and fabrication procedure was standardized wherever possible.

#### (a) Rolled Material

Both super-purity- and commercial-purity-base alloys were prepared in rolled form. They were made up from either super-purity or 99.5% pure

TABLE I.—Composition and Properties of Aluminium-Magnesium-Silicon Alloys.

(a) 0.036-in. Sheet, 99.5%-Purity-Base Alloys.

Composition			Free-Cone Bend-Test Results (Aged at 175° C. for 8 hr.)						Classification *	Mechanical Properties			Grain-Size for Samples Solution-Treated at 540° C.
			Solution-Treated at 500° C.		Solution-Treated at 520° C.		Solution-Treated at 540° C.			Solution-Treated at 540° C. Aged at 175° C. for 8 hr.			
Mg, %	Si, %	Fe, %	Length of Crack, cm.	Length of Surface Crack, cm.	Length of Crack, cm.	Length of Surface Crack, cm.	Length of Crack, cm.	Length of Surface Crack, cm.		0.1% P.S., tons/in. <sup>2</sup>	U.T.S., tons/in. <sup>2</sup>	Elong. % on 2 in.	
0.32	1.30	0.21	Nil	1.0	Nil	4.0	Nil	4.0	Transition	13.60	17.50	13.0	
0.36	0.62	0.21	"	Nil	"	Nil	"	Nil	Ductile	10.72	14.18	10.0	
0.38	0.84	0.22	"	"	"	"	"	"	"	13.62	16.31	11.0	
0.43	1.00	0.23	"	4.1	"	5.4	1.5	2.0	Transition	13.61	16.40	10.5	
0.41	1.20	0.23	"	4.0	"	4.0	6.0	2.0	Brittle	14.80	19.11	13.0	
0.50	1.04	0.22	"	Nil	3.0	3.0	6.0	1.0	"	14.75	19.45	13.0	
0.56	0.77	0.21	"	"	6.0	4.0	7.0	2.0	"	14.47	17.70	11.0	
0.56	1.20	0.23	"	3.0	10.5	Nil	Complete fracture		"	16.65	20.55	10.5	
0.65	0.42	0.22	"	Nil	Nil	"	Nil	Nil	Ductile	8.44	11.4	11.0	
0.65	0.69	0.22	"	"	"	6.0	"	6.0	Transition	13.95	16.68	12.0	
0.64	0.91	0.23	"	1.5	8.0	3.0	12.0	Nil	Brittle	16.11	19.33	11.5	
0.67	0.94	0.22	"	1.2	3.0	4.5	6.0	4.0	"	15.40	19.22	13.0	
0.63	0.97	0.23	"	1.0	3.0	4.0	6.0	4.0	"	15.47	19.23	12.0	
0.62	1.45	0.23	1.0	3.2	6.0	Nil	12.5	Nil	"	16.00	20.45	10.5	
0.71	0.69	0.22	Nil	Nil	Nil	"	Nil	1.5	Transition	12.11	16.34	15.0	
0.79	0.61	0.21	"	"	"	"	"	Nil	Ductile	11.78	15.90	12.0	
0.83	0.85	0.23	"	1.0	"	3.0	11.0	"	Brittle	14.55	19.06	14.0	
0.86	0.98	0.23	"	1.0	4.0	2.0	6.0	4.0	"	15.20	19.47	13.0	
0.85	1.20	0.23	"	1.0	7.0	Nil	7.0	Nil	"	17.80	21.51	13.5	
0.94	0.49	0.21	"	Nil	Nil	"	Nil	"	Ductile	11.40	16.05	15.0	
0.99	0.72	0.21	"	"	"	4.0	3.0	3.0	Brittle	12.95	18.30	17.0	
0.96	0.42	0.21	"	"	"	Nil	Nil	Nil	Ductile	11.02	16.18	15.0	
0.92	0.67	0.22	"	"	"	3.0	"	4.0	Transition	12.18	16.90	16.0	
1.04	1.15	0.21	"	1.0	2.0	4.0	12.0	Nil	Brittle	17.70	20.90	12.0	
1.11	1.02	0.23	"	1.0	Nil	2.0	6.0	2.5	"	14.68	19.18	14.0	
1.15	1.27	0.23	3.5	1.5	7.5	2.0	12.5	Nil	"	17.90	21.38	10.5	
1.08	1.54	0.23	2.0	2.3	7.0	2.0	9.0	2.0	"	16.83	21.58	11.0	
1.20	0.91	0.21	Nil	Nil	Nil	1.0	Nil	6.0	Transition	14.02	18.70	15.5	
1.20	1.03	0.23	"	"	"	5.0	6.0	4.0	Brittle	15.08	18.85	12.0	
1.40	1.36	0.23	"	2.0	6.0	3.0	10.0	Nil	"	15.94	20.79	14.5	
2.10	1.20	0.22	"	Nil	Nil	2.0	Nil	6.0	Transition	12.43	17.75	16.0	

\* See text, p. 382.



## (b) 0.036-in. Sheet, Super-Purity-Base Alloys.

Composition			Mechanical Properties												Grain-Size, mm.
			Quenched from 540° C., Aged Immediately at 175° C. for 8 hr.						Quenched from 540° C., After 3 Days Aged at 175° C. for 8 hr.						
			0.1% P.S., tons/in. <sup>2</sup>	U.T.S., tons/in. <sup>2</sup>	Elong. % on 2 in.	Free-Cone Bend Performance			0.1% P.S., tons/in. <sup>2</sup>	U.T.S., tons/in. <sup>2</sup>	Elong. % on 2 in.	Free-Cone Bend Performance			
C, cm.	SC, cm.	SB, cm.				C, cm.	SC, cm.	SB, cm.							
Mg, %	Si, %	Cu, %													
0.84	0.56	...	15.65	16.79	2.0	12.5	Nil	Nil	10.70	13.15	5.0	Nil	Nil	7.0	0.2-0.6
0.84	0.56	0.65	17.78	20.20	4.0	Nil	„	7.0	9.55	13.31	10.5	„	„	5.0 (very slight)	0.2-0.6
0.93	0.52	...	13.62	16.30	3.0	12.7 (whole length)	...	...	9.36	13.39	9.0	„	„	2.0	0.3-0.7
0.96	0.77	...	17.25	19.79	1.5	Complete fracture	...	...	13.1	16.48	5.5	12.0	„	„	0.2-0.4
0.40	0.50	...	8.81	10.78	5.5	Nil	Nil	12.0 (slight)	7.62	10.90	13.5	Nil	„	„	0.8-1.0
0.44	0.50	0.29	14.21	15.18	2.5	„	„	12.0 (slight)	11.15	14.0	9.0	„	„	10.0 (slight)	0.8-1.0
0.42	0.75	...	12.9	20.70	2.0	12.7 (whole length)	...	...	10.92	13.18	5.0	„	6.0	5.0	0.3-0.4
0.48	1.22	...	14.18	17.12	3.0	12.7 (whole length)	...	...	12.08	15.45	3.0	11.5	Nil	Nil	0.2-0.3
0.34	1.19	...	11.2	14.05	6.0	Nil	2.5	5.0 (very slight)	9.8	13.72	8.0	Nil	„	6.0	0.2-0.3

C = Cracked.

S.C. = Surface cracking.

S.B. = Surface bursts.

## (c) 0.25-in.-dia. Rod, Super-Purity-Base Alloys.

Composition		Mechanical Properties										Grain-Size, mm.
		Immediate Precipitation-Treatment at 175° C. for 8 hr.										
		Quenched from 540° C.					Air-Cooled from 540° C.					
Mg, %	Si, %	0.1% P.S., tons/in. <sup>2</sup>	U.T.S., tons/in. <sup>2</sup>	Elong. % on 2 in.	Approx. Redn. of Area, %	Angle of Bend	0.1% P.S., tons/in. <sup>2</sup>	U.T.S., tons/in. <sup>2</sup>	Elong. % on 2 in.	Approx. Redn. of Area, %	Angle of Bend	
0.27	0.24	2.80	4.85	22.0	...	180°	1.32 *	4.80	23.0	98.5	180°	Mainly 2.0
0.29	0.62	11.01	13.40	9.5	20.6	180°	8.26 *	11.70	12.0	32.8	60°	Mainly 2.0
0.22	0.97	10.75	13.40	10.0	21.9	180°	10.28	13.35	7.0	9.39	60°	1.0-1.5
0.34	0.42	6.72	9.30	15.0	...	180°	5.75 *	11.20	20.0	94.0	180°	1.0-1.5
0.39	0.52	10.78	12.50	8.5	44.9	180°	7.99	11.72	13.0	61.2	180°	1.0-1.5
0.57	0.42	13.40	14.90	6.0	18.4	56°	9.78 *	13.0	9.0	19.7	70°	1.5-2.0
0.67	0.50	16.42	17.50	3.0	14.7	25°	12.84 *	14.90	4.0	15.5	14°	1.5-2.0
0.62	0.67	17.20	18.49	4.0	13.2	24°	14.55	16.21	2.0	7.1	25°	Mixed 0.3-2.5
0.96	0.42	14.90	18.50	13.5	35.0	180°	11.10	15.32	7.0	19.85	90°	1.0-1.5
0.98	0.52	14.65	16.91	17.5	5.5	45°	10.85 *	14.90	12.0	42.0	90°	Mainly fine 0.3-1.5
0.89	0.64	17.90	19.00	2.0	10.92	32°	13.50	17.25	4.0	10.2	56°	0.2-0.6
1.26	0.72	14.32	20.30	14.0	25.3	73°	11.02	15.62	12.0	32.8	180°	} Centre, Elongated grains 2.0-3.0 Outside 0.3
1.26	0.82	18.10	23.85	10.0	24.0	26°	12.90	16.95	12.0	32.2	180°	
1.22	0.92	16.89	19.52	11.5	32.2	110°	15.72	19.72	15.0	50.7	47°	

Composition		Mechanical Properties										Grain-Size, mm.
		3 Days' Interval at Room Temperature before Precipitation-Treatment at 175° C. for 8 hr.										
		Quenched from 540° C.					Air-Cooled from 540° C.					
Mg, %	Si, %	0.1% P.S., tons/in. <sup>2</sup>	U.T.S., tons/in. <sup>2</sup>	Elong. % on 2 in.	Approx. Redn. of Area, %	Angle of Bend	0.1% P.S., tons/in. <sup>2</sup>	U.T.S., tons/in. <sup>2</sup>	Elong. % on 2 in.	Approx. Redn. of Area, %	Angle of Bend	
0.27	0.24	...	...	...	...	180°	...	...	...	...	180°	Mainly 2.0
0.29	0.62	...	...	...	...	180°	...	...	...	...	180°	Mainly 2.0
0.22	0.97	8.95	12.85	16.0	46.2	180°	6.38	11.02	19.0	47.3	180°	1.0-1.5
0.34	0.42	...	...	...	...	180°	...	...	...	...	180°	1.0-1.5
0.39	0.52	...	...	...	...	180°	...	...	...	...	180°	1.0-1.5
0.57	0.42	...	...	...	...	180°	...	...	...	...	90°	1.5-2.0
0.67	0.50	...	...	...	...	90°	...	...	...	...	33°	1.5-2.0
0.62	0.67	12.62	15.7	8.5	16.2	36°	12.03	15.20	7.0	14.0	34°	Mixed 0.3-2.5
0.96	0.42	9.84	15.02	25.0	53.0	180°	9.25	13.89	15.0	29.0	180°	1.0-1.5
0.98	0.52	...	...	...	...	180°	...	...	...	...	180°	Mainly fine 0.3-1.5
0.89	0.64	11.4	16.51	18.0	28.3	90°	11.5	15.89	10.5	21.9	110°	0.2-0.6
1.26	0.72	...	...	...	...	180°	...	...	...	...	180°	} Centre, Elongated grains 2.0-3.0 Outside 0.3
1.26	0.82	12.18	17.43	17.0	58.3	180°	10.7	15.50	15.5	46.2	180°	
1.22	0.92	...	...	...	...	90°	...	...	...	...	54°	

\* Results after 8-hr. interval.

aluminium and super-purity-base hardeners melted in a gas-fired furnace, degassed with hexachlorethane, and semi-continuously cast at 700° C. and 8 in./min. into 12 × 6 × 1-in. rolling blocks. The blocks were scalped to remove any surface defects, soaked at 500° C. for 2-4 hr., and then hot rolled at this temperature to blanks 0.1 in. thick × 8 in. wide. After annealing at 360° C. for 1 hr., the material was cold rolled to a final thickness of 0.036 in.

### (b) Extruded Material

Several super-purity-base alloys were prepared, using the melting procedure outlined above, and semi-continuously cast into small experimental extrusion billets 12 × 1 $\frac{3}{4}$  in. in dia. The billets were machined to 1.45 in. dia. and cut into 3-in. lengths. Each length was then extruded at 540° C. and a speed of 24 in./min. to  $\frac{1}{4}$ -in.-dia. rod. The container temperature was also 540° C.

Particulars of factory-produced extrusions are given in Table II. In this case, 5-in.-dia. billets were extruded to 0.5-in.-dia. rods.

### (c) Heat-Treatment

Heat-treatments were carried out in air-circulation furnaces controlled with an accuracy of  $\pm 2^\circ$  C. For purposes of comparison, a standard solution-treatment temperature of 540° C. was employed, which is 11° C. below the lowest ternary solidus temperature (551° C.) for super-purity-base alloys under equilibrium conditions, and a precipitation-treatment of 8 hr. at 175° C., which is sufficient to produce the maximum mechanical properties.

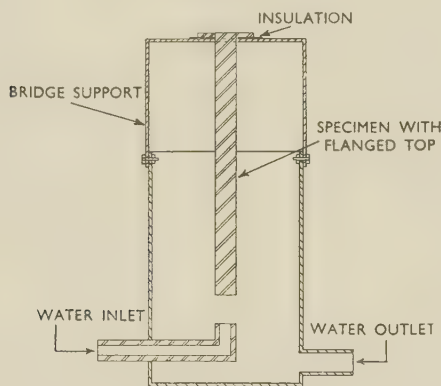


Fig. 1.—Sectional Diagram of Apparatus Used for Cooling-Rate Experiments.

A modified Jominy apparatus was found to be useful for obtaining a gradation of the cooling rate in the same specimen. A sketch of the apparatus is shown in Fig. 1. Thermocouples were peened to the surface of the specimen at regular intervals along its length to determine the rates of cooling. The specimen was subsequently machined and notched, so that Izod determinations could be made along its length. From the cooling curves obtained, and also by an independent mathematical calculation, it was possible to correlate brittleness with rate of cooling.

## 2. METHOD OF TESTING

Since most of the alloys were in the form of 0.036-in.-thick sheet, the most convenient method of assessing relative brittleness was found to be by the free-cone bend-test apparatus<sup>19</sup> shown in Fig. 14 (Plate LV). The specimens were always taken transverse to the rolling direction. As illustrated, the specimen is in

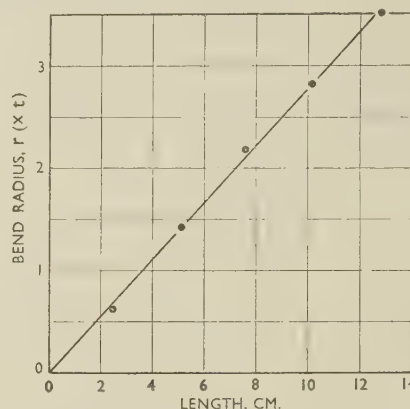


Fig. 2.—Relation Between Length and Bend Radius in the Free-Cone Bend Test.

the form of a trapezium so that, by suitable adjustment of the screws *A*, the bend radius may be made to vary along the length of the specimen from a flat bend at one end to  $3\frac{1}{2}t$  at the other, as shown in Fig. 2. These limits of bend radius were found to be the most satisfactory for the investigation. Various ranges of bend radius may be obtained by adjustment of the four corner screws indicated by *A* in Fig. 14. Originally, the test was designed to provide a rapid method of determining the minimum bend radius for alloys in sheet form. Quantitatively, however, the test has been found to be inadequate, mainly because the designation of minimum bend radius for a specimen showing only slight surface cracking and for one fracturing completely for the same distance, would be identical. For these reasons, the test has been used merely as a qualitative method for determining brittleness, and the type as well as the length of cracking produced on bending has been considered. In fully heat-treated alloys of commercial purity, specimens free from cracking were regarded as ductile, those with only surface cracks as transition, and those with definite cracking giving separation, as brittle. In super-purity-base alloys, this method of classification is more difficult on account of spasmodic bursts produced along the entire length even in more ductile alloys. This feature is found to be associated with the exceptionally coarse grains formed during solution-treatment and subsequent precipitation along certain of the grain boundaries.

Simple bending in a vice is a useful practical test, particularly for material in rod form, brittleness being related to the angle of the bend produced before failure. Alloys in the form of extruded rod which gave a bend in excess of 90° were considered ductile.



This test, however, is in certain instances extremely sensitive to variations in grain-size, as shown in Fig. 15 (Plate LV), which compares the angles of bend obtained for press-quenched extrusions having a fine-grained equiaxed structure with those for the same alloys after separate heat-treatment, which resulted in much larger grain-size.

The results given in Table III indicate that there is also a general tendency for the proof stress to be

possibly related to differences in deformation mechanism.

The difference in microstructure is illustrated in Figs. 17 and 18 (Plate LV). From these observations it is apparent that the vice bend test is applicable only if the grain-size is maintained roughly constant, and it is therefore only approximate for comparing the brittleness of a series of alloys of various compositions and grain-sizes.

TABLE II.—*Production Details for Factory-Extruded 0.5-in.-Dia. Rod.*

Alloy No.	Composition							Extrusion Temp., °C.	Extrusion Time, sec.	Mean Ram Pressure, lb./in. <sup>2</sup>	Heat-Treatment
	Mg, %	Si, %	Fe, %	Mn, %	Cr, %	Cu, %	Ti, %				
6	1.00	0.73	0.29	...	...	...	...	565	94	3100	Press-Quenched and Precipitation-Treated at 175° C. for 6 hr.
7	1.00	1.00	0.29	...	...	...	...	565	91	2900	
8	0.99	0.99	0.50	...	...	...	...	570	94	2800	
10	0.53	0.63	0.30	...	...	...	...	570	64	2500	
11	0.61	0.83	0.26	...	...	...	...	570	91	2600	
12	0.54	0.82	0.54	...	...	...	...	575	114	2600	
13	0.35	1.07	0.26	...	...	...	...	575	100	2300	
14	0.50	1.11	0.26	...	...	...	...	575	115	2400	
15	0.46	1.11	0.53	...	...	...	...	570	106	2400	
16	0.67	1.02	0.45	...	0.32	...	...	570	106	2800	
21	0.66	0.97	0.24	0.40	...	...	...	590	80	2700	Unquenched Press-Quenched and Precipitation-Treated as above
C	0.70	0.95	0.38	0.82	...	0.12	...	575	206	3300	
A	0.47	1.41	0.40	...	...	0.12	...	570	155	2400	
19	0.96	0.61	0.30	...	0.22	0.30	0.11	570	99	3000	
18	0.68	1.25	0.49	...	0.17	0.29	...	565	102	2800	

TABLE III.—*The Effect of Silicon, Magnesium, and Iron on the Izod Values and Tensile Properties.*

Alloy No.	Composition				Extrusion Temp., °C.	Mechanical Properties														
						Press-Quenched and Aged at 175° C. for 6 Hr.					Solution-Treated, Water-Quenched, and Aged *					Solution-Treated, Air-Cooled, and Aged *				
	Mg, %	Si, %	Fe, %	0.1% P.S., tons/in. <sup>2</sup>		U.T.S., tons/in. <sup>2</sup>	Elong. % on 1.5 in.	R. of A., %	Mean Izod Value, ft.-lb.	0.1% P.S., tons/in. <sup>2</sup>	U.T.S., tons/in. <sup>2</sup>	Elong. % on 1.5 in.	R. of A., %	Mean Izod Value, ft.-lb.	0.1% P.S., tons/in. <sup>2</sup>	U.T.S., tons/in. <sup>2</sup>	Elong. % on 1.5 in.	R. of A., %	Mean Izod Value, ft.-lb.	
AR	0.72	0.96	0.38	...	...	...	...	...	19.55	21.00	8.0	11.85	4.6	15.90	19.10	4.0	9.6	3.0		
6	1.00	0.73	0.29	565	12.69	17.60	28.0	55.5	11.3	16.00	18.00	14.5	36.4	11.1	14.50	17.65	14.0	21.4	5.8	
7	1.00	1.00	0.29	565	16.55	20.50	21.5	34.4	7.1	17.80	20.39	13.0	26.7	8.1	14.00	17.80	12.0	21.4	3.5	
8	0.99	0.99	0.50	570	16.89	21.20	20.0	32.2	6.6	16.92	19.70	14.0	33.5	9.6	15.47	18.80	10.0	22.6	4.1	
10	0.53	0.63	0.30	570	12.70	16.40	26.0	69.2	17.4	14.80	16.60	11.0	45.5	18.5	13.35	15.70	14.5	27.2	10.6	
11	0.61	0.83	0.26	570	15.00	18.70	24.0	44.8	9.9	17.40	19.25	12.0	19.5	9.6	15.70	18.47	11.0	18.3	4.3	
12	0.54	0.82	0.54	575	14.69	18.40	26.0	53.4	14.1	16.08	18.10	16.0	51.8	12.8	14.87	17.55	16.5	27.4	7.6	
13	0.35	1.07	0.26	575	14.35	18.30	24.0	53.6	13.1	15.29	17.55	17.0	34.1	11.8	13.90	17.55	14.5	12.7	7.8	
14	0.50	1.11	0.26	575	16.50	20.10	21.0	28.3	7.4	15.79	17.85	13.0	26.7	7.3	15.65	18.97	12.5	14.0	5.1	
15	0.46	1.11	0.53	570	15.78	19.32	24.0	58.2	11.7	16.55	19.00	16.0	35.0	11.5	14.91	18.50	14.0	15.8	7.3	

\* Solution-treatment : 540° C. for 30 min. Precipitation-treatment : 175° C. for 8 hr.

lower in the press-quenched material. This lower proof stress must undoubtedly be taken into account when comparing the angles of bend. Apart from this variation, however, it would appear that grain-size has a much greater influence on the bendability of alloys 13, 6, and 11, which represent limiting brittleness, than on that of the more brittle alloys 7 and 14. The fact that there is no corresponding difference in Izod value suggests that variations in bending performance are not in this instance associated with any difference in grain-boundary precipitation. The explanation of this anomaly is

Bending round a fixed radius was also found to be inadequate for the assessment of brittleness, since some alloys known to give very low Izod values passed a bend radius of 3*t* and in some instances 2*t*. This behaviour is understandable when it is remembered that reduction of area and elongation, which are closely related to bendability, are not always a measure of notch-sensitivity. It also appears that, within limits, the Izod value and proof stress are independent of grain-size, although the reduction of area and elongation may change considerably. This is illustrated by a comparison of the mechanical

properties of the as-extruded and solution-treated material given in Table III. The variation in reduction of area due to differences in grain-size for any given proof stress is shown in Fig. 3. The Izod impact test figure, which gives an accurate measure of notch-sensitivity, probably depends to a large extent on grain-boundary weakness, and only to a very small extent on the slip within the grains which occurs during bending and in the tensile test. The Izod result appears to be affected only by the presence

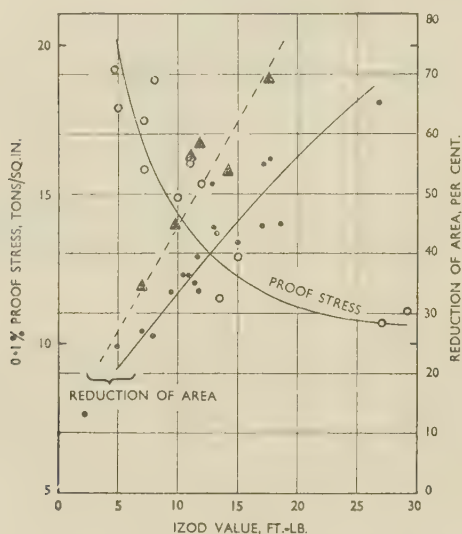


FIG. 3.—Relationship Between 0.1% Proof Stress, Reduction of Area, and Izod Value for Al-Mg-Si Alloys Containing 0.21-0.23% Iron, Solution-Treated at 540° C. and Artificially Aged. (Prepared mainly from results in Table III.)

#### KEY.

- ▲ Reduction of area (grain-size mainly 0.03-0.05 mm.).
- Reduction of area (grain-size mainly 0.15-0.20 mm.).
- Proof stress.

of very large or irregular grains, which are seldom encountered in practice, and is therefore considered to be the most satisfactory test for brittleness.

### III.—EXPERIMENTAL RESULTS

#### 1. EFFECT OF MAGNESIUM, SILICON, AND IRON

In discussing the experimental results, it will be necessary to consider them in relation to the constitution of the aluminium-magnesium-silicon system. Fig. 4 represents the solid-solution relationships at the aluminium corner, and has been drawn to represent the best available information at the present time. It is based largely on the work of Phillips,<sup>20</sup> and of Dix<sup>21</sup> and Keller<sup>22</sup> and their colleagues.

In this diagram, the full lines *PRST* represent the extreme limit of solid solubility under equilibrium conditions, while *SM* and *SN* are the boundaries of the three-phase field at the eutectic temperature. For lower temperatures, the boundaries of the  $\alpha$  solid solution and of the three-phase field are indicated

by the various dotted lines. For example, at 540° C. the limit of solid solubility is indicated by the dotted lines *AB* and *BC*, and the three-phase field is bounded by the lines *BE* and *BD*. These latter are, for all practical purposes, parallel to the quasi-binary line *OR* and to the silicon axis, respectively. The locus of the apex of the three-phase field, as it moves with decreasing temperature, is the curved line *SBG*.

If an alloy having a composition to the left of the line *PRST* is heated to a temperature high enough to ensure a homogeneous  $\alpha$  solid solution and is then slowly cooled to room temperature, precipitation takes place, the nature of the precipitate depending on the composition of the alloy. Thus, with alloys lying above the quasi-binary line *OR*, the precipitate will be  $Mg_2Si$  only and the composition of the solid solution will change by moving along a line parallel to *OR*. With relatively high magnesium contents and at low temperatures, there will be some precipitation of  $Mg_2Al_3$ .

Alloys represented by points below the quasi-binary line *OR*, will behave differently, according as their compositions lie above or below the line *SBG*. Below this line, the initial precipitate will be silicon and the composition of the solid solution will change along a line parallel to the silicon axis until it meets the line *SBG*. Thereafter, there will be simultaneous precipitation of silicon and  $Mg_2Si$ , the composition of the solid solution changing as the temperature is reduced in the direction of the arrows. Above the line *SBG*, the initial precipitate will be  $Mg_2Si$ , and the composition of the solid solution will change along a line parallel to *OR* until it meets the line *SBG*, when simultaneous precipitation of silicon and  $Mg_2Si$  will begin.

In practice, when the alloy is first quenched from the solution-treatment temperature and then reheated to the ageing temperature, it is probable that all these processes take place simultaneously and that for any alloy below the quasi-binary line, i.e. with silicon in excess of that required for the formation of  $Mg_2Si$ , some simultaneous precipitation of silicon and  $Mg_2Si$  will take place. The amount of this simultaneous precipitation will, however, depend on the considerations discussed above.

In Figs. 5 and 6 are plotted the normal mechanical properties obtained after solution-treatment at 540° C., followed by 8 hours' precipitation-treatment at 175° C. The plotted points and the associated figures indicate the 0.1% proof stress values. Through these points contours have been drawn at a number of different levels, with an indication against each of the approximate level of both proof stress and ultimate tensile stress (U.T.S.).

In Fig. 5, which is for alloys containing approximately 0.2% iron, the contours are hyperbolic in form, the asymptotes being parallel to the silicon axis and to the  $Mg_2Si$  line, respectively, while the vertices lie roughly on the line *GBS* (Fig. 4), which represents the locus of the apex of the three-phase field (Al, Si,  $Mg_2Si$ ) with falling temperature.



Fig. 6, which is for alloys made up with aluminium of super purity, is similar in general appearance, but the curves are all shifted, parallel to the silicon axis, in the direction of decreasing silicon. It would thus appear that the effect of iron is, at least in part, equivalent to a reduction in the effective silicon content.

Figs. 7 and 8 show similar contours for the ductility of the alloys as determined by Izod and bend tests. The contours are of the same form and fall in the same position on the diagram as those for proof

treatment temperature of 540° C. The slight difference in shape between the contour of maximum brittleness and the boundaries of the three-phase field is, no doubt, due to a departure from equilibrium conditions.

Under the light microscope there is a clear difference between a ductile and a brittle alloy within a certain range of composition. After etching for the same time, the grain boundaries in a ductile alloy are only faintly visible, whereas in a brittle alloy they are clear and distinct. The difference in microstructure is well shown in Figs. 20 and 21 (Plate LVI), while

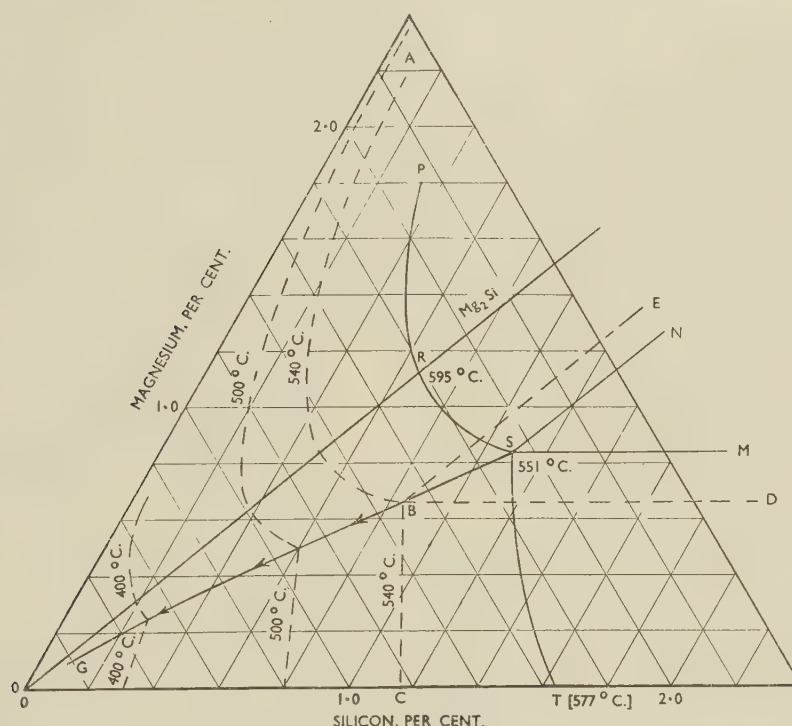


FIG. 4.—Solid-Solution Relationships at the Aluminium Corner of the Al-Mg-Si System.

stress (Figs. 5 and 6). Thus it would appear that, in the simple aluminium-magnesium-silicon alloys with incidental iron, it is impossible to achieve high strength without correspondingly reducing ductility. Alloys with magnesium contents in excess of that needed to form  $Mg_2Si$  are in general ductile, but their strength is low. Increasing the silicon for a given magnesium content, raises the strength, but results in an alloy with low impact resistance and poor bending properties. A similar result is obtained if magnesium is added to a straight silicon alloy.

In alloys whose compositions lie below the quasi-binary line  $OR$ , simultaneous precipitation of silicon and  $Mg_2Si$  takes place on cooling, and the shape of the contours suggests that both strength and ductility are dependent upon the amount of this simultaneous precipitation. Thus maximum strength and minimum ductility are obtained on alloys within the boundaries of the three-phase field at the heat-

treatment temperature of 540° C. The slight difference in shape between the contour of maximum brittleness and the boundaries of the three-phase field is, no doubt, due to a departure from equilibrium conditions.

Under the light microscope there is a clear difference between a ductile and a brittle alloy within a certain range of composition. After etching for the same time, the grain boundaries in a ductile alloy are only faintly visible, whereas in a brittle alloy they are clear and distinct. The difference in microstructure is well shown in Figs. 20 and 21 (Plate LVI), while

The range of composition for which these differences in microstructure may be observed is strictly limited, and appears to be confined to ductile alloys of balanced or  $Mg_2Si$  composition containing approximately 0.5–1.0% magnesium, when compared with brittle alloys containing the same amount of magnesium and an excess of silicon. Alloys containing a large excess of silicon with low magnesium, those with a considerable excess of magnesium, and others containing copper all show distinct grain boundaries after etching, although they are ductile.

It is therefore not always possible to assess brittle-





ness microscopically, although, after etching, alloys in this system showing only very faint grain boundaries are invariably ductile and brittle alloys invariably show distinct grain boundaries.

## 2. EFFECT OF HEAT-TREATMENT CONDITIONS

As might be expected from the foregoing discussion, the temperature of solution-treatment has a marked influence on the properties of the alloys. At higher temperatures more magnesium and silicon are taken into solution, and the extent of subsequent precipitation is therefore increased, resulting in both higher mechanical properties and a greater tendency to intercrystalline weakness. The curves in Fig. 9 show that, for an alloy within the range of composition which is susceptible to intercrystalline weakness, it is not possible, by adjustment of the solution-treatment temperature, to obtain satisfactory mechanical properties without a correspondingly low Izod value.

Similarly, with regard to precipitation-treatment, it has been found that, over the range 140°–200° C.,

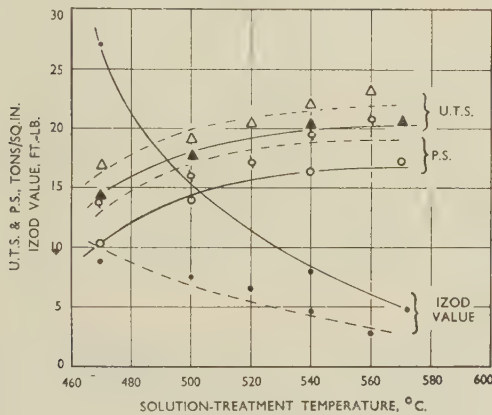


FIG. 9.—Effect of Solution-Treatment Temperature on the Tensile Properties and Izod Values of Two H10-Type Alloys, Precipitation-Treated at 175° C. for 8 Hr.

KEY.	
--- Δ ---	U.T.S.
--- ○ ---	P.S.
--- ● ---	Izod
--- ▲ ---	U.T.S.
--- ○ ---	P.S.
--- ● ---	Izod
Si 0.98, Mg 0.76, Fe 0.35%.	
Si 1.0, Mg 1.0, Fe 0.29%.	

adjustment of neither time nor temperature will give the desired values of proof stress and U.T.S. without the development of the intercrystalline weakness as shown by a low Izod value; outside this temperature range the times of treatment become either inconveniently long or inconveniently short. The curves obtained at 140° and 200° C. are shown in Figs. 10 (a) and (b).

In certain super-purity-base aluminium-magnesium-silicide alloys, the time interval between quenching and precipitation has a very pronounced effect on both the normal mechanical properties and the brittleness. With an interval of 24 hr., the proof and ultimate stresses may be lowered by as

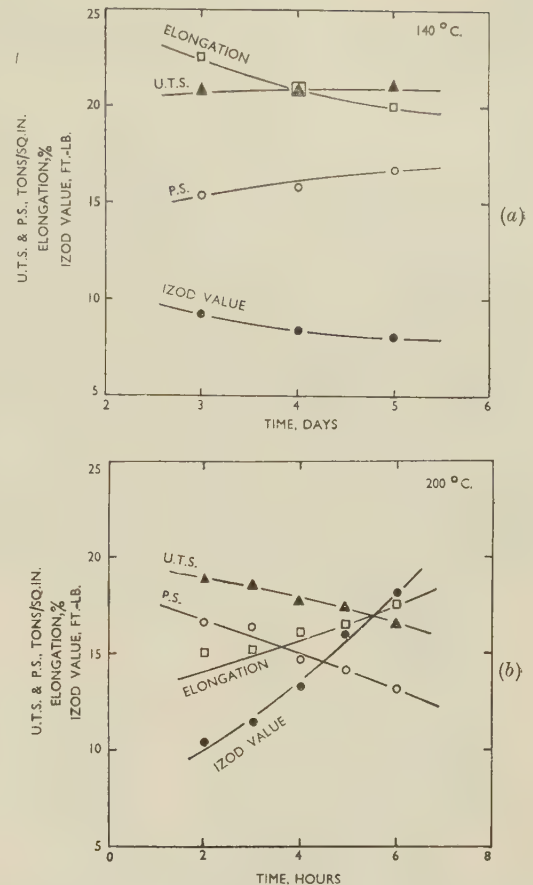


FIG. 10.—Effect of Precipitation-Treatment at (a) 140° C. and (b) 200° C. on the Tensile Properties and Izod Values of an H10-Type Alloy (Mg 0.69, Si 1.00, Fe 0.55%).

much as 4 tons/in.<sup>2</sup>, and in some alloys, after a three-day interval, by 6 tons/in.<sup>2</sup>. In commercial-purity-base alloys, this effect is not nearly so marked, as is shown in Fig. 11. It will be seen that in alloys of normal commercial purity the changes associated with varying interval between quenching and pre-

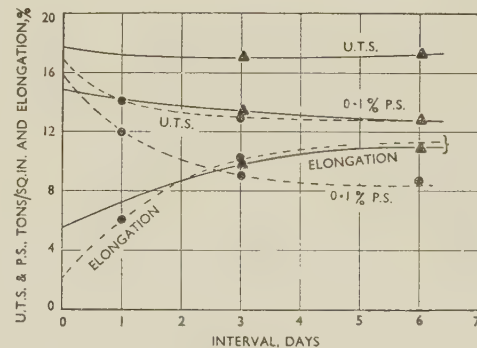


FIG. 11.—Effect of Interval Between Solution-Treatment at 540° C. and Precipitation-Treatment at 175° C. for 8 Hr. on the Tensile Properties of Sheet 0.036 in. Thick.

KEY.		
Mg, %	Si, %	Fe, %
--- ● ---	0.84	0.56
--- ▲ ---	0.79	0.61
---	---	0.21

precipitation-treatment are not of sufficient magnitude to have any influence on the intercrystalline weakness of the alloys.

### 3. EFFECT OF COOLING RATE

When a magnesium-silicide alloy is quenched from the solution-treatment temperature, the solid solution is retained in a supersaturated state because the rate of cooling is such that little if any precipitation takes place. On the other hand, with air-cooling or delayed quenching, the amount of precipitation can be appreciable. Precipitation starts as soon as the temperature drops below that necessary for complete solution of the  $Mg_2Si$ , and is, of course, more rapid at high temperatures than at low ones. For this reason delays in quenching may have serious effects.

To study the possible influence of rate of cooling on the brittleness of these alloys, a modified Jominy apparatus was constructed (Fig. 1). The specimen

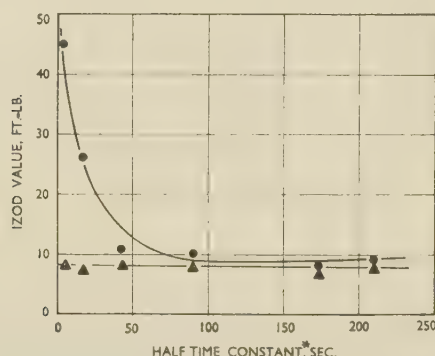


FIG. 12.—Effect of Cooling Rate on the Izod Value as Determined by the Quenched-End Specimen Solution-Treated at 540° C. and Precipitation-Treated at 175° C. for 8 Hr.

#### KEY.

	Si, %	Mg, %	Cu, %	Fe, %
—●—	0.29	0.69	0.25	...
—▲—	0.96	0.72	...	0.38

\* Time taken to cool through 270° C.

was heated to the solution-treatment temperature and placed in position. The water was then turned on so that the specimen was quenched from one end. The rate of cooling was determined by means of thermocouples embedded at various points in the specimen, and was also estimated mathematically. The calculated and experimental figures were in good agreement.

Izod determinations were made at selected distances from the quenched end, and the values obtained plotted against cooling rate. Two typical curves are shown in Fig. 12, from which it can be seen that, for alloys in the brittle range of composition, slow cooling does not have much influence upon the Izod value, but that slow cooling can be very damaging to alloys which are normally ductile. There is clearly no chance that by careful choice of cooling rate a brittle alloy can be converted into a ductile one. All the alloys will, of course, be ductile when

the rate of cooling is slow enough for annealing to take place.

Micro-examination shows that slowly cooled samples have a much more well-defined grain-boundary network than quenched specimens. This is illustrated in Figs. 22 and 23 (Plate LVI). It is interesting to note the analogous behaviour on air-cooling of the aluminium-4% copper alloy, as described and illustrated by Gayler.<sup>23</sup> In this alloy also the grain-boundary precipitate is much thicker and more continuous when air-cooled.

Besides its influence upon the ductility of the alloys, as shown by the Izod values, air-cooling also results in somewhat lower figures for proof stress and U.T.S. (see Tables I and III).

### 4. THE EFFECT OF STRUCTURE

The energy required to produce fracture, as measured by the Izod impact test, is mainly dependent on the ease, and hence the rate, with which a crack can propagate from the point of highest

TABLE IV.—Effect of Directionality on Izod Impact Value.

Composition			Solution-Treatment Temp. (°C.) before Ageing at 175° C., 8 hr.	Izod Impact Value, ft.-lb.		
				Notched in the X Direction *	Notched in the Y Direction *	Notched in the Z Direction *
Mg, %	Si, %	Fe, %				
0.76	0.98	0.35	520 540	8 5	8 5	6 3
0.75 Cu, 0.27% Cr, 0.22%	1.30	0.50	520 540	12 7	13 7	6 3

\* The three axes X, Y, and Z are mutually perpendicular, X and Y being in the plane of the plate and Z at right angles to this plane. Y is in the direction of rolling and X transverse to this direction.

TABLE V.—Mechanical Properties of 0.5-in-Dia. Extruded Rod.

Dia. of Extrusion Billet, in.	Composition			Mechanical Properties				Izod Value, ft.-lb.		
	Mg, %	Si, %	Fe, %	0.1% P.S., tons/in. <sup>2</sup>	U.T.S., tons/in. <sup>2</sup>	Elong. % on 1.5 in.	Redn. of Area, %			
1½	0.83	1.05	0.42	20.2	21.7	14.5	43.0	19.0	20.0	19.0
5	0.69	1.00	0.55	17.4	20.45	18.0	27.8	6.8	6.7	7.3

stress concentration across the section. This rate is largely a function of: (a) the existence of planes of weakness or a path of low resistance along which a crack may travel, and (b) the length of the path of least resistance. In the brittle aluminium-magnesium-silicon alloys, (a) is satisfied by the weakness at the grain boundaries, but the length through which the crack travels may vary according to the size and shape of the grains.

Recrystallized grains elongated in the rolling



direction are occasionally found in hot-worked material, such as hot-rolled blank, and may give rise to considerable variations in Izod value, as shown in Table IV.

unaffected by variations in grain-size within the limits normally encountered in practice. If, however, exceedingly large grains are produced by stretching before solution-treatment, the impact value for the

TABLE VI.—*The Effect of Cold Work on Tensile Properties of Al-Mg-Si Alloys.*

Solution-Treatment : 540° C. for 30 min. Precipitation-Treatment : 175° C. for 6 hr.

Alloy No.	Composition						Solution-Treated, Water-Quenched, and Aged (P)				Stretched 10%, then as in (P) (U)				Solution-Treated, Water-Quenched, Stretched 10%, and Aged (R)			
	Mg, %	Si, %	Fe, %	Mn, %	Cr, %	Cu, %	0.1% P.S., tons/in. <sup>2</sup>	U.T.S., tons/in. <sup>2</sup>	Elong. % on 1.5 in.	R. of A., %	0.1% P.S., tons/in. <sup>2</sup>	U.T.S., tons/in. <sup>2</sup>	Elong. % on 1.5 in.	R. of A., %	0.1% P.S., tons/in. <sup>2</sup>	U.T.S., tons/in. <sup>2</sup>	Elong. % on 1.5 in.	R. of A., %
A	0.47	1.14	0.40	...	...	0.12	16.61	20.48	19.0	27.2	14.18	18.30	12.5	16.75	19.5	21.5	14.0	25.1
15	0.46	1.11	0.53	...	...	...	16.8	20.08	17.0	32.7	14.4	18.42	10.5	15.45	18.35	20.3	16.0	39.4
6	1.00	0.73	0.29	...	...	...	12.65	17.61	22.0	37.0	12.25	16.82	16.0	25.1	16.7	18.4	17.0	44.4
17	0.96	0.61	0.30	...	0.22	0.30	20.0	23.3	25.0	...	15.9	19.65	24.5	42.3	19.4	20.7	20.7	57.5
						(Ti 0.11)												
21	0.66	0.97	0.24	0.40	...	...	16.5	20.02	24.0	56.0	14.58	17.75	26.0	59.9	19.31	21.4	19.0	69.0
C	0.70	0.95	0.38	0.82	...	0.12	15.5	19.2	20.0	59.0	13.60	17.8	26.5	51.0	17.90	19.3	21.0	65.5
16	0.67	1.02	0.45	...	0.32	...	24.9	26.5	17.0	45.5	23.8	25.2	15.0	44.2	21.5	22.6	16.5	56.6
18	0.68	1.25	0.49	...	0.17	0.29	22.8	25.2	17.0	44.2	20.7	23.3	16.0	50.5	23.1	24.6	16.5	50.9

Alloy No.	Composition						Solution-Treated, Air-Cooled, and Aged (S)				Stretched 10%, then as in (S) (V)				Solution-Treated, Air-Cooled, Stretched 10%, and Aged (L)			
	Mg, %	Si, %	Fe, %	Mn, %	Cr, %	Cu, %	0.1% P.S., tons/in. <sup>2</sup>	U.T.S., tons/in. <sup>2</sup>	Elong. % on 1.5 in.	R. of A., %	0.1% P.S., tons/in. <sup>2</sup>	U.T.S., tons/in. <sup>2</sup>	Elong. % on 1.5 in.	R. of A., %	0.1% P.S., tons/in. <sup>2</sup>	U.T.S., tons/in. <sup>2</sup>	Elong. % on 1.5 in.	R. of A., %
A	0.47	1.14	0.40	...	...	0.12	15.25	19.2	10.0	10.09	13.94	17.32	5.0	7.37	16.3	19.4	12.5	17.1
15	0.46	1.11	0.53	...	...	...	14.8	19.15	18.5	24.7	13.85	17.4	6.5	1.37	16.55	19.32	14.5	27.8
6	1.00	0.73	0.29	...	...	...	12.02	16.78	19.0	28.4	12.22	15.15	11.0	11.9	15.42	17.6	16.5	49.6
17	0.96	0.61	0.30	...	0.22	0.30	9.33	14.7	22.5	61.2	10.52	15.1	25.0	57.2	13.7	16.25	22.5	68.8
						(Ti 0.11)												
21	0.66	0.97	0.24	0.40	...	...	11.1	15.55	23.0	64.7	11.59	15.05	21.0	60.5	14.15	16.5	19.0	58.8
C	0.70	0.95	0.38	0.82	...	0.12	11.6	16.51	21.5	50.7	11.45	15.98	21.0	54.2	15.32	17.15	18.5	53.2
16	0.67	1.02	0.45	...	0.32	...	6.48	12.0	25.0	69.5	8.71	12.55	23.0	62.1	12.7	15.0	23.0	66.0
18	0.68	1.25	0.49	...	0.17	0.29	7.44	13.4	22.5	63.5	6.94	12.69	24.5	63.0	13.09	15.42	20.0	27.7

TABLE VII.—*The Effect of Cold Work on Mean Izod Values (ft.-lb.) of Al-Mg-Si Alloys.*

Solution-Treatment : 540° C. for 30 min.

Precipitation-Treatment : 175° C. for 6 hr.

Alloy No.	Composition						Solution-Treated, Water-Quenched, and Aged (P)	Stretched 10%, then as in (P) (U)	Solution-Treated, Water-Quenched, Stretched 10%, and Aged (R)	Solution-Treated, Air-Cooled, and Aged (S)	Stretched 10%, then as in (S) (V)	Solution-Treated, Air-Cooled, Stretched 10%, and Aged (L)
	Mg, %	Si, %	Fe, %	Mn, %	Cr, %	Cu, %						
A	0.47	1.14	0.40	...	...	0.12	8.7	12.9	7.5	6.2	8.9	5.9
15	0.46	1.11	0.53	...	...	...	8.7	15.1	9.6	6.4	10.4	6.2
6	1.0	0.73	0.29	...	...	...	11.3	17.0	8.8	9.4	13.0	8.8
17	0.96	0.61	0.30	...	0.22	0.30	23.0	22.8	20.8	29.6	26.0	33.5
						(Ti 0.11)						
21	0.66	0.97	0.24	0.40	...	...	27.5	36.5	38.0	22.0	25.3	25.0
C	0.70	0.95	0.38	0.82	...	0.12	28.0	31.0	24.0	24.6	23.8	22.8
16	0.67	1.02	0.45	...	0.32	...	38.5	32.0	25.0	33.2	34.5	30.5
18	0.68	1.25	0.49	...	0.17	0.29	15.5	17.3	12.6	28.0	31.6	23.8

Very pronounced elongation of the grains, produced by extruding with a low reduction ratio, leads to a considerable increase in Izod value. The mechanical properties of 0.5-in.-dia. rod extruded from 1½- and 5-in.-dia. billets are compared in Table V.

For alloys of commercial purity, the Izod value is

fully heat-treated alloy is considerably increased. On the other hand, very large grains reduce the mechanical properties, including the reduction of area and elongation. This applies to both air-cooled and quenched samples, as illustrated in Tables VI and VII for alloys stretched 10%.

## 5. THE EFFECT OF COLD WORK

Stretching 10% before precipitation-treatment does not appear to influence the grain-boundary precipitation, since there is very little change in Izod value. Quenched and air-cooled samples behave similarly in that the mechanical properties are considerably improved without any increase in brittleness. The mechanical properties given in Tables VI and VII indicate that any increase in proof stress in the range obtaining for the more

magnesium-silicon alloys in the fully heat-treated condition are increased by the addition of 0.3% copper, which has no adverse effect on brittleness, and 0.3% chromium to balance the tendency for decreased corrosion-resistance.

Copper also increases the rate of precipitation during natural ageing, as illustrated in Table VIII.

The exact role of copper in this respect is not fully understood, since according to solid-solubility data recently published by Axon,<sup>24</sup> it remains completely in solid solution. A possible explanation may be

TABLE VIII.—*Effect of Copper on Natural Ageing of Al-Mg-Si Alloys Quenched from 540° C.*

Composition			Mechanical Properties								
			Tested within 30 Min.			Aged 3 Days at 18° C.			Aged 11 Days at 18° C.		
Mg, %	Si, %	Cu, %	0.1% P.S., tons/in. <sup>2</sup>	U.T.S., tons/in. <sup>2</sup>	Elong. % on 2 in.	0.1% P.S., tons/in. <sup>2</sup>	U.T.S., tons/in. <sup>2</sup>	Elong. % on 2 in.	0.1% P.S., tons/in. <sup>2</sup>	U.T.S., tons/in. <sup>2</sup>	Elong. % on 2 in.
0.40	0.50	...	1.70	6.14	20.0	3.25	8.27	20.5	3.61	8.62	19.0
0.44	0.50	0.29	1.78	6.54	19.5	3.37	9.45	23.5	4.05	10.05	22.0
0.84	0.56	...	4.02	9.13	15.0	6.59	12.61	17.0	7.12	12.35	13.0
0.84	0.56	0.65	3.16	9.40	20.0	6.1	13.5	21.5	7.31	14.57	24.0

TABLE IX.—*Comparison of Mechanical Properties of Alloys Quenched and Air-Cooled from 540° C.*

Composition			Mechanical Properties							
			Quenched from 540° C. and Immediately Aged at 175° C. for 8 hr.				Air-Cooled from 540° C. at 6° C./sec. and Immediately Aged at 175° C. for 8 hr.			
Mg, %	Si, %	Cu, %	0.1% P.S., tons/in. <sup>2</sup>	U.T.S., tons/in. <sup>2</sup>	Elong. % on 2 in.	Free-Cone Bend Test Results	0.1% P.S., tons/in. <sup>2</sup>	U.T.S., tons/in. <sup>2</sup>	Elong. % on 2 in.	Free-Cone Bend Test Results
0.40	0.50	...	8.81	10.8	5.5	Surface cracking 1.0 cm.	6.68	9.37	9.5	Satisfactory
0.44	0.50	0.29	14.21	15.2	2.5	Intermittent bursting from end to end	13.40	14.65	2.0	Cracked 12.5 cm.
0.84	0.56	...	15.65	16.8	2.0	Intermittent bursting 7.0 cm.	13.40	14.72	2.0	Cracked 12.0 cm.
0.84	0.56	0.65	17.78	20.2	4.0	Slight surface cracking 5.0 cm.	17.78	18.75	1.5	Complete fracture at 20° bend

brittle alloys (13–18 tons/in.<sup>2</sup>) has little effect on the Izod value, and it may therefore be inferred that brittleness is more dependent on the precipitation characteristics of the alloy.

## 6. THE EFFECT OF COPPER

Additions of copper have an extremely beneficial effect on the mechanical properties of the aluminium-magnesium-silicon alloys in the quenched and artificially aged condition. In alloys of the H10 type, an addition of 0.3% copper is sufficient to raise the proof and ultimate stresses by about 3 tons/in.<sup>2</sup>. This advantage is, however, offset by a decrease in corrosion-resistance unless chromium or manganese is also present. Full advantage of the effect of copper is achieved in certain North American alloys in which the mechanical properties of the more ductile aluminium-

connected with the increase in the degree of supersaturation of the solid solution.

Further, as a result of the increased rate of precipitation, alloys containing copper in the absence of manganese and chromium appear to be more susceptible to preferential grain-boundary precipitation during air-cooling. A comparison of the free-cone bend tests for the alloys listed in Table VIII, quenched and air-cooled (approx. 6° C./sec.) from 540° C. and precipitation-treated, is made in Table IX. It must be borne in mind, however, that complete inter-crystalline fracture would not occur with the low-proof-stress alloy, owing to the relative ease of grain deformation, even assuming considerable grain-boundary weakness. On the other hand, there is little evidence of any large variations in brittleness in the samples quenched and artificially aged,



although copper increases the proof stress by as much as 5.40 tons/in.<sup>2</sup> in the alloy containing 0.40% magnesium and 0.50% silicon. Microscopically, employing the standard etching procedure (1½ min. in 10% H<sub>2</sub>SO<sub>4</sub> + 5% HF), it was not possible to detect any difference in microstructure between the air-cooled samples, with and without additions of copper. However, the former were strongly attacked at the grain boundaries after prolonged etching (2–2½ min.). This is in agreement with the fact that aluminium-magnesium-silicon alloys containing copper alone are more susceptible to inter-

in order to ensure a fine-grained product. The degree of recrystallization taking place during extrusion depends on factors such as cast structure of the billet, homogenization, reduction ratio, and speed and temperature of extrusion. Normally, larger extruded sections are only partly recrystallized, and therefore on account of these structural variations it is extremely difficult to assess the true notch-sensitivity of manganese-containing alloys by the Izod test. Izod values have been found to vary from 11 to 40 ft.-lb. Typical properties of H10WP alloys in the form of 0.5-in.-dia. extruded rod, with and

TABLE X.—The Effect of Manganese and Chromium on the Mechanical Properties of an H10WP Alloy (0.036-in. Sheet).

Solution-treated at 540° C. Aged at 175° C. for 8 hr.

Composition						Mechanical Properties			Free-Cone Bend Test	
Mg, %	Si, %	Fe, %	Cu, %	Mn, %	Cr, %	0.1% P.S., tons/in. <sup>2</sup>	U.T.S., tons/in. <sup>2</sup>	Elong. % on 2 in.	Cracking, cm.	Surface Cracking, cm.
0.84	1.10	...	...	...	...	16.35	19.25	6.5	Complete fracture	...
0.76	1.05	0.31	...	...	...	16.68	20.36	13.0	8.0	Nil
0.84	1.05	...	...	0.41	...	17.75	21.44	12.5	Nil	7.0
0.74	0.95	0.24	...	0.34	...	18.42	21.31	9.5	"	5.5
0.68	0.95	0.27	...	0.71	...	17.40	20.42	10.0	"	3.0
0.68	0.95	0.25	...	0.90	...	16.50	19.70	10.0	"	3.8
0.66	0.94	0.31	...	1.15	...	15.20	19.20	14.5	"	Nil
0.72	1.09	0.36	...	...	0.21	18.55	21.72	13.5	"	6.0
0.89	0.72	0.42	0.30	0.16	0.30	17.60	21.80	11.5	"	3.5

crystalline corrosive attack. This behaviour suggests that copper does influence grain-boundary precipitation or the diffusion of atoms to the grain boundaries.

#### 7. THE EFFECT OF MANGANESE AND CHROMIUM

Additions of manganese in the approximate range 0.4–0.7% to brittle aluminium-magnesium-silicon alloys have the important effect of inhibiting preferential grain-boundary precipitation, with the result that the alloys are no longer notch-sensitive. The mechanical properties are little affected by manganese if the addition is restricted to a maximum of approximately 0.8%, as shown in Table X, which also illustrates the corresponding marked improvement in bending performance.

The microstructure of a solution-treated and artificially aged alloy is characterized by the presence of many minute specks or dispersoids in the matrix (Fig. 19, Plate LV), but there is generally a complete absence of any grain-boundary precipitate. A possible explanation for this phenomenon is that the specks, which are presumably (Mn,Fe)Al<sub>6</sub>, act as nuclei for the subsequent precipitation of the Mg<sub>2</sub>Si and silicon, thus largely preventing their preferential grain-boundary precipitation.

The main disadvantage of adding manganese lies in the fact that the recrystallization temperature is considerably raised, with the result that special precautions are necessary during extrusion and rolling

without manganese, are given in Tables III, VI, and VII.

The minimum addition of manganese necessary to suppress preferential grain-boundary precipitation is not known, but alloys containing 0.4 and 0.7% manganese appear to be equally satisfactory.

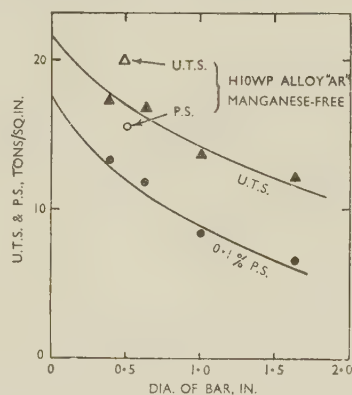


FIG. 13.—Effect of Cooling Rate from the Solution-Treatment Temperature (540° C.) on the Mechanical Properties of an H10-Type Alloy Containing Manganese, Precipitation-Treated at 175° C. for 8 Hr. Composition: Mg 0.69, Si 1.01, Fe 0.35, Mn 0.42%.

In an alloy containing manganese, rapid general precipitation, with a consequent large decrease in mechanical properties, occurs if the rate of cooling from the solution-treatment temperature is decreased,

as shown in Fig. 13. In this experiment, the cooling rate was varied by air-cooling rods 8 in. long of varying diameter. For purposes of comparison, points representing the properties of an air-cooled 0.5-in.-rod for a manganese-free alloy have been included.

The behaviour of chromium is similar in every respect to that of manganese, with the exception that on a weight percentage basis it appears to be approximately twice as effective and the maximum addition is usually 0.3%. The mechanical properties of rolled and extruded H10WP alloys containing chromium, and of similar American-type alloys containing copper and chromium, are given in Tables X, VI, and VII, respectively.

#### IV.—CONCLUSIONS

The criterion of ductility adopted arbitrarily for this investigation was the ability of an alloy in the form of 0.036-in. sheet, quenched and artificially aged, to produce the maximum properties to withstand a flat bend on the standard free-cone bend test without cracking. Alloys satisfying this condition were found to have a minimum Izod value of about 11 ft.-lb., which was considered to be a reasonable figure for dividing ductile and brittle alloys.

Using this criterion, brittleness in aluminium-magnesium-silicon alloys, solution-treated at 540° C. and precipitation-treated at 175° C. for 8 hr., was found to be dependent on both the magnesium and the silicon content of the alloy. For instance, in super-purity-base alloys with magnesium contents of 0.7% or higher, a very small percentage of silicon in excess of that required to form the compound  $Mg_2Si$  is sufficient to produce a considerable increase in brittleness. Similarly, with silicon contents of 1.2% or higher, a very small percentage of magnesium in excess of about 0.35% is sufficient to produce a similar increase in brittleness. The effect of iron is to displace the brittleness contour slightly further to the excess silicon side of the quasi-binary line, and thus, other factors remaining equal, a greater percentage of excess silicon is required to produce the same degree of brittleness in commercial-purity alloys.

For the same composition, increase in brittleness has been related to increased continuity of the grain-boundary network, continuity being assessed by the number of grains enveloped by the precipitate and not by the appearance of the latter at high magnifications. However, as in the case of alloys with copper additions, alloys containing an excess of silicon are more severely attacked at the grain boundaries on etching. Therefore, variations in brittleness as a result of compositional changes cannot always be associated with a corresponding difference in microstructure. Moreover, brittleness is not determined by grain-boundary weakness alone, but by the strength within the grains relative to that

at the boundaries. For any alloy in this series, it has been found that as the strength of the grains increases so the grain-boundary network generally becomes more continuous. Each of these phenomena depends on composition and heat-treatment, and they appear to be inseparable in quenched and artificially aged alloys. This is clearly illustrated by the similar form of the contours for brittleness and mechanical properties. It has been shown, however, that large variations in brittleness, not always accompanied by significant differences in proof stress, can be achieved by other treatments. Moreover, the converse is true when the effect of stretching 10% before artificial ageing is considered, and it would therefore appear that in the higher ranges of proof stress changes in grain-boundary precipitation are of greatest importance.

The relationship between composition and brittleness for a constant solution-treatment temperature of 540° C. can be associated with the degree of supersaturation of the solid solution, with respect to both silicon and magnesium. The importance of the latter is also illustrated by the effect of solution-treatment temperature.

The precipitation-treatment is also of paramount importance in relation to brittleness, and artificial ageing is necessary for preferential precipitation on the grain boundaries. Brittleness cannot be produced by natural ageing, although A. Sendorek (unpublished work) has shown that air-cooled super-purity-base alloys decrease in ductility after several weeks' ageing at room temperature. The lowest Izod value can again be associated with the most continuous network, combined with the maximum mechanical properties.

In contrast to the commercial-purity-base alloys, the mechanical properties and brittleness of the higher-strength super-purity-base alloys in the fully heat-treated condition decrease rapidly with increase in the time interval at room temperature between quenching and artificial ageing.

Within certain limits of cooling rate, a decrease in the rate of cooling from the solution-treatment temperature gives rise to the formation of a more continuous grain-boundary precipitate, which appears to be thicker than that produced by artificial ageing and increases the brittleness. This phenomenon appears to be more pronounced in the coarser-grained super-purity-base alloys, particularly those with a highly supersaturated solid solution of approximately  $Mg_2Si$  composition.

Additions of copper increase the proof and ultimate stresses by several tons/in.<sup>2</sup> in the quenched and artificially aged condition without any sacrifice of ductility. Impaired corrosion-resistance limits the copper addition to about 0.3%. Copper appears to increase the brittleness on air-cooling from the solution-treatment temperature as before, within certain limits of cooling rate.

No attempt has yet been made to identify the brittle grain-boundary film. The grain-boundary precipitate



produced on air-cooling is most probably  $Mg_2Si$ , but that produced in artificially aged brittle alloys which contain an excess of silicon cannot be resolved under the light microscope.

The results are of considerable practical value in that the limitation of the aluminium-magnesium-silicon alloys in respect of notch-sensitivity is clearly illustrated. In particular, satisfactory mechanical properties in the H10WP alloy cannot be obtained without accompanying notch-sensitivity in the absence of chromium or manganese.

Additions of 0.4–0.7% manganese or approximately 0.3% chromium inhibit preferential grain-boundary precipitation during artificial ageing and air-cooling. Instead, precipitation appears to be of a more general nature within the grains, and to occur rapidly on

air-cooling with an accompanying large drop in 0.1% proof stress after artificial ageing. Maximum strength, together with good ductility, may be obtained by adding both copper and chromium or copper and manganese. The combination of a magnesium content of 0.7% or over with a large excess of silicon should be avoided, even in the presence of manganese or chromium, if maximum ductility is desired.

*Note Added in Proof.*—Since this paper was prepared, Chadwick, Muir, and Grainger<sup>25</sup> have published work on the effect of iron, manganese, and chromium on an alloy of this type. Their conclusions with regard to the effect of these additions are in substantial agreement with those reached by the present authors.

## REFERENCES

1. K. Yokoyama, *Nippon Kinzoku Gakkai-Si* (Trans. Inst. Metals Japan), 1937, **1**, 43, 92.
2. T. Mishima, *World Eng. Congress, Tokyo* (1929), *Proc.*, 1931, **36**, (4), 215.
3. R. Buehl, J. H. Hollomon, and J. Wulff, *Amer. Inst. Min. Met. Eng., Tech. Publ. No. 1120* (in *Metals Technol.*, 1939, **6**, (7)).
4. J. Hérenghuel and P. Lacombe, *Compt. rend.*, 1944, **218**, 404; also *Métaux, Corrosion-Usure*, 1944, **19**, 39.
5. J. D. Grogan and R. J. Pleasance, *J. Inst. Metals*, 1939, **64**, 57.
6. E. C. W. Perryman, *Compt. rend.*, 1952, **235**, 884.
7. G. L. Bailey, *J. Inst. Metals*, 1951, **79**, 243.
8. D. McLean, *ibid.*, 1952–53, **81**, 121.
9. D. McLean and L. Northcott, *J. Iron Steel Inst.*, 1948, **158**, 169.
10. E. C. W. Perryman, *Symposium on Internal Stresses in Metals and Alloys* (Inst. Metals Monograph Rep. Series No. 5), p. 251. 1948: London (Institute of Metals).
11. P. Brenner and G. J. Metcalfe, *J. Inst. Metals*, 1952–53, **81**, 261.
12. G. J. Metcalfe, *ibid.*, 1952–53, **81**, 269.
13. A. H. Geisler and F. Keller, *Trans. Amer. Inst. Min. Met. Eng.*, 1947, **171**, 192.
14. W. Hume-Rothery, "Structure of Metals and Alloys" (*Inst. Metals Monograph Rep. Series No. 1*), p. 65. 1950: London (Institute of Metals).
15. W. Geller, *Z. Metallkunde*, 1939, **31**, 9.
16. P. Brenner and H. Kostron, *ibid.*, 1939, **31**, 89.
17. C. Panseri and M. Monticelli, *Alluminio*, 1945, **14**, 51.
18. Ministry of Supply Rep. No. A.I.D./Met. **9** (1947).
19. A. Benkő, *Aluminium* (Budapest), 1952, **4**, 97.
20. H. W. L. Phillips, *J. Inst. Metals*, 1946, **72**, 156.
21. E. H. Dix, Jr., F. Keller, and R. W. Graham, *Trans. Amer. Inst. Min. Met. Eng., Inst. Metals Div.*, 1931, 404.
22. F. Keller and C. M. Craighead, *ibid.*, 1936, **122**, 315.
23. M. L. V. Gayler, *J. Inst. Metals*, 1946, **72**, 243.
24. H. J. Axon, *ibid.*, 1952–53, **81**, 209.
25. R. Chadwick, N. B. Muir, and H. B. Grainger, *ibid.*, 1953–54, **82**, 75.





# TECHNIQUES FOR THE INVESTIGATION OF THERMAL CONDITIONS IN CONTINUOUS CASTING \*

By D. M. LEWIS,† B.Sc., A.I.M., MEMBER

## SYNOPSIS

An account is given of the apparatus and techniques employed for a study of thermal conditions in the continuous casting of aluminium alloys. Methods used for determining the solidification contour include pour-out or "dumping", dip-stick measurements, tracer additions of copper, and radioactive-tracer additions. The measurement of temperatures in solidifying billets and ingots is outlined, details being given of the thermocouple layout and of the equipment for amplification and high-speed recording of the signals. The method of producing isothermal distributions from the recorder charts is described. The limited information available from the thermal analyses is supplemented by calculations in which the Liebmann iteration method is employed, and by use of an electrical tank analogue in which various features of the casting process can be simulated. The possible value of the conducting-paper-field plotter is mentioned.

Information on heat-transfer conditions, both in the mould and when the metal enters the sub-mould cooling area, is of importance in mould design and for process control, and an experimental method of measuring heat transfer by means of thermocouple plugs is described. Heat-transfer values are also derived from temperature gradients in calculated temperature fields or may be measured directly by using a slight modification of the analogue technique.

## I.—INTRODUCTION

THE process of continuous casting, at present used almost exclusively for the production of extrusion billets and rolling ingots in aluminium alloys, and which is now showing signs of increasing importance in the steel industry, developed very largely as a result of practical experience. Even to-day, nearly a century after the first published reference to the method, the theory is only partially understood, and little information is available to allow the successful application of the technique under new conditions.

Considerable experimental work is necessary to devise satisfactory casting processes for new alloys or for new sizes of ingot or billet, e.g. it is not yet possible to translate a practice for 10-in.-dia. billets directly into one suitable for billets of appreciably larger diameter, say, 16 or 30 in., and the repeated trial and error necessary for evolving an appropriate procedure is expensive both in time and material.

The special requirements desirable in continuously cast metal have been listed by Scheuer<sup>1</sup> as follows: (a) absence of inclusions and flaws, (b) uniform composition, i.e. absence of segregation, (c) fine and regular distribution of constituents, (d) small grain-size of the matrix, and (e) a clean and smooth surface.

These requirements can be met only by conflicting procedures, particularly in regard to casting speed. Better surfaces can usually be obtained by raising the speed, but this increases the depth of the liquid metal pool, and thereby creates a condition of unsatisfactory feeding at the centre line. Insufficient liquid-metal supply causes porosity and spider-web cracking.

The importance of cooling rates draws attention to one of the main difficulties encountered in continuous casting, viz. the tendency of the metal mass to crack during the casting operation or after removal of the billet or ingot from the casting machine. Severe temperature gradients exist in the surface layers after casting, and an unfavourable stress condition develops with a cold, rigid, outer skin opposing the natural tendency for the core to contract in volume as its temperature falls. When the shrinkage stresses become too high, cracking takes place. Very little is known of the mechanism of the internal-stress systems in billets and ingots.

Practical methods of reducing the cracking tendency have been worked out, but at present they offer only a partial cure. Very low casting rates are normally recommended as essential to reduce the internal stresses to small values, but complications then arise owing to the need for casting at economic rates.

For the majority of alloys, the very rapid cooling from the liquid phase, obtained by fast casting, results in fine grain structures with reduced segregation as compared with normal statically cast ingots. Slow casting, however, can produce severe surface lapping due to excessively rapid solidification of the surface skin near the mould wall. Lapping greatly increases the thickness of metal to be scalped off, and can have serious effects in the later fabricating processes, particularly extrusion and rolling.

Practical experience shows that the continuous-casting process, as operated commercially, must satisfy four basic requirements. A good surface must be combined with a fine grain structure and minimum porosity and segregation; there must be

\* Manuscript received 3 December 1953.

† Aluminium Laboratories, Ltd., Banbury, Oxon.

little or no cracking during or after casting; and the casting rate must be as high as possible. These conflicting demands illustrate that investigations of the physical aspects of the process may usefully concentrate on two main variables, heat-transfer conditions and the internal-stress system. Although, to a large extent, the stress distribution is a function of heat transfer, it can be regarded as a separate study. The present paper introduces techniques for the investigation of the thermal conditions only in continuously cast light alloys.

## II.—PREVIOUS WORK

The literature of the continuous-casting process, although voluminous, contains few references to physical investigations of the process itself. Mathematical studies of the rate of solidification have been made by Roth,<sup>2</sup> Tikhonov and Shvidkovsky,<sup>3</sup> and Bingel,<sup>4\*</sup> while Doyle<sup>5</sup> has given figures for temperature distribution and internal-stress values for large-diameter aluminium alloy billets. The purely metallurgical aspects of the process have been the subject of papers by Scheuer,<sup>1</sup> Hérenguel,<sup>6, 7</sup> Waters,<sup>8</sup> and others, and in the last few years some valuable accounts have appeared of the actual operation of casting units. Those of Krainer and Tarmann,<sup>9</sup> Speith and Bungeroth,<sup>10</sup> and Pierce,<sup>11</sup> although referring to steel practice, contain basic information of value in the general study of the process.

The purely mathematical investigation of the solidification behaviour of the metal in continuous casting yields useful results, although the accuracy is of a relatively low order. The errors can be traced to the numerous assumptions made for dealing with the known behaviour of the metal in the mould, e.g. Roth<sup>2</sup> makes the following assumptions in his calculations: (i) that solidification begins only when the metal reaches the water bath or the sub-mould sprays, (ii) that there is a linear radial temperature gradient, (iii) that there is negligible longitudinal heat flow in the billet or ingot, (iv) that the metal is poured with zero super heat, (v) that after entering the spray-cooling region, the billet acquires a constant surface temperature, and (vi) that on solidification no change occurs in the thermal properties of the metal.

The errors in most of these assumptions are quite obvious, although in some cases the effects are not serious. Assumption (i) has been shown by recent experimental work to be approximately valid for some types of mould if very low casting speeds are excluded. Apart from the formation of the initial skin, almost negligible skin thickening takes place in the mould, the main process of freezing occurring in the spray-cooled sub-mould region.

Using these simplifications, Roth derived two

expressions for the growth behaviour of the metal skin, viz:

(a) *For a rectangular ingot:*

$$x = v [L\rho + \frac{1}{2}c\rho(\theta_f - \theta_s)] \frac{y^2}{2K(\theta_f - \theta_s)}. \quad (1)$$

(b) *For a cylindrical ingot having a radius, R:*

$$x = \frac{v \left[ \left( \frac{R^3}{3} - r^3 \log_e \frac{R}{r} - \frac{r^3}{3} \right) (L\rho + \frac{1}{2}c\rho(\theta_f - \theta_s)) \right]}{3RK(\theta_f - \theta_s)}. \quad (2)$$

$x$  being the depth of the liquid pool,  $y$  the thickness solidified, and  $r$  the radius of the liquid pool at the depth  $x$ .

When casting 99.2% aluminium, these equations can be simplified by inserting the following values for the constants:

$L$ , latent heat of fusion	92.4 cal./g.
$\rho$ , density	2.71 g./c.c.
$c$ , specific heat (20°–400°C.)	0.24 cal. (average)
$K$ , thermal conductivity (average)	0.555 cal./cm. <sup>2</sup> /°C./sec.
$\theta_f$ , melting temperature	660° C.
$\theta_s$ , surface temperature of metal	20° C.
$v$ , casting speed	$V \times \frac{2.54}{60}$ cm./sec.

( $V$  is casting speed in in./min.)

Then, for a rectangular ingot,

$$x = 0.0263 V^2 \dots \dots \dots (3)$$

where  $x$  is the distance of a point on the solidification front below the free liquid surface.

In the case of a cylindrical billet, equation (2) reduces to:

$$x = 0.0016 V \left[ \frac{R^3}{3} - r^3 \log_e \left( \frac{R}{r} \right) - \frac{r^3}{3} \right] \quad (4)$$

The calculation of these basic equations was taken a step further by Tikhonov and Shvidkovsky,<sup>3</sup> who, by introducing the concept of finite heat-transfer values in the cooling system, have partially eliminated a serious source of error in Roth's work. No account was taken, by these investigators, of the effect of metal temperature or mould size. The equations of Tikhonov and Shvidkovsky, as reproduced by Ruddle,<sup>12</sup> take the basic forms shown in equations (5) and (6).

*Rectangular ingot:*

$$x = v \left\{ \frac{(L\rho + \frac{1}{2}c\rho\phi)y^2}{2K\phi} + \frac{[L\rho + \frac{1}{2}c\rho\phi]y}{h\phi} - \frac{\left[ \frac{1}{2}Kc\rho \log_e \left( 1 + \frac{h}{2K} \right) \right]}{2h^2} \right\} \dots \dots (5)$$

\* A recent paper by Klein<sup>45</sup> shows a new approach to the theory of the solidification process in continuous casting. A complete translation of the paper was not available when the present account was written.



Cylindrical ingot:

$$x = v \left\{ - \frac{\left( L\rho + \frac{c\rho\phi}{6} \right) y^3}{3KR\phi} + \left[ \frac{\left( L\rho + \frac{c\rho\phi}{4} \right)}{2K\phi} + \frac{\left( L\rho + \frac{c\rho\phi}{12} \right)}{2hR\phi} \right] y^2 + \left[ \frac{\left( L\rho + \frac{c\rho\phi}{4} \right)}{h\phi} + \frac{Kc\rho}{12h^2R} \right] y - \left[ Kc\rho \left( 1 + \frac{K}{3hR} \right) \log_e \left( 1 + \frac{hy}{K} \right) \right] 4h^2 \right\} \quad (6)$$

In both expressions the symbol  $\phi$  represents  $(\theta_f - \theta_s)$  and  $h$  is the Newtonian heat-transfer coefficient.

In considering mould solidification, appropriate values of  $h$  can be used to take into account air-gap formation when heat transfer is predominantly by radiation and convection, conduction being negligible.

of the elapsed time. It also shows that the thickness is inversely proportional to the square root of the casting speed.

The expressions for the cylindrical billet cannot be derived in the same way. If, however, values are substituted for  $x$ ,  $y$ , and  $r$ , in the case of a typical billet where  $R = 11.45$  cm., the following is obtained:

$$t = 0.0423V\{0.473T^2 - 0.026T^3\} \quad (9)$$

This expression is considerably more cumbersome to manipulate than the relatively simple relationship existing between  $t$ ,  $T$ , and  $V$  in equation (8).

When the various expressions are compared with figures obtained from typical casts, the agreement, as can be seen from Figs. 1 (a) and (b), is particularly poor. The results are obviously of very restricted value in practical studies of the casting of billets

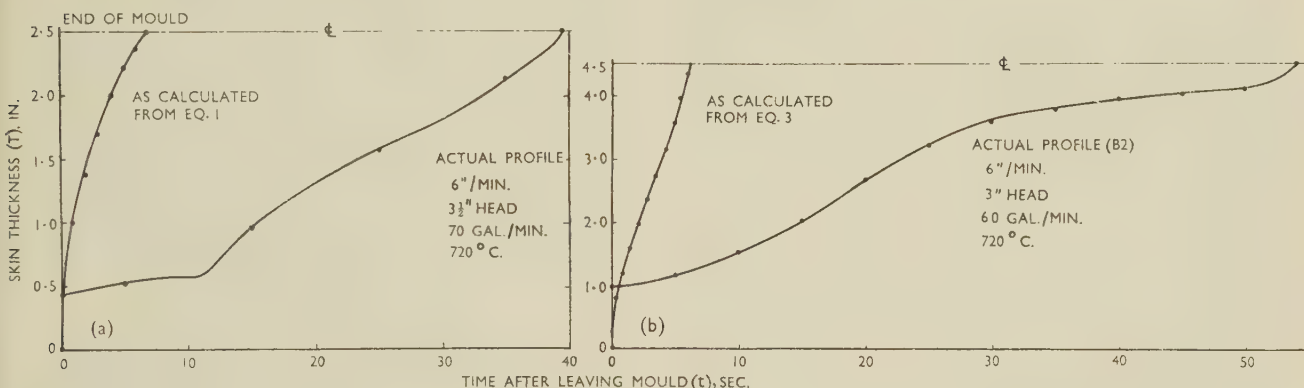


Fig. 1.—Curves Showing Lack of Agreement Between Calculated and Experimentally Determined Solidification Contours. (a) Rectangular ingot, 20 x 6 in. (b) Cylindrical billet, 9 in. dia.

When the metal emerges from the mould into the cooling sprays, the value of  $h$  increases and approximates to infinity when the outside surface is submerged in the cooling water. In this case ( $h \rightarrow \infty$ ), equation (5) reduces to the same form as that of Roth (equation (1)). It is also possible to obtain some simplification of equation (6) for a cylindrical billet:

$$x = v \left\{ - \frac{\left[ L\rho + \frac{c\rho\phi}{6} \right] y^3}{3KR\phi} + \frac{\left[ L\rho + \frac{c\rho\phi}{4} \right] y^2}{2K\phi} \right\} \quad (7)$$

So that these calculations may be considered in terms of practical aspects of the casting process, the expressions have been re-written to give the skin thickness,  $T$ , in terms of time,  $t$ , after the start of casting, values being substituted for the various constants. The vertical co-ordinate,  $x$ , is then replaced by  $t$ , and the horizontal co-ordinate,  $y$ , by the thickness,  $T$ . Roth's expression for the rectangular ingot, equation (3), then changes to:

$$T = \sqrt{\frac{38.02 t}{V}} \quad (8)$$

which confirms the accepted theory that skin thickness at any point is proportional to the square root

and ingots. It is noticeable, however, that the calculated times for complete solidification are excessively short; this can probably be explained by the fact that a perfect quench has been assumed ( $h \rightarrow \infty$ ). Experimental results show that the quench conditions call for a value of  $h$  of a very low order. The lack of agreement between calculated and experimental results has been noticed by other investigators, and it is normally found that the rate of solidification derived from actual heat-transfer determinations is consistently lower than that calculated by both the Roth and the Tikhonov formulæ.

The unreliability of the equations defining the solidification behaviour makes it almost impossible to use calculated figures in an investigation of the interrelationship between the kinetics of solidification and the metallurgical features of the metal. It therefore becomes essential to study the process by experimental methods, and from the results obtained to endeavour to correct the discrepancies in the calculated figures.

The work introduced in the present paper is designed to give information on the shape and position of the solid/liquid interface, the temperature distribution in billets and ingots, and the heat-transfer relationships

in the cooling systems normally employed. It is intended to consider these factors in relation to the metallurgical effects produced in the metal, particularly grain-size and orientation, distribution of segregation and porosity, frequency of occurrence of bleed bands, existence of blebbing, &c. As the present paper deals only with the physical techniques employed in the research, few references are made to experimental results except in cases where these can clarify the description of the method.

### III.—DETERMINATION OF THE SOLIDIFICATION CONTOUR

The whole principle of the continuous-casting process can be said to be explained by reference to the shape of the solidification front or the sump-contour, as it is frequently termed. A shallow pool or sump is a prime requisite for reasonably stress-free castings, but the contour also exerts a strong effect on segregation in the ingot or billet. The sump shape is also important in showing the rate of thickening (or remelting) of the solid skin, both inside the mould and when the ingot emerges into the extra chilling zone below the mould. Knowledge of the depth of the pool, although not essential in aluminium casting, has an extremely important influence on the design of equipment for the continuous casting of steels; reference to the paper by Speith and Bungeroth<sup>10</sup> shows that, in the casting of steel ingot sections ( $6 \times 7$  in.), the pool depth can exceed 20 ft.

The orientation of the columnar crystals in any cast metal ingot or billet depends upon the contour shape, as at all points the major axis of the grains lies in the direction of heat flow, i.e. normal to the isothermal planes. The solidification front can, of course, be regarded as an isothermal front, both in the case of pure metal, where it is a single isotherm, or in the case of alloys having a solidification range, as two planes, at the liquidus and solidus temperatures, respectively.

The rate of thickening of the metal skin indicates the efficiency of heat removal both in the mould and the sub-mould cooling area. Although considerable experimental work has been done to derive laws for metal-solidification rates in static castings, examination of the literature indicates only one attempt to measure the solidification rate of continuously cast metal,<sup>2</sup> when the measurement was made to check the validity of previously derived mathematical expressions.

In order to obtain information on the extent and shape of the sump contour, four methods have been employed in the present work: (1) the pour-out method, (2) dip-stick measurements, (3) the addition of a copper tracer, and (4) radioactive-tracer additions.

#### 1. THE POUR-OUT METHOD

This technique, known as "dumping" in American accounts of solidification investigations, has been

discussed in some detail by Ruddle.<sup>12</sup> The reasoned arguments there put forward to show the uncertainty of the results have been confirmed by Pellini,<sup>13</sup> who quotes examples of work in which serious errors have been made by relying on pour-out tests.

In continuous casting, numerous practical difficulties interfere with ready operation of the technique, and these probably account for the unusual results obtained by Roth.<sup>2</sup> The very rapid chilling results in considerable solidification taking place in the time interval before the liquid interior of the billet can be poured out. The sump contour then indicates a pool depth considerably less than that existing during the casting operation.

It is, however, important to mention one case where the pour-out method does give some useful information. When casting at particularly high speeds, fracture of the billet skin frequently occurs at about the level of the bottom of the mould, the liquid interior running out through the hole so produced and leaving a profile of the solid skin inside the mould. The shape of this profile invariably shows that considerable remelting has occurred inside the mould after the air gap has formed. It is probable that fracture of the skin occurred when its thickness became too slight to withstand the frictional force of the metal against the mould wall combined with the hydrostatic pressure of the liquid interior.

#### 2. DIP-STICK MEASUREMENTS

Few references to the use of this technique appear in the published literature, although it can yield useful information in the case of pure metals. There is, however, one serious drawback, for accurate measurements cannot be obtained on the steeply sloping surfaces of the sump. Reasonably accurate results are obtained only for the rather flat base of the solidification pool.

The value of dip-stick measurements increases considerably when applied to large billets and ingots. Here the rate of casting is relatively low, there are negligible fluctuations of liquid level in the mould, and the base of the sump is relatively flat.

In the present work, dip-stick readings have been taken as an approximate check on the results indicated by the embedded thermocouples in the thermal-analysis experiments, and to show the extent of the billet requiring examination when tracer additions have been made.

#### 3. TRACER ADDITIONS

Although the application of this technique to continuous casting does not appear to have been previously described, it is well-known in the light-alloy industry. At a late stage in the casting operation, a few pounds of a liquid aluminium alloy containing about 20% copper are added to the liquid metal entering the billet. To avoid unnecessary interference with the thermal conditions, the temperature of this "tracer" metal should not differ



appreciably from that of the main metal stream. The copper-rich alloy rapidly becomes distributed through the liquid pool and immediately freezes when it reaches the solidus line, a sharp boundary being formed between the two metal zones. After sectioning the billet, one face is rough machined; this operation usually makes obvious the shape of the sump contour, owing to the difference in machinability between the two alloys, as shown in Fig. 17 (a) (Plate LVII). The contour can be made considerably plainer by rough polishing and macro-etching the surface (Fig. 17 (b), Plate LVII).

The addition of a copper tracer can, of course, be used only to investigate the solidification of non-copper-bearing alloys.

#### 4. RADIOACTIVE-TRACER ADDITIONS

A technique employing extremely small additions of a tracer that can always be distinguished from

materials. In the latter, serious interference is to be expected from the activity acquired by the various alloying elements, but it appears likely that by the selection of suitable irradiation and decay periods, useful contour autoradiographs can be obtained.

It is of the greatest importance to realize the difference between the contours determined by the various techniques. The pour-out method, as has been stressed by Ruddle<sup>12</sup> and by Pellini,<sup>13</sup> gives information on the position of the liquidus. That the dip-stick technique gives similar readings will be clear from Fig. 2 (a), where the relatively large-sized end of the dip-stick is shown supported on the extreme tips of the growing dendrites. The tracer procedures, however, probably show the position of the solidus boundary as, at the instant of mixing, the tracer-bearing metal penetrates into the liquid-filled spaces between the dendrites, as shown in Fig. 2 (b).

Careful examination of the microstructure of the boundary between the differently etched portions of the tracer-bearing sections shows a possible second change of structure corresponding to the liquidus line. In the case of commercial-purity aluminium, however, the freezing temperature range is particularly small, and the liquidus and solidus boundaries are consequently close together, but with alloys having appreciable solidification ranges, the border zone extends over a considerable distance. There is a possibility that the radioactive-tracer method will enable this zone to be studied in considerable detail.

#### IV.—MEASUREMENT OF TEMPERATURES IN SOLIDIFYING INGOTS AND BILLETS

##### 1. GENERAL CONSIDERATIONS

The importance of knowing the temperature conditions at all points in the metal during the whole of the casting process has become recognized largely as a result of the recent work of Ruddle,<sup>15</sup> and of Pellini and his associates.<sup>16, 17</sup>

The thermal-analysis technique involves placing a number of thermocouples in the mould cavity to record the temperatures at known points in the metal mass during solidification. When dealing with static casting, it is usual to have additional thermocouples embedded in the mould walls to obtain information on heat flow into the mould material.

Arrangements for locating the couples, such as those employed by Bishop, Brandt, and Pellini,<sup>16</sup> can be used only for static casting in sand and chill moulds, where considerable accuracy of location is possible. Locating and supporting the couples in continuous casting is, however, much more difficult, and, moreover, the presence of the couples can interfere with the actual casting process. In addition, the thermal gradients in the continuous process are considerably steeper and the rates of temperature change very much greater than in normal sand or chill moulds. Useful temperature surveys can only be obtained, therefore, by using a number of couples, each of which is read at very short time-intervals.

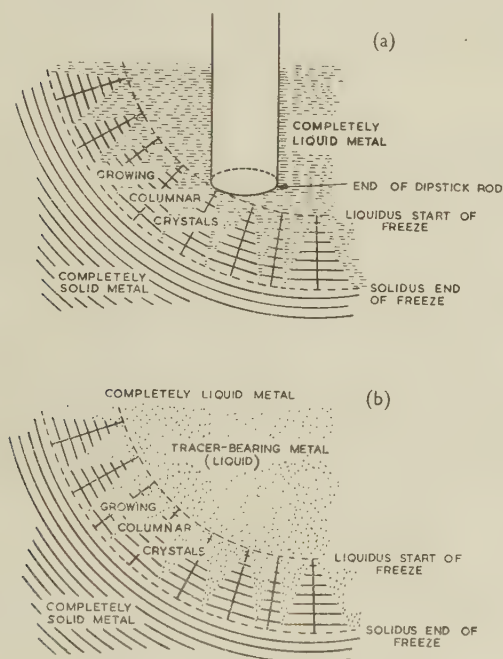


FIG. 2.—Determination of Solidification Contours.

- (a) Probable effect when a dip-stick rests on the dendrite tips.  
(b) Penetration of tracer-bearing metal into the interdendritic spaces.

alloying elements and impurities in the basis metal appears to be of great value. Experimental work, carried out in conjunction with the Isotopes Division of the Atomic Energy Research Establishment, Harwell, has resulted in a suitable procedure being developed in which a tracer content of 1 or 2 p.p.m. radioactive gold  $Au^{198}$  can delineate the solid/liquid front. The technique has been described in detail by Putman.<sup>14</sup>

The method used at present is applicable to the study of solidification in commercially pure aluminium, but work is proceeding on its application to alloy

Published information on high-speed recording of thermocouple readings appears restricted to methods in which cathode-ray-tube displays are obtained, the traces being recorded photographically,<sup>18</sup> or in which a number of pen recorders are employed, each connected to its own thermocouple.

An examination of cathode-ray-tube presentation techniques<sup>18</sup> indicated numerous disadvantages and showed that the methods required considerable development before becoming suitable for foundry use.

Equipment using two high-speed pen recorders in association with a thermocouple-scanning method has been described by Watson and Dixon.<sup>19</sup> This apparatus, later improved by Fowler,<sup>20</sup> has been employed for recording temperature changes in ingot moulds in steel works.<sup>21</sup> It is important, however, to note that the maximum reading rate of this equipment is considerably lower than that required for studying the temperature distributions in continuously-cast ingots. Scanning and recording speeds of at least 3 thermocouples/sec. are essential for the latter application, compared with 10 thermocouples/min. which can be regarded as a useful maximum figure in investigating ingot-mould temperatures.

Brief details of the method used at the British Non-Ferrous Metals Research Association for recording the distribution of temperature in sand castings have been given by Ruddle,<sup>15</sup> who employed a motor-driven thermocouple selector-switch, feeding signals to a D.C. amplifier, and thence to a high-speed twin-channel recorder. The maximum recording rate of the equipment was 3 thermocouples/sec., but for the most efficient operation very good electrical screening of all the equipment was essential.

## 2. TEMPERATURE-RECORDING EQUIPMENT DEVELOPED FOR USE IN CONTINUOUS CASTING

As no apparatus was commercially available for working at the required scanning speed, a suitable recorder was designed, arrangements being made to incorporate various desirable features of the instruments described by other investigators. In its final form the temperature-recording equipment consists of 5 units, viz.:

(a) the thermocouple selector-switch, calibration, and backing-off sources;

(b) the timing unit controlling the thermocouple selector-switch;

(c) a balanced "chopper"-type D.C. amplifier and its associated power supplies;

(d) the condenser storage unit maintaining the indication on the first channel of the recorder, while the second channel is taking up the indication from the next thermocouple; and

(e) a high-speed twin-channel pen recorder with a  $3\frac{1}{2}$ -in. scale on each channel.

A detailed description of the principles of operation of the whole equipment will be given in a forthcoming paper by Taylor and Farley, but brief remarks on

the various units may be appropriate in the present account. An indication of the layout of the instrument can be obtained from Fig. 19 (Plate LVIII), which shows the apparatus connected up for use on the continuous-casting machine.

### (a) *Thermocouple Selector System, Calibration, and Backing-Off Sources*

As preliminary investigations showed that temperature errors of up to 20° C., as a result of contact e.m.f.s, can be expected from both rotary thermocouple switches and uni-selectors, individual relays are fitted in the present apparatus for connection to each thermocouple. The relay coils are energized in turn by a uni-selector controlled by the timer unit. Extensive testing has shown that contact e.m.f.s are not developed in these relays.

### (b) *Timing Unit*

The scanning rates required in the equipment which lie in the range 10 thermocouples/sec. to 4 thermocouples/min., call for a timing unit of considerable accuracy and extreme flexibility. Both qualities are obtained by a resistance-condenser combination exerting control over the striking of a thyatron valve which operates a uni-selector switch and steps it on to the next position. Two functions are performed by the uni-selector switch: consecutive energizing of the individual relays for connection of the thermocouples to the amplifier input, and alternate operation of the relays for connection of the two condenser storing circuits to the amplifier output.

The timing unit can operate continuously or make one complete circuit of the twenty-four thermocouple positions and then stop. Continuous scanning is employed for investigation of the casting process, while the second scheme has proved useful for rapid surveys of temperature distribution inside furnaces at different time intervals.

### (c) *Amplifier*

This unit consists of a chopper-type D.C. amplifier with a balanced input stage which almost entirely eliminates hum pick-up on the thermocouple leads. The final amplifier design has seven stages.

### (d) *Condenser Storage Circuit*

In initial tests, using the Evershed and Vignoles duplex high-speed recorder, it was arranged that the amplified thermocouple voltage should be connected alternately to each pen, which meant that while one pen was recording the second pen returned to zero. The disadvantages of this system, viz. excessive pen travel and reduced recording time on the chart, soon indicated that a circuit which would maintain the correct indication on pen *A*, while pen *B* was taking up its new indication, and vice versa, would have several advantages. First, the pen would travel direct from one thermocouple reading to the next, with a consequent reduction in wear on the instrument, and secondly, the recording time per chart length would increase to 100%. This modification,



when included, made it possible to run the chart at half-speed and still obtain equal ease of interpretation.

The circuit employed for the condenser storage system is particularly simple, consisting of a twin triode valve connected in two cathode follower-circuits. The output from the D.C. amplifier is switched alternately by Siemens high-speed relays to condensers connected between grid and earth of each cathode follower-stage, the output voltage for the recording pens being taken from the cathodes of the twin triode valve. Each grid condenser maintains constant current in its respective cathode follower-circuits while the other pen is taking up its new indication.

#### (e) Evershed and Vignoles Quick-Response Recorder

This instrument, a twin-pen unit, each pen being driven by amplifiers, is arranged to record on Teledeltos paper, using a spark discharge. A third pen can be deflected by a solenoid to record on the centre of the chart and give a mark for easy identification of the recordings or to indicate the positions of other events on the chart time scale.

### 3. ARRANGEMENT OF THERMOCOUPLES

When deciding on methods of locating the required thermocouples in the billets, a number of factors require consideration; these include the means of obtaining the maximum thermo-e.m.f.s, accurate location of the couples at the desired positions in the metal, the use of wires of the minimum thermal capacity compatible with robust construction, and adequate electrical insulation when immersed in liquid and later embedded in solid metal.

The first experiments employed Chromel/Alumel couple wires insulated from the melt by  $\frac{1}{4}$ -in.-dia. twin-bore silica tubing, over practically their whole length. The silica tubes were inserted into  $\frac{1}{4}$ -in.-dia. holes drilled in the steel base of the stool and held upright by a locating spider laid across the top of the mould. For insulation, the thermocouple junctions were sprayed with Dycote, a proprietary mould wash.

Results obtained by this technique were very disappointing, as the couples frequently gave no readings, indicating that the insulation had broken down at an early stage in the experiment. Radiographic examination of slices cut from the billets showed that failure was due to crushing of the silica tube by stresses induced in the interior of the billet during contraction, and in numerous cases this crushing action had completely cut the thermocouple wires. Another frequent source of trouble was the tendency of the liquid metal to penetrate the bore of the tubing before solidifying and so short-circuit the couple bead. This resulted in the actual location of an indicated temperature being considerably below that of the thermo-junction.

It was found impossible to obtain reliable readings from the majority of the twelve or fourteen couples employed in this arrangement and it was decided,

in view of the difficulties, to dispense with silica tubes and insulate the wires with a layer of Dycote only. It is essential that the layer of Dycote be extremely thin, as otherwise the coating rapidly flakes off to expose the bare wires. A further alteration in procedure was a change in the stool thermocouple mounting-arrangement, Fig. 3 illustrating the principle of the improved system employed in all later experiments. The original  $\frac{1}{4}$ -in.-dia. holes have been enlarged to  $\frac{3}{4}$  in., leaving the profile as shown. A short length of twin-bore silica tube is then inserted into the hole and well packed in place with asbestos wool. A spiral cone, formed from

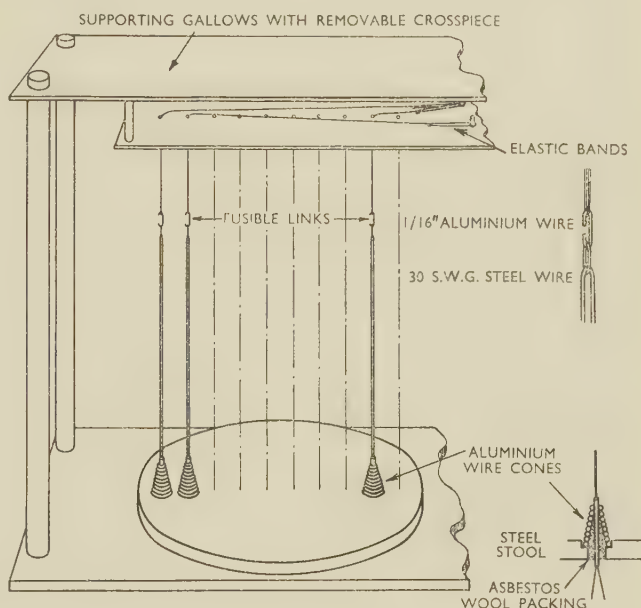


FIG. 3.—Details of the Thermocouple Supporting System.

aluminium wire and pushed over the silica tube, presses the asbestos wool around the silica, thus ensuring that the tubing is held firmly in position. To prevent leakage of the metal, the holes in the short length of silica tube through which the wires emerge are plugged with a thick layer of Dycote. The thermocouple wires of measured length are supported fairly loosely in position by means of fine vertical steel wires attached to a gantry mounted on the ram platform of the casting unit. By interposing a number of fusible links in the supporting system (see Fig. 3), the wires are released immediately the thermocouples become completely immersed in the liquid metal.

Much better results have been obtained using these improved techniques, and the average mortality rate among the thermocouples has been reduced to approximately one in ten. It is believed that the improvement in performance results largely from the use of the aluminium-wire cones. As the metal cools, these cones prevent any contraction stresses from cracking the supporting silica tubing and shearing the couple wires.

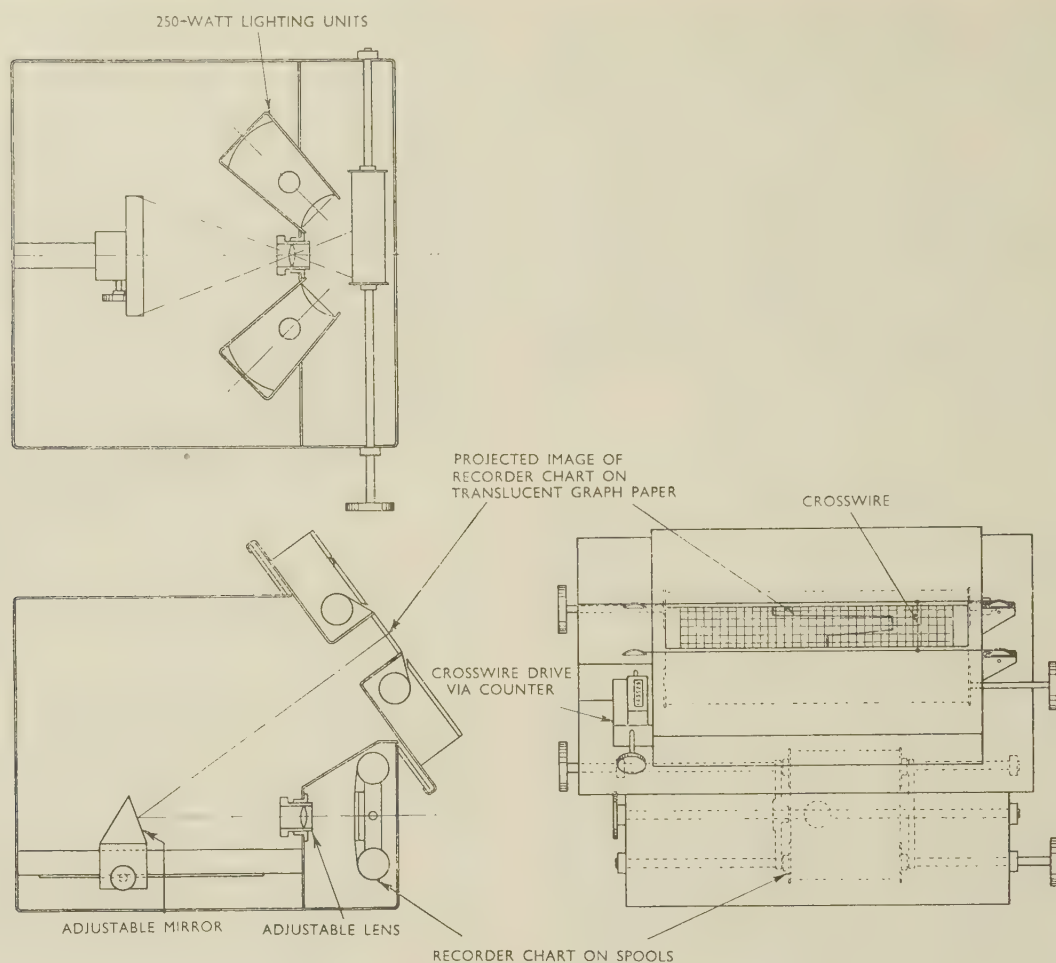


FIG. 4.—Outline Drawing of Projection Reader.

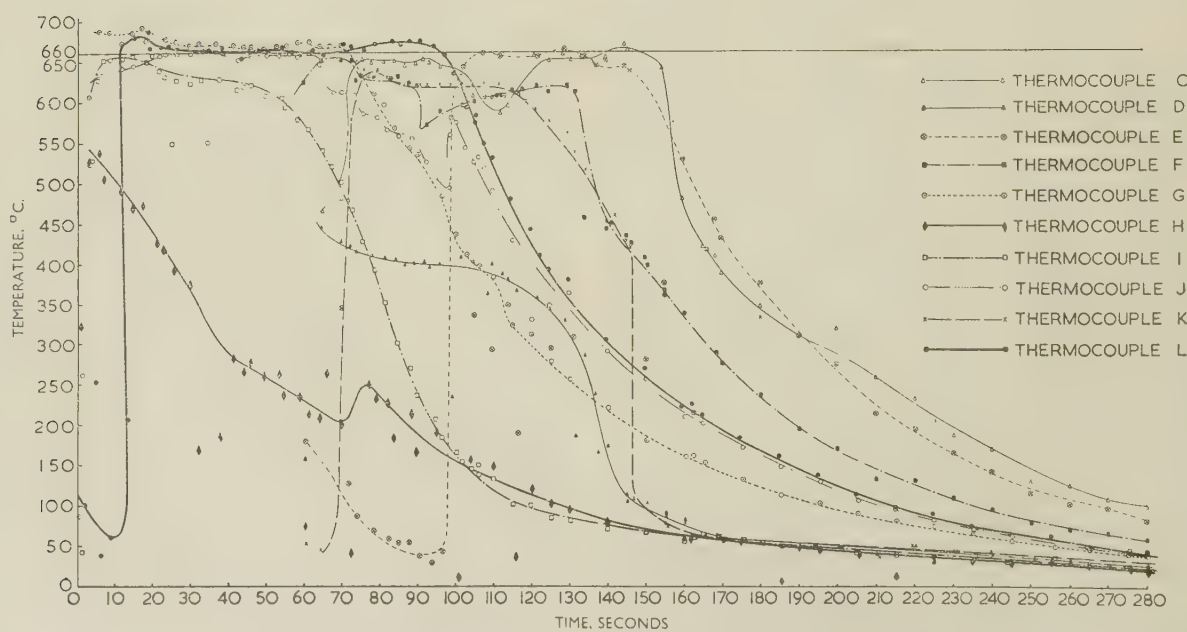


FIG. 5.—Typical Cooling Curves Plotted from a Temperature Chart.



At the conclusion of each cast in which thermocouples are employed, the billet is sectioned to produce a length about 10 cm. long containing the thermojunctions. As the majority of the couples are located

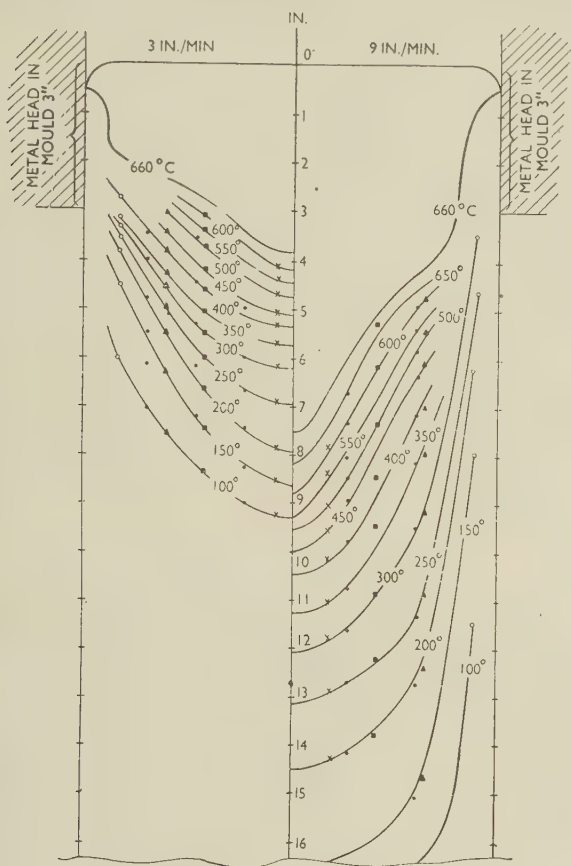


FIG. 6.—Examples of Isothermal Fields in Billets Cast at 3 and 9 in./min.

along a diameter, a flat slice is prepared which contains all the couples within a 2-cm. thickness of metal. This is radiographed to ascertain the final positions of the couple junctions (Fig. 18, Plate LVII). Correction lines can be inserted on the radiograph to ensure that the time scale is determined from the instant when the majority of couples entered the metal simultaneously.

As interpretation of the chart from the high-speed recorder occupies considerable time when done by conventional methods, it has been necessary to develop more rapid means of deriving the time/temperature curves for each thermocouple. One procedure adopted was to mount a sheet of semi-transparent graph paper on a vertical glass plate and rule two lines on the paper to represent 0° and 800° C., respectively. The chart obtained during the actual casting experiment was placed on the stage of an epidiascope, whose projection magnification was adjusted until the zero of the record and the 800° C. calibration points coincided with the equivalent

lines drawn on the graph paper. While the chart was wound slowly across the epidiascope stage, the projected image of each thermocouple deflection was marked against the appropriate time position on the graph paper. By using this technique, complete time/temperature curves for a run lasting 280 sec. and involving the use of ten thermocouples scanned at a rate of 4/sec. could be plotted in one day.

Although this represented a very considerable improvement on the early method of interpreting the records, viz. measuring each deflection on a transparent scale, further time-saving in the reading operation was necessary, and new projection equipment was therefore designed for this purpose. The principle of operation of the reader is somewhat analogous to that of the Vickers projection microscope, as can be seen from Fig. 4. Arrangements are incorporated for actual measurement of the temperature value at any time interval by means of a cross wire operating through a gearing system and indicating on a counter mechanism. These digital readings of temperature are of considerable value when use is made of mathematical techniques (see Section V) for deriving the temperature distributions in more detail.

Plotting the temperature results on the projection reader produces a set of cooling curves similar to that in Fig. 5. By taking into account the casting rate and the positions of the various thermocouples, it then becomes possible to draw in the positions of the isotherms. The number of points yielding useful results is necessarily small, but by transferring the readings from the opposite side of the axis by a "mirror-image" method reasonably regular isothermal curves can be obtained.

In order to illustrate the effect of changing casting conditions upon the temperature distributions, two typical isothermal fields are reproduced in Fig. 6. These indicate the effect of an increase in casting speed from 3 to 9 in./min., other variables being unchanged.

## V.—DETERMINATION OF COMPLETE TEMPERATURE FIELDS IN INGOTS AND BILLETS

### 1. LIMITATIONS OF PRACTICAL DETERMINATIONS OF TEMPERATURE CONDITIONS

The experimental determination of the temperature conditions in the interior of continuously-cast billets and ingots, although providing information of great value, suffers from severe practical limitations, and it is doubtful whether these can be overcome by refinements of technique. A major difficulty lies in placing the thermocouples accurately in portions of the ingot metal where the temperature conditions are of greatest interest, e.g. in the surface layers of the metal skin. It can be seen from Fig. 7 that the location of thermocouples in appropriate positions in this type of field, where temperature gradients are

particularly steep, calls for a high degree of precision, as any slight misplacement produces erroneous temperature indications quite valueless as experimental results. Very slight shifts of the couple wires due to vibration or similar causes can lead to considerable error.

A second difficulty arises from the fact that although the thermocouple wires may be of very low heat capacity, their presence in the outer layers of the skin can easily upset the sensitive solidification process and result in tears in the metal.

Probably the most serious disadvantage of the thermal-analysis type of experiment is the difficulty

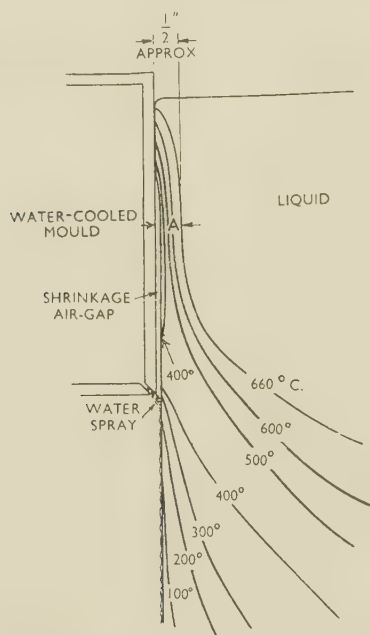


FIG. 7.—Diagram Showing the Difficulty of Locating Thermocouples in the Thin Skin in the Mould.

of casting continuously under extreme conditions. At normal casting speeds many of the effects resulting from various factor-changes may not be apparent, and it becomes essential to employ excessive alterations in the levels of these variables in order to produce measurable results. In most cases these changes cannot be attempted on an actual cast, as they would produce early failure. An illustrative example of this is the investigation of effects produced by extremely short moulds, where experimental tests of this change in practice would be exceedingly difficult. It thus becomes plain that the information obtained from experimental casts requires to be supplemented from other sources.

## 2. MATHEMATICAL METHODS

Mathematical solution of the heat-flow problem, as treated by Carslaw and Jaeger,<sup>22</sup> is a matter of complexity even in bodies of relatively simple geometrical shapes having regular boundary conditions. In the case of most practical problems, the difficulties

become too serious and exact solutions cannot be obtained by present-day methods. This situation has consequently stimulated the development of methods of obtaining approximate solutions. Before describing some of these techniques, it is necessary to examine the differential equations that refer to heat conduction.

In any solid through which there is a three-dimensional flow of heat, the temperature field at the point  $P(x, y, z)$  is a continuous function of  $x$ ,  $y$ , and  $z$  and also of the time  $t$ . From this the heat flow in a homogeneous isotropic solid can be written as:

$$\frac{\partial \phi}{\partial t} = k \left( \frac{\partial^2 \phi}{\partial x^2} + \frac{\partial^2 \phi}{\partial y^2} + \frac{\partial^2 \phi}{\partial z^2} \right) \quad (10)$$

in which  $\phi$  is the value of temperature, and  $k$  represents the diffusivity,  $\frac{K}{\rho c}$ , where  $K$  = thermal conductivity,  $\rho$  = density, and  $c$  = specific heat.

Where steady-state conditions are being examined, the value of  $\frac{\partial \phi}{\partial t}$  becomes zero, and the equation is reduced to the form:

$$\Delta^2 \phi = \left( \frac{\partial^2 \phi}{\partial x^2} + \frac{\partial^2 \phi}{\partial y^2} + \frac{\partial^2 \phi}{\partial z^2} \right) = 0 \quad (11)$$

Heat flow in any solid thus becomes an example of that large class of natural phenomena known as Laplacian or harmonic fields. For any given set of boundary conditions, in whatever medium, there is a unique solution satisfying the Laplace equation. Calculation of this solution from the differential equation above is particularly difficult, and various approximation methods must be employed. These can be classified as: (i) mathematical procedures, e.g. the use of conjugate complex functions, the separation of variables, graphical methods, the use of iteration procedures, and the relaxation process; and (ii) experimental methods, particularly the electrolytic tank, the electrical network analogy, hydraulic analogies, and the use of a stretched rubber membrane. A most valuable discussion of the various methods of field investigation, particularly those used in electron physics but applicable also to problems in many other fields of physics, has been given by Green.<sup>23</sup>

In the work described in the present paper, both mathematical and experimental techniques have been applied with considerable success. Brief accounts will be given of the iteration procedure and the use of the electrical tank analogy.

## 3. LIEBMANN ITERATION TECHNIQUE

The field-plotting procedure, devised by Liebmann<sup>24</sup> in 1918, depends on the property of any two-dimensional harmonic function having its potential at a point equal to the average of that of the four equidistant points at a small distance,  $h$  (Fig. 8). Liebmann's basic method has been very greatly improved by the work of Shortley and Weller,<sup>25</sup> and their co-



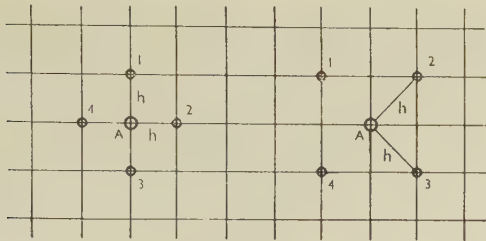


FIG. 8.—Principle of Liebmann Iteration Calculation.

$$\phi_A = \frac{1}{4}(\phi_1 + \phi_2 + \phi_3 + \phi_4)$$

workers,<sup>26</sup> who have evolved a number of special techniques for reducing the amount of arithmetical computation required for solution of the problem. From the field of photoelastic stress analysis, there

possible, estimated values of temperature are inserted at the mesh points. It is useful to sub-divide the whole area as shown, so that the values along rows 1, 3, and 4 give subsidiary boundaries. Fig. 9 (b) shows the scheme when calculation begins.

Starting now at point (a2), the values of the four known surrounding points (a1, b2, a3, &c.) are averaged to give an approximate value for the centre point. The process is repeated for points (b2) and (c2) and so on. A new set of values in this area thus results. The process is repeated in the other areas to give additional values, but care must be taken that calculation follows the same geometrical pattern in each case. Points (a2) and (b2), &c., can now be employed for the calculation of improved values at a1, b1, &c., and also along a3, b3, &c. It is then

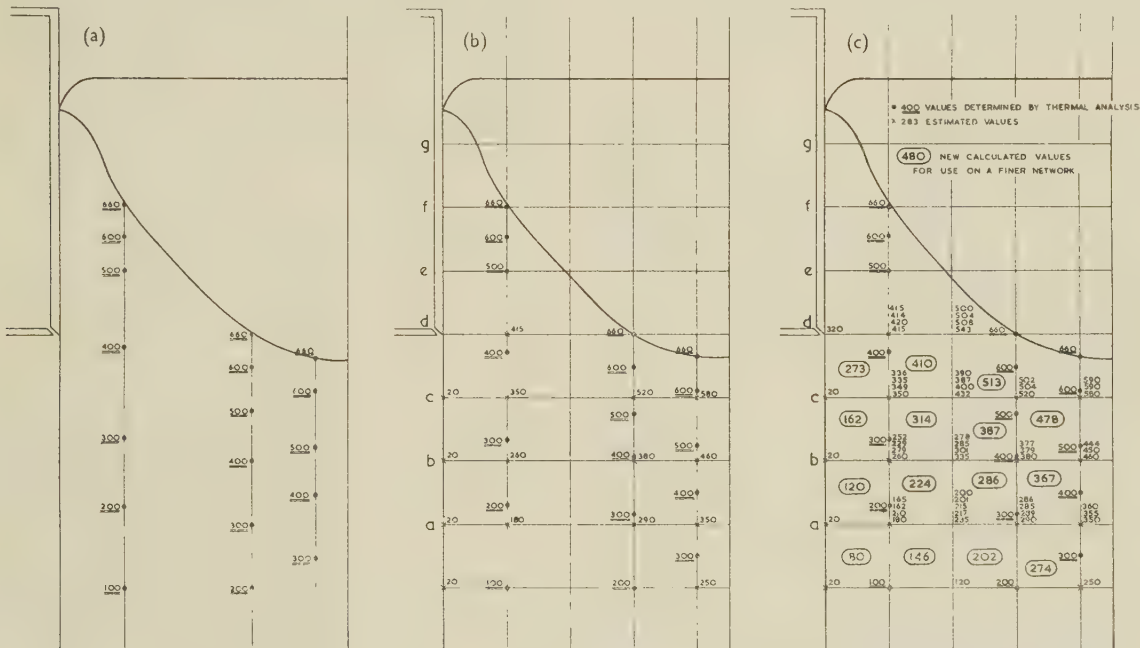


FIG. 9.—Development of an Iteration Calculation.

- (a) Basic information. (b) Mesh inserted and estimated values put in. (c) Completed computation. The ringed numbers give computed values for the centre of each mesh square.

have originated the numerous refinements proposed by Frocht and his associates.<sup>27, 29</sup>

The procedure in solving the field distributions by the iteration method can be illustrated by reference to Fig. 9 (a), which shows the known information for a typical casting condition. The figures given are the temperatures at the points indicated, determined in each case by thermal analysis. Along the field edge the surface temperature is estimated as being that of the spray water impinging on the metal when it emerges from the mould. Along the solidification boundary the temperature is constant, being that of the solid/liquid interface (660° C. in the case of pure aluminium).

A coarse net is drawn over the area to split it into convenient squares, as shown in Fig. 9 (b). Whenever

advisable to proceed with the iteration in a definite geometrical sequence; in Fig. 9 (c) this was a1, b1, c1, d1, e1, d2, c2, b2, a2, a3, b3, c3, c4, b4, a4, a3, a2, a1, and repeat. The way the values converge can be seen from Fig. 9 (c), where the successively corrected values after each traverse are placed one above the other. Traversing is continued until the change of value at each of the points in successive operations is less than the degree of accuracy required for the solution.

For those fields where rapid potential (temperature) changes exist, e.g. at the billet surface, the necessary accuracy can be obtained only by having a fine mesh size. Even halving the mesh size, however, increases the arithmetical work to a formidable extent, the magnitude of which can be appreciated when it is

realized that a very coarse network frequently contains over 100 points, and that six repeated traverses may be required to obtain values of the necessary accuracy.

The need for reducing arithmetical computation has been realized for many years, and numerous

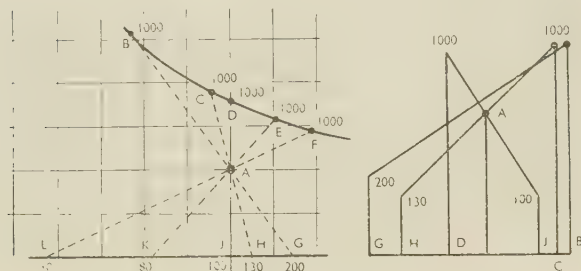


FIG. 10.—Principle of the "Linear Rosette".

simplifications, intended to lead to early convergence of the results, have been developed. Some examples of these important methods are the block formulæ of Shortley and Weller,<sup>25, 26</sup> and the linear rosette evolved by Frocht.<sup>28, 29</sup> Some formulæ, which allow calculation of the final accurate values without the necessity of iteration, have been proposed by Moskovitz,<sup>30</sup> but these are difficult to apply in the examination of complex fields. In the latter case, iteration appears to be less complex than the use of the special formulæ.

The linear rosette, originally suggested for calculating starting values in the analysis of photoelastic fringe patterns, has been found to be of considerable value in working out temperature distributions. The method of use can be understood by reference to Fig. 10. The line *BCDEF* represents a boundary having a uniform potential of 1000 units, while boundary *LKJHG* has a potential gradient along its length with the values indicated at the marked points. It is required to ascertain an approximate value for the potential at *A* in order to start the iteration procedure.

The value at *A* can be estimated in the case of line *BAG* by measuring the distances *BG* and *AG* and calculating as follows:

$$\phi_A \simeq 200 + \left[ \frac{AG}{BG} \times (1000 - 200) \right]$$

$$\text{Similarly, } \phi_A \simeq 100 + \left[ \frac{AJ}{DJ} \times (1000 - 100) \right]$$

$$\text{and } \phi_A \simeq 30 + \left[ \frac{AL}{FL} \times (1000 - 30) \right]$$

It is advisable to obtain at least four values for  $\phi_A$  from rosette lines arranged as shown. The mean of these values can be a very close approximation to the correct figure, particularly where a large number of rosette lines are employed for the calculation. High accuracy is also obtained when the point *A* lies relatively close to the high-potential boundary. By

using a number of linear rosettes at suitable points in the field being examined, particularly good values of potential can be estimated at a few key points before the iteration process is started. Accurate final values for most points in the field can then normally be obtained after only two traverses.

A difficulty with the iteration methods of solving partial differential equations lies in the fact that unknown boundary conditions cannot normally be determined, the only exception being values for potential along the axis of an axi-symmetric field. That it is of some importance to be able to calculate unknown values in the system under consideration can be seen from Fig. 11, where known values of temperature have been inserted. The surface temperature of the billet or ingot inside the mould is not known, and it is therefore difficult to calculate, by the conventional techniques, a temperature distribution in the solid metal which is first solidified (shown shaded in Fig. 11).

Evaluation of the potentials in those cases where the boundary values are not known in their entirety has been discussed by Kuo-Chu Ho and Moon,<sup>31</sup>

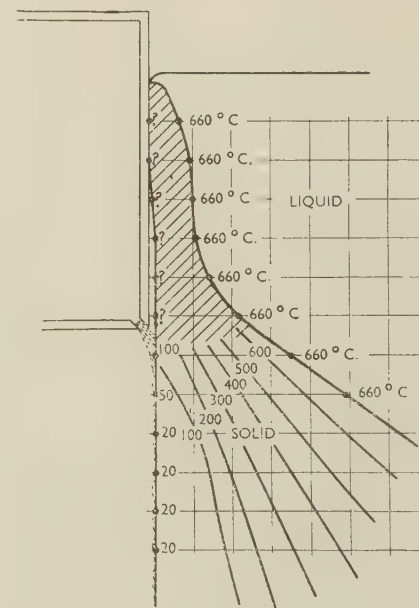


FIG. 11.—Diagram Showing Area Where Temperature Conditions are Not Known.

who have proposed a mathematical method which does not employ the iteration technique. Although its use gives the required values to a high degree of accuracy, the extra labour involved seems unnecessary in this problem, as reasonably good results can be obtained from an extension of the normal iteration procedure by calculating values forward into the unknown field. Useful values suitable for studies of temperature conditions in the solidified metal can be obtained in this way.



## 4. THE ELECTRICAL TANK ANALOGUE

The fact that the Laplace equation which defines the steady-state flow of heat in a conductor can also define the electrical potential in a dielectric or current field can now be discussed in fuller detail.

Heat transmission at any point under steady-state conditions can be expressed by the following:

$$\frac{dQ}{dA} = -k \text{ grad } \phi \quad . \quad . \quad . \quad (12)$$

where  $dQ$  is the amount of heat passing in unit time over an element of surface  $dA$ , at right angles to the direction of the temperature gradient,  $\phi$  is the temperature of the point, and  $k$  is the thermal conductivity of the medium. The value of  $\phi$  is a harmonic function of the points in the field and is defined by the Laplace equation.

Examining now the expression for electrical current flow, it is found that:

$$\frac{dQ}{dA} = -\frac{1}{\rho} \text{ grad } V \quad . \quad . \quad . \quad (13)$$

in which  $\frac{dQ}{dA}$  represents the current density at a point,

$\rho$  is the resistivity of the medium, and  $V$  is the potential at the point considered. The similarity between the two expressions is obvious, it being seen that there

is correspondence between  $\frac{dQ}{dA}$  (thermal) and  $\frac{dQ}{dA}$

(electrical), between  $Q$  and  $V$  and between  $k$  and  $\frac{1}{\rho}$ .

The simple thermal problem can thus be simulated by an electrical system. In the present case the temperature  $\phi$  is made to correspond with the potential

$V$ , and the value of  $\frac{dQ}{dA}$  with the current  $I$ . When

required, zones of different thermal conductivity can be represented by differences in resistivity in the electric model.

The use of a flat metallic sheet as a conductor representing a cross-section of the thermal model is not normally feasible, as extremely high currents will be required to give any measurable voltages on its surface. An exception to this will be described at a later stage, but for the majority of work a liquid conductor is employed. This allows 20–30 V., or even more, to be applied from a source producing only 2–5 W.

The electrical tank analogue, although traceable in principle to the early work of Kirchoff, has been employed widely in many branches of physics and engineering since about 1910. That its use has extended into many fields is plain from the diversity of applications described by Dadda in a comprehensive survey of the technique.<sup>32</sup> A great deal of information on the development and improvement of the technique, particularly in aerodynamic and hydrodynamic problems can be obtained from the papers of Peres<sup>33</sup> and Malavard,<sup>34</sup> while the work of Dadda in the electrical-engineering field is also of value. Little

research on heat transfer<sup>35</sup> appears to have been done by means of the tank analogy, probably because there are relatively few examples of steady-state heat transfer. For the present research it has, therefore, been necessary to study the use of the analogy in the various engineering fields.

The apparatus used is illustrated in Fig. 12, in which the thermal and electrical systems have been drawn side by side. In addition, the photographs of the equipment in Figs. 20 and 21 (Plates LVIII and LIX) show the arrangement of the traversing mechanism, electrode system, plotting table, &c.

The wedge-shaped shallow tank, built of an insulating material (in the present case a cast paraffin-wax tray 4 ft. 6 in. long  $\times$  2 ft. wide  $\times$  5 in. deep along one edge) represents a section of a cylinder between two median planes forming an angle of a few degrees. The electrolyte level in the tank is adjusted to rise

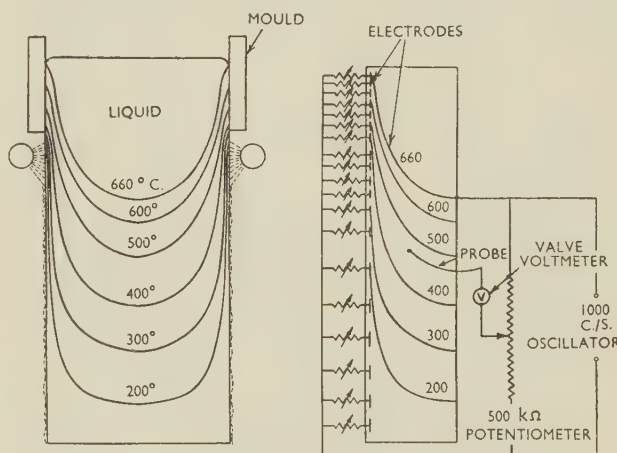


FIG. 12.—Basic Principle of Electrical Tank Analogue.

to a shore line marked on the bottom when it is equivalent to the billet radius represented at the appropriate magnification. Normal tap-water has been found satisfactory as the conductor in the tank.

The shape and position of the solidification front, obtained by the various methods described in Section III, is represented in the analogue by a shaped electrode shown as a continuous line in Fig. 12, but actually made up of adjustable electrode wires visible in the photograph. These are maintained at a potential equivalent to 660°C. The electrodes representing the cooling surface of the billet are arranged along the side of the tank, being connected, via a bank of adjustable resistors, to the supply point at zero potential. The values of the various resistances are adjusted to give currents in each electrode circuit equivalent to the heat flow in zones of corresponding size in the mould and sub-mould cooling areas. The electrodes in all cases are copper wires, or strips coated with a colloidal graphite film for reducing the contact resistance and polarization effects.

As direct current cannot be used to energize the

tank because of the polarization effects then present at the electrodes, the power supply is taken from a 1000-c./s. oscillator capable of delivering 5 W. at 70 V., the normal potential difference across the tank, however, being 15 V. The oscillator output is fed to the electrode system via screened cable in order

corporate a lamp to project an illuminated image of cross wires on to the plotting screen on the plate-glass tank-cover. The probe-traversing mechanism gives movement in two directions at right angles and allows scanning of the whole of the water surface in the tank. By using this method of indicating the

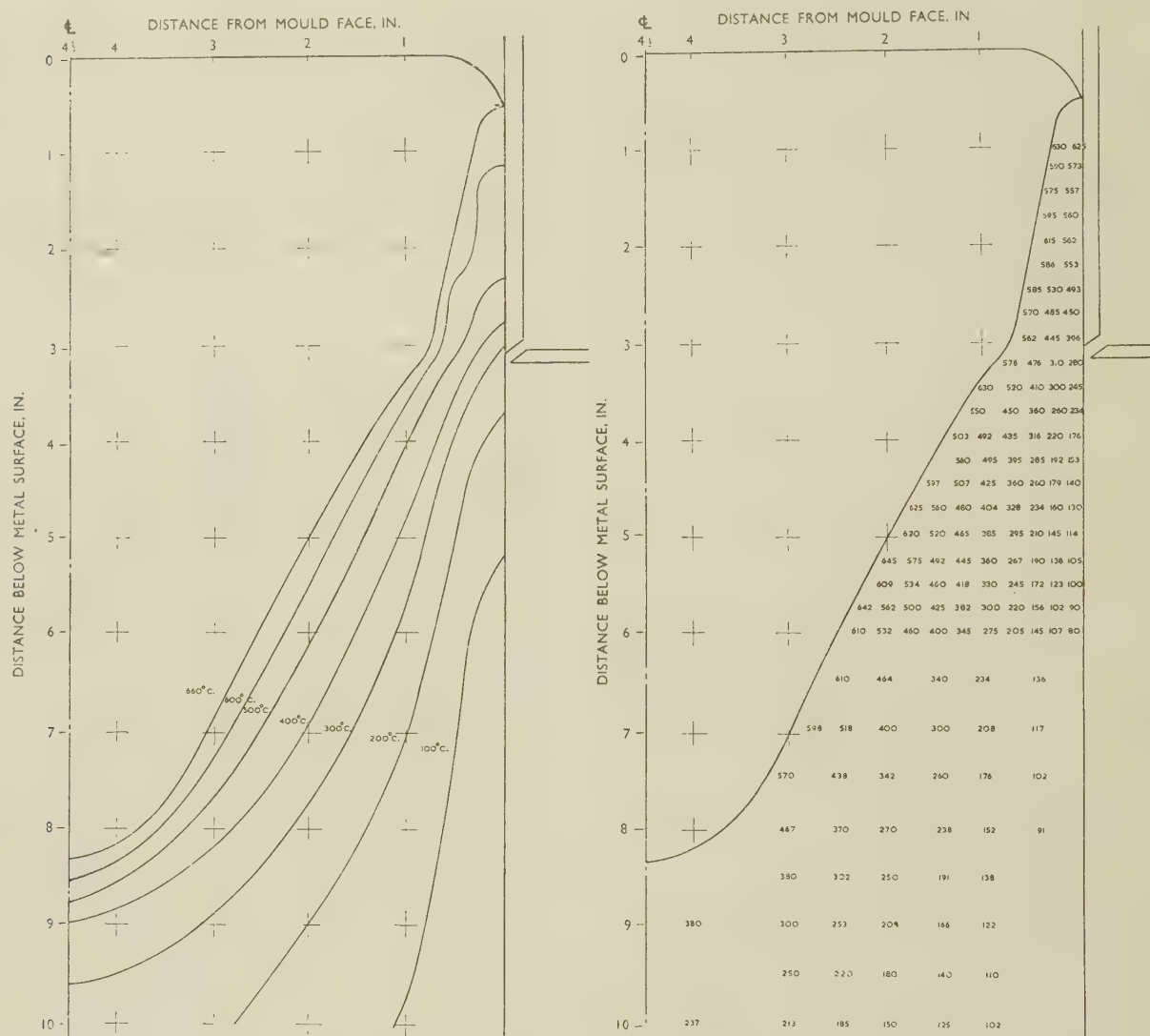


FIG. 13.—Temperature Fields Plotted in the Tank Analogue.

(a) Determination of isothermals. (b) Measurement of temperatures at fixed points.

to minimize mains pick-up. A precision potentiometer of high resistance, connected across the main tank supply, serves for measurement or for setting the potential values.

The probe, for measuring the voltage at all points in the tank, consists of a steel needle mounted in a chuck in order to dip 3 mm. below the water surface, and connected by a screened cable to the moving arm of the potentiometer. The probe holder in-

probe position, there are negligible errors due to backlash in the traversing system, an advantage compensating fully for the slight difficulty experienced in observing the probe position as it moves between the electrodes.

Indication of potentiometer balance has been obtained by using earphones, and also a cathode-ray tube, but the present work has shown that the use of a special valve voltmeter having a very high input



impedance gives results of the greatest precision. The instrument employed possesses ranges of 0–50 V., 0–5 V., 0–1 V., and 0–0.1 V. The probe lead is in series with a 5:1 step-up transformer to amplify the out-of-balance voltage before application to the valve-voltmeter circuit. Final balancing of the potentiometer is done with the voltmeter set to the most sensitive range.

The equipment is operated by moving the probe into close contact with the curved electrode and arranging its position to be on the line joining two of the electrode wires. The resulting points when marked on the plotting screen are joined up by pencilled lines to give a very close approximation to the shape and position of the curved electrode. At the same time the probe potential is read from the potentiometer and plotted on squared paper to give a potentiometer-reading/potential-value calibration curve. The probe needle is now brought into contact with the individual electrodes along the edge of the tank to mark the position of the line representing the billet surface. By marking the positions of these boundaries on the plotting table, limits can be set on the area to be scanned by the probe, this precaution being of special value in cases where the electrical model is made up of complicated electrode shapes.

There are two basic methods of proceeding with the field plotting; the potentiometer can be set to a definite potential value from the calibration curve and the probe carriage moved to find positions where the voltmeter gives null readings, or the probe can be moved to definite positions in the tank, e.g. to special mesh points, and the potentiometer adjusted each time to obtain the actual potential values. Each method has its advantages, the former allowing rapid plotting of isothermal positions, while the latter can give values for potential in areas where the slight temperature gradients make isotherm plotting difficult. The second method is particularly useful in providing figures for checking the results of iteration calculations. An example of a typical potential field plotted by both these procedures is given in Fig. 13.

The equipment described is large enough to allow the temperature fields in 9-in.-dia. billets to be studied as complete radial sections at magnifications up to  $\times 4$ , but special areas of interest can be modelled at a considerably larger magnification if required. For these experiments the potential conditions at the boundaries of the appropriate area must be defined with some degree of accuracy, but the results give values for the interior conditions with considerable precision.

A valuable feature of the electrical tank is the ease with which changes in conditions can be simulated, e.g. the overall effect of changing the mould length or the heat-transfer conditions can be introduced by altering the value of a few series resistances. Experience has shown that by using the electrical tank a temperature field of useful accuracy can be plotted

in about 3 hr., which compares with about 120 man-hr. required for a thermal analysis of one set of conditions in continuous casting.

Experiments with the electrical-tank technique for studying the casting process are in a very early stage, but work now in progress is intended to simulate the effects of superheat, latent heat, and also of the solidification temperature range in the case of alloy systems. Electrical arrangements for this purpose, when incorporated, should allow investigation of the complete casting process, but at the price of introducing some complexity into the equipment.

The electrical tank analogue can provide other information apart from direct potential (temperature) values in the interior of the metal. The potential at each electrode at the edge of the tank gives very good values for the temperature at points on the billet surface, while the current in each electrode circuit is equivalent to the heat-transfer rate at that area on the surface of the billet or ingot. An addi-

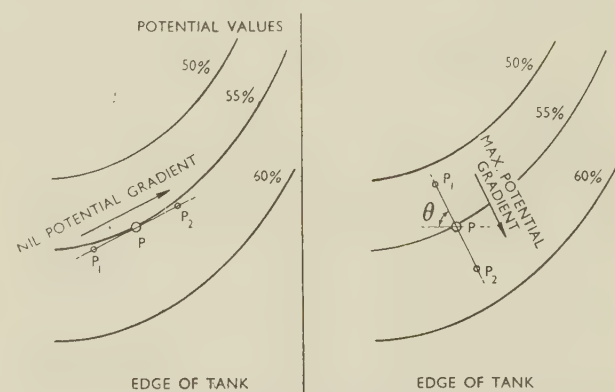


FIG. 14.—Principle of the Triple Probe for Gradient Measurement.

tional technique of value is the determination of potential gradients within the electrolyte. The method, developed mainly because of its importance in electron optics, has been discussed by Dadda,<sup>36</sup> Malavard,<sup>37</sup> and Sander and Yates,<sup>38</sup> who have each proposed modifications of the basic multiple-probe technique.

In principle the single probe is replaced by a double or triple probe having points a known fixed distance apart. The electrical circuits are arranged to measure the potential difference between the probe points in addition to determining the potential level of the probe unit within the tank. After the probe assembly has been moved into a position where the main point  $P$  is at a position of known potential (Fig. 14), the unit is rotated around  $P$  as a centre. The outer points,  $p_1$  and  $p_2$ , can take up the positions as shown where both points lie, together with  $P$ , on the isothermal at that point, or they can be turned to the other position where the line,  $p_1Pp_2$ , is normal to the isothermal. For this position there is maximum

potential difference between  $p_1$  and  $p_2$ , and the value of the gradient is given by:

$$\frac{\phi_{p_1} - \phi_{p_2}}{p_1 - p_2},$$

where  $\phi_{p_1} - \phi_{p_2}$  represents the potential difference. The direction of the maximum potential gradient gives the line of current flow which has an angle  $\theta$  with the axis of the model. Although from this it is possible to derive the vectors of radial and longitudinal heat flow, the technique is also useful in indicating the direction of crystal growth. In addition to this, a complete knowledge of the temperature gradients appears to be of the greatest importance in studying stress distributions in ingots and billets.

## 5. CONDUCTING-PAPER FIELD PLOTTING

A recent development of considerable importance in heat-flow studies is the use of electrically conducting paper for field plotting. The technique, which has been described briefly by Malavard,<sup>39</sup> consists of cutting a sheet of Teledeltos paper to the shape of the field under study and joining electrodes to it, at the appropriate points, by means of conducting silver paint. Direct current is employed with an ordinary pencil acting as the probe, having the lead connected in series with a microammeter and the potentiometer. Various suggestions have been made for improving the basic technique by forming boundary resistances of known values integrally with the conducting paper. Tests using this method have given results of considerable promise, while the convenience of the technique is a particular advantage; the apparatus is simple, there are no complicating phase or polarization effects, and the speed of operation can be very high. It is, however, at present applicable only to two-dimensional problems.

## VI.—DETERMINATION OF HEAT-TRANSFER CONDITIONS

During the operation of the continuous-casting process under works conditions, cases frequently arise where successful casting of an alloy mass becomes possible only by alteration of the cooling conditions, e.g. the difference in practice between aluminium and copper moulds and the reduction of cooling-water volume, the variation in both cases being mainly change of heat-transfer conditions. The changes introduced are, however, completely empirical, owing to the lack of data on the effects of the heat-transfer variable in the casting process. No reference can be traced in the literature to any determinations of heat transfer in the continuous casting of aluminium alloys.

At first sight it would appear that the ideal condition for casting would be a very high heat-transfer rate in the mould, to give very rapid chilling and solidification, followed by a moderate heat removal in a longitudinal direction from the billet or ingot.

The characteristics of metals prevent these desirable features being realized, as the diffusivity of the metal imparts a finite limit to the rate of heat removal. The mould, by its physical form, combined with the solidification and cooling contraction of the metal, produces an air gap with a consequent severe reduction in heat transfer. Depending on various other factors, this can mean a temporary cessation of skin thickening or even partial remelting of the previously solidified skin.

These effects, of such importance in the casting process, require investigation in order to provide information for mould design and for determination of efficient operating procedures.

Investigation of heat-transfer conditions within the mould itself presents no real difficulty, but this does not apply to the sub-mould cooling area, particularly when water sprays are employed, as the problem is then one of spray-quenching. Little work has been done to evaluate the actual cooling efficiency of sprays of various types, and the papers by Wallace and Manes,<sup>40</sup> and Wallace and Newton,<sup>41</sup> outline what appears to be the only metallurgical investigation of the subject. A comprehensive research programme is now in operation, however, at Columbia University.<sup>42</sup>

## 1. EXPERIMENTAL METHODS OF HEAT-TRANSFER DETERMINATION

Practical methods of obtaining the required heat-transfer data during casting operations have been used by numerous investigators, usually as part of a study of the heating-up of sand or chill moulds. The work of Savage and Fowler<sup>21</sup> on temperature cycles experienced by ingot moulds in steel works included an investigation of the heat loss from the solidifying ingot, and also the heat-transfer conditions in the ingot and mould system as a function of its position in the casting pit. In this work thermocouples were inserted at known positions in the mould walls, and from the resulting readings the temperature gradients and then the rates of heat flow were calculated. By taking into account the heat loss from the mould surface the total heat loss from the steel was obtained in terms of time from the start of teeming.

The only published information on heat-transfer determinations in continuous casting appears in the paper by Krainer and Tarmann,<sup>9</sup> in which details are given of the results obtained during the casting of steel. The steel mould in their experiments served as one wire of a thermocouple system, the other element being fine Constantan wires welded into small cavities in the wall. In addition, the temperature rise of the cooling water was determined throughout the experiment. Very valuable practical information was obtained from this arrangement.

In the present work it was not possible to use the aluminium mould as one element of a thermocouple, owing to its poor thermoelectric characteristics against other metals. To overcome this difficulty, small



thermocouples were made up for insertion into the mould wall, the plugs, shown in Fig. 15, consisting of 2 B.A. aluminium bolts. Two sets of grooves are cut in the bolts as shown, and a  $\frac{1}{16}$ -in. hole drilled

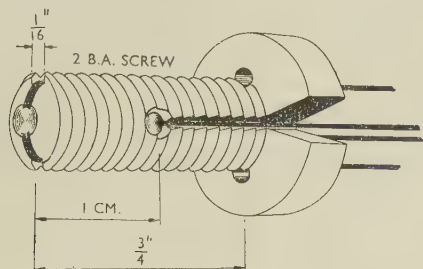


FIG. 15.—Thermocouple Plugs.

with its centre exactly 1 cm. from the screwed end of the rod. The Chromel/Alumel couple wires, each of 36 S.W.G., welded to form the couple, are threaded into position with the junction in the centre hole of the plug, the two wires and the junction being held in position by means of Quigley's cement. The second couple is arranged over the end of the rod with the junction located in a slight depression. Wires leaving the plug are insulated with Durotube sleeving. The plugs are screwed into the mould wall until the projecting end of the first junction lies flush with the wall. In some cases it is possible to employ a couple projecting very slightly into the mould cavity, when some indication of billet surface temperature inside the mould can be obtained. This practice cannot, however, be recommended owing to the tendency for the projecting junction to tear the thin solidified metal skin.

In order to cover the full used length of the mould and yet interfere as little as possible with cooling conditions, the plugs are arranged in a spiral around the outer face, each plug being 1 cm. below its neighbour and also 5 cm. apart along the circumference.

The wires from the plugs are brought out to a multi-position switch which connects each couple in turn to the temperature indicator. During the casting operation, the complete set of couples is normally scanned 3 or 4 times.

The considerable scatter in the resulting temperature measurements due to fluctuations of the metal level may be rendered more serious by the unknown movements, inside the mould, of the newly solidified skin after formation of the air gap. Krainer and Tarmann<sup>9</sup> have mentioned a scatter of up to 10% in experimental results due to level changes of 3–5 cm. Although in the present work changes of level were controlled to  $\pm \frac{1}{4}$  in., the resulting errors may be quite serious. Modifications now being made to the apparatus, in order to reduce the fluctuations to less than  $\pm \frac{1}{16}$  in. and to eradicate any sudden surges of flow, are expected to improve the heat-transfer results appreciably.

The thermocouple plugs produce better results than sectional moulds, and an added advantage—the mould-cooling conditions are undisturbed. A sectional mould, in which the rise of temperature of the water in each zone is measured, gives integrated values only for heat transfer over the zone area, indicating, in this way, values considerably lower than the maximum figures.

## 2. DERIVATION OF HEAT-TRANSFER RESULTS

Mathematical methods are available for calculating heat-transfer rates for hot ingots contained in cold moulds, but the uncertainties regarding the high-temperature properties of each metal and of the exact cooling mechanism can introduce serious errors.

When fairly complete temperature conditions inside the ingot or billet are known, there is little difficulty in obtaining heat-transfer rates from the known thermal gradients. Temperature fields plotted either from the iteration procedure or on the electrical

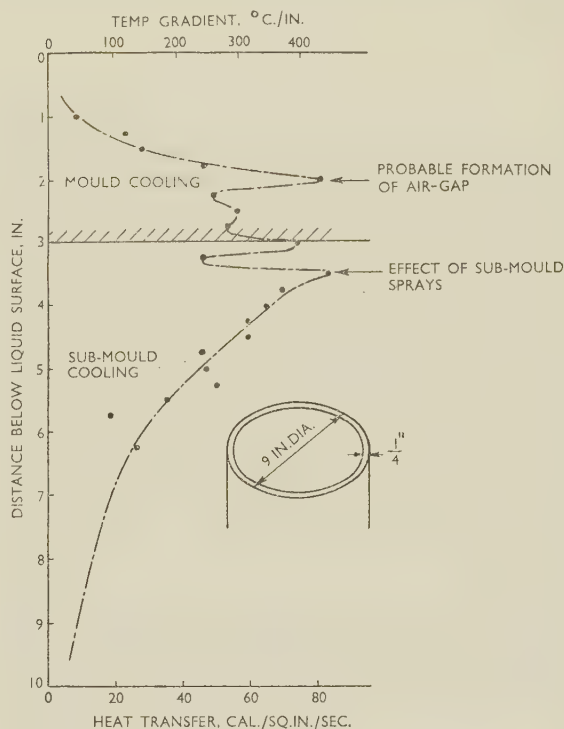


FIG. 16.—Curve Showing Temperature Gradient and Heat Transfer in Outer  $\frac{1}{4}$  in. Skin of Billet as a Function of Distance from the Liquid Surface. Heat transfer is calculated for the  $\frac{1}{4}$ -in.-thick skin of a 9-in.-dia. billet.

tank analogue give the required information in a readily usable form. Taking Fig. 13 as an example, the temperature gradient in the outer  $\frac{1}{4}$ -in. skin of the billet can be obtained directly from the skin temperatures and the values existing  $\frac{1}{4}$  in. inside the metal. From the expression:

$$\frac{dQ}{dA} = -k \text{ grad } \phi,$$

the rate of heat flow is a product of the thermal conductivity and the temperature gradients. Although the mean temperature level influences the value of the thermal conductivity, no very great error is introduced by regarding the latter as a constant,  $k = 0.5$  cal./sec./°C./cm. The resulting heat-transfer rates for a typical field are shown in Fig. 16.

In the electrical analogue, determination of the potential gradients by means of the multiple probe is a simple technique, but the gradient must be measured normally to the model edge representing the billet surface, as surface heat transfer takes no account of longitudinal heat flow. When the analogue is connected up as shown in Fig. 12, a useful estimate of the heat-transfer conditions below the mould can be obtained from measurements of the current flowing in each electrode circuit. For electrodes of equal area the electrode currents are proportional to the heat transfer at the equivalent point on the billet or ingot.

## VII.—CONCLUSIONS

The apparatus and techniques described in this paper have been developed for studying various physical aspects of the continuous-casting process. Although they emphasize examination of the thermal problems, it is not implied that these are the only ones requiring study. Other important features of the process are the stress conditions in the ingots and billets resulting from the steep thermal gradients, the mode of distribution of the incoming metal in the liquid pool, and—although it does not appear to be of extreme importance in light-alloy casting—the friction between the solidified skin and the mould wall. The last factor assumes considerable importance in the casting of higher-melting-point metals, where the formation of the air gap does not result in such an appreciable reduction of friction as in the case of aluminium alloys.

The effect of physical variables on the metallurgical features has not been explored to any extent and many unusual effects, e.g. the unusual periodicity of structure mentioned by the author,<sup>43</sup> cannot at present be explained satisfactorily in terms of heat flow. Recent work by Siebel, Altenpohl, and Cohen,<sup>44</sup> which discusses the banding effect common on most aluminium alloy ingot and billet surfaces, proposes an explanation, in terms of heat-transfer effects, that can probably be extended to describe the periodic variations in grain structure.

From recent metallurgical work certain evidence questions the validity of the steady-state assumption in the continuous-casting process, this applying particularly to mould solidification. For the major portion of the solidification process, which occurs below the mould as a result of the spray cooling or immersion in the water bath, no such doubts exist.

In view of this uncertainty regarding the *state* of the process, it may be asked whether there is justification for using the various techniques described. By regarding the problem as one of steady state, the information obtained shows the average thermal conditions which can form the basis for closer study of detailed conditions at various times and positions. This method is being used to study the solidification rates of  $20 \times 5$ -in. ingots. The sump contours show some lack of symmetry, but the mean values give smooth even curves easily compared one with the other. Deviations of the actual contours from the mean curve then appear to throw light on the subsidiary movements of the metal in the mould while solidification is proceeding. This work is pursued to elucidate the manner in which the metal gives up its contained heat after air-gap formation.

The various mathematical expressions for the solidification behaviour of the metal do not appear to be valid in many practical cases. If it becomes possible to propose corrections to the solidification equations, it must be borne in mind that only the mean conditions may then be defined. These mean conditions, under a steady-state régime, are those given by the various methods of solution of the Laplace equation.

The dip-stick and tracer techniques for delineation of the sump contour can easily be applied as control tests. The radioactive-tracer method, although developed for a restricted purpose, is now being extended to investigate the liquid-metal flow through various types of baffles. In addition, it can probably be employed for studying the solidification rates and metal behaviour in static castings.

The equipment described in this paper for the measurement of temperature in solidifying billets and ingots would appear to be useful in other fields of study, particularly where rapid temperature changes make the use of conventional recorders impossible. The thermal-analysis experiments, although subject to very many practical errors, give results that act as checks on the figures obtained from arithmetical computation and the analogue techniques.

The descriptions given of the Liebmann iteration technique and of the electrical tank will, it is hoped, stimulate use of these methods in other metallurgical researches. These two methods of solving (approximately) the Laplacian equation can be complementary to the well-known "relaxation" techniques, but do not suffer from the latter's disadvantage of being sometimes difficult to apply.

The work on heat-transfer conditions aims at obtaining information likely to be of value in mould design and in arranging cooling methods to give less steep temperature gradients in the billet or ingot while still producing desirable metallurgical structures.

Increased research into the fundamentals of the complex metallurgical problem of continuous casting is urgently required, particularly in view of its increasing importance in both non-ferrous and ferrous fields.



# ACKNOWLEDGEMENTS

In expressing indebtedness to the Directors of Aluminium Laboratories, Ltd., for permission to publish this paper, the author also records his appreciation of their interest and encouragement in work involving the application of a number of unfamiliar physical techniques. The assistance of very many of the author's colleagues in the Metallurgy and Physics Divisions of Aluminium Laboratories, Ltd., has resulted in the successful introduction and operation of these techniques. In this connection, special thanks are due to Mr. H. W. Taylor, who was responsible for the design and construction of the

temperature recorder, and to Mr. R. W. Gilkes, who arranged all the actual experimental casts.

Information on apparatus and techniques has been most readily given by numerous firms and individuals, and the author thanks all those with whom he has had fruitful discussions, particularly, Professor A. Preece, King's College, Newcastle-on-Tyne; Mr. E. Markland, Nottingham University; Mr. E. R. Hartill, Metropolitan-Vickers Electrical, Co., Ltd., Manchester; Mr. D. McDonald, British Thomson-Houston, Co., Ltd., Rugby; Mr. J. L. Putman, Atomic Energy Research Establishment, Harwell; and Dr. L. Dadda, Milan Polytechnic, Milan.

# REFERENCES

1. E. Scheuer, *J. Inst. Metals*, 1949-50, **76**, 103.
2. W. Roth, *Aluminium*, 1943, **25**, 283.
3. A. N. Tikhonov and E. G. Shvidkovsky, *Zhur. Tekhn. Fiziki*, 1947, **17**, 161.
4. J. Bingel, *Arch. Metallkunde*, 1949, **3**, 174.
5. W. M. Doyle, *Metal Ind.*, 1945, **66**, 370, 390.
6. J. Héréguel, *Rev. Mét.*, 1949, **46**, 309.
7. J. Héréguel, *Metal Treatment*, 1949, **16**, 133.
8. B. H. C. Waters, *Metal Treatment*, 1952, **19**, (84), 379; (85), 433; (86), 474; (87), 527; 1953, **20**, (88), 3; (89), 79; (90), 103.
9. H. Krainer and B. Tarmann, *Stahl u. Eisen*, 1949, **69**, 813; *Metal Treatment*, 1950, **17**, 3.
10. K. G. Speith and A. Bungeroth, *Stahl u. Eisen*, 1952, **72**, 869.
11. W. B. Pierce, *Steel*, 1953, **133**, (15), 256.
12. R. W. Ruddle, "The Solidification of Castings. A Review of the Literature". (Inst. Metals, Monograph Rep. Series No. 7.) 1950: London (Institute of Metals).
13. W. S. Pellini, *Amer. Foundryman*, 1953, **23**, (2), 69; (3), 59.
14. J. L. Putman, *J. Inst. Metals*, 1953-54, **82**, 414.
15. R. W. Ruddle, *ibid.*, 1950, **77**, 1.
16. H. F. Bishop, F. A. Brandt, and W. S. Pellini, *Trans. Amer. Found. Soc.*, 1951, **59**, 435.
17. R. P. Dunphy and W. S. Pellini, *ibid.*, 1951, **59**, 425.
18. H. Staiger and E. Neher, *Jahrb. deut. Luftfahrtforschung*, 1940, (II), 449.
19. J. D. Watson and H. E. Dixon, *J. Sci. Instruments*, 1949, **26**, 17.
20. R. T. Fowler, *Instrument Practice*, 1952, **6**, 233.
21. L. H. W. Savage and R. T. Fowler, *J. Iron Steel Inst.*, 1953, **173**, 119.
22. H. S. Carslaw and J. C. Jaeger, "The Conduction of Heat in Solids". 1947: Oxford (Clarendon Press).
23. P. E. Green, Jr., *Eng. School Bull. N. Carolina State Coll.*, 1949, (45).
24. H. Liebmman, *Sitz. ber. math.-physikal. Klasse K. Bayer. Akad. Wiss. München*, 1918, 385.
25. G. H. Shortley and R. Weller, *J. Appl. Physics*, 1938, **9**, 334.
26. G. H. Shortley, R. Weller, P. Darby, and E. G. Gamble, *ibid.*, 1947, **18**, 116.
27. M. M. Frocht, *ibid.*, 1946, **17**, 730.
28. M. M. Frocht, "Photoelasticity", Vol. 2, p. 239. 1948: New York (John Wiley and Sons, Inc.); London (Chapman and Hall, Ltd.).
29. M. M. Frocht and M. M. Leven, *J. Appl. Physics*, 1941, **12**, 596.
30. D. Moskovitz, *Quart. Appl. Math.*, 1944, **2**, 148.
31. Kuo-Chu Ho and R. J. Moon, *J. Appl. Physics*, 1953, **24**, 1186.
32. L. Dadda, *Energia Elett.*, 1951, **28**, 23.
33. J. Peres, *Proc. 5th Internat. Congress Appl. Mechanics, Harvard*, 1939, 9.
34. L. Malavard, *J. Roy. Aeronaut. Soc.*, 1947, **51**, 739.
35. L. Malavard and J. Miroux, *Proc. IVe Congrès Internat. Chauffage Indust., Paris*, 1952, Group I, Sect. 13, Paper No. 82.
36. L. Dadda, *Energia Elett.*, 1949, **26**, 469.
37. G. L. Malavard, "Techniques Générales du Laboratoire de Physique", Vol. 2, p. 223. 1950: Paris (Editions du C.N.R.S.).
38. K. F. Sander and J. G. Yates, *Proc. Inst. Elect. Eng.*, 1953, [II], **100**, (74), 167.
39. L. Malavard, *Recherche aéronaut.*, 1951, (20), 61.
40. W. P. Wallace and C. E. Manes, *Iron Age*, 1952, **169**, (5), 112.
41. W. P. Wallace and T. L. Newton, *ibid.*, 1952, **169**, (15), 121.
42. V. Paschkis, *Metal Progress*, 1952, **62**, (6), 93.
43. D. M. Lewis, *J. Inst. Metals*, 1952-53, **81**, (12), 712 (discussion).
44. G. Siebel, D. Altenpohl, and H. M. Cohen, *Z. Metallkunde*, 1953, **44**, (5), 173.
45. H. Klein, *Giesserei (Techn.-Wiss. Beihefte)*, 1953, (10), 441.

# 1532 THE USE OF AUTORADIOGRAPHY FOR FINDING THE SOLIDIFICATION BOUNDARY IN CONTINUOUSLY CAST ALUMINIUM \*

By J. L. PUTMAN,† M.A.

## SYNOPSIS

A brief account is given of experimental work carried out to determine whether  $\text{Au}^{198}$  and  $\text{Cu}^{64}$  are suitable for use as radioactive tracers for the delineation of the liquid/solid interface in continuously cast aluminium billets. Very good results were obtained with the gold additions.

A very small amount of a non-active gold alloy is added to the incoming stream to the billet, and the gold is distributed throughout the liquid pool. A suitable section of the solid billet is prepared and irradiated in a neutron flux. After a suitable decay period has elapsed, autoradiographs are produced from the polished surface.

Unusual striations on the autoradiograph appear to be due to some mixing phenomenon not yet explained.

## I.—INTRODUCTION

IN the continuous casting of aluminium, the cooling conditions in an ingot can be calculated only if the shape of the solidification boundary is accurately known. The approximate shape of the boundary can be calculated, but the results are not sufficiently reliable for the cooling conditions in the interior of the ingot to be deduced.

The shape of the boundary may also be determined by experiment, the stream of molten aluminium entering the crater being replaced, at a late stage, by a copper-bearing hardener-alloy. The copper is distributed in the molten metal around the solidification boundary, and can subsequently be detected in a section of the cast ingot by differential etching. Unfortunately, it is necessary to raise the copper concentration in the liquid pool to about 4%. This is sufficient to affect the metallurgical properties of the aluminium cast after the copper addition, and may also affect the cooling conditions to an extent that will vitiate the experiment.

## II.—PRINCIPLES OF THE RADIOACTIVE METHOD

It was, therefore, proposed that the solidification boundary should be determined by the addition of a contaminant which could be raised to a high level of radioactivity by irradiation in an atomic pile, and which could afterwards be detected photographically in the ingot. The great sensitivity of detection available with such methods was expected to enable very much smaller quantities of contaminant to be used.

Two experimental methods were considered:

(1) To add to the molten aluminium a contaminant

already made radioactive; this method suffers from the disadvantage that handling precautions are necessary when adding the radioactive material to the molten stream of aluminium.

(2) To add the contaminant as ordinary inactive material and subsequently to irradiate portions of the cast ingot in the pile to induce activity in the contaminant after casting. This method has the advantage that it does not involve the handling of radioactive material in the casting operation, but it does slightly increase the difficulties of pile irradiation, since much larger samples have to be irradiated. The second method also relies on the possibility of obtaining a much higher radioactivity in the contaminant material than in the aluminium ingot, or in any impurities in the ingot. It was decided, however, to use the second method in order to avoid radioactivity in the casting operation.

## III.—PRELIMINARY TESTS

To establish the best contaminant for use as a tracer material and to find the best conditions for irradiation and exposure to a photographic plate, two samples were made up; each consisted of a circular disc of aluminium,  $\frac{1}{2}$  in. in dia. and  $\frac{1}{2}$  in. thick, surrounded by a fitting annulus of outside dia.  $\frac{7}{8}$  in., composed of the same type of aluminium to which a known percentage of contaminant had been added in the melt.

The aluminium forming the disc material contained: copper 0.008, magnesium 0.001–0.003, silicon 0.06–0.07, iron 0.24–0.28, titanium 0.007%, manganese traces. Copper and gold were chosen as the most suitable contaminants for use as tracers, because of their high activation cross-sections (i.e. their ability to become radioactive in the pile) and their convenient

\* Manuscript received 3 December 1953.

† Head of Physics Group, Isotopes Division, Atomic Energy Research Establishment, Harwell, Berks.



radioactive decay periods. The half-life for decay of  $\text{Cu}^{64}$  is 12.9 hr. and that for  $\text{Au}^{198}$  is 2.69 days. In the copper-bearing material the percentage of copper was raised to 0.06% and in the gold-bearing material an addition of 0.0048% gold was made. The samples were arranged to have one perfectly flat polished face.

The samples were then irradiated in a pile, in a flux of  $10^{12}$  neutrons/cm.<sup>2</sup>/sec. The copper-bearing sample was irradiated for 2 days and the gold-bearing sample for 4 days. During this irradiation the aluminium base metal and its contaminants would also be expected to become radioactive. The half-life for decay of  $\text{Al}^{28}$ , however, is only 2.3 min., so that its activity rapidly decayed after irradiation, to reach a negligible level compared with that of the long-lived contaminants. Of these, only  $\text{Cu}^{64}$  would be expected to have an appreciable activity after a decay period of about 12 hr. Because the half-life of radioactive decay of iron is very much longer than the irradiation period, no very significant activity was introduced into the iron.

After waiting for the radioactivity of the impurities to decay, photographic exposures were made by laying the smooth surfaces of the samples on Industrial B X-ray film for measured periods. Fig. 1 (Plate LX) shows prints from the exposures obtained for the gold-bearing sample after decay periods of (a) 1 day and (b) 7 days. The exposure times were 20 sec. and 4 min., respectively.

In the copper-bearing sample, the contrast was reduced by the copper impurities already present in the aluminium. In the gold-bearing sample this background, which appears in Fig. 1 (a), could be eliminated because, owing to the longer period of radioactive decay of  $\text{Au}^{198}$ , time could be allowed for the copper activity to decay to a low level (see Fig. 1 (b)). The gold, of course, does not enter into solid solution, but is distributed in discrete particles around the grain boundaries of the aluminium. These particles, however, are small enough and closely enough spaced to allow good resolution of the boundary of the gold-bearing material. In both exposures the definition of the edges is much clearer where they are in contact with the relatively inactive aluminium, than at the outside of the discs where stray radiations falling upon the photographic plate, produced a fogging effect. The range of this fogging was reduced by surrounding the specimens with thick-walled brass tubes.

#### IV.—DELINEATION OF THE SOLID BOUNDARY

Gold was used as a tracer in the final experiments, both because of the good contrast obtainable and because of the smaller quantities needed for detection. The addition was made in the form of 0.5 g. of 8%-gold hardener, containing 40 mg. gold, diluted with 200 g. liquid aluminium. This mixture was poured into the input stream of molten aluminium as it

flowed into the crater during the casting of an 8.6-in.-dia. billet. A mean gold content of 0.0007% was found in the final metal by subsequent spectrographic analysis. The base metal contained: aluminium 99.576, copper 0.15, magnesium 0.001, silicon 0.12, iron 0.27, manganese 0.009, and titanium 0.009%.

After casting, a transverse section of the billet was cut and polished, and then further divided into three pieces convenient for irradiation in a pile. These pieces were irradiated for  $6\frac{1}{2}$  days in a neutron flux of  $10^{12}$  neutrons/cm.<sup>2</sup>/sec. The first autoradiograph was taken after allowing 3 days for the short-lived radioactive contaminants to decay away; the exposure time was 10 min. Further exposures were made on an Industrial B X-ray film, after decay periods of 7 and 10 days. Exposure times were adjusted to compensate for decay of the  $\text{Au}^{198}$ . For these exposures, the irradiated portions were placed side by side on the photographic film, and separated by 0.1 in.-thick aluminium spacers to simulate the spacing of the saw cuts. These spacers also had a screening effect which prevented blurring of the photographic plate between the samples.

The autoradiograph of which Fig. 2 (Plate LX) is a print is the result of a 43-min. exposure after a decay period of 10 days. There was very little difference between this and all other autoradiographs taken after the initial decay period of 3 days. The shape of the solidification boundary is clearly indicated by the blackening of the photographic film, i.e. white areas in the print.

#### V.—DISCUSSION

A striking feature of Fig. 2 is the strong intensity of exposure at the solidification boundary. This heavily exposed region is followed by another region of very little exposure and then by a further exposed region apparently parallel to the first. This alternation of dark and light regions is repeated several times, with gradually decreasing contrast until a fairly uniform exposure of the film is obtained. The reasons for these striations are now being studied. They are obviously related to the conditions of flow in the liquid aluminium in the crater, and correspond to successive arrivals of the gold-bearing material at the solidification boundary before this material has had time to become uniformly mixed with the pool of liquid aluminium.

Because of the uneven distribution of the tracer impurity, as shown in Fig. 2, it is evident that even smaller quantities of gold could have been used to mark the boundary. The mean gold content in the crater in this experiment was 7 p.p.m., but local concentrations of gold are much higher than that deduced by assuming that the gold is evenly distributed through the molten metal. This argument also applies to non-radioactive methods of determining the solidification boundary, and local concentrations may be many times higher than those expected if complete mixing is assumed.

The method of radioactivation followed by autoradiography appears to afford a convenient research method for measuring the solidification boundary, and one in which much lower contamination of pure aluminium occurs than in the use of any non-radioactive method. There is no doubt that autoradiography may be extended to other metals and particularly to alloys of aluminium, provided that periods of pile irradiation and of subsequent decay can be so chosen that the alloying materials have a lower activity than the tracer materials.

For high-alloy materials the more straightforward tracer method is applicable, and the radioactive material may be added in the melt. In the absence of background activities, no waiting period is necessary before making the autoradiographs, which can be made as soon as the ingot is cool. Moreover, longer exposures of the X-ray film can be made, permitting the use of proportionally smaller quantities of tracer material. If 10 mg. of 8%-gold hardener were irradiated in the pile under similar conditions to those used for the samples in the radioactivation tests and introduced in 200 g. of molten aluminium alloy, results

similar to those shown in Fig. 2 are to be expected from a  $3\frac{1}{2}$ -hr. exposure to the X-ray film within 1 day of irradiating the sample. The highest radioactivity of the gold at any time would be about 10 millicuries, and only the minimum of handling precautions would be necessary. In practice, it would probably be found more convenient to use a larger, more diluted sample for irradiation, e.g. 1 g. of pure aluminium containing 0.08% gold.

#### ACKNOWLEDGEMENTS

This investigation was made at the request of Aluminium Laboratories, Ltd., Banbury, who also made and cut all the metal specimens. The author wishes particularly to thank Mr. D. M. Lewis, of Aluminium Laboratories, Ltd., for helpful discussions in the preparation of this paper. Thanks are also due to Mr. R. Peart and Mr. E. W. Solomon of the Atomic Energy Research Establishment, who made the autoradiographs. This report is published by permission of the Director, Atomic Energy Research Establishment.



MICROSTRUCTURES OF MOLYBDENUM AND MOLYBDENUM ALLOYS.

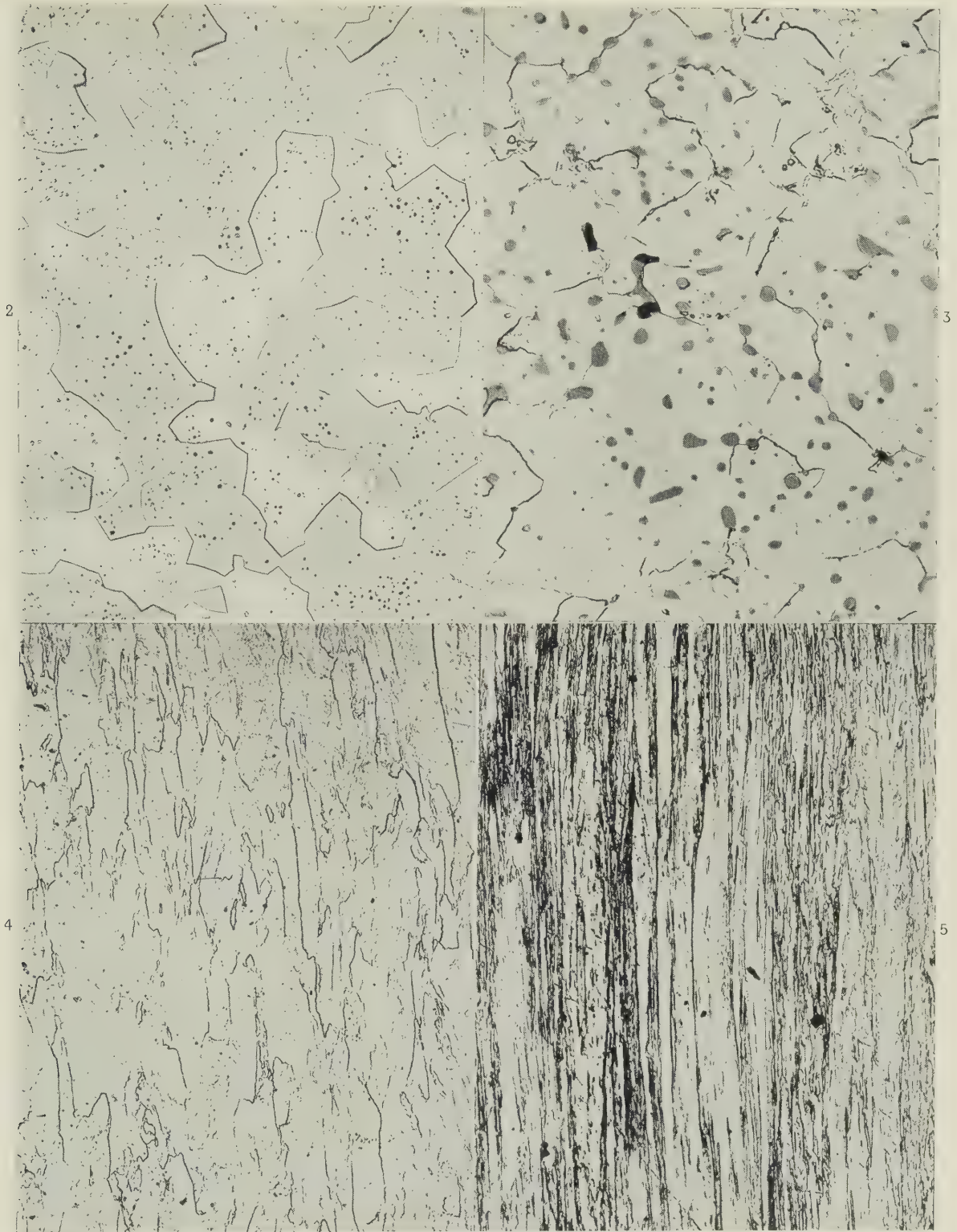
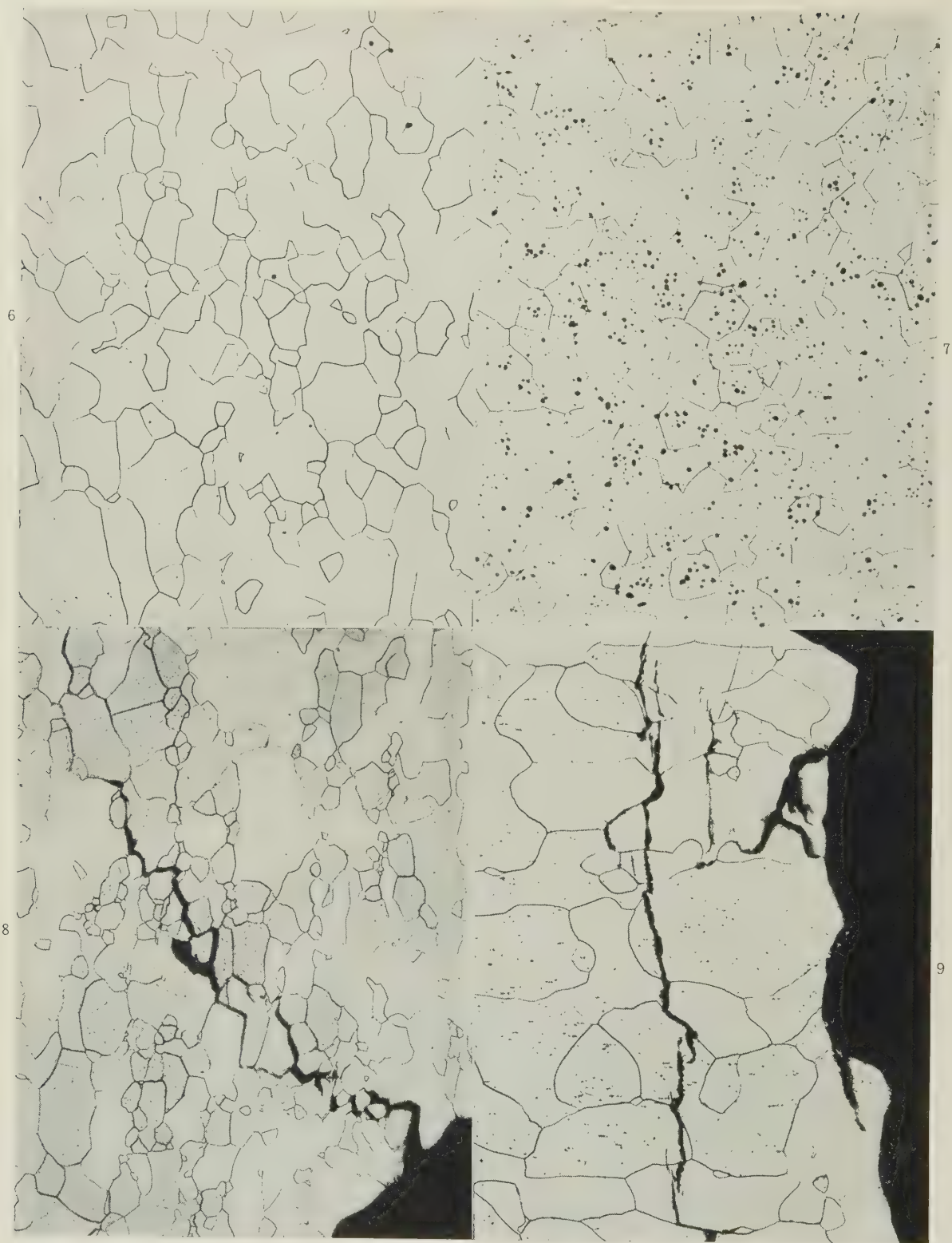


FIG. 2.—20% Tungsten Alloy (RDJ), As Sintered.  $\times 150$ .  
 FIG. 3.—8% Titanium Alloy (RDS), Swaged Through Three Dies.  $\times 500$ .  
 FIG. 4.—10% Tantalum Alloy (RHE), As Swaged.  $\times 150$ .  
 FIG. 5.—Swaged Molybdenum (RIP), As Received.  $\times 150$ .

## MICROSTRUCTURES OF MOLYBDENUM.

FIG. 6.—Molybdenum As Annealed at 1500° C. (RKJ).  $\times 150$ .FIG. 7.—Molybdenum As Sintered (RLY).  $\times 150$ .FIG. 8.—Intergranular Fracture in Molybdenum (RIP).  $\times 150$ .FIG. 9.—Mixed Intergranular/Transgranular Fracture in Molybdenum (RKA).  $\times 150$ .



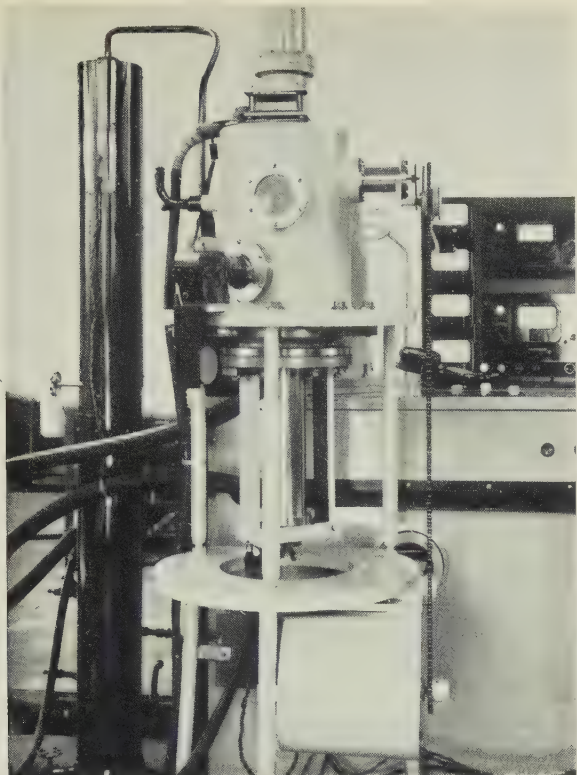


FIG. 3.—Arc-Melting Plant Assembled for Operation.



FIG. 4.—Macrostructure of Ingot of Molybdenum Containing 0.052% Carbon. Etched in 50%  $\text{HNO}_3$ .  $\times 2$ .



FIG. 5.—Pure Molybdenum.

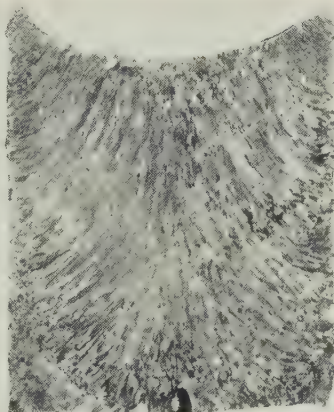


FIG. 6.—42% Tungsten.

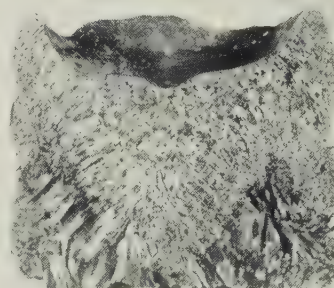


FIG. 7.—3.5% Iron.

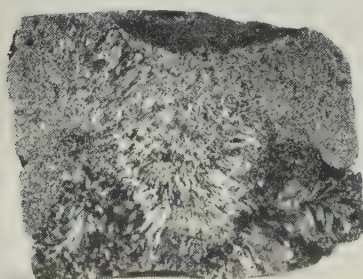


FIG. 8.—2% Cobalt.

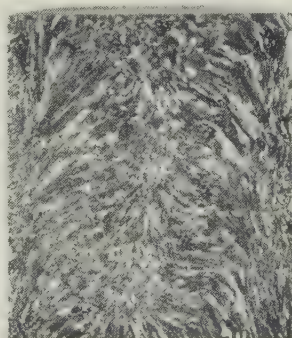


FIG. 9.—1% Aluminium.

FIGS. 5-9.—Macrostructures of Ingots of Molybdenum with Alloying Additions. Etched in 50%  $\text{HNO}_3$ .  $\times 1$ .





FIG. 10.—Illustrating Surface Condition of Molybdenum Ingot Melted in Vacuum with D.C. (negative), 1250 amp., 33 V.



FIG. 11.—Illustrating Surface Condition of Molybdenum Ingot Melted in Argon with D.C. (positive), 1700 amp., 20 V. (Melted on base plug cast in vacuum.)

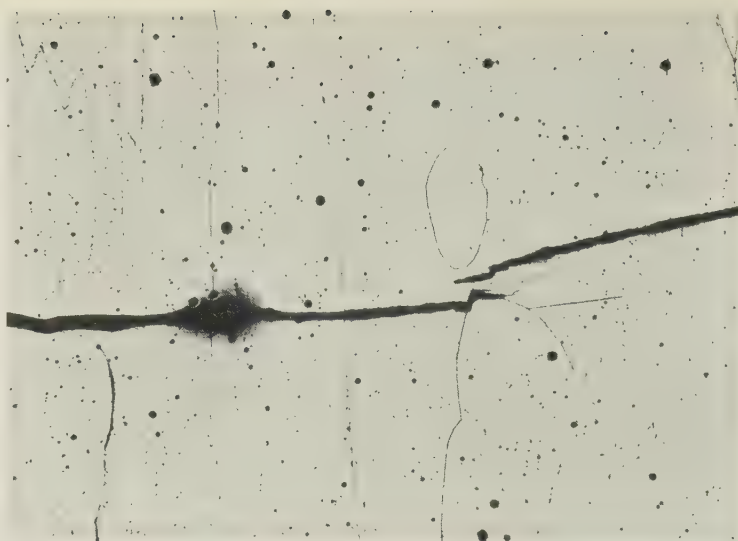


FIG. 12.—Photomicrograph Showing Internal Crack in Incompletely Deoxidized Vacuum-Melted Molybdenum Ingot. Polished electrolytically in  $H_2SO_4$ -methyl alcohol solution and etched in alkaline potassium ferricyanide solution.  $\times 100$ .

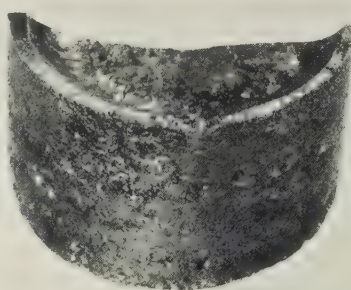


FIG. 13.—Section Showing Concavity of Crater in Vacuum-Melted Ingot.  $\times 1$ .

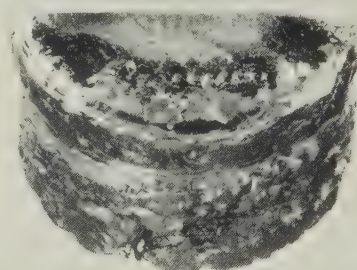


FIG. 14.—Section Showing Almost Flat Crater in Argon-Melted Ingot.  $\times 1$ .

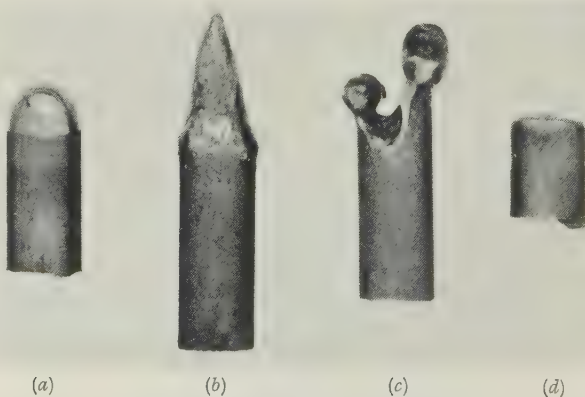


FIG. 15.—Showing Shapes of Electrode Burn-Offs: (a) D.C. (positive); (b) and (c) D.C. (negative); (d) A.C.



## GENERAL CONSTRUCTION OF IMPACT PRESSURE-WELDING APPARATUS.

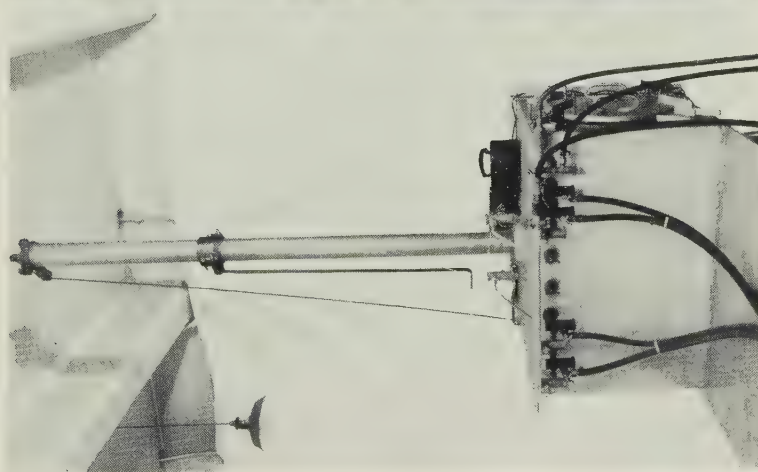


FIG. 1.—Rear View of Welding Chamber, Showing Back-Pressure Valves and Outlet Manifold.

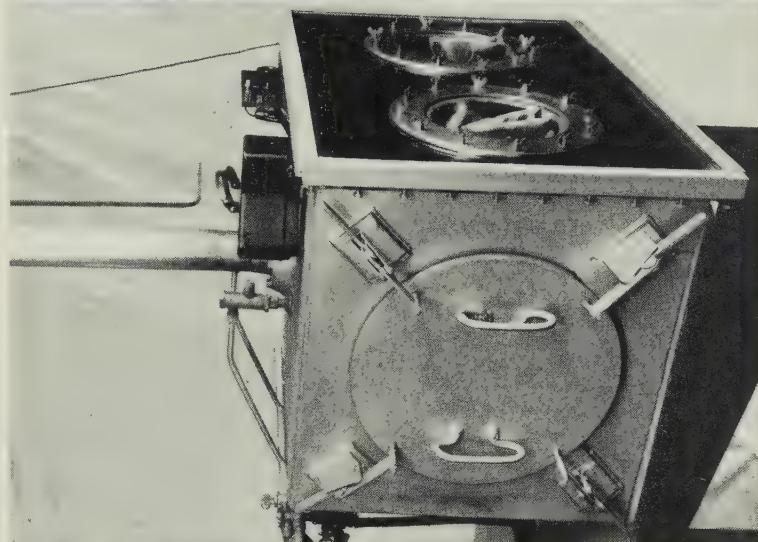


FIG. 2.—End View of Chamber, Showing Original Manhole Cover and Clamping Arrangements.

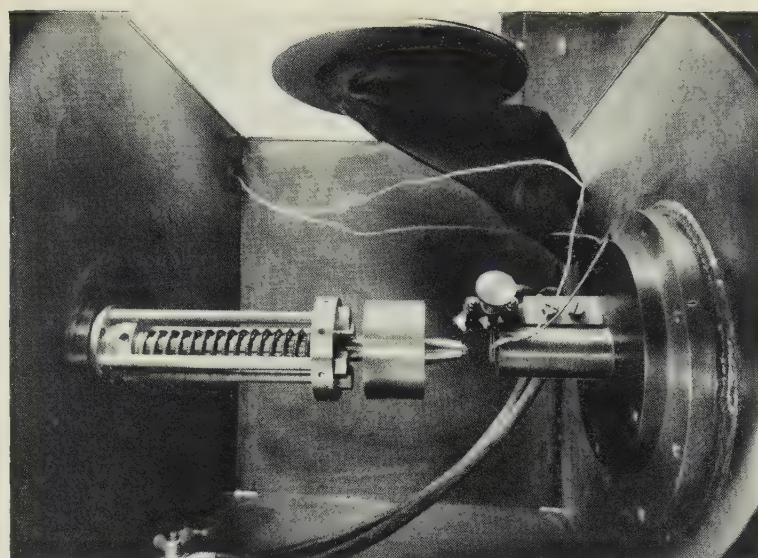


FIG. 3.—The Impact-Loading Device. A test-piece is clamped in position ready for welding.

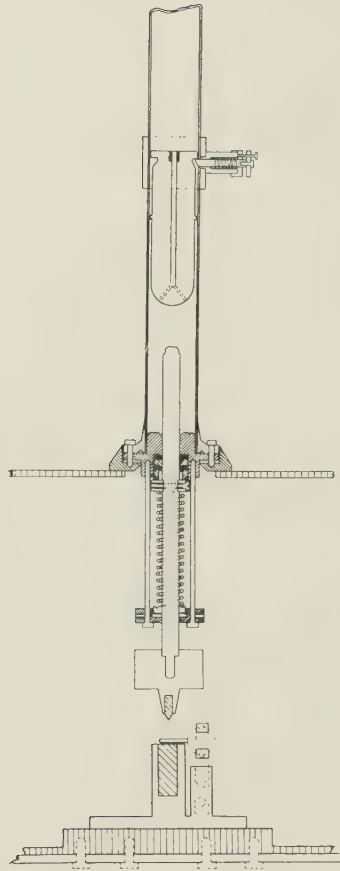


FIG. 4.—Schematic Cross-Section of Impact-Loading Device. The weight and its release mechanism and anvil are also shown.



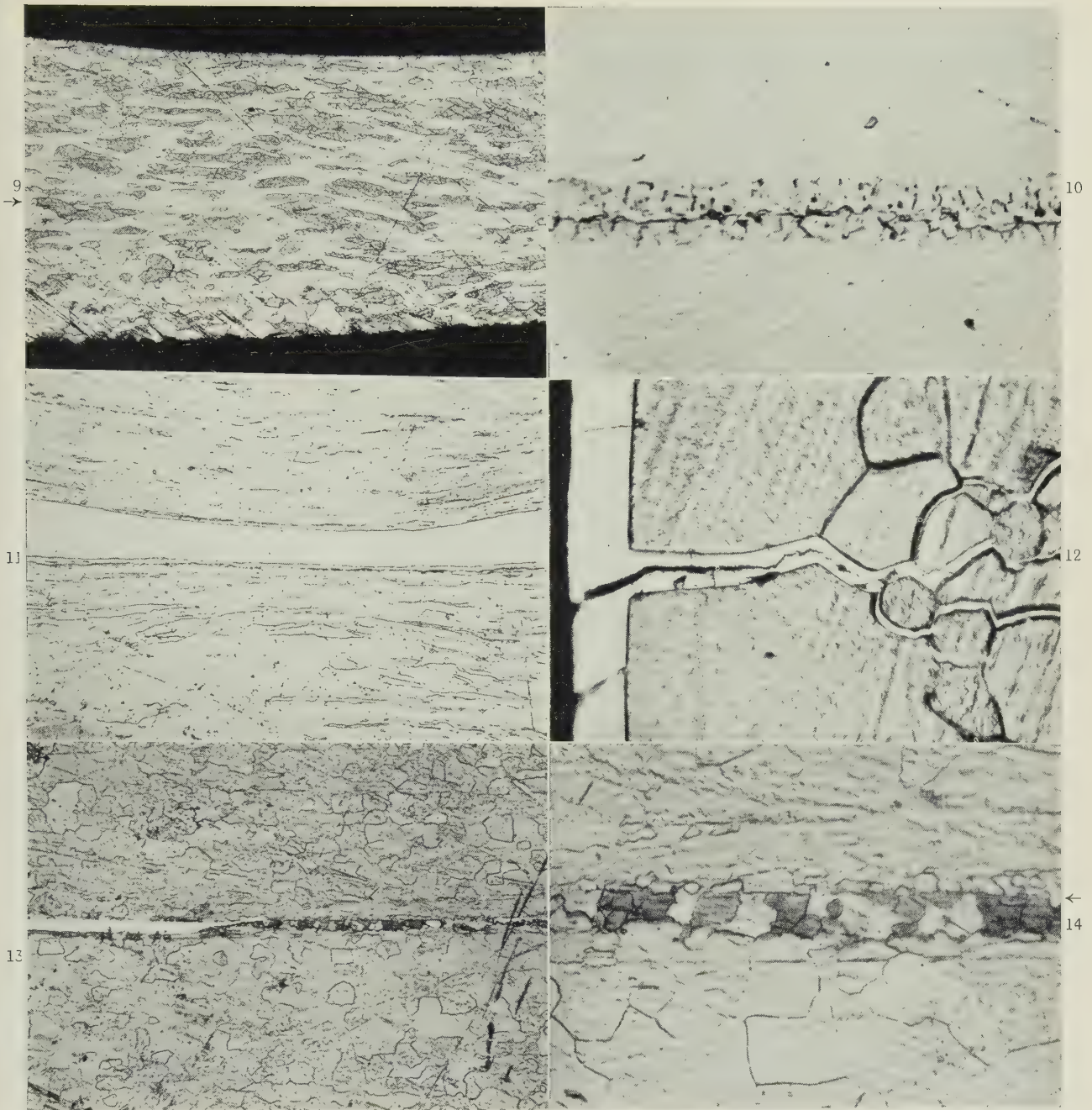


FIG. 9.—Cross-Section of a Molybdenum/Molybdenum Pressure Weld Made at 1000° C. Etched.  $\times 100$ .

FIG. 10.—Cross-Section of an Iron Insert Weld Made at 1400° C. and 5% Deformation. Unetched.  $\times 750$ .

FIG. 11.—Austenitic Stainless Steel Insert Weld Made at 900° C. and 51% Deformation. Lightly etched.  $\times 250$ .

FIG. 12.—Showing Extensive Grain-Boundary Infiltration of Stainless Steel into Molybdenum. Etched.  $\times 500$ .

FIG. 13.—Nickel Insert Weld Made at 1400° C. and 5% Deformation, Showing Two Different Adjacent Modes of Junction. Etched.  $\times 150$ .

FIG. 14.—Part of Weld Illustrated in Fig. 13, Showing Interface in Greater Detail. Etched.  $\times 750$ .

(All reduced by  $\frac{1}{10}$  in reproduction.)

15

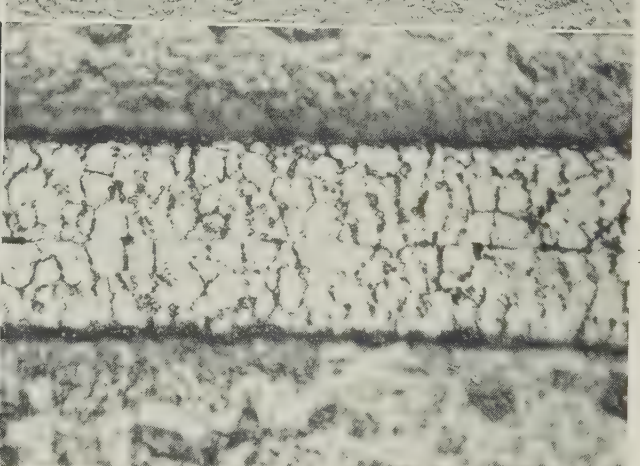
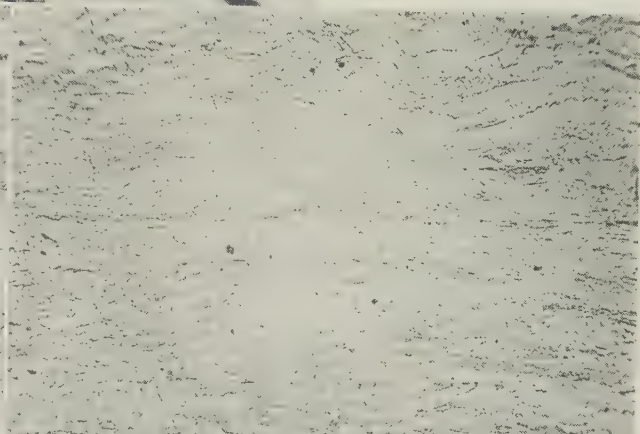
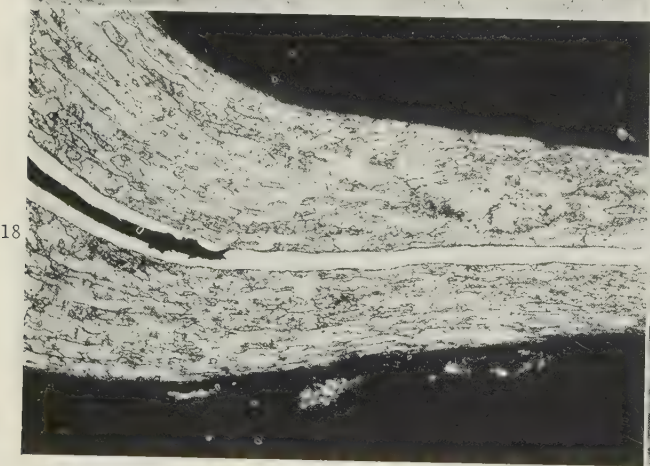
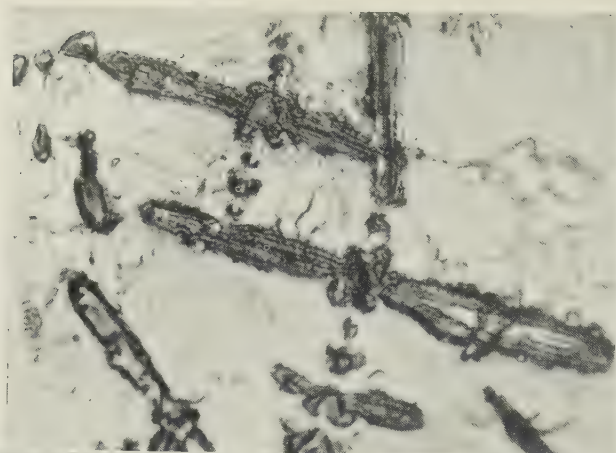


FIG. 15.—Fractograph of Interface of Weld Shown in Fig. 13. Unetched.  $\times 750$ .

FIG. 16.—Niobium Insert Weld Made at  $1400^{\circ}\text{C}$ . and 20% Deformation. Etched.  $\times 250$ .

FIG. 17.—Tantalum Insert Weld Made at  $900^{\circ}\text{C}$ . and 41% Deformation. Etched.  $\times 250$ .

FIG. 18.—Electrodeposited Chromium Insert Weld Made at  $900^{\circ}\text{C}$ . and 37% Deformation. On the left is the undeformed portion of the weld. The chromium/chromium interface cannot be detected. Etched.  $\times 100$ .

FIG. 19.—Part of the Weld Shown in Fig. 18. Chromium/chromium interface revealed by electrolytic etching. Note grain growth across the interface.  $\times 500$ .

(All reduced by  $\frac{1}{10}$  in reproduction.)



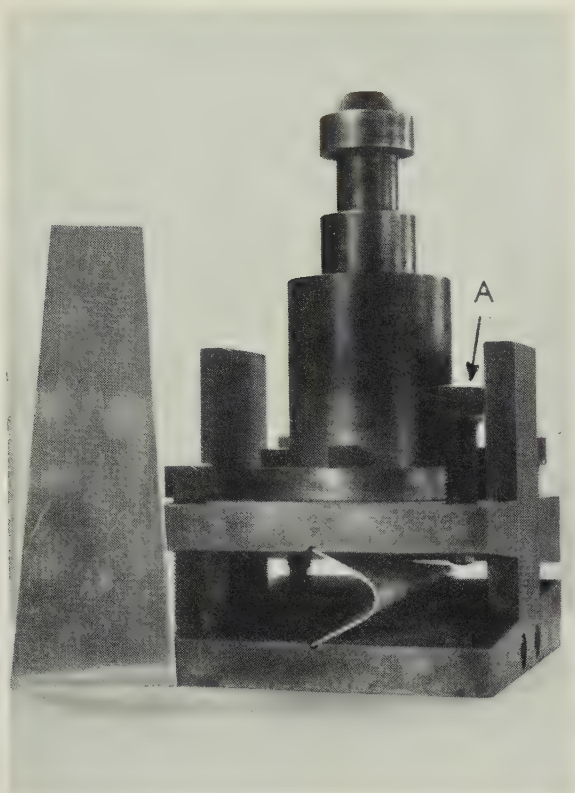


FIG. 14.—Free-Cone Bend Apparatus, Showing the Specimen Before and After Bending.

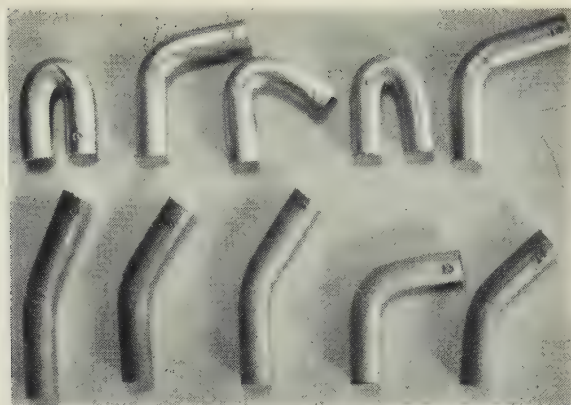


FIG. 15.—Vice Bends on 0.5-in.-dia. Extruded Rod.

Top : Press-quenched and aged at 175° C. for 6 hr.

Bottom : Solution-treated at 540° C. and aged at 175° C. for 6 hr.

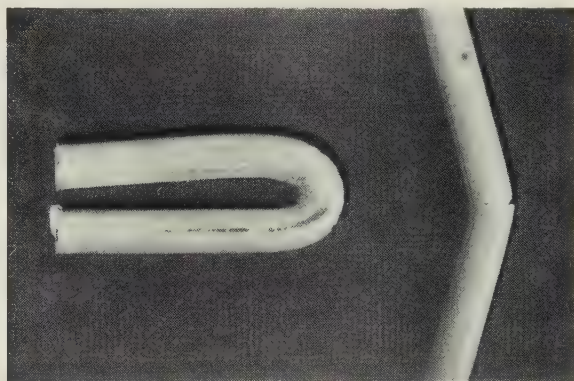


FIG. 16.—Vice Tests on Alloys Shown in Figs. 20 and 21. Ductile alloy contained Mg 0.96, Si 0.42%; brittle alloy, Mg 0.89, Si 0.64%.



FIG. 17.—Alloy No. 6, Press-Quenched and Aged at 175° C. for 6 Hr.  $\times 100$ .

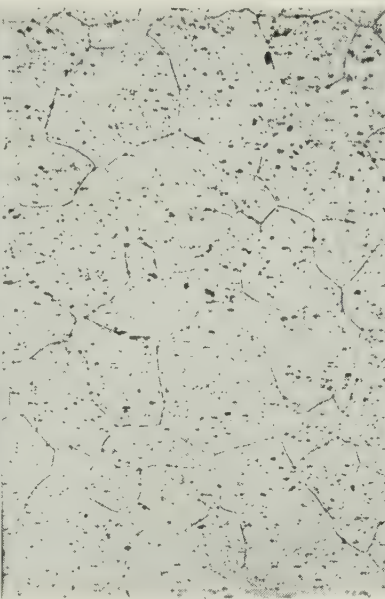


FIG. 18.—Alloy No. 6, Solution-Treated at 540° C. and Aged at 175° C. for 6 Hr.  $\times 100$ .

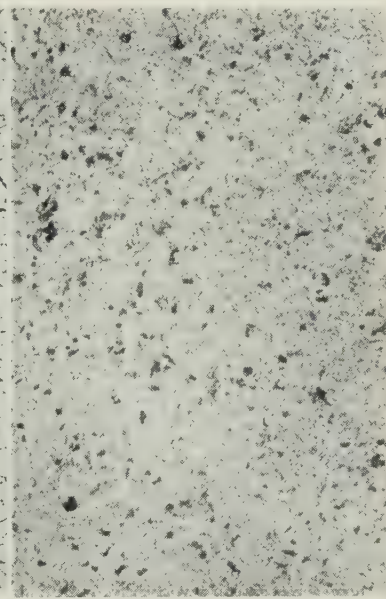
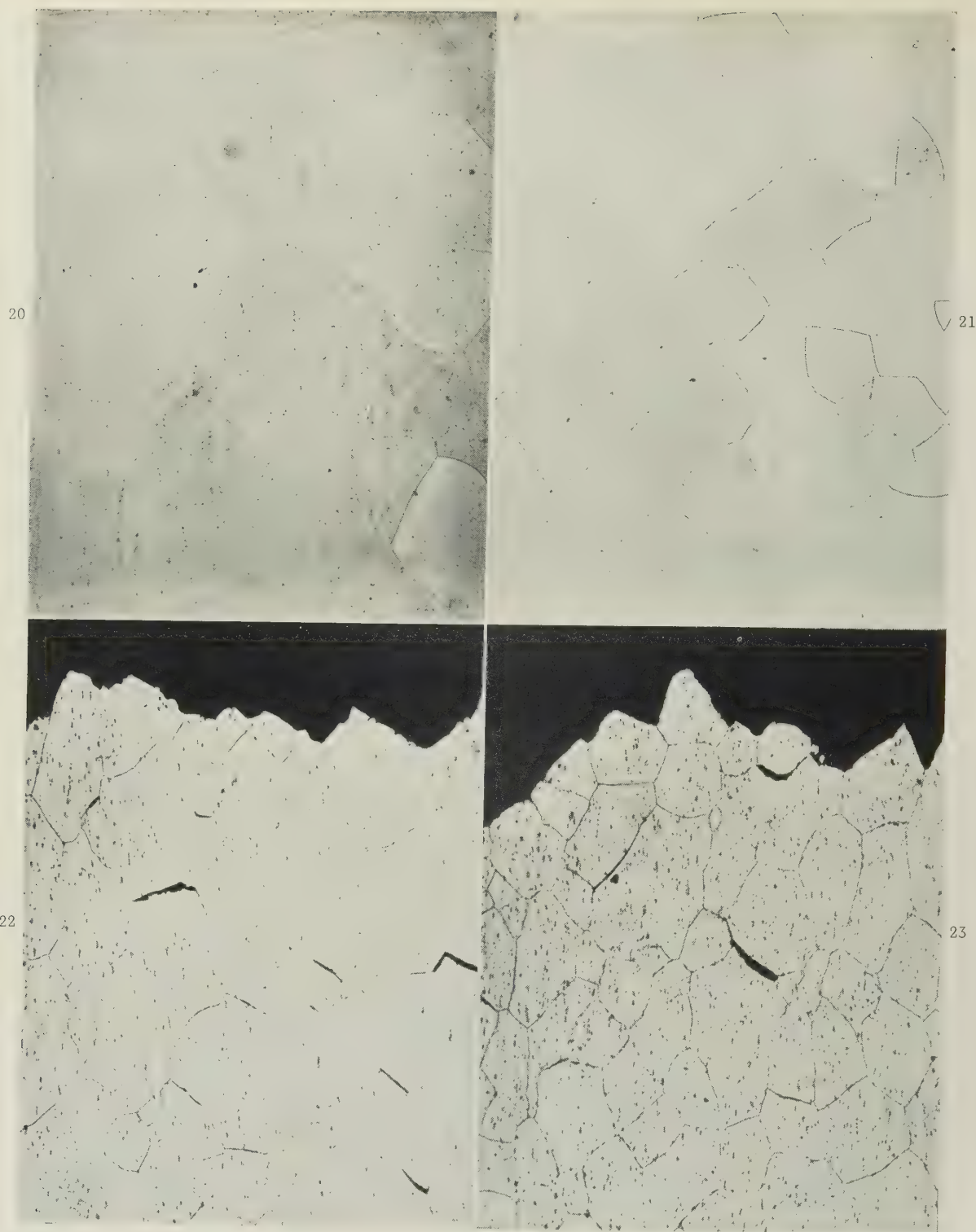


FIG. 19.—H10WP Alloy No. 21 Containing 0.4% Manganese, Solution-Treated at 540° C. and Aged at 175° C. for 8 Hr.  $\times 200$ .

FIGS. 17-19.—Etched for 30 sec. in solution of 5% HF and 10%  $\text{H}_2\text{SO}_4$  in water.



FIGS. 20 and 21.—Super-Purity-Base Alloys, Solution-Treated at 540° C. and Aged at 175° C. for 8 Hr. Etched for 90 sec. in solution of 5% HF and 10% H<sub>2</sub>SO<sub>4</sub> in water. × 75.

FIG. 20.—Alloy containing Mg 0.96, Si 0.42%.

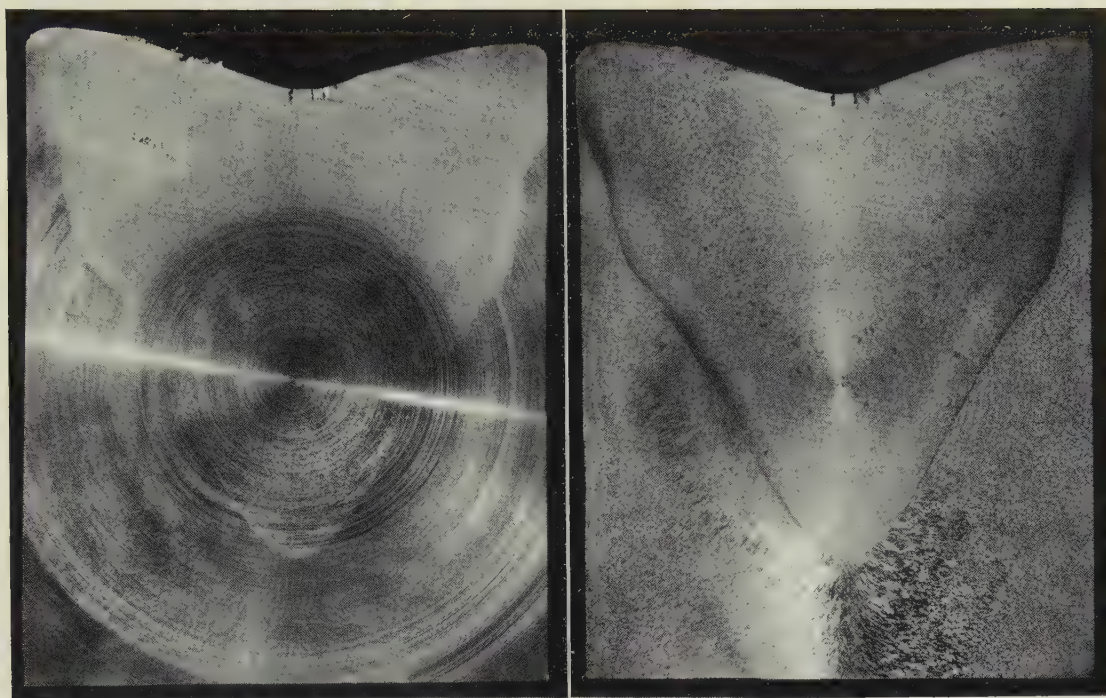
FIG. 21.—Alloy containing Mg 0.89, Si 0.64%.

FIGS. 22 and 23.—Tensile Fracture in H10WP Alloy No. 7, Solution-Treated at 540° C. and Aged at 175° C. for 8 Hr. Etched for 30 sec. in solution of 5% HF and 10% H<sub>2</sub>SO<sub>4</sub> in water. × 100.

FIG. 22.—Quenched from 540° C.

FIG. 23.—Air-cooled from 540° C.





(a) Machined surface.

(b) Macro-etched face.

FIG. 17.—Tracer Method of Indicating Solidification Contours.

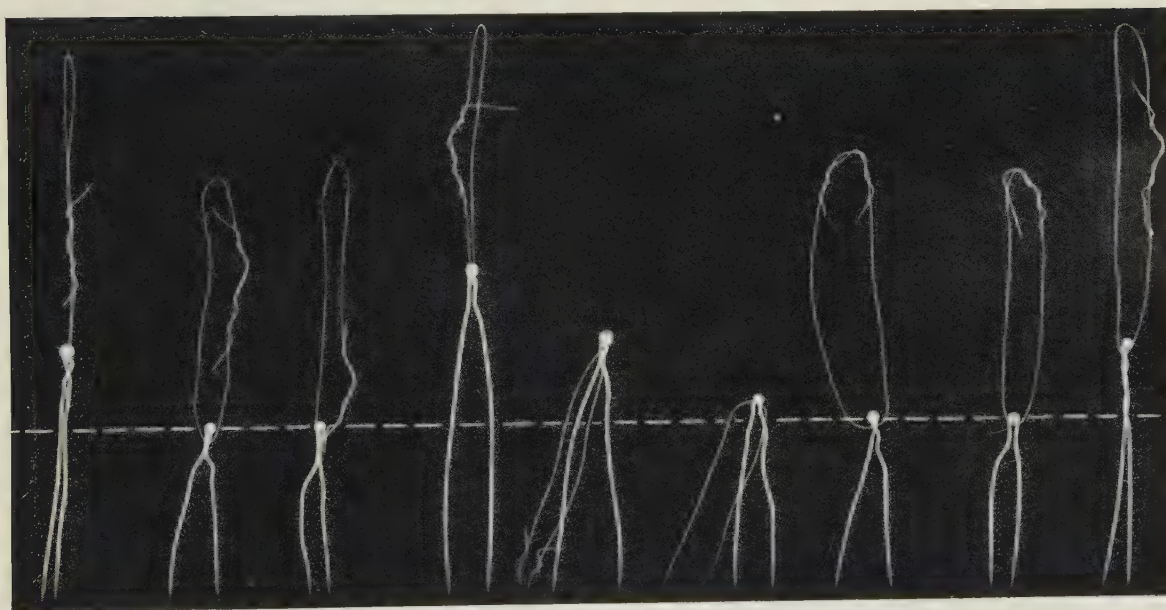


FIG. 18.—Radiograph of a Billet Slice, Showing Final Position of Thermocouples.

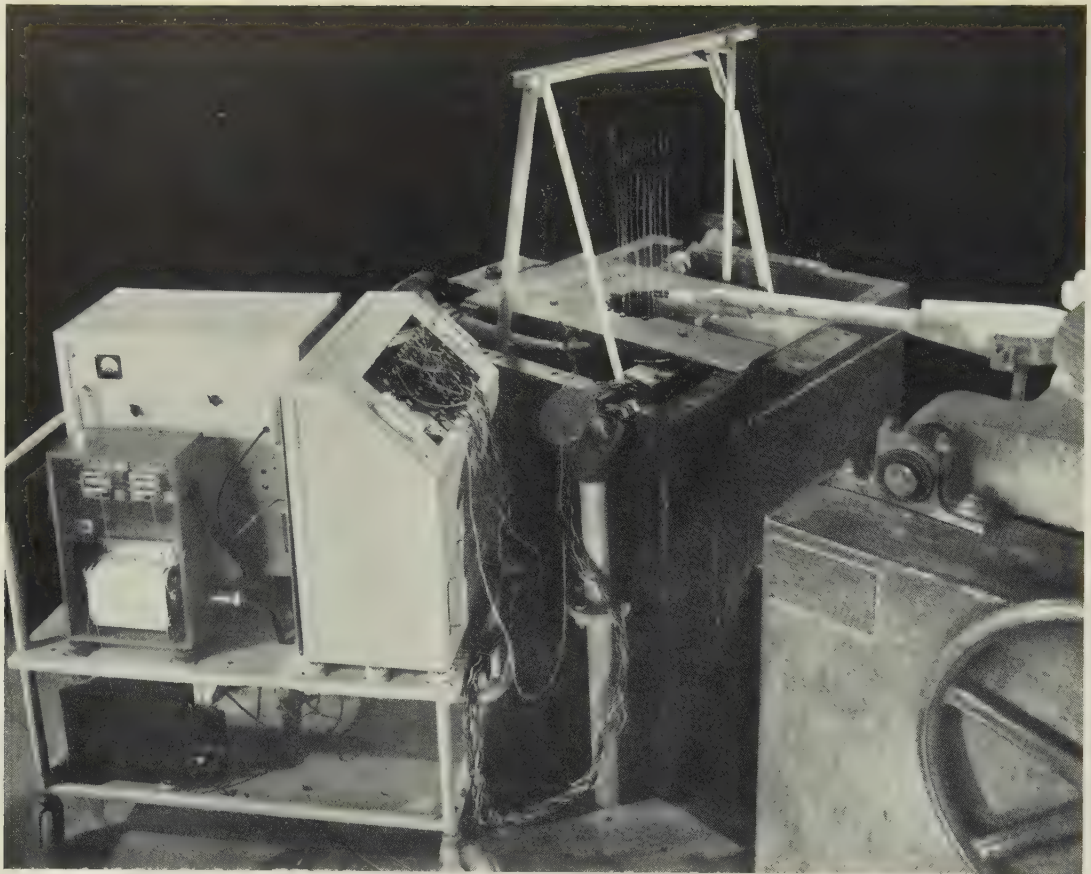


FIG. 19.—The High-Speed Temperature Recorder in Use During an Experimental Cast.

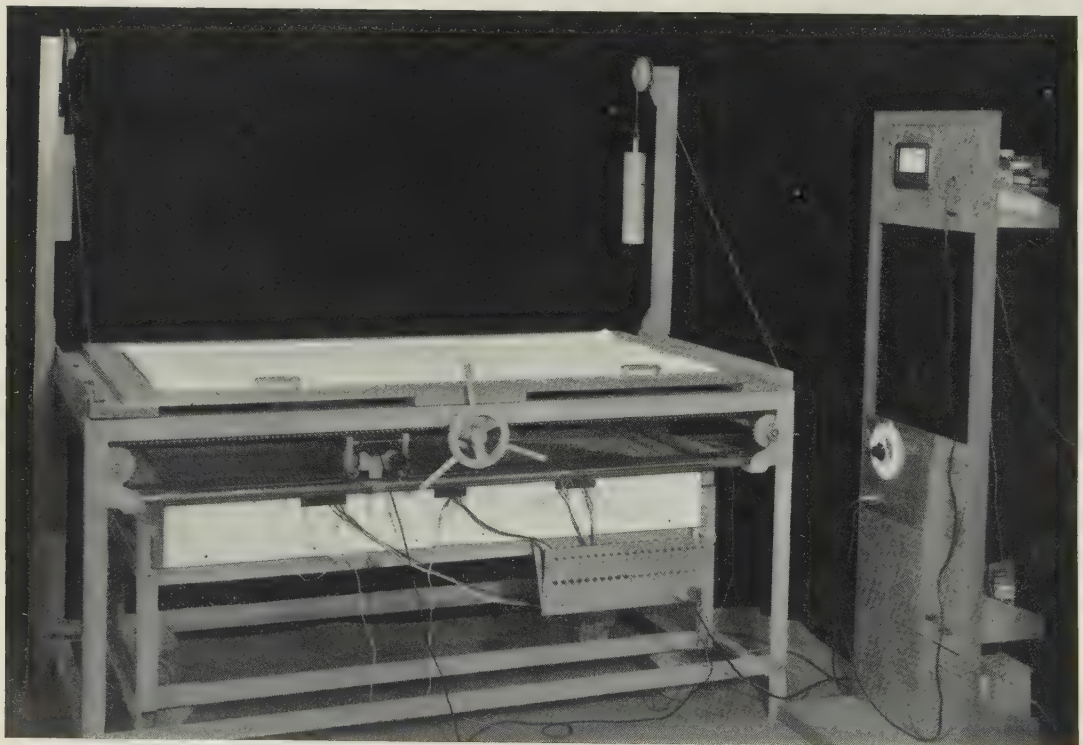


FIG. 20.—General View of Electrical Tank Analogue. The rack on the right contains the oscillator and power packs, precision potentiometer, and the valve voltmeter.



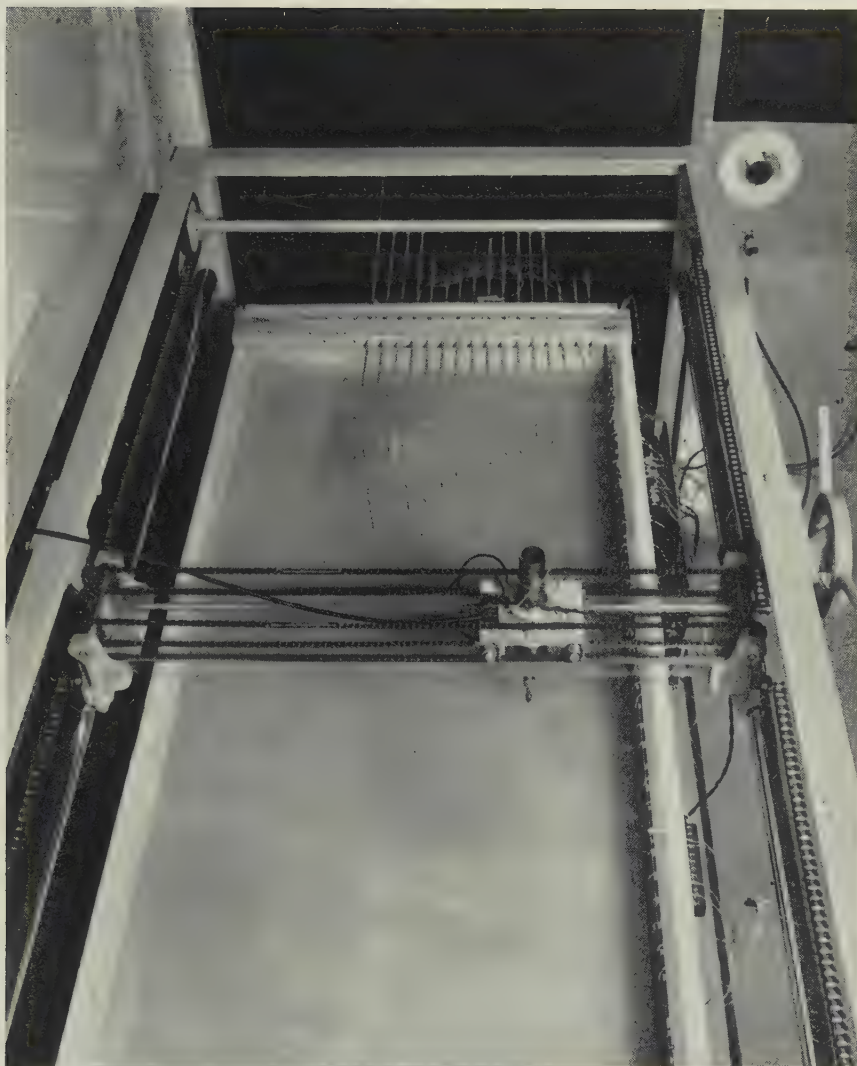
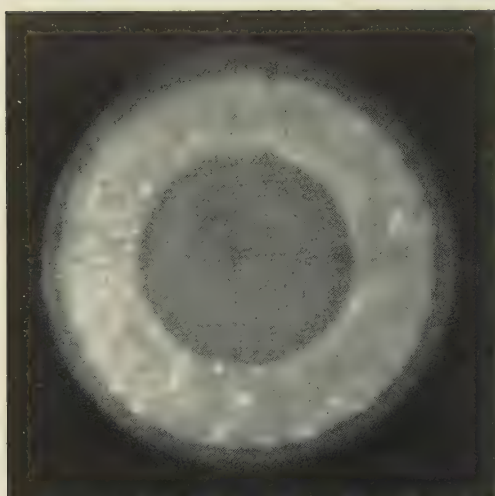


FIG. 21.—Probe Traversing Gear and Electrode System of the Tank Analogue.



(a) After One-Day Decay Period.



(b) After Seven-Day Decay Period.

FIG. 1.—Preliminary Exposures of Irradiated Gold-Bearing Sample of Aluminium.

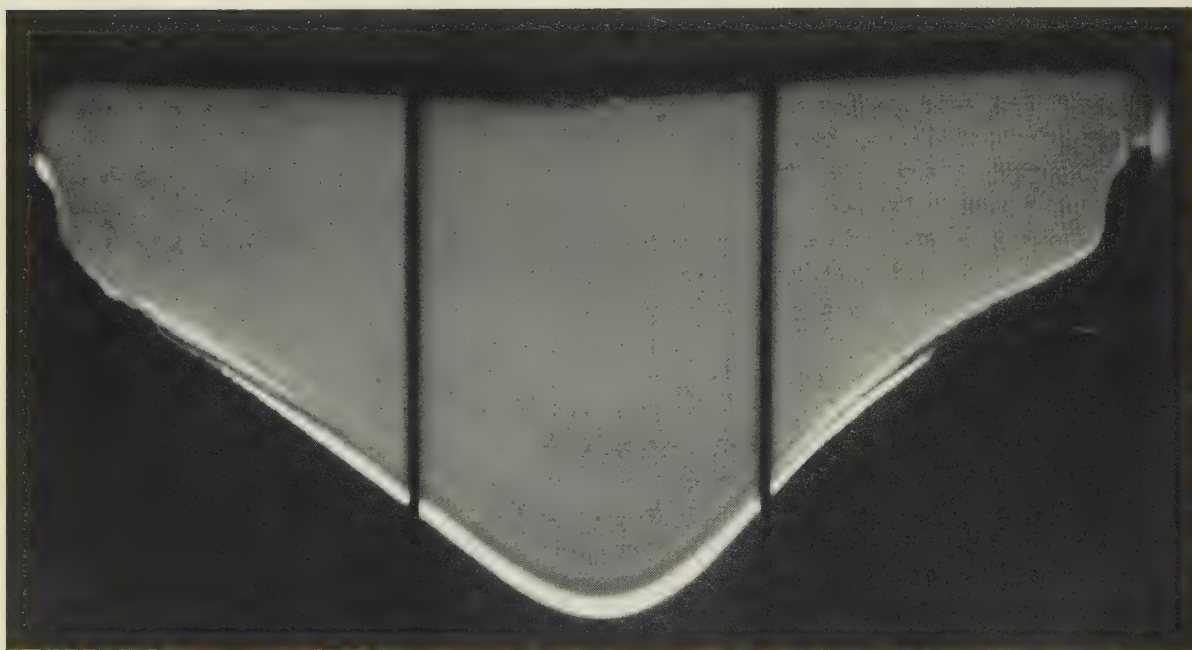


FIG. 2.—Autoradiograph Showing Solidification Boundary of Continuously Cast Aluminium Ingot. (Positive print.)



# THE DOMAIN STRUCTURE OF FERROMAGNETIC METALS \*

By PROFESSOR L. F. BATES,† Ph.D., D.Sc., F.R.S.

## SYNOPSIS

A brief outline is given of the domain concept as applied to ferromagnetic metals and their alloys. This is followed by a description of the powder-pattern technique which permits the mapping of the intersections of domain boundaries with suitably prepared surfaces of ferromagnetic metals; the methods of preparing the surfaces are described. The powder patterns are often of great beauty and have led to new knowledge concerning important magnetization processes, and made possible certain fundamental experiments on these processes. In particular, they have enabled the predictions of modern domain theory to be checked quantitatively. By their means it is possible to follow the motion of domain boundaries under the influence of magnetic fields and thus to study the effects of impurities or inclusions on magnetic hysteresis phenomena.

## I.—INTRODUCTION

I WANT to deal with a number of concepts and many experiments which are of great importance to all who are concerned with the study of ferromagnetism and which should, therefore, be of general interest to metallurgists. I begin with the concept originally advanced by Pierre Weiss to explain the fact that we may take a piece of unmagnetized iron and by the application of a field of a few oersteds magnetize it to technical saturation. The examination of single crystals of ferromagnetic substances shows that such crystals exhibit directions of easy and of difficult magnetization, and we say that such crystals are magnetically anisotropic. For example, we may magnetize with ease a single-crystal specimen of iron parallel to the [100] direction, less easily along the [110], and still less easily along the [111] direction. We have no difficulty in accepting the Weiss concept that an unmagnetized crystal is made up of small regions or domains, each magnetized to a degree of magnetic saturation which is determined by its temperature and state of strain, &c., along an easy direction of magnetization.

If, however, each domain in an unmagnetized iron crystal is actually magnetized parallel to one of the cube edges of the crystal, why does not the whole specimen automatically form one single, large domain? This was the question answered by Landau and Lifshitz<sup>1</sup> in 1935, following their examination of the magnetostatic energy associated with the free poles on the ends or sides of such a completely magnetized specimen. They showed by means of a series of simple diagrams that the magnetostatic energy could

be greatly reduced by replacing the single, large domain block magnetized in one direction only by a series of smaller domain blocks magnetized consecutively in antiparallel directions, so that the positive and negative magnetizations, or free poles, at the ends of the many smaller domains more or less neutralized one another. And, with a little thought, small triangular subsidiary domains, termed closure domains, could be devised to ensure that practically no flux at all escaped from the specimen.

Adjacent domains are, of course, magnetized in opposite directions, and these 180° domains, as we will now call them, have to be separated by boundaries or regions of gradual transition from one direction of magnetization to the other. We therefore speak of a 180° boundary or wall, in which the magnetic spin vectors along a line of atoms gradually change from one direction to the antiparallel one as we pass through the wall. As the exchange coupling energy between two neighbouring electron spins depends on the square of the angle between their spin vectors, it follows that there is a tendency for the wall to be as wide or as thick as possible. Indeed, in some nickel-iron alloys of low anisotropy, these boundaries, or Bloch walls as we often call them, are really comparatively wide, so that experiments of the type which would easily reveal their presence in the case of pure iron crystals fail with crystals of these alloys.

But a 180° wall cannot have an unrestricted thickness, for only a very little of the material inside the wall can be magnetized along an easy direction; consequently exchange energy decreases with increase in wall thickness and magnetic anisotropy energy increases therewith. The result is that the overall

\* Delivered at the Annual Spring Meeting, London, 26 April 1954.

† Lancashire-Spencer Professor of Physics and Deputy Vice-Chancellor, University of Nottingham.

wall thickness is determined by the two conflicting energy claims, and an approximate expression for the thickness in terms of the two energies may easily be derived. In the case of iron, a  $180^\circ$  wall is about  $10^{-5}$  cm. or 300 atoms thick.

## II.—THE DOMAIN STRUCTURE OF COBALT

If a circular disc is removed from one of the sides of a hexagonal crystal of cobalt, an ideal specimen is obtained for the investigation of the simplest domain structure, and I propose to treat this case in some detail. I am fortunate in possessing such a disc, about 8.5 mm. in dia. and 0.9 mm. thick, kindly presented to me by Professor Sucksmith. The domain structure in the unmagnetized state is easily made visible; the surface is first polished mechanically down to 0000 grade emery, and then polished electrolytically in a bath of orthophosphoric acid. During the polishing, a black powder, which is thought to be ferromagnetic, tries to form a deposit on the surface and has to be continuously swabbed away.

On placing the polished surface under a metallurgical microscope, with light field setting and with the instrument slightly out of focus, Fig. 1 (a) (Plate LXI) was obtained. It is emphasized that the specimen is unmagnetized and attention is directed to the two transverse slip lines in the picture which act as fiducial marks. There is little doubt here about the reality of a domain structure, without further proof. But, following a technique due to Bitter, by placing on the surface a drop of a solution of colloidal magnetite prepared according to Elmore's or Bozorth's recipe,<sup>2</sup> Fig. 1 (b) was obtained with the microscope properly focused. The dark lines of colloid lie above the  $180^\circ$  walls, and we note also some "daggers" or "spikes" which actually give the outlines of closure domains produced because the surface of the specimen is not an exact crystal plane.

By applying the same methods of photography to a damaged portion of the surface near the edge of the specimen where three crystal grains meet, Figs. 2 (a) and 2 (b) (Plate LXI) were obtained. The star-spangled portion of Fig. 2 (b) is typical of the basal plane of cobalt. Finally, with a magnetic field applied parallel to the long edge of the picture we obtained Figs. 3 (a) and 3 (b) (Plate LXI), the field for Fig. 3 (b) being substantially higher than that for Fig. 3 (a). In the latter pictures the black deposits actually represent whole domain surfaces, and in Fig. 3 (b) they have disappeared in the interior of the surface of the specimen, i.e. in the right-hand upper portion of the picture, because with increase of field that portion of the specimen becomes magnetically saturated. In the lower portion of the pictures the very heavy black deposits tell us that the surface of this particular crystal grain is by no means parallel to a true crystal plane, and we have therefore a heavy colloid deposit covering a sheet of free magnetic poles.

Now, the case of cobalt is peculiarly simple. It

possesses only two easy directions of magnetization, perpendicular to the basal plane, whereas iron possesses six such directions parallel to the cube edges, and nickel has eight such directions parallel to the cube diagonals. Consequently, whilst  $180^\circ$  domain walls are very important in iron and in nickel, boundaries between neighbouring domains magnetized along directions which are perpendicular to one another, or  $90^\circ$  boundaries, are also very important in iron. Similarly,  $70^\circ$  and  $110^\circ$  boundaries are very important in nickel.

It must be emphasized that boundaries are always formed in such a way that free magnetism is reduced to a minimum. For example, for many years Fig. 16 (a) was used to illustrate simple descriptions of the



Fig. 16.—Diagrammatic Representation of the Domain Structure of a Demagnetized Iron Crystal.

main domain structure supposed to exist in the middle portion of a (100) surface of an unmagnetized single crystal of iron, and it was considered that on the application of a magnetic field magnetization occurred first because of boundary displacements between adjacent domains and later by rotation of the domain vectors. We now know, however, that Fig. 16 (b) represents iron in the unmagnetized state very much more adequately, for there is here no free magnetism at any internal boundary.

## III.—PREPARATION OF CRYSTAL SURFACES

It is now appropriate to give more details of the preparation of crystal surfaces for this work. We have already seen, in the case of cobalt, that it is desirable to have a true crystal plane as the specimen surface, and this is established by optical and eventually by X-ray examinations. The surface is mechanically polished down to 0000 emery, and then the Beilby layer is removed by electrolytic polishing, followed if necessary by annealing *in vacuo*. We have made several devices for ensuring excellent mechanically polished surfaces of small specimens, and a few words about electrolytic polishing may not be out of place here.

Fig. 17 is a diagram of a simple electrolytic cell in which both anode and cathode are simultaneously rotated. Whether successful electrolytic polishing occurs because of the exceptionally high resistance of the film of liquid over the anode or because of the peculiar denudation of the ions in such a film is immaterial to this description; we find that with iron and nickel the best results are obtained when both



electrodes are rotated, so that the electrolyte is kept as homogeneous as possible. The single crystal forming the anode was formerly sunk in a polystyrene

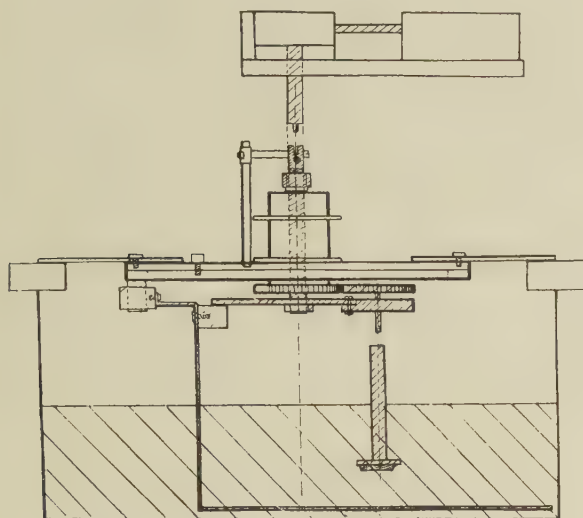


FIG. 17.—Apparatus for Electrolytic Polishing.

mould and fixed in position with polystyrene glue, electrical contact with the back of the specimen being made by impregnating the glue with graphite. More recently, a small Alnico magnet has been used as a kind of magnetic chuck without glue, and both the magnet and the specimen are polished. The latter

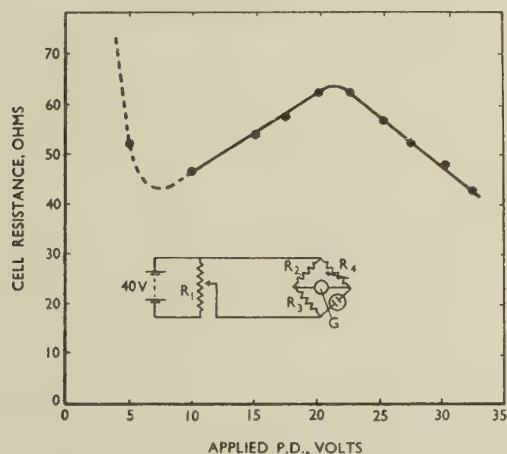


FIG. 18.—Bridge Circuit for Electrolytic Polishing, and Set of Results. Electrolyte: chromic + acetic acids; anode = 1.8 cm.<sup>2</sup> iron. Electrode separation = 2 cm. Cathode: iron.

$R_1 = 12 \Omega$ ,  $R_2 = 500 \Omega$ ,  $R_3 = 5000 \Omega$ ,  $R_4 = 0-1000 \Omega$ .  
 $G =$  microammeter.

method, of course, permits much more rapid removal of the specimens from the bath.

Fig. 18 shows a simple bridge arrangement by which the current supplied to the bridge can be fixed precisely at the value which gives maximum cell resistance,

and the curve of cell resistance plotted against the potential difference between the cell terminals obtained when a mixture of acetic acid and chromic acid is used as electrolyte. This bridge arrangement works extremely well.

#### IV.—CLOSURE DOMAINS ON IRON AND SILICON-IRON

I am now going to suppose that we have a relatively long rectangular parallelepiped formed from a single-crystal specimen of pure iron or of silicon-iron, cut with its upper and lower surfaces parallel to a (100) plane and its long side faces parallel to a (110) plane. Let us first consider what we might expect to see on the upper surface when the material is in the unmagnetized state and we examine it by the Bitter-figure technique. If the surface is strained, we shall see a wonderful maze pattern which is simply characteristic of strain and which is easily reproducible; i.e. however often we magnetize and demagnetize the specimen, we always recover the same maze pattern. Moreover the pattern is easily reversed, i.e. black becomes white in the pattern, by the application of a small magnetic field perpendicular to the surface. With an unstrained surface, identical patterns are never obtained with successive demagnetizations.

Next, if the unstrained surface is unblemished and is a true crystal plane, we shall see comparatively few deposits; we may occasionally observe a 180° boundary and a few daggers or spikes near the edges of the specimen. If there is an inclusion or a tiny pit in the surface, we shall find peculiar patterns which I will deal with later. Generally, however, the surface is not a true (100) plane and we observe a complicated "fir-tree" pattern, as shown in Fig. 4 (a) (Plate LXII). This structure was very beautifully explained by Williams, Bozorth, and Shockley<sup>3</sup> in a paper remarkable for both its elegance and its range of new facts. The trunks of the "fir-trees" are here 180° boundaries, while the branches are special closure domain patterns, formed as it were by shallow, ellipsoidal-shaped closure domains running out from the walls of the principal main domains and intersecting the surface. The sole purpose of these closure domains is to prevent as much magnetic flux as possible from leaving the surface. They do not, of course, produce complete flux closure. Fig. 4 (b) shows in diagrammatic form the way in which the magnetic vectors are distributed in these domains. If the trunks are 90° walls, the branches leave perpendicularly to the trunk, as in Fig. 4 (c).

The essential correctness of the vector distributions can readily be proved, for if a very narrow line is scratched in the surface by means of a fine glass fibre, we thus dig a kind of microscopic trench across which lines of force can jump when the trench runs at right angles to the direction of prevailing magnetization, and deposits of colloid will form along the trench. In fact, in the surface, however carefully it is prepared,

we usually find unwanted trenches provided by very slight undulations formed during polishing. If these undulations are at right angles to the magnetization, then deposits of colloid will form along them; but scratches or undulations running parallel to the magnetization will not attract the colloid. In many of the figures (especially Plates LXIV and LXV), randomly scattered line deposits may be noticed, each indicative of departure from surface perfection, but each serving to manifest a direction of magnetization. It is said to be helpful in certain rare cases to examine the surface with a fine wire probe of some permanently magnetized material, but I have no personal experience of this technique.

Now, the degree of departure of the surface from a perfect (100) plane and the type of curvature of the surface greatly affect the "fir-tree" pattern. The greater the angle the surface makes with a true crystal plane, the heavier the colloid deposits. On a nearly true crystal surface we find very little colloid; with a small angle of inclination or departure, the branches of the "fir-trees" appear long and faint, decreasing in size but increasing in deposit intensity with increase in angle of inclination, until they become indistinct and very dense. The Bozorth explanation of their formation requires that the branches always point downhill with respect to the (100) plane, and this is found to be the case. Many of these statements can be supported by noting the effects of a small magnetic field on the branches.

An account of the demagnetized state would be incomplete without a reference to the beautiful work of Williams and Shockley,<sup>4</sup> who shaped a single-crystal specimen of silicon-iron in the form of a picture frame whose sides were parallel to [100] directions and whose main surfaces were (100) planes. In a demagnetized state, a single 180° domain boundary ran down the middle of the surface of each side of the frame, and when a magnetizing field was supplied by a coil wound on one side of the frame, the boundary could be displaced sideways to an extent directly proportional to the change in overall magnetization.

A special type of boundary is very occasionally observed with silicon-iron specimens demagnetized by heating them *in vacuo* above the Curie point. Fig. 5 (Plate LXII) shows two fine examples of what we term a "wiggly boundary". The line deposits of colloid indicate that the two regions separated by the wiggly boundary are magnetized in anti-parallel directions; in other words, the magnetization vectors appear to meet head-on at the boundary. While this view is likely to be correct, it may well be that we have here a special kind of flux closure, the lines of magnetization on opposite sides of the boundary forming closed loops or rings so that the lines of force turn inwards as they approach the boundary. This phenomenon is now being carefully investigated, because we should like to know how the number of wiggly boundaries and, indeed, the number of domain boundaries of any kind, depends upon the rate of cooling through the Curie point, and so on.

## V.—QUANTITATIVE ASPECTS OF DOMAIN STRUCTURE

It is often helpful in dealing with domain theory to have in mind a scheme of magnetization processes suggested by Néel. Starting with the view that in an unmagnetized iron crystal each domain vector is aligned parallel to one of the six directions represented by the cube edges and their extensions in the negative directions, we picture a six-phase state of magnetization, termed Mode I magnetization. When we apply a small external field to the crystal, supposing the latter to be ellipsoidal in shape both for convenience and for ease in understanding, then before an effective field can be established *inside* the crystal three of the phases must disappear, because otherwise they would entirely oppose the internal field; we are then left with a three-phase, or Mode II, magnetization. On

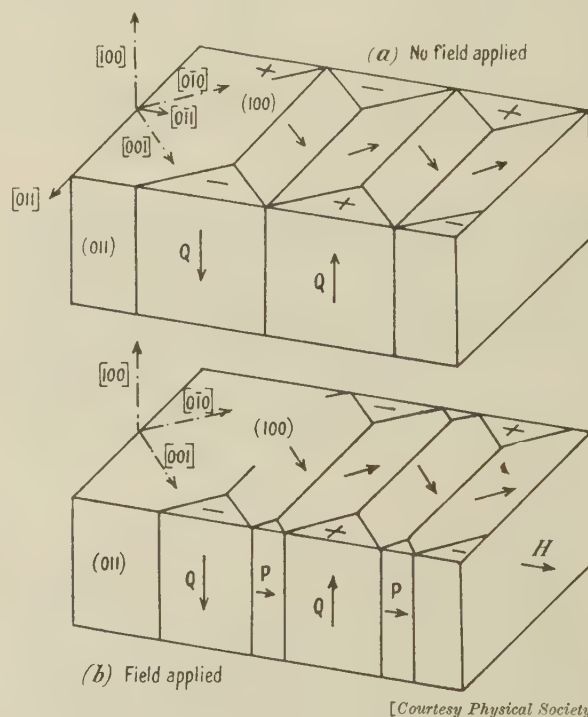


FIG. 19.—Domain Structure Proposed by Néel.

increasing the applied field further, we can really establish a field *within* the crystal itself, and eventually make one of the remaining phases so unfavoured that it fades away, so leaving only a two-phase or Mode III magnetization. Finally, as the applied field is increased without limit, a single-phase or Mode IV magnetization alone can exist.

The Bitter-figure technique has been most successfully applied to the quantitative examination of Mode III magnetization, using crystals of iron or silicon-iron cut in the special manner shown in Fig. 19 (a). Here we have what we frequently describe as the Néel cut, a crystal in the shape of a rectangular parallelepiped with its upper and lower surface (100) planes

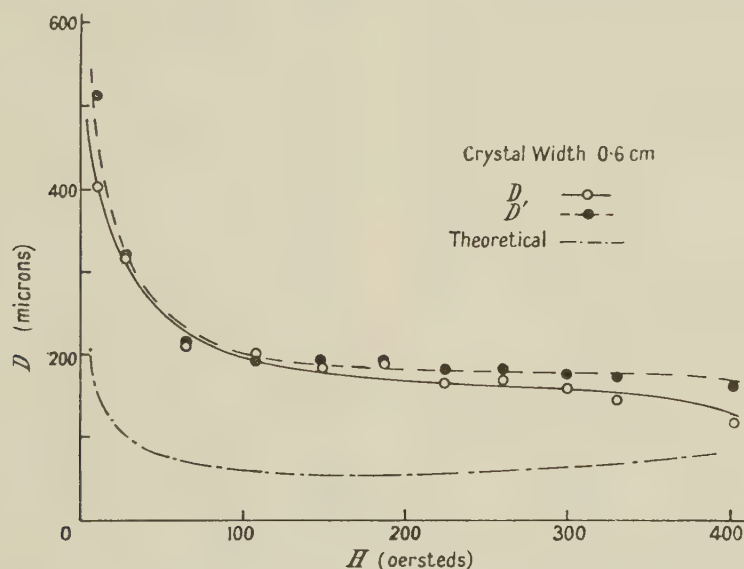


and its sides (110) planes. In the upper surface there are two easy directions of magnetization with the [110] direction running midway between them. When an extremely small field acts inside the crystal and Mode II just gives way to Mode III magnetization, a common-sense argument shows us that the principal domains must be leaf-like, with their planes perpendicular to the [110] direction and with the magnetic vectors of adjacent domains directed parallel to the  $[0\bar{1}0]$  and  $[00\bar{1}]$  easy directions of magnetization. In other words, adjacent domains are separated by  $90^\circ$  boundaries. Néel postulated that at the sides of the crystal there existed certain closure domains, the antiparallel, or  $Q$ , domains which are also magnetized along easy directions.

On the establishment of a finite field *within* the

We have  $D = \sqrt{\gamma L(W_p + W_q)/W_p W_q}$ , where  $L$  is the width of the specimen,  $\gamma$  is the energy/cm.<sup>2</sup> of a domain wall, and  $W_p$  and  $W_q$  are, respectively, the energy/c.c. of the parallel and antiparallel domains.

Several of my research workers, in particular Drs. F. E. Neale and C. D. Mee, have made measurements of  $D$  and  $H$  for crystals of silicon-iron cut in the prescribed manner. Typical records from which  $D$  was determined are shown in Fig. 7 (Plate LXIII);  $H$  was measured with a magnetic potentiometer. The lines of deposit run at right angles to the effective magnetic field, and it is the average distance between these lines which gives the period,  $D$ . One would, *a priori*, expect to observe twice as many lines as are actually observed, but we find that alternate domain boundaries are missing from the patterns because the stray fields



[Courtesy Physical Society.]

Fig. 20.—Variation of Domain Spacings on (100) and (110) Planes with Field.

—○— (100) plane —●— (110) plane

crystal, a field such as one could measure with a magnetic potentiometer, several domain changes occur. First the main vectors turn inwards towards the [110] direction, but always in such a way that the normal component of magnetization is continuous across the domain walls, and a new set of closure domains, the parallel, or  $P$ , domains appear as shown in Fig. 19 (b), and Mode III magnetization obtains. We do not, of course, include the small, subsidiary closure domains when describing a mode of magnetization.

Néel showed that it is relatively easy to calculate the period or spacing,  $D$ , between successive pairs of domains as a function of the effective magnetic field,  $H$ , within the crystal. From the expression for the total energy/unit volume of the specimen in terms of the magnetic anisotropies and the volumes of the several domains, together with the energies of the individual domain boundaries, one calculates the value of  $D$  for which this expression is a minimum with a stated value of  $H$ .

above them are in opposition to the applied magnetic field.

The deposits found on the (110) sides of a Néel cut are often surprisingly beautiful and complex; in Nottingham, for obvious reasons, we refer to them as lace patterns. In the example shown in Fig. 8 (a), (Plate LXIII), attention is directed to a kind of St. Andrew's Cross pattern which is frequently observed, and which is thought to be of special significance, although we cannot provide an adequate explanation for its occurrence.

If we do not understand the significance of the St. Andrew's Cross, still less do we understand one peculiar difference which we observed between the lace patterns obtained on crystals of silicon-iron and those on pure iron. In Fig. 8 (a) for silicon-iron, the lace patterns run vertically, i.e. perpendicular to the applied field. But in the case of pure iron exposed to approximately the same field (Fig. 8 (b), Plate LXIII), they are inclined at an angle of about  $14^\circ$  to the

vertical. A further example for a smaller field is given in Fig. 8 (d) (Plate LXIII). The experiments have now been carried out with two different crystals of pure iron and have been frequently repeated. The phenomenon may be due to hidden imperfection in the crystals, or it may be an effect due to differences in crystal dimensions, for the iron crystals were rather thin, and this feature is being investigated further. In Fig. 8 (c) are reproduced some lace patterns photographed by Mr. Hart on large-grained polycrystalline silicon-iron; the strange slope should be noted. The polycrystalline material was very thin.

Turning now to Fig. 20, we have some typical  $D/H$  results obtained by Dr. Mee on a silicon-iron crystal some 13 mm. long and  $6 \times 6$  mm. in cross-section both for the (100) and (110) surfaces, together with the theoretical curve for pure iron calculated on Néel's theory. There ought not to be much difference between the theoretical curve for silicon-iron and that for pure iron, since the anisotropy constant,  $K$ , enters into the expression for the period,  $D$ , as  $K^{-1/4}$ ; and we have recently found that experiments on pure iron

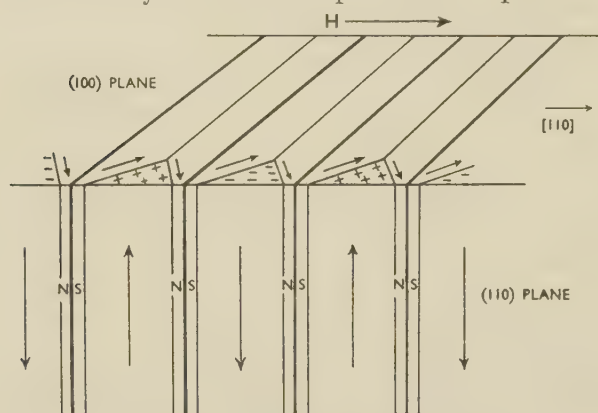


FIG. 21.—Suggested Explanation of Formation of a Lace Pattern on a (110) Surface of Silicon-Iron.

and on silicon-iron are in accord. The results show that there is no doubt about the essential correctness of Néel's ideas, but there is certainly some numerical discrepancy. However, this discrepancy need not unduly disturb us, for Néel's calculation certainly does not envisage a lace pattern on the (110) surface. Indeed, we think that the state of affairs on the (110) surface is more adequately given by Fig. 21 than by Fig. 19 (b).

Now, you may have observed some feather-like or branch-like projections on one side of the line deposits on the (100) surface, the side presumably favoured by the applied field conditions. These projections ought theoretically to make the same angle with the line deposit as the domain vectors make with the domain boundaries in the Néel diagram. Dr. Mee measured a series of these angles as a function of the effective magnetic field and compared them with the values expected on Néel's theory. Again, experiment showed that Néel's results are essentially correct, though exact numerical agreement is not obtained.

## VI.—THE DOMAIN STRUCTURE OF NICKEL

The straight-line patterns such as one observes with the Néel cut appear to be more widespread than would be imagined, for such a pattern was found by Dr. G. W. Wilson on the (111) plane of a single crystal of nickel;<sup>5</sup> it is reproduced in Fig. 6 (b) (Plate LXII). One would hardly expect this pattern at all, for nickel with its eight easy directions of magnetization generally gives patterns which are very difficult to interpret, and in the case in point there is no easy direction in the surface of the crystal. Yet, even for the (111) nickel surface, we obtain a curve of  $D/H$  which strongly reminds us of similar curves for the Néel cut with silicon-iron, and it is probable that the nickel line patterns are due to small triangular closure domains in the surface, which are magnetized parallel to the applied field. The scratch and mound techniques fail in the case of nickel.

In the case of a nickel (110) surface with a [100] direction running down the middle, we would expect a domain structure very similar to that of the Néel cut for iron, and Dr. Wilson managed to obtain the line patterns of Fig. 6 (a) (Plate LXII). They are however, thin and diffuse compared with those found on cobalt and on iron, presumably because the magnetic anisotropy constant of nickel is so much smaller and its saturation intensity of magnetization so much less. It is difficult to take into account the effects of strain, to which nickel is extraordinarily sensitive, in computing theoretical  $D/H$  curves for this metal. However, such pictures certainly provide food for thought, as may be realized from a study of the patterns obtained by Wilson on a nickel (112) plane with an applied field along the [100] direction, and Wilson's suggested model of the corresponding domain structure.

I have already said that nickel is extraordinarily sensitive to strain. Now, in Nottingham, we have paid much attention to obtaining nickel surfaces as nearly as possible true crystal planes and we took reasonable care, as we thought, to avoid straining them. However, from some work very recently published by Yamamoto and Iwata,<sup>6</sup> it appears that we should have discovered much more about the domain structure of nickel if we had confined our attention to less perfectly shaped but very much more carefully annealed crystals. On unmagnetized (110) nickel surfaces, these workers found "fir-tree" patterns with their branches set at  $35^\circ$  on one side of a trunk and at  $55^\circ$  on the other, since the trunks follow the [111] directions and the branches the [110] or [001] directions. Again, branches were often found to occur singly on one side or the other of the trunk, and this resulted in some bending of the  $180^\circ$  boundary.

In silicon-iron, tree patterns are sometimes found whose trunks are  $90^\circ$  walls with branches at  $45^\circ$ , as shown in Fig. 4 (c). On a nickel (110) surface, Yamamoto and Iwata obtained analogous patterns, but the trunks were  $71^\circ$  walls with branches at about



35° on both sides of the trunk, when the surface was inclined to the (110) plane by rotation about a [100] direction. When, however, the surface was rotated about the [110] direction, they found 109° trunks with *P* domain branches perpendicular to the wall and ending externally in small extension pieces, and *Q* domain branches making angles of 55° with the trunk. In addition, special types of tree pattern were obtained by slight rotation of the crystal surface from the (110) plane about the direction of the 71° walls.

An interesting parallelogram-net pattern was obtained when the (110) surface, instead of being truly plane, was somewhat rounded during polishing to form a spherical surface with a radius of curvature of about 2 cm. The net was thought to be formed of 180° and 109° walls or, alternatively, of 180° and 71° walls, and it was thought too that magnetostrictive energy had much to do with the pattern obtained. Further, it was found that the crystal direction along which an alternating-current demagnetizing field was applied was important, as 180° boundaries tended to form parallel to that direction. Obviously, so far only the surface of the nickel phenomena has been scratched!

## VII.—THE EFFECTS OF INCLUSIONS

As a result of the powder technique, we are quickly learning the important part which small inclusions such as impurities or small defects such as accidental pits or deliberately made tiny deformations may play in magnetization processes. Let us consider, for example, the effects which a small inclusion in the shape of a square may have upon the magnetization of the main domain configuration in which it is situated. As Néel first showed, we cannot admit that free poles may form over its sides, for otherwise the magnetostatic energy associated with them would be, relatively speaking, enormous. Consequently, a system of closure domains must form around the inclusion.

Two cases are of particular interest. In the first, the inclusion lies wholly within a main domain, and we can devise a closure system like that of Fig. 9 (a) (Plate LXIV). Such a closure system is often observed, and an example is given in Fig. 9 (b) (Plate LXIV). The spikes are never, to my knowledge, found in the same line as, but always at 45° to, the direction of magnetization in the main domain. In the second case, a 180° boundary passes straight through the inclusion, and Néel suggested the very simple closure system of Fig. 9 (c). Now this structure is certainly observed, if only rarely, and has been photographed by Dr. Mee (Fig. 9 (d), Plate LXIV), and by Mr. Martin (Fig. 10 (d), Plate LXIV). This structure is probably rare because imperfections are usually round instead of square, and because the small triangular closure domains could so easily be obscured by the imperfection itself and by the liquid colloid around it.

It is especially interesting to observe what happens

when a boundary strikes an inclusion as it moves across a crystal surface under an increasing magnetic field. An interesting series of pictures taken by D. H. Martin is shown in Fig. 10 as a 180° boundary was caused to move across an inclusion. These pictures drive home the importance of imperfections in magnetization processes. They also make us consider whether the tiny imperfections evident on the surfaces of our specimens are produced during polishing and whether similar imperfections are present within the body of a crystal. They must cause other thoughts in the minds of those who make transformer materials!

In Fig. 10 the field is gradually being increased from (a) to (h) in such a way that the large domain on the right-hand side of each picture decreases to the advantage of its neighbours, so that a 180° boundary is being pushed more and more to the right of the picture. If we wish to think in terms of the hysteresis cycle, we may imagine that we are on an ascending portion of the loop a little below the knee, where irreversible phenomena are much in evidence. Now, an imperfection of some kind stands in the way of the free movement of the boundary, and we see the way in which the Néel closure structure of Fig 9 (c) is established. The triangular areas on opposite sides of the imperfection are very clear in certain of the photographs, but perhaps what is particularly interesting is the convincing proof of the existence of irreversible processes, i.e. of hysteresis, which they provide. We cannot imagine that such changes in domain configuration can possibly be reversible. Figs. 10 (c) to (f) to some extent give us an idea of what may occur when we attempt to measure reversible permeability, which we think is a measure of the ability of a boundary to suffer displacement without rupture. Figs. 10 (g) and (h) show what happens when we apply fields too great for reversible changes only, fields which produce rupture of a boundary, and which, therefore, give a measure of the coercivity.

In Fig. 11 (Plate LXV) we have four pictures, again taken by D. H. Martin, which show how a 90° boundary, moving from left to right, behaves when it strikes an imperfection. We note the interesting way in which a dagger closure domain collapses and merges into the boundary and how another dagger is later formed on the opposite side of the imperfection. Again, if we wish to think in terms of hysteresis cycle, we are witnessing one of the irreversible phenomena which occur on a downward portion of the loop below the knee.

Recently we have made many records when studying what we term the domains of reverse magnetization which arise when an initially saturated crystal of silicon-iron is slowly demagnetized.<sup>7</sup> We used a 3% silicon-iron specimen, some  $8 \times 2 \times 1.5$  mm., cut so that each surface was a true (100) plane with its long axis parallel to a [100] direction along which a magnetic field was applied. When a strong magnetic field, sufficient to saturate the specimen, was slowly reduced to zero and then increased in the

reverse sense, we recorded the sequence of events shown in Fig. 12 (Plate LXV).

The first departure from the saturated, single-domain condition was the appearance of closure domains at imperfections in the surface. At first they were very small, but they grew in size so that when the applied field was approximately zero they were of the usual size of tree patterns. Thus, in Fig. 12 (a) we have the closure structure around a large imperfection when a small reverse field acted, while Fig. 12 (b) shows how the structure increased in size with an increase in the field. Fig. 12 (c), obtained with further increase in reverse field, shows a breakdown of a 90° closure domain producing a new structure running upwards and obviously magnetized in the opposite sense to the initial saturation direction; the new structure was in a region of some slight surface imperfection. We call this new structure a domain of reverse magnetization. Such domains grow very rapidly with change in field, as shown by Fig. 12 (d) and the composite picture Fig. 12 (e), which were obtained following an increase in field of less than 1 Oe. above that used for Fig. 12 (c). Once again, we get an idea of how hysteresis may arise and we also see why any theoretical difficulties which may be encountered<sup>8</sup> in trying to explain how an ideal, saturated crystal can eventually become demagnetized, do not appeal to the experimenter who deals with crystals in which there are bound to be surface and other imperfections.

One naturally asks, can a small strained portion of a crystal which is otherwise properly annealed act as an imperfection? Fig. 13 (Plate LXVI), taken by Martin, shows very convincingly that it can. Each "wiggly" patch in Fig. 13 (a) and 13 (c) with its suggestion of an embryo maze pattern is a region of strain, and closure domains form around it in the same way as around a pit or inclusion. In Fig. 13 (c) the long line of dots sloping upwards from right to left, above the patch of strained material, provides a good example of the sets of very tiny pits which are often found after electrolytic polishing.

## VIII.—EXPERIMENTS WITH POLYCRYSTALS

Metallurgists may possibly become impatient with the many references made to work with single crystals only, and may wonder whether polycrystalline material is ever investigated. Relatively few experiments have been made on polycrystalline material, because a specimen must possess a grain structure sufficiently coarse to allow reasonably undisturbed powder patterns to be formed, and it is advisable that individual grains subjected to examination should have a definite crystal plane located in the surface of the specimen. The behaviour of polycrystalline cobalt, given in Fig. 2 (a), illustrates these points.

Among recent experiments are those of Martius, Gow, and Chalmers,<sup>9</sup> who photographed the behaviour of domain walls in the neighbourhood of grain boundaries in a bicrystal of nickel. Dijkstra and

Martius<sup>10</sup> examined the changes in the domain pattern of grain-oriented silicon-iron with large grain-size when the specimen was put under various tensions within the elastic range. They made observations on a crystal grain with a (110) plane in the surface of the specimen and applied tension along the [110] direction. They found that at a load of approximately 1 kg./mm.<sup>2</sup> the original domain pattern vanished, and that after a transition stage with increasing load a new stress-induced domain pattern appeared. Nesbitt and Williams<sup>11</sup> obtained patterns on polycrystalline Alnico V (Alcomax) in an attempt to explain the mode of action of a magnetic field applied during heat-treatment of such materials.

We recently tried to see how far patterns found on polycrystalline surfaces had their counterpart in patterns on single crystal surfaces.<sup>12</sup> It can be seen at once from Fig. 14 (Plate LXVI) that the patterns give clear indications of the orientations of the polycrystal grains. With adjacent grains of closely similar orientation (as Chalmers and his collaborators found<sup>9</sup>), the patterns are often continuous from one grain to the other, while grains of widely differing orientations have distinctive patterns, with a sharp line of demarcation at the grain boundary. We were able to compare the spacings of a lace pattern on single-crystal and polycrystalline specimens of approximately the same thickness and we found good agreement between the two. It is very interesting that some of the lace patterns found on grains of a polycrystalline specimen did not run parallel to the [100] direction, but at an angle thereto. For example, in Fig. 8 (c), we have such a pattern for a field of 35 Oe., approximately the same magnitude as that used by Dr. Mee in obtaining the pattern of Fig. 8 (d), namely 45 Oe. Perhaps it should be added that we have no real proof that a field of 35 Oe., as measured by a magnetic potentiometer set over several crystal grains, is precisely the field within the particular grain in which one is interested.

I mention this point because of some experiments made with a single-crystal (100) disc of silicon-iron, some 14 mm. in dia. and 0.75 mm. deep, with a small central hole. We magnetized the disc by sending a current through a long straight wire threaded through the hole perpendicular to the disc. We found Néel line patterns in the four possible regions on the disc where one would expect them; but, whereas we feel sure that the magnetizing field falls off inversely as the distance from the centre of the disc, the line spacing appears to remain constant as one moves across the disc from the centre to the perimeter, as shown in Fig. 15 (Plate LXVI) which is made from some fourteen superimposed pictures.

The reason for this strange constancy is not far to seek. It lies in the complicated closure structures which are found at the borders of the line systems, i.e. from the rim and the edges of the holes, and which penetrate into the domains between the lines. In other words, instead of the Néel lines being forced to fall closer together as we approach the centre of the disc,



the closure structure alters instead in such a way as to maintain the total energy of the whole system at a minimum. This result seems to me to be of great importance, for it is reasonable to deduce from it that leaf-shaped domains tend to form whenever possible, and that they must be much more widespread than we formerly imagined them to be. In addition, we see here complete Néel lines, i.e. every alternate line is not now missing. We note particularly the hatched appearance of a set of  $90^\circ$  domains, separated by domains relatively clear of colloid, and the way in which the former taper towards the edge of the hole.

There are many interesting features here which warrant further examination.

## ACKNOWLEDGEMENTS

I should like to express my thanks to my research students and to all who have helped us in our work by the provision of specimens and in other ways; my thanks are due particularly to the British Iron and Steel Research Association, the Department of Industrial and Scientific Research, the British Electrical and Allied Industries Research Association, Dr. Rohn Truell, and Dr. D. Shoenberg.

## REFERENCES

Many references to work published up to the end of 1950 will be found in "Modern Magnetism" by L. F. Bates. 1951: Cambridge (University Press).

1. L. Landau and E. Lifshitz, *Physikal. Z. Sowjetunion*, 1935, **8**, 153.
2. R. M. Bozorth, "Ferromagnetism", p. 533. 1951: New York (D. Van Nostrand Co.).
3. H. J. Williams, R. M. Bozorth, and W. Shockley, *Phys. Rev.*, 1948, [ii], **75**, 155.
4. H. J. Williams and W. Shockley, *ibid.*, 1948, [ii], **75**, 178.
5. L. F. Bates and G. W. Wilson, *Proc. Phys. Soc.*, 1953, [A], **66**, 819.
6. M. Yamamoto and T. Iwata, *Sci. Rep. Research Inst. Tohoku Univ.*, 1953, [A], **5**, 433.
7. L. F. Bates and D. H. Martin, *Proc. Phys. Soc.*, 1953, [A], **66**, 162.
8. W. F. Brown, Jr., *Rev. Modern Physics*, 1945, **17**, 15.
9. U. M. Martius, K. V. Gow, and B. Chalmers, *Phys. Rev.*, 1951, [ii], **82**, 106.
10. L. J. Dijkstra and U. M. Martius, *Rev. Modern Physics*, 1953, **25**, 146.
11. E. A. Nesbitt and H. J. Williams, *Phys. Rev.*, 1950, [ii], **80**, 112.
12. L. F. Bates and A. Hart, *Proc. Phys. Soc.*, 1953, [A], **66**, 813.

# 1534 THE INFLUENCE OF EXTRUSION DIRECTION ON THE CORROSION AND STRESS-CORROSION OF ALUMINIUM-COPPER-MAGNESIUM ALLOYS \*

By E. A. G. LIDDIARD,† M.A., F.I.M., MEMBER, and WINIFRED A. BELL,‡ B.A.

## SYNOPSIS

Stress-corrosion tests were carried out on extrusions and sheet made from the same billet of aluminium-4% copper-0.5% magnesium-0.8% manganese alloy and on sheet rolled from an extruded bar. In the fully heat-treated condition, extrusions show little, if any, susceptibility to stress-corrosion when the stress is parallel with the direction of extrusion, whereas sheet is susceptible whether stressed parallel with or normal to the rolling direction. Specimens cut transversely from extruded bar show susceptibility to stress-corrosion equal to that of sheet material. Variation in susceptibility is attributed to directionality in structure which is less marked in low-manganese material. Stress-corrosion is not influenced by the thickness of the specimen and is prevented by spraying with commercial-purity aluminium or aluminium-1% zinc alloy.

## I.—INTRODUCTION

PREVIOUS study of the corrosion behaviour of aluminium-copper-magnesium alloy (HE15-WP, British Standard No. 1476) extrusions when exposed to various field tests has shown that the material is not susceptible to stress-corrosion when stressed under constant-strain bending in either industrial or marine atmospheres or in a 3% salt spray.<sup>1</sup> In sheet form, the aluminium-copper-magnesium alloys of this type, in the solution-treated and elevated-temperature-aged condition, are susceptible to stress-corrosion in salt spray. In laboratory salt-spray tests, normal commercial material extruded in the solution-treated and elevated-temperature-aged condition withstood stresses as high as the minimum 0.1% proof stress specified for this material, i.e., 24 tons/in.<sup>2</sup>, for 12 months without any failures occurring.

The high stress-corrosion resistance is attributed to the occurrence of preferential attack along planes parallel to the direction of extrusion. This results in a redistribution of stress at the base of a corrosion pit or crevice and prevents the penetration of cracks or intercrystalline fissures normal to the direction of stressing. Corrosion, particularly in the early stages, usually takes the form of attack at grain boundaries that run longitudinally to the direction of extrusion. In contrast, rolled sheet in the heat-treated and elevated-temperature-aged condition suffers intercrystalline corrosion which tends to penetrate through the thickness of the sheet.

In the earlier paper,<sup>1</sup> it was suggested that the

composition of the material might have a pronounced influence on the structural inhomogeneities, particularly in the absence of full recrystallization, as it is well known that the presence of manganese raises the recrystallization temperature of aluminium-copper-magnesium alloys and, in extrusions, manganese-rich particles tend to string out into bands. These two factors militate against the complete homogenization of the alloy during solution-treatment.<sup>2,3</sup> The work described in the present paper was, therefore, undertaken to investigate further the effects of direction of stressing in relation to working direction, and the susceptibility of rolled and extruded material to the simultaneous application of stress and corrosion.

## II.—EXPERIMENTAL PROCEDURE

### 1. PREPARATION OF MATERIALS

Two separate casts of aluminium-copper-magnesium alloys were made, one containing the normal 0.76% manganese, and the second, of otherwise similar composition, containing 0.08% manganese. These two materials will be referred to as "normal manganese" and "low manganese". Continuously cast billets of these alloys were cut in half, one portion being extruded to 2-in.-dia. bar and the other portion forged into slabs which were subsequently rolled to sheet of various thicknesses. Details of composition and of the extrusion, forging, and rolling procedures are given in an Appendix (p. 432). All the materials were cast and worked in accordance with normal commercial practice.

\* Manuscript received 23 June 1953; in revised form 30 October 1953.

† Director of Research, Fulmer Research Institute, Stoke

Poges, Bucks.

‡ Formerly Investigator, Fulmer Research Institute, Stoke Poges, Bucks.



The specimens of sheet and extrusion were subjected to corrosion and stress-corrosion tests in order to determine: (1) the stress-corrosion properties in bending of sheet and extrusion made from the same cast billet; (2) the behaviour of the material in direct-tension stress-corrosion tests, and when stressed normal and parallel to the direction of extrusion; and (3) the influence of manganese on the stress-corrosion properties.

## 2. STRESS-CORROSION BEND TESTS ON SHEET AND EXTRUSION MADE FROM THE SAME BILLET

Specimens, 0.1 in. thick  $\times \frac{3}{4}$  in. wide  $\times$  12 in. long, were cut longitudinally from the 2-in.-dia. extruded bars, from four positions approximately  $\frac{1}{4}$  in. below the surface at diametrically opposite places, as shown in Fig. 1 (a). Specimens of the

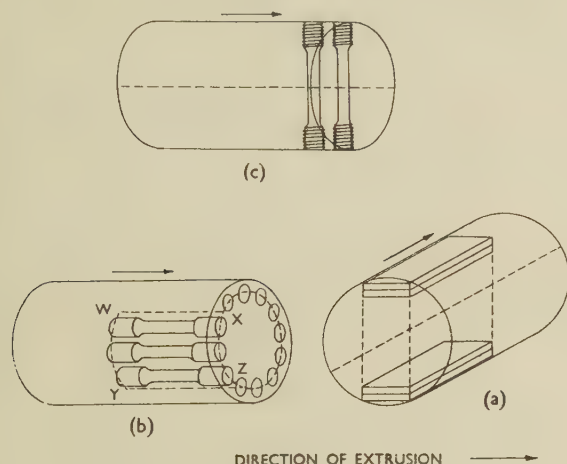


FIG. 1.—Specimen Taken from Extruded Bar.

same width and length, of three thicknesses (0.2, 0.1, and 0.05 in.) were also cut from the rolled sheet. The specimens were subjected to stress-corrosion bend tests at constant load, using four-point loading, and not under constant-strain bending as in the earlier work on atmospheric corrosion.<sup>1</sup>

The specimens were sprayed with 3% sodium chloride solution five times per week. The results of the tests given in Table I (a) show that only one failure occurred with extruded material. The low-manganese extruded specimen stressed at 20 tons/in.<sup>2</sup> broke after 362 days' exposure, but the unstressed, corroded specimens exposed for periods of approximately one year had an average breaking strength of only 20.6 tons/in.<sup>2</sup>. There is, therefore, no evidence of acceleration of corrosion by stress. If these results are compared with those reported in Table I (b), (c), and (d), which were obtained on sheet test-pieces made from sheet rolled from the same billets, the superiority in stress-corrosion resistance of the extruded material is very marked. Failures occurred rapidly in sheet of both alloys in thicknesses ranging from 0.05 to 0.20 in., except in the case of the normal-manganese 0.2-in. sheet, stressed at 16 tons/in.<sup>2</sup>, but

TABLE I.—Results of Stress-Corrosion Tests in Bending.

Material	Stressed And Corroded		Unstressed, Corroded Same Time As Stressed Specimens		Unstressed, Un-corroded Controls	
	Stress, tons/in. <sup>2</sup>	Time To Failure, days	U.T.S., tons/in. <sup>2</sup>	Elong., %	U.T.S., tons/in. <sup>2</sup>	Elong., %
(a) Specimens 0.1 in. Thick Cut from Extruded Bar						
Low manganese	20	362	21.6	3	...	...
	16	> 350*	19.1	4	23.7	11
	16	> 375*	21.2	5	25.6	10
Normal manganese	20	> 363*	25.9	2.5	33.5	8
	20	> 257*	27.1	6	32.3	8
(b) Specimens Cut from 0.2-in. Sheet						
Low manganese	24	5-7	...	...	...	...
	24	8	28.8	8	27.8	10
	20	11	29.1	11	...	...
	20	7	27.8	6	27.8	10
	16	6	25.2	5	...	...
	16	8	25.8	5	...	...
Normal manganese	24	12	29.5	7.5	...	...
	24	12	30.9	8	28.0	10
	20	20	30.4	7	29.0	10
	20	174	27.9	4	...	...
	16	> 418*	(18.8)†	(1)†	...	...
	16		21.8	1	...	...
	16	> 358*	(17.0)†	(1)†	...	...
			21.6	1	...	...
(c) Specimens Cut from 0.1-in. Sheet						
Low manganese	24	4	26.7	5	...	...
	20	2-5	27.3	7.5	28.3	10
	20	5-7	31.6	6.0	...	...
	20	9	28.4	8.0	...	...
	20	14	29.2	13.0	29.1	10
	20	13	28.0	13.0	...	...
	16	9-12	26.9	3	...	...
Normal manganese	24	3	29.2	6	...	...
	24	7	29.8	6	...	...
	20	7	25.2	5	30.1	10
	20	5-7	32.0	6.5	...	...
	20	20	25.5	4	30.4	8
	16	30	28.8	2	...	...
	16	13	28.0	7	...	...
(d) Specimens Cut from 0.05-in. Sheet						
Low manganese	20	15	26.4	3	...	...
	20	6	27.1	6	27.8	12
	17.65	15	27.4	4.5	...	...
	17.65	15	27.4	5.0	28.8	12
	16	15	23.6	...	28.4	13
	16	14	23.4	...	...	...
Normal manganese	20	5	30.9	5	...	...
	20	5	27.8	4	29.0	10
	16	28	27.9	2	30.2	10
	16	25	28.2	1	30.8	10
(e) Specimens 0.1 in. Thick Cut from Sheet Rolled from Extruded 2-in.-Dia. Bar						
Low manganese	20	7	...	...	...	...
	20	18	27.2	4	30.1	11
	20	12	28.5	9	29.8	12
	16	45	27.3	7	29.9	12
	16	40	27.3	4	...	...
Normal manganese	20	27	32.1	10.0	...	...
	20	49	30.8	5	32.5	11
	16	195	27.1	2	32.5	11
	16	223	21.7	...	32.4	11

\* Removed unbroken.

† Tensile tests on stressed corroded specimen after removal unbroken.

even here there was evidence of slight acceleration of corrosion damage by the stress.

X-ray pole figures were determined by the British Non-Ferrous Metals Research Association on specimens of sheet and extrusion. The sheet specimen showed little, if any, preferred texture, but the extruded sample of normal manganese content showed marked preferred orientation. The [100] fibre texture was present with a preference for (110) planes in the surface. The [111] fibre texture was also present, though not to such an extent as the [100], and again showed a preference for (110) planes in the surface.

Since the corrosion-resisting properties of sheet and extruded bar from the same billet differed so widely, the effect of rolling sheet from a sample of 2-in.-dia. bar was also investigated. Samples of bar in both alloys were rolled to sheet 0.1 in. thick, with intermediate annealing. Pieces of sheet were solution-treated, quenched in cold water, and aged at 170° C., as for previous batches of material. Standard 0.75-in.-wide test-strips were cut from the sheets and subjected to the normal 3% sodium chloride spray stress-corrosion bend test. The results, given in Table I (e), should be compared with those in Table I (a). It was found that at a stress of 20 tons/in.<sup>2</sup>, failure of the low-manganese sheet material occurred in 7 and 18 days, and that the normal-manganese sheet material failed after 27 and 49 days' exposure at the same stress. It is clear that the rolling of the extruded bar reduced the stress-corrosion resistance almost to that of sheet rolled from the original cast billet (see Table I (c)). X-ray pole figures showed no preferred orientation.

### 3. INFLUENCE OF DIRECTION OF STRESSING

The influence of the method of stressing was investigated, using specimens stressed in direct tension by lever-operated jigs. The specimens were small cylindrical bar-type test-pieces with threaded ends and a gauge-length of 1 in., the diameter of the gauge portion being 0.179 in. The specimens were held in a vertical position in the testing unit, the gauge-lengths being sprayed once daily with 3% sodium chloride solution. Similar unstressed specimens were exposed to the same corroding conditions and were subjected to tensile tests when the corresponding test-piece failed in the stress-corrosion testing-jig.

The specimens were cut from 2-in.-dia. extruded bar in both alloys. One series in each alloy was machined with the longitudinal axis parallel to the longitudinal axis of the original bar (see Fig. 1 (b)), the specimens being cut from a zone about 0.15 in. below the surface. A second series in each alloy was machined with the longitudinal axis perpendicular to the longitudinal axis of the bar (see Fig. 1 (c)). During testing, therefore, the direction of stress was generally parallel to the fibre structure of the bar in the first series, and perpendicular to it in the second series.

The results of the stress-corrosion tests are shown in Tables II (a) and (b), together with the results of tensile tests made on unstressed corroded specimens and unstressed uncorroded control specimens. Comparing first the effect of direction of stressing, it is immediately obvious that the specimens cut transversely failed much more rapidly than those cut longitudinally, and there was rapid failure of the transversely cut specimens, even at the lowest stresses of 16 tons/in.<sup>2</sup>.

In contrast to the results obtained on flat specimens cut from extruded bar and tested in bending (see Table I (a)), there is evidence of some stress-corrosion in the longitudinal cylindrical specimens tested in direct tension. It must, however, be kept in mind that the specimens were cut from extrusions in such

TABLE II.—Results of Stress-Corrosion Tests by Direct Tension.

Material	Stressed and Corroded		Unstressed, Corroded Same Time As Stressed Specimens		Unstressed, Uncorroded Controls	
	Stress, tons/in. <sup>2</sup>	Time To Failure, days	U.T.S., tons/in. <sup>2</sup>	Elong., %	U.T.S., tons/in. <sup>2</sup>	Elong., %
(a) 0.179-in.-Dia. Cylindrical Specimens Cut Longitudinally from 2-in.-Dia. Extruded Bar						
Low manganese	24	17	25.5	12	...	...
	24	20	24.5	10	...	...
	20	47	24.3	10	25.6	12
	20	46	24.5	10	25.6	16
	16	117	24.4	12	...	...
	16	160	23.5	10	...	...
Normal manganese	24	77	30.0	5	...	...
	20	60	30.4	5	32.6	9
	16	125	28.8	1	32.8	10
(b) 0.179-in.-Dia. Cylindrical Specimens Cut Transversely from 2-in.-Dia. Extruded Bar						
Low manganese	24	3	23.9	3	...	...
	24	6	24.4	3.5	...	...
	20	4	27.6	5.5	25.7	3.5
	20	6	24.6	3	...	...
	16	7	24.6	3	26.5	4
	16	10	24.2	2	...	...
Normal manganese	24	4	27.8	3	...	...
	24	3	28.1	3.5	...	...
	20	4	26.5	3	28.2	4
	20	5	27.0	3	...	...
	16	7	27.7	3	28.4	4
	16	7	26.4	2	...	...
(c) 0.179-in.-Dia. Specimens Cut Longitudinally from 0.2-in.-Thick Sheet						
Low manganese	24	2-4	26.2	7	...	...
	24	2	26.9	9	27.8	10
	20	3	26.6	8	27.8	10
	20	3-5	26.4	5	...	...
	16	8	...	...	...	...
	16	5-7	25.0	4	...	...
Normal manganese	24	2	28.2	5	...	...
	24	3	28.1	6	30.1	10
	20	3	28.4	8	...	...
	20	2-7	25.8	4	30.4	8
	16	3-5	28.9	12.5	...	...
	16	13	27.8	8	...	...



TABLE II.—*continued.*

Material	Stressed and Corroded		Unstressed, Corroded Same Time As Stressed Specimens		Unstressed, Un-corroded Controls	
	Stress, tons/in. <sup>2</sup>	Time To Failure, days	U.T.S., tons/in. <sup>2</sup>	Elong., %	U.T.S., tons/in. <sup>2</sup>	Elong., %
(d) Flat Specimens Cut Longitudinally from 0.1-in.-Thick Sheet						
Low manganese	24	1-3	26.2	8	...	...
	24	2	27.3	15	28.3	10
	20	2	27.0	12	...	...
	20	4	24.7	4	29.1	10
	16	3	26.6	9	...	...
	16	3	26.9	3	...	...
Normal manganese	24	2	28.9	9	...	...
	24	4	28.6	7	30.1	10
	20	7	28.0	7	...	...
	20	3	28.7	7	30.4	8
	16	6	27.2	5	...	...
	16	8	26.4	4	...	...
(e) Flat Specimens Cut Longitudinally from 0.05-in.-Thick Sheet						
Low manganese	24	2-4	23.5	4	...	...
	24	2	27.1	8	27.8	12
	20	1-3	25.4	6	...	...
	20	2	...	...	28.8	12
	16	3	...	...	28.4	13
	16	4-6	...	...	...	...
	16	2-4	...	...	...	...
	16	2-4	...	...	...	...
Normal manganese	24	2	27.6	5	...	...
	24	2	...	...	...	...
	24	4-7	...	...	29.0	10
	20	2-5	...	...	...	...
	20	2	...	...	30.2	10
	16	2-4	...	...	30.8	10
	16	3	...	...	...	...
	16	4-6	...	...	...	...
(f) 0.179-in.-Dia. Specimens Cut Transversely from 0.2-in.-Thick Sheet						
Low manganese	24	2	26.8	8	...	...
	24	3-5	24.9	3	...	...
	20	1-3	27.3	8	27.4	11
	20	2-4	25.2	5	27.1	11
	16	7	23.3	4	...	...
	16	7	23.8	3	...	...
Normal manganese	24	1-3	27.4	5	...	...
	24	5	28.4	6	...	...
	20	1	28.7	7	29.6	9
	20	2-7	25.4	3	29.2	7
	16	8	23.6	2	...	...
	16	6	25.1	2	...	...

a way that the planes parallel to the surface of the original extrusion (*W*, *X*, *Y*, *Z* in Fig. 1 (*b*)) emerged at opposite sides of the specimens, and corrosion could proceed down them in a way that would not have been possible if the specimens had been concentric with the surfaces of the original extrusion. The specimens did not, therefore, allow full advantage to be taken of structural directionality. Specimens cut from sheet of various thicknesses were also tested in direct tension, and the results are given in Table II (*c*)-(f). It is immediately obvious that the stress-corrosion susceptibility of transverse specimens cut from extrusions is similar to that of sheet specimens.

Microsections were cut at monthly intervals from unstressed sheet specimens exposed to similar corro-

ding conditions. Both the low- and normal-manganese alloys were found to be very susceptible to inter-crystalline corrosion, and there was a very slight tendency in the normal-manganese alloy for the corrosion to occur longitudinally owing to slight elongation of the grains in the direction of rolling. The difference in corrosion behaviour of the two alloys in sheet form, however, is not very marked. Fig. 2 (Plate LXVII) shows photomicrographs of 0.2 in. (*a*) normal- and (*b*) low-manganese sheet specimens exhibiting such intercrystalline corrosion after 3 months' exposure to 3% sodium chloride solution sprayed once daily.

### III.—DISCUSSION OF RESULTS

A rapid comparative assessment of the results can be made by examining Table III, which gives the average results of all the tests made.

TABLE III.—*Average Time (Days) To Failure Under Various Stresses.*

Type of Test	Extrusions			Sheet		
	Direction of Stressing	Low Mn	Normal Mn	Low Mn	Normal Mn	Thickness, in.
(a) Stress = 24 tons/in. <sup>2</sup>						
Direct tension	Longitudinal to extrusion direction	19	77	3	3	0.2
				3	3	0.2*
				2	3	0.1
	Transverse to extrusion direction	5	4	...	...	0.05
4-Point-load bend test	Longitudinal to extrusion direction	...	...	7	12	0.2
				4	5	0.1
(b) Stress = 20 tons/in. <sup>2</sup>						
Direct tension	Longitudinal to extrusion direction	46	60	2	2	0.2
				3	3	0.2*
				3	5	0.1
	Transverse to extrusion direction	5	4	...	...	0.05
4-Point-load bend test	Longitudinal to extrusion direction	362	> 363 †	9	97	0.2
				9	11	0.1
				10	5	0.05
				12 ‡	38 ‡	0.1 ‡
(c) Stress = 16 tons/in. <sup>2</sup>						
Direct tension	Longitudinal to extrusion direction	139	125	7	9	0.2
				7	7	0.2*
				3	7	0.1
	Transverse to extrusion direction	8	7	...	...	0.05
4-Point-load bend test	Longitudinal to extrusion direction	> 375 †		7	> 418 †	0.2
				11	22	0.1
				15	27	0.05
				43 ‡	209 ‡	0.1 ‡

\* Stressed normal to rolling direction.

† Removed unbroken.

‡ Sheet rolled from extruded bar.

In comparing the relative susceptibility of low- and normal-manganese-containing material, it must be remembered that tests carried out at similar stresses are not strictly comparable, since the ultimate tensile strength of the normal-manganese material is 2-7 tons/in.<sup>2</sup> higher than that of the low-manganese

material, the exact figure depending on whether the specimens are from sheet or extrusions and on whether they were cut transversely or longitudinally (see Appendix).

The low-manganese material exhibits less directionality, and any apparent effect of manganese in reducing susceptibility in sheet material may be due to the higher ultimate strength and greater directionality which may be expected even in sheet material (see Figs. 2 and 3, Plate LXVII).

In only one set of results, viz. bending tests on normal-manganese material, is there any evidence of a systematic variation in life with the thickness of the sheet, and it must be concluded that susceptibility to stress-corrosion cannot be minimized by increasing the thickness of the material unless the stress per unit area is also reduced. In sheet material the direction of stressing, either parallel or normal to the direction of rolling, has no marked effect upon the stress-corrosion properties (cf. Tables II (c) and (f)).

From a comparison of the results obtained in constant-load bending and in direct tension, it is clear that direct tension is a more stringent test than bending. This may seem surprising at first sight, since the stress concentration expected at the base of crevices should, other things being equal, be greater in bending than in tension. Two factors, however, may operate in opposite directions. In bending tests only one face of the specimen is in tension and, since compressive stresses normally decrease rather than increase corrosion damage, the specimens can be regarded as being exposed to stress-corrosion from one side only, whereas the tensile specimens are subject to stress-corrosion from both surfaces. In addition, structural directionality may assist the lateral spread of corrosion more in bending than in direct tension.

It is clear, both from previous work and from the microscopic examination of the corroded specimens in the present work, that the attack occurring on extruded aluminium-copper-magnesium alloy proceeds along planes parallel to the original surfaces of the extrusion. This effect is particularly marked in material of normal manganese content. The directionality of structure is probably responsible for the lower susceptibility of these materials to stress-corrosion in constant-load bending, since the shear between the planes of structural inhomogeneity will tend to assist the lateral spread of corrosion and so reduce the stress concentration. Some support for this view is given by the relatively small differences in the lives of low-manganese and normal-manganese material when stressed in direct tension. Figs. 3 (a) and 3 (b) are photomicrographs showing the banded structure after etching in Keller's reagent. The bands are more distinct and much narrower in the normal-manganese than in the low-manganese alloy extrusions.

Although extrusions when stressed in bending parallel to the extrusion direction are not susceptible

to stress-corrosion, they are susceptible to layer or exfoliation corrosion, which may be serious. An example of this type of corrosion is shown in Fig. 4 (Plate LXVII), a photograph of the compression side of an extruded specimen which has been stressed by bending, and corroded by exposure to the industrial atmosphere at Sheffield for two years. It can be seen that the attack runs in planes parallel to the surface or extrusion direction, and that layers exfoliate from the surface.

The most striking and important result of the present investigation is, however, the very marked effect of structural directionality on stress-corrosion behaviour of material of identical composition and final heat-treatment, particularly in materials fabricated by extrusion as compared with rolling. Although the direct-tension stress-corrosion test is probably less sensitive to structural directionality than the bend test, the difference in the lives of specimens cut longitudinally and transversely to the direction of extrusion is striking. This is of particular interest as the small test specimens cut longitudinally were not concentric with the plane of the original surface of the extrusion, and the gauge-length of the transverse specimens lay in the central portion of the original bar, where directional effects were likely to be less marked. The transverse specimens tended to fail at, or near, the shoulder of the specimen, where the flow in the original extrusion would be greater than at the centre.

#### IV.—PREVENTION OF STRESS-CORROSION

In view of these results, it is obvious that some kind of protection is necessary before this type of aluminium-copper-magnesium alloy sheet or extrusion, stressed normal to the direction of extrusion, can safely be used for structural work in corrosive atmospheres. Some preliminary tests have been carried out in order to see whether protection can be given by metallic sprayed or painted coatings which, if anodic to the basis alloy, will protect it sacrificially, in a similar manner to cladding on sheet.

Sheet specimens (0.036 in. thick) of the normal-manganese alloy have been sprayed with commercial-purity (99.7%) aluminium, aluminium-1% zinc alloy, and zinc. Similar specimens were painted with two brush coats of metallic zinc paint. These, together with unprotected control specimens, were stressed in a cantilever or one-point-load type of jig. In this type of jig, a size A flat test-piece, in accordance with British Standard No. 18 (1950), is bolted at one end and a weight suspended from the other. This has been used as a simple quick-sorting test for preliminary work because of its convenience when a great number of specimens are entailed. The stress is not constant over the gauge-length, as in the four-point-load bend test, but is concentrated at one end of the gauge-length and decreases down the length of the specimen. The probability of a particularly susceptible area being located in the zone of maximum stress is,



therefore, less in this type of test than in either of the other two tests used in the investigation.

The results, given in Table IV, show that metallic-

TABLE IV.—*Stress-Corrosion Tests on Coated-Sheet Specimens Stressed in Cantilever Type of Jig.*

Type and Thickness of Coating	Stress, tons/in. <sup>2</sup>	Days to Failure
Sprayed commercial-purity aluminium (99.7%) 0.002 in. (nominal)	24	> 265 *
	18	> 476 *
Sprayed aluminium-1% zinc alloy 0.002 in. (nominal)	24	> 265 *
	18	> 476 *
Sprayed zinc 0.002 in. (nominal)	24	265
	18	> 354 *
	18	129
	15	132
	15	> 290 *
Metallic zinc paint, two brush coats	24	131
	18	71
	18	41
	15	108
	15	61
Controls, shot-blasted surface	24	4
	24	11
	18	14
	15	34

\* Not broken.

zinc paint lengthens the life of the specimens, but that zinc spraying gives longer protection. Both, however, are inferior to 99.7% aluminium or aluminium-1% zinc alloy sprayed coatings, for which there have been, so far, no failures.

## V.—PRACTICAL IMPLICATIONS

Since, in practice, extrusions in their original form are likely to be stressed in the direction of extrusion, or at least in a direction parallel to the surfaces of the original extrusion, failure by stress-corrosion is unlikely to occur in extruded aluminium-copper-magnesium alloys heat-treated in the normal way. Where parts are machined or forged from extrusions, however, stress-corrosion is likely to be a serious risk if the direction of stressing is normal to the flow planes of the original extrusions. Attention is also drawn to the layer type of corrosion which previous work <sup>1</sup> has shown may be associated with structural directionality in an extruded aluminium-copper-magnesium alloy.

Alloying additions which increase directionality of structure either by raising the recrystallization temperature, or by forming banded precipitates, will increase the resistance to stress-corrosion when the stress is longitudinal to the direction of extrusion, but will tend to increase susceptibility when the stress is normal to the extrusion planes.

Peripheral grain growth and practices which tend to destroy directional effects, e.g. welding or solution-treatment after critical amounts of cold work, are

likely to render extrusions comparable in stress-corrosion behaviour to unclad sheet. Since protection can be given to sheet material by metallic aluminium or aluminium-1% zinc alloy sprayed coatings, extrusions are also likely to be protected by these coatings. Increasing the thickness of parts subject to stress-corrosion will not reduce susceptibility to failure unless the stress per unit area of cross-section is reduced thereby.

## VI.—CONCLUSIONS

(1) The susceptibility to stress-corrosion of fully heat-treated extrusions of aluminium-copper-magnesium alloys is strikingly dependent on the mode and direction of stressing in relation to the direction of extrusion.

(2) When stressed in bending longitudinally to the extrusion direction, extrusions are practically free from stress-corrosion.

(3) When the specimen is stressed in direct tension longitudinally to the direction of extrusion, stress-corrosion susceptibility is markedly less than that of unclad sheet of the same composition and heat-treatment.

(4) When the specimen is stressed in direct tension normal to the direction of extrusion, the stress-corrosion susceptibility of extrusions is marked, and is as great as that of unclad sheet of the same composition and heat-treatment.

(5) The directional effects noted above are increased by the presence of normal quantities of manganese.

(6) Tests in direct tension on both low-manganese and normal-manganese material and bending tests on low-manganese material have shown no evidence that the stress-corrosion susceptibility is, in any way, influenced by the thickness of the specimen. Bend tests on material of normal-manganese content have shown some increased life with increasing thickness of sheet, which is probably associated with decreasing directionality of structure as the amount of working and the degree of recrystallization on heat-treatment are increased.

(7) Aluminium or aluminium-1% zinc alloy sprayed coatings minimize or entirely suppress stress-corrosion in sheet material. Slightly less protection is given by sprayed-zinc coatings and somewhat less by metallic-zinc paint.

## ACKNOWLEDGEMENTS

This paper is published by permission of the Ministry of Supply and of Almin, Ltd., the joint sponsors of the work.

Some of the experimental work described was started by Mr. G. J. Metcalfe when in charge of the Corrosion Section at the Fulmer Research Institute. The authors wish to thank International Alloys, Ltd., who cast the experimental billets; Southern

Forge, Ltd., who made the extrusions; the Royal Aircraft Establishment, who carried out the rolling of the sheet from the extruded billet; and the British Non-Ferrous Metals Research Association, who provided the X-ray pole figures.

## REFERENCES

1. G. J. Metcalfe, *J. Inst. Metals*, 1952-53, **81**, 269.
2. H. J. Seemann and M. Dudek, *Aluminium*, 1940, **22**, 521.
3. H. Kostron, *ibid.*, 1941, **23**, 195.

## APPENDIX

## PREPARATION OF SPECIAL BILLETS OF NORMAL- AND LOW-MANGANESE CONTENT

Cast billets were made in two alloys of almost identical chemical compositions, apart from manganese content, as follows:

	Cu, %	Mg, %	Si, %	Fe, %	Mn, %	Ni, %	Zn, %	Pb, %	Sn, %	Ti, %
Low manganese	4.08	0.54	0.87	0.32	0.08	0.03	0.02	0.02	0.02	<0.02
Normal manganese	4.00	0.53	0.93	0.32	0.76	<0.02	0.03	0.02	0.03	<0.02

The billets were approximately  $6\frac{1}{2}$  in. in dia.,  $\times$  12 in. long. One billet in each alloy was cut in half, one half being rolled into sheet and the other half being extruded to 2-in.-dia. bar. The half-billets that were rolled to sheet were first skimmed to 6 in. dia.  $\times$  6 in. long, then forged to  $2\frac{1}{2}$ – $2\frac{3}{8}$  in. thick and 5–6 in. wide, with the major axis parallel to that of the original billet. At the start of forging, the temperature of the billets was 430° C., and at the finish, 380°–395° C.

The original bars were upset to approximately

3 in. in height without spreading. They were then cubed and drawn out on the original axis; the slabs were rolled to sheet. Hot rolling was carried out at 480° C. in four stages with approximately 40% reduction in thickness at each stage down to the thickness required, i.e. 0.2, 0.1, 0.05, and 0.036 in. thick. After rolling, all the strips were annealed at 360° C. for 1 hr. and were then cooled slowly in the furnace overnight. Samples from these sheets were stored in this condition and were solution-treated at  $505 \pm 5^\circ$  C., quenched in cold water, and aged for 8 hr. at 170°–175° C.

There was some variation in the properties of the material in different forms, but the average properties obtained on test-pieces of the same form as those used for corrosion testing were as follows:

		U.T.S., tons/in. <sup>2</sup>	Elong., %
2-in. Extruded Bar (sub-standard test-pieces):			
Low manganese	{ Longitudinal	25.1	12
	{ Transverse	26.1	4
Normal manganese	{ Longitudinal	32.8	9
	{ Transverse	28.3	4
0.2-in. Sheet			
Low manganese	{ Longitudinal	27.8	10
	{ Transverse	27.2	11
Normal manganese	{ Longitudinal	29.4	9
	{ Transverse	29.4	8
0.1-in. Sheet			
Low manganese	. . . .	28.7	10
Normal manganese	. . . .	30.2	9
0.05-in. Sheet			
Low manganese	. . . .	28.3	12
Normal manganese	. . . .	30.0	10
0.1-in. Sheet Rolled from 2-in. Extruded Bar			
Low manganese	. . . .	29.9	12
Normal manganese	. . . .	32.5	11



# A REDETERMINATION AND INTERPRETATION OF THE TITANIUM-RICH REGION OF THE TITANIUM-CHROMIUM SYSTEM\*

1535

By (MRS.) M. K. McQUILLAN,† M.A., MEMBER

## SYNOPSIS

Conflicting evidence in the literature has led to a redetermination of the phase boundaries in the composition range 0–14 at.-% chromium, using techniques designed to eliminate all likely sources of error. The results differ from those previously obtained by micrographic methods, and agree with those obtained in the range 0–4 at.-% chromium by the hydrogen-pressure method. The eutectoid temperature has been found to be much lower than hitherto supposed.

The difference between the present and previous micrographic results has been found to be due to insufficiently rapid quenching in the earlier experiments. A new interpretation of the behaviour of titanium alloys, based on the postulate of the aggregation of like atoms in the  $\beta$  solid solution, has been put forward, and a reason for this behaviour, in terms of a change with temperature in the electronic structure of the titanium atom, is suggested. It is believed that similar considerations may apply in other titanium alloy systems.

## I.—INTRODUCTION

SINCE the publication of the author's original survey<sup>1</sup> of the constitutional diagram of the titanium-chromium binary system, several other groups of workers<sup>2-4</sup> have reported micrographic investigations on this system. The later work, though providing general confirmation of the original diagram, has been concentrated more particularly on the titanium-rich region of the system, and detailed studies have been made on the position of the  $\beta/(\alpha + \beta)$  boundary, a feature which had not been investigated by the present author, to whom titanium metal of sufficiently high purity was not at that time available. It has been observed, however, that the boundaries presented as a result of these studies not only differ in varying degrees among themselves, but also differ appreciably from the partial  $\beta/(\alpha + \beta)$  boundary determined by (A. D.) McQuillan,<sup>5</sup> who, using very pure starting materials, studied alloys containing up to 5 at.-% chromium by the hydrogen-pressure method.† The present work was intended to clear up the position by reinvestigating the boundary, using techniques designed to eliminate all the more obvious sources of error, and has resulted in the confirmation of the hydrogen-pressure work. In continuing the investigation beyond the composition range covered by the hydrogen-pressure experiments, a boundary has been determined, the shape and direction of which cannot be reconciled with the previously determined position of the eutectoid point, and the work has, therefore, been extended to include

an investigation of the eutectoid reaction. The results obtained have given rise to a new concept of the behaviour of alloys of titanium with  $\beta$ -stabilizing elements.

## II.—EXPERIMENTAL PROCEDURE

It was considered that the reasons for the differences between the observations of the various previous workers must lie among the following: (1) that the starting materials used were not always sufficiently pure, (2) that some of the alloys were contaminated in the course of the work, (3) that insufficient time was allowed for the attainment of equilibrium, and (4) that, in the case of quenching experiments, the quenching rate was not sufficiently rapid to ensure the retention of the high-temperature structure. The experimental methods adopted in the present work were planned with the object of eliminating, as far as possible, all these potential sources of error.

### 1. MATERIALS USED

The titanium used was the purest available, i.e. iodide material prepared by the Foote Mineral Co. of America. Both chemical and spectrographic analyses showed that the only appreciable impurity present was zirconium of the order of 0.5 at.-%. The transformation range of the unalloyed material (which is the most useful criterion of its purity) was 872°–880° C. The chromium used was prepared electrolytically by Johnson, Matthey and Co., Ltd., and was subse-

\* Manuscript received 11 August 1953.

† Imperial Chemical Industries, Ltd., Metals Division, Birmingham.

‡ In this method phase changes occurring in titanium alloys are followed by plotting against temperature the pressure of the hydrogen in equilibrium with the alloy when

a specimen is heated in a closed system containing a quantity of hydrogen equivalent to a hydrogen content in the alloy of about 0.05 at.-%. Marked discontinuities occur in the pressure/temperature curves when the  $\alpha \rightleftharpoons \beta$  transformation begins and ends.

quently deoxidized. It contained less than 0.01% oxygen and 0.05% nitrogen.

## 2. MAKING UP THE ALLOYS

Six-gramme buttons of a series of titanium-chromium alloys were prepared by melting in an arc furnace on a water-cooled copper hearth, under an atmosphere of argon at reduced pressure. Each alloy was melted, turned over, and remelted several times. No appreciable weight change was found to occur during melting, and nominal compositions have, therefore, been taken to be the actual compositions. The buttons appeared to be satisfactorily uniform in composition, but as an additional precaution, those having the highest chromium contents were homogenized for 3 days at 1000° C. Atmospheric contamination during this period was prevented by heating the buttons inside a stoppered titanium cylinder in a continuously evacuated clear silica tube in which the pressure was lower than  $10^{-5}$  mm. of mercury. An outer envelope of clear silica evacuated to a pressure of  $5 \times 10^{-3}$  mm. of mercury served to reduce the rate of diffusion of air into the system. A check on the vacuum conditions inside the homogenizing apparatus was kept by means of a control specimen of pure titanium. The conditions were accepted as satisfactory only if no increase in the hardness of the control specimen had occurred during heat-treatment.

## 3. HEAT-TREATMENT

A very high degree of vacuum and a very rapid quench were the essential features of the heat-treatment apparatus used for this work. The type of apparatus used has already been described.<sup>1</sup> It consists of an evacuated water-cooled metal bell sealed on to a base-plate, through which pass two water-cooled electrodes about 3 in. apart. The heating element is formed by two metal strips arranged between the electrodes in the form of a bow, and is supplied with a current in the range 100–400 amp. The small alloy specimen is supported on a platinum/platinum-rhodium thermocouple in the space between the heaters. The thermocouple, which is sealed into a silica insulator passing out of the vacuum chamber through an O-ring seal in the base, serves to measure the temperature of the specimen as well as to support it, and since the hot junction is in direct contact with the specimen, a very accurate temperature reading is obtained. No reaction between specimen and thermocouple has been observed at the temperatures involved in these experiments. A metal tube, ending just above the specimen, passes through the bell and is connected through a vacuum tap to a water reservoir. The specimen is quenched by a stream of water which impinges directly upon it when the vacuum tap is turned, the heating current being switched off simultaneously. This results in almost instantaneous cooling to room temperature. After quenching, the apparatus is rinsed in alcohol and dried in warm air.

The vacuum attainable within this apparatus is better than  $10^{-5}$  mm. of mercury, but since titanium will take up oxygen and nitrogen even at such pressures the danger of contamination was further reduced by using titanium strips for the heater elements, which, being always at a higher temperature than the specimen and having a much greater surface area, act as getters and considerably improve the vacuum conditions. Titanium heaters have the additional advantage that they introduce no danger of metallic contamination.

The specimen temperature, which was controlled manually by varying the heater current, was dependent on the voltage fluctuations of a private mains supply. The effect of such fluctuations was overcome to a considerable extent by the continuous use of a temperature recorder, which ensured that the thermal history of each specimen was known in detail, and could be allowed for in interpreting the results. The temperatures quoted are estimated to be accurate to  $\pm 5^\circ$  C.

The alloy specimens were pickled in hydrofluoric acid before being mounted in the heating apparatus, and were degreased in ether after mounting. An outgassing period at about 400° C. was usually allowed at the beginning of the heat-treatment, followed by a homogenizing treatment of about 1 hr. in the range 900°–1000° C. The heating periods required for the attainment of equilibrium in any temperature range were determined by trial and error. At 660° C. a week was found to be sufficient for specimens containing up to 10 at.-% chromium. After polishing, the quenched specimens were etched in either 4% nitric acid and 3% hydrofluoric acid in water, or 40% hydrofluoric acid in glycerine.

## III.—EXPERIMENTAL RESULTS

### 1. THE $\beta/(\alpha + \beta)$ BOUNDARY

From quenching experiments carried out as described above, it was possible to determine the  $\beta/(\alpha + \beta)$  boundary indicated by the heavy line in Fig. 1, in which the results of previous workers have also been plotted. It will be observed that the present results agree very well with the experimental points obtained by the hydrogen-pressure method, and it now becomes clear that it would have been better to plot the boundary by joining up these points instead of by drawing what appeared to be the best curve through them, as was done in the original paper. The agreement between the present micrographic results and the hydrogen-pressure work has been further checked by (A. D.) McQuillan, who, at the author's request, has recently examined a 6.5 at.-% chromium alloy and has found a discontinuity in the pressure/temperature curve corresponding to the  $\beta/(\alpha + \beta)$  boundary at 735° C., thus confirming the existence of the bulge in the boundary established by micrographic methods. That the true boundary lies



appreciably below those previously reported on micrographic evidence is illustrated by Fig. 2 (Plate LXVIII), which shows the structure of a 4.1 at.-% chromium alloy water-quenched from 765° C., a temperature well within the  $(\alpha + \beta)$  region in the diagrams presented by Duwez and Taylor,<sup>2</sup> Van Thyne, Kessler, and Hansen,<sup>3</sup> and Cuff, Grant, and Floe.<sup>4</sup> The specimen shows the transformed  $\beta$  solid solution, and no equilibrium  $\alpha$  phase could have been present at the heat-treatment temperature.

The most probable reason for the difference between the observations of the above-mentioned workers and

librium nucleated  $\alpha$ , and that the apparent position of the  $\beta/(\alpha + \beta)$  boundary given by these experiments would be above the true one.

## 2. THE EUTECTOID TRANSFORMATION

The difficulty of reconciling the shape of the new  $\beta/(\alpha + \beta)$  boundary with the existence of a eutectoid point at about 14 at.-% chromium and 670°–685° C., the position indicated by previous work, made necessary an investigation of the eutectoid reaction. Since two specimens at the most could be heat-treated

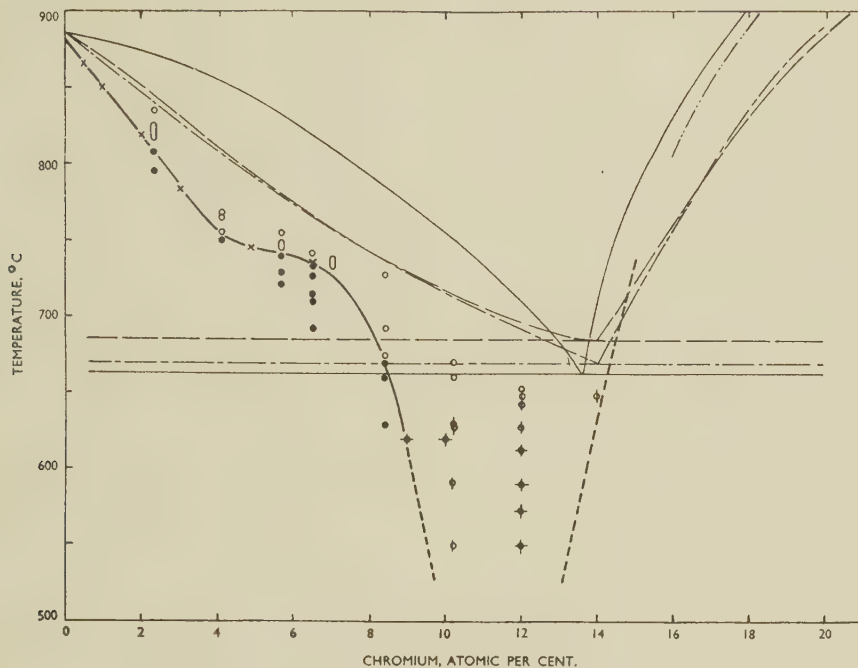


FIG. 1.—The Titanium-Chromium Phase Diagram.

### KEY.

— Present work.  
 — Duwez and Taylor.<sup>2</sup>  
 - - - Cuff, Grant, and Floe.<sup>4</sup>  
 - - - Van Thyne, Kessler, and Hansen.<sup>3</sup>  
 - - - Previous work by present author.<sup>1</sup>

× A. D. McQuillan, hydrogen-pressure determinations.<sup>6</sup>  
 ●  $\alpha + \beta$  alloys.  
 ○ Retained  $\beta$  alloys.  
 ⊙ Partially transformed  $\beta$  alloys.  
 ⊕ Completely transformed  $\beta$  alloys.

the present ones has been brought to light by some recent work done by (A. D.) McQuillan<sup>6</sup> on a titanium-nickel alloy, in which he found that considerable amounts of nucleated  $\alpha$  phase were formed during cooling from temperatures just above the  $\beta/(\alpha + \beta)$  boundary unless the quenching process was very rapid indeed. Nucleated  $\alpha$  phase was formed if the quench was delayed by as little as 0.4 sec. Titanium-chromium alloys have been found to behave in a similar way. Since it appears from published micrographic work that the specimens examined were invariably enclosed in a protective container, and were quenched by dropping both container and specimen into a quenching medium, it is fairly certain that the quenching rate would not have been sufficiently rapid to prevent the formation of non-equilibrium

in the quenching apparatus at any one time, its use in the eutectoid work, for which very long heating periods were reported to be necessary, appeared to be impracticable, and in order to hasten the work, rapid quenching (which at this stage was thought to be less important for eutectoid specimens) was sacrificed, and a conventional tube furnace used. Specimens containing 10.2 and 12 at.-% chromium were heated for 1000 hr. at temperatures ranging from 540° to 650° C. in the hope that the reportedly sluggish eutectoid reaction would approach completion in those cases in which the heat-treatment temperature was below the eutectoid temperature. At the end of this period, the specimens, which were sealed individually into small clear silica tubes, were removed from the furnace with the least possible delay. The cooling

process was complete within a minute or two, and it was not expected that any change would take place in a eutectoid structure during this short period.

Micro-examination of the specimens after heat-treatment showed that no simple explanation based on the existence of a eutectoid line within or above the temperature range of the heat-treatments could be applied to their structures. Considerable metallurgical reaction seemed to have occurred in the 12 at.-% chromium specimens, whereas 10.2 at.-% specimens heated at the same temperatures showed only grain-boundary breakdown. An appreciable amount of the compound  $\text{TiCr}_2$ , which can easily be identified by etching in an alkaline 10% solution of potassium ferricyanide, appeared in all the 12 at.-% chromium specimens, and a smaller amount was observed in the grain boundaries of the 10 at.-% chromium specimens. It appeared in a variety of forms, as very small rounded particles, as larger equiaxed crystals, as needles, or as a constituent of an unresolvable matrix, but it was in every case associated with the  $\alpha$  phase. Careful consideration of these structures led to the conclusion that they could not be accepted as equilibrium structures or even as structures tending towards equilibrium, and the only alternative, unlikely as it seemed at the time, was that they were breakdown structures due to insufficiently rapid cooling at the end of the heat-treatment.

In order to test this point, pieces of several of the 12 at.-% chromium specimens were reheated in the quenching apparatus for periods varying from a few hours to several days at the temperature at which they had been heated during the 1000-hr. treatment, and were then quenched. Care was taken to reach the required temperature as rapidly as possible without exceeding it. The times involved were of the order of 3 or 4 min. It is reasonable to suppose that if the structures observed after the 1000-hr. heat-treatment were the equilibrium structures corresponding to the temperatures at which the specimens were heated during this period, no significant change would occur during a further short period of heating at the same temperature. If, on the other hand, the observed structures were formed during cooling, a further period of heating might be expected to restore them to their former state, which would probably be retained after the very rapid quench undergone in the quenching apparatus.

In each case considerable changes were found to have occurred on reheating and quenching, as may be seen by comparing Fig. 3 with Fig. 4 and Fig. 5 with Fig. 6 (Plate LXVIII). Fig. 3 shows the structure of a 12 at.-% chromium specimen heated at  $652^\circ\text{C}$ . for 1000 hr. and cooled. Fig. 4 represents the same specimen after reheating at  $652^\circ\text{C}$ . for 24 hr., followed by rapid quenching. It will be observed that the  $\alpha$  phase and the  $\text{TiCr}_2$  present in the specimen on cooling after the 1000-hr. treatment are, on reheating, disappearing, and are being replaced by small new crystals of the  $\beta$  phase. This is conclusive evidence that the original structure was not an equilibrium

structure, and it is clear that the alloy was actually in the single-phase  $\beta$  region at  $652^\circ\text{C}$ .

Figs. 5 and 6 illustrate the effect of reheating at the same temperature and quenching a 12 at.-% chromium alloy originally heated at  $590^\circ\text{C}$ . On quenching after reheating for 4 days, the needles and equiaxed particles of  $\text{TiCr}_2$  and the needles of the  $\alpha$  phase seen in Fig. 5 have disappeared, and have been replaced by the fine uniform structure of Fig. 6. The only reasonable interpretation of this change is that the equilibrium structure at  $590^\circ\text{C}$ . is again single-phase  $\beta$  solid solution which breaks down even during the rapid water-quench. Under such conditions, however, there is insufficient time for any appreciable growth of the precipitating phases, and a very fine structure results. The structure observed in Fig. 6 is very similar to those of the 12 at.-% chromium alloys more slowly cooled after prolonged heating at  $567^\circ$  and  $548^\circ\text{C}$ ., and it is evident, therefore, that these specimens cannot safely be regarded as having retained their high-temperature equilibrium structures on cooling, in spite of their eutectoid-like appearance. The fact that the 10.2 at.-% chromium specimen heated at  $548^\circ\text{C}$ . shows large  $\beta$  grains with only a small amount of breakdown in some of the boundaries supports this point of view, and it is likely that all these alloys were heated in the single-phase  $\beta$  region.

In the light of this evidence, the equilibrium diagram of the titanium-rich end of the titanium-chromium system has been re-drawn in the way indicated in Fig. 1. The eutectoid temperature has not yet been determined with any certainty, but it must lie somewhere between  $548^\circ\text{C}$ . and room temperature.

Attempts have been made to fix the position of the lower part of the  $\beta/(\alpha + \beta)$  boundary by heat-treatment in the quenching apparatus, but the instability of the  $\beta$  solid solution after prolonged heating at the low temperatures involved causes considerable difficulty. Some information has been gained from specimens cold worked before heat-treatment in order to provide a means of distinguishing between the  $\alpha$  phase present at the heat-treatment temperature (which will have recrystallized) and that produced on quenching (which would be of Widmannstätten form), but the application of this technique is limited by the requirement that the heat-treatment temperature must be above the recrystallization temperature.

#### IV.—DISCUSSION OF RESULTS

The experimental results described present a number of problems. It has been established, for instance, that the heat-treatment times required to produce equilibrium nucleated  $\alpha$  phase in  $(\alpha + \beta)$  alloys range from 4–20 hr. at  $800^\circ\text{C}$ . to about a week at  $660^\circ\text{C}$ ., and yet considerable quantities of this same material, in a form indistinguishable from the equi-



librium phase, are produced during rapid cooling. Furthermore, quite large particles of phases as different in composition as the  $\alpha$  solid solution (virtually chromium-free) and  $\text{TiCr}_2$  (containing about 60% chromium) can be formed during rapid cooling from very low temperatures. Thus, there is evidence in the behaviour of these alloys which implies quite slow rates of diffusion on one hand, and exceptionally high rates of diffusion on the other. Another fact for which it is difficult to account is that the  $\beta$  solid solution is retained on quenching with increasing difficulty the lower the heat-treatment temperature. A theory has, however, been developed which can explain these apparent contradictions, and throws light on the general behaviour of titanium alloys.

It is considered that at lower temperatures the  $\beta$  phase is far from being an ideal solution, and that the titanium-titanium bonds and chromium-chromium bonds are very much stronger than the titanium-chromium bonds. This results in a strong tendency towards the separation, during heat-treatment, of titanium-rich and chromium-rich regions, or, in other words, a clustering of like atoms. For each alloy composition and temperature there will be an equilibrium state of clustering at which the number of atoms attaching themselves to an existing group of similar atoms will be equal to the number breaking away as a result of thermal fluctuations. The rate at which this equilibrium state is achieved would be expected to depend on the rate of diffusion of the atoms through the lattice, and, on the evidence of the rate of nucleation of equilibrium  $\alpha$  phase, the time required for its attainment would be expected to be of the order of hours at about 800° C. and weeks below 650° C. Within these limits, therefore, the degree of clustering existing in any alloy would be dependent upon heat-treatment time, as well as upon the temperature and composition of the specimen. From general considerations it would be expected that the equilibrium degree of clustering corresponding to lower temperatures, though reached more slowly, would be greater than that at high temperatures, since fewer atoms among those becoming attached to a group of like atoms would possess sufficient energy to break away again. It is thought, however, that there is probably an additional reason for the occurrence of more severe clustering effects at lower temperatures, as will be explained when the background to the behaviour of titanium-chromium alloys is discussed in the next section.

On the clustering hypothesis, therefore, a  $\beta$  solid solution consists, after heat-treatment within a certain critical range of temperature, of titanium-rich and chromium-rich regions whose number, size, and composition depend on the alloy composition and the heat-treatment time and temperature. Such a solid solution, on cooling to a temperature below that at which it can exist in equilibrium, would be expected to break down into titanium-rich and chromium-rich phases far more easily than would a homogeneous solution of the same overall composition. Thus very

rapid diffusion rates need not be postulated in order to explain the formation of the  $\alpha$  phase and  $\text{TiCr}_2$  on cooling alloys submitted to long heat-treatments at low temperatures, since most of the necessary diffusion would have occurred during the heat-treatment. The reason for the increasing difficulty experienced in retaining the  $\beta$  phase after long heating at low temperatures also becomes clear when it is realized that specimens treated in this way would be clustered to the greatest degree.

The formation of nucleated  $\alpha$  phase during cooling from temperatures just above the  $\beta/(\alpha + \beta)$  boundary has a similar explanation in terms of the clustering theory. Clustering occurring during heat-treatment would result in the formation of titanium-rich regions from which the  $\alpha$  phase would readily precipitate during cooling. If this is so, a preliminary period of heating in the  $\beta$ -phase region is essential to the formation of nucleated  $\alpha$  phase during cooling, and this is a point which has been tested experimentally. Two specimens of a titanium-chromium alloy containing 2.4 at.-% chromium were homogenized at 1000° C. and cooled to 820° C., a temperature just within the single-phase  $\beta$  region. One of them was then cooled directly to room temperature. The other was held at 820° C. for a week before being cooled, at the same rate as the first, to room temperature. As predicted by the theory outlined, nucleated  $\alpha$  phase was observed in the microstructure only of the specimen held at 820° C. for a week. The alloy cooled directly to room temperature consisted entirely of martensitically transformed  $\beta$  phase. Additional confirmation has been provided by (A. D.) McQuillan, who, at the author's suggestion, repeated his recent experiments<sup>6</sup> on a 2.4 at.-% nickel alloy, and found that nucleated  $\alpha$  was formed during cooling only if the specimens were held for an appreciable time at a temperature within the  $\beta$  region, and not if they were cooled immediately from that temperature.

The success of these ideas in explaining the experimental results of the present work led to their application to the observations of other workers on the titanium-chromium system. An explanation of the high  $\beta/(\alpha + \beta)$  boundaries reported has already been presented, but it is of interest to note here that the highest boundary (that of Duwez and Taylor<sup>2</sup>) is the result of the most prolonged heat-treatments, which is what would be expected from the clustering theory. It is also significant that none of the previous workers obtained direct evidence for the existence of the eutectoid at 670°–685° C. Their hypo-eutectoid specimens had  $(\alpha + \beta)$  structures with some evidence of the compound  $\text{TiCr}_2$  in the grain boundaries, and the hypereutectoid alloys consisted of partially transformed  $\beta$  phase, most of the transformation having again occurred in the grain boundaries. These observations are consistent with the new diagram if it is considered that the alloys examined after heat-treatment at 650°–700° C. had been, when at temperature, in the  $(\alpha + \beta)$ ,  $\beta$ , or  $(\beta + \text{TiCr}_2)$  regions, according to chromium content, and that the  $\beta$  solid

solution, in which clustering would have occurred to a degree varying from specimen to specimen, partially transformed on cooling, producing  $\alpha$  or  $\alpha + \text{TiCr}_2$ . The incomplete nature of the transformation has been ascribed in the published work to the sluggishness of the eutectoid reaction. It is now suggested that once the equilibrium degree of clustering is achieved, further heating in the temperature range 650°–680° C., even if continued indefinitely would produce no greater amount of transformation.

Further points of interest are the reports that Duwez and Taylor<sup>2</sup> found no evidence for the eutectoid transformation at 670°–685° C. by thermal-analysis methods, and that Cuff, Grant, and Floe<sup>4</sup> found a dilatometric effect in this temperature region only on heating. The explanation of the latter observation is believed to be as follows. Having detected no reaction on cooling, Cuff, Grant, and Floe heated their specimens for a prolonged period at a temperature considered to be below the eutectoid line before carrying out further dilatometric work, in the hope that they would in this way ensure the presence in their alloys of sufficient  $\alpha$  and  $\text{TiCr}_2$  to cause appreciable dimensional changes on reacting together to form the  $\beta$  solid solution when heated through the eutectoid temperature. According to the new concept of the behaviour of titanium–chromium alloys, this heat-treatment would permit the occurrence of clustering, which would result in the breakdown of the  $\beta$  solid solution on cooling. Thus, the specimen used in the dilatometer would contain  $\alpha$  and  $\text{TiCr}_2$  as intended, but as a result of a different process. These phases would redissolve in the  $\beta$  phase on heating, and in so doing might be expected to cause the volume changes observed at 670°–685° C., which is probably the lowest temperature region in which sufficient diffusion can occur. No effect would be observed on cooling because the breakdown of the  $\beta$  solution would not occur until the true eutectoid temperature, which is now believed to be below the temperature range studied, was reached.

A review of the published work on other titanium alloy systems shows that in all binary systems of titanium with a transition element in which the existence of a eutectoid reaction in the titanium-rich region has been reported, no direct evidence for the eutectoid has been presented. In each case the so-called hypo-eutectoid alloys have ( $\alpha + \beta$ ) structures, and the hypereutectoid alloys consist of partially transformed  $\beta$  solutions in which the greater part of the reaction has occurred in the grain boundaries. The marked similarity between the observations reported for these systems (titanium–manganese,<sup>7</sup> titanium–tungsten,<sup>8</sup> titanium–nickel,<sup>9</sup> and titanium–iron<sup>3, 10</sup>) and those made on the titanium–chromium system suggests that they may be subject to the same influences, and that re-examination, using methods which permit very rapid quenching, would show that the eutectoid lines, and, perhaps, the  $\beta/(\alpha + \beta)$  boundaries too, in these systems are lower than those reported.

## V.—THEORETICAL CONSIDERATIONS

The clustering hypothesis put forward in this paper explains many apparently anomalous features of titanium-alloy behaviour. In taking the discussion further and considering possible reasons for clustering, a concept of the general nature and behaviour of titanium has emerged which, though empirical and, no doubt, over-simplified as presented here, links up most of the unusual properties of the metal, and appears to be capable of refinement and extension. The key to the problem lies in the anomalous resistivity/temperature curves of titanium,<sup>11</sup> zirconium,<sup>12</sup> and hafnium,<sup>13</sup> the shape of which suggests that the electronic structure of these elements undergoes on heating, as a result of thermal excitation, a reversible change from a low-temperature form to a high-temperature form. The change begins in each instance some hundreds of degrees below the temperature of the phase transformation from a hexagonal lattice to a cubic lattice, and is not completed until a temperature appreciably above that of the transformation is reached. Thus, the phase transformation appears to be a result of the electronic change rather than the cause of it, and it would be expected, therefore, that the electronic change would occur in a similar way in titanium-rich solid solutions, even though the phase transformation may have been suppressed.

On the evidence of the resistivity/temperature curves alone, it is not possible to say whether the electronic change occurs gradually in all the atoms at once, or whether it goes to completion in a gradually increasing number of atoms, but the latter appears more probable and fits the greater number of facts, at least as far as systems of the type of the titanium–chromium system are concerned. In this case, titanium or a titanium-rich solid solution will, at any temperature within the wide range throughout which the change occurs, consist of a mixture of two types of titanium atom in different electronic states, which would be expected to have different binding energies. If the experimental facts that there is virtually no solubility of chromium in  $\alpha$ -titanium and that titanium and chromium are completely mutually soluble in the  $\beta$  form at higher temperatures are now considered, it will be seen that there is good reason to suppose that the low-temperature electronic structure of the titanium atom results in very unfavourable titanium–chromium interaction, whereas the high-temperature electronic structure results in favourable interaction between titanium and chromium atoms. Thus a single-phase titanium–chromium alloy existing within the critical temperature region (from below 400° to above 1100° C.) will contain some titanium atoms which attract chromium atoms and some which repel them, the number of those which repel chromium increasing markedly with decreasing temperature. Here, therefore, appears to lie the explanation of the clustering phenomenon observed in the  $\beta$  solid solution—one which accounts both for its occurrence



and its strong temperature-dependence. A reason for the rather surprising stability of the highly clustered  $\beta$  solution may be found in the stabilizing effect of a statistical interchange of titanium atoms between the two types of bonding.

The type of behaviour outlined here would obviously have a fundamental influence on alloy systems of titanium with elements other than chromium, and the nature of the postulated electronic change is a matter of considerable interest from this and other points of view. It is, however, one which can probably be discussed to greatest advantage at a later date. At present it is perhaps sufficient to point out that if this approach to the problem of the behaviour of titanium proves to be a sound one, it means that the outer electron shells of the titanium atoms in a metallic lattice cannot be considered as forming a common

electron band, and that titanium cannot be treated in terms of the band theory. It is possible, however, that this is only true of alloys of titanium with elements of the same type as chromium.

#### ACKNOWLEDGEMENTS

The author wishes to express her thanks to Dr. N. P. Inglis and Dr. J. W. Rodgers of the Research Department, Imperial Chemical Industries, Ltd., Metals Division, for their encouragement of the work; to Dr. A. D. McQuillan of Birmingham University, for carrying out the confirmatory hydrogen-pressure experiment; and to Mr. J. Lumby of the Research Department, Imperial Chemical Industries, Ltd., Metals Division, for his assistance with the experimental work.

#### REFERENCES

1. M. K. McQuillan, *J. Inst. Metals*, 1951, **79**, 379.
2. P. Duwez and J. L. Taylor, *Trans. Amer. Soc. Metals*, 1952, **44**, 495.
3. R. J. Van Thyne, H. D. Kessler, and M. Hansen, *ibid.*, 1952, **44**, 974.
4. F. B. Cuff, N. J. Grant, and C. F. Floe, *Trans. Amer. Inst. Min. Met. Eng.*, 1952, **194**, 848.
5. A. D. McQuillan, *J. Inst. Metals*, 1951-52, **80**, 363.
6. A. D. McQuillan, *ibid.*, 1953-54, **82**, 47.
7. D. J. Maykuth, H. R. Ogden, and R. I. Jaffee, *Trans. Amer. Inst. Min. Met. Eng.*, 1953, **197**, 225.
8. D. J. Maykuth, H. R. Ogden, and R. I. Jaffee, *ibid.*, 1953, **197**, 231.
9. H. Margolin, E. Ence, and J. P. Nielsen, *ibid.*, 1953, **197**, 243.
10. H. W. Worner, *J. Inst. Metals*, 1951, **79**, 173.
11. A. D. McQuillan, *ibid.*, 1950-51, **78**, 249.
12. H. K. Adenstedt, *Trans. Amer. Soc. Metals*, 1952, **44**, 949.
13. J. D. Fast, *J. Appl. Physics*, 1952, **23**, 350.

# 1536 RESISTIVITY ANOMALIES IN THE NICKEL-CHROMIUM SYSTEM AS EVIDENCE OF ORDERING REACTIONS\*

By ROLF NORDHEIM,† Chem.Eng., Sc.D., and NICHOLAS J. GRANT,‡ B.S., Sc.D.

## SYNOPSIS

The electrical-resistivity anomaly in the nickel-chromium system is considered on the basis of new data and of Taylor and Hinton's results (*J. Inst. Metals*, 1952-53, **81**, 169). It is shown that the explanation of the effect is more consistent with short-range than long-range order. During long-time annealing at temperatures below 500° C., the resistivity of alloys with more than 30 at.-% chromium decreases markedly. This effect is associated with long-range ordering, possibly of the CuAu type.

## I.—INTRODUCTION

THE resistivity anomaly in the nickel-chromium system, tentatively attributed by Yano<sup>1</sup> and by Thomas<sup>2</sup> to an ordering reaction, has recently been considered in detail by Taylor and Hinton.<sup>3</sup> The characteristic feature of this anomaly is that during annealing after non-equilibrium cooling the resistivity increases towards an equilibrium value, this increase being marked enough to cause a minimum on the resistivity/temperature curve.

The suggestion that the increasing resistivity below 700°–800° C. is caused by ordering is supported by the fact that the effect is strongest for the alloy with a composition corresponding to Ni<sub>3</sub>Cr,<sup>1,2</sup> and that the phenomenon is associated with a lattice contraction and an evolution of heat.<sup>1,3</sup> Although ordering normally causes a decrease in the resistivity, Taylor and Hinton attempted to show that in the nickel-chromium system the change in the Brillouin zones during ordering may cause the resistivity to increase. Neither earlier investigators nor Taylor and Hinton were able to detect positively any superstructure lines in the X-ray pattern of annealed alloys. But such lines were definitely observed in the pattern of an alloy having one-fifth of its chromium atoms replaced by aluminium (which would tend to increase the intensity of the superstructure diffractions). From specific-heat data the critical ordering temperature was determined to be 544° C.

As part of a more extensive investigation of the ageing characteristics of complex nickel-chromium-base alloys, the present authors have studied this resistivity anomaly in the nickel-chromium system. Some of the results of these studies will be presented here, and the phenomenon will be discussed on the basis of these data and of those published by Taylor and Hinton.

## II.—EXPERIMENTAL PROCEDURE

The materials used were Mond nickel and electrolytic chromium. To decrease its oxygen and carbon content, the chromium was annealed in a hydrogen atmosphere at 1250° C. for 100 hr. The alloys were melted by the cold-crucible method, using a water-cooled tungsten electrode and an atmosphere of purified helium. The chromium contents of the experimental Alloys Nos. 1–5 were:

Alloy no.	1	2	3	4	5
Cr,* at.-%	10.9	22.2	25.0	32.0	35.7

\* Nickel by difference.

Alloy No. 2 contained carbon <0.002, sulphur <0.002, oxygen 0.03, nitrogen <0.005 wt.-%.

Alloys No. 1, 2, and 4 were forged at 1100°–1000° C. and, subsequently, machined to bars of 3 mm. dia. Alloys No. 3 and 5 were cold forged to 50% reduction in area, and after annealing in helium at 1100° C. for 20 hr., were machined to bars of 3 mm. dia.

The 3-mm. bars were used for electrical-resistance measurements with a Kelvin double bridge, nickel wire (spot welded to the specimen) serving as the current and potential leads. Changes of 0.05% of the total gauge resistance could be detected. The temperature was measured with Chromel/Alumel thermocouples attached to the specimen. The heat-treatments were carried out in vertical-tube furnaces having a long-time temperature variation of not more than  $\pm 1.5^\circ$  C. The temperature difference over the gauge-length was less than  $\pm 1.5^\circ$  C. The following heat-treatments were used:

(a) Isothermal annealing at 289°–593° C. after water-quenching from 980° C.

(b) Stepwise heating after water-quenching from 980° C.

(c) Stepwise furnace cooling from 980° C.

\* Manuscript received 18 July 1953.

† Formerly Research Assistant, Department of Metallurgy, Massachusetts Institute of Technology; now associated with the Department of Chemistry and Metallurgy, Norwegian

Defence Research Establishment, Lilleström, Norway.

‡ Associate Professor, Department of Metallurgy, Massachusetts Institute of Technology, Cambridge, Mass., U.S.A.



The specimens were always held for  $\frac{1}{2}$  hr. at  $980^{\circ}\text{C}$ . before quenching or furnace-cooling. All heat-treatments took place in purified helium.

For the isothermal runs the annealing period was timed from the moment the thermocouples reached the chosen annealing temperature. This usually occurred within 3 min. During the first 10 or 15 min., the temperature difference over the gauge-length was more than  $1.5^{\circ}\text{C}$ .; the thermal e.m.f., however, was always less than the reading accuracy of the bridge. For each alloy all the runs were performed with the same specimen. The resistance at  $980^{\circ}\text{C}$ . served as a check to make sure that the alloys did not undergo any permanent change in the course of the tests. After completion of the last test, the resistivity at room temperature was measured by making contact for the potential leads with sharp needles.

Samples for microstructural examination were mechanically polished and given an anodic etch in an aqueous solution of 10% glycerine and 5% hydrofluoric acid. For X-ray examinations heat-treated bars were electrolytically polished to 0.4 mm. dia, and rotated in a 57.3-mm. Debye-Scherrer camera, using monochromatic  $\text{CrK}_{\alpha}$  radiation ((200) reflection from a plane rock-salt crystal).

Rockwell B hardness measurements were made on discs of 3–4 mm. thickness, the discs being given the same forging and heat-treatment as the resistivity bars. The same disc was used for a complete isothermal run.

### III.—EXPERIMENTAL RESULTS

By isothermal annealing, stepwise heating, and stepwise cooling the equilibrium resistivity of Alloys

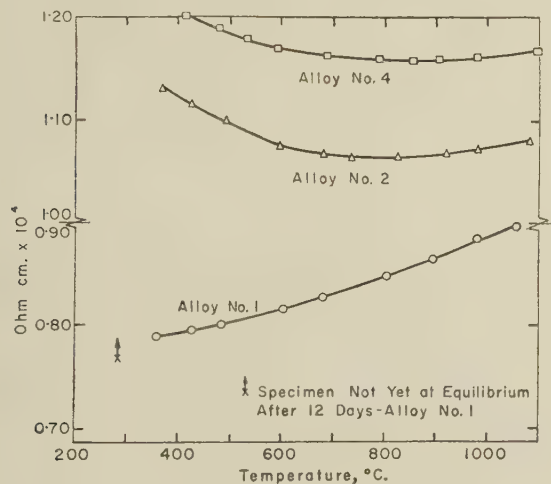


FIG. 1.—Equilibrium Values of the Electrical Resistivity of Alloys No. 1, 2, and 4.

No. 1 (10.9% Cr), 2 (22.2% Cr), 3 (25.0% Cr), and 4 (32.0% Cr) was determined. The equilibrium curves for Alloys No. 1, 2, and 4 are reproduced in Fig. 1. The curve for Alloy No. 3 was practically identical with the curve obtained for a similar alloy by Taylor

and Hinton, except that the equilibrium resistivity for Alloy No. 3 continued to increase with cooling below  $480^{\circ}\text{C}$ ., but equilibrium was approached

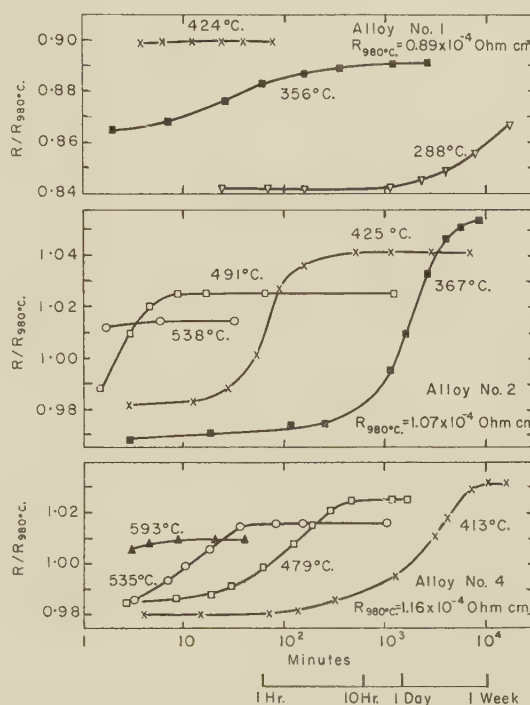


FIG. 2.—Change in the Electrical Resistance of Alloys No. 1, 2, and 4 during Isothermal Annealing after Water-Quenching from  $980^{\circ}\text{C}$ .

more and more slowly. These equilibrium values were independent of the thermal history.

Fig. 2 shows the change in the electrical resistance of Alloys No. 1, 2, and 4 during isothermal annealing after water-quenching. It is observed that the rate of approach towards the equilibrium state is strongly dependent on both temperature and composition.

According to Fig. 2, the resistivity of Alloy No. 4 (32.0% Cr) remained unchanged between the seventh and the twenty-seventh hr. at  $479^{\circ}\text{C}$ . With continued annealing, however, the resistivity started to

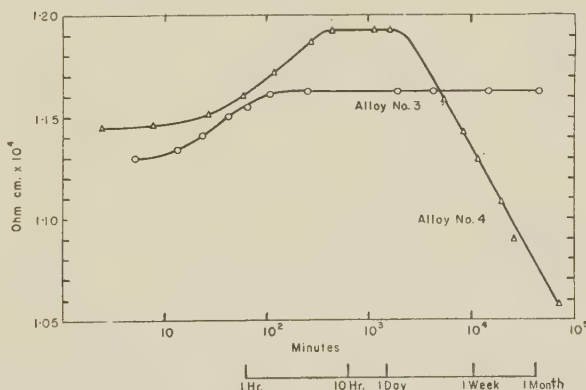


FIG. 3.—Change in the Electrical Resistivity of Alloys No. 3 and 4 during Annealing at  $479^{\circ}\text{C}$ .

decrease, as shown in Fig. 3. At the same time the temperature coefficient of the electrical resistivity increased markedly (Fig. 4). After 1190 hr. at

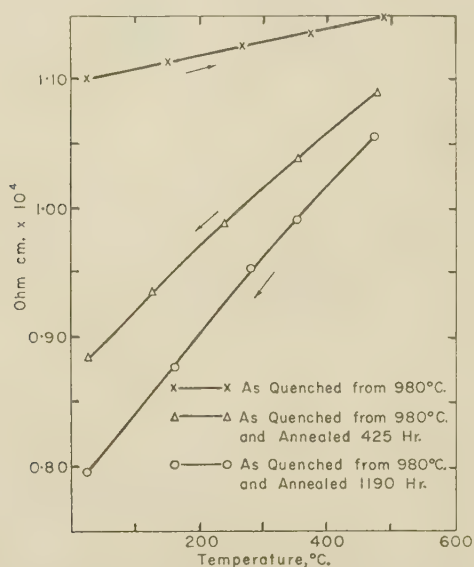


FIG. 4.—Electrical Resistivity of Alloy No. 4 Before and After Annealing at 479° C. The resistivity was measured during both heating and cooling at a rate of approximately 10° C./min.

479° C., the average coefficient between 25° and 479° C. had increased by approximately 435%, corresponding to a drop in the room-temperature resistivity of 28%. This effect was not caused by any permanent change such as the loss of chromium reported by Holler<sup>4</sup> for Nichrome. In fact, the room-temperature resistivity of Alloy No. 4, after water-quenching from 980° C. a sample that had been exposed for 1 week at 479° C., was the same as before the isothermal treatment at 479° C. In Fig. 5 is shown the change in the resistivity of Alloy No. 5

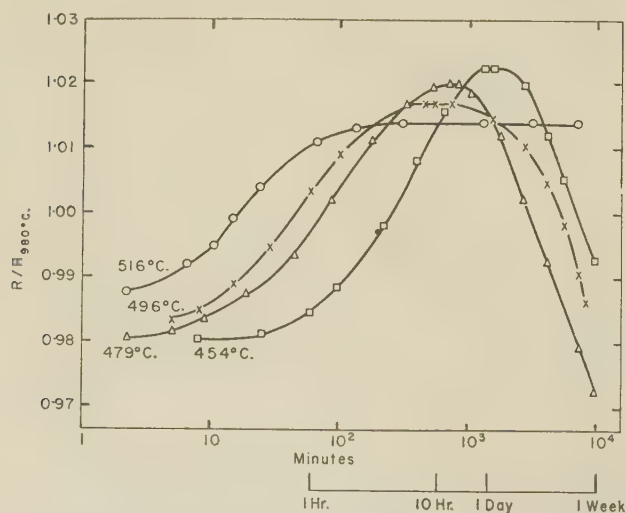


FIG. 5.—Change in the Electrical Resistance of Alloy No. 5 during Isothermal Annealing After Water-Quenching from 980° C. ( $R_{980^\circ\text{C.}} = 1.18 \times 10^{-4}$  ohm. cm.).

(35.7% Cr) during annealing at temperatures ranging from 454° to 516° C. It is observed that the decrease in resistivity occurred most rapidly at 480°–490° C. Such a decrease in the resistivity was not observed for the alloys with lower chromium content than Alloy No. 4 (see Fig. 3, showing the change in the resistivity of Alloy No. 3 (25.0% Cr) during annealing at 479° C.).

The decrease in the electrical resistivity of Alloys No. 4 and 5 during long-time annealing was not accompanied by any microstructural changes, and the only change revealed by X-ray examination was a rather marked lattice contraction. Associated with the 28% decrease in the room-temperature resistivity of Alloy No. 4 was a decrease in the lattice parameter of approximately 0.5%.

Fig. 6 shows the change in the hardness of Alloys No. 3 and 4 during annealing at 479° C. The hardness of Alloy No. 4 increased in two steps which nearly correspond to the increase and the subsequent decrease in the electrical resistivity. Only the first of these steps could be recognized in the hardness curve for Alloy No. 3.

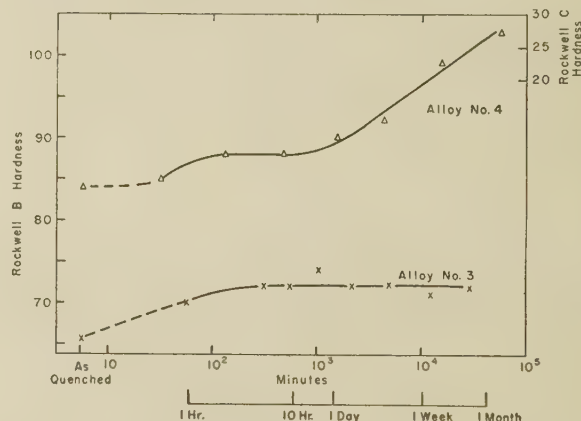


FIG. 6.—Change in Hardness of Alloys No. 3 and 4 During Annealing at 479° C.

#### IV.—DISCUSSION

In the following discussion the two resistivity changes described in the previous section will be treated separately. The increase in resistivity during annealing after non-equilibrium cooling will be referred to as Change 1, whereas the subsequent decrease in the resistivity of the alloys with more than 30% chromium will be called Change 2.

##### 1. CHANGE 1

In the previous section, it was pointed out that the rate of approach towards the equilibrium resistivity was strongly temperature-dependent. From the time/resistivity curves in Fig. 2, the activation energy for the phenomenon causing Change 1 was calculated to be about 50,000 cal. Applying this value to Alloy No. 2 (22.2% Cr), it is estimated that the times to



attain equilibrium resistivity at 300°, 500°, and 600° C. are about one year, a few minutes, and one second, respectively. At the highest temperature, it is therefore very difficult to observe Change 1. However, its existence can be recognized by the deviation of the equilibrium-resistivity curve from a normally sloping line. Fig. 1 thus shows that Change 1, noticeable already at 800°–900° C., becomes gradually stronger with decreasing temperature.

As has been pointed out by earlier investigators,<sup>1-3</sup> there is good reason for associating Change 1 with an ordering reaction. There are two alternatives to consider: (i) long-range and (ii) short-range order. If long-range order corresponding to  $\text{Ni}_3\text{Cr}$  develops below a certain temperature, the equilibrium resistivity of an alloy with 25% chromium would be expected to change discontinuously at this temperature. Taylor and Hinton explained the smooth shape of the resistivity curve by assuming the existence, not of a homogeneously ordered material, but of a mixture of highly ordered and partially ordered regions. If this were the case, the mixture should be different in a slowly cooled specimen from that in a quenched and annealed specimen, so that the resistivity below the proposed critical temperature (544° C.) would depend on the thermal history. As was pointed out in the previous section, this was not observed to be the case.

The critical temperature of 544° C. was obtained by Taylor and Hinton from the maximum in their specific-heat curve, measured during the heating of a previously very slowly cooled and, presumably, highly ordered material. The significance of these measurements is, however, open to some question. Under equilibrium conditions the magnitude of Change 1 increases gradually with decreasing temperature and on subsequent heating the effect is gradually reversed. At low temperatures the approach toward the equilibrium state is a very slow process, so that with a heating rate of 2°/min., as used by Taylor and Hinton, no substantial reversal of Change 1 will take place until a temperature is reached at which the relaxation time for this process becomes of the order of a few minutes. For an alloy with 25% chromium, this temperature will be approximately 500° C. At this temperature a fairly strong reaction will occur, with a correspondingly high heat absorption. The maximum in the specific-heat curve determined by Taylor and Hinton may thus be a result of the relative rate of heating and the rate of reaction for the reversal of Change 1, and reliance on the equilibrium-resistivity data, which give no evidence of a critical ordering temperature for the nickel-chromium alloys studied in the present instance, may be preferable.

Although the difference between the atomic scattering factors of nickel and chromium is rather small, it should be possible to detect superstructure diffractions from an ordered (long-range)  $\text{Ni}_3\text{Cr}$  phase by use of suitable radiation such as  $\text{MnK}_\alpha$  radiation. But Taylor and Hinton, using such radiation, were able to observe, positively, only superstructure lines

in the pattern of an alloy having one-fifth of the chromium atoms replaced by aluminium. Since Change 1 was also observed for this aluminium-modified alloy, Taylor and Hinton concluded that the resistivity change was related to the occurrence of superstructure lines in the X-ray pattern, i.e. to the presence of long-range order. The sample used for the X-ray examinations, however, was given a "long soaking" at 480° C., whereas the resistivity curve was obtained during cooling in one day. The results obtained in this way do not, therefore, necessarily prove that Change 1 is associated with the presence of superstructure lines in the X-ray pattern.

Although the partial substitution of aluminium for chromium did not significantly change the specific-heat and the electrical-resistivity curves (measured during cooling in one day), Taylor and Floyd,<sup>5</sup> on the basis of X-ray determinations, reported that such substitution raised the critical ordering temperature rapidly. In alloys containing more than 10% aluminium, long-range order persisted even at 1150° C. This indicates quite clearly that the superstructure lines observed in the pattern of the alloy containing 5% aluminium and 20% chromium were not associated with Change 1.

Taking into account the absence of a discontinuity in the equilibrium-resistivity curve and the absence of superstructure lines in the X-ray pattern of  $\text{Ni}_3\text{Cr}$ , the existence of long-range order seems very improbable. Short-range order, on the other hand, which explains the lattice contraction and heat evolution associated with Change 1 just as well as long-range order does, is quite consistent with this absence of superstructure lines in the X-ray pattern and the smooth resistivity curve.

A phenomenon similar to Change 1 has also been observed in iron-aluminium alloys containing up to 18% aluminium.<sup>6</sup> The iron-aluminium system has the advantage of being well suited for X-ray examinations. Comparing the results of Thomas' resistivity measurements<sup>6</sup> and Bradley and Jay's X-ray examinations,<sup>7</sup> it may be concluded that when the aluminium content is increased to the extent that superstructure lines can be detected in the X-ray pattern of annealed alloys, Change 1 disappears and the resistivity decreases during annealing, which is normal for long-range ordering. These observations support the suggestion that Change 1 in the nickel-chromium system is caused by short-range rather than long-range ordering.

## 2. CHANGE 2

Change 2, which is marked enough to decrease the resistivity of Alloys No. 4 (32.0% Cr) and 5 (35.7% Cr) below that for Alloy No. 2 (22.0% Cr), cannot be explained by precipitation of either the chromium-rich  $\alpha$  phase or impurities. The fact that the rate of decrease of resistivity reached a maximum at 480°–490° C., indicates that ordering, if present, is of the long-range rather than the short-range type. However, the effect cannot be long-range ordering

corresponding to  $\text{Ni}_3\text{Cr}$ , since it was not observed in Alloy No. 3 (25% Cr). On the other hand, the CuAu type of ordering, in which the symmetry changes from cubic to tetragonal, is usually accompanied by a marked increase in hardness,<sup>8,9</sup> and as shown in Fig. 6, Change 2 was associated with such an increase in hardness.

Ordering of the CuAu type should give rise to superstructure lines as well as splitting (or broadening) of the main lattice reflections (200) and (220) in the X-ray-diffraction pattern. Although none of these effects was observed during annealing of Alloys No. 4 and 5, this does not necessarily exclude the alternative of the CuAu type of ordering. For the copper-gold system, Harker<sup>9</sup> has found that the greater part of the hardness increase occurred before any superstructure lines and broadening and splitting of the main lattice reflections could be detected in the X-ray pattern. In particular, it was hard to observe any superstructure lines for alloys with compositions deviating appreciably from the ideal stoichiometric ratio. Unfortunately, the solubility limit for chromium in nickel does not allow an increase in chromium content beyond that for Alloy No. 5. Precipitation of the chromium solid-solution phase during annealing would complicate the reactions. However, the decrease in the resistivity of Alloy No. 4 was associated with a relatively strong decrease in lattice parameter. Such a decrease in lattice parameter gives further support to the theory of ordering.

#### V.—SUMMARY

During annealing after non-equilibrium cooling, the electrical resistivity of nickel-chromium alloys increases towards an equilibrium value which is independent of the thermal history. The effect, first noticeable at 800°–900° C., becomes gradually stronger with decreasing temperature. Since the effect is strongest for alloys with compositions corresponding to  $\text{NiCr}_3$  and is associated with a lattice contraction and heat evolution, there is good reason to believe

that ordering is taking place. However, the facts that no superstructure lines have been detected in the X-ray pattern of annealed nickel-chromium alloys and that no discontinuity in the equilibrium-resistivity curve for alloys with 25% chromium has been observed, make the choice of long-range order seem very improbable. On the other hand, the gradual increase in the magnitude of the effect with falling temperature gives strong support to the theory of short-range order.

During long-time annealing at about 500° C., the resistivity of alloys with more than 30% chromium decreased markedly. This effect was accompanied by a large increase in hardness and a considerable lattice contraction, but no microstructural changes were detected. Although no superstructure lines could be observed in the X-ray pattern, the decrease in the resistivity and the lattice contraction give evidence of long-range order. The increase in hardness, being characteristic of the CuAu type of ordering, supports this view.

#### ACKNOWLEDGEMENTS

The authors wish to acknowledge support of this research by the United States Bureau of Ships, which initiated the programme of work, and by the Office of Naval Research, which is the present sponsor of the programme.

#### REFERENCES

1. Z. Yano, *Japan Nickel Rev.*, 1941, **9**, 17.
2. H. Thomas, *Z. Physik*, 1951, **129**, 219.
3. A. Taylor and K. G. Hinton, *J. Inst. Metals*, 1952–53, **81**, 169.
4. H. D. Holler, *Trans. Electrochem. Soc.*, 1947, **92**, 91.
5. A. Taylor and R. W. Floyd, *J. Inst. Metals*, 1952–53, **81**, 451.
6. H. Thomas, *Z. Metallkunde*, 1950, **41**, 185.
7. A. J. Bradley and A. H. Jay, *Proc. Roy. Soc.*, 1932, [A], **136**, 210.
8. W. Köster, *Z. Metallkunde*, 1940, **32**, 277.
9. D. Harker, *Trans. Amer. Soc. Metals*, 1944, **32**, 210.



# X-RAY DETERMINATION OF THE ALPHA-PHASE BOUNDARY OF THE COPPER-INDIUM ALLOY SYSTEM\*

1537

By R. O. JONES,† B.Sc., and PROFESSOR E. A. OWEN,† M.A.,  
D.Sc., MEMBER

## SYNOPSIS

The  $\alpha$ -phase boundary of the system copper-indium has been determined by the X-ray method from the peritectic temperature (710° C.) down to 250° C. The maximum solubility of indium in copper is 10.8<sub>5</sub> at.-% and is found to occur at 575° C. The solubility at 710° C. is 10.0<sub>5</sub> at.-% indium. The boundary below 575° C. shows a point of inflection, suggesting a transformation at about 470° C. The solubility of indium in copper decreases rapidly below this temperature, reaching 1.1 at.-% at 250° C.

## I—INTRODUCTION

THE alloy system copper-indium has not been extensively studied; two groups of workers only have devoted attention to it, both at a comparatively recent date.<sup>1,2</sup> Work had been carried out in this laboratory on the solubility of indium in copper in 1938, and was referred to in a paper by Owen and Morris<sup>3</sup> without any data being given on which the figures for the solubility were based. A paper giving this information has now been published,<sup>4</sup> but the range of temperature over which the solubility was examined was restricted and did not extend to temperatures lower than about 470° C. Moreover, the purity of the copper used to make the alloys was not as high as it is possible to obtain. In the present paper an account will be given of work undertaken with copper of 99.999% purity and indium of 99.98% purity and in which the temperature range is extended down to 250° C. It is necessary to survey the whole boundary in some detail because metallurgists find that in the range 520°–575° C. the solution of indium in copper is less than that found by X-ray investigation, a result which is somewhat unexpected, since X-ray measurements usually show, at the lower temperatures, less solubility than that found in metallurgical investigations.

In the first investigation, Weibke and Eggers<sup>1</sup> used thermal, microscopic, and X-ray methods, whereas the second investigation, by Hume-Rothery, Raynor, Reynolds, and Packer,<sup>2</sup> was carried out entirely by the ordinary metallurgical methods, excluding the X-ray method. The present investigation has been made entirely by the X-ray method, following the technique developed in this laboratory.

## II.—EXPERIMENTAL PROCEDURE

A detailed account of the method used in determining phase boundaries in equilibrium diagrams has

already been published<sup>3,5</sup> and fully discussed;<sup>6</sup> only very brief reference to experimental work is needed here, therefore, since the same technique as that used previously was adopted.

Weighed quantities of the two metals, copper and indium, were fused in evacuated silica capsules at about 1100° C.; the capsules were vigorously shaken during fusion for about 20 min. by means of a specially designed mechanism. The alloys were then quenched in cold water and lump-annealed at 575° C. for 14 days in the unopened capsules in which they had been prepared. The alloy ingots weighed between 1 and 1.5 g.; in no case did the change in weight during preparation exceed 0.001 g. and usually it was about 0.0005 g.

The focusing camera used to take the precision photographs was provided with a mechanism by which the powder specimen could be moved backwards and forwards along the circumference of the camera during the X-ray exposure. By this means more crystallites contribute to the lines in the photographs, thereby producing lines that are better defined and freer from the unevenness of intensity that is sometimes observed when the powder specimen is stationary and the grains are not very fine. The improved lines were much easier to measure, with the result that the accuracy of lattice-parameter measurement was substantially increased.

## III.—LATTICE PARAMETER/COMPOSITION CURVE

Eight alloys, the compositions of which fell within the range of the pure  $\alpha$  phase, were prepared in the form of cylinders about 5 mm. high and about 4 mm. in dia. From each ingot three powder specimens were taken, from the bottom and from the top of the ingot and from one of the cut faces produced by sawing the ingot along a central longitudinal section. These were annealed overnight at a temperature

\* Manuscript received 20 May 1953; in revised form 1 December 1953.

† Physics Department, University College of North Wales, Bangor.

within the range 500°–600° C. in small evacuated silica capsules. The maximum difference in lattice-parameter value in any set of three samples was about 0.0004 kX, which corresponds to a difference of 0.05 at.-% in composition; this was accepted as sufficient evidence that the ingots were practically free from segregation.

The lattice-parameter values for alloys of different

TABLE I.—*Lattice-Parameter Values Corresponding to Different Alloy Compositions in the  $\alpha$ -Phase Region.*

Indium, at.-%	Lattice Parameter	
	kX at 18° C.	Å. at 18° C.
0.00	3.6074 <sub>5</sub>	3.6147 <sub>4</sub>
2.0 <sub>6</sub>	3.6269 <sub>8</sub>	3.6343 <sub>6</sub>
4.0 <sub>1</sub>	3.6455 <sub>7</sub>	3.6529 <sub>3</sub>
5.8 <sub>7</sub>	3.6623 <sub>8</sub>	3.6697 <sub>8</sub>
7.6 <sub>1</sub>	3.6786 <sub>1</sub>	3.6860 <sub>4</sub>
8.4 <sub>3</sub>	3.6974 <sub>4</sub>	3.6948 <sub>9</sub>
9.0 <sub>6</sub>	3.6913 <sub>8</sub>	3.6988 <sub>4</sub>
9.8 <sub>2</sub>	3.6991 <sub>8</sub>	3.7066 <sub>5</sub>
10.5 <sub>6</sub>	3.7046 <sub>6</sub>	3.7120 <sub>8</sub>

compositions in the  $\alpha$ -phase region, given in Table I, agree closely with those of Weibke and Eggers<sup>1</sup> and of Owen and Roberts.<sup>4</sup>

#### IV.—THE $\alpha$ -PHASE BOUNDARY BETWEEN 710° AND 250° C.

To arrive at the position of the boundary, an additional alloy of composition 11.4 at.-% indium was prepared; this alloy is in two-phase regions from the lowest temperature (250° C.) to the temperature of the peritectic (710° C.). Other alloys already prepared were also used at temperatures at which it was possible to employ them, that is, temperatures at which annealing produced precipitation of a phase, thus avoiding the need for diffusion to take place from one grain to another in reaching the equilibrium condition. At each temperature under consideration, two samples were usually taken of the appropriate alloy, one sample being annealed for double the period of the other, although this practice was not always followed if it was considered that the first period of annealing was sufficient to produce the equilibrium condition by comparison with the results obtained with alloys at adjacent temperatures. All samples were quenched in iced water in the special furnace designed for rapid quenching.<sup>7</sup> If there was agreement between the lattice-spacing values yielded by the two samples, it was assumed that equilibrium had been established. If no agreement was found, further periods of annealing were adopted. It is important that these lattice-parameter values should be recorded, as from them the degree of equilibrium attained at each temperature can be judged; they are therefore given in Table II, together with details of the annealing treatment in each case.

This table also gives the boundary point corresponding to each temperature of annealing. It will be observed that the lattice-parameter values after different times of annealing at any temperature agree satisfactorily, with but few exceptions. The greatest deviation is that between the parameter values at 261° and 263° C.; these are not plotted separately, since the mean value lies within 0.2 at.-% of the individual values. The determination of the position of the boundary is not as accurate at the lowest temperatures as it is at the higher temperatures, where the accuracy is slightly better than  $\pm 0.2$  at.-%.

In Fig. 1 the position of the  $\alpha$ -phase boundary is shown over the whole range of temperature investigated, and with it are shown the boundaries determined by the other investigators of this system.

In the earliest work on the copper-indium system carried out by Weibke and Eggers,<sup>1</sup> the parameter/composition curve was determined with five alloys which did not cover the whole range of solid solution, so that for the more concentrated solutions a long extrapolation was necessary. Furthermore, the estimated error in lattice parameter was  $\pm 0.001$  kX, and in some cases  $\pm 0.002$  kX, so that the location of the boundary was not considered to have been determined to a high degree of accuracy. They found the maximum solubility of 11.63 at.-% indium to occur at 574° C.; at the peritectic temperature of 715° C. determined by them, the solubility was about 9.5 at.-% indium. The position of the boundary can, however, be regarded as having been only approximately determined.

In the work of Hume-Rothery, Raynor, Reynolds, and Packer,<sup>2</sup> the peritectic temperature was found to lie between 709.4° and 710.6° C., i.e. definitely lower than the temperature stated by Weibke and Eggers, but the eutectoid transformation at 574° C. was confirmed; the maximum solubility at this temperature was, however, estimated to be 10.9 at.-% indium. The boundary between 574° and 710° C. was now found to be steeper, whereas the boundary below 574° C. down to about 516° C. was very near to that determined by Weibke and Eggers. The amount of solution at 710° C. was also found to be slightly more than before, namely 9.95 at.-% indium.

The X-ray determination of the position of the  $\alpha$ -phase boundary over the range between 710° and 470° C. by Owen and Roberts<sup>4</sup> shows very close agreement with the results of Hume-Rothery and his co-workers<sup>2</sup> for temperatures above the transformation at 574° C., but, contrary to the statement made by these workers<sup>3</sup> that there is substantial agreement, below this temperature there is a marked divergence between the results; the later results of Owen and Roberts show a distinctly higher solubility over this range of temperature, the difference amounting to about 2 at.-% at 516° C.

The most recently published work on the  $\alpha$ -phase boundary of the copper-indium system is that of Owen and Roberts<sup>4</sup> over the restricted range from



TABLE II.—Data for the X-Ray Determination of the  $\alpha$ -Phase Boundary of Copper-Indium Alloys.

Annealing Treatment		Lattice Parameter, kX units at 18° C.					Boundary Point, at.-% In.	
Time, hr.	Temp., ° C.	Indium Content, at.-%						
		4.0 <sub>1</sub>	7.6 <sub>1</sub>	8.4 <sub>9</sub>	10.5 <sub>0</sub>	11.4 <sub>1</sub>		
1	689	...	...	...	...	3.7022 <sub>9</sub>	10.2 <sub>1</sub>	} 10.2 <sub>2</sub>
2	693	...	...	...	...	3.7023 <sub>4</sub>	10.2 <sub>3</sub>	
1	642	...	...	...	...	3.7054 <sub>2</sub>	10.5 <sub>9</sub>	} 10.5 <sub>6</sub>
2	644	...	...	...	...	3.7052 <sub>0</sub>	10.5 <sub>4</sub>	
17	595	...	...	...	...	3.7068 <sub>3</sub>	10.7 <sub>8</sub>	} 10.7 <sub>9</sub>
16.5	597	...	...	...	...	3.7070 <sub>0</sub>	10.7 <sub>9</sub>	
41	597	...	...	...	...	3.7071 <sub>9</sub>	10.8 <sub>0</sub>	
7	579	...	...	...	...	3.7074 <sub>3</sub>	10.8 <sub>2</sub>	} 10.8 <sub>3</sub>
18	578	...	...	...	...	3.7074 <sub>3</sub>	10.8 <sub>4</sub>	
2	564	...	...	...	...	3.7036 <sub>9</sub>	10.3 <sub>8</sub>	} 10.3 <sub>8</sub>
4	565	...	...	...	...	3.7037 <sub>2</sub>	10.3 <sub>9</sub>	
2	557	...	...	...	...	3.7027 <sub>5</sub>	10.2 <sub>6</sub>	} 10.2 <sub>2</sub>
4	557	...	...	...	...	3.7018 <sub>0</sub>	10.1 <sub>6</sub>	
19	557	...	...	...	...	3.7026 <sub>3</sub>	10.2 <sub>4</sub>	
5.5	549	...	...	...	...	3.6974 <sub>6</sub>	9.6 <sub>4</sub>	} 9.6 <sub>4</sub>
18	547	...	...	...	...	3.6977 <sub>2</sub>	9.6 <sub>6</sub>	
18	547	...	...	...	...	3.6972 <sub>2</sub>	9.6 <sub>1</sub>	} 9.6 <sub>3</sub>
1.75	543	...	...	...	...	3.6972 <sub>7</sub>	9.6 <sub>3</sub>	
3.5	544	...	...	...	...	3.6974 <sub>6</sub>	9.6 <sub>4</sub>	} 9.4 <sub>1</sub>
66	535	...	...	...	...	3.6952 <sub>6</sub>	9.4 <sub>0</sub>	
41	537	...	...	...	...	3.6954 <sub>4</sub>	9.4 <sub>2</sub>	} 9.4 <sub>1</sub>
4	531	...	...	...	...	3.6934 <sub>6</sub>	9.1 <sub>8</sub>	
6	531	...	...	...	...	3.6932 <sub>3</sub>	9.1 <sub>6</sub>	} 9.1 <sub>7</sub>
17	522	...	...	...	3.6911 <sub>1</sub>	...	8.9 <sub>2</sub>	
34	526	...	...	...	...	3.6930 <sub>6</sub>	9.1 <sub>4</sub>	} 9.0 <sub>3</sub>
4.5	517	...	...	...	...	3.6880 <sub>6</sub>	8.5 <sub>9</sub>	
44.5	515	...	...	...	...	3.6882 <sub>4</sub>	8.6 <sub>1</sub>	} 8.5 <sub>8</sub>
46	517	...	...	...	...	3.6876 <sub>6</sub>	8.5 <sub>4</sub>	
2	497	...	...	...	...	3.6819 <sub>7</sub>	7.9 <sub>4</sub>	} 7.8 <sub>8</sub>
4	497	...	...	...	...	3.6810 <sub>0</sub>	7.8 <sub>2</sub>	
19	484	...	...	...	...	3.6775 <sub>1</sub>	7.4 <sub>8</sub>	} 7.4 <sub>8</sub>
18	477	...	...	...	3.6733 <sub>6</sub>	...	7.0 <sub>4</sub>	
36	478	...	...	...	...	3.6746 <sub>0</sub>	7.1 <sub>7</sub>	} 7.1 <sub>0</sub>
17	464	...	...	...	...	3.6631 <sub>5</sub>	5.9 <sub>6</sub>	
92	465	...	...	...	...	3.6638 <sub>0</sub>	6.0 <sub>2</sub>	} 5.9 <sub>9</sub>
3	459	...	...	...	...	3.6606 <sub>3</sub>	5.6 <sub>8</sub>	
6	459	...	...	...	...	3.6604 <sub>3</sub>	5.6 <sub>6</sub>	} 5.6 <sub>7</sub>
48	457	...	...	...	...	3.6564 <sub>3</sub>	5.2 <sub>5</sub>	
20	443	...	...	...	...	3.6502 <sub>6</sub>	4.5 <sub>7</sub>	} 4.5 <sub>3</sub>
41	443	...	...	...	...	3.6511 <sub>2</sub>	4.6 <sub>6</sub>	
73	442	...	...	...	...	3.6482 <sub>1</sub>	4.3 <sub>6</sub>	} 3.0 <sub>0</sub>
51.5	418	...	...	...	...	3.6352 <sub>9</sub>	2.9 <sub>8</sub>	
94	413	...	...	...	...	3.6353 <sub>1</sub>	2.9 <sub>8</sub>	} 3.0 <sub>0</sub>
144	415	...	...	...	...	3.6358 <sub>4</sub>	3.0 <sub>3</sub>	
18	377	...	...	3.6256 <sub>2</sub>	...	...	1.9 <sub>5</sub>	} 1.9 <sub>4</sub>
70	376	...	...	3.6254 <sub>8</sub>	...	...	1.9 <sub>4</sub>	
26	366	3.6231 <sub>1</sub>	...	...	...	...	1.6 <sub>8</sub>	} 1.6 <sub>0</sub>
50	360	...	...	3.6217 <sub>6</sub>	...	...	1.5 <sub>3</sub>	
66	338	3.6200 <sub>5</sub>	...	...	...	...	1.3 <sub>5</sub>	} 1.3 <sub>5</sub>
48	302	...	...	...	...	3.6173 <sub>1</sub>	1.0 <sub>6</sub>	
144	290	...	3.6191 <sub>7</sub>	...	...	...	1.2 <sub>5</sub>	} 1.1 <sub>5</sub>
6 days	261	3.6200 <sub>8</sub>	...	...	...	...	1.3 <sub>6</sub>	
12 "	263	...	3.6166 <sub>1</sub>	...	...	...	0.9 <sub>5</sub>	

710° to 470° C. In Fig. 1 it will be seen that the present results agree with those of Owen and Roberts within the error of measurement. All over the range from 710° to 470° C. the difference between the positions allocated to the boundary does not exceed 0.2 at.-%, and at most temperatures it is less than this. The transformation temperature where maximum solu-

350° and 250° C. a big change in temperature corresponds to only a small change in composition, so that at the lowest temperatures the boundary becomes almost parallel to the temperature axis. The form of the boundary in this region of temperature is very similar to that proposed by Weibke and Eggers, but the present results fix the boundary at much lower

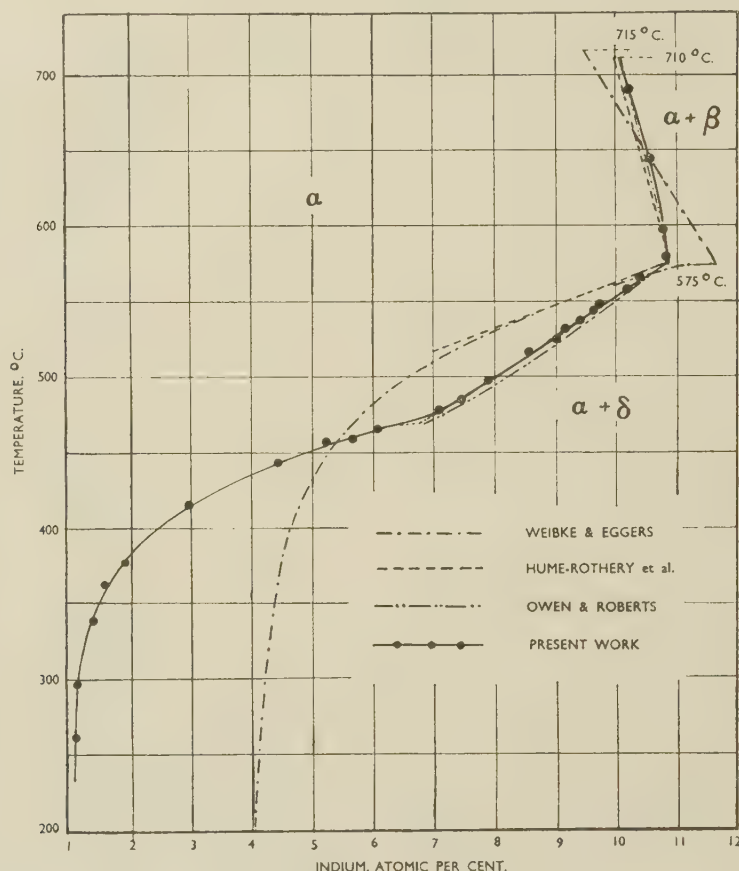


FIG. 1.— $\alpha$ -Phase Boundary in Copper-Indium System.

bility (10.8 at.-% indium) occurs, is 575° C., both the maximum solubility and the transformation temperature agreeing closely with the results of Hume-Rothery *et al.* and of Owen and Roberts.

The present investigation extends the boundary down to 250° C. At 470° C. the boundary shows a point of inflection, the rate of change of composition per unit change of temperature displaying a sharp increase in this vicinity; but as the temperature is lowered, the boundary changes course, and between

indium contents. Whereas Weibke and Eggers place the boundary at about 4.2 at.-% indium at 300° C., the corresponding value from the present work is about 1.2, a difference of 3 at.-%.

The point of inflection at 470° C. is so definite that the boundary below 575° C. could be drawn in two parts, as shown dotted in Fig. 1, which would lead one to expect a transformation also at 470° C., but we have not investigated the point with sufficient thoroughness to arrive at a definite conclusion.

#### REFERENCES

1. F. Weibke and H. Eggers, *Z. anorg. Chem.*, 1934, **220**, 273.
2. W. Hume-Rothery, G. V. Raynor, P. W. Reynolds, and H. K. Packer, *J. Inst. Metals*, 1940, **66**, 209.
3. E. A. Owen and D. P. Morris, *ibid.*, 1949-50, **76**, 145.
4. E. A. Owen and E. A. O'D. Roberts, *ibid.*, 1952-53, **81**, 479.
5. E. A. Owen and E. A. O'D. Roberts, *ibid.*, 1945, **71**, 213.
6. E. A. Owen and D. P. Morris, *ibid.*, 1949-50, **76**, 677 (discussion).
7. E. A. Owen, *J. Sci. Instruments*, 1944, **21**, 65.
8. J. Reynolds, W. A. Wiseman, and W. Hume-Rothery, *J. Inst. Metals*, 1951-52, **80**, 637.



# SOME FURTHER OBSERVATIONS ON THE FATIGUE PROCESS IN PURE ALUMINIUM \*

By P. J. E. FORSYTH, A.I.M., MEMBER

## SYNOPSIS

The fatigue process in pure aluminium has been more fully studied (cf. *J. Inst. Metals*, 1951-52, **80**, 181) with special reference to the mechanism of slip under cyclic stresses. The similarities and differences of deformation produced by cyclic and static stressing have been investigated both microscopically and by the multiple-beam interference technique. The effect of cyclic stressing at a higher frequency has been investigated, and it is concluded that cyclic stressing may produce a considerable rise in temperature in the region of slip bands, which become more localized at higher frequencies.

## I.—INTRODUCTION

EARLIER work <sup>1</sup> has shown how the stress level can influence the mode of deformation and subsequent cracking of pure aluminium and aluminium- $\frac{1}{2}$ % silver alloy. The complications of kink bands and polygonization have been experienced at high stresses, but the failure occurring at lower stresses is more characteristic of the fatigue process experienced in higher-strength materials, where slip alone is the only visible sign of deformation. The process of slip under fatigue stresses has now been more fully studied by interferometric as well as microscopic techniques.

The work of Heidenreich and Shockley,<sup>2</sup> Brown,<sup>3</sup> and others has shown that the slip lines or bands which can be observed on the polished surface of metal crystals after plastic deformation are the traces of packets of finely spaced slip lamellæ appearing on the crystal surface. This fine structure, within what appears as a single band under the light microscope, can be successfully resolved into fine lamellæ only by the electron microscope. These lamellæ have a remarkably constant width (approximately 200 Å. for aluminium).

In the present paper, a packet of fine slip lamellæ will be referred to as a slip band, in accordance with the generally accepted nomenclature. Under cyclic stressing, slip bands often form groups which may be spaced fairly regularly across any particular grain. These groups will be called "striations".

## II.—EXPERIMENTAL PROCEDURE

### 1. INTERFEROMETRIC EXAMINATION

In order to examine the topography of the surface of a fatigued specimen in more detail than can be achieved by the usual microscopic methods, the Tolansky method of multiple-beam interferometry was used on the polished surfaces of 99.99% pure aluminium specimens. Such an examination gives quantitative

information about the surface topography; the interferometric fringes can be regarded as surface contour lines, the vertical difference in level between adjacent fringes being  $\lambda/2$ . Monochromatic light was used, a convenient source being a mercury arc with a mercury green filter ( $\lambda = 5460$  Å.). The vertical resolution of this method is very great, and depends only on the definition of the fringes formed. This in turn depends on many factors of technique, but it is not experimentally difficult to obtain a high degree of vertical resolution. Any type of deformation which produces surface irregularities greater than the resolution limit may be detected unless the disturbed region is small enough to lie completely within fringes.

Slip bands lend themselves well to this technique, as they usually extend across microscopically large areas, and the vertical displacements at the steps are usually conveniently similar to the fringe spacing, i.e.  $\lambda/2$ . Sudden displacements of the fringes represent surface steps or ledges, while changes in fringe direction represent changes in surface slope; and surface grooves are revealed as greatly exaggerated notches along the fringes. They are, therefore, similar in their interpretation to surface contours on a map where the contours are placed at  $\lambda/2$  differences in level, the reference plane in the case of the fringes being the optical flat used in the technique.

Fig. 8 (Plate LXIX) shows a fringe pattern of the surface of an electropolished polycrystalline super-pure aluminium specimen after applying a direct stress, and Fig. 9 (Plate LXIX) shows the microscopic appearance of the same area. Fig. 1 shows schematically a possible cause of this corrugated form of deformation which has already been observed under alternating stress,<sup>1</sup> but which could not then be explained. As can be seen from Fig. 1, this form of slip is likely to occur only in a polycrystalline specimen, for the linked ends of the interleaved layers represent the boundary restraint which is present in polycrystalline material, and it can be seen

\* Manuscript received 20 August 1953.

† Metallurgy Department, Royal Aircraft Establishment, Farnborough, Hants.

that no general crystalline rotation will occur under these conditions. This mode of deformation of grains in polycrystalline aggregates has often been observed in the present work. It is interesting to note that kinking is absent from grains which slip in this manner. Fig. 8 (Plate LXIX) indicates that

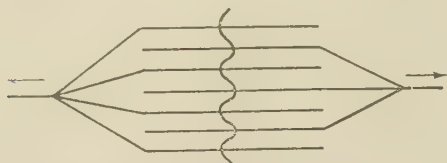


FIG. 1.—Schematic Diagram Illustrating the Type of Deformation Which Could Cause Surface Corrugations.

large-scale movement of material has occurred, since the fringes show marked undulations. Fig. 9 (Plate LXIX) shows that, apart from a few widely spaced slip bands, this large-scale movement cannot be detected microscopically.

The simple case of a set of slip bands produced by direct stress on a single crystal was next examined. The fringe pattern observed showed saw-toothed fringes indicating that the normal type of slip displacement was accompanied by a rotation of the crystal. If such a crystal was then strained in the opposite direction, i.e. to reverse the slip direction, most of the slip occurred on or very near the original bands, and the fringe pattern of such a surface showed that the bands were now grooves and no longer steps. The mechanism of this change is illustrated in Fig. 2 (a), (b), and (c). The grooves were almost as deep as the steps, suggesting that very little reverse slip occurs on the original planes.

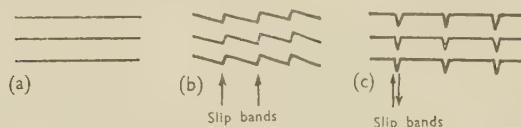


FIG. 2.—Effect of Reversal of Stress on Slip Bands as Indicated by Fringes. (a) Before Stressing, (b) After Static Stress, and (c) After Cyclic Stress.

When a single-crystal specimen of pure aluminium was subjected to repeated cyclic stresses at a frequency of 6000 c./min., the type of slip deformation produced continued to be of the general form shown in Fig. 2, i.e. the crystal showed rotation combined with the slip and conditions were not as illustrated in Fig. 1. The specimen was continuously observed while being vibrated, and it was found that the slip bands appeared to be fairly regularly spaced along the crystal, the spacing becoming slightly less towards the fixed end of the cantilever, where the stress was greater. On further cyclic stressing, the new bands appeared close to the original ones, producing striations. These striations, illustrated in Fig. 10 (Plate LXIX), were observed to maintain the original slip-band spacing. This sequence is shown diagrammatically in Fig. 3 (a), (b), and (c). Although the first few stress reversals may produce a set of slip bands, each subsequent

reversal does not necessarily produce new bands, although the striations grow steadily in width during the fatigue life. This will be referred to in Section III, where the particular case of kink bands is considered.

Fig. 11 (Plate LXIX) shows a region in the same specimen where a kink band has developed; this band is characterized by the absence of visible slip and shows up in contrast with the heavily marked surface. Fig. 12 (Plate LXIX) shows the irregular nature of the surfaces of the striations, and also reveals that the regions apparently free from visible slip have in fact undulating surfaces. It can also be seen that some of the fringes actually enclose small areas, indicating that short furrows and ridges have been produced, the ends of which taper off the general surface level. Fig. 13 (Plate LXIX), on the other

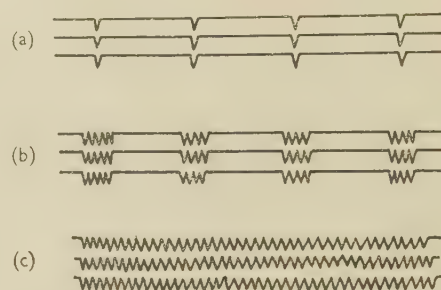


FIG. 3.—Changes in Slip-Band Distribution Which May Be Produced by Continued Cyclic Stressing.

hand, shows that the slip bands produced by static stressing are usually steps or ledges.

Fig. 4 (a) shows the method of formation of slip bands under the action of a direct stress with accompanying rotation of the crystal, Fig. 4 (b) shows how striations can be produced by the action of cyclic stresses, and Fig. 4 (c) indicates how a region of constraint to the free rotation of the crystal may produce a kink band. The formation of these structures in pure aluminium under the action of fatigue stresses has been described in earlier work.<sup>1</sup> Further observations which have been made on 99.5% purity aluminium show it to be more susceptible to kinking than is pure aluminium.

The fringe patterns reveal that the striations are regions of very irregular slip, producing many minute hills and valleys. It is noticeable that under cyclic stressing the slip displacements very rarely exceed  $\lambda/2$  (fringe spacing), i.e. approximately  $0.2\mu$  ( $2000 \text{ \AA.}$ ); even the larger-scale displacements, although often taking place over band widths of  $100 \mu$ , very rarely exceed this figure. It can, therefore, be concluded that the slip displacements are not comparable with those discussed by Brown,<sup>3</sup> because there seems to be no constant value in any particular grain. It might be assumed that the bands contain only one lamella, but the band widths suggest that small slip displacements are probably occurring over many lamellæ; indeed, it seems likely that every possible plane is being brought into action within the striations.



The fringe patterns also show that even the regions with no visible slip are corrugated. These corrugations seem to be due to very fine slip which has been observed with the electron microscope, and may also be due to elastic internal strains. These regions are seen to exist between striations and also in the kink bands already described, i.e. they exist as elastically

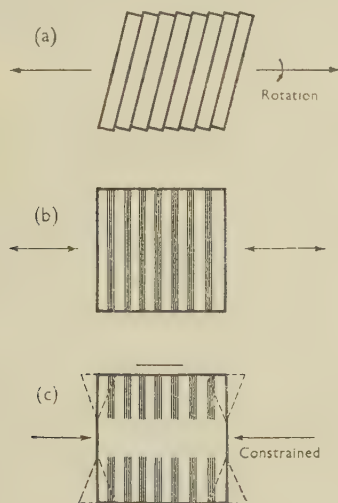


FIG. 4.—Formation of Slip Bands (a), Striations (b), and Kink Bands (c).

strained regions connecting all the plastically deformed regions. Fig. 14 (Plate LXIX) shows a fringe pattern of a surface where striations and kink bands exist together.

## 2. ELECTRON-MICROGRAPHIC OBSERVATIONS

The electron microscope was used to examine these regions more thoroughly. Specimens of pure aluminium were electropolished without preliminary grinding and subjected to fatigue at 6000 c./min. to give the effects just described. An oxide replica was then taken from the surface and examined under the electron microscope. The most noticeable feature was that the slip bands which could easily be resolved within the striations with the light microscope themselves contained many finer bands. These are shown in Fig. 15 (Plate LXIX) and Fig. 16 (Plate LXX). It was not possible to resolve these bands to find out whether they consisted of lamellæ similar to those described by Brown and others. The bands could no doubt have been further resolved with improved techniques, but the very fine spacing (of the order of 1000 Å.) made this impossible with the methods being used.

The so-called "slipless" regions are also seen to be covered with lamellæ so fine that they are beyond the resolution limit of the light microscope (see Fig. 15 (Plate LXIX)). These observations were in agreement with the interferometric investigations, which also suggested that movement of a more homogeneous kind was occurring, but they do not provide evidence for or against elastic strains in the

surface material. The electron micrography showed the existence of very fine cross slip and also regions of high lattice curvature (Fig. 16, Plate LXX).

## 3. HIGHER-FREQUENCY FATIGUE TESTS (20,000 c./min.)

To investigate the type of deformation occurring at higher frequencies, the apparatus described in the Appendix (p. 455) was constructed. Specimens of electropolished super-pure (99.99%) aluminium were fatigued at 20,000 c./min. Fig. 17 (Plate LXX)—a typical microstructure—shows that slip striations are more definite and often very straight and continuous across any particular grain. These striations frequently consist of deep channels or sometimes ridges where the slip cannot be clearly resolved (Fig. 18, Plate LXX). The depth of the channels was often such that no light from the vertical illuminator was reflected back. Repolishing showed that they were in fact shallow, with short cracks often appearing along the bottom. Fig. 17 also shows that appreciable disturbance occurs at or near the grain boundaries at these higher frequencies. The form of this disturbance can be seen more clearly in Fig. 19 (Plate LXX). The general darkening visible in some of the grains in Fig. 17 can be seen in Fig. 19 to be due to a fine network structure similar to that previously discussed, but of a finer nature. Fig. 20 (Plate LXX) also shows this network and, in addition, a striation that has propagated the deformation across the boundary into a neighbouring grain. Fig. 21 (Plate LXX) shows a similar occurrence and the appearance of a region of network structure produced by the disturbance. The regions where striations meet the grain boundary often show boundary migration (see Figs. 22, 23, and 24, Plates LXX and LXXI).

The specimens in Figs. 23 and 24 have been repolished and etched to reveal the boundaries. This removes the slip striations. The result of this treatment and of subsequent fatigue for a further period in order to produce the striations again is shown in Fig. 22. This movement of boundaries has been observed at all frequencies used, and has already been reported. The present observations are believed to throw more light on the nature of this movement. The specimens fatigued at higher frequencies were also examined by means of the electron microscope. Figs. 25 and 26 (Plate LXXI) show that very fine slip bands of a spacing of approximately 1000 Å. were common, and the bands were generally very much straighter than those obtained at lower stresses (Figs. 15 and 16); there were also fewer regions of local curvature.

## 4. THE INITIATION OF FATIGUE CRACKS IN SILVER CHLORIDE

Earlier observations on the initiation of fatigue cracks<sup>1</sup> produced no definite conclusions as to the part played by crystallite boundaries in crack

initiation. Nye<sup>4</sup> has demonstrated that silver chloride may be used for photoelastic observations, the stress pattern being examined by polarized light. Silver chloride consisting of an aggregate of small crystals having plastic properties in many ways similar to those of metals can be used to demonstrate the effect of grain boundaries and slip bands on the stress pattern. It was at first thought that this technique could be applied to fatigue specimens during the test, but this was found to be impracticable in the existing experimental arrangement, as very thin specimens are essential.

It was, however, considered that a transparent substance such as silver chloride might throw some light on the initiation of cracks if the material could be fatigued, and if the fatigue process was comparable with that of aluminium. The silver chloride was cast *in vacuo* in a Pyrex tube, pressed into sheet form between platens, and then annealed at 400° C. for 1 hr. It was found that the surface could be simply prepared by grinding on a ground-glass surface; this produced a surface finish with fine scratches which could be removed by dissolving away the surface in ordinary photographic fixer. This also etched the grain boundaries and produced a very satisfactory surface for a microscopical examination. Suitable test-pieces were prepared and fatigued in the small high-frequency machine described in the Appendix. After continuous examination with transmitted light, it was found that the silver chloride test-pieces behaved in much the same way as pure aluminium. Slip bands and kink bands were observed (Figs. 27 and 28, Plate LXXI). After a period of fatigue stressing, the slip bands were cleared from the surface by dissolving a layer away. This treatment was found to etch the boundaries of small crystallites which had been produced by fatigue stressing. It can be seen from Fig. 29 (Plate LXXI) that small cracks have started at these crystallite boundaries.

### III.—DISCUSSION

#### 1. SLIP PRODUCED BY CYCLIC STRESSES

Most of the observations on slip deformation and work-hardening have hitherto been made on statically stressed crystals, and it is not surprising to find that cyclic stressing modifies the slip mechanism. Two mechanisms suggest themselves, viz. slip back on the original planes or slip on neighbouring planes. The effect of stress reversals on a metal specimen has recently been investigated in the X-ray work of Wood and Head.<sup>5</sup> They showed that a large amount of the deformation produced by the positive half of the stress cycle was "recoverable" when the other half of the cycle was completed. The higher the frequency of cyclic stressing, the less was the initial deformation and the more complete the recovery on completion of the cycle. The implications of these observations are: (i) that slip in one direction can be partially restored by a stress reversal, and (ii)

that the strain as detected by X-rays is almost completely removed. These observations cannot, however, distinguish by which of the two slip mechanisms this recovery occurs. If a slip plane after moving a certain distance hardens to such an extent that it is unlikely to slip again, it seems inevitable that a reversal of stress in the opposite direction will cause slip on a neighbouring plane. It has been confirmed during the present investigation that, in fact, the stress reversal causes further slip, producing an adjacent band.

The concept of the slip process in metals may be over-simplified by the classical picture of glide and accompanying crystal rotation, as this implies that all crystal layers are gliding in the same direction relative to some external point. If we imagine that some layers glide in the opposite direction, or if we take the case when approximately equal numbers of layers move in each direction and when these two sets of layers are fairly regularly interleaved with one another, glide will take place without any large-scale rotation. The interferometric observations in the present work show that in polycrystalline specimens where the crystals are invariably restrained by their neighbours this form of glide is very common (see Fig. 1). The external shape of such a grain will not be changed to any great extent and it does not interfere with its neighbours to the same degree as one that glides and rotates, although the amount of glide that has occurred in each may be the same. In spite of this macroscopic difference in modes of glide, it is considered unlikely that there will be any difference in the basic slip mechanism and that considerations based on the behaviour of a single crystal, free to rotate and glide, are of general application.

The microscopic and interferometric observations have shown that plastic strain occurs as glide on certain planes. These movements can be observed as surface steps, and a reversal of slip direction can be brought about by a reversal of stress. It has been demonstrated in Section II that slip does not necessarily occur on the same crystal planes during the reversal of strain, but that new planes are used up and the original step becomes a groove. It is emphasized, however, that this reversal will reduce the internal strain set up by the first half of the cycle, in much the same way as the deformation described in the previous paragraph and illustrated in Fig. 2. This suggests that macro-bending stresses which produce kink bands are relieved by the stress reversal, but that plastic strain in the form of a slip displacement occurs and remains on very localized planes. If the first half of the cycle has produced a kink band, the outline of the band will be accentuated by further reversals of strain with the production of many other slip bands, each one stopping short at the kink band.

Jillson<sup>6</sup> has described kinking as the movement of lattice curvatures of opposite signs until they become locked. Many of them will cancel one another out,



but if, owing to local impedances, some become locked, others moving across the crystal will also be stopped and thus the kink will become more marked. Jillson considers these curvatures as the basic form of deformation and the slip process as a logical result of two curvatures of opposite signs meeting and

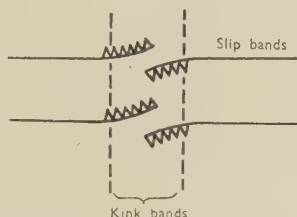


FIG. 5.—Production of Kink Bands. Condition produced by the first half of the first stress cycle.

cancelling one another. Mott<sup>7</sup> has illustrated the same phenomenon by a series of dislocations of the same sign that have been prevented from moving freely across the crystal and have piled up in certain regions to produce local hardening as the result of local lattice curvatures. These will exist in pairs, and, as can be seen from Fig. 5, they will produce kink bands.

Fig. 5 represents the condition produced by the first half of the first stress cycle; if now the cycle is reversed, experimental evidence suggests that the reverse slip occurs very near the original bands and the condition shown in Fig. 6 is produced. The dislocations piled up in the first half of the cycle will be to a great extent cancelled out or dissipated by the production of the neighbouring slip band. The complete elimination of the curvature is, however, unlikely; observations have indicated that a drift in one direction or the other occurs. These observations are in agreement with those of Wood and Head. Although the macro-stresses may be relieved, the crystal has nevertheless suffered additional slip under the action of the reverse half of the stress cycle. More and more slip bands appear, usually associated in striations, and eventually the whole bulk of the crystal may

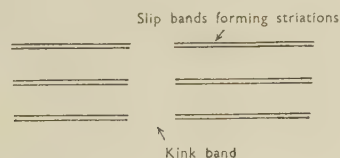


FIG. 6.—Production of Kink Bands. Condition on completion of first stress cycle.

have slipped, though just how many slip lamellæ this involves it is hard to estimate. It is interesting to observe that cracking can occur in the crystal before the whole crystal is covered with slip bands.

The striations produced by fatigue at high frequencies are more clearly defined than those produced at low frequencies. Many shorter slip bands are also

formed, often in the conjugate position to the main slip-band direction. The microscopical appearance of the slip bands in the aluminium specimens suggests that they may have experienced a considerable rise in temperature, because a stain, or what appears to be a granular oxide film, is formed along these marked striations. This staining or heat-tinting was also observed in copper and Armco iron even at the lower frequencies. If there is a heating effect, it is not surprising that it becomes more noticeable at the higher frequencies, as the temperature gradient between the slip bands and the surrounding matrix must be greater as a result of the shorter time cycle in which heat energy can be dissipated. The fact that copper and Armco iron exhibit these effects at lower frequencies may be due only to their greater tendency to show heat-tinting. That slip bands or striations were attaining temperatures considerably above room temperature would explain the fact that slip is confined chiefly to the striations where considerable thermal softening has occurred. These elevated temperatures may also be enough to lower considerably the cohesive strength of the metal in these regions.

## 2. BOUNDARY MIGRATION AT THE ENDS OF SLIP STRIATIONS

It has been seen that appreciable boundary movement may occur in either direction at the ends of

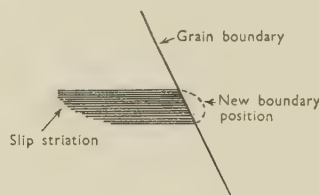


FIG. 7.—Conditions at the End of a Slip Striation.

slip striations. Such migration produces irregular serrated boundaries. It had been observed earlier and had been thought to be partly due to the movement of the crystal itself. This may often be the case, but there is now evidence for a true boundary migration as well as a mechanical movement. If we consider the end of a slip striation as shown in Fig. 7, the movement of dislocations along the slip bands will continually agitate the boundary region. Dislocations may be trapped at the boundary, and others will return from the boundary regions under the action of the cyclic stresses. This condition of continual agitation might produce boundary migration. The specimens illustrated in Figs. 22–24 showed this to be a true migration, as the earlier boundary positions were often still visible, and the part of the crystal which had been swept by the moving boundary often etched differently from the unaffected material. It was also noticed that particles of impurity in the boundary sometimes impeded the movement as

shown in Fig. 24. The fact that these striations may have reached temperatures considerably above room temperature may help the migration process.

Although a general work-hardening of the specimen may be found, it is considered that work-hardening and embrittlement are not the causes of fatigue cracking. The fact that cracks are initiated in the sub-boundaries in silver chloride suggests that a similar mode of failure may occur in aluminium, although it is difficult to substantiate this. It is, however, certain that the cracks are initiated in regions where these boundaries are most noticeable after etching.

#### IV.—CONCLUSIONS

(1) Interferometric observations show that cyclic stresses produce slip on many closely spaced bands in aluminium. These bands have a grooved contour rather than the step form which is obtained by static stressing.

(2) Cyclic stressing produces slip bands congregated in striations. These striations increase in width with continuous cyclic stressing by the process of the formation of increasing numbers of slip bands. Eventually the whole grain surface may be covered with bands.

(3) The spacing of the striations is that of the set of slip bands produced by the first stress cycle, and the number of striations is proportional to the stress level in any particular region.

(4) Because all striations grow wider at approximately the same rate, the more heavily stressed grains will be completely covered by slip bands in a shorter time than the lightly stressed grains, because their original slip-band spacing was more dense.

(5) Kink bands may appear as regions containing very few slip bands and, therefore, show up in marked contrast to the remainder of the crystal, which may be densely covered with bands.

(6) There is no evidence that each stress cycle produces additional bands. The number of visible slip bands is not directly proportional to the number of stress reversals the specimen has experienced. As the first few stress cycles of a fatigue test may produce a relatively large number of bands, it seems that the formation of a slip band or even a slip lamella may be either an avalanche process or the integration of a number of small movements. The latter process may be very much more common.

(7) Between slip bands and striations, the surface of the crystal often undulates, the corrugations running in the direction of the slip bands. This can be detected by the multiple-beam interferometer after cyclic or static stressing. These corrugations may be due to a more homogeneous form of slip which leaves no microscopically visible bands, or due to internal stresses which produce small amounts of strain. Very fine slip bands can be observed by the electron microscope in these so-called "slipless"

regions. They are often of the order of 1000 Å. spacing, and, if the slip distance on each was small, they might give the fringe pattern which is often observed.

(8) Tests at higher frequencies (20,000–30,000 c./min.) produced slip bands that formed themselves to a very marked degree into striations, which in many cases were resolvable into slip bands only by using the electron microscope.

(9) The striations produced at higher frequencies often showed a granular surface film which gave a slightly stained appearance to the surface, suggesting than an increase in temperature had occurred.

(10) Many very short slip bands were also found in the specimens fatigued at high frequencies, and conjugate slip was often evident in the form of "feather edges" to the main slip bands.

(11) Boundary migration which had been noticed in earlier observations was shown to be a true boundary movement and occurred usually at the ends of striations. It could progress either into the striated grain or its neighbour, and always left a disturbed region behind it.

(12) The boundary migration would seem to be due to the continual movement of dislocations to and from the boundary region.

(13) It is possible that a considerable temperature rise occurs within the striations produced by cyclic stressing, especially at higher frequencies; this would account for the confinement of slip to these regions, and might also increase the possibility of polygonization.

(14) The higher frequencies caused marked disturbance near the grain boundaries and also a fine network structure.

(15) Fatigue tests on silver chloride showed clearly that considerable polygonization had occurred and that fatigue cracks had started at the new crystallite boundaries. Earlier work had suggested that the same phenomenon occurred in pure aluminium.

#### ACKNOWLEDGEMENTS

Acknowledgement is made to the Chief Scientist, Ministry of Supply, and to the Comptroller, H.M. Stationery Office, for permission to publish this paper. The author is also indebted to Mr. D. Lewis for the electron-microscope work, including the electron micrographs Figs. 15, 16, 25, and 26.

#### REFERENCES

1. P. J. E. Forsyth, *J. Inst. Metals*, 1951–52, **80**, 181.
2. R. D. Heidenreich and W. Shockley, *J. Appl. Physics*, 1947, **18**, 1029.
3. A. F. Brown, *J. Inst. Metals*, 1951–52, **80**, 115.
4. J. F. Nye, *Proc. Roy. Soc.*, 1949, [A], **198**, 190; **200**, 48.
5. W. A. Wood and A. K. Head, *J. Inst. Metals*, 1951, **79**, 89.
6. D. C. Jillson, *Trans. Amer. Inst. Min. Met. Eng.*, 1950, **188**, 1009.
7. N. F. Mott, Summer School Lectures (Bristol), 1951, (not published).



## APPENDIX

## HIGH-FREQUENCY FATIGUE MACHINE

The machine constructed for the continuous examination of specimens under the microscope is illustrated in Fig. 30 (Plate LXXI). The specimen, in the form of a rectangular-section cantilever (*A*), was examined on its wide surface near the root end, which was electropolished. Usually a stress raiser in the form of a groove was machined on the under surface of the specimen opposite the spot to be examined.

At magnifications of approximately  $100\times$ , ordinary illumination could be used instead of stroboscopic light, as movement was small and in the direction of the optical axis. Resolution was not as good, but it was sufficient for the advent of slip bands, &c., to be seen.

The specimen was driven at resonance by an audio-frequency oscillator, the resonant frequency for the specimens being between 25,000 and 30,000 c./min. The specimen-drive was in the form of a moving coil fixed to the free end of the specimen in the field of a loudspeaker permanent magnet.

Experiments with the conventional tubular moving coil working in the annular air gap showed that this method was impracticable when the specimen had to be changed periodically, because of the necessity

of accurate centring of the coil. It was also found that the fragile nature of such a coil was a great disadvantage. It was therefore decided to wind a flat coil between formers (*B*). This coil was positioned in the weaker field which existed above the annular gap, but because the design allowed for a greater number of turns on the coil, a sufficient vibration amplitude could be induced in the specimen. It is obvious that this design could be much improved by using a permanent magnet with a differently shaped air gap, so that the coil could work in a stronger part of the field. The generated wave form was transmitted to an oscilloscope from a crystal pick-up. The movement was not taken direct from the specimen but as a transmitted vibration in the body of the machine. This method was found to give ample sensitivity and allowed a more simple design to be used without the necessity of some form of removable coupling between specimen and crystal pick-up.

The quartz crystal head (*C*) was mounted on a rubber pad fixed to the body of the machine. The movement was transmitted to the "free" end of the crystal via a short rod of polyvinyl chloride from the bridge (*D*). This linkage permitted the transmission of the necessary movement. It would be a great improvement to use the quartz crystal as an exciter, the output voltage of which could be amplified to drive the specimen, thus maintaining the vibrations on the resonance peak.

# 1539 THE SYSTEM URANIUM-MERCURY \*

By B. R. T. FROST,† B.Sc., Ph.D., JUNIOR MEMBER

## SYNOPSIS

The uranium-mercury alloy system has been examined over the whole composition range from  $-40^{\circ}$  to  $1000^{\circ}$  C., by means of X-ray, thermal, and low-temperature micrographical analysis. The high volatility of mercury necessitated the development of a method of preparation of the alloys at relatively low temperatures by the use of pyrophoric uranium. Three types of thermal-analysis apparatus were used to suit the varying conditions over the  $1100^{\circ}$  C. temperature range. At all except very dilute concentrations the alloys were pyrophoric, and all operations had to be carried out *in vacuo*.

The solid solubility of uranium in mercury and that of mercury in uranium are both very small. The addition of mercury to uranium has no detectable effect on the transformation temperatures of uranium. Three intermetallic compounds, with the formulæ  $\text{UHg}_2$ ,  $\text{UHg}_3$ , and  $\text{UHg}_4$ , have been identified, and the crystal structures of  $\text{UHg}_2$  and  $\text{UHg}_3$  have been confirmed. From a consideration of these structures and of the melting points of the compounds, it is concluded that the high electrochemical factor between mercury and uranium is not operating with its maximum effect in the compounds.

## I.—INTRODUCTION

THE examination of the uranium-mercury system formed part of a general investigation of the alloys of uranium.<sup>1, 2, 3</sup> It was known, at the beginning of this work, that the system had been examined in the United States, and that three compounds,  $\text{UHg}_2$ ,  $\text{UHg}_3$ , and  $\text{UHg}_4$ , had been identified. The crystallographic structures of these compounds were published in 1949,<sup>4</sup> and have been discussed by Raynor.<sup>5</sup> Since, however, full details of the equilibrium diagram were lacking, it was decided to continue the investigation at Harwell.

The development of a number of special experimental techniques was necessary to overcome the difficulties in preparation and examination of the alloys. In the first place, the high melting point of uranium ( $1133^{\circ}$  C.) and the low boiling point of mercury ( $358^{\circ}$  C.) made simple liquid metal mixing for alloying impossible, and secondly, mercury exerts a vapour pressure of several hundred atmospheres at the melting point of uranium, so that all experiments at temperatures exceeding the boiling point of mercury (e.g. thermal analysis) had to be performed in sealed pressure vessels. Although the formation of compounds leads to a reduction in vapour pressure, the latter is still appreciable above  $400^{\circ}$  C. A third complicating factor was the highly pyrophoric nature of the alloys at all except very low concentrations of uranium.

Uranium has three allotropic modifications; the  $\alpha$  form, stable from room temperature to  $665^{\circ}$  C., has an orthorhombic crystal structure, the  $\beta$  form, stable from  $665^{\circ}$  to  $772^{\circ}$  C., has a complex structure, and the  $\gamma$  form, stable from  $772^{\circ}$  to  $1133^{\circ}$  C., has the body-centred cubic structure. The  $\gamma$  structure is the only one which is truly metallic, and the closest distance of approach of the atoms in this structure

( $3.0 \text{ \AA.}$ ) is the value used in size-factor calculations. Uranium is a fairly electropositive metal, lying between aluminium and beryllium in the electrochemical series.<sup>6</sup> Mercury has a rhombohedral crystal structure, the closest distance of approach of the atoms being  $3.0 \text{ \AA.}$ , and the Goldschmidt atomic diameter  $3.1 \text{ \AA.}$  The metal is electronegative in character, having an electrode potential similar to that of silver.

## II.—EXPERIMENTAL METHODS

### 1. MATERIALS

Two samples of uranium were used, one having a purity of 99.97 wt.-% and the other 99.84%, the latter containing more aluminium and carbon than the former. No difference in alloying behaviour of the two samples could be detected. The principal impurities were iron, carbon, silicon, aluminium, oxygen, and nickel.

The mercury, which was supplied by Johnson, Matthey and Co., Ltd., was triple distilled and spectrographically pure.

### 2. PREPARATION OF THE ALLOYS

The alloys could not be prepared by melting together the two metals and stirring, as is the normal practice. Superheating mercury to the melting point of uranium yields a vapour which, besides exerting a very high pressure if confined, reacts only slowly with solid or liquid uranium.

Initially, to overcome this difficulty, clean uranium in the form of electropolished rod or turnings was heated at  $300^{\circ}$  C. in mercury, which attacked the uranium to form the first mercury-rich compound,  $\text{UHg}_4$ . The reaction then ceased, and the product,

\* Manuscript received 12 August 1953.

† Metallurgy Division, Atomic Energy Research Establishment, Harwell, Berkshire.



when cooled to room temperature, consisted of the uranium encrusted with  $\text{UHg}_4$  crystals surrounded by mercury. Isolation of the crystals of  $\text{UHg}_4$  by filtration showed these to be pyrophoric, so that most alloys in this range of composition had to be handled *in vacuo* or in an inert atmosphere. Two techniques were developed which would meet this need and at the same time improve the alloying reaction between uranium and mercury.

It is well known that dangerous or pyrophoric materials may be handled quite safely under vacuum

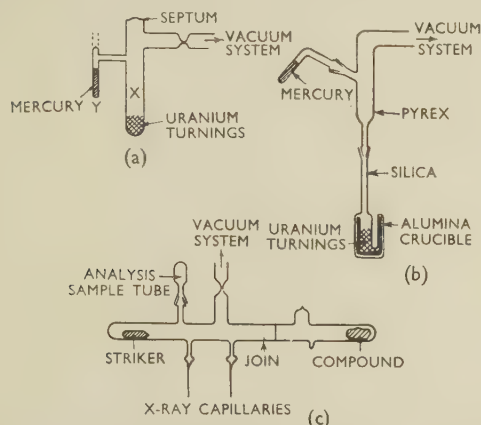


FIG. 1.—Tubes for Hydriding Process.

in glass tubes sealed by septums or glass membranes. Anderson and D'Eye<sup>7</sup> have applied this technique at Harwell to the examination of the halides of thorium. It is also well known that uranium can be rendered more reactive by converting the massive metal to a fine powder hydride  $\text{UH}_3$ , and then heating *in vacuo* to re-form the metal. On the basis of this experience, the alloying reactions were carried out in Pyrex tubes of the type shown in Fig. 1.

A weighed amount of clean uranium turnings was placed in the bottom of the larger tube (X) shown in Fig. 1 (a), and a weighed quantity of pure mercury in the side tube (Y), which was then sealed off. The uranium was converted to the hydride,  $\text{UH}_3$ , by admitting pure hydrogen to the system and heating the tube X at  $250^\circ\text{C}$ . for  $\frac{1}{2}$  hr. At the end of this time the system was opened to the vacuum pumps and the heating continued, so that the hydride decomposed, leaving uranium in the form of a grey, pyrophoric powder. When the tube was cool, it was sealed at the constriction, the mercury run from Y into X and the side arm Y sealed and removed by means of an oxy-gas torch. The main tube X was held in a furnace at  $300^\circ\text{C}$ . for several hours to allow the contents to react. Specimens for X-ray and chemical analysis were obtained by attaching a second Pyrex tube (Fig. 1 (c)) to the reaction tube. This analysis tube, to which were attached X-ray capillary and sample tubes, was evacuated and sealed. A glass striker in the analysis tube was made to pierce the septum, and the powdered alloy was shaken into the capillaries and sample tubes, which were sealed and removed.

Specimens for thermal analysis were prepared in a tube of the type shown in Fig. 1 (b). The hydriding process was carried out as detailed above, and the uranium allowed to cool after its conversion from the hydride. The mercury was added while the tube was still attached to the system, and the narrow silica tube was sealed in a very hot flame. In a modified procedure, the alloy was prepared in the type of tube shown in Fig. 1 (a) and transferred to the thermal-analysis tube, which was attached to the reaction tube by a silica-Pyrex graded seal. The attachment was achieved in a manner similar to that in which the "analysis" tube was sealed on in the first method, (Fig. 1 (c)).

### 3. METALLOGRAPHY

The major part of the alloy system was determined by X-ray and thermal-analysis methods, microscopic examination being difficult (if not impossible) except for the mercury-rich alloys, which have to be examined at low temperatures. For this purpose a cold microscope stage, similar to that described by Rosenhain and Murphy,<sup>8</sup> was constructed.

The specimen was prepared by pouring the liquid alloy into an open-ended glass tube which rested on a microscope slide, the tube and slide being surrounded by a mixture of acetone and solid carbon dioxide. A sharp tap on the slide removed it from the solid metal and supporting glass tube, leaving a flat surface for examination. The tube containing the solidified alloy was placed in an insulated dish of cooling mixture with the metal surface uppermost under a microscope as shown in Fig. 2. A metal cover attached to the microscope objective dipped into the liquid below. To prevent frosting of the lens, a stream of air dried by anhydrous calcium chloride and cooled by

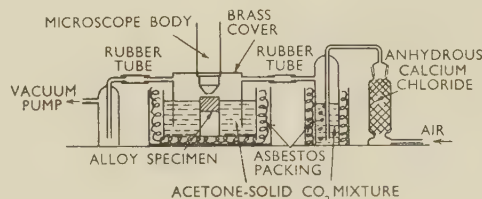


FIG. 2.—Cold Microscope Stage.

bubbling through an acetone-solid  $\text{CO}_2$  mixture, was passed through the compartment containing the specimen. The compound phase in the mercury-rich alloys was readily distinguished owing to its high oxidation rate, so that etching was unnecessary.

### 4. X-RAY METHODS

The specimens, sealed in Pyrex capillary tubes, were examined by conventional X-ray techniques. The capillaries were mounted in 9- or 19-cm. Debye-Scherrer cameras and exposed to  $\text{CuK}_\alpha$  radiation (nickel filtered). Long exposure times were necessary because of the high absorption by mercury and uranium, and there was a high background owing to fluorescence.

A Unicam high-temperature camera, which had been modified in accordance with the recommendations of Berry, Henry, and Raynor,<sup>9</sup> to give accurate temperature control and measurement, was used for exposures from 350° C. to room temperature.

### 5. THERMAL ANALYSIS.

The difficulties involved in thermal analysis arose mainly from the high vapour pressure of mercury above 450° C., and the occurrence of the liquid phase at room temperature in the mercury-rich alloys.

Thermal analysis of the uranium-mercury alloys was divided into three stages:

- (a) low-temperature analysis (−60° C. to room temperature);
- (b) medium-temperature analysis (room temperature to 450° C.);
- (c) high-temperature analysis (450°–1000° C.).

#### (a) Low-Temperature Analysis

A very simple but accurate thermal-analysis apparatus for low-temperature ranges was constructed from a tall, narrow Dewar flask, 18 in. long, with an internal dia. of 2 in. This was mounted in a box and surrounded by asbestos wool (Fig. 3 (a)). The bottom 3 in. of the flask were filled with liquid nitrogen to provide a suitable temperature gradient. As shown by a large number of experiments, in half an hour the temperature between the top of the flask and the liquid level fell linearly, the gradient remaining constant.

The specimen was poured into a Pyrex tube which had a thermocouple sheath sealed into it. An iron/Constantan thermocouple was inserted in the sheath,

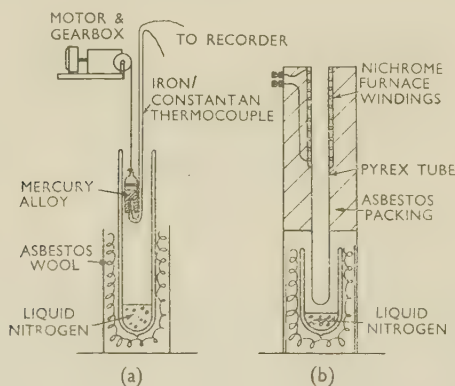


FIG. 3.—Apparatus for Low-Temperature Thermal Analysis.

the ends being connected to a recording potentiometer. This thermocouple was of fine-gauge wire insulated with glass fibre, which made it flexible and allowed it to follow freely the descent of the specimen tube into the Dewar flask. The rate of descent, controlled by a synchronous motor, was 1° C./min., which gave reproducible results for the cooling curves.

Fig. 3 (b) shows a modified form of apparatus for the examination of alloys over a wider range of tempera-

ture, viz. −100° to +200° C. In this arrangement the specimen was lowered down the long, 1½-in.-dia. Pyrex tube, round the top of which was wound a Nichrome furnace. Adjustment of the furnace current and of the level of liquid nitrogen in the Dewar flask gave a smooth temperature gradient.

#### (b) Medium-Temperature Analysis

Specimens obtained by the hydride method and already sealed in a vacuum were used for thermal analysis in this range. The sample tube was placed inside a small steel container, closed by a steel screw-on cap through which passed the Chromel/Alumel thermocouple wires (Fig. 4). The purpose of this

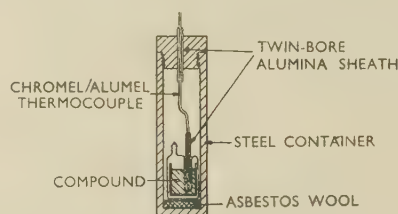


FIG. 4.—Apparatus for Medium-Temperature Thermal Analysis.

container was to keep the temperature fluctuations as low as possible and to minimize damage should the mercury vapour pressure become sufficient to burst the specimen tube. This arrangement was mounted inside a Nichrome-wound tube furnace which was connected to a Variac auto-transformer. The brushes of the Variac were driven around the coil at a constant speed by a motor driving a train of gears. The gear train ended in a solid Sindanyo wheel which bore on a large-diameter, rubber-rimmed disc, attached to the brush spindle of the Variac. This gave a smooth time/temperature curve without the "hunting" produced by a programme controller. By using a suitably designed cam in place of the large-diameter disc, the time/temperature curve can be maintained linear.<sup>10</sup>

#### (c) High-Temperature Analysis

The methods previously used for the thermal analysis of mercury alloys in the high-temperature range include measurements at constant pressure and measurements in a confined space where the internal mercury vapour pressure is opposed by an external gas pressure. Thermal-analysis measurements at constant pressure are somewhat restricted. Murphy<sup>11</sup> has shown that the second method, however, even when pressures are of the order of hundreds of atmospheres, does not give rise to an erroneous phase diagram, since the effect on the liquidus is within the limits of experimental error, even at 1000° C. It was decided to determine the upper region of the liquidus curve of the system uranium-mercury by the method employed by Murphy, i.e. to place the specimen in a small furnace fixed inside a stout, steel, gas-tight container and to admit a suitable gas to the system to balance the mercury vapour pressure.



Murphy has stated that a well-constructed silica specimen tube can withstand the vapour pressure of mercury up to 960° C., but the type of tube employed for the uranium-mercury alloys was not sufficiently strong, since it had been designed with the hydride process in mind.

The pressure vessel used in this investigation, shown in Fig. 5, was constructed of mild steel. The end caps were bolted down on to Neoprene gaskets which kept the vessel pressure-tight.

An attachment to the lower cap connected with a 10,000-lb./in.<sup>2</sup> flexible gas line; in the upper cap were

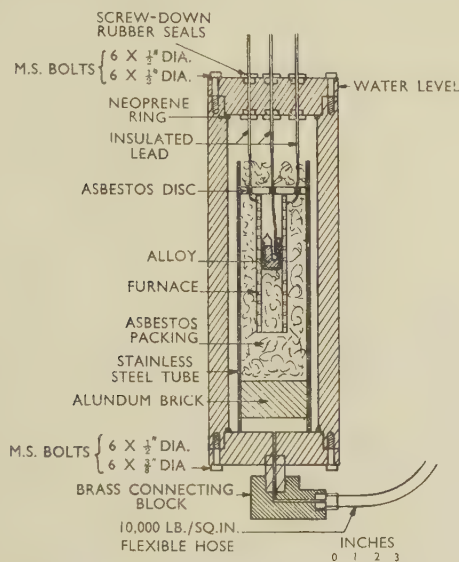


FIG. 5.—Pressure Vessel for High-Temperature Thermal Analysis.

fixed five small rubber gaskets through which passed the leads to the furnace and the thermocouple.

A silica specimen tube with a thermocouple attached was placed inside a 1-in. outside-dia. Mullite tube, wound with Kanthal "A" wire and insulated with asbestos wool. This was placed in a 2-in. inside-dia. stainless-steel tube which rested on a refractory block in the bottom of the pressure vessel. Flexible insulated wires were connected from the furnace and the thermocouple to the leads in the top cap of the pressure vessel, which was then firmly attached. The tube was mounted in a steel cradle which stood inside a tank filled with water to within an inch of the top of the pressure vessel to keep the body of the vessel cool. The gas inlet was connected with a line from a 120-atm. nitrogen cylinder which included a suitable bursting disc, a release valve, and a steel-tube Budenberg gauge. The current for the furnace was supplied from the motor-driven Variac described in Section II, 5 (b), and a Chromel/Alumel thermocouple was connected to a potentiometric recorder or to a potentiometer circuit. During heating it was found preferable to allow the nitrogen to trickle into the vessel, rather than to increase the pressure at temperature intervals, since the sudden admission of cold gas seriously affected the shape of the time/temperature curve.

Experiments showed that the silica specimen tubes could withstand the internal pressure at 1000° C. with an external pressure of 120 atm.

## 6. ELECTRICAL-RESISTIVITY MEASUREMENTS

The shape of the mercury-rich liquidus was determined by resistivity measurements. The validity of this method for liquidus determinations has been discussed by Frost and Maskrey.<sup>3</sup> The apparatus consisted of a U-tube, the capillary bore of which was of uniform section, filled with a mercury-rich alloy of known composition. Platinum wires dipped into the liquid column. The tube was immersed in an oil bath, the temperature of which was controlled by a toluene thermostat or by a Sunvic helical control, depending on the temperature range. The resistivity of a series of alloys of varying composition was determined potentiometrically over the range 20°–250° C.

## 7. CHEMICAL ANALYSIS

Initially the method of analysis of the alloys was to drive off the mercury by heating *in vacuo* and weigh the uranium as oxide. The mercury could also be condensed and weighed.<sup>12</sup> In a later method the mercury was precipitated and weighed as the iodate, the uranium being estimated as the di-uranate.

## III. EXPERIMENTAL RESULTS

### 1. THE FORM OF THE DIAGRAM

The thermal-analysis and X-ray-diffraction results are detailed in Tables I and II. These results, and

TABLE I.—*Thermal-Analysis Results* ( $\pm 2^\circ$  C.).

U, at.-%	Arrests, °C.		Thermal-Analysis Method *
2.5	−38.0	...	Low temp.
...	...	252	Med. temp.
7.5	−41	315	Low and med. temp.
12.5	−40	348	" " "
17.5	−42	365	" " "
22.5	365	389	" " "
25	392	407	" " "
30	390	455	" " "
35	450	515	Med. temp. and high temp.
45	457	698	High temp.
55	455	850	" "
62.5	925	...	" "
0.08	−40	...	Low temp.
0.07	−43	...	" "
0.06	−41	...	" "
0.10	100	...	" " (mod.)

\* See p. 458.

TABLE II.—*X-Ray Diffraction Results.*

U, at.-%	Temp., °C.	Pattern
10	Room (20)	Diffuse (liquid Hg)
22.5	20	UHg <sub>4</sub> + UHg <sub>3</sub>
25	20	UHg <sub>3</sub>
25	300	UHg <sub>3</sub>
30	20	UHg <sub>3</sub> + UHg <sub>2</sub>
33	20	UHg <sub>2</sub>
45	20	UHg <sub>2</sub> + U

those obtained by micrographic and resistivity methods, are assembled in the complete diagram in Fig. 6. The results of the resistivity experiments are shown graphically in Fig. 7, in which the proposed liquidus curve is drawn.

The diagram contains three compounds whose compositions are, as far as can be ascertained, invariable. The formulæ  $\text{UHg}_2$ ,  $\text{UHg}_3$ , and  $\text{UHg}_4$  have been assigned to the compounds, the structures of which are described in Section III, 2. The compounds are all formed peritectically;  $\text{UHg}_2$  at  $455^\circ\text{C}$ .,  $\text{UHg}_3$  at  $390^\circ\text{C}$ ., and  $\text{UHg}_4$  at  $365^\circ\text{C}$ .. The liquidus is represented by smooth curves falling from the uranium axis at  $1133^\circ\text{C}$ . to the mercury-rich eutectic at  $-40^\circ\text{C}$ . The curve from  $1133^\circ$  to  $455^\circ\text{C}$ . was determined by the high-temperature thermal-analysis method in which the highest attainable temperature was about  $1000^\circ\text{C}$ . Four reliable arrests, accurate to  $\pm 5^\circ\text{C}$ ., were obtained out of a large number of experiments, and as the two ends of the curve are defined by  $1133^\circ$  and  $455^\circ\text{C}$ ., a fairly accurate liquidus curve can be drawn.

The liquidus curves between  $455^\circ$  and  $250^\circ\text{C}$ . have been drawn in their most probable forms, having regard to the small number of arrests obtained. From  $160^\circ$  to  $-40^\circ\text{C}$ . the liquidus curve is based on the results of the resistivity measurements given in Fig. 7. Alloys were examined up to  $250^\circ\text{C}$ ., but the uranium in solution tended to be oxidized at the exposed

of uranium in solid mercury. It was not possible to devise a means of determining the actual solubility of mercury in solid uranium. The similar atomic sizes of the two elements meant that there would be little lattice distortion by solution, and diffraction patterns

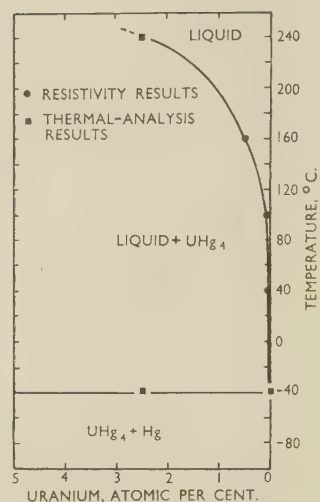


FIG. 7.—Solubility of Uranium in Liquid Mercury.

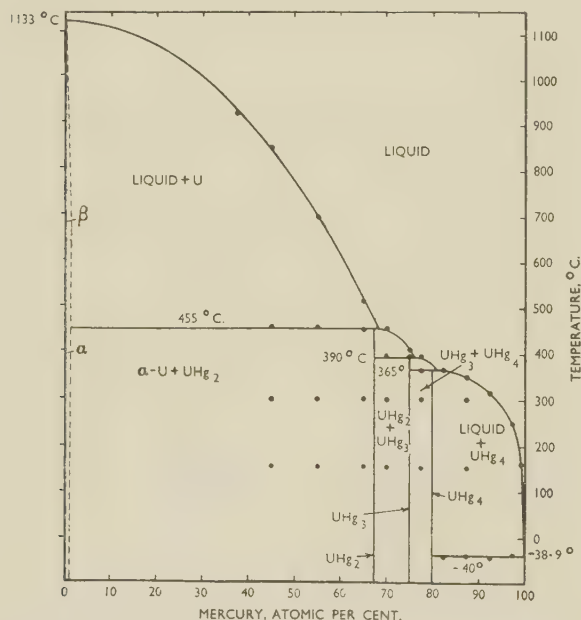


FIG. 6.—The System Uranium-Mercury, Showing Critical Alloys.

surfaces of the liquid at temperatures above  $200^\circ\text{C}$ ., and these results had to be discounted.

Thermal analysis established the eutectic horizontal at  $-40^\circ\text{C}$ . fairly accurately, and this was confirmed by low-temperature metallography, which also showed that there is an extremely small solubility

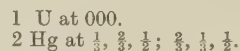
would not show whether solid solubility were extensive or not. Thermal analysis of uranium-rich alloys tended to show that there was little solid solubility at this end of the diagram.

Experiments on an alloy containing 2 at.-% mercury showed that the uranium in equilibrium with the liquid phase above  $455^\circ\text{C}$ . transformed from  $\alpha \rightarrow \beta \rightarrow \gamma$  and  $\gamma \rightarrow \beta \rightarrow \alpha$ , at the normal transformation temperatures of  $665^\circ$  and  $770^\circ\text{C}$ . for the  $\alpha/\beta$  and  $\beta/\gamma$  changes, respectively.

## 2. THE STRUCTURES OF THE COMPOUNDS

The structures of the compounds were determined from X-ray-diffraction patterns. The author's results are in fair agreement with those of the American workers,<sup>4</sup> viz.:

(a)  $\text{UHg}_2$ .—This compound has a hexagonal structure for which  $a = 4.976$ ,  $c = 3.218 \text{ \AA}$ .,  $c/a = 0.65$ . The unit cell, referred to co-ordinate axes, is:



The structure is represented diagrammatically in Fig. 8.

(b)  $\text{UHg}_3$ .—This compound has a hexagonal structure with  $a = 3.320$ ,  $c = 4.875 \text{ \AA}$ .,  $c/a = 1.47$ .

(c)  $\text{UHg}_4$ .—The Americans failed to obtain a pure pattern of  $\text{UHg}_4$ , and a similar difficulty was encountered by the author. The closeness in composition of  $\text{UHg}_4$  and  $\text{UHg}_3$  means that an error of 1 at.-% in the composition of a sample will result in the appearance of a two-phase pattern. The method adopted was, therefore, to start with a mercury-rich



alloy and to remove excess mercury by evaporation. Not until all the excess mercury had been driven off did the specimen become sufficiently brittle to be broken up and shaken into a Pyrex capillary tube. As these operations were all performed *in vacuo*, it was never found possible so to adjust conditions that the exact composition of  $\text{UHg}_4$  was obtained in the capillary. With excess mercury present, the liquid was forced to the outside of the capillary tube, next to the walls, and caused blackening of the film due to

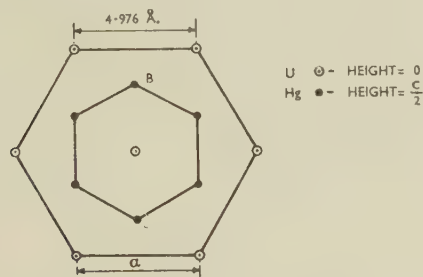


FIG. 8.—Unit Cell of  $\text{UHg}_2$ .

fluorescence. With excess uranium, extra lines of  $\text{UHg}_3$  were present in the pattern, some overlapping the  $\text{UHg}_4$  lines, and it was not possible to identify the structure unambiguously.

All attempts by the author to index the impure patterns gave unit cells with inacceptably high values for the density.

#### IV.—DISCUSSION

The form of equilibrium in the system under discussion is influenced by two factors: the large difference in melting points of the two elements and the formation of three size-factor compounds. The first factor gives rise to the steeply rising liquidus curve across the whole diagram. The three compounds are formed peritectically, and so affect the shape of this liquidus but little. Since the electrochemical factor between uranium and mercury is high, it might have been expected that the compounds would have high melting points; the possible reasons why this does not happen are discussed below.

The terminal solid solutions are both very limited in range of homogeneity. At the mercury-rich end, the compound  $\text{UHg}_4$  has a relatively high melting point compared with mercury, and tends to restrict solid solubility by the well-known relative free-energy effect,<sup>13</sup> i.e. the lower the free energy of the compound relative to the free energy of the solid solution, the more restricted is the solubility.

Although the sizes of the two species of atom are very similar, there are no other common features. The latent heats of vaporization are very different, a condition which, according to Hildebrand and Scott,<sup>14</sup> tends to promote liquid immiscibility and restriction of solid solubility. This may also help to account for the small solubility of mercury in uranium.

The fact that the three compounds formed in this system are of the size-factor type was established by Rundle and Wilson.<sup>4</sup> In a private communication, Raynor<sup>5</sup> commented on their results as follows: "The compounds (of uranium) with mercury have crystal structures which, where known, do not show analogies with known size-factor compounds, but it is known that the atomic volumes of uranium and mercury in the three compounds are, within their limits of accuracy, additive. This would indicate the virtual absence of any type of binding other than the purely metallic, and the probability is that atomic-size relationships are the main factors governing their formation. The fact that true Laves phases are not found may possibly be attributed to the close similarity between the atomic sizes of uranium and mercury." In Rundle and Wilson's paper,<sup>4</sup> the atomic volumes of the two elements in the compounds are compared with those in the elemental state. The agreement is good in every case, including that of their postulated pseudo-b.c.c. for  $\text{UHg}_4$ .

A detailed analysis of inter-atomic distances is possible only for  $\text{UHg}_2$ , in which the U-U distance is 3.2 Å., the Hg-Hg distance 2.82 Å., and the U-Hg distance 3.38 Å. The closest distances of approach of the elements in their respective crystal structures are 3.10 Å. for mercury and 3.0 Å. for uranium. In  $\text{UHg}_2$ , therefore, the mercury atoms are compressed and the uranium atoms are spaced more widely apart. With the high electrochemical factor operating, a contraction of the mean U-Hg distance would be expected, but in fact the atoms do not even touch one another. It is possible to rearrange the atoms in the  $\text{UHg}_2$  unit cell so that the electrochemical factor is satisfied. One mercury atom is in the 000 position, and the other occupies either the  $\frac{1}{3}$ ,  $\frac{2}{3}$ ,  $\frac{1}{2}$  or the  $\frac{2}{3}$ ,  $\frac{1}{3}$ ,  $\frac{1}{2}$  positions, the remaining position being occupied by the uranium atom. This gives a U-Hg distance of 2.82 Å., i.e. a bond contraction. The X-ray intensities which such an arrangement would produce were calculated, and did not agree quite as well with the observed intensities as those calculated for the original cell. However, the scattering factors of uranium and mercury are too similar for definite conclusions to be drawn. It was hoped to overcome this difficulty by the use of neutron diffraction, since the scattering factors of uranium and mercury for neutrons differ considerably. Unfortunately, mercury has an abnormally high linear absorption coefficient for neutrons, which means that with the neutron sources at present available a specimen would fail to give a pattern of sufficient intensity to resolve the problem.

The properties of compounds formed in other mercury alloy systems were examined to assess the importance of the electrochemical factor. These properties,<sup>15</sup> which include the melting points, heats of formation,  $H_f$ , electrochemical factors, and  $R$ , the melting points of the compounds divided by the melting points of the corresponding second element, are listed in Table III. The small amount of crystallo-

graphic data available indicates that the type of compound formed is governed by size-factor considerations. These data do not permit the calculation of interatomic distances in the compounds, but the "relative melting points"  $R$  (column 5 of Table III)

TABLE III.—*Properties of Binary Mercury Compounds.*

Compound (A-Hg)	Heat of Formation ( $H_f$ ) in k.cal./g.-atom	Electrochemical Factor	M.P., °K.	$R = \frac{\text{M.P. Compound}}{\text{M.P. of A (°K.)}}$
LiHg .	— 10.4	+ 3.85	873	1.9
LiHg <sub>2</sub> .	— 8.3	3.85	611	1.35
LiHg <sub>3</sub> .	— 6.7	3.85	513	1.1
Na <sub>3</sub> Hg .	— 2.8	3.5	307	0.8
Na <sub>3</sub> Hg <sub>2</sub> .	— 4.5	3.5	396	1.05
NaHg .	— 5.5	3.5	492	1.3
Na <sub>7</sub> Hg <sub>8</sub> .	— 5.6	3.5	500	1.35
NaHg <sub>2</sub> .	— 6.2	3.5	628	1.7
NaHg <sub>4</sub> .	— 4.4	3.5	431	1.15
KHg .	— 5.5	3.6	451	1.35
KHg <sub>3</sub> .	— 6.5	3.6	477	1.40
KHg <sub>10</sub> .	— 3.0	3.6	230	0.68
MgHg <sub>4</sub> .	— 3.5	3.2	233	0.25
CeHg <sub>4</sub> .	— 4.6	...	887	0.97
Ag <sub>3</sub> Hg <sub>4</sub> .	— 0.1	0	400	0.32
AuHg .	— 0.7	— 0.8	675	0.5
Cd <sub>3</sub> Hg .	— 0.2	1.2	461	0.78
CdHg .	— 1.0	1.2	398	0.67
CdHg <sub>3</sub> .	— 1.0	1.2	298	0.5
CdHg <sub>4</sub> .	— 0.8	1.2	280	0.47
CdHg <sub>19</sub> .	— 0.03	1.2	239	0.4
Tl <sub>2</sub> Hg <sub>5</sub> .	— 0.34	1.1	288	0.67
Pb <sub>2</sub> Hg .	— 0.02	0.9	273	0.64
UHg <sub>2</sub> .	...	2.4	728	0.52
UHg <sub>3</sub> .	...	2.4	663	0.47
UHg <sub>4</sub> .	...	2.4	638	0.45

show that the electrochemical factor is operating in a qualitative manner. Where several compounds are formed in a system, the compound having the highest melting point is obviously the one in which the electrochemical factor has its maximum effect, and, for the present argument, is selected for comparison with other systems. The strongly electropositive alkali metals form compounds which have high heats of formation and high values of  $R$ . Calcium, lead, and thallium are less electropositive and form compounds

with lower values of  $H_f$  and  $R$ , while the silver and gold compounds have even lower values. It has already been remarked that the electrochemical factor between uranium and mercury is high. The values of  $R$  for the compounds in the system are, however, comparable with those in the system silver-mercury, which are much lower than would be expected from the above considerations. This behaviour is, nevertheless, consistent with the crystallographic data, which seems to indicate that there is no U-Hg bond contraction in UHg<sub>2</sub>, and this may mean that the electrochemical factor is not fully operative in the system. This behaviour is not unique, since the so-called "size-factor compounds" of the formula UX<sub>3</sub>, which have a face-centred cubic ordered structure, do not show U-X bond contractions, although their melting points are high.<sup>3</sup> No reasonable explanation of this behaviour in terms of current alloy theory is possible at present.

#### ACKNOWLEDGEMENTS

Grateful acknowledgement is due to Mr. J. T. Maskrey for assistance in some of the experimental work and to Mr. C. E. Austing and Miss M. Hocking for the chemical analyses. The author also wishes to thank Dr. H. M. Finnieston, Professor G. V. Raynor, and many of his colleagues at A.E.R.E. for advice and constructive criticism throughout this work.

#### REFERENCES

1. P. C. L. Pfeil, *J. Inst. Metals*, 1950, **77**, 553.
2. J. D. Grogan, *ibid.*, 1950, **77**, 571.
3. B. R. T. Frost and J. T. Maskrey, *ibid.*, 1953-54, **82**, (4), 171.
4. R. E. Rundle and A. S. Wilson, *Acta Cryst.*, 1949, **2**, 148.
5. G. V. Raynor, private communication.
6. A. R. Gibson, private communication.
7. J. S. Anderson and R. W. M. D'Eye, *J. Chem. Soc.*, **1949**, S.244.
8. W. Rosenhain and A. J. Murphy, *Proc. Roy. Soc.*, 1926, [A], **113**, 1.
9. R. L. Berry, W. G. Henry, and G. V. Raynor, *J. Inst. Metals*, 1950-51, **78**, 643.
10. J. G. Ball and E. Adams, *J. Sci. Instruments*, 1951, **28**, 47.
11. A. J. Murphy, *J. Inst. Metals*, 1931, **46**, 507.
12. M. Gibson, *A.E.R.E. Rep.*, 1950, (C/M 65).
13. W. Hume-Rothery, "The Structure of Metals and Alloys" (Inst. Metals Monograph and Report Series No. 1). 1950: London.
14. J. H. Hildebrand and R. L. Scott, "The Solubility of Non-Electrolytes". 1950: New York (Reinhold Publishing Corp.).
15. C. J. Smithells, "Metals Reference Book". 1949: London (Butterworths Scientific Publications).



# THE TERNARY COMPOUND *E* IN THE SYSTEM ALUMINIUM-CHROMIUM-MAGNESIUM \*

1540

By (Miss) K. LITTLE,† M.A., D.Phil.

## SYNOPSIS

Single crystals of the aluminium-rich ternary compound phase *E*, in the system aluminium-chromium-magnesium, of approximate composition  $\text{CrMg}_{1.5}\text{Al}_{12}$ , have been examined goniometrically and by X-rays. The crystals are face-centred cubic, with  $a = 14.65 \text{ \AA}$ . Lines on the powder photograph correspond with strong reflections observed on oscillation photographs. Compound *E* is believed to be a member of a group of closely related phases that includes the aluminium-rich compounds  $\text{MnMg}_2\text{Al}_{10}$ ,  $\beta(\text{Fe-Si})$ , and the metastable phase  $\text{MnAl}_{13}$ , which is made stable by solution of chromium to give  $\text{CrMn}_4\text{Al}_{65}$ .

## I.—INTRODUCTION

An intermetallic compound in the system aluminium-chromium-magnesium was first described by Erdmann-Jesnitzner,<sup>1</sup> who suggested a composition corresponding roughly with  $\text{Cr}_3\text{Mg}_3\text{Al}_{24}$ . A more complete micrographic examination of the system<sup>2</sup> showed that the compound phase actually has a range of composition and contains a smaller proportion of chromium. The approximate limits of composition were shown to be  $\text{Cr}_2\text{Mg}_3\text{Al}_{23}$  and  $\text{Cr}_2\text{Mg}_3\text{Al}_{25}$ . Values obtained by direct chemical analysis of extracted crystals are represented by the formulæ  $\text{Cr}_2\text{Mg}_3\text{Al}_{25}$  (2 samples) and  $\text{Cr}_2\text{Mg}_4\text{Al}_{24}$  (1 sample). An account is given of an incomplete crystallographic examination of some of these extracted compound crystals.

## II.—CRYSTAL HABIT

Crystals were prepared by annealing alloys in the (liquid + *E*) region and then quenching. They were extracted electrolytically. The majority of crystals appeared to be small hexagonal plates, and as a preliminary measure extracted crystals of *E* were examined goniometrically by Dr. M. Porter. Her report was as follows :

Crystals are cubic. There are two habits :

(1) Simple octahedral, showing unmeasurable traces of  $(110)$  and  $(100)$ .

(2) Twins of spinel type, a juxtaposition twin of octahedra, twinned upon the octahedral plane. These crystals have the appearance of hexagonal plates.

## III.—CELL DIMENSIONS AND SPACE GROUP

From oscillation photographs of untwinned crystals the unit cell side was found to be approximately  $14.6 \text{ \AA}$ .

To obtain a more accurate value of the lattice constant for any given specimen, the main reflections on the powder photograph were measured. Thus, for a specimen of composition  $\text{Cr}_2\text{Mg}_3\text{Al}_{25}$ , the side of the unit cell was  $14.65 \text{ \AA}$ . Owing to the very small number of crystals available, the density has not been measured, but if it is assumed to be in the region of 2.9 the calculated number of "molecules" of  $\text{Cr}(\text{MgAl})_{14}$  is 12.

Inspection of oscillation photographs showed many clear reflections, some being of considerable intensity. The distribution of these very intense reflections gave no indication that the structure might be regarded as a distortion of any simpler unit.

From the indices of reflections obtained the compound was found to be face-centred, and all possible values were present for  $\{hhl\}$  and  $\{hk0\}$ . This left as possibilities the following space groups :  $F23$ ,  $F43m$ ,  $Fm3$ ,  $F4_13$ ,  $F43$ ,  $Fm3m$ . Both the morphological evidence and the fact that reflections such as  $(026)$  and  $(620)$  or  $(\bar{1}5 \ 7 \ 1)$  and  $(\bar{7} \ 15 \ 1)$  have equal intensities point to an octahedral space group. The octahedral space groups are  $F43$  or  $Fm3m$ , and since the formation of twinned crystals implies the presence of a plane of symmetry, the most probable space group is  $Fm3m$ . The positions of the chromium atoms are :

$$(000 : 0\frac{1}{2}\frac{1}{2} : \frac{1}{2}0\frac{1}{2} : \frac{1}{2}\frac{1}{2}0) + (000 : \frac{1}{4}\frac{1}{4}\frac{1}{4} : \frac{3}{4}\frac{3}{4}\frac{3}{4})$$

## IV.—DISCUSSION

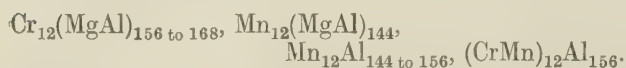
Wakeman and Raynor<sup>3</sup> have compared the ternary compounds  $T(\text{MnMg})$ , of approximate composition  $\text{MnMg}_2\text{Al}_{10}$ , *E*, and  $\beta(\text{Fe-Si})$ . The compounds are analogous in appearance, hardness, and etching characteristics, and would appear to be members of a definite group of related phases. Another compound whose appearance and etching properties are very similar to those of *E* is the compound *G* in the system aluminium-manganese,<sup>4, 5</sup> which probably belongs to

\* Manuscript received 15 August, 1953.

† Inorganic Chemistry Laboratory, Oxford; now at Atomic Energy Research Establishment, Harwell, Berks.

the same group. In the binary alloys it is metastable, but addition of chromium (with a consequent decrease in the electron:atom ratio) causes the formation of what is apparently a stable ternary compound phase of composition  $\text{CrMn}_4\text{Al}_{65}$ .

The approximate formulæ are:



The variation in ratio of (MnCr) to (MgAl) could be accounted for by the presence of vacant atomic sites. Such a phenomenon has been observed in the compounds  $\text{CrAl}_7$  and  $\text{Cr}_2\text{Al}_{11}$ , but with these the "holes" are in positions occupied by transition-metal atoms, whereas in the present series it seems more probable that the "holes" are in aluminium positions in the lattice. This would be in accordance with the observation that *G* is metastable unless it has some chromium in solution, since substitution of

chromium for manganese, magnesium for aluminium, or "holes" for aluminium all result in the reduction of the electron:atom ratio.

#### ACKNOWLEDGEMENTS

The author wishes to thank Mrs. D. Hodgkin for help and advice given in the interpretation of the photographs, Mr. H. M. Powell for the use of apparatus, and Dr. W. Hume-Rothery, in whose laboratory the crystals were prepared.

#### REFERENCES

1. F. Erdmann-Jesnitzer, *Aluminium Archiv.*, 1940, (29).
2. K. Little, H. J. Axon, and W. Hume-Rothery, *J. Inst. Metals*, 1948-49, **75**, 39.
3. D. W. Wakeman and G. V. Raynor, *ibid.*, 1948-49, **75**, 131.
4. K. Little, G. V. Raynor, and W. Hume-Rothery, *ibid.*, 1947, **73**, 83.
5. K. Little and W. Hume-Rothery, *ibid.*, 1948, **74**, 521.



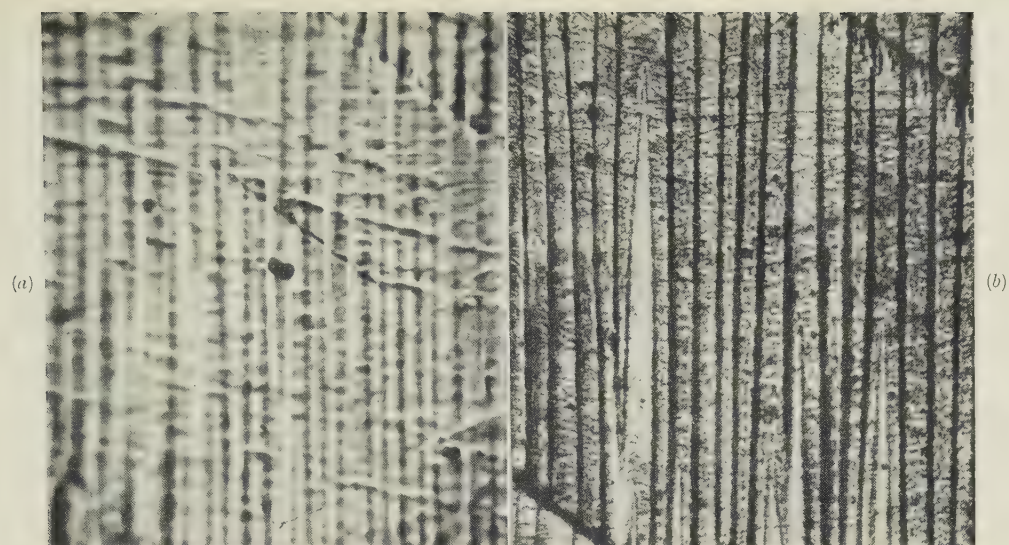


FIG. 1.—Unmagnetized Cobalt (*a*) without Colloid, and (*b*) with Colloid.

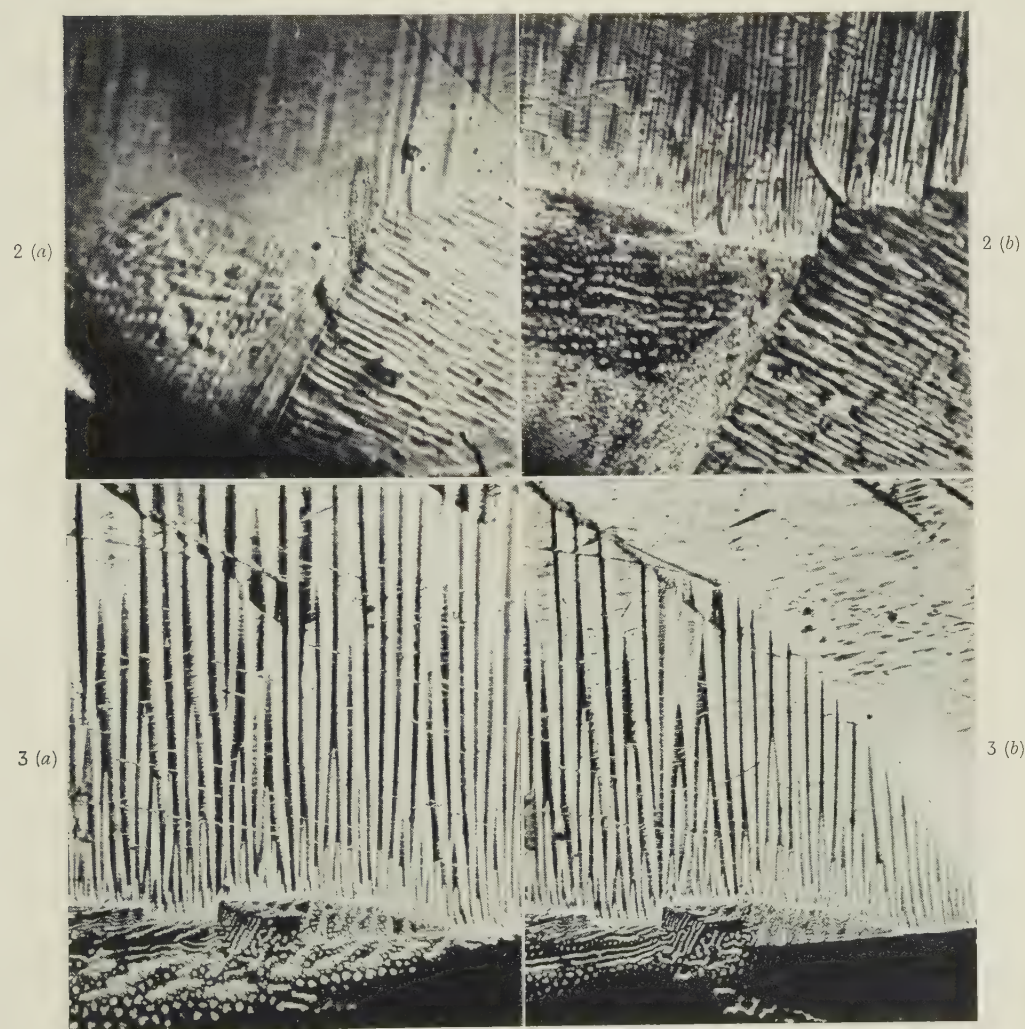


FIG. 2.—Polycrystalline Cobalt, Unmagnetized, (*a*) without Colloid, and (*b*) with Colloid.

FIG. 3.—Colloid Deposits on a Multigrain Surface of Cobalt. Magnetic field applied  $\uparrow$ . The field in (*b*) was substantially higher than in (*a*).

[To face p. 464.



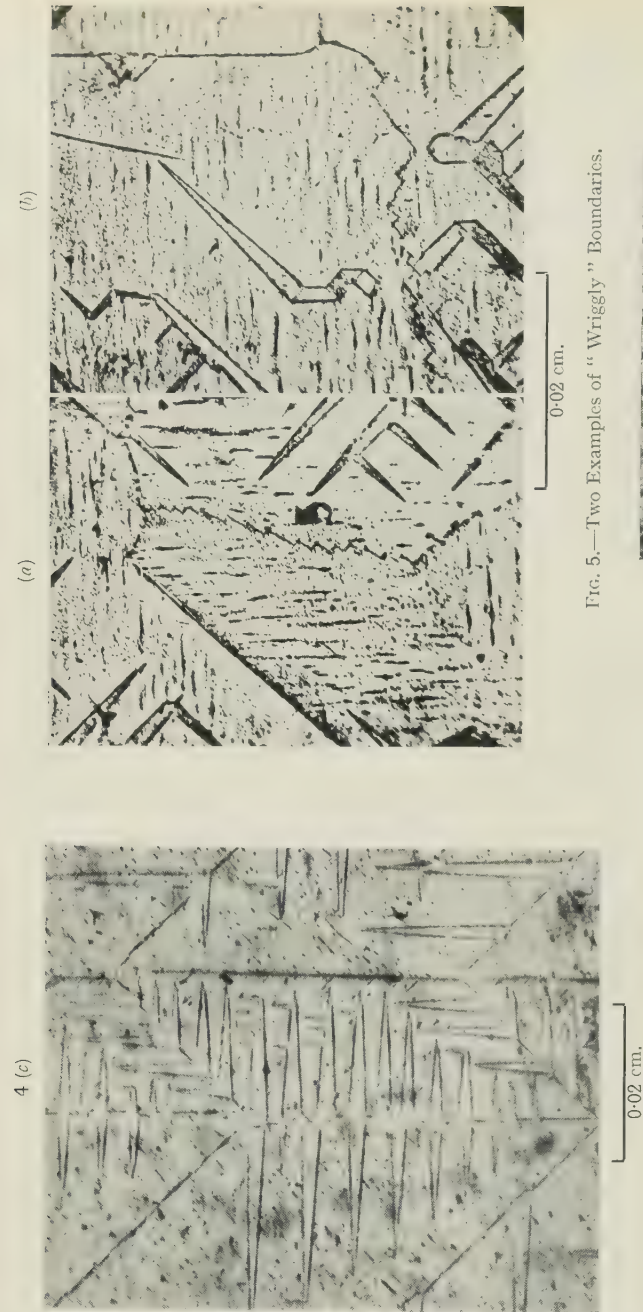


FIG. 5.—Two Examples of "Wiggly" Boundaries.

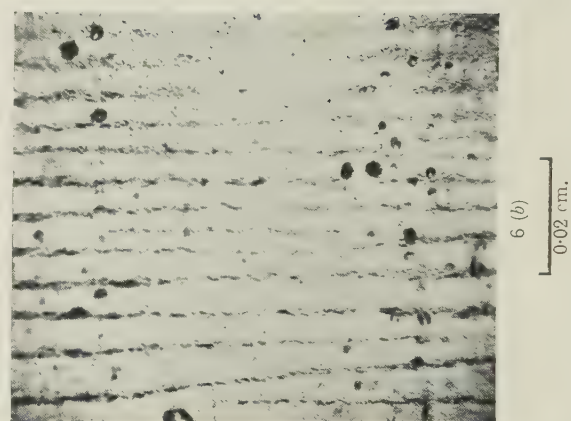


FIG. 6.—Patterns on Nickel.

(a) On (110) Surface,  $H = 100$  Oe. (b) On (111) Surface,  $H = 25$  Oe.

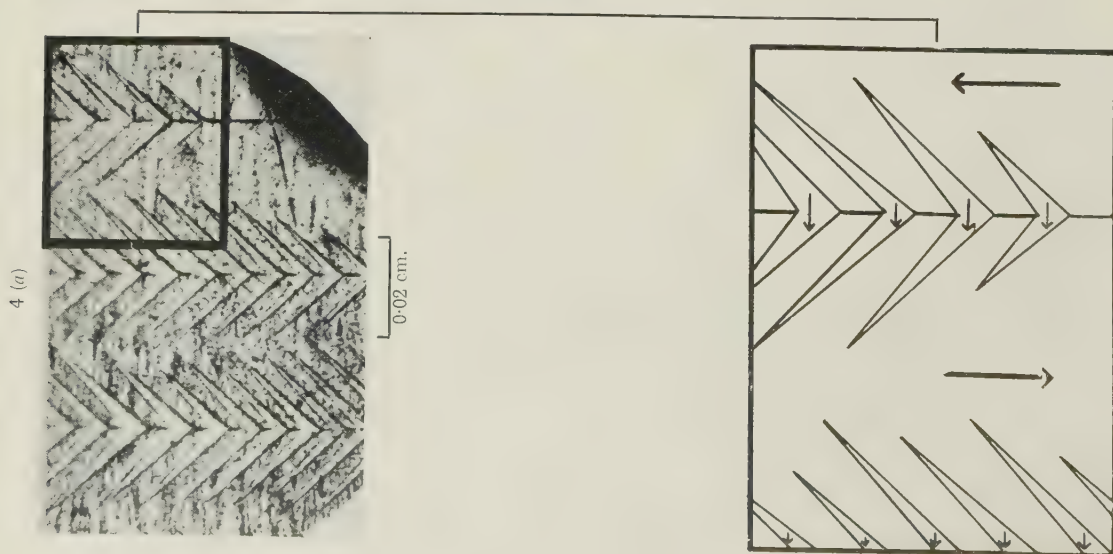


FIG. 4.—"Fir-Tree" Patterns.

(a) On (100) Plane of Silicon-Iron. (b) Interpretation of Patterns,  $180^\circ$  Domain Walls. (c) Tree Patterns,  $90^\circ$  Domain Walls.



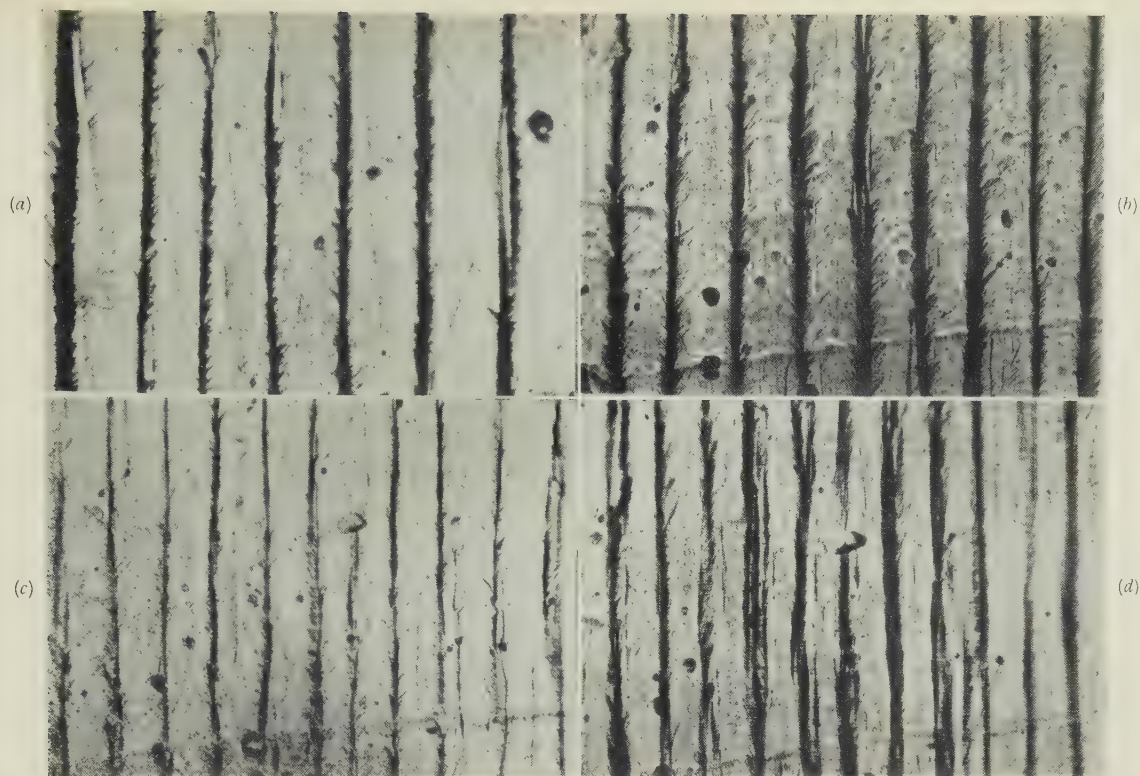


FIG. 7.—Line Patterns on a (100) Surface (Néel cut) of Silicon-Iron (a) 11 Oe., (b) 50 Oe., (c) 133 Oe., (d) 350 Oe.  
 $H \rightarrow$ .

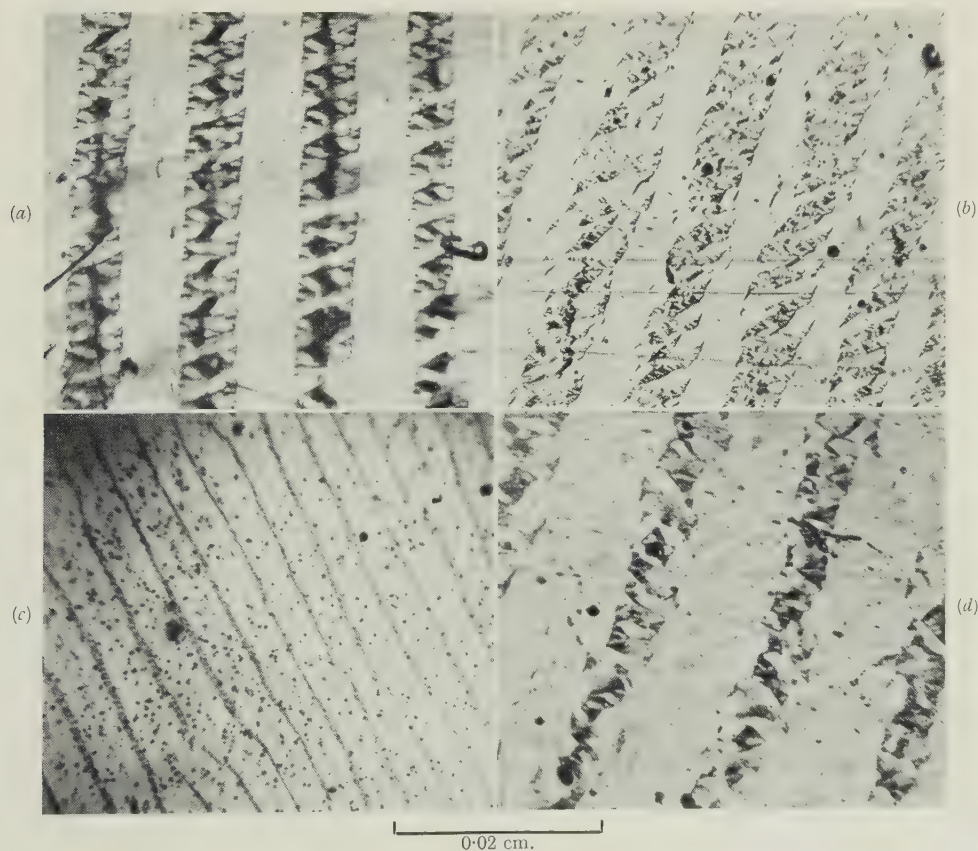


FIG. 8.—Examples of Lace Patterns.

- (a) (110) Surface of Silicon-Iron Crystal, Width 0.13 cm., [011] Direction  $\rightarrow$ .  $H = 45$  Oe.  $\rightarrow$ .  
 (b) (110) Surface of Pure Iron Crystal, Width 0.1 cm., [011] Direction  $\rightarrow$ .  $H = 45$  Oe.  $\rightarrow$ .  
 (c) Polycrystal of Silicon-Iron, Thickness 0.035 cm.,  $H = 35$  Oe.  $\rightarrow$ .  
 (d) (110) Surface of Pure Iron.  $H = 20$  Oe.  $\rightarrow$ .

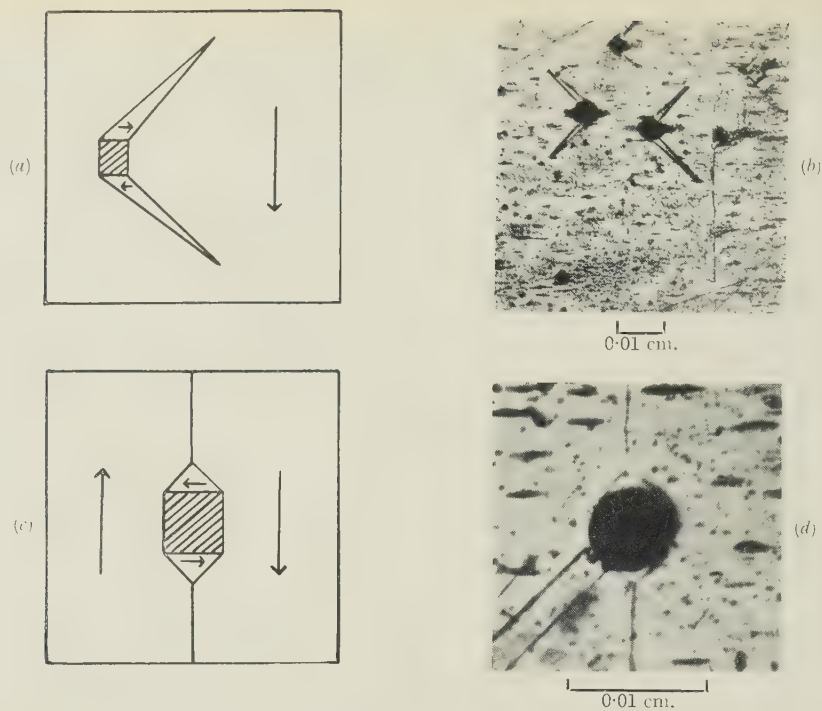
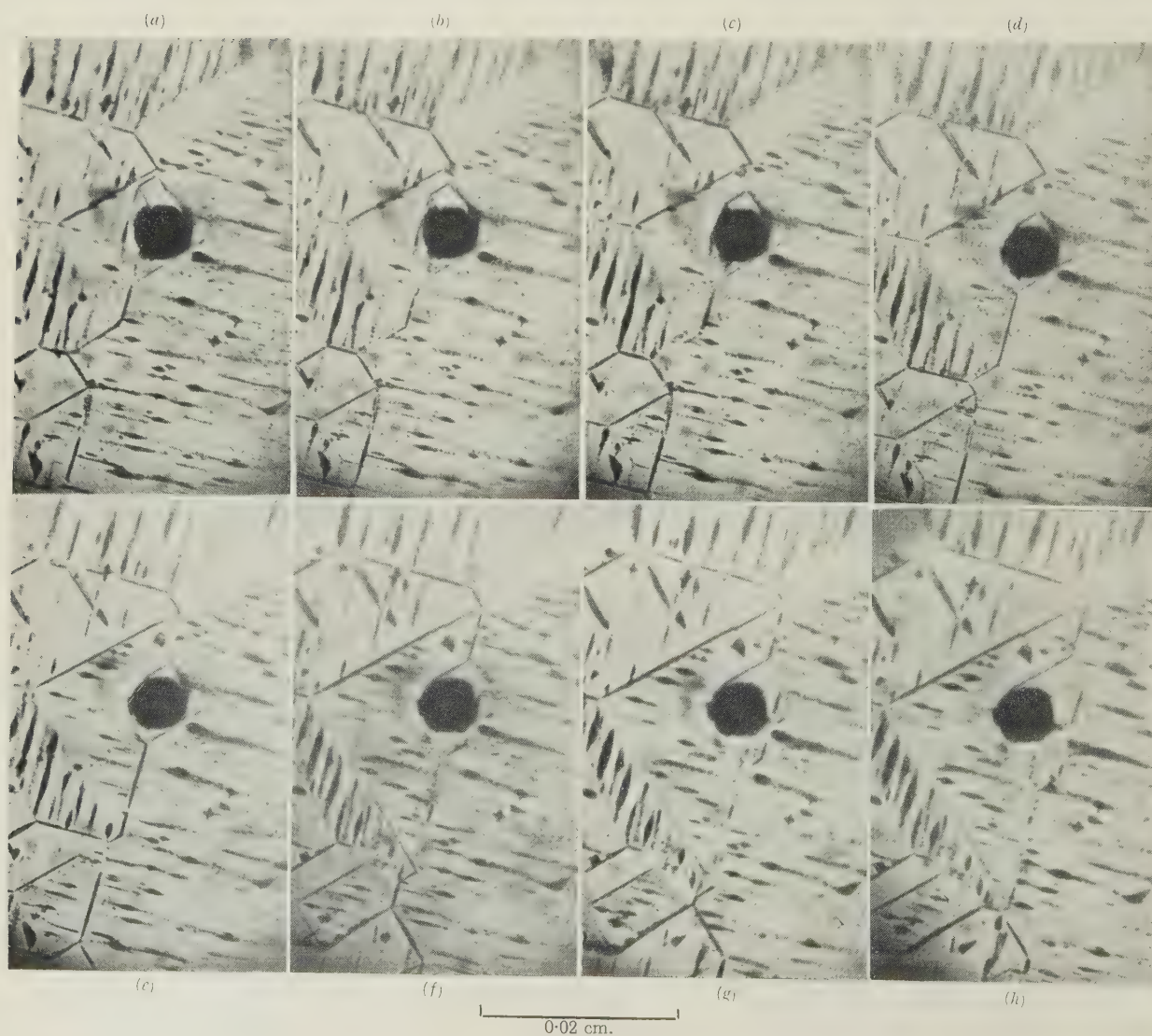


FIG. 9.—Examples of Closure Domains Around Imperfections.

FIG. 10.—Passage of a 180° Boundary Across an Inclusion; Field Applied  $\uparrow$  and Increasing from (a) to (h).



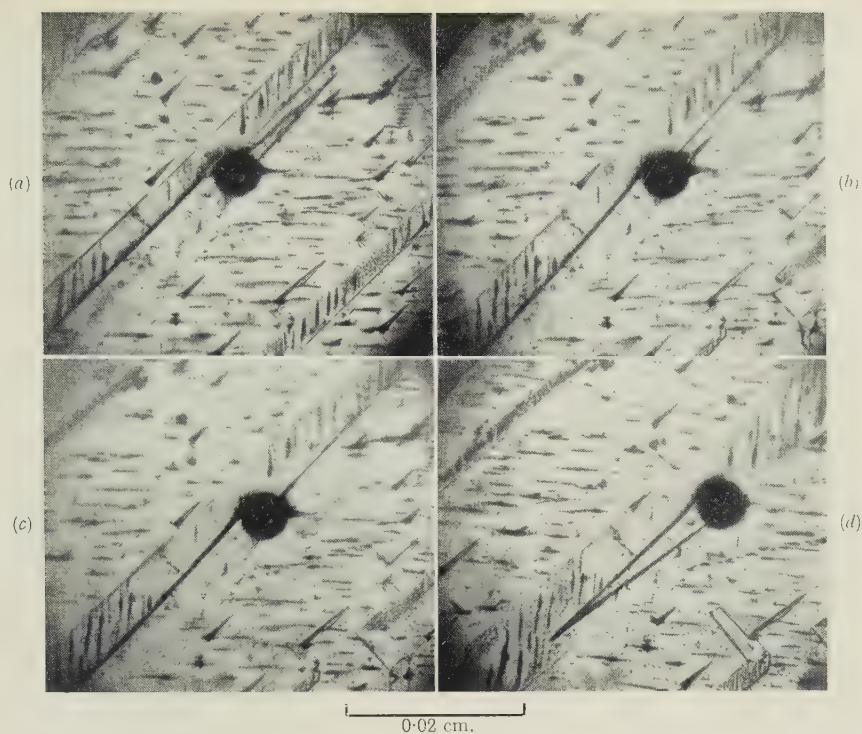


FIG. 11.—Passage of a  $90^\circ$  Boundary Across an Inclusion, Field Applied  $\uparrow$  and Decreasing from (a) to (d).

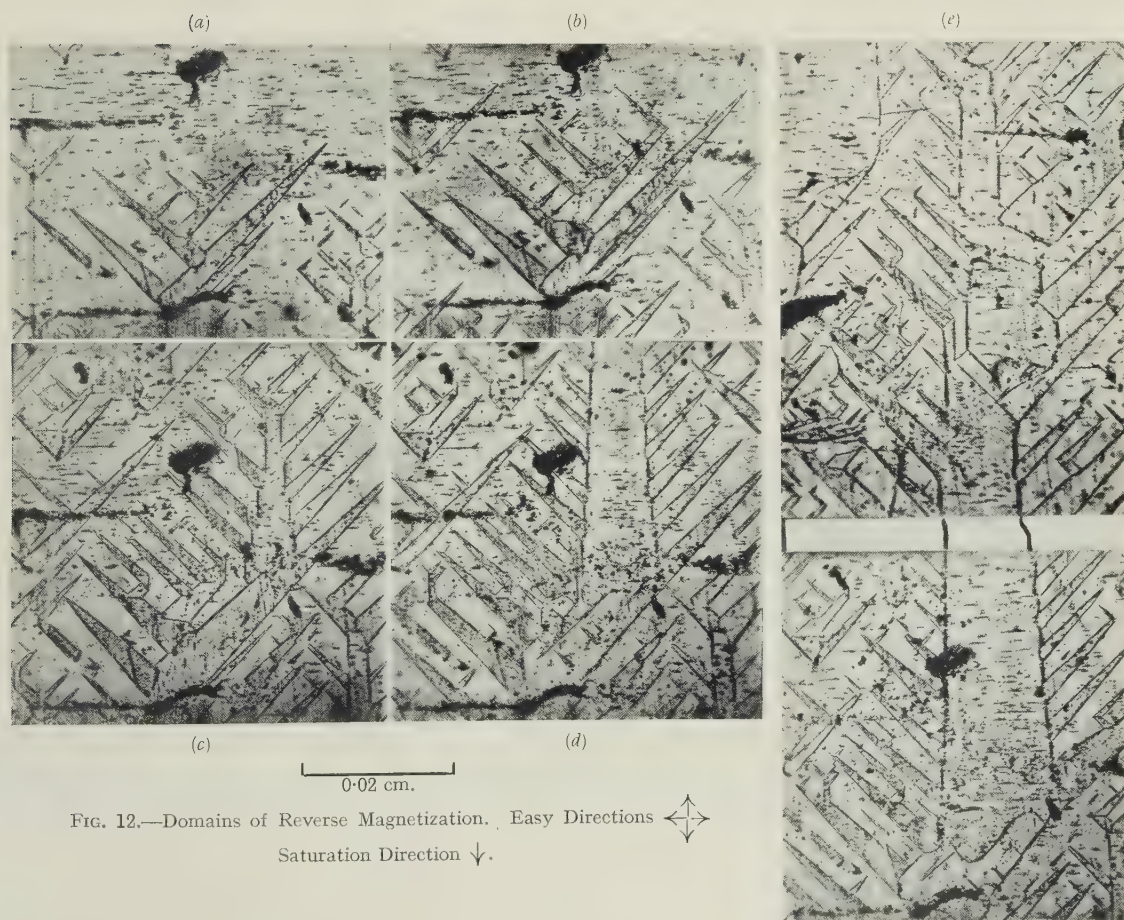


FIG. 12.—Domains of Reverse Magnetization. Easy Directions  $\star$   
Saturation Direction  $\downarrow$ .

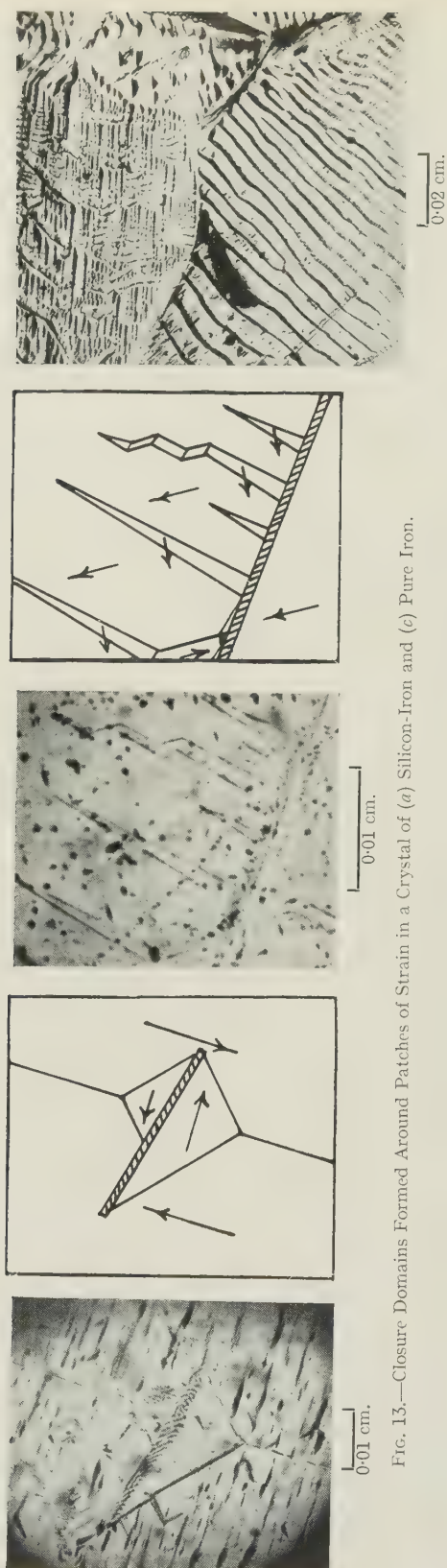


FIG. 13.—Closure Domains Formed Around Patches of Strain in a Crystal of (a) Silicon-Iron and (c) Pure Iron.

FIG. 14.—Domain Patterns on Polycrystalline Silicon-Iron.

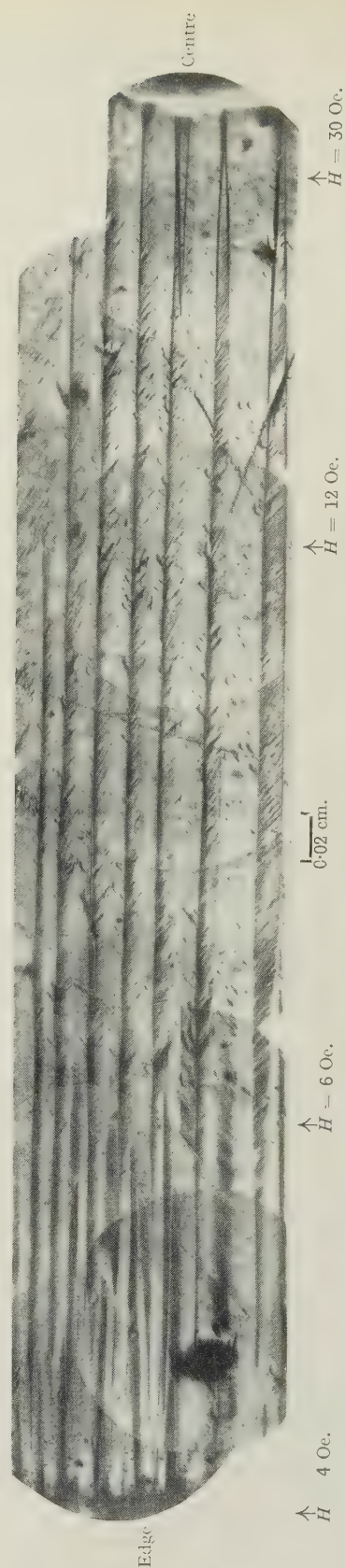


FIG. 15.—Néel Lines on a Circular Disc of Silicon-Iron Magnetized Circularly by a Current Passing through a Wire, Perpendicular to the Disc, through a Central Hole on the Right of the Photograph.



## ALUMINIUM-COPPER-MAGNESIUM ALLOYS.

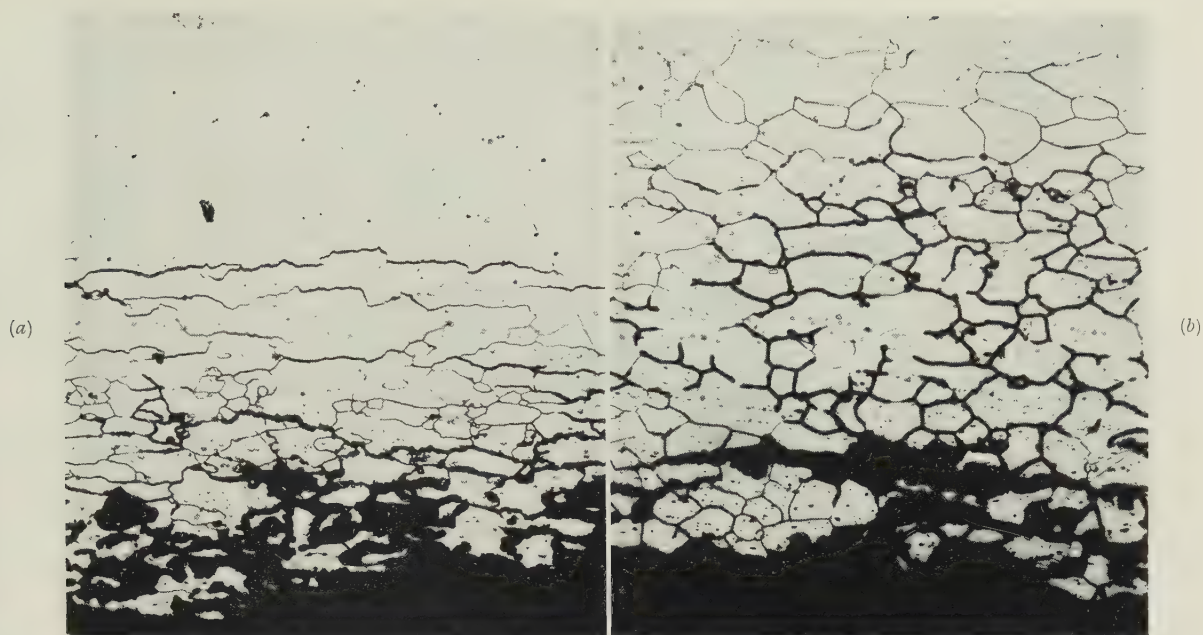


FIG. 2.—Inter crystalline Corrosion of (a) Normal-Manganese and (b) Low-Manganese Unstressed 0.2-in.-Thick Sheet Specimens After Exposure to 3% NaCl Solution Sprayed Once Daily for 3 Months.  $\times 100$ .



FIG. 3.—Banded Structure of (a) Normal-Manganese and (b) Low-Manganese Extruded Specimens. Etched in Keller's reagent.  $\times 100$ .

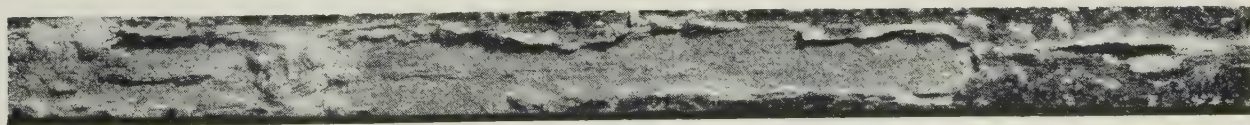


FIG. 4.—Layer Foliation from Specimen of HE15-WP After 2 Years' Exposure at Sheffield.

## TITANIUM-CHROMIUM ALLOYS.

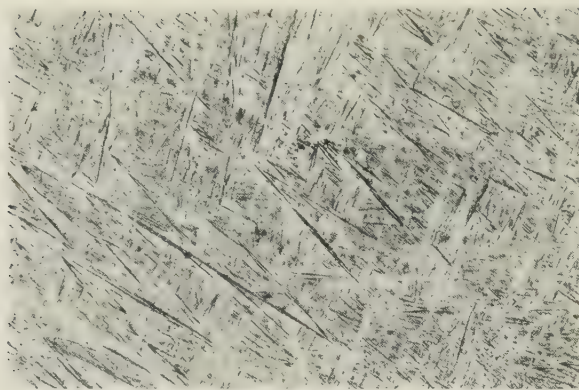


FIG. 2.—4.1 At.-% Chromium Alloy, Water-Quenched from 765° C. Transformed  $\beta$ .  $\times 100$ .

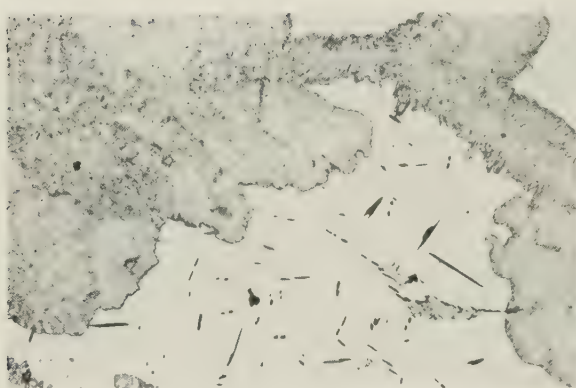


FIG. 3.—12 At.-% Chromium Alloy Cooled after 1000 Hr. at 652° C.  $\beta$  solid solution partially transformed to  $\alpha$  and  $\text{TiCr}_2$ .  $\times 100$ .

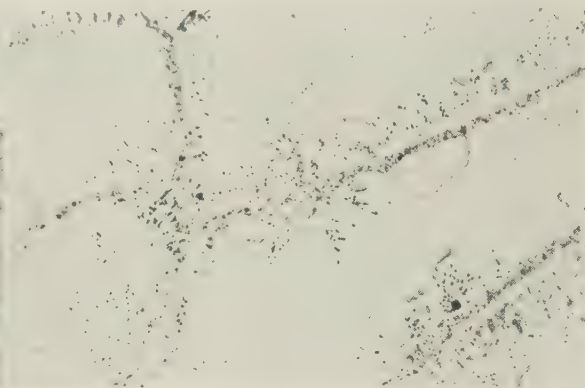


FIG. 4.—Same Specimen as Fig. 3, Re-Heated to 652° C. for 24 Hr. and Water-Quenched. New crystals of  $\beta$  + remains of  $\alpha$  and  $\text{TiCr}_2$ .  $\times 100$ .

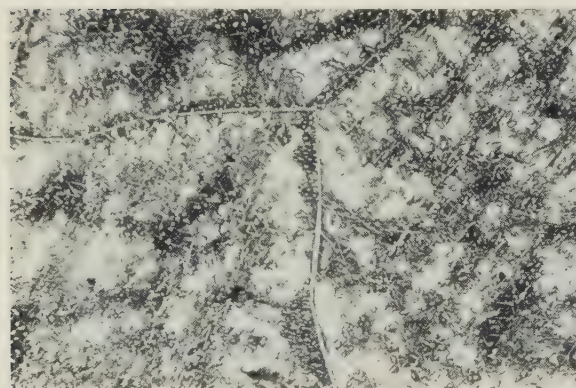


FIG. 5.—12 At.-% Chromium Alloy Cooled After 1000 Hr. at 590° C. Partially transformed  $\beta$ , showing precipitated  $\alpha$  and  $\text{TiCr}_2$ .  $\times 100$ .

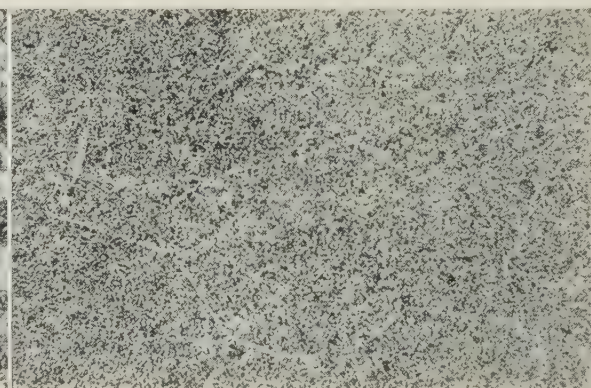


FIG. 6.—Same Specimen as Fig. 5 Reheated for 4 Days at 590° C. and Water-Quenched.  $\times 100$ .



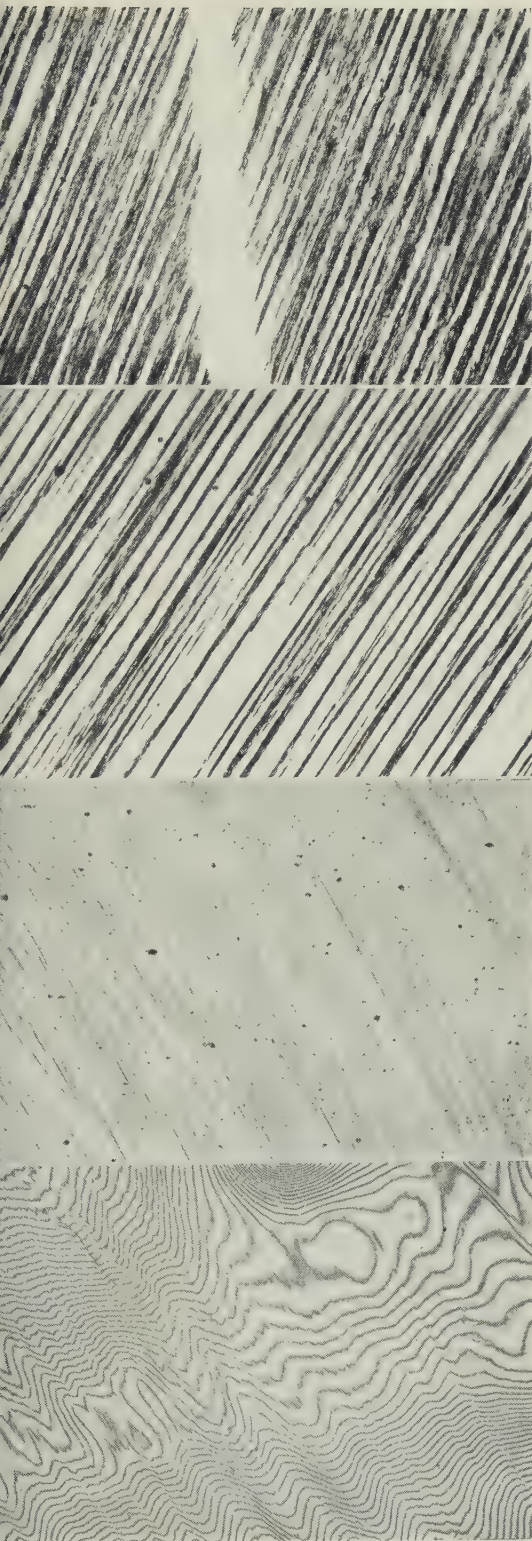


FIG. 8.—Interference Fringe Pattern of Aluminum Surface After Tensile Stressing,  $\times 125$ .  
 FIG. 9.—Optical Micrograph of Area Shown in Fig. 8.  $\times 125$ .  
 FIG. 10.—Slip Striations Produced by Cyclic Stresses,  $\times 125$ .  
 FIG. 11.—Kink Band Produced by Cyclic Stresses,  $\times 125$ .

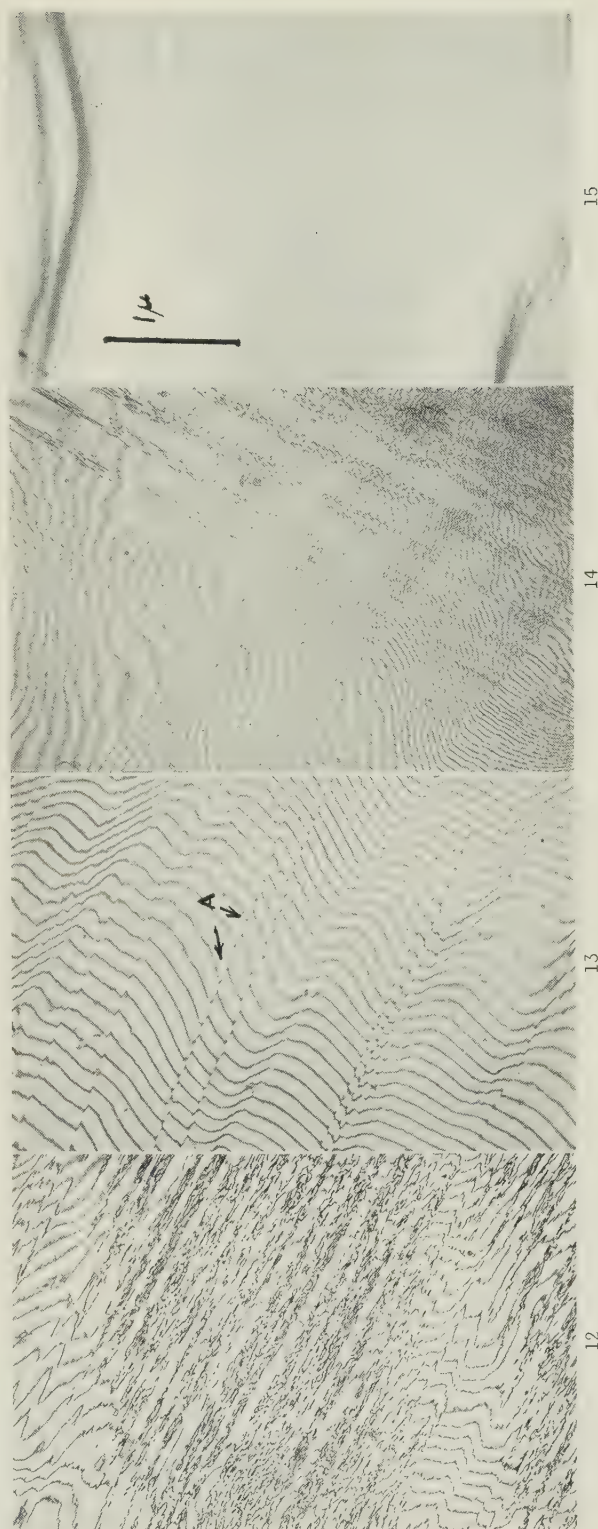


FIG. 12.—Fringe Patterns of Striated Regions,  $\times 125$ .  
 FIG. 13.—Fringe Pattern of the Surface of a Static Stressed Pure Aluminum Specimen,  $\times 200$ . A indicates position of a slip-band surface ledge.  
 FIG. 14.—Fringe Pattern of Striations and Kink Bands,  $\times 125$ .  
 FIG. 15.—Electron Micrograph of Slip Produced by Cyclic Stresses,  $\times 125$ .



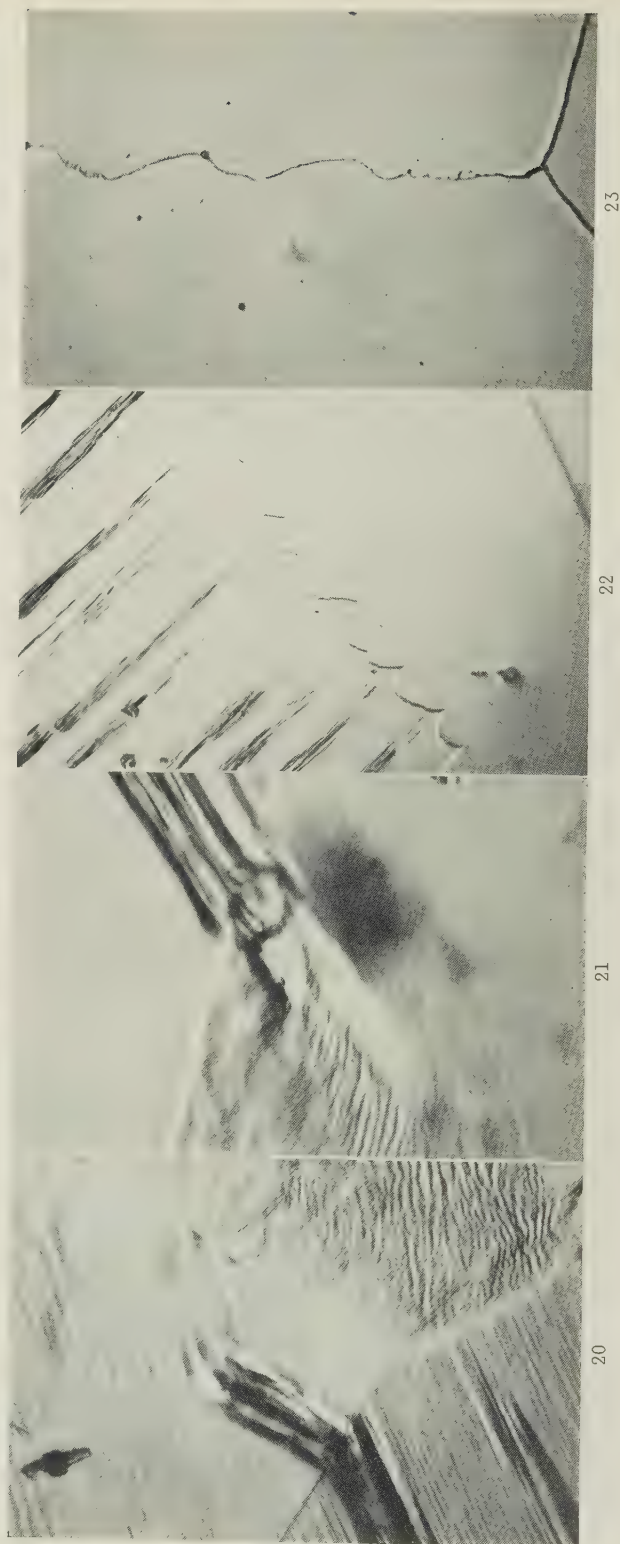
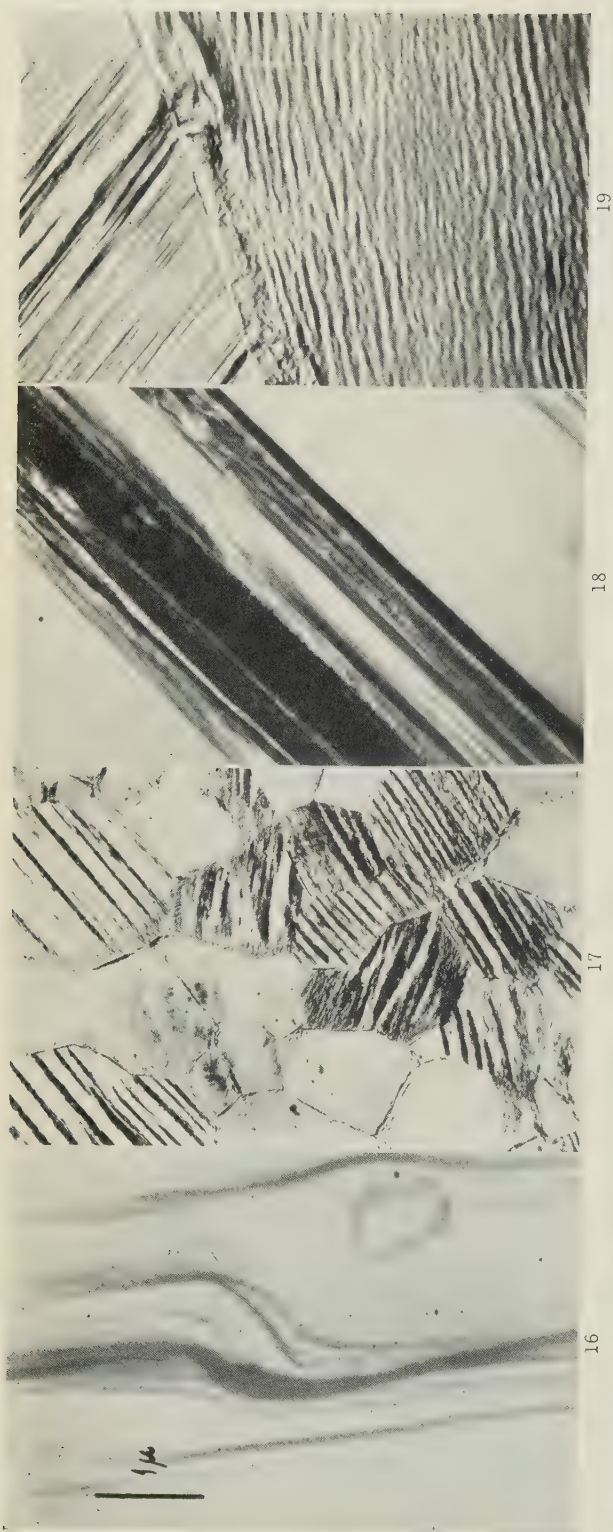


FIG. 16. Electron Micrograph of Slip Produced by Cyclic Stresses.

FIGS. 17-21.—Photomicrographs of Specimens Fatigued at 20,000 c./min.

FIG. 17.—Striations and Deformed Boundary Regions.  $\times 80$ .

FIG. 18.—Heavily Defined Striation Produced by Fatigue Stresses.  $\times 2000$ .

FIG. 19.—Boundary Region Showing Deformed Structure.  $\times 2000$ .

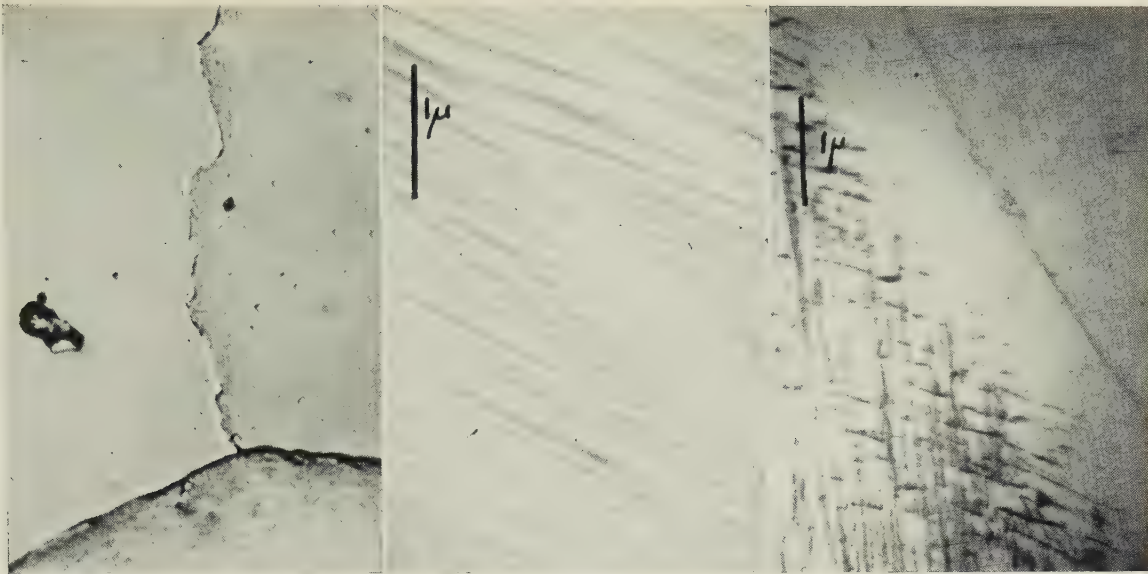
FIG. 22.—Boundary Migration at Regions Corresponding to the Ends of Striations.  $\times 1000$ .

FIG. 20.—Slip Striation Crossing Grain Boundary.  $\times 2000$ .

FIG. 21.—Disturbance Produced in Adjoining Grain by a Slip Striation.  $\times 2000$ .

FIG. 23.—Boundary Migration.  $\times 2000$ .





24

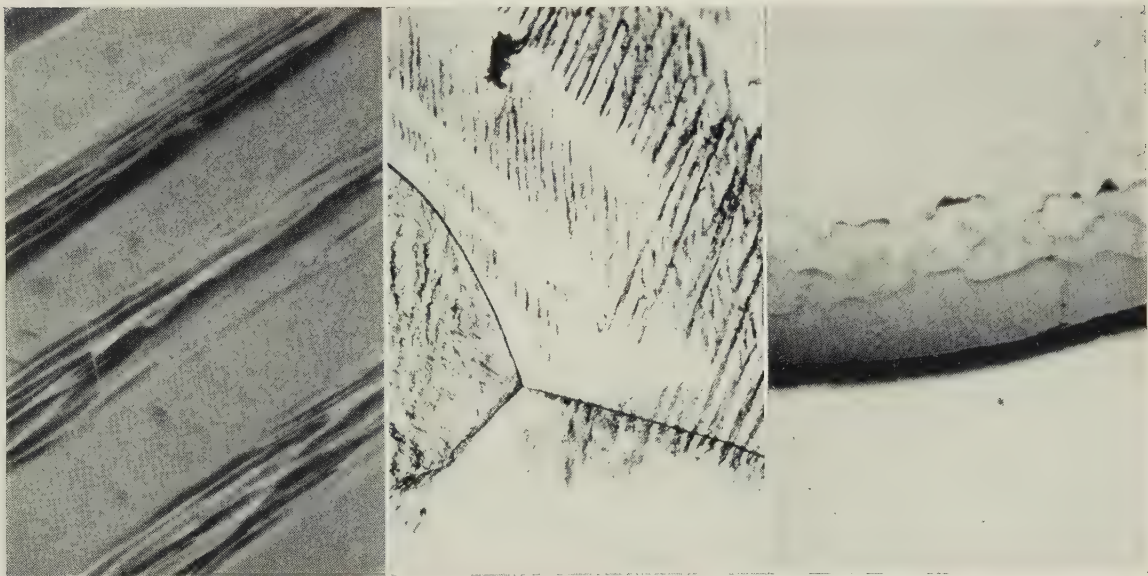
25

26

FIG. 24.—Boundary Migration.  $\times 2000$ .

FIG. 25.—Electron Micrograph Showing Fine Slip Produced at High Frequency.

FIG. 26.—Electron Micrograph Showing Boundary Region.



27

28

29

FIGS. 27-29.—Silver Chloride.

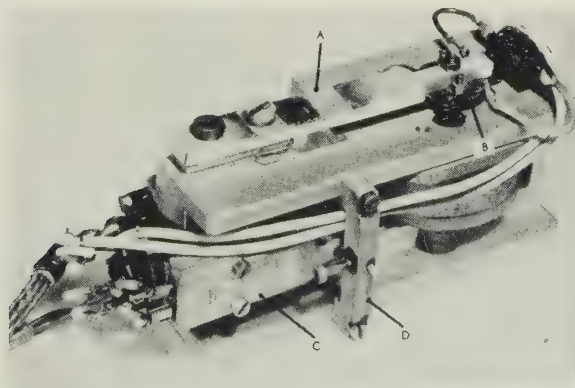
FIG. 27.—Striations in AgCl Subjected to Cyclic Stresses.  $\times 1500$ .FIG. 28.—AgCl After a Period of Cyclic Stresses.  $\times 125$ .FIG. 29.—AgCl After a Period of Cyclic Stresses, Showing Polygonization and Fatigue Cracks.  $\times 500$ .

FIG. 30.—High-Frequency Fatigue Machine.





# STAINING OF CLAD ALUMINIUM ALLOY SHEETS DURING SALT-BATH HEAT-TREATMENT\*

1541

By E. C. WILLIAMS,† M.Sc., A.Inst.P., MEMBER, and H. J. G. CHALLIS,‡ F.R.I.C., A.I.M., MEMBER

## SYNOPSIS

Staining of clad aluminium alloy sheets in baths of molten sodium nitrate at 500° C. is primarily associated with abnormal amounts of free alkali in the salt. When salt containing more than 0.03% of free alkali (expressed as Na<sub>2</sub>O) is chilled at the surface of a sheet entering the bath, alumina is formed and staining occurs almost instantaneously. At concentrations of free alkali above 0.10%, a stain consisting of sodium aluminate is formed on prolonged immersion. Under production conditions, staining is mostly of the instantaneous kind.

Factors tending to increase alkalinity are discussed, and a method of neutralizing excessive free alkali by passing carbon dioxide through the molten salt is described.

## I.—INTRODUCTION

HEAT-TREATMENT of clad aluminium alloy sheets in molten sodium nitrate baths is common practice and, amongst other advantages, notably short heat-treatment time, it does not greatly impair the surface finish produced by cold rolling. Staining, however, may be experienced spasmodically when a bath becomes slightly alkaline, and its incidence may be sufficient to cause rejection of appreciable quantities of finished sheet. The present paper gives an account of an investigation into the causes of staining and of methods for its elimination in practice.

The type of staining concerned is illustrated in Fig. 1 (Plate LXXII). The stained areas usually appear light-grey in colour and sometimes give faint interference effects. Baths in which staining occurs have been found on analysis to be slightly more alkaline than those in which it does not occur, and typical analyses are given in Table I. Addition of

molten sodium nitrate baths should include regular determination of both total alkali and nitrite contents in order to keep check of abnormal decomposition.<sup>2-4</sup> The test consists of a straight acid-alkali titration,<sup>2, 5, 6</sup> which estimates any free alkali together with carbonate, but it is important that free alkali should be determined separately for reasons which will be discussed later. A suitable method of analysis is described in the Appendix (p. 470). Although the form in which free alkali actually exists in the molten salt is unknown, it is conveniently expressed as the oxide Na<sub>2</sub>O.

A survey of routine analyses of this nature carried out over a period of 7 years, during which no serious staining was reported, indicated that an appreciable concentration of carbonate, at least up to 0.3% expressed as Na<sub>2</sub>O, could be tolerated and that the free-alkali content seldom exceeded 0.01%. When staining did occur, the rise in free alkali was significant, and it seemed that a concentration of 0.03% in a molten bath at 500° C. might be responsible.

Other possible causes of staining were considered, including (i) diffusion of alloying elements to the surface of the pure aluminium coating on clad sheets, (ii) contamination with oil, and (iii) stray electric currents between the sheets and the bath; these, however, were discounted on further investigation.

Apart from the differences in alkalinity referred to above, analysis of salt in baths prone to staining (Table I) revealed no abnormal contents of potentially detrimental impurities such as chlorides or sulphates.<sup>1, 2</sup>

TABLE I.—*Analysis of Non-Staining and Staining Baths.*

Constituent	Non-Staining Salt, %	Staining Salt, %
Sodium nitrite . . . . .	9.5	9.6
Combined alkali (as Na <sub>2</sub> O) . . . . .	0.28	0.22
Free alkali (as Na <sub>2</sub> O) . . . . .	0.009	0.06
Sulphate . . . . .	Nil	Nil
Chloride . . . . .	0.06	0.04
Iron . . . . .	0.0072	0.0009
Silica . . . . .	Nil	Nil
Aluminium . . . . .	0.002	0.002

up to 10% sodium nitrite with the object of preventing corrosion of iron containers<sup>1</sup> tends to increase alkalinity.

The usual test for alkalinity in the control of

## II.—EFFECTS OF ABNORMAL FREE-ALKALI CONTENTS

In order to study the effects of abnormal amounts of free alkali, small specimens of 18 S.W.G. cold-

\* Manuscript received 18 July 1953; in revised form 15 October 1953.

† Technical Officer, Imperial Chemical Industries, Ltd.,

Metals Division, Birmingham.

‡ Division Chief Analyst, Imperial Chemical Industries, Ltd., Metals Division, Birmingham.

rolled D.T.D. 390 sheet were immersed in a laboratory salt bath (at 500° C.), which was charged with salt taken from a non-staining production bath that initially contained 0.30% carbonate and less than 0.01% free alkali, both expressed as Na<sub>2</sub>O. Deliberate increases in the free-alkali content were effected by adding pure caustic soda pellets.

Staining was not observed until the free alkali was increased to 0.06% (Table II). Above this

TABLE II.—Results of Removal of Free Alkali with Carbon Dioxide (Laboratory Bath).

Expt.	Additions	Free Alkali (as Na <sub>2</sub> O), %	Carbonate (as Na <sub>2</sub> O), %	Appearance of Sheet
1	Salt from non-staining bath *	0.009	0.30	No stains
2	0.1% NaOH added	0.06	0.40	Slight stains
3	0.25% NaOH added	0.16	0.41	Definite stains
4	As Expt. 3 after 2 hr.	0.13	0.44	" "
5	As Expt. 3 after 20 hr.	0.075	0.48	" "
6	As Expt. 5 + CO <sub>2</sub> for 1 hr.	0.036	0.50	No stains

\* Sodium nitrite content = 9.9%.

value it became more extensive, but it was evident from repeated experiments that at least 0.10% of free alkali was required to induce appreciable staining, a figure exceeding the limit of 0.03% inferred from routine analysis of production baths. The discrepancy was resolved when the observation was made that if a specimen was momentarily immersed in a bath and quickly withdrawn, stains appeared under patches of salt adhering to the surface. Chilling of the salt when it came into contact with a cold surface was thus suggested as an important factor. It was subsequently found that staining under such conditions could be induced when the free-alkali content was only 0.045%, a figure in better agreement with the 0.03% limit for production baths.

These experiments thus indicated that staining could occur (a) on prolonged immersion at a minimum free-alkali content of about 0.10%, and (b) at the moment of immersion if the salt were chilled by the cold metal surface and at a free-alkali content exceeding 0.03%. The stains produced under these two different sets of conditions had not the same appearance, and from the results of electron-diffraction examination described in Section III it must be concluded that they are fundamentally different in character. They will therefore be referred to as "immersion" and "instantaneous" stains, respectively.

The difference in appearance between the stains is evident in Fig. 2 (Plate LXXII), which shows a sample of clean, pure aluminium sheet partly immersed in, and quickly withdrawn from, a bath at 500° C. containing 0.25% free alkali, and afterwards re-immersed to a greater depth for 10 min. The pro-

nounced horizontal line across the centre of the specimen, which corresponds to the level of the first immersion, and the dark patches below it, are instantaneous stains. Immersion stains, which are more uniform and whiter in appearance, occur on parts of the lower half of the specimen not stained during the first treatment and also above the horizontal line up to the level of the second immersion. Fig. 3 (Plate LXXII) illustrates an instantaneous "salt-line" stain, similar to that of Fig. 2, found in a rejected production batch.

### III.—ELECTRON-DIFFRACTION EXAMINATION OF STAINED SURFACES

Good transmission electron-diffraction patterns were obtained from films prepared by thinly varnishing specimens with collodion, and stripping in a saturated aqueous solution of mercuric chloride. Slight contamination of films with mercurous chloride sometimes occurred, but it was always possible to distinguish between the diffraction rings due to mercurous chloride and those produced by other substances. Some of the patterns obtained are reproduced in Figs. 4–9 (Plate LXXIII).

#### 1. PRODUCTION STAINING

Surfaces of D.T.D. 390 sheets stained in production baths after heat-treatment for 20 min. at

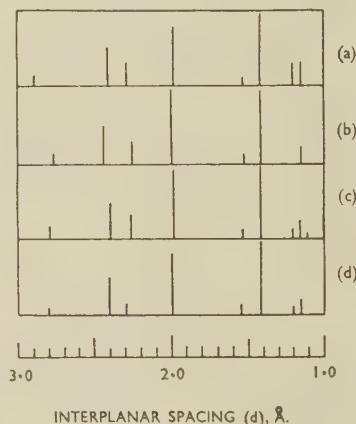


FIG. 10.—Identification of  $\eta$ -Al<sub>2</sub>O<sub>3</sub>.

- (a) Production staining.
- (b) Experimental salt-bath staining.
- (c) Aluminium foil heated for 15 min. at 700° C. in air.
- (d)  $\eta$ -Al<sub>2</sub>O<sub>3</sub>: data of Stumpf, *et al.*<sup>7</sup>

500° C. gave patterns (Figs. 4 and 5) consisting of continuous rings sometimes slightly arced, and a few cross-grating spots. Relative intensities and interplanar spacings, or *d*-values, for the rings agreed with those obtained by Stumpf, Russell, Newsome, and Tucker,<sup>7</sup> using the X-ray powder method, for certain forms of anhydrous alumina, as indicated in Figs. 10 and 11, in which vertical lines of lengths



proportional to relative intensities are drawn on a horizontal scale of  $d$ . The agreement is least satisfactory with the  $\delta$ - $\text{Al}_2\text{O}_3$  of Stumpf, *et al.*, although for strong reflections by planes of  $d = 2.00$  and  $1.40 \text{ \AA}$ , there is almost exact correspondence. It is therefore possible to identify the constituents of the stains with two of six different modifications of alumina which Stumpf, *et al.*, claim to have distinguished, namely

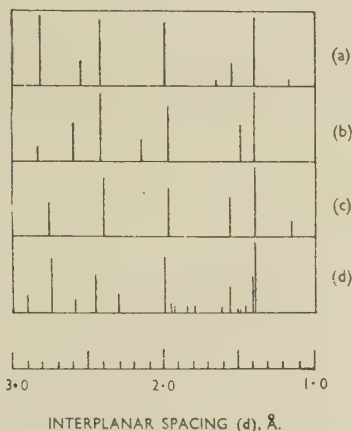


FIG. 11.—Identification of  $\delta$ - $\text{Al}_2\text{O}_3$ .

- (a) Production staining.
- (b) " " "
- (c) Experimental salt-bath staining.
- (d)  $\delta$ - $\text{Al}_2\text{O}_3$ : data of Stumpf, *et al.*<sup>7</sup>

$\eta$ - $\text{Al}_2\text{O}_3$ , which has a spinel structure of parameter  $a = 7.94 \text{ \AA}$ , and  $\delta$ - $\text{Al}_2\text{O}_3$  of unknown structure. It is of interest to note that  $\eta$ - $\text{Al}_2\text{O}_3$  is identical with the form listed as  $\gamma$ - $\text{Al}_2\text{O}_3$  in the A.S.T.M. Index of Diffraction Patterns and with the oxide formed by heating aluminium foil in air for 15 min. at  $700^\circ \text{C}$ . (Fig. 10 (c)).

## 2. INSTANTANEOUS AND IMMERSION STAINING

Instantaneous stains in their original state, i.e. as formed by momentary immersion and rapid withdrawal from a bath, the samples not being subjected to further heating, consisted of an amorphous substance according to the diffraction pattern obtained (Fig. 6). Similar stains were produced both in a laboratory bath containing 0.25% free alkali and in a production bath. When samples bearing such stains were subsequently immersed in a non-staining bath at  $500^\circ \text{C}$ . for several minutes, with the object of reheating, the stains were unchanged in appearance, though diffraction patterns indicated that the amorphous constituent had been almost completely converted to crystalline  $\delta$ - $\text{Al}_2\text{O}_3$  (Fig. 7). Other stains, similarly prepared, consisted of  $\delta$ - $\text{Al}_2\text{O}_3$  and others of  $\eta$ - $\text{Al}_2\text{O}_3$ . It was therefore concluded that instantaneous stains initially consist of amorphous alumina and are transformed to a crystalline modification on further heating.

Immersion stains gave patterns (Fig. 8) quite different from those given by the instantaneous type,

and compared fairly well (Fig. 12) with an X-ray powder pattern of sodium aluminate ( $\text{NaAlO}_2$ ). Several specimens gave patterns made up of rings corresponding to both sodium aluminate and  $\eta$ - $\text{Al}_2\text{O}_3$  (Figs. 9 and 12 (c)).

These observations establish that the stains occurring under production conditions are generally of the instantaneous type. The sodium aluminate, or immersion stain, has not been clearly observed on any of the production samples investigated, and in general it is not expected, because free alkalinity in production baths is unlikely to reach 0.1%. A careful re-interpretation of the electron-diffraction plates has indicated, however, that a few of the production stains did contain small quantities of sodium aluminate.

## 3. EFFECT OF SALT TEMPERATURE ON NATURE OF STAIN

The temperature at the interface between aluminium and salt provides one obvious difference between the conditions leading to the two types of staining. To investigate this factor, specimens of pure aluminium sheet which were purposely thin and of small mass to avoid chilling were immersed for 5 min. in a bath containing 0.25% free alkali at temperatures between  $500^\circ$  and  $320^\circ \text{C}$ ., the latter being the lowest temperature at which the bath remained fluid.

Stains formed at  $400^\circ \text{C}$ . and above had the appearance of the immersion type, whereas those formed below  $400^\circ \text{C}$ . resembled the instantaneous

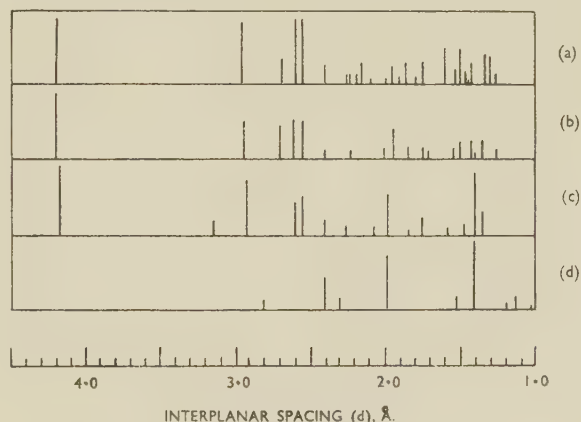


FIG. 12.—Identification of  $\text{NaAlO}_2$  and  $\eta$ - $\text{Al}_2\text{O}_3$ .

- (a)  $\text{NaAlO}_2$  from X-ray diffraction data.
- (b) Immersion staining in experimental bath.
- (c) Immersion and instantaneous staining ( $\text{NaAlO}_2 + \eta$ - $\text{Al}_2\text{O}_3$ ).
- (d)  $\eta$ - $\text{Al}_2\text{O}_3$ : data of Stumpf, *et al.*<sup>7</sup>

type. The immersion stain formed at  $400^\circ \text{C}$ . and above consisted of sodium aluminate, but in specimens stained below  $400^\circ \text{C}$ . the amount of this compound, as judged by the intensities of diffraction rings, became progressively less with decreasing temperature, an amorphous phase (haloes) becoming predominant. By further heating of stained specimens

in pure sodium nitrate at 500° C., the amorphous substance was converted to crystalline alumina, confirming that stains formed at the lower temperature were mainly of the type formed instantaneously by sudden immersion in a bath at 500° C. The lowering of the temperature of the salt when it came into contact with the surface of a cold sheet was thus confirmed as a prime factor in instantaneous staining.

It is not possible to base a complete theory of staining on the above observations. The underlying surface reactions cannot be defined without further, more detailed, investigation, but it is clear that free alkali is an essential factor. Its action may be either a direct attack on the metal to form the substance of stains or a disruption of the very thin, natural protective film of alumina characteristic of aluminium surfaces, thus exposing the metal to attack by sodium nitrate.

#### IV.—PRACTICAL ASPECTS OF STAINING

Most features of staining under production conditions in alkaline baths are explained by what may be considered the essential factor in instantaneous staining, viz. that salt is chilled at the sheet surface. Reference has already been made to staining along a line corresponding to the salt level when a sheet is partially immersed, and this effect, as is shown by actual trials, arises when the lowering of sheets into a bath by an overhead crane is suddenly arrested. Local chilling of salt at certain parts accounts for the streaky appearance (Fig. 1, Plate LXXII). In heat-treating strip in coil form, only the outermost laps are stained. The salt probably does not immediately penetrate between the inner laps on immersion, and it is supposed that the whole coil is heated sufficiently to preclude chilling of salt before it does come into contact with the inner surfaces. Because coils require longer heat-treatment than a batch of sheets held in a cradle and separated slightly from each other, immersion staining is more likely to occur with coils, though only if the free-alkali content is near 0.10%. Occasionally perfect mirror-image stains have been obtained on adjacent sheets in a batch. This effect also is a consequence of instantaneous staining, which occurs when salt is momentarily solidified in the gap between sheets.

##### 1. NEUTRALIZATION OF ALKALINE BATHS

The reconditioning of salt which is unsatisfactory is an important problem when baths may contain up to 30 tons of salt and replacement by fresh salt is obviously uneconomical. Continental and American workers<sup>6, 8</sup> claim that alkalinity may be corrected by addition of acid salts such as sodium bichromate or acid bisulphate, but obviously these cannot be used where baths contain added nitrite. The ideal additive is one which will result in a neutral or inactive product that has no deleterious effects on

aluminium or on the salt. Dry carbon dioxide appears to meet these requirements, since it converts the free alkali to carbonate, which, even in appreciable amounts, as discussed in Section I, is innocuous.

Encouraging results were obtained in laboratory tests in which gaseous carbon dioxide was bubbled through an experimental bath at 500° C., which had been made alkaline as before by additions of sodium hydroxide, the bath becoming non-staining after 1 hr. (Table II). Tests on a production scale have proved the efficacy of the method. A 30-ton bath in a staining condition was treated by passing carbon dioxide through an iron pipe with the outlet immersed in the salt (Table III). Initially the free-alkali

TABLE III.—*Reconditioning of Production Bath with Carbon Dioxide.*

Total CO <sub>2</sub> Added, lb.	Analysis of Salt			Notes on Condition of Sheets
	NaNO <sub>2</sub> , %	Free Alkali (as Na <sub>2</sub> O), %	Carbonate (as Na <sub>2</sub> O), %	
...	9.6	0.055	0.19	Random stains all over sheets
17	9.6	0.04	0.22	Progressive reduction to slight patches of stain
28	9.8	0.04	0.21	Slight staining
36	9.7	0.037	0.22	" " "
40	9.7	0.035	0.23	Very slight staining
62	10.0	0.030	0.24	" " "
100	9.7	0.020 0.017	0.26	No stains apparent

(1) Capacity of bath—approximately 30 tons of sodium nitrate-nitrite mixture.

(2) Reconditioning was intermittent between production heat-treatment, which was spread over a period of 28 days and included 4 days at 525° C.

(3) Sheets suspended from iron cradle by iron clips, and held in position by retaining chains.

content of the bath was 0.055% and the carbonate content 0.20% (both expressed as Na<sub>2</sub>O). During a 7½-hr. treatment about 17 lb. of carbon dioxide was used and a marked decrease in the severity and extent of staining was achieved, the free-alkali content having dropped to 0.04%. Gassing of the bath was continued whenever possible between production heat-treatments, and staining was prevented almost entirely, the free alkali progressively diminishing.

Elimination of the last traces of staining, involving neutralization of the remaining free alkali to below 0.03%, necessitated treatment over a much longer time than was required to effect the marked early improvement. The staining at this stage was faint, however, and confined to areas which had been moistened and cooled by water remaining in the cradles and retaining chains after quenching of previous batches. Eventually the salt was reconditioned sufficiently to provide completely stain-free sheets. The efficacy of this remedy depends upon the uniform distribution of the gas throughout the molten salt, and conditions in the above test were not



ideal. The method of reconditioning alkaline baths by carbon dioxide is the subject of a provisional patent<sup>9</sup> and has been used to correct spasmodic staining.

Finely ground silica powder was also tested as a reconditioning additive. It was found that, although this additive produced a rapid decrease in alkalinity, a small amount of free alkali persistently remained, even though stoichiometric quantities were used. This method was not applied in practice, however, because of possible damage through abrasion to the surface of the aluminium sheets, which are very soft at the temperature of heat-treatment.

## 2. CONTROL OF ALKALINITY

Factors tending to increase the free-alkali content of a bath include high working temperatures, addition of sodium nitrite, and contamination by organic matter which accelerates decomposition of the salt. Free-alkali content decreases when fresh salt is added to compensate for drag-out, and a large through-put of material, necessitating frequent topping-up to the working level, normally keeps the alkalinity at a low value. Conversion of free alkali to carbonate by absorption of atmospheric carbon dioxide occurs slowly and cannot be relied upon to prevent an abnormal increase.

Sodium nitrite in large concentrations appears to be the most important factor in promoting high alkalinity, and it should be maintained at the minimum concentration compatible with satisfactory life of the iron containers. Addition of nitrite is probably necessary when using externally heated gas- or oil-fired baths, but baths of the electric immersion-heater type are far less susceptible to this type of attack, and may be operated with straight sodium nitrate.

Close observation of sodium nitrate baths to which no nitrite was added has been maintained over a period of twelve months. The nitrite content built up to about 1% in the first two months and then remained constant; free alkali rarely attained 0.025% and no staining occurred. On the other hand, a bath containing 10% added nitrite developed a content of 0.03% free alkali within a few days and caused slight staining. It is significant that with a 10% addition of nitrite, the total alkalinity (free alkali + carbonate) rose to 0.1% (expressed as  $\text{Na}_2\text{O}$ ) after 3 months, whereas in a straight nitrate bath it did not exceed 0.05% after twelve months.

## V.—CONCLUSIONS

(1) Staining of clad aluminium alloy sheets during heat-treatment at 500° C. in molten sodium nitrate baths occurs when the free-alkali content of the salt exceeds 0.03% by weight expressed as  $\text{Na}_2\text{O}$ . Combined alkali in the form of carbonate is not a factor in staining, and amounts up to 0.3% by weight expressed as  $\text{Na}_2\text{O}$  may be tolerated.

(2) Two kinds of staining are possible: so-called "instantaneous" staining occurs almost immediately on immersion at those parts of a sheet where the salt is momentarily chilled and solidified on the surface. "Immersion" staining results in stains which are whiter in appearance and more general in character than instantaneous stains and which occur only at a free-alkali content exceeding 0.10%  $\text{Na}_2\text{O}$ . Instantaneous staining can occur when the free-alkali content is below 0.10%  $\text{Na}_2\text{O}$ , provided that it is greater than 0.03%  $\text{Na}_2\text{O}$ .

(3) Electron-diffraction examination has established that instantaneous stains when first formed consist of amorphous alumina, which is converted to various crystalline modifications on further heating at the heat-treatment temperature of 500° C. Immersion stains consist of sodium aluminate,  $\text{NaAlO}_2$ .

(4) Since free alkali is the prime cause of staining, control of this factor is essential for its prevention. Conditions which tend to accelerate decomposition of salt and to increase free alkali must be avoided. It is recommended in particular that the amount of sodium nitrite addition to baths be restricted to the minimum compatible with a satisfactory life of the iron containers. Accidental contamination of baths with foreign matter, such as oil or grease, likely to accelerate decomposition should be kept to a minimum. Periods of heat-treatment above 500° C. should be as short as possible.

(5) Baths that are liable to stain may be reconditioned by treatment with gaseous carbon dioxide until the free-alkali content is brought below 0.03%  $\text{Na}_2\text{O}$ . This treatment permits reconditioning of baths containing added nitrite.

## ACKNOWLEDGEMENTS

The authors wish to express their thanks to Dr. N. P. Inglis and Dr. W. O. Alexander for their interest and encouragement in this investigation, and to Mr. A. Blewitt and Mr. A. R. Holland for assistance in the experimental work. Their thanks are also due to Dr. J. F. Brown and Mr. D. Clark of Imperial Chemical Industries, Ltd., Billingham Division, for helpful advice and criticism during the course of this work.

## REFERENCES

1. P. Lloyd and E. A. C. Chamberlain, *J. Iron Steel Inst.*, 1940, **142**, 141p.
2. A. C. Finch, *Sheet Metal Ind.*, 1940, **14**, 1286.
3. B. Pretsch, *Metallwirtschaft*, 1935, **14**, 703.
4. "Recommendations for the Installation and Maintenance of Nitrate Baths". 1944: London (The Fire Officers Committee).
5. R. J. Box and B. A. Middleton, *J. Iron Steel Inst.*, 1945, **151**, 71p.
6. French Patent No. 821,726 (1937).
7. H. C. Stumpf, A. S. Russell, J. W. Newsome, and C. M. Tucker, *Indust. Eng. Chem.*, 1950, **42**, 1398.
8. W. M. Sutherland, *Iron Age*, 1945, **156**, (14), 82.
9. British Patent Application No. 19517/50.

## APPENDIX

## DETERMINATION OF FREE ALKALI IN SODIUM NITRATE BATHS

(a) *Reagents Required*

(i) Distilled water (free from carbon dioxide). The water is boiled for 30 min. in a flask, the flask stoppered lightly, and the water allowed to cool slightly. The stopper is then placed in the flask more firmly and the water allowed to cool to room temperature. The flask must be kept stoppered to prevent any absorption of carbon dioxide.

(ii) Barium chloride.

(iii) Hydrochloric acid, (*N*/10).

(iv) Phenolphthalein, 1% solution in alcohol.

(b) *Method*

Weigh out approximately 10 g. of the sample, which should not be finely powdered, and transfer quickly

to a 500-ml. Erlenmeyer flask, which should be kept stoppered when not in use so as to exclude carbon dioxide. Add 50 ml. of the carbon-dioxide-free distilled water and immediately replace the stopper in the flask. Shake the flask to dissolve the sample. When the sample has dissolved, remove the stopper, add approximately 1 g. barium chloride, replace the stopper, shake to dissolve the barium chloride, and allow the flask and solution to stand for 5 min.

Remove the stopper, add a few drops of phenolphthalein, and titrate with *N*/10 hydrochloric acid, adding the acid drop by drop until the pink colour is discharged.

$$1 \text{ ml. } N/10 \text{ HCl} = 0.0031 \text{ g. Na}_2\text{O}$$

Hence, on a 10-g. sample :

$$\text{ml. } N/10 \text{ HCl required} \times 0.031 = \% \text{ Na}_2\text{O}$$



# THE CONSTITUTION OF GOLD-MOLYBDENUM ALLOYS, WITH PARTICULAR REFERENCE TO THE SOLUBILITY OF MOLYBDENUM IN GOLD\*

1542

By G. A. GEACH,† M.Sc., Ph.D., F.I.M., MEMBER, and  
D. SUMMERS-SMITH,† B.Sc., Ph.D., A.R.T.C., MEMBER

## SYNOPSIS

The gold-molybdenum system has been investigated by X-ray powder photography, and the solubility of molybdenum in gold determined by lattice-parameter measurements up to 800° C. The solubility has also been derived from parameter measurements on quenched specimens. A eutectic between gold and molybdenum occurs at 1054° C.; at this temperature the solubility of molybdenum in gold is 1.25 at.-%, falling to 0.7 at.-% at room temperature. The solubilities of the transition metals in gold are discussed.

## I.—INTRODUCTION

No investigation of the gold-molybdenum system has been published, though a brief reference by Dreiholz<sup>1</sup> suggested that molybdenum was insoluble in solid gold. Owen and Roberts<sup>2</sup> have investigated the solubilities of a number of the normal metals in gold, and have shown that the electron concentration of the gold solid solution at maximum solubility lies in the range 1.05–1.33, provided that the size-factors are favourable. The atomic diameter of molybdenum differs by only 5% from that of gold, and a small solubility of molybdenum in gold would therefore be expected on the assumption that the transition elements behave similarly to the normal elements when dissolved in the univalent metals of Group IB.

## II.—EXPERIMENTAL METHODS

### 1. PREPARATION OF THE ALLOYS

The alloys were prepared from gold and molybdenum powders of purities 99.999 and 99.8%, respectively. Samples (1 g.) of these were mixed for 24 hr. in a small ball mill,<sup>3</sup> compacted in a small mould 5.0 mm. in dia., and sintered for 7 days at 1000° C. in evacuated silica capsules. A few of the alloys were analysed for molybdenum. The values found did not differ from the nominal compositions in the gold-rich alloys by more than 0.1 wt.-%, which was within the limit of the experimental errors of the analysis owing to the small quantity of material available, and therefore nominal compositions have been assumed for all of the alloys. The prolonged mixing ensures homogeneity, and in no case did the parameter measurements obtained from powder samples from different portions of the pellet differ significantly.

### 2. HIGH-TEMPERATURE X-RAY PHOTOGRAPHY

A 19-cm. Unicam high-temperature X-ray camera was modified in a way similar to that described by Berry, Henry, and Raynor.<sup>4</sup> The temperature of the specimen was calibrated against a thermocouple fixed

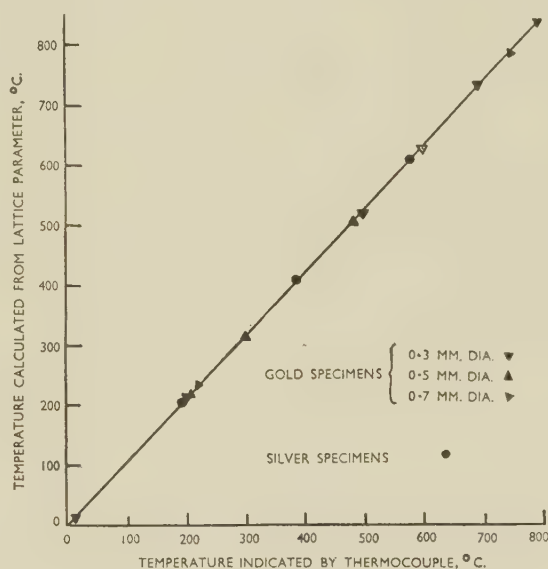


FIG. 1.—Calibration of High-Temperature X-Ray Camera.

close to it, using specimens of pure gold and silver. Specimens were sealed in silica tubes with a wall thickness of about 20  $\mu$ . To ensure uniformity of conditions, a specimen length of 5 mm. was adopted and specimen tubes of 0.3 mm. dia. were selected.

The results of the calibration for various gold and silver specimens are given in Fig. 1.

\* Manuscript received 9 October 1953.

† Formerly Research Metallurgist, Associated Electrical Industries Research Laboratory, Aldermaston, Berks.; now

with Imperial Chemical Industries, Billingham Division.

† Physical Metallurgy Section Leader, Associated Electrical Industries Research Laboratory, Aldermaston, Berks.

## III.—EXPERIMENTAL RESULTS

## 1. X-RAY ANALYSIS

Initially nine alloys at intervals across the diagram were sintered, with pellets of the pure metals, and examined by X-rays. Filings from the pellets were annealed for 2 hr. at 600° C. and slowly cooled to room temperature. Photographs were taken in a 9-cm. Unicam powder camera, using Cu  $K_{\alpha}$  radiation. The powder photographs showed two phases: one face-centred cubic and the other body-centred cubic. Sharp diffraction photographs were obtained, and the results of the parameter measurements are given in Table I. Lattice spacings are reported in kX units, using the wave-lengths from the Siegbahn Tables. All values have been corrected to 20° C., using the

TABLE I.—*Lattice-Parameter Measurements on Gold-Molybdenum Alloys.*

Mo Content, at.-%	Lattice Parameter Corrected to 20° C., kX		Mo Content, at.-%	Lattice Parameter Corrected to 20° C., kX	
	F.c.c. Phase	B.c.c. Phase		F.c.c. Phase	B.c.c. Phase
0	4.0700	...	67.2	4.0692	3.1404
9.8	4.0691	*	75.5	4.0692	3.1403
18.6	4.0692	*	82.7	4.0693	3.1404
33.9	4.0692	3.1405	89.2	*	3.1404
46.8	4.0693	3.1403	94.9	*	3.1403
57.8	4.0691	3.1404	100	...	3.1404

\* Pattern detected but too faint to be measured.

thermal coefficients of expansion for the pure metals. The values given in the table are the mean of two parameter determinations on different samples from the pellets; in no case did these results differ by more than 0.0001 kX.

These preliminary experiments indicated that, while there is a small solubility of molybdenum in gold, there appears to be no solubility of gold in molybdenum. The remainder of the 89.2% and 94.9% molybdenum alloy pellets were melted in an argon-arc furnace, annealed at 1000° C. for 7 days and water-quenched to ensure that equilibrium had been attained in the molybdenum-rich alloys. The lattice parameters of the body-centred cubic phase in these alloys were:

Molybdenum, %	Lattice Parameter at 20° C., kX
89.2	3.1404
94.9	3.1404

These values show no variation from the lattice parameter of pure molybdenum, confirming that the solubility of gold in molybdenum must be very small. The results of these preliminary experiments also suggest that no intermediate phases are formed.

The constancy of the lattice parameters of the face-centred cubic phase in Table I shows that the solubility of molybdenum in gold is less than 9.8 at.-%. A further series of alloys was made in the range up to 9.8% molybdenum and examined in the high-

temperature camera. After the initial sintering treatment, all subsequent heat-treatments were given in the camera; photographs of each alloy were taken at approximately 800°, 600°, 400°, and 200° C., and at room temperature.

To determine the time required for equilibrium to be attained, the following experiment was carried out. A specimen from the 3.0% molybdenum alloy was maintained at 420° C. in the camera for 25 hr. and photographed after 1, 5, and 24 hr. The lattice parameters, which show no significant change over the 24-hr. period, were:

Time of Anneal before Exposure, hr.	Lattice Parameter, kX
1	4.0933
5	4.0932
24	4.0934

The following procedure was then adopted for all alloys. The specimens were heated in the camera to approximately 800° C., annealed for 1 hr., and then photographed. The specimen was then slowly cooled to 600° C., annealed there for 1 hr., and photographed; and so on for the other temperatures. Duplicate specimens were examined for the 0.6% molybdenum alloy; both sets of data lie on the same parameter/temperature curve, showing that homogeneity and probably equilibrium had been obtained. The parameter determinations for all the alloys are given in Table II.

TABLE II.—*Lattice-Parameter Measurements at Various Temperatures.*

Mo, at.-%	Temp., °C.	Parameter, kX	Mo, at.-%	Temp., °C.	Parameter, kX
0.2	8	4.0692	0.4	12	4.0692
	210	4.0813		183	4.0795
	403	4.0935		394	4.0924
	601	4.1063		584	4.1048
	813	4.1197		793	4.1193
0.6	8	4.0685	0.6		
	227	4.0820		207	4.0807
	410	4.0936		409	4.0935
	608	4.1063		507	4.1062
	804	4.1194			
0.8	14	4.0690	1.2	17	4.0689
	184	4.0792			
	397	4.0918		425	4.0934
	594	4.1050		632	4.1075
	792	4.1186		848	4.1229
1.6	16	4.0689	3.1	23	4.0694
	190	4.0794		199	4.0800
				419	4.0933
	592	4.1045		602	4.1054
	791	4.1188		799	4.1195
5.0	20	4.0692			
	187	4.0793			
	418	4.0933			
	604	4.1055			
	806	4.1202			

As a further check that equilibrium had been attained in the specimens after annealing in the camera, a sample of the 1.6% molybdenum alloy was annealed



in a furnace for 7 days at 600° C. and water-quenched. It was then heated as quickly as possible in the camera to 600° C. (the time required for heating being approximately 30 min.), annealed in the camera for 1 hr., and photographed. A value of  $a = 4.1059$  kX

given in Table IV. Agreement at 600° and 800° C. is good. The mean value of the lattice parameter of the gold solution at 20° C., as given in Table IV,

TABLE III.—Lattice Parameters of Quenched Alloys.

Mo, at.-%	Parameter (kX) of Alloys Quenched from:		
	1000° C.	800° C.	600° C.
0.4	4.0696	...	...
0.6	4.0693	...	...
0.8	4.0687	...	...
1.2	4.0678	...	...
1.6	...	4.0683	4.0684
2.0	4.0679	4.0681	4.0685
3.0	4.0679	4.0681	4.0685

TABLE IV.—Solubility of Molybdenum in Gold.

Temp., °C.	Solubility of Molybdenum, at.-%	
	High-Temperature-Camera Results	Quenched-Specimen Results
20	0.7	0.65
200	0.7	...
400	0.9	...
600	0.9	0.95
800	1.1	1.05
1000	...	1.2

indicates a solubility of 0.7 at.-% molybdenum at that temperature.

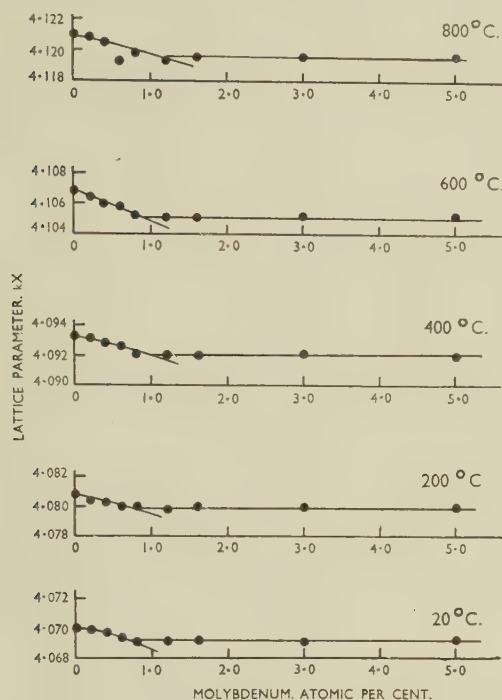


FIG. 2.—Composition/Parameter Curves at Various Temperatures.

was obtained at 604° C. This falls on the lattice-parameter/temperature curve previously described for the 1.6% molybdenum alloy and suggests that the annealing periods given in the camera were sufficient for equilibrium to be obtained.

Composition/parameter curves at 800°, 600°, 400°, 200°, and 20° C. are drawn in Fig. 2, the parameter values at these temperatures having been read off the curves obtained from the data in Table II. These composition/parameter curves indicate that the solubility of molybdenum in gold increases from 0.7 at.-% at 20° C. to 1.1% at 800° C.

Experiments were not carried out in the high-temperature camera above 800° C., owing to the failure of the cellophane window at temperatures above this. Instead, a series of alloys was quenched from 1000° C. to determine the maximum solubility of molybdenum in gold. A small number of alloys was also quenched from 800° and 600° C. to see whether the value obtained in this way agreed with that determined by the high-temperature camera. The alloys at 1000° C. were annealed for 4 days, those at 800° C. for 7 days, and those at 600° C. for 10 days before quenching. The lattice parameters for these alloys are given in Table III. The solubility of molybdenum at different temperatures as determined by the high-temperature camera and the results obtained from the quenched specimens are

## 2. MISCELLANEOUS RESULTS

Although the remainder of the diagram was not investigated in detail, a few experiments were carried out on the melting points of the gold-rich alloys.

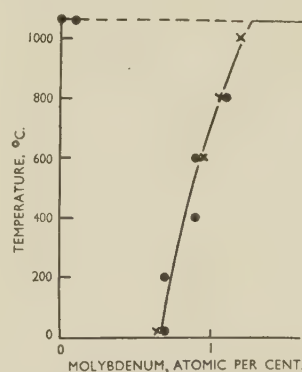


FIG. 3.—The Solubility of Molybdenum in Gold.

### KEY.

- High-temperature X-ray results.
- x Results from quenched specimens.

Thermal analysis of 2% and 10% molybdenum alloys revealed an arrest at 1054° C., which is interpreted as a eutectic. The solidus temperature of a 0.1% molybdenum alloy was detected at 1058° C. and the melting point of gold at 1063° C.

The solubility of molybdenum in gold as determined by both X-ray methods is given in Fig. 3.

This shows a maximum solubility of 1.25 at.-% molybdenum at the eutectic temperature of 1054° C.

#### IV.—DISCUSSION

Owen and Roberts<sup>2</sup> have shown that the electron concentrations of the solid solutions of the normal elements in gold lie in the range 1.05–1.33 at maximum solubility. The maximum solubilities of the transition elements in gold are given in Table V.

TABLE V.—Maximum Solubilities of the Transition Elements in Gold.

Alloy System	Max. Solubility of Transition Metal, at.-%	Postulated "Valency"	Electron Concentration	Reference
Au-Ti .	10.6	4	1.32	5
Au-Cr .	23.5	2	1.24	6
Au-Mn .	30.8	2	1.31	7
Au-Fe .	74.5	1	1.10	8
Au-Co .	23.5	2	1.24	8
Au-Ni .	100	1	...	6
Au-Zr .	7.3	4	1.22	9
Au-Mo .	1.25	6	1.06	...
Au-Pd .	100	1	...	6
Au-Pt .	100	1	...	6

Possible values of the "valencies" of these metals in solution in gold, which give electron concentrations in the range found by Owen and Roberts, are also

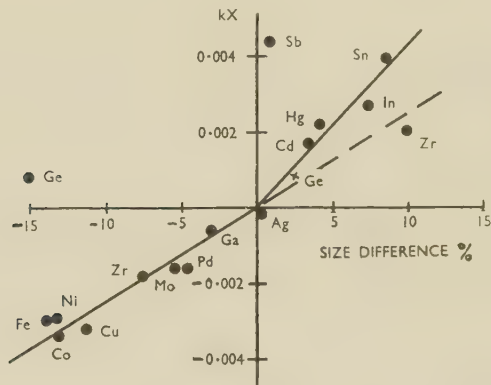


FIG. 4.—The Change of Lattice Parameter of Gold per 1 at.-% of Solvent Plotted Against Percentage Size Difference.

shown in the table. It is interesting that, whereas titanium, zirconium, and molybdenum exhibit their group valencies, all the metals of the later groups have low values. The data are too incomplete for

it to be decided whether they support the subdivision of the transition metals into the two classes suggested by Hume-Rothery, Irvine, and Williams,<sup>10</sup> but the marked difference between chromium and molybdenum is suggestive.

One at.-% molybdenum causes a change of  $-0.0016$  kX in the lattice parameter of gold. The change per atomic-% solute for a number of metals is plotted against their size difference from gold in Fig. 4. It would appear that the distortion is proportional to the size difference, being less for atoms smaller than gold. Zirconium, the only transition element larger than gold for which there is information, behaves like the remainder of the transition elements, causing only half the distortion of the larger normal elements. The normal metals germanium and antimony do not obey the relationship. Their atomic diameters, however, were obtained from structures of low co-ordination number, and are thus probably low. If we use the atomic diameter which Axon and Hume-Rothery<sup>11</sup> obtained for germanium in aluminium solution, much better agreement is obtained (point marked X in Fig. 4). On the other hand, Owen and Roberts have suggested that the large distortion caused by antimony might be due to a "valency" effect; if this is the case, it is surprising that molybdenum with 6 valency electrons causes only one-third of the distortion found with antimony.

#### ACKNOWLEDGEMENTS

The authors wish to express their thanks to Mr. R. A. J. Shelton, who carried out the chemical analyses, and to Dr. T. E. Allibone, F.R.S., for permission to publish this paper.

#### REFERENCES

1. — Dreibholz, *Z. physikal. Chem.*, 1924, **108**, 1.
2. E. A. Owen and E. A. O'Donnell Roberts, *J. Inst. Metals*, 1945, **71**, 213.
3. D. Summers-Smith, *Metallurgia*, 1949, **39**, 309.
4. R. L. Berry, W. G. Henry, and G. V. Raynor, *J. Inst. Metals*, 1950–51, **78**, 643.
5. E. Raub, P. Walter, and M. Engel, *Z. Metallkunde*, 1952, **43**, 112.
6. M. Hansen, "Der Aufbau der Zweistofflegierungen", 1936: Berlin (Springer).
7. E. Raub, U. Zwicker, and H. Bauer, *Z. Metallkunde*, 1953, **44**, 312.
8. E. Raub and P. Walter, *ibid.*, 1950, **41**, 234.
9. E. Raub and M. Engel, *ibid.*, 1948, **39**, 172.
10. W. Hume-Rothery, H. M. Irvine, and R. J. P. Williams, *Proc. Roy. Soc.*, 1951, [A], **208**, 431.
11. H. J. Axon and W. Hume-Rothery, *ibid.*, 1948, [A], **193**, 1.



# METALLOGRAPHIC OBSERVATIONS ON CELL FORMATION AND DEVELOPMENT IN ALUMINIUM\*

1543

By J. W. KELLY,† M.Sc., and R. C. GIFKINS,‡ B.Sc., A.I.M.,  
MEMBER

## SYNOPSIS

Features associated with the cell sub-structure in high-purity aluminium have been examined by a number of microscopical techniques and by the X-ray back-reflection method. The scope and sensitivity of the techniques have been critically examined. Fine- and coarse-grained specimens were deformed at various rates and at various temperatures up to 325° C. The white-line pattern obtained by narrow-pencil illumination with the microscope out of focus does not appear to give an unambiguous indication of cell boundaries, particularly at low rates of strain at the higher temperatures. Etch-pits did not delineate either boundaries of cells or the sub-structure of polygonized single crystals, whereas deep etching did.

Examination of specimens repolished and anodized at various stages of deformation showed that in a significant proportion of grains, in both coarse- and fine-grained specimens, kink and deformation bands formed first across the whole grain and then broke down with the development of cells, both along and across the bands. This also occurred at 300° C., when slip could not be detected with the phase-contrast microscope, but cell-boundary migration often took place rapidly during small strain intervals at 300° C., and tended to mask the banded structure. At extensions up to 20% there was no evidence of relative movement of cells, but there was some tilting, and their orientation differences progressively increased. These observations are discussed in relation to recent models for deformation during creep.

## I.—INTRODUCTION

DURING the last few years, a considerable amount of evidence has accumulated for the existence of sub-structures in metals deformed under various conditions.<sup>1</sup> Particular interest has been shown in the conditions for the formation of sub-structures in aluminium; Wood and his collaborators<sup>2</sup> have indicated the dependence of the size of the sub-structures, which they termed "cells", on rate and temperature of deformation. In discussions on papers by Wood *et al.*,<sup>3</sup> and in papers by other authors,<sup>4,5</sup> it has been suggested that the mechanism of cell formation is the same as that for polygonization, the type of sub-structure investigated by Cahn<sup>6</sup> in aluminium and other metals. During the course of the present investigation, a number of papers by various authors have been published which support the polygonization hypothesis,<sup>7-10</sup> and particular attention has been directed to observations which showed the formation of cells in bands.<sup>11-12</sup>

At the start of this investigation, however, the evidence for cells rested on X-ray-diffraction observations and the appearance of the deformed surface when viewed with narrow-pencil illumination and the microscope slightly out of focus. There appeared to be a marked difference between both the appearance and orientation distribution of cells and of sub-grains

formed by polygonization, only the similarity of the X-ray sub-reflections being indisputable. It seemed worthwhile, therefore, to attempt a re-examination of the formation and development of cells in aluminium using the latest available techniques. These methods included the use of the out-of-focus technique, etch-pits, deep etching, multiple-beam interferometry, phase-contrast microscopy, and polarized light on anodized surfaces; the metallographic observations were corroborated by X-ray back-reflection photographs.

The main results of this re-examination have confirmed and extended those of other workers, particularly of Rachinger,<sup>11</sup> McLean,<sup>12</sup> and Gervais, Norton, and Grant,<sup>13-14</sup> and show that cells form from kink and deformation bands in many grains, at various rates at temperatures up to 300° C., in both fine- and coarse-grained specimens.

## II.—MATERIALS AND EXPERIMENTAL METHODS

### 1. GENERAL OBSERVATIONS

The material consisted of cold-rolled aluminium strip of 99.98% purity. Tensile specimens were made from this with a gauge-length of 1.4 in. and a cross-section  $\frac{1}{2} \times \frac{1}{8}$  in.; the specimens were suitably treated to give either a fine grain-size (about  $10^{-1}$  mm. dia.) or

\* Manuscript received 15 June 1953; in revised form 15 October 1953.

† Research Student; ‡ Senior Research Officer, Common-

wealth Scientific and Industrial Research Organization, The Baillieu Laboratory, University of Melbourne, Australia.

a coarse one (about 2 mm. dia.). After annealing, the specimens were strained under constant load at temperatures up to  $325^{\circ} \pm 3^{\circ} \text{C}$ . Loads were adjusted to give minimum creep rates between 0.15 and 0.2%/hr. Some fine-grained specimens were strained at 20%/hr. and 11%/min. (the latter speed being obtained with a hand-operated machine), and others were loaded at  $325^{\circ} \text{C}$ . to give a minimum creep rate of 1%/hr. In all, about 30 specimens were examined, usually at 3% intervals of strain up to 20% extension, using several of the techniques for the examination of selected areas at each stage.

Specimens were polished electrolytically in orthophosphoric acid and the surface film was removed. Deep etching for 10 min. at  $30^{\circ} \text{C}$ . in the standard solution for etching aluminium (73% water, 25% nitric, and 2% hydrofluoric acid) was necessary to reveal cell boundaries. Etch-pits were developed using the three-acid reagent of Lacombe and Beaujard<sup>15</sup> or modifications of it at various temperatures.

Multiple-beam interference fringes were produced from the deformed specimens as previously described.<sup>16</sup> Both positive and negative phase-contrast microscopes were employed.

The anodizing solution recommended by Sperry<sup>17</sup> was found to be the most satisfactory, and after electropolishing and micro-etching, specimens were anodized in this solution in a standard manner. After examination with polarized light, the anodic film was loosened in the way recommended by Sperry and finally removed by electropolishing lightly. After further extension the specimen was electropolished to smooth out the roughened surface and anodized again for further examination.

The optical arrangement was such that colour variations dependent on the underlying orientation were obtained with polarized light and the anodized specimens. This was found to give more information than variations of intensity alone, so that although photographs were taken by a standard procedure on colour-sensitive film, notes of colours were kept. Contrast was found to be greatest in the blue part of the spectrum, and specimens were rotated to bring particular grains into this range. Moreover, it was during rotation that the best impression of detail was obtained, so that photographs represent a "still" from the sequence.

## 2. VALIDITY AND SENSITIVITY OF THE ANODIC-FILM AND POLARIZED-LIGHT METHOD

There appears to be general agreement<sup>7, 17, 18</sup> that this method gives a true representation of the variations of orientation in aluminium however the detailed optical mechanism may vary. Experiments showed that the colours did not change significantly with time of anodizing until the striated structure<sup>18</sup> appeared; the colours in a given area were thus reproducible. A standard petrological test demonstrated that the colours were all due to first-order

interference, i.e. each represented a unique orientation.

Unfortunately, the microscope used could not be adapted to make accurate measurements of extinction angle, but an estimate of the sensitivity was made in the following way. The number of cells (four or less) in a small marked area was determined, using the anodic-film method, and then the total orientation spread of this group of cells was obtained from an X-ray back-reflection photograph. By division, the detectable orientation difference\* between cells was found to be  $\frac{1}{2}^{\circ}$  to  $1^{\circ}$ ; this is in agreement with the value quoted by McLean.<sup>12</sup>

Polishing and anodizing a specimen five times did not change the colours or the configuration of the cells noticeably; Figs. 1 and 2 (Plate LXXIV) show the first and last photographs taken on an area of such a specimen. It was clear, therefore, that the technique could be used to follow changes in an area without ambiguity. The depth of material removed at each stage was about 0.0002 in. Good correspondence between cells revealed by this technique and by deep etching is shown in Figs. 3 and 4 (Plate LXXIV).

## 3. THE USE OF ETCH PITS TO REVEAL SUB-BOUNDARIES

The sub-boundaries in polygonized aluminium were revealed by Cahn,<sup>6</sup> using the three-acid reagent of Lacombe and Beaujard,<sup>15</sup> and as earlier (unreported) attempts to reveal cell boundaries in the specimens used by Wilms and Wood<sup>19</sup> had been unsuccessful, a direct comparison between cell and polygonization sub-boundaries was made.

Both fine- and coarse-grained specimens known to contain a well-developed cell structure were etched in the three-acid reagent and in several modifications of it at various temperatures. Although it was occasionally possible to imagine networks of pits which could be presumed to outline cells, it was found that there was no relation between these and the cells revealed by the anodic-film technique. An illustration of this has been given elsewhere.<sup>20</sup>

An aluminium single crystal was prepared and polygonized in the manner described by Cahn,<sup>6</sup> and the typical break-up of X-ray reflections was observed. Portions of the specimen were polished flat and etched in the three-acid reagent or a modification of it. A typical area is shown in Fig. 5 (Plate LXXIV), where there is no indication of boundaries. However, after repolishing and deep etching with the standard reagent, straight polygonization boundaries were observed (Fig. 6, Plate LXXIV). It appears, therefore, that cell and polygonization boundaries behave in the same way with respect to etching reagents. No satisfactory explanation<sup>20</sup> of the failure of the three-acid reagent to reveal sub-boundaries seems to have been advanced; other workers,<sup>5, 9, 14</sup> using coarse-grained specimens and generally much higher temperatures of straining, have successfully used the three-acid reagent to reveal cell boundaries.

\* Strictly, the minimum, but with only 3 or 4 cells this would equal the actual orientation difference.



### III.—THE SURFACE TOPOGRAPHY OF STRAINED SPECIMENS

#### 1. OBSERVATIONS WITH THE PHASE-CONTRAST MICROSCOPE

The use of the phase-contrast microscope, even at extensions below 3%, failed to reveal any evidence of slip traces on specimens strained at a rate of 0.15%/hr. at 300° C., but at 200° C. McLean's<sup>7</sup> observation of fine slip at less than 1% extension was confirmed. Fine slip was also detected in specimens strained at a higher rate (1%/hr.) at 325° C., when normal slip traces were absent. With extensions greater than 6%, the specimen surface was usually too distorted to obtain a true phase-contrast image with the 4-mm. objective available.

When the out-of-focus technique showed white or black lines (usually presumed to be cell boundaries<sup>2, 7</sup>) and when these were isolated from other features, the phase-contrast image revealed them as diffuse bands of different intensity from that of the background. This suggests that these boundaries did not consist of sharp discontinuities.<sup>21</sup> There was no evidence of relative movement of cells to produce steps at their boundaries, at extensions up to 20%.

#### 2. THE WHITE-LINE PATTERNS

The pattern of white and black lines which is obtained from deformed crystals when narrow-pencil illumination and slight defocusing are employed will be referred to as the white-line pattern. At 200° C. this pattern corresponds to features associated with slip, deformation bands, and cell boundaries.<sup>21</sup> At higher temperatures, the cellular nature of the pattern becomes more obvious,<sup>19</sup> but, although there is often a close association between marked white lines and cell boundaries revealed by other methods, many lines appear to have no sub-boundary as counterpart. This is illustrated in Figs. 7 and 8 (Plate LXXIV). Figs. 13–20 (Plate LXXV) show how the white lines arise from surface tilts, ridges, or troughs. Cellular networks shown in previous papers<sup>5, 22</sup> are very similar to those obtained from undulations caused by the smoothing action of electropolishing on scratches and surface defects. The white-line pattern does not appear to be an unambiguous way of detecting cell boundaries on the surface of specimens deformed slowly at 300° C. Nevertheless, with a low rate of strain at 200° C or a higher rate at 300° C., the white lines did correspond reasonably well to the long edges of bands of cells (see Figs. 29 and 30, Plate LXXVII), though it was difficult to detect the boundaries within the bands by this method.

The white-line pattern from deformed zinc was in good agreement with the facets formed by cells; Ramsey<sup>23</sup> has shown that these facets correspond to true sub-grains. With zinc there was usually an alternation of slope of the cells,<sup>24</sup> so the black-and-white pattern interchanged very clearly on moving from inside to outside true focus (see Figs. 25 and 26, Plate LXXVI).

#### 3. FEATURES REVEALED BY INTERFEROMETRY

In aluminium specimens strained so that normal slip was absent, multiple-beam interference fringes showed that there was no tilting of surface areas comparable to the facets formed in zinc;<sup>24</sup> tilting was in fact often associated with dome-like areas which appeared to be the result of "drag" at grain boundaries where relative movement occurred, as in lead.<sup>25</sup> This feature is illustrated in Figs. 15, 16, 19, and 20 (Plate LXXV). Tilting did not increase markedly with increased deformation. The white-line pattern sometimes corresponded to a small kink in the fringes, and more rarely to the intersection of tilted areas; some white lines did not appear to be associated with any distinct feature of the fringe pattern. All of these points are illustrated in Figs. 13–20 (Plate LXXV).

At the relatively high rate of strain (1%/hr.) used at 325° C., besides the fine slip previously noted in Section III. 1, some coarse, roughly parallel, marks were noted in some grains, and these also appeared most clearly at an early stage of deformation. A group of such markings is shown in Figs. 17 and 18 (Plate LXXV); the fringe pattern is very similar to that obtained with some types of slip, indicating fairly abrupt changes in slope but not definite steps. After further deformation it was not easy to detect these marks with bright-field illumination (Fig. 19), but the fringe pattern revealed them as broad undulations. This phenomenon resembles the fading of prominent slip bands observed by McLean<sup>26</sup> at 200° C.

Other effects, some of which have been noted previously in lead<sup>25</sup> and also when using other methods, were clearly demonstrated by the fringes illustrated in Figs. 13–20. The broadened grain boundaries were shown to consist of areas slightly inclined to the surface and often to be of a step-like character due to alternations of boundary sliding and migration.<sup>5, 8, 27</sup> Triple-point steps were frequently observed, and the fringe patterns confirm previous suggestions of their formation.<sup>5, 8, 22, 25</sup> When slip was present at lower temperatures (200° C. or lower), triple-point steps were often replaced by emphasized slip, similar to that found in lead.<sup>25</sup>

#### 4. CONTINUED DEFORMATION OF REPOLISHED SPECIMENS

The general complexity of the surface of specimens after about 10% extension was such that small tilts or relative displacements of cells would be masked. A specimen which had been deformed to 15% in the "slipless" range of conditions was therefore repolished flat and then creep was allowed to continue at the same rate and temperature. After 4% further deformation, the white-line pattern consisted of a clear network of black and white lines, sometimes separated and at others close together. The latter corresponded to a sinusoidal topography, as shown in Figs. 9 and 10 (Plate LXXIV); although there was some tilting there was no relative movement of cells.

#### IV.—ORIENTATION CHANGES WITHIN GRAINS

Selected areas on a number of specimens, strained at various rates and temperatures, were observed by using the process of repolishing, anodizing, and examination with polarized light at various stages of deformation. Some specimens were also sectioned parallel to the surface, polished, and anodized; the general appearance of these areas was similar to that of the surface grains.

##### 1. FORMATION OF BANDED SUB-STRUCTURE

With this technique it was not possible to detect cells during the early stages of deformation, although the white-line patterns suggested, and X-ray photographs confirmed, that they were present; e.g. at the low rate of deformation at 300° C., cells were usually ill-defined up to extensions of about 10%, as shown in Fig. 21 (Plate LXXVI).

In many grains it was noted that the first indication of breakdown was the formation of bands across the grain (see Fig. 21); the bands subsequently became more distinct and at the same time broke up into cells. Figs. 21–23 (Plate LXXVI) represent three of a series of photographs taken at extensions between about 10 and 20% on one of the coarse-grained specimens slowly strained at 300° C. In the fine-grained specimens the banding was not so apparent, because the band width was comparable to the grain-size; it could, however, be detected by observation of alternations of colour and it was concluded that possibly two-thirds and certainly one-third of the grains in both kinds of specimen were banded. Fig. 24 (Plate LXXVI) shows banding in a fine-grained specimen; without the aid of the colours it is not easy to see this, but the alternation of dark and light groups of cells can be seen fairly clearly in one grain.

The bands were of several distinct types in specimens slowly deformed at 300° C. Sometimes they were of approximately equal width but alternating in colour (and thus orientation); Fig. 31 (Plate LXXVII), although taken on a specimen deformed at 200° C., is typical. In other grains, the same orientation relationships existed, but the bands were alternately wide and narrow (Fig. 27, Plate LXXVII). Figs. 28, 29, and 32 (Plate LXXVII) show that this type of banding is very common both at higher rates of strain at 300° C. and at lower temperatures. In yet other grains, instead of alternating, the orientation of the bands changed through a number of stages and then back again, giving a terraced impression, as in Fig. 34 (Plate LXXVII).

##### 2. EFFECT OF DEFORMATION ON CELL SIZE AND SHAPE

It is clear from the illustrations that the cell size varies over quite a wide range for each set of conditions of deformation, and this point should be noted when considering references to cell size, particularly those obtained from X-ray evidence. The mean cell

size, however, appears to vary with temperature and strain rate in the usual manner.<sup>2</sup>

An increase in the number of cells with continued deformation seems to be shown by Figs. 21–23 (Plate LXXVI), but evidence from X-ray photographs by various workers<sup>10, 29</sup> appears to conflict with this indication, which will be discussed in Section V, 2.

It was found that the cell-boundary configuration in many grains could change greatly over a small interval of extension without change in the orientation relationships of the cells. This was particularly marked in the smaller grains and in those showing least tendency to banding, and it is illustrated by Figs. 11 and 12 (Plate LXXIV), which were taken on a specimen at extensions of 11.4 and 12.3%, respectively (0.15%/hr. at 300° C.). This process would tend to obscure the evidence of the formation of cells in bands, particularly in the absence of the polarized-light colours.

##### 3. THE EFFECTS OF STRAIN RATE AND TEMPERATURE ON BAND WIDTH

In view of the established dependence of mean cell size on rate of strain and temperature,<sup>2, 11</sup> it seemed of interest to determine the effect of these variables on the width of bands observed with polarized light. Figs. 27–29 (Plate LXXVII) are typical of the results obtained at 300° C. with various rates of strain after about 10% extension. Fig. 27 was obtained at the low rate of 0.15%/hr., whilst Figs. 28 and 29 were taken on specimens extended in  $\frac{1}{2}$  hr. and 1 min., respectively. The decrease in band width is clearly shown, and by rotation of the specimens it was possible to see that there was a corresponding decrease in cell size; 2–4 cells were usually present across a band. At the higher rates of strain, the slip traces which were visible before polishing and anodizing were always at a high angle to the bands. This is illustrated by Fig. 30 (Plate LXXVII), which shows the same area as Fig. 29 before polishing and anodizing.

Figs. 31–33 (Plate LXXVII) show the effect of decreasing the temperature whilst maintaining the strain rate at about 0.15%/hr., and they show areas taken after 10–15% extension at 200°, 100°, and 22° C., respectively. Again the decrease in band width is apparent. At 100° C. and higher temperatures, 2–4 cells were present across each band and cells were

TABLE I.—*Effect of Temperature and Strain Rate on Band Width.*

Temp., ° C.	Strain Rate, % per hr.	Band Width, cm. $\times 10^{-3}$	Temp., ° C.	Strain Rate, % per hr.	Band Width, cm. $\times 10^{-3}$
22	0.1	1.3	300	0.1	12.4
100	0.1	3.2	300	20.0	6.4
200	0.1	6.1	300	660.0	2.1

present at 22° C., although only clearly detected on rotation of the specimen; the serration along the bands gives an indication of cell size. Table I



illustrates the variation of band width (and hence cell size) with strain rate and temperature.

At the low rate at 22° C. the X-ray reflections consisted of a continuous ring around the Debye circle; Wood and Rachinger<sup>29</sup> and others have suggested that this indicates a fine sub-structure, and Kellar, Hirsch, and Thorp<sup>30</sup> have advanced evidence from work using an X-ray micro-beam to support this. The polarized-light technique revealed this sub-structure metallographically, though only clearly on rotation of the specimen.

#### 4. DEFORMATION AT ROOM TEMPERATURE FOLLOWED BY ANNEALING AT 300° C.

Simultaneous straining and annealing gave a different structure from straining at low temperature and then annealing, as previous X-ray results have indicated.<sup>31</sup> After selected areas had been photographed by the polarized-light technique, some specimens were slowly deformed at room temperature and then annealed at 300° C. for the time they had been extending (142 hr.). After repolishing and anodizing again, it was found that there were considerable changes in grain boundaries, but the band and cell sizes were unaltered.

#### 5. STRESS-RECOVERY

Suiter and Wood<sup>31</sup> have shown, and Hino, Shewmon, and Beck<sup>32</sup> have confirmed, that cells of an equilibrium size form from cold-worked specimens subsequently deformed at a given temperature and strain rate. In the present investigation, the presence of bands of cells was looked for after stress-recovery. A cold-worked specimen (8% in tension) was extended a further 6% at 0.18%/hr. at 300° C. Cells of a size appropriate to these conditions were revealed by the anodic technique, but only one grain in 20 showed a possible tendency to banding; otherwise there appeared to be complete randomness of orientation of cells.

### V.—DISCUSSION AND CONCLUSIONS

The results of the present investigation are discussed in the following sections; some of these results confirm and extend recent suggestions on cell formation and the part played by polygonization.

#### 1. FORMATION OF CELLS FROM KINK AND DEFORMATION BANDS

When aluminium is strained at temperatures up to 300° C. a significant proportion of cells are formed from some type of deformation band. There is no evidence that this cell formation is associated with fine slip lines at 300° C. and low rates of strain. At lower temperatures, however, fine and normal slip were observed, confirming and extending recent suggestions that the cells develop from deformation bands. Wyon and Crussard<sup>5</sup> suggested this mechanism on the basis of X-ray evidence, and Rachinger<sup>11</sup> has arrived at the same conclusion.

McLean<sup>12</sup> made detailed observations at 200° C. when slip was present and put forward a model in which deformation bands form first near the boundaries and then spread to the whole grain; subsequently the bands polygonize to form rows of subgrains, and eventually small relative movements between these take place. Gervais, Norton, and Grant<sup>14</sup> have recently found the formation of kink bands, as distinct from deformation bands,<sup>33</sup> to precede the breakdown into cells in coarse-grained specimens deformed at temperatures near the melting point.

The present results do not seem to confirm McLean's<sup>12</sup> suggestion that dislocations pile up at grain boundaries and form deformation bands there first, for the bands appear to develop across the whole grain simultaneously. A more sensitive technique for the metallographic examination of the early stages of creep is needed, however, to settle this point.

If the bands do form simultaneously, or almost so, across the grain, they may be kink bands, as suggested by Gervais, Norton, and Grant;<sup>14</sup> the presence of bands which are alternately wide and narrow would seem to support this, particularly as this type of banding predominated at lower temperatures or higher strain rates. As Rachinger<sup>11</sup> has pointed out, no satisfactory explanation of the dependence of cell and band width on temperature and strain rate has yet been given. It seems that the simpler crystallographic nature of kink bands could form a promising line of approach to this problem. It would be possible to speculate on the significance of the other types of banding where "terraced" bands or bands of equal width occurred, but it seems better at this stage to note that any truly comprehensive hypothesis must also take them into account.

The fact that the bands appear to break down into 2-4 cells across their width is another modification to McLean's model; presumably these cells are formed by polygonization across as well as along the bands.

#### 2. INCREASE OF THE NUMBER OF CELLS WITH DEFORMATION

Consideration of the banded nature of cells shows that care must be exercised in the interpretation of X-ray photographs. There is a periodicity in the orientation of cells across a grain, and within each band cells are surrounded by neighbours of similar orientation. Thus reflections from cells in various parts of a grain are likely to be superposed, and this could lead to an underestimate of the number of cells, particularly at relatively low extensions of the specimen. Neither the rapid attainment of an equilibrium cell size<sup>28</sup> nor the direct dependence of cell size on strain<sup>10</sup> would appear to give a true picture, at least until polygonization is complete. The latter apparently occurs at extensions of above 20% under the conditions of the present experiments at 200° or 300° C., as sliding at cell boundaries was not observed up to a strain of 20%. McLean<sup>12</sup> found little displacement at cell boundaries before a strain of 20% and mentioned that the white-line pattern only be-

came distinct at 20% strain and 200° C.; on the other hand, in the present investigation, the white-line pattern was clear at much lower strains, despite the absence of relative movement of cells.

### 3. PROPERTIES OF CELLS AND CELL BOUNDARIES

A number of the properties of cells and their boundaries have been revealed or emphasized by the present investigation:

(a) Phase-contrast and multiple-beam interference fringes showed that cell boundaries on the surface consisted of ridges or troughs which are broad compared with their vertical extension.

(b) Besides being less clearly defined than in zinc, facets formed by cells showed little tendency to progressive tilting.

(c) There was marked migration of many cell boundaries over small intervals of strain, especially in grains which did not show banding of cells. Migration of a similar character has been observed by Washburn and Parker,<sup>34</sup> and is an accepted property of polygonization boundaries.

(d) The absence of relative movement of cells in the present investigation and the smallness of the movement found by McLean<sup>12</sup> may be accounted for by the banding of cells rather than by any difference in kind between cell boundaries and ordinary low-angle grain boundaries. For relative movement to occur at cells along the edges of bands, it is necessary for complete rows or lamellae of cells to move past one another; moreover, each of these cells has neighbours of very close orientation to itself both along and across the band (in three dimensions), so that cells do not in general have orientation relationships which are similar to normal grains. These considerations might also apply to the explanation of the resistance to creep found by McLean and Tate<sup>35</sup> in polygonized aluminium.

### 4. STRESS-RECOVERY AND POLYGONIZATION

The absence of banding of cells in stress-recovered specimens suggests that cells, similar to those formed by polygonization of kink or deformation bands, can be formed by another process, namely, the selective growth of cells formed during cold working.<sup>32</sup>

However, the process of creep at room temperature followed by heating at 300° C. does not give any increase in the size of the small cells formed during this cold working. This appears to happen only under the conditions used by Cahn<sup>6</sup> or Guinier and Tennevin<sup>36</sup> when cold work at high rates is followed by annealing at elevated temperatures. It is suggested, therefore, that the lamellae found by Cahn were the result of a two-stage process: (i) polygonization at room temperature to form very fine lamellae, and (ii) selective growth at high temperature. This is polygonization followed by "recrystallization *in situ*" as suggested by Lacombe<sup>37</sup> and as adopted by the present authors in discussing the formation of cells in zinc.<sup>24</sup> The existence of this process has been clearly demonstrated in silicon-iron single crystals by Dunn and Daniels.<sup>38</sup>

### ACKNOWLEDGEMENTS

The investigation formed part of the joint programme of research of the Metallurgy Research Department of the University of Melbourne and the Physical Metallurgy Section of the Commonwealth Scientific and Industrial Research Organization, and was carried out at the Baillieu Laboratory under the general direction of Professor J. Neill Greenwood, whose advice and encouragement are gratefully acknowledged. The authors also wish to thank their colleagues for helpful discussions and suggestions.

### REFERENCES

1. A. Guinier, "Imperfections in Nearly Perfect Crystals", p. 402. 1952: New York (John Wiley and Sons, Inc.); London (Chapman and Hall, Ltd.).
2. W. A. Wood, G. R. Wilms, and W. A. Rachinger, *J. Inst. Metals*, 1951, **79**, 159.
3. C. Crussard, *ibid.*, 1948-49, **75**, 1125 (discussion).
4. G. B. Greenough and E. M. Smith, *ibid.*, 1950, **77**, 435.
5. G. Wyon and C. Crussard, *Rev. Mét.*, 1951, **48**, 121.
6. R. W. Cahn, *J. Inst. Metals*, 1949-50, **76**, 121.
7. D. McLean, *ibid.*, 1951-52, **80**, 507.
8. H. C. Chang and N. J. Grant, *Trans. Amer. Inst. Min. Met. Eng.*, 1952, **194**, 619.
9. I. S. Servi, J. T. Norton, and N. J. Grant, *ibid.*, 1952, **194**, 965.
10. G. B. Greenough, C. M. Bateman, and E. M. Smith, *J. Inst. Metals*, 1951-52, **80**, 545.
11. W. A. Rachinger, *Bull. Inst. Metals*, 1952, **1**, (15), 125.
12. D. McLean, *J. Inst. Metals*, 1952-53, **81**, 287.
13. A. M. Gervais, J. T. Norton, and N. J. Grant, *Trans. Amer. Inst. Min. Met. Eng.*, 1953, **197**, 1166.
14. A. M. Gervais, J. T. Norton, and N. J. Grant, *ibid.*, 1953, **197**, 1487.
15. P. Lacombe and L. Beaujard, *J. Inst. Metals*, 1948, **74**, 1.
16. R. C. Gifkins, *Australasian Eng.*, 1952, (May), 63.
17. P. R. Sperry, *Trans. Amer. Inst. Min. Met. Eng.*, 1950, **188**, 103.
18. A. Hone and E. C. Pearson, *Metal Progress*, 1950, **58**, 713.
19. G. R. Wilms and W. A. Wood, *J. Inst. Metals*, 1948-49, **75**, 693.
20. R. C. Gifkins and J. W. Kelly, *Trans. Amer. Inst. Min. Met. Eng.*, 1953, **197**, 730 (discussion).
21. R. C. Gifkins and J. W. Kelly, *J. Inst. Metals*, 1952-53, **81**, 717 (discussion).
22. W. Betteridge and A. W. Franklin, *ibid.*, 1951-52, **80**, 147.
23. J. A. Ramsey, *ibid.*, 1951-52, **80**, 167.
24. R. C. Gifkins and J. W. Kelly, *Acta Met.*, 1953, **1**, 320.
25. R. C. Gifkins, *J. Inst. Metals*, 1953-54, **82**, 39.
26. D. McLean, *ibid.*, 1952-53, **81**, 133.
27. W. A. Rachinger, *ibid.*, 1951-52, **80**, 415.
28. W. A. Wood and R. F. Scrutton, *ibid.*, 1950, **77**, 423.
29. W. A. Wood and W. A. Rachinger, *ibid.*, 1948-49, **75**, 571.
30. J. N. Kellar, P. B. Hirsch, and J. S. Thorp, *Nature*, 1950, **165**, 554.
31. W. A. Wood and J. W. Suiter, *J. Inst. Metals*, 1951-52, **80**, 501.
32. J. Hino, P. G. Shewmon, and P. A. Beck, *Trans. Amer. Inst. Min. Met. Eng.*, 1952, **194**, 873.
33. R. W. K. Honeycombe, *J. Inst. Metals*, 1951-52, **80**, 45.
34. J. Washburn and E. R. Parker, *Trans. Amer. Inst. Min. Met. Eng.*, 1952, **194**, 1076.
35. D. McLean and A. E. L. Tate, *Rev. Mét.*, 1951, **48**, 765.
36. A. Guinier and J. Tennevin, "Progress in Metal Physics". Vol. II, p. 177. 1950: London (Butterworths Scientific Publications).
37. P. Lacombe, quoted by R. W. Cahn, *ibid.*, p. 156.
38. C. G. Dunn and F. H. Daniels, *Trans. Amer. Inst. Min. Met. Eng.*, 1951, **191**, 147.



# SOME OBSERVATIONS ON THE DEFORMATION OF ZINC AT HIGH TEMPERATURES \*

1544

By R. W. CAHN,<sup>†</sup> Ph.D., MEMBER, (MISS) I. J. BEAR,<sup>‡</sup>  
A.M.T.C., and R. L. BELL,<sup>†</sup> B.Sc., STUDENT MEMBER

## SYNOPSIS

The orientation relationships between neighbouring units of sub-structure (cells) in grains of hot-deformed polycrystalline zinc were determined by a new micro-beam X-ray-diffraction technique. The axis about which neighbouring cells are mutually tilted, derived from the Laue photographs by a new analytical technique, was always nearly parallel to the basal plane after creep at 250° C., but not always after creep at 350° C. This tilt axis was also parallel to the cell boundary. Tensile experiments with single crystals of zinc revealed non-basal slip at 350° but not at 250° C., which is consistent with the observed positions of the tilt axis if the cell boundaries are built up of edge dislocations. An attempt is made to systematize the temperature-dependence of slip crystallography. Some observations are reported on the growth of existing cells during continued creep.

Indirect evidence is presented that the growth sub-structure present in cast zinc is due mainly to impurity segregation alone and that any orientation differences present must be very small.

## I.—INTRODUCTION

EVER since the discovery by Wilms and Wood <sup>1</sup> that creep caused the grains of polycrystalline aluminium to divide into cells, there has been controversy about the origin and nature of this sub-structure. The original interpretation put forward by Wilms and Wood was that the individual grains broke down, in an unspecified manner, into smaller units which slid over each other during further deformation. Critics of this interpretation maintained that the formation of cells was a special instance of polygonization,<sup>2</sup> but Wood and his collaborators <sup>3</sup> in reply made the valid point that for a given temperature and a particular time at that temperature, a much more pronounced sub-structure resulted if stress was simultaneously applied than if annealing followed cold deformation. It was discovered at a later date that coarsening of an existing cell structure at a high temperature could be greatly accelerated by simultaneously applying a stress.<sup>4, 5</sup> Nevertheless, the metallographic similarities between a cell structure and a structure produced by cold deformation and subsequent annealing prompted the conclusion that the two types of structure do not differ basically in origin,<sup>6, 7</sup> and recently published letters <sup>8, 9</sup> suggest that there is now general agreement on this point.

The only matter about which scope for disagreement seems to remain is in the suggested relative displacement of neighbouring cells. This displacement does sometimes occur, but it is very restricted and cannot normally be responsible for any important part of the total deformation, except possibly at very high temperatures, as suggested by McLean.<sup>10, 11</sup> He has

presented quantitative evidence to support his contention that, under conditions leading to cell formation, much of the deformation is actually accomplished by very finely distributed slip which is caused by the movement of dislocations over distances which are small compared with the grain diameter. The dislocations, having contributed to the deformation, join a cell boundary, which thereby becomes gradually enriched in dislocations; this causes an increased angle of tilt between the cells on either side. The present work, which was undertaken in a search for fresh evidence of the dislocation structure of cell boundaries, provides indirect confirmation of McLean's formulation.

By the determination of the relative orientation of neighbouring cells in grains of hot-deformed polycrystalline zinc, it was hoped to see whether the orientation was consistent with the idea that the cell boundaries consisted of dislocations. So far as is known, only edge dislocations have a tendency to collect into a stable array, and the axis about which the cells bordering such an array are mutually tilted is parallel to the slip plane and normal to the slip direction (the so-called "roller axis"). Zinc was chosen for this work because when slip occurs it is normally restricted to a single lattice plane, so that the tilt axis should always be parallel to the basal plane even when no slip lines are visible. Moreover, Ramsey <sup>12</sup> has shown that a clearly defined cell structure is generated in zinc during creep at 200° C.

Previous attempts have been made to determine tilt axes for creep cells in aluminium by means of Laue photographs.<sup>13, 14</sup> Calnan and Burns <sup>13</sup> found that the direction of the tilt axis varied considerably across

\* Manuscript received 22 July 1953; in revised form 19 September 1953.

<sup>†</sup> Department of Metallurgy, University of Birmingham.

<sup>‡</sup> Formerly of Department of Metallurgy, University of Birmingham; now with C.S.I.R.O., Fisherman's Bend, Vic., Australia.

a grain, being only locally parallel to the expected roller axis. Servi, Norton, and Grant,<sup>14</sup> who worked with single crystals of aluminium, found the tilt and roller axes to be coincident in the two instances they quote; here slip had taken place on (112) planes. Servi, *et al.* emphasized, as did Calnan and Burns, that the numerous fine sub-spots constituting each Laue spot were arranged along a single arc only exceptionally. It was not possible to find out which spots were due to neighbouring cells, or, therefore, to determine the tilt axes unambiguously. In the present work it was thought essential to use an X-ray beam small enough to straddle two cells only.

## II.—EXPERIMENTAL METHODS

### 1. PREPARATION OF SPECIMENS

Specimens with a square cross-section,  $0.5 \times 0.5$  cm., and with enlarged ends, were cast in a split graphite mould from high-purity zinc (spectroscopic analysis: lead 0.002, cadmium 0.0002, copper 0.0005, iron 0.003, and silver 0.00001%). A suitable grain-size was obtained by preheating the mould above the melting point of zinc. The specimens used had 20–30 grains/cm.<sup>2</sup>. One surface of each specimen was ground and then given a prolonged electrolytic polish in a solution of potassium hydroxide.<sup>15</sup> The grain boundaries became deeply grooved, and in addition a cellular structure reminiscent of a honeycomb was seen in some grains, as shown in Fig. 2 (Plate LXXVIII). This structure seems to be identical with that first reported by Buerger<sup>16</sup> in single crystals of zinc grown from the melt, and studied more fully by Smialowski,<sup>17</sup> who showed that it was proof against long periods of annealing. This structure, which did not impede the development of creep cells, is distinct from a lineage or macro-mosaic, which is an altogether coarser structure associated with quite large orientation differences; to avoid confusion with creep cells, we shall refer to it as the Smialowski structure.

### 2. DEFORMATION

Deformation was effected by dead loading in a furnace through which a slow stream of nitrogen was passed to minimize oxidation. This precaution was effective for short creep periods at 200°–250° C., but after several hours at 350° C. oxidation became severe. The elongation was measured by means of inscribed gauge-marks, although the figures so obtained had little significance, as the elongation was usually uneven.

At a later stage it proved desirable to carry out high-temperature experiments with zinc single crystals. These crystals, grown by the Andrade method and seeded to fix the orientation, were deformed on a Polanyi machine at a strain rate of several %/min. During extension, the electrolytically polished crystals were kept immersed in a salt-bath at the requisite

temperature. The extension was interrupted for Laue photographs to be taken.

### 3. DETERMINATION OF TILT AXES

A Laue back-reflection camera was used, providing an X-ray beam of 0.02 cm. dia. at the specimen, which was 1.7 cm. from the film. The area to be irradiated was first selected under a microscope, and then accurately aligned in the beam by a method recently described by Cahn.<sup>18</sup> Although well-defined cells at least 0.02 cm. in dia. were selected, on some of the photographs each spot of the Laue pattern was subdivided into more than the expected two sub-spots. In such cases there must have been several cells with slightly differing orientations, the boundaries between them not being visible. Out of a large number of photographs only those having two sharp sub-spots per Laue spot were selected, or else three sharp sub-spots well resolved; in this last case, the sub-spots were taken in pairs. Even patterns on which pairs of sub-

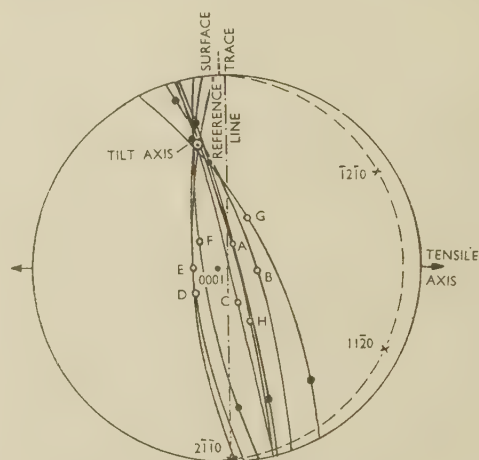


FIG. 17.—Stereogram of Laue Photograph Reproduced in Fig. 1 (Plate LXXVIII).

spots were only about 0.2 mm. apart could be accurately interpreted if the spots were fairly sharp. Before analysis, one emulsion of the double-sided film was removed by chemical means to eliminate spurious sub-structure in the Laue spots. Fig. 1 (Plate LXXVIII) shows a specimen Laue photograph, which has a rather larger separation of sub-spots than was normal.

The analytical method used to determine the tilt axis in each case is explained in an Appendix (p. 488). The orientation of the grain is first determined, and on a stereographic projection of the grain a separate great circle is drawn through each of a number of poles corresponding to selected spots on the Laue photograph. Strictly, each such pole refers to a particular sub-spot, e.g. the left-hand one of each Laue spot; see Fig. 24 (b) (Appendix). Each great circle is a locus of all possible positions of the tilt axis which are consistent with the relative positions of a corresponding pair of sub-spots; consequently all the



great circles intersect at the pole of the true tilt axis. Fig. 17 is the stereogram relevant to the Laue photograph of Fig. 1 (laterally reversed). The open circles are poles corresponding to Laue spots, while the full circles are calculated poles used for constructing the great circles. The margin of error is arbitrarily represented by the small circle which has been positioned so as to be as small as possible and yet cut or touch each great circle.

### III.—EXPERIMENTAL RESULTS

#### 1. METALLOGRAPHIC OBSERVATIONS

Specimens were deformed at temperatures from 200° to 350° C., and extended in creep by up to 50%. At all temperatures a proportion of grains showed slip lines and no cells, but the slip was more distinct at the lower temperatures. Care had to be taken to distinguish cracks in the thick oxide films, which formed from slip at the higher temperatures. Such cracks are visible in Fig. 9 (Plate LXXIX). Only a minority of grains at any temperature had well-developed cells, and these, as previously remarked by Ramsey, were entirely or almost free of slip lines.

Detailed investigation was restricted to Specimens No. 4 and 10. Specimen No. 4 was initially loaded at 200° C., and the temperature was then raised to 250° C., when the greater part of the elongation took place. The specimen fractured at an elongation of several per cent., which could not be accurately measured. Specimen No. 10 crept to fracture at 350° C., being elongated about 10%; the elongation was very uneven. Some photomicrographs were also taken of Specimen No. 9, which had crept 9% at 250° C.

Fig. 3 (Plate LXXVIII) shows a grain in Specimen No. 4 which had both slip lines and a single bend plane. This was generally the nearest approach to cell formation in grains with well-developed slip. The configuration in Fig. 3 is reminiscent of the bend planes observed together with slip lines in single-crystal creep specimens by Washburn and Parker.<sup>19</sup> Exceptions to the mutual exclusiveness of slip and cell formation were sometimes found, as in Fig. 4 (Plate LXXVIII), where a projecting tongue of a grain was evidently constrained by its neighbours.

Attention was given to cases of apparent double or multiple slip, because the X-ray evidence (Section III, 2) gave reason for expecting it. Thus Fig. 5 (Plate LXXVIII) shows a group of grains, two of which appear to have undergone double slip; this is illusory, however, since the grain boundary on the left has actually advanced in jerks (each position of the boundary being marked by viscous displacement) and the regions swept by the boundary then slipped on the basal plane of the new orientation. The bottom grain has behaved in a similar fashion. All instances of apparent double slip could be accounted for in this way. One puzzling configuration (Fig. 6, Plate LXXVIII) was interpreted after Laue photographs had been taken of various areas. Basal slip had occurred in the

original single grain (slip lines *A*), followed by twinning and slip in the twin (lines *B*), followed in turn by the growth of new or neighbouring grains and slip in these grains (lines *C* and *D*). It was thus established that only basal slip occurred on a visible scale at 250° C. Little well-defined slip was seen after creep at 350° C., and no double slip.

Figs. 7-9 (Plates LXXVIII and LXXIX) show cells in grains which also have a well-marked Smialowski structure. The cell boundaries do not deviate at all where they cross the boundaries of the Smialowski structure, and no such deviation was ever observed. It follows that the individual components or cells of the Smialowski structure are of identical orientation, or very nearly so. The fact that the structure is nevertheless chemically attacked by the electrolytic polishing medium must then be due to segregation of impurities, and this conclusion is in agreement with Rutter and Chalmers' <sup>20</sup> recent work on this type of imperfection in tin. The thickness of the Smialowski boundaries (see especially Fig. 2, Plate LXXVIII) is consistent with such segregation. Rutter and Chalmers, however, found that in addition small orientation differences of up to 15' existed between the Smialowski cells.

#### 2. X-RAY OBSERVATIONS

Eight Laue photographs of grains in Specimen No. 4 and seven photographs of grains in Specimen

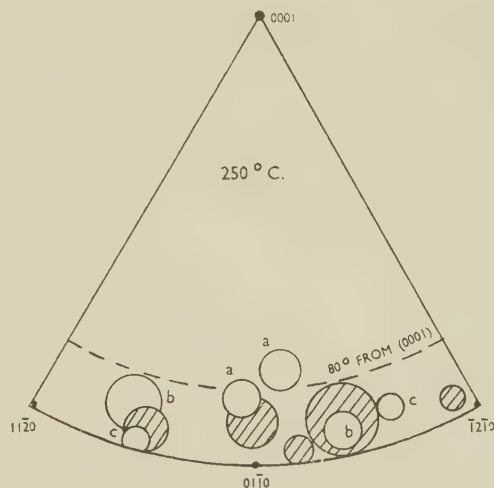


FIG. 18.—Tilt Axes in Specimen No. 4, after Creep at 250° C.

No. 10 were suitable for analysis. The tilt axes found are collected together in Figs. 18 and 19. The circles represent the limits of error, and those which are shaded refer to photographs with only two sub-spots to each Laue spot. These are the axes on which the most reliance can be placed. Pairs of axes referring to photographs with three sub-spots are indicated by the same letter.

It is striking that all tilt axes for the specimen deformed at 200°-250° C. are within a few degrees of being parallel to the basal plane and that this is not

true for the specimen deformed at 350° C. On the dislocation model for cell boundaries this implies that this specimen had undergone fine slip on a non-basal plane. Though no coarse slip had been found on

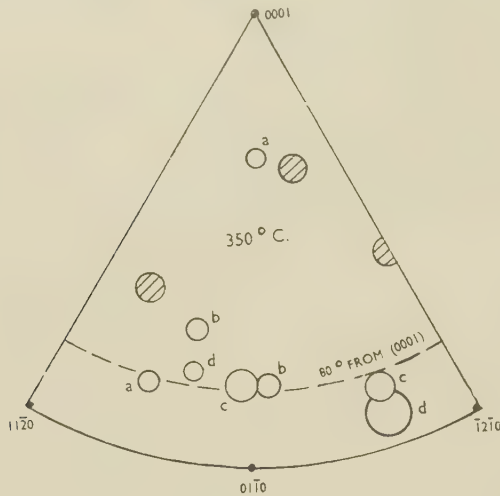


FIG. 19.—Tilt Axes in Specimen No. 10, after Creep at 350° C.

any plane but (0001), evidence for non-basal slip at 350° C. was obtained with single crystals (see Section III, 3).

An attempt was made to correlate X-ray data with microscopic observations. The angle,  $\alpha$ , between the tensile direction and the basal plane of each of the grains investigated is given in Table I. The basis

TABLE I.—Positions of Basal Planes Relative to Tensile Axis ( $\alpha$ ) and the Specimen Surface ( $\beta$ ).

Specimen/ Grain No.	$\alpha$ , in °	$\beta$ , in °	Remarks
4/1	8	8	Very little slip, localized. Many cells.
4/5	39	47	Much slip, some large bend planes, no cells.
4/7	23	25	A little slip, some cells.
4/8	7	16	No slip, many cells.
10/1	5	5	" " "
10/2	2	2	" " "
10/3	0	0	" " "

for the selection of grains (except No. 4/5) was that they should show marked cells. It follows from the values of  $\alpha$  in Table I that cells are formed most easily when a grain is oriented so that the resolved shear stress in the basal plane is small, making basal slip difficult. (One might also expect them to form if  $\alpha \cong 90^\circ$ , but this was not found.) Specimen No. 4/7 seems to have a limiting orientation for cell formation. The discrete bend planes in 4/5 are not regarded as cells, and the rule does not apply to them. The angles between the tilt axes and the tensile axis had no obvious preferred value, but there was a tendency for this angle to be fairly high.

It was desirable to examine the relationship between a tilt axis and the plane of the corresponding cell boundary. The difficulty was that the inclination of a boundary to the specimen surface could not be determined. This difficulty was overcome by selecting for examination grains in which the tilt axes were nearly parallel to the specimen surface. If a tilt axis in such a grain should prove to be parallel to the surface trace of the corresponding cell boundary, it follows that the axis must be parallel to the boundary itself (irrespective of the angle of inclination of the latter to the surface). Since at 250° C., the tilt axes were parallel to the basal plane, it was sufficient to look for grains with small or zero angle between basal plane and specimen surface ( $\beta$  in Table I). No. 4/1 was such a grain. It proved that each tilt axis was indeed parallel to the surface trace of the corresponding cell boundary. This is illustrated by a stereogram (Fig. 20 (a)) on which the direction of the axes and boundary traces are plotted. Fig. 20 (b) shows the actual boundary configuration. (The boundary between cells B and G was so faint that its direction could only be estimated; the boundary between C and D was curved.) Four of the five axes were derived from Laue photographs with two sub-spots only and were not therefore liable to any ambiguity in interpretation.

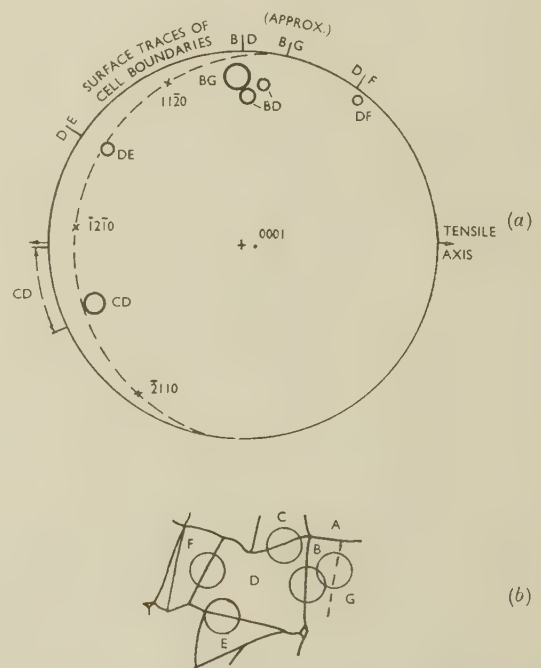


FIG. 20.—(a) Tilt Axes and Surface Traces of Cell Boundaries in a Grain in Specimen No. 4, after Creep at 250° C. (b) Sketch of Cell Configuration and Sites at Which the X-Ray Beam Impinged. (No optical inversion.)

A similar analysis for the grains of Specimen No. 10 was made difficult by the fact that so many of the Laue photographs had sets of three sub-spots. On two of the photographs of grain 10/1 which had two sub-spots only, the tilt axes by good fortune made fairly



small angles with the specimen surface. These cell boundaries, again, were almost parallel to the associated tilt axes. Fig. 17 refers to one of these photographs.

### 3. SLIP SYSTEMS ACTIVE AT HIGH TEMPERATURES

The suggestion that the observed orientations of the tilt axes for Specimen No. 10 imply the existence of non-basal slip, needs amplification. If slip occurs only on the prismatic plane  $(10\bar{1}0)$ , in the usual slip direction  $[\bar{1}210]$ , then the associated roller axis would be  $[0001]$ , which lies in  $(10\bar{1}0)$  and is normal to  $[\bar{1}210]$ . If there is co-operative slip on the basal and prismatic planes (after the manner of pencil glide or cross-slip as known in various cubic metals), an intermediate roller axis would result. Similar arguments would apply to co-operative slip on  $\{0001\}$  and the pyramidal plane  $\{10\bar{1}1\}$ . Now  $\{10\bar{1}0\}$  and  $\{10\bar{1}1\}$  are the most closely packed planes after the basal plane, and any non-basal slip would be expected on one or other of these two planes.

No true double slip was observed on any of the polycrystalline creep specimens, but this was felt to be inconclusive, for the following reason. Grains favourably oriented to form cells (basal plane almost parallel to the tensile axis) had only sub-microscopically fine slip, and other grains could deform exclusively by basal slip (non-basal slip being associated with a high critical shear stress), so that there was no reason to expect double slip in these.

A search was made of the literature for evidence of non-basal slip in single crystals of zinc. Mark, Polanyi, and Schmid<sup>21</sup> observed apparent prismatic slip lines in zinc crystals locally pulled into ribbons (*Nachdehnung*), but later Schmid and Wassermann<sup>22</sup> recognized these markings as being due to basal slip in twinned material. Boas and Schmid<sup>23</sup> reported some rather hazy markings on hot-stretched zinc crystals which may have been due to prismatic slip.

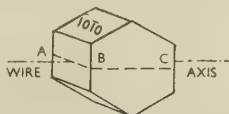


FIG. 21.—Final Orientation of Zinc Crystal after Slip at High Temperature. *ABC* is Plane of Flattened Band.

Some better evidence was published in a little-known paper by Kolesnikov.<sup>24</sup> Single-crystal wires, in which the basal plane was parallel to the wire axis, were stretched at various temperatures. Above 300° C., the crystals necked down, the necked portion being flattened in a plane which was normal to the basal plane. The orientation tended towards that shown in Fig. 21; a crystal of this type eventually broke with a knife-edge fracture along a line parallel to *AB*. Kolesnikov deduced that the crystal had deformed by prismatic slip, although slip lines were not visible. The knife-edge fracture was attributed to slipping apart of the crystal on one or more of the four (cozonal)

prismatic planes which were equally inclined to the wire axis. Kolesnikov concluded that if the crystal had undergone pyramidal slip the crystal would have been drawn to a point, because the six pyramidal planes are not cozonal.

To put the matter beyond doubt some further experiments have been performed. Cylindrical crystals of the critical orientation shown in Fig. 22 were made. The basal plane was inclined at  $2^\circ$  to the wire axis so that basal slip was possible although a high tensile stress would be needed. In Fig. 22 the slip direction subject to the highest resolved shear stress is

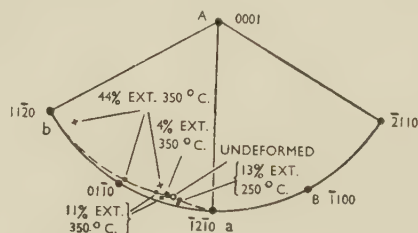


FIG. 22.—Orientations of Two Zinc Crystals of Identical Initial Orientation. Pulled at 250° and 350° C.

KEY.

● Calculated Orientations.      × Observed Orientations.

*a* if the slip plane is the basal plane A. If slip is on a first-order prismatic plane, however, the most highly stressed slip plane is *B*, with *b* as slip direction. In the first case the wire axis would in effect rotate towards *a*, in the other towards *b*, and this constituted a test between the alternatives.

The results for two crystals pulled at 350° and 250° C. are shown in Fig. 22. The first crystal was pulled in stages to a total extension of 44% without fracture. After the final extension, several Laue photographs at different points were taken, but only two of these were sufficiently free of asterism to be capable of interpretation. The widely different orientations derived from these two photographs shows how inhomogeneous the deformation had been. The crystal was flattened in the way described by Kolesnikov. The second crystal, pulled at 250° C., elongated uniformly in the middle portion, but the grips completely restrained the end portions, as would be expected for this orientation if slip was purely basal. The specimen twinned and failed by slipping apart in the twin, after 13% extension. The sense of rotation of the lattice relative to the tensile axes in the two cases was consistent with basal slip at the lower temperature, and prismatic slip at the higher. Figs. 10-13 (Plate LXXIX) are photomicrographs of these two specimens. Fig. 10 is of the specimen deformed at 250° C., and shows characteristic basal slip lines. Their waviness is due to undulations of the surface. Figs. 11-13 are of the specimen pulled 44% at 350° C. Fig. 11 shows prismatic slip with a great deal of cross-slip on the basal plane; this was typical, prismatic slip being invariably accompanied by much basal cross-slip. The beaded aspect of some slip lines is attri-

buted to attack by the salt bath. Figs. 12 and 13 show an extra set of slip lines, seen only after the last extension, and then only in a few places. These are probably due to pyramidal slip combined with cross-slip on the basal plane, but the orientation was so variable at this late stage of deformation that this could not be confirmed. The identity of the prevalent prismatic slip, however, was firmly established from measurements of the slip lines at various azimuths after only 11% extension, when the orientation was still fairly uniform.

The shear stress required for prismatic slip has not yet been determined, but it is certainly much greater than the stress for basal slip at the same temperature. Thus the crystal pulled at 250° C., which became twinned, thereafter continued to slip on the basal plane in the twin at a much reduced load.

#### 4. THE GROWTH OF CELLS

In further search of evidence on the nature of cell boundaries, the following experiment was carried out. Specimen No. 16 was given a small extension in creep at 330° C. and various fields with well-developed cells were photographed. Fig. 14 (Plate LXXIX) is one such field. The specimen surface was now ground lightly and repolished, only about 0.2 mm. thickness of metal being taken off. The specimen was made to



FIG. 23.—(a) Migration of a Cell Boundary. (b) Migration of a Cell Boundary as Viewed on a Repolished Surface.

creep further at the same temperature, and rephotographed at intervals. Figs. 15 and 16 (Plate LXXIX) show the same field as Fig. 14 after repolishing and further creep. The dark (tilted) bands in these two photographs represent regions traversed by cell boundaries. (In the absence of the intermediate polish, only the new position of the cell boundaries would have been visible.)

The change of shape associated with the migration of cell boundaries, and accentuated in this experiment, can only be understood if the boundaries are simple dislocation arrays. Areas traversed by ordinary large-angle grain boundaries do not become tilted, although there is viscous slip at the various positions assumed by the boundaries. Fig. 23 is intended to show graphically what is seen in the microscope: (a) when the specimen is not given a repolish and (b) when it is repolished.

The tilted bands of Figs. 15 and 16 (Plate LXXIX) cannot be due to viscous displacement at cell boundaries combined with continuous migration, because a boundary which does not migrate, such as *AB* in Figs. 14 and 15, hardly shows in the later photographs. On the viscous-flow hypothesis, a high step should develop at such a place.

#### IV.—DISCUSSION AND CONCLUSIONS

(1) At creep temperatures below about 300° C. the tilt axes relating the orientations of neighbouring cells are approximately parallel to the basal plane.

(2) At temperatures above about 300° C., the tilt axes are not always parallel to the basal plane, though there is a tendency for this to be so.

(3) At all temperatures, the observed tilt axes are consistent with the hypothesis that the cell boundaries are ordinary bend planes, that is, they consist of arrays of edge dislocations. Generally, the tilt axis is not normal to a slip direction, and it follows that the boundary contains two sets of dislocations in such cases.

(4) The observation that the tilt axis is approximately parallel to the cell boundary, where this can be unambiguously tested, is also consistent with (3).

(5) Cell structures form most readily in grains so oriented with respect to the tensile axis that they cannot easily slip on the basal plane. Under these circumstances small obstacles can arrest a sufficiently large number of dislocations to nucleate cell boundaries; dislocations do not get a chance to travel far from their sources, and the back-pressure of the arrested dislocations soon blocks the sources. In more favourably oriented grains dislocations tend to move right to the grain boundaries, forming no cells, which allows each dislocation source to produce a visible slip line. On this basis it is possible to account for the fact that slip and cell formation are mutually exclusive.

In this hypothesis the constraint exerted by neighbouring grains is neglected. The main effect of the complicated interaction must be a greatly increased complexity of the cell pattern, differentiating it from isolated bend planes or kink bands (pairs of bend planes) such as are found in single-crystal zinc creep specimens.<sup>19</sup> Grains in a polycrystal which are favourably oriented for slip do not form cells in spite of the constraint exerted by their neighbours; the constraint seems to be taken up by continuous bending of the slip lines.

It can be argued that the mode and degree of deformation of a grain in a polycrystal is determined primarily by the stresses imposed upon it by its neighbours, the resultant of which may be quite different from the simple tension which is applied externally. In the absence of preferred orientation, however, the assumption that this tension acts directly on each grain taken as a whole, must be at least an approximation to the truth. In this case the deductions made from Table I remain valid.

The foregoing conclusions are consistent with the interferometric studies of cell formation in zinc published by Gifkins and Kelly<sup>25</sup> at the time of writing. These investigators confirmed an earlier suggestion of Ramsey<sup>6</sup> that cells are formed when the lattice becomes very unevenly bent, the sites of most severe curvature acting as dislocation traps and so turning into cell boundaries. Ramsey thought that uniformly bent grains would have difficulty in becom-



ing polygonized afterwards, and this may well be the reason why grains favourably oriented for slip form no cells.

(6) Cell boundaries migrate readily under stress, producing thereby a change in the shape of the grain. This is consistent with the hypothesis proposed in (3). The observations made exclude the possibility that any viscous slip occurred at the cell boundaries. It also serves to explain why, as Wood and Suiter<sup>4</sup> have emphasized, cells can grow appreciably only when stress is applied. In the absence of an external stress, the change in shape of some grains, occasioned by cell growth, would soon set up a back stress in neighbouring grains which would arrest further growth.

Cottrell<sup>26</sup> has put forward an alternative explanation based on the ease with which dislocations can climb out of their slip planes if they are moving through a field of other dislocations. The great distances, on an atomic scale, through which dislocations have to climb<sup>27</sup> to form uniform arrays when they are initially concentrated in a few coarse slip bands, can be suggested as a reason why grains containing such bands do not form cells.

(7) Above about 300° C. zinc can slip on {10 $\bar{1}$ 0} planes in the close-packed [12 $\bar{1}$ 0] direction, and there is some evidence that slip on {10 $\bar{1}$ 1} planes is also possible, though rare. Such abnormal slip is always accompanied by cross-slip on the basal plane. Metallographic evidence of such slip has been restricted to single crystals; polycrystals showed little visible slip of any kind at 350° C. Non-basal slip is consistent with observation (2), above.

The observation that zinc is capable of non-basal slip at sufficiently high temperatures links neatly with observations on some other hexagonal close-packed metals. Magnesium crystals are known to slip on the pyramidal planes {10 $\bar{1}$ 1} as well as on the basal planes, at room temperature, if the tensile axis is inclined at less than 6° to the basal plane,<sup>28</sup> and at higher temperatures pyramidal slip becomes more prevalent.<sup>29</sup> No prismatic slip has been detected. Titanium slips preferentially on {10 $\bar{1}$ 0} and {10 $\bar{1}$ 1} planes, the former being predominant.<sup>30</sup> Basal slip in suitably oriented titanium crystals has also been observed, but it has a higher critical shear stress than the other planes.<sup>31</sup> A recent paper,<sup>32</sup> however, gives grounds for supposing that basal slip may be easier than pyramidal slip. At higher temperatures pyramidal slip becomes more common.<sup>33</sup> These observations can be related to the relative densities of atomic packing on the various planes which are given in Table II (columns 3–5).

Column 6 lists the observed slip planes in the order of critical shear stresses, the plane in bold type being far the most important. The observations in Table II may be interpreted to a first approximation, by making two assumptions: (i) the more densely packed a lattice plane, the more easily it can act as slip plane, and (ii) as the temperature is raised, the less densely packed planes acquire a better chance of acting as slip planes.

The first hypothesis is necessarily inexact because of

the ambiguity of the concept of packing density when applied to the puckered sheets which make up {10 $\bar{1}$ 0} and {10 $\bar{1}$ 1} planes. In a "puckered" sheet some rows of atoms form zigzag lines; the packing densities in Table II were obtained by projecting the positions of all atoms in the puckered sheets into the lattice plane. The idea behind the hypothesis is, of course, that dense packing inside a sheet of atoms goes with loose binding between neighbouring planes and, therefore, easier slip. Puckering of a sheet of atoms counteracts the effect of close packing; this no doubt accounts for the fact that {10 $\bar{1}$ 1} is more favoured, in comparison with {10 $\bar{1}$ 0}, than the listed packing densities would lead one to expect, for {10 $\bar{1}$ 0} is more puckered than {10 $\bar{1}$ 1} in all cases.

TABLE II.—*Packing Densities on Slip Planes in Close-Packed Hexagonal Metals.*

Metal	<i>c/a</i>	Packing Densities of :			Observed Slip Planes in Order of Ease of Operation		
		{0001}	{10 $\bar{1}$ 0}	{10 $\bar{1}$ 1}			
Titanium .	1.587	1.000	1.092	0.959	{10 $\bar{1}$ 0}	{10 $\bar{1}$ 1}	{0001}
Magnesium	1.624	1.000	1.066	0.940	{10 $\bar{1}$ 0}	{0001}	{10 $\bar{1}$ 1}
Zinc .	1.856	1.000	0.933	0.846	{0001}	{10 $\bar{1}$ 1}	{10 $\bar{1}$ 0}
Cadmium .	1.886	1.000	0.918	0.816	{0001}	{10 $\bar{1}$ 0}	{10 $\bar{1}$ 1}?
					{0001} + ?		

No indications of non-basal slip exist for cadmium, except for an isolated electron micrograph of cross-slip on a cadmium crystal, published by Brown.<sup>34</sup> Arguing purely from the listed packing densities, prismatic slip would seem to be unlikely and pyramidal slip virtually impossible.

It is possible to justify the second hypothesis in the following manner. The width of a dislocation (i.e. the number of dislocated atoms measured parallel to the slip direction) would be expected to increase with temperature, because the periodicity of the lattice is increasingly impaired by thermal vibrations. Mathematical treatment has confirmed this supposition.<sup>35</sup> The wider a dislocation is, the smaller is the intrinsic resistance of the lattice to its motion (the influence of any neighbouring defects being here ignored).<sup>26</sup> This intrinsic resistance also depends sensitively on the density of packing in the slip plane.<sup>26</sup> At a low temperature, then, the actual critical shear stress for the closest-packed plane (which is conditioned by the defect pattern in the unstrained crystal) will exceed the intrinsic resistance to dislocation motion in that plane, but will be smaller than the high intrinsic resistance to dislocation motion in the next most closely packed plane. At a higher temperature, dislocation widths will have increased and the intrinsic resistances to dislocation motion in each of the two planes will have sharply diminished to the point where the actual critical shear stress will be greater than either. The second slip plane then begins to take a part.

#### ACKNOWLEDGEMENTS

The untimely death of Professor Daniel Hanson does not prevent the authors from expressing their

appreciation of his encouragement and support. Professor A. H. Cottrell read the manuscript and suggested a number of improvements, for which the authors are grateful. The zinc used was kindly donated by the National Smelting Co., Ltd., Avonmouth, who also carried out the spectrographic analysis. The paper is published by permission of the Director of the Atomic Energy Research Establishment.

## REFERENCES

1. G. R. Wilms and W. A. Wood, *J. Inst. Metals*, 1948-49, **75**, 693.
2. R. W. Cahn, *ibid.*, 1949-50, **76**, 121.
3. W. A. Wood and W. A. Rachinger, *ibid.*, 1949-50, **76**, 237.
4. W. A. Wood and J. W. Suiter, *ibid.*, 1951-52, **80**, 501.
5. J. Hino, P. G. Shewmon, and P. A. Beck, *Trans. Amer. Inst. Min. Met. Eng.*, 1952, **194**, 873.
6. J. A. Ramsey, *J. Inst. Metals*, 1952-53, **81**, 61.
7. J. A. Ramsey, *ibid.*, 1952-53, **81**, 215.
8. W. A. Rachinger, *Bull. Inst. Metals*, 1952, **1**, (15), 125.
9. W. A. Wood, *ibid.*, 1953, **1**, (21), 198.
10. D. McLean, *J. Inst. Metals*, 1952-53, **81**, 133.
11. D. McLean, *ibid.*, 1952-53, **81**, 287.
12. J. A. Ramsey, *ibid.*, 1951-52, **80**, 167.
13. E. A. Calnan and B. D. Burns, *ibid.*, 1950, **77**, 445.
14. I. S. Servi, J. T. Norton, and N. J. Grant, *Trans. Amer. Inst. Min. Met. Eng.*, 1952, **194**, 965.
15. W. H. J. Vernon and E. G. Stroud, *Nature*, 1938, **142**, 477.
16. M. J. Buerger, *Z. Krist.*, 1934, **89**, 195.
17. M. Smialowski, *Z. Metallkunde*, 1937, **29**, 133.
18. R. W. Cahn, *J. Sci. Instruments*, 1953, **30**, 201.
19. J. Washburn and E. R. Parker, *Trans. Amer. Inst. Min. Met. Eng.*, 1952, **194**, 1076.
20. J. W. Rutter and B. Chalmers, *Canad. J. Physics*, 1953, **31**, 15.
21. H. Mark, M. Polanyi, and E. Schmid, *Z. Physik*, 1923, **12**, 58, 78, 111.
22. E. Schmid and G. Wassermann, *ibid.*, 1928, **48**, 370.
23. W. Boas and E. Schmid, *ibid.*, 1930, **61**, 767.
24. A. F. Kolesnikov, *Zhur. Eksper. Teoret. Fiziki*, 1938, **8**, 1031.
25. R. C. Giffins and J. W. Kelly, *Acta Met.*, 1953, **1**, 320.
26. A. H. Cottrell, "Dislocations and Plastic Flow in Crystals", pp. 64 and 185. 1953: Oxford (Clarendon Press).
27. N. F. Mott, *Phil. Mag.*, 1953, [vii], **44**, 741.
28. E. C. Burke and W. R. Hibbard, Jr., *Trans. Amer. Inst. Min. Met. Eng.*, 1952, **194**, 295.
29. E. Schmid, *Z. Elektrochem.*, 1931, **37**, 447.
30. F. D. Rosi, C. A. Dube, and B. H. Alexander, *Trans. Amer. Inst. Min. Met. Eng.*, 1953, **197**, 257.
31. A. T. Churchman, *Nature*, 1953, **171**, 706.
32. E. A. Anderson, D. C. Jillson, and S. R. Dunbar, *Trans. Amer. Inst. Min. Met. Eng.*, 1953, **197**, 1191.
33. F. D. Rosi and F. C. Perkins, *ibid.*, 1953, **197**, 1083.
34. A. F. Brown, *Advances in Physics*, 1952, **1**, 427.
35. H.-D. Dietze, *Z. Physik*, 1952, **132**, 107.

## APPENDIX

## DERIVATION OF TILT AXIS FROM A LAUE PHOTOGRAPH

Fig. 24 (a) represents a back-reflection Laue photograph on which only one Laue spot, sub-divided into two sub-spots X and Y, is shown. OQ is an arbitrary reference line inscribed on the film. Fig. 24 (b) is the corresponding stereogram, projected along the X-ray beam. A, B are the poles corresponding to X, Y,

respectively. D is the film-to-specimen distance,  $\theta$  is the angle between the incident X-ray beam and the lattice planes responsible for spot X. The other

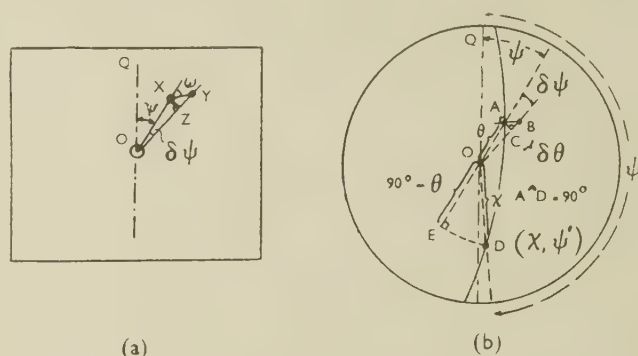


FIG. 24.—(a) Two Sub-Spots on a Back-Reflection Laue Photograph. (b) Construction for Deriving Tilt Axis from Positions of Sub-Spots.

symbols are included in the figures. It is assumed that  $\delta\psi$ ,  $\delta\theta$  are small angles.

Then 
$$XZ \sim OX \cdot \delta\psi = D \cdot \tan 2\theta \cdot \delta\psi$$
 and

$$\begin{aligned} YZ &\sim OY - OX = D[\tan 2(\theta + \delta\theta) - \tan 2\theta] \\ &= D[\tan 2\delta\theta\{1 + \tan 2(\theta + \delta\theta) \cdot \tan 2\theta\}] \\ &\sim 2D \cdot \delta\theta(1 + \tan^2 2\theta) \\ &\sim 2D \cdot \delta\theta \cdot \sec^2 2\theta \end{aligned}$$

Therefore

$$\begin{aligned} \omega &\sim \text{angle } XYZ = \tan^{-1} XZ/YZ \\ &\sim \tan^{-1} (D \cdot \tan 2\theta \cdot \delta\psi / 2D \cdot \delta\theta \cdot \sec^2 2\theta) \end{aligned}$$

$$\begin{aligned} &\sim \tan^{-1} \left( \frac{\sin 4\theta}{4} \cdot \frac{\delta\psi}{\delta\theta} \right) \\ \therefore \frac{\delta\psi}{\delta\theta} &\sim \frac{4 \tan \omega}{\sin 4\theta} \quad \dots (1) \end{aligned}$$

On the stereogram, Fig. 24 (b), a great circle is now entered through A to intersect the arc AB at right angles. A small tilt about an axis, the stereographic projection of which lies anywhere along this great circle, will bring pole A into coincidence with pole B. This great circle is therefore the locus of all tilt axes consistent with the observed positions of X and Y; it is constructed by locating a point D on it which is  $90^\circ$  from A. To derive the necessary formulæ we extrapolate AO to E so that E is  $90^\circ$  from A, and join ED by a great circle. Let D be at an angular distance  $\chi$  from O. An expression may then be obtained for  $\chi$  by solving the spherical triangle OED. A is the pole of the great circle ED, so that

$$\begin{aligned} \angle EAD &= \text{angle } EAD \sim \text{angle } CAB \\ (\text{because angle } BAD &= 90^\circ \sim \text{angle } CAE) \\ &\sim \tan^{-1} BC/AC \sim \tan^{-1} \{\delta\theta/(\delta\psi \sin \theta)\} \\ \text{Angle } EOD &= 180^\circ + \text{angle } QOA - \text{angle } QOD = \\ &180^\circ + \psi - \psi'. \end{aligned}$$



Solving triangle  $OED$  in which angle  $OED = 90^\circ$ :

$$\sin(90^\circ - O\hat{D}) = \cos(E\hat{O}) \cdot \cos(E\hat{D})$$

or

$$\begin{aligned} \sin(90^\circ - \chi) \\ \sim \cos(90^\circ - \theta) \cdot \cos \left[ \tan^{-1} \left( \frac{\delta\theta}{\delta\psi} \cdot \frac{1}{\sin \theta} \right) \right], \end{aligned}$$

so that from equation (1)

$$\begin{aligned} \cos \chi &\sim \sin \theta / \left[ 1 + \left( \frac{\delta\theta}{\delta\psi} \cdot \frac{1}{\sin \theta} \right)^2 \right]^{\frac{1}{2}} \\ &\sim \sin \theta / \left[ 1 + \frac{\sin^2 4\theta}{16 \tan^2 \omega} \cdot \frac{1}{\sin^2 \theta} \right]^{\frac{1}{2}} \quad (2) \end{aligned}$$

It is possible to solve triangle  $OED$  using a second method, i.e.

$$\sin(E\hat{O}) = \tan(90^\circ - \text{angle } EOD) \cdot \tan(E\hat{D})$$

or

$$\sin(90^\circ - \theta) \sim \cot(\psi - \psi') \cdot \delta\theta / (\delta\psi \cdot \sin \theta)$$

so that from equation (1),

$$\cot(\psi - \psi') \sim \frac{\tan \omega}{\cos 2\theta} \quad (3)$$

$\theta$ ,  $\psi$ , and  $\omega$  are measured from the film, and by substituting these in equations (2) and (3),  $\chi$  and  $\psi'$  are calculated. These angles define  $D$ , which can now be plotted, and the great circle joining  $A$  and  $D$  is drawn.

This procedure is repeated for several pairs of sub-spots, and the intersection of the great circles then locates the tilt axis. If the angle of rotation about the tilt axis,  $\lambda$ , is desired, this can be calculated from the equation

$$\lambda = A\hat{B} / \sin(A\hat{T})$$

where  $T$  is the stereographic plot of the tilt axis.  $A\hat{T}$  is measured on the stereogram, and it can be shown that

$$A\hat{B} = \frac{\delta\psi}{4 \tan \omega} (16 \sin^2 \theta \cdot \tan^2 \omega + \sin^2 4\theta)^{\frac{1}{2}}$$

$\delta\psi$  can either be measured directly or, somewhat more accurately, calculated from

$$\delta\psi = XY \cdot \sin \omega / OX.$$

# 1545 METHODS FOR DETERMINING THE LIQUIDUS POINTS OF TITANIUM-RICH ALLOYS\*

By W. HUME-ROTHERY,† O.B.E., F.R.S., MEMBER, and  
D. M. POOLE,‡ B.Sc., M.Sc., STUDENT MEMBER

## SYNOPSIS

Two methods are described for determining the liquidus points of alloys of titanium or other metals which are too reactive for the use of conventional thermal analysis. In one method, the alloy is first prepared in an argon-arc furnace, and small specimens, in titanium containers, are heated to successive temperatures and quenched. Microscopical examination will then usually permit distinction between specimens quenched from the totally liquid or partly liquid field, and the liquidus point of a titanium-nickel alloy has been determined as lying within a temperature bracket of 4° C. In the second method, specimens of varying composition are quenched from a fixed temperature in a container whose composition lies on the solidus curve at the temperature concerned. The liquidus point is thus determined by a composition bracket, and the totally and partly liquid specimens are distinguished both microscopically, and by the fact that the container is attacked much more rapidly when the totally liquid field is reached.

## I.—INTRODUCTION

THE determination of the liquidus points of reactive alloys of high melting point, such as those of titanium, is a matter of great difficulty. The conventional methods of thermal analysis require a relatively large amount of metal, which in the pure state is costly, whilst the long periods involved by slow cooling from high temperatures result in contamination by almost all refractories. The present note describes two methods for determining the liquidus points of such alloys, which involve the use of relatively small quantities of material under conditions in which contamination is unlikely to occur.

## II.—PRINCIPLE OF METHOD

The principle underlying the first method can be understood from Fig. 1. Suppose that  $TL$  and  $TS$  are the liquidus and solidus curves for a solid solution in a metal  $T$ . Consider an alloy of composition  $x$ , whose solidus point is at  $S_x$ . This point can be found by conventional methods of quenching and microscopical examination, using specimens which have been prepared in an argon-arc melting furnace, or in an H.F. induction furnace if suitable refractories are available. Suppose now that a number of small containers of composition  $x$  are prepared with the shape shown in Fig. 2, and that a small pellet of alloy of composition  $S_1$  is placed in one of these, and then heated to the temperature of  $S_x$  in a vacuum or suitable inert atmosphere. At this temperature the alloy of composition  $S_1$  will partly melt to give solid of composition  $S_x$  and liquid of composition  $L_x$ . Since the container itself has the composition  $S_x$ , we

may expect the reaction between the liquid and the container to be slow, and if the specimen is rapidly cooled after a period of, say, 15 min., we may expect little attack of the container, whilst the micro-

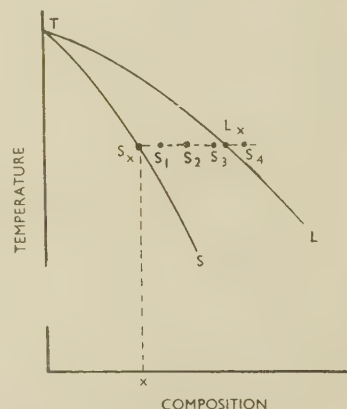


FIG. 1.—Hypothetical Phase Diagram Illustrating the Principle of the Method.



FIG. 2.—Sketch of Container.

structure of the alloy will enable the chilled liquid to be distinguished from the portion of the pellet remaining unmelted at the temperature of  $S_x$ . The experiment can be repeated with pellets of compositions  $S_2$ ,  $S_3$ , and  $S_4$ . If these have the compositions shown in Fig. 1, the alloy  $S_4$  will be the

\* Manuscript received 4 November 1953.

† Royal Society Warren Research Fellow, and University

Lecturer in Metallurgical Chemistry, Oxford.

‡ Inorganic Chemistry Laboratory, Oxford.



first alloy lying outside the liquidus, and with this alloy we may expect a relatively rapid attack of the container, whilst the microstructure should show only chilled liquid inside the container. In this way the liquidus point is determined by a composition bracket, and there is a double indication of the stage at which the alloy inside the container has been heated within the totally liquid field.

### III.—EXPERIMENTS WITH COPPER-TIN ALLOYS

The above method was tested by experiments on copper-tin alloys, using containers drilled from a bar containing 5 wt.-% tin, which was kindly presented by the British Non-Ferrous Metals Research Association. After annealing to equilibrium, the solidus point of the container was found to be 926° C., and the liquidus point at this temperature is at 17.4 wt.-% tin. Alloys containing 10, 15, and 20 wt.-% tin were prepared, and a small slug of each alloy was heated in one of the containers in a sealed silica tube for 30 min. at 926° C., after which the tube was rapidly cooled by quenching in water. The containers with their inserts were then sectioned, ground, polished, and etched, and the experiments showed that the liquidus could easily be placed within a composition bracket of 5%, and that both the microstructure and the attack of the container indicated when the insert had reached the totally liquid field.

Fig. 3 (Plate LXXX) shows a section through the 15% tin alloy at a place where there was a sharp angle in the container. The alloy is in the partly liquid state at 926° C., and there is comparatively little rounding at the corner, whilst the unmelted solid is clearly distinguished from the chilled liquid. Fig. 4 (Plate LXXX) is a similar photograph of the 20% tin alloy after quenching from 926° C., and here the much greater rounding of the previously sharp corner is apparent, indicating a greater attack of the container; the internal structure is entirely of chilled liquid. A much closer bracket could undoubtedly have been obtained, but as the interest of the work was in titanium alloys, these experiments with copper alloys were not carried further.

It then appeared possible that, provided the rates of diffusion were not too great, the liquidus might be obtained directly from the microstructures, by heating alloys of a given composition in pure copper containers to successive temperatures, followed by quenching and microscopical examination. The theory of this method is less certain, because some reaction between the copper container and the semi-liquid insert may occur. The method was tested with copper-tin alloys, and was again found to be satisfactory. The microstructures of the semi-liquid and totally liquid alloys were readily distinguished, and the method was then applied to titanium alloys.

### IV.—EXPERIMENTS WITH TITANIUM-NICKEL ALLOYS

A specimen of a titanium-nickel alloy containing ~23.5 wt.-% nickel was prepared in an argon-arc furnace, using the purest I.C.I. iodide titanium, and pure nickel shot.\* Small containers were made out of I.C.I. Grade II iodide titanium, the internal diameter of the hole being approximately  $\frac{5}{32}$  in. Specimens were heated at successive temperatures in an atmosphere of argon in sealed silica tubes, and were then quenched in air, and examined microscopically. Fig. 5 (Plate LXXX) illustrating the structure obtained after quenching from 1184° C., shows relatively large crystals of undissolved solid together with chilled liquid. The latter consists of a fine structure of dendrites of  $\beta$ -titanium † in a light background, which on further etching showed the ( $\beta$ -Ti + Ti<sub>2</sub>Ni) eutectic when examined at high magnification. Fig. 6 (Plate LXXX) shows the same alloy after quenching from 1206° C.; at this temperature a very few crystals of undissolved solid remain, most of which have floated to the upper half of the ingot. Fig. 7 (Plate LXXX) shows the structure after quenching from 1210° C., and here there is no sign of undissolved solid. The containers underwent little or no attack from the inserts, and the liquidus point was determined by a temperature bracket of 6° C. After the experiments, the containers of the two critical alloys were filed away from the inserts, and the latter were analysed by Johnson, Matthey and Co., Ltd., with the following results:

	Quenched from 1206° C. Partly Solid	Quenched from 1210° C. Totally Liquid
Titanium, %	78.49	78.70
Nickel, %	21.49	21.24

The closely agreeing values for the two specimens showed that the method was consistent, and that relatively little attack of the container had occurred. In view of the small size of the specimens any marked attack of the container would have caused a large increase in the titanium content.

The use of a sealed silica tube is possible only up to temperatures of the order of 1200°–1300° C., and for higher temperatures the following arrangement has proved satisfactory. The container of Grade II iodide titanium is supported on a sling of sheet titanium, and is covered with a piece of titanium foil; alternatively, the container is provided with a titanium plug cap. The assembly is hung by means of molybdenum wire in a vertical platinum-wound resistance furnace of the type described by Harris and Hume-Rothery.<sup>1</sup> The molybdenum wire passes through a vertical glass tube at the top of the furnace, and is attached to a small iron cylinder which can be moved up and down by means of a magnet. The temperature is measured by means of a thermo-

\* This work was done at the Atomic Energy Research Establishment, Harwell, and we must thank Dr. H. M.

Finniston and Dr. M. B. Waldron for their kind help.

† This has, of course, changed to  $\alpha$ -titanium on cooling.

couple, and at the end of the experiment, the container is lowered rapidly\* into the cold part of the furnace assembly, and from the high temperatures concerned, this produces a "quench" which in some cases is sufficiently drastic for a distinction to be made between alloys cooled from the totally liquid and from the partly liquid state. Where more rapid cooling is required, we have succeeded in quenching into a container of silicone oil placed in the cold part of the furnace. At temperatures approaching that of the melting point of pure titanium ( $1660^{\circ}\text{C.}$ ), the titanium sling may be replaced by one of zirconium or molybdenum, and the plug cap should be used.

#### V.—DISCUSSION

Experiment alone can determine whether the simple method of heating an alloy in a container of the pure solvent metal is suitable for a given system. Where it is applicable, the method is simple and economical, whilst the danger of contamination from refractories is avoided. If the system is such that rapid attack of a pure metal container occurs, the alternative method of using a container whose composition is that of the solidus point at the temperature concerned

should be applicable. This method is equally simple and economical, but involves the additional labour of preparing a series of containers. It also involves a knowledge of the solidus curve, but this, of course, will generally be required if an equilibrium diagram is being determined. Many alternative devices for the rapid cooling of a container from high temperatures can be devised, and it is suggested that one or other of the above methods should permit a reasonably accurate measurement of many liquidus curves which have previously been regarded as too difficult for determination.

#### ACKNOWLEDGEMENTS

The authors must express their thanks to Professor Sir Cyril Hinshelwood, F.R.S., and to Dr. F. M. Brewer for laboratory accommodation and many other facilities which have encouraged their researches.

#### REFERENCE

1. G. B. Harris and W. Hume-Rothery, *J. Iron Steel Inst.*, 1953, **174**, 212.

---

\* This operation can be carried out in a fraction of a second.



# ISOTHERMAL TRANSFORMATIONS OF HYPO-EUTECTOID ALUMINIUM BRONZES \*

1546

By R. HAYNES,† B.Met., Ph.D., A.I.M., JUNIOR MEMBER

## SYNOPSIS

A binary hypo-eutectoid copper-aluminium alloy and similar alloys containing small amounts of nickel have been transformed isothermally in the range 350°–560° C., and the results have been plotted as time/temperature/transformation diagrams. The course of the transformations is described, and the mechanism of formation of the cellular eutectoid is discussed.

Nickel has little effect on the rates of transformation, but 3% nickel results in the formation of a double knee in the curve representing the start of the eutectoid reaction.

An ordered martensitic phase is obtained when the high-temperature phase,  $\beta$ , is quenched. Neither a microstructural change associated with an ordering reaction, nor the temperature at which martensite first forms, has been detected in the range 560°–350° C.

## I.—INTRODUCTION

INVESTIGATIONS of the isothermal transformations of non-ferrous alloys have been few,<sup>1-8</sup> and have been concerned mainly with copper-aluminium alloys. With the exception of one study of a hypereutectoid alloy, the investigations have been confined to alloys of eutectoid composition; the behaviour of both eutectoid and hypereutectoid alloys is complicated. The work described in the present paper was undertaken to investigate the behaviour of hypo-eutectoid alloys during isothermal transformation and to study the effect of small additions of nickel to a binary hypo-eutectoid alloy.

## II.—ALLOYS AND METHOD

Alloys, whose compositions are given in Table I, were prepared from electrolytic copper, super-purity aluminium, and Mond nickel shot. These were melted in a gas-fired furnace, using a plumbago crucible and a cover of charcoal to protect the metal from oxidation. The alloy was cast into a warm cast-iron mould of 2-in.-square cross-section, and ingots weighing about 10 lb. were produced. Casting temperatures, which were about 200° C. above the respective melting points of the alloys, are shown in Table I.

TABLE I.—*Compositions of Experimental Alloys.*

Alloy No.	Casting Temp., °C.	Copper, %	Aluminium,* %	Nickel, %	Iron, %	Silicon, %
0	1220	88.59	11.40	Nil	0.01	Nil
1	1225	88.39	10.57	1.02	0.02	Trace
3	1172	86.43	10.54	3.03	Trace	Nil

\* By difference.

After the ingot had been heated to a temperature between 850° C. and 900° C., the metal was forged,

with one reheating, to a 1-in.-square cross-section. At this stage the head of the ingot was cut off and the metal was hot rolled to  $\frac{5}{16}$ -in. bar. The hot-rolling temperature was about the same as that used for the forging.

Samples for analysis, taken from the ends and the middle of the bars, showed that the bars were reasonably uniform in composition. The figures in Table I are the mean of the three analyses on each bar. The major impurities liable to be present have also been determined.

Specimens, approximately  $\frac{3}{16}$ -in. thick, of Alloys 0 and 1 were annealed at 900°  $\pm$  10° C. for 1 hr. in air before immersion in a molten bath containing about 100 lb. of pure lead, which was held within  $\pm$  2° C. of the desired transformation temperature. Since a small amount of the  $\alpha$  phase remained out of solution after treatment at 900° C., Alloy 3 was annealed at 950° C. Several specimens on a jig were introduced into the lead bath simultaneously. Individual specimens were removed by hand and quenched in water after predetermined time intervals, and were examined microscopically. Specimens were etched electrolytically in 1% aqueous chromic acid, as recommended by Coons and Blickwede.<sup>9</sup> The grains of  $\beta$  after annealing at 900° or 950° C. were about 1 mm. in dia.

## III.—EXPERIMENTAL RESULTS

For binary alloys containing 9.4–15.6% aluminium, the phases present below the eutectoid temperature (565° C.) are  $\alpha$  and  $\gamma_2$ , according to Raynor's annotated equilibrium diagram.<sup>10</sup> Below the eutectoid temperature, Alloy 1, containing 1% nickel, lies within the ( $\alpha + \gamma_2$ ) field of the ternary system and Alloy 3, containing 3% nickel, lies on the edge of the ( $\alpha + \gamma_2 + \text{NiAl}$ ) field. When Alloy 3 is cooled slowly, a few particles of the NiAl solid solution are observed,

\* Manuscript received 4 June 1953; in revised form 30 October 1953.

† Assistant Lecturer in Metallurgy, University of Leeds.

but none of this phase has been detected in isothermally transformed specimens. The maximum temperature at which the eutectoid transformation can occur in Alloy 3 is that of the four-phase plane associated with the phases  $\alpha$ ,  $\beta$ ,  $\gamma_2$ , and  $\text{NiAl}$ . This

the Widmannstätten form (Fig. 5, Plate LXXXI). During the initial period, precipitation of  $\alpha$  is very rapid, and an inhomogeneous structure is observed in the  $\beta$  regions (Fig. 6, Plate LXXXI). This quickly disappears and is not observed in specimens which

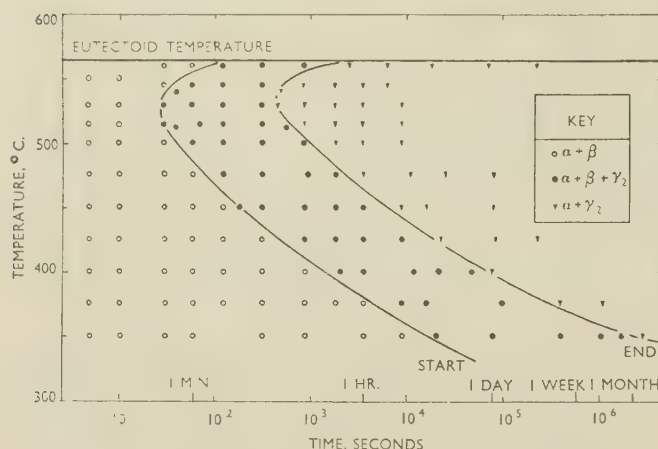


FIG. 9.—Time/Temperature/Transformation Diagram for Alloy 0.

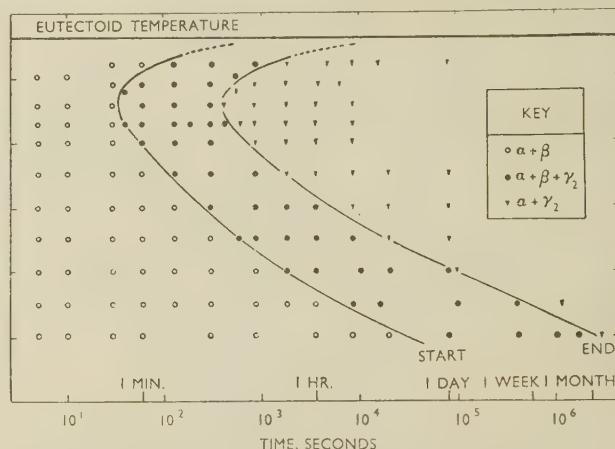


FIG. 10.—Time/Temperature/Transformation Diagram for Alloy 1.

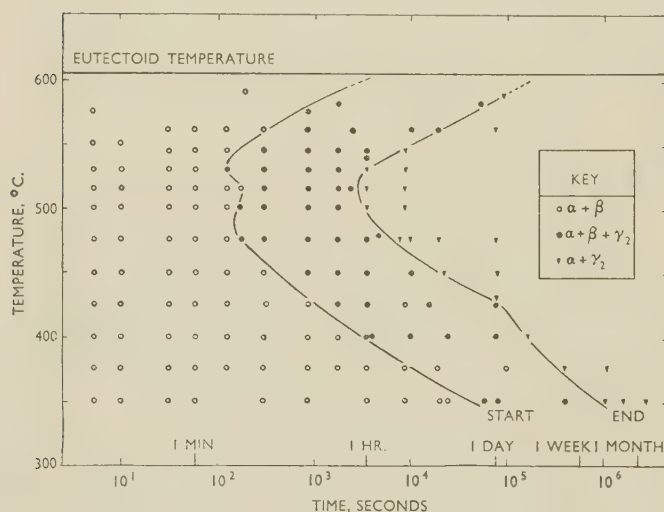


FIG. 11.—Time/Temperature/Transformation Diagram for Alloy 3.

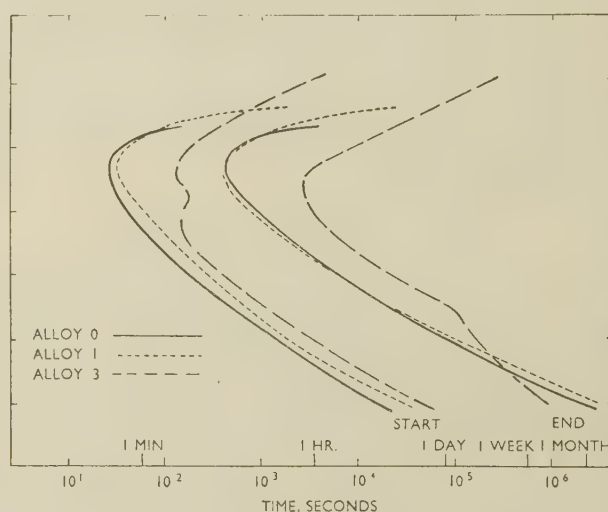


FIG. 12.—Comparison of the Time/Temperature/Transformation Diagrams for Alloys 0, 1, and 3.

temperature has been determined as  $605^\circ \pm 2^\circ \text{C}$ . (unpublished work).

Isothermal transformations in the alloys follow a common pattern, but the rates of the various processes depend upon the temperature of the transformation and the composition of the alloy. The first stage in the transformation is the precipitation of the pro-eutectoid  $\alpha$  which occurs as a precipitate at the grain boundaries and as a Widmannstätten "structure" within the grains (Fig. 1, Plate LXXXI). At transformation temperatures  $100^\circ \text{C}$ . or more below the eutectoid temperature, the  $\alpha$  phase also occurs in a fine acicular form within the grains, side by side with

have been transformed for periods greater than about 1 min. The pro-eutectoid  $\alpha$  formed during isothermal transformation shows a "cored" appearance.

Later in the transformation, the  $\gamma_2$  appears, and this may be regarded as the beginning of the formation of eutectoid. At first the  $\gamma_2$  occurs at the surface of the pro-eutectoid  $\alpha$ , which has precipitated at the grain boundaries of the original  $\beta$  (Fig. 3, Plate LXXXI) and subsequently  $\gamma_2$  appears at the surface of particles of pro-eutectoid  $\alpha$  within the original  $\beta$  grains. The first stage of eutectoid formation consists in the growth of an envelope of  $\gamma_2$  around the pro-eutectoid  $\alpha$ . The envelope seems to start from a point on the surface



of the  $\alpha$  and spreads over the surface in a layer of fairly uniform thickness. Later the envelope thickens in an irregular way and eventually grains of both  $\alpha$  and  $\gamma_2$  grow, irregularly and simultaneously, into the remaining  $\beta$  (Fig. 7, Plate LXXXI), until the latter is all consumed.

Dark points appear in  $\alpha$  during the period in which eutectoid is forming (Fig. 4, Plate LXXXI). Typical micrographs of specimens of Alloy 0, illustrating the progressive change in the microstructure after increasing periods of transformation at 530° C., are shown in Figs. 1, 2, 3, and 4 after 5 sec., 10 sec., 2 min., and 15 min. respectively.

The structure of the eutectoid is mainly cellular, whereas that formed in an alloy of approximately eutectoid composition is lamellar.<sup>1-3</sup> The fineness of

the curves is due to the increasing fineness of the pro-eutectoid  $\alpha$  formed as the transformation temperature is lowered.

#### IV.—DISCUSSION OF RESULTS

The precipitation of a large amount of pro-eutectoid  $\alpha$  is accompanied by considerable diffusion, and it is probable that concentration gradients form within the phases. Eventually  $\gamma_2$  is nucleated at the interface between  $\alpha$  and  $\beta$ , and the  $\gamma_2$  precipitate grows by spreading over the surface of the  $\alpha$ . Probably the growing  $\gamma_2$  precipitate will follow the contour of highest aluminium concentration, since a minimum amount of diffusion is needed to allow this to occur. After the formation of a sheath of  $\gamma_2$  around pro-eutectoid  $\alpha$ ,  $\alpha$  and  $\gamma_2$  grow into the  $\beta$  and  $\alpha$  will relieve any supersaturation by precipitation of  $\gamma_2$  either on the  $\gamma_2$  sheath or on nuclei within the  $\alpha$ .

Eutectoid which forms in alloys of approximately eutectoid composition (12% aluminium) is lamellar,<sup>1-3</sup> while the eutectoid formed in the alloys containing 10.5% aluminium is cellular. The alloy containing 11.4% aluminium forms both kinds of eutectoid. Lamellar eutectoid can be formed in these alloys by slow cooling, and it is possible that lamellar eutectoid cannot form from a phase in which there are considerable concentration gradients.

Nickel has little effect on the rate of transformation, as shown in Fig. 12, but with the addition of 3% nickel there are indications that a double knee is developing in the curve representing the start of the eutectoid reaction.

Comparison of C curves for hypo-eutectoid Alloy 0 and for eutectoid copper-aluminium alloys<sup>1-3</sup> shows that the knee of the curve for Alloy 0 is at a higher temperature (530° C.) than that for eutectoid alloys (500° C.). The induction periods ("eutectoid start") and times to completion of reaction ("eutectoid end") are of the same order of magnitude, but both induction period and time to completion of reaction are shorter for Alloy 0. This may be due to the larger number of interfaces at which  $\gamma_2$  precipitate can be nucleated and the smaller amount of material to transform to eutectoid.

When specimens of the alloys are quenched from the range of temperatures in which the  $\beta$  exists, the  $\beta$  undergoes a martensitic transformation. The martensitic phase,  $\beta'$ , has been shown always to be ordered,<sup>11</sup> and it may be inferred that the ordering occurs before the martensitic reaction. In alloys of eutectoid composition, the ordering reaction has been associated with a change in the microstructure of the  $\beta$  (i.e. the formation of the  $\beta + \beta_1$  structure<sup>2</sup>) which occurs during isothermal transformations in a certain range of temperatures, and the  $M_s$  temperature has been determined.<sup>1-3, 12</sup> Neither of these reactions has been identified in the present examination. The reactions may occur at lower temperatures than those investigated, i.e. 560°–350° C., or the method adopted for investigating the transformations may be in-

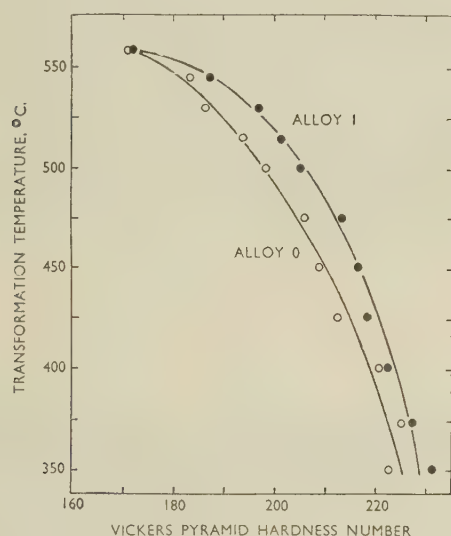


FIG. 13.—Hardness/Temperature Curves for Alloys 0 and 1.

the cellular structure does not vary greatly with temperature, but in specimens transformed at the lower temperatures the acicular  $\alpha$  limits the development of the cellular structure owing to the fineness of the  $\alpha$ . In Alloy 0 containing 11.4% aluminium, a little lamellar eutectoid forms (Fig. 8, Plate LXXXI), but none is observed in the other alloys whose aluminium contents are about 10.5%. If specimens of the alloys are slowly cooled from the annealing temperature to the eutectoid temperature and then isothermally transformed, the eutectoid is lamellar, although a thin envelope of  $\gamma_2$  occasionally surrounds the pro-eutectoid  $\alpha$ .

Results of the studies of the isothermal transformations are shown in the time/temperature/transformation diagrams (Figs. 9–12).

Hardness values of the completely transformed specimens were measured for Alloys 0 and 1, and the results are shown in Fig. 13. The rate at which hardness increases, with respect to degree of undercooling, becomes smaller as the degree of undercooling increases. It is concluded that the shape of

adequate. Earlier investigators<sup>12</sup> observed arrests in the cooling curves of a number of alloys, taken during rapid cooling, in the range 380°–500° C., which were attributed to the martensitic reaction.

#### ACKNOWLEDGEMENTS

The work described in this paper was carried out in the Department of Metallurgy, University of Sheffield.

The author wishes to thank Emeritus Professor J. H. Andrew, Professor A. G. Quarrell, and Mr. A. J. MacDougall for their interest and encouragement; Mr. C. Wollerton for carrying out the analyses; Messrs. Jonas and Colver, Ltd., Sheffield, for forging and rolling the material, and the Department of Scientific and Industrial Research for a maintenance grant, which enabled the research to be carried out.

#### REFERENCES

1. C. S. Smith and W. E. Lindlie, *Trans. Amer. Inst. Min. Met. Eng.*, 1933, **104**, 69.
2. D. J. Mack, *ibid.*, 1948, **175**, 240.
3. E. P. Klier and S. M. Grymko, *ibid.*, 1949, **185**, 611.
4. W. R. Hibbard, Jr., G. H. Eichelman, Jr., and W. P. Saunders, *ibid.*, 1949, **180**, 92.
5. R. H. Fillnow and D. J. Mack, *ibid.*, 1950, **188**, 1229.
6. A. H. Kasberg, Jr., and D. J. Mack, *ibid.*, 1951, **191**, 903.
7. G. R. Speich and D. J. Mack, *ibid.*, 1953, **197**, 549.
8. R. D. Garwood and A. D. Hopkins, *J. Inst. Metals*, 1952–53, **81**, 407.
9. W. C. Coons and D. J. Blickwede, *Trans. Amer. Soc. Metals*, 1945, **35**, 284.
10. G. V. Raynor, *Inst. Metals Annotated Equilib. Diagr. Series*, No. **4**, 1944.
11. A. B. Greninger, *Trans. Amer. Inst. Min. Met. Eng.*, 1939, **133**, 206.
12. V. Gawranek, E. Kaminsky, and G. Kurdjumow, *Metallwirtschaft*, 1936, **15**, 370.



STAINING OF CLAD ALUMINIUM ALLOY SHEETS.

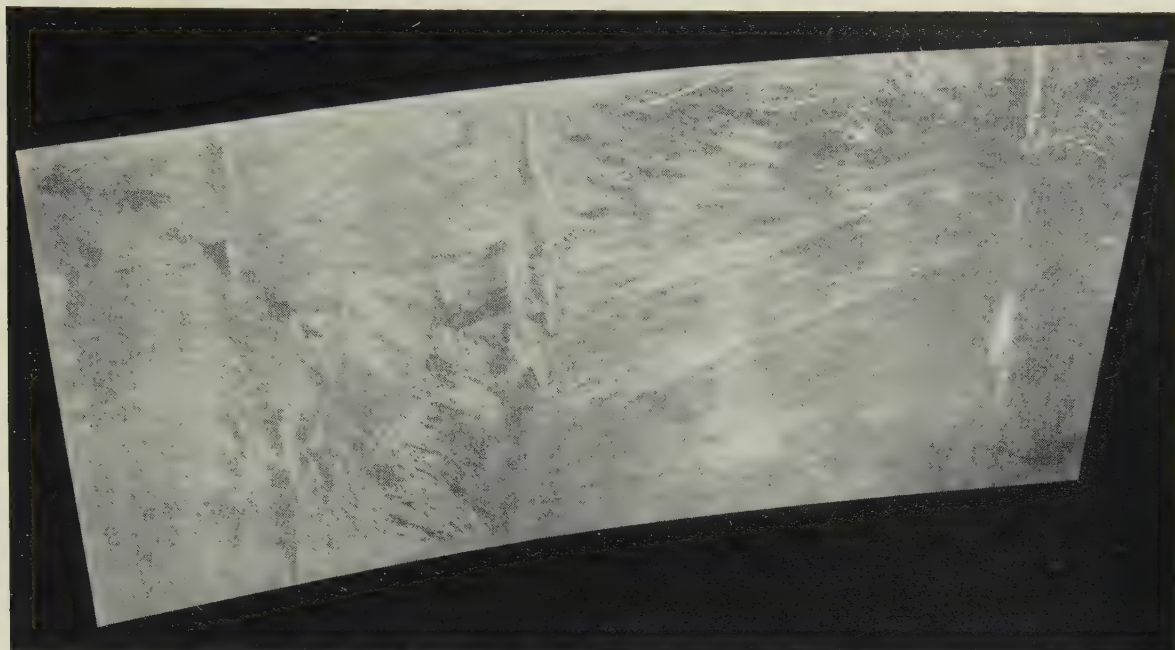


FIG. 1.—Typical Example of Staining.

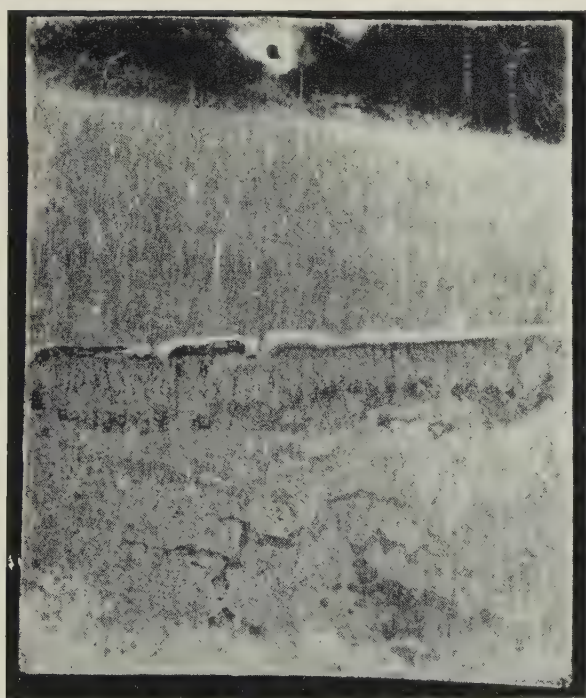


FIG. 2.—Immersion and Instantaneous Staining Produced in an Experimental Bath.  $\times 2$ .

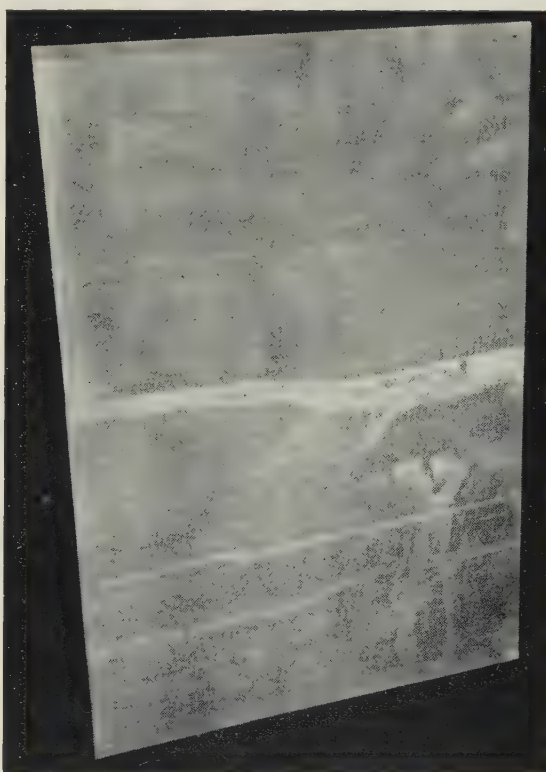
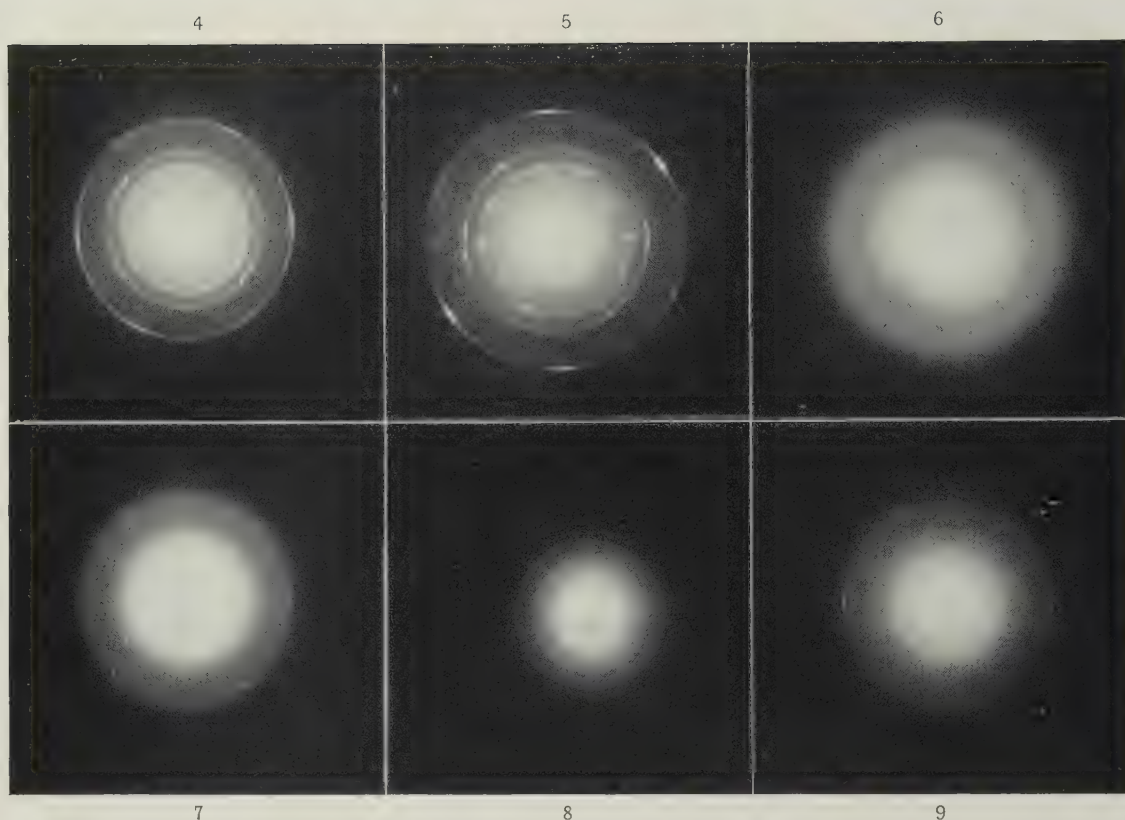


FIG. 3.—Pronounced Staining at the "Salt-Line".



FIGS. 4-9.—Transmission Electron-Diffraction Patterns of Films Stripped from Stained Surfaces of Clad Aluminium.

FIGS. 4 and 5.—Production Stains :  $\eta$ - $\text{Al}_2\text{O}_3$ .

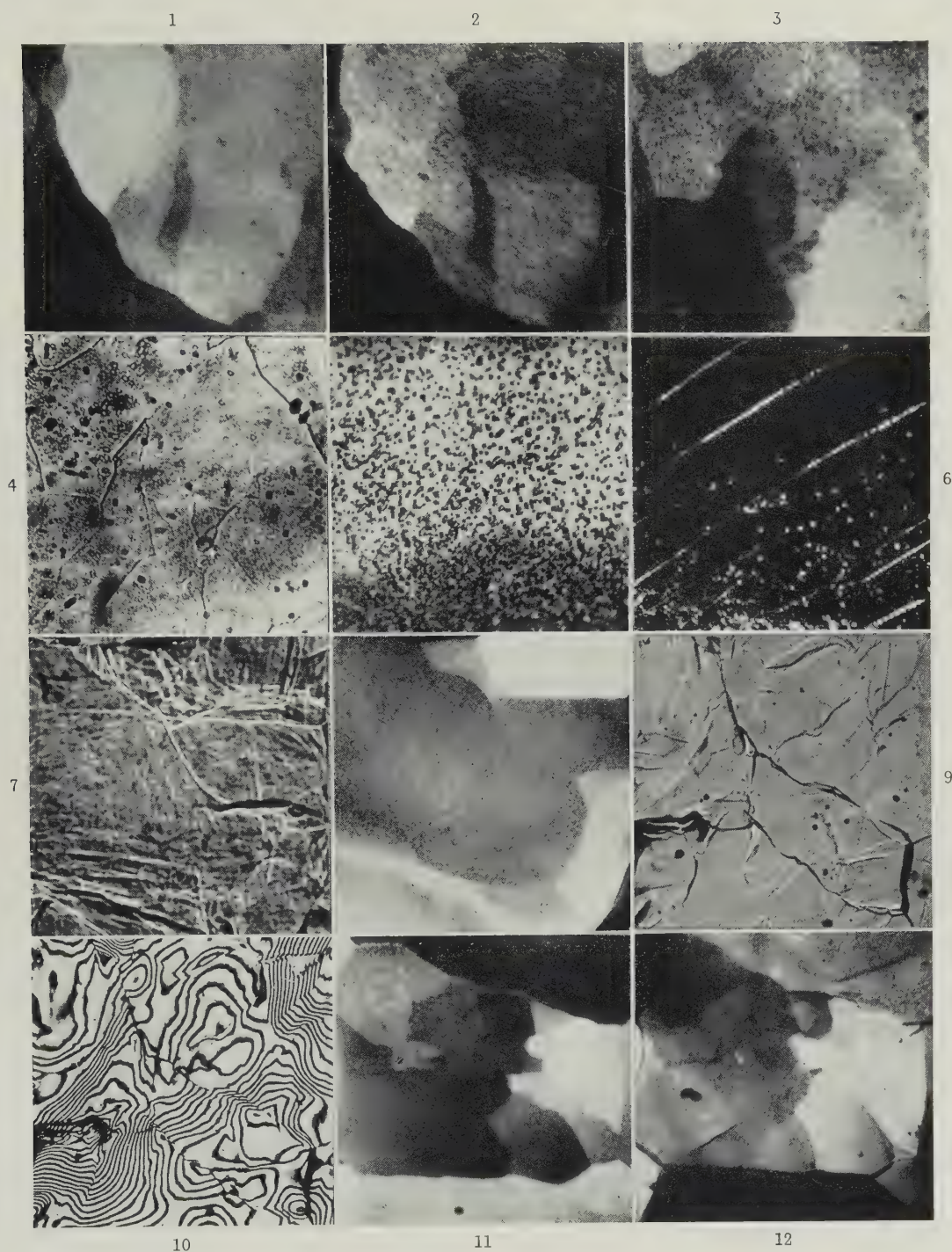
FIG. 6.—Instantaneous Stain as Formed : Amorphous  $\text{Al}_2\text{O}_3$ .

FIG. 7.—Instantaneous Stain Reheated at  $500^\circ\text{C}$ . :  $\delta$ - $\text{Al}_2\text{O}_3$ .

FIG. 8.—Immersion Stain : Sodium Aluminate ( $\text{NaAlO}_2$ ).

FIG. 9.—Composite Stain :  $\eta$ - $\text{Al}_2\text{O}_3$  +  $\text{NaAlO}_2$ .





FIGS. 1 and 2.—Same Area of Aluminium Specimen before and after Polishing and Anodizing Five Times. Photographed with polarized light and wave-plate.  $\times 150$ .

FIGS. 3 and 4.—Specimen Slowly Deformed 15% at 300° C., Showing Correspondence between Cells Revealed by Polarized-Light Method (Fig. 3) and by Deep Etching (Fig. 4).  $\times 150$ .

FIG. 5.—Polygonized Single Crystal of Aluminium, Etched in Lacombe and Beaujard's Reagent.  $\times 110$ .

FIG. 6.—Same Crystal as Fig. 5; Another Area Deeply Etched. Oblique illumination.  $\times 110$ .

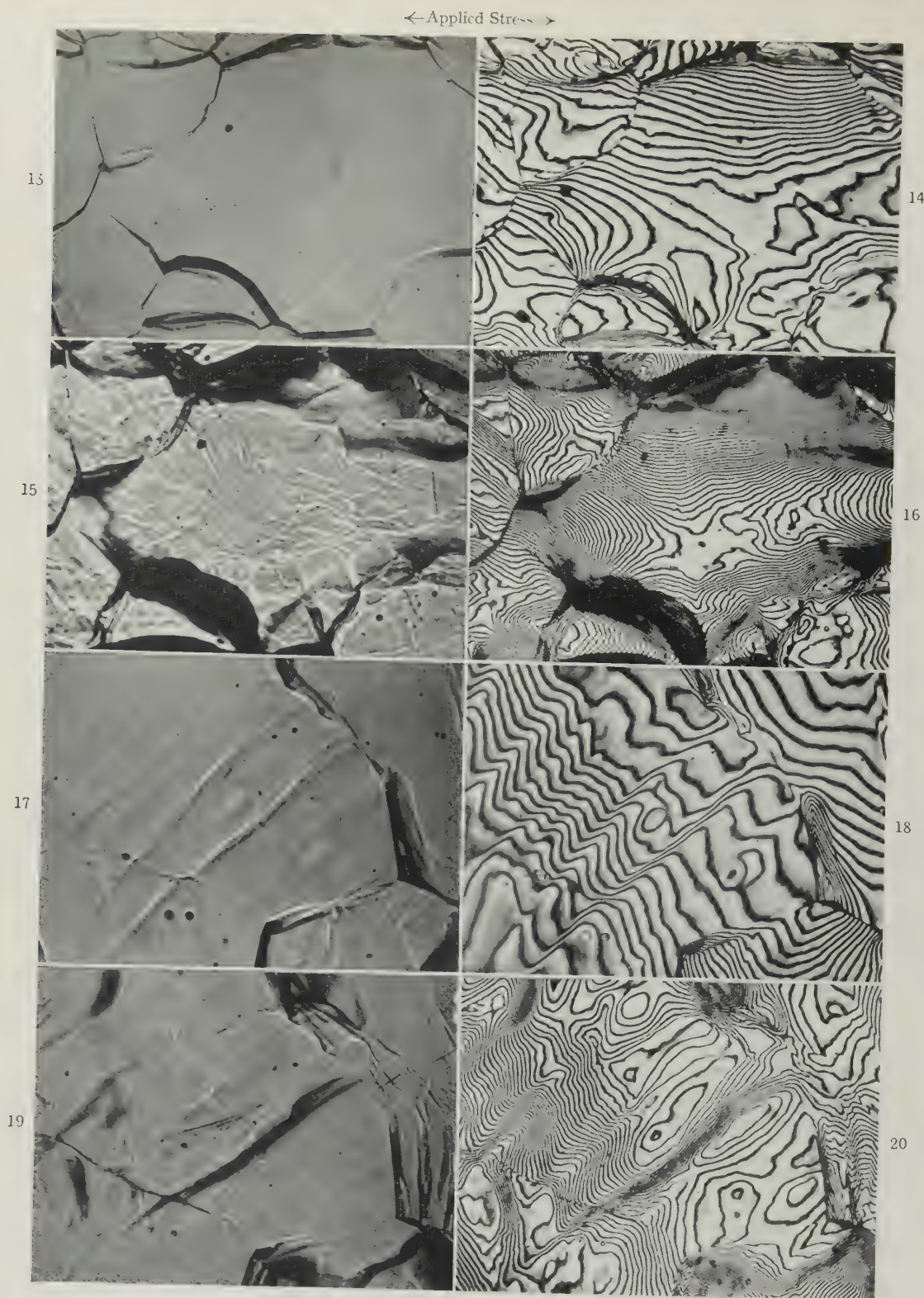
FIGS. 7 and 8.—Specimen Slowly Deformed 15% at 300° C. Surface pattern obtained by out-of-focus method (Fig. 7) compared with the same area after repolishing, anodizing, and photography with polarized light (Fig. 8).  $\times 100$ .

FIGS. 9 and 10.—“White-Line” Pattern and Multiple-Beam Interferogram, Respectively, of Specimen Deformed at 1%/hr. at 325° C., Repolished Flat after 16% Extension, and Further Deformed to 20% at the Same Rate.  $\times 150$ .

FIGS. 11 and 12.—Specimen Deformed at 0.15%/hr. at 300° C. Same area at 11.4 and 12.3% extension, respectively. Polarized-light method. Showing changes in cell configuration.  $\times 100$ .

Reduced by  $\frac{1}{10}$  in reproduction.





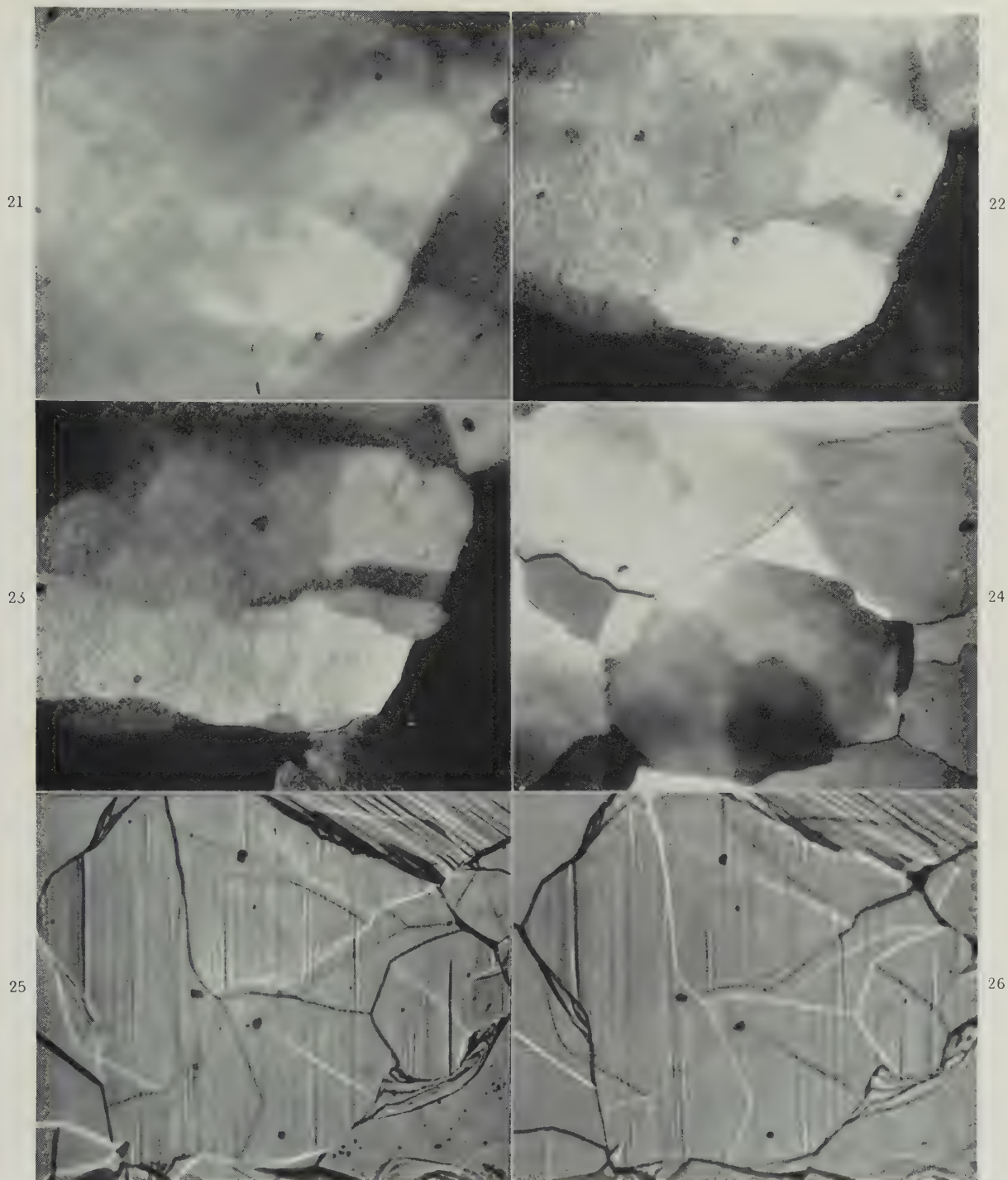
FIGS. 13-20.—Surface Features of Deformed Aluminium, Revealed by White-Line Patterns and Interferometry.  $\times 100$ .

FIGS. 13-16.—Area on a specimen deformed at 1%/hr. at 325° C.; white-line patterns and corresponding interferograms at 2% and 11% extension. Showing surface tilts, grain-boundary "broadening", and triple-point steps.

FIGS. 17-20.—As Figs. 13-16; another area to show slip-like markings, grain-boundary migration, and absence of cell movements.

Reduced by  $\frac{1}{10}$  in reproduction.

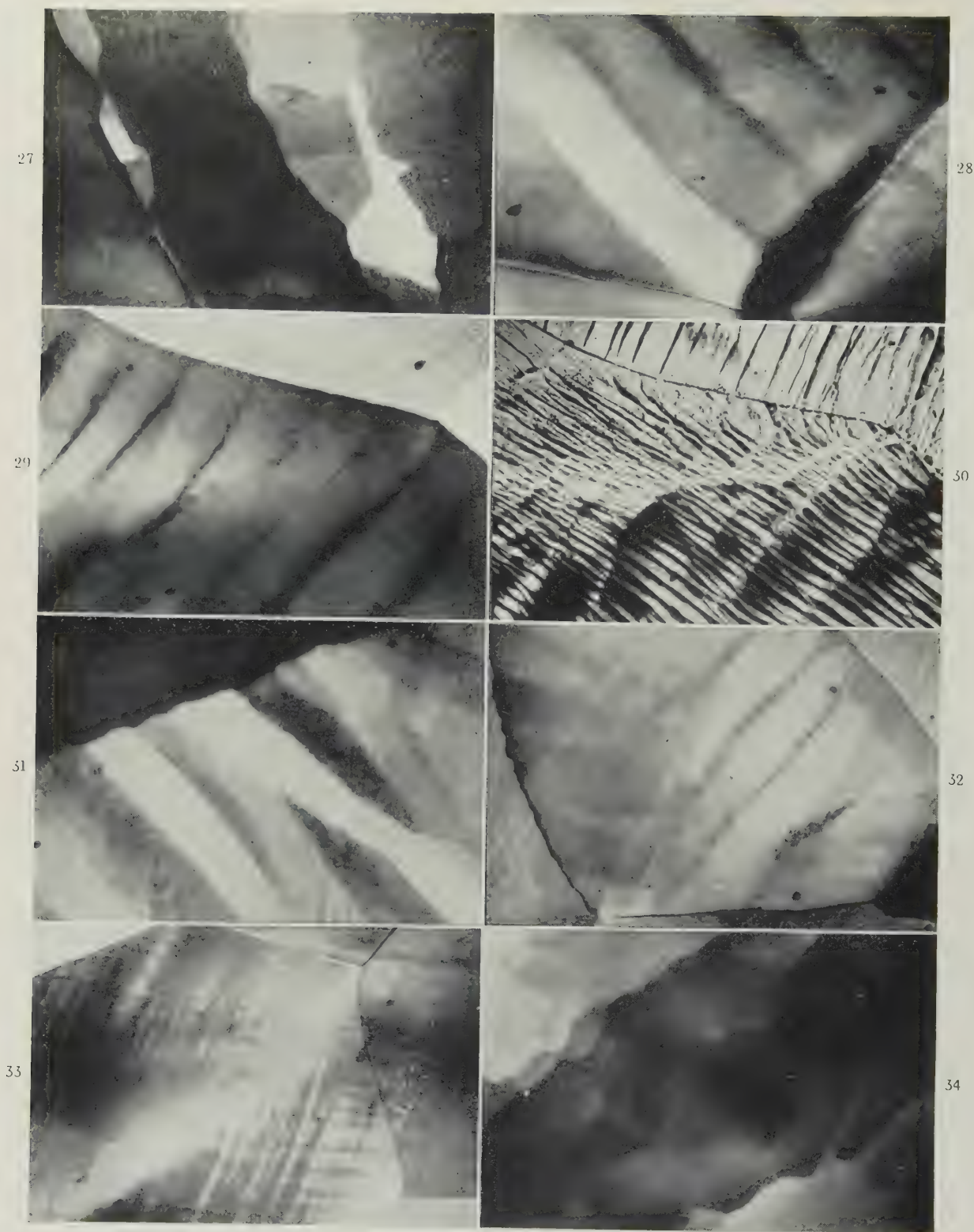




FIGS. 21-23.—Development of Bands and Cells in Coarse-Grained Aluminium Strained at 0.15%/hr. at 300° C. Extensions of 12.2, 16.4, and 18.2%, respectively. Polarized light.  $\times 150$ .

FIG. 24.—Cells in Fine-Grained Specimen, Strained at 0.15%/hr. at 300° C.; 12.8% Extension. Polarized light.  $\times 150$ .

FIGS. 25 and 26.—Pure Zinc. Slowly deformed at rate of 4.5% in 18 hr. at 200° C. Showing white-and-black-line patterns inside and outside focus, respectively.  $\times 200$ .



FIGS. 27-29.—Effect of Rate of Strain on Width of Bands of Cells at 300° C.; 0.15, 21, and 660%/hr., respectively. About 10% extension. Polarized light.  $\times 150$ .

FIG. 30.—Same Specimen Area as in Fig. 29 before Repolishing and Anodizing.  $\times 150$ .

FIGS. 31-33.—Effect of Temperature on Width of Bands of Cells, Deformed at 0.15%/hr. at 200°, 100°, and 22° C.; 10-15% Extension. Polarized light.  $\times 150$ .

FIG. 34.—“Terraced” Band in Coarse-Grained Specimen, Deformed at 0.15%/hr. at 300° C. after 13% Extension. Polarized light.  $\times 150$ .



## CELL STRUCTURES IN HIGH-PURITY ZINC.

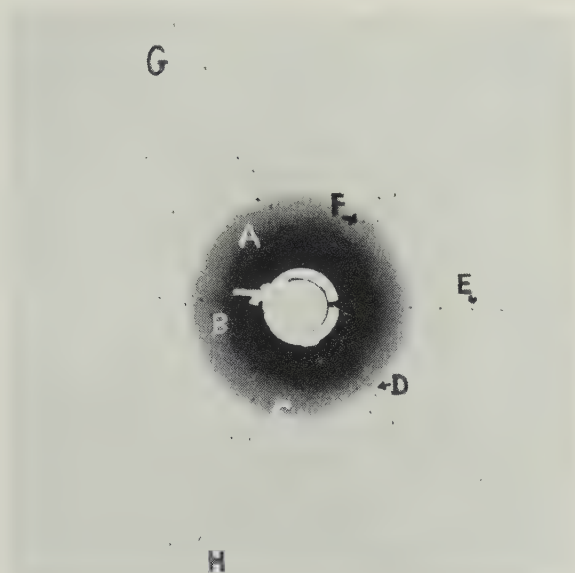


FIG. 1.—Back-Reflection Laue Photograph of a Pair of Creep Cells.

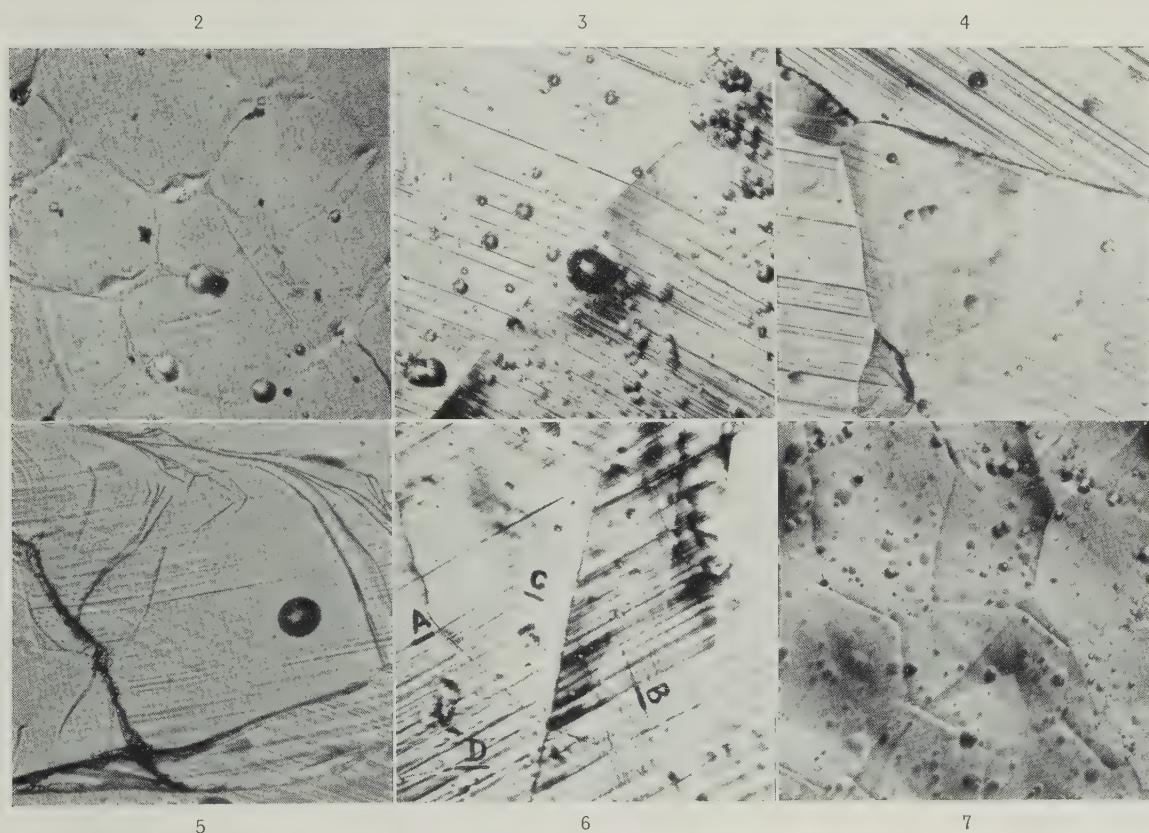


FIG. 2.—Smialowski Structure Revealed by Electrolytic Polishing.  $\times 120$ .

FIG. 3.—Bend Plane and Slip. Specimen No. 4.  $250^{\circ}\text{C}$ .  $\times 90$ .

FIG. 4.—Cell in Corner of Grain. Specimen No. 9.  $250^{\circ}\text{C}$ .  $\times 90$ .

FIG. 5.—Apparent Double Slip. Specimen No. 9.  $250^{\circ}\text{C}$ .  $\times 120$ .

FIG. 6.—Apparent Double Slip. Specimen No. 4.  $250^{\circ}\text{C}$ .  $\times 120$ .

FIG. 7.—Cells Superimposed on Smialowski Structure. Specimen No. 4.  $250^{\circ}\text{C}$ .  $\times 90$ .

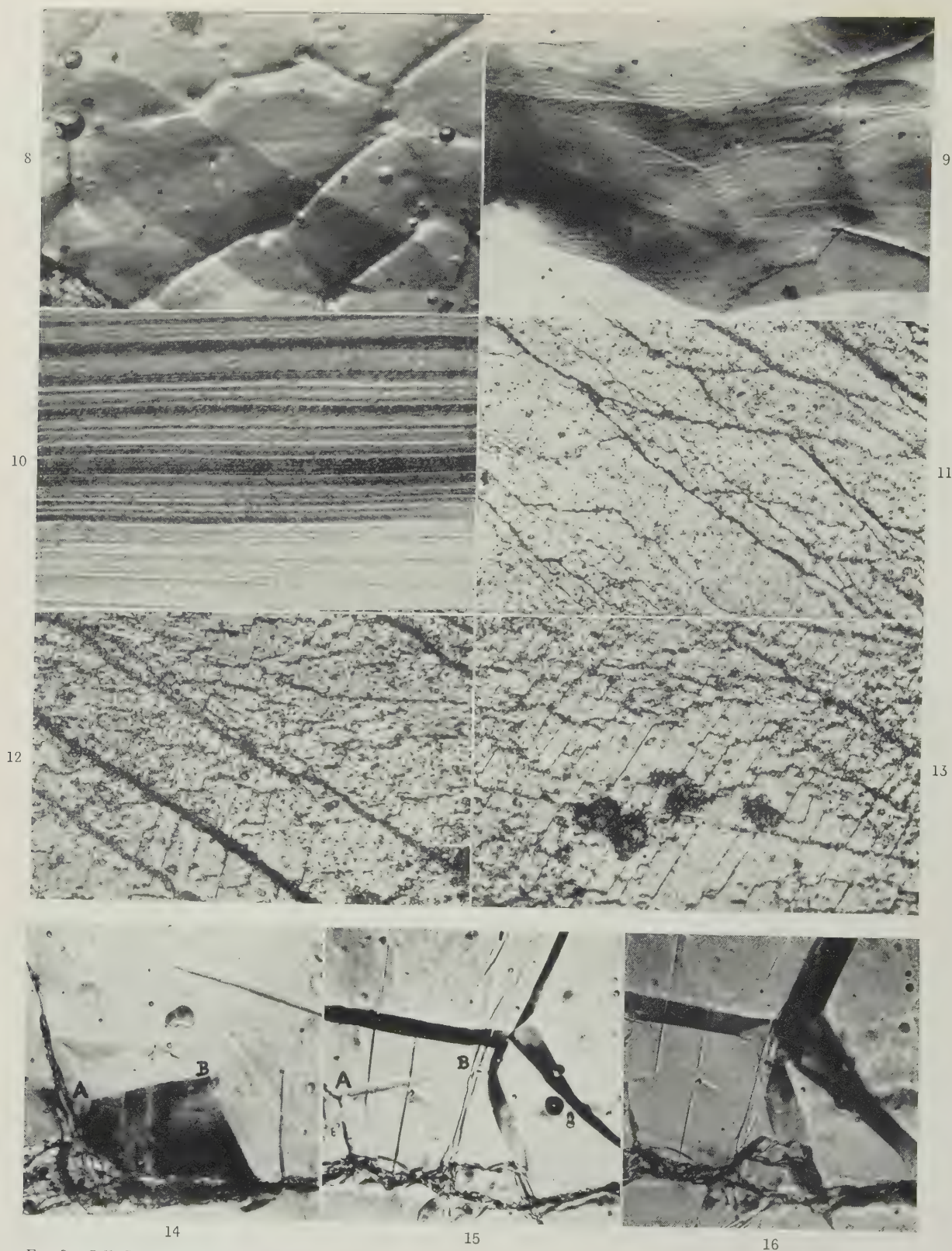


FIG. 8.—Cells Superimposed on Smailowski Structure. Specimen No. 16. 330° C.  $\times 120$ .

FIG. 10.—Basal Slip. 250° C.  $\times 150$ .

FIG. 12.—Pyramidal (?) and Prismatic Slip. 350° C.  $\times 500$ .

FIG. 9.—Cells and Cracks in Oxide Film Superimposed on Smailowski Structure. Specimen No. 10. 350° C.  $\times 90$ .

FIG. 11.—Prismatic Slip. 350° C.  $\times 500$ .

FIG. 13.—Pyramidal (?) and Prismatic Slip. 350° C.  $\times 500$ .

FIGS. 14-16.—Specimen No. 16. 330° C.  $\times 120$ .

FIG. 14.—Cells on Original Surface.

FIG. 15.—Same Cells, after Repolishing and Further Creep.

FIG. 16.—Same Cells, after Repolishing and Further Creep.



## COPPER-TIN ALLOYS.

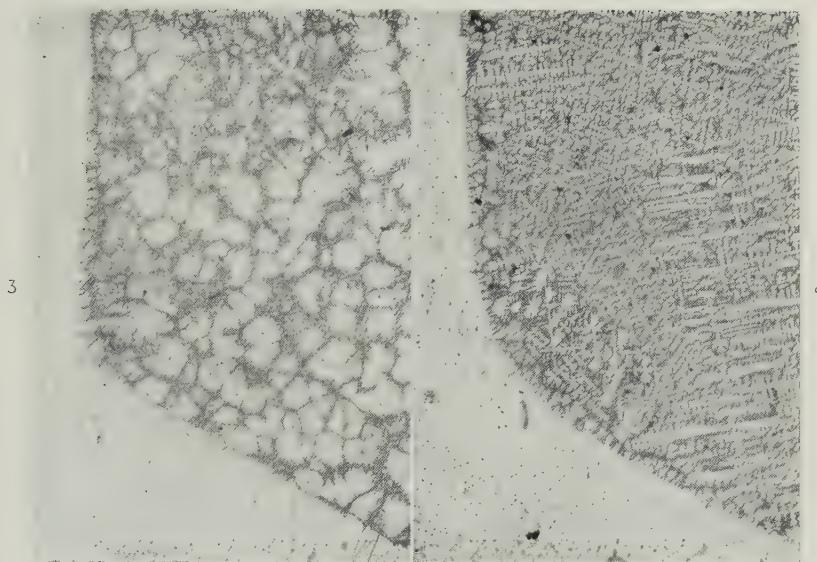


FIG. 3.—Cu-15 wt.-% Sn Insert, Annealed for 30 Min. in Cu-5 wt.-% Sn Container at 926° C. and Quenched. Semi-liquid.  $\times 40$ .

FIG. 4.—Cu-20 wt.-% Sn Insert, Annealed for 30 Min. in Cu-5 wt.-% Sn Container at 926° C. and Quenched. Totally liquid.  $\times 40$ .

Etched in acid alcoholic  $\text{FeCl}_3$ .

## TITANIUM-NICKEL ALLOYS.

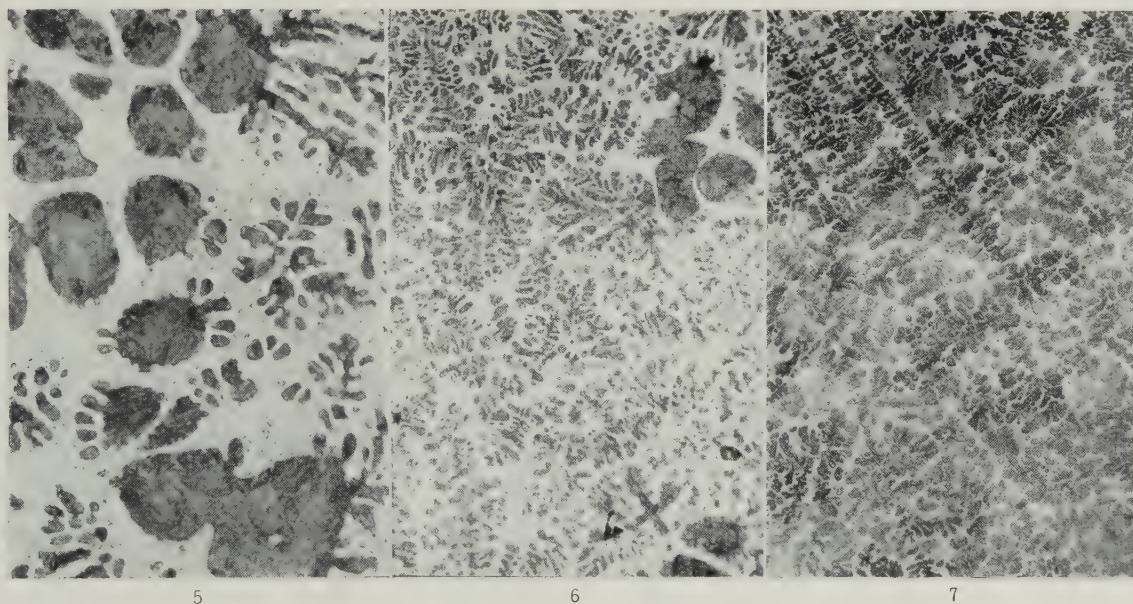


FIG. 5.—Ti-23.5 wt.-% Ni, Annealed at 1184° C. for 20 Min. in Ti Container and Quenched. Solid + chilled liquid.  $\times 250$ .

FIG. 6.—Ti-23.5 wt.-% Ni, Annealed at 1206° C. for 20 Min. in Ti Container and Quenched. Trace solid + chilled liquid.  $\times 250$ .

FIG. 7.—Ti-23.5 wt.-% Ni, Annealed at 1210° C. for 20 Min. in Ti Container and Quenched. Chilled liquid.  $\times 250$ .

Etched in 2%  $\text{HF}$  + 2%  $\text{HNO}_3$  in water.



## MICROSTRUCTURES OF COPPER-11.4% ALUMINIUM ALLOY.



- FIG. 1.—Transformed for 5 Sec. at 530° C. Pro-eutectoid  $\alpha$  in matrix of  $\beta$ .  $\times 150$ .  
 FIG. 2.—Transformed for 10 Sec. at 530° C. Pro-eutectoid  $\alpha$  in matrix of  $\beta$ .  $\alpha$  precipitation is heaviest adjacent to the boundary of the original  $\beta$  grains.  $\times 150$ .  
 FIG. 3.—Transformed for 2 Min. at 530° C. Pro-eutectoid  $\alpha$  in matrix of  $\beta$  + eutectoid. The dark areas of eutectoid are growing into the  $\beta$  matrix, especially adjacent to the original  $\beta$  grain boundary.  $\times 150$ .  
 FIG. 4.—Completely Transformed at 530° C. Pro-eutectoid  $\alpha$  in a matrix of eutectoid.  $\times 600$ .  
 FIG. 5.—Transformed for 5 Weeks at 350° C. "Blocky" Widmannstätten and "acicular"  $\alpha$  in an eutectoid matrix.  $\times 150$ .  
 FIG. 6.—Transformed for 10 Sec. at 530° C. Pro-eutectoid  $\alpha$  and inhomogeneous  $\beta$ .  $\times 600$ .  
 FIG. 7.—Transformed for 5 Min. at 530° C. Growth of non-lamellar eutectoid into  $\beta$ . Note the sheath of  $\gamma_2$  around the pro-eutectoid  $\alpha$ .  $\times 3000$ .  
 FIG. 8.—Transformed for 5 Min. at 530° C. Lamellar eutectoid.  $\times 3000$ .



## METALS AND MARINE ENGINEERING \*

1547

By S. F. DOREY,† C.B.E., D.Sc., F.R.S.

## SYNOPSIS

A review is given of the more important aspects of applying non-ferrous metals and alloys in modern marine engineering. Some of the problems associated with the uses of existing alloys are discussed, and the trends for future developments are indicated.

## I.—INTRODUCTION

As an engineer I am most conscious of the honour you have conferred in electing me to the Presidential Chair. In the course of the Institute's history there have been twenty-six previous Presidents renowned in the fields of research, industry, and the application of metals. Six of these distinguished gentlemen have been members of the engineering profession, and no less than three of them also attained the position of President of the Institution of Mechanical Engineers. I, therefore, count myself even more fortunate that you have honoured me as your choice to follow such noted engineers and maintain this important link with the metallurgist.

The development and extension of the applications of non-ferrous metals and alloys are dependent on the close co-operation between all who are directly and indirectly concerned with the various phases of research, production, and utilization of these materials. This axiom was appreciated by the founders and pioneers of the Institute, who also recognized that stimulation of interest in non-ferrous metals was dependent on ensuring that the interests of all members should be regularly and systematically covered by contributions to the *Journal*. In recent years there has been a tendency for the theoretical and scientific aspects to be overstressed at the expense of practical considerations.

Let me say at once that I feel sure no one would ever associate me with belittling the achievements of those engaged on pure or applied scientific research. Rather would I encourage these men, whose achievements have built up the high international status of the Institute. Nevertheless, there is a large proportion of the members whose interests and activities are associated with the industrial and service aspects of metals. It is undesirable that these members should be neglected, as their observations and opinions of the behaviour of metals in practice can offer guidance for research and development, in addition to assisting others concerned with similar

problems. The inclusion in the *Journal* of a greater number of contributions relating to metals in service is, therefore, essential. It is with this knowledge that I have devoted my Presidential Address to more practical matters which may be of appeal to all sections of the Institute's membership.

The publications of the Institute provide one of the main channels for the transmission of information relating to metallurgical developments. The proposal of the Council to publish *Metallurgical Reviews*, consisting of reports of progress in metallurgy, can therefore be regarded as a step in the right direction. I should point out that it has been arranged to include subjects having an appeal to all members, and in particular to those less familiar with scientific jargon. This new publication should increase interest in the Institute and, in my opinion, thereby ensure its greater economic stability, as well as offering an important advantage to anyone becoming a member.

## II.—HISTORICAL SURVEY

Before considering applications of non-ferrous metals in marine engineering, it might perhaps be as well for me to give a brief outline of the outstanding developments made in this field since the foundation of the Institute in 1908.

During that time, steam conditions have increased, on an average, from pressures and temperatures of 240 lb./in.<sup>2</sup> and 400° F. to 625 lb./in.<sup>2</sup> and 950° F., respectively.<sup>1</sup> Associated with this progress have been the change over from coal to oil fuel and the displacement of the steam engine by the steam turbine for high-powered propulsion purposes. Following the experiments on the *Turbinia* in 1894–96, the steam turbine developed rapidly.<sup>2</sup> The adoption of this type of main propulsion machinery for H.M. Battleship *Dreadnought* in 1906 became a ruling factor in the establishment of the turbine for large ships, and the close of 1907 saw the completion of the steam-turbined liner *Mauretania*. Subsequent developments have greatly increased the efficiencies

\* Delivered at the Annual General Meeting, London, 27 April 1954.

† Chief Engineer Surveyor, Lloyd's Register of Shipping, London.

of these machines, and powers of the order of over 40,000 H.P. are now transmitted by single shafts in large ships.

The oil engine, which has almost displaced the steam reciprocating engine as a prime mover, was at a very early stage of development in 1908, 250 H.P. being the maximum power available, for marine purposes,<sup>3</sup> from engines constructed in this country. The gas engine,<sup>4</sup> which was well established for land purposes, offered opposition to the oil engine in the marine industry, though it attained little more than experimental operation on the gunboat *Rattler*. However, the advance of the oil engine has been remarkable, power outputs per cylinder increasing from 80 H.P. to an existing value of over 1500 H.P., and exceeding 2000 H.P. for engines at present under construction.

The operation of a gas turbine at St. Denis in Paris aroused the interest of the marine engineer in 1908,<sup>5</sup> and as late as 1910<sup>6</sup> the opinion was expressed that engines of this type might be developed for marine installations. Their high temperatures (although reduced at this time by water injection) and low efficiencies presented such formidable difficulties that the gas turbine has been applied as a marine prime mover only in recent years.

Oxy-acetylene welding<sup>7</sup> was, at this early date, employed only for certain limited hull, boiler, and machinery repairs. Steel and copper were considered as suitable for welding, whereas aluminium was regarded as unsuitable for fusion jointing, soldering being preferred. Controversy existed as to whether the blacksmith or the boilermaker should be employed as the welder, in view of their differing knowledge of the fabrication of metals. The extensive use of fusion welding, in engine and boiler shops and in shipyards for constructional purposes at the present time, appears remarkable in comparison with these early practices.

These few examples, selected from an astonishingly large number of developments made in marine engineering, illustrate the progress achieved during the history of this Institute. This progress has been allied with that of the metallurgical industries, which have provided the essential materials of construction and have developed improved methods of fabrication. With the increased security of operating conditions, the low proportion of failures attributable to the quality of the materials employed is indicative of the progress made and standards maintained by the metallurgist.

To-day economic considerations, in conjunction with limitations of supply, still restrict the uses of non-ferrous metals for engineering and constructional purposes. In consequence, where static or dynamic stresses alone control design and service requirements, non-ferrous metals are rarely included in the materials selected. Since the foregoing remarks impose such strict limitations on non-ferrous metal development and usage, it is obvious that for these metals and alloys to be practical propositions, only markedly en-

hanced properties, offering manufacturing superiority or resistance to adverse service features, will be of consequence.

The wide range of metals included in the non-ferrous group have many and varied inherent qualities which render them of major industrial importance. It must be admitted that single outstanding features rarely constitute sufficient grounds for the selection of a metal for service, but suitable alloying, in conjunction with fabrication and heat-treatment, has largely provided a solution by enhancing overall qualities. In consequence, these alloys serve a most vital role in ensuring efficient operation and adequate service life of machinery and structures, although the proportion employed in relation to other materials may be relatively small.

Such is the case in marine engineering, and although the uses of non-ferrous metals in this field have been reviewed previously,<sup>8</sup> recent improvements and developments have increased the number and types of alloys in service, in addition to widening their general field of application. A further review is, therefore, not unwarranted, and since manufacturing and operating conditions create the demands for existing and improved alloys, this more logical basis of examination will be adopted. Many of the service problems experienced are of long standing and, whilst a trend towards minimization has been in progress, satisfactory solutions have not yet been attained. If, therefore, somewhat archaic aspects are referred to, justification is founded on lack of a practical solution.

### III.—CORROSION

In the first place, the corrosive nature of marine environments constitutes one of the most arduous service conditions metals are required to withstand in their many applications. The long-term appreciation of this fact is indicative of the formidable nature of the problems presented, in which non-ferrous metals have played an important alleviating role.

At the beginning of this century the corrosion problems associated with marine condensers were of a sufficiently serious character for this Institute to found, in 1910, a Corrosion Research Committee, whose purpose was to investigate the causes leading to the failures encountered. The series of eight reports subsequently published, and the guidance they afforded, were valuable contributions towards the solution of a most serious problem. The marine engineer has derived great benefit as a result of these investigations and their continuation by the British Non-Ferrous Metals Research Association since 1930.

The forms of corrosion observed comprised dezincification, impingement attack, pitting, and galvanic action.<sup>9</sup> The benefits conferred by additions of up to 0.05% arsenic in minimizing dezincification of  $\alpha$ -brasses and aluminium brasses are now well established.<sup>10</sup> Since the  $(\alpha + \beta)$  60:40 brass does not respond to such additions, the use of this alloy has been confined to components of working sections



which have sufficient thickness to tolerate reasonable amounts of dezincification.

Impingement attack or corrosion erosion was observed to result in rapid deterioration of the alloys then employed. The high local liquid velocities, associated with air bubbles in excess of a critical size, produced a scouring action capable of removing protective scales and deposits, thereby accelerating corrosion. Increase of temperature and any form of local obstruction, which increased liquid velocities, enhanced this effect. Since copper undergoes erosion due to liquid velocity alone, it has now been confined to less arduous services in water systems. The arsenic-bearing 70:30 brass is still employed for condensers in which liquid velocities do not exceed 7 ft./sec. and provides suitable service life in these applications. Where higher velocities are associated with aeration, 70:30 cupro-nickel tubes, with iron contents of 0.4–1.0% and manganese 0.5–1.5%, are widely employed or, alternatively, 76:22:2 aluminium brass inhibited with arsenic is used.

In view of the benefits obtained from small additions of iron and manganese to 70:30 cupro-nickel, the influence of iron on alloys of lower nickel content was investigated.<sup>11</sup> Marked improvements of both impingement-resistance and attack experienced under stagnant conditions were obtained from iron additions of 1–2% to alloys containing 5–10% nickel. Alloys of this type with 5% nickel and 1.05–1.35% iron have prospects of being widely employed for condenser and other purposes. The 10% nickel, 2% iron alloy is, however, preferred in the U.S.A.

Tin-bearing copper alloys with tin contents below 8% have so far proved inferior to these alloys, although when the content is of the order of 12% good resistance to erosion has been observed. Coatings of zinc, tin, nickel, or chromium have been applied to the surface of non-ferrous tubes, but have not been considered worthy of continued use. Duplex tubing, in which different alloys are utilized for bore and external surfaces, have frequently been considered for specific purposes. In America this form of tube is again receiving consideration, combinations of copper, various brasses, aluminium bronze, or cupro-nickel being supplied with aluminium, Monel, nickel, or steel external contact metals. Chemical and refrigeration plant represent the greatest application of these forms of tubing, but as yet few data are available on the service experience obtained.

Existing normal service conditions of marine condensers are well within the estimated limits of the improved alloys. However, operation involving polluted cooling waters still presents an important problem. Cupro-nickels have been proposed as the most suitable tube materials for this type of service, as both 70:30 and aluminium brasses have proved unreliable. It must be admitted, however, that this proposal does not offer an entirely satisfactory solution, and it is desirable that investigations of deterioration in polluted waters should be continued.

Associated with this problem are those involving severe pitting of these alloys due to marine growths. Bio-fouling tends to be more severe on alloys having enhanced corrosion-resistance. In addition to causing pitting by its own action, the growth tends to trap decaying debris, thereby increasing the attack on the metal surface. Adequate water velocities and careful maintenance assist in reducing these forms of deterioration, but as polluted-water and bio-fouling effects are allied, investigations should serve a dual purpose.

The use of dissimilar metals, whether in contact or in different parts of a continuous system in contact with sea water, inevitably leads to cathodic corrosion. The relative value of the electrode potential for each metal or alloy, immersed in sea water, indicates the liability of marine corrosion occurring in the more anodic metal, when two or more are involved. As a preliminary precaution, therefore, metals and alloys of widely differing potentials should be avoided in these instances, although severe restrictions may thus be imposed on the range of suitable materials available.

Steel-to-aluminium alloy jointing is becoming increasingly frequent with the extension of the usage of aluminium alloys to structural and machinery applications. Local contact at faying surfaces of structures is usually avoided by interposing galvanized strip or non-metallic packing and bolting with surface-protected steel bolts and by the application of zinc chromate paint.<sup>12</sup> In some instances unprotected local steel-to-aluminium contact has resulted in rapid corrosion of the aluminium. In machinery applications, when the necessity arises, zinc coating of the steel is usually adopted as the most feasible method of protection. However, when extruded aluminium alloy hollow sections were employed for cooling grids with brine circulations in refrigeration plant, avoidance of corrosion at steel-bodied shut-off valve connections was not achieved, and these grids have been dispensed with.

Steel riveting of aluminium structures exposed to marine atmospheres is, therefore, undesirable, although in other respects it offers a suitable jointing method. In addition, the liability of steel-cored aluminium overhead-line conductors,<sup>13</sup> in similar atmospheres, to bulging, which is considered essentially of electrolytic origin, also illustrates the difficulties of combining these two alloys. In this instance bitumen coatings were found of little value owing to cracking, hardening, or disintegration, and periodical application of suitable greases provided the best protection.

Copper and nickel alloys are avoided in contact with aluminium and its alloys, and the effects of copper-to-steel contacts are minimized by zinc coating the steel surfaces or by the employment of protection blocks which corrode sacrificially. Zinc is widely used in this connection, the high-purity form being considered the most effective. However, owing to the ineffective bonding of zinc to steel and to the

semi-impervious layer of corrosion product formed on the zinc surface after short-time operation, doubt has been cast on the value of this metal as a protector for marine purposes.<sup>14</sup> Despite the possible validity of these criticisms, however, zinc is still extensively used and must be of some merit. Addition of  $\frac{1}{2}\%$  lithium to the zinc has been suggested<sup>15</sup> as a means of obtaining a less-insulating corrosion product, but no record has so far been observed of this alloy finding use in service.

Iron or steel affords protection to copper alloys and is not only beneficial in reducing the corrosion due to electrolytic action, but also it enhances the corrosion-resistance of aluminium brass.<sup>16</sup> Nickel-base alloys, being more noble, are generally confined to applications with stainless steels or to components where the sections are such that some degree of corrosion may be tolerated.

Protective coatings or blocks of more anodic characteristics therefore form the most common method of limiting these forms of corrosion. In recent years the economic and practical value of cathodic protection of buried pipelines and structures has offered an alternative means of minimizing corrosion.<sup>17</sup> High-purity magnesium anodes have proved most effective and, in conjunction with suitable impressed potentials and current densities, have been extended in use to protect marine pipelines, structures, and the submerged surfaces of ships laid up in reserve. Only limited experience has been obtained with sea-going vessels, as many as 106 magnesium anodes being located on the bilge keel. Whilst such refinements might prove effective in extending docking periods for operational warships, the benefits afforded to merchantmen are doubtful, as these vessels are docked at frequent intervals for many purposes.

A most serious corrosion problem exists in oil-tankers, which carry alternately oil cargo and sea-water ballast<sup>18</sup> in the same tanks. Flat surfaces and other regions which do not drain efficiently undergo rapid corrosion. The combined influence of the oil and the sea water promotes this extreme deterioration, the high oxygen contents of the oils being mainly responsible, although the sulphur content has also been suggested as an additional contributory factor. Steaming out of the tanks aggravates these conditions by loosening adhering scale and increasing the chlorine-ion concentration at the higher temperatures involved. Although cathodic protection, involving the use of an active magnesium or other type of anode, has been applied in limited instances, controversy exists as to the economic and practical advantages obtained.

Aluminium alloys are claimed to have a high resistance to corrosion under these conditions and might offer alternative means of reducing deterioration either as spray coatings, linings, or complete tank units. So far these alloys have not been tried, but future development may involve their use.

The deposition of minute quantities of one metal

from solution on to another of more anodic characteristics in water-carrying systems in whose construction dissimilar metals have been used, has been observed<sup>19</sup> to accelerate corrosion failure. Copper transmitted in this form to galvanized steel or aluminium components was the metal mainly concerned, but this example demonstrates the further need of careful material selection for the conditions appertaining.

The high rate of corrosion of metals which can be associated with electrolytic action presented marine engineers with major problems over 100 years ago. For example, the severity of corrosion of iron screw-shafts running in sea-water-lubricated brass bushes and in the vicinity of copper sheathing, led to the fitting of brass sleeves or liners to the shaft as a means of protection. At the present time, limitations on the selection of the wide range of metals and alloys available to the engineer are imposed by similar problems. Solutions offered by surface coatings, wastage blocks, or impressed cathodic protection cannot always be employed, or are not entirely efficient. An effective solution appears to be far from obvious, and the engineer can only hope that the metallurgist, in his researches, may develop more efficient methods of passivation.

#### IV.—CAVITATION EROSION

One of the most severe forms of metallic-surface deterioration is associated with damage sustained by cavitation erosion. Under the suction conditions of dynamic fluid flow, the surfaces of propellers, impellers, and similar hydraulic-machinery components may suffer this form of erosion. The collapse of cavities formed on these surfaces is considered to release quantities of energy in the form of localized forces, similar in nature to water hammer. The magnitude of these forces may be sufficient to bend propeller blades, but their confined character more commonly induces highly localized stresses in the metal, producing surface rupture and severe distortion of the crystal structure. Damaged surfaces tend to increase local turbulence, enhancing cavitation tendencies and extending the depth and area of the eroded zone. The mechanism of failure is not fully understood, and controversy exists as to the part played by corrosion.

Marine propellers experience this form of damage to varying extents, depending on the design, the conditions of operation, and the material of which they are made. Cast iron and cast steel are prone to have local regions of porosity which are easily eroded and give rise to a deeply pitted form of attack. Bronzes, which are of a more resistant nature, exhibit eroded regions having the appearance of areas that have been subjected to intense local sand-blasting. Despite their more resistant nature, however, bronze propellers have been known to decrease in weight during service by as much as 10%, attributable to overall corrosion and erosion losses.



Such losses not only impair the propeller's efficiency, but also reduce its inertia. In consequence, the one-node mode of torsional vibration of the machinery dynamic system will be raised, and critical vibrations may be placed out of barred speed ranges or brought in close proximity to service or operational speeds.

Improved propeller designs based on extensive hydrodynamic studies are expected to reduce cavitation conditions, but the higher powers transmitted and the turbulent flow imparted by the stern of the ship will limit the benefits likely to be obtained. The application of alloys having the maximum resistance to this form of cavitation erosion has therefore been considered. In order that the relative merits of the available alloys might be ascertained, experimental techniques simulating extreme cavitation conditions on the surfaces of suitable specimens have been adopted.<sup>20-23</sup> Erosion-resistances were based on weight losses in standard exposure times and, whilst some degree of variation of results is inevitable, good guidance is given to the relative resistance of the alloys involved. A reasonable assessment of the erosion-resistance of an alloy is given by the product of the surface Brinell hardness number and the corrosion-fatigue resistance expressed in tons/in.<sup>2</sup> for 50 million cycles of reverse bending. The more highly resistant alloys have values in excess of 800, and in descending order of merit they include austenitic stainless steels, aluminium bronzes, with or without nickel additions, low-nickel stainless steels, silicon Monel, Monel metal, high-tensile bronze, and Turbadium bronze. Below 800, the normal manganese bronzes, silicon bronzes, phosphor bronzes, gun-metals, cast irons, and aluminium alloys are placed. This does not imply that the manganese bronzes which have given such good service have poor resistance, but they are used purely as a basis of comparison.

Cast iron, which is still widely used as a propeller material, should have its surface skin intact, as this increases its resistance to erosion, as do additions of copper, nickel, and chromium. Soft alloy "stopper" metals employed to plug local casting defects are of negligible value.

Nickel deposits, applied to the surfaces of cast-iron propellers of trawlers,<sup>24-25</sup> have provided increased corrosion- and erosion-resistance in service. The severe corrosion, which occurred at fractured sections, and the high cost of the deposit caused this practice to be abandoned, however. Similar deposits applied to bronze propellers have also proved uneconomical. Spray coatings of zinc, lead, and aluminium have been applied to cast-iron propellers in service.<sup>26</sup> Of these metals, pure aluminium was found to be the most reliable, although respraying of exposed areas became necessary at intervals.

Erosion losses were found to increase with increase of sea-water temperature, up to 50° C., used in laboratory tests, and this feature must be taken into account when comparing the merits of the metals in service. Of the alloys tested showing cavitation-

erosion characteristics superior to those generally used, the stainless steels and aluminium bronzes appear the most suitable for manufacture and service purposes. Since uniformity of cast structure is advantageous in providing homogeneous properties throughout the propeller mass, the grain refinement obtained from iron and manganese additions to 9-12% aluminium bronzes should be beneficial.<sup>27</sup>

Beeching's experiments<sup>22</sup> clearly indicated that aluminium, nickel, or both, as additions to copper or copper-zinc-base metal, resulted in alloys having low cavitation-erosion-loss characteristics. The latest materials used for large marine propellers are copper-aluminium alloys with nickel and iron additions, resembling that specified in B.S. 1400 A.B.2, and the more recent copper alloy with high aluminium and manganese content. Castings having maximum weights of 25 and 35 tons have been made in these alloys, respectively, and even larger castings are under consideration.

Impellers of pumps are invariably of gun-metal, manganese bronze, aluminium bronze, Monel metal, or stainless steel. Cast surfaces can frequently be retained, thereby offering superior resistance to corrosion and erosion. The last three materials quoted are usually employed where the conditions are most severe in respect of temperature, stress, and erosion.

The exceedingly low erosion-resistance of aluminium alloys<sup>21</sup> cannot be neglected if these materials are to be used for hull construction and for small-sized propeller castings. The service experience under conditions of erosion has not yet been sufficient to establish the resistance of these alloys, but, should the experimental evidence be borne out, alternative materials may have to be used for hull sections that experience cavitation.

Sprayed-metal deposits applied for the protection or reclamation of surfaces experiencing cavitation erosion have been found to be of only temporary value, both experimentally<sup>21</sup> and in service. The porosity associated with these deposits is probably responsible, and sound fusion welds represent the best method of repair and surfacing.

Both hydrodynamic and metallurgical researches are leading to a reduction of cavitation damage. Assessment of the factors governing metallic failure by this kind of erosion will undoubtedly lead to an improved understanding of the essential qualities of alloys necessary to resist rupture. In consequence, control in the manufacture and requirements of improved alloys may be established on a more scientific basis.

## V.—FATIGUE

Alternating stresses, arising from the excitation of natural modes of vibration of machinery and component mass-elastic dynamic systems, have resulted in many service failures.<sup>28</sup> Mathematical analysis in conjunction with dynamic stress measurements,

obtained during operation of machinery installations, has led to a reduction in failures of this type, either by the avoidance of critical vibrations in the vicinity of operating speeds, or by limiting vibration stresses to values below the fatigue strength of the materials employed.<sup>29</sup>

Alloys having enhanced fatigue strength are advantageous where these conditions are involved, in that they permit higher stress levels to be tolerated. In addition, where the actual magnitudes of the stresses are indeterminable, higher-strength alloys can extend service life by increasing the number of cycles to rupture, and may even provide a complete solution. Such improvements were simply demonstrated by the radical reduction in failures of lead cable sheathing, subjected to vibratory conditions in service, by improving the poor fatigue characteristics of pure lead with small alloying additions of tin, antimony, and cadmium.<sup>30</sup> These alloys are now in general use, although aluminium has also been employed for land purposes, as it provides weight reduction and further improved fatigue strength. However, aluminium-sheathed cables are not used for marine purposes, the cathodic quality of lead being more favourable.

Whilst cold working is readily employed for improving the mechanical properties of non-ferrous alloys, the availability of many alloys capable of acquiring enhanced strength by heat-treatment, has offered marked advantages. In many instances, precipitation-hardening or quenching to obtain structures of the acicular martensitic type, has had such a marked influence as to render non-ferrous alloys competitive with ferrous materials in many applications. In addition, consideration has been given to the development of strength by the precipitation of ordered phases, but as yet this feature has not been of marked industrial importance.

The low corrosion-fatigue strength of plain carbon and many low-alloy steels, confirmed by reverse-bending salt-spray tests of 50–100 million cycles' duration, at less than 4000 lb./in.<sup>2</sup> has been responsible for machinery failures.<sup>31</sup> Copper- and nickel-base alloys, in particular, offer excellent corrosion-fatigue characteristics, and manganese, aluminium, and phosphor bronzes, Monel metal, and K Monel metal have all been used in preference to these steels for many shafting applications, including screwshafts of limited size. In addition, these alloys are frequently preferred to the chromium stainless steels because of the tendency of this material to pitting, especially in the presence of graphite grease.

Corrosion-fatigue strengths of many alloys have been determined experimentally for cycles of stress in excess of 50 million, and they provide the engineer with useful design data. However, with the exception of steels, there is a lack of information relating to the influence on the corrosion-fatigue strength<sup>32–34</sup> of mean stress, stress concentration, and combined-stress conditions.

At elevated temperatures the influence of mean

stress in relation to fatigue is of marked importance, owing to the deformation due to creep. At a given elevated temperature, the limitations imposed by fatigue strength and creep strength form individual extremities. A method of computing the limiting strength<sup>35</sup> under their combined influence has been suggested as a basis for design. The reliability of this method, however, still requires confirmation by experiment.

The magnitude of vibratory stresses, occurring when natural frequencies of components are excited by external influences, is dependent on the degree of damping available. Whilst the significance of the damping capacity of material has not yet been fully assessed, in instances where accurate determinations have been made low values have been recorded for many metals and alloys.<sup>36</sup> Internal damping cannot, therefore, be relied on to limit alternating stresses to values below the fatigue strength. This does not necessarily imply that the inherent damping properties of metals are insignificant, for, in similar application, a metal of superior damping characteristics might give longer service life.

## VI.—USE OF METALS AT ELEVATED TEMPERATURES

The advent of the gas turbine focused attention on the requirements of alloys for service at elevated temperatures. The development of both ferrous and non-ferrous alloys to meet these needs has been indeed remarkable. As operating temperatures even higher than those at present employed would be desirable, the search for superior materials continues. In this country, with the exception of the well-established Nimonic series of alloys, ferritic and austenitic steels have so far proved most suitable for these purposes. In the U.S.A. similar conditions prevail, although more extensive use has been made of cobalt-base alloys and alloys containing high proportions of this metal. Both heat- and creep-resisting steels contain high total contents of nickel, chromium, cobalt, molybdenum, titanium, niobium, tungsten, and manganese, thus demonstrating the importance of non-ferrous metals in these applications. Indeed, the total content of these metals frequently exceeds 45%, and for heat-resisting purposes the higher the temperature, the greater the amount of non-ferrous metals present.

To a large extent, gas-turbine alloys have been based on three primary metals, typical being nickel-chromium-iron and nickel-cobalt-iron alloys and, more recently considered in Canada, nickel-aluminium-molybdenum alloys.<sup>37</sup> Stiffening against creep depends in these alloys on the precipitation of constituents, provided in some instances by small additions of other elements. With the possible limits of these types of alloy being approached, materials based on higher-melting-point metals have been receiving greater attention. Chromium, titanium, and molybdenum are the metals mainly involved



and, although the purer forms of these metals are not themselves suitable for high-temperature application, alloys may be developed with more favourable characteristics. One alloy,<sup>38</sup> containing chromium 60, molybdenum 25, and iron 15%, withstood a stress of 9 tons/in.<sup>2</sup> at 870° C. for more than 1000 hr., indicating the potentialities of alloys of these types.

With extensive research programmes in progress throughout the world, embracing both metallic and non-metallic materials, in an endeavour to raise operating temperatures as high as possible, the engineer can only await further developments made by the metallurgist.

The search for high-temperature materials has tended to mask the desirability of determining the operational limits of many familiar alloys used at less-elevated temperatures. Information provided by short-time tests is undesirable, as doubts remain as to the degree of stability of structure and as to the reliability of stress assessment based on these findings, when applied to components of installations constructed for long-duration service.

Copper shortening which occurred in rotor windings of large turbo-alternators<sup>39</sup> aggravated by shift working to cope with peak-hour loads, illustrates the necessity for a knowledge of creep characteristics of materials in service at more moderate temperatures. Copper with additions of up to 0.1% silver to increase the creep strength and reduce the softening tendencies following cold work, or alternatively the introduction of suitable aluminium alloys, has provided a solution to these present problems.

Copper-base alloys used in steam-plant applications have received little attention in long-term investigational work, and suitable pressure-temperature design criteria are based on very limited experimental data. Tests of not less than 10,000 hours' duration are essential on many of these alloys, and the failure of copper alloys in gas-turbine heat-exchangers also demonstrates the lack of knowledge of their scaling qualities in many atmospheres.

Metal-to-metal contact is not uncommon at elevated temperatures, and galling has frequently been encountered at steam-valve faces and guides. All steels are susceptible to this form of surface rupture, and the use of Stellite surface deposits has proved the most feasible method of overcoming these difficulties. Silicon Monel metal has good anti-seizing properties at these temperatures, but low ductility and high hardness of the cast 3.75% silicon alloys can lead to thermal cracking with temperature gradients.

Surface deposits of Stellite are widely used for I.C. engine exhaust-valve faces to extend the service life at the high temperatures encountered. Oxy-acetylene flame-welded deposits of 80:20 nickel-chromium alloy are being increasingly employed for the repair of Diesel-engine valves and provide high resistance to corrosion and cracking.

For steam-turbine blading the ferrous alloys have almost completely replaced non-ferrous alloys in new

construction. Stainless iron and nickel-chromium ferritic and austenitic steels are the most commonly employed, replacing existing copper and nickel-copper alloys. Non-ferrous materials are widely used for gland purposes, and the most suitable alloys for the various operating temperatures have been quoted by Brown<sup>40</sup> as being: brass up to 850° F., S Monel (3.5% silicon) below 1300° F., and Nimonic 75 for higher temperatures.

Although the engineer can usually make suitable allowance for the expansion of metals with temperature, the use of dissimilar metals presents many complex problems. The joint application of aluminium and steel to ship construction has been receiving attention, mainly from the point of view of achieving a suitable design to minimize induced stresses.<sup>41</sup>

Temperature gradients, involving thermal conductivity in addition to expansion, are of a more serious nature. Distortion and thermal-fatigue failures are becoming more common with increased operating temperatures. Data provided by metallurgists on mechanical and physical properties of alloys and their variation with temperature have been useful in design, but the factors controlling thermal shock and fatigue failure require greater attention if these are to be avoided in service.

For piston heads of I.C. engines, cast iron has given excellent service and is still preferred by many engineers. Its replacement in heavy-oil engines by forged steel was mainly based on increased soundness and pressure-tightness, although the use of centrifugal-spun 13% chromium cast steel is based partly on its superior heat-resisting properties. Whilst 20% chromium steel is considered superior, as yet this material has not been tried. Aluminium deposits on cast-iron heads have been applied to reduce the heat-absorption characteristics, but opinion differs as to the value of such measures. For heavy slow-speed engines, light-alloy piston heads have not been used, as the saving in reciprocating masses is insufficient to warrant them.

High-speed engines, however, employ cast aluminium-alloy pistons to a great extent, as the reduction in reciprocating masses is of great value. Well-established "Y" alloy and R.R. alloys are used, and reliability has been sufficiently good to merit their continued service.<sup>42</sup>

## VII.—APPLICATIONS OF LIGHT ALLOYS

The advantages of light-weight construction, employing aluminium alloys of suitably high specific strength and good corrosion-resistance, are not so marked in shipbuilding as in other transport industries. In addition, the extensive experience obtained in steel construction and the equipment of yards to handle steel fabrication have militated against the use of light alloys when the latter are not readily adaptable to similar processes. The extension of light alloys to ship construction has, therefore, been

based more on long-term policy, and extension of their application is increasing with design and practical experience.

Scantlings of aluminium structures have been based on somewhat greater values than those given by the strength ratios of the equivalent in steel. Weight-saving, therefore, amounts to approximately 50% of a normal steel structure. The advantages for the present use of light-weight construction have been summed up as: <sup>43</sup>

(1) A reduction in topside weight which increases the stability of the vessel, offering advantages not only in new construction, but in reconversion work.

(2) Greatly increased corrosion-resistance of aluminium alloys, particularly against the detrimental effects of petroleum and its products.

(3) Greater flexibility in the design of vessels operating in conditions which impose limitations on draft, beam, and length.

(4) Reduction in contamination of cargo and ease of cleansing refrigeration and other holds.

(5) For Naval vessels, the non-magnetic characteristics and weight-saving are important, the latter permitting increased armour and armament.

(6) Greater flexibility in hull design, permitting increased speed with the same machinery power or less power for equivalent speeds.

Of these items the first has been the most important in merchant-ship construction, finding application mainly in passenger vessels. Topside weight-saving has been effected by manufacturing masts, superstructures, funnels, davits, lifeboats, and accommodation fittings in aluminium alloys. The S.S. *United States* has incorporated in its construction a total of some 2000 tons of these alloys, and a total weight-saving of 15–20% of the original displacement is claimed as a result of the direct and indirect influence of these materials. <sup>44</sup> With the exception of this ship, such extensive quantities of light alloys are not encountered in the many other merchant ships of composite construction. For these ships the quantities used range up to 250 tons.

For structural purposes aluminium alloys with up to 5½% magnesium are considered most suitable. With this maximum magnesium content and small additions of manganese and chromium, the tendency for precipitation of the  $\beta$  phase has been obviated, and so has the stress-corrosion associated with the presence of this phase. Aluminium–4% magnesium alloys (N.P. 5/6) are used for plate manufacture, as they are more suitable for hot working than those of higher magnesium content. The mechanical properties are generally good and meet the maximum stress requirements of 17 tons/in.<sup>2</sup> with comparative ease. Further, their good welding characteristics render alloys of this composition superior to those of the heat-treatable type of alloy. There is, therefore, a tendency for this material to be more widely used,

and in America alloys of similar composition may in future be employed in preference to the existing 61S-T6 alloy. Details of the light alloys used in ship construction are given in Table I, taken from a paper by Corlett. <sup>44</sup>

Alloy N6 (5% magnesium) is used for rivets, as well as H10 (1.0% magnesium, 1% silicon), the latter having superior extrusion qualities to the former alloy and being, therefore, more favoured. However, it is usually employed in the heat-treated (WP) condition, as is the corresponding American alloy 61S-T4. These alloys do not work-harden to the same extent as N6, but age-harden to give higher proof stresses. Age-hardening of rivets after quenching is a drawback in shipyard practice, but it was overcome during construction of the S.S. *United States* by adopting the aircraft industry's practice of refrigerated storage. A temperature of –10° F. was employed, the rivets being wrapped in aluminium foil or other insulating material to assist in delaying precipitation-hardening between the time of removal from storage and the actual time of driving. <sup>12</sup>

TABLE I.—*Aluminium Alloys Used in Ship Construction.* <sup>44</sup>

(a) Percentage Compositions (Nominal)

	Cu	Mg	Si	Fe	Mn	Cr	Zn	Al
N5/6	...	3.9	...	...	0.8	...	...	Rest
N6	...	5	...	...	0.5	...	...	"
H10	...	0.7	1.0	...	0.4	...	...	"
61S-T (U.S.A.)	0.25	1.0	0.6	...	...	0.25	...	"
Lloyd's re-quirements	0.1	5.5	0.60	0.75	1.0	0.5	0.1	"
	0.1	1.5	1.30	0.60	1.0	0.5	0.03	"

(b) Mechanical Properties (Minimo)

(Typical values are given in parentheses)

Alloy	Size or Condition	0.1% Proof Stress, tons/in. <sup>2</sup>	U.T.S., tons/in. <sup>2</sup>	Elongation, %	
				On 2 in.	On 8 in.
N5/6	$\frac{1}{8}$ – $\frac{1}{4}$ in.	8 (15.5)	17 (20.5)	12 (13.8)	(10.1)
	$\frac{1}{4}$ – $\frac{1}{2}$ in.	8 (12.0)	17 (19.5)	12 (22.3)	(15.4)
NE6	Up to 2 in.	8 (8.5)	16 (17.0)	18 (25)	...
	Over 2 in.	7 (8)	16 (17.0)	18 (25)	...
HE10	W	7 (10.0)	12 (15.5)	18 (25)	...
	WP	15 (18.0)	18 (20.0)	10 (13)	...
61S-T6	Plate	15.6 (17.4)	18.7 (20.0)	10 (15)	...
	Bar	15.6 (17.4)	16.9 (20.0)	10 (15)	...
Lloyd's re-quirements	All	8	17	...	10

\* Non-heat-treated.

† Heat-treated.

Rivets are driven both hot and cold, pneumatic methods being used for N6 rivets of the order of  $\frac{1}{2}$  in. dia. (cold) and  $\frac{3}{4}$  in. dia. (hot). The heating of aluminium alloy rivets requires greater attention than is usual in steel-rivet practice. Light alloy rivets are worked in a temperature range of 400°–500° C., higher temperatures being most undesirable.

The high-strength, heat-treated Duralumin and aluminium–magnesium–zinc types of alloy are not employed in marine construction owing to their inferior corrosion-resistance. In the clad condition



these alloys are not economic propositions, although they have been employed in some German Naval vessels.

Many small craft have been constructed entirely of light alloys, using normal and stressed-skin techniques. They provide means of gaining general experience of fabrication methods, as illustrated by the recent manufacture of a 72-ft. yacht of light alloy welded construction. For the aluminium alloys to be extensively used in ship construction, efficient welding techniques must be developed. The self-adjusting inert-arc method, as used in the fabrication of this yacht, at present provides the most suitable method of fusion welding. However, as yet, this method is severely limited for general shipyard use by the degree of penetration obtained, the need to maintain a clean and corrosion-free filler wire, and the difficulties of maintaining an inert atmosphere during open-air welding. The high degree of reliability attained in the fusion welding of steels has, therefore, placed aluminium alloys at present in a less favourable position.

Ease of handling gives the light alloys great advantages for hatch covers, crankcase doors, and similar applications. In the engine room, however, apart from these uses and piston castings, light alloys are not extensively employed, as the savings in weight are not sufficiently vital. Where these alloys are employed for crankcase, sump, and cylinder castings, the engines concerned are generally used for other land purposes where these features are advantageous. Some engine builders have even considered offering cast iron as an alternative for marine purposes. In consequence, the cast aluminium alloys containing silicon and magnesium find only limited scope in the machinery of merchant ships.

The ultimate tensile strength of aluminium alloys used in ship construction is still relatively low, 20 tons/in.<sup>2</sup> being an almost limiting value for normal plates and sections. It must, therefore, be appreciated that the development of alloys having superior strength while retaining the other desirable properties of existing alloys, remains an important consideration.

### VIII.—USE OF TITANIUM

The remarkable resistance of titanium, in the high-purity form or with small alloy additions, to severe attack by both hot and cold sea water has aroused the interest of the marine engineer. Although this metal has not so far been used for marine purposes, the mechanical properties and corrosion-resistance are of such a high order as to render it very suitable for many applications in this industry. The problems associated with its production and fabrication, in addition to its exceedingly high cost, as discussed by Dr. Maurice Cook in his recent Autumn Lecture,<sup>45</sup> impose severe limitations on the engineering importance of the metal. In addition, the elevated-

temperature properties are disappointing, and until greatly improved alloys are developed, little competition will be offered to existing high-temperature materials.

The resources of this metal are sufficiently great and readily accessible to warrant its consideration for the requirements of engineering industries. If conservation of some less abundant metals becomes necessary, titanium may offer a suitable alternative in many applications. The metallurgist has adequate scope and opportunity to develop this metal, and its future clearly rests with him and his endeavours.

### IX.—BEARING METALS

The maintenance of film-lubrication conditions between metal surfaces in relative movement constitutes the ideal requirements of service. Advances in lubrication theory and practice have been responsible for the efficient operation of machinery by limiting surface contact to a minimum. Load and velocity variations may still result in changes from film to boundary lubrication, and the short-time contacts between the metal surfaces are minimized in their effect by suitable selection of the mating materials. Non-ferrous metals which exhibit a low friction coefficient and a high resistance to local seizure, in relationship to journal materials, perform a most important function in this connection.

Whilst these qualities are of major importance, the bearing metal must also have adequate mechanical strength at the operating temperatures to withstand the applied bearing loads and sufficient ductility to tolerate normal amounts of malalignment. In addition, the rate of wear undergone by shaft and bearing surfaces must be exceedingly low and the corrosion-resistance must be of a high order. A great deal is, therefore, required of a bearing metal, and it is not surprising that no ideal alloy exists and actual selection for particular service represents a compromise or an ingenious combination.

Methods of assessing the relative merits of bearing metals with any degree of reliability have not yet been established, and controversy as to the controlling qualities still exists. The maximum loading per unit area forms a major feature in relation to both the strength of the metal and the degree of wear which may be tolerated. The product of this load and the surface velocity, often quoted as a criterion, leaves much to be desired, as variation within this product of either factor may be too wide. Further, the influence of bearing metals on the critical  $ZN/P$  value, expressing change from film to boundary conditions, is not of great significance, as the related function is also dependent on bearing dimensions, clearance, surface conditions, lubrication method, and surface and lubricant characteristics.<sup>46</sup> In effect, gains shown in experiments involving lubrication may be attributed to, or dependent on, the mechanical and not the metallurgical features involved.

In practice, two main types of plain bearings are used, thin- and thick-shelled. For heavy-engineering purposes, where heavy loads, low speeds, and flexibility occur, thick-shelled bearings are employed. Moreover, in I.C. engine practice, when line boring is preferred, thick-shell practice is obviously involved. The shell thicknesses vary from 8–12 mm. at a journal diameter of 600 mm. to 2–4 mm. for small-diameter shafts. Although thinner shells may appear to be more favourable for the larger bearing diameters, this has not been confirmed in practice, and war-time economy measures involving reduced shell thicknesses proved unsuccessful.<sup>47</sup>

Marine engines in many instances have shafting of normalized plain-carbon steel with Brinell hardness values between 121 and 173, the lower hardness being more commonly used. White-metal bearings, therefore, are employed of the high-tin Babbitt types, containing 80–93% tin. The large surface areas which may be involved in bonding these bearing metals to copper alloys, cast iron, or cast steel present difficulties in obtaining entirely effective union over the whole surface. In the absence of suitable methods for proving the bond—other than hammer testing—keying of the metal is still widely employed as an added precaution, although it offers little improvement against fatigue failure.

Higher-speed engines, with increased bearing loads, high oil temperatures, shaft journals of heat-treated steel with a Brinell hardness of 300 and line-bored bearings employ thick-shelled lead-bronze, usually tin-backed to steel. The refinement of using top and bottom half-shells of different metals (i.e. white metal on the lightly loaded side and lead-bronze on the highly loaded side) is no longer widely employed. Such refinement was based more on considerations of economy than on bearing theory, and hence the change to all-lead-bronze bearings and the disappearance of this technique.

In practice, failures of thick-shelled bearings are divided evenly between (a) wiping and running of the metals, and (b) cracking or breaking up of the surface. A high percentage of failures of type (a) were due to oil starvation arising from neglect. Cracking of bearing metals by fatigue is exceedingly common, and may be associated with high oil temperature or simply with the inability of the metal to resist the loading conditions.

These failures are invariably associated with the bearing halves supporting the high loads in reciprocating machinery. Bottom halves of main and cross-head bearings and top halves of bottom-end bearings, therefore, are most susceptible to cracking, although bottom halves of bottom ends also suffer a fair proportion of failures in practice.

Alternative bearing metals having increased strength while retaining the other qualities of the high-tin Babbitt metals have not yet been produced, and engineers must, therefore, contend with the failures as best they can. Whether the aluminium–20% tin alloys or the 30 : 30 : 40 copper–silver–lead

alloy, exhibiting higher fatigue properties, will prove superior to either of those described in thick-shell applications has yet to be demonstrated.

More lightly loaded bearings for line shafting and similar purposes utilize lead-base Babbitt metals. These give excellent service, especially in view of the flexibility of marine-shafting installations and the variation in alignment with loading conditions of the ship.

The realization that greatly increased fatigue strength is a feature of very thin layers of bearing metals has led to the development of thin-shell bearing practice. These bearings are not extensively employed in marine engineering, but are found in some high-speed main and auxiliary engines. Shafts hardened by surface methods are most commonly used with bearings of this type. White metals and lead-bronze layers cast-bonded to steel shells are both favoured, although the latter find greatest usage, with or without lead and indium coatings. The excellent anti-friction properties of lead and indium reduce engine frictional losses, and extended use of these metals in bearing applications is expected.

Top-end bearings are made of white metal, lead-bronze or, more commonly, phosphor-bronze bushes, depending on the type of engine, pin hardness, lubrication, and temperature. Bearing metals of similar type are used in pumps, in addition to other bronzes, whilst for under-water service an alloy of zinc 30, tin 68, and copper 2% is frequently preferred.

Stern-tube and rudder bearings are salt-water lubricated, being of lignum vitæ and gun-metal mating materials. The stern-tube bearing supporting the tailshaft and propeller is of vital importance, as the ship must be docked for examination or repair to be carried out. Wear of the lignum vitæ must be kept to a minimum, and as gun-metal has provided a suitable contact metal in this respect, alternatives have not been greatly considered.

Gun-metals within the range 88 : 10 : 2 to 87 : 8 : 5 or leaded gun-metals of the 85 : 5 : 5 : 5 type are generally employed in the static or centrispun cast forms for these cylindrical liners. Where facilities are inadequate for casting in the entirety, sections may be cast and joined after shrinkage on to the shaft, by fusion-jointing methods. On completion of machining, the liner may be tested to 30 lb./in.<sup>2</sup> pressure to ensure soundness before shrinking on to the shaft. Contraction stresses in the longitudinal direction are reduced during shrinking by leaving a region of the bore at the liner centre with clearance and preferentially cooling this section first, after sliding on the shaft. Such regions are pumped up with red lead or similar compound, and the necessary holes, drilled for this purpose, are plugged.

Over a period of 15 months the recorded failures of gun-metal liners were as follows :

Severe Cracking	Severe Porosity	Cracking at Neck Ring	Corrosion— Bronson Scoring	Total
10	2	2	6	20



Penetration of sea water between liner and steel shaft may promote corrosion-fatigue failure of the shaft and certainly electrolytic corrosion will occur. Of the liner failures by cracking, cracks of the order of less than 1 ft. in length were found in all but two instances. Splitting from end to end occurred in one of these two liners and in the other two cracks approaching 3 ft. in length were evident. Local cracking and disintegration in the region of the neck ring could have been due to lack of adequate running clearance, but the full explanation of these failures was not found.

## X.—ELECTRICAL FEATURES OF METALS

The high electrical conductivity of copper has placed it in an almost indispensable position in the manufacture of equipment for the generation, transmission, and distribution of electricity. However, in recent years aluminium and its alloys have encroached to an increasing extent upon this field, owing to the need to conserve copper and to the greater specific strength and lower density of these alloys. Electrical-conductor grade aluminium, having a favourable ratio of weight to electrical conductivity, was suitably employed for high-tension transmission lines. More recently alloys of this metal have been used as the windings of transformers, motors, and generators for land purposes. However, copper is still preferred to aluminium alloys for marine purposes, as are lead alloys for the cable sheathing.

The influence of alloy additions has been determined in relation to the reduction in conductivity of pure copper. Silver additions of up to 1% result in only small reductions, but offer enhanced resistance to copper shortening.

High-resistance alloys are for preference solid solutions and Constantan (copper 55, nickel 45%) and Manganin (copper 88, nickel 12%) are widely employed; in addition, nickel-chromium alloys are used for high-temperature operation, with or without aluminium, at compositions within the solid-solution region.

Non-ferrous metals offer a wide range of magnetic characteristics which find extensive usage. Nickel forms an important alloying element with iron as a soft magnetic material, the high permeability peaks, at compositions of the order of 50 and 80% nickel, being the most suitable. Permanent-magnet alloys contain a number of non-ferrous metals, principally cobalt, nickel, aluminium, copper, and tungsten. These alloys contain iron as a major constituent, but there are a number of entirely non-ferrous alloys which exhibit useful ferromagnetic properties, although of only limited industrial importance. However, they are sufficient to demonstrate the potential possibilities of non-ferrous alloys in this capacity and, indeed, the overall electrical field offers one of the most important for non-ferrous metal research and development.

## XI.—RADIOGRAPHY

Casting and welding inspection, involving radiographic techniques, have been established as unparalleled proving methods. The merits of  $\gamma$ -radiography need little comment, with the exception of improvements afforded by the introduction and application of radioactive isotopes. Iridium 192 as applied to steel thicknesses of  $\frac{1}{2}$ –2 in. has resulted in high-quality radiographs comparable with those obtained by X-ray methods, particularly at the higher thicknesses. The main disadvantage of this isotope consists of its short half-life period of some 70 days. Cobalt 60, having a half-life of 5.3 years and used on thicknesses of steel up to 6 in., is widely employed for castings and weldments of thicker section.<sup>48</sup> Light alloys are more frequently radiographed by thulium 170, which has a lower equivalent kV. and is, therefore, more adaptable to these metals.

Thickness gauging using thallium 204, strontium 90, and iridium 192, in addition to applying back-scattering methods for the measurement of coating thicknesses or gauging plates and tubes for internal surface corrosion and wastage,<sup>49</sup> illustrate a few of the many applications of non-ferrous metals in radioactive condition.

## XII.—FUSION JOINTING AND DEPOSITION OF METALS

The jointing, rectification, and repair of metals by fusion methods now form a major industrial process, and the adaptability of alloys to this type of union has become an almost essential feature. A wide range of methods have been developed for fusion jointing, including many having specific applications. Metallurgical soundness and physical properties equivalent to the parent metal provide the desired object of fusion-welding processes, although when high strength is not a primary feature, other forms of joint involving fused filler metal are available.

Low-strength joints, in which fusion of the parent metal is not attained, have wide application. Soft and hard soldering, brazing, and bronze welding represent the chief such methods. Soft soldering with tin-lead alloys, with or without antimony and silver additions, is applied where temperature and stress conditions are of a low order. Strength investigations on these forms of joint have indicated maximum values for a 50:50 tin-antimony alloy which solidifies over a wide range of temperature.<sup>50</sup> The extensive use of soft soldering for iron, copper, zinc, lead, tin, nickel, and their alloys is sufficiently well known to require little comment.

Brazing, or hard soldering, involving deposits of copper-zinc alloys or copper-zinc-silver alloys (the familiar silver solders), provides alloys of superior strength capable of service at higher temperatures. Gas-torch, furnace, and pot-dipping processes, for jointing copper and its alloys, steels and stainless

steels, nickel, silver, and tungsten carbide, form extensive assembly processes. Monypenny<sup>51</sup> has discussed these methods in relation to turbine-blade segment assemblies and lacing wire attachment. The detrimental effects of a tensile stress, initiating cracking in steels during hard soldering,<sup>51,52</sup> cannot be overlooked, and influences of the higher jointing temperature requirements must be considered in relationship to possible physical and structural changes in the parent steels. Monel metal is not appreciably impaired by brazing, slight reduction in strength only occurring.

The application of these methods to copper steam-pipe flange attachment, providing many years of efficient service, and the jointing of steel shells to copper alloy tube-plates in heat-exchanger practice, demonstrate their reliability. Bronze welding with filler rods having fusion points exceeding 920° C. imposes limits on the parent metals, of which copper, copper-silicon alloys, cast iron, and steels are the most suitable. Although providing good joints, bronze welding is not widely employed, as methods involving fusion of the parent metal are frequently preferred.

In marine engineering the efficient welding of thick sections is essential, and many processes perfected for thin-gauge material have very restricted application. The degree of perfection attained in jointing steels by electric arc-welding processes has not been approached by any method applied to non-ferrous metals. Less extensive usage may be partly responsible for this fact, although greater complications of oxidization, melting points, thermal conductivity, and solidification characteristics have presented more formidable difficulties in these applications. In all instances, the degree of success obtained in fusion welding is greatly dependent on suitable preparation, fluxing, the development of efficient techniques, the operator's skill, and pre- and post-heating requirements. The quality of welds cannot be directly attributed to the unsuitability of a particular process without foundation on extensive experience. However, by elimination of some of the sources which could be responsible for error, simplification is achieved. Inert arc-welding processes, therefore, offer marked advantages when applied to many non-ferrous metals. The self-adjusting electrodes and argon atmosphere used in these processes have stimulated increased interest in this technique.

Despite the advances in welding processes, the practice of poured welding or "burning on", first established in the foundry, is still used. Repairs to castings of copper alloys, aluminium alloys, and ferrous materials are most commonly encountered, and with careful procedure and suitable fluxing satisfactory repairs, with metal of similar analysis to the base casting, can be achieved.

Deposits of metals and alloys may be applied by fusion methods for reclamation and repair of worn and damaged surfaces or for corrosion-resisting

purposes. Depending on the thickness required, either one of the methods referred to may be used or, alternatively, metal spraying may be adopted. The latter method offers advantages of simplicity, and any metal, except chromium, that can be produced in wire form may be deposited. However, since fusion of the parent metal is rarely achieved and the strength of the deposit is doubtful, reclaimed parts should possess scantlings sufficient to withstand the applied loads before rectification. The building-up of bearing surfaces and worn shaft surfaces has been extensively undertaken by this process with good results.

Surface spraying of zinc or aluminium for corrosion-resisting purposes has been applied to steel, zinc being applied to the hulls of small ships and tank surfaces.<sup>53</sup> The tendency for coatings to be porous requires that deposited metals should be anodic to the base metal, and fusion welding is preferable where severe erosion conditions prevail.

Electrodeposition of non-ferrous metal for reclamation, corrosion protection, and decorative purposes has become so well established as to require little comment. Nickel and chromium deposits have proved reliable for the reclamation of worn surfaces and in some cases have been preferred. Of the two metals, nickel has been most favoured, and for steel shafting continuous deposits in the form of bands obviate any possibility of the metal flaking off the surface.

Cadmium plating of steel in contact with aluminium has been proposed in constructions involving these two metals. The favourable electrode potential of cadmium could be utilized on the surfaces of steel bolts and similar items in contact with aluminium. Cadmium may, therefore, be used in this form to an increasing extent, engine builders in other industries having already proved its merits in reducing these dissimilar-metal problems.

Non-ferrous metals are readily used in all these deposition processes, but fusion-welding methods have not yet attained the desired efficiency required for marine purposes, particularly in regard to aluminium alloys, some alloys with aluminium contents, and many high-temperature materials. The use of these materials is being influenced by this feature and can be increased only by the introduction and development of more efficient and reliable welding methods.

### XIII.—FABRICATION FEATURES

A high proportion of non-ferrous metals is used in the cast condition for marine-engineering purposes, copper alloys being the principal materials concerned. A large number of these castings having weights less than 10 cwt. are used for valve bodies and components, pump parts, bushes, brasses, and similar items, whilst stern-tube parts, tailshaft liners, larger pump casings, impellers, and turbine-nozzle castings



more commonly weigh between  $\frac{1}{2}$  and 5 tons. Propeller castings are frequently of 30–40 tons weight in the cast condition, of which some 25–35% may be removed in machining operations. These items comprise some of the largest castings made in non-ferrous alloys and demonstrate the castability of these alloys and the high degree of foundry control employed. Although castings of 50 tons weight represent the largest produced for marine purposes in manganese-bronzes, the size limitations are imposed by machining facilities and design requirements.

Propeller castings of high-tensile ( $\alpha + \beta$ ) brasses or manganese bronzes are still extensively used, although aluminium bronzes are increasing in popularity as a result of their superior erosion qualities and increased strength, which permit greater flexibility in design. Although modified  $\beta$ -brasses of the high-tensile type offer excellent strength qualities, the liability of these alloys to intercrystalline cracking in sea water forms an undesirable feature. However, a limited number of propellers has been cast in alloys of this structure containing 2% nickel and having tensile strengths of 35 tons/in.<sup>2</sup>. Nickel additions of this order to normal manganese bronzes increase the erosion-resistance, but tend to increase difficulties of repair and rectification. Turbadium bronze, an alloy of this type, has been employed fairly extensively, the propellers of the *Queen Mary* of some 32 tons finished weight being typical examples.

Few propellers complete their service life without some repairs being necessary to eroded areas or to make good damage sustained by striking submerged objects. Failures due to defective castings are comparatively infrequent, indicating the generally high quality obtained.

Improvements in foundry control, casting methods, and inspection techniques have enhanced the soundness and uniformity of properties of all castings. Although welding methods have provided simple means of reclaiming and repairing defective castings, it is essential that this fact should not be reflected in relaxation of control or of efforts to improve the casting procedure and so reduce the defects encountered.

The improvement in pressure-tightness<sup>54</sup> of bronze castings effected by lead additions has resulted in a preference for this form of alloy. Low-pressure valve bodies and parts, sea connections, liners, and similar parts have, therefore, been cast in both these materials.

Manganese, nickel, and aluminium bronzes have been extensively employed for higher-pressure parts and more severe temperature conditions, although for steam chests steels are being more extensively used, as the upper operating limits of these non-ferrous alloys are being exceeded or have not been sufficiently well established to warrant their use.

Centrifugal-casting methods are extensively employed where the form of the components is adaptable to the process. Both chill and sand moulds are used, the former for gear blanks and bushes, where the improved structures at the chilled surfaces are of

importance; sand moulds are employed for tailshaft liners and stainless-steel piston crowns.

The higher-strength alloys are taking precedence for cast machinery parts, the aluminium bronzes being the most popular. Difficulties due to the aluminium content do not appear to be unduly severe for casting or welding, provided that reasonable precautions are taken. Vulcan hydraulic coupling rotor and clutch parts have been cast in these alloys, the intricate oil passages being readily reproduced and the strength being adequate for rotational speeds in excess of 750 r.p.m.

Aluminium alloy castings are most commonly used for lower-strength parts where ease of handling is essential. Sand- and die-cast pistons of these alloys are widely used for the smaller oil engines, as in other industries. Die-casting and precision investment-casting of non-ferrous alloys have not been extensively used in marine engineering, although high machining costs have led to consideration of these methods for low-stressed turbine and other machinery parts, at present machined from wrought materials.

Wrought alloys are used for shafting purposes in extruded, rolled, and, less frequently, forged form. The convenience of rolled or extruded round bar is useful for shafting having loose steel couplings. In consequence, as a result of the generally available sections and economic considerations, shaft diameters in excess of 5 in. are rarely used.

Aluminium alloys used in ship construction are not made in such convenient sizes and sections as steels, and a tendency to increase the sizes of plates, in particular, has been in progress to meet these demands. Cold working of plates and sections to obtain more favourable mechanical properties imposes limitations on welding, in that the weld and fusion zone will be inferior in strength to the remaining parent metal.

The use of the plasticity of non-ferrous metals is of value for jointing purposes. Metal gaskets are most commonly of lead, aluminium, tin, nickel, Monel metal, and copper. Selection of the metal depends on the pressure, temperature, type of joint, and possibility of galvanic action with the flange material.

#### XIV.—CONCLUSIONS

Within the scope of this survey some of the merits and limitations of non-ferrous metals in marine engineering have been considered. Combating corrosion still provides the most important function of these metals, and although improved alloys have reduced the rate of deterioration against some forms of this attack, there is still plenty of scope for further developments.

For elevated-temperature applications, low- and high-alloy steels have replaced non-ferrous metals in steam plant and in steam-turbine and gas-turbine compressor components. The Nimonic alloys, how-

ever, are preferred by many manufacturers for gas-turbine blading and similar stressed components.

Light alloys are still at an early stage of development for shipbuilding purposes. Their future progress is largely dependent on a reduction in cost for the equivalent steel structure, and this can be related to the necessities of improvements in both material and fabrication methods.

Whilst there is a trend for plain bearings of steam turbines to be of the steel-backed, thin-shell, white-metal types in place of the existing thick-shelled, bronze-backed types, similar trends are impossible in heavy-oil engines. Fatigue failures of the thick-shelled, white-metal bearings used in these engines are not infrequent, and bearing metals of improved strength and capable of use with plain carbon steel journals would be advantageous.

Many of the non-ferrous metals used have limitations of resources and production. In consequence it is undesirable that either the engineer or the metallurgist should restrict his views too greatly in considering alloys for particular service. With the large number of existing alloys and the prospect of further increases in the future, close co-operation between engineer and metallurgist is desirable in order that the most efficient and economical selections of material may be made.

#### ACKNOWLEDGEMENTS

I desire to express my thanks to many of my colleagues and others who have assisted me in the preparation of this Address and, in particular, to Mr. G. P. Smedley, B.Eng., B.Met., an Engineer Surveyor on my staff.

#### REFERENCES

1. C. E. Meyer, *Trans. Soc. Naval Arch. Marine Eng.*, 1949, **57**, 379.
2. C. A. Parsons and R. J. Walker, *Trans. N.E. Coast Inst. Eng. Ship.*, 1906-7, **23**, 157.
3. F. M. Timponson, *Trans. Inst. Marine Eng.*, 1906-7, **18**, 3.
4. E. Shackleton, *ibid.*, 1908-9, **20**, 3.
5. T. D. Kelly, *ibid.*, 1907-8, **19**, 3.
6. W. R. Cummins, *ibid.*, 1910-11, **22**, 112.
7. L. M. Fox, *ibid.*, 1910-11, **22**, 3.
8. F. G. Martin, *J. Inst. Metals*, 1928, **40**, 7.
9. R. May, *ibid.*, 1928, **40**, 141.
10. P. T. Gilbert, *Trans. Inst. Marine Eng.*, 1954, **66**, 1.
11. G. L. Bailey, *J. Inst. Metals*, 1951, **79**, 243.
12. C. V. Boykin and M. L. Sellers, *Trans. Soc. Naval Arch. Marine Eng.*, 1953, **61**.
13. J. S. Forrest and J. M. Ward, *Inst. Elect. Eng. Preprint*, 1954.
14. J. T. Crennell, *Chem. and Ind.*, 1954, (8), 204.
15. R. R. Rogers and W. R. G. Stewart, *Trans. Canad. Inst. Min. Met.*, 1949, **52**, 107.
16. P. T. Gilbert and R. May, *Trans. Inst. Marine Eng.*, 1950, **62**, 291.
17. Symposium on "Cathodic Protection" (Soc. Chem. Ind.), 1953; see *Chem. and Ind.*, 1954, (3), 56; (4), 93; (7), 172; (8), 204.
18. J. Lamb, E. V. Mathias, and W. G. Waite, *Trans. N.E. Coast Inst. Eng. Ship.*, 1954, **70**, 377.
19. L. Kenworthy, *J. Inst. Metals*, 1943, **69**, 67.
20. S. Logan Kerr, *Trans. Amer. Soc. Mech. Eng.*, 1937, **59**, 373.
21. J. M. Mousson, *ibid.*, 1937, **59**, 399.
22. R. Beeching, *Trans. Inst. Eng. Ship. Scotland*, 1946, **90**, 203.
23. W. C. Stewart and W. L. Williams, *Proc. Amer. Soc. Test. Mat.*, 1946, **46**, 836.
24. J. McNeil, *Trans. Inst. Marine Eng.*, 1931, **43**, 561.
25. R. E. Wilson, *ibid.*, 1942-43, **54**, 152.
26. W. E. Ballard, G. F. Fairbairn, and F. S. Pilkington, *ibid.*, 1942-43, **54**, 1.
27. G. T. Callis, *Metal Ind.*, 1951, **79**, 167.
28. S. F. Dorey, *Trans. Inst. Marine Eng.*, 1935-36, **47**, 305.
29. S. F. Dorey, *Trans. N.E. Coast Inst. Eng. Ship.*, 1938-39, **55**, 203.
30. R. S. Dean and J. E. Ryjord, *Metals and Alloys*, 1930, **1**, 410.
31. N. P. Inglis and G. F. Lake, *Trans. Faraday Soc.*, 1931, **27**, 803.
32. H. J. Gough and D. G. Sopwith, *J. Iron Steel Inst.*, 1937, **135**, 293p.
33. A. J. Gould, *ibid.*, 1949, **161**, 11.
34. T. J. Dolan, *J. Appl. Mechanics*, 1938, **5**, 140.
35. H. J. Tapsell, *Iron Steel Inst. Special Rep.* 1952, (43), 169.
36. R. G. Voysey, *Proc. Inst. Mech. Eng.*, 1945, **153**, 483.
37. H. V. Kinsey and M. T. Stewart, *Trans. Amer. Soc. Metals*, 1951, **43**, 193.
38. R. M. Parke and F. P. Bens, *Symposium on Materials for Gas Turbines (Amer. Soc. Test. Mat.)*, 1946, 80.
39. N. D. Benson, J. McKeown, and D. N. Mends, *J. Inst. Metals*, 1951-2, **80**, 131.
40. T. W. F. Brown, *Proc. Inst. Mech. Eng., Preprint*, 1954.
41. E. C. B. Corlett, *Trans. Inst. Naval Arch.*, 1950, **92**, 376.
42. A. J. Murphy, *Trans. Inst. Marine Eng.*, 1945-46, **57**, 31.
43. M. G. Forrest, *Trans. Soc. Naval Arch. Marine Eng.*, 1947, **55**, 305.
44. E. C. B. Corlett, *Trans. N.E. Coast Inst. Eng. Ship.*, 1951-52, **68**, 221.
45. M. Cook, *J. Inst. Metals*, 1953-54, **82**, 93.
46. H. W. Swift, *Proc. Inst. Mech. Eng.*, 1935, **129**, 399.
47. C. C. Pounder, *ibid.*, 1949, **160**, 312.
48. J. D. Hislop, *Trans. Inst. Marine Eng.*, 1951, **63**, 83.
49. (Sir) J. Cockcroft, *J. Inst. Prod. Eng.*, 1953, **32**, 342.
50. "The Welding, Brazing, and Soldering of Copper and Its Alloys" (Copper Development Assoc. Publ. No. 47), p. 147. 1951.
51. J. H. G. Monypenny, *Trans. Inst. Marine Eng.*, 1945-46, **57**, 129.
52. R. Genders, *J. Inst. Metals*, 1927, **37**, 215.
53. J. Barrington Stiles, *Trans. Inst. Marine Eng.*, 1948, **60**, 239.
54. F. Hudson, *J. Inst. Metals*, 1944, **70**, 407.



# NOTE ON THE CONSTITUTION OF THE TITANIUM-GOLD SYSTEM IN THE REGION 0-6 ATOMIC PER CENT. GOLD\*

1548

By (MRS.) M. K. McQUILLAN,† M.A., MEMBER

## SYNOPSIS

Micrographic examination of quenched specimens has shown that the titanium-gold system is of the eutectoid type. The eutectoid temperature has been found to be  $830^{\circ} \pm 2^{\circ} \text{C.}$ , and the solubility of gold in the  $\alpha$  solid solution at this temperature is approximately 3 at.-%. The second constituent is  $\text{Ti}_3\text{Au}$ .

## I.—INTRODUCTION

ALTHOUGH much constitutional work has been done on titanium alloy systems in recent years, some of the gaps still remaining in our knowledge hinder any systematic approach to the problem of titanium-alloy behaviour. As part of a general attack on this problem, a micrographic study of the titanium-rich region of the titanium-gold system has been carried out, the chief points of interest being the effect of gold on the  $\alpha \rightleftharpoons \beta$  transformation temperature and the degree of solubility of gold in  $\alpha$ -titanium. The general nature of this part of the system has been established, although the phase boundaries have not yet been located with final precision.

## II.—EXPERIMENTAL PROCEDURE

Iodide titanium, containing no appreciable impurity other than zirconium of the order of 0.5 at.-%, and having a transformation range in the unalloyed condition of  $872^{\circ}$ – $880^{\circ} \text{C.}$ , was melted with gold of 99.99% purity on a water-cooled copper hearth in an arc furnace under argon at reduced pressure. No appreciable weight change occurred during melting, and nominal compositions, which were in fairly good agreement with analysed compositions, have been used.

Heat-treatments were carried out as described in an earlier paper,<sup>1</sup> direct quenching in a stream of water being used whenever rapid cooling appeared to be important, e.g. for alloys heated in the  $\beta$ -phase region. Stringent precautions were taken against contamination of the alloys during heat-treatment. Except where otherwise stated, temperatures may be assumed to be correct to  $\pm 5^{\circ} \text{C.}$

## III.—EXPERIMENTAL RESULTS

Difficulty was experienced in determining accurately the  $\beta/(\alpha + \beta)$  and  $\alpha/(\alpha + \beta)$  boundaries, owing to

the fact that the  $\beta$ -phase, which could not be retained by quenching at any of the compositions covered by this work, transformed in such a way that the trans-

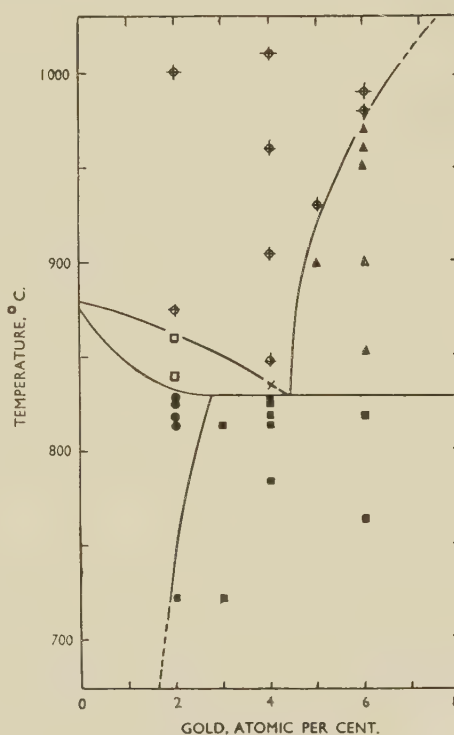


Fig. 1.—Partial Constitutional Diagram for the Titanium-Gold System.

- KEY.
- ⊕ Transformed  $\beta$ .
  - ▲ Transformed  $\beta + \text{Ti}_3\text{Au}$ .
  - $\alpha + \text{transformed } \beta$ .
  - $\alpha$ .
  - $\alpha + \text{Ti}_3\text{Au}$ .
  - × Point given by hydrogen-pressure experiment.

formation product differed very little in appearance from  $\alpha$  formed from  $\beta$  by nucleation and growth under equilibrium conditions. No true martensite

\* Manuscript received 23 December 1953.

† Imperial Chemical Industries, Ltd., Metals Division, Birmingham.

was formed, although the quenched structures became rather more martensitic in appearance, and also harder, the higher the temperature from which the  $\beta$  was quenched. The interpretation of the microstructures was aided by information obtained from an experiment carried out by the hydrogen-pressure method<sup>2</sup> on a 4 at.-% gold alloy, which began to transform from  $\beta$  to  $\alpha$  at 835° C., thus confirming that additions of gold to titanium depress the transformation.

The constitutional diagram as determined by this work is seen in Fig. 1. The eutectoid temperature has been found to be  $830 \pm 2^\circ$  C. and the eutectoid composition  $4.4 \pm 0.2$  at.-%. The compound which is formed, together with the  $\alpha$  solid solution, by eutectoidal decomposition of the  $\beta$  phase, has been shown by X-ray diffraction methods to be  $\text{Ti}_3\text{Au}$ , as described by Duwez and Jordan.<sup>3</sup> It has a  $\beta$ -tungsten structure with  $a = 5.096$  Å. The maximum solubility of gold in  $\alpha$ -titanium is approximately 3 at.-%.

#### IV.—DISCUSSION

Gold is one of the few  $\beta$ -stabilizing elements which is soluble to any appreciable extent in  $\alpha$ -titanium. In this it resembles copper,<sup>2,4</sup> which is a member of

the same group in the Periodic Table. There is, however, a significant difference between the atomic size-factors, relative to titanium, of copper (12.9%) and gold (2%). Since the size-factors of a number of the  $\beta$ -stabilizing elements which have no appreciable solubility in the  $\alpha$  phase lie within this same range, it is probable that electronic factors rather than atomic sizes exert the controlling influence on  $\alpha$  solubility.

#### ACKNOWLEDGEMENTS

Among her colleagues at Imperial Chemical Industries, Ltd., Metals Division, the author wishes to thank Dr. N. P. Inglis for his encouragement of the work on titanium-alloy behaviour, Mr. E. Yeomans for carrying out the X-ray work, and Mr. J. Lumby for assistance with the experimental work. Her thanks are also due to Dr. A. D. McQuillan, of Birmingham University, for carrying out the hydrogen-pressure experiment.

#### REFERENCES

1. M. K. McQuillan, *J. Inst. Metals*, 1953–54, **82**, (9), 433.
2. A. D. McQuillan, *ibid.*, 1951, **79**, 73.
3. P. Duwez and C. B. Jordan, *Acta Cryst.*, 1952, **5**, 213.
4. A. Joukainen, N. J. Grant, and C. F. Floe, *Trans. Amer. Inst. Min. Met. Eng.*, 1952, **194**, 766.



# GRAIN-REFINING ADDITIONS FOR CAST COPPER ALLOYS\*

1549

By A. CIBULA,† M.A., A.I.M., MEMBER

(Communication from The British Non-Ferrous Metals Research Association)

## SYNOPSIS

The object of the work described was to develop a method of grain-refining cast copper alloys, using the theory of the grain-refining mechanism deduced from earlier work on aluminium and other alloys (*J. Inst. Metals*, 1949–50, **76**, 321). A number of borides, nitrides, and carbides of transition metals were selected as possible nuclei for the solidification of copper-rich solid solutions, as they appeared to have suitably high melting points and stabilities, with lattice structures similar to that of copper. The influence of the possible grain-refiners was studied mostly upon sand-cast copper-tin alloys, though a few experiments were made on alloys containing aluminium, lead, and zinc. Undercooling measurements were also made during the solidification of several coarse-grained and fine-grained alloys.

Several of the additions proved to be effective grain-refiners. The presence of nuclei was confirmed by the much-reduced undercooling detected in copper-tin alloys refined by niobium boride. In bronzes and gun-metals, however, the nuclei produced fine equiaxial structures only when sufficient tin or lead or tin + lead was present to restrict the growth of the first-formed grains by establishing concentration gradients around them and thus to allow new grains to be nucleated.

The most effective grain-refining additions in commercial bronzes and gun-metals were found to be: (i) 0.03% zirconium with carbon and/or nitrogen in the absence of sulphur, (ii) 0.2% titanium with 0.03% boron, and (iii) 0.1% iron or cobalt with 0.03% boron. In iron-free  $\beta$ -brass, 0.03% zirconium and 0.02% boron together caused marked grain-refinement.

## I.—INTRODUCTION

THERE is at present no commercial method of grain-refinement which is of more than limited application to copper-base casting alloys, for although fine grain-sizes may be produced in most copper alloys by the use of very low casting temperatures or by the addition of up to 2% iron, there are often serious objections to both methods in practice. The theory of grain-refinement developed in earlier work<sup>1</sup> on cast light alloys, however, appeared to be of quite general application, and an attempt has been made to use it in the present research to produce a method of grain-refining copper alloys.

The earlier observations on the grain-refinement of light alloys suggested that the most profitable approach would be the introduction of fine particles into copper-alloy melts, which could act as nuclei during solidification. The most important property required in a nucleating compound appeared to be that its lattice should be similar in structure and dimensions, at least in certain planes, to that of the crystals to be refined, and it was concluded from this that the nitrides, carbides, and borides of several transition metals might form suitable nucleating particles. This conclusion has been tested by undercooling and grain-size measurements in castings of various copper alloys, using the techniques described in Section III.

The effects of several of the refining compounds

were compared by adding them to 7-kg. melts of phosphorus-deoxidized bronzes and gun-metals, from which  $\frac{3}{4}$ - and  $2\frac{1}{4}$ -in.-dia. bars were sand-cast for grain-size measurements. Finally, a few experiments were made to select grain-refining additions for cast  $\alpha/\beta$  brass and an iron-free  $\beta$ -brass containing aluminium.

## II.—PREVIOUS WORK

### 1. THE GRAIN-REFINEMENT MECHANISM IN CAST ALLOYS

In previous work<sup>1</sup> on high-purity castings, it was observed that marked undercooling occurred near the mould wall before the first dendrites could form there, but that these grains subsequently grew without hindrance (as shown by the rapid and complete recalescence which followed undercooling) and a wholly columnar structure resulted.

When a suitable alloying element, e.g. copper or nickel, was dissolved in the melt, recalescence after undercooling at the surface of the casting became slower and incomplete; undercooling then spread into the interior of the casting as it cooled and, if sufficient of the alloying element had been added, became great enough to cause new grains to grow there and a coarse equiaxial structure to be formed. The more extensive undercooling and slower recalescence in these castings indicated that the release of latent heat had become

\* Manuscript received 21 January 1954. The work described in this paper was made available to members of The British Non-Ferrous Metals Research Association in con-

fidential research reports issued during 1951–53.

† Research Investigator, British Non-Ferrous Metals Research Association, London.

too slow to balance the abstraction of heat by the mould during the first stages of solidification; as the number of crystals growing in the melt was greater than in the pure metal, the slower release of heat of fusion implied that crystal growth had been retarded by the solute metal.

This deduction was consistent with suggestions<sup>2-6</sup> that in alloys where the initial solid differs greatly from the melt in composition, a layer of low-melting-point liquid forms round the first dendrites, owing to incomplete diffusion, and hinders their further growth; it has been suggested<sup>6</sup> that the effects of the solute-rich barrier is reinforced in some alloys by the precipitation of a second phase round the dendrites. However, although this or a similar mechanism may produce equiaxial instead of columnar structures, the grain-size remains large.<sup>1</sup>

Experiments on iron,<sup>7</sup> magnesium,<sup>8,9</sup> and aluminium<sup>1,10,11</sup> alloys have shown that the finest macrostructures are obtained when, in addition to a solute which hinders crystal growth, nucleating particles are present in the melt, which assist the formation of solid-solution crystallites and enable them to form after very little undercooling. In the absence of a solute, most of the added nuclei may be ineffective because the grains nucleated at the surface of the casting can grow towards the centre unimpeded by concentration gradients and thus produce a narrow columnar structure; with a suitable solute, on the other hand, crystal growth is sufficiently retarded to allow further crystallites to be nucleated in large numbers and a fine structure to result.<sup>1</sup>

Turnbull<sup>12</sup> and others have shown that even high-purity metals contain a few stray nuclei, but these particles differ greatly in effectiveness and are seldom numerous or effective enough to reduce the grain-size very much; in contrast, the grain-refining nuclei discussed above are specific compounds which have powerful nucleation effects and can easily be dispersed in the melt in large numbers. Consideration of the properties of nuclei which have already been identified in metals and other materials<sup>13-17</sup> suggests that the following properties in a compound favour strong nucleation: (i) a similarity of lattice structure and dimensions to that of the phase to be nucleated, at least in certain lattice planes; (ii) strong adsorption bonds between the atoms of the phase to be nucleated and atoms or ions of one of the constituents of the nucleating compound; (iii) a sufficiently high melting point and stability for the particles to remain solid and undecomposed in the melt. The extent to which the first two conditions are satisfied presumably controls the effectiveness of the nuclei; the stronger the adsorption bonds, for example, the greater the lattice misfit which can be tolerated.

The minimum degree of lattice fit which allows efficient nucleation cannot be easily assessed at present, but misfits of up to 20% have been observed in a number of effective nuclei and even greater misfits, up to 30%, do not prevent nucleation in other instances.

The existence of strong adsorption bonds can be deduced only indirectly; e.g. from the formation of a stable compound between a constituent of the nucleus and, in the present case, copper. There is evidence that the nature of the interatomic bonds in the nucleating compound may influence the strength of the adsorption bonds, an important component of which appears to be electrostatic forces;<sup>14</sup> it has been suggested that ionic compounds, or those with strongly metallic properties, are more effective as nuclei in metallic and ionic melts or solutions than are homopolar compounds, which are only slightly ionized. Because of the lack of data on the formation of adsorption bonds, grain-refining additions for copper alloys have been mainly selected in the present work according to their structures, melting points, and stabilities. To assess the commercial value of a grain-refining addition, other properties such as its effect on casting properties must, of course, be considered.

## 2. GRAIN-REFINEMENT OF COPPER ALLOYS

The marked grain-refinement obtainable by the use of low pouring temperatures has been pointed out in earlier papers<sup>2,18</sup> and is often used in casting ingots for working. The refinement is probably due to the formation of crystallites of solid metal in the pouring stream or in the mould; these become distributed by turbulence and act as nuclei for continuing solidification.<sup>2,19</sup> Grain-refinement has been similarly produced by means of metallic wires placed in the mould before casting.<sup>20</sup> The maximum casting temperature at which a fine macrostructure can be obtained decreases as the size of the casting increases and as turbulence during pouring decreases; for example, very low pouring temperatures have to be used in the Durville casting process, in the absence of a grain-refining element, owing to the small degree of turbulence.<sup>2,21</sup> In the present work, a casting temperature was used which was high enough to avoid refinement by this means, to prevent possible confusion with the effects of the added elements.

Marked grain-refinement has been obtained in a large number of copper alloys by means of iron additions.<sup>22-24</sup> In several of these alloys, the iron is precipitated as primary dendrites of  $\gamma$ -iron when its concentration is greater than the peritectic-point composition, and there is evidence that these primary crystals nucleate the solidification of copper-rich solid solutions.<sup>23,24</sup> The difference between the interatomic distances in the face-centred cubic lattices of copper and  $\gamma$ -iron is little greater than 1% (compared at room temperature). The additions of iron required for grain-refinement are large (1-3%) and the resulting oxide skin in some alloys is objectionable; the refining effects are mostly used in practice in the aluminium-containing alloys. Even larger additions of cobalt act in a similar way to iron.

Additions of up to 1.5% nickel,<sup>25</sup> 5% lead,<sup>26</sup> 0.02% lithium,<sup>27</sup> 1% vanadium or chromium,<sup>28</sup> 0.25%



zirconium,<sup>29</sup> and 0.5% titanium<sup>30</sup> have also been claimed to produce grain-refinement in cast copper alloys, although in several cases the reduction in grain-size indicated was small. Boron additions (up to 4.5%) have been advocated for grain-size control in copper alloys;<sup>31, 32</sup> in one paper,<sup>32</sup> it has been suggested that grain-refinement is due to nucleation of a  $\beta$ -phase by  $B_4C$  particles.

Northcott<sup>33</sup> studied the influence of small additions of many elements on the growth of columnar grains in copper alloys. He found that the influence of the added elements showed a pronounced periodicity corresponding to their positions in the Periodic Table, some of the elements which most strongly restricted columnar growth being oxygen, sulphur, phosphorus, titanium, nickel, selenium, tin, tellurium, and lead. It was suggested that the influence of low concentrations of these alloying elements was caused primarily by their adsorption on to the surfaces of dendrites in the melt, and that the periodicity in the consequent interference with crystal growth was due to variations in the strength of the adsorption bonds; other physical properties of the alloying elements might have varied in the same way,<sup>34</sup> however, and in the absence of any specific evidence that adsorption had occurred, the possibility exists that differences in the rates of diffusion in molten copper, for example, or nucleation by compounds of the additions, were responsible for the effects observed. It is significant that several of the elements which had marked effects in the rapidly cooled ingots studied by Northcott have only a slight influence on the structure of sand castings; this suggests that, if adsorption does occur, its effect can be important only at high rates of crystal growth.

### 3. SELECTION OF NUCLEI FOR COPPER ALLOYS

Many of the carbides, nitrides, and borides formed by the transition metals have simple lattice structures in which the non-metallic atoms occupy interstitial positions.<sup>35</sup> For this reason these compounds are very similar to the metals in structure and have other strongly metallic properties; they are therefore likely to nucleate metallic melts. This probably explains not only why many of the compounds form nuclei in aluminium alloys,<sup>1, 11</sup> but also the fact that several addition elements which might be expected to form carbides, nitrides, and borides have been noted as grain-refiners in ferrous alloys (although other explanations have been given): e.g. zirconium and titanium in iron-carbon alloys<sup>36</sup> and boron in iron<sup>3</sup> and iron-chromium alloys.<sup>37</sup>

The use of carbides, nitrides, and borides (including aluminium diboride) as grain-refiners in copper alloys was therefore considered first in the present work. The known lattice structures, densities, and stabilities of the most suitable of these compounds are given in Table I. Several of the transition metals form other borides with apparently less suitable structures, and these may precipitate in preference to those listed in the table, thus preventing grain-refinement.

All the compounds have melting points above the liquidus temperatures of cast copper-base alloys. Their stabilities, where known, are high and they are likely to exist without decomposition in molten copper

TABLE I.—*Properties of the Most Suitable Nucleating Compounds for Copper-Base Alloys.*<sup>38-47</sup>

Cu structure and lattice dimensions: f.c.c.,  $a_0 = 2.55$ ; interatomic distance on closest-packed plane: 2.55 Å; density at 20° C.: 8.94 g./c.c.

Formula	Structure and Lattice Dimensions, Å.	Inter-atomic Distance on Closest Packed Plane, Å.	Misfit with Lattice of Solid Copper (at 20° C.), %	Density (at 20° C.), g./c.c.	Free Energy of Formation at 1400° K., k.cal./g.-atom C or N
TiC	Interstitial f.c.c. lattice structures $\left\{ \begin{array}{l} a_0 = 4.32 \\ a_0 = 4.23 \end{array} \right.$ AlB <sub>2</sub> -type hexagonal. Metal atoms on simple hexagonal lattice, $a_0 = 3.03$ , $c_0 = 3.23$	3.05	+20	4.3	-39
TiN		2.99	+17	...	-43
TiB <sub>2</sub>		3.03	+19	4.5	...
VC	Interstitial f.c.c. structure, $a_0 = 4.15$ or 4.30	2.94 or 3.04	+15 or 19	5.4	-10
VN	Interstitial f.c.c. structure, $a_0 = 4.13$	2.92	+14	...	-8
VB <sub>2</sub>	AlB <sub>2</sub> -type hexagonal, $a_0 = 3.00$ , $c_0 = 3.06$	3.00	+18	4.6	...
CrB <sub>2</sub>	AlB <sub>2</sub> -type hexagonal, $a_0 = 2.97$ , $c_0 = 3.07$	2.97	+16	6.1	...
FeB	Orthorhombic. Metal atoms in distorted hexagonal layers	2.7-3.0	+18	...	...
MnB	Orthorhombic (FeB type). Metal atoms in distorted hexagonal layers	2.7-3.0	+18	6.5	...
ZrC	{ Interstitial f.c.c. structures $\left\{ \begin{array}{l} a_0 = 4.69 \\ a_0 = 4.63 \end{array} \right.$ AlB <sub>2</sub> -type hexagonal, $a_0 = 3.17$ , $c_0 = 3.53$	3.32	+30	6.9	-37
ZrN		3.27	+28	...	-45
ZrB <sub>2</sub>		3.17	+24	6.2	...
NbC	{ Interstitial f.c.c. structures $\left\{ \begin{array}{l} a_0 = 4.44 \\ a_0 = 4.36 \end{array} \right.$ AlB <sub>2</sub> -type hexagonal, $a_0 = 3.09$ , $c_0 = 3.31$	3.14	+23	7.8	...
NbN		3.08	+21	...	...
NbB <sub>2</sub>		3.09	+21	6.6	...
Mo <sub>2</sub> C	{ Interstitial h.c.p. structures $\left\{ \begin{array}{l} a_0 = 2.99, \\ c_0 = 4.71 \end{array} \right.$ Trigonal; hexagonal cell $a_0 = 3.01$ , $c_0 = 20.9$ . Metal atoms in close-packed planes in layers	2.99	+17	8.9	-7
MoC		2.88	+13	8.6	...
MoB <sub>2</sub> ·3(e)		3.01	+18	7.0	...
WC	{ Hexagonal close-packed interstitial structures $\left\{ \begin{array}{l} a_0 = 2.89, \\ c_0 = 2.82 \end{array} \right.$ Hexagonal, $a_0 = 2.98$ , $c_0 = 13.9$ . Metal atoms in close-packed planes in layers	2.89	+13	15.5	...
W <sub>2</sub> C		2.99	+17	17.2	...
WB <sub>2</sub> ·3(e)		2.98	+17	11.0	...
AlB <sub>2</sub>	Hexagonal, $a_0 = 3.00$ , $c_0 = 3.25$	3.00	+18	3.2	...

alloys, particularly as the compounds of the non-metals (carbon, nitrogen, and boron) with copper and its common alloying elements are generally unstable or non-existent. Many of the components of the borides, nitrides, and carbides form stable oxides, however, and efficient deoxidation of the melts before the additions are made would be necessary.

The metal atoms in almost all these compounds are in cubic or hexagonal lattices in which the distances between metal atoms are up to 30% greater than the corresponding distances in the copper lattice (com-

pared with misfits of 0-16% with the aluminium lattice); many of the differences in the lattice dimensions seemed likely to be less than the limit for efficient nucleation.

For these reasons, several of the compounds listed in Table I appeared to be suitable for the grain-refinement of copper alloys in which the primary phase is an  $\alpha$  solid solution. Other compounds which were considered in a similar manner included the

## 2. PREPARATION OF MELTS

The melts were prepared in alumina-coated Salamander crucibles in gas-fired injector furnaces. The copper was melted under a slightly oxidizing flame and, except where otherwise stated, no other degassing treatment was used. After the major alloying elements had been dissolved, the melts were deoxidized with 0.03% phosphorus—sufficient to leave a small

TABLE II.—Composition and Preparation of Alloys.

Metal or Alloy	Purity or Alloy Content, %	Impurities, %	Source or Method of Preparation
(a) <i>Pure Metals</i>			
Copper . . .	>99.99% (excl. oxygen and sulphur)	Only As ( $\sim 0.001$ ) detected spectrographically in several batches	Commercial electrolytic
Tin . . .	Approx. 99.8	0.065 Pb, 0.028 Sb, 0.01 Bi, 0.005 Fe, 0.025 As in typical batch	Refined stick tin
Zinc . . .	99.99	...	" "
Lead . . .	>99.99	0.001 Fe, 0.002 Cd	Crown Special
Nickel . . .	>99.99	...	Tadanac ingot
Aluminium . .	>99.99	0.03 Fe, 0.055 C, 0.001 S in typical batch	Carbonyl pellets
		...	Super-purity
(b) <i>Aluminothermic Master Alloys</i>			
Al-B . . .	Approx. 19 B	1.53 Fe, 0.48 Si	Commercial aluminothermic alloy
Al-Ti . . .	" 9 B	1.45 Fe, 0.57 Si	
Al-V . . .	50.5 Ti	1.35 Fe, 1.1 Si	" " " "
Al-V . . .	Approx. 28 V	1.18 Fe, 0.44 Si	" " " "
Al-Nb	10 V		
	17.4 Nb + Ta	6.04 Fe, 0.48 Si	
	15.0 Nb + Ta	0.45 Fe, 0.61 Si	Commercial "Al-70%" Nb + "Ta dissolved in molten Al at $\sim 1500^\circ$ C.
Al-Zr . . .	(Ta approx. 5% Nb) 32 Zr	5.42 Fe, 4.57 Si	Commercial aluminothermic alloy
(c) <i>Aluminium-Free Master Alloys</i>			
Cu-B . . .	5.2 B	0.45 Mg, 0.15 Fe, 0.1 Si	Commercial alloy
	1.4 B	0.14 Mg, 0.3 Fe	} Prepared by reduction of $B_2O_3$ over copper melt by plunging Mg at $1300^\circ$ C.
	6.3 B	0.33 Mg, 0.08 Fe, 0.4 Si, 0.06 C	
Cu-Ti . . .	24.8 Ti	...	Vacuum-melted Ti dissolved in molten Cu at $1100^\circ$ C.
Cu-Zr . . .	9.6 Zr	0.1 Fe, 0.01 each Al, Mn, Si, and Sn	Commercial Zr sheet dissolved in molten Cu at $1100^\circ$ C.
Cu-Fe . . .	12.0 Fe	...	Swedish ingot iron dissolved in molten Cu at $1400^\circ$ C.
Cu-Cr . . .	9.4 Cr	<0.2 Al	Commercial alloy
Cu-Nb . . .	5.6 Nb	$\sim 0.1$ Fe, 0.03 Ti, 0.02 Si	Commercial Cu-70 Nb alloy dissolved in molten Cu at $1900^\circ$ C. <i>in vacuo</i>
Cu-Co . . .	13.9 Co	...	Electrolytic Co (99.9%) dissolved in molten Cu at $1300^\circ$ C.
Cu-Mn . . .	33.4 Mn	...	Electrolytic Mn (99.9%) dissolved in molten Cu at $1100^\circ$ C.

transition-metal silicides, arsenides, tellurides, and phosphides, but these seemed less suitable for the initial experiments.

## III.—EXPERIMENTAL METHODS

### 1. MATERIALS

The compositions of the materials and the sources or methods of preparation of the master alloys are given in Table II. The aluminothermic master alloys, which were impure and sometimes badly segregated, were used only in the preliminary experiments.

residue of phosphorus after removal of oxygen—and the refining additions were made immediately before casting. The phosphorus was omitted from melts to which aluminium-containing alloys were added because aluminium is itself an effective deoxidizer; other departures from the general melting practice are described below.

It was found that the borides could be precipitated as small crystals in the melts by adding the master alloys of boron and the transition metals listed in Table II. Attempts to use a nickel-5% boron alloy were unsuccessful, apparently because nickel boride is not soluble in copper-rich melts and remains undecomposed.



The addition of the carbides (and nitrides) was less straightforward and the following methods were studied:

(i) A copper-26% titanium alloy containing 1.5% titanium carbide, prepared by dissolving titanium in copper under a charcoal cover, was added to the melts just before casting. Dendrites of the carbide in the master alloy are shown in Fig. 7 (Plate LXXXII).

(ii) Pellets of titanium carbide, bonded with 20–66% nickel by sintering *in vacuo* at 1400° C., were added to the melts. The carbide was successfully dispersed only in melts containing 80% or more nickel, at temperatures above 1450° C.; the remainder of the copper and other alloying elements was added subsequently. The carbide particles grew from about 1 to 10  $\mu$  during this treatment and were badly segregated in the final casting, as shown in Fig. 8 (Plate LXXXII).

(iii) Carbon was dissolved in the melts by heating them under a charcoal cover or in contact with graphite before the addition of titanium or zirconium. The precipitated carbide crystals were large and numerous only in nickel-containing alloys, in which the solubility of carbon is high.

Although each of the methods was effective in reducing the grain-size, (i) and (ii) were objectionable because of the high temperatures and large excess of the transition metal required. The third method of introducing carbides was eventually used, as described in Section V.

### 3. METHOD OF CASTING

Bars of  $\frac{3}{4}$ - and  $2\frac{1}{4}$ -in. dia. and 4 in. long were sand-cast, the feeder heads being, respectively,  $1\frac{3}{8}$  in. dia.  $\times$   $1\frac{1}{2}$  in. and  $3\frac{1}{4}$  in. dia.  $\times$  3 in. The moulds were of Mansfield sand and were used green, except in the experiments on the measurement of undercooling for which the moulds were dried. Pouring temperatures are given in the appropriate sections.

### 4. UNDERCOOLING MEASUREMENTS

The technique previously used<sup>1</sup> to measure undercooling in solidifying castings was only slightly modified for the present work. Briefly, the method consisted in introducing thermocouples into the mould cavity before the melt was poured, the  $2\frac{1}{4}$ -in.-dia. sand casting being used. One thermocouple junction was placed 1.5–2.0 mm. from the mould wall to detect undercooling close to where solidification began; the second thermocouple junction was placed midway between the central axis and the surface of the casting, to detect undercooling in front of the dendrites growing from the mould wall.

The cooling curves obtained in this work were similar to those reproduced in an earlier paper.<sup>1</sup> When the rate of cooling was slow, as in the interior of the casting, it was assumed that recalescence after undercooling was virtually complete and therefore equal to the degree of undercooling. This method of measuring undercooling was subject to an error due to the separation of solid metal during recalescence and a

corresponding change in the liquidus temperature of the residual melt, but the error was significant only when undercooling was large.

At the surface of the casting, the rate of cooling was so great that recalescence after undercooling was incomplete in most alloys, and the above method could not be used. If partial recalescence occurred, the degree of undercooling was taken as the difference between the minimum temperature before recalescence at the surface and the liquidus temperature recorded by the internal couple. When even partial recalescence did not occur (as in the alloys containing 10% tin), the inflection in the cooling curve near the liquidus temperature was too indistinct to allow an estimate of undercooling at the surface to be made.

Alloys prepared for undercooling measurements were cast at 150° C. superheat; this was sufficient to allow turbulence, indicated by fluctuations in the cooling curves, largely to subside before the liquidus temperature was reached.

### 5. EXAMINATION OF CASTINGS

Transverse sections were taken from the middle of the bars and were etched in alcoholic ferric chloride solution. The grain-sizes were measured to  $\pm 25\%$  with a rule, at a convenient magnification, at points half-way along the radii.

Sections for micro-examination were taken from the  $\frac{3}{4}$ -in.-dia. sand-cast bar, next to the surface prepared for grain-size estimation. The use of diamond dust<sup>48</sup> was found to be essential for polishing these specimens, owing to the hardness of the boride and carbide crystals.

## IV.—MECHANISM OF GRAIN-REFINEMENT IN CAST COPPER ALLOYS

To determine whether the theory of grain-refinement of light alloys<sup>1</sup> is applicable to copper-base alloys, castings were made in copper deoxidized with 0.03% phosphorus and in alloys containing up to 3% aluminium or 10% tin. The influence of boride particles on the undercooling and grain-size of the 10% tin alloy was studied by adding 0.05% niobium and 0.1% boron before casting; the aluminium contents of the tin-containing alloys were made up to 1% to avoid variations in aluminium content due to the aluminothermic master alloys.

The results of undercooling measurements and details of the macrostructures of the castings are given in Table III; the scatter in the results of undercooling measurements in each series of the 10% tin alloys is to be expected, in view of the random nature of nucleation, but the probability of an effect arising simply by chance, equal to that apparently produced by the boride additions, was calculated to be less than 1 in 100.

Melts containing only small concentrations of phosphorus and aluminium undercooled 1°–2° C. before solidification began at the surface of the casting, and rapid and complete recalescence then followed. No undercooling was detected in the interior of these

castings and, in accordance with this, the structure was almost entirely columnar.

The addition of 3% aluminium resulted in only partial recalescence (0.9° C.) after undercooling at the surface, but detectable undercooling did not spread far into the interior and the structure remained columnar.

TABLE III.—Undercooling and Macrostructures of Castings in Copper-Base Alloys, Poured at 150° C. Superheat.

Nominal Composition, %	Thermocouple at Interface		Undercooling at Internal Thermocouple, °C.	Macrostructure of Casting
	Undercooling, °C.	Recalescence, °C.		
0.03 P	1.3	1.3	<0.1	Predominantly columnar
0.2 Al	1.6	1.6	<0.1	Columnar
3 Al	About 2	0.9	<0.1	"
2 Sn, 1 Al	About 2	0.3	0.5	Columnar + 8 mm. equiaxial
4 Sn, 1 Al	"	0.3	0.5	" + 7 mm. equiaxial
10 Sn, 1 Al	"	0	1.4, 1.0, 0.6, 0.8	Predominantly 5-6 mm. equiaxial
10 Sn, 1 Al + 0.05 Nb + 0.1 B	"	0	0.4, <0.1, <0.1, 0.3	1.0, 0.8, 1.3, and 2.3 mm. equiaxial

Additions of 2 or 4% tin had a greater effect than 3% aluminium; not only was recalescence at the surface less complete (only 0.3° C.), but a small degree of undercooling (0.5° C.) was also detected in the interior of the castings and the columnar structures were partially broken up by equiaxial grains. When the tin content was increased to 10%, recalescence at the surface was completely prevented and undercooling was increased to about 1° C. in the interiors of the castings, the structures of which were predominantly equiaxial although of large grain-size.

The addition of the boride-forming elements to the 10% tin alloy considerably diminished undercooling, though it was still detectable in two castings. The grain-sizes of the boride-containing alloys were also much less than those of the untreated 10% tin alloys.

The results described are very similar to those previously obtained in aluminium alloy castings,<sup>1</sup> and indicate that the description of the grain-refining mechanism in those alloys is also applicable to copper-base alloys. There was one important difference, however, for whereas no undercooling could be detected in the fine-grained aluminium alloys, a small degree of undercooling was still detectable in the copper-tin alloys containing niobium boride; this indicates that boride crystals are less effective as nuclei in copper alloys than in aluminium alloys, probably owing to their greater misfit with the copper lattice.

## V.—GRAIN-REFINEMENT OF BRONZES AND GUN-METALS

### 1. COMPARISON OF GRAIN-REFINERS

To compare the grain-refinement produced by the possible nucleating compounds, additions of several transition metals were made, either alone or with

boron, to copper-10% tin melts from which bars were then cast at 1150° C.

Preliminary experiments with the aluminothermic alloys showed that several of the transition metals (titanium, vanadium, niobium, zirconium, and iron) produced marked grain-refinement when present in sufficient quantities, but the simultaneous addition of boron resulted in refinement at much smaller concentrations in all cases. As aluminium would be objectionable in commercial bronzes and gun-metals, further experiments were carried out using aluminium-free alloys; additions of cobalt, nickel, manganese, titanium, zirconium, niobium, chromium, and iron were made, with and without 0.06% boron. Suitable vanadium, molybdenum, and tungsten alloys were not available.

The coarse macrostructures of the 2½-in.-dia. bars of the unrefined alloys were similar to that shown in

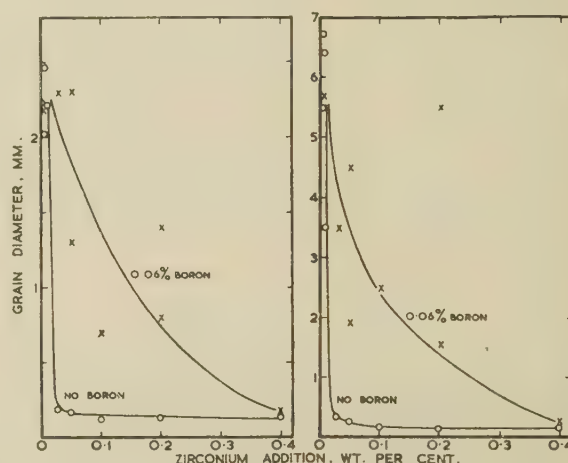


FIG. 1.—Effect of Zirconium and Boron Additions on the Grain-Size of Sand-Cast Bars of Copper-10% Tin Alloys, Cast at 1150° C.

(a) ¾-in.-dia. sand-cast bars. (b) 2¼-in.-dia. sand-cast bars.

Fig. 9 (Plate LXXXII). The grain-sizes produced by the most effective grain-refiners are plotted in Figs. 1-4 (see also Figs. 10 and 11, Plate LXXXII). The compositions quoted are the nominal contents; analyses of several alloys showed that the losses of transition-metal additions were 30% or less, but the loss of boron was about 70%.

#### (a) Metal Additions Without Boron

Additions of manganese (up to 1%) and nickel (up to 2%) had only very slight effects on the grain-size, largely confined to the columnar grains at the surface of the bars. Chromium (1%) produced moderate grain-refinement, the grain diameter being reduced by 60-80%. Zirconium, iron, and, to a smaller extent, titanium greatly reduced the grain-size, though much more iron was required (more than 1.6%) than of the other elements.

The grain-refinement produced by zirconium was much greater than that observed in the aluminium-



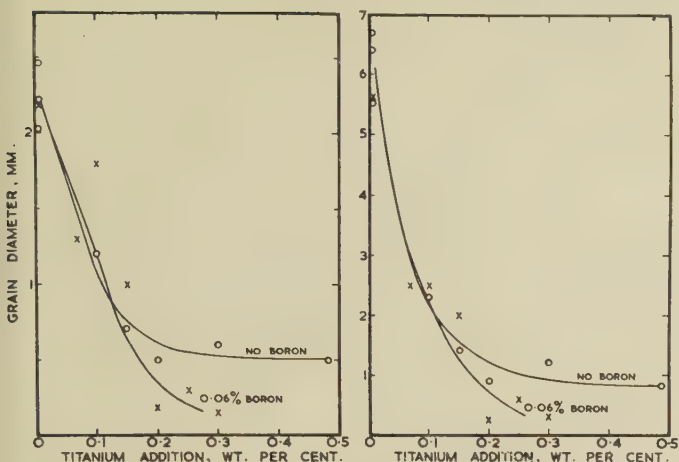


FIG. 2.—Effect of Titanium and Boron Additions on the Grain-Size of Sand-Cast Bars of Copper-10% Tin Alloys, Cast at 1150° C.

(a)  $\frac{3}{4}$ -in.-dia. sand-cast bars. (b)  $2\frac{1}{4}$ -in.-dia. sand-cast bars.

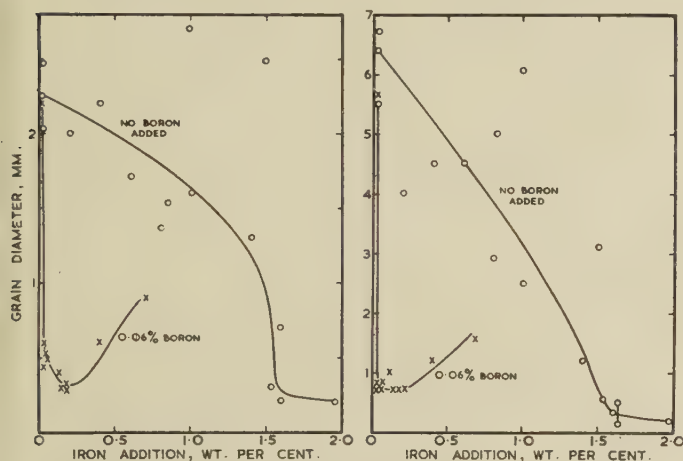


FIG. 3.—Effect of Iron and Boron Additions on the Grain-Size of Sand-Cast Bars of Copper-10% Tin Alloy, Cast at 1150° C.

(a)  $\frac{3}{4}$ -in.-dia. sand-cast bars. (b)  $2\frac{1}{4}$ -in.-dia. sand-cast bars.

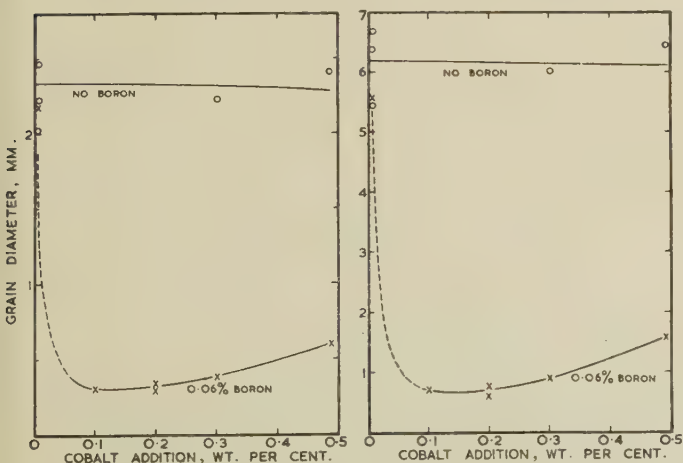


FIG. 4.—Effect of Cobalt and Boron Additions on the Grain-Size of Sand-Cast Bars of Copper-10% Tin Alloys, Cast at 1150° C.

(a)  $\frac{3}{4}$ -in.-dia. sand-cast bars. (b)  $2\frac{1}{4}$ -in.-dia. sand-cast bars.

containing alloys, but was strongly influenced by melting conditions, as shown by several experimental results summarized in Table IV.

TABLE IV.—Influence of Melting Conditions on the Grain-Refinement Produced by the Addition of Zirconium to Bronzes and Gun-Metals Containing 5–10% Tin.

Zirconium Addition, %	Size of Melt, lb.	Melting Conditions	Grain-Size, mm.
0.06	100	No N <sub>2</sub> -degassing; contact with graphite and charcoal avoided or strongly oxidizing conditions maintained until deoxidation and addition of Zr	2–3
0.05–0.1	15		0.3 to columnar
>0.02	15	Graphite present during de-oxidation; no N <sub>2</sub> -degassing	0.1–0.2
0.05	100	Graphite and nitrogen present during degassing	0.1–0.2

The maximum effect was produced by as little as 0.02–0.03% zirconium if carbon was in intimate contact with the melt during or after deoxidation, whereas under continuously oxidizing conditions, which would eliminate carbon, and in the absence of N<sub>2</sub>-degassing, very coarse grain-sizes were obtained even with 0.12% zirconium. The effect of titanium additions was similarly influenced by melting conditions. These results support the suggestion that zirconium and titanium carbide form effective nuclei in copper alloys.

TABLE V.—The Effect of Carbon and Nitrogen on the Grain-Refinement of Copper-8% Tin-0.08% Phosphorus Alloys by Zirconium.<sup>49</sup>

Casting temperature 1150° C.

Treatment	Grain-Size of D.T.D. Bar, mm.
(a) Melted in gas furnace in oxidizing atmosphere, in Sillimanite crucible	3–6
(b) As (a) but degassed with N <sub>2</sub> through silica tube	0.23
(c) As (a) but degassed with N <sub>2</sub> under charcoal cover	0.08

Further research <sup>49</sup> summarized in Table V indicates that nitrogen has an influence similar to, though apparently smaller than, that of carbon.

#### (b) Effect of Sulphur on the Grain-Refinement Produced by Zirconium Additions

As sulphide inclusions appear to be quite common in commercial gun-metal castings, a study was made of the influence of sulphur on the grain-refinement produced by zirconium additions. The results given in Table VI for 85:5:5 gun-metal show that sulphur can entirely prevent grain-refinement, but it was found that the addition of magnesium before the zirconium

eliminates interference by the sulphur. Further experiments with a commercial 86 : 7 : 5 : 2 gun-metal containing 0.1% sulphur indicated that only small magnesium additions (0.05–0.1%) were necessary to permit the grain-refining action of zirconium; excessive additions of magnesium (0.2%) made the metal stream sluggish. The effect of sulphur is presumably due to its reaction with the added zirconium to form zirconium sulphide (in place of the nitride or carbide); magnesium evidently prevents this reaction by precipitating the sulphur as the more stable magnesium sulphide, in accordance with the microstructures described in Table VI.

TABLE VI.—*Influence of Sulphur on the Grain-Refinement Produced by Zirconium in 85 : 5 : 5 : 5 Gun-Metal.*

7-kg. melts were heated under a charcoal cover, degassed with nitrogen, and sand-cast at 1150° C. after deoxidation with 0.03% phosphorus and addition of 0.06% zirconium.

Treatment of Melt		Grain-Size of $\frac{3}{4}$ -in.-dia. Bar, mm.	Microstructure
(a)	Zirconium addition only	0.1	Normal zirconium-containing inclusions
(b)	0.3% Sulphur (as cuprous sulphide) added before degassing	Columnar + coarse equiaxial	Numerous slate-grey sulphide inclusions, often associated with the lead particles (probably lead sulphide)
(c)	0.3% Sulphur added before degassing and 0.4% magnesium plunged before zirconium addition	0.1	Pale blue cubes or plates present (probably magnesium sulphide)

pitating the sulphur as the more stable magnesium sulphide, in accordance with the microstructures described in Table VI.

#### (c) Metal Additions with Boron

Boron alone had no effect on the grain-size of these alloys, but greatly increased the grain-refinement produced by several of the transition metals, notably titanium, iron, and cobalt, as shown in Figs. 2, 3, and 4. In castings of various boron contents made from 40-kg. melts in later experiments, the greatest refinement was produced by a boron addition of 0.03% (corresponding to 0.01% boron retained in the melt) when the iron or cobalt content was 0.1–0.2%.

An addition of boron with 0.05% niobium resulted in as much grain-refinement as that produced by titanium boride. Manganese (0.3% or more) with boron produced no grain-refinement in  $\frac{3}{4}$ -in.-dia. bars, but considerable refinement in patches in the larger bars, suggesting that the nuclei responsible for refinement had incompletely precipitated before solidification began. Additions of boron only slightly reduced the grain-size of nickel-containing alloys, again largely in the areas of columnar structure, and did not affect the moderate degree of refinement produced by chromium additions.

The grain-refinement produced in the copper-tin alloys by the additions of zirconium with boron, although marked, was considerably less than that produced by zirconium additions with carbon but no boron. This indicates that zirconium boride crystals

are more stable than the carbide but that they are less effective as nuclei.

## 2. MICROSTRUCTURES AND IDENTIFICATION OF PRIMARY PARTICLES

The maximum grain-refinement produced by about 1.6% iron (see Fig. 3) coincided with the appearance of primary iron-rich dendrites, which supports the suggestion that these may have acted efficiently as nuclei. At lower iron contents, angular particles of the iron-rich phase occurred, which, as they appeared to have formed by secondary precipitation, often in association with the eutectoid, could have had little influence on the nucleation of primary copper-rich dendrites.

In the absence of boron, several other transition metals produced constituents associated with the  $\alpha + \delta$  eutectoid. The fine-grained zirconium-containing alloys, however, contained large numbers of hard, angular particles (often cubic or hexagonal) throughout the solid solution, which were absent from the coarse-grained zirconium alloys; these particles were not identified, but may have been carbide particles which had acted as nuclei. Very few particles of this type were observed in other boron-free alloys, except in those containing chromium in which numerous crystals of an intermetallic constituent could be seen.

Boron, in the absence of transition metals, formed eutectic structures containing equiaxial particles in aluminium-free alloys and needles or plates in those containing aluminium. When the transition metals were also present, all alloys contained numerous hard, angular particles, as shown in Fig. 12 (Plate LXXXII). Boride crystals extracted electrolytically from a fine-grained alloy containing niobium and boron were found to have an  $\text{AlB}_2$ -type structure ( $a_0 = 3.09$ ,  $c_0 = 3.29$  Å.), apparently identical with that of  $\text{NbB}_2$  ( $a_0 = 3.086$  and  $c_0 = 3.306$  Å. for one composition within the range of homogeneity of this compound).<sup>38, 42</sup> Two borides were observed in alloys containing iron (illustrated in Fig. 13, Plate LXXXII) which were probably  $\text{Fe}_2\text{B}$  and  $\text{FeB}$ , as these are the stable borides formed in the iron-boron system. The boride precipitated in the nickel-containing alloys appeared to be identical with the stable  $\text{Ni}_2\text{B}$  phase examined in a nickel-5% boron alloy.

In the titanium alloys the influence of boron and titanium contents on microstructures was studied more fully and boride crystals were found to appear only in fine-grained alloys.

Although these results indicate that many of the borides can act as nuclei, the grain-size measurements showed that their effectiveness varies; in those cases where some indication of their identity was obtained, the borides can be placed in the following order of decreasing effect: (i)  $\text{TiB}_2$ ,  $\text{NbB}_2$  (and probably  $\text{ZrB}_2$ ); (ii)  $\text{FeB}$ ; (iii)  $\text{Ni}_2\text{B}$ . It is significant that this order of effectiveness is the same as that indicated by the similarity of the lattice structures of the borides to



that of copper, for, although the interatomic distances are similar in these compounds, their complexity increases from the simple hexagonal lattice of metal atoms in  $AlB_2$ -type borides to a distorted hexagonal lattice in  $FeB$  and a tetragonal  $CuAl_2$ -type structure in  $Ni_2B$ .<sup>35</sup>

### 3. INFLUENCE OF ALLOY COMPOSITION

It was suggested in Section II that the grain-refinement produced by nuclei may be influenced by the concentrations of other alloying elements. Alloys of various tin, lead, and zinc contents were, therefore, cast at 1150°–1170° C. after additions of iron boride, niobium boride, or zirconium to investigate this suggestion. The grain-size measurements shown in Fig. 5 confirm the important influence of alloy composition with each nucleating compound, and indicate that nuclei which produce the greatest refinement also require the lowest concentration of solutes to be made effective. Lead had an influence similar to tin, but somewhat smaller: a 5% tin–5% lead alloy, for instance, had the same grain-size as a 7 or 8% tin alloy after additions of iron boride. Zinc contents up to 5% had no appreciable influence in a 5% tin alloy refined with iron boride.

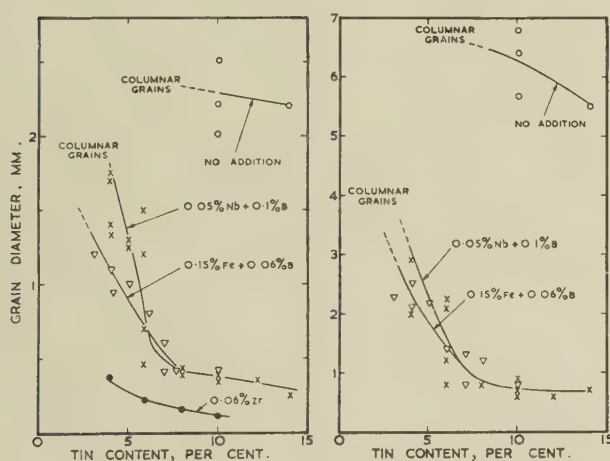


Fig. 5.—Effect of the Variation in Tin Content on the Grain-Refinement Produced by Several Refining Additions in Copper-Tin Alloys Sand-Cast at 1150° C.

(a)  $\frac{3}{4}$ -in.-dia. sand-cast bars. (b)  $2\frac{1}{4}$ -in.-dia. sand-cast bars.

KEY.

- No addition.
- ×—× 0.05% Nb + 0.1% B in Al-containing alloys.
- ▽—▽ 0.15% Fe + 0.06% B } in Al-free alloys.
- 0.06% Zr

### 4. INFLUENCE OF CASTING TEMPERATURE

The stability of the grain-refining nuclei at high temperatures was examined by casting copper–10% tin alloys containing niobium boride at temperatures up to 1325° C., one group of alloys being poured after the minimum of superheating, while a second was superheated to 1300°–1350° C. after the grain-refining addition. Series of boride-free alloys were made similarly for comparison.

The results plotted in Fig. 6 show that the grain-size of the boride-containing alloys increased only to a small extent as the casting temperature was raised,

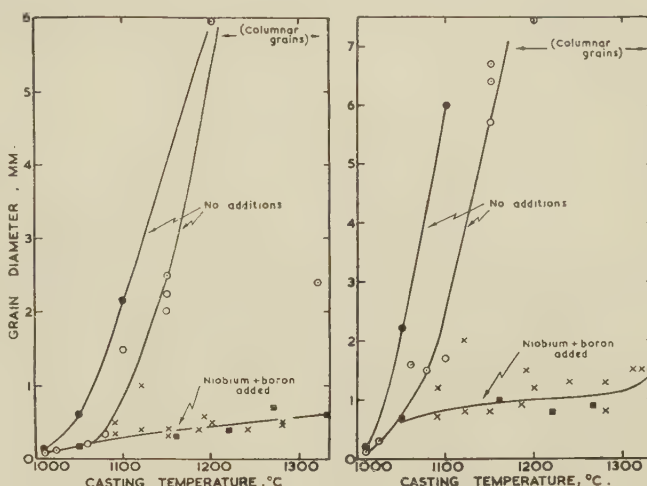


Fig. 6.—Effect of Casting Temperature on the Grain-Size of Sand-Castings of Copper–10% Tin Alloys, Showing the Influence of Niobium + Boron Additions.

(a)  $\frac{3}{4}$ -in.-dia. sand-cast bars. (b)  $2\frac{1}{4}$ -in.-dia. sand-cast bars.

KEY.

- No additions } Not heated more than 80° C. above casting
- ×—× 0.05% Nb + 0.1% B } temperature.
- No additions } Superheated to 1300°–1350° C. before
- 0.05% Nb + 0.1% B } casting.

whereas the alloys free from grain-refiners became very coarse-grained when the pouring temperature exceeded 1000°–1050° C. Superheating before casting had no significant effect in either series. Iron boride and zirconium additions were also found to be effective with casting temperatures up to at least 1180° C.

### 5. SELECTION OF GRAIN-REFINERS FOR BRONZES AND GUN-METALS

As commercial gun-metal castings are often poured with considerable turbulence, it is important to avoid alloying elements which create tenacious oxide skins. It was observed in the present work that iron, cobalt, zirconium, and titanium all increased the tendency for oxide skins to form on molten bronzes when added in approximately the following (or greater) amounts: zirconium 0.03%, titanium 0.1%, iron 0.2%, cobalt 0.5%. Only with excess of these metals, however, were the oxide films more tenacious than, for example, zinc oxide on gun-metal melts. When boron was also present, the oxide films were even less continuous, owing to the formation of globules of molten borates.

Comparison of the above figures with the amounts of these elements required for grain-refinement shows that solid oxidation products can be avoided on grain-refined alloys by using boron (>0.02%) with iron (0.05–0.2%) or cobalt (0.1–0.5%). Greater refinement can be obtained, although with some formation of solid oxides, by using zirconium (>0.03%) with carbon and/or nitrogen treatment; several such zirconium-

refined alloys which were examined contained very fine, rounded particles of oxide inclusions which did not seem likely to be harmful.

These additions have been used in other unpublished work on the influence of grain-size on the properties of gun-metal castings,<sup>50, 51</sup> including both sand-cast and chill-cast alloys.

## VI.—REFINEMENT OF CAST BRASSES

### 1. IRON-FREE $\beta$ -BRASS

Commercial castings of  $\beta$ -brass are normally fine-grained, owing to their high iron content. Iron-free alloys are, however, required for some purposes and the influence of zirconium and boron additions on the grain-size of such alloys was therefore studied. Grain-size measurements were made on bars cast at 1070° C. from melts containing 33% zinc and 4% aluminium; the results are listed in Table VII.

TABLE VII.—*Grain-Refinement by Additions of Zirconium and Boron to Copper-33% Zinc-4% Aluminium Alloys Sand-Cast at 1070° C.*

Nominal Zr Addition, %	Nominal B Addition, %	Grain-Size	
		$\frac{3}{4}$ -in.-dia. Bar, mm.	$2\frac{1}{4}$ -in.-dia. Bar, mm.
Up to 0.14	...	Large columnar	4 + columnar
0.06	0.008	0.5	0.9
0.06	0.024	0.4	0.7
0.02	0.02	0.6	1.2
...	0.02	1.8	3.0

Zirconium was quite ineffective as a grain-refiner in these alloys unless boron was added simultaneously to precipitate zirconium boride particles. These proved to be effective nuclei, although the primary solid phase has a  $\beta$  (b.c.c.) structure less similar than that of the  $\alpha$ -solid solution to the lattice of  $ZrB_2$ .

### 2. BRASS CONTAINING 67% COPPER, 33% ZINC

The mainly columnar macrostructure of this alloy when cast at 1050° C. was not completely eliminated by additions of iron or zirconium borides; the width of the columnar grains was reduced from 1.3 to 0.4 mm. in the smaller bar and from 4 to 1.2 mm. in the larger bar by addition of 0.05% of zirconium and 0.03% boron. Boron additions without zirconium produced about half this reduction in grain-size.

## VII.—SUMMARY AND CONCLUSIONS

### 1. MECHANISM OF GRAIN-REFINEMENT IN CAST COPPER ALLOYS

The mechanism of grain-refinement in the cast copper alloys studied in this work resembles that proposed in previous experiments on light alloy castings.<sup>1</sup> Grain-refinement may be produced in

several cast copper alloys by the introduction of fine particles which nucleate crystallization; a number of suitable nucleating compounds have been selected having lattice structures similar to that of copper-rich solid solutions, which cause marked refinement in both sand-cast and chill-cast alloys.

Measurements of grain-size and undercooling have shown that the nuclei are fully effective only when alloying elements are present which retard the growth of solid-solution dendrites by establishing concentration gradients round them in the melt, and allow further crystallites to be nucleated.

### 2. GRAIN-REFINEMENT OF BRONZES AND GUN-METALS

#### (a) Boron-Free Additions

Marked grain-refinement is produced in bronze and gun-metal castings by additions of 0.03% or more zirconium, 0.2% or more titanium, or 1.0% or more iron. The effect of zirconium additions is almost independent of casting temperature up to at least 1180° C. and is greatest when the tin or tin + lead contents exceed 2–4% and carbon or nitrogen is intimately in contact with the melt during or after deoxidation. Small hard particles have been observed in fine-grained zirconium-containing alloys, which have not been identified, but may have been carbide or nitride particles which act as nuclei during solidification. The effect of titanium additions is similarly influenced by the presence of carbon. In iron-containing alloys, the greatest grain-refinement occurs when primary iron-rich dendrites are present.

Moderate grain-refinement is produced by additions of 1% or more of chromium, but little or no refinement (less than 50% reduction in grain diameters) by additions of up to 2% nickel, up to 1% manganese, or up to 0.5% cobalt.

#### (b) Boron-Containing Additions

Boron additions (0.01–0.02% by analysis) have little effect alone, but increase the grain-refinement produced in bronzes and gun-metals by titanium, iron, cobalt, and (to a smaller extent) manganese and nickel; boron has no influence on the effect of chromium and reduces the strong effect of zirconium additions.

The results of the present research support the view that crystals of several of the borides are effective nuclei in copper-rich melts, the grain-refinement obtainable depending on the similarity of the boride lattices to that of solid copper. Iron boride nuclei are effective only in alloys containing more than 5–7% tin or tin + lead but when effective are almost uninfluenced by casting temperatures up to at least 1180° C.; the effect of niobium boride additions is almost independent of pouring temperature up to at least 1325° C.

### 3. GRAIN-REFINEMENT OF BRASSES

Additions of zirconium alone to an  $\alpha/\beta$ -brass and an iron-free  $\beta$ -brass containing aluminium did not cause



TABLE VIII.—Grain-Refiners for Sand-Cast Bronzes, Gun-Metals, and Brasses.\*

Refining Addition, (Nom.), %	Grain-Size Produced, mm.		Other Effects *	Estimated Present Cost of Addition/100 lb.
	$\frac{3}{4}$ -in.-Dia. Bar	$2\frac{1}{4}$ -in.-Dia. Bar		
(a) <i>Bronzes and Gun-Metals Containing 10% Sn, Cast at 1150° C.</i>				
None . . . .	2.3 + columnar	6.4 + columnar	...	...
Zr (0.03) . . .	<0.2	0.2	Thin oxide skins formed on pouring stream, more pronounced than on untreated bronzes, but easily broken up during pouring. Thick oxide skin on pouring stream; hard spots sometimes found in castings and rusting occurs on surface of casting.	6s.
Ti (0.25) . . .	0.5	0.9		5s.
Fe (1.8) . . .	0.2	0.2		Small
Ti (0.2) and B (0.03)	0.2	0.4	Thin, easily broken oxide skin on pouring stream.	4s. + (?) 6s.
Fe (0.1) and B (0.03)	0.4	0.7	Pouring stream clear of solid oxides; poorly adhering oxide on casting. Pronounced mould-reaction in sand moulds.	6s.
Co (0.1) and B (0.03)	0.4	0.7		2s. + (?) 6s.
(b) <i>β-Brass (33% Zn, 4% Al, 0% Fe), Cast at 1070° C.</i>				
None . . . .	Large columnar		...	...
Zr (0.03) and B (0.02)	0.5	0.7	No effect on oxidation of pouring stream; no mould-reaction observed.	...
(c) <i>α/β-Brass (67% Cu, 33% Zn), Cast at 1050° C.</i>				
None . . . .	Columnar (1.3 wide)	Columnar (4 wide) + 8 equiaxial	...	...
Zr (0.03) and B (0.02)	Columnar (0.4 wide) + some 0.4 equiaxial	Columnar (1.2 wide) + 2.5 equiaxial	Cleaner surface on melt; mould-reaction in sand moulds.	...

\* The results of mould-reaction effects which were studied in unpublished work, are summarized here.

grain-refinement under normal melting conditions; the addition of zirconium boride, however, resulted in a fine equiaxial structure in the  $\beta$ -brass although in the  $\alpha/\beta$ -brass only a reduction in width of the columnar grains could be produced.

The most effective grain-refiners found in this work are compared in Table VIII, in which their influence on mould reaction and the oxidation of the pouring stream and their approximate cost are also noted.

#### ACKNOWLEDGEMENTS

The author is indebted to the Director and Council of The British Non-Ferrous Metals Research Association for permission to publish this paper. He gratefully acknowledges the co-operation of Mr. T. Burchell and Dr. G. L. Miller, of Messrs. Murex, Ltd., in the preparation and supply of several master alloys, and the assistance of Mr. J. Fox (who made the X-ray examinations) and Mr. E. Owden.

#### REFERENCES

1. A. Cibula, *J. Inst. Metals*, 1949–50, **76**, 321.
2. R. Genders and G. L. Bailey, "The Casting of Brass Ingots" (B.N.F.M.R.A. Research Monograph No. 3), p. 59. 1934: London (B.N.F.M.R.A.).
3. C. Benedicks and H. Löfquist, "Non-Metallic Inclusions in Iron and Steel", p. 231. 1930: London (Chapman and Hall, Ltd.).
4. L. Northcott, *J. Iron Steel Inst.*, 1934, **129**, 171f.
5. H. Hanemann and W. Hofmann, *Z. Metallkunde*, 1937, **29**, 149.
6. L. Northcott, *J. Inst. Metals*, 1939, **65**, 173.
7. P. Bardenheuer and R. Bleckmann, *Stahl u. Eisen*, 1941, **61**, 49.
8. K. Achenbach, H. A. Nipper, and E. Piwowarsky, *Giesserei*, 1939, **26**, 597.
9. N. Tiner, *Trans. Amer. Inst. Min. Met. Eng.*, 1946, **166**, 242.
10. V. Kondic and D. Shutt, *J. Inst. Metals*, 1950–51, **78**, 105.
11. A. Cibula, *ibid.*, 1951–52, **80**, 1.
12. D. Turnbull, *Trans. Amer. Inst. Min. Met. Eng.*, 1950, **188**, 1144.
13. B. Vonnegut, *J. Appl. Physics*, 1947, **18**, 593.
14. J. H. van der Merwe, *Discussions Faraday Soc.*, 1949, (5), 201.
15. D. Turnbull and B. Vonnegut, *Indust. Eng. Chem.*, 1952, **44**, 1292.
16. M. Telkes, *ibid.*, 1308.
17. G. W. Preckshot and G. G. Brown, *ibid.*, 1314.
18. B. N. Ames and N. A. Kahn, *Trans. Amer. Found. Soc.*, 1950, **58**, 229.
19. H. Kostron, *Z. Metallkunde*, 1949, **40**, 321.
20. E. Scheil, *ibid.*, 1936, **28**, 228.
21. A. J. Murphy and G. T. Callis, *J. Inst. Metals*, 1948–49, **75**, 325.
22. S. F. Hermann and F. T. Sisco, *Trans. Amer. Inst. Min. Met. Eng.*, 1931, **93**, 262.
23. K. Iwasé, Ju-n Asato, and N. Nasu, *Sci. Rep. Tōhoku Imp. Univ.*, 1936, [j], Honda Anniv. Vol., 652.
24. F. C. Child, *Brit. Non-Ferrous Metals Research Assoc. Rep. R.R.E.* **235** (1943).
25. J. S. Vanick, *Foundry*, 1950, **78**, 86.
26. R. A. Colton and M. Margolis, *Trans. Amer. Found. Soc.*, 1951, **59**, 360.

27. P. E. Landolt and F. R. Pyne, *Foundry*, 1949, **77**, 90.
28. Brit. Patent No. **445,620**.
29. F. R. Hensel, E. I. Larsen, and A. S. Doty, *Trans. Amer. Inst. Min. Met. Eng.*, 1941, **143**, 212.
30. Metal Hydrides, Inc. (U.S.A.), Trade Pamphlet. **1947**: Beverly, Mass.
31. Brit. Patent No. **530,447**, **536,980**, and **537,225**.
32. J. P. Dennison and E. V. Tull, *J. Inst. Metals*, 1952-53, **81**, 513.
33. L. Northcott, *ibid.*, 1938, **62**, 101.
34. W. Hume-Rothery, *ibid.*, 1938, **62**, 121 (discussion).
35. R. Kiessling, *J. Electrochem. Soc.*, 1951, **98**, 166.
36. R. E. Bannon, *Trans. Amer. Soc. Metals*, 1937, **25**, 737.
37. Yu. A. Klyachko, L. L. Kunin, N. S. Khreshchanovsky, and E. S. Ginzburg, *Doklady Akad. Nauk S.S.S.R.*, 1950, **72**, 927.
38. R. Kiessling, *Acta Chem. Scand.*, 1947, **1**, 893.
39. R. Kiessling, *ibid.*, 1949, **3**, 90.
40. R. Kiessling, *ibid.*, 1950, **4**, 146.
41. L. H. Anderson and R. Kiessling, *ibid.*, 1950, **4**, 160.
42. J. T. Norton, H. Blumenthal, and S. J. Sindeband, *Trans. Amer. Inst. Min. Met. Eng.*, 1949, **185**, 749.
43. H. J. Goldschmidt, *J. Iron Steel Inst.*, 1948, **160**, 345.
44. R. W. G. Wyckoff, "Crystal Structures", Vol. 1. **1948**: New York and London (Interscience Publishers).
45. K. K. Kelley, *U.S. Bur. Mines Bull.*, 1937, (**407**).
46. F. D. Richardson, *J. Iron Steel Inst.*, 1953, **175**, 33.
47. J. Pearson and U. J. C. Ende, *ibid.*, 1953, **175**, 52.
48. E. C. W. Perryman, *J. Inst. Metals*, 1950, **77**, 61.
49. P. Gregory, unpublished work.
50. A. R. French and A. Cibula, unpublished work.
51. A. Cibula, unpublished work.



# EXPLORATORY CREEP TESTS ON METALS OF HIGH MELTING POINT\*

1550

By N. P. ALLEN,† M.Met., D.Sc., MEMBER, and W. E. CARRINGTON †

(Communication from the National Physical Laboratory.)

## SYNOPSIS

The strength at 1000° C. of a number of metals, in their purest available form, with melting points above that of iron, was assessed by compression creep tests *in vacuo*, the criterion being the stress needed to give 1% creep strain in 24 hr. Titanium, zirconium, vanadium, niobium, tantalum, chromium, molybdenum, tungsten, platinum, palladium, rhodium, iridium, iron, cobalt, and nickel and certain sintered carbides were tested. When high-temperature strength was plotted against atomic number, a periodicity similar to that given by the melting points and elastic constants of the metals was obtained. The materials tested are discussed in the light of their usefulness for high-temperature service.

## I.—INTRODUCTION

THE creep-resisting alloys that have been used in gas turbines during the past ten years have almost all been based on the face-centred solid solutions of iron, nickel, chromium, and cobalt, stiffened with additions of other elements. They maintain useful strength up to 800° C. and are slowly being developed so as to be serviceable up to 900° C. The exploitation of their potentialities is not yet complete. Nevertheless, a time will come when their capabilities will have been fully used, and further progress will then depend on finding materials able to withstand stress at still higher temperatures. The slowness of the advance of the blade temperature in turbines above 800° C. suggests that present types of alloy may not be capable of much further development.

It seemed, therefore, desirable to explore the strength at high temperatures of metals having higher melting points than that of iron and, in particular, to find out how the possible materials would compare at a service temperature of 1000° C. When the work was started, many of the metals with melting points above 1500° C. were available only in small quantity, and pieces large enough for test-bars of the usual size could not be obtained. It was necessary to devise a method of test that was applicable to such small pieces as could be procured. The purity and soundness of the samples were not always high, nor under control. Little was known about the technology of the less-familiar metals, and the influence of the many important factors that might affect their properties could not be explored without unduly extending the investigation. Under these circumstances it is impossible to expect finality, and any conclusions must be more or less tentative. Nevertheless, it has been possible to obtain a useful picture of the general situation. Some of the metals that were difficult to procure when the work began have since

become more abundant; and in some cases it has been interesting to observe the differences in purity and performance between samples of the same metal from different sources.

## II.—METHOD OF TEST

For the assessment of strength at high temperatures, a compression creep test on a cylindrical sample  $\frac{1}{4}$  in. long  $\times$   $\frac{1}{8}$  in. dia. was adopted. The apparatus is illustrated in Fig. 1. The specimen, with its ends accurately ground flat and parallel, was compressed between two alumina rods, loaded by means of a lever. It was heated in a small platinum resistance furnace, evacuated to a pressure of about 0.02 mm. of mercury, the pressure of the lever being transmitted to the alumina push-rods within the furnace through Sylphon bellows. The compression of the specimen was derived from the drop of the lever as measured by a dial gauge. The temperature of the specimen was measured by a thermocouple placed in a nickel-chromium alloy block which surrounded the specimen and push-rods, and also served to keep the push-rods and specimen in their correct relative positions. The outer case of the furnace was water-cooled, in order to protect the base-plate and lever from temperature fluctuations which might result in spurious changes of the apparent length of the specimen. The heating current was supplied from a battery, and was sufficiently uniform to maintain the temperature of the specimen uniform to  $\pm 5^\circ$  C. after steady conditions had been reached. The apparatus was assembled and evacuated at room temperature, and heated to 1000° C. in 1–3 hr. When the temperature was steady, the load was applied and the instantaneous compression of the test-piece and loading column were noted, a correction being made for the bending of the lever, which had been determined previously. Further readings of the dial gauge were made at

\* Manuscript received 1 December 1953.

† Metallurgy Division, National Physical Laboratory, Teddington, Middlesex.

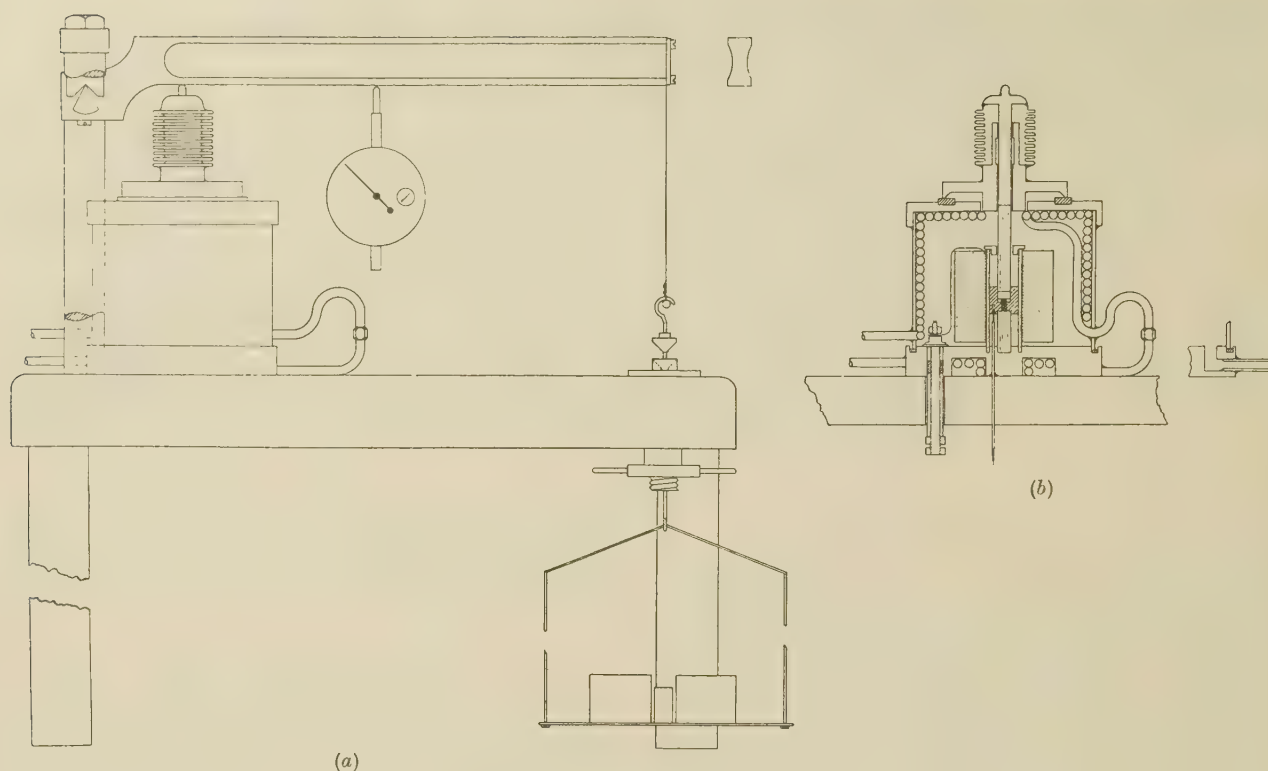


FIG. 1.—Diagram of Compression Creep Apparatus.

(a) Side view.

(b) Cross-section through furnace unit.

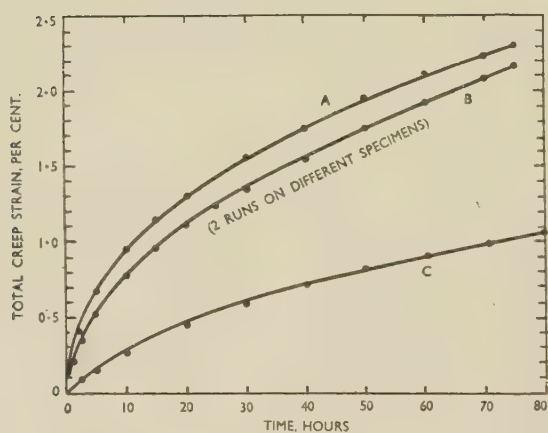


FIG. 2.—Comparison of Tests on Heat-Resisting Alloy in Compression *in Vacuo* (Curves A and B) and in Tension in Air (Curve C) at 1000° C., all under Stress of 0.44 ton/in.<sup>2</sup>.

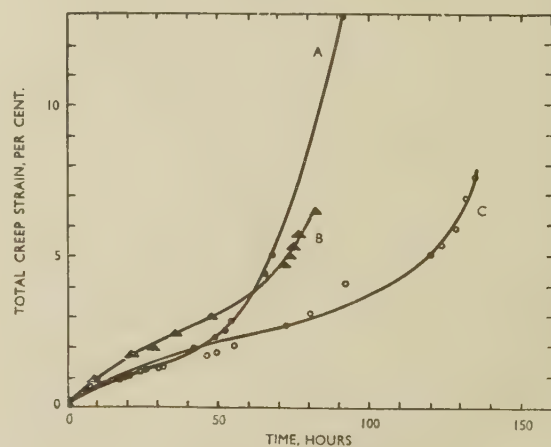


FIG. 3.—Comparison of Tests in Compression (Curves B and C) and Tension (Curve A) on Aluminium at 200° C., all under Stress of 1 ton/in.<sup>2</sup>.



3- or 6-min. intervals at first, and then at longer intervals, the test being continued as a rule for 24 hr.

An alternative way of using the equipment was to raise the temperature by steps of 50° C. and measure the creep resulting from the application of a fixed load for 10 min. at each temperature. This procedure was continued until the temperature reached 1000° C. or until the deformation became too rapid to measure. The rate of creep, when plotted against the temperature, yielded a curve which was usually flat in the lower temperature range and rose steeply at higher temperatures. Tests of this kind are referred to as "step tests".

The equipment gave smooth time/strain curves which were reproducible with many materials, but experience showed that it was easy to over-estimate their accuracy. Comparison of the curves with those obtained in tensile creep tests on the same material showed that agreement was good provided that the strain was above 1% (Fig. 2), but that the first 0.5% of strain occurred much faster in the compression creep test than in the tensile test (Fig. 3). This initial creep appeared to take place mainly at the two ends of the specimen, and to be associated with the deviations from perfect flatness in the ends

technical interest will centre round a commercial form of rather lower purity. For comparison, pure iron, nickel, and cobalt have been examined, and also one or two creep-resisting alloys and some sintered products consisting of a hard carbide bonded with a metal or mixture of metals of the iron group. The samples will now be considered in detail, the metals being taken in the order of their groups in the Periodic Table.

### 1. TITANIUM

The first samples were sheet and bar rolled from sintered powder prepared by the U.S. Bureau of Mines by the Kroll process. Later, titanium cast from Kroll-process metal melted in an induction furnace in a graphite crucible became available, and subsequently bar made from sponge metal melted in an arc furnace. The analyses of these materials are given in Table I.

It soon became apparent that none of the samples would withstand any appreciable stress at 1000° C., and attention was turned to determining the maximum temperature at which useful strength was maintained. The sintered and rolled sheet from the U.S. Bureau of Mines would not withstand a stress

TABLE I.—*Analyses of Titanium.*

Material	Composition, %										
	Fe	Si	Mg	Ca	Al	V	Cu	C	O	N	H
U.S. Bureau of Mines, sheet . .	0.19	0.045	<0.005	<0.01	0.006	0.012	n.d.	0.064	0.18	0.027	0.002
bar . .	0.15	0.005	0.30	0.036	n.d.	<0.01	n.d.	n.d.	0.16	0.02	0.001
Cast bar, melted in graphite . .	0.075	0.30	n.d.	n.d.	0.72	n.d.	0.035	0.47	n.d.	n.d.	n.d.
Kroll sponge, melted in graphite, as cast . . . . .	0.11	0.03	0.30	0.012	0.026	n.d.	n.d.	0.15	0.31	0.031	0.009
Kroll sponge, induction-melted . .	0.11	0.02	<0.01	n.d.	0.007	n.d.	0.003	0.10	0.17	0.01	0.008

n.d. = not determined.

of the test-piece and push-rods. Conclusions were therefore based upon deformations substantially greater than 0.5%. The stress necessary to produce a strain of 1% in 24 hr. was recorded, this stress being derived as a rule from the results of three or four experiments in which the total strain varied between 0.5 and 1.5%. A strain of 1% in 24 hr. is greater than could be tolerated in most creep-resisting components, and the stress producing it may be regarded as the upper limit of stress that could be applied in practice to the material in question.

### III.—SCOPE OF THE WORK

The original intention was to examine all metals with melting points above that of iron, but as yet hafnium, osmium, and ruthenium have not been procured in suitable form, and no attention has been given to certain other metals that are so little known that even their melting points are still uncertain. In general, the purest available form of the metal has been examined, except in the cases of titanium and zirconium, in which it is already clear that

of 1 ton/in.<sup>2</sup> at 500° C. for 24 hr. without deforming more than 1%, but graphite-melted material in the cast state was appreciably stronger, being capable of withstanding 1 ton/in.<sup>2</sup> at 600° C. The bar rolled from arc-melted sponge titanium, which had a Vickers diamond pyramid hardness number of about 200 and a tensile strength of 38.5 tons/in.<sup>2</sup> at room temperature, would withstand 7.5 tons/in.<sup>2</sup> at 400° C., but not more than 1 ton/in.<sup>2</sup> at 600° C.

The effect of additions of oxygen and carbon was studied by means of "step tests". Fig. 4 gives some typical results. Curve *A* relates to a sample of remelted van Arkel titanium of rather high purity tested in the cast state, and curves *B* and *C* to the same material with 0.1 and 0.5% oxygen, respectively, added during melting. Addition of oxygen raises the temperature up to which useful strength is maintained, but, as is well known, this rise is accompanied by a serious loss of toughness. Pure van Arkel titanium in the cast state was appreciably stronger at high temperatures than rolled material of quite ordinary purity (curve *D*). Curve *E* is typical of cast material that has been induction-

melted in graphite crucibles. Such material, containing both oxygen and carbon, is relatively strong at high temperatures, and it seems probable that the carbon as well as the oxygen contributes to the strength.

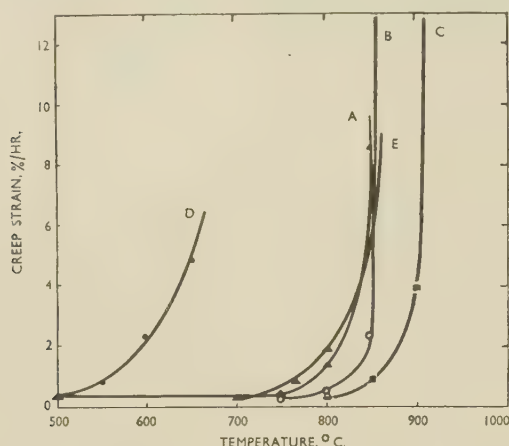


Fig. 4.—Percentage Creep/Hr. of Five Samples of Titanium of Varying Oxygen and Carbon Contents. Stress = 1 ton/in.<sup>2</sup>.

KEY.

Material	Analysis, %							
	O	N	C	Fe	Al	Ca	Mg	Si
A. Cast van Arkel	0.02	0.005	...	0.059	0.22	<0.001	<0.001	0.06
B. " "	0.10	0.005	...	...	...	...	...	0.04
C. " "	0.50	0.005	...	...	...	...	...	0.012
D. Rolled bar	0.16	0.02	...	0.15	...	0.036	0.30	0.005
E. Cast in graphite	0.20	0.01	0.66	0.11	0.026	0.012	0.30	0.032

## 2. ZIRCONIUM

Like titanium, zirconium was far too weak to be tested at 1000° C. A sample of swaged bar \* obtained from the United States and probably made by the Kroll process had a stress for 1% strain in 24 hr. of about 2 tons/in.<sup>2</sup> at 600° C. and 6 tons/in.<sup>2</sup> at 400° C. It thus maintained its strength rather better at high temperatures than rolled titanium of corresponding purity. Unworked cast zirconium,† supplied by the U.S. Bureau of Mines and made by melting van Arkel zirconium in a graphite crucible, was rather stronger, the corresponding stress at 600° C. being 2½–3 tons/in.<sup>2</sup>. Fig. 5 gives the results of "step tests" on a series of cast zirconium samples of varying oxygen contents, and shows that oxygen appreciably raises the temperature at which the metal loses its strength. The effect of oxygen on zirconium is very similar to its effect on titanium. All these samples were melted in a graphite crucible and contained about 0.2% carbon. Zirconium dissolves appreciably less carbon when melted in graphite crucibles than does titanium.

## 3. VANADIUM

Two samples of vanadium were examined, both in the cast state. One consisted of large metallic beads supplied by Johnson, Matthey and Co., Ltd., and made by reduction of vanadium pentoxide with

calcium. The other was an ingot supplied by the Union Carbide Co., U.S.A. The method of reduction has not been disclosed, but a general description of this material has been published.<sup>1</sup> The analyses of the samples are given in Table II.

Both samples yielded rapidly under 1 ton/in.<sup>2</sup> at 1000° C., the rate of deformation being rather greater than in pure iron or nickel under the same conditions. At 800° C., the stress for 1% strain in 24 hr. was somewhat above 2 tons/in.<sup>2</sup> for the bead sample, and somewhat below for the ingot sample. At 600° C., this stress was about 7 tons/in.<sup>2</sup> for the ingot sample, and the behaviour was not appreciably altered by annealing the sample for 7½ hr. at 1400° C.

Vanadium was thus rather similar at 800° C. to zirconium at 600° C., and at 600° C. it resembled zirconium at 400° C.

## 4. NIOBIUM

Niobium was tested in the form of swaged bars—one ¼ in. square and the other ⅛ in. round—both made by the Fansteel Corp., U.S.A. The former was of ordinary purity, and contained 0.23% tantalum, 0.07% carbon, 0.11% iron, and spectroscopic traces of copper and titanium. The latter was a special grade made for, and supplied by, Johnson, Matthey and Co., Ltd., and was regarded as "spectroscopically

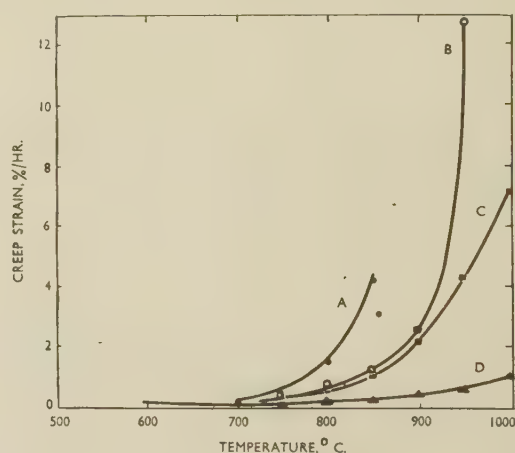


Fig. 5.—Percentage Creep/Hr. of Four Samples of Cast Zirconium of Varying Oxygen Contents. Stress = 1 ton/in.<sup>2</sup>.

KEY.

Material	Analysis, %			
	O	N	C	Fe
A. Iodide process	0.01	0.01	0.14	0.077
B. Bureau of Mines stock	0.07	0.01	0.18	0.03
C. } Bureau of Mines stock, {	0.27	0.03	0.14	0.065
D. } with added oxygen {	0.60	0.02	0.29	0.067

pure". Traces of aluminium and silicon could be found spectroscopically, but no tantalum or any other metallic element.

The samples behaved in much the same way when tested at 1000° C. The less-pure sample deformed at the necessary rate when the stress was about

\* Analysis: Fe 0.065, Si 0.06, Cu 0.018, Ca 0.042, Ni 0.03%.

† For analysis, see material A in Fig. 5.



6 tons/in.<sup>2</sup>, and the purer sample seemed a little stronger. Both materials were found to be considerably hardened at the end of the test, the initial hardness ranging from 158 to 194 Vickers diamond pyramid hardness number, and the final hardness ranging from 244 to 320. The hardening was not confined to the surface and was accompanied by noticeable embrittlement, but the samples at the end of the test were still sufficiently tough to withstand several blows from a hammer and to bend a little before they broke.

There was little doubt that the hardening was due to absorption of gas, in spite of the relatively low pressure maintained during the tests. The experiments were therefore repeated, using a more perfect vacuum, and a shorter time of exposure at a high temperature. Conditions were not quite perfect, but the increase of hardness was limited to 20 or

purity swaged rod supplied by Murex, Ltd. The analyses and initial hardnesses are given in Table III.

These materials, when tested without special precaution, underwent the same kind of hardening as was experienced with niobium, and their strength at 1000° C. was similar, a stress of 4 or 5 tons/in.<sup>2</sup> being required to produce the standard rate of deformation.

When tested under improved conditions such that the hardening was less than 30 Vickers hardness units, the stress was between 3 and 4 tons/in.<sup>2</sup> and the metal was still ductile after test. The Murex tantalum had a higher initial hardness than that of Fansteel. Even under the best vacuum obtainable in the test, the stress for the standard deformation of the Murex sample was much higher than the Fansteel metal. The material gas-hardened very readily under the conditions of the test.

TABLE II.—*Analyses of Vanadium.*

Material	Composition, %											
	Chemical						Spectrographic					
	O	N	H	C	Fe	Si	Fe	Si	Al	Cr	Cu	Mn
Ingot (Union Carbide)	0.085	0.017	...	0.075	0.082	0.075	...	...	0.002–0.02	0.001–0.01	0.002–0.02	0.002–0.02
Beads (Johnson, Matthey)	0.025	0.12	0.002	n.d.	...	...	0.001–0.01	0.05–0.5	0.01–0.1	...	...	0.005–0.05

n.d. = not determined.

TABLE III.—*Analyses of Tantalum.*

Material	Composition, %									Vickers Hardness No.
	Nb	C	Fe	Cu	Al	Ca	Si	Mg	Ti	
Fansteel . . .	0.26	0.05	0.14	<0.01	n.d.	n.d.	n.d.	n.d.	n.d.	130
Murex . . .	<0.05	n.d.	0.01	<0.01	0.02	<0.01	<0.02	<0.02	<0.01	185

n.d. = not detected.

30 hardness units, and the stress necessary to cause 1% deformation in 1 hr. was found to be 2.8 tons/in.<sup>2</sup> for the purer sample of niobium. Niobium is thus stronger at 1000° C. than vanadium, very much stronger than zirconium, which is the element that precedes it in the Periodic Table, and comparable in strength with molybdenum, which follows it in the Table. Absorption of gas contributes to its strength and, if maintained within limits, might not reduce the ductility to such an extent as to render the metal useless for engineering purposes.

The high ductility of niobium at room temperature is a great advantage. In a single test, a sample which had been reduced 63% in thickness by cold rolling proved capable of withstanding a compressive stress of 5 tons/in.<sup>2</sup> for 24 hr. at 1000° C. with less than 0.5% deformation.

## 5. TANTALUM

The tantalum consisted of a swaged rod of ordinary purity supplied by the Fansteel Corp. and a high-

Tantalum is, therefore, stronger at 1000° C. than niobium, but it is considerably more dense. Consequently, if both were equally available, niobium would generally be preferred.

## 6. CHROMIUM

The most reliable sample of chromium was a vacuum-melted ingot prepared at the National Physical Laboratory by Adcock<sup>2</sup> from electrolytic chromium, and containing 0.018% nitrogen and 0.200% insoluble matter, mostly chromic oxide in the form of large inclusions. This yielded consistent results, and the stress for 1% strain in 24 hr. was between 2 and 3 tons/in.<sup>2</sup>. This figure was supported by the results from a sample obtained from Mr. Marden of Westinghouse, and sintered from pure chromium powder made by the Marden and Rich process.<sup>3</sup> This sample, when examined spectroscopically, showed the presence of iron, silicon, and calcium in quantities between 0.01 and 0.1%, and of manganese, aluminium, tungsten, and copper between 0.001 and 0.01%. It

was a little porous, and would therefore be expected to give results rather below the value for dense chromium, and it was compressed by 1% under a stress of 2 tons/in.<sup>2</sup> in 3 hr.

Mr. Marden also provided a second sample of chromium which had been both sintered and swaged to a  $\frac{1}{8}$ -in.-dia. rod. It was by no means so pure, containing 0.30% silicon, 0.44% iron, 0.15% aluminium, and 0.05% manganese, but it was appreciably stronger, being able to carry loads up to 6 tons/in.<sup>2</sup> at 1000° C. without deforming more than 1%, although its behaviour was irregular. A sample of electrolytic chromium, melted at the N.P.L. in an argon-arc furnace, but contaminated with 0.11% nitrogen and rather porous, was also irregular in its behaviour. Some of the test-pieces taken from it carried stresses of 4 tons/in.<sup>2</sup> for 24 hr. with less than 1% strain. Chromium seems therefore to be rather easily strengthened by impurities, but all the samples,

this may have been the result of the working conditions rather than of the high carbon content. The  $\frac{1}{2}$ -in.-dia. sintered and swaged bar required a stress of about 4 tons/in.<sup>2</sup> as swaged. After being annealed for 2 hr. at 2000° C., it was softer; the required stress was above 2 tons/in.<sup>2</sup> but appreciably lower than 4 tons/in.<sup>2</sup>. The behaviour of the  $\frac{3}{16}$ -in.-dia. bar was irregular, and some samples withstood 5 tons/in.<sup>2</sup> without deforming much more than 0.5% in 24 hr. On the whole the differences between samples were not great. The conclusion to be drawn is that the stress for a fully softened sample is 3–4 tons/in.<sup>2</sup>, but that work-hardening may be retained at 1000° C. and may raise the stress for the required rate of deformation to at least 5 tons/in.<sup>2</sup>.

## 8. TUNGSTEN

The samples of tungsten were all sintered and swaged from powder in the usual way. One rod,

TABLE IV.—*Analyses of Molybdenum.*

Material	Composition, %						Vickers Hardness No.
	C	Si	Fe	Al	Ni	Mn	
$\frac{1}{8}$ -in. swaged bar from ingot . .	0.026–0.17	0.004	0.013	0.020	0.006	<0.005	204–240
$\frac{1}{2}$ -in. sintered and swaged bar . .	0.001	<0.02 *	0.028	0.002 *	<0.01 *	0.002 *	208
$\frac{3}{16}$ -in. sintered and swaged bar . .	n.d.	<0.01	<0.01	...	...	...	254

n.d. = not determined.

\* Spectrographically determined.

TABLE V.—*Analyses of Tungsten.*

Material	Composition, %								
	Cu	Fe	Al	Ti	Ca	Mg	Ni	Cr	C
5-mm.-dia. rod . .	0.015	0.18	0.02	0.018	0.056	0.015	<0.01	...	0.013
8-mm.-dia. rod . .	0.001–0.01	0.067	<0.002	...	<0.002	<0.002	0.005	0.011	0.003

whether pure or not, are brittle at room temperature, and this is an objection to its use.

## 7. MOLYBDENUM

Molybdenum has recently become available in larger masses than hitherto. Bars are either rolled or swaged at 1200°–1250° C. from ingots made by arc melting in the manner described by Parke and Ham,<sup>4</sup> or swaged from blocks of pressed and sintered powder. Several examples of bars made by both methods were examined. Those made from ingots were  $\frac{1}{8}$  in. in dia. Table IV contains a typical analysis. Samples representative of the highest (0.17%) and lowest (0.026%) carbon contents resulting from the melting process were supplied by the Climax Molybdenum Company. The sintered and swaged bars were of two sizes,  $\frac{1}{2}$  and  $\frac{3}{16}$  in. in dia., and their analyses are also given in the table.

The bar obtained from the ingot deformed at the rate of 1% in 24 hr. under stresses of 4–5 tons/in.<sup>2</sup>. The high-carbon sample required a rather lower stress than the others (less than 4 tons/in.<sup>2</sup>), though

supplied by the Research Laboratory of the General Electric Co., Ltd., was described as spectroscopically pure, and a purity of 99.995% was claimed. The others were not quite so pure; Table V contains some analyses.

Test-pieces from these rods as swaged did not creep rapidly at 1000° C. under stresses below 5 tons/in.<sup>2</sup>, and it was necessary to raise the stress to  $7\frac{1}{2}$  tons/in.<sup>2</sup> before it was certain that they were creeping appreciably throughout their length. The 8-mm. rod, after being annealed for 7 hr. at 1500° C., which reduced the Vickers hardness number from 442 to 388, yielded at the required rate of deformation under a stress of 6 tons/in.<sup>2</sup>.

## 9. IRON, NICKEL, AND COBALT

Three varieties of iron were tested: a typical Swedish wrought-iron bar, a sample rolled from sintered carbonyl-iron powder, and a normalized bar of iron prepared by vacuum-melting at the National Physical Laboratory<sup>5</sup> and containing 99.96% iron.

The nickel samples were an ingot made by melting



pure nickel powder in a vacuum, and a bar prepared by sintering similar powder and swaging at room temperature.

A cobalt rod was prepared by swaging at 1100° C. a pure sintered bar provided by Johnson, Matthey and Co., Ltd., and a sample of cast cobalt was prepared by melting cobalt powder of similar purity in a vacuum.

The analyses of these samples, together with the results of the compression tests and the hardness values before and after testing, are given in Table VI. The swaged nickel bar was initially somewhat work-hardened, but it softened during heating, and behaved under test in much the same way as the cast nickel.

were prepared. The samples were made by melting and processing into wire form and were subsequently annealed.

The rhodium and iridium were prepared by powder metallurgy from the purest commercially available powders, and were supplied in the swaged form. The samples consisted of 99.99% rhodium and 99.97% iridium; the analyses given are approximate, and were made spectroscopically.

Platinum crept very rapidly under the lowest load applied, which was 0.5 ton/in.<sup>2</sup>. Palladium gave the required creep rate under 0.3 ton/in.<sup>2</sup>. They both softened during test, and in view of the known recrystallization temperatures of these metals, there

TABLE VI.—*Analyses of Iron, Nickel, and Cobalt.*

Material	Composition, %									Stress (tons/in. <sup>2</sup> ) for 1% Creep Strain in 24 Hr.	Vickers Hardness No.	
	C	Si	Mn	P	S	O	N	Ni	Fe		Before Test	After Test
Iron :												
Swedish iron. .	0.017	0.05	0.005	0.036	0.003	0.35	0.016	...	...	<0.33	...	...
Carbonyl sintered and rolled . .	0.015	<0.002	<0.005	<0.0005	<0.0005	0.0019	0.003	0.011	...	0.35	...	...
N.P.L. pure rolled .	0.0026	0.007	0.008	0.001	0.004	0.0037	0.0015	0.007	...	0.48	63	64
Nickel :												
N.P.L. vacuum- melted . .	0.096 *	0.004 *	...	...	...	0.1 *	...	...	0.001 *	<0.33	...	...
Sintered, swaged .	...	...	...	...	...	...	...	...	...	0.25	232	63
Cobalt :												
Sintered, swaged .	...	>0.015	0.005	...	...	...	...	>0.005	>0.005	0.62	176	149
N.P.L. vacuum- melted . .	...	0.003	...	...	...	...	...	0.0007	0.001	0.30	127	120

\* Analysis of powder from which ingot was made.

TABLE VII.—*Analyses of the Platinum Metals.*

Material	Composition, %								Vickers Hardness No.	
	Ir	Pd	Rh	Pb	Fe	Au	Insoluble	Si	Before Test	After Test
Platinum . . .	...	0.002	0.016	0.005	0.001	0.001	...	...	49	34-36
Palladium . . .	...	...	0.035 *	...	0.011	...	0.005	...	58	39-52
Rhodium . . .	0.005-0.05	<0.001	...	0.002	0.01	<0.001	...	0.01-0.10	269	198-201
Iridium . . .	...	<0.001	<0.005	<0.002	0.01	<0.001	...	0.01-0.10	...	268-305

\* Rh + Au.

All these metals were weak at 1000° C., and though the sintered and swaged cobalt bar was rather stronger than the rest, it was not possible to conclude that the differences between the metals were greater than the differences between individual samples of each metal.

#### 10. THE PLATINUM METALS

Material sufficient to make 4-6 test-pieces of platinum, palladium, rhodium, and iridium were available, the platinum and palladium from The Mond Nickel Co., Ltd., and the others from Johnson, Matthey and Co., Ltd. The analyses and hardness values before and after testing are given in Table VII.

The analyses quoted for platinum and palladium are those of the swaged metal from which the samples

is little possibility of greater strength being obtained by cold working.

The rhodium as received underwent 1% strain in 24 hr. at a stress between 3 and 4 tons/in.<sup>2</sup>. This strength could probably not be relied upon for long periods, since the metal softened appreciably during test. The specimens after test were annealed at 1500° C. for 4 hr., after which their Vickers hardness number was 157. The stress they were able to carry was then somewhat less than 3 tons/in.<sup>2</sup>, showing that the metal in the annealed state was still very much stronger than platinum and palladium.

The iridium as received was also work-hardened. A stress of 5 tons/in.<sup>2</sup> could be applied for 24 hr. without producing a deformation of more than 0.5%. The deformation under the same stress was rather

greater, but still not above 1%, after the metal had been annealed at 1500° C. for 2 hr. It was therefore re-annealed for 1 hr. at 2000° C., after which the hardness was 217 and approximately equal to that reported for cast iridium.<sup>6</sup> After this treatment, the stress giving 1% strain in 24 hr. was about 6 tons/in.<sup>2</sup>.

#### 11. MISCELLANEOUS ALLOYS

A rolled bar of 80:20 nickel-chromium alloy and a bar of typical Nimonic 80, as supplied to the National Physical Laboratory for creep tests at 650°–750° C., were both very weak at 1000° C. The strain was well over 1% in 24 hr. under 0.5 ton/in.<sup>2</sup>. The strength in this test was not much greater than that of pure nickel.

A typical 18% tungsten high-speed steel in the annealed condition was decidedly stronger than pure iron, giving about the same rate of deformation (1.3% in 24 hr.) under 1 ton/in.<sup>2</sup> as pure iron showed under  $\frac{1}{2}$  ton/in.<sup>2</sup>. In view of the small effect of chromium in solid solution in nickel, this effect is more probably attributable to the dispersed carbides than to the dissolved tungsten and chromium in the alloy.

The effect of interspersed hard compounds was seen more clearly in Stellite and sintered carbides. Two cast samples of Stellite were examined, one with 5% tungsten and 25% chromium, the other with 9% tungsten and 29% chromium. Both could be regarded as consisting metallographically of a network of carbides set in a matrix of cobalt-chromium solid solution, and both would carry 2 tons/in.<sup>2</sup> under the standard conditions. A sintered tungsten carbide, consisting essentially of 95% tungsten carbide bonded with 5% cobalt, had a corresponding strength of just under 1 ton/in.<sup>2</sup>, whereas another consisting of a mixture of tungsten and tantalum carbides bonded with 10% cobalt had a strength of 3 tons/in.<sup>2</sup>. The highest strength obtained in materials of this kind was given by samples of titanium carbide bonded with 40 or 50% of nickel-chromium-cobalt alloy, some of which deformed by 0.7–1.4% during 24 hr. under 4 tons/in.<sup>2</sup>. These materials differ markedly

in strength, and since it is unlikely that the hard compound itself undergoes any considerable deformation, the strength would appear to be influenced principally by the composition of the bond and the quantity and distribution of the hard compound. Although the bond itself is relatively weak, the load-carrying capacity of these mixtures appears to be comparable with that of the strongest of the pure metals, with the exception perhaps of tungsten.

The details of composition and hardness of these alloys are recorded in Table VIII.

#### IV.—DISCUSSION

The relative strengths of the pure metals, in the soft condition (free from the effects of cold work) are summarized in Table IX.

TABLE IX.—*Properties of Pure Metals in the Soft Condition.*

Metal	Stress (tons/in. <sup>2</sup> ) for 1% Deformation in 24 Hr.				Density, g./ml.	Stress/Density at 1000° C.
	400° C.	600° C.	800° C.	1000° C.		
Titanium . .	7.5	...	...	~0.1	4.5	0.022
Zirconium . .	5.6	1.6	...	~0.1	6.5	0.015
Vanadium . .	...	7.5	1.6	0.3	6.1	0.05
Niobium . .	...	...	...	2.8	8.4	0.33
Tantalum . .	...	...	...	3.4	16.6	0.18–0.24
Chromium . .	...	...	...	2.3	7.1	0.28–0.42
Molybdenum . .	...	...	...	3.4	10.4	0.29–0.38
Tungsten . .	...	...	...	6	19.3	0.31
Platinum . .	...	...	...	~0.1	21.4	0.005
Palladium . .	...	...	...	0.3	11.9	0.03
Rhodium . .	...	...	...	3	12.4	0.24
Iridium . .	...	...	...	6	22.4	0.27
Iron . .	...	...	...	0.48	7.87	0.06
Cobalt . .	...	...	...	0.62	8.9	0.07
Nickel . .	...	...	...	0.25	8.9	0.03

Since in aircraft applications, and especially in turbine rotors, the density is important, the ratio of the strength at 1000° C. to the density is also given. The stresses in rotor blades are rarely less than 2 tons/in.<sup>2</sup>, and may be as high as 10 or 15 tons/in.<sup>2</sup>. There are very few metals so strong at 1000° C. that they are likely to be sufficiently improved by alloying to withstand stresses of this order. Of these, iridium seems to have most of the properties required, but it is far too costly. Chromium would be very promising on a strength-to-weight basis if it were not so brittle. Molybdenum and tungsten both need to be protected from oxidation; of the two, molybdenum would be preferred on account of its lower density. Niobium has a good strength-to-weight ratio and is also ductile. If it can be protected from oxidation, it should be a very promising material indeed, particularly as it is capable of considerable hardening. But the uses of niobium are so many, and the supplies so uncertain, that it is doubtful whether the development of an alloy based on niobium would prove the best use of the metal.

When the strengths of the metals at 1000° C. are plotted against their atomic numbers, a very marked periodicity is observed, which parallels the well-known periodicity of melting point and elastic constants (Fig. 6). The height of the peaks increases

TABLE VIII.—*Analyses and Properties of Miscellaneous Alloys.*

Material	Composition, %	Vickers Hardness No.	Stress (tons/in. <sup>2</sup> ) for 1% Creep Strain in 24 Hr.
Tungsten carbide/cobalt alloy	Co 4.7, Fe 0.5	1160	<1
" " " " " "	Co 12, Fe 0.5	1050	1.5
Tungsten carbide with TiO and TaO	Co 10.3, Ti 8.1, Ta 6.3, Fe 0.5	1400	3
Cast Stellite G8	Co 64.5, W 5, Cr 25.5	350–425	2
" " " " " "	Co 58, W 9, Cr 29	480–550	2
Titanium carbide/Ni–Cr–Co alloy	Co 7.75, Ni 31.75, Cr 10.5, TiO 50	775	3–4
" " " " " "	Co 6.25, Ni 25.25, Cr 8.5, TiO 60	1120	3–4
Nimonic 80	W 18.4, Cr 4.3, V 1.1, C 0.7, Si 0.3	...	About 0.4
Tungsten steel	Ni 76.8, Cr 20.8, Fe 0.6, Si 0.6, Mn 0.5	...	0.9
Nickel–chromium alloy		...	About 0.2



progressively on passing from the first to the third Long Period. There is no precise relation between the measured creep strengths and either the melting points or the elastic constants, but this is not to be expected in view of the approximate nature of the measurements. There is, however, a closer parallelism between the strengths at 1000° C. and the elastic constants at room temperature than between the strengths and the melting points in that the elastic constants fall more sharply on the low-atomic-number side of the peaks than do the melting points. Thus titanium and zirconium, which are weaker than cobalt and palladium, have lower elastic constants but higher melting points. There is a very sharp fall of strength between rhodium and palladium in the second Long Period, and between iridium and platinum in the third. This fall is continued to silver in the second Long Period and to gold in the third, and is accompanied by very little change of density. It suggests that as orbital electrons are added, the ionic core of the atom shrinks and the tenuous mantle of valency electrons extends.

The high creep strength of the sintered carbides is of considerable interest. These materials are in general brittle at room temperature; even the best require very careful design to avoid sudden changes

These considerations, which are largely geometrical, arise at any temperature, and it is readily understandable that at room temperature, when the yield point of the bonding material under simple tension is relatively high, its effective yield point in the channels between the hard particles may be so high as to exceed the fracture stress. The material will

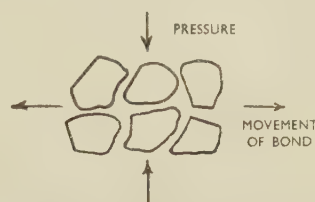


FIG. 7.—Effect of Pressure on Bonded Material.

then break without deforming, exhibit sensitivity to notches, and have all the disadvantages of a brittle material.

There are in fact three fracture stresses to consider: that of the bonding material, that of the hard particle, and that of the junction between them. Fig. 8 (Plate LXXXIII) illustrates a case in which it is clearly the carbide crystal that has broken first. A degree of restraint upon the shear of the bonding material which is sufficient to raise the general stress level before deformation above any of these fracture stresses will result in a brittle material. But restraint upon the shear of the bond is precisely the effect that has to be produced if these composite bodies are to have good creep-resistance at high temperature. There is no point in raising the shear strength of the bond to such an extent that the material becomes unusably brittle, and the only course is to maintain the shear strength of the bond in balance with the fracture stresses. Consequently, hard crystals of high cleavage strength must be chosen; they must be united firmly with the bonding material, and the bonding material itself must have a high fracture stress. Fortunately, the fracture stresses of materials can be influenced by metallurgical means, and there is reason to hope that the potentialities in this direction are not yet exhausted.

#### ACKNOWLEDGEMENTS

The work described above has been carried out under the Research Programme of the National Physical Laboratory. This paper is published by permission of the Director of the Laboratory.

#### REFERENCES

1. A. B. Kinzel, *Metal Progress*, 1950, **58**, 315.
2. F. Adcock, *J. Iron Steel Inst.*, 1927, **115**, 369.
3. J. W. Marden and M. N. Rich, U.S. Patent No. **1,760,367** (1930).
4. R. M. Parke and J. L. Ham, *Trans. Amer. Inst. Min. Met. Eng.*, 1947, **171**, 416.
5. B. E. Hopkins, G. C. H. Jenkins, and H. E. N. Stone, *J. Iron Steel Inst.*, 1951, **168**, 377.
6. R. F. Vines, "The Platinum Metals and Their Alloys". 1941: New York (International Nickel Co.).

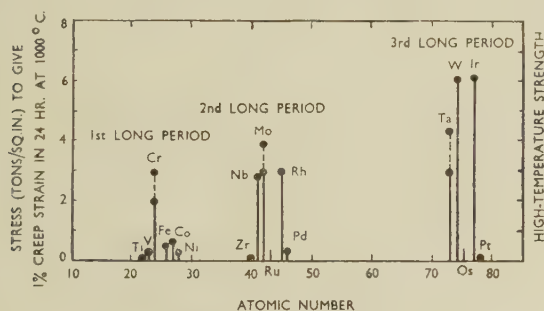


FIG. 6.—Relation Between High-Temperature Strength and Atomic Number of Metals Investigated.

of section before they can be used in moving parts. They present the problem of maintaining or improving the creep strength at 1000° C., whilst very considerably improving the ductility at all other temperatures.

The source of their creep strength is the same as that of their brittleness. Deformation takes place principally in the bonding material between the carbides. The tests on the 80:20 nickel-chromium alloy, Nimonic 80, and cobalt suggest that this material by itself is very weak. The composite bodies deform slowly under high pressures because the hard particles cannot approach each other without squeezing the bonding material out sideways (Fig. 7). The bonding material is restrained from making this movement by its contact with the hard particles, and a state of triaxial stress is set up which in effect raises the yield point of the binding material. The difference in strength between Nimonic 80 and titanium carbide bonded with nickel-chromium-cobalt alloy suggests that the yield point may be raised by a factor of 5-10.

# 1551 THE CONSTITUTION OF THE TITANIUM-RICH ALLOYS OF TITANIUM, IRON, AND OXYGEN \*

By N. P. ALLEN,† D.Sc., M.Met., F.I.M., MEMBER, T. H. SCHOFIELD,† M.Sc., F.I.M., MEMBER, and (Mrs.) B. MELLISH,† B.Sc.

(Communication from the National Physical Laboratory.)

## SYNOPSIS

The constitution of the titanium-rich alloys of titanium, iron, and oxygen has been investigated between 550° and 1100° C. by microscopical and X-ray methods. Alloys containing up to 5% oxygen and 5% iron have been prepared by arc-melting. The  $\alpha$  and  $\beta$  phase fields are restricted at all temperatures, and the extent of the  $(\alpha + \beta)$  field decreases with falling temperature between 1100° and 650° C. owing to the progression of the  $(\alpha + \beta + x)$  and the  $(\alpha + x)$  fields, where  $x$  is a complex oxide of titanium and iron. At 550° C. all the alloys investigated, except for a restricted  $\alpha$  field, consist of  $(\alpha + \text{FeTi})$ .

## I.—INTRODUCTION

THE titanium-rich alloys of both the titanium-iron and the titanium-oxygen systems have been studied in detail and reported in the literature,<sup>1-13</sup> but no work has yet been published on the constitution of the titanium-rich titanium-iron-oxygen alloys. Iron and oxygen are normally present as impurities in commercial titanium (Kroll-process sponge); oxygen may also be introduced during the preparation of alloys, and both iron and small amounts of oxygen have been purposely added to increase the strength of titanium. It is therefore important to investigate the combined effect of these two elements on the microstructure and mechanical properties of titanium.

The present paper describes an investigation of the constitution of alloys containing up to 5 wt.-% oxygen and iron in the temperature range 550°–1100° C.

## II.—REVIEW OF PREVIOUS WORK

### 1. TITANIUM-IRON SYSTEM

The constitution of the titanium-rich alloys of titanium and iron has been investigated by Craighead, Simmons, and Eastwood,<sup>1</sup> Worner,<sup>2</sup> and Van Thyne, Kessler, and Hansen,<sup>3</sup> and the results of these different workers show substantial agreement.

The addition of iron to titanium depresses the  $\alpha \rightarrow \beta$  transformation temperature and results in an eutectoid decomposition of the  $\beta$  phase, at 15–16% iron and 585° C., into TiFe and an  $\alpha$  phase containing less than 0.5% iron. The melting point of titanium is also depressed and the liquidus and solidus curves fall steeply to the eutectic horizontal at 1080° C. The eutectic occurs at 32% iron, and consists of  $\beta$  containing 25% iron and TiFe.

### 2. THE TITANIUM-OXYGEN SYSTEM

Investigations of the titanium-rich titanium-oxygen alloys at temperatures below 1200° C. have been carried out by Ehrlich,<sup>4,5</sup> Jaffee, Ogden, and Maykuth,<sup>6</sup> Jaffee and Campbell,<sup>7</sup> Finlay and Snyder,<sup>8</sup> Sutcliffe,<sup>9</sup> Worner,<sup>10</sup> Jenkins and Worner,<sup>11</sup> and Clark.<sup>12</sup>

Bumps, Kessler, and Hansen<sup>13</sup> have investigated the system up to and including the melting points on alloys containing 0–30 wt.-% oxygen. Their phase diagram agrees substantially with the work carried out in the Metallurgy Division of the National Physical Laboratory.

## III.—EXPERIMENTAL METHODS

### 1. MATERIALS USED

The alloys were prepared from sponge titanium (manufactured by the Kroll process by E. I. du Pont de Nemours), pure iron, and pure titanium dioxide. An analysis of the sponge titanium gave the following results: oxygen 0.2, hydrogen 0.02, nitrogen 0.01, carbon 0.05, iron 0.3, magnesium 0.035, and silicon 0.025%.

The iron was a mixture of turnings from several samples prepared in the Metallurgy Division, and gave an average analysis of: carbon 0.007, silicon 0.003, sulphur 0.005, manganese 0.003, aluminium 0.003%. A spectrographic analysis of the titanium dioxide gave the following results: silicon 0.06, iron 0.04 (variable 0.03–0.07), aluminium <0.001, magnesium <0.05%.

### 2. ANALYSIS OF THE ALLOYS

The gas content of alloys low in oxygen was determined by vacuum fusion.<sup>14</sup> The titanium contents of alloys higher in oxygen were determined by a

\* Manuscript received 3 November 1953.

† Metallurgy Division, National Physical Laboratory, Teddington, Middlesex.



precision absorptiometric<sup>15</sup> method, and the oxygen content was obtained by difference. For this purpose the content of other elements, silicon, &c., was taken as 0.1% and that of hydrogen and nitrogen as 0.15% (based on vacuum-fusion analysis). Some of these determinations were confirmed gravimetrically, and the agreement between the two methods showed that the difference figures for oxygen had an accuracy of the order of  $\pm 0.2\%$ . The iron content of all alloys was determined colorimetrically with thioglycolic acid in citrate solution.

The analyses in general showed good agreement with the nominal compositions.

### 3. PREPARATION OF THE ALLOYS

The requisite amount of material for each 75-g. charge was briquetted under a load of 20 tons/in.<sup>2</sup> in case-hardened steel dies. Melting was carried out in a small arc furnace in an atmosphere of 12 cm. of argon (99.8% purity). To ensure homogeneity, each ingot was melted four times. Between each melting operation the ingot was turned over by means of a spade-shaped probe fitted into the top of the furnace.

### 4. ANNEALING TREATMENTS

All alloys intended for metallographic and X-ray examination were homogenized by heating at 1300° C. for 6 hr. in a vacuum furnace (10<sup>-3</sup> mm. mercury), followed by furnace-cooling to room temperature at an average rate of 1.5° C./min. The specimens for all further heat-treatments were sealed into evacuated silica tubes, heated to the desired temperature, and maintained there for a definite time to permit an approach to equilibrium. The silica tubes were then simultaneously broken and quenched in water. The times and temperatures of the heat-treatments were as follows:

Annealing Temp., °C.	Annealing Time, hr.
1100	1
1000	4
900	8
800	8
650	820
550	820

The microstructures of selected alloys heat-treated at 800° C. for twice and 45 times the original annealing time were compared, and since no significant changes were observed, it was concluded that equilibrium conditions had been attained.

The specimens were prepared for microscopical examination by rubbing down on emery papers to the 00 grade and then polishing with alumina (160 mesh) and finally with chromic oxide. The etching reagent used consisted of an aqueous solution of  $\frac{1}{2}\%$  hydrofluoric acid and  $\frac{3}{4}\%$  nitric acid.

### 5. X-RAY-DIFFRACTION TECHNIQUE

X-ray-diffraction examination of certain alloys was undertaken to confirm the metallographic observa-

tions. The diffraction patterns were obtained from powder (200 mesh) with a 9- or 19-cm.-dia. Debye-Scherrer powder camera, using filtered  $\text{CuK}_\alpha$  radiation.

## IV.—THE EFFECT OF THERMAL TREATMENTS ON THE PHASE BOUNDARIES

All the alloys were examined for segregation in the as-cast condition, and also after the homogenizing treatment, before heat-treatment at the specified temperatures.

Very fine Widmanstätten structures were observed in the as-cast titanium-iron alloys; the structures were coarsened by the addition of oxygen, and the well-known "basket weave" structure was observed. Typical as-cast and homogenized structures are shown in Figs. 2-5 (Plate LXXXIV). The slowly cooled alloys of higher iron and oxygen contents showed evidence of a slow breakdown of the  $\beta$  solid solution into a finely dispersed mixture of  $(\alpha + x)$  (where  $x$  is probably a complex oxide of iron and titanium) which does not occur uniformly but in isolated regions, particularly along the grain boundaries (Fig. 5). It was noticed that the microstructure of specimens furnace-cooled from 1300° C. tended to be similar to the microstructures of the same alloys quenched from 800° C.

### 1. THE 1100° C. ISOTHERMAL

The results of metallographic and X-ray examinations of specimens quenched from 1100° C. are shown in Fig. 1 (a). The microstructures of the single-phase alloys indicated that the grain-size of the specimens was relatively large.

The  $\beta$  phase field extends to somewhat less than 1% oxygen with iron contents up to at least 5%. Alloys containing less than 4% iron quenched from the  $\beta$  phase field show typical transformation structures; and with more than 4% iron present the  $\beta$  phase is retained by quenching. This was confirmed by X-ray examination. The existence of sub-boundaries in some  $\beta$  grains was noticed.

The solubility of iron in the  $\alpha$  phase is about 0.2%, and thus the  $\alpha$  phase field, which starts at 2.85% oxygen, is even more restricted than the  $\beta$  phase field. The alloy containing 5.28% oxygen and 0.17% iron showed, in the grains and grain boundaries, very slight traces of retained  $\beta$ , which increased slightly in number as the annealing temperature was lowered to 900° C.

Between the  $\alpha$  and  $\beta$  phase fields, an extensive duplex ( $\alpha + \beta$ ) region occurs, and adjacent to it a three-phase field consisting of  $(\alpha + \beta + x)$ . Evidence of a three-phase field at 1100° C. is based on one specimen, but its existence at lower temperatures is well established. Some doubt as to the precise position of the boundaries of this three-phase field exists at all temperatures; consequently, the boundaries are shown dotted in Fig. 1 (a)-(e). Further

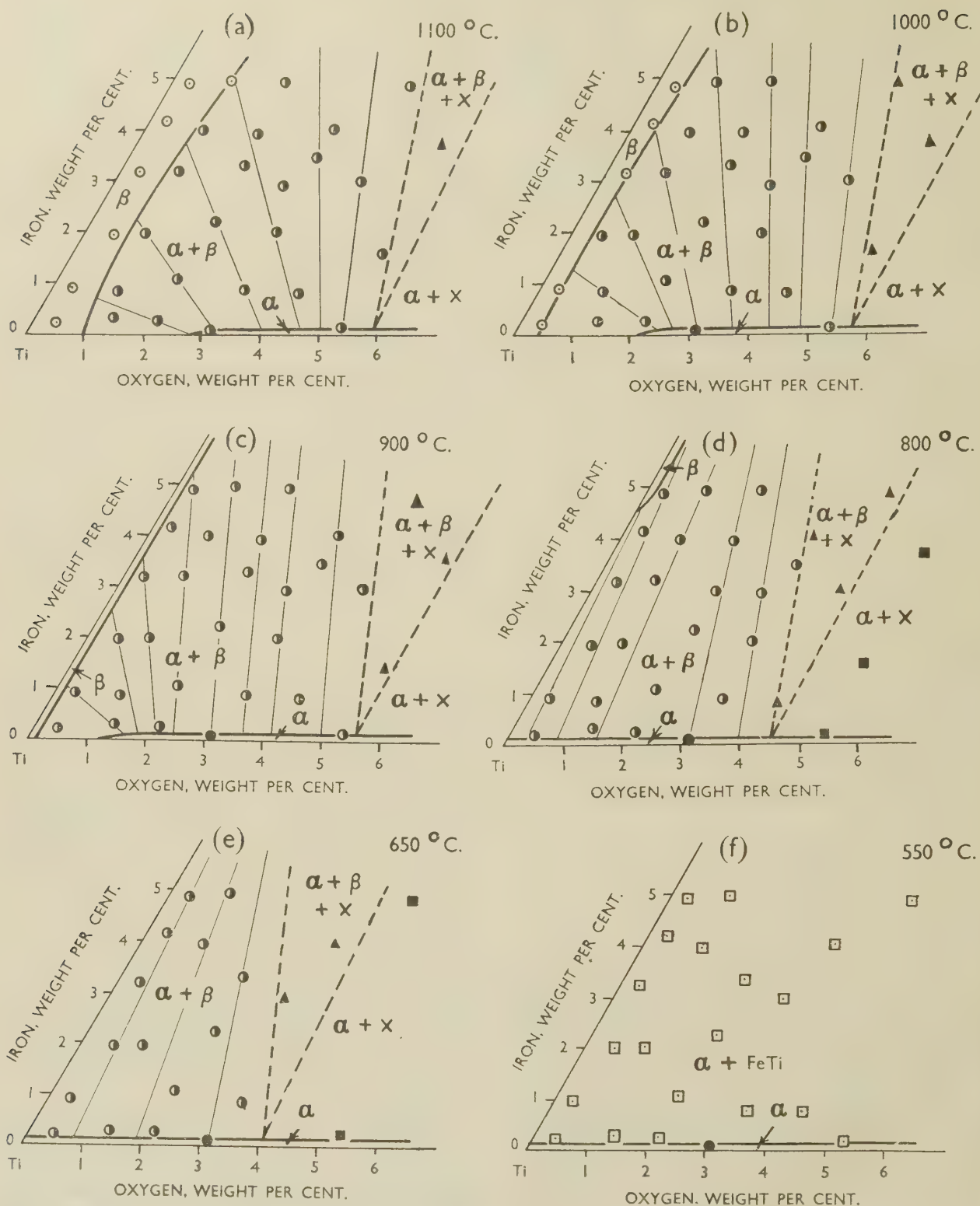


FIG. 1.—Isothermal Sections for Titanium-Iron-Oxygen Alloys at (a) 1100° C., (b) 1000° C., (c) 900° C., (d) 800° C., (e) 650° C., and (f) 550° C., as Determined by X-Ray and Metallographic Examination.



experiments are required to establish its limits precisely.

The constituent  $x$  appears to be a complex oxide of titanium, iron, and oxygen of the ideal composition  $\text{Fe}_3\text{Ti}_3\text{O}$ , as proposed by Karlsson.<sup>16</sup> With increase of oxygen content, the  $\beta$  phase of the three-phase field is suppressed, and adjacent to it a binary ( $\alpha + x$ ) field appears. In fixing tentatively the boundaries of the ( $\alpha + \beta + x$ ) field it has been assumed that the ( $\alpha + \beta + x$ )/( $\alpha + x$ ) boundary ends at a composition approximating to  $\text{Fe}_3\text{Ti}_3\text{O}$ . The position of the ( $\alpha + \beta$ )/( $\alpha + \beta + x$ ) boundary has been fixed from microscopical evidence and phase-rule considerations.

## 2. THE 1000° C. ISOTHERMAL

The isothermal diagram shown in Fig. 1 (b) is very similar to that at 1100° C., except that all the boundaries are slightly displaced towards the titanium-iron isothermal.

The  $\beta$  phase field now extends only to approximately 0.45% oxygen with iron contents up to 5%. The  $\alpha$  phase field contains approximately 0.15% iron in solution and begins at 2.2% oxygen. The alloy containing 3.05% oxygen and 0.10% iron consists entirely of  $\alpha$ , whilst that containing 5.28% oxygen and 0.17% iron shows traces of spheroidal retained  $\beta$  in the grains and grain boundaries. The microstructures of alloys quenched from the ( $\alpha + \beta$ ) phase field close to the  $\beta$  phase boundary showed the white-etching  $\alpha$  phase in the darker matrix of transformed  $\beta$ . In alloys of higher oxygen content the  $\beta$  phase did not generally darken on etching. Fig. 6 (Plate LXXXIV) shows an alloy containing 4.1% oxygen and 4.9% iron quenched from 1000° C., which is near the boundary of the three-phase field. Traces of the  $x$  constituent can be seen where the  $\beta$  phase has transformed along the  $\alpha$  and  $\beta$  grain boundaries.

## 3. THE 900° C. ISOTHERMAL

As shown in Fig. 1 (c), the  $\beta$  phase field at this temperature is very restricted and the  $\beta$ /( $\alpha + \beta$ ) phase boundary is practically constant at about 0.1% oxygen. The  $\alpha$  phase field is extended slightly and begins at 1.2% oxygen, but the solubility of iron in this phase remains about the same. Fig. 7 (Plate LXXXIV) shows a typical microstructure of alloys quenched from the duplex ( $\alpha + \beta$ ) field, and illustrates the "needle-like" appearance of the isothermally formed  $\alpha$  phase in a matrix of  $\alpha$  (transformed  $\beta$ ) formed during the quench.

Fig. 7 and Figs. 8–9 (Plate LXXXV) show the effect of increase in oxygen content on the microstructures of alloys containing approximately 4% iron after annealing and quenching from 900° C. The  $\alpha$  phase separates on the crystal planes of  $\beta$  (Fig. 7), the amount increasing with increase in oxygen content, until at 5.2% oxygen the microstructures consist of an  $\alpha$  matrix with small islands of  $\beta$  partly decomposed to ( $\alpha + x$ ) (see Fig. 9).

## 4. THE 800° C. ISOTHERMAL

At 800° C. the  $\beta$  phase field does not appear until the iron content is about 4.5% (Fig. 1 (d)). The  $\alpha$  phase boundary intersects the titanium-iron isothermal at about 0.15% iron. The solubility of iron in the  $\alpha$  phase does not change significantly with increase in oxygen content. The three-phase field ( $\alpha + \beta + x$ ) has moved towards the titanium-iron isothermal, and the apex of this field on the  $\alpha$  phase boundary occurs at about 4.5% oxygen.

Fig. 10 (Plate LXXXV) illustrates the mode of separation of  $x$  in the grain boundaries and apparently along certain crystallographic planes in an alloy containing 5.28% oxygen and 0.17% iron. The 3.05% oxygen, 0.10% iron alloy was single-phase at this temperature. A specimen of the alloy containing 4.1% oxygen and 4.9% iron was reheated for 6 and 45 times the initial annealing period of 8 hr., but no significant change in the proportion of the phases present occurred, thus confirming that equilibrium conditions were attained after 8 hr. at this temperature. The X-ray powder diffraction-pattern of this alloy showed a number of new, faint lines that could not be accounted for by FeTi or any of the oxides of titanium, but they were consistent with some of the stronger lines of the complex oxide of titanium, iron, and oxygen of composition  $\text{Fe}_2\text{Ti}_4\text{O}$  and cell size  $a = 11.31 \text{ \AA.}$ , as suggested by Karlsson.<sup>16</sup> This complex oxide is isomorphous with the high-speed-steel carbide  $\text{Fe}_3\text{W}_3\text{C}$ , and has a range of composition between  $\text{Fe}_3\text{Ti}_3\text{O}$  and  $\text{Fe}_2\text{Ti}_4\text{O}$ . The diffraction pattern of the alloy containing 5.21% oxygen and 3.74% iron was duplex, and consisted of  $\alpha$ -titanium and the complex oxide.

## 5. THE 650° C. ISOTHERMAL

The isothermal diagram for this temperature is shown in Fig. 1 (e). The  $\beta$  phase field does not appear in the portion of the ternary system under consideration, the  $\alpha$ /( $\alpha + \beta$ ) phase boundary remains unaltered, and the three-phase field is displaced towards the titanium-iron isothermal. Fig. 11 (Plate LXXXV) illustrates an alloy quenched from the ( $\alpha + \beta$ ) field, and Fig. 12 (Plate LXXXV) shows the same alloy quenched from 550° C., i.e. from the ( $\alpha + \text{FeTi}$ ) field.

## 6. THE 550° C. ISOTHERMAL

The isothermal diagram (Fig. 1 (f)) consists of a restricted  $\alpha$  phase field and an extensive duplex ( $\alpha + \text{FeTi}$ ) region. X-ray-diffraction experiments on two alloys (2.95% oxygen and 2.90% iron; 4.10% oxygen and 4.9% iron) confirmed the presence of the intermetallic compound FeTi at this temperature. The lattice parameter of FeTi was found to be  $a = 2.98 \text{ \AA.}$ , which is in good agreement with the values reported by Van Thyne, *et al.*<sup>3</sup> All the diffraction lines were identified as  $\alpha$ -titanium or FeTi, and no lines corresponding to the complex oxide of titanium, iron, and oxygen were found.

The appearance of the eutectoid ( $\alpha + \text{FeTi}$ ) is shown in Figs. 12 and 13 (Plate LXXXV). The compound  $x$  and  $\text{FeTi}$  could not be distinguished microscopically, and the formation and transformation of these compounds has not been studied in detail.

#### V.—SUMMARY AND DISCUSSION

The results of this metallographic examination of annealed and quenched specimens show that the somewhat restricted ( $\alpha + \beta$ ) phase field which occurs in the titanium-oxygen binary alloys is increased considerably by the addition of iron at all temperatures between 650° and 1100° C. (In the titanium-oxygen binary alloys the ( $\alpha + \beta$ ) phase field does not exist below the transformation temperature, 882° C.). The extent of the ( $\alpha + \beta$ ) phase field decreases with falling temperature by the gradual advance of the phase fields ( $\alpha + \beta + x$ ) and ( $\alpha + x$ ), where  $x$  is a complex oxide of titanium and iron.

As the extent of the ( $\alpha + \beta$ ) phase field increases with the addition of iron, so the extent of the  $\alpha$  phase field is markedly decreased, and this field does not exist at any of the temperatures investigated if the iron content is greater than about 0.2%.

Although the  $\beta$  phase field becomes less extensive with falling temperatures between 1100° and 900° C., the extent of the field within this range remains almost independent of the iron content up to 5%. At 800° C. the  $\beta$  phase field does not occur until about 4.5% iron is present, but the precise position of the  $\beta/(\alpha + \beta)$  boundary at this temperature has not been investigated. At some temperature below 800° C. the  $\beta$  phase becomes unstable and slowly decomposes into  $\alpha$  and  $\text{FeTi}$ . In the binary titanium-iron alloys, this decomposition occurs at about 600° C. In the ternary alloys, however, it is not certain whether the  $\beta$  phase decomposes directly to ( $\alpha + \text{FeTi}$ ) or whether the complex oxide  $x$  is involved. Thus, one alloy in the three-phase field, quenched from 800° C., on X-ray examination showed ( $\alpha + \beta + x(\text{Fe}_2\text{Ti}_4\text{O})$ ); the same alloy quenched after prolonged

annealing at 650° C. consisted of both  $x$  and  $\text{FeTi}$  as well as  $\alpha$ , whilst after quenching from 550° C. only  $\alpha$  and  $\text{FeTi}$  were present. All alloys in the range investigated after prolonged annealing at 550° C. consisted of ( $\alpha + \text{FeTi}$ ) except for a very restricted  $\alpha$  phase field.

Since the  $\alpha$  phase in the ( $\alpha + \beta$ ) phase field is dispersed in the form of "islands" in a  $\beta$  phase matrix, it is easy to estimate approximately by visual examination of the photomicrographs the relative areas of the  $\alpha$  and  $\beta$  phases present at each temperature investigated. From these estimations and the known compositions of the alloys, it is possible to mark the position of the tie-lines by application of the lever principle. The directions of the tie-lines determined in this way are shown in the isothermal diagrams (Figs. 1 (a)-(f)).

The direction of the tie-lines determines the composition of the  $\alpha$  and  $\beta$  phases present in an alloy at a given temperature, and since the  $\alpha$  phase becomes increasingly hard and brittle with increase in oxygen content, the oxygen content of this phase may have an important effect on the mechanical properties of the alloy. For example, an alloy containing about 4% iron and 0.3% oxygen quenched from 900° C. consists of  $\alpha$  containing about 2.0% oxygen in a matrix of  $\beta$ . Since the brittle  $\alpha$  phase separates in the form of long plates (Fig. 7), it is conceivable that this structure might give rise to brittleness in the alloy. It is intended to investigate this aspect in future work.

#### ACKNOWLEDGEMENTS

The work described above has been carried out as part of the Research Programme of the National Physical Laboratory, and this paper is published by permission of the Director of the Laboratory.

The authors wish to acknowledge the assistance given by their colleagues in carrying out the analyses, and also that of Mr. A. E. Bacon in the preparation of the alloys.

#### REFERENCES

1. C. M. Craighead, O. W. Simmons, and L. W. Eastwood, *Trans. Amer. Inst. Min. Met. Eng.*, 1950, **188**, 485.
2. H. W. Worner, *J. Inst. Metals*, 1951, **79**, 173.
3. R. J. Van Thyne, H. D. Kessler, and M. Hansen, *Trans. Amer. Soc. Metals*, 1952, **44**, 974.
4. P. Ehrlich, *Z. Elektrochem.*, 1939, **45**, 362.
5. P. Ehrlich, *Z. anorg. Chem.*, 1941, **247**, 53.
6. R. I. Jaffee, H. R. Odgen, and D. J. Maykuth, *Trans. Amer. Inst. Min. Met. Eng.*, 1950, **188**, 1261.
7. R. I. Jaffee and I. E. Campbell, *ibid.*, 1949, **185**, 646.
8. W. L. Finlay and J. A. Snyder, *ibid.*, 1950, **188**, 277.
9. D. A. Sutcliffe, *R.A.E. Tech. Note No. MET.141*.
10. H. W. Worner, *Australasian Eng.*, 1950, (Nov.), 52.
11. A. E. Jenkins and H. W. Worner, *J. Inst. Metals*, 1951-52, **80**, 157.
12. H. T. Clark, Jr., *Trans. Amer. Inst. Min. Met. Eng.*, 1949, **185**, 588.
13. E. S. Bumps, H. D. Kessler, and M. Hansen, *Trans. Amer. Soc. Metals*, 1953, **45**, 1008.
14. H. A. Sloman and C. A. Harvey, *J. Inst. Metals*, 1951-52, **80**, 391.
15. W. T. L. Neal, *Analyst* (in the press).
16. N. Karlsson, *Nature*, 1951, **163**, 558.



# THE CONSTITUTION OF THE COPPER-RICH COPPER-ZINC-GALLIUM ALLOYS\*

1552

By T. B. MASSALSKI,† B.Sc., STUDENT MEMBER, and PROFESSOR  
G. V. RAYNOR,‡ M.A., D.Sc., VICE-PRESIDENT

## SYNOPSIS

For comparison with previous work, the system copper-zinc-gallium has been examined by metallographic and X-ray methods, and isothermal sections for the copper-rich alloys have been established at 725°, 625°, 580°, and 400° C. At all four temperatures, the 21/13 electron compounds ( $\gamma$  phases) of the copper-zinc and copper-gallium alloys form a complete series of solid solutions. The 3/2 electron compounds ( $\beta$  phases) of the two systems form complete series of solid solutions at 725° and 625° C. At 580° C. the copper-gallium  $\beta$  phase is not stable, but the copper-zinc  $\beta$  phase persists to the composition 11 at.-% zinc and 17.5 at.-% gallium. The copper-gallium  $\zeta_1$  phase, which is stable at this temperature, dissolves only approximately 0.5 at.-% zinc, and at zinc contents between 1 and 10 at.-%, the primary  $\alpha$  solid-solubility isothermal corresponds with equilibrium between  $\alpha$  and the  $\gamma$  phase. The form of the equilibrium is similar at 400° C., at which temperature the copper-gallium  $\zeta_2$  phase is stable; the ( $\alpha + \gamma$ ) phase field extends to much higher zinc contents (27–28.5 at.-%) and the ordered  $\beta'$  phase of the copper-zinc system extends only to the composition 32.2 at.-% zinc and 7.6 at.-% gallium.

The bearing of the results on general alloy theory is briefly discussed, and it is suggested that the hexagonal phases of restricted homogeneity range formed by transformation in the solid state from body-centred cubic 3/2 electron compounds may have different characteristics from the hexagonal close-packed 3/2 electron compounds which are stable from room temperature to the melting point.

## I.—INTRODUCTION

MAJOR developments in the theory of binary-alloy formation were made possible by the detailed comparison of accurately established equilibrium diagrams. Similarly detailed comparison of a large number of ternary equilibrium diagrams is necessary for the development of a theory of ternary-alloy formation, and experiments have been in progress over a number of years in the authors' laboratory, with the aim of providing data for this purpose. The present paper describes the results of an examination of the system copper-zinc-gallium, undertaken for comparison with previous work.

The binary systems upon which the ternary system is based are well established. The details of the copper-zinc equilibrium diagram have been reviewed by Raynor,<sup>1</sup> and for the copper-gallium system the work of Hume-Rothery and Raynor<sup>2</sup> and of Betterton and Hume-Rothery<sup>3</sup> has been accepted. The zinc-gallium system is of the simple eutectiferous type, in which very restricted mutual solid solutions are in equilibrium in the solid state,<sup>4, 5</sup> and it is thus of little importance to the present work.

In the course of the research, isothermal partial equilibrium diagrams, covering the composition ranges 0–30 at.-% gallium and 0–60 at.-% zinc, have been established at 725°, 625°, 580°, and 400° C. by metallographic and X-ray methods.

## II.—MATERIALS AND METHODS

All alloys were prepared from the following materials: (i) Oxygen-free, high-conductivity copper. (ii) Spectrographically pure zinc, in which the only elements detected spectrographically were: lead 0.0001, cadmium <0.0001, copper <0.0001, iron <0.0005, and tin <0.0005%. (iii) Spectrographically standardized gallium, supplied by Johnson, Matthey and Co., Ltd.

In all respects except the preparation of alloys, the experimental methods were identical with those reported in previous communications from the authors' laboratory; it is considered unnecessary to repeat this information, therefore, and reference may be made to the work of Greenfield and Raynor on copper-zinc-germanium alloys.<sup>6</sup> The volatility of zinc and the relative scarcity of gallium, however, dictated special melting and casting techniques. In the earlier part of the work, alloys were prepared in quantities of 3 g., using a small-scale induction melting unit constructed by Mr. P. H. Stirling. Copper and gallium were melted together in a graphite crucible under an argon atmosphere, and the zinc added in the form of a master alloy with copper. After the melt had been stirred with a preheated alumina rod, a mild-steel split mould was placed mouth downwards on the crucible and clamped in position. Rotation of the furnace unit then allowed

\* Manuscript received 17 December 1953.

† Research Student, University of Birmingham.

‡ Professor of Physical Metallurgy, University of Birmingham.

the molten metal to fill the mould. By this means sound ingots with fine chill-cast microstructures were produced, measuring approximately 4 mm. in dia. and 1.5-2.0 cm. in length. The whole melting and casting process could be completed in 1 min., but in spite of this, small zinc losses occurred, and casting of alloys to predetermined compositions was difficult.

All critical alloys, and many others in addition, were chemically analysed, either in the authors' laboratory or by Johnson, Matthey and Co., Ltd.; results from the two laboratories were in excellent agreement, and the totals of the analytically determined percentages of the three metals were satisfactory ( $100 \pm 0.06$ ). By comparison of intended and analysed compositions, it was later possible to make allowance in weighing materials for the probable zinc loss on melting and casting, and with experience compositions very close to those intended were obtained. In the later stages of the work, however, when it was desired to prepare alloys of accurately predetermined composition for the precise location of narrowly separated phase boundaries, even greater control was necessary. This was obtained by a method based on that used by Owen and Roberts.<sup>7</sup> Carefully weighed amounts of the three metals were placed in narrow transparent silica tubes fitted with silica-rod handles, and each tube, after repeated evacuation and flushing with argon, was sealed with a reduced pressure of argon inside it. By means of the handle, the container was then held in an oxy-acetylene flame and shaken vigorously for 5 min. after the contents had melted. The tubes were quenched in water, and, since the containers did not in general shatter, homogenization annealing treatments were carried out without change of container. The initial weights of materials (approximately 1 g.) differed from those of the fully annealed ingots only by 1 part in 5000 to 1 part in 2000, so that very accurate control of composition was obtained. As a test of the method, six of the alloys prepared in silica were chemically analysed by Johnson, Matthey and Co.,

synthetic compositions of alloys prepared in silica may be accepted, provided that no abnormal weight loss is detected after preparation and annealing.

### III.—EXPERIMENTAL RESULTS

The results obtained are best represented as isothermal diagrams, involving the  $\alpha$ ,  $\beta$ , and  $\gamma$  phases of the copper-zinc and copper-gallium systems, the  $\beta'$  phase of the copper-zinc system, and the  $\zeta_1$  and



FIG. 1.—The 725° C. Isothermal. Unanalysed alloys are distinguished by vertical bars.

KEY TO FIGS. 1-6

$\alpha$  ■;  $\beta$  OR  $\beta'$  ●;  $\gamma$  ▲;  $\zeta_1$  □,  $\alpha + \beta(\beta')$  △;  $\beta + \gamma$  OR  $\beta' + \gamma$  □;  $\alpha + \gamma$  ○;  $\alpha + \zeta_1$  ▢;  
 $\alpha + \beta + \gamma$  ▤;  $\alpha + \beta' + \gamma$  ▥;  $\alpha + \zeta_1 + \gamma$  ▦;  $\alpha + \zeta_2 + \gamma$  ▧;  $\zeta_1 + \gamma$  ▨;  $\zeta_2 + \gamma$  ▩

TABLE I.—Comparison of Synthetic and Analysed Compositions.

Alloy	Synthetic Composition, at.-%			Analysed Composition, at.-%		
	Cu	Zn	Ga	Cu	Zn	Ga
W3 *	71.4	18.1	10.5	71.25	18.20	10.56
T4 .	65.9	27.1	7.0	65.89	27.14	6.97
T5 .	76.7	4.1	19.2	76.65	4.13	19.21
U9 *	71.0	10.8	18.2	71.06	10.64	18.30
U10 *	72.5	9.8	17.6	72.67	9.79	17.54
V7 *	77.4	1.0	21.6	77.41	1.06	21.53

\* These alloys were also analysed for silicon; this was found to be present in no greater amount than could be accounted for by analytical reagent blanks.

Ltd., and the agreement between synthetic and analysed compositions was excellent, as shown in Table I.

It may justifiably be claimed, therefore, that the

$\zeta_2$  phases of the copper-gallium system. It must be emphasized that many more alloys were examined than are represented in the isothermal diagrams, which contain mainly critical alloys that have been analysed or prepared in silica. In certain cases, no analysis was carried out; these alloys are distinguished in the equilibrium diagrams by vertical bars. The results which are not reported were in all cases consistent with the diagrams as presented.

In the following sections, individual alloys are



referred to where necessary in terms of their atomic percentages of zinc and gallium in that order. Thus an alloy containing 2.74 at.-% zinc and 22.93 at.-% gallium is denoted 2.74/22.93.

### 1. THE 725° C. ISOTHERMAL (FIG. 1)

At 725° C. the body-centred cubic  $\beta$  phases in the systems copper-zinc and copper-gallium are stable. Fig. 1 shows that these phases form complete solid solutions with each other. The complex cubic  $\gamma$  phases in the two binary systems are also mutually soluble. Though the  $(\beta + \gamma)/\gamma$  boundary is accurately a straight line joining the two binary limits, the boundaries of the ternary  $\beta$  phase are slightly curved. The primary solid-solubility isothermal is slightly convex towards the copper-rich corner of the diagram, and the  $(\alpha + \beta)$  phase field is of constant width.

### 2. THE 625° C. ISOTHERMAL (FIG. 2)

This temperature is only slightly above that of the eutectoidal decomposition of the copper-gallium  $\beta$  phase into  $\zeta_1$  and  $\gamma$ ; consequently the extent of the



FIG. 2.—The 625° C. Isothermal.

$\beta$  phase on the copper-gallium axis of the ternary diagram is restricted. Otherwise, the equilibrium

relationships in the ternary system are identical with those at 725° C. The ternary  $\beta$  phase area has, however, diminished considerably, and the  $\alpha$  solid

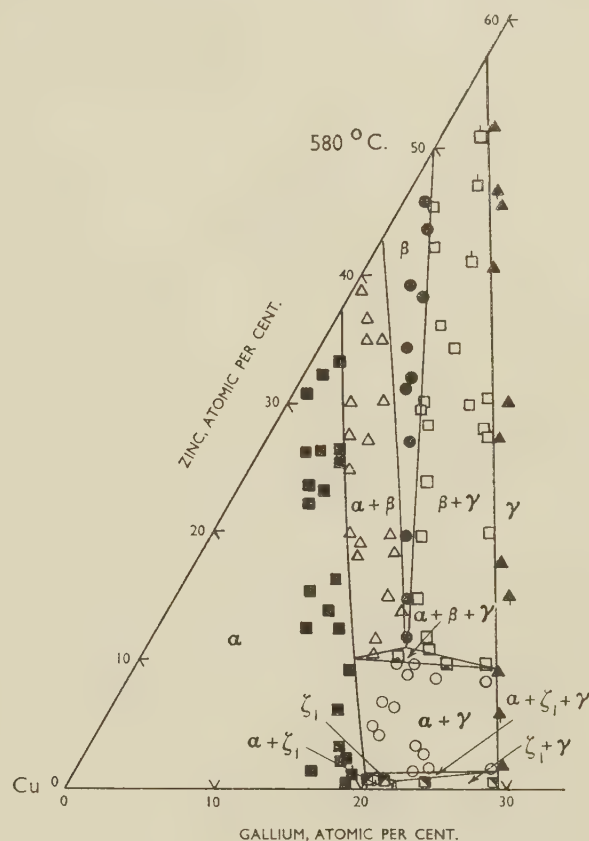


FIG. 3.—The 580° C. Isothermal.

solution is more extensive. The  $(\alpha + \beta)$  and  $(\beta + \gamma)$  areas are slightly wider than at the higher temperature.

### 3. THE 580° C. ISOTHERMAL (FIG. 3)

The copper-gallium  $\beta$  phase decomposes at 616° C. into the  $\gamma$  and  $\zeta_1$  phases.  $\zeta_1$  has a close-packed hexagonal crystal structure, and appears on the copper-gallium axis of the ternary diagram, in place of  $\beta$ , in Fig. 3. As at higher temperatures, the  $(\beta + \gamma)/\gamma$  boundary is a straight line. The copper-zinc  $\beta$  phase dissolves a considerable amount of gallium and penetrates, as a narrowing phase field, well into the ternary diagram. The two  $3/2$  electron compounds  $\beta$  and  $\zeta_1$  do not, however, enter into simple equilibrium with each other. This is in striking contrast to the behaviour of the copper-aluminium-germanium system,<sup>8</sup> where the body-centred cubic copper-aluminium  $\beta$  phase and the copper-germanium  $\zeta$  phase (close-packed hexagonal) are in equilibrium with each other over a wide temperature range. In the present case, equilibrium is established between the  $\alpha$  and  $\gamma$  phases, and the diagram contains narrow  $(\alpha + \beta + \gamma)$  and  $(\alpha + \zeta_1 + \gamma)$

three-phase triangles, both of which were metallographically confirmed. The penetration of the copper-gallium  $\zeta_1$  phase into the ternary diagram is very limited, and the  $(\alpha + \zeta_1 + \gamma)$  triangle occurs very close to the binary copper-gallium axis. This region of the diagram is shown on a larger scale in Fig. 4; the three-phase regions are adequately

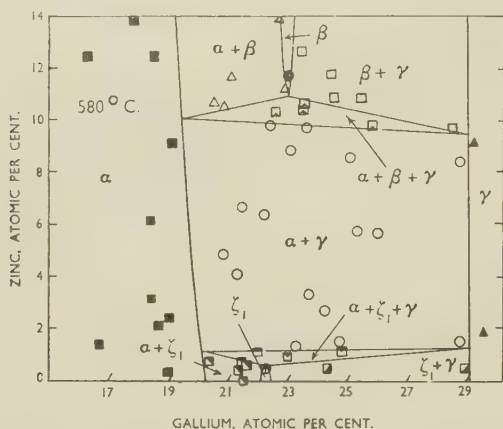


FIG. 4.—Enlarged Portion of the 580° C. Isothermal.

defined, but only one alloy (0.5/22.0) could be placed in the homogeneous  $\zeta_1$  area.

The primary  $\alpha$  boundary is again slightly convex towards the origin of the diagram.

#### 4. THE 400° C. ISOTHERMAL (FIG. 5)

The  $\zeta_1$  phase of the copper-gallium system breaks down at 475° C. into the  $\gamma$  and  $\zeta_2$  phases. The latter, which is also close-packed hexagonal in crystal structure, is stable at 400° C. In the copper-zinc system, the appropriate 3/2 electron compound is  $\beta'$ , an ordered body-centred cubic structure formed from the disordered  $\beta$  phase at 454–468° C. Fig. 5 shows that though the two binary  $\gamma$  phases still form a complete series of solid solutions across the diagram, the ordered  $\beta'$  phase can dissolve much less gallium than the disordered  $\beta$  phase at 580° C. The  $\beta'$  area has shrunk considerably, while the  $(\alpha + \gamma)$  phase field, relatively narrow at 580° C., has greatly expanded. There is also an enlargement of the  $(\alpha + \beta' + \gamma)$  triangle as compared with the  $(\alpha + \beta + \gamma)$  triangle at 580° C. As in the case of  $\zeta_1$  at 580° C., the  $\zeta_2$  phase at 400° C. dissolves very little zinc, and the  $(\alpha + \zeta_2 + \gamma)$  three-phase triangle, which is shown on an enlarged scale in Fig. 6, is very close to the binary copper-gallium axis.

#### 5. X-RAY CONFIRMATION

Whenever possible, confirmation of the metallographic work was obtained by X-ray-diffraction methods, using quenched filings. The use of these methods was complicated by decomposition on quenching of the ternary  $\beta$  phase in certain composi-

tion ranges; in these ranges, however, unambiguous interpretation of quenched microstructures presented no difficulty, owing to the familiar form of the decom-

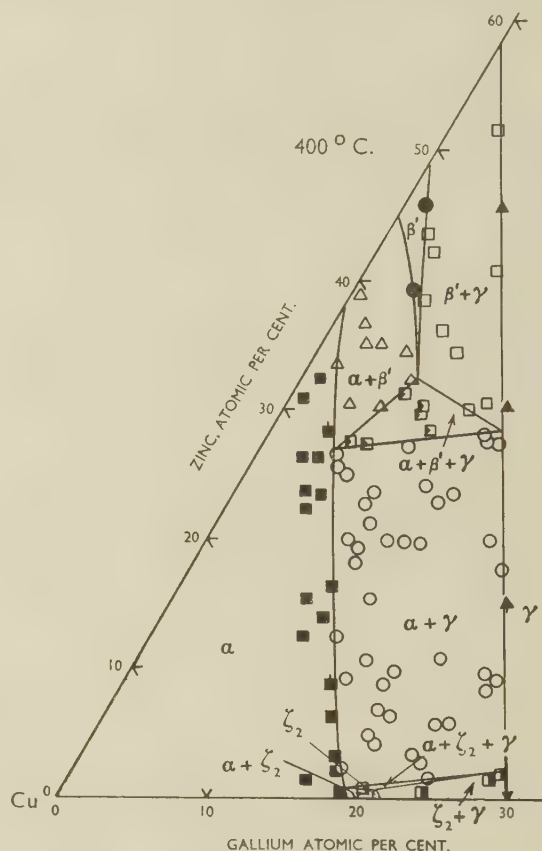


FIG. 5.—The 400° C. Isothermal.

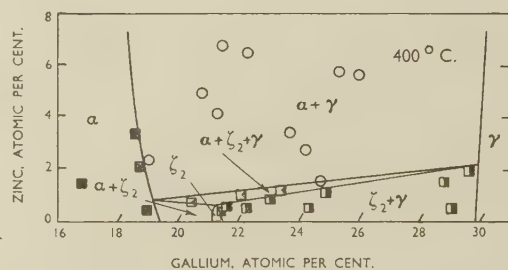


FIG. 6.—Enlarged Portion of the 400° C. Isothermal.

position, which gave rise either to a very fine precipitate or a martensitic appearance according to composition.

#### IV.—DISCUSSION

The outstanding features of the constitution of the copper-zinc-gallium alloys are the very restricted solubility of zinc in the copper-gallium  $\zeta_1$  and  $\zeta_2$  phases, the absence of simple equilibrium between  $\beta$  and  $\zeta_1$  or  $\zeta_2$  and the existence of  $\alpha$  and  $\gamma$  in equilibrium



at temperatures below that of the eutectoidal decomposition of the copper-gallium  $\beta$  phase. It is not possible to say at the present time whether the ( $\alpha + \gamma$ ) equilibrium is due to a marked stabilization (lowering of free energy) of the  $\gamma$  structure on the formation of the ternary solid solution, or whether it is due to the inability of the  $\zeta_1$  and  $\zeta_2$  phases to dissolve sufficient zinc to prevent the  $\alpha$  and  $\gamma$  phases from entering into equilibrium. It is of interest to note that in the system silver-magnesium-zinc<sup>9</sup> the complex close-packed hexagonal  $\zeta$  phase stable at low temperatures in the binary silver-zinc alloys also has a very restricted solubility for the third metal. In this case the restriction was attributed to the large difference between the size-factors\* of magnesium and zinc with respect to silver (+10.7 and -7.8%, respectively). The same factor, however, cannot account for the restriction of  $\zeta_1$  and  $\zeta_2$  in the copper-zinc-gallium alloys, because the difference between the size-factors with respect to copper of zinc and gallium is well within the range for which simple equilibrium between body-centred cubic and close-packed hexagonal 3/2 electron compounds has been previously observed.<sup>6,8</sup> In all cases where such a simple equilibrium has been noted, however, it is significant that the hexagonal phase involved is stable from the melting point to room temperature, and is not formed from the body-centred cubic 3/2 electron compound by a reaction in the solid state. This suggests that the hexagonal phases formed at low temperatures, and approximating in composition to that corresponding with 3/2 electrons per atom, may be a different type of phase (i.e. owing their limited stability to factors other than electron concentration) from those which are hexagonal, but stable over the whole temperature range from room temperature to the melting point. This view is strengthened by the fact that the crystal structures of the low-temperature forms are frequently complex, and not simple close-packed structures; it is also significant that these low-temperature phases are usually of limited homogeneity range even in the binary systems.

The discussion of the equilibria in the copper-zinc-gallium system in terms of atomic size-factors is difficult, in view of the complexity of the crystal structure for gallium. If the atomic diameter of gallium is defined as the closest distance of approach of atoms in the crystal of the element (2.44 Å.), the size-factor of gallium with respect to copper is -4.47%. There is evidence,<sup>10</sup> however, that the effective atomic diameter of gallium in solid solution in copper or silver is larger than the closest distance of approach of atoms in the crystal, and an analysis of lattice-spacing relationships for copper-rich alloys suggests that a value of 2.6 Å. for the effective diameter of gallium is more appropriate.<sup>11</sup> The size-factor with respect to copper is then approximately +1.7%.

The form of the equilibria in the present case is not inconsistent with this small positive value; if the effective size-factor in the ternary system varies linearly from -4.47% on the copper-gallium axis to +4.23% on the copper-zinc axis, then, provided that the  $\zeta_1$  and  $\zeta_2$  phases may be regarded as normal 3/2 electron compounds, they would be expected<sup>6,10</sup> to persist in the ternary model at least until an effective size-factor in the region of zero was reached at approximately equal percentages of gallium and zinc. If, on the other hand, the effective size-factor varies only from +1.7% for copper-gallium to +4.23% for copper-zinc, no such extensive penetration of the  $\zeta_1$  and  $\zeta_2$  phases into the ternary model would be expected, as the size-factor for gallium with respect to copper is already near the positive borderline of the size-factor range within which hexagonal 3/2 electron compounds are favoured. The very restricted solubility of zinc in  $\zeta_1$  and  $\zeta_2$ , however, suggests that these phases are not to be regarded as normal 3/2 electron compounds, and it is doubtful how far the application of simple size-factor considerations is justified.

As shown in Figs. 1, 2, 3, and 5, the various phase boundaries in the isothermal sections deviate only slightly from straight lines, which is consistent with a favourable size-factor throughout the ternary system. They do not, however, occur at exactly constant electron:atom ratios. The form of the primary solid-solubility isothermals is of interest, since the same type of convexity towards the copper-rich corner of the ternary diagram is shown by the copper-zinc-germanium alloys, but to a rather greater extent. When zinc is substituted for germanium at the solid-solubility limit of the latter in copper, approximately three zinc atoms replace one of germanium; thus both the number of centres of distortion in the lattice and the overall distortion increase, since the expansion produced in copper by three atoms of zinc is approximately 1.8 times that produced by one germanium atom. The decrease in solubility represented by the convex solubility isothermals may be interpreted in terms of a tendency to reduce this increased distortion.<sup>8</sup> In the present case, when three zinc atoms replace two gallium atoms, in order to maintain an approximately constant electron:atom ratio of 1.4 at the solubility limit, the number of centres of distortion and the overall distortion again increase, since three zinc atoms cause 1.13 times as much expansion of the copper lattice as two gallium atoms. The increase in the distortion is, however, much smaller than in the copper-zinc-germanium system, and the convexity developed in the solubility isothermal is correspondingly reduced. At the solid-solubility limit of zinc in copper, the lattice is already heavily distorted by a high concentration of zinc atoms, so that although the overall distortion is slightly reduced on substituting

\* The size-factor of a given metal  $M$  with respect to a solvent  $A$  is measured by the difference between the atomic

diameters of  $M$  and  $A$ , expressed as a percentage of that of the latter.

two gallium atoms for three zinc atoms, the lattice may be regarded as unable to accommodate the centres of increased expansion corresponding to the introduced gallium atoms. The slight restriction of solid solubility may thus be understood, as in the system copper-zinc-germanium, where the distortion effects on substituting germanium for zinc are more serious and the solubility restrictions more marked.

## ACKNOWLEDGEMENTS

This work forms part of a general survey of ternary equilibrium diagrams based on copper or silver as solvents, and grateful acknowledgement for generous financial assistance is made to the Department of Scientific and Industrial Research, the Royal Society, the Chemical Society, and Imperial Chemical Industries, Ltd.

## REFERENCES

1. G. V. Raynor, *Inst. Metals Annotated Equilib. Diagr. Series*, 1944, (3).
2. W. Hume-Rothery and G. V. Raynor, *J. Inst. Metals*, 1937, **61**, 205.
3. J. O. Betterton, Jr., and W. Hume-Rothery, *ibid.*, 1951-52, **80**, 459.
4. N. A. Puschin, S. Stephanowić, and V. Stajić, *Z. anorg. Chem.*, 1932, **209**, 329.
5. W. Kroll, *Metallwirtschaft*, 1932, **11**, 435.
6. P. Greenfield and G. V. Raynor, *J. Inst. Metals*, 1951-52, **80**, 375.
7. E. A. Owen and E. A. O'Donnell Roberts, *ibid.*, 1945, **71**, 213.
8. G. V. Raynor and P. Greenfield, *ibid.*, 1953-54, **82**, 59.
9. G. V. Raynor and R. A. Smith, *ibid.*, 1949-50, **76**, 389.
10. W. Hume-Rothery, P. W. Reynolds, and G. V. Raynor, *ibid.*, 1940, **66**, 191.
11. G. V. Raynor, *Trans. Faraday Soc.*, 1949, **46**, 698.



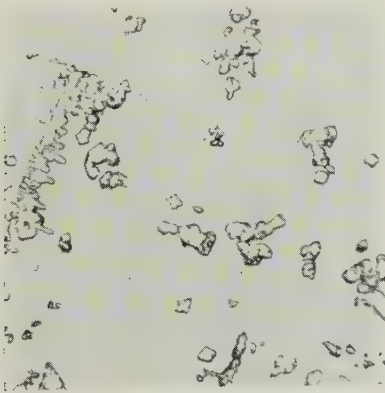


FIG. 7.—Titanium Carbide Dendrites in Copper 25.9% Titanium-0.29% Carbon Alloy. Unetched.  $\times 500$ .

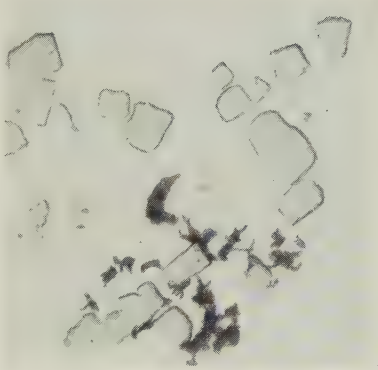


FIG. 8.—Titanium Carbide Particles (and Graphite) in Copper 20% Nickel Alloy to Which 1% Titanium Carbide was Added as Sintered 33% Nickel Pellets. Original size of particles =  $1\mu$ . Unetched.  $\times 600$ .

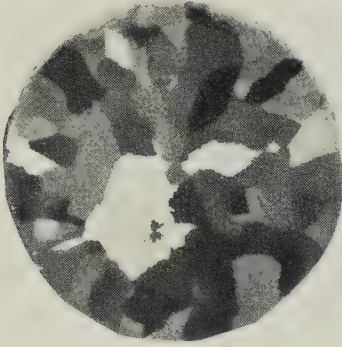


FIG. 9.—Coarse Macrostructure of  $2\frac{1}{4}$ -in.-dia. Bar of Copper-10% Tin-0.5% Cobalt Alloy, Sand Cast at  $1150^{\circ}\text{C}$ . Typical of unrefined alloys. Etched in alcoholic  $\text{FeCl}_3$  solution.  $\times \frac{1}{4}$ .

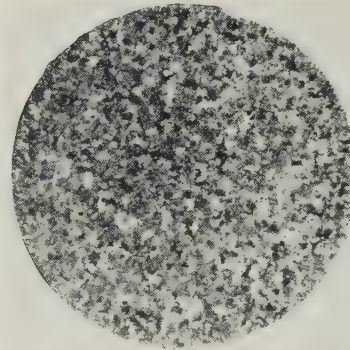


FIG. 10.—Fine Macrostructure of  $2\frac{1}{4}$ -in.-dia. Bar of Copper-10% Tin-0.1% Cobalt-0.06% Boron Alloy, Sand Cast at  $1150^{\circ}\text{C}$ . Etched in alcoholic  $\text{FeCl}_3$ .  $\times \frac{1}{4}$ .

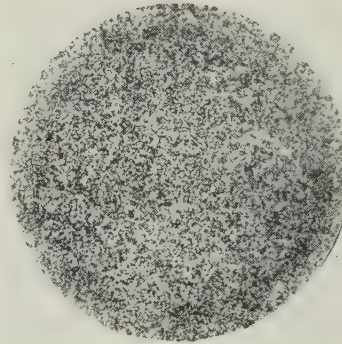


FIG. 11.—Very Fine Macrostructure of  $2\frac{1}{4}$ -in.-dia. Bar of Copper-10% Tin-0.05% Zirconium Alloy Sand Cast at  $1150^{\circ}\text{C}$ . Etched in alcoholic  $\text{FeCl}_3$  solution.  $\times \frac{1}{4}$ .

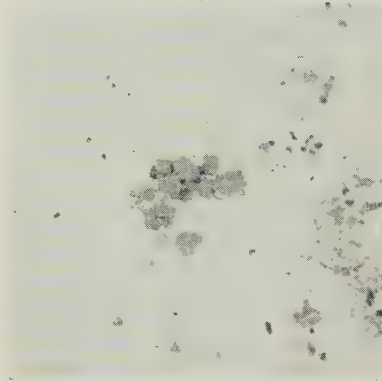


FIG. 12.—Particles of Titanium-Boron Constituent, Probably  $\text{TiB}_2$ , in Copper-10% Tin-0.3% Titanium-0.2% Boron Alloy, Sand Cast at  $1150^{\circ}\text{C}$ . Unetched.  $\times 1500$ .



FIG. 13.—Two Iron-Boron Constituents, (Probably Iron Borides) in Copper-10% Tin-0.96% Iron-0.2% Boron Alloy, Sand Cast at  $1150^{\circ}\text{C}$ . Unetched.  $\times 1000$ .

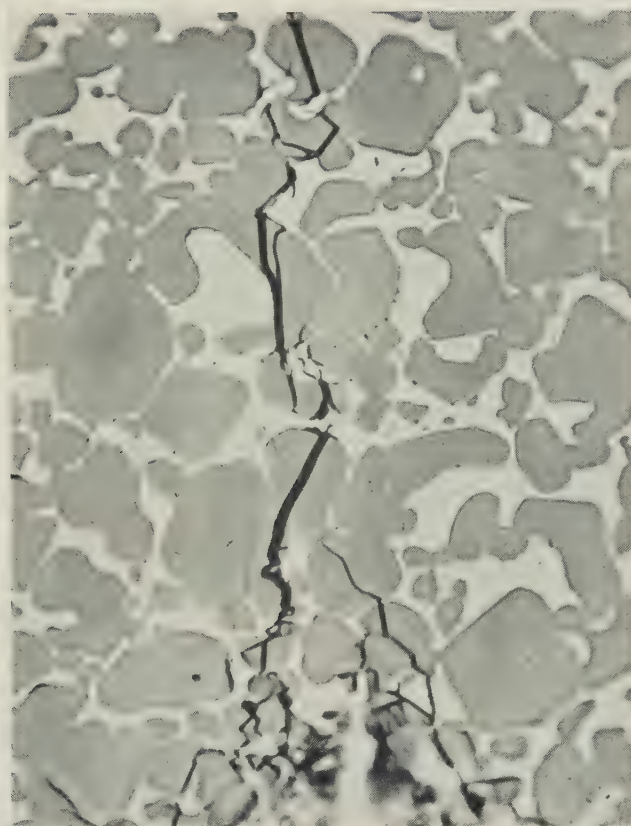


FIG. 8.—Crack Arising from Point of Diamond Hardness Impression  
Made on Nickel-Bonded Titanium Carbide.  $\times 1500$ .



## MICROSTRUCTURES OF TITANIUM-IRON-OXYGEN ALLOYS.

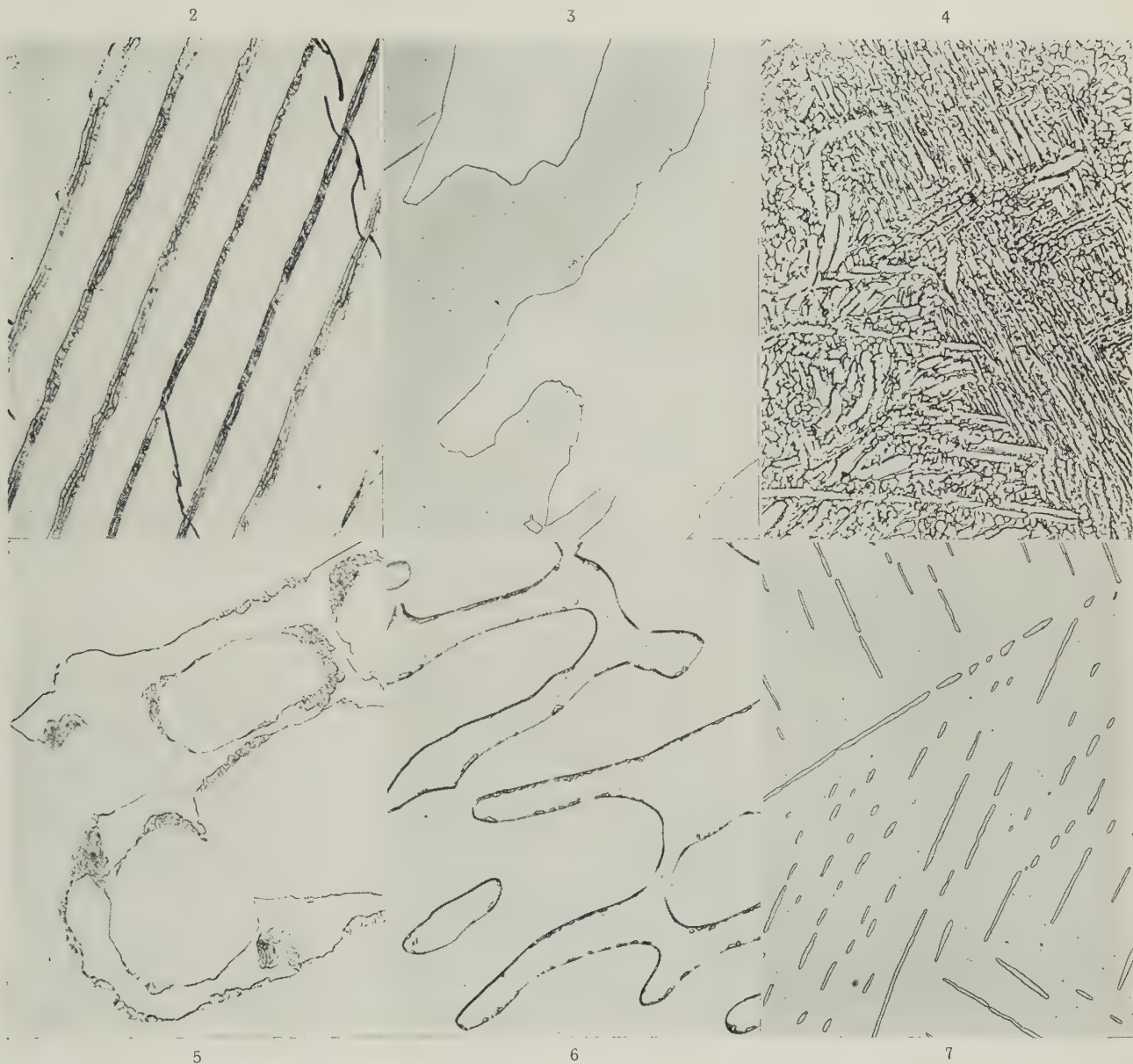


FIG. 2.—0.10% Iron, 3.05% Oxygen. As cast. Large elongated grains of  $\alpha$  in transformed  $\beta$  matrix.  $\times 150$ .

FIG. 3.—0.10% Iron, 3.05% Oxygen. Homogenized at  $1300^{\circ}\text{C}$ . and furnace-cooled.  $\alpha$  solid solution.  $\times 150$ .

FIG. 4.—4.9% Iron, 4.1% Oxygen. As cast.  $\times 150$ .

FIG. 5.—4.9% Iron, 4.1% Oxygen. Homogenized at  $1300^{\circ}\text{C}$ . and furnace-cooled. ( $\alpha + \beta + x$ ).  $\times 500$ .

FIG. 6.—4.9% Iron, 4.1% Oxygen. Homogenized at  $1300^{\circ}\text{C}$ . and furnace-cooled, annealed for 4 hr. at  $1000^{\circ}\text{C}$ ., and water-quenched.  $\alpha + \beta +$  traces of  $x$  at grain boundaries.  $\times 500$ .

FIG. 7.—4.17% Iron, 0.37% Oxygen. Homogenized at  $1300^{\circ}\text{C}$ . and furnace-cooled, annealed for 8 hr. at  $900^{\circ}\text{C}$ ., and water-quenched.  $\alpha$  "needles" in  $\beta$  matrix.  $\times 150$ .

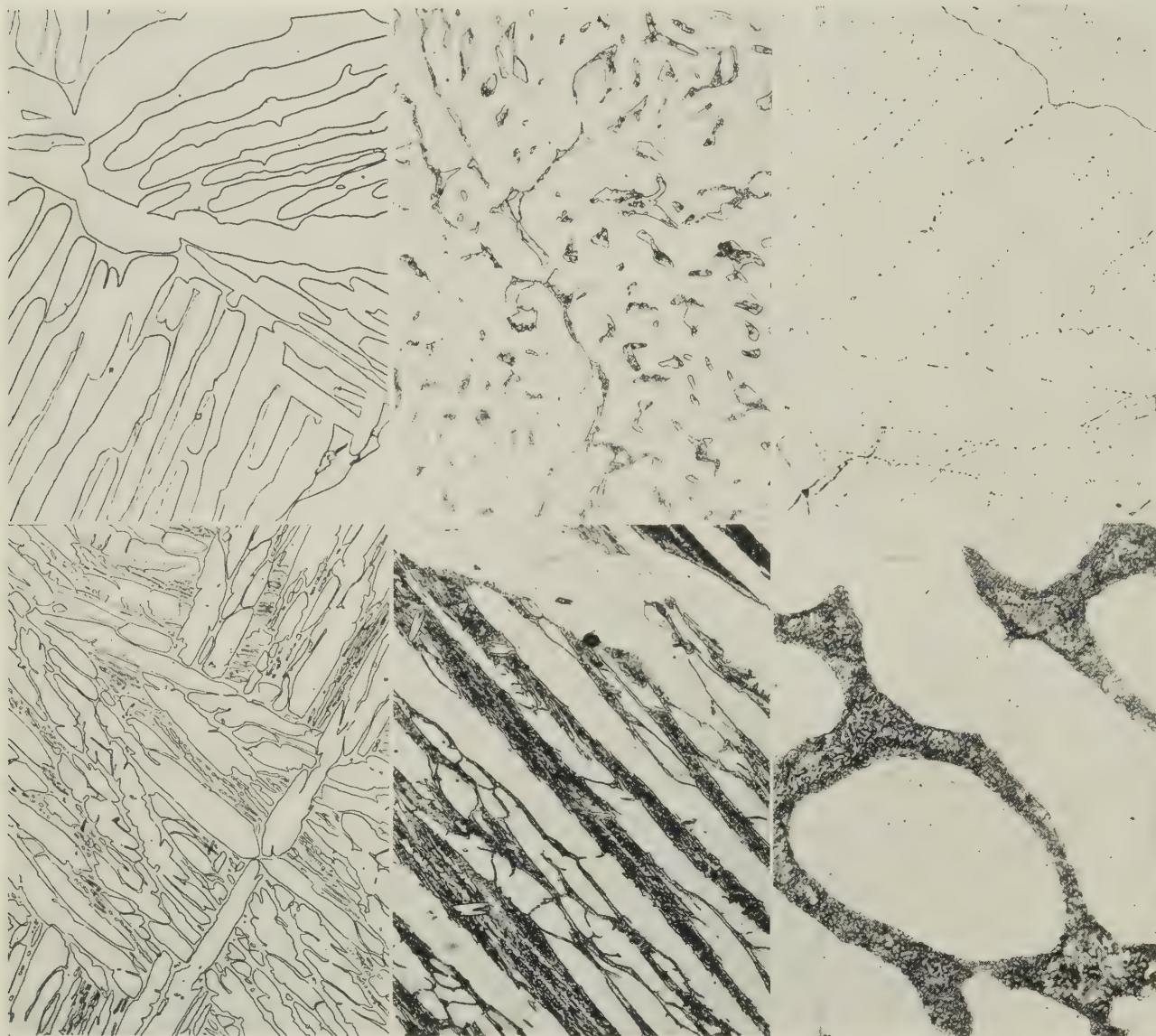
Etched in aqueous solution of  $\frac{1}{2}\%$  HF +  $\frac{1}{4}\%$   $\text{HNO}_3$ .

## MICROSTRUCTURES OF TITANIUM-IRON-OXYGEN ALLOYS.

8

9

10



11

12

13

FIG. 8.—4.1% Iron, 3.25% Oxygen. Homogenized at 1300° C. and furnace-cooled, annealed for 8 hr. at 900° C., and water-quenched.  $\alpha$  in  $\beta$  matrix.  $\times 150$ .

FIG. 9.—3.74% Iron, 5.21% Oxygen. Homogenized at 1300° C. and furnace-cooled, annealed for 8 hr. at 900° C., and water-quenched.  $\alpha + \beta + \alpha$ .  $\times 150$ .

FIG. 10.—0.17% Iron, 5.28% Oxygen. Homogenized at 1300° C. and furnace-cooled, annealed for 8 hr. at 800° C., and water-quenched. Traces of  $\alpha$  in  $\alpha$  matrix.  $\times 150$ .

FIG. 11.—4.91% Iron, 0.95% Oxygen. Homogenized at 1300° C. and furnace-cooled, annealed for 820 hr. at 650° C., and water-quenched. ( $\alpha + \beta$ ).  $\times 150$ .

FIG. 12.—4.91% Iron, 0.95% Oxygen. Homogenized at 1300° C. and furnace-cooled, annealed for 820 hr. at 550° C., and water-quenched.  $\alpha$  in eutectoid matrix of ( $\alpha + \text{FeTi}$ ).  $\times 150$ .

FIG. 13.—4.9% Iron, 4.1% Oxygen. Homogenized at 1300° C. and furnace-cooled, annealed for 820 hr. at 550° C., and water-quenched. ( $\alpha + \text{FeTi}$ ).  $\times 500$ .

Etched in aqueous solution of  $\frac{1}{2}\%$  HF +  $\frac{3}{4}\%$  HNO<sub>3</sub>.



# A STUDY OF PREFERRED ORIENTATION IN EXTRUDED, DRAWN, AND ANNEALED COPPER \*

1553

By PROFESSOR PAUL G. BASTIEN,† Dr. ès Sci., MEMBER, and  
DR. J. POKORNY‡

## SYNOPSIS

An X-ray study of the texture produced by the extrusion and cold drawing of pure copper and copper containing small amounts of alloying elements, indicates that the double  $\langle 111 \rangle + \langle 100 \rangle$  texture is always found. On recrystallization at progressively increasing temperatures, the  $\langle 100 \rangle$  texture becomes steadily weaker, while the  $\langle 111 \rangle$  texture first becomes weaker and then grows much more marked at high annealing temperatures. This phenomenon is less apparent in copper alloys containing soluble additions.

The orientation of the first grains to recrystallize is governed by the method and degree of cold deformation.

## I.—INTRODUCTION

A NUMBER of face-centred cubic metals (e.g. copper, gold, and silver) in the form of wire have a double  $\langle 111 \rangle + \langle 100 \rangle$  texture, whether the wire is produced by drawing, rolling, or forging<sup>1</sup> or by extrusion,<sup>2</sup> the texture in the surface layers being slightly different. The mechanism of the formation of such textures has been studied<sup>3</sup> in relation to the direction of flow of the metal and the appearance of deformation bands.<sup>4</sup> A theory recently put forward<sup>5</sup> to account for the behaviour of cubic metals is based upon the relation of the slip directions to the deformation axis.

For copper, the drawing texture seems to be always double and well developed, with the  $\langle 111 \rangle$  direction predominating, and with certain modifications in intensity and direction occurring in the outer layers of the wire.<sup>1</sup> Severe working may, however, give rise to a single  $\langle 111 \rangle$  texture.<sup>6</sup> In the drawn and recrystallized state, results are conflicting. The deformation textures may be maintained up to 1000° C.<sup>7</sup> or may be modified<sup>8</sup>; single  $\langle 111 \rangle$ ,  $\langle 100 \rangle$ , and  $\langle 112 \rangle$  textures have been reported, and so have random orientations. It should be noted, however, that these observations were made on relatively fine wires not exceeding 3 mm. in dia., and on specimens of copper of varying degrees of purity. The methods of preparation (semi-finished drawn, rolled, or machined material, with and without intermediate annealing) also differed, so that it is not surprising that possible explanations of the phenomena observed are but rarely included in the papers.

The present investigation was directed towards determining the orientations produced in copper by extrusion and cold drawing, and the influence of such factors as degree of working, added elements, and

temperature of annealing after deformation, as well as to establishing the connection between deformation and recrystallization textures.

Various grades of copper were examined, and it would appear that small percentages of added elements, at least with copper of the degree of purity employed as the basis metal, had no substantial effect on the textures formed, nor, therefore, on the mode of deformation of the crystals.

## II.—PREPARATION AND WORKING OF MATERIALS

A series of copper alloys containing small additions of bismuth, silver, arsenic, or antimony, were prepared by the following method. Electrolytic copper was melted in an oil-fired crucible furnace, the surface of the liquid metal being protected against oxidation by a layer of wood charcoal; when the alloying additions had been made, the melt was deoxidized with phosphor copper and the metal poured direct into a circular mould, 120 mm. in dia. and 800 mm. deep. After cropping and skimming, the billet was extruded to a dia. of 27 mm. and the rod thus obtained was cold drawn, with intermediate anneals, to 14 mm. (73% reduction of area). Some of the rod was examined in this form, while in other cases a further reduction to 2 mm. dia. (93% reduction of area) was effected by wire drawing.

The compositions of the alloys, as determined by chemical analysis, are given in Table I.

The equilibrium diagrams of the binary alloys of copper with the various addition elements (bismuth, silver, arsenic, or antimony) show that copper containing up to 1% arsenic or up to 0.45% antimony is

\* Manuscript received 25 February 1953; in revised form 12 October 1953.

† Director of Scientific Research and Professor, Ecole

Centrale des Arts et Manufactures, Paris.

‡ Ingénieur-Chef de Travaux, Centre d'Etudes Supérieures de la Sidérurgie, Metz.

single-phase up to above 1000° C., and that copper containing up to 0.47% silver (below 350°–400° C.) or up to 0.009% bismuth (the bismuth is liquid above 271° C.) is two-phase.

TABLE I.—Composition of Materials Studied.

	Cu, %	As, %	Sb, %	Bi, %	Ag, %	P, %	O, %	S, %
Pure copper	100.0	0.008	Nil	Nil	Nil	0.016	0.014	0.027
Cu-Sb alloy	99.55	0.007	0.45	"	"	0.011	0.011	0.026
Cu-Bi alloy	99.85	0.005	Nil	0.009	"	0.011	0.010	0.021
Cu-Ag alloy	99.50	0.005	"	Nil	0.47	0.016	0.009	0.024
Cu-As alloy	99.00	1.000	"	"	Nil	0.013	0.006	0.022

Slight traces of Pb were detected in all the materials, but no Fe, Ni, Se, Sn, Te, or Zn was found.

As carbon is practically insoluble in copper, it was used in most of the experiments to protect the latter from oxidation during annealing. A check made by vacuum annealing showed that neither the grain growth nor the texture obtained was affected by annealing in air or in powdered charcoal.

Annealing at 300°, 400°, 500°, 700°, and 1000° C. for 1 hr. was carried out in an electric furnace. Great care was taken in handling the material to avoid any unwanted nucleation in grains accidentally cold worked between the various anneals. Identical results were obtained with the samples which had undergone all the successive anneals and those which had been raised directly to the final annealing temperature. The rate of heating had no effect either on the orientation texture or on the grain-size, at least in the usual restricted range of heating rates.

The specimens which had undergone the mechanical and annealing treatments described were studied by various methods—X-ray-diffraction patterns, mechanical testing, and micrographical examination—to determine the nature and extent of the orientation texture thus developed. Investigations on the drawn rods were supplemented by observations on the drawn wires, in order to obtain results that could be compared with those of other authors, and also to determine the degree of disorder of the crystal lattice resulting from severe cold work.

### III.—X-RAY-DIFFRACTION STUDY

#### 1. TECHNIQUE

For the X-ray-diffraction study of orientation, unfiltered copper radiation was employed. It was not convenient to use a bent quartz-crystal monochromator, since this would have introduced an exaggerated elongation of the intensity maxima on the diffraction rings. However, this device was employed later to follow the disappearance of certain reflections in patterns of various texture specimens.

Under the experimental conditions adopted, specimens having an average grain-size exceeding 30  $\mu$  were mounted in a scanning device which maintained a constant angle between the fibre axis and the incident X-ray beam during the movement of the specimen.

Two types of specimen were used, needles of  $\frac{3}{10}$  mm. dia. cut longitudinally from the centre, at mid-radius, and at the edge of the rod, and flat cross-sections of the rod. Each needle specimen was rotated about its own axis and sometimes traversed along it. The flat specimens were moved in their own plane, the inclination of the latter to the beam having been selected in advance. The film, in a cylindrical holder, could be adjusted to be at right angles to the incident beam, as for normal diffraction-ring photographs, or to be coaxial with the beam, the pattern in this case being recorded as straight parallel lines on the unrolled film. These straight lines could then be measured by means of the Vassy recording microdensitometer<sup>9</sup> and their intensity evaluated by integration.<sup>10</sup>

It should be noted that, when using  $\text{CuK}\alpha$  radiation, the overall uniform intensity of the (331) ring is due to crystals oriented according to the  $\langle 111 \rangle$  texture, while the (400) and (420) rings are due to the crystals in a different orientation, provided, of course, that the fibre axis is parallel to the incident beam. The absence of diffraction maxima in this particular case permits the use of a monochromator and makes it possible to follow the variations in intensity of the  $\langle 111 \rangle$  texture (Fig. 3 (a) and (b), Plate LXXXVI).

#### 2. RESULTS

The orientation textures present were determined first by calculation and by stereographic projection of

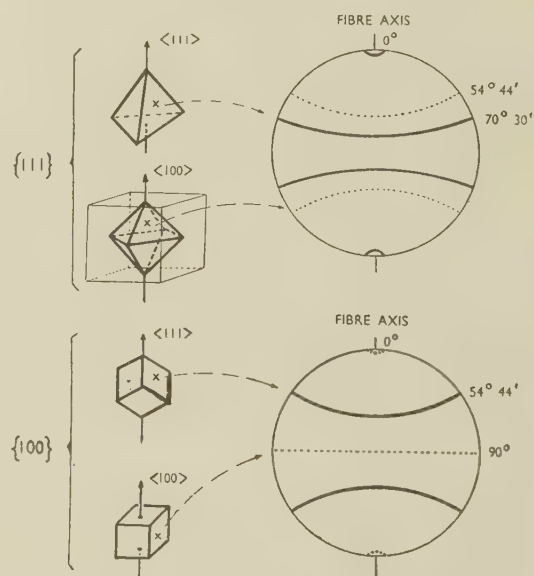


FIG. 1.—Pole Figures for Ideal  $\langle 100 \rangle$  (---) and  $\langle 111 \rangle$  (—) Textures.

the diagrams obtained with the needle specimens, and then confirmed by the existence of equatorial spots on the reflection photographs of the flat specimens (Fig. 4, Plate LXXXVI).

Generally speaking, the  $\langle 111 \rangle$  and  $\langle 100 \rangle$  textures were found in the central portion of all the rods, either



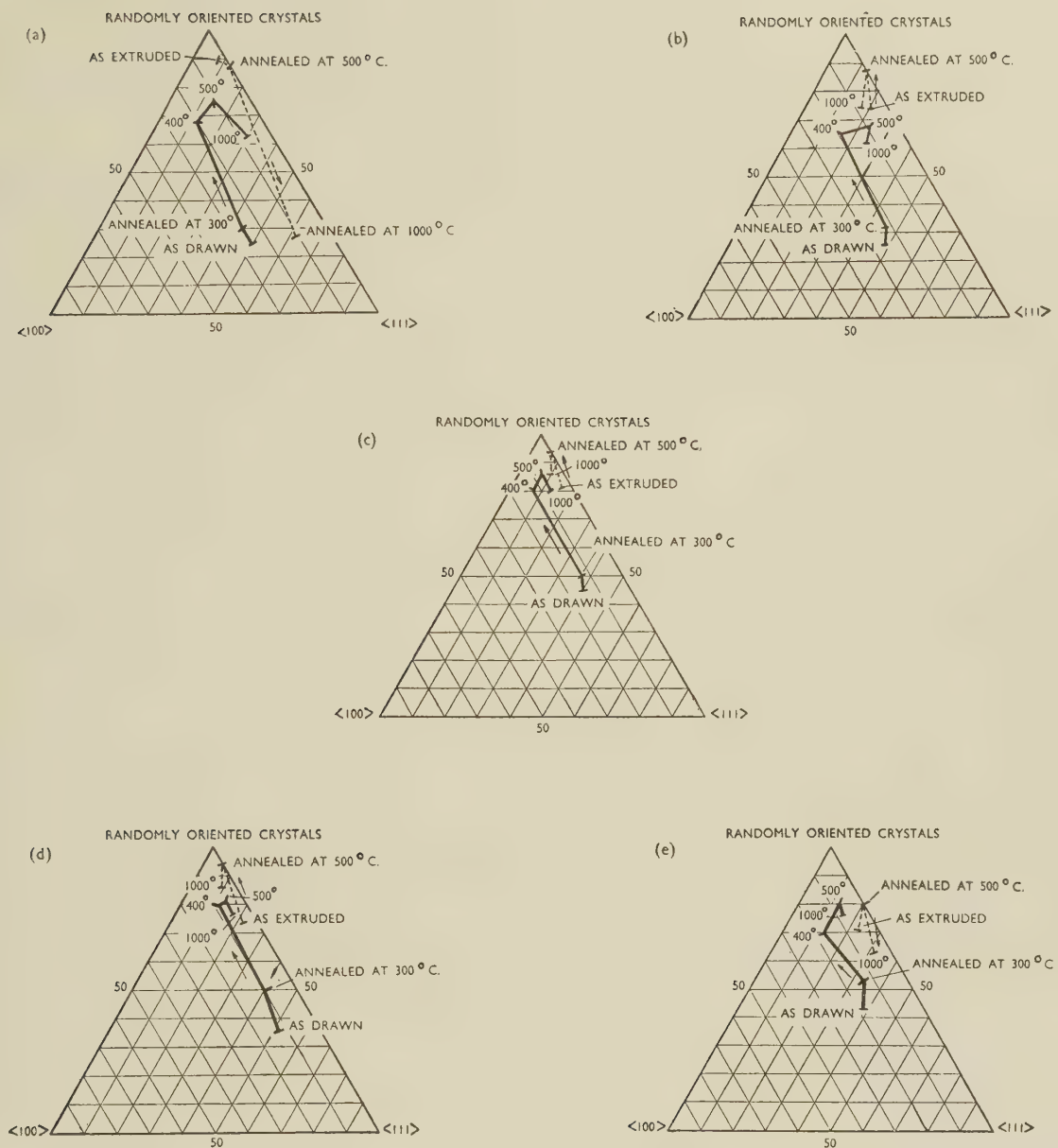


FIG. 2.—Showing Proportion of Material Oriented in the  $\langle 111 \rangle$  and  $\langle 100 \rangle$  Directions and of Randomly Oriented Material in Rods of (a) Pure Copper, (b) Cu-0.009% Bi, (c) Cu-0.45% Sb, (d) Cu-1% As, and (e) Cu-0.47% Ag Alloys.

separately or superimposed, to the exclusion of any other orientation. The  $\langle 112 \rangle$  texture occurs only at the extreme surface of the rods drawn and annealed at  $1000^\circ\text{C}$ . and is entirely absent from the cold-drawn rods; it is always very weak.<sup>11</sup>

As stated above, in order to obtain results that would be comparable with those of other authors, experiments were also carried out with material in the form of 2-mm.-dia. wire. The double texture was again found, but was more pronounced. On annealing for 1 hr. at  $500^\circ\text{C}$ ., these wires exhibited primary recrystallization grains having an exclusively  $\langle 100 \rangle$  orientation. On approaching  $700^\circ\text{C}$ . this orientation was gradually replaced by the  $\langle 112 \rangle$  orientation, and at  $1000^\circ\text{C}$ . the change-over was practically complete.

Fig. 1 shows the ideal pole figures for the  $\langle 111 \rangle$  and  $\langle 100 \rangle$  textures. In practice the lines are expanded into bands, for all the crystals included in the  $\langle u, v, w \rangle$  orientation (see next section) are not exactly oriented in the drawing direction.

### 3. QUANTITATIVE EVALUATION

From the relative intensities of the maxima due to the  $\langle 111 \rangle$  and  $\langle 100 \rangle$  spots on the (200) diffraction line, and from the uniform background intensity of the (200) line due to the non-oriented crystals, it was possible to calculate the respective volumes occupied by the randomly oriented crystals ( $x\%$ ), those oriented in the  $\langle 111 \rangle$  direction ( $y\%$ ), and those oriented in the  $\langle 100 \rangle$  direction ( $z\%$ ). Certain corrections had to be made, principally to take account of the multiplicity factor of the  $\{100\}$  faces likely to occur in the three types of crystal mentioned above, and a correction for speed, the spots not all being on the same level. For the purpose of these calculations, it was necessary to define standard lengths of spot for photometry corresponding to deviation ranges of  $2\delta$  for the orientations concerned. Crystals in orientations  $\langle u, v, w \rangle$  were accordingly considered to be contained in a cone within an angle of  $2\delta$ , chosen to be equal, respectively, to  $1^\circ 30'$ ,  $10^\circ$ , and  $25^\circ$ , and corresponding to three degrees of perfection of texture.

For rods extruded and drawn to 73% reduction of area the results were as given in Table II.

TABLE II.—Percentages  $x$ ,  $y$ , and  $z$ , of the Various Textures Occurring in Rods of Copper and Copper Alloys with  $2\delta = 25^\circ$ .

Texture, %	Pure Cu	Cu-Sb	Cu-Bi	Cu-Ag	Cu-As
$x$ (randomly oriented)	25	45	27	42	36
$y$ (oriented in $\langle 111 \rangle$ direction)	50	40	48	39	52
$z$ (oriented in $\langle 100 \rangle$ direction)	25	15	25	19	12

The ratios of  $y\langle 111 \rangle : z\langle 100 \rangle$  textures for the three degrees of perfection were as given in Table III.

The quantitative results for all the rods in all the

states considered are collected in the triangular diagrams (Fig. 2 (a)–(e)). The arrows on the figures indicate the development by recrystallization of the various orientations at increasing temperature.

TABLE III.—Ratios of  $\langle 111 \rangle : \langle 100 \rangle$  Texture in Rods of Copper and Copper Alloys for Varying Degrees of Perfection of Orientation.

Value of $2\delta$	Pure Cu	Cu-Sb	Cu-Bi	Cu-Ag	Cu-As
$25^\circ$	2	2.7	1.9	2.1	4.3
$10^\circ$	2.6	3.1	2.6	3.6	5.3
$1^\circ 30'$	3	3.1	3.2	3.1	5.9

### IV.—MEASUREMENT OF THE ELASTICITY MODULUS OF ORIENTED COPPER

By virtue of the elastic anisotropy of the copper crystal, textures in copper bars can be assessed from elasticity measurements. The maximum value for the elastic modulus ( $E$ ) is  $19,400\text{ kg./mm.}^2$  (in the  $\langle 111 \rangle$  direction); the minimum value is  $6800\text{ kg./mm.}^2$  (in the  $\langle 100 \rangle$  direction); while a random polycrystalline orientation gives an average value of about  $12,000\text{ kg./mm.}^2$ . The  $\langle 111 \rangle$  texture increases the value of  $E$ , while the  $\langle 100 \rangle$  texture diminishes it, in both cases in the direction of the axis of the rod.

The results given in Table IV were obtained with

TABLE IV.—Values of  $E$  for Pure Copper and Copper Alloy Rods in Various Conditions.

Material	Condition	$E$ , $\text{kg./mm.}^2$
Drawn copper	Cold worked	14,830
	Annealed at $500^\circ\text{C}$ .	13,205
	„ $1000^\circ\text{C}$ .	14,223
Drawn copper-0.09% silver alloy	Cold worked	14,795
	Annealed at $500^\circ\text{C}$ .	13,121
	„ $1000^\circ\text{C}$ .	14,150
Extruded copper	Cold worked	12,930
	Annealed at $500^\circ\text{C}$ .	13,373
	„ $1000^\circ\text{C}$ .	14,150
Extruded copper-0.45% antimony alloy	Cold worked	12,479
	Annealed at $500^\circ\text{C}$ .	12,570
	„ $1000^\circ\text{C}$ .	13,272

Cabarat's apparatus,<sup>12</sup> by means of which elasticity values can be determined by observation of longitudinal vibrations in vacuum.

It is interesting to note the fall in the value of  $E$  produced in the drawn rods by annealing at  $500^\circ\text{C}$ . and the increase in value obtained on raising the annealing temperature from  $500^\circ$  to  $1000^\circ\text{C}$ . These variations were less marked for the extruded rods. The highest values were obtained with pure copper, while extruded rods containing antimony gave the lowest values.



## VI.—CONCLUSIONS

(1) *Effect of Cold Work.*

In general, the double  $\langle 111 \rangle + \langle 100 \rangle$  texture, whose existence is already well-established,<sup>13</sup> was found to occur at the centre of the drawn rods. The single  $\langle 111 \rangle$  texture was present throughout the extruded rods and in the outer layers of the drawn rods. In the latter case the fibre axis was slightly inclined to the axis of drawing. This layer of different texture extended as far as the mid-radius in rods of copper-1% arsenic alloy.

The prominence of these textures increased with the degree of cold work. In all the rods examined the  $\langle 111 \rangle$  texture was much stronger than the  $\langle 100 \rangle$  texture; the volume of the metal having a  $\langle 111 \rangle$  orientation in the drawing direction was almost double that having the  $\langle 100 \rangle$  orientation (see Tables above).

(2) *Effect of Additions.*

The elements added—antimony, bismuth, silver, and arsenic—had very little effect on the deformation texture, which remained of the double type at the centre of the rods. However, with copper containing arsenic or bismuth in solid solution the volume of material oriented in the  $\langle 111 \rangle$  direction was almost treble that with the  $\langle 100 \rangle$  orientation (as compared with double the amount for pure copper).

(3) *Effect of Annealing Temperature.*

Recrystallization had a considerable effect on the distribution of the crystals between the two orientations. Heating to 300° C., then to 400° and 500° C., caused a progressive weakening of both the  $\langle 111 \rangle$  and  $\langle 100 \rangle$  orientations, the latter diminishing appreciably less than the former. Around 500° C. the intensity of the two orientations was about the same, while the volume of randomly oriented crystals was at a maximum, and was particularly high in rods containing the added elements, antimony, arsenic, or silver, in solid solution. Recrystallization at 1000° C., in general, brought about an increase in all the rods in the proportion of  $\langle 111 \rangle$  texture, particularly in pure copper.

Elements in solid solution gave rise to the highest proportion of random orientations (75–80% of the total volume of the crystals, as against about 60% for pure copper or copper with an addition of bismuth). Fig. 2 (e), the triangular diagram for copper alloyed with silver, shows between 300° and 400° C. an increase in the amount of  $\langle 100 \rangle$  texture coincident with the solution of the silver in the copper.

These results are in line with those obtained by other authors<sup>14</sup> relating to various types of copper subjected to severe cold work by rolling and annealing at low temperatures (500°–600° C.), and summed up by Barrett<sup>15</sup> as follows: "The recrystallization texture of copper is changed by smaller additions of alloying elements than the additions required to change the deformation texture." The results of the present study confirm this view. Again, Barrett writes: "Soluble elements that have the more marked solution-hardening effect on copper seem to generate the more complex recrystallization textures." This reveals itself by a greater degree of randomness, e.g. in the present case with silver and antimony. The degree of randomness produced by antimony was the highest recorded (80%). It may also be noted that silver greatly restricts the development of the  $\langle 111 \rangle$  texture between 500° and 1000° C. (Fig. 2 (e)).

As regards the orientation of the first crystals resulting from primary recrystallization, Fig. 5 (a) and (b) (Plate LXXXVII) shows the presence of large crystals in the  $\langle 100 \rangle$  and random orientations, in copper rod drawn to 73% reduction of area and annealed at 300° C. However, wires made of the same copper drawn to 93% reduction of area and annealed at the same temperature show large recrystallized grains in the  $\langle 100 \rangle$  orientation only. (Fig. 6, Plate LXXXVII).

The elastic modulus in the longitudinal direction varied with the character and degree of orientation of the rods, in agreement with the results obtained by X-ray methods. Micrographic studies, made later, have confirmed that the reappearance of a pronounced  $\langle 111 \rangle$  texture on annealing above 500° C. is attributable to the growth of grains with a preferred orientation.

## REFERENCES

1. E. Schmid and G. Wassermann, *Z. Physik*, 1927, **42**, 779.
2. W. Hofmann, *Z. Metallkunde*, 1937, **29**, 266.
3. C. S. Barrett and L. H. Levenson, *Trans. Amer. Inst. Min. Met. Eng.*, 1939, **135**, 327.
4. C. S. Barrett and L. H. Levenson, *ibid.*, 1940, **137**, 112.
5. W. R. Hibbard, Jr., and M.-K. Yen, *ibid.*, 1948, **175**, 126.
6. W. R. Hibbard, Jr., *ibid.*, 1949, **185**, 598.
7. E. Schmid and G. Wassermann, *Z. Physik*, 1926, **40**, 451.
8. C. S. Barrett, "The Structure of Metals", 2nd edn., p. 486. 1952: New York and London (McGraw-Hill).
9. E. Vassy, *Rep. 8me Congr. Groupement Avancement Méthodes Anal. Spectrograph. Produits Métallurg.*, 1947, 27; also *Science et Ind. phot.*, 1945, **16**, 1, 65; 1948, **19**, 56.
10. A. Guinier, "Radiocrystallographie", p. 100. 1945: Paris (Dunod).
11. P. Bastien and J. Pokorny, *Compt. rend.*, 1952, **234**, 1780.
12. R. Cabarat, P. Gence, L. Guillet, and R. Le Roux, *J. Inst. Metals*, 1951–52, **80**, 151.
13. P. Bastien and J. Pokorny, *Compt. rend.*, 1951, **232**, 2447.
14. R. M. Brick, D. L. Martin, and R. P. Angier, *Trans. Amer. Soc. Metals*, 1943, **31**, 675.
15. C. S. Barrett, "The Structure of Metals", p. 499.

# NOTICE TO AUTHORS OF PAPERS FOR THE "JOURNAL" AND CONTRIBUTORS TO DISCUSSIONS

1. **Papers will be considered for publication from non-members as well as members of the Institute.** They are accepted for publication in the *Journal* and not necessarily for presentation at any meeting of the Institute. MSS. should be addressed to The Editor of Publications, The Institute of Metals, 4 Grosvenor Gardens, London, S.W.1.

2. **Papers suitable for publication** may be classified as:

(a) Papers recording the results of original research.  
(b) First-class reviews of, or accounts of progress in, a particular field.

(c) Papers descriptive of works methods, or recent developments in metallurgical plant and practice.

(d) Papers in classes (a), (b), and (c) above, previously published in languages other than English, French, German, or Italian, if of sufficient merit.

3. **Manuscripts and illustrations** should be submitted in duplicate. MSS. must be typewritten (*double-line spacing*) on one side of the paper only, and authors are requested to sign a declaration that neither the paper nor a substantial part thereof has been published elsewhere. Exceptions may be made in certain cases where a paper has been published in a language other than English, French, German, or Italian (see 2(d) above). MSS. not accepted are normally returned within 6 months of receipt.

In the interests of economy, all papers must be written as concisely as possible; in general, internal research reports are not in suitable form for publication as papers in the *Journal*. All but the simplest mathematical expressions should be written by hand, with capital and small letters clearly distinguished. Superscript and subscript letters should also be plainly indicated. Greek letters and special signs should be identified in the margin. For style, spelling, and abbreviations used, any recent issue of the *Journal* may be consulted.

4. **Synopsis.** Every paper must have a synopsis (not exceeding 250 words in length) which, in the case of a paper reporting original research, should state its objects, the ground covered, and the nature of the results. The synopsis will appear at the beginning of the paper, and should be in a form suitable for use by abstracting organizations. Extracts from a "Guide for the Preparation of Synopses" drawn up by the Abstracting Services Consultative Committee are reproduced below.

5. **References** must be collected at the end of the paper and must be numbered in the order in which they occur in the MS. Initials of authors must be given, and the Institute's official abbreviations for periodical titles (as used in *Metallurgical Abstracts*) should be employed, where known. References to papers should be set out in the style:

A. L. Dighton and H. A. Miley, *Trans. Electrochem. Soc.*, 1942, 81, 321 (i.e. year, volume, page).

References to books should be in the following style:

C. Zener, "Elasticity and Anelasticity of Metals". 1948: Chicago (University of Chicago Press).

6. **Illustrations.** Each illustration must have a number and description; only one set of numbers must be used in one paper, and it is desirable to number the half-tone illustrations consecutively, rather than to intersperse them with the line figures. The captions should be typed on a separate sheet.

The set of **line figures** sent for reproduction must be drawn (about twice the size to appear in the *Journal*) in Indian ink on smooth white Bristol board, good-quality drawing paper, co-ordinate paper, or tracing cloth, which are preferred in the order given. Co-ordinate paper, if used, must be blue-lined, with the co-ordinates to be reproduced finely drawn in Indian ink. Curves should be drawn boldly (i.e. at least twice the thickness of the frame). Experimental points should be indicated by open or closed circles, triangles, squares, &c. (preferably not crosses). Curves should be broken on each side of such symbols and plenty of allowance should be made for closing up in blockmaking. All lettering and numerals, &c., should preferably be in *pencil*, so that the Institute's standard lettering may be affixed, and ample margins must be left outside the framework of the figures to enable this to be done. The second set of line illustrations may be photostat copies.

**Photographs** must be restricted in number, owing to the expense of reproduction, and photomicrographs should be trimmed to the smallest possible of the following sizes consistent with adequate representation of the subject: 4 in. deep by 3 in. wide: 2 in. deep by 3 in. wide: 2 in. square. Magnifications of photomicrographs must be given in each case. Photographs for reproduction should be loose, not pasted down (and not fastened together with a clip, which damages them), and the figure number and author's name should be written on the back of each. Captions should be given to the photomicrographs, but these should be kept as brief as possible.

Because of the present high cost of printing and paper it is imperative that authors restrict illustrations (particularly photographs) to the absolute minimum deemed necessary to support their argument. Only in exceptional cases will illustrations be reproduced if already printed and readily available elsewhere.

7. **Tables or Diagrams.** Results of experiments, &c., may be given in the form of tables or figures, *but* (unless there are exceptional reasons) *not both*. Tables should bear Roman numbers, and each should have a heading that will make the data intelligible without reference to the text.

8. **Corrections.** A certain number of corrections in proof are inevitable, but any modification of the original text is to be avoided. Since corrections are very expensive, the Institute reserves the right to require authors to contribute towards their cost if the Editor deems them to be excessive. The Institute also reserves the right to require a contribution to the cost of remaking any block where this is necessitated by an error on the author's part.

9. **Reprints.** Individual authors are presented with a maximum of 25, and two or more authors with a maximum of 50 reprints from the *Journal*, without covers. Limited numbers of additional reprints can be supplied at the author's expense, if ordered before proofs are passed for press. (Orders should preferably be placed when submitting MSS.)

10. **Discussion.** Except in the case of special symposia, shorthand records of discussions are not taken at meetings. Written discussion may be submitted on any paper, preferably typewritten (*double-line spacing*). References should be given in the form of footnotes. Paragraphs 6 and 7 above are also applicable to such contributions. Reprints of discussion cannot be supplied to contributors.

## GUIDE FOR THE PREPARATION OF SYNOPSES

(As recommended by the Abstracting Services Consultative Committee)

1. **Purpose.** The synopsis is not part of the paper; it is intended to convey briefly the content of the paper, to draw attention to all new information, and to the main conclusions. It should be factual.

2. **Style of writing.** The synopsis should be written concisely and in normal rather than abbreviated English. It is preferable to use the third person. Where possible use standard rather than proprietary terms, and avoid unnecessary contracting.

It should be presumed that the reader has some knowledge of the subject, but has not read the paper. The synopsis should therefore be intelligible in itself without reference to the paper; for example, it should not cite sections or illustrations by their numerical references in the text.

3. **Content.** The title of the paper is usually read as part of the synopsis. The opening sentence should be framed accordingly and repetition of the title avoided. If the title is insufficiently comprehensive, the opening should indicate the subjects covered. Usually the beginning of a synopsis should state the objective of the investigation.

It is sometimes valuable to indicate the treatment of the subject by such words as: brief, exhaustive, theoretical, &c.

The synopsis should indicate newly observed facts, conclusions of an

experiment or argument and, if possible, the essential parts of any new theory, treatment, apparatus, technique, &c.

It should contain the names of any new compound, mineral species, &c., and any new numerical data, such as physical constants; if this is not possible, it should draw attention to them. It is important to refer to new items and observations, even though some are incidental to the main purpose of the paper; such information may otherwise be hidden, though it is often very useful.

When giving experimental results the synopsis should indicate the methods used; for new methods the basic principle, range of operation, and degree of accuracy should be given.

4. **References.** If it is necessary to refer to earlier work in the summary, the reference should always be given in full and not by number. Otherwise references should be left out.

When a synopsis is completed, the author is urged to revise it carefully, removing redundant words, clarifying obscurities, and rectifying errors in copying from the paper. Particular attention should be paid by him to scientific and proper names, numerical data, and chemical and mathematical formulae.



# THE CLEAVAGE FRACTURE OF PURE POLY-CRYSTALLINE ZINC IN TENSION\*

1554

By G. W. GREENWOOD,† B.Sc., Ph.D., JUNIOR MEMBER, and  
PROFESSOR A. G. QUARRELL,‡ D.Sc., Ph.D., A.R.C.S.,  
MEMBER

## SYNOPSIS

A study has been made of some of the cleavage properties of zinc; the effects of grain-size, temperature, strain rate, and plastic deformation on the type of fracture and the true fracture stress have been investigated.

The true fracture stress has been shown to be inversely proportional to the square root of the mean grain diameter in tests at  $-196^{\circ}\text{C}$ . This relationship was found to be valid at higher temperatures if a correction was made for the effect of deformation before fracture. The constant of proportionality increased with increasing temperature. An activation energy for elongation to fracture was determined from the related effects of temperature and strain rate.

It is concluded that a dislocation theory can be developed to account for the build-up of large internal stresses from which cracks leading to cleavage can result.

## I.—INTRODUCTION

PURE zinc has long been known to show a well-defined cleavage fracture along the basal (0001) planes, and this metal has often been used in experiments for the study of the cleavage mechanism.<sup>1</sup> Little quantitative work has, however, been reported on the properties of the pure polycrystalline material.

Experiments of Masing and Polanyi<sup>2</sup> showed a marked increase in true fracture stress with decrease in grain-size in tension tests carried out in liquid air, although only two grain-sizes were investigated. The results were interpreted by Orowan,<sup>3</sup> on the basis of the Griffith crack theory,<sup>4</sup> to show that if cracks could be assumed to exist whose size was of the order of the mean grain diameter,  $d$ , then the true fracture stress,  $\sigma$ , would be expected to be proportional to  $1/\sqrt{d}$ . From present concepts of defects in metals, however, such an explanation would appear much oversimplified, and an analysis by Elliott<sup>5</sup> has shown that it could hardly explain the phenomenon in pure metals because cracks of length  $> 10$ -20 interatomic distances would be unstable and would be expected to close spontaneously under thermal fluctuations and plastic flow.

The present work was undertaken to investigate the effects of grain-size, temperature, strain rate and plastic deformation on the occurrence of cleavage fracture, so that the mechanism might be better understood. Preliminary experiments were made to determine the most suitable procedure. Since, for most grain-sizes considered, zinc was found to show cleavage in simple tension even up to room temperature, there was no need to introduce arbitrary notches. This was a great advantage, since the precise "notch

effect" is still incompletely understood quantitatively and accurate stress calculations cannot be made. The fact that true cleavage-fracture stresses could be measured directly in simple tension permitted the effects of variables on this quantity to be determined.

The aims of the present work were therefore resolved into determining the relation between  $\sigma$  and the grain-size,  $d$ , over a range of grain-sizes. The effects of temperature,  $T$ , strain rate,  $\dot{\epsilon}$ , and plastic deformation,  $\epsilon$ , on the type of fracture and the value of  $\sigma$  were also investigated. In addition, reasons were sought for the sharp transition temperature between brittle and ductile fracture which was reported by Agnor and Shank<sup>6</sup> from impact tests on polycrystalline zinc.

## II.—EXPERIMENTAL METHODS

### 1. MATERIAL AND SPECIMEN PREPARATION

The material used was zinc of 99.99+ % purity. "Crown Special" (distilled) and "Tadanac" (electrolytic) varieties were used and both gave identical results under test. Spectrographic analyses showed that the impurity contents in the two varieties were:

	Pb, %	Cd, %	Cu, %	Fe, %
Crown Special	0.0003	0.001	0.0001	0.002
Tadanac	0.0003	0.0015	0.0001	0.001

The material was used in the form of extruded bars,  $\frac{7}{8}$  in. in dia. It was found possible to obtain a range of grain-sizes by the selection of specimens from different parts of the bars. Material was specially extruded to form a fine grain-size range from 100 to 500 grains/in. Larger grain-sizes were obtained by

\* Manuscript received 10 December 1953.

† Scientific Officer, Metallurgy Division, Atomic Energy

Research Establishment, Harwell, Berks.; formerly University of Sheffield.

‡ University of Sheffield.

annealing treatments which extended the range of grain-sizes to 25 grains/in.

Great care was taken in the machining of the specimens, which were of  $\frac{1}{16}$  in.<sup>2</sup> cross-section and 1.264 in. gauge-length. The surface of the gauge-length was polished with 000 emery paper cooled with paraffin to remove the last 0.002 in.

## 2. TENSOMETER METHODS

To determine the values of the true fracture stresses, stress/strain curves were plotted, using a Hounsfield tensometer. The instrument had a maximum load capacity of 2 tons, thus providing a maximum stress of 20 tons/in.<sup>2</sup> in a specimen of the size used. This was found to be adequate in all the tests. The tensometer was driven by an electric motor which gave a range of strain rates from 0.002 to 1%. True fracture stresses could be measured to an accuracy of  $\pm 0.2$  ton/in.<sup>2</sup>.

The tensometer was arranged with its axis vertical, and the specimen was surrounded by a cylindrical insulated container open at the top but attached with a liquid-tight seal to the moving member below the lower grip. By filling the container with suitable coolants, tensile tests could be made in the range  $-196^\circ$  to  $+50^\circ$  C.

For the temperatures  $-196^\circ$ ,  $-77^\circ$ , and  $0^\circ$  C., the usual coolants were used, namely liquid nitrogen, solid  $\text{CO}_2$ -acetone mixture, and ice and water. A temperature of  $-160^\circ$  C. was obtained by filling the bath with liquid nitrogen and then slowly pouring in *isopentane* alternately with more liquid nitrogen until the bath was almost filled with solidified *isopentane*. Time was allowed for the liquid nitrogen to evaporate, and the test was started when the *isopentane* began to melt. The temperature of the specimen was checked with a copper/Constantan couple and did not vary by more than  $3^\circ$  from  $-160^\circ$  C. during the test. In a similar manner, tests were made at the melting point of ethyl alcohol,  $-117^\circ$  C.

The procedure adopted in obtaining temperatures of  $-160^\circ$  and  $-117^\circ$  C. involved preliminary cooling of the specimens to  $-196^\circ$  C.

## 3. GRAIN-SIZE COUNTING

Preliminary experiments indicated the necessity for accurate grain-size measurements. A check on the grain-size could be obtained easily by grain counts along the cleavage surface. However, it was desirable to choose specimens of a given grain-size before they were tested.

Each specimen was electropolished on both end surfaces, and grain-size counting was carried out by viewing under a microscope with polarized light. The numbers of grains lying along two perpendicular diameters of the field of view were counted. Eight fields of view were taken in all for each specimen. Grain-size was found to be uniform, and calculations of the mean grain diameters could be considered accurate

to  $\pm 4\%$ . For the few specimens of very large grain-size obtained by annealing, however, the error could be as much as  $\pm 20\%$  because of the relatively few grains across the gauge diameter.

## III.—EXPERIMENTAL RESULTS

### 1. THE EFFECT OF GRAIN-SIZE ON CLEAVAGE AT LOW TEMPERATURES

#### (a) Measurements at $-196^\circ$ C.

Stress/strain curves, at  $-196^\circ$  C., to the point of fracture were plotted for specimens over the range of grain-sizes available. The fractures always occurred suddenly. Variation in strain rate over the limits of the apparatus had no effect on results at this temperature, and 0.053%/sec. was chosen as a convenient rate. The stress/strain curves showed no overall plastic deformation at this temperature; this point was also checked by measurements of gauge diameter before and after test.

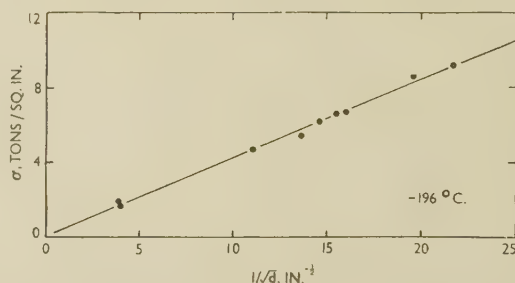


FIG. 1.—Relation Between True Fracture Stress,  $\sigma$ , and Mean Grain Diameter,  $d$ , at  $-196^\circ$  C.

Examination of the cleavage facets showed them to be crossed by parallel striations as in Fig. 15 (Plate LXXXVIII). Highly reflecting long narrow areas were observed in each grain. The dark striations were steps of varying depths. The long narrow areas were easily demonstrated to be sections of basal (0001) planes by observing them under a microscope, using polarized light. Using crossed nicols, the specimen was rotated, keeping any particular facet in view; the areas remained dark on rotation, thus indicating that they were sections of basal planes. Electropolishing the gauge-length showed twins in grains adjacent to the fracture surface, and it appeared that localized twinning caused the striated structure of the cleavage facets. The remainder of the gauge-length was twin-free. This was typical of all specimens fractured at  $-196^\circ$  C.

By plotting the true fracture stress,  $\sigma$ , against  $1/\sqrt{d}$ , a straight line passing through the origin was obtained, as shown in Fig. 1. This provided confirmation over a range of grain-sizes of the relation originally suggested from the work of Masing and Polanyi.<sup>2</sup> The deviation of results from this line is seen to be small. In Fig. 1, the two specimens



showing lowest  $\sigma$  values, corresponding to large grain diameters,  $d$ , and low values of  $1/\sqrt{d}$ , were obtained from the annealed material. The remaining seven specimens were chosen from sections of the extruded rods. The result for a specimen cycled three times between room temperature and  $-196^\circ\text{C}$ . was also found to lie on the line.

Since the tests at  $-196^\circ\text{C}$ . gave fractures in tension without overall plastic deformation, though with some localized twinning associated with the process of fracture, it might be expected that the experimental values of the true fracture stresses would have some significance. The fractures obtained at this temperature could be regarded as the closest approach for pure metals to the idealized condition of fracture in the elastic range.

(b) *The Interpretation of Experimental Values Obtained for True Fracture Stresses at  $-196^\circ\text{C}$ .*

The  $\sigma$  values at  $-196^\circ\text{C}$ . plotted in Fig. 1 are very much less, by a factor of 100 to 1000, than the estimates of fracture stress calculated from the cohesion theory of flawless materials.<sup>7-9</sup> The relationship between  $\sigma$  and  $d$  illustrated in Fig. 1 is  $\sigma\sqrt{d} = 0.42$  (ton/in.<sup>2</sup>) in.<sup>1/2</sup>.

If this relationship is assumed to hold down to grain sizes approaching atomic dimensions, the limiting value of the true fracture stress becomes approximately 4000 tons/in.<sup>2</sup>. The present experimental results can be more directly compared with the predictions from the Griffith crack theory if the assumption is made that cracks exist of the order of the mean grain diameter  $d$ . The Griffith formula can be written :

$$\sigma = \sqrt{\alpha E / 2c}$$

where  $\alpha$  is the surface energy,  $E$  is Young's modulus, and  $2c$  the crack length.

If the crack length,  $2c$ , is identified with the mean grain diameter,  $d$ , then the formula becomes :

$$\sigma = \sqrt{\alpha E / d}$$

Since  $\alpha$  and  $E$  are constant at a given temperature, the formula immediately provides the experimentally observed relationship  $\sigma \propto 1/\sqrt{d}$ . The formula also predicts that fracture will occur on planes perpendicular to the direction for which Young's modulus has the least value. In zinc the maximum and minimum values are :<sup>1</sup>

$$\begin{aligned} E \text{ at } 70^\circ \text{ to the } c \text{ axis} &= 12,130 \text{ kg./mm.}^2 \\ E \text{ parallel } &,, \quad ,, = 3560 \text{ kg./mm.}^2 \end{aligned}$$

These values are in keeping with the observation that the (0001) plane is the most favourable cleavage plane.

To compare the numerical value of  $\sigma\sqrt{d}$  as determined by experiment with the value from the Griffith theory, a value of  $\alpha$  must be assumed. This has not yet been measured for zinc in the solid state, but extrapolation from surface-tension measurements suggests that its value is about  $10^3$  ergs/cm.<sup>2</sup>.

From the Griffith theory,

$$\begin{aligned} \sigma\sqrt{d} &= \sqrt{\alpha E} \approx \sqrt{10^3 \times 3.56 \times 10^{11}} \\ &\approx 1.9 \times 10^7 \text{ (dynes/cm.}^2\text{)cm.}^{1/2} \\ &\approx 0.08 \text{ (ton/in.}^2\text{)in.}^{1/2} \end{aligned}$$

which may be compared with the experimental value from Fig. 1 of  $\approx 0.42$  (ton/in.<sup>2</sup>)in.<sup>1/2</sup>.

The Griffith formula thus provides numerical values of roughly the required order of magnitude as well as indicating the correct  $\sigma$  to  $1/\sqrt{d}$  relationship if cracks can be assumed to exist of the order of the mean grain diameter.

(c) *The Relationship between True Fracture Stress and Grain-Size at  $-160^\circ\text{C}$ .*

The variation of  $\sigma$  with temperature,  $T$ , is of some importance. The results at  $-196^\circ\text{C}$ . indicated that in considering this variation the effect of different values of  $d$  must be taken into account. Provided that no

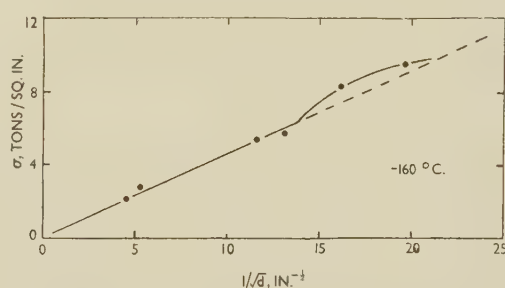


FIG. 2.—Relation Between True Fracture Stress and Mean Grain Diameter at  $-160^\circ\text{C}$ . The two specimens of smallest grain-size showed measurable elongation before fracture.

overall plastic deformation occurs before fracture, the Griffith theory appears to predict a small decrease in  $\sigma$  with increase in  $T$ , because the values of the surface energy  $\alpha$  and Young's modulus  $E$  are both expected to decrease slowly with increase in  $T$ .

A graph was plotted of  $\sigma$  against  $1/\sqrt{d}$  at  $-160^\circ\text{C}$ ., and the results are shown in Fig. 2. The four specimens of largest  $d$  (and therefore of smallest  $\sigma$ ) fractured without overall deformation. The stress/strain curves and careful measurements of gauge diameter showed that in the two specimens of smallest  $d$  some slight overall deformation had occurred before fracture. An examination of all the fracture surfaces showed them to be similar to that in Fig. 15 (Plate LXXXVIII). In the two specimens where some deformation had occurred by slip and twinning before fracture along the gauge-length, there was no apparent difference in the appearance of the cleavage facets.

Fig. 2 shows the line of  $\sigma$  against  $1/\sqrt{d}$  drawn through zero and the four points which correspond to the specimens fractured without overall prior deformation. It appeared possible that the  $\sigma$  values of the two specimens of smallest grain-size were slightly increased by the deformation which occurred before fracture. The dotted portion of the  $\sigma$  against  $1/\sqrt{d}$  line might be

considered to represent hypothetical  $\sigma$  values which would be obtained in the absence of prior deformation.

The graph for  $-160^\circ\text{C}$ . (Fig. 2) can profitably be compared with that for  $-196^\circ\text{C}$ . (Fig. 1). The relative slopes of the two lines of  $\sigma$  against  $1/\sqrt{d}$  are also included for ease of comparison in Fig. 10. The line gradient at  $-160^\circ\text{C}$ . is slightly greater than that at  $-196^\circ\text{C}$ ., the difference being larger than the experimental errors. Thus  $\sigma$  is found to be greater at  $-160^\circ$  than at  $-196^\circ\text{C}$ . for specimens of similar grain-size and in the absence of overall deformation before fracture. The apparent effect of raising the temperature is, therefore, in opposition to the predictions of the Griffith crack theory. To confirm these results it was thought desirable to carry out further experiments at higher temperatures. As it seemed likely that at higher temperatures specimens would undergo increasing amounts of plastic flow before fracture, it was decided to attempt to determine the effects of such flow upon the fracture stress.

## 2. THE EFFECT OF PLASTIC DEFORMATION BEFORE FRACTURE

### (a) General Observations

Investigations of fracture properties are almost invariably complicated by the fact that different specimens undergo different amounts of cold work before fracture. The problem therefore arises of how to deduce the effects of cold work occurring during the test. It is clear that a study of the fracture characteristics must involve a knowledge of the flow properties and mechanisms by which plastic deformation occurs.

In many previous studies of fracture, attempts have been made to obtain a value for  $\sigma$  by extrapolation to a suitable value at zero deformation, although this quantity would seem to be of only hypothetical interest. The attempts have usually taken one of two forms: (i) the introduction of arbitrary notches whereby plastic deformation could be largely inhibited and (ii) pre-straining the metal at temperatures where it was ductile and then testing at some lower temperature where relatively little or no further deformation occurred.

Both methods are open to objections. The notch effect is still incompletely understood in an exact quantitative form, though some calculations have been made of the effective stresses at a notch. There is also the further difficulty that it is not possible to be certain that plastic deformation at the notch does not occur. The prestrain method can be criticized, since the effect of deformation is well known to be dependent on the temperature at which it is carried out.

In the present work the prestrain method was used. To counter the objection of the effect of variation in temperature, the prior deformation was carried out at three temperatures. The form of the deformation and the effects of its variation on the cleavage facets were also studied metallographically after the various

prestrains had been given; in no case did further deformation occur during the tests at  $-196^\circ\text{C}$ .

### (b) The Effect of Prestrain at $50^\circ\text{C}$ . on the True Fracture Stress at $-196^\circ\text{C}$ .

To obtain a sufficient number of specimens of grain-size as nearly equal as possible from the material available, they were chosen from lengths of extruded rod having about 120 grains/in. In order that a conveniently large range of prestrains could be given without the specimens fracturing during prestraining, the prestrain temperature was chosen as  $50^\circ\text{C}$ ., with the strain rate  $0.053\%/ \text{sec}$ . Even small variations in strain rate had appreciable effects at this temperature. In measuring the value of the prestrain (denoted by  $\epsilon_p$ ), the units of "natural strain" were used.  $\epsilon_p$  was defined as  $\log_e(A_0/A)$ , where  $A_0$  and  $A$  are the initial and final areas of cross-section, respectively.

In each case, when the required value of prestrain at  $50^\circ\text{C}$ . had been given, the specimen was unloaded, and the true fracture stress was measured at  $-196^\circ\text{C}$ .

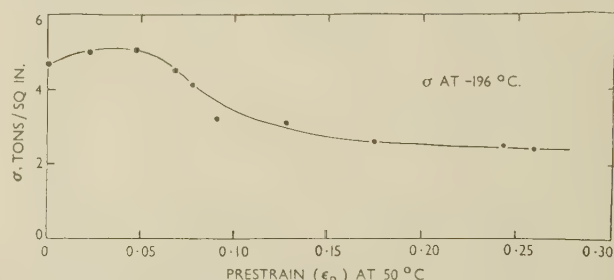


Fig. 3.—Variation of True Fracture Stress for Specimens of Nearly Equal Grain-Size ( $\sim 120$  grains/in.) at  $-196^\circ\text{C}$ ., with Prestrain,  $\epsilon_p$ , Given at  $50^\circ\text{C}$ .

The results obtained are shown in Fig. 3. The value of  $\sigma$  measured at  $-196^\circ\text{C}$ . increases to a maximum at about 0.04 prestrain and the further prestrain causes a steady fall in the value of  $\sigma$ . Comparable experiments by McAdam *et al.*<sup>10</sup> on the effect of prestrain on the true fracture stress of steels indicate that a continuous increase is caused.

The cleavage facets were examined metallographically, and considerable changes in their appearance for different values of prestrain were observed. Specimens which were given a prestrain  $< \sim 0.07$  showed the cleavage facets striated with twin markings and had an appearance similar to that shown in Fig. 15 (Plate LXXXVIII). An increasing number of grains were observed without striations due to twinning in specimens given prestrains  $> \sim 0.07$ . Non-crystallographic markings became increasingly apparent. A typical cleavage facet from a specimen having a prestrain  $> 0.07$  is shown in Fig. 16 (Plate LXXXVIII). The facet is seen to be flat and the polarized-light test previously described identified it as a basal plane.

### (c) Further Experiments on the Effects of Prestrain

It appeared desirable to determine whether the form of the curve of Fig. 3 was similar for specimens



of different grain-sizes. Specimens were therefore prestrained at 20° C., and Fig. 4 indicates that specimens over a range of grain-sizes could be fitted on the same curve of  $\sigma\sqrt{d}$  against  $\epsilon_p$ . The results did not depend on the time between prestraining and test. Two specimens were prestrained in compression before machining for test at -196° C. and the results are included in Fig. 4. It appears that prestrain in compression has similar effects to prestrain in tension in the range employed.

Observations of the cleavage facets of the specimens indicated that their appearance depended chiefly on the amount of prestrain given before fracture. When  $\epsilon_p$  was  $< \sim 0.07$ , all the cleavage facets were crossed by striations due to twinning. For greater pre-

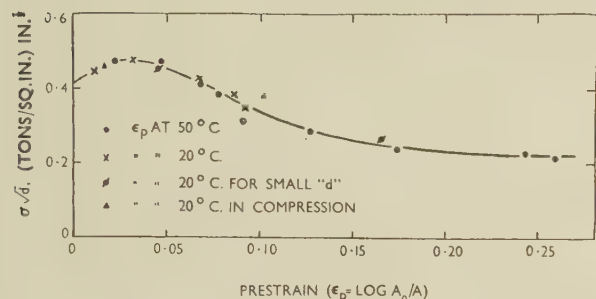


FIG. 4.—Effect of Prestrain at 50° and 20° C. on True Fracture Stress at -196° C. for Specimens of Various Grain-Sizes.

strains increasing numbers of facets were without striations, but showed structures similar to the one in Fig. 16 (Plate LXXXVIII).

#### (d) The Effect of Prestrain at -77° C.

Since the effects of deformation are dependent on temperature, it was necessary to examine the effect of prestrain at a temperature lower than 20° C.

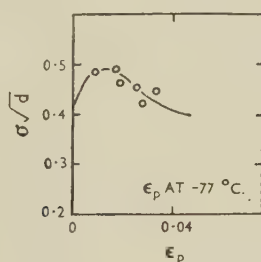


FIG. 5.—Effect of Prestrain at -77° C. on True Fracture Stress at -196° C.

Specimens of various grain-sizes were prestrained at -77° C., although only small amounts of prestrain could be given at this temperature. The results obtained are shown in the graph of  $\sigma\sqrt{d}$  against  $\epsilon_p$  in Fig. 5. Over the small range of values it is difficult to obtain a precise curve, but Fig. 5 shows a maximum of  $\sigma\sqrt{d}$  at a value of  $\sim 0.015$  for  $\epsilon_p$ . The shape of the curve is similar to the one of Fig. 4 for prestrain at

higher temperatures, except that the same variation in  $\sigma\sqrt{d}$  is brought about by relatively smaller values of  $\epsilon_p$  at -77° C.

At -77° C. a given prestrain had a greater effect

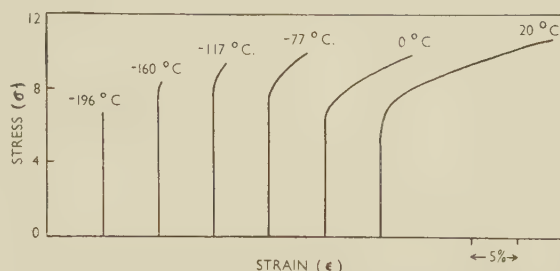


FIG. 6.—True Stress/Strain Curves to Fracture at Various Temperatures for Specimens of Nearly Equal Grain-Size ( $\sim 250$  grains/in.).

than the same value of prestrain given at 20° C. This might be expected from a consideration of the stress/strain curves at -77° and 20° C. These curves are shown in Fig. 6, which represents the true-stress/natural-strain relationships, for specimens of nearly equal grain-size (250 grains/in.), to their points of fracture in tests at various temperatures. The curves show increasing rates of strain-hardening with decrease in temperature.

Thus, from a consideration of the effects of prestrain at 50°, 20°, and -77° C. on true fracture stress at -196° C., a given prestrain at any temperature is equivalent to a rather larger prestrain at a higher temperature.

### 3. TRUE FRACTURE-STRESS MEASUREMENTS AT -77° C. AND THE EXTRAPOLATION TO VALUES CORRESPONDING TO FRACTURE WITHOUT DEFORMATION

Stress/strain curves were plotted to fracture at -77° C. for specimens over a range of grain-sizes. The graph of  $\sigma$  against  $1/\sqrt{d}$  is shown in Fig. 7, and the  $\sigma$  values measured are represented by circles. At this temperature only the specimen of largest grain-size fractured without measurable overall deformation. The specimens showed increasing ductility before fracture with decreasing grain-size, as shown in Table I.

The points obtained for true fracture stresses at -77° C. in Fig. 7 are seen to lie on a curve, but if it can be assumed that the effect of deformation before fracture at this temperature has the same percentage effect on  $\sigma$  as the changes brought about by prestrain at -77° C. on  $\sigma$ , measured at -196° C., as shown in Fig. 5, then an extrapolation can be made to a hypothetical value of  $\sigma$  at -77° C. corresponding to fracture without deformation. This form of extrapolation has been much used in experiments on steels.<sup>10, 11</sup>

The method of extrapolation is indicated in Table I, and when the extrapolated values of  $\sigma$ , shown in Fig. 7, are plotted against  $1/\sqrt{d}$ , the results lie

on a straight line through the origin. It appears that  $\sigma$  can be considered proportional to  $1/\sqrt{d}$  at  $-77^\circ\text{C}$ . if the correction is made for the plastic de-

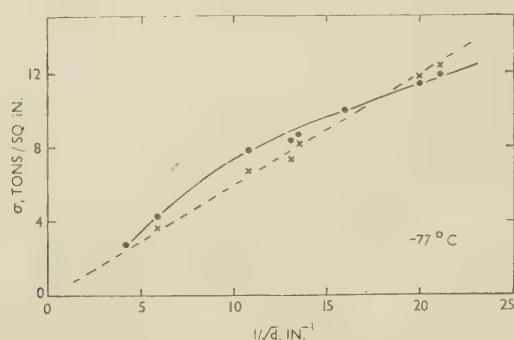


FIG. 7.—The Relation Between True Fracture Stress and Mean Grain Diameter at  $-77^\circ\text{C}$ . The measured  $\sigma$  values are shown by circles. The values corrected for deformation (on the basis of Fig. 5) are shown by crosses.

formation which occurs before fracture. The lines drawn for comparison in Fig. 10 show increasing slope with increasing temperature of test.

TABLE I.—The Effect of Prestrain on Fracture Stress at  $-77^\circ\text{C}$ .

Measured Value of $\sigma$ at $-77^\circ\text{C}$ , tons/in. <sup>2</sup>	Strain Before Fracture in Test, $\epsilon_c$	Grains/in., $1/d$	% Change in $\sigma$ Due to $\epsilon_p$ (see Fig. 5)	Value of $\sigma$ Extrapolated to Zero Deformation, tons/in. <sup>2</sup>
2.7	0	18	0	2.7
4.2	0.006	35	+11	3.6
7.8	0.016	116	+15	6.6
8.3	0.022	171	+12	7.3
8.6	0.032	182	+6	8.1
9.9	0.043	257	0	9.9
11.3	0.046	402	-3	11.6
11.8	0.048	443	-4	12.3

#### 4. TRUE-FRACTURE-STRESS MEASUREMENTS AT $0^\circ$ AND $20^\circ\text{C}$ .

Stress/strain curves were plotted at  $0^\circ$  and  $20^\circ\text{C}$ ., and at these temperatures the effects of deformation became increasingly important. Even the annealed specimens of largest grain-size showed some ductility before fracture, and increasing ductility with decreasing grain-size was very marked. Small variations in strain rate had considerable effect, and the rate was therefore maintained constant at  $0.053\%/sec$ .

At  $0^\circ\text{C}$ . the results plotted on the  $\sigma$  versus  $1/\sqrt{d}$  graph shown by circles in Fig. 8 can apparently be represented by a straight line not passing through the origin when no correction is made for the effect of deformation. The elongation of all the specimens tested at  $0^\circ\text{C}$ . was greater than that which gives the maximum  $\sigma$  value as shown in Fig. 4. If the effect of deformation is now taken into account exactly as in the previous section and the  $\sigma$  values are extrapolated to the hypothetical values corresponding to zero

deformation on the basis of the prestrain curve in Fig. 4, then the results are as indicated by crosses in Fig. 8. The specimens of large grain-size had low ductilities, and the amount of deformation they received during test was therefore relatively small and increased the value of  $\sigma$ . The specimens of smaller grain-size, on the other hand, showed greater ductility before fracture, and the amount of deformation in them corresponded to the late stages of the curve in Fig. 4 and so caused the  $\sigma$  values to be reduced.

A change in appearance of the cleavage facets was noted with different amounts of deformation. In the three specimens of largest grain-size in Fig. 8 (where the elongation to fracture was less than 0.07, the cleavage facets were crossed by twins, as shown in Fig. 15 (Plate LXXXVIII). For the smaller grain-sizes, the specimens fracturing after greater strains had an increasing number of facets with an appearance

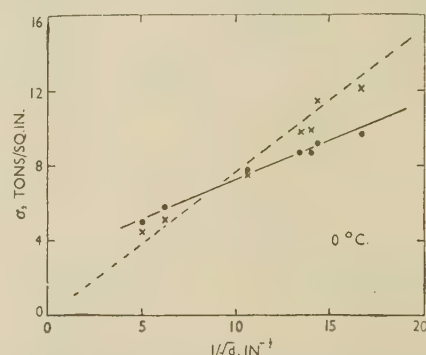


FIG. 8.—Relation at  $0^\circ\text{C}$ . Between True Fracture Stress and Mean Grain Diameter. Measured  $\sigma$  values are shown by circles. Values corrected for deformation (from Fig. 4) are shown by crosses.

similar to that shown in Fig. 16. This provided further evidence that the strain  $\epsilon_c$  in the tests to cause fracture had comparable effects to the prestrain  $\epsilon_p$  given at the same temperature followed by fracture at  $-196^\circ\text{C}$ . Thus the observations of the cleavage facets supported the arguments used for the correction of the  $\sigma$  values for the deformation occurring before fracture.

In the tensile tests at  $20^\circ\text{C}$ . the specimens showed much greater ductility before fracture than in the tests at  $0^\circ\text{C}$ . The specimens of smaller grain-size tested at  $20^\circ\text{C}$ . showed ductile fractures after necking. This represented fracture above the transition temperature. Fig. 13 (Plate LXXXVIII) illustrates the types of fracture; two specimens show cleavage fracture perpendicular to their axes after different amounts of deformation. The ductile fracture is seen to have occurred after considerable necking; for comparison of lengths, an unbroken specimen is included. No fracture-stress measurements were made on specimens giving ductile fractures.

For the specimens of larger grain-size which gave cleavage fractures at  $20^\circ\text{C}$ ., the  $\sigma$  values plotted against  $1/\sqrt{d}$  are shown by circles in Fig. 9. The crosses represent the values corrected for the effect of



deformation on the basis of Fig. 4. It appears that the corrected  $\sigma$  values again lie approximately on a straight line through the origin. The gradient of the dotted line is also shown in Fig. 10, which can now be

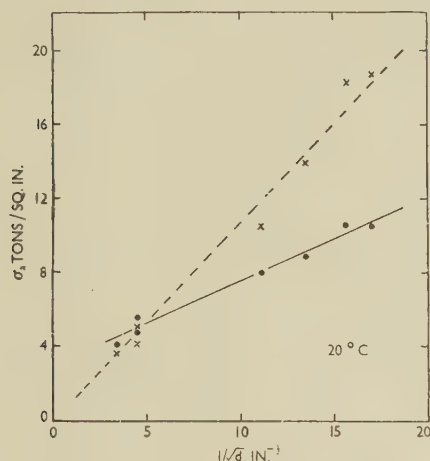


Fig. 9.—Relation at 20° C. Between True Fracture Stress and Mean Grain Diameter. Measured and corrected values (from Fig. 4) are shown by circles and crosses, respectively.

considered to give the relationship  $\sigma$ , corrected for deformation, proportional to  $1/\sqrt{d}$  for the various temperatures of test.

At 20° C. the cleavage facets of the three specimens which fractured after  $< 0.07$  natural strain again showed striations due to twinning. For increasing strain at fracture, fewer facets showed twins; Fig. 17 (Plate LXXXVIII) shows a facet of a specimen when

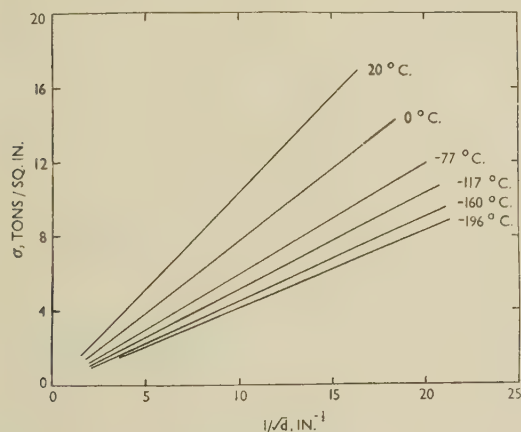


Fig. 10.—Relation Between True Fracture Stress and Mean Grain Diameter at a Series of Temperatures when Correction is Made for Deformation Occurring before Fracture.

fracture occurred after 0.175 natural strain. Figs. 16 and 17 (both  $\times 250$ ), can be directly compared, since both represent similar strain at fracture. It appears that twinning which causes stepping of the cleavage facets is largely inhibited during fracture if the strain at fracture is greater than about 0.07. Cleavage frac-

tures invariably occurred before a strain of about 0.30 was reached. Otherwise, specimens having a sufficiently small grain-size and greater ductility necked down completely after further elongation which proceeded until a slow ductile fracture occurred. There would seem to be difficulty in producing cleavage in zinc which has been deformed by more than about 0.30 strain.

In view of this, a specimen of small grain-size was elongated to 0.40 strain at 20° C. and then tested to fracture at  $-196^\circ$  C. The rather striking feature shown in Fig. 14 (Plate LXXXVIII) is that cleavage is found to occur outside the neck in a position where the natural strain is less than 0.30. The experiments indicate that heavily worked specimens are less likely to show cleavage even at low temperatures. This links up with the observations in the tests at higher temperatures, namely that, if deformation can proceed to more than 0.30 strain, the specimens continue to deform and give ductile fractures.

It would seem that these observations can be identified with the phenomenon termed "rheotropic brittleness" by Ripling and Baldwin,<sup>12, 13</sup> who found that specimens of steel and zinc were less liable to fracture after heavy deformation than without. When high prestrain was given, the ductility was found to be increased in tests at lower temperatures. Unfortunately Ripling and Baldwin did not measure true fracture stresses or examine the types of fracture.

##### 5. THE EFFECT OF STRAIN RATE

The rate of straining could be varied from 1 to  $\frac{1}{500}$  %/sec. The effect of variation within this range was too small to be detectable below  $-77^\circ$  C. Its effect, however, became increasingly marked at higher temperatures. The elongation before cleavage  $\epsilon_c$  was markedly dependent upon the strain rates employed and also upon the grain-size of the specimens under the given conditions of test. Thus, in determining the influence of strain rate, it was particularly necessary to choose specimens having grain-sizes as nearly equal as possible. To obtain the required number of specimens, an average grain-size of  $210 \pm 30$  grains/in. was selected.

Tests were carried out over the range of strain rates at 0°, 10°, and 20° C., and the strains  $\epsilon_c$  occurring before cleavage were measured. The results are given in Fig. 11, which shows the curves of  $\epsilon_c$  against  $\log \dot{\epsilon}$ . The scatter of results is due to the small grain-size variation, and the curves have been drawn as far as possible to represent those which would have been obtained for specimens of equal grain-size.

The results indicate that the elongations before cleavage in tests at high strain rates at 20° C. are of similar value to those obtained with lower strain rates at 0° C. An examination of the stress/strain curves indicated that the flow properties, such as approximate yield stress and strain-hardening, were also similar for specimens which showed similar elongations before fracture.

The form of the curves in Fig. 11 suggested that an "activation-type" process was occurring. A graph was therefore drawn of  $1/T$  against  $\log \dot{\epsilon}$ , as shown in Fig. 12, for the conditions of constant elongation before fracture for the values  $\epsilon_c = 0.11$  and  $0.20$

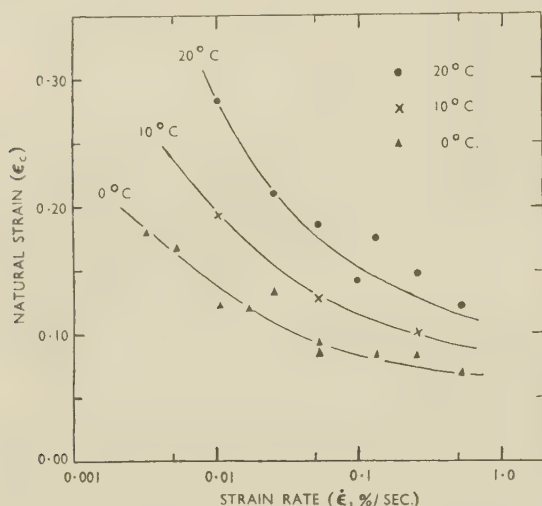


FIG. 11.—Variation of Elongation before Cleavage,  $\epsilon_c$ , at Three Temperatures, with Strain Rate  $\dot{\epsilon}$ .

taken from Fig. 11. From the graphs, the activation energy can be expected to lie within the range  $21 \pm 5$  kg.cal./g.-mol. This is similar to the activation energy for self-diffusion of zinc. The values for single crystals<sup>14</sup> are 20.4 and 31.0 kg.cal./g.-mol., parallel and perpendicular to the  $c$  axis, respectively.

Specimens having similar elongations before fracture also had similar stress/strain curves. Hence it would seem that the plastic deformation as well as the

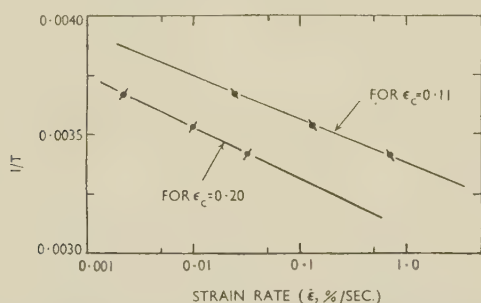


FIG. 12.—A Graph of  $1/T$  ( $T$  = Temperature, °K.) Against  $\dot{\epsilon}$  ( $\epsilon$  = Strain Rate) to Determine the Activation Energy.

fracture process is governed by an activation law. The effects of temperature  $T$  and strain rate  $\dot{\epsilon}$  can thus be combined in a parameter of the form  $f(\dot{\epsilon} \cdot e^{QK/T})$ .

## 6. THE TRANSITION TEMPERATURE

In previous studies of fracture, many definitions have been given of the term "transition temperature". Usually, however, the term has been used in notched-bar impact tests, and it has been defined as a tempera-

ture at which a certain energy has been absorbed by a change in type of fracture. Such a transition temperature was first quantitatively reported by Agnor and Shank<sup>6</sup> for zinc.

In the present work, the transition temperature was clearly defined in simple tension. The change from typical cleavage to ductile fracture was very precise and, for specimens of the same grain-size tested at the same strain rate, it occurred over a temperature range of only a few degrees. Fig. 6 shows a series of typical stress/strain curves for specimens of nearly equal grain-size. If the temperature was sufficiently high for a strain of 0.30 to be reached without fracture, the specimens continued to deform and considerable necking took place, ending in a ductile fracture, and this represented fracture above the transition temperature.

The effect of grain-size was clearly apparent. For any given temperature, the smaller the grain-size, the more ductile was the specimen. Thus decrease in grain-size depressed the transition temperature.

From the effects of strain rate previously described, it was seen that higher strain rates were equivalent to lower temperatures and vice versa. Hence the transition temperature was raised in tests at higher strain rates. The results of the previous section gave quantitative data confirming that "shock" or rapid stressing increases the likelihood of cleavage failure.

## IV.—DISCUSSION OF RESULTS

To summarize, the observations for which an explanation is sought are: (1) the low value of the cleavage stress  $\sigma$ , (2) the existence of the sharp transition temperature, (3) the proportionality between  $\sigma$  and  $1/\sqrt{d}$ , (4) the increase of  $\sigma$  with increase of temperature, (5) the effects of strain on fracture, and (6) the mutual relationship of temperature and strain rate.

The low cleavage-fracture stress of zinc has been shown to be less than the theoretical cohesive strength by a factor of the order of 100 to 1000.<sup>7-9</sup> This remains the fundamental problem of cleavage, and it is in consequence of this that many failures of metals in service have been traced to cleavage fracture.

It has been shown that the Griffith crack theory<sup>4</sup> can be used directly to explain the results at  $-196^\circ\text{C}$ . shown in Fig. 1. The increase of  $\sigma$  with temperature was, however, against the predictions of the Griffith theory, and there are theoretical objections to the assumption of the existence of large cracks in pure metals.<sup>5</sup> Moreover, the effects of strain on fracture shown in Figs. 4, 5, and 14 are too complex to admit of interpretation in terms of simple mechanisms based on pre-existing cracks.

The objection to the direct application of the Griffith crack theory to pure metals is that it appears wrong to assume that cracks can always be present. The solution of the problem of cleavage in pure metals therefore resolves itself into a search for a mechanism whereby high internal stresses can be built up to give rise to cracks sufficiently large to be propagated under



the applied stress. It is thus necessary to determine the origin of the cracks which ultimately lead to fracture, since they cannot be considered to exist before the stress is applied.

Elementary ideas of crack formation when dislocations are piled up at a barrier have been given by Zener.<sup>15</sup> In a pure polycrystalline metal this condition is most likely to be developed at the end of a slip line, when the dislocations, moving in the slip direction under the applied stress, are halted by a grain boundary. Recently, the theory has been further developed and, in particular, Petch<sup>16</sup> has used it to explain cleavage in steels for which he obtained the relationship  $\sigma = \sigma_0 + f/\sqrt{d}$ , where  $\sigma_0$  and  $f$  are constants. This relationship is similar to that found for zinc in the present work; for zinc, however,  $\sigma_0 = 0$  and  $f$  has about half the value obtained for steel.

It would be of considerable interest to know whether the relationship is valid for other metals which show cleavage. Experiments by the present authors have shown that it does not hold for magnesium.

The dislocation theory of cleavage will now be briefly presented, and it will be shown to predict values of  $\sigma$  for zinc which are of the correct order of magnitude. The number of dislocations,  $n$ , which can be piled up in a length  $L$  of slip line between the source and barrier under an applied shear stress  $\sigma_s$ , has been calculated by Eshelby, Frank, and Nabarro.<sup>17</sup> It is found that :

$$n = L\sigma_s/2A \quad . \quad . \quad . \quad (1)$$

where  $A = \mu b/2\pi(1-\nu)$  for edge dislocations,  $\mu$  being the shear modulus,  $b$  the strength of a dislocation, and  $\nu$  Poisson's ratio.

An analysis by Koehler<sup>18</sup> has shown that, in addition to large shear stresses, large tensile stresses are also produced. He calculated the tensile stress,  $\sigma_T$ , across a plane perpendicular to the slip direction and obtained the relationship :

$$\sigma_T = k n \sigma_s \quad . \quad . \quad . \quad (2)$$

where  $k$  is a constant of the order of unity. Substituting the value of  $n$  from equation (1) gives :

$$\sigma_T = k L \sigma_s^2 / 2A$$

If  $\sigma_T$  is greater than the theoretical cohesive strength,  $\sigma_m$ , fracture should occur. Thus the criterion for fracture is :

$$k L \sigma_s^2 / 2A \geq \sigma_m$$

Since  $k$ ,  $A$ , and  $\sigma_m$  are constants, the shear stress,  $\sigma_s$ , necessary for fracture is seen to depend on the length  $L$  available for dislocation pile-up, or on the grain diameter,  $d$ , if the array of dislocations can be assumed

to occupy the entire length of a slip line in a grain. Furthermore, since

$$\sigma_s = \sigma/\sqrt{2},$$

we have :

$$\sigma_s = \sigma/\sqrt{2} \propto 1/\sqrt{L} \propto 1/\sqrt{d}$$

Thus, on dislocation theory, a formula is obtained which gives the experimentally observed relationship  $\sigma \propto 1/\sqrt{d}$ . The present work has provided results from which the formula may be tested numerically.

Considering, for example, a specimen of grain-size  $d = 10^{-2}$  cm., the shear stress in the most favourably orientated grain at fracture is of the order of  $10^9$  dynes/cm.<sup>2</sup> from Fig. 1. It is known that  $A$  is of the order of  $10^4$  dynes/cm. and  $k$  is of the order of unity.

$$\therefore \sigma_T = k L \sigma_s^2 \times 10^{-4} = 1 \times 10^{-2} \times 10^{18} \times 10^{-4} = 10^{12} \text{ dynes/cm.}^2$$

The tensile stress near the tip of the dislocation pile-up is therefore of the order of the theoretical cohesive strength, and the formula gives approximately correct numerical values for fracture.

To calculate the number of dislocations which must, if cleavage occurs, be piled up on the slip lines of specimens of this grain-size,

$$n = L\sigma_s/2A = 10^{-2} \times 10^9 \times 10^{-4} = 10^3$$

Thus, on the dislocation mechanism, for cleavage to occur in a specimen of mean grain diameter  $10^{-2}$  cm., it would be necessary for 1000 dislocations to be piled up between the source and grain boundary.

On a dislocation mechanism, two reasons can be advanced to explain the increase of  $\sigma$  with temperature: (i) If the pile-up of dislocations occurred sufficiently slowly, at the higher temperatures their increased mobility might allow them to diffuse out of their slip planes; hence it would be necessary to apply a higher overall stress  $\sigma$  before the pile-up was large enough to provide the stress concentration necessary for cleavage. (ii) Increased stress relaxation from neighbouring dislocation sources is to be expected at higher temperatures, particularly if the dislocation sources are affected by nitrogen.\*

The above reasoning indicates why flow would be expected to occur at higher temperatures and in particular for the smaller grain-sizes. A general yielding of the grains would take place before an internal stress sufficient for cleavage could be built up. The build-up of the internal stresses leading to crack formation at the higher temperatures is possible only at sufficiently high strain rates, where the time allowed for stress relaxation is short. Here we have a direct interpretation of the transition temperature. It also appears

\* H. L. Wain and A. H. Cottrell (*Proc. Phys. Soc.*, 1950, [B], 63, 339) have shown that the presence of nitrogen in single crystals of zinc causes a yield point similar to that found in mild steel. In the present work, yield points in polycrystalline zinc at low temperatures were not observed, nor could they be developed by strain-ageing treatments.

However, discontinuous yielding was observed in polycrystalline zinc specimens when they were strained at 50° C. at a constant strain rate of 0.053%/sec. The effect appears to be analogous to the "blue brittleness" of mild steel tested at about 300° C.

that after heavy deformation there are no slip lines long enough to permit the pile-up of a number of dislocations sufficient to cause cleavage.

The observed effects of strain on  $\sigma$  are difficult to explain at present. The effects of prestrain on  $\sigma$ , shown in Figs. 3-5 are seen to be too complex to admit of interpretation on simple theories of pre-existing cracks. On the dislocation theory, the effect of prestrains in the range 0.05-0.25 in decreasing the  $\sigma$  value at  $-196^\circ\text{C}$ . must be explained in terms of the structures obtained after varying amounts of deformation.

Twinning was shown to be associated with fractures which occurred after small deformations, but after larger deformations the cleavage facets were relatively twin-free. It may be that the decrease in  $\sigma$  caused by strain was connected with the lack of twinning at fracture. Apart from this observation, no further effects were found of a connection between twinning and fracture. The whole problem of the effect of strain on  $\sigma$  for zinc is likely to present difficulties in interpretation until the modes of deformation are better understood.

In conclusion, it appears that a dislocation mechanism for the build-up of large internal stresses leading to cracks which cause cleavage can be successfully applied to some of the phenomena in the cleavage of polycrystalline zinc. Further development of the dislocation theory is, however, necessary to complete the explanations of the cleavage fracture of zinc under tension.

#### ACKNOWLEDGEMENTS

The authors' thanks are due to the University of Sheffield for the award of a George Senior Research Fellowship which enabled one of them (G. W. G.) to devote his whole time to this research. Thanks are also due to Charles Clifford and Son, Ltd., Birmingham, for preparing and presenting the extruded bars of high-purity zinc and to Mr. S. W. K. Morgan of the Imperial Smelting Corporation, Ltd., Avonmouth, for arranging for the spectrographic analyses. The authors are also grateful to their colleagues for many helpful discussions during the course of the work.

#### REFERENCES

1. E. Schmid and W. Boas, "Plasticity of Crystals". 1950: London (F. A. Hughes and Co., Ltd.).
2. G. Masing and M. Polanyi, *Z. Physik*, 1924, **28**, 169.
3. E. Orowan, *Z. Physik*, 1933, **86**, 195.
4. A. A. Griffith, *Phil. Trans. Roy. Soc.*, 1920, [A], **221**, 163.
5. H. A. Elliott, *Proc. Phys. Soc.*, 1947, **59**, 208.
6. T. J. Agnor and M. E. Shank, *J. Appl. Physics*, 1950, **21**, 939.
7. M. Polanyi, *Z. Physik*, 1921, **8**, 323.
8. E. Orowan, *Z. Krist.*, 1934, **89**, 327.
9. F. Seitz, "Physics of Metals". 1943: New York (McGraw-Hill Book Co., Inc.).
10. D. J. McAdam, G. W. Geil, and R. W. Mebs, *Trans. Amer. Inst. Min. Met. Eng.*, 1947, **172**, 323.
11. M. Gensamer, E. Saibel, and J. T. Ransom, *Weld. J.*, 1947, **26**, 443s.
12. E. J. Ripling and W. M. Baldwin, *Proc. Amer. Soc. Test. Mat.*, 1951, **51**, 1028.
13. E. J. Ripling and W. M. Baldwin, *Trans. Amer. Soc. Metals*, 1951, **43**, 778.
14. C. J. Smithells, "Metals Reference Book". 1949: London (Butterworths Scientific Publications).
15. C. Zener, "Fracturing of Metals", p. 1. 1948: Cleveland, O. (American Society for Metals).
16. N. J. Petch, *J. Iron Steel Inst.*, 1953, **174**, 25.
17. J. D. Eshelby, F. C. Frank, and F. R. N. Nabarro, *Phil. Mag.*, 1951, [vii], **42**, 351.
18. J. S. Koehler, *Phys. Rev.*, 1952, [iii], **85**, 480.



# PREFERRED ORIENTATION IN ROLLED URANIUM SHEET\*

1555

By J. ADAM,† B.Sc., Ph.D., A.Inst.P., and J. STEPHENSON,‡  
B.Met., A.I.M., MEMBER

## SYNOPSIS

Preferred orientations produced in flat uranium plates rolled in the  $\alpha$  range with light or heavy total reductions, are reported. A simple description of the deformation texture of rolled uranium as a mixture of grains with (010) and (110) planes oriented perpendicular to the rolling direction is accurate for high temperatures and a high total rolling reduction.

Textures observed in plates rolled below 500° C. agree with predictions of Calnan and Clews (*Phil. Mag.*, 1952, [vii], 43, 93), based on twinning modes of deformation found by Cahn (*Atomic Energy Research Establishment Rep.*, 1951, (M/R 740).

## I.—INTRODUCTION

APART from its technological importance in the construction of nuclear reactors, uranium attracts the attention of crystallographers and metallurgists because of its complicated  $\alpha$  and  $\beta$  crystal structures, which are unusual among metallic elements. Three phases occur between room temperature and the melting point of uranium. At 650° C. the orthorhombic  $\alpha$ -uranium<sup>1,2</sup> transforms into a complex tetragonal  $\beta$  phase,<sup>3,4</sup> which in turn changes at 775° C. to a simple body-centred cubic  $\gamma$  phase.

The results of X-ray studies of the deformation textures of polycrystalline uranium after rolling have been reported by Harris.<sup>5</sup> He observed that low total reduction during hot rolling resulted in a much greater density of (010) poles compared with the (110) poles in the rolling direction, and that this condition was reversed by heavier total reduction. In certain cases (130) poles were found in the rolling direction. Harris also established that (113) planes were sometimes strongly oriented parallel to the rolling direction.

## II.—EXPERIMENTAL TECHNIQUES

Two main experimental difficulties are encountered in the X-ray study of preferred orientation in uranium. First, the transmission technique, which is ordinarily the most useful in the determination of preferred orientation, is ruled out owing to the heavy absorption of X-rays of wave-lengths suitable for diffraction work. The second difficulty lies in the diffraction pattern of uranium, the reflections of particular importance in the study of textures being either very weak or occurring in barely-resolved triplets or doublets.

Two experimental techniques were used for the determination of the intensity of the diffracted beam;

a photographic method and one involving the use of a Geiger counter.

### 1. PHOTOGRAPHIC METHOD

The photographic technique is based essentially on a method developed by Custers,<sup>6</sup> the principle of which can be seen from Figs. 1 and 2. Fig. 1 illustrates the experimental arrangement. A flat sample is

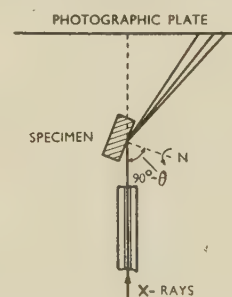


FIG. 1.—Illustrating Technique Employed with Photographic Apparatus.

placed at an angle  $\theta_{hkl}$  to the X-ray beam and a glancing-angle photograph of the  $hkl$  reflection is obtained on a flat photographic film. The observed intensity maxima and minima are plotted on a circle of reflection which passes through the centre of the standard stereographic projection, the normal to the face of the sample being at the centre of the projection. The specimen is rotated stepwise in its own plane, and a series of photographs is obtained which furnish a partial pole figure. Fig. 2 shows a series of circles of reflection corresponding to 30° rotations for the reflection at  $\theta_{hkl} = 18^\circ$ . These circles can be used for the 110, 021, and 002 reflections of uranium, since  $\theta_{110} = 17.5^\circ$ ,  $\theta_{021} = 17.8^\circ$ , and  $\theta_{002} = 18.1^\circ$ , when Cu radiation is used.

\* Manuscript received 19 February 1954.

† Principal Scientific Officer, and ‡ Senior Scientific

Officer, Atomic Energy Research Establishment, Harwell, Berks.

Ideally, nearly 60° of the pole figure could be covered by this method; in practice it is difficult to get beyond 40°, owing to geometrical broadening of the lines which causes overlapping of the three reflections mentioned. Photometry of the films, even in the central regions of the photograph, is very uncertain because the three reflections are not completely resolved. The positions of the maxima and minima must therefore be estimated by eye. Examination of three prepared surfaces of a sample which are respectively perpendicular to the rolling direction (R.D.), to the normal direction (N.D.), and to the transverse direction (T.D.), gives a substantial

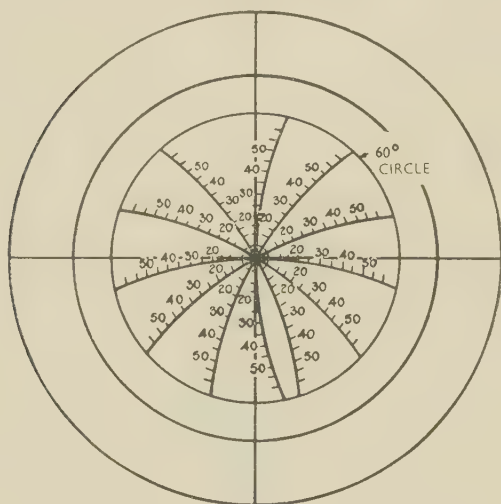


FIG. 2.—Chart for Plotting Pole Figures. ( $\theta = 18^\circ$ )

portion of the pole figure. Owing to the partial overlapping of the important reflections, the method is not very accurate for uranium, although it yields an approximate picture of the distribution of the poles.

In the present work, X-ray photographs were taken in a scanning camera <sup>7</sup> to eliminate the "spottiness" of the lines. A set of photographs was obtained for each face (R.D., N.D., and T.D.) of each sample at a glancing angle of 18°. These photographs were used for plotting qualitative pole figures for the (001), (110), and (021) planes. The presence or absence of the 020 reflection, nearly "in focus", in the same set of photographs was recorded, but because of its low intensity no attempt was made to obtain a more detailed (010) pole figure.

To gain some information about the distribution of the (100) planes, photographs were taken at a glancing angle of 33°, corresponding to the 200 reflection. The information obtained was very limited, because the 200 reflection is weak and barely resolved from the 023 line. Two photographs were taken from each face of all samples, the orientations of the sample being so chosen that the corresponding reflection circles were tangential to the axes of the stereographic projection at R.D., N.D. and T.D.

## 2. GEIGER-COUNTER METHOD

The Geiger-counter method used in this work was developed by Harris.<sup>5</sup> Intensities of all reflections within the range of the spectrometer ( $2\theta = 0-90^\circ$ ) are measured from the three prepared surfaces of the sample. These intensities are compared with measured intensities from a randomly oriented specimen. If  $I_{hkl}$  is the measured intensity of the  $hkl$  reflection from an oriented sample and  $A_{hkl}$  is the intensity of the same reflection from a random sample, the quantity  $p$  is defined as:

$$p = \frac{I_{hkl}}{\sum I_{hkl}} \cdot \frac{\sum A_{hkl}}{A_{hkl}}$$

$\sum I_{hkl}$  and  $\sum A_{hkl}$  are the sums of all the measured intensities from an oriented and a random sample, respectively. These factors come out as certain constants in an expression for  $p$  derived by Harris and are useful as normalizing factors.

The quantity  $p$  is a measure of the abundance of the ( $hkl$ ) planes parallel to a particular surface of the sample relative to the random distribution. Thus  $p = 1$  for a random distribution, while  $p < 1$  indicates a deficiency and  $p > 1$  an excess of particular planes parallel to the surface examined. The measured  $p$  values are marked on a standard stereographic projection of uranium, and three such projections are made for each rolled plate, showing the relative abundance or scarcity of various planes in the rolling, normal, and transverse directions.

TABLE I.—Values of  $\sum A_{hkl}/A_{hkl}$  for a Randomly Oriented Sample.

Line	Harris <sup>5</sup>	Present Work	Jacob and Warren <sup>1</sup>
020	0.99	1.0	1.1
110	13.6	17.0	15.0
021	12.9	16.1	21.0
002	9.5	12.0	10.0
111	10.8	11.5	12.0
022	0.92	...	0.51
112	11.6	8.5	8.5
130	0.71	...	0.77
131	8.8	8.2	7.3
040	1.6	1.4	1.3
023	2.9	3.4	3.2
200	1.67	2.5	1.6
041	1.61	...	0.68
113	2.46	2.6	2.3
132	0.90	...	0.77
042	1.38	1.8	1.7
221	10.7	8.3	7.6
004			
202			
133			
114	3.7	3.6	2.9
	3.26	2.1	1.8
	100	100	100

The method is rapid and reasonably accurate when the degree of preferred orientation is not very high, the main sources of inaccuracies being the weakness of several important reflections (see Table I) and the difficulty of resolving others which occur in doublets or triplets. Harris <sup>5</sup> estimated the error in individual  $p$  values at 20%, and this is probably correct in most



cases. The errors in  $p$  values become appreciably higher when the sample examined is highly oriented, owing to the relatively small number of strong reflections.

A North-American Philips X-ray spectrometer was employed for the work now described. The input voltage and the tube current were stabilized. The specimens were mounted in a fast-scanning mechanism specially designed for use with Geiger-counter X-ray spectrometers.<sup>8</sup>

A fine-grained random bar was used for the measurements of  $A_{hkl}$  and  $\Sigma A_{hkl}$ , and good agreement was found between results from various sections of the bar. The final values adopted agreed in general with Harris's measurements on a cast bar.<sup>5</sup> Table I shows the values of the normalized intensities from various crystallographic planes in unoriented uranium; Harris's values and Jacob and Warren's<sup>1</sup> calculated intensities are given for comparison.

### III.—PREPARATION OF SPECIMENS

The investigations reported by Harris<sup>5</sup> were made on round bars which, because of their geometry, yielded little information about the preferred orientation in directions other than the rolling axis. In addition, the bars examined were, in the main, rolled without intermediate reheating to ensure temperature control. For the present study flat plates were rolled by the following technique.

Cast plates,  $5 \times 3 \times \frac{3}{4}$  in., taken from the same melt to ensure uniformity of composition, were preheated singly in a horizontal vacuum furnace to the selected rolling temperature, the vacuum broken, and the plate taken out, reduced by one pass, its new thickness measured, and the plate returned to the furnace to regain the rolling temperature. The process was repeated until the desired reduction had been obtained. The operation from breaking the vacuum to re-starting the pumps lasted about  $1\frac{1}{2}$  min., and reheating times were about 15 min. After the last pass the sheet was water-quenched. The transfer of the plate from the furnace to the rolls was rapid (15 sec. or less), and experiment established that the temperature of the plate as it entered the rolls was effectively that of the furnace.

Specimens for X-ray examination were cut from the approximate centre of the plate. Three samples, cut at right angles to the rolling direction, the normal direction, and the transverse direction, respectively, were polished mechanically and electrolytically.<sup>9</sup> After polishing, the specimens were examined microscopically by polarized light to see whether any recrystallization had occurred, and then macro-etched before X-ray examination.

Plates which had undergone a high reduction (80%) had a final thickness of  $\frac{1}{8}$  in., which was not great enough for efficient scanning in the X-ray camera in T.D. and R.D. This difficulty was overcome by cutting two neighbouring specimens and mounting them together before polishing.

The variables in the rolling process were the temperature, the total deformation, and the effect of individual high reductions. Below 500° C. it was impracticable to reduce the plates by more than 15% per pass, as the load required was too great for the mill. Accordingly, all reductions were limited to 15%.

Above 500° C., although the basic reduction was in general held at 15% per pass, two plates were rolled with reductions of 15%, 20%, 25%, 33%, and 50%.

TABLE II.—Rolling Details.

Rolling Temperature, °C.	Total Reduction			
	50-60%		80%	
	Sample Letter	Remarks	Sample Letter	Remarks
300	$\begin{smallmatrix} H \\ L \end{smallmatrix}$	15% reduction per pass. " 60% " " Total	... ...	... Failure of plate at 62%.
350	...	...	$M$	Initial rolling 32% at 600° C.; then 73% at 12% per pass. Total 81%.
400	$K$	15% reduction per pass.	$P$	15% reduction per pass.
500	$J$	15% reduction per pass.	$T$	Increasing reductions.
600	$\begin{smallmatrix} S \\ F \end{smallmatrix}$	15% reduction per pass. Last pass 35%.	... $Q$	... Last pass 35%.
640	...	...	$N$	Increasing reductions.

This treatment is described in Table II as "increasing reductions".

The total reduction given was held at two levels, viz.: about 50-60% and about 80%. The treatment given to the individual plates from which specimens were taken is shown in Table II.

### IV.—EXPERIMENTAL RESULTS

The results obtained are summarized in Figs. 3-6, which illustrate pole figures, and in Figs. 7-10, which are stereographic projections on which the  $p$  values have been plotted. Only four of the most typical results are reproduced in each case. The pole figures have been idealized, any asymmetry due to accidents of rolling and sampling being eliminated. Fig. 11 is a "key" stereographic projection of uranium. The following summary of results is divided for convenience into low- and high-reduction rolling, each of these sections being sub-divided into low- and high-temperature rolling.

#### 1. LOW-REDUCTION ROLLING (UP TO 60% TOTAL)

##### (a) Rolling Temperatures 300° and 400° C.

The observed texture is complex, as can be seen from the  $p$  values (Fig. 7) and typical pole figure (Fig. 3) reproduced. All plates rolled at these temperatures showed high  $p$  values ranging from 4 to 8 for the (010) planes perpendicular to the rolling

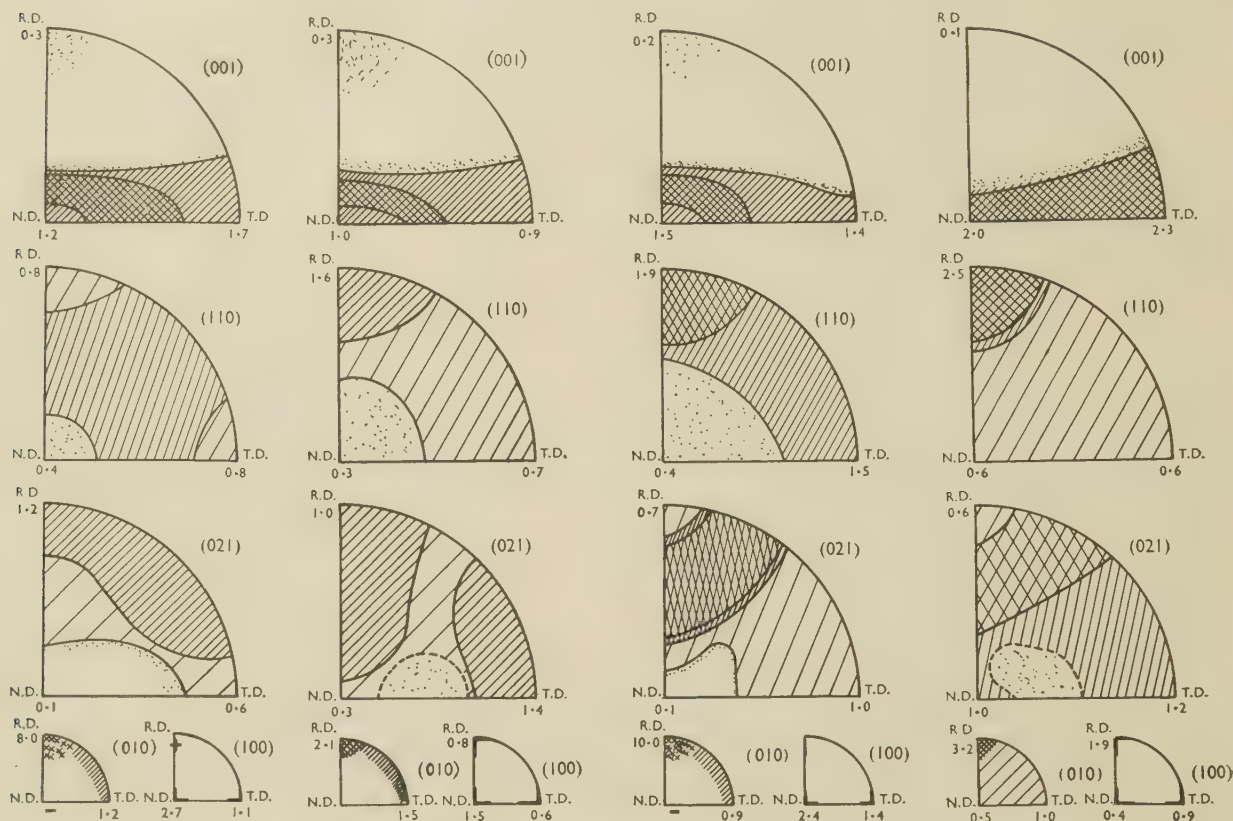
direction. Other planes giving  $p$  values greater than 1 in the R.D. are the (041), (021), (131), and (130).

In the N.D., i.e. the rolling plane, high  $p$  values are observed for the (114) and (113) planes, and appreciable preferred orientation is exhibited by the (001), (100), (023), and (112) planes. The distribution of the (001), (110), and (021) poles is shown in Fig. 3.

T.D. are frequently zero, even when the 020 reflection can be seen on the photographs.

#### (b) Rolling Temperatures 500° and 600° C.

Plates rolled at 500° and 600° C. differ from samples rolled at the lower temperatures. The  $p$  values for the (010) poles in the R.D. are considerably weaker



FIGS. 3-6.—Typical Pole Figures.

FIG. 3.—Sample L. Rolled at 300° C.; total reduction 60%.  
FIG. 4.—Sample S. Rolled at 600° C.; total reduction 50%.

FIG. 5.—Sample P. Rolled at 400° C.; total reduction 80%.  
FIG. 6.—Sample N. Rolled at 650° C.; total reduction 80%.

The (010) and (100) pole figures, also given, are very approximate for the reasons given in Section II, 1. The plus sign on the (100) pole figure indicates that intensity maxima have been observed on photographs within a few degrees of the R.D.

The distribution of (001) poles in a "doughnut" surrounding the R.D. is particularly interesting, because it shows that a simple model based on [010] and [001] directions will not describe the texture adequately.

The (021) pole figure shows a large spread around the R.D. and the distribution of the (110) planes is fairly uniform, although weak maxima were observed on some photographs.

As very weak lines can be more readily discerned on a photograph than on a recorded trace, it is not surprising that the  $p$  values for (010) planes in the

(1.7–2.8 in various samples), while the 110 reflections become more intense (Fig. 8). The typical pole figure (Fig. 4) shows a definite concentration of the (110) poles in the R.D. The (001) "doughnut" was sometimes incomplete and occasionally in samples rolled at 600° C. the (001) poles were concentrated in the N.D.

In general, the  $p$  values in the N.D. were similar for all plates rolled with low reduction, although samples rolled at higher temperatures showed lower values for the (100) planes.

## 2. HIGH-REDUCTION ROLLING (ABOUT 80% TOTAL)

### (a) Rolling Temperatures 350° and 400° C.

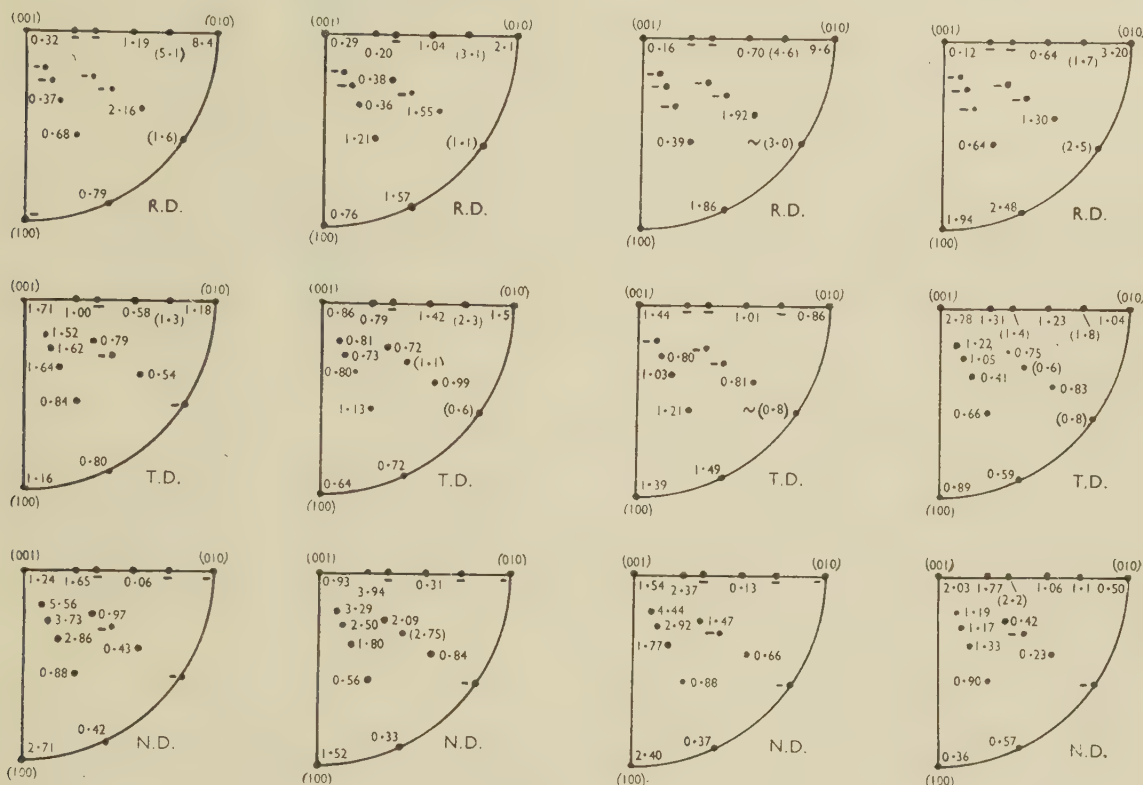
As was to be expected, the degree of preferred orientation obtained in all these samples was con-



siderably higher than in the case of samples rolled with a low reduction. Very high  $p$  values are found for the (010) planes in the R.D. (Fig. 9) and the spread towards the (001) is quite small (see the low  $p$  values for the (021) and (133) planes, suggesting a well-developed texture). The (110) planes also show a certain amount of preferred orientation perpendicular

(b) Rolling Temperatures 500° and 640° C.

The texture of these samples closely resembles a mixture of two fibre textures with the (110) and (010) planes perpendicular to the R.D. Both the  $p$  values and pole figures (Figs. 10 and 6) support this view.



FIGS. 7-10.—Typical Plots of  $p$  Values on Stereographic Projections.

FIG. 7.—Sample *L*. Rolled at 300° C. Reduction: 15% per pass, 60% total.  
 FIG. 8.—Sample *S*. Rolled at 600° C. Reduction: 15% per pass, 50% total.  
 FIG. 9.—Sample *P*. Rolled at 400° C. Reduction: 15% per pass, 80% total.  
 FIG. 10.—Sample *N*. Rolled at 650° C. Reduction: increasing, 80% total.

to the rolling direction. The typical pole figure (Fig. 5) shows a well-developed texture. The (110) poles show a definite concentration in the R.D.

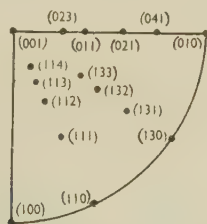


FIG. 11.—Standard Stereographic Projection of Uranium.

Again, the (001) "doughnut" indicates that the preferred orientation is complex, although in some samples this "doughnut" was found to be incomplete.

It is noteworthy that one of the samples (not reported in this paper) rolled at 600° C. had almost completely recrystallized, and a marked concentration of (001) poles in the T.D. had resulted.

Examination of microsections from the samples reported on revealed some recrystallization in plate *N* rolled at 640° C. but not in other samples.

## V.—DISCUSSION

### 1. INTERPRETATION OF RESULTS

Although, strictly speaking, the only impartial and complete method of describing preferred orientation is by pole figures, it is generally accepted that a texture may be approximately depicted by a model of crystallites oriented in a particular manner. In some cases it is possible to relate the results to the known modes

of plastic deformation of single crystals. When an adequate description of a texture is given, some quantity may be derived giving a measure of preferred orientation.

The plastic deformation of single crystals of  $\alpha$ -uranium has been studied and discussed in detail by Cahn.<sup>10</sup> He established the existence of two slip planes and four twinning systems (Table III).

TABLE III.—*Slip and Twinning Modes in Uranium* (Cahn<sup>10</sup>).

Type of Twinning	Twinning Elements			
	$K_1$	$K_2$	$\eta_1$	$\eta_2$
<i>a</i>	(130)	(1 $\bar{1}$ 0)	[3 $\bar{1}$ 0]	[110]
<i>b</i>	Irrational approx. (1 $\bar{7}$ 2)	(112)	[312]	Irrational
<i>c</i>	(112)	Irrational approx. (172)	Irrational	[312]
<i>d</i>	(121)	Irrational	Irrational	[311]
Type of Slip	Slip Plane		Slip Direction	
<i>e</i>	(010)	Probably [1 $\bar{1}$ 0], [1 $\bar{1}$ 2] also possible.	[100]	
<i>f</i>	(110)			

Cahn<sup>10</sup> finds that slip of type (f) and twinning of type (d) are infrequent and that consideration of the first three twinning systems suggests stress directions in which a crystal will be unable to twin in either compression or tension (Fig. 12).

Assuming the four most frequent modes of deformation found by Cahn, Calnan and Clews<sup>11</sup> predicted qualitatively the deformation texture which would be produced by rolling uranium. They have derived textures resulting from deformation by twinning, and demonstrated the effect on these textures of varying amounts of slip (see Fig. 13).

Comparison of these predictions with the experimental results indicates that the textures produced by rolling below 500° C. could be described as typical of twinning. This does not exclude slip as a mode of deformation at low temperatures; the effect of such

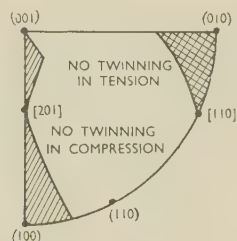


FIG. 12.—Forbidden Regions for Twinning. (Cahn.<sup>10</sup>)

slip upon the final texture appears to be masked, however, by profuse twinning.

The effect of the (010) [100] slip shows itself, according to Calnan and Clews, as preferred orientation of the (110) planes perpendicular to the rolling direction (Fig. 13 (b) and (c)). It seems very probable

that  $p$  values of about 1.9 observed for the (110) planes in samples rolled below 500° C. with high reduction (Fig. 9) are due to the reorientation of crystallites caused by slip. The compression texture

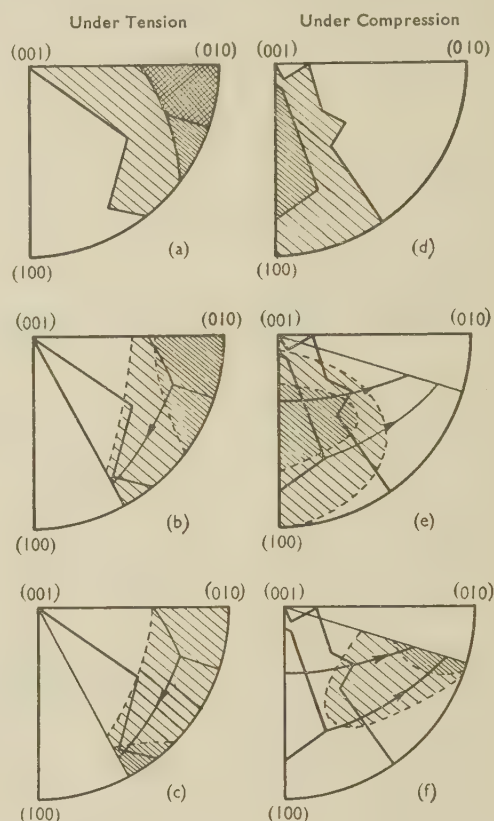


FIG. 13.—Twinning Textures in Uranium. (Calnan and Clews.<sup>11</sup>)

(a) and (d). Resulting from twinning alone.  
(b) and (e). Resulting from twinning and some slip.  
(c) and (f). Resulting from twinning and a large amount of slip.

The shading shows the densities of orientation. The arrows indicate slip rotation.

observed (N.D. in Fig. 9) is not in very good agreement with predictions as shown in Fig. 13 (f), i.e. for a large amount of slip, but if less slip were assumed (e.g. Fig. 13 (e)) the agreement is reasonably good.

According to Cahn, twinning mechanism does not operate at high temperatures in uranium, and consequently the textures of bars rolled above about 500° C. cannot reasonably be expected to fit Calnan and Clews' predictions.

The preferred orientation of plates rolled at temperatures between about 500° and 650° C. with high reduction resembles a double fibre texture as described below. In the case of low reduction at these temperatures, the preferred orientation observed showed variations from plate to plate, and could not be fitted into any consistent scheme.

## 2. THE DOUBLE-FIBRE-TEXTURE MODEL

The observed pole figures and the  $p$  values for plates rolled with heavy reduction in the temperature region



from about 500° to 650° C. are quite similar in N.D. and T.D. This feature, coupled with the great intensity of the 010 and 110 reflections observed in R.D., suggests that the rolling texture can be described as a mixture of two sets of crystallites oriented with the (010) and (110) planes perpendicular to the rolling direction.

### 3. MECHANISM FOR HIGH-TEMPERATURE TEXTURES

It is not possible to determine the deformation modes which have combined to yield a given texture, but it is possible to demonstrate the validity of suggested models by an application of the Calnan and Clews procedure. It is suggested that, in the absence of twinning, a combination of the two slip systems observed by Cahn (010) [110] and (110) [ $\bar{1}\bar{1}0$ ] could yield, by a process of duplex slip, a similar high-temperature texture to that obtained. A detailed analysis has not, however, been made.

## VI.—CONCLUSIONS

Rolling of uranium at temperatures below the  $\alpha$ - $\beta$  transformation produces preferred orientation.

Preferred orientations observed in plates rolled below about 500° C. agree well with predictions made by Calnan and Clews based on known twinning and slip systems. In bars rolled with low total reduction,

the effect of slip is almost completely masked by profuse twinning, and the texture can be best described as typical of twinning. In bars rolled with high total reduction there is evidence of the effect of slip on the final texture.

Preferred orientation observed in bars rolled in the 500°–650° C. range with high reduction resembles a double fibre texture in which (010) and (110) planes are perpendicular to the rolling direction. In bars rolled with low reduction, various textures were observed which have not been fitted into a consistent scheme.

### ACKNOWLEDGEMENTS

This work was carried out at the Atomic Energy Research Establishment, Harwell. Thanks are due to the Director of the Establishment for permission to publish the paper.

Mr. D. H. Walker of Atomic Energy of Canada, Ltd., while working at Harwell, took a major part in this investigation in its early stages.

The authors would like to thank Dr. H. M. Finnieston, Mr. L. M. Wyatt, and Dr. J. Thewlis for their continued interest in the work and for helpful discussions. They are grateful to Mr. P. G. Dawson and Mr. D. W. K. Collins for their assistance on the experimental side, and to Mr. E. C. Sykes, who examined the samples metallographically.

### REFERENCES

1. C. W. Jacob and B. E. Warren, *J. Amer. Chem. Soc.*, 1937, **59**, 2588.
2. J. S. Lukesh, *Acta Cryst.*, 1949, **2**, 420.
3. C. W. Tucker, Jr., *U.S. Atomic Energy Commission Publ.*, 1950, (AECD-2957); and *Acta Cryst.*, 1951, **4**, 425.
4. J. Thewlis, *Nature*, 1951, **168**, 198; and *Acta Cryst.*, 1952, **5**, 790.
5. G. B. Harris, *Phil. Mag.*, 1952, [vii], **43**, 113.
6. J. F. H. Custers, *Physica*, 1948, **14**, 453.
7. J. Thewlis and A. R. Pollock, *J. Sci. Instruments*, 1950, **27**, 72.
8. J. Adam, *ibid.*, 1952, **29**, 324.
9. B. W. Mott and H. R. Haines, *Metallurgia*, 1951, **43**, 255.
10. R. W. Cahn, *Atomic Energy Research Establishment Rep.*, 1951, (M/R 740); see also *Acta Met.*, 1953, **1**, 49 and *Acta Cryst.*, 1951, **4**, 470.
11. E. A. Calnan and C. J. B. Clews, *Phil. Mag.*, 1952, [vii], **43**, 93.

# The Constitution of Alloys of Aluminium, Copper, and Iron

By H. W. L. PHILLIPS

(*Journal*, this vol., p. 197.)

MR. P. R. SPERRY\*: The disagreement over the existence of the  $\alpha$  phase in the aluminium-copper-iron system came to my notice while conducting a metallographic study of some commercial aluminium alloys, during which it became necessary to examine certain alloys in order to confirm the presence of the  $\alpha$  phase as proposed by Phragmén† and to establish its metallographic characteristics. The experimental work was very limited. Therefore, it is gratifying to find confirmation in the work of Mr. Phillips and to have the aluminium corner of the system expounded more completely than it had been previously.

For the experimental work mentioned, two alloys were made, having the following compositions:

Alloy	Iron, %	Copper, %	Silicon, %	Aluminium
1	1.03	4.68	0.02	Balance
2	1.04	15.16	0.01	Balance

The cooling-curve arrests obtained with an average cooling rate of about 3° C./min. were as follows (accuracy  $\pm 3^\circ$  C.):

Alloy	Arrest Temperature, °C.			
	648	637	593	548
1	(643)		(590)	(548)
(Phillips)				
2	615	598	593	548
(Phillips)	(610)		(590)	(548)

For comparison, the corresponding temperatures from the liquidus surface diagram of Mr. Phillips (Fig. 4, p. 203) are also listed. The agreement is reasonable in all cases.

The arrest at 637° C. in alloy 1 was apparently where secondary  $\text{FeAl}_3$  began to form from the melt. There was no indication of an arrest at the invariant point at 620° C., where the  $\alpha$  phase should form from  $\text{FeAl}_3$ . Metallographic examination showed that this reaction had been suppressed and that the  $\beta$  phase was forming directly from  $\text{FeAl}_3$  as in Fig. A (Plate LXXXIX). An extremely small amount of  $\alpha$  eutectic was present in this sample. The microstructure, in the order of formation from the melt, consisted of primary Al, Al +  $\text{FeAl}_3$  eutectic, Al +  $\alpha$  eutectic, ( $\text{FeAl}_3$  and  $\alpha$ )  $\rightarrow$   $\beta$  peritectic, Al +  $\beta$  eutectic, and Al +  $\beta$  +  $\text{CuAl}_2$  eutectic.

When alloy 1 was heated at 540° C. for 120 hr., all the  $\text{CuAl}_2$  went into solution, all  $\alpha$  disappeared, and only a few residual cores of  $\text{FeAl}_3$  remained in the  $\beta$ , so that the alloy could be considered as belonging in the Al +  $\beta$  phase field at that temperature.

Alloy 2 contained no  $\text{FeAl}_3$  at all, but rather it had a substantial quantity of eutectic  $\alpha$ . The latter apparently began precipitating from the melt at 598° C., and when the temperature had dropped about 5° C. further the peritectic reaction involving the change from  $\alpha$  to  $\beta$  was initiated. Fig. B (Plate

LXXXIX) illustrates the envelopment of  $\alpha$  by  $\beta$ , and it shows the striking resemblance that  $\alpha$  has to its isomorph,  $\text{MnAl}_6$ . Heating of alloy 2 at 540° C. for 120 hr. brought about the complete disappearance of  $\alpha$  and only partial solution of  $\text{CuAl}_2$ , indicating that this alloy belongs in the Al +  $\beta$  +  $\text{CuAl}_2$  field.

It would be of interest to determine if the addition of manganese to aluminium-copper-iron alloys would enlarge the Al +  $\alpha$  field at the expense of the Al +  $\beta$  and the Al +  $\text{FeAl}_3$  fields. From a practical standpoint, silicon should also be present. It has been my observation that, in ingots of commercial alloys of various types containing 1.5–5% copper, the iron is usually present in the form of  $\alpha(\text{AlFeSi})$  (Chinese script) and that subsequent heating causes some transformation to another phase. This new phase turns out to be  $\beta(\text{AlCuFe})$ , if there is little or no manganese present, or ( $\text{Mn,Fe})\text{Al}_6$ , if the manganese content is about equal to, or greater than, that of the iron. Just what ratio of manganese to iron is necessary to avoid completely the formation of  $\beta(\text{AlCuFe})$  has not been determined.

MR. PHILLIPS (*in reply*): It is very satisfactory to find such close agreement between Mr. Sperry's work on these alloys and my own, as regards the constituents formed during solidification, the temperature at which the various reactions take place, and the constituents present under conditions of equilibrium. In his table of arrest temperatures for alloys 1 and 2, Mr. Sperry implies that I did not observe the 637° C. arrest in alloy 1 due to the separation of the  $\text{FeAl}_3$  + Al eutectic, and that at 598° C. in alloy 2 due to the Al +  $\alpha$  eutectic. These secondary arrest temperatures are given in Fig. 16 (p. 207) of my paper: I should estimate the arrest in question in alloy 1 to occur at 635° C., and that in alloy 2 at 602° C., in reasonably good agreement with the temperatures which Mr. Sperry determined. He mentions that he was unable to detect the  $\text{FeAl}_3 \rightarrow \alpha$  arrest at 620° C. in alloy 1, and suggests that the peritectic reaction had been suppressed and that  $\beta$  had formed directly from  $\text{FeAl}_3$ . This may well have been the case, but the arrest itself is easily missed, even when the reaction has undoubtedly occurred. I was never able to detect it on an inverse-rate cooling curve taken in the usual way, and only succeeded in doing so by the use of a constant-gradient furnace.

I should like to congratulate Mr. Sperry on his excellent micrographs, which show the differences in habit and etching behaviour between  $\text{FeAl}_3$ ,  $\alpha$ , and  $\beta$  in a most convincing way.

I was very interested in Mr. Sperry's observations on the effect of manganese additions on the structure of these alloys. Unfortunately, it is a subject on which I have no first-hand experience.

\* Research Metallurgist, Kaiser Aluminum and Chemical Corporation, Department of Metallurgical Research, Spokane,

Washington, U.S.A.

† G. Phragmén, *J. Inst. Metals*, 1950, 77, 489.



# THE CONSTITUTION OF THE SYSTEM SILVER-LITHIUM\*

1556

By W. E. FREETH,† Ph.D., B.Sc., MEMBER, and PROFESSOR  
G. V. RAYNOR,‡ M.A., D.Sc., VICE-PRESIDENT

## SYNOPSIS

The system silver-lithium has been examined by the methods of thermal analysis, metallography, and X-ray diffraction. The equilibrium diagram differs considerably from that previously accepted. The liquidus curve falls relatively smoothly from the freezing point of silver to a eutectic at 89.2 at.-% lithium and 145.5° C. The lithium-rich branch of the liquidus curve rises smoothly from the eutectic point to the freezing point of lithium. The determination of the solidus curve, annealing and quenching experiments, and X-ray investigations together reveal that the solubility of lithium in silver ( $\alpha$ ) is extensive (46.6 at.-% lithium at room temperature) and that four intermediate phases exist. The  $\beta$  phase is formed from  $\alpha$  by a solid-state reaction or by the reaction  $\alpha \rightleftharpoons \beta + \text{liq.}$  (317° C.), according to composition. The  $\gamma_3$  phase is similarly formed by a reaction in the solid state from  $\beta$ , or by the reaction  $\beta \rightleftharpoons \gamma_3 + \text{liq.}$  (164° C.). At 154° C.,  $\gamma_3$  and the liquid react together to form  $\gamma_2$ . At higher lithium contents, the  $\gamma_1$  phase is formed in the solid state. The  $\beta$ ,  $\gamma_3$ ,  $\gamma_2$ , and  $\gamma_1$  phases respectively include the compositions  $\text{AgLi}$ ,  $\text{Ag}_4\text{Li}_3$ ,  $\text{Ag}_3\text{Li}_{10}$ , and  $\text{AgLi}_{12}$ . The crystal structure of  $\beta$  is body-centred cubic (caesium chloride type), while the structures of  $\gamma_3$ ,  $\gamma_2$ , and  $\gamma_1$  are of the  $\gamma$ -brass type. The results are briefly discussed.

## I.—INTRODUCTION

In the course of experimental work on ternary magnesium-silver-lithium alloys, results were obtained which could not be reconciled with the previously accepted equilibrium diagram for the silver-lithium system. For this reason, and also because of the existence of an intermediate phase reported as  $\text{Ag}_3\text{Li}_{10}$ , which crystallizes in the  $\gamma$ -brass structure in circumstances precluding the attainment of an electron : atom ratio of 21/13, the system silver-lithium has been reinvestigated in the authors' laboratory.

The equilibrium diagram proposed by Pastorello,<sup>1,2</sup> on the basis of experiments on alloys prepared in stainless-steel crucibles under an argon atmosphere, is given in Fig. 1; the phase  $\text{AgLi}$  was reported as having a caesium chloride type of crystal structure ( $a = 3.222 \text{ \AA.}$ ). No variation of the lattice spacing of lithium was observed. According to the X-ray work of Zintl and Brauer,<sup>3</sup> the lattice spacing of  $\text{AgLi}$  at 53 at.-% silver is  $3.17 \text{ \AA.}$  The structure of the phase denoted  $\text{AgLi}_3$  by Pastorello was examined by Perlitz,<sup>4</sup> who obtained identical diffraction patterns from alloys containing 76–80 at.-% lithium, which were indexed in terms of a  $\gamma$ -brass structure of spacing  $9.94 \text{ \AA.}$  On the basis of this work, the phase was more properly denoted  $\text{Ag}_3\text{Li}_{10}$ , with 52 atoms per unit cell.

In the present work, the methods of thermal analysis, metallography, and X-ray diffraction have been used together. Though based on standard procedures, the experimental arrangements were modified where necessary owing to the marked reactivity of

the lithium-rich alloys. Specimens were prepared from assay silver of purity 99.99% (Johnson, Matthey and Co., Ltd.), and from high-purity lithium metal with a sodium content less than 0.02% (New Metals

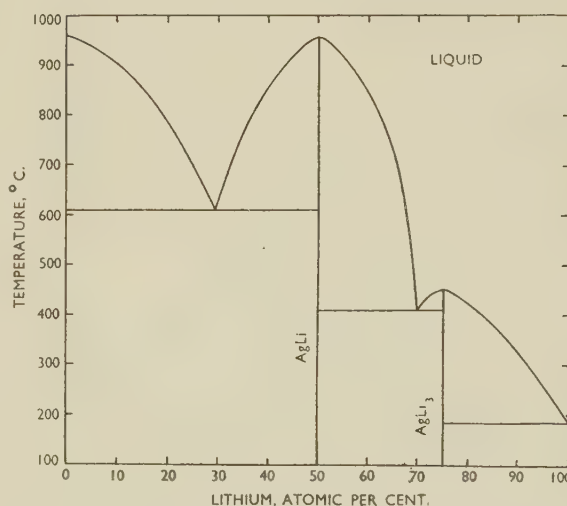


FIG. 1.—Equilibrium Diagram of Silver-Lithium System, According to Pastorello.<sup>1,2</sup>

and Chemicals, Ltd.). Apart from some preliminary specimens, alloys were melted and cast in a furnace unit specially developed for the purpose and for accurate cooling-curve work, using mild steel as the crucible material, and an atmosphere of purified argon.

\* Manuscript received 25 January 1954.

† Department of Metallurgy, University of Birmingham.

‡ Professor of Physical Metallurgy, University of Birmingham.

The furnace assembly is illustrated in Fig. 2, which is self-explanatory. When melting and casting, carefully weighed quantities of silver were placed in the crucible unit, and the whole apparatus evacuated and flushed with purified argon several times before melting under a positive pressure of 5 cm. of argon. Lithium was then added through the appropriate tube, G, and the alloy well stirred by the mechanical stirrer, A. Casting was effected by rapid rotation of the whole assembly so that the metal entered the mould V. All ingots for metallographic work were homogenized *in vacuo*, and in general the following times were employed:

Composition, at.-% Li	Temp., °C.	Time, days
<25	600	7
25-45	500	4
45-50	450	2
50-55	375	2
>55	Several hours at a temperature just below solidus.	

The decrease of annealing time at the higher lithium contents was necessitated by the volatility of lithium; tests showed, however, that the periods were sufficiently long for the attainment of equilibrium. Annealing treatments were ended by quenching the ingots into water or into liquid paraffin, according to the compositions of the alloys. Microspecimens were prepared by grinding under liquid paraffin and polishing either with "Globe" or "Silvo" metal polish (silver-rich material) or with a suspension of red lead in liquid paraffin (lithium-rich alloys). Etching proved difficult, and in the course of the work many reagents were used; the usual method of application was by means of a Selvyt pad moistened with the reagent.

For cooling-curve experiments, silver was melted in the furnace unit as above, and a Chromel/Alumel thermocouple was calibrated against the melting point of silver before the addition of lithium. Cooling curves were begun approximately 50° C. above the liquidus temperature, at a rate such that the alloys cooled to the arrest point at about 4° C./min. During the taking of the whole cooling curve a positive pressure of argon was maintained, and the temperature difference between the alloy and the inner furnace winding was maintained constant by means of automatic control. Under these conditions excellent liquidus arrests were obtained, together with an indication of the solidus temperature. In many cases arrests in the solid state were also clearly revealed. For solidus temperatures, heating curves were carried out only after homogenizing the specimen in the furnace; certain of the solid-state arrests were also examined by the slow heating or cooling of specimens homogenized to equilibrium after the completion of the original cooling-curve experiment. X-ray-diffraction experiments were made difficult by the volatility and reactivity of lithium. Specimens composed of filings could be used only for alloys containing less than 60 at.-% lithium, and even then no stress-relief annealing of the powder was possible. Lattice-spacing measurements could therefore not be made to

the highest degree of accuracy. For alloys containing more than 60 at.-% lithium, rods of small diameter proved suitable, but again no stress-relief anneal could

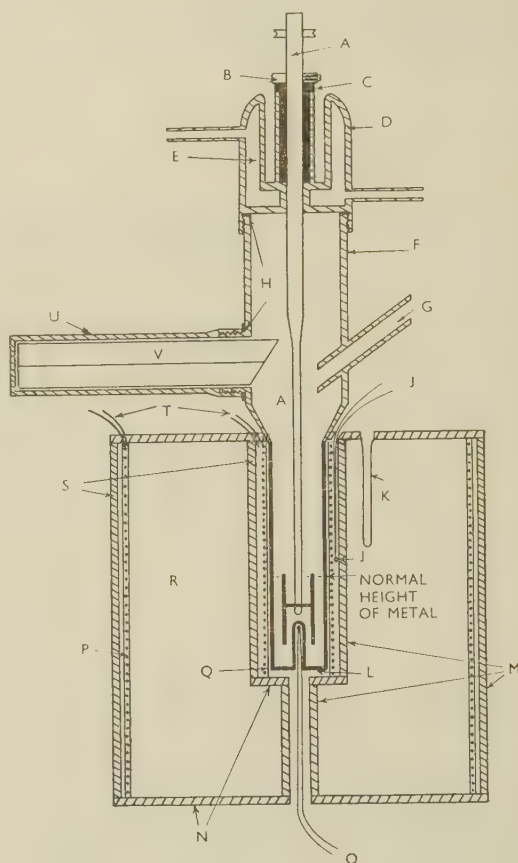


FIG. 2.—Cooling-Curve and Casting Furnace.

KEY.

- A. Stirrer driven by an electric motor (100 r.p.m.).
- B. Stirrer-adjustment platform.
- C. Stirrer sleeve.
- D. Furnace cooling head (mild steel).
- E. Water chamber.
- F. Furnace body.
- G. Argon inlet (also used for adding metal).
- H. Hallite washers.
- J. Thermocouple for indicating the temperature of the winding coil.
- K. External thermocouple sheath.
- L.  $\frac{1}{8}$ -in.-thick mild-steel crucible, welded to furnace body.
- M. Mild-steel sheet casing.
- N. Asbestos floor.
- O. Thermocouple for indicating the temperature of the specimen.
- P. Electrical heating winding embedded in Alundum cement.
- Q. Mild-steel heating tube insulated from electrical winding by thin mica.
- R. Iron core.
- S. Asbestos wool.
- T. Heating elements.
- U. Mould arm.
- V. Mild-steel split mould.

be given. In some cases the specimens were brittle enough to be powdered in a mortar under a dilute solution of Canada balsam in xylol, which was then used as the mounting medium for the powder specimen. All specimens were exposed to copper  $K_{\alpha}$  radiation in an 11-cm. Philips powder camera of the Straumanis pattern; the wave-lengths assumed were:

$$\begin{aligned}\text{Cu}K\alpha_1 &= 1.537395 \text{ kX} \\ \text{Cu}K\alpha_2 &= 1.541232 \text{ kX}\end{aligned}$$



All alloys examined in the solid state were chemically analysed. In the liquidus-curve determination, owing to the large number of alloys involved, it proved more convenient to determine the freezing points of a series of alloys made by adding carefully weighed amounts of metal to silver, lithium, or an alloy of known composition, only the last member of the series being analysed. The compositions of intermediate alloys could then be estimated within very close limits (see below).

## II.—EXPERIMENTAL RESULTS

The equilibrium diagram deduced from the present work is shown in Fig. 3. In addition to the terminal solid solutions, four intermediate phases, denoted respectively  $\beta$ ,  $\gamma_3$ ,  $\gamma_2$ , and  $\gamma_1$ , have been observed. For ease in description, the various features of the diagram may be considered in turn.

### 1. THE LIQUIDUS

The form of the liquidus curve was first established by preliminary experiments on unanalysed alloys, not included in Fig. 3. All the points finally plotted refer either to analysed alloys (full circles) or to series of alloys formed by adding metal to silver, lithium, or an analysed alloy (open circles). In the latter case the terminal alloy of each series was analysed, and the difference between the actual and intended compositions was recorded, and used to apply small corrections to the intended compositions of the intermediate alloys. The assumption was made that the small lithium losses occurred continuously and uniformly throughout the series of experiments, and Fig. 3 shows that there is excellent agreement between the points obtained in this way and those supported by chemical analysis. The liquidus falls smoothly and continuously from the freezing point of silver to a eutectic at  $145.5^\circ\text{C}$ . and a composition of 89.2 at.-% lithium. It then rises smoothly to the freezing point of lithium. Clear indications were obtained of an invariant reaction at  $317^\circ\text{C}$ . and 61.0–67.6 at.-% lithium. In alloys containing approximately 76–85 at.-% lithium, two distinct arrests were observed between the temperature of the liquidus and that of the eutectic. Initially these could not be interpreted, but as work proceeded it became clear that they were connected with reactions in the solid state, as shown in Fig. 3; their significance is discussed below.

### 2. THE SOLIDUS

For alloys containing up to approximately 85 at.-% lithium, the solidus was established by the method of annealing and quenching. Above this composition limit, heating curves, carried out on well-annealed alloys, were employed. The results are included in Fig. 3, and show that the melting points of silver-lithium alloys fall steadily from that of silver to  $164^\circ\text{C}$ . at 77 at.-% lithium. At this stage a marked dis-

continuity occurs, and the succeeding branch of the solidus curve is flat, falling slowly to the eutectic temperature of  $145.5^\circ\text{C}$ . From 91 at.-% lithium, the solidus curve rises smoothly to the melting point of lithium.

### 3. CONSTITUTION IN THE SOLID STATE

As noted above, an invariant reaction occurs in the partially liquid region, between 61.0 and 67.6 at.-% lithium, at a temperature of  $317^\circ\text{C}$ . Thermal curves of alloys containing 49.0–61.0 at.-% of lithium showed well-marked arrests at similar temperatures ( $330^\circ$ – $317^\circ\text{C}$ ., according to composition). The points plotted in Fig. 3 refer mostly to thermal arrests for alloys annealed in the solid state before cooling or heating, but are confirmed by preliminary work carried out by cooling directly from the melt. These arrests in the solid state are clearly connected with the invariant reaction at  $317^\circ\text{C}$ . A further set of thermal arrests in the solid state was observed for alloys containing 58.1–76 at.-% lithium. The observed temperatures increased from  $182^\circ\text{C}$ . at 58.1 at.-% lithium to a maximum of  $201^\circ\text{C}$ . at 65.5 at.-% lithium, and then decreased to  $164^\circ\text{C}$ ., the temperature of the higher of the two invariant reactions noted during the determination of the liquidus curve.

The existence of these two series of thermal arrests indicated the presence of reactions in the solid state, and to investigate the nature of these the annealing and quenching experiments summarized in Fig. 3 were carried out. Up to 46.4 at.-% lithium, alloys quenched from the annealing temperature or slowly cooled to room temperature gave rise to homogeneous microstructures consisting of twinned polygonal grains. X-ray-diffraction patterns of both quenched and slowly cooled alloys were characteristic of the face-centred cubic structure of silver. Alloy 46.88,\* however, on quenching from  $400^\circ\text{C}$ . and from  $300^\circ\text{C}$ . showed the homogeneous  $\alpha$  microstructure with a fine precipitate of dark-etching phase at the grain boundaries; experience showed that this type of structure was characteristic of slight decomposition of homogeneous  $\alpha$  alloys on quenching. After cooling to room temperature, the face-centred cubic structure was found to be mixed with a small amount of a phase having an ordered caesium chloride structure. Similar indications were given for alloy 48.04, except that on quenching from  $280^\circ\text{C}$ . a two-phase structure, easily differentiated from that produced by quenching from above  $330^\circ\text{C}$ ., was observed. By furnace-cooling alloys containing 46.8–50 at.-% lithium from temperatures above  $330^\circ\text{C}$ ., it was possible to obtain the  $\beta$  phase in a Widmanstätten type of distribution, which considerably assisted the phase identification. Thus the solubility of lithium in silver extends up to approximately 46.6 at.-% at low temperatures, and to the composition of the solidus above  $330^\circ\text{C}$ . The interpretation of the thermal arrests in the solid state is that they mark the transformation of  $\alpha$  into the

\* Individual alloys are referred to in terms of their atomic percentage of lithium.

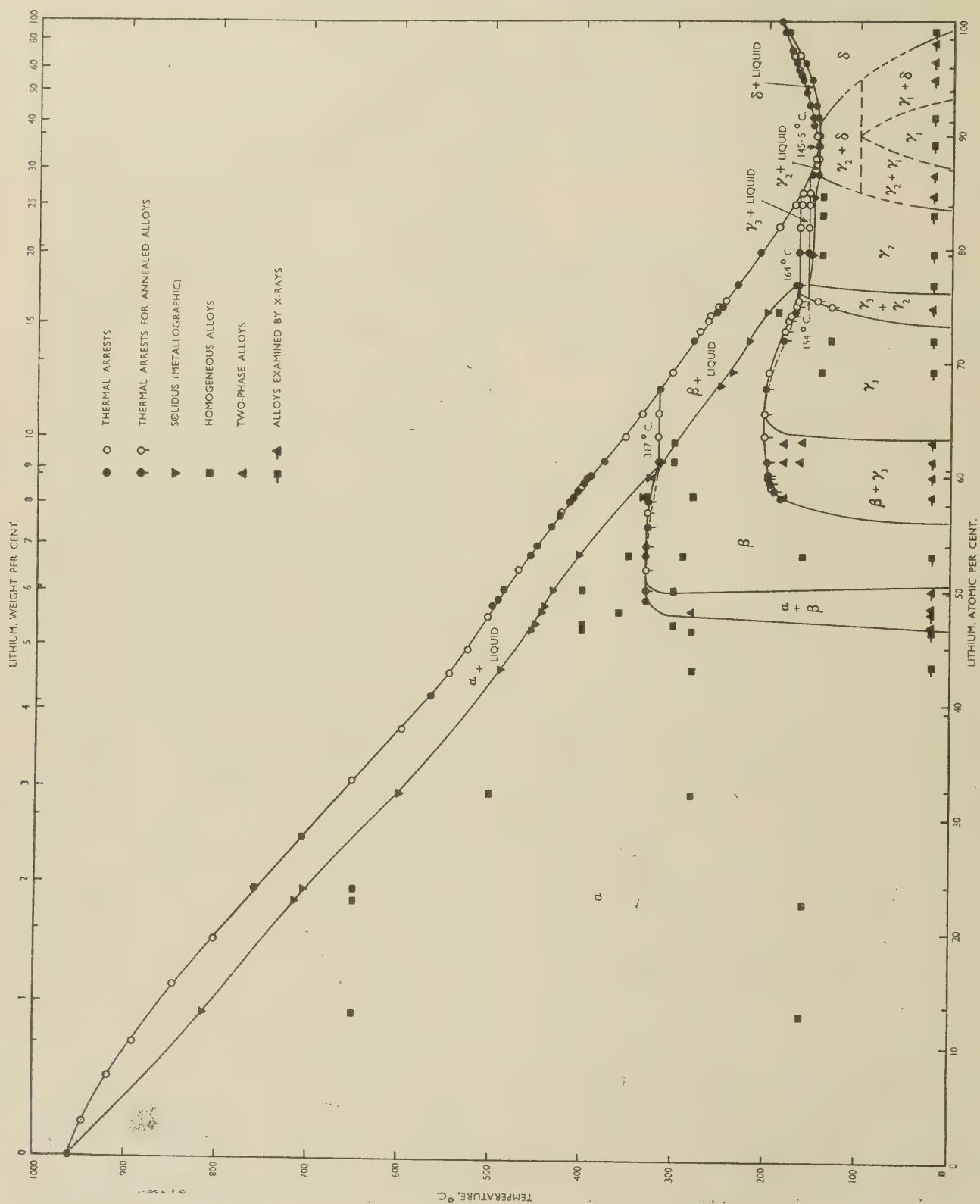


Fig. 3.—Equilibrium Diagram of Silver-Lithium System, According to Present Work.



cæsium chloride-type phase ( $\beta$ ) with falling temperature; the thermal arrests at 317° C. are then due to the reaction  $\alpha \rightleftharpoons \beta + \text{liq.}$  The X-ray-diffraction patterns of alloys 49.88 and 53.00 showed lines characteristic of a cæsium chloride structure, with a very slight admixture of  $\alpha$  in the former. Measurement of the film from alloy 49.88 gave  $a = 3.163$  kX.

With further increase in lithium content, a two-phase area occurs below 201° C. Thus alloy 58.2, annealed at 280° C., was micrographically homogeneous, but after quenching from 180° C. a dark-etching phase, denoted  $\gamma_3$ , appeared in addition to the  $\beta$  phase. It is of interest that after quenching from 330° C. the microstructure was of the decomposed  $\alpha$  type, thus confirming the persistence of the  $\alpha$  phase above the  $\beta$  region in the equilibrium diagram. A specimen furnace-cooled from 330° C. gave a duplex microstructure containing approximately 30% of the dark-etching  $\gamma_3$  constituent, and X-ray-diffraction experiments showed that the alloy contained the cæsium chloride structure of  $\beta$ , together with a  $\gamma$ -brass structure. Similar indications were given by alloys 59.79, 61.30, and 63.0, so that the thermal arrests which occur in the solid state from 58.1 to 76% lithium are to be identified with the transformation of  $\beta$  into  $\gamma_3$ , while the invariant reaction at 164° C. corresponds to  $\beta \rightleftharpoons \gamma_3 + \text{liq.}$  This interpretation is supported by the homogeneous  $\gamma_3$  structures plotted in Fig. 3, which were confirmed by X-ray-diffraction experiments.

Between 76 and 83 at.-% lithium homogeneous microstructures were again obtained by quenching from 140° C. or by slow cooling. The diffraction patterns of this phase ( $\gamma_2$ ) were very similar to those of  $\gamma_3$ , but the intensities of the diffraction lines showed characteristic differences on careful comparison. The presence of a two-phase region between  $\gamma_3$  and  $\gamma_2$  was revealed by the X-ray pattern of alloy 74.46, which contained the lines due to both structures; the occurrence of two thermal arrests in the solid state (alloy 75.0 at 130° C.; alloy 75.5 at 144° C.) is consistent with the boundary as drawn in Fig. 3. The thermal arrests at 154° C. are thus associated with the reaction  $\gamma_3 + \text{liq.} \rightleftharpoons \gamma_2$ .

The region from 83 to 100 at.-% lithium is somewhat complex. Thermal analysis shows clearly that only one invariant reaction, the eutectic at 145.5° C., exists between 86.6 and 91 at.-% lithium. The reaction involved is  $\text{liq.} \rightleftharpoons \gamma_2 + \text{Li-rich solid solution } (\delta)$ , which extends, at the eutectic temperature, from 91 to 100 at.-% lithium. Of the eight alloys plotted in this region, all of which were annealed at 140° C., air-cooled, and examined metallographically and by X-rays, only alloy 1.0 possessed the homogeneous body-centred cubic structure of the lithium-rich solution. Alloys 91.65 and 89.11 gave rise to diffraction patterns very similar to those of  $\gamma_3$ , which could be satisfactorily indexed in terms of a homogeneous structure. Alloys 86.42 and 84.7 gave diffraction patterns in which the lines due to the new phase ( $\gamma_1$ ) were admixed with those of  $\gamma_2$ , while the diffraction patterns of

alloys 97.99, 96.39, and 94.85 showed admixture of the  $\gamma_1$  and lithium-rich solid-solution lines. The  $\gamma_1$  phase therefore exists at room temperature from approximately 87 to 93 at.-% lithium. Attempts to define the maximum temperature of stability of  $\gamma_1$  were inconclusive, owing to the difficulty of the metallography of quenched lithium-rich alloys, the fact that decomposition structures were observed after quenching, and the impracticability of high-temperature X-ray methods. No indications of a thermal arrest in the solid state in the region from 86 to 95 at.-% lithium could be obtained. This portion of the equilibrium diagram has therefore been drawn with broken lines to indicate the uncertainty of the temperature of the reaction  $\gamma_2 + \text{Li-rich solid solution} \rightleftharpoons \gamma_1$ .

#### 4. THE CRYSTAL STRUCTURES OF THE INTERMEDIATE PHASES

The diffraction pattern of the  $\beta$  phase is characteristic of the cæsium chloride structure, in agreement with the work of earlier investigators.<sup>1-3</sup> The intermediate phase examined by Perlitz,<sup>4</sup> which was observed between 76 and 80 at.-% lithium, corresponds with the  $\gamma_2$  phase of the present investigation. The diffraction pattern of the  $\gamma_2$  phase, the range of homogeneity of which includes the composition  $\text{Ag}_3\text{Li}_{10}$ , was satisfactorily indexed in terms of the  $\gamma$ -brass structure proposed by Perlitz, with the side of the unit cell equal to 9.68 kX at 79.56 at.-% lithium. It was noted, however, that all the observed diffraction lines could also be accounted for on the basis of a face-centred cubic unit cell of side  $a = 6.50$  kX. The newly discovered  $\gamma_3$  phase includes the composition  $\text{Ag}_4\text{Li}_9$ ; all the lines in the diffraction pattern of  $\gamma_3$  were satisfactorily indexed in terms of a large cubic unit cell of side  $a = 9.49$  kX at the silver-rich composition limit. From this, and the general similarity of the diffraction patterns of  $\gamma_2$  and  $\gamma_3$ , it is clear that the crystal structure of  $\gamma_3$  is basically that of  $\gamma$ -brass also. The diffraction pattern of the  $\gamma_1$  phase is again similar to that of  $\gamma_2$ , and all the lines may be accounted for on the assumption of a large cubic unit cell of side  $a = 9.80$  kX at 91.65 at.-% lithium. It may be noted that the side of the unit cell is not much smaller than three times the lattice spacing of lithium. From the diffraction patterns obtained, the  $\gamma_3$ ,  $\gamma_2$ , and  $\gamma_1$  phases appear to be closely related both to each other and to the  $\gamma$ -brass structure, and it is probable that they are based respectively on the compositions  $\text{Ag}_4\text{Li}_9$ ,  $\text{Ag}_3\text{Li}_{10}$ , and  $\text{AgLi}_{12}$ . In the diffraction patterns, the most marked differences are those due to variations in the intensities of corresponding lines. Differences must therefore exist in the distributions of silver and lithium atoms on the various atomic sites available.

### III.—DISCUSSION

The equilibrium diagram shown in Fig. 3 is strikingly different from that due to Pastorello (Fig. 1); no explanation of this can be advanced unless the earlier

experiments made use of inhomogeneous melts. According to the present work, the solid solubility of lithium in silver extends to a maximum of 60.8 at.-% at 317° C. and has a value of 46.6 at.-% at room temperature. The solid solubility of silver in lithium falls from 9 at.-% at 145.5° C. to approximately 1 at.-% at room temperature. Lithium, which is univalent, is the only one of the alkali metals which has a favourable size-factor with regard to silver, while the size-factor of silver with respect to lithium is also favourable. The existence of mutual solid solutions is therefore understandable, but the very extensive solubility of lithium in silver is remarkable. It is probable that this is connected with the very small size of the ion of lithium, which enables it to replace silver on the solvent lattice without the introduction of large repulsive forces due to the overlapping of ionic atmospheres.

The  $\beta$  phase, the silver-rich limit of which corresponds almost exactly with the equiatomic position, has the caesium chloride structure, and is to be interpreted as based upon the arrangement LiAg. At this composition, the centres of the silver atoms are 3.163 kX apart; if any increase in the silver content were to

occur, Ag-Ag distances of  $\frac{3.163\sqrt{3}}{2}$  kX would be introduced. Since this distance is smaller than the interatomic distance in the crystal of silver, and also smaller than the atomic diameter of silver for co-ordination number 8, repulsive forces between silver ions would occur; the inability of LiAg to support an excess of silver may therefore be understood. Over the composition range 50–60.8 at.-% lithium,  $\beta$  is formed from  $\alpha$  by a reaction in the solid state, while from 60.8 to 77.0 at.-% lithium it enters into equilibrium with the liquid. Experiments show that  $\alpha$  cannot be quenched unchanged from above the  $\beta$  region; metallographically recognizable decomposition structures are produced. The  $\beta$  phase can support a considerable replacement of silver by lithium above 201° C., but below this temperature the  $\gamma_3$  phase occurs. Again it is not possible to quench  $\beta$  unchanged from above 201° C. As the lithium percentage is increased, the phases  $\gamma_2$  and  $\gamma_1$  successively occur.

The  $\gamma_3$ ,  $\gamma_2$ , and  $\gamma_1$  phases all appear to be closely related structurally, and to possess  $\gamma$ -brass type structures. The  $\gamma$ -brass structure was discussed by Bradley and Thewlis,<sup>5</sup> who showed that four types of crystallographically equivalent atomic sites occur, able to accommodate the following numbers of atoms:

Type of Site	No. of Atoms/Unit Cell
A	8
B	8
C	12
D	24

The atomic arrangement is complex, but may be regarded as a repetition in space of clusters of 26 atoms each; the clusters are disposed relatively to

each other like the atoms of a body-centred cubic structure. There may thus be two types of cluster; Type 1 occurring at the body centres, and Type 2 occurring at the cube corners of the body-centred cubic arrangement of clusters. The atomic distribution in the two types of cluster need not be identical. It is thus usual to differentiate the atomic sites as follows:

Cluster of Type 1	Cluster of Type 2	No. of Atoms/Unit Cell
$A_1$	...	4
...	$A_2$	4
$B_1$	...	4
...	$B_2$	4
$C_1$	...	6
...	$C_2$	6
$D_1$	...	12
...	$D_2$	12

In terms of this scheme, the  $Pb_3Li_{10}$  phase in the system lead-lithium, investigated by Rollier and Arregghini,<sup>6</sup> contains 12 lead atoms in  $D_1$  sites, with the remaining 40 sites occupied by lithium atoms. If it be assumed that the similar phase  $Ag_3Li_{10}$  ( $\gamma_2$ ) has the same structure with 12 silver atoms in the  $D_1$  sites, then the  $\gamma_3$  phase ( $Ag_4Li_9$ ) may be regarded as derived from it by replacing four lithium atoms in  $A_2$  sites by silver, thus giving a structure analogous to  $Cu_6Al_4$ .  $\gamma_1$  may be regarded as derived from  $\gamma_2$  by the replacement of the 12 silver atoms in  $D_1$  sites by lithium, together with the replacement of four lithium atoms in  $A_2$  sites by silver, to give the structure  $AgLi_{12}$ . The latter rearrangement is not a simple one, and the existence of a two-phase region between  $\gamma_2$  and  $\gamma_1$  is understandable on the basis of this interpretation. On the other hand, the  $\gamma_2 \rightarrow \gamma_3$  rearrangement which, if the above interpretation is correct, involves only a difference in the population of the  $A_2$  sites, might be expected to be continuous; as shown in Fig. 3, however, a two-phase region exists. It would be of considerable interest to confirm the atomic positions in these three closely related structures.

#### ACKNOWLEDGEMENTS

The authors gratefully acknowledge generous financial assistance, towards the researches of which the present work forms a part, from the Royal Society, the Department of Scientific and Industrial Research, the Chemical Society, and Imperial Chemical Industries, Ltd.

#### REFERENCES

1. S. Pastorello, *Gazz. Chim. Ital.*, 1930, **60**, 493.
2. S. Pastorello, *ibid.*, 1931, **61**, 47.
3. E. Zintl and G. Brauer, *Z. physikal. Chem.*, 1933, [B], **20**, 245.
4. H. Perlitz, *Z. Krist.*, 1933, **86**, 155.
5. A. J. Bradley and J. Thewlis, *Proc. Roy. Soc.*, 1926, [A], **112**, 678.
6. M. A. Rollier and E. Arregghini, *Z. Krist.*, 1939, **101**, 470.



# THE SYSTEMS MAGNESIUM-LITHIUM AND MAGNESIUM-LITHIUM-SILVER \*

1557

By W. E. FREETH,† Ph.D., B.Sc., MEMBER, and PROFESSOR  
G. V. RAYNOR,‡ M.A., D.Sc., VICE-PRESIDENT

## SYNOPSIS

The system magnesium-lithium has been re-examined by thermal and metallographic methods, and it has been confirmed that there is a maximum on the  $\beta$  liquidus (29.0–29.4 at.-% lithium, 594° C.). The invariant reaction involving the magnesium-rich solid solution ( $\alpha$ ),  $\beta$ , and the liquid is therefore a eutectic reaction (588° C.). Detailed study of the form of the ( $\alpha + \beta$ )/ $\beta$  boundary shows that although the boundary is almost vertical from 100° C. (29.9 at.-% lithium) to 500° C. (29.0 at.-% lithium), it bends sharply towards lower lithium contents above 500° C. and intersects the liq.  $\rightleftharpoons \alpha + \beta$  eutectic horizontal at 24.5 at.-% lithium.

Metallographic experiments were carried out on the magnesium-lithium-silver system, with special reference to the form of the ( $\alpha + \beta$ )/ $\beta$  phase boundary, at temperatures between 208° and 500° C. Isothermal diagrams indicate that the ternary  $\beta$  phase enters into equilibrium with  $\alpha$ ,  $\text{Mg}_3\text{Ag}$ , and  $\text{MgAg}$ . The lithium-rich corner of the ( $\alpha + \beta + \text{Mg}_3\text{Ag}$ ) phase triangle occurs at the following compositions for the temperatures studied:

208° C.	4.5 at.-% silver; 25.5 at.-% lithium.
305° C.	10.0    „    ; 20.3    „    .
410° C.	14.3    „    ; 12.5    „    .

At 495° C.  $\beta$  and liquid coexist, and experiments at 500° C. indicate that approximately 20 at.-% silver dissolves in  $\beta$  at this temperature. A wide solid solution of lithium in  $\text{MgAg}$  is also indicated by the various phase boundaries determined.

The results are briefly discussed.

## I.—INTRODUCTION

IN 1945, Hume-Rothery, Raynor, and Butchers<sup>1</sup> published an account of the magnesium-lithium-silver system, work on which was undertaken in connection with the possibility of developing a heat-treatable magnesium-rich alloy of low density. The boundaries of the primary magnesium-rich solid solution were accurately determined at 205°, 321°, and 421° C., and the positions of the ( $\alpha + \text{Mg}_3\text{Ag} + \beta$ ) triangle were established for the same three temperatures. More recently, arising out of work carried out at the Battelle Memorial Institute,<sup>2</sup> interest has concentrated on complex alloys based upon the more lithium-rich body-centred cubic  $\beta$  phase of the magnesium-lithium system, and a series of experimental age-hardenable alloys containing relatively small amounts of aluminium, zinc, silver, and cadmium has been investigated. Although the properties of high-strength alloys based on the magnesium-lithium system are reasonably stable at room temperature, they begin to deteriorate above about 70° C.; silver as a solute, however, appears to have a stabilizing effect on the age-hardened alloys, so that improved performance at 70° C. was attainable. It is therefore of interest to know the effect of silver on the magnesium-lithium  $\beta$  phase alloys, and on the duplex ( $\alpha + \beta$ ) alloys. A detailed investigation has accord-

ingly been made of the magnesium-lithium-silver alloy system at higher solute concentrations than were studied by Hume-Rothery, Raynor, and Butchers; in particular, the course of the ( $\alpha + \beta$ )/ $\beta$  boundary in the ternary alloys has been determined. Owing to inconsistencies in the literature, the binary magnesium-lithium system has also been re-examined.

The general form of the magnesium-lithium equilibrium diagram has been established, but certain features remain in doubt. The  $\alpha$  solid-solubility curve determined metallographically by Hume-Rothery, Raynor, and Butchers<sup>1</sup> agrees excellently with the X-ray determinations of Hofmann,<sup>3</sup> and has been accepted in the present work. The ( $\alpha + \beta$ )/ $\beta$  boundary, however, is less certain; according to Henry and Cordiano,<sup>4</sup> it lies at 29.4 at.-% lithium at room temperature, and 27.8 at.-% at 591° C., where  $\alpha$  and liquid react peritectically to give  $\beta$ . Grube, von Zeppelin, and Bumm<sup>5</sup> give values of 30.8 at.-% lithium at 860° C. and 28.6 at.-% at 587.5° C., at which temperature they report a eutectic (liq.  $\rightleftharpoons \alpha + \beta$ ). The ( $\alpha + \beta$ )/ $\beta$  boundary suggested by Saldau and Schamray<sup>6</sup> is almost vertical at 30 at.-%, with a eutectic reaction liq.  $\rightleftharpoons \alpha + \beta$  at 588° C. More recently Catterall<sup>7</sup> has obtained values ranging from 24.1 at.-% lithium at 588° C. to 28.3 at.-% at 350° C., implying that the invariant reaction involving  $\alpha$ ,  $\beta$ , and the liquid did not persist above 24.1 at.-% lithium, in

\* Manuscript received 25 January 1954.

† Department of Metallurgy, University of Birmingham.

‡ Professor of Physical Metallurgy, University of Birmingham.

marked contrast to the earlier work. This invariant reaction has been described as a peritectic by Henry and Cordiano, but Grube and his associates agree with Saldau and Schamray in finding a eutectic reaction. This implies a maximum in the liquidus and solidus curves at some composition on the lithium-rich side of the intersection of the ( $\alpha + \beta$ )/ $\beta$  boundary and the eutectic horizontal. Grube, von Zeppelin, and Bumm place this maximum at the composition  $\text{Li}_2\text{Mg}_5$  ( $592^\circ\text{C.}$ ), but Saldau and Schamray suggest the composition  $\text{LiMg}_2$  at  $600^\circ\text{C.}$  A further complication is that the latter workers report a peritectic reaction and a two-phase region at high lithium contents.

The only previous work on the ternary magnesium-lithium-silver system is that by Hume-Rothery, Raynor, and Butchers mentioned above.

## II.—MATERIALS AND METHODS

The alloys used in the present investigation were prepared from magnesium of purity 99.99% supplied by the Dominion Magnesium Company, Toronto, from lithium guaranteed to contain less than 0.02% sodium (New Metals and Chemicals, Ltd.), and from assay silver, 99.99% pure, supplied by Johnson, Matthey and Co., Ltd. Initially, alloys for metallographic work were made up using a modification of the casting apparatus described by Hume-Rothery, Raynor, and Butchers,<sup>1</sup> with an atmosphere of specially purified argon. Crucibles of mild steel, washed internally with magnesia, were found to be the most satisfactory, since alumina-lined crucibles were rapidly attacked by alloys relatively rich in lithium. Since this apparatus is not well adapted for thermal analysis, a new thermal-analysis furnace, incorporating mechanical stirring, inert atmosphere, and controlled temperature differences between specimen and winding, was developed and used for all thermal-analysis experiments. By the provision of a mould in a side arm, the apparatus was adapted for melting and casting of specimens for metallographic work, and most of the alloys discussed in this paper were prepared in this way. As the furnace is being separately described,<sup>8</sup> no further reference is made to it here. The techniques employed for metallographic examination were closely similar to those described earlier,<sup>1</sup> and standard X-ray techniques were used for confirmatory purposes. Throughout the annealing processes, temperatures were accurately controlled by automatic regulators, and measured by standardized thermocouples; specimens were sealed *in vacuo* in hard-glass tubes, and reaction between the alloy and the container was prevented by mild-steel tubing surrounding the specimen. Owing to the reactivity of the alloys, ethylene glycol was used as the quenching medium for lithium contents greater than 35 at.-%; below this limit, water could be used safely when quenching from below  $550^\circ\text{C.}$ , but for quenching from higher temperatures ethylene glycol was again used. All critical alloys were analysed chemically after the metallographic examination was complete, either by

Johnson, Matthey and Co., Ltd., or in the authors' laboratory; results from the two sources were satisfactorily consistent.

## III.—EXPERIMENTAL RESULTS

### 1. THE SYSTEM MAGNESIUM-LITHIUM

#### (a) *Thermal Analysis*

Exploratory experiments with the thermal-analysis apparatus showed that alloys could be prepared to accurately predetermined compositions, and also that thermal-analysis results obtained with a given alloy were reproducible after several remeltings. It was therefore considered justifiable to survey the liquidus curve by the thermal analysis of a series of alloys made by successive additions of lithium to magnesium, or to a freshly made alloy, the terminal alloy of the series being analysed for comparison of nominal and actual compositions. The entire composition range was covered in three main series. First, twelve alloys were prepared by the successive addition of lithium to magnesium; the terminal alloy, whose nominal composition was 29.25 at.-% lithium, proved to contain 29.4 at.-% by analysis, so that the nominal compositions of the intermediate alloys may be accepted within close limits. The second series was made by adding lithium to an alloy containing 22.5 at.-% until a nominal composition of 54 at.-% lithium was reached; analysis of this alloy gave 54.2 at.-% lithium. The third series was obtained by adding magnesium to pure lithium up to a nominal lithium percentage of 70.0 by atoms, which was confirmed exactly by analysis. The results obtained are shown in Fig. 1. The primary arrests were in all cases very marked, and it was also found that the end of the arrest, under the conditions employed, was sharp, giving an approximate solidus temperature. To investigate the reliability of regarding the end of the cooling-curve arrest in this system as an indication of the solidus, several alloys were slowly cooled and the apparent solidus temperature recorded. After annealing below the solidus for approximately 1 hr, heating curves were taken. In all cases, the heating-curve arrest occurred at the temperature indicated by the end of the cooling-curve arrest. The solidus temperatures have thus been included in Fig. 1, together with heating-curve results in the critical region from 25 to 30 at.-% lithium, obtained from analysed alloys.

#### (b) *The $\beta$ Solidus*

The reliability of the solidus temperature indicated by the end of the primary arrests decreases as the liquidus-solidus separation increases. Thus, nine alloys were used in the region 32.7–70.0 at.-% lithium to establish the solidus metallographically. The results (Fig. 1) are in good agreement with the approximate solidus temperatures from cooling curves; each point plotted represents a temperature midway between that at which no chilled liquid was visible in



the microstructure, and that ( $3^{\circ}$ – $6^{\circ}$  C. higher) at which chilled liquid was observed.

(c) *The  $(\alpha + \beta)/\beta$  Boundary*

According to the thermal-analysis work, the lithium-rich end of the eutectic horizontal occurs at 24.5 at.-% lithium, whereas previous metallographic

appearance, which could be mistaken for a structure denoting the presence of two phases at the quenching temperature. In the present case particular attention was paid to the speed of quenching, and it was possible to distinguish with ease the fine structure produced by quenching from the massive particles of  $\alpha$  present in equilibrium at the quenching temperature.

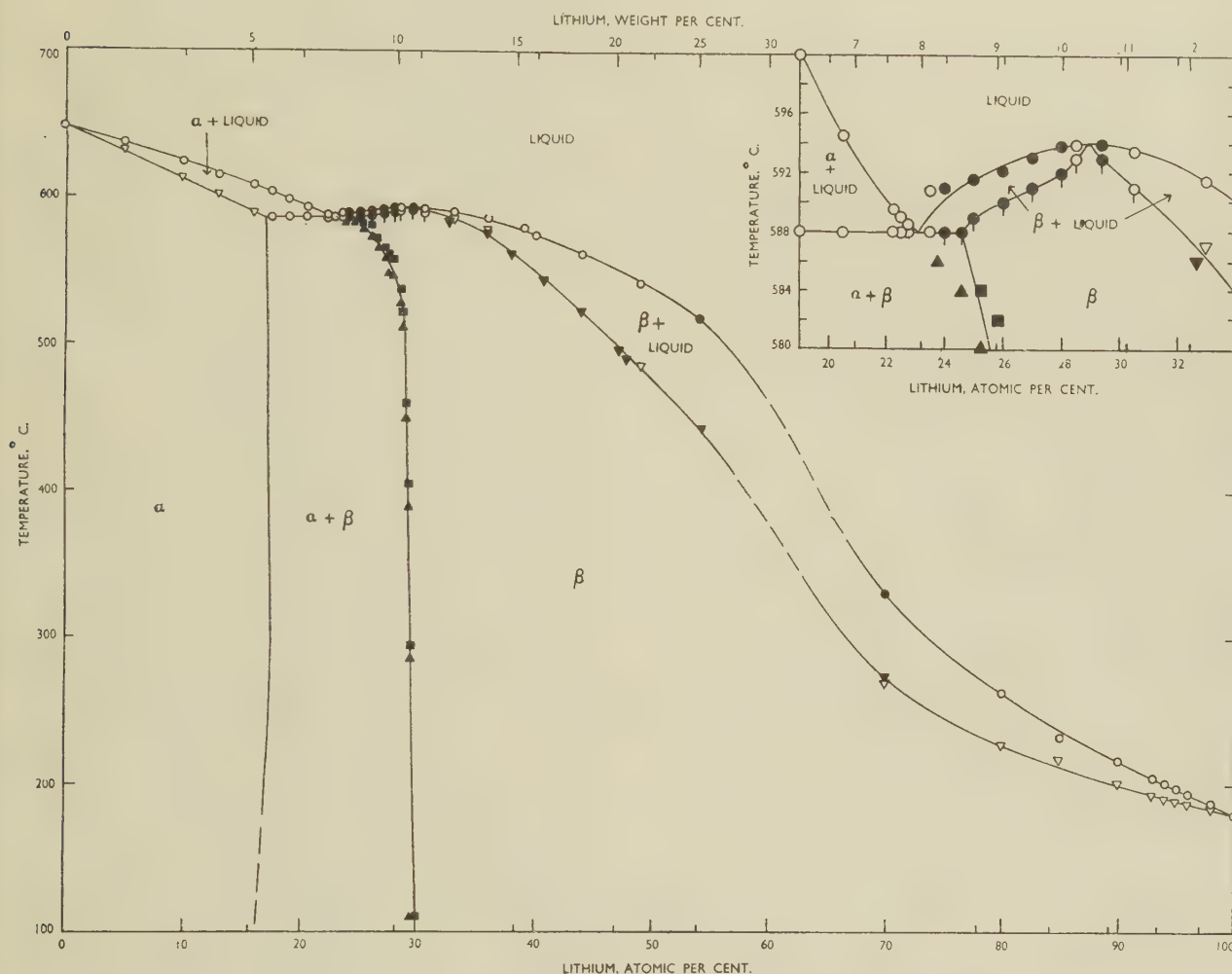


FIG. 1.—The Equilibrium Diagram of the Magnesium-Lithium System.

KEY.

Thermal Arrests  $\circ, \bullet$ ; solidus points from heating curves  $\circ, \bullet$ ; approximate solidus from end of cooling-curve arrest  $\nabla$ ; solidus from metallography  $\blacktriangledown$ ;  $(\alpha + \beta)$  alloys  $\blacktriangle$ ;  $\beta$  alloys  $\blacksquare$ ; black symbols represent analysed alloys.

investigations indicated an intersection of the eutectic horizontal and the  $(\alpha + \beta)/\beta$  boundary at 27.8–29 at.-% lithium. The present work suggests the reason for this discrepancy. Although the  $\beta$  phase, of such a composition that it crosses the  $(\alpha + \beta)/\beta$  boundary on cooling to room temperature, may be retained by drastic quenching from temperatures below  $520^{\circ}$  C., quenching from above  $520^{\circ}$  C. gives rise to the precipitation of  $\alpha$  in a fine Widmanstätten type of structure. Relatively slow quenching leads to a coarser

The technique adopted was to anneal alloys in the two-phase region until the  $\alpha$  particles had coalesced into large crystals, and then to anneal specimens at successively higher temperatures until the only feature in the quenched microsection was the fine precipitate formed on quenching. The results are incorporated in Fig. 1; the boundary bends round above  $500^{\circ}$  C. to join satisfactorily with the eutectic horizontal.

The equilibrium diagram determined in the present work confirms that there is a maximum on the  $\beta$

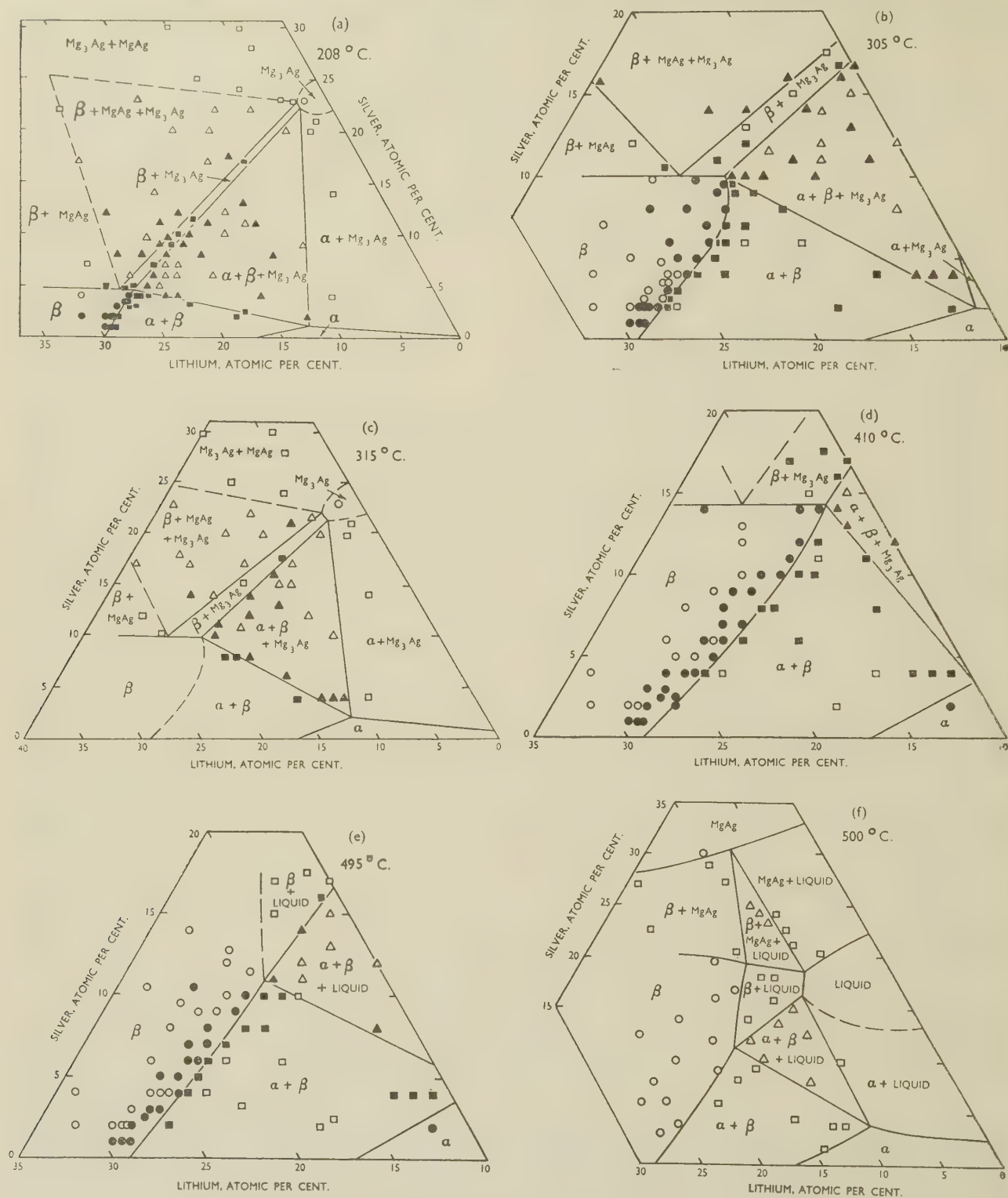


FIG. 2.—System Magnesium-Lithium-Silver: Partial Isothermals at (a) 208° C., (b) 305° C., (c) 315° C., (d) 410° C., (e) 495° C., (f) 500° C.

#### KEY.

One-phase alloys, ○, ●; two-phase alloys □, ■; three-phase alloys △, ▲; black symbols represent analysed alloys.  
 (a)–(c) Alloys annealed for 7 days after homogenization for 7 days at 410° C. (d) Alloys annealed for 4 days after homogenization for 7 days at 410° C.  
 (e) and (f) Alloys annealed for 3 hr. after homogenization for 7 days at 410° C.



liquidus; it occurs at 29.0–29.4 at.-% lithium and a temperature of 594° C. The liq.  $\rightleftharpoons \alpha + \beta$  eutectic temperature is 588° C., in agreement with Saldau and Schamray,<sup>6</sup> but there is no sign of the invariant reaction in the lithium-rich alloys which they reported.

## 2. THE SYSTEM MAGNESIUM-LITHIUM-SILVER

A large number of alloys, of compositions in the range 10–40 at.-% lithium and 0–20 at.-% silver, was examined by metallographic methods at 208°, 305°, 410°, and 495° C. Supplementary experiments with alloys richer in silver were carried out at 208°, 315°, and 500° C. All the annealing temperatures were below that at which decomposition on rapid quenching interferes, and no difficulty was experienced on this account.

The results are presented in the form of isothermal diagrams (Figs. 2 (a)–(f)), which are self-explanatory; open symbols represent unanalysed alloys. At 208° C. approximately 4.5 at.-% silver dissolves in the magnesium-rich  $\beta$  phase; the  $(\alpha + \beta)/\beta$  boundary lies at an almost constant magnesium content. The position of the  $(\beta + \text{Mg}_3\text{Ag} + \text{MgAg})$  triangle implies a considerable solid solubility of lithium in the ordered body-centred cubic MgAg phase, which is confirmed by the six  $(\text{Mg}_3\text{Ag} + \text{MgAg})$  microstructures observed. The 305° C. isothermal (Fig. 2 (b)) shows that the solubility of silver in the  $\beta$  phase has increased considerably, and a slight curvature has been introduced into the  $(\alpha + \beta)/\beta$  boundary. The 315° C. isothermal, which was examined in less detail, is similar (Fig. 2 (c)) and indicates a solubility of lithium in MgAg similar to that at 208° C. At 410° C. (Fig. 2 (d)), the solubility of silver in  $\beta$  has again increased, and the  $(\alpha + \beta)/\beta$  boundary ends at 12.5 at.-% lithium and 14.3 at.-% silver.

In the binary silver-magnesium alloys, a eutectic (liq.  $\rightleftharpoons \alpha + \text{Mg}_3\text{Ag}$ ) occurs at 471.5° C., and at 494.5° C. the reaction  $\text{MgAg} + \text{liq.} \rightleftharpoons \text{Mg}_3\text{Ag}$  takes place. As shown by thermal-analysis experiments on selected alloys, the eutectic is depressed to 462° C. by lithium, while the peritectic is depressed to 482° C. Thus at 495° C. (Fig. 2 (e)),  $\text{Mg}_3\text{Ag}$  is no longer present, and  $\beta$  enters into equilibrium with liquid rich in magnesium and silver. The limiting solubility of silver in  $\beta$  at this temperature was not determined, but the less-detailed survey carried out at 500° C. indicates a solubility exceeding 20 at.-% silver at this temperature (Fig. 2 (f)).

In order to confirm the metallographic results, many of the quenched alloys were examined by X-ray-diffraction methods, and the results were in all cases consistent with the phase fields indicated in Fig. 2.

## IV.—DISCUSSION

The experiments described show that, in the composition range of interest to the present work, no ternary compound exists in the system magnesium-

lithium-silver. There is, however, a wide solid solution of silver in the body-centred cubic  $\beta$  phase of the magnesium-lithium system, extending up to approximately 20 at.-% at 500° C. The solubility is 4.5 at.-% at 208° C., so that the solubility surface moves rapidly towards the magnesium-lithium wall of the ternary model with decreasing temperature. A wide solubility of lithium in the MgAg phase has also been observed.

The form of the  $(\alpha + \beta)/\beta$  boundary in the ternary system is of interest. Although at 208° C. the boundary occurs at an almost constant magnesium content, at the higher temperatures the magnesium percentage decreases as the silver content rises along the boundary. Thus, although a binary alloy containing 17.5 at.-% lithium lies at the solubility limit of lithium in close-packed hexagonal magnesium at 495° C., a ternary alloy containing the same amount of lithium but with 10 at.-% magnesium replaced by silver is in the body-centred cubic region. Similarly, at lower temperatures, body-centred cubic structures may be obtained at lithium contents which correspond in binary magnesium-lithium alloys to duplex structures containing a large proportion of the close-packed hexagonal phase. This may be of importance where hot-forming operations are under consideration. Reference to the isothermal diagrams shows that alloys containing small amounts of silver (up to 5 at.-%) may easily be obtained in the homogeneous  $\beta$  region if they contain 30 or more at.-% lithium. On cooling, the phase precipitated is the MgAg phase, which can contain a considerable proportion of lithium, except for compositions close to those of the  $(\alpha + \beta)/\beta$  phase boundary, where  $\text{Mg}_3\text{Ag}$  or  $(\text{MgAg} + \text{Mg}_3\text{Ag})$  are precipitated.

According to Jackson and his co-workers,<sup>2</sup> the ageing of magnesium-lithium-silver alloys having sufficient lithium to consist of the  $\beta$  phase, and a sufficient quantity of silver, is accompanied by the precipitation of a phase which they denoted  $\theta$ . This phase was tentatively assigned the composition  $\text{MgLi.LiAg}$ , and was regarded as a transitional structure. It is of interest to note that very similar, apparently transitional phases were observed<sup>2</sup> in suitably aged ternary alloys of magnesium and lithium with zinc, aluminium, and cadmium, and in each case the provisional composition  $\text{MgLi.LiX}$  was assigned ( $X = \text{Zn, Al, or Cd}$ ). Approximate lattice spacings ranging from  $a_0 = 6.66 \text{ \AA.}$  for  $\text{MgLi.LiZn}$  to  $a_0 = 6.78 \text{ \AA.}$  for  $\text{MgLi.LiAg}$  were quoted, so that the structure may be presumed cubic. According to the work of Busk, Leman, and Casey,<sup>9</sup> the  $\text{MgLi.LiAl}$  phase is body-centred cubic, and based upon a structure of the NaTl type (*B* 32), so that a similar structure is probable for  $\text{MgLi.LiAg}$ . This suggests that the  $\theta$  phase may be associated in the present case with the wide solid solution of lithium in MgAg. The suggested composition of  $\theta$  may be attained merely by dissolving sufficient lithium in the MgAg phase. The reported lattice spacing is approximately twice that of MgAg, so that the appropriate composition would result if, in

a cubic unit consisting of eight unit cells of MgAg, the silver atoms at the corners and face centres of the unit and the magnesium atoms at the centres of alternate small unit cells were replaced by lithium. It is possible that an ordered arrangement of this type has a provisional stability and is precipitated on ageing, later relaxing towards equilibrium by rejecting lithium atoms so that the composition of the phase moves towards that corresponding to the equilibrium tie-line for the appropriate temperature. This would be con-

sistent with the observation <sup>2</sup> that the lattice spacing of (MgLi.LiAg) decreases as ageing proceeds.

#### ACKNOWLEDGEMENTS

The authors wish to acknowledge gratefully the financial assistance given by the Royal Society, the Department of Scientific and Industrial Research, the Chemical Society, and Imperial Chemical Industries, Ltd.

#### REFERENCES

1. W. Hume-Rothery, G. V. Raynor, and E. Butchers, *J. Inst. Metals*, 1945, **71**, 589.
2. J. H. Jackson, P. D. Frost, A. C. Loonam, L. W. Eastwood, and C. H. Lorig, *Trans. Amer. Inst. Min. Met. Eng.*, 1949, **185**, 149.
3. W. Hofmann, *Z. Metallkunde*, 1936, **28**, 160.
4. O. H. Henry and H. V. Cordiano, *Trans. Amer. Inst. Min. Met. Eng.*, 1934, **111**, 139.
5. G. Grube, H. von Zeppelin, and H. Bumm, *Z. Elektrochem.*, 1934, **40**, 160.
6. P. Saldau and F. Schamray, *Z. anorg. Chem.*, 1935, **224**, 388.
7. J. A. Catterall, *Nature*, 1952, **169**, 336.
8. W. E. Freeth and G. V. Raynor, *J. Inst. Metals*, 1953-54, **82**, 569.
9. R. S. Busk, D. L. Leman, and J. J. Casey, *Trans. Amer. Inst. Min. Met. Eng.*, 1950, **188**, 945.



## Discussion

# The Control of Quality in the Production of Wrought Non-Ferrous Metals and Alloys. II.—The Control of Quality in Working Operations \*

Professor A. J. MURPHY,† M.Sc., F.I.M. (Past-President) (*rapporteur*): In the first part of this Symposium, held last year, there were five papers devoted to the production of ingots and billets in brass, copper and high-conductivity copper-base alloys, zinc and zinc alloys, aluminium alloys, and magnesium alloys. I will say no more about them except to recall that there was an introductory paper to the series by Dr. Singer, who discussed "The Principles of Technical Control in Metallurgical Manufacture". The scope of his paper was wider than the range of specific topics covered last year, and I believe that the principles which he enunciated, whether right or wrong, are equally relevant to the papers now under consideration and that we may well have occasion to examine how far these papers exemplify, ignore, or disobey them.

Professor Ford and Mr. Wistreich, who deal with sheet and strip rolling and drawing of wire, enunciate the following basic principles. The degree to which a property can be controlled depends upon the methods available for measuring it and for correcting any departure from the desired value. The degree of control actually realized then depends upon the accuracy and speed of measurement and the particular methods adopted for exercising the control. The choice of methods is influenced by both technical and economic considerations. The tolerance allowable from the standard of reference is dictated not only by the importance of the property in question but also by the cost of exercising control within the fixed limits of tolerance.

They conclude that prevention of error is the best form of control, and this demands care to maintain steady conditions of temperature, hardness, and thickness during hot rolling; strip tension, roll temperature, and roll pressure during cold rolling.

Surface finish is said to be the most important single factor determining the sales value of strip and wire, but it is not readily amenable to measurement and, therefore, to control. This view, that if you cannot measure a property, then it is very difficult to control, might be a subject for argument.

In their paper on hot and cold rolling of aluminium and its alloys Mr. King and Dr. Turner list the significant properties which have to be maintained at acceptable standards as being the tensile properties, the bending and pressing properties (in which are included earing and grain-size), corrosion-resistance, surface finish, flatness, and uniformity of gauge. One gains the impression that their approach to the problem of control is to build up an ever-increasing knowledge of the interactions between variables in processing and the characteristics of the materials at successive stages. Practical manufacturing operations are so complex that the authors distrust the efficacy of controlled experiments to reproduce all the significant factors, even though the data from such controlled experiments can be recorded with a higher degree of accuracy than observations in actual production.

This leads them to commend the statistical analysis of production results over a limited period of time without

planned experimentation. Data normally recorded may usefully be supplemented by other data reported only for the purpose of the analysis. Apparently Mr. King and Dr. Turner find this treatment helpful mainly in revealing the influence of factors which might otherwise have been overlooked or underrated. They evidently attach more importance to this than to the close examination of the relation between ranges of tolerance and the cost of maintaining them.

In his paper on hot and cold rolling of copper and copper-base alloys, Mr. Kee favours, of the methods available for gauge control, strip tension—applicable in cold rolling, and pre-determined roll setting—applicable to hot and cold rolling of sheet and strip. Both methods counter the effects of variable ingoing gauge, temperature variations, speed effects, and differences in conditions of lubrication. The paper makes a notable contribution on control during annealing, and the outline of requirements for controlled atmospheres in the case of copper and brass is particularly valuable.

Finally, the author mentions the importance of standardizing production schedules so far as possible. A number of standard breakdown gauges are adopted, and production to this stage follows an invariable sequence. From the appropriate break-down stage, further reductions follow one of several standard sequences of cold reduction and annealing cycles known to give definite tempers and grain-size and freedom from directionality. It seems to me that only in the case of gauge control does the author see a prospect of rigid mechanical control. Other characteristics are the result of numerous interacting factors, and a measure of flexibility in control methods is necessary to cope with the variations in history of the material coming forward.

Mr. Smith and Dr. Swindells attach great importance to the skilful judgment required to produce extruded material of an adequate standard in the most economical manner, especially as extrusion does not lend itself to the precise control attainable with other processes such as rolling and tube drawing. The greatest safeguards of quality are still believed to be constant vigilance, intelligent enthusiasm, and attention to apparently insignificant detail. One might sense in their introduction something in the nature of a challenge to the conception of automatic control and a shade of disrespect in the warning against substituting technological mythologies for the more old-fashioned variety.

The authors discuss in most interesting fashion the related influences of extrusion speed, extrusion temperature, and design of press, and call attention to some features where improvement of equipment would facilitate closer control of the product. It is pointed out that the really significant temperature is that of the section as it emerges from the die, and in the interests of quality it would be most valuable if this temperature could be strictly controlled. Various methods have been suggested and tried, but no satisfactory solution has yet been reached.

Mr. Whyte discusses statistical control in metal-working operations. He holds that it is seldom true that the problems

\* Joint discussion on papers Nos. 1522–1526 (*Journal*, this vol., pp. 281–344) held in London on 28 April 1954. Part I of the Symposium took place on 25 March 1953, and the papers

and discussion are printed in Vol. 81 of the *Journal*.

† Professor of Industrial Metallurgy, Birmingham University.

of an industry are not amenable to statistical treatment, and quotes examples from actual practice. He urges that sampling rates should be related to the observed indications of quality—diminishing on clear evidence of high or low quality and intensifying when quality is doubtful, and comments that this flexibility is unpopular in the non-ferrous industry, which prefers to have sampling rates firmly laid down in specifications.

The efficacy of a method of testing is not merely a function of its characteristics in respect of cost and precision, but depends also upon the variability of the production which is being tested and on the sampling procedure which is possible. The author concludes that the more heterogeneous the product, the less reproducible need be the test used to measure it, and the wider the range of samples that can be covered by repeat tests, the less is the need for a test of high precision. The trend of technical developments in metal working towards more streamlined production, increased output, and reduced costs, makes it increasingly difficult to establish error-actuated mechanical control. Statistical control provides an alternative.

In the topic which we are discussing, "control of quality" and "quality control" are not necessarily synonymous terms. It is under the former, and much broader term, that the authors involved in actual manufacture have described what they recognize as the technical factors influencing the quality of their products and how they set about controlling the quality through regulation of the variables. Little has been said about quality control in the specialized sense used by Dr. Singer and Mr. Whyte.

One gains the impression that it is in the aspect of dimensional characteristics that there is the best prospect of extending automatic control, but that in the apparently more complex field of general metallurgical qualities, good results could be obtained by a well-directed application of statistical methods.

Last year Dr. Singer reminded us that technical control was not an end in itself and enumerated the following principles:

- (i) Physical measurement of quality characteristics should be made wherever possible in order to control production with certainty at economic tolerances and rejection rates.
- (ii) A better understanding of all industrial processes involving a human operator will result from applying the principles derived from the study of automatic control mechanisms.
- (iii) A greater use of statistical methods involving a small number of products may be forecast.
- (iv) It is anticipated that advances in control of quality will be made by extending technical control to cover more of the primary variables in manufacture.

I suggest that we might usefully take as themes in the present discussion, these questions:

- (1) Has the knowledge of the nature of the processes involved in rolling and extruding metals now reached the stage where (a) automatic control of quality and (b) statistical control of quality, can be applied much more extensively?
- (2) If such an extension is feasible and desirable, what would be the consequences or requirements in a reorientation of inspectional techniques and procedures?
- (3) Is the further extension of these methods of control dependent upon superior techniques in instrumentation compared with those now available?

Mr. E. A. BOLTON,\* M.Sc., F.I.M. (Member): I should like to pay a tribute to the excellence of the papers from a practical point of view, and this is true even of such an apparently theoretical paper as that by Mr. Whyte. I find of particular interest the papers by Professor Ford and Mr. Wistreich and by Mr. Kee, where the subjects fall more within my own field of experience.

Mr. Kee rightly points out that the demands of the fabricat-

ing process often impose closer limits of impurity content than do the specifications or the needs of the finished job. This is particularly so with hot working. With hot rolling, in my own experience, it may be necessary to exercise stricter control with round billets than with flat strip in the same alloy. In the latter case, cracked edges, within reason, may be removed in the shearing discard and slight surface cracking may be eliminated by a scalping operation at, of course, some increase of cost. With a round billet intended for rod or wire, there is no remedy except the scalping of the rod, which is very costly and somewhat uncertain in its results. I believe, also, that there is a greater tendency for round billets to acquire cracked surfaces on hot rolling than is the case with flat strips, other conditions being equal.

On p. 309, Mr. Kee mentions the combined effect of tin and iron in causing fire-cracking in 70:30 brass. It would be appreciated if he could quote figures in this case. He also refers to certain elements which may restrict grain growth during the annealing of brass, thereby disturbing normal mill procedure. Something akin to this can occur with copper. It is well known that certain brands of copper wire-bars will produce rod which is appreciably harder to draw than the normal product, and this property is easily recognized by the skilled operative. Nevertheless, the resulting wire satisfies the normal tests, including that of electrical conductivity.

Several of the papers lay stress on the need for accuracy of dimensions and good shape of the hot-worked product, and it must be agreed that faulty material at this stage can be rectified in the subsequent cold working only by costly means and the expenditure of extra time, with the result that productivity is lessened, production schedules are disturbed, costs are increased, and profits are lowered—or perhaps I should say, losses are increased. Such special processing may include extra passes in cold rolling or machining operations such as scalping of strip or rod.

Professor Ford and Mr. Wistreich mention the formation of fins and laps in rod rolling and give the chief cause as incorrect roll-pass design. This is true, but accuracy of roll setting is also important and the setting and adjustment may well be in the hands of the operative. Where a rod mill is rolling a variety of alloys, the tendency to spread will vary with different alloys or even with the same alloy under different temperature conditions, which must therefore be kept under careful control. Incidentally, although on p. 282 Ford and Wistreich state that hot rolling is the first forming operation, one must not forget the importance of extrusion for the production of wire rod. Such rod may in some cases be more costly, but it is free from laps and fins and extrusion is an alternative to be considered where special surface quality is required.

With regard to the shape of hot-rolled strip, it is essential that conditions of hot rolling shall yield a strip with a cross-section suitable for cold rolling. Mr. King and Dr. Turner make some useful remarks on this point on p. 302. Control of shape and gauge of cross-section in cold rolling by cambering of rolls has been well studied for many years, and the present authors give much interesting information on the subject. Surely, however, Professor Ford and Mr. Wistreich are in error at the beginning of their last paragraph on p. 288. It is too much camber which gives a ripple in the centre of the strip, which is over-elongated. Mill operatives would say that such strip is "spouty". Too little camber would result in over-elongation of the edges, and the strip would be said to be "wavy-edged". I am sure that the authors fully understand this, but I think that there has been a slight error in the recording and that a little explanation is desirable. It is very interesting that in two of the papers there is a reference to the use of jets on the surface of the rolls to give local control of temperature and so of camber. This is a very old practice, and here, above all, the skill and experience of the roller count.

I have made reference to certain rollers' terms. The

\* Factory Manager, Elliott Works, Imperial Chemical Industries, Ltd., Metals Division, Birmingham.



roller also speaks of having a "knob" or a "gutter" on his rolls, or he may have both on the same rolls at different places, especially if the rolls are of a length which is greater than the width of strip normally produced upon them. These terms are well understood in the trade, but may be somewhat startling to a newcomer, who may expect to see something spectacular. These "gutters" and "knobs" are, however, part of the roller's means of obtaining strip of satisfactory shape coupled with evenness of gauge over the cross-section.

With round wire there is only one dimension to consider, and there is nothing to correspond with the shape of strip, provided, of course, that the wire is truly circular. This is mainly a matter of attention to the die and its contour. The die must not be allowed to become impregnated with even a trace of foreign matter, while the contour can be taken care of by inspection with one of a number of instruments developed over the last few years. We now know much more about the dies which we are using than was formerly the case, and some of the credit for this must go to B.I.S.R.A., and notably to Mr. Wistreich.

I am glad that Professor Ford and Mr. Wistreich have called attention to the need for maintaining intermediate die size on slip-type machines. Further to the reasons which they give for this, it should be added that enlargement by wear of one die throws undue work on the following one, and early failure may result. This is often given as a reason for not employing both tungsten carbide and diamond dies on the same run, as the more rapid wear of the tungsten carbide may cause the first diamond die to fail prematurely. However, provided that the danger is appreciated, they may be used in combination.

On p. 287, Professor Ford and Mr. Wistreich call attention to the possible use of a pneumatic method for the continuous gauging of wire on lines already applied in the textile industry. I should like to ask them if the method has actually been employed in wire drawing, the reference being to work which is now about four years old. Have there been any recent developments, since they mention a possible use in the case of pinion wire? Some tentative experiments using a diamond die as the orifice tended to show that vibration of the wire would be too great and that wear of the orifice might be expected to occur. It also seemed doubtful if the method would give a sufficiently quick response at the speeds used in wire drawing. In any case, the point should be noted that it is not really the wire diameter but an effect of the wire area that is measured in this method of control.

With regard to shaped wire, I would agree with the authors that we are still largely in the hands of the skilled workman. It may be noted that on p. 327 of their paper Mr. Smith and Dr. Swindells in a rather different sphere refer to the need for skilled experience in die-making.

Mr. King and Dr. Turner and also Mr. Kee have much to say on the control of temper and grain-size, with special reference to the means of attaining tempers intermediate between hard and soft. The respective merits of temper-rolling and temper-annealing are compared in both papers, and, although one refers to light alloys and the other to copper and copper-base alloys, there is agreement that a better combination of the properties of strength and ductility is obtained by temper-annealing. The latter process depends upon both time and temperature. In my view, the temperature of annealing is the primary factor and the time has to be varied in accordance with the nature of the annealing furnace and to accommodate the weight and bulk of the charge. The temperature should be as low as possible, but due regard must be paid to the avoidance of excessive time in the interests of cost of production and of productivity. The virtual impossibility of temper-annealing pure copper is pointed out by Mr. Kee, and I would agree with his view so far as any practical annealing temperature is concerned. In the annealing of certain very large coils of narrow copper strip, the centres of some of the coils remained fully hard although the outsides were completely softened. Probably

the annealing time was too short for the centres to attain the desired temperature. The point that I want to emphasize is that the margin of conditions between the outsides and insides of the coils was very narrow and yet one part was fully hard and the other part fully soft.

Referring now to temper-rolling, and, it may be added, temper-drawing, the process becomes more difficult as the final gauge of the work decreases on account of the need for greater precision, as pointed out by Mr. Kee on p. 316. The variables are as follows:

- (a) Grain-size (or degree of softness) at the ready-for-finishing size.
- (b) Strip thickness or wire diameter at the ready-for-finishing size.
- (c) Strip thickness or wire diameter at the finished size.

All these factors are subject to working tolerances.

To obtain the required temper, the amount of final reduction must be related to the grain-size before finishing, and to some extent there is a choice to be made. If the initial grain-size before finishing is reduced, the final reduction must be decreased accordingly. It is usually desirable to have a fine grain, but this entails accuracy of dimensions both before and after the final reduction, otherwise the amount of cold work and the final temper may vary widely. For this reason, with thin-gauge material, I would agree with Mr. Kee's statement on p. 316 that it may be better to use temper-annealing to obtain quarter-hard temper, and, of course, with brass this can be done. I do not think that the effect of variability of grain-size before finishing is always fully realized, but it is important both for the reasons given above and for its effect on the final product where bending or forming has to take place. We should do well to pay more attention to the grain-size of quarter-hard and annealed material. Someone has remarked upon the virtual absence of this requirement in British Standard specifications. I should be the last to urge that it should be inserted, but I think that it is of considerable importance.

I note with interest the statement by Mr. King and Dr. Turner on p. 296 that a fast rate of heating to annealing temperature generally gives a fine grain. They are referring to light alloy, but it may also be true of brass. In some experiments to obtain bright-annealed brass wire through the medium of salt-bath annealing, we found that while the wire remained bright, the very rapid heating had caused it to develop an exceedingly fine grain-size, and the temper of the final wire was quarter-hard and not soft as intended. Variations of bath temperature were without any appreciable effect on the results.

With regard to bright annealing and pickling, on p. 317 Mr. Kee states that when using burnt cracked ammonia the hydrogen content of the furnace atmosphere must not greatly exceed 4%, if embrittlement of tough-pitch copper containing 0.015-0.05% of oxygen is to be avoided. Could he say how far the relationship between permissible hydrogen content and the temperature, depends upon the temperature of annealing? In his excellent summary of the precautions to be taken in bright-annealing processes, Mr. Kee states quite categorically on p. 318 that bright annealing of the common brasses is not possible. This may be a somewhat dangerous statement to make, but so far as my own experience is concerned, I am inclined to agree with him. There seems to be a choice between material which is fully soft but not quite bright and that which is quite bright but not fully soft. The gap is a very narrow one, but I think it nevertheless exists. On the other hand, completely bright and soft nickel silver wire may be obtained, but even so, it is advantageous to introduce a light pickle after the bright annealing, as this assists the further drawing of the wire, probably for reasons similar to those quoted by Mr. Kee in the case of brass for deep drawing.

On pp. 318 and 319, Mr. Kee refers to the regeneration of pickle solutions by electrolytic means, and goes on to state

that similar solutions are used for the pickling of both brass and copper. Is regeneration by electrolytic means practised on brass pickling solutions, or is it used only in the case of copper? If not applied in the case of brass, this would necessitate different baths and different pickling solutions for the two products.

Regarding the formation of red stains in the pickling of brass if the scale contains cuprous oxide, it must not be overlooked that cupric oxide can also cause red stains through the setting up of concentration cell effects. However, in most cases if cupric oxide is present, so also will be cuprous oxide, so that the point may be a little academic.

Taken in conjunction with the statements of Mr. King and Dr. Turner on p. 305, the paper by Mr. Whyte gives much food for thought. His Fig. 2 (p. 335) points the way to a solution of problems which are constantly facing those in charge of production. For example, it appears in principle to be relevant to the matters discussed by Mr. Smith and Dr. Swindells in their first paragraph on p. 324.

In conclusion, I should like to stress the part played in the control of quality by skilled, experienced, and conscientious operatives working under enlightened supervision. This is not lost sight of by the authors of the papers. Faults

warning given by the gauge-meter may be premature; the chance that the gauge-meter will fail to give a timely warning is negligible. Operational experience will help to reduce to a minimum the interval between gauge-meter warning and the real need for action. At the moment, the point to bear in mind is that a continuous supply of information about the wire gauge, even though it may be imprecise, would be preferable to precise, but intermittent information which is being obtained at the expense of stopping the machine and which frequently is not available when required. For similar reasons vibrations of the wire, though reducing the precision of the gauge, should not seriously detract from its usefulness.

The results of laboratory work on the pneumatic gauge are distinctly promising, but works' tests are needed before final judgment on the method is passed.

Mr. J. F. KAYSER,† F.I.M., Assoc. Met.: The most important thing to remember about statistical methods of quality control is that they must be used and appreciated not only by gentlemen with academic qualifications, but must also be considered by men in the works. It is possible to educate workers, and not only skilled workers, so that they can readily understand what a histogram means. It is not wise to refer

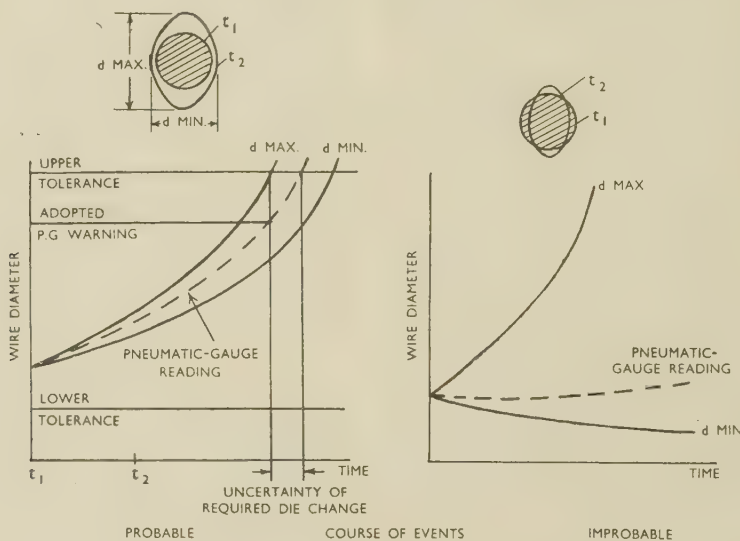


FIG. A.

can develop which, while obvious at the time to the operative, become covered up by subsequent processing. They may not be apparent in the final product, but may reappear with disastrous results when the material is in the hands of the user. However far mechanization proceeds and however far inspection methods may be developed, much of their value may be lost unless the co-operation of the operatives and lower grades of supervision is fostered to the utmost extent.

Mr. J. G. WISTREICH,\* M.Sc.(Eng.), D.I.C.: With reference to the points raised by Mr. Bolton, I agree that control of size of the intermediate die in a multi-hole slip-cone machine is important. An instrument permanently mounted inside the machine is needed, because the die is not accessible to the operator during running of the machine.

I am afraid that I cannot help Mr. Bolton with information about routine use of the pneumatic gauge, beyond what is stated in the paper. He is quite right in assuming that the pneumatic-gauge signal depends on the cross-sectional area of the wire, so that it measures the average diameter, whereas, admittedly, the maximum diameter is wanted. However, as shown in Fig. A, the consequence of this is merely that the

to standard deviation, mode, and the like; it is preferable to say "You must push it to the right", or "You must push it to the left", and whenever possible use betting terms. There are very few production procedures that cannot be statistically controlled. One problem that evaded us for a long time was its application in the control of plating baths, but that has now been achieved, and has placed the plating department on a completely new footing.

I have always been under the impression that there is nothing easier than to measure surface finish by one or other of the profilometers that are now available. We are interested mainly in strip used for making razor blades, and we have no difficulty at all in measuring its surface finish. It is indeed a simple matter to measure the surface finish of the three tiny facets which build up the edge of a safety-razor blade.

I would urge that consumers of raw materials should not labour under the impression that the cheapness of their finished product is directly dependent upon the cheapness of their raw material. Often the more expensive materials allow one to produce the cheapest goods.

I do think that it is important that the producer should take the consumer completely into his confidence so that it is

\* Head of Metal Working Laboratories, British Iron and Steel Research Association, Sheffield.

† Chief Technician, Gillette Industries, Ltd., Isleworth.



unnecessary for the latter to examine raw material when he receives it. We have established such good relationships and are so much in the confidence of most of our suppliers of raw materials, that we find it unnecessary exhaustively to examine their products. We know their methods of inspection because we have worked them out together, and we know that their production is under control. It is only when production methods are not under control, and by control, I mean statistical control, that two inspection departments are needed, one at the producer's end and the other at the consumer's end.

Dr. BØRGE LUNN,\* M.Sc., F.I.M. (Member): I would like to refer to the paper by Professor Ford and Mr. Wistreich. In the cold rolling of thin strip or foil the coefficient of friction is of very great importance. With increased speed the coefficient of friction becomes less, causing a reduction in thickness of the rolled strip (the so-called "speed effect").

We might compare the conditions in the rolling process with those in a journal bearing, the roll being the journal and the strip the bearing metal. Taking the well-known curve of Stribeck † (see Fig. E, p. 596), which shows the relation between speed and coefficient of friction, it is obvious that increased speed will decrease the coefficient of friction in the region of boundary lubrication, which is the prevalent state during cold rolling. What we need is exact information about the slope of the curve in this region. Unfortunately, very little is known about the compounds responsible for the formation of the boundary-lubrication film, even by the suppliers of lubricants!

In boundary lubrication the coefficient of friction seems to depend on the chemical reactivity of the components in the lubricant, and recent research on the rolling of foil shows that the lubricant has to contain both fatty materials and small amounts of large molecules in a mineral oil. Through boundary chemical reactions, in which the surrounding atmosphere plays a part, films of complex compounds are formed on the sliding surfaces and a quasi-hydrodynamic state is obtained—a condition which is responsible for the decreased coefficient of friction.

The problems are very complex and are further complicated by the different elastic properties of the rolling mills. To obtain full control on the shape of rolled products it is necessary to investigate more thoroughly the frictional properties of the lubricants.

Professor Dr.-Ing. P. BRENNER ‡ (Member): With regard to the paper by Mr. King and Dr. Turner, I wish to refer to the problem of earing and especially in its relation to casting. I agree with the authors that the casting process has some influence upon earing characteristics, but, naturally, it represents only one factor. I feel that the view that sheet rolled from permanent-mould ingots gives a narrower range of earing than sheet rolled from continuously-cast ingots should not be generalized, because the earing characteristics, especially of sheets produced from continuously-cast ingots, depend in a high degree on the casting conditions. It is true that continuously-cast ingots usually show a more pronounced directionality, but this can be equalized by adjustments in the subsequent operations, such as temperature of hot rolling, degree of cold rolling, and annealing.

The main trouble, in my opinion, originates from the variations in the structure and especially the preferred textures which sometimes occur in continuously-cast ingots. It is found that, after rolling, the earing characteristics vary over the length and width of the sheet in accordance with the differences of structure within the original ingot.§ It is pos-

sible to reduce the directionality as well as the non-uniformity of the structure by determining suitable casting conditions; for example, the casting temperature, the casting speed, the height of the mould, and last but not least, the distribution of the metal when poured into the mould. In our experience, continuously-cast ingots poured under such conditions give satisfactory earing characteristics even in the case of aluminium of 99.5% purity. Therefore, it is not necessary to use permanent-mould ingots when sheets with good earing characteristics are required; it may even be undesirable to do so, because their use may entail blister formation, coarse grain, segregation, and so on.

I suggest that a great advantage of the continuous-casting process is that the casting conditions can be varied and, in particular, better controlled over a much wider range than in the case of permanent-mould casting. For different types of alloy and shapes and dimensions of the ingots, casting conditions have, of course, to be selected in order to achieve the optimum quality. This problem has not yet been completely solved, and much work remains to be done in the field.

Professor H. FORD,|| D.Sc., Ph.D. (Member): I am interested in the remarks of Mr. Kee about the effect of grain-size in the cold rolling of copper. It is important to point out that the effect of grain-size on hardness or yield stress is not a simple function of grain-size alone, as far as mechanical working is concerned; it is a combined effect of grain-size and thickness of strip.

This is clearly demonstrated by the plane compression test.¶ In this test plastically deforming material is forced to move according to a certain pattern, depending upon the number of grains in the cross-section of the strip, so the resulting yield-stress curve may be modified. The effect becomes noticeable after about 40% reduction, the curve beyond this point being lower the greater the number of grains relative to the strip thickness. The difference can be as much as  $1\frac{1}{2}$  tons/in.<sup>2</sup> at about 80% reduction, but at higher reductions the curves tend to coalesce. This effect was first pointed out by Cook and Richards.\*\*

Mr. W. K. J. PEARSON,†† B.Sc. (Member): Mr. King and Dr. Turner present an excellent general account of earing, but with many qualifications. We understand their caution because, in our experience, it would be quite easy to provide exceptions to almost any assertion that one cared to make on the problem. However, we are in agreement with the general effect of many of the factors discussed.

Interactions between those factors are difficult to sort out experimentally because the influence of some of them tends to persist throughout the process. As an example of this, earing in the final sheet can be affected by very coarse-grained ingots, as mentioned by Dr. Brenner; we have even found patterns of earing in the final sheet which corresponded exactly with the positions of large grains in the original ingots.

We must agree also on the effect of casting temperature; in fact, any of the conditions in the casting stage which influence the rate of freezing of the structure, and particularly the constitutional state rather than the grain-size. Constitution, which has such a controlling influence on later-stage earing, seems to affect the recrystallization texture rather than the rolling texture. This is particularly evident when studying binary alloys. For example, binary alloys with iron, silicon, manganese, copper, or magnesium show profound effects on earing of quite small solute additions. Eventually, with sufficient addition, rolling textures can be completely retained; that is, the normal change on annealing is sup-

\* Technical Director, A/S Nordiske Kabel- og Traadfabriker (Northern Cable and Wire Works), Copenhagen.

† F. P. Bowden and D. Tabor, "The Friction and Lubrication of Solids", p. 257. 1950: Oxford (University Press).

‡ Director of Research, Vereinigte Aluminium-Werke A.G. and Vereinigte Leichtmetall-Werke G.m.b.H., Bonn (Rhein).

§ F. Plattner, *Z. Metallkunde*, 1954, 45, 254.

|| Imperial College of Science and Technology, London.

¶ A. B. Watts and H. Ford, *Proc. Inst. Mech. Eng.*, 1952-53, [B], 1, (10), 448.

\*\* M. Cook and T. Ll. Richards, *J. Inst. Metals*, 1940, 66, 1.

†† Research Laboratories, The British Aluminium Co., Ltd., Gerrards Cross, Bucks.

pressed. The influence of composition under commercial rolling conditions is also well shown by super-purity aluminium, which is quite unaffected by rolling temperature—in marked contrast to normal-purity aluminium.

Although high earing can be avoided in super-purity aluminium, the other elements in normal-purity and manganese-containing alloys considerably assist earing control, when the right processing conditions are determined. Mr. King and Dr. Turner find these conditions readily when ingot quality is constant, but it is now generally agreed that some treatment such as a long preheat is advisable to counteract casting variables.

Although the reasons for this behaviour of aluminium alloys are little understood, empirical methods now enable a low level of earing to be achieved in continuously cast metal, or even a given degree and type of earing to be predicted with some certainty. The only simple solution to the problem seems to be a very old one practised by a competitor of ours in India. Chill-cast ingots, about the size and shape of a pancake, are rolled "round the clock" into circles; they

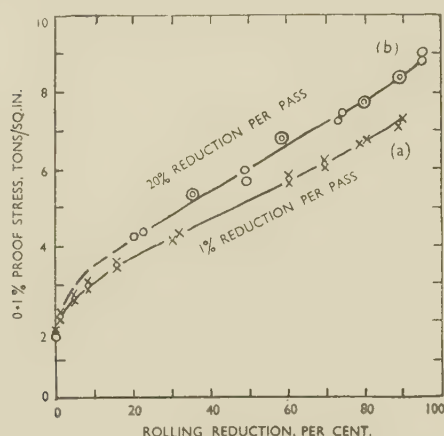


FIG. B.—Curves Obtained in Rolling 99.99% Aluminium Sheet 0.254 in.  $\times$  8 in. wide; roll radius = 7.0 in.

give no earing at all, but the middle of the circle is more than twice as thick as the edge.

With regard to control of surface finish, Professor Ford and Mr. Wistreich on p. 289 of their paper consider the effect of roll smoothness. Hot rolling of aluminium is, of course, an exception to the authors' general statement, because of the formation of a roll coating. The surface finish is determined by the coating on the roll rather than by the underlying roll condition. For example, a roll with an initial Talysurf roughness in an axial direction of about 10 micro-in. may develop an aluminium coating of many times this roughness, with corresponding roughness on the blank rolled from it. Quite stable coatings can be very thin relative to normal roll finishes, but, generally speaking, they exercise a controlling effect on the blank finish. The stability of the coating is of more importance than its roughness, because, if large pieces of the coating become detached, they may cause objectionable defects throughout subsequent rolling, whereas moderate blank roughness can be rolled out.

The observations of these authors on lubricants are very interesting and curious. Their statements on p. 290 as to the effect of lubricants with a low coefficient of friction are rather surprising, and it would be interesting to have more details of the tearing of particles from the surface. I wonder whether the phenomenon involved is the same as that we have observed in strip and have called a "matt-surface

effect". Close examination shows no removal of material, but only a depression of the surface by a matter of  $1\mu$ . Slip bands are visible in these depressions, and I believe they always occur but usually become obscured by the smearing action of the rolls between the neutral and exit planes. We know that high back tension and high contact angles promote the matt finish, presumably because they reduce forward slip. The authors show in their Fig. 4 (Plate XLIV) a somewhat similar effect in wire. It is also known in drawn tube, and in drawn sheet it is referred to as "orange peel".

I should like to add to Professor Ford's remarks about the effect of the geometry and grain-size in the plane compression test. We have found that something rather similar occurs in connection with the percentage reduction per pass in rolling. Curve (a) in Fig. B is for super-purity aluminium rolled without tension, and represents the tensile proof stress with a 1% reduction per pass. With a 20% reduction per pass one gets a somewhat different curve (b), which can be as much as 20% higher than (a). Is that because the angle of contact is not the same in the two cases and a different geometry prevails, as Professor Ford suggests?

Dr. F. A. CHAMPION,\* B.Sc., A.R.C.S., F.I.M. (Member): On p. 303 Mr. King and Dr. Turner refer to relations between the appearance of aluminium-magnesium alloys and the temperature of annealing. They give  $380^{\circ}\text{C}$ . as the temperature above which a black oxide coating is formed, but the value of  $350^{\circ}\text{C}$ . given by de Brouckère† is more in line with my own experience, and I would suggest "visible" rather than "black" oxide, since the appearance is often white rather than black, especially after pick-up of  $\text{CO}_2$  by the  $\text{MgO}$  during storage. The main difficulty in keeping the temperature down seems to be the attainment of full recrystallization, and hence the required mechanical properties in the final product.

In spite of the remark by Professor Ford and Mr. Wistreich at the beginning of Section IV of their paper (p. 289), which was interpreted even more strongly by Professor Murphy, my impression is that customers pay more attention to mechanical properties, which can be assessed numerically, than to surface finish. The proportion of reflection which is specular, as measured, for example, by the Guild photometer, does provide a valuable assessment of surface appearance for laboratory purposes. Perhaps Mr. King and Dr. Turner could give their experience on the compromise between surface appearance and mechanical properties. I should also like to know if they have found that the thin sheet envelope does in fact reduce oil staining, since in our experience the worst oil staining occurs with limited oxygen supply, which causes partial oxidation and leaves a very thin carboniferous residue.

Dr. A. N. TURNER,‡ B.Sc., A.R.S.M., A.I.M. (Member): I would like to correct any impression Professor Murphy may have gained that we have given up classical laboratory experimentation in favour of the statistical investigation of works results. That is not correct. The two methods are complementary. Laboratory work alone is often not sufficient. It is of little use, for example, developing a method for the control of earing quality for a particular commodity in the laboratory and trying to apply it directly in the works. Differences in equipment and the scale of operation would almost certainly preclude a satisfactory result being obtained. Laboratory investigations are, however, necessary in arriving at an understanding of the processes that are occurring and are absolutely essential in the planning of statistical studies in the works and in helping in their interpretation.

I was interested in Mr. Bolton's remarks about grain-size and rate of heating to annealing temperature. I should like to ask if the effect of grain-size on the tensile properties of brass is considerably greater than it is on those of aluminium.

\* Research Laboratories, The British Aluminium Co., Ltd., Gerrards Cross, Bucks.

† L. de Brouckère, *J. Inst. Metals*, 1945, **71**, 131.

‡ Head of Metallurgical Division, Aluminium Laboratories Limited, Banbury, Oxon.



I am sure that a variation in grain-size in an aluminium alloy, within normal commercial limits, would not lead to such a considerable alteration in ultimate tensile strength as to bring its properties from those of the annealed to those of the quarter-hard condition. In Mr. Bolton's experiment on the annealing of brass wire, was the increase in strength due to grain-size alone or because the material had not been fully softened?

Mr. Bolton also refers to the need for skill on the part of operatives and for enlightened technical supervision. I agree. The skill of the men in the works is very much to be admired, and is indispensable, but I suggest that the need to rely on it is a confession of lack of technological knowledge and incapacity to control the process by other means. Is it desirable to rely implicitly on the acquired skill of an operative to achieve a product? Would not some alternative, more impersonal, if not automatic, means of control, be preferable?

I agree with Dr. Brenner that the influence of the casting operation on earing characteristics is most marked, although I do not think it necessarily of overwhelming importance, as much can be done to control earing in the subsequent stages of manufacture. I suggest further that the ingot texture is not the only important factor resulting from the casting operation. Indeed, Mr. Pearson has already pointed out that constitution plays a very large part. As an illustration of this I can quote some work in which we poured ingots of commercial- and super-purity aluminium by the permanent-mould and by the direct-casting method. In the case of the commercial-purity aluminium there was a very considerable difference in the earing of the final sheet under the conditions of fabrication used, the direct-cast ingot giving the wider range. With the super-purity aluminium, which had in any case a higher earing level, there was very little difference between the casting methods. This suggests that a very important factor is the interaction between the rate of chilling and the constitution—a high rate of chilling allowing more impurities to be retained in solid solution. Composition also has an effect, interacting with rate of chilling and texture.

I agree that it may be possible to get "patterns" of earing from large as-cast grains. I suggest that this is the same effect as that noted in our paper and termed by us "ghost" structure, where we found, in the aluminium-1.25% manganese alloy, that blocks of very fine crystal size but similar orientation might be enclosed within a sheath of an elongated grain existing from a previous stage of manufacture. More information is needed about the effects of alloying elements on recrystallization characteristics. Mr. Pearson's remark that it is possible to make additions to aluminium such that the texture after annealing is similar to that existing before annealing is particularly interesting, and I should appreciate further details.

Dr. T. W. FARTHING\*: Mr. Bolton has asked for the levels of tin and iron necessary to cause fire-cracking in  $\alpha$ -brass. What are Mr. Kee's views regarding the tendency to fire-cracking in Admiralty brass? If tin and iron contents are important in  $\alpha$ -brass, presumably of 70:30 composition, does it mean that the iron content is much more vital in Admiralty brass, which already contains 1% tin?

Although in this symposium we are considering quality and the difficulties of controlling quality in only two main fields, rolling and wire drawing, I must express surprise at the notable omission of tube drawing. The rolling and wire-drawing problems reported apply equally to tubes, but do not seem to be capable of such direct correction, largely because, with a fixed die and an internal plug or mandrel, which is to all intents and purposes "floating" inside the die, it is very difficult to impose automatic methods of control. One has the same surface area in a tube as with

strip of a similar size, but one side is virtually inaccessible and therefore, particularly with small-diameter tubes, inspection is not always easy.

This matter may be more important with tubes than strip and sheet, because the conditions of acceptance are possibly rather more rigid. The condenser-tube specification, for instance, is very strict indeed. I appreciate that with sheet, one encounters the deep-drawing problem, but with tubes also drifting is frequently called for, and defects such as score-marks from the mandrel can lead to splitting during this operation. Again, tubes are, on the whole, subject to more intense conditions of corrosion than are strip and sheet: severe attack can be initiated by the trapping of a deposit, such as sand, at a lap or other defect, and irregularities in the bore of a condenser tube can lead to serious problems of impingement attack and other common phenomena. On conditions of use alone, therefore, tube quality is of vital importance.

Finally, quite apart from quality, there is the actual mechanism of tube drawing. One can do three things in drawing a tube: sink it with no control over the gauge; reduce the gauge without appreciably reducing the diameter; or reduce both gauge and outside diameter. These methods produce tubes with very different properties, for example, a sunk tube is much more susceptible to season-cracking than one in which wall and outside diameter have been reduced together.

I feel that there is a definite need for an up-to-date appraisal of the techniques and problems of tube drawing, and consider that the scope of the present symposium could have been profitably enlarged by a paper on this subject.

Mr. L. O. CARTWRIGHT,\* A.I.M. (Member): In connection with the annealing of H.C. copper, Mr. Kee refers to varying types of charge annealed in atmospheres containing 2-3% hydrogen at temperatures up to 550°C. I should like to know if, in dealing with finer sizes of H.C. copper wire and strip, he met with difficulty in regard to "stickiness" in the annealed coils, as this can be a serious factor in subsequent operations involving decoiling. Our own experience is that annealing temperatures must be kept low to avoid this trouble, and I wonder whether Mr. Kee can give us any further pointer as to how it may be avoided.

Mr. Kee also refers to annealing of lubricant-contaminated materials in controlled atmospheres. This problem confronts most of us when using this type of annealing equipment, but in Mr. Kee's paper the treatment represents accommodation of an undesirable alien. The charge is heated for  $\frac{1}{2}$  hr. at 200°C. in order to drive off the lubricant and the temperature is then raised for annealing the charge. This must represent inefficient use of the annealing plant, because of the extended time required for dealing with a charge in this manner, and some residual of the lubricant would be left on the material. The vapours from the lubricant would collect in the filters of the plant, and this would occasion very frequent changing of the filters.

With regard to the pickling of brass, I shall be pleased to hear Mr. Kee's reply to Mr. Bolton's point, as it has always been our contention that saturation of the solution with zinc would occur and that electrolytic pickling of brass would be uneconomical from that point of view.

Comments have been made about co-operation between the consumer and the producer from which some beneficial effects are said to have been derived. We are always praying for co-operation in the reverse direction, and I sincerely wish that any consumers present will take note of this plea for co-operation, especially in regard to their end uses of our products.

Mr. W. W. KEE,† B.Sc., F.I.M. (Member): In discussing my paper, Mr. Bolton and Dr. Farthing have raised the

\* Imperial Chemical Industries, Ltd., Metals Division, Birmingham.

† Director, Enfield Copper Refining Co., Ltd., Brimsdown, Middlesex.

question of the influence of tin and iron on the fire-cracking of brass. In the paper reference will be found to the effects of individual impurities, and I cited the case of tin and iron as one where individually they may be harmless but combined they can be harmful in promoting fire-cracking. This factor does not give rise to serious trouble in practice with the straight brasses, and we have no direct experience in the working of Admiralty brass as mentioned by Dr. Farthing. I am sorry that I cannot quote any upper limits for tin in the presence of iron. The matter has also been reported upon by Gibbs,\* but I do not think he quotes any figures.

I have been asked about the permissible hydrogen content of burnt cracked-ammonia atmospheres at various temperature levels. In the case of tough-pitch copper annealed at 350°–400° C. the hydrogen content may be, say, 5%, and I know of one plant where up to 6% hydrogen has been used without any trouble. At 500°–550° C. the hydrogen content should be reduced to less than 3%. In general, as the temperature rises, the amount of hydrogen that can be tolerated decreases. The conditions are also influenced by the quantity and type of rolling lubricant present on the stock being annealed.

Another question concerned the electrolytic regeneration of brass and copper pickling liquors. Our practice is to have a single circulating system to which are fed pickling liquors for both materials. Zinc build-up in solution controls itself by drag-out losses from the whole system, and has never given any trouble at all. The zinc content averages between 4.5 and 6 g./l. The copper is recovered as cathodes from the electrolytic cells. These may be expected to become powdery if the zinc content becomes excessive, and then the current density must be reduced.

In reply to Mr. Cartwright's enquiry about the sticking of copper coils during annealing, we do not encounter any serious trouble. As far as H.C. copper is concerned, there are only rare instances of trouble with tightly-wound coils during annealing; with phosphorus-deoxidized copper sticking sometimes occurs, and we have found no solution so far.

Mr. Cartwright also queried the inefficiency represented by the furnace time lost in removing the rolling lubricant. I agree that more frequent cleaning of oil scrubbers is involved, but this causes little inconvenience or expense. If one has, for one reason or another, to deal with excessively oily stock, there appears to be no satisfactory alternative.

Mr. K. E. THOMPSON,† B.Sc., A.I.M. (Member): I propose to confine my remarks to the paper by Mr. Smith and Dr. Swindells.

It is gratifying to know that aluminium can stand comparison with copper, except perhaps in the type of metal flow produced during extrusion. Copper can apparently take care of itself, since it is self-lubricating, but aluminium alloys which extrude with a non-lubricating type of flow present some difficulties.

The authors state that pure aluminium is effective as a lubricant for strong alloys. I understand that glass has been used in a similar manner, and it would be interesting to know whether it can be regarded as a serious rival to aluminium in this field.

It is true that there are definite advantages in ensuring effective lubrication, but the authors do not pretend that their method is an easy one to apply. Furthermore, it would appear to have two disadvantages, one being a thin aluminium clad surface on the extruded section and the other an increasing tendency for the presence of sub-surface defects, as in the case of copper. On the other hand, the normal practice in extruding strong alloys provides comparative freedom from

sub-surface defects, but gives an outer band of coarse grain after heat-treatment.

Have we, therefore, reached a stage with the lubricated extrusion of aluminium alloys where any further development will increase the difficulties of obtaining products free from sub-surface defects? If this is the case, ought we to re-assess the possibility of producing strong alloys by quenching at the press to overcome these difficulties? One suggestion is that the strong alloys could be extruded by the normal practice, followed immediately by a rapid boost to heat-treatment temperature in an induction furnace, and, finally, water-quenched. Such a method presents enough advantages to justify its serious consideration, and I should be glad to know if the authors have already considered this possibility, and, if so, what conclusions they have reached.

Mr. R. W. ELKINGTON,‡ B.Sc., A.R.S.M. (Member): Mr. Smith and Dr. Swindells mention on p. 329 the value of controlling the egress temperature of an extrusion. There appears to be no satisfactory direct way of doing this. It may be pointed out, however, that for alloys of the Duralumin type this temperature is often related inversely to the temperature of the billet before entry into the container, all other factors being equal. Experiments have shown that a fair measure of control of the egress temperature can be obtained by a rigid control of the billet temperature and the extrusion speed.

The effects of contaminated furnace atmospheres mentioned on pp. 331 and 332 are particularly interesting and important. Independent work by Stroup§ and by Barker,|| presumably well known to the authors, has drawn attention to this. These workers have shown, in particular, the effects of sulphur compounds and moisture in the furnace atmosphere. In the case of those extrusions which usually exhibit the coarse-grained peripheral zones after solution-treatment, the effects are shown as deterioration at and near these grain boundaries, which markedly affects mechanical properties. The defects are apparent after quenching, and are believed to cause cracking similar to that resulting from overheating. Whilst, in dealing with the effects of furnace atmospheres, the authors have confined themselves to blister formation, it would be interesting to know if they have observed such cracking in the Duralumin-type alloys which could not be readily attributed to prior overheating.

In discussing heat-treatment, the authors refer to the "hot humid atmosphere" of the furnace. Could they perhaps give figures in this connection indicating some critical moisture content, together with sulphur content, above which quality is impaired? They provoke discussion on the difficulty of obtaining reproducible results from experiments on the effects of furnace atmospheres carried out in laboratory furnaces. This is an interesting point, since we have experienced similar difficulties, and may indicate either that the conditions existing in the larger furnaces are not readily reproduced or that they are not fully understood.

Dr. C. E. RANSLEY,¶ M.Sc., F.I.M. (Member): I would like to comment on the point, raised by Mr. Smith and Dr. Swindells on pp. 331 and 332 of their paper, regarding the somewhat obscure effects of furnace atmosphere in relation to the blistering of extruded aluminium alloy sections and, particularly, alloys containing magnesium. Mr. King and Dr. Turner also refer to this question briefly in their paper.

Leaving out of account the possibility of overheating, which can be recognized without any difficulty, it has been known for a long time that heat-treatment can produce deleterious effects under certain conditions. It has equally

\* L. E. Gibbs, "Cold Working of Brass". 1946: Cleveland, O. (American Society for Metals).

† Northern Aluminium Co., Ltd., Rogerstone, Mon.

‡ Aluminium Laboratories Limited, Banbury, Oxon.

§ P. T. Stroup, *Symposium on Controlled Atmospheres:*

*Amer. Soc. Metals*, 1942, 207.

|| L. J. Barker, *Iron Age*, 1946, 157, (19), 60.

¶ Research Laboratories, The British Aluminium Co., Ltd., Gerrards Cross, Bucks.



been recognized that certain fluoride vapours can have a very beneficial effect in offsetting these conditions, and Aluminium Laboratories Limited, have an early patent in which various compounds suitable for introduction into the furnace for this purpose have been described. There is no doubt that only very small amounts of fluoride are necessary to produce the desired results.

Both the present papers quite rightly stress the importance of protecting the material as far as possible from the products of combustion in fuel-fired furnaces. I would like to emphasize that, in addition, these deleterious effects can also occur in electric furnaces, and stem from the same cause. Some quantitative data we have obtained in experimental work on this subject may be of general interest.

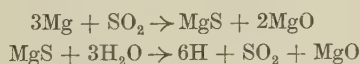
The blistering is caused by an excessive pick-up of hydrogen from the atmosphere in the heat-treatment furnace. The main point is that although water vapour by itself can lead to some absorption of gas, the real trouble with which we are concerned is caused by traces of sulphur, which appear to act in a catalytic capacity. The remarkable effect of sulphur may be illustrated by the results we obtained in some tests on H10 alloy (an  $Mg_2Si$ -type alloy) in the form of extruded and drawn tubing. This material was solution-treated in an electrically heated laboratory furnace under very carefully controlled conditions. The standard atmosphere in the furnace was clean air, moistened by passing through a water-bubbler at room temperature, and into this we injected various percentages of sulphur dioxide. The hydrogen content of the metal, after solution treatment at 540° C. for 30 min., was determined by vacuum extraction, with the following results:

$SO_2$ , %	Nil	0.2	2.0	8.0
$H_2$ , c.c./100 g.	0.16	2.4	3.0	2.6

The same effects were produced by traces of sulphuretted hydrogen. In the entire absence of sulphur, however, the gas pick-up even in 100% steam was only about 1.0 c.c./100 g.

When it is remembered that the solubility of hydrogen at atmospheric pressure is only about 0.02 c.c./100 g. at 540° C., the amount of gas absorbed in the presence of sulphur is extraordinarily high, and represents the possible development of internal pressures of many tons/in.<sup>2</sup>. But although we have found that the gas-absorption effects are very reproducible, it does not follow that blistering of the metal always takes place. This depends upon the quality of the metal being treated, i.e. whether there is any porosity in it inherited from the cast ingot or billet, and the control of this factor was discussed in the symposium last year.

The mechanism of the reaction can probably be represented as:



It is a characteristic of this reaction that a certain amount of staining of the alloy takes place, and if the material is allowed to air-cool to room temperature, by a slight but distinct smell of  $H_2S$ . Magnesium sulphide is very readily hydrolysed and the smell fades away fairly rapidly. Quenching, of course, destroys it immediately.

Pre-exposure of the metal to HF vapour or the introduction into the furnace of a fluoride slightly volatile at the heat-treatment temperature completely inhibits the reaction, presumably by the preferential formation of a stable magnesium fluoride film.

As mentioned earlier, these deleterious effects can occur in electric furnaces and are accompanied by the same characteristics. The source of sulphur in this case is very probably the oils used for drawing and rolling, and some control over this factor might be possible.

Mr. F. KASZ,\* B.Sc., A.R.Ae.S. (Member): We are indebted to the authors of these valuable papers for further advancing our knowledge of what we do. Perhaps one may be forgiven

for wishing that, in places, greater emphasis had been laid on control of what we do.

For example, preheating may involve, or be preceded by, a long soak at temperature—the so-called homogenization treatment. Such treatment may be deliberate to relieve internal stresses, to promote a closer approach to constitutional equilibrium, and to facilitate hot working. To achieve the aims, both temperature and time must be controlled, since these determine the rate and extent at, and to which, the diffusion processes proceed.

But just as homogenization may be beneficial in some cases, it may be undesirable in others. For example, if gas control has been inadequate, homogenization may accentuate blisters; it may cause giant grains in commercial-purity aluminium after high reductions and an anneal at 480° C. (some 70° lower than suggested by Mr. King and Dr. Turner); and it may lower the proof and ultimate tensile stresses of heat-treated strong alloys by 0.3–0.7 tons/in.<sup>2</sup>. Even when it is sought, for these reasons, to avoid homogenization, it may occur, in some degree, inadvertently—for example through two-staging. We should welcome more specific information on the kind of control exercised to obtain the desired results of homogenization and to avoid the unwanted effects.

Mr. Kee avoids homogenization and prefers to heat as rapidly as possible, for fairly obvious reasons. It would be interesting to learn whether the introduction elsewhere of semi-continuous casting of copper alloys has created a need for homogenization.

Mr. King and Dr. Turner favour the large, continuous preheating furnace on the ground that it gives closer temperature control. Providing long runs on the same alloy and slab size are possible that is so; but if frequent changes of programme are required, as Mr. Smith and Dr. Swindells have indicated, there is a great deal to be said for a larger number of small batch furnaces.

While the copper-base alloys are normally heated as rapidly as possible, internal stresses and non-equilibrium eutectics often limit the heating rates used for light alloys—a point to which Mr. Smith and Dr. Swindells refer. Are they able to say what those limiting rates should be on the different alloys?

Mr. King and Dr. Turner state that after homogenization the fastest possible heating helps to avoid crocodiling and edge cracking. It is not clear why this should be so. We have observed rapid heating of 48 in. × 8 in. slabs to cause temperature differences up to 50° C.; and the associated temperature gradients might be expected to lead to just the sort of deformation that would aggravate these defects. Would the authors care to comment further on this?

The same authors also state that wide ingots take longer to reach soaking temperature than narrow ones. This is to be expected if length and thickness remain the same, but it is somewhat misleading if applied to a second reheat after first-stage cross rolling. In this case the wider—and thinner—slab will demonstrably heat faster owing to the greater surface-area : volume ratio.

Another point which is a little puzzling in King and Turner's paper is the observation that a longer preheat time increases 45° earing, while two-staging increases 90° earing. In so far as two-staging involves a longer preheat time, the statements appear to be in contradiction. Could the authors clear up this point?

In hot working, the difficulty of control is accentuated by the fact that operations are rarely completed above the recrystallization temperature. As an example, we find that, even with the closest control, the temperature at 0.25-in. hot-rolled gauge may vary from 160° to 300° C., and 0.1% proof stress from 11 to 15 tons/in.<sup>2</sup> in the case of a 3.5% magnesium alloy.

These problems of controlling temperature and associated properties seem likely to be most accentuated in extrusion, where temperatures may fall or rise, and it would be interest-

\* Head, Experimental Department, The British Aluminium Co., Ltd., Falkirk.

ing to learn from Mr. Smith and Dr. Swindells whether there is any hope of better control through more effective heating or cooling of containers.

The drafts used are relevant to this question of temperature control. These drafts are normally limited by the mill horse-power, having regard to shape control, but some control can be exercised within limits, and is important in respect to crocodiling and edge cracking, as well as to other defects. It would be interesting to learn what those drafts are and how they and their effects compare for the different alloys and slab sizes based on aluminium and copper.

It is the practice in some light alloy works to control edge cracking by edge rolling, but not a great deal appears to have been published about this. Can Mr. King and Dr. Turner enlighten us further on its success? The same authors also deal with cladding and suggest that it is adequately controlled by using clean cover plates of correct thickness. I suggest—and I am sure they are aware—that there is much more to it, if we are to have a uniform and undiffused coating on both sides of the finished sheet. The covers themselves must be of appropriate quality, and their size, the rolling-pass schedules, and mill pass-line height are all relevant.

A point which has been the subject of comment by Mr. Pearson (p. 586) was raised by Professor Ford and Mr. Wistreich, i.e. the importance of the roll's smoothness to surface finish. Mr. Pearson points out that in the case of light alloys, roughness is conditioned by the coating of aluminium. Dr. Turner and Mr. King rather suggest that the control of that coating is almost entirely a matter of the control of the soluble oil. Do they consider that current control methods are adequate? With heavier drafting and high outputs, do they think that we should have recourse to supplementary means of coating control, such as wipers and rotary wire brushes, which are used in some cases? Could Mr. Kee advise whether similar problems of coating control arise in the copper industry, even though in that case the hot-rolled blank is scalped and the question of surface defects probably does not arise?

Professor Ford and Mr. Wistreich have also stressed, as have other authors, the importance of regulating the mechanical properties, shape, gauge, surface condition, of the hot-rolled blank, if subsequent cold rolling is to be adequately controlled. In this connection, I might mention an interesting example of inadequate control which we encountered some years ago. In one works, hot rolling could be completed at 0.25 in. on a two-high mill, or the part-rolled slab could be passed straight on, at some intermediate thickness without reheating, to a four-high mill, where the reduction to 0.25 in. was completed. Pure unannealed blanks from the four-high mill required 20% more power than corresponding blanks from the two-high mill, when subsequently cold rolled from 0.250 to 0.180 in. But on tensile testing, the blanks finished on the four-high mill showed proof stresses significantly lower by 1 ton/in.<sup>2</sup> than those finished on the two-high mill. The question arose, therefore, whether the 20% increased power requirement was due to some internal metal characteristic not reflected in the tensile test, or to some surface-finish characteristic associated with the different mills. Perhaps the various authors would care to comment on this.

In cold working, the primary aim is to reduce the cross-sectional area to the required shape and size; but the methods are controllably varied to give acceptable finish and other qualities, such as strength, grain-size, and directionality in the finished product.

In temper-hardening, the practice of controlling final reductions to give different work-hardened tempers is common to the aluminium and copper sheet industries. Figs. 1 and 2 (p. 292) and Table I (p. 294) of King and Turner's paper illustrate the sort of control which can be exercised. I would agree with most of the figures in Table I, but would question the bend radii for the as-rolled condition, which seem far too high. For example, on the same alloy given 50% reduction to 0.064 in. gauge we obtain 2.5–3T instead of the 9T shown.

Precise gauge control is, of course, important to work-hardened property control, and to subsequent forming operations on the sheet. The demand for close weight control in modern aircraft has accentuated the need with strong light alloy sheets. The weaknesses of manual control and the need for precise automatic methods have become increasingly apparent as strip-rolling speeds have increased. The methods described by Professor Ford and Mr. Wistreich, initiating the error signal in roll-force meters, seem promising. Could the authors advise whether such control systems would require recalibration for different alloys of different yield points and work-hardening characteristics?

That cold work affects both grain-size and the tensile properties is generally true. But I suggest that it is perhaps a little misleading to say, as Mr. King and Dr. Turner do on p. 297, that the grain-size of batch-annealed strong alloy is progressively higher, the higher the finishing reduction. This is true in some cases, but there is here an undoubted interaction with the annealing conditions, as for the copper alloys mentioned by Mr. Kee; and with the slow heating rates common to normal annealing muffles, the effect of reductions may be negligible. The following figures for an Al-Cu-Mg-Mn alloy illustrate this point:

TABLE A

Finishing Reduction, %	Grains/Linear In.	
	Time to 360° C. 2 min.	Time to 360° C. 3 hr.
20	240	230
30	240	270
50	450	260
80	960	250

Even when finishing reductions are the same, it has been observed on more than one occasion that the same composition, strip-mill rolled, will give different tensile properties from that sheet-mill rolled. Mr. Pearson has perhaps brought one factor to our attention in showing that after a given total reduction, the yield point may vary according to the reductions on the individual drafts. Measurements have shown that the coiled strip, after rolling, may have a temperature of up to 100° C. and the temperatures on leaving the roll gap must be much higher. In strip rolling, do we in many cases cold work and follow by immediate recovery to some degree? Are the effects of any such recovery further reaching than the mere tensile properties would reveal? It would be interesting to have further comments on that point.

In controlling the shape and size of any forming orifice, be it roll-gap, extrusion, or wire-drawing die, many effects of the vital friction force are still not certain. It is not very clear why increased speed reduces the friction coefficient, although one contributor has attributed it to improved lubrication. Is some factor such as increased acceptance angle involved?

Annealing in particular is an operation whose control is subject to the influence of earlier processing and subsequent requirements. Primarily aimed at softening, annealing conditions must be set with a regard for grain-size, earing, and oil staining. To achieve the required results, heating rate, maximum temperature, time at temperature, cooling rate, and in some cases atmosphere composition, all call for control.

Unfortunately, too many industrial furnaces give quite inadequate control of heating and cooling rates, and even in the regulation of maximum temperature and time-at-temperature, the common practice, mentioned by Mr. Kee, of calibrating a furnace to run for a certain time with controlled heat inputs is not altogether satisfactory. The error signal is not usually initiated in the metal temperature itself; and the relationship between metal temperature at different parts of the charge and the error-correcting linkage varies widely with the nature and weight of the charge. The difficulties are further accentuated when we come to low-temperature treat-



ment, such as partial annealing or precipitation treatments. The difficulties are largely inherent in having to transmit heat down a temperature gradient, and it would be interesting to learn whether any real progress has been made to give controlled precision heating with induction or resistance methods generating the heat where it is wanted—in the metal itself.

Reverting to grain-size and tensile property control, Mr. Kee's industry uses grain-size assessment as a control over properties. Professor Ford (p. 585) has shown one point where that might go astray. I might mention another aspect. Some time ago we carried out experiments in which hot-rolled blanks of an Al-Cu-Mg-Mn alloy were sheet-mill rolled to give sheets at 0.051 in. gauge with finishing reductions from 10 to 80%. Halves of the sheets were muffle-annealed at 365° C. for  $\frac{1}{2}$  hr., the time-to-temperature being 3.5 hr. The remaining halves were salt-bath annealed at 365° C. for  $\frac{1}{2}$  hr., the time-to-temperature being only a few seconds. In each group, the tensile 0.1% proof stress was greater the finer the grain. But the two groups of plots did not lie on the same curve. The indication was that even when the grain-size was the same, the salt-bath annealed material had a 0.1% P.S. about 0.75 ton/in.<sup>2</sup> higher than that of the muffle-annealed samples. The figures suggest that something more than grain-size is involved, and it would not seem to be Professor Ford's gauge effect, in so far as gauge was constant. Perhaps members would care to comment on this.

Mr. King and Dr. Turner suggest that atmosphere control might be responsible for blistering in unclad alloys, and I think there is no doubt that this can be so. But are they satisfied that the material under observation had a sufficiently low gas content? Many years ago we experienced blister trouble with unclad D.T.D. 603B, and in the course of investigation, an ingot was clad over only half its surfaces. After rolling down to sheets, there was therefore one sheet in the middle, half of which was unclad, the other half being clad with a coating the thickness of which varied from near nil at the junction to the full 5% further along the length. After heat-treatment, it was observed that the number of blisters/ft.<sup>2</sup> decreased steadily from quite a high value at the unclad portion, through the region of thickening cladding, to nil where the cladding thickness was 5%. It seemed that the cladding would inhibit a certain amount of porosity from developing into blister, and that unclad metal therefore demanded a lower gas content. Action based on that interpretation has been reasonably successful.

The practicability of partial annealing depends, as Mr. Kee rightly observes, on the rapidity with which the required property falls with increasing time-at-temperature. It is true, as Mr. King and Dr. Turner say, that there is a certain amount of latitude in controlling the process, but I certainly do not think that that latitude justifies the adjective "considerable" which they attach to it. For example, with commercial-purity aluminium, whose process-history has been controlled much more rigidly than is normally necessary, an increase of 5° C. in partial annealing temperature will completely alter the temper from half-hard to quarter-hard. The problems of controlling industrial-sized loads to these limits need no emphasis. The softer the temper aimed at, the nearer is the approach to recrystallization temperature and the rapid property fall mentioned by Mr. Kee. This may make partial annealing difficult to control adequately, even for the aluminium-magnesium alloys, which are normally less sensitive. On occasion, one can find control rather knife-edged.

It has been stressed in discussion that the partially annealed product has the best combination of strength and ductility. Notwithstanding the advantages, I feel that that is something which should be weighed with caution. Although the ductility, as measured by general elongation on the 2-in. gauge-length of a tensile test-piece is better than that on

temper-rolled material, the bending and forming behaviour of partially annealed material, depending on local elongation—as mentioned by Mr. King and Dr. Turner—may be markedly inferior.

In his excellent paper, Mr. Whyte pleads for extended use of statistical methods in quality control, and in compelling examples shows how usefully they can be applied. The author has amply demonstrated the value of such methods in our own organization, and it is clear that Mr. King and Dr. Turner are equally alive to their advantages.

But if in other quarters there is some resistance to their wider adoption, as Mr. Whyte suggests, perhaps it arises from their advocates' enthusiastic over-emphasis of certain aspects.

A particular method of handling process data may do no more than evaluate the uncertainty inherent in the process. That is, of course, a vital first step towards improving the process, but of itself it may do nothing to increase the certainty of obtaining a desired result. An executive will rarely be satisfied that a process is in control if it merely satisfies Shewhart's definition as being one whose future behaviour can be predicted within calculable limits. A process may meet this criterion while yet having too low an average and too widely variable an achievement to satisfy him. For example, Mr. Whyte's method of calculating the most economical input weights is the most satisfactory, even if the average recovery is 30%, with individuals scattered between 10 and 60%. But the executive's real worry would be to raise the average recovery to, say, 70%, with individuals scattered only between 69 and 71%. Thus, the executive will consider his process in *adequate* control only when the *desired* result can be predicted with *high* certainty. In other words, he will be happier to know, relatively imprecisely, how precise his processes are than to know precisely how imprecise they are.

It may be that some executives will remain unconvinced by statistical control of processes which they consider inadequate, until they appreciate that that control, allied to statistics' other techniques and to the normal research methods, can be a powerful aid in raising process performance to an adequate level of precision and achievement.

The basic materials for the statistician are, of course, the arithmetical data collected on the process, and Mr. King and Dr. Turner plead for the recording of "as much information as possible". Intelligently done, as I am sure in their case it would be, I agree; but otherwise there may be grounds for reserve.

The process data contain the error signal. But it is in code. And the brains of the statistician and his colleagues must be used to decipher it and to initiate the correction. General observation suggests that so long as the human mind is as it is, it is only necessary to feed enough information into it fast enough to paralyse its powers of thought. I sincerely believe that in this paper-ridden world there is a grave danger of substituting masses of paper for incisive thought; and it may be that our industries, sometimes accused of failing to do enough, are failing in places through trying to do too much. There can be no doubt whatever that a day may be well spent in calculating that the average rejection has been 10%; but I suggest that on occasions, the day might be better spent in reducing the rejections to, say, 5%.

Mr. F. KING,\* A.I.M. (Member): Mr. Kasz has asked some questions on the hot rolling and cold rolling of aluminium, with reference to our paper. As regards the earing effect, the long preheat is a 45° factor and the two-stage preheating is a 90° factor. In the case quoted, there had been some hot work between the first and second preheat or reheat, and in this respect the second reheat had much the same effect as an anneal of the hot slab, which is a 90° effect.

We find that one of the most important factors affecting the uniformity of Alclad coating, i.e. thickness of coating, is the initial hot-mill reduction. It is necessary to measure the

\* Works Metallurgist, Northern Aluminium Co., Ltd., Rogerstone, Mon.



ingot before preheating, to note the overall thickness of ingot and plate, and to adjust the first pass in accordance with the total thickness of the sandwich.

As regards coating on the surface of hot-mill rolls, we favour control by soluble oil emulsions which are used for roll cooling and roll lubrication. Other methods are available, such as wire brushes. The objection to these is that they disintegrate during use, and although one can control the coating, in the end the slab may have iron wire rolled into its surface. Wipers or scrapers offer another alternative. A fairly rigid scraper is needed to remove the aluminium coating from a hot-mill roll. One may succeed in removing the aluminium coating but in the process produce grooves in the rolls, so that the final stage is worse than the initial stage.

Mr. Kasz has stated that in certain cases he found partial annealing to be a question of knife-edge control; a matter of 5° C. would result in the difference between obtaining quarter-hard material and a fully annealed material. This is true, particularly in trying to partially anneal a material which has been heavily cold worked, but in trying to get the softer tempers, such as quarter-hard, it is better not to give very heavy reductions. Another way of avoiding knife-edge control is to sacrifice fast annealing and to use a lower temperature and a longer time.

Mr. N. I. BOND-WILLIAMS,\* B.Sc., A.I.M. (Member of Council): As Mr. Smith and Dr. Swindells say, there is a considerable factor of ignorance on extrusion. Probably the most dangerous thing they say in the paper is that "modern practice has been built up on the basis of experience and by any standard must be regarded as reasonably satisfactory." When I read that, I asked myself what standard they were using. There was no standard that I could find. As I felt the paper might have been improved by the incorporation of numerical information which would help us to formulate some standards, it seemed that the simplest thing was to go to our factory and discover the figures which I thought the authors should have included.

Unfortunately, I was forced to the same conclusion, there are no standards and the factor of ignorance is very great indeed. It seems to me that we might attempt to continue the good work which they have started by pooling such information as we can, in order to reduce this area of ignorance.

Mr. Smith and Dr. Swindells refer, first, to the quality of the original billet. My interest is essentially in high-copper alloys and particularly in high-conductivity copper, and I will refer only to that fraction of the paper which deals with those two materials. Our company has found that a valuable aid in achieving control over the quality of billets is a fairly recent development in non-destructive testing—electronic conductivity testing. We believe that this alone has reduced our rejections at subsequent stages by something like 1%, which is quite significant.

Next, there is a structural effect arising from the method of casting to which Mr. Smith and Dr. Swindells have not referred, but on which they might be able to give some enlightenment. We have repeatedly noticed, and believe it to be a fact, that whereas copper behaves similarly in extrusion whether it is cast in a water-cooled mould or an iron mould, the high-copper alloys, particularly brasses containing between 65 and 68% copper, with lead or tin additions, are easier to extrude when cast in a chilled iron mould than when cast in a water-cooled copper mould. In order to overcome the disadvantage of the billet cast in the water-cooled mould, we have found it necessary to give it very extended heat-treatment before extrusion.

I am afraid that I cannot entirely agree with the authors' remarks on furnace control. This may be due to the unreasonable attitude of the executive and not to the reason of the metallurgist. We are being pressed all the time, in order to reduce cost and increase output, to increase the extrusion ratio; and as this is increased it appears to narrow

the tolerance of the other factors to which the authors refer, particularly the factor of temperature. In some cases we are working in a tolerance range of about  $\pm 5^\circ\text{C}$ . If we go over the top, the stuff melts as it comes out of the die and is of little use; it makes a mess of the press and takes a long time to clear up. If we go 5° C. down, it sticks and there is no product. We believe it to be virtually impossible, at the temperature which we are using, for manual operation of the furnace to work within those limits, and we feel obliged to control the furnace by automatic means. We appear to have achieved some success in doing so, because we are now able to operate economically, with high extrusion ratios, whereas previously, with manual operation, that was impossible.

A further consideration which justifies automatic control at this stage is atmosphere control. Auto-control aids production of a regular atmosphere in a furnace running at about 950° C., oil-fired with 24 burners, which is virtually impossible with manual operation. With automatic control designed to give a long cycle on one level of control and a short cycle on the other, the unbalance in the generation of atmosphere from the burners is considerably reduced. I quarrel with the authors on that point and would ask them for more up-to-date information about it.

A further factor which they do not mention as affecting extrusion quality is that of fatigue on the part of the operator, or team of operators. Mr. Kasz has referred at greater length than did Mr. Smith and Dr. Swindells to the choice between personal and impersonal controls. I have cited a case where it was necessary to make the control impersonal because it appeared to be beyond the capacity of a man to operate the controls. With fatigue, we have a separate problem, in that the team are able to operate the controls when they are fresh, but are not able to do so when they are tired and the performance then lags both in quantity and in quality. We believe that under the heading of press design a great deal more could be done to improve the type of control system, particularly in the case of hydraulic presses. For example, speed control is an important variable in production of good work, and yet almost every accumulator system has a speed-control device which demands a very great deal of physical output by the operator. It is not surprising if, towards the end of a long shift by a hot machine, and generally in front of a hot furnace, the lever is not moved with quite the vigour which is required. It is the experience of my company that this sort of work should have a great deal more power assistance and that with such assistance it is possible to achieve a very much higher quality. That also applies to some of the auxiliary operations, such as the separation of pads from butts.

Finally, the billets themselves should be handled by power. In many small presses even today it is customary for quite large billets to be handled by a man with tongs. That has the disadvantage that the transfer time between the furnace and the press is extended, and further damage to the billet surface takes place.

As to the use of statistical quality control to isolate damaging factors, I can give a precise example. A section of copper which we were producing was found to vary considerably in size. By taking out a series of statistical records we discovered a fact which had hitherto escaped us—we were stretching the material by applying too much torque to the coiling machines. This aspect had not been entirely overlooked in the design, for the coiling machine was built with an air motor in order that there could be control, that the coiler could adjust itself to the speed of the press, and that it could be stalled, which is impossible with most electrical machines. But we established through statistical study that, despite these precautions, we were still stretching the material. The difficulty was cured simply by the addition of a reducing valve.

Very little reference is made by Mr. Smith and Dr. Swindells to container liners, their shape, and the effect of the

\* Managing Director, Aston Chain and Hook Co., Ltd., Birmingham.



shape on quality. Life is an aspect we are not discussing, but it interests people who buy this expensive equipment. Experience has brought a puzzling feature to our attention. We employ a liner about 50% longer than the billet which is at present our standard, and in the course of use these liners become barrel-shaped at one end. After some time, we reverse them and they become barrel-shaped at the other end. Then we reverse them again and they begin to assume a very curious shape, but as the shape becomes more curious the proportion of good work becomes higher. I wonder whether anyone else has noticed a similar effect.

Very little has been said in the paper about the need for frequent die changes, and it would be interesting to know whether that is due to the fact that in the extrusion of copper the die is inclined to foul more readily than in the case of brass. We feel that in dealing with press design the authors should have commented on the importance of making die changing a reasonably easy and rapid operation.

Have Mr. Smith and Dr. Swindells any views or opinions on the possibility of inspecting extruded material, in particular extruded copper, for surface and sub-surface defects? A solution to that problem has so far eluded us.

In conclusion I should like to congratulate the authors, not only of this paper but of all the papers, on producing a symposium which demonstrates that the metal industry in this country is alive to the need for the interchange of information. There was a time when the Institute of Metals was criticized for not being sufficiently practical. Earlier symposia have dealt with practical problems, but I think never before have I seen a series of papers which have been of so much value to me personally and to my company.

Dr. I. G. SLATER,\* M.Sc., C.I.Mech.E., F.I.M. (Member): I will content myself by asking one general question. These papers are primarily of intense practical interest, and it is appropriate that we should examine the economic side in some detail. A stranger reading them would be literally amazed at the complexities and the ramifications which we find in our light alloy industry and the various processes involved in cold working. These are duly reflected in the control of quality.

This leads me to suggest that in looking at this matter of economic significance in a broad way, we should recognize the three limitations imposed upon us. First, we have the limitations in cold-working operations arising from the present status of the various engineering sciences and skills. These are perhaps the most dominant of all limitations, but are capable of much further exploitation. The second limitation is the exact nature of user requirements, which has been barely touched on during the discussion. They should be recognized as a leading issue. Are user requirements logical and sensible in relation to the economics of what we can now produce?

The third limitation—possibly it is not a limitation—is the metallurgist's knowledge and imagination. Perhaps we may say that the metallurgist has rather over-run his potentialities; he has given industry far more than it can digest either from the engineering-sciences aspect or the user aspect, and it is appropriate that the metallurgist should examine his own conscience in this matter and find out whether or not he has overplayed his hand.

The question I want to pose is this: What would the authors care to do in the way of rationalizing the procedures which presently burden all work and operational control with a view to effecting economies—radical economies—in the products which are made? These will impose limitations in the materials which we produce—not necessarily in quality but certainly in type. We are burdened by the fact that most other metals can usefully alloy with aluminium, and in consequence possible commercial products are legion.

Mr. CHRISTOPHER SMITH,† F.I.M. (Member of Council): Dr. Swindells and I decided that, in replying to comments on our paper, I should deal with aluminium and he with the heavier metals. Mr. Thompson wants to know if there is any reason why glass should not be used as a lubricant in the extrusion of light alloys. Provided that a glass with the appropriate characteristics can be found, I think it would be quite suitable.

There is no danger of causing an increase in the number of sub-surface defects by employing lubricated extrusion, provided lubrication is perfect. It may be of interest to show what happens in lubricated extrusion when using aluminium as a lubricant. It is important to surround all surfaces of the billet (except the back end) which come in contact with the tools, and for fully efficient lubrication it is necessary to use an entry such as that shown in Fig. C. Under these tool conditions, with a thickness of aluminium as little as 20 thousandths of an inch, lubrication is perfect and fully lubricated flow of the alloy occurs. If the more usual square-entry die is used (Fig. D), it is impossible adequately to lubricate across the corners, and the aluminium coating actually penetrates the alloy billet at the point where lubrication breaks down and follows the course indicated in the figure. In that case there is a coating of aluminium on the outside of the rod, plus an infinitesimally thin coating of alloy outside that. If the lubrication breaks down elsewhere, the aluminium will penetrate the billet at that point and become aggregated into quite a large blob (see Fig. D).

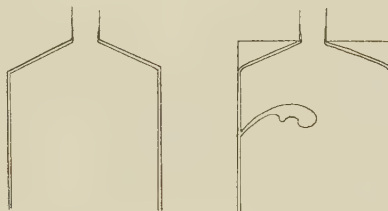


FIG. C.

FIG. D.

I have been asked about egress temperatures. I think it is not fully realized how greatly temperatures increase during the extrusion operation. A patent has recently been taken out in which it is shown that magnesium can be extruded without preheating, provided one starts with a hot billet, extrudes half of it, and then follows on for the whole shift with cold billets, using the energy of deformation to heat them up. In complicated aluminium alloy extrusions a great deal of heat is generated, and controlling the temperature of the billet is only one factor in controlling egress temperatures. In reply to a question, I have not experienced inter-crystalline cracking in the outer zone of an extrusion in the absence of overheating.

As regards the relationship between humidity and blistering in furnace atmospheres, I am indebted to Dr. Ransley for virtually answering the question, but I think there may well be more to the problem than he suggests. I have found that treating sections with a variety of substances will inhibit blistering, among them tea from the ever-present tea-can! For many years we prevented the development of blisters by the application of tallow.

Mr. Kasz has made his usual brilliant contribution to the discussion and has asked questions which are not easy to answer. As regards the limit of rate of heating to avoid trouble with non-equilibrium eutectics, our reference was to the use of induction heating, which imparts a near-instantaneous rate of heating. Under normal heating conditions I think a rate of about 10° C./min. is not injurious, but I

\* Director of Research and Development, T.I. Aluminium, Ltd., Birmingham.

R R

† Works Superintendent, James Booth and Co., Ltd., Birmingham.

have no knowledge of what is the limiting rate of heating to prevent harm from that cause.

Dr. N. SWINDELLS,\* M.A., F.I.M. (Member): Professor Murphy has taken us to task for not paying sufficient lip service in our paper to scientific techniques. We are aware of these techniques and have carried out some statistical work on determining the optimum billet length for extrusion. Our results agreed entirely with those obtained by the practical men in the works, so that everybody was happy. It has been suggested that control of quality by skilled operatives is not altogether satisfactory. Whilst this is true, there are so many minor points of detail which can affect the quality that proper acknowledgment is due to the practical men who have developed a fair amount of low cunning in coping with these problems.

It is interesting to know that Mr. Bond-Williams is testing the electrical conductivity of copper billets using electronic equipment. With the 60:40-type brasses, the conductivity is insensitive to significant changes in composition and impurities, apart from manganese. We have therefore not developed such measures for control purposes with these alloys.

With regard to the control of billet preheating temperature,  $\pm 5^\circ\text{C}$ . is an outstanding achievement, and is presumably obtained by using a furnace with an adequate soaking zone. Such a furnace would not be particularly suitable for the extrusion of batches of different alloys where various extrusion temperatures are required without undue delay between alloys.

The influence of the state of the container liner on the amount of scrap produced during extrusion is of considerable interest. We have investigated this point recently by keeping accurate detailed records of batches of extrusions throughout the life of a liner. No change in the scrap was observed during a life of 25,000 billets, after which it became necessary to remove the liner because of cracking.

Eddy-current methods may prove useful for the detection of sub-surface defects in copper, although such methods do not seem to be applicable to the normal central defect in brass.

Mr. A. H. WAINE,† A.I.Mech.E., F.I.M.: As one who assists in their manufacture, I suggest some consideration might be given to the tools employed in the non-ferrous metal industry.

The importance of the dimensional requirements demanded from these tools has been illustrated by a reference to the rolling of aluminium foil of about a  $\frac{1}{4}$  thou. thick, the tolerance thereon being unstated; and again when mention was made of roll surfaces having "knobs" and "gutters." In simple terms the metal is forced, by both rolling and extrusion, to assume a new shape as a result of its inability to pass without deformation through an aperture of smaller dimensions. Apart from wear, distortion, and other allied characteristics, the control of the shape of that aperture must be of paramount importance from every practical and economic point of view and with all operational speeds.

Whilst in the case of rolls initial cambers constitute an endeavour to produce the suitable shape by mechanical means, there can be serious disturbances due to thermal effects. The practical significance lies in the fact that hardened steel is approximately 30% stronger in compression than in tension and, therefore, the retention of curvatures of a convex type when the mill is loaded ensures conditions more favourable for optimum tool behaviour than when the contours become akin to sine curves. It would be interesting if the authors would indicate what further steps are being taken in modern practice to control "shape".

Mr. Smith referred to the high temperatures generated

during the deformation of stock, and it may be of practical value to users to indicate that hardened steel rolls of 100 Shore Scleroscope hardness (equivalent roughly to 950 V.D.H.) begin to lose this high intrinsic hardness at about  $85^\circ\text{C}$ . The operator who conditions his rolls by superficial work-hardening should, therefore, realize that his efforts can be nullified by operating temperatures of this order.

Mr. E. A. BOLTON: Dr. Turner has referred to the brass wire mentioned in my earlier contribution, which had been flash-annealed, to use the term employed by Mr. Kasz, by means of a salt-bath treatment, and asks whether it was annealed or not. I have no figures for the hardness of the wire or the strength, but I believe that the grain-size was of the order of 0.01 mm. It was annealed, but it had a very fine grain-size.

The figures given by Mr. Kasz are relevant in this matter, I think they refer to strip which had suffered something like 80% reduction. The wire had inevitably undergone heavy cold work; I do not know the percentage, but it might have been as much as 80%. I used the term "quarter-hard" somewhat loosely, and the wire would not be quarter-hard in the sense in which Dr. Turner terms it, but it was not sufficiently soft for satisfactory delivery to a customer. On the other hand, had we ourselves intended to process that wire further, to a smaller size, we should have had no hesitation in doing so.

Dr. Turner has taken me somewhat to task for my emphasis on the part played by the workman. I am quite unrepentant. I did not suggest that we should abandon or lessen scientific control and substitute that of the workman. That is far from my thoughts.

Perhaps it will clarify the matter if I give an illustration of the sort of thing I have in mind. A workman on the job may notice that a particular bar is finned slightly, owing to some possible variation of temperature which ought to be under control. If the bar goes forward for rolling that defect may be invisible—unless there are special, and expensive, methods of inspection in use—but it is still present in the wire. It does not give the slightest trouble in the drawing process. The wire receives a normal inspection at the end and is sent to a customer. He puts it through an operation and immediately the laps or fins open out—and there is rejected material. If the workman is trained to pick out such faults—he is the only person to have seen them—a lot of expense and vexation can be avoided.

Mr. C. B. H. DE WINTON,‡: I am more the man responsible for running the mills than a technician. However, we have carried out one or two experiments which may be of interest.

It will be remembered that a paper was presented recently by Hessenberg and Sims§ on the practice of gauge control by tension. We welcomed it as a simple way of overcoming the gauge control problem, and tried to put it into operation on a fast temper mill doing about 30% reduction and rolling at high speeds, where gauge control is rather important. I am sorry to report that by varying the tension we could make no appreciable difference to the gauge of the strip. In considering this result, we came to the conclusion that there was insufficient friction in the roll-bite under the trial conditions to be able to use this variable to control the gauge. We would be glad of Professor Ford's comments on this matter.

We have read with interest the paper by Professor Ford and Mr. Wistreich, but there are two comments we would like to make. We do not feel that the authors have sufficiently stressed the importance of thermal control of the roll. This is a big problem, bigger in many cases than gauge control, and much more work could usefully be concentrated on methods of improving the position. Then they discuss the effect of lubrication on surface finish of the product. In

\* Chief Metallurgist, McKechnie Bros., Ltd., Birmingham.

† Hadfields, Ltd., Sheffield.

‡ Rolling Mill Superintendent, Northern Aluminium Co.,

Ltd., Rogerstone, Mon.

§ W. C. F. Hessenberg and R. B. Sims, *Proc. Inst. Mech. Eng.*, 1952, [A], 166, 75.



common with other manufacturers, we are interested in that problem, but some of the facts and figures given do not tie up with our practical experience, particularly in connection with the remarks on the lower coefficient of friction.

Mention has been made of the skilled operator's position. It is of the utmost importance to utilize his knowledge. We must help him to do the job more easily by reducing the number of variables which he has to control, so that he gets bored with pressing buttons rather than tears his heart out trying to control all the variables that exist in rolling.

Mr. A. J. FIELD,\* M.C., B.Sc., F.I.M. (Member): For control of gauge in strip rolling, three well-known methods are suggested. First, variation of speed will give a measure of inverse variation of gauge, owing, supposedly, to the direct variation of oil-film thickness at the roll/strip interface and in the roll bearings. For economy of production, however, maximum speed is required. Secondly, variation of tension gives a measure of inverse gauge variation, this being most effective with back- or ingoing tension; but tension can break strip, and while a certain amount is necessary for stable rolling, too high a tension may be detrimental for this reason. Furthermore, excessive outgoing tension is undesirable for the strip, as the great build-up of compressive force in the coil often causes a collapse of the interior laps. Thirdly, screwdown can provide whatever gauge variation is required, and this appears to be the best means for automatic gauge control, being in the case of tandem mills applied to free screws.

In regard to speed, experience with tandem mills is that increase of mill speed decreases inter-stand tension. At first sight it appears as if the statement by Professor Ford and Mr. Wistreich (Section II, 1 (e), p. 285) is contrary to this, but apparently it is to the last stand only that speed increase is applied by these authors, and would increase the ingoing tension at that stand.

With regard to the relation between strip/roll friction and what might best be called normal roll force, it is difficult to see, from the triangle of forces, how variations in friction can greatly affect the normal roll force directly. Such increase in normal roll force as is found to coincide with increased friction must be an indirect effect, arising from the increase of gauge with friction for a given roll setting. Perhaps, as well as considering the "friction hill", we should include the "normal roll force hill", although in general it is sufficient to take into account the total of each force.

One effect of combined high friction and draft is the formation of "herringbone ripple" on the strip, as referred to by Mr. King and Dr. Turner (p. 299). This is a roughly  $\frac{1}{2}$ -in.-pitch ripple, in transverse zig-zag chevron pattern, covering the entire strip. In my opinion, this is the impression on the strip of a standing-wave sonic vibration in the roll barrel, generated by the rolling friction under the conditions in use at the time.

The important quality of flatness in strip is cumulative. Flatness must be right at each pass, and depends on the material fed into the rolls as well as on the correctness of roll profiles and setting at the particular pass. It is also dependent on uniformity of friction across the width of the strip in the pass.

The profile or camber of the rolls is a very important factor in rolling flat strip, as the rolls must be deflected truly flat by the strip. In my experience, the best shape for roll camber is that of the deflection curve for a uniformly loaded beam, which can be written as:

$$y = K \left[ \frac{L^2 x^2}{2} - \frac{x^4}{3} \right]$$

with the origin at the centre of the roll barrel of length  $L$ ,  $x$  being the lateral distance from the centre and  $y$  the ordinate

distance between the abscissa and the roll surface. This profile is similar to the sine curve and rather more pointed than the parabolic, or its near relation, the circular arc, which tends to give two slack bands on thin strip.

With regard to the control of quality in extrusion, there is one point that may be important. One puts a billet in an extrusion-press container and brings up the plunger with a tight plate in front of it; this squeezes the billet up to the die. At that point there are two substances hermetically enclosed in the container—metal and air. What happens to the air? Does it pass out through the die in the section, sometimes forming blisters for which the casting shop is blamed? It seems for this reason to be advisable to keep the amount of entrapped air to a minimum by using billets of the largest diameter that can be got into the container.

Mr. W. J. THOMAS,† M.I.Mech.E. (Member of Council): I should like a better appreciation of what is a good and what is a bad lubricant, and for what purposes it is good and for what purposes it is bad. What happens to the asperities and why are they flattened with a bad lubricant and not with a good lubricant? Mr. Bolton has mentioned "wavy edge" on rolled strip. When I first saw strip with this wavy edge, I enquired to what it was due. I was told that there was "not enough pinch on the rolls", so I erroneously assumed there was insufficient camber on the roll, and it took me some time to realize that what was meant was that the rolls had not been screwed down sufficiently to damp out the camber.

Professor FORD: Mr. Pearson has referred to the shape of the stress/strain curve of cold-rolled material, and quotes figures based on a 0.1% proof stress (Fig. B, p. 586). There are a number of factors involved which decide the shape of the curve: one is the size of the individual passes; another is the ratio of grain-size to strip thickness and length of the contact arc; and a third is the basis of assessing yield stress. In making a large number of light passes yet other factors may be involved; non-uniform deformation is one of them, the plastic deformation being mainly confined to the surface material.

Mr. Kasz has also made some comments on the yield-stress curve developed from values of the 0.1% proof stress. The true yield-stress curve may not (and usually will not) be given by plotting the proof stress readings of progressively rolled material. In the earlier stages, at least, the proof stress will occur in the elastic-plastic range, not the completely plastic range, that is, the proof stress will be lower than the true yield stress of the material at the point in question. It is therefore necessary to interpret curves based on proof stresses with some care.

The statement about camber on p. 288 of our paper is incorrect and we are grateful to Mr. Bolton for pointing out the error: the effect of camber is, of course, the reverse of that stated. The slip occurred in transcribing notes.

Mr. Field questions our statement about the relationship between speed and inter-stand tension (p. 285). Taken in its context the statement is correct: if the speed of the last stand is varied without varying the speed of the previous stand, then an increase in speed will increase the inter-stand tension, and vice versa.

Mr. WISTREICH: As an alternative to Professor Ford's explanation of Mr. Pearson's curves, I would suggest that the effect is associated with differences in deformation textures. Three years ago I drew attention to a similar phenomenon occurring in wire drawing.† It was evident from the curves then shown (Fig. E, *loc. cit.*) that work-hardening of copper wire was less rapid with small passes than with large ones, and it appeared that the surface texture of the wire depended on the drafting. My colleague, Mr. P. W. Wright, has

\* Works Manager, The British Aluminium Co., Ltd., Falkirk.

† Assistant Managing Director, The British Aluminium

Co., Ltd., London.

‡ *J. Inst. Metals*, 1950-51, 78, 687 (discussion).

recently demonstrated\* that the surface texture of steel strip varies with small differences in cold-rolling treatment; indeed, he has been able to distinguish between  $\frac{1}{2}$  and 1% temper-rolling passes. In his case the effect on the mechanical properties of such small differences in treatment became apparent only after ageing of the steel. One may well imagine that Mr. Pearson's two rolling treatments have produced more substantial differences in texture and mechanical properties.

I should like to reply briefly to questions about automatic control of strip gauge. Mr. Kasz has asked whether there is any need for recalibration for different alloys. The answer is "no", because the system corrects for changes of mill-housing stretch and of roll deformation, and does not depend on how these changes are brought about, i.e. it does not matter whether they are caused by changes in ingoing gauge or hardness of the material or by changes in friction or tension. In one method control of gauge is achieved by keeping the roll force constant; this is done by adjusting the tension. Mr. de Winton has pointed out one limitation of this method, namely, that in some instances even appreciable changes of

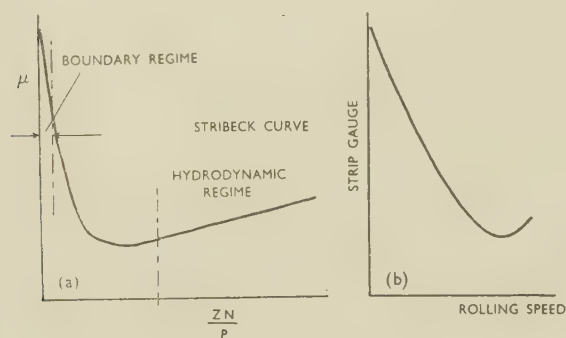


FIG. E.

tension will not bring about the desired correction of gauge. An even more important limitation of this method is that coiler drives more powerful than is customary may be needed, and, of course, it cannot be applied in hot rolling. Thus, the scope for automatic control by tension is limited. However, the alternative method put forward by Hessenberg and Sims,† that is automatic control of screwdown, is applicable to all flat rolling. This method has been tried under both laboratory and works conditions, and the equipment will shortly be available commercially. One system of this screw-down control is in current use in the B.I.S.R.A. laboratories in Sheffield; this is a system which can be installed in most existing mills with very little modification. Anyone who would like to see it in operation is welcome to do so.

It has been questioned whether the speed effect is due to friction. That this is indeed so, is now established conclusively.‡

Billigmann and Pomp show that the effect is a "hydrodynamic" one, i.e. it is related to what is observed in bearing lubrication. Referring to the curves in Fig. E, on starting and at low speeds the boundary régime of lubrication predominates but as the speed is raised it tends to give way to the hydrodynamic régime. The " $\mu$ " curve is a familiar and ancient signpost of lubrication theory §; for rolling, the speed parameter depends on draft and the ratio of roll diameter to strip thickness, and on the viscosity of the lubricant.

Generally speaking, only the left half of the Stribeck curve is relevant to rolling practice, but it is interesting to note that on occasions one does pass the point of minimum friction || so that the gauge after having decreased on acceleration from standstill may actually increase somewhat on further speeding up. The point which I should like to make is that inasmuch as non-viscous lubricants, such as graphite, are not usually acceptable, the speed effect will always be with us and must be corrected for. The most efficient method of correction is automatic gauge control.

Mr. Waine has raised the question of tool shape. I should like to comment on the shape of wire-drawing dies. I strongly believe that closer control of die shape will lead to more consistent die performance; recent results of industrial trials point in this direction. There is still a great deal to be learnt about which is the best shape for a given job, but it is already clear that it is worth while keeping the shape constant, even if it is not the best one. This brings me to the subject of the skill of the craftsman, which has been so much discussed. Surely the heart of the matter is this; the present-day consumer calls for such a high degree of consistency in the quality of the product, and modern fabricating processes are so fast and so complicated, that the skilled craftsman needs better tools—in the form of instruments and controls. Even automatic control is but a tool which needs the sure hand, eye, and brain of a highly skilled worker.

Mr. G. E. G. TUCKER,¶ B.Sc. (Junior Member): I am disappointed that there have been no direct contributions to the discussion of Mr. Whyte's paper, and I should like to point out two slight inaccuracies. First, the suggestion is made that a sampling procedure exists which will ensure that 95% of a batch will meet certain grain-size requirements. In fact, it is impossible to ensure anything by a sampling procedure without sampling the whole batch, since determination of the mean gives no information about the distribution of individuals. Another point which the author makes is that his equation (9) (p. 343) is increasingly true for any symmetrical unimodal distribution as  $n$  increases. This is correct only if the standard deviation exists initially.

I look forward to papers dealing with the use of statistics from the metallurgist's point of view. Mr. Whyte has admirably demonstrated what can be done with statistics when they are available, but many people are deterred from using statistics because they do not know what to calculate or how to calculate it. In that respect the text-books are not of much use, because the metallurgist's data are seldom as well-behaved as text-book examples. This is particularly true when data are uncontrolled or incomplete. One normally has to use multiple-regression techniques which suffer from several disadvantages, such as the necessity for assuming a particular mathematical form for the regression equation and the impossibility of accommodating discrete, or non-numerical, factors at more than two levels. In spite of that, as Mr. King and Dr. Turner have said, we have found multiple-regression techniques extremely useful in examining works data.

I should like to hear Mr. Whyte's comments on the analysis of uncontrolled and incomplete data, and on the defects of multiple-regression techniques.

Mr. M. WHYTE,\*\* B.Sc. (Member): Mr. Tucker has made the point, in connection with my paper, that it is impossible, without 100% sampling, to ensure that no batch is released which contains less than 95% of acceptable items. This is true, but although I used the word *ensure* in discriminating

\* In the press.

† W. C. F. Hessenberg and R. B. Sims, *Proc. Inst. Mech. Eng.*, 1952, [A], 166, 75.

‡ R. B. Sims, *Inst. Petroleum: Symposium on Metal-Working Oils*, 1954, Preprint.

J. Billigmann and A. Pomp, *Stahl u. Eisen*, 1954, 75, 441.

R. B. Sims and D. F. Arthur, *J. Iron Steel Inst.*, 1952, 172, 285.

§ R. Stribeck, *Z. v.d.I.*, 1902, 46, 1341, 1432, 1463.

|| G. E. Stoltz and J. W. Brinks, *Iron Steel Eng.*, 1950, 27, (10), 69.

¶ Research Metallurgist, Aluminium Laboratories Limited, Banbury, Oxon.

\*\* Research Laboratories, The British Aluminium Co., Ltd., Gerrards Cross, Bucks.



between two possible criteria—that the mean of a batch passes the specification or that 95% of the individual items in the batch pass the specification—the sampling scheme finally derived is based on odds 20-1 against accepting a batch which does not satisfy the acceptance criteria adopted. The mean of a batch gives no information regarding the distribution of the individual items but, in the example quoted, the distribution within batches is shown to be known from the analysis of past results.

The formula for the standard error of a mean is valid for almost all unimodal distributions met with in practice. The Cauchy distribution is an exception, but is seldom encountered.

Multiple-regression techniques applied to works data have in our experience proved very useful. It is important, however, that the statistician should work in close collaboration with the technical staff concerned. Care has to be taken to exclude "freak" results which arise from effects not at all representative of the technical process.

I suspect that Mr. Kasz had his tongue in his cheek when commenting on the statistical approach. The statistician distinguishes two types of variation. First, there is that due to assignable causes. These are the causes which fix mean levels. Sub-standard levels usually indicate inadequacy of technical plant or knowledge, and the statistician cannot accept responsibility for this. The statistical analysis of process data, may, however, reveal adverse factors which are easily rectified, and this may lead to immediate improvements. An example has been quoted by Mr. Bond-Williams and another by Andrew is quoted in my paper.

The second type of variation distinguished by the statistician is not assignable to specific causes. Here the statistician defines the variability quantitatively and ensures that full economic advantage is taken of the situation as it stands. In so doing the variation due to non-assignable causes is often, in practice, reduced. It may be more important to improve levels, but if this cannot be done, it is as important to take full advantage of the circumstances as they are.

Mr. Kayser has made a plea for simple statistical methods. I agree that quality control should be simple and should extend right down to the operators on the plant. In this way the operator's sense of responsibility is enhanced and his technical skill and knowledge fed back to the man in charge. Improved control usually results. A successful application of this nature in which the introduction of control charts on melting furnaces led to an immediate improvement in composition control has been described by Hood.\*

Mr. W. J. THOMAS: Changes in production methods are taking place all the time, and we continually have to review

the methods we adopt for control of quality. In particular, since the war, in the light metals industry we have gone in more for direct casting and we handle bigger shapes and roll at higher speeds. All these new factors, which apply to the non-ferrous metals industry in general, bring their own problems, and what may have given control years ago does not necessarily do so now.

From the operators in the mill we may not expect quite the same degree of craftsmanship as in years gone by, but we expect greater vigilance. They have different and more complicated tools and control is very largely in their hands. If you ask for too much from the human element in the works you will not get a consistent performance and I think that much still remains to be done in providing tools which will make operations more regular and more standardized. Collaboration between the technical staff and the craftsmen therefore remains one of the most promising methods of improving and maintaining quality control.

Mr. F. KING, A.I.M., (Member) and Dr. A. N. TURNER, B.Sc., A.R.S.M., A.I.M., (Member) (*in further reply*): With regard to Dr. Champion's comments on our paper, we agree that a visible oxide film may be produced when aluminium-magnesium alloys are annealed at temperatures above 350°C. As the annealing temperature is increased above 350°C., so the appearance of the film changes from a whitish discoloration or bloom to the dark or black oxide referred to in our paper. Enveloping will reduce the tendency towards this defect. If very oily material is enveloped for annealing, staining will result. It is for this reason that we stipulate that annealing loads must be clean. We believe, however, that the staining is due to thermal decomposition of the oil rather than to partial oxidation, the important factor being not limitation of oxygen supply, but the prevention of free circulation of furnace gases.

It is our opinion that for many applications, surface appearance is as important as tensile properties and earing characteristics, this being true of circle material and container sheet materials used for decorative purposes, which are to be coated with transparent lacquers. Surface finish is also important for sheet used for the building of civil aircraft on which camouflage paint is not used. In our experience any compromise affecting surface appearance does not involve mechanical properties so much as cost of production. It is also a matter which is governed by the availability of equipment. The products of high-speed flood-lubricated strip mills are generally duller than those of slower-speed strip mills and flat sheet mills. The rolling schedule for these various types of mill can be adjusted to give products having similar mechanical properties but of widely different surface finish, the brighter surface finish generally being the more costly to produce.

---

\* J. W. Hood, *Metal Progress*, 1953, 64, (5), 84.

## The Behaviour of the Crystal Boundaries of Aluminium at Temperatures Near the Melting Point

By W. I. PUMPHREY and J. V. LYONS

(*Journal*, this vol., p. 33.)

Mr. A. P. GREENOUGH,\* M.A. (Member): In the discussion of their interesting experimental results given on p. 35, the authors state: "It seems probable that the observed occurrence of intercrystalline fracture, unaccompanied by any sudden fall in strength, is due to viscous flow at the crystal boundaries, and that the sudden fall in strength and the total loss of ductility (accompanied by the glazed type of fracture) with progressive increase in the temperature of testing is associated with incipient melting of the crystal boundaries. . . ." It is difficult to accept this statement without more evidence than that provided.

The results of Ké, mentioned in the paper, and later results in the same field, all indicate that the apparent viscosity of the crystal boundaries falls continuously with increasing temperature, until at the melting point of the metal in the mass the apparent viscosity is the same as that of the liquid. On this basis, therefore, the melting of the grain boundaries should produce no sudden fall in the strength of the specimens. However, it is difficult to see the relevance of Ké's results to the present discussion, since they imply a shear strain across the crystal boundary of sub-microscopic dimensions. The danger of applying these results to cases where the shear strain is large has been very well illustrated by the work of Puttick and King.† Further, Dr. Pumphrey and Dr. Lyons give no details of the shape of the fractured surfaces, nor even of the grain-size of their specimens, but if these were similar to those illustrated by Singer and Cottrell, whose work is mentioned, it is quite obvious that the fracture does not take place simply by the two ends of the specimen shearing apart across a plane grain boundary.

In that case, the fracture must involve some normal separation of the surfaces. Pumphrey and Lyons assume that the thickness of the crystal boundary in aluminium is 10–15 Å. That being so, the thickness of the liquid layer formed by the melting of the boundary would be expected to be of the same order of magnitude. Have the authors any evidence of the tensile properties of so thin a layer of liquid aluminium? Such evidence as I have leads me to expect that they will be very different from the properties of the same liquid in bulk. For example, a layer of water, many times the thickness suggested for the grain boundary, between two optical flats, can be made to support a considerable tensile load.

The AUTHORS (*in reply*): Mr. Greenough suggests that, since the apparent viscosity of the crystal boundary decreases continuously with increasing temperature and is the same as that of the liquid metal at the melting point of the metal in the mass, the occurrence of melting in the crystal boundaries should not cause a sudden fall in the observed strength of a tensile specimen.

On the basis of Ké's findings, we would agree that the melting of the crystal boundaries should produce no sudden fall in the strength of a polycrystalline specimen provided that the crystal boundaries and the crystals melt at the same bulk

melting point. If, however, the boundaries become molten at a temperature below the bulk melting point, then the viscosity at the crystal boundaries will fall suddenly to that lower value which is characteristic of the molten liquid in the mass at the higher bulk melting point, and the strength of the specimen will fall correspondingly to the strength which would be associated with the metal at its melting point under the ideal conditions where the crystal boundaries and the crystals melt simultaneously. It must also be borne in mind that melting is progressive with rise in temperature, so that further increase in the temperature of the mass once melting has begun, produces an increase in the thickness of liquid at the crystal boundary. This must be taken as the criterion of the instant at which melting can be said to have started, since otherwise there would be no means of distinguishing between a boundary which had melted and one which was still solid but was behaving in a viscous manner with a viscosity similar to that of the liquid. Thus, when melting begins, the decrease in strength with increase in temperature is determined chiefly by the increase in thickness of the film of liquid at the crystal boundary and not by the decrease in boundary viscosity. Since melting in pure aluminium occurs over a very limited temperature range, then a small increase in temperature above that at which melting first occurs will produce a considerable increase in the thickness of the liquid film at the crystal boundary and a corresponding rapid fall in strength will follow. It seems reasonable to postulate that at lower temperatures the thickness of the solid crystal boundary which is behaving in a viscous manner does not increase with increase in temperature, so that the fall in strength is then a function of the gradual fall in viscosity.

In answer to the second point raised by Mr. Greenough, it is known that at suitably slow rates of straining, at temperatures well below the melting point, intercrystalline fractures can occur in pure aluminium specimens which can be attributed to the viscous flow of the crystal boundaries under such conditions. It is not obvious why considerations of the viscous behaviour of a crystal boundary can be applied only to shear strains of sub-microscopic dimensions, as Mr. Greenough suggests.

In their work, Puttick and King (*loc. cit.*) found that beyond a certain small deformation the strain was no longer linear with time under constant load. They did not suggest, however, that the crystal boundary ceases to behave in a viscous manner for large deformations, but rather that the departure from linearity is probably due to irregularities at the crystal boundary. Thus, there appears to be no real objection to considering large deformations as occurring by a process of viscous boundary flow.

The grain-size of the specimens which we tested was very similar to that of the specimens tested by Singer and Cottrell. We agree, of course, that fracture must have occurred in our specimens by movement of the crystals normal to the crystal boundaries as well as by a shear movement, but while we have no detailed information on the tensile properties of a

\* Metallurgy Department, University College, Swansea.

† K. E. Puttick and R. King, *J. Inst. Metals*, 1951–52, **80**, 537.  
598



thin film of liquid between two supporting solid pieces, we should have thought that the adherence of two optical flats with a liquid film between them was associated, largely, with the effects of external atmospheric pressure, rather than with the properties of the film.

While we are most appreciative of Mr. Greenough's comments, we feel that his observations do not, in any way, invalidate our consideration of the results recorded, since we have, in fact, made no use of the tensile-strength figures obtained in our tests in any subsequent calculations. Our

suggestions are based on the observation that, in the tensile testing of pure aluminium specimens at temperatures near the melting point, intercrystalline fracture can occur (i) unaccompanied by, and (ii) at high temperatures accompanied by, a sudden fall in tensile strength. Our suggestions are based upon the observed temperatures associated with these phenomena, and although we agree that the final mechanism of fracture is more complex than a simple shear-strain process, this does not materially affect our arguments.

## Discussion

# Molybdenum and Molybdenum Alloys and the Arc Melting of Metals\*

Mr. A. J. HERZIG,† M.S.E. (Member): The evolution of a new engineering material invariably requires the simultaneous solution of several problems not necessarily technologically interdependent from a research point of view. The evolution of molybdenum and molybdenum-base alloys as engineering materials involves the development of four major aspects of the overall problem: (i) The establishment of the properties obtainable in the new materials. (ii) Development of commercial methods of producing and fabricating them. (iii) The discovery of methods of protecting them from oxidation at elevated temperatures. (iv) The design of machines and equipment to use the new materials in our complicated technology.

The present status of arc-cast molybdenum and its alloys in the United States on these four counts may be summarized as follows:

(i) The metallurgical foundation for the technological development of a new series of metallic alloys is virtually assured under the research programme which began in the United States in 1947. Wrought alloys amenable to many of the current fabrication processes and having strengths at elevated temperatures well above those of the present so-called "super-alloys" have been produced and are becoming available for development purposes.

(ii) Pilot operations at the Climax Molybdenum Company of Michigan over a period of several years have confirmed that the commercial production of molybdenum and molybdenum-base alloys by the arc-casting process is feasible. Recent developments in powder-metallurgy techniques have extended the applications to which molybdenum produced by that process can be applied. However, for large sections of molybdenum and for molybdenum to meet special requirements, preference is being shown in several quarters for arc-cast molybdenum.

(iii) The difficult problem of protecting molybdenum from oxidation has been receiving the attention of many well-qualified investigators, both at the fundamental and the practical levels. This problem has already been reduced to a question of feasibility rather than possibility. Although a universally applicable method of protection may still be a long way off, results of research at the present time suggest that the solution to the problem for special strategic applications is probably not far away.

(iv) Substantial quantities of the alloys are being made available for experimentation and for limited production where oxidation-resistance is not a prerequisite to performance. Most, if not all, of the applications require developments in design to derive full benefit from the new material.

It is to be expected that with the solution of the problem of oxidation-resistance, revolutionary engineering developments will be forthcoming.

Mr. A. J. HERZIG, M.S.E. (Member), and Mr. BRINLEY JONES,‡ M.Met.: Progress in the field of preparing forgeable aggregates of molybdenum and molybdenum-base alloys has been so rapid since 1950 that one must at the present time employ great caution in ascribing to them properties characteristic only of the materials with which one research group has concerned itself.

Apparently, the authors of the paper on forgeability, &c., have not had access to much of the recent work on molybdenum. In the United States, laboratories investigating the properties of molybdenum and its alloys, produced either by the powder-sintering or the arc-casting procedures, have been in close co-operation. This close communication has, indeed, revealed some difference in the characteristics of molybdenum produced by the two processes. On the other hand, it has also shown good agreement on certain basic matters of great significance and in contradiction to some of the conclusions reached in the paper.

There is good agreement in the United States that in wrought molybdenum, produced either by powder-metallurgy or arc-casting methods, the stress-rupture strength in tension can be at least doubled by proper alloying. Also, that the effect of alloying is to increase the elevated-temperature hardness, strength, and recrystallization temperature.

In dealing with vacuum arc-cast, carbon-deoxidized, unalloyed molybdenum, it has been established that the commercial working of 250 lb., 6½-in.-dia., ingot sections of molybdenum is feasible by extrusion at 2300° F. (1260° C.) and subsequent rolling. In pilot operations to date, upwards of 75,000 lb. of molybdenum ingots have been handled in this way.

In the case of arc-cast alloyed molybdenum, and with compositions showing from 1.5 to 2.0 times the stress-rupture strength of pure molybdenum, extrusion at 2600° F. (1426° C.) and subsequent rolling has been proved to be commercially feasible. Upwards of 5000 lb. of experimental product have been thus produced.

It is, therefore, submitted that the authors' conclusion (2) (p. 358) not only "may not" apply to arc-cast molybdenum, but actually "does not" apply to molybdenum as now produced in the United States.

It is further held that conclusion (9) (p. 359) is not applicable to arc-cast molybdenum and is unduly pessimistic in view of the rapid advances taking place in this field.

\* Joint discussion on the papers by G. L. Hopkin, (Mrs.) J. E. Jones, A. R. Moss, and D. O. Pickman (*Journal*, this vol., p. 361); J. H. Rendall, S. T. M. Johnstone, and W. E. Carrington (p. 345); and A. R. Moss (p. 374).

† Vice-President and Director, Climax Molybdenum Co., Detroit, Mich., U.S.A.

‡ Director, Climax Molybdenum Co. of Europe, Ltd.

Dr. L. NORTHCOTT,\* F.I.C., F.I.M. (Member): It is true that we are getting near the limit for high-temperature use of iron- and nickel-base alloys. Excluding the platinum-type metals, the alternative materials are tungsten, tantalum, molybdenum, chromium, vanadium, titanium, and zirconium. The last two are hexagonal and the others body-centred cubic metals. With few exceptions (tantalum being only a partial exception) all these materials suffer from the tough-to-brittle transition, and in that sense behave similarly to iron. The N.P.L. work has been carried out with a view to determining whether alloying additions can be made to lower the transition temperature, and the authors have concluded on the basis of their investigations that such additions raise the transition temperature. I think it desirable to bear in mind that their conclusions refer solely to the conditions under which the experimental work was carried out, and particularly the fact that the powder-metallurgy technique was used. From work at the Armament Research Establishment, and more especially in America, it is clear that, by employing arc melting, additions of certain elements can usefully be made on the basis of their behaviour as deoxidants. Adequate additions of titanium, for example, have been found by American workers to eliminate entirely embrittlement due to continuous oxide inclusions between the crystals.

Although the results of the work at the N.P.L. are rather negative, alternative methods of lowering the transition temperature must exist, and in fact the results so far obtained are sufficiently promising to warrant continuation of the search.

Mr. R. EBORALL,† M.A. (Member): I congratulate the authors of the paper on arc melting on the very fine furnace which they have developed, and on their full and lucid exposition of the subtleties of its operation. It is clear that the difficulties encountered were great, yet the solutions reached appear complete and are certainly elegant.

It is rather impressive that the thermal efficiency is around 25%, when it is considered that metal is being held molten against a directly cooled copper surface; it shows that it pays to have a large power input and get the job done quickly.

I am a little surprised that the authors should have adopted a deep fixed mould, rather than a short mould with a falling base; the latter has the advantages that the surface of the melt is kept in view and that the arc is always above the mould. Is there some difficulty connected with adjusting the rate of the downward withdrawal, or with the spatter from the arc? No mechanical difficulties have come to light when the falling-hearth arrangement is used for titanium.

Can the authors say anything about segregation in alloys? When melting titanium alloys in our furnace we have found it desirable to melt everything twice, once to make a series of homogeneous buttons and then to remelt the buttons into bar. I believe that double melting is now frequently practised in the United States when titanium alloys are arc-melted on a large scale. In the authors' practice the molten pool is considerably deeper than in our own, but it cannot be very deep at the edge, and even at the deepest part the metal would be molten for less than a minute.

For some purposes, including the production of titanium alloys, there would be an advantage in using green compacts for the consumable electrode. Is the only difficulty here that of obtaining electrical contact to a rather fragile material, or are there others?

Mr. D. O. PICKMAN (*in reply*): The high efficiency of the consumable-electrode arc-melting process may be attributed to the fact that the metal is heated mainly before and during its passage through the arc, when the cooling effect of the mould is very slight. This means that the rate of melting, or melting efficiency, is not appreciably affected by the severity of the mould cooling. In the non-consumable-electrode process, on the other hand, the rate of melting is influenced

much more by mould cooling and, hence, the efficiency will be less.

No particular mechanical difficulty is anticipated in the use of a retractable mould-base. We share Mr. Eborall's view that it is advantageous to have the arc either above or close to the top of the mould. There is the possibility that, with arcs operating in high vacuum, the wider scattering of spatter under these conditions may lead to more trouble with spatter-initiated discharges. It has been our experience that arcs running in argon at atmospheric pressure produce much less spatter and are, in any event, not liable to this type of discharge.

Segregation of alloys is not thought to be serious, but little precise information is available. Provided that the alloying addition is made at a uniform rate and in a form readily soluble in the melt (small particles), the high temperature and turbulence undoubtedly help very much to promote uniformity. Some segregation of volatile alloys to the outer skin has been found. This is thought to be due to condensation of the alloy on the cool mould above the ingot and subsequent re-solution as the ingot advances up the mould.

We have never attempted to use green compacts as a consumable electrode, but are of the opinion that the joining of the compacts would present great difficulty apart from that of obtaining electrical contact. It may well be possible to melt single green bars attached to the end of an electrode, but the length of such bars is limited by manufacturing and handling difficulties.

MESSRS. RENDALL, JOHNSTONE, and CARRINGTON (*in reply*): We are aware of the large volume of work on molybdenum and its alloys that is being carried out in the U.S.A. However, the results of the greater part of this work have not been published in the usual scientific journals, and we thought it to be more satisfactory to refer only to results which are generally available. It is gratifying to hear from Mr. Herzig that substantial progress is being made.

It appears that the main point of difference between Messrs. Herzig and Brinley Jones and ourselves is the effect of alloying elements on the high-temperature strength of molybdenum. Herzig and Brinley Jones report that alloying appears to double the stress-rupture tensile strength, whereas we find only a slight improvement due to alloying in our compression creep tests.

We would like to point out that in their tests the Americans were measuring the greatest stress that the alloy would carry without undergoing more than a certain quite small amount (1%) of plastic deformation in a given time, and that this stress may be substantially less than the stress that produces rupture in an equal time, and bears no simple relation to it.

There are two reasons for preferring our method of test. Whilst there are no doubt cases in which a component at high temperatures may be allowed to undergo substantial deformation during service, the majority of the applications of creep-resistant alloys are such that the component becomes unserviceable when it deforms. The stress that may be applied is limited to the stress which will not produce appreciable deformation during the expected life of the component. In the case of molybdenum alloys, the poor oxidation-resistance of the material generally requires that a protective coating be employed, and since all such protective coatings are brittle, the components cannot be allowed to deform to such an extent that the protective coating cracks, for the protection will then be lost.

The work of the Climax Molybdenum Company has shown that the stress-rupture properties of molybdenum can be improved by alloying, but the degree to which the resistance to slow deformation has been improved is not yet clear. In view of the large amount of excellent investigation that is being carried out, it is to be hoped that more information on this point will be available in the near future.

We are in general agreement with Dr. Northcott's remarks.

\* Armament Research Establishment, Fort Halstead.

† Head of the General Metallurgy Section, British Non-Ferrous Metals Research Association, London.



## Discussion

# An Investigation of Thickening and Metal Entrapment in a Light Alloy Melting Flux

By A. H. SULLY, H. K. HARDY, and T. J. HEAL

(Journal, this vol., p. 49.)

Dr. E. F. EMLEY,\* F.R.I.C., F.I.M. (Member): The authors support the view that the action of the flux in assisting agglomeration of metal is due not to dissolution of oxide films by the flux, but rather to stripping of the films by surface-tension forces. Dissolution of oxide films can play no appreciable part in the recovery of fine magnesium scrap, for the solubility of MgO in the usual fluxes does not exceed about 0.1%. With magnesium, however, it appears that the flux action is less simple, and surface-tension forces alone are insufficient to effect recovery.

Some years ago a process for recovering magnesium sawings and powder was developed in which the magnesium was pelleted with anhydrous carnallite and fed into a stirred flux bath. The temperature was subsequently raised and  $\text{CaF}_2$  added to coagulate the metal.† In investigating the best composition for the flux bath laboratory experiments were made in which standard pellets were fed into NaCl-KCl baths containing increasing additions of  $\text{MgCl}_2$ .‡ It was noted that very low recoveries were obtained in the absence of  $\text{MgCl}_2$ , but that the metal recovery rose up to a certain point and then fell slowly as successively larger additions of  $\text{MgCl}_2$  were used. In the absence of  $\text{MgCl}_2$  little hydrogen was evolved on adding the pellets, but with  $\text{MgCl}_2$  present vigorous evolution of hydrogen occurred, presumably owing to removal of the last traces of moisture from the nominally anhydrous  $\text{MgCl}_2$ . A similar result was obtained with additions of (anhydrous)  $\text{CaCl}_2$ . It was also noticed that as the  $\text{MgCl}_2$  (and  $\text{CaCl}_2$ ) contents were increased, the residue of uncoagulated metal left in the flux phase fell steadily. These observations suggested that adequate stripping of oxide films was not effected by NaCl-KCl mixtures alone, despite their low surface tension and high wetting power, but that addition of a hydrolysible chloride caused stripping of adherent oxide films by chemical attack on the underlying metal with consequent evolution of hydrogen, and presumably disruption of adherent films. When sufficient  $\text{MgCl}_2$  to strip all the metal had been added, further addition merely resulted in metal losses through chemical attack, and metal recovery fell accordingly.

There is a threshold concentration of  $\text{CaF}_2$  which must be reached in the flux bath before appreciable coagulation occurs. In the above experiments  $\text{CaF}_2$  was added until no further coagulation of the dispersed metal took place. It was observed that the threshold concentration fell with increasing  $\text{MgCl}_2$  content of the flux bath, and the reason for this is not clear. The phenomenon of coagulation by  $\text{CaF}_2$  appears, however, to involve contact angle, and it is evident to the eye that when the threshold concentration of  $\text{CaF}_2$  has been reached the flux no longer wets the metal globules easily, and coagulation at the surface of the metal proceeds quite readily. This effect of  $\text{CaF}_2$  in reducing the wetting power of a chloride flux is in accordance with the observation that a stoicheio-

metric excess of  $\text{CaF}_2$  in relation to  $\text{MgCl}_2$  promotes non-wetting in magnesium alloy fluxes.§ The threshold  $\text{CaF}_2$  concentration for coagulation also depends on the alloy content of the magnesium.

The authors used a flux of 90% NaCl and 10%  $\text{CaF}_2$  in a number of their experiments, and it is thus possible that the fluxing action may be similar to that with magnesium, but that stripping of films, in this case by wetting alone, and coagulation are here taking place simultaneously. Can the authors say whether satisfactory aluminium recovery can be achieved if the  $\text{CaF}_2$  is omitted, and KCl added, if desired, to reduce the melting point? There is also the possibility of a small amount of  $\text{CaCl}_2$  being formed from reaction of  $\text{CaF}_2$  and NaCl.

What was the composition of the flux used for metal-content determination and remelting experiments? The authors identified  $\text{CaF}_2$  in the product, so it may have been of the NaCl- $\text{CaF}_2$  type. Did the authors try large additions of KCl and  $\text{CaCl}_2$ ? It is not thought that these would dissolve any alumina, but they might be more effective than NaCl in increasing the fluidity of the slag. If the flux used originally contained any calcium chloride it is possible that some stiffening may have taken place owing to hydrolysis by residual water and by moist air. The presence of  $\text{MgCl}_2$  and  $\text{CaCl}_2$  in magnesium alloy fluxes causes stiffening through hydrolysis, particularly in thin layers, the phenomenon being accentuated when the flux is wet or the content of alkali metal chloride low.

The authors' remarks about viscosity and metal entrapment are generally applicable also to magnesium, although the proportion of finely divided metal remaining in the thickened magnesium fluxes is less. The viscosity measurements are interesting, and the authors are to be congratulated on the apparatus they have constructed for determining the viscosity of their fluxes and the effects on it of variable shear rate.

Dr. E. SCHEUER || (Member): We asked the Fulmer Research Institute to do some work on the mechanism of the fluxing action in aluminium melting because we had formed the opinion that the development of fluxes had gone about as far as could be expected by pure trial-and-error methods. Further progress could be anticipated only through new discoveries, which cannot be produced at will, or by the slow and laborious method of getting to understand the fundamental mechanism of the fluxing action.

The authors have made progress in the right direction on two points. They have confirmed and elaborated the view held by us and others for some time, namely, that surface forces are mainly responsible for the removal of the oxide skin from the liquid aluminium which forms the basis of the fluxing action.

They have further brought to light the fact that the viscosity

\* Chief Metallurgist, Magnesium Elektron, Ltd., Clifton Junction, Manchester.

† British Patent No. 555,412.

‡ Prepared in anhydrous form by chlorination of MgO in

the presence of carbon.

§ E. F. Emley, *J. Inst. Metals*, 1948-49, 75, 457.

|| Chief Metallurgist and Head of Laboratories, International Alloys, Ltd., Aylesbury, Bucks.

of the slag is abnormally high for a suspension of aluminium in liquid salt, and have found a plausible explanation for this fact. They have also discovered the thixotropic effect, which so far, however, is too small to be utilized industrially.

The authors, I am sure, will be the first to admit that the paper deals with only a small part of the total problem. What seems to be most desirable now is to measure the surface tensions on the pairs of substances operating in the fluxing process, namely: metal/oxide; metal/flux; and oxide/flux.

The determination of surface tensions at the temperatures and under the conditions involved is certainly not easy. There are contradictory observations, for instance, regarding the surface tension between alumina and liquid aluminium. A drop of liquid aluminium on an alumina surface will not wet that surface, but on the other hand, if the alumina film is lifted from the top of a body of liquid aluminium one finds a film of aluminium attached to it. It seems unavoidable that measurement of surface tensions will have to be carried out in order to make progress in understanding the mechanism of fluxing, if it is admitted that surface tension is the decisive agent.

Here is a challenging field for work. It may be difficult, but it will yield interesting and, in the long run, also useful results.

Mr. R. CHADWICK,\* M.A., F.I.M. (Member): While the general conclusions of the authors with regard to the thickening effect of aluminium on the flux mixtures examined can hardly be disputed, it does appear that the possible slow reaction with water of some of the constituent salts might be an additional factor affecting the amount of thickening. The hydrolysis of liquid magnesium chloride with the formation of volatile hydrogen chloride and a solid oxychloride is, of course, well known. In the study of low-melting mixtures of chlorides and fluorides, however, we have found that mixtures containing alkaline earths, which retain their fluid conditions over periods of days or even weeks, may eventually thicken and solidify by the formation of oxychlorides. It is not generally realized that water is very tenaciously held in such salt mixtures, and is not normally completely removed by heating in air even at the melting point. Apparently water vapour can either be retained in solution or may cause slow hydrolysis, depending upon the composition. Commercial grades of salts seem to be particularly prone to slow reaction in the fused state, and it is possible that magnesium chloride is the impurity responsible for promoting hydrolysis.

Lithium chloride is frequently present in welding fluxes, and is sometimes added to the cleansing fluxes used in melting. This salt seems to have an important beneficial effect in preventing the thickening of the molten mixture. It is interesting to observe, however, that lithium is used up in the fluxing reaction, and this appears to be due to the formation of a complex of  $\gamma$ -alumina of approximate composition  $\text{Li}_2\text{O} \cdot 5\text{Al}_2\text{O}_3$ , which forms a dense aggregate so that oxide is removed from suspension.

Nothing is said in the paper about the mechanism involved in cleansing a liquid aluminium bath by means of a small flux addition, which is a common industrial practice. Before the flux addition oxide particles are normally present in the melt, so that after tapping of the upper layers without prior fluxing there remains a thick sludge of metallic appearance, consisting of metal intimately mixed with oxide. The addition of flux causes the oxide to separate and float on the surface and the metal regains its fluidity. The mechanism involved in the separation is probably the change in surface-tension relationships described by the authors, the result of which is that liquid metal ceases to be capable of wetting the oxide particles. This fluxing action is accompanied by considerable heat evolution, and unless careful control is exercised, the rise in temperature may lead to a substantial increase in metal losses. This observed thermal effect is probably complex in

its origin. For example, when the oxide separates it entrains finely divided metal, and under the action of flux, which continually removes newly formed oxide layers, this burns vigorously in air and may even reach incandescence.

Dr. R. T. PARKER (Member): I am interested to note the work which has been done to determine the rate of fall of aluminium particles in flux mixtures, and in particular would like to hear a little more about the effect of stirring. It seems possible that some other means of agitation of the melt, such as is afforded by ultrasonic vibration, might bring about an accelerated separation. However, the authors may be able to state definitely whether it is necessary to have some particular form of motion in the melt to obtain the effect they desire. My suggestion that ultrasonic vibration may be of assistance is based on the fact that when we have used it we have noted that segregation of aluminium dendrites results in a solidifying aluminium-silicon alloy of slightly less than eutectic silicon content. In this case the difference in density between the aluminium dendrite and the melt is quite small.

The AUTHORS (*in reply*): Dr. Emley's remarks are very interesting. The reactions which he describes illustrate the complex nature of the reactions between flux systems, metal, and metal oxide. Probably these reactions are rather more complex for magnesium than for aluminium. Although the flux, as used in commercial practice, contained 90% NaCl and 10%  $\text{CaF}_2$ , our measurements of viscosity were made on NaCl only, since  $\text{CaF}_2$  did not appreciably alter the viscosity of the flux. In small-scale experiments the omission of  $\text{CaF}_2$  did not significantly affect film stripping or metal agglomeration and recovery, but we have no information on the effect in large-scale production of omission of  $\text{CaF}_2$  from the flux. Neither have we any knowledge of the effect of addition of KCl or  $\text{CaCl}_2$  to the flux. The most efficient thinning agent which we discovered was fresh NaCl.

A point particularly worthy of note is that even a grossly thickened flux is quite capable of stripping alumina films from aluminium. If a bead of aluminium is melted on top of a sample of flux which is so thickened by alumina that the aluminium bead does not sink through it, the flux penetrates the oxide film on the metal bead and is drawn by surface-tension forces up over the bead between the metal and the oxide film, thus detaching the oxide film which floats on the flux film. Consequently we are fairly confident that the thickening of the flux and consequent metal entrapment are not related to any loss of efficiency of the flux in separating oxide films from the metal.

We fully agree with Dr. Scheuer that this investigation deals with only one of several problems relating to the action of melting fluxes. The investigation was carried out primarily to discover why the fluxes became thickened and entrapped so much aluminium. Answers to these points were obtained, but though advantage can be taken of the thixotropic breakdown on stirring to effect recovery of some of the trapped aluminium, at least in small-scale experiments, over half the trapped metal remains as globules that are too small to settle at sufficient rates to ensure recovery. Many wider problems remain to be investigated. Surface-tension studies are important, since surface-tension forces determine not only the ability of fluxes to strip oxide films, but may also assist agglomeration both of metal and stripped films. We share Dr. Scheuer's opinion that much useful work remains to be carried out.

Mr. Chadwick suggests that hydrolysis of the flux constituents might be responsible for some degree of flux thickening, and the experiments which he describes on fluxes containing alkaline earths confirm that this may occur. Our experiments were of much shorter duration than his, and we found that the viscosity of the 90% NaCl, 10%  $\text{CaF}_2$  flux was not increased by allowing it to stand molten in air for periods of up to 24

\* Assistant Research Manager, Imperial Chemical Industries, Ltd., Metals Division, Birmingham.



hr., which was much longer than the time of an individual experiment. Some degree of thickening of flux suspensions containing alumina occurred because of volatilization of flux constituents during the experiment, which increased the effective alumina content. This effect was, however, negligible by comparison with the effect produced by the particle shape of the alumina. It was our common practice to measure the amount of alumina in the flux at the end of an experiment in order to allow for this effect.

Dr. Parker's point is interesting, but we do not think that

ultrasonic vibration would assist agglomeration in thickened flux suspensions. Stirring assists settling, because the films of alumina align themselves normal to the shear gradient, thus effectively decreasing the viscosity in a vertical direction. We do not think that a short-wavelength vibration would achieve this end. In the case of the settling of aluminium dendrites, the effect is probably due to the fact that growing dendritic crystals are disrupted and can settle, whereas in a melt which is not vibrated settling is hindered by interlocking dendrites.

## Discussion

### Creep \*

Dr. P. FELTHAM †: One of the principal difficulties in the interpretation of creep in polycrystals in terms of the theory of dislocations is the rather incomplete understanding of the rôle of grain boundaries. How important that rôle may be is clearly shown in Fig. 3 (p. 230) of the paper by Dr. Chang and Dr. Grant.

Creep resulting from slip which does not encounter boundaries, or encounters only boundaries which do not present obstacles to the propagation of the slip bands, i.e. which may be considered to take place in effect in a single crystal, can be seen to be about 15 times faster (curve I) than the average creep rate (curve IV) as measured for the whole gauge-length of the specimen. Curves II and III, representing creep due to slip in which the bands have encountered boundaries acting as obstacles, seem to be of a character intermediate between that of curves I and IV.

Now, composite curves such as IV are of the type generally obtained in conventional creep experiments, and it is clear that by themselves they cannot provide an adequate basis for the study of the creep mechanisms. The complexity of the creep process comes to light by observations such as those shown by the curves in Fig. 3. These seem to indicate the occurrence of at least two rate-determining mechanisms, and raise the question as to their nature and mutual relation.

Dealing first with curve I, I suggest that it can be adequately interpreted on the assumption that slip took place at first in one single slip plane, and that some of the edge dislocations remaining within it diffused out of that slip plane, bit by bit, in a direction perpendicular to it in a manner described by Mott.‡ Any such segment, on reaching a definite length  $l$ , determined by  $l = Gb/\sigma$  (where  $\sigma$  is the shear stress acting in the slip plane containing the segment,  $G$  is the shear modulus, and  $b$  the Burgers vector) in turn generates dislocations § in its own plane of slip, and so on. Such a process would require an activation energy somewhat in excess of that of self-diffusion.† I have not been able to find data on aluminium suitable for the comparisons I wish to make, but in single crystals of zinc, for example, an activation energy of about 35 k.cal./g. atom was found by Cottrell and Aytakin || for creep at low stresses, in good agreement with about 31 k.cal./g. atom for self-diffusion in a direction perpendicular to the basal planes, which are also those of easy slip.

If the local shear stresses in the vicinity of the first-formed slip band, or bands, are not relaxed, or only incompletely relaxed, soon after their formation, because the dislocations at the leading edges are held up by an impermeable boundary and cannot escape from the crystal, quite a different process

seems to operate. Then the addition of slip bands close to the original one continues, and they pile up next to one another like packs of cards, giving rise to heavy slip bands such as  $K-K$  in Fig. 10 (Plate XXXIV). These are much broader than the slip bands, such as  $S-S$  in Fig. 7 (Plate XXXIV), which have not been impeded by unfavourably oriented boundaries.

Owing to the large and increasing forces acting on the boundary where it is met by the "pack" of slip bands, ¶ severe distortion of the lattice followed by disordering akin to local melting would probably take place, and give rise to the observed recrystallization manifest in boundary migration. The resulting reorientation of the boundary would eventually facilitate the continuance of slip into adjacent grains, as can be seen in the bottom left-hand corner of Figs. 9 and 10 (Plate XXXIV). After such a local relief of stress, diffusion of dislocations out of the heavy slip band would not necessarily lead to further slip, but might result in some kind of sub-grain formation by a polygonization mechanism.

An elementary disordering process, equivalent to the momentary melting of a small group of atoms, should have an activation energy equal to about  $nL$ , where  $n$  is the number of atoms in the molten group and  $L$  the latent heat of melting per atom. On taking  $n = 8$  one obtains a value of about 17 k.cal./g. atom for polycrystalline zinc, such as is required to fit the creep results of Cottrell and Aytakin. ||

Although this value is only about one-half of that of the activation energy for self-diffusion perpendicular to the basal planes, it would not necessarily occur with greater ease than the diffusion of dislocations, because the probability of the occurrence of such a highly co-operative process is small owing to the geometric requirements involved. If, therefore, the steady creep rate is expressed by the equation :

$$\dot{\epsilon} = A \exp(-Q/RT) \cdot \exp(q\sigma/RT)$$

where  $A$ ,  $Q$ , and  $q$  are constants, both  $A$  and  $Q$  can be expected to be lower for slow creep in polycrystals than in single crystals. The temperature-independent entropy term  $\exp(-nL/RT_{\text{melt}})$  (which would be comprised in the constant  $A$  in the case in which the equation describes the creep rate controlled by the remelting of groups of  $n$  atoms) is of the order of  $10^{-5}$  in zinc, so that, apart from any other factors,  $A$  would be expected to be at least  $10^5$  times smaller if the equation refers to polycrystalline creep than if it refers to creep in single crystals. In fact, Cottrell and Aytakin find  $A$  to be about  $10^{10}$  times smaller in that particular case. This large factor is of course to a great extent counteracted by the

\* Joint discussion on the following papers published in the *Journal*: A. Latin (1952-53, **81**, 529); R. C. Gifkins (this vol., p. 39); J. P. Dennison (this vol., p. 117); W. Betteridge (this vol., p. 149); L. M. T. Hopkin and C. J. Thwaites (this vol., p. 181); H. C. Chang and N. J. Grant (this vol., p. 229).

† Standard Telecommunication Research Laboratories, Enfield, Middlesex.

‡ N. F. Mott, *Proc. Phys. Soc.*, 1951, [B], **64**, 729.

§ F. C. Frank and W. T. Read, Jr., *Phys. Rev.*, 1950, [ii], **79**, 722.

|| A. H. Cottrell and V. Aytakin, *J. Inst. Metals*, 1950, **77**, 389.

¶ D. McLean, *Nature*, 1953, **172**, 300.

associated halving of the activation energy. (That the activation energy of creep in aluminium alloys and steels can be very far removed from the corresponding activation energies for self-diffusion is shown by recent experiments.\*)

It seems therefore that the coarseness of the observed slip bands will depend to a large extent upon the ability of the boundary to withstand the mounting force acting on it, without permitting appreciable local stress relaxation facilitated by the melting of small groups of atoms, polygonization, or fracture, of which the last may occur under fatigue conditions. The ability of a boundary to hold up the propagation of slip bands would decrease with increasing temperature, and at a given, constant strain rate the coarseness of the bands would be found to diminish in polycrystals on raising the temperature, until eventually they would cease to be altogether resolvable by ordinary optical means. This phenomenon, and the associated disappearance of asterism, which follow from such an interpretation, have been the subject of many investigations, particularly in the last few years, and need no further comment.

A two-stage mechanism of the type I have sketched in broad outlines, seems not only to account quite well for the very beautiful evidence obtained by Dr. Chang and Dr. Grant, but also to provide a basis for the interpretation of the relation between the principal manifestations of creep and of their mutual relations, in particular of the rôle of boundaries and of the phenomenon of "equicohesion".

Professor Dr. phil. E. SCHMID † (Member): I should like to refer to the effect of  $\alpha$  and  $\beta$  radiation on the creep of metal crystals. Andrade ‡ has reported an experiment in which cadmium crystals were exposed to bombardment by  $\alpha$  particles. He found, within a certain range of small extensions, that there was a considerable increase in the rate of creep (up to about 500%). Similar experiments carried out by Dr. Lintner and myself § have not corroborated these results, but on the contrary have shown a hardening of zinc crystals exposed to  $\alpha$  radiation from polonium (ca. 40 mC.) during creep. An example is given in Fig. A, which shows elonga-

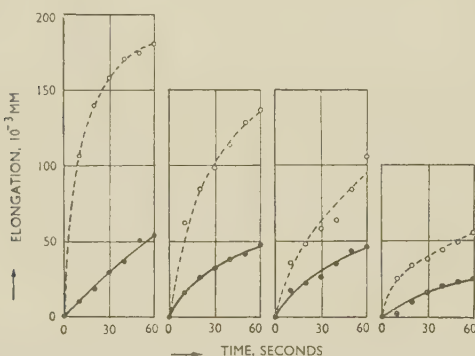


FIG. A.—Creep Curves for a Zinc Crystal ●—● Exposed and ○—○ Not Exposed to  $\alpha$  Radiation. Stress 178 g./mm.<sup>2</sup>.

tion/time curves for a zinc crystal (initial orientation of the glide elements  $\chi_0 = 27^\circ$ ,  $\lambda_0 = 32^\circ$ ) under a stress of 178 g./mm.<sup>2</sup>.

The experiments were carried out in the following way. After undergoing creep for 1 min., the crystal was unloaded and exposed to radiation from a nearby source of  $\alpha$  rays. After 3 min. the crystal was subjected to creep a second time, while still being irradiated. The resulting elongation/time curve is plotted in Fig. A with the same zero point as the first curve. The extension amounts to little more than  $50 \times 10^{-3}$  mm., as compared with  $180 \times 10^{-3}$  mm. in the first test. The

crystal was again unloaded, the  $\alpha$  source removed, and a recovery time of 3 min. allowed; the next creep experiment was then begun. After a further 3 min. the specimen was once more irradiated, and so on. In all cases hardening was apparently caused by the radiation and partly offset by subsequent recovery. As the  $\alpha$  particles do not penetrate more than approximately  $13 \mu$  into the metal, the results observed are probably due to effects in a thin surface layer, the hardening of which may be expected to be much greater than that of

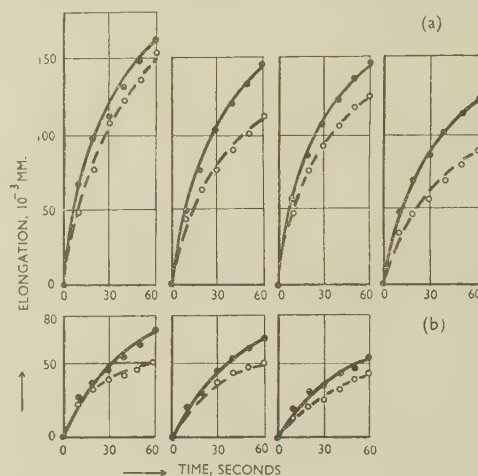


FIG. B.—Creep Curves for a Zinc Crystal ●—● Exposed and ○—○ Not Exposed to  $\beta$  Radiation. (a) Stress 140 g./mm.<sup>2</sup>. (b) Stress 160 g./mm.<sup>2</sup>.

the average cross-section which is effective in the creep experiment. Accordingly, the effect decreases with increasing diameter of the crystal samples used.

When zinc crystals were exposed in exactly the same manner to  $\beta$  radiation, following on some initial hardening by a small amount of creep, the bombardment caused softening. Fig. B gives results for a zinc crystal ( $\chi_0 = 29^\circ$ ,  $\lambda_0 = 32^\circ$ ), which was exposed to  $\beta$  radiation from  $P^{32}$  (ca. 75 mC.). In contrast to the results obtained with  $\alpha$  radiation, the elongation/time curves show greater extensions for the irradiated specimens.

No exact theoretical interpretation of the results is yet possible, but they may be explained with reference to the widely differing effects of  $\alpha$  and  $\beta$  particles on the lattice. While in the first case it is mainly a question of atom repulsion (occupation of interstitial sites), in the second case local temperature increases are principally involved.

Experiments of this kind would appear to be of interest in connection with studies of the solid state, because they afford a means of producing definite amounts of lattice distortion and of observing their influence on physical properties.

Mr. T. B. MARSDEN, || B.Sc. (Student Member): My remarks are concerned with creep-rupture tests performed on binary age-hardenable copper alloys and are intended to be complementary to Dr. Dennison's paper.

A copper-2.42% magnesium alloy has been tested in what might be termed three "limiting states":

- (1) As solution-treated (3 hr. at  $700^\circ\text{C}$ .).
- (2) Aged to maximum hardness (solution-treated for 3 hr. at  $700^\circ\text{C}$ ., aged for 16 hr. at  $500^\circ\text{C}$ .).
- (3) Slowly cooled from the solution-treatment temperature to precipitate the second phase in massive form.

On ageing this alloy the second phase is distributed as a fine continuous lattice and boundary precipitate, visible at mag-

\* P. Feltham, *Proc. Phys. Soc.*, 1953, [B], **66**, 865; *Phil. Mag.*, 1954, [vii], **45**, 9.

† II Physikalisches Institut der Universität, Wien.

‡ E. N. da C. Andrade, *Nature*, 1945, **156**, 113.

§ E. Schmid and K. Lintner, *Österr. Akad. Wiss., Anz.*, 1954, (3); *Österr. Akad. Wiss., Sitzber.*, 1954, **163** (in the press).  
|| University College, Swansea.



nifications greater than about 400 (Fig. C, Plate LXXXIX). Slow cooling produces a similar distribution of second phase in an extremely massive form (Figs. D and E, Plate LXXXIX).

It seems probable that the effect of particle-size on creep-rupture properties, i.e. time to fracture and elongation per cent. under a given stress, is entirely dependent on testing conditions.

Considerable variation of properties between the three states is experienced at 250° C., but upon raising the testing temperature to 400° C., the properties show a distinct similarity, as indicated by the data given in Table A.

TABLE A.—Stress to Cause Fracture in 100 Hr. of Copper-2.42% Magnesium Alloy in Various Heat-Treatment States and at Different Temperatures.

Condition	Temp., °C.	Stress, tons/in. <sup>2</sup>
Solution-treated . . . . .	250	16
Aged to maximum hardness . . . . .	250	13.5
Slowly cooled . . . . .	250	9.5
Solution-treated . . . . .	400	6.2
Aged to maximum hardness . . . . .	400	5.8
Slowly cooled . . . . .	400	5.9

The precipitating phase in this alloy is said to be the inter-metallic compound Cu<sub>2</sub>Mg, the brittle nature of which is probably the cause of its relatively poor performance in the slowly cooled state at 250° C. At 400° C. the embrittling effect does not seem to be in evidence, since elongations of the order of 10% can occur at fracture, and it appears likely that at this temperature the precipitate has little effect on the deformation processes, whatever its particle-size may be. It should be mentioned that, since the ageing heat-treatment was carried out at 500° C., no precipitation during test is experienced with the material in the fully hardened and slowly cooled states, although some will occur with material solution-treated before testing.

Binary copper alloys having chromium contents of 0.45% and 0.67% exhibit considerable similarity in creep-rupture properties, although the 0.45% alloy has a grain size four times larger than that of the 0.67% alloy. This indicates that grain-size is not as important a factor as is often alleged. It would appear from the comparison of the various alloys examined that the solution-treatment temperature may be a more critical factor in determining the creep-rupture properties.

Mr. R. C. GIFFKINS,\* B.Sc., A.I.M. (Member): I have read Dr. Latin's paper with great interest, because it covers a wide field of results and ideas in a stimulating manner. The comments I have to make concern some of the many points of contact between Dr. Latin's paper and my own on the creep of lead.

I believe that one of the most important factors in the creep of lead is grain-size, particularly in relation to the cross-sectional area of the specimen. Dr. Latin's specimens all contained grains of the order of  $\frac{1}{2}$  mm. dia., so that only a few grains were present through the section. This would tend to limit the opportunity for extensive movement at grain boundaries and cause increased slip or other local intragranular changes, as I have suggested elsewhere †; some experiments with pure lead specimens of different cross-section but similar grain-sizes, at present in progress, confirm this suggestion. I wonder whether this partly accounts for the upper limit of ~20% extension at fracture found by Dr. Latin for his specimens; if so, the correspondence of this strain with the theoretical one for atom-pair rupture would seem to be

fortuitous. Further, it should be recalled that Greenwood and Worner,‡ for example, have reported intercrystalline failures of tellurium-lead alloys at as much as 50–90% extension.

The influence of grain-size and creep rate on ductility seems to be much more complex than Dr. Latin suggests, and his hypothesis does not appear to cover other experimental evidence. I have found that very pure lead (99.9992%) does show the predicted invariance of ductility with rate of strain; extruded specimens fracture at 30–40% over the range  $3.5 \times 10^{-1}$  to  $4.6 \times 10^{-6}$  mm./mm./day. However, Table B indicates that the behaviour of alloys varies in this respect.

With alloys in which thallium is in solid solution:

(a) There is a marked increase in ductility with lower rates of strain for a given alloy (cf. specimens A and B, C and D). Visible slip tends to be eliminated at the lower strain rates.

(b) A decrease in grain-size for a given alloy also results in an increase in ductility, but the mechanism of creep becomes increasingly that of movement at grain boundaries without visible slip (cf. specimens D and E).

With a 0.05 tellurium alloy:

(c) Ductility drops with decreased rate of strain and visible slip becomes less (cf. specimens K and L).

(d) A decrease in grain-size has the same effect as in (b) (cf. specimens F and H).

Thus, thallium alloys, which have been found to behave as if they were fine-grained pure lead,§ do not show the invariance of ductility with rate of strain; further, both thallium and the two-phase tellurium alloys exhibit an increase in ductility

TABLE B.—Creep and Fracture of Lead-Thallium and Lead-Tellurium Alloys.

Alloy	Specimen	Stress, lb./in. <sup>2</sup>	Mean Grain Dia., mm.	Fracture at:		Type of Deformation Mechanism
				%	Days	
8% Thallium (extruded)	A	1500	0.04	70	1	Much visible slip
	B	300	0.04	372	220	Very little visible slip
4.35% Thallium (extruded)	C	500	0.04	180	55	Some visible slip
	D	300	0.04	273	198	Very little visible slip
	E	300	0.07	188	880	As C
0.05% Tellurium (extruded)	F	500	Finer than G	223	54	Slightly more slip than C
	G	500	~0.04	114	65	More slip than F
	H	500	Coarser than G	83	160	More slip than G
0.05% * Tellurium (rolled)	K	2000	~0.1	40	10 hr.	Some visible slip
	L	500	~0.1	16	137	Much less slip than K

\* Results from H. C. Coe, M.Sc. Thesis, Melbourne University, 1952.

with finer grain-sizes, which is in agreement with Dr. Latin's results but does not support his theory, because this increase in ductility is accompanied by the progressive elimination of ordinary visible slip.

These results seem to indicate that low ductility and the tendency to intercrystalline fracture are associated with tests of longer duration in a series, and that this factor of long time might co-operate with or replace the effect of mechanism of deformation in some circumstances. Time would be impor-

\* Senior Research Officer, Physical Metallurgy Section, Commonwealth Scientific and Industrial Research Organization, The Baillieu Laboratory, University of Melbourne, Australia.

† R. C. Giffkins, *J. Inst. Metals*, 1952–53, 81, 417.

‡ J. N. Greenwood and H. K. Worner, *Proc. Australasian Inst. Min. Met.*, 1936, (101), 57.

§ R. C. Giffkins, *J. Inst. Metals*, 1953–54, 82, 39.

tant in a process such as the agglomeration of vacancies (or other lattice defects) as suggested by Dr. Latin (p. 536) and also by Greenwood.\*

Contrary to the suggestion made by Dr. Latin (p. 534), I believe that evidence favours the idea that, other things being equal, recrystallization during creep is favoured by a grain-size which is large compared to the specimen cross-section (see the results of tests with thallium alloys †). The experiments with pure lead of large cross-sectional area, mentioned above, support this also. In connection with the reference to Andrade ‡ in the same paragraph, I would like to point out that Greenwood § anticipated Andrade's results by fifteen years; he noted the effect of recrystallization during creep of lead and a number of alloys. It should be noted, moreover, that Andrade also used Tadanac lead, and it was not therefore more "highly pure" than that used by Dr. Latin. Again, it is probably relevant to any discussion of this phenomenon that the creep rates studied by Andrade were much higher than those of Dr. Latin; they were about 7 mm./mm./day, at which rate I feel sure glide-plane slip predominates.

Finally, I would like to ask some questions about Fig. 7 (Plate LXXXII), which interests me because of its similarity to structures I have encountered with tellurium-lead alloys. Is the structure shown developed on a polished surface during creep, or only after polishing and etching subsequent to creep? I am not quite clear as regards the specific changes at the boundaries which are illustrated, and would be glad of further details. Also, are the stripes the remains of extrusion marks or do they represent segregation revealed by etching?

I would like to express agreement with some of the main conclusions drawn by Dr. Hopkin and Mr. Thwaites from their work on the creep of lead and lead alloys, but wish to discuss a number of points which seem to be less well sustained.

A major item of agreement is the great effect of grain-size on creep. I feel, however, that the criticism of Greenwood and his collaborators on this score is not entirely justified. They showed their awareness of this factor, but accepted it as a modification inherent in additions of solute; consequently, the strain-anneal history of specimens was standardized. Perhaps the only really fundamental approach is to try to show that creep is practically unaffected, whatever the particular combination of straining and annealing used to attain a given grain-size.

Similarly, the conditions for comparing the effect of solute atoms might be more fundamentally acceptable if atomic percentage of each element were compared, rather than weight percentage as has been done by the authors. Where the authors have used atomic percentage, in Section V, 4 (p. 185), I believe a case could be made for comparing the same proportion of maximum solid solubility. However, on the authors' basis of comparison, Fig. 6\* (p. 186) seems to show the correlation between melting point and creep which they have denied, for the creep strains for indium, tin, and antimony are in the order of increasing melting point. Thus, the indication of a correlation between atomic diameter and creep-resistance is not invalid.

It is interesting to note the use of constant stress in such a large programme of long-term tests. Do the authors think it was worth the extra complexity of apparatus to employ this rather than constant load?

It is asserted fairly strongly on p. 192, but with reservations elsewhere, that Dr. Hopkin and Mr. Thwaites believe the fragmentation to result from polygonization. In this connection, I should like to raise the following points: (a) There does not

seem to be any relevance to the authors' thesis that the fragments, which are somewhat indirectly inferred from X-ray results, should be formed by the mechanism of polygonization. (b) Further, X-ray diagrams could indicate the presence, not of fragments, but of relatively perfect areas of grains separated from each other by less-perfect zones, as I have suggested elsewhere. (c) Again, if the structure is one similar to cells or polygonized sub-grains, I should expect there to be a change to an equilibrium sub-grain size during creep of pre-strained specimens, as in aluminium. ¶\*\* This change is also associated with a return to a creep rate similar to that of an annealed specimen. †† (d) The authors seem to me to leave out the strongest evidence for fragmentation or polygonization, namely the metallographic. Apart from this, I am most interested to know the technique used to show up the fragments metallographically, since I have not been able to relate a very definite spottiness of the X-ray reflections to any sub-structure. ||

Thus, on the subject of polygonization it seems that Dr. Hopkin and Mr. Thwaites, in common with others, have used polygonization as a popular synonym for fragmentation or sub-grain formation, advancing neither clear evidence for sub-grains nor reasons why they should be formed by polygonization if they are present. It would seem sufficient to describe the effect in terms of fragments of the kind discussed by Kellar, Hirsch, and Thorp. ‡‡

My own work inclines me to believe that high-purity lead does show an inflection in the creep curve due to recrystallization, even at high stresses, and Andrade ‡ has also found it at the high stresses he used. Do the authors think that the inflection might be revealed if frequent readings of creep strain were taken and plotted with an extended time scale, or have they theoretical reasons for believing the effect to be suppressed at high stresses?

The work in Melbourne has given rather conflicting evidence on the authors' statement that a smaller grain-size gives a lower recrystallization strain. Is the general evidence on this more clear-cut than that shown in Fig. 1 (p. 183)?

It is not easy to see the justification for giving 0.02 mm.<sup>2</sup> as the critical value for the grain-size effect (Fig. 2, p. 183), especially for alloys of lower tin content. If there is a critical value, are there any suggested reasons for it, as this seems a matter of some theoretical interest?

I would also welcome some remarks on the choice of total strain in a given time as an index of creep behaviour. It seems a good practical index, but in theoretical discussions (particularly Fig. 6, p. 186) less sound, since it contains some or all of the initial extension, transient creep, minimum creep, recrystallization strain, and varying proportions of tertiary creep.

I should be glad if Dr. Betteridge would amplify one section of his argument or perhaps show me where I have missed a point. From the argument in Section III, 2 (p. 152) alone, I am not sure why it should be concluded that either grain-boundary viscosity or internal changes in the grain are the only possibilities. Are combinations of the two, or even of viscosity with internal changes limited to a zone near the boundary, excluded by the analysis of the shape of the creep curves?

A second question concerns the forthright conclusion in the last paragraph (p. 161). I feel it would be of great help and interest to all in this field of work if Dr. Betteridge would be prepared to suggest what he considers to be the best way of investigating the problem of grain-boundary viscosity (or its absence) at high stresses.

\* J. N. Greenwood, *Bull. Inst. Metals*, 1952, 1, 104.

† R. C. Gifkins, *J. Inst. Metals*, 1952-53, 81, 417.

‡ E. N. da C. Andrade, *Nature*, 1948, 162, 410.

§ J. N. Greenwood, *Proc. Australasian Inst. Min. Met.*, 1934, (95), 79.

|| R. C. Gifkins, *J. Inst. Metals*, 1953-54, 82, 39.

¶ W. A. Wood and J. W. Suiter, *ibid.*, 1951-52, 80,

501.

\*\* J. Hino, P. G. Shewmon, and P. A. Beck, *Trans. Amer. Inst. Min. Met. Eng.*, 1952, 194, 873.

†† G. R. Wilms, Ph.D. Thesis, University of Melbourne, 1951.

‡‡ J. N. Kellar, P. B. Hirsch, and J. S. Thorp, *Nature*, 1950, 165, 554.



Mr. D. McLEAN,\* B.Sc. (Member): I should like to discuss some points raised by Dr. Betteridge. Dr. Betteridge points out that Kê-type experimental results do not correspond to a single relaxation time, as assumed in the original theory. This is very true, as Fig. F, which compares various published experimental results with those which would be obtained for a single relaxation time, makes clear. The abscissa is ( $2\pi \times$  frequency  $\times$  relaxation time), i.e.  $\omega\tau$ , which is the appropriate variable, plotted on a logarithmic scale, and the ordinate is the shear modulus. The curves show that for the pure aluminium investigated by Kê, the modulus change covers a range of  $\omega\tau$  about  $10^4$  times wider than would a single relaxation time. For the aluminium-magnesium alloy the range is about  $10^8$  times wider. There is therefore a spread of relaxation times of at least  $10^4:1$  in the pure metal and of at least  $10^8:1$  in the alloy.

These are wide ranges, so wide that Dr. Betteridge concludes that the process Kê assumed to be responsible—that of grains sliding bodily over each other—cannot explain them.

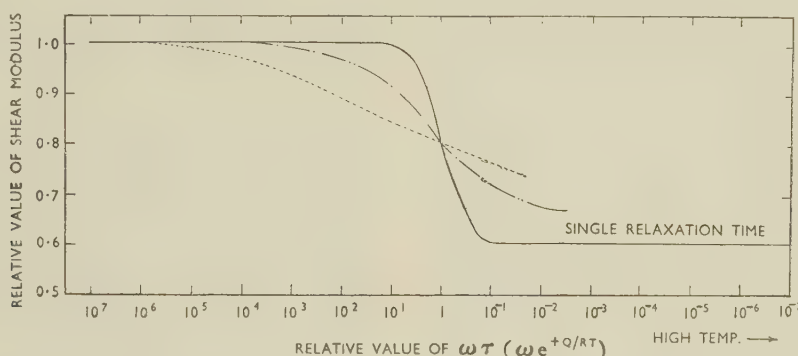


FIG. F.—Generalized Plots of Shear Modulus against Temperature for Pure Aluminium — — — (Kê†) and Aluminium-1.617% Magnesium Alloy - - - - (Starr, Vicars, Goldberg, and Dorn‡).

However, the following argument suggests that such wide ranges are not unreasonable on Kê's basis in a real polycrystalline aggregate. Kê† finds that the activation energy in pure aluminium for damping and for shear modulus relaxation is 34,000 cal./mol.; Starr, Vicars, Goldberg, and Dorn‡ find that the value in the aluminium-magnesium alloy used for the curve in Fig. F is 58,000 cal./mol. A simple calculation shows that in the former case a band of activation energies of  $\pm 4000$  cal./mol. and in the latter of  $\pm 9000$  cal./mol. would produce the observed range. Are such bands, which are moderate compared with the absolute value of the activation energy, reasonable? The answer is surely yes, because it is known that free energies at crystal boundaries vary over a wide range, depending on the degree of fit; this, for example, depends on the difference in orientation between the two crystals on either side of the boundary, and the ease of sliding must also depend on the degree of fit. When the fit is perfect or nearly perfect, as in a single crystal or at a twin boundary, sliding will be difficult; when it is bad, sliding should be easier. The suggestion arising from this is, therefore, that Kê's model is fundamentally correct, but that in a real polycrystalline aggregate a range of relaxation times must be expected.

Dr. Betteridge then points out that in Kê-type torsion creep experiments the strain does not asymptotically approach a constant value, as it should according to the original Kê model, but continues, albeit perhaps more and more slowly. Kê's suggestion, of course, was that creep at these low strains was due to the crystals sliding over each other. His reason

for expecting a limiting value, approached asymptotically, was derived from the assumption that at the end of a sliding boundary a purely elastic strain was set up, which could not help but impose a definite limit on the strain. It seems that here a feature of the real situation was overlooked. This is that at the end of a sliding boundary a large stress concentration arises like that at the end of a crack. The stress applied in a typical Kê experiment is small, but not far below that required to induce plastic flow. It therefore seems probable that the stress concentration mentioned does cause plastic deformation at grain corners. If so, there is no reason to expect an asymptotic limit to the strain. One would expect instead that creep would continue at a slower and slower rate, and this, as Dr. Betteridge points out, is what actually happens.

I suggest therefore that the Kê model is fundamentally correct, but that two small modifications are needed to make it resemble more exactly the real situation; the recognition of (a) a wide range of relaxation times on account of the different

properties of individual boundaries, (b) the occurrence of plastic strain in the crystal at each end of a sliding boundary.

Dr. N. P. ALLEN,\* M.Met., F.I.M. (Member): This discussion leaves me with the impression that the creep mechanism is agreed to be very complex and that investigators who have drawn attention to the different types of process are beginning to come together in their assessment of the relative importance of the processes. Slip, grain fragmentation, crystal rotation, grain-boundary sliding, and grain-boundary migration all play a part, but the material yields as a whole, and the rate at which any one process can take place is not independent of the rates of the other processes.

Three different views on the factor that controls the overall speed of the deformation appear to be developing. One is that the rate of flow is determined primarily by the rate of dispersal of the groups of dislocations that are held to be responsible for work-hardening, this rate of dispersal being in turn a function of the availability and mobility of vacancies. The second is that the important factor is the clogging of the movement of dislocations by dissolved atoms or precipitates that may become attached to them. The third view is that the mobility at the grain boundary controls everything, by making possible the grain rotation that is a necessary accompaniment of slip. Critical experiments enabling us to decide between these views will be most welcome.

Insufficient attention appears to be given to the importance of precipitates. Most useful creep-resisting materials are in fact precipitation-hardened, and their usefulness seems to be

\* Metallurgy Division, National Physical Laboratory, Teddington.

† T. S. Kê, *Phys. Rev.*, 1947, [ii], 71, 533.

‡ C. D. Starr, E. C. Vicars, A. Goldberg, and J. E. Dorn, *Trans. Amer. Soc. Metals*, 1953, 45, 275.

associated with the resistance that the precipitate offers to coagulation and solution at the temperature of service. We do not yet know how to select a precipitate having the desired properties.

Dr. LATIN (*in reply*): I thank Mr. Gifkins for his useful comments on my paper. I am somewhat out of touch at present with this field of work, but will do my best to reply to his points.

I fully endorse Mr. Gifkins's view on the importance of grain-size. As regards my own specimens, I suggest that the grain-size was such as to favour the growth of elastic strains at the grain boundaries and that this would be encouraged rather than diminished by the limitation of extensive boundary movement. The extension reached at fracture depends upon so many factors that it is not at all surprising that a very wide range of values can be obtained. My own suggestion from my results merely amounts to the view that there could be some significant relationship between the extension found under the conditions of my tests (in particular the tests on pipe) and elastic strains produced at the grain boundaries. That complications in the mode of deformation could readily arise, which would either limit or enhance the growth of elastic strains is, however, well realized.

With regard to the comment on the complexity of the influence of grain-size on creep rate and ductility, I do not think I have suggested that this is not likely to be very complex, especially when alloying additions are present. I deliberately attempted to simplify the issues in order to try to arrive at general principles; perhaps I over-simplified, but in any case I would suggest that there is perhaps rather too great a tendency, in work on creep, towards the study of the trees, to the detriment of a clear picture of the wood. On the other hand, of course, one must not forget the variety of complications that can occur. The data on the thallium alloys are of great interest and I would suggest that these are probably at least in part explained by Mr. Gifkins's own finding that they behave as if they were fine-grained, and as such need not necessarily show a decrease or constancy of ductility with decrease of rate of strain. The results on the tellurium alloy are similar in nature to my own on this type of material but I cannot see that they are necessarily in disagreement with my theoretical considerations, which do not imply that increase in ductility must of necessity be accompanied by ordinary visible slip.

I take it that Mr. Gifkins's suggestion with regard to the factor of long time amounts to the view that intercrystalline fracture is largely the result of purely time-dependent effects. That such effects may co-operate with effects resulting from deformation processes may well be likely but it is difficult to believe that they could be of primary significance, in view, for example, of the fact that in some of the materials (e.g. antimonial alloys) intercrystalline fracture can occur at fairly rapid creep rates. There are of course, again, complicating effects here, but I suggest that the fundamental mechanism of fracture is in all probability the same, namely the development of critical elastic-strain energies.

I note with interest Mr. Gifkins's findings with regard to the relationship between grain-size and recrystallization; I think he will agree that, in general, recrystallization in other processes is undoubtedly favoured by fine grain-size. It is difficult to see why this should not be broadly true of creep also, although there may well be conditions in which recrystallization resulting from the effects of, say, particularly large local strains may result readily in large-grained alloys. This is an aspect of importance which I am afraid I was unable to study as fully as I would have wished; I can merely report that in most cases in my work no marked change in grain-size occurred during creep and I was unable to observe any very definite recrystallization effects. In pure lead certainly I consider it quite likely that some did occur and its occurrence would well explain the considerable scatter in the extensions at fracture

obtained. I am of course aware of Greenwood's experiments on recrystallization; I referred to those of Andrade as being more closely allied to my own work. I am afraid that I was under the false impression that Andrade had used a specially purified lead. I agree that his tests were at comparatively rapid creep rates and the difference in observations may well be connected with this fact.

Fig. 7 (Plate LXXXII) of my paper is a photomicrograph of an etched longitudinal section of extruded strip subsequent to creep. The precise nature of the changes at the boundaries was not fully settled; from observations at a later stage of deformation, which showed signs of some dispersed second phase in specimens examined under the microscope, I think that the changes were of not dissimilar nature to those which occur in coarse-grained alloy *E*. The stripes were revealed only by etching. They correspond in direction to the direction of extrusion, and examination, again on samples from later stages of deformation, indicated that they finally disappeared at what appeared to correspond to complete structural change of the alloy. This alloy exhibited ductile fracture at small creep rates and an increase of extension, an effect probably connected with its fineness of grain, which I believe results in a release of or retardation in the development of grain-boundary elastic strains.

Dr. HOPKIN and Mr. THWAITES (*in reply*): Although we believe that our results show the true effect of grain-size on creep-resistance, we agree with Mr. Gifkins that the only way of being sure of this is to prove that the relationship between creep-resistance and grain-size remains the same no matter what combinations of straining and annealing are used to vary the grain-size. We would like to point out, however, that different combinations of straining and annealing might also affect the irregularity of grain boundaries and the extent of twinning, which also affects creep-resistance as shown in Table V (p. 187) of our paper.

It is true, of course, that the use of atomic percentages is more fundamentally acceptable than weight percentages, but since no detailed relationships with composition are attempted and only the general effect of composition is illustrated, e.g. in Fig. 4 (p. 184), it does not matter whether atomic or weight percentages are used.

In Section V, 4 (p. 185) we do not see the point of Mr. Gifkins's suggestion of comparing alloys of the same proportion of their maximum solid solubility. Assuming that valency and electrochemical effects do not influence these alloys, then alloys containing the same proportion of their maximum solid solubility would probably exhibit similar lattice distortions because of their respective size-factors. There would, then, be two variables; different numbers of atoms of different size-factors contributing to the arbitrary lattice distortion. This complicates rather than simplifies the interpretation of results.

We agree that the text relating to Fig. 6 (p. 186) is inadequate. There is no significant difference between the creep-resistance of the antimony and tin alloys, although the melting points of these elements differ considerably. The difference in melting point between indium and tin, however, is much less, yet there is a marked difference between their creep-resistances. Clearly, an uncontrolled factor is present which invalidates any conclusion as to the effect of size-factor.

When our work was planned it was decided to use constant-stress tests in the hope that analysis by the Andrade equation of the creep curves obtained would facilitate interpretation of the results, but this was found not to be the case.\* The only other reason for employing constant-stress tests is that reliable comparisons of creep-resistance can be made after any arbitrary time during the tests without the complication of increased stress which occurs in tests at constant load.

In our paper the term "fragmentation" has been used merely to describe a disordered structure and was suggested by the fragmented appearance of the X-ray reflections. It

\* L. M. T. Hopkin, *J. Inst. Metals*, 1952-53, **81**, 443.



was not intended that the term should describe the precise nature of the disordered structure or the mechanism by which it was formed. We have used the term "polygonization" to describe a relatively perfect cell structure with distinct boundaries. In our present state of knowledge the terms "polygonized" and "cell" structures are synonymous, since it is most likely that they can result only from the diffusion of dislocations. On p. 192 of the paper it is argued that since the creep curves of the as-extruded specimens with fragmented structures and the plastically overstrained specimens had different characteristics (see Appendix III), despite some similarities in the X-ray photographs, then the structures were different. The results suggest that the as-extruded copper-bearing alloys had fragmented structures which were more perfect than those of the plastically strained specimens, and it was considered likely that the as-extruded specimens were in a polygonized condition, especially as a polygonized structure had been observed metallographically in as-extruded lead-arsenic alloys, which also gave fragmented X-ray reflections. Conventional methods of polishing the lead-arsenic alloys were used but we suspect that the reason for the polygonized structure being revealed was because precipitation occurred along the cell boundaries. The fact that polygonized structures can be obtained by hot working has been clearly established by McLean and Tate.\*

As regards recrystallization in high-purity lead, we can assure Mr. Gifkins that sufficiently frequent readings of creep strain were taken to preclude the possibility of having missed the characteristic inflection in this material. The presence of an inflection is likely to be associated with a suitable rate of strain relative to that of recrystallization, and probably by a difference of grain-size before and after recrystallization. It seems likely that recrystallization can occur slowly and continuously without much change of grain-size and produce tertiary creep. It was in fact in the coarse-grained specimens, where recrystallization should be slower than in fine-grained specimens, that the inflection was less distinct or absent.

The evidence for recrystallization occurring at lower strains the finer the grain-size, was extensive. For instance, the following figures are for the pure lead tested at 300 lb./in.<sup>2</sup>:

Average Grain-Size, mm. <sup>2</sup>	Approx. Strain at the Beginning of Recrystallization, %
0.15	0.9
0.38	1.5
0.86	2.5
1.8	3.3

Although creep-resistance was shown to increase markedly with grain-size for grain-sizes below 0.02 mm.<sup>2</sup>, the effect was small above this value. We do not think that there is any fundamental reason for this abrupt change in behaviour. For instance, if relative grain-boundary area per unit volume is plotted against creep strain, a reasonable straight line is obtained with no critical value at a grain-size of 0.02 mm.<sup>2</sup>. Reference to this grain-size as a critical value emphasizes the fact that for values greater than this there is little effect of grain-size on creep-resistance.

The choice of total strain as an index of creep behaviour was made in the absence of a better one. The use of minimum creep rates is difficult at low stresses, which are the most important, where it cannot be certain that the minimum

rate of creep has been reached unless the stage of tertiary creep is present.

Dr. W. BETTERIDGE (*in reply*): With regard to Mr. Gifkins's comments, the conclusions I drew from the shape of the creep curve described in Section III, 2 (p. 152) only included the fact that the creep was unlikely to be due solely to grain-boundary viscous flow. The evidence that the creep was more likely to be due to grain distortion is provided by the results described in Sections III, 3 and 4 (pp. 155 and 159), particularly the linear relationship illustrated in Fig. 7 (p. 156). It is, of course, possible that the observed strain is due to a combination of grain distortion and of grain-boundary flow, but the simple power law would seem to imply a single mechanism rather than a combination of two, probably interdependent, mechanisms. The term viscous grain-boundary flow is regarded as embracing the relative movement of two grains, even though the shear strain is not concentrated at a plane but is distributed throughout a narrow zone in the vicinity of the boundary; it is only necessary that, with a constant shear stress across a boundary, the rate of displacement should remain constant with time.

It is agreed that the statement in the last sentence is perhaps too pessimistic, as it was intended to refer only to torsional tests on solid samples, as described in the paper. It was explained in Section III, 1 (p. 151) that the interpretation of the results of such tests is only straightforward when the stress is low. A torsional test in which a hollow test-piece is used, so that the shear stress is essentially constant across the section, would enable the true stress/strain relationship to be studied. Furthermore, most interesting results are now being obtained by a combined tensile-torsional technique, low-stress torsional tests of the type described in this paper being carried out at intervals during the progress of high-stress tensile creep tests. Preliminary results by this technique have already been described.†

Mr. McLean's comments serve to indicate that, as was stated in the final section of the paper, the available evidence is not sufficient to permit a conclusive interpretation of the observations to be made. Mr. McLean shows that a very wide range of relaxation times is necessary to explain the shear-modulus determinations of other workers, but suggests that such a range could be due to a moderate range in activation energies, which, in view of the known free energies of crystal boundaries, he regards as reasonable. While it is agreed that the range of grain-boundary properties can be very wide, an equally important factor in determining the shape of the various curves is the distribution of properties within this range. In a completely random arrangement of orientations, only a small proportion of boundaries will separate crystals with small orientation differences (and, therefore, with properties deviating at all widely from those of the average boundary) and this would not be expected to affect the shape of the curves significantly. It is possible, however, that polygon boundaries in strained and annealed metals will act in this manner and have an important influence.

Plastic strain at the end of sliding boundaries has, of course, been observed in creep tests at a normal stress level,‡ and may be of significance in low-stress tests, but calculations made on such an assumption show that the creep strain still tends to an asymptotic value, at a higher strain level than in the purely elastic case, provided that the applied stress is below the limiting stress at which plastic flow of the crystals is assumed to begin.

\* D. McLean and A. E. L. Tate, *Rev. Mét.*, 1952, **48**, 763.

† W. Betteridge, *N.P.L. Symposium on Creep*, 1954, Paper No. 15.

‡ W. Betteridge and A. W. Franklin, *J. Inst. Metals*, 1951-52, **80**, 147.

## Discussion

## Precipitation-Hardening\*

Dr. J. NUTTING,† B.Sc. (Member): From their metallographic examination of the ageing process in aluminium-4% copper alloys, Mr. Polmear and Dr. Hardy conclude that the presence of the  $\theta'$  phase is associated with the platelets visible in the electron micrographs. They have been unable to detect any changes associated with the formation of G.P.[1] or G.P.[2], although they think there may be a dot-like structure associated with G.P.[2].

Mr. G. Thomas and I have examined metallographically the early stages in the ageing of aluminium-4% copper alloys, using a technique similar to that of Mr. Polmear and Dr. Hardy and we have also studied metallographically many of the specimens used by Miss Silcock, Mr. Heal, and Dr. Hardy. We have been able to detect metallographic changes at an earlier stage than that reported by Mr. Polmear and Dr. Hardy. It has also been possible to correlate the microstructural changes with structural changes determined by X-ray-diffraction methods. The alterations in structure noted are:

(1) The appearance of dots which seem to be associated with the presence of G.P.[1]. A typical electron micrograph is shown in Fig. A (Plate XC). As ageing proceeds, the number of dots in a given area increases greatly, but the size of the dots varies only slightly. The actual size is 80–160 Å. in dia., i.e. 30–60 atom spacings.

(2) With increasing ageing temperatures the dots are still present, but are now aligned in rows along the [100] directions. Fig. B (Plate XC) is a typical electron micrograph. This microstructure is associated with the formation of G.P.[2].

(3) At still higher ageing temperatures, or longer ageing times, clearly defined rod-like markings are seen along the [100] directions. It is assumed that these are the traces of platelets intersecting the free surface. An electron micrograph is reproduced in Fig C (Plate XC). As stated by Mr. Polmear and Dr. Hardy, this is the microstructure associated with the presence of the  $\theta'$  phase.

The electron microscope shows the G.P.[1] to take the form of spheres, or sometimes ellipsoids, but certainly not the platelets required to account for the X-ray-diffraction results of Miss Silcock, Mr. Heal, and Dr. Hardy. Another interesting observation is that the dot markings are always present in the microstructure immediately after quenching. In this condition the size of the dots may be varied by changing the solution-treatment temperature and the rate of cooling.

The results may be taken to indicate that in these alloys a homogeneous solid solution does not exist, but that there are always micro-regions rich in copper. The G.P.[1] may then form from these regions by a kind of ordering effect. A somewhat similar effect has been reported by Walker and Guinier‡ in the ageing of aluminium-silver alloys.

The microstructural changes give some indication of the answers to the questions raised by Miss Silcock, Mr. Heal, and Dr. Hardy with regard to the mode of formation of the precipitates G.P.[1], G.P.[2], and  $\theta'$  (p. 247 of their paper). The evidence suggests that after formation of G.P.[1], G.P.[2] is nucleated and grows, the G.P.[1] then going back into

solution. After growth, the G.P.[2] may change directly into  $\theta'$ .

Miss Silcock, Mr. Heal, and Dr. Hardy, in describing these various possible changes, have used the term "allotropic". Allotropy is generally used to describe reversible changes of stable phases. In the present case none of the phases is stable, and it is believed that the changes are irreversible. Monotropic may be employed to describe the change from G.P.[2] to  $\theta'$ , but, strictly, monotropic should be applied only to a change from a metastable to a stable phase. In view of this difficulty perhaps it would be better to describe the changes as diffusionless transformations.

Dr. M. L. V. GAYLER§ (Member): Mr. Polmear and Dr. Hardy have observed the "light phenomenon" at an earlier stage in the course of ageing than I did, but, on the other hand, they did not detect it within the grains. They consider that the "light phenomenon" originates as a crystallization process, probably the result of strains arising from cold-water quenching and precipitation on ageing, contrary to my conclusion that it formed an integral part of the ageing process of aluminium-copper alloys.

In view of Dr. Hardy's thermodynamical theory of ageing,|| I would like to express agreement with the interpretation of the formation of the "light phenomenon" now put forward. I am not, however, convinced that it is not formed within the grains. Under certain conditions of ageing ¶ there is no doubt that this is the case, but possibly an alternative explanation of its presence may be forthcoming.

I have also shown\*\* that the "light phenomenon" is formed in great quantity on cold working the quenched 4% copper alloy before and after ageing, and I deduced that the mechanism of relief of strain caused by cold work was similar to that occurring in relief of strains set up during age-hardening. I still think that my deduction is correct, though it needs qualifying in view of the present authors' theory of the formation of the "light phenomenon".

Dr. Hardy has summed up all his records on the ageing of binary aluminium-copper alloys in Fig. 3 (p. 238) of his own paper, and has shown that with low concentrations of copper single-stage ageing alone takes place but that with 2.5–4% copper the alloys exhibit two stages separated by a flat plateau. Fig. 3 (p. 238) of this paper and also Fig. 24 (p. 248) of his paper with Miss Silcock and Mr. Heal, obtained by X-ray analysis of Dr. Hardy's specimens, put before us a picture of what takes place during the ageing process in terms of phase changes. This work represents a perfect example of the right type of co-operation between the metallurgist and the X-ray physicist, and Dr. Hardy and his colleagues at the Fulmer Research Institute are to be congratulated on their valuable contribution to the solution of the problem of age-hardening.

M. A. SAULNIER†† (Member): A study of the extensive literature relating to the aluminium-4% copper alloys reveals a certain lack of agreement between the physicists, who base themselves on X-ray-diffusion photographs, and the metal-

\* Joint discussion on the following papers published in the *Journal*: L. M. T. Hopkin and C. J. Thwaites (1952–53, **81**, 255); I. J. Polmear and H. K. Hardy (1952–53, **81**, 427); H. K. Hardy (this vol., p. 236); J. M. Silcock, T. J. Heal, and H. K. Hardy (this vol., p. 239); K. M. Entwistle (this vol., p. 249).

† Department of Metallurgy, Cambridge University.

‡ C. B. Walker and A. Guinier, *Acta Met.*, 1953, **1**, 568.

§ Consultant, Fulmer Research Institute, Stoke Poges, Bucks.

|| H. K. Hardy, *J. Inst. Metals*, 1950, **77**, 457.

¶ E.g. M. L. V. Gayler, *ibid.*, 1946, **72**, Figs. 5 and 6 (Plate XIII), Figs. 17 and 18 (Plate XVI).

\*\* M. L. V. Gayler, *ibid.*, 1946, **72**, 543.

†† Chef de la Section de Micrographie et de Rayons-X, Service de Recherches et d'Essais Physiques, Cie. Pêchiney, Chambéry (Savoie), France.



lographers, who rely upon their microscopic observations. It is, however, clear that advances in knowledge of the structural changes in these alloys can be achieved only through the joint use of these complementary methods. Owing to the necessity of using replicas, the resolving power of the electron microscope is insufficient to give a direct picture of the transformations in the early stages of hardening, and the special X-ray-diffusion techniques employed also have their limitations. Whatever may be the precautions taken to ensure identity of composition, a single crystal does not behave under heat-treatment in the same way as a polycrystalline aggregate, and moreover, X-rays can provide only an overall impression of the phenomena taking place in the interior of the specimen being examined. Thus, when X-ray photographs have revealed the presence of the  $\theta'$  phase, it would be most helpful to be able to establish by means of the electron microscope whether these first platelets of  $\theta'$  occur only at discontinuities in the lattice, or alternatively whether they are surrounded by zones of "recrystallized" matrix.

From this point of view, the paper by Miss Silcock, Mr. Heal, and Dr. Hardy does not seem to conflict in any serious respect with the theory which we have advanced as the result of a study\* based on dilatometry and electron microscopy, and which can be summed up, at the stage now reached, as follows:

(1) In the quenched state a supersaturated solid solution is said to be homogeneous. In fact, it is heterogeneous by reason of the lattice imperfections in it, and it is also heterogeneous on a scale of several hundred atoms because of statistical fluctuations. As a result, there is present at any given moment a number of nuclei sufficient, if they become stable, to give rise to crystallites of intermetallic compounds.

(2) These conditions of relative stability are brought about by natural or artificial ageing in the case of nuclei which have a given approximate atomic composition, e.g. one copper atom to two or three aluminium atoms. These nuclei are rejected from the solid solution and may be considered as copper-rich aggregates, having a very imperfect crystalline structure continuous with the matrix. It is a question merely of terminology whether one regards them as zones, in accordance with Guinier's modified interpretation,† or as the  $\theta''$  phase already in being, since "there is a continuous transition from the original zone to the  $\theta''$  phase".‡ This interpretation is satisfactorily confirmed by dilatometry. The rejection of  $\theta''$  from the saturated solid solution should be accompanied by a decrease in volume, if there is no rearrangement of the matrix, and by an increase if such rearrangement takes place. The fact that a decrease in volume is observed makes it probable that precipitation occurs without rearrangement of the matrix, and thus takes the form of precipitation of a nucleus without migration in the usual sense in the body of the solid solution.

(3) In the course of artificial ageing the aggregates precipitated become progressively better ordered, taking on a definite crystal structure and becoming richer in copper by the customary processes of growth of precipitates. The matrix suffers considerable impoverishment in copper atoms and increases in volume (at the end of several hours at 150° C., for instance).

We therefore connect the increase in hardness due to artificial ageing with "precipitation", growth, and progressive ordering of the structure of the  $\theta''$  phase.

Miss Silcock, Mr. Heal, and Dr. Hardy have observed that the growth of precipitates is accentuated after the flat plateaux on the ageing curves. On the basis of the variations of volume recorded in dilatometry, we agree that the first increase in hardness corresponds with the nucleation and the second increase of hardness with the growth of the  $\theta''$  phase. This

growth is associated with a rearrangement in the direction of a better-defined crystal structure and with the variations in parameter observed by the authors. But it is also possible to connect the plateaux with the precipitation of the  $\theta'$  phase at discontinuities in the lattice (grain boundaries, slip lines, &c.) and with local "recrystallization" of the matrix.

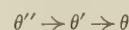
(4) At the peak hardness reached on artificial ageing, the electron microscope reveals general precipitation of a phase other than  $\theta'$ , which we have termed the X phase (this is the phase whose structure has been determined by Guinier and which he has called  $\theta''$ ). At the same time platelets of  $\theta'$  appear, concentrated mainly at lattice discontinuities.

Figs. E and F (Plate XCI) which are electron micrographs of aluminium-4% copper alloy at its peak hardness after ageing at 190° C. for 28 hr., show heavy precipitation of  $\theta''$ , the "light phenomenon" at the boundaries in Fig. F, and the growth of platelets of  $\theta'$  in certain "recrystallized" zones.

(5) As regards  $\theta'$ , numerous micrographs have been published elsewhere which establish the chief features of its mode of precipitation. Fig. D (Plate XC) is of an aluminium-4% copper alloy near the peak of its hardness on ageing at 150° C. and shows white platelets of  $\theta'$ , parallel to one another and concentrated on curious swellings of the matrix which we are inclined to regard as zones in course of "recrystallization".

### Conclusions.

(a) We suggest that the sequence of precipitation is:



The term "G.P. zone" has served, in the theory of hardening in a homogeneous phase, to designate flat clusters in which the copper atoms remain for the most part at lattice points of the matrix. The current conception of aggregates differs considerably from this, since they are regarded as made up of atoms of aluminium and of copper which have left the matrix lattice. To retain the term "zone" is to risk causing confusion.

The  $\theta''$  phase at first shows serious departures from periodicity (G.P.[1]), then becomes progressively better ordered (G.P.[2]). By calling the phase  $\theta''$  throughout all stages of its development, account is taken of this progressive ordering, and the special character of the chemistry of alloys is also emphasized.

(b) Under conditions of artificial ageing, i.e. for isothermal treatments at temperatures below about 300° C., the  $\theta'$  phase, surrounded by recrystallized matrix, appears in the regions where there is a certain amount of stored-up energy due to work-hardening; first at lattice discontinuities, then in the interior of the grains where these have undergone spontaneous hardening by reason of precipitation of  $\theta''$ . The resulting effect is a softening; at first localized, then becoming general. Above 300° C., the  $\theta'$  phase is precipitated directly without preliminary hardening, and softening takes place.

(c) The sequence in which the structural changes occur is indissolubly bound up with the phenomena of lattice distortion, spontaneous plastic deformation (dislocations and voids), and recrystallization. Although undoubted progress has been made in recent years with regard to the establishment of the precipitation sequence, the hardening processes themselves remain obscure.

Dr. A. BERGHÉZAN ||: I should like to congratulate Mr. Polmear and Dr. Hardy on the very elegant microscopical technique by means of which they have achieved such remarkable results. I have applied ¶ the same techniques (electron and optical microscopy) to a study of the subject, in an

\* A. Saulnier, *Compt. rend. 1<sup>re</sup> Congr. Internat. Microscopie Electronique, Paris (1950)*, 1953, 424.

A. Saulnier and R. Syre, *Rev. Mét.*, 1952, 49, 1.

† A. Guinier, *Compt. rend.*, 1950, 231, 655.

‡ A. Guinier, *Acta Cryst.*, 1952, 5, 121.

§ Celluloid-silica replicas were employed, with a view to

checking results previously obtained using the oxide-film technique.

¶ Centre de Recherches d'Antony (Seine), France.

¶ A. Berghézan, *Publ. Sci. Tech. Ministère de l'Air*, 1953, (283).

attempt to explain the mechanism of the "light phenomenon" found by Dr. Gayler in aluminium-4% copper alloys.

(A) Mechanism of Formation of the "Light Phenomenon".

I agree that the "light phenomenon" is due to "recrystallization" at the grain-boundary interface. This "recrystallization", though it may result from strains set up by quenching and subsequent ageing, as the authors suggest, is not always produced in this way, since it occurs also in their absence. Such strains may be essential to promote grain-boundary recrystallization in pure metals, but this is not necessarily the case with alloys. In fact, I have noted the appearance of the "light phenomenon" immediately after cooling in air, without ageing, and also after even slower cooling, where there could be no question of cooling strains, and the theory of their effect is no longer applicable.

Numerous observations have shown that, in the case of alloys, precipitation takes place first at the grain boundaries and that by reason of the impoverishment thus created, "recrystallization" then occurs at the boundaries. The electron micrograph of an aluminium-4% copper alloy, shown in Fig. G (Plate XCII) illustrates this fact very well. It can be seen that the precipitate takes the form of an S, on account of the growth of two crystallites of the "light phenomenon" in opposite directions. As the boundary was originally straight, the precipitate had no alternative but to form in a straight line. Growth of the crystallites followed, and the precipitate was forced to follow the new interface thus created and to take its shape. Although the two phenomena of precipitation and "recrystallization" occur successively, they can take place very rapidly during air-cooling or slow cooling. The very short period for which the alloy remains at a high temperature during these slow-cooling treatments is sufficient to cause the appearance of the "light phenomenon". There is nothing unusual about this. It is well known that at grain boundaries the crystal lattice is in a state of considerable disorder, and that in consequence the free energy available is higher than in the body of the matrix. This renders very much easier the interchange of atoms between one part of the interface and another, especially at high temperatures. The rate of diffusion along the boundaries is therefore much higher than in the remainder of the matrix, as has been shown by a number of authors. Hence, it is not surprising that on passing through the precipitation temperature in the course of air-cooling, rapid precipitation from the supersaturated solid solutions should take place. This precipitation impoverishes the neighbouring regions and, as is always the case in such a transformation, energy is liberated. A non-equilibrium state is set up at the boundary—it has, in fact, more or less existed there since the solution heat-treatment. Competition between the lattices of the two adjoining crystals then begins afresh, each trying to grow at the expense of its neighbour. This gives rise to the appearance of the "light phenomenon".

When the relative disorientation of the two adjoining crystals is great, one of them absorbs the other. Alternatively, when the orientations are similar, both may develop (Figs. G and H, Plate XCII). This is rendered possible by the fact that on account of a variation of orientation along the interface itself, each of the crystals possesses weak spots.

(B) Crystal Orientation of the "Light Phenomenon".

Dr. Gayler has stated that the "light phenomenon," as revealed by chemical attack, has an orientation identical with that of the crystal from which it has grown, and different from that of the crystal into which it advances. As a result, the edges of the "light phenomenon" appear to be differently attacked; the attack being hardly discernible on the side

bordering on the matrix crystal whose orientation is identical with it, and very marked on the other side.

Electron microscopy has shown that this is not always strictly true. Sometimes the orientation of the "light phenomenon" seems to differ slightly. This is indicated by the change in direction of the white dots on crossing the slightly attacked edge of the matrix crystal and passing into the "light phenomenon". As has been shown elsewhere,\* the change in direction of the white dots is related to the crystal orientation of the adjacent grains (Figs. J and K, Plate XCII).

Optical microscopy has confirmed the findings of the electron microscope. Examination by polarized light of thin films on an anodically oxidized specimen giving interference colours, shows a change of colour which might be due to a simultaneous change in orientation and composition. The results obtained with the electron microscope make it possible to resolve this ambiguity.

(C) Nature of the Phases Present.

In the case of aluminium-copper alloys, examination with the electron microscope makes it possible to identify the precipitated phase as being unquestionably the equilibrium phase  $\theta$  ( $\text{Al}_2\text{Cu}$ ) (Figs. G and H, Plate XCII). However, the white crystallites of the "light phenomenon" do not always consist of the solid solution stable at the ageing temperature concerned. The whole range of solid solutions may occur, from the initial supersaturated solid solution to the solid solution stable at the ageing temperature, since decomposition takes place gradually and not suddenly. This applies also to the matrix crystals, as I have shown elsewhere.† Quite frequently electron micrographs show that there is also expulsion of atoms, even in the phase impoverished in copper.

Dr. V. A. PHILLIPS,‡ B.Sc., A.R.S.M., A.I.M. (Member): Mr. Polmear and Dr. Hardy attribute the formation of the "light phenomenon" to a recrystallization process. Do the authors mean "recrystallization", or have they in mind a process of grain-boundary migration? In recrystallization strained material is replaced by strain-free grains, normally of a different orientation from that of the matrix, which form by a process of nucleation and growth. There is no indication in the authors' work that the light zones have an orientation differing from that of the neighbouring grains. Evidence exists § that in an aluminium-6% copper alloy the zones have the same orientation as the grain from which they start to grow. This is supported by work on aluminium-10% zinc alloy in which similar zones are formed.|| The evidence thus points to the fact that the light zones form by grain-boundary migration. The process does not appear to be recrystallization as defined above, nor does it appear to be grain growth under the influence of surface tension, since the curved interface migrates away from its centre of curvature. The main driving force for grain-boundary migration seems to be the change in free energy associated with the formation of a more stable precipitate or pre-precipitate from a less stable form. Loss of coherency between "precipitate" and matrix results, for example, in a big release of energy.

Changarnier and Calvet § found that the temperature at which light zones were most pronounced was raised, up to a certain point, by addition of manganese. In the binary aluminium-6% copper alloy, it rose from 150° to ~300° C. when 0.075% manganese was present; <0.01% manganese suppressed their formation at low temperatures. Thus, small amounts of manganese appear to have a considerable effect on the occurrence of the "light phenomenon", unlike small additions of indium or tin, which, according to the present authors, greatly facilitated nucleation during the ageing of an aluminium-4% copper alloy but had little effect on the "light

\* P. Bussy and G. Chaudron, *Compt. rend.*, 1953, **236**, 2323.

† A. Berghézan, *loc. cit.*

‡ Investigator, British Non-Ferrous Metals Research Association, London.

§ (Mlle.) C. Changarnier and J. Calvet, *Compt. rend.*, 1953, **237**, 179.

|| E. C. W. Perryman and J. C. Blade, *J. Inst. Metals*, 1950, **77**, 263.



phenomenon". Such small amounts of manganese are almost certainly in solution; moreover, the rate of diffusion of manganese in aluminium is extremely slow even at 300°C. At lower temperatures atoms of manganese are virtually anchored in the lattice, producing centres of strain and presumably impeding grain-boundary migration of any kind.

Mr. C. J. THWAITES,\* B.Sc., A.R.S.M. (Junior Member): During the course of the work which Dr. Hopkin and I carried out on the effect of minor additions on the age-hardening of lead-antimony alloys,† we constantly observed the "light phenomenon" referred to by Mr. Polmear and Dr. Hardy. We found that the extent of the phenomenon became greater with increasing solute concentration. When the lead-0.85% antimony binary alloy was extruded at different temperatures, at all of which it was single-phased, the rods extruded at the lowest temperature showed a significantly greater amount of decomposition at the grain boundaries than those extruded at the highest temperature. This was probably due to the greater amount of retained plastic deformation in the materials extruded at the lowest temperature, where less complete recrystallization would occur during the extrusion process.

Mr. Polmear and Dr. Hardy suggest that quenching strains may be responsible for the phenomenon. However, we found that by water-quenching, instead of air-cooling, less decomposition was obtained and it was further reduced, but not eliminated, by quenching in a solid carbon dioxide/acetone mixture.

While in most instances where the "light phenomenon" was observed the new solid-solution interface was looped, as shown by Mr. Polmear and Dr. Hardy (Fig. 2, Plate LXVI) in other cases we found that the particles of precipitate formed in the grain boundary first and the new solid solution, with its characteristic looped interface, was observed only after ageing for a period. I should like to hear from anyone who has observed a similar phenomenon.

Dr. P. FELTHAM‡: Dr. Entwistle finds two damping effects, one with an activation energy of 38 k.cal./g.-atom, and one with an activation energy of about one-third this value, namely 13 k.cal./g.-atom. The latter occurred in Duralumin and in the quaternary alloy, but not in the other alloys.

These results raise three distinct questions. First, what is the nature of the principal mechanisms that give rise to these two manifestations; secondly, what is the origin of the spectrum of relaxation times that seems necessary to account for the spread of the damping curve characterized by the lower activation energy (Fig. 7, p. 256); and, finally, why have damping peaks associated with activation energies of the order of 13 k.cal./g.-atom not been observed in all the alloys?

Before making some suggestions on these points I want to emphasize that one must not lose sight of the important fact that all the alloys studied were supersaturated after quenching, and therefore not in thermodynamic equilibrium. Consequently there are within them vacancies, interstitial atoms of the solutes and of the solvent phase in excess of equilibrium concentrations, as well as concentration gradients. It is therefore highly probable that the principal sources of the damping would have to be sought in the diffusion of interstitial atoms and of vacancies, taking place in essentially the same way as suggested by Gorsky § on the basis of his studies of copper-gold alloys.

The activation energy associated with vacancy diffusion should be approximately the same as that for volume self-diffusion in aluminium, and this is in fact the case, both being

about 38 k.cal./g.-atom.¶ This activation energy is composed of two parts, of which one, equal to about two-thirds of the total, is required for the generation of the vacancy in the lattice, and the other for its movement. Mott || estimates the latter to be 13 k.cal./g.-atom in aluminium. In cubic metals it is therefore likely that diffusion by the movement of already-existing vacancies originally "frozen in" by quenching from the solution-treatment temperature, is, in the main, responsible for the 13 k.cal./g.-atom damping peak. Contributions to the damping from the movement of double vacancies, which are more mobile than single ones,¶ and from interstitial diffusion, the activation energy of which is also to be expected to be of the right order of magnitude,\*\* are also likely.

Now, the relaxation time  $\tau$  corresponding to frequencies of a few thousand cycles/sec., such as lead to the peak in the damping-capacity curve with the lower activation energy (13 k.cal./g.-atom) in Duralumin, should be of the order of  $10^{-4}$  sec. at room temperature. If this value is substituted into Einstein's expression:

$$\tau \approx \lambda^2 / D_0 \exp(-H/RT)$$

and the diffusion coefficient  $D_0$  is taken to be of the order of 0.1, which is reasonable,†† while  $\lambda$  for a vacancy jump is taken as the interatomic spacing in aluminium, then a value of about 13 k.cal./g.-atom is obtained for  $H$ , as required.

The answer to the second question, as to the origin of the spectrum of relaxation times, then follows quite naturally from this interpretation of the 13 k.cal./g.-atom damping peak, for the energy barrier  $H$ , which a given existing vacancy has to surmount in moving to an adjacent position, will depend upon the type and concentration of atoms in its immediate vicinity and upon the nature of the atom with which it interchanges position. On the basis of available data on the diffusion of copper, magnesium, silicon, and zinc into aluminium, it seems reasonable to assume that the separate  $H$  values corresponding to the diffusion of atoms of these elements in aluminium, facilitated by place interchange with existing vacancies, will be distributed around the measured mean value of approximately 13 k.cal./g.-atom with deviations of up to  $\pm 2$  k.cal./g.-atom at low concentrations.

Finally, there remains the question why a damping peak of the 13 k.cal./g.-atom type has not been found in all the alloys. I think that the answer is that in the alloys which, by comparison with Duralumin and the quaternary alloy, are rather poorer in alloy content, measured in at.-%, the corresponding values of  $H$  are either somewhat greater or somewhat smaller than 13 k.cal./g.-atom and that, in view of the fact that  $\tau$  would increase or decrease by a factor of about a hundred if  $H$  changed by only as much as plus or minus 2 k.cal./g.-atom, respectively, the damping peak is displaced to frequencies entirely outside the ranges experimentally investigated by Dr. Entwistle.

It can also be understood that changes in the damping capacity occurring after quenching, due to the type of diffusion I have mentioned, need not be related in an immediately obvious way to changes in hardness, except in so far as the diffusion leads to precipitation.

Dr. ENTWISTLE (in reply): The analysis which leads Dr. Feltham to the conclusion that atom interchange with vacancies can explain the observed damping changes is based on the assumption that  $D_0$  is identical for diffusion in the quenched and annealed alloy; that is, that it is independent of vacancy concentration. No experimental data are available to check this point for the aluminium alloys under dis-

\* Tin Research Institute, Greenford, Middlesex.

† *J. Inst. Metals*, 1953-54, **82**, 181.

‡ Standard Telecommunication Research Laboratories, Enfield, Middlesex.

§ W. S. Gorsky, *Physikal. Z. Sowjetunion*, 1935, **8**, 457.

|| N. F. Mott, *Phil. Mag.*, 1952, [vii], **43**, 1151.

¶ J. H. Bartlett and G. J. Dienes, *Phys. Rev.*, 1953, [ii],

s s 2

89, 848.

\*\* F. Seitz, "Phase Transformations in Solids", edited by R. Smoluchowski, J. E. Meyer, and W. A. Weyl, p. 77. 1951: New York (J. Wiley and Sons); London (Chapman and Hall).

†† W. Jost, "Diffusion in Solids, Liquids, and Gases". 1952: New York (Academic Press).

cussion, but the results of Nowick and Sladek\* on a silver-zinc alloy indicate the general effect to be expected. The diffusion coefficient  $D$  can be determined from the relaxation time  $\tau$  for stress-induced atom migration, where  $\tau = \tau_0 \exp(H/RT)$

Then  $D_0 \propto \frac{1}{\tau_0}$  and the constant of proportionality is identical for the quenched and annealed states. On this basis it can be shown from the measured relaxation times for the quenched and annealed silver-zinc alloys that:

$$\frac{D_0 \text{ (quenched)}}{D_0 \text{ (annealed)}} \simeq 10^{-4}$$

Thus the value of  $D_0$  is much lower in the quenched condition. If the value of  $D_0$  is substituted in the Einstein equation quoted by Dr. Feltham  $\tau$  is increased by this factor, and a predicted relaxation time of about 1 sec. results. This supports the opinion expressed in the paper that the observed relaxation time is too short to be explained by atom migration over an interatomic distance, and that the Einstein equation yields reasonable values only if  $\lambda$  is reduced, that is, if diffusion over less than one interatomic distance is considered.

In any event, the main objection to a simple vacancy-interchange mechanism is the absence of any observed rise of relaxation time during ageing which would result from the inevitable decay of vacancies. There is, too, the difficulty of explaining why the temperature dependence of  $\tau$  is governed by a different law from the rate of attainment of maximum damping. It may be that the latter is governed by long-range atom migration and the former by diffusion over at most one inter-atom distance, but further information on this point is required before any definite picture can be established.

I support Dr. Feltham in his general conclusion that atom migration is most likely to be in some way responsible for the observed effects—as he rightly points out, a distribution of relaxation time is to be expected in these circumstances—but I feel that more experimental data are required before it is possible to form a clear picture of the detailed mechanism operating.

Dr. Feltham's view that damping peaks might exist outside the range of experimental conditions attained in the work, reiterates the view expressed in the paper.

Miss SILCOCK, Mr. HEAL, and Dr. HARDY (*in reply*): Much of the discussion is concerned with the "light phenomenon" and with the lack of agreement between the X-ray studies and the structures observed with the electron microscope.

The electron micrographs of the "light phenomenon", presented by Dr. Berghézan, are extremely interesting. Further experimental results will be found in the work of his compatriots Changarnier and Calvet.† Dr. Berghézan regards the grain-boundary migration as a result of the competition between the adjoining grains when energy is liberated in the precipitation process. Dr. Phillips's view is rather similar, since the grain-boundary movement, with a consequent extension of the grain-boundary area, is thought to provide a means of absorbing some of the energy liberated when a more stable precipitate is formed.

We hold the view that the "light phenomenon" involves grain-boundary movements to allow relief of strain. The strains may arise in quenching or during the precipitation process. Diffusion is more rapid in the grain boundaries than within the grains and migration of the interface across a small volume of the metal will provide a path for easy diffusion and hence rapid precipitation. In practice, a few large particles of  $\theta'$  or  $\theta$  are formed. Re-solution of the initial precipitates is inevitable,‡ because the more stable precipitates are in metastable or stable equilibrium with a solid solution of lower copper content. The relative freedom from precipitate and the comparatively low copper content over the "swept-out" region accounts for the light-etching characteristics. We will

add the new suggestion that once the grain interface has moved to take up the precipitation strains, the growth of the bulges becomes possible since the migration of the boundary into a region of higher free energy greatly accelerates the precipitation process. On this basis, it is reasonable that the grain advances away from its radius of curvature (like any growing particle) and that the boundary shifts into either of the neighbouring grains. Recrystallization leading to typical discontinuous precipitation will occur when the lattice strains associated with precipitation are sufficiently high.§

It is indisputable that lattice strain facilitates grain-boundary movements and that quenching introduces strains. Even on relatively slow cooling, precipitation at the grain boundaries, which always occurs more rapidly, must set up lattice strains (due to the volume changes) which may be relieved either by plastic flow or grain-boundary adjustments.

Unfortunately, electron microscopy does not offer a direct method of studying the nature of the precipitates present, and this must be inferred by comparison with the results of X-ray analysis. We are very hesitant in following the positive identifications made by Dr. Nutting (and Mr. Thomas); whilst we can see only general mottling and no clear plates of precipitate within the grains of M. Saulnier's electron micrographs at about  $\times 20,000$ . At peak hardness at  $190^\circ\text{C}$ ., the X-ray results predict particles larger than  $500\text{ \AA}$ . dia. (1 mm. in Figs. E and F, Plate XCI), when Polmear and Hardy observed plates of  $900\text{--}5500\text{ \AA}$ . (2–10 mm.).

If the quenched solid solution contained essentially spherical regions rich in copper of  $150\text{ \AA}$ . dia., they would be too large to be detected by the small-angle scatter techniques used. Such regions, therefore, could exist. Dr. Nutting interprets his electron micrographs of the quenched alloys in terms of such regions, but finds no modification in the appearance of the replicas for ageing treatments which produce X-ray evidence (streaks) interpreted by us as G.P.[1] platelets. These streaks in the X-ray patterns of Figs. 1 (Plate XXXIX), 13, and 14 (Plate XLI) (rods in reciprocal space) are unambiguously due to a structure in which one Laue condition has been relaxed, that is, a structure which is disordered in one direction only or has an insufficient number of repeat units in that direction, i.e. a thin platelet. It remains to consider how such a structure could develop within a single postulated spherical copper-rich region. The possibilities are:

(a) That the copper atoms concentrate to form one copper-rich platelet. This does not conflict with the observed X-ray evidence, except that increasing ageing temperatures produce platelets of increasing diameter.

(b) That the copper atoms concentrate to form several copper-rich platelets within one spherical region. Such an assumption could explain the shortening of the streaks on the small-angle scatter patterns with increasing ageing temperature. But in these circumstances additional diffraction effects due to inter-platelet interference would be expected and have not been observed.

(c) That the regions develop a structure which is completely disordered in one direction. We regard this picture as being physically unlikely.

In view of the above we would like to have more concrete evidence that the interpretation of the electron micrographs advanced by Dr. Nutting is unambiguous. For example, can he rule out the possibility that the white points are due to the solution of copper-rich regions during anodizing leading to thin spots in the replica film whose shape and size are not governed by those of the original copper segregate?

In reply to M. Saulnier, we can only reiterate the remarks we have made in our paper on the structural-ageing characteristics. We prefer to regard G.P.[1] and G.P.[2] as separate structures. This is the only way in which one can account satisfactorily for the very marked discontinuity in the growth process corresponding to the flat plateau on the ageing curve.

\* A. S. Nowick and R. J. Sladek, *Acta Met.*, 1953, **1**, 131.

† (Mlle.) C. Changarnier and J. Calvet, *Recherche Aéronaut.*, 1953, **36**, 25.

‡ H. K. Hardy, *J. Inst. Metals*, 1950, **77**, 547; 1951, **79**, 321.

§ H. K. Hardy, *ibid.*, 1948–49, **75**, 707.



If G.P.[1] streaks were due to thin platelets of G.P.[2], there seems no reason why they should not increase in size monotonically. The classical theories of nucleation require that the particles shall grow, once the critical size has been exceeded.

One major difficulty which still has to be explained is the mechanism by which the G.P. zones [1] form so rapidly. There is a large discrepancy between the diffusion coefficient calculated by extrapolation from measurements at high temperatures and the value calculated from the sizes of the plates as set up by X-ray analysis.\* Part, at least, of this anomaly could be removed by the existence of copper-rich regions within the solid solution from which the G.P. zones [1] could be formed.

The question of whether the appearance of G.P.[2] and  $\theta'$  is due to allotropic (or monotropic) changes or whether they arise by direct nucleation in the matrix is still unsolved. Even if the changes are monotropic they could arise by nucleation

of the new phase within the particles of the old phase. On the other hand, Dr. Nutting assumes that the transformation would be diffusionless; this would occur only if, on reaching a critical size, the particles broke away from the matrix with a form of "click-over" reaction. The mechanism of the formation of the "next-more-stable phase" does not affect the necessary re-solution of the previous precipitate which, happily, is shown both by theory and experiment.

We would like to conclude by thanking all who took part in the discussion. We have been glad to supply our hardness specimens to the workers at Cambridge and our divergencies of opinion in no way detract from the pleasure derived from the collaboration. We share the hopes of the electron microscopists that their techniques will be developed further. We are pleased to receive Dr. Gayler's commendation, although we are keenly aware that our knowledge of the ageing process is still in the qualitative stage.

## Discussion

### Continuous Casting†

Mr. R. W. RUDDLE,‡ M.A., A.I.M. (Member): In the last decade or so considerable progress has been made in transforming the manufacture of castings from an age-old art into a science. The steps taken by the founder to secure castings of high quality—the preparation of the metal, the way of introducing it into the mould, and the feeding techniques and other devices employed to minimize unsoundness—are beginning to be governed by scientific considerations and are becoming less and less a matter for the individual foundryman's skill and experience, important though these still are. One direction in which considerable advances have been made in recent years is the study of the mechanism of freezing and the flow of heat during the solidification period, a matter of high importance, since the rates at which the different parts of a casting freeze govern its soundness and the incidence of segregation and cracking. Much work has already been done on this subject in this country, in the U.S.A., and on the Continent, and in view of the increasing interest being shown in many places, the papers under consideration, which deal with experimental techniques used in work of this kind, are indeed timely. Although they are concerned only with continuous casting, much of the matter is of quite general applicability. The paper by Mr. Lewis gives an admirable account of certain methods and techniques which have so far been applied little or not at all in foundry work, for example, that using the electrical tank analogue.

From time to time various workers have attempted to calculate the movement of the solidification front in freezing castings by purely mathematical reasoning, and Section II (p. 396) of the paper by Mr. Lewis is instructive in showing just how difficult such calculations are and how misleading the results can be, if they are not checked by experiment. I mention this because the example quoted highlights the limitations of mathematical calculation and serves as a warning to those who may be prepared to trust the mathematician too implicitly.

I am glad that in Section III (p. 398), on the determination of the solidification front, a distinction has been drawn between the methods which show the liquidus isotherm and those which reveal the solidus isotherm, for, even in continuous casting, where solidification rates are high, there may be a considerable difference between the two when an alloy of long freezing range

is cast. I imagine that in the continuous casting of alloys of long freezing range the distance between these two isotherms may be several inches, but perhaps the author can give us some more precise information.

The technique involving the addition of a copper-containing alloy appears to be a very simple way of ascertaining the position of the solidification front in continuous castings in copper-free alloys. Mr. Lewis states that this method cannot be used with copper-containing alloys, but I wonder whether he is correct in this. I should have thought it possible to reverse the process and add pure aluminium to a casting in a copper-containing alloy. The author suggests that this "addition" technique reveals the position of the solidus isotherm, but I feel a little doubtful whether, in the case of an alloy of long freezing range, the added liquid really does penetrate into the mushy zone quite as far as the solidus isothermal plane. The elegant radioactive tracer method described by Mr. Lewis, and in greater detail by Mr. Putman, although more time-consuming, is clearly most valuable, since it gives information about both the liquidus and solidus isotherms.

The temperature-measurement method is undoubtedly the most generally useful way of studying the solidification of castings, and Mr. Lewis has included a detailed description of the varied techniques he has employed. Little indication is given however, of the accuracy of measurement, and I hope he will say something about this in his reply. In the diagrams reproduced in the paper, the thermocouple leads often appear to intersect the isothermal planes at a considerable angle, and this makes me wonder whether some error may not have been introduced as a result of conduction up the thermocouple wires. In work which my colleagues and I carried out some years ago in the laboratories of the B.N.F.M.R.A., we found that alignment of the thermocouple leads approximately parallel to the isotherms was vital, if these conduction errors were to be avoided.

I cannot leave the subject of temperature-measurement technique without expressing my admiration of the ingenious optical methods used by the author to facilitate the wearisome task of interpreting the recorder charts. I know from personal experience just how large an expenditure of time and labour is involved in this.

Section V (p. 403) of Mr. Lewis's paper, on the interpreta-

\* H. Jagodzinski and F. Laves, *Z. Metallkunde*, 1949, **40**, 296.

H. K. Hardy, *J. Inst. Metals*, 1951, **79**, 321.

† Joint Discussion on the papers by D. M. Lewis (*Journal*,

this vol., p. 395) and J. L. Putman (p. 414).

‡ Head of Melting and Casting Section, British Non-Ferrous Metals Research Association, London.

tion of temperature measurements and the plotting of the thermal field within the casting, is most helpful, particularly the application of the Liebmann iteration technique, which, so far as I know, has not been used before in connection with casting solidification. The author states that this technique may be used to extrapolate the isotherms to that awkward and important region of the casting near the mould surface where the boundary conditions are not known. It is, however, not entirely clear how he has done this, and I should be grateful if he could enlarge on this point.

I am particularly interested in the electrical analogue, for it is an especially simple and time-saving technique which must be of great value as an adjunct to actual temperature measurements in continuous castings, where approximately steady-state heat flow obtains. It is unfortunate that this technique is inapplicable to other casting methods where the heat flow is unsteady. I gather that at the beginning of each experiment with the analogue, Mr. Lewis adjusts to suitable values the resistances which govern the boundary conditions and which represent the heat-transfer coefficients at the surface of the ingot, but I am not at all clear how these adjustments are arrived at and how he knows whether the assumed boundary conditions are in fact correct. Admittedly, in the

which the author has obtained with his various techniques and feel disappointed that so little indication is given in the present paper. No doubt there are good reasons for this, but I hope that in the not too distant future he will feel able to give us another paper dealing with this aspect. Application of the techniques described will, I have no doubt, lead to far-reaching conclusions which should permit optimum cooling conditions for continuous-casting operations to be computed precisely, instead of being determined by trial and error as at present.

Professor Dr. Ing. P. BRENNER\* (Member): Mr. Lewis's paper forms an excellent contribution to the literature of continuous casting, but I feel that the mathematical studies of Roth, published in 1943, are criticized too unfavourably. Very possibly there is an error in equations (3) and (4) of the paper. We have checked the solidification contours calculated from his equations (1) and (2), illustrated in Fig. 1 (a) and 1(b)† (p. 397), and found a better agreement with the experimentally determined contours than Mr. Lewis did. His Fig. 1 is reproduced as Fig. A and includes the curves which we obtained.

We are quite aware of the deficiencies of our equations. On

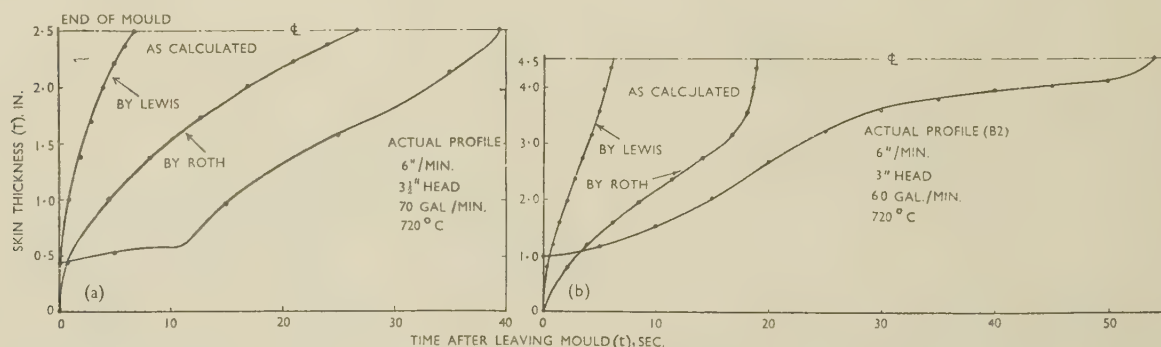


FIG. A.—Reproduction of Fig. 1 (a) and (b) of the Paper by Lewis, Including Curves Calculated from Equations (1) (left) and (2) (right) of the Paper on the Basis of Roth's Theory.

following Section he describes how he attempted the difficult problem of measuring the heat transfer in the mould, but these attempts seem so far to have been attended by only moderate success. In fact, he seems to prefer the results of calculations based on the positions of the isotherms in the interior of the casting, or those obtained with the electrical analogue (he states elsewhere that the analogue can be used to determine the boundary conditions). I do not see how the analogue, which depends for its accurate functioning on feeding in the correct boundary conditions, can be used to determine these boundary conditions, and it almost appears as if the author has here been arguing in a circle. I hope he will clear this matter up and tell us exactly how he arrived at his boundary conditions.

In his conclusions (p. 412), Mr. Lewis emphasizes the necessity for linking up the heat-flow data revealed by his methods with metallurgical phenomena which occur during solidification and subsequent cooling. This cannot be too strongly stressed, since the aim of work of this kind is improvement of the quality of the casting by careful adjustment of the cooling conditions. Unless precise information is available on the effects of a given change in cooling conditions on the metallurgical events occurring during and after freezing, attempts to apply heat-flow data in practice may be dangerous and lead to unsuspected complications.

I confess that I am filled with curiosity as to the results

the other hand, they represent the first attempts to calculate the solidification front, and they show clearly some basic facts which we were anxious to bring out; for instance, that the depth of the liquid sump is proportional to the casting speed and to the second power of the ingot diameter, and so on. Of course the calculations given in more recent papers, such as that of Klein,‡ are much more exact than those of Roth.

Mr. B. J. ELSON,§ B.Sc.: There are several points in Mr. Lewis's paper which appear to be mathematically incorrect. The whole basis of the iteration technique and electrical tank analogue depends on the fact that the temperature  $\phi$  is a harmonic function. This is not the case in this problem. The heat-conduction equation (eq. (10), p. 404) is correct relative to axes fixed in the solid considered. By transforming to axes fixed at the mould the equation becomes:

$$k \left( \frac{\partial^2 \phi}{\partial x^2} + \frac{\partial^2 \phi}{\partial y^2} + \frac{\partial^2 \phi}{\partial z^2} \right) = \frac{\partial \phi}{\partial t} + v \frac{\partial \phi}{\partial z}$$

where  $z$  is the depth of a point below the mould and  $v$  is the speed of casting. A steady-state condition exists relative to the mould, and hence  $\frac{\partial \phi}{\partial t}$  can now be taken as zero. The resulting equation shows that  $\phi$  is not a harmonic function.

However, an iteration technique may still be used to interpolate between the basic information, but it would be very

\* Director of Research, Vereinigte Aluminium-Werke A.G. and Vereinigte Leichtmetall-Werke G.m.b.H., Bonn/Rhein, Germany.

† Corrigendum: In this figure "Calculated from Eq. 3"

should read "Calculated from Eq. 2."

‡ H. Klein, *Giesserei (Techn. wiss. Beihefte)*, 1953, (10), 441.

§ Research Laboratories, The British Aluminium Co., Ltd., Gerrards Cross, Bucks.



unwieldy and also a function of the diffusivity of the metal, which varies with temperature.

Still referring to the iteration technique, as has been stated, Liebmann's formula refers to a plane harmonic function. For a cylindrical billet a quasi-plane harmonic function should have been used, i.e. one which satisfied the equation :

$$\frac{\partial^2 \phi}{\partial r^2} + \frac{1}{r} \frac{\partial \phi}{\partial r} + \frac{\partial^2 \phi}{\partial z^2} = 0$$

On deriving the iteration technique for this equation, it will be found that each temperature should be weighted according to its distance from the axis. This can introduce differences of about 10° C. at high-temperature axial points.

Turning now to the analogue solution with the solidification front and boundary conditions imposed, the method again assumes that  $\phi$  is a solution of Laplace's equation. Apart from the solidus face-boundary condition, the analogue solution does not depend on the rate of casting. Allowing for this, the effect would be to extend the isotherms in the direction of casting, and the temperatures would be higher than those predicted by the analogue technique. This appears to be the case on comparing Figs. 6 (p. 403) and 13 (p. 408). As an approximate example, consider the temperature at a point of the axis 2 in. below the solidification front. From Fig. 6, the measured temperatures for speeds of 3 in./min. and 9 in./min. are 350° and 500° C., respectively. The solidification front in Fig. 13 has a deeper profile than either of these, and therefore it would be expected that the temperature gradient would be lower and the temperature at a point 2 in. below the front would be greater than 500° C. In actual fact, from Fig. 13 the temperature at this point is only approximately 250° C.—a difference of more than 250° C. Can the author give any simple explanation of this difference, or must it be attributed to omitting the casting speed from the equation of heat conduction?

Dr. E. SCHEUER\* (Member): The paper by Mr. Lewis describes a very useful, if not a very simple, method of determining the temperature distribution in solidifying billets in the continuous-casting process, which is, of course, the most important measurement in this connection.

Evidently some desirable objectives have still to be achieved. The measurement of the temperature gradient on the liquid side of the solidification zone will be difficult because of the comparatively small temperature differences, which, however, may form comparatively steep gradients in a narrow zone immediately adjacent to the zone of solidification. If measurements of these gradients could be carried out, useful information would be obtained. Further, the method as it stands takes no account of the fluctuations in heat flow connected with the forming of the first thin shell of solid metal, which have serious repercussions on the structure of the billet, and indications of which can be found in Fig. 16 (p. 411).

It would also be interesting to study carefully the temperature field in the solid lower part of the billet for information on the setting up of the internal stresses which prove so troublesome with larger-diameter billets. This can, of course, be done by the method as it now exists, provided that the experiment is carried on through a sufficient length of billet.

One cannot help speculating on the implications of certain features revealed by the measurements given in the paper, though they are published only as illustrations of the method. There is, for example, the convex portion of the isotherms in Fig. 6 (p. 403) about halfway between the centre and the surface of the billet, evidently due to the impingement of the spray on the billet when it leaves the mould. The effect of this inflection is to produce a much more steeply inclined solidification front in this important part of the cross-section, with a corresponding tendency to increased inverse segregation and internal stresses. This emphasizes the importance

of controlling the rate and position of the cooling action below the mould proper, and of connecting it with the condition in the lower part of the mould.

Some conclusions may also be drawn from the temperature distribution along the axis of the billet as shown in Fig. 6. The temperature gradient in the region of 600° C. is ~70°/in. for a pouring rate of 9 in./min. and 170°/in. for a pouring rate of 3 in./min. Considering an alloy of the Duralumin type, having a solidification range of about 70°–80° C. between about 620° and 540° C., one can foresee a considerably smaller temperature gradient owing to the influence of the latent heat of fusion, which, spread evenly over the interval, would amount to an increase in the specific heat of the order of 300%. This leads one to expect a thickness of the solidification zone of the order of 1–3 in. under the range of cooling and pouring conditions covered in Fig. 6. Can the author give any figures relating to alloys having a substantial range of solidification?

The application of the radioisotope tracer technique as described by Mr. Putman raises great hopes as to the possibilities of gaining by relatively simple means more insight into the details of the mechanism of solidification in alloys.

Mr. J. F. HOBBS,† B.Sc., A.I.M. (Member): As one who has obtained a considerable number of recordings of temperature conditions within continuous castings by an inserted-thermocouple technique, I am very interested in Mr. Lewis's paper. I would like to enquire the diameter of thermocouple which was used and would query the necessity or desirability of coating the actual junctions with Dycote. It is obviously important to have the best possible contact between the couple junction and the surrounding metal of the casting, and in my experiments I have obtained satisfactory results using a bare junction.

Mr. Lewis's technique differs from my own in that his couples enter the casting from below while I have always inserted them from the top of the casting. I should welcome his comments on the respective merits of the two procedures. One obvious disadvantage of Mr. Lewis's arrangement is that it could not be applied in fully continuous operation, as on the Junghans-Rossi machine.

I feel that Mr. Lewis has been somewhat harsh in his assessment of the merits of the inserted-thermocouple technique and would query his statement that slight displacement of the couples makes the results obtained quite valueless. Although the final position of the couples does not always correspond precisely with that intended, it is always possible to determine the position by X-ray examination and make the appropriate correction. I am wondering if Mr. Lewis has been prejudiced by his evident difficulties in insulation of the couples inserted in the ingot. Even under the best conditions, he experiences a couple mortality of about 1 in 10, when using 24 S.W.G. Chromel/Alumel wires insulated with woven asbestos sleeving, with a short length of closely fitting twin-bore insulator at the junction. In my work, I have experienced a mortality figure of around 1 in 50.

M. A. KOHN‡: I would like to make some suggestions about one point concerning the autoradiographic technique described by Mr. Putman, when used with metallic samples. Where high resolution is desired, the choice of a suitable emulsion is of great importance. The autoradiographic method has been used at IRSID for more than four years, and from our experience, the French emulsion known as Pathelith seems to be one of the best for such work; I think that a similar emulsion, called Kodolith, is made in England.

I have not had an opportunity of employing the Industrial B X-ray film used by the author; but last year we carried out some experiments on fifteen different commercial emulsions, including the Industrial G, which, from the maker's description, is very similar in contrast to Industrial B, but has a

\* Chief Metallurgist and Head of Laboratories, International Alloys, Ltd., Aylesbury, Bucks.

† Research Department, Imperial Chemical Industries,

Ltd., Metals Division, Birmingham.

‡ Chef du Service de Radioactivité, Institut de Recherches de la Sidérurgie, Saint-Germain-en-Laye (S. et O.), France.

slightly coarser grain and is faster. Our tests were made in order to compare these emulsions from the point of view of contrast, background, speed, and resolution, when darkened by the  $\beta$ -rays of radio-copper and radio-arsenic. The results confirmed that X-ray films are generally not suitable; they are fast, but they have a high background and are coarse-grained. We found that some emulsions used for photostat copying or for lantern slides were better, and produced autoradiographs of good contrast and high resolution.

Dr. C. E. RANSLEY,\* M.Sc., F.I.M. (Member): There is still a good deal we do not know about the continuous-casting process, and there are two distinct facets to the problem. These are the effects of various casting parameters on (i) the surface quality of the extrusion billet or rolling block, and on (ii) the residual stresses left in the completed casting.

The surface quality is undoubtedly mainly influenced by the conditions of shell formation within the mould itself, and possibly immediately below the mould exit, and Mr. Lewis points out the very considerable difficulties in exploring this region of the casting by a buried-thermocouple technique. Our experience suggests that the conditions within the mould are actually very unstable from moment to moment, and we feel a little dubious as to whether any very useful results will be obtained by the thermocouple-plug method described on p. 411 of the paper, even if a very close control of metal level in the mould is achieved.

The residual stresses in the casting are, of course, determined by the thermal gradients existing in the metal throughout the freezing process, but I should not have thought it necessary to locate the isotherms with extreme accuracy for an examination of this aspect. Slight variations in the speed of withdrawal, water flow, and so on are bound to lead to some small irregularities in heat extraction, and will thus tend to make a minute analysis of the experimental results rather unprofitable. I am not clear, in fact, why Mr. Lewis is dissatisfied with the excellent practical values shown in his Fig. 6 (p. 403), which needs only a few observations of surface temperature on the emergent casting (which should not be difficult to carry out) in order to allow the complete isotherms to be drawn in below the mould with reasonable accuracy. It is difficult to see what advantage accrues from the adoption of a more critical treatment, such as an iteration technique, when the data are considered in relation to their final application, and perhaps the author would care to comment on this aspect of his work.

Dr. W. A. BAKER,† F.I.M. (Member): Regarding the precision of temperature measurement necessary to obtain useful information about the solidification of the metal in the vicinity of the mould, I suggest that interpretation of temperature measurements of a given accuracy is very much easier when the material being cast has a fairly long freezing range and when the relation between the percentage of metal solidified and the temperature, within the liquidus-solidus interval, is roughly linear. When pure metal is cast, or when most of the metal solidifies within a few degrees of the liquidus temperature, it becomes very difficult to determine the end of solidification from a cooling curve. The effects of air-gap formation on the shape and position of liquidus and solidus isotherms might be determined with greater precision by direct-temperature measurement if alloys of suitable constitution were chosen for such experiments.

Dr. F. R. MORRAL,‡ B.S. (Member): Mr. Lewis points out that the whole principle of the continuous-casting process can be explained by reference to the shape of the solidification front, also called the sump contour. He discusses four techniques. One of them, the tracer technique, is well illustrated by Mr. Putman.

The accompanying photomacrograph (Fig. B, Plate XCIII) and reproduction of a radiograph (Fig. C, Plate XCIII) taken through a  $\frac{1}{2}$ -in.-thick vertical section of the top of a 13-in. rectangular ingot of 2S aluminium show well the solidification front and disturbances occurring on continuous casting. Staples and Hurst § presented only a short longitudinal section, insufficient to show the possibilities of the macrographic technique. The radiograph, which has lost some detail in reproduction, shows by diffraction the longitudinal grains and their direction of growth. The solidification front can be drawn by tracing perpendiculars to these crystals. The radiograph also gives an indication of events in casting which caused a change in the growth direction of the crystals.

A combination of these two techniques shows more than the autoradiographic technique, although the latter will remain unique for fine-grained alloys.

Dr. V. PASCHKIS ||: Mr. Lewis's paper deals with a subject of great practical importance in an unusually comprehensive and clear way. The author states correctly that experimentation on actual casting is difficult to carry out, particularly if unusual conditions regarding casting speed and cooling are to be explored. Therefore, it is important to seek for methods of analysing conditions without extensive experimentation.

The author's Section V (p. 403) presents a number of different techniques used to explore the temperature field in a casting. However, all his techniques are predicated on knowing the temperature distribution at least in part by direct observation. These temperatures, moreover, must be measured in the solid zone, because equations (10) and (11) (p. 404) hold only for the case that no heat sources occur; but prior to solidification heat sources do occur in form of the heat of fusion being liberated.

In view of this limitation it becomes very important to explore methods of computing the entire process, i.e. without relying on direct measurements. In Section VI, 2, (p. 411) Mr. Lewis discusses mathematical methods for calculating the cooling rates of hot ingots and refers to the lack of knowledge of high-temperature properties as alone limiting the usefulness of this approach. In order to be usable, the conventional mathematical methods require, as the author himself states in his Section II (p. 396), intolerably sweeping assumptions. However, use of an electrical analogue computer ¶ has led to an excellent check with thermal-analysis data. The results obtained by Pellini to which Mr. Lewis refers have been predicted by means of the analogue computer. Good correlation with experimental data was obtained both in the case of steel castings \*\* and of aluminium castings.††

The application of the analogue-computer technique to continuous casting is still in its early stages and has to overcome two difficulties.

(i) Continuous casting presents a special mathematical problem, since it is one of "moving heat sources".

(ii) As in all computations, the thermal properties must be known, and these properties here include some which are particularly poorly established. It seems that the thermal contact resistance between casting and mould prior to the

\* Research Laboratories, The British Aluminium Co., Ltd., Gerrards Cross, Bucks.

† Research Manager, British Non-Ferrous Metals Research Association, London.

‡ Department of Metallurgical Research, Kaiser Aluminum and Chemical Corp., Spokane, Washington, U.S.A.

§ R. T. Staples and H. J. Hurst, *J. Inst. Metals*, 1952-53, **81**, Plate LV, Fig. 5; also *Inst. Metals Monograph and Rep. Series*, No. 15, 1953, Plate X, Fig. 5.

|| Department of Mechanical Engineering, Columbia University, New York.

¶ V. Paschkis and H. D. Baker, *Trans. Amer. Soc. Mech. Eng.*, 1942, **64**, 105.

V. Paschkis, *Metal Progress*, 1947, **52**, 813.

\*\* V. Paschkis, *Trans. Amer. Found. Assoc.*, 1945, **53**, 90; *Proc. Inst. Brit. Found.*, 1951, **44**, A32.

†† V. Paschkis, *Trans. Amer. Found. Soc.*, 1948, **56**, 366.



formation of the air-gap, as well as the resistance after its formation and in the separate zone, are very important.

In this connection the computer offers valuable possibilities. It permits of varying all the properties which enter into a problem over a wide range, thus determining which of the several variables are of critical importance.

The work done so far with the analogue computer in the field of continuous casting was on brass and will be published in due course. Unfortunately, there are insufficient experimental data available with which to compare the results of the computations.

One additional item deserves mention. In Section IV, 3 (p. 403) of the paper a method is described for transferring the thermocouple recordings to a common graph. From the figures quoted in the paper, a speed of 25 sec. per point transferred seems to have been achieved. The method used by the author is a very ingenious one, solving a problem widely encountered. Dr. F. Freudenstein has developed in this laboratory a transferring device based on mechanical linkage. This is nearing completion, and it is hoped that it will provide a still more rapid rate.

Mr. LEWIS (*in reply*): The paper under discussion was put forward to introduce some of the work on continuous casting now being done at Aluminium Laboratories Limited, Banbury. It was hoped that a useful discussion of the subject would be stimulated, even though no account of our results was being presented at that time. As is well known to all who have worked on continuous casting, the process is so complex that any programme of investigation only yields results very slowly, even when use is made of the important statistical techniques. We felt that an account of our techniques would be a better introduction than a premature discussion of the results.

It will be appropriate here to point out two misprints on p. 396 of the paper. Equation (3) should read  $x = 0.0263Vy^2$ , and in the next paragraph the correct statement should read as follows:

... "equation (2) reduces to

$$x = 0.018_2 \frac{V}{R} \left[ \frac{R^3}{3} - r^3 \log_e \left( \frac{R}{r} \right) - \frac{r^3}{3} \right].$$

Mr. Ruddle's remarks are of the greatest interest in view of his own important work on the subject of metal solidification. Our investigations of the solidification profile have, up to the present, been confined mainly to commercial-purity aluminium, but even here some rather striking discrepancies appear between dip-stick readings and the profiles given by either of the tracer techniques. Measurements taken on cooling curves have shown a difference of about  $\frac{1}{4}$  in. between the liquidus and solidus lines for metal of 99.2% purity. I agree with Mr. Ruddle that this probably extends to some inches for alloys with a long solidification range. This point will be investigated in later work.

My statement that the copper-tracer method of showing the solidification front would be unsuitable for copper-containing alloys was based on the fact that the profile is shown clearly owing to contrast between the two etched zones. In the work described contrast is between Al + nil Cu and an Al-4% (approx.) Cu alloy. It is then relatively easy to show the difference by etching. The addition of pure aluminium to an aluminium-copper alloy would result only in dilution of liquid alloy in the pool. There would, of course, be a difference in composition at the boundary, but this would be between one aluminium-copper alloy and another with a somewhat higher value for the aluminium content. Etching would probably show the solidification front, but not with any great clarity.

There is a possibility that the tracer-bearing metal may not actually penetrate into the mushy zone as far as the solidus, but this will be tested at a later stage in the work, when it becomes possible to check a number of autoradiographs against the corresponding cooling curves.

Since the papers under discussion were written, the radio-

active tracer technique has been further developed and cannot now be described as "time consuming", as the specimens do not require irradiation in an atomic pile. The tracer addition of about 1 millicurie of an aluminium-gold alloy is made to the metal during casting, this level of activity requiring only the very simplest protective measures. This addition gives about 0.0001% gold in the metal in the pool. The sections can be prepared and examined without delay, while sufficient activity is present for very good autoradiographs to be produced for the 5-6 days following the experiment. This technique and its results will be described in a later paper.

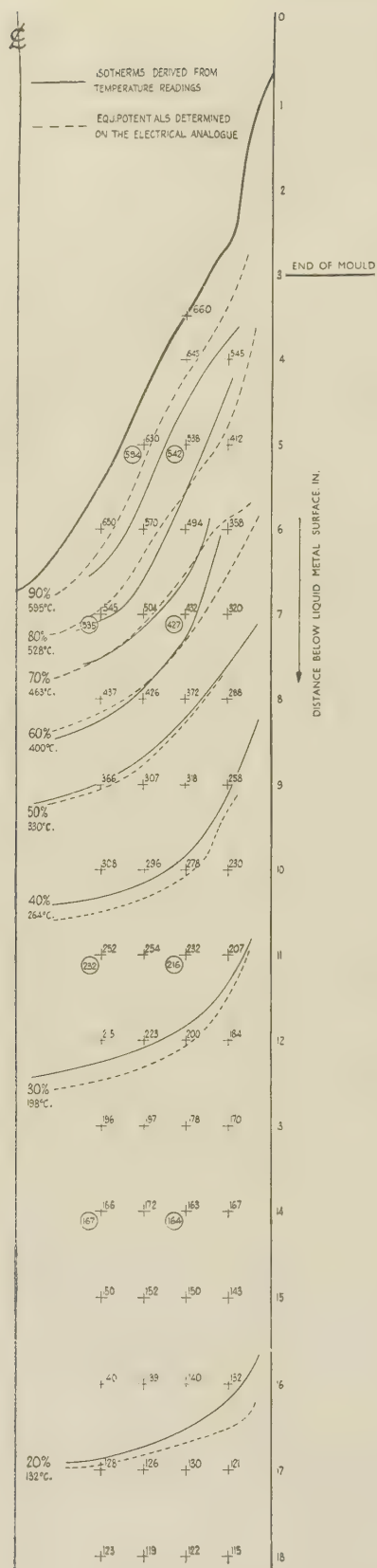
The error in the thermal-analysis experiments has been reduced to reasonable proportions and now results mainly from errors in the positions and levels of the thermocouples and of electrical and thermal short-circuit effects below the thermo-junctions. Laying the couple wires parallel to the isotherms, as Mr. Ruddle has done, is an ideal method of overcoming conduction errors, but we feel that we have achieved a similar result by supporting the couples from the ingot base. The wires warm up steadily as they pass into the pool, and when the junctions enter the liquid there can be little difference between their temperatures and that of the surrounding metal. The couple wires then act as a high-resistance path to heat flow in comparison to the low-resistance path through the solid aluminium.

The use of the Liebmann iteration method for getting a picture of conditions in the mould depends on having good measured temperature values for positions as close as possible to the casting surface, in order to approximate to the correct boundary conditions. A grid can then usually be made up from: (1) the solidification profile, i.e. the 660°C. isotherm, (2) the line of determined temperatures, (3) the point of initial contact of the metal and the mould, assumed to be 660°C., and (4) the temperature distribution worked out for the remainder of the ingot. Calculations can then proceed in the normal manner.

Mr. Ruddle's question on setting up the electrical analogue touches on a point not covered in sufficient detail in the paper. The analogue must be set up on known boundary conditions, but in the case of surface heat transfer few values are known. If there is taken one set of temperature readings in the interior of the metal (say, obtained from one thermocouple only) under similar casting conditions, the resistance values connected to analogue surface electrodes can be altered to give the required potential (temperature) values at equivalent positions in the tank. Thus, from a known partial solution of the expression for heat flow in the ingot there are derived surface-resistance conditions which give a good approximation of the temperature field. The probe can then trace out all the isotherms and cover the complete ingot section in some detail. The accuracy of this technique should be clear from Fig. D.

There was no intention to show Dr. Roth's results in too unfavourable a manner, and I can assure Dr. Brenner that my sole purpose was to illustrate a case where the calculated values for the profiles differed appreciably from the experimental results. I am indebted to Dr. Brenner for showing that these differences are not as great as those illustrated in my Fig. 1. It is, however, still clear that agreement in not good between the two profiles, either in the depth of the pool or in the profile outline. Dr. Roth's work is, in spite of this limitation, the foundation on which all subsequent calculations on continuous casting are based.

In preparing the paper it was thought desirable to reduce the essential mathematics to a minimum, but this resulted, as pointed out by Mr. Elson, in the actual heat conduction equation being omitted in favour of the Laplace equation. Continuous casting certainly is an example of a system having a moving heat source, but, as Mr. Elson will admit, consideration of this would have introduced into the problem an analysis of considerable complexity. What has been done, in the case of the analogue, is to impose upon it the shape of the solidification front and a series of experimentally determined temperatures, both of which take into account the rate of casting and hence depend on the solution to the differential equation involving the velocity. The result obtained from



the analogue is a solution of the Laplace equation but it approximates closely to the true solution of the problem, as can be seen from Fig. D.

In the iteration calculations the modified equation quoted by Mr. Elson was in fact employed for all work done on cylindrical billets; to facilitate calculation the tables given by Shortley, Weller, Darby, and Gamble \* were used, as these take into account the radial distance of the points. It is true that neglect of this effect will give quite considerable temperature differences near the axis.

In order to take into account the effect of the velocity, the iteration calculation has been done for the casting conditions shown in Fig. D by two methods, (a) a velocity term being considered, the diffusivity taken as constant, and (b) the normal Liebmann method. The results of both are shown in Table A.

TABLE A.—Comparison of Temperature Values Between Measured Figures and those Determined by a Modified Iteration and the Normal Liebmann Method.

The figures refer to the cast shown in Fig. D.

Distance Below Mould Exit Level, In.	Distance from Ingot Surface, In.						
	0.53	1.06			1.59		2.12
	Measured	Measured	Modified Iteration	Normal Iteration	Measured	Modified Iteration	Measured
0.533	620	...	...	...	...	...	...
1.066	520	...	607	606	...	...	...
1.60	442	540	557	549	640	645	639
2.133	403	...	516	507	617	607	600
2.666	375	...	484	475	588	578	569
3.20	350	470	455	447	558	551	541
3.733	329	...	426	417	...	515	504
4.266	310	...	394	385	...	465	453
4.80	293	380	364	355	436	421	410
5.333	278	...	337	329	...	384	374
5.866	262	...	313	305	...	352	343
6.40	248	301	290	284	330	323	316
6.933	234	...	269	264	...	297	290
7.466	219	...	249	244	...	271	264
8.0	207	232	231	226	250	248	241
9.066	183	...	200	197	...	211	207
9.60	174	186	188	185	205	196	193
10.666	160	...	168	166	...	172	170
11.2	153	160	160	158	170	163	161
12.27	142	...	147	145	...	148	147
13.33	129	138	134	134	...	137	136
14.40	120	...	124	123	...	127	126
16.0	110	114	112	112	110	112	112

It is clear that there is close approximation between the values obtained by each technique, the final values being well within the experimental error of the whole experiment. In view of the minor effect resulting from changes of diffusivity with temperature, it was not considered necessary to make an extra correction.

It was not intended that Figs. 6 and 13 of the paper should be compared as, apart from casting speed, they refer to two completely different experiments. The diagrams were reproduced in the paper to illustrate different points, and we would ask Mr. Elson not to draw any special conclusions from them at this stage.

Dr. Scheuer draws attention to some of the many features in the solidification process which are, at present, not clear. It is our hope that the work described will assist in explaining some of these phenomena.

It is interesting to know of Mr. Hobbs's experiments and

FIG. D.—Temperature Fields Showing Close Agreement Between Measured Values and Electrical Analogue Readings. Thermocouple values shown thus:  $\pm 288$  and analogue readings 216. The values are for a  $20 \times 6$  in. ingot in 2S alloy cast at  $670^\circ \text{C}$ ., 6 in./min., 3 in. metal depth in mould and 60 gal./min. of cooling water.

\* G. Shortley, R. Weller, P. Darby, and E. H. Gamble, *J. Appl. Physics*, 1947, 18, 116.



the results on a fully continuous process of the Junghans-Rossi type. In answer to his enquiry, the thermocouple wires used by us are 22 S.W.G. and are coated with Dycote wash up to the junctions. The welded junction itself is left bare, as we have found that electrical troubles occur at the amplifier when a coating is used.

I feel that feeding the thermocouples into the top of the mould, as Mr. Hobbs has done, calls for some anchoring method within the ingot, while the conduction losses up to the wires must always be appreciable. These considerations made us arrange our equipment for the thermocouples to stand from the base of the ingot. Mr. Hobbs's mortality rate of one thermocouple in fifty must be regarded as an achievement and is a figure we have not yet attained.

Dr. Ransley mentions the probable unsteadiness of conditions within the mould and the difficulties in obtaining information about these conditions. The thermocouple-plug procedure was used to get some integrated values of heat flow over zones in the mould, but the disadvantages and inaccuracies of the method were appreciated, although up to the present it has not been possible to try any other improved techniques.

Our reasons for using the iteration method are to fill in detail into what is sometimes a very inadequate skeleton of temperature values gained from thermo-analysis experiments. It is agreed that it is pointless to strive for very high accuracy in the final temperature values when the measured values used as a basis for the calculation can contain a fair degree of error.

Dr. Baker's valuable suggestion that more information on mould phenomena might be obtained by using alloys of wide solidification range is of interest and will be investigated in the near future.

The contribution from Dr. Paschke mentions how another type of analogue, the Heat and Mass Flow Analyser, can be applied to investigating the continuous-casting process. We look forward with interest to the paper describing the results obtained. There is so little fundamental information on the

casting process that each investigation of some facet of the problem is of extreme value.

It was with interest that I read Dr. Morral's contribution in which he describes a technique that seems to have received no attention. The effect described has often been evident to us in the radiographs of sections such as that shown in Fig. 18 (Plate LVII) of the paper. The grain structure is shown fairly clearly in the original radiograph of Fig. 18 but has been completely lost in reproduction. We have not examined the section near the head of the ingot, however, and thus have not encountered the change of structure shown by Dr. Morral. I agree that the solidification profile can be drawn from the perpendiculars to the crystals, but the operation is accompanied by a chance of serious error, as it is difficult to decide on the main grain axis.

Mr. PUTMAN (*in reply*): With regard to Mr. Kohn's remarks, no special virtue is claimed for Industrial B X-ray film in this work. We use it as a medium-grain emulsion for  $\gamma$ -radiography and therefore had films available. High resolution and contrast were not necessary in the application described, but may well be important in more detailed investigation of the properties which these experiments have revealed. I thank M. Kohn for drawing our attention to his valuable work on the choice of emulsions for autoradiography.

The photomicrograph and radiograph shown by Dr. Morral are certainly impressive, and together give information which could not be expected from the radioactive-tracer technique. It seems to me, however, that the methods are to some extent complementary. Whilst Dr. Morral's figures beautifully illustrate the grain structure, which the tracer method does not, the autoradiographic method gives a measure of the deposition of material as a function of time and a direct picture of the solidification boundary. It is to be expected that further investigation by tracer methods might yield new information about the flow of molten metal within the crater to which the striations in my Fig. 1 (Plate LX) are related.

## Discussion

# The Properties of Aluminium-Magnesium-Silicon Alloys \*

Mr. J. CROWTHER,† M.Sc., F.I.M. (Member): In discussing these two stimulating papers I should like to confine myself to the general picture they present. The aluminium-magnesium-silicon alloys are of great industrial importance; they have in general excellent corrosion-resistance coupled with useful strength and are readily produced as sheet or as thin or complicated extrusions. A wide range of strengths is available, but unfortunately highest strength goes with a ductility which, although adequate for straightforward use, does not allow of much forming in the fully heat-treated condition. Because of the wide range of application of this type of alloy it has proved difficult to standardize on a small number of alloy compositions, and various magnesium and silicon contents have been used, often with manganese and more recently with chromium and copper.

In a few specialized applications cases of "brittle" fracture have been encountered. These have occurred in alloys which must be regarded as brittle only in comparison with the high general level of ductility of the class as a whole. Of the two papers under discussion, that by Mr. Harris and Mr. Varley deals more specifically with the conditions under which low ductility can be developed in straight ternary alloys; Mr. Chadwick, Mr. Muir, and Mr. Grainger are concerned with the effects of adding iron, manganese, and chromium to a chosen

Al-Mg-Si alloy, but they also deal largely with levels of ductility and the two papers fit together very well.

The papers are important in at least two fields. First, they have a sound practical value, because together they give a good general background for the consideration of the many industrial alloys based on the Al-Mg-Si system. Mr. Harris and Mr. Varley relate the mechanical properties of a wide range of ternary alloys to the phase diagrams already established, and here it may be noted how rapidly the properties change with magnesium content in the region commonly used.

Both sets of investigations are particularly concerned with the factors affecting ductility in fully precipitated alloys. Harris and Varley describe the composition range in ternary alloys in which ductility is lowest, which unfortunately is also the region of highest strength, and how this brittleness is affected to only a minor degree by permissible variations in heat-treatment. An important finding is that alloys outside the so-called brittle range can be rendered brittle by too slow a cooling rate after solution-treatment.

Mr. Chadwick and his co-workers demonstrate the very marked effect of manganese and chromium, and to a lesser degree iron, in eliminating this tendency to brittle fracture.

The second important aspect of the two papers is their examination of the reasons for such behaviour. It is shown

\* Joint discussion on the papers by R. Chadwick, N. B. Muir, and H. B. Grainger (*Journal*, this vol., p. 75) and I. R. Harris and P. C. Varley (p. 379).

† Chief Metallurgist, James Booth and Co., Ltd., Birmingham.

that low ductility in the pure ternary alloys is associated with intercrystalline cracking and can be connected with a mode of low-temperature precipitation which allows grain boundaries to be revealed clearly on etching. Chadwick, Muir, and Grainger show that manganese and chromium additions cause a localized high-temperature precipitate which is generated within the cast grains and persists in bands in the wrought structure. Their demonstration that harmful grain-boundary precipitation of  $Mg_2Si$  or silicon at low temperatures is prevented by a fine dispersion of this high-temperature precipitate, but can occur in the same alloy if the high-temperature precipitate is coarsened, seems to me to be of fundamental importance.

Similar high-temperature precipitates can be obtained in other alloys containing manganese, including the high-strength alloys based on Al-Cu-Mg-Si and particularly on Al-Cu-Mg-Zn, in both of which manganese (or chromium) is an essential ingredient. In the latter group, at least, it can be demonstrated that coarsening of this precipitate drastically alters the recrystallization and precipitation characteristics of the alloy.

The accompanying micrographs (Figs. A and B, Plate XCIV) show the high-temperature precipitate in:

- (i) Al-7% Mg-0.3% Mn alloy, homogenized for 100 hr. at 450° C., water-quenched, and reheated for 20 hr. at 200° C.
- (ii) Al-6% Zn-3% Mg-0.6% Cu-0.4% Mn alloy, homogenized for 1000 hr. at 460° C., water-quenched, and reheated for 16 hr. at 135° C.

Manganese and chromium are very important addition elements in industrial high-strength alloys and a full understanding of their effects awaits an examination of the way in which the high-temperature precipitate they form controls the precipitation of hardening compounds at low temperatures. I hope someone will be stimulated by these papers to investigate this kind of effect further in several aluminium-base alloy systems.

The final question thrown out by Chadwick, Muir, and Grainger is also important: Does the brittle fracture result from an inherently brittle or weak grain-boundary film, or is it a secondary corrosion effect of a boundary film? The authors seem to favour the first explanation and are supported by the evidence of the other paper and by the way in which this type of alloy is normally regarded as not susceptible to stress-corrosion. Here again a parallel problem exists in the Al-Cu-Mg-Zn system, where failures in highly stressed components have been ascribed to "stress-corrosion" but may well be due to a similar "brittle" phenomenon in a highly directional structure.

Mr. R. CHADWICK,\* M.A., F.I.M. (Member): The two papers show very clearly the importance and also the complexity of precipitation effects in the metallurgy of aluminium-magnesium-silicon alloys. Quite apart from the age-hardening process itself, at least four precipitation stages can occur and not less than two precipitate phases are involved, but observations have so far been rather superficial in character and incidental to the main investigations, which are concerned with mechanical properties. The need for detailed metallographic studies is clearly indicated.

The demarcation of brittle zones in alloys without manganese or chromium is shown by Mr. Harris and Mr. Varley in their Figs. 7 and 8 (p. 386) by reference to Izod values. Data relating to bending properties of alloys containing 0.7% magnesium with varying silicon, manganese, and iron are shown in the form of a solid diagram in Fig. C (Plate XCIV), in which a high  $R/T$  value (plotted vertically) is associated with low ductility. The position of the hump in this diagram, representing minimum ductility in the ternary alloy at 1% silicon content, is in close agreement with the data presented in Fig. 8, where for a 0.7% magnesium content minimum ductility occurs with 0.9% silicon. It will be seen in Fig. C that

at little as 0.2% iron + manganese produces a useful improvement in ductility, and that with 0.4% iron + manganese there is scarcely any evidence of a hump. The brittleness hump in the manganese-free alloys, acute though it is at one specific magnesium : silicon ratio, is nevertheless sufficiently broad to affect almost the whole range of useful compositions. The final conclusion of Harris and Varley (p. 393) that: "In particular, satisfactory mechanical properties in the H10-WP alloy cannot be obtained without accompanying notch-sensitivity in the absence of chromium or manganese" does, therefore, deserve repetition and should have been underlined. Indeed, if this is now to be regarded as generally accepted, there would seem to be no further obstacle to making additions of chromium or manganese obligatory in B.S. specifications.

Mr. Harris and Mr. Varley have provided only limited data on the effect of manganese on tensile properties (Table X), from which they draw the conclusion (p. 391) that: "The mechanical properties are little affected by manganese if the addition is restricted to a maximum of approximately 0.8%." That manganese additions have a beneficial effect on ductility, however measured, is surely not in dispute, and it is assumed that this remark is intended to refer to proof stress and U.T.S. However, detailed examination and comparison of figures quoted in Table X does not bear out this contention. For example, alloys 1 and 3 have practically identical magnesium and silicon contents, the latter having 0.41% manganese by virtue of which the proof stress is increased by 1.4 tons/in.<sup>2</sup> and the U.T.S. by 2.2 tons/in.<sup>2</sup>. Alloys 2 and 4 may also be compared with a somewhat similar result, although here the greater increase is in the proof stress. Other alloys of higher-manganese are of lower-magnesium content, and comparison is therefore invalid. However, the results now quoted are in substantial agreement with our own.

On the question of copper it is still more difficult to find the basis for the deductions made by Harris and Varley, who, on p. 390, state that: "an addition of 0.3% copper is sufficient to raise the proof and ultimate tensile stresses by about 3 tons/in.<sup>2</sup>". In Table X the copper-free alloys matching most nearly the composition of the copper-bearing alloy No. 9 are Nos. 3, 4, and 8, all three of which have mechanical properties very close indeed to those of No. 9. Other possible comparisons in Table VI (p. 389) of alloys 15 with A, 21 with C, and 16 with 18, seem to indicate that copper has the effect of lowering slightly both proof and tensile stress values.

Harris and Varley present no data on corrosion-resisting properties, although they state that the advantage to mechanical properties of a copper addition is offset by a decrease in corrosion-resistance unless chromium or manganese is also present. It is surely well established that copper additions adversely affect corrosion-resistance in alloys both with and without manganese. Whether anything is gained on balance by obtaining a small increase in mechanical strength at the expense of diminished corrosion-resistance is highly questionable, because such strength cannot be fully utilized in engineering design if extra allowances have to be made for corrosion within the lifetime of a structure.

Dr. F. A. CHAMPION,† B.Sc., A.R.C.S., F.I.M. (Member): The brief reference to corrosion-resistance in the conclusions of Mr. Harris and Mr. Varley is perhaps misleading. The second sentence in the penultimate paragraph of p. 392 may suggest a marked increase in corrosion above 0.3% copper. The available evidence seems to me to indicate a fairly gradual harmful effect of increasing copper content which is minimized by the presence of manganese or chromium. One must therefore strike a balance between the required mechanical and corrosion properties. I would suggest that the figure of 0.3% copper has become significant more from its common usage in America in these alloys than from any special effect on corrosion.

\* Assistant Research Manager, Imperial Chemical Industries, Ltd., Metals Division, Birmingham.

† Research Laboratories, The British Aluminium Co., Ltd., Gerrards Cross, Bucks.



Mr. D. L. W. COLLINS,\* B.Sc., A.R.S.M. (Member): The two papers are of great interest to us, not only on their own merits, but because we have been carrying out substantially similar studies at Banbury; in general, we agree with the authors, but there are some differences in our programme and results which it may be worth while summarizing.

Briefly, our programme was as follows: Ternary alloys within the range 0.3–1.2% silicon, 0.5–2.0% magnesium were prepared with a super-purity aluminium base, and the same basic compositions were used for alloys with additions of iron,

we used. Further, the properties are only slightly increased by the presence of iron; this does not agree with the results in either paper, since Chadwick, Muir, and Grainger report a substantial increase with iron, and Harris and Varley a decrease. The apparent anomaly is possibly explained by the different casting techniques used in the three investigations; it has been shown by Phillips† that the rate of cooling can substantially affect the form in which iron occurs, and this is supported by our own observation, so that there may well be a difference in the free silicon remaining after casting under

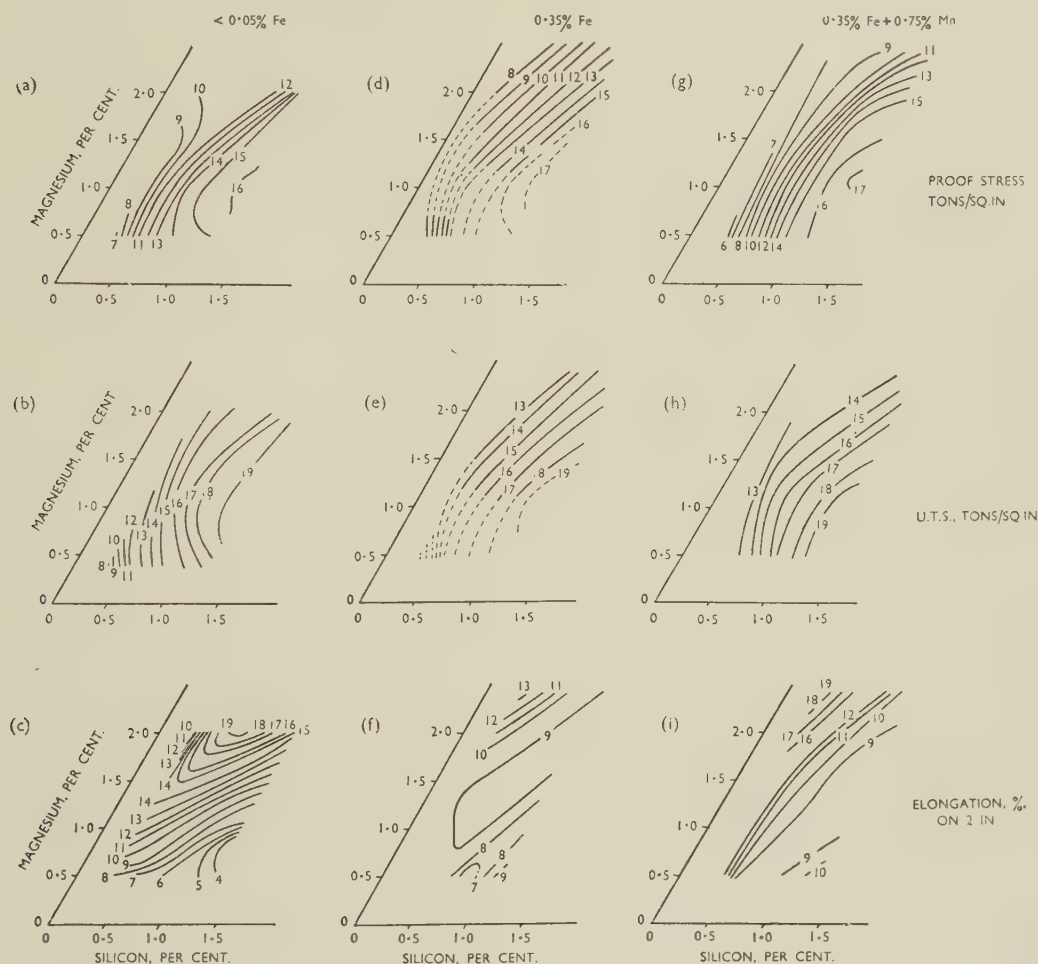


FIG. D.—Properties of Al-Mg-Si Alloys with <0.05% Fe, 0.35% Fe, and 0.35% Fe + 0.75% Mn, in the Fully Heat-Treated Condition.

iron + manganese, or copper. The alloys were tested as 0.036-in. sheet and 1-in.-dia. extrusions. Rolling ingots were cast in a permanent mould, extrusion billets semi-continuously in an 8 $\frac{1}{8}$ -in.-dia. mould. A solution heat-treatment temperature of 520° C. was used in all cases. All sheet and some extrusions were heat-treated in a salt bath, the remainder in an air furnace.

Fig. D shows contour diagrams of the tensile properties of alloys without iron, with 0.35% iron, and with 0.35% iron + 0.75% manganese, in the form of 0.036-in. sheet. It can be seen that these are very similar to Fig. 6 (p. 386) of the paper by Mr. Harris and Mr. Varley, which gives the properties of super-purity-based alloys. This in itself is somewhat surprising in view of the lower heat-treatment temperature which

various conditions. The difference does not appear to arise from the casting process as such, since in our own work neither sheet from permanent-mould ingots nor 1-in.-dia. extrusions from semi-continuously cast billets showed a significant variation in properties with iron contents from 0.05 to 0.5%.

It appears well established that brittleness and intercrystalline fracture are associated with the occurrence of a grain-boundary precipitate, probably of  $Mg_2Si$ , but there is evidence which indicates that the weakness may be due to a region of depleted solid solution immediately adjacent to the grain boundary, rather than to the precipitate itself; Figs. E and F (Plate XCIV) are photomicrographs of an HE10-type alloy which was held at 280° C. for 22 days, etched in ammoniacal

\* Aluminium Laboratories Limited, Banbury, Oxon.

† H. W. L. Phillips, *J. Inst. Metals*, 1946, **72**, 151.

ammonium oxalate solution, and show what appears to be a denuded zone at each of the grain boundaries which remained unetched. This view is also supported by purely mechanical considerations; in our own work almost completely intergranular fractures in tensile tests, with little or no distortion of the grains, was observed in alloys with a range of tensile strength values, and it is clear that in these cases the strength of the materials was determined by the strength of the grain boundaries. If the intergranular weakness were due to a brittle film of precipitate, it would be expected that as the continuity of this film increased the strength would diminish, but in fact the reverse occurred, the strength increasing as the continuity of the film increased. The results are consistent, however, with the presence of a peripheral "over-aged" region, slightly weaker than the material of the main body of the grains.

The observed effect of manganese in reducing the brittleness of fully heat-treated alloys is probably due in the main to the reason suggested by the authors, that the manganese forms nuclei for the precipitation of  $Mg_2Si$  and silicon within the grains, but a reduction in the age-hardening properties due to the presence of manganese may be a contributory cause. It is probable that the solubility of magnesium and silicon is reduced by the presence of manganese (the solubilities of the individual elements are certainly reduced in the ternary Al-Si-Mn and Al-Mg-Mn systems) so that there is less  $Mg_2Si$  precipitated during ageing, and thus proportionately less tendency for precipitation at the grain boundaries; the solution-hardening effect of manganese is, however, sufficient to compensate for the reduction in precipitation-hardening. There is some experimental support for this hypothesis, in that the increase in strength from the annealed to the fully heat-treated state is less in the manganese-containing alloys than in the manganese-free alloys; this increase is presumably due almost entirely to precipitation-hardening, since the solution-hardening effects in the two conditions may be taken as approximately equal.

In the case of additions of copper, our experimental work and experience with 65S alloy again confirm that of Harris and Varley, but here I must point out that the solubility data given by Axon\* are for alloys at  $460^\circ C$ ; the solubility of copper at room temperature and at the ageing temperature will presumably not be in excess of that in binary aluminium-copper alloys, i.e. about 0.2%, so that the effect of copper in excess of this amount is explicable quite simply by precipitation-hardening. Results consistent with this assumption have been obtained with additions of  $\frac{1}{2}\%$  and  $1\frac{1}{2}\%$  of copper; in general, it appears that the precipitation effects of copper and of magnesium and silicon are independent, additive factors. The increase in grain-boundary precipitation on air-cooling which was observed in copper-containing alloys may thus be the same phenomenon as was reported by Gayler,† rather than an analogy.

With reference to the work on the effect of quenching rate, I should like to ask Mr. Harris and Mr. Varley if they have any direct evidence on the effect of air-quenching on the brittleness of commercial H9-type alloys; in our experience air-quenching of thin sheet gives satisfactory tensile properties, and in Table IX (p. 390) of their paper, the bending properties of the alloy containing 0.4% Mg, 0.5% Si appear to be improved by air-quenching.

Mr. E. A. G. LIDDIARD,‡ M.A., F.I.M. (Member): One might conclude from reading these papers that the H10-WP alloy suffers from an alarming intercrystalline weakness unless it contains additions of chromium and manganese. Manganese and chromium raise the recrystallization temperature of this alloy, and in so doing they increase the amount of work necessary to deform it and increase the directionality of its structure. The effect of these additions is therefore to lower

the ease of hot working, particularly the extrusion rate, and to raise fabricating costs. If, therefore, the same degree of working and the same annealing or recrystallization temperatures are used in alloys with and without manganese and chromium additions, there is likely to be a marked difference in grain-size and texture. In practice, the ease with which the manganese- and chromium-free alloy can be deformed allows greater or more rapid reductions and the use of a lower annealing temperature. The authors have in general used similar working schedules and an annealing temperature of  $540^\circ C$  for both alloys. Manufacturers who make the manganese- and chromium-free alloy habitually use an annealing temperature of  $520^\circ C$ , and it is a pity that closer comparison has not been made between alloys of appropriate but different working and annealing treatments.

Mr. Chadwick and his collaborators state on p. 79 that: "in the absence of the banded structure, manganese as an alloying element was ineffective". Mr. Harris and Mr. Varley, in their Table IV (p. 388), show that the Izod impact values of a straight magnesium-silicon alloy annealed at  $520^\circ C$  were 8, 8, and 6 ft.-lb., as compared with 7, 7, and 3 ft.-lb. for an alloy containing 0.27% Cu and 0.22% Cr annealed at  $540^\circ C$ . In commenting on the directional effects shown by this table Harris and Varley do not point out that, in the short transverse (Z) direction, chromium and copper additions bring about no improvement in impact values, even when the same annealing temperatures were used, and it may well be significant that the ratio of X or Y to the Z values is greater than 2 in the case of the chromium + copper alloy and is only about  $1\frac{1}{2}$  in the straight alloy. This suggests that these alloying additions may have no advantage and perhaps may even be disadvantageous to the properties of material at the flash line in forgings, or in some components machined from extrusions and stressed transverse to the original extrusion direction.

A paper discussing the influence of structural directionality on corrosion and stress-corrosion behaviour of HE15-WP alloy by Miss Bell and myself§ shows that manganese in these alloys performs the important function of increasing directionality and increases resistance to stress-corrosion when the stress is parallel with the plane of working. On the other hand, manganese additions, if anything, increase susceptibility in the short transverse direction. It is also shown in this paper and in earlier work by Metcalfe|| that severe directionality of structure can cause layer-type corrosion, which takes some time to develop and appears to become auto-accelerating when it reaches a certain stage. The results of some atmospheric corrosion tests on 0.10-in.-thick extruded sections in secondary (211) alloy, showing marked directionality of structure and containing Cu 2.00, Mg 0.70, Si 0.85, Fe 0.40, Mn 0.36, Pb 0.05, Zn 0.2%, and less than 0.03% Ni, Ti, and Sn, press-quenched and naturally aged, emphasize this. Specimens were exposed at Sheffield in parallel with the HE10-WP alloy free from chromium and manganese, described in Metcalfe's paper. The results of mechanical tests after 3, 6, 12, and 24 months are given in Fig. G and show an average rate of corrosion damage of the 211 alloy, as judged by loss in strength, to be about one-third of that of the HE10-WP alloy exposed simultaneously, and to be equivalent to a loss in thickness of only 0.002 in. from each side in two years. At the end of this period, however, one specimen was missing and was presumed to have failed. Layer-type corrosion was observed on 6 of the remaining specimens. After three years' exposure, all specimens of the 211 alloy show layer foliation, which is severe in all specimens except one. In contrast, the HE10-WP specimens appear still to be in good condition, with the rate of corrosion damage decreasing with time. An evaluation of the relative corrosion-resistance of the two alloys after one year's exposure would have suggested that both

\* H. J. Axon, *J. Inst. Metals*, 1952-53, **81**, 209.

† M. L. V. Gayler, *ibid.*, 1946, **72**, 243.

‡ Director, Fulmer Research Institute, Ltd., Stoke Poges, Bucks.

§ E. A. G. Liddiard and (Miss) W. A. Bell, *J. Inst. Metals*, 1953-54, **82**, (9), 426.

|| G. J. Metcalfe, *ibid.*, 1952-53, **81**, 269.



alloys were good, but that the 211 alloy, with marked structural directionality, was appreciably better than HE10-WP. Now, after three years, it is clear that the 211 alloy would be a dangerous material to use unprotected for structural work in corrosive atmospheres. It follows that short-time corrosion tests, whether in the laboratory or in the field, are not reliable in cases where corrosion damage may be influenced by directionality of structure.

The short-time accelerated corrosion tests which Chadwick, Muir, and Grainger have used, and from which they conclude that manganese and chromium, particularly the latter, reduce intercrystalline attack, are probably a reflection of the effects of these addition agents on directionality and grain-size and may bear no relation to the behaviour of these alloys in service. Reference to Figs. 34-39 (Plate XIII) of their paper shows that the grain-size of the alloy free from chromium and

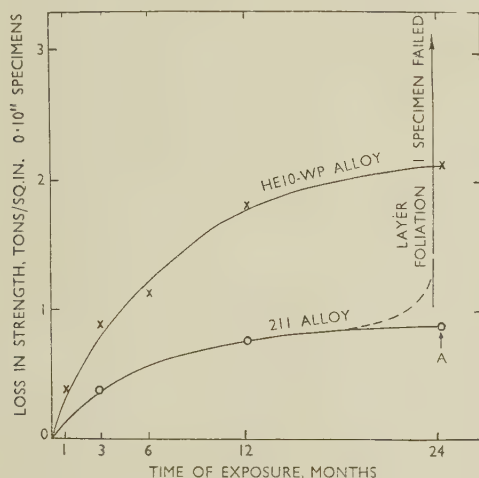


FIG. G.—Results of Atmospheric Corrosion Tests at Sheffield on HE10-WP and 211 Alloy. All points are the average of 9 specimens, except A which is the average of 8 specimens (1 specimen missing, presumed failed).

manganese additions is about three times as great as that of the other materials, so that, other factors being equal, the same area of grain-boundary attack will penetrate three times deeper into the chromium- and manganese-free alloy, quite apart from any directional effects.

The paper by Metcalfe\* to which Harris and Varley refer, and which surveyed the resistance to atmospheric corrosion of HE10-WP alloy free from manganese or chromium, showed that the corrosion rate decreased with time and that, even in the worst atmospheric conditions, sections of thicknesses exceeding 0.10 in. could be expected to withstand a stress equal to the original proof stress indefinitely. Although the point is not mentioned in Metcalfe's paper, no evidence of serious embrittlement as a result of intercrystalline corrosion was found. In fact, the lowest elongation on any specimen 0.10 in. in thickness after two years' exposure in the worst atmosphere was 6%. In addition to this evidence we have the experience of many years of good service given by structures made in the chromium- and manganese-free alloy.

Our knowledge of the mechanism of layer corrosion is at present inadequate, and I am not aware of any case of this type of corrosion in the copper-free aluminium-magnesium silicide alloys. It may well be that their intrinsically high

resistance to corrosion will delay the incidence of layer-type attack indefinitely. If so, structural directionality will be advantageous in sheet and in extrusions stressed in the direction of working. Nevertheless, insistence on chromium and manganese additions in specifications for alloys of this type, particularly for use in structures not subject to impact loading, would seem to be unjustified on the evidence so far available.

Dr. V. A. PHILLIPS, A.R.S.M., B.Sc., A.I.M. (Member): At the British Non-Ferrous Metals Research Association an extensive study has been made of the factors governing the properties of small commercial extrusions in a wide variety of magnesium-silicide-type alloys. While there are some points on which we differ, our general conclusions agree in most respects with those of the present authors. We find that aluminium-magnesium-silicon alloys containing  $\frac{1}{2}$ – $\frac{3}{4}$ % magnesium and without other additions have comparatively poor bending properties in the artificially aged condition if free silicon, that is silicon in excess of that required to form  $Mg_2Si$  and to combine with iron impurity, is present. The presence of excess silicon also causes tensile fracture to occur in an intercrystalline instead of in a normal trans-crystalline fashion. Micrographic examination of artificially aged materials indicates that preferential precipitation occurs at grain boundaries in alloys containing excess silicon. After suitable etching, a number of the grain boundaries appear wide and diffuse and contain particles (or pits). The number of such boundaries and their width increases as ageing progresses (Figs. H–M (Plate XCV)). In our experience, materials which fracture in an intercrystalline manner always exhibit abnormal boundary structures of this type. On the other hand, materials showing such structures do not always fracture in an intercrystalline fashion, over-aged materials being a case in point (Fig. M).

This phenomenon appears to be analogous to the "light phenomenon" previously observed in aluminium-4% copper,† aluminium-6% copper,‡ and in aluminium-10% zinc alloys.|| As in the work of Gayler† and of Perryman and Blade,|| and in agreement with the views of Geisler¶ on aluminium-magnesium-silicon alloys, it is considered that the wide diffuse zones represent regions of the denuded solid solution in equilibrium at the ageing temperature, formed as the result of localized precipitation at grain boundaries. The type of fracture will depend on the relative strengths of the interior of the grain and of the boundary region. A tendency to intercrystalline fracture would not be expected to develop until a stage is reached where the boundary regions, initially strengthened by ageing, become over-aged and weak while the interior of the grain is still hardening.

It seems probable that the black spots in the wide diffuse boundaries which were not evident in the unetched state, represent etching effects centred about submicroscopic particles of precipitate or about concentrations of magnesium and silicon atoms prior to the formation of actual particles of precipitate.

We have examined the effect of manganese, copper + manganese, and copper + chromium on the grain-boundary structure. A 0.23% manganese, excess-silicon alloy (Fig. N, Plate XCV) showed normal grain boundaries, and examination of tensile specimens indicated that the tendency to intercrystalline fracture was slight; larger additions of 0.6–0.7% manganese apparently completely eliminated it.

Commercial alloys with no excess silicon, but containing sufficient copper + manganese or copper + chromium to give a strength equal to or better than that obtainable in the excess-silicon alloys, showed normal grain boundaries (Figs. O and P, Plate XCV) and were free from any tendency to intercrystalline fracture.

\* G. J. Metcalfe, *J. Inst. Metals*, 1952–53, **81**, 269.

† M. L. V. Gayler, *ibid.*, 1946, **72**, 243.

‡ I. J. Polmear and H. K. Hardy, *ibid.*, 1952–53, **81**, 427.

§ (Mlle.) C. Changarnier and J. Calvet, *Compt. rend.*, 1953, **237**, 179.

|| E. C. W. Perryman and J. C. Blade, *J. Inst. Metals*, 1950, **77**, 263.

¶ A. H. Geisler, *Trans. Amer. Inst. Min. Met. Eng.*, 1949, **180**, 230.

On p. 392 of their paper, Mr. Harris and Mr. Varley state that the behaviour of chromium is similar in every respect to that of manganese, except that on a weight-percentage basis it appears to be approximately twice as effective. In our experience, in small extrusions the fibrous grain structure obtained when 0.6–0.7% manganese is present persists after heat-treatment, whereas extrusions containing  $\frac{1}{4}$ % copper +  $\frac{1}{4}$ % chromium commonly recrystallize during extrusion or subsequent heat-treatment, so that one would expect to lose the advantages of the press-effect.

Intercrystalline weakness is unlikely to be apparent when material having a fibrous grain structure is tested parallel to

TABLE A.—Effect of Period of Storage at Room Temperature Before Artificial Ageing on the Properties of Two HE10 Alloys.

Over-strain, %	Period of Storage, hr.	0.1% Proof Stress, tons/ in. <sup>2</sup>	Tensile Strength, tons/ in. <sup>2</sup>	Elonga- tion (Total on 2 in.), %	Bend-Test Value (Minimum Radius/ Thickness)	Tendency to Inter-crystal- line Tensile Fracture §
<i>Alloy 1. Containing Magnesium 0.62, Silicon 0.95, Iron 0.38%, Solution-Treated at 530° C. and Aged 6 hr. at 170° C.</i>						
0	<1	14.2	18.6	16.5	1.2	Pronounced
	3	13.3	18.5	19 †	1.2	Moderate
	24	13.1	18.0	21	>0.7, <1.0	Pronounced
	168	11.5	17.4	24	Fairly deep cracks in vice test ‡	Moderate
2	<1	18.5	20.6	12.5	1.8–2.0	Pronounced
	3	18.0	20.2	13	>1.8, <2.0	"
	24	15.9	19.0	18	1.6	"
	168	13.9	18.2	19	0.7	"
10	<1	19.3	21.1	11	2.2	Pronounced
	3	19.4	21.2	11	2.2	"
	24	18.4	20.5	13	1.8	"
	168	17.1	20.0	14.5	1.6	"
<i>Alloy 2. Containing Magnesium 0.68, Silicon 1.01, Iron 0.28%, Solution-Treated at 520° C. and Aged 5 hr. at 175° C.</i>						
0	<1	17.9	20.7	14	2.0	...
	3	17.8	20.5	15	1.4	...
	24	17.7	20.4	11.5 †	>1.2, <1.7	...
	168	16.5	20.2	18	1.6	...
2	<1	19.4	21.2	12	2.0	...
	3	19.1	21.2	13.5	>1.4, <1.8	...
	24	18.9	20.6	11.5	2.0	...
	168	18.2	20.7	15	1.2	...
10	<1	20.4	22.4	10	2.2	...
	3	19.8	21.6	10	2.3	...
	24	19.4	21.2	9.5 †	2.0	...
	168	19.2	21.1	12	1.8	...

§ Overstrained immediately after solution-treatment.

† Broke near shoulder.

‡ Specimen bent flat on itself in a vice.

§ Specimens mechanically polished, etched in ammonium oxalate.

the fibre direction and, as is well known, manganese tends to stabilize the fibrous structure and associated deformation texture produced by extrusion. However, samples of two H10 alloy extrusions containing 0.6–0.7% manganese still fractured in a predominantly transcrystalline fashion in a tensile test when cross-rolled to 50% reduction before heat-treatment to cause recrystallization. The beneficial effect of manganese therefore appears to be due to the inhibition of discontinuous precipitation, and this is confirmed by the fact that the bending properties of a similar artificially aged extrusion, with a fibrous structure, were almost the same whether the axis of bending was parallel or perpendicular to the fibre direction.

Contrary to the results of Mr. Harris and Mr. Varley, we

have found that in alloys of normal commercial purity there may be a very marked effect of varying interval between quenching and precipitation-hardening on the properties obtained (see Table A). The magnitude of this effect is quite as large as they observed on high-purity alloys. The reason for the discrepancy between their results on commercial materials and our own is uncertain, but may be due to minor impurities.

I would like to ask these authors whether they have made any comparison of the behaviour of notched and plain Izod and tensile specimens which would enable them to say whether it is the speed of impact or the notch effect which is responsible for the particularly low Izod values obtained on some of the materials?

In the case of fully heat-treated excess-silicon alloys of 0.04–0.06 mm. grain-size we obtained bend-test values (minimum radius/thickness) ranging from  $\frac{3}{4}$  to  $2\frac{1}{2}$ . Straightening by stretching before solution-treatment gave exceedingly large grains and bend values greater than 6 were then obtained. According to Fig. 41 (p. 78) of their paper, Mr. Chadwick, Mr. Muir, and Mr. Grainger obtained a limiting bend value of 7 on their high-purity iron-free basis alloy. From their photomicrographs (Figs. 7, 16, 32, 33) it would appear that this alloy had a coarser grain-size than is usually found in commercial material and that additions of iron and manganese had a considerable grain-refining effect. Can the authors say what part of the observed changes in mechanical properties are attributable to grain refinement and what part are attributable to a reduction in tendency to discontinuous precipitation?

Mr. A. SENDOREK,\* Dipl.Ing. (Member): I should like to make some comments on the grain-boundary phenomena described in these two papers.

Under Mr. Varley's direction, I have been investigating the effect of different forms of precipitation on the strength and ductility of super-purity-base aluminium-magnesium silicide and aluminium-magnesium-zinc alloys. This work may be considered as an extension of that already published by Dix, Keller, and Graham,† by Geisler‡ and by Chaudron, Hérenguel, and Lacombe.§ In the sense that it deals with the aluminium-magnesium-silicon alloys with no excess of silicon it is complementary to the work of Harris and Varley.

In the simple fully heat-treated aluminium-magnesium-silicon alloys I have found that as the amount of  $Mg_2Si$  in solution at the quench is increased, so the ductility is reduced and grain-boundary weakness appears. With 0.9%  $Mg_2Si$  in solution the tensile fracture is transcrystalline and ductile; at 1.15%  $Mg_2Si$  the fracture is still ductile though partly intercrystalline; while with 1.4%  $Mg_2Si$  in solution at the quench the fracture is completely intergranular and the material nearly as brittle as an excess-silicon alloy of equal strength. Thus it would appear that the presence of excess silicon is not necessarily essential for the development of brittleness.

In agreement with Chaudron, Hérenguel, and Lacombe, similar results have been obtained with the aluminium-magnesium-zinc alloys. This work together with that of Grogan and Pleasance|| on aluminium-zinc alloys, and some work of my own on aluminium-copper alloys, shows that in many age-hardening alloys of aluminium embrittlement may take place owing to intergranular weakness developing as the degree of supersaturation of the solid solution is increased.

Although it is possible to follow the gradual development of intergranular weakness or decohesion by the increase which takes place at room temperature in the number of shiny facets on the tensile fracture of the naturally aged aluminium-magnesium-zinc alloys, nothing can be seen unetched under

\* Research Laboratories, The British Aluminium Co., Ltd., Gerrards Cross, Bucks.

† E. H. Dix, Jr., F. Keller, and R. W. Graham, *Trans. Amer. Inst. Min. Met. Eng., Inst. Metals Div.*, 1931, 404.

‡ A. H. Geisler, *Trans. Amer. Inst. Min. Met. Eng.*, 1949, 180, 245.

§ J. Hérenguel and G. Chaudron, *Métaux et Corrosion*, 1941, 16, 33, 49.

|| J. Hérenguel and P. Lacombe, *Métaux, Corrosion-Ussure*, 1944, 19, 39.

J. Hérenguel, *Rev. Mét.*, 1947, 44, 77.

|| J. D. Grogan and R. J. Pleasance, *J. Inst. Metals*, 1939, 64, 57.



the microscope either in these alloys or in aluminium-magnesium silicide alloys naturally or artificially aged. Samples air-cooled from the quenching temperature, however, show a network of grain-boundary precipitation easily resolvable under the microscope even without etching.

This is illustrated in Figs. Q and R (Plate XCVI), which relate to an alloy with 1.4%  $Mg_2Si$ , in the form of  $\frac{1}{2}$ -in.-dia. extrusion, solution-treated at 540° C. and aged at 175° C. for 12 hr. The first sample (Fig. Q) has been water-quenched and the grain boundaries are visible after electropolishing as faint bright lines, turning to dark when the focus changes slightly, due to a difference in level between the grain-boundary zones and the grains. The second sample (Fig. R) was air-cooled from 540° C. and shows a very distinct precipitate embedded in a narrow, light-coloured, grain-boundary zone. This structure was formed on air-cooling and was unchanged by subsequent ageing. The strength of both samples is almost identical, with the mean value of 13.7 tons/in.<sup>2</sup> for the 0.1% proof stress and 16.5 tons/in.<sup>2</sup> for the ultimate tensile stress. The water-quenched sample has 13% elongation and an Izod value of 13, and the air-cooled one 4% elongation and an Izod value of 3 $\frac{1}{2}$ . An equivalent microstructure obtained by air-cooling from 460° C. an aluminium alloy containing 2.60% magnesium and 5.45% zinc (in the form of  $\frac{3}{4}$ -in.-dia. extrusion) is shown in Fig. S (Plate XCVI).

Similar grain-boundary networks can also be produced in the same alloys by over-ageing, as illustrated by Fig. T (Plate XCVI) for an aluminium-magnesium silicide alloy aged at 300° C. for 6 hr.

It seems likely that the continuous bright band along the grain boundaries is a zone impoverished in solute atoms, such as was found by Gayler\* in the aluminium-copper alloys and by Perryman and Blade† in the aluminium-zinc alloys, and judging by its effects on the properties of the material it may well be an exaggerated form of the network revealed by etching the artificially aged brittle alloys.

In view of this I consider that brittleness in these alloys is not due to brittleness of precipitate, which seldom forms a continuous film along the grain boundary, but rather to the weakness of the continuous zone of impoverished metal formed as a result of precipitation.

M. G. M. RENOUDARD‡ (Member) and M. M. TOURNAIRE§ (Member): The authors of both the papers have stressed the importance of the precipitates formed at the grain boundaries during artificial ageing, but the exact nature of these precipitates is not known. Mr. Harris and Mr. Varley, for instance, state that in the brittle alloys containing excess silicon the precipitate cannot be resolved by the optical microscope.

We should like to suggest a method which we feel might help in its identification. The method is a chemical one and consists in dissolving the alloy in cold solute hydrochloric acid. In this process the free silicon seems to remain unaltered, the silicon present in solid solution is largely transformed into volatile hydrides, and most of the silicon contained in the  $Mg_2Si$  is transformed into an insoluble compound which appears to be a hydrate of the silicon monoxide. The silicon occurring in the submicroscopic structures (which do not cause brittleness) seems to react in the same way as the silicon in solid solution.

All the compounds formed during the reaction can be collected and analysed, thus making possible an approximate determination of the proportions of the phases present in the alloys.

The method does not, of course, permit discrimination between the precipitates formed within the grains and those located at the grain boundaries. However, as there seems to be no reason to think that these differ in nature, the

information to be gained by this method would probably prove valuable.

Using this method, we have observed that the proportion of  $Mg_2Si$  formed during artificial ageing increases as ageing proceeds. In alloys containing a very large excess of silicon, some free silicon also appears during ageing, but in the industrial alloys the proportion of free silicon formed remains very low. This is in agreement with the opinion expressed in both papers that the precipitate formed at the grain boundaries during artificial ageing is probably  $Mg_2Si$ . We are shortly publishing a paper dealing with this matter in greater detail.

Mr. H. W. L. PHILLIPS,¶ M.A., F.R.I.C., F.Inst.P., F.I.M. (Member): If Fig. 7 (p. 386) of the paper by Mr. Harris and Mr. Varley is superposed upon Fig. 5 (p. 386), it will be found that the boundary of the zone of maximum brittleness coincides fairly closely with the curve for 17 tons/in.<sup>2</sup> proof stress. I should like to ask the authors whether a change in the solution-treatment temperature or in the time or temperature of the precipitation treatment would cause both curves to be displaced to an equal extent. Is it, in fact, possible, by any form of heat-treatment, to obtain a proof stress of 17 tons/in.<sup>2</sup> without encountering brittleness? In Fig. 7, the alloys highly susceptible to brittleness under the specified heat-treatment conditions are confined to a comparatively small range of compositions. It would seem, however, that composition is not primarily the factor responsible for brittleness, and that it would be possible, by appropriate heat-treatment, to render an alloy lying in this apparent danger zone free from brittleness, with, of course, a concomitant decrease in the proof and ultimate tensile stress. Will the authors confirm that this is a correct deduction? If an alloy, the composition of which lies well outside the zone of maximum brittleness of Fig. 7, is fabricated and heat-treated, would it be possible by subsequent rolling or drawing to increase its proof stress to, say, 17 tons/in.<sup>2</sup> without encountering brittleness, or would working be likely to lead to brittleness at an even lower value of the proof stress?

Dr. A. N. TURNER,¶ B.Sc., A.R.S.M., A.I.M. (Member): In the conclusions to their paper Mr. Harris and Mr. Varley state that "... satisfactory mechanical properties in the H10-WP alloy cannot be obtained without accompanying notch-sensitivity in the absence of chromium or manganese". One may be permitted to ask: "Satisfactory for what?" As a criterion of "satisfactory notch-sensitivity", the authors have chosen a minimum Izod impact value of 11 ft.-lb., but there are many applications in which H10-WP alloy may be used, for which an impact strength of this order is totally unnecessary. It would be most unwise, therefore, to insist on a modification to the composition of the alloy group with the object of ensuring such a high impact strength if, by so doing, the ease with which the material is fabricated were to be appreciably decreased. It is suggested, therefore, that the sentence quoted would be better for some qualification.

I should also like to correct any impression there may be that a magnesium silicide alloy containing copper and chromium has a substantially inferior corrosion-resistance to a copper-free alloy of the same type containing manganese. The corrosion properties are, in fact, very similar.

Mr. HARRIS and Mr. VARLEY (*in reply*): Mr. Crowther, in presenting an excellent review of the two papers, has mentioned the similar behaviour of the Al-Cu-Mg-Zn alloys in which manganese or chromium is again an essential ingredient. In these alloys, also, high-temperature precipitates may be obtained which govern the low-temperature precipitation char-

\* M. L. V. Gayler, *J. Inst. Metals*, 1946, **72**, 243.

† E. C. W. Perryman and J. C. Blade, *ibid.*, 1950, **77**, 263.

‡ Chef du Laboratoire de Recherches, Cie. Générale du Duralumin et du Cuivre, Rive de Gier (Loire), France.

§ Chef des Recherches et des Laboratoires, Cie. Générale du

Duralumin et du Cuivre, Paris, France.

¶ Research Laboratories, The British Aluminium Co., Ltd., Gerrards Cross, Bucks.

¶ Head of Metallurgical Division, Aluminium Laboratories Limited, Banbury, Oxon.



acteristics, and it has been suggested that failures in highly stressed Al-Cu-Mg-Zn alloys ascribed to "stress corrosion" may well be due to a similar "brittle" phenomenon in a highly directional structure. This latter possibility cannot be overlooked, but it would appear from our recent research that brittle fractures in Al-Cu-Mg-Zn alloys containing manganese or chromium are entirely transcrystalline and therefore not associated with grain-boundary precipitation.

Mr. Crowther's statement that: "In a few specialized applications cases of brittle fracture have been encountered in alloys which must be regarded as brittle only in comparison with the high general level of ductility of the class as a whole" may give the impression that the straight H10-WP alloy could be considered less brittle in comparison with other standards. This view is, of course, erroneous, since the impact value for an alloy of this type solution-treated at 540° C. and precipitation-treated at 175° C. for 8 hr. is 3-4 ft.-lb. and for a solution-treatment at 520° C. 6-7 ft.-lb. We would therefore consider the alloy as brittle, irrespective of the comparison made. Without the addition of manganese the ductility of these alloys could be classified as similar to that of grey cast iron and certain brasses, which are common engineering materials with restricted applications because of their brittle behaviour.

We would agree with Mr. Chadwick's suggestion that a more detailed fundamental approach to the mechanism of precipitation in these alloys is required. A detailed metallographic study would undoubtedly be of great assistance, but in our experience the grain-boundary precipitate in quenched and artificially aged alloys cannot be identified microscopically even with the aid of the electron microscope and changes in the region of the grain boundaries can be detected microscopically only by observing the etching characteristics.

Our comments with regard to Table X may have been a little misleading, and in referring to 0.8% manganese as a safe maximum we meant to point out that a manganese addition in excess of this figure would lower the proof stress and ultimate tensile stress with a corresponding increase in elongation and ductility. From a comparison of the two papers under discussion there appears to have been some difference in opinion with regard to the effect of iron on the mechanical properties of the ternary Al-Mg-Si alloys. This difference is only apparent, and support of this is given by Mr. Collins's results. In alloys in which all the silicon and magnesium takes part in the precipitation-hardening, iron has the effect of reducing the amount of silicon available by the formation of (Fe-Si) insoluble constituent and so reduces the mechanical properties. Thus the maximum mechanical properties and minimum ductility are obtained with lower (Mg + Si)% in the alloys free from iron. Once the maximum properties have been attained, as in alloys with 0.7% Mg, 1.0% Si, the properties are not decreased by iron but rather the reverse, as illustrated by Mr. Chadwick and his colleagues and by ourselves in Table X. This slight increase in mechanical properties may be due partly to the solution-hardening effect of the iron and partly to the grain-refining effect of this element.

With regard to the effect of copper, alloy 9 in Table X was selected merely to illustrate the tensile properties and ductility of the 61S type of alloy, and not for comparison with the other alloys given in the table. We have illustrated in Table IX (p. 390) that the mechanical properties are increased by adding copper, but the statement that "in alloys of the H10 type an addition of 0.3% copper is sufficient to raise the proof and ultimate stresses by about 3 tons/in.<sup>2</sup>" refers to the results of unpublished work.

One of the main points raised by Mr. Collins is in connection with the apparent anomaly with regard to the effect of iron. It has been stated that the rate of cooling during casting has an influence on the form in which the iron occurs and that this may be an important factor. On the other hand, Mr. Collins says: "The difference does not appear to arise from the casting process as such, since in our own work neither sheet from permanent-mould ingots nor 1-in.-dia. extrusions from semi-continuously cast billets showed a significant variation in properties with iron contents from 0.05 to 0.5%." It would therefore appear that the casting factor is a very minor

one and the explanation we have already advanced seems to be the most logical one.

In the light of our recent research, to which Mr. Sendorek has referred, we would agree entirely with Mr. Collins's and Dr. V. A. Phillips's explanation of brittleness in these alloys. All three investigators have been able to associate intercrystalline fracture with a region of depleted solid solution adjacent to the grain boundary, rather than with a film of precipitate a few atoms thick. We have not observed that manganese reduces the age-hardening properties of these alloys, nor that the increase in strength from the annealed to the fully heat-treated state is less in alloys containing manganese. We are therefore doubtful whether the theory suggested by Mr. Collins, which is based on the solution-hardening influence of manganese and its effect on the solid solubility of magnesium and silicon, is correct, particularly when there is no solid-solubility data for the system Al-Mg-Si-Mn available to support this view. His observation that "the precipitation effects of copper and of magnesium and silicon are independent additive factors" is most likely the correct one and the increase in proof stress and ultimate tensile stress is undoubtedly due to the precipitation-hardening effect of copper.

If an H9-type alloy is air-cooled before precipitation treatment, the Izod value is reduced from 16 to 10 ft.-lb., but the increase in brittleness is not considered sufficiently serious to condemn this method of heat-treatment.

Mr. Liddiard has pointed out that manganese and chromium raise the recrystallization temperature, and in consequence they increase the directionality of the structure. Therefore, if the same degree of working and the same annealing or recrystallization temperatures are used in alloys with and without manganese and chromium additions, there is likely to be a marked difference in grain-size and texture. This is perfectly true and precisely why it is not possible to determine the primary influence of manganese on grain-boundary precipitation by comparison of Izod values for extruded sections. The structure of extrusions in the alloy containing manganese consists of an outer zone which has fully recrystallized but is highly directional, and an inner unrecrystallized zone, so that Izod impact tests on such material indicate only the secondary structural effect of manganese. Very often in the manganese-bearing alloy a fully recrystallized structure cannot be obtained even by raising the annealing temperature to that of the solidus, and a structure approaching that of the manganese-free alloy can exist only in sheet or extrusion, fully recrystallized after cold working. We are therefore of the opinion that it is of greater importance to compare similar structures in alloys solution-treated at the same temperature, with the same degree of supersaturation of the solid solution with magnesium and silicon, than to attempt to follow the manufacturer's procedure. The free-cone bend-test results for alloys in sheet form given in Tables I (a) (p. 380) and X (p. 391) illustrate quite clearly that an H10-WP alloy containing manganese, solution-treated at 540° C., is more ductile than a manganese-free alloy of similar composition solution-treated at 520° C. The results we have given in Table IV (p. 388), although illustrating the directionality effect, should not be considered from any other point of view, since the material used was 0.5-in.-thick hot-rolled blank, which is not a standard product, and, secondly, the beneficial effect of manganese and chromium is known to be reduced in the presence of a large excess of silicon. Normally we would not expect such low Izod values in the Z direction, and there are no reasons for believing that additions of manganese and chromium would have no advantage when components machined from forgings or extrusions were stressed in the transverse direction.

We note Mr. Liddiard's evidence on the ill effects of copper on the corrosion-resistance of aluminium alloys and would not disagree with this. We do not propose to discuss the relative merits or demerits of intercrystalline and exfoliating (or "layer") corrosion, but we are surprised that Mr. Liddiard should suggest a form of corrosion in H10 alloys for which he has no direct evidence. He apparently attributes the lack of evidence to short exposure in the corrosion tests involved and the photograph reproduced in Fig. U (Plate XCVII) may



therefore be of interest. The specimens shown had the composition given in Table B.

TABLE B.

Form	Specimen No.	Analysis, %				
		Si	Fe	Cu	Mn	Mg
Sheet Extrusion	1, 2	1.08	0.40	0.002	0.75	0.57
	3	1.16	0.37	0.04	0.85	0.66

Exposure up to seven years has failed to give any indication of exfoliation (or "layer") corrosion.

The results of Dr. Phillips's metallographic examination are most interesting and, although a different etching reagent has been used, the results are in substantial agreement with our own in that there is a distinct difference between the structure of the naturally aged and artificially aged alloys after etching. Reference has been made to the press effect in an alloy containing 0.6-0.7% manganese and one with  $\frac{1}{4}$ % copper +  $\frac{1}{4}$ % chromium. In our experience, although the latter alloy would tend to recrystallize during extrusion, it would not do so if copper was absent, and the press effect in an alloy containing  $\frac{1}{4}$ % chromium is very pronounced. A most important point which has been raised is that fully recrystallized extruded material fractures in a transcrystalline manner, indicating that the beneficial effect of manganese is due to the inhibition of discontinuous precipitation and not merely to a directionality effect. This confirms our own results on fully recrystallized sheet.

The decrease in mechanical properties with long periods of storage is remarkable, but it is evident from the results given by Dr. Phillips that there is very little decrease in proof stress and ultimate tensile stress after 3 days' interval and in this respect the results are in substantial agreement with our own. We have not yet had occasion to investigate the effect of such long precipitation intervals. With regard to the influence of testing speed, we have carried out several Hounsfield notched-bar tests the results of which could be related linearly with the corresponding Izod values, and there appears to be little doubt that the notch effect is responsible for the low Izod values.

The research carried out by Mr. Sendorek has involved a very detailed metallographic study of age-hardening aluminium alloys exhibiting intercrystalline fracture, and the characteristics which are described apply equally well to Al-Mg-Si, Al-Mg-Zn, and Al-Cu alloys. A most important observation is that the intergranular weakness increases as the degree of supersaturation is increased. According to the solubility data represented in our Fig. 4 (p. 385) it is possible to have about 1.55% magnesium + silicon in solid solution at 540° C. corresponding to the point *B* in the figure. In the fully heat-treated condition an alloy of this composition with excess of silicon will give an Izod value of about 3 ft.-lb. Similarly, an alloy of balanced composition containing 1.0% Mg and 0.6% Si will be supersaturated to the same degree if a solution-treatment temperature of 580° C. is employed, and in the fully heat-treated condition this alloy also gives an Izod value of about 3 ft.-lb. with a similar intercrystalline fracture. Thus brittleness in Al-Mg-Si alloys, as in other age-hardening alloys, depends on the degree of supersaturation of the solid solution and in this instance not merely on the amount of excess silicon.

The chemical method described by M. Renouard and M. Tournaire is most interesting and by a careful examination of the results of this method it appears that the investigators may be able to determine the relative amounts of Mg<sub>2</sub>Si and excess silicon precipitated during artificial ageing. Unfortunately, it will not be possible to discriminate between that precipitated within the grains and at the grain boundaries, but the information should be quite useful.

In reply to the queries made by Mr. H. W. L. Phillips, we would say with reference to Figs. 5 and 7, that any change in

the solution-treatment temperature or in the time or temperature of the precipitation-treatment would cause both curves to be displaced to an equal extent. There is therefore no method of heat-treatment for manganese-free alloys which would enable a proof stress of 17 tons/in.<sup>2</sup> to be obtained without encountering brittleness. It is also possible by adjusting the heat-treatment conditions to improve the ductility with a simultaneous reduction in proof stress and ultimate tensile stress. We would like to point out that it is difficult to apply the term "freedom from brittleness", since only an arbitrary brittleness-ductility transition has been considered. If 11 ft.-lb. is selected as the limiting Izod value, then an alloy "free" from brittleness would have a proof stress of about 12 tons/in.<sup>2</sup> and an ultimate tensile stress of 16-17 tons/in.<sup>2</sup>. The possibility of cold working a fully heat-treated alloy has not been considered, but it is our impression that there would be little improvement in the proof stress : ductility ratio by using this method.

Dr. Turner has stated that there are many applications for H10-WP alloys where an impact strength of the order of 11 ft.-lb. is totally unnecessary. We would not agree on this point; in our opinion, if the application justifies the use of a higher-proof-stress alloy such as H10-WP, then it is also desirable that the alloy should not be notch-sensitive.

Mr. CHADWICK, Mr. MUIR, and Mr. GRAINGER (*in reply*): We are extremely gratified to see the wide interest in the theoretical aspects of precipitation phenomena in the aluminium-magnesium-silicon alloys, as well as in more practical implications. By far the most interesting topic, and the one with which we propose to deal first, concerns grain-boundary fracture in artificially-aged alloys in the absence of manganese or chromium. It is true that, as Dr. V. A. Phillips remarks, brittleness occurs only in alloys on the silicon side of the Mg<sub>2</sub>Si line in the ternary diagram. This is clearly brought out by Harris and Varley (Fig. 7, p. 386), but these authors also point out that in ternary alloys useful mechanical properties cannot be obtained outside the range of compositions in which brittleness occurs. However, Mr. Sendorek observes that even with magnesium and silicon in a stoichiometric ratio, fracture tends to become intergranular with increasing proportions of Mg<sub>2</sub>Si and deduces that excess silicon is not essential to the development of brittleness. Also MM. Renouard and Tournaire put forward evidence that the precipitate formed at the grain boundaries during artificial ageing is Mg<sub>2</sub>Si rather than silicon. Again, in the same connection, we cannot see what new point Dr. Phillips is trying to make in his fourth and fifth paragraphs, illustrated in Figs. N, O, and P (Plate XCV). The manganese is varied in these alloys as well as the magnesium and silicon contents, and the change in boundary structure would appear to be progressive rather than sharply defined.

Alternative theories have been put forward with regard to the nature of the grain-boundary weakness leading to intercrystalline fracture. Dr. V. A. Phillips, Mr. Sendorek, and Mr. Collins all suggest that weakness is associated with the denuding of the grain boundaries during artificial ageing, and Mr. Collins shows photographs of etched specimens which support this contention. We do not feel that in the present state of knowledge it is possible to draw any definite conclusions as to the actual mechanism of fracture, but we would like to put forward some further evidence and arguments which have a bearing on this subject. In the first place, it is interesting to compare the mechanical properties in the room-temperature and artificially-aged conditions of alloys with and without manganese but otherwise of the same composition. An example taken from our plotted data is shown in Table C. It will be noted that the effect of manganese on the U.T.S. in the room-temperature aged condition, i.e. where the fracture is ductile in both alloys, is to raise the tensile strength by 2.2 tons/in.<sup>2</sup>. In the artificially-aged alloys, where the manganese-free alloy has a brittle fracture and the manganese-bearing alloy a ductile fracture, the manganese has exactly the same effect on U.T.S. which is again raised by 2.2 tons/in.<sup>2</sup>. In other words, although in the manganese-free alloy the fracture is brittle, there is no premature failure and the full mechanical

properties of the grains themselves are realized. A second interesting piece of evidence on the question of intergranular rupture was obtained by fracturing a polished specimen of a high-purity manganese-free alloy and observing the grains in the neighbourhood of the fracture. Figs. V and W (Plate XCVII) illustrate the early stages of fracture. It will be noted that at the tip of cracks advancing along grain boundaries there is, in each case, considerable distortion of the neighbouring grain material. Thirdly, grain-size appears to be highly

TABLE C.—Influence of Manganese on the Mechanical Properties of High-purity Aluminium-0.7% Magnesium-1.0% Silicon Alloy.

	Room-Temperature Aged		Fully Heat-Treated	
	Mn nil	Mn 0.6%	Mn nil	Mn 0.6%
0.1% Proof Stress, tons/in. <sup>2</sup>	7.7	9.6	18.0	20.1
U.T.S., tons/in. <sup>2</sup>	16.2	18.4	20.5	22.7
Elongation on 2 in., %	25	20	3	10

significant, and indeed Dr. V. A. Phillips and Mr. Liddiard have already pointed this out. The well-established classical theory of the triaxial stress system at the advancing tip of a crack clearly indicates that where the crack width is large, as in a large-grain specimen, a higher stress is developed than where the crack width is small. It may well be, therefore, that the reduced tendency to intercrystalline fracture which accompanies the addition of iron (Fig. 41, p. 78, of our paper), is explained by the refinement of grain-size, since other structural differences appear to be absent. Fig. Z shows grain-

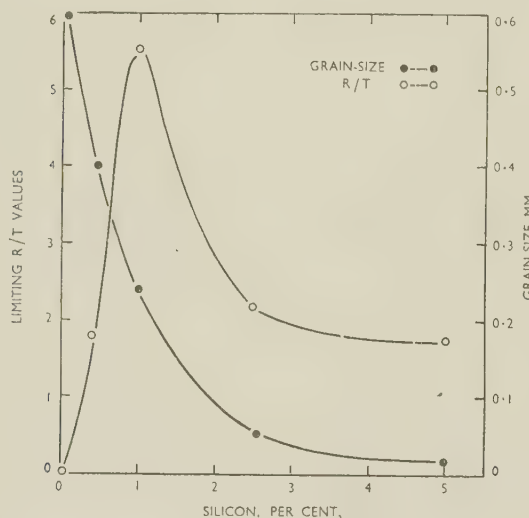


FIG. Z

sizes and limiting  $R/T$  values for a series of alloys containing 0.7% magnesium, with negligible iron and manganese, and silicon ranging from 0 to 5%. With small amounts of silicon grain-size is large but there is no precipitation; with intermediate silicon content, i.e. 1% or so, precipitation occurs and grain-size is still large, so that brittleness develops; while, finally, as the silicon is increased the grain-size is refined and so brittleness diminishes, although precipitation is still present. It would indeed seem to be quite clear that, since in all the work carried out so far these differences in grain-size obtain, the grain-size effect cannot, in fact, be separated from the other structural changes. In answer to Dr. Phillips's final

question, therefore, it is impossible to separate grain-size and precipitation effects.

Variations in grain-size seem to be of considerable significance in other respects; for example, Mr. Collins refers to the different effects of iron additions in three alloy series described, respectively, in the paper by Harris and Varley, in our own paper, and in the data illustrated in Fig. D of this discussion. Mr. Collins attributes these differences to the condition of the iron associated with the method of casting, although he gives no explanation of how this arises. It is, however, interesting to note that in our own data, Figs. 40 and 41 (p. 78), the effect of iron on ultimate tensile stress is highest (an increase of 2 tons/in.<sup>2</sup>) in alloys free from manganese and chromium, where there is very considerable reduction in grain-size as a result of the iron addition. Where substantial amounts of manganese or chromium are present, the effect of iron on grain-size is much smaller and the increase in tensile strength is generally less than 1 ton/in.<sup>2</sup>, and, in one series at least, is probably not significant. It is, therefore, quite possible that any increase of strength which we found by the addition of iron could be ascribed to its grain-refining effect. Dr. Phillips describes other experiments on the grain-size effect, in the course of which he cold rolled an extruded H10 alloy containing manganese and then heat-treated it so that recrystallization occurred. Presumably this cold-rolled and heat-treated material had an equiaxed structure similar to that of our own sheet material, and therefore it would be expected to show good ductility in all directions of testing.

Mr. Liddiard has drawn attention to the fact that manganese increases the recrystallization temperature of the alloy and thus makes extrusion more difficult, but he has failed to mention the advantage to be gained by its inclusion in material intended for sheet and strip manufacture. The presence of either manganese or chromium in the latter is most desirable in order to restrict the formation of the  $\beta$  aluminium-iron-silicon phase which has such a detrimental effect on hot-rolling behaviour. Admittedly the structures of extrusions in the manganese-bearing materials are more directional than those of the straight ternary alloys, but the suggestion that they may consequently be prone to serious corrosion of the layer or exfoliation type is, in our opinion, not borne out in practice.

In the matter of corrosion-resistance, grain-size again appears to be an important factor and Mr. Liddiard points out that in our Figs. 34-39 (Plate XIII) differences in depth of attack in corrosive media may be ascribed almost entirely to differences in grain-size. We agree that this deduction is probably correct and indeed our observations in actual service trials, as well as in laboratory tests, indicate that the more severe attack experienced by manganese-free alloys is in general associated with a coarse-grained structure. On the other hand, iron, which refines the grain, has an adverse effect on corrosion-resistance and in manganese-free alloys attack is increased ten times by the addition of 0.25% of iron, in spite of the reduced grain-size.

The alloys on which we carried out our studies were substantially free from directionality, but we cannot agree that the results of accelerated corrosion tests bear no relation to the behaviour of similar alloys in service. It is, of course, true that these tests are used mainly as a means of making a rapid comparison of the susceptibility to corrosion of a large number of alloys and, in particular, to attack of an intercrystalline nature, but with the alloys in question we have found that the salt-peroxide test produces results which compare well with the effects of extended exposure to industrial atmospheres. Some examples taken from a piece of light alloy equipment made from extruded components of alloy HE10 and subjected to 2 years' service in an industrial atmosphere will illustrate this point. Microsections through the surface of various component parts include one, Fig. X (Plate XCVII), which, on chemical analysis, proved to be free from manganese or chromium, while the other, Fig. Y (Plate XCVII), contained 0.6% manganese. The similarity in degree and mode of attack between these samples and the corresponding alloy specimens subjected to salt-peroxide accelerated tests which are illustrated in Figs. 34 and 36 in our paper is obvious.



## X-RAY-DIFFRACTION PHOTOGRAPHS.

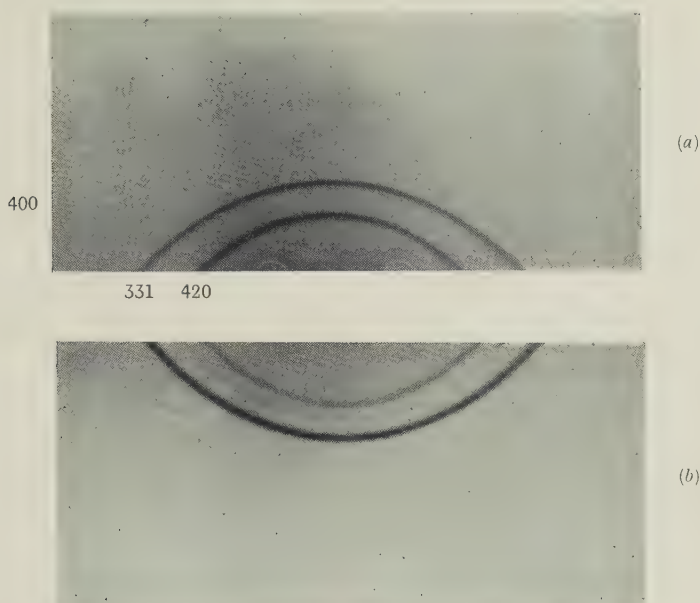


FIG. 3.—Copper-0.009% Bismuth Alloy Rod. (a) As extruded.  $\langle 111 \rangle$  texture very weak, giving normal intensity of the (400), (331), and (420) lines similar to those from a randomly oriented specimen. (b) As drawn to 73% reduction of area. The intensity of the lines remains uniform, but growth of the  $\langle 111 \rangle$  texture has caused the (400) line to disappear, has weakened the (420) line, and strengthened the (331) line. Cross-section of rod at right angles to the incident beam.  $\text{CuK}_\alpha$  radiation.

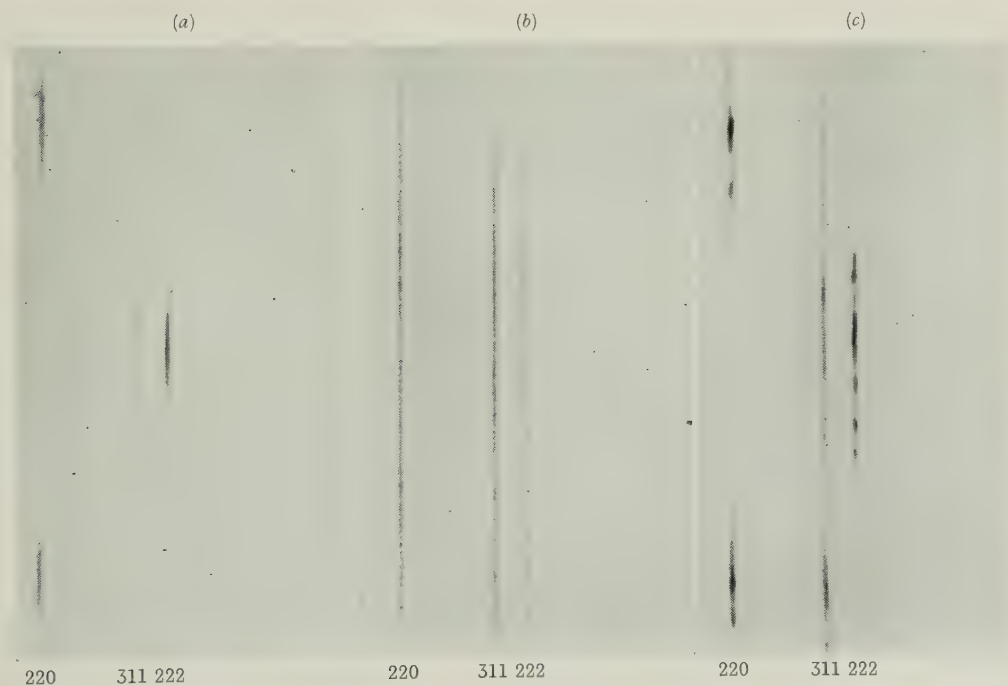


FIG. 4.—Pure Copper Rod Cold Drawn to 73% Reduction of Area. (a) As cold worked.  $\langle 111 \rangle$  texture very marked. (b) As recrystallized after annealing for 1 hr. at 500°C.  $\langle 111 \rangle$  texture very weak. (c) As recrystallized after annealing for 1 hr. at 1000°C.  $\langle 111 \rangle$  texture again very marked. Cross-section of rod inclined at a Bragg angle corresponding to the (222) reflection. Film-holder horizontal.  $\text{CuK}_\alpha$  radiation.

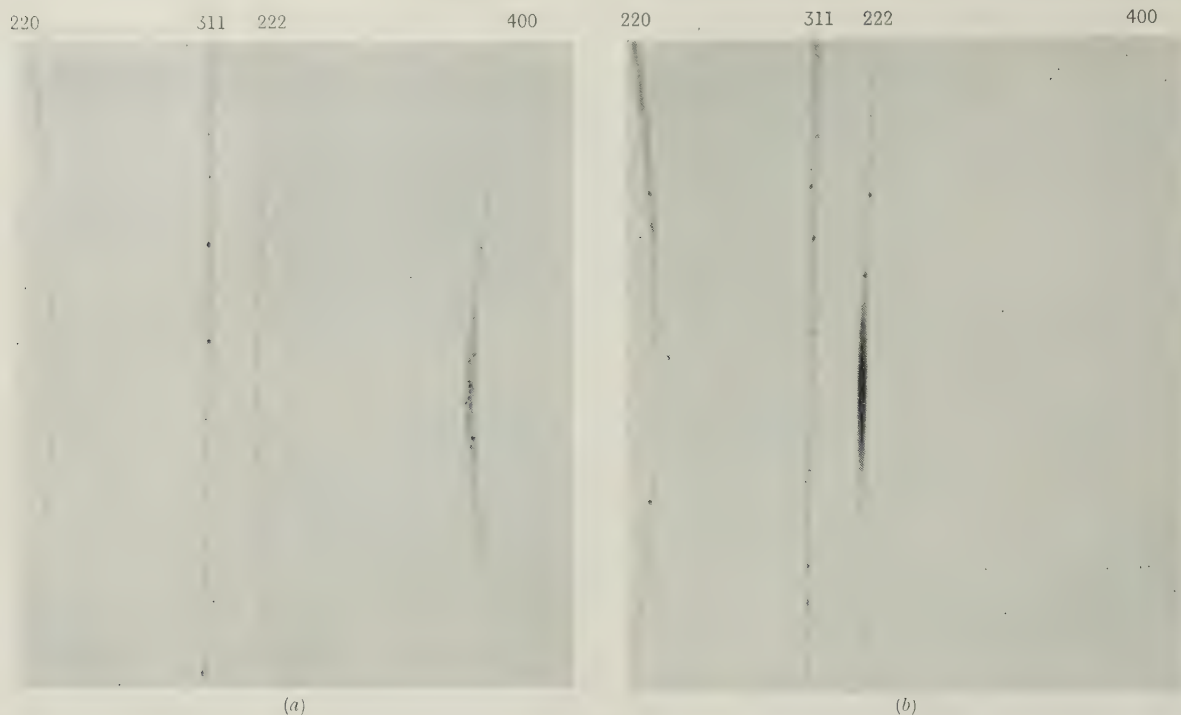


FIG. 5.—Pure Copper Rod Drawn to 73% Reduction of Area and Annealed for 1 Hr. at 300° C. (a) Cross-section inclined at a Bragg angle corresponding to the (400) reflection. Grains recrystallized in the  $\langle 100 \rangle$  direction or randomly oriented. (b) Corresponding to the (222) reflection. Few, if any, of the grains recrystallized in the  $\langle 111 \rangle$  direction. Film-holder vertical.  $\text{CuK}_\alpha$  radiation.

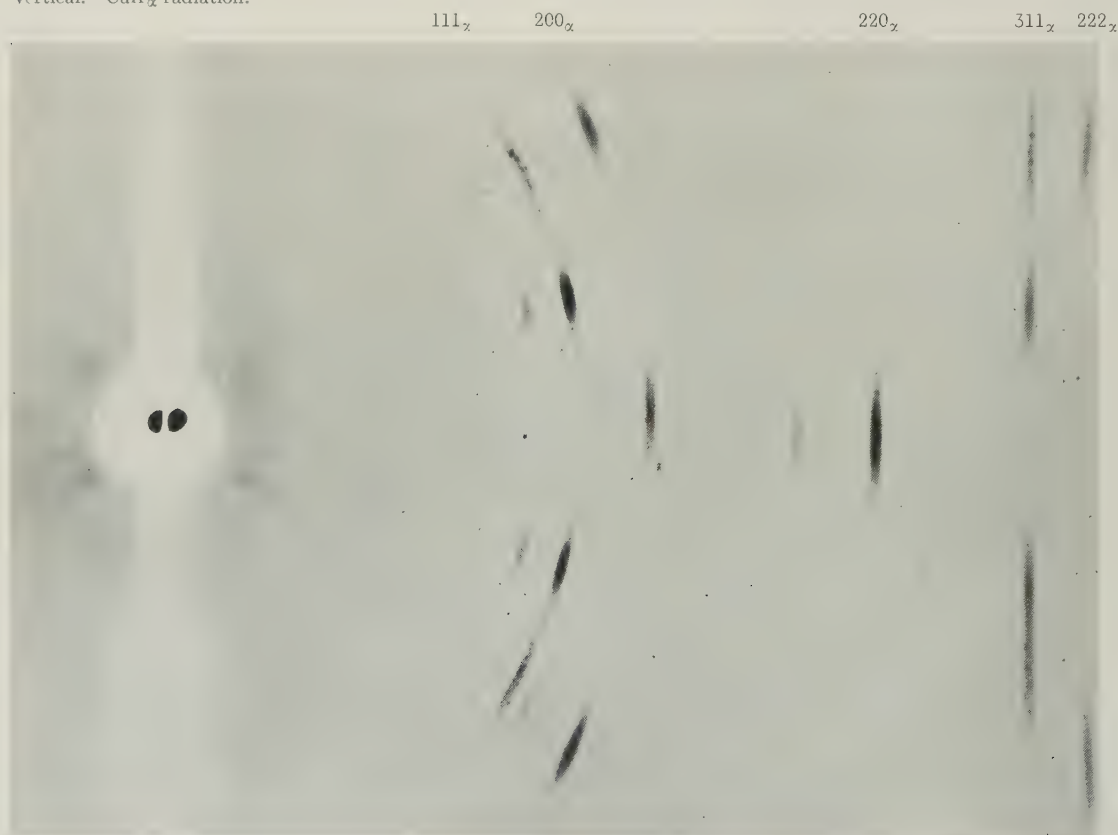


FIG. 6.—Pure Copper Wire Cold Drawn to 93% Reduction of Area and Annealed for 1 Hr. at 300° C. The recrystallized grains have an exclusively  $\langle 100 \rangle$  orientation. Specimen in the form of a needle. Film-holder vertical.  $\text{CuK}_\alpha$  and  $K_\beta$  radiation.



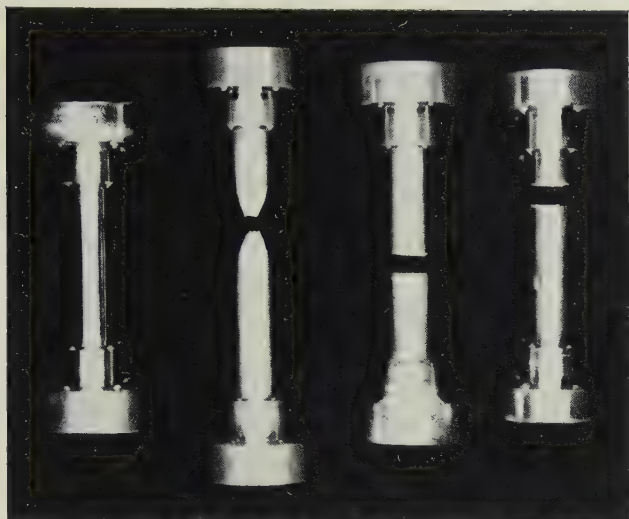


FIG. 13.—Tensile Specimens of Zinc. Showing (left to right) a specimen before fracture, a specimen giving a ductile fracture above the transition temperature, and two specimens with cleavage fractures after different amounts of deformation.

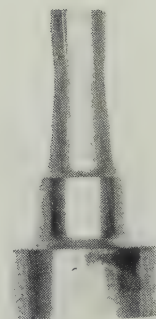


FIG. 14.—Zinc Specimen Fractured at  $-196^{\circ}\text{C}$ . after Heavy Prestrain at  $20^{\circ}\text{C}$ . The cleavage fracture has occurred outside the neck.

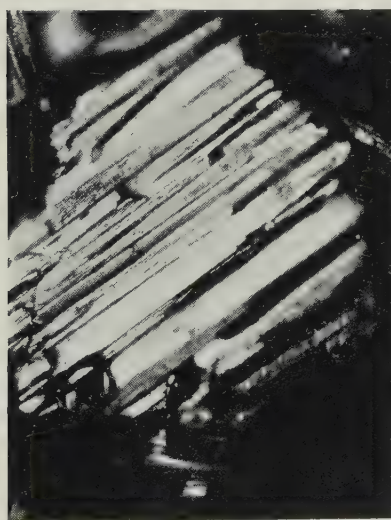


FIG. 15.—Specimen Fractured at  $-196^{\circ}\text{C}$ .  
 $\times 200$ .



FIG. 16.—Specimen Fractured at  $-196^{\circ}\text{C}$ . after a Prestrain of 0.174 Given at  $50^{\circ}\text{C}$ .  $\times 250$ .

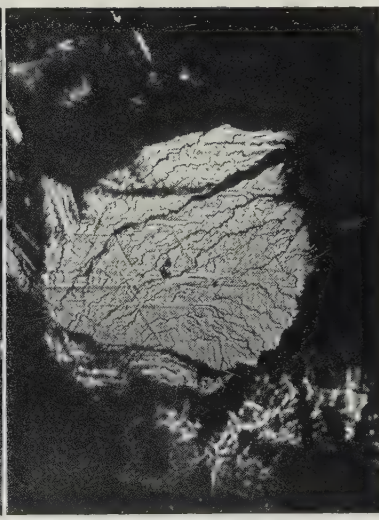


FIG. 17.—Specimen Fractured at  $20^{\circ}\text{C}$ . after Undergoing 0.175 Strain before Fracture. This is comparable with Fig. 16.  $\times 250$ .

Reduced by  $\frac{1}{3}$  in reproduction.



FIG. A.—Aluminium-1% Iron-5% Copper Alloy (Alloy 1), As Cast. The  $\text{FeAl}_3$  (dark grey) and the  $\alpha$  phase (arrow) are both enveloped by  $\beta$  phase.  $\times 400$ .

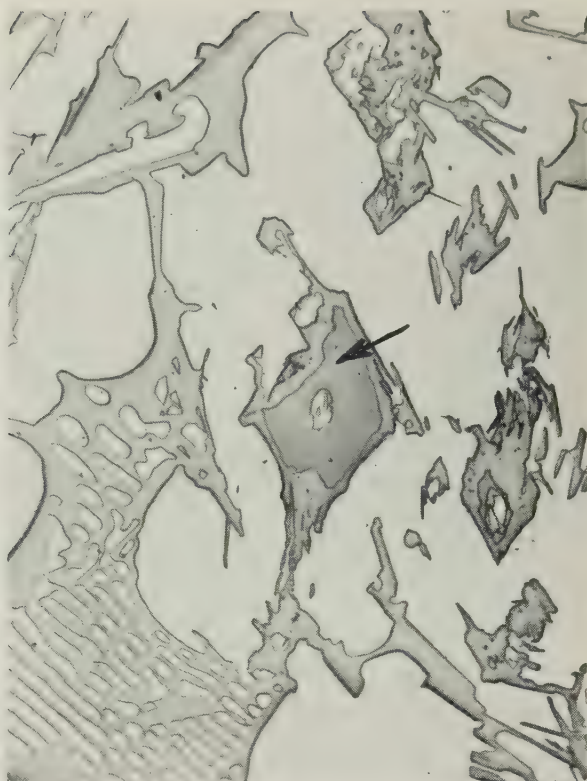


FIG. B.—Aluminium-1% Iron-15% Copper Alloy (Alloy 2), As Cast. The  $\alpha$  phase (arrow) is enveloped by  $\beta$ . There is very little contrast between the  $\text{CuAl}_2$  and the  $\beta$  in the eutectic structure on the left-hand side of the photomicrograph.  $\times 400$ .

Etch: 10%  $\text{H}_3\text{PO}_4$ , 50° C., 1 min.  
(Sperry on Phillips.)

MICROSTRUCTURES IN COPPER-2.42% MAGNESIUM ALLOYS IN RELATION TO CREEP.

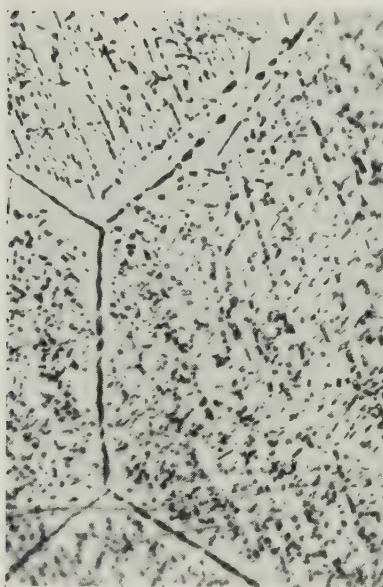


FIG. C.—Aged for 16 hr. at 500° C. (maximum D.P.H.).  $\times 1500$ .

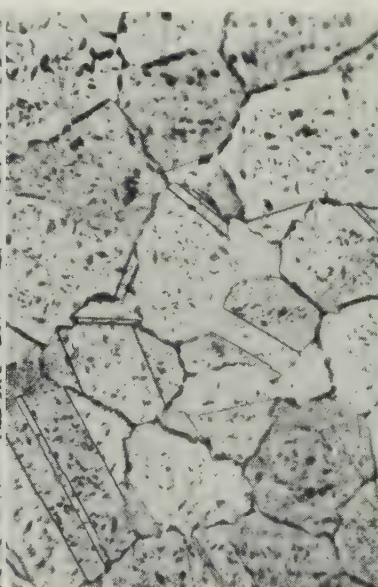


FIG. D.—Slowly cooled at 5° C./hr. from 700° C.  $\times 100$ .

(Marsden.)

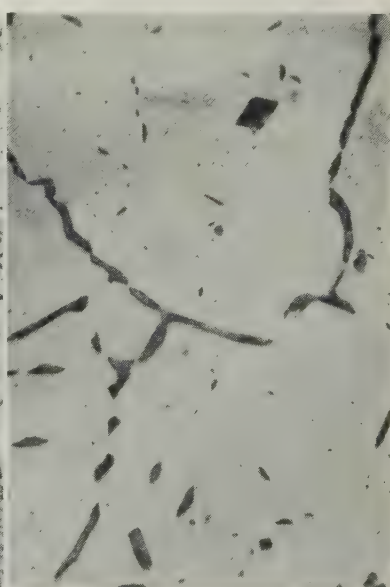
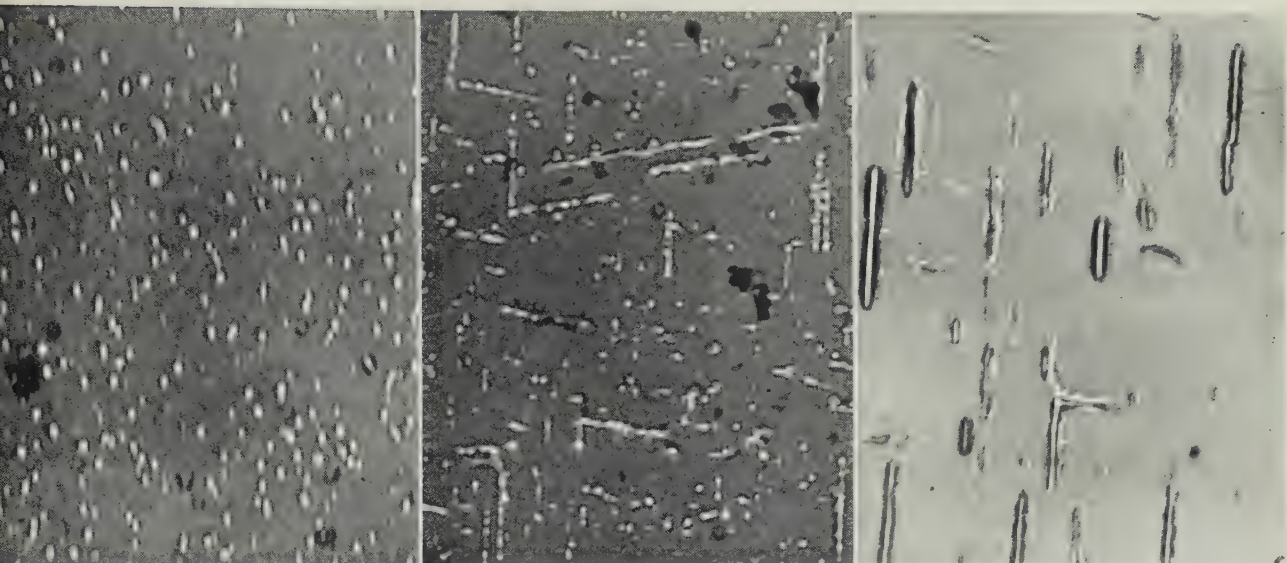


FIG. E.—As Fig. D.  $\times 500$ .



PRECIPITATION-HARDENING.



FIGS. A-C.—Electron Micrographs of Al-4% Cu Alloy. (*Nutting.*)

FIG. A.—Aged for 50 hr. at 100° C. Showing presence of G.P. [1].  $\times 60,000$ .

FIG. B.—Aged for 100 days at 130° C. Showing presence of G.P. [2].  $\times 60,000$ .

FIG. C.—Aged for 300 days at 190° C. Showing presence of  $\theta'$ .  $\times 30,000$ .

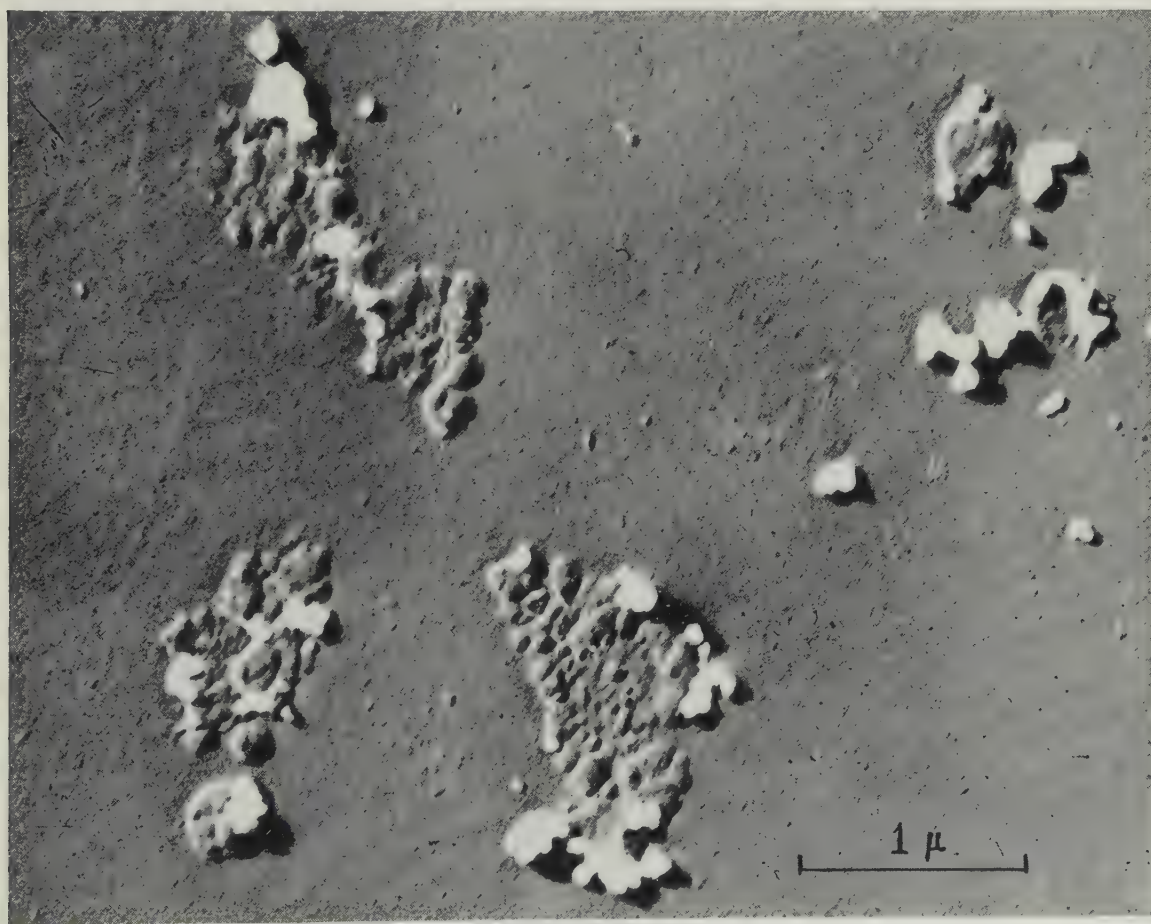


FIG. D.—Electron Micrograph of Al-4% Cu Alloy, Showing the Structure Attained at Maximum Hardness on Ageing at 150° C. Celluloid-silica replica, shadowed. (*Saulnier, after M. E. Kellenberger.*)





E

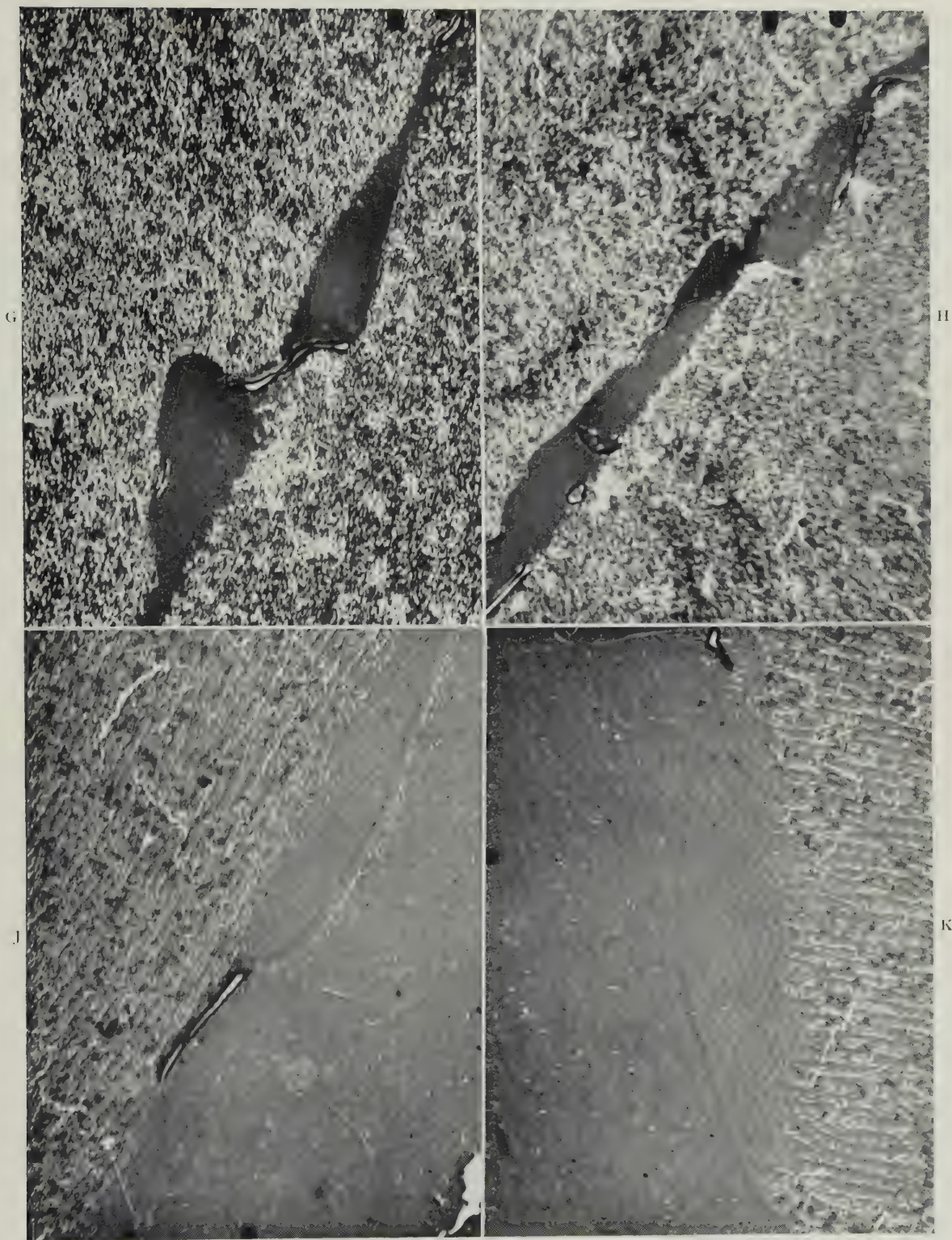


F

FIGS. E and F.—Electron Micrographs of Al-4% Cu Alloy, Showing the Structures Attained at Maximum Hardness on Ageing at 190° C. Celluloid-silica replicas, unshadowed. (Saulnier.)



## PRECIPITATION-HARDENING.



FIGS. G-K.—Electron Micrographs of an Air-Cooled Al-4% Cu Alloy. (Berghézan.)

- FIG. G.—Aged for 12 hr. at  $168^{\circ}\text{C}$ ., showing the “light phenomenon” developed in two neighbouring crystals. The initially straight boundary becomes curved and the particle of precipitate takes on the form of an S, as a result of the growth of the two crystallites of the “light phenomenon” in opposite directions.  $\times 17,000$ .
- FIG. H.—Aged for 12 hr. at  $168^{\circ}\text{C}$ . The “light phenomenon” completely separates the two neighbouring grains, but the mechanism of formation is still easily seen. The precipitate in the centre is curved, as in Fig. G.  $\times 10,000$ .
- FIG. J.—The lines of white dots in the crystallite of the “light phenomenon” run practically parallel to the similar lines of white dots in the matrix crystal, indicating that they have the same or a very similar orientation.  $\times 18,000$ .
- FIG. K.—The direction of the lines of white dots in the crystallite of the “light phenomenon” has changed, indicating a difference in orientation between it and the matrix crystal.  $\times 18,000$ .

CONTINUOUS CASTING.

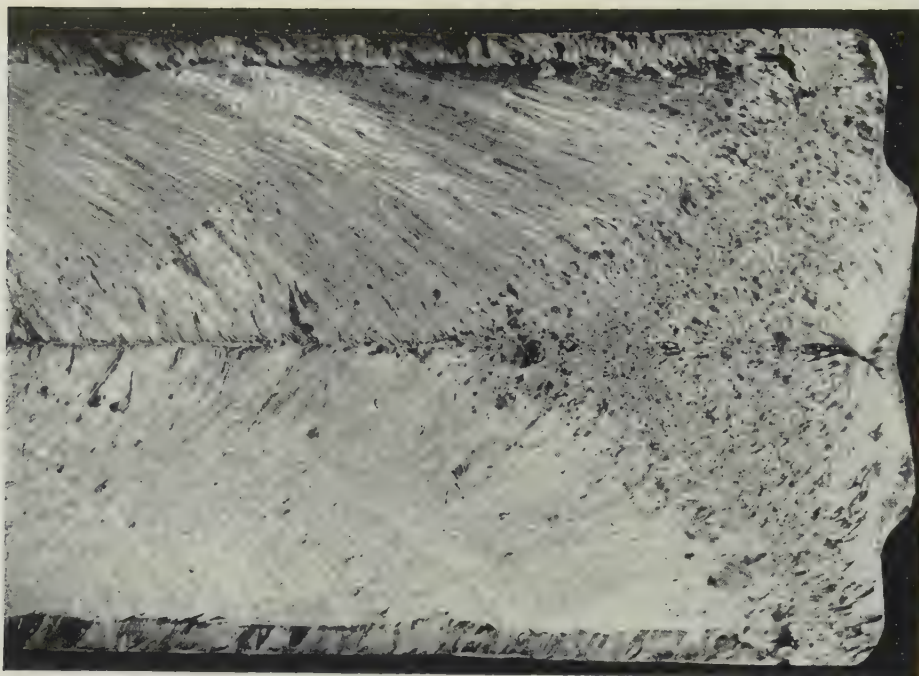


FIG. B. Photomicrograph of vertical section of 13-in. ingot. Caustic etch.  $\times 4$ .



FIG. C.—Radiograph taken through  $\frac{1}{2}$ -in.-thick section of same ingot.  $\times 4$ .

FIGS. B and C.—Illustrating Information Regarding the Solidification Front and Structure, &c., Resulting from Continuous Casting of 2S Aluminium. (*Morral.*)



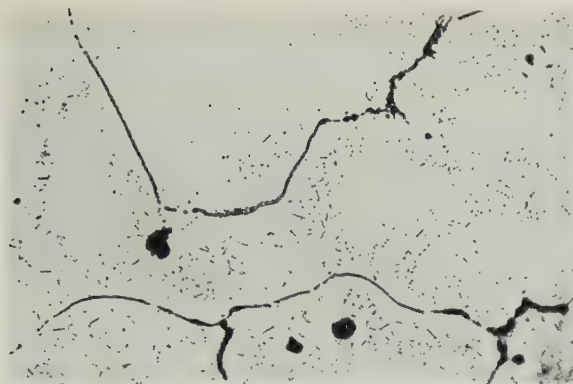


FIG. A.—High-Temperature Precipitate in Al-7% Mg-0.3% Mn Alloy, homogenized for 100 hr. at 450° C., water-quenched, and reheated for 20 hr. at 200° C.  $\times 300$ . (Crowther.)

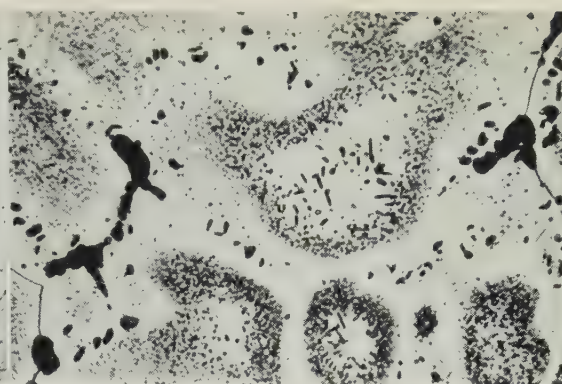


FIG. B.—High-Temperature Precipitate in Al-6% Zn-3% Mg-0.6% Cu-0.4% Mn Alloy, homogenized for 1000 hr. at 460° C., water-quenched, and reheated for 16 hr. at 135° C.  $\times 350$ . (Crowther.)

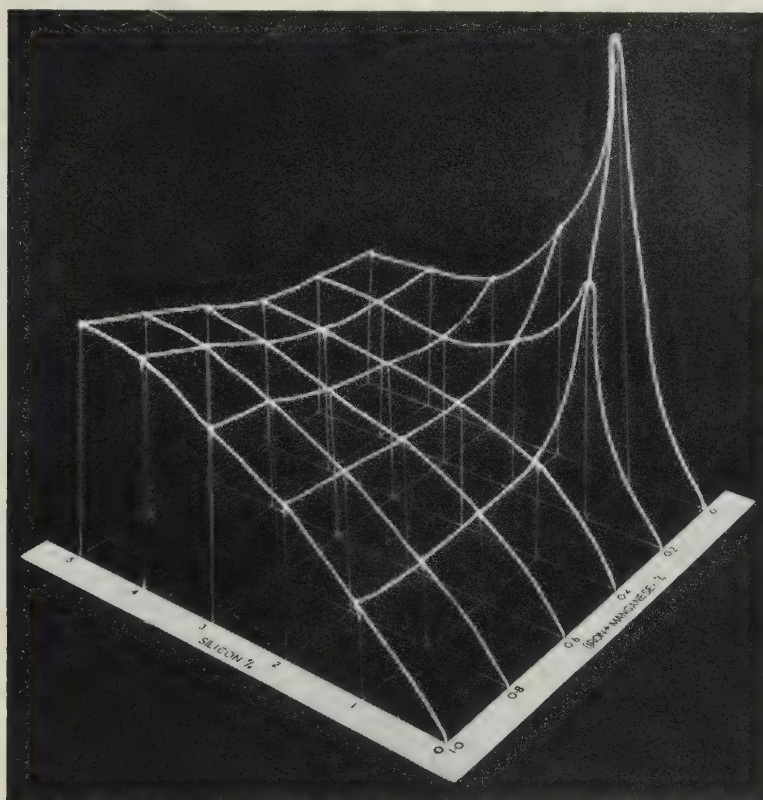


FIG. C.—Solid Diagram Illustrating Bending Properties of Al-0.7% Magnesium Sheet Alloys with Varying Silicon and Iron + Manganese Contents. Vertical scale: minimum radius of bending ( $R$ )/thickness ( $T$ ). (Chadwick.)

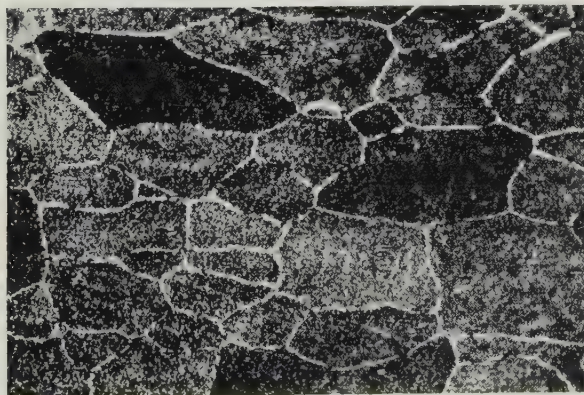


FIG. E.—HE10 Alloy, held at 280° C. for 22 days, showing unetched zone at grain boundaries. Etched in ammoniacal ammonium oxalate.  $\times 150$ . (Collins.)

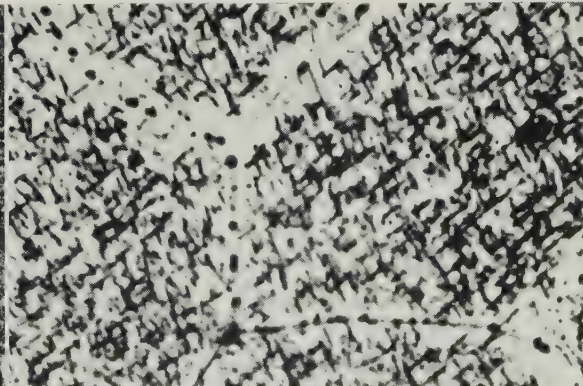
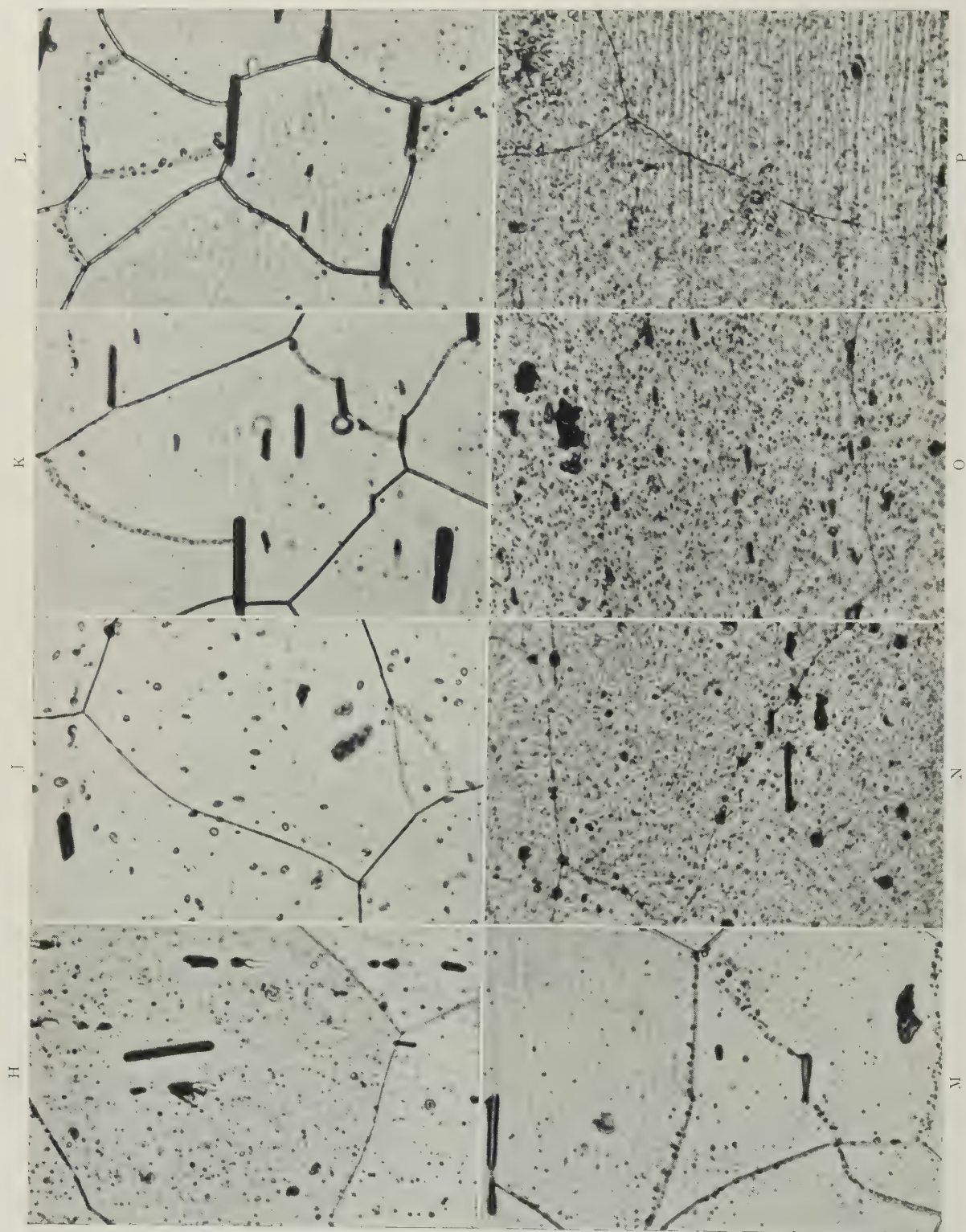


FIG. F.—As Fig. E, showing grain-boundary precipitate.  $\times 2000$ . (Collins.)



## PROPERTIES OF ALUMINUM-MAGNESIUM-SILICON ALLOYS.



FIGS. H-P.—Grain Boundaries in Specimens Electropolished and Etched in Ammonium Oxalate.  $\times 1000$ . (Phillips.)

FIG. H.—Al-0.60% Mg-1.05% Si-0.29% Fe Alloy, as quenched from 535° C., D.P.H. 46.

FIG. J.—Aged  $\frac{1}{2}$  hr. at 185° C., D.P.H. 104.

FIG. K.—Aged 4 hr. at 185° C., D.P.H. 127.

FIG. L.—Aged 8 hr. at 185° C., D.P.H. 127.

FIG. M.—Aged 48 hr. at 185° C., D.P.H. 109.

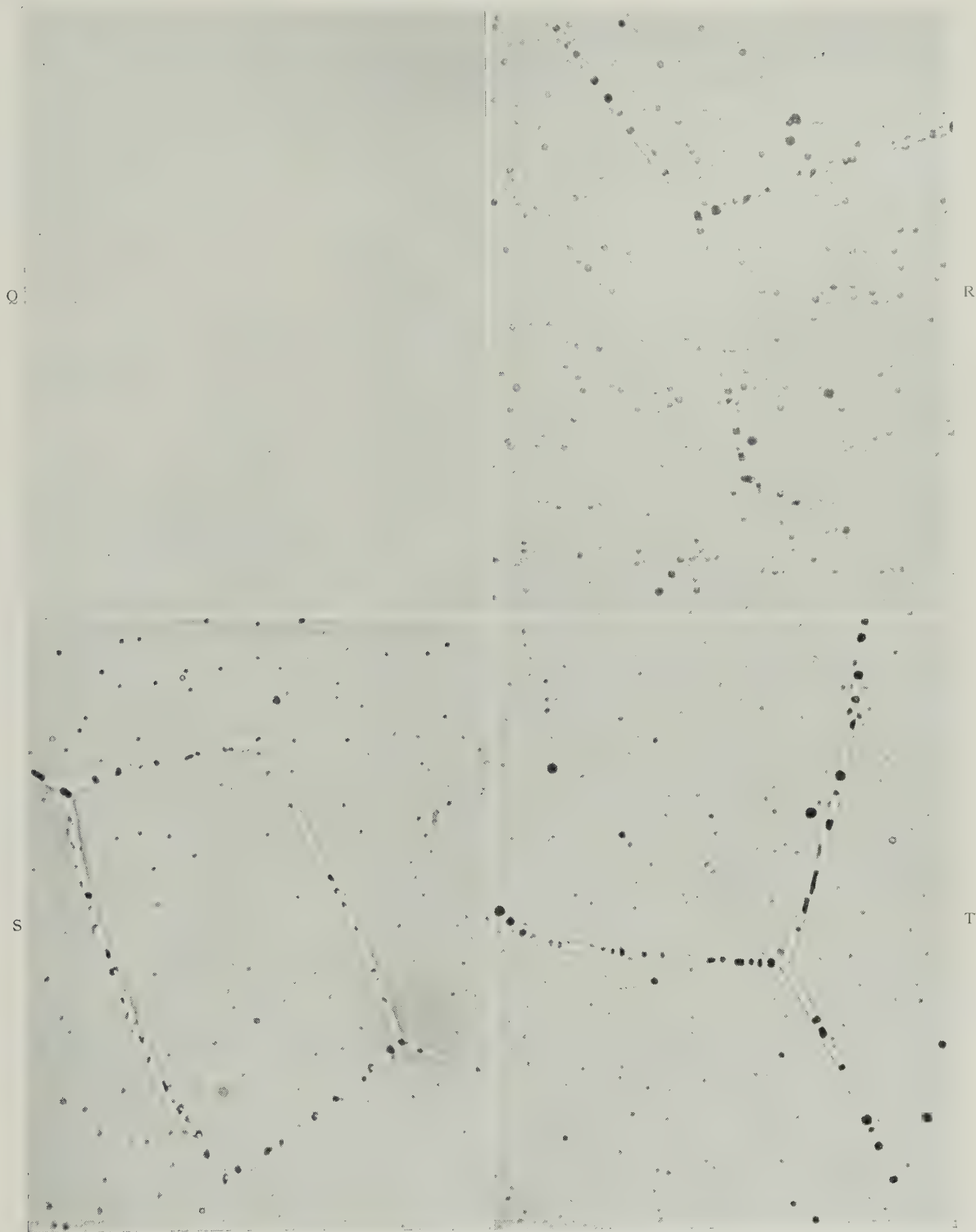
FIGS. N-P.—Artificially aged alloys.

FIG. N.—Al 0.57% Mg-1.13% Si-0.23% Mn-0.26% Fe.

FIG. O.—Al 1.14% Mg-0.55% Si-0.48% Mn-0.50% Fe.

FIG. P.—





FIGS. Q-T.—Grain Boundaries in Electrolytically Polished Specimens. (*Sendorek.*)

FIGS. Q and R.—Super-purity-base Al alloy containing 0.96% Mg and 0.5% Si, solution-treated at 540° C. and aged at 175° C. for 12 hr.

Fig. Q.—Quenched from 540° C.  $\times 400$ .

Fig. R.—Air-cooled from 540° C.  $\times 800$ .

FIG. S.—Super-purity-base Al alloy containing 2.60% Mg and 5.45% Zn, air-cooled from 460° C., naturally aged for 3 months.  $\times 800$ .

FIG. T.—Alloy as in Figs. Q and R, solution-treated at 540° C., quenched and aged at 300° C. for 6 hr.  $\times 800$ .

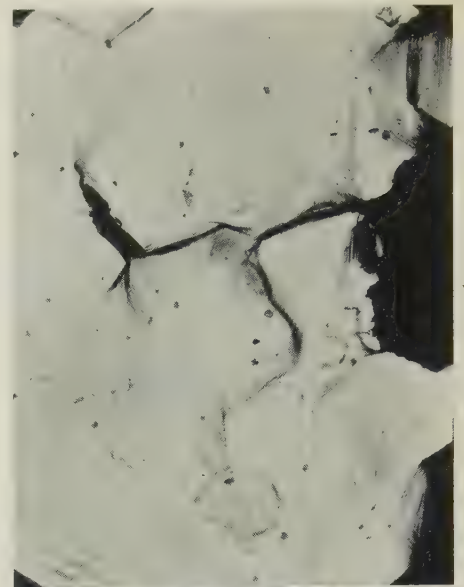


Rolled metal; 5½ years salt spray.

Rolled metal; 7 years industrial atmosphere.

Extruded metal; 7 years industrial atmosphere.

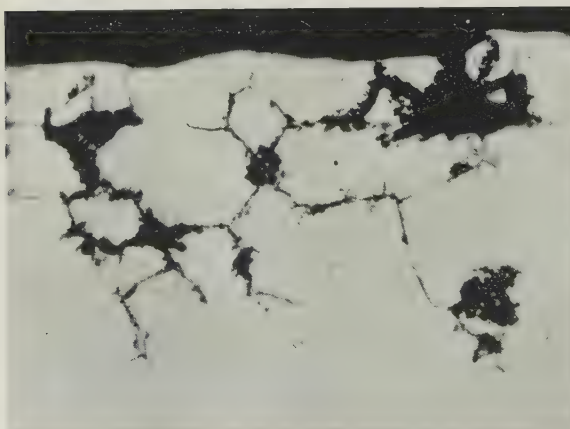
FIG. U.—Corrosion Effects in H10 Alloy. (*Harris and Varley.*)



FIGS. V and W.—Unetched Surface of High-Purity Al-0.7% Mg-1% Si Alloy After Tensile Fracture Showing Crack Propagation.

FIG. V.— $\times 100$ . FIG. W.— $\times 500$ .

Reduced by  $\frac{1}{3}$  in reproduction. (*Chadwick et al.*)



FIGS. X and Y.—Sections from Different Portions of Light Alloy Equipment Showing Corrosion After 2 Years' Service in an Industrial Atmosphere.

FIG. X.—Mn-free. FIG. Y.—0.6% Mn. Unetched.  $\times 100$ . (*Chadwick et al.*)



## Additional discussion.

Mr. L. E. SAMUELS,\* B.Met.E. (Member): I should like to comment on the assumption made by Mr. Harris and Mr. Varley that the etching effects found at the grain boundaries of their brittle alloys indicate the presence of almost continuous films of precipitate. There is now a considerable amount of evidence to suggest that this is not necessarily so.

Perhaps the first relevant case reported was that of the antimonial brasses investigated by McLean and Northcott,† where etching effects which might be thought to indicate the presence of precipitation could be developed at the grain boundaries of brittle alloys. Although McLean and Northcott did in fact suggest that the presence of a continuous precipitate could be adopted as a working hypothesis, they clearly had some doubts on the matter. A little later, Voce and Hallows‡ reported an examination of brittle bismuth-containing coppers. They found that continuous dark lines developed at many grain boundaries of brittle material during electrolytic polishing, and stated their belief that this indicated the presence of continuous films of bismuth. This conclusion was criticized by McLean,§ who, by comparison with his antimonial brasses, suggested that the contour of the grain-boundary lines constituted in reality a groove on one side of the grain boundary and a ridge on the other, a contour difficult to reconcile with precipitation. I re-examined Voce and Hallows' specimens, and was able to establish by a metallographic taper-sectioning method that McLean's suggestion as to the grain-boundary contour was correct.|| Further, it was found that deep grooves could be developed at the grain boundaries of mechanically polished specimens by using suitable etching reagents, and that various reagents differed appreciably in their effects. No positive evidence of precipitation was found. These results, combined with a re-assessment of the electron-microscope examination of the same specimens conducted by Schofield and Cuckow,¶ suggested that the presence of discrete precipitates was most unlikely. In order to explain the brittleness, I adopted a suggestion previously advanced by McLean and Northcott\*\* to explain the temper-brittleness of steels, and mentioned by the present authors in the Introduction to their paper. This phenomenon—the segregation of solute atoms at the grain boundary without actual precipitation—has come to be known as “equilibrium segregation”.

A number of similar cases of this type have now been reported, viz. in copper-tin alloys (Perryman ††), aluminium-iron alloys (Perryman ‡‡), and copper-antimony alloys (McLean §§). All these alloys show peculiar etching effects at the grain boundaries under conditions where precipitation is thought to be absent; the investigation of the copper-tin alloys included electron-microscope examination. The  $\beta$ -brasses which I studied ||| may represent another example of the same effect, although this examination introduced a further complication in that the ridge-and-groove contour referred to above was also developed during electrolytic polishing at grain boundaries known to contain precipitates of  $\gamma$  phase. I would also classify temper-brittle steels in this

group. Mr. Harris and Mr. Varley have interpreted McLean and Northcott's\*\* results on temper-brittle steels as suggesting that the networks which can be developed in these steels by suitable etching reagents indicate actual precipitation, although McLean and Northcott themselves did not believe that precipitation was present. Moreover, careful electron-microscope examination by both Maloof ¶¶ and Woodfine\*\*\* failed to detect any evidence that networks of precipitated carbide are present in such steels. After a critical review of the subject, Woodfine agrees with McLean and Northcott that the most likely explanation of temper-brittleness is a segregation at the grain boundaries, rather than precipitation.

Unless some concept such as an equilibrium segregation is accepted to explain these grain-boundary etching effects, it is necessary to postulate “submicroscopic” precipitation; submicroscopic, it is to be noted, with respect to the electron microscope. Not only is this an artificial distinction, but it still will not account for the observations on the copper-antimony alloys of McLean, §§ which were specifically chosen for investigation because their constitution is such that there is no possibility of precipitation.

I suggest, therefore, that it must now be admitted that there are two possible explanations of grain-boundary etching effects of the type found by Mr. Harris and Mr. Varley. First, the presence of precipitation and, secondly, a change in the solid solution which does not involve actual precipitation. There would seem to be no justification for adopting the first explanation and ignoring the second, as these authors have done, unless some positive evidence of precipitation is obtained. This virtually means that it is not safe to assume precipitation unless the precipitate can be seen and discretely resolved microscopically.

The AUTHORS (*in reply*): Mr. Samuels has raised the very important point that grain-boundary weakness in many alloys has been ascribed to “equilibrium segregation”, or the segregation of solute atoms at the grain boundaries without actual precipitation. Whether this is happening in the case under consideration is, we think, more a matter of terminology than of fact. The very excellent photographs published in the discussion of our paper ††† by Dr. V. A. Phillips and by Mr. A. Sendorek show conclusively that, at any rate at a later stage, precipitation takes place at an accelerated rate along the crystal boundaries, and that this results in a continuous zone of impoverished solid solution. It is now generally agreed that this is the cause of the observed brittleness.

Our own observations and those of Dr. Phillips and Mr. Sendorek suggest that there is a continuous gradation between the apparently uniform solid solution of the quenched alloy and the obviously overaged grain boundaries of Fig. M (Plate XCV) and Fig. T (Plate XCVI). Whether the initial stages (Fig. 21, Plate LVI, of our paper) are ascribed to submicroscopic precipitate or to equilibrium segregation, seems to be largely a question of nomenclature. The difficulty of drawing a line between equilibrium segregation and the initial stages of precipitation is particularly great in an age-hardening alloy, where the eventual precipitate is a compound of two solute elements.

\* Senior Scientific Officer, Defence Standards Laboratories, N.S.W. Branch, Sydney, Australia.

† D. McLean and L. Northcott, *J. Inst. Metals*, 1946, **62**, 583.

‡ E. Voce and A. P. C. Hallows, *ibid.*, 1947, **73**, 323.

§ D. McLean, *ibid.*, 1947, **73**, 791 (discussion).

|| L. E. Samuels, *ibid.*, 1949–50, **76**, 91.

¶ T. H. Schofield and F. W. Cuckow, *ibid.*, 1947, **73**, 377.

\*\* D. McLean and L. Northcott, *J. Iron Steel Inst.*, 1948,

158, 169.

†† E. C. W. Perryman, *Trans. Amer. Inst. Min. Met. Eng.*, 1953, **197**, 906.

‡† E. C. W. Perryman, *ibid.*, p. 911.

§§ D. McLean, *J. Inst. Metals*, 1952–53, **81**, 121.

||| L. E. Samuels, *ibid.*, this vol., p. 227.

¶¶ S. R. Maloof, *Trans. Amer. Soc. Metals*, 1952, **44**, 264.

\*\*\* B. C. Woodfine, *J. Iron Steel Inst.*, 1953, **173**, 240.

††† *J. Inst. Metals*, this vol., Plates XCV and XCVI.

## Discussion

## Grain Refinement of Cast Copper-Base Alloys\*

Dr. J. C. CHASTON,† A.R.S.M., A.Inst.P., F.I.M. (Member): The general idea that crystallization from a melt may be started at a number of centres of nucleation is, of course, an old one, but it has long been evident that not all forms of solid matter can act as nuclei. It is suggested by Mr. Cibula that if nucleation is to occur, the particles must: (a) possess a crystal structure that fits the structure of the solid to be nucleated within certain limits, and (b) be wetted by the molten metal. From the results quoted, it does not seem that the question of fit is really of great importance. The best inoculant found, zirconium carbide, had a misfit of 30% at 20° C., whereas tungsten carbide, which was not of great value, had a misfit of only 13%. It would appear that other factors, such as the ability of the nuclei to be formed by reaction within the melt itself so that the free surfaces are completely free from films of foreign matter and are easily wetted, are much more important. It is significant here that so much effort was required in the experimental work to obtain the inoculant in the right form. Such compounds as zirconium carbide, for instance, are obviously difficult to add in what might be called an active state.

The best results were obtained with a zirconium-copper alloy made by dissolving zirconium in copper in the presence of carbon. Has Mr. Cibula tried heating zirconium-copper alloy and carbon to a high temperature for prolonged periods to produce a master alloy?

It is evident that the addition of inoculants cannot always in itself be sufficient to produce fine grain. Heat is evolved during solidification, and concentration gradients tend to be set up which stop the growth of the crystals that form on the mould surface and allow new ones to be formed elsewhere. Refining by nucleation obviously cannot be expected to succeed in all environments at all rates of cooling and with ingots of every possible size. Dr. Dennison and Mr. Tull worked with metal moulds and Mr. Cibula with sand. It is interesting to look at the results with a view to deciding how far these complicating factors may have affected grain-refinement. Fig. 4 (Plate LXXX) of the paper by Dennison and Tull shows the structure produced by modifying the all-β 12.5% aluminium alloy with 0.01% boron. In the experimental ingot the thin rim of fine-grain material is seen to surround an extensive columnar region, but in the larger commercial 10% aluminium ingot with a corresponding boron addition (Fig. 8, Plate LXXX) only small regions of large grain-size are visible. Could that be a mould effect?

Incidentally, did a columnar region occur in the ingot shown in Fig. 7 (Plate LXXX)? The reproduction suggests that grain-refinement is much better with 0.0025% boron (Fig. 7) than with 0.01% (Fig. 8, Plate LXXX). Was this so?

With regard to the effect of remelting, Dr. Dennison and Mr. Tull state that remelting the 12.5% aluminium alloy containing 0.01% boron did not impair the grain refinement. Was the columnar region of similar extent on both occasions?

Dr. R. T. PARKER,‡ B.Sc., A.R.S.M., F.R.I.C., F.I.M. (Member): Although the point is not directly relevant to the subject of Mr. Cibula's paper, I feel that Dr. Chaston's remarks suggest one avenue for further work which needs emphasizing. That is, the relationship between rate of chilling and the effect of grain-refining elements. We are now well used to thinking of certain levels of added titanium or boron

elements which act reasonably consistently in sand castings, particularly when these are of regular reproducible shape. However, it is known that differing rates of chill in themselves have some effect on grain-size. Metal which is rapidly water-chilled, as during granulation, has a very fine structure. Metal in the thin outer skin of a continuously cast ingot also possesses a fine grain structure, while the interior of such billets often solidifies with a reasonably fine-grained equiaxed structure. The material between these two zones is frequently coarsely columnar. A certain amount of observation of such materials leads me to suggest—without very much evidence—that not enough is known about the levels of grain-refining elements needed to alter the grain-size in these different zones, where the thermal gradients on solidification are so vastly different.

I would suggest, therefore, that this is an aspect which should receive attention, since it is possible that varying threshold values of elements might be disclosed as necessary with different rates of chill.

Dr. N. P. ALLEN,§ M.Met., F.I.M. (Member): Views about the solidification process must be profoundly influenced by ideas on the nature of the liquid state, but hitherto little attention has been paid to the peculiarities of the liquid state when nucleation and crystal growth have been discussed.

The crystalline state is characterized by great regularity, extending over long distances, in the arrangement of the atoms. Occasional atomic sites are left vacant, but the total amount of free space is small. The liquid state is not very different: the atoms are about the same distance apart and at equal temperature are vibrating with much the same amplitude. The neighbours of any one atom are arranged around it in much the same pattern as in the solid state. It differs however, from the solid state in three essential respects: (1) The regularity of the pattern is less in the liquid state so that, moving away from a given atom, the atoms are found in positions that diverge increasingly from the positions that would be expected if the pattern were regularly repeated. (2) The amount of free space is greater in the liquid state (corresponding to the increase in volume on melting) and it is more evenly distributed through the mass, so that it cannot be properly thought of as consisting of a number of definite vacant sites, though no doubt a number of spaces of roughly the size of an atom are present. (3) The configuration is not constant, as it is in the crystal, but is continually fluctuating, this fluctuation being a consequence of the freedom of movement that the atoms acquire as a result of the greater proportion of free space.

Fig. A may be considered to represent the boundary between solid and liquid at the melting point, the region to the left of XY having a regular array of atoms, whilst that to the right is composed of a number of vaguely defined regions in which an approximation to a regular array exists, together with regions in which little trace of regularity can be found. These regions change continuously in outline and orientation.

In an array of this kind solidification would proceed as a result of regions such as 1 or 2 in Fig. A finding themselves by chance in a position and orientation favourable for union with the crystalline material on the left-hand side of XY. Alignment of these regions with the crystal lattice then results in a local contraction, accompanied by the production of free

\* Joint discussion on the papers by J. P. Dennison and E. V. Tull (*J. Inst. Metals*, 1952-53, **81**, 513) and by A. Cibula (this vol., p. 513).

† Manager, Research Laboratories, Johnson, Matthey and Co., Ltd., Wembley.

‡ Director of Research, Aluminium Laboratories Limited, Banbury, Oxon.

§ Superintendent, Metallurgy Division, National Physical Laboratory, Teddington.



space in adjacent regions such as *a* in Fig. B. The free spaces have high energy (this energy being the latent heat of fusion), and the alignment can be permanent only if (i) the atoms from the liquid diffuse into the spaces, (ii) the latent heat of fusion is conducted away, and (iii) the consequent loss of energy is greater on the average than the increase in surface energy due to the increase of the area of the liquid/solid interface.

The chief function of a solidification nucleus is to provide a foundation on to which the temporary regions such as 1 and 2 (Fig. A) can anchor themselves, for if they remain in one position long enough, and the system as a whole is losing energy, there is a chance for the free space at the periphery of the regions (the "peripheral free space") and its associated

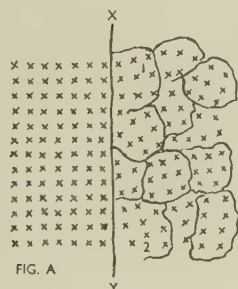


FIG. A



FIG. B

energy to diffuse away, rendering the position permanent. The essential condition for a surface to act as a nucleus is that the average energy of the bonds between the atoms of the surface and those of the liquid be sufficiently greater than the average energy of bonds between the atoms of the liquid.

The chance that any given part of a surface will act as a nucleus depends on the magnitude of the difference between these two average energies.

The rate at which solidification can proceed is influenced by the rate at which the peripheral free space can diffuse away. Any impurity atoms in the liquid capable of attaching themselves to the free spaces and reducing their mobility, will consequently reduce the rate of advance of the solidification front. The opportunity for another surface to function as a nucleus will thereby be increased, and the resulting grain-size may be decreased.

These considerations apply to a simple metal. In an alloy the regions 1 and 2 in Fig. A must satisfy an additional condition before they can become permanently attached to the crystal. Besides having, by chance, about the right spacing and orientation to match the crystal, they must also have a composition similar to that of the crystal in equilibrium with the liquid at the prevailing temperature. This is usually substantially different from the mean composition of the liquid, and the probability that the region has the necessary composition is small. It is to be expected therefore that rates of crystal growth will generally be less in alloys than in pure metals. The continuous selection for attachment to the crystal of regions having less than the average proportion of solute, results in the liquid near the solidification front becoming enriched in solute. This decreases the probability of the formation of regions of suitable composition, and retards crystal growth. Diffusion of the solute away from the

solidification front tends to restore the situation, and may become a controlling factor.

Professor A. PREECE,\* M.Sc., F.I.M. (Member): Since grain growth in metals occurs in both the liquid and solid state and in each case involves the migration of grain boundaries, the mechanism operating must surely be the same for the two conditions. In this connection one may refer, for example, to the influence of aluminium in producing inherently fine-grained steel, as an instance of grain refinement in the solid state.

Dr. BØRGE LUNN,† M.Sc., F.I.M. (Member): Will the addition of grain-refining agents have any influence on the grain growth at recrystallization of the cold-worked material?

Mr. K. EICKHOFF,‡ Dipl.-Phys.: With regard to Mr. Cibula's paper, it may be of interest to point out that a similar grain-refining effect can be achieved during the recrystallization of wrought  $\alpha$ -brass. A preliminary study was carried out by making additions of up to 0.1% of various elements to an  $\alpha$ -brass containing about 64% copper. After recrystallization treatment of the cold-worked specimens, a markedly smaller grain-size was observed in samples containing zirconium, iron, or phosphorus, as compared with those without any addition. No investigation was made as to the form in which the additions were most effective, but as carbon crucibles were used, at least in the case of zirconium, the presence of the carbide might be expected.

Dr.-Ing. H. VOSSKÜHLER †: I have two questions of practical interest to ask regarding refining by boron. Dr. Dennison and Mr. Tull have examined the grain-size of cast alloys. Do the boron compounds also influence the recrystallization grain-size of wrought alloys? It is known that some compounds of boron, e.g. boron carbide, are very hard, and for this reason are used for cutting tools. If these compounds are present in a copper-alloy matrix, it is possible therefore that the alloys so formed may be difficult to machine by turning, drilling, &c. Have any observations been made on this point?

Dr. DENNISON and Mr. TULL (*in reply*): The comparison of size-effect made by Dr. Chaston should have been between Figs. 2 and 8 (Plate LXXX of our paper,) which illustrate, respectively, laboratory and commercial billets of equivalent aluminium content. We agree that the chilling effect, being proportionately greater in the smaller billets, may be responsible for the extensive columnar zone shown in Fig. 2. The outer rim of fine-grained material occurred only in laboratory casts of the 12.5% aluminium alloy.

Table V (p. 519) of our paper, which gives details of crystal sizes for the commercial billets, shows that the refinement produced by 0.0025% boron was distinctly inferior to that resulting from 0.01% boron. With the latter addition, the extent of the columnar zone was considerably reduced.

Dr. B. Lunn, Mr. Eickhoff, and Dr. Vosskübler infer that boron additions may also have a refining effect on the recrystallized grain-size. Whilst we have not carried out such recrystallization experiments, we have observed grain-growth effects during hot rolling.

For a given (10%) reduction per pass, at 800° and 900° C., the final grain-size of a section from the unrefined commercial billet containing 10% aluminium was much greater than that of a similar section from the refined billet. At 950° C., however, considerable grain-growth occurred in the refined material, which then had the larger final grain-size.

No particles of boron carbide could be detected by microscopic examination at a magnification of  $\times 1000$ . The machining properties of grain-refined material appeared to

\* Professor of Metallurgy, King's College, University of Durham.

† Nordiske Kabel-og Traadfabriker (Northern Cable and Wire Works), Copenhagen.

‡ Wieland-Werke A.G., Ulm/Donau, Germany.

be superior to those of untreated billets, probably owing to the absence of long columnar-crystal boundaries.

Mr. A. CIBULA (*in reply*): Dr. Allen has provided a useful picture of nucleation and the progress of solidification, and it would be of considerable advantage if this picture were extended quantitatively, in the manner attempted by Turnbull and Vonnegut\* for example. It might then be possible to elucidate the factors which enable the surface of a foreign particle to act as a nucleus in a melt and, in particular, to evaluate the importance of lattice fit, a problem which has been pointed out by Dr. Chaston. The fact that the order of lattice fit was not the same as the order of effectiveness of the several types of nuclei used in copper alloys, indicates that another factor is also important in nucleation, as suggested in the paper. In view of the considerable evidence available from other examples of nucleation,† however, it seems unreasonable to conclude that lattice fit is of only slight importance. Simple wetting hardly seems to be sufficient to bring about nucleation, as so few types of particles are effective as nuclei in melts; in an aluminium-1.3% chromium alloy, for instance, the primary crystals of intermetallic compound precipitated during freezing did not prevent undercooling of solid-solution crystallites at the peritectic temperature and, in accordance with this observation, did not cause grain refinement.‡

Whatever controls the effectiveness of a nucleus, the grain-refining compound must in practice be dispersed as fine particles throughout the molten metal in such a way that they are wetted by the melt, as pointed out by Dr. Chaston. However, if a zirconium-copper-carbon alloy were used as a refining addition, as he suggests, the difficulty might arise that the zirconium carbide particles in this concentrated master alloy would be too large and could not subsequently be broken up when dispersed in the melt. In the work described in the paper, an attempt was made to use a titanium-copper-carbon alloy, but effective refinement was obtained only when an excess of the alloy was added, presumably owing to the large size of the titanium carbide dendrites; in subsequent experiments, therefore, the constituents of the grain-refining compounds were added separately, as this procedure resulted in the precipitation of fine particles in the melt.

Dr. Parker has pointed out that little is known about the influence of the rate of chilling on the effectiveness of grain refiners. It might be expected that a more severe chill would make concentration gradients steeper, and thus accentuate the solute-rich barrier of low melting point which surrounds the growing dendrite and restricts its growth; in contrast with this effect, however, an increased chill would render steeper the (rising) temperature gradient in front of the solid/liquid interface and thus tend to reduce the extent

of undercooling in the melt on the opposite side of the low-melting-point barrier. Therefore, the influence of rate of chilling on the effectiveness of the added nuclei would depend upon the relative diffusivities of heat and solute atoms. It seems unlikely, however, that the size of the refining addition would vary greatly with the rate of chill, as it has been estimated that only a small proportion of the particles added in a normal grain-refining addition become centres of crystallization, even when the finest grain-sizes are obtained.‡ Should a grain-refining addition prove to be ineffective at the rate of chilling employed, it would probably be necessary to select a different and more effective grain refiner. A similar choice may be required if the concentration of alloying elements in the metal is reduced, and in this case some indication of the alternatives available for bronzes is given in the paper; it is shown that at high tin contents both zirconium carbide (or nitride) and iron boride cause marked grain refinement, whereas in a 4% alloy only the former compound may be used.

A number of contributors have referred to the possible influence of grain-refining particles on recrystallization and grain growth in the solid metal. No conclusive evidence has been published of the nucleation of recrystallization by impurity particles, though it has been claimed that such particles may nucleate the precipitation of a new phase in the solid (e.g. Dennis§ has suggested that alumina particles may nucleate graphitization in hypo-eutectoid steel). However, it is possible that many of the grain-refining particles introduced into the melt to control the as-cast grain-size may subsequently become anchored at grain boundaries, particularly as most of the added particles are not required as nuclei during solidification. Such particles may presumably stabilize the grain boundaries, but would probably be no more effective than other types of inclusion. The stabilization of grain boundaries by embedded particles appears to be more important during changes in the solid metal (during heat-treatment, for example) than during crystallization from the melt, presumably because the energy changes during solidification are far greater than during recrystallization and grain growth. This difference can be illustrated by the influence of plates of *N*-AlCuFe on the grain-size of aluminium-4½% copper alloys.|| In the as-cast structure, these crystals usually lie within the grains, where they are formed by secondary crystallization, and show little evidence of restricting grain growth during solidification, as, in the absence of a grain refiner, the grain-size may be large. During solution-treatment, however, the grain boundaries migrate until they coincide with the *N*-AlCuFe plates, which then appear to stabilize the grain-size; if a high-purity alloy free from *N*-AlCuFe plates is solution-treated, grain growth occurs, in the absence of the grain-boundary inclusions, and the grain-size increases from 0.15 to 3 mm. or more.

\* D. Turnbull and B. Vonnegut, *Indust. and Eng. Chem.*, 1952, **44**, 1292.

† J. H. van der Merwe, *Discussions Faraday Soc.*, 1949, (5), 201.

‡ A. Cibula, *J. Inst. Metals*, 1949-50, **76**, 321.

§ W. E. Dennis, *J. Iron-Steel Inst.*, 1952, **171**, 59.

|| A. Cibula, unpublished work, 1951.



## Discussion

## The Influence of Extrusion Direction on the Corrosion and Stress-Corrosion of Aluminium-Copper-Magnesium Alloys

By E. A. G. LIDDIARD and WINIFRED A. BELL

(Journal, this vol., p. 426)

Dr. U. R. EVANS,\* M.A., Sc.D., F.R.S., F.I.M. (Member): This paper should do much to bring home to designers the importance of taking directional properties into consideration. Doubtless, in certain cases, they have long done so. When timber is the material of construction, the direction of the grain receives due attention; again, in welding metals the fact that the tensile strength at right angles to the surface of a plate is different from that parallel to the length, is known to be a matter of great moment. It may be doubted, however, whether designers always realize the marked effect of directional properties on the elongation values of certain materials or on their susceptibility to stress-corrosion—features brought out clearly in Table II (p. 428) of the paper.

Directional properties play a part in the corrosion-susceptibility of many materials, and an example from ferrous metallurgy may perhaps be permissible. Wrought iron consists of alternate parallel layers, which in our work at Cambridge † we term *Q* (quickly corroding) and *R* (resistant) zones; lately, *V* (very resistant) zones have been discovered. If the face of a flat slab consists of *R* or *V* material, serious corrosion may be prevented over long periods; if the zones do not lie strictly parallel, so that certain *Q* zones curve outwards and cut the surface, corrosion will soon start to penetrate along such zones. Finally, if the sheared edges of a plate, which are practically sure to be cut by *Q* zones, are insufficiently protected, then corrosion is almost certain to penetrate along them. The first effect will be an *increase* in thickness of the plate, since the corrosion product formed internally occupies a larger volume than the metal destroyed; later this swelling may cause layers of relatively unchanged metal to split off, and the thickness will *diminish*. The whole change is insidious, and may well escape observation until the splitting off of surface layers starts, since the attack is internal and gives rise to black magnetite instead of hydrated ferric oxide (rust) with its familiar red warning colour.

Certain aluminium alloys—especially in the extruded state—also contain layers along which corrosion can penetrate easily, with internal formation of a corrosion product which occupies a larger volume than the original alloy. If such a change starts at the sheared edge of a plate, the first result will be an increase in thickness, and thus it may easily escape the attention of the inspectors; later, layers of the unchanged alloy may be forced away, carrying with them any protective material which may have been applied to the face. Such examples—displaying both swelling and flaking—have been met with on material taken from an aircraft. They represent an exceptional behaviour, possibly due to corrosive substances from the cargo carried, but the specimens examined serve to show what may occur if the areas where layer corrosion can start receive insufficient protection.

It should be noted that sheared edges are the parts least well placed to receive sacrificial protection from cladding of the face. Undeniably, when the whole surface is very wet with a highly conducting liquid (such as concentrated salt solution), the cathodic protection afforded by cladding with unalloyed aluminium may extend for a surprising distance

over the bare alloy surface. But conditions under which the wetting liquid is only a tenuous film containing little salt are less favourable to cathodic protection. The use of a spray test in which specimens are kept thoroughly and permanently wet with concentrated salt solution is not a rigorous test for the efficacy of protection by a sacrificial coating, whether cladding, spraying, or metal-pigmented paint. Intermittent wetting, with alternate dry periods, and the use of very dilute solutions alternating with strong solutions, might form a more stringent test, which could be designed to represent more faithfully the conditions of service. It may be complained that dilute salt solutions would corrode very slowly and that such tests would occupy too long a time, but it is worth noticing that Beck, Keihn, and Gold ‡ have recently recorded that—at least under conditions of immersion—dilute salt solution is much more corrosive (to unalloyed aluminium) than is concentrated solution, apparently because the aluminium can pass away as a colloidal solution instead of building up a protective film. It would be interesting to know whether the results recorded in Table IV (p. 431) of the paper would have been equally favourable if very dilute salt solution had been chosen instead of the 3% sodium chloride apparently used.

It should be noted that in layer corrosion the swelling involved in conversion of the metal into oxide or hydroxide itself produces stresses, and if the penetration is along a layer close to the surface, those stresses will push away the unchanged layer outside, and thus corrosion can progress continuously. Applied tension is not needed, although where tension is applied in a direction calculated to help in pulling apart the layers, it will enhance destruction, as indicated in Table II of the paper.

Whether the face of an extrusion is protected by cladding, spraying, painting, or otherwise, it would seem that the designer and maintenance personnel should be warned to direct special attention to all places where the susceptible zones of the alloy can cut the surface; also that the designer should be careful not to cut away the original surface in such a way as to expose susceptible zones without making proper provision for the protection of the danger-points.

At such places spraying may sometimes be possible; where it is not, metal-pigmented paints, though less effective than spraying (as shown in Table IV), are better than nothing. At Cambridge considerable work has been done on metal-pigmented paints, mainly metallic zinc paints. It has long been felt, however, that aluminium-pigmented paints, if and when they were capable of protecting at all, would in general last for a longer time. The difficulty has been that, in order to provide protection at gaps, however narrow, metal-to-metal contact between the pigment particles is essential; whereas most samples of zinc powder fulfil this condition, ordinary aluminium powder, whether in the form of flakes or round particles, does not. Mr. C. E. Bird, under the auspices of the Ministry of Supply, is now working at Cambridge to overcome this difficulty and has had more than a modicum of success. While it is too soon to make far-reaching claims, it seems

\* Reader in the Science of Metallic Corrosion, Cambridge University.

† U. R. Evans, *J. Soc. Chem. Ind.*, 1928, 47, 62T.

K. G. Lewis and U. R. Evans, *Iron and Steel Inst. Special Rep.*, 1934, (5), 209.

J. P. Chilton and U. R. Evans, *J. Iron Steel Inst.*, 1955 (in the press).

‡ W. Beck, F. G. Keihn, and R. G. Gold, *J. Electrochem. Soc.*, 1954, 101, (8), 393.

possible that a new material may in due course become available for protecting areas where the swelling and flaking process termed layer corrosion normally starts.

The existence of susceptible zones in aluminium alloys may cause errors in testing for ordinary stress-corrosion cracking. Tests were recently being carried out here by Mr. H. K. Farmery on strips of a certain alloy, in a condition very susceptible to stress-corrosion cracking. He found that certain specimens did not fracture when stressed in a salt solution under a load which caused rapid failure in other—nominally identical—specimens. Read blindly, the results would appear to suggest that such long-lived specimens were more resistant than the others. The real difference, however, was that in these exceptional specimens the cracking, instead of penetrating through the thickness of the specimen, turned parallel to the surface along a susceptible plane, so that breaking under the conditions of the test did not occur; if later, the specimen was removed from the testing machine, and subjected to twisting, it broke up quite readily, showing that it had not really been resistant.

Directional properties, if fully recognized and understood by the designer, need not prove a serious danger; indeed a skilful designer can take advantage of them. If, however, the facts are not fully exposed to all concerned, there is a real danger. That is one of many reasons why this paper is extremely welcome.

Mr. R. CHADWICK,\* M.A., F.I.M. (Member): The susceptibility to stress-corrosion of heat-treated and artificially aged aluminium-copper-magnesium alloys is, of course, well known, and the poor performance of the rolled alloys examined by Mr. Liddiard and Miss Bell therefore occasions no surprise. On the other hand, the remarkable degree of anisotropy of the extruded material in its stress-corrosion behaviour has not hitherto been realized and is quite outstanding, having regard to the much smaller differences in normal tensile properties in the two directions of testing.

In interpreting and applying the authors' results, regard should be paid to the exceedingly complex and heterogeneous structures existing in different parts of extruded bar as normally produced. The fibrous structure, in which crystal length may be one hundred times or so greater than diameter, is normally present, it is true, over most of the area. However, at the surface there is generally a layer, which varies from paper thickness to several millimetres, having a coarse equiaxed crystal structure of low resistance to stress-corrosion. If this outer layer is present on a component, therefore, transverse strength where corrosion is involved is likely to be much lower than that reported by the authors. In other words the results now obtained on specimens machined out of a bar, and therefore excluding the surface layers, may not be applicable to unmachined components and stampings.

Another factor to be guarded against is the possibility of cold work having been applied before heat-treatment, arising either from room-temperature manipulation or even from a hot-working operation, such as stamping, carried out at too low a temperature. If the total cold deformation from all operations exceeds a critical amount, involving generally about a 10% change in cross-section, final heat-treatment will lead to recrystallization, whereupon the stress-corrosion behaviour will be similar to that of sheet. Although such possible causes of reduced resistance to stress-corrosion are briefly mentioned by the authors under "Practical Implications" (p. 431), they would appear to have received insufficient emphasis. It is indeed extremely doubtful whether any aircraft constructor could be sufficiently sure of having only the fibrous extruded structure present in any particular component, to enable stressing to be based on the high values found in this series of experiments.

A recent related paper by Hooker and Waisman,† dealing with more practical aspects of stress-corrosion cracking in aircraft components, has a special bearing on the present discussion, since it deals in some detail with remedies, including the application of protective coatings. While the expected protection afforded by metal spraying was in fact achieved, where the sprayed coating bore a suitable electro-potential relationship to the underlying alloy, the procedure proved to be impracticable for various reasons. For example, it interfered with consistent and accurate tensioning of bolts, while the coating tended to crack under bolt-head pressure. The most serious objection, however, was the masking of defects so that inspection became impossible. This last aspect clearly deserves serious attention and is something on which metallurgists with experience of airframe engineering problems might well express more detailed and authoritative views.

Dr. F. A. CHAMPION,‡ A.R.C.S., F.I.M. (Member): The sheet for this work was produced from the same billet as was used for the extrusions, the hot rolling being preceded by forging. This was fully justified as a means of minimizing extraneous factors, but in consequence it seems that even the manganese-bearing alloy cannot be regarded as a typical commercial product.

The authors point out the negligible effect of initial thickness on stress-corrosion susceptibility generally shown in this work, but can they explain why the thinner sheet was much more susceptible than the 0.2-in. manganese-bearing sheet (see Table I, p. 427)?

Mr. Liddiard and Miss Bell give the impression that they prefer to exclude manganese, in order to get stress-corrosion rather than exfoliation, but the reverse seems preferable in view of the more insidious character of stress-corrosion. I have shown § that sprayed coatings of aluminium give effective protection against structural corrosion of these copper-bearing alloys, while experiments in other laboratories and the success of cladding on rolled alloys point to the value of cathodic protection against stress-corrosion. It is therefore to be expected that appropriate sprayed coatings will provide good protection against all these forms of corrosion and I am glad to see that the present work confirms this. Hooker and Waisman † have also obtained encouraging results, although their conclusions are biased by their tendency to concentrate on zinc instead of aluminium sprayed coatings and to ignore confusion caused probably in their tests by notch effects resulting from machining.

Experience has shown, however, that good adhesion of sprayed coatings of aluminium is more difficult to achieve with the higher purities; 99.5% therefore seems preferable for sprayed coatings compared with the 99.7% used by the authors and for rolled-on cladding. On the other hand, alloying with zinc should be necessary only for coatings on copper-free alloys and may be expected to prove a disadvantage eventually on copper-bearing alloys owing to the high potential difference between core and cladding and the consequent undue wastage of cladding at any exposure of the core.

Dr. W. M. DOYLE,|| M.Eng., F.I.M. (Member): The results recorded are most interesting and valuable in so far as they add to the accumulation of knowledge on this subject, which some designers find it rather difficult to understand. The authors are very fortunate in being able to arrive at certain fundamental conclusions with such a small number of tests, and doubly fortunate in being able to record a high degree of consistency in the tests at the individual stress levels, using both the four-point-loading bend test and the direct-tension test. There is no indication in the paper whether the tests

\* Assistant Research Manager, Imperial Chemical Industries, Ltd., Metals Division, Birmingham.

† R. N. Hooker and J. L. Waisman, *Corrosion*, 1954, 10, (10), 325.

‡ Research Laboratories of The British Aluminium Co., Ltd., Gerrards Cross, Bucks.

§ F. A. Champion, *Metal Ind.*, 1951, 79, 355, 384.

|| Chief Research Metallurgist, High Duty Alloys, Ltd., Slough, Bucks.



were carried out under controlled temperature and humidity conditions, which Perryman and Hadden\* in their work at the B.N.F.M.R.A. proved to have a marked influence on the consistency of the results. Normally, in my experience, even under such controlled conditions, the results of direct-tension tests on susceptible materials, stressed at loads approximately between 50 and 75% of the 0.1% proof stress, show a considerable degree of scatter. In this connection, also, I note that neither in the paper nor the appendix is there any mention of the 0.1% proof stress of the extruded bars and sheet. I suggest that the authors should consider quoting these values in their reply. It is probable that tests carried out at 24 tons/in.<sup>2</sup>, in the case of the bending tests, may have produced a permanent set, especially in the low-manganese alloy in the form of the 0.1-in.-thick sheet.

It is rather unfortunate that Table III (p. 429), which gives the average time-to-failure under various stresses, does not indicate that the results are, in some cases, single results and in others the average of two, and in a few instances, three and five tests. This, however, may not be significant in view of the very high degree of consistency which it has been possible to obtain.

The very large differences in the actual results obtained from the bending tests, compared with the direct-tension tests, need further detailed consideration, because of the implication that slight differences in relative superiority of one form of alloy compared with another—for example, extrusions versus sheet—or in a comparison of alloys with one another, may be greatly exaggerated if assessed by means of the bending technique. I would appreciate the authors' opinion as to whether these differences are in part due to the fact that in any form of bend test, used for the assessment of stress-corrosion susceptibility, it is only the surface fibres on the tensile side that are stressed at the stated load.

In tests on other materials, which I have carried out, small cracks were noted in some cases of tests under bending, which did not lead to failure of the specimens in as long a period as 120 days. It would be of interest if Mr. Liddiard and Miss Bell could state whether their unfailed bend-test specimens were examined for such cracks.

Were the longitudinal specimens, tested in direct tension and machined, as stated by the authors, "from a zone about 0.15 in. below the surface" (p. 428), in the area of coarse peripheral grains normally associated with extrusions in this type of alloy? If they were machined from the affected zone, then their grain-size and fibre structure would differ very materially from the centre of the extrusion.

It is important to note that the authors have indicated the differences in relative susceptibility to stress-corrosion under salt-water conditions only, of two varieties of the same alloy, due to three factors: (1) the form of the alloy, (2) the method of test, and (3) the direction of stressing relative to the fibre structure. These are only some of the factors connected with the problem of stress-corrosion, and as this phenomenon is associated with the potential differences between grain-boundary constituents and the adjacent grains, the problems must be associated with quenching and ageing conditions, which, in turn, provide a very fruitful field for future research.

Mr. H. B. GRAINGER,† B.Sc., A.I.M. (Member): The paper illustrates an important principle, namely that stress-corrosion characteristics are determined not only by composition but by structure, and furthermore, that changes of composition may influence these characteristics indirectly by bringing about some structural change. I should like to amplify the authors' findings by means of some stress-corrosion data obtained in the I.C.I. laboratories, using an aluminium-7% zinc-2.2% magnesium-1.3% copper alloy in the form of fully heat-treated rolled sheet. The resistance to stress-corrosion of this alloy is very low and is not markedly influenced by an

addition of 0.25% manganese, but when a similar amount of chromium is also added, a remarkable improvement is effected. This is illustrated in Fig. A, where applied tensile stress is plotted against the time to failure of specimens sprayed twice daily with 3% sodium chloride solution.

It is of interest to compare the structures of these materials, for whereas that containing manganese has a uniform equiaxed structure (Fig. B, Plate XCVIII), that with chromium in addition, has long, flat grains elongated in the rolling direction (Fig. C, Plate XCVIII).

The propagation of stress-corrosion cracks in these alloys has been studied by means of bend tests on sheet specimens immersed in salt-peroxide solution. In the equiaxed, manganese-bearing alloy a single intergranular fissure develops rapidly in a direction at right angles to the direction of applied stress (Fig. D, Plate XCVIII). With chromium present, however, although corrosion starts in the same direction, there is a marked tendency for the advancing fissure to develop along the elongated grain boundaries parallel to the surface (Fig. E, Plate XCVIII). Furthermore, when corrosion begins at the edge of a sheet specimen, very deep fissures develop along the elongated grain boundaries, as illustrated in Fig. F (Plate

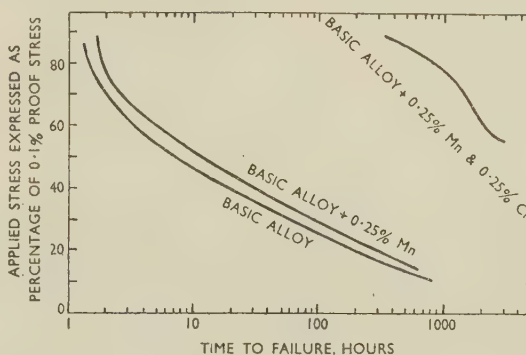


FIG. A.—Influence of Manganese and Chromium on the Stress-Corrosion Behaviour of an Aluminium-7% Zinc-2.2% Magnesium-1.3% Copper Alloy.

XCVIII). This specimen was not subjected to any externally applied stress, and it appears probable that in this instance residual internal stresses were sufficient to initiate stress-corrosion in the preferred direction.

It would appear that the improved behaviour of the chromium-bearing alloys is not due to any substantial change in the susceptibility to corrosion of the grain-boundary regions, but arises from the lack of suitably disposed inter-crystalline paths normal to the surface, which limits the development of stress-corrosion cracks in that direction.

Dr. R. T. PARKER,‡ B.Sc., A.R.S.M., F.R.I.C., F.I.M. (Member): I should like to comment on the results presented in Tables III and II. In particular, I feel that although the authors say at the bottom of p. 429: "In comparing the relative susceptibility of low- and normal-manganese-containing material, it must be remembered that tests carried out at similar stresses are not strictly comparable, since the ultimate tensile strength of the normal-manganese material is 2.7 tons/in.<sup>2</sup> higher than that of the low-manganese material," the results given in Table III are somewhat misleading. The U.T.S. values of the extruded materials vary from about 26 to 33 tons/in.<sup>2</sup>, and in view of this it would appear that the stresses of 24 and 20 tons/in.<sup>2</sup> are more liable to give misleading results on stress-corrosion testing than the stress of 16 tons/in.<sup>2</sup>. In fact, as the lower stress is approached, the differences between the extruded materials (see Table III, cols. 3 and 4), whether

\* E. C. W. Perryman and S. E. Hadden, *J. Inst. Metals*, 1950, 77, 207.

† Technical Officer, Imperial Chemical Industries, Ltd.,

Metals Division, Birmingham.

‡ Director of Research, Aluminium Laboratories Limited, Banbury, Oxon.

in the longitudinal or transverse direction of testing, become quite small.

Apart from this, however, it would appear that there is a marked difference in the ordinary corrosion characteristics of the two extruded materials. Table A gives results, abstracted mainly from Table II (p. 428), for applied stresses of 16 tons/in.<sup>2</sup> and for the low- and normal-manganese materials tested in both directions. (For purposes of comparison some figures for unstressed, uncorroded controls have been taken from the appendix (p. 432).)

TABLE A

Material	Unstressed, Corroded		Unstressed, Un-corroded	
	U.T.S., tons/in. <sup>2</sup>	Elong., %	U.T.S., tons/in. <sup>2</sup>	Elong., %
<i>Longitudinal Tests</i>				
Normal manganese	28.8	1	32.8	10
Low manganese	24.4	12	25.1 *	12 *
	23.5	10		
<i>Transverse Tests</i>				
Normal manganese	27.7	3	28.4	4
	26.4	2	28.3 *	4 *
Low manganese	24.6	3	26.5	4
	24.2	2	26.1 *	4 *

\* From Appendix (p. 432).

Examination of these results shows that in transverse testing hardly any difference exists between the two materials, particularly if loss of elongation is taken as an indication of behaviour. In the longitudinal direction, however, there is a vast difference; the low-manganese material showing very little alteration in properties whether corroded or not. The normal-manganese material, however, has lost an appreciable proportion of its ultimate tensile strength and an unexpectedly high proportion of its elongation. It does not appear that this is pure chance, since results for the other specimens of the normal-manganese alloy tested at 24 and 20 tons/in.<sup>2</sup> in the longitudinal direction (Section (a) of Table II) confirm that appreciable proportions of the properties have been lost in as little as 77 or 60 days. To my mind this indicates that the two materials are of such differing ordinary corrosion characteristics that the stress-corrosion results may be clouded in consequence.

Dr. F. ROHNER\* (Member): The difference in stress-corrosion susceptibility of specimens cut longitudinally and transversely from extruded bar of aluminium-copper-magnesium alloys has two aspects. From a directly practical point of view one may say that extrusions lend themselves preferentially to longitudinal straining, and therefore no severe restriction in their practical application results from this directional difference. Regarded from a more theoretical angle, the effect throws valuable light on the mechanism of stress-corrosion.

Similar investigations to those of the present authors have been made in Germany by Bollenrath † and by Brenner.‡ § Bollenrath experimented with aluminium-copper-magnesium and aluminium-zinc-magnesium alloys. In addition to the fact that longitudinal specimens proved less susceptible to stress-corrosion than transverse specimens, two other findings are worth mentioning. Specimens from extrusions of small

cross-section were less susceptible to stress-corrosion than those from extrusions of larger cross-section. The difference in stress-corrosion susceptibility between longitudinal and transverse specimens was found to be greater for alloys with high than for those with low contents of alloying elements. Bollenrath used the fork-test (*Gabelprobe*) originated by Matthaes.† ||

Brenner§ found that with sheets the stress-corrosion susceptibility is slightly higher for specimens taken parallel than for those taken transverse to the rolling direction. On aluminium-zinc-magnesium sheet we have made the same observation.

Dr. E. SCHEUER ¶ (Member): In the past, most observers have been led to the conclusion that the weakness of extruded material in the transverse direction was connected primarily with the eutectic network, traces of which remained even after heat-treatment. This view was supported by the fact that fracture under mechanical stress and the direction of corrosion paths reveal a pattern very much the same as that which this network would assume under deformation during extrusion.

From the micrographs shown in Fig. 2 (Plate LXVII) of the paper, the path of corrosion in sheet seems to have little or no connection with the distribution of the copper-rich constituent present, but follows the recrystallization grain boundaries. These seem, however, still slightly elongated in the plane of rolling.

The results of the stress-corrosion tests raise the question as to whether in the extruded material the actual aluminium grain boundaries are still identical with the eutectic meshwork, or whether corrosion attack follows a different, only geometrically similar, path connected with the recrystallization structure. Are the authors in a position to provide evidence on this point?

I would like to mention that exfoliation attack in sheet is by no means unknown.

Dr. H. SUTTON,\*\* C.B.E., F.R.Ae.S., F.I.M. (Member of Council): The authors have described useful experiments on a matter of considerable technical importance, and have presented conclusions which are probably reasonable in relation to the scope of the work. It is, of course, a problem of very great difficulty in corrosion work to make experiments in a comparatively short period of time and in such a way that they can bear a direct relationship to behaviour in service over much longer periods. The time factor is especially important. Twelve months' exposure to severe conditions in laboratory work could be regarded as fairly rigorous and not unduly hasty in comparison with much of the published laboratory results on stress-corrosion in light alloys. But users frequently desire the materials to last much longer than a year, and even when they would, if possible, arrange for the main tensile stresses on extruded material in service to be applied in the direction of extrusion, this cannot always be done. Sometimes users of equipment expose it to conditions of service which are quite severe as regards corrosion, stress-corrosion, &c.

A good deal of the early experience of wrought light alloys in engineering applications was obtained on Duralumin, and in the course of this its high resistance to stress-cracking and stress-corrosion cracking in the solution heat-treated, quenched, and naturally aged condition came to be recognized. Many investigators, including my colleagues and myself, have taken the performance of this material as a useful basis for comparison with that of other materials. In such work there

\* Research Laboratories, Société Anonyme pour l'Industrie de l'Aluminium, Neuhausen, Switzerland.

† F. Bollenrath, W. Bungardt, and H. Cornelius, *Z. Metallkunde*, 1944, **36**, 73.

‡ F. Bollenrath and H. Gröber, *ibid.*, 1944, **36**, 187.

§ P. Brenner, *Aluminium*, 1943, **25**, 346.

§ P. Brenner, *Z. Metallkunde*, 1953, **44**, 85.

|| K. Matthaes, *Jahrbuch Lilienthal-Ges. Luftfahrt.*, 1936, 404.

¶ Chief Metallurgist and Head of Laboratories, International Alloys, Ltd., Aylesbury, Bucks.

\*\* Director of Materials, Research and Development (Air). Ministry of Supply.



is scope for arranging similarity of shape, form, and general method of manufacture. Details, such as the application of tensile over-strain for purposes of straightening, may be found to be of significance.

Long experience of quenched and naturally aged Duralumins indicates that material having intrinsically high resistance to intercrystalline corrosion under the influence of marine conditions, also has the capacity to withstand high stresses applied in directions normal to that of extrusion under those conditions. No doubt the authors intend conclusion (2) (p. 431) to be understood to apply only to the material and conditions of the work which they now describe, but it is to be hoped that it will not be taken otherwise. In relation to the material studied and the prevailing conditions, the results obtained are both interesting and useful, especially as the applied stresses were under control throughout. The authors' results on sprayed coatings certainly indicate a considerable degree of protection to be achievable by the use of commercial aluminium or 1% zinc alloy coatings applied by spraying.

Dr.-Ing. H. VOSSKÜHLER\*: I read the paper with much interest since I have worked for many years in this field.

As regards the effect of working direction, my own investigations have shown the importance of *Korngränzendichte*, that is, the number of grain boundaries cut by a line of definite length in the direction of stress on the surface of a specimen.

In general, grains become stretched in the working direction and are longer in this direction than in the transverse one. By stressing in the longitudinal direction, therefore, only a few grain boundaries are involved, while in the transverse direction many more are affected. Therefore the susceptibility to stress-corrosion is much greater in the transverse than in the longitudinal direction.

Furthermore, the material becomes more susceptible in the transverse direction if elongated compounds of manganese, silicon, &c., are present, but this is a matter of structural weakness only and not one of stress-corrosion.

Matthaes has demonstrated the influence of the *Korngränzendichte* in a convincing manner. He painted several stress-corrosion specimens of the same material in such a way that each specimen had an uncoated area, the length of which differed from one specimen to another. Stress-corrosion experiments showed that the greater the length of the uncoated area, the shorter was the life. The explanation is that only a few out of a large number of grain boundaries are susceptible, and that if the number of grain boundaries increases with the greater length of the uncoated area, the tendency to failure increases also.

There is another point I should like to mention, that is, the very marked difference in stress-corrosion behaviour between extruded and rolled material of identical composition. I think the varying degree of recrystallization is responsible for this.

We investigated the effect of chromium on the stress-corrosion behaviour of aluminium-zinc-magnesium and found that low chromium contents did not increase the life of specimens, whereas larger additions did so. X-ray patterns showed that the specimens with a short life had recrystallized, whereas those with a long life had not done so.

In my opinion many factors influence stress-corrosion behaviour, *Korngränzendichte* and recrystallization being only two of them.

Mr. LIDDIARD (*in reply*): I regret that it has not been possible to consult with my co-author, Miss Bell, in formulating this reply.

Dr. Evans's comments are much appreciated, and I agree with all the opinions expressed. However, the suggestion that a more dilute salt solution might form a more stringent test may not be valid, since there would be no opportunity for the aluminium corrosion products to pass away as a

colloidal solution, as in the experiments of Beck, Keihn, and Gold. In any case, the conditions of exposure using a daily salt spray would tend to cause a concentration of salt solution by evaporation, even if one started with a relatively dilute solution.

Dr. Evans's remarks on the susceptible zones are particularly interesting, but I believe that more work is necessary to identify the nature of these zones. Mr. Chadwick, in his contribution, obviously assumes that the zones are essentially crystal boundaries and that if recrystallization takes place which results in an equiaxed crystal structure, the susceptible zones disappear. I have some doubt on this point. The photomicrograph reproduced as Fig. G (Plate XCVIII) shows that there can be marked directionality of transcrystalline attack in an extruded aluminium-copper alloy. This photomicrograph was obtained in the course of an investigation into the corrosion and stress-corrosion characteristics of specimens of an extruded 2% copper-1% magnesium-1% silicon alloy, on the surface of which there was the familiar zone of coarse equiaxed crystal structure of varying thicknesses mentioned by Mr. Chadwick. No case of stress-corrosion failure was observed in this material, which was stressed at a load corresponding to the 0.1% proof stress in four-point bending, despite the presence of the coarse recrystallized zone on the outside. Several specimens, however, showed marked layer corrosion. The most severe layer corrosion seems to occur only when susceptible zones coincide with grain boundaries. The time to onset of severe layer corrosion appeared to be longer with greater thicknesses of the equiaxed zone. In other words, this coarse structure on the outside acted as a barrier to severe layer-type corrosion and was not sufficiently thick in relation to the cross-section of the specimen to cause any appreciable stress-corrosion. While we agree fully with Mr. Chadwick's remarks about the important influence of recrystallization on the tendency to directional stress-corrosion, our experience suggests that once corrosion has penetrated through the coarse equiaxed zone on a normal extrusion, attack then spreads out and stress-corrosion virtually ceases, although layer corrosion can be serious.

The paper by Hooker and Waisman offers a most useful confirmation of the suggestion that both layer and stress-corrosion can be prevented by metal spraying, a point initially brought out by Dr. Champion, who asked if we could explain why the thinner sheet was more susceptible than the 0.2-in. manganese-bearing sheet. The tendency with the normal manganese-type sheet was for the susceptibility to stress-corrosion to decrease slightly with increasing thickness, but no such tendency was found with the low-manganese material. It was observed, as illustrated in Fig. 2 (Plate LXVII) of the paper, that the 0.2-in. manganese-containing sheet retained some degree of directionality, and we formed the opinion that the intermediate working and annealing which took place on rolling down the thin-gauge sheet tended to reduce the directionality. In my opinion, the susceptible zones are due partly to variations in composition from layer to layer, particularly in copper content, and partly to preferential grain-boundary orientation. The former, I believe, arises from the original ingot and tends to be evened out with repeated working and annealing. The experiments on manganese-free material were carried out solely to study the effects of an alloying constituent which raised the recrystallization temperature and thereby favoured directionality. If the impression was given that directionality was necessarily undesirable, this was because we were anxious to emphasize the fact that even if susceptibility to stress-corrosion is avoided by conferring marked directionality, as, for example, by extrusion, in so doing one may increase the susceptibility to another form of attack which under unstressed corrosive conditions can be more serious, namely, exfoliation or layer corrosion.

\* Wieland-Werke A.G., Ulm/Donau, Germany.

Dr. Doyle commented on the good reproducibility of the results. His doubts arose from tests which he had carried out on the aluminium-zinc-magnesium alloys, and he may be relieved to know that we also have experienced a very much greater scatter of results with this class of alloy, under the same conditions of test. We do not use controlled temperature and humidity conditions because in our experience such controls decrease the severity of testing and make this less similar to practical conditions. The ideal testing conditions would probably be with controlled variations in both temperature and humidity. We think that the degree of reproducibility obtained was due partly to the use of material from the same initial cast throughout. We did not measure the 0.1% proof values of our materials, because corroded material may break with little or no elongation, and the measurement of proof stress becomes difficult. There seemed therefore to be little point in ascertaining these values in the uncorroded condition. The differences between the results of bending and direct-tension tests are attributed to the fact that the flat bend specimens were more nearly parallel to the surfaces of extrusions than the longitudinal tensile specimens, and susceptible zones therefore rarely cut the surface of the bend specimens at points of maximum stress. With cylindrical specimens, on the other hand, all the susceptible planes would cut the cylindrical surface at some point. In cases where flat specimens were used, the differences between direct tension and four-point loading are rather less marked, but still appear to be significant, and this is attributed to shear stress in bending which tends to assist the lateral spread of attack whenever there is directionality. It was not possible to examine the unfailed bend-test specimens for cracks, because the amount of general corrosion that took place was fairly considerable, and any specimens which had been exposed for a year showed sufficient corrosion from the surface to mask any cracking.

Mr. Grainger's results are of great interest and emphasize how necessary it is to take into account the possible influence of alloying additions on the directionality of structure, and to keep this in mind in assessing the effect of these additions on susceptibility to stress-corrosion. The addition of chromium to the aluminium-zinc-magnesium-type alloys has often been stated to improve corrosion- and stress-corrosion-resistance, but Mr. Grainger's photographs show that this may not be true if stress is applied normal to the direction of working.

I agree with Dr. Parker that when comparing stress-corrosion susceptibility of different materials, results obtained at the lower stresses may be a little more discriminating, but I am of the opinion that the results obtained using relatively high stresses on both the low- and normal-manganese materials provide useful and unclouded evidence of the difference between the stress-corrosion behaviour in the longitudinal and transverse directions of each material.

The main object in carrying out tensile tests on specimens corroded unstressed was to provide evidence of true stress-corrosion and to show that the material when corroded unstressed for a similar period would support a higher load than the specimen stressed and corroded simultaneously. The object was not primarily to explore the difference between low- and normal-manganese material. In fact, care has been taken

not to draw any comparisons or conclusions as to the desirability or otherwise of manganese additions. The very low figure for elongation recorded for one specimen of the normal-manganese material corroded unstressed is, we believe, abnormal, and due perhaps to localized corrosion. With the relatively high-strength, normal-manganese material there is likely to be a greater susceptibility to notch effect as a result of localized corrosion, and we should expect a corrosion pit of identical geometry to have a greater effect on the strength and elongation of the higher-strength material than on the softer and more ductile low-manganese alloy.

I am grateful for Dr. Rohner's contribution. The methods of stress-corrosion testing adopted by Bollenrath and his collaborators were rather different from those which we employed, and no direct comparison was made between extruded and sheet material from the same original billet. The conclusion, quoted by Dr. Rohner, that specimens cut from extrusions of small cross-section were less susceptible to stress-corrosion than those from extrusions of larger cross-section, also agrees with our findings. In both atmospheric and laboratory tests we have found complete resistance to stress-corrosion in cases where 0.1-in.-thick extrusions were tested in bending. Taking specimens from an extrusion always results in susceptible zones cutting the surface in the way described by Dr. Evans. Furthermore, in the absence of recrystallization, there is a tendency for directional effects to be more marked near the surface of the extrusion than in the centre.

Dr. Scheuer raises the question whether susceptibility to stress-corrosion is due to directionality of recrystallized grain boundaries or to the original eutectic network. In our opinion, both factors can play a part and much will depend upon whether or not the material is in a condition of grain-boundary susceptibility.

With regard to Dr. Sutton's remarks, I would emphasize that this paper forms part of an investigation on the corrosion of aluminium-copper-magnesium alloys and aluminium-magnesium-silicon alloys which has already extended over four years and will continue for eight years, and which includes atmospheric tests at Sheffield and Hayling Island. In these tests, hundreds of extruded specimens have been stressed in four-point bending at stresses corresponding to the 0.1% proof stress, and in no case has there been any evidence of stress-corrosion failure or of accelerated corrosion damage by stress. In his original paper, Metcalfe\* attributed this result to the strong directionality of the extruded material, and the object of the work described in our paper was to demonstrate in laboratory tests the effect of this directionality. We are of the opinion that conclusion (2) (p. 431) is of general applicability to these alloys, provided that they are stressed in the form of extrusions and that pieces are not cut out of them, and provided also that they are not treated in such a way as to destroy their directional properties, e.g. by straining and recrystallizing in the manner suggested by Mr. Chadwick, or by welding. Nevertheless, extruded material showing marked directionality may be susceptible to the severe exfoliation (layer corrosion) which can, in some circumstances, be as dangerous as stress-corrosion.

I fully agree with Dr. Vosskuhler's remarks.

\* G. J. Metcalfe, *J. Inst. Metals*, 1952-53, **81**, 269.



## Discussion

## Staining of Clad Aluminium Alloy Sheets During Salt-Bath Heat-Treatment

By E. C. WILLIAMS and H. J. G. CHALLIS

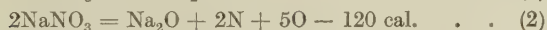
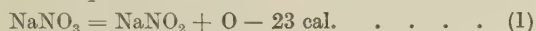
(Journal, this vol., p. 465)

Dr. F. ROHNER\* (Member): There are considerable differences in the composition of salt baths used in different plants, and it is to be hoped that the discussion of this paper will lead to an evaluation of their merits. Mr. Williams and Mr. Challis advocate straight sodium nitrate baths. They have shown that in their case the free alkali content, developed by decomposition of the nitrate, is responsible for the staining. It is, however, not yet clear whether for other bath compositions and working conditions the same is true. It is to be hoped that the simple method for the determination of free alkali given in the appendix to the paper will encourage work in this direction.

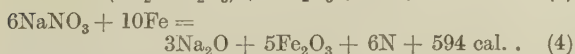
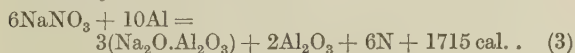
I am much interested in the authors' electron-diffraction examination of the stained surfaces. The fine diffraction patterns reproduced in the paper indicate that the instantaneous type of stain consists of amorphous alumina, while the immersion type consists of sodium aluminate. The application of electron diffraction to metallurgical problems is still infrequent, and some details about the apparatus and the technique used would be welcome. I assume the diffraction patterns illustrating this paper have been taken with a hot-cathode diffractograph.

In their introduction, the authors state that "the form in which free alkali actually exists in the molten salt is unknown". I think, however, that any thermal decomposition or reduction leads primarily to the oxide  $\text{Na}_2\text{O}$ , which by reaction with moisture in the air may be partially or wholly hydrated to form  $\text{NaOH}$ :

## Thermal decomposition:



## Reduction by Al or Fe:



I admit that chemical formulæ always represent idealizations, but I should not hesitate to describe the free alkali in this case as  $\text{Na}_2\text{O}$ , which may be partially hydrated to  $\text{NaOH}$ .

Some twenty years ago over-heating of salt baths or other inappropriate working conditions from time to time caused explosions. Modern salt baths with electric immersion-heaters and up-to-date temperature control are, however, free from such hazards.

The composition we originally used for salt baths was 50% sodium nitrate plus 50% potassium nitrate, with a melting point of  $220^\circ\text{C}$ . Potassium nitrate is much more expensive than sodium nitrate. A change was therefore made to an 80:20 composition, with a melting point of  $270^\circ\text{C}$ . Later, we added 5% potassium bichromate to this nitrate mixture. Staining of sheets, which was not insignificant at that time, could be considerably reduced by this bichromate addition. This effect may be due to the well-known inhibiting effect of chromates, or to a neutralization of alkali effected by the bichromate. At present we are working with 90% sodium

nitrate plus 10% sodium nitrite. Troubles with staining are not serious but in the light of Mr. Williams and Mr. Challis's paper we envisage a change to straight sodium nitrate baths.

Mr. R. CHADWICK,† M.A., F.I.M. (Member): As so often happens, the operation of salt baths involves two complementary requirements. From the point of view of preserving the mild-steel bath and internal fittings, nitrite additions are invaluable but, as the authors point out, decomposition products are detrimental to the light alloy, causing staining. To indicate just how valuable nitrite additions can some-

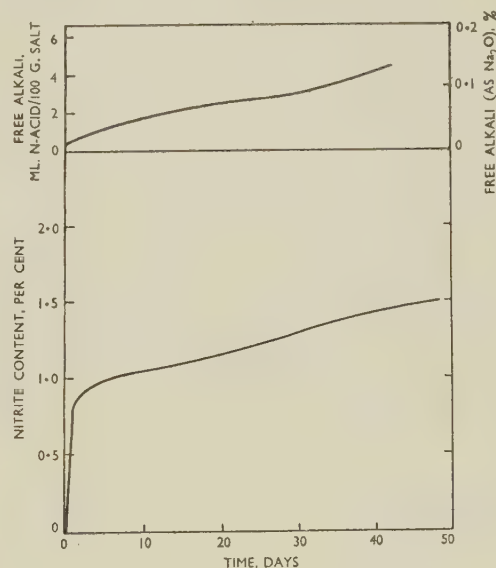


FIG. A.—Decomposition of Fresh Sodium Nitrate in 15-Ton Gas-Fired Salt Bath at  $500^\circ\text{C}$ . (Chadwick.)

times be, it is interesting to recall experience with a particular salt bath which was started up during the war, using straight sodium nitrate. The 26-ft.-long bath, fabricated from  $1\frac{1}{8}$ -in. mild-steel plate and fired by a double bank of gas burners, was severely attacked on the side walls, and had to be taken out of commission after 95 days' continuous operation, while a replacement bath suffered similar damage after only 65 days. From studies of the known chemistry of the thermal decomposition of sodium nitrate, and from laboratory-scale experiments with nitrate/nitrite mixtures, it seemed clear that the oxidizing tendency of nitrate would be reduced by a nitrite addition, and in fact a third steel bath installed under the same operating conditions, except for the addition of 6% of sodium nitrite, remained virtually unattacked after a year.

Mr. Williams and Mr. Challis on p. 469 state that the presence of sodium nitrite appears to be the factor promoting high alkalinity, but they do not draw the obvious inference. Decomposition, which has been studied by Pretsch‡ and by

\* Research Laboratories, Société Anonyme pour l'Industrie de l'Aluminium, Neuhausen, Switzerland.

† Assistant Research Manager, Imperial Chemical Industries Ltd., Metals Division, Birmingham.

‡ B. Pretsch, *Metallwirtschaft*, 1935, 14, 703.

Leschewski and Degenhard,\* is a two-stage process, the nitrate first of all losing oxygen, evolved normally as a gas, to give nitrite, and the nitrite decomposing further to give sodium oxide with the evolution of nitrous oxide fumes. Some data which I obtained on a large gas-fired salt bath are reproduced in Fig. A. A concentration of 0.75% of nitrite was attained in the first 24 hr., with visible evolution of oxygen gas. Thereafter the nitrite content quickly settled down to a steady value of about 1% under normal conditions, involving some drag-out and daily replenishment with fresh sodium nitrate. As would be expected, however, alkali content increased in a steady manner, and showed no sharp initial rise. It is also interesting to note from other small-scale experiments that in nitrate/nitrite mixtures heated in air, a balanced reaction occurs, so that if more than about 10% of nitrite is present, oxidation to nitrate takes place as indicated in Fig. B. Similar but slower changes occur in industrial salt baths, and attempts to maintain nitrite contents of 20% and over proved completely unsuccessful.

These data indicate that the oxidizing character of the bath is diminished by quite a small nitrite addition, and it is probable that, except in the most severe cases, some 2-3% of nitrite would be sufficient to protect steelwork from scaling, without seriously raising the alkali content, since 1% or so of nitrite is likely to be present anyway. Data on the relative decomposition of sodium and potassium salts (Fig. C),\* show that in respect of alkali formation, the potassium salt is to be preferred, indicating a further possible means of controlling alkalinity, although of course at considerably enhanced cost.

While the role of free alkali in staining is clearly demonstrated, one wonders whether there are not good grounds for thinking that water also plays an important part. There would appear, indeed, to be a strong analogy with the fused chloride/fluoride baths used in the brazing of aluminium. Part of the water in the solid salts is retained on melting, and in fact water is picked up from the atmosphere at a temperature as high as 600° C., aluminium components being severely attacked unless very careful and thorough dehydration is first carried out. It seems highly probable that a similar retention of water occurs in sodium nitrate/nitrite mixtures and, by analogy, plays a part in the staining. Indeed, the addition of caustic soda shown by Mr. Williams and Mr. Challis to

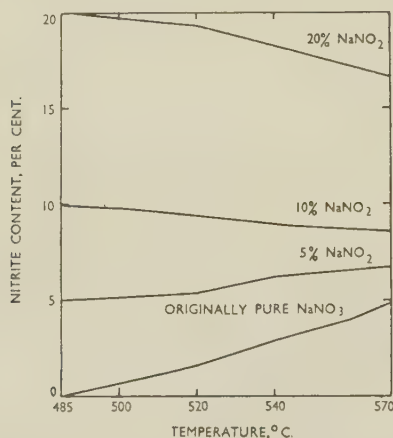


FIG. B.—Change in Composition of Sodium Nitrate/Sodium Nitrite Mixture, 8-kg. Charges, After 24 Hr. in Iron Container. (Chadwick.)

cause staining involves a water addition. Adsorbed water may also be present on thin sheet surfaces and is likely to prove of at least equal significance. For example, sheets splashed with water shortly before heat-treatment are known

to stain more readily, and the splash pattern may even be revealed by salt-bath heat-treatment; again, the authors refer to the staining effect of moisture on chains and cradle fittings. Furthermore, the negative temperature coefficient of the staining reaction would appear to require further

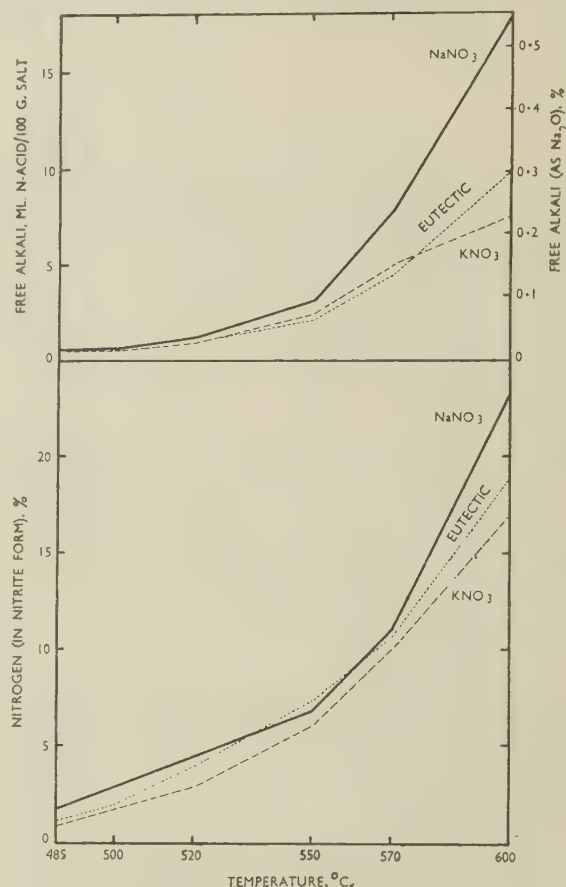


FIG. C.—Decomposition of Sodium and Potassium Nitrates, 80-g. Charges, After 8 Days in Iron Containers. (Leschewski and Degenhard cited by Chadwick.)

explanation than the authors' somewhat doubtful differentiation of "instantaneous" and "immersion" types of staining, especially since the reaction between sodium nitrate and aluminium at higher temperatures has, in fact, a positive temperature coefficient. However, if water is assumed to take part, then it would clearly be dispelled or diffuse away more slowly at low than at high temperatures, allowing a longer period for attack to occur.

Dr. F. A. CHAMPION,† A.R.C.S., F.I.M. (Member): I agree with the authors that nitrite has only a slight direct effect on staining and that its importance lies in generating alkali, but I do not think that the general alkalinity of the bath provides a satisfactory measure of the latter effect. Our experience suggests that staining occurs where sheets are in very close proximity as a result of distortion. Under these local conditions the ratio of metal surface to salt volume is high, and consequently the alkalinity developed must be locally much higher than the general level in the bath. This also accounts for the irregularity of the staining. Oil is discounted by the authors in their introduction, but included as a factor in their conclusions. We find that it is important and assume that,

\* K. Leschewski and W. Degenhard, *Z. anorg. Chem.*, 1938, 239, 17.

† Research Laboratories of The British Aluminium Co., Ltd., Gerrards Cross, Bucks.



under the local high metal-surface: salt-volume ratio referred to above, the oil produces a local high nitrite concentration.

I agree that the use of bichromates or bisulphates is impractical owing to the consequent increase in evolution of nitrous fumes, but have the authors any experience on the use of chromates to prevent nitrite formation and hence the development of alkalinity?

Mr. Williams and Mr. Challis discount diffusion as a factor in staining. I suggest that, as with all corrosion phenomena, staining is dependent both on the conditions in the bath (e.g. alkalinity) and on the susceptibility of the metal, and that the effects of these two classes of factor are, in a qualitative sense, additive. The presence of  $\text{CuAl}_2$  or  $\text{Mg}_2\text{Si}$  in the alloy heightens the susceptibility of the metal to staining, and hence diffusion of these phases to the surface of clad metal increases the risk of its occurring. Conversely, the absence of staining does not show absence of diffusion, since staining conditions may not prevail in the bath.

Mr. A. J. FIELD,\* M.C., B.Sc., F.I.M. (Member): The authors refer to "instantaneous" and "immersion" staining, the former caused at the moment of immersion and the latter on prolonged immersion. Heating of the aluminium sheets on descending into the salt is very rapid, and, although sheets are not usually closely observed at this stage, owing to the risk of splashing, there appears to be little solidification of salt. Furthermore, if the sheet has a uniform surface, and is free from contact with other sheets, it is not easy to see how patchy stains occur in the molten salt, which is of uniform composition. The formation of a line of stain when the descent is stopped is understandable, as staining occurs at any "water-line". Sheets entering the salt, which are in contact with one another at certain points may tend to stain at these areas, but this does not invariably occur.

The authors draw attention to a difference in the type of staining at lower and higher salt-bath temperatures. We have noticed that patchy films of oil left on a sheet tend to cause slight corresponding stains at the lower temperatures, and that the effect is much less at the normal heat-treatment temperature of about 500° C.

In the factory with which I am connected, we have long adopted the simple method of making only 100% nitrate of soda additions to the salt bath, after the original make-up with 10% sodium nitrite, and we experience very little trouble with staining on clad alloys. Even after many months of use with 100% nitrate additions, the iron plate of the tanks and the nickel of the heater tubes does not appear to be attacked to any detrimental extent.

The paper refers to staining on clad alloys only. These constitute the bulk of the strong-alloy business, and staining with this material is not a serious problem, provided that adequate washing is carried out afterwards. Staining in 100% nitrate baths of unclad alloys, covering large broken areas, is of much more common occurrence, and it would be of interest to know how this might be avoided.

Mr. H. TAYLOR † (Member): This paper is most interesting and valuable in that it has provoked new thought upon what is an expensive, although spasmodic, problem with most manufacturers of strong-alloy sheet.

Since the paper was published we have repeated a great deal of work described in it, with one major difference, namely that Mr. Williams and Mr. Challis operated a salt bath which included an addition of 10% sodium nitrite, whereas we used a straight sodium nitrate bath. Incidentally, to-day there seems to be no case for the addition of sodium nitrite, since the majority of the salt baths in operation are of the electric-immersion type, with which an extremely long life of bath can be obtained, using straight sodium nitrate. It has long been understood that the presence of nitrite very greatly increases the tendency to staining, and that it is probably

cheaper to use straight sodium nitrate and so maintain the staining at a low level, with possibly some shortening of the life of the container.

In general, the results working with a 5-cwt. test-piece salt bath containing straight sodium nitrate are similar to those obtained by the authors. The analysis of the salt in this furnace, which had been in use for a long time, showed sodium nitrite 1.6 and combined alkali 1.8%. Staining was found to occur at a minimum level of 0.06% free alkali. This content was attained by the addition of caustic soda pellets and was checked by the method of analysis provided by Mr. Williams and Mr. Challis.

This tolerable free-alkali content in a straight sodium nitrate bath is approximately twice as great as that found by the authors for the onset of staining in sodium nitrate with nitrite addition.

Now it is known that spasmodic staining occurs with straight sodium nitrate heat-treatment baths, where the free-alkali content seldom exceeds 0.01%, and it is suggested by the authors (p. 468) that staining at this level is "confined to areas which had been moistened and cooled by water remaining in the cradles and retaining chains after quenching previous batches". We confirm that the presence of moisture will induce stains from an otherwise non-staining bath, but suggest that this is because of the formation of free alkali as a result of some reaction with the steam produced. Steam, superheated to about 500° C., was passed through molten salt held at about the same temperature, and it was found that with small effort the free alkali was increased from zero to 0.01%. It is also confirmed that passing carbon dioxide reduces the free-alkali content, but if the salt bath is merely allowed to stand, then the free-alkali content falls. In a period of six days' standing, the free-alkali content fell from 0.25 to 0.04%. It was also found that bubbling air through the bath accelerates the normal tendency towards a reduction of the free-alkali content.

Summarizing all the evidence now available, the following conclusions can be drawn:

- (1) It is preferable to use straight sodium nitrate baths, i.e. without sodium nitrite additions.
- (2) Care should be taken to see that all cradles and loads are free of moisture before they are immersed in the heat-treatment furnace; if this is done, there will be no increase in the free-alkali content and no staining will occur.
- (3) If the free-alkali content of a straight sodium nitrate bath increases to such an extent that staining of Alclad sheet ensues, the content can be reduced in the manner indicated by the authors or by the two slower methods of allowing the bath to stand un-used or of bubbling air through the molten salt.

Mr. H. T. ROBERTS,‡ A.I.M. (Member): The particular plant with which I have been associated for a number of years is in the fortunate position of operating salt baths with electric-immersion heating, using sodium nitrate as the heat-transfer medium. This is a combination which the authors infer will give the greatest freedom from white stains. Our own experience of heat-treating Alclad strong alloys agrees with their findings.

For the most part difficulties were confined to a time when supplies of super-refined or synthetic sodium nitrate were difficult to obtain. During this period less highly refined natural nitrate was used and this gave rise to great a deal of staining trouble. Contrary to the authors' experience, however, we found that staining was most pronounced on the first load heat-treated immediately after making additions of fresh salt, and decreased in intensity as subsequent loads were treated. In fact, it was possible to relieve the situation by treating scrap loads immediately after topping-up, production batches being treated only when the bath had been allowed time to settle down.

It was thought at the time that staining might have been

\* Works Manager, The British Aluminium Co., Ltd., Falkirk.

† Chief Metallurgist, Northern Aluminium Co., Ltd.,

Banbury, Oxon.

‡ Metallurgist, Northern Aluminium Co., Ltd., Rogerstone, Mon.



attributable to undesirable impurities in the natural salt, but routine chemical analysis of the bath samples did not reveal any abnormalities. It would be interesting to hear the authors' views on this point.

I should also like to comment on the authors' omission of the presence of water from their list of the possible causes of staining.

The AUTHORS (*in reply*): Dr. Rohner suggests that we have been diffident in associating free alkali, as determined by titration, with sodium oxide, but that we nevertheless expressed the results of analysis as if it consisted entirely of this compound. We were not prepared to dogmatize on this point in the absence of clear evidence pointing to the existence of sodium in salt baths.

Mr. Chadwick has provided valuable information concerning equilibria in salt mixtures, and this indicates that alkalinity arises simply from decomposition of nitrite. He suggests that water may play a part in staining to a greater extent than we have thought. In particular, he considers that the inverse temperature-dependence of staining which we observed may be explained by the more rapid expulsion of adsorbed moisture from the surface of sheets at the higher temperatures. We argue that since the presence of free alkali is an essential condition and, furthermore, since staining is very rapid, any preliminary reaction of the salt with water, which might raise the alkalinity to a level sufficient to cause staining, would have to occur at an equally rapid rate. From our experience it can be said that if the bath is in a non-staining condition, i.e. without a high free-alkali content, moisture on the sheets does not produce staining. On the other hand, if the free alkali exceeds a certain value, then moisture on the sheet surface can aggravate the effect. We prefer to regard the effect of temperature in terms of the adsorption on the surface of the alkaline constituent, which should be greater at the lower temperature, rather than the converse desorption of water. No reference has been made to this view in the paper, because we did not set out to investigate the ultimate reaction.

Dr. Champion disagrees with us concerning the importance we attach to a general level of alkalinity and quotes from his experience that staining is more probable when sheets are in close proximity. He then suggests that the high ratio of metal surface to salt volume leads to a local increase in alkalinity. Again, we can reply by referring to the rapidity of the staining reaction; this seems to preclude the suggested localized formation of alkali which, in our opinion, would have to occur at an equally rapid rate. The fact that staining is more noticeable when sheets are close together in the bath is explained, we believe, not by the metal-surface : salt-volume ratio, but by the greater mass of cold metal and the resulting faster fall in temperature. Instantaneous staining does not occur unless the salt in contact with the metal is rapidly

chilled. We discounted oil as a direct factor in staining as a result of experiments in which oiled sheets were treated in a non-staining bath and on withdrawal were found to be quite clean and not stained, but we have included it as a factor which tends to increase alkalinity by its action on the salt. With regard to diffusion of alloying elements, careful spectrographic and metallographic examination was carried out in an attempt to detect diffusion into the cladding, but the results were negative. It is not denied that with over-long heat-treatments the surface may be more liable to staining and corrosion after treatment. We do not believe that diffusion of alloying elements aggravates the type of staining in salt-baths which we have called instantaneous, because we are satisfied that aluminium is the major metallic radical in the substance of the stains. In fact, similar stains were obtained on sheets of pure aluminium. We have no experience regarding the possible effect of chromates in preventing the formation of nitrite.

Mr. Field entertains some doubts regarding the chilling effect on the salt of clad sheets entering a bath. He says that the metal will be heated very rapidly, but we may well ask, how rapidly? The remarkable feature of this staining is its rapidity, and it was this which led us to use the term "instantaneous" in describing it. We do not agree that it is difficult to conceive of patchy stains occurring when the sheets appear to have a uniform surface finish. Metal surface phenomena are often heterogeneous and the appearance of surfaces to the unaided eye is a poor criterion of uniformity in respect of physical or chemical properties. Mr. Field refers to the staining of unclad sheets during heat-treatment. Alkali staining is of less significance with such materials, which are stained mainly as a result of diffusion of alloying elements, such as magnesium and copper, to the surface. This effect is difficult to avoid and can be minimized only by careful adjustment of immersion time relative to the heat-treatment temperature. Adequate spacing of sheets avoids contact stains and ensures a more uniform surface finish.

We are particularly pleased to learn from Mr. Taylor that he has confirmed our work. We note with interest that spasmodic staining can occur even in straight nitrate baths. He has also established that moisture in the form of superheated steam increases the free-alkali content, and it would be of further interest to know the rate at which this increase occurs. In his summarized conclusions, however, Mr. Taylor has omitted one of the most important factors leading to increased alkalinity, that is, overheating of salt, which should be avoided when using either straight nitrate or nitrate/nitrite mixtures.

Mr. Roberts refers to the interesting observation that staining was most pronounced, in his experience, immediately after making additions of fresh salt. We suggest that since unrefined salt was used impurities, possibly in the form of free alkali, were responsible.

## Discussion

# The Constitution of Titanium Alloys \*

Dr. N. P. ALLEN,† M.Met., F.I.M. (Member): An interesting method has been used by Mr. T. H. Schofield at the National Physical Laboratory for determining the liquidus of titanium-oxygen alloys. It is a variant of his method ‡ for determining the melting point of pure titanium, in which a small cylinder of the metal with a centrally drilled hole is heated rapidly, whilst the temperature of the central hole is

observed with an optical pyrometer. The melting point of the metal is taken to be the temperature at which liquid metal is first seen to rise in the hole. When this experiment is made with an alloy, the temperature at which liquid metal rises in the hole can be clearly observed, but examination of the sample after cooling shows that the metal filling the hole differs in composition from the average of the alloy. Its composition

(Mrs.) B. Mellish (this vol., p. 534).

† Superintendent, Metallurgy Division, National Physical Laboratory, Teddington.

‡ T. H. Schofield and A. E. Bacon, *J. Inst. Metals*, this vol., p. 167.

\* Joint discussion on the following papers published in the *Journal*: H. W. Wornor (1952-53, 81, 521, and this vol., p. 222); A. D. McQuillan (this vol., p. 47); (Mrs.) M. K. McQuillan (this vol., pp. 433 and 511); O. Kubaschewski and W. A. Dench (this vol., p. 87); W. Hume-Rothery and D. M. Poole (this vol., p. 490); N. P. Allen, T. H. Schofield, and



can, however, be estimated by hardness testing or otherwise, and can be regarded as the composition in equilibrium with solid metal at the observed temperature.

Many of the discrepancies between the equilibrium diagrams reported by various observers are no doubt due to the differences in purity of the titanium employed. The oxygen and nitrogen contents have varied, and any failure of the very troublesome experimental precautions is apt to introduce further quantities of these elements. Both elements have a marked tendency to increase the extent of the  $(\alpha + \beta)$  range, and to raise the temperature at which  $\alpha$  first appears, so that in general the results that give the shortest  $(\alpha + \beta)$  range and the lowest temperature of the  $\beta/(\alpha + \beta)$  boundary are most likely to be correct.

The work is further complicated by the fact that the alloys may transform either by a nucleation-and-growth mechanism, or by a martensitic transformation. Conditions may be similar to those that exist in the iron-nickel system, in which an alloy may change entirely from  $\gamma$  to martensitic  $\alpha$  on normal cooling, but revert partly to  $\gamma$  on reheating to a temperature well below that at which  $\gamma$  is the sole equilibrium constituent. The formation of  $\beta$  in Mrs. McQuillan's 12% chromium alloy reheated to 652° C. (Fig. 4, Plate LXVIII) does not show that 652° C. is above the  $\beta/(\alpha + \beta)$  boundary at this composition, but only that it is above the  $\alpha/(\alpha + \beta)$  boundary.

The suggestion that clustering accounts for the rapid separation of  $\alpha$  from  $\beta$  during quenching in alloys in which diffusion is slow, is difficult to reconcile with the structures in Figs. 2 and 3 (Plate VII) of Dr. A. D. McQuillan's paper. For clusters of the size of the  $\alpha$  plates shown in these figures would be extremely improbable; and if the clusters are a good deal smaller than the plates, diffusion is still necessary to permit the plates to form. Unless, indeed, the composition of the plates is substantially the same as that of the matrix, in which case there is no need for the clustering hypothesis. Clusters of the size indicated in Fig. 2 should be detectable by X-ray observations at the relevant temperature.

Mrs. M. K. McQUILLAN,\* M.A. (Member): I think that all those who have worked with titanium will agree that one of the outstanding things we have learned in the course of our work is the importance of experimental techniques. The most obvious difficulty is, of course, the prevention of atmospheric contamination at elevated temperatures. Oxygen pick-up is naturally less important when oxygen is one of the constituents of the alloys studied, but considering the readiness with which titanium will take up oxygen, it would be of interest to know to what extent the compositions of the ternary alloys studied by Dr. Allen, Mr. Schofield, and Mrs. Mellish were moved along the oxygen axis by their 6-hr. treatment at 1300° C. in a vacuum of  $10^{-3}$  mm. of mercury. One wonders also whether any nitrogen could have been taken up at the same time. A further difficulty encountered at Birmingham when adding controlled amounts of oxygen to titanium in the form of titanium dioxide, is that of obtaining an oxide free from nitrogen. It has been found that, even when using titanium dioxide of allegedly very high purity, the nitrogen content of the alloys has increased progressively with the oxygen content. Since the oxygen content of the higher-oxygen alloys used in the work on the titanium-iron-oxygen system was obtained by difference, the authors' assurance that no nitrogen contamination could have occurred in this way would be valuable. One more point concerning experimental techniques which may be relevant to the titanium-iron-oxygen alloys is the question of precipitation of phases during quite rapid cooling. We have found that breaking silica specimen tubes under water is not a sufficiently rapid method of quenching to prevent the precipitation of

quite large amounts of non-equilibrium phases in some binary systems of titanium with  $\beta$ -stabilizing elements, and it is possible that the same factors influence the ternary systems. Could there, for instance, be any connection between the precipitation of apparently nucleated  $\alpha$  during quenching after heating at temperatures just above the  $\beta/(\alpha + \beta)$  boundary, observed in the titanium-nickel and titanium-chromium systems, and the statement made by Allen, Schofield, and Mellish (p. 535) to the effect that the microstructure of their specimens cooled from 1300° C. tended to be similar to those quenched from 800° C.?

The question of experimental techniques also arises in connection with Dr. Worner's paper on the titanium-tin system. He himself has drawn attention to the fact that his heat-treatment of these alloys in the temperature range 800°-900° C. was probably of insufficiently long duration. Work now in progress at Birmingham indicates that this was indeed the case. We have investigated the question of heat-treatment time in the titanium-tin system by heating together alloys which have the same composition but, as a result of previous heat-treatment at higher temperatures, have different microstructures, i.e. one is in a single-phase condition and the other in a two-phase condition. When equilibrium is reached, both specimens must contain the same phases. After periods of 2 weeks at 800° C. neither specimen appeared to have changed. Some titanium-tin specimens have now been heated for as long as 5 months at 890° C., and slow changes still seem to be taking place. We suspect that when equilibrium is eventually achieved, our structures will indicate that some modification of present ideas on the equilibrium diagram is necessary.

Dr. H. W. WORNER,† M.Sc. (Member): Dr. A. D. McQuillan's results are of interest to me because I have frequently studied the microstructures of quenched alloys as a means of locating phase boundaries in titanium-rich alloys. Using a technique of quenching described in an earlier paper,‡ I have found that the  $\beta/(\alpha + \beta)$  boundary for an alloy containing 3.7 at.-% nickel (by analysis) lies between 790° and 785° C. The alloy was made by melting iodide-refined titanium with 99.9% grade nickel in an argon-atmosphere arc-furnace. Before the quenching experiments, the alloy was heavily forged at about 800° C., then pickled to remove the surface-oxide layer and heated *in vacuo* for 4 hr. at 1000°-1050° C. Each specimen used in the series of quenching experiments was rapidly reheated into the range 1000°-1050° C., held in this range for an hour, then slowly cooled to the desired temperature, which was maintained for  $\frac{3}{4}$ -1 hr. before quenching.

My result for this 3.7 at.-% nickel alloy is in reasonable agreement with the value of 780° C. reported by Dr. McQuillan § for an alloy containing 3.6 at.-% nickel. The few particles of  $\alpha$  phase observed in the alloy quenched from 785° C. were very much coarser than those shown in Fig. 2, (Plate VII, this vol.) of the paper now under discussion.

Dr. McQuillan has focused attention on an important consideration, and I welcome his paper because it has given me an opportunity of making an additional check on the efficacy of a technique of quenching which I have used extensively.

I am definitely in favour of quoting the temperature range of the  $\alpha \rightleftharpoons \beta$  transformation as a criterion of the purity of titanium used in alloy research. However, certain possible impurities, for example, tin, zirconium, and silver, do not cause a marked spread of the  $(\alpha + \beta)$  field. I therefore consider it advisable to report all the analytical data available, together with the transformation range. The hardness of the metal is also worth reporting, since it may have some significance when considered in relation to the content of impurities.

\* Imperial Chemical Industries, Ltd., Metals Division, Birmingham.

† Physical Metallurgy Section, C.S.I.R.O., Baillieu Laboratory, University of Melbourne.

‡ H. W. Worner, *J. Inst. Metals*, 1952-53, **81**, 521.

§ A. D. McQuillan, *ibid.*, 1951-52, **80**, 363 (Fig. 5, Plate LV).



Dr. W. A. BAKER,\* F.I.M. (Member of Council): Special difficulties are encountered in the melting and heat-treatment of titanium-rich alloys. Simple hardness tests on titanium specimens remelted or re-heat-treated by the techniques used, provide reliable evidence on the adequacy of the precautions taken to avoid contamination, and papers in this field should include the results of such tests or equivalent tests, to demonstrate that the experimental techniques used are above suspicion. In this connection I suggest that specimens heat-treated in conventional furnaces could be rapidly quenched by using longer evacuated silica tubes than usual and arranging for one end to project from the furnace and dip into a bath of Wood's metal, which could be sucked quickly into the tube to produce the drastic quench required, by breaking the end of the tube at the appropriate time.

I entertain some misgivings about the clustering mechanism which Mrs. McQuillan has proposed to account for her observations on the rapidity with which certain  $\beta$ -phase alloys can undergo changes during rapid cooling, because it seems to me that the microstructures developed in such alloys are not readily reconcilable with the hypothesis. The hypothesis would readily explain rapid nucleation of the  $\alpha$  phase, but in its present form it does not account satisfactorily for the growth of the  $\alpha$  particles. The photomicrograph of Fig. 6 (Plate LXVIII) suggests that the least linear dimension of the  $\alpha$  phase in the quenched specimen was about 5  $\mu$ . Is it to be supposed that the chromium-rich clusters are separated by distances of this order of magnitude, or is some other mechanism available to account for the growth of the  $\alpha$ -phase particles from similar titanium-rich regions? It seems to me that if long-range diffusion is to be excluded in accounting for these structures, the microstructure observed in the quenched alloy should reflect the nature of the clustering immediately before the quenching, in which case the microstructure should remain unchanged in a series of specimens quenched at different, but relatively rapid, rates. I would invite Mrs. McQuillan to enlarge on her hypothesis to account for the observed structure in greater detail.

Dr. H. K. HARDY,† M.Sc., A.R.S.M., A.I.M. (Member): The questions I wish to raise concern the new titanium-chromium phase diagram put forward by Mrs. McQuillan. The equilibrium structures at 650° C. are now stated to be: up to 9% chromium,  $\alpha + \beta$ ; 9 to 14% chromium,  $\beta$ ; more than 14% chromium,  $\beta + \text{TiCr}_2$ .

Duwez and Taylor,‡ also using high-purity materials, found that alloys containing 6–8% chromium, heat-treated for 28 days at 650° C., had structures consisting of  $\alpha + \beta + \text{TiCr}_2$ , according to room-temperature X-ray examination. Their alloy with 17% chromium had a microstructure identical with that of Mrs. McQuillan's Fig. 6 (Plate LXVIII) for a 12 at.-% chromium alloy heat-treated for about 6–7 weeks at 590° C. The author's earlier paper§ gives the microstructure (Fig. 9, Plate XLIX) of a titanium–27.5 at.-% chromium alloy quenched from 650° C. as  $\alpha + \text{TiCr}_2$ , although in this case the basis material was of rather lower purity.

Mrs. McQuillan holds the view that titanium–chromium alloys, when quenched from 650° C., undergo a (eutectoid) decomposition at some fairly low temperature. Part of the  $\beta$  is retained, and the remainder decomposes to  $\alpha$  and  $\text{TiCr}_2$ . Whilst the rate of formation of  $\alpha$  may be quite rapid, it is equally necessary that  $\text{TiCr}_2$  should be formed on quite rapid quenching. The isothermal transformation characteristics of some titanium–chromium alloys made from titanium sponge have been reported by Frost *et al.*|| An alloy with 7.5 wt.-%

chromium did not form  $\text{TiCr}_2$  in less than 1 hr. at 570° C. This appears incompatible with the presence of  $\text{TiCr}_2$  in the 6–8% chromium and 27.5% chromium alloys quenched from 650° C., if they had then been in the  $\beta$  field.

I suspect that a titanium–12% chromium alloy has yet to be annealed for a sufficiently long time to reach equilibrium at 650° C. It is possible that the  $\omega$  phase found by Frost,|| or some other metastable phase, becomes very persistent in the region of 10–15% chromium.

Whilst high-temperature X-ray studies are certainly needed to check the equilibrium presence of  $\beta$  below 650° C., I would enter a plea that the understanding of any complex constitutional diagram benefits from a combination of metallographic and X-ray work, even when limited to room temperature.

The hypothesis of clusters in the  $\beta$  solid solution, whether they are titanium-rich or chromium-rich, stands greatly in need of experimental verification. If the atoms remain on the  $\beta$  lattice sites, the small-angle-scatter X-ray method is about the only choice available. Three conditions would have to be fulfilled: (i) the technique must be adapted for the high-temperature examination of reactive materials; (ii) the clusters would have to be within a suitable size-range; and (iii) there must be sufficient difference in scattering power between the solvent and solute atoms. The last condition is not met by titanium–chromium alloy. It would be necessary to choose a system in which the transition element came from the Second Long Period and which, in the author's opinion, exhibits the clustering phenomena.

Dr. P. HERASYMENKO¶ (Member): Dr. A. D. McQuillan has shown previously\*\* that the  $\beta/(\alpha + \beta)$  boundaries for binary alloys containing up to 5 at.-% of chromium, manganese cobalt, and nickel follow a course very close to the idealized boundary for the ideal  $\beta$  solid solution in equilibrium with  $\alpha$  phase containing negligible amounts of solute atoms. In the titanium–iron system, the  $\beta/(\alpha + \beta)$  boundary is higher than the idealized one, and therefore the  $\beta$  phase should considerably deviate from the behaviour of ideal solid solutions.

The course of the  $\beta/(\alpha + \beta)$  boundary for the titanium–chromium system established by Mrs. McQuillan indicates that the behaviour of the  $\beta$  phase in this case shows a deviation from ideality for a solid solution at chromium contents above about 4.5%. The following thermodynamic analysis of the  $\beta/(\alpha + \beta)$  boundaries for the titanium–chromium and titanium–iron systems may be of general interest to the theory of titanium alloys. The data used for this analysis were as follows:

- (1) Heat capacities of pure  $\alpha$ - and  $\beta$ -titanium:

$$\begin{aligned}\alpha\text{-Ti } \dagger\dagger: C_p &= 5.9 \times 2.96 \times 10^{-3} T \\ \beta\text{-Ti } \dagger\dagger: C_p &= 7.525\end{aligned}$$

- (2) Heat of  $\alpha$ - $\beta$  transformation §§:

$$\Delta H^{\circ}_{882.5^{\circ}\text{C.}} = 678 \text{ cal./g.-atom}$$

- (3) The solubility of chromium and iron in the  $\alpha$  phase is assumed negligibly small.

From these data, the free energy of  $\alpha$ -titanium relative to  $\beta$  was found to be:

$$\Delta F^{\circ} = 824 + 9.040T - 2.303 \times 1.625T \log T + 1.48 \times 10^{-3} T^2$$

Applying this equation to the  $\beta/(\alpha + \beta)$  boundaries as found by Dr. A. D. McQuillan and Mrs. McQuillan for the titanium–

\* Research Manager, British Non-Ferrous Metals Research Association, London.

† Senior Metallurgist, Fulmer Research Institute, Ltd., Stoke Poges, Bucks.

‡ P. Duwez and J. L. Taylor, *Trans. Amer. Soc. Metals*, 1952, **44**, 495, 516.

§ M. K. McQuillan, *J. Inst. Metals*, 1951, **79**, 379.

|| P. D. Frost, W. M. Parris, L. L. Hirsch, J. R. Doig, and C. M. Schwartz, *Trans. Amer. Soc. Metals*, 1954, **46**, 231.

¶ Research Division, New York University, U.S.A.

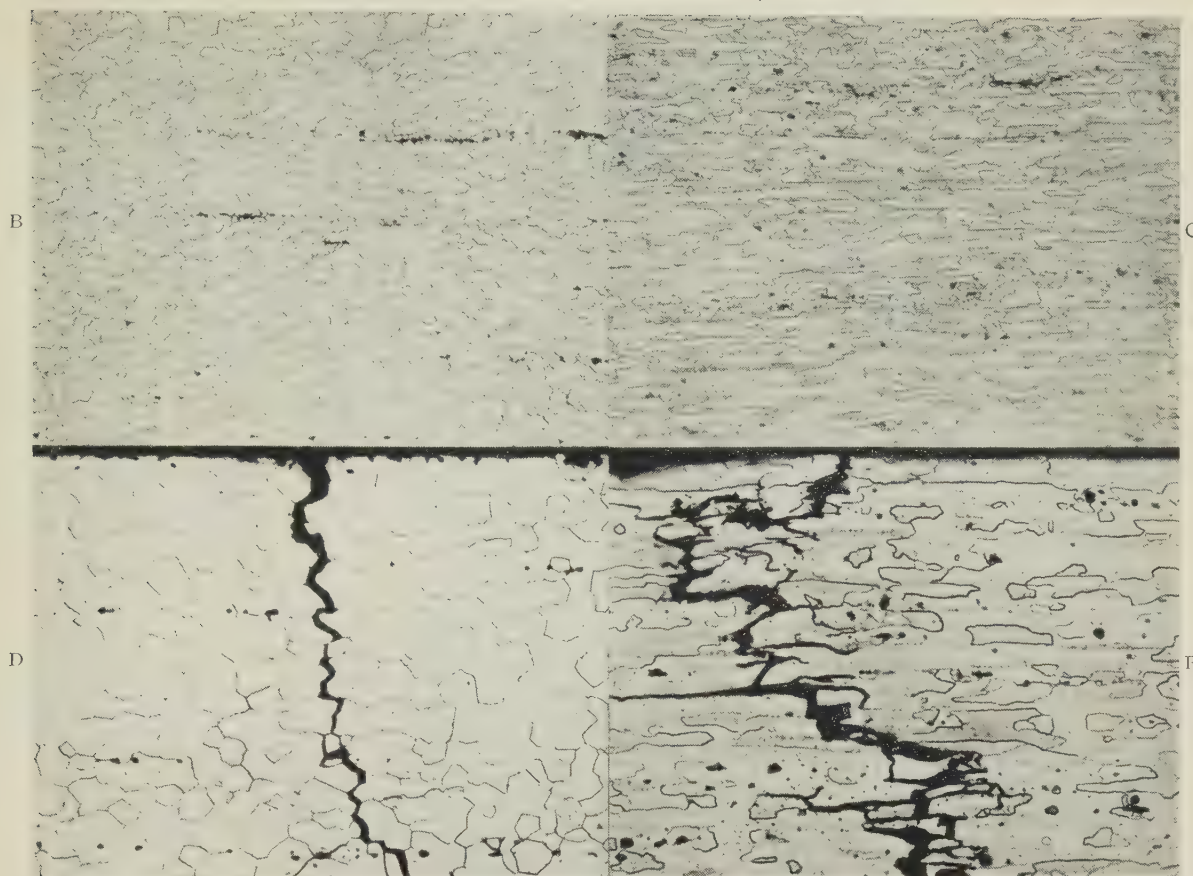
\*\* A. D. McQuillan, *J. Inst. Metals*, 1951–52, **80**, 363.

†† O. Kubaschewski and E. L. Evans "Metallurgical Thermochemistry." 1951: London (Butterworth-Springer, Ltd.).

‡‡ F. M. Jaeger, E. Rosenbohm, and R. Fonteyne, *Proc. K. Acad. Wet. Amsterdam*, 1936, **39**, 445; *Rec. Trav. Chim.*, 1936, **55**, 618.

§§ A. D. McQuillan, *Proc. Roy. Soc.*, 1950, [A], **204**, 309.





FIGS. B-F.—Influences of Manganese and Chromium on the Stress-Corrosion Behaviour of an Aluminium-7% Zinc-2.2% Magnesium-1.3% Copper Alloy. (*Grainger.*)

FIG. B.—Microstructure of alloy containing 0.25% Mn.  $\times 100$ .

FIG. C.—Microstructure of alloy containing 0.25% Mn, 0.25% Cr.  $\times 100$ .

FIG. D.—Stress-corrosion crack in alloy containing 0.25% Mn.  $\times 250$ .

FIG. E.—Stress-corrosion crack in alloy containing 0.25% Mn, 0.25% Cr.  $\times 250$ .

All etched in Keller's reagent.

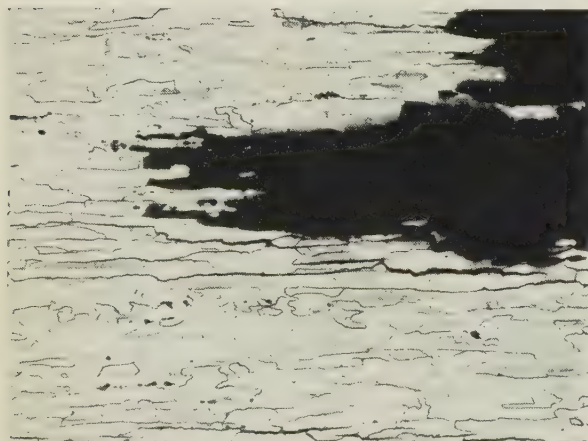


FIG. F.—Corrosion from the Edge of Unstressed Sheet in Alloy Containing 0.25% Mn, 0.25% Cr. Unetched.  $\times 100$ .

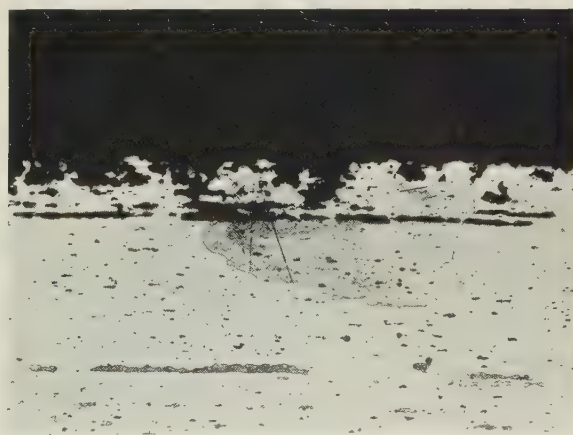


FIG. G.—Transcrystalline Layer Corrosion in Secondary Aluminium Alloy Extrusion (Cu 2.0, Mg 0.70, Si 0.85, Fe 0.40, Mn 0.36%), Press-Quenched and Naturally Aged, After 3 Years' Exposure at Sheffield. Etched in Keller's reagent.  $\times 100$ . (*Authors' reply.*)

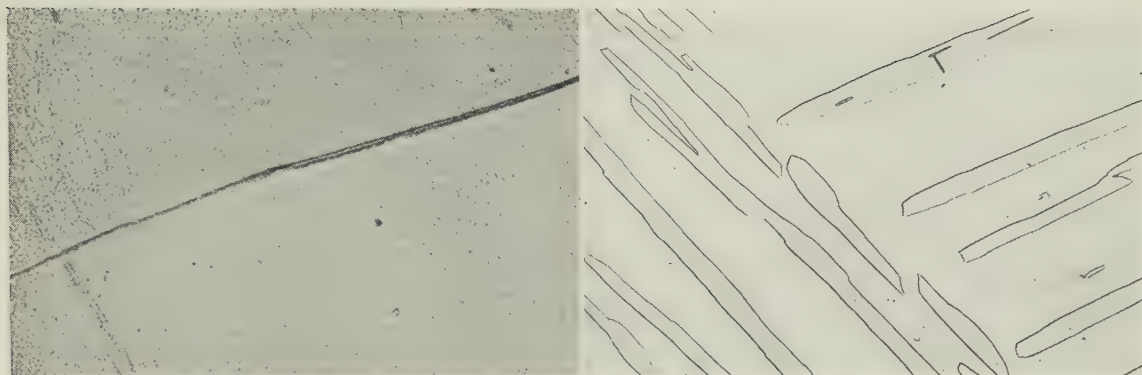
[To face p. 646.



Figs. B-D.—Photomicrographs of Titanium-6 Wt.-% Chromium Alloy, Annealed at 700° C. and Water-Quenched. Etched in 60% glycerine, 20% HF, 20% HNO<sub>3</sub>.  $\times$  250.  
 (*Van Thyne and Rostoker.*)

FIG. B.—Annealed 2 hr. Fine platelets of  $\alpha$  in matrix of retained  $\beta$ .  
 FIG. C.—Annealed 42 hr. Coarsening of  $(\alpha + \beta)$  structure in Fig. B.  
 FIG. D.—Annealed 72 hr. Pronounced coarsening of  $(\alpha + \beta)$  structure.





FIGS. E and F.—Specimens of Titanium-Iron-Oxygen Alloys Water-Quenched from  $1000^{\circ}\text{C}$ . Etched in  $\frac{1}{2}\%$  HF,  $\frac{3}{4}\%$   $\text{HNO}_3$ .  $\times 150$ . (*Allen's reply.*)

FIG. E.—4.17% Fe, 0.37% O.

FIG. F.—3.21% Fe, 1.02% O.

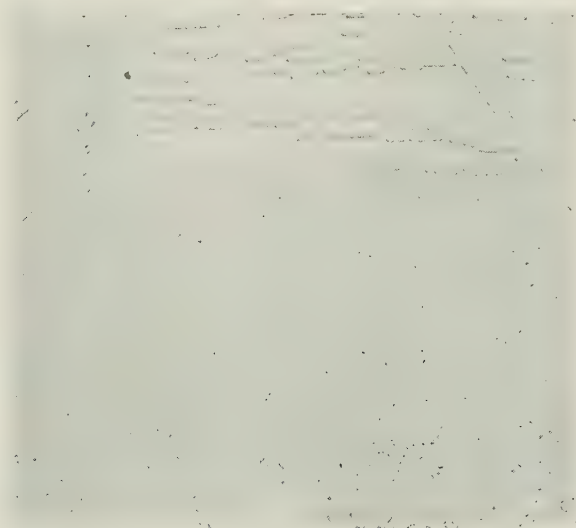


FIG. G.—Titanium-6.5 At.-% Chromium Alloy, Heated at  $693^{\circ}\text{C}$ . for Approx. 1 Week. Rapidly quenched.  $\times 250$ . (*M. K. McQuillan's reply.*)



FIG. B.—Longitudinal Section of Copper Strip Rolled 70%,  
Showing Intense Shear Markings.  $\times 450$ . (*Roberts.*)



iron and titanium-chromium systems, the activities and activity coefficients of titanium in  $\beta$  solid solutions at the temperatures of the  $\beta/(\alpha + \beta)$  boundaries have been calculated for the range of concentrations investigated by both authors. The course of the free energies and of the activity coefficients of titanium in these two systems are shown in the upper sections of Fig. A.

It is seen that the activity coefficient of titanium in the  $\beta$  phase of titanium-chromium alloys is practically equal to unity up to about 4.5 at.-% chromium; the  $\beta$  phase can thus be regarded in this composition range as a nearly ideal solution. Above 4.5 at.-% chromium, the activity coefficient rapidly increases and attains a maximum value,  $\gamma_{Ti} = 1.016$ , at about 7 at.-% chromium. In the interval from 7 to 9 at.-% chromium the activity coefficient decreases below unity. In the titanium-iron system the activity coefficient of titanium in the  $\beta$  phase increases above unity at the smallest

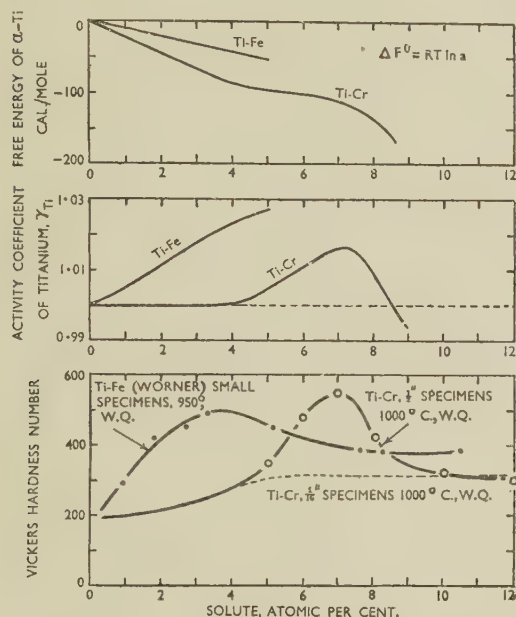


FIG. A.—Free Energy and Activity Coefficient of Titanium and Hardness of Water-Quenched Specimens as a Function of the Solute Content in Titanium-Chromium and Titanium-Iron Alloys.

additions of iron. The value of the activity coefficient of titanium in the  $\beta$  phase can be taken as an approximate measure of the tendency to  $\alpha$  precipitation. Alloys having a low activity coefficient are more likely to retain  $\beta$  on quenching from high temperatures than alloys with  $\gamma_{Ti} > 1$ . In the titanium-chromium system one would expect the tendency to precipitate  $\alpha$  to be higher in the range from 4.5 to 8 at.-% chromium than at chromium contents lower than 4.5 at.-% or higher than 8 at.-%. (Actually  $\beta$  transforms to martensite at low chromium contents, but this reaction, being a diffusionless one, involves only a minor displacement of atoms in the lattice, and not the formation of two new phases by a long-distance diffusion process.)

It was observed that the martensitic phase in those cases where its formation was not accompanied or followed by the nucleation and growth of  $\alpha$  particles, had a low hardness comparable to that of retained  $\beta$ . The formation of a fine precipitate of  $\alpha$  in the  $\beta$  matrix or in the martensitic structure becomes evident through a considerable increase of hardness, although in many cases  $\alpha$  cannot be detected metallographically.

The above conclusion, that alloys having  $\gamma_{Ti} > 1$  should exhibit a greater tendency to nucleate  $\alpha$ , is corroborated by experimental data.

The lower section of Fig. A shows that  $\frac{1}{2}$ -in. square rods of titanium-chromium alloys, when quenched from 1000° C. in water, have an increased hardness in the range between 5 and 9 at.-% chromium, with a maximum at about 7 at.-%, which corresponds to the maximum on the curve of the activity coefficient for this system.\* The hardness measurements by Worner† on thin specimens of titanium-iron alloys quenched in water from 950° C. show that the tendency for the nucleation of  $\alpha$  becomes evident in thinner sections and at a much lower content of alloying element than in titanium-chromium alloys. This fact also conforms with the course of the activity coefficient of titanium in titanium-iron alloys.

The conclusions arrived at above are difficult to reconcile with the assumption expressed by Mrs. McQuillan (p. 437) that "at lower temperatures the  $\beta$  phase (in the titanium-chromium system) is far from being an ideal solution". As was shown above, this can be true in the region above 4 at.-% chromium, but not at lower chromium contents. I am inclined to believe that the nucleation of  $\alpha$  phase in the specimen containing 2.4 at.-% chromium and held for a week just above the  $\beta/(\alpha + \beta)$  boundary could have been produced by extraneous causes rather than by an inherent change of the properties of the  $\beta$  phase itself. One such possible extraneous cause could have been the evaporation of titanium from the titanium-heater element on to the specimen and the resulting change in the composition of the surface layers of the specimen, displacing them into the  $(\alpha + \beta)$  field. Has the author considered this possibility?

Dr. P. H. MORTON,‡ B.A., M.S. (Member): When one considers the crystallographic mechanism whereby the clustering described in Mrs. McQuillan's very illuminating paper can take place, some interesting possibilities arise. These centre around the great similarity between the structures of  $\beta$  titanium and the compound  $TiCr_2$ , which has the  $C_{15}$  Laves-phase structure. The  $TiCr_2$  unit cell contains eight titanium atoms arranged on a diamond-type sub-lattice. Interpenetrating with these are sixteen chromium atoms, which are in groups of four, each atom located at the corner of a tetrahedron, the tetrahedra being joined corner to corner. If, however, each tetrahedron is replaced by a titanium atom situated at its centre, the result is a second diamond-type sub-lattice of eight titanium atoms, which combined with the first would produce sixteen titanium atoms arranged precisely as eight body-centred cubic unit cells. Furthermore, the distance between titanium atoms in  $TiCr_2$  is only 4% different from the interatomic spacing of  $\beta$ -titanium.

The compound  $TiCr_2$  is most stable at a composition richer in titanium than the stoichiometric value. Duwez and Taylor§ have suggested that this may be achieved by an excess titanium atom replacing, not an individual much smaller chromium atom, but rather a tetrahedron of four chromium atoms. The converse of this is equally likely, namely that under certain conditions, four chromium atoms in a  $\beta$  solid solution of titanium may arrange themselves in the form of a tetrahedron and replace a single titanium atom—a sort of cross between substitutional and interstitial solid solution. Clustering would then take place by the arrangement of chromium tetrahedra into the form of the compound  $TiCr_2$ , whose structure is dependent largely on considerations of geometrical packing rather than on interatomic forces. The chromium-rich  $TiCr_2$  cluster would, however, have no grain boundary, but would be continuous with the  $\beta$  lattice. This is not, then, a precipitation process, but rather an ordering reaction, in that a new structure is built up within the parent  $\beta$  phase, in the same orientation, and bearing a close relation to it. The precipitation both of pure  $\alpha$ -titanium and of the compound  $TiCr_2$  from the same 12% chromium alloy

Birmingham.

§ P. Duwez and J. L. Taylor, *Trans. Amer. Soc. Metals*, 1952, **44**, 495.

\* P. Herasymenko, data from unpublished work.

† H. W. Worner, *J. Inst. Metals*, 1951-52, **80**, 213.

‡ Imperial Chemical Industries, Ltd., Metals Division, U U

during rapid cooling is now more readily explained; not only has the diffusion required taken place during the prior solution-treatment, but the  $\text{TiCr}_2$  structure has already been formed also.

This mechanism provides a possible explanation why chromium with a size-factor of 13% should form a complete range of solution with  $\beta$ -titanium in spite of very low solubility in  $\alpha$ -titanium. The answer proposed is that the chromium atom is too small to dissolve substitutionally in  $\beta$ -titanium (at least above relatively low chromium contents) and dissolves instead in groups of four with an effective size-factor of only 8%. In  $\alpha$ -titanium, however, no such mechanism is possible and the solubility remains extremely low.

It is perhaps worth remark that apart from titanium the only other  $A$  components of  $AB_2$  Laves phases which have a body-centred cubic structure are zirconium, niobium, and tantalum. It is therefore not surprising that such a mechanism has not been postulated before. It is unfortunate that direct confirmation of these suggestions can be obtained only by means of a high-temperature X-ray or electron-diffraction camera operating *in vacuo*.

Dr. H. SUTTON,\* C.B.E., F.R.Ae.S., F.I.M. (Member of Council): Mrs. McQuillan has indicated the probability of the eutectoid temperature in the titanium-chromium system being much lower than has been suggested by earlier work. Her observations on the effects of soaking at different temperatures in the  $\beta$  field before cooling to normal temperature, are certainly illuminating.

As regards the effects of cooling from temperatures just above the  $\beta$ -phase-field boundary, is it not probable that the cooling velocity through a range of temperature not much below that of the boundary is very critical, and that when cooling starts not much above that range the cooling velocity through the range will tend to be much lower than when cooling is started from an appreciably higher temperature, when the operating conditions of cooling are similar in the two cases?

Quenching of alloys such as titanium-chromium, titanium-manganese, titanium-iron from the  $\beta$  field, and the behaviour on reheating to temperatures below the hitherto reported eutectoid temperature, suggests that precipitation-hardening by a dispersed phase occurs under appropriate conditions. Is it not possible that the  $\omega$  intermediate phase is playing an important part?

Mr. R. J. VAN THYNE† and Dr. W. ROSTOKER‡: We should like to offer some comment on the results and the logical deductions of Mrs. McQuillan's paper. Inasmuch as one of the titanium-chromium diagrams criticized by the author is based on work performed by one of us (R. J. V.), we can here elaborate in more detail on the analysis of the data than was permitted or thought necessary in the original paper.

It would appear to us that there is nothing in the author's description of her melting and heat-treatment methods that would indicate more stringent limitation of contamination by oxygen and nitrogen than in our own case. In our opinion the specimens we studied were no more contaminated than were Mrs. McQuillan's. No measurable hardness increase was found on remelting small control ingots of iodide titanium. The quality of starting materials is always a point of uncertainty, and in this instance the matter cannot easily be resolved. It is obvious from the form of the titanium-oxygen and titanium-nitrogen phase diagrams that minor amounts of these elements can have a considerable influence on the disposition of the  $\beta/(\alpha + \beta)$  boundary. It would not be incredible, therefore, that with a fortuitously low total interstitial content the  $\beta/(\alpha + \beta)$  boundary could be depressed to somewhere approaching the curve of the author's Fig. 1

(p. 435) up to about 6% chromium. The constitution shown for chromium contents greater than 6%, however, could not reasonably be accommodated by such a rationalization.

The author makes a vigorous case for effectiveness of quenching as a basic requisite for accurate estimation of  $\alpha$  produced during prior annealing. We hold that the efficiency of quenching is a relatively minor consideration. The reasons are quite simple:  $\alpha$  nucleated and grown from a  $\beta$  matrix generally appears as long, thin platelets arrayed in the familiar Widmanstätten configuration; with continued annealing at the transformation temperature, the platelets coarsen progressively. A typical sequence of microstructures is presented in Figs. B-D (Plate XCIX). Accordingly, we submit that it is possible to distinguish metallographically between  $\alpha$  formed isothermally and that which forms anisothermally.

Mrs. McQuillan states that none of the previous workers obtained direct evidence for the existence of the eutectoid. We would call attention to the eutectoid structure illustrated in Fig. 3 of the paper by Van Thynne, Kessler, and Hansen.† This was developed by annealing at 675° C. for 360 hr. The same paper (Fig. 9) shows a eutectoid structure in a titanium-iron alloy. We are of the opinion that these structures are characteristic of eutectoid configurations. The fact that these eutectoid colonies occur only at grain boundaries is indicative only that the transformations are far from complete. We would not accept an interpretation that the eutectoid colonies formed on cooling, since the structure is too coarse.

We find the discussion of the so-called non-equilibrium precipitation of  $\alpha$  and  $\text{TiCr}_2$  extremely vague. The reader cannot evaluate the author's reasons for deciding whether a particular ( $\alpha + \text{TiCr}_2$ ) configuration is eutectoid or not. Actually, the co-precipitation of  $\alpha$  and  $\text{TiCr}_2$  by a condition of double supersaturation could be expected in alloys in the region of the eutectoid composition. It is mandatory, however, that a double supersaturation condition can exist only below the eutectoid temperature. Upper bainite in steel provides a perfectly good example of a coincident formation of two new phases in a non-lamellar, but equilibrium, configuration. Sheehan, Julien, and Troiano§ cite examples of steels which show no pearlite under any condition of isothermal transformation. If the author chooses to place the eutectoid temperature very much below 548° C., then the precipitates in Figs. 3 and 5 of her paper (Plate LXVIII) must have been rejected below that temperature. Our experience with isothermal-transformation characteristics would lead us to believe that the microstructure in Fig. 5 is far too coarse to have been developed at such temperatures, especially as a result of cooling through the temperature range.

It seems more than surprising to us that if, for a 12 at.-% chromium alloy, 590° C. is within the  $\beta$  field, the subsequent reheating and rapid quenching did not yield an all- $\beta$  structure instead of the phase mixture apparent in Fig. 6 (Plate LXVIII). In fact, there could be even more transformation products in the rapidly quenched specimen than in the slowly cooled specimen.

Mrs. McQuillan's interpretation of her results has necessitated the conception of a rather involved theory. One cannot help getting the impression that the theory is quite empirical. The argument regarding the time-dependency of the occurrence of nucleated  $\alpha$  in a 2.4 at.-% chromium alloy need not be applicable to the proposed theory. The results can easily be understood in terms of the normal shape of  $TTT$  curves. At temperatures just below the  $\beta/(\alpha + \beta)$  transus, it is to be expected that  $\alpha$  nucleation will be slower than at larger degrees of undercooling. We have encountered instances where, metallographically and resistometrically, apparent nucleation of  $\alpha$  at only a few degrees of undercooling requires more than an hour.

If the author is seriously concerned with invalidating the

\* Director of Materials, Research and Development (Air), Ministry of Supply.

† Armour Research Foundation, Chicago, Ill., U.S.A.

‡ R. J. Van Thynne, H. D. Kessler, and M. Hansen, *Trans. Amer. Soc. Metals*, 1952, **44**, 974.

§ J. P. Sheehan, C. A. Julien, and A. R. Troiano, *ibid.*, 1949, **41**, 1165.



disposition of  $\beta/(\alpha + \beta)$  boundaries, might we suggest that a more direct and unambiguous experimental technique be used, such as plotting electrical resistivity or linear expansion against temperature on a careful stepwise cooling cycle?

Dr. ALLEN, Mr. SCHOFIELD, and Mrs. MELLISH (*in reply*): In reply to Mrs. McQuillan, the gas contents of the specimens were determined by vacuum fusion after heat-treatment at 1300° C. During heat-treatment a specimen of the alloy approximately  $1 \times \frac{3}{8} \times \frac{3}{8}$  in. was enclosed in a crucible fitted with a lid made from commercial titanium; loose titanium turnings were also placed round the specimen. Before analysis and cutting up into smaller sections for further heat-treatment, the specimen was ground on all faces.

In all, eighteen specimens were analysed for gas content. The nitrogen contents of specimens prepared from melts without addition of titanium dioxide but with different amounts of iron varied between 0.02 and 0.05 wt.-%. The nitrogen contents of specimens containing nominally 1 and 2 wt.-% oxygen were between 0.09 and 0.25 wt.-%. Similar increases in nitrogen content with oxygen content have also occurred in an investigation of the constitution of titanium-oxygen alloys. The hydrogen contents of all alloys varied between 0.004 and 0.009 wt.-%. As stated in the paper, when estimating the oxygen contents of titanium-oxygen alloys which were not analysed for gas content, a mean value was allowed of 0.15% for nitrogen plus hydrogen.

These results indicate that little if any nitrogen was introduced during heat-treatment at 1300° C., but that nitrogen appears to have been introduced during melting of those alloys made with additions of titanium dioxide. A complication arises in the accurate determination of nitrogen in titanium alloys, since the nitrogen contents obtained by vacuum fusion are generally much higher than those obtained by the chemical (Kjeldahl) method. The source of nitrogen in titanium alloys and its accurate determination are at present under investigation at the National Physical Laboratory, and it is hoped to publish the results of this work in due course.

Decomposition of  $\beta$  during quenching can affect only the position of the  $\beta/(\alpha + \beta)$  boundaries, and in the duplex ( $\alpha + \beta$ ) region the rate of decomposition of  $\beta$  is determined by the transformation rate of the  $\beta$  in equilibrium with the  $\alpha$ . This transformation rate is affected by the quenching temperature and the iron and oxygen contents. In Figs. E and F (Plate C) are shown the microstructure of two alloys whose compositions lie near the same tie-line and which have been quenched at the same temperature. The composition of the  $\beta$  constituent is therefore the same in both alloys at the moment of quenching. The quenching rate has clearly been sufficient to suppress decomposition of  $\beta$  in the alloy in Fig. E, and consequently also that in Fig. F. The  $\alpha$  constituent seen in Fig. F therefore represents the quantity of  $\alpha$  in equilibrium at the moment of quenching. Application of the lever principle then fixes the  $\beta/(\alpha + \beta)$  boundary near the position drawn, and this cannot be seriously in error, though more exact experiments might show that a little  $\alpha$  in some cases forms during the quenching operation.

Dr. KUBASCHEWSKI (*in reply*): There are two points in Dr. Herasymenko's contribution on which I would like to comment. Dr. Herasymenko has calculated in Fig. A the free energies and activity coefficients of titanium in the systems titanium-iron and titanium-chromium. In general, the conversion of phase boundaries into free energies does not yield any additional information, unless independent thermodynamic data are available which permit calculation of heats and entropies. In the particular case of titanium-

iron, however, Dr. Herasymenko's calculation reveals an appreciable deviation of the activity from Raoult's law. Since this law is generally obeyed in alloy systems at atom fractions approaching unity, one cannot help feeling suspicious about the position of the phase boundary used for the calculation. An experimental check seems to be advisable, and conclusions should not be drawn from the present free-energy data.

It is also not clear how conclusions with respect to the oxidation-resistance of titanium alloys could be arrived at from the activity coefficients. The change in oxidation rate depends primarily on the effect of the added metal on the number of vacancies in the titanium oxides. The activity coefficients play a part in that they affect the equilibrium fraction of titanium at the metal/oxide interface,\* but this effect should be negligible at the compositions under consideration.

Dr. A. D. MCQUILLAN (*in reply*): The fact that, by using conventional quenching methods, Dr. Worner has been able to obtain a value for the temperature of the  $\beta/(\alpha + \beta)$  boundary in a 3.7 at.-% nickel alloy which is in good agreement with my boundary, is extremely interesting. It is indeed difficult to see on thermodynamic grounds how the  $\beta/(\alpha + \beta)$  boundary in titanium-rich binary alloy systems which show little  $\alpha$ -phase solubility, can depart very markedly from the idealized boundary presented in an earlier paper of mine,† especially where the amount of addition element is small. The value of 678 cal./mole for the latent heat of the transformation in titanium‡ cannot be in error by more than  $\pm 70$  cal./mole, and it would be necessary to assume a value of at least 1350 cal./mole to explain the form of the boundary in dilute alloys of chromium in titanium as presented by Van Thyne, Kessler, and Hansen.§ and by Cuff, Grant, and Floe.|| Unless, therefore, the disagreement between the various positions reported for the  $\beta/(\alpha + \beta)$  boundaries in systems of titanium with transitional elements can be explained in terms of the effect of impurity elements or  $\alpha$ -phase precipitation during quenching, we are faced with a rather formidable thermodynamic problem.

Mrs. M. K. MCQUILLAN (*in reply*): The most general and valid criticism of my paper on the titanium-chromium system concerns the mechanism of the formation of large-scale precipitates from a  $\beta$  solid solution during quenching. In spite of the contrary opinions of one or two contributors to the discussion, I think that in view of the evidence produced by Dr. A. D. McQuillan's work on titanium-nickel alloys and mine on the titanium-chromium alloys it must be accepted that such precipitation does occur, and it remains to discover the means whereby it does so. Explanations based solely on very rapid long-range diffusion fail, because under isothermal conditions diffusion rates in the alloys in question appear to be rather slow, and also because the occurrence of precipitation and the nature of the precipitate depend on the temperature and duration of the isothermal heat-treatment preceding the quench. Some process must, therefore, be occurring in the solid solution, from which the non-equilibrium phases precipitate, during the heat-treatment, and there is no alternative but to postulate ordering or clustering. How the transition from the clustered solution to the massive precipitate takes place is not yet clear, but it is hoped that current experimental work will bring us closer to the solution, and it seems most likely at the present stage that it is a complex process in which the aggregation of like atoms plays an important part. Until more is known about the mechanism of precipitation I do not think it is possible to say whether or not it is to be expected, as proposed by Dr. Baker,

\* C. Wagner, *J. Electrochem. Soc.*, 1952, **99**, 369.

† A. D. McQuillan, *J. Inst. Metals*, 1951-52, **80**, 363.

‡ A. D. McQuillan, *Proc. Roy. Soc.*, 1950, [A], **204**, 309.

§ R. J. Van Thyne, H. D. Kessler, and M. Hansen, *Trans. Amer. Soc. Metals*, 1952, **44**, 974.

|| F. B. Cuff, N. J. Grant, and C. F. Floe, *Trans. Amer. Inst. Min. Met. Eng.*, 1952, **194**, 848.



that the visual appearance of the microstructure after quenching will be directly related to the nature of the clustering which has occurred before quenching. I agree with Dr. Allen that high-temperature X-ray work could throw considerable light on this problem, and look forward to the development of experimental techniques which will allow such work to be carried out on titanium alloys without the complications introduced by gas contamination. The other points raised by the various contributors to the discussion are concerned with various aspects of my work, and are perhaps most conveniently dealt with individually.

In drawing an analogy between the titanium-chromium and iron-nickel systems Dr. Allen appears to be assuming that the decomposition of the titanium-chromium  $\beta$  solid solution on quenching is a martensitic process in which one phase transforms to another by a shear mechanism. The 12 at.-% chromium alloy under discussion, however, does not transform directly from  $\beta$  containing 12 at.-% chromium to  $\alpha$  of the same composition; the  $\beta$  phase decomposes, forming two new phases of appreciably different compositions. Analogies with normal martensitic reactions appear, therefore, to be somewhat misleading. Dr. Allen's analogy again breaks down in that the phase boundaries with which we are concerned in the titanium-chromium system are the  $\beta/(\alpha + \beta)$  boundary and the eutectoid horizontal, and not, as in the iron-nickel system, the  $\alpha/(\alpha + \gamma)$  and  $\gamma/(\alpha + \gamma)$  boundaries. In view of these marked differences between the two cases, I do not fully understand Dr. Allen's point. He appears to say that if one quenched a  $\beta$  solid solution and reheated it in the  $(\alpha + \beta)$  field, the martensite formed on quenching would partly revert to  $\beta$  during the reheating process. This may be so, but it does not seem to be directly relevant to the case in question, in which the specimen was reheated at the same temperature as that from which it was quenched. I can see that if it is assumed that the precipitation of  $\alpha$  and  $\text{TiCr}_2$  from the  $\beta$  phase occurs martensitically, one could account for my observations by arguing that although 652° C. is below the eutectoid temperature in the titanium-chromium system, 1000 hours' heating at this temperature is insufficient to initiate the eutectoid decomposition of the  $\beta$  phase, and that in spite of the fact that both  $\alpha$  and  $\text{TiCr}_2$  are equilibrium phases at this temperature, their martensitic mode of formation causes them to redissolve on further heating at the same temperature. The essential implication in such an argument, however (i.e. that at 652° C. isothermal eutectoid decomposition has not started in 1000 hr.) destroys immediately any evidence ever put forward for the existence of the eutectoid horizontal at temperatures above 652° C., since in no other work on the titanium-chromium system have the heating times been as long as 1000 hr., and consequently no equilibrium  $\alpha + \text{TiCr}_2$  could ever have been observed.

I fully concur with Dr. Baker in emphasizing the importance of constant checks on experimental techniques, and as mentioned in the paper, hardness measurements on unalloyed iodide titanium were used to check oxygen contamination in the experimental work. The differences between my experimental results and those of other workers in the same field cannot be attributed to atmospheric contamination of my alloys, since, as Dr. Allen has pointed out, oxygen and nitrogen raise the phase boundaries in the titanium-rich region of titanium alloy systems rather than depress them. There would obviously be considerable advantages in a conventional tube furnace which permitted really rapid quenching, but I foresee experimental difficulties in the technique proposed by Dr. Baker, and fear that it may not be compatible with adequate protection of the specimens.

In order to answer the questions raised by Dr. Hardy, I am afraid that I must cover much the same ground as that already covered in the paper, where I pointed out that in my opinion the difference between my present results concerning the position of the eutectoid line and those obtained in all previous work on the titanium-rich region of the titanium-chromium system, including my own, is due to the fact that structures closely similar to those formed by isothermal eutectoid decomposition can appear during quenching,

and that such structures have hitherto been accepted as those which were present before quenching took place. Unless it is believed that the products of an isothermal eutectoid decomposition can redissolve in the matrix from which they were precipitated, on further heating at the temperature at which they were first formed, I consider it impossible to evade the conclusion that structures of the type shown in Figs. 3 and 5 (Plate LXVIII) of the paper can be formed during quenching, and that we cannot, therefore, regard any similar structures produced in these alloys by techniques akin to mine as being the result of isothermal decomposition during heat-treatment. Dr. Hardy points out that it is difficult to accept the fact that  $\text{TiCr}_2$  can be formed from a solution containing only 12 at.-% chromium in the short period of a fairly rapid quench. With this I fully agree, but not for the reasons put forward by Dr. Hardy, who has not taken into consideration the fact that one would expect all micrographic work on the isothermal transformation of  $\beta$ -phase titanium alloys to be as much affected by precipitates formed during cooling from the heat-treatment temperature as are the constitutional studies, and that evidence proving  $\text{TiCr}_2$  to be present in a structure after quenching cannot be accepted as evidence that it was there at temperature. As pointed out at the beginning of Section IV (p. 436) of the paper, the clustering hypothesis was put forward in order to account for the kind of difficulties mentioned by Dr. Hardy.

In expressing the view that no 12 at.-% chromium alloy has yet been annealed long enough to attain equilibrium at 650° C., I suspect that Dr. Hardy has shifted his ground a little. If in making this statement, he is accepting the fact that the eutectoid-like phases shown in Fig. 3 of the paper (considered by other workers to be evidence of heat-treatment below the eutectoid temperature) were formed during cooling, then he has no longer any reason for believing that the eutectoid temperature is above 650° C. If he does not accept this fact, how can he explain the observed effect of heating these structures for a further period at the same temperature in terms of an insufficiently prolonged initial heat-treatment? I must again draw attention to the fact that my original heat-treatment at 650° C. was of longer duration than any applied by other workers. Dr. Hardy's suggestion that the  $\omega$  phase may be playing a part in the decomposition of  $\beta$ -phase titanium-chromium alloys in the region of 10–15% chromium, once more appears to imply acceptance of the fact that the  $\alpha$  and  $\text{TiCr}_2$  seen in the microstructures after quenching are not there at temperature, and consequently does away with any need to suppose that the  $\beta$  phase should decompose at 650° C. in these alloys. I am rather surprised that Dr. Hardy should feel it necessary to plead for the use of X-rays in metallurgy at this stage of the development of the science, and although, as I have said already, I would welcome the possibility of using reliable high-temperature X-ray techniques in the study of titanium alloys, room-temperature X-ray work can be of little help in the present instance, since the point at issue is not what phases are present in our alloys (on which all workers are agreed) but how these phases were formed.

Dr. Herasymenko's thermodynamic consideration of the  $\beta/(\alpha + \beta)$  boundaries in the systems titanium-chromium and titanium-iron is very interesting, but I do not agree that the calculated values of the activity coefficients for the dilute titanium-chromium alloys necessarily mean that the solutions are ideal, since in very dilute solutions activity coefficients are usually close to unity. I can assure Dr. Herasymenko that the results which I obtained on titanium-chromium alloys were not affected by titanium deposited from the heaters, and I have no doubt that he will appreciate the point when he realizes that the  $\beta/(\alpha + \beta)$  boundary on which he bases his calculations is derived from experiments precisely similar to those which he is criticizing. If, therefore, the method is in doubt, his calculations are invalidated.

Dr. Morton has put forward an interesting idea which may well help to explain part of the unusual behaviour of the titanium-chromium system, and it is to be hoped that



experimental techniques capable of testing his hypothesis directly will soon become available.

Recent measurements of the quenching rate attainable in the apparatus used for the titanium-chromium work suggest that Dr. Sutton is right in saying that at the very beginning of the quench the cooling rate is a little slower than at slightly lower temperatures. I think, however, that such an effect alone could not account for the influence of heat-treatment temperature on the precipitation occurring during cooling, since, if the temperature is sufficiently high, widely different cooling rates will not produce precipitates of the kind discussed in the paper. Furthermore, the effect of the time for which the specimens are held at any given temperature within a critical range suggests strongly that precipitation is controlled by some process occurring during heat-treatment. In answer to Dr. Sutton's question concerning the  $\omega$  phase, I can only suggest that any speculation in this direction is hampered by the fact that it is not yet known with certainty whether or not the  $\omega$  phase is present at the heat-treatment temperature or is formed during cooling from it. So far, I believe, it has only been observed at room temperature. This is another point which high-temperature X-ray work should be able to resolve.

I am very glad to have a contribution to the discussion from Mr. Van Thyne and Dr. Rostoker, the former being associated with work discussed in my paper, and I note with interest that they consider it possible that oxygen and nitrogen impurities could account for the differences in our results up to 6 at.-% chromium. I do not fully understand, however, their point concerning the possibility of distinguishing micrographically between isothermal  $\alpha$  and  $\alpha$  formed during quenching. Figs. 1-5 (Plate VII) in the paper on the titanium-nickel system by Dr. A. D. McQuillan\* show clearly that the  $\alpha$  formed during quenching is just such as that described by Mr. Van Thyne and Dr. Rostoker as being isothermal  $\alpha$ . Their photomicrographs (Figs. B-D, Plate XCIX), which illustrate the development of an  $\alpha$  precipitate when a quenched  $\beta$  alloy is heated for successively longer periods in the  $(\alpha + \beta)$  region, scarcely help their argument. It is clearly to be expected that the equilibrium isothermal  $\alpha$  produced during the heat-treatment will coarsen with time. It is equally clear that the size of any non-equilibrium  $\alpha$  precipitated from the remaining  $\beta$  phase will be controlled by the distribution of the  $\alpha$ -phase material already present. Thus, when the equilibrium structure is coarse, large  $\beta$  regions exist between the  $\alpha$  plates, and large  $\alpha$  plates can be precipitated from these regions on cooling. The size of the  $\alpha$  plates, therefore, provides no means of distinguishing between the isothermal precipitate and that formed on quenching. I have not myself found any really reliable method of recognizing non-equilibrium precipitates in quenched titanium alloys other than ascertaining whether they disappear or change markedly after reheating and very rapid quenching, but I have observed that in specimens in which non-equilibrium  $\alpha$  may be present, some of the  $\alpha$  phase often appears to etch rather differently from the rest in spite of being of the same crystallographic orientation, and I have tended to associate the different appearances with the different methods of formation of equilibrium and non-equilibrium  $\alpha$ . Differences of the kind in question may be observed in the microstructures presented by Mr. Van Thyne and Dr. Rostoker (Figs. C and D). It may be of interest to compare these structures with that of the most closely similar of my rapidly quenched alloys, presented in Fig. G (Plate C). The alloy, which had a chromium content of 6.5 at.-%, and was heated for about a week at 693° C., should, according to the constitutional diagram proposed by Mr. Van Thyne and his fellow workers,† contain about 55% of the  $\alpha$  phase. An 8 at.-% chromium alloy heated at the same temperature for the same time and also rapidly quenched, showed only retained  $\beta$ , instead of the 35%  $\alpha$  expected from the diagram of Van Thyne *et al.*

Mr. Van Thyne and Dr. Rostoker claim that the microstructure of an 18% chromium alloy, heated for 360 hr. at 675° C., which shows a structure closely similar to that represented by my Fig. 3 (Plate LXVIII) is positive evidence of the occurrence of the eutectoid. I agree that the structures are eutectoid-like in appearance and result from the decomposition of the  $\beta$  phase, but since my work has shown conclusively that such structures are re-absorbed by the  $\beta$  phase on reheating to temperatures below 675° C., and are not, therefore, the products of isothermal eutectoid decomposition, they cannot be used as evidence for the position of the eutectoid line. It has been stated that it is impossible to evaluate my reasons for deciding whether a given  $\alpha + \text{TiCr}_2$  configuration is eutectoid or not. I must, therefore, say once more that there is no reason why a eutectoid structure produced isothermally in the course of a 1000-hr. heat-treatment should disappear or be radically altered by a few more hours of heat-treatment at the same temperature, and that if such a change occurs I consider that the structure originally observed cannot be that produced by the isothermal heat-treatment. As I have already pointed out in connection with Dr. Hardy's contribution to the discussion, the use of conclusions based on isothermal-transformation experiments in discussing the present results is illogical, since any micrographic results obtained from such experiments are open to precisely the same objections as the constitutional studies, and I think we may have to revise our opinions on the types of precipitate which may be formed at very low temperatures in titanium alloy systems. Large particles of titanium hydride, for instance, can be produced at about 100° C., and although it may be argued that hydrogen moves more easily through the titanium lattice than does a substitutional alloying element, appreciable movement of the titanium atoms must occur, nevertheless, in order to produce the face-centred cubic hydride structure. The need for large-scale long-range diffusion in the production of the observed precipitates in titanium-chromium alloys is obviated by the clustering mechanism I have proposed.

I cannot see why Mr. Van Thyne and Dr. Rostoker find the structure of my Fig. 6 (Plate LXVIII) so surprising, in view of the clear indication of the dissolution of the  $\alpha$  and  $\text{TiCr}_2$  phases on reheating given by Figs. 3 and 4 (Plate LXVIII). I consider that the structure of Fig. 6 is a reasonable result of a breakdown of the  $\beta$  phase during a quench more rapid than that which produced the structure of Fig. 5, yet insufficiently rapid to retain the  $\beta$  phase. It would, I think, be considerably more surprising if the structure of Fig. 5 could be converted to that of Fig. 6 merely by heating for an additional short period at the same temperature, without dissolution of the phases present in the structure of Fig. 5.

The explanation of the time dependency of the precipitation of  $\alpha$  during cooling on the basis of nucleation time, suggested by Mr. Van Thyne and Dr. Rostoker, assumes that the heat-treatments following which  $\alpha$  was precipitated were carried out in the  $(\alpha + \beta)$  region, although, according to my results, the temperatures concerned lay within the single-phase  $\beta$  field. Since the experiments on which my boundary is based involved heat-treatment times greatly in excess of those considered by Mr. Van Thyne and Dr. Rostoker to be necessary for nucleation, it is difficult to see why no  $\alpha$  formed in the alloys which they believe to be in the two-phase region.

In reading the last sentence of Mr. Van Thyne and Dr. Rostoker's contribution I could not help wondering what our classical metallographers would think on hearing straightforward microscopy described as an "indirect and ambiguous experimental technique" for the determination of phase boundaries in constitutional diagrams. The comment is even more surprising when one considers that the work of Mr. Van Thyne and his associates on the titanium-chromium

\* A. D. McQuillan, *J. Inst. Metals*, this vol. p. 47.

† R. J. Van Thyne, H. D. Kessler, and M. Hansen, *Trans. Amer. Soc. Metals*, 1952, **44**, 974.

system employed just such a technique. I feel that one could hardly do worse than choose electrical-resistivity methods as a means of studying phase changes in titanium alloys, since electrical resistivity is one of the most anomalous of all the properties of titanium, and marked discontinuities can appear in the resistivity/temperature curves of indisputably single-phase titanium alloys. Resistivity methods have already been tried in several constitutional investigations on titanium alloys, such as, for instance, that of Maykuth, Ogden, and Jaffee\* on the titanium-manganese system, but have not been found to yield useful results. Dilatometry as applied to titanium-base materials at high temperatures also presents a number of difficult problems,

both concerning the reliability of the experimental techniques and the interpretation of the results.

I would like to thank all those who have contributed to the discussion of my paper for their comments. In reviewing what has been said I find that no explanation of my observations has been put forward which does not invalidate all previous micrographic evidence for the existence of the eutectoid at 670°–685° C. and I feel, therefore, that although we do not yet completely understand the behaviour of the systems of titanium with the transition elements, my work has shown that there is something in that behaviour which requires understanding, and has, I hope, indicated the direction in which an explanation might be sought.

## Discussion

# Exploratory Creep Tests on Metals of High Melting Point

By N. P. ALLEN and W. E. CARRINGTON

(*Journal*, this vol., p. 525)

Dr. A. H. SULLY,† M.Sc., F.Inst.P., F.I.M. (Member): Dr. Allen and Mr. Carrington's paper is a nice example of the use of a simple technique to give roughly quantitative data of a survey nature as a guide to further work. The compressive creep test is simply conducted and specimens are easily prepared. We have used similar equipment to assess the creep-resistance of chromium alloys. On the whole we hold a better view of the accuracy of this type of test, perhaps because we take more precautions to eliminate at least some sources of error. For example, localized deformation at the ends of the test-piece can be minimized by using a specimen with shoulders at either end of larger diameter than the centre portion, and lapping the ends of the push-rods and the specimen to ensure good superficial contact.

Even with these precautions, however, certain differences between tensile and compression tests persist, the most striking difference being in the primary stage of creep. The initial creep deformation is always higher in the compression test for reasons which are not clear to us. Dr. Allen and Mr. Carrington cautiously state that the first 0.5% of strain occurred much faster in the compression creep test. In our experience, using a slightly different type of specimen, the difference occurs almost entirely in the primary stage. Steady-state creep rates and the time to onset of tertiary creep agree well between compression and tension tests provided that the total deformation is low. The last proviso is important. Where strains of the order of several per cent. are involved, as in the authors' Fig. 3 (p. 526), good agreement cannot be expected because of stress intensification in tension and stress reduction in compression due to the sectional change of the specimen.

I would caution very strongly against the use of the compression test to assess the creep properties of bodies such as metal-ceramic aggregates. In tests on bonded carbides we

have found no correlation at all between compression and tension tests. In compression, creep decreases continuously and finally stops, whereas in tension a more normal creep curve, leading to fracture, occurs. The reason lies in the dispersion of hard particles in a relatively soft matrix. In compression, interference between particles leads to a cessation of flow, whereas in tension creep can occur continuously in the matrix, leading to fracture.

The compression test is most suitable for purely metallic alloys of relatively small grain-size. Errors may arise if the grain-size becomes comparable with the gauge diameter. Perhaps the major advantage of the test is that for brittle or notch-sensitive materials it enables the intrinsic creep-resistance to be assessed without the complications arising from stress-raisers which may lead to premature fracture in a tensile creep test. To this extent the results may be misleading, but they are nevertheless extremely valuable when properly interpreted.

The AUTHORS (*in reply*): We are in agreement with Dr. Sully's view that caution is needed in assessing the properties of metal-ceramic bodies on the compression creep test alone. These tests give some idea of the order of strength to be expected, but should not be carried so far that interference between the hard particles is to be expected. The tests were necessarily of short duration, but they showed clearly that relatively weak metals and alloys were much stronger when acting as bonding materials for carbides.

The comparison between compression and tension tests on aluminium at 200° C. (Fig. 3) was extended to the micro-structure, and it was found that in both types of test the degree of polygonization of the grains could be correlated with the total creep strain of the test-piece.

\* D. J. Maykuth, H. R. Ogden, and R. I. Jaffee, *Trans. Amer. Inst. Min. Met. Eng.*, 1953, **197**, 225.

† Principal Physicist, Fulmer Research Institute, Stoke Poges, Bucks.



## Discussion

## Preferred Orientation \*

Dr. T. LL. RICHARDS,† B.Sc., F.I.M. (Member): The study of preferred orientation in metals is of considerable technical importance and, consequently, we have, at the Metals Division of I.C.I., paid a great deal of attention to it. The main reason for our interest is that preferred orientation is nearly always associated with anisotropy and therefore with directionality, which is very undesirable in strip required for the manufacture of pressings. Directionality, indeed, leads to reduced ductility and consequent likelihood of fracture and to unevenness in metal flow, resulting in pronounced earing of drawn products. It is therefore essential that, as manufacturers, we should know how to deal with this problem. Makers of transformer laminations, on the other hand, seek to develop preferred orientation, in order to take advantage of the high magnetic permeability in a certain crystallographic direction. Most non-ferrous metals and alloys are elastically anisotropic, and it may be that for certain applications there would be some advantage in developing preferred orientation in these metals also.

The production of wrought metal in the form of wire, tubes, or strip is essentially a matter of deformation and annealing, and we have therefore focused much of our attention on these processes and on the resulting deformation and annealing textures.

Study of the development of preferred orientation in deformed and annealed metal, however, can yield information not only of direct technical value but also of real significance in the effort to understand the basic principles underlying the properties and behaviour of metals.

These three papers are concerned with metals having very different structures, and in discussing them it would probably be most appropriate to deal with preferred orientation in a very general way and try to point out common characteristics.

The obvious common link between copper, titanium, and uranium is that they are all metals, and so, for the purpose of discussion, may be regarded as assemblies of large positive ions in a cloud of free electrons. Thus, whatever the metal structure and mode of deformation, it might be expected that the atoms would move relative to each other and the crystal lattice to take up orientations in which the atoms are, as it were, separated in the direction of maximum extension and brought together in directions of maximum contraction. Thus, in deformation of a face-centred cubic single crystal, one would expect to end up with the  $\langle 112 \rangle$  axis parallel to the tension axis and the  $\langle 110 \rangle$  axis parallel to the axis of compression, as is in fact observed. In rolling, which is usually regarded as a combination of tension and compression, one would by the same argument predict the primary rolling texture  $\{110\} \langle 112 \rangle$  for face-centred cubic metals.

A common feature of the rolling textures of a number of metals of different structure is now apparent. In the face-centred cubic primary texture  $\{110\} \langle 112 \rangle$ , the atomically close-packed  $\{111\}$  plane lies with a  $\langle 112 \rangle$  direction in the rolling direction. A similar atomic arrangement is found in the  $\{100\} \langle 110 \rangle$  texture of body-centred cubic iron, and also in those of hexagonal titanium and orthorhombic  $\alpha$ -uranium. All these textures have considerable spread, mainly about the rolling direction, and clearly factors other than simple atomic re-arrangement determine whether the atomically close-packed plane lies perpendicular to the strip surface, as for the face-centred and body-centred cubic textures, or is inclined, as for the titanium and uranium textures. From considerations of atomic packing one would expect the close-packed layers to lie normal to the strip, as for the face-

centred and body-centred cubic textures, provided that there are other shear planes in orientations which allow plastic deformation to occur. For both the hexagonal and the  $\alpha$ -uranium layer-like structures, the close-packed layers have a tendency to lie parallel to the strip surface, but settle in symmetry positions at which deformation by compression can still take place on the layers.

Considerations of atomic arrangement, symmetry, and availability of shear systems can account for the  $\langle 111 \rangle$  and  $\langle 100 \rangle$  textures of drawn copper observed by Professor Bastien and Dr. Pokorny. This is so obvious that I do not propose to elaborate further, although Mr. Yeomans in his contribution explains why the  $\langle 111 \rangle$  texture is ultimately predominant.

In the principal theories of textures, Professor Mathewson and Dr. Pickus have adopted symmetry of slip systems as the main criterion. Sir Geoffrey Taylor, and later Dr. Calnan and Dr. Clews, have developed treatments for dealing with the deformation of polycrystalline aggregates. All these theories presuppose that the shear elements are known, particularly those operative in the later stages of heavy deformation. As Dr. Roberts shows below, while ordinary slip occurs in the initial stages of rolling of copper and brass, a different form of shear is operative at later stages. It therefore seems more appropriate to use the Calnan and Clews theory in reverse, as Dr. Williams and Professor Eppelsheimer have suggested in their paper.

In concluding, I would emphasize that I prefer a general unified theory which derives the possible shear modes and ultimate texture purely from a knowledge of the crystal structure, and our ideas along these lines are developing.

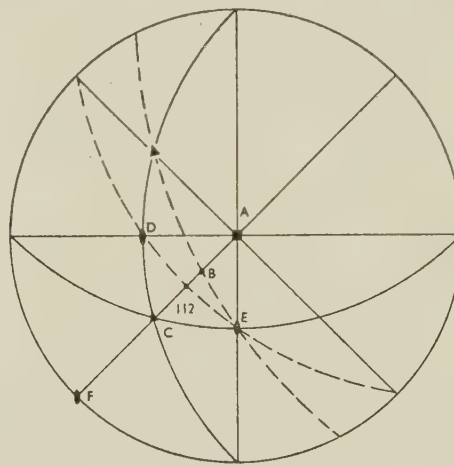


FIG. A.

Mr. D. E. YEOMANS,† B.Sc., A.I.M. (Member): I hope to throw some light on the development of  $\langle 111 \rangle$  texture with heavy deformations in the wire drawing of face-centred cubic metals. In so doing, I shall introduce and make use of an unconventional deformation mechanism, and this really is the main feature of my contribution.

By way of introduction, I should mention that the  $\langle 111 \rangle$  texture appears when deformation takes place in pure tension, as well as in wire drawing. Thus, when polycrystalline copper extended, the preferred orientation is predominantly

\* Joint discussion on the papers by D. N. Williams and D. S. Eppelsheimer (*J. Inst. Metals*, 1952-53, **81**, 553); P. G. Bastien and J. Pokorny (this vol., p. 545); and J. Adam and

J. Stephenson (this vol., p. 561).

† Technical Officer, Research Department, Imperial Chemical Industries, Ltd., Metals Division, Birmingham.

$\langle 100 \rangle$  in the early stages of deformation, but there is a progressive increase in the amount of  $\langle 111 \rangle$  texture until, at the end of uniform elongation, the proportions of the two types are approximately equal. The question is: Why is the  $\langle 111 \rangle$  texture developed when, by simple slip theory, we should expect  $\langle 112 \rangle$ . The idea now proposed is that, after some degree of deformation during which conventional slip mechanisms have been operative, another slip or shear mechanism becomes operative, namely, slip on  $\{100\}$  planes in  $\langle 110 \rangle$  directions. Thus, referring to Fig. A, a tension axis within the unit triangle  $ACD$  would rotate towards the slip direction  $E$  until side  $AC$  was reached. Duplex slip on  $\{111\}$  planes in  $\langle 110 \rangle$  directions would then take the tension axis towards  $\langle 112 \rangle$ . However, if shear on  $\{100\}$  plane  $A$  in the  $\langle 110 \rangle$  direction  $F$  occurs, the tension axis will rotate towards  $F$  until stability is reached at  $C$ , when the  $\langle 111 \rangle$  texture is developed.

It can easily be calculated that between  $A$  and  $B$  the resolved shear stress for conventional slip on  $\{111\}$  planes is greater than that for slip on  $\{100\}$  planes, but between  $B$  and  $C$  the reverse is true and, on this basis alone, there is a possibility that  $\langle 110 \rangle \{100\}$  shear will occur.

Dr. W. T. ROBERTS,\* M.Sc. (Junior Member): Theories of rolling textures based on the assumption that deformation occurs only by the usual crystallographic slip or twinning modes are generally regarded as adequate to explain the observed preferred orientation. These shear modes have been determined in large crystals which have not undergone very severe deformation, but there is evidence that, after heavy reductions, other shear mechanisms are operative. As experimental texture determinations are usually made on material which has been very heavily rolled, it is important that some consideration should be given to these mechanisms. On this basis, it is possible to offer an explanation for the difference between the rolling textures developed in copper and 70:30 brass, other than those already suggested by Professor Cottrell, viz. slip overshoot and the effect of solutes on recrystallization temperature.

Photomicrographs of longitudinal sections of 70:30 brass rolled by different amounts up to 95% † show that up to 40% reduction markings typical of the normal slip process are predominant, and so it may be expected that, at this stage, the material will have a somewhat poorly developed  $\langle 110 \rangle \langle 112 \rangle$  texture, as predicted by consideration of slip alone. After heavier reductions, however, a more intense type of marking appears, and there is a noticeable difference between the markings on brass and copper. In brass, each crystal contains two sets of markings and, because these are two symmetrical systems, it is argued that the orientation remains essentially the same, so that after heavy reductions a sharper  $\{110\} \langle 112 \rangle$  texture is obtained. In copper, however, each crystal contains only one set of heavy markings (Fig. B, Plate CI). These are evidently not traces of the same type of plane as in brass, for otherwise two sets would be found; Mr. Yeomans has suggested that shear might occur on  $\{100\}$  planes, and this would be quite consistent with the observed traces. The spread which accompanies the rotation of  $\{100\}$  planes to an equilibrium position could account for the observed texture in copper.

Dr. E. G. STANFORD, M.Sc.‡: The theoretical work on the formation of textures takes into account the mechanism of slip only, and, as a means of verifying the results, X-ray measurements are made, involving the construction of pole figures. X-ray measurements of this type lack precision, and provide a poor means of checking the theory.

The question in my mind is whether theoretical work should

not take into consideration these other mechanisms which Dr. Richards has mentioned. Would such a study lead to an explanation of the fact that, when sheet is rolled by different procedures and then annealed, the recrystallization textures obtained on annealing vary with the rolling procedure, although the cold-rolled texture, as measured by X-ray diffraction, is the same in each case? I cannot believe that the cold-rolled texture is, in fact, exactly the same in each case, and it is my opinion that a lack of precision in the X-ray method is responsible for giving an erroneous impression. Is it therefore possible that similar erroneous impressions arise in theoretical work where the results of the theory cannot be checked with sufficient precision? It would be instructive to hear this point argued by Dr. Richards and his co-workers and those who tell us that texture formation takes place by slip alone.

Dr. K. W. ANDREWS,§ B.Sc., F.I.M. (Member): Some of the general principles which these papers underline apply to other metals, and in this connection I should like to refer to some work we have been doing on stainless steel containing 18% chromium and 8% nickel. This is a face-centred cubic alloy, and the rolling textures are similar to those obtained with other face-centred metals, although we have not so far carried out much detailed work on rolled material.

Wires of this stainless steel show textures similar to those reported by Professor Bastien and Dr. Pokorny for copper and some alloys of copper. It is interesting to find the  $\langle 111 \rangle$  and the  $\langle 100 \rangle$  texture both in the ferrous and in the non-ferrous material. It seems, however, that in stainless steel the  $\langle 111 \rangle$  texture more definitely predominates. We were dealing with smaller-diameter wire and in addition we found a considerably smaller proportion of crystals which could properly be described as "randomly oriented". The  $\langle 111 \rangle$  orientation, when once established, tends to persist through subsequent stages of drawing and annealing. It was not possible to find any evidence of a zonal texture as usually defined, but there was a greater spread of orientation in the outer layers of both annealed and drawn wires. No evidence was obtained for a  $\langle 112 \rangle$  texture.

Since annealed face-centred cubic metals show a twinned structure, it follows that if the bulk of a crystal is oriented with  $\langle 111 \rangle$  parallel to the wire axis, parts of the crystal having a twin relationship to the rest will not have the  $\langle 111 \rangle$  orientation if the twin plane is one of the  $\{111\}$  set which lies at an angle to the wire. Faint extra diffraction maxima would therefore be expected, and these have in fact been observed both for the annealed wires and for the same wires after further drawing. This is not quite the same thing as the so-called "twinned texture" of rolled sheet, but is perhaps analogous to some of the effects described by Dr. Richards || for annealed brass strip. The correct interpretation of diffraction patterns is facilitated by simple relationships between the indices of a plane in the twin fragment and the plane in the parent crystal to which it lies parallel.

The work of Dr. Adam and Mr. Stephenson leads them to describe the preferred orientation of uranium sheet rolled between 500° and 600° C. in terms of two sets of crystallites with (010) and (110) planes perpendicular to the rolling direction. Apparently these orientations are not quite the same as the orientation effects described by Seymour ¶ for uranium foil. The extent of the discrepancy is not very great and might arise from the differences in temperature and degree of reduction. I mention this work in view of Seymour's rather interesting suggestion that the textures could be explained by reference to the similarity between the orthorhombic  $\alpha$ -uranium structure and the close-packed hexagonal structure. The major component in the texture resembled that obtained with close-packed hexagonal metals with

\* Technical Officer, Research Department, Imperial Chemical Industries, Ltd., Metals Division, Birmingham.

† M. Cook and T. Ll. Richards, *J. Inst. Metals*, 1943, **69**, 351, Plate XXVI, Figs. 2-7.

‡ Aluminium Laboratories Limited, Banbury, Oxon.

§ Research and Development Department, The United Steel Companies, Ltd., Rotherham, Yorks.

|| T. Ll. Richards, "Progress in Metal Physics", Vol. I, p. 299. 1949: London (Butterworths Scientific Publications).

¶ W. Seymour, *Trans. Amer. Inst. Min. Met. Eng.*, 1954, **200**, 999 (in *J. Metals*, 1954, **6**, (9)).



$c/a < 1.633$  and the minor component corresponded to  $c/a > 1.633$ . Some of the slip planes and twin planes for  $\alpha$ -uranium had already been interpreted in terms of this structural relationship. This kind of approach is valuable, and it provides a further example of the way in which textures may be understood by considering similarities between different structures.

Dr. E. A. CALNAN\*: In connection with the paper by Professor Bastien and Dr. Pokorny, it is possible to explain the different drawing textures in copper and copper alloys on the basis of the "overshoot" observed in the slip behaviour of alloy single crystals.†

On the question of the different rolling textures of copper and  $\alpha$ -brass, a tentative explanation might be proposed on the basis of the movement of stacking faults on  $\{111\}$  planes. Growth faults, i.e. twin faults, or deformation faults, would in moving perpendicular to themselves produce orientation rotations of  $180^\circ$  and  $60^\circ$ , respectively, about the  $[111]$  plane normal. Owing to the three-fold symmetry about the  $[111]$ , these rotations produce identical preferred orientations. It may be shown that a  $(110)[\bar{1}\bar{1}2]$  texture rotated in turn about the two most favourable  $\{111\}$  poles reaches an orientation very close to the "irrational" texture observed in copper by Hu, Sperry, and Beck.‡ It might be suggested that in the alloys the solute atoms inhibit the fault movements, and hence the  $(110)[\bar{1}\bar{1}2]$  texture resulting from slip is the end-point.

Mr. G. E. G. TUCKER,§ B.Sc. (Junior Member): I should like to make a specific remark arising from the very interesting paper by Dr. Williams and Professor Eppelsheimer. In considering  $\{10\bar{1}1\} \langle 11\bar{2}0 \rangle$  slip, the authors state (p. 555 of their paper) that each  $\{10\bar{1}1\}$  plane has two slip directions, but in fact there is only one  $\langle 11\bar{2}0 \rangle$  direction in any  $\{10\bar{1}1\}$  plane.

It is obvious from these papers that a knowledge of critical shear stresses for slip and twinning on various systems would be of very great value. It is possible, of course, to make inspired guesses based on the experimental results, but this seems to be a very dangerous procedure, especially if the

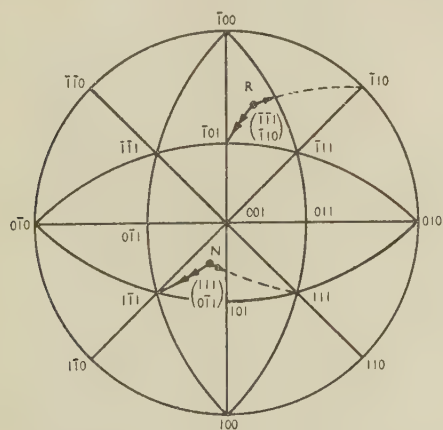


FIG. C.—Active Slip Systems in Rolling a Face-Centred Cubic Crystal of Orientation  $(215)[924]$ .

→ Uniaxial stress rotations.  
 - - -> Triaxial stress rotations.

actual deformation modes are not well established. I am especially interested in the results obtained by Dr. Adam and Mr. Stephenson for  $\alpha$ -uranium, because in this case the

principal type of slip, according to Cahn,|| i.e.  $(010)[100]$ , is not on the most closely packed plane, and the experimental results for compression suggest that not much slip has taken place. If, however, the slip system were  $(001)[100]$ , which is the "natural" system (i.e. closest-packed plane, closest-packed direction), then the compression results could be adequately explained.

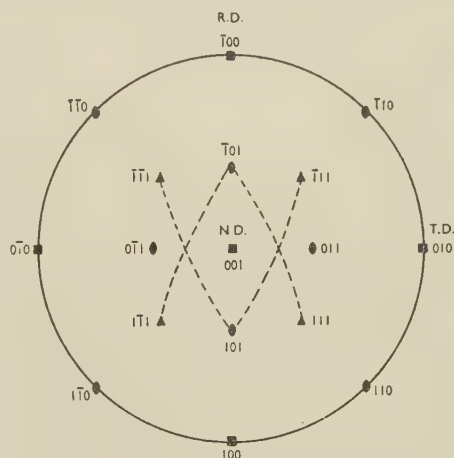


FIG. D.—Active Slip Systems in Rolling a Face-Centred Cubic Crystal of Orientation  $(001)[100]$ .

A factor often ignored in explaining rolling textures is that the actual deformation modes operating during rolling are not necessarily the same as those during uniaxial tension and compression. For this reason a texture which simultaneously satisfies the tension and compression results, will not necessarily be the correct rolling texture (although it often is so) and such a texture is not necessarily reached by a combination of the uniaxial crystal rotations. In Fig. C a hypothetical case for a face-centred cubic metal is plotted. The points  $N$  and  $R$  represent the rolling plane and rolling direction, respectively, and the slip systems operative in the unit triangles containing these points are marked. The system which has the maximum resolved shear stress is, however, neither of these when the triaxial stress system:

$$\begin{aligned}\sigma_1 &= \sigma & (\text{normal to rolling plane}) \\ \sigma_2 &= -n\sigma & (\text{parallel to rolling direction}) \\ \sigma_3 &= \left(\frac{1-n}{2}\right)\sigma & (\text{parallel to transverse direction})\end{aligned}$$

is considered; instead it is  $(11\bar{1})[\bar{1}01]$ . Thus, the actual rotations of points  $N$  and  $R$  towards  $(11\bar{1})$  and  $[\bar{1}01]$  are completely different from the uniaxial stress rotations towards  $(111)$  and  $[\bar{1}10]$ .

Finally, I should like to say a few words about so-called stable orientations. It is very tempting to describe an orientation as stable when its operative slip systems are symmetrically disposed relative to the principal stress directions. It is not, however, usually realized that many such positions represent cases of unstable equilibrium. Fig. D illustrates again a theoretical case for a face-centred cubic metal, in which the rolling plane is  $(001)$  and the rolling direction  $[100]$ . The four symmetrically disposed, equally stressed, slip systems are shown by linking the plane and direction of each by a dotted arc. This orientation thus appears stable. However, the real test of stability is to determine whether orientations displaced a little from the ideal, such as must occur in practice by slightly unbalanced

\* Metallurgy Division, National Physical Laboratory, Teddington.

† E. A. Calnan, *Acta Met.*, 1954, 2, (6), 865.

‡ H. Hu, P. R. Sperry and P. A. Beck, *Trans. Amer. Inst. Min. Met. Eng.*, 1952, 194, 76.

§ Aluminium Laboratories Limited, Banbury, Oxon.

|| R. W. Cahn, *Acta Cryst.*, 1951, 4, 470.

slip, tend to rotate into, or away from, the ideal position. For each such displaced orientation the resolved shear stresses on the various slip systems must be recalculated and the rotation tendency due to the now active systems determined. In the particular case considered it is found that if the orientation is altered by rotation about the rolling direction, then the tendency is for this rotation to continue, rather than be reversed. Such rotations have been observed in polycrystalline super-purity aluminium sheet with a high proportion of the "cube texture", right from the beginning of deformation.

Dr. WILLIAMS and Professor EPPELSHEIMER (*in reply*): The discussion on preferred orientation has shown that there are still a large number of unsolved problems relating to the development of textures in deformed metals. In our opinion, many of these problems will be solved when Calnan and Clews' method of texture analysis is more extensively applied. We were gratified, therefore, to see Dr. Richards' comments on the potential value of this method.

The question raised regarding the number of slip directions in the  $\{10\bar{1}1\}$  slip system is chiefly one of nomenclature. There is only one active  $\langle 11\bar{2}0 \rangle$  slip direction in any  $\{10\bar{1}1\}$  slip plane. However, there are two potential slip directions, one  $180^\circ$  opposed to the other. For example, the  $\{10\bar{1}1\}$  plane might exhibit slip in either the  $[1\bar{2}10]$  or the  $[12\bar{1}0]$  direction. In most cases, once a stress is applied to the system, one of the directions is immediately favoured over the other. Both directions were necessarily considered in all resolved-shear-stress calculations, however, which led us to refer to the number of slip directions in a manner slightly more inclusive than that in common practice. We hope that Mr. Tucker, and all others who noticed this lapse from accepted terminology, were not unduly confused.

Dr. ADAM and Mr. STEPHENSON (*in reply*): There appears to be a certain amount of confusion regarding the indices of the closest-packed planes in  $\alpha$ -uranium. This arises from the fact that atoms in the structure do not lie at the lattice points. If it is desired to find a crystallographic plane containing the largest number of lattice points per unit area, the answer is clearly (010) (the spacing  $d_{020}$  being the largest), but the atoms associated with this plane form a surface which can be described as a corrugated sheet, the corrugations being parallel to the  $\langle 100 \rangle$  direction. If, however, we wish to find the most closely packed flat sheets of atoms, the answer is either the (021) or, a very close second, the (001) plane.

Since the distances between the atoms within each corrugated sheet are the shortest in the structure (thus suggesting the strongest bonding) it is justifiable to regard  $\alpha$ -uranium as a stack of corrugated sheets\* parallel to the (010) plane. The predominating slip system found by Cahn, viz. (010)  $\langle 100 \rangle$ , conforms therefore to the usual rules of the closest-packed plane and the closest-packed direction, and there is no need to regard the hypothetical slip on the (001) plane as a more "natural" system. This, we, hope answers Mr. Tucker's remark.

It is understandable, however, that one should speculate on the similarity between the  $\alpha$ -uranium structure and hexagonal close packing, and in the absence of evidence to the contrary, it may be supposed that uranium slips on the (001) plane as pointed out by Mr. Tucker and Dr. Andrews (reference to work by Seymour). The small discrepancies between Seymour's results and ours are mainly due to different rolling conditions. Seymour's results do not contradict ours although his interpretation is different. He says that his findings do not agree with the predictions of Calnan and Clews,† but in fact they agree quite well with the predicted texture for twinning alone or for twinning with some slip, and our interpretation of the preferred orientation at low tempera-

tures is that, owing to profuse twinning, the effect of slip is largely masked by twinning texture.

Recently published work by Winogradski‡ is of great interest. The asymmetries found in his patterns, obtained from foils rolled at room temperature, in our opinion support the interpretation of the texture on the basis of a twinning mechanism, because when looking at the Calnan and Clews pictures of predicted intensity maxima for twinning alone or for twinning with some slip, it appears that any pole round about (010) is likely to appear in the rolling direction and any pole around (102) or (101) is likely to appear in the compression direction, hence asymmetries varying from foil to foil or even from place to place in the same foil can be expected.

The explanation of the cold-rolled textures therefore does not call, in our opinion, for assuming a slip on the (001) plane; it is admitted, however, that such a slip would also account for the observed preferred orientation.

This brings us to a remark of a general nature made by Dr. Richards, who says that he prefers the application of the Calnan and Clews procedure in reverse, i.e. to determine the modes of plastic deformation from observed preferred orientation. Although in some cases such an application is justified, as for example in the work of Dr. Williams and Professor Eppelsheimer, it seems to us that the generalization should not be made here, because more than one answer will probably be found.

We agree with Dr. Stanford's comment that the X-ray determinations of preferred orientation are not sufficiently precise to show minor components of textures with accuracy. In addition, the effects of sampling and accidental variations in rolling conditions can be eliminated only by examining large numbers of specimens, an extremely laborious and time-consuming process that can be justified only in very special cases.

Professor BASTIEN and Dr. POKORNY (*in reply*): Our knowledge of the mechanism of texture formation is based principally on the results of X-ray work, and although these give a reasonably clear picture of the distribution of the crystals in a deformed metal, the final state of distortion of the crystal lattice, which depends on a number of factors, is still not well understood.

The major deformation textures resulting from small amounts of cold work, can, in general, be adequately accounted for from considerations of the symmetry of the deforming stresses (a symmetry which differs, for example, in drawing from that in rolling, or in the case of the extension of a single crystal from that of a polycrystalline aggregate) and of the active slip planes. For heavy deformations, however, the state of distortion of the metal lattice assumes such importance that new theories have to be introduced. These distortions depend, for example, on the exact mode of deformation (its geometry, speed, and temperature) and on the amount of alloying additions present and the form in which they exist. They can be detected and studied in cold-worked metals during and after recrystallization, by X-ray methods—which show that nucleation and grain growth do not take place at random (see Figs. 5 and 6, Plate LXXXVII, of our paper) but determine the recrystallization textures—supplemented by microscopic examination; such combined studies, though difficult to carry out on cold-worked metal, may easily be done on recrystallized metal (examination of twins and corrosion figures).

It is therefore useful to study both recrystallization textures and deformation textures in order to explain the different orientations that are obtained, as Dr. Stanford points out, from identical deformation textures. The phenomena of nucleation and grain growth, although not yet completely understood, can thus assist in the working out of satisfactory general theories of the mechanism of the deformation of metals.

\* C. W. Tucker, *Trans. Amer. Soc. Metals*, 1950, **42**, 762.

† E. A. Calnan and C. J. B. Clews, *Phil. Mag.*, 1952, [vii],

43, 93.

‡ A. Winogradski, *Rev. Mét.*, 1954, **51**, 597.





## OBITUARY

COLONEL SIR PAUL GUETERBOCK

(*Past-President*)

Colonel Sir Paul Gueterbock, K.C.B., D.S.O., M.C., T.D., D.L., J.P., M.A., died at his home, George's Plot, Abbots Leigh, near Bristol, on 8 March 1954, at the age of 67. By his death, the Institute lost one of its greatest Past-Presidents.

Sir Paul was an outstanding leader, both in public service and in industry. Quiet, reserved, and competent in all he undertook, he had a most lovable personality and the gift of inspiring, encouraging, and getting the best out of his subordinates. Within the small circle of his friends, he was a delightful companion.

His research work and his great administrative gifts contributed in a large measure to the success and prosperity of the Company of tin and lead smelters of which he was Managing Director.

Paul Gottlieb Julius Gueterbock was born in 1886, and was educated at Rugby (Scholar) and Trinity College, Cambridge (Scholar), where he was a student of C. T. Heycock.

After graduating at Cambridge, he joined the firm of Capper Pass and Sons, Ltd., tin and lead smelters, in 1909, and from that time his technical interests were confined to the non-ferrous metals. From 1909 to 1914 he worked on the constitution of the antimony-tin-lead alloys and, on his return from military service in the First World War, he was again mainly engaged on research for the company. Although most of this later work was on methods of extraction, in 1925 he published, jointly with Nicklin, a paper on the effect of very small amounts of impurities in tin. He developed and invented new processes for the recovery and refining of tin, and published scientific papers on tin and tin alloys. When an electrolytic refinery for lead was needed quickly during the Second World War, he and his assistants produced a workable alkaline process so that the plant could be fabricated in mild steel.

Because of his outstanding administrative ability, however, he was required to take up positions of greater authority with the Company, until in 1924 he was made a Director, and in 1937 Managing Director, a position he held until his death. He was also Chairman of Victor G. Stevens, Ltd., Gateshead; Chairman of Geo. Pizey and Son, Ltd., London; a former Chairman of the British Non-Ferrous Smelters' Association; and a Member of Council of the British Non-Ferrous Metals Research Association for many years. In 1948 he was appointed Deputy Chairman of the South-west Regional Council of the Federation of British Industries.

From the time of his youth, Sir Paul set a very high example of devotion to the duties of citizenship and public work, and the great services that he rendered to the nation were recognized in the various honours that were bestowed on him.

He enlisted in the Cambridge University Rifle Volunteer

Corps in 1905 and was commissioned in the Corps in 1907. In 1908 he transferred to the Cambridge University Officers' Training Corps and in 1909 to the 4th Bn. The Gloucestershire Regiment. He served with distinction in this Battalion in France during the First World War, and was awarded the M.C. in 1916, in which year he was wounded on the Somme. He served as Assistant Staff Captain, 145 Infantry Brigade in 1916 and G.S.O. II, 48th Division in 1917. From June 1917 to March 1919 he was Brigade Major, 36 Infantry Brigade in the 12th Division, which was heavily engaged at Cambrai and in a long series of battles up to the time of the Armistice in 1918. He was three times mentioned in dispatches and was awarded the D.S.O. in 1919.

After the war, he was appointed Second in Command of the 4th Bn. The Gloucestershire Regiment, which he commanded from 1924 to 1929, when he was promoted Colonel on the General List of the Territorial Army. He served as a member of the Gloucestershire Territorial and Air Force Association from 1923 to 1936, Vice-Chairman from 1936 to 1938, and as Chairman of the Association from 1938 until 1952, when he relinquished the appointment owing to ill-health. He was County Army Welfare Officer for Gloucestershire from 1939 to 1949; Honorary Colonel of the 50th Royal Tank Regiment 1939 to 1946; Member of the Territorial Army Advisory Committee in 1947; and Honorary Colonel of the 44th/50th Royal Tank Regiment from 1947 until his death.

He was awarded the C.B. in 1943, was appointed an A.D.C. (additional) to the King in 1947, and was knighted (K.C.B.) in 1949. In 1946 he was appointed a Deputy Lieutenant for the County of Gloucestershire and he was a Justice of the Peace.

One of his recreations was rifle shooting. He captained the Rugby and Cambridge University teams and was Chairman of the Gloucestershire County Rifle Association from 1923 to 1934.

Sir Paul was elected a Member of the Institute of Metals in 1922. He served as a Member of Council from 1940 to 1943, as Vice-President from 1943 to 1946, and as President from 1946 to 1948. In recognition of his great services to the Institute, he was elected a Fellow in 1949. He was a Vice-President of the Institution of Mining and Metallurgy and a Fellow of the Institution of Metallurgists.

Sir Paul is survived by Lady Gueterbock, a son, a daughter, and two stepdaughters. In all his public and professional activities, he was fortunate in the happiness of his family life and the understanding and sympathy of Lady Gueterbock in his work. Lady Gueterbock attended the Institute's meetings frequently and will be remembered for the gracious way in which she supported her husband in his Presidential duties.

G.





The Late COLONEL SIR PAUL GUETERBOCK, K.C.B., D.S.O., M.C., T.D., D.L., J.P.,  
M.A., F.Inst.Met.  
(*Past-President*)





## NAME INDEX

- Adam, J., and J. Stephenson. Paper: "Preferred Orientation in Rolled Uranium Sheet", 561; reply to discussion, 656.
- Allen, N. P. Discussion on "Creep", 607; discussion on "Grain Refinement of Cast Copper-Base Alloys", 632; discussion on "The Constitution of Titanium Alloys", 644.
- and W. E. Carrington. Paper: "Exploratory Creep Tests on Metals of High Melting Point", 525; reply to discussion, 652.
- T. H. Schofield, and (Mrs.) B. Mellish. Paper: "The Constitution of the Titanium-Rich Alloys of Titanium, Iron, and Oxygen", 534; reply to discussion, 649.
- Andrews, K. W. Discussion on "Preferred Orientation", 654.
- Bacon, A. E. See Schofield, T. H.
- Baker, W. A. Discussion on "Continuous Casting", 618; discussion on "The Constitution of Titanium Alloys", 646.
- Bastien, Paul G., and J. Pokorny. Paper: "A Study of Preferred Orientation in Extruded, Drawn, and Annealed Copper", 545; reply to discussion, 656.
- Bates, L. F. May Lecture: "The Domain Structure of Ferromagnetic Metals", 417.
- Bear, (Miss) I. J. See Cahn, R. W.
- Bell, R. L. See Cahn, R. W.
- Beil, Winifred A. See Liddiard, E. A. G.
- Berghézan, A. Discussion on "Precipitation-Hardening", 611.
- Betteridge, W. Paper: "The Low-Stress Torsional Creep Properties of Pure Aluminium", 149; reply to discussion, 609.
- Blade, J. C., and J. W. Cuthbertson. Paper: "The Structure and Mechanical Properties of Copper-Manganese-Tin Alloys", 17.
- Bolton, E. A. Discussion on "The Control of Quality in Working Operations", 582, 594.
- Bond-Williams, N. I. Discussion on "The Control of Quality in Working Operations", 592.
- Brenner, P. Discussion on "Continuous Casting", 616; discussion on "The Control of Quality in Working Operations", 585.
- Cahn, R. W., (Miss) I. J. Bear, and R. L. Bell. Paper: "Some Observations on the Deformation of Zinc at High Temperatures", 481.
- Calnan, E. A. Discussion on "Preferred Orientation", 655.
- Carrington, W. E. Note: "Lamellæ in Chromium", 170; see also Allen, N. P.; Rendall, J. H.
- Cartwright, L. O. Discussion on "The Control of Quality in Working Operations", 587.
- Chadwick, R. Discussion on "An Investigation of Thickening and Metal Entrapment in a Light Alloy Melting Flux", 602; discussion on "Staining of Clad Aluminium Alloy Sheet During Salt-Bath Heat-Treatment", 641; discussion on "The Influence of Extrusion Direction on the Corrosion and Stress-Corrosion of Aluminium-Copper-Magnesium Alloys", 636; discussion on "The Properties of Aluminium-Magnesium-Silicon Alloys", 622.
- N. B. Muir, and H. B. Grainger. Paper: "The Effect of Iron, Manganese, and Chromium on the Properties in Sheet Form of Aluminium Alloys Containing 0.7% Magnesium and 1.0% Silicon", 75; reply to discussion, 629.
- Challis, H. J. G. See Williams, E. C.
- Champion, F. A. Discussion on "Staining of Clad Aluminium Alloy Sheet During Salt-Bath Heat-Treatment", 642; discussion on "The Control of Quality in Working Operations", 586; discussion on "The Influence of Extrusion Direction on the Corrosion and Stress-Corrosion of Aluminium-Copper-Magnesium Alloys", 636; discussion on "The Properties of Aluminium-Magnesium-Silicon Alloys", 622.
- Chang, Hsing C., and Nicholas J. Grant. Paper: "Mechanism of Creep Deformation in High-Purity Aluminium at High Temperatures", 229.
- Chaston, J. C. Discussion on "Grain Refinement of Cast Copper-Base Alloys", 632.
- Cibula, A. Paper: "Grain-Refining Additions for Cast Copper Alloys", 513; reply to discussion, 634.
- Cole, H. G., A. E. L. Tate, and B. Walters. Paper: "The Preparation and Properties of Magnesium Alloy Sheets of Controlled Impurity Content", 25.
- Collins, D. L. W. Discussion on "The Properties of Aluminium-Magnesium-Silicon Alloys", 623.
- Cook, Maurice. Autumn Lecture: "The New Metal Titanium", 93.
- and R. J. Parker. Paper: "The Computation of Loads in Metal Strip Rolling by Methods Involving the Use of Dimensional Analysis", 129.
- Cowan, A. See Parkins, R. N.
- Crowther, J. Discussion on: "The Properties of Aluminium-Magnesium-Silicon Alloys", 621.
- Cuthbertson, J. W. See Blade, J. C.
- Dench, W. A. See Kubaschewski, O.
- Dennison, J. P. Paper: "Some Creep Characteristics of a Group of Precipitation-Hardening Alloys Based on the Alpha-Copper-Aluminium Phase", 117.
- and E. V. Tull. Reply to discussion on "The Application of Grain-Refinement to Cast Copper-Aluminium Alloys Containing the Beta Phase", 633.
- Dorey, S. F. Presidential Address: "Metals and Marine Engineering", 497.
- Doyle, W. M. Discussion on "The Influence of Extrusion Direction on the Corrosion and Stress-Corrosion of Aluminium-Copper-Magnesium Alloys", 636.
- Eborall, R. Discussion on "Molybdenum and Molybdenum Alloys and the Arc Melting of Metals", 600.
- Eickhoff, K. Discussion on "Grain Refinement of Cast Copper-Base Alloys", 633.
- Elkington, R. W. Discussion on "The Control of Quality in Working Operations", 588.
- Elson, B. J. Discussion on "Continuous Casting", 616.
- Emley, E. F. Discussion on "An Investigation of Thickening and Metal Entrapment in a Light Alloy Melting Flux", 601.
- Entwistle, K. M. Paper: "Changes of Damping Capacity in Quench-Ageing Aluminium-Rich Alloys", 249; reply to discussion, 613.
- Eppelsheimer, D. S. See Williams, D. N.
- Evans, U. R. Discussion on "The Influence of Extrusion Direction on the Corrosion and Stress-Corrosion of Aluminium-Copper-Magnesium Alloys", 635.
- Farthing, T. W. Discussion on "The Control of Quality in Working Operations", 587.
- Feltham, P. Discussion on "Creep", 603; discussion on "Precipitation-Hardening", 613.
- Field, A. J. Discussion on "Staining of Clad Aluminium Alloy Sheet During Salt-Bath Heat-Treatment", 643; discussion on "The Control of Quality in Working Operations", 595.
- Ford, Hugh. Discussion on "The Control of Quality in Working Operations", 585, 595.
- Ford, Hugh, and J. G. Wistreich. Paper: "Problems of the Control of Dimension, Shape, and Finish in the Rolling of Sheet and Strip and in the Drawing of Wire", 281; reply to discussion, 584, 595.
- Forsyth, P. J. E. Paper: "Some Further Observations on the Fatigue Process in Pure Aluminium", 449.
- Freeth, W. E., and G. V. Raynor. Papers: "The Constitution of the System Silver-Lithium", 569; "The Systems Magnesium-Lithium and Magnesium-Lithium-Silver", 575.
- Frost, B. R. T. Paper: "The System Uranium-Mercury", 456.
- and J. T. Maskrey. Paper: "The System Uranium-Lead", 171.
- Gayler, M. L. V. Discussion on "Precipitation-Hardening", 610.
- Geach, G. A., and D. Summers-Smith. Paper: "The Constitution of Gold-Molybdenum Alloys, with Particular Reference to the Solubility of Molybdenum in Gold", 471.
- Gifkins, R. C. Discussion on "Creep", 605; paper: "Structural Studies of the Creep of Lead", 39; see also Kelly, J. W.
- Grainger, H. B. Discussion on "The Influence of Extrusion Direction on the Corrosion and Stress-Corrosion of Aluminium-Copper-Magnesium Alloys", 637; see also Chadwick, R.
- Grant, Nicholas J. See Chang, Hsing C.; Nordheim, Rolf.
- Greenfield, P. See Raynor, G. V.
- Greenough, A. P. Discussion on "The Behaviour of the Crystal Boundaries of Aluminium at Temperatures Near the Melting Point", 598.
- Greenwood, G. W., and A. G. Quarrell. Paper: "The Cleavage Fracture of Pure Polycrystalline Zinc in Tension", 551.
- Grogan, J. D., and R. J. Pleasance. Paper: "A Survey of the Uranium-Nickel System", with an Appendix (by Betty E. Williams): "An X-Ray Examination of Some Uranium-Nickel Alloys", 141.
- Hardy, H. K. Discussion on "The Constitution of Titanium Alloys", 646; paper: "Ageing Curves at 110°C. on Binary and Ternary Aluminium-Copper Alloys", 236; reply to discussion, 614; see also Silcock, (Miss) J. M.; Sully, A. H.
- Harris, I. R., and P. C. Varley. Paper: "Factors Influencing Brittleness in Aluminium-Magnesium-Silicon Alloys", 379; reply to discussion, 627, 631.
- Haynes, R. Paper: "Isothermal Transformations of Hypo-Eutectoid Aluminium Bronzes", 493.
- Heal, T. J. See Silcock, (Miss) J. M.; Sully, A. H.
- Heath, A. R. See Whitaker, Marjorie.
- Herasymentko, P. Discussion on "The Constitution of Titanium Alloys", 616.
- Herzig, A. J. Discussion on "Molybdenum and Molybdenum Alloys and the Arc Melting of Metals", 599.
- and Brinley Jones. Discussion on "Molybdenum and Molybdenum Alloys and the Arc Melting of Metals", 599.
- Hobbs, J. F. Discussion on "Continuous Casting", 617.
- Hopkin, G. L., (Mrs.) J. E. Jones, A. R. Moss, and D. O. Pickman. Paper: "The Arc Melting of Metals and Its Application to the Casting of Molybdenum", 361; reply to discussion, 600.
- Hopkin, L. M. T., and C. J. Thwaites. Paper: "The Effects of Some Constitutional Factors on the Creep and Fatigue Properties of Lead and Lead Alloys", 181; reply to discussion, 608.



- Hopkins, A. D. Paper: "The Copper-Silicon Eutectoid Transformation", 163.
- Hume-Rothery, W., and D. M. Poole. Paper: "Methods for Determining the Liquidus Points of Titanium-Rich Alloys", 490.
- Jenkins, A. E. Paper: "The Oxidation of Titanium at High Temperatures in an Atmosphere of Pure Oxygen", 213.
- Johnstone, S. T. M. See Rendall, J. H.
- Jones, Brinley. See Herzog, A. J.
- Jones, (Mrs.) J. E. See Hopkin, G. L.
- Jones, R. O., and E. A. Owen. Paper: "X-Ray Determination of the Alpha-Phase Boundary of the Copper-Indium System", 445.
- Kasz, F. Discussion on "The Control of Quality in Working Operations", 589.
- Kayser, J. F. Discussion on "The Control of Quality in Working Operations", 584.
- Kee, W. W. Paper: "The Control of Properties and Structure in the Hot and Cold Rolling of Copper and Copper-Base Alloys", 307; reply to discussion, 587.
- Kelly, J. W., and R. C. Giffkins. Paper: "Metallographic Observations on Cell Formation and Development in Aluminium", 475.
- King, F., and A. N. Turner. Paper: "The Control of Quality in the Hot and Cold Rolling of Aluminium and Aluminium Alloys", 291; reply to discussion, 586, 591, 597.
- Kohn, A. Discussion on "Continuous Casting", 617.
- Kubaschewski, O., and W. A. Dench. Paper: "The Free-Energy Diagram of the System Titanium-Oxygen", 87; reply to discussion, 649.
- Latin, A. Reply to discussion on "Some Observations on Creep and Fracture from Investigations on Lead Cable-Sheath Alloys", 608.
- Lewis, D. M. Paper: "Techniques for the Investigation of Thermal Conditions in Continuous Casting", 395; reply to discussion, 619.
- Liddiard, E. A. G. Discussion on "The Properties of Aluminium-Magnesium-Silicon Alloys", 624.
- and Winifred A. Bell. Paper: "The Influence of Extrusion Direction on the Corrosion and Stress-Corrosion of Aluminium-Copper-Magnesium Alloys", 426; reply to discussion, 639.
- Little, (Miss) K. Paper: "The Ternary Compound *E* in the System Aluminium-Chromium-Magnesium", 463.
- Lunn, B. Discussion on "Grain Refinement of Cast Copper-Base Alloys", 633; discussion on "The Control of Quality in Working Operations", 585.
- Lyons, J. V. See Pumphrey, W. I.
- Mack, David J. See Spencer, Chester W.
- McLean, D. Discussion on "Creep", 607.
- McQuillan, A. D. Paper: "The Re-Investigation of a Nickel-Titanium Alloy and Observations on  $\beta(\alpha + \beta)$  Boundaries in Titanium Systems", 47; reply to discussion, 649.
- McQuillan, (Mrs.) M. K. Discussion on "The Constitution of Titanium Alloys", 645; paper: "A Redetermination and Interpretation of the Titanium-Rich Region of the Titanium-Chromium System", 433; reply to discussion, 649; paper: "Note on the Constitution of the Titanium-Gold System in the Region 0-6 Atomic Per Cent. Gold", 511.
- Marsden, T. B. Discussion on "Creep", 604.
- Maskrey, J. T. See Frost, B. R. T.
- Massalski, T. B., and G. V. Raynor. Paper: "The Constitution of the Copper-Rich Copper-Zinc-Gallium Alloys", 539.
- May, R. Paper: "Some Observations on the Mechanism of Pitting Corrosion", 65.
- Mellish, (Mrs.) B. See Allen, N. P.
- Morton, P. H. Discussion on "The Constitution of Titanium Alloys", 647.
- Moss, A. R. Paper: "The Pressure Welding of Molybdenum", 374; see also Hopkin, G. L.
- Muir, N. B. See Chadwick, R.
- Murphy, A. J. Discussion on "The Control of Quality in Working Operations", 581.
- Nordheim, Rolf, and Nicholas J. Grant. Paper: "Resistivity Anomalies in the Nickel-Chromium System as Evidence of Ordering Reactions", 440.
- Northcott, L. Discussion on "Molybdenum and Molybdenum Alloys and the Arc Melting of Metals", 600.
- Nutting, J. Discussion on "Precipitation-Hardening", 610.
- Owen, E. A. See Jones, R. O.
- Parker, R. J. See Cook, Maurice.
- Parker, R. T. Discussion on "An Investigation of Thickening and Metal Entrapment in a Light Alloy Melting Flux", 602; discussion on "Grain Refinement of Cast Copper-Base Alloys", 632; discussion on "The Influence of Extrusion Direction on the Corrosion and Stress-Corrosion of Aluminium-Copper-Magnesium Alloys", 637.
- Parkins, R. N., and A. Cowan. Paper: "The Mechanism of Residual Stress Formation in Sand Castings", 1.
- Parr, J. Gordon. Note: "The Effect of Cold Work on an Iron-Manganese Alloy", 92.
- Paschke, V. Discussion on "Continuous Casting", 618.
- Pearson, W. K. J. Discussion on "The Control of Quality in Working Operations", 585.
- Phillips, H. W. L. Papers: "The Constitution of Alloys of Aluminium, Copper, and Iron", 197; reply to discussion, 568; "The Constitution of Aluminium-Copper-Silicon Alloys", 9.
- Phillips, V. A. Discussion on "Precipitation-Hardening", 612; discussion on "The Properties of Aluminium-Magnesium-Silicon Alloys", 625.
- Pickman, D. O. See Hopkin, G. L.
- Pleasant, R. J. See Grogan, J. D.
- Pokorny, J. See Bastien, Paul G.
- Poole, D. M. See Hume-Rothery, W.
- Preece, A. Discussion on "Grain Refinement of Cast Copper-Base Alloys", 633.
- Pumphrey, W. I., and J. V. Lyons. Paper: "The Behaviour of the Crystal Boundaries of Aluminium at Temperatures Near the Melting Point", 33; reply to discussion, 598.
- Putman, J. L. Paper: "The Use of Autoradiography for Finding the Solidification Boundary in Continuously Cast Aluminium", 395; reply to discussion, 621.
- Quarrell, A. G. See Greenwood, G. W.
- Rachinger, W. A. Note: "A Slide-Rule for the Interconversion of Atomic and Weight Percentages for Any Binary Alloy System", 38.
- Ransley, C. E. Discussion on "Continuous Casting", 618; discussion on "The Control of Quality in Working Operations", 588.
- Raynor, G. V. See Freeth, W. E.; Massalski, T. B.
- and P. Greenfield. Paper: "Constitution of the Copper-Rich Copper-Aluminium-Germanium Alloys", 59.
- Rendall, J. H., S. T. M. Johnstone, and W. E. Carrington. Paper: "The Forgeability, Creep Strength, and Ductility of Molybdenum and Some of Its Alloys", 345; reply to discussion, 600.
- Renouard, G. M., and M. Tournaire. Discussion on "The Properties of Aluminium-Magnesium-Silicon Alloys", 627.
- Richards, T. Ll. Discussion on "Preferred Orientation", 653.
- Roberts, H. T. Discussion on "Staining of Clad Aluminium Alloy Sheet During Salt-Bath Heat-Treatment", 643.
- Roberts, W. T. Discussion on "Preferred Orientation", 654.
- Rohner, F. Discussion on "Staining of Clad Aluminium Alloy Sheets During Salt-Bath Heat-Treatment", 641; discussion on "The Influence of Extrusion Direction on the Corrosion and Stress-Corrosion of Aluminium-Copper-Magnesium Alloys", 638.
- Rostoker, W. See Van Thyne, R. J.
- Ruddle, R. W. Discussion on "Continuous Casting", 615.
- Samuels, L. E. Discussion on "The Properties of Aluminium-Magnesium-Silicon Alloys", 631; paper: "The Metallographic Detection of Gamma Phase in Beta-Brass", 227.
- Saulnier, A. Discussion on "Precipitation-Hardening", 610.
- Scheuer, E. Discussion on "An Investigation of Thickening and Metal Entrapment in a Light Alloy Melting Flux", 601; discussion on "Continuous Casting", 617; discussion on "The Influence of Extrusion Direction on the Corrosion and Stress-Corrosion of Aluminium-Copper-Magnesium Alloys", 638.
- Schmid, E. Discussion on "Creep", 604.
- Schofield, T. H. See Allen, N. P.
- and A. E. Bacon. Paper: "The Melting Point of Titanium", 167.
- Sendorek, A. Discussion on "The Properties of Aluminium-Magnesium-Silicon Alloys", 626.
- Silcock, (Miss) J. M., T. J. Heal, and H. K. Hardy. Paper: "Structural Ageing Characteristics of Binary Aluminium-Copper Alloys", 239; reply to discussion, 614.
- Slater, I. G. Discussion on "The Control of Quality in Working Operations", 593.
- Smith, Christopher, and Norman Swindells. Paper: "Some Factors Affecting the Quality of Extrusions", 323; reply to discussion, 593, 594.
- Spencer, Chester W., and David J. Mack. Paper: "The Copper-Indium Eutectoid at 31.36 Weight Per Cent. Indium", 81.
- Sperry, P. R. Discussion on "The Constitution of Alloys of Aluminium, Copper, and Iron", 568.
- Stanford, E. G. Discussion on "Preferred Orientation", 654.
- Stephenson, J. See Adam, J.
- Sully, A. H. Discussion on "Exploratory Creep Tests on Metals of High Melting Point", 652.
- and H. K. Hardy. Paper: "Some Metallographic Observations of the Creep of Aluminium-Copper Alloys", 264.
- H. K. Hardy, and T. J. Heal. Paper: "An Investigation of Thickening and Metal Entrapment in a Light Alloy Melting Flux", 49; reply to discussion, 602.
- Summers-Smith, D. See Geach, G. A.
- Sutton, H. Discussion on "The Constitution of Titanium Alloys", 648; discussion on "The Influence of Extrusion Direction on the Corrosion and Stress-Corrosion of Aluminium-Copper-Magnesium Alloys", 638.
- Swindells, Norman. See Smith, Christopher.
- Tate, A. E. L. See Cole, H. G.
- Taylor, H. Discussion on "Staining of Clad Aluminium Alloy Sheet During Salt-Bath Heat-Treatment", 643.
- Thomas, W. J. Discussion on "The Control of Quality in Working Operations", 595, 597.
- Thompson, K. E. Discussion on "The Control of Quality in Working Operations", 588.
- Thwaites, C. J. Discussion on "Precipitation-Hardening", 613; reply to discussion on "The Effect of Minor Additions on the Age-Hardening of a High-Purity Lead-Antimony Alloy", 613; see also Hopkin, L. M. T.
- Tournaire, M. See Renouard, G. M.
- Tucker, G. E. G. Discussion on "Preferred Orientation", 655; discussion on "The Control of Quality in Working Operations", 596.
- Tull, E. V. See Dennison, J. P.
- Turner, A. N. Discussion on "The Properties of Aluminium-Magnesium-Silicon Alloys", 627; see also King, F.



- Van Thyne, R. J., and W. Rostoker.** Discussion on "The Constitution of Titanium Alloys", 648.
- Varley, P. C.** *See* Harris, I. R.
- Vosskuhler, H.** Discussion on "Grain Refinement of Cast Copper-Base Alloys", 633; discussion on "The Influence of Extrusion Direction on the Corrosion and Stress-Corrosion of Aluminium-Copper-Magnesium Alloys", 639.
- Waine, A. H.** Discussion on "The Control of Quality in Working Operations", 594.
- Walters, B.** *See* Cole, H. G.

- Whitaker, Marjorie.** Paper: "The Oxidation of Aluminium-Magnesium Alloys in Steam. A Contribution to Research on Mould Reaction", with an Appendix (by A. R. Heath): "The Constitution of Oxide Films Formed at High Temperature on Aluminium-Magnesium-Beryllium Alloys", 107.
- Whyte, M.** Paper: "Statistical Control in Metal-Working Operations", 335; reply to discussion, 597.
- Williams, Betty E.** *See* Grogan, J. D.
- Williams, D. N., and D. S. Eppelsheimer.** Reply to discussion on "A Theoretical Investigation of the Deformation Textures of Pure Titanium", 656.
- Williams, E. C., and H. J. G. Challis.** Paper: "Staining of Clad Aluminium

- Alloy Sheets During Salt-Bath Heat-Treatment", 465; reply to discussion, 644.
- de Winton, C. B. H.** Discussion on "The Control of Quality in Working Operations", 594.
- Wistreich, J. G.** Discussion on "The Control of Quality in Working Operations", 595; *see also* Ford, Hugh.
- Worner, H. W.** Discussion on "The Constitution of Titanium Alloys", 645; paper: "The Structure of Titanium-Silver Alloys in the Range 0-30 Atomic Per Cent. Silver", 222.
- Yeomans, D. E.** Discussion on "Preferred Orientation", 653.













UNIVERSITY OF ILLINOIS AT CHICAGO  
3 8198 316 018 520



